nature

INTERNATIONAL WEEKLY JOURNAL OF SCIENCE

Volume 319 No 6048 2 – 8 January 1986 £1.90

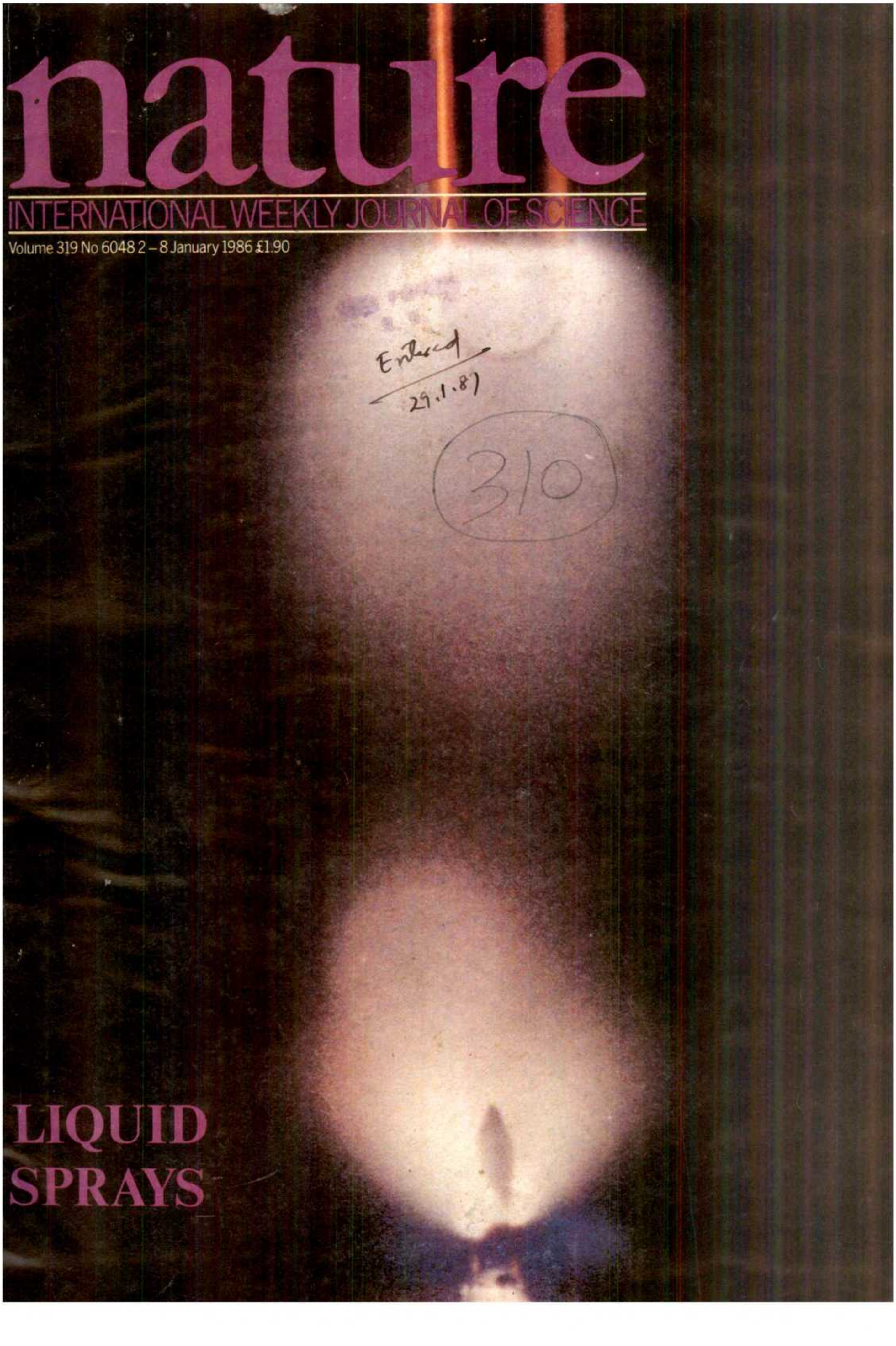

Entered
29.1.87

310

LIQUID
SPRAYS

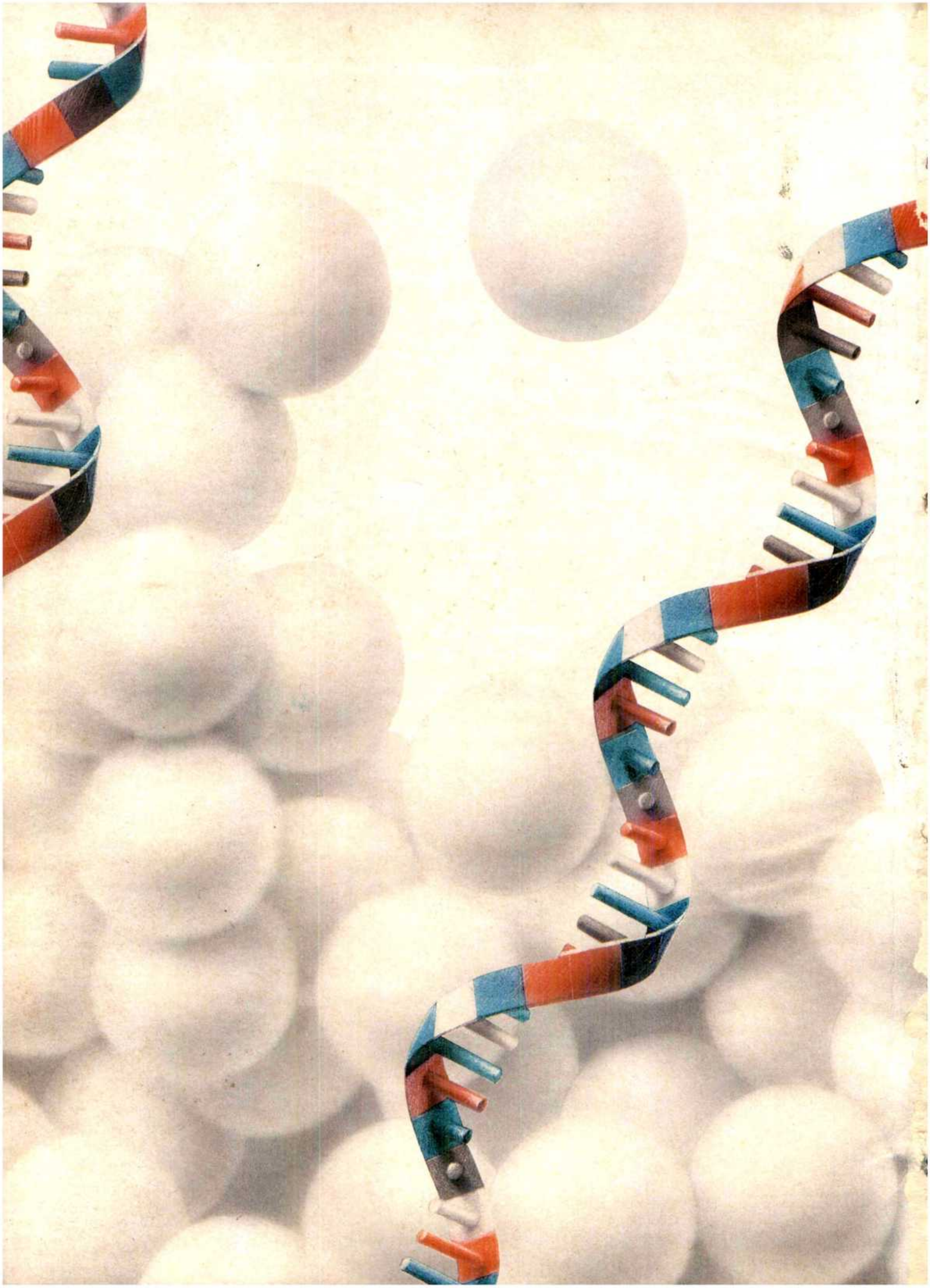

OUK - H06857 - 310 - RP 437.

nature

NATURE VOL. 319 2 JANUARY 1986

29.5.86

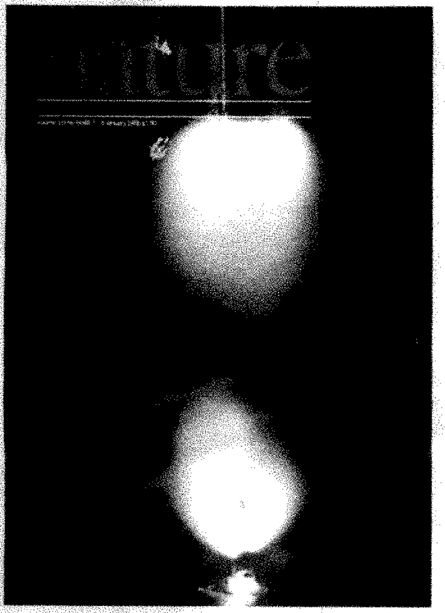

Glow discharge around an oil drop suspended under a high potential in a chamber filled with helium. When the helium is replaced with air, a stable jet issues from the drop due to electrohydrodynamic forces. See p.41.

OPINION

Who will regulate the bankers? 1
OPEC is not yet dead 2

NEWS

Japanese public health 3
Australian science
Remote sensing 4
French science
Japanese communications 5
Red greens on Yellow River?
Space science
Argentine science 6
Laboratory animals 7
Bhopal disaster

CORRESPONDENCE

AIDS hazard in brain/Earnshaw's theory/etc. 8

NEWS AND VIEWS

Further anxieties about AIDS 9
Approaches to AIDS therapy
David Klatzmann
& Luc Montagnier 10
Weather forecasting: Storm hunting with fractals
A Hollingsworth 11
Immunoglobulin genes: Inversion for gene construction
David Baltimore 12
Plate tectonics: Global thermal histories
Mike Bickle 13
Protein structure: Polar pocket with nonpolar lining
David J Cowley 14
Obituary: Glynn Isaac
Bernard Wood 15
The fate of the California condor
David S Wilcove
& Robert M May 16

SCIENTIFIC CORRESPONDENCE

Trialkyl lead in rain in the Black Forest
H Faulstich
& C Stournaras 17
An anniversary for the lipid bilayer
J A Kint
& J G Leroy 17
X chromosomes and dosage compensation
H S Chandra 18
The Grand Menhir re-examined
R L Merritt 18

310

BOOK REVIEWS

Evolution: Essays in Honour of John Maynard Smith
P J Greenwood, P H Harvey and M Slatkin, eds
Douglas J Futuyma 19
Einstein in America
by J Sayen
Joseph Haberer 20
Biology of Fertilization
C B Metz and A Monroy, eds
Jack Cohen
Seeds of Change: Five Plants that Transformed Mankind
by H Hobhouse
Janet Browne 21
Model Neural Networks and Behavior
A I Selverston, ed.
Adrian Horridge 22
Calcium in Biological Systems
R P Rubin, G B Weiss and J W Putney, eds
P F Baker

ARTICLES

Rim syncline volume estimation and salt diapirism
K Sørensen 23
Direct evidence for chromosomal inversion during T-cell receptor β-gene rearrangements
M Malissen, C McCoy, D Blanc, J Trucy, C Devaux, A–M Schmitt-Verhulst, F Fitch, L Hood & B Malissen 28
Molecular structure of an aspartic proteinase zymogen, porcine pepsinogen, at 1.8 Å resolution
M N G James
& A R Sielecki 33

LETTERS TO NATURE

A radio outburst and jet from the symbiotic star CH CyG
A R Taylor, E R Seaquist
& J A Mattei 38
Mechanism of stable jet formation in electrohydrodynamic atomization
I Hayati, A I Bailey
& Th F Tadros 41
Fractal characterization of inhomogeneous geophysical measuring networks
S Lovejoy, D Schertzer
& P Ladoy 43
Archaean magmatic sulphate
K Hattori & E M Cameron 45
Carbon isotope excursions in Precambrian/Cambrian boundary beds, Morocco
M E Tucker 48
Planktonic foraminiferal ontogeny and new perspectives for micropalaeontology
G-J A Brummer, C Hemleben
& M Spindler 50
Acoustic cavitation generated by microsecond pulses of ultrasound
L A Crum & J B Fowlkes 52
Potent ulcerogenic actions of platelet-activating factor on the stomach
A-C Rosam, J L Wallace
& B J R Whittle 54
1-Methyl-4-phenylpyridine is neurotoxic to the nigrostriatal dopamine pathway
A J Bradbury, B Costall, A M Domeney, P Jenner, M E Kelly, C D Marsden
& R J Naylor 56

Contents continued overleaf

Nature® (ISSN 0028-0836) is published weekly on Thursday, except the last week in December, by Macmillan Journals Ltd and includes the Annual Index (mailed in February). Annual subscription for USA and Canada US $240. USA and Canadian orders to: *Nature*, Subscription Dept, PO Box 1501, Neptune, NJ 07753, USA. Other orders to *Nature*, Brunel Road, Basingstoke, Hants RG21 2XS, UK. Second class postage paid at New York, NY 10012 and additional mailing offices. Authorization to photocopy material for internal or personal use, or internal or personal use of specific clients, is granted by *Nature* to libraries and others registered with the Copyright Clearance Center (CCC) Transactional Reporting Service, provided the base fee of $1.00 a copy plus $0.10 a page is paid directly to CCC, 21 Congress Street, Salem, Massachusetts 01970, USA. Identification code for *Nature*: 0028-0836/86 $1.00 + $0.10. US Postmaster send address changes to: *Nature*, 65 Bleecker Street, New York, NY 10012. Published in Japan by Macmillan Shuppan K.K., Eikow Building, 1-10-9 Hongo, Bunkyo-ku, Tokyo, Japan. © 1986 Macmillan Journals Ltd

MULTI-SAMPLE/LARGE VOLUME

200 VIAL SPEED VAC®
EVAPORATOR/CONCENTRATOR

FOR RESEARCH AND CLINICAL LAB

- Virtually 100% solids recovery
- No bumping or foaming losses
- Handles oversize containers
- Special microplate rotor

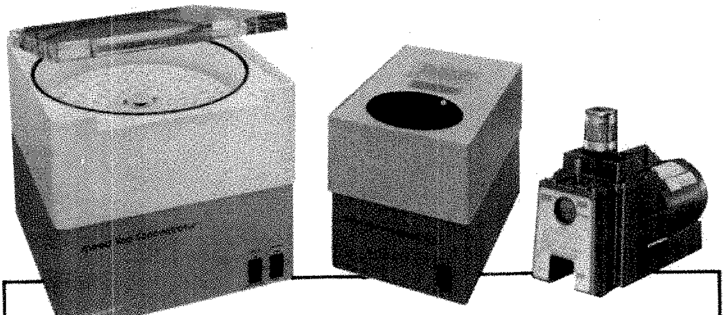

SVC200H Speed Vac® Concentrator for hormones, anti-depressants, acetaminophen, prostaglandins, antibodies, concentration and harvesting

Applies both vacuum and centrifugal force to hold solids while evaporating solvent. Proven over years of reliable service. Complete line of accessories includes vacuum, traps to −90°C, heating, switchover-to-vacuum pump system, and extensive rotor library including our special 8-Microplate Rotor. For complete details and ordering information, call or write:

Savant
INSTRUMENTS, INC.
110-103 Bi-County Blvd., Farmingdale, NY 11735 • (516) 249-4600

Reader Service No.1

RP437

·NEW FROM·
MACMILLAN PRESS
SCIENTIFIC & MEDICAL

THE MUSCLE SPINDLE

Edited by I A Boyd and M H Gladden

Muscle spindles are modified muscle fibres with both sensory and motor functions that have a key role in both dynamic and static muscle function. Research suggests that the muscle spindle is far more complex in terms of structure and function than was previously thought. This book, based on an international meeting attended by the world's foremost authorities, provides an up-to-date account of the main features of spindle structure and physiology in mammals.

☐ Edited proceedings of the first full international meeting on muscle spindle.
☐ Includes new research which shows this to be an area of great importance to neurophsysiologists.
☐ Edited by two acknowledged experts on the subject.
☐ Will be of interest to all neurophysiologists, pharmacologists and physiologists.

CONTENTS

The Contributors Preface PART 1: Morphology of Mammalian Muscle Spindles (Chapters 1–17) Review – I A Boyd and M H Gladden PART 2: Internal Working of Muscle Spindles (Chapters 18–35) Review – I A Boyd and U Proske PART 3: Static and Dynamic Fusimotor Neurones and their Reflex Control (Chapters 36–47) Review – M H Gladden and P R Murphy PART 4: Novel Experimental and Analytical Methods Used to Examine Behaviour of the Muscle Spindle (Chapters 48–57) Review – I A Boyd and J R Rosenberg

360pp 234 x 156 mm £40.00
ISBN 0 333 38446 6

Please order this title from your bookseller or from Judy Chappell, Marketing Assistant, Macmillan Press, Houndmills, Basingstoke, Hants RG21 2XS, UK.

MACMILLAN PRESS

NATURE'S 1986
CALENDAR!

12 cover photographs superbly reproduced in full colour. Send for your calendar now.

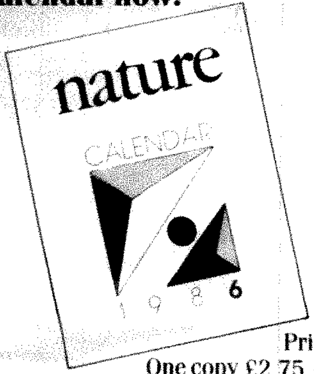

Prices:
One copy £2.75 (UK)
£3.75 (REST OF WORLD)
Three or more copies £2.50 (UK)
£3.20 (REST OF WORLD) each

Send orders to:
Circulation Manager, Macmillan Journals Ltd., FREEPOST (UK ONLY) Brunel Road, Houndmills, Basingstoke, Hants., RG21 2XS UK.

Annual Subscription Prices

UK & Irish Republic		£104
USA & Canada		US$240
Australia, NZ & S. Africa	Airspeed	£150
	Airmail	£190
Continental Europe	Airspeed	£125
India	Airspeed	£120
	Airmail	£190
Japan	Airspeed	Y90000
Rest of World	Surface	£120
	Airmail	£180

Orders (with remittance) to:

USA & Canada
Nature
Subscription Dept
PO Box 1501
Neptune
NJ 07753
USA

UK & Rest of World
Nature
Circulation Dept
Brunel Road
Basingstoke
Hants RG21 2XS, UK
Tel: 0256 29242

(The addresses of Nature's editorial offices are shown facing the first editorial page)

Japanese subscription enquiries to:
Japan Publications Trading Company Ltd
2-1 Sarugaku-cho 1-chome
Chiyoda-ku, Tokyo, Japan
Tel: (03) 292 3755

Personal subscription rates: These are available in some countries to subscribers paying by personal cheque or credit card. Details from:

USA & Canada
Nature
65 Bleecker Street
New York
NY 10012, USA
Tel: (212) 477-9600

UK & Europe
Felicity Parker
Nature
4 Little Essex Street
London WC2R 3LF, UK
Tel: 01-836 6633

Back issues: UK, £2.50; USA & Canada, US$6.00 (surface), US$9.00 (air); Rest of World, £3.00 (surface), £4.00 (air)

Binders
Single binders: UK, £5.25; USA & Canada $11.50; Rest of World, £7.75. Set of four: UK, £15.00; USA & Canada $32.00; Rest of World, £22.00

nnual indexes (1971-1985)
K, £5.00 each; Rest of World, $10.00

ure First Issue Facsimile
75p; Rest of World (surface), $1.50; (air) $2.00

re in microform
e to University Microfilms International, 300
h Zeeb Road, Ann Arbor, MI 48106, USA

A large anion-selective channel has seven conductance levels
M E Krouse, G T Schneider & P W Gage 58

Permanent distortion of positional systems of *Xenopus* embryo by brief early perturbation in gravity
J Cooke 60

Human T-cell clones recognize a major *M. leprae* protein antigen expressed in *E. coli*
A S Mustafa, H K Gill, A Nerland, W J Britton, V Mehra, B R Bloom, R A Young & T Godal 63

***Mycobacterium leprae*-specific protein antigens defined by cloned human helper T cells**
T H M Ottenhoff, P R Klatser, J Ivanyi, D G Elferink, M Y L de Wit & R R P de Vries 66

Identification of a secretory granule-binding protein as caldesmon
R D Burgoyne, T R Cheek & K-M Norman 68

Estimation of the polarity of the protein interior by optical spectroscopy
R B Macgregor & G Weber 70

Human N- *myc* is closely related in organization and nucleotide sequence to c- *myc*
N E Kohl, E Legouy, R A DePinho, P D Nisen, R K Smith, C E Gee & F W Alt 73

MATTERS ARISING

Mapping of general anaesthetic target sites
J R Elliott & D A Haydon
Reply: N P Franks & W R Lieb 77

MISCELLANY

100 years ago 13
Books received 79
New on the market 81
Employment: The brain drain is here again
R Pearson 84

NATURE CLASSIFIED

Professional appointments — Research posts — Studentships — Fellowships — Conferences — Courses — Seminars — Symposia:
Back Pages

Next week in *Nature*:

- Falklands rotation
- Global warming ahead
- Ages of sedimentary rocks
- Masses of Uranus's moons
- Gamma-burst from Crab pulsar
- Model for promoter gene
- PDGF from monocytes?
- Immunoglobulin gene transcription
- Synapsin I bundles microtubules
- Peripheral action of CRF
- Light quality and phytoplankta
- Bird cries wolf

GUIDE TO AUTHORS

Authors should be aware of the diversity of *Nature*'s readership and should strive to be as widely understood as possible.

Review articles should be accessible to the whole readership. Most are commissioned, but unsolicited reviews are welcome (in which case prior consultation with the office is desirable).

Scientific articles are research reports whose conclusions are of general interest or which represent substantial advances of understanding. The text should not exceed 3,000 words and six displayed items (figures plus tables). The article should include an italic heading of about 50 words.

Letters to *Nature* are ordinarily 1,000 words long with no more than four displayed items. The first paragraph (not exceeding 150 words) should say what the letter is about, why the study it reports was undertaken and what the conclusions are.

Matters arising are brief comments (up to 500 words) on articles and letters recently published in *Nature*. The originator of a Matters Arising contribution should initially send his manuscript to the author of the original paper and both parties should, wherever possible, agree on what is to be submitted.

Manuscripts may be submitted either to London or Washington). Manuscripts should be typed (double spacing) on one side of the paper only. Four copies are required, each accompanied by copies of lettered artwork. No title should exceed 80 characters in length. Reference lists, figure legends, etc, should be on seperate sheets, all of which should be numbered. Abbreviations, symbols, units, etc, should be identified on one copy of the manuscript at their first appearance.

References should appear sequentially indicated by superscripts, in the text and should be abbreviated according to the *World List of Scientific Periodicals*, fourth edition (Butterworth 1963-65). The first and last page numbers of each reference should be cited. Reference to books should clearly indicate the publisher and the date and place of publication. Unpublished articles should not be formally referred to unless accepted or submitted for publication, but may be mentioned in the text.

Each piece of artwork should be clearly marked with the author's name and the figure number. Original artwork should be unlettered. Suggestions for cover illustrations are welcome. Original artwork (and one copy of the manuscript) will be returned when manuscripts cannot be published.

Requests for permission to reproduce material from Nature *should be accompanied by a self-addressed (and, in the case of the United Kingdom and United States, stamped) envelope.*

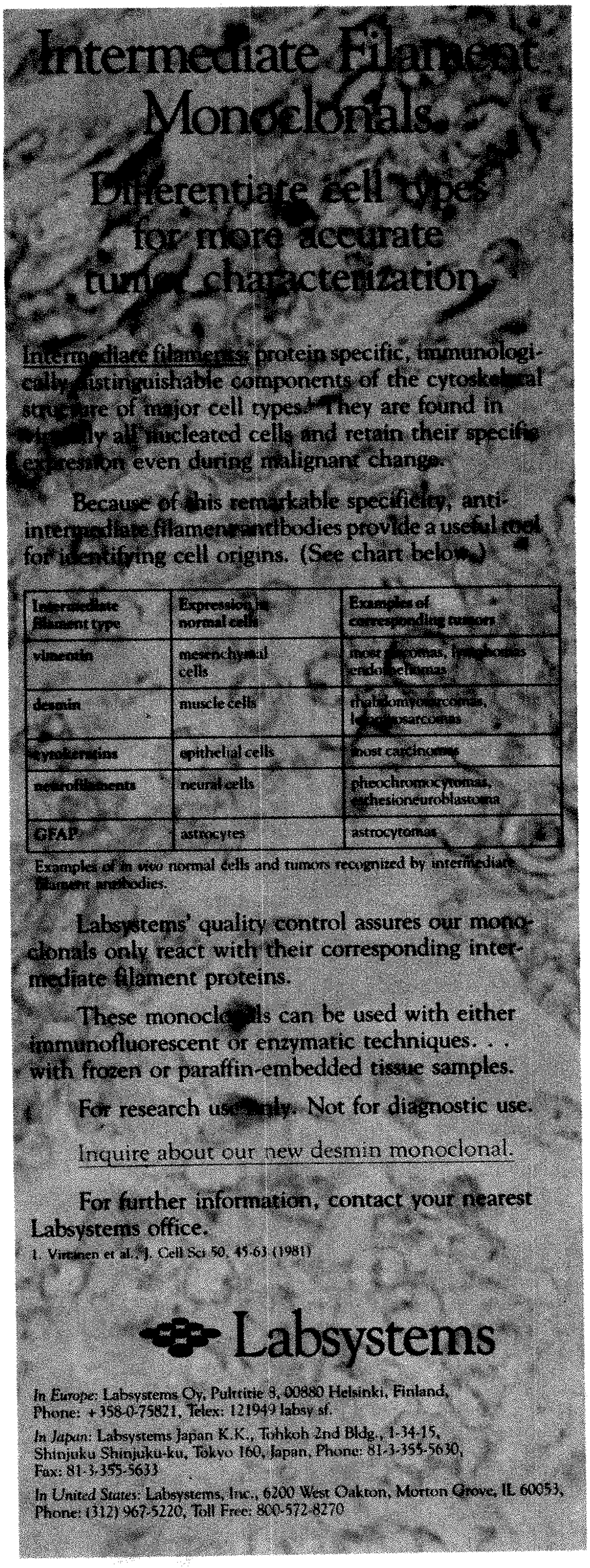

Intermediate Filament Monoclonals.

Differentiate cell types for more accurate tumor characterization.

Intermediate filaments: protein specific, immunologically distinguishable components of the cytoskeletal structure of major cell types.[1] They are found in virtually all nucleated cells and retain their specific expression even during malignant change.

Because of this remarkable specificity, anti-intermediate filament antibodies provide a useful tool for identifying cell origins. (See chart below.)

Intermediate filament type	Expression in normal cells	Examples of corresponding tumors
vimentin	mesenchymal cells	most sarcomas, lymphomas endotheliomas
desmin	muscle cells	rhabdomyosarcomas, leiomyosarcomas
cytokeratins	epithelial cells	most carcinomas
neurofilaments	neural cells	pheochromocytomas, esthesioneuroblastoma
GFAP	astrocytes	astrocytomas

Examples of *in vivo* normal cells and tumors recognized by intermediate filament antibodies.

Labsystems' quality control assures our monoclonals only react with their corresponding intermediate filament proteins.

These monoclonals can be used with either immunofluorescent or enzymatic techniques. . . with frozen or paraffin-embedded tissue samples.

For research use only. Not for diagnostic use.

Inquire about our new desmin monoclonal.

For further information, contact your nearest Labsystems office.

1. Virtanen et al., J. Cell Sci 50, 45-63 (1981)

Labsystems

In Europe: Labsystems Oy, Pulttitie 8, 00880 Helsinki, Finland,
Phone: +358-0-75821, Telex: 121949 labsy sf.

In Japan: Labsystems Japan K.K., Tohkoh 2nd Bldg., 1-34-15,
Shinjuku Shinjuku-ku, Tokyo 160, Japan, Phone: 81-3-355-5630,
Fax: 81-3-355-5633

In United States: Labsystems, Inc., 6200 West Oakton, Morton Grove, IL 60053,
Phone: (312) 967-5220, Toll Free: 800-572-8270

Reader Service No.6

EDITORIAL OFFICES

London Office
4 Little Essex Street, WC2R 3LF
Telephone: (01) 836 6633 Telex: 262024

Washington Office
1134 National Press Building, DC 20045
Telephone: (202) 737-2355

Tokyo Office
Eikow Building, 10-9, Hongo 1-Chome, Bunkyo-ku, Tokyo 113
Telephone: (03) 816 3756/7 Telex: 2722634 MSKKJ

Editor: John Maddox

Deputy Editor: Peter Newmark

Editorial Staff: Jennifer Altman, Philip Campbell, Maxine Clarke, Isobel Collins, Peter Gambles, Tim Lincoln, Geoffrey North, Peta Pickering, Miranda Robertson (Washington), Charles Wenz, Nigel Williams and Karen Wright (Washington)

Washington Correspondents: Tim Beardsley and Joe Palca

Tokyo Correspondent: Alun Anderson

France Correspondent (in London): Robert Walgate

Art and Design: Julie Busby, Joel Chernin, Julia Ward, Marie Xeridat

Administration: Mary Sheehan, Michèlle Ashman, Juliette Bedborough, Joanna Czechowska, Geraldene Lambert, Rosanna Mallett, Maureen Palmer, Lorraine Prendergast (Washington), Meg Taylor, and Penelope Walker (Washington)

Publisher: Elizabeth Hughes

Managing Director: Ray Barker

Promotion Manager: Felicity Parker

International Advertising Manager: Andy Sutherland

European Display Advertising Manager: Hilary Turnbull

Classified Advertising Manager: Mark Pearson

Nature New York Office
65 Bleecker Street, New York, NY 10012
Telephone: (212) 477-9600 Telex: 668497 UW

President: Gary M. Rekstad

American Advertising Manager: Henry Dale

Classified Advertising Manager: Marianne Ettisch

Circulation Director: Paul E. Siman

Canadian Display and Classified: Peter Drake, 17 Pine Crescent, Toronto, Ontario M4E 1L1—(416) 690-2423

Display Advertising Representatives

New York: Nature Office

Chicago: Didier & Broderick, Inc.—(312) 498-4520

San Francisco: Jobson/Jordan/Harrison/Schulz, Inc-(415) 392-6794

Los Angeles & Pasadena: Jobson/Jordan/Harrison/Schulz, Inc.—(818) 796-9200

New England: Denis J. O'Malley (212) 477-9623

Mid-Atlantic: Denis J. O'Malley (212) 477-9623

Southeast: Nature New York Office

Spring, Texas: Jobson/Jordan/Harrison/Schulz, Inc.—(713) 376-2368

France: Françoise Teisseyre Paris—(1) 46 22 51 54

West Germany and Austria: Franz Schrecklinger TMW Top Media Werbegesellschaft GmbH Frankfurt—(69) 726046

Holland and Belgium: Adele Struyck Holland—(034) 04 23265

Scandinavia: Andrew Karnig
Andrew Karnig & Associates AB
Finnbodavagen, 1, 131 31 Nacka
Sweden—Telephone: 08 44 00 05 Telex: 89101755

Japan: Mashy Yoshikawa
Orient Echo Inc. Tokyo—(03) 235 5961

Australia: Gus Bartel & Associates PO Box 1755, Southport, Queensland 42158—(075) 466 577

Nature® ISSN 0028-0836
Registered as a newspaper at the British Post Office © 1986 Macmillan Journals Ltd

Vol. 319 No. 6048 2 January

nature

NATURE VOL. 319 9 JANUARY 1986

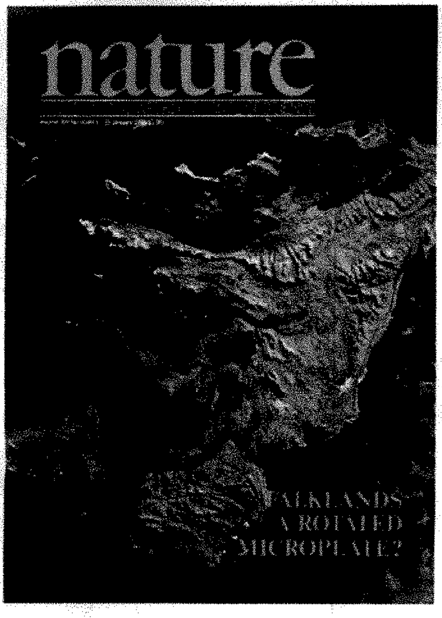

Palaeomagnetic evidence suggests that the Falkland Islands underwent a rotation of approximately 120° during the early stages of the break-up of Gondwanaland, and that they were originally adjacent to the Transkei area of South Africa. The islands probably first moved as a microplate while Antarctica was separating from southern Africa, and drifted to their present position, undergoing further rotation, during the opening of the South Atlantic. See p.131.

OPINION

Discrimination is not cricket 85
Chopper politics 86

NEWS

Japanese technology 87
US science adviser
British computing 88
Siberian river scheme
Soviet request for collaboration
Synthetic fuels 89
British biotechnology
Bell Labs 90
Israeli–Egyptian cooperation 91
Comecon technology 92
West German space

CORRESPONDENCE

Sakharov's recognition/Velikovsky/ Room for feet/Nuclear weapons 93

NEWS AND VIEWS

Voyager 2 swings by Uranus 95
Light and ultraphytoplankton
G E Fogg 96
Cell biology: Life without clathrin
James E Rothman 96
Are komatiitic lavas voracious?
Robert W Nesbitt 97
A supernova for a neighbour
Arnold Wolfendale 99
Gene regulation: Importance of helical periodicity
Tariq Enver and Roger Patient 99
Microplates in Antarctica
A K Martin 100

SCIENTIFIC CORRESPONDENCE

Pauling's model not universally accepted
J W Cahn, D Gratias & D Shechtman; A L Mackay; 102
P A Bancel, P A Heiney, P W Stephens & A I Goldman; A A Berezin

BOOK REVIEWS

Culture and the Evolutionary Process
by R Boyd and P J Richerson
Philip Kitcher 105
Pattern Recognition: Human and Mechanical
by S Watanabe
P W Hawkes 107
Molecular Bases of Neural Development
G M Edelman, W E Gall and W M Cowan, eds
Raymond D Lund
The Carbon Cycle and Atmospheric CO$_2$: Natural Variations Archean to Present
E T Sundquist and W S Broecker, eds
Michael Whitfield 108
The Physical Chemistry of Membranes: An Introduction to the Structure and Dynamics of Biological Membranes
by B L Silver
Charles Tanford

REVIEW ARTICLE

Future global warming from atmospheric trace gases
R E Dickinson & R J Cicerone 109

ARTICLES

Masses of the satellites of Uranus
S F Dermott & P D Nicholson 115
Requirement of stereospecific alignments for initiation from the simian virus 40 early promoter
K Takahashi, M Vigneron, H Matthes, A Wildeman, M Zenke & P Chambon 121

LETTERS TO NATURE

A very high energy γ-ray burst from the Crab pulsar
P N Bhat, P V Ramanamurthy, B V Sreekantan & P R Vishwanath 127
Solar ellipticity fluctuations yield no evidence of *g*-modes
J R Kuhn, K G Libbrecht & R H Dicke 128
Are the Falkland Islands a rotated microplate?
C Mitchell, G K Taylor, K G Cox & J Shaw 131
Production of ^{10}Be and ^{26}Al by cosmic rays in terrestrial quartz *in situ* and implications for erosion rates
K Nishiizumi, D Lal, J Klein, R Middleton & J R Arnold 134
Thermal erosion by komatiites at Kambalda, Western Australia and the genesis of nickel ores
D I Groves, E A Korkiakoski, N J McNaughton, C M Lesher & A Cowden 136
Estimating the error of age interpolation in sedimentary rocks
C Badgley, L Tauxe & F L Bookstein 139
Light quality and oceanic ultraphytoplankters
H E Glover, M D Keller & R R L Guillard 142
Birds that 'cry wolf'
C A Munn 143
Synapsin I is a microtubule-bundling protein
A J Baines & V Bennett 145

Contents continued overleaf

UK
Nat (ISSN 0028-0836) is published weekly on Thursday, except the last week in December, by Macmillan Journals Ltd and includes the Annual Index (mailed in February). Annual subscription
Writ A and Canada US $240. USA and Canadian orders to: *Nature*, Subscription Dept, PO Box 1501, Neptune, NJ 07753, USA. Other orders to *Nature*, Brunel Road, Basingstoke, Hants RG21
Nort UK. Second class postage paid at New York, NY 10012 and additional mailing offices. Authorization to photocopy material for internal or personal use, or internal or personal use of specific
is granted by *Nature* to libraries and others registered with the Copyright Clearance Center (CCC) Transactional Reporting Service, provided the base fee of $1.00 a copy plus $0.10 a page is
ectly to CCC, 21 Congress Street, Salem, Massachusetts 01970, USA. Identification code for *Nature*: 0028-0836/86 $1.00 + $0.10. US Postmaster send address changes to: *Nature*, 65 Bleecker
New York, NY 10012. Published in Japan by Macmillan Shuppan K.K., Eikow Building, 1-10-9 Hongo, Bunkyo-ku, Tokyo, Japan. © 1986 Macmillan Journals Ltd

TGF-BETA

TRANSFORMING GROWTH FACTOR TYPE BETA

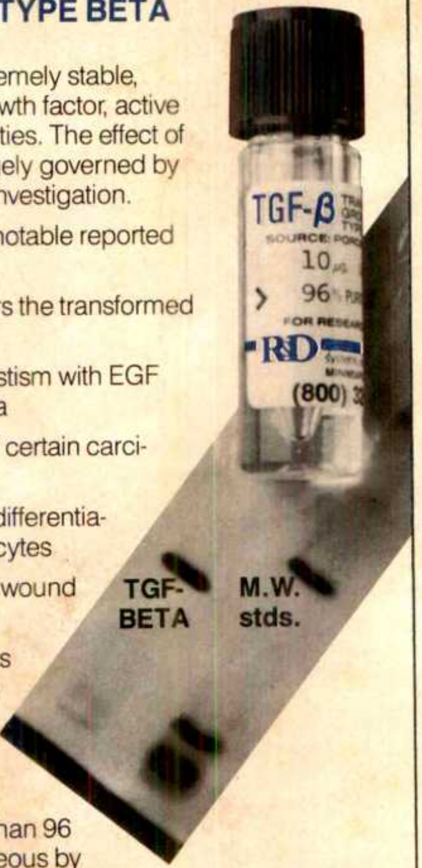
TGF-β
SOURCE: POR
10 µg
> 96% PUR
FOR RESEA
R&D
(800) 3
TGF-BETA
M.W. stds.

TGF-beta is an extremely stable, multi-functional growth factor, active in picomolar quantities. The effect of the molecule is largely governed by the cell line under investigation.

Some of the more notable reported effects are:[1]

- Reversibly confers the transformed phenotype
- Provides synergistism with EGF and/or TGF-alpha
- Inhibits growth of certain carcinoma cell lines
- Inhibits terminal differentiation of pre-adipocytes
- Promotes *in vivo* wound healing
- Mimics the effects of *ras* oncogene transfection
- Induces *c-sis* expression

PURITY: greater than 96 percent homogeneous by silver-stained gels, amino acid analysis and N-terminus sequencing.

ACTIVITY: Approximate ED_{50} of 1 ng/ml for the stimulation of colony formation of AKR-2B (clone 84A) cells in soft agar and 0.1 ng/ml for NRK (clone 49F) cells.

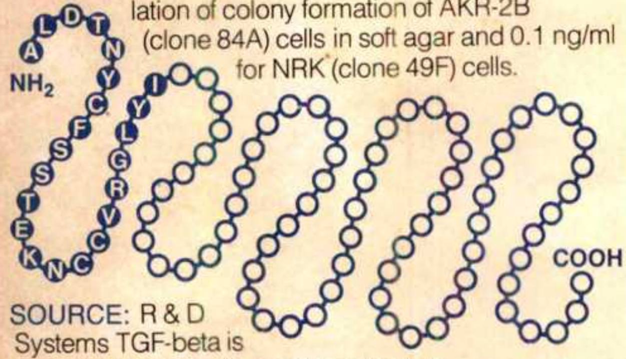
NH2
A
L
D
T
N
Y
C
F
S
S
T
E
K
N
C
C
V
R
G
Y
L
Y
I
D
COOH

SOURCE: R & D Systems TGF-beta is prepared from fresh porcine platelets. Based on its molecular weight, amino acid analysis and N-terminus sequencing (22 a.a.), it is indistinguishable from TGF-beta prepared from human sources.

TO ORDER: Call 1 (800) 328-2400 or to request information or technical bulletins (In Minnesota call 612-379-2956).

---

[1] For a more complete description and list of references, request R & D Systems Technical Bulletin, GFB-1085 on TGF-beta.

R&D

R & D Systems, Inc.
614 McKinley Place N.E.
Minneapolis, MN 55413

Reader Service No.4

● NEWS ● FEATURES
● ORIGINAL RESEARCH
● PRODUCT EVALUATIONS
● INDUSTRIAL APPLICATIONS
● JOB OPENINGS
● BOOK and PRODUCT REVIEWS and more!

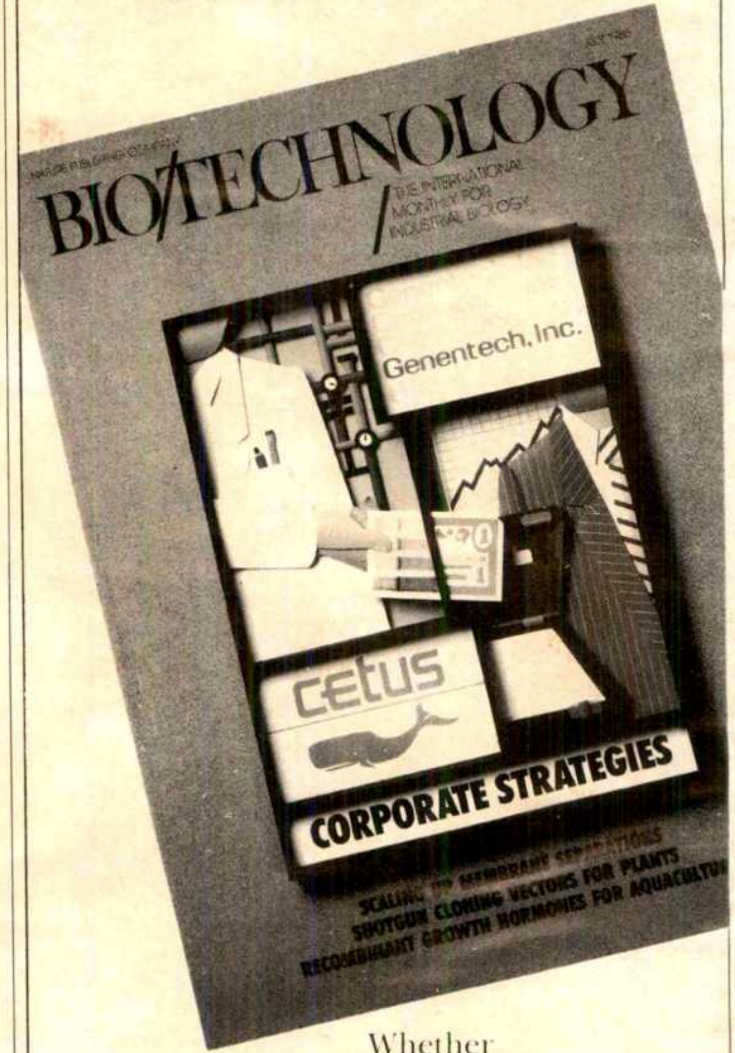
BIO/TECHNOLOGY
THE INTERNATIONAL MONTHLY FOR INDUSTRIAL BIOLOGY
Genentech, Inc.
cetus
CORPORATE STRATEGIES
SCALING UP MEMBRANE SEPARATIONS
SHOTGUN CLONING VECTORS FOR PLANTS
RECOMBINANT GROWTH HORMONES FOR AQUACULTURE

Whether you are involved in the engineering, scientific or commercial aspects of biotechnology, this is the one magazine you can't afford to be without.

For details of our special 2-year subscription offer and a FREE SAMPLE COPY phone Za Dale on (01) 836 6633 (UK) or Paige Beaver (212) 477 9600 (US) OR write to

Bio/Technology
Macmillan Journals Ltd
4 Little Essex Street
London WC2R 3LF
UK

Bio/Technology
65 Bleeker Street
New York
NY 10012
USA

CONTENTS

NATURE'S 1986

CALENDAR!

12 cover photographs superbly reproduced in full colour. Send for your calendar now.

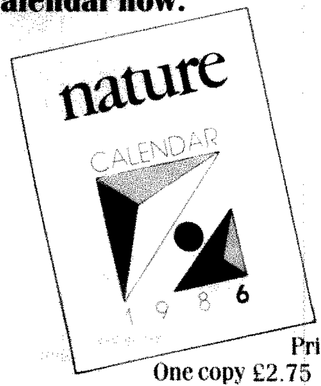

Prices:
One copy £2.75 (UK)
£3.75 (REST OF WORLD)
Three or more copies £2.50 (UK)
£3.20 (REST OF WORLD) each

Send orders to:
Circulation Manager, Macmillan Journals Ltd., FREEPOST (UK ONLY)
Brunel Road, Houndmills, Basingstoke, Hants., RG21 2XS UK.

Annual Subscription Prices

UK & Irish Republic		£104
USA & Canada		US$240
Australia, NZ & S. Africa	Airspeed	£150
	Airmail	£190
Continental Europe	Airspeed	£125
India	Airspeed	£120
	Airmail	£190
Japan	Airspeed	Y90000
Rest of World	Surface	£120
	Airmail	£180

Orders (with remittance) to:

USA & Canada	**UK & Rest of World**
Nature	Nature
Subscription Dept	Circulation Dept
PO Box 1501	Brunel Road
Neptune	Basingstoke
NJ 07753	Hants RG21 2XS, UK
USA	Tel: 0256 29242

(The addresses of Nature's editorial offices are shown facing the first editorial page)

Japanese subscription enquiries to:
Japan Publications Trading Company Ltd
2-1 Sarugaku-cho 1-chome
Chiyoda-ku, Tokyo, Japan
Tel: (03) 292 3755

Personal subscription rates: These are available in some countries to subscribers paying by personal cheque or credit card. Details from:

USA & Canada	**UK & Europe**
Nature	Felicity Parker
65 Bleecker Street	Nature
New York	4 Little Essex Street
NY 10012, USA	London WC2R 3LF, UK
Tel: (212) 477-9600	Tel: 01-836 6633

Back issues: UK, £2.50; USA & Canada, US$6.00 (surface), US$9.00 (air); Rest of World, £3.00 (surface), £4.00 (air)

Binders
Single binders: UK, £5.25; USA & Canada $11.50; Rest of World, £7.75. Set of four: UK, £15.00; USA & Canada $32.00; Rest of World, £22.00

Annual indexes (1971-1985)
UK, £5.00 each; Rest of World, $10.00

Nature First Issue Facsimile
UK, 75p; Rest of World (surface), $1.50; (air) $2.00

Nature in microform
Write to University Microfilms International, 300 North Zeeb Road, Ann Arbor, MI 48106, USA

Functional corticotropin releasing factor receptors in the primate peripheral sympathetic nervous system
R Udelsman, J P Harwood, M A Millan, G P Chrousos, D S Goldstein, R Zimlichman, K J Catt & G Aguilera **147**

IgE-mediated degranulation of mast cells does not require opening of ion channels
M Lindau & J M Fernandez **150**

Murine cells expressing an HLA molecule are specifically lysed by HLA-restricted antiviral human T cells
E Gomard, B Begue, S Sodoyer, J L Maryanski, B R Jordan & J P Levy **153**

A nuclear factor that binds to a conserved sequence motif in transcriptional control elements of immunoglobulin genes
H Singh, R Sen, D Baltimore & P A Sharp **154**

Activated human monocytes express the c-*sis* proto-oncogene and release a mediator showing PDGF-like activity
Y Martinet, P B Bitterman, J-F Mornex, G R Grotendorst, G R Martin & R G Crystal **158**

Erratum . . . page 160
A closely linked genetic marker for cystic fibrosis
R White, S Woodward, M Leppert, P O'Connell, Y Nakamura, M Hoff, J Herbst, J-M Lalouel, M Dean & G Vande Woude

MISCELLANY

100 years ago **98**
Books received **162**

NATURE CLASSIFIED

Professional appointments — Research posts — Studentships — Fellowships — Conferences — Courses — Seminars — Symposia: **Back Pages**

Next week in *Nature*:

- Dwarf black hole at galactic centre
- CO_2 and vegetation
- Coulomb's law wanting
- Secondary antiprotons
- Palaeomagnetic measurement
- Continental growth
- Protein kinase C affects K^+ conductance
- *neu* oncogene
- Man's place among great apes
- Expression of cauliflower mosaic virus
- Advocacy in science

GUIDE TO AUTHORS

Authors should be aware of the diversity of *Nature*'s readership and should strive to be as widely understood as possible.

Review articles should be accessible to the whole readership. Most are commissioned, but unsolicited reviews are welcome (in which case prior consultation with the office is desirable).

Scientific articles are research reports whose conclusions are of general interest or which represent substantial advances of understanding. The text should not exceed 3,000 words and six displayed items (figures plus tables). The article should include an italic heading of about 50 words.

Letters to *Nature* are ordinarily 1,000 words long with no more than four displayed items. The first paragraph (not exceeding 150 words) should say what the letter is about, why the study it reports was undertaken and what the conclusions are.

Matters arising are brief comments (up to 500 words) on articles and letters recently published in *Nature*. The originator of a Matters Arising contribution should initially send his manuscript to the author of the original paper and both parties should, wherever possible, agree on what is to be submitted.

Manuscripts may be submitted either to London or Washington). Manuscripts should be typed (double spacing) on one side of the paper only. Four copies are required, each accompanied by copies of lettered artwork. No title should exceed 80 characters in length. Reference lists, figure legends, etc, should be on seperate sheets, all of which should be numbered. Abbreviations, symbols, units, etc, should be identified on one copy of the manuscript at their first appearance.

References should appear sequentially indicated by superscripts, in the text and should be abbreviated according to the *World List of Scientific Periodicals*, fourth edition (Butterworth 1963-65). The first and last page numbers of each reference should be cited. Reference to books should clearly indicate the publisher and the date and place of publication. Unpublished articles should not be formally referred to unless accepted or submitted for publication, but may be mentioned in the text.

Each piece of artwork should be clearly marked with the author's name and the figure number. Original artwork should be unlettered. Suggestions for cover illustrations are welcome. Original artwork (and one copy of the manuscript) will be returned when manuscripts cannot be published.

Requests for permission to reproduce material from Nature *should be accompanied by a self-addressed (and, in the case of the United Kingdom and United States, stamped) envelope.*

BIO/TECHNOLOGY INVITES YOU TO ATTEND ITS

PREMIER CONFERENCE

BIO/TECHNOLOGY

LOOKS TO THE NEXT DECADE

January 20-22, 1986—New Orleans

BIO/TECHNOLOGY Looks to the Next Decade will go beyond most scientific symposia. First and foremost, the conference will bring together some of the world's leading authorities in molecular biology and process technology in a setting modeled after the very best of the invitation-only conferences. Everything is designed to provide a maximum exchange of ideas and information.

A look at the roster of keynote speakers, all leading researchers in their fields, demonstrates at a glance that only the highest level of scientific information will be presented.

To insure the greatest possible interaction and exchange, each afternoon will be devoted to roundtable discussions chaired by the keynote speakers, and featuring panelists of the highest calibre. There will be opportunity for all attendees to make brief presentations during these sessions, and participants are urged to bring their own slides.

If you want to get a jump on the ideas and techniques that will guide biotechnology through the '80s and '90s—this conference is for you.

Participation will be limited to provide maximum opportunity for fruitful exchange. So don't delay. Register now to guarantee your place.

CONFERENCE PROGRAM & SPEAKERS

JANUARY 20—MORNING

THE MOLECULAR BIOLOGY OF PLANTS AND ANIMALS: A VIEW FROM THE FRONTIER

SPEAKERS:

David Goeddel
Director, Molecular Biology, Genentech

Richard Flavell
President, Biogen Research Corp.

Norman Borlaug
CIMMYT, Mexico City and Professor, Dept. of Soil and Crop Science, Texas A&M

JANUARY 20—AFTERNOON

SEMINAR IN MOLECULAR BIOLOGY

PANELISTS

David Goeddel, Co-Chairman

Richard Flavell, Co-Chairman

Budd Colby
Director, Technology Development,
Triton Biosciences

SEMINAR IN AGRICULTURAL BIOTECHNOLOGY

PANELISTS

Norman Borlaug, Chairman

Robert Fraley
Manager of Plant Molecular Biology,
Monsanto

David Evans
Vice President for Research,
DNA Plant Technology, Inc.

Charles Arntzen
Associate Director of Central Research and Development,
E.I. Du Pont de Nemours and Co.

JANUARY 21—MORNING

COMMERCIAL PRODUCTION PROCESSES

SPEAKERS:

Malcolm Lilly
Professor of Biochemical Engineering, University College London

Robert Herschberg
Department of Process Development,
Genentech

Yukio Sugino, Director
Biotechnology Labs, Takeda Chemical,
Japan

Ephraim Katchalski-Katzir
Professor of Biophysics and Biotechnology, Tel Aviv University, Israel

nature

NATURE VOL. 319 16 JANUARY 1986

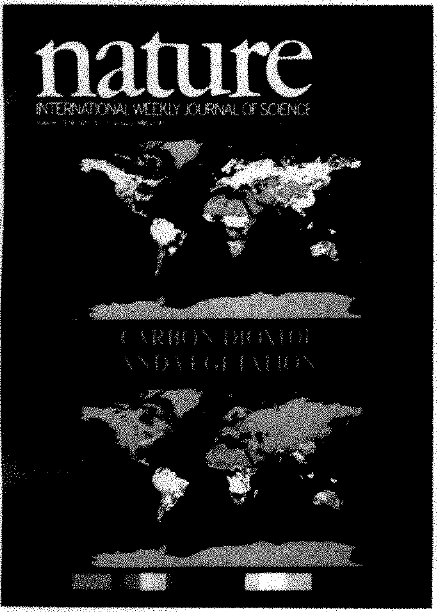

Satellite-derived data showing the amount of photosynthetically active radiation absorbed by terrestrial vegetation for August 1982 (top) and February 1983. Brown/orange represent zero absorbance, cream/light green represent low absorbance, dark green is medium absorbance and red/violet high absorbance. See p.195, and News and Views p.181. (Photo: NASA/Goddard Space Flight Center.)

OPINION

British research scrutinized again 163
Agenda for Geneva 164

NEWS

French research strategy 165
Nuclear winter
German research agency 166
Seibold in Europe
Antarctic treaty
Nuclear safety 167
Neutron research sources
US/Canada acid rain 168
Fusion research
British science 169
***Refusnik* scientists**
Viral cancers 170
Infection mechanism?
Polish astronomers
British veterinarians 171
DNA fingerprinting
Romanian mathematics

CORRESPONDENCE

Japanese psychiatry/Animal intelligence/Extraterrestrials/etc. 172

NEWS AND VIEWS

Newtonian gravitation corrected 173
Does Uranus have a magnetic field?
A J Dessler 174
Obituary: Jacques Oudin
Guy Bordenave 174
Perovskites and plate tectonics
Geoffrey D Price 175
Inositol phosphates: Profusion and confusion
Bob Michell 176
Limits to Coulomb's law
Robert W Cahn 177
Where do antiprotons come from?
Andrew Buffington 178
Lifestyle of plesiosaurs
Michael A Taylor 179
Neuroendocrinology: Molecular approach appraised
Stafford Lightman 180
Photosynthesis seen from above
R A Warrick 181
Hydrogenases: From chemistry to legume growth
R Cammack and M G Yates 182

SCIENTIFIC CORRESPONDENCE

The real cause of Ethiopia's problems
B D Perry 183
Major groove or minor groove?
W Jia-Huai
The facts on cystic fibrosis testing
D J H Brock & V van Heyningen 184
Long running experiments
S Toby

BOOK REVIEWS

Artificial Intelligence: The Very Idea
by J Haugeland
John A Campbell 185
The Duality of the Mind
by A L Wigan
John C Marshall 186
Shackleton
by R Huntford
Derek Fordham
Changes in Eukaryotic Gene Expression in Response to Environmental Stress
B G Atkinson and D B Walden, eds
and
The Adaptive Role of Lipids in Biological Systems
by N Hadley
C Ladd Prosser 187
Design and Performance of Muscular Systems
C R Taylor, E Weibel and L Bolis, eds
R M Simmons 188

COMMENTARY

Edwin Hubble: legal eagle
N Hetherington 189

ARTICLES

Is the galactic centre black hole a dwarf?
D A Allen & R H Sanders 191
Relationship between atmospheric CO_2 variations and a satellite-derived vegetation index
C J Tucker, I Y Fung, C D Keeling & R H Gammon 195
Solvation energy in protein folding and binding
D Eisenberg & A D McLachlan 199

LETTERS TO NATURE

Inadequacy of Coulomb's friction law for particle assemblies
K Kendall 203
Secondary antiproton production in relativistic plasmas
C D Dermer & R Ramaty 205
Specific role of transient O^- (s) at Mg(0001) surfaces in activation of ammonia by dioxygen and nitrous oxide
C T Au & M W Roberts 206
A new method for measuring palaeomagnetic intensities
M Boyd 208
Seismic reflection imaging of the subducting Juan de Fuca plate
A G Green, R M Clowes, C J Yorath, C Spencer, E R Kanasewich, M T Brandon & A Sutherland Brown 210
Thermal expansion of silicate perovskite and stratification of the Earth's mantle
E Knittle, R Jeanloz & G L Smith 214
$^{187}Os/^{186}Os$ in marine manganese nodules and the constraints on the crustal geochemistries of rhenium and osmium
M R Palmer & K K Turekian 216
Protein kinase C activation induces conductance changes in *Hermissenda* photoreceptors like those seen in associative learning
J Farley & S Auerbach 220

Contents continued overleaf

Nature® (ISSN 0028-0836) is published weekly on Thursday, except the last week in December, by Macmillan Journals Ltd and includes the Annual Index (mailed in February). Annual subscription for USA and Canada US $240. USA and Canadian orders to: *Nature*, Subscription Dept, PO Box 1501, Neptune, NJ 07753, USA. Other orders to *Nature*, Brunel Road, Basingstoke, Hants RG21 2XS, UK. Second class postage paid at New York, NY 10012 and additional mailing offices. Authorization to photocopy material for internal or personal use, or internal or personal use of specific clients, is granted by *Nature* to libraries and others registered with the Copyright Clearance Center (CCC) Transactional Reporting Service, provided the base fee of $1.00 a copy plus $0.10 a page is paid directly to CCC, 21 Congress Street, Salem, Massachusetts 01970, USA. Identification code for *Nature*: 0028-0836/86 $1.00 + $0.10. US Postmaster send address changes to: *Nature*, 65 Bleecker Street, New York, NY 10012. Published in Japan by Macmillan Shuppan K.K., Eikow Building, 1-10-9 Hongo, Bunkyo-ku, Tokyo, Japan. © 1986 Macmillan Journals Ltd.

CULTURE CONTROL
from
Sci ERA™
Sci
QUAD DRIVE SYSTEM
DUAL OVERHEAD DRIVE SYSTEM
BELLCO

BELLCO ANNOUNCE *THE* MOST ADVANCED RANGE OF MAGNETIC STIRRERS AND ROLLER APPARATUS AVAILABLE

Now you can achieve greater reproducibility and protect valuable cell cultures better than ever before with Bellco's brand new Sci-ERA range of instrumentation.
The **Quad Drive System** gives you precise control over up to four remote stirring platforms, with optional **Power Pack** in case of power failure. The **Cell Production Roller Apparatus** offers back-up power *plus* secondary motor, alarms and space for up to 50 vessels.
Other new products from Bellco include high-precision non-heating **Magnetic Stirrer, Mass Media Dispenser** and **Dual Overhead Drive Culture System** – all designed to give you increased productivity and the ultimate in culture control.
Send for full information today.

BELLCO
INTERNATIONAL

Reader Service No.173

Sterilin House, Clockhouse Lane, Feltham, Middx, England TW14 8QS. Tel: Ashford (07842) 51155. Telex: 8812910 STERI-G.

CONTENTS

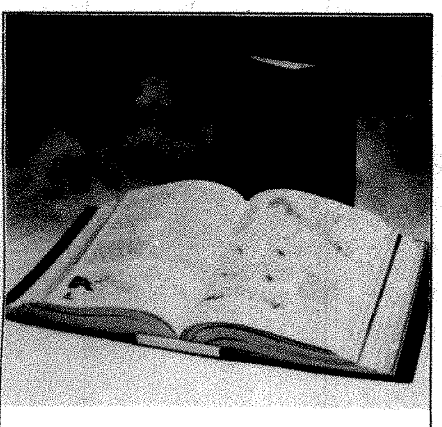

NATURE BINDERS

Your copies of Nature are invaluable for future reference so why not give them the treatment they deserve and file them neatly in our special Nature binders?

Ordering address and prices for one or a set of four are listed below.

Annual Subscription Prices

UK & Irish Republic		£104
USA & Canada		US$240
Australia, NZ & S. Africa	Airspeed	£150
	Airmail	£190
Continental Europe	Airspeed	£125
India	Airspeed	£120
	Airmail	£190
Japan	Airspeed	Y90000
Rest of World	Surface	£120
	Airmail	£180

Orders (with remittance) to:

USA & Canada
Nature
Subscription Dept
PO Box 1501
Neptune
NJ 07753
USA

UK & Rest of World
Nature
Circulation Dept
Brunel Road
Basingstoke
Hants RG21 2XS, UK
Tel: 0256 29242

(The addresses of Nature's editorial offices are shown facing the first editorial page)

Japanese subscription enquiries to:
Japan Publications Trading Company Ltd
2-1 Sarugaku-cho 1-chome
Chiyoda-ku, Tokyo, Japan
Tel: (03) 292 3755

Personal subscription rates: These are available in some countries to subscribers paying by personal cheque or credit card. Details from:

USA & Canada
Nature
65 Bleecker Street
New York
NY 10012, USA
Tel: (212) 477-9600

UK & Europe
Felicity Parker
Nature
4 Little Essex Street
London WC2R 3LF, UK
Tel: 01-836 6633

Back issues: UK, £2.50; USA & Canada, US$6.00 (surface), US$9.00 (air); Rest of World, £3.00 (surface), £4.00 (air)

Binders
Single binders: UK, £5.25; USA & Canada $11.50; Rest of World, £7.75. Set of four: UK, £15.00; USA & Canada $32.00; Rest of World, £22.00

Annual indexes (1971-1985)
UK, £5.00 each; Rest of World, $10.00

Nature First Issue Facsimile
UK, 75p; Rest of World (surface), $1.50; (air) $2.00

Nature in microform
Write to University Microfilms International, 300 North Zeeb Road, Ann Arbor, MI 48106, USA

Differential expression of α-fetoprotein genes on the inactive X chromosome in extraembryonic and somatic tissues of a transgenic mouse line
R Krumlauf, V M Chapman, R E Hammer, R Brinster & S M Tilghman 224

The *neu* oncogene encodes an epidermal growth factor receptor-related protein
C I Bargmann, M-C Hung & R A Weinberg 226

Similarity of protein encoded by the human c-*erb-B*-2 gene to epidermal growth factor receptor
T Yamamoto, S Ikawa, T Akiyama, K Semba, N Nomura, N Miyajima, T Saito & K Toyoshima 230

Primate η-globin DNA sequences and man's place among the great apes
B F Koop, M Goodman, P Xu, K Chan & J L Slightom 234

***fgr* proto-oncogene mRNA induced in B lymphocytes by Epstein–Barr virus infection**
M S C Cheah, T J Ley, S R Tronick & K C Robbins 238

Expression of cauliflower mosaic virus reverse transcriptase in yeast
H Takatsuji, H Hirochika, T Fukushi & J-E Ikeda 240

Detection of cytosine methylation in the maize alcohol dehydrogenase gene by genomic sequencing
H Nick, B Bowen, R J Ferl & W Gilbert 243

Transcription factor Sp1 recognizes a DNA sequence in the mouse dihydrofolate reductase promoter
W S Dynan, S Sazer, R Tjian & R T Schimke 246

MISCELLANY

100 years ago 177

NATURE CLASSIFIED

Professional appointments — Research posts — Studentships — Fellowships — Conferences — Courses — Seminars — Symposia: Back Pages

Next week in *Nature*:

- Voyager nears Uranus
- Solar magnetism
- El Niño's impact on life
- Smoke in nuclear winter
- Classical nuclear deterrence strategy
- Isoleucine stereoisomers on Earth
- Thirty-carbon pentacyclic hydrocarbon in oil
- Early North American primate
- Prehistoric diet reconstruction
- Stomatal opening
- Vasopressin in neurones
- Viral DNA in feline AIDS

GUIDE TO AUTHORS

Authors should be aware of the diversity of *Nature*'s readership and should strive to be as widely understood as possible.

Review articles should be accessible to the whole readership. Most are commissioned, but unsolicited reviews are welcome (in which case prior consultation with the office is desirable).

Scientific articles are research reports whose conclusions are of general interest or which represent substantial advances of understanding. The text should not exceed 3,000 words and six displayed items (figures plus tables). The article should include an italic heading of about 50 words.

Letters to *Nature* are ordinarily 1,000 words long with no more than four displayed items. The first paragraph (not exceeding 150 words) should say what the letter is about, why the study it reports was undertaken and what the conclusions are.

Matters arising are brief comments (up to 500 words) on articles and letters recently published in *Nature*. The originator of a Matters Arising contribution should initially send his manuscript to the author of the original paper and both parties should, wherever possible, agree on what is to be submitted.

Manuscripts may be submitted either to London or Washington). Manuscripts should be typed (double spacing) on one side of the paper only. Four copies are required, each accompanied by copies of lettered artwork. No title should exceed 80 characters in length. Reference lists, figure legends, etc, should be on seperate sheets, all of which should be numbered. Abbreviations, symbols, units, etc, should be identified on one copy of the manuscript at their first appearance.

References should appear sequentially indicated by superscripts, in the text and should be abbreviated according to the *World List of Scientific Periodicals*, fourth edition (Butterworth 1963-65). The first and last page numbers of each reference should be cited. Reference to books should clearly indicate the publisher and the date and place of publication. Unpublished articles should not be formally referred to unless accepted or submitted for publication, but may be mentioned in the text.

Each piece of artwork should be clearly marked with the author's name and the figure number. Original artwork should be unlettered. Suggestions for cover illustrations are welcome. Original artwork (and one copy of the manuscript) will be returned when manuscripts cannot be published.

Requests for permission to reproduce material from Nature *should be accompanied by a self-addressed (and, in the case of the United Kingdom and United States, stamped) envelope.*

Now You Have A Choice of Two Benchtop Ultracentrifuges

For spinning small samples at 100,000 rpm

For a decade, researchers have been using the economical little Airfuge® Ultracentrifuge to pellet microsamples quickly at high centrifugal forces. It accelerates to 100,000 rpm, pellets, and gently stops before a floor-model ultracentrifuge can even get to speed.

Now Beckman offers yet another advance in ultracentrifuge technology — the TL-100. This microprocessor-controlled benchtop model with refrigeration does a lot more than pellet. It can isolate plasmid DNA in a 2-mL tube using precious little CsCl. It makes rate zonal separations just like big ultracentrifuges but in 2.2-mL tubes in its own miniature swinging bucket rotor. It even offers a vertical tube rotor with 2-mL tubes.

Use the Airfuge for quickly pelleting small sample volumes and for special jobs like preparing particles for electron microscopy. Use the TL-100 for any other separation technique on microsamples. Save your floor-model ultracentrifuge for larger volumes.

BECKMAN
BECKMAN
TL-100
BECKMAN
Airfuge

nature

NATURE VOL. 319 23 JANUARY 1986

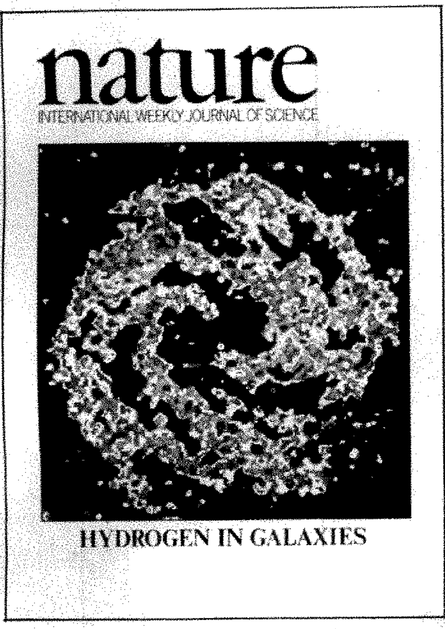

A pseudo-colour picture showing the distribution of neutral atomic hydrogen within 5 arc minutes of the centre of the southern spiral galaxy M83 = NGC 5236. The highest column densities are coloured red. The observations were made at a resolution of 10 arc minutes with the Very Large Array telescope. The analysis and display were performed with the Groningen Image Processing System. See p.296.

OPINION

Europe still unsure of itself 249
No more numbers game 250
Scribes in space

NEWS

Archaeologists 251
Searle's UK research lab closes
Channel tunnel
Japanese science budget 252
Space research
Television 253
UK public spending
Gramm–Rudman Act 254
Genetic engineering
Soviet Union 255
West German schools

CORRESPONDENCE

West German universities/German prizes/UK physics/AFRC cuts 256

NEWS AND VIEWS

Growth by cannibalization 257
Sex chromosomes: Mammalian X and Y crossover
Paul S Burgoyne 258
Nuclear winter: Towards a scientific exercise
K A Emanuel 259
Reconstructing ancient diets
Richard Burleigh 259
Ecology: Tundra river transformation
S I Heaney 260
Developmental biology: Unscrambling egg structure
Hugh Woodland & Elizabeth Jones 261
What causes the solar cycle?
Douglas Gough 263
Nucleic acid-binding proteins: More metal-binding fingers
Jeremy M Berg 264
The mammoth's last migration
Jared Diamond 265
Is there lightning on Venus?
Janet G Luhmann & Andrew F Nagy 266

SCIENTIFIC CORRESPONDENCE

Cerebral damage and functional localization
J C Marshall 267
The magnetic field of Uranus
W I Axford & V M Vasiliunas
Solar wind interaction with Uranus' atmosphere
W-H Ip 268
Archaebacterial terminator
A Klein
Reply: R A Garrett
How to test special relativity
M Psimopoulos & T Theocharis 269
Ontogeny of natural killer cells
L L Lanier & J H Phillips
The search for extraterrestrials
D G Blair 270
Clone controversy at Immunex
S M Wolff, P E Auron, C A Dinarello, L J Rosenwasser, A C Webb & A Rich

BOOK REVIEWS

The Descent of Woman: A New Edition
by E Morgan and
Myths of Gender: Biological Theories About Women and Men
by A Fausto-Sterling
Robert Attenborough 271
Scientific Communications and Informatics
by A I Mikhailov et al.
Eugene Garfield, Henry Small and George Vladutz 272
Archaebacteria
C R Woese and R S Wolfe, eds
D B Nedwell 273
On the Track of Ice Age Mammals
by A J Sutcliffe
Paul G Bahn
Changing Order: Replication and Induction in Scientific Practice
by H M Collins
Augustine Brannigan 274

COMMENTARY

Uncertainty and the Strategic Defense Initiative
J Wright 275

REVIEW ARTICLE

Ocean variability in relation to living resources during the 1982–83 El Niño
R T Barber & F P Chávez 279

ARTICLES

Global resonances in the evolution of solar magnetic fields
J O Stenflo & M Vogel 285
A gradient of sex linkage in the pseudoautosomal region of the human sex chromosomes
F Rouyer, M-C Simmler, C Johnsson, G Vergnaud, H J Cooke & J Weissenbach 291

LETTERS TO NATURE

Large-scale dissociation of molecular gas in galaxies by newly formed stars
R J Allen, P D Atherton & R P J Tilanus 296
Astrophysical implications of amorphous ice — a microporous solid
E Mayer & R Pletzer 298
Importance of local mesoscale factors in any assessment of nuclear winter
B W Golding, P Goldsmith, N A Machin & A Slingo 301
Evolution of an impact-induced atmosphere and magma ocean on the accreting Earth
T Matsui & Y Abe 303
Chemical effects of large impacts on the Earth's primitive atmosphere
B Fegley Jr, R G Prinn, H Hartman & G H Watkins 305
Direct conversion of methane to methanol, chloromethane and dichloromethane at room temperature
K Ogura & K Takamagari 308

Contents continued overleaf

Nature® (ISSN 0028-0836) is published weekly on Thursday, except the last week in December, by Macmillan Journals Ltd and includes the Annual Index (mailed in February). Annual subscription for USA and Canada US $240. USA and Canadian orders to: *Nature*, Subscription Dept, PO Box 1501, Neptune, NJ 07753, USA. Other orders to *Nature*, Brunel Road, Basingstoke, Hants RG21 2XS, UK. Second class postage paid at New York, NY 10012 and additional mailing offices. Authorization to photocopy material for internal or personal use, or internal or personal use of specific clients, is granted by *Nature* to libraries and others registered with the Copyright Clearance Center (CCC) Transactional Reporting Service, provided the base fee of $1.00 a copy plus $0.10 a page is paid directly to CCC, 21 Congress Street, Salem, Massachusetts 01970, USA. Identification code for *Nature*: 0028-0836/86 $1.00 + $0.10. US Postmaster send address changes to: *Nature*, 65 Bleecker Street, New York, NY 10012. Published in Japan by Macmillan Shuppan K.K., Eikow Building, 1-10-9 Hongo, Bunkyo-ku, Tokyo, Japan. © 1986 Macmillan Journals Ltd

Scale-up with FPL
from Pharmacia

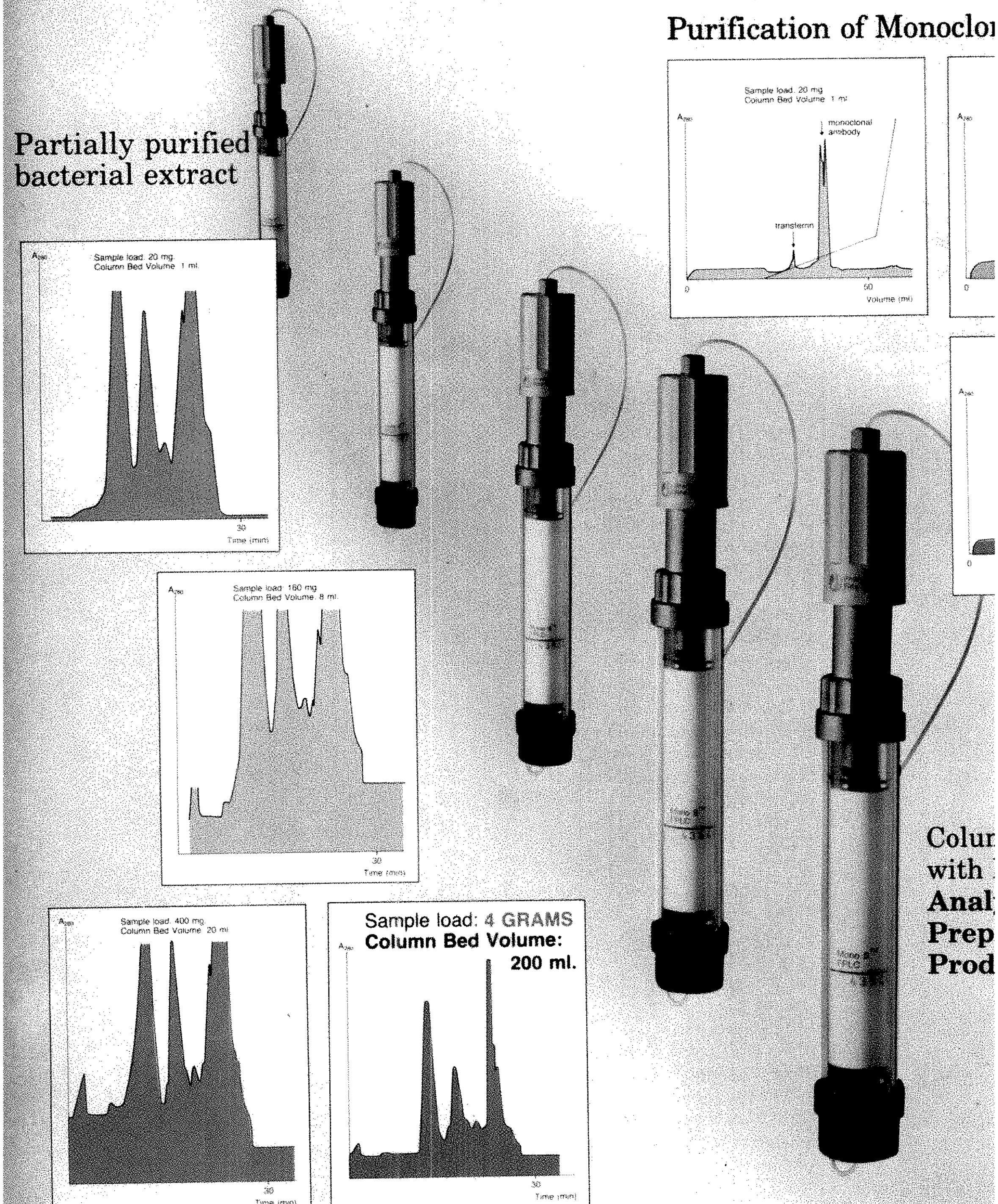
Purification of Monoclo
Sample load: 20 mg
Column Bed Volume: 1 ml
A_{280}
monoclonal antibody
transferrin
0
50
Volume (ml)
Partially purified bacterial extract
Sample load: 20 mg.
Column Bed Volume: 1 ml.
30
Time (min)
Sample load: 160 mg
Column Bed Volume: 8 ml.
Sample load: 400 mg
Column Bed Volume: 20 ml
Sample load: 4 GRAMS
Column Bed Volume: 200 ml.
Colu
with
Anal
Prep
Prod

For more information on chromatographic scale-up possibilities contact your local Pharmacia representative.

Laborat
S-751 8
Reader

That important research article you've been looking for located instantly!

nature
1984 index
Volumes 307-312

If you store your copies of Nature for future reference, then the annual index of subject and author is an essential part of your collection. These comprehensive annual indexes are available for all issues of Nature from 1971 to 1985.
Prices and address for orders are set out below.

Annual Subscription Prices

UK & Irish Republic		£104
USA & Canada		US$240
Australia, NZ & S. Africa	Airspeed	£150
	Airmail	£190
Continental Europe	Airspeed	£125
India	Airspeed	£120
	Airmail	£190
Japan	Airspeed	Y90000
Rest of World	Surface	£120
	Airmail	£180

Orders (with remittance) to:

USA & Canada
Nature
Subscription Dept
PO Box 1501
Neptune
NJ 07753
USA

UK & Rest of World
Nature
Circulation Dept
Brunel Road
Basingstoke
Hants RG21 2XS, UK
Tel: 0256 29242

(The addresses of Nature's editorial offices are shown facing the first editorial page)

Japanese subscription enquiries to:
Japan Publications Trading Company Ltd
2-1 Sarugaku-cho 1-chome
Chiyoda-ku, Tokyo, Japan
Tel: (03) 292 3755

Personal subscription rates: These are available in some countries to subscribers paying by personal cheque or credit card. Details from:

USA & Canada
Nature
65 Bleecker Street
New York
NY 10012, USA
Tel: (212) 477-9600

UK & Europe
Felicity Parker
Nature
4 Little Essex Street
London WC2R 3LF, UK
Tel: 01-836 6633

Back issues: UK, £2.50; USA & Canada, US$6.00 (surface), US$9.00 (air); Rest of World, £3.00 (surface), £4.00 (air)

Binders
Single binders: UK, £5.25; USA & Canada $11.50; Rest of World, £7.75. Set of four: UK, £15.00; USA & Canada $32.00; Rest of World, £22.00

Annual indexes (1971-1985)
UK, £5.00 each; Rest of World, $10.00

Nature First Issue Facsimile
UK, 75p; Rest of World (surface), $1.50; (air) $2.00

Nature in microform
Write to University Microfilms International, 300

Does partial melting reduce the creep strength of the upper mantle?
S Karato 309

Partial melting zones in the crust in southern Tibet from magnetotelluric results
V N Pham, D Boyer, P Therme, X C Yuan, L Li & G Y Jin 310

Isoleucine stereoisomers on the Earth
J L Bada, M Zhao, S Steinberg & E Ruth 314

Bicadinane, a C_{30} pentacyclic isoprenoid hydrocarbon found in crude oil
H C Cox, J W de Leeuw, P A Schenck, H van Koningsveld, J C Jansen, B van de Graaf, V J van Geerestein, J A Kanters, C Kruk & A W H Jans 316

Early Eocene *Cantius torresi* — oldest primate of modern aspect from North America
P D Gingerich 319

Reconstruction of African human diet using bone collagen carbon and nitrogen isotope ratios
S H Ambrose & M J DeNiro 321

Blue light-dependent proton extrusion by guard-cell protoplasts of *Vicia faba*
K Shimazaki, M Iino & E Zeiger 324

Magnocellular axons in passage through the median eminence release vasopressin
M C Holmes, F A Antoni, G Aguilera & K J Catt 326

Excitatory amino acids inhibit stimulation of phosphatidylinositol metabolism by aminergic agonists in hippocampus
M Baudry, J Evans & G Lynch 329

Expression of a translocated c-*abl* gene in hybrids of mouse fibroblasts and chronic myelogenous leukaemia cells
D Kozbor, A Giallongo, M E Sierzega, J B Konopka, O N Witte, L C Showe & C M Croce 331

Disease-specific and tissue-specific production of unintegrated feline leukaemia virus variant DNA in feline AIDS
J I Mullins, C S Chen & E A Hoover 333

Structural homology of the product of the *Drosophila Krüppel* gene with *Xenopus* transcription factor IIIA
U B Rosenberg, C Schröder, A Preiss,

Induction of yeast Ty ele transcription by ultravio
R Rolfe, A Spanos & G Banks

MISCELL

100 years ago
Books received

NATURE CLA

Professional appointmen
Research posts — Studer
Fellowships — Conferen
Courses — Seminars —

Next week in

- Creationists slant
- Pulsar evolution
- Titan's atmosphe
- Antarctic meteor different
- Photochemical m
- Electrolocation in platypus
- Neonatal immun
- Proto-oncogene c cell proliferation
- Neuropeptide fu
- Latest in peptide

GUIDE TO AU

Authors should be aware of the diver
and should strive to be as widely und

Review articles should be accessible
Most are commissioned, but unsolic
(in which case prior consultation with

Scientific articles are research report
general interest or which represent
understanding. The text should not e
displayed items (figures plus tables).
an italic heading of about 50 words.

Letters to *Nature* are ordinarily 1,000
than four displayed items. The first
150 words) should say what the letter
reports was undertaken and what the

Matters arising are brief comments (u
and letters recently published in *Na*
Matters Arising contribution should
script to the author of the original
should, wherever possible, agree on

Manuscripts may be submitted eithe
ton). Manuscripts should be typed (d
of the paper only. Four copies are req
by copies of lettered artwork. No title
ters in length. Reference lists, figure l
seperate sheets, all of which should
tions, symbols, units, etc, should be
the manuscript at their first appearan

References should appear sequenti
scripts, in the text and should be abb
World List of Scientific Periodicals, fo
1963-65). The first and last page nu
should be cited. Reference to books s
publisher and the date and place of
articles should not be formally refer
submitted for publication, but may be

Each piece of artwork should be
author's name and the figure number

biozyme
LABORATORIES LIMITED
GREAT BRITAIN

ALKALINE PHOSPHATASE

(Calf Intestine)

Form:
A highly purified salt-free stabilised solution in 50% Glycerol/ 0.5mM $MgCl_2$/0.05 mM $ZnCl_2$

The solution requires no dialysis before commencement of the coupling procedure.

Protein concentration
10–20 mgs per ml.

SPECIFIC ACTIVITIES (U/mg Protein)

Product Code	Glycine Buffer pH 9.6 25°C Biozyme Assay	Glycine Buffer pH 10.4 37°C	Diethanolamine Buffer pH 9.8 37°C
ALPI-10G	>1300	>1700	>4200
ALPI-9G	>1100	>1400	>3500
ALPI-8G	> 800	>1000	>2500

Unit 6, Gilchrist-Thomas Estate,
Blaenavon,
GWENT NP4 9RL,
South Wales, Great Britain
Tel. No: 0495 790678
Telex: 497731 A/B
"BIOZYM G"

EDITORIAL OFFICES

London Office
4 Little Essex Street, WC2R 3LF
Telephone: (01) 836 6633 Telex: 262024

Washington Office
1134 National Press Building, DC 20045
Telephone: (202) 737-2355

Tokyo Office
Eikow Building, 10-9, Hongo 1-Chome, Bunkyo-ku, Tokyo 113
Telephone: (03) 816 3756/7 Telex: 2722634 MSKKJ

Editor: John Maddox

Deputy Editor: Peter Newmark

Editorial Staff: Jennifer Altman, Philip Campbell, Maxine Clarke, Isobel Collins, Peter Gambles, Laura Garwin, Tim Lincoln, Geoffrey North, Peta Pickering, Miranda Robertson (Washington), Charles Wenz, Nigel Williams and Karen Wright (Washington)

Washington Correspondents: Tim Beardsley and Joseph Palca

Tokyo Correspondent: Alun Anderson

France Correspondent (in London): Robert Walgate

Art and Design: Joel Chernin, Elizabeth Terrell, Julia Ward and Marie Xeridat

Administration: Mary Sheehan, Michèlle Ashman, Juliette Bedborough, Joanna Czechowska, Geraldene Lambert, Rosanna Mallett, Maureen Palmer, Lorraine Prendergast (Washington), Meg Taylor and Penelope Walker (Washington)

Publisher: Elizabeth Hughes

Managing Director: Ray Barker

Promotion Manager: Felicity Parker

International Advertising Manager: Andy Sutherland

European Display Advertising Manager: Hilary Turnbull

Group Classified Advertising Manager: Mark Pearson

Nature New York Office
65 Bleecker Street, New York, NY 10012
Telephone: (212) 477-9600 Telex: 668497 UW

President: Gary M. Rekstad

American Advertising Manager: Henry Dale

Classified Advertising Manager: Marianne Ettisch

Circulation Director: Paul E. Siman

Canadian Display and Classified: Peter Drake, 17 Pine Crescent, Toronto, Ontario M4E 1L1—(416) 690-2423

Display Advertising Representatives

New York: Nature Office

Chicago: Didier & Broderick, Inc.—(312) 498-4520

San Francisco: Jobson/Jordan/Harrison/Schulz, Inc–(415) 392-6794

Los Angeles & Pasadena: Jobson/Jordan/Harrison/Schulz, Inc.—(818) 796-9200

New England: Denis J. O'Malley (212) 477-9623

Mid-Atlantic: Denis J. O'Malley (212) 477-9623

Southeast: Nature New York Office

Spring, Texas: Jobson/Jordan/Harrison/Schulz, Inc.—(713) 376-2368

France: Françoise Teisseyre Paris—(1) 46 22 51 54

West Germany and Austria: Franz Schrecklinger TMW Top Media Werbegesellschaft GmbH Frankfurt—(69) 726046

Holland and Belgium: Adele Struyck Holland—(034) 04 23265

Scandinavia: Andrew Karnig Andrew Karnig & Associates AB Finnbodavagen, 1, 131 31 Nacka Sweden—Telephone: 08 44 00 05 Telex: 89101755

Japan: Mashy Yoshikawa Orient Echo Inc. Tokyo—(03) 235 5961

Australia: Gus Bartel & Associates PO Box 1755, Southport, Queensland 42158—(075) 466 577

Nature® ISSN 0028-0836
Registered as a newspaper
at the British Post Office © 1986

nature

NATURE VOL. 319 30 JANUARY 1986

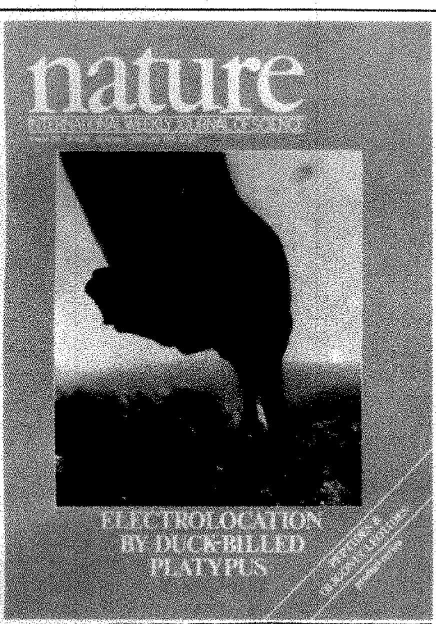

A trained duck-billed platypus attracted by the dipole field of a battery. During its dive the platypus closes its eyes, ears and nose by reflex action, relying totally on electrical somatosensory and chemical sensors in the bill. The battery, at a distance of 10 cm, sets up a field strength similar to that produced by the muscle potentials of live prey. See p.401. (Photo: G. Langer)

OPINION

How governments should be run 343

Max-Planck survives 344

NEWS

Solar System 345

Asbestos ban?

SDI

US research costs 346

Panel's prescription

Poles sentenced

Japanese education 347

US animal drugs

British universities 348

SFC defies Congress

IVF 349

Academic redundancies

US research grants

French nuclear power 350

Nuclear power

French science 351

Hungarian dam

Marine Science

CORRESPONDENCE

Free will etc. 352

NEWS AND VIEWS

Molecular biology in Japan 353

Shortcomings of an eagle's eye
Graham R Martin 357

Unexpected chemistry of Antarctic meteorites
George W Wetherill 357

Acetylcholine and brain cells
David Brown 358

Testing Solar System stability
P J Message 359

Ocean Drilling Programme: Formation of the Norwegian Sea
The Leg 104 shipboard scientific party 360

Clues to prehistoric ecology from the pollen record
Peter D Moore 361

Physics of liquids: Are diameters rectilinear?
J S Rowlinson 362

BOOK REVIEWS

The Life of Ernst Chain: Penicillin and Beyond ***by R W Clark***
Gwyn Macfarlane 363

Biology of Amphibians
by W E Duellman and L Trueb
Tim Halliday 364

Neuropsychology of Memory
L R Squire and N Butters, eds
Patrick Rabbitt 365

An Illustrated Guide to the Protozoa
J J Lee, S H Hutner and E C Bovee, eds
F E G Cox 366

Fiber Optics: Technology and Applications *by S D Personick*
John J O'Reilly

COMMENTARY

The fight for science textbooks
T H Jukes 367

ARTICLES

Isolation of a cDNA clone coding for a possible neural nicotinic acetylcholine receptor α-subunit
J Boulter, K Evans, D Goldman, G Martin, D Treco, S Heinemann & J Patrick 368

Expression of the c-*myb* proto-oncogene during cellular proliferation
C B Thompson, P B Challoner, P E Neiman & M Groudine 374

LETTERS TO NATURE

Origin of ultra-high-energy γ-rays from Cygnus X-3 and related sources
D Kazanas & D C Ellison 380

Period derivative and orbital eccentricity of binary pulsar 1953+29
L A Rawley, J H Taylor & M M Davis 383

Feasibility of a low-mass binary source progenitor for PSR1937+214
L C Jeffrey 384

Long-term changes in the semimajor axes of the outer planets
A Milani, A M Nobili, K Fox & M Carpino 386

D to H ratio and the origin and evolution of Titan's atmosphere
J P Pinto, J I Lunine, S-J Kim & Y L Yung 388

Antarctic and non-Antarctic meteorites form different populations
J E Dennison, D W Lingner & M E Lipschutz 390

A new optical photochemical memory device in a light-sensitive chemically active medium
L Kuhnert 393

A plate tectonic model of the eastern Indonesia collision zone
T R Charlton 394

Tectonics of the westernmost Gulf of Aden and the Gulf of Tadjoura from submersible observations
P Choukroune, B Auvray, J Francheteau, J C Lepine, F Arthaud, J P Brun, J M Auzende, B Sichler & Y Khobar 396

Formation of cubic structures in microemulsions containing equal volumes of oil and water
J Tabony 400

Electroreception and electrolocation in platypus
H Scheich, G Langner, C Tidemann, R B Coles & A Guppy 401

Acetylcholine induces burst firing in thalamic reticular neurones by activating a potassium conductance
D A McCormick & D A Prince 402

Acetylcholine hyperpolarizes central neurones by acting on an M_2 muscarinic receptor
T M Egan & R A North 405

Contents continued overleaf

Nature® (ISSN 0028-0836) is published weekly on Thursday, except the last week in December, by Macmillan Journals Ltd and includes the Annual Index (mailed in February). Annual subscription for USA and Canada US $240. USA and Canadian orders to: *Nature*, Subscription Dept, PO Box 1501, Neptune, NJ 07753, USA. Other orders to *Nature*, Brunel Road, Basingstoke, Hants RG21 2XS, UK. Second class postage paid at New York, NY 10012 and additional mailing offices. Authorization to photocopy material for internal or personal use, or internal or personal use of specific clients, is granted by *Nature* to libraries and others registered with the Copyright Clearance Center (CCC) Transactional Reporting Service, provided the base fee of $1.00 a copy plus $0.10 a page is paid directly to CCC, 21 Congress Street, Salem, Massachusetts 01970, USA. Identification code for *Nature*: 0028-0836/86 $1.00 + $0.10. US Postmaster send address changes to: *Nature*, 65 Bleecker Street, New York, NY 10012. Published in Japan by Macmillan Shuppan K.K., Eikow Building, 1-10-9 Hongo, Bunkyo-ku, Tokyo, Japan. © 1986 Macmillan Journals Ltd.

INTRODUC
THE RAPID RC
CUSTOM PE
FOR ANTIPEPTIDE ANTIBOD

CRB CUSTC
EXPRE

CRB have developed great experience in the **Selection** and
generation of **Antipeptide Antibodies** to oncogenes, growth
proteins etc., together with expertise in Peptide Conjugation T
and Assay Procedures.

As an addition to our existing services for molecular biology,
(2-3 weeks) for the custom synthesis of such peptides. These **Gu**
are supplied at **Low Cost** with **Comprehensive Analytical Da**
fast atom bombardment mass spectrometric analysis).

Peptide-carrier protein **Conjugates** may also be prepared ra
variety of methods directed to the production of more careft

Other CRB services include Hydrophilicity Analysis, Epitop
Antibody Specificities, synthesis of internally Radiolab
developing a New Immunisation Protocol for the h
antibodies.

For further details, or for any information c
of, synthetic peptides please cont
Research Director.

CRB
CAMBRIDGE
RESEARCH
BIOCHEMICALS

Cambridge Research Biochemicals Ltd. Button End Harston, Cambridge
CB2 5NX England Telephone: Cambridge (0223) 871674 Telex: 817694 CRBLTD G

Cambridge Research Biochemicals Ltd. PO Box 58, 2003 Park Street, Atlantic Beach,
New York 11509 USA. Telephone: (516) 239 3831 Telex: 971398

Reader Servic

NATURE'S 1986
CALENDAR!

12 cover photographs superbly reproduced in full colour. Send for your calendar now.

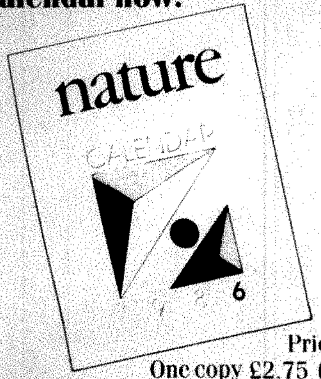

Prices:
One copy £2.75 (UK)
£3.75 (REST OF WORLD)
Three or more copies £2.50 (UK)
£3.20 (REST OF WORLD) each

Send orders to:
Circulation Manager, Macmillan Journals Ltd., FREEPOST (UK ONLY) Brunel Road, Houndmills, Basingstoke, Hants., RG21 2XS UK.

Annual Subscription Prices

UK & Irish Republic		£104
USA & Canada		US$240
Australia, NZ & S. Africa	Airspeed	£150
	Airmail	£190
Continental Europe	Airspeed	£125
India	Airspeed	£120
	Airmail	£190
Japan	Airspeed	Y90000
Rest of World	Surface	£120
	Airmail	£180

Orders (with remittance) to:

USA & Canada	UK & Rest of World
Nature	Nature
Subscription Dept	Circulation Dept
PO Box 1501	Brunel Road
Neptune	Basingstoke
NJ 07753	Hants RG21 2XS, UK
USA	Tel: 0256 29242

(The addresses of Nature's editorial offices are shown facing the first editorial page)

Japanese subscription enquiries to:
Japan Publications Trading Company Ltd
2-1 Sarugaku-cho 1-chome
Chiyoda-ku, Tokyo, Japan
Tel: (03) 292 3755

Personal subscription rates: These are available in some countries to subscribers paying by personal cheque or credit card. Details from:

USA & Canada	UK & Europe
Nature	Felicity Parker
65 Bleecker Street	Nature
New York	4 Little Essex Street
NY 10012, USA	London WC2R 3LF, UK
Tel: (212) 477-9600	Tel: 01-836 6633

Back issues: UK, £2.50; USA & Canada, US$6.00 (surface), US$9.00 (air); Rest of World, £3.00 (surface), £4.00 (air)

Binders
Single binders: UK, £5.25; USA & Canada $11.50; Rest of World, £7.75. Set of four: UK, £15.00; USA & Canada $32.00; Rest of World, £22.00

Annual indexes (1971-1985)
UK, £5.00 each; Rest of World, $10.00

Nature First Issue Facsimile
UK, 75p; Rest of World (surface), $1.50; (air) $2.00

Nature in microform
Write to University Microfilms International, 300 North Zeeb Road, Ann Arbor, MI 48106, USA

Primary structure of *Torpedo californica* acetylcholinesterase deduced from its cDNA sequence
M Schumacher, S Camp, Y Maulet, M Newton, K MacPhee-Quigley, S S Taylor, T Friedmann & P Taylor 407

Single channels and ionic currents in peptidergic nerve terminals
J R Lemos, J J Nordmann, I M Cooke & E L Stuenkel 410

Neonatal T-cell tolerance to minimal immunogenic peptides is caused by clonal inactivation
G Gammon, K Dunn, N Shastri, A Oki, S Wilbur & E E Sercarz 413

Molecular cloning and expression of cDNA for human granulocyte colony-stimulating factor
S Nagata, M Tsuchiya, S Asano, Y Kaziro, T Yamazaki, O Yamamoto, Y Hirata, N Kubota, M Oheda, H Nomura & M Ono 415

'Brain-specific' transcription and evolution of the identifier sequence
C Sapienza & B St-Jacques 418

Rearrangement of two distinct T-cell γ-chain variable-region genes in human DNA
M-P Lefranc, A Forster & T H Rabbitts 420

An *Agrobacterium* transformation in the evolution of the genus *Nicotiana*
I J Furner, G A Huffman, R M Amasino, D J Garfinkel, M P Gordon & E W Nester 422

Erratum . . . page **427**
***Mycobacterium leprae*-specific protein antigens defined by cloned human helper T cells**
T H M Ottenhoff, P R Klatser, J Ivani, D G Elferink, M Y L de Wit & R R P de Vries

Corridendum . . . page **427**
Efficiency of petroleum expulsion from shale source rocks
D Leythaeuser, M Radke & R G Schaefer

MATTERS ARISING

Palaeontological and molecular views of panda phylogeny
L M Van Valen
Reply: S J O'Brien, W G Nash, R E Benveniste, D E Wildt & M E Bush 428

Oncofetal antigens
J H Coggin Jr 428
Reply: T Feizi 428

PRODUCT REVIEW

Automated continuous flow peptide synthesis
R P Andrews 429

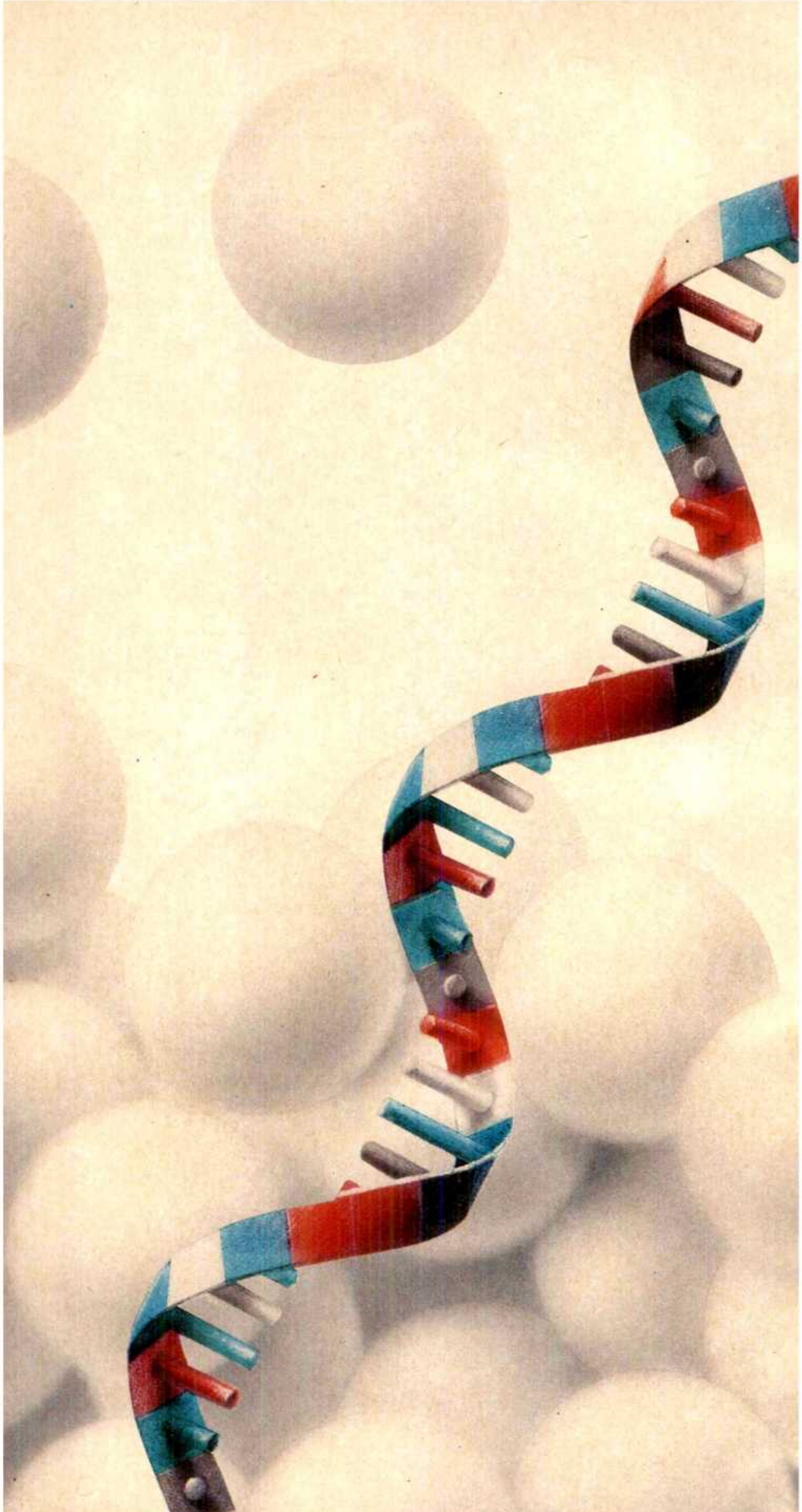

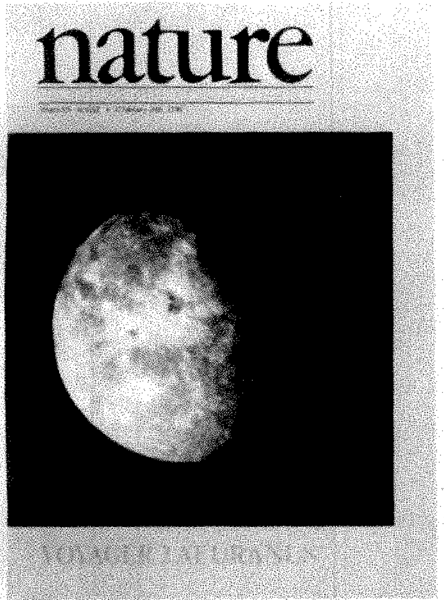

A Voyager 2 picture of Oberon, Uranus' outermost moon, taken from a distance of 410,000 miles. The colour was reconstructed from images taken through the narrow-angle camera's violet, clear and green filters. Features as small as 7 miles on the moon's surface are visible, as are several large impact craters. For more Voyager photographs, see p.453.

OPINION

Why did Challenger matter? 435
End of the road 436
Giving bugs the vote

NEWS

US space research 437
SDI on campus
Ariane 438
Marine satellites
Voyager 2 439
Soviet environment
Animal welfare 440
Guidelines off
Preaching to converts
Pacific volcano 441
AIDS
Trials on ice
British clinical research 442
MRC attacked
Budget of INSERM grows
Bulgar identity 443
Marine science
EPA expansion urged

CORRESPONDENCE

Remote viewing/Sexism/ UNESCO/etc. 444

NEWS AND VIEWS

Galactic voids may be statistical 445
New fossil finds in old rocks
S M Awramik 446
Are developmental genes mediators of cell communication?
Michael Akam 447
Sources of basic magmas
R N Thompson 448
Human evolution: How small was the bottleneck?
J S Jones & S Rouhani 449
X-ray astronomy: New results from Exosat
A C Fabian 451
Neurobiology: Microcircuits to see by
Gordon M Shepherd 452

SCIENTIFIC CORRESPONDENCE

Large computers key to aggregation phenomena
R Botet & R Jullien 454
Minimum energy configurations
M G Calkin, D Kiang & D A Tindall 454

BOOK REVIEWS

The Royal Institution: An Informal History
by G Caroe
Roy Porter 455
Quantum Fluctuations
by E Nelson
Philip Pearle 456
Theoretical Biology and Complexity
R Rosen, ed.
Lee A Segel 457
On the track of an epidemic — three books on AIDS
Richard S Tedder
Molecular Semiconductors: Photoelectrical Properties and Solar Cells
by J Simon and J-J André
Daniel D Eley 458

ARTICLES

Optical synchrotron emission in the southern lobe of 3C33
K Meisenheimer & H-J Röser 459
Homologies in both primary and secondary structure between nuclear envelope and intermediate filament proteins
F D McKeon, M W Kirschner & D Caput 463

LETTERS TO NATURE

Quasi-periodic oscillations in the X-ray flux of Cyg X-2
G Hasinger, A Langmeier, M Sztajno, J Trümper, W H G Lewin & N E White 469
How old is Cygnus A?
M J Spinks, W G Rees & P J Duffett-Smith 471
Ionic origins of carbenes in space
D K Bohme 473
An intense cold core eddy in the North-East Atlantic
S L Kupferman, G A Becker, W F Simmons, U Schauer, M G Marietta & H Nies 474
Nd–Sr–Pb isotope constraints on the sources of West Maui volcano, Hawaii
E Hegner, D Unruh & M Tatsumoto 478
Carbon and sulphur isotopic composition of Kilauea parental magma
T M Gerlach & D M Thomas 480
Calcium anomalies in the mantle and a subducted metaserpentinite origin for diamonds
D J Schulze 483
Mechanism of aqueous dissolution of silicate glasses yielded by fission tracks
J-C Dran, J-C Petit & C Brousse 485
Pb–Pb systematics of Lewisian gneisses — implications for crustal differentiation
M J Whitehouse & S Moorbath 488
Stromatolites from the 3,300–3,500-Myr Swaziland Supergroup, Barberton Mountain Land, South Africa
G R Byerly, D R Lower & M M Walsh 489
Evolutionary relationships of human populations from an analysis of nuclear DNA polymorphisms
J S Wainscoat, A V S Hill, A L Boyce, J Flint, M Hernandez, S L Thein, J M Old, J R Lynch, Y Falusi, D J Weatherall & J B Clegg 491
Crabs that breathe air with their legs — *Scopimera* and *Dotilla*
D P Maitland 493
Ganglion cell dendrites are presynaptic in catfish retina
H M Sakai, KI Naka & J E Dowling 495

Contents continued overleaf

Nature® (ISSN 0028-0836) is published weekly on Thursday, except the last week in December, by Macmillan Journals Ltd and includes the Annual Index (mailed in February). Annual subscription for USA and Canada US $240. USA and Canadian orders to: *Nature*, Subscription Dept, PO Box 1501, Neptune, NJ 07753, USA. Other orders to *Nature*, Brunel Road, Basingstoke, Hants RG21 2XS, UK. Second class postage paid at New York, NY 10012 and additional mailing offices. Authorization to photocopy material for internal or personal use, or internal or personal use of specific clients, is granted by *Nature* to libraries and others registered with the Copyright Clearance Center (CCC) Transactional Reporting Service, provided the base fee of $1.00 a copy plus $0.10 a page is paid directly to CCC, 21 Congress Street, Salem, Massachusetts 01970, USA. Identification code for *Nature*: 0028-0836/86 $1.00 + $0.10. US Postmaster send address changes to: *Nature*, 65 Bleecker Street, New York, NY 10012. Published in Japan by Macmillan Shuppan K.K., Eikow Building, 1-10-9 Hongo, Bunkyo-ku, Tokyo, Japan. © 1986 Macmillan Journals Ltd

FROM NEW ENGLAND BIOLABS

KINASE KINASE KIN
KINASE KINASE KIN
KINASE KINASE KIN
KINASE KINASE KIN
KINASE KINASE KI

T4 POLYNUCLEOTIDE KINASE
CLONED AT NEW ENGLAND BIOLABS *
OFFERS YOU THE HIGHEST QUALITY AT THE LOWEST PRICE

#201

500 units $30   2,500 units $100

UST RELEASED

Avr II
#174
5′...C▼CTAGG...3′
3′...GGATC▲C...5′
0 units
00 units

BspM I
#502
5′...ACCTGC(N)$_4$...3′
3′...TGGACG(N)$_8$...5′
100 units
500 units

BspM II
#504
5′...T▼CCGGA...3′
3′...AGGCC▲T...5′
20 units
100 units

Eag I
#505
Xma III isoschizomer
5′...C▼GGCCG...3′
3′...GCCGG▲C...5′
100 units
500 units

EcoO109
#503
Dra II isoschizomer
5′...PuG▼GNCCPy...3′
3′...PyCCNG▲GPu...5′
2,000 units
10,000 units

PpuM I
#506
5′...PuG▼G${}^{A}_{T}$CCPy...3′
3′...PyCC${}^{A}_{T}$G▲GPu...5′
50 units
250 units

Rsr II
#501
5′...CG▼G${}^{A}_{T}$CCG...3′
3′...GCC${}^{A}_{T}$G▲GC...5′
25 units
125 units

T7 RNA Polymerase
#251
5,000 units
25,000 units

Discovered and characterized at New England Biolabs

**Constructed in a manner first described by C.A. Midgley and N.E. Murray (1985).*

NEW ENGLAND Biolabs INC.

32 Tozer Road, Beverly, MA 01915-9990/USA, TEL. 617-927-5054 TELEX 6817316
England Biolabs GmbH, Postfach 2750, 6321 Schwalbach/Taunus, Federal Republic of Germany, TEL. (06 196) 3031 TELEX 410989 NEB D

Reader Service No.195

CONTENTS

NATURE'S 1986 CALENDAR!

12 cover photographs superbly reproduced in full colour. Send for your calendar now.

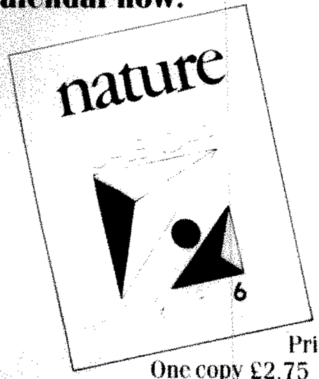

Prices:
One copy £2.75 (UK)
£3.75 (REST OF WORLD)
Three or more copies £2.50 (UK)
£3.20 (REST OF WORLD) each

Send orders to:
Circulation Manager, Macmillan Journals Ltd., FREEPOST (UK ONLY) Brunel Road, Houndmills, Basingstoke, Hants., RG21 2XS UK.

Annual Subscription Prices

UK & Irish Republic		£104
USA & Canada		US$240
Australia, NZ & S. Africa	Airspeed	£150
	Airmail	£190
Continental Europe	Airspeed	£125
India	Airspeed	£120
	Airmail	£190
Japan	Airspeed	Y90000
Rest of World	Surface	£120
	Airmail	£180

Orders (with remittance) to:

USA & Canada
Nature
Subscription Dept
PO Box 1501
Neptune
NJ 07753
USA

UK & Rest of World
Nature
Circulation Dept
Brunel Road
Basingstoke
Hants RG21 2XS, UK
Tel: 0256 29242

(The addresses of Nature's editorial offices are shown facing the first editorial page)

Japanese subscription enquiries to:
Japan Publications Trading Company Ltd
2-1 Sarugaku-cho 1-chome
Chiyoda-ku, Tokyo, Japan
Tel: (03) 292 3755

Personal subscription rates: These are available in some countries to subscribers paying by personal cheque or credit card. Details from:

USA & Canada
Nature
65 Bleecker Street
New York
NY 10012, USA
Tel: (212) 477-9600

UK & Europe
Felicity Parker
Nature
4 Little Essex Street
London WC2R 3LF, UK
Tel: 01-836 6633

Back issues: UK, £2.50; USA & Canada, US$6.00 (surface), US$9.00 (air); Rest of World, £3.00 (surface), £4.00 (air)

Binders
Single binders. UK, £5.25; USA & Canada $11.50; Rest of World, £7.75. Set of four: UK, £15.00; USA & Canada $32.00; Rest of World, £22.00

Annual indexes (1971-1985)
UK, £5.00 each; Rest of World, $10.00

Nature First Issue Facsimile
UK, 75p; Rest of World (surface), $1.50; (air) $2.00

Nature in microform
Write to University Microfilms International, 300 North Zeeb Road, Ann Arbor, MI 48106, USA

Different factors from the central nervous system and periphery regulate the survival of sensory neurones
A M Davies, H Thoenen & Y A Barde 497

Proliferating bipotential glial progenitor cells in adult rat optic nerve
C ffrenchConstant & M C Raff 499

Restricted recognition of β_2-microglobulin by cytotoxic T lymphocytes
HG Rammensee, P J Robinson, A Crisanti & M J Bevan 502

Two roles for guanine nucleotides in the stimulus–secretion sequence of neutrophils
M M Barrowman, S Cockcroft & B D Gomperts 504

Clonal origin of haematopoietic colonies in the postnatal mouse liver
J Rossant, K M Vijh, C E Grossi & M D Cooper 507

A human osteosarcoma cell line secretes a growth factor structurally related to a homodimer of PDGF A-chains
CH Heldin, A Johnsson, S Wennergren, C Wernstedt, C Betsholtz & B Westermark 511

A saturable receptor for ^{32}P-inositol-1,4,5-trisphosphate in hepatocytes and neutrophils
A Spät, P G Bradford, J S McKinney, R P Rubin & J W Putney Jr 514

Stimulation of bone resorption and inhibition of bone formation *in vitro* by human tumour necrosis factors
D R Bertolini, G E Nedwin, T S Bringman, D D Smith & G R Mundy 516

MISCELLANY

New on the market 519

Employment: Breaks in career — What chance for women?
R Pearson 522

NATURE CLASSIFIED

Professional appointments — Research posts — Studentships — Fellowships — Conferences — Courses — Seminars — Symposia: **Back Pages**

Next week in *Nature*:

- Cosmic string discovery?
- High-redshift quasars
- Irradiation history of meteorites
- Stratospheric dinitrogen pentoxide
- Sargasso Sea pollution
- Quaternary volcanic eruption
- Gulls' feeding tactics
- Recombinant vaccinia a universal vaccine?
- AIDS virus replication
- Pathophysiology of Alzheimer's disease
- Electron microscope tomography of ribonucleoprotein

GUIDE TO AUTHORS

Authors should be aware of the diversity of *Nature*'s readership and should strive to be as widely understood as possible.

Review articles should be accessible to the whole readership. Most are commissioned, but unsolicited reviews are welcome (in which case prior consultation with the office is desirable).

Scientific articles are research reports whose conclusions are of general interest or which represent substantial advances of understanding. The text should not exceed 3,000 words and six displayed items (figures plus tables). The article should include an italic heading of about 50 words.

Letters to *Nature* are ordinarily 1,000 words long with no more than four displayed items. The first paragraph (not exceeding 150 words) should say what the letter is about, why the study it reports was undertaken and what the conclusions are.

Matters arising are brief comments (up to 500 words) on articles and letters recently published in *Nature*. The originator of a Matters Arising contribution should initially send his manuscript to the author of the original paper and both parties should, wherever possible, agree on what is to be submitted.

Manuscripts may be submitted either to London or Washington). Manuscripts should be typed (double spacing) on one side of the paper only. Four copies are required, each accompanied by copies of lettered artwork. No title should exceed 80 characters in length. Reference lists, figure legends, etc, should be on seperate sheets, all of which should be numbered. Abbreviations, symbols, units, etc, should be identified on one copy of the manuscript at their first appearance.

References should appear sequentially indicated by superscripts, in the text and should be abbreviated according to the *World List of Scientific Periodicals*, fourth edition (Butterworth 1963-65). The first and last page numbers of each reference should be cited. Reference to books should clearly indicate the publisher and the date and place of publication. Unpublished articles should not be formally referred to unless accepted or submitted for publication, but may be mentioned in the text.

Each piece of artwork should be clearly marked with the author's name and the figure number. Original artwork should be unlettered. Suggestions for cover illustrations are welcome. Original artwork (and one copy of the manuscript) will be returned when manuscripts cannot be published.

Requests for permission to reproduce material from Nature *should be accompanied by a self-addressed (and, in the case of the United Kingdom and United States, stamped) envelope.*

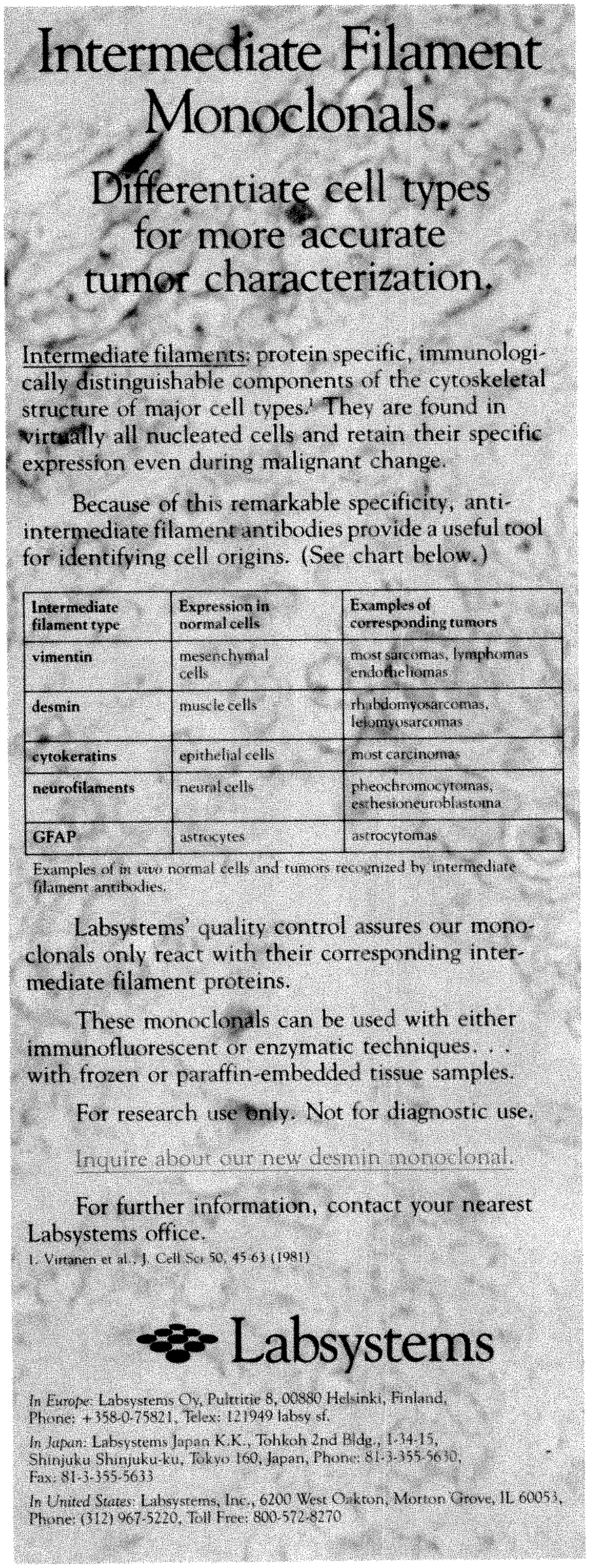

Intermediate Filament Monoclonals.

Differentiate cell types for more accurate tumor characterization.

Intermediate filaments: protein specific, immunologically distinguishable components of the cytoskeletal structure of major cell types.[1] They are found in virtually all nucleated cells and retain their specific expression even during malignant change.

Because of this remarkable specificity, anti-intermediate filament antibodies provide a useful tool for identifying cell origins. (See chart below.)

Intermediate filament type	Expression in normal cells	Examples of corresponding tumors
vimentin	mesenchymal cells	most sarcomas, lymphomas endotheliomas
desmin	muscle cells	rhabdomyosarcomas, leiomyosarcomas
cytokeratins	epithelial cells	most carcinomas
neurofilaments	neural cells	pheochromocytomas, esthesioneuroblastoma
GFAP	astrocytes	astrocytomas

Examples of *in vivo* normal cells and tumors recognized by intermediate filament antibodies.

Labsystems' quality control assures our monoclonals only react with their corresponding intermediate filament proteins.

These monoclonals can be used with either immunofluorescent or enzymatic techniques. . . with frozen or paraffin-embedded tissue samples.

For research use only. Not for diagnostic use.

Inquire about our new desmin monoclonal.

For further information, contact your nearest Labsystems office.

1. Virtanen et al., J. Cell Sci 50, 45-63 (1981)

Labsystems

In Europe: Labsystems Oy, Pulttitie 8, 00880 Helsinki, Finland, Phone: +358-0-75821, Telex: 121949 labsy sf.

In Japan: Labsystems Japan K.K., Tohkoh 2nd Bldg., 1-34-15, Shinjuku Shinjuku-ku, Tokyo 160, Japan, Phone: 81-3-355-5630, Fax: 81-3-355-5633

In United States: Labsystems, Inc., 6200 West Oakton, Morton Grove, IL 60053, Phone: (312) 967-5220, Toll Free: 800-572-8270

Reader Service No.7

JOURNALS FROM MACMILLAN

NEW JOURNAL LAUNCHED DECEMBER 1984

☐ **PHARMACEUTICAL MEDICINE** Quarterly

Editor: R. N. Smith. Assistant Editor: P. J. Keen

"a quarterly journal, which includes papers on the validation of new and established methods of testing drugs in man written by investigators both inside and outside the pharmaceutical industry. It also provides a forum for the exchange of ideas about issues affecting drug development. These new developments merit support from all involved in the management, sale and use of drugs." ***Lancet***

☐ ***BRITISH JOURNAL OF PHARMACOLOGY*** Monthly

THE JOURNAL OF THE BRITISH PHARMACOLOGICAL SOCIETY

Chairman: J. F. Mitchell

Secretary to the Editorial Board: G. M. Lees

One of the top five most cited pharmacology journals in the world.

A vital source of relevant information for physiologists, immunologists, molecular biologists

☐ ***PUBLIC HEALTH*** Monthly

THE JOURNAL OF THE SOCIETY OF COMMUNITY MEDICINE

Editor: J. S. Robertson

From the beginning of 1986 Macmillan will be publishing ***Public Health.*** Now in its 100th volume, the journal publishes studies in preventive and social medicine and all aspects of public health and particularly welcomes reports of original epidemiological studies

☐ ***POSTGRADUATE MEDICAL JOURNAL*** Monthly

JOURNAL OF THE FELLOWSHIP OF POSTGRADUATE MEDICINE

Editor: B. I. Hoffbrand

A monthly compendium of current clinical research and practice invaluable to the graduate in training

☐ ***HUMAN TOXICOLOGY*** Bi-monthly

Secretary to the Editorial Board: P. Turner

Covers all aspects of human toxicology embracing both animal research with particular relevance to man and studies with humans

SAMPLE COPY ORDER FORM

Please tick the titles you would like to receive, fill in details and return to the address shown.

Name ....

Position ....

Address ....

....

....

Return to
Alison Baverstock,
Macmillan Press, Houndmills,
Basingstoke, Hants
RG21 2XS, UK.

Macmillan Press
Scientific & Medical

nature

NATURE VOL. 319 13 FEBRUARY 1986

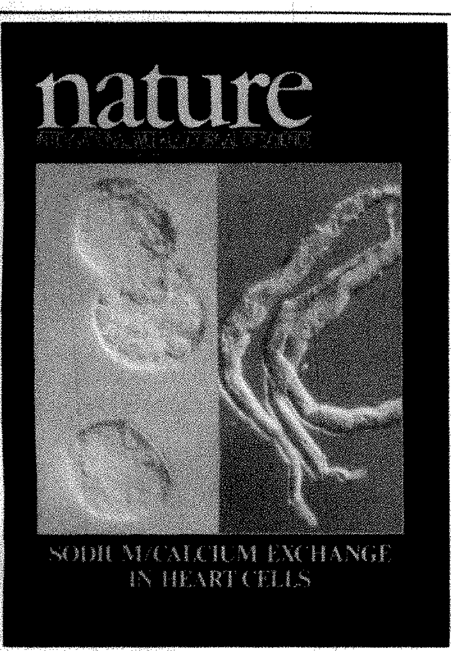

Cultured cardiac myocytes. Cyclic activation of the Na–Ca exchange current in cardiac myocytes by the release of Ca from the sarcoplasmic reticulum can cause maintained spontaneous activity. This process may contribute to some forms of cardiac pacemaking. See page 597.

OPINION

Prospect of US budget chaos 523

NEWS

World Archaeological Congress 524
Animal welfare
European particle physics 525
AIDS protein made
US budget 526
Japanese research 528
Gorbachev purge reaches researchers
Pharmaceuticals in Britain 529
West German forests
Eureka 530
European neutrons
Sir Keith Joseph regrets. . . 531

CORRESPONDENCE

World Archaeological Congress/ Stellar colours/Radiation 532

NEWS AND VIEWS

More tests of special relativity 533
Polyribonucleic acids as enzymes
F H Westheimer 534
Biological rhythms: Sleep researchers caught napping
N Mrosovsky 536
Peptides and Alzheimer's disease
Alan Fine 537
Reservoir species discovered in the stratosphere
Donald J Wuebbles 538
Distant galaxies: Pushing back the redshift limit
C Martin Gaskell 539
Limits of visual resolution
Graham Martin 540
First results from Spacelab 2
Eugene W Urban 540

SCIENTIFIC CORRESPONDENCE

Accidental human vaccination with vaccinia virus expressing nucleoprotein gene
L Jones, S Ristow, T Yilma & B Moss 543
Malaria — mitogens or super antigens?
G O Oyeyinka 543
The riddle of the magnetic doors
L C Tai 544

BOOK REVIEWS

The Mind's New Science: A History of the Cognitive Revolution
by H Gardner
Donald Broadbent 545
The Old Brown Dog: Women, Workers and Vivisection in Edwardian England
by C Lansbury
W F Bynum 546
Earthquake Prediction
by K Mogi
Chi-Yu King 547
An Atlas of Immunofluorescence in Cultured Cells
by M C Willingham and I Pastan
Julian Heath
Alfred North Whitehead: The Man and His Work, Vol. I 1861–1910
by V Lowe and
Science and the Modern World
by A N Whitehead
George Gale 548

COMMENTARY

Recombinant vaccinia viruses as vaccines
F Brown, G C Schild & G L Ada 549

ARTICLES

Horizontal shear flow in the mantle beneath the Tonga arc
D Giardini & J H Woodhouse 551
Post-transcriptional regulation accounts for the *trans*-activation of the human T-lymphotropic virus type III
C A Rosen, J G Sodroski, W C Goh, A I Dayton, J Lippke & W A Haseltine 555
Three-dimensional structure of a specific pre-messenger RNP particle established by electron microscope tomography
U Skoglund, K Andersson, B Strandberg & B Daneholt 560

LETTERS TO NATURE

A quasar with $z=3.71$ and limits on the number of more distant objects
J S Dunlop, A J B Downes, J A Peacock, A Savage, S J Lilly, F G Watson & M S Longair 564
Will cosmic strings be discovered using the Space Telescope?
B Paczyński 567
Determination of cosmogenic ^{41}Ca in a meteorite with tandem accelerator mass spectrometry
P W Kubik, D Elmore, N J Conard, K Nishiizumi & J R Arnold 568
Detection of stratospheric N_2O_5 by infrared remote sounding
G C Toon, C B Farmer & R H Norton 570
Synthetic organic chemicals in the deep Sargasso Sea
A H Knap, K S Binkley & W G Deuser 572
A lagrangian mixed layer model of Atlantic 18°C water formation
J D Woods & W Barkmann 574
Isotope anomalies induced in laboratory distillation
T M Esat, R H Spear & S R Taylor 576
An exceptionally large late Quaternary eruption from New Zealand
P C Froggatt, C S Nelson, L Carter, G Griggs & K P Black 578
Aeromagnetic anomalies and tectonic trends in and around the Benue Trough, Nigeria
D E Ajakaiye, D H Hall, T W Millar, P J T Verheijen, M B Awad & S B Ojo 582
High-pressure transformation of eclogite to garnetite in subducted oceanic crust
T Sekine, T Irifune, A E Ringwood & W O Hibberson 584

Contents continued overleaf

Nature® (ISSN 0028-0836) is published weekly on Thursday, except the last week in December, by Macmillan Journals Ltd and includes the Annual Index (mailed in February). Annual subscription for USA and Canada US $240. USA and Canadian orders to: *Nature*, Subscription Dept, PO Box 1501, Neptune, NJ 07753, USA. Other orders to *Nature*, Brunel Road, Basingstoke, Hants RG21 2XS, UK. Second class postage paid at New York, NY 10012 and additional mailing offices. Authorization to photocopy material for internal or personal use, or internal or personal use of specific clients, is granted by *Nature* to libraries and others registered with the Copyright Clearance Center (CCC) Transactional Reporting Service, provided the base fee of $1.00 a copy plus $0.10 a page is paid directly to CCC, 21 Congress Street, Salem, Massachusetts 01970, USA. Identification code for *Nature*: 0028-0836/86 $1.00 + $0.10. US Postmaster send address changes to: *Nature*, 65 Bleecker Street, New York, NY 10012. Published in Japan by Macmillan Shuppan K.K., Eikow Building, 1-10-9 Hongo, Bunkyo-ku, Tokyo, Japan. © 1986 Macmillan Journals Ltd.

Amersham provides the perfect match

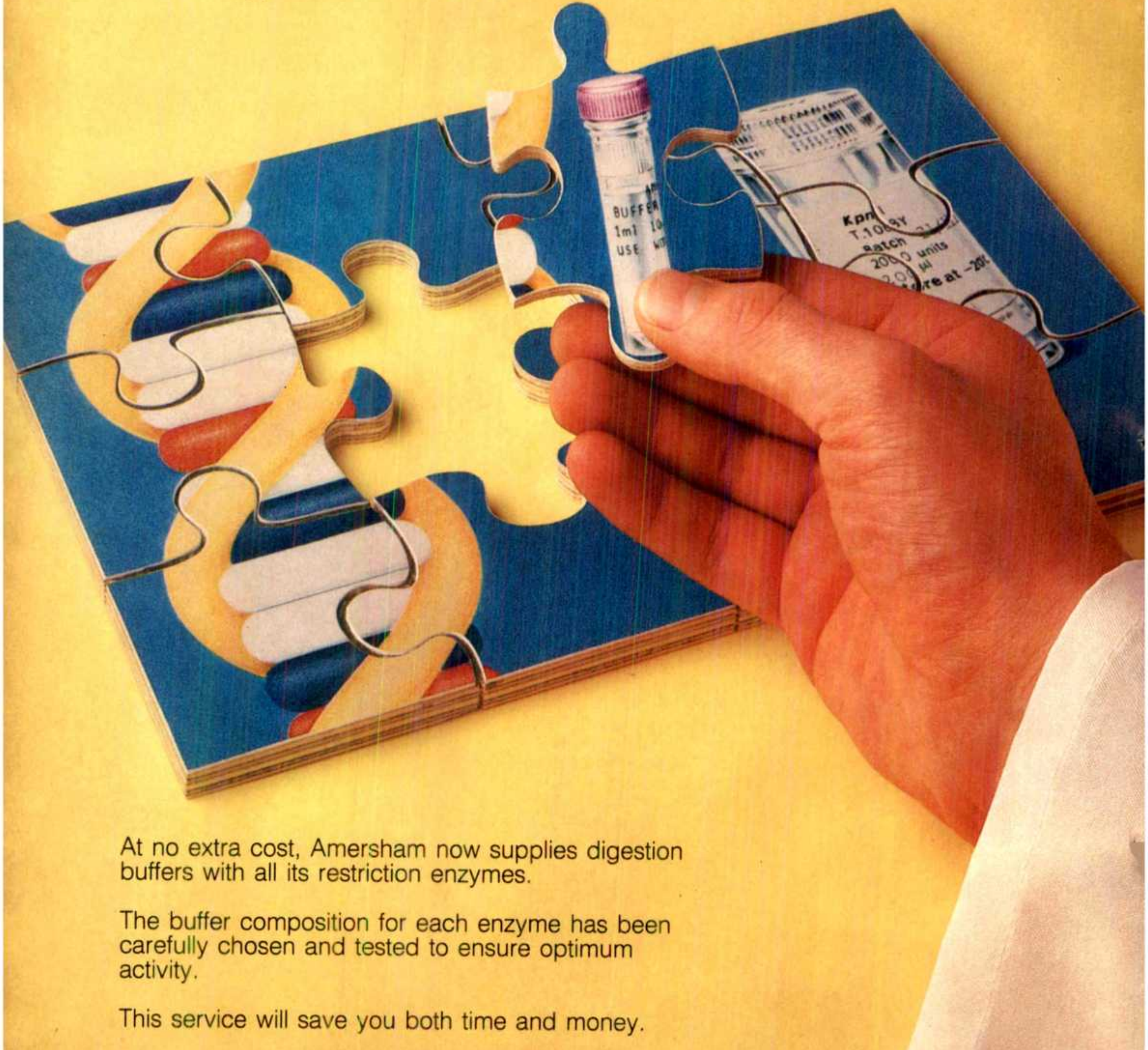

At no extra cost, Amersham now supplies digestion buffers with all its restriction enzymes.

The buffer composition for each enzyme has been carefully chosen and tested to ensure optimum activity.

This service will save you both time and money.

So when it comes to DNA cleavage, remember it's only Amersham who provides the correct buffer with each enzyme—a perfectly matched pair.

Amersham Corporation
2636 South Clearbrook Drive, Arlington Heights, IL 60005
(312) 364-7100 or (800) 323-9750 (Toll Free)

Amersham

In Canada 505 Iroquois Shore Road, Oakville ONT L6H 2R3 (416) 842-2720/(800) 268-5061

Reader Service No.5

CONTENTS

NATURE'S FIRST ISSUE FACSIMILE

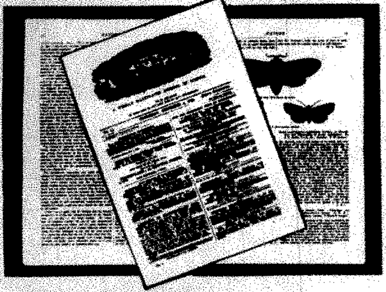

.....40-PAGES OF INTRIGUING SCIENTIFIC HISTORY REPRODUCED.

ORDER YOUR OWN COPY AND DISCOVER HOW SCIENCE HAS ADVANCED SINCE 1869!

PRICES AND ADDRESS FOR ORDERS ARE SET OUT BELOW.

Annual Subscription Rates (including Index)
USA & Canada US$240

Orders (with remittance), subscription inquiries and change of address to:
Nature
Order Department
PO Box 1501
Neptune
NJ 07753
USA
Call toll-free (USA only); (800) 524-0384
Please allow 6-8 weeks for your subscription to start.

Personal subscription rates
These are available in the USA and Canada to subscribers paying by personal check or credit card. For details contact the New York Circulation Offices (address below).

Back issues
US$6.00

Binders
Single binder US$11.50; set of four binders US$32.00

Annual indexes (1971–1985)
US$10.00

Nature first issue facsimile
US$4.00

Orders (with remittance) to:
Circulation Offices
Nature
65 Bleecker Street
New York
NY 10012
USA
Tel: (212) 477-9628
Details of subscription rates in all other countries are available from this address

Nature in microform
For information contact:
University Microfilms International
300 North Zeeb Road
Ann Arbor
MI 48106
USA

Washington Editorial Office
Nature
1134 National Press Building
DC 20045
USA
Tel: (202) 737-2355

The pyroxene paradox in MORB glasses — a signature of picritic parental magmas?
D Francis 586

Flock-feeding on fish schools increases individual success in gulls
F Götmark, D W Winkler & M Andersson 589

Vernier acuity of neurones in cat visual cortex
N V Swindale & M S Cynader 591

Reciprocal changes in corticotropin-releasing factor (CRF)-like immunoreactivity and CRF receptors in cerebral cortex of Alzheimer's disease
E B De Souza, P J Whitehouse, M J Kuhar, D L Price & W W Vale 593

Na–Ca exchange current in mammalian heart cells
J Kimura, A Noma & H Irisawa 596

Identification of Na–Ca exchange current in single cardiac myocytes
S Mechmann & L Pott 597

Repetitive transient rises in cytoplasmic free calcium in hormone-stimulated hepatocytes
N M Woods, K S R Cuthbertson & P H Cobbold 600

Stable expression of two variable surface glycoproteins by cloned *Trypanosoma equiperdum*
T Baltz, C Giroud, D Baltz, C Roth, A Raibaud & H Eisen 602

Nucleotide sequence of chicken c-*myb* complementary DNA and implications for *myb* oncogene activation
D Rosson & E P Reddy 604

Corrigendum . . . page 606
Major shear zones and autochthonous Dalradian in the north-east Scottish Caledonides
W.A. Ashcroft, B.C. Kneller, A.G. Leslie & M. Munro

MISCELLANY

100 years ago 536

NATURE CLASSIFIED

Professional appointments — Research posts — Studentships — Fellowships — Conferences — Courses — Seminars — Symposia:
Back Pages

Next week in *Nature*:

- X rays from black holes and binaries
- Neptune's ring
- Ozone in the Northern Hemisphere
- Poly-iron aggregates
- Energetics of load carrying
- Electron micrographs of frozen-hydrated material
- Apamin receptor in myotonic muscular dystrophy
- Ribosomal exit channel for nascent protein
- Calcium channel modulation
- Natural killers in immune defence

GUIDE TO AUTHORS

Authors should be aware of the diversity of *Nature*'s readership and should strive to be as widely understood as possible.

Review articles should be accessible to the whole readership. Most are commissioned, but unsolicited reviews are welcome (in which case prior consultation with the office is desirable).

Scientific articles are research reports whose conclusions are of general interest or which represent substantial advances of understanding. The text should not exceed 3,000 words and six displayed items (figures plus tables). The article should include an italic heading of about 50 words.

Letters to *Nature* are ordinarily 1,000 words long with no more than four displayed items. The first paragraph (not exceeding 150 words) should say what the letter is about, why the study it reports was undertaken and what the conclusions are.

Matters arising are brief comments (up to 500 words) on articles and letters recently published in *Nature*. The originator of a Matters Arising contribution should initially send his manuscript to the author of the original paper and both parties should, wherever possible, agree on what is to be submitted.

Manuscripts may be submitted either to London or Washington). Manuscripts should be typed (double spacing) on one side of the paper only. Four copies are required, each accompanied by copies of lettered artwork. No title should exceed 80 characters in length. Reference lists, figure legends, etc, should be on seperate sheets, all of which should be numbered. Abbreviations, symbols, units, etc, should be identified on one copy of the manuscript at their first appearance.

References should appear sequentially indicated by superscripts, in the text and should be abbreviated according to the *World List of Scientific Periodicals*, fourth edition (Butterworth 1963-65). The first and last page numbers of each reference should be cited. Reference to books should clearly indicate the publisher and the date and place of publication. Unpublished articles should not be formally referred to unless accepted or submitted for publication, but may be mentioned in the text.

Each piece of artwork should be clearly marked with the author's name and the figure number. Original artwork should be unlettered. Suggestions for cover illustrations are welcome. Original artwork (and one copy of the manuscript) will be returned when manuscripts cannot be published.

Requests for permission to reproduce material from Nature *should be accompanied by a self-addressed (and, in the case of the United Kingdom and United States, stamped) envelope.*

New journal
launched
December 1984

A NEW JOURNAL FROM MACMILLAN PRESS

Pharmaceutical Medicine

Editor Dr R. N. Smith
Assistant Editor P. J. Keen

. . . "a quarterly journal, which includes papers on the validation of new and established methods of testing drugs in man written by investigators both inside and outside the pharmaceutical industry. It also provides a forum for the exchange of ideas about issues affecting drug development. These new developments merit support from all involved in the management, sale and use of drugs." *Lancet*

Contents of issue one:

EDITORIAL – Pharmaceutical Medicine – Promoting a Discipline. **COMMENTARY** – The Orphaned Clinical Trials. How Many Authors Make a Paper? Balancing Therapeutic Risks and Benefits. New Testament. **REGULATORY SCENE – *N. Mattison*** Unexpected Side-effects: The Regulatory Implications of the Oraflex and Zomax Withdrawals in the USA. **PAPERS – *G. T. McInnes, J. R. Shelton, I. R. Harrison, J. M. Clarke and R. M. Perkins*** Assessment of the Long Term Effects of Aldosterone Antagonists by a Short Term Assay. ***Z. Subhan and I. Hindmarch*** Assessing Residual Effects of Benzo-diazepines on Short Term Memory. ***C. Y. Hong, B. N. Chiang and P. Wu*** *In Vitro* Spermicidal Potencies of the Dosage Forms and Active Ingredients of Some Vaginal Contraceptives: Measured with a Trans-Membrane Migration Method. ***R. J. Tallarida, T. M. Smith, A. F. Johnson and R. C. Blodgett*** Non-Physicians and Physicians Assess Severity of Disease States and Adverse Drug Reactions: Application to Drug Benefit – Risk Measurement. ***M. J. VandenBurg, K. A. Young, J. Wojtulewski, R. Jenkins, G. Kimber and W. J. C. Currie*** Does It Matter how Visual Analogue Scales Are Used in Clinical Studies? **BOOK REVIEWS** – Drug Dosage and Administration Strong Medicine. **ABSTRACTS. Instructions for Authors.**

Contents of issue two:

OBITUARY – Derek C. Quantock, PhD, MD. **EDITORIAL** – Therapeutic Trials – Responsibility and Accountability. **COMMENTARY** – Death Certificates and Drug Safety. Dr Derek Quantock – an Appreciation. Dr Graham Dukes – a Chair. Diploma in Pharmaceutical Medicine. Where Do We All Come From? Eyeing Adverse Events. Successful Candidates (Dip. Phar. Med.). **REGULATORY SCENE – *N. Mattison*** Sources of Change Affecting the US Pharmaceutical Industry in the 1980s. **PAPERS – *S. B. Banes and P. Turner*** Ophthalmic Opticians and Ocular Adverse Drug Reactions. ***K. P. Hinchcliffe, K. E. Surrall and J. S. Dixon*** Reproducibility of Pain Measurements in Rheumatoid Arthritis by Patients using Visual Analogue Scales. ***A. Johnston, S. Warrington and P. Turner*** An Attempt to Estimate the Absolute Bioavailability of Flecainide without Reference to a Parenteral Dose. **REVIEW – *B. Whiting and A. W. Kelman*** The Population Approach to Kinetic Parameter Estimation. **OCCASIONAL LECTURE – *M. N. G. Dukes*** Pharmaceuticals: Take Another Look. **BOOK REVIEWS** – Guide to Clinical Studies and Developing Protocols. A Manual of Adverse Drug Interactions, 3rd edn. Development of Anti-asthma Drugs. Pharmaceutical Medicine. Whose Body Is It? **LETTERS TO THE EDITOR – *A. E. F. Chandler*** The Comings and Goings of Medical Advisers. ***C. Maxwell*** Orphaned Clinical Trials. **ABSTRACTS. Instructions for Authors.**

Issue three will include:

ABSTRACTS. *W. F. McGhan and L. H. Block* An analysis of drug recalls and court actions in the US pharmaceutical industry. ***J. Hill and H. A. Bird*** Clinical assessments in rheumatoid arthritis. ***N. Mattison*** Pharmaceutical innovation and generic drug competition in the US.

*For a sample copy of **Pharmaceutical Medicine** issue one please fill in the details below and return to the address shown.*

NAME ______________________________

POSITION ______________________________

ADDRESS ______________________________

____

Return to Alison Baverstock, Macmillan Press,
Houndmills, Basingstoke, Hants RG21 2XS, UK.

Macmillan Press
Scientific & Medical

nature

Who will regulate the bankers?

That financial institutions should be trustworthy is a necessary condition for their continued sponsorship of innovation. Banks, in other words, need laws.

Not so long ago, banks were the epitome of stability in society. Grave sober-suited men (there were hardly any women) would move around marbled banking halls confident that even if they were not much liked, they were at least respected, veritable pillars of society. Now all that has changed. On both sides of the Atlantic and in the Far East as well, banks have taken to going bust. Last year, there were more banking failures in the United States than in any previous year since the great depression. During the same year, in Britain, the Bank of England moved quickly to rescue from impending collapse the Johnson Matthey Bank. Why has there been this rash of banking failures? Do they matter? And, if so, what can be done to prevent them?

A bank is an institution that makes a business of looking after other people's money. It will borrow money from one group of people and lend that same money on to other people. Its lenders are recompensed by the payment of part of the interest the borrowers are required to pay; the remainder goes to the owners of the bank, a reward for their time, trouble and expense. A banking system is an essential ingredient of an industrial society; if people had no choice but to keep personal wealth in gold, hidden perhaps in a mattress, there would be no means by which one person's wealth could finance another's innovation. The social function of the banks is to make some people's personal wealth accessible to others who may make better use of it, the creation of credit as it is called.

The only other way of financing innovation so far devised entails the embodiment of most wealth in the state, and the subsequent investment of the same funds by civil servants, as attempted in countries such as the Soviet Union. In the West, technology as it has become is as much the creation of the banking system as of technologists. Certainly the collapse of the banking system would bring technology to a halt. One of the great conceptual developments of the past few years has been the discovery that all financial institutions that take in money from some people and lend it to others have exactly the same economic function as those formally called banks.

Fraud

Obviously, such a system is open to abuse, most simply by the crude device in which the bankers convert depositors' money to their own use, paying enough interest to keep the victims happy and being prepared to decamp when all the funds have gone. In most places, bankers who operate in this fashion are considered criminals, and may finish up in gaol. Others may run into trouble innocently, by lending their deposits unwisely, either because they too readily share their borrowers' optimism (which partly accounts for the troubles of banks in the US Middle West that, two years ago, found themselves over-committed to oil exploration) or because of unexpected changes in the economic climate. Between these extremes of fraud and innocence, the unhappy experience of the past few years has revealed a wealth of ingenious schemes by which bankers, in the pursuit of profit, can run into trouble. Lending money to borrowers unlikely ever to repay the funds may seem profitable until the period of the loan runs out.

Banks and other financial institutions are also vulnerable to fraud, by individuals or even other institutions. Embezzlement, the device by which bank officers siphon off deposits for their own use (often with the conviction that it can be repaid) was once the most common reason why some bankers would be drummed out of their community; it has become a means by which financial institutions can be busted, as with those sections of the Lloyds insurance market in London that have been affected by the scandals of the past few years. Among the tricks that institutions have learned to play on each other are the use of the same collateral to raise more than a single loan, one of the devices by which the Florida company EMS Securities kept itself afloat while insolvent until, last year, it collapsed, bringing down a string of Ohio banks with it. The collapse of the Singapore stock market in the past few weeks has been brought about by yet another device, essentially one by which present credit was traded against future obligations (which could not be met).

Fear

What now worries Western governments, and should worry the rest of us, is the fear that the financial troubles of the past few months will get out of hand. Governments are in a nasty fix. Having recognized that all financial institutions are banks of a kind, and recognizing the importance of banks as a means of stimulating economic activity, they have moved quickly to remove regulations preventing one set of financial institutions from competing with another. The technology the banking institutions have helped to stimulate has brought further complications; dealing in financial securities (debt obligations) has become literally a 24-hour business. The rewards of success are greater than ever. The risks of failure are similarly unprecedented, as is the suspicion that a large part of the debt hanging over the markets, the obligations of the debtor nations of Latin America in particular, may be worth not much more than the paper (or silicon) on which it is recorded. And the much-publicized misdemeanours of the heirs of the black-suited men of a previous generation has raised the question whether bank officers can be trusted with the future of the world's prosperity.

So enthusiam for deregulation is being overlaid by enthusiam for further regulation. In Britain, a curious situation has arisen. Since the early 1970s, successive governments have rightly encouraged changes of the rules by which institutions of different kinds must live. Competition among financial institutions has indeed increased, while London has strengthened its place on the international scene, roughly half-way between Tokyo and New York. Two years ago, the stock market (in exchange for the government's agreement not to pursue a complaint that its internal rules were restraints on competition) agreed to dispense with the most irksome of these restraints, the rules regulating those who may trade in stocks. The result now is that there are powerful and newly created financial institutions, many of them offshoots of conventional banks, waiting for the day next October, called the "big bang", when competition is to be free. The only certainty is that not all the hopeful institutions can hope to succeed, or even survive.

The dangers in such a prospect should be plain for all to see. The social function of the London stock market, like that of other stock markets, is to provide a means of buying and selling the debt obligations of governments and commercial companies, essential if lenders are to be persuaded to lend. But stockbrokers, with the help of banks of different kinds, also function as a means of bringing new money into the system, in which respect they function as if they were banks in the more familiar sense. The London stock exchange (like others) sets out to regulate the securities that may be bought or sold and even the terms on which trading is allowed, yet there is no means by which lenders (called investors) can be protected against their own poor judgement (nor should there be). But the unprecendented circumstances in which, later this year, much enlarged stockbroking firms will be fighting each other for business that will not expand overnight to match their ambitions are plainly full of risk; the London stock market (like others) maintains a fund to compensate investors who lose money when stockbrokers fail, but there are plainly arithmetical limits to what the collective power of commission-men can do to safeguard the assets belonging to those on whose behalf they deal.

That is only one of the reasons why the British government should be more active in the regulation of its financial institutions. The issue has been bubbling away for two years, since the publication of the report on the steps needed to safeguard investors by Sir Jim Gower. The government has already created a Securities Investment Board whose function will be to superintend the working of financial institutions other than banks (looked after by the Bank of England), the stock market (which superintends itself) and the Lloyds insurance market (which purports to do the same). While the new board will require all those who take in money to be registered, it will ordinarily agree that groups of like-minded institutions should look after themselves. Similarly, the supervision of ordinary banks by the Bank of England is to be overseen by another new board, but one nominated by the Bank of England itself. Before this intended legislation becomes law, it may easily be amended. It should be toughened, and for a simple reason.

However well-deserved may have been the reputation for probity of past bankers, the sanctions they used to apply to keep each other on the straight and narrow path no longer apply. A fraudster who knows that he can move easily from one financial centre to another will not be much deterred by knowing that he will be disinvited from the better golf clubs in the place at which his activities are first discovered. The financial community in Britain is nevertheless offended that there should be talk of explicit external regulation of its affairs, while the government is over-inclined to listen to these arguments. But in the long run, there will be no alternative to explicit regulation. The British government had better bite that bullet now, before too much damage is done. Financial institutions are too important to the economy to be left solely in the hands of financiers. □

OPEC is not yet dead

The oil producers will now be less powerful unless the oil consumers invite further discomfort.

OPEC, the Organization of Oil Exporting Countries, continues to exist, but only just. That is the simplest reading of the meeting at Geneva early in December, when the member states decided that they could no longer by *fiat* fix the world price for crude oil. This development has been on the cards for at least the past two years, for as long as OPEC's fixed price has been greater than the price at which oil was to be had on the Rotterdam spot market, and while OPEC members have themselves been selling oil at prices below the official price. So is it possible now to celebrate the end of an awkward period in the affairs of the industrialized West and then to forget?

That is what complacency suggests, but complacency is a poor guide. OPEC came into being a quarter of a century ago because the oil-exporting countries quite rightly tumbled to the fact that they were being exploited. In the 1950s, crude oil was being taken from Saudi Arabia at less than one US dollar a barrel, of which less than a half found its way to the government of that kingdom. During that period, in the United States, it was necessary artificially to prop up the price of domestically produced oil by means of cumbersome sponsored devices such as the Texas Railroad Commission, a federally sponsored carte. But OPEC showed its strength only in 1969, when Libya cancelled the concessions previously let to multinational oil companies, and began selling its own oil to those prepared to buy it. From that point, the developments of 1973, when the official price of OPEC's crude oil was multiplied roughly five times, were inevitable. The further but smaller increases of price in 1979, ostensibly compensation for inflation in oil-consuming states, were a proof that OPEC was still in a strong position.

What has happened since was also predictable. In the oil-consuming states, the intensity of energy consumption has decreased steadily and dramatically, partly because of greater efficiency but also because of the changing pattern of goods manufactured in the industrialized West. It could easily come about that energy consumption, and oil consumption in particular, will increase again if economic growth accelerates, but many old inefficient ways have probably gone for good.

But none of this implies that OPEC, too, has gone for good. In the long run, the present period of OPEC's weakness, brought about by the declining demand for oil by the industrialized economies and the success of exploration for oil (at OPEC's high price) elswhere in the world, has been accentuated by the urgent need of some oil-producing governments to maintain their oil revenues at the high levels to which they have been overfortunately accustomed. Iran and Nigeria, importunately compelled to sacrifice their long-term interests for the immediate need for cash, have done as much to weaken OPEC as the compensatory market mechanisms at work elsewhere.

For the years immediately ahead, the course of events is predictable enough. Now that oil prices have fallen (to not much more than $25 a barrel or $175 a tonne), the incentives to exploration will be diminished (but not much), economic activity in the industrialized economies should be stimulated (but, again, not spectacularly) and the price of oil will find a new level at which the interests of the producers and the consumers are balanced. But further ahead, early in the next century perhaps, there will be a different setting for the oil market. By then, no doubt, there will have been further important discoveries of oil in parts of the world still unexplored, so that the potential membership of OPEC will have been enlarged or at least changed (for some oil producers will also have used up their reserves). Similarly, there may then also be now unexpected developments in energy technology that could have transformed the pattern of consumption. But what will stand out, at the turn of the century, is that Saudi Arabia will almost certainly remain in the unique position it occupies at present, as the country most richly endowed with plentiful reserves of crude oil that differs in the most radical respect from that available elsewhere — its production cost is very much less.

This is the sense in which December's events do not spell the end of OPEC. Even if in the years ahead it is destined to become a not particularly congenial dining club, there is every reason to expect that the market for petroleum will change in such a way that Saudi Arabia will again be in a position to play a leading part in sharpening OPEC's teeth. For the oil consumers, the lesson should be clear. Whatever new discoveries there may be, and whatever the fluctuations of the price of crude oil, there are the strongest strategic reasons for strengthening the influences that have induced the energy economies of the past few years. Artificial restraints are inappropriate, as are subsidies of any kind. The better rationalization of industrial production internationally may be more important. Nobody wants OPEC to become a tyrannical influence on the world economy again, but the safeguards are in the hands of the oil consumers. □

Japanese public health

New campaign launched against hepatitis B

Tokyo

JAPAN'S Ministry of Health and Welfare launched the world's first public hepatitis-B immunization campaign on 1 January. Funds have been provided to immunize 10,000 babies each year identified as being at risk by the presence of hepatitis Be (HBe) antigens in their mothers.

The go-ahead for the programme follows by a few weeks the commercial release of hepatitis-B vaccines from two domestic manufacturers, the Kitasato Research Institute and Green Cross. A third manufacturer, the Chemo-thero Therapeutic Institute, will have a similar product available in May. Licences to produce the vaccines were granted in April after clinical trials were completed. The vaccines are derived from the plasma of hepatitis-B virus carriers inactivated by heat and formalin treatment and are essentially the same as those licensed in the United States in 1982.

Carrying out the programme is very expensive. Each of the three injections required costs around 5,000 yen (US$25) and this is added on to the high cost of identifying mothers whose babies are at risk. One thousand million yen ($5 million) has been allocated by the government for the first year of the campaign. Hepatitis B is a major public health problem in Japan not only because of the seriousness of hepatitis itself but also because it can lead to cirrhosis and cancer of the liver. Hepatitis-B virus infection has been linked to more than 80 per cent of all casses of primary hepatocellular cancer: the immunization campaign may thus fairly claim to be the first that might wipe out one form of cancer. Mother-to-child transmission of hepatitis B is the most important route of production of hepatitis B carriers; 85–90 per cent of babies borne to HBe-antigen-positive mothers will have become carriers by the time they are three months old. Clinical trials of the immunization method on 3,000 babies in Japan have already shown that transmission can be virtually wiped out.

Japan's selective immunization campaign is not, however, likely to serve immediately as a model for other countries. First, Japan is one of the few affected nations wealthy enough to bear the costs of immunization and with the expensive procedures for testing for HBe antigen established as routine at health centres. Again, although the overall frequency of hepatitis-B carriers is, at 2.6 per cent (rising to 5 per cent in some areas of Kyushu), quite high compared to Europe and North America, it is still sufficiently low that idenfifying those at risk is cheaper than a mass immunization campaign.

In the developing countries of Asia, the problems are of a different magnitude. In both Taiwan and Korea, around 15 per cent of the population are carriers and in mainland China around 10 per cent. Chinese officials say that the cost of vaccine would have to fall by one to two orders of magnitude before any mass immunization campaign could be contemplated.

Hopes for a fall in costs lie with the genetically engineered vaccines now just coming onto the market. The vaccines, produced by the Pasteur Institute and Genentech in mammalian cells and by Merck in yeasts, are still very expensive. But the potential market is huge and Japanese companies are in the race to produce cheap vaccines. **Alun Anderson**

Australian science

Radical shakeup planned

THE Australian Science and Technology Council (ASTEC), the world's most prolific source of recommendations on the management of publicly supported research, has advocated radical changes in the organization of the Commonwealth Scientific and Industrial Research Organization (CSIRO). The recommendations are put forward by a subcommittee of ASTEC under its chairman, Professor R.O. Slatyer of the Australian National University, Canberra.

In a report* to the federal prime minister published at the end of last year, ASTEC advocated the replacement of the present top management of the organization, called the "executive" and consisting of three full-time and two part-time members, by a board of seven part-timers and a single full-time official, which would be the source of research policy for the organization. The most startling aspect of this proposal is that the full-time official, to be called the Chief Executive, would be appointed by the board (rather than by the government) and would be liable to dismissal by the board.

According to the report, the chief purpose of the proposed changes would be to ensure that the lines of responsibility for research policy and for management within CSIRO are unambiguous. The Slatyer committee has considered but rejected arguments that CSIRO should be split up into separate organizations responsible for research in different fields, on the grounds that Australia needs a strong central (and flexible) research organization but the committee urges that CSIRO's strategy should be more closely directed towards the needs of existing and emerging industries, saying that CSIRO programmes exclusively concerned with basic research should be hived off to other institutions, most probably universities, "perhaps in conjunction with a scheme to identify national centres for research in which a number of universities might participate".

The starting point for many of the Slatyer committee's proposals is a sense of regret that the last reform of CSIRO eight years ago has not produced the benefits expected of it. The report says that CSIRO's advisory council has not been able to influence policy as intended (and that it should be abolished), and that the same conclusions apply to the state and territory committees that at present formally have a role in guiding research policy. The Slatyer committee is especially regretful that the 1977 reform that grouped CSIRO research laboratories (called divisions) into three institutions, each with a separate director, has blunted rather than strengthened the links between top management and the divisions.

Although the Slatyer report does not say so explicitly, its recommendations reflect the evolution of Australian research institutions and in particular the increasing strength of the universities in research. But the sustained emphasis in the Slatyer report on the need that CSIRO should concentrate its efforts and resources on providing assistance for industry (including the traditional industries of agriculture and mining) will, if accepted, bring about a considerable change both in the pattern of research at many of the well-established research divisions and in the ethos of CSIRO as Australia's chief employer of those bent on a career in research.

On the last point, the report says that CSIRO should give up its now common practice of employing most of its new recruits on indefinite contracts (there is also at present a one-year probationary contract) and that it should instead switch to a system in which an initial period of employment on a short-term contract would be the general rule, with an understanding that only a proportion of those thus hired would win permanent appointment. The committee says this pattern would, among other things, serve to provide opportunities for postdoctoral scientists, especially those returning from abroad. □

**Future directions for CSIRO*. Australian Government Printing Office, Canberra.

Remote sensing

US agencies blamed for muddle

Washington

An outspoken study of the "crisis" in the 13-year-old US Earth remote sensing programme by the National Academy of Sciences has concluded that US pre-eminence in the field is now seriously threatened by "not-so-benign neglect". The academy says that substantially increased government resources will be needed if the potential of the technique is to be realized, and knocks some agency heads together for letting the area fall into disarray.

The academy's report emphasizes that the present situation is urgent. The only civilian Earth remote-sensing satellite in service, Landsat 5, is expected to fail before private industry can launch a replacement. No improvement is likely unless the government increases the $250 million ceiling it has placed on remote sensing while the programme is being transferred to the private sector.

Although negotiations with an industrial consortium to take over the programme are at an advanced stage, there are still no definite arrangements for the future, and during the probable hiatus in the US service, the French company SPOT (Systeme Probatoire d'Observation de la Terre) can be expected to secure a large part of the market for remotely-sensed Earth data: although customers would prefer continuity of data, SPOT's data will be available and will have some technical advantages.

The academy's report* was produced by its research arm, the National Research Council (NRC), under the chairmanship of George Harter. The report has been more than two years in preparation and seems to have engendered some controversy: an earlier draft by a specially appointed committee was rejected by NRC's Space Applications Board, which then set about producing a better version. The work of the earlier committee is acknowledged only in passing.

NRC is enthusiastic about the ultimate potential of data sensed from space, while pointing out that data must in future (not as at present) be made available to users in processed form if they are to be saleable products. Oil companies, which now use remotely-sensed data for prospecting, have spent years and large research budgets in discovering how to use it. (Oceanographic remote sensing, according to NRC, should remain within the government as a "public good" service.)

Although NRC supports the government's basic strategy of turning Earth remote sensing over to the private sector while keeping meteorological satellites under its own wing, it is harsh in its criticism of how the strategy was carried out.

NRC stresses that technical problems are no part of the reason why the programme has done so badly. Rather, parochialism is to blame: the programme fell between the twin stools of the National Aeronautics and Space Administration (NASA) and the National Oceanic and Atmospheric Administration (NOAA).

Although the two agencies worked together for many years on remote sensing, after NOAA was officially placed in charge of the programme and NASA faced a budget crisis in the early 1980s, NASA threw the ball over to NOAA, which was apparently unready to catch it. Part of the reason, according to NRC, was NOAA's disadvantageous and often-criticized bureaucratic niche within the Department of Commerce. NRC accordingly recommends that NOAA be found a more suitable home.

Even if NOAA stays where it is, however, NRC is not so pessimistic as to believe the two agencies could never again work together constructively. NRC wants to abandon the present arrangements whereby institutional rather than technical considerations dictate what sensors are flown on a given spacecraft, and proposes a single coordinated effort, with NOAA remaining in charge of applied and market research for Earth data, and NASA providing technical support for the development of new sensors, for example. Finally, NRC tells the two agencies in future to allow each other to use space on their platforms and also to make this available to industry.

Tim Beardsley

**Remote Sensing of the Earth from Space: A Program in Crisis* (National Academy Press, 1985).

French science

CNRS faces political change

Should the Centre National de la Recherche Scientifique (CNRS), the principal French research council, be split up? This seems to be the question of the month in right-wing scientific circles in France, where the general election due in March is expected to return a government of the right. It is difficult to establish exactly where the idea comes from, although *Le Monde* picks on "sources close to Jacques Chirac", the mayor of Paris, expected to become France's next prime minister.

CNRS has had to contend with some criticism of late. The council is certainly big, supporting more than 10,000 academics in disciplines from physics to history, and its multidisciplinary nature has given it considerable flexibility in meeting the challenge of new sciences such as materials, microelectronics, robotics and biotechnology. But in responding to these new goals and in its policy of "*overture*", openings up the hallowed halls of academic institutions to the public, to industry and to other research bodies, CNRS "has changed profoundly" over the past 3–4 years, says its director-general Pierre Papon.

In so doing CNRS may have created enemies, particularly among more traditional academics used to the old somewhat feudal continental system of professorial fiefdoms that were once prevalent in France. CNRS has attempted to cross these barriers where they still exist — Papon still feels it necessary to preach the values of the British and US departmental system — and has also used its budgetary muscle, in concert with the ministry of education, to concentrate resources on priority areas. The prospect of a right-wing government has given some of those affected a chance to complain, and there is a growing clamour in France for a return of power to the professor, at the expense of that of the science political apparatus such as CNRS. A fragmentation of CNRS into disciplinary subsections would clearly serve this cause well.

To confuse matters, however, the present research minister in the socialist administration, Hubert Curien, speaking just before Christmas at a prize-giving at CNRS, was ambiguous in his reply to criticisms of the centre. He described the criticisms as "a typical French exercise in self-flagellation", and said that if CNRS did not exist, he would have to invent it; but he also said that "one must not be deaf to criticism" and talked of "a new mode of scientific organization" in "networks" of projects rather than isolated grants.

In the circumstances, one might expect M. Papon to feel somewhat isolated and exposed, but he finds no policy conflict with M. Curien. "Networks", for example, correspond to his own concept of interdisciplinarity. And moreover Papon was re-appointed for a second three-year term of office in October. He fully intends to continue his work under a new government, "unless it shifts policy by 90 or 180 degrees". Also, Papon's appointment was made by the President of France, and François Mitterrand does not face re-election until 1988. Papon also believes that "no responsible government could contemplate a dismemberment of CNRS", or retreat from the present government's policy of harnessing science for the economy, of which he himself has been a major architect. By the middle of the year, when a new government will be preparing its budget and policies for 1987, he should know if he is right.

Robert Walgate

Japanese communications

What band-rate for psi?

Tokyo

WHEN it comes to new methods of telecommunication, Japan's Ministry of Posts and Telecommunications believes in looking at even the long shots. The ministry's fanciful new "Research Committee on Future Telecommunications Media" is, among other things, to look into the prospects for telepathy as a communications medium.

The new eight-member committee has been established on the recommendation of a private advisory panel to the Minister of Posts and Telecommunications. It will be headed by Shigemichi Sonoyama, vice-president of the National Space Development Agency, and to add weight to the panel's discussions, another of its members is Tadahiro Sekimoto, president of the giant electronics company NEC.

Japan is not, of course, the only country in the world to think of the potential of telepathy; it has long been rumoured that the Soviet Union is taking the subject very seriously. But perhaps this is the first time that a posts and telecommunications ministry has taken up the idea. True to Japan's vigorous commercial spirit, the ministry has in mind practical application. An attractive feature of telepathy is that transmission is instantaneous, or so some claim. Dr Ootani, a psychologist at the Self-Defence Forces University, will be the principal scientist to investigate "superhuman abilities", although anyone with such abilities might be expected to avoid research panels and the possibility of being turned into a kind of living telephone exchange.

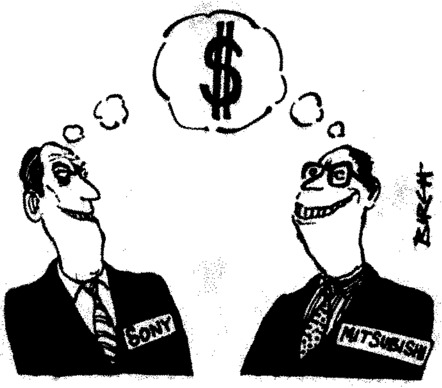

Telepathy will not be the only new telecommunications medium to be investigated. One professor from Kanagawa University will take a look at the potential of neutrinos. And another professor from Tohoku University will assess gravity waves, even though ministry officials agree that their existence is scarcely more certain than that of telepathic waves. Backing up their investigations are experts on brain physiology, electrical communication and computer intelligent management systems.

The committee is expected to hold four meetings by the spring for an initial exchange of views. Although the hopes of practical application of the new media might seem very far off, the ministry says it is not "too early to start study".

Alun Anderson

Red greens on Yellow River?

A BELIEF is growing in China that the proposed hydroengineering works on the Yangtze (Yellow) river will "spoil the scenery", the New China News Agency reports. But an unnamed official of the Yangtze river valley planning office maintains that construction of the proposed hydroelectric power station, which will substantially raise the water level in the Yangtze gorges, will not greatly harm the scenery. In fact the authorities are looking forward to improved amenities and, according to a planning office spokesman, "some new scenery will emerge".

The purpose of the project is threefold. The hydroelectric plant will have a capacity of 13 m kWh, said the spokesman, and will supply power to cities as far away as Beijing, Tianjin and Tangshan in the north, Shanghai in the east, Canton in the south, and Sischuan in the west. The new, higher water level will submerge more than 90 per cent of the dangerous shoals in the three gorges, thereby reducing hazards to navigation and increasing the number of vessels that can safely be carried on the middle Yangtze and the Chuan river, with a substantial saving in the cost of transport.

At the same time, flood control measures in the three gorges will substantially reduce the risk of flooding to the Dongtin Hu, Poyang Hu and Jianghan plains, densely populated areas which are China's commodity grain and cotton base. At present, more than 1 million people, the spokesman said, are needed to protect the existing dykes during the flood season each year, and according to archives going back to the end of the Han dynasty, some 2,000 years ago, there was major flooding until the beginning of this century in one year out of ten.

What form Chinese concern over the three gorges has taken is unclear. There is no suggestion of mass protests, but anxiety is clearly sufficiently acute and widespread for the planning office to find it necessary to issue a statement to reassure the public.

Vera Rich

Space science

British head for French lab

FRANCE is building a new £4-million laboratory for space sciences at the Université de Paris Sud (Orsay), and has attracted a leading British space scientist as its first director.

But Dr Alan Gabriel, now head of the space and astrophysics division of the Rutherford Appleton Laboratory near Oxford, who will direct the new Institut de Physique Spatiale d'Orsay (IPSO), says he does not feel part of a brain-drain. "I don't want to be negative about British space science", he said. "It's not true to say things are much better in France than they are here." The new British National Space Centre for the coordination of the UK space effort "offers most exciting possibilities" and it was "not at all" true to say British space science is not well-enough supported. Moreover space science is international, and Gabriel expects much cooperation between IPSO and his British colleagues.

However, Gabriel implies that he feels more cramped at the Rutherford Appleton Laboratory than he expects to be in Paris. Gabriel's present division of around 150 is merely one part of a 1,500-strong multidisciplinary laboratory; in Paris, IPSO will be no bigger than the space and astrophysics division but it will be independent, except for some support from the research councils and the university. "I shall be able to play a more creative role", Gabriel says.

At the new Paris laboratory, two-thirds of the staff will come from an existing French group housed in an overcrowded old laboratory in nearby Verrier-le-Buisson. The Laboratoire de Physique Stellaire et Planetaire has experiments on both the European and Soviet Halley probes (Giotto and Vega).

The new IPSO will also form a focus for a number of space science groups now scattered around the Paris area, and will take advantage of the proximity to LURE, the Orsay synchroton radiation source, for calibration of optical instruments from the X-ray region to the visible.

IPSO's initial research programme will concentrate on solar physics, infrared studies of the interstellar medium to shed light on mechanisms of star formation and Solar System studies including dust, comets and asteroids. (France is planning for a mission to the asteroids either within the European Space Agency or bilaterally with the Soviet Union.) Gabriel is also interested in developing a capability at IPSO for X-ray astronomy. He expects IPSO to become one of the major centres for space sciences in France.

Robert Walgate

Argentine science

Slow return to openness

Buenos Aires

ARGENTINE science is recovering slowly from the traumas of the past decade. In contrast with 1973, on the eve of the return of Peron, and 1979, after the military had finally repressed the opposition, it is evident that the morale of the people has been uplifted and that there is a strong desire for political stability under democratic rule.

The severe repression by the military dictatorship afflicted all scientists, depriving many of their jobs and some of their lives. One biochemist, apparently considered too outspoken, had a bomb planted in his house and telephone threats which compelled him to leave his university and to move with his family to a remote part of Argentina.

Another outspoken biochemist became a victim of the mindless repression apparently only because he was Jewish. His home was visited one day at five in the morning by men in plain clothes, who had come to arrest him. Fortunately, his wife's mother answered the door and screamed out that the men were thieves. So he escaped with his pregnant wife and young children over the roof tops.

The Israeli government, to its honour, acted as a Scarlet Pimpernel by providing passports for such refugees, irrespective of their religion; a general escape route was organized with the cooperation of the Belgian airline Sabena.

The exodus of Argentine scientists during the repression and their enrichment of the culture of other countries has been documented by Budiansky (*Nature* **311**, 201; 1984). Few of those expatriates have yet returned, probably because they cannot afford to; salaries in the universitites and government institutes remain depressed. Industrial salaries are relatively remunerative, three or four times those of academics. The low salaries in the state sector (see Budiansky's article) and the general economic malaise are professional people's chief preoccupation.

In the aftermath of the repressions, demands for retribution continue, but scientists are divided. Some, partly out of self-interest or envy, are accusing those who prospered under the military of criminality; others, including many who suffered under the despotism, support the call for a "full stop" to recrimination.

In the universities, a commission is examining the credentials of all professors appointed during the past 20 years, when the normal procedures for appointment were suspended. This is time-consuming for university staff and probably diverts attention from the need to renew the resources of the universities so as to meet the challenges of the future.

Argentina, in common with the developed countries, has greatly expanded its university system in the past two decades. (Cordoba, founded about 1650, is probably the oldest university in the Western Hemisphere.) Although the old universities are still dominant, such extra resources as there have been seem to have been concentrated on the new universities, so that there has been little renovation of the older universities, which are now dilapidated and inadequately equipped to strengthen or maintain their position as centres of science.

Nevertheless, scientists are pressing on in reasonably good spirits, although they seen no way out of the impasse caused by Argentina's economic problems. Subscriptions to journals have been cancelled wholesale; support for assistants has to come from professors' personal salaries. Buildings are in an appalling state, but all new building schemes have been frozen by the government.

There is a lack of campuses in the older universities, so that departments are widely scattered, and thus isolated from interaction with others and prevented from sharing equipment, libraries and overheads generally. Apparently, the authorities in the past have been suspicious of campuses as foci of political action by students. Surely such fears of criticism could be abandoned by the democratic government, even if the concentration of resources in campuses will have to be a long-term aim.

One move towards the concentration of resources was the inauguration of research centres by the national research council, CONICET. Buildings, staff and equipment were funded on a modest scale, but again these are dispersed and isolated. They have successfully encouraged good basic science, but now the government intends to transfer them from CONICET to the universities, which leaves researchers fearing that their centres will be reduced to a state of academic deprivation. Integration of the centres, with protection of their resources, is essential if their work is to expand.

In the biosciences, it is striking that, as elsewhere, the emphasis is now heavily on technology. The size of the Argentinian agricultural industry offers much scope for biotechnology to improve plant and animal crops, and eventually to exploit the arid regions and their solar energy. As in Brazil, 10–15 per cent of ethanol must be added to motor fuel to promote the exploitation of sugar by fermentation. Health care products are being developed through innovation in biotechnology. For instance, the Polichaco pharmaceutical company has announced a contract worth US$3 million to supply to Brazil diagnostic reagents for pregnancy testing. Excellent molecular biology towards characterizing the virus of Argentinian haemorraghic fever is being done at the University of La Plata, in laboratories which in Britain would be condemned as unsuitable. With resignation, the researcher says, "This shows that expensive facilities are not essential for success in molecular biology".

The government has set up a committee to develop a policy for biotechnology, and many groups seem to be competing for access to any funds that may be made available. But the government is still searching for a formula to define biotechnology. Yet a policy is needed urgently because of the momentum of research in this field elsewhere in the world and to offer the Argentinian scientists the opportunities they deserve.

Academic scientists have even begun to entertain the idea of obtaining support from industry and other entrepreneurs, but this approach may need legislation; the universities have traditionally prevented academics from having links with industry.

The transfer of technology from university to industry is beset with difficulty. In the fermentation field, despite its rapid expansion to produce ethanol, there is a marked reluctance by industry to take advantage of scientific innovation which Argentine scientists are developing, even in ethanol fermentation.

Remedies may yet emerge from the changing politiacal climate. Both the radical party government under Alfonsin and the recent Austral currency reform seem to be winning confidence. It is a pity that the Falklands (Malvinas) problem remains unsolved. The slogan "The Malvinas islands belong to Argentina" remains conspicuous in public places, even though serious comment recognizes the historical realities and the need for flexibility in Argentinian policy.

There is also a new spirit of cooperation in South America. Chile and Argentina have settled their territorial disagreement and, in the past weeks, there have been agreements between Argentina and Brazil and between Chile and Peru on friendship and cooperation.

The lack of normal relations between Britain and Argentina continues to affect trade. For instance, the supply of radioactive chemicals from Britain has been made difficult. One molecular biologist has resorted to making his own labelled nucleotides, with a cost saving of over 80 per cent on his reckoning if technician's time is discounted. There is an historical affinity between Britain and Argentina that surely requires Britain to settle its differences with Argentina with chivalry and thus to help ensure that despotism never returns there again.

S.J. Pirt

Laboratory animals

US protection act approved

Washington

SHORTLY before its Christmas break, the US Congress passed legislation supported both by animal welfare campaigners and by researchers' organizations designed to improved standards of care for laboratory animals. The Improved Standards for Laboratory Animals Act requires painful experiments to be justified to a committee that includes at least one disinterested member of the public charged with ensuring that pain and distress are minimized.

The new act was introduced by Senator Robert Dole (Republican, Kansas) and Representative George Brown (Democrat, California) with 136 co-sponsors. Animal welfare workers, chiefly the Society for Protective Animal Legislation, worked for two years with researchers' organizations to find acceptable compromise provisions. The bill as passed was supported by, among others, the America Society for the Protection of Cruelty to Animals, the Humane Society of the United States, the American Physiological Society and the Association of Professors of Medicine.

The chief effect of the new act is to require the creation of Institutional Animal Committees that must include one external member; at present, many but not all institutions which carry out research on animals have such committees. The committees will be required to conduct semiannual inspections of research facilities and to report violations of regulations to institutional and federal authorities. The Secretary of Agriculture is empowered to promulgate regulations on care, treatment and practices to minimize pain and distress, but not on the conduct of experiments.

The new act also requires institutions to provide training in the humane treatment of animals, encourages alternatives to animal testing where possible and requires principal investigators to certify that alternatives have been considered. Exercise for laboratory dogs, use of anaesthesia with paralysants and limitations on repeated major operations on the same animal are also specified.

A new information service at the National Agricultural Library is established under the act, in order to minimize unintended duplication of experiments, and both federal and private laboratories are subject to its provisions. Although the act makes clear that experimental protocols will be respected, it is required to suspend federal support if an agency determines that animal care in a particular project has been persistently unacceptable.

Tim Beardsley

Bhopal disaster

India blames Union Carbide

New Dehli

INDIA's official report on the events leading to the Bhopal disaster last year says that about half a tonne of water had entered the tank containing methyl isocyanate (MIC), thus confirming the findings of Union Carbide. But the report says that the chemical reaction leading to a catastrophic increase of temperature was caused by contamination of the tank by metal ions, which acted catalytically.

The report is the work of a 16-member committee led by Dr S. Varadarajan, the chemist who is now the secretary-general of the Department of Scientific and Industrial Research. It specifically disputes Union Carbide's claim that entry of large quantities of water alone was responsible for the ghastly accident on 2 December 1984, saying that the runaway reaction leading to a rapid rise of temperature and pressure in the storage tank could have been triggered by water only if the MIC inside the tank had also been contaminated with metallic impurities.

The report, by implication, rules out sabotage, alleged by Union Carbide, and instead puts the blame on the US company for its choice of unsuitable corrodable materials for the piping thought to have been the source of the contamination.

Varadarajan's committee reached its conclusions on the basis of experiments carried out on a second undamaged storage tank at Bhopal. The experiments included heating MIC alone and reacting it in the presence of water, chloroform and traces of ferric salts and sealed containers at temperatures up to 250 degrees centigrade. These simulations yielded all the twelve or so different types of solid residues found inside the damaged tank.

Based on these experimental data and an actual inventory of the tank residues, it was estimated that 12,087 kg of MIC and 595 kg of chloroform (used as a solvent) reacted with 512 kg of water, producing enough heat to vapourize the remaining 28 tonnes of MIC in the tank. The report says that the escaped gas also included 80 kg of ammonia and 1.25 tonnes of carbon dioxide.

The Varadarajan report has incidentally put to rest the controversy over whether the gas that leaked was MIC, cyanide or both. Union Carbide had from the beginning insisted that cyanide was not present, but Indian doctors who carried out autopsies on gas victims suspected otherwise. The report agrees with Union Carbide on the basis of the experimental evidence it has collected.

The most important finding of the Varadarajan committee relates to the role of water. Union Carbide maintains that the runaway reaction was due to the addition of large amounts of water to MIC containing chloroform. The Indian report says that ingress of 500 kg of water would at best have consumed four tonnes of MIC and raised the tank temperature to just 70 degrees centigrade, below the boiling point of MIC (at the safety valve pressure). The report also says that chloroform could not have catalysed the reaction below 200 degrees centigrade, whence the conclusion that some other catalyst must have been involved.

From the products of tank residues, calculated heats of chemical reactions and the extent of bulging in the tank, the committee estimated that the tank reached a temperature above 250 degrees centigrade. According to the report, only "the onset of metal-ion catalysed polymerization of MIC" could account for this rapid increase of temperature.

The Varadarajan committee says that the metallic contaminants (iron and sodium) came from corroded pipes and the tank itself and catalysed the trimerization of MIC. Subsequent entry of water hydrolysed the MIC, producing heat and carbon dioxide and allowing "trimerization to take off with explosive violence".

In support of this theory, the report lists iron, sodium, chromium and nickel among the metallic contaminants found inside the exhumed tank. Sodium was present at a level of 60 p.p.m., equivalent to 25 litres of 5 per cent sodium hydroxide. According to the report, the contaminants most probably came from tank accessories made of materials such as carbon steel and copper.

The source of sodium is identified as the vent gas scrubber. One source of iron was found to be the tank itself, probably released as ferric iron as a result of corrosion caused by hydrochloric acid formed by the hydrolysis of phosgene.

Exactly how the contaminants and half a tonne of water came to enter the tank, the report can only guess. Indirectly, the report rules out sabotage by the argument that while it may be easy to pour water into the tank, a saboteur would not know the role of metallic contaminants.

The report concludes that the gas leak would have been avoided had the 42 tonnes of MIC been stored in several small steel drums. "The needless storage of large quantities of MIC for long periods, as well as insufficient caution in design, choice of materials for construction and provision of measuring and alarm instruments, together with inadequate controls on systems of storage and quality of stored materials as well as lack of necessary facilities for quick and effective disposal material exhibiting instability led to the accident."

K. S. Jayaraman

AIDS in the human brain

THE causative agent of acquired immune deficiency syndrome or AIDS (variously known as LAV, HTLV-III or ARV virus) is akin to the lentiviruses[1]. It would appear, on current estimates of AIDS virus prevalence in the US population (about 0·5 per cent), that between 10^5 and 10^6 persons may develop lentivirus-like encephalopathies during the next fifteen years. When other animals are infected with similar lentiviruses (maedi–visna virus in sheep), the disease is progressive and fatal, with an incubation period of one to six years. The duration of AIDS encephalopathies already known in humans is not well established but may range from one to 14 years.

The similarities between the two diseases and their causative agents are established experimentally. Both of them, RNA retroviruses, are integrated into the genome of the host's cells as proviral DNA. Efforts to treat the viral DNA must include protection for the host's DNA, a task of which we are at present incapable. Both AIDS virus and the lentiviruses possess the properties of "antigenic drift", lessening the likelihood of a vaccine as we now understand vaccines. Thus, the burden of disease control falls on epidemiology and prevention.

The implications of such a large number of men, women and children with progressive disease for the economy, health care system and emotional state of society are unprecedented. The scientific necessities, the need to develop strategies for dealing with a new type of human infection and producing a lifetime viraemia pose scientific puzzles of dizzying proportions. Even if my estimates of clinical neurological disease are in error by one or more orders of magnitude, the tragedy is still shocking, especially as it comes on top of the already manifest deaths due to AIDS immune suppression. If AIDS is a lentivirus disease, the immune-suppressed AIDS patients may be only the tip of the iceberg.

The threat of AIDS as a lentivirus disease should motivate politicians, public health workers and scientists to establish a unified plan for AIDS prevention on local, national and international scales. Since the mechanics of transmission of AIDS-lentivirus are known, the great risk associated with anal intercourse, promiscuous heterosexual encounters, blood to blood contact and the use of shared drug injection paraphernalia must be explained in the most specific terms to all levels of society. Those already infected must be included in the strategy. Universal blood testing should not be ruled out. If AIDS is a lentivirus epidemic, to err on the side of caution would be prudent.

CECIL H. FOX
M. COTTLER-FOX

8708 First Avenue,
Silver Spring, Maryland 20910, USA

[1] Seale, J.R. *J. R. Soc. Med.* **78**, 613–615 (1985).

Homochiral creationism

SIR—
Cried God, making Adam from clay
In a dexterous left-handed way,
"Bring me PVED
ΔE_{pv}
Or I can't get it done in a day!"[1]

HILTON STOWELL

ERPB Laboratory,
120 Nature Creek SW,
Milledgeville, Georgia 31061, USA

[1] Tranter, G.E. *Nature* **318**, 172–173 (1985).

Earnshaw's theorem

SIR—This theorem is not often mentioned in scientific journals. It denies the possibility that an electric charge can be held stable solely under the electrostatic influence of other electric charge. It was used in a recent letter (*Nature* **317**, 208; 1985) to refute a case put earlier by Berezin (*Nature* **315**, 104; 1985). It is as well to keep in mind that the Reverend Samuel Earnshaw developed his theorem with an eye to the constitution of the aether as a medium comprising a structured system of electric charges, separated by what, presumably, would be regarded as a truly void state of the vacuum. The theorem fails if the charges permeate a charge plenum or continuum having a charge density, because displacement can then be subject to a linear restoring force rate, owing to interaction with this continuum.

We have now come to accept that the vacuum medium does have some rather special characteristics and a possible structure, so it is not unlikely that it comprises electric charges permeating a charge plenum, notwithstanding the Earnshaw theorem.

If this is the case, then the theorem cannot even be applied without some reservation when considering the mutual stability of charge in matter. The support for the structured vacuum is enhanced by the related theoretical derivation of the fine-structure constant in terms of the geometrical features of an electrical charge system neutralized by a charge continuum. A value of the fine-structure constant in matching accord with its measurement at the level of one part in ten million has recently been reported from such analysis (*Phys. Lett.* **110**A, 113; 1985).

H. ASPDEN

Department of Electrical Engineering,
The University,
Southampton SO9 5NH, UK

Price of star wars

SIR—R. V. Harrowell (*Nature* **317**, 470; 1985) criticized the proposed Strategic Defense Initiative on the grounds that if it is successful it will supposedly release deadly amounts of unexploded plutonium into the atmosphere.

Let us compare the radioactivity of this plutonium with that of the radioactive material already present in the air. According to that arcane source of data, *The Handbook of Chemistry and Physics* (66th edition), the atmosphere masses 5.136 hexillion grams, its mean relative molecular mass is 28.966, and the molecular fraction of radon is one part per hexillion. If we combine this information we see there are 0.18 moles of radon in the atmosphere. The half-life of radon is 3.82 days and that of plutonium is 24,110 years; radion is therefore 2.3 million times as radioactive as plutonium. The equivalent of 400,000 moles (about 100 tons) of plutonium is already present in the air in the form of radon. We can compare that with the mass of 5,000 warheads at 10 kg of plutonium each, that is, 50 tons.

JOSEPH HERTZLINGER

16 Warren Lane,
Jericho, New York 11753, USA

Metric system

SIR—There is a further problem to be considered in the controversy about ambiguities in metric notation, affecting the acquisition of mathematical concepts by school children.

In the days of Imperial measures, areas used to be denoted in units of square inches, square feet, etc. Such quantities were usually written in the form: "16 square inches" or "16 sq. ins". This was naturally read by the child as "sixteen square inches", and was quite unambiguous.

Nowadays it is common to denote areas in the metric system as follows: "16 cm^2" which is naturally read as "sixteen centimetres squared". A very understandable confusion then arises in a young mind between "16 centimetres squared", which is just acceptable as a way of expressing 16 cm^2, and "sixteen centimetres square" which can only mean 256 cm^2.

The meaning of "sixteen square centimetres" is thus obscured, and is not easy to clarify in verbal terms.

The fault arises, of course, from the linguistic confusion between "square" and "squared" which employs minimal coding to represent an important difference. However this confusion is not helped by a system of notation which itself confuses units and quantities.

R.J. BIRD

50 Highbury,
Jesmond,
Newcastle upon Tyne NE2 3EA, UK

Further anxieties about AIDS

AIDS has been a serious problem of public health since it was first recognized. The realization that it may affect the human nervous system gives a new twist. But the remedies are the same.

The letter from the Drs Fox on page 8 has plainly been written to scare, but it should be taken seriously for all that. Since AIDS (acquired immune deficiency syndrome) was first recognized, it has been seen as a serious threat to public health. It is intractable and infectious, although not especially so. What the Drs Fox (respectively a pathologist and a physician) are saying is that the threat is probably more serious than has been thought, now that it has been demonstrated that infection by the AIDS virus, HTLV-III or LAV, can damage the central nervous system. But it is too soon to know how much more serious.

While so much remains to be understood about the consequences of infection by the AIDS virus, it is not surprising that uncertainty abounds. But the wonder is that so much has been learned about AIDS and its causes in a mere four years.

The immune deficiency that marks out AIDS arises because of the depletion of the sub-class of T (for thymus) lymphocytes known as "helper" cells. Infected people produce characteristic antibodies, by means of which diagnostic tests have been developed and put into service. Their most immediate use is in the screening of blood for transfusions; it is too early to know how effective they will be.

Two lessons have emerged from the determination in the past year of the nucleotide sequence of several isolates of the virus. Viruses recovered from different sources differ — suggesting antigenic variability like that which makes the influenza virus variable — and the AIDS virus is less like HLTV-I (recovered from patients with apparently infectious adult T-cell leukaemia) than visna virus, responsible for a progressive (demyelinating) disease of the nervous system of sheep.

A great deal has also been learned about the nature of AIDS itself. That only some, perhaps 10 per cent or so, of those with HLTV-III antibodies succumb to one of the infections or other conditions that characterize the disease is not surprising. Other viruses may affect people subclinically, causing them little trouble but stimulating the production of antibodies which protect against further infection.

Much has also been learned about the mechanism of the spread of AIDS. Homosexuals, haemophiliacs given contaminated blood-clotting factor and syringe-using drug addicts are the groups chiefly at risk, but the disease has also been transmitted to heterosexual partners of homosexual men and by infected women to their children *in utero*. Blood-to-blood transmission is the surest route to infection. Little is known about the effectiveness of other methods of transmission, but the AIDS virus is plainly not particularly infectious. Even so, it is reasonable to expect that in due course the infection will spread through the general population in the narrow sense that the groups now most at risk will be less conspicuous. This is what seems to have happened in some parts of Central Africa.

It is a triumph that questions like these have been successfully answered in so short a time. Even so, there remain some curious puzzles. If, for example, the underlying defect in AIDS patients is immunosuppression, why should the rare skin cancer called Kaposi's sarcoma, believed by some to involve cytomegalovirus as a kind of co-carcinogen, be such a common sequel to infection by HTLV-III? Why not other kinds of cancer? And what is the status of those who carry antibodies against HTLV-III but show no overt AIDS? Are they patients in waiting, just lucky or is there an explanation of their apparent immunity?

This is the point from which the Drs Fox start. What, they ask, if those without overt AIDS who have been infected by the virus are at risk of succumbing instead to one of the neurological conditions associated with overt AIDS? What would happen if psychiatric hospitals were refilled with relatively young people suffering from conditions at present associated with old age, dementia for example? Could we shoulder the social burden? The question is chilling. Is it fair?

Over the past few months, there has been a trickle of articles in the clinical journals pointing to a neurological component of AIDS. From the outset, physicians have recognized what is vaguely called "AIDS-related encephalopathy" in some overt infections. The new development (see, for example, Ho *et al.* and Resnick *et al.*, both in *New. Engl. J. Med.*, **313**, 1493 & 1498; 1985) is the recognition that HTLV-III virus may infect brain tissue (promoting the formation of antibodies in the cerebrospinal fluid) and that it may be directly responsible for some of the damage done to the nervous systems of people with AIDS. More ominously, some of those in whose nervous tissue HTLV-III has been found are people without overt AIDS.

These investigations are still few and far between. Knowledge of the neurological complications of AIDS itself is only sketchy. As yet, there is no factual basis for an attempt to guess at the frequency with which virus reaches the brains of those who have merely been infected with the virus. But if the apparent similarity between HTLV-III and visna virus is sustained by further investigations, and because HTLV-III is a retrovirus that may become a part of the genome of somatic cells and nervous tissue in particular, there is a danger that AIDS infection may be hidden in the brains of human beings much as the herpes simplex virus (which causes "cold sores") may linger dormantly in the peripheral nervous system, bursting out only from time to time.

This is the background against which the Drs Fox have written their scary letter. There is a possibility that HTLV-III will lodge in infected people's brains, serving both as a cause of direct neurological damage and as a reservoir for the infection of others. Plainly there is an urgent need that this possibility should be explored, not least because virus in the brain may be less accessible to therapeutic drugs. Plainly, that will take time.

What, in the meantime, should be done? Reactions to the emergence of AIDS as a public health problem in industrialized communities has spanned the usual spectrum from panic to complacency. Many have responded with exaggerated fear to the notion that casual contact may infect them, while the primitive response of those who believe that Lot's wife met her deserved fate on the escape from Sodom and Gomorrah has been distasteful and unhelpful.

A strategy for containing AIDS can consist only of two components — some means of decelerating the spread of infection (which is a short-term measure) and, later, some means of preventing infection of those at risk. Infection by contaminated blood products should soon be halted. No doubt the fear of infection has already had an important influence on the behaviour of homosexuals, perhaps even drug addicts. But the benefits will emerge only slowly and the prospects for prophylaxis and cure are still distant. The recognition that there are probably neurological consequences of infection by HTLV-III makes a serious problem of public health still worse.

John Maddox

Immunology

Approaches to AIDS therapy

from David Klatzmann and Luc Montagnier

MUCH publicity has been given to the announcement by a group of French physicians of their treatment of acquired immune deficiency syndrome (AIDS) with cyclosporin A, an immunosuppressant. After four days of treatment with the drug, the T4 lymphocyte count of one patient rose from 4 to 250 cells per microlitre (900 ± 400 being the normal value), most of which seemed to be immature lymphocytes[1]. But it was later announced that whereas 10 patients with AIDS or the AIDS-related complex had shown similar initial improvements in T-lymphocyte counts, the original patient had died 15 days after treatment began. At first sight, it may well seem counterproductive to treat an immune deficiency disease with an immunosuppressant. There is some theoretical basis[2-4] for such treatment if AIDS is considered to be a virus-induced autoimmune disease but, because of the hazards of immunosuppressive treatment, the evidence for and against AIDS as an autoimmune disease needs to be carefully considered.

The most frequent clinical expression of AIDS is the occurrence of severe opportunistic infections, reflecting a profound defect of cellular immunity. Laboratory analysis demonstrates a broad spectrum of immune abnormalities[5], among which is a drastic reduction in the numbers of T4 lymphocytes in peripheral blood and secondary lymphoid organs as well as an impairment of their functions[6,7]. This may be accounted for by the biological properties of the AIDS virus, LAV[2] (also known as HTLV-III or ARV) which displays a selective tropism for normal T4 lymphocytes both *in vitro* and *in vivo*[8]. Intensive replication of the virus in cultured T4 lymphocytes is accompanied by a cytopathic effect which includes inhibition of cell growth, virus-induced fusion of the plasma membrane and, eventually, destruction of the cells[8].

It is unlikely, however, that AIDS is the result of a direct progressive destruction of T4 cells by the virus for at least two reasons. The first is that the replication and cytopathic effect of LAV can only be observed in activated T4 cells[2,9]. Indeed, LAV infection of resting T4 cells does not lead to viral replication or to expression of viral antigen on the cell surface, while stimulation by lectins or antigens of the same cells results in the production of viral particles, antigenic expression and the cytopathic effect. An equivalent phenomenon has been extensively documented for visna virus[10], the expression of which is associated with the activation of latently infected macrophages[11]. Visna virus is the prototype of the lentivirus family of retroviruses and comparison of LAV and visna virus nucleotide sequences strongly suggests that LAV is also a lentivirus. Indeed, comparison of protein and nucleotide sequences of various retroviruses generates phylogenetic trees demonstrating that not only LAV and visna but also caprine arthritis-encephalitis virus and equine infectious anaemia virus (the latter being antigenically related to LAV[12]) are members of a subfamily of retrovirus that diverged early from other retroviruses such as oncoviruses[3,13].

The second reason to doubt that the destruction of T4 cells by LAV is the cause of AIDS is that only a small proportion of these cells is infected by the virus. It is not clear why this is so because, by definition, all T4 cells carry T4 molecules on their surface and these molecules seem to act as the receptor by which LAV enters the cells[14,15]. And yet in purified T4-cell cultures, even at the peak of virus replication only 5–10 per cent of the cells express viral antigen and are subsequently lysed by the cytopathic effect[8]. Furthermore, only 10–20 per cent of clones derived from the CEM T4 cell line are susceptible to LAV infection, even though they all express the T4 molecule on their surface[16]. A similar picture emerges from studying patients: *in situ* hybridization with viral DNA probes indicates that less than 1 in 10,000 lymphocytes are replicating LAV at a given time[17] and the Southern blot hybridization technique, which can detect as little as one copy of viral DNA per cell, yields negative results on fresh peripheral blood lymphocytes of AIDS patients[18].

Taken together, these observations provide evidence against direct destruction of the T4-cell system by virus infection and replication. Therefore, one has to envisage alternative theories that explain the impairment in T4-cell number and function that characterizes AIDS. What could these be?

Immunosuppressive proteins

One possibility could be that LAV, like human T-cell leukaemia viruses I and II[19] as well as mouse and cat leukaemia viruses, possesses a protein in its envelope (p15E) that is able to induce immune depression of T-cell function. But no such protein seems to be produced by LAV. Various reports have suggested that sera of AIDS patients contain soluble factors that can suppress *in vitro* T-cell functions[20]. Such factors have not been characterized and their viral origin has not been proven but at least the observation that viral proteins are released during *in vitro* LAV production by lymphocytes[21] is consistent with the idea. The availability through genetic engineering of viral purified proteins should help in testing this hypothesis in the near future.

Autoimmune mechanisms

The role of viral infections in triggering autoimmune diseases is well documented. For instance, diabetes in mice can be caused by an immune destruction of Langerhans cells following their infection by viruses such as coxsackie strains[22]. In retroviral infections, such a mechanism has been invoked for the encephalitis induced by visna virus and the haemolysis induced by equine infectious anaemia virus. AIDS patients often display signs of autoimmune reactions that are probably secondary to cell destruction caused by various opportunistic infections, but a more specific autoimmune process may be triggered by the ability of LAV envelope proteins to bind to T4 molecules. Indeed, not only virions but also free LAV proteins released from LAV-producing lymphocytes may bind to T4 molecules on the surface of uninfected lymphocytes. This could explain the general disappearance of detectable T4 molecules on the surface of LAV-infected cultured T4 lymphocytes in which only 10 per cent of cells seem to express viral antigens.

Whether this also occurs *in vivo* is not known, but if it does, the result could be that non-infected lymphocytes become highly immunogenic because of their surface-bound T4 molecules. This could account for a general destruction of the T4-cell system by classical cellular and antibody-mediated cytotoxicity[4]. The whole pathophysiology of AIDS would then be the result of a situation in which the few LAV-infected cells in the resting state are invisible to the immune system because they do not express viral antigens. Each time these cells are stimulated, not only they but also many non-infected cells will be destroyed by the immune system because they have become coated by LAV proteins. Thus, the immune deficiency induced by LAV infection would be the result of an active autoimmune destruction of the T4 lymphocytes, probably enhanced by the repeated stimulation of the immune system by antigens or alloantigens.

Rational therapy

According to the pathophysiology of the disease, three therapeutic approaches to AIDS can be distinguished. The first is the development of drugs to destroy viral particles and infected cells, or at least stop the virus spreading. After *in vitro* screening, drugs such as HPA23, suramin and ribavirin have demonstrated antiviral activity and are now being tested in controlled clinical trials. Preliminary results indicate that LAV cannot be isolated from patients' lymphocytes during treatment but that the virus reappears at the end of treatment; moreover, the control of virus spreading is not associated with an immune or clinical improvement[23,24].

A second approach involves immune stimulation or reconstruction. Immunostimulators alone, even pure interleukin-2, seem to fail to reconstitute the immune system of AIDS patients. Interferon, which has both antiviral and immunostimulant effects, seems to be of value in the treatment only of Kaposi's sarcoma, which is often associated with AIDS. In any case, since cell activation probably contributes to virus spreading and T4 depletion, the use of such drugs in patients with minor symptoms of LAV infection may be dangerous in that it could accelerate progression of the disease unless antiviral drugs were used at the same time. Immune reconstitution by bone-marrow graft or leukocyte transfusion has been found not to work because the grafted cells are rapidly reinfected by the virus[25].

The third approach would be based on the view that AIDS is an autoimmune disease. This would suggest that immunosuppressive drugs, which can limit both cell stimulation and cytotoxic mechanisms, have a role in the treatment of AIDS. In that case, treatment would be designed first to control virus replications and then to 'tolerate' non-infected cells coated with viral proteins, in the way an allograft can be tolerated. Since there is still no firm basis for such a therapeutic approach, which is potentially dangerous, caution is required before clinical trials. While immunosuppressive treatment has been used in visna-infected animals with clinical improvement of early brain lesions without any adverse results[26], there are descriptions in the literature of patients who have died of fulminant *Pneumocyctis carinii* pneumonia after being treated with immunosuppressive drugs in ignorance that they were LAV-infected[27]. Even if cyclosporin A has some potential use in virus-induced autoimmune disease, its use in AIDS patients should await more experimental knowledge about its action on T cells, which may be highly complex[28].

Finally, because of the complexity of the pathophysiology of AIDS, only active and constant cooperation between biologists and clinicians will lead to an effective therapy, probably involving a combination of drugs and other treatments. ☐

David Klatzmann is at the Hospital La Pitié-Salpêtrière, 75634 Paris Cédex 13; Luc Montagnier is at the Institut Pasteur, 75724 Paris Cedex 15, France.

---

1. see *Nature* **318**, 3 (1985).
2. Montagnier, L. *et al. Human T Cell Leukamia Lymphoma Viruses* (eds Gallo, R.C., Essex, M.E. & Gross, L.) 363 (Cold Spring Harbor Laboratory, New York, 1984).
3. Sonigo, P. *et al. Cell* **42**, 369 (1985).
4. Klatzmann, D. thesis, Univ. Paris (1985).
5. Seligmann, M. *et al. N. Engl. J. Med.* **15**, 1286 (1984).
6. Gluckman, J.C. *et al. Clin. exp. Immun.* **60**, 8 (1985).
7. Fauci, A.S. *et al. Ann. intern. Med.* **102**, 800 (1985).
8. Klatzmann, D. *et al. Science* **225**, 59 (1984).
9. McDougal, J.S. *et al. J. Immun.* **135**, 3151 (1985).
10. Haase, A.T. *et al. Science* **195**, 175 (1977).
11. Narayan, O. *et al. Infect. Immunity* **41**, 67 (1983).
12. Montagnier, L. *et al. Ann. Virol. (Inst. Pasteur)* **135E**, 119 (1984).
13. Chiu, I.M. *et al. Nature* **317**, 366 (1985).
14. Klatzmann, D. *et al. Nature* **312**, 767 (1984).
15. Dagleish, A. *et al. Nature* **312**, 764 (1984).
16. Klatzmann, D. *et al. Abstr. RNA Tumour Viruses Conf.* Cold Spring Harbor Laboratory (1985).
17. Harper, M.E. *et al. Abstr. int. Conf. AIDS*, Atlanta, 27 (1985).
18. Shaw, G.M. *et al. Science* **226**, 1165 (1984).
19. Cianciolo, G.J. *et al. Science* **230**, 453 (1985).
20. Cunningham-Rundles, S. *et al. J. clin. Immun.* **3**, 156 (1983).
21. Montagnier, L. *et al. Virology* **144** 283 (1985).
22. Rossini, A.A. *et al. A. Rev. Immun.* **3**, 289 (1985).
23. Rozenbaum, W. *et al. Lancet* i, 450 (1985).
24. Lane, M.C. *et al. Cancer Res. Suppl.* **45**, 4674 (1985).
25. Lane, M.C. *et al. N. Engl. J. Med.* **311**, 1099 (1985).
26. Nathanson, N. *et al. Lab. Invest.* **35**, 444 (1976).
27. Moffat, E.H. *et al. Lancet.* **i**, 935 (1985).
28. Shevach, E.M. *A. Rev. Immun.* **3**, 397 (1985).

Weather forecasting

Storm hunting with fractals

from A. Hollingsworth

MRS BEETON might well have observed that to make tiger soup, first catch your tiger. Tigers for a weather forecaster are vigorous storms that put life or property at risk. They occur on scales ranging from the tornado (~1 km) to mid-latitude cyclones (~2,500 km). Locating the whereabouts of a storm and estimating its ferocity are the first steps in making a useful forecast, but the surface meteorological network is very inhomogenous, with holes of many sizes where storms can lurk undetected.

On page 43 of this issue, Lovejoy *et al.* describe this problem in the language of fractal analysis. They give a definition of the dimension of an observing network, and argue that if the dimension of the network is lower than the dimension of the field being observed, many of the most energetic entities will never be detected. Many geophysical networks including the surface weather network are patchy in coverage and therefore lack dimensional resolution. Lovejoy *et al.* argue that long-term averages of geophysical fields derived from such dimensionally incomplete networks may be substantially biased: because of the inhomogeneity of the surface network, rare but vigorous events can be missed.

This suggests a bleak view of the feasibility of useful weather forecasting, a view which is belied by the fact that economically useful forecasts are routinely made out to perhaps 3 days in the tropics, 4 or 5 days in the southern hemisphere, and 6 or 7 days in the northern hemisphere extratropics. The success of the forecasts depends heavily on data sources other than the surface network as well as on sophisticated data-assimilation systems; ultimately success depends on the fact that scale separation is a meaningful concept for many practical purposes.

Data from polar orbiting and geostationary satellites, from the balloon network and from ships and aircraft provide the main basis for routine forecasting. The geostationary satellites, of which four are currently operational, provide multichannel measurements every half-hour over their field of view, which is roughly within 55′ of the nadir point at the equator (Fig.1). Cloud track winds can be derived from successive half-hourly scans in the visible and infrared. The satellites have a resolution of 1 km at nadir, and are invaluable for surveillance of tropical disturbances on all important scales. Two polar orbiting satellites provide radiometric soundings with good horizontal resolution four times a day, for most parts of the globe (Fig.2). Vertical structure in humidity and temperature can be derived from the soundings; in middle and high lati-

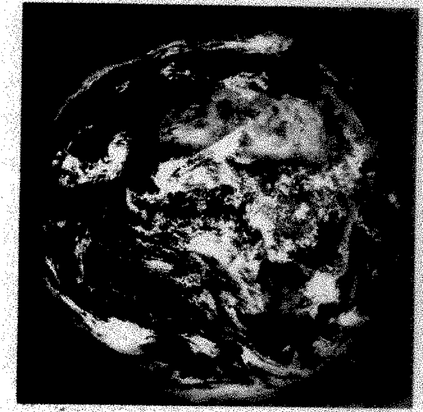

Fig. 1 Meteosat picture for 12.00 on 17 September 1985. The disturbance off the West African coast is the African wave that eventually developed into Hurricane Gloria. Cloud track winds can be estimated from successive half-hourly scans. The infrared channels enable one to estimate the height of the clouds. Pixel resolution at nadir corresponds to 1 km.

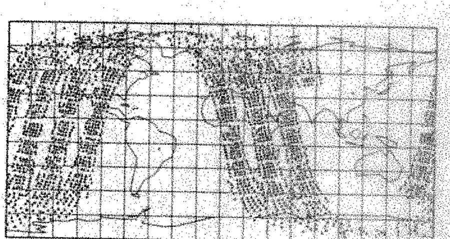

Fig. 2 Data coverage from a polar orbiter in a single six-hour period, covering about three orbits. A single orbiter can monitor every point on Earth twice a day.

tudes, the temperature soundings are valuable in inferring the winds.

The data from these diverse sources are integrated in a coherent view of atmospheric structure in space and time using four-dimensional data-assimilation methods. At the core of these techniques is a sophisticated global forecast model which provides rather accurate estimates of the expected state of the atmosphere, based on earlier observations. At any given time the observations are insufficient to determine the atmospheric structure.

Information from the forecast model is used in conjunction with the latest observations in a Bayesian estimation of the true state of the atmosphere; the forecast model is essential to resolve the underdeterminacy of the observations. There are many analogies between the methods used in this field and those used, for example, in computational vision (see Poggio, T., Torre, V. & Koch, C. *Nature* **317**, 314; 1985) or the applications of the Kalman–Bucy filter in control theory (see *Data Assimilation Methods* eds Bengtsson, L., Ghil, M. & Kallen, E., 330; Springer, 1981).

Global weather forecast models solve a version of the Navier–Stokes equations for fluid flow on a grid which has a horizontal resolution of about 150 km and a vertical resolution of 1–2 km. Some important weather cannot be resolved on such a grid. The fact that one can nevertheless make useful forecasts suggests that the simplification of treating the atmosphere as smoothly varying on the smallest resolved scales is not a serious error. Statistical methods can, if necessary, be used to interpret the forecast in such a way as to recover useful local detail. ☐

A. Hollingsworth is at the European Centre for Medium Range Weather Forecasts, Shinfield Park, Reading, Berkshire RG2 9AX, UK.

Immunoglobulin genes

Inversion for gene construction

from David Baltimore

JOINING of immunoglobulin genes as an event of immunodifferentiation is not unique in the biological world. Recombination of DNA molecules is commonplace and serves many functions, including meiotic recombination, post-replicative repair, phase variation in *Salmonella* bacteria and the generation of transcribable surface antigen genes in trypanosomes. Although DNA recombination frequently occurs, somatic rearrangement of gene fragments to produce functional genes is at present known to be used only by the immune system. This specificity implies that the rearrangement process should be active only in particular cells and be targeted only to well-defined DNA segments. On page 28 of this issue Malissen *et al.*[1] have extended our understanding of the rearrangement process by their analysis of the T-cell receptor gene complex.

The nature of the enzymes involved in the immunoglobulin gene rearrangement process, their control and their targeting specificity remain mysterious — we are still trying to understand the ground rules. One of the more obscure aspects is the relative placement and orientation of the gene fragments to be recombined to produce the immunoglobulin molecule. Although textbooks and the diagramatic slides shown by many immunologists blithely display strings of variable (*V*), diversity (*D*) and joining (*J*) segments, the only situation where a complete physical linkage has been achieved for all the elements of an immunoglobulin gene-segment joining system is with chicken lambda genes[2]. For all mammalian systems, the relative positions and orientations of the elements to be joined are incompletely established. Various arguments give a strong indication of the organization and orientation of the immunoglobulin heavy-chain gene segments[3,4], but the situation for the kappa light-chain genes is uncertain. The joining of kappa-chain gene segments involves a recombination between one of many hundreds of *V* segments with one of four *J* segments.

Although the *V* and *J* segments have not been physically linked in recombinant DNA clones, Lewis *et al.* in 1982 proposed that at least some of the kappa *V* regions occur in the DNA chain in the opposite transcriptional orientation to the *J* segments[5]. This proposal was based on the observation that in certain cells that have productively rearranged their DNA, segments of DNA remain that should have been deleted if both *V* and *J* were found in the same orientation[5-7]. If a *V* segment were in the opposite orientation to a *J* segment, joining the two elements would have to invert the intervening DNA rather than deleting it. Such an inversion would not remove any large segments of DNA from the cell but would simply reconfigure the existing DNA. This proposal met with much disbelief largely, I believe, because the DNA gymnastics involved seemed formidable although, in fact, they are quite ordinary (see the figure).

A decision about whether inversional joining is a mechanism of rearrangement was approached in two further papers by Lewis *et al.*, who used an artificial DNA construct with inverted *V* and *J* segments that would rearrange after integration into certain cells[8,9]. This work showed that inversional joining is a feasible mechanism, but left open the question of whether it actually occurs in normal B-cell maturation. Two indirect pieces of data argued for inversional joining[10,11], but both involved abnormal events. The direct demonstration of inversional joining in the kappa gene of a plasmacytoma was made by Feddersen and Van Ness[12], who found that they could recover both products of a natural joint and showed that the two had to arise by inversional joining. This directly implied that some *V* regions are in opposite orientation to the *J* regions.

Malissen *et al.* have now extended the analysis to the *V* regions of the T-cell receptor gene complex. Here they have uncovered a most surprising situation (one that could as easily have been true of kappa light-chain genes and may yet turn out to be). They have shown that at least one *V* segment is downstream of the constant (*C*) regions. In all previously characterized systems of immunoglobulin-related genes, the *V* segments have been thought to be upstream of the other segments. For immunoglobulin heavy-chain genes, joining is accompanied by deletion of the intervening DNA[3] and this requires that the

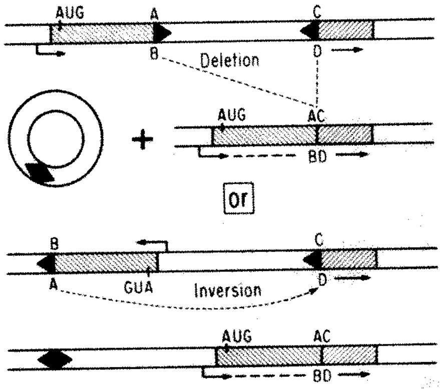

The difference between deletional and inversional joining. The difference is solely in topological orientation of the two participating pieces of DNA. The units to be joined (the *V* and *J* units shown here) are identical but in one case they are located in the DNA in the same transcriptional orientation and in the other in opposite orientation. The biochemistry of joining is identical in both: the same sequences are joined to one another. This can be seen by following the locations of the hypothetical sequences A, B, C and D. In both cases of joining, A is joined to C and B is joined to D. The consequences of deletional and inversional joining are quite different. In the first, a segment of DNA containing the joining signals is released as a circle and discarded from the cell. In the second, no segment of DNA is lost from the cell but the inversion causes the back-to-back apposition of the joining signals. ↳, Site of initiation of transcription with direction indicated; AUG, codon in *V* region that initiates translation; ▶, signal encoded in the DNA that specifies a site for joining (a conserved heptamer and nonamer).

V regions be upstream of the *C* regions (if they were downstream, the *C* region itself would become part of the deleted DNA).

For a *V* region to be downstream of the *C* region, topological considerations dictate that the *V* region must be in opposite transcriptional orientation to the *C* region. Malissen *et al.* were able to verify this because the *V* and *C* regions are near enough to each other to be physically linked in cloned DNA. The structure that they uncovered, in fact, implies that the joined segment in the T-cell clone arose by an initial deletional join of an upstream *D* segment to a *J* segment followed by a *V*-to-*D* – *J* inversional join in the downstream direction.

It should be emphasized that all of the DNA mechanics that have been found to underlie T-cell receptor gene rearrangement are congruent to the events of immunoglobulin gene rearrangement. The DNA signals thought to direct the rearrangement process are indistinguishable in the two systems. Malissen *et al.*[1] reinforce this perspective by showing that *D*-to-*J* rearrangement precedes *V*-to-*D* – *J* rearrangement as found for immunoglobulin heavy chains. They also note that the joined genes have lost potential coding nucleotides found near the joining signals in the germline DNA elements and that new nucleotides (constituting an *N* region) are found between the joined *V* and *D* segments. The only surprise is that the reciprocal joint formed during the recombination retains three nucleotides between the heptamers. In all cases of immunoglobulin gene joining yet studied, the heptamers are joined back-to-back with no intervening nucleotides (in one case a join with one nucleotide missing was found; ref. 9).

With this demonstration of inversional joining of a T-cell receptor *V* gene segment, most of what we want to know about the topology of joining is available. All we now need is to understand the sequence requirements for joining; then we can turn to enzymology, a task already begun in many laboratories but with little reported success. □

1. Malissen *et al. Nature* **319**, 28 (1986).
2. Reynaud, C.-A., Anquez, V., Dahan, A. & Weill, J.-C. *Cell* **40**, 283 (1985).
3. Alt, F.W. *et al. EMBO J.* **3**, 1209 (1984).
4. Brodeur, P.H. & Riblet, R. *Eur. J. Immun.* **10**, 922 (1984).
5. Lewis, S., Rosenberg, N., Alt, F. & Baltimore, D. *Cell* **30**, 807 (1982).
6. Steinmetz, M., Altenburger, W. & Zachau, H. *Nucleic Acids Res.* **8**, 1709 (1980).
7. Van Ness, B., Coleclough, C., Perry, R. & Weigert, M. *Proc. natn. Acad. Sci. U.S.A.* **79**, 262 (1982).
8. Lewis, S., Gifford, A. & Baltimore, D. *Nature* **308**, 425 (1984).
9. Lewis, S., Gifford, A. & Baltimore, D. *Science* **228**, 677 (1985).
10. Alt, F.W. & Baltimore, D. *Proc. natn. Acad. Sci. U.S.A.* **79**, 4118 (1982).
11. Hochtl, J. & Zachau, H. *Nature* **302**, 260 (1983).
12. Feddersen, R.T.M. & Van Ness, B.G. *Proc. natn. Acad. Sci. U.S.A.* **82**, 4792 (1985).

David Baltimore is at the Whitehead Institute, 9 Cambridge Center, Cambridge, Massachusetts 02142, and the Department of Biology, Massachusetts Institute of Technology, Cambridge, Massachusetts 02139, USA.

100 years ago

PHYSICS AT JOHNS HOPKINS

The large and well appointed laboratories recently erected by the Trustees of the Johns Hopkins University for the Chemical and Biological Departments have by contrast made the more evident the needs of the Physical Department, which has been obliged to occupy temporarily parts of four different buildings for a physical laboratory. The new laboratory is to be a handsome building of red brick, trimmed with brown sandstone, and will occupy a fine site about a block from the other University buildings, on the corner of a quiet little street midway between the more important streets, which carry the bulk of the traffic. It will therefore be as free from disturbance from the earth-vibrations as could be expected in a city. The building will be 115 feet long by 70 feet broad and will have four stories besides the basement. In the centre of the building, and below the basement, are several vaults for instruments requiring to be used at constant temperature, also a fireproof vault for storage. In these vaults will be placed Prof. Rowland's dividing-engine, by which the diffraction-gratings are ruled, and the Rogers-Bond comparator, which has recently become the property of the University. There will be a tower on the south-east corner which will be provided with telescope and dome, and will be a convenient observatory when great steadiness in the instruments is not required.

from *Nature* **33** 236, 7 January 1886.

Plate tectonics

Global thermal histories

from Mike Bickle

Tectonic geology is a manifestation of the thermal evolution of the interior of the Earth. Surprisingly, models for this thermal evolution have proved difficult to reconcile with a geological record that extends over three-quarters of the history of the Earth. The relatively low crustal thermal gradients recorded in the earliest rocks are incompatible with the higher gradients predicted by convection models that incorporate the higher radiogenic heat production that must have then prevailed. After re-examining this problem, F.M. Richter (*Earth planet. Sci. Lett.* **73**, 350; 1985) concludes that low continental thermal gradients could only have been maintained in the Archaean if the continental lithosphere was stabilized by chemical means (that is, was less dense), rather than being a simple thermal boundary layer as seems appropriate for much of the present-day lithosphere. The concept of a chemically stabilized lithosphere is not new (see, for example Jordan, T.H. *Nature* **274**, 544; 1978) but it now seems that such stabilization was of greater importance in the past and may have had a profound effect on the evolution and preservation of ancient continental crust.

Models for global thermal evolution allow calculation of the temperature dependence of heat loss for a spherical, layered and convecting Earth. To be successful, a model must not only yield a plausible range of present-day interior temperatures (given an appropriate initial state), but must also account for the higher radiogenic heat production and loss of initial heat formation that must have occurred in the past. Successful models achieve this by generating internal temperatures higher than at present and thinner boundary layers with steeper thermal gradients.

Good evidence for higher internal temperatures is provided by komatiitic lavas, which are restricted to the Archaean and were erupted at temperatures about 200°C higher than any recent lavas. However, the geological evidence from metamorphic rocks, crustal thickness and sedimentary basin subsidence indicates that the range of crustal thermal gradients in the Archaean may not have differed significantly from the range of modern continental thermal gradients. This inference is strongly supported by the demonstration of Archaean ages for diamonds (Richardson, S.H. *et al. Nature* **310**, 198; 1984). The diamonds must have been preserved since roughly 3,200 Myr ago at depths greater than 150 km in continental lithosphere of at least similar thickness to present day continental lithosphere.

The problem addressed by Richter is how to allow higher interior temperatures without affecting that part of the boundary layer under the continents. Previous solutions have noted that heat is lost from the Earth's interior by two mechanisms: an unsteady small-scale convection of sinking and rising jets transporting heat to the base of the lithosphere through which it is subsequently lost by conduction; and larger scale recirculation of the whole lithosphere in oceanic regions, that is, plate tectonics. The driving and resisting forces involved in the second mechanism are difficult to quantify and there has been a temptation to assume that plate tectonics can transport any necessary extra heat. Richter has developed regional models to try to account for heat lost by both mechanisms as a function of internal temperatures. He looks particularly at the interdependence of the mechanisms. All his models with thermal boundary-layer definitions for the lithosphere result in boundary-layer thermal gradients that in-

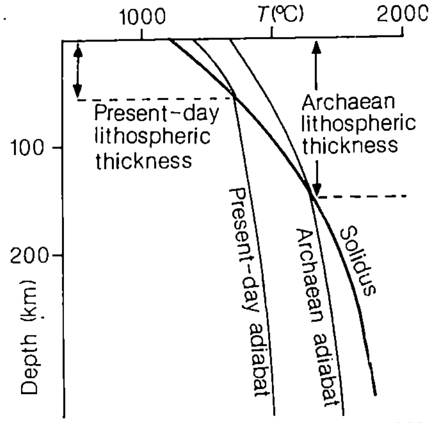

Depth–temperature plot for the upper 200 km of the Earth, showing the intersection of the present-day and supposed Archaean temperature profiles with the mantle solidus (the locus of the onset of melting). Because of the increased depth of initiation of melting in the Archaean, the depleted lithosphere would have been thicker than today.

crease at a rate faster than the increase in heat production. This is because the effectiveness of plate-tectonic heat loss decreases as temperatures increase and plate thicknesses decrease. The only viable resolution of this problem is that the continental lithosphere is stabilized chemically rather than thermally.

How robust is this conclusion? All convection calculations involve a series of assumptions. U.R. Christensen (*J. geophys. Res.* **90**, 2995; 1985) has performed numerical calculations of convection in a fluid with a temperature-sensitive viscosity and raised some important questions about the validity of the parameterized calculations used by Richter. Such calculations estimate the temperature dependence of heat loss by comparing numerical convection models run at various newtonian viscosities, but with constant viscosity in each model. Christensen's experiments with viscosity as a function of temperature indicate that heat flux is less sensitive to temperature than previously thought. This is because the cooler higher-viscosity upper boundary layer controls convection rates; hence the heat flux is related to some temperature in the upper boundary layer rather than the substantially higher interior temperature used as a scaling factor in the parameterized calculations. Christensen's calculations indicate how much has to be learnt about convection in variable viscosity and non-newtonian fluids appropriate to the Earth's mantle.

Nevertheless, such complexities seem unlikely to affect Richter's basic conclusions. Heat flux from the Earth is necessarily fixed at a rate sufficient to allow the Earth to cool to its present state from initial temperatures high enough to allow substantial but incomplete outgassing. In addition, Richter's calculations span a range of viscosity–temperature relationships including the limiting case of viscosity independent of temperature. Interior temperatures are less well constrained by parameterized models, but no model based on the lithosphere as a simple thermal boundary layer allows global heat to rise without increased heat input into the continental lithosphere.

The heat loss considerations allow some interesting speculations about Archaean tectonics, which are important because they lead to possible tests of the hypothesis of a chemically depleted continental lithosphere. Increased mantle temperatures cause melting to be initiated at greater depths. For example, at 1,600°C, appropriate to the Archaean mantle, melting might be initiated at about 150 km under mid-ocean ridges compared with depths of roughly 60 km for modern mantle (at approximately 1,350°C). This could yield a depleted lithosphere 150 km thick with 25 km of oceanic crust (see figure). The former might be converted to continental lithosphere by accretion of island arcs. Stabilization of the lithosphere by depletion to the depth at which melting is initiated seems essential to preserve Archaean crust from an alternative tectonic mode postulated by Richter. If convection penetrated into regions of partial melt below continental lithosphere the overlying crust would be continuously buried beneath copious volcanicity. This would lead to subsidence, stablization of a cool dynamically thickened thermal boundary layer and continous recycling of the volcanic material down into the underlying mantle. Such a process is incompatible with preservation of Archaean crust and if it operated must have been restricted to a pre-Archaean period or perhaps to those areas of Archaean crust not preserved.

The postulate of a thick chemically depleted continental lithosphere is testable. Isotope data, including those yielding the age of garnet inclusions in diamond, can demonstrate the antiquity of periodotite xenoliths (such as are found in kimberlite pipes) putatively derived from the continental lithosphere. Their chemistry can indicate the degree of chemical depletion. A critical point yet to be resolved is whether the density decrease due to chemical changes is adequate to stabilize the lithosphere against the thermally induced density increase which limits the thickness of modern oceanic lithosphere (Houseman, G. & McKenzie, D.P. *Geophys. J.R. astr. Soc.* **68**, 133; 1982). ☐

Mike Bickle is in the Department of Earth Sciences, University of Cambridge, Downing Street, Cambridge CB2 3EQ, UK.

Protein structure

Polar pocket with nonpolar lining

from David J. Cowley

CLASSICAL crystallographic studies of the globular protein myoglobin (Kendrew, J.C. *et al. Nature* **185**, 422; 1960) showed the oxygen-carrying plate-like haem group to be embedded in a pocket that is lined largely with nonpolar amino acids. But on page 70 of this issue R.B. MacGregor and G. Weber report optical spectroscopy studies with a new fluorescent probe, which indicate that the haem cleft has a polar interior.

Like the commonly used probe amino-naphthalene sulphonate, the new probe DANCA* has spectroscopic properties that reflect the polarity of its environment. But it has the advantage that the dipole moment on electronic excitation changes markedly in strength but not in direction. Such changes, detected spectroscopically and compared with the probe's optical properties in a series of homogenous solutions of defined polarity, allow the ready estimation of the local polarity of a biological macromolecule enveloping the rigid probe chromophore.

DANCA has a high affinity (dissociation constant 1.2×10^{-5} M at 24°C) for apomyoglobin because its carboxylic acid group mimicks that of haem itself. PRODAN*, which has neither the high affinity for apomyoglobin nor the carboxylate group of DANCA, nevertheless has nearly identical absorption and fluorescent properties and can therefore be used for calibration purposes for solvents in which DANCA is insoluble.

Bound DANCA can be displaced stoichiometrically from apomyoglobin by one equivalent of haemin, showing that the probe is not loosely associated at a variety of sites but is located only in the protein pocket. On binding of DANCA to apomyoglobin in aqueous buffer at *p*H 6.0, the fluorescent emission intensity increases fourfold and the emission band shifts to higher energy. The emission spectrum is similar to that of DANCA in the very highly polar solvent *NN*-dimethylformamide at 20°C or in glycerol at −40°C. It is the gross redshift of the emission band relative to PRODAN in nonpolar cyclohexane solvent that reveals the high effective polarity of the interior of the myoglobin pocket.

The apparent paradox of a pocket lined with nonpolar amino acids and yet with a high effective polarity is resolved if the amide dipoles (C=O...H–N) disposed around the rim of the segments of alpha

---

*DANCA is 2′-(*N*,*N*-dimethyl)amino-6′-naphthoyl-4-*trans*-cyclohexanoic acid; PRODAN is 6-propionyl 2-(*N*,*N*-dimethyl)aminonaphthalene.

helix forming the haem pocket can exert substantial electric fields inside the pocket despite the attenuation by the insulating lining of hydrocarbon side chains (see figure). Calculations confirm the feasibility of this explanation, which may apply to many enzyme interiors.

To infer environmental polarity from fluorescence band positions requires that the surrounding medium has had the opportunity to undergo a full adjustment to the excited chromophore before the latter emits light. Otherwise the emission spectrum shifts to longer wavelengths as longer wavelengths of light are used to excite selectively more stabilized solvated chromophores. This 'red edge effect' is observed for PRODAN in glycerol at −42°C but is absent above 1°C. Since 'solvent' relaxation must be complete, dependence of the emission of DANCA-myoglobin on the wavelength of excitation at room temperature is attributed to a heterogeneity of probe orientations within the haem pocket. Haem itself binds in two distinct orientations. The reported steady-state fluorescence studies provide limited information. Time-resolved spectra and fluorescence anisotropy decay data would enable the rotational constraints on the bound probe and the exchange rates between probe configurations to be evaluated.

An additional redshift of fluorescence, above the expected solvent relaxation shift, incipient at −35°C and almost fully developed at 4°C, is intriguing. Despite the claimed merits of DANCA as a probe of well-defined geometry and electronic nature, the initial excited state may transform to a more polar, lower-energy excited state by twisting about the dimethylamino-naphthalene bond, with a likelihood that depends on the polarity and viscosity of the constraining medium. Such processes have been documented for many intramolecular charge-transfer systems analogous to DANCA, the classic example being *p*-*N*,*N*-dimethylaminobenzonitrile (Kosower, E.M. *Acc. Chem. Res*, **15**, 259; 1982 and Grabowski, Z.R. *et al. Nouv. J. Chim.* **3**, 443; 1979). If this were to be the case the 'environment polarity' would be overestimated. Notwithstanding, the high polarity of the myoglobin haem pocket is real.

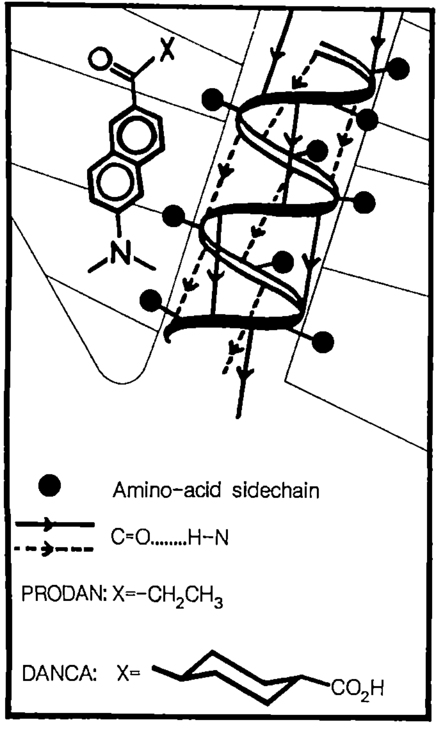

The haem cleft of apomyoglobin

MacGregor and Weber calculate electrostatic interaction energies of a monopole charge within a square grid of locations in the haem plane, together with the partial charges of nitrogen and oxygen centres of the peptide backbone in the known crystallographic positions of deoxymyoglobin, on the assumption that the intervening nonpolar sidechains form a dielectric of relative permitivity 3. Several orientations of the probe molecule, represented by a pair of opposite charges 0.84 nm apart on the grid, were found to be capable of producing spectral shifts in excess of the observed shifts of ~1,000 cm^{-1}.

On the basis of the often minor changes in acid dissociation constants of protic groups in water and inside certain proteins, it has been deduced that many protein cavities have a high effective polarity despite the lining of 'nonpolar amino-acid residues' (Warshel, A. *Proc. natn. Acad Sci. U.S.A.* **81**, 4785; 1984). These deductions are corroborated by the calculations and optical evidence of MacGregor and Weber. ☐

David J. Cowley is in the Chemistry Department, University of Ulster, Coleraine, County Londonderry BT52 1SA, Northern Ireland.

Glynn Isaac 1937–1985

GLYNN ISAAC died in a hospital in Japan on 5 October after a brave fight against a vicious, and as yet unidentified, infectious illness. Although 'officially' an archaeologist, he drew no boundaries between disciplines in his pursuit of evidence about the origins and early stages of human behaviour. His field contributions are important enough in their own right, but Isaac will mainly be remembered for his eclectic use of evidence and for his passionate insistence that the hypothetico-deductive method can, and should, be applied to problems of prehistory.

Glynn Isaac's introduction to archaeology began as a schoolboy and continued as a student in Cape Town, and came from A.J. Goodwin and Monica Wilson. His mentors at Cambridge were Graham Clark and the late Charles McBurney. In 1961 he accepted a research post with Louis Leakey in Kenya which was the beginning of his professional association with African prehistory. Louis and Mary Leakey had investigated the site of Olorgesailie between 1942 and 1954 and, with typical generosity and perspicacity, Leakey gave Isaac the responsibility of further excavating and analysing the site. Isaac's monograph on Olorgesailie is a classic of its kind, and contains clear evidence of his sensitivity to the confounding problems that the geological context can bring to the interpretation of archaeological sites.

Field work in Nakuru and in the Natron Basin followed and it was at Natron, at Penini, that Isaac began his association with Richard Leakey. In 1969, Leakey invited Isaac to investigate the archaeological evidence which had then been recently discovered at the KBS site, at what was then East Rudolph, now Koobi Fora, in northern Kenya. However, Issac's contribution to the work at Koobi Fora was much wider, for he joined Leakey as co-director of the Koobi Fora research project and was instrumental in the development of nearly all aspects of the research that flowed from that area. His broad training in zoology and geology was crucial for this task. His strength as a scientist was most evident at the time when there was a conflict between the isotope and palaeontological evidence for the age of the KBS tuff. Isaac was determined to see, and was instrumental in achieving, the reassessment of the evidence. The apparent resolution of this problem proved to be the stimulus to important geochemical research which has resulted in more precise and accurate correlations of ash layers at four of the major East African sites.

Isaac was an inveterate hypothesis maker. His hypotheses about early hominid land use, behaviour and subsistence were mostly based on evidence that he and his collaborators had painstakingly recovered at Koobi Fora and elsewhere. The diverse and pertinent projects undertaken by his students, from studies of food availability to contemporary hunter-gatherers to the factors which disturb contemporary archaeological sites, speak for his willingness to put his own ideas to the test.

Isaac loved Africa and its people and he, more than any other, saw the need and the obligation to involve Africans in prehistory research. Prehistory is a field not usually noted for the humility of its practitioners but Isaac stood out as being wholly without self interest. His enthusiasms and influence spread far, and his impact on palaeontology, dating and on the conduct of anthropological field and laboratory research, as well as prehistoric archaeology, were more profound than I suspect we presently realize.

Bernard Wood

Endangered species

The fate of the California condor

from David S. Wilcove and Robert M. May

CALIFORNIA condors (*Gymnogyps californianus*) have soared over the foothills and valleys of the western United States since the Pleistocene. Whether they will survive the twentieth century is another matter. Recent counts indicate that only six condors remain in the wild, with another 21 in captivity. The future of North America's largest bird rests with these 27 individuals.

The heyday of the condor is long past. Fossil remains indicate they once occurred from British Columbia in Canada to the southern extent of Baja California in Mexico, and eastwards across the southern United States to Florida. The rich Pleistocene mammal fauna as revealed in the Rancho LaBrea tarpits must have provided abundant food (carrion) and one can imagine the condors squabbling over the carcass of a mammoth. At that time, there were a number of giant scavenging birds in North America, of which the condor is the only surviving species.

Within historical memory, condors still occurred all along the Pacific coast of North America, yet almost as far back as the records go, they have been in decline. By 1850 they had almost disappeared north of California; by 1940 there were none left in Baja California. For most of the past 50 years, they have occupied a U-shaped area of about 45,000 km^2 from Santa Barbara south along the coastal range to San Jose and along the western foothills of the Sierra Nevadas to southern Madera county.

The first condor census, published in 1953 (ref. 1), gave an estimate of 60 birds, but this was obtained without marking individuals and is now believed to have been far too low[2]. By 1978, only 25 – 35 condors were thought to remain in the wild. Four years later, some of the wild birds were brought into captivity and eggs were collected for captive hatching. The captive population has grown steadily but so far only by supplementary wild eggs and birds, because it will be several years before most of the captive birds are old enough to breed. The wild population, meanwhile, had dropped to 15 by October 1984 and another six birds had disappeared by May 1985, when three of the survivors were brought into captivity. All the wild birds today are radio-collared, which should allow biologists to monitor them closely.

Many explanations have been offered for the decline of the condor. In the vivid but teleological language of some earlier ecologists, it was termed a senile species: a bird whose low reproductive rate (one offspring every two years), lengthy adolescence (six or more years) and vast home range ill-suit it for life in modern-day southern California. The demise of the condor may, therefore, be simply a protracted coda to the larger extinctions that occurred about 10,000 years ago as recorded at Rancho LaBrea. Although there is some truth in this, for conservation purposes it is more useful to focus on the specific environmental problems that plague the condor, including molestation by humans, food shortages, environmental pollution and habitat destruction.

At the turn of the century, when a condor egg was worth as much as $300, many of the nests were robbed. Federal protection has eliminated this threat but it has not prevented the occasional loss of adult birds to hunters. There is debate about the extent to which such vandalism is responsible for recent losses.

End of the line? (Frank Lane picture agency).

Some have suggested that the extinction of the Pleistocene megafauna resulted in a food shortage for the condor, but there were large herds of antelope and elk in the San Joaquin and Sacramento Valleys until the mid-nineteenth century. The expansion of ranching in this region provided the condors with abundant livestock, chiefly cattle, sheep and horses[3], although the switch to agriculture in the early 1900s probably did reduce their food supply. A programme providing food supplements was started in 1971 (ref. 4).

A far more serious problem has been contamination of the food supply. Condors ingest lead when they dine on animals that have been shot by hunters[5]; at least two birds have died in the past three years from lead poisoning and lead levels in the remaining wild condors are alarmingly high. Levels of DDE in tissue samples from wild condors are high enough to cause reproductive problems, assuming that condors are as sensitive as most birds of prey to DDE[5]. Eggshells of California condors from 1964 – 1969 were 33 per cent thinner than in the pre-DDT era[6].

As the condors live in one of the nation's fastest growing areas, not surprisingly their habitat is under assault. Oil production and urbanization are continually extending into the grasslands where the birds forage, and mining and timber interests would like greater access to the mountainous regions where the birds roost and nest.

The US Department of the Interior must weigh all of these factors when deciding what to do with the remaining condors. Some scientists have recommended that the remaining wild birds be brought into captivity for safe-keeping. Their argument, which seems unanswerable to us, is that a programme of breeding captive birds is the only thing that can save the species, but others think that removing wild birds will eliminate any chances for re-introducing captive-bred individuals to the wild. Without older birds to show them where to roost, nest and forage, new recruits have little chance of surviving.

This argument epitomizes the choice that is likely to face us increasingly often, as more species are driven to the brink by human population expansion: do we settle for preserving specimens of each species in some form of zoo or do we strive, possibly hopelessly, to preserve the ecological entity with its full panoply of behaviour in the wild? In the case of the condor, some urge that a few be left wild, because it may be politically impossible to fend off the assaults on their habitat if there are no wild birds left[7]. The most recent agreement hammered out between the State of California and the Department of the Interior proposes the capture of three of the six remaining wild condors with simultaneous release of three captive birds, but the agreement is contingent on the department purchasing a 14,000-acre tract of land needed for condor conservation, and will probably collapse if any more wild birds die in the next four months.

California condors were around long before the first humans colonized the New World. It may be a measure of the success of our own species that we have all but eliminated the condor. Another measure will be whether we can now save it. ☐

1. Koford, C.B. *Nat. Audubon Soc. Res. Rep.* 4 (1953).
2. King, W.B. *ICBP Bird Red Data Book* (Smithsonian Institution, Washington, DC 1981).
3. Grossman, M.L. & Hamler, J. *Birds of Prey of the World* (Bonanza Books, London, 1964).
4. American Ornithologists' Union *Auk* 94, suppl. (1977).
5. Wiemeyer, S.N. Krynitsky, A.J. & Wilbur, S.R. in *Vulture Biology and Management* (University of California Press, Berkeley 1983).
6. Kiff, L.F., *et al. Condor* 81, 166 (1979).
7. Crawford, M. *Science* 229, 884 (1985).

David S. Wilcove and Robert M. May are in the Department of Biology, Princeton University, Princeton, New Jersey 08544, USA.

Trialkyl lead in rain in the Black Forest

SIR—We have recently suggested that high concentrations of trialkyl lead, R$_3$Pb$^+$, as detected, for example, in rainwater samples from the Black Forest, may be harmful to the forests of Central Europe[1]. The theory has been seriously questioned by M.H. Unsworth and R.M. Harrison[2]. We wish to provide some new and supplementary data, which we believe can help to remove their doubts.

The most serious questions posed by the authors concerned the bioassay used for quantitation of R$_3$Pb$^+$. In continuing our study for several months of this year on behalf of the government of Baden-Württemberg, two independent methods have been employed for the determination of R$_3$Pb$^+$ in rain water. In addition to the tubulin assay, all samples were submitted to a chemical separation procedure[3] which was also used for the determination of some of the concentration values cited by Unsworth and Harrison. The results of both assays were the same within the limits of experimental error. Again, four of the samples collected at two locations in the Black Forest had trialkyl lead concentrations higher than 0.2 μM.

Unsworth and Harrison were concerned about the likelihood of the occurrence of such high concentrations of R$_3$Pb$^+$ in rain. The concentrations are indeed 100–1,000 times higher than those reported by others. So far, however, analytical data on trialkyl lead in rain are scarce. The few data known are from locations with a typical sea climate, which may not be comparable to locations on the Continent. Moreover, the occurrence of trialkyl-lead-polluted rain seems to be confined to small areas, as shown by the analytical results obtained from one of our sampling stations which, although located only 100 km east of the Feldberg, has never given R$_3$Pb$^+$ values above the limit of detection. Sampling at this site alone would have led to different conclusions. Finally, the Antwerp data mentioned by Unsworth and Harrison were one-sample measurements, and therefore statistically insignificant. In 1984, it took us 4 months of uninterrupted observation before we recorded a single toxic event.

Unsworth and Harrison argue that the low concentrations of R$_3$Pb$^+$ in the atmosphere cannot account for the high concentrations of R$_3$Pb$^+$ in rain. For the undegraded compound R$_4$Pb, Harrison and coworkers[4] reported atmospheric concentrations at rural sites of up to 230 ng m^{-3}. After degradation, the distribution of R$_3$PbX can be expected to remain unchanged, at least for some period of time. However, values of R$_3$PbX were reported to be as low as 2 ng m^{-3}. So where is the rest? The loss is most easily explained by the high instability of salts when dispersed in air. They may be captured by polar media, such as surfaces of particulate matter, and would therefore be analysed together with the inorganic lead. Indeed, in most of the studies of atmospheric lead pollution, the term "inorganic lead" stands for the lead fraction removed by filters. R$_3$PbX could be washed off the surface of such particles, on contact with rain or fog. In our example, 230 ng of R$_3$PbX would be dissolved in about 10 ml (10 g m^{-3} is the typical atmospheric humidity in Europe). The resulting concentration would be about 10^{-7}M, which is within the range of R$_3$PbX found in the Black Forest. This value does not consider the R$_3$PbX that may be taken up by rain on its way from clouds to the surface.

Fortunately, we do not disagree on controversial theories but on a finding that can be examined experimentally. Therefore, we suggest that further discussion should be postponed until our results have been confirmed by others. Twin samples were taken of most of the rainwater samples collected in 1985 in the Black Forest. They are waiting to be analysed.

H. FAULSTICH
C. STOURNARAS

Man-Planck-Institut für Medizinsche Forschung,
D-6900 Heidelberg 1,
Postfach 10 38 20, FRG

1. Faulstich, H. & Stournaras, C. *Nature* 317, 714–715 (1985).
2. Unsworth, M.H. & Harrison, R.M., *Nature* 317, 674 (1985).
3. De Jonghe, W.R.A., Van Mol, W.E. & Adams, F.C. *Analyt. Chem.* 55, 1050–1054 (1983).
4. Birch, J., Harrison, R.M. & Laxen, D.P.H. *Sci. Tot. Envir.* 14, 31–42 (1980).

An anniversary for the lipid bilayer

SIR—The year 1985 marked the sixtieth anniversary of the proposal by Gorter and Grendel[1] that biological membranes consist of a double layer of lipid molecules, as appropriately mentioned by Bretscher[2]. In 1925 E. Gorter, a pediatrician with a strong interest in chemical pathology, and F. Grendel, a chemist in the laboratory of the University Children's Hospital at Leiden, The Netherlands, derived their cell membrane model from observations made with rather simple experimental techniques. The lipid extracted with acetone from a known amount of erythrocytes was spread as a monolayer on a water surface. The ratio of monolayer lipid area to total erythrocyte surface turned out to be close to 2: 1 for red blood cells from different mammalian species. Thus the investigators concluded with the suggestion that in the cell membrane of erythrocytes sufficient lipid is present for constituting a molecular bilayer. The structural model is the more remarkable because it was derived without any modern instrumental method such as infrared spectrometry, gas chromatography or electron spin resonance. Already 10 years ago, the Gorter-Grendel model was considered by Bretscher and Raff[3] a major breakthrough in cell biology, comparable to that of the double DNA helix. In 1934 Danielli and Davson[4] improved on the model by allowing for proteins to be additional components of plasma membranes. The fluid mosaic model proposed in 1972 by Singer and Nicolson[5], viewing functional biological membranes as bidimensional solutions of integral proteins in a liquid phospholipid matrix, remains the current basis for experimental work.

In 1966, Bar *et al.*[6] repeated the Gorter-Grendel experiments and discovered two major errors. First, acetone treatment extracts membrane lipids, and cholesterol in particular, incompletely. Second, more refined measurements of the surface area of the human erythrocyte yield the value of 145 ± 8 μm^2 instead of 99 μm^2, the value used in 1925. The Dutch investigators had in fact made two mutually compensating errors of about 40%.

We are proud that in 1935 Dr E. Gorter, at that time chairman of the pediatrics department at Leiden, accepted an invitation from Ghent State University to come and found the first university children's hospital in Flanders, Belgium. The strong interaction between pediatric observation and biochemical research, kindled by Professor Gorter, and promoted continually by his pupil and successor, Professor Hooft, who died in 1980, remedied effectively the developmental delay of pediatrics in Belgium. We owe much to Evert Gorter, who was once called: 'The best chemist among all pediatricians and the best pediatrician among all chemists.'

J.A. KINT
J.G. LEROY

Department of Pediatrics,
State University of Ghent,
De Pintelaan 185,
B–9000, Ghent, Belgium

1. Gorter, E. & Grendel, F. *J. Exp. Med.* 41, 439–443 (1925).
2. Bretscher, M.S. *Scientific American* 253, [illegible] 92, (1985).
3. Bretscher, M.S. & Raff, M.C. *Nature* 258, 43–49 (1975).
4. Danielli, J.F. & Davson, H. *J. cell. comp. Physiol.* 5, 495–508, (1934).
5. Singer, S.J. & Nicolson, G.L. *Science* 175, 720–[illegible] (1972).
6. Bar, R.S., Deamer, D.W. & Cornwell, D.G. *Science* 153, 1010–1012, (1966).

Scientific Correspondence

Scientific Correspondence is intended to provide a forum in which readers may raise points of a rather technical character which are not provoked by articles or letters previously published (where the Matters Arising section remains appropriate).

X chromosomes and dosage compensation

Sir—D.A. Smith (*Nature* **315**, 103; 1985) uses the term "dosage compensation" to mean that effect on the rate of transcription of X-linked genes in the male which enables it to survive the lack of one X chromosome; X inactivation in the female is, then, a further compensatory step to enable *it* to get over the problem of overactive X-linked genes. By suggesting that evolution could have somehow "resolved" the situation arising from aneuploidy for an entire X chromosome in the mammalian male, G.P. Maroni (*Nature* **317**, 22; 1985) asks whether the inferences drawn by Smith are valid. Purely in terms of the physiology of gene action, precisely what evolution had to "resolve" is not clear: in the course of their extensive analysis of the problem of dominance, Kacser and Burns[1] have shown that — special cases apart — metabolic fluxes are extremely insensititve to whether an enzyme is represented by one structural gene or two.

I wish to draw attention to a point that usually is not taken into account. Sex chromosomes are expected to include one or more sex-determining genes. If the mammalian X chromosome indeed contains genes determining primary sex, what such genes might require is not dosage compensation but full expression, or even exaggeration, of the difference in dosage between XX and XY genotypes. Thus it can be argued that dosage compensation (in the usual phenotypic sense) is unlikely to be the primary reason for X inactivation. Is it possible that X inactivation has a function more vital than dosage compensation? I have suggested that sex determination may be such a function[2]. The observed dosage compensation of *G6PD*, *HPRT*, *PGK* and such other X-linked housekeeping genes would then be, in the evolutionary sense used by Maynard Smith[3], an effect of X inactivation, not its function. This model requires that a distinction be made between dosage compensation at the level of the phenotype and that which might render the effective copy number of particular X-linked genes equal between XX and XY genotypes. Details are given in ref.2.

In *Drosophila melanogaster*, the Bridges ratio, X/A, is central to both sex determination and X-chromosome dosage compensation. Sex-specific lethal mutations such as *mle* and *Sxl*^{f1} affect both sex determination and dosage compensation, demonstrating that some genetic elements are common to the two processes[4,5]. Thus it appears that sex determination and dosage compensation may be two facets of the same regulatory process. A plausible genetic regulatory model has been proposed for intracellular measurement of the X/A ratio and the remarkable phenotypic effects of certain of these mutations[6]. An attempt has been made to interpret mammalian X inactivation in terms of this model, on the assumption that X inactivation also is based on some type of ratio measurement or intracellular counting of chromosomes[7].

H. Sharat Chandra

MCBL & ICMR Centre,
Indian Institute of Science,
Bangalore 560 012, India

1. Kacser, H. & Burns, J.A. *Genetics* **97**, 639--666 (1981).
2. Chandra, H.S. *Proc. natn. Acad. Sci. U.S.A.* **82**, 6947-6949 (1985).
3. Maynard Smith, J. in *Genome Evolution*, (eds Dover, G.A. & Flavell, R.B.) 375–382 (Academic, London, 1982).
4. Belote, J.A. & Lucchesi, J.C. *Nature* **285**, 573–575 (1980).
5. Lucchesi, J.C. & Skripsky, T. *Chromosoma* **82**, 217--227 (1981).
6. Gadagkar, R., Nanjundiah, V., Joshi, N.V. & Chandra, H.S. *J. Biosci.* **4**, 393–415 (1982).
7 Gartler, S.M. & Riggs, A.D. *A. Rev. Genet.* **17**, 155-190 (1983).

The Grand Menhir re-examined

Sir—Commenting on P.G. Bahn's alerting us[1] to C. T. LeRoux's discovery that the capstones of three tombs in Brittany once formed a single decorated 14m long menhir, one of the decorations being a carving of a *hache-charrue* (axe-plough), I suggested in *Scientific Correspondence*[2] that Le Roux's discovery requires a reexamination of the date and function of the over 20m long now fallen and broken menhir called the Grand Menhir Brisé. My suggestion assumed the validity of the assertion first made by R.S. Minot[3] and then by E. Twohig[4] that there is also a *hache-charrue* carved on the latter menhir.

I recently examined the Grand Menhir Brisé and could not discern a *hache-charrue* carved on it even after I checked my observations against the sketch by Minot in his 1965 article and against the small scale drawing furnished to me by Twohig. There are unevennesses on the surface of the granite of the second fragment of the Grand Menhir Brisé (counting the largest fragment as the first fragment) which may be interpreted as possibly depicting an axe head, but there is no indication that these are man-made rather than natural, and the presence of the rest of the alleged *hache-charrue* seems to depend upon the imagination of the beholder[5] (See *Hamlet*, Act 3, Scene 2, "Shape of cloud").

Twohig, in the course of her careful and thorough research, did not always find carvings reported by Minot to be genuine, (personal communication) and Minot's sketch of the alleged *hache-charrue* differs from Twohig's drawing in substantial ways, including not showing a loop on the haft. Because of its size and weathered nature, Twohig did not make a rubbing, photograph or full-scale tracing of the alleged carving, and the small scale drawing on which she bases the drawing in her book reflects what she saw but does not necessarily record what others will see.

One further observation should be made. LeRoux interprets the three granite fragment now serving as capstones of La Table des Marchands, the tomb of Gavrinis, and the tumulus of "er-Vinglé", as having once formed a single carved *menhir*. R.J.C. Atkinson suggests that the three granite fragments determined by LeRoux to once have been a single standing stone was a very long *capstone* which was later broken, its fragments then used as capstones in three separate tombs (personal communication). A very long capstone would be consistent with the shape of the stone when unbroken, and we know that dolmens were constructed which could utilize very long capstones, such as Le Grand Dolmen at Bagneux (Maine-et-Loire).

Atkinson points out that menhirs, unlike upright stones and capstones used in tomb construction, do not have carvings on them, except, in rare instances, for some markings at the base, and certainly not halfway up the menhir. In such event the date of construction of the Gavrinis tomb of about 5200 to 5000 BP would be irrelevant to the determination of the date of erection of the Grand Menhir, and a possible date of about 3600 BP initially proposed by Alexander Thom[6] and A.S. Thom in connection with their lunar observatory hypothesis would not be affected by LeRoux's discovery.

Robert L. Merritt

2 Bratenahl Place,
Bratenahl,
Cleveland, Ohio 44108, USA

1. Bahn, P.G. *Nature* **314**, 671 (1985).
2. Merritt, R.L. *Nature* **316**, 396 (1985).
3. Minot, R.S. *Bull. Soc. polymathique Morbihan*, 89–98(1965).
4. Twohig, E.S. *The Megalithic Art of Western Europe*, 190, Fig. 171 (Clarendon, Oxford, 1981).
5. Thom, A. & A.S. *J. Hist. Astr.*, 147–160 (1971).

Nature's Guide to How Britain Runs its Science

The latest edition of this popular wallchart is now available. The guide provides a comprehensive survey of the administration of British science, showing at a glance the functions, key personnel and finance of government departments, public and independent bodies, and the research councils. It has been thoroughly updated to take account of the many changes in structure and personnel that have occurred since the previous edition was published in 1983.

Copies are available from: Nature, Brunel Road, Houndmills, Basingstoke, Hants, RG21 2XS, UK. Prices: £4.75 (UK), US$8.50 (USA and Canada), £5.75 (all other countries). Airmail despatch outside the UK. Payment with order please. □

Intellect in evolution

Douglas J. Futuyma

Evolution: Essays in Honour of John Maynard Smith. Edited by P.J. Greenwood, P.H. Harvey and M. Slatkin.
Cambridge University Press: 1985. Pp.328. £30, $49.50.

By the fertility and originality of his thought, the variety of his interests and contributions, and the influence of his effervescent personality on his colleagues and students, John Maynard Smith has taken his place as one of this era's leading evolutionary biologists. His empirical and theoretical contributions have included functional morphology, *Drosophila* genetics and cytology, the genetics of developmental patterns, the evolution of senescence, the theory of polymorphism, speciation, evolutionary rates, and kin and group selection, the evolution of sex, and the evolution of behaviour. This *Festschrift* in honour of Maynard Smith on his imminent retirement from Sussex University therefore marks the end of an era.

Maynard Smith, perhaps more than any other single individual, has embraced both major strategies of explanation of evolutionary change: the formal theory of population genetics, including natural selection; and the phenotypic theory of adaptations. This second theory of adaptive strategies is largely devoid of genetics, but attempts to predict, for real phenotypic characters, the ordering of fitness values that appear as abstract constructs in population genetics. Both of these approaches, between which there is considerable tension, are represented in this collection.

The power of population genetics is revealed in Slatkin's theoretical treatment of the role somatic mutation might play in defending plants against attack by creating genetic mosaics (he concludes it will usually have little effect), and by Bengtsson's review of the number of underdominant loci required to establish a sterility barrier to gene flow between incipient species (generally many are required). These essays exemplify Lewontin's point that the role of population genetic theory is not to predict evolution, but to delineate the prohibited and the possible. Lewontin is less encouraging on the ability of theory to explain observations (for example to specify causes for gene frequency distributions), but is hopeful that variation at the nucleotide level may "give a finer structure of genetic detail corresponding to the detail that is built into the theory". Yet the theory includes elements such as population size, gene flow and linkage disequilibrium that surely will never be known in such detail, so the scope for such optimism may be rather narrow.

Representing the population genetic approach to adaptations, Felsenstein provides an intriguing distillation of theories of recombination, with some surprising conclusions (for example, the sib-competition model of Williams is a special case of Fisher and Muller's theory). Michod and Sanderson develop a theory of behavioural structure that obviates the need for kin selection as a necessary explanation of cooperation. Rose reviews his work on the genetics of senescence.

Maynard Smith: a view of both major strategies of explanation of evolutionary change.

Strategic analysis has become one of the chief tools in the study of adaptations, and Maynard Smith's introduction of the evolutionary stable strategy (ESS) concept is surely one of his most important contributions. The pitfalls lie not so much in the theory, which like population genetics theory varies in the realism of its assumptions, but in the testing, especially by the comparative method. Charnov shows the power of ESS theory to predict sex ratio and related phenomena, and uses the comparative method to good advantage. Packer and Pusey make a fairly convincing case for the ability of ESS theory to predict the outcome of asymmetrical contests in social mammals.

But observations do not always conform to the theory, as both Clutton-Brock and Parker and Hammerstein note, or they may conform for the wrong reasons. For example, Silvertown cites the composite *Hypochoeris glabra* in support of the hypothesis that the proportion of far-dispersing fruits should increase with fruit number because of density-dependent competition. But because near-dispersed fruits develop only on the circumference of the capitulum, the conformity to expectations is a necessary allometric consequence of the ratio of circumference to the area.

In other instances, the sensitivity of the test is inadequate. For example, D. Charlesworth attempts an admirably careful test of the hypothesis that dioecy has evolved in angiosperms as an outcrossing mechanism, by seeing if it is negatively correlated with self-incompatibility across families and genera. The data are inadequate for the test, but even if they were adequate, a census of this kind is not sufficient, because a phylogenetic analysis is required in each case to infer whether dioecy arose in a self-compatible or self-incompatible ancestor.

We are now all aware of the excess of overenthusiastic adaptationism, and of the difficulties of testing strategic theories of adaptation. But the theory itself may prove to have important limitations, as Parker and Hammerstein point out in an excellent review of evolutionary game theory. For example, realistic extensive games in which the current decision depends on previous events typically have multiple stable solutions. Thus the historical contingency of evolution is inescapable, even in optimality models. Parker and Hammerstein also note that the necessary synthesis of strategic theory with population genetics has not yet occurred and may prove difficult – as the schism within this book bears witness

Among the remaining essays, some fall within these two approaches: Seger presents a very restricted genetic model of sympatric speciation, León theorizes on seed germination, Gittleman reviews possible advantages of aggregated placing of young by mammals, and Greenwood and Wheeler offer a highly speculative physiological explanation of sexual size dimorphism in homeotherms.

A potpourri of other contributions includes an exemplary exercise in adaptive hypothesis testing by Harvey and Ralls concerning body size in weasels, an intriguing failure by Bradbury, Vehrencamp and Gibson to find a mechanistic basis for the variance in male reproductive success in lek-forming species, an elaboration by Stenseth of Maynard Smith and Stenseth's theory of lag-load and evolutionary rates, and a benediction by May.

This well-edited volume offers a nicely balanced overview of some of the most active areas of investigation of adaptation. Like most honorary volumes, it is neither deep nor comprehensive, but several of the essays, as I have described, are important and thoughtful, and will surely be cited widely.

Douglas J. Futuyma is in the Department of Ecology and Evolution, State University of New York, Stony Brook, New York 11794, USA

Action at a distance in public affairs

Joseph Haberer

Einstein in America. By Jamie Sayen. *Crown: 1985. Pp.340. $17.95.*

OF Einstein it may be said that "fame was the spur" for his life-long involvement in matters relating to political and social issues. In 1920, with his sudden and unanticipated emergence as a world figure, he recognized that his name and celebrity status could be used as a means to shape public opinion and influence those who made decisions on issues with which he was concerned: notably, war and peace; Zionism and the Jewish people; social and economic justice; the threat of fascism and Hitler; the responsible and humane use of scientific knowledge.

Einstein's fame took hold first and especially in America. It is his relationship to the country of his eventual adoption that is at the centre of this biography. In 20 chapters Sayen explores thoroughly and with great acumen the many aspects of Einstein's experience with and in America: from the first journey in 1921 (with Chaim Weizmann, to raise money for the Hebrew University and publicize the Zionist cause) to his last effort in 1955 with Bertrand Russell through a Manifesto to warn against the dangers of the arms race. Most of the book deals with the years after Einstein settled in America in 1933, but three chapters cover the years prior to his arrival and provide an excellent background to the American phase.

Sayen's book is the first to deal primarily with Einstein's various political activities during his mature years, and since there was no intention of writing a complete biography little attention is given to Einstein's scientific work (Abraham Pais's *Subtle is the Lord*, published in 1982 by Oxford University Press, has done this superbly). Sayen demonstrates a thorough grasp of the Einstein materials and literature; evident throughout is his careful and impressive use of the large correspondence from the Einstein Archives. Earlier biographies, most notably Ronald Clark's *Einstein: The Life and Times* (World Publishing, 1971) were clearly deficient in this regard, and are quite misleading on several important aspects of Einstein's political life.

The Einstein that emerges in these pages is a brilliant scientist, as one would expect; a man with a finely honed sense of social responsibility; a person of great warmth, kindness and modesty. We know however, remarkably little about his deeper self and he seems to have gone to considerable lengths to keep it that way. But we know of some problems, most notably his life-long failure to establish intimate personal relationships. Sayen shows Einstein with some of his flaws, and thus avoids the all-too-frequent hagiographic accounts that have come our way.

There is a widely held view that Einstein's political perceptions and activities were those of a man filled with good intentions but characterized by a rather naive grasp of politics and social issues. Sayen lays this myth to rest. Einstein clearly made it his business to be well-informed on those matters on which he took a public stand or in which he became otherwise engaged; he would not, for example, sign petitions, write references or support causes unless he had satisfied himself thoroughly that the facts were such that he could in good conscience do so. He was fully aware that his name was his credit, and he made every effort not to squander it. To be sure he made some mistakes, but he learned quickly to be more careful, and it is remarkable how seldom he erred in his assessments of people and events.

Einstein was the progenitor of the scientist as a publicist for the causes with which he identifies. He wrote (for a scientist of his day) extensively in the press on social and political subjects, and kept up a flow of correspondence in which he addressed important questions of the time. Sayen's book demonstrates that Einstein's understanding of the political and social realities of the twentieth century, as well as his underlying philosophical positions, were much keener and showed a better grasp of the emerging forces than those of most of his critics. For example, his attitude towards the Soviet Union was sympathetic towards its socialist objectives, but from the early 1920s — long before the Stalinist excesses — he was quite aware of the human rights abuses. He refused in the 1920s to sign petitions attacking right-wing excesses unless they included criticism of those of the left also. But he argued in the post-1945 period that an accommodation with the Soviet Union was imperative for a lasting peace, though he recognized the obstacles on both sides that stood in the way. His reluctance to criticize the Soviet Union publicly during the Cold War period was based on complicated reasoning, but came down essentially to an unwillingness to add fuel to the anti-communist hysteria in America.

Although Einstein understood politics, he appears to have thoroughly disliked the activity and the process. He took positions, but avoided choosing parties, or becoming a partisan. Perhaps he resembled somewhat the platonic philosopher-king, who reluctantly, but out of perceived necessity, enters the tainted and turmoil ridden world of the political. He sought to influence while keeping his distance. ☐

Joseph Haberer is Professor of Political Science, Purdue University, West Lafayette, Indiana 47907, USA.

Close considerations

Jack Cohen

Biology of Fertilization. Edited by Charles B. Metz and Alberto Monroy. *Academic: 1985. Three volumes, pp.391, 475 and 469. $75, £75 each volume.*

IN THE late 1960s, a number of people, myself among them, moved from other fields of developmental biology into research on fertilization, partly because electron microscopical techniques were dramatically illuminating the magic moments of membrane fusion but also because mammalian gametes were just becoming accessible to experiment. *Concepts of Fertilization*, edited by Monroy and Metz and published in 1967, was a guide book to the territory for us. That collection of authoritative, and revelatory, review articles by all the "big names" put the subject in context and provided both opinion and forecasts; it did not have the now-fashionable tone that "for each expert there is an equal-and-opposite expert", with each disagreement referenced and written in the dense prose which now seems mandatory for the professional review. The editors were daring, for that time, in assembling biochemists, botanists and electron-microscopists, as well as fertilization specialists, and in suggesting that work upon bacteria, algae and *Paramecium* could illuminate sea urchin and mammal fertilizations.

This new collection, which comes in three volumes entitled *Model Systems and Oogenesis, Biology of the Sperm* and *The Fertilization Response of the Egg,* looks very different. We have all got older, and we now know much more. But beyond that I believe there is a much more basic and serious difference. As an area of science develops, knowledge should not simply accumulate; generally accepted theories should encompass large areas of previously disparate observations and bring them into a coherent framework. New textbooks then reflect this coherence in their examples for students. There have been several attempts in the area addressed by this collection, of which Austin and Short's series *Reproduction in Mammals*, now going through a second edition, has probably been the most successful.

For me, this new collection of reviews fails because it gives only sporadic indications of the larger view. The density of information, argument and referencing of most of the articles is appropriate to the subjects they consider, and these articles could well have been found in the *Advances in . . .* or *Current Topics in . . .* sort of book. What is missing is the ultimate rather than the proximate consideration. All the authors, even those considering polyspermy and its prevention, write of *the* sperm and *the* egg, and the failure of the vast majority of gametes to fertilize is never invoked in arguments about the few which do and the mechanisms they seem to use. Similarly, the enormous variety of mRNA elaborated by the oocyte's diploid (maternal) genome and stored in mysterious ways for use by the cleaving embryo is explained as the proximate mechanism to supplement the mRNA-synthetic abilities of the single zygote nucleus, in the immense egg cytoplasm, until such time as the nuclei have multiplied. Surely the theoretical importance of early development being controlled by maternal genome, only mentioned by Monroy, could have been expanded somewhere? The titles of the individual reviews often promise such a general approach — "Nucleo-cytoplasmic interactions . . .", "Activation of DNA synthesis . . .", "Regulation of mammalian spermatogenesis", "Vertebrate sex determination" — but each focuses down on one problem and doesn't usually generalize in the Discussion section either; there are too many "More work is needed before meaningful generalizations . . ." conclusions. If this is so, then this is not the time to review that subject.

The reviews seem mostly to have been written in about 1981, and to have been updated in 1983–1984; later references are nearly always to the author's own work. This is inevitable in such a grand compilation, but it makes the previous criticisms much more serious. Generalities, indeed prejudices, of workers of this eminence will usually keep their interest for some years, but these minor issues lose immediacy much sooner. Particularly unfortunate in this context is the absence of the inositol triphosphate (IP3) story of 1984, which provided a new second messenger with close affiliations to the cell membrane; it rendered incomplete nearly all of the controversy about Ca^{++}, much of that about membrane receptors of egg or sperm, and all of that about phospholipid involvement in sperm maturation. An attempt by Whitaker and Steinhardt to make good this particular deficiency by way of an addendum to their Chapter 5, printed at the end of Vol. 3, only succeeds in emptying this can of worms among all the other contributors: tangled discussions of cytoplasmic pH, Na$^+$/H$^+$ exchange and egg activation/cortical reactions, and even the bindin story, are shown to have been incomplete, needing identification of this crucial thread. If theories had been proposed, IP3 would have added mechanism; as it is, for most of the articles subsequent discovery invalidates much of their content.

There is certainly a place for this collection in university libraries, and even in the more specialized collections of directors of (rich) *in vitro* fertilization units, while individual articles will be very valuable, especially for research students. But what a pity it is that they will miss the real expansion of mental horizons which we gained from the first edition. ☐

Jack Cohen is Senior Lecturer in the Department of Zoology and Comparative Physiology, University of Birmingham, Birmingham B15 2TT, UK.

Products of history

Janet Browne

Seeds of Change: Five Plants that Transformed Mankind. By Henry Hobhouse. *Sidgwick & Jackson: 1985. Pp.245. £15. To be published in the United States later this year by Harper & Row.*

POTATOES are not usually given much thought beyond the kitchen table, yet in Henry Hobhouse's *Seeds of Change* they take on a starring role. Rightly so, for these humble tubers have had a dramatic part in world events. The blight of 1845 meant nothing less than starvation for the Irish nation; economic crisis erupted in Britain, forcing rapid tax reform, repeal of the Corn Laws and a temporary halt to restrictive trading practices; and on a larger scale, one more wave of hopeful settlers emigrated to the United States where they then went on to become a recognizable force in the shaping of modern America.

There are other plants, other commodities that have changed the course of history and, of these, Hobhouse selects a further four to illustrate his general theme that plants matter more than one might think. Sugar cane in the West Indies, a crop supported by an economic and social superstructure of plantations and slavery, was, by his account, responsible for the infamies of the slave trade and for nearly half of all the seagoing effort, naval and civil, of western European countries before 1830. It gave Britain commitments in the Caribbean that Hobhouse feels she could well have done without (and an irredeemably sweet tooth). Cotton, on the other hand, made the American south rich and confident. This too was a cash crop based on slavery, contributing to a lifestyle that was ripped apart by the Civil War and yet, ironically, feeding the first great industrial revolution with raw material for newly mechanized processes of textile production.

Then there is tea. The British tea trade with China during the eighteenth century heralded not only imports of porcelain ("china"), opium and redesigned "clipper" ships, but also a fight for economic supremacy with the Dutch East India Company, encouraging Britain to concentrate primarily on India, and the opium wars of 1840–1842 that finally opened up two British footholds in China — Shanghai and Hong Kong. Last of all, although first in his book and undoubtedly Hobhouse's most interesting chapter, there was the hunt for quinine, the bark of a South American tree which prevents and cures malaria, thereby allowing the opening up of great tracts of central Africa and India to European colonial powers.

There is much here that will be fresh, surprising and intriguing to most readers whatever their background. The stories of these staple products are extraordinarily rich, containing within them all kinds of repercussions that echo through to the present day. But for professional historians, perhaps for scientists too, the book is hampered by Hobhouse's all-pervading sense of moral outrage at the activities of our ancestors, and his implicit assumption that things are better now. Perhaps his forthcoming sequel (on corn, oil and wine) will be less Anglocentric and less judgemental. Many readers will surely wish for something more of an analysis of the actual causes involved in, for example, the colonization of India; the ability to control malaria through quinine, critical as it may have been, is hardly a reason for India's emergence as the jewel in the British Crown, any more than it is an explanation for the scramble for Africa. Hobhouse's breezy good sense is no match for the deeper causes lurking here. ☐

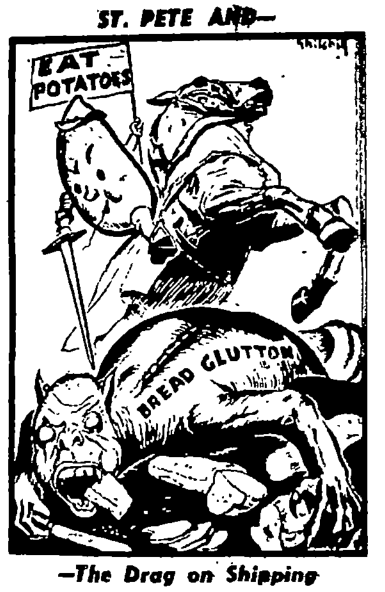

Wartime exhortation in the Daily Express *of 18 January 1943. The cartoon is reproduced in the revised impression of* The History and Social Influence of the Potato *by Redcliffe Salaman, which has been edited and is introduced by J.G. Hawkes. Publisher is Cambridge University Press, price is hbk £35, $49.50; pbk £12.50, $16.95*

Janet Browne is a historian of science at the Darwin Archives, University Library, Cambridge CB3 9DR, UK.

R437

Connecting with the invertebrates

Adrian Horridge

Model Neural Networks and Behavior. Edited by Allen I. Selverston. *Plenum:1985. Pp.548. $69.50, £66.03.*

THE scope of this book is less than the title suggests and limited largely to central nervous mechanisms in invertebrates. More than 20 of the contributors are from the US west coast and the same number work during summers at Wood's Hole. The dedication to Graham Hoyle is apt. In some sense it represents a panegyric of collective achievement as the topic has developed several important cutting edges, because, in Selverston's words, these invertebrate systems have "characteristics especially suitable for answering specific questions".

The qualitative analysis of real connections between actual neurones in favoured invertebrate preparations, and the origin of these patterns in development and inheritance dominate the scene. Fundamentally the book is an expression of the reductionist approach, in which analysis goes from detail to detail, down to actual mechanical causes by every available technique. The chase leads into topics such as the "activity-dependent enhancement of synaptic facilitation" as the mechanism at the point where learning actually occurs, to long-lasting effects of synaptic modulators, to cyclic AMP and calcium ions. In the growth studies, the editor has selected accounts of marking membranes with antibodies which reveal that neurone surfaces differ chemically, but the reductionism is non-quantitative, an interesting paradox.

With this type of analysis, an important feature is the commonality of the results. Almost every one of the 27 papers concentrates on a different preparation but the results seem to be comparable. We begin to understand that there are only a limited number of mechanisms, presumably based on a limited number of conserved DNA sequences, which generate channels, transmitters, receptors on membranes, hormones, and units in a construction set. After a century of effort, we understand many of these components; by contrast, we are just at the threshold of the chemical mechanisms that bring and hold the pattern of connections together. The final chapters on neurogenetics are excellent snippets of a fast-moving and fascinating topic.

As an exercise to demonstrate the importance of invertebrate preparations to our understanding of nervous systems, the volume is a great success. Identifiable neurones, large enough to be dissected out singly and analysed for chemical content, have pushed our understanding much further than is possible with vertebrates.

That statement applies to much besides the contents of this book, notably to sense organs and sensory processing. For this volume has nothing on information flow, signal-to-noise ratios, or on the optimization of the neural networks. The software is all molluscan: the hardware chitinous. Those recording from anonymous mammalian neurones of medical interest get on-line computers whereas those slogging to elucidate the exactly identified invertebrate neural circuits pursue a task which one of them rightly recognizes as "a long and irksome process". But neural networks, surface-specific molecular interactions in growth, and polypeptide sequences are also topics where an enormous amount of tedious fact-finding must be done before elegant generalizations can be reached, simply because the human understanding has no ready-made models for ordering these new bodies of data.

There are seven chapters dealing with neural circuitry, nicely spread between leech, molluscs, locust flight motor and the lobster pyloric ganglion. Again this is essential foundation work, defining the components, that opens up studies of growth, learning, plasticity, transmitters and membrane biophysics. Later sections in the book deal with all these topics. Development studies, cellular chemistry and membrane biophysics are again spread between insects, a mollusc and leech. Analysis of learning in circuits of identified neurones is restricted to molluscs, where work has consolidated over the past decade. Even neurogenetics now spans three phyla.

Unfortunately the presentation is often lack-lustre; lacking any introductory concessions, lacking spice, lacking a real philosophical backing, and certainly lacking a historical perspective or even a decent index. Essentially a result of lack of thought, it is today characteristic of much scientific writing done as an account of ongoing activity, out of date in five years. I suspect many of the circuits described are oversimplifications. Nowhere in the book is there a consideration of how to analyse neurone function. I am frustrated however that my own student, whom I have tried to interest in this problem, states that "this is the wrong type of question".

There are 60 contributors, among them most of the best specialists in the field, and there are many excellent contributions. The whole book is a splendid summary of ongoing activity at an expert level contributing to the understanding of many aspects of all nervous systems. The book should be read by all who try to make sense of how central nervous systems are really put together in the non-mathematical non-engineering sense. □

Adrian Horridge is Professor of Neurobiology, Australian National University, Box 475, ACT 2601, Australia.

Delayed responses

P.F. Baker

Calcium in Biological Systems. Edited by R.P. Rubin, G.B. Weiss and J.W. Putney. *Plenum:1985. Pp.737. $89.50, £85.03.*

COMING to grips with the many roles of calcium is just another task the modern biologist must master. This volume is based on the proceedings of a "calcium theme" included in the 67th Annual FASEB meeting held in Chicago in April, 1983. It includes 80 contributions divided into three sections: metabolic and functional aspects, regulation of muscle contractility, and nutritional and pathophysiological aspects of calcium action..

In general, the choice of contributors and contributions — which range from calcium chemistry and biochemistry to clinical medicine — are excellent, although readers would have benefited from a few more overviews setting specific topics in perspective. A far more important criticism, however, is that the meeting was held in 1983 and the book only appeared in 1985, two whole years later.

For a field that is changing as fast as calcium such a delay is unacceptably long and, unfortunately, robs the book of much of its value. This is very sad as the book contains a great deal that would have been highly topical in 1983 or even 1984, but by now has largely reached the scientific community by other means. Nevertheless, it says much for the editors' choice that there is still material of considerable interest and the volume clearly delineates the ubiquitous and pivotal role of calcium in diverse physiological and pathological states. It is only a pity they did not convince their publishers that for those intending to purchase a book of this type, its value is inversely related to the delay between the meeting and its publication.

P.F. Baker is Professor of Physiology at King's College London (KQC), Strand, London WC2R 2LS, UK.

- A recent volume in Humana's *Contemporary Biomedicine* series is *Calcium and Contractility: Smooth Muscle,* edited by A.K. Grover and E.E. Daniel. The book is a collection of reviews by well-known figures in the field and contains, says the publisher, "Incisive synthesizing summaries of the powerful outpouring of research on cell contractility today". Price is $64.50 in the United States, $74.50 elsewhere.

Rim syncline volume estimation and salt diapirism

Kai Sørensen*

Geologisk Institut, Aarhus Universitet, DK-8000 Århus C, Denmark

Quantitative studies of salt structures are based on the assumption of a simple relationship between excess sediment volumes and the volumetric growth of salt structures. This assumption is inadequate and, instead, this article shows how the excess volume relates to the volume swept out by the deforming sediment surface and the moving salt/sediment interface. The use of this new basis for volume reckoning is demonstrated, and its implications for waste disposal, hydrocarbon exploration and tectonic subsidence studies are emphasized.

SALT pillows and salt diapirs occur in great numbers in several sedimentary basins. The movement of salt dramatically changes the depositional geometry of its enclosing basin, creating, for example, structural traps for hydrocarbons. Salt structures are also considered suitable sites for the disposal of high-level nuclear waste. Thus, there are compelling reasons for studying such structures.

Studies of natural salt diapirism are built on the classic work of Trusheim[1,2] who demonstrated how the history of a diapir can be unravelled by observing the location and timing of excessive sediment thicknesses, assuming these to be caused by subsidence over a depleting source layer. The main features of Trusheim's model are illustrated in Fig. 1 (*b*, *c*). In the pillow phase[1], excess sediment volumes are deposited in the primary rim syncline (V^1_{rs}), far from the centre of the structure (Fig. 1*b*). The excess volume (V_{ex}) is defined as the rim syncline volume (V^1_{rs}) minus the 'regional normal' (V_{rn}). 'As measured' sediment volumes must be corrected for compactional effects. The amount of finitely displaced salt (V_{st}) is the volume of salt above the original source layer (of thickness s_0). The diapiric-phase rim syncline (V^2_{rs}), the secondary rim syncline[1], is characterized by excess volumes adjacent to the diapir (Fig. 1*c*). It is overlain by an only slightly structured rim syncline (V^3_{rs}) of the post-diapiric phase, the tertiary rim syncline. Trusheim's model is qualitative, but its quantitative potential was realized "*Das Volumen des akkumulierten bzw. extrudierten Salzes entspricht in jeder Phase dem der Sedimente, die diese Bewegungen kompensieren, sofern man die epirogene Absenkung subtrahiert*" (ref. 1, p. 145). Although Trusheim's 'volume rule' has been used by several authors[3-7], there has been no systematic discussion of volume estimation. This article aims to start such a discussion and, using an example, to demonstrate its relevance. The volume discussion is generally valid, but the diagrams illustrating it (Figs 2, 3) are two-dimensional, that is, areas sum in the figures as volumes in the general discussion.

Pillow phase

Analogous with experimental diapirism[8], it is hypothesized that a salt pillow outlines the growth stages (Fig. 2*a*) whose surface expression is a laterally extending sink and narrowing source. The salt and sediment displacement volumes are laterally extended and do not overlap vertically, so that the following equation can be considered valid for volumes summed over the entire salt intake area (Σ_a) and over time (Σ_t)

$$\Sigma_a\Sigma_t V^1_{sk}(=\Sigma_a\Sigma_t V^1_{sc})=\Sigma_a\Sigma_t V^1_{sdd}(=\Sigma_a\Sigma_t V^1_{std}) \qquad (1)$$

where the superscripts designate the pillow phase. Complexities in volume estimation arise because such physically real volumes as, for example, the sink volume, have to be related to the measurable excess volume, which is an operationally defined construction.

The growth stages envelop an 'overlap volume', acting first as a sediment source and then as a sediment sink (surface overlap volume, V_{so}). A corresponding overlap volume (displacement overlap volume, V_{do}) is enveloped by the subsurface salt-sediment interface. Within the displacement overlap volume, sediments are first displaced by salt, then salt by sediments.

The overlap volumes 'measure' the path of the structure (Fig. 2*a*). Whether the surface overlap volume is reflected in the excess rim syncline volume depends on the regional rate of sedimentation. Two extremes can be envisaged.

First, when the regional rate of sedimentation (v_{sd}) is zero (Fig. 2*b*), uplift within the surface overlap volume leads to erosion of the pre-pillow series ('pre' of Fig. 2*a*), so that the cumulative excess sediment volume is equal to the cumulative sink volume (Fig. 2*a*, sum of arrowed prisms). This, in turn, is larger than the volume of finitely displaced salt (V_{st}) by an amount equal to the surface overlap volume (Fig. 2*a*), so that

$$\Sigma_a\Sigma_t V^1_{ex}=\Sigma_a\Sigma_t V^1_{sk}=V^1_{st}+\Sigma_a\Sigma_t V^1_{so} \qquad (v_{sd}=0) \qquad (2)$$

Second, when the regional rate of sedimentation exceeds the rise rate of the structure (v_{up}), the uplift within the surface

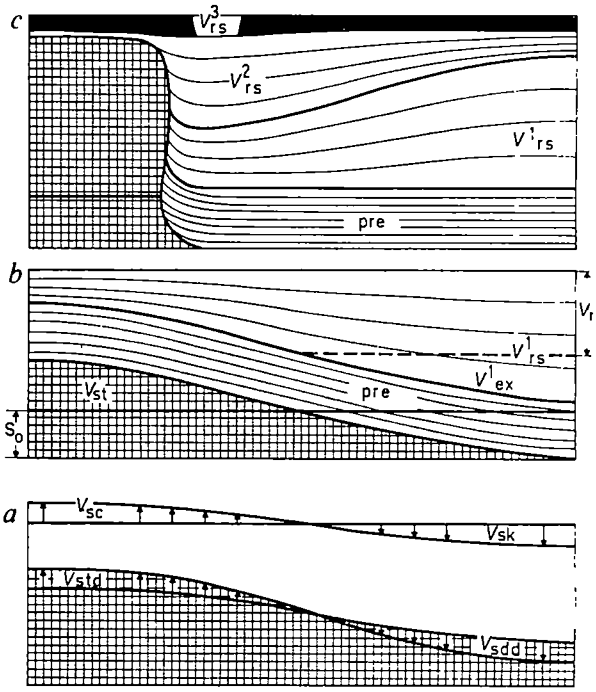

Fig. 1 Volume terms and Trusheim's model[1]. *a*, Salt displacement volume (V_{std}) and sediment displacement volume (V_{sdd}) overlain by sediment source (V_{sc}) and sediment sink (V_{sk}), respectively. *b*, Trusheim's pillow phase with the primary rim syncline (V^1_{rs}) overlying the pre-pillow series (pre). V^1_{ex}, Excess rim syncline volume; V_{rn}, regional normal volume; V_{st}, volume of finitely displaced salt. *c*, Trusheim's diapiric and post-diapiric phases. V^2_{rs}, Secondary rim syncline; V^3_{rs}, tertiary rim syncline; source layer thickness, s_0.

---

[*] Present address: Statoil, PO Box 300, N 4001 Stavanger, Norway.

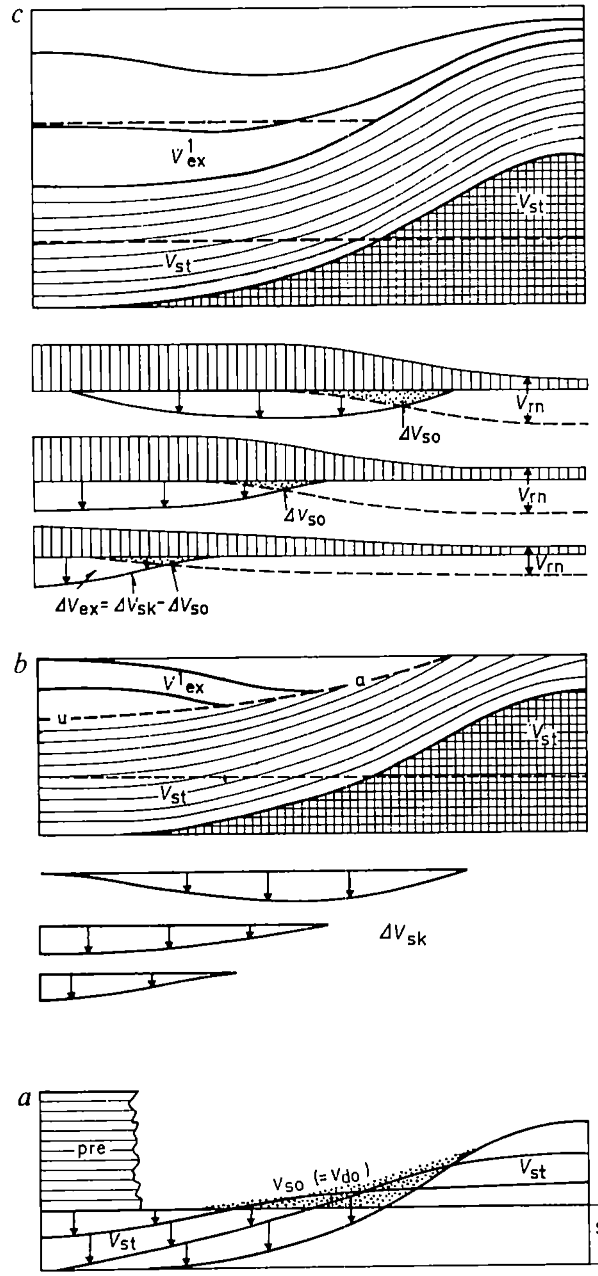

Fig. 2 Pillow phase volume estimation. *a*, V_{so}, surface overlap volume; V_{do}, subsurface displacement overlap volume. Pre-pillow series (pre) and source layer thickness (s_0). *b*, Pillow formation with no regional sedimentation. The excess volume (V^1_{ex}) is equal to the sink volume ($\Sigma\Delta V_{sk}$) but larger than the displaced salt volume (V_{st}). Note the angular unconformity (au) between rim syncline layering and the pre-pillow series. *c*, Pillow formation with the regional rate of sedimentation larger than the salt uplift rate. The excess volume (V^1_{ex}) is smaller than the sink volume ($\Sigma\Delta V_{sk}$) by an amount equal to the overlap volume ($\Sigma\Delta V_{so}$) but equal to the displaced salt volume (V_{st}). This limiting case is similar to the pillow phase of Trusheim's model (see Fig. 1*b*). Note the absence of angular unconformities. Arrows define cut-out volumes.

overlap volume causes a regional sedimentation (Fig. 2*c*, vertical ruling) less than normal (V_{rn}, Fig. 2*c*). When deriving the excess volume by subtracting a constant regional normal (Fig. 2*c*, vertical ruling plus stippled) from the rim syncline volume (the "epirogene Absenkung" of Trusheim[1]), the excess volume becomes (see Fig. 2*c*)

$$\Sigma_a\Sigma_t V^1_{ex} = \Sigma_a\Sigma_t V^1_{sk} - \Sigma_a\Sigma_t V^1_{so} = V^1_{st} \qquad (v_{sd} > v_{up}) \tag{3}$$

Only in this case will the compaction-corrected excess volume be equal to the finite amount of displaced salt. For the pillow phase, in general, equations (2) and (3) combine to give

$$V^1_{st} + \Sigma_a\Sigma_t V^1_{so} \geq \Sigma_a\Sigma_t V^1_{ex} \geq V^1_{st} \tag{4}$$

As illustrated in Fig. 2, the internal structures of the primary rim syncline can be expected to differ significantly in the two cases, although the sink volumes of both cases, Fig. 2*b*, *c*, (triangular prisms with arrows) are equal. In the first case, angular unconformities between the layering of the primary rim syncline and the layering of the pre-pillow series develop. In the second case, the primary rim syncline will be characterized by converging and diverging layering. It should therefore be possible to decide which side of equation (4) the excess sediment volume of a specific structure approaches.

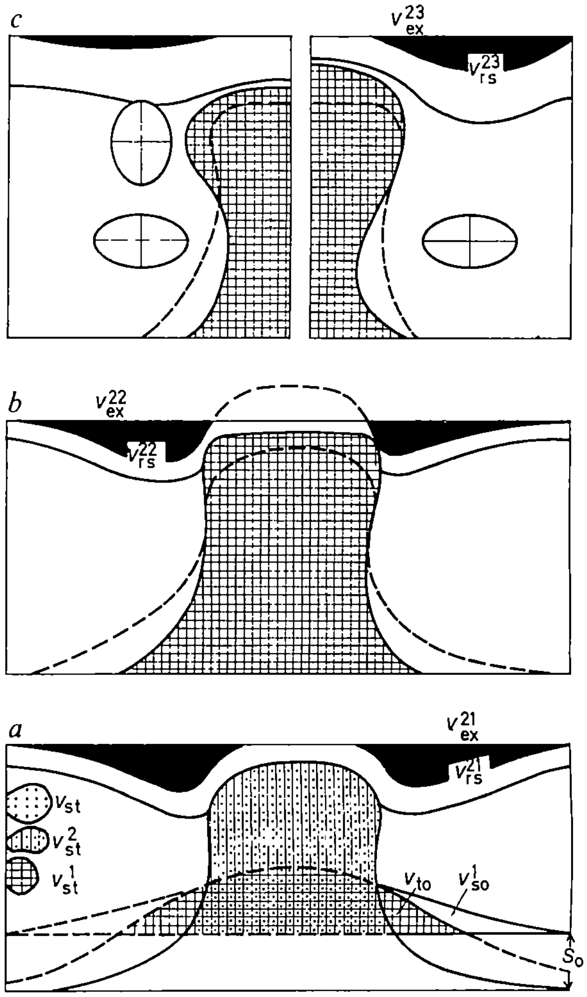

Fig. 3 Three modes of the diapiric phase. *a*, Intrusion mode; its rim syncline (V^{21}_{rs}) and its excess volume (V^{21}_{ex}). V_{so}, Surface overlap volume; V_{to}, transition overlap volume; V_{st}, salt volumes. *b*, Dissolution mode; its rim syncline (V^{22}_{rs}) and its excess volume (V^{22}_{ex}). *c*, Overhang mode; its rim syncline (V^{23}_{rs}) and its excess volume (V^{23}_{ex}). Right, overhang formation by necking. Left, overhang formation by combined necking and top spreading.

Diapiric phase

Trusheim suggested that the transition from the pillow to the diapiric phase was discontinuous, the pillow formation leading eventually to a fault-controlled breakthrough. If the diapir develops without significant lateral movements, overlap volumes are not formed. In this phase, the excess volume therefore corresponds to the sink volume. But other types of volumetric discordances may develop. They can be described with reference to three 'modes' of diapirism (Fig. 3). Real diapirs are likely to alternate between the intrusion and dissolution modes after

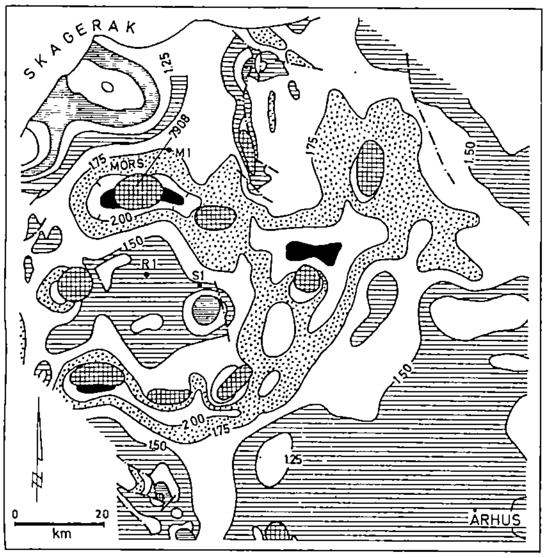

Fig. 4 The Danish onshore salt structure province. Cross-hatched, salt diapirs. Contours, two-way-travel time in seconds to the Gassum Formation reflector. The Gassum reflector is undisturbed under the Århus-Silkeborg Flat (west of Århus)[19] and under the Rødding Flat (south of the well R1)[14]. Deep wells mentioned in the text: R1 (Rødding 1), M1 (Mors 1) and S1 (Skive 1). 7908, seismic profile discussed in the text. Simplified after a map by Baartman, Olsen and Woodward (in ref. 20).

initial intrusion, and overhang formation may occur in combination with both intrusion and dissolution.

In the 'intrusion mode' (Fig. 3*a*) the following equalities hold

$$\Sigma_a\Sigma_t V^{21}_{\mathrm{ex}} = \Sigma_a\Sigma_t V^{21}_{\mathrm{sk}} (= \Sigma_a\Sigma_t V^{21}_{\mathrm{sc}}) = \Sigma_a\Sigma_t V^{21}_{\mathrm{sdd}} (= \Sigma_a\Sigma_t V^{21}_{\mathrm{std}}) \qquad \text{(intrusion mode)} \quad (5)$$

Because, by definition, no material transfer occurs across the fault plane, the sink volume must also be equal to the displacement volume (provided intrusion is fault-controlled). The first superscript designates the diapiric phase, the second, the mode.

For some combinations of overburden thickness, regional sedimentation rate and diapiric rise rate, diapirism leads to breakthrough (Fig. 3*b*) to the surface (extrusion) or to near-surface dissolution. In both cases, salt is dissolved, so that the surface source and sink volumes are no longer equal. The volume estimation formula for the 'dissolution mode' of diapirism must include this inequality which can become significant in two respects. If distant sources cannot supply material, lack of a nearby sediment source will lead to a deepening sink. In this stage, depositional patterns, which are entirely different from the regional pattern, may develop. Under some circumstances, petroleum source rocks can be anticipated in the rim syncline, in other conditions evaporite (re)deposition[9]. In this mode, salt diapirism may have a generic influence on sedimentation, and not the merely moderating influence suggested recently[6]. The discordance between source and sink volumes may also lead to delayed filling of the sink, in which case the possibility of excess sediments post-dating the age of the sink arises. The complete volume formula is therefore

$$\begin{aligned} &\Sigma_a\Sigma_t V^{22}_{\mathrm{sdd}} = \Sigma_a\Sigma_t V^{22}_{\mathrm{sk}} > \Sigma_a\Sigma_t V^{22}_{\mathrm{sc}} \geq 0 \\ &\Sigma_a\Sigma_t V^{22}_{\mathrm{ex}} \leq \Sigma_a\Sigma_t V^{22}_{\mathrm{sk}} \end{aligned} \qquad \text{(dissolution mode)} \quad (6)$$

Many diapirs are characterized by significant overhangs. In the Trusheim model[1], overhang formation is supposed to occur by spreading of the diapir top. Alternatively, its formation can be thought of as a consequence of source layer depletion leading to 'necking' (Fig. 3*c*, right)[10]. Finally, overhang formation may be the result of combined necking and top spreading (Fig. 3*c*, left). If so, the positive and negative displacement volumes are vertically superposed and the surface sink will be less than the subsurface displacement volume. If necking is the dominant process, a surface sink will develop. To the 'overhang mode' of diapirism the following relation applies

$$0 \leq \Sigma_a\Sigma_t V^{23}_{\mathrm{sk}} = \Sigma_a\Sigma_t V^{23}_{\mathrm{ex}} \leq \Sigma_a\Sigma_t V^{23}_{\mathrm{sdd}} \qquad \text{(overhang mode)} \quad (7)$$

Significant lateral movements during overhang formation must be accommodated by deformation of pre-existing rim synclines. The strain ellipses (Fig. 3*c*) illustrate, in a general way, the state of finite strain imposed on the rim syncline by the overhang formation. Consequently, accurate volume estimation for salt diapirs with significant overhangs requires identification of the mechanism of overhang formation.

Let us consider a diapir (say that of Fig. 3*a*) and apply Trusheim's volume rule to its entire development. His rule asserts that the total excess volume is equal to the amount of finitely

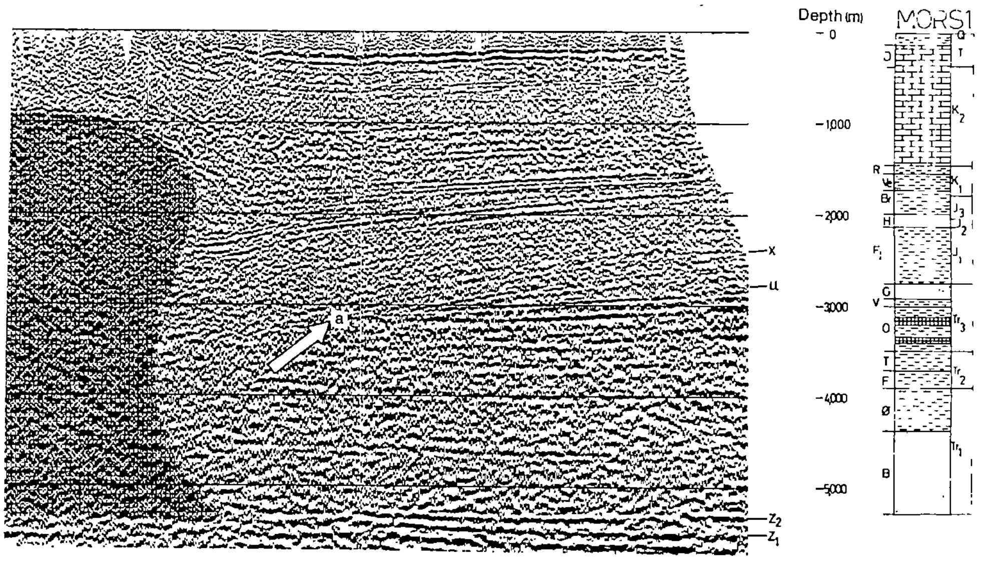

Fig. 5 Migrated and depth-converted seismic reflection profile 7908 (Fig. 4). Acquisition and data processing by Prakla Seismos. The horizontal layering below the on-lap unconformity (au) signifies the pre-pillow series on top of a depleted source layer. Reflectors z_1 and z_2 probably originate from carbonatic and sulphatic source layer remnants. The line 'au' marks an on-lap and truncation structure which is interpreted as marking the onset of source layer depletion (see Fig. 2*b*). The Mors well, terminated at a depth of 5,303 m below sea level, is located close to the northeastern termination of line 7908. Stratigraphy and lithology from refs 20-23. Lithology: dots, sandstone; bars, shale; dots and bars, sandy shale; bricks, chalk. Cross-hatched, evaporites. Lithostratigraphy: Bunter Formation (B); Ørslev Formation (Ø); Falster Formation (F); Tønder Formation (T); Oddesund Formation (O); Vinding Formation (V); Gassum Formation (G); Fjerritslev Formation (Fj); Haldager Formation (H); Bream Formation (Br); Vedsted Formation (Ve); Rødby Formation (R). Chronostratigraphy: T_1, T_2, T_3, Lower, Middle and Upper Triassic, respectively; J_1, J_2, J_3, Lower, Middle and Upper Jurassic, respectively; K_1, K_2, Lower and Upper Cretaceous, respectively; D, Danian. T, Tertiary. Q, Quaternary.

displaced salt (V_{st}, Fig. 3*a*). Following the volume estimation of this work, however, the total excess volume is

$$V^1_{st}+\Sigma_a\Sigma_t V^1_{so}+V^2_{st}\geq\Sigma_a\Sigma_t V^{1+2}_{ex}\geq V^1_{st}+V^2_{st} \quad (8)$$

in which $V^1_{st}+V^2_{st}$ is seen to exceed V_{st} by an amount equal to the volume defined by the original source layer surface, the pillow surface and the diapir surface. Terming this volume the 'transition overlap volume' (V_{to}), equation (8) becomes

$$V_{st}+\Sigma_a\Sigma_t V^1_{so}+V_{to}\geq\Sigma_a\Sigma_t V^{1+2}_{ex}\geq V_{st}+V_{to} \quad (9)$$

The excess volume is always larger than the volume of the salt which moved into the structure, so that Trusheim's volume rule, applied to a diapir, is incorrect, and only correct in the limit $v_{sed}>v_{up}$ when applied to a pillow structure (see equation (3)).

To obtain the excess volume as estimated above, it is necessary to correct the 'as measured' volumes ('am') for compaction: a correction due to the post-depositional compaction (post-correction, post(cc)) and a correction due to the syn-depositional compaction of the underlying sediments (pre-correction, pre(cc)). Post-depositional compaction leads to a positive post-correction equal in magnitude to the expansion of the unit in response to decompaction. Part of a unit under consideration is due to compaction of the underlying sediments, leading to a negative pre-correction. Then the compaction-corrected rim syncline volume (V_{rs}(cc)) is

$$V_{rs}(\mathrm{cc})=V_{rs}(\mathrm{am})+\mathrm{post(cc)}-\mathrm{pre(cc)}+\mathrm{er(c)} \quad (10)$$

including an erosional correction (er(c)). The excess volume, in its corrected form, is

$$V_{ex}=V_{rs}(\mathrm{cc})-V_{rn}(\mathrm{cc}) \quad (11)$$

where V_{rn}(cc) is the regional normal corrected by a procedure similar to that of equation (10). Depending on lithology and position within the sequence, the total correction may be negative, positive or zero. The correction to any interval including the surface will be negative if erosional effects are negligible.

Mors post-diapirism

From uncorrected rim synclines[1,5,7] it has been inferred that diapiric rates of 0.1-0.5 mm y^{-1} are typically followed by rise rates at least one magnitude less[5,7]. Trusheim[1] designated this 'slow tail' to diapirism as the post-diapiric phase, and its associated rim syncline as the tertiary rim syncline (see Fig. 1). Taking compactional effects into consideration, the question arises as to whether the excess volume of the post-diapiric rim syncline reflects salt structuring or whether it results from differential compaction.

The Mors salt diapir (Fig. 4) developed from a Zechstein source layer of unknown thickness (z_0). The profile to be discussed is derived from the seismic reflection profile 7908 (Fig. 5) which connects the Mors diapir with the deep well, Mors 1. The regional geology implies that the post-Oligocene history of the Mors area has been one of net erosion. It is therefore necessary to consider the effects of compaction on the 'post-diapiric' history, allowing for a non-vanishing erosion correction in equation (10). The decompaction calculations have been performed according to ref. 11. Maximum post-Oligocene erosion could have been ~300 m. Removal of the Upper Cretaceous (UC) section leads to an 'expansion' of the pre-UC section of Mors 1 of 596 m assuming zero post-Oligocene erosion and 676 m assuming an erosion of 300 m. The corresponding expansions of the section through the secondary rim syncline (Fig. 6) are 679 and 749 m, respectively. The difference in expansion between the primary (Mors 1) and secondary rim synclines (83 m and 73 m, respectively) is not very sensitive to variations in the erosion correction of the relevant magnitude. This difference in expansion constitutes the negative pre-correction to the 'as measured' excess thickness. The latter has a maximum magnitude of 200-250 m, so that the compaction correction does not eliminate the 'as measured' excess thickness of the post-LC rim syncline. Further calculations indicate that excess thicknesses persist through the entire UC and Danian chalk intervals, so that Mors did undergo extended, slow post-diapirism.

Neglecting compactional effects, the post-burial history of diapirs has been inferred in several studies[7,12] on the basis of

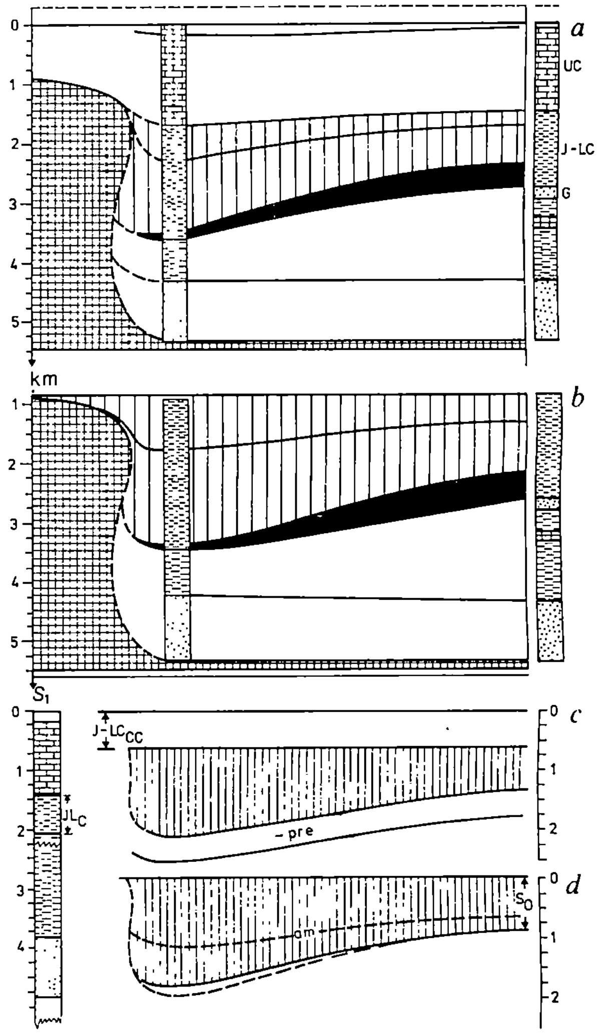

Fig. 6 Depletion history along 7908 and the total excess rim syncline. *a*, Present configuration. Black, the primary rim syncline. The lower boundary to the primary rim syncline corresponds to line au of Fig. 5. Vertical ruling, the secondary rim syncline. The lower boundary to the secondary rim syncline corresponds to reflector x of Fig. 5. White above ruling: the tertiary rim syncline. UC, Upper Cretaceous. J-LC, Jurassic and Lower Cretaceous. G, Gassum Formation. The upper stippled line indicates the maximum possible post-Oligocene erosion. Lithology symbols as in Fig. 5. *b*, End Lower Cretaceous configuration. Decompaction has been performed assuming an exponential decay of porosity (f) with depth (z), $f=f_0\exp(-cz)$, where $1/c$ is the depth constant, the depth at which the porosity has decreased to $1/e$ of its original value), and the following material parameters[11]: sandstone ($c=0.27$; $f_0=0.49$), sandy shale ($c=0.39$; $f_0=0.56$), shale ($c=0.51$; $f_0=0.63$). Measuring z in km, c is in units of km^{-1}. *c*, Primary and secondary rim syncline (vertical ruling) after subtraction of a compaction-corrected Jurassic–Lower Cretaceous thickness (J-LC$_{cc}$) derived from J-LC of Skive 1(S1) and after subtraction of the pre-correction (-pre). Skive 1 was terminated at a depth of 2,300 m below sea level; the Skive 1 column below this level was derived by a depth conversion of reflection data[14]. *d*, The compaction-corrected excess rim syncline (between zero level and the lower stippled line). Vertical ruling: the pre-UC part of the excess rim syncline. The excess thickness derived from uncorrected data: between zero level and am. All depth scales in km below sea level.

thickness differences between layers above and outside the diapir. The very large expansion of the pre-UC sections after removal of the post-Lower Cretaceous (LC) section at Mors shows that neglect of compactional effects in this procedure will lead to completely false conclusions as to post-burial rise rates. At Mors, this procedure[13] would indicate a post-LC rise of 700 m, to which should be added an unknown height equivalent of dissolved salt. The excess volume shows that the true post-LC rise of the diapir at a maximum (with no dissolution) could have been ~100 m.

Mors total excess volume

The volume estimation leading to equation (9) will now be applied to profile 7908 in order to derive the total excess volume along it. The reflection profile (Fig. 5) shows a pronounced on-lap sequence of Gassum and lower Fjerritslev formation times. This angular unconformity ('au', Fig. 5) suggests fast pillow growth, similar to the model of Fig. 2*b*. There are only slight indications of pre-Gassum time salt depletion along 7908, so that au can be taken as the lower boundary to the primary rim syncline (Fig. 6*a*). In the preceding discussion of volume, the choice of a pillow phase growth model (Fig. 2*a*) was 'justified' by analogy with experimental work[8]. The on-lap sequence above the angular unconformity au (Fig. 5) shows that this choice is realistic in the case of Mors. The occurrence of similar on-lap structures adjacent to other salt structures in the Danish basin suggests a wider applicability of this pillow growth model.

Reflector x of Fig. 5 has been chosen to represent the pillow to diapir transition of Mors. When allowing for compactional effects, an abrupt change to excess thicknesses adjacent to the diapir takes place at approximately this level (corresponding to mid-Lower Jurassic time). The post-diapiric, diapiric, pillow and pre-pillow phases of the basin north of Mors can now be delineated (Fig. 6*a*), acknowledging that the diapiric to post-diapiric transition is arbitrarily positioned at the LC–UC transition.

The geometry of the 'total' rim syncline (encompassing the total structure development), except for minor post-LC movements, is shown in its positively post-corrected form in Fig. 6*b*. The negative pre-correction is calculated by decompaction to the lower boundary of the total rim syncline, giving the corrected, total rim syncline (Fig. 6*c*). The total excess volume can now be derived by subtraction of the regional normal. The original source layer thickness, s_0, will then appear as the minimum height of the excess rim syncline. The crucial point of this process is the derivation of the 'regional normal', because this thickness exists nowhere near Mors. The choice of the 'regional normal' will be explained below.

A comparison of seismic sections over the Rødding Flat (Fig. 4) and sections crossing the Skive 1 well and the Skive structure indicates that the J-LC of Skive 1 is similar to the J-LC of the Rødding Flat west of the Skive pillow structure where no J-LC salt movement occurred[14]. The J-LC thickness in Skive, being 549 m, can therefore be used as the 'regional normal'. To find the total excess thickness, the compaction-corrected regional normal (J-LC_{cc}, Fig. 6*c*) is subtracted from the 'top' of the total rim syncline, while the negative pre-correction is subtracted from the 'bottom'. Subsequently, the remaining part of the rim syncline (Fig. 6*c*, ruled) is decompacted to give the compaction-corrected excess thickness (Fig. 6*d*, ruled). The lower stippled line of Fig. 6*d* shows the thickness to be added due to post-diapiric movements. This gives a source layer depletion of 850 ± 50 m (s_0 of Fig. 6*d*). Adding to this the remaining Zechstein thickness (probably a basal carbonatic and sulphatic facies, 250 ± 50 m thick) yields an original Zechstein thickness (z_0) of 1,100 ± 100 m.

The total excess volume is clearly as much as 50% larger than the total salt volume (allowing for three-dimensional effects[15]), illustrating the significance of the overlap volumes (equation (9) and Figs 2*a*, 3*a*) in the volume estimation. Following Trusheim, this would lead to erroneous conclusions about the amount of dissolved salt. It is also seen (Fig. 6*d*) that the true excess volume is considerably larger (again ~50%) than the 'as measured' excess volume.

Conclusions and implications

The discussion of volume estimation for salt diapirism leads to the conclusion that the total excess volume cannot be simply related to the amount of salt as claimed by Trusheim's[1] volume rule. It is necessary to account for the interrelation of several volume terms—surface sink and source volumes, subsurface displacement volumes and overlap volumes—and to relate these to the excess volume, taking into account the fact that the latter can vary with varying rates of regional sedimentation.

For the discussion of the disposal of high-level waste in salt structures, it is essential to have maximum confidence in both growth histories and growth rates. The example of Mors shows that this goal can only be reached by the use of rigorous volume estimation, for without it, diapiric rise rates may be considerably underestimated (Fig. 6*d*). The discussion of the post-burial history of Mors shows, on the other hand, that it is possible to document very long periods of vanishingly small post-diapiric movement, a period whose growth rate in previous studies has been grossly overestimated due to the neglect of compactional effects.

The discussion of volume estimation is of relevance to another applied aspect of salt structures, petroleum exploration. In this context, sink and source volume relations should be emphasized. In the 'dissolution mode' of diapiric movement the diapir itself does not provide a source to fill the sink volume. In this mode, accumulation of source material for petroleum generation may be enhanced in the sink, in contrast to the diapiric periods without dissolution.

Finally, to perform trustworthy analyses of tectonic subsidence histories of sedimentary basins containing salt structures, it is essential to allow for salt-induced thickness variations. In recent studies[11,16,17] of North Sea subsidence, salt-induced sedimentation has been neglected, despite the fact that many exploration wells have been located on strongly salt-influenced structures. This aspect is exemplified in ref. 18.

I thank I. Madirazza for helpful discussions at all stages of this work, and L. Jans and E. M. Nielsen for assistance with figures and manuscript.

Received 9 July; accepted 7 October 1985.

1. Trusheim, F. *Z. dt. geol. Ges.* **109**, 111–151 (1957).
2. Trusheim, F. *Bull. Am. Ass. petrol. Geol.* **44**, 1519–1540 (1960).
3. Sannemann, D. *Mem. Am. Ass. petrol. Geol.* **8**, 261–270 (1968).
4. Rühberg, N. *Z. angew. Geol.* **22**, 413–420 (1976).
5. Jaritz, W. *Z. dt. geol. Ges.* **131**, 387–408 (1980).
6. Seni, S. J. & Jackson, M. P. A. *Bull. Am. Ass. petrol. Geol.* **67**, 1219–1244 (1983).
7. Seni, S. J. & Jackson, M. P. A. *Bull. Am. Ass. petrol. Geol.* **67**, 1245–1274 (1983).
8. Berner, H., Ramberg, H. & Stephansson, O. *Tectonophysics* **15**, 197–218 (1972).
9. Trusheim, F. *Beih. geol. Jb.* **112** (1971).
0. Whitehead, J. A. & Luther, D. S. *J. geophys. Res.* **80**, 705–717 (1975).
1. Sclater, J. G. & Christie, P. A. F. *J. geophys. Res.* **85**, 3711–3739 (1980).
12. Roll, A., in *Geotektonische Symp. zu Ehren von Hans Stille* (ed. Lotze, F.) 228–245 (Ferd Enke, Stuttgart, 1956).
13. Larsen, G. & Baumann, J. *Dansk geol. Foren., Årsskr. f. 1981*, 151–155 (1982)
14. Møller, J. J. Thesis, Aarhus Univ. (1982).
15. Sørensen, K. *Rep. Danish envir. Protection Agency* (ITG, Danish Technical University, Lyngby, 1984).
16. Wood, R. & Barton, P. *Nature* **302**, 134–136 (1983).
17. Barton, P. & Wood, R. *Geophys. J. R. astr. Soc.* **79**, 987–1022 (1984).
18. Sørensen, K. *Nature* (in the press).
19. Madirazza, I. & Petersen, S. A. (in preparation).
20. Michelsen, O. *et al. Geol. Surv. Denmark* Ser. B, No. 5 (1981).
21. Elkraft & Elsam (Danish Utilities) *Salthorstundersøgelser*, I–V (Elsam, Fredericia, 1981)
22. Berthelsen, F. *Geol. Surv. Denmark*, Ser. B, No. 4 (1980).
23. Michelsen, O. *Geol. Surv. Denmark* Ser. B, No. 2 (1978).

Direct evidence for chromosomal inversion during T-cell receptor β-gene rearrangements

Marie Malissen*, Candice McCoy*, Dominique Blanc*, Jeannine Trucy*, Christian Devaux*, Anne-Marie Schmitt-Verhulst*, Frank Fitch†, Leroy Hood‡ & Bernard Malissen*

* Centre d'Immunologie INSERM-CNRS de Marseille-Luminy, Case 906, 13288 Marseille, Cedex 9, France
† Department of Pathology, University of Chicago, Chicago, Illinois 60637, USA
‡ Division of Biology, California Institute of Technology, Pasadena, California 91125, USA

A germline T-cell receptor variable region (V_β) *gene segment* ($V_\beta 14$) *has been mapped 10 kilobases to the 3′ side of the constant region* ($C_\beta 2$) *gene. The* $V_\beta 14$ *gene segment is in an inverted transcriptional polarity relative to the diversity-region* (D_β) *and joining-region* (J_β) *gene segments and the* C_β *genes. Analyses of a T-cell clone (J6.19), which has productively rearranged the* $V_\beta 14$ *gene segment, indicate that the productive* V_β–D_β–J_β *rearrangement and its reciprocal flank recombination product are linked and located at either border of a chromosomal inversion. These data demonstrate for the first time a linkage between mammalian V and C genes and verify that a functional T-cell receptor* V_β *gene can be constructed through a chromosomal inversion.*

T-CELL antigen receptors are disulphide-linked heterodimers constituted of two chains designated α and β (refs 1–3), each divided into variable (V) and constant (C) regions[4]. The T-cell receptor V_β region is encoded by three distinct sets of DNA segments designated variable (V_β), diversity (D_β) and joining (J_β)[5-9] which join during T-cell differentiation to generate a complete V_β gene[5]. The β-gene family contains two closely linked constant-region (C_β) genes denoted $C_\beta 1$ and $C_\beta 2$, each of which is preceded by a cluster of six functional joining-region (J_β) gene segments[5-7], at least one diversity-region (D_β) gene segment[8,9] and an unknown number of V_β gene segments.

Before somatic rearrangements, the 3′ side of the V_β gene segments, the 5′ side of the J_β gene segments and both sides of the D_β gene segments are flanked by recognition sequences for DNA rearrangement. These recombination signal sequences are comprised of three components—a conserved heptamer, a non-conserved spacer sequence of 12 or 23 nucleotides and a conserved A+T-rich nonamer[5-9]. As in immunoglobulin genes, DNA rearrangement occurs only when one gene segment has a 12-base-pair (bp) recognition sequence and the second has a 23-nucleotide signal sequence.

Several mechanisms have been suggested for the joining process[10,11]. First, the DNA between the two gene segments may loop out and be deleted by virtue of a site-specific recombination event joining the two gene segments (looping out-excision model)[12,13]. Second, during mitotic duplication of a chromosome, an unequal crossing-over may occur between the 3′ end of a gene segment on one sister chromatid and the 5′ end of the second gene segment on the second sister chromatid. The two resulting chromatids would be segregated at the next cell division, giving rise to two types of daughter cells. One cell would contain the joined gene segments; this cell and its progeny would appear to have deleted all the DNA between the recombined gene segments. The second cell would contain a reciprocal flank recombination product with the two recombination signals fused back-to-back at their coding-proximal borders. This model is denoted unequal sister chromatid exchange[14,15]. A third model, particularly relevant to the data presented in this article, requires that the two gene segments to be joined are oriented in opposite transcriptional polarity in the germline DNA. Inversion of the stretch of chromosomal DNA between the 3′ (or the 5′) ends of these two gene segments would result in the formation of (1) an appropriate coding joint with both gene segments in the same transcriptional direction and (2) a reciprocal flank recombination joint. This inversion model does not lead to the loss or gain of intervening sequences between the joined gene segments but merely to their rearrangement[15-18]. Finally, the looping out-excision model may have an alternative form in which the excised loop is reintegrated back into the genomic (looping out-excision-reintegration model)[19,20]. However, since recombination events may occur in several steps during ontogeny[17,21-24], a combination of inversion or sister chromatid

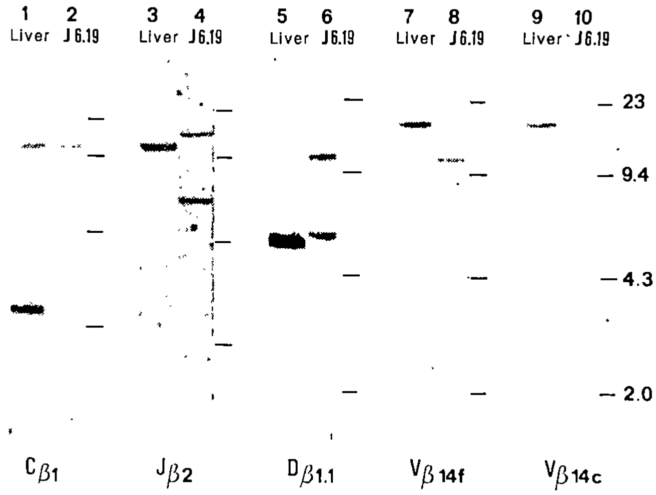

Fig. 1 Southern blot analyses of J6.19 T-cell DNA. DNAs from B10.A liver and J6.19 T cells were digested to completion with *Eco*RI (lanes 1, 2) or *Bam*HI (lanes 3–10) and after gel electrophoresis and transfer, hybridized to ^{32}P-labelled single copy probes. Probes were isolated from either the germline β-chain gene cosmid 2.3W7 (ref. 6) or the λ genomic clones 47.1 J6.19 and 46.1 J6.19 (this paper). The $C_\beta 1$ probe is a 2.5-kb *Eco*RI fragment that hybridizes to $C_\beta 1$ as well as to $C_\beta 2$ sequences because of homology between these two genes. Probe $J_\beta 2$ is a 2.3-kb *Eco*RI fragment which contains all of the $J_\beta 2$ gene segments. Probe $D_\beta 1.1$ is a 3.2-kb *Hin*dIII-*Bam*HI fragment which detects sequences 5′ to $D_\beta 1.1$, the $D_\beta 1.1$ and the two 5′ $J_\beta 1$ gene segments. Two probes were used to analyse the $V_\beta 14$ gene segment. The first one, denoted $V_\beta 14$c, corresponds to a 250-bp *Mbo*II fragment contained entirely within the $V_\beta 14$ coding sequence. The second probe, denoted $V_\beta 14$f, is a 4-kb *Eco*RI-*Sal*I fragment corresponding to the non-coding 3′ side of the $V_\beta 14$ gene segment. The parental B10.A strain liver DNA is included in each analysis for comparison of the rearrangements with the germline pattern. Size markers are indicated in kb.

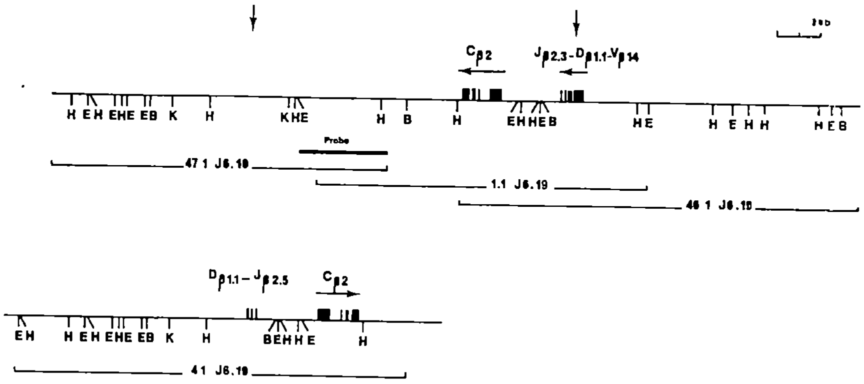

Fig. 2 Restriction maps of the genomic clones containing the β-gene rearrangements observed in J6.19 T lymphocytes. Exons encoding V_β, D_β and J_β gene segments and C_β genes are indicated by vertical lines or boxes above the horizontal line. Cleavage sites are indicated by vertical lines below the horizontal line. Restriction enzyme abbreviations are as follows: B, *Bam*HI; E, *Eco*RI; H, *Hin*dIII; K, *Kpn*I. A genomic library was constructed from *Sau*3A partially digested J6.19 DNA using the λ bacteriophage vector EMBL-3 (ref. 41). Screening of the library was carried out according to Maniatis *et al.*[42] using probes specific for D_β 1.1, C_β1, J_β2 and C_β2 sequences (see below). DNA was prepared from the isolated genomic clones and mapped with the restriction enzymes indicated. The location of the V_β, D_β, J_β and C_β sequences was determined by Southern blot analyses of restriction fragments from the genomic clones. Some hybridization probes have been described previously; they correspond either to subclones made from the germline β cosmid 2.3W7[6,11] or to oligonucleotides specific (1) for each of the 12 functional J_β gene segments, (2) for the 5'-flanking sequences of the D_β1.1 and D_β2.1 gene segments and (3) for the D_β1.1 and D_β2.1 gene segments[27,35]. The restriction fragments contained in these clones account for all the rearrangements detected in the Southern blot analysis of KB5-C20 DNA (see Fig. 1). The position of the 4-kb *Eco*RI-*Sal*I fragment isolated from clone 47.1 J6.19 and used to probe the J6.19 genomic library is indicated by a filled box. Vertical arrows indicate the border of the chromosomal inversion. Horizontal arrows indicate 5' to 3' orientation.

exchange and deletion can explain all existing observations[11,17,25].

We report here the molecular linkage of a germline T-cell receptor V_β gene segment 3' to the C_β locus. This V_β gene segment (V_β14) is oriented in opposite transcriptional polarity relative to the D_β and J_β gene segments and the C_β genes. Analyses by chromosomal walking techniques of a T-cell clone that has productively rearranged the V_β14 gene segment demonstrate that the productive V_β-D_β-J_β rearrangement and its reciprocal flank recombination product are linked on the same piece of DNA and located at either border of a chromosomal inversion. Taken together, these data represent to our knowledge the first formal demonstration of a chromosomal inversion mechanism operating during V_β to D_β-J_β joining.

β-Gene rearrangements in T cell J6.19

J6.19 is a proliferative T-cell clone that originates from a B10.A mouse and responds to hen egg ovalbumin presented by I-A^k-bearing cells[26]. DNA from J6.19 cells was digested with *Eco*RI and *Bam*HI and Southern blots of the digested DNA were then hybridized with the probes described in Fig. 1. Hybridization of the C_β1 probe to *Eco*RI-digested B10.A liver DNA shows the C_β1 (lower band) and C_β2 (upper band) genes in their germline configurations. *Eco*RI digests of J6.19 DNA hybridized to the C_β1 probe demonstrate that both C_β1 genes are deleted and that at least one C_β2 gene is present. Hybridization with the J_β2 probe shows that the J_β2 cluster is rearranged on both chromosomes of J6.19 T cells. Finally, hybridization with the D_β1.1-J_β1.1-J_β1.2 probe indicates that this region is twice rearranged in J6.19 cells.

To further delineate the nature of the β-gene rearrangements in J6.19 T cells, we have constructed a complete λ phase genomic library and isolated the clones encompassing all of the β-gene rearrangements observed during Southern blot analyses. Three classes of clones were found for J6.19 DNA, represented by clones 4.1, 46.1 and 47.1 (Fig. 2). The localization within the clones of the D_β and J_β gene segments and the C_β genes was determined using the hybridization probes described in Fig. 2 legend. Clone 46.1 has no C_β1 gene. Oligonucleotide probes show that the D_β1.1 gene segment is joined to the J_β2.3 gene segment and that the 5'-flanking sequence for the D_β1.1 gene segment is absent—therefore, this clone contains a V_β-D_β1.1-J_β2.3 rearrangement. Clone 4.1 has a D_β1.1 gene segment joint to a J_β2.5 gene segment and does contain 5'-flanking sequence for the D_β1.1 gene segment—therefore, this clone encodes a partial D_β1.1-J_β2.5 rearrangement. Clone 47.1 is novel in that it contains the rearranged 5'-flanking D_β1.1 sequence and does not hybridize to the J_β or C_β probes. A vertical arrow indicates the localization of the 5'-flanking D_β1.1 sequence inside clone 47.1 (Fig. 2). This clone will be discussed later as it has important implications for β-gene rearrangement mechanisms. These three β-gene rearrangements represent all of those observed by Southern blot analyses in the J6.19 T cells (Fig. 1).

The complete variable gene and novel rearrangements have been subcloned and sequenced (Fig. 3). The V_β rearrangement in λ clone 46.1 appears functional in that it has appropriate leader and V_β gene segment sequences and a V_β-D_β-J_β joining that maintains the proper translational reading frame (Fig. 3). The sequence of the V_β gene segment from clone 46.1 of the J6.19 cells is reported here for the first time. This V_β segment detects a single hybridizing band when used to probe a Southern blot of B10.1 liver DNA (Fig. 1) and, accordingly, defines a new single-member V_β subfamily. According to the nomenclature introduced by Barth *et al.*[27] and Kronenberg *et al.*[10], this V_β gene segment will be denoted V_β14.

The novel rearrangement observed in clone 47.1 corresponds to a flank recombination product with the heptamer sequences of V_β and D_β rearrangement signals joined in a back-to-back orientation (Fig. 3). Similar rearrangements have been reported for some immunoglobulin genes[14–20]. Does the flank recombination product of clone 47.1 correspond to the reciprocal of the V_β-D_β rearrangement defined by clone 46.1? If so, 5' D_β1.1 recognition sequences for DNA rearrangement should be joined to the 3' V_β14 recognition sequences. To answer this question we have isolated (see below) and determined the nucleotide sequence of the germline V_β14 gene segment (Fig. 3). Comparison of the coding sequences of the germline V_β14 gene segment and its rearranged counterpart found in J6.19 T cells demonstrates no nucleotide differences and further illustrates the lack of somatic hypermutation in T-cell receptor β genes. Moreover, comparison of the 3'-flanking sequence of the germline V_β14 gene segment and of the V_β recognition sequence of the V_β-D_β flank recombination product found in J6.19 T cells demonstrates a complete nucleotide identity (Fig. 3). Therefore, these data indicate that the V_β14 gene segment rearranged in J6.19 T cells has not segregated away from its reciprocal flank recombination product. Since the sister chromatid exchange model requires that the reciprocal events segregate independently in the two daughter cells, the β-gene rearrangement data obtained with J6.19 T cells are only consistent with either an inversion model or with the looping out-excision-reintegration model.

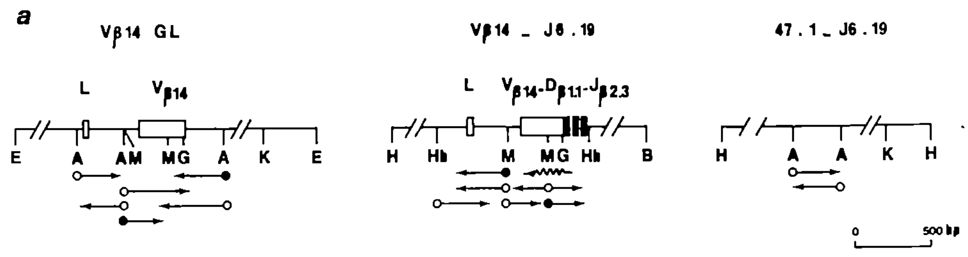

b

```
                                    M  L  Y  S  L  L  A  F  L  L  G  M  F  L
  1 AGACAAGCCTAGACAAAGACCATCTTGAACTATGCTGTACTCTCTCCTTGCCTTTCTCCTGGGCATGTTCTTGGGTGGGT  80  VB14 GL
    --------------------------------------------------------------------------------      VB14-J6.19

 81 GCATTCCCCTGTTGAAAACCTACTTTCAAATTGTTGCTTCCATCTCTCCACCTGTTAAAGGTGTAGATTCTTTGGTACTG 160  VB14 GL
    --------------------------------------------------------------------------------      VB14-J6.19

161 GCTTGCCTCTCTTGACCACAGTCCTCCAATTACTGAGATATGGGCATTTCACACTCTTTCAGTATTGACTCTCAGTTTTG 240  VB14 GL
    --------------------------------------------------------------------------------      VB14-J6.19

241 TATCTTTTAGAAAGGATTTGTCTCCCCTTGCCCTGTAACATTTTTCATCCTTGGCTCTTCTAGTATACTCCCTGAGACTG 320  VB14 GL
    --------------------------------------------------------------------------------      VB14-J6.19

321 ATTACATGTAACCCCTTCAGAGGGAAGGCAAGCAAGCTGGTGTGTGTGTATGTGTAGAGGTGTGTGTTTCTACTCTAAAT 400  VB14 GL
    --------------------------------------------------------------------------------      VB14-J6.19

                       G  V  S  A  Q  T  I  H  Q  W  P  V  A  E  I  K  A  V  G  S  P
401 GACTCTATTTCTTTACAGGTGTTAGTGCTCAGACTATCCATCAATGGCCAGTTGCCGAGATCAAGGCTGTGGGCAGCCCA 480  VB14 GL
    --------------------------------------------------------------------------------      VB14-J6.19

     L  S  L  G  C  T  I  K  G  K  S  S  P  N  L  Y  W  Y  W  Q  A  T  G  G  T  L  Q
481 CTGTCTCTGGGGTGTACCATAAAGGGGAAATCAAGCCCTAACCTCTACTGGTACTGGCAGGCCACAGGAGGCACCCTCCA 560  VB14 GL
    --------------------------------------------------------------------------------      VB14-J6.19

      Q  L  F  Y  S  I  T  V  G  Q  V  E  S  V  V  Q  L  N  L  S  A  S  R  P  K  D
561 GCAACTCTTCTACTCTATTACTGTTGGCCAGGTAGAGTCGGTGGTGCAACTGAACCTCTCAGCTTCCAGGCCGAAGGACG 640  VB14 GL
    --------------------------------------------------------------------------------      VB14-J6.19

     D  Q  F  I  L  S  T  E  K  L  L  L  S  H  S  G  F  Y  L  C  A  W  S
641 ACCAATTCATCCTAAGCACGGAGAAGCTGCTTCTCAGCCACTCTGGCTTCTACCTCTGTGCCTGGAGTCTCACACTGAGT 720  VB14 GL
    --------------------------------------------------------------------CCACAGGGGGCA      VB14-J6.19
                                  GGGAGGGTCCTTTTTTGTATAAAGCTGTAACATTGTGG------------      47.1-J6.19

721 AGGGTGGGGCAGACATCTGTGCAAAAACCACACCCTCTCTTTAGTCCTTCCTCCCTCACTAGGAACCCTCACTAGGGATG 800  VB14 GL
    GCAGAAACGCTGTATTTTGGCTCAGGAACCAGACTGACTGTTCTCGGTAAGTTGGGAGCTAG                        VB14-J6.19
    --------------------------------------------------------------------------------      47.1-J6.19

801 GGTGGAGGGGGTTTGCCACTGAATTTCTGGCTGATAGTCAAGTTGAAGTCTGGAAAACAACATGATTCAAGTCAGAAGTC 880  VB14 GL
    --------------------------------------------------------------------------------      47.1-J6.19

881 ACCAAAGACATTTATTAAACTCGTTATCAGTGACTCACATATGCAGAACCTGTGAGTTGCCTACACACAGTAAAATTTCC 960  VB14 GL
    --------------------------------------------------------------------------------      47.1-J6.19

961 AGTTTGTAGTAT                                                                     972  VB14 GL
    ------------                                                                          47.1-J6.19
```

Fig. 3 Sequencing strategies (*a*) and sequences (*b*) of the $V_\beta 14$ germline segment, the $V_\beta 14$–J6.19 coding joint and the 47.1–J6.19 reciprocal flanking joint. The sequence of the $V_\beta 14$ germline segment denoted $V_\beta 14$ GL was obtained from a 5-kb *Eco*RI fragment derived from cosmid 40.1 W7 (see Fig. 4). The $V_\beta 14$–$J6.19$ sequence corresponds to the rearranged $V_\beta 14$ gene segment found in J6.19 T cells. The sequence denoted 47.1–J6.19 corresponds to the $V_\beta 14$–$D_\beta 1.1$ flank recombination product found in J6.19 T cells. This latter sequence was obtained from a 300-bp *Acc*I fragment hybridizing to a $D_\beta 1.1$ flanking oligonucleotide probe. *a*, The sequences were obtained by either the dideoxy-chain termination methods (wavy arrows) or by the procedure of Maxam and Gilbert. Closed circles indicate a 5′ end labelling and open circles a 3′-end labelling. The following abbreviations are used: L, leader; V_β, variable gene segment. The restriction enzyme abbreviations are as follows: A, *Acc*I; E, *Eco*RI; G, *Bgl*I; H, *Hin*dIII; Hh, *Hha*I; K, *Kpn*I; M, *Mbo*II. *b*, Comparison of the $V_\beta 14$ GL nucleotide sequence with the $V_\beta 14$-J6.19 and 47.1–J6.19 sequences. The predicted amino-acid sequence encoded by the $V_\beta 14$ exons is indicated above using the one-letter amino-acid code. Nucleotide identities with the upper line are shown with dashes. The D_β and V_β recognition sequences have been boxed. Note that the 3′ side of the germline $V_\beta 14$ gene segment is flanked by the sequence CACACTG-(23 nucleotides)-GCAAAAACC which is similar to the recognition signals found 3′ to the immunoglobulin *V* region genes[10].

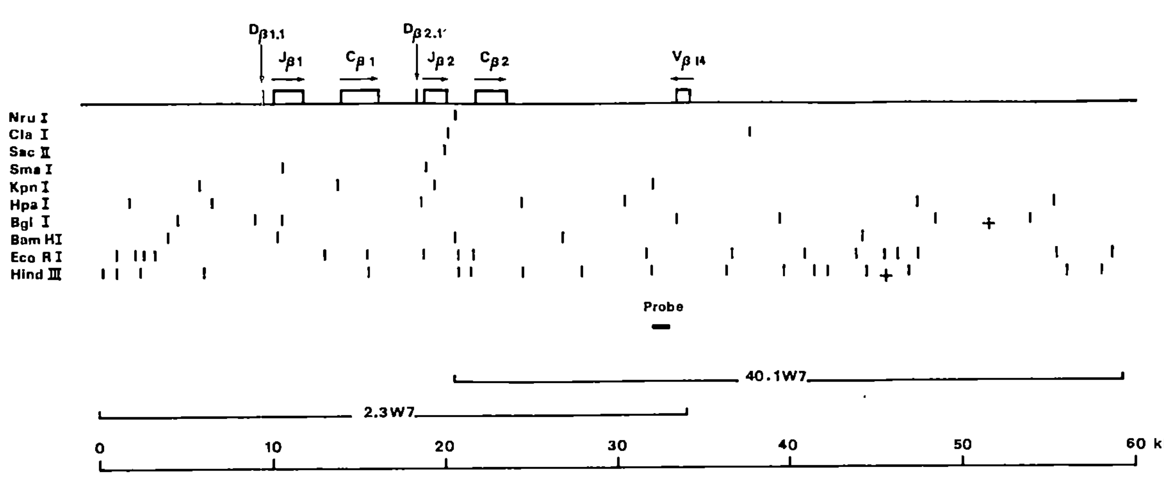

Fig. 4 Restriction map of the clones 2.3W7 and 40.1W7 isolated from a cosmid library constructed with DNA from the livers of B10.WR7 mice. Boxes or vertical lines above the horizontal line indicate the exons encoding V_β, D_β, J_β and C_β sequences. The cosmid clone 2.3W7 has been described previously[6]. The position of the 900-bp *Kpn*I-*Sau*3A probe used to isolate the cosmid 40.1W7 is indicated by a filled box. The cosmid clone 40.1W7 was mapped with the restriction enzymes indicated by single and double digestions. A (+) between two restriction sites indicates the presence of unassigned sites in this region for the same enzyme. The orientation and the location of the different gene segments were determined by Southern blot analyses of restriction fragments. The hybridization probes are described in the legend to Fig. 2. Arrows indicate 5′ to 3′ transcriptional orientation.

V_β14 gene segment lies 10 kb 3′ to C_β2

Further clues concerning the location of the V_β14 gene segment were unexpectedly obtained during analysis of the KB5-C20 alloreactive cytotoxic T-cell clone generated from a B10.BR mouse and directed against the H-2K^b molecule[28]. KB5-C20 T cells present two incomplete D_β–J_β rearrangements on one chromosome and a complete V_β–D_β–J_β rearrangement on the second chromosome (data not shown). In order to determine whether the V_β gene segment used in KB5-C20 T cells had been reported previously, the λ genomic clone corresponding to a complete V_β–D_β–J_β rearrangement (clone 28.1 KB5) was hybridized with a panel of probes specific for various V_β gene segments. Unexpectedly, clone 28.1 KB5 hybridized with two different V_β probes corresponding to V_β (refs 27, 29) and V_β14 (this paper). These two V_β gene segments show less than 20% homology. We have subsequently determined the relative positions of the V_β2 and V_β14 gene segments within the 28.1 KB5 clone. The V_β2 gene segment mapped to the 5′ side of the J_β2–C_β2 sequences. Surprisingly, the V_β14 gene segment mapped about 10 kilobases (kb) to the 3′ side of the C_β2 gene. However, T lymphocytes undergo complex β-gene rearrangements during T-cell differentiation[11] and these may have brought the V_β14 gene segment to its position in clone 28.1 KB5. We have therefore analysed the germline localization of the V_β14 gene segment before any β-gene rearrangement.

We have described previously a 34-kb mouse cosmid clone denoted 2.3W7 containing the C_β1 and C_β2 genes with their associated D_β and J_β gene segments[6]. This clone was isolated from a cosmid genomic library constructed from B10.WR7 liver DNA. We have now extended the molecular map to the 3′ side of the C_β2 gene by chromosomal walking. The single-copy probe used for that purpose corresponds to a 900-bp *Kpn*I-*Sau*3A fragment derived from the 3′ end of the cosmid clone 2.3W7 (Fig. 4). This procedure yielded the cosmid clone 401.1 W7 and allowed us to extend our map about 35 kb to the 3′ side of the C_β2 gene (Fig. 4). Southern blots of the 40.1 W7 cosmid clone were then hybridized with the V_β14 gene segment probe. This probe was found to hybridize strongly to a 5-kb *Eco*RI fragment located to the 3′ side of the C_β2 gene. Direct confirmation that this 5-kb *Eco*RI fragment does indeed encode the V_β14 gene segment was provided by DNA sequence analysis (see above). Interestingly, the germline V_β14 gene segment has a 5′ to 3′ transcriptional orientation that is opposite to that found for the D_β and J_β gene segments and the C_β genes (Fig. 4). Thus, these results demonstrate that in germline DNA the V_β14 gene segment lies 10 kb to the 3′ side of the C_β2 gene and is oriented in opposite transcriptional polarity relative to the D_β and J_β gene segments and the C_β genes.

V_β14 rearrangement by chromosomal inversion

The V_β14 gene segment constitutes to our knowledge the first example in which a germline V_β segment has been linked to the locus encoding the D_β and J_β gene segments and the C_β genes. Therefore, further analysis of the DNA rearrangements accompanying the productive V_β14 joining event observed in J6.19 T cells has provided additional insights into the mechanism of V_β to D_β–J_β joining. Because the germline V_β14 segment is oriented in an opposite polarity relative to the D_β and J_β gene segments and the C_β genes, one way to interpret the reciprocal recombination products found in J6.19 T cells involves a chromosomal inversion event. As outlined in Fig. 5, if the V_β14 gene segment joins to the D_β1.1–J_β2.3 segment by chromosomal inversion, the reciprocal flank recombination product would be formed and retained on the same chromosome bearing the productive V_β14–D_β–J_β rearrangement. Furthermore, because we have shown that the V_β14 gene segment is located about 10 kb to the 3′ side of the C_β2 gene, the reciprocal flank recombination product should be found about 10 kb to the 3′ side of the C_β2 gene. To test this supposition, we attempted to link the genomic clone encompassing the V_β14–D_β1.1–J_β2.3 rearrangement (clone 46.1 J6.19, Fig. 2) to the V_β–D_β1.1 flank recombination product (clone 47.1 J6.19, Fig. 2). For that purpose we rescreened a complete λ genomic library made from J6.19 T cells using a single-copy probe derived from the genomic clone 47.1 J6.19 (Fig. 2) and isolated one clone, denoted 1.1 J6.19. Subsequent mapping with restriction enzymes and Southern blot analyses of restriction fragments established that the 1.1 J6.19 clone does indeed overlap with the 46.1 J6.19 and 47.1 J6.19 genomic clones (Fig. 2). Therefore, we conclude that the V_β14–D_β1.1–J_β2.3 rearrangement and its reciprocal flank recombination product are linked on the same piece of DNA and located at either border of a chromosomal inversion. It was possible to determine the extent of the inversion region by comparing the restriction map shown in Fig. 2 with the one corresponding to the germline configuration (Fig. 4). Moreover, as predicted by the inverted joining model depicted in Fig. 5, the reciprocal flank recombination product is indeed located 10 kb to the 3′ side of the C_β2 gene. Integrity of the molecular map presented in Fig. 2 was confirmed by Southern blot analyses of J6.19 T-cell DNA cleaved with *Bam*HI and hybridized with four single-copy probes encompassing the inversion (Fig. 1). This analysis also indicates that the V_β14 segment located on the homologous chromosome lies in the germline configuration 10 kb to the 3′

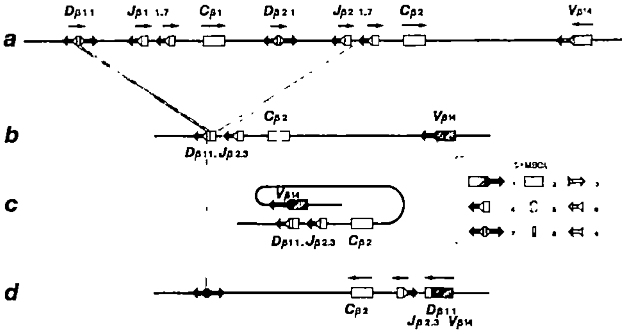

Fig. 5 Model explaining the presence in J6.19 T cells of the productive V_β–D_β–J_β rearrangement and of its reciprocal recombination product at either border of a chromosomal inversion. The chromosomal structures depicted in *a* and *d* are based on the data presented in Figs 4 and 2, respectively. Intermediate structures generated during the proposed pathway of rearrangement are illustrated in *b* and *c*. *a*, Organization of the germline C_β1 and C_β2 genes with their associated D_β (D_β1.1 and D_β1.2) and J_β (J_β1.1-7 and J_β2.1-7) gene segments. The germline V_β14 segment lies 10 kb to the 3′ side of the C_β2 gene and is oriented in opposite transcriptional polarity relative to the D_β, J_β and C_β sequences. Two stepwise recombinations must have occurred to form the final structure. *b*, An initial D_β1.1–J_β2.3 rearrangement occurred on the chromosome. This scheme is consistent with recent data suggesting that D_β to J_β rearrangements occur prior to V_β to $D_\beta J_\beta$ rearrangements (ref. 24 and R. Haars, M. Kronenberg and L.H., in preparation). The absence of both J_β1 clusters and both C_β1 genes in J6.19 T cells supports the concept that D_β to J_β rearrangement occurs either by the looping out–excision or by the sister chromatid exchange model. *c*, The V_β14 segment is recombined with the D_β1.1–J_β2.3 segment much as in the model of inverted joining hypothesized in refs 16, 18 and 25. During this process the V_β14 gene segment uses its 3′ recognition sequence to mediate joining with the D_β1.1 segment. *d*, The resulting product would have kept the entire DNA stretch located between the recombination points. A productive V_β14–D_β1.1–J_β2.3 joining would be formed with segments in the same transcriptional polarity. The reciprocal flank recombination product is also formed and lies 10 kb to the 3′ side of the C_β2 gene. The homologous chromosome is not shown; it presents a partial D_β1.1–J_β2.5 rearrangement and a V_β14 gene segment in germline configuration (see text). Arrows indicate 5′ to 3′ transcriptional orientation. Distances are not drawn to scale. Symbol for gene segments are as follows: 1, germline V_β14 segment; 2, V_β coding sequences; 3, V_β14 joining signal; 4, germline J_β segment; 5, J_β coding sequences; 6, J_β joining signal; 7, germline D_β segment; 8, D_β coding sequences and 9, D_β joining signals.

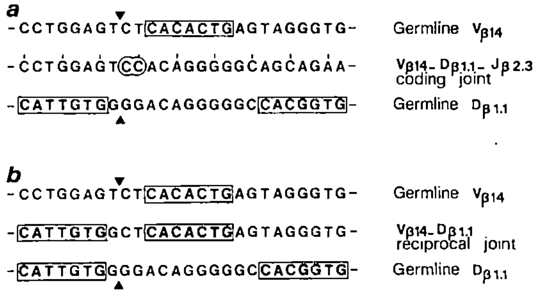
a
-CCTGGAGTCTCACACTGAGTAGGGTG-
Germline Vβ14
-CCTGGAGTCCACAGGGGGCAGCAGAA-
Vβ14-Dβ1.1-Jβ2.3 coding joint
-CATTGTGGGGACAGGGGGCCACGGTG-
Germline Dβ1.1
b
-CCTGGAGTCTCACACTGAGTAGGGTG-
Germline Vβ14
-CATTGTGGCTCACACTGAGTAGGGTG-
Vβ14-Dβ1.1 reciprocal joint
-CATTGTGGGGACAGGGGGCCACGGTG-
Germline Dβ1.1

Fig. 6 Comparison of the sequences of the coding (*a*) and reciprocal (*b*) junctions located at either border of the J6.19 inversion. Heptameric elements of the joining signals are boxed; the spacer regions and nonamer elements of the joining signals are not included in the sequence shown. Nucleotide regions not accounted for by germline V_β or D_β sequences (N region) are enclosed in circles. The sites of crossing-over are shown by black triangles. The $V_\beta14$-$D_\beta1.1$-$J_\beta2.3$ reading frame is indicated by ticks above the first base of each codon. The sequences corresponding to the $V_\beta14$-$D_\beta1.1$-$J_\beta2.3$ coding joint, the $V_\beta14$-$D_\beta1.1$ reciprocal joint and the $V_\beta14$ germline segments are from this article (Fig. 3). The germline $D_\beta1.1$ segment has been reported previously[9,28].

end of the $C_\beta2$ gene. Taken together, these results demonstrate unequivocally that the $V_\beta14$ to D_β-J_β rearrangement observed in J6.19 T cells has occurred through a 14-kb chromosomal inversion.

DNA joints not precisely recombined

The 14-kb inversion observed in J6.19 T cells creates two new DNA joints. One is the V_β-D_β coding joint and the other is the reciprocal flank recombination signal joint. Analysis of the sequence of the $V_\beta14$-$D_\beta1.1$ reciprocal joint indicates that three nucleotides separate the two heptamers (Fig. 6*b*). Two of these intervening nucleotides appear to be derived from germline sequences 5′ to the $V_\beta14$ heptamer whereas the third one may originate from the 3′ side of the $D_\beta1.1$ heptamer. Thus, all three intervening bases could be accounted for by germline sequences. This observation suggests that the recognition sequences need not be precisely joined in the rearrangement process[18,25]. Such an intervening triplet of nucleotides has not been found in V_κ to J_κ reciprocal joints. In fact, in each κ example reported to date, the two heptamers are joined precisely back to back[15,18,19,23,24,30]. Unfortunately there is no way of knowing on the basis of a single example if the nucleotide triplet separating the two heptamers should be considered as a characteristic feature of the V_β-D_β reciprocal joint.

Analysis of the coding joint (Fig. 6*a*) indicates that two nucleotides have been deleted from the coding sequences of the $D_\beta1.1$ gene segment. Because the germline $D_\beta1.1$ gene segment sequence is derived from B10.A, the same strain from which J6.19 T-cell clone is derived, we may conclude that two nucleotides have been deleted from the coding sequences of the $D_\beta1.1$ gene segment. Therefore, joining does not conserve all of the sequences present in the precursor elements. Furthermore, two bases between the joined $V_\beta14$ and $D_\beta1.1$ gene segments cannot be accounted for in either germline gene segment and may represent an N region. N regions consist of short stretches of random nucleotides appearing as insertions at V-D and D-J junctions of both immunoglobulin heavy-chain[16,31-34] and T-cell receptor β genes[8,9,35]. A direct conclusion obtained from the comparison of the reciprocal recombination products and of their precursor sequences is that DNA elements are asymmetrically joined during the V_β-D_β recombination event. The reciprocal joint sequence arises entirely from the precursor germline sequences, whereas the coding joint sequence shows both an N region and a small number of base pairs missing relative to the precursor sequences. Similar conclusions have been reached during the analysis of the products formed during V_κ to J_κ joining events[18,25].

Discussion

We have mapped the germline $V_\beta14$ gene segment 10 kb to the 3′ side of the $C_\beta2$ gene and shown that it presents an inverted transcriptional polarity relative to the D_β and J_β gene segments and the C_β genes. Having examined a productive $V_\beta14$ joining event, we present evidence that V_β-D_β joining can occur via chromosomal inversion. These results have been obtained from genomic libraries constructed from B10.A, B10.BR or B10.WR7 DNA. These three strains of mice share the same chromosome 6 derived from the B10 background[36]. To extend our results to other strains of laboratory mice, we have performed Southern blot analyses of AKR, BALB/c, C3H and C57BL/6 liver DNA cleaved with seven different restriction enzymes (*Bam*HI, *Bgl*II, *Eco*RI, *Hin*dIII, *Pst*I and *Pvu*II) and hybridized these DNAs with probes $C_\beta2$, $V_\beta14$c and $V_\beta14$f (see legend to Fig. 2). In all cases the sizes of the genomic fragments correspond with those predicted by the map obtained from B10.WR7 mice. Further support for this model was obtained by the direct analysis of a β-genomic clone derived from A.TL DNA (D.B. and C.D., unpublished observations).

An analysis of the β-gene rearrangements in the T J6.19 cells suggests they occurred in the following manner. Initial $D_\beta1.1$-$J_\beta2$ rearrangements occurred on both β-locus chromosomes. This contention is consistent with recent data suggesting that D_β-J_β rearrangements occur before V_β to $D_\beta J_\beta$ rearrangements[24] (R. Haars, M. Kronenberg and L.H., in preparation). Since the $J_\beta1$ clusters and $C_\beta1$ gene have been deleted from both chromosomes in the J6.19 cells, the $D_\beta1$-$J_\beta2$ joining events must have occurred by the looping out-excision or by the sister chromatid exchange mechanisms. The chromosome 6 represented by clone 4.1 presumably did not undergo any further β rearrangement (Fig. 2). The $V\beta$ to $D_\beta J_\beta$ rearrangement on the other chromosome 6 presumably led to the V_β-D_β flank recombination products of clone 47.1, thus requiring an inversional mechanism for DNA rearrangements (Fig. 5). Indeed, the inversion model would predict that each time the $V_\beta14$ gene segment of the J6.19 cells is used, there should be a flank recombinational product present in that T cell. Thus, T cell J6.19 must use two distinct mechanisms for DNA rearrangement—one for $D_\beta J_\beta$ joining and a second for V_β to D_β-J_β joining.

We have shown that the joining signals of $V_\beta14$ and $D_\beta1.1$ have recombined, leading to an inversion of a region of the T-cell receptor β locus. Such a V_β-D_β joining could not have occurred by unequal sister chromatid exchange, because a dicentric and an acentric chromosome would have resulted from such an event. In fact, each time the $V_\beta14$ gene segment is used because of its inverted translational orientation, it should be joined by chromosomal inversion and there should be a flank recombination product present in that cell. It is interesting that in immunoglobulin genes, the reciprocal joints apparently do not accumulate at the λ or heavy-chain gene loci with the same frequency with which they are found at the κ locus[18,25]. In fact, the feasibility of an inversion model for κ-gene joining has recently been established by the *in vitro* joining experiments of Lewis *et al.*[18,25]. Because we have demonstrated that the presence of a V_β-D_β reciprocal joint is a consequence of the topological relationships between β-gene segments, we believe that in a similar way some V_κ gene segments will be found in an inverted orientation either 5′ or 3′ relative to the C_κ gene.

The T-cell receptor β-chain locus constitutes a striking example in which the gene segments to be joined have different transcriptional polarities. How many additional V_β gene segments have the same transcriptional polarity as the $V_\beta14$ gene segment? To date, a number of T cells have been examined for all of their T-cell receptor gene rearrangements. However, analyses of 15 helper T-cell clones (refs 35, 37 and J. Kobori and N.

Shastri, unpublished data) did not reveal any flank recombination products, a finding consistent only with V_β-D_β joining occurring via the looping out-excision or the sister chromatid exchange models. Therefore, we believe that most V_β gene segments will be in the same transcriptional polarity as the D_β-J_β-C_β gene clusters.

The β genes of the human T-cell receptor have been located on the long arm of chromosome 7, band q35 (refs 38, 39). Cytogenetic studies of lymphocyte cultures stimulated with T-cell mitogens and derived from patients with ataxia telangiectasia indicate increased chromosome breakage and various abnormalities of chromosomes 7 and 14. Particularly interesting is the observation[40] of a pericentric inversion of chromosome 7 with breakpoints at p13 and q35. It is tempting to speculate, in relation to our data, that this chromosome inversion mimics a normal site-specific V_β-D_β rearrangement by inverted joining. It should be noted with regard to this possibility that the t(11; 14) chromosomal translocation recently observed in two separate cases of B-cell neoplasms has involved a heavy-chain segment on chromosome 14 and a heptamer-nonamer signal-like sequence on the normal chromosome 11[40]. In a similar way, a mouse nonproductive κ rearrangement has been shown to involve the joining of a J_κ segment to a sequence unrelated to any V, which is flanked in the germ line by a recombination signal sequence resembling those found to the 3′ side of V gene segments[30]. Whether the pericentric inversion of chromosome 7 observed in ataxia telangiectasia involves the T-cell receptor β-chain locus and is mediated by a mechanism similar to the V_β-D_β inversion mechanism described in this article will require the molecular characterization of the chromosomal breakpoints.

We thank Drs J.-F. Brunet and P. Golstein for making available KB5-C20 RNA samples and C. Bellegarde-Kourilsky for typing the manuscript. C.McC. is supported by a fellowship from the Fondation pour la Recherche Médicale. D.B. is supported by a predoctoral training grant from Ministère de la Recherche et de la Technologie. This work was supported by institutional grants from CNRS, INSERM and NIH.

Received 2 July; accepted 1 October 1985.

1. Allison, J. P., McIntyre, B. W. & Bloch, D. *J. Immun.* **129**, 2293–2300 (1982).
2. Haskins, K. *et al. J. exp. Med.* **157**, 1149–1169 (1983).
3. Meuer, S. C. *et al. Nature* **303**, 808–810 (1983).
4. Hood, L., Kronenberg, M. & Hunkapiller, T. *Cell* **40**, 225–229 (1985).
5. Chien, Y., Gascoigne, N. R. J., Kavaler, J., Lee, N. E. & Davis, M. M. *Nature* **309**, 322–326 (1984).
6. Malissen, M. *et al. Cell* **37**, 1101–1110 (1984).
7. Gascoigne, N. R. J., Chien, Y., Becker, D. M., Kavaler, J. & Davis, M. M. *Nature* **311**, 387-391 1(984).
8. Kavaler, J., Davis, M. M. & Chien, Y. *Nature* **310**, 421–423 (1984).
9. Sium, G. *Nature* **311**, 344-350 (1984).
10. Kronenberg, M., Siu, G., Shastri, N. & Hood, L. *A. Rev. Immun.* (in the press).
11. Kronenberg, M. *et al. Nature* **313**, 647–653 (1985).
12. Max, E. E., Siedman, J. G. & Leder, P. *Proc. natn. Acad. Sci. U.S.A.* **76**, 3450–3454 (1979).
13. Sakano, H., Hüppi, K., Heinrich, G. & Tonegawa, S. *Nature* **280**, 288–294 (1979).
14. Van Ness, B. G., Coleclough, C., Perry, R. & Weigert, M. *Proc. natn. Acad. Sci. U.S.A.* **79**, 262–266 (1982).
15. Höchtl, J., Müller, C. R. & Zachau, H. G. *Proc. natn. Acad. Sci. U.S.A.* **79**, 1383–1387 (1982).
16. Alt, F. W. & Baltimore, D. *Proc. natn. Acad. Sci. U.S.A.* **79**, 4118–4122 (1982).
17. Lewis, S., Rosenberg, N., Alt, F. & Baltimore, D. *Cell* **30**, 807–816 (1982).
18. Lewis, S., Gifford, A. & Baltimore, D. *Nature* **308**, 425–428 (1984).
19. Steinmetz, M., Altenburger, W. & Zachau, H. G. *Nucleic Acids Res.* **8**, 1709–1720 (1980).
20. Selsing, E. & Storb, U. *Nucleic Acids Res.* **9**, 5725–5735 (1981).
21. Yaoita, Y., Matsunami, N., Choi, C. Y., Sugiyama, H., Hishimoto, T. & Honjo, T. *Nucleic Acids Res.* **11**, 7303–7316 (1983).
22. Alt, F. W. *et al. EMBO J.* **3**, 1209–1219 (1984).
23. Selding, E., Voss, J. & Storb, U. *Nucleic Acids Res.* **12**, 4229–4256 (1984).
24. Born, W., Yagüe, J., Palmer, E., Kappler, J. & Marrack, P. *Proc. natn. Acad. Sci. U.S.A.* **82**, 2925–2929 (1985).
25. Lewis, S., Gifford, A. & Baltimore, D. *Science* **228**, 677–685 (1985).
26. Wilde, D. B. *et al. J. Immun.* **133**, 1992–1995 (1984).
27. Barth, R. K. *et al. Nature* **316**, 517–523 (1985).
28. Albert, F., Buferne, M., Boyer, C. & Schmitt-Verhulst, A.-M. *Immunogenetics* 16, 553-559 (1982).
29. Patten, P. *et al. Nature* **312**, 40–46 (1984).
30. Höchtl, J. & Zachau, H. G. *Nature* **302**, 260–263 (1983).
31. Sakano, H., Kurosawa, Y., Weigert, M. & Tonegawa, S. *Nature* **290**, 562–565 (1981)
32. Kurosawa, Y. *et al. Nature* **290**, 565–570 (1981).
33. Kurosawa, Y. & Tonegawa, S. *J. exp. Med.* **155**, 201–218 (1982).
34. Desiderio, S. V. *et al. Nature* **311**, 752–755 (1984).
35. Goverman, J. *et al. Cell* **40**, 859–867 (1985).
36. Klein, J., Figueroa, F. & David, C. S. *Immunogenetics* **17**, 553–596 (1983)
37. Malissen, M., Trucy, J., Mjolsness, S., Ma, D., Firch, F. & Hood, L. (in preparation)
38. Collins, M. K. L. *et al. EMBO J.* **3**, 2347–2350 (1984).
39. Isobe, M., Erikson, J., Emanuel, B. S., Nowell, P. C. & Croce, C. M. *Science* **228**, 580–582 (1985).
40. Tsujimoto, Y. *et al. Nature* **315**, 340–343 (1985).
41. Frischauf, A., Lehrach, H., Poustka, A. & Murray, N. *J. molec. Biol.* **170**, 827–842 (1983)
42. Maniatis, T., Fritsch, E. F. & Sambrook, J. *Molecular Cloning: A Laboratory Manual* (Cold Spring Harbor Laboratory, New York, 1982).

Molecular structure of an aspartic proteinase zymogen, porcine pepsinogen, at 1.8 Å resolution

Michael N. G. James & Anita R. Sielecki

Medical Research Council of Canada Group in Protein Structure and Function, Department of Biochemistry, University of Alberta, Edmonton, Alberta, Canada T6G 2H7

The only well-understood mechanism of zymogen activation is that of the serine proteinases, in which proteolytic cleavage leads to conformational changes resulting in a functional active site. A different mechanism is now unveiled by the crystal structure of pepsinogen. Salt bridges that stabilize the positioning of the N-terminal proenzyme segment across the active site of pepsin are disrupted at low p*H, releasing the amino-terminal segment and thereby exposing the catalytic apparatus and the substrate-binding sites.*

THE specialized cells and tissues of eukaryotic organisms which produce proteolytic enzymes protect themselves from digestion by synthesizing inactive precursors of the active enzymes[1]. These zymogens have lengths of polypeptide that are N-terminal extensions of the active proteinases. Activation of a zymogen is commonly accomplished by limited proteolysis that removes the proenzyme segment extension. Many biologically important processes, such as the blood clotting cascade, are critically dependent upon this precursor to active enzyme conversion[2].

The zymogens of the pancreatic serine proteinases are usually activated upon cleavage by other proteolytic enzymes. For example, the removal of an N-terminal hexapeptide from trypsinogen by enterokinase or trypsin is accompanied by a conformational change that completes the formation of the primary substrate-binding cavity of trypsin[3]. In contrast, the zymogens of the gastric aspartic proteinases only require H^+ ions (pH <5.0) to initiate the activation process[4]. These pioneering observations of Herriott indicated that at pH 4.0–4.6 the formation of pepsin from the inactive precursor is autocatalytic.

a

1P 5P
LEU-VAL-LYS-VAL-PRO-

6P 10P
LEU-VAL-ARG-LYS-LYS-

11P 15P
SER-LEU-ARG-GLN-ASN-

16P 20P
LEU-ILE-LYS-ASP-GLY-

21P 25P
LYS-LEU-LYS-ASP-PHE-

26P 30P
LEU-LYS-THR-HIS-LYS-

31P 35P
HIS-ASN-PRO-ALA-SER-

36P 40P
LYS-TYR-PHE-PRO-GLU-

41P 44P
ALA-ALA-ALA-LEU-

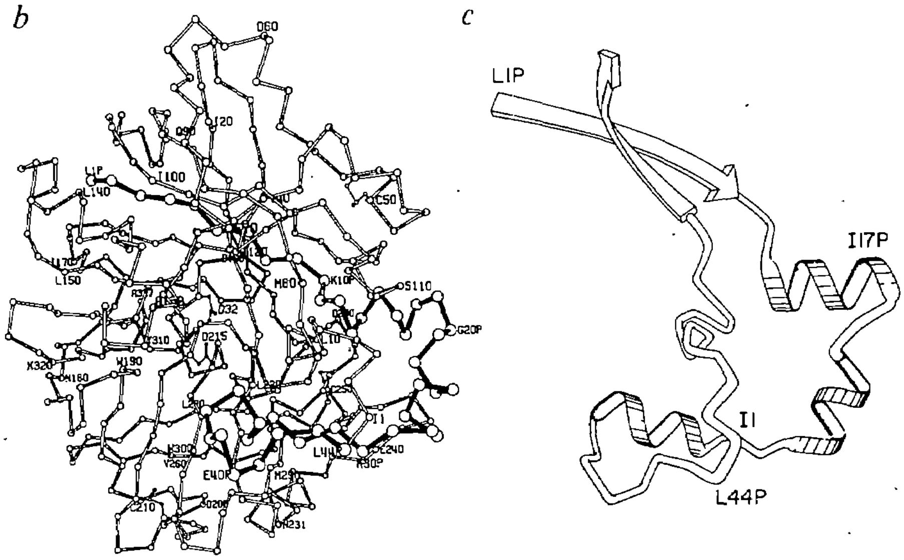

Fig. 1 ***a***, Amino-acid sequence of the proenzyme segment of pepsinogen. The 44 residues are numbered sequentially from 1 followed by the suffix P as suggested by Foltmann[13]. The residues of the active portion of the molecule are numbered according to the porcine pepsin amino-acid sequence[14,15]. ***b***, Representation of the α-carbon atom positions of porcine pepsinogen (ORTEP, C. Johnson, Oak Ridge National Laboratories). The 44 residues of the proenzyme segment have the virtual bonds that connect C^{α} atoms in thick black lines; the pepsin portion of the molecule is indicated by open bonds. The side-chain positions of Asp 32, Asp 215 and the three disulphide bridges are indicated. Every 10th residue is labelled with the single-letter code for the residue name and the sequence number. Large crystals of porcine pepsinogen suitable for high-resolution crystallographic analysis were grown by the hanging-drop, vapour-diffusion method. The protein solution contained 10 mg ml^{-1} pepsinogen (Sigma, lot 98C-0451), 1.8 M Li_2SO_4 buffered with 50 mM [*N*-morpholino]ethane sulphonic acid to a *p*H of 6.1. The crystals of the native protein are monoclinic, space group C2, with unit cell dimensions $a = 105.8$, $b = 43.4$, $c = 88.6$ Å and $\beta = 91.4°$. There are four molecules of pepsinogen, relative molecular mass ≃ 39,600, per unit cell ($V_m = 2.57$ Å^3 per dalton). The crystals used for this structure solution are similar to those of porcine pepsinogen reported previously[20] except for a 1% difference in the *a* axial length. Intensity data to 1.8 Å resolution (37,575 unique reflections) for the native pepsinogen crystals were collected on an Enraf-Nonius CAD4 diffractometer using a data collection protocol described previously[21]. The structure was solved by a combination of multiple isomorphous replacement[22] and molecular replacement[23] techniques. The molecular replacement used a search model based on the 1.8 Å resolution refined coordinates of penicillopepsin[19]. Details of this structure solution will be reported elsewhere (A.R.S., M. Fujinaga, R. J. Read and M.N.G.J., in preparation). ***c***, A ribbon drawing of the secondary structural features of the proenzyme segment (residues Leu 1P–Leu 44P of pepsinogen) along with the first 17 residues of active pepsin. Two of the scissile bonds cleaved during zymogen processing, Leu 16P–Ile 17P and Leu 44P–Ile 1, are labelled. There are three short helical stretches in the proenzyme segment, Ser 11P–Asp 19P, Lys 21P–Thr 28P, approximately orthogonal to one another, and Pro 33P–Tyr 37P. The side chains of Leu 12P, Leu 16P, Leu 22P, Phe 25P and Leu 26P contribute to the hydrophobic core of this small domain. The chain from His 29P to Asn 32P has an extended conformation. The remaining segment of the proenzyme peptide, from Pro 39P to Leu 44P, seems to have few secondary structural features. The electron density for the segment from Ala 42P to Ile 1 is relatively weak at the present refinement stage. The peptide bond between Leu 44P and Ile 1 is exposed on the surface of the molecule.

Many elegant chemical, spectrophotometric and kinetic studies have been designed to elucidate the pathway of the conversion of porcine pepsinogen to pepsin. Optical rotatory dispersion studies of pepsinogen[5] showed that the zymogen exhibits characteristics of α-helical structure not present in pepsin. Furthermore, the conformation of the zymogen is stabilized by electrostatic interactions involving the basic amino acids of the proenzyme segment and carboxylate groups on the enzyme[5]. Ultraviolet spectroscopy detects a rapid conformational change in the molecule as a solution of pepsinogen is acidified to *p*H 2.85 (ref. 6). If the *p*H of the solution is returned to neutrality after a short time, this conformational change is fully reversible and no formation of pepsin is observed; this is consistent with a possible intermediate in the reaction[6]. It has also been shown that the activation of pepsinogen in a dilute acidic solution containing an excess of substrate, haemoglobin, is independent of pepsinogen concentration, suggesting an intramolecular activation process in which the unproteolysed zymogen cleaves itself[7]. Similar deductions of a unimolecular mechanism have been made independently by Funatsu *et al.*[8,9]. Further support for an intramolecular activation comes from kinetic experiments showing that the rate of conversion of pepsinogen is a first-order reaction at *p*H values below 3, that is, independent of zymogen concentration[10]. At higher *p*H values, however, the observed kinetics are consistent with a mixed reaction mechanism in which pepsin-catalysed activation predominates[10].

The proenzyme segment of pepsinogen consists of 44 amino acids of known sequence[11,12] (Fig. 1*a*). It has not been possible to isolate the intact peptide Leu 1P–Leu 44P from activation solutions. Instead, several shorter peptides resulting from multiple proteolytic cleavages can be isolated, suggesting a sequential mechanism for the conversion. The first peptide to be observed results from the hydrolysis of the Leu 16P–Ile 17P bond, with the concomitant formation of an enzymatically active pseudopepsin molecule[16,17]. The subsequent formation of mature pepsin is concentration dependent and may represent the bimolecular component important in the activation process at relatively higher *p*H values[18].

Comparison of the crystallographic solution of the molecular structure of pepsinogen with that of an active aspartic proteinase, penicillopepsin[19], reveals the reasons for the catalytic incompetence of the intact zymogen. In addition, the observed structure (Fig. 1*b*, *c*) sheds new light on the interpretations of the many solution studies.

Molecular structure of pepsinogen

The model of pepsinogen reported here has been subjected to restrained-parameter least-squares refinement[24], following the same strategy used in this laboratory for other protein structures[25]. Whereas detailed hydrogen bonding interactions may change on further refinement and inclusion of all ordered solvent, interpretations based on the present structure should not change substantially. The high quality of the electron density

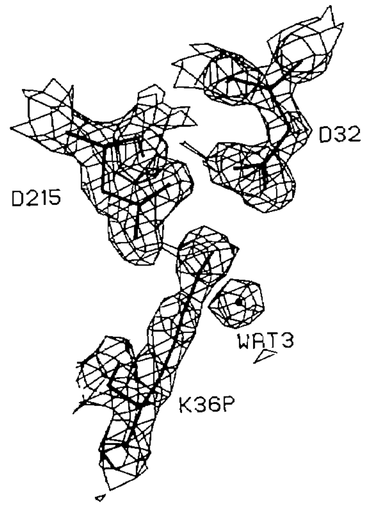

Fig. 2 Electron density contour surfaces in the vicinity of the active site of pepsinogen (Asp 32 and Asp 215). The current agreement factor between observed structure factor amplitudes, $|F_0|$, and calculated ones based on the refined atomic coordinates, $|F_c|$, is 0.167 ($R=\Sigma||F_0|-|F_c||/\Sigma|F_0|$) for the 26,191 reflections with $I \geqslant 2\sigma(I)$ in the 6.0–1.8-Å resolution range (I is the measured intensity of the reflection, $\sigma(I)$ its estimated standard deviation). The molecular model includes 110 ordered solvent molecules. The root-mean-square deviations from expected geometry are acceptably small, 0.016 Å for covalent bond lengths, 0.037 Å for bond angle-related distances, 0.025 Å for out-of-plane deviations and 4.0° for deviations from 180° for the *trans* peptide bonds. The contour level on this $2F_0-F_c$ map is 0.60 eÅ^{-3}. Full thick lines correspond to the molecular model at this stage of the refinement. Solvent molecule Wat 3 is hydrogen bonded to N^{ζ} of Lys 36P.

map at the current stage of refinement can be seen in Fig. 2. The present agreement factor is 0.167.

The crystallographic structures of four aspartic proteinases have been reported previously[19,26–28]. All four structures are highly homologous and have a general overall shape that resembles a croissant. The N-terminal domains, residues 1–170, are folded in a similar fashion to the C-terminal domains (residues ~180–327), suggesting gene duplication, divergence and subsequent fusion in the evolutionary history of these enzymes[29]. Most residues of the aspartic proteinases adopt a β-sheet conformation. The secondary and tertiary structural interactions in penicillopepsin at 1.8 Å resolution have been discussed elsewhere[19]. In all of these enzymes, the active-site aspartate residues, Asp 32 and Asp 215, are located at the junction of the two domains in an extended substrate-binding cleft. Possible modes of productive binding of substrates have been established by crystallographic studies of inhibitor binding to penicillopepsin[21,30–32] and to rhizopuspepsin[33,34].

The polypeptide chain of the pepsin portion of pepsinogen (residues Ile 1–Ala 327) folds in a fashion that is highly homologous to those of the several aspartic proteinases of known structure mentioned above. Visual comparison of the α-carbon atom chain tracing of pepsinogen (Fig. 1*b*) with that of the active pepsin molecule[28] certainly confirms this. A more detailed comparison must await the completion of the refinement of both molecular structures. Nevertheless, there is clearly a major conformational difference between the N-terminal 12 residues of pepsin and the corresponding 12 residues in pepsinogen. In pepsin, residues Ile 1–Leu 6 form strand 1 of a large six-stranded antiparallel β-sheet, a common feature of all aspartic proteinases[19]. The next five residues form a reverse turn that changes the polypeptide chain direction[28].

In contrast, these residues in pepsinogen are intimately associated with the inactivation domain, on the opposite side of the molecule (Fig. 1b). The side chain of Ile 1 in the zymogen is ~40 Å from its final position in the active enzyme. Residues Ile 1–Asp 3 are in an extended conformation, followed by a series of reverse turns from Glu 4 to Asp 11 which give the chain an irregular helical conformation. From Pro 39P to Asn 8, the polypeptide chain forms a large loop into the centre of which fits the tip of the flap (a β-hairpin loop, residues 72–82). The side chain of Leu 10 contributes to the hydrophobic core of the inactivation domain.

The overall shape of the inactivation domain of pepsinogen (residues Lys 9P–Glu 13) is that of a flattened disk with a long N-terminal extension formed by the first 8 residues, Leu 1P–Arg 8P (Fig. 1*c*). This disk-like domain fits neatly into the part of the structure that corresponds to the substrate-binding cleft in pepsin with apparently little distortion of the conformation of the active enzyme. The first six residues of pepsinogen form the first strand of the same large, centrally located six-stranded antiparallel β-sheet as do the N-termini of the active aspartic proteinases.

Mechanism of inhibition

The present molecular structure of pepsinogen clearly shows why the zymogens of the aspartyl proteinases are inactive. Part of the proenzyme segment, residues Ser 11P–Leu 44P, occupies the substrate-binding cleft of the pepsin portion of the zymogen, competitively blocking access to the two catalytically important aspartyl residues (Figs 1*b*, 2). Lys 36P has a pivotal role in the inhibition of the intact zymogen at high *p*H. This residue is in

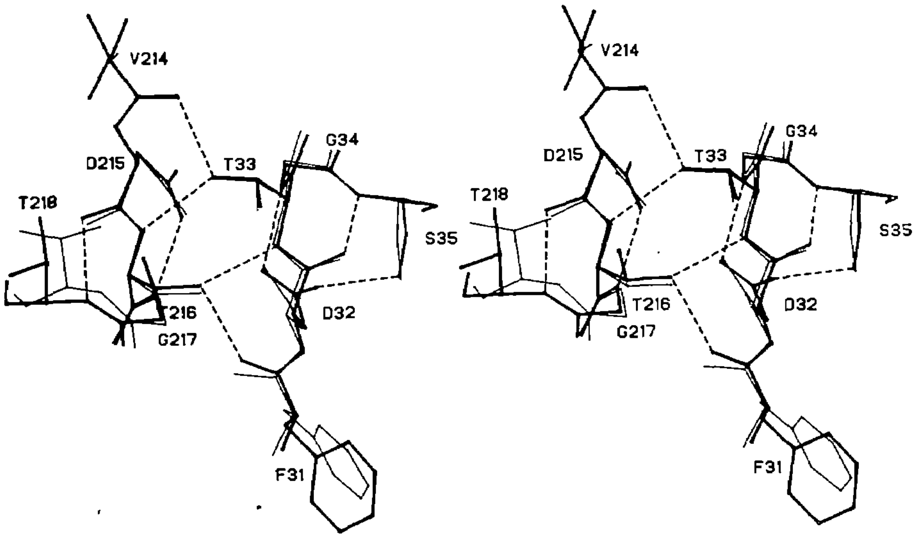

Fig. 3 A stereo representation of the two active-site strands: Phe 31–Ser 35 and Val 214–Thr 218 of pepsinogen (drawn in thick lines), superimposed on the equivalent residues of penicillopepsin[19]: Phe 32–Ser 36 and Ala 212–Thr 216 (in thin lines). Hydrogen-bonding interactions involving atoms of pepsinogen are indicated by dashed lines. The least-squares superposition of the coordinates of the main-chain atoms (N, C^{α}, C^{β}, C, O) of these residues yields a root-mean-square deviation of 0.36 Å for the 48 common atom pairs. The largest difference is associated with the main chain of Thr 218 (Thr 216 in penicillopepsin). The hydrogen bond that the $O^{\gamma 1}$ side-chain atom of this residue forms with the side-chain carboxyl group of Asp 213 in penicillopepsin has no equivalent in pepsinogen. All other hydrogen-bonding interactions for this region of the zymogen are as observed for active penicillopepsin.

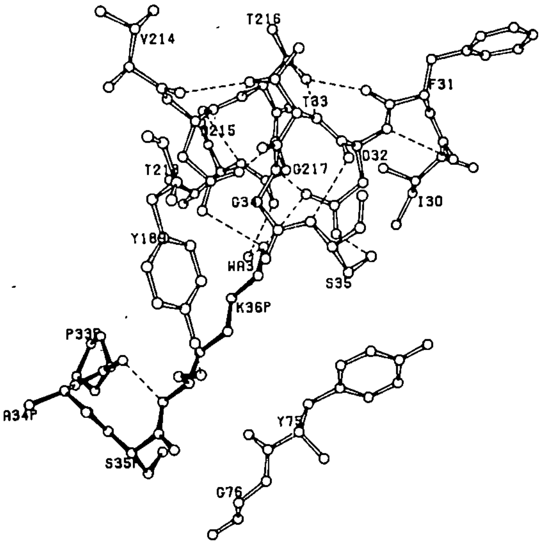

Fig. 4 A rendering of the active-site region of pepsinogen with four residues of the proenzyme segment, Pro 33P–Lys 36P (PLUTO, S. Motherwell, University Chemical Laboratory, Cambridge, UK). Hydrogen-bonding interactions are shown by dashed lines. The residues of the proenzyme segment are drawn with filled bonds, the pepsin portion with open bonds, both in this figure and in Fig. 5. The molecule labelled WA3 corresponds to water 3, depicted in Fig. 2 with its associated electron density.

a highly conserved region of the zymogens of the vertebrate aspartic proteinases[35].

We suggest that the residues of pepsinogen in the immediate vicinity of the two catalytic aspartyl residues are in, or very close to, their active conformation. It is not possible to consolidate this hypothesis by direct comparison with the known structure of pepsin[28]. Crystals of porcine pepsin have been grown from ethanol, a compound known to inhibit this enzyme. Ethanol molecules have been tentatively identified in close proximity to the aspartyl residues, a binding that could induce conformational changes[28]. In any event, only the pepsin α-carbon coordinates are available in the Brookhaven Protein Data Bank[36]. Another member of the aspartyl proteinase family, penicillopepsin, has had its crystal structure determined at its pH optimum. The details of the conformation of the active site, with its intricate hydrogen bonding, have been described elsewhere[19]. A least-squares superposition of the active-site regions of penicillopepsin and pepsinogen is depicted in Fig. 3. The small rotation of the side chain of Asp 32 relative to the native conformation of penicillopepsin, as can be seen in Fig. 3 for pepsinogen, has also been observed in the crystal structure of the complex of penicillopepsin with the inhibitor Iva-Val-Val-StaOEt (refs 21, 30).

In the active conformation of penicillopepsin, the two carboxyl groups of Asp 33 and Asp 213 are the recipients of several strong hydrogen bonding interactions[19]. Asp 32 and Asp 215 in pepsinogen have most of these hydrogen bonds present (Fig. 3) but, in addition, the positively charged N^{ζ} of Lys 36P provides electrostatic stabilization through hydrogen bonding for one of the formal net negative charges on these residues (Fig. 4). This interaction must also be an important factor in the inhibition of the inherent activity of the zymogen. It is likely that the net charge at the active site of pepsinogen is −2, as the pH of the crystals is 6.1 and the higher pK_a of the pepsin active site is 4.7. Stabilization of the second formal negative charge must come from the other favourable hydrogen bonds and dipole interactions. The position of N^{ζ} of Lys 36P relative to the two aspartic acid side chains in pepsinogen is within 0.5 Å of the refined position of a solvent molecule, 039, in penicillopepsin. We have interpreted this solvent as a bound ammonium or hydronium ion with a possible electrophilic role in the catalytic mechanism[32]. The disposition of Lys 36P provides additional evidence that the 039 site of penicillopepsin is a favourable position for the binding of positively charged groups to aspartyl proteinases, an important yet unresolved issue in the elucidation of the mechanism of the active enzymes[19,32].

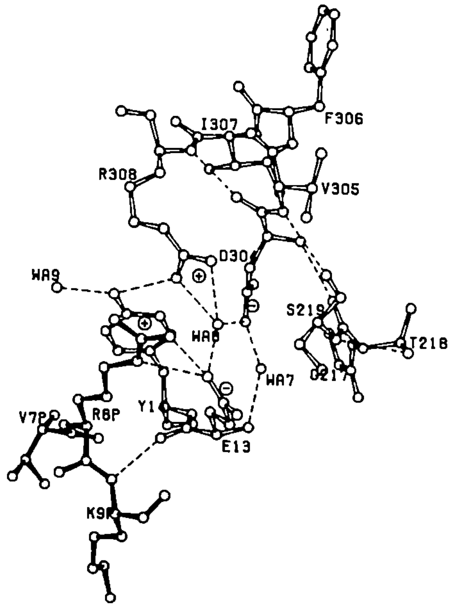

Fig. 5 The residues neighbouring the unusual interaction of Arg 8P and Arg 308 are shown (PLUTO, S. Motherwell, University Chemical Lab., Cambridge, UK). Possible hydrogen bonds are represented by dashed lines. The close proximity of the carboxylate groups of Glu 13 and Asp 304 are important in stabilizing the disposition of the two arginine residues at high pH. Protonation of Glu 13 and Asp 304 on lowering the pH below 4 would remove these stabilizing electrostatic effects and strong repulsion of the two positively charged guanidinium groups could trigger a conformational change. Water WA8 bridges the interaction between Asp 304 and Arg 308.

There are four aromatic rings in the vicinity of this electrostatic interaction of Lys 36P and the two aspartic acid carboxyl groups, Tyr 37P, Tyr 9, Tyr 75 and Tyr 189. The side chain of Tyr 75 on the flap is stacked with its aromatic plane almost perpendicular to that of Tyr 9. One of the first events detected spectrophotometrically on lowering the pH of a solution of pepsinogen from neutrality to 2–4 is an ultraviolet spectral change that can be associated with tyrosyl and tryptophan absorbance bands[6]. As the active-site carboxyl groups take up a proton, the complicated hydrogen bonding network involving Asp 32 and Asp 215 would be disrupted with a concomitant alteration in the environment of these several tyrosine side chains, as observed in the spectrophotometric experiments.

Intramolecular ionic interactions

It has been suggested that, at neutral pH, the highly positively charged proenzyme segment is bound to the pepsin portion of the molecule via ionic interactions with negatively charged carboxylate groups[5]. This early suggestion is now confirmed by the crystal structure. In addition to the ionic attractions between the Lys 36P side chain and the carboxylate groups of Asp 32 and Asp 215 that we have discussed (Fig. 4), several other electrostatic interactions contribute to this stabilization (Table 1).

A cluster of two positively charged groups (Arg 8P and Arg 308) and two negatively charged carboxylate groups (Glu 13 and Asp 304) is shown in Fig. 5. Also included in the environment of these charged groups are several highly ordered water

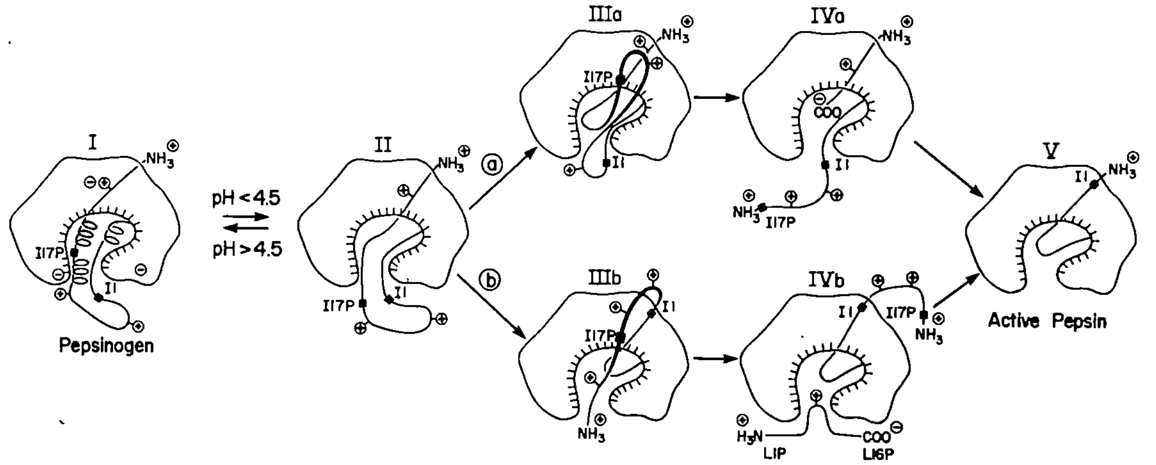

Fig. 6 Proposed steps in the activation of pepsinogen. Interconversion of structures I and II is a reversible, *p*H-dependent process. Structures III*a* and III*b* are two possible alternatives that would place the first scissile bond Leu 16P–Ile 17P at the catalytic site. In pathway *a*, the N-terminus of the zymogen remains in its crystallographically observed position; in pathway *b* the N-terminal residues of pepsin (Ile 1–Asn 8) occupy their final position by replacing the N-terminus of the proenzyme segment. The segment of polypeptide chain from Ile 17P to Ile 1 is sufficiently long to wrap around the back of the molecule, allowing the scissile bond Leu 16P–Ile 17P to approach and bind in a productive mode analogous to that shown in structure III*a*. A unimolecular reaction would release peptide Leu 1P–Leu 16P to yield structures IV*a* or IV*b*. This peptide is a known inhibitor of porcine pepsin[37] and therefore probably also inhibits pseudopepsin, as indicated schematically in structure IV*b*. Conversion of structure IV*a* or IV*b* to active pepsin probably occurs by an intermolecular pepsin cleavage to release peptide Ile 17P–Leu 44P.

molecules, WAT 7, 8 and 9, which mediate additional interactions. The positively charged guanidinium groups of the two arginine side chains stack with their planes approximately parallel, but separated by a van der Waals contact distance of ≈3.5 Å. This surprising interaction is stabilized by the close proximity of the two carboxylate groups of Glu 13 and Asp 304 (Fig. 5). A possible sequence of events on lowering the *p*H of a solution of pepsinogen is the protonation of these carboxylate groups, thus removing the charge stabilization. The two guanidinium side chains would be electrostatically repelled, inducing a changed conformation in the proenzyme segment. Similar arguments apply to protonation of the several other carboxylate groups listed in Table 1. This leads to the disruption of the conformation of the zymogen as the *p*H is lowered.

Steps in activation

The molecular structure of the zymogen of porcine pepsin places limitations on the sequence of events required to convert the inactive precursor to the activated enzyme. Structure I in Fig. 6 is a diagrammatic representation of the conformation of pepsinogen that we have determined crystallographically at $pH > 6$. On lowering the *p*H of a solution of pepsinogen, conversion of structure I to structure II (Fig. 6) is accompanied by the following known events. The carboxylate groups involved in stabilizing ion pairs (Table 1) become protonated, facilitating a conformational change in the proenzyme segment. This change can be fully reversed by raising the *p*H of the solution after a short time[6]. However, prolonged incubation results in irreversible activation with the intramolecular cleavage of the peptide bond Leu 16P–Ile 17P[16,17], a bond favoured for hydrolysis because pepsin has a specificity for hydrophobic side chains[38]. This scissile bond is part of the first helix of the proenzyme segment (Fig. 1) and residues Leu 16P and Ile 17P must move ≈18 Å to reach the active site. In addition, this bond must approach the two aspartate groups Asp 32 and Asp 215 to bind in the manner of a good substrate[31,32].

Table 1 Electrostatic interactions of the proenzyme segment with the pepsin part of pepsinogen

Positively charged residue*	Negatively charged residue	Hydrogen-bonding distances (Å)
Lys 3P ε-NH_3^+	Asp 171 COO^-	3.5
Arg 8P Guan$^+$	Glu 13 COO^-	2.9, 2.8
Arg 13P Guan$^+$	Asp 11 COO^-	2.8, 2.8
His 29P Imid$^+$	Asp 3 COO^-	2.8
His 31P Imid$^+$	Glu 7 COO^-	2.5
Lys 36P ε-NH_3^+	Asp 32 COO^-	3.0
	Asp 215 COO^-	2.8

* Guan$^+$ and Imid$^+$ stand for the guanidinium and imidazolium groups of arginine and histidine, respectively.

There are two ways in which the scissile bond Leu 16P-Ile 17P can be positioned in the substrate-binding cleft (pathways *a* and *b* of Fig. 6). Structure III*a* results when Leu 1P-Leu 6P, the extended polypeptide preceding the first helix of the proenzyme segment, remains in the zymogen conformation as part of the six-stranded antiparallel β-sheet (Fig. 1). The N-terminal to C-terminal direction of the polypeptide corresponds to that proposed for productive substrate binding to aspartyl proteinases[31–34,39]. The second mode of binding, represented by structure III*b*, occurs if the segment Leu 1P-Leu 6P is displaced by the N-terminal residues of pepsin (Ile 1-Leu 6). In both cases, intramolecularly catalysed cleavage of the bond Leu 16P-Ile 17P would yield structures IV*a* and IV*b*, respectively.

The most likely path in the conversion of intermediate structures IV*a* and IV*b* to active pepsin, structure V, is via an intermolecular cleavage step in which the peptide bond Leu 44P-Ile 1 is bound in the active site of a second activated pepsinogen (or active pepsin) molecule. These two structures, IV*a* and IV*b*, are quite analogous and are differentiated only by how peptide Leu 1P-Leu 16P is bound to the enzyme. Further degradation of the two major peptides released during the activation process takes place, resulting in many short segments[37].

The activation of mammalian aspartic proteinases from their inactive precursors is accompanied by some spectacular conformational changes. We have shown that the residues in the active site of pepsinogen are in a conformation remarkably close to the active conformation of penicillopepsin (Fig. 3). The *p*H-induced conformational upheavals involve the movement of the competitive proenzyme segment out of the active-site cleft of pepsin, exposing the catalytic apparatus and freeing the substrate-binding sites. The position of the N-terminal Ile 1 residue of active pepsin is ≃40 Å from the observed position of this residue in pepsinogen. The activation steps we propose in order to rationalize how this remarkable conformational change can take place are entirely consistent with the low *p*H unimolecular activation process that has been suggested to occur in solution.

Dr Y. Nakagawa supplied us with our initial sample of highly purified porcine pepsinogen. Koto Hayakawa has grown the pepsinogen crystals and carried out the heavy-atom search. Randy Read and Masao Fujinaga provided their expertise with the molecular replacement and phase combination methods. This research has been generously supported by the MRC of Canada in a grant to the MRC Group in Protein Structure and Function.

Received 8 July; accepted 26 September 1985.

1. Kassell, B. & Kay, J. *Science* **180**, 1022–1027 (1973).
2. Neurath, H. *Science* **224**, 350–357 (1984).
3. Huber, R. & Bode, W. *Acc. chem. Res.* **11**, 114–121 (1978).
4. Herriott, R. M. *J. gen. Physiol.* **22**, 65–78 (1939).
5. Perlmann, G. E. *J. molec. Biol.* **6**, 452–464 (1963).
6. McPhie, P. *J. biol. Chem.* **247**, 4277–4281 (1972).
7. Bustin, M. & Conway-Jacobs, A. *J. biol. Chem.* **246**, 615–620 (1971).
8. Funatsu, M., Harada, Y., Hayashi, K. & Jirgensons, B. *Agric. biol. Chem.* **35**, 566–572 (1971).
9. Funatsu, M., Harada, Y., Hayashi, K. & Kaneda, T. *Agric. biol. Chem.* **36**, 305–312 (1972).
10. Al-Janabi, J., Hartsuck, J. A. & Tang, J. *J. biol. Chem.* **247**, 4628–4632 (1972).
11. Ong, E. B. & Perlmann, G. E. *J. biol. Chem.* **243**, 6104–6109 (1968).
12. Pedersen, V. B. & Foltmann, B. *FEBS Lett.* **35**, 255–256 (1973).
13. Foltmann, B. *Essays Biochem.* **17**, 52–84 (1981).
14. Tang, J. *et al. Proc. natn. Acad. Sci. U.S.A.* **70**, 3437–3439 (1973).
15. Sepulveda, P., Marciniszyn, J., Liu, D. & Tang, J. *J. biol. Chem.* **250**, 5082–5088 (1975).
16. Dykes, C. W. & Kay, J. *Biochem. J.* **153**, 141–144 (1976).
17. Kay, J. & Dykes, C. W. in *Acid Proteases, Structure, Function, and Biology* (ed. Tang, J.) 103–127 (Plenum, New York, 1977).
18. Christensen, K. A., Pedersen, V. B. & Foltmann, B. *FEBS Lett.* **76**, 214–218 (1977).
19. James, M. N. G. & Sielecki, A. R. *J. molec. Biol.* **163**, 299–361 (1983).
20. Rao, S. N., Koszelak, S. N. & Hartsuck, J. A. *J. biol. Chem.* **252**, 8728–8730 (1977).
21. James, M. N. G., Sielecki, A. R., Salituro, F., Rich, D. H. & Hofmann, T. *Proc. natn. Acad. Sci. U.S.A.* **79**, 6137–6141 (1982).
22. Green, D. W., Ingram, V. M. & Perutz, M. F. *Proc. R. Soc.* **A225**, 287–295 (1954).
23. Rossmann, M. G. *The Molecular Replacement Method* (Gordon & Breach, New York, 1972).
24. Hendrickson, W. A. & Konnert, J. H. in *Computing in Crystallography* (eds Diamond, R., Ramaseshan, S. & Venkatesan, K.) 13.01–13.23 (Indian Academy of Sciences, International Union of Crystallography, Bangalore, 1980).
25. Sielecki, A. R. *et al. J. molec. Biol.* **134**, 781–804 (1979).
26. Hsu, I.-N., Delbaere, L. T. J., James, M. N. G. & Hofmann, T. *Nature* **266**, 140–145 (1977).
27. Subramanian, E. *et al. Proc. natn. Acad. Sci. U.S.A.* **74**, 556–559 (1977).
28. Andreeva, N. S., Zdanov, A. S., Gustchina, A. E. & Fedorov, A. A. *J. biol. Chem.* **259**, 11353–11365 (1984).
29. Tang, J., James, M. N. G., Hsu, I.-N., Jenkins, J. A. & Blundell, T. L. *Nature* **271**, 618–621 (1978).
30. James, M. N. G., Sielecki, A. R. & Moult, J. in *Peptides, Structure and Function* (eds Hruby, V. & Rich, D.) 521–530 (Pierce Chemical Company, Rockford, Illinois, 1983).
31. Hofmann, T., Hodges, R. S. & James, M. N. G. *Biochemistry* **23**, 635–643 (1984).
32. James, M. N. G. & Sielecki, A. R. *Biochemistry* **24**, 3701–3713 (1985).
33. Bott, R., Subramanian, E. & Davies, D. R. *Biochemistry* **21**, 6956–6962 (1982).
34. Bott, R. R. & Davies, D. R. in *Peptides, Structure and Function* (eds Hruby, V. & Rich, D.) 531–540 (Pierce Chemical Company, Rockford, Illinois, 1983).
35. Foltmann, B. & Pedersen, V. B. in *Acid Proteases, Structure, Function and Biology* (ed. Tang, J.) 3–22 (Plenum, New York, 1977).
36. Bernstein, F. C. *et al. J. molec. Biol.* **112**, 535–542 (1977).
37. Dunn, B. M. *et al. J. biol. Chem.* **253**, 7269–7275 (1978).
38. Powers, J. C., Harley, A. D. & Myers, D. V. in *Acid Proteases, Structure, Function, and Biology* (ed. Tang, J.) 141–157 (Plenum, New York, 1977).
39. James, M. N. G., Hsu, I.-N. & Delbaere, L. T. J. *Nature* **267**, 808–813 (1977).

LETTERS TO NATURE

A radio outburst and jet from the symbiotic star CH Cyg

A. R. Taylor*, E. R. Seaquist† & J. A. Mattei‡

* Kapteyn Astronomical Institute, University of Groningen,
9700 AV Groningen, The Netherlands
† Department of Astronomy, University of Toronto, Toronto,
Ontario, Canada M5S 1A7
‡ American Association of Variable Star Observers, 187 Concord Ave,
Cambridge, Massachusetts 02138, USA

CH Cyg is an M7 III star that is known to undergo periods of brightening in the blue-violet continuum at irregular intervals of a few years[1–3]. During the active phase, the spectrum also exhibits strong Balmer emission and emission lines from He I, Fe II and various forbidden transitions, giving it the appearance of a symbiotic star. As part of a monitoring programme on symbiotic stars, observations with the National Radio Astronomy Observatory Very Large Array (VLA) have been made on CH Cyg over the past year at intervals of a few months. During the period April 1984 to May 1985 this monitoring revealed a strong radio outburst coincident with the production of a multi-component jet, and a comparison of high-resolution maps at two epochs separated by 75 days shows that the jet is expanding at a rate of 1.1 arc s yr^{-1}. The onset of the radio outburst coincides in time with a remarkable decline in the visual brightness of the star. The luminosity of the star during the optically active state and the energetics of the mass loss suggest that the outburst is the result of accretion at, or near, the Eddington limit onto the surface of a white dwarf.

The observations of CH Cyg trace the evolution of a radio outburst during which the flux density increased by a factor of 30. Figure 1 shows the radio light curve at $\lambda = 2$ cm. The outburst was continuing at the time of our last observation on 3 May 1985, and the radio spectrum during the outburst has remained essentially constant. Figure 2 shows radio spectra obtained at three epochs. The spectral index between 5 and 14.9 GHz is +1.2. This is typical (although slightly high) for radio-detected symbiotic stars[4], and is consistent with emission through optically thick thermal bremsstrahlung.

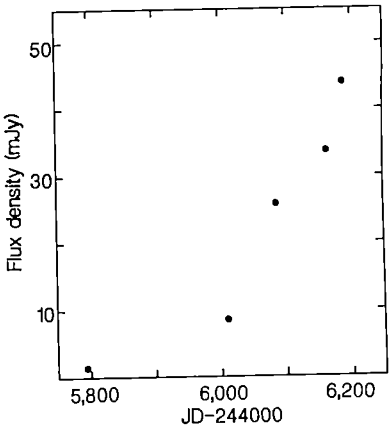

Fig. 1 The radio light curve of CH Cyg at $\lambda = 2$ cm from April 1984 to May 1985.

The radio brightening illustrated by Fig. 1 is reminiscent of symbiotic novae. About six such objects are known, for example, HM Sge, V1016Cyg, RR Tel, and high-resolution maps show shell-like geometries on the sub-arc second scale[5,6]. In contrast, our high-resolution maps of CH Cyg reveal a jet-like feature. Moreover, the 'jet' is clearly expanding at a high velocity. This effect is shown in Fig. 3, where we present maps of CH Cyg at $\lambda = 2$ cm obtained at two epochs with the highest resolution configuration of the VLA. The Smithsonian Astrophysical Observatory catalogue position of CH Cyg, with 1 σ error bars, is shown by the cross on each map. The first map from 8 November 1984 shows two radio components (labelled A and C) with roughly equal flux density separated by 0.18 arc s. On 22 January 1985, 75 days later, the source exhibits an additional component (B), and the separation of A and C appears to have increased to 0.4 arc s. The position of the midpoint between A and C on the two dates agrees to within 0.02 arc s, which is the same to within the accuracy of the measurements and implies that the jet feature is a bipolar phenomenon originating from a point near the position of component B. Extrapolating the rate of expansion backwards in time indicates that components A and C were produced between 22 July and 7 September 1984. This agrees well with the time of onset of radio outburst shown in Fig. 1, and is about 5 months after our first observation in April 1984. This earlier detection might thus be interpreted as a quiescent level of emission or an earlier, weak outburst.

The position, flux density and angular extent of each component in Fig. 2, based on elliptical gaussian fits, are listed in Table 1. From the flux densities and angular sizes, the brightness temperature at 14.9 GHz is about the same for each component and equal to 7×10^3 K, consistent with the equilibrium temperature of a photoionized gas cooled primarily by forbidden line emission. The optical depth of a fully ionized gas at radio wavelengths is given by

$$\tau(\nu)=2.7\times10^{-20}\,\nu^{-2.1}\,T_e^{-1.35}\int_0^w n_e^2\,\mathrm{d}l$$

where ν is the radiation frequency (GHz), T_e and n_e are the electron temperature (K) and density (cm^{-3}), w is, in this case, the width of the jet (cm) and l is the path link. Estimates of the distance to CH Cyg range from less than 200 to 600 pc. Adopting an intermediate value of 400 pc, the typical component width of 0.06 arc s on 22 January, corresponds to $w=3\times10^{15}$ cm. Because the jet is partially optically thick up to 22 GHz, under the assumption of cylindrical symmetry, we can place a lower limit of $2\times10^6\,\mathrm{cm}^{-3}$ on the r.m.s. electron density, yielding masses $M_A > 6\times10^{-7}\,M_\odot$, $M_B > 1.3\times10^{-6}\,M_\odot$ and $M_C > 5\times10^{-7}\,M_\odot$. For distance $D=400$ pc the rate of elongation of the jet corresponds to a projected velocity of 2,100 km s^{-1}. The bipolar expansion velocity is thus $V_e = 1{,}050/\sin i$ km s^{-1}, where i is the inclination of the jet axis to the line-of-sight.

Table 1 CH Cyg jet components

	RA(1950)	Dec.(1950)	S(14.9 GHz) (mJy)	a_{maj} (arc ms)	a_{min} (arc ms)	PA (°)
8 November 1984						
A	19 23 14.121	50 08 30.79	4.2±0.3	71±7	55±8	115±10
C	14.133	30.65	5.1±0.3	75±5	30±9	175±15
22 January 1985						
A	14.111	30.88	6.2±0.16	94±2	74±3	95±7
B	14.123	30.76	12.2±0.18	196±2	66±4	141±1
C	14.139	30.59	7.4±0.17	146±2	52±4	149±1

Figure 4 shows the visual light curve of CH Cyg observed by the American Association of Variable Star Observers (AAVSO) from April 1981 to May 1985. Beginning about 1977 the star had been in an optically active state, reaching a peak visual magnitude of about 5.8. This is the highest brightness level observed since monitoring began in 1935. However, the start of the radio outburst coincides with a remarkable decline of 1.5 mag in the visual brightness to the pre-1977 level. This decline of July 1984 was also noted by Tomov[7], who attributed it to a decrease in the blue continuum source based on the fact that the TiO molecular bands of the red giant, which are almost completely filled in by the continuum in earlier spectra, are clearly visible in August and September. He also notes that the Balmer emission had become very wide, expanding to ~2,500 km s^{-1} in Hβ. Selvelli and Hack[8] also observed a large increase in the Balmer line widths between July and November 1984. They report a full width of 3,950 km s^{-1} for Lyα in November 1984 and January 1985.

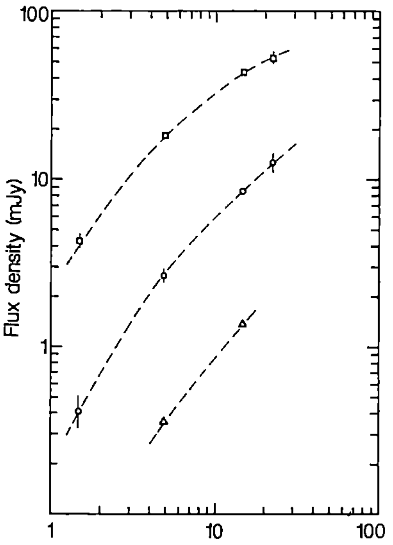

Fig. 2 Radio continuum spectra of CH Cyg at three epochs: □, 3 May 1985; ○, 8 November 1984; △, 6 April 1984.

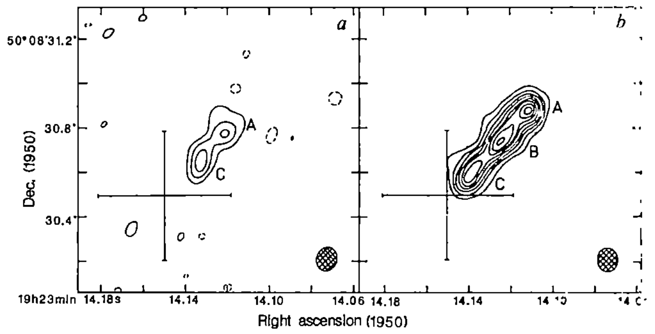

Fig. 3 VLA radio maps at $\lambda=2$ cm separated by 75 days (*a*, 8 November 1984; *b*, 22 January 1985) showing the evolution of the jet. The half-power ellipse of the synthesized beam is indicated at lower right.

We have considered two possible explanations for the expanding jet feature: (1) the propagation of an ionization front from a highly directional source of ionizing photons; and (2) the outward motion of ionized material along an axis defined by the central power source. The sudden turn on of a hot source that emits L_{ph} ionizing photons per second will produce an ionization front propagating outward at a velocity roughly given by $v=L_{ph}/4\pi r^2 n_H$, where n_H is the constant number density of hydrogen atoms. Taking $n_H=2\times10^6\,\mathrm{cm}^{-3}$ and L_{ph} sufficient to ionize material to an angular distance of 0.2 arc s yields $v\simeq$ 2,000 km s^{-1} for $D=400$ pc. A model of this type can thus account for the observed expansion rate. It seems, however, unlikely that a rapidly propagating front should be produced at a time when the optical luminosity is decreasing; although it is possible that most of the flux has shifted to the ultraviolet, as is observed during the optical decay of novae. Another difficulty is that, in the case of a propagating front, one expects the structure of material behind the ionization front to remain roughly constant. Such a model is therefore difficult to reconcile, in a straightforward manner, with the appearance, at a later date, of a third component interior to the front. If the material of component B were present on 8 November, it should have been visible.

The radio data thus favour a material flow model. Such an interpretation is further strongly supported by the appearance of high-velocity Balmer emission at the time of the onset of the optical decline and radio outburst. If the radio jet represents outflowing material, a lower limit on the rate of mass ejection is provided by the fact that component B is absent on 8 November. The mass M_B must have been ejected over an interval of <75 days, yielding a mass ejection rate $\dot{M}_e > 7\times10^{-6}\,M_\odot\,\mathrm{yr}^{-1}$ for $V_e > 1{,}050$ km s^{-1}. The energy flow involved in the mass loss

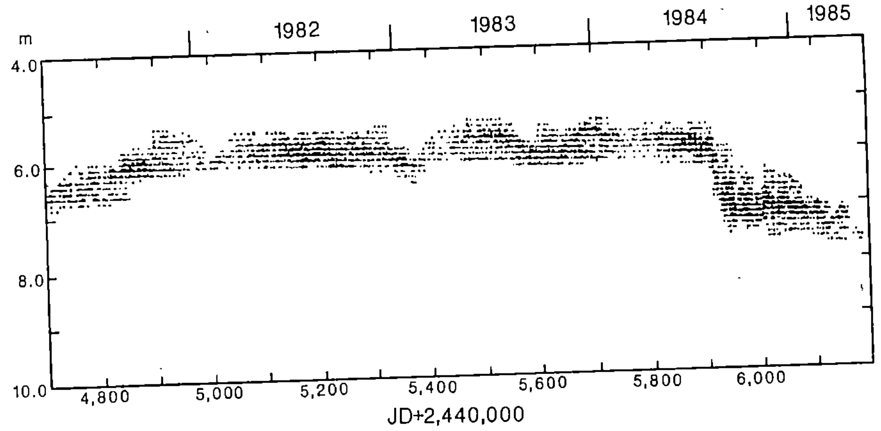

Fig. 4 The AAVSO visual light curve of CH Cyg from April 1981 to May 1985. Each dot represents one observation.

is $>3\times10^{36}$ erg s^{-1}, and the total kinetic energy of the bulk motion is $\geqslant10^{43}$ erg. The energetics of the mass flow is thus similar to that observed in nova shells, and points to an origin in an event having total luminosity of the order of at least 10^{37} erg s^{-1}. Luud *et al.*[9] pointed out that the integrated ultraviolet flux measured in September 1981 yields a luminosity of $\sim10^{38}$ erg s^{-1}. The total radiative luminosity at maximum light is thus sufficient to power the outflow.

It has been suggested previously that the CH Cyg system contains an accretion disk[10,11]. Most notably, Slovak and Africano[10] have observed optical continuum flickering on a timescale of a few minutes. Such flickering is common among cataclysmic variables, where it is attributed to a hotspot on an accretion disk around a white dwarf. In the case of CH Cyg, the timescale of the flickering implies an upper limit of $\sim10^{10}$ cm in the radius of the accreting object. We are therefore led to the suggestion that the energy required for the creation of the jet feature is produced by accretion onto the surface of a compact object. For a $1 M_\odot$ object with radius R the critical rate at which the accretion-generated luminosity exceeds the Eddington limit is given by

$$\dot{M}_{\rm cr}\simeq10^{-3}\left(\frac{R}{R_\odot}\right)\qquad M_\odot\,{\rm yr}^{-1}$$

For $R<10^{10}$ cm, $\dot{M}_{\rm cr}\leqslant10^{-4}\,M_\odot\,{\rm yr}^{-1}$, and for a white dwarf $\dot{M}_{\rm cr}\simeq10^{-5}\,M_\odot\,{\rm yr}^{-1}$. These accretion rates are comparable to the mass loss rate in the jet. Since during an accretion driven outburst $\dot{M}_{\rm e}$ will be less than or, at most, equal to the rate of accretion, $\dot{M}_{\rm acc}$, onto the central object, we infer that for the event leading to the CH Cyg jet $\dot{M}_{\rm acc}\geqslant\dot{M}_{\rm cr}$. From the calculations of Shakura and Sunyaev[12], accretion through a disk at a rate close to, or exceeding, the Eddington limit can produce a radiation-driven outflow of matter along the angular momentum axis of the disk. Bath[13] has modelled such an outflow and finds that outflow velocities of a few thousand km s^{-1} can be obtained from supercritical accretion onto a white dwarf, and expected mass ejection rates are $<0.5\,\dot{M}_{\rm cr}$, in excellent agreement with the observations. The ultraviolet luminosity before the radio outburst suggests that the accretion rate has been near, or at, supercritical since 1981.

The formation of a massive disk and accretion rates of the order $10^{-5}\,M_\odot\,{\rm yr}^{-1}$ imply that mass transfer occurs through Roche lobe overflow from the red giant. Accretion rates from the red giant wind alone will be much too small, typically $10^{-8}\,M_\odot\,{\rm yr}^{-1}$ or less. A number of periods, both spectroscopic and photometric, have been reported for CH Cyg, ranging from about a month to many years. The fact that since 1977 CH Cyg seems to spend most of the time in an optically active state, that the luminosity has been near supercritical since at least 1981 and that flickering has been observed at many epochs, indicates that a high accretion rate persists for a large fraction of the orbital period. For a radius of the M7III primary of $R_*=200\,R_\odot$ (ref. 14), a maximum orbital separation of about $2R_*$ (for high mass transfer rate through the inner lagrangian point) would require an orbital period of $\leqslant3$ yr.

An object with radius typical of a white dwarf and luminosity $L\sim10^{38}$ erg s^{-1} will have a surface temperature $T=10^5$–10^6 K, and might be detectable as an X-ray source. In this regard, it is noteworthy that CH Cyg lies near the centre of the error box of the HEAO A-2 hard X-ray source H1926+503 (ref. 15). If the X-ray flux is associated with CH Cyg, the luminosity, measured in November 1977 when the source was entering the optically active state, is $\sim10^{33}$ erg s^{-1}, consistent with optically thick accretion through a disk onto a white dwarf at a rate $\geqslant10^{-7}\,M_\odot\,{\rm yr}^{-1}$ (ref. 16). X-ray observations of CH Cyg during the outburst will be very important.

The radio outburst from CH Cyg is an unusual and complex event, and, while we have presented a preliminary picture to account for the phenomenon, some problems remain. Although the observational evidence strongly supports a material flow model, a propagating ionization front cannot be ruled out. In either case, it is difficult to reconcile the optical decline with either the radiation required for the ionization or the energy for the mass flow. Further observations are clearly needed. A measurement of the ultraviolet luminosity will be particularly valuable. The spectral evolution during the decay of the radi outbursts will also provide important clues. The radio deca should be accompanied by a flattening of the radio spectra index as the material expands and becomes optically thin.

The only other symbiotic star known to exhibit a jet-lik feature is R Aqr[17]. This feature, which appeared some tim between 1970 and 1977, was first detected optically as a emission spike[18,19]. An ejection model for this source[20] has bee questioned because no proper motion of the components ha been observed[21]. Spergel *et al.*[22] have suggested instead that th appearance of the 'R Aqr jet' was the result of sudden photoio ization of condensations in the red giant wind. More recentl Solf and Ulrich[23] have successfully modelled the kinematics the nebulosity about R Aqr in terms of two episodes of bipol shell ejection 185 and 640 yr ago, with total shell mass $\sim10^{-5}\,M_\odot$ and expansion velocity of the order of 100 km s^{-} The CH Cyg outburst provides the first opportunity to obser an event giving rise to a radio jet from a symbiotic star. It w be important to follow the evolution of the CH Cyg jet at rad and other wavelengths, both to clarify the nature of the outbu and jet formation and to study the kinematics of the jet co ponents at large radii.

This research was partially supported by a postdoctoral f lowship (to A.R.T.) and a grant (to E.R.S.) from the Natu Sciences and Engineering Research Council of Canada. J.A. acknowledges the support of National Science Foundati grant no. AST 7910S76. The National Radio Astrono Observatory is operated by Associated Universities Inc., un contract from the NSF.

Received 12 September; accepted 7 October 1985.

1. Deutsch, A. J., Lowen, L., Morris, S. C. & Wallerstein, G. *Publ. astr. Soc. Pacif.* **86**, 233-236 (1974).
2. Faraggiana, R. & Hack, M. *Astr. Astrophys.* **15**, 55-76 (1971).
3. Hack, M. & Selvelli, P. L. *IAU Colloq.* No. 70, 131-136 (1982).
4. Seaquist, E. R., Taylor, A. R. & Button, S. *Astrophys. J.* **284**, 202-210 (1984).
5. Kwok, S., Bignell, R. C. & Purton, C. R. *Astrophys. J.* **279**, 188-196 (1984).
6. Newell, R. T. thesis, New Mexico Inst. Mining and Technology (1981).
7. Tomov, T. *Imform. Bul. Variable Stars, IAU Commun.* **27**, No. 2610 (1984).
8. Selvelli, P. L. & Hack, M. *Astr. Express.* **1**, 115-126 (1985).
9. Luud, L., Tomov, T., Vennik, J. & Panov, K. *Soviet Astr. Lett.* **8**, 257-260 (1982).
10. Slovak, M. H. & Africano, J. *Mon. Not. R. astr. Soc.* **185**, 591-606 (1978).
11. Anderson, C. M., Oliverson, N. A. & Nordsieck, K. H. *Astrophys. J.* **242**, 188-194 (1980).
12. Shakura, N. I. & Sunyaev, R. A. *Astr. Astrophys.* **24**, 337-355 (1973).
13. Bath, G. T. *Mon. Not. R. astr. Soc.* **178**, 203-217 (1977).
14. Wilson, L. A. in *Physical Processes in Red Giants* (eds Iben, I. & Renzini, A.) 225-229 (Reidel, Dordrecht, 1981).
15. Marshall, F. E. *et al. Astrophys. J. Suppl.* **40**, 657-665 (1979).
16. Patterson, J. & Raymond, J. C. *Astrophys. J.* **292**, 535-549 (1985).
17. Sopka, R. J., Herbig, G., Kafatos, M. & Michalitsianos, A. G. *Astrophys. J. Lett.* **258**, L35-L39 (1982).
18. Herbig, G. H. *IAU Circ.* No. 3535 (1980).
19. Wallerstein, G. & Greenstin, J. L. *Publications of the Astronomical Soc. of the Pacific,* Vol. 92, 275-283 (1980).
20. Kafatos, M. & Michalitsianos, A. G. *Nature* **298**, 540-542 (1982).
21. Mauron, N., Nieto, J. L., Picat, J. P., Lelievre, G. & Sol, H. *Astr. Astrophys. Lett.* **142**, L13-L15 (1985).
22. Spergel, D. N., Giuliani, J. L. & Knapp, G. R. *Astrophys. J.* **275**, 330-341 (1983).
23. Solf, J. & Ulrich, H. *Astr. Astrophys.* **148**, 274-288 (1985).

Mechanism of stable jet formation in electrohydrodynamic atomization

I. Hayati*, A. I. Bailey* & Th. F. Tadros†‡

* Department of Chemical Engineering and Chemical Technology,
Imperial College of Science and Technology, Prince Consort Road,
London SW7 2BY, UK
† ICI plc, Plant Protection Division, Jealotts Hill Research Station,
Bracknell, Berkshire RG12 6EY, UK

The disruption of a liquid into a spray of charged droplets, when subjected to an intense electric field, has attracted considerable interest from both a fundamental and applied point of view. On the applied side, the process has been used in paint spraying, electrostatic printing, electrostatic emulsification, fuel atomization in combustion systems and in space vehicle propulsion systems. More recently, the phenomenon has found potential application in crop spraying because of the low energies required, the ability to produce fine sprays within a narrow size distribution and the preferential deposition on the target surfaces. Despite its wide range of applications, the mechanism of liquid disruption is only poorly understood. At a critical potential, the so-called Taylor[1] cone develops, with a fine stable jet issuing from its tip. The formation of such cones and jets is essential for the production of an electrohydrodynamic spray. Most previous work aimed at understanding jet formation has been based on high-speed photographic techniques. We have made direct observations of jet formation and our results, presented here, demonstrate the role of electrical shear effects in this process, and invalidate those theories that assume a uniform velocity profile[2] for the liquid in the conical base of the jet.

If a large potential (up to ~15 kV) is gradually applied to a capillary through which a semiconducting liquid is flowing slowly, the size of the emergent drop decreases while the dripping rate increases. At a certain potential the drop at the end of the capillary ejects a small drop or a long filament. This filament breaks off and the meniscus of the drop relaxes back to its initial shape in a pulsating fashion, the rate of which increases with an increase of potential. At a critical potential, depending on the conductivity of the liquid, the main drop develops into a cone—the Taylor[1] cone—with a fine stable jet issuing from its tip; this is a prerequisite for the production of an electrohydrodynamic spray, which consists of a symmetrical assembly of such jets around the capillary or nozzle. Despite the importance of stable jets, their mechanism of formation remains unclear. It is known, for example, that not all liquids form such stable jets and that effective atomization can only be achieved if the conductivity of the liquid is within the limits 10^{-6}-$10^{-8}\ \Omega^{-1}\ \mathrm{m}^{-1}$ (that is, a semiconducting liquid). In previous work aimed at understanding jet formation, theoretical treatments assumed a uniform velocity profile within the Taylor cone and certain authors[1,3] regarded the cone as an equipotential surface. Here we decided to study the movement of the liquid as it emerges from the capillary and forms the Taylor cone.

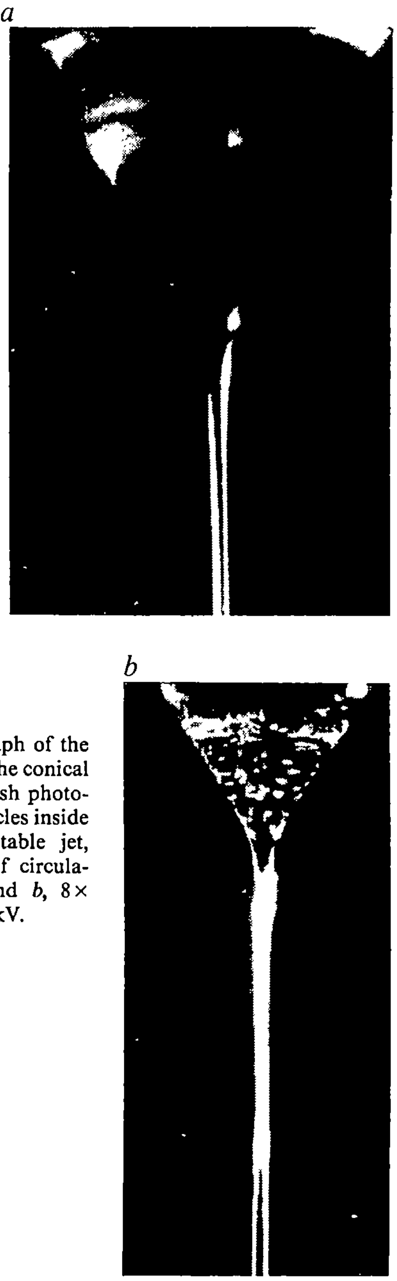

Fig. 1 *a*, Streak photograph of the circulation pattern within the conical base of a stable jet. *b*, Flash photograph of lycopodium particles inside the conical base of a stable jet, indicating the direction of circulation. Flow rate for *a* and *b*, $8\times10^{-9}\ \mathrm{m}^3\ \mathrm{s}^{-1}$ at 10.5 kV.

To observe the movement of the liquid at the base of the jet, we chose a relatively large capillary, of 1-2 mm diameter, so that the dimensions of the cone were not too small, and tracer particles, lycopodium powder, were added to the liquid. The region of interest was observed and simultaneously photographed at a magnification of about ×30 using a microscope. The experimental set-up consisted of a metal capillary, to which

---

‡ To whom correspondence should be addressed.

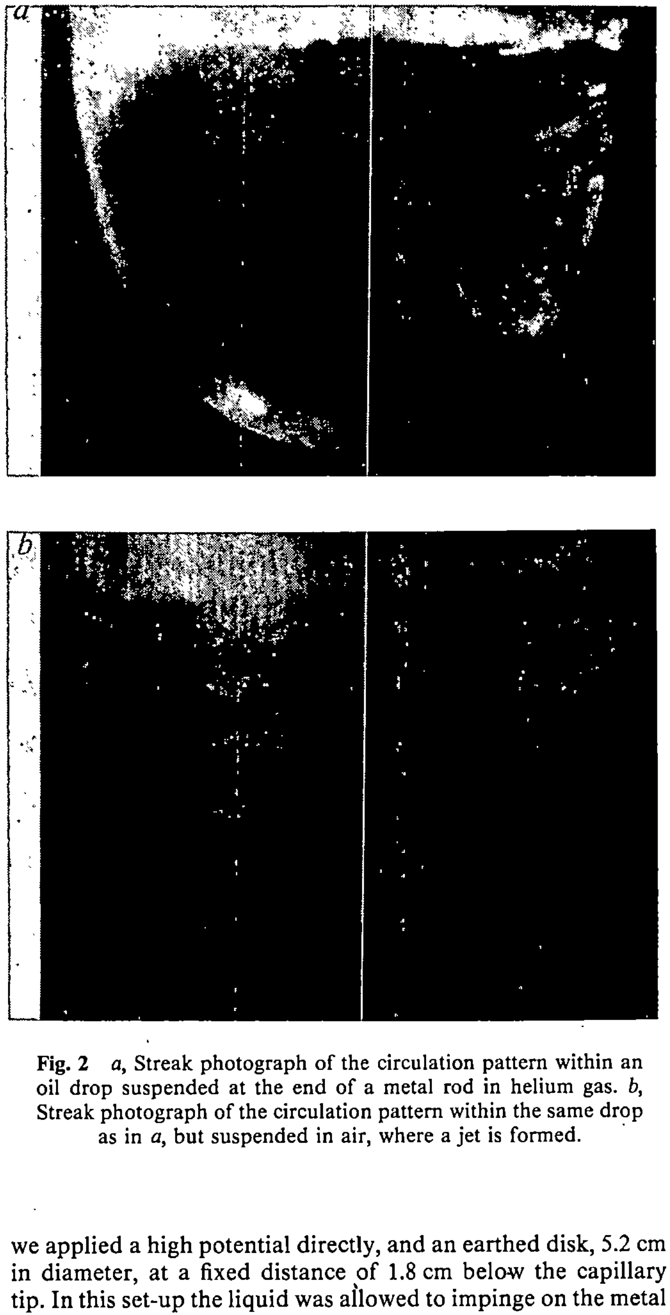

Fig. 2 *a*, Streak photograph of the circulation pattern within an oil drop suspended at the end of a metal rod in helium gas. *b*, Streak photograph of the circulation pattern within the same drop as in *a*, but suspended in air, where a jet is formed.

we applied a high potential directly, and an earthed disk, 5.2 cm in diameter, at a fixed distance of 1.8 cm below the capillary tip. In this set-up the liquid was allowed to impinge on the metal disk. The liquid used was an isoparaffin oil, Isopar M, to which we added *n*-butanol to bring the conductivity within the required limits (see above). The rate of flow of the liquid (8×10^{-11} to 88×10^{-8} m^3 s^{-1}) was controlled using a perfusor pump. The jets were illuminated with white light and photographed using a camera.

As the potential was applied and a stable jet was formed, we observed a very clear axisymmetric circulation of the particles in the conical base of the jet. Good streak photographs of this motion were difficult to obtain, but Fig. 1*a* shows this circulation pattern, produced at a flow rate of 8×10^{-9} m^3 s^{-1} (10.5 kV). The direction of motion, which could be identified easily by looking through the microscope, is of great interest. The particles were seen to come down the surface of the cone and reverse upwards along its axis; this was confirmed by taking photographs using a flash light. The light generated by the flash fades after it is triggered so that a moving particle will develop a faint streak in the direction of its motion. Such a photograph is shown in Fig. 1*b*; particles near the axis of the cone have a faint streak pointing upwards. This result is of great significance because it indicates that there is a backflow at the centre whereas the velocity is greatest at the surface of the liquid. This represents almost the opposite of the velocity distribution for laminar flow in a tube, where the velocity is zero at the wall of the tube and maximum at the centre. This direct observation of circulatory flow invalidates those theories which assume a uniform velocity profile[2] for the liquid in the Taylor cone.

The origin of this circulation may be understood by reference to a review by Melcher and Taylor[4] on electrohydrodynamic shear stresses; they pointed out that for an interface to be subjected to a shear stress, the surface must simultaneously support surface charge and be subjected to a tangential electric field. These two conditions are both satisfied in the present system. The electric field within the liquid will drive free charges to the surface of the cone, hence the surface is charged and is subjected to a normal electric field, E_n. Because of the semiconducting nature of the liquid, a potential difference will exist between the base of the cone at the end of the capillary and the tip of the cone. This potential difference ensures that the interface is subjected to a tangential electric field, E_t, in the direction of flow, and hence an electric shear stress on the surface of the cone

$$\tau_t = \varepsilon_0 E_n E_t$$

where ε_0 is the permittivity of free space. This shear stress causes the axisymmetric convection currents within the Taylor cone that are reported here for the first time.

The velocity profile within the cone was analysed by solving analytically the equations of motion for creeping flow in axisymmetric spherical coordinates. The solution of these equations will be given elsewhere[5]. It is sufficient to mention here that the calculated velocity profiles are consistent with those shown in Fig. 1. Such convection currents were not detected within a water cone, because the high conductivity of water ensures that the cone is almost an equipotential surface. Although the surface is charged it is not subjected to a tangential electric field and shear stress.

Another demonstration of the circulatory motion due to electrohydrodynamic shear stresses was provided by observations of pendant drops inside a glass chamber which could be filled with various gases. We observed that the distortion of a drop hanging from a metal rod connected to a high potential depends on the breakdown potential of the gas. If the breakdown potential is lower than that required to cause instability of the liquid, the atmosphere becomes conducting and no stable jet can be formed. Examples of such gases are He and Ne. For these gases, glow discharges were observed in the dark, and with a semiconducting liquid the flow extended from the edges of the rod down to the earthed plate. The drop was enveloped by the electric discharge. The addition of lycopodium powder to the liquid revealed an axisymmetric circulatory motion but in the opposite direction to that observed within the cone of Fig. 1—that is, near the surface the particles moved upwards and near the centre line of the drop they moved downwards. Figure 2*a* shows the circulation within an oil drop surrounded by He gas.

Again this circulation can be explained as being due to electrical shear effects. The surface of the drop supports free charge due to the field applied, which drives the charges from the bulk to the surface. Hence the first condition for shear stresses to occur is satisfied. The discharge at the edge of the rod where it is in contact with the liquid creates a local potential drop near that region. Hence, the potential at the tip of the drop will be higher than at its edges. This potential difference produces a tangential field and hence a tangential stress across the surface of the drop in the upward direction, and creates the convection currents observed within the drop. If the voltage is increased slightly, a stronger discharge is produced and the motion becomes faster, sometimes causing the drop to climb up the metal rod. If the helium input is stopped and air gradually fills the glass chamber, the discharge disappears and the circulation stops. On further increase in the voltage, the drop develops into a Taylor cone and from its tip a thin jet is ejected. As soon as this occurs, a circulation pattern is observed (Fig. 2*b*), the direction of the circulation being the same as that in Fig. 1.

When a pendant drop of a conducting liquid such as water was surrounded by helium, the discharge originated at the surface of the drop itself rather than at the rod, and extended to the earth plate. When tracer particles were introduced into this water drop, no motion of the particles could be observed. Instead, all the particles settled at the bottom of the drop. Again, this result is attributed to the high conductivity of water, which forms an equipotential surface; hence the surface is not subjected to a tangential field.

The above observations clearly demonstrate the role of electrical shear effects in the process of formation of a stable jet. These shear stresses resulting from the electric field within the cone and further down the jet produce a downward longitudinal force which stabilizes the jet by smoothing any perturbations on the surface. As one moves downwards from the cone, the electric field within the jet gradually decreases and so does the shear stress. A point is reached at which the radial force exceeds the shear force, thus causing disruption of the jet into a brush of thin jets which ultimately break into a monodisperse spray; this was confirmed by careful observations of the jet at the point of break-up for semiconducting liquids. With conducting liquids such as water, there is no build-up of electric field within the jet and hence there will be no tangential stress; the jet suffers only the destabilizing effect of the radial stresses and an unstable spray is produced.

The direction of the circular motion within the liquid cone, as demonstrated here, indicates that the jet is formed by the stripping of the drop surface rather than by the pulling of the liquid from the bulk of the drop or the detachment of small droplets from the liquid apex[6]. Thus, it seems that the movement of the thin surface layer of liquid relative to the bulk of the cone under the effect of surface-charge gradients is analogous to the Gibbs–Marangoni effect[7,8] where the movement of a thin liquid film occurs under the effect of surface-pressure gradients.

We thank Mr D. Maw for taking the flash photograph.

Received 1 August; accepted 30 September 1985.

1. Taylor, G. I. *Proc. R. Soc.* **A280,** 383-397 (1964).
2. Horning, D. W. & Hendricks, C. D. *J. appl. Phys.* **50,**(4), 2614-2617 (1979).
3. Bailey, A. G. *Phys. Bull.* **35,** 146-148 (1984)
4. Melcher, J. R. & Taylor, G. I. *A. Rev. Fluid Mech.* **1,** 111-146 (1969).
5. Hayati, I. *J. Fluid Mech.* (submitted).
6. Kozhenkov, V. I. & Fuks, N. A. *Russ. Chem. Rev.* **45,** 1179-1184 (1976).
7. Gibbs, J. W. *Collected Works* Vol. 1, 301 (Dover, New York, 1961).
8. Adamson, A. W. *Physical Chemistry of Surfaces,* 110 (Wiley, New York, 1976).

Fractal characterization of inhomogeneous geophysical measuring networks

S. Lovejoy*, D. Schertzer* & P. Ladoy†

* Physics Department, McGill University, 3600 University Street, Montreal, Quebec, Canada H3A 2TB
† EERM/CLIM, Météorologie Nationale, 2 Ave Rapp, Paris, 75007, France

The measuring stations of most *in situ* geophysical networks are spatially distributed in a highly inhomogeneous manner, being mainly concentrated on continents and population centres. When inhomogeneity occurs over a wide range of scales in a space of dimension E, it can be characterized by a fractal dimension D_m. For measuring networks, there is no reason to assume *a priori* that D_m equals E; it will usually be less than E. The world meteorological network studied here is an example on a surface for which $E=2$ (the surface of the Earth) whereas, the network has an empirical dimension $D_m \simeq 1.75$. Whenever $D_m < E$, any sufficiently sparsely distributed phenomena (with dimension $D_p < E - D_m$, here 0.25), cannot be detected—even if the network is infinite. Because these rare phenomena are the most intense, this insufficient dimensional resolution is associated with biases in geophysical statistics, serious difficulties in interpolating measurements to a uniform grid, and problems in calibrating remotely-sensed information.

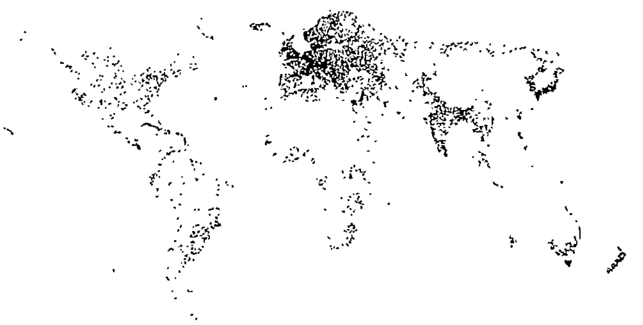

Fig. 1 The locations of the 9,563 stations in the global meteorological measuring network (defined as the stations which the World Meteorological Organisation lists as performing at least one meterological measurement per day), showing their high degree of non-uniformity. Most are clustered on the continents and major industrial areas. The dimension (D_m) is ~1.75.

The intuitive notion of dimension D_m of a set (whether fractal or otherwise) is given by the variation of the number of points ($\langle n(L)\rangle$) with the size of the region (L):

$$\langle n(L)\rangle \propto L^{D_m}$$

When D_m is less than the dimension (E) of the space in which the set is embedded, when L increases, the volume of space available increases as L^E which is faster than the number of points of the set that are available to fill it ($\langle n(L)\rangle$). Hence, larger and larger 'holes' (empty regions) appear and the set is concentrated on a decreasing fraction of the total space. Furthermore, at a given scale, sets with lower D_m are more dominated by holes, and are hence more sparse.

Although there are many ways of estimating the dimension of sets of points, many of which have been developed for studying strange attractors[2–5] they generally yield similar results. The method used here, actually determines a particular dimension called the correlation dimension[6]. To apply this method to a geophysical network (considered here as a set of points), determine, for each station in the network, the number ($n(L)$) of other stations within various radii L of the point, and its average $\langle n(L)\rangle$ over all the stations. We then obtain D_m as the slope of $\log\langle n(L)\rangle$ against $\log L$. Scales over which $\langle n(L)\rangle$ varies non-algebraically, define the characteristic lengths of the network.

To apply this technique to a surface network (such as the highly clustered world meteorological network, Fig. 1), we must discuss a complication that takes into account the curvature of the Earth's surface. If the latter is covered uniformly with stations in a region of area S, then $\langle n(L)\rangle \propto S$. Taking $S(\theta)$ as the area of the spherical cap defined by two points subtending an angle θ at the Earth's centre (radius r) we may define the corresponding scale $L(\theta)$ by:

$$S(\theta) = (\pi/4)L^2(\theta) = 2\pi r^2(1-\cos\theta/2)$$

Note that with this definition of L, for small θ, the formula reduces to the usual great circle distance ($= r\theta$), and we recover $D_m = 2$ when the stations are homogeneously distributed.

Figure 2 shows $\langle n(L)\rangle$ calculated using the above L, for the 9,563 stations in this network separated by at least 0.01° of arc

(~1 km, the accuracy of the data). Avoiding double counting, each station defines 9,562/2 = 4,781 values of L, hence there are 9,563 × 4,781 = 45,720,703 independent values that go into the histogram for estimating $\langle n(L)\rangle$. Figure 2 shows that roughly between the minimum resolvable scale, (~1 km) and ~2,000 km, $\langle n(L)\rangle \propto L^{1.75}$, hence $D_m \sim 1.75$. The size of the scaling regime is limited as the number of points is finite: $\langle n(L)\rangle_{\max} = 4{,}781$ and $\langle n(L)\rangle_{\min} \sim 1/9{,}563 \sim 10^{-4}$. Assuming $L^{1.75}$ between these limits implies $L_{\max} \sim 7{,}500$ km, $L_{\min} \sim 0.3$ km, which shows that the scaling observed in Fig. 2 spans a range nearly as large as is possible. Similar analysis of the French climatological network (3,593) stations yielded $D_m \sim 1.8$, while the Canadian meteorological network (414 stations) yielded $D_m \sim 1.5$.

The fact that $D_m < E$, sets new detectability limits. A network, dimension D_m can detect a phenomenon with dimension D_p, only if the two sets intersect. However, a theorem in geometry shows that this is certain to occur only when $D_p > E - D_m$. Two sets, dimension = D_1, D_2 embedded in a space dimension = E, intersect on a set dimension = $D_\cap$. (With the co-dimension $C = E - D$) according to the following rule:

$$C_\cap = \mathrm{Inf}((C_1 + C_2), E)$$

Example. Intersection in space ($E = 3$) of two planes

$$(D_1 = D_2 = 2 \Rightarrow C_1 = C_2 = 1)$$

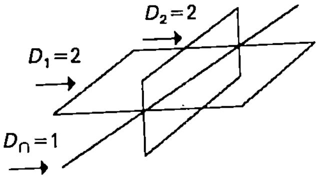

$$C_\cap = C_1 + C_2 = 2 \Rightarrow D_\cap = E - C_I = 1$$

Although the example is for two standard sets (planes) it holds for most fractal sets. Note that if $C_m + C_p > E$, the intersection set probably has dimension zero ($C_\cap = E$), hence, the sets typically miss each other. Hence, in the case studied here, sparse surface phenomena with $D_p < 2 - 1.75 = 0.25$, cannot be detected. In analogy with the network's spatial resolution, which is the minimum detectable scale, we may define, its dimensional resolution as $E - D_m$ which is the minimum resolvable dimension.

The inability to detect sparse phenomena is serious because, in general, we expect geophysical fields to be characterized by multiple fractal dimensions[6-9]. In turbulence, fields are generally characterized by multiple fractal dimensions[10-13]. In geophysics, there is empirical evidence for multidimensionality in the rainfield[14,15]. If a field is multidimensional, then regions exceeding a threshold T define fractal sets with dimension $D_p(T)$ decreasing with T. Thus, whenever averages are taken over sets with $D_m < E$, then, by the intersection theorem, the most intense fractals (with $D_p(T) < E - D_m$) are missed. While both mono- and multidimensional fields have statistical properties that are functions of scale, multidimensional fields are in addition dependent on the dimension (for example, line, plane, volume or fractal set) over which they are averaged.

We have argued that the characterization of network inhomogeneity by the fractal dimension (D_m) raises new problems concerning the detectability of sparse phenomena. Since phenomena (of any size) with $D_p < E - D_m$ will not intersect the network, we have obtained a new criterion for evaluating measuring networks: to detect phenomena, not only must a network have sufficient spatial resolution it must also have sufficient dimensional resolution. In general, we expect the fractal dimension of geophysical fields to be a decreasing function of intensity: thus, any lack of dimensional resolution leads to biases in the spatial averages. Finally, as information on the lowest dimensional fractals is lost, similar biases will arise when measurements are interpolated to uniform grids with dimension E.

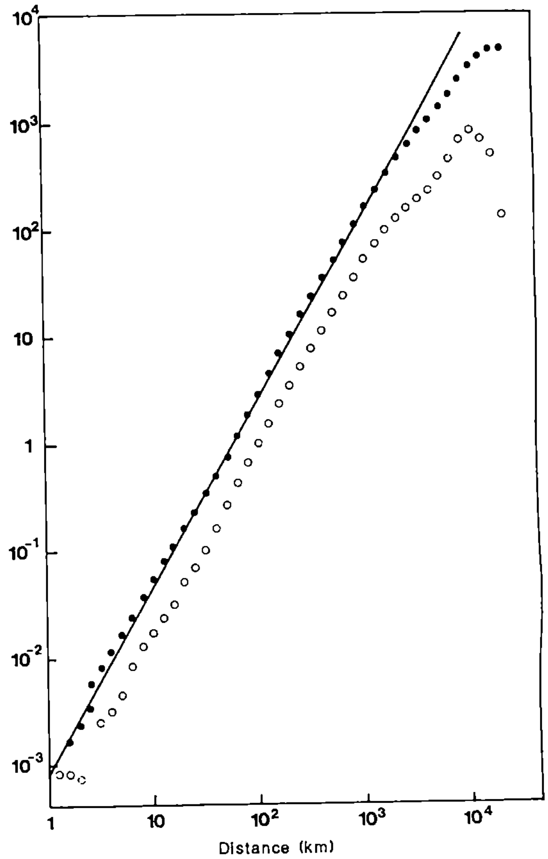

Fig. 2 ○, The average number of stations within annuli of geometrically increasing radii; ● (the integral of the previous function), the function $\langle n(L)\rangle$ described in the text. Over the scaling regime, both should be parallel and straight: the $L^{1.75}$ function is shown for reference. The scaling regime apparently continues down to scales comparable with the accuracy of the geographical locations used to determine L(~1 km) which is, therefore, the spatial resolution of the network. For comparison, the standard analysis method (which assumes $D_m = 2$, a surface area of ~10^8 km^2, and 10^4 stations), attributes an average area of $10^8/10^4 = 10^4$ km^2 per station hence a spatial resolution of ~10^2 km^2 which is about 100 times larger than its true resolution.

We thank B. Luneau for help in preparing Fig. 1. We acknowledge the CNRS (France), ATP (RA) for partial financial support.

Received 2 June; accepted 21 October 1985.

1. Mandelbrot, B. *The Fractal Geometry of Nature.* (Freeman, San Francisco).
2. Roux, J. C., Simoy, R. H. & Swinney, H. L. *Physica* **8D**, 257-266 (1983).
3. Grassberger, P. & Procaccia, I. *Phys. Rev. Lett.* **50**, 346-349 (1983).
4. Grassberger, P. & Procaccia, I. *Physica* **9D**, 189-208 (1983).
5. Nicolis, C. & Nicolis, G. *Nature* **311**, 529-532 (1984).
6. Hentschel, H. G. E. & Procaccia, I. *Physica*, **8D**, 435-444 (1983).
7. Grassberger, P. *Phys. Lett.* **97**, 227-230 (1983).
8. Schertzer, D. & Lovejoy, S. *Symp. on Turbulence and Chaotic Phenomena in Fluids*, 141-144 (*IUTAM*, Kyoto, Japan, 1983).
9. Mandelbrot, B. *J. Stat. Phys.* **34**, 895-930 (1984).
10. Parisi, O. & Frisch, O. *Turbulence and predictability in geophysical fluid dynamics and climate dynamics* (eds. Ghil, M. *et al.*) 84-88 (International School of Physics, Enrico Fermi, Varenna, Italy, 1985).
11. Shertzer, D. & Lovejoy, S. *Turbulent Shear Flow*, Vol. 4 (ed. Launder, B.) 7-33 (Springer, New York, 1985).
12. Schertzer, D. & Lovejoy, S. *PCH J.* (in the press).
13. Lovejoy, S., Schertzer, D. *AMS Bull.* (in the press).
14. Lovejoy, S. & Schertzer, D. *Digital Image Processing in Remote Sensing*, Ch. 14 (ed. Muller, P. J.) (Taylor and Francis, London, 1985).
15. Tsonis, A. A. Preprint (Univ. Wisconsin).

Archaean magmatic sulphate

Keiko Hattori*† & Eion M. Cameron*†‡

* Department of Geology, University of Ottawa, Ontario, Canada K1N 6N5
† Derry Laboratory for Sedimentary Geochemistry and Ore Deposits, Ottawa-Carleton Centre for Geoscience Studies, Ottawa, Ontario, Canada K1N 6N5
‡ Geological Survey of Canada, Ottawa, Ontario, Canada K1A 0E8

The absence of redbeds, the occurrence of readily oxidizable minerals in placers, and the rarity of sulphate minerals are some features which suggest generally reduced conditions on the Earth's surface during Archaean time[1]. Supporting this conjecture are $\delta^{34}S$ values near 0‰ for sulphides of sedimentary rocks[2–4] and massive sulphide deposits[5], since isotopic fractionation requires oxidation–reduction reactions. The flux of oxidized species during the Archaean produced by fixation of organic carbon was, however, comparable with modern levels[6], but was largely consumed by reactions with a large supply of reduced mantle material[4,7]. Notable occurrences of Archaean sulphate are ~3,400-Myr stratiform barites in Australia[8,9], South Africa[10] and India[11], with $\delta^{34}S$ ~+4‰ (refs 8–10) which are believed to have formed by bacterial oxidation of primary (0‰) sulphide[10]. Consideration of the Archaean sulphur cycle has focused on sulphate of this origin. We draw attention here to sulphate of different isotopic composition, +8 to +14‰, of magmatic origin, that contributed to the total flux of oxidized species during the Archaean.

Occurrences of sulphate minerals in Archaean terrane (Table 1) have been divided into vein and stratiform types. These are mainly barite or anhydrite. Where gypsum is found, it appears to have formed by hydration of primary anhydrite at low temperatures. It is important to establish first that these sulphates are of Archaean age and were not introduced by later processes. We have used Sr isotope determinations for this purpose. As both barite and anhydrite generally contain >1,000 p.p.m. (parts per 10^6) Sr and negligible Rb, measured and initial $^{87}Sr/^{86}Sr$ ratios are the same. Most samples are of late Archaean age (2,800–2,600 Myr) and have ratios in the range 0.7013–0.7021 (Table 1). This is comparable with initial ratios of magmatic rocks of this age, for example, 0.7014 to 0.7018 for mafic volcanic rocks from the Abitibi belt, Canada[12] and 0.7013 for mafic volcanic rocks from Kambalda, Australia[13]. Values for felsic intrusives are in a similar range[14,15] except for higher ratios for intrusives derived by partial melting of pre-existing rock[16].

The low $^{87}Sr/^{86}Sr$ ratios of sulphate minerals are taken to indicate that these sulphate minerals formed during volcanism or during the following plutonism and metamorphism of the belts. Because of the secular increase in the Sr isotopic composition of ocean water[17] and igneous rocks[14], their formation at a later time, that is, in the Proterozoic, from either of these sources, would produce higher $^{87}Sr/^{86}Sr$ ratios. Furthermore, solutions passing through Archaean rocks at a later time may gain ^{87}Sr produced by decay of ^{87}Rb. Based on their Sr isotope values, we have eliminated some occurrences within Archaean rocks, for example, barite veins in volcanic rocks in the Thunder Bay district with values >0.710 (ref. 18) and barite veins in the Timmins–Matachewan area with ratios of 0.7030 to 0.7050 (ref. 18). In both cases, some of the veins of similar occurrences in the areas cut Proterozoic rocks, confirming their post-Archaean origin.

Most of the vein occurrences referenced in Table 1 are associated with gold mineralization. The time relationship of the sulphate veins with gold mineralization varies from pre-gold and penecontemporaneous with the host intrusive (McIntyre Mine[19]); contemporaneous with the gold mineralization (Golden Mile, Kalgoorlie (J. M. F. Clout and E.M.C., unpublished data), Lac Shortt[20]); to post-gold (Lake Shore and Macassa Mines[21]). At Lake Shore and Macassa in Kirkland Lake the sulphates occur in shear zones. Since mineralization and igneous activity took place during the Archaean, the associated sulphate also probably formed at this time. The continuous movement of the shear zones during the late Archaean and Proterozoic may explain their high $^{87}Sr/^{86}Sr$ ratios (Table 1), by incorporation of radiogenic Sr.

Reported occurrences of stratiform barite have been from older (≥3,000 Myr) Archaean rocks. Until recently there was no known occurrence in Archaean strata of North America, which are mostly 3,000–2,670 Myr (ref. 22). Elsewhere, the only barites that may be stratiform and late Archaean are in the Bulawayan Group of Zimbabwe, but their genesis and age are uncertain[23]. In 1981, the large Hemlo gold deposit, near Marathon, Ontario, was discovered. The tabular ore bodies appear to be stratiform near the facies contact between volcaniclastic and epiclastic sedimentary rocks. The main ore zone and footwall rocks contain massive barite layers and lenses up to 10 m in thickness[24]. More recently, massive barite bands, which are discontinuous but on strike >6 km within a metasedimentary sequence, have been found 21–26 km west from the Hemlo mineralization[25].

Whereas $\delta^{34}S$ values for the Barberton and North Pole barites are ~+4‰, most of the other sulphate minerals are in a range of +7 to +14‰. This is too large to be explained by simple oxidation of primary magmatic sulphide. Sulphates of this composition could only have formed by two processes: ^{34}S-enrichment of biologically-produced sulphate of ~4‰ by its partial reduction to ^{34}S-depleted sulphide; or formation by magmatic or magmatic–hydrothermal processes with $\delta^{34}S$ values being determined by inorganic isotopic exchange reactions at high temperature.

Sulphate in igneous rocks is formed by two processes: oxidation of primary sulphide in silicate magma (magmatic sulphate) and hydrolysis of SO_2 gas in aqueous fluids (magmatic–hydrothermal sulphate). The solubility of sulphur in silicate melts depends on oxygen fugacity (f_{O_2}) as well as temperature and pressure[26], and the contents usually range from ~800 to ~1,100 p.p.m. in mafic volcanic rocks[27–29]. Felsic magmas may have contained more[30], although they tend to lose most of the sulphur during intrusion and solidification. Most of this sulphur is present as sulphide and sulphate with the relative proportions controlled by f_{O_2} (ref. 26). The f_{O_2} is determined by the mineral assemblages[26,28], principally the Fe^{3+}/Fe^{2+} ratios, as the amount of iron is far larger than that of sulphur. Overall reaction for the oxidation of sulphur in silicate magma is expressed as[28]

$$S^{2-}(\text{melt}) + 4H_2O = SO_4^{2-}(\text{melt}) + H_2 \tag{1}$$

Evidence for this process is a correlation between the water and sulphate contents in basaltic glass[28] and an increase in δD values of water in pillowed basalt due to degassing of low δD gas, such as CH_4 and/or H_2 (ref. 31). Selective degassing of H_2 from magma causes reaction (1) to move to the right, oxidizing the magma[28]. Such magmatic sulphate comprises 15–36% of the total sulphur[28,29]. The magmatic sulphate is retained in the glass phase on solidification.

In a more open system, such as subaerial extrusives, much of the sulphur is lost as gas, SO_2 (refs 29, 32), reducing the magmatic sulphate content in the remaining silicate melt, often to <30 p.p.m., and f_{O_2}. The escaping SO_2 gas from magma is eventually hydrated to SO_4 in the atmosphere by the following reactions, even in low p_{O_2} (partial pressure of O_2) conditions:

$$SO_2 + H_2O + 1/2\,O_2 = H_2SO_4 \tag{2}$$

SO_2 gas dissolved in an aqueous fluid in igneous rocks at high temperatures will hydrolyse to form sulphate in the magmatic-hydrothermal system[33]:

$$SO_2(\text{gas}) + 2H_2O = H_2SO_4 + H_2(\text{gas}) \tag{3}$$

Table 1 Sulphate minerals in Archaean greenstone belts

Locality	Mineral*	Age†	Occurrence‡	Mineralization§	^{87}Sr/^{86}Sr‖	$\delta^{34}S_{CD}$‰
Massive stratiform						
Barberton, South Africa	BR	~3.4	Some are replacement of GY[46]		0.7009 to 0.7017 ($N=8$)[10]	av. +3.4±0.3 ($N=7$)[10] av. +3.8±0.4 ($N=11$)[9]
North Pole, Western Australia	BR	~3.4	Some are replacement of GY[9]		0.7004 ($N=2$)[8]	+3.6 to +4.9 ($N=6$)[8] av. +3.6±0.5 ($N=32$)[9]
Big Stubby, Western Australia	BR	~3.4	In felsic volcanics[52]	Cu, Zn, Pb		+11, +13, +13[9]
Bien Venue, South Africa	BR	~3.1	In felsic volcanics	Cu, Zn, Pb	0.7011 ($N=1$)‡‡	+3 to +13 ($N=4$)‡‡
Hemlo, Ontario	BR	~2.7	Base of Au mineralization and in footwall rocks	Au, Mo	0.7017 to 0.7018 ($N=5$)[24]	+8 to +12 ($N=40$)[24]¶
Northern Eagle, Padre, Kadrey, Ontario	BR	~2.7	West and on strike from Hemlo	(Mo, As)††	0.7017 to 0.702 ($N=3$)[24]	+2, +8, +10‡‡
Stratiform disseminated						
Lac Shortt, Quebec	BR	~2.6	Minor amount in ore[20]	Au		
Stratabound disseminated or discontinuous lenses						
Hemio, Ontario	AN	~2.7	Disseminated or small lens in footwall rocks	Au	0.7013[25]	+8 ($N=3$)‡‡
Monomineralic vein (lens)						
McIntyre, Ontario	AN	~2.6	In Q-F-P[19]	Au, Cu	0.7011‡‡	+8, +10‡‡
Lake Shore, Ontario	BR	~2.6	In syenite	Au	0.7048, 0.7056‡‡	+12, +13, +14, +14‡‡
	AN		In ore vein in syenite[21]			
Macassa, Ontario	BR	~2.6	In syenite[21]	Au	0.7073, 0.7078‡‡	+14‡‡
	AN		In syenite			
Lamaque, Quebec	AN	~2.6	In Q-F-P[47]	Au		+13 to +14[47]
Young-Davidson, Ontario	BR	~2.6	In syenite[48]	Au		
Ross, Ontario	AN	~2.6	In andesite, dacite, syenite	Au	0.7023 ($N=2$)‡‡	+8, +9, +10‡‡
	BR		In ore veins[21]			
Golden Mile, Western Australia	AN	~2.7	In granophyre unit of Golden Mile Dolerite	Au	0.7015 ($N=2$)# (J. H. F. Clout and E.M.C. unpublished)	+12 ($N=2$)#
Eye-Dashwa Lake, Ontario	GY	~2.7	In granite[49,50]		0.7045 ($N=1$)[49]	av. +7.1±0.4 ($N=8$)[49]
Lac du Bonnet, Manitoba	GY	~2.7	In granite[50]			+7.3, +8.2[50]
Others not well known						
Con Mine, Northwest Territories	AN	~3.1**	Disseminated in tonalite boulder in shear zone[51]	Au		+6.8, +7.0, +7.2[51]
Heron Bay, Ontario	AN BR	~2.7	Monomineralic lens in volcanics	Au, Mo	0.7021 ($N=2$)‡‡	+9‡‡

* BR, barite; AN, anhydrite; GY, gypsum.
† Age of the host rocks.
‡ Q-F-P; quartz feldspar porphyry; vol, volcanic rocks; sed, sedimentary rocks.
§ Precious and base metal mineralizations in the area.
‖ The minimum value was listed for anhydrite. See text for explanation.
¶ Values for the massive basal barite.
# The data are taken for anhydrite closely associated with gold mineralization since late stage sulphates have higher values.
** The ^{207}Pb/^{205}Pb age of zircon in the boulder containing anhydrite.
†† Minor amounts associated with the massive barite.
‡‡ This study.

Diffusive loss of H_2 gas will move the reaction to the right. At temperatures below the H_2O-saturated solidus, hydrolysis of SO_2 can also yield H_2S gas and sulphate[33]:

$$4SO_2(\text{gas}) + 4H_2O = H_2S(\text{gas}) + 3H_2SO_4 \qquad (4)$$

Precipitation of the sulphate by reaction with Ca^{2+} to form anhydrite in aqueous fluid moves the reaction to right.

Epizonal intrusives are particularly suitable for developing sulphate of this latter origin. The low lithostatic pressure facilitates the exsolution of H_2O and S from silicate magmas; brecciation due to the secondary boiling, which allows escape of gas phases; and ready access to surface water. The occurrence of sulphate minerals in the hydrothermal system of porphyry copper mineralization is well documented[34,35].

The sulphur isotopic composition of magmatic sulphate will depend on the temperature, the ratio S^{2-}/SO_4^{2-}, and the primary S isotopic compositions of the magma, which is ~0‰ for Archaean magmas because of lack of contamination of sedimentary rocks containing sulphide of $\delta^{34}S$ different from 0‰. The isotopic fractionation factor, α, in melts[36] at 600–1,000 °C is:

$$1{,}000 \ln(\alpha_{SO_4^{2-}-S^{2-}}) = 7.4 \times 10^6/T^2 - 0.19$$

where T is in K. $\alpha_{SO_4^{2-}-S^{2-}}$ is 5‰ at 900 °C, 8‰ at 700 °C and 9‰ at 600 °C. There may be re-equilibration in silicate glass during cooling after solidification, giving lower apparent formation temperatures[28]. Because sulphide is dominant in most magmas, it will show the least departure from the primary isotopic composition of 0‰, with sulphate being in the range of +7 to +12‰ (refs 28, 29). However, degassing of H_2 can increase the sulphate content, causing $\delta^{34}S$ for the latter to decline, for example, Hawaiian subaerial flows[29]. $\delta^{34}S$ for sulphate in magmatic-hydrothermal fluids are larger than that of magmatic sulphate because of lower temperatures of the fluids compared with melts.

When $\delta^{34}S$ for total S is ~0‰, $\delta^{34}S$ values of magmatic sulphate will mostly be in a range of +7 to +10‰ for mafic rocks formed at ~1,000 °C and higher, to ~+12‰ in felsic rocks with lower solidification temperatures. The values of magmatic-hydrothermal sulphate formed in aqueous fluids is mostly in the range of +8 to +14‰ (refs 35, 37). An important point is that the rate of formation of magmatic and magmatic-hydrothermal sulphate is independent of the atmospheric oxygen pressure. It is dependent on the intensity of volcanism over a given time and the tectonic conditions in which this takes place.

For the vein sulphates listed in Table 1, which are mostly associated with intrusions and which have δ^{34}S values of +8 to +13‰, it is reasonable to suggest that these are of magmatic-hydrothermal origin. They are analogous to the veins of anhydrite on Phanerozoic porphyry mineralization. What is less certain is the origin of the +8 to +13‰, tabular sulphate body parallel to bedding, such as that at the Hemlo main deposit and barite occurrences west of Hemlo. These appear to have precipitated by the interaction of Ba^{2+}-rich fluid and sulphate-rich water[24]. This requires the earlier accumulation of sulphate in the surface water since sulphate was generally poor in the Archaean, both in continental and submarine environments.

There are two possible origins for this sulphate: (1) biological oxidation of primary sulphide to form ~0 to ~+5‰ sulphate in a basin, followed by (1*a*) biological or (1*b*) abiological enrichment in ^{34}S; or (2) introduction of magmatic and/or magmatic-hydrothermal sulphate. In both cases, there is a requirement that the basin be restricted to prevent its dissipation within the sulphate-poor Archaean ocean waters[4].

Option (1*a*) can be largely disregarded since there is a general lack of pyritic graphitic shale in the footwall rocks of the Hemlo succession. Six samples of pyrite from the limited occurrences of graphitic shale have δ^{34}S values ranging from +1.8 to +3.5‰. It is not possible to identify whether options (1*b*) or (2) was dominant. However, a magmatic or magmatic-hydrothermal contribution of sulphate from high-level magma seems possible, considering the intense volcanism in the region[38]; the abundance of high level intrusives, including porphyries; the essential lack of sedimentary rocks in the footwall; and the overall association between sulphates and gold mineralization demonstrated above.

How important might the flux of magmatic and magmatic-hydrothermal sulphate be during the Archaean? The oxidation condition of magmas is thought to have been similar since Archaean time, judging from similar mineral assemblages[39]. Assuming ~900 p.p.m. S in magmas, of which 20% is sulphate, an evaluation may be made of the production rate of magmatic sulphate. At present, the total output of volcanic rocks is estimated to be ~26 to ~34 $km^3 yr^{-1}$, 23 $km^3 yr^{-1}$ in the oceanic environment and 3-10 $km^3 yr^{-1}$ in the continental environment[40]. Using these values, the total amount of sulphate presently produced by submarine magma can be calculated: 23×10^{15} (volume of rocks) × 2.4 (specific gravity) × 900×10^{-6} (content of S) × 0.2 (proportion of SO_4^{2-}) × 96/32 (conversion from S to SO_4^{2-}) = ~3×10^{13} g yr^{-1}. The formation of SO_4 in continental environments is difficult to evaluate because the high rate of SO_2 production from present-day volcanoes, $1.2 \times 96/64 \times 10^{13}$ g $= 1.8 \times 10^{13}$ g (ref. 41) may reflect contamination and assimilation of magma by sulphur-rich sedimentary rocks and because the size of continents in Archaean time is uncertain[42]. If we assume that continental volcanism has been similar throughout geological time, the total production of magmatic sulphate is calculated to be 4.8×10^{13} g yr^{-1}. This compares with ~1.8×10^{14} g yr^{-1} produced by weathering processes[43], so that ~27% of the annual production is magmatic sulphate. Even if we ignore the continental supply, the magmatic sulphate would constitute ~17%.

If magmatic and magmatic-hydrothermal sulphate were to accumulate in the Archaean ocean, the present concentration in sea water, 4×10^{21} g (ref. 43), would have been reached in ~100 Myr. The quantity estimated is a minimum, since volcanism may have been several times more intense at 2,700 Myr (ref. 44) and an undefined quantity of magmatic-hydrothermal sulphate must be added. It can thus be concluded that there was a significant contribution of the magmatic sulphate to the flux of oxidized species in the surface environments in the Archaean and, indeed, in later periods.

Intense volcanism and fast seafloor spreading during the Archaean[42,45] provided a large quantity of reduced mantle material to the Earth's surface. Because of the high rate of interaction between the reduced iron and manganese from the mantle and the hydrosphere at the spreading ridges and subduction zones, the oxidized species formed in the hydrosphere were removed from the Archaean ocean[4,7]. The prevailing reduced conditions in the Earth's surface both in continental and submarine environments was, thus, maintained in Archaean time, and evidence for the presence of sulphate in the hydrosphere, therefore, will be generally lacking. Evidence of magmatic sulphate will only be retained locally in rocks which escaped subduction, such as back-arc basins and rift systems in continents. Preserved continental magmatic-hydrothermal systems, as described above, are other examples.

This study was supported by NSERC grant (grant no: A0616) and the Rector's fund to K.H. We thank Anglo American Corp. of South Africa; Derry, Michener, Booth and Wahl; Lac Minerals; Noranda Mines; Ore Quest Consultants; Pamour Porcupine Mines; Teck Corporation; and Western Mining Corporation for permission to collect samples. We thank R. H. Kirkham for unpublished data, R. W. Sullivan and O. Van Breemen for strontium isotope analyses, and Hitoshi Sakai and Akira Ueda for helpful comments.

Received 5 July; accepted 30 September 1985.

1. Cloud, P. E. *Science* **160**, 729-736 (1968).
2. Cameron, E. M. & Garrels, R. M. *Chem. Geol.* **28**, 181-197 (1980).
3. Hattori, K., Campbell, F. A. & Krouse, H. R. *Nature* **302**, 323-326 (1983).
4. Cameron, E. M. *Nature* **296**, 145-148 (1982).
5. Sangster, D. F. *Geol. Ass. Can. Spec. Pap.* **20**, 723-739 (1980).
6. Junge, C. E., Schidlowski, M., Eichman, R. & Pietrek, H. *J. geophys. Res.* **80**, 4542-4552 (1975).
7. Veizer, J., Compston, W., Hoefs, J. & Nielsen, H. *Naturwissenschaften* **69**, 173-180 (1982).
8. Perry, E. C. Jr., Hickman, A. H. & Barnes, I. L. *Geol. Soc. Am. Abst. Prog.* 1226 (1975).
9. Lambert, I. B., Donnelly, T. H., Dunlop, J. S. R. & Groves, D. I. *Nature* **276**, 808-810 (1978).
10. Perry, E. C., Monster, J. & Reimer, T. *Science* **171**, 1015-1016 (1971).
11. Radhakrishna, B. P. & Vasudev, V. N. *J. geol. Soc. Ind.* **18**, 525-541 (1977).
12. Hart, S. R. & Brooks, C. *Contr. Miner. Petrol.* **61**, 109-128 (1977).
13. Roddick, J. C. *Geochim. cosmochim Acta* **48**, 1305-1318 (1984).
14. Fauer, G. & Powell, J. L. *Strontium Isotope Geology* (Springer, New York, 1972).
15. Turek, A., Smith, T. E. & Huang, C. H. *Can. J. Earth Sci.* **18**, 323-329 (1981).
16. Glikson, A. Y. *Earth Sci. Rev.* **15**, 1-73 (1979).
17. Veizer, J. & Compston, W. *Geochim. cosmochim. Acta* **40**, 905-914 (1976).
18. Cameron, E. M., Hattori, K. & Sullivan. R. W. *Geol. Surv. Can. Paper 84-8* 3 (1984).
19. Mason, R. O. *Geol. Surv. Can. Paper 85-8* 6 (1985).
20. Cormier, M., Gauthier, A. & Muir, J. E. *Can. Inst. Min. Metal. Spec.* **34**, 393-411 (1984).
21. Thomson, J. E. *et al. Ont. Dept. Min. A.* Rep. **57**, part 5, (1950).
22. Percival, J. A. & Krogh, T. E. *Can. J. Earth Sci.* **20**, 830-843 (1983).
23. Morrison, E. R. *Rhodesia Geol. Surv. Miner. Resourc. Ser.* **15** (1970).
24. Cameron, E. M. & Hattori, K. *Geochim. cosmochim. Acta* **49**, 2041-2051 (1985).
25. Hattori, K., Cameron, E. M. & Smith, R. *Abstr. geol. Ass. Can.* **10**, A-25 (1985).
26. Katsura, T. & Nagashima, S. *Geochim. cosmochim. Acta* **38**, 517-531 (1974).
27. Moore, J. G. & Fabbi, B. P. *Contr. Miner. Petrol.* **33**, 118-127 (1971).
28. Sakai, H., DesMarais, D. J., Ueda, A. & Moore, J. G. *Geochim. cosmochim. Acta* **48**, 2433-2441 (1984).
29. Sakai, H., Casadevall, T. J. & Moore, J. G. *Geochim. cosmochim. Acta* **46**, 729-738 (1982).
30. Anderson, A. T. *Rev. Geophys. Space Phys.* **13**, 37-55 (1974).
31. Kyser, T. K. & O'Neil, J. R. *Geochim. cosmochim. Acta* **48**, 2123-2133 (1984).
32. Ueda, A. & Sakai, H. *Geochim. cosmochim. Acta* **48**, 1837-1848 (1984).
33. Burnham C. W. in *Geochemistry of Hydrothermal Ore Deposits* 2nd edn (ed. Barnes, H. L.) 71-136 (Wiley, New York, 1979).
34. Heberlein, D. R. & Godwin, C. I. *Econ. Geol.* **79**, 902-918 (1984).
35. Beane, R. E. & Titley, S R. *Econ. Geol. 75th Ann. Vol.* 235-269 (1981).
36. Miyoshi, T., Sakai, H. & Chiba, H. *Geochem. J.* **18**, 75-84 (1984).
37. Field, C. W. & Gustafson, L. B. *Econ. Geol.* **71**, 1533-1548 (1976).
38. Muir, T. L. *Ont. geol. Surv. Rep.* No. 217 (1982).
39. Holland, H. D. *The Chemical Evolution of the Atmosphere and the Ocean* (Princeton University Press, 1984).
40. Crisp, J. A. *J. Volcan. Geotherm. Res.* **20**, 177-211 (1984).
41. Berresheim, H. & Jaeschke, W. *J. geophys. Res.* **88**, 3732-3740 (1983).
42. Richter, F. M. *Earth planet. Sci. Lett.* **73**, 350-360 (1985).
43. Holser, W. T. & Kaplan, I. R. *Chem. Geol.* **1**, 93-135 (1966).
44. Turek, A., Smith, P. E. & Van Schmus, W. R. *Can. J. Earth Sci.* **21**, 457-464 (1984).
45. Bickle, M. J. *Earth planet. Sci. Lett.* **40**, 301-315 (1978).
46. Hickman, A. H. *Geol. Surv. A. Rep. 1972*, 57-60 (1973).
47. Kerrich, R. *Can.. Inst. Min. Met. Spec. Vol.* 27 (1983).
48. Dyer, W. S. *Ont. Dep. Mines 44th A. Rep.* (1935).
49. Kamineni, D. C. *Chem. Geol.* **39**, 263-272 (1983).
50. Kamineni, D. C. & Stone, D. C. *Contr. Miner. Petrol.* **83**, 237-246 (1983).
51. Nikic, Z., Baadsgaard, H., Folinsbee, R. E., Krupicka, J., Leech, A. P. & Sasaki, A. *Geol. Soc. Am. Spec. Pap.* **182**, 169-175 (1980).
52. Hickman, A. H. *Geol. surv. West Austral. Bull.* **127** (1983).

Carbon isotope excursions in Precambrian/Cambrian boundary beds, Morocco

Maurice E. Tucker

Department of Geological Sciences, University of Durham, Durham DH1 3LE, UK

The Precambrian/Cambrian boundary is one of the most significant points on the geological timescale, because it marks the change in the fossil record from soft-bodied organisms to skeletonized faunas. The Cambrian explosion or radiation event[1] saw the evolution of many new life forms, especially various molluscs and archaeocyathids from the base of the Cambrian (Tommotian stage). Others, including the trilobites and bivalves, evolved a little later in the succeeding Atdabanian stage[2,3]. A massive increase in the biomass of the photic zone through phytoplankton blooms has also been postulated for this time[4], particularly in the late Riphean/early Vendian and in the early Cambrian[5]. There has been much discussion concerning where precisely to place the boundary[6,7] and there are several contenders in the world for the type section[8]. I present here a carbon isotope profile, from the Precambrian/Cambrian boundary beds in Morocco, where two distinctive positive $\delta^{13}C$ excursions are revealed. These are interpreted as records of increased organic productivity as part of the Precambrian/Cambrian explosion of life. $\delta^{13}C$ excursions could be useful points for correlation between boundary sections.

The late Precambrian/Cambrian strata are extensively exposed on the northern slopes of the Anti-Atlas mountains in southern Morocco[9]. The 'classic' section occurs near the village of Tiout, 25 km south-east of Taroudannt, 80 km east of Agadir (Fig. 1). The sequence begins with the Dolomie Inferieur, 200 m of dolomite with local cryptalgal, grainstone and replaced evaporite horizons. The succeeding Serie Lie de Vin (950 m) consists of cyclically arranged limestones, dolomites and fine clastics which represent rhythmic fluctuations in the position of the shoreline[10]. Algal thrombolites and stromatolites occur throughout the sequence and include the genera *Tungussia*, *Patomia* and *Nimbophyton*[11,12]. The Calcaire Superieur (220 m) consists of massive limestones (some black, some oolitic), dolostones, chert nodules and the stromatolite *Acaciella*. The first trilobites (small opisthoparians[13]) appear towards the top of the Calcaire Superieur, and within a few metres there are archaeocyathid bioherms[14]. The upper, fossiliferous 130 m of the Calcaire Superieur have been separated off to form the Transition Beds[10,12] (Fig. 2). Shales with the trilobite *Fallotaspis* mark the beginning of the Serie Schisto-Calcaire[13], which consists of many transgressive oolite-shale cycles[15]. Overall, the Moroccan sequence reflects mostly shallow-water shelf sedimentation on the subsiding north-west margin of the Saharan Craton, adjacent to the opening Iapetus (Proto-Atlantic) Ocean[16].

There has been much discussion on the position of the Precambrian/Cambrian boundary at Tiout, as at other boundary candidates, but there now appers to be a consensus. On the basis of a detailed study of the stromatolites, notoriously difficult to use for dating, the Serie Lie de Vin is placed in the Vendian (latest Precambrian)[11]. An alternative view on the stromatolites suggests that they are lowest Cambrian[17] but a similar Vendian age for the Lie de Vin is derived from acritarchs[18]. The archaeocyathids indicate a mid-Atdabanian age for the Transition Beds[14], suggesting that the Calcaire Superieur is lower Atdabanian and Tommotian. The Tommotian is recognized by the occurrence of small shelly fossils[1], which are mostly phosphatic, but unfortunately these have not yet been found in the Anti-Atlas despite acid digestion of many samples[11]. The Tommotian stage was generally a regressive time[2] so that its deposits may be thin or even absent. The Precambrian/Cambrian boundary is thus likely to occur in the Lower Calcaire Superieur or Upper Serie Lie de Vin. The Dolomie Inferieur is attributed to the late Riphean[10,18]. A tilloid of probable glacial origin occurs in the Tiddiline Formation, unconformably beneath the Dolomie Inferieur[19].

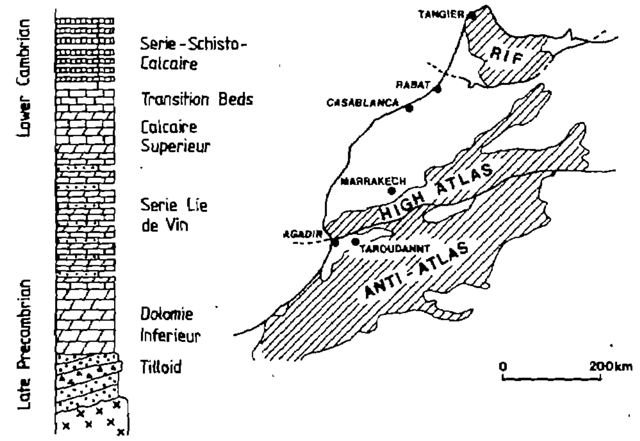

Fig. 1 Location map of Morocco, showing the three principal tectonic units, the Anti-Atlas, High Atlas and Rif, and the stratigraphy of the late Precambrian/Cambrian beds in the Anti-Atlas.

The results of whole-rock, carbon stable-isotope analyses of limestones and dolomites from the Anti-Atlas boundary beds are presented in Fig. 2. With such determinations, there is always the possibility that the values have a diagenetic component through cement precipitation, calcite neomorphism or dolomitization, so that the values do not reflect the isotopic composition of contemporaneous sea water. However, it is generally held that the marine carbon-isotope signature is less prone to alteration during diagenesis than the oxygen isotope as the reservoir of carbon is very much smaller than that of oxygen in diagenetic porewaters[20]. When recrystallization and dolomitization of calcite or aragonite grains and muds take place, in most cases the carbon-isotope ratio is altered little because the carbon atoms are almost entirely derived from the original carbonate.

In organic-rich sediments, diagenetic calcites and dolomites can be very light to quite heavy (-20 to $+10‰ \delta^{13}C$), as a result of the various diagenetic breakdown processes affecting organic matter[21]. However, organic-rich carbonates were not analysed in this study, and in fact, other late Precambrian organic-rich limestones (from Norway[22] and California; unpublished data) analysed have typical marine $\delta^{13}C$ values (average 1.7 and 2.0‰ respectively). Meteoric waters with soil-derived CO_2 can give extreme $\delta^{13}C$ signatures to carbonate precipitates, but these are typically negative, rather than positive, and can be expected to relate to prominent emergence horizons (absent in the Precambrian/Cambrian of the Anti-Atlas). Finally, there is little isotopic fractionation of carbon isotopes with temperature.

The profile in Fig. 2 is derived from limestones and dolomites from a variety of open, shallow-marine facies and degrees of diagenesis, but the broad pattern of $\delta^{13}C$ change is considered to be a genuine record of changes in $\delta^{13}C$ of the original marine precipitates. As an example, there is no significant difference between the $\delta^{13}C$ values of oolites and stromatolites in the Serie Schisto-Calcaire, or between bioclastic and oolitic limestones in the Transition Beds at the top of the Calcaire Superieur. The oxygen-isotope data, not presented here, show more scatter; this is expected as diagenesis can affect the $\delta^{18}O$ considerably, mainly through the precipitation of ^{18}O-depleted calcite spar cement[23], and there can be a several per mil difference between limestones and dolomites. The validity of the very positive $\delta^{13}C$ values of the Dolomie Inferieur might be questioned but, in fact, their oxygen-isotope values (M.E.T., unpublished data) are

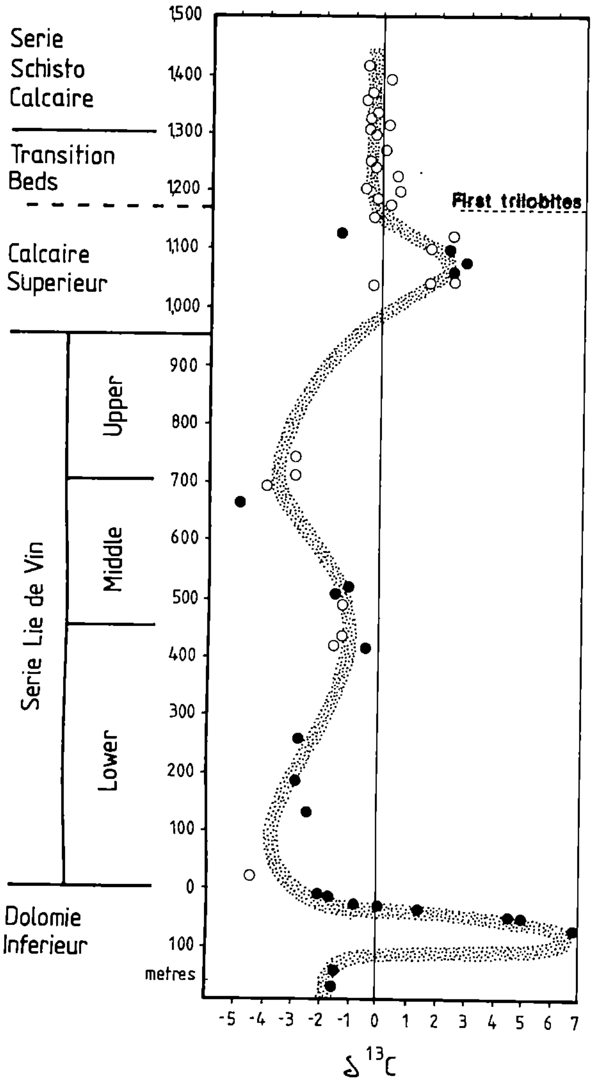

Fig. 2 Carbon-isotope stratigraphy from the late Precambrian/Cambrian boundary beds, Tiout, near Taroudannt, Anti-Atlas. Closed symbols are dolomites; open symbols are limestones.

in the same range (−6 to −9‰ PDB) as the samples above and below, suggesting no major difference in the diagenesis. This deduction is supported by microscopic studies. Thus, the $\delta^{13}C$ isotope profile of Fig. 2 is considered to be a reflection of changes in the carbon-isotopic composition of sea water during the critical late Precambrian/Cambrian time.

The carbon-isotope profile shows two positive excursions in $\delta^{13}C$, one near the top of the Dolomie Inferieur and the other within the Calcaire Superieur. The Serie Lie de Vin has a moderately negative signature, and the limestones of the Transition Beds and Serie Schisto-Calcaire are close to 0‰ PDB. The carbon-isotope signature of marine limestones (and many dolomites) tends to reflect the $\delta^{13}C$ of total dissolved inorganic carbon (TDC) in sea water. Average oceanic $\delta^{13}C$ TDC today is ~0‰ and shallow marine carbonate precipitates are in the range 0 to 4‰ PDB (refs 20, 23). Organic carbon, on the other hand, has very negative $\delta^{13}C$, in the range −20 to −30‰, since the lighter ^{12}C is preferentially incorporated into organic matter. It is generally assumed that the input of carbon to the oceans has remained relatively constant through time and that the ocean carbon reservoir mass had changed little. Changes in oceanic $\delta^{13}C$ TDC are thus thought to be caused by variations in the carbon output to the organic carbon (C_{org}) and carbonate carbon (C_{carb}) reservoirs[24,25]. At present, a C_{org}/C_{carb} output ratio of around 1:4 maintains the steady-state $\delta^{13}C$ of ~0‰ in oceanic water. Increases in the burial rate of the ^{12}C-enriched organic carbon, relative to the amount of carbonate carbon being precipitated, thus lead to a positive or heavier isotopic composition of seawater TDC, and of carbonate precipitates therefrom. Higher rates of organic carbon burial could result from increases in organic productivity. Alternatively, they could reflect an increase in the preservation potential of the organic carbon; this could result from oceanographic effects, such as the development or expansion of oxygen-depleted oceanic water masses. Positive excursions of $\delta^{13}C$ have been detected in Cretaceous and Jurassic limestones[26,27], and correlate with oceanic anoxic events (OAEs), when increased organic productivity through eustatic sea-level rises leads to the burial of much organic matter and depletion of the oceanic TDC in ^{12}C.

The two positive $\delta^{13}C$ excursions revealed in the Morocco boundary beds can be interpreted as indicating increased levels of organic productivity, resulting in the preferential extraction of ^{12}C from the oceanic carbonate reservoir. The excursion at the top of the Dolomie Inferieur is probably close to the Riphean/Vendian boundary, a time of radiation of eukaryotic plankton[5]; it could reflect a major increase in the microplankton in the oceans, perhaps an evolutionary event related to a post-glacial climatic warming or more vigorous oceanic circulation connected with the opening of Iapetus, which took place around this time[16]. There are no major facies changes through the peritidal Dolomie Inferieur, so that the $\delta^{13}C$ event is unlikely to reflect increased productivity through a eustatic sea-level rise, as is generally the case with the Cretaceous OAEs[28]. The Dolomie Inferieur is not particularly organic-rich but the organic matter would probably be buried in deeper water sediments of contemporaneous basins and oceans. Such organic-rich deposits occur in the early Vendian of the Sparagmite Basin, south Norway[22]. The second positive excursion, in the Calcaire Superieur, is not so extreme but occurs in strata probably containing the Tommotian/Atdabanian boundary. This was a time of rapid metazoan evolution[1,2] and a second radiation event of the microplankton[5]. These increased levels of organic productivity can be expected to have affected the oceanic carbon budget. After each $\delta^{13}C$ excursion, the sea water returned to more normal values as recycling of the organic matter restored the balance of the organic carbon/carbonate carbon reservoirs.

The late Precambrian/early Cambrian was a time of oceanic chemical events. An extreme rise in the sulphur-isotope ($\delta^{34}S$) curve has been termed the Yudomski Event[29] and attributed to the catastrophic mixing of brine in local basins with the surface ocean water. An OAE and a phosphogenic event have been postulated for this time[4], along with catastrophic mixing of deep anoxic waters with aerated surface waters[4,30]. These chemical events have been invoked as major factors in organic evolution (as well as extinction), and they can be expected to have had an effect on the carbon-isotopic signature of sea water. It is possible that the $\delta^{13}C$ excursions reported here are connected with the other chemical events which took place around the Precambrian/Cambrian boundary and which were probably instrumental in the Cambrian metazoan radiation event.

If, as contended, the $\delta^{13}C$ excursions reported here are due to fluctuations in oceanic $\delta^{13}C$, they should be recorded in other boundary sections and could be a means of correlation, independent of the palaeontology, in a similar way to that proposed for magnetic polarity stratigraphy[31]. This could be very useful with some boundary profiles where, because of the facies developed, fossils are poorly represented.

This project is supported by the NERC. I thank John Rouse, formerly of the British Geological Survey, for organizing the isotope analyses; the Ministère de l'Energie et des Mines, Rabat, for permission to undertake fieldwork in Morocco; Martin Brasier, John Cowie, John Hudson, John Rouse, Mike Arthur and Phil Sandberg for comments; and Andy for artwork, and Nicola for wordprocessing.

Received 27 June; accepted 11 October 1985.

1. Brasier, M. D. *Systematics Ass. Spec. Vol.* **12,** 103-159 (1979).
2. Brasier, M. D. *Precambr. Res.* **17,** 105-124 (1982).
3. Stanley, S. M. *Am. J. Sci.* **276,** 56-76 (1975).
4. Cook, P. J. & Shergold, J. H. *Nature* **308,** 231-236 (1984).
5. Vidal, G. & Knoll, A. H. *Nature* **297,** 57-60 (1982).
6. Cowie, J. W. *Geol. Mag.* **115,** 151-152 (1978).
7. Bjørlykke, K. *Precambr. Res.* **17,** 99-104 (1982).
8. Cowie, J. W. *Episodes* **8,** 93-97 (1985).
9. Choubert, G. *Congr. Geol. Int. 19e, Alger, Monogr. region.* **6,** 77-194 (1952).
10. Monninger, W. E. W. *Arb. Palont. Inst. Wurzburg* **1,** 1-289 (1979).
11. Schmitt, M. O. & Monninger, W. E. W. in *Fossil Algae* (ed. Flugel, E.) 80-85 (Springer, Berlin, 1977).
12. Schmitt, M. O. *Arb. Palaont. Inst. Wurzburg* **2,** 1-188 (1979).
13. Sdzuy, K. *Geol. Mag.* **115,** 83-94 (1978).
14. Debrenne, F. & Debrenne, M. *Geol. Mag.* **115,** 101-119 (1978).
15. Tucker, M. E. *Proc. int. Ass. Sedim. Eur. Meet.,* Lerida, 467-469 (1985).
16. Schenk, P. E. *Can. J. Earth Sci.* **8,** 1218-1251 (1971).
17. Bertrand-Sarfati, J. *Newslett. Stratigr.* **10,** 20-26 (1981).
18. Choubert, G., Faure-Muret, A. & Timofeiev, B. K. *C.r. hebd Séanc. Acad. Sci., Paris* **288D,** 191-194 (1979).
19. Leblanc, M. in *Earth's Pre-Pleistocene Glacial Record* (eds Hambrey, M. J. & Harland, W. B.) 120-122 (Cambridge University Press, 1981).
20. Anderson, T. F. & Arthur, M. A. *Soc. Econ. Paleont. Miner. Short Course* **10,** 1-151 (1983).
21. Irwin, H., Curtis, C. D. & Coleman, M. *Nature* **269,** 209-213 (1977).
22. Tucker, M. E. *Precambr. Res.* **22,** 295-315 (1983).
23. Hudson, J. D. *J. geol. Soc. Lond.* **133,** 637-660 (1977).
24. Broecker, W. S. *Chemical Oceanography* (Harcourt Brace Jovanovich, 1974).
25. Mackenzie, F. T. & Pigott, J. D. *J. geol. Soc. Lond.* **138,** 183-196 (1981).
26. Scholle, P. A. & Arthur, M. A. *Bull. Am. Ass. petrol. Geol.* **64,** 67-87 (1980).
27. Clayton, C. & Jenkyns, H. C. *Sdimentology* 32 (in the press).
28. Jenkyns, H. C. *J. geol. Soc. Lond.* **137,** 171-185 (1980).
29. Holser, W. T. *Nature* **267,** 403-408 (1977).
30. Keith, M. L. *Geochim. cosmochim. Acta* **46,** 2621-2637 (1982).
31. Kirschvink, J. L. & Rozanov, A. Yu. *Geol. Mag.* **121,** 189-203 (1984).

Planktonic foraminiferal ontogeny and new perspectives for micropalaeontology

Geert-Jan A. Brummer*, Christoph Hemleben† & Michael Spindler‡

* Institute of Earth Sciences, Free University, PO Box 7161, 1007 MC Amsterdam, The Netherlands
† Institut und Museum für Geologie und Paläontologie, Universität Tübingen, Sigwartstr. 10, 7400 Tübingen, FRG
‡ Alfred-Wegener-Institute for Polar Research, Columbus-Center, 2850 Bremerhaven, FRG

Planktonic foraminifers are some of the most widely used microfossils for dating marine sedimentary rocks and the calcareous test has been used to reconstruct their depositional history over the past 120 million years[1]. By tracing the successive growth stages of extant representatives of this group, we have obtained criteria which identify pre-adult forms that, traditionally, have been disregarded in foraminiferal research. Thus, large quantities of "... unidentifiable miscellaneous juveniles ..."[2] have become available to help decipher the fossil record of marine environments. Comparative studies of growth series at species and supraspecific levels allowed the identification of three major species groups, each showing three different developmental stages. Their recognition introduces new possibilities for establishing a natural classification of planktonic foraminifers, for disclosing their evolutionary history and for testing evolutionary models in general.

Despite the early recognition of the importance of reconstructing the sequence of events during planktonic foraminiferal growth[3-8], only recently has the first comprehensive and comparative work appeared[9]. Departing from previous procedures, we followed an ontogenetic approach by considering the complete series of individual ontogenetic stages of each of the 10 species present in our samples. We used pre-adult tests collected from the living plankton offshore Barbados to minimize interference by additional carbonate layers secreted during later growth stages[7], and to exclude post-lifetime alterations of the test[1].

Initially, the pre-adult morphology of a species had to be learned by backtracking the successive growth stages of transparent adult specimens under the light microscope (Fig. 1*c*, *d*). This enabled us to determine the taxonomic identity of the individual pre-adult stages and to reverse the backtracking process in order to document morphological change during ontogeny.

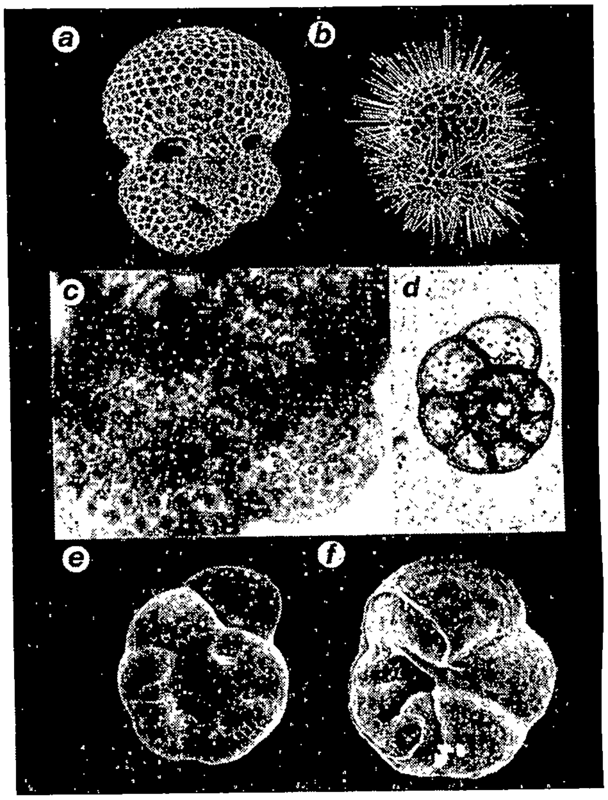

Fig. 1 Scanning electron (*a*, *b*, *e*, *f*) and transmission light (*c*, *d*) micrographs, illustrating the pre-adult morphology of *G. sacculifer* (Brady) as obtained from backtracking the successive growth stages of transparent adult specimens. *a*, Spiral view of adult specimen (×88). *b*, Umbilical view of adult specimen (×79). *c*, Same specimen as in *a*, showing the pre-adult growth stages contained in the adult test (×194). *d*, Spiral view of a typical juvenile (×321). *e*, Spiral view of a juvenile, compare with *c* and *d* (×429). *f*, Umbilical view of an early neanic form, showing the abrupt morphological transition from the juvenile stage (penultimate chamber) to the neanic stage (last chamber; ×352).

Most species completed at least three phases of growth. During the initial (juvenile) stage, as well as the final (adult) stage, growth is morphologically conservative. Confined by rather spasmodic morphological changes, the intermediate (neanic) stage shows rapid transformation of virtually all features during its development.

Three species groups exhibiting characteristic ontogenetic morphology could be discerned (Fig. 2). Their distinction is essentially based on the same criteria used in traditional foraminiferal classification: gross shape of the test and constituent chambers, presence or absence of spines, position of the aperture(s) and texture of the test wall[10]. Remarkably the species groups distinguished here coincide with a subdivision in adult wall-textural types as conceived recently[11].

Group 1, comprising the species *Globigerinella aequilateralis* (Brady), *Globigerinoides conglobatus* (Brady), *Globigerinoides ruber* (d'Orbigny), *Globigerinoides sacculifer* (Brady) and *Orbulina universa* (d'Orbigny), shows striking morphological changes during ontogeny (Fig. 2*a*-*d*). Juveniles of this group have few large pores concentrated along sutures, a smooth test wall with sparse, sparsely distributed delicate spines and an extra-umbilical aperture. Then, when a size of ~80 μm is reached, abrupt morphological changes occur, marking the onset of the neanic stage. Well-defined, densely distributed spines appear on all chambers, pores spread over the entire chamber surface and the cancellate wall texture emerges (Fig. 1*f*). During the neanic phase, the number of chambers per whorl decreases and the main aperture shifts towards its ultimate position. Finally, at a size of ~200 μm, advanced features such as secondary apertures herald the transition from the neanic to the adult stage of growth.

Group 2, which includes the species *Globorotalia menardii* (Parker, Jones and Brady) and *Neogloboquadrina dutertrei* (d'Orbigny), ontogenetically resembles group 1 (Fig. 2*e*–*h*). Consistent differences are the pustulate instead of spinose wall texture, the less-pronounced apertural shift during the neanic stage and a morphologically gradual neanic–adult transition. Additional characteristics of *G. menardii* comprise the development of a keel during the neanic stage and the absence of a cancellate wall texture.

Group 3, consisting of *Candeina nitida* (d'Orbigny), *Globigerinita glutinata* (Egger) and *Globigerinita juvenilis* (Bolli), retains most morphological features throughout ontogeny (Fig. 2*i*–*l*). Numerous minute pores may cover the non-spinose, pustulate test from as early as the second chamber. The apertural shift is a prominent feature of the neanic stage but the neanic–adult transition could be defined only in *C. nitida*, where chambers provided with numerous sutural apertures cover the umbilicus.

Planktonic foraminiferal classification, taxonomy and phylogeny has relied solely on adult morphological features[9–12]. Our study of growth series of species reveals that major taxonomic characters change during the ontogeny of individual species. If the present, adult-based taxonomy were applied to the successive ontogenetic stages of, for instance *G. ruber*, it would have to be assigned to three different genera. As integral

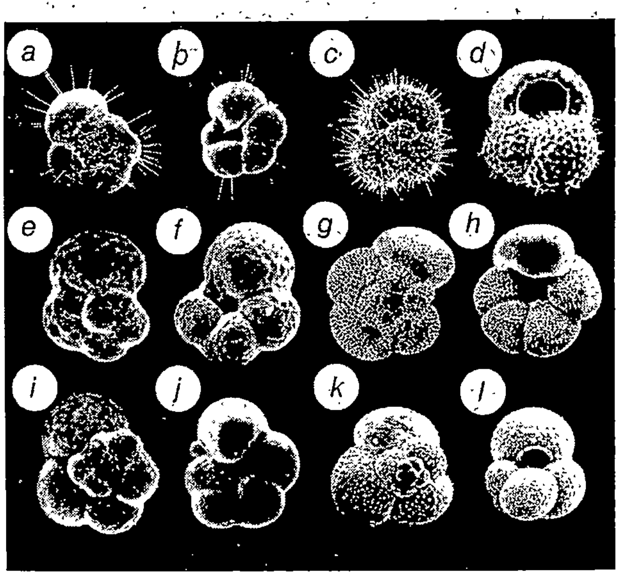

Fig. 2 Scanning electron micrographs of the adult versus pre-adult morphology of three species representing the three species groups distinguished by their ontogeny. *a*–*d*, *G. ruber* (group 1); *a*, *b*, spiral (×449) and umbilical (×469) view of juvenile, *c*, *d*, same views (×120, ×147) of adult specimens. *e*–*h*, *N. dutertrei* (group 2); *e*, *f*, spiral (×290) and umbilical (×304) view of early neanic forms, *g*, *h*, same views (×74, ×62) of adult specimens. *i*–*l*, *G. juvenilis* (group 3); *i*, *j*, spiral (×653) and umbilical (×805) view of early juvenile, *k*, *l*, same views (×143, ×136) of adult specimens. Striking differences between ontogenetic phases are observed, involving taxonomically important characteristics such as wall texture, spine and pore distribution, shape and number of chambers in the last whorl, and position of the aperture.

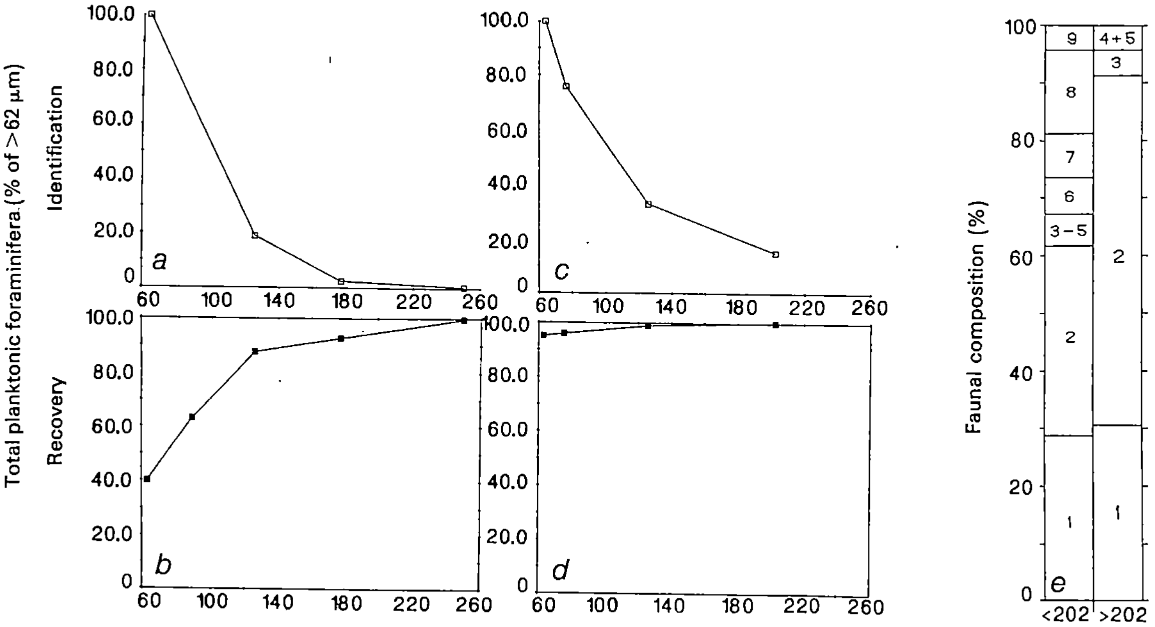

Fig. 3 Effect of the ontogenetic analytical approach on recovery, identification and species composition of planktonic foraminifers in relation to sieve mesh size. Sediment sample preparation methods traditionally use 125-μm or larger-sized sieve mesh fractions[2]. Living plankton is usually collected by plankton nets of 202 μm or greater mesh size[16]. *a*, Recovery in sediment surface samples from the Santa Barbara Basin, Pacific Ocean, demonstrating the exponential growth of the recovery of specimens with decreasing mesh-size (after ref. 16). *b*, Single sediment surface sample from offshore Madagascar, Indian Ocean, showing rapidly diminishing identification frequencies towards the fine fractions when conventional identification criteria are used (modified after ref. 2). *c*, Surface water, 10-μm plankton net samples from offshore Barbados, Caribbean Sea. Recovery frequency runs parallel to that of sediment surface samples in *a*. *d*, Same sample as in *c*, using identification criteria based on ontogenetic morphology. The identification frequency remains very high in contrast to low values attained by using conventional (adult) morphological criteria (*b*). *e*, Changed species composition in the >202-μm compared with the <202-μm sieve fraction of a 10-μm plankton net sample (same as in *c*, *d*). 1, *G. ruber*; 2, *G. sacculifer*; 3, *N. dutertrei*; 4, *Globigerinella aequilateralis*; 5, *O. universa*; 6, *Globorotalia anfracta*, 7, *Globigerinita glutinata*; 8, *G. juvenilis*; 9, unidentified. Note the absence of *G. anfracta*, *G. glutinata* and *G. juvenilis* in the >202-μm fraction and the greatly reduced relative frequency of *G. sacculifer* in the <202-μm fraction.

parts of ontogeny, the morphology of the juvenile, neanic and adult phases together provide a new and comprehensive set of distinguishing features, evoking a reconsideration of our theory about planktonic foraminiferal species.

Although phylogeny has essentially been considered as a series of ontogenies[13,14], the comparison of adult morphological characteristics has traditionally been used to reconstruct planktonic foraminiferal evolutionary lineages[9,12]. We expect that comparative ontogeny, rather than adult morphology alone, will produce a balanced and natural classification, taxonomy and phylogeny[1,3] which, at present, suffers from adaptive adult morphological convergences and repetitive evolution[1,12]. Using comparative ontogeny to infer evolutionary lineages reliably, we can more accurately define lineage-zones, regarded as "... one of the best assurancies of reliable time correlation on a biostratigraphic basis"[15].

Most importantly, ontogenetic morphology allows the identification of the pre-adult forms which constitute the bulk of a foraminiferal sample[2,16]. The 125-μm, 149-μm or 202-μm sieves generally used to recover adult forms also induce the single most critical artefact in faunal analyses[2]. With decreasing mesh size, recovery of specimens from a sample increases exponentially, identification frequencies decline correspondingly and marked shifts in faunal composition occur (Fig. 3). A pilot survey of a 10-μm plankton net sample from offshore Barbados shows an exponentially increasing specimen recovery, similar to that reported elsewhere[2,16]. However, when ontogenetic morphology is used as a tool for identification, 95% of the small (62–125 μm) sieve-size fraction is still identifiable (Fig. 3*d*). Faunal analysis of the same sample shows marked changes in species composition relative to sieve mesh size (Fig. 3*e*). Large species dominating the >202-μm fraction have greatly diminished relative frequencies in the <202-μm fraction, whereas small species start to appear in considerable quantities.

Small species, accounting for about one-third of all extant taxa[1], have a largely unexplored potential due to their hidden occurrence among unidentified pre-adult forms. Together, their abundance and great diversity may give a detailed biostratigraphical analysis of fossil, adult-poor, shallow marine sediments. Faunal composition, as recognized in the small-sized fraction, will lead to more accurate and stable reconstructions of late Tertiary palaeoceanography and palaeoclimatology[16], which rely mainly on patterns of foraminiferal distribution[1].

Planktonic foraminiferal ontogeny yields a new and penetrating micropalaeontological approach which will contribute towards a better understanding of planktonic foraminifers as a group and their application in biostratigraphy, palaeoceanography and palaeoclimatology.

We thank O. R. Anderson, Y. A. Baumfalk, G. M. Ganssen, D. Kroon, S. R. Troelstra and J. E. van Hinte for critically reading the manuscript; the staff of the Bellairs Research Institute for help during the fieldwork; and H. Hüttemann (Geological Institute, Tübingen) for operating the scanning electron microscope. This study was supported by the Netherlands Organization for the Advancement of pure Research (ZWO) and the Sonderforschungsbereich (SFB 53) 'Palökologie' (D30) of the Deutsche Forschungsgemeinschaft. It is contribution 7 of the UvAVU-Werkgroep Mariene Geologie and SFB 53 Konstruktionsmorphologie 186.

Received 17 June; accepted 17 October 1985.

1. Vincent, E. & Berger, W. H. in *The Oceanic Lithosphere* Vol. 7 (ed. Emiliani, C.) 1025–1119 (Wiley, New York, 1981).
2. Bé, A. W. H. & Hutson, W. H. *Micropaleontology* **23**, 369–414 (1977).
3. Parker, F. L. *Bull. Am. Palaeont.* **52**, 111–208 (1967).
4. Banner, F. T. & Blow, W. H. *Micropaleontology* **13**, 133–162 (1967).
5. Olsson, R. K. *Trans. Gulf Cst Ass. geol. Soc.* **21**, 419–432 (1971).
6. Olsson, R. K. *Eclog. geol. Helv.* **65**, 185–195 (1972).
7. Parker, F. L. *J. Foram. Res.* **3**, 70–77 (1973).
8. Parker, F. L. in *Progress in Micropaleontology* (eds Takayanagi, Y. & Saito, T.) 258–262 (Micropaleontology Press, New York, 1976).
9. Huang, C. Y. *J. Foram. Res.* **11**, 173–190 (1981).
10. Stainforth, R. M., Lamb, J. L., Luterbacher, H., Beard, J. H. & Jeffords, R. M. *Paleont. Contr. Univ. Kans.* **62**, 1–425 (1975).
11. Steineck, P. L. & Fleischer, R. L. *J. Paleont.* **52**, 618–635 (1978).
12. Kennett, J. P. & Srinivasan, M. S. *Neogene Planktonic Foraminifera* (Hutchinson & Ross, Stroudsburg, 1983).
13. Gould, S. J. *Ontogeny and Phylogeny* (Harvard University Press, Cambridge, 1977).
14. Stanley, S. M. *Macroevolution* (Freeman, San Francisco, 1979).
15. Hedberg, H. D. (ed.) *International Stratigraphic Guide* (Wiley, New York, 1976).
16. Berger, W. H. *Mar. Geol.* **11**, 325–358 (1971).

Acoustic cavitation generated by microsecond pulses of ultrasound

L. A. Crum* & J. B. Fowlkes

Physical Acoustics Research Laboratory, Department of
Physics and Astronomy, University of Mississippi, Oxford,
Mississippi 38677, USA

Under extreme acoustic stress, liquids can be caused to rupture, with the transient generation of a vapour cavity. The subsequent collapse of these cavities is normally violent enough to be observed with the unaided eye or ear, and often generates free radicals due to the high temperatures and pressures associated with the collapse. Flynn[1] has calculated that microsecond pulses of ultrasound with peak intensities in the range 10–30 W cm^{-2} can generate transient cavitation in water. Because some diagnostic ultrasound systems[2,3] now in clinical use generate microsecond length pulses with temporal peak intensities >100 W cm^{-2}, there is reason to believe that this mechanism could operate in diagnostic conditions in aqueous media. We show here that ultrasonic pulses as short as one cycle at a frequency of 1.0 MHz give rise to luminescence flashes characteristic of violent cavitation. This provides the first experimental confirmation of Flynn's theoretical calculations.

Because the pulses produced by diagnostic ultrasound generators are rich in harmonics and short in time, we decided not to utilize the commonly used cavitation detection criterion—the acoustic detection of a shock wave or subharmonic frequency components—as there is little evidence that cavitation collapses in this short pulse regime can be detected acoustically. Rather, we have used a photometric detection system based on the observation, through a photomultiplier tube, of light produced by the cavitation bubble. This light emission results from the oxidation of luminol by the free radicals generated during the collapse of a cavity and should properly be termed chemiluminescence.

An essential ingredient of the cavitation generation system is that the acoustic pressure amplitude of the sound field is increased linearly with time, at a reproducible rate, until cavitation occurs. The experimental system will be described in more detail in a later report, a similar apparatus is described elsewhere[4]. The heart of the system is a ramp generator that drives both a strip recorder and the amplitude modulation input of a function generator. The d.c. voltage level on the strip chart record is linearly related to the peak-to-peak output of the function generator. This signal is amplified and delivered to a focused transducer (resonance frequency 1.0 MHz) that radiates into an echo-free chamber (wall lined with acoustic absorber) filled with distilled water saturated with argon, and containing luminol. The chart record is calibrated in units of megapascals by inserting a small, calibrated hydrophone (Medicoteknisk Institut, PVDF ultrasonic probe, outer diameter, 1.0 mm) into the focal region of the sound field during simulated measurements at low amplitudes.

Light generated by a cavity collapsing in the focal region is detected by a photomultiplier tube and the resulting pulse is preamplified and fed into a pulse height discriminator. The

---

* Present address. Anatomy Department, Guy's Hospital Medical School, London Bridge, London SE1 9RT, UK.

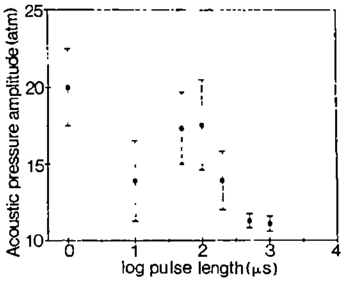

Fig. 1 Variation of the acoustic cavitation threshold of water containing luminol with pulse length for a duty cycle of 1:10. The points are the average of at least 10 independent measurements and the error bars represent ± one standard deviation. The carrier frequency was 1.0 MHz and the liquid was saturated with argon. The abscissa plots the logarithm (to the base 10) of the pulse length to compress the scale. Thus, an abscissa value of 3 implies that about 1,000 cycles were contained in the pulse, 2 means 100, 1 means 10, and 0 indicates that the pulse contained essentially one cycle.

discriminator level determines the sensitivity of the apparatus and is set to 600 mV, which is well above the average electrical background level (~150 mV) but below the typical chemiluminescence pulse height (~1.0 V). After discrimination, the signal passes through a noise gating network that either ignores the signal (no decision) or resets the system (cavitation detected). The noise gating network is a type of coincidence counter that requires that two pulses be observed within a 100-ms time interval. The reason for this criterion is that we have discovered through experience that a cavitation 'event' typically generates several optical flashes during 100 ms while the background noise is randomly distributed in time. The noise gating thus significantly lowers the false count rate. The system is reset by an immediate reduction of the acoustic pressure amplitude to zero for a quiescent period of 300 s; after this resting period is over, the acoustic pressure is again ramped until a cavitation event occurs and the sequence is repeated.

We have taken measurements of the cavitation threshold as a function of pulse length and of the length of time between pulses (duty cycle). A duty cycle of 1:10 means that the sound field is on for 1 time unit and off for the succeeding 9 time units. (This is a much longer duty cycle than used clinically by one to two orders of magnitude.)

Figure 1 shows the measured values of the threshold acoustic pressure amplitude required to initiate cavitation in distilled water containing luminol, as a function of pulse length, with a duty cycle of 1:10. Similar behaviour is observed for duty cycles of 1:3, 1:5 and 1:20. It is the temporal peak acoustic pressure rather than the average intensity that is important in the generation of cavitation effects[5]. An approximate value of the temporal peak intensity can be obtained by assuming a plane wave and using the relation $I = P_a^2/2\rho c$, where P_a is the temporal peak acoustic pressure, ρ is the density of the liquid and c the velocity of sound in the liquid.

Each data point presented is the average of at least 10 individual measurements. For the critical data point at an abscissa value of 0 (corresponding to pulses generated by a diagnostic ultrasound generator), we have taken more than 30 separate measurements on three different days with three different liquid samples. On one occasion, a second operator made the measurements (although the system is essentially automated). We thus have confidence in the validity of this measurement. Furthermore, at a duty cycle of 1:10, and at values of the temporal peak acoustic pressure only slightly higher than that determined as the threshold, single cycle pulses of 1-MHz ultrasound give light emission that is easily visible to the naked eye.

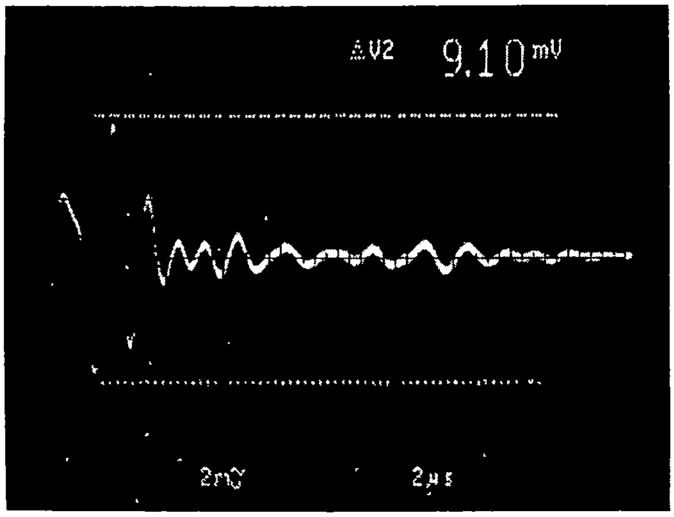

Fig. 2 An oscilloscope photograph of the temporal variation of the acoustic pressure near the focus of the sound field as measured by a calibrated miniature hydrophone. This pulse is intended to mimic those used in diagnostic ultrasound scanners.

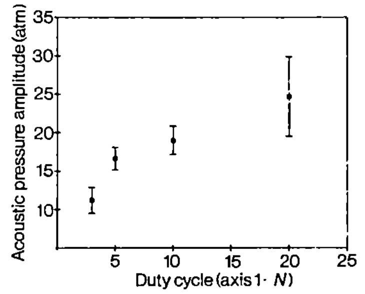

Fig. 3 Variation of the acoustic cavitation threshold of water containing luminol with duty cycle for a pulse length of ~1μs. The carrier frequency was 1.0 MHz and the liquid was saturated with argon.

Figure 2 shows a photograph of the temporal variation of the acoustic pressure as measured by our miniature probe hydrophone. Note that there is some ringing of the transducer but only at a much reduced amplitude. This pulse closely resembles the scanning mode pulse of a diagnostic ultrasound system which typically has a large negative cycle followed by a large positive cycle. Furthermore, this pulse is also similar to that used by Flynn[1] in his theoretical studies.

We have also examined the dependence of the cavitation threshold on duty cycle for the 'one cycle' pulse. These data are shown in Fig. 3. We have been concerned that the cavitation nuclei may respond to the pulse repetition frequency rather than the individual pulses. However, since the acoustic pulse used here dies out within a few microseconds, (well before the beginning of the next pulse), there is good reason to believe that these pulses act independently of each other. The data in Fig. 3 essentially confirm this fact showing an asymptotic behaviour at larger duty cycles. Furthermore, Marston and Unger[6] have presented evidence that single pulses of negative pressure can produce cavitation in water.

Note that we have established an arbitrary definition of the cavitation threshold as that value of the peak temporal acoustic pressure at which the output pulses reaching the pulse height discriminator from the photomultiplier tube have values of 600 mV or larger. This requirement is a working definition in that this discriminator setting permits us to obtain a desirable signal-to-noise ratio. It is quite conceivable that a more sensitive detection system would indicate lower values of the threshold. Our definition of cavitation involves the production of light by the collapsing cavity. Sonoluminescence is a reasonably well understood phenomenon[7,8] that is apparently the result of the radiative recombination of free radicals produced by the collapsing cavity[9]. However, the light emission that we observe is probably not sonoluminescence from within the cavity itself (produced by the recombination of free radicals); rather, it is light from the bulk of the liquid resulting from free radicals which 'escape' from the cavity and react with the luminol. Luminol has been used by several researchers (see, for example, ref. 10) to increase the output of light emissions from acoustic cavitation and the specific oxidation reactions that lead to light emission have been studied in some detail[11,12]. What is most important, and relevant to this work, is that the presence of free radicals are required for light emission to occur. Because these free radicals are highly reactive, and pose a threat to biological tissues, it is their presence that is important, not the light emission *per se*.

The light emission from the insonified area we observed can be seen by the naked eye, and appears in the form of 'streaks' rather than 'flashes'. We interpret this as being due to the relatively long lifetime of the oxidation reaction (as long as 50 ms according to Finch[10] and the rapid movement of collapsing cavities through the focal region due to radiation pressure forces. However, we have recently observed intense light emission from a form of 'stable' cavitation, in which bubbles pulsate violently for many cycles, with the use of an image intensifier tube as a light detector[13]. Because the temporal peak acoustic pressures are quite large, we should not expect that individual cavitation bubbles would survive the collapse phase and remain intact. It is possible, however, that the collapse and bubble breakup would effectively 'seed' the liquid with several new microbubbles that could act as cavitation nuclei[14]. The nearly continuous light emission suggests this form of 'steady' cavitation.

Finally, we draw attention to the fact that biological systems possess stabilized gas nuclei that can be activated by reduced pressures, either statically, as in the case of decompression sickness[15,16], or dynamically, as in the case of the biological effects of ultrasound[17–21]. These nuclei seem to exist in appreciable numbers in a variety of biological tissues, and our new evidence gives reason to believe that single cycle pulses of ultrasound could activate these nuclei in a violent manner. Accordingly, the data presented here may have important implications for clinical use of such ultrasound systems and imply that extensive risk assessment studies ought to be carried out.

We gratefully acknowledge the financial support of the NSF and the Department of Health and Human Services (Federal Drug Administration, Center for Devices and Radiological Health), the assistance of R. Massey in data acquisition and helpful conversations with A. Atchley, K. Commander, F. Gaitan and R. Holt.

Received 23 April; accepted 11 November 1985.

1. Flynn, H. G. *J. acoust. Soc. Am.* **72**, 1926–1931 (1982).
2. Carstensen, E. L. & Flynn, H. G. *Ultrasound Med. Biol.* **8**, 1720–1723 (1982).
3. Kremkau, F. W. *Clinics Obstet. Gyn.* **10**, 395–401 (1983).
4. Roy, R. A., Atchley, A. A., Crum, L. A., Fowlkes, J. B. & Reidy, J. J. *J. acoust. Soc. Am.* (in the press).
5. Carstensen, E. L., Parker, K. J. & Barbee, D. B. *J. acoust. Soc. Am.* **74**, 1057–1061 (1983).
6. Marston, P. L. & Unger, R. T. *Shock Waves in Condensed Matter* (Plenum, New York, in the press).
7. Jarman, P. *J. acoust. Soc. Am.* **32**, 1459–1464 (1960).
8. Walton, A. J. & Reynolds, G. T. *Adv. Phys.* **33**, 595–660 (1984).
9. Sehgal, C., Sutherland, R. G. & Verrall, R. E. *J. phys. Chem.* **84**, 396–398 (1980).
10. Finch, R. D. *Ultrasonics* **1**, 87–95 (1964).
11. White, E. H. & Roswele, D. F. *Accts. chem. Res.* **3**, 54–61 (1970).
12. Burdo, E. G. & Seitz, W. R. *Analyt. Chem.* **47**, 1643–1648 (1975).
13. Crum, L. A. & Reynolds, G. T. *J. acoust. Soc. Am.* **78**, 137–139 (1985).
14. Crum, L. A. *Appl. Sci. Res.* **38**, 101–111 (1982).
15. Evans, A. & Walder, D. N. *Nature* **222**, 251–254 (1969).
16. McDonough, P. M. & Hemmingsen, E. A. *J. appl. Physiol.* **56**, 513–521 (1984).
17. ter Haar, G. R. & Daniels, S. *Phys. Med. Biol.* **26**, 1145–1150 (1981).
18. Berg, K. B., Child, S. Z. & Carstensen, E. L. *Ultrasound Med. Biol.* **9**, 1448–1453 (1983).
19. Sommer, F. G. & Pounds, D. *Med. Phys.* **9**, 1–11 (1982).
20. Williams, A. R. & Miller, D. L. *Ultrasound Med. Biol.* **6**, 251–260 (1980).
21. Dyson, M. & Suckling, J. *Physiotherapy.* **64**, 105–111 (1978).

Potent ulcerogenic actions of platelet-activating factor on the stomach

Ann-Charlotte Rosam, John L. Wallace & Brendan J. R. Whittle

Department of Mediator Pharmacology,
Wellcome Research Laboratories, Beckenham, Kent BR3 3BS, UK

Platelet-activating factor (PAF) is an endogenous phospholipid which has been implicated as a mediator of allergic and inflammatory processes[1]. It is synthesized and released by neutrophils, platelets, macrophages, monocytes, basophils and endothelial cells[2–8], and is a potent platelet-aggregating agent, a vasodilator, increases vascular permeability, stimulates neutrophil aggregation and degranulation[9] and induces release of lysosomal enzymes[10]. A role for PAF in the hypotension associated with endotoxin shock[11,12] and in necrotizing enterocolitis[13] has recently been suggested. As there is an association between septic shock and acute gastric damage[14], we propose that PAF is an endogenous mediator of ulceration in the stomach. Indeed, as reported here, intravenous (i.v.) infusion of PAF to rats, at doses of 20–200 pmol per kg per min, resulted in the formation of extensive haemorrhagic erosions in the gastric mucosa. The ulcerogenic actions of PAF are not attributable solely to its hypotensive actions and were not mediated via effects on platelets or cyclooxygenase products, nor via histamine H_1, H_2 or α-adrenergic receptors. PAF is the most potent gastric ulcerogen yet described and its endogenous release may underlie or contribute to certain forms of gastric ulceration.

PAF (1-*O*-alkyl-2-*O*-acetyl-*sn*-glyceryl-3-phosphorylcholine; Sigma) was infused i.v. (100 ng per kg per min) to pentobarbitone-anaesthetized male Wistar rats for periods of 5–20 min. The stomachs were removed immediately after the PAF infusion or at 30–180 min after the infusion. With this dose, macroscopically visible gastric erosions were present in all of the treatment groups. As the most consistent level of damage was produced in the group infused with PAF for 20 min with the stomach removed 60 min later, this protocol was used in all subsequent experiments. To test the relationship between dose of PAF and the extent of gastric damage, PAF was infused i.v. at doses of 10–100 ng per kg per min (20–200 pmol per kg per min); 1 h later the stomachs were removed, opened and the mucosa was photographed using colour transparency film. Samples from the fundic region were fixed in neutral-buffered formalin for subsequent histological analysis. The severity of macroscopically visible damage was scored, independently, by two observers in a randomized, blind manner and assigned a score on a scale from 0 (normal) to 3 (severe) (see Fig. 1 legend).

All doses of PAF produced areas of macroscopically visible gastric hyperaemia, with doses of 30–100 ng per kg per min producing extensive, severe hyperaemia and haemorrhage (Fig. 1). As evaluated histologically, the damage caused by these doses of PAF was characterized by extensive vascular congestion, extravasation of erythrocytes, destruction of the surface epithelium, dilatation of glands and focal regions of necrosis extending throughout the depth of the mucosa (Fig. 2). The incidence of these effects increased with an increase of the dose of PAF infused. In addition to congestion of mucosal and submucosal blood vessels with erythrocytes, aggregates of polymorphonuclear leukocytes were frequently observed, particularly at the base of the mucosal glands.

As has been reported previously[9], infusion of PAF had significant dose-related hypotensive effects. At doses of 10, 30, 50 and 100 ng per kg per min, PAF produced decreases in mean systemic arterial blood pressure of 18±4, 48±4, 62±4 and 64±9 mm Hg, respectively ($n = 5$ per group). Although it is well established that both clinical and experimental shock are associated with acute gastric ulceration[15], a reduction in blood pressure

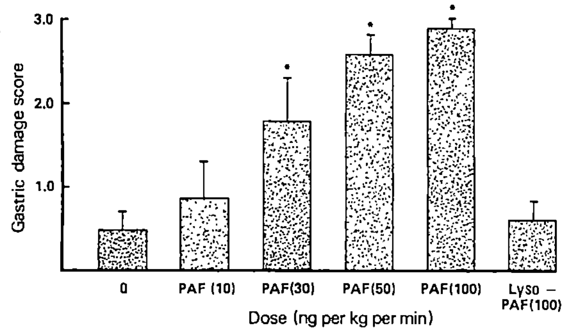

Fig. 1 Gastric damage scores for rats given PAF, lyso-PAF or vehicle alone i.v. for 20 min. Damage was assessed from colour transparencies taken 1 h after completion of the infusion. A score of 0 was assigned if the mucosa appeared normal. A stomach exhibiting haemorrhage or erythaema was assigned a score of 1 (diffuse), 2 (moderate, multiple sites) or 3 (severe, extensive). The scoring was done independently by two observers in a randomized, blind manner and there was a highly significant correlation ($r = 0.87$; $P < 0.001$) between the scores assigned by the two observers. Asterisks indicate groups which differ significantly ($P < 0.05$) from the control group.

Table 1 Effects of hypotensive agents on gastric mucosal damage

Compound	Dose (μg per kg per min)	Damage score	% With haemorrhage	Δ *BP* (mm Hg)
Vehicle	—	0.5 ± 0.2	0	1 ± 2
PAF	0.05	2.6 ± 0.2*	75	62 ± 4*
Prostacyclin	0.5	0.6 ± 0.2	0	55 ± 4*
Isoprenaline	0.5	0.3 ± 0.2	0	50 ± 3*
Nitroprusside	10.0	1.4 ± 0.4†	0	72 ± 2*

Hypotensive agents were administered i.v. for 20 min; 1 h after completion of the infusion, the stomach was removed and the damage assessed as described in Fig. 1 legend. The presence of haemorrhage was determined histologically and is expressed here as the per cent of the total number of rats in which haemorrhage was observed. In the control group, vehicle (0.25% bovine serum albumin in normal saline) alone was infused. Isoprenaline hydrochloride (Sigma) and sodium nitroprusside (BDH) were dissolved in normal saline. Prostacyclin (Wellcome Foundation Ltd) was dissolved initially in 1 M Tris buffer (*p*H 8.5) then diluted in 1.25% sodium bicarbonate. Results are the mean ±s.e.m. for 5–8 rats per group. Δ *BP* represents the decrease in mean arterial blood pressure during the infusion of the compound. With all agents, the peak fall in blood pressure was observed within 1 min of the start of the infusion and the depression of blood pressure was maintained throughout the infusion period. After termination of the infusion, the blood pressure returned to control levels within 10 min.

* $P < 0.01$; † $P < 0.05$, significant difference compared with the control group.

by pharmacological vasodilators is not generally associated with such mucosal damage. However, to determine whether the fall in blood pressure produced by PAF was itself sufficient to induce gastric damage in the present study, some other hypotensive agents were administered i.v. according to the same protocol. Isoprenaline (0.5 μg per kg per min), prostacyclin (0.5 μg per kg per min) and nitroprusside (10 μg per kg per min) each produced a rapid fall in blood pressure of 50–70 mm Hg which was comparable to that induced by high doses of PAF and was maintained throughout the period of infusion (Table 1). Only infusion of nitroprusside produced macroscopic gastric damage, but this was significantly less severe ($P < 0.05$) than that produced by a dose of PAF (30 ng per kg per min) which elicited a significantly smaller ($P < 0.05$) fall in blood pressure. Furthermore, histological evaluation revealed that none of these hypotensive agents produced haemorrhagic erosions in the gastric mucosa. Thus, the fall in blood pressure induced by PAF would be insufficient alone to produce the observed mucosal damage.

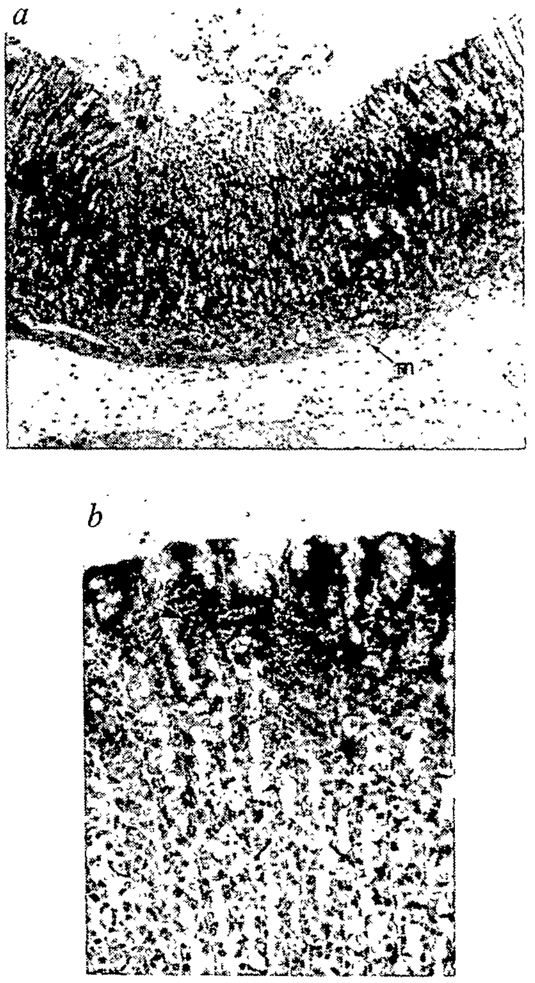

Fig. 2 *a*, Haemorrhagic erosion in the gastric mucosa of a rat given PAF (100 ng per kg per min) for 20 min. The tissue was fixed 1 h after completion of the infusion. Note that the necrotic region extends down to half the depth of the mucosa and does not penetrate the muscularis mucosae (m). Extruded cells (e) can be seen in the lumen. (Haematoxylin and eosin stain. ×39.) *b*, Mucosal vasocongestion (arrows) in gastric mucosa of rat given PAF as for *a*. This engorgement extended throughout the entire depth of the mucosa. Macroscopically, this region appeared hyperaemic. (Haematoxylin and eosin stain. ×96.)

We investigated whether the effects of PAF are shared by its structurally similar precursor and breakdown product, lyso-PAF (1-*O*-alkyl-*sn*-glyceryl-3-phosphorylcholine). Lyso-PAF (100 ng per kg per min) given i.v. had no significant effect on the gastric mucosa, as assessed either macroscopically (mean score of 0.6 ± 0.2) or histologically, nor did it affect blood pressure. A higher dose of lyso-PAF (10 μg per kg per min), which also failed to alter the blood pressure, produced diffuse mucosal hyperaemia (mean score of 1.4 ± 0.3). The level of damage was less than that produced by PAF at 30 ng per kg per min, indicating a difference in ulcerogenic potency of over 3,000-fold, while a dissociation between the gastric-damaging actions and any hypotensive actions of lyso-PAF was clearly demonstrated.

Although PAF has been shown to be a vasodilator in most organs and to increase vascular permeability, its actions on the gastric vasculature are not yet known. Histamine, a vasodilator, has been suggested to have pro-ulcerogenic actions[16], perhaps through its ability to increase capillary permeability. Several agents which have vasconstrictor actions in the gastric mucosa have also been shown to be pro-ulcerogenic: for example, thromboxane A_2 (ref. 17) and noradrenaline[18]. Release of these endogeneous mediators could, therefore, be involved in the ulcerogenic actions of PAF. To test for any such role, an inhibitor of cyclooxygenase (indomethacin), an α-adrenergic receptor antagonist (phentolamine) or a histamine H_1-receptor antagonist (mepyramine) was administered before i.v. infusion of PAF (50 ng per kg per min) at a dose yielding a damage score of 2.6 ± 0.2. Indomethacin (5 mg per kg subcutaneous) administered 45 min before PAF caused a significant ($P < 0.001$) increase in the damage score (3.0 ± 0; $n = 4$). Pretreatment with phentolamine (10 mg per kg i.v.) or mepyramine (5 mg per kg i.p.) did not significantly affect the extent of damage induced by PAF (mean score 2.0 ± 0.2, $n = 5$ and 2.0 ± 0, $n = 3$, respectively). The ulcerogenic actions of PAF therefore appear to be independent of the release of these mediators.

Although resting gastric acid secretion in the anaesthetized rat is low, intragastric instillation of 0.1 M HCl (3 ml) before PAF infusion (50 ng per kg per min) did not significantly augment the severity of macroscopic damage, although the regions of mucosal haemorrhage were stained black. Furthermore, i.v. administration of antisecretory doses of the H_2-receptor antagonist cimetidine (50 mg per kg) 15 min before infusion of PAF (100 ng per kg per min) did not significantly reduce the severity of the gastric damage (mean score of 2.8 ± 0.3; $n = 4$). Thus, unlike the case with many experimental models of gastric damage, the presence of a high intraluminal concentration of acid is not a prerequisite for PAF-induced ulceration.

Despite its name, PAF does not cause platelet aggregation in the rat, nor does it cause the thrombocytopenia that is associated with infusion of PAF in other species[9]. However, it might stimulate the release of biologically active mediators from platelets which could contribute to the ulcerogenesis. This possibility was studied in rats made thrombocytopenic 24 h previously by i.v. injection of an anti-platelet serum raised in rabbits against rat washed platelets[19]. Reduction of the number of circulating platelets by 85–90% below that of control rats treated with normal rabbit serum did not reduce the damage (mean score 2.2 ± 0.6; $n = 3$) produced by PAF (50 ng per kg per min).

Our studies demonstrate that PAF is a potent ulcerogenic agent in the rat stomach. In a previous study on ischaemic bowel necrosis, haemorrhagic lesions were observed in the rat gastric mucosa after i.v. injections of very high doses of PAF in combination with endotoxin[13]. While the hypotensive actions of PAF could contribute to its ulcerogenic actions, especially at the higher doses, this is unlikely to be the sole mechanism. However, a local vascular action of PAF may well be important. Indeed, the histological observations of vascular congestion suggest that stasis may be a precipitating event in the ulceration process. Stasis could occur as a result of vasoconstriction, exudation of plasma, or through aggregation of one or more of the cellular components of blood. PAF has potent pro-aggregatory and degranulatory effects on neutrophils both *in vivo*[20] and *in vitro*[21]. Infusion of PAF to rabbits leads to substantial neutropenia, perhaps as a result of sequestration of neutrophil aggregates in the lung and other tissues[20,22]. Sequestration of neutrophil aggregates in the stomach, as observed in the histological sections taken after PAF administration, could thus contribute to congestion of the mucosal vasculature. Generation of free radicals and release of lysosomal enzymes following neutrophil aggregation could also contribute to the tissue damage induced by PAF.

Gastric damage was observed with a dose of PAF as low as 20 pmol per kg per min, the total dose administered over 20 min being 400 pmol per kg. Concentrations of PAF of 4.7 nM have been found in the blood of rats during endotoxin shock; this concentration could be achieved by an infusion of PAF at 300 pmol per kg[12]. Hence, the doses of PAF which produced extensive gastric damage in the present model are within the range of concentrations found *in vivo* in a model of a disease associated with acute gastric ulceration. The use of specific PAF antagonists will help to clarify the contribution of endogeno PAF to such gastric damage. Whether the release of PAF fr circulating or entrapped blood cells under other circumstanc such as after haemorrhagic shock, also contributes to gast damage is not yet clear. It is conceivable that in conditio characterized by infiltration of inflammatory cells, or in sequence of events following local tissue damage, PAF may released directly into the mucosa. Thus, both systemic and lo release of PAF could initiate or further amplify gastric ulcerati under pathological conditions.

J.L.W. is the recipient of a fellowship from the MRC Canada.

Received 13 September; accepted 31 October 1985.

1. Benveniste, J., Henson, P. M. & Cochrane, C. G. *J. exp. Med.* **136,** 1356–1377 (1972).
2. Lynch, J. M., Lotner, G. Z., Betz, S. J. & Henson, P. M. *J. Immun.* **123,** 1219–1226 (19
3. Chignard, M., LeCoudic, J. P., Tence, M., Vargaftig, B. B. & Benveniste, J. *Nature* 799–800 (1979).
4. Mencia-Huerta, J. M. & Benveniste, J. *Eur. J. Immun.* **9,** 409–415 (1979).
5. Camussi, G. *et al. J. Immun.* **131,** 1802–1807 (1983).
6. Camussi, G. *et al. Immunology* **42,** 191–199 (1981).
7. Benveniste, J. *Nature* **249,** 581–582 (1974).
8. Prescott, S. M., Zimmerman, G. A. & McIntyre, T. M. *Proc. natn. Acad. Sci. U.S.A.* 3534–3538 (1984).
9. Vargaftig, B. B., Chignard, M., Benveniste, J., Lefort, J. & Wal, F. *Ann. N.Y. Acad.* **3710,** 119–137 (1981).
10. Doebber, T. W., Wu, M. S. & Shen, T. Y. *Biochem. biophys. Res. Commun.* **125,** 980- (1984).
11. Terashita, Z., Imura, Y., Nishikawa, K. & Sumida, S. *Eur. J. Pharmac.* **109,** 257–261 (19
12. Doebber, T. W. *et al. Biochem. biophys. Res. Commun.* **127,** 799–808 (1985).
13. Gonzalez-Crussi, F. & Hsueh, W. *Am. J. Path.* **112,** 127–135 (1983).
14. Skillman, J. J., Gould, S. M., Chung, R. S. K. & Silen, W. *Ann. Surg.* **172,** 564–584 (19
15. Harjora, P. T. & Sivula, A. *Ann. Surg.* **163,** 21–28 (1966).
16. Davenport, H. *New Engl. J. Med.* 1307–1312 (1967).
17. Whittle, B. J. R., Kaufmann, G. L. & Moncada, S. *Nature* **292,** 472–474 (1981).
18. Whittle, B. J. R. *Br. J. Pharmac.* **80,** 545–551 (1983).
19. Whittle, B. J. R. *Mechanisms of Mucosal Protection in the Upper Gastrointestinal Tract* Allen, A., Flemstrom, G., Garner, A., Silen, W. & Turnberg, L. A.) 295–301 (Raven, York, 1984).
20. McManus, L. M., Hanahan, D. J., Demopoulos, C. A. & Pinckard, R. N. *J. Immun.* 2919–2924 (1980).
21. Camussi, G. *et al. Int. Archs Allergy appl. Immun.* **64,** 25–41 (1981).
22. Camussi, G., Tetta, C. & Bussolino, F. *Prostaglandins* **25,** 343–351 (1983).

1-Methyl-4-phenylpyridine is neurotoxic to the nigrostriatal dopamine pathway

A. J. Bradbury*, B. Costall*, A. M. Domeney*, P. Jenner†, M. E. Kelly*, C. D. Marsden† & R. J. Naylor*

* Postgraduate School of Studies in Pharmacology, University of Bradford, Bradford BD7 1DP, UK
† MRC Movement Disorders Research Group, University Department of Neurology and Parkinson's Disease Society Researc Centre, Institute of Psychiatry and King's College Hospital Medica School, Denmark Hill, London SE5 8AF, UK

Systemic administration of 1-methyl-4-phenyl-1,2,3,6-tetrahyd pyridine (MPTP) is neurotoxic to cerebral dopaminergic neuro in several animal species, and can cause parkinsonism in man[1] The mechanism of this action may be indirect. MPTP is oxidi in the brain to a pyridinium species, 1-methyl-4-phenylpyrid (MPP^+)[6]. This oxidation is greatly decreased by inhibition monoamine oxidase B[6], as are the biochemical effects of MP in the mouse[7] and its neurotoxicity in the monkey[8]. We now s that MPP^+ exerts a powerful neurotoxic action on the nigrostria dopamine system of the rodent.

The neurotoxic potential of MPP^+ in the mouse was initia investigated by injecting MPP^+ (10 μg) dissolved in distil water into the ventricular system, a route selected to avoid difficulties of penetrating the blood–brain barrier. Mice recei one injection daily for 3 days, via chronically in-dwelling gu

Table 1 Neurotoxic action of MPP^+ and MPTP infused into rat substantia nigra revealed as depletions of dopamine/metabolites in posterior striatum

Treatment	Dopamine (ng per mg tissue)	DOPAC	HVA (pg per mg tissue)	Serotonin	5-HIAA
Vehicle	2.70 ± 0.4	242 ± 23	166 ± 36	338 ± 62	281 ± 24
MPTP	2.44 ± 0.2	281 ± 17	144 ± 78	485 ± 41	307 ± 22
MPP^+	0.74 ± 0.1*	87 ± 9*	44 ± 8†	414 ± 44	274 ± 15

Male Sprague-Dawley rats (300-325 g) were implanted with chronically in-dwelling guide cannulae aimed at the substantia nigra zona compacta (Ant.2.2, Vert.1.8, Lat. ± 2.0)[11,12] and were subsequently implanted subcutaneously (in the interscapular region) with two Alzet osmotic minipumps. MPTP (Research Biochemicals Inc.) or MPP^+ dissolved in distilled water was continuously infused bilaterally via injection units connected to the pumps at a rate of 0.48 μl h^{-1}, containing 10 μg per day, for 4 days. Levels of dopamine, serotonin and their metabolites in the posterior striatum were determined by high-pressure liquid chromatography. Values are expressed as the mean ±1 s.e.m.; $n = 5$.

* $P < 0.01$ and † $P < 0.05$ compared with vehicle treatment; Mann-Whitney *U*-test.

cannulae, and were killed on day 4. At this time, striatal dopamine levels were reduced by 35%, and 3,4-dihydroxyphenylacetic acid (DOPAC) levels by 27%, with no reductions in levels of homovanillic acid (HVA), serotonin or 5-hydroxyindoleacetic acid (5-HIAA). Thus, MPP^+ was shown to have actions on dopaminergic neurones, the modest reductions perhaps reflecting the difficulties encountered by MPP^+ in penetrating the neostriatal complex from the ventricular system.

Consequently, in a second series of experiments, MPTP and MPP^+ were infused directly into the dopaminergic cell body group in the substantia nigra of the rat. The rat was a particularly suitable species for these studies because it is relatively insensitive to the neurotoxic actions of MPTP[6,9]. To minimize problems of nonspecific damage, MPTP and MPP^+ (10 μg per 24 h) were infused bilaterally into the substantia nigra via chronically in-dwelling guides and injection units. Motor functions, including locomotor response, ability to climb and grip on a vertical wire grid, and the presence of rigidity in the limbs and trunk were recorded daily during 4 days of infusion. Rats were killed 1 day and 1 month after the infusions and the striatum was dissected for analysis of the content of dopamine and serotonin, and their metabolites, and for estimates of ^{3}H-dopamine uptake into striatal synaptosomes.

Even when MPTP was infused continuously into the substantia nigra, there was no loss of striatal dopamine or its metabolites (Table 1). There was a small decrease in ^{3}H-dopamine uptake into striatal synaptosomes 1 day after cessation of MPTP administration (vehicle, 0.91 ± 0.01; MPTP, 0.62 ± 0.15 pmol ^{3}H-dopamine per mg protein per 6 min, $P < 0.05$, $n = 4$), but this was not present 1 month after MPTP treatment (vehicle, 1.05 ± 0.17; MPTP, 0.82 ± 0.08 pmol ^{3}H-dopamine per mg protein per 6 min, $P > 0.05$, $n = 4$).

In contrast, MPP^+ infused into the rat substantia nigra was markedly neurotoxic to dopamine function; striatal dopamine levels 1 day after the infusion were reduced by 73%, DOPAC levels by 64% and HVA by 27%, with no change in levels of serotonin or 5-HIAA (Table 1). Infusion of MPP^+ caused a large decrease in ^{3}H-dopamine uptake at both 1 day and 1 month post-infusion (1 day, 0.27 ± 0.04; 1 month, 0.36 ± 0.04 pmol ^{3}H-dopamine per mg protein, both $P < 0.001$ compared with vehicle controls (results above), $n = 4$).

MPP^+ infused into the substantia nigra caused profound motor deficits, in contrast to the less severe effects of MPTP. Both neurotoxins caused reductions in locomotion and loss of ability to coordinate movements of the front limbs, seen as an inability to grip on a vertical wire grid and so climb on the grid. However, the effects of MPP^+ were more severe, with additional loss of the ability to use the hindlimbs to grip and climb on the vertical grid, and the development of rigidity in forelimbs, hindlimbs and trunk (Table 2). These effects developed within 12 h of the start of MPP^+ infusion into the substantia nigra and were maximal by day 2. The overall impression of the effects of MPP^+ treatment was the appearance of a severe motor impairment.

Table 2 Motor impairment caused by the bilateral infusion of MPTP and MPP^+ into rat substantia nigra

Treatment	Locomotor activity	Grid test	Rigidity
Vehicle	92 ± 10.0	20 ± 0.0	0.0 ± 0.0
MPTP	40 ± 5.1*	9.3 ± 0.8*	0.0 ± 0.0
MPP^+	13 ± 1.4*	0.0 ± 0.0*	15.0 ± 0.0*

Locomotor activity was measured daily in individual photocell cages; interruptions of beams were recorded every 5 min and summed to give counts per 60 min. Locomotor depression was maximal by day 2; data are given for day 3 (±1 s.e.m.). Deficits in limb movement were assessed using a vertical wire grid and scored as follows: (1) climbing upwards or sideways on grid; (2) maintaining position on grid for 30 s; (3) gripping grid with forepaws; (4) gripping grid with hind paws. Results are expressed as the total score (±1 s.e.m.) for five test sessions on days 2-4 of infusion. Rigidity was noted as being present or absent in the forelimbs, the hindlimbs and the trunk, giving a maximum score of 3 for each animal. Results are expressed as the total score (±1 s.e.m.) determined during five test sessions on days 2-4 of infusion. $n = 5$.

* $P < 0.001$ compared with vehicle treatment; one-way ANOVA followed by Dunnett's test.

These studies in the rodent emphasize that the oxidative metabolism of MPTP is required for expression of its neurotoxic action, and that one metabolite, MPP^+, found in monkey and mouse brain after MPTP administration[6], has powerful neurotoxic action on the nigrostriatal dopaminergic system. The previous uncertainty as to whether MPTP neurotoxicity results from the formation of MPP^+ or from the oxidative processes forming MPP^+ is thus partly resolved; MPP^+ itself appears neurotoxic, although histological assessment of the extent and specificity of the neuronal damage caused by MPP^+ is required. It remains possible that the oxidative processes forming MPP^+ also have neurotoxic potential. However, the nature of the motor deficits and severity of the loss of striatal dopaminergic function caused by MPP^+ may provide clues to the pathogenesis of Parkinson's disease.

This work was supported by the MRC, the Parkinson's Disease Society, the Wellcome Trust and the SERC. We thank Dr W. Langston for the gift of MPP^+.

Received 7 May; accepted 10 October 1985.

1. Langston, J. W., Forno, L. S., Rebert, C. S. & Irwin, I. *Brain Res.* **292**, 390-394 (1984)
2. Langston, J. W. & Ballard, P. *Can. J. neurol. Sci.* **11**, 160-165 (1984).
3. Burns, R. S. *et al. Proc. natn. Acad. Sci. U.S.A.* **80**, 4546-4550 (1983).
4. Heikkila, R. E., Cabbat, F. S., Manzino, L. & Duvoisin, R. C. *Neuropharmacology* **23**, 711-713 (1984).
5. Chiueh, C. C. *et al. Eur. J. Pharmac.* **100**, 189-194 (1984).
6. Markey, S. P., Johannessen, J. N., Chiueh, C. C., Burns, R. S. & Herkenham, M. A. *Nature* **311**, 464-467 (1984).
7. Heikkila, R. E., Manzino, L., Cabbot, F. S. & Duvoisin, R. C. *Nature* **311**, 467-469 (1984)
8. Langston, J. W., Irwin, I. & Langston, E. B. *Science* **225**, 1480-1482 (1984).
9. Bradbury, A. J. *et al. Br. J. Pharmac.* **83**, 395P (1984).
10. Bradbury, A. J., Costall, B. & Naylor, R. J. *Neuropharmacology* **22**, 1172-1176 (1983)
11. de Groot, J. *Verh. K. Akad. Wet.* **52**, 14-40 (1967).
12. Domeney, A. M., Costall, B. & Naylor, R. J. *Neuropharmacology* **21**, 327-335 (1982).

A large anion-selective channel has seven conductance levels

Mauri E. Krouse, Gavan T. Schneider & Peter W. Gage

Department of Physiology, John Curtin School of Medical Research, Australian National University, ACT 2601, Australia

Ion channels have generally been found to have two predominant conductance levels thought to be associated with 'open' and 'closed' states, but intermediate (subconductance) states have also been reported[1-3]. We have now found that a large conductance, anion-selective channel in pulmonary alveolar epithelial cells[4] can adopt any of six open levels of conductance that are integer multiples of 60–70 pS. The channel is usually either fully open or fully closed. The frequencies of the different conductance levels are inconsistent with the notion that there are six independent channels. We suggest that the channel consists of six conducting pathways in parallel, 'co-channels', with a shared gating mechanism that can synchronously render all of them non-conducting. Other channels with lower maximum conductance may operate in a similar way but multiple conductance levels would not easily be detected because of a less favourable signal-to-noise ratio.

Currents were recorded at room temperature (21-25 °C) from inside-out patches excised from the apical surface of cultured mouse alveolar type II cells. Recording procedures are described elsewhere[4]. Excised patches were held at 0 mV and then stepped to positive or negative potentials to record currents. Following a step in potential, patches are seen to contain from 0 to 4 channels, each with a conductance of ~400 pS. In most patches, channels become inactivated with time, becoming completely inactivated within 6 s to 10 min and inactivating more rapidly the further the potential is stepped away from 0 mV. Inactivation could be reversed by returning to 0 mV. Thus, the large conductance anion channel in pulmonary epithelial cells has characteristics in common with large conductance anion channels described in other tissues[5-7].

Selected current records, obtained from an excised patch in which there appears to be only one 400-pS channel following a voltage step from 0 to 57 mV, are shown in Fig. 1. This channel displays rapid inactivation so that no full openings are observed after 10 s. The records shown in Fig. 1 were chosen to illustrate the different current levels and types of channel behaviour. In Fig. 1*A*, the channel is open most of the time, closing several times near the middle of the record. The mean current through the open channel (upper level) is 23 pA, corresponding to a conductance of 404 pS (holding potential 57 mV, null potential 0 mV), similar to previous reports[4] of the conductance for this channel. The noise level (flickering) is greater when the channel is open than when it is closed. This phenomenon is even more noticeable in Fig. 1*B*, *C*; *B* shows the current fluctuating between 21 and 15 pA, the latter being about two-thirds of the open current, whereas *C* shows the current fluctuating between 23 and 12 pA, the lower level being about half the maximum current. Occasionally, the current fluctuates between 0 and 7.5 pA (Fig. 1*D*) and, less frequently, clear steps occur from the closed state to the lowest level, which is about one-sixth of the maximum current (Fig. 1*E*). In all 41 patches studied, only transitions between the fully open and closed states are seen at first, followed by the invariable appearance of subconductance levels.

Records such as those shown in Fig. 1*A*–*E* strongly suggest that there are several subconductance states of these channels. Clearer examples of the six current levels recorded in several different patches are shown in Fig. 1*F*. The levels are always approximately an integer multiple (up to six) of one-sixth of the maximum current, although it is often difficult to differentiate between the maximum and five-sixth maximum levels because of rapid transitions between the two. Furthermore, the average current at the lowest level is often less than one-sixth

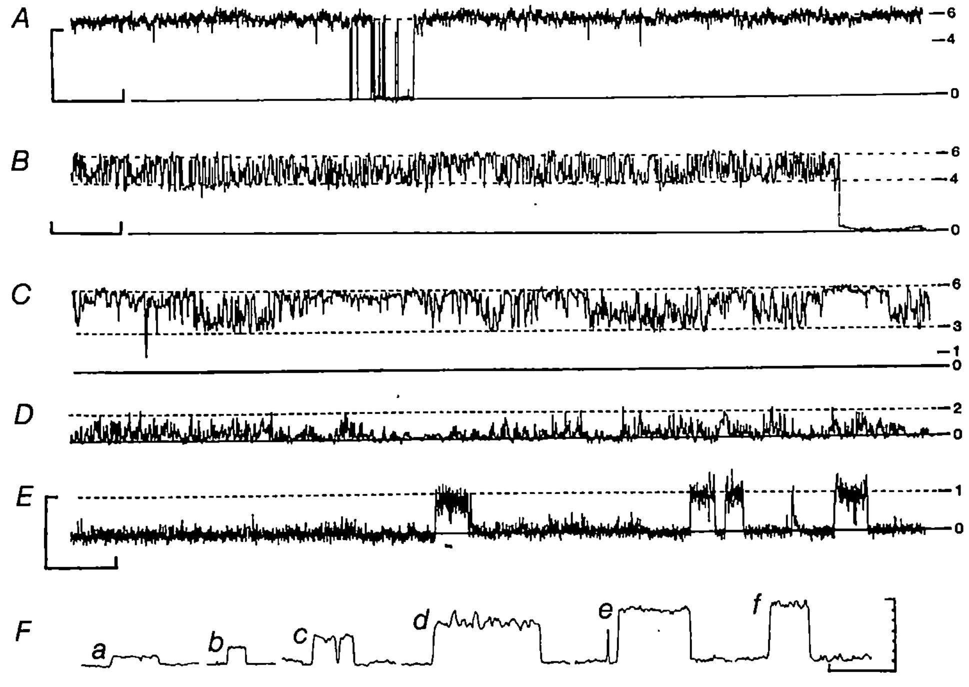

Fig. 1 *A*–*E*, Records of currents from an excised, inside-out patch of membrane following a voltage step from 0 to +57 mV (voltage of the bath solution on the cytoplasmic surface of the membrane with respect to the pipette solution). The bath and pipette contained the same solution (140 mM NaCl, 3 mM CsCl, 1 mM $MgCl_2$, 2 mM $CaCl_2$, 10 mM glucose, 10 mM Na^+-HEPES, *p*H 7.3). Upward deflections represent positive current flowing from the bath into the pipette (chloride ions moving in the opposite direction). Current was recorded on an FM tape recorder and subsequently played back through a 4-pole Bessel filter (−3 dB at 5.3 kHz), digitized at 25 μs per point and analysed by computer. Records were selected to show different current levels. Numbers on the right of each record and the broken lines show integer multiples of the lowest level seen (*E*); solid lines show the baseline (closed channel) current level. *A*, Transitions between fully open and closed levels (the commonest transitions). *B*, Transitions between the fully open and fourth levels (followed by a transition to the closed level) with the fifth level also present. *C*, Transitions between the fully open and third levels with the fourth and fifth levels also present. *D*, Transitions between the closed and second level with the first level also present. *E*, Transitions between the closed and first level. The dotted line was drawn at one-sixth of the maximum current level. Scale bars: *A*, 20 pA and 100 ms; *B*–*D*, 20 pA and 20 ms; *E*, 7 pA and 500 ms. *F*, Records obtained from five different patches clearly showing maintained current levels at 1, 2, 3, 4, 5 and 6 (*a*–*f*) times the first (lowest) current level (*a*). The Bessel filter cutoff (−3 dB) was set in the range 0.7–3.3 kHz.

of the maximum level (see Fig. 1*E*), presumably because of rapid flickering between open and closed states[10].

Amplitude histograms of currents recorded from individual patches also provide evidence for multiple conductance levels. Figure 2 shows an amplitude histogram of a 91-s record from the same patch as in Fig. 1. The period was chosen because it contained several lowest-level openings, including those in Fig. 1*E*. The histogram has peaks showing that there is a significant probability that the current could be at several levels between the fully open and closed levels. The units in the lower abscissa are one-sixth of the current between the first and last peaks. The second peak at ~5 pA gives a first-level current less than one-sixth of the maximum current level, as expected if there is rapid flickering between the first level and the closed state.

One simple model for the multiple current levels is that they are caused by contributions from six channels opening and closing independently. However, two characteristics of the currents exclude this possibility. First, following a shift in potential, some patches have conductances that are integer multiples of 400 pS and the conductance decreases in 400-pS steps. It would be a remarkable coincidence if all the 41 patches studied here contain an integer multiple of six independent channels and if the channels then dropped out in groups of six. Second, more than half of 1,000 measured transitions between clearly distinguishable levels appear to be (within less than 100 μs) between the fully open and closed states, with no sign of an intermediate level even at 4 kHz bandwidth. If a single channel has a mean open time of 3 ms (approximately the mean duration of the first conductance level; see Table 1), the probability of six channels closing within a 100-μs period would be $(1-\exp(-100/3{,}000))^6$, that is, less than 10^{-8}. It seems very unlikely, therefore, that independent channels with a conductance of ~70 pS could produce the patterns of current levels we have observed.

Several other models to explain our observations proved unsatisfactory. For example, there could be six sequential open conformations of a single channel, each with a different conductance. This model requires the unlikely assumption that the difference in conductance is the same between each state. Moreover, we were unable to find a set of rate constants linking such states which would give rapid transitions between the closed and fully open states and still allow persistent intermediate states such as those observed. Alternatively, there could be six open states of a channel connected via a single closed state but this would suggest that different current levels should be separated by a closed level, which was seldom seen.

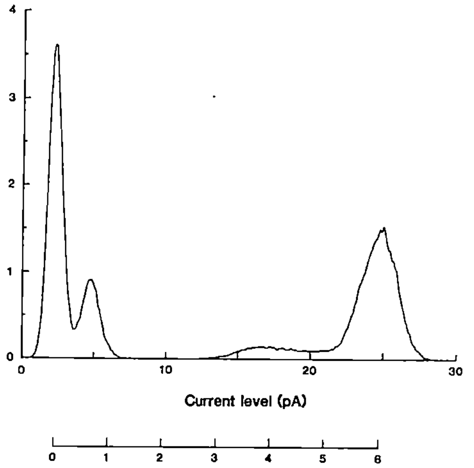

Fig. 2 Current amplitude during a 91-s recording period from the same patch as in Fig. 1*A–E*. The section of record was chosen for analysis because it contained examples of the first (lowest) current level and, for this reason, the histogram shows a peak at ~5 pA. Generally, only three peaks are seen (0, 4, 6), the peak for the lowest current being spread out and covering the 0, 1 and 2 current levels. The lower abscissa has units that are one-sixth of the difference between the peaks of the lowest and highest current amplitude. The probability of residing in each of the levels is given by the area under each of the peaks. The offset of the first peak from zero indicates a seal resistance of ~25 GΩ.

The appearance of seven equally spaced conductance levels together with step changes between the closed and fully open states suggests that the channel consists of six identical conducting units (co-channels) that function cooperatively to form a single channel. We believe that our results can be explained by a model in which the channel consists of a cluster of six co-channels sharing a common regulatory 'gate' that can occlude all six simultaneously. A similar model with two conducting units has been proposed previously by Miller to explain the behaviour of a small chloride channel in electroplaques[8]. It has also been suggested that the selectivity of high-conductance potassium channels arises in a similar way[9].

To test this model, we analysed currents from two patches that exhibited fully open states at the end of recording periods of 30–100 s. Measurements were made of the time spent at each of the seven levels (0, 1, 2, 3, 4, 5 and 6 times one-sixth of maximum). To exclude noisy transitions between levels, we only accepted those levels maintained for ⩾0.3 ms. Because of the

Table 1 Results of analysis to test for the presence of co-channels

Level	No. of events	Observed open time	Observed occupancy	Open-state occupancy	Predicted occupancy	Predicted open time
0	101	2.50	0.145	—	0.001	—
1	5	3.02	0.009	0.010	0.009	3.32
2	34	4.07	0.079	0.092	0.053	3.72
3	45	4.24	0.110	0.129	0.175	4.25
4	89	5.56	0.284	0.332	0.321	4.94
5						
6	104	6.25	0.373	0.436	0.442	6.25

Measurements of current levels lasting longer than 0.3 ms in recordings of current from two patches in which the channel continued to show full openings at the end of a recording period. Because of difficulty in distinguishing the fifth and sixth levels, the two are taken together. Observed occupancy gives the fraction of the total measurement time that a channel was at a given current level, including closed. The fraction of the total measurement time that co-channels were open (excluding the closed times that were considered to be due, primarily, to the presence of a regulatory gate) is given by open-state occupancy. Predictions of the occupancy of any of the current levels are given in the sixth column. To calculate the probabilities, it was assumed that there were six identical, independent co-channels, each with a p of 0.71. The predicted occupancies were calculated from the binomial equation $P_k=\binom{6}{k}p^k(1-p)^{6-k}$ (that is, $P_0=(1-p)^6$, $P_1=6p(1-p)^5 \ldots P_{5+6}=6p^5(1-p)+p^6$). Deviations between predicted and observed occupancies at the lower levels are not surprising because: (1) the smaller number of events increases the measurement error; and (2) the exclusion of rapid flickering from the data would affect measured mean open time. The predicted open times were obtained from the assumption of a simple two-state model, a co-channel open probability of 0.71 and the observed open time of the 5+6 level (see text).

continuous flickering between the five-sixth and six-sixth level, the two were difficult to distinguish so were taken together and treated as a single level. The frequency of the closed state is an underestimate because we included only those times between two clearly identified open states: we excluded closed states showing rapid flickering. We have not included long closed periods (often of several seconds duration) which occur between bursts of channel openings. Results of our analysis are shown in Table 1. The fraction of the total time for which a current level was observed is given in column 4 (observed occupancy). The open-state occupancies, obtained by excluding the closed state (0 level), are also shown in Table 1.

If we assume that we are observing current flowing through six co-channels opening and closing independently (except when the channel is closed by a shared gate), the open-state occupancies should conform with a binomial distribution. Occupancies predicted for six co-channels, each with an open probability (p) of 0.71, are given in Table 1. There is good agreement between the observed and predicted open-state occupancies. Again, the discrepancy between the observed and predicted 0-level occupancies highlights the need to propose a superimposed shared gating mechanism that occludes all six co-channels at least 14.5% of the time.

Such a binomial scheme can be used to predict the probability of transitions between current levels[8]. If the behaviour of each co-channel can be described by

$$\mathrm{C} \underset{b}{\overset{a}{\rightleftharpoons}} \mathrm{O}$$

where C and O are the closed and open states of each co-channel, a is the opening rate and b the closing rate, it is possible to predict open times of multiple co-channel states. For example, the rate of leaving the state associated with four open co-channels is $4b+2a$, where $4b$ is the rate for one of four open co-channels closing and $2a$ the rate for one of two closed co-channels opening. If the probability of each co-channel being open is 0.71, as before, then $a/b=p/1-p=2.45$ and the rate of a channel leaving the four-co-channel state is $8.9b$. Rates of leaving each of the other multiple-co-channel states can be calculated in a similar way. The predicted open times (reciprocals of the rates) of each multiple-co-channel state were calculated from a value of b obtained from the mean duration of the $5+6$ level (for which most data were available, see Table 1). There is clearly good agreement between observed open and predicted open times (Table 1).

Thus, evidence for our co-channel model is: (1) channels of high conductance that show seven equally spaced conductance levels; (2) a high percentage of rapid transitions between closed and fully open states; (3) open-state probabilities and open times consistent with the existence of six identical, independent co-channels; and (4) a closed-state probability and closed time greater than expected from six independent co-channels.

This kind of channel behaviour is probably not confined to pulmonary alveolar cells. Records of currents from high-conductance chloride channels in a variety of tissues[5-7] show subconductance states and transitions similar to those described here. Furthermore, multiple conductance levels between fully open and closed levels have been noted in other large-conductance channels[11-13] and single subconductance states have been seen in smaller channels[1-3]. Indeed, it has been reported recently that a potassium channel in an *Aplysia* neurone[14] displays both equally spaced conductance levels and rapid transitions between fully open and closed states. Such observations raise the possibility that a mechanism involving clusters of co-channels with a shared gate functions in a wide variety of channels in other preparations. If so, the phenomenon is important in channel assembly and function and must be taken into account during analysis of single-channel currents and in the formulation of theories of ion permeation through membranes.

After submission of this paper, a high-conductance chloride channel with 17 conductance levels in a molluscan neurone has been reported[15] and we have observed channels with more than seven current levels.

We thank John Dempster for allowing us to use some of his analysis programs, Mark Rogers for help with analysis and Dr Alasdair Gibb for helpful comments on the manuscript.

Received 23 July; accepted 28 October 1985.

1. Hamill, O. P. & Sakmann, B. *Nature* **294**, 462-464 (1981).
2. Labarca, P. & Miller, C. *J. Membrane Biol.* **61**, 31-38 (1981).
3. Pallotta, B., Magleby, K. & Barret, J. *Nature* **298**, 576-578 (1981).
4. Schneider, G. T., Cook, D. I., Gage, P. W. & Young, J. A. *Pflügers Arch. ges. Physiol.* **404**, 354-357 (1985).
5. Blatz, A. L. & Magleby, K. L. *Biophys. J.* **43**, 237-241 (1983).
6. Nelson, D. J., Tang, J. M. & Palmer, L. G. *J. Membrane Biol.* **80**, 81-89 (1984).
7. Gray, P. T. A., Bevan, S. & Ritchie, J. M. *Proc. R. Soc.* **B221**, 395-409 (1984).
8. Miller, C. *Phil. Trans. R. Soc.* **B299**, 401-411 (1982).
9. Latorre, R. & Miller, C. *J. Membrane Biol.* **71**, 11-30 (1983).
10. Yellen, G. *J. gen. Physiol.* 157-186 (1984).
11. Rae, J. & Levis, R. *Molec. Physiol.* **6**, 115-162 (1984).
12. Kolb, H. A., Brown, C. D. A. & Murer, H. *Pflügers Arch. ges Physiol.* **403**, 262-265 (1985).
13. Gibb, A. J. *Proc. Aust. physiol. pharmac. Soc.* **16** (1985).
14. Kazachenko, V. N. & Geletyuk, V. I. *Biochim. biophys. Acta* **773**, 132-142 (1984).
15. Geletyuk, V. I. & Kazachenko, V. N. *J. Membrane Biol.* **86**, 9-15 (1985).

Permanent distortion of positional system of *Xenopus* embryo by brief early perturbation in gravity

Jonathan Cooke

Laboratory of Embryogenesis, National Institute for Medical Research, The Ridgeway, Mill Hill, London NW7 1AA, UK

The formation of a body plan from an initially radially symmetrical egg during animal development is presumed to involve a 'positional system'[1,2] and a subsequent mechanism of local response to position values provided by this system. Early gene products intimately connected with the latter response mechanism have been identified in *Drosophila*[3-5], and because these share conserved sequences with possible counterparts in vertebrates, there is renewed interest in understanding the physiological nature of the positional system itself in a vertebrate embryo. In the frog *Xenopus*, body position value appears to be specified in outline across much of the egg material by stages comprising a few cells, after only ~2 h of development[6-10]. This is already suggestive of a structural or mechanical recording system rather than a diffusion-controlled gradient. I describe here an experiment aimed at perturbing the positional system by causing gravity-driven rearrangements within eggs which conflict with their own, self-organizing rearrangements near the time of first cleavage. The system appears to retain its full regulatory properties during only a brief time interval, so that records of positional profiles disturbed at the close of that interval are permanent, and give rise to systematically abnormal body patterns in otherwise healthy larvae. The results are inconsistent with the notion that *Xenopus* primary pattern results from a set of determinant 'plasms' in the egg, or from a mechanism dominated by long-range diffusion of molecules[11,12].

The direct action of the positional system occurs mainly in the yolky, endodermal part of the egg. Coordinated mesodermal and ectodermal body contributions are set up later by appropriately balanced spatial patterns of inductive activity emanating from the endoderm[13-16]. The deviant bodies that I shall describe here are detectable on external form alone (top row, Fig. 1), but I have also analysed the mesoderm, whose anatomy is sufficiently differentiated at early larval stages. After 48 h of development (stage 29-30; ref. 17), all mesoderm cells can be scored histologically as members of the different axial pattern elements (see Fig. 2), but there has been little growth to obscure the proportions in which the tissue was originally partitioned

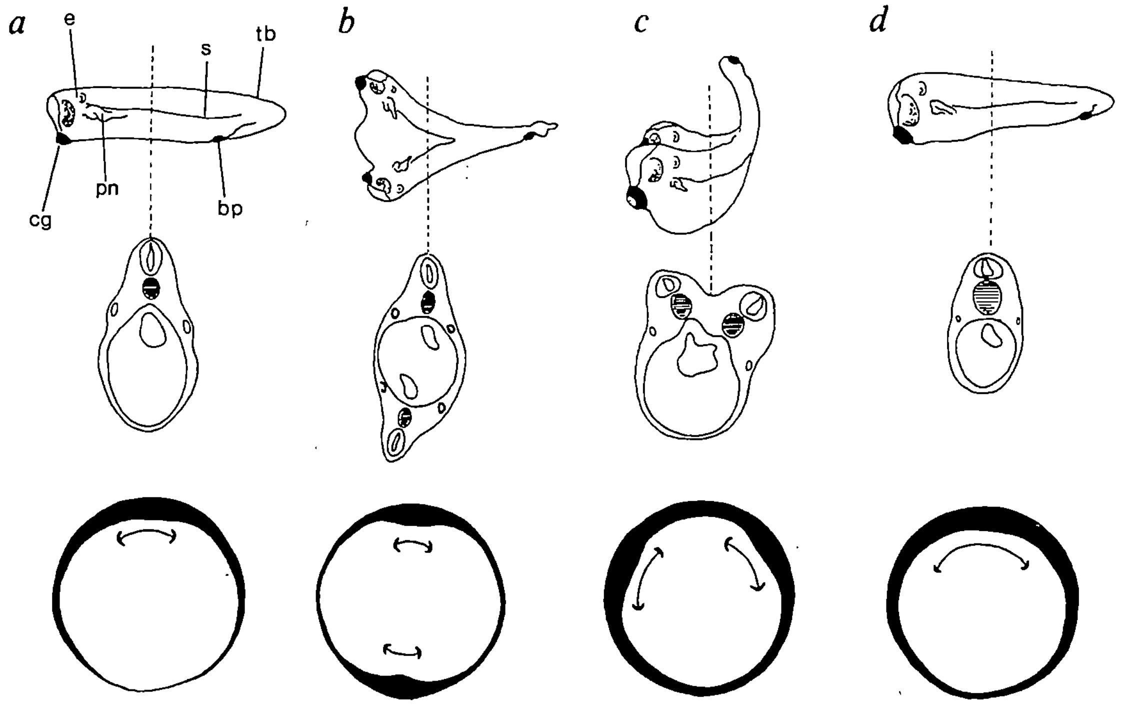

Fig. 1 Twinned and imbalanced body patterns seen after tilting eggs in gravity, and a suggested interpretation. The top row shows camera lucida sketches of the normal body form (*a*) and of three typical experimentally produced body forms (*b*–*d*) at the larval stage used for pattern analysis. *b*, A twinned pattern with approximately equal and opposite partial axes and moderate deficiency of posterior pattern. *c*, A twinned pattern with adjacent and massively constructed partial axes but an extreme deficiency of posterior pattern. *d*, An imbalanced single pattern with systematic over-allocation to dorsal and anterior structure at the expense of posterior structure. The second row shows schematic transverse sections of each body form, at approximately 8th somite level. Neural tubes, notochords (shaded) and the yolky gut mass with a single or double archenteric cavity are shown. Note the relative sizes of the notochord in cross-section. The third row shows corresponding egg outlines in the horizontal plane relative to normal gravity orientation. The thickness of the outline represents the profile around the egg yielding each body form, with respect to levels of activation, or 'body position values', recorded by the early-acting positional system. With the normal, complete profile (*a*), the mes-endodermal body plan is built essentially from head plus notochord towards tail, around the egg meridians from top to bottom of the outline, the position of sperm entry being near the bottom. The separate internal arc opposite the thickest part of the outline represents arbitrarily the normal extent of an egg sector specified for allocation to notochord production. The outlines of *b* and *c* suggest how, when two such peaks of activation arise in one egg after early perturbation of the plasm shifts, interactive effects due to their relative positioning may influence greatly the profile attained by each, and hence the relative amount of the system allocated to notochord and anterior structure. There is a corresponding variable sacrifice of the posterior pattern complement. Such variation is observed (see text). Outline *d*, corresponding to a single but incorrectly proportioned axial pattern, is perhaps an extreme version of type *c* with partial regulation fusing the original centres of activation. Externally visible larval features: e, eyecup; cg, cement gland; pn, pronephros; s, line of lateral edges of somites; bp, proctodaeum (original blastopore); tb, tailbud.

into founder territories for these structures[18]. Mesodermal pattern balance in individuals is therefore assayed by scoring the nuclei encountered on every fifth 7-μm section of the transverse series, and sampling $\sim 10^4$ cells (or one-third of the total when nuclear size and section thickness are properly considered[19]).

The mesodermal pattern is highly consistent among individual normal embryos, and is subtle in the sense that characteristic proportions of the totals of somite and lateral plate cells are allocated to these structures at each level in the axis[9]. This feature, a measure of the relative 'head-' or 'tail-heaviness' of tissue distribution along the normal series of somite segments, can be quantified as the 'somite index' (see Table 1), which has a certain range of normal variation.

My attempt to force the system outside its normally regulated performance was based on recently published work concerning mechanical aspects of the pre-cleavage events[6,7,20–22]. After fertilization, a system of spontaneous sliding displacements between deep egg regions and the surface structure, driven in relation to the position at which the sperm aster is developing, normally orientates and activates the development of the body from the egg's substance. Any artificially maintained tilt of the eggs away from their natural orientation in gravity, at times when their self-generated movements are occurring, can override the orientating effect of the sperm. Normal patterns then develop, but are symmetrical around that plane in which gravity has caused the egg contents to rearrange. There is much to suggest[10,23] that the total set of movements within the normal egg, more than merely orientating its pattern formation, is quantitatively related to normal completeness and proportioning of the pattern itself.

Towards the end of the pre-cleavage interval, progressive 'gelling' of some egg component appears to record unalterably the net results of all preceding reorganizations in setting up a pattern, whether these were dominated by the natural mechanism or by artificial tilt. Therefore, tilting in gravity at a late stage in this sensitive period, in directions calculated to conflict widely with the system of activation orientated by sperm entry in each egg, might lead to the recording of positional profiles different from those resulting from either natural or imposed systems when acting alone. Such a regime tilt through 70–100° in planes that raised the sperm entry point (s.e.p.) very high in gravity, beginning at 65–85% of the time from fertilization to first cleavage, was accordingly applied to experimental populations of eggs from synchronously fertilized clutches. At the chosen temperature (19 °C), this involved tilting at between 65 and 85 min after fertilization. The eggs were released to orientate freely in gravity at the 8-cell stage after 1 h. Control eggs were subjected to identical conditions except that they were not tilted (for production and handling of eggs in such experiments, see refs 8, 20, 21).

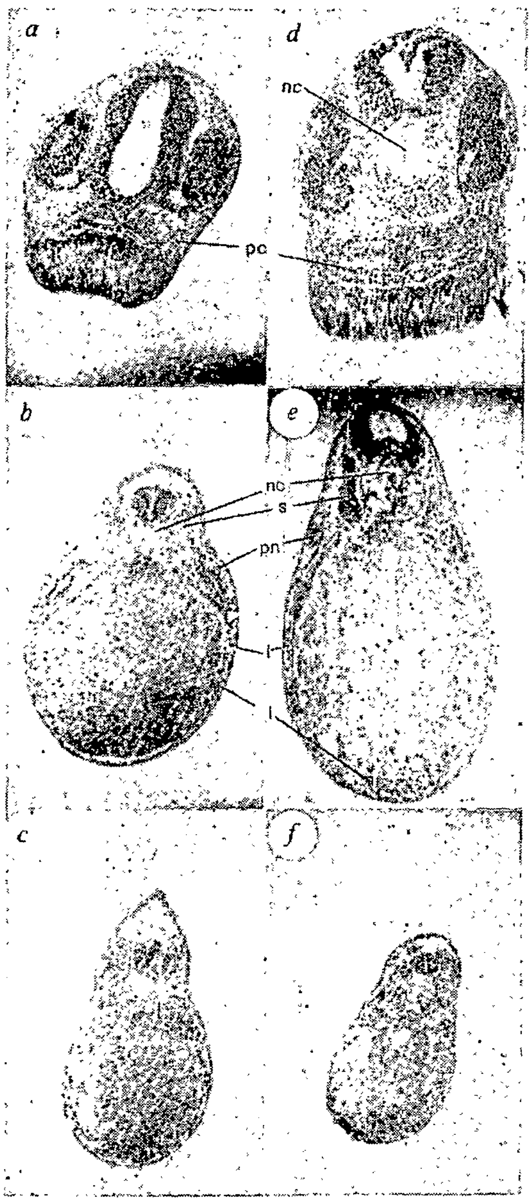

Fig. 2 Internal structure of normal and pattern-imbalance imbalanced larvae. *a–c*, Sections taken at different levels in control larva at stage 29; *d–f*, equivalent sections in a sibling morphologically 'disturbed' after pre-cleavage tilt. *a*, *d*, Level of forebrain, eyecups, ventral prechordal mesoderm and cement gland. Note the massive size of the latter two regions in the disturbed case, and the intrusion of the massive notochord cross-section into this anterior level. *b*, *e*, Level of highest cell count in pronephros (approximately opposite somite 5). Note the greater cross-sectional area of the gut mass, under-allocation to pronephros, the massive notochord and wide floor plate of the neural tube, and the large lateral plate population in the disturbed case. *c*, *f*, Level just anterior to the proctodaeum (blastopore). Note the small cross-section and diminished scale of construction of the entire mesoderm in the disturbed case. Only at this level does the cell number in the notochord cross-section return to normal values. nc, Notochord; pc, prechordal mesoderm; pn, pronephros; l, lateral plate; s, somite.

Six populations of ~80 eggs each were subjected to the experimental regime, with tilting of each individual in sequence being completed across the 20-min period. Synchronously fertilized siblings in similar numbers were used as controls for each population. After 2 days, five of the experimental populations included instances of twinned or mirror-duplicated pattern and of a characteristic, 'imbalanced' single body pattern, in normally healthy larvae. The single-body pattern involved large ventral
head and anterior trunk regions but small, slender poste
parts (Fig. 1*d*). There were between 2 and 6 twins per populat
(26 in total), in contrast to only one among the 450 contr
Affected populations showed between 4 and 12 imbalan
single bodies (39 in all), whereas none was seen either am
the controls, in three populations where s.e.p. up tilt was impo
before the midpoint of pre-cleavage, or in three populati
where this tilt was applied for 1 h between the 4- and 32-
stages.

Larvae showing the externally deviant morphology all
quite abnormal balances of mesoderm pattern in relation t
the controls, or to apparently normal members of their exp
mental batches. This is illustrated for two typical sets of s
bodies in Table 1. That the control/experimental differe
shown in Figs 1*a*, *d* (camera lucida) and 2*a–f* (transv
section) may appear undramatic to the non-specialist, i
measure of the precision of performance of the normal pat
formation under study. As in previous work of this kin
Xenopus, an abnormal pattern *per se* is not associated
abnormal numbers of mesoderm cells[18]. Internal features of
syndrome (for 20 abnormal mesoderms analysed complet
are as follows: (1) The cellular allocation to notochord is 1.5
times normal, the excess being concentrated towards the ante
of the axis. (2) The allocation to the ventral pre-chordal st
ture, and particularly the anterior lateral plate, is enhan
while that to the total somite is usually somewhat reduced.
pre-chordal imbalance is reflected in the deep, broad head
excessive area of cement gland induced in the head ectode
(3) Although the total somite segment number is correct,
axis is anterior-heavy. While the slender anterior somites
allocated at least their normal cell numbers, the cross-secti
of those in the trunk and tail are progressively reduced be
the norm (Fig. 2*b*, *c*, *e*, *f*; see also Table 1). The posterior lat
plate and tailbud tissues are also under-represented in rela
to the massive 'chest' tissue. (4) The allocation to the proneph
is frequently abnormally small, down to less than half the nor
6–9% of mesoderm (Fig. 2*b*, *e*), or is even absent.

The twinned bodies turn out to represent opposed pairs
partial body patterns, the regions represented in each axis be
the entire notochord and those other parts of the plan that
over-represented in the imbalanced singles. The pronephros
those parts of the somite pattern normally contributed from n
the s.e.p. meridians, are reduced or absent. Two features of
variation seen among these twin patterns are particularly in
mative concerning the dynamical properties of the early p
tional systems. The first concerns notochord allocation. In m
cases the two notochords lie relatively close together, suggest
that the centres of 'activation' of two positional systems aris
in the egg were situated considerably less than 180° apart. Th
is then normal or supranormal cellular allocation to e
notochord, and thus twice or more the normal allocation to
structure (Fig. 1*c*, second and third rows). In other cases, wh
the midlines of the twinned system are equal and opposed
the egg, there is a diminished allocation to each notochord s
that the total allocation is little above normal (Fig. 1*b*).
second noteworthy feature (not represented in Fig. 1) is t
one or both patterns may be locally incomplete at the extremi
of the head and anterior notochord, and there may be a la
asymmetry in partitioning of the total cell population to sma
and larger, complete or anteriorly incomplete patterns.

Figure 1 (third line) offers an interpretation of the patte
in terms of profiles with respect to some variable that could
termed position value for pattern contribution, encoded into
structure around the egg margin. All the imbalances produ
are systematic over-allocations of egg meridians to those posit
values which are normally specified relatively far from the p
of sperm entry, and are associated with the fastest develop
meridians of the egg and gastrula.

It is clear that abnormal profiles of the primary positio
variable, recorded at an essentially pre-cellularized stage,

be maintained for many hours and cell cycles; they are ultimately transmitted from endodermal regions as aberrations in the balance of mesoderm specification. Positional systems that are incomplete in the opposite sense—that is, lacking dorso-anterior values entirely—show similar stability from egg to larva[6,22,23]. Such behaviour, and the rapidity with which the system is set up, is very different from what would be expected from a reaction/diffusion or source/diffusion morphogen landscape, with substance concentration being registered as the position value[11,12]. The various stably maintained asymmetries that are seen in twinned positional profiles also deviate from the behaviour expected of reaction/diffusion. On the other hand, the fact that simple mechanical manipulation can alter drastically the relative allocations to different parts of the pattern in the egg as a whole, is scarcely compatible with the idea that a set of determinant plasmas is simply deployed by the pre-cleavage events.

Table 1 Pattern balance in sibling sets after exposure of eggs to an experimental regime of gravity re-orientation

		% Mesoderm cells in:				Somite
		NC	S	PN	LPL	ratio
Set 1						
Controls (no tilt s.e.p. up)	1	5.6	43.4	6.0	45.0	3.4
	2	6.3	47.1	5.3	41.3	3.1
	3	5.7	45.6	5.5	43.2	3.5
Controls (tilt, but normal morphology)	4	5.7	46.7	5.0	42.6	2.9
	5	6.0	44.1	5.6	44.3	3.5
Experimentals (tilt, then deviant morphology)	1	8.9	37.4	3.2	50.5	2.1
	2	9.8	44.0	4.3	41.0	2.4
	3	10.1	38.6	3.9	47.4	1.7
	4	11.4	35.0	2.1	51.5	1.0
	5	9.5	39.5	3.8	49.2	1.8
Set 2						
Controls (no tilt s.e.p. up)	1	5.6	44.2	5.7	44.5	2.9
	2	5.8	47.4	6.6	40.2	2.8
	3	6.0	41.9	7.2	44.9	2.5
Controls (tilt, but normal morphology)	4	4.9	44.5	5.4	45.2	2.7
	5	5.4	46.2	6.1	42.3	2.4
Experimentals (tilt, then deviant morphology	1	11.0	32.5	3.5	53.0	1.5
	2	14.6	38.5	1.5	45.4	0.9
	3	8.5	37.7	5.0	48.8	2.0
	4	9.6	32.7	6.2	51.5	2.0

Somite ratio is the mean maximum number of nuclei seen in transverse sections through somites 14-16 inclusive, divided by the equivalent value for sections of somites 4-6 inclusive. This ratio is indicative of the way in which mesoderm has been allocated to form the pattern of different axial levels, and values between 2.0 and 3.5 characterize the normal embryos from various ovulations. S, somite; PN, pronephros; NC, notochord; LPL, lateral plate.

Mechanochemical models of pattern production (see, for example, ref. 24), invoking the generation of local variations in some non-fluid aspect of the egg's structure that are then inherited by the blastomeres, may have relevance to this relatively small yet rapidly developing vertebrate egg. A long-term research goal must be the elucidation of ways in which structural or physiological modulation of early cellular material can stably affect the local developmental rate[6,7,23] and, ultimately, set position-specific modes of transcription in nuclei. Possible reasons for the previous report of prolonged regulatory ability for body pattern formation, following other operations carried out on *Xenopus* blastula stages[25], have been discussed elsewhere[8].

I thank Wendy Hatton for histology, and John Gerhart and George Oster for fruitful discussions.

Received 10 June; accepted 13 November 1985.

1. Wolpert, L. *Curr. Topics Dev.* **6**, 183-223 (1971).
2. Lewis, J. & Wolpert, L. *J. theor. Biol.* **62**, 478-490 (1976).
3. McGinnis, W., Levin, M. S., Hafen, E., Kuroiwa, A. & Gehring, W. J. *Nature* **308**, 428-433 (1984).
4. Muller, M. M., Carrasco, A. E. & De Robertis, E. M. *Cell* **39**, 157-162 (1984).
5. Slack, J. M. W. *Nature* **310**, 364-365 (1984).
6. Sharf, S. R. & Gerhart, J. C. *Devl Biol.* **99**, 75-87 (1983).
7. Vincent, J. P., Oster, G. F. & Gerhart, J. C. *Devl Biol.* (in the press).
8. Cooke, J. & Webber, J. A. *J. Embryol. exp. Morph.* **88**, 85-112 (1985).
9. Cooke, J. & Webber, J. A. *J. Embryol, exp. Morph.* **88**, 113-133 (1985).
10. Cooke, J. *Cell. Differ.* **17**, 1-12 (1985).
11. Gierer, A. & Meinhardt, H. *Kybernetik* **12**, 30-39 (1972).
12. Gierer, A. *Phil. Trans. R. Soc.* **B295**, 429-440 (1981).
13. Sudarwati, S. & Nieuwkoop, P. D. *Wilhelm Roux Arch. dev. Biol.* **16**, 189-201 (1971).
14. Gimlich, R. L. & Gerhart, J. *Devl Biol* **104**, 117-130 (1984).
15. Dale, L., Smith, J. C. & Slack, J. M. W. *J. Embryol. exp. Morph.* **89**, 289-312 (1985).
16. Gimlich, R. L. & Cooke, J. *Nature* **306**, 417-473 (1983).
17. Nieuwkoop, P. D. & Faber, J. *Normal Table of* Xenopus laevis (*Daudin*) (Elsevier, Amsterdam, 1967).
18. Cooke, J. *J. Embryol. exp. Morph.* **53**, 269-289 (1979).
19. Abercrombie, M. *Anat. Rec.* **94**, 239-247 (1946).
20. Gerhart, J., Ubbels, G., Black, S., Hara, K. & Kirschner, M. *Nature* **292**, 511-516 (1981).
21. Black, S. D. & Gerhart, J. C. *Devl Biol.* **108**, 310-324 (1985).
22. Scharf, S. R., Vincent, J. P. & Gerhart, J. C. in *Molecular Biology of Development*, 51 73 (Liss, New York, 1984).
23. Cooke, J. *J. Embryol. exp. Morph.* **88**, 135-151 (1985).
24. Oster, G. & Odell, G. in *Fronts, Interfaces and Patterns* (ed. Bishop, A.) (Elsevier, Amsterdam, 1983).
25. Cooke, J. *Nature* **290**, 775-778 (1981).

Human T-cell clones recognize a major *M. leprae* protein antigen expressed in *E. coli*

Abu Salim Mustafa*, Harvindar Kaur Gill*||, Audun Nerland*, Warwick J. Britton†, Vijay Mehra‡§, Barry R. Bloom§, Richard A. Young‡ & Tore Godal*

* Laboratory for Immunology, Department of Pathology and the Norwegian Cancer Society, Norsk Hydro's Institute for Cancer Research, Montebello, N-0310 Oslo 3, Norway
† Clinical Immunology Research Centre, University of Sydney, Sydney 2006 New South Wales, Australia
‡ Whitehead Institute for Biomedical Research, Nine Cambridge Centre, Cambridge Massachusetts 02142, and Department of Biology, Massachusetts Institute of Technology, Cambridge, Massachusetts 02139, USA
§ Department of Microbiology and Immunology, and Irvington House Institute for Medical Research, Albert Einstein College of Medicine, Bronx, New York 10461, USA
|| Present address: Division of Immunology and Serology, Institute for Medical Research, Jalan Pahang, Kuala Lumpur, Malaysia

Leprosy is a chronic infectious disease caused by *Mycobacterium leprae*. As with other intracellular parasites, protective immunity is dependent on T cells and cell-mediated immunity[1]. In animal models, immunization with killed armadillo-derived *M. leprae* elicits strong T-cell responses, delayed-type hypersensitivity and protection against viable challenge[2-5]. We have recently shown that killed *M. leprae* can induce delayed-type hypersensitivity in healthy human volunteers[6]. Identification of the *M. leprae* antigens that are recognized by T cells and may be involved in protection has been hampered by the inability to cultivate the organism *in vitro* and by difficulties in antigen purification from limited quantities of armadillo-derived bacillus. Because genes for the major protein antigens of *M. leprae* as seen by mouse monoclonal antibodies have been isolated[7,8], it has become possible to test whether these individual antigens are recognized by T cells. We screened crude λ gtll phage lysates of *Escherichia coli* containing individual *M. leprae* antigens using *M. leprae*-specific T-cell clones isolated from *M. leprae*-vaccinated volunteers. Using this method, we find that nearly half of the *M. leprae*-specific T-cell clones are stimulated to proliferate by lysates containing an epitope of a *M. leprae* protein of relative molecular mass 18,000 (18K).

Healthy human volunteers vaccinated with killed *M. leprae* were sensitized to soluble *M. leprae* antigens[6]. Forty-two T-cell

Table 1 Antigen reactivity and surface phenotype of *M. leprae*-specific and cross-reactive T-cell clones

Clones:	AF/6C8	AF/5C10	ATT 1/10B	ATT 2/5A	ATT 2/4F	ATT 6/10F	ATT 5/1D	NHH 2/2F	NHH 1/E7	NHH 5/1D	WR 7/F6	ATT 2/6E	ATT 4/1F	ATT 4/
Antigens														
Control	120	150	139	561	435	291	149	380	251	139	564	612	409	57
Soluble *M. leprae* (CD45)*	5,590	22,065	5,773	4,027	5,300	1,615	6,068	9,585	3,607	4,858	29,065	15,177	5,424	17,12
PPD	374	261	257	696	589	140	142	681	318	200	322	23,586	2,919	6,48
BCG	108	237	270	436	278	298	128	271	178	287	479	ND	16,114	N
SPA 30†	39,562	26,638	3,441	3,194	ND	1,273	ND	4,658	ND	1,943	28,982	ND	ND	N
Whole *M. leprae* (CD45)	3,565	17,957	7,076	3,334	ND	2,010	ND	10,471	3,205	5,774	ND	ND	ND	N
Human *M. leprae*	4,177	8,466	2,558	2,605	ND	1,525	ND	8,311	2,810	4,681	4,102	ND	ND	N
Armadillo protein	115	273	106	223	ND	183	ND	295	224	ND	ND	ND	ND	N
M. tuberculosis (H37Rv)	ND	171	125	710	ND	117	ND	259	488	221	ND	11,982	ND	16,64
M. vaccae	ND	754	103	169	ND	183	ND	78	96	186	ND	809	ND	3,74
Nonchromogenin	325	277	162	304	495	115	221	134	146	337	5,363	616	2,092	64
Vaccin	325	422	125	254	469	135	356	107	498	296	109	864	917	1,41
Xenopin	131	375	140	321	417	87	246	146	99	326	332	1,009	5,818	5,89
Schrofulin	520	435	2,526	1,453	2,694	1,862	522	2,985	281	478	126	2,452	3,165	2,74
Kansasin	261	89	267	597	564	125	171	206	81	389	118	3,492	5,266	3,69
Tuberculin	215	550	89	527	ND	153	ND	585	196	419	120	1,806	ND	2,00
Duvalin	358	498	112	317	272	145	263	183	192	251	516	1.430	2,164	82
Neoaurumin	806	806	45	255	653	316	448	106	133	749	449	520	319	47
Flavescin	243	142	313	414	420	569	631	58	63	ND	345	900	2,050	57
Aviumin A	192	324	140	1,169	147	98	294	137	164	ND	226	2,568	2,986	2,65
Aviumin C	295	376	505	566	ND	173	ND	202	420	ND	299	631	ND	48
Glaxo BCG sonicate	540	337	176	342	ND	210	ND	720	402	ND	166	12,009	ND	14,92
Phenotype CD4	+	+	+	+	+	+	+	+	+	ND	+	+	+	+
CD8	−	−	−	−	−	−	−	−	−	ND	−	−	−	−

Peripheral blood mononuclear cells (PBMC) were separated from five healthy volunteers vaccinated with 1.5×10^8 or 4.5×10^8 killed *M. leprae*[6]. 20×10^6 PB (2×10^6 cells ml^{-1}) in complete medium (RPMI 1640+15% human AB serum+1% penicillin/streptomycin) were cultured with 10 $\mu g\,ml^{-1}$ soluble *M. leprae* anti (Batch CD45 from R. J. W. Rees through WHO/IMMLEP Bank) in 25-cm^2 flasks (Costar). Flasks were incubated at 37 °C in an atmosphere of 5% CO_2 and 95% On day 6, cells were washed and recultured with fresh autologous irradiated (2,500 rad) feeder cells+antigen. On day 9, viable cells were recovered on Lympho gradient and cloned in 60-well Microtest plates (Falcon) by limiting dilution[11]. After 7–10 days, cells from growing wells were transferred to 96-well flat-bottom p (Nunc) with fresh autologous feeders+antigen+recombinant interleukin-2 (IL-2; Cetus). After further incubation at 37 °C for 7–10 days, growing cultures were transfe to 24-well plates (Nunc) with 1×10^6 ml^{-1} autologous irradiated PBMC as feeder+10 $\mu g\,ml^{-1}$ soluble antigens of sonicated *M. leprae*+100 U ml^{-1} recombinant Recombinant IL-2 alone was added on day 4. The cycle was repeated every seventh day. When T cells reached 1–2×10^6 ml^{-1}, they were subcultured at 2×10^5 cell well. After 4–8 weeks of cloning, sufficient cells were available for antigen testing. To test antigen reactivity of the clones in a proliferative assay, adherent cells 10^5 irradiated PBMC were distributed into each well of 96-well flat-bottom trays and used as antigen-presenting cells; 10^4 cloned T cells and antigens at opt concentration were added. Antigens were either whole bacilli or soluble sonicates of mycobacteria[12]. Cells were incubated for 48–72 h at 37 °C in 5% CO_2 and air. At 4 h before collection, cultures were pulsed with 0.045 MBq ^3H-thymidine (specific activity 185×10^3 MBq mol^{-1}), incorporated radioactivity was measured[13] median values of counts per minute (c.p.m.) determined. A clone was considered to be proliferating in response to a given antigen when incorporated c.p.m. in cult with antigen minus c.p.m. in cultures without antigen was ≥1,000 and $T/C>2$ (such values in the table are underlined) where T/C = (c.p.m. in cultures with antigen/c. in cultures without antigen). Phenotypes of the T cells (CD4 or CD8) are also listed.

* Soluble *M. leprae* was an ultrasonicated and Millipore membrane (0.22 μm)-filtered preparation of whole bacilli batch CD45 (from R. J. W. Rees).

† SPA 30 was the filtrate of soluble *M. leprae* filtered through Amicon ultramembranes with 30,000 relative molecular moles cut-off (from J. Convit).

clones raised against *M. leprae* soluble extracts were established from five volunteers. These cells were screened for reactivity to antigens prepared from *M. leprae*, BCG, *Mycobacterium tuberculosis*, PPD (purified protein derivative) and other mycobacteria. Eleven of the 42 T-cell clones reacted with *M. leprae* antigens derived from humans or armadillos, but not with BCG or PPD; the responses of these 11 clones to various antigen preparations are shown in Table 1. The response to antigen preparations from other mycobacteria was absent or low, restricted to *Mycobacterium scrofulaceum* (5 clones) and *Mycobacterium nonchromogenicum* (1 clone). The responses of three T-cell clones that exhibit broad mycobacterial cross-reactivity (ATT 2/6E, ATT 4/1F, and ATT 4/4C) are included for comparison.

Five abundant *M. leprae* proteins with relative molecular masses of 65K, 36K, 28K, 18K and 12K have been identified through the use of monoclonal antibodies[7–9]. Each of the genes encoding these proteins has been cloned in *E. coli* Y1089 (ref. 7). Lysogens of λ gtll recombinant phage carrying each of the five *M. leprae* genes were constructed and used to express the antigen of interest in a crude lysate[10]. Similar amounts of *M. leprae* antigen were produced in each of the five lysates. The crude lysates were tested for their ability to stimulate 10 of the *M. leprae*-specific T-cell clones (Table 2); 5 of 10 *M. leprae*-specific T-cell clones responded to *E. coli* lysates containing antigen expressed from the recombinant phage Y3179 (ref. 7). Four of these reactive T-cell clones were established from one volunteer, the other came from a second volunteer. The patt of reactivity of the T-cell clones suggests that the λ gtll ph Y3179 expresses an *M. leprae* epitope that is absent in BC *M. tuberculosis* and other cultivable mycobacteria, but is sha with *M. scrofulaceum*.

The λ gtll clone Y3179 expresses an antigenic determin

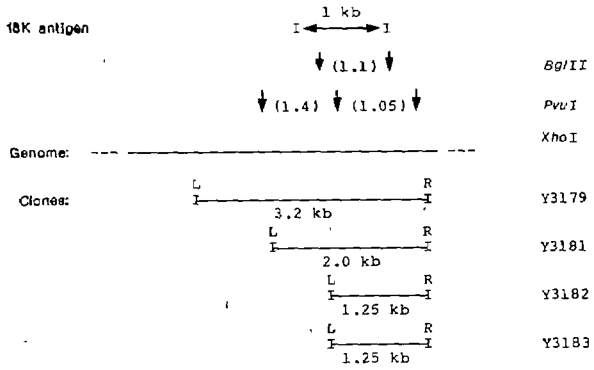

Fig. 1 Restriction endonuclease mapping and *M. leprae* DN size of recombinant phage Y3179, Y3181, Y3182 and Y318 expressing epitope of an 18K protein antigen recognized by a singl *M. leprae*-specific monoclonal antibody L.7.17[7–9]. Arrows (↓ show the sites of restriction endonuclease action, and the size o *M. leprae* DNA thus produced is given in parentheses.

Table 2 Proliferation of T-cell clones in response to the recombinant *M. leprae* antigens from phage vector λ gtll expressed in *E. coli*

				Lysates from *E. coli* infected with				
				Y3178	Y3180	Y3164	Y3179	Y3184
				M. leprae specific antigens expressed				
T-cell clones	—*	Soluble *M. leprae* (CD45)	λ gtll control	64K	36K	28K	18K	12K
Specific clones								
AF/6C8	201	35,331	345	328	51	160	169	100
AF/5C10	271	5,718	579	259	98	627	387	127
ATT 1/10B	554	29,379	326	424	1,009	295	2,926	384
ATT 2/5A	320	24,532	550	133	187	146	8,225	175
ATT 2/4F		31,505	218	115	304	136	11,382	165
ATT 5/1D	318	23,411	275	181	212	422	101	158
ATT 6/10F	110	29,928	215	114	106	117	8,746	156
NHH 2/2F	91	23,761	109	201	161	76	10,389	101
NHH 1/E7	148	4,461	350	143	167	209	208	246
WR 7/F6	530	12,291	202	186	170	131	132	71
Cross-reactive clones								
ATT 4/1F	808	30,246	858	496	455	691	430	680
ATT 2/6E	803	25,626	876	1,366	965	1,071	634	691
ATT 4/4C	511	6,953	779	734	548	596	643	592

Crude *E. coli* lysates containing individual *M. leprae* antigens were prepared by inducing λ gtll recombinant lysogens of the strain Y1089[10]. Single colonies of recombinant lysogens were inoculated into 100 ml of LB medium (*p*H 7.5) and cultures were incubated at 32 °C. When cells had grown to $A_{600} = 0.5$, cultures were transferred to 45 °C and incubated for 20 min. Isopropyl β-D-thiogalactopyranoside (IPTG) was added to 10 mM and the cultures were further incubated at 38 °C for 1 h. All incubations were carried out with good aeration. The cell pellet obtained after centrifugation was resuspended in saline 1/20 of original culture volume and frozen immediately in liquid nitrogen. Thawing of frozen cells resulted in lysis of induced lysogen. To reduce viscosity, crude lysates were briefly sonicated (3 × 10 s) on ice, and then sterilized by Millipore filtration. Lysates were then frozen at −70 °C in aliquots until used. Antigenic activity was lost rapidly on storage at +4 °C, so new vials were used when stimulating T-cell clones. Expression was confirmed by probing crude lysates with the appropriate monoclonal antibodies[7,8]. T-cell clones were tested with different doses of crude lysates as described for other antigens in Table 1. Results are given for 10 μg ml^{-1} of crude lysate and expressed as in Table 1.

* Control cultures without antigen.

Table 3 Proliferation of T-cell clones to Y3179 and other recombinant antigens recognized by L.7.15 antibody

		E. coli lysate containing expressed antigens from:							
		Y3179		Y3181		Y3182		Y3183	
T-cell clones	—*	10 μg	50 μg	10 μg	50 μg	10 μg	50 μg	10 μg	50 μg
2/4F	541	22,370	31,728	2,839	6,425	751	2,580	753	2,527
2/5A	445	21,266	16,224	2,510	10,368	1,178	3,009	1,290	5,727
6/10F	471	12,415	11,638	1,873	6,592	1,167	3,016	1,625	5,073

Crude lysates containing antigens expressed by phage Y3179, T3181, Y3182 and Y3183 were prepared as described for Table 2. Responses of the T-cell clones to two lysate concentrations (10 μg ml^{-1} and 50 μg ml^{-1}) are given as in Table 1.

* Control cultures without antigen.

of an 18K *M. leprae* protein recognized by the monoclonal antibody L7.15 (refs 7, 8). Y3179 contains 3.2 kilobases (kb) of *M. leprae* DNA, sufficient to encode additional polypeptides that might be fortuitously expressed in the Y3179 lysate and which could conceivably be responsible for stimulation of the T-cell clones. However, two lines of evidence favour the idea that some portion of the 18K protein is responsible for T-cell stimulation. Additional λ gtll clones containing smaller inserts and sharing only 1.25 kb of DNA produce the epitope recognized by L7.15 (Fig. 1); *E. coli* lysates of these phage stimulate the same T-cell clones that respond to Y3179 (Table 3). More importantly, while most *M. leprae* proteins exhibit immunological cross-reactivity with proteins from other mycobacteria, the L7.15 epitope is specific to *M. leprae*[8,9], as is the response of the five *M. leprae*-specific T-cell clones. The precise nature of the stimulatory epitope is being investigated.

These results establish that vaccination of normal volunteers with killed *M. leprae* induced a population of CD4-positive T cells that could be cloned *in vitro* and which exhibited *M. leprae*-specific reactivity. In addition, T-cell clones from two volunteers were capable of responding to an *M. leprae* antigen expressed in crude λ gtll phage lysates of *E. coli*. This and possibly other *M. leprae* antigens recognized by T-cell clones may be relevant to protection against leprosy.

The methods used here should be generally applicable to the identification of parasite polypeptide antigens recognized by T cells. While there is a high background of nonspecific reactivity of normal peripheral blood lymphocytes to crude phage lysates, antigen-specific T-cell clones produce a relatively minor background response, making it possible to test their reactivity to individual antigens in crude lysates.

For leprosy, these methods should facilitate further identification and characterization of *M. leprae* antigens recognized by T cells. Once these antigens are purified, it should be possible to evaluate their relative importance to the T-cell repertoire of *M. leprae*-immune individuals and to examine their role in protection against infection.

We thank Drs T. M. Buchanan, A. H. J. Kolk, J. Ivanyi and O. Closs for anti-*M. leprae* monoclonal antibodies and J. L. Stanford, J. Convit, G. Rook, R. J. W. Rees, O. Closs and J. Bennedsen for mycobacterial antigens. Recombinant human interlerleukin-2 was kindly provided by Cetus. We also thank D. Baltimore, M. Gefter and N. Oliver for discussion and critical comments. Technical assistance was provided by Inger Natvig and D. Sweetser. Secretarial assistance was provided by Heidi Andersen. This work was supported by the UNDP/World Bank/WHO Special Programme for Research and Training in Tropical Diseases.

Received 27 August; accepted 14 October 1985.

1. Bloom, B. R. & Godal, T. *Rev. infect. Dis.* **5**, 765–780 (1983).
2. Shepard, C. C. *Int. J. Lepr.* **44**, 222–226 (1976).
3. Patel, P. J. & Lefford, M. J. *Infect. Immun.* **19**, 87–93 (1978).
4. Mehra, V. & Bloom, B. R. *Infect. Immun.* **23**, 787–794 (1979).
5. Shepard, C. C., Van Landingham, R. & Walker, L. L. *Infect. Immun.* **29**, 1034–1039 (1980).
6. Gill, H. K., Mustafa, A. S. & Godal, T. *Bull. Wld Hlth Org.* (in the press).
7. Young, R. A. *et al. Nature* **316**, 450–452 (1985).
8. Engers, H. *et al. Infect. Immun.* **48**, 603–605 (1985).
9. Britton, W. J., Hellqvist, L., Basten, A. & Raison, R. L. *J. Immun.* (in the press).
10. Huynh, T. V., Young, R. A. & Davis, R. W. in *DNA Cloning Techniques: A Practical Approach* (ed. Glover, D.) (IRL Press, Oxford, in the press).
11. Qvigstad, E., Digranes, S. & Thorsby, E. *Scand. J. Immun.* **18**, 291–297 (1983).
12. Stanford, J. L. *et al. Lepr. Rev.* **51**, 303–314 (1980).
13. Mustafa, A. S. & Godal, T. *Clin. exp. Immun.* **52**, 29–37 (1983).

Mycobacterium leprae-specific protein antigens defined by cloned human helper T cells

Tom H. M. Ottenhoff*, Paul R. Klatser†, Juraj Ivanyi‡, Diènne G. Elferink*, Madeleine Y. L. de Wit† & René R. P. de Vries*

* Department of Immunohaematology and Blood Bank,
University Hospital of Leiden, 2333 AA Leiden, The Netherlands
† Laboratory of Tropical Hygiene, Royal Tropical Institute,
1105 Az Amsterdam, The Netherlands
‡ MRC Tuberculosis and Related Infections Unit,
Hammersmith Hospital, London W12 0HS, UK

Leprosy displays a remarkable spectrum of symptoms correlating with the T-cell-mediated immune reactivity of the host against the causative organism, *Mycobacterium leprae*[1]. At one pole of this spectrum are lepromatous leprosy patients showing a *M. leprae*-specific T-cell unresponsiveness[2]; at the other are tuberculoid leprosy patients displaying both acquired immunity and delayed-type hypersensitivity against *M. leprae* which are thought to be conferred by helper T (T_h) cells[1,3–5]. Because well-defined *M. leprae* antigens are crucial for the prevention and control of leprosy[1,6,7], we have cloned *M. leprae*-reactive T cells (TLC) of the helper phenotype from a tuberculoid leprosy patient. As reported here, these TLC show an unexpected diversity in the recognition of *M. leprae* and related mycobacteria, which is different from that exhibited by monoclonal antibodies[8,9]. Half of these TLC are completely or almost *M. leprae*-specific, whereas the other half are cross-reactive with most or all other mycobacteria. A *M. leprae* protein of relative molecular mass (M_r) 36,000 (36K) defined by a *M. leprae*-specific monoclonal antibody[7,8,10] stimulates 4 out of 6 TLC tested. Each of these TLC recognizes a different antigenic determinant, one of which is *M. leprae*-specific. The previous paper describes other *M. leprae*-specific T-cell clones half of which recognize an epitope on a *M. leprae* protein of M_r 18 K.

Whereas the *M. leprae*-specific unresponsiveness in lepromatous leprosy patients may be triggered by specific immunosuppression-inducing determinants on the bacillus[11], virtually nothing is known about the antigens recognized by T_h cells responsible for the cell-mediated immune reactivity against *M. leprae* in tuberculoid leprosy patients. To study the antigenic determinants involved in activating these T cells in more detail, we have cloned *M. leprae*-reactive T cells of a tuberculoid leprosy patient.

Peripheral blood mononuclear cells of a tuberculoid leprosy patient were restimulated *in vitro* with *M. leprae* antigen, cloned and propagated as described elsewhere[12]. Autologous Epstein-Barr virus (EBV)-transformed B cells (EBV-BC) were used as antigen-presenting cells (APC), as evidence suggests that these cells can effectively present *M. leprae* antigens to primed T cells (for review see ref. 13). One advantage of using EBV-BC as APC is that such cells provide a continuous and unlimited source

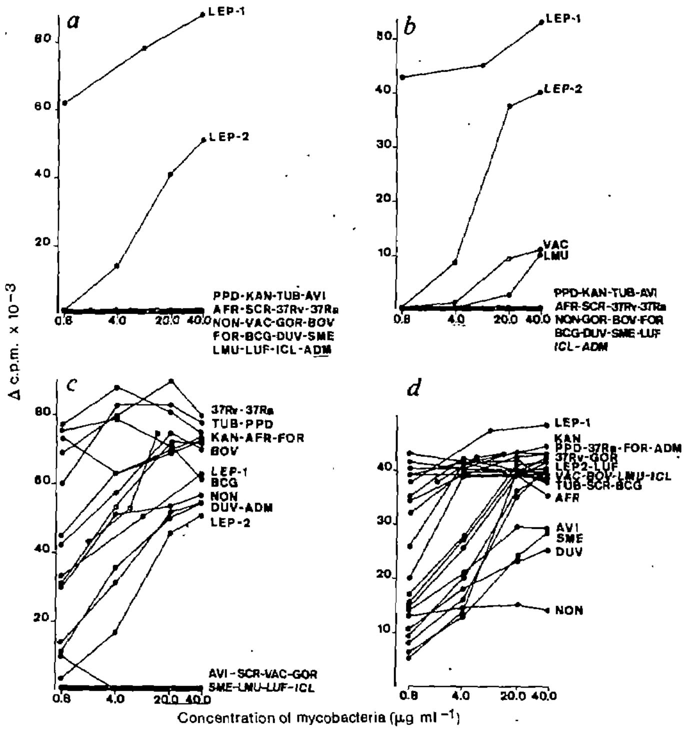

Fig. 1 Antigen specificity of *M. leprae*-reactive cloned T cells. Mycobacterial antigens were presented via autologous or HLA class II-compatible APC to 23 different *M. leprae*-reactive TLC from a tuberculoid leprosy patient. Four different patterns of reactivity were observed, and a representative example of each pattern is shown (*a–d*) (pattern *a*: $n=6$, *b*: $n=5$, *c*: $n=2$, *d*: $n=10$). The antigens tested were: LEP-1, Dharmendra lepromin, consisting of bacilli isolated from human lepromas; LEP-2, armadillo-derived *M. leprae*; PPD, purified protein derivative of *M. tuberculosis* (obtained from Statens Serum Institute, Copenhagen); KAN, *M. kansasii*; TUB, *M. tuberculosis*; AVI, *M. avium*; AFR, *M. africanum*; SCR, *M. scrofulaceum*; 37Rv, *M. tuberculosis* H37Rv; 37Ra, *M. tuberculosis* H37Ra; NON, *M. nonchromogenicum*; VAC, *M. vaccae*; GOR, *M. gordonae*; BOV, *M. bovis*; FOR, *M. fortuitum*; BCG, *M. bovis* BCG; DUV, *M. duvalii*; SME, *M. smegmatis*; LMU, *M. lepraemurium*; LUF, *M. lufu*; ICL, *M. avium intracellulare*; ADM, armadillo-derived aspecific mycobacteria. Dharmendra lepromin was tested in dilutions of 1:240, 1:120 and 1:60. PPD was tested at concentrations of 1.7, 5.0 and 16.7 μg ml^{-1}. All other mycobacteria had been ultrasonicated as described in ref. 21, and were tested at 0.8, 4.0, 20.0 and 40.0 μg ml^{-1}. Results are mean Δ c.p.m. × 10^{-3} (^{3}H-thymidine incorporation) of duplicate cultures (standard deviations mostly <10%), as assessed by subtracting background proliferation in the absence of antigen from responses in the presence of antigen.

Methods. Antigen reactivation, cloning, expansion and proliferative assays were performed as described elsewhere[12]. Briefly, peripheral blood mononuclear cells were isolated by Ficoll-Isopaque density gradient centrifugation and restimulated *in vitro* with an optimal concentration of Dharmendra lepromin (1:120–1:60) in 24-well tissue culture plates. T-cell blasts, enriched for by Percoll density centrifugation, were then cloned by limiting dilution on a feeder cell mixture consisting of irradiated autologous EBV-BC (10^5 cells ml^{-1}), peripheral blood mononuclear cells from 3–4 random donors (10^6 cells ml^{-1}), and Dharmendra lepromin (1:120–1:60). Of the original 295 microwells seeded, 56 contained growing cultures, and 34 of these showed proliferative responses. Growing cultures were restimulated once a week with the feeder mixture, supplemented with Leuko Agglutinin A (1 μg ml^{-1}) (Pharmacia) and expanded in the presence of interleukin-2-containing supernatants. In proliferative assays, 10^4 TLC, 5×10^4 irradiated autologous or HLA class II-compatible peripheral blood mononuclear cells as APC, and antigen were co-cultured in flat-bottomed 96-well microtitre plates (Greiner, FRG). After 72 h, 1.0 μCi ^{3}H-thymidine was added to each well; cultures were collected 16 h later on glass-fibre filters using a semi-automatic sample harvester. ^{3}H-Tdr incorporation assessed by liquid scintillation counting.

Table 1 *M. leprae*-specific and cross-reactive TLC recognize different determinants on a 36K protein purified by a *M. leprae*-specific monoclonal antibody

	T cell:	1G5	1E4	2F9	3B4	1F9	3E8	TLB1	TLB2
Antigen	Antigen specificity:	LEP (*a*)*	LEP (*a*)	LEP-VAC-LMU (*b*)	Partly cross-reactive (*c*)	Completely cross-reactive (*d*)	Completely cross-reactive (*d*)		
M. leprae		14.2±4.3	57.9±0.1	88.4±6.2	42.2±2.1	10.0±2.0	70.5±3.5	53.7±5.0	46.7±0.9
36K *M. leprae* protein		0.1±0.0	24.0±5.5	26.8±0.5	21.4±0.6	0.2±0.0	20.0±0.2	18.2±4.9	17.2±3.4
12K *M. leprae* protein		0.1±0.1	0.1±0.0	48.8±5.4	0.2±0.1	0.1±0.0	5.9±1.4	0.2±0.0	3.9±0.9
Medium		0.0±0.0	0.1±0.1	0.1±0.1	0.2±0.1	0.1±0.0	2.3±1.8	0.1±0.1	0.3±0.0

The results are the mean c.p.m. ($\times 10^{-3}$) ± s.d. of duplicate cultures. Positive cultures are boxed and are defined as exceeding the mean background proliferation by at least 3×s.d. and in addition giving $>10^3$ c.p.m. Proliferation assays were carried out as described in Fig. 1 legend. *M. leprae* antigen is Dharmendra lepromin. The 36K protein was purified by the fast protein liquid chromatography system (FPLC; Pharmacia, Sweden) (P.R.K. *et al.*, manuscript in preparation). Briefly, *M. leprae* sonicate was applied to an anion-exchange column (Mono Q, HR5/5; Pharmacia) and eluted with a linear salt gradient. Further purification was carried out on a gel permeation column (TSK G3000 SW; LKB, Sweden). The purity of the antigen was analysed by SDS-polyacrylamide gel electrophoresis and SDS-polyacrylamide gel electrophoresis immunoperoxidase assay[11]. The 12K protein was purified by affinity chromatography using monoclonal antibody ML06A1 coupled to cyanogen bromide-activated Sepharose 4B, followed by elution with 3 M NaSCN[9]. The optimal stimulatory concentration for the 36K protein was 16 μg ml^{-1}, and that for the 12K protein, 0.4 μg ml^{-1}. TLB1 and TLB2 were generated as described in ref. 15.

* For abbreviations see Fig. 1 legend.

of APC, which drastically reduces the number of autologous peripheral blood mononuclear cells needed for the cloning and propagation of antigen-specific T cells.

Twenty-three *M. leprae*-reactive proliferative TLC were selected at random and studied in more detail with regard to their antigen specificity. All 23 TLC were of the $T3^+$ $T4^+$ $T8^-$ phenotype, and were strongly positive for HLA-DR antigens. Twenty-two TLC were restricted in their response by HLA-DR determinants and one was restricted by a hitherto unknown polymorphic HLA-DQ determinant, as assessed by panel and inhibition studies (T.H.M.O. *et al.*, manuscript in preparation).

Two *M. leprae* preparations of different origin, ultrasonicates from 19 other mycobacteria, and the purified protein derivative (PPD) of *Mycobacterium tuberculosis* were presented to these TLC via autologous or HLA (histocompatibility locus antigen) class II-compatible APC. The results (Fig. 1) reveal four patterns of antigen reactivity: (1) TLC recognizing determinants expressed exclusively by *M. leprae* ($n=6$); (2) TLC activated by determinants present on *M. leprae* and cross-reactive with one or two other mycobacterial strains, mainly *Mycobacterium vaccae* and *Mycobacterium lepraemurium* ($n=5$); (3) TLC reactive with several but not all mycobacteria ($n=2$); and (4) TLC triggered by cross-reactive determinants present on all mycobacteria, sometimes with the exception of *Mycobacterium nonchromogenicum* ($n=10$). None of the TLC showed a proliferative response in the presence of APC and either tetanus toxoid or *Candida albicans*, which represented non-mycobacterial control antigens. Similar data were obtained with TLC from two other patients (data not shown).

Recently, five *M. leprae* proteins have been described that contain *M. leprae*-specific antigens recognized by murine monoclonal antibodies[7-9,14]. The M_rs of these proteins are 12K, 18K, 28K, 36K and (55-)65K. To investigate whether these antibody-defined *M. leprae* proteins are also recognized by human T cells, we tested the 12K and 36K *M. leprae* proteins which had been purified by using, respectively, the *M. leprae*-specific monoclonal antibodies MLO6A1 (refs 8, 9) and F47-9-1 (refs 8, 10). Six different *M. leprae*-reactive TLC, and a *M. leprae*-generated polyclonal T-lymphoblast culture (TLB)[15] from the same patient (TLB1) and from a second tuberculoid leprosy patient (TLB2) were tested.

The data presented in Table 1 show that the *M. leprae*-specific 36K protein is recognized by four of the six TLC tested and by both TLB1 and TLB2, whereas the *M. leprae*-specific 12K purified protein is recognized by only one TLC and (weakly) by one TLB, each of which is also reactive with the 36K protein. As all four TLC reacting with the 36K protein display different antigen-specificity patterns (Fig. 1), they must recognize four different antigenic determinants on the 36K protein, only one of which is clearly *M. leprae*-specific. The finding that only one of the two *M. leprae*-specific TLC (1E4, see Table 1) recognized the 36K protein suggests that the other *M. leprae*-specific TLC tested (1G5) reacts with another *M. leprae*-specific determinant not expressed on the 36K protein. In addition, as only one of the two completely cross-reactive TLC (3E8) tested reacts with the 36K protein, at least two common mycobacterial determinants are defined by these TLC, one of which resides on the 36K protein.

The six TLC and the two TLB have so far failed to respond to 3,6-di-*O*-methylglucose-$(CH_2)_8$-bovine serum albumin (BSA), when tested at a wide range of concentrations (5×10^{-3}–2×10^3 μg ml^{-1}). This synthetic antigen contains a *M. leprae*-specific monosaccharide component which forms the terminal part of the trisaccharide complex on *M. leprae* phenolic glycolipid. This glycolipid has been shown to trigger *M. leprae*-specific suppressor T cells in lepromatous but not in tuberculoid patients, as measured by inhibition of concanavalin A-stimulated peripheral blood mononuclear cell cultures[13].

Thus, 6 out of 23 human helper TLC recognized at least two separate determinants that are uniquely expressed by *M. leprae*, but which are distinct from those defined by murine monoclonal antibodies, only a few of which have been found to recognize *M. leprae*-specific protein antigens[7-10,14]. So far, all murine *M. leprae*-reactive TLC cross-react with other mycobacteria[16,17]. The finding that 3 out of 5 nearly *M. leprae*-specific human TLC also react with *M. vaccae* is in accord with the results of *in vivo* skin tests which revealed a selective cross-reactivity between *M. leprae* and *M. vaccae*[18].

The TLC described here define antigenic determinants on purified *M. leprae* proteins which are capable of triggering T cells. It remains to be elucidated which *M. leprae* antigenic determinants recognized by these helper TLC are involved in protective immunity as opposed to immunopathology. A comparison of the antigenic determinants defined by TLC from healthy contacts with those defined by TLC from tuberculoid leprosy patients may be helpful in distinguishing between the two groups of *M. leprae* antigens. In addition to these two groups, a third group of antigens may be involved in the induction of *M. leprae*-specific suppression[6,11]. Recently, we have cloned *M. leprae*-reactive suppressor T cells. Thus, we will be able to study whether different antigenic determinants are recognized by cloned helper and suppressor T cells.

Thus the use of TLC and purified *M. leprae* proteins will enable us to define the *M. leprae* antigens involved in T-cell-mediated protective immunity, immunopathology and possibly suppression; these, therefore, are exquisite tools for the rational design of a *M. leprae* vaccine and skin-test reagents[1,6].

The T-cell responses against these proteins cannot be inhibited by the relevant monoclonal antibodies (data not shown); this was not unexpected because, as a rule, antibodies and T cells react with different epitopes of the same antigen (see, for example, ref. 19). It is interesting that four out of the six TLC and both TLB react with the 36K protein, whereas only one of these TLC and one TLB respond to one of the four other *M. leprae*-specific proteins known—that is, the 12K protein. This result suggests that T_h cells preferentially recognize immunodominant antigenic determinants[20] expressed on the 36K protein. Recently, the genes for the major proteins of *M. leprae* have been cloned and expressed[7] and indeed the five abovementioned *M. leprae*-specific proteins have been formed. Therefore, it should now be possible to determine whether one or more of the antigenic determinants on the 36K protein defined by these TLC is formed—in part—by lipid or carbohydrate components.

We thank Dr R. J. W. Rees and the late Dr C. C. Shepard for providing us with *M. leprae* antigens; Dr D. L. Leiker for his help in obtaining blood samples from leprosy patients; Arend Kolk and Frits Koning for monoclonal antibodies; Teunis Eggelte for synthetic saccharide antigens; John Haanen and Earl Johanns for technical assistance; and Tiny van Westerop for drawing part of the figure and preparing the manuscript. This study was supported in part by the Foundation for Medical Research (FUNGO grant 13-83-01), the Immunology of Leprosy (IMMLEP) component of the UNDP/WORLD Bank/WHO Special Programme for Research and Training in Tropical Diseases, and the Netherlands Leprosy Relief Association (NSL).

Note added in proof: Recent experiments show that analysis of a recombinant 36K *M. leprae*-specific protein, expressed in *Escherichia coli*, reveals that different *M. leprae*-specific protein determinants are detected by these *M. leprae*-specific TLC.

Received 4 September; accepted 29 October 1985.

1. Bloom, B. R. & Godal, T. *Rev. infect. Dis.* **5,** 765-780 (1983).
2. Bloom, B. R. & Mehra, V. *Immun. Rev.* **80,** 5-28 (1984).
3. Rees, R. J. W. *Nature* **211,** 576 (1966).
4. Patel, P. J. & Lefford, M. J. *Infect. Immunity* **19,** 87-93 (1978).
5. Lowe, C., Brett, S. J. & Rees, R. J. W. *Clin. exp. Immun.* **61,** 336-342 (1985).
6. Mitchison, N. A. *Nature* **308,** 112-113 (1984).
7. Young, R. A. *et al. Nature* **316,** 450-452 (1985).
8. Engers, H. D. *et al. Infect. Immunity* **48,** 603-605 (1985).
9. Ivanyi, J., Morris, J. A. & Keen, M. in *Monoclonal Antibodies Against Bacteria* (eds Macario, A. J. L. & Macario, E. C.) (Academic, New York, in the press).
10. Klatser, P. R., de Wit, M. Y. L. & Kolk, A. H. J. *Clin. exp. Immun.* (in the press).
11. Mehra, V., Brennan, P. J., Rada, E., Convit, J. & Bloom, B. R. *Nature* **308,** 194-196 (1984).
12. Haanen, J. B. A. G. *et al. Scand. J. Immun.* (in the press).
13. Elferink, B. G., Ottenhoff, T. H. M. & de Vries, R. R. P. *Scand. J. Immun.* **22,** 585-589 (1985).
14. Young, D. B., Fohn, M. J., Khanolkar, S. R. & Buchanan, T. M. *Clin. exp. Immun.* **60,** 546-552 (1985).
15. Ottenhoff, T. H. M., Elferink, B. G., Hermans, J. & de Vries, R. R. P. *Hum. Immun.* **13,** 105-116 (1985).
16. Kaufmann, S. H. E. *Cell Immun.* **83,** 215-220 (1984).
17. Kingston, A. E. & Colston, M. J. *Acta leprologica* **2,** 369-377 (1984).
18. Stanford, J. L. in *Biology of Mycobacteria* Vol. 2 (eds Ratledge, C. & Stanford, J. L.) 85-127 (Academic, London, 1983).
19. Lamb, J. R., Eckels, D. D., Lake, P., Woody, J. N. & Green, N. *Nature* **300,** 66-69 (1982).
20. Manca, F., Clarke, J. A., Miller, A., Sercarz, E. E. & Shastri, N. *J. Immun.* **133,** 2075-2078 (1984).
21. Klatser, P. R., van Rens, M. M. & Eggelte, T. A. *Clin. exp. Immun.* **56,** 537-544 (1984).

Identification of a secretory granule-binding protein as caldesmon

Robert D. Burgoyne, Timothy R. Cheek & Kathryn-Marie Norman

MRC Secretory Control Group, The Physiological Laboratory, University of Liverpool, PO Box 147, Liverpool L69 3BX, UK

Stimulation of adrenal chromaffin cells results in a rise in the concentration of intracellular free calcium[1-3] which initiates catecholamine secretion by exocytosis[4,5]. An understanding of the molecular basis of exocytosis will require knowledge of the sites of action of calcium. A role for calmodulin has been implicated in secretion from chromaffin cells[6,7], and isolated granule membranes bind both calmodulin[8] and a series of cytosolic proteins[9-12] in a calcium-dependent fashion. Here, we demonstrate that one of the cytosolic granule-binding proteins with a relative molecular mass (M_r) of 70,000 (70K) is a form of the calmodulin-regulated actin-binding protein caldesmon, first isolated from smooth muscle[13]. Cytoplasmic gels assembled from an adrenal medullary extract in the absence of Ca^{2+} contained actin and the 70K protein. The association of both of these proteins with the cytoplasmic gel was inhibited by a micromolar concentration of Ca^{2+}. In addition, we have demonstrated that the 70K protein is localized at the periphery of chromaffin cells. These results are consistent with the notion that 70K protein (caldesmon) has a role in regulating the organization of actin filaments of the cell periphery during the secretory process.

A number of bovine medullary cytosolic proteins bind to chromaffin granule membranes with a range of affinities for Ca^{2+} (refs 9-12). Among those that bind with the highest affinity (Fig. 1*a*, *b*) is a polypeptide with an approximate M_r of 70,000. This major granule-binding protein was used as an immunogen in the preparation of specific antisera (Fig. 1). Anti-70K antiserum recognized the 70K polypeptide on immunoblots of granule-binding proteins (Fig. 1*c*) and adrenal medulla homogenates. In immunoblots of homogenates of a variety of rat tissues, anti-70K antiserum recognized a 70K polypeptide in brain, pancreas, heart and liver but not in skeletal muscle (Fig. 1*f*–*i*). An additional 130K polypeptide was recognized by anti-70K antiserum in brain and liver. A non-immune mouse antiserum did not recognize any polypeptides on immunoblotting. The 70K polypeptide in the adrenal homogenate (Fig. 1*d*, *e*) and the granule-binding protein fraction, and the 70K and 130K polypeptides recognized by anti-70K in brain homogenates, were found to be heat-stable.

The protein caldesmon was first isolated from chicken gizzard as a 150K calmodulin-binding F-actin regulatory protein[13]. Subsequently, caldesmon was shown to be present in a range of tissues and cell types[14,15] but absent from skeletal muscle[14]. Caldesmon is now known to exist in a 120–140K form and a 71–77K form; both forms bind to calmodulin and F-actin and are heat-stable[15,16]. There is a remarkable similarity between these caldesmon forms and the polypeptides recognized here by anti-70K, including the ability of 70K from the granule-binding preparation to bind to calmodulin[11]. That the 70K and 130K proteins are forms of caldesmon was confirmed by the finding that anti-70K recognized the purified turkey gizzard 140K caldesmon on immunoblotting (Fig. 2*a*, *b*).

Extracts from adrenal medulla incubated at 25 °C in the absence of Ca^{2+} form supramolecular cytoplasmic gels. Using peptide mapping in comparisons with skeletal muscle proteins, we have shown that actin and myosin are major constituents of these gels (our unpublished observations). Gels assembled from extracts containing $>1\ \mu M$ free Ca^{2+} were depleted of both actin and a 70K polypeptide (Fig. 2*c*–*i*). Immunoblotting with

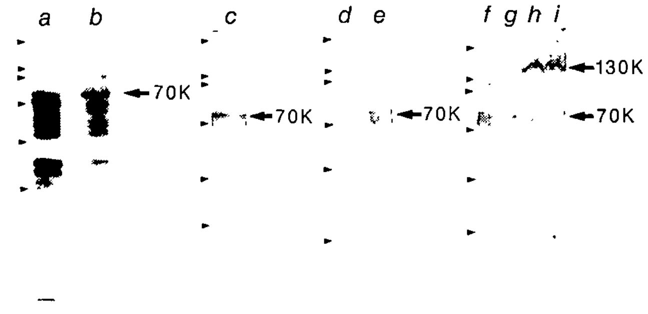

Fig. 1 Characterization of anti-70K antiserum. Granule-binding proteins were prepared[9] by binding from bovine medullary cytosol in the presence of 1 mM Ca^{2+} and elution at 100 μM free Ca^{2+} (*a*), followed by elution with EGTA (*b*). *c–i*, Immunoblotting with anti-70K antiserum of: granule-binding protein fraction, eluted with EGTA (*c*), and the heat-precipitated (*d*) and heat-stable (*e*) fractions of bovine adrenal medullary homogenate; and homogenates of rat heart (*f*), pancreas (*g*), liver (*h*) and brain (*i*). Differences in the apparent migration of the 70K polypeptide between gels are due to differences in electrophoretic conditions. In each case the positions of M_r markers are indicated by arrowheads on the left (M_r, from the top: 205K, 116K, 94K, 67K, 43K and 29K). **Methods.** Anti-70K antiserum was prepared by excising gel bands from tracks of granule-binding proteins as in *b*. The gel slices were homogenized in phosphate-buffered saline (PBS) and injected into mice with Freund's complete adjuvant three times, with intervals of 14 days between injections. The mice were killed and bled 14 days after the last injection and a γ-globulin fraction prepared from the serum by sodium sulphate precipitation. Antisera produced in two different mice gave essentially identical results. For immunoblotting, proteins were separated on 10 or 12.5% polyacrylamide slab gels and transferred to nitrocellulose sheets. After staining the proteins with Ponceau S, the nitrocellulose was washed in PBS, incubated in 3% bovine serum albumin (BSA), 0.2% Triton X-100 in PBS for 10 min, then incubated overnight at 4 °C with anti-70K (1:50 dilution). Bound antibody was detected by incubation with anti-mouse biotin (diluted 1:50; Amersham) for 60 min, followed by incubation with horseradish peroxidase (HRP)-streptavidin (diluted 1:150; Amersham) for 30 min and development with diaminobenzidine. All antibodies were diluted in 3% BSA, 0.2% Triton X-100 in PBS. Homogenates were prepared by homogenization in 5 mM Tris-HCl, 4 mM EGTA, *p*H 8.0 and 180 μg protein was electrophoresed per track. Adrenal medullary homogenate was boiled for 3 min before separation, by centrifugation, into heat-precipitable and heat-stable fractions.

anti-70K demonstrated that the antiserum recognized the Ca^{2+}-regulated 70K polypeptide of the gel as well as a minor 130K polypeptide (Fig. 2*k*, *l*); this provides additional confirmation that the 70K protein is the actin-binding protein caldesmon and demonstrates that the assembly of actin and 70K into supramolecular gels is inhibited by micromolar Ca^{2+} concentrations.

The localization of 70K in bovine adrenal chromaffin cells was determined by immunoperoxidase staining of bovine chromaffin cells in primary culture (Fig. 3). The cultures also contained flat non-chromaffin cells[17] which showed weak, diffuse staining with anti-70K. In chromaffin cells, anti-70K antiserum produced intense staining of regions at the cell periphery. We have also found that on cryostat sections anti-70K stains the periphery of rat adrenal chromaffin cells as well as cells from a wide range of other tissues (R.D.B. and K.-M.N., unpublished observations). Anti-70K stained stress fibres in fibroblasts in culture[15,18] and gave a pattern of staining in small intestine that was indistinguishable from that described for antibody to gizzard caldesmon[14]. The localization of 70K in chromaffin cells resembles that of α-fodrin[19], which suggests that these two proteins may form part of a subplasmalemmal cytoskeleton. However, α-fodrin was localized as a continuous ring around the cell periphery in control cells and as patches following stimulation, whereas 70K was already localized along patches of the cell periphery in control cells (Fig. 3). We detected no effect of stimulation on the localization of 70K in chromaffin cells.

Thus, we have demonstrated that a protein isolated on the basis of its ability to bind reversibly to chromaffin granule membranes in the presence of Ca^{2+} is a form of the actin-binding protein caldesmon. Furthermore, caldesmon and actin assemble from adrenal medullary extracts into supramolecular gels only when the free Ca^{2+} concentration is <1 μM. It has been shown previously that, in the absence of Ca^{2+}, caldesmon stimulates actin assembly[20], crosslinks F-actin[16] and inhibits the regulation of F-actin gelation by filamin[21,22]. All these functions of caldesmon are inhibited by Ca^{2+} in the presence of calmodulin, to which caldesmon then binds preferentially[13,16,20,22]. In the adrenal chromaffin cell, caldesmon may be expected to control a reorganization of F-actin at the cell periphery, including solation of the subplasmalemmal actin network following the rise in intracellular free Ca^{2+} concentration during stimulation.

A role for changes of cytoskeletal organization in secretion from chromaffin cells has previously been suggested from the observations that chromaffin granules bind F-actin[23] and increase the viscosity of F-actin in a Ca^{2+}-inhibitable manner[24]

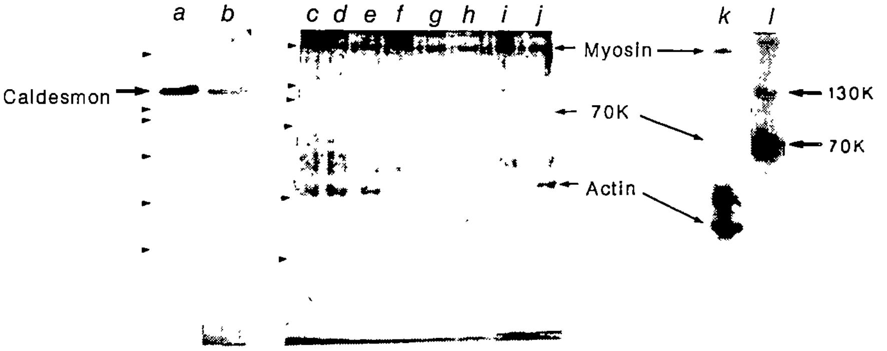

Fig. 2 Recognition by anti-70K antiserum of turkey gizzard caldesmon and a Ca^{2+}-regulated protein in medullary cytoplasmic gels. Turkey gizzard 140K caldesmon was transferred to nitrocellulose and revealed by Ponceau S staining (*a*) and immunoperoxidase staining with anti-70K (*b*). Cytoplasmic gels assembled from medullary extracts in the presence of 0.1 (*c*), 0.5 (*d*), 1.0 (*e*), 2.5 (*f*), 5.0 (*g*), 7.5 (*h*) or 10 μM (*i*) free Ca^{2+} or EGTA (*j*) are shown on a Coomassie blue-stained gel, and in the presence of EGTA after transfer to nitrocellulose and staining by Ponceau S (*k*), followed by anti-70K (*l*). The positions of M_r markers are indicated by arrowheads on the left (M_r, from the top: 205K, 116K, 94K, 67K, 43K, 29K).

Methods. Caldesmon was prepared from turkey gizzard as described previously[16]. For the preparation of cytoplasmic gels, adrenal medullae were homogenized in 1 mM EDTA, 10 mM mercaptoethanol, 0.5 mM ATP, 40 mM Tris-HCl *p*H 7.4 and centrifuged at 100,000*g* for 90 min at 4 °C. Aliquots were dialysed against 5 mM EGTA, 10 mM mercaptoethanol, 0.5 mM ATP, 40 mM Tris-HCl *p*H 7.0, with $CaCl_2$ added to give a calculated free $[Ca^{2+}]$ of 0.1–10 μM. Cytoplasmic gels were assembled after addition of $MgCl_2$ to 8 mM by incubation at 25 °C for 60 min, harvested by centrifugation at 13,000*g* for 7 min at room temperature, and contaminating membranous material was removed by washing with buffer containing 0.5% Triton X-100.

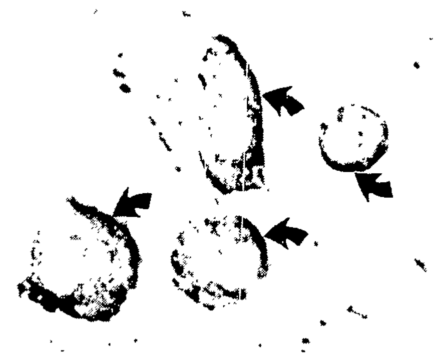

Fig. 3 Immunoperoxidase staining of bovine chromaffin cells in primary culture by anti-70K antiserum. Non-chromaffin cells in the culture[17] were only weakly stained. Chromaffin cells (arrowed) have intense staining around the internal periphery of the cells which in most cases does not form a continuous ring.

Methods. Bovine adrenal chromaffin cells were dissociated and maintained in monolayer culture for 2 days as described previously[17], after which they were fixed with 4% formaldehyde in PBS and air-dried. After washing in PBS, immunoperoxidase staining with anti-70K antiserum was done using essentially the same conditions as those used for immunoblotting (see Fig. 1 legend).

and that stimulation of chromaffin cells results in a redistribution of α-fodrin[19]. Of importance for future investigations is the relationship between caldesmon and α-fodrin at the cell periphery during exocytosis. The demonstration of a reversible association of caldesmon with granule membranes suggests an additional function for caldesmon in regulating the interaction of secretory granules with the cytoskeleton during the secretory process.

This work was supported by a project grant from the MRC. T.R.C. was in receipt of a MRC Research Studentship.

Received 4 September; accepted 4 November 1985.

1. Burgoyne, R. D. *Biosci. Rep.* **4**, 605-611 (1984).
2. Burgoyne, R. D. & Cheek, T. R. *FEBS Lett.* **182**, 115-118 (1985).
3. Knight, D. E. & Kesteven, N. T. *Proc. R. Soc.* **B218**, 177-199 (1983).
4. Burgoyne, R. D. *Biochim. biophys. Acta* **779**, 201-216 (1984).
5. Baker, P. F. & Knight, D. E. *Phil. Trans. R. Soc.* **B296**, 83-103 (1981).
6. Burgoyne, R. D., Geisow, M. J. & Barron, J. *Proc. R. Soc.* **B216**, 111-115 (1982).
7. Kenigsberg, R. L. & Trifaro, J. M. *Neuroscience* **14**, 335-347 (1985).
8. Burgoyne, R. D. & Geisow, M. J. *FEBS Lett.* **131**, 127-131 (1981).
9. Geisow, M. J. & Burgoyne, R. D. *J. Neurochem.* **38**, 1735-1741 (1982).
10. Creutz, C. E. *et al. J. biol. Chem.* **258**, 14664-14674 (1983).
11. Geisow, M. J. & Burgoyne, R. D. *Nature* **301**, 432-435 (1983).
12. Sudhof, T. C., Ebbecke, M., Walker, J. H., Fritsche, U. & Baustead, C. *Biochemistry* **23**, 1103-1109 (1984).
13. Sobue, K., Muramoto, Y., Fujita, M. & Kakiuchi, S. *Proc. natn. Acad. Sci. U.S.A.* **78**, 5652-5655 (1981).
14. Ishimura, K. *et al. Cell Tissue Res.* **235**, 207-209 (1984).
15. Bretscher, A. & Lynch, W. *J. Cell Biol.* **100**, 1656-1663 (1985).
16. Bretscher, A. *J. biol. Chem.* **259**, 12873-12880 (1984).
17. Burgoyne, R. D. & Norman, K. M. *Neuroscience* **14**, 955-962 (1985).
18. Owada, M. K. *et al. Proc. natn. Acad. Sci. U.S.A.* **81**, 3133-3137 (1984).
19. Perrin, D. & Aunis, D. *Nature* **315**, 589-592 (1985).
20. Galazkiewicz, B., Mossakowska, M., Osinska, H. & Dabrowska, R. *FEBS Lett.* **184**, 144-149 (1985).
21. Sobue, K. *et al. FEBS Lett.* **182**, 201-204 (1985).
22. Maruyama, K., Morimoto, K., Kijima, Y., Sobue, K. & Kakiuchi, S. *J. Biochem., Tokyo* **97**, 1517-1520 (1985).
23. Burridge, K. & Phillips, J. H. *Nature* **254**, 526-529 (1975).
24. Fowler, V. M. & Pollard, H. B. *Nature* **295**, 336-339 (1982).

Estimation of the polarity of the protein interior by optical spectroscopy

Robert B. Macgregor[*] **& Gregorio Weber**

Department of Biochemistry, School of Chemical Sciences,
University of Illinois, Urbana, Illinois 61801, USA

Crystallographic studies of myoglobin have shown that the haem pocket is lined with nonpolar amino-acid residues[1]. In order to estimate the true polarity of the interior of proteins, certain studies have used bound fluorophores[2–7], the spectroscopic properties of which reflect the polarity of their environment. These studies have most often used 1-amino-8-naphthalene sulphonate (ANS) as a probe, but a more suitable probe, in principle, is 6-propionyl 2-(*N*,*N*-dimethyl)aminonaphthalene (PRODAN)[8]. We have synthesized a molecule with the advantageous spectroscopic properties of PRODAN but with a higher affinity for apomyoglobin: 2′-(*N*,*N*-dimenthyl)amino-6-naphthopyl-4-*trans*-cyclohexanoic acid (DANCA), and report here its use to determine the polarity of the myoglobin haem pocket. Our results show that the pocket is actually a polar environment, and the polarity can be accounted for by peptide amide dipoles.

Polar chromophores and fluorophores are molecules that exhibit large differences in the electronic distribution of the ground and fluorescent states. The local polarity of a biological system harbouring such molecules can be estimated by comparison of the spectral properties in that environment with those of the probe in solvents of known polar characteristics. The ideal polar fluorescent probe should have no sources of charge besides two readily identifiable monopoles, and the dipole moment that they determine should change strength but not direction in the excited state. Most important, the probe should be soluble in a range of solvents that cover the polarity scale, from apolar solvents like cycohexane to the most polar ones like alcohol or water. PRODAN is a fluorophore probe which approaches this standard (Fig. 1); its synthesis and spectral properties have been described elsewhere[8]. The positive monopole resides at the amino nitrogen and the negative one at the keto oxygen. The dipole moment in the ground state is ~2 D and that of the fluorescent state 18-20 D. In cyclohexane the absorption and emission are centred at 341 and 401 nm respectively, in water they are located at 364 and 531 nm. The absorption and emission bands in water are much broader than in cyclohexane.

Attempts to observe the changes in spectra that result when PRODAN is bound to apomyoglobin are hampered by the relatively low affinity of this molecule for this binding site. To improve the binding affinity while keeping the spectral characteristics of PRODAN intact, we synthesized DANCA (Fig. 1 and G.W. and F. J. Farris, unpublished data). The negatively charged carboxyl was introduced to improve the affinity for the apoprotein, following the example of haem itself, while the cyclohexane ring was intended to hold the carboxyl group away from the spectrally relevant aminoaphthoyl moiety. This isolation reveals itself in the spectral identity of PRODAN and DANCA in media in which their common solubility permits comparison.

At 24 °C apomyoglobin binds one DANCA molecule with $K_D = 1.2 \times 10^{-5}$ M. Bound DANCA is stoichiometrically displaced by the addition of one equivalent of haemin, indicating a unique location in the haem pocket of myoglobin[3]. The absorption spectrum of the protein-dye complex (Fig. 1) is centred at 362 nm (27,620 cm^{-1}) and has a halfwidth of 2,790 cm^{-1}. Cooling the sample to 4 °C shifts the absorption to 366 nm (27,320 cm^{-1}) and causes it to narrow to 2,480 cm^{-1}. The spectrum of DANCA in buffer is centred at 360 nm (27,780 cm^{-1}), with a halfwidth of ~3,600 cm^{-1} and no appreciable temperature dependence. In cyclohexane the absorption of PRODAN is centred at 341 nm (29,326 cm^{-1}) and has a halfwidth of 2,100 cm^{-1}. The shift in absorption with respect to cyclohexane is direct evidence of the considerable polarity of the haem pocket. The temperature dependence of the absorption indicates

---

[*] Present address: Max-Planck-Institut fur biophysikalische Chemie, Abteilung molekulare Biologie, D-3400 Goettingen, FRG.

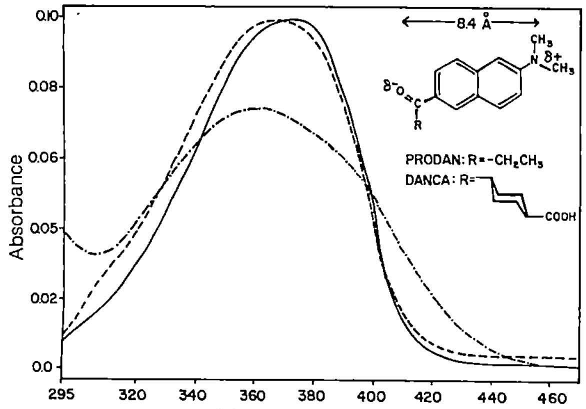

Fig. 1 The absorption spectra of a solution containing 200 μM apomyoglobin and 5.7 μM DANCA (95% bound) at 4 °C (——) and at 24 °C (- - -). Also shown is the absorption spectrum of a 5.7-μM solution of DANCA in buffere at 24 °C -·-·-). Inset: structure of PRODAN and DANCA. DANCA was synthesized in this laboratory; purity was verified using HPLC. The concentration of DANCA in water was determined spectrophotometrically using $E = 14{,}000\ \text{cm}^2\ \text{mmol}^{-1}$ at 360 nm. Haemin and sperm whale myoglobin were purchased from Sigma. Apomyoglobin was prepared according to the method of Teale[13]. All experiments involving protein were carried out in 20 mM bis-Tris buffer, *p*H 6.0. Before an experiment, the apomyoglobin was centrifuged at 20,000 *g* at 4 °C for 40 min to remove aggregates. The concentration of apomyoglobin was determined from the absorbance at 280 nm using $E = 13{,}500\ \text{cm}^2\ \text{mmol}^{-1}$ (ref. 14).

that the population becomes more heterogeneous with increasing temperature. This can result from small changes in the binding site or from the appearance of new fluorophore orientations in an unchanged binding site. Regardless of origin, it is clear that the bound dye has, at either temperature, a much narrower distribution of interactions than in the aqueous buffer.

The fluorescence of DANCA in *p*H 6.0, 20 mM bis-Tris buffer at room temperature has an average wavenumber of 18,826 cm^{-1} (531 nm). On titration with apomyoglobin, this fluorescence is replaced by a new one centred at 21,755 cm^{-1} (459 nm) (Fig. 2) and the intensity increases by a factor of four. This emission spectrum is almost identical to those of PRODAN or DANCA in *N*,*N*-dimethylformamide (DMF) at room temperature[8] or in a glycerol at −40 °C[9,10]; it is also strongly redshifted with respect to the fluorescence spectra in nonpolar media like cyclohexane (401 nm), or weakly polar ones like chloroform (440 nm) or even acetone (452 nm).

The heterogeneity of the probe interaction is revealed by the dependence of the fluorescence spectrum on the excitation wavelength and the changes in interaction in the excited state are revealed by its temperature dependence[9,10]. Figure 3[9] shows the average fluorescence energy and bandwidth of PRODAN in glycerol as a function of excitation wavelength at −42 °C and at 1 °C. At the lower temperature, glycerol is a vitrified solid and its interactions with the dye at emission are determined by the ground state charge distribution about the fluorophore. In this condition, excitation at the longer wavelengths selects fluorophore populations possessing more favourable energies of interaction with solvent and therefore results in progressively redder emissions; the fluoroscence excited at the red edge of the absorption shows the largest shift and the smallest bandwidth. At the higher temperature, 1 °C, the rate of solvent dipole reorientation exceeds the rate of emission and causes the fluorescence spectrum to become almost independent of the excitation wavelength. The emission of DANCA-apomyoglobin (Table 1) also shows dependence on excitation wavelength but, in contrast to the data in Fig. 3, the spectral changes are not diminished by raising the temperature within the range in which the protein remains in its native conformation.

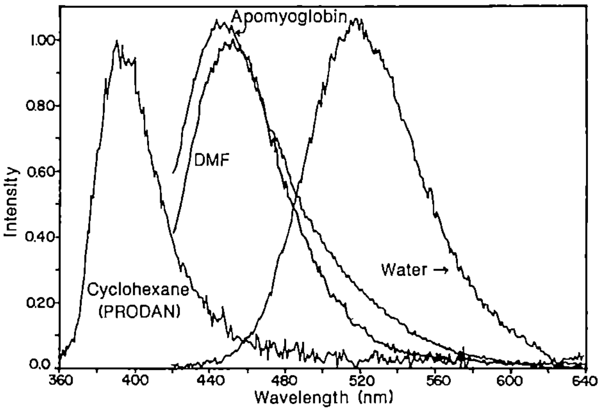

Fig. 2 The fluorescence of DANCA bound to apomyoglobin and in three solvents of different polarity.

The dependence of the fluorescence spectrum on the exciting wavelength shows that we are dealing with a heterogeneous population of DANCA-apomyoglobin complexes, although occupation is restricted to a single molecule. This result is not surprising as haem itself binds in two orientations within its pocket[11].

At 24 °C, the absorption of DANCA-apomyoglobin is shifted −1,706 cm^{-1} and the emission −2,751 cm^{-1} with respect to the corresponding values of PRODAN in cyclohexane. In the complete absence of relaxation of the polar surroundings, we expect equal displacements of the absorption and emission with respect to those observed in an apolar solvent like cyclohexane. The observed difference discloses the existence of a relaxation that increases the Stokes shift expected in a rigid medium by about −1,000 cm^{-1} and is substantially complete at 4 °C. Its course at lower temperatures was explored by observations of the fluorescence of DANCA-apomyoglobin in 60% glycerol-aqueous buffer. We found that the characteristic spectrum of DANCA-apomyoglobin at room temperature is not disturbed by addition of glycerol. At −34 °C the spectral relaxation observed in buffer at higher temperatures is reduced to −200 cm^{-1} and at −74 °C it has disappeared altogether.

Table 1 Dependence of the fluorescence of DANCA bound to apomyoglobin on excitation wavelength

Excitation (nm)	Low temperature* $\Delta\bar{\nu}_g$	Low temperature* Halfwidth	High temperature* $\Delta\bar{\nu}_g$	High temperature* Halfwidth
359	21,818	1,652	21,755	1,707
427	21,119	1,552	20,985	1,636
Difference	−699	−100	−770	−71

All energies are given in wavenumbers (cm^{-1}).

* At 359 nm, low temperature is 4 °C and high temperature is 24 °C; on excitation at 427 nm, low temperature is 6 °C and high temperature is 22 °C.

We draw two conclusions from our observations. First, the protein provides a polar environment that induces a shift in the average absorption of ~ −1,700 cm^{-1} with respect to the unperturbed absorption of the probe; this environment is therefore quantitatively similar to that observed in solutions of PRODAN or DANCA in DMF. At −74 °C the fluorescence is similarly displaced. Second, a relaxation process takes place during the excited state and results in an additional redshift of the fluorescence of ~1,000 cm^{-1}. It is already incipient at −35 °C and virtually complete at 4 °C.

The origin of the relaxation is obscure; however, it seems clear that the time-independent effects on the absorption, and the emission of the probe at the lowest temperature can be

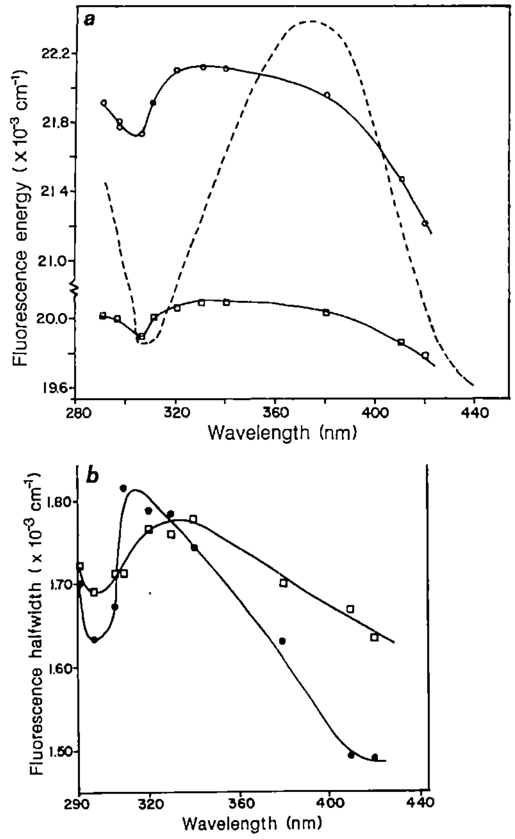

Fig. 3 The excitation wavelength dependence of the emission of PRODAN in glycerol at two temperatures. *a*, Average energy of the fluorescence against excitation wavelength at −42 °C (○) and 1 °C (□). The fluorescence excitation spectrum of PRODAN in glycerol at −42 °C is given by the broken line. *b*, Fluorescence bandwidth against excitation wavelength at −42 °C (●) and 1 °C (□). All fluorescence spectra were recorded on a modified version of the single-photon counting spectrofluorimeter described by Jameson *et al.*[15], and were corrected for monochromator transmission and photomultiplier tube response. The fluorescence spectra of the DANCA-apomyoglobin complex were deconvolved from the total spectra, which included contributions from free DANCA, by using a nonlinear least-squares fitting procedure[16].

explained in terms of discrete electrostatic interactions between the probe and protein and that the strength of these interactions corresponds to a medium of considerable polarity. This result is at variance with previous conclusions on the polarity of the haem pocket based on the ANS-apomyoglobin complex[3]. We note that the virtual insolubility of ANS in truly nonpolar solvents excludes the possibility of establishing a reliable polarity scale for this probe. Additionally, the absorption spectrum and the effect of temperature on the absorption and emission were not evaluated.

Crystallographic studies of myoglobin have shown that the haem pocket is lined with nonpolar amino-acid residues[1], yet our results indicate that the binding site is strongly polar. This inconsistency is only apparent; the fluorophore monopoles can readily interact with the protein amide dipoles through the low dielectric medium provided by the nonpolar amino acids. As a direct test of this supposition, we have calculated the electrostatic interaction energy of DANCA with the partial charges at each of the nitrogen and oxygen atoms of the peptide backbone. In this calculation it was assumed that the probe molecule is located in the plane defined by the haem in the crystallographic structure of deoxymyoglobin and that the coordinates of the other atoms in the molecule are unchanged when the haem is substituted by the probe molecule. Figure 4 shows a contour map of calculated interaction energies of the peptide bond

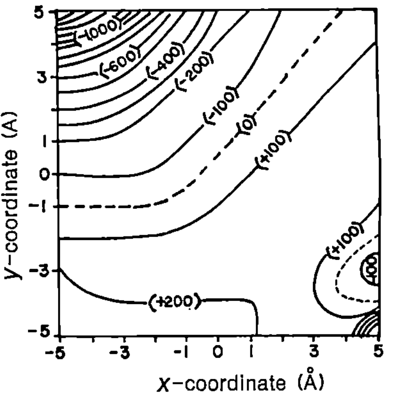

Fig. 4 Map of the electrostatic interaction energy of the peptide bond dipoles with a partial charge located in the plane occupied by the haem in the crystallographic structure of deoxymyoglobin. The partial charge equals the charge of the positive monopole of DANCA in the excited electronic state (∼−0.56 e) minus its charge in the ground state (∼−0.06 e); the strength of the DANCA monopoles follows from the known dipole moments in ground and excited state, 2 and 18 D, respectively, and the distance between the monopoles, 8.4 Å. The x-coordinate is the direction defined by a line drawn from Fe^{2+} and N-1 of the porphyrin ring, the y-coordinate is along the line between Fe^{2+} and N-2, and the z-coordinate is perpendicular to the ring. The energies are given in units of cm^{-1} to facilitate comparison with the spectroscopic results. Contour lines represent changes of 100 cm^{-1} in the interaction energy. Energies were calculated assuming a dielectric constant of 3 for the interior of the protein, and a dipole moment of 3.7 D for the peptide bond.

charges with a positive monopole successively placed at the nodes of an 11 × 11-Å grid situated in the haem plane. A dielectric constant of 3 was assumed for the intervening medium. The contour lines show calculated differences between the electrostatic interaction energies of all the protein peptide dipoles with the amino nitrogen of DANCA, in both the ground and excited states, expressed in wavenumbers to permit direct comparison with the spectral shifts. The values for the negative monopole (DANCA keto oxygen) are equal in magnitude but with opposite sign. For each position that can be chosen as a location for the amino nitrogen of the probe, the total change in interaction energy on excitation equals the energy shown at that point plus the negative of the energy at a point placed 8.4 Å away. Several probe orientations yield spectral displacements well in excess of −1,000 cm^{-1}. These values are close to the difference between the absorption of DANCA-apomyoglobin at room temperature or that of the emission at −74 °C, and the respective values for PRODAN in cyclohexane. However, we do not wish to stress the coincidence of observation and calculation; no exact calculation could be made without knowing the atomic structure of the DANCA-apomyoglobin complex. Our intention here is to demonstrate qualitatively the contribution of the peptide bonds to the polarity of the interior of proteins rather than to analyse particular properties of myoglobin.

Warshel *et al.*[12], in re-examing the theories concerning the interactions of charges located within proteins, point out that the similarity of the dissociation constants of proton-bearing groups within the protein and in water force the conclusion that the protein is polar in their immediate vicinity, and that previous theoretical treatments had neglected the role of peptide bonds in the stabilization of charges. Our results corroborate these considerations by demonstrating that a large portion of the polarity registered by a spectroscopic probe placed in the haem pocket of myoglobin must be attributed to the peptide dipoles.

We thank Dr George Phillips for providing us with the crystallographic coordinates of deoxymoglobin. This work was supported in part by PHS grant GM 11223.

Received 6 May; accepted 2 October 1985.

1. Kendrew, J. C. *et al. Nature* **185**, 422-427 (1960).
2. Weber, G. in *Light and Life* (eds McElroy, W. D. & Glass, B. 82-106 (Johns Hopkins University Press, Baltimore, 1961).
3. Stryer, L. *J. molec. Biol.* **13**, 482-495 (1965).
4. McClure, W. O. & Edelman, G. M. *Biochemistry* **5**, 1908-1919 (1966).
5. Gafni, A., DeToma, R. P., Manrow, R. E. & Brand, L. *Biophys. J.* **17**, 155-168 (1977).
6. Brand, L. & Gohlke, J. *A. Rev. Biochem.* **41**, 843-868 (1972).
7. Anufrieva, E. V., Volkhenstein, N. V. & Samokish, V. A. *Dokl. Biophys.* **195**, 159-162 (1972).
8. Weber, G. & Farris, F. *Biochemistry* **18**, 3075-3078 (1979).
9. Macgregor, R. B. thesis, Univ. Illinois-Urbana (1983).
10. Macgregor, R. B. & Weber, G. *Ann. N.Y. Acad. Sci.* **366**, 140-154 (1981).
11. La Mar, G. N., Toi, H. & Krishnamoorthi, R. *J. Am. chem. Soc.* **106**, 6395-6401 (1984).
12. Warshel, A., Russell, S. T. & Churg, A. K. *Proc. natn. Acad. Sci. U.S.A.* **81**, 4785-4789 (1984).
13. Teale, F. W. J. *Biochim. biophys. Acta* **35**, 543 (1959).
14. Colonna, G., Irace, G., Parlato, G., Aloj, S. M. & Balestrieri, C. *Biochim. biophys. Acta* **532**, 354-367(1978).
15. Jameson, D. M., Spencer, R. D. & Weber, G. *Rev. Scient. Instrum.* **47**, 1034-fi038 (1976).
16. Torgerson, P., Drickamer,. H. G. & Weber, G. *Biochemistry* **18**, 3079-3083 (1979).

Human N-*myc* is closely related in organization and nucleotide sequence to c-*myc*

Nancy E. Kohl, Edith Legouy, Ronald A. DePinho, Perry D. Nisen, Russell K. Smith, Connie E. Gee* & Frederick W. Alt

Department of Biochemistry and Molecular Biophysics,
Columbia University, College of Physicians and Surgeons,
New York, New York 10032, USA
*Department of Pathology, Dana Farber Cancer Institute, Harvard
University Medical School, Boston, Massachusetts 02115, USA

N-*myc*, a cellular gene related to the c-*myc* proto-oncogene[1-4], was originally identified on the basis of its very frequent amplification and overexpression in a restricted set of tumours, most notably human neuroblastomas[1,2]. That N-*myc* may have a causal role in the genesis of these tumours is suggested by the observation that in the rat embryo fibroblast co-transformation assay[5,6] it has a transforming potential similar to that of c-*myc*[7,8]. The apparent structural and functional homology of N-*myc* and c-*myc* suggests that they may be members of the same proto-oncogene family. However, despite these apparent similarities, expression of the two genes appears to be dramatically different with respect to tumour specificity, as well as tissue and developmental stage specificity[9,10]. To further elucidate the common and unique aspects of N-*myc* and c-*myc* gene structure and function in normal and transformed cells, we have determined the organization of human N-*myc* and the nucleotide sequence of its messenger product, and we report here that N-*myc* and c-*myc* have a similar intron/exon structure and that their protein products share regions of significant homology.

To isolate an N-*myc*-specific complementary DNA clone, we prepared a λ phage Charon 16A cDNA library from total poly(A)$^+$ RNA of the IMR-32 human neuroblastoma cell line and screened the library for hybridization to various N-*myc* genomic probes. Initial screenings with the N-*myc* genomic probe NB-19-21 which derives from the more 5′ region of the gene (see Fig. 1*a*) yielded no clones. Thus, we isolated a genomic clone containing regions of the gene both 5′ and 3′ to NB-19-21 (Fig. 1*a*), identified restriction fragments from the 3′ portions which contained coding sequences but not repetitive sequences, and used these to further screen the library. This approach yielded multiple N-*myc*-specific cDNA clones, the longest of which was ~1 kilobase (kb) (pI1-1; Fig. 1*b*). To obtain longer cDNA sequences we hybridized a primer prepared from pI1-1 (Fig. 1*b*) to mRNA from the human neuroblastoma cell line NB-16, extended the primer with reverse transcriptase, prepared a Charon 16A library of the primer-extended cDNA, and screened the resulting library with NB-19-21 (see Fig. 1 legend). In this way we isolated an additional cDNA clone, p9D (Fig. 1*b*), which when combined with pI1-1 represents 1.7 kb of unique sequence.

Attempts to extend primers isolated from the 5′ end of clone 9D were unsuccessful due to a strong stop in the reverse transcription reaction; various analyses indicated that this strong stop resulted from extensive secondary structure in this region of the sequence (see Fig. 2). To bridge this strong stop, we used S_1 nuclease mapping (fragments 7,7′ and 8; see Fig. 1*c*) to identify coding sequences in the corresponding region of the genomic clone. A primer isolated from these coding sequences (a 500-base pair (bp) *Xho*I-*Bam*HI fragment from NB-19-21; Fig. 1*a*) was hybridized to NB-16 mRNA, extended and cloned. Screening the library with a 1-kb *Bam*HI-*Eco*RI genomic fragment shown by S_1 nuclease analysis to contain N-*myc* coding sequences (BR-1; Fig. 1*a*) yielded several clones, the longest of ~1 kb (p0; Fig. 1*b*). Colinearity of these cDNA sequences with the mRNA was confirmed by S_1 nuclease protection experiments (probes 1-5; Fig. 1*c*). Together, the cDNA clones and the genomic fragment bridging them represent 2.7 kb of unique sequence, almost enough to encode the entire N-*myc* message (~3.0 kb). Additional transcribed sequences lie upstream of the 5′ end of the cDNA clone (see below).

Comparison of the nucleic acid sequence of the N-*myc* cDNA and genomic clones, coupled with various S_1 nuclease mapping experiments, indicated that N-*myc* has three exons; in analogy to c-*myc* gene, we refer to these exons as 5′-exon 1-exon 2-exon 3-3′ (Fig. 1*a*). Figure 2 shows the nucleotide sequences of the N-*myc* cDNA clones and of selected regions of the genomic clone containing sequences complementary to N-*myc* mRNA (as defined by S_1 protection). The presence of a poly(A) tail and an adenylation signal confirms the orientation of the genomic and cDNA clones and defines approximately the 3′ terminus of the N-*myc* gene (Figs 1*a*, *b*, 2).

Restriction endonuclease mapping and Southern blot analyses (data not shown) indicate that the 5′ portion of the 9D cDNA clone spans a discontinuous region in the genomic clone. Comparison of the nucleotide sequence of this region of the cDNA clone with the relevant regions of the N-*myc* genomic clone confirms that sequences contiguous in cDNA are separated by an intron of ~2,500 bp in the genomic clone (Figs 1*a*, *b*, 2). That this discontinuity was not a cloning artefact was confirmed by appropriate S_1 nuclease protection experiments (using fragment 8 in Fig. 1*c*). The sequences CAG/GTAAAG, spanning the 3′ boundary of exon 2, and TCTTTCTCTCAG/AT, spanning the 5′ boundary of exon 3, are in agreement with the predicted consensus sequences for the donor and acceptor splice junctions[11]. Extensive restriction endonuclease analyses (not shown) confirm the colinearity of the cDNA and genomic clone within the proposed exon 3 sequence. Thus, exon 3 extends for 1,526 bp between the splice site and the poly(A) tail (Fig. 2). The 5′ boundary of exon 2, located by S_1 nuclease protection analyses, lies ~170 bp 5′ to the *Xho*I site within the NB-19-21 region (analyses used fragments 7 and 7′ of Fig. 1*c*); the exact boundary (nucleotide 680, Fig. 2) was determined by comparing the nucleotide sequences of the corresponding regions of the genomic clone and cDNA clone p0. Thus, exon 2 extends 902 bp from this upstream boundary to the 3′ splice donor site. The sequences TTGCAG/TGT, spanning the 5′ boundary of exon 2, and CCG/GTGCGT, spanning the 3′ boundary of exon 1, correspond respectively to the acceptor and donor splice junction consensus sequences[11]. Sequences in the 5′ cDNA clone p0 extend 314 bp upstream of the splice donor site at the 3′ boundary of exon 1.

Because S_1 nuclease protection experiments (using fragment 6 of Fig. 1*c*) indicated that additional transcribed sequences lie upstream of the end of this clone, we used primer extension to define the 5′ boundary of exon 1. Primer extension of a *Nar*I fragment isolated from the 5′ end of p0 (nucleotides 309-375;

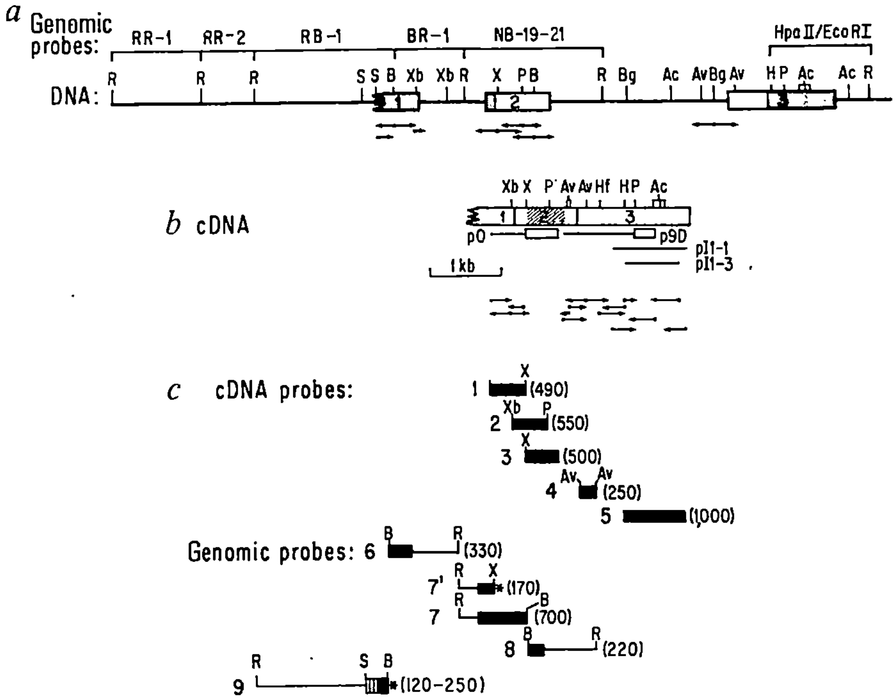

Fig. 1 Organization of human N-*myc*. *a*, Partial restriction map of the N-*myc* genomic clone NG-2. Boxes are exons: shaded boxes denote untranslated sequences, open boxes translated sequences. The heterogeneity of the 5′ terminus of exon 1 is indicated by sawtoothing. Genomic fragments used as probes to screen the cDNA libraries and in Northern blot analyses are indicated at the top. Arrows below the map indicate genomic fragments that have been sequenced. Restriction sites: Ac, *Acc*I; Av, *Ava*I; B, *Bam*HI; Bg, *Bgl*II; H, *Hin*cII; Hf, *Hin*fI; P, *Pst*I; R, *Eco*RI; S, *Sma*I; X, *Xho*I; Xb, *Xba*I (not all sites are shown). *b*, Partial restriction map of the N-*myc* cDNA. Open box denotes the structure of the N-*myc* cDNA deduced from the cDNA clones, S_1 nuclease mapping of relevant regions of the genomic clone and primer extension. The numbers within the boxes indicate the positions of the three exons. The shaded area within exon 2 represents the region of composite cDNA derived from genomic coding sequences; the stippled area in exon 1 represents the region derived by primer extension and S_1 nuclease mapping. The heterogeneity of the 5′ end of the mRNA is indicated by sawtoothing. The cDNA clones are shown beneath the map. The boxed portion of cDNA clones p9D and p0 indicates the position of the primer used in the construction of these clones. Arrows indicate sequencing strategies. *c*, S_1 nuclease mapping of the coding regions of the genomic clone and of the cDNA clones. Fragments used as probes in the S_1 protection experiments are shown. The locations of the protected fragments are indicated by solid boxes; for probes 6 and 8, the location was confirmed by sequence analysis and cDNA cloning. For probe 9, the multiplicity of the protected fragments is indicated by a hatched box. The size of the protected fragment is given in parentheses. An asterisk at the end of a fragment indicates that the probe was terminally labelled; all other probes were uniformly labelled.

Methods. The N-*myc* genomic clone NG-2 was obtained by screening a Charon 35 recombinant phage library (prepared from size-fractionated, *Mbo*I partially-digested DNA[44] from the LA-N-5 human neuroblastoma cell line[45]) with the 2-kb *Eco*RI fragment NB-19-21 (ref. 1). cDNA clones pI1-1 and pI1-3 were isolated from a cDNA library[46] prepared from total poly(A)$^+$ RNA from the IMR-32 cell line[47] and screened with a 1.6-kb *Hpa*II-*Eco*RI fragment of the genomic clone which was shown to contain coding sequences but not repetitive sequences as follows. *Eco*RI fragments from the genomic clone 3′ of NB-19-21 were further digested with various restriction enzymes, the DNA fractionated on agarose gels and transferred to nitrocellulose. Duplicate blots were probed with either nick-translated human DNA (to detect repetitive sequences) or first-strand cDNA synthesized from RNA from the NB-16 human neuroblastoma cell line[48] (to detect coding sequences). cDNA clone 9D was derived as follows. A terminally labelled, single-stranded *Hae*III fragment isolated from pI1-1 (nucleotides 2,481–2,745 in Fig. 2) was used in a primer extension reaction[49] with cytoplasmic poly(A)$^+$ RNA[46] from the NB-16 cell line. This DNA/RNA hybrid was converted to double-stranded (ds) DNA[50] and cloned into the λ phage vector Charon 16A[46]. The library was screened with the NB-19-21 probe. The cDNA clone p0 was obtained by primer extension of a 500-bp *Xho*I-*Bam*HI genomic fragment (nucleotides 852–1,357 in Fig. 2) and cloning of the ds-cDNA as described above. The library was screened with the 1-kb *Bam*HI-*Eco*RI genomic fragment, BR-1. For S_1 nuclease mapping, fragments were subcloned into the M13 phage vector mp8 or mp19 and single-stranded, uniformly labelled DNA probes were prepared as described previously[51]. Alternatively, the DNA was terminally labelled after restriction endonuclease digestion and single-stranded probes were isolated from a strand separation gel[46]. Labelled probes were hybridized with 20–250 ng of NB-16 cytoplasmic poly(A)$^+$ RNA in 80% formamide, 400 mM NaCl, 40 mM PIPES *p*H 6.4, 1 mM EDTA at 42 °C or 50 °C overnight, and digested with 6,000 units S_1 nuclease (Boehringer). For pI1-1, the 1-kb *Eco*RI insert was subcloned into pSP64 and the plasmid linearized with *Pvu*II. Transcription, hybridization and RNase digestion were performed as described elsewhere[52], except that 20 μCi of ^{32}P-CTP (760 Ci mol^{-1}) was used in a 10-μl reaction containing unlabelled CTP at a final concentration of 30 μM. Protected fragments were analysed on 5% polyacrylamide/7 M urea sequencing gels.

Fig. 2) localized the upstream boundary of exon 1 at ~200 bp 5′ of the primer (data not shown). To define this boundary more accurately, we repeated the primer extension analysis with a primer from an even more 5′ region (a 91 bp *Hae*II-*Bam*HI fragment, nucleotides 167–257 in Fig. 2; Fig. 3*c*). Numerous bands of varying intensity extending 35–165 nucleotides 5′ of the primer were observed (Fig. 3*a*). S_1 nuclease analysis using genomic fragment RB-1 labelled at the *Bam*HI site (probe 9 of Fig. 1*c*; see Fig. 3*c*) yielded multiple protected fragments corresponding to those observed in the primer extension assay (Fig. 3*b*), demonstrating that these products represent multiple transcription initiation sites and not strong stops in the reverse transcription reaction. Identical fragments were protected by RNAs from a variety of human neuroblastoma cell lines in which N-*myc* is present in single and multiple copies (not shown), indicating that the heterogeneity of the 5′ end of exon 1 is not a result of amplification. Northern blot analysis using probes RR-1 and RR-2 (see Fig. 1*a*) failed to detect additional coding sequences in the 5′ region of the genomic clone (not shown). Thus, exon 1 appears to vary from 450 to almost 600 nucleotides long as a result of multiple sites of transcription initiation.

In summary, these data demonstrate that the N-*myc* gene is encoded by three exons. In support of this conclusion, it is notable that the combined size of the three exons is approximately enough to encode the entire N-*myc* mRNA, and the overall size of the N-*myc* gene (~7 kb) is consistent with the size predicted from transfection studies of the murine gene[7]. Thus, N-*myc* and c-*myc* appear to have a remarkably similar organization, the most prominent difference being the increased size of exon 3 (1.5 kb for N-*myc* as opposed to 0.9 kb for c-*myc*[12]; Fig. 2).

The apparent similarities in the organization of the N- and c-*myc* genes suggest the possibility of additional conserved features. Exon 1 of c-*myc* represents a long, untranslated leader sequence[13–16]. Although the exon 1 of N-*myc* contains two potential translation initiation codons (nucleotides 385 and 521; Fig. 2), termination codons in all three reading frames render it untranslatable. Thus, the N-*myc* and c-*myc* genes appear to have in common a large untranslated first exon (Fig. 2). Furthermore, it has been suggested that regulation of c-*myc* expression is mediated by hairpin-loop structures within the first exon[13] or between exons 1 and 2 (ref. 15). In this regard, it is notable that numerous potential stem-loop structures with significant standard free energy changes exist between exons 1 and 2 and within exon 2 of N-*myc*, although none is exactly homologous to those found in c-*myc* (see Fig. 2 legend).

As translation of the c-*myc* protein initiates near the 5′ end of exon 2 (ref. 12), we searched for a translation initiation codon in the 5′ region of exon 2 of N-*myc*. We found three ATGs within this region, at positions 797, 821 and 830 (see Fig. 2), all within the same translational reading frame. From the first ATG within exon 2, an open reading frame continues for 1,392 nucleotides (allowing for proper splicing) before reaching the termination codon TAG at position 2,280. Multiple termination codons interrupt this sequence in the other two translational

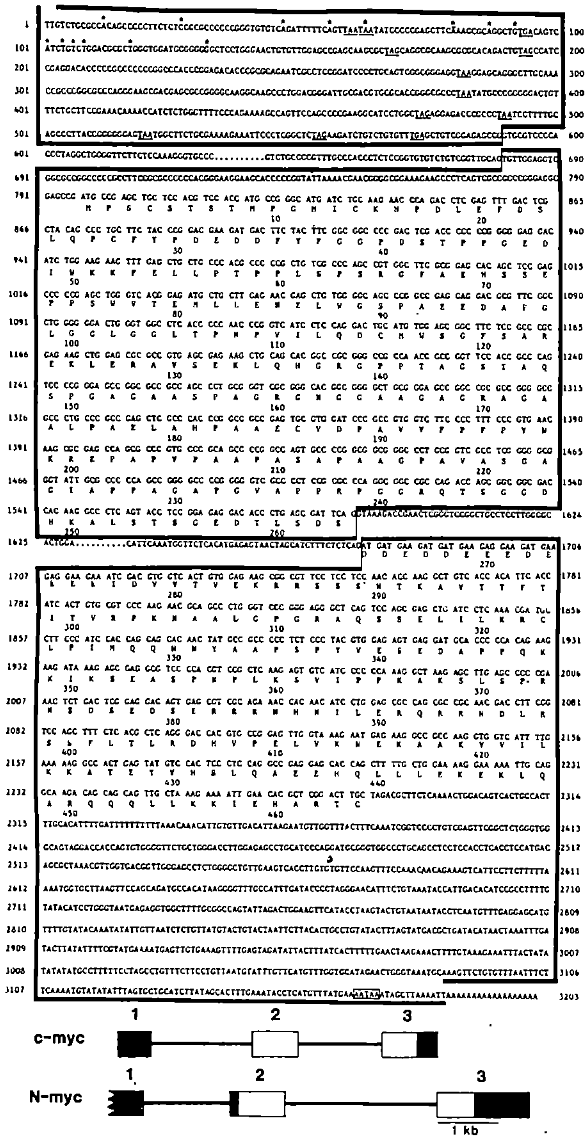

Fig. 2 Nucleotide sequence of human N-*myc*. Restriction fragments were isolated from the cDNA and genomic clones and terminally labelled. Sequencing was by the Maxam and Gilbert[53] method using the strategy described in Fig. 1*a*, *b*. Boxes around the sequence indicate the positions of the three exons; the open box defining exon 3 indicates that the precise 3′ end of the gene has not been determined. However, homology between human and murine genes in this region defines approximately the 3′ end of the gene. The open box around exon 1 indicates the heterogeneity of the 5′ boundary of this exon. Asterisks indicate transcription initiation sites; the locations of these sites, determined by primer extension and S_1 nuclease analyses, are accurate to within 5 bp. Gaps indicate regions of the introns that were not sequenced. The deduced amino-acid sequence of the putative N-*myc* protein is shown for nucleotides 797–2,279. The adenylation signal (AATAAA) is boxed[54]. Termination codons in exon 1 are underlined. Potential stem-loop structures in mature RNA were identified by computer analyses. The positions and free energy[55] of the 10 most stable structures are as follows (position indicated by the bases in the stem): 1,274–1,296 versus 1,413–1,439, $\Delta G_0 = -72.2\ \mathrm{kcal\ mol^{-1}}$; 211–231 versus 1,269–1,296, $\Delta G_0 = -65.6\ \mathrm{kcal\ mol^{-1}}$; 778–808 versus 1,198–1,227, $\Delta G_0 = -55.7\ \mathrm{kcal\ mol^{-1}}$; 1,082–1,107 versus 1,230–1,257, $\Delta G_0 = -52.1\ \mathrm{kcal\ mol^{-1}}$; 689–715 versus 780–803, $\Delta G_0 = -51.1\ \mathrm{kcal\ mol^{-1}}$; 320–345 versus 958–983, $\Delta G_0 = -48.9\ \mathrm{kcal\ mol^{-1}}$; 110–141 versus 1,243–1,274, $\Delta G_0 = -47.1\ \mathrm{kcal\ mol^{-1}}$; 719–740 versus 1,362–1,387, $\Delta G_0 = -32.3\ \mathrm{kcal\ mol^{-1}}$; 799–821 versus 2,525–2,548, $\Delta G_0 = -31.7\ \mathrm{kcal\ mol^{-1}}$; 582–697 versus 1,513–1,552, $\Delta G_0 = -29.7\ \mathrm{kcal\ mol^{-1}}$. Several of these structures occur in the area of the strong stop to reverse transcription (near the 5′ end of cDNA clone p9D, at base 1,403). Additional evidence for secondary structure in exon 2 derives from heteroduplexing experiments and difficulty in sequencing the region. A region of nucleotide sequence homology (60–70%) between the N-*myc* and r-*fos*[21] and c-*fos*[20] genes occurs between nucleotides 1,677 and 1,712. A structural comparison of N-*myc* and c-*myc* is shown at the bottom of the figure. Exons are indicated by boxes: open boxes represent translated sequences, solid boxes represent untranslated sequences. Heterogeneity of the 5′ end of N-*myc* is indicated by sawtoothing. The genes are oriented 5′-exon 1-exon 2-exon 3-3′.

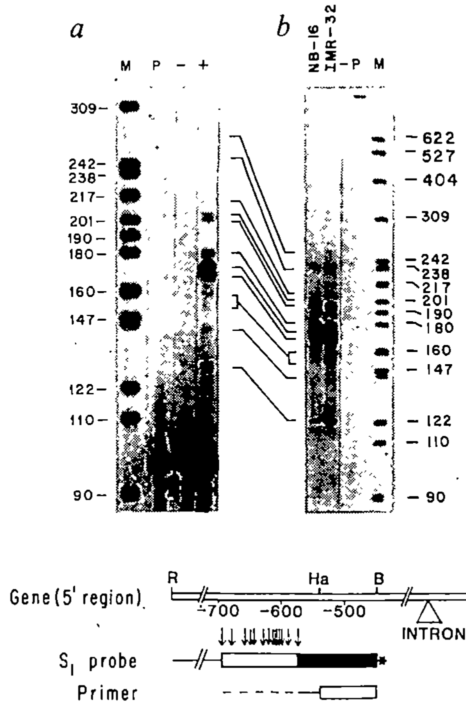

Fig. 3 Localization of the 5′ end of N-*myc*. *a*, Primer extension analysis. A 91-bp *Hae*II-*Bam*HI fragment isolated from the 3′ end of the genomic subclone RB-1 (nucleotides 167–257 in Fig. 2) was annealed to 2 μg of NB-16 cytoplasmic poly(A)$^+$ RNA and extended with reverse transcriptase[49]. *b*, S_1 nuclease mapping. Genomic fragment RB-1 labelled at the *Bam*HI site was annealed to 0.5 μg NB-16 cytoplasmic poly(A)$^+$ RNA or 25 μg of IMR-32 total RNA and digested with S_1 nuclease as described in Fig. 1 legend. The products of both assays (*a* and *b*) were analysed on 5% acrylamide/7M urea sequencing gels. Corresponding fragments in the two assays are indicated. Lane M, pBR322 DNA digested with *Hpa*II; P, probe; −, control reaction containing no RNA; + or NB-16, reaction containing NB-16 cytoplasmic RNA; IMR-32, reaction containing total RNA from the IMR-32 human neuroblastoma cell line. *c*, The 5′ end of N-*myc*, represented by the thin box. Numbering is with respect to the translation initiation signal, with the A of the ATG being +1. The probe used in the S_1 nuclease analysis is shown at the bottom. The protected fragment is indicated by a thick box; vertical arrows indicate the position of the 5′ termini. The primer used in the primer extension analysis is indicated by the open box beneath the probe. The extended products are indicated by the broken line. B, *Bam*HI; Ha, *Hae*II; R, *Eco*RI.

reading frames. Although we cannot say unequivocally that the ATG at 797 is the N-*myc* translation initiation codon, this seems likely because it is the first ATG of the open reading frame. In addition, this ATG initiation codon and the downstream coding sequence are conserved in murine N-*myc*[17].

Several observations indicate that the proposed N-*myc* coding region is correct, most notably the striking homology of the putative N-*myc* protein to the c- and v-*myc* proteins throughout their amino-acid sequences (discussed in detail below). In addition, *in vitro* translation of purified N-*myc* mRNA yielded a diffuse product of relative molecular mass (M_r) 50,000 (50K)–55K (data not shown), a size in accord with the M_r of 50K predicted from the nucleotide sequence of the putative N-*myc* coding region (Fig. 2). Thus, the putative N-*myc* protein is similar in size to the c-*myc* protein; the larger size of the N-*myc* mRNA appears to result primarily from its larger 3′-untranslated region (~900 bp compared with ~350 bp for the c-*myc* mRNA)[12].

Comparison of the deduced amino-acid sequence of the putative N-*myc* protein with that of the human and viral *myc* proteins indicates regions of significant homology in the domains encoded by both exons 2 and 3 (Fig. 4). When the protein products of N-*myc* and c-*myc* are compared with the product of the viral gene, the homology in both cases is higher in the exon 3-encoded domain. In the exon 2-encoded domain, the

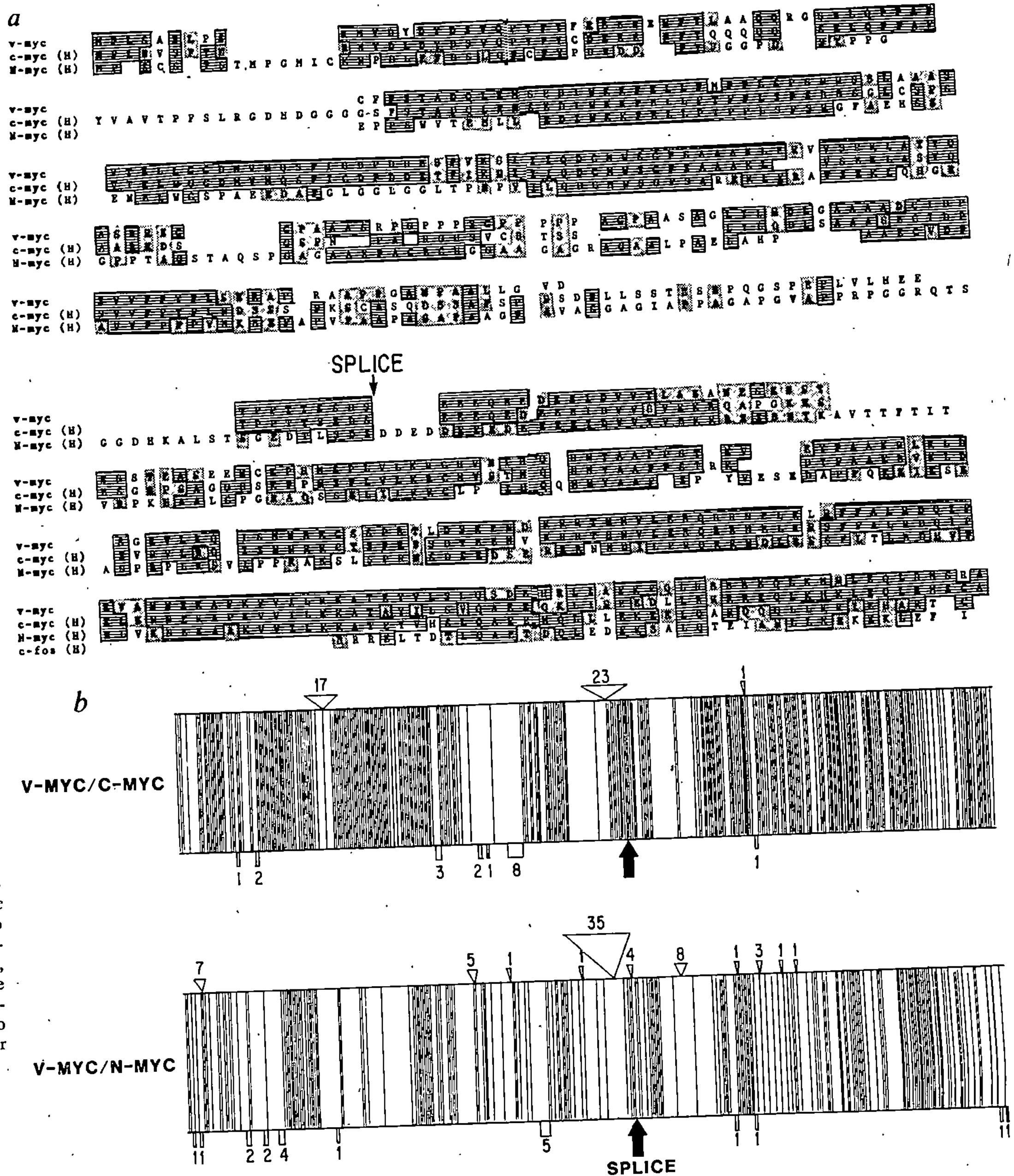

Fig. 4 Comparison of the amino-acid sequences of the putative N-*myc*, c-*myc* and v-*myc* proteins. ***a***, The amino acids were aligned by inspection, with gaps introduced to achieve maximum homology. Homologous amino acids are boxed and shaded. Amino-acid substitutions judged by McLachlan[56] to occur at higher than average frequencies are indicated by shading alone. The region of the human *fos* protein[20] found in a computer-assisted search of the 3,061 sequences in the NIH protein database (the Protein Identification Resources of the NIH) to be homologous with a region of the putative N-*myc* gene product is shown. The amino-acid sequence of the c-*myc* protein is from ref. 12; that of the v-*myc* protein from ref. 57. ***b***, Homology between amino-acid sequences of the v-*myc* protein and the c-*myc* and N-*myc* proteins is shown schematically. The sequence of the v-*myc* protein was used as a template on which either the N-*myc* or c-*myc* protein sequence was superimposed. Homologous amino acids are indicated by a line. Amino-acid insertions in the N-*myc* and c-*myc* proteins relative to the v-*myc* protein are indicated by triangles at the top, deletions by rectangles at the bottom of the grid; the numbers indicate the size, in amino acids, of the insertion or deletion.

homology between v-*myc* and c-*myc* is ~65%, that between v-*myc* and N-*myc* ~40%; in the exon 3-encoded domain these homologies are ~70% and 50%, respectively. A comparison of the v-*myc* and N-*myc* proteins (Fig. 4*b*) shows that there are clusters of highly conserved amino acids in both coding domains. Within the first protein-coding exon, c-*myc* diverges significantly from v-*myc* in three areas, including two large insertions and an 8-amino acid deletion[12]. In two of these regions N-*myc* more closely resembles v-*myc*; however, N-*myc* contains a 35-amino-acid insertion in the region where c-*myc* contains a 23-amino-acid insertion (see Fig. 4). In general, insertions and deletions of amino acids in N-*myc* relative to v-*myc* are in regions previously noted to be subject to such structural variations between *myc*-related proteins[18], in agreement with the notion that these are regions that can tolerate changes in length.

We have demonstrated that the structure of human N-*myc* resembles that of c-*myc* (Fig. 2), and that significant nucleotide and amino-acid sequence homology exists between these genes and between their gene products (Fig. 4). The data presented here support the notion that N-*myc* and c-*myc* are members of the same cellular proto-oncogene family[7]. c-*myc* encodes a nuclear protein which has DNA-binding capacity *in vitro*, a property attributed to the abundance of basic amino acids a the carboxy terminus of this protein[19]. This feature is share by the putative N-*myc* gene product; thus, the N-*myc* protei may also be a nuclear, DNA-binding protein. When the deduce amino-acid sequence of the N-*myc* protein was compared wit those of the over 3,000 proteins in the NIH protein database the most significant region of homology detected (excluding v and c-*myc* genes) was between the putative N-*myc* and c-*fo* proteins: when residues 425-464 of the predicted N-*myc* protei are aligned with residues 157-196 of the c-*fos* protein[20], 15 c the 40 amino acids are homologous, with many other conserva tive substitutions (Fig. 4). In addition, a region of notab nucleotide sequence homology between the N-*myc* and r-*fos* and c-*fos*[20] genes occurs at the beginning of exon 3 (see Fig. legend). Although any significance of these homologies remai to be determined, it is notable that the c-*fos* protein has al been localized to the nucleus[22].

In addition to the structural and functional similariti between the *myc* genes and their respective products, so regulatory similarities have also been observed, most notab the reduced expression of the N- and c-*myc* genes in certa tumour lines following chemical differentiation[23-26]. Howev other aspects of the regulation of the two genes appear to be drastically different. The c-*myc* gene product is expressed in a wide variety of normal and transformed cells where it is probably involved in growth and division[23,27-30]. In addition, deregulated expression of c-*myc* has been implicated as contributing to the development of numerous classes of tumours[31-35]. However, expression of N-*myc* is detectable in a very restricted set of normal or transformed cells and deregulated expression of N-*myc* has been implicated only in a limited set of tumours[9,10]. Neither the control nor the function of the differences in expression of the two *myc* genes is understood. However, it is notable that the promoter regions of the two genes appear to differ. Whereas transcription of c-*myc* mRNA initiates at two cap sites located ~150 bp from one another, each of which is preceded by a classical TATA motif[13-16], transcription of N-*myc* mRNA appears to initiate at multiple sites, most of which occur in the absence of an upstream TATA-like sequence. Such initiation heterogeneity has also been observed for the dihydrofolate reductase[36] and 3-hydroxy-3-methylglutaryl coenzyme A reductase (HMG CoA reductase)[37] genes and for the early and late regions of simian virus 40 (SV40)[38,39]. Significantly, sequences upstream of the major N-*myc* initiation sites show several similarities to the promoter of SV40. This region is G+C-rich (~70% G+C) and contains a 9/10-nucleotide match with the imperfect 21-bp repeat of the SV40 promoter, including the hexanucleotide CCGCCC, which is important in transcription of the viral early and late genes[40-42]. This 'GC' motif has also been observed in the promoter of the herpes thymidine kinase gene[43] and in the control region of several housekeeping genes including HMG CoA reductase[37]. An additional property that the HMG CoA reductase[37] gene has in common with N-*myc* and c-*myc*[13-16] is the presence of an exceptionally long 5'-untranslated leader sequence, most of which derives from a 5' noncoding exon. The strong conservation of the 5' noncoding exon between the c-*myc* genes of mouse and human suggests a significant functional role for this exon: one proposed function is a regulatory role with respect to c-*myc* expression[13,15,31]. Although no homology is detectable between the 5' exon of N-*myc* and that of c-*myc*, the 5' exons of human and murine N-*myc* show 85% homology (not including insertions and deletions)[17]; this evolutionary conservation of the 5' exon of N-*myc* also suggests a significant functional role for the exon (in analogy to c-*myc* this may be a regulatory role). If so, the lack of homology between the 5' exons of N-*myc* and c-*myc* would be consistent with divergent regulatory patterns of the two genes.

We thank P. Madaule for assistance with the computer analyses. This work was supported by NIH grant 2-POI CA 23767-06 and a Searle Scholars Award to F.W.A. F.W.A. is a Mallinkrodt Scholar. C.E.G. is a fellow of the Anna Fuller Cancer Fund and E.L. is an EMBO fellow.

Received 17 September; accepted 23 October 1985.

1. Kohl, N. E. *et al. Cell* **35**, 359-367 (1983).
2. Schwab, M. *et al. Nature* **305**, 245-248 (1983).
3. Michitsch, R. W., Montgomery, K. T. & Melera, P. W. *Molec. cell. Biol.* **4**, 2370-2380 (1984).
4. Michitsch, R. W. & Melera, P. W. *Nucleic Acids Res.* **13**, 2545-2558 (1985).
5. Land, H., Parada, L. F. & Weinberg, R. A. *Nature* **304**, 596-602 (1983).
6. Ruley, H. E. *Nature* **304**, 602-606 (1983).
7. Yancopoulos, G. D. *et al. Proc. natn. Acad. Sci. U.S.A.* **82**, 5455-5459 (1985).
8. Schwab, M., Varmus, H. E. & Bishop, J. M. *Nature* **316**, 160-162 (1985).
9. Kohl, N. E., Gee, C. E. & Alt, F. W. *Science* **226**, 1335-1337 (1984).
10. Zimmerman, K. A. *et al. Nature* (in the press).
11. Mount, S. M. *Nucleic Acids Res.* **10**, 459-472 (1982).
12. Colby, W. W. *et al. Nature* **301**, 722-725 (1983).
13. Battey, J. *et al. Cell* **34**, 779-787 (1983).
14. Watt, R. *et al. Proc. natn. Acad. Sci. U.S.A.* **80**, 6307-6311 (1983).
15. Saito, H. *et al. Proc. natn. Acad. Sci. U.S.A.* **80**, 7476-7480 (1983).
16. Bernard, O. *et al. EMBO J.* **2**, 2375-2383 (1983).
17. DePinho, R. *et al. Proc. natn. Acad. Sci. U.S.A.* (in the press).
18. Ralston, R. & Bishop, J. M. *Nature* **306**, 803-806 (1983).
19. Persson, H. & Leder, P. *Science* **225**, 718-721 (1984).
20. van Straaten, F. *et al. Proc. natn. Acad. Sci. U.S.A.* **80**, 3183-3187 (1983).
21. Cochran, B. *et al. Science* **226**, 1080-1082 (1984).
22. Curran, T. *et al. Cell* **36**, 259-268 (1984).
23. Westin, E. H. *et al. Proc. natn. Acad. Sci. U.S.A.* **79**, 2490-2494 (1982).
24. Reitsma, P. H. *et al. Nature* **306**, 492-494 (1983).
25. Campisi, J. *et al. Cell* **36**, 241-247 (1984).
26. Thiele, C. J., Reynolds, C. P. & Israel, M. A. *Nature* **313**, 404-406 (1985).
27. Gonda, T. J., Sheiness, D. K. & Bishop, J. M. *Molec. cell Biol.* **2**, 617-624 (1982).
28. Kelly, K. *et al. Cell* **35**, 603-610 (1983).
29. Makino, R., Hayashi, K. & Sugimura, T. *Nature* **310**, 697-698 (1984).
30. Pfeifer-Ohlsson, S. *et al. Cell* **38**, 585-596 (1984).
31. Leder, P. *Science* **222**, 765-771 (1983).
32. Collins, S. & Groudine, M. *Nature* **298**, 679-681 (1982).
33. Dalla Favera, R., Wong-Staal, F. & Gallo, R. C. *Nature* **299**, 61-63 (1982).
34. Alitalo, K. *et al. Proc. natn. Acad. Sci. U.S.A.* **80**, 1707-1711 (1983).
35. Little, C. D. *et al. Nature* **36**, 194-196 (1983).
36. McGrogan, M. *et al. J. biol. Chem.* **260**, 2307-2314 (1985).
37. Reynolds, G. A. *et al. Cell* **38**, 275-285 (1984).
38. Ghosh, P. K. & Lebowitz, P. *J. Virol.* **40**, 224-240 (1981).
39. Ghosh, P. K. *et al. J. molec. Biol.* **126**, 813-846 (1978).
40. Everett, R. D., Baty, D. & Chambon, P. *Nucleic Acids Res.* **11**, 2447-2464 (1983).
41. Baty, D. *et al. Nucleic Acids Res.* **12**, 915-932 (1984).
42. Vigneron, M. *et al. EMBO J.* **3**, 2373-2382 (1984).
43. McKnight, S. L. & Kingsbury, R. *Science* **217**, 316-324 (1982).
44. DePinho, R. *et al. Molec. cell. Biol.* **4**, 2905-2910 (1984).
45. Seeger, R. C. *et al. J. Immun.* **128**, 983-989 (1982).
46. Yancopoulos, G. D. & Alt, F. W. *Cell* **40**, 271-281 (1985).
47. Tumilowicz, J. J. *et al. Cancer Res.* **30**, 2110-2118 (1970).
48. Gilbert, F. *et al. Cancer Genet. Cytogenet.* **7**, 33-42 (1982).
49. Reth, M. G. & Alt, F. W. *Nature* **312**, 418-423 (1984).
50. Gubler, U. & Hoffman, B. J. *Gene* **25**, 263-269 (1983).
51. Biggin, M., Farrell, P. J. & Barrell, B. G. *EMBO J.* **3**, 1083-1090 (1984).
52. Zinn, K., DiMaio, D. & Maniatis, T. *Cell* **34**, 865-879 (1983).
53. Maxam, A. M. & Gilbert, W. *Meth. Enzym.* **65**, 499-560 (1980).
54. Proodfoot, N. J. & Brownlee, G. G. *Nature* **263**, 211-214 (1976).
55. Tinoco, I. Jr. *et al. Nature new Biol.* **246**, 40-41 (1973).
56. McLachlan, A. D. *J. molec. Biol.* **61**, 409-424 (1971).
57. Alitalo, K. *et al. Proc. natn. Acad. Sci. U.S.A.* **80**, 100-104 (1983).

MATTERS ARISING

Mapping of general anaesthetic target sites

FRANKS and Lieb[1] have suggested that the comparative effectiveness as general anaesthetics of members of the *n*-alkane and *n*-alkanol homologous series may be understood in terms of their effects on the activity of a water-soluble protein, firefly luciferase. In particular, they propose the following: "When general anaesthetic target sites in animals and the luciferase protein are mapped out using the fine details of the potency data, remarkable similarities are revealed'. We disagree. Consider first the *n*-alkane results. Figure 2 of Franks and Lieb indicates that roughly equal aqueous concentrations of *n*-pentane, *n*-hexane, *n*-heptane and *n*-octane are required for 50% inhibition of luciferase activity. However, there are data available on the effectiveness of these compounds as general anaesthetics. The data of Fuhner (see Table 4 of Ferguson[2]) and Crisp *et al.*[3] on alkane-induced narcosis in mice and barnacle larvae respectively show very clearly (given knowledge of the saturated aqueous concentrations[4]) that in both these widely disparate species, the effective aqueous concentration decreases progressively from *n*-pentane to *n*-octane; this is shown here in Fig. 1*a*. Thus alkane activity as a general anaesthetic and as an inhibitor of firefly luciferase could be said not to correlate at all.

For the *n*-alkanol system, Franks and Lieb compare luciferase data with their chosen combination of data from the studies of Vernon[5] and Meyer and Hemmi[6] on anaesthesia in tadpoles. These three sets of results are plotted in their original form in Fig. 1*b* (the plots have been displaced from each other vertically so as to show more clearly the variations in slope which are to be compared). The data of Meyer and Hemmi show no correlation with the luciferase results. The usefulness of Vernon's much earlier results is marred by the fact that, for the C_5 experiment, Vernon used not *n*-pentanol but an isopentanol of unspecified structure (perhaps even a mixture of the two isopentanols) and arbitrarily divided his result by two. The correct position of this point (shown in parentheses in Fig. 1*b*) is thus unclear, a feature which Franks and Lieb do not mention. Given also that Vernon says nothing about the purity of his *n*-alkanols—which, in 1913, was probably not very high—such correlation as might be claimed between the luciferase data and Vernon's results is, to say the least, unconvincing, and does not justify Franks and Lieb's Fig. 3.

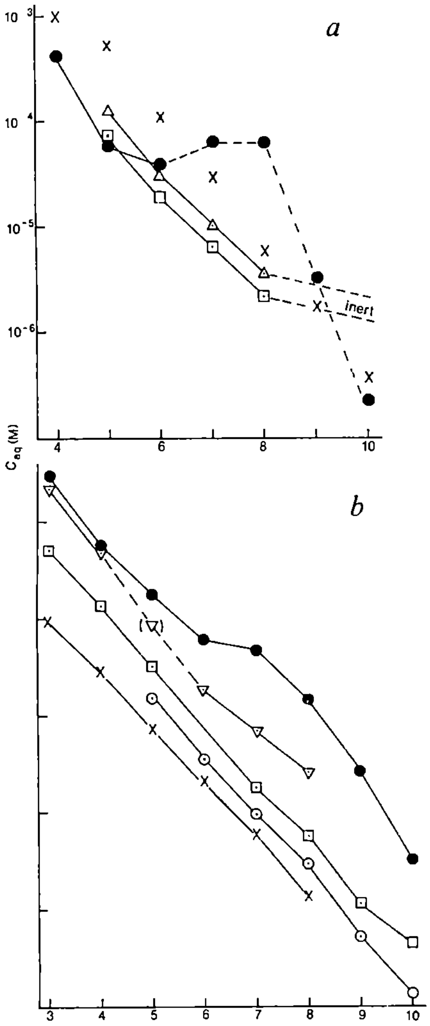

Fig. 1 The dependence on chain length of aqueous concentrations of *n*-alkanes (*a*) and *n*-alkanols (*b*) required to produce a given endpoint in various systems. The abscissa shows the number of carbon atoms in the molecule. The ordinate for *a* gives the aqueous concentrations (C_{aq}) of *n*-alkane required to produce a saturated solution in pure water[1] (×); inhibit luciferase activity by 50%[1] (●); induce narcosis in mice[2] (△), and induce narcosis in barnacle larvae[3] (⊡). The data for mice are given as the concentration in Ringer's solution at 20 °C which would be in equilibrium with the blood of the mouse. The ordinate for *b* again gives the required concentrations but the plots for each system have been displaced vertically to an arbitrary extent in order that the slopes may be more readily compared. The systems are: ●, 50% reduction of luciferase activity[1]; ∇, reversible suppression of spontaneous movement in tadpoles (the point in parentheses is derived from data for an undefined iso-derivative)[5]; ⊡, reversible suppression of reflex movement in tadpoles[6]; ⊙, 50% reduction of Na current in a voltage-clamped squid giant axon[7]; ×, reversible inhibition of luminescence in bacteria[8].

While their relevance to general anaesthesia is debatable, similar experiments examining the effects of alcohols on the sodium current of the squid giant axon[7] and on bacterial luminescence[8] (Fig. 1*b*) show no significant irregularities in the range pentanol to heptanol and exhibit clear similarities to the data of Meyer and Hemmi on anaesthesia in tadpoles.

For the two families of *n*-alkanes and *n*-alkanols there remains the one similarity that, for the alkanols, the anaesthetic potency and the binding to luciferase decline beyond *n*-dodecanol. But there is thought to be little luciferase in the central nervous system.

J. R. ELLIOTT
D. A. HAYDON
Physiological Laboratory,
University of Cambridge,
Cambridge CB2 3EG, UK

1. Franks, N. P. & Lieb, W. R. *Nature* **316**, 349-351 (1985).
2. Ferguson, J. *Proc. R. Soc.* **B127**, 387-404 (1939).
3. Crisp, D. J., Christie, A. O. & Ghobashy, A. F. A. *Comp. Biochem. Physiol.* **22**, 629-649 (1968).
4. Haydon, D. A., Hendry, B. M., Levinson, S. R. & Requena, J. *Biochim. biophys. Acta* **470**, 17-34 (1977).
5. Vernon, H. M. *J. Physiol., Lond.* **47**, 15-29 (1913).
6. Meyer, K. H. & Hemmi, H. *Biochem. Z.* **277**, 39-71 (1935).
7. Haydon, D. A. & Urban, B. W. *J. Physiol., Lond.* **341**, 411-427 (1983).
8. Taylor, G. W. *J. cell. Physiol.* **4**, 329-348 (1933).

FRANKS AND LIEB REPLY—We disagree with the criticisms of Elliott and Haydon. The purpose of our paper[1] was to demonstrate that the abrupt cut-offs in general anaesthetic potencies observed when ascending homologous series of *n*-alkanes and *n*-alcohols can be mimicked by a pure soluble protein, thus lending further support to the idea that the primary target sites in general anaesthesia are proteins. These cut-offs occur at very different positions in the alkane and alcohol series, when anaesthetic ED_{50} (50% effective dose) concentrations become greater than saturated aqueous concentrations.

For the *n*-alkanes, we found[1] that the luciferase cut-off occurs between C_6 and C_7. In animals, the cut-off point is species-dependent[1], occurring between C_6 and C_{10}. In view of the different cut-off positions, it is quite wrong to expect a point-to-point correlation in potency data in this transition region: Elliott and Haydon are comparing (luciferase) data just past the cut-off with (animal) data just before the cut-off. They have also ignored data for fish, which show a cut-off very similar to that for luciferase[1]. What is important is that the luciferase enzyme exhibits an alkane cut-off at a position similar to those observed in animals.

For the *n*-alcohols, we found that, in common with general anaesthesia, the luciferase cut-off occurs much later than it does for the *n*-alkanes and this is due to a levelling-off of ED_{50} s for the higher alcohols. These points are clear from Fig. 2, where data for general anaesthesia and luciferase inhibition are compared directly. (Elliott and Haydon have obscured these points by choosing to plot only data between C_3 and C_{10} and by offsetting their curves on a relative scale. Also, their inclusion of data for bacteria and squid axons seems to us a red herring.) The close correspondence between the data of Vernon[2] and those of Meyer and Hemmi[3] shows that the worries of Elliott and Haydon are unfounded. As for the inflection at about C_6, it is clear that, although small, it is a real feature of the combined general anaesthesia data. (Elliott and Haydon's concern about Vernon's C_5 data point is not relevant, as the same feature is found even if this is disregarded.) However, this minor feature has no bearing on the mechanism of the alcohol cut-offs, which are due to the much larger changes in slope at about C_{11}.

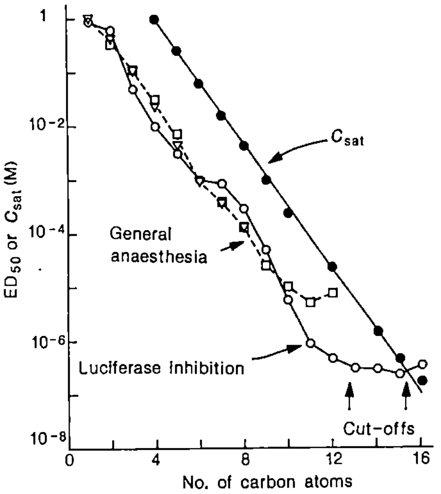

Fig. 2 The effectiveness of the *n*-alcohols as general anaesthetics and as inhibitors of firefly luciferase. ○, ED_{50} s for luciferase[1]; ∇ and □, general anaesthesia ED_{50} s for tadpoles, from refs 2 and 3, respectively; ●, maximum aqueous concentrations (solubilities)[4].

In summary, we feel that, in contrast to lipid bilayers, protein pockets similar to that found on firefly luciferase provide both a plausible and an economic explanation of cut-off effects in general anaesthesia. Despite our disagreements with Elliott and Haydon, we can at least concur with their final sentence!

N. P. FRANKS
W. R. LIEB
Biophysics Section,
The Blackett Laboratory,
Imperial College of Science
and Technology,
London SW7 2BZ

1. Franks, N. P. & Lieb, W. R. *Nature* **316**, 349-351 (1985).
2. Vernon, H. M. *J. Physiol., Lond.* **47**, 15-29 (1913).
3. Meyer, K. H. & Hemmi, H. *Biochem. Z.* **277**, 39-71 (1935).
4. Bell, G. H. *Chem. Phys. Lipids* **10**, 1-10 (1973).

BOOKS RECEIVED

Mathematics

Functions and Graphs: A Precalculus Course. By RAYMOND A. BARNETT. *McGraw-Hill: 1985. Pp.644. ISBN 0-07-003896-1. £27.95.*

Handbook of Applicable Mathematics, Vol. V, Parts A & B. Combinatorics and Geometry. WALTER LEDERMANN and STEVEN VAJDA (eds). *Wiley: 1985. Part A, pp.327, ISBN 0471-90567-4. Part B, pp.732, ISBN 0-471-90568-2. Complete set £88.*

A History of Algebra; From al-Khwarizmi to Emmy Noether. By B.L. VAN DER WAERDEN. *Springer-Verlag: 1985. Pp.271. Hbk ISBN 3-540-13610-X. DM 98.*

The Mathematics of Finite Elements and Applications, Volume V. J.R. WHITEMAN (ed.). *Academic: 1985. Pp.650. Hbk ISBN 0-12-747255-X. $59.00, £53.00.*

Mathematics and the Search for Knowledge. By MORRIS KLINE. *Oxford University Press: 1985. Pp.257. Hbk ISBN 0-19-503533-X. £21.00.*

Partial Differential Equations for Scientists and Engineers, 3rd Edn. By G. STEPHENSON. *Longman: 1985. Pp.161. ISBN 0-582-44696-1. £6.95.*

Recursive Aspects of Descriptive Set Theory. By RICHARD MANSFEILD and GALEN WEITKAMP. *Oxford University Press: 1985. Pp.144. ISBN 0-19-5036026. £15.*

Astronomy

Astronomy and the Imagination: A New Approach to Man's Experience of the Stars. By NORMAN DAVIDSON. *Routledge & Kegan Paul: 1985. Pp.237. ISBN 0-7102-0371-3. £12.95.*

The Milky Way Galaxy. HUGO VAN WOERDEN, RONALD J. ALLEN and W. BUTLER BURTON (eds). *Reidel: 1985. Pp.660. Hbk ISBN 90-277-1919-5; pbk ISBN 90-277-1920-9. Hbk Dfl. 195, $69; pbk Dfl. 90, $32.50.*

Stargazing: Astronomy Without a Telescope. By PATRICK MOORE. *Barrons: 1985. Pp.176. ISBN 0-8120-5644-2. $19.95.*

Space Science

From Spacelab to Space Station. H. STOEWER and PETER M. BAINUM (eds). *American Astronautical Society: 1985. Pp.259. Hbk ISBN 0-87703-209-2; pbk ISBN 0-87703-210-6. Hbk $50; pbk $40.*

Interstellar Migration and the Human Experience. BEN R. FINNEY and ERIC M. JONES (eds). *University of California Press: 1985. Pp.354. Hbk ISBN 0-520-05349-4. Hbk $28.75, £21.25.*

Permanent Presence — Making it Work. IVAN BEKEY (ed.). *American Astronautical Society: 1985. Pp.177. Hbk ISBN 0-87703-207-6; pbk ISBN 0-87703-208-4. Hbk $40; pbk $30.*

Spacefarers of the '80s and '90s. The Next Thousand People in Space. By ALCESTIS R. OBERG. *Columbia University Press: 1985. Pp.238. Hbk ISBN 0-231-05906-X. $24.95.*

Technology

Advances in Solar Energy: An Annual Review of Research and Development. KARL W. BÖER *et al.* (eds). *American Solar Energy Society/Plenum: 1983. Pp.310. ISBN 0-306-42019-8. Np.*

Pop-11: A Practical Language for Artificial Intelligence. By R. BARRETT. A. RAMSAY and A. SLOMAN. *Ellis Horwood: 1985. Pp.232. Pbk ISBN 0-85312-924-X. £9.50.*

Science and Technology in World Development. By ROBIN CLARKE. *Oxford University Press: 1985. Pp.216. Hbk ISBN 0-19-219195-0; pbk ISBN 0-19-289176-6. Hbk £12.50; pbk £4.95.*

Solid State Chemical Sensors. JIŘÍ JANATA and ROBERT J. HUBER (eds). *Academic: 1985. Pp.211. ISBN 0-12-380210-5. $49, £49.*

Solid State Protonic Conductors III-for Fuel Coals and Sensors. J.B. GOODENOUGH, J. JENSEN and A. POTIER (eds). *Odense University Press: 1985. Pp.284. ISBN 87-7492-517-2. $20.*

Spectral Techniques and Fault Detection. MARK G. KARPOVSKY (ed.). *Academic: 1985. Pp.608. Hbk ISBN 0-12-400060-6. $44.50, £39.00.*

Technology, Institutions and Government Policies. JEFFREY JAMES and SUSUMU WATANABE (eds). *Macmillan: 1985. Pp.265. Hbk ISBN 0-333-38562-4. £25.00.*

Computer Science

Computing for Biologists: An Introduction to BASIC Programming with Applications in the Life Sciences. By ALAN FIELDING. *Addison-Wesley: 1985. Pp.190. Pbk ISBN 0-201-14574-X. Pbk £8.95.*

Introduction to Computer Systems: A User-View. By BRIAN MOLINARI. *Cambridge University Press: 1985. Pp.274. ISBN 0-521-24962-7. Hbk £22.50, $39.50; pbk £7.95, $14.95.*

Microcomputers. By D.G.C. JONES. *Adam Hilger: 1985. Pp.64. Pbk ISBN 0-85274-770-5. Pbk £2.95.*

Environmental Sciences

Air Pollution by Photochemical Oxidants: Formation, Transport, Control and Effects on Plants. R. GUDERIAN (ed.). *Springer-Verlag: 1985. Pp.346. ISBN 3-540-13966-4/0-387-13966-4. DM 158.*

Black Carbon in the Environment: Properties and Distribution. By EDWARD D. GOLDBERG. *Wiley: 1985. Pp.198. ISBN 0-471-81979-4. Np.*

Chemosphere: Chemistry, Biology and Toxicology as Related to Environmental Problems. Vol. 14, No. 6/7. *Pergamon: 1985. Pp.989.2/yr. $250.*

Chlorinated Dioxins and Dibenzofurans in the Total Environment II. LAWRENCE H. KEITH, CHRISTOFFER CHOUDHARY (eds). *Ann Arbor Science: 1985. Pp.547. Hbk ISBN 250-40646-2. £65.00.*

Earth Sciences

Categorical Data Analysis for Geographers and Environmental Scientists. By NEIL WRIGLEY. *Longman: 1985. Pp.392. ISBN 0-582-30127-0. £45.*

Changes in Global Climate: A Study of the Effect of Radiation and Other Factors during the Present Century. By K. Ya KONDRAT'EV. *Balkema: 1985. Pp.288. ISBN 90-6191-442-6. $29.50, £22.*

Humic Substances in Soil, Sediment and Water. Geochemistry. Isolation, and Characterization. GEORGE R. AIKEN, DIANE M. McKNIGHT, ROBERT L. WERSHAW and PATRICK MacCARTHY (eds). *John Wiley: 1985. Pp.692. Hbk ISBN 0-471-88274-7. £61.35.*

Karst Geomorphology. By J.N. JENNINGS. *Basil Blackwell: 1985. Pp.293. Hbk ISBN 0-631-14031-X; pbk ISBN 0-631-14032-8. Hbk £27.50; pbk £9.50.*

Mastodon-bearing Springs and Late Quaternary Geochronology of the Lower Pomme de Terre Valley, Missouri. By C. VANCE HAYNES Jr. *The Geological Society of America/Special Paper 204: 1985. Pp.35. Pbk ISBN 0-8137-2204-7. $10.00.*

Minerals Resources and Engineering Geology. AKIRA SASAKI, SHUNSO ISHIHARA and YOTARO SEKI (eds). *Wiley: 1985. Pp.299. ISBN 0-471-10536-8. £27.95.*

The Polar Cusp. JAN A. HOLTET and ALVENGELAND (eds). *Reidiel: 1985. Pp.422. ISBN 90-2771923-3. Dfl.160, $55, £40.75.*

Preferred Orientation in Deformed Metals and Rocks: An Introduction to Modern Texture Analysis. HANS–RUDOLF WENK (ed.). *Academic: 1985. Pp.610. ISBN 0-12-744020-8. $59.50, £59.50.*

The Puzzle of the Plates: Spilhaus Repeating World Map. (Educational Jigsaw.) Created by ATHELSTAN SPILHAUS. *American Geophysical Union: 1985. Np.*

Quaternary Environments: Eastern Canadian Arctic, Baffin Bay and Western Greenland. J.T. ANDREWS (ed.). *George Allen & Unwin: 1985. Pp.774. ISBN 0-04-551094-6. £50, $75.*

Soil Reclamation Processes: Microbiological Analyses and Applications. ROBERT L. TATE III and DONALD A. KLEIN (eds). *Marcel Dekker: 1985. Pp.368. ISBN 0-8247-7286-5. $71.25.*

Syngenesis and Epigenesis in the Formation of Mineral Deposits. A. WAUSCHKUHN, C. KLUTH and R.A. ZIMMERMANN (eds). *Springer-Verlag: 1985. Pp.653. ISBN 3-540-13845-5 0-387-13845-5. DM 175.*

Biological Sciences

Advances in Prostaglandin, Thromboxane, and Leukotriene Research: Platelets, Prostaglandins and the Cardiovascular System. GIAN G. NERI SERNERI *et al.* (eds). *Raven: 1985. Pp.393 ISBN 0-88167-062-6. $35.*

AIDS-Associated Syndromes. S. GUPTA (ed.). *Plenum: 1985. Pp.181. Hbk ISBN 0-306-42016-3 Np*

Alternative Immunoassays. W.P. COLLINS (ed.). *Wiley: 1985. Pp.244. ISBN 0-471-90669-7. £28.*

Behavioral Evolution and Integrative Levels. GARY GREENBERG and ETHEL TOBACH (eds). *Lawrence Erlbaum: 1984. Pp.307. ISBN 0-89859-363-8. £28.75.*

Biochemistry of Plant Cell Walls. C.T. BRETT and J.R. HILLMAN (eds). *Cambridge University Press. 1985. Pp.312. ISBN 0-521-30487-3. £19.50.*

Biology of the Nerve Growth Cone. STANLEY KATER and PAUL LETOURNEAU (eds). *Alan R. Liss: 1985. Pp.351. ISBN 0-8451-0242-7. £34.00*

Biology of Pteridophytes: Proceedings of the Symposium held at Edinburgh, Sept. 12-16 1983. A.F. DYER and C.N. PAGE (eds). *The Royal Society of Edinburgh: 1985. Pp.474. £17.*

Brain Imaging and Brain Function. LOUIS SOKOLOFF (ed.) *Raven: 1985. Pp.308 ISBN 0-88167-084-7. $70.50.*

Catecholamines as Hormone Regulators. NIRA BEN-JONATHAN, JANICE M. BAHR and RICHARD I. WEINER (eds). *Raven: 1985 Pp.396. ISBN 0-89004-607-7. $47.*

Color Atlas of Kidney Biopsy: Pathology of Glomerular Diseases. By W. ROTTER.*Alan R. Liss 1985. Pp.280. ISBN 0-8451-0239-7. £95.*

Computer-assisted Bacterial Systematics. M. GOODFELLOW, D. JONES and F.G. PRIEST (eds). *Academic: 1985. Pp.443. Hbk ISBN 0-12-289665-3. $75.00, £55.00.*

Current Primate Researches. M.L. ROONWAL S.M. MOHNOT and N.S. RATHORE (eds) *Department of Zoology, University of Jodhpur, Jodhpur-342001, India: 1984. Pp.626. Np.*

Developments in Ophthalmology, Vol. 12: Visual Field in Glaucoma. Cellular Proliferation. W STRAUB and B.P. GLOOR (eds). *Karger: 1985 Pp.134. ISBN 3-8055-4022-1. SwFr. 93, DM 111 $39.75.*

Diseases of Marine Animals. Vol. IV, Part 1 Introduction, Pisces. O. KINNE (ed.). *Biologische Anstalt Helgoland, Hamburg, Federal Republic of Germany: 1984. Pp.541. ISBN 3-98008183-4. Np.*

Ecosystem Theory for Biological Oceanography. ROBERT E. ULANOWICZ and TREVOR PLATT (eds). *Department of Fisheries and Oceans, Ottawa, Canada: 1985. Pp.260. Pbk ISBN 0-660-11900-5 (Canada) $14.95, (other countries) $17.95.*

The Endocrine System and the Environment. BRIAN K. FOLLET, SUSUMU ISHII and ASHA CHANDOLA (eds). *Springer-Verlag: 1985. Pp 329 ISBN 3-540-15101-X/0-387-15101-X. DM 118.*

Environmental Regulation of Microbial Metabolism. I.S. KULAEV, E.A. DAWES and D.W TEMPEST (eds). *Academic: 1985. Pp.515. ISBN 0-12-428580-5. $49, £38.*

The Epigenetic Nature of Early Chordate Development: Inductive Interaction and Competence. By P.D. NIEUWKOOP, A.G. JOHNEN and B ALBERS. *Cambridge University Press: 1985. Pp.373 Hbk ISBN 0-521-25107-9. Np.*

Experimental Approaches for the Study of Hemoglobin Switching. GEORGE STAMATOYANNOPOULOS and ARTHUR W. NIENHIUS (eds) *Alan R. Liss: 1085. Pp.514. Hbk ISBN 0-8451-5041-3 £59.00.*

Fish and Shellfish Pathology. ANTHONY E ELLIS (ed.). *Academic: 1985. Pp.412. Hbk ISBN 0-12-237490-8. $69.50, £53.50.*

Flowering Plants of the World. V.H. HEYWOOD (ed.). *Croom Helm: 1985. Pp.335. Hbk 0-7099-3778-4. Hbk £19.95.*

Fragile Sites on Human Chromosomes. By GRANT R. SUTHERLAND and FREDERICK HECHT. *Oxford University Press: 1985. Pp.280. ISBN 0-19-503542-9. £40.*

Genetics, 3rd Edn. By MONROE W. STRICKBERGER. *Macmillan, NY: 1985. Pp.842. Pbk ISBN 0-02-946740-3. Pbk £15.95.*

Global Ecology. CHARLES H. SOUTHWICK (ed.). *Blackwell Scientific: 1985. Pp.323. Pbk ISBN 0-87893-810-9. Pbk £14.80.*

Hematopoietic Stem Cell Physiology. EUGENE P. CRONKITE, NICHOLAS DAINIAK, RONALD P. McCAFFREY, JIRI PALEK and PETER J. QUESENBERRY (eds). *Alan R. Liss: 1985. Pp.489. ISBN 0-8451-5034-0. £64.00.*

Higher Plant Cell Respiration. R. DOUCE and D.A. DAY (eds). *Springer-Verlag: 1985. Pp.522. ISBN 3-540-13935-4/0-387-13935-4. DM 298.*

Hormones and Human Behaviour. By BERNARD T. DONOVAN. *Cambridge University Press: 1985. Pp.223. Hbk ISBN 0-521-25881-2. Np.*

How The Dinosaurs Became Extinct. By S.N.U. FERNANDO. *Merlin Books: 1985. Pp.47. ISBN 0-86303-196-X. £1.25.*

Immobilised Cells and Enzymes: A Practical Approach. J. WOODWARD (ed.). *IRL Press: 1985. Pp.177. Pbk ISBN 0-947946-21-7. Np.*

In Search of the Double Helix: Darwin, DNA and Beyond. By JOHN GRIBBIN. *Wildwood House: 1985. Pp.369. Hbk ISBN 0-7045-3077-5. £12.95.*

The Intelligent Universe: A New View of Creation and Evolution. By FRED HOYLE. *Michael Joseph: 1985. Pp.256. Hbk ISBN 0-7181-2298-4; pbk ISBN 0-7181-2613-0. £8.95.*

The Interphotoreceptor Matrix in Health and Disease. C. DAVID BRIDGES and ALICE J. ADLER (eds). *Alan R. Liss: 1985. Pp.287. Hbk ISBN 0-8451-5040-5. £37.00.*

Intracellular Protein Catabolism. EDWARD A. KHAIRALLAH, JUDITH S. BOND and JOHN W.C. BIRD (eds). *Alan R. Liss: 1985. Pp.702. ISBN 0-8451-5030-8. Np.*

Isolation and Identification of Micro-Organisms of Medical and Veterinary Importance. C.H. COLLINS and J.M. GRANGE (eds). *Academic: 1985. Pp.387. ISBN 0-12-181460-2. $55, £45.*

Jones's Animal Nursing, 4th Edn. D.R. LANE (ed.). *Permagon: 1985. Pp.706. ISBN 0-08-031983-1. $38, £19.50.*

The Lactoperoxidase System: Chemistry and Biological Significance. KENNETH M. PRUITT and JORMA O. TENOVUO (eds). *Marcel Dekker: 1985. Pp.272. ISBN 0-8247-7298-8. $66.*

Linear Models in Biology. Linear Systems Analysis with Biological Applications. By M. R. CULLEN. *Ellis Horwood: 1985. Pp.213. Pbk ISBN 0-85312-905-3. $10.50.*

Membrane Fluidity in Biology, Vol. 3. Disease Processes. RONALD C. ALOIA and JOAN M. BOGGS (eds). *Academic: 1985. Pp.316. Hbk ISBN 0-12-053003-1. $64.50, £56.00.*

Membrane Protein Biosynthesis and Turnover. P.A. KNAUF and J.S. COOK (eds). *Academic. 1985. Pp.531. ISBN 0-12-153324-7. $89, £89.*

Methods in Enzymology. Vol. 112: Drug and Enzyme Targeting. KENNETH J. WIDDER and RALPH GREEN (eds). *Academic: 1985. Pp.589. ISBN 0-12-182012-2. $69.*

Microencapsulation and Artificial Cells. T.M.S. CHANG (ed.). *Humana: 1985. Pp.320. ISBN 0-89603-073-3. $65.*

Applied Biological Sciences

Advances in Cancer Research, Volume 44. GEORGE KLEIN and SIDNEY WEINHOUSE (eds). *Academic:1985. Pp.355. ISBN 0-12-006644-0. $55.00, £48.00.*

Alcohol and the Brain: Chronic Effects. RALPH E. TARTER and DAVID H. VAN THIEL (eds). *Plenum:1985. Pp.349. Hbk ISBN 0-306-41998-X. Np.*

Aldehyde Adducts in Alcoholism. MICHAEL A. COLLINS (ed.). *Alan R. Liss:1985. Pp.230. ISBN 0-8451-5033-2. £35.*

Basic Mechanisms and Clinical Treatment of Tumor Metastasis. MOTOMICHI TORISU and TAKESHI YOSHIDA (eds). *Academic:1985. Pp.661. ISBN 0-12-695680-4. $59.50, £59.50.*

Biological Control in Agricultural IPM Systems. MARJORIE A. HOY and DONALD C. HERZOG (eds). *Academic:1985. Pp.589. Hbk ISBN 0-12-357030-1. $49.50, £43.50.*

Calcitonin 1984: Chemistry, Physiology, Pharmacology and Clinical Aspects. A. PECILE (ed.). *Elsevier Biomedical Press:1985. Pp.485. Hbk ISBN 0-444-80690-3. $92.50, Dfl.250.00*

Carcinogenesis: The Role of Chemicals and Radiation in the Etiology of Cancer. ELIEZER HUBERMAN and SUSAN H. BARR (eds). *Raven:1985. Pp.538. ISBN 0-88167-130-4. $76.*

Circulatory Shock: Basic and Clinical Implications. H.F. JANSSEN and C.D. BARNES (eds). *Academic: 1985. Pp.242. ISBN 0-12-380240-7. $39.00, £35.00.*

Contributions of Modern Biology to Medicine. U. BERTAZZONI, F.J. BOLLUM and M. GHIONE (eds). *Raven:1985. Pp.261. ISBN 0-88167-029-8.$40.50.*

Current Issues in Toxicology: The Use of Short-Term Tests for Mutagenicity and Carcinogenicity in Chemical Hazard Evaluation. H.C. GRICE (ed.) *Springer-Verlag:1984. Pp.197. Pbk ISBN 3-540-13696-7/0-387-13696-7. Pbk DM 52.*

Drug Fate and Metabolism. Methods and Techniques, Vol. 5. EDWARD R. GARRETT and JEAN L. HIRTZ. *Marcel Dekker, New York and Basel:1985. Pp.345. Hbk ISBN 0-8247-7423-X. $79.50 (US and Canada), $95.25 (other countries).*

Encyclopedia of Medical Radiology. F. HEUCK and E. SCHERER (eds). *Springer-Verlag:1985. Pp.843. ISBN 3-540-13155-8/0-387-13155-8. DM 880.*

Germfree Research: Microflora Control and its Application to the Biomedical Sciences. BERNARD S. WOSTMANN *et al.* (eds). *Alan R. Liss:1985. Pp.512. ISBN 0-8451-5031-6. £60.*

Hyperthermic Oncology 1984, 2 Vols. JENS OVERGAARD (ed.). *Taylor & Francis: 1984. Vol. 1 pp.870, ISBN 0-85066-273-7. Vol. 2 pp.385, ISBN 0-85066-281-8. Vol.1 £70; Vol. 2 £40.*

Immunity to Cancer. ARNOLD E. REIF and MALCOLM S. MITCHELL (eds). *Academic:1985. Pp.659. Hbk ISBN 0-12-586270-9. $43.00, £38.00.*

Interferon Alpha-2: Pre-clinical and Clinical Evaluation. DANIEL L. KISNER and J.F. SMYTH (eds). *Martinus Nijhoff:1985. Pp.111. ISBN 0-89838-701-9. Dfl. 84, $19.95, £18.95.*

***In Vivo* Perfusion and Release of Neuroactive Substances: Methods and Strategies.** ALEJANDRO BAYON and RENE DRUCKER-COLIN (eds). *Academic:1985. Pp.322. Hbk ISBN 0-12-083350-6. $62.50, £54.50.*

Magnesium Deficiency: Physiopathology and Treatment Implications. M.J. HALPERN and J. DURLACH (eds). *Karger:1985. Pp.248. ISBN 3-8055-3979-7. $79.75, £58.50.*

Manual of Drug Therapy. DAVID A. SCHEINBER and LABE SCHEINBERG (eds). *Raven.1985. Pp.400. ISBN 0-88167-074-X. $21.*

Manual of Radiographic Interpretation for General Practitioners. By P.E.S. PALMER *et al. World Health Organization:1984. Pp.216. Pbk ISBN 92-4-154177-6. SwFr. 23.*

Monitoring for Adverse Drug Reactions. S.R. WALKER and A. GOLDBERG (eds). *MTP Press:1985. Pp.152. ISBN 0-85200-876-7. £29.95.*

Monitoring Human Exposure to Carcinogenic and Mutagenic Agents. A. BERLIN, M. DRAPER, K. HEMMINKI and H. VAINIO (eds). *Oxford University Press:1985. Pp.457. Hbk ISBN 0-19-723056-3. £25.00.*

Monoclonal Antibodies in Cancer. STEWART SELL and RALPH REISFELD (eds). *Humana: 1985. Pp.448. ISBN 0-89603-068-7. D 74.50.*

Neuroendocrine Correlates of Stress. KENNETH W. McKERNS and VLADIMIR PANTIC (eds). *Plenum:1985. Pp.345. Hbk ISBN 0-306-42072-4. Np.*

Novel Biochemical, Pharmacological and Clinical Aspects of Cytidinediphosphocholine. V. ZAPPIA *et al.* (eds). *Elsevier:1985. Pp.406. ISBN 0-444-00967-1. $78.*

P-450 and Chemical Carcinogenesis. YUSAKU TAGASHIRA and TSUNEO OMURA (eds) *Japan Scientific Societies Press/Plenum:1985. Pp.175. ISBN 0-306-42123-2. Np.*

The Patient, Biological, Psychological, and Social Dimensions of Medical Practice, 2nd Edn. By HOYLE LEIGH and MORTON F. REISER. *Plenum: 1985. Pp.457. ISBN 0-306-41985-8. Np.*

Postoperative Pain: Understanding its Nature and How to Treat it. By JANE HOSKING and EDWARD WELCHEW. *Faber & Faber:1985. Pp.175. ISBN 0-571-13538-2. £4.95.*

Practical Fow Cytometry. By HOWARD M. SHAPIRO. *Alan R. Liss:1985. Pp.295. ISBN 0-8451-0243-5. £37.50.*

Prevention of Head Injuries in Skiing: Mechanisms, Experimental Study, and Prevention. By SOOYOUNG OH. *Karger:1985. Pp.164. Pbk ISBN 3-8055-3978-9. SwFr. 49, DM 59, $21.00, £15.40.*

Principles of Medical Therapy in Pregnancy. NORBERT GLEICHER (ed.). *Plenum:1985. Pp.1290. ISBN 0-306-41845-2. Np.*

Principles of Plant Biotechnology: An Introduction to Genetic Engineering in Plants. By S.H. MANTELL, J.A. MATTHEWS and R.A. MCKEE. *Blackwell Scientific:1985. Pp.269. Pbk ISBN 0-632-01215-3. Pbk £10.80.*

Progress in Medical Radiation Physics. COLIN G. ORTON (ed.) *Plenum:1985. Pp.254. ISBN 0-306-41789-8. Np.*

Progress in Pesticide Biochemistry and Toxicology. D.H. HUTSON and T.R. ROBERTS (eds). *Wiley: 1985. Pp.368. ISBN 0-471-90460-0. £42.*

Psychological and Behavioural Treatments For Disorders of the Heart and Blood Vessels. MADY HORNIG-ROHAN and STEVEN E. LOCKE (eds). *Institute for the Advancement of Health:1985. Pp.180. Hbk ISBN 0-914533-01-0. $45.00.*

Raynaud Update: Pathophysiology and Treatment. E. DAVIS (ed.) *Karger:1985. Pp.160. ISBN 3-8055-3992-4. DM 165, $58.75.*

Recent Results in Cancer Research: Predictive Drug Testing on Human Tumor Cells. V. HOFMANN, M.E. BERENS and G. MARTZ (eds). *Springer-Verlag: 1984. Pp.285. ISBN 3-540-13497-2/0-387-13497-2. DM98, $35.70.*

Recombinant DNA Research and Viruses: Cloning and Expression of Viral Genes. YECHIEL BECKER (ed.) *Martinus Nijhoff:1985. Pp.373. ISBN 0-89838-683-7. Dfl. 219, $59.95, £45.50.*

Screening for Cancer. ANTHONY B. MILLER (ed.) *Academic:1985. Pp.458. ISBN 0-12-496720-5. $65, £65.*

Seedling Physiology and Reforestation Success. MARY L. DURYEA and GREGORY N. BROWN (eds). *Martinus Nijhoff: 1984. Pp.339. ISBN 90-247-2949-1. Dfl.120, $45.50, £30.50.*

Tumor Markers: Clinical and Laboratory Studies. By JANIS V. KLAVINS. *Alan R. Liss:1985. Pp.198. Hbk ISBN 0-8451-0248-6. Hbk £37.00.*

Sociology

American Freedom and the Social Sciences. By JAMES DEESE. *Columbia University Press: 1985. Pp.237. ISBN 0-231-05914-0. $32.50.*

Applying the Humanities. DANIEL CALLAHAN, ARTHUR L. CAPLAN and BRUCE JENNINGS (eds). *Plenum: 1985. Pp.329. Hbk ISBN 0-306-41968-8. Np.*

Cities and Services: The Geography of Collective Consumption. By STEPHEN PINCH. *Routledge & Kegan Paul: 1985. Pp.213. Pbk ISBN 7102-0493-0; hbk ISBN 7102-0054-4. Pbk £7.95; hbk £18.50.*

Essays in Human Sociobiology. JAN WIND (ed.). *Academic: 1985. Pp.164. Pbk. $16.*

Racial and Cultural Minorities: An Analysis of Prejudice and Discrimination, 5th Edn. By GEORGE EATON SIMPSON and J. MILTON YINGER. *Plenum: 1985. Pp.491. ISBN 0-306-41777-4. Np.*

Strengthening Urban Management: International Perspectives and Issues. THOMAS L. BLAIR (ed.). *Plenum: 1985. Pp.358. Hbk ISBN 0-306-42081-3. Np.*

History of Science

The Ashmolean Museum and Oxford Science 1683–1983. By A.V. SIMCOCK. *Museum of the History of Science, Broad Street, Oxford OX1 3AZ, England: 1984. Pp.48. Pbk ISBN 0-903364-03-4. Pbk £3.*

Robert T. Gunther and the Old Ashmolean. A.V. SIMCOCK (ed.). *Museum of the History of Science, Broad Street, Oxford OX1 3AZ, England: 1985. Pp.99. Pbk ISBN 0-903364-04-2. £4.*

Western blotting kit for AIDS virus

The latest batch of new products includes a touch-sensitive video display from Zenith and from Bio-Rad a kit for analysis of the AIDS virus

- New from Enzo-Biochem is a ready-to-use nick-translation kit which includes all the necessary reagents and a detailed protocol for the biotinylation of DNA probes. A biotin-labelled nucleotide, Bio-II-dUTP, replaces TTP in the standard nick-translation reaction. Standard procedures for nick-translation are used and result in substitution of 20–70% of the available thymidine residues with biotinylated dUTP. The Enzo nick-translation kit produces stable biotinylated DNA probes and is recommended for dot blots, Southern blots and for *in situ* hybridization. Detection systems are also available from Enzo-Biochem for immediate visualization of the probe.
Reader Service No. 100.

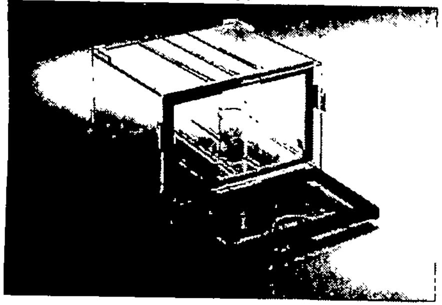

Bel-Art's fully transparent desiccator.

- Bel-Art airtight desiccator cabinets provide a dust and moisture free environment for the storage and protection of samples, chemicals, specimens or electronic components. These economical cabinets are injection-moulded in high impact polystyrene for full transparency, rigidity, and strength. They are easily stacked which saves valuable bench space and are also suitable for refrigerator applications.
Reader Service No. 101.

- Accurate and convenient pH measurement of low ionic strength solutions is now possible with the introduction of two new ranges of high-definition pH indicator sticks by May & Baker Laboratory Products of Manchester. Specially designed for use in weak solutions and part of the Dosatest range of pH indicators, the three zone and single zone sticks each consist of indicator pads firmly bonded to a plastic support allowing extended immersion times without solution contamination. The entire pH range is covered by the three zone sticks, one stick covers pH 0.0 to 6.0, another pH 4.5 to 10.0 and finally pH 7.0 – 14.0. Each of the three zone sticks has three hydrophobically separated indicator pads which change colour when immersed in the solution. A simple comparision of the new colour for each zone to that of the reference scale gives the pH of the solution to within 0.5 pH units. For very high definition pH measurements, May & Baker produce a range of one-zone plastic sticks which together cover a pH range of 0.3 to 9.5. The single indicator zone records the solution pH to within 0.2 to 0.5 pH units.
Reader Service No. 102.

- The ProtoBlot immunoscreening system allows the use of rabbit or mouse primary antibodies as probes to detect λgt11 recombinants containing DNA sequences of interest. The system consists of the highest quality affinity purified second antibody, alkaline phosphatase conjugates and the necessary colour development substrates. A positive control is included, consisting of a recombinant λgt11 ovalbumin clone and mouse monoclonal antibody. Also included is an *E. coli* extract for background reduction in cases where primary anisera contain cross-reacting nonspecific antibodies. ProtBlot is produced by Promega Biotec.
Reader Service No. 103.

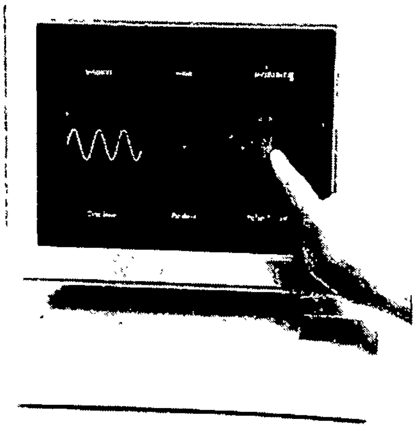

Acoustic waves actuate the Zenith touch-sensitive video screen.

- Zenith's acoustic touch system, a unique new system for interactive video displays, is based on surface acoustic wave (SAW) technology. SAWs are inaudible waves of high-frequency sound that are generated electrically and move across a solid surface like waves on water. In the acoustic touch system, two inexpensive piezoelectric elements mounted on the surface of a cathode ray tube or a glass overlay are electrically 'excited' and emit SAWs. Acoustic reflector strips along each edge of the tube face send the SAWs across the screen, creating an invisible matrix of touchpoints. When a finger interrupts the soundwaves, two more transducers sense it and a microprocessor locates the source of the break at a horizontal and vertical crosspoint. Because SAWs are affected by the amount of finger pressure applied, the Zenith system can also define pressure levels, a depth coordinate that makes acoustic touch the first 'three-dimensional' touch-screen system.
Reader Service No. 104.

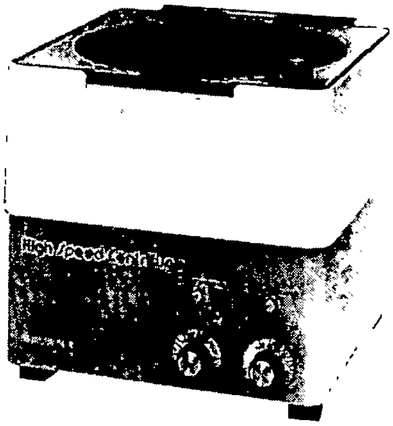

The HSC10000 bench-top centrifuge.

- Savant Instruments' new microcentrifuge, the HSC10000, is a table-top high-speed unit featuring accurate temperature control to ±1°C and speeds to 12,800 r.c.f. (10,000 r.p.m.) to rapidly bring down suspensions and colloids, precipitates and other flocs. An adjustable timer selects the interval for centrifugal action and a speed control permits settings in 20 increments of 500 r.p.m. The HSC10000 maintains any temperature between 5°C and 80°C within ±1°C and as many as 40 samples (0.4 ml microcentrifuge tubes) can be inserted into one of the nine available rotors for tubes from 0.4 ml to 15 ml. The heavy-duty Lexan cover is locked into place and the timer set. Centrifugal action separates the precipitate while the thermal system holds the temperature at the desired level for both product stability and repeatability. For the HSC10000, Savant offers a range of interconnecting tubing, hardware and accessories including a space-saving instrument cart.
Reader Service No. 105.

These notes are based on information provided by the manufacturers. To obtain further details about these products use the reader service card bound inside the journal.

- A rapid and simple new radioimmunoassay kit for measuring rat atriopeptin III and other rat atriopeptins has been introduced by Upjohn Diagnostics. The simple four-step procedure provides results in a day and a half, and is available in a variety of formats for different levels of sensitivity. The assay antibody cross-reacts with atriopeptins I and II and rat alpha-atrial natriuretic peptide. *Reader Service No. 106.*

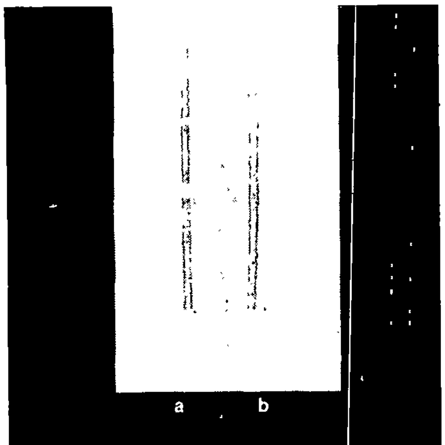

a) HTLV III/LAV Antibody Positive Human Serum.
b) HTLV III/LAV Antibody Negative Human Serum.

- Bio-Rad has introduced a range of products for AIDS Western blotting, a highly specific and sensitive technique for the serological analysis of HTLV-III/LAV virus and characterization of viral gene products. The enzyme-linked immunoelectrotransfer blot technique (EITB), developed at the Center for Disease Control, Atlanta, USA is a highly standardized method, utilizing high field intensity Western blotting after electrophoresis of viral proteins in SDS-PAGE. Two systems are available: one for rapid separation using miniature gels, the other provides high capacity, high resolution separations on standard gels. *Reader Service No. 107.*
- Laserspec, from Spectrolab, is a new, very high transmission tunable filter designed specifically for lasers. It interfaces directly with any laser and is suitable for beam widths of 0.5–5 mm diameter. Overall specifications are 80% transmission, 2Å bandwidth, 170 nm – 4 µm wavelength range. Being continously tunable, Laserspec can be used in laser spectroscopy, Raman, and wavelength rejection. *Reader Service No. 108.*

ADVERTISEMENT

PHORBOL ESTERS
99 + % PURE
MPMA
4-0-METHYLPHORBOL 12-MYRISTATE 13-ACETATE
Cat. #M2550 .... 5mg/\$65^{00}
L C SERVICES CORPORATION
165 New Boston Street
Woburn MA 01801
(617) 938-1700

Circle No.53 on Reader Service Card.

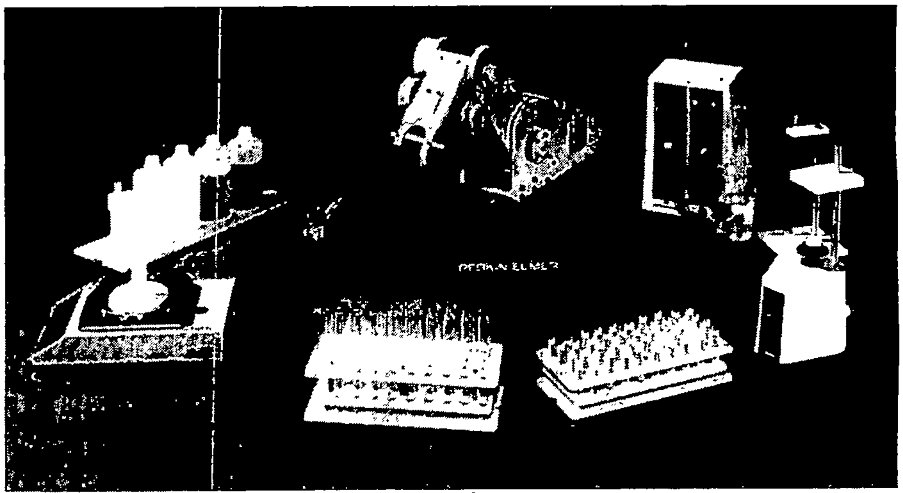

The Perkin-Elmer robot surrounded by its potential targets.

- The MasterLab robotics system from Perkin-Elmer provides the missing link in the entirely automated and integrated analytical laboratory: automatic sample preparation. The basic MasterLab system comprises a robot, a robot electronics module, a communications interface and an IBM PC. Each system can be designed to meet the automation requirements of a specific application or sample preparation procedure. Depending on the application, accessory modules such as mixers, dispensers or balances may be required to interface with the system. Several levels of automation are possible with the MasterLab system, for example: total automation which integrates robotic sample preparation with analysis and a laboratory information management system; sample preparation for subsequent transfer to instruments for analysis; specific applications, such as weighing samples, filtering, dispensing or handling dangerous substances. *Reader Service No. 109.*
- The latest freeze dryer from Martin Christ Gmbh is a unit in which the ice condenser is integrated with the drying chamber. During the drying process the water vapour is frozen, taking the shortest way over the ice condenser surfaces which can be cooled to −75° C, and are sited right and left of the product shelves. The drying period can be reduced by 30% compared with conventional devices, where the drying chamber is separated from the ice condenser compartment. *Reader Service No. 110.*

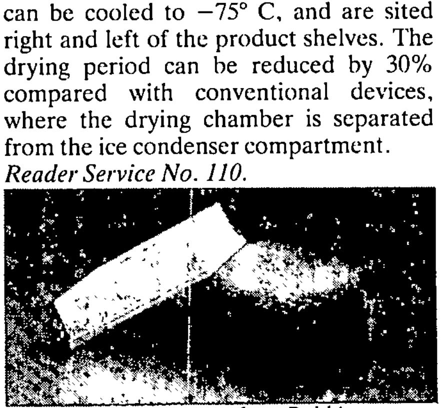

A rack of 125 pipette tips from Robbins.

- The disposable Titer-Pak II, from Robbins Scientific, consists of a box with telescoping cover and a sturdy, non-flex rack pre-loaded with 125 pipette tips. The tips are made of virgin polypropylene and can be used with Pipetman, Eppendorf and Excalibur pipettors up to 1,000 µl. This entire unit is disposable or can be autoclaved repeatedly without any distortion resulting. It is also available sterilized by cobalt irradiation. *Reader Service No. 111.*

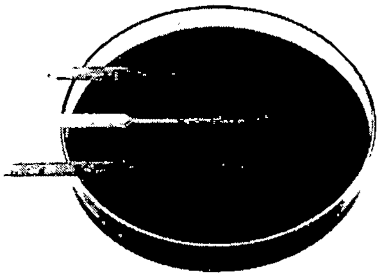

Disposable 'Bioloops' come ready-sterilized.

- Elkay disposable Bioloop inoculating loops and needles are now available in a choice of four sterile packaging options: individually wrapped, 10-pack, 30-pack and 50-pack. Bioloops are pre-sterilized so there is no need for flaming prior to use, reducing risk of spreading pathogenic aerosols and saving time. Bioloops are available with a needle at one end and a 10 µl or 1 µl loop at the other. The third type has both a 10 µl and 1 µl loop. Each model is colour-coded for easy identification. *Reader Service No. 112.*
- New from Jasco Inc. is a research-grade spectrofluorometer, the Model FP-770. The instrument features *f*/2.5 optics permitting scanning from 200 to 850 nm (optional) at 1,000 nm per min. A computer data station for all user interaction provides functional keys for extreme ease of operation. The dedicated software program with its built-in self-diagnostic capability offers a 19-function range of computerized luminescence spectroscopy. The FP-770, a dual-beam with reference photomultiplier system corrected for light source fluctuation, has a wavelength accuracy of ±1.5 nm and repeatability of ±0.3 nm. *Reader Service No. 113.*

Damage is kept to a minimum by the Microfluidics continuous-flow cell disruption system.

- Controllable continuous-flow cell disruption with a minimum of damage to cell contents is achieved with the Microfluidics M-110 B. Self-contained, compact and light-weight, the M-110 B can be run on an open bench or placed in a laminar flow hood if required. The unit provides the option of processing dilute or concentrated cell suspensions as small as 10 ml through to 1 litre per minute pilot production runs. The M-110 B temperature-controlled models can operate down to −25° C, and full-scale models up to 20 gallons per minute are available.

Reader Service No. 114.

A program for the determination of dry weight and moisture content is available from Mettler.

- The dry weight and moisture content of samples taken from the drying oven can now be determined quickly and easily with a new program from Mettler LabWare—DRYING. It is stored on a microcassette and used as application-specific software in combination with a hand-held Epson HX-20 computer and a Mettler analytical or precision balance. DRYING stores the weight values and codes of up to 300 samples. After drying in the drying chamber, the samples are identified through their codes during back-weighing and the desired values are determined automatically. DRYING automatically records every every determination. In the case of a whole sample series, it even determines the mean value. The program uses a dialogue to guide the operator through the determination, and instructions appear on the 4-line computer display in English, French or German, or any desired fourth language.

Reader Service No. 115.

- Two different designs are available in the Nordia fume cupboard range. The fume cupboards are fitted with toughened glass in a variety of timber and metal fabrications. The Nimrod range of aerodynamically designed compensated airflow fume cupboards, complying with the performance and safety requirements of DD80, is available in four widths. Standard features of the Nimrod range include a control panel incorporating a key-operated panel isolator with remote push button station for the extract fan motor, showing visual motor running/failed conditions. Other safety features include an optional audio-visual sash high and airflow failure alarms, a sash locking system and a heat sensor alarm/extinguisher. The economical Harrier fume cupboard range has been designed primarily for work involving lower levels of toxicity. Mason Nordia also provides and installs fume extraction systems, mechanical and electrical services and special gas installations.

Reader Service No. 116.

- Two new columns for the analysis of amino acids by ion chromatography are now available from Dionex. The HPIC-CS4 cation exchange and the HPIC-AS8 anion exchange columns provide complementary selectivities for the confirmation of amino acids, using advanced pellicular resin technology which allows high efficiency and high-speed separations without the limitations of traditional, totally porous ion exchange columns. The columns provide the specificity of classical ion exchange and the speed of pre-column derivatization. The Dionex ion chromatograph for amino acids is ideally suited for the analysis of amino acids in complex matrices with minimal sample pretreatment. The same system can perform state-of-the-art ion chromatography including the analysis of other ionic organic compounds and an extensive range of inorganic ions.

Reader Service No. 117.

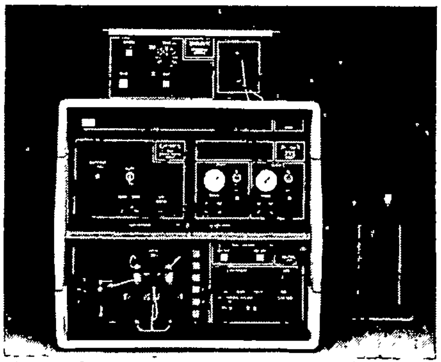

A complete amino-acid chromatography system from Dionex.

- Packard Instrument Company has developed a new software program, COMBICEPT, for steroid receptor assays. Using a single assay, COMBICEPT provides simultaneous calculations of the oestrogen and progesterone receptor concentrations in tissue cytosols. Designed as part of Packard's Personal Computer Data Acquisition and Analysis System (PC-DAAS). COMBICEPT provides simultaneous dual-lable receptor assay calculations (oestrogen and progesterone), on-screen curve editing, multi-assay, multi-tissue data reduction, and on-line/off-line processing. Receptor data are stored on a floppy disk, and up to nine assay protocols can be stored. Each tissue is identified by a name, and the final results calculated using the individual protein concentrations. The software can be implemented on all present production models of Packard Tri-Carb and Auto-Gamma counters. Data for other systems can be processed manually.

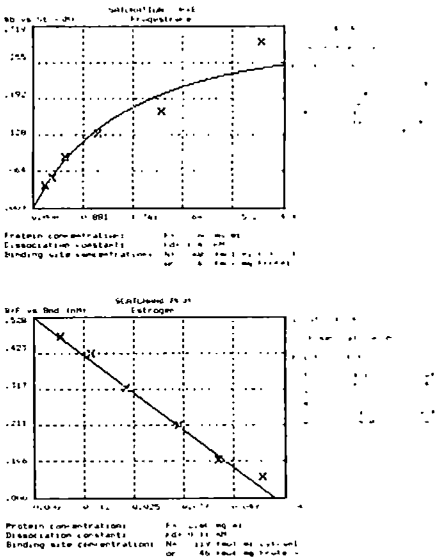

Packard's latest steroid receptor assay program at work.

Reader Service No. 118.

- AMOR, from Spark of Holland is a new AMperometric detectOR for HPLC. This new electrochemical detector features a solid-state *in situ* reference electrode which is entirely maintenance-free. The working electrode is constructed so that the edge of the glassy carbon material is extraneous to the cell. The edge of the working electrode often causes noises and drift problems in EC detection. The cell is thermally insulated and electrically shielded. The cell volume may be varied by applying different (Teflon) spacers (0.4 – 1.0µl). Sensitivity range is from 0.1 nA to 1000 nA, and potential setting from −2 to +2V.

Reader Service No. 119.

- CelsiDot single level temperature sensitive labels are now available on rolls with 1,200 pieces of identical dots. There are 40 different temperature ratings available between 40°C (105°F) and 260°C (550°F). The white temperature sensitive indicating triangle turns permanently black when exposed above its rated temperature level. The self-adhesive labels can be applied to any clean, dry surface.

Reader Service No. 120.

The brain drain is here again

from Richard Pearson

Much is made of the 'brain drain' of UK scientists to overseas posts, but little is known about the extent of the proble

THE brain drain is back in the news in the United Kingdom. The Civil Service is trying to plug the leakage of computer scientists to industry. The UK scientific community is worried about losses overseas. The universities complain about losses of academic lecturers to industry. There are some hopes that the Strategic Defense Initiative will reduce the brain drain from the United Kingdom. But in Ireland emigration remains an emotive subject with some educationalists seeking to play down talk about a brain drain. It is clear from these recent examples that the term 'brain drain' itself embraces a number of different flows and any assessment of its scale or impact depends on the perspective of the reporter.

Last year the Advisory Board for the Research Councils (ABRC) reported to the government its growing concern about the increasing losses of talented British scientists overseas. Its subsequent detailed enquiry, based on 40 leading research groups, showed that departments were gravely concerned about the losses not only of their most talented students and postdoctoral research workers but also of outstanding senior scientists. However, because the departments usually only employed small numbers of scientists they found it hard to present a statistical assessment of the flow or of the trends over time. They did, however, note a growing loss of senior chemists, materials scientists, biochemists and molecular biologists. The physicists and to a lesser extent the engineers reported far fewer problems. ABRC was able to identify 45 British senior scientists working overseas.

A more detailed study of biotechnology two years ago (*Nature* **309**, 654; 1984) revealed an estimated 250 UK nationals who had gone overseas in the previous decade, a total which excluded newly qualifying postgraduates[1]. The biotechnologists had gone to a wide range of countries and employing sectors. Typically leavers were aged 26–30 although one in three was aged over 30. The leavers went from industry, higher education and research institutes. The majority went however to jobs with commercial organizations. Nearly half went to the United States, with Switzerland and other European destinations for another one in three. In all, UK personnel went to 13 different countries and were working for over 65 different organizations. One new overseas biotechnology venture company had recruited over 16 UK nationals.

The reasons for losses overseas have been more related to improved job prospects and research opportunities overseas than salary, although the latter has usually come as a healthy bonus, and can be a major barrier for those thinking about returning. ABRC reported a growing frustration by senior scientists over the improved level of facilities, both recurrent support and equipment, available overseas, and the frustration over the difficulties in getting research funding approved in the United Kingdom. For younger scientists and those newly qualifying, then the flow overseas is seen as part of a more regular pattern of broadening their experience, usually in the United States, although growing numbers are thought to be going because of the lack of jobs in the United Kingdom. The recent restrictions on work permits in the United States may be restricting the scale of this potential outflow. The 'New Blood' scheme designed by the University Grants Committee (UGC) was thought to be helpful in the latter case, while additional UGC research funding is helpful with the former. The government has also cited the opportunities for 'star wars' research now available in the United Kingdom as another inducement to stem the flow. Two other factors aggravating the flow overseas are seen to be aggressive recruiting in the United Kingdom on the part of US universities and industry, and the greater receptiveness of US industry to novel and untried ideas. Where British laboratories have world class facilities, as at the Science and Engineering Research Council Nuclear Structure Facility or the Cambridge Laboratory of Molecular Biology, then they seem able to attract staff back from overseas and losses are not a significant problem. However, growing concern is reported over the level of funding and the lowering of morale which can only encourage further losses in the future.

Losses overseas are, however, usually

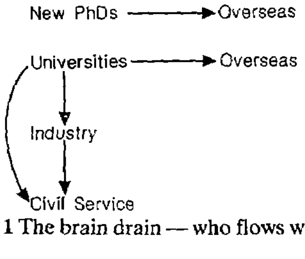

Fig. 1 The brain drain — who flows where?

only a very small part of mobility bet
sectors and its direct effect has been
to evaluate. Rather it has been seen
as a loss of potential. ABRC also re
growing concern about losses
academia to industry, particularl
chemists. However, one person's lo
another's gain and flows between se
within a country have not tended t
classified as a 'brain drain' in the pa
common international problem in tim
skill shortages is that there will nor
be a flow from academia to industry
latter usually being quicker to respo
staff shortages by raising salaries an
proving conditions. Any shortag
academic, and more specifically, teac
staff will however undermine the f
supply of suitably qualified graduate
so reinforce the longer-term impa
shortages.

Ironically, while ABRC was repo
concern about the universities' inabil
compete with employers in industry
the scientific civil service, the latter,
information technology area, is
creasingly suffering from an outflow
specialist staff to industry.

The Civil Service has histori
trained all its own computer staff, ra
if ever, recruiting experienced staff
the open market. Information techn
is now being increasingly used in the
Service, pushing up the number of sk
staff needed, while at the same time
cial policy has been to hold down the
of growth in public sector pay levels.
result there has been an increasing
out of the Civil Service into better
jobs in industry and commerce. Resp
ing to the growing problems, the go
ment and the trades unions have
agreed increases in pay levels in
grades of up to 26% to help stem this
drain.

There are many dimensions to the
drain, the range and direction of 'mo
covered widening as concern about
shortages and funding has incre
Quantification in this complex ar
rarely attempted, more qualitative a
ments and key names are usuall
prime ammunition of those seeking
fluence policy.

*Richard Pearson is at the Institute of Man
Studies, Mantell Building, University of S
Brighton BN1 9RF, UK.*

---

[1] Pearson, R. & Parsons, D. *The Biotechnology Brai* (Science and Engineering Research Council, 1984).

nature

Discrimination is not cricket

A meeting in Paris on 17 January will decide whether to persist with the ban on South Africans at this year's archaeology congress in Southampton. The organizers should cut their losses and cancel.

WHAT connection can there be between the exclusion of people from South Africa from the planned congress of the International Union of Prehistoric and Protohistoric Sciences (IUPPS) at Southampton later in the year and the demand, a week ago, by the government of Bangladesh for a public denunciation of apartheid from a group of not particularly distinguished English cricketers? Or, for that matter, with some of the reactions there have been to the continued scandalous detention of Dr Andrei Sakharov in Gor'kii? These questions are not riddles left over from the holiday season, but should directly concern the members of the executive committee of IUPPS, which will be meeting next week in Paris to decide whether the ban on South African participation at the congress should stand.

What can happen? The best outcome would be some ingenious means by which the congress could go ahead without the academic community inflicting permanent damage on itself and the rest of us, but the chances of that are slim. The next best course would be to abandon the congress, acknowledging that the organizers are in an impossible position from which there is no honourable escape. To continue with the arrangements that have been made, or further to fudge the issue, will be intolerable.

The circumstances leading to the mess in prospect have been fully catalogued (see *Nature* **318**, 195; 1985). Briefly, responsibility for this year's congress was delegated by IUPPS to British archaeologists and anthropologists on the usual rota basis, but enthusiasm at Southampton for making the affair intellectually interesting and commercially successful must originally have seemed a plus. Planning fell to the British national committee, whose chairman, Professor John Evans, is also president of IUPPS, but most of the donkey work seems to have fallen to Professor Peter Ucko, secretary of the committee and also head of archaeology at the University of Southampton, the chief venue for the congress. By early last summer, the organizers had come under pressure to ban participants from South Africa. Pressure came from four different sources — students at Southampton (whose communal facilities were to provide space for a registration desk), the Association of University Teachers (AUT) which has a "national policy" that its members should not indulge in "academic relations" with South Africa, the British Anti-Apartheid Movement (which threatened to write to the embassies of anti-apartheid governments in London, and which may even have done so) and the Southampton City Council (which threatened to withdraw financial support and hospitality if South Africans were present at the congress). In September last year, the British committee capitulated, and South Africans were told they would not be eligible. There have been ructions ever since.

Cricket

Superficially, what happened last week in Bangladesh is not very different. As the English "B" team was gathering at London airport, the government of Bangladesh discovered that the names of three members of the party appear on a list, maintained by the United Nations in New York, of sportsmen who have played games in South Africa. The government demanded that those concerned should denounce apartheid and promise never to go to South Africa again. The English cricket authorities, offended by the blackmail and fearful about the precedents that would be set, refused, and the tour of Bangladesh is cancelled. Cricket enthusiasts now fear that the games planned for West Indies in the summer of this year (to which the English would have to send an "AAA" team to stand any chance of winning) will similarly be wrecked.

Scholarship

If cricketers placed in an impossible position find it prudent to cancel planned events, why should not archaeologists do likewise? That is the obvious parallel, even if the reality is more complicated. Both cricket and scholarship have separately been offered as ingredients of the cultural cement that holds international society together, helping to provide hope that contemporary problems in international relations will one day be solved amicably, by reason. Although practitioners of both kinds are fond of saying that scholarship (or cricket) should be kept away from politics, their international doings unavoidably have political consequences, usually beneficial. The practical question, that cricketers and scholars must separately ask, is how best to conduct their international affairs so as not to compromise desirable objectives, among which the disappearance of the tragically wrongheaded policies of apartheid from South Africa must be one.

Circumstances matter. One reason why national sporting teams no longer go to South Africa is the fear that to do so would be read in South Africa as tacit approval for a distasteful system. Just how to balance that argument against the calculation that going will help to loosen the system is not easy, but the sportsmen are probably correct in the decision they have reached. In much the same spirit, it is unthinkable that one of the scientific unions would now arrange an international conference in Pretoria. By the same test, it would be wrong for a scholar to accept an invitation from the government of South Africa to embark on a lecture tour or for some other purpose that could be misrepresented. But it does not follow that South African scholars, as people, are no longer a part of the international community, or that they have nothing to contribute to its wellbeing. One of the ironies of the Southampton ban is that it will affect some of those who, by the accidents of palaeontology, have the most to contribute. To the extent that some of those affected are from the Universities of Witwatersrand and Cape Town, which have been bastions of liberality for the past three decades, the ban is also a cruel way of dealing with courageous people.

Mishandling

This is only part of the reason why IUPPS should next week overrule its British committee's decision on South Africa. No amount of agonizing by a group of archaeologists, anthropologists and ethnologists can make much difference to the course of events in South Africa, but the mishandling of the Southampton congress could do damage that will persist for longer than apartheid can. The invitations (in reality, they were advertisements) originally sent to South African scientists were addressed to them as individuals, which was right and proper. The organizers have larded their ban with varying expressions of regret that the course they have felt compelled to follow will interfere with the free flow of ideas in science (and also infringe the statutes of IUPPS). There is wide sympathy for the position in which they find themselves, having to choose between the application of a principle they espouse and their understandable wish not to see months of careful planning wasted, perhaps at substantial cost. But there is no basis on which a group of scholars can exclude from an otherwise public meeting people who are qualified to attend, but whose government is socially unjust. To be the first in the field is a dubious distinction.

This is where the case of Dr Sakharov is relevant. Sakharov was an outspoken critic of the Soviet system a decade ago. He has not been charged with criminal activities, but merely sent to live in isolation from his friends and colleagues. Senior members of the Soviet academy say that Sakharov has been dealt with leniently, given the sharpness of his criticisms, but to their credit they have not expelled him from the academy, which would remove both his salary and his present degree of protection from administrative harassment. Even so, the case of Sakharov, like those of many other Soviet citizens who have suffered harsh administrative and legal penalties, has clouded scientific collaboration between Western and Soviet institutions. Yet at no stage has it been seriously suggested in the West that Soviet scientists as such are not welcome in the international community. If anything, the decay of formal collaboration has intensified the sense of loss that Soviet colleagues are absent from meetings at which they would naturally be found. Mercifully, but inconsistently, Soviet scientists have not been banned from Southampton. So why pick on South Africans?

The organizers say they have no choice, but they are wrong. Those who arrange meetings are always free to cancel them. Far better to stomach the embarrassment of wasted advertising literature than to be the first to introduce the principle of discrimination on the grounds of nationality into the conduct of intellectual affairs. Unless something can be done to make this congress respectable, it will probably be a tarnished affair, not merely on account of the notoriety it has attracted but because of the numbers of people who are threatening to stay away in sympathy with the handful of South Africans who will be excluded. The executive committee of IUPPS should bite the bullet and appeal to other scientific unions for help with the money problems left over.

Meanwhile, others must worry about the damage already done. The reputation of British academic institutions will have been harmed by this general advertisement of the power of campus demagogues, students and, lamentably, teachers. Does this mean that South Africans will be banned from all future international meetings in Britain? Does AUT's famous national policy deliberately invite this consequence, or is it merely a licence for local initiative by sporadic vigilantes? In their own interests, British academics should insist that the position of their representative body is clarified. AUT rightly spends most of its energy on academic pay and conditions of service, but its annual conferences may also adopt resolutions on more general matters. AUT's policy on South Africa is badly thought out.

More generally, there are international forces to be reckoned with. Although the constitution of IUPPS itself is explicitly non-discriminatory, the union is affiliated to UNESCO, which adopted a policy of deliberate discrimination against South Africans four years ago. Does that make sense? There is a more sinister threat in the statement by one of the Southampton organizers that it is no longer possible to organize an international conference to which "third world" scientists are invited without discriminating against South Africans. That cannot be the whole truth (witness the attendance of several South African astronomers at last December's meeting of the International Astronomical Union in Delhi), but even if it were a part of the truth, it would be a bad business for us all. □

Chopper politics

The British government seems bent on making a muddle of its policy on helicopter manufacture.

WESTLAND, a small manufacturer of helicopters based in south-west England, has become the centre of a bewildering row between British cabinet ministers for all the wrong reasons, which between them should provide a salutary warning for high-technology industries dependent on defence departments for their survival. The troubles stem from the nature of the helicopter as a means of transport. Although it was once commonly supposed that such machines had a bright future as means of almost personal transport, experience has shown them to be an expensive means of getting about, uncompetitive with fixed-wing aircraft over distances much greater than 100 kilometres and with surface transport over shorter distances. The only civil markets for the machines that matter are tiny, and are confined to circumstances where other means of transport do not exist (as in the servicing of oil-rigs at sea) or where a few minutes saved on a journey time may command a high price. (There is still a market for helicopter journeys between New York's principal international airport and Manhattan.) Otherwise, the helicopter has become almost exclusively a military vehicle, a means of transport and a battle-station.

Westland has known this for some time. For the past year, it has been pleading with the British Ministry of Defence under Mr Michael Heseltine for extra projects on which to work, and has been refused. So, under pressure from its bankers, Westland has been seeking larger companies willing to mount what is called in the trade a "rescue". The US corporation United Technologies, which owns Sikorski, another helicopter manufacturer, in conjunction with Italian Fiat, was the first in the field. Mr Heseltine has since organized a bid from a European consortium of aircraft manufacturers which differs chiefly in the amount of employment it offers the labour force at Westland. Members of the British cabinet have fallen out among themselves because some (including the Prime Minister) rightly say that the company should decide on commercial ground which bid to accept, while Mr Heseltine (who is not alone) threatens that Westland will not again win European orders for helicopters unless it accepts the bid he has organized (which it is within the power of European governments to ensure).

The piquancy of the resulting row derives from its bearing on British domestic politics. What the participants have forgotten is that Westland's problems of a year ago were a sign that there were then more helicopter manufacturers than the world's defence ministries could employ. Nothing much seems to have changed since then. And nothing has happened to suggest that Westland's technical dependence on other manufacturers (Sikorski in particular) will have been replaced by technical adventurousness in an admittedly difficult field. Mr Heseltine's European bid smells too much of an attempt to keep in being a company that is otherwise not viable by means of a redistribution of helicopter work among European governments.

The lesson to be learned from this should in reality have been learned a long time ago. The prizes now go to those who make technically advanced products of high quality. In civilian markets, to be second or third best is to invite disaster, but in the military field, chauvinism can keep projects afloat for longer than logic would allow. The fate of Westland has become an issue largely because the British government has resolved to let economic logic apply more rigorously than will other European governments. Mr Heseltine's laudable ambition that European defence forces should have access to the best equipment could just as well be satisfied by letting Westland go to the highest bidder and, quite separately, planning with European governments a strategy for buying (not necessarily making) the next generation of military helicopters. That way, he would discover, British taxpayers would find themselves paying less. □

Japanese technology

First sale overseas of military equipment

Tokyo

JUST before Japan's companies closed for the new year holiday, a small but potentially momentous technology deal was completed between the United States and Japan. The price of the deal is secret, but even if rumours that the US side moaned at having to shell out $40 million are correct, it will hardly add much to a mountainous trade deficit. The significance of the deal is that it is the first sale of military equipment by Japan to a foreign country since the Korean war.

The equipment sold to the United States consisted of anti-aircraft homing devices that, in contrast to the usual heat-seeking technology, guide missiles to their targets through visual tracking. The equipment employs charge-coupled devices similar to those used in the "seeing eye" sensors of autofocus video cameras. Japan has long been a leader in such research. The homing device was developed by the Technical Research and Development Institute, the government research body responsible for the development of weaponry for Japan's Self Defense Forces.

"Self-defence forces" is what they have to be called because Article 9 of the Japanese constitution specifically states that "land, sea and air forces as well as other war potential, will never be maintained. The right of belligerency of the state will not be recognised." Even self-defence forces are of doubtful constitutionality and must be as non-belligerent as possible. Defence is an extremely sensitive issue and a subject of continuous national controversy. The present government, which favours expansion, is hamstrung by the actions of Prime Minister Miki's government ten years ago. Back in 1976, it was decided that defence spending should be kept within 1 per cent of gross national product (GNP). (In contrast, the United Kingdom spends 5.6 per cent of GNP, a difference that has helped the development of Japan's non-military technology.)

This guideline, for it is nothing more, has now become an impenetrable barrier. Over the past year, Prime Minister Yasuhiro Nakasone has tried a hundred different roundabout ways of saying the limit would have to go, but without success. This year's defence budget is set at 0.993 per cent of GNP, provided the economy grows as well as is hoped. If UK accounting methods were used, Japan would already be spending 1.6 per cent of GNP. Over the years, some defence-related items have vanished from the defence budget; there was even once a suggestion that the troops' food was not strictly a defence item and could be taken out of the budget.

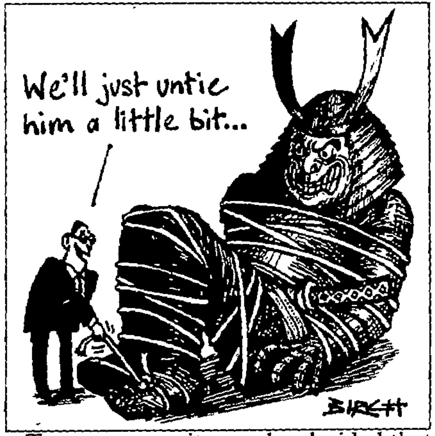
We'll just untie him a little bit...
BIRCH

Ten years ago, it was also decided that export of any kind of weapon or weapons component to any country, friendly or unfriendly, would be prohibited. This ruling has been enforced: when a company exported a metal component for a hand grenade trigger, the police took action. But that has not altogether prevented some bending of the rules. Japan, after all, manufactured the floating dock moored in Vladivostock for the massive Soviet aircraft carrier *Minsk*, on the grounds it was not necessarily for military use. More recently, under pressure from Washington, the United States alone has been excepted from restrictions. In November last year, the first Joint Military Technology Commission meeting was held to promote the transfer of military technology to the United States. Interest was apparently shown in high-speed gallium arsenide microchips and optical fibre communications equipment. Now the first technology sale has gone ahead.

The next big question for the Japanese government will be whether or not to participate in the US Strategic Defense Initiative (SDI). The decision by the United Kingdom to join the project is felt to have put the heat on Japan — it will have to say yes or no, rather than just trying to pretend that it had never been asked. Prime Minister Nakasone is known to be in favour of the project and the Foreign Minister has recently stated that the United States cannot be kept waiting too long for a decision. Both have repeatedly stressed that SDI is "defensive" and "non-nuclear". Government experts say participation would not be unconstitutional.

Business circles, on the other hand, cannot make up their minds whether they might be really missing out on some totally new technology if they do not join the project. But when all is said and done, it will still require an enormous push for Japan to join SDI. There is still only one issue that really unites the great mass of the people against the government that has been in power for 30 years — any hint of a move back towards militarism.

Alun Anderson

US science adviser

McTague fills Keyworth's shoes

Washington

JOHN McTague has been named acting director of the White House Office of Science and Technology Policy (OSTP), replacing George Keyworth II who resigned at the end of last year. McTague has been with OSTP since 1983 as deputy director.

McTague's temporary appointment has surprised many, as it was widely expected that Erich Bloch, director of the National Science Foundation, would be given the additional title of acting director of OSTP until a permanent replacement could be chosen. Indeed, that had been Keyworth's recommendation, but according to OSTP spokesman Maurice Roesch, acting director for defence programmes, "the idea was considered and rejected". McTague's interim appointment was a "collective decision" of the White House personnel office and OSTP.

McTague is a physical chemist. He was at the Institute of Geophysics and Planetary Physics at the University of California at Los Angeles from 1970 to 1982, after which he served as chairman of the National Synchrotron Light Source Department at Brookhaven National Laboratory until he joined OSTP.

McTague has enjoyed a good working relationship with Congress. Ezra Heitowit, staff director for the House of Representatives subcommittee on science, research and technology, describes him as "helpful and forthcoming with staff members".

A public supporter of the Strategic Defense Initiative (SDI) proposed by President Reagan, McTague is nevertheless unlikely to be as actively involved in promoting SDI as his predecessor.

The failure to name a permanent replacement for Keyworth will keep alive rumours about the possible demise of OSTP. But Roesch insists that the search for a permanent director is being carried out "as rapidly and expeditiously as possible", although he could suggest no timetable for when that permanent appointment could be expected.

Joseph Palca

British computing

Cooperative research spends up

The Alvey Programme, Britain's answer to the Japanese fifth-generation computing programme and the US integrated circuit programme, has now committed almost all of its £350 million budget. The money is being spent on "cooperative pre-competitive research in information technology" through the Department of Trade and Industry (DTI), the Ministry of Defence (MoD) and the Science and Engineering Research Council (SERC).

Alvey's director, Brian Oakley, says that a "very useful programme" has been mounted in the past two years, although he is not impressed by some of the government's financial restrictions; for example, no extra posts were provided for the programme, meaning that it is run on "the proverbial shoestring". Money for Alvey comes from funds that each department had already earmarked for other uses.

Alvey projects fall into five main categories: intelligent knowledge-based systems (23 approved projects); man-machine interface; very-large-scale integration (VLSI, exclusively focusing on silicon technology) and computer-aided design; software engineering (16 approved projects); and computer architecture. Of 550 proposals submitted to Alvey, 102 have been approved, 6 per cent of which are long-range speculative projects in universities. Each approved project includes an average of two or three industrial teams and one or two academic teams, ranging from two to eight partners per project.

Oakley admits that some mistakes have been made. One example is the Alvey requirement that, once a project has been technically approved, a collaborative agreement covering industrial property rights is required before money is paid. But the lack of advice or guidelines from Alvey has resulted in delays while arguments between partners were sorted out. "Quite inexcusable bureaucracy" resulted from the decision to divide up administrative duties — VLSI contracts to MoD and academic grants to SERC. The intention was to minimize the central administration team and to involve all participants in administrative decisions, but in fact bureaucratic differences and delays resulted. Oakley recommends that a non-governmental body should administer future collaborative schemes. Ten per cent of approved Alvey projects are also delayed by SERC's cash-flow problems, but Oakley foresees an end to these problems early in 1986.

Despite the problems, Alvey's annual report* provides evidence that a strong technology base is being provided in Britain by a directed collaboration between government, industry and academic research institutions. Alvey is halfway through its five-year life; the future of information technology research after this time is uncertain. Should Britain maintain its own attempt to compete with the United States and Japan or combine forces formally with ESPRIT, the European Strategic Programme of Research and Development in Information Technology?

Oakley is in no doubt that there is a strong need for both a national and an international programme. Geoffrey Pattie, minister for industry and information technology, hopes that a working group will be set up, with industry playing a "leading role" in deciding what is to be done.

Maxine Clarke

*Alvey Programme annual report and poster supplement 1985. Price £10 each from Institute of Electrical Engineers, PO Box 8, Southgate House, Stevenage, Herts SG1 1HQ, UK.

Siberian river scheme

Russian party demands caution

A group of eminent Russian writers has called for the cancellation of the proposed southward diversion of the Siberian rivers. In a letter published last week by the daily *Sovetskaya Rossiya*, they say that the scheme "threatens serious consequences not only for future generations but also for those alive today". They condemn the project as an interference in "natural conditions that have built up over millions of years" and claim that the ecological, economic and social consequences have been insufficiently considered. Although opposition to the project has been voiced by Soviet environmentalists since the idea was revived in the mid-1970s, the writers' letter is unusually outspoken, attacking as "premature" the inclusion of the diversion scheme in the "Draft Guidelines" of the new five-year plan. Although the guidelines will formally remain open for public comment until the Party Congress next month, this remark questions the professional expertise of the high-level team responsible for this part of the plan, suggesting not so much a general relaxation of press censorship as the seriousness of concern over the diversion scheme. The appearance of such a letter, signed not by professional environmentalists, but by literary figures who in the West might be expected to show "green" tendencies, is itself significant.

The group includes Dmitrii Likhachev, perhaps the most eminent Soviet literary critic on the mediaeval period, and Leonid Leonov, whose literary career dates back to the early days of the Soviet Union. For several of them, this is not their first expression of hostility to the scheme — Vasilii Belov, one of the best known of the group, actually published a letter attacking the scheme in the Paris emigré newspaper *Russkaya Mysl'*, but it is their first public statement on the matter in the Soviet press.

Although they span three literary generations, the writers are all strongly committed to the traditions of old Russia. Some consider that the group constitutes a potentially significant political force, dubbed it the "Russian Party".

The fortunes of the group during the past few years have not been unclouded — during the June 1983 Plenum of the Central Committee, their views were attacked by Konstantin Chernenko, at the time propaganda secretary under General Secretary Yurii Andropov. Nevertheless, they have been largely responsible for the government's pledge that "monuments of Russian antiquity" should not be damaged. Such an assurance is significant in the context of Soviet hydroengineering, which before the Second World War submerged, among other places, the Dnieper rapids (analogous, for a Ukrainian, to drowning Runnymede or Harper's Ferry), and also the important archaeological site of Ithil, capital of the Khazars, the one gentile nation in the past 2,000 years to have converted to Judaism.

Vera Rich

Soviets ask for space

Academician Anatolii Aleksandrov, president of the Soviet Academy of Sciences, has called for a world space organization for international cooperation in the peaceful study and use of space. Such an organization, he said in an interview in *Pravda*, would ensure access for all states "on the basis of mutual advantage" to the data from meteorological, Earthscan and navigational satellites, and would be particularly beneficial to developing countries that cannot afford their own space programme. It would, furthermore, provide a framework for major cooperation in space research, and would also, by its very existence, "epitomize peaceful intentions in space".

The proposed organization, Aleksandrov suggested, would coordinate the activities of existing international bodies. He spoke glowingly of Soviet participation in the international KOSPAS–SARSAT experimental sea-rescue service jointly with the United States, Canada, France and Norway, and in the 10-nation Venus-Halley's comet programme.

Not all space cooperation, however runs auspiciously for the Soviet Union. A few weeks ago, there were reports of a major rebuff by the council of Inmarsat

Synthetic fuels

US Synfuels narrowly bites dust

Washington

THE Synthetic Fuels ("Synfuels") Corporation (SFC), willed into existence by Congress in 1980 with an annual spending power of $20,000 million, was legislated out of existence just before Christmas. But the controversial corporation's end was only narrowly prevented from turning into a $600 million spending spree.

SFC was formed when oil and natural gas prices were expected to continue to rise sharply, making the development of other sources of such fuels economically realistic. SFC's job was to support companies attempting to develop these alternatives. But reality turned out differently from expectations. Oil and natural gas prices did not rise precipitously, while large-scale projects for producing fuel from oil shale and natural gas from coal encountered technical problems for which expensive solutions were required.

In more than five years, only one of SFC's projects actually reached the point of producing energy on a commercially usable scale — the Cool Water coal gasification plant in California, which feeds into a combined cycle generator to produce electricity.

As its future came to seem less and less bright, members of Congress began to attack SFC as a rogue elephant, claiming that it was poorly managed and that its goals had in any case receded out of reach. Congress has also known that the Reagan administration has been sceptical of SFC since its inception towards the end of the Carter presidency. After fierce negotiations last year, by the end of the summer it was clear that SFC's days were numbered.

That prospect spelt disaster for two of SFC's projects, the Union shale plant at Parachute Creek in Colorado and the Seep Ridge oil shale project in Utah, both of which are still in need of SFC backing if they are ever to be viable. This dire prospect seems to have provoked the high drama in the days and hours before and after the congressional vote on 16 December.

Two interested senators, Jake Garn (Republican, Utah) and William Armstrong (Republican, Colorado) appear to have taken the initiative in asking the White House to allow the SFC board to meet and to provide the funds for the projects at risk before Congress had finally voted the corporation out of existence. If that had happened, the government would still have been liable for the commitments, in excess of $600 million.

Reports of what was afoot reached Capitol Hill together with the intelligence that the President's chief of staff, Donald T. Regan, has blessed the plan for a final meeting of the board, and even that the president might delay signing an abolition bill so as to give SFC a last chance to act.

The board of governors of SFC seems to have been in a difficult position. On the one hand, there were signals from the White House apparently authorizing new spending, but, on the other, clear indications that Congress wanted to call a halt to synthetic fuels development. In the end, the board decided not to act without written instructions. There appear to have followed several heated telephone conversations between members of the Congress and the White House, at the end of which the board was instructed to spend no more public money.

Ironically, the measure abolishing SFC was appended to a larger financial bill which was, in the end, defeated in the vote on 16 December. For a while, SFC was back in limbo, but supporters of SFC were unable to engineer a last-minute reprieve for the corporation, which was finally abolished when the larger financial measure was passed on 19 December. **Joseph Palca**

collaboration

the international programme for establishing a system of geostationary navigational satellites. According to the Soviet side, the list of rocket launchers initially accepted by Inmarsat includes the Soviet *Proton* rocket, which, the Soviet participants claim, is cheap and meets the programme's requirements. The United States has now opposed the use of the *Proton*, on the grounds that a launch from the Baikonur site would give the Soviet team the chance to acquaint themselves with the US equipment aboard the satellites, and remains unconvinced by Soviet assurances that the delivery of the rocket to the aunch-site, preparations for launching and the launch itself would be carried out n conditions that would exclude any "information leaks" about the on-board equipment.

The dispute over the abandonment of he *Proton*, which the Soviet side claims will mean a loss to Inmarsat of several million US dollars, was not mentioned by Aleksandrov. His vigorous urging of the benefits of pooling knowhow and economic assets in global space organization acquires, in the light of the Inmarsat disagreement, an additional topical note.

Vera Rich

British biotechnology

Celltech within sight of profit

CELLTECH, Britain's budding biotechnology corporation, greeted the new year with an annual report showing a 27 per cent decrease in losses and a forecast of profitability by 1987. In the year ending 30 September 1985, Celltech's £3.8 million turnover more than doubled the previous year's. Chief executive Gerard Fairtlough reckons his company is the world leader in the bulk production of monoclonal antibodies, and is looking to Japanese and US markets, which account for about 85 per cent of Celltech's customers.

Although Celltech's cash balance fell from £9.8 million to £5.7 million during the year, Fairtlough says there is no present need to increase the company's equity base. Rather, Celltech is likely to rely on joint ventures of the kind that established Boots–Celltech Ltd in 1983 and Apcel Ltd in 1984. At its outset in 1980, Celltech gained impetus from an exclusive and widely-criticized agreement with the Medical Research Council (MRC) for first rights of refusal on all pertinent research. Although the five-year agreement was significantly qualified in 1983, Celltech's finance director Hugh Perrott says that the group still enjoys close collaboration with the council's laboratories.

Celltech's crowning accomplishment so far has been the development of a 1,000-litre fermentation tank, which churns out kilogram quantities of the antibodies that the US company Ortho Diagnostic Systems Inc. will market worldwide as blood group reagents.

Monoclonal antibody production occupies most of Celltech's culture products division, which also supplies antibodies for the purification of interferon and interleukin-2. Last year Celltech spent £2.4 million on expanding these facilities.

The health care division has agreed with the Japanese pharmaceutical firm Sankyo to develop calcitonin, potentially a treatment for osteoporosis and Paget's disease, and tissue plasminogen activator, which dissolves blood clots, for commercial availability. In the United States, Serono Laboratories Inc. has contracted Celltech to produce human growth hormone in mammalian cells and is already conducting clinical trials.

Fairtlough says he has suffered only one disappointment in his company's short history: chymosin, Celltech's first recombinant DNA product, had to be shelved because of patent difficulties and an over-estimation of the demand. Fairtlough contends that the dwindling (50 to 15 per cent) shareholdings of the British Technology Group (BTG), which provided the financial catalysis for Celltech's beginnings, does not reflect a lack of faith on BTG's part. He says that Celltech's shareholders are as satisfied as its customers.

Karen Wright

Bell Labs

From monopoly to competition

Murray Hill, New Jersey

REPORTS of the death of research at AT&T Bell Laboratories have been exaggerated. Since AT&T spun off seven regional telephone operating companies representing two-thirds of its assets at the start of 1984 in settlement of an anti-trust case, Bell Laboratories have indeed changed. But fears that the new slimmed-down AT&T would be unable or unwilling to support basic research in the style of the past have not materialized.

For 60 years, Bell Labs have been the world's foremost electronic research laboratories. Ian Ross, Bell Labs' president, argues that with a budget of $2,000 million and a staff of 19,000, the laboratories are of the scale expected of a company the size of AT&T (operating revenues in 1984: $33,000 million), and that basic research is now more important to AT&T than ever. What has changed is that the development staff, representing (as it did before 1984) some 90 per cent of the total, is now working more efficiently and with increased urgency to exploit usable research results to develop what he calls "killer technologies": technologies that will, like the transistor, lead to the demise of what went before. Basic research, he insists, remains untouched.

The corporate restructuring has, however, been far from painless. In the year following divestiture, Bell Labs lost 4,000 of their then 24,000 staff to AT&T information systems, which manufactures computers, and a further 4,000 to Bell Communications Research, the company set up to conduct research for the newly liberated local telephone companies. Some of the lost ground has since been regained, and Ross has used the opportunity to push Bell Labs in what he sees as the direction of AT&T's future: "we are", he says, "running like hell to change the technology mix".

The 1982 settlement that led to the break-up of AT&T also affirmed an earlier ruling of the Federal Communications Commission that allowed it to enter unregulated markets in information-handling. Ross's greatest hope for Bell Labs is that they will achieve a "fundamental solution to the problem of how to handle software", in which progress worldwide has been less spectacular than in hardware. Almost half of Bell Labs' employees are now producing software as their end-product, and Ross expects to see the proportion rise.

The Strategic Defense Initiative (SDI) is one area that would benefit from fundamental software advances and Ross is making bids on SDI contracts. Solid-state physics and chemistry, once at the forefront of Bell Labs' research, are by comparison now taking a back seat, while only a handful of researchers in economics and psychology remain to keep AT&T with a "window" in that field.

Not that Ross has abandoned physics; there are, he says, still two orders of magnitude of improvement in the circuit density of silicon integrated circuits to be achieved before fundamental constraints are reached, and three orders of magnitude of improvement in optical data transmission rates. Ross clearly intends that Bell Labs should maintain their pre-eminence in this area.

But for all Ross's enthusiasm, it is plain that the uncertainty of 1984 did cause a crisis of morale among Bell Labs' researchers. The losses to Bell Communications Research (Bellcore) and AT&T Information Systems were keenly felt; in Bell Labs' photonics research laboratory, for example, Bell Labs researchers work alongside Bellcore staff but are forbidden to share their research results. That irritation should soon be removed, when the Bellcore workers move into a new building now under construction. But AT&T's uncertain finances, which have caused large lay-offs in some manufacturing divisions, have led to what Ross calls a "salary structure freeze" across the company, including Bell Labs, meaning that salary increases are not awarded automatically. Ross says the "expectation" is that salaries "will be unfrozen" before long.

Many researchers, however, go to work at Bell Labs in part because of their reputation for having an easy collegiate atmosphere with the freedom to pursue academic interests. The introduction of symbols of corporate formality such as security checks for visitors and identification badges for staff therefore caused much resentment, and some took the changes as a cue to leave, most to go to universities.

One who did leave Bell Labs, Terry Miller, went to become professor of chemistry at Ohio State University; he says his decision was the result of a tempting offer and uncertainty about the climate for research at Bell Labs, but he remains in contact with former colleagues and does not now hesitate to recommend a research career there to inquiring students.

Not all divisions seem to have experienced attrition. Kumar Patel, executive director of research for physics and academic affairs, noted no change, but said the changed circumstances of AT&T meant that he had to "do more explaining" to hire promising researchers. But Patel's division has not been untouched by the changes to AT&T. Physicists in the division have shown the possibility of building a positron microscope, which would be an analytical tool with unique properties. "In the old environment, we would have done nothing about it", said Patel. Now, development staff are watching progress closely, and within two years a business decision will be taken on whether the positron microscope should be the target of a major Bell Labs development effort.

Arno Penzias, Bell Labs' vice president for research, is clearly stung by suggestions that AT&T's new competitive spirit will mean an end to the sort of unfettered basic research that led, for example, to his Nobel-prize-winning discovery of the cosmic microwave background radiation. Penzias defiantly points out that astrophysicists still work at Bell Labs, the justification being that the tools of their research may have applications to AT&T's technological base. High-energy physicists, by the same logic, are not employed. And Penzias insists that basic research staff, who now number about 1,000 ("crudely where it's been for a long time") are still encouraged to pursue long-term projects that might bring benefits in five to 20 years rather than more short-term gains. Researchers realize that they are protected as far as possible from the effects of fluctuating budgets, and most feel the worst of the crisis is over.

Penzias says that long-term strategic research at Bell Labs has always been important because, even before divestiture and despite the appearance of monopoly, AT&T always faced pressure to be competitive on prices. (Penzias cites AT&T's response to the establishment of COMSAT, which was to develop optical transmissions.) The change represented by divestiture for Bell Labs is merely in the way it benefits from successful research; before, it was mainly through cross-licensing agreements (the old AT&T was forbidden from benefiting directly from spin-off from its research), while now "one can envisage a script where AT&T cannot afford to pay its dividend". The effect is that research has "moved from being an important part of AT&T's prospects to a vital part".

Laboratory managers have been told to work harder to identify promising research breakthroughs at an early stage in order to alert promising development workers; while the development division has been totally reorganized into product line groupings that correspond to the activities of AT&T's other subsidiaries. Before divestiture, a researcher who found a result of possible interest would "write a memo, throw it over a wall and wait fo someone to answer", according to Davi Lang, head of semiconductor and electronics research: "Now they answer the telephones".

Penzias says the salary scheme for basi researchers at Bell Labs continues to encourage excellence in research, which i assessed and closely monitored by laboratory managers. (Efforts by researchers to ensure that their ideas are taken up by development staff are, however, now rewarded by salary bonuses, an innovation to reflect the changing times.) And Penzias believes in allowing researchers total freedom of inquiry. Mitchell Marcus, a linguistics and artificial intelligence researcher, agrees that he is given "more freedom than in a university". Alan Huang, who heads what may be the only corporate optical computing research department in the world, says he was "startled" shortly after divestiture to be told to take more risks in his research.

Huang's futuristic theorems on pattern recognition algorithms that might one day form the basic logical operations in optical computers are clearly exceptional, but his upbeat assessment of the post-divestiture working environment at Bell Labs is shared by many others. However, there is a niggle: Bell Labs have made a decision to be more careful about the information they will allow researchers to publish.

The irritation arises because recognition by peers is an important form of feedback, not entirely compensated for by the knowledge that permission to publish is being denied because of the possible importance to AT&T of the results being reported. Ross says he favours publishing more, but with "more on what we've done and less on how we did it". Fewer than one per cent of the 4,000 papers submitted for publication clearance each year are turned back for revision, but it seems to be accepted that irritation over this has increased: Ross says he is watching the subject "closely". Penzias cites the case of Narendra Karmarkar's celebrated algorithm in linear programming, now being used by AT&T for designing Pacific basin communication networks, as an example of the successful and judicious application of the policy: although Karmarkar's particular implementation of the algorithm remains proprietary, enough details were released for publication for Karmarkar to receive public recognition and win academic prizes.

Ross opposed divestiture at the time the question was being examined in court, and says he still believes the decision was a mistake. But it has allowed — or obliged — Bell Labs to be more responsive to technical developments. Ross complains that Bell Labs' most famous invention, the transistor, was brought into every home in transistor radios by other companies while AT&T spent 20 years in developing a version reliable enough for use in its only permitted application: telephone switching equiment. When the next "transistor" is invented, Ross says, "we can take it wherever we want". And, perhaps with good reason, he seems to have no doubt that there will be a next time.

Tim Beardsley

Israeli–Egyptian cooperation

Minor relic of Camp David

Rehovot

THE grandiose dreams of large-scale scientific cooperation between Egypt and Israel that flowered in the wake of Anwar Sadat's visit to Jerusalem in November 1977 and the peace treaty of March 1979 have not materialized. Nevertheless, despite intervening political storms, joint research projects in agriculture, mariculture and medicine have been quietly taking place.

As with the Camp David negotiations, US go-betweens have played an important role; the trilateral Cooperative Arid Lands Agriculture Research Programme (CALAR) was set up by researchers from Egypt, Israel and the United States at the University of San Diego, California, in June 1981, with financial support from the US Agency for International Development.

Although research programmes are developed and carried out independently in each participating country to suit specific conditions and needs, experience has shown that lessons learned in one are generally applicable in the other. This is certainly true of the exploitation for agricultural purposes of the abundant quantities of saline water in both Israel and Egypt.

One of the participating scientists, Professor Jehoshua Rudich of the Hebrew University's Faculty of Agriculture in Rehovot, points out that the Israeli practice until now has been to dilute saline water found in its desert regions (normally some five times as salty as ordinary irrigation water) with fresh water until it is only twice as saline. It is then used to irrigate salt-tolerant crops, notably cotton and melons.

More recently, within the framework of the CALAR programme, undiluted brackish water has been used to grow tomatoes (following the use of small quantities of sweet water to reach the flowering stage). The yields were slightly below normal, but the tomatoes were of high quality colour, acidity and flavour.

In parallel work in Egypt, Dr Adel S. El-Beltagy and his colleagues have shown, according to a recent CALAR report, that the local Edkawy variety of tomato is highly suitable for cultivation with saline water. They are, at the same time, producing water of various degrees of salinity and testing it with different methods of irrigation (drip, furrow), as well as studying how yields are affected by such factors as planting distances, windbreaks and fertilizers.

Another CALAR project in both countries involves the development of drought-resistant forage shrubs to feed sheep and goats. While the exploitation of brackish water is naturally emphasized, Dr Dov Pasternak of Israel's Ben-Gurion University, has set his sights on using water taken directly from the Mediterranean. His team has achieved encouraging results with approximately 50 plant species, most of them from the parched interior of Australia.

The Egyptians, meanwhile, have achieved significant progress in cross-breeding the Barki goat, a hardy native of their desert regions but a low producer of milk, with the high-producing Damascus goat.

A third sphere under investigation is the cultivation of crops that can be used as industrial raw materials. Successful results have been achieved in the deserts of both countries with jojoba, guayule and buffalo gourd.

Although political factors have kept cooperation out of the headlines, it has been reflected in more than a dozen joint Israeli-Egyptian presentations at international gatherings as well as joint papers in international scientific journals, mostly on the endemic parasitic afflictions leishmaniasis and malaria.

Medical cooperation began, however, with the mosquito-borne viral disease called Rift Valley fever. Ordinarily confined to central and southern Africa, it has killed 598 people and thousands of animals in Egypt since 1978. Israeli experts, fearing a further spread of the disease, readily agreed to a suggestion by the United States of discussions with their Egyptian counterparts.

Israel's main contribution has been made by a team led by Professor Rachel Galun of the Hebrew University's Kuvin Centre for the Study of Infectious and Tropical Diseases, which carried out studies on the behaviour of the mosquitoes that transmit the virus to cattle, sheep and man. Her findings were almost certainly of use in helping Dr Sherif El-Said of Ain Shams University and his colleagues in their successful efforts first to monitor and then to stamp out Rift Valley fever in Egypt.

Hebrew University researchers also worked together with Egyptian doctors and scientists after an outbreak of visceral leishmaniasis in Egypt. On that occasion, efforts in Jerusalem centred on the detection of antileishmanial antibodies by use of a new method that was developed there.

"Like all good cooperation", Professor Galun explains, "that between the Egyptians and ourselves has been based on mutual self-interest. For we both realize that infectious diseases and the vectors that carry them do not respect national boundaries."

Nechemia Meyers

Comecon technology

Plans laid for collaboration

THE Soviet bloc seems on the brink of novel schemes for technical collaboration. The Comecon economic summit in Moscow last month outlined five key areas of cooperation in its "Comprehensive programme" for collaboration among member countries "up to the year 2000". The five priorities, electronics, automation, nuclear power, new materials and biotechnology, hold no surprises — they were already earmarked for "integrated" cooperation at a previous summit in June 1984. More interesting, however, are the measures proposed for implementing cooperation, and the suggestion that the new programme could be the basis for cooperation outside Comecon itself.

The programme notes that the member countries have decided to translate the priorities "immediately" into specific agreements and contracts, embracing all stages of the "science/technology/production/market" process. The programme provides for direct relationships between scientific organizations and production enterprises in the member countries. Such relationships have until now usually been channelled through high-level organizations situated in the capitals of the countries concerned. This organizational development may fit in with the interest expressed by some Comecon countries in technical collaboration with West European governments. Direct relations of the kind now proposed would thus facilitate possible cooperation between the "comprehensive programme" and the West European Eureka programme, in which companies rather than governments will be the principal actors.

Comecon interest in Eureka has not been great, and the Czechoslovak party daily *Rude Pravo* has been downright hostile, alleging that Eureka and the US Strategic Defense Initiative (SDI) are closely linked, and that many companies likely to be involved in Eureka have already been contacted by the Pentagon, and will work simultaneously for both projects.

The one Comecon country to show real interest in a possible link-up with Eureka is East Germany, an interest that dates back to the visit of French Prime Minister Laurent Fabius to East Germany in June 1985. Perhaps significantly, the main Western interest in such cooperation seems to be coming from West Germany. Last month, Rudi Arndt, chairman of the socialist group in the European Parliament and himself a member of the West German Socialist Party (SPD), told a Moscow press conference that the delegation he had brought to Moscow might "smoothe the way for a formal agreement between the EEC and Comecon", and noted that the prospects for cooperation between the "comprehensive programme" and Eureka were "good".

The Soviet response to Eureka has so far been noncommittal. A Moscow television press conference after the Comecon summit noted that "there are a number of spheres of research and development of new technologies which are to be found in our programme and in the Eureka programme", but pointed out that the decisions leading to the Comecon programme were taken in June 1984, "at a time when no one had yet heard of Eureka".

Such an emphasis on the priority of the comprehensive programme is not, however, without its risks. President Ceaucescu of Romania has already criticized the programme, suggesting that the planners should first have implemented what they undertook to do in June 1984.

What Ceaucescu was referring to is not entirely clear, but he may well have meant the much publicized decision in 1984 to raise the economies and technological bases of the "less developed" Comecon countries (Mongolia, Cuba and Vietnam), to the level of the rest; the comprehensive programme says nothing specifically about these countries although the benefits they might expect were mentioned at the press conference afterwards. **Vera Rich**

West German space

Ministers at odds about Hermes

Bonn

THE federal ministers for research and foreign affairs are sharply in conflict over the proposal that West Germany should participate in the French plan to develop a space shuttle called Hermes. Heinz Riesenhuber, the Christian Democrat (CDU) Minister for Research and Technology, has set his face against collaboration in the project, saying that this could not be justified within the framework of his ministry's strategy for research and development. But the Free Democrat (FDP) foreign minister, Hans-Dietrich Genscher, is keen that West Germany should collaborate in the French project for the sake of Franco-German relations.

Riesenhuber's objections to collaboration have their root in budgetary problems. The minister says that German collaboration could not be financed out of the research budget as it stands, and that if West Germany is to take part in the Hermes project, the federal government will have to allocate extra funds for the work. This position is consistent with the decision of the federal cabinet a year ago that it would support no further large research projects until the 1990s.

Riesenhuber also argues, in further support of his unwillingness to participate in Hermes, that it would be senseless to invest in an "outdated technology", implying that Hermes is a copy of the US shuttle system. He compares the Hermes concept unfavourably with other schemes for the development of reusable space vehicles, such as the British Aerospace HOTOL concept. There is also, in Riesenhuber's mind, anxiety that the French project assumes continued use of the launching site at Kourou, in French Guiana, despite the "explosiveness" of the political climate there.

The dispute between the ministers appears to spring from the decision at the most recent meeting between the federal Chancellor, Helmut Kohl (CDU), and the President of France, François Mitterrand, that the two governments should sponsor a joint study project aimed at turning Hermes into a practical machine.

Riesenhuber's coolness on Hermes conflicts with the technical opinion given to him some months ago by the German Air and Space Research Institute (DFVLR), which recommended participation. But the minister points out that the DFVLR report drew attention to several technical defects of the French proposal such as the inability of the new Ariane V rocket system to compete economically with the new US shuttle-based technology and the intended polar orbit of Hermes, which would be incompatible with the orbits of the US space stations. The French plan would also require new emergency landing sites and data transmission networks. But Riesenhuber may have been chiefly influenced by the consideration that West German hopes to influence the development of an independent European space technology would be undermined if the funds were to be paid directly to the French.

The DFVLR proposals for a new West German initiative in advanced space technology are ambitious. The institute recommended spending about DM600 million a year on a three-cornered programme including both Hermes and the proposed European space vehicle "Columbus", intended as an adjunct to the proposed US space station.

Riesenhuber says that his research budget cannot cover costs on this scale, and is urging that any programme of this kind sponsored by the federal government should be partly financed by industrial sources, perhaps to the tune of 20 or 30 per cent. Riesenhuber points out that many of the proposed experiments could be of industrial value to German industry.

Jürgen Neffe

Sakharov's scientific legacy

Sir—Erast B. Gliner is right to say that Sakharov's contribution to science[1] should be emphasized in the campaign to end his exile and to save his life. However, Gliner's statement that Sakharov "is not considered as a head of some scientific school inside of the Soviet Union or abroad" is not entirely correct. Sakharov's pioneering work on the problem of a controlled thermonuclear reaction, which began the well known tokamak project, was the main reason for his election as a full member of the Academy of Sciences of the USSR in 1953, together with his co-author Igor Tamm. More than 20 years later, Sakharov was elected as a member of the US National Academy of Sciences for similar reasons. In a brief autobiography[2] published in 1974, Sakharov made a special point about two projects that he considered the most important of his contributions to nuclear physics:

> In the summer of 1950, almost simultaneously with the beginning of work on the thermonuclear weapon, I. E. Tamm and I began work on the problem of a controlled thermonuclear reaction; i.e., on the utilization of the nuclear energy of light elements for purposes of industrial power. In 1950 we formulated the idea of the magnetic thermo-isolation of high-temperature plasma, and completed estimates on the parameters for thermonuclear synthesis installations. This research, which became known abroad through a paper read by I. V. Kurchatov at Harwell in 1956 and through the materials of the First Geneva Conference on the Peaceful Use of Atomic Energy, was recognized as pioneering. In 1961 I proposed, for the same purposes, the heating of deuterium with a beam from a pulse laser. I mention these things here by way of explaining that my contributions were not limited to military problems.

In the Soviet Union, acknowledgment of Sakharov's work has been made only in publications from before 1968. Even though the tokamak project for which I. Tamm and A. Sakharov laid the foundations is continuing in the Soviet Union (the tenth, eleventh and twelfth tokamaks are now operating for research purposes), Sakharov's name has been omitted from the history of this field. Sakharov's role was last acknowledged in two official biographies of Igor Kurchatov published in 1967[3,4]. I. Golovin, a close colleague of Kurchatov (the head of the Soviet atomic project), recorded Kurchatov's reaction to Sakharov's theory in a very clear way: "Kurchatov was sitting in his study on New Year's Eve 1950 when he turned [to Golovin] and said: 'Sakharov has boosted us to tackle the second atomic problem of the twentieth century which is no less magnificent [than fission] — obtaining boundless energy by burning the waters of the ocean' "[4]. In some Western histories of Soviet science, the role of Sakharov in the tokamak project is fully acknowledged[5].

When asked about Sakharov's fate, some Soviet officials (including Anatoly Alexandrov, president of the Academy of Sciences of the USSR) normally answer that Sakharov is restricted to Gorky because he is in the possession of important military secrets and that this exile is made in strict observance of Soviet laws. Neither reason is correct. Sakharov was exiled to Gorky on the basis of an "individual" decree signed by the late President Leonid Brezhnev in 1980 as a reprisal for Sakharov's protest over the Soviet invasion of Afghanistan. There are no provisions in Soviet law for such a form of punishment, and the exile was imposed without any trial or decision of the court. Sakharov had had no access to classified information since 1968.

Now, when the new leadership clearly considers many aspects of Brezhnev's internal policy in a very unfavourable light, his legal actions may also be re-examined more carefully and critically. Gorbachev's intention to accelerate scientific and technological cooperation between East and West could not be served better than by restoration of full freedom to Sakharov.

Zhores A. Medvedev
National Institute for Medical Research,
Mill Hill, London NW7 1AA, UK

1. Gliner, E.B. *Nature* **318**, 513 (1985).
2. Sakharov, A.D. *Sakharov Speaks*, 30-31 (Knopf, New York, 1974).
3. Astashenkov, P. *Kurchatov*, 173 (Moldaya Gvardija, Moscow, 1967).
4. Golovin I.N. *Kurchatov* (Atomizdat, Moscow, 1967).
5. Parry, A. *The Russian Scientist*, 172-173 (Collier Macmillan, London, 1973).

Velikovsky

Sir—In his letter (*Nature* 10 October, p.470) criticizing the discussion of the Babylonian Venus observations in my review of Bauer's *Beyond Velikovsky*, Lynn E. Rose claims that he and Vaughan have worked to vindicate these data whereas Huber has rejected two-thirds of them.

The Babylonian texts in question were copied a millennium after the observations; there are so many variants between the copies as well as self-contradictions within individual tablets that at least 20 per cent of the data is suspect from the outset. As one of the most enthusiastic Velikovskians, Rose wishes to use these questionable data to prove that the Earth's orbit has changed dramatically in the past three millennia. Huber, as a scientist inclined to believe in the stability of the Earth's orbit, wishes instead to show that this corpus of material is statistically consistent with modern parameters, and even after throwing out the demonstrably bad sections of the text, over half of the 49 observations agree with modern values within the accuracy of the Babylonian observations.

C. Leroy Ellenberger, no longer a convinced Velikovskian, has pointed out to me that I might nevertheless have even better cited the uniformity of Greenland ice core Dye 3 as a way in which science could actually demonstrate that Velikovsky's scenario did not happen. This 2,000-metre sample is continuous and datable for the past 10,000 years and shows no dust or acid layers that would signal the sort of universal catastrophe predicted by Velikovsky.

Owen Gingerich
Harvard-Smithsonian Center for Astrophysics,
Cambridge, Massachusetts 02183, USA

Metric system

Sir—While endorsing all the comments made by your correspondent Alex Berezin (*Nature* **317**, 762; 1985), I hope that a mixture of different systems of units, including some nonmetric ones, will be retained, at least in the field of aviation. It is a major contribution to safety for a pilot to know that data quoted by radio in feet refer to altitude, while data quoted in metres refer to visibility, and that nautical miles are used to refer to distance along a route, from a radio beacon or airport, etc.

This system is standard throughout the world, the only exception being, characteristically, the United States, where statute miles are thrown in for measuring both visibility and distances, runways are measured in feet instead of metres and air pressure is quoted in inches (of mercury) instead of hectopascals.

If one overlooks this idiosyncrasy, the system works most satisfactorily and is very well suited to be used throughout international airspace, a space which is non-Euclidean, anisotropic and subject to changes of scaling factors (wind, air-pressure and so on) at any time.

Robert Bywater
Department of Cell Research,
Wallenberg Laboratory,
University of Uppsala,
Uppsala, Sweden

Nuclear weapons

Sir—Edward Teller's letter (*Nature* **318**, 99; 1985) is accompanied by two graphs, one of relative numbers and the other of relative yields of US nuclear weapons. In both cases, the data presented end in 1980, before President Reagan's accelerated weapons programme, with which Dr Teller was closely associated and of which he should be in a position to present the consequences, both for numbers and yield. What are the figures for the past two years?

A. J. McEvoy
1015 Ecublens,
Lausanne, Switzerland

Pragmatism is not enough

SIR—It is a well-publicized fact that many species of organisms are in danger of extinction from human activities, especially in the humid tropics where massive deforestation threatens to exterminate countless forms not yet discovered by science. Fortunately, many individuals and organizations have risen to oppose the shortsighted economic and social behaviour that causes this problem — above all, the continued growth of human populations. Many arguments have been adduced for the importance of species preservation, including the actual or potential value of species as food or genetic resources, agents of biological control, components of healthy ecosystems and of our own life-support systems, or objects of aesthetic or intellectual interest. E. O. Wilson, in his recent book *Biophilia*, offers a more subtle argument: the innate affinity of man with other living things, and the fundamental connection between the value we place on them and the value we place on ourselves.

All these arguments are valid, and worth making at every opportunity. However, I suggest that we make a serious and possibly fatal tactical error when we rely solely on such justifications for species preservation. They are all based on the same flawed assumption: that the survival of a species is ultimately justified by its usefulness to man.

Take, for example, the popular argument that the humid tropics are vast untapped reservoirs of potentially valuable genetic diversity. This is true, and among the better reasons for preserving the rainforests. But what will happen to this justification if advances in genetic engineering in the next century make wild gene pools superfluous (or seemingly superfluous) for practical applications? The universal tendency of our technology, after all, is to replace natural products with synthetic ones, and to reduce our dependence on wild species of every sort.

When scientists try to oppose polluters, exploiters and developers solely with these kinds of pragmatic arguments about the value of species, ecosystems or gene pools to human well-being, we have already been manoeuvred into fighting on the ground they have chosen. Our pragmatic arguments for the long-term value of species will be weighed against their pragmatic arguments for the immediate needs of human beings. If an impartial judge rules that their arguments are more compelling and that a flood-control dam will objectively provide more tangible benefits to humanity than will an endangered species, to whom will scientists appeal?

If man's momentary need is allowed to decide the fate of other species, then in the long run the odds are stacked against them. Yet as scientists we owe our allegiance to objectivity and therefore to pragmatism. This, in my view, is why we cannot afford to speak only as scientists, or to let ourselves be limited by that label. We are scientists second and human beings first, and therefore must judge and act and justify our actions according to criteria that transcend science and pragmatism; namely, moral criteria.

If we are ultimately to preserve our biological inheritance, the only position we can take that is sufficiently strong — the only ground that is sufficiently high to be defended against the pragmatists, the economists, the politicians and the exploiters — is that we humans, as the *de facto* stewards of nature, are morally accountable for our stewardship. At the very least, we are accountable to posterity, and for such blunders as we have already committed with toxic and radioactive wastes, we may even live to be cursed by our own children. Those who acknowledge an authority above and beyond this world have still more reason to fear judgement. But if we pride ourselves on any claim to morality at all, whatever, its philosophical basis, that morality must lead is to use nature in a way that will preserve its diversity permanently intact.

This, admittedly, is a moral principle that is more implicit than explicit in many of the theologies and philosophies of the past. But just as there is progress in scientific understanding, there is also progress in moral philosophy and in what we are pleased to call "civilization". Little by little, the human race has grudgingly come to admit that certain things are simply wrong — such as murder, theft, slavery, torture, racism, genocide and even cruelty to animals. Though still committed, these are generally acknowledged, at least, to be crimes. Extermination of a species is also a crime. It is murder of a unique and irreplaceable evolutionary "individual"; it is theft at the expense of our own posterity; and it is a form of genocide as indefensible as any other.

These are the facts we must force mankind to admit, and ultimately to codify in enforceable international law; and there is no time to waste.

DARYL P. DOMNING

Department of Anatomy,
Howard University,
Washington, DC 20059, USA

Bees in SE Asia

SIR—As people of, we believe, "some importance", we read with dismay your editorial on "Bees in South-East Asia" (*Nature* **317**, 190; 1985). Scientific thinking on this issue is clouded by political rhetoric on both sides. We wish to protes about a different matter — your judgement that "nobody of much importance seems to have taken the biological warfare scare seriously".

We take it seriously, as do some of our patients — the H'Mong people of Laos. I is our privilege to work at a hospital which cares for these surviving refugees. They know, perhaps better than any of us, jus how seriously to take it.

Atrocities are indeed hard to imagine To suggest that these people, who believe that biological warfare has been used against them, are "nobody of much importance", rings of past atrocities which also were denied.

We call on you to be more circumspect in conferring the mantle of importance on some people and not on others. And we caution that science is not well served by the assumption that the "important" people are more likely to be astute observers or logical thinkers.

KAREN R. REEVES
WILLIAM H. ANDERSON

St Elizabeth's Hospital,
736 Cambridge Street,
Boston, Massachusetts 02135, USA

Leprosy vaccine

SIR—Your report (*Nature* **317**, 665; 1985) about the proposed test of the World Health Organization (WHO) leprosy vaccine in India does not accurately represent the status of the method used to prepare the vaccine. Although this has not been formally published, the protocol is freely available from WHO and elsewhere and involves no proprietary or patented processes. Further, I have demonstrated the process in two separate laboratories in India, both of which have all the necessary apparatus and chemicals. Several visitors from India have also been shown how to purify *M. leprae* by the process. So it is not clear what technology needs to be transferred. The involvement of the company Wellcome in the matter is simply because materials for use in man must be prepared in licensed permises; there is no question of either development or exploitation of the process by Wellcome.

Your correspondent correctly comments that the main problem of indigenous production of the WHO-type vaccine is that the armadillo colony set up by the Indian Council for Medical Research failed to thrive. These are difficult animals to keep, but there is no restriction on advice and training on how to keep them.

There may indeed be instances where "multinationals" have restricted access to products by developing countries, but the leprosy vaccine is not such an instance.

PHILIP DRAPER

National Institute
for Medical Research,
Mill Hill, London NW7 1AA, UK

Voyager 2 swings by Uranus

The US spacecraft launched towards Jupiter 8.5 years ago is about to encounter Uranus, a planet that has completed only two of its orbits since it was first discovered. The event could be exciting.

THIS time two weeks from now, on 24 January, the US space probe Voyager 2 will make its closest approach to the planet Uranus, providing many people with a reminder of a truth too easily forgotten, that for all its supposed familiarity, the Solar System is huge. The most striking sign of that is that Voyager 2 will have been on its way for more than eight years by the time it passes within 81,500 km of Uranus. Another is that Uranus, unlike both Jupiter and Saturn, is so far away (3×10^9 km) that it remains a bundle of conjectures that are unlikely to be resolved by a single spacecraft.

Nobody should be surprised. That it is just two centuries since Uranus was discovered gives the show away. In an orbit whose radius is 19.18 times greater than that of the Earth, Uranus intercepts only four per cent of the sunlight reaching the Earth even though its radius is 4.02 times as great. At that distance, the image is tiny (1.8 arc seconds across), small enough to fit inside the Great Red Spot on the surface of Jupiter.

The real surprise is what it was in 1781, that the discovery of Uranus should have fallen to German-born William Herschel, the professional oboe-player and musician who (like Handel) had followed the Hanoverians to Britain in search of a living, and who seems to have become an amateur astronomer by accident. The tale of how Herschel's gifted amateurism, which turned on his flair for making accurate mirrors from speculum metal, excited the enthusiasm of Georgian England was nicely told at the International Astronomical Union's symposium at Bath on the bicentenary. The way in which the irregularities in the orbit of Uranus led directly to the discovery of Neptune is another heroic tale. But for the rest, nobody is much wiser about Uranus than in Herschel's time.

Inference rather than direct observation remains the chief source of what little is known; none of the occasional reports of surface features on the planet is regarded seriously. Even the still startling intelligence that the spin axis of the planet is virtually parallel to the plane of its orbit derives most directly from the observation that the orbits of the five known satellites (the first two found by Herschel) lie in planes that are virtually perpendicular to the plane of the planet's orbit, although the measured oblateness (0.022, with an uncertainty of about 5 per cent), which varies with the phase of the planet at observation, fits in with the supposed spin axis. More recent attempts to learn something of the motion of the planet from Doppler measurements of atmospheric emission lines have helped only to pin down the period of rotation to about 15 hours (and few will be surprised if Voyager 2 recovers a different value).

This is why the next few weeks may bring more information about Uranus than the whole of the past two centuries. The hope is that the set of eleven experiments that gathered a rich harvest of information from the successive encounters with Jupiter (in 1980) and Saturn (in 1981) will still be functioning at Uranus (and at Neptune, which will be encountered on 24 August 1989, almost exactly twelve years after Voyager 2 was launched).

The visual observations may be even more telling on this occasion than at the previous encounters with outer planets. For if there are recognizable features on the surface of Uranus, it should at least be possible to learn directly something about the speed of revolution of the atmosphere of the planet (which is not necessarily that of the bulk). Indeed, the three cameras on Voyager 2 should be capable of yielding a resolution of better than 700 km for 700 hours before and after the encounter, which means that the daily newspapers may have splashed the first photographs of Uranus before this issue of *Nature* has appeared.

Another of the planned routes to a direct measurement of the speed of revolution may be a disappointment. If Uranus has a permanent magnetic field like that of the Earth, there will also be a magnetosphere that dominates the solar wind and, within that, a store of charged particles trapped in the magnetic field whose interaction with the atmosphere will give radio emissions varying with the rotation of the planet (if the magnetic and rotation axes are different). The first reports from what is called the Planetary Radio Astronomy Experiment suggest only meagre radio emission, at best. Perhaps there is no magnetic field worth speaking of. The next few days should tell.

This question has a bearing on the chemical constitution of Uranus and thus on current versions of the theory of how the planets were originally formed. Outwardly, Uranus and Neptune are similar. Uranus has 14.6 Earth masses, Neptune has 16.78. But the radii are oppositely related, at 4.02 and 3.89 Earth radii respectively. The difference of density may not be great, but it requires an explanation.

The standard assumption is that, even at these great distances from the Sun, planets will contain substantial quantities of the elements whose refractory oxides finish up as rocks on planets like the Earth. But Uranus and Neptune will have two other kinds of materials, those that form ices at the temperatures that reign (the atmosphere of Uranus, colder than that of Neptune, appears to be at a mere 65 K) but also materials that are still gaseous under those conditions, hydrogen and helium most significantly.

Given such a model, together with the mass and radius of the planet, it is possible to work out the relationship of pressure and density with depth beneath the surface. If the planet is spinning on an axis, it is also possible to relate the equatorial bulge and the aspherical components of the gravitational field to the speed of rotation, whence several attempts to calculate the rotational speed. (The shape of the gravitational field is inferred from, for example, the motion of the satellites or the shapes of the rings, of which, at Uranus, there are nine.) But here again, the data are not good enough to settle unambiguously the several persisting uncertainties. Here again, Voyager 2 should help enormously, not simply because its trajectory near Uranus is well designed for helping to pin down the gravitational field but because there will be direct measurements of the composition of the atmosphere

That raises several questions. The ratio of deuterium to hydrogen should be greater than on the Sun, but its measured value may be a guide to the temperature at which these planets formed. Why there is virtually no ammonia in the atmosphere of Uranus is another puzzle. (Methane is abundant.) The narrowness of the nine rings, and their apparent opacity, is another problem (but see this issue, p. 115) on which some light may be thrown by the very close approach to the innermost satellite Miranda expected for Voyager 2, a mere 15,000 kilometres. Whether there is an internal source of heat other than that of energy released by minor gravitational readjustments within an apparently stable planet may also be determined. The way things have turned out, the spacecraft is an instrument of which even Herschel would have been proud.

John Maddox

Ocean ecology

Light and ultraphytoplankton

from G. E. Fogg

H. Lohmann, studying filter mechanisms used by planktonic appendicularians to collect extremely fine particulate matter from sea water, pointed out the inadequacy of the conventional fine silk net for sampling plankton. He suggested that the small organisms which pass through the net could be important in the economy of the oceans because they might multiply much faster than the larger forms. The smallest of the phytoplankton, bacteria and tiny protozoa, are now grouped as picoplankton (diameter 0.2–2.0 μm) or ultraplankton (diameter less than 10 μm). The behaviour of these microorganisms is analysed in this issue (Glover, H.E., Keller, M.D. & Guillard, R.R.L. *Nature* **319**, 142; 1986) and was the subject of a recent NATO advanced study workshop. The conclusions support Lohmann's 75-year-old suggestion and mean that our ideas about ocean ecosystems will have to be revised.

Although it has often been noted that much of the photosynthetic activity of water samples is contained in the fraction that passes through the phytoplankton net, these minute organisms have remained largely unconsidered because they are so difficult to identify and count. Picoplankton only leaped into prominence when the value of the epifluorescence microscope for counting tiny coccoid cyanobacteria (blue-green algae) was realized (Johnson, P.W. & Sieburth, J. McN. *Limnol. Oceanogr.* **24**, 928; 1979 and Waterbury, J.B., Watson, S.W., Guillard, R.L. & Brand, L.E. *Nature* **277**, 293; 1979). Because they contain biliprotein pigments, these organisms are easily recognized by their strong and characteristic autofluorescence. Epifluorescence shows that they are abundant in most, if not all, the world's oceans, and the filter fraction in which they are collected contains most of the total photosynthetic capacity.

Physical considerations suggest that organisms of this size are peculiarly suited to planktonic life. Their sinking rates are negligible compared with the scale of the turbulence found in even the calmest seas. They have high surface/volume ratios which, combined with the steep diffusion gradients that are set up around very small sinks, allow them to take up nutrients at a high rate. Furthermore, a given amount of photosynthetic pigment dispersed in small cells absorbs light more effectively than an equivalent amount packaged in large cells. The strains examined in laboratory culture grow best at low light intensities of less than one fiftieth of full sunlight. Perhaps the only disadvantages of small size for a phytoplankter are the difficulties of moving into waters richer in nutrients or more favourably illuminated, and a greater vulnerability to predators.

Picoplanktonic cyanobacteria are generally found in concentrations of 10^4 cells per ml in inshore and offshore waters but are more evident in nutrient-poor offshore waters where larger phytoplankton, less able to use low concentrations of nutrients, are not successful. Although they are found throughout the water column in the euphotic zone, these cyanobacteria are concentrated at the bottom of the zone. This is not because they sediment out but is rather because they grow best in these conditions, using the low irradiance efficiently to support growth and benefiting from nutrients transported up from richer waters below. The oceanic picoplanktonic cyanobacteria contain large amounts of phycoerythrin, a pigment which seems admirably suited to absorb the blue-green light penetrating into deep water, but most of this pigment seems to be photosynthetically inactive, as demonstrated by its high fluorescence yield. Phycoerythrin may be more important as a nitrogen reserve than as an accessory photosynthetic pigment (Wyman, M., Gregory, R.P.F. & Carr, N.G. *Science* **230**, 818; 1985).

As well as cyanobacteria, there are eukaryotic ultraphytoplankton, detectable by the autofluorescence of their chlorophylls. These have so far scarcely been characterized and are difficult to grow in culture, but they are sometimes more abundant than the cyanobacteria in deep water and seem to grow best at even lower irradiances. Glover and her colleagues have now examined the photosynthetic performances and growth efficiencies of such forms at different irradiance levels and in different wavebands and find that the eukaryotes do better than the cyanobacteria in the dim blue-violet light that penetrates to the bottom of the euphotic zone in clear oceanic waters. Chlorophylls *b* or *c*, the major accessory pigments of these organisms, promote absorption in this region of the spectrum. In contrast, cyanobacteria grow best in green light. The larger eukaryotic phytoplankton have lower efficiencies at low irradiances than the ultraplanktonic species, probably as a result of the size effect discussed above.

It appears that eukaryotic ultraplankton, being adapted to low light intensities, can occupy a zone in which an ample nutrient supply is maintained by transport upwards from deeper water whereas the cyanobacteria need higher irradiances but can persist in waters which are sometimes depleted of combined nitrogen, and perhaps phosphorus, because of their high storage capacity. Further investigation of the physiology of these highly successful tiny organisms, together with increasing knowledge of the activities of the heterotrophic ultraplankton, will help to complete a picture of one component of an ecosystem that is probably responsible for most of the energy transformations and recycling of materials taking place in the oceans. □

G.E. Fogg is at the Marine Science Laboratories, University College of North Wales, Menai Bridge, Anglesey LL59 5EH, UK.

Cell biology

Life without clathrin

from James E. Rothman

During receptor-mediated endocytosis, the process by which many macromolecules are taken up from the extracellular fluid into cells, receptors cluster in specialized regions of the cell surface, which invaginate to form coated vesicles. The coating is made of protein and the best characterized of the proteins is clathrin. It has always been assumed that the spontaneous assembly of clathrin molecules into a polygonal array on the surface of the budding vesicle is responsible for driving the budding process. This has also been seen as attractive paradigm for the mechanism of vesicular transport between intracellular compartments. But does clathrin play that role in intracellular transport? Do clathrin-coated vesicles mediate biosynthetic intercompartmental protein transport, such as the distribution of newly synthesized proteins from the endoplasmic reticulum via the Golgi stacks to plasma membranes, secretory granules and lysosomes? Three recent papers offer some new and surprising answers to these fundamental questions[1-3].

From immunofluoresence studies using antibodies to clathrin it has been clear that clathrin is localized both to the Golgi complex and to the plasma membrane, suggesting a role for clathrin in both biosynthetic and endocytic protein traffic. But an important extension of such studies by Griffiths *et al.*[1] and Orci *et al.*[2] has now greatly limited the steps in biosynthetic protein traffic that might be mediated by clathrin-coated vesicles and has led to the discovery of a new type of morphologically coated vesicle, which seems not to contain clathrin. Using colloidal gold-based immunocytochemistry combined with electron microscopy to localize clathrin antigens in the Golgi complex, both groups find that clathrin is mostly concentrated at the trans-most cisterna of the Golgi stack.

The Golgi stack is an asymmetrical structure comprizing a series of distinct compartments or cisternae. Proteins arrive from the endoplasmic reticulum at one end (the 'cis' face) of this stack, pass from one compartment to the next, and finally emerge from the last cisterna at the opposite ('trans') end. Thus, the restriction of clathrin-coated vesicles to the trans-most cisterna suggests that, at most, clathrin-coated membranes serve as carriers from this location to terminal destinations, such as the cell surface, secretory granules and lysosomes.

It is generally agreed that clathrin probably coats primary lysosomes and newly formed secretory granules in the cell. By contrast, a protein that is known to be destined for the plasma membrane (the vesicular stomatis virus-encoded G protein) could not be detected by Griffiths *et al.*[1] in the clathrin-coated buds forming from the trans-cisterna. The picture that seems to be emerging is that clathrin-coated vesicles are restricted to routes connecting the Golgi with some terminal destinations of biosynthetic traffic, but perhaps not the plasma membrane. Lysosomal enzymes and secretory proteins destined for storage granules may be selectively removed from the Golgi in clathrin-coated membranes. Perhaps the left-overs — consisting of cell-surface proteins and constitutive (unregulated) secretions — are transported to the plasma membrane by other types of vesicles, whose content may not be nearly so selective. Of course, the picture may be still more complicated, with polarized cells having multiple surface domains.

Given that clathrin is restricted to the Golgi exit point, how do transported proteins move from the endoplasmic reticulum to the Golgi, and from one cisterna to another across the stack? Another surprise described by Griffiths *et al.*[1] is that although there are morphologically coated vesicles or buds at all levels of the Golgi, they are not labelled by antibodies to clathrin. As the authors point out, the simplest explanation is that these coated structures are not made up of clathrin. The clear and exciting implication is that a new type of coated vesicle, whose coat protein is yet to be discovered, carries biosynthetic protein traffic up to the trans-most Golgi cisterna. A number of mysteries are created. Why is the same type of clathrin coat not used at all stages of biosynthetic protein transport? Are the new type of coated vesicles capable of selective protein transport, like clathrin-coated vesicles, or might they have quite different functions, perhaps even as bulk carriers? In this connection, note that the first station where a choice of destination must be made along the biosynthetic protein-transport pathway is probably in the trans-most cisterna of the Golgi stack, which is where clathrin is first found.

Clathrin-coated vesicles from chicken oocytes. × 125,000, 1% uranyl acetate stain. Photograph courtesy of B. Pearse.

Yet another surprise is that some cells can manage quite well without any clathrin at all. This sobering finding emerged when Payne and Schekman[3] deleted the single clathrin gene from yeast. Yeast has coated vesicles and its clathrin, like mammalian clathrin[4], is composed of three-legged 'triskelions' containing equimolar amounts of a heavy chain (190 kD in yeast) and a light chain (36 kD)[3]. Payne and Schekman prepared an antibody against the yeast heavy chain and used this to isolate the heavy-chain gene from a library of yeast DNA in a phage lambda expression vector. Using what are now standard methods in yeast genetics, they replaced the normal clathrin heavy-chain gene of yeast with a grossly deleted version, prepared *in vitro* using restriction enzymes. Spores carrying only the deleted clathrin gene do not synthesize any clathrin heavy chain or even any immunologically cross-reactive material, yet they are quite unexpectedly viable, although they grow more slowly than wild-type cells. The only indication of a defect in the cells is an accumulation of vesicular structures in the cytoplasm and the presence of a larger than usual intracellular pool of invertase, which, however, is secreted at essentially normal rates.

What could this mean? As the authors suggest, one possibility is that although biosynthetic transport does not require clathrin-coated vesicles in yeast, endocytosis still does. If so, this would fit well with the evidence from animal cells that clathrin may not be needed for constitutive transport from the endoplasmic reticulum through the Golgi complex to the cell surface. (It is not known whether proper vacuole formation is needed for yeast to grow; also, yeast does not store secretory products.) Another possibility would be that there is a 'back-up' system — an alternative clathrin-like molecule that can replace clathrin when needed, or an alternative pathway that can salvage transport. If so, the back-up coat protein must be structurally dissimilar from clathrin proper, since there is but a single clathrin gene and no cross-hybridizing DNA even under conditions of low stringency, nor any other polypeptide that cross-reacts with antibodies to clathrin. A final, and even less comfortable, possibility is that clathrin is not required to form the vesicles that it normally coats, nor for their utilization. This would be truly heretical but cannot be dismissed out of hand.

These unexpected developments add a breath of fresh air and excitement, and suggest that we are about to obtain a more sophisticated view of the process of protein sorting. They also serve as a reminder that generalizations in cell biology can be more dangerous to the health of the investigator than to that of the organism. □

1. Griffiths, G., Pfeiffer, S., Simons, K & Matlin, K. *J. Cell Biol.* **101**, 949 (1985).
2. Orci, L., Ravazzola, M., Amherdt, M., Louvard, D & Perrelet, A. *Proc. natn. Acad. Sci. U.S.A.* **82**, 5385 (1985).
3. Payne, G. & Schekman, R. *Science* **230**, 1005 (1985).
4. Mueller, S. & Branton, D.J. *J. Cell Biol.* **98**, 341 (1984).

James E. Rothman is in the Department of Biochemistry, Stanford University, California 94305, USA.

Geology

Are komatiitic lavas voracious?

from Robert W. Nesbitt

KOMATIITE lavas are highly magnesian silicate rocks which are mainly restricted to the first half of the Earth's history. First recognized less than twenty years ago, in the 3,500-Myr-old Barberton greenstone belt in South Africa[1], they have since been identified in most continents where volcanic greenstones are exposed. They are particularly interesting for their restricted but economically important association with Fe–Ni–Cu sulphides: the most important deposits always occur at the base of the first flow of any komatiite lava pile[2]. Huppert *et al.*[3] have put forward a model in which this association is explained by thermal erosion. In a paper on page 136 of this issue, D.I. Groves and colleagues provide an example of this but one which, paradoxically, reinforces previous criticisms of the model[5].

Komatiite flows consist of an underlying olivine cumulate zone overlain by a zone of skeletal (or spinifex-texture[6]) olivine — that is, olivine set in a matrix of skeletal clinopyroxene and glass. Overall, the grain size and morphology of the olivine changes from a random arrangement of olivine plates with fine-grain size at the top of the flow to a coarse-grained parallel plate-like arrangement just above the cumulate zone (Fig. 1*a*, *b*). These textures, together with geochemical and experimental data, have led to the concept that komatiitic liquids erupted at temperatures of 1,600 °C, some 300–400 °C above those observed for basaltic flows[7].

Based on these data, Huppert *et al.*[3] speculated that, because of their low viscosity, komatiite liquids would display turbulent flow rather than the laminar flow typical of lower-temperature silicate melts. Their calculations suggested that this would result in high temperatures being maintained at the base of flows, so that the komatiite liquids would be capable of thermally eroding the underlying rocks. Consequently, the komatiite flows might create their own channels and, as a result, assimilation of underlying material could take place.

This new concept also provided an explanation for the occurrence of Ni–Fe–Cu sulphides at the base of komatiite flows. If sulphide-bearing sediments were assimilated they would immediately form an immiscible sulphide liquid, because sulphur has low solubility in silicate melts. The liquid would then scavange Ni and Cu out of the komatiite melt and the resultant Ni–Fe–Cu sulphide liquid would settle into topographical lows at the base of the komatiite flow, which itself was still molten. Although the sulphide–silicate immiscibility model was not new, this scheme provided an explanation for the origin of the sulphur and for the channel or trough-like structures, which are a prominent feature of almost all komatiitic nickel sulphide deposits.

In a further twist to the complexities of komatiite-sulphide genesis, Groves *et al.*[4] now suggest that the thermal-erosion model only works if a pool of sulphide liquid already exists — the sulphide providing the high thermal-conductivity medium necessary to intitiate melting in the underlying rock. Their evidence comes from the hanging-wall ore bodies at Kambalda, Australia, which are unusual in that they are found between flows higher in the section rather than at the base of the first flow. Groves and colleagues have examined spinifex-textured olivine–sulphide associations that occur in komatiite flow-top zones, just below the massive hanging-wall ore bodies. In these occurrences (Fig.1*c*), sulphide occupies the inter-olivine areas; the authors claim that this represents a replacement of the pyroxene and glass that normally occurs there. The main evidence sems to be the occurrence of types transitional between all-sulphide and all-silicate inter-olivine material, interpreted as the result of selective melting in the spinifex zone of the komatiite flow by the transference of heat through the sulphide pool from the overlying komatiite flow. The resulting silicate liquid was then displaced upwards from between the olivine grains by the overlying heavier sulphide, which settled into the space that was previously occupied by pyroxene and glass.

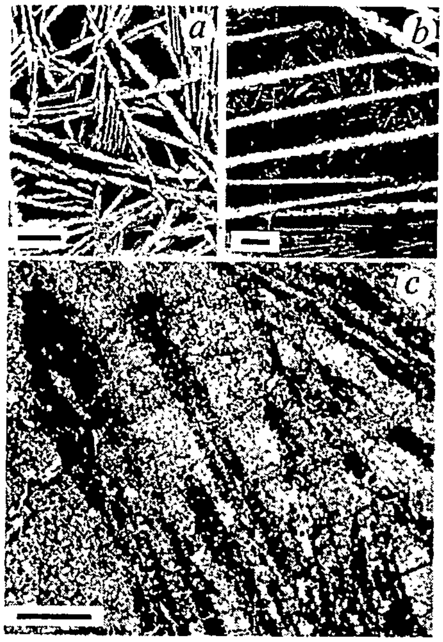

Fig.1 *a*, Thin section of a komatiite with random spinifex texture. Olivine (white) plates separate areas of glass and clinopyroxene (dark areas). This textural type is commonly found close to the upper surface of flows. *b*, Thin section of a komatiite with plate spinifex texture. The long light-coloured crystals are olivine with the inter-olivine areas occupied by clinopyroxene and glass. This is found near the upper surface of komatiite flows but below the random spinifex type shown in *a*. *c*, Polished rock slab showing skeletal olivine crystals (dark) and Fe–Ni–Cu sulphide. These may represent pre-existing plate spinifex-textured komatiite[4].

Furthermore, the fact that the olivine texture in the sulphide is always of the plate type, indicates that the fine-grained random spinifex (commonly found above the plate-type) must have been thermally eroded by the overlying flow. This is a particularly critical observation because Groves *et al.* claim that along strike from the sulphide occurrence, the younger komatiite flow directly overlies either a sediment or a spinifex-textured komatiite with random olivine. In other words, thermal erosion occurred only if a pool of sulphide liquid was present. Hence the paradox — although they provide an example of thermal erosion, Groves *et al.* at the same time caution against the general application of the model.

If komatiite flow on older komatiite does not produce melting without the intervention of sulphide liquid, what about komatiite liquid flowing on to basalt or sediment? Groves *et al.*[4] have looked again at the major nickel ore environment at Kambalda, where massive sulphides occur in trough-structures separating pillow basalts (footwall) from komatiites. Here the evidence for thermal erosion is less definite, despite the undoubted presence of a major pool of sulphide liquid. The problem lies in the lack of specific marker horizons in the underlying pillow basalt sequence that would indicate whether there has been removal of the basalt. Although they admit that the trough structures almost certainly focused thermal erosion through the presence of the sulphides, the authors insist that such troughs are first-order volcanic/topographical features and not the products of thermal erosion

We are thus faced with a major dilemma. According to Huppert *et al.*[3], sulphide pools are generated by thermal erosion in surface channels through assimilation of sedimentary sulphur, whereas Groves *et al.*[4] claim that such erosion takes place only under pre-existing sulphide pools. A possible resolution of the problem may be that thermal erosion took place within the crust — evidence from other lines of investigation, particularly studies of zircon ages in the Kamalda area[8], indicate the influence of crustal contamination. So sulphide contamination of komatiites may have occurred *en route* rather than at the surface.

This solution, however, brings us full circle back to the problem of how to transport a dense sulphide liquid to the surface in a lower-density silicate medium — the outstanding problem in previous models involving mantle-derived sulphide liquids. For academic earth scientists, the tangle of contradictions provides a fascinating research challenge, while exploration geologists continue to puzzle over the problem of why Kambalda komatiites are so richly endowed in nickel sulphides when elsewhere there are only komatiites and sulphidic sediments. □

1. Viljoen, M.J. & Viljoen, R.P. *Spec. Publ. geol. Soc. S. Afr.* **2,** 1221 (1969).
2. Gresham, J.J. & Loftus-Hill, G.D. *Econ. Geol.* **76,** 1373 (1981).
3. Huppert, H.E., Sparks, R.S.J., Turner, J.S. & Arndt, N.T. *Nature* **309,** 19 (1984).
4. Groves, D.I., Korkiakoski, E.A., McNaughton, N.J., Lesher, C.M. & Cowden, A. *Nature* **319,** 316 (1986).
5. Claoue-Long, J.C. & Nesbitt, R.W. *Nature* **313,** 247 (1985).
6. Nesbitt, R.W. *Geol. Soc. Aust. Spec. Publ.* **3,** 331 (1971).
7. Green, D.H. *Geology* **3,** 15 (1975)
8. Compston, W., Williams, I.S., Campbell, I.H. & Gresham, J.J. *Earth planet. Sci. Lett.* (in the press).

Robert W. Nesbitt is Professor of Geology at the University of Southampton, Highfield, Southampton SO9 5NH, UK.

---

100 years ago

In the twentieth volume of the *American Journal of Science* I gave a preliminary account of my search for the trans-Neptunian planet. I regard the evidence of its existence as well-founded, and nothing has weakened my conviction as to its existence in about that part of the sky assigned; while the independent researches by Prof. Forbes conducted him to an identical result. That five years have elapsed, and the planet is still unfound, is not sufficient assurance to me that its existence is merely fanciful. From *Nature* **33** 258, 14 January 1886.

Cosmic rays

A supernova for a neighbour?

from Arnold Wolfendale

COULD a supernova have exploded recently on our doorsteps? Don Clayton, D.P. Cox and F.C. Curtis think so. In *The Galaxy and the Solar System* (University of Arizona Press, in the press), they suggest that a supernova explosion occured 15 pc away — only ten times the distance to the nearest star — about 10^5 years ago. If this controversial claim is correct, it could help to explain the origin of cosmic rays.

It is remarkable that 75 years after they were discovered by Victor Hess, researchers still argue about where cosmic rays come from. The seemingly incessant rain of cosmic rays that bombard the Earth consists of atomic nuclei, protons, electrons and about one part per million of γ rays. This tiny γ-ray component is proving of considerable value to researchers because γ rays travel in straight lines, unlike the particles, which follow tortuous paths in the tangled magnetic fields of the Galaxy. Because many of the γ rays seem to be produced by the cosmic-ray particles interacting with the gas in the interstellar medium (ISM), they can be used to probe the spatial distribution of the particles and thus give a hint as to their sources.

Although some particles achieve enormous energies — up to 10^{20} eV, compared with about 10^{12} eV in the giant accelerators — it is the lower-energy particles that are of concern here. Among the many contenders for their generation, supernovae (SN) — exploding stars, typified by the well-documented Crab Nebula of 1054 — are currently the favourite. Although they were first suggested as cosmic-ray sources in 1934, problems arose because the cosmic ray particles were supposed to lose energy in the ensuing supernova remnant (SNR). Recent advances have, however, included clever ideas on how shock waves can transform shock energy into cosmic rays with high efficiency so that the cosmic-ray energy in a SNR increases rather than falls with time. Support has come from claims that a comparatively nearby old remnant, termed the Loop I SNR, has within it a higher cosmic-ray intensity than elsewhere (Bhat, C.L. *et al. Nature* **314**, 515; 1985).

The ideas of Clayton and colleagues on the thorny question of the environment and history of the Solar System are the most recent developments bearing on the origin of cosmic rays. Gone are the days when the ISM was considered to have a uniform density of 1 atom cm^{-3}; now it is thought to have at least three phases differing in density and temperature. Clayton *et al.* propose that the Solar System is immersed in a 'cloudlet', with a density of 0.1 atom cm^{-3} and temperature 10^4 K extending about 1 pc from the Sun, residing in a medium of much lower density and considerably higher temperature (4×10^{-3} atom cm^{-3}, 10^6 K), that extends approximately 100 pc from the Sun. It is in this lower-density medium that a SN is assumed to have occurred only 15 pc away about 10^5 years ago.

The authors point out two factors favouring their proposals: the argument of D.P. Cox and P.R. Anderson (*Astrophys. J.* **253**, 268; 1982) that this could explain the observed soft X-ray flux, and Clayton's own suggestion that the comparatively strong γ-ray line from the unstable ^{26}Al nucleus in the ISM comes from the debris of the SN explosion. This γ-ray line is very interesting as it is the first clear case of a line from radioactive nuclei in the general ISM; it was detected by the HEAO-3 and Solar Maximum Mission spacecraft, both of which recorded fluxes in excess of expectation. ^{26}Al has a half life of about 10^5 years and some is doubtless produced in SN explosions; if a SN were so close and had exploded so recently, little ^{26}Al would have been lost by decay, so that the γ-ray flux could be entirely explained.

What effect would such a SN have on the ambient cosmic-ray flux? The authors expect the present value to be twice the average but I find this difficult to accept. There is now a wealth of data on the gradients of cosmic-ray intensity in the Galaxy, obtained by satellite studies of γ rays above 100 MeV, and an excess much more than 30 per cent would be difficult to accommodate, at least in the important proton component. Problems also arise with the relative numbers of cosmic-ray 'nuclei' more massive than protons, in particular with the 'grammage' distribution, which is an indicator of the amount of ISM through which the cosmic rays have passed. Clayton's group are able to get round these difficulties by involving four components of the cosmic radiation that have achieved their energies in different ways in the remnant and in the supernova itself — but this seems a rather contrived solution.

Where, then, does all this leave the problem of cosmic-ray origin? It seems increasingly possible that supernova shocks accelerate a significant fraction of the low-energy cosmic-rays. Although a supernova as recent as 10^5 years ago and as close as 15 pc seems unlikely, some of the ideas put forward by Clayton *et al.* for explaining outstanding anomalies in related areas are worthy of much more detailed study. □

Arnold Wolfendale is Professor of Physics in the University of Durham, South Road, Durham DH1 3LE, UK.

Gene regulation

Importance of helical periodicity

from Tariq Enver and Roger Patient

ATTEMPTS to understand transcription of eukaryotic genes by the enzyme RNA polymerase II have so far focused either on the identification of the sequences that together constitute the gene promoter or on the proteins (*trans*-acting factors) that recognize these sequences and are necessary for transcription. A paper by Takahashi *et al.* on page 121 of this issue[1] demonstrates that the static arrangement of the promoter sequences is an important parameter for transcription. The authors suggest this may best be interpreted as reflecting a role for protein – protein contacts in promoter activation.

Broadly speaking, RNA polymerase II promoters are organized according to a common modular plan[2]. The 'TATA box' specifies accurate initiation of transcription from a position 25–30 base pairs (bp) downstream (of itself). Additional 'upstream elements' important for efficient transcription are located within 100 bp of the transcription start. And transcriptional activity may be further modulated by an enhancer element. As shown in the figure, the 'early' promoter of simian virus 40 (SV40) conforms to this general scheme. The upstream elements appear in the form of six GC-rich sequence motifs, two each within the three 21 / 22 bp repeats; a pair of 72 bp repeats constitute the enhancer element.

Takahashi *et al.*[1] have tested the effects of altering the stereospecific relationships of these three promoter elements of SV40 by making insertions of odd or even multiples of 5 bp — about half a turn of the DNA helix — either between the enhancer and 21 bp repeats (site P in the figure) or between the 21 bp repeats and the TATA box (site Q). Strikingly, insertions at either site that maintain the helical pitch relationships of the promoter have little effect on transcriptional efficiency, whereas those that alter it reduce transcriptional efficiency by up to 10-fold. One interpretation of the importance of the helical disposition of the promoter elements is that it facilitates contacts between the *trans*-acting factors that bind at the SV40 promoter elements[2,3], and/or that it provides the appropriate recognition surface for RNA polymerase II.

Precedent for the involvement of protein – protein contacts in the regulation of gene expression comes from studies on *Escherichia coli*. The elegant work of Ptashne and coworkers[4] has clearly demonstrated that whereas repression by bacteriophage lambda repressor (cl) protein is mediated by steric exclusion of RNA polymerase, the simultaneous stimulation of the adjacent, divergently transcribing promoter for the *cl* gene itself is mediated by protein – protein contacts between the repressor and RNA polymerase. The proximity of the binding sites for activator proteins and RNA polymerase in the galactose[5] and arabinose[6] operons also suggests that activation occurs by protein – protein contacts. However, one of these activator proteins, the cyclic AMP receptor protein, acts on several operons, and the portions of its binding sites relative to the promoters are variable, thus calling into question whether induction always works by protein – protein contacts.

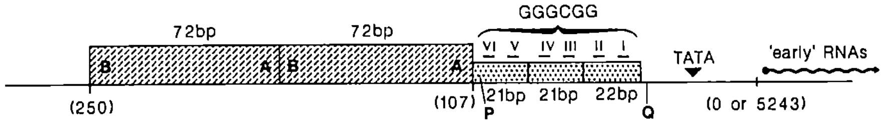

Schematic diagram of the simian virus 40 'early' promoter.

What other explanations are possible for the helical periodicity observed by Takahashi *et al.*? One possibility currently attracting attention is DNA bending. From studies of trypanosome kinetoplast DNA, Wu and Crothers have pointed out that the sequence elements causing the axis of the helix to deviate must be arranged at intervals approaching 10.5 bp if the sum of the helical deviations is to result in a bend[7]. Bending may be an important component in defining the binding site of a *trans*-acting factor. Work on the positioning of nucleosomes on DNA[8] provides evidence that bending is important for protein – DNA interactions and it may well also act to facilitate protein – protein contacts. Such a mechanism has been suggested for the induction of the lactose operon of *E.coli* by cyclic AMP receptor protein, which induces DNA bending on binding to its recognition site and may thereby facilitate contacts with RNA polymerase[7].

Alternatively, the observed helical periodicity may reflect a requirement in factor binding for the stereospecific alignment of two or more altered DNA structures. Possibly relevant in this context is the identification of Z-DNA segments in the SV40 72 bp repeats[9]. Another quite attractive explanation would involve the interaction of the promoter with the nucleoskeleton[10]. Attachment along one face of the helix could block access of transcription factors to that face and the extent of blockage would vary with periodicity.

Particularly intriguing is the requirement for stereospecific alignment between the enhancer of SV40 and its 21 bp repeats. Might this shed light on enhancer mechanisms, and can it be reconciled with the fact that enhancers potentiate transcription from their promoters in a way that is essentially independent of orientation, distance or position relative to the gene[11]? In their paper, Takahashi *et al.* cite as yet unpublished evidence from their group[12] that each 72 bp enhancer motif contains two distinct binding domains (A and B in the figure). If, as their data imply, the important protein – protein interaction is between factors bound at A and the 21 bp repeats, then reversing the orientation of the enhancer with respect to the 21 bp repeats might be expected to perturb the critical factor interaction.

Takahashi *et al.* suggest that action at a distance could still be mediated by protein – protein contacts if the interposing DNA is looped out[2,11]. Possible examples of this type of mechanism have been found in the galactose and arabinose operons of *E.coli*, where it has been suggested that repressor monomers bind at two well-separated sites and monomer – monomer interactions facilitate DNA loop formation[13,6]. Interestingly, insertions between the two binding sites in the arabinose operon show the same helical periodicity as described by Takahashi *et al.* for SV40.

Although DNA loop-out seems a reasonable model for enhancer action from a distance upstream of the promoter, the model is sterically unattractive for a downstream enhancer. An attractive modification to the model is that the loop forms only transiently to facilitate intramolecular factor transfer. But, although upstream enhancement has been demonstrated *in vitro*, downstream enhancement has not, suggesting that simple factor transfer cannot be the whole story. The magnitude of enhancement *in vitro* is only about 10-fold[14] whereas it is 100–1,000-fold *in vivo*. Interestingly, the transcription level seen *in vivo* by Takahashi *et al.* varies with insert size over the range of variation seen *in vitro*. Thus, it is possible that both may be reflecting only one component of the proposed biphasic nature of the 72 bp repeats, whereby they act as both an enhancer and an upstream promoter element at short range but just as an enhancer at long range[15]. The helical periodicity and *in vitro* effects may be due to their action solely as a promoter element. It is tempting to suggest that domain A in the 72 bp repeats is the promoter element and domain B is the enhancer. One could then predict that domain B could be completely separated from domain A with little loss of activity; in fact, 50 bp seems to be the upper limit[12]. ☐

1. Takahashi, K. *et al. Nature* **319**, 121 (1986).
2. Dynan, W.S. & Tjian, R. *Nature* **316**, 774 (1985).
3. Wildeman, A.G. *et al.* cited in ref. 1 as ref. 16.
4. Ptashne, M. *Trends biochem. Sci.* **9**, 142 (1984).
5. Adhya, S. & Garges, S. *Cell* **29**, 287 (1982).
6. Dunn, T.M. *et al. Proc. natn. Acad. Sci. U.S.A.* **81**, 5017 (1984).
7. Wu, H.-M. & Crothers, D.M. *Nature* **308**, 509 (1984).
8. Drew, H.R. & Travers, A.A. *J. molec. Biol.* **186**, 1 (1985).
9. Nordheim, A. & Rich, A. *Nature* **303**, 674 (1983).
10. Jackson, D.A. & Cook, P.R. *EMBO. J.* **4**, 919 (1985).
11. Serfling, E. *et al. Trends genet. Sci.* **1** 224 (1985).
12. Zenke, M. *et al. EMBO J.* (in the press).
13. Irani, M.H. *et al. Cell* **32**, 783 (1983).
14. Sergeant, A. *et al. J. molec. Biol.* **180**, 577 (1984).
15. Wasylyk, B. *et al. Nucleic Acids Res.* **12**, 5589 (1984).

Tariq Enver and Roger Patient are in the Department of Biophysics, Kings College London (KQC), 26–29 Drury Lane, London WC2B 5RL, UK.

Plate tectonics

Microplates in Antarctica

from A.K. Martin

Two basic schools of thought have emerged on how Antarctica, and particularly West Antarctica, fitted against southern South America before the break-up of Gondwanaland. One suggests that Patagonia and the Falkland Plateau fit into the Weddell Sea, implying that East and West Antarctica have formed one plate since the Jurassic[1,2]. The other places East Antarctica against Mozambique and overlaps West Antarctica with the Falkland Plateau[3,4]. This overlap, which was considered unacceptable, implies that West Antarctica has moved relative to East Antarctica and thus formed a separate plate or several microplates during early break-up[5]. Palaeomagnetic evidence supported the existence of West Antarctica microplates[6]; in this issue, Mitchell *et al.*[7] provide more evidence for microplates in this region, not from West Antarctica but from the Falkland Islands on the present-day South American plate.

A wealth of seafloor spreading and fracture zone data substantiate that the Falkland Plateau has been part of the South American plate since the initiation of the South Atlantic[8,9] — its palaeoposition 125 Myr ago is well constrained. The new palaeomagnetic work, however, suggests that more than 190 Myr ago the Falkland Islands were adjacent to the Transkei coast of South Africa and that a rotation of 180° occurred between 190 and 125 Myr. As originally suggested by Adie[10], this palaeoposition aligns the Lafonian diamictite of the Falklands with the Dwyka tillite of South Africa, which forms the effective demarcation of the northern front of the Cape Fold Belt.

Although the authors concede that much more palaeomagnetic, geochronological and structural work is required to confirm the reconstruction[7], their work has much wider implications for the geology of the area. First, if the Mozambique palaeoposition for East Antarctica is adopted, then a curvilinear mountain belt (the Gondwanide orogen of Du Toit[3]) would have stretched from the Sierre de la Ventana in South America across the Cape Fold Belt in South Africa to the Trans-Antarctic mountains[3,11] (see figure). In their rotated positions, the Falkland Islands and the Ellsworth Block complete the chain — if left unrotated, they would necessitate large re-entrants in the mountain belt. Proponents of a more southerly palaeoposition of a single-plate Antarctica used such re-entrants as criticisms both of this refit and of the philosophy of aligning mountain belts[12]. Their objections now fall away.

Debate has also centred around the plate-tectonic nature of the Gondwanide orogeny. The Cape Fold Belt and its intercontinental correlates are seen as constituting a back-arc basin, with the fore-arc and magmatic terranes extending from Chile through Tierra del Fuego to the West Antarctic peninsula[11]. These latter areas are considered the source of volcanic detritus found in foreland basins on the Gondwanide continents. An alternative view is that the Cape Fold Belt, in particular, represents an intracratonic orogeny; there is a lack of nearby fore-arc or magmatic features, the metamorphic grade is low, and the small amount of crustal shortening is considered incompatible with fast-moving colliding plates[13,14].

But the stable craton of Gondwanaland must include the 1,000-Myr-old Cape Meredith complex in the Falkland Islands. The Lower Cretaceous palaeoposition of the Falklands implies a south-westward bulge in the craton and the fore-arc terranes of Tierra del Fuego — 1,500 km from the Cape Fold Belt — is considered too distant for the two areas to be linked by subduction-related orogeny[13], unless some extreme form of 'flat-plate' or low-angle subduction occurred. The rotation of the Falkland Islands to the eastern margin of South Africa removes the bulge in the craton, opening up a space in the Jurassic reconstruction (see figure) that may have been occupied by West Antarctic microplates. The distance between fore-arc terranes and the Cape Fold Belt may therefore be considerably reduced. The alignment of the fold vergences of the Falkland Plateau and the Ellsworth Block with the rest of the Gondwanide orogeny also weakens the argument[14] that large variations in fold vergences are more typical of mobile belts within continental crust than subduction-related orogenies.

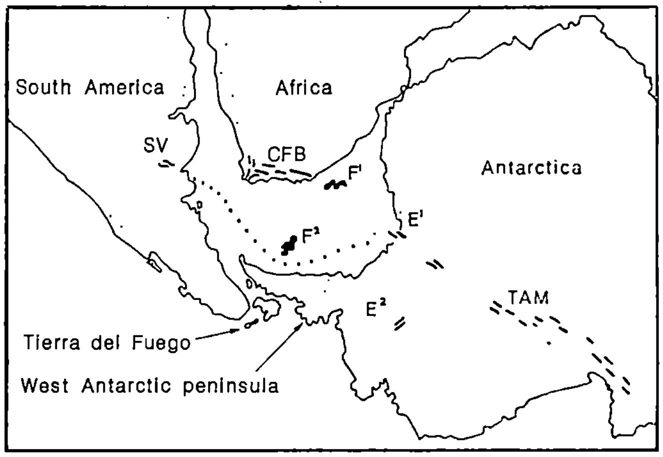

A new reconstruction of Gondwanaland[19] showing the Lower Jurassic (F^1) and Lower Cretaceous[9] (F^2) palaeopositions of the Falkland Islands. Also shown are the rotated (E^1) and unrotated (E^2) positions of the Ellsworth Block within Antarctica[6]. The dashes represent the Gondwanide Orogeny: SV, Sierra de la Ventana; CFB, Cape Fold Belt; TAM, Trans-Antarctica Mountains. The dotted line represents the southwestern bulge of the Gondwanide craton caused by the Falkland Islands in their Lower Cretaceous (F^2) palaeoposition, which is removed if the rotated (F^1) position is adopted. Note that the West Antarctic peninsula is shown in its present day position.

Although the rotation of the Falkland microplate solves some problems in south-western Gondwanaland, it raises a whole batch of new questions. How did the Falkland Islands move south-westward and rotate to their Lower Cretaceous palaeoposition? Was the movement associated with the mid-Jurassic–Cretaceous formation of the Outeniqua Basin that underlies the southern continental margin of South Africa and its apparent continuation in the central basin of the Falkland Plateau[15]? Is there some oceanic crust under the central Falkland Plateau[16]? In short, how was the Lower Cretaceous Falkland Plateau constituted?

There is evidence that some movement occurred between the South American mainland and Africa shortly before the South Atlantic opened. Pre-mid-Jurassic palaeomagnetic poles[17] suggest that South America occupied a position about 300 km west of its palaeoposition next to Africa, as shown in the figure, a position almost identical to the one it occupied in the mid-Cretaceous after 10–12 Myr of seafloor spreading in the South Atlantic[9]. This suggests that there may have been separation between the two continents followed by closure before the Lower Cretaceous opening of the South Atlantic. Did such movements involve all of South America or was there relative movement between additional microplates within southern South America? Were these movements similar to or even associated with mid-Jurassic–lowermost Cretaceous (pre-Barremian) back-arc basins in Patagonia and Tierra del Fuego?[18].

All the microplates in the area have still to be identified and their palaeopositions solved. Moreover the configuration of the Patagonian and West Antarctic subduction zones and their relationship to Gondwanaland break-up is not yet known. The subduction of varied oceanic features could have led to the offset of spreading ridges around southern Africa by long transform faults, or complicated microplate tectonics and subduction could provide an explanation for the change in vergence between the Cedarberg and southern limbs of the Cape Fold Belt.

Answers may lie in new marine geophysical data from key areas of the southern ocean and in comprehensive palaeomagnetic, petrological, structural and geochronological studies of the various plates. The new work on the Falklands microplate shows that a different approach to an apparently simple reconstruction reveals a more complicated reality. ☐

1. Harrison, C.G.A., Barron, E.J. & Hay, W.W. *Geology* 7, 374 (1979).
2. Veevers, J.J., Powell, C. McA. & Johnson, B.D. *Earth planet. Sci. Lett.* **51**, 435 (1980)
3. Du Toit, A.L. *Our Wanderering Continents* (Oliver & Boyd, Edinburgh, 1937).
4. Norton, I.O. & Sclater, J.G. *J. geophys. Res.* **84**, 6803 (1979).
5. Dalziel, I.W.D. & Elliott, D.H. *Tectonics* **1**, 3 (1982)
6. Watts, D.R. & Bramall, A.M. *Nature* **293**, 638 (1981).
7. Mitchell, C., Taylor, G.K., Cox, K.G. & Shaw, J. *Nature* **319**, 131 (1986).
8. Rabinowitz, P.D. & Labrecque, J.L. *J. geophys. Res.* **84**, 5973 (1979).
9. Martin, A.K., Goodlad, S.W., Hartnady, C.J.H. & du Plessis, A. *Geophys. J.R. astr. Soc.* **71**, 567 (1982)
10. Adie, R.J. *Geol. Mag.* **89**, 401 (1952)
11. Dalziel, I.W.D. *Geology*, **8**, 260 (1980)
12. Harrison, C.G.A., Barron, E.J. & Hay, W.W. *Geology* **8**, 262 (1980).
13. Dingle, R.V., Siesser, W.G. & Newton, A.R. *Mesozoic and Tertiary Geology of Southern Africa* (Balkema, Rotterdam, 1983).
14. Halbich, I.W. in *Geodynamics of the Cape Fold Belt* (eds Sohnge, A.P.G. & Halbich, I.W.) 177 (Geology Society of South Africa, 1983).
15. Martin, A.K., Hartnady, C.J.H. & Goodlad, S.W. *Earth planet. Sci. Lett.* **54**, 293 (1981).
16. Rabinowitz, P.D. *Geol. Soc. Am. Bull.* **91**, 655 (1980)
17. Valencio, D.A., Vilas, J.F. & Pacca, I.G. *Geophys. J. R. astr. Soc.* **73**, 135 (1983).
18. De Wit, M.J. & Stern, C.R. *Tectonophysics* **72**, 229 (1981)
19. Martin, A.K. & Hartnady, C.J.H. *J. geophys. Res.* (in the press).

A.K. Martin is at the National Research Institute for Oceanology, PO Box 320, Stellenbosch 7600, South Africa.

Pauling's model not universally accepted

SIR—John Maddox[1] has announced that Linus Pauling "has once more thrown a cat among some pigeons". This cat is a model of directed multiple twinning of a cubic crystal that Pauling[2] insists is the explanation of quasiperiodic crystals with icosahedral symmetry. Pauling's model is specific enough to be contradicted by many experimental observations from high resolution and dark-field transmissions electron microscopy, field ion microscopy, Mössbauer spectroscopy and various electron diffraction methods, most of which have been published.

For a twin model to be meaningful, the size of the individual crystals of the twin must be at least as large as the lattice parameter of 26.73 Å proposed by Pauling. The model is thereby trivially dismissed through a careful examination of the evidence already published of the high resolution (2 Å) transmission electron micrographs[3-7] which show neither twins nor cubic unit cells. There are also detailed companion diffraction data from single icosahedral orientations akin to a conventional single-crystal pattern[3-9]. Had Pauling taken the single crystal diffraction pattern of his predicted structure, rotated it into the 20 different orientations of his twinning model, and superimposed them, he would have seen immediately that his model fails to reproduce these observed diffraction patterns. Happily, contemporary crystallography has these exacting tools available to develop and verify proposed structures.

One of the most compelling observations to contradict the twinning hypothesis comes from field ion microscopy in which individual atoms are resolved[10]. The icosahedral symmetry is seen to extend over the entire field of view. Any twinning of crystals would have been observed and would have altered the symmetry.

From the beginning we viewed twinning as the obvious model within conventional crystallography[8,9] for explaining our observations. Five-fold twins of the equilibrium orthorhombic Al_6Mn phase are occasionally seen in electron microscopy and easily identified as such (D. Shechtman, unpublished data and ref. 11). Micro-diffraction from areas containing equal amounts of all the twins gives a five-fold pattern, which is clearly indexable as coming from periodic crystals and which is different from that of the icosahedral phase. As predicted, dark-field imaging from different spots in turn highlights each twin separately. Microdiffraction away from the twin boundaries clearly reveals single-crystal diffraction. However, for the icosahedral solid dark-field imaging from any spot highlights the entire grain[9]. With such evidence, supplemented by convergent beam diffraction[9,12], twinning has, for some time, ceased to be a tenable hypothesis, even for small unit cells.

Pauling has nonetheless highlighted, however inadvertently, both the ongoing intense search for models of this structure and the basic questions this poses about crystallography. Crystal periodicity has been elevated from a nineteenth century hypothesis of crystallography to the status of a law or an axiom in spite of the well-known existence of incommensurately modulated crystals. In a thought experiment any finite structure can be reproduced and stacked in a periodic array. We could make a periodic model of a glass or of the icosahedral solid by taking a large enough cube, reproducing it exactly and stacking it. If the "unit cell" is large enough, this "periodic crystal" would be experimentally indistinguishable from a glass or the icosahedral solid. Such a large unit cell model would not need to be twinned as it contains internally the required symmetry approximately.

As an aside it should be noted that, because of defects, most conventional real crystals are not truly periodic, but crystallography ignores this and recognizes the ideal. Would it then matter if the artificial periodicity of the large unit cell models was also destroyed by defects?

We have in our own work[13] used the cut and projection methods[14-17] to generate in a systematic way a sequence of periodic structures of ever-increasing periods which in the limit become truly quasiperiodic. In such a sequence, the order and structural units are apparent on a scale which remains constant once the cell dimensions have become large — that is, as the cell dimension increases, the mesh of the diffraction pattern naturally becomes finer and the diffraction pattern deviates less and less from its quasiperiodic limit. Through these studies we can examine various categories of observable differences between the quasiperiodic phase and its long periodic approximant. This enables us to see which of these are the best indicators of large unit cells. The observations on the icosahedral phase are remarkably accurately fitted by the quasiperiodic limit. Pauling's model, and its attendant requirement for *post facto* twinning, simply does not fit anywhere in this sequence.

The nth member of the cubic approximants has a unit cell which is $4.8281\,\tau^n$ Å, where $\tau=1.618034=2\cos(\pi/5)$ is the golden mean which is an important geometric constant with 5-fold axes. Lattice constants of successive approximants increase by a factor of τ. Many d-spacings in the same direction are observed to increase with this ratio, for example, 1.2765 and 2.060 Å which Pauling incorrectly assigns nonparallel indexings of 20 6 2 and 10 8 2. The fifth approximant is interesting for comparing with Pauling's model. Its lattice parameter is 53.545 Å, exactly twice Pauling's. In this cell the 2.168-Å d-spacing which is known to lie along the 5-fold axes has indexes 13 21 0, and for the m3 cubic point group has the 12-fold multiplicity required for icosahedral 5-fold axes. The exact 5-fold direction for icosahedral symmetry is $\langle 1\ \tau\ 0\rangle$. The ratio 21/13 of two successive Fibonacci numbers is an approximant to τ. The angles between the $\langle 13\ 21\ 0\rangle$ are close to what is required for icosahedral symmetry. There is no need to twin this structure to approximate icosahedral symmetry! On the other hand, Pauling assigns 12 2 2 to this spacing, that is, 24 4 4 on the doubled cell. It occurs in 24 different directions in just one of his 20 crystals. In his twinned structure the 480 spots with this d-spacing would occur in either 60 or 120 clusters depending on how much strain he allows. There are too many of them and they do not lie along the twelve 5-fold directions. Comparison with all the fifth approximant indexing shows that only the first two of Pauling's assignments are correct.

Because powder patterns are obtained from many crystals of all orientations, they do not reveal the rotational symmetries as graphically as do single-crystal patterns. By focusing on powder patterns alone, Pauling could attempt to ignore the 5-fold axes. But even the powder diffraction method reveals that many pairs of d-spacings are in ratio of the golden mean and more exact patterns would have required him to keep increasing his unit cell.

John Maddox[1] marvels at "how intuition, experience and apparently universal knowledge can be used to fashion a complicated and unknown crystal structure out of thin air". Unfortunately, complicated crystal structures cannot be fashioned out of thin air. However, Pauling's stochastic method is justly famous when the proper building blocks are used. Pauling's basic building block of aluminium dodecahedra containing the transition element at its centre was wrong chemically. It has been ruled out by Mössbauer measurement on the icosahedral phase[18]. This building block does not occur in any of the known structures of periodic crystals of aluminium with manganese, or with manganese and silicon. The ternary combination may indeed contain packing units quite similar to those that occur in the icosahedral phase[6,19], and Pauling's method using these units may be more successful.

Experimental evidence is a convincing tool for ruling out models. There is by now a wide variety of experimental evidence to rule out both twinning of any sort and all structures of conventional periodic crystals except for those near the limit mentioned above. Pauling's model can only claim a reasonable fit to the X-ray powder pattern data and is contradicted by everything else. The cat was dead. In spite of the commotion, the pigeons will endure.

JOHN W. CAHN
Institute for Materials Science and Engineering,
National Bureau of Standards,
Gaithersburg, Maryland 20899, USA
DENIS GRATIAS
C.E.C.M./C.N.R.S.,
15 rue Georges Urbain,
94400 Vitry-sur-Seine, France
DAN SHECHTMAN
Department of Materials Engineering,
Israel Institute of Technology,
Technion, 32000 Haifa, Israel

1. Maddox, J. *Nature* **317**, 417 (1985).
2. Pauling, L. *Nature* **317**, 512 (1985).
3. Hiraga, K., Hirabayashi, M., Inoue, A. & Masumoto, T. *Sci. Rep. RITU, A* **32**, 309 (1985).
4. Bursill, L. & Lin, J. *Nature* **316**, 50 (1985).
5. Portier, R., Shechtman, D., Gratias, D. & Cahn, J.W. *J. Mic. Spectro. Elec.* **10**, 107 (1985).
6. Guyot, P. & Audier, M. *Phil. Mag.* **B 52**, L15 (1985).
7. Knowles, K.M., Greer, A.L., Saxton, W.O. & Stobbs, W.M. *Phil. Mag.* **B 52**, L31 (1985).
8. Shechtman, D., Blech, I., Gratias, D. & Cahn, J.W. *Phys. Rev. Lett.* **53**, 1951 (1984).
9. Shechtman, D. & Blech, I. *Met. Trans. 16A*, 1005 (1985).
10. Melmed, A. & Klein, R. *Phys. Rev. Lett.* (submitted).
11. Zhang, Z., Ye, H.Q. & Kuo, K.H. preprint.
12. Bendersky, L. *Phys. Rev. Lett.* **55**, 1461 (1985).
13. Gratias, D. & Cahn, J.W. *Scripta Met.* (in the press).
14. Elser. V. *Phys. Rev. Lett.* **54**,1730 (1985)
15. Elser, V. *An Introduction to Quasicrystal Diffraction*, preprint (1985), AT&T Bell Lab.
16. Duneau, M. & Katz, A. *Phys. Rev. Lett.* **54**,2688 (1985).
17. Duneau, M. & Katz, A. *Quasiperiodic Patterns and Icosahedral Symmetry* preprint Ecole Polytechnique (France, 1985).
18. Swartzendruber, L., Shechtman, D., Bendersky, L. & Cahn, J.W. *Phys. Rev.* **B 32**, 1383 (1985).
19. Henley, C. & Elser, V. *Phys. Rev. Lett.* (in the press).

SIR—The icosahedral phases of alloys such as Al/Mn recently reported by Shechtman and others[1] and amply confirmed by several other groups, present many problems which are compounded by Pauling's demonstration[2] that the powder patterns can be explained as being due to a cubic structure (with $a = 26.74$ Å) which he postulates in some detail. I believe that some puzzling aspects of the situation can now be resolved.

There are two major viewpoints: (1) that the icosahedral phase is a materialization of the Penrose pattern and (2) Pauling's view, that the phase is a result of the twinning of cubic crystallites. I sketch here my reasons for preferring the former.

Normal crystal phases fall into one or other of the 230 space groups. Their diffraction effects have the three-dimensional point symmetries which are one or other of the 32 crystallographic point groups. The diffraction symmetry of the icosahedral phases is m35, which is not one of the 32 crystallographic point groups and thus the real space structure giving rise to the diffraction cannot be that of a normal crystal. What then is it? I assert that it is a particularly fine-grained and highly ordered texture corresponding to what might be called an 'icosahedral coincidence site lattice'. This might also be seen[3] as an icosahedral nematic, again perhaps the most ordered possible.

High resolution electron micrographs produced by several groups show no signs of the twin boundaries which would be necessary for Pauling's model. Twinning must therefore be at a near to atomic level.

The basic physical observation[4] is that the diffraction patterns show that there are three strong coplanar reciprocal lattice vectors (corresponding to planes of spacings 2.168, 2.060, 1.2765 Å) which lie in the directions of the 5-fold, 2-fold, 2-fold axes of a dodecahedron, respectively, and that the first is half the vector sum of the others. The indices (12,2,2), (10,8,2) and (20,6,2), allocated by Pauling, are incompatible with this. Further, Pauling allocates to strong reflections in the ratio of $1{:}\tau{:}\tau^2$ the cubic cell indices with $n = 64$, 168 and 440 which are close to the squares of 8, 13 and 21 from the Fibonacci series, but he neglects the angular relationships between the strong reflections. (Note: τ is the golden number $(1 + \sqrt{5})/2$.)

The effect of strong structure factors for planes, which would be the $(\tau, 1, 0)$ planes in a cubic cell (parallel to the faces of a regular dodecahedron), is to produce two periodicities, in the incommensurable ratio of τ, along the 2-fold axes. The published electron micrographs clearly show this irregularity. From this, everything else flows. In order to have a material structure with two such overlapping periodicities there must be a determinate or statistical rule to decide which has precedence at a particular site. The Penrose tiling is such a determinate rule.

The Penrose tiling gives a convincing indexing of the diffraction patterns[4,5], but leaves open the problem of placing atoms in the quasi-unit-cells, for which various suggestions have been made.

The essential geometry is to be found in the demonstration by Euclid that five cubes may be inscribed in a regular dodecahedron. Pauling emphasizes the cubic nature of the twinning, but gives no guidance as to how it may be continued indefinitely. The quasi-crystal view emphasizes the icosahedral quasi-lattice and provides an algorithm for indefinitely great extension.

The twin relationship arising from seeing five cubes inscribed in a dodecahedron, means that along the 5-fold axis all five cubes are viewed in the $[\tau, 1, 0]$ direction. In the three-fold view, two cubes (related as a $\Sigma = 3$ coincidence site lattice) are viewed along [111] and three along $[(1 + \tau), 1, 0]$ and in the 2-fold direction [100] for one cube and $[\tau, 1, 1/\tau]$ for four cubes. We may ask how the five structures intersect as a finite grouping and how such an arrangement may be extended.

The diffraction effects of the icosahedral phase thus resemble those of a twinned cubic texture, of a Penrose tiling and of an incommensurate structure. A quasi-lattice in N-dimensions was originally defined[6] as one where lattice points are arranged with integral coordinates with respect to more than N axes. The hexagonal Miller–Bravais system is a familiar case, but if the axial lattice vectors are incommensurate with each other, then incommensurate periods in the same direction can occur.

We assert that the Penrose tiling can be regarded as: (i) an icosahedral nematic structure, (ii) an icosahedral coincidence site lattice and (iii) a generator of homometric structures. Two structures are homometric if they have the same diffraction pattern but different structures (spatial arrangements of the scattering matter). Thus they have the same set of amplitudes for the Fourier terms but different sets of phases. (We wish to point out that these sets of phases may have symmetries different from that of the point group of the diffraction amplitudes.)

If we take threads along the 2-fold axes then the Penrose tiling may be covered (three times over) by the 15 threads, each rhombohedron being crossed by three threads, each entering through one face and leaving through the face opposite. From this it follows that the spacing of the planes of tiles with a common edge is twice the unit rhombohedral edge. In the Penrose tiling these are planes across the structure parallel to the faces of a regular dodecahedron and at these uniform intervals. The strongest diffraction line corresponds to a spacing of 2.170 Å for these planes. With the indices of Bancel *et al.*[4], this strongest plane would correspond to the layers of tiles, but the edge of the fundamental rhombohedra would be only 1.085 Å. They could thus occur only statistically. On Elser's indexing[5] the fundamental edge would be τ^3 times this, namely 4.60 Å, but the layers would then be 9.20 Å apart and it is then necessary to explain why the strongest Bragg planes have a spacing of $1/\tau^3$ times this.

The nature of the threads remains open but they may be imagined, for example, as icosahedra (of Al around Mn) sharing edges. The Penrose pattern would describe how one set of threads can pass through another.

In view of the production of the icosahedral phase by rapid cooling it is unlikely that the potentiality of the Penrose pattern to prescribe an exactly determinate structure of infinite extent is used. The problem is the classical one of packing dodecahedra which almost fit to fill space.

The diffraction properties of a quasi-lattice are subtle and unexpected. The Fourier transform of an extended one-dimensional Fibonacci series of long and short intervals (in the ratio of τ) is the same as the series itself. This is also the case in more than one dimension, and holds for those arrays of lattice points which can be derived by bounded projection from a lattice of higher dimensionality (an alternative definition of a quasi-lattice)[5]. Determination of the atomic arrangement still, as far as we know, waits for the development of a method of calculating structure factors and for the apportionment of statistical and determinate features of the texture.

Alan L. Mackay
Department of Crystallography,
Birkbeck College,
University of London,
Malet Street, London WC1E 7HX, UK

1. Shechtman, D., Blech, I., Gratias, D. & Cahn, J.W. *Phys. Rev. Lett.* **53,** 1951 (1984).
2. Pauling, L. *Nature* **317,** 512–514 (1985).
3. Nelson, D. & Sachdev, S. *Phys. Rev.* **B32,** 689–695.
4. Bancel, P.A., Heiney, P.A., Stephens, P.W. Goldman, A.I. & Horn, P.M. *Phys. Rev. Lett.* **54,** 2422–2425 (1985).
5. Elser, V. *Acta crystallogr.* (in the press).
6. Mackay, A.L. *Sov. Phys. Cryst.* **26,** 517–522 (1981) *Physica* **114A,** 609–613 (1982)

Sir—We recently presented X-ray and electron diffraction data on the icosahedral phase of rapidly quenched Al–Mn and introduced a simple indexing scheme based on the symmetry of an icosahedron (Bancel *et al.*, ref. 1 and in the press). We used our X-ray diffraction measurements to argue against models for the structure of this material that require multiple scattering from different crystallites to explain the electron diffraction patterns. Linus Pauling has proposed[2] a new crystalline model for the icosahedral phase, which he compares with X-ray powder diffraction data obtained from Shechtman and Blech[3].

In Pauling's model, the icosahedral symmetry observed in the electron diffraction patterns is accommodated by multiple twinning of cubic crystals. Although twinning makes the analysis more complicated, it is still possible to check whether the (hkl) indices given in Table 1 of Pauling's paper can be consistent with the observed electron diffraction patterns. Consider any two of Pauling's cubic vectors, which are separated by some angle ϕ. Upon twinning, each vector is rotated via a set of icosahedral symmetry operations to a new set of positions. The same twinning operations act upon both cubic vectors, so that the angle ϕ is preserved during rotation. If one now calculates the angle that the vectors of one icosahedral set make with the vectors of the other set, the angle ϕ should certainly appear. Pauling's model fails this test on nearly all counts[1]. Thus, the icosahedral diffraction spots cannot be attributed to rotations of the cubic structure which Pauling proposes.

Pauling states that the agreement between the X-ray peak positions of Shechtman's data and the d-spacings predicted by his model provides compelling evidence that his structure is the correct one. We are not convinced by this argument because we believe that seven of the peaks he indexes are actually due to a different phase present in the sample. We have measured X-ray powder diffraction patterns from a large number of rapidly quenched icosahedral alloys, and find that reflections 3,4,6,8,10,15, and 16 listed in Pauling's Table are due to a contaminant phase that appears when excess Si is present in the sample. These peaks are not found in the electron diffraction patterns. (Note that Shechtman's sample contained several atomic % Si). We feel that this fortuitous agreement of several spurious peaks is an argument for the hypothesis that *any* powder diffraction pattern can be indexed via a sufficiently large cubic unit cell.

The question remains as to whether a crystal structure incorporating a large unit cell might still describe the electron and X-ray diffraction data. Based on recent low angle electron and X-ray diffraction data we can specify a minimum size for any proposed cubic unit cell. For any periodic structure the squares of any two d-spacings must be in integer ratios unless the corresponding diffraction spots have the same symmetry (so are collinear) in which case the ratio of the d-spacings is a ratio of integers. We have observed two such spots which lie along the major axes of the 2-, 3-, and 5-fold symmetry planes with d-spacings of 8.85(7) and 5.42(3)Å, the ratio of which is 1.633. The lowest rational approximate, within experimental error, to this number, is 13/8. This implies a minimum cell size of a_0=8(8.85Å)=71Å. A 27Å cubic unit cell cannot produce two *collinear* spots with these radii even with the inclusion of multiple twinning. Although our arguments are stated in the context of a twinning model, numerous high resolution microscopy measurements vitiate the possibility of twins in these structures. In the absence of twinning our limit of 70Å as a minimum cell size holds and is valid for any crystal symmetry. A crystal structure adhering to this criterion would have to include well over 10,000 atoms in its unit cell.

Finally, we find somewhat curious Pauling's statement that "Crystallographers can now cease to worry that the validity of one of the accepted bases of their science has been questioned". No one has seriously questioned the premise that fivefold or icosahedral symmetry is inconsistent with periodic translational order. Rather, it has been observed that particular arrangements of atoms without simple periodic translational order and with crystallographically disallowed symmetries may nonetheless give rise to sharp diffraction patterns[4]. The study of "quasicrystalline" structures is mathematically intriguing. Furthermore, even if all the phases of Al–Mn should turn out to be crystalline, the theory of quasicrystalline materials may well provide clues to the properties of materials that have local icosahedral symmetry.

Peter A. Bancel
Paul A. Heiney
Department of Physics and Laboratory
for Research on the Study of Matter,
University of Pennsylvania,
Philadelphia, Pennsylvania 19104, USA
Peter W. Stephens
Department of Physics,
State University of New York,
Stony Brook, New York 11794, USA
Alan I. Goldman
Physics Department,
Brookhaven National Laboratory,
Upton, New York 11973, USA

1. Bancel, P.A. Heiney, P.A. Stephens, P.W., Goldman, A.I. & Horn, P.M. *Phys. Rev. Lett.* **54,** 2422 (1985).
2. Pauling, L. *Nature* **317,** 512 (1985).
3. Shechtman, D. & Blech, I. *Metal Trans,* **16**A, 1005 (1985).
4. Levine, D. & Steinhardt, P.J. *Phys. Rev. Lett.* **53,** 2477 (1984).

Sir—In the analysis of apparent icosahedral symmetry of Al–(Mn–,Fe–) alloys by Pauling[1] one observation remained unaccounted for. Mössbauer data of Swartzendruber *et al.*[2] indicate the presence of two type of sites for the transition metal. The occurrence ratio was found to be close to the golden mean $(\sqrt{5}+1)/2=1.61803$. In the model of an aperiodic "icosahedral phase" this can be easily explained by two types of differently distorted icosahedra. In order to fill the three-dimensional space in the sense of the 5-fold Penrose tile the occurrence ratio of two different elements should be exactly the golden mean.

On the other hand, in the Pauling's picture of multiple twinning of cubic crystal the growth process can be seen as starting from the 12-vertex icosahedral seed (Fig. 1 of ref. 3), with the next layer being dodecahedral (20 atoms). In any structure based on these two mutually complementary polyhedra the occurrence ratio of 20/12=1.667 could be expected for different types of lattice sites. But this ratio differs from the golden mean by only 3%.

A plausible suggestion is, therefore, that Swartzendruber *et al.*[2] did, in fact, observe the above ratio (20/12) rather than the golden mean. If this is the case, then the dilemma between the "icosahedral phase" and Pauling's model based on a cubic cell could be resolved by the Mössbauer experiment with the peak intensity resolution greater than 3%.

A.A. Berezin
Department of Engineering Physics,
McMaster University,
Hamilton, Ontario,
Canada L8S 4M1

1. Pauling, L. *Nature* **317**, 512 (1985).
2. Swatzendruber, L.J., Shechtman, D., Bendersky, L. & Cahn, J.W. *Phys. Rev.* B **32**, 1383 (1985).
3. Bergman, G. Waugh, J.L.T. & Pauling, L. *Acta crystallogr.* **10**, 254 (1957)

Taking culture seriously

Philip Kitcher

Culture and the Evolutionary Process. By Robert Boyd and Peter J. Richerson.
Chicago University Press: 1985. Pp.331. $30, £25.50.

FOR true believers in biology as the key to understanding human behaviour, "culture" is a word that cowards use. Sociobiological zealots maintain that the invocation of culture as an evolutionary force obfuscates Darwin's insight that human behaviour is the product of evolution. At the other extreme are those who refuse to commit social science, protesting that the combined efforts of anthropologists, sociologists and mislocated biologists teach us far less about human nature and human conduct than the observations of a Shakespeare or a Stendhal. Human culture, they declare, is too complex for analysis, and it radically transforms the simple forms of behaviour we have inherited from hominid or prehominid ancestors. Between the militant sociobiologists and the despondent sceptics lies a large territory, explored by a small number of scholars who hope to take human culture seriously and to analyse its evolutionary effects. Robert Boyd and Peter Richerson have charted some of this territory with exemplary skill and determination.

Culture and the Evolutionary Process addresses two general problems. Boyd and Richerson want to understand the evolutionary effects of various systems of cultural transmission, conceived as systems in which individuals may acquire phenotypic characteristics at least partly as a result of imitating any number of cultural "parents" or "models". They attempt to identify the various forces that can preserve or change the distribution of traits across the generations of a population having a system of cultural transmission. Their second general question concerns the possibility of maintaining systems of cultural transmission under ordinary selection.

The second question arises because Boyd and Richerson see their book as a (polite) debate with conventional human sociobiologists. (In my view, the deference is overdone and the differences understated.) If it were shown merely that certain conditions of cultural transmission might lead members of a population to forms of behaviour distinct from the sociobiological optima, then there would be a simple retort: where cultural transmission proves maladaptive, selection will work to eliminate it; hence culture can only be maintained when it helps to amass evolutionary capital; we may fathom human behaviour by looking at reproductive uccess and forgetting culture.

The book tackles its main questions by mathematical analyses and discursive reviews of findings from psychology, anthropology and sociology. The mathematics is intended to pinpoint the conditions under which various kinds of evolutionary processes can occur. In particular, the authors want to specify the circumstances that would allow for characteristics detracting from genetic fitness to become prevalent. Their surveys of the social sciences are to provide motivation for the mathematical models they construct and to suggest that it is possible, even likely, that the conditions for the maintenance of genetically maladaptive behaviour may be met.

Inspired by Lewontin's well-known account of the structure of population genetics, Boyd and Richerson begin with a representation of an idealized life-cycle in which genetic and cultural transmission jointly affect the distributions of genotypes and phenotypes in descendant generations (pp.5–6). The representation raises at once the obvious possibilities that the book will explore. Does the existence of more than two cultural "parents" make a difference? What are the features of blending and non-blending cultural inheritance? How does imitation interact with individual learning? What happens if the traits that make someone culturally influential differ from those that promote reproductive success? Should we expect that people will be more likely to be influenced by those who have fitness-enhancing characteristics? When will it pay to follow the majority?

The authors develop their basic account of cultural transmission by simplifying ideas worked out in great detail by Cavalli-Sforza and Feldman. Imagine that people are "enculturated" by a fixed number of individuals playing different roles, and that each role has a weight in the transmission of a characteristic. The occupant of each role may have or lack the characteristic. Consider any possible combination. There will be a probability that a person "enculturated" by that sequence of cultural parents will acquire the characteristic. The system of cultural transmission may be identified by specifying the probabilities for all the possible combinations. As the authors note, this approach to systems of cultural transmission allows them to represent both blending and non-blending inheritance.

Analogues of genetic mutation and drift are easily introduced into the basic picture (pp.67–69). But the interesting disruptive forces are those to which Boyd and Richerson devote most attention. The first involves a contrast between individual and social learning. Imagine that the young acquire their adult behaviour by striking a compromise between imitation and individual attempts to learn. If cultural transmission operated unconstrained it would lead them to adopt a certain value of a behavioural parameter; their own efforts lead them to an estimate (possibly error-infected) of the optimal value of the parameter; the adult behaviour expresses a weighted average of the two. Boyd and Richerson show that this scenario involves a force that will increase the frequency of traits favoured by learning, a force they call "guided variation" (pp.95–97). Since the effect of guided variation is adaptive when the individuals are good at determining the best value of the behavioural parameter, it is natural to ask if natural selection will allow for a non-zero weight to be assigned to cultural transmission. The authors give a rigorous demonstration of the intuitive idea that errors in learning and costs of learning may outweigh possible benefits of distrusting tradition. Sometimes the wise child should agree that teachers know best.

Just as guided variation can mimic natural selection, so too can another force that Boyd and Richerson discuss at length. Suppose there is genetic variation with respect to the propensity for imitating traits that lead to reproductive success. Then we can expect selection to favour alleles whose bearers follow the fit. As the authors put it, if guided variation and direct bias were the only forces that shape cultural evolution, then ". . . with the usual caveats, we would be able to predict cultural variation by asking what increases genetic fitness" (p.157).

But it is the power of other forces that is the central theme of the story. Boyd and Richerson propose three ways in which culture can favour the genetically maladaptive. Individuals may base their behaviour on the conduct of those around them. If this occurs, the authors suggest, there may be an analogue of group selection which allows for the evolution of cooperative arrangements. Second, there may be indirect bias, in which some forms of behaviour give a person high status as a model, with the result that other, correlated, traits are also imitated. (Intuitively, the process is analogous to genetic linkage.) Boyd and Richerson offer an analysis of indirect bias, arguing that it can have effects like those of runaway sexual selection. The third force is the simplest. Transmission systems are said to be "asymmetric" if they favour different traits. If the characteristics that make one a successful cultural "parent" are incom-

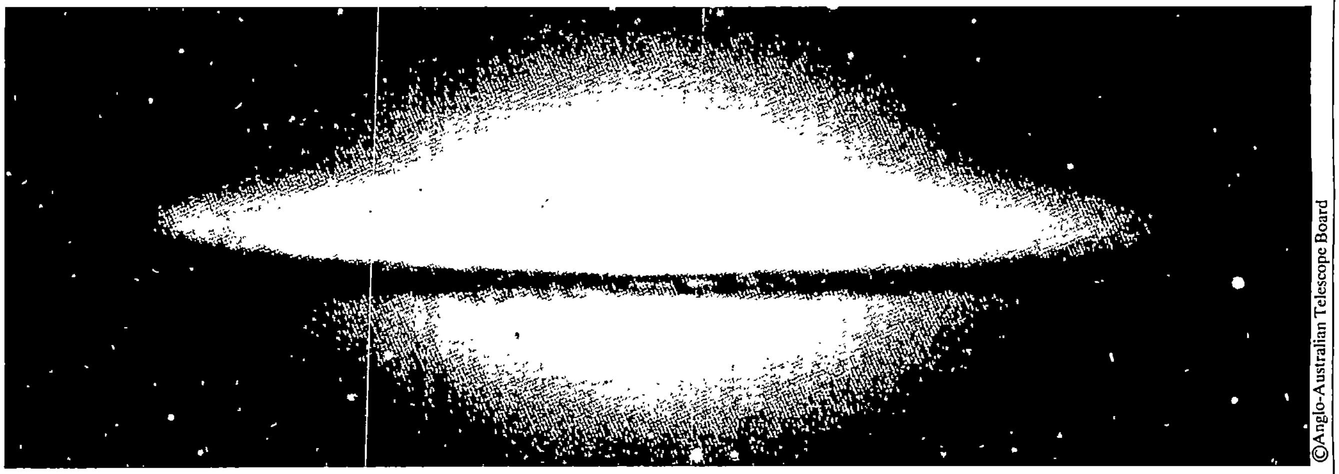

Edge of darkness: the aptly named Sombrero Galaxy, in Virgo (the "brim" is the dust lanes of the galaxy's central plane). The photograph is reproduced from Peter Cadogan's From Quark to Quasar: Notes on the Scale of the Universe, *recently published by Cambridge University Press, a highly illustrated journey from the human scale to the very large and the very small. Price of the book is £12.95, $24.95.*

patible with some that promote reproductive success, then it is possible for culture to disrupt the smooth workings of natural selection.

The main thrust of *Culture and the Evolutionary Process* can be appreciated by focusing on this last force. Boyd and Richerson construct a sequence of analyses (purchasing decreases in artificiality with increasing complexity) in which they identify precise conditions for the maintenance of a maladaptive trait. As we might expect, selection against the trait has to be relatively weak and the competition for dominant cultural role relatively intense. (The authors tell us *how* weak and *how* intense.) Now comes the sociobiologists' challenge: if cultural transmission is asymmetric with respect to genetic transmission, will selection eliminate it in favour of a system that will reward reproductive success? Not necessarily, claim Boyd and Richerson. For there may be indirect constraints that force certain reproductively successful individuals out of the competition for cultural influence, as well as direct benefits deriving from "enculturation" by a large sample of the local population (pp.188–190).

The authors sum up in a typically modest and cautious way. After noting that their analyses "suggest that asymmetric cultural transmission may cause human evolution to diverge from the predictions of sociobiological theory", they add: "Whether and to what extent it does is an empirical problem" (p.199). More self-congratulatory writers might have seen themselves as constructing a framework within which alternative hypotheses about human behaviour and its evolution could at last be formulated and tested against one another. For what Boyd and Richerson do is to show that there are far more things in the evolutionary process than are dreamed of by most sociobiologists.

Perhaps the chief danger is not that this book will languish unread but that it will serve as the gospel for a new social scientific creed. Reformed sociobiologists may confute their sceptical opponents by announcing that Boyd and Richerson have solved the problem of culture. But the authors themselves claim far less, and rightly so, for there are important questions on which they touch either scantily or not at all.

Consider the focus on cultural transmission. Quite early on, Boyd and Richerson commit themselves to the idea that "culture can profitably be viewed as a system of inheritance" (p.19). But is the entire effect of culture on human evolution to be represented in terms of the transmission of traits that individuals can acquire or reject? Many social institutions are hard to represent in such terms (think of apartheid). Moreover, such institutions frequently have the effect of assigning the members of certain subpopulations to radically different microenvironments with large consequences both for the phenotypes that develop and for the determinants of fitness (again, think of apartheid). Boyd and Richerson step gingerly around the controversy about holism and reductionism without explaining how they plan to treat features of human society such as these.

A second limitation concerns the issue of linkage among cultural traits. One of the banal facts of life is that choices constrain. Certain forms of behaviour preclude others. Moreover, the choices that a person makes are affected both by the actual constraints and those that are perceived to exist. Once these truisms are given their due, we see that there is a type of linkage, possibly important, besides that captured in Boyd and Richerson's indirect bias. To adapt the analogy, the course of evolution at one cultural "locus" may have effects on what happens elsewhere. Further, the ability to free oneself from some constraints might itself be shaped by selection. Perhaps there are adaptive advantages in being able to perceive certain logical and probabilistic connections.

Culture and the Evolutionary Process inherits from traditional sociobiology the habit of treating particular pieces of human behaviour as if they were individually shaped by the evolutionary process. In presenting new mathematical ideas this may simply be pardonable simplification (although the discussion of challenges to adaptationism on pp.282–283 is uncharacteristically superficial). Nevertheless, as social scientists consider the possibility of applying these ideas to aspects of human behaviour, it is crucial to appreciate the possibility that the proximate mechanisms of a piece of behaviour may be implicated in many areas of our social lives. Informative recent studies in descriptive anthropology have sometimes been accompanied by a superfluous and irritating descant to the effect that minute details of behaviour enhance reproductive success. It would be sad if Boyd and Richerson's pioneering efforts spawned a mindless pseudo-adaptationist programme, in which developmental and proximate constraints were ignored and the optima of the new mathematical analyses perceived everywhere.

This book does not iron out a minor wrinkle in the biology of human social behaviour. Rather it addresses one major part of an enormous problem, and it does so with erudition, rigour and imagination. *Culture and the Evolutionary Process* is not easy going, but it deserves a broad readership and a lasting influence. With luck we may one day transcend the dialogue between simplistic reductionism and despairing scepticism. ☐

Philip Kitcher is Director of the Minnesota Center for the Philosophy of Science, University of Minnesota, Minneapolis, Minnesota 55455, USA. His most recent book is Vaulting Ambition: Sociobiology and the Quest for Human Nature *(MIT Press, 1985).*

nature

FIRST CONFERENCE IN JAPAN

◎January 20 ⇛ 22, 1986
◎Keio Plaza Hotel, Tokyo, Japan

ture is pleased to
nounce a conference on
future of molecular
logy and its applications
iotechnology and
dicine, to be held at the
io Plaza Hotel, Tokyo,
January 20-22, 1986.
conference will be
dressed by distinguished
lecular biologists from
United States, Europe
Japan.

e speakers from the
ited States will include
bel Prize winners **James
Watson** *(Cold Spring
rbor)*, who (with F.H.C.
ck) first suggested the
ucture of DNA, and
lter Gilbert *(Harvard
iversity)*.
ier speakers include:
nley Cohen *(Stanford
iversity)*
m Blundell *(Birkbeck
lege, London)*
J. Peacock *(CSIRO,
berra)*
Walter Gehring *(University of Basel)*
Richard Lerner *(Scripps Clinic, La Jolla)*
Sydney Brenner *(Laboratory of Molecular Biology, Cambridge)*
Susumu Tonegawa *(Massachusetts Institute of Technology)*
Shosaku Numa *(Kyoto University)*
Tasuku Honjo *(Kyoto University)*
Ken-ichi Matsubara *(Osaka University)*
Yoshiki Hotta *(University of Tokyo)*
Mitsuaki Yoshida *(Cancer Research Institute)*
Tadatsugu Taniguchi *(Osaka University)*
Hisayuki Matsuo *(Miyazaki Medical College)*
Tokindo Okada *(National Institute for Basic Biology)*
Hal Weintraub *(Hutchinson Cancer Center, Seattle)*

The three main topics to be covered by the conference are

- **Molecular biotechnology**
- **Development and regulation**
- **Immunology and virology**

and the programme is being designed to provide an opportunity for those working in industry, medicine or academic research to bring themselves up to the forefront of research through discussion with world leaders. There will be ample time for questions and discussion. Simultaneous translation services into English and Japanese will be available.

Registration fees:
Y100,000

Full details are available from:
Nature Conference Secretariat
International Conference Organizers, Inc.
103, Crescent Plaza
4-6, Minami-Aoyama 2-chome
Minato-ku
Tokyo 107 Japan
Tel: 03-470-3766
Cable: CONFERENCEORGAN TOKYO

Bursaries for young people have been graciously donated by the following companies:

Ajinomoto Co., Inc.
Asahi Chemical Industry Co., Ltd.
Chugai Pharmaceutical Co., Ltd.
Daiichi Seiyaku Co., Ltd.
Dainippon Pharmaceutical Co., Ltd.
Eisai Co., Ltd.
Fujisawa Pharmaceutical Co., Ltd.
Kanebo Ltd.
Kureha Chemical Industry Co., Ltd.
Kyowa Hakko Kogyo
Meiji Milk Products Co., Ltd.
Mitsubishi Chemical Industries Ltd.
Nippon Kayaku Co., Ltd.
Nitto Chemical Industry Co., Ltd.
Sankyo Co., Ltd.
Shionogi & Co., Ltd.
Sumitomo Chemical Co., Ltd.
Suntory Ltd.
Taisho Pharmaceutical Co., Ltd.
Takeda Chemical Industries Ltd.
Teijin Ltd.
Toray Industries Inc.
Yakult Honsha Co., Ltd.
Yamanouchi Pharmaceutical Co., Ltd.

MOLECULAR BIOLOGY BECOMES BIOTECHNOLOGY

Announcing the first issue of an exciting new journal. . .

Biology & Philosophy

Editor: MICHAEL RUSE, *University of Guelph, Canada*

The First Issue Contains:

John Collier: Entropy in Evolution. **Paul M. Churchland:** Cognitive Neurobiology: A Computational Hypothesis for Laminar Cortex. **Ullica Segerstrale:** Colleagues in Conflict: An 'In Vivo' Analysis of the Sociobiology Controversy. **Ivan T. Frolov:** Genes or Culture? A Marxist Perspective on Humankind. **The Editors:** Review Article: The Nature of Selection: Evolutionary Theory in Philosophical Focus by Elliott Sober. **George G. Williams:** Comments on 'The Nature of Selection'. **Elliott Sober:** Reply to George Williams. **Michael Ruse:** Booknotes.

Subscription Information ISSN 0169-3867
Volume 1 (4 issues)
Institutional rate: Dfl. 196.00/US $ 70.00 incl. postage/handling
Private rate: Dfl. 72.00/US $ 26.00 incl. postage/handling

Free sample copies available on request.

D. Reidel Publishing Company

P.O. Box 322
3300 AH Dordrecht
Holland

Falcon House
Queen Square
Lancaster, LA1 1RN
England

Reader Service No.3

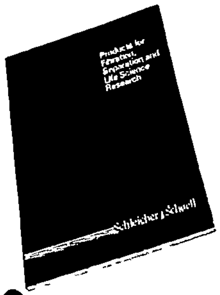
Products for Filtration, Separation and Life Science Research
Schleicher & Schuell

Free.
And easy.

The all new 100-page full-color catalog from S&S.

Get your free S&S catalog, "Products for Filtration, Separation and Life Science Research". This easy-to-use reference guide includes complete descriptions and ordering information for all S&S products—for nucleic acid and protein research, clinical research and diagnostics, and analytical and general laboratory filtration and separation. Send or call for your copy today.

Name__________ Title__________
Organization__________ Dept.__________
Street__________
City__________ State______ Zip______
Phone (____)__________

Schleicher & Schuell
Keene, New Hampshire 03431
(800) 245-4024 • (603) 352-3810

Reader Service No.1

MACMILLAN 1985/6 ACADEMIC BOOK SALE

The following selection of books at greatly reduced prices may now be ordered from all major bookstores. This offer is open until 28th February 1986 only. Order now using the spaces provided below.

____**International Mortality Statistics**	P. Alderson	23969 5	(£47.00) £14.95
____**Biochemistry of Parasitic Helminths**	John Barrett	25669 7	(£12.95) £3.95 (paperback)
____**Urban Air-Pollution Modelling**	Michael M. Benarie	23391 3	£35.00 £17.50
____**Birth Defects Compendium**	Daniel Bergsma (ed.)	27876 3	(£50.00) £25.00
____**Polar Dielectrics and Their Applications**	Jack C. Burfoot and George W. Taylor	17958 7	(£20.00) £6.95
____**The Ultimate Software Selector**	Federation of Micro System Centres	37556 4	(£9.95) £2.95
____**Environmental Factors in Mammal Reproduction**	Desmond Gilmore and Brian Cook (eds.)	24150 9	(£25.00) £8.95
____**X-Ray Microanalysis**	M. A. Hayat	32355 6	(£30.00) £9.95
____**Horticultural Reviews Volume 4**	Jules Janick (ed.)	34192 9	(£25.00) £8.95
____**The RAE Table of Earth Satellites, 1959-1982, 2nd Ed.**	D. G. King-Hele, J. A. Pilkington, D. M. C. Walker, H Hillier and A. N. Winterbottom	35374 9	(£50.00) £25.00
____**Hydrogen and Energy**	Charles A. McAuliffe (ed.)	18432 7	(£12.00) £4.95
____**Plant Galls of India**	M. S. Mani	18067 4	(£12.50) £3.95
____**The Design of Air Quality Monitoring Networks**	R. E. Munn	30460 8	(£20.00) £6.95
____**Growth Without Ecodisasters?**	Nicholas Polunin (ed.)	23521 5	(£22.50) £5.95
____**The Arctic Ocean: The Hydrographic Environment and the Fate of Pollutants**	Louis Rey (ed.)	31017 9	(£45.00) £12.50
____**Developmental Psychology and Society**	John Sants (ed.)	21340 8	(£20.00) £6.95
____**Cancer and the Environment**	L. A. Sobel (ed.)	28591 3	(£15.00) £4.95
____**The Fast Breeder Reactor – Need? Cost? Risk?**	Colin Sweet (ed.)	27973 5	(£20.00) £6.95

Please complete and return this form to your bookseller, or in case of difficulty to: **Macmillan Distribution Ltd, Houndmills, Basingstoke, Hampshire RG21 2XS, UK.**

Please supply ______ titles as indicated

☐ Please invoice me. Postage and packing £1.00 per title.

☐ I enclose a cheque for £__________

☐ Charge £______ to my credit card as shown. Access/Visa/Amex/Diners Club

Card No. __________ Expiry Date ______
Signature __________
Name (capitals) __________
Address (capitals) __________

This offer is not applicable in USA.

M MACMILLAN PRESS LTD.
Houndmills, Basingstoke, Hants RG21 2XS, UK. M

More than perceptive

P.W. Hawkes

Pattern Recognition: Human and Mechanical. By Satosi Watanabe. *Wiley: 1985. Pp.570. $44.95, £46.*

PATTERN recognition has always been an uneasy subject. There is no obvious definition of "pattern" to fit everything that is grouped within the subject—letters and numbers and the characters of such languages as Chinese and Japanese, chromosomes, ship or aircraft profiles, types of terrain as seen from above, human cell categories, the list is as long as it is varied. It is even more difficult to tie down "recognition", for the idea is closely linked to the human faculty of recognition; the latter is so extraordinary that any attempt to emulate or simulate it at other than a trivial level seems inconceivable. Typists perform stupefying feats of pattern recognition on hand-written material; and once one begins really to think about the problems, it seems that the schoolteacher is performing a much more formidable task in recognizing his new intake of pupils each year than in acquiring his diplomas and degrees.

These difficulties have meant that, unlike most subjects of a primarily mathematical nature, pattern recognition has generated a considerable literature of a philosophical kind, devoted not so much to methods of performing pattern recognition tasks by computer as to understanding what such tasks involve, indeed, to understanding what the brain is doing as it tries to perform them. In this large and difficult book, Professor Watanabe has gone more deeply than most into such questions.

The volume is dedicated "To Dorothea for her patience and cheerful encouragement" and the reader may well sigh for a similar companion for the text is very difficult going, largely because of the language employed: it is inevitable that a young and complicated subject will need some new vocabulary, but it is not necessary to adopt the habits of the least literate kind of sociological writing. All too often Professor Watanabe falls into this style, with the result that some passages are so (linguistically) opaque as to be almost impenetrable. This is sad because, even if obscured by the language in which they are conveyed, the ideas brought together here deserve to be pondered carefully by practitioners of the subject. We are led through a number of ways of regarding the notion of pattern, with a host of down-to-earth examples, ranging from the conceptual (pattern recognition as seeing-one-in-many, as perception, as value-orientated ponderation) to the more overtly mathematical (pattern recognition as entropy minimization, as covariance diagonalization, as discrimination, as structure analysis).

Watanabe expects his readers to work hard, for they must not be daunted by encounters with sensory physiology, classical philosophy or thermodynamic reasoning; they must be at ease with the formidable notation of formal logic; and they must be happy with linear algebra and statistical decision theory. The author does try very hard to explain everything as he goes along, but the more the reader knows beforehand of the tools employed, the more benefit he will gain from the text and the greater will be his admiration for the way the numerous threads are woven together to produce — the metaphor is well-deserved — a very impressive pattern.

This, then, is a rich and densely filled book, occasionally verbose and unconsciously elliptical but exciting and definitely worth the effort demanded in reading it. Pattern recognition will presumably be tamed over the decades as our understanding of the mathematical and cognitive processes involved advances. I suspect that readers who then turn back to their precursors' books will be impressed by the ability of Watanabe to see where the problems lie and to shed some light on their nature at so primitive a stage of the subject. □

P.W. Hawkes is Maître de Recherche at the Laboratoire d'Optique Electronique du CNRS, BP 4347, F-31055 Toulouse Cedex, France.

Developing concepts

Raymond D. Lund

Molecular Bases of Neural Development. Edited by Gerald M. Edelman, W. Einar Gall and W. Maxwell Cowan. *Wiley: 1985. Pp.606. $85, £87.50.*

RESEARCH on the development of the nervous system has for many years been constrained by techniques which are largely inadequate, especially when compared with the richness of theories offered by early generations of scientists. Now, however, we have the exciting opportunity to define and sequence antigens of developmental significance, to collect cDNA libraries and to study the molecules responsible for assembling the extraordinary structures which make up the nervous system.

There was, therefore, good reason for the Neurosciences Institute of New York, a leading body in the world of the neurosciences, to assemble a symposium around this new research initiative, and to prepare this, its fourth major publication since its inception in 1981.

The book is divided into six sections concerning early development, glia and neurone guidance, neural crest, formation of neurites and synapses, maps and retinotectal system and, finally, gene expression, "primary processes" and behaviour. An elegant introduction by Cowan summarizes the history of work on neural development, and in the last few sentences emphasizes the excitement ahead as this field increasingly becomes the province of molecular biologists.

The introduction is followed by a well-written set of essays by some of the most distinguished investigators currently working in this area. A wide variety of material is covered. For example, given the new insight provided by studies of the adhesion molecule, N-CAM, Rakic has re-examined the field of cerebellar development in which he was heavily involved some years ago. Many articles such as those of Edelman, Letournean, Goodman, Gershon and Schmidt review the current thrust of research in their laboratories. Yet others have reviewed fields to which they have contributed a smaller part. The diversity of approaches and the content of many of the articles make for interesting reading. None of them is dull and most are easily accessible to readers with only a limited background in developmental neurobiology.

As with all volumes which arise from a meeting, the book cannot hope to be comprehensive. However, one wonders, despite the justifications offered, why a fifth of it is devoted to the retinotectal system, a topic that has perhaps suffered from overexposure (and one ironically in which the developmentally significant molecules suggested over 40 years ago still elude identification). Surprisingly, little space is devoted to areas such as transmitter modulation, growth factors, acetylcholine receptor ontogeny, development of cell identity and genetic controls of development.

Indeed the amount of space devoted to molecular biology is quite small. This is in marked contrast to the Cold Spring Harbor Symposium of 1983 on molecular neurobiology. It is a pity also that no one thought to write a summary to balance Cowan's introduction, outlining how our present state of knowledge might be extended and how the approaches presented at the symposium might develop in the light of the recent technical and conceptual advances.

To summarize, it must have been a marvellous symposium and the book presents an elegant set of essays on neural development — among the best of their kind — but it only rarely enlightens on the molecular bases of development. □

Raymond D. Lund is in the Department of Anatomy and Cell Biology, University of Pittsburgh School of Medicine, Pittsburgh, Pennsylvania 15261, USA.

Cycling back to the beginning

Michael Whitfield

The Carbon Cycle and Atmospheric CO_2: Natural Variations Archean to Present. Edited by E.T. Sundquist and W.S. Broecker. *American Geophysical Union: 1985. Pp.627. $28.*

It is refreshing — although somewhat disconcerting — for someone involved in the investigation of the contemporary global CO_2 cycle and its possible climatic effects to view the problem from a much broader perspective. This volume jolts the reader into considering such a wider view by presenting a stimulating potpourri of ideas on the direction, cause and consequences of natural fluctuations in atmospheric CO_2 levels over the past 3.5×10^9 yr.

There are more than 40 papers, replete with useful data and providing intriguing insights into the response of different feedback systems to perturbations in the global carbon cycle over timescales varying from tens of thousands to hundreds of millions of years. The papers themselves have been edited thoroughly, and the text is clearly presented and well illustrated. The overall structure, too, is well conceived, in that the contents list is organized into five sections which move progressively further back in time. The first section is intended to link present-day concerns to the geological perspective while subsequent sections take the reader in turn through the last glaciation, the Pleistocene, the Cenozoic, and finally the Phanerozoic and Precambrian. There is a wealth of information here which, however, is unfortunately difficult to dig out because the book has no index and the papers within each section do not necessarily follow a logical sequence. Furthermore the sections identified in the contents list are not explicitly identified in the text, so that the browser finds himself slipping unwittingly from one timescale to another.

The first three sections cover the past 5×10^5 yr and mainly deal with the use of the carbon and oxygen isotope records in ice cores and in deep-sea sediments to elucidate the role of the oceans in controlling fluctuations in atmospheric CO_2 levels. Only one paper deals with the influence of the terrestrial biota on carbon storage. There are many absorbing accounts here of the potential and pitfalls of isotopic techniques for estimating atmospheric CO_2 levels, ice volumes, palaeoproductivity and palaeocirculation patterns. Over this timescale, orbital variations appear to trigger changes in atmospheric CO_2 levels which are, in turn, followed by changes in ice volume.

During the Cenozoic (10^8 yr), processes such as volcanism, tectonic movement, continental weathering and organic carbon burial begin to assume a dominant role. In addition to isotopic clues, crises in the biological record characterized by mass extinctions provide useful markers against which to assess the interaction between the biota and the atmosphere. Surprisingly, only the Cretaceous/Tertiary event is considered here, although the discussion is spiced by the presentation of two conflicting hypotheses (planetismal impact and mantle outgassing).

Geochemical models for CO_2 control in the Phanerozoic are covered in some detail in the final section, but the treatment of the Precambrian is rather sketchy so that only 15 per cent of the book as a whole considers the first 99.75 per cent of geological time! The overall picture suggested is of a punctuated fall from atmospheric CO_2 concentrations one hundred times the present level 3×10^9 yr ago, through a value approximately ten times the present level 10^8 yr ago, to a pre-industrial value only 80 per cent of the present level. The burial and preservation of organic carbon has played a primary role in this decline — a factor which geochemical modellers are now taking into account.

This is a fascinating collection of papers which will repay the effort required for specialist readers to pick their way through such a variety of information. The cost is very reasonable, and one can hope that many individuals will buy the book and use it to help them place the current ferment in atmospheric CO_2 research into a proper perspective. ☐

Michael Whitfield is a Senior Principal Scientific Officer at the Marine Biological Association of the UK, The Laboratory, Citadel Hill, Plymouth PL1 2PB, UK.

Uncertain alliance

Charles Tanford

The Physical Chemistry of Membranes: An Introduction to the Structure and Dynamics of Biological Membranes. By Brian L. Silver. *Allen & Unwin: 1985. Pp.396. £45, $60.*

To present a concise account of all physico-chemical aspects of membranes in a single book, suitable for students and beginning researchers, is difficult because membrane physical chemistry comprises two quite different bodies of knowledge. One centres on the structure and molecular dynamics of the membrane, and includes the physical methods (nuclear magnetic resonance, neutron scattering etc.) used for structural investigations but should also include some account of the molecular interactions that hold the membrane together. The other part centres on the physical chemistry of membrane function, and is chiefly thermodynamic and kinetic in its approach to questions of membrane potential, permeability, and carrier or protein mediated transport. Conventional wisdom suggests that these two fields might be better tackled by separate authors in separate books.

Dr Silver's book attempts to include all these topics but regrettably cannot be recommended for either structural or functional information. Its broad organization is good: 18 chapters with appropriate titles. Within each chapter, unfortunately, there is insufficiency, often chaos, sometimes error, and always a flippant haphazardness as to what is selected for discussion and what is omitted, who is cited and who is not. The entire book has only 378 pages of text which includes 125 figures, many of them full page.

The better chapters are one that deals with order and disorder, as seen by nuclear magnetic resonance and electron spin resonance; one on intermolecular forces, which includes a mathematically detailed section on van der Waals' forces; and one on fluctuations, which includes an introduction to stochastic processes. Order/disorder is in part explained by picturesque images (a box of uncooked spaghetti, a pile of sleepy earthworms) that may be helpful to some students.

The poorer chapters are those that deal with solution physical chemistry (thermodynamics, kinetics, diffusion, membrane potential etc.). For example, the "celebrated Nernst equilibrium equation" is derived, properly limited to boundaries with the same solvent on both sides, only to be applied on the very next page to the equilibrium distribution of an ion between the *membrane interior* and the adjacent solution.

In the next chapter, on passive transport, the author argues as to whether or not diffusion can be regarded as arising from the action of a force. His conclusion is not clear but a subsequent parenthetical statement — "The theoretically inclined will perhaps remember that the diffusion coefficient is related to the autocorrelation function for the random force beating on the molecule" — implies perhaps that diffusion can be regarded in this way. The following chapter is centred on Eyring's absolute rate theory for diffusion, but misrepresents the basic ideas behind the theory by confusing energy and free energy of the activated state.

Silver has a lively style and an instinct for apt imagery. Combination of these assets with more careful theoretical analysis could produce a truly useful book. ☐

Charles Tanford is J.B. Duke Professor of Physiology at Duke University, Box 3709-P, Durham, North Carolina 27710, USA.

Future global warming from atmospheric trace gases

Robert E. Dickinson & Ralph J. Cicerone

National Center for Atmospheric Research, Boulder, Colorado 80307, USA

Human activity this century has increased the concentrations of atmospheric trace gases, which in turn has elevated global surface temperatures by blocking the escape of thermal infrared radiation. Natural climate variations are masking this temperature increase, but further additions of trace gases during the next 65 years could double or even quadruple the present effects, causing the global average temperature to rise by at least 1 °C and possibly by more than 5 °C. If the rise continues into the twenty-second century, the global average temperature may reach higher values than have occurred in the past 10 million years.

THE likelihood of global climate change from increasing concentrations of carbon dioxide is now well known[1-10]. Much more recent is the realization that other less-abundant trace gases are also increasing and that their change is likely in total to have an effect on climate comparable with that of carbon dioxide[11-21]. These include CH_4, tropospheric O_3, N_2O and the chlorofluorocarbons (CFCs) CCl_3F and CCl_2F_2. What do we know about the effect of these gases on climate, their temporal trends, and the implications of these increases? To see how such climate change can occur, we first consider the energy-exchange processes of the Earth–atmosphere system. The relative contribution of the various trace gases to climate change will be determined by their relative contributions to these energy processes.

Solar radiation is absorbed by the atmosphere and the Earth's surface, providing the energy required by many terrestrial processes. Figure 1 shows the amount of energy involved, on a global and annual average. For climate to be in equilibrium, this absorbed solar radiation must be balanced by outgoing thermal radiation. The partial trapping of this thermal radiation by radiatively-absorbing particles or molecules helps to increase surface temperatures by several tens of degrees compared with what they would be without the atmosphere. This process, sometimes called the 'greenhouse effect', occurs largely in the first 10–15 km of the atmosphere, that is, the troposphere. Radiatively active constituents both absorb and emit thermal radiation, depending on their effective cross-sections and on temperature. Their emission varies with the local atmospheric temperature, whereas their absorption depends on the temperatures of the other atmospheric layers and of the Earth's surface where the radiation was initially emitted. Because tropospheric temperatures decrease with increasing altitude, typically by 5–7 °C km^{-1}, the active atmospheric constituents absorb more upward radiative flux than they emit. Clouds and water vapour are the dominant contributors to this process.

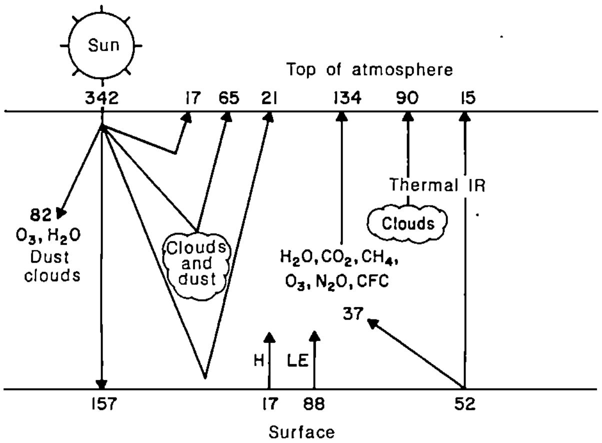

Fig. 1 Schematic depiction of the global and annual average fluxes of radiation within the climate system. Incident solar radiation is either absorbed or reflected as indicated on the left side. Most of the reflection occurs in the atmosphere and most of the absorption at the Earth's surface. Evapotranspiration (LE) and sensible heat fluxes (H) transfer much of the absorbed solar energy to the atmosphere. The absorbed solar energy must ultimately be returned to space as thermal infrared radiation as indicated on the right side. Only the net thermal flux between the surface and atmosphere is shown. Reductions of thermal flux to space from increasing concentrations of trace gases warm the global atmosphere.

What is surprising is that other atmospheric gases, present in minute amounts, in some cases in concentrations <1 part per 10^9 (p.p.b.), also contribute significantly to this trapping of thermal radiation. These gases include, in particular, carbon dioxide, tropospheric ozone, methane, nitrous oxide, and certain chlorocarbons, in order of their present contributions to atmospheric radiative processes. Without the atmosphere's radiatively active constituents, the Earth would lose thermal radiation essentially as a black body at the temperature of its surface, $T_s = 287.5$ K, that is, ~ 387 W m^{-2}, neglecting corrections for the nonlinearity of the black-body emission, surface emissivities <1, and stratospheric effects. The actual radiative flux from the top of the atmosphere is 239 W m^{-2}, so the total amount of trapped radiation is ~ 148 W m^{-2}. Sustained changes in this trapping by as little as 1 W m^{-2} change the Earth's radiative balance sufficiently to be of considerable importance for the climate system. Table 1 shows the current concentrations of atmospheric trace gases and contributions to this radiative trapping.

Table 1 The current 1985 trapping of thermal infrared radiation (ΔQ) by current tropospheric trace constituents

Gas	Current concentration	ΔQ_{total} (W m^{-2})	Ref.
Carbon dioxide	345 p.p.m.	~50	63
Methane	1.7 p.p.m.	1.7	16
Ozone	10–100 p.p.b.	1.3	
Nitrous oxide	304 p.p.b.	1.3	16
CFC-11	0.22 p.p.b.	0.06	19
CFC-12	0.38 p.p.b.	0.12	19

The term ΔQ_{total} is the change of net radiation at the tropopause if the given constituent is removed, but the atmosphere is otherwise held fixed.

The contribution to the Earth's thermal budget of such minute concentrations of trace gases is of considerable interest in its own right. However, the changing concentrations of these gases as a result of human activities[20,21] add a considerable sense of urgency to their study. We review here our current understanding of the radiative properties of the relevant gases, their sources, sinks, and changing concentrations, and the implications of these changes for future climate.

Radiative properties of the atmosphere

Solar radiation of wavelengths from ~0.3 to ~4 μm heats the climate system. Thermal emission at wavelengths from ~4 to ~100 μm, in turn, cools the Earth's surface and atmosphere, ultimately returning the absorbed solar energy to space. The solar radiation is scattered (reflected in all directions) by clouds, aerosols, the Earth's surface, and the major atmospheric molecules (Fig. 1) and absorbed by all but the last of these. Thick clouds act nearly as black bodies in absorbing and emitting thermal infrared radiation, as do also most terrestrial surfaces (an exception is quartz sand with relatively low emissivities[22]).

Of the radiatively active gases in the current atmosphere, only H_2O, CO_2, CH_4, O_3, N_2O and the chlorofluorocarbons (CFC-11 and CFC-12) are in sufficient concentrations to be important in Earth's overall thermal budget. Of these, the strongest absorber by far is water vapour. Indeed, much of tropospheric radiation can be described with water vapour as the only gaseous absorber. Water in either vapour or in cloud form absorbs solar radiation and absorbs and emits thermal radiation. These water vapour states are internal to the climate system, that is, their distributions are controlled by climate processes themselves (that is, the atmospheric hydrological cycle) rather than by sources uncoupled to the climate system. Understanding how water vapour concentrations and cloud radiative properties might change in the future thus requires knowledge of how these terms function as feedbacks in the climate system (a question we shall return to later). Our primary thrust here is to review the role of the other less-abundant trace gases, whose concentrations are being directly perturbed by human activities. Understanding the radiative properties of these gases and their future concentrations is the key to understanding the relative contributions of these gases to climate change.

Ozone is the only other atmospheric gas which absorbs much solar radiation, primarily in the stratosphere. Atmospheric carbon dioxide is but a very weak absorber of solar radiation. The other atmospheric trace gases only affect the atmospheric heat budget through their absorption and emission of the thermal infrared radiation, primarily over the wavelength range ~6–16 μm. Furthermore, at the wavelengths where water vapour strongly absorbs and emits radiation, the effect of other gases is minimal. The vibrational-rotational bands of water vapour thus block radiation at wavelengths <8 μm and rotational bands block wavelengths >18 μm. Carbon dioxide, in turn, dominates the absorption of radiation between 12 and 18 μm.

The remaining spectral region from 8 to 12 μm is known as the 'window' because of the atmosphere's relative transparency to radiation over these wavelengths. The intensity of black-body radiation depends on wavelength according to the Planck function; at the temperatures of the Earth's surface, this function has its maximum values in the window region. Consequently, ~25% of the thermal emission from the Earth's surface (~100 W m^{-2}) is at wavelengths of 8–12 μm. A larger fraction of the emission from the top of the atmosphere is in this spectral range. In this wavelength region, emission varies with temperature T approximately as $\exp(-1{,}500/T)$. A trace gas at a temperature ~33 °C less than that of Earth's emission temperature will thus only re-emit about half as much energy as it absorbs. Because of the presence of clouds, the maximum increase of trapping in the window region is ~30 W m^{-2}.

Interestingly enough, CH_4, O_3, N_2O, CFC-11 (CCl_3F) and CFC-12 (CCl_2F_2) all have strong absorption bands in the atmospheric window region. These trace gases absorb and emit as functions of wavelength in discrete lines with extended wings. These lines occur in bands and result from the rotational splitting of individual vibrational energy transitions of the molecules. Their strength is determined from the strength of the band transitions, from the concentration of the trace gas, and from the rotational partitioning of the band into individual lines. The emission rate of a line depends on its absorption strength and on local atmospheric temperature.

The weakest lines absorb radiation significantly only in their line cores, and this absorption increases essentially linearly with concentration of the absorber gas. Somewhat stronger lines absorb radiation mostly in the wings, with only relatively small amounts absorbed by their saturated cores. Increasing absorber concentration pushes the peak absorption farther into the line wings so that wing absorption increases with the square root of the product of atmospheric pressure and absorber concentration. With even stronger line strengths, the peak absorption is pushed so far into line wings that other lines within the band overlap the absorbing wings and absorption only increases logarithmically with increasing absorber concentration. The absorption of a band varies with absorber concentration according to the variation of its stronger absorbing lines.

The chlorofluorocarbons CFC-11 and CFC-12 and tropospheric ozone are present in such small concentrations and have so many individual lines that their absorption of thermal radiation is nearly proportional to their concentration. Methane and nitrous oxide, being relatively more abundant, increase their absorption essentially according to the square root of their concentrations, whereas carbon dioxide absorption is proportional to the logarithm of its concentration. All the trace gases absorb not in single bands but in multiple bands, and weaker hot and isotopic bands are also present. The above scaling arguments are only approximate and are especially prone to error if applied to large changes in concentration where either the stronger bands may change their dependence on absorber amount, or previously unimportant weaker bands of a given gas may become relatively more important.

Increases in the concentrations of atmospheric trace gases since pre-industrial times and the consequent trapping of thermal radiation are shown in Table 2. The trapping by ozone and the CFCs, whose stronger bands are in the middle of the window region, is affected very little (~15%) by overlap with water vapour and with carbon dioxide absorption. Methane and nitrous oxide, whose strongest bands are on the short wavelength edge of the window region, lose about half of their trapping[20] by such overlap. Since much of the effect of increases in the trace gases is to make the atmospheric window region more opaque, this trapping might be called the 'dirty window' effect.

Table 2 Estimated pre-industrial trace gas concentrations and implied change in thermal trapping to 1985

Gas	Pre-industrial concentration	$\Delta Q_{\text{pre-industrial}}$ (W m^{-2})
Carbon dioxide	275 p.p.m.	1.3
Methane	0.7 p.p.m.	0.6
Tropospheric ozone (below 9 km)	0–25% less	0.0–0.2
Nitrous oxide	285 p.p.b.	0.05
CFC-11	0.00 p.p.b.	0.06
CFC-12	0.00 p.p.b.	0.12
Total		~2.2

Trapping is inferred from refs 19 and 20, scaling approximately logarithmically, with CO_2 concentration, with the square root of N_2O and CH_4 concentration, and linearly with O_3 and CFC-11 and -12 concentrations.

Atmospheric trace gases

Carbon dioxide: Atmospheric carbon dioxide concentrations are now ~25% higher than they were 200 yr ago before the age of extensive industrialization and forest clearing. Current concentrations (1985) are about 345 p.p.m. (parts per 10^6) and are increasing by 1–1.5 p.p.m. yr^{-1}, mostly as a result of continued burning of fossil fuel (adding ~5.2×10^{12} kg yr^{-1} of carbon) and forest removal (continuing to add about 10^{12} kg yr^{-1} of carbon)[10]. The basic features of the global carbon cycle are well known, but questions remain as to the contributions of land soils and forests and the rate of uptake of carbon by the oceans. The largest source of uncertainty in projecting future atmospheric carbon dioxide concentrations, however, lies in the future rates of fossil fuel combustion.

Halocarbons: Halogenated hydrocarbons (halocarbons) are now widely produced and widely used. These include fluorocarbons, chlorofluorocarbons, chlorocarbons and bromocarbons. Most scientific attention has focused on the potential role of chlorine and bromine atoms from these molecules as ozone-destroying catalysts in Earth's stratosphere[23-25]. Certain of these chemicals have also been recognized to be potent greenhouse gases[11,20].

The chlorofluorocarbons, often referred to popularly by their trade name of 'Freons', CCl_3F (CFC-11) and CCl_2F_2 (CFC-12), were measured first in the atmosphere in 1971 (ref. 26) and 1973 (see, for example, ref. 27), respectively. Since then, increasingly accurate and precise measurements have shown that their atmospheric concentrations have grown at about the same rate as would be expected from industrial production and release into the atmosphere[24,28], after minor corrections for the amounts produced but not yet released and for the quantities destroyed in the stratosphere and dissolved in oceans. In 1981, there were about 6.0×10^9 kg of CFC-12 in the atmosphere together with 5.0×10^9 kg of CFC-11. At 1981 release rates, these amounts represent the cumulative results of 15–20 yr of global emissions. (Unpublished data from several investigators give 1985 mixing ratios of CFC-11 of at least 0.22 p.p.b. and for CFC-12 of at least 0.38 p.p.b.). Indeed, atmospheric concentrations of these compounds were observed to have increased by ~6% yr^{-1} during 1978–81 (refs 29, 30). In the early 1970s, annual emissions were a larger fraction of the amounts already in the atmosphere, and larger percentage annual increases were observed, along with considerably more CFCs in the Northern Hemisphere than in the Southern Hemisphere. Although most of the release continues to be in the Northern Hemisphere, the hemispheric difference has decreased to <10%.

A projection of concentrations of atmospheric CFC-11 and CFC-12 beyond the present requires some knowledge about future industrial production and release rates. Current releases annually increase mixing ratios of CFC-11 by about 12 p.p.t. (parts per 10^{12}) and CFC-12 by 21 p.p.t., as estimated from changing atmospheric concentrations. A recent report[31] attempts to estimate their future production and release rates and that of several other similar chemicals; it recognizes the dynamics of changing industrial usages, competitive products and world and regional populations. Worldwide CFC-11 emissions are projected to increase by between 2.8 and 5.1% yr^{-1} from 1980 until 2000; corresponding figures for CFC-12 are 2.5–3.5% yr^{-1}. Between AD 2000 and 2025, CFC-11 emissions could change by −1% to +4.7% yr^{-1} and CFC-12 emissions would increase by between 1.0 and 4.6% yr^{-1}. Beyond the year 2025, growth estimates are less well-based, but Quinn *et al.*[31] suggest annual increases of 0.6–2.0% for CFC-11 and 1.1–2.1% yr^{-1} for CFC-12.

Even if future release rates of CFC-11 and CFC-12 remained at present levels, their atmospheric concentrations would continue to increase for the next century because of the relatively long residence times, τ_i, for these species, at least 60 and 100 yr, respectively[32]. In general, for a well-mixed chemical with sources $S(t)$

$$\frac{dN(t)}{dt}=S(t)-N(t)/\tau \qquad (1)$$

where $N(t)$ is the total number of molecules (or mass) of the given species in the global atmosphere at time t. Even if we were to assume that present emissions remained constant, equation (1) shows that concentrations of CFC-11 and CFC-12 would more than double, to values of ~0.5 and 1.0 p.p.b. respectively, within the next 40 yr and eventually rise to values of ~0.7 and 2.1 p.p.b., using 60- and 100-yr lifetimes, respectively.

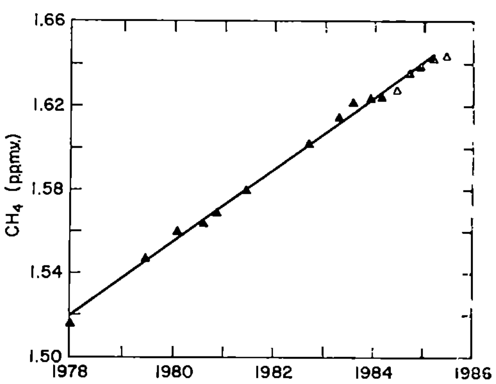

Fig. 2 Globally averaged methane concentrations in surface air from January 1978 to June 1985 as measured by Blake and Rowland[42]. Air samples were collected simultaneously from northern and southern latitudes. In computing global averages, measured values were weighted by the Earth's area in latitude belts. In 1985, there are 4.8×10^{15} g CH_4 in the atmosphere; annual sources (sinks) are $(3–7)\times10^{14}$ g.

Other halocarbons requiring attention include CCl_4, $CClF_3$, CF_4, $CHClF_2$, $CHCl_2F$, $C_2H_3Cl_3$, $C_2Cl_3F_3$, $C_2Cl_2F_4$, C_2ClF_5, C_2F_6, $CBrF_3$ and $CBrClF_2$. Because of the location of the absorption bands of these species and their rapid rates of accumulation in the atmosphere, they represent potentially important greenhouse gases. Research is needed to quantify their band absorbances and atmospheric concentrations with special attention to $CHCl_2F$ and $C_2Cl_3F_3$.

Nitrous oxide: Atmospheric N_2O is increasing in concentration globally, although the record of its past change is not as extensive as that for methane, and the reasons for this increase are less clear than those for halocarbons. Weiss[33] measured a global increase of ~0.6 p.p.b. yr^{-1} (0.2% yr^{-1}) between 1976 and 1980, whereas Khalil and Rasmussen[34] find an 0.8 p.p.b. yr^{-1} increase between 1979 and 1982. The mid-1980 N_2O concentration in the Northern Hemisphere was 301 p.p.b. and in the Southern Hemisphere it was ~0.8 p.p.b. less. Weiss fits his 1976–80 data with one of two curves; either one that assumes an added combustion source of N_2O growing at 3.5% yr^{-1} or one that assumes an agricultural-fertilizer source growing at 6% yr^{-1} (ref. 33) with an atmospheric residence time of 100 yr in both cases. Weiss, in extending his N_2O monitoring through 1984, finds that global concentrations continue to rise by 0.6 p.p.b. yr^{-1} (personal communication), but that it is not yet possible to distinguish between the two source-growth curves that fit the data. Earlier data from 1961–74 showed similar rates of N_2O increase[35].

Although the present observed and projected rates of N_2O increase may seem small, they imply that total global sources of N_2O are now elevated by ~30% over unperturbed steady-state sources, assuming a growth rate of 0.2% yr^{-1} and a 150-yr lifetime for N_2O. If the N_2O increase is due to either increased microbial nitrification and denitrification of agricultural fertilizers, or combustion, then much of this imbalance has developed in the past few decades and it may continue to grow rapidly.

Concentrations of N_2O of 320–330 p.p.b. are likely by AD 2000, regardless of which anthropogenic source is assumed to be growing[33,34]. Better future projections require determination of whether increased combustion of nitrogen-containing fuels[36,37] and biomass[21] or increased application of nitrogen fertilizers[38] is primarily responsible for the continuing N_2O increase. Both sources are difficult to quantify; field losses of N_2O due to microbial nitrification and denitrification of nitrogen fertilizers are variable[38,39] and candidate elementary reactions

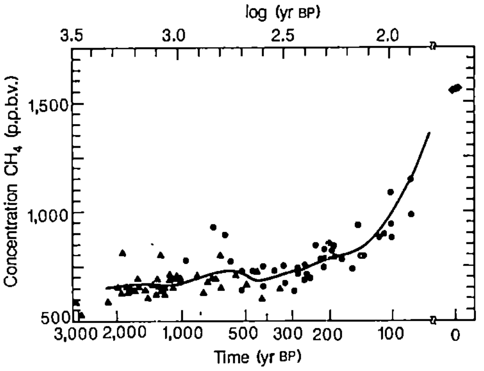

Fig. 3 Concentrations of atmospheric methane (100-300 yr BP) from ref. 44. ●, Data from polar ice cores obtained from Greenland; ▲, data from ice cores at the South Pole. The present concentration of methane is shown on the right (◆). The solid line is the smoothed average concentration based on the data; it is the average concentration in successive overlapping periods of 0.3 units each in the log (l) scale at the top of the figure.

that can produce N_2O in combustion have been identified only recently[40].

Methane: Methane is of considerable scientific interest because of its relatively rapid growth and the diverse possible causes of this increase. Global concentrations have increased by $>1\%$ yr^{-1} since 1978, as shown by Fig. 2, based on data from flame-ionization gas chromatography. A reanalysis[41] of ground-based solar absorption infrared spectroscopic data concludes that the concentration of tropospheric CH_4 in 1951 was 1.15 p.p.m., about 30% below that of 1985 (ref. 42). An earlier re-examination of infrared data from the 1950s and 1960s had concluded[43] that the rate of methane increase was slower.

The increase in global methane apparently began in previous centuries. Figure 3 shows an analysis of gases trapped in dated ice cores[44], indicating that methane concentrations have doubled since the eighteenth century, but that they were relatively constant for the previous 2,000-3,000 yr. Selective diffusion of CH_4 out of old ice cores may have biased the data of Fig. 3 (ref. 43), but H. B. Craig, who earlier found similar results[45], considers this unlikely (personal communication) based on his tests. Further confirmation has been reported[46]. Methane-consuming microbes may have lived in the ice, but we consider this unlikely.

Why has atmospheric methane increased in the past, and what is its future? Answering these questions requires knowledge of both the sources and sinks of methane. Ehhalt[47] summarized five measurements of ^{14}C in samples from air liquefication plants in the 1950s. These samples had a ^{14}C content of about 80% of that of standard wood, or equivalently 20% 'dead carbon' from fossil fuels. He suggested that this value of 20% should only be used as an upper limit since air liquefication plants are usually situated in heavily industrialized areas so that the samples were subject to contamination from local fossil-fuel-derived methane. Various authors over the past decade have constructed methane-source inventories subject to this constraint. A recent examination[21] lists rice paddies, ruminant animals, biomass burning, swamps and marshes, natural gas, and coal mining losses as the major sources, in decreasing order of importance. However, serious questions of mechanisms and related ecological variability remain[48-51]. Further, we should be cautious about conclusions drawn from the 1950s ^{14}C data because: first, the relative sizes of ^{14}C-rich and ^{14}C-poor sources are probably changing with time; and second, the old samples, collected by liquefying air, may not be representative of the $^{14}CH_4/^{12}CH_4$ in air. Unfortunately, few conclusions can be drawn about methane sources from ^{14}C analyses today in view of the bomb-produced ^{14}C in the contemporary biota and sediments. It might be useful to examine the concentrations of the ^{13}C stable isotope; such research is just beginning[52].

The principal known sink of atmospheric methane is the gas-phase reaction $OH + CH_4 \rightarrow CH_3 + H_2O$ (ref. 72). Some tantalizing but indirect evidence suggests that atmospheric OH concentrations are decreasing[53], at least in NO poor regions—the lower and middle troposphere; increasing methane and increasing CO concentrations (not yet proven) should act to suppress OH (ref. 54) through nonlinear atmospheric chemistry.

Ozone: Ozone is of considerable interest because of its important roles, its complex behaviour, and its susceptibility to human-induced global change. Near the ground in urban areas, ozone is a pollutant. Throughout the global troposphere, ozone photolysis initiates free-radical chemistry. In the middle and upper stratosphere, where the largest concentrations are found, ozone strongly attenuates solar ultraviolet light and in doing so drives stratospheric wind systems.

Tropospheric ozone increases are difficult to discern with extant observing systems, but increases have been indicated. A recent critical analysis[55] of ozone data finds that, on average over Europe and North America from the late 1960s to the early 1980s, near-surface ozone has increased by 1-3% yr^{-1} and ozone in the middle troposphere (700-500 mbar) by 1-2% yr^{-1}. These increases occur largely during the summer, especially in industrialized areas. Such increases might have begun in the 1940s, as is suggested by shifts in the seasonal cycle of ozone concentrations and other scattered observations[55]. There is considerable variability and little evidence for change in the upper troposphere.

Theoretical models of tropospheric chemistry predict that increasing anthropogenic releases of hydrocarbon and nitrogen oxide (NO_x) gases should be increasing tropospheric ozone[55-57,15]. Such increases depend on poorly known atmospheric NO_x concentrations and on some meteorological processes such as vertical transport and chemical roles of clouds, but changes in the Northern Hemisphere should be larger than those in the Southern Hemisphere, as is evidently observed. Future changes in the stratosphere may also lead to increases of tropospheric ozone.

As discussed previously[20], most studies of the latitudinal variation of tropospheric ozone indicate that concentrations in the Northern Hemisphere are at least 50% higher than in the Southern Hemisphere. However, a recent aircraft survey has given contradictory results[58], possibly because of seasonal or longitudinal variations. Furthermore, latitudinal variations may be due to transport[59].

An association of observed trends of ozone in the Northern Hemisphere with increases in total fossil fuel use would also support the possibility of an increase of tropospheric ozone in the Northern Hemisphere of up to 50% over pre-industrial values. We indicate in Table 2 that global average tropospheric ozone (below 9 km) is estimated to have increased by between 0 and 25% since pre-industrial time. Improving estimates of past or future ozone change will require a better understanding of the contributions of ground and high-level pollution.

Global stratospheric ozone changes are likely to occur because of continuing and accelerating human activities[24,25]. Increasing concentrations of chlorofluorocarbons and nitrous oxide decrease stratospheric O_3 at altitudes above 30 km. Changes of ozone in the lower stratosphere are more complex and difficult to project; they will depend on latitude and altitude and on wind systems[59,60]. A variety of chemical reactions involving polyatomic species (many of which have yet to be measured in the atmosphere) also affect this response.

Future scenarios

For comparing the future climate effects of the various trace gases, we take the year 2050 as a reference point and assume the ranges indicated in Table 3. The question of possible future concentrations for CO_2 has been extensively studied, and we have adopted values from the latest such study[10].

A range of possible future emissions for CFC-11 and CFC-12 has been obtained from economic analysis[31], and we have used these emissions together with equation (1) to obtain the concentrations shown in Fig. 4. Concentration scenarios have taken $\tau = 60$ yr for CFC-11 and $\tau = 100$ yr for CFC-12, near the low end of most previously inferred values[32]. Lifetimes are likely to lie in the range 50–80 yr and 90–130 yr, respectively. These lifetimes will decrease in the future, as increased concentrations of chlorine atoms lower the ozone concentrations above 30 km, and hence increase the fluxes of ultraviolet that photolyse the CFCs. Obvious decreases in the total column ozone following stratospheric ozone decrease are likely to trigger political constraints on further increases in the production of the CFCs. Our projections neglect the uncertainty in CFC lifetimes and their decrease with increasing burden and also neglect possible emission reductions from future regulation of CFC production.

Table 2 shows that the radiative effect of the CFCs which have been added to the atmosphere up to 1985 is only ~11% of that from CO_2 increases. However, the CO_2 increase has occurred over the past two centuries, and the current burden of CFCs has been added almost entirely within the past 30 yr. The radiative effect of these CFCs added over the past 30 yr is about one-third that of the CO_2 added over the same period. Table 3 indicates that for the assumed future scenario the additional radiative trapping by the CFCs between 1985 and 2050 is likely to be ~70% that of CO_2. This increase in the relative importance of the CFCs in the future follows from the near-linear dependence on concentration of the CFC radiative effects versus the logarithmic dependence of the effects of CO_2.

Because of our current relatively poor understanding of the reasons for the increases in methane concentrations, a wide range of possible futures appears in Table 3. A continuation of the current growth rate of 1.2% yr^{-1} to the year 2050, assuming present methane lifetimes, would give 3.7 p.p.m. at that time. Increases in methane will probably be amplified by decreasing OH, but will be diminished by slowdown in population growth and required resources. Another recent analysis[21] argues that increases from pre-industrial concentrations are likely to be proportional to projected future populations. They accordingly infer concentrations of 2.5 p.p.m. by 2050; values this small would require a large reduction in methane growth rates within the next few decades. We judge that in the year 2050 concentrations will lie between 2.1 and 4.0 p.p.m. The upper limit is inferred from the extrapolation of current growth plus a small decrease (8%) of methane lifetimes. Methane lifetimes may decrease by much more[54]. The lower limit is inferred by arguing that the current trend should last at least 20 yr but that, considering our ignorance of the processes involved, we cannot exclude absence of further growth after that. Table 3 suggests that from now to 2050 the radiative effects of increasing methane are likely to be about one-quarter that of CO_2. Table 2 indicates that the increase in radiative trapping from past methane increases has been about the same as that expected from future methane increases and is about half of that inferred from past CO_2 increases. Methane has already increased to ~250% of pre-industrial values and probably will not repeat this relative increase by 2050. The relative increase of CO_2, on the other hand, will probably be greater in the next 65 yr than it has been up to now[10].

If the anthropogenic source of nitrous oxide were to continue to grow at 3.5% yr^{-1}, it would increase by a factor of 10 by the year 2050 and N_2O concentrations would rise above 500 p.p.b. (ref. 33). Such rapid future growth is probably excluded by economic and population constraints[21]. Assuming that a quadrupling of the current emission rates over the next 65 yr is not impossible, we infer an upper limit for N_2O concentrations of 450 p.p.b. for the year 2050. We infer a lower limit of 350 p.p.b. for the year 2050 using an average annual increase similar to that now observed.

A likely upper limit to fossil-fuel consumption over the next century is about four times current consumption rates[10]. With such consumption and an upper limit of 20% of current ozone associated with fossil-fuel pollution, global tropospheric ozone could conceivably increase by 60% over current values. Ozone will also increase in the upper troposphere and lower stratosphere in response to increases of the CFCs and to oxides of nitrogen from increasing jet aircraft traffic. The details of latitudinal and especially vertical distribution of ozone change are important for any accurate estimate of climate effects. Lacking such details, we estimate the likely radiative trapping of changing ozone concentrations by the year 2050 as that given by a change in ozone between 0 and 50% uniformly over the altitude range 0–12 km.

To determine the net contribution to radiative trapping included in Table 3, we have simply summed separately the upper and lower limits of the projected contributions of the individual gases. Although all contributions are unlikely to achieve their upper or lower limits simultaneously, this assumption probably does not overestimate the likely range of total trapping for two reasons. First, the rates of increase of the different trace gases are more likely to be highly correlated than not—their sources all depend heavily on fossil-fuel utilization; methane and nitrous oxide emissions both also depend on agricultural development and that of the CFCs on general technological development. Second, past experience with similar uncertain environmental questions indicates that actual uncertainties are likely to be larger than can be judged from simple arguments such as those used here. In particular, there are many other trace gases present in small but rapidly growing concentrations[20], some of which will add significantly to global warming by the year 2050.

Table 3 Scenario for trace gas concentrations in the year 2050 and implied increased trapping of thermal radiation from 1985 (ref. 19)

Gas	Year 2050 scenario	ΔQ_{2050} ($W\,m^{-2}$)
Carbon dioxide	400–600 p.p.m.	0.9–3.2
Methane	2.1–4.0 p.p.m.	0.2–0.9
Tropospheric ozone (0–12 km)	15–50% more	0.2–0.6
Nitrous oxide	350–450 p.p.b.	0.1–0.3
CFC-11	0.7–3.0 p.p.b.	0.23–0.7
CFC-12	2.0–4.8 p.p.b.	0.6–1.4
Total		2.2–7.2

Referring to either the lower or the upper limit totals in Table 3, we infer that the total contribution of the other trace gases is more likely than not to exceed the contribution from CO_2.

Implications for climate change

We have aimed to provide an overall framework for considering the relative contributions of various trace gases to climate change. Relatively realistic three-dimensional climate models have been used to study only a very limited number of scenarios for future climate; that is, scenarios assuming a steady-state doubling or quadrupling of atmospheric carbon dioxide concentrations. The radiative forcing for the latter is about double that for the former.

The future climate change from likely increases of all trace gases will undoubtedly differ in detail from that inferred from the superposition of the climate changes that would occur, assuming that each trace gas changes separately. Furthermore, the climate change from individual trace gases depends not only on the global average trapping of radiation as discussed here, but also on the latitudinal and especially vertical distributions of atmospheric heating or cooling changes implied by the trace gas change. However, the implications of these details have not yet been satisfactorily resolved, and so our estimates of the climate change resulting from the various trace gases assume that the dependence of this climate change on external forcing can simply be represented by the global radiative trapping alone.

Indeed, the radiative trapping values given in Tables 1-3 are only approximate estimates. Their precise values depend not only on (somewhat uncertain) band strengths but also on the temporally and spatially varying distributions of cloudiness and atmospheric temperatures. The values used here have been inferred mostly from simple one-dimensional models of the atmosphere. Recognizing these caveats, we suggest that at present the most useful way to estimate the future climate change from CO_2 and the other trace gases is to scale from the studies that have been done on climate change from CO_2 increases, allowing for the time lag required for the oceans to warm up.

Three-dimensional general circulation models (GCMs) represent the climate system as the sum of the day-to-day weather systems integrated over many years of simulated time. In doing so, they can include realistically all the feedbacks of simpler models plus those that depend on the details they generate. They include, in particular, albedo feedbacks from seasonally varying snow and sea ice, lapse rate feedbacks involving adjustment to moist adiabatic lapse rates in tropical latitudes, controls by baroclinic disturbances in mid-latitudes, and feedbacks by the highly stable stratification of polar latitudes. Cloud feedbacks are potentially very important for amplifying global temperature change, but they cannot be inferred yet with confidence, and negative feedbacks on solar radiation absorption from changes in cloud liquid water have not been included[61].

Because of the difficulty in isolating individual feedbacks in GCMs, and the expense of examining all trace gases of possible significance, simpler energy balance[62] and convective adjustment models[63] have also proved valuable.

Recent GCM simulations[3,6,7] give for steady-state CO_2 doubling ($\Delta Q \simeq 4.0\ \mathrm{W\,m^{-2}}$) a global average temperature increase of between 2.1 °C (ref. 3) and 4.8 °C (ref. 6). Consideration of uncertain model feedbacks suggests that a value as low as 1.5 °C or as high as 5.5 °C is possible[10].

Because several decades or more are required for the oceans to equilibrate with changes in global radiation[64-69], we cannot convert the heating rates given in Tables 2 and 3 directly into expected temperature changes for the same dates. However, continuing the current burden of trace gases added by human activities indefinitely implies an eventual increase from pre-industrial temperatures of 0.5-2° C. Global mean temperatures can only be estimated with any confidence back to 1900. About two-thirds of the anthropogenic forcing has developed since that time. Oceanic thermal inertia is currently reducing the temperature response by (very roughly) half of what it would be in a steady state. Allowing for this factor, we infer a temperature increase of 0.3-1.0 °C from 1900 to the present[10,70]. The observed increase is about 0.5 °C (refs 10, 70) which would seem to confirm the present analysis. However, global temperatures around 1940 were nearly as warm as now and they declined in the 1960s. Thus, unexplained climate variations occur that will probably confound unambiguous identification of the trace gas signal for at least another decade or two.

The scenarios given in Table 3 imply that by the year 2050 there will be a global average temperature increase of 1 °C to >5 °C, depending on the extent of positive feedbacks in the climate system and on reduction of the response by oceanic heat uptake. Global temperatures will probably continue to grow well into the twenty-second century as the atmospheric loading of trace gases and ocean heat content increases further.

The GCMs simulate not only global conditions but also the detailed geographical distribution of many climate parameters including the atmospheric hydrological cycle. Implications of future climate change from trace gases for agriculture and natural ecosystems require establishing these details with some confidence. All the GCM simulations indicate largest temperature changes in high latitudes. Some models strongly suggest a significant mid-latitude, mid-continent summer drying. Past model studies have inspired a wide range of climate-impact 'what if' studies, examining the potential implications of the range of possible future climates[73]. However, practical analyse will require a new generation of climate models whose globa feedbacks and regional simulations can be accepted wit confidence. They will also require allowance for the large-scal adjustments of human systems that can occur on the timescale involved[71].

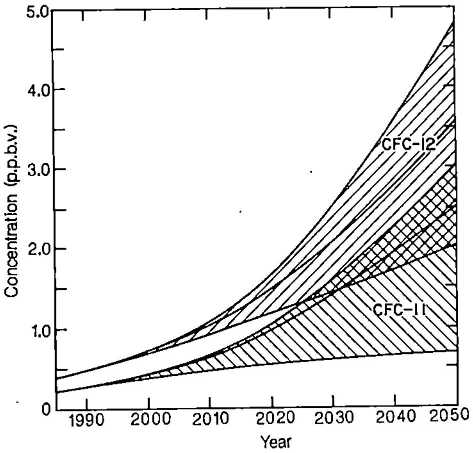

Fig. 4 Range of possible scenarios of the concentrations of CFC-11 and CFC-12 between 1985 and 2050 as inferred from future sources projected from an economic analysis[31]. Upper, lower and middle scenarios are shown for each gas and their ranges are indicated by the slanted line patterns.

Accurate model predictions may take more than a decade t arrive. Meanwhile, further emphasis should be given to definin and bounding the uncertainties in future climate change[7 Without a better understanding of the extreme upper limits t possible future climate change, we must view with considerabl concern this global experiment now under way.

We thank Drs J. Kiehl, W. Clark, and P. Crutzen for helpf comments. The National Center for Atmospheric Research i sponsored by the NSF.

1. Callendar, G. S. *Q. Jl R. met. Soc.* **64**, 223-240 (1938).
2. Manabe, S. & Wetherald, R. T. *J. atmos. Sci.* **24**, 241-259 (1967).
3. Manabe, S. & Stouffer, R. J. *J. geophys. Res.* **85**, 5529-5554 (1980).
4. Climate Research Board *Carbon Dioxide and Climate: Scientific Assessment* (Nation Academy of Sciences, Washington DC, 1979).
5. Dickinson, R. E. *Carbon Dioxide Review 1982* (ed. Clark, W. C.) 101-133 (Oxford Universi Press, 1982).
6. Hansen, J. *et al. Maurice Ewing Symp. 5* (eds Hansen, J. & Takahashi, T.) (Americ Geophysical Union, Washington DC, 1984).
7. Washington, W. M. & Meehl, G. A. *J. geophys. Res.* **89**, 9475-9503 (1984).
8. Carbon Dioxide Assessment Committee *Changing Climate* (National Academy of Scienc Washington DC, 1983).
9. Mitchell, J. F. B. *Q. Jl R. met. Soc.* **109**, 112-152 (1984).
10. Bolin, B., Döös, B. R., Jager, J. & Warrick, R. A. (eds) *The Greenhouse Effect, Clima Change and Ecosystems. A Synthesis of the Present Knowledge* (Wiley, Chichester, in t press).
11. Ramanathan, V. *Science* **190**, 50-52 (1975).
12. Wang, W. C., Yung, Y. L., Lacis, A. A., Mo, T. & Hansen, J. E. *Science* **194**, 685-690 (197
13. Dickinson, R. E., Liu, S. C. & Donahue, T. M. *J. atmos. Sci.* **35**, 2142-2152 (1978).
14. Flohn, H. *Carbon Dioxide, Climate and Society* (ed. Williams, J.) 227-238 (Pergam London, 1978).
15. Fishman, J., Ramanathan, V., Crutzen, P. J. & Liu, S. C. *Nature* **282**, 818-820 (1979).
16. Donner, L. & Ramanathan, V. *J. atmos. Sci.* **37**, 119-124 (1980).
17. Hameed, S., Cess, R. D. & Hogan, J. *J. geophys. Res.* **85**, 7537-7545 (1980).
18. Lacis, A., Hansen, J., Lee, P., Mitchell, P. & Lebedeff, S. *Geophys. Res. Lett.* **8**, 1035-10 (1981).
19. World Meteorological Organization *WMO Global Ozone Research and Monitoring Proj Rep. No. 14 of the Meeting of Experts on Potential Climatic Effects of Ozone and O Minor Trace Gases* (World Meteorological Organization, Geneva, 1982).
20. Ramanathan, V., Cicerone, R. J., Singh, H. B. & Kiehl, J. T. *J. geophys. Res.* **90**, 5547-5566 (1985).
21. Bolle, H.-J., Seiler, W. & Bolin, B. *The Greenhouse Effect, Climatic Change, and Ecosyste A Synthesis of the Present Knowledge* Ch. 4 (Wiley, Chichester, in the press).
22. Prabhakara, C. & Dalu, G. *J. geophys. Res.* **81**, 3719-3724 (1976).
23. Molina, M. J. & Rowland, F. S. *Nature* **249**, 810-812 (1974).
24. National Academy of Sciences/National Research Council *Stratospheric Ozone Deple by Halocarbons: Chemistry and Transport* (Washington DC, 1979).
25. Prather, M. J., McElroy, M. B. & Wofsy, S. C. *Nature* **312**, 227-231 (1984).
26. Lovelock, J. E., Maggs, R. J. & Wade, R. J. *Nature* **241**, 194-196 (1973).
27. Hester, N. E., Stephens, E. R. & Taylor, O. C. *J. Air Pollut. Control Ass.* **24**, 491-595 (197
28. Penkett, S. A., Brice, K. A., Derwent, R. G. & Eggleton, A. E. J. *Atmos. Envir.* **13**, 1011-1 (1979).
29. Cunnold, D. M. *et al. J. geophys. Res.* **88**, C13, 8379-8400 (1983).
30. Cunnold, D. M. *et al. J. geophys. Res.* **88**, C13, 8401-8414 (1983).
31. Quinn, T. H. *et al. Projected Use, Emissions and Banks of Potential Ozone-Depleting S stances* WD-2483-1-EPA (Rand Corp., Santa Monica, 1985).

32. Stordal, F., Isaksen, I. S. A. & Horntveth, K. *J. geophys. Res.* **90**, D3, 5757–5776 (1985).
33. Weiss, R. F. *J. geophys. Res.* **86**, C8, 7185–7195 (1981).
34. Khalil, M. A. & Rasmussen, R. A. *Tellus* **35B**, 161–169 (1983).
35. Craig, H., Weiss, R. F. & Dowd, W. L. *Pap. at Symp. on the Terrestrial Nitrogen Cycle and Possible Atmospheric Effects* (American Geophysical Union, Washington DC, 1976).
36. Pierrotti, D. & Rasmussen, R. A. *Geophys. Res. Lett.* **3**, 265–268 (1976).
37. Weiss, R. F. & Craig, H. *Geophys. Res. Lett.* **3**, 751–754 (1976).
38. Delwiche, C. C. (ed.) *Denitrification, Nitrification, and Atmospheric Nitrous Oxide* (Wiley, New York, 1981).
39. Mosier, A. R., Parton, W. J. & Hutchinson, G. L. *Environmental Biogeochemistry* (ed. Hallberg, R.) (1982).
40. Perry, R. A. *J. chem. Phys.* **82**, 5485–5488 (1985).
41. Rinsland, C. P., Levine, J. S. & Miles, T. *Nature* **318**, 245–249 (1985).
42. Blake, D. R. & Rowland, F. S. *J. atmos. Chem.* (in the press).
43. Ehhalt, D. H., Zander, R. J. & Lamontagne, R. A. *J. geophys. Res.* **88**, C13, 8442–8446 (1983).
44. Rasmussen, R. A. & Khalil, M. A. K. *J. geophys. Res.* **89**, D7, 11599–11605 (1984).
45. Craig, H. & Chou, C. C. *Geophys. Res. Lett.* **9**, 1221–1224 (1982).
46. Stauffer, B., Fischer, G., Neftel, A. & Oeschger, H. *Science* **229**, 1386–1387 (1985).
47. Ehhalt, D. H. *Tellus* **26**, 58–70 (1974).
48. Rasmussen, R. A. & Khalil, M. A. K. *J. geophys. Res.* **86**, C10, 9826–9832 (1981).
49. Cicerone, R. J., Shetter, J. D. & Delwiche, C. C. *J. geophys. Res.* **88**, C15, 11022–11024 (1983).
50. Seiler, W., Holzapfel-Pschorn, A., Conrad, R. & Scharfe, D. *J. atmos. Chem.* **1**, 241–268 (1984).
51. Harriss, R. C., Gorham, E., Sebacher, D. I., Bartlett, K. B. & Flebbe, P. A. *Nature* **315**, 652–654 (1985).
52. Stevens, C. M. & Rust, F. E. *J. geophys. Res.* **87**, C7, 4879–4882 (1982).
53. Khalil, M. A. K. & Rasmussen, R. A. *Atmos. Envir.* **19**, 397–407 (1985).
54. Thompson, A. M. & Cicerone, R. J. *Nature* (submitted).
55. Logan, J. A. *J. geophys. Res.* **90**, 10463, 10482 (1985).
56. Liu, S. C., Kley, D., McFarland, M., Mahlman, J. D. & Levy, H. II *J. geophys. Res.* **85**, 7546–7552 (1980).
57. Crutzen, P. J. & Gidel, L. T. *J. geophys. Res.* **88**, 6641–6661 (1983).
58. Gregory, G. L., Beck, S. M. & Williams, J. A. *J. geophys. Res.* **89**, 9642–9648 (1984).
59. Levy, H., Mahlman, J. D., Moxim, W. J. & Liu, S. C. *J. geophys. Res.* **90**, 3753–3772 (1985)
60. Isaksen, I. S. A. & Stordal, F. *J. geophys. Res.* **90** (in the press).
61. Somerville, R. C. J. & Rener, L. A. *J. geophys. Res.* **89**, 9668–9672 (1984).
62. North, G. R., Cahalan, R. G. & Coakley, J. A. *Rev. Geophys. Space Phys.* **19**, 91–122 (1981)
63. Ramanathan, V. & Coakley, J. A. *Rev. Geophys. Space Phys.* **16**, 465–489 (1978).
64. Bretherton, F. P. *Prog. Oceanogr.* **11**, 93–129 (1982).
65. Spelman, M. J. & Manabe, S. J. *J. geophys. Res.* **89**, 571–586 (1984).
66. Bryan, K., Komro, F. G., Manabe, S. & Spelman, M. J. *Science* **215**, 56–68 (1982).
67. Thompson, S. L. & Schneider, S. H. *Science* **217**, 1031–1033 (1982).
68. Schneider, S. H. & Thompson, S. L. *J. geophys. Res.* **6**, 3135–3147 (1981)
69. Wigley, T. M. L. & Schlesinger, M. E. *Nature* **315**, 646–652 (1985).
70. Wigley, T. M. L. *Climate Monitor* **13**, 133–148 (1985).
71. Clark, W. C. *Ecologically Sustainable Development of the Biosphere* (Publ. No. 26, IIASA, 1985).
72. Crutzen, P. J. *The Geophysiology of Amazonia* (ed. Dickinson, R. E.) Ch 8 (Wiley, New York, in the press).
73. Parry, M. L. (ed.) *Climatic Change* (Spec. Issue) 7 (1985).

ARTICLES

Masses of the satellites of Uranus

S. F. Dermott & P. D. Nicholson

Center for Radiophysics and Space Research, Space Sciences Building, Cornell University, Ithaca, New York 14853, USA

The dynamical theory used to obtain the masses of the uranian satellites from their orbital precession rates contains a fundamental error. The masses can be derived from the precession rates, but a correct analysis of the available data must allow for the fact that the eccentricities, inclinations and precession rates all vary considerably with time, due to mutual secular perturbations.

THE Voyager 2 spacecraft should encounter Uranus on 24 January 1986 and we will then obtain the first detailed images of this puzzling and poorly understood system. Visual observations by Sir William Herschel in 1781 and Lassel in 1851 revealed the presence of four major satellites of similar size: Ariel, Umbriel, Titania and Oberon[1]. The comparatively small and innermost satellite, Miranda, was discovered photographically by Kuiper in 1948 (ref. 1). All of these satellites orbit the planet in direct, near-equatorial, near-circular orbits, but the dynamics of the system appear to be quite different from those of the satellite systems of Jupiter and Saturn. This difference has been insufficiently recognized, which has led to serious misinterpretations of the available observational information.

The radii and the masses of the satellites are presented in Table 1. Brown *et al.*[2] and Brown and Clark[3] determined the satellite radii from photometric and radiometric measurements using a version of the standard radiometric model developed for asteroids. The latest and most complete derivation of the satellites' orbital elements (Table 2) is due to Veillet[4], who has also determined the masses of the four larger satellites from the observed pericentre precession rates[5,6]. The striking feature of these results is the marked dichotomy in the derived satellite densities; the densities of Ariel and Umbriel are similar to those of the inner satellites of Saturn, and are consistent with a composition of 40% rock and 60% water-ice, but Titania and Oberon appear to have much higher densities, suggesting that the water-ice constitutes little more than a thin outer shell. Near-infrared reflectance spectra show that all five satellites have surfaces of water-ice contaminated with a dark spectrally neutral material showing spectral characteristics similar to those of, for example, carbonaceous chondritic material[7].

Table 1 Masses of the uranian satellites

j	Satellite	Radius* (km)	m/M† $\times 10^5$	m/M‡ $\times 10^5$	Densities§ (g cm^{-3})
1	Miranda	250±110	~0.1	0.2±0.2	—
2	Ariel	665±65	1.8±0.6	1.8±0.4	1.3±0.5
3	Umbriel	555±50	1.1±0.3	1.2±0.5	1.4±0.6
4	Titania	800±60	3.2±0.8	6.8±0.8	2.7±0.6
5	Oberon	815±70	3.4±1.0	6.9±0.8	2.6±0.6

* From ref. 2.

† Derived from the radii of Brown *et al.*[2] using a nominal density of .3 g cm^{-3}. The quoted uncertainties in the masses take no account of he uncertainties in the densities.

‡ From ref. 4.

§ Derived from the radii of Brown *et al.*[2] and the masses of Veillet.

A second unusual feature of the Uranus system is the fact that all five satellites have comparable non-zero orbital eccentricities. Since the prediction[8] and discovery[9] of active volcanism on Jupiter's satellite Io, it has been realized that tidal heating due to eccentricity damping may dominate the internal heat budgets of some satellites, so that the thermal evolution of some satellites cannot be understood without a concomitant understanding of their orbital evolution. This is certainly true for Io and may also be for Europa[10-12] and for the saturnian satellite Enceladus[13]. The observed orbital eccentricities and the calculated tidal damping timescales of the uranian satellites are shown in Table 2. It is puzzling that the inner satellites have tidal damping timescales much shorter than those of the outer satellites, probably much shorter than the age of the Solar System, even though all the orbital eccentricities are both finite and of similar magnitude[14,15].

We argue here that the problem posed by the satellite density distribution arises from a misunderstanding of the orbital dynamics and may be imaginary. We also show that the observed eccentricities of the inner satellites, Miranda and Ariel, may be partly forced by the outer satellites and that these forced eccentricities may be maintained despite strong tidal damping.

Secular perturbations

In the jovian and saturnian systems, the orbital elements of many of the satellites (Io, Europa and Ganymede; Mimas, Enceladus, Tethys, Dione and Hyperion) are affected by orbit-orbit resonances. With the exception of a near-commensurability involving Miranda, Ariel and Umbriel, the Uranus system exhibits no true resonances of this type. In the absence of such resonant interactions, the long-term variations in the orbital eccentricity, e, and the inclination, I, of a satellite are largely determined by the secular terms in the satellite's disturbing function, that is, by those terms in the disturbing function that do not depend on the mean longitudes of any of the satellites. If we number the satellites from 1 to n in order of increasing semimajor axis, a, then the secular part of the truncated disturbing function, R_j, for the jth satellite can be written[16]

$$R_j = n_j a_j^2\left[\frac{1}{2}A_{jj}e_j^2 + \sum_{\substack{k=1\\k\neq j}}^{n} A_{jk}e_je_k\cos(\tilde{\omega}_j-\tilde{\omega}_k)\right.$$
$$\left.+\frac{1}{2}B_{jj}I_j^2+\sum_{\substack{k=1\\k\neq j}}^{n} B_{jk}I_jI_k\cos(\Omega_j-\Omega_k)\right] \tag{1}$$

where

$$A_{jj} = n_j\left[\frac{3}{2}J_2\left(\frac{R_p}{a_j}\right)^2-\frac{9}{8}J_2^2\left(\frac{R_p}{a_j}\right)^4-\frac{15}{4}J_4\left(\frac{R_p}{a_j}\right)^4\right.$$
$$\left.+\frac{1}{4}\sum_{\substack{k=1\\k\neq j}}^{n}\frac{m_k}{M}\alpha_{jk}\bar{\alpha}_{jk}b_{3/2}^{(1)}(\alpha_{jk})\right] \tag{2}$$

$$B_{ij} = -n_j\left[\frac{3}{2}J_2\left(\frac{R_p}{a_j}\right)^2-\frac{27}{8}J_2^2\left(\frac{R_p}{a_j}\right)^4-\frac{15}{4}J_4\left(\frac{R_p}{a_j}\right)^4\right.$$
$$\left.+\frac{1}{4}\sum_{\substack{k=1\\k\neq j}}^{n}\frac{m_k}{M}\alpha_{jk}\bar{\alpha}_{jk}b_{3/2}^{(1)}(\alpha_{jk})\right] \tag{3}$$

$$A_{jk} = -\frac{1}{4}\frac{m_k}{M}n_j\alpha_{jk}\bar{\alpha}_{jk}b_{3/2}^{(2)}(\alpha_{jk}) \tag{4}$$

and

$$B_{jk} = \frac{1}{4}\frac{m_k}{M}n_j\alpha_{jk}\bar{\alpha}_{jk}b_{3/2}^{(1)}(\alpha_{jk}) \tag{5}$$

In these expressions

$$\alpha_{jk} = \begin{cases} a_k/a_j & \text{if } k<j \\ a_j/a_k & \text{if } k>j \end{cases} \tag{6}$$

$$\bar{\alpha}_{jk} = \begin{cases} 1 & \text{if } k<j \\ \alpha_{jk} & \text{if } k>j \end{cases} \tag{7}$$

n_j is the mean motion, $\tilde{\omega}_j$ is the longitude of pericentre, Ω_j is the longitude of the ascending node, and m_j is the mass, all for the jth satellite. M, R, J_2 and J_4, are, respectively, the mass, the radius and the first two zonal gravity coefficients of the planet, and the $b_s^{(k)}$ are Laplace coefficients[16]. Since J_2 is non-zero, the orbital inclinations of the satellites must be referred to the equatorial plane of the planet. In writing these expressions, we have neglected solar perturbations (negligible for the uranian satellites), terms of fourth order and higher in the satellite eccentricities and inclinations, and terms of second order in the masses.

The solution of Lagrange's equations for the orbital element variations produced by this disturbing function follows the method described by Brouwer and Clemence[16]. It is convenient to transform the conventional orbital elements into the symmetrical forms

$$\begin{aligned} h &= e\sin\tilde{\omega} \\ k &= e\cos\tilde{\omega} \end{aligned} \tag{8}$$

and

$$\begin{aligned} p &= \sin I\sin\Omega \\ q &= \sin I\cos\Omega \end{aligned} \tag{9}$$

in terms of which the solutions take the simple harmonic form:

$$\begin{matrix} h_j \\ k_j \end{matrix} = \sum_{i=1}^{n} e_{ji} \begin{matrix} \sin \\ \cos \end{matrix}\left(g_it+\beta_i\right) \tag{10}$$

and

$$\begin{matrix} p_j \\ q_j \end{matrix} = \sum_{i=1}^{n} I_{ji} \begin{matrix} \sin \\ \cos \end{matrix}\left(f_it+\gamma_i\right) \tag{11}$$

The eccentricity eigenfrequencies, g_i, are the roots of the determinant

$$\begin{vmatrix} A_{11}-g & A_{12} & \cdots & A_{1n} \\ A_{21} & A_{22}-g & \cdots & A_{2n} \\ A_{n1} & \cdot & \cdots & A_{nn}-g \end{vmatrix} = 0 \tag{12}$$

while the inclination eigenfrequencies, f_i, are the roots of a similar determinant involving the elements B_{jk}. The coefficients e_{ji} are components of the ith eigenvector of the matrix A, with corresponding eigenvalue g_i:

$$\sum_{k=1}^{n} A_{jk}e_{ki} = g_ie_{ji}, \qquad (j=1,2,\ldots,n) \tag{13}$$

Similarly, the coefficients I_{ji} $(j=1,2,\ldots,n)$ are components of the ith eigenvector of the matrix B, corresponding to the eigenvalue f_i. A complete solution of this form involves a total of $4n$ arbitrary constants—the magnitudes of the $2n$ eigenvectors, and the corresponding phases, β_i or γ_i, which, in turn, are determined by a complete set of $4n$ initial conditions (e_j, $\tilde{\omega}_j$, I_j, Ω_j; $j=1,2,\ldots,n$) at some epoch. Note that the solutions for the eccentricity/pericentre variations are completely decoupled from the inclination/node solutions, thus considerably simplifying the analysis.

There are two circumstances in which the variations of e and $\tilde{\omega}$ (or I and Ω) for a particular satellite are relatively simple. In the first of these two cases, the planetary term in equations (2) and (3), involving J_2 and J_4, are much larger than the satellite terms. Since all of the Laplace coefficients are comparable in size, it follows that the off-diagonal matrix elements A_{jk} $(k\neq j)$ are much smaller than the diagonal elements A_{jj}, so that the eigenfrequencies $g_i \simeq A_{ii}$ and the eigenvectors have only small off-diagonal components e_{ji} $(j\neq i)$. As a result, the eccentricities are essentially constant and the pericentre precession rates, $\dot{\tilde{\omega}}_j$, are equal to the eigenfrequencies g_j. This is true for all of the inner satellites of Jupiter and Saturn, except Rhea[17], because of these planets' large oblatenesses. In this case, $\dot{\tilde{\omega}}_j \simeq g_j \simeq A_{jj}$, and $\dot{\Omega}_j \simeq f_j \simeq B_{jj} \simeq -A_{jj}$, so that the nodal precession rate is equal, but of opposite sign, to the pericentre precession rate.

In the second case, the mass of one satellite (j, say) is sufficiently small that its perturbations on the other satellites may be neglected. In consequence, all off-diagonal terms in the jth column of matrix A may be set to zero, and the jth eigenfrequency is again given by $g_j = A_{jj}$ (or $f_j = B_{jj}$). The remaining $n-1$ eigenfrequencies are not, however, necessarily close to the diagonal terms. The eccentricity of satellite j is usually considered as comprising a 'free' component, of frequency g_j, and several 'forced' components, the latter being due to the perturbations by the other satellites. In situations where the free eccentricity is much larger than any of the forced components, the total eccentricity is again virtually constant and the pericentre precision rate is g_j. Examples of this case are provided by the asteroids, for which the (derived) free eccentricities and inclinations are known as 'proper' elements, and the forced components due to the planets are typically ~30% of the free components.

Neither of these two situations applies in the uranian satellite system: Uranus' J_2 is comparatively small[18], and all five satellites have similar masses. Rather, the uranian system is likely to be more closely analogous to the planetary system, for which J_2 (Sun) = 0, and in which all eccentricities and inclinations experience significant secular variations about their mean values. Large variations in e and I, and in $\tilde{\omega}$ and Ω, are to be expected for each of these satellites, on timescales of decades to centuries. A special case is Miranda, whose proximity to Uranus and relatively small mass are reminiscent of both cases discussed above, and which shows an anomalously large 'free' inclination (see Table 2).

Satellite masses

Because of the lack of orbit-orbit resonances in the uranian satellite system, the mutual gravitational perturbations of the satellites' mean longitudes are small and the satellite masses cannot be determined by methods that have proved useful for many jovian and saturnian satellites. The masses of the uranian satellites are, at present, determined from observations of the motions of their pericentres. Harris[5], Dunham[6] and, more recently, Veillet[4] assume that the forced eccentricities of the uranian satellites are negligible compared with their free eccentricities, and that the pericentre precession rates are constant and given by

$$\dot{\tilde{\omega}}_j = A_{jj} \tag{14}$$

Since all the a_j and n_j values are easily determined, the only significant unknowns in equation (14) are J_2 and the five satellite masses. Before the discovery of the narrow uranian rings, J_2 was not known with useful accuracy and thus Harris and Dunham were able to obtain only poor estimates of the satellite masses. However, the uncertainty in J_2 is now effectively negligible[18] and Veillet has used this fact and his own observational programme to derive the satellite masses from the five observed precession rates (see Tables 1, 2). For Titania and Oberon, in particular, the quoted uncertainties in the masses are smaller than 12%. In Table 2, the observed precession rates, $\dot{\tilde{\omega}}_{\rm obs}$, are also compared with those that would be produced by the planet alone, $\dot{\tilde{\omega}}_{\rm P}$. We see that the pericentre rates of Oberon, Titania and even Umbriel are largely determined by the mutual perturbations.

Since the coefficients $b_{3/2}^{(1)}$ and $b_{3/2}^{(2)}$ in equations (2-5) have comparable magnitudes, it follows that if the satellite masses are sufficient to increase significantly $\dot{\tilde{\omega}}_{\rm obs}$ above $\dot{\tilde{\omega}}_{\rm p}$, then the off-diagonal terms, A_{jk} and B_{jk}, must make significant contributions to the eigenfrequencies, thus rendering equation (14) inapplicable. It also follows that, if the initial eccentricities of the satellites have comparable magnitudes, then the forced eccentricities are not negligible and e_j and $\tilde{\omega}_j$ must suffer significant periodic variations. Such variations have been neglected in all published analyses of the observational data although their potential importance was mentioned by Greenberg in 1975 (ref. 17).

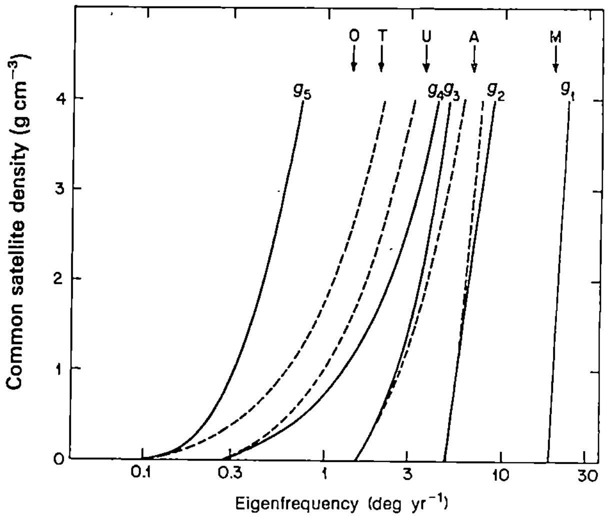

Fig. 1 The solid lines show the variations of the eccentricity eigenfrequencies with the common density of the Uranian satellites. The broken lines are the frequencies associated with the principal diagonal terms of the eigenfrequency matrix. M, A, U, T, and O denote the pericentre precession rates observed by Veillet[4] for, respectively, Miranda, Ariel, Umbriel, Titania and Oberon.

To illustrate the above statements, we consider an heuristic model in which the satellites have a common density ρ. If the off-diagonal terms, A_{jk}, in equation (12) are arbitrarily set to zero, then the forced eccentricities are also zero and the eigenfrequencies are given by the terms, A_{jj}, on the principal diagonal. Figure 1 shows these frequencies as a function of increasing density ρ (the dashed curves) compared with actual eigenfrequencies obtained by solving the full equation (the solid curves). The numbering of the five eigenmodes is chosen so that $g_i \rightarrow A_{ii}$ as $\rho \rightarrow 0$. For the first three modes, the true eigenfrequencies differ only slightly from the dashed curves for all plausible densities. The remaining two eigenmodes, however, which largely reflect interactions between the outer satellites, Titania and Oberon, deviate significantly from the dashed curves for densities as small as 0.5 g cm^{-3}. It is clear then that, at least for these two satellites, equation (14) must be seriously in error.

Table 2 Orbital elements, precession rates and eccentricity damping timescales

j	Satellite	a* (km)	e	$\tilde{\omega}_0$† (deg)	I (deg)	Ω_0† (deg)	$\dot{\tilde{\omega}}_{\rm obs}$ (deg yr^{-1})	$\dot{\tilde{\omega}}_{\rm P}$* (deg yr^{-1})	T_e/Q‡ (Myr)
1	Miranda	129775	0.0027 ± 0.0006	111 ± 14	4.22 ± 0.16	21 ± 5	19.8 ± 0.2	19.04	2
2	Ariel	190822	0.0034 ± 0.0003	120 ± 5	0.31 ± 0.11	263 ± 21	6.8 ± 0.3	4.94	0.5
3	Umbriel	265832	0.0050 ± 0.0003	193 ± 3	0.36 ± 0.08	279 ± 12	3.6 ± 0.2	1.55	8
4	Titania	436035	0.0022 ± 0.0001	147 ± 3	0.142 ± 0.031	311 ± 11	2.0 ± 0.1	0.27	50
5	Oberon	583117	0.0008 ± 0.0001	212 ± 7	0.101 ± 0.024	234 ± 16	1.4 ± 0.2	0.10	300

* Calculated from the observed orbital periods, with $GM = 5.784184 \times 10^6$ km^3 s^{-2}, $J_2 = 3.3450 \times 10^{-3}$, $J_4 = -3.21 \times 10^{-5}$ and $R_p = 26{,}200$ km (ref. 18). Note that the published value of J_2 has been adjusted to Veillet's determination of $M_\odot/M = 22{,}945$.

† At epoch 0 January 1950, 12 h UT. e, I, $\tilde{\omega}_0$, Ω_0 and the observed precession rates, $\dot{\tilde{\omega}}_{\rm obs}$, are from ref. 4.

‡ The calculated tidal damping timescales, T_e, assume that the satellites are icy and have rigidities of 4×10^{10} dyn cm^{-2} and densities of 1.3 g cm^{-3}. Q is the tidal dissipation function and probably has a value ~10^2 (ref. 26).

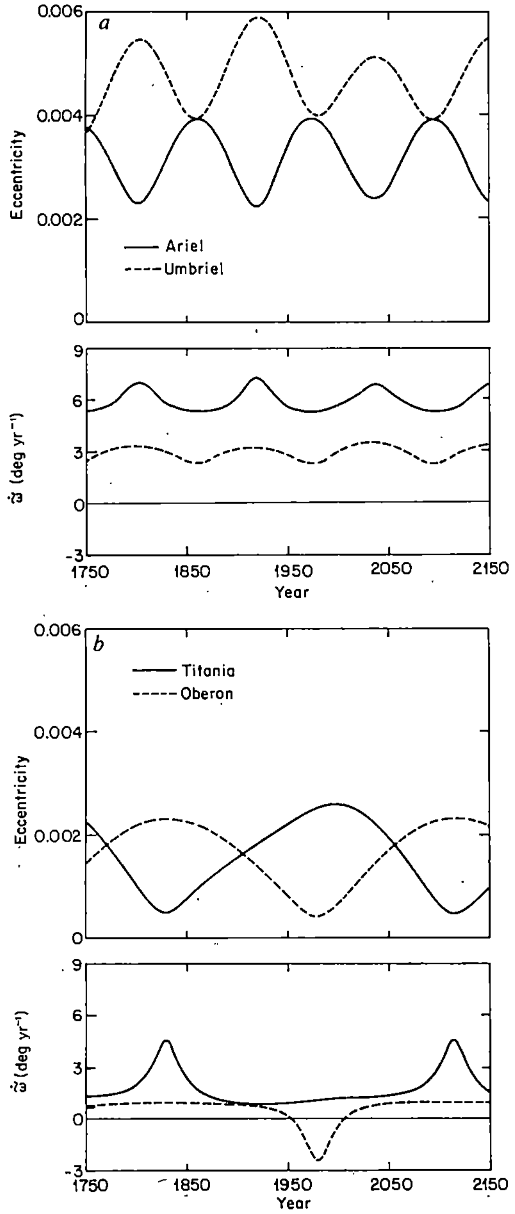

Fig. 2 Possible variations of the eccentricities and the pericentre precession rates of Ariel and Umbriel (*a*) and Titania and Oberon (*b*). We assume that the uranian satellites have a common density of 1.3 g cm^{-3}. The initial conditions are the orbital elements listed by Veillet[4] for the epoch 1950.0 (see Table 2).

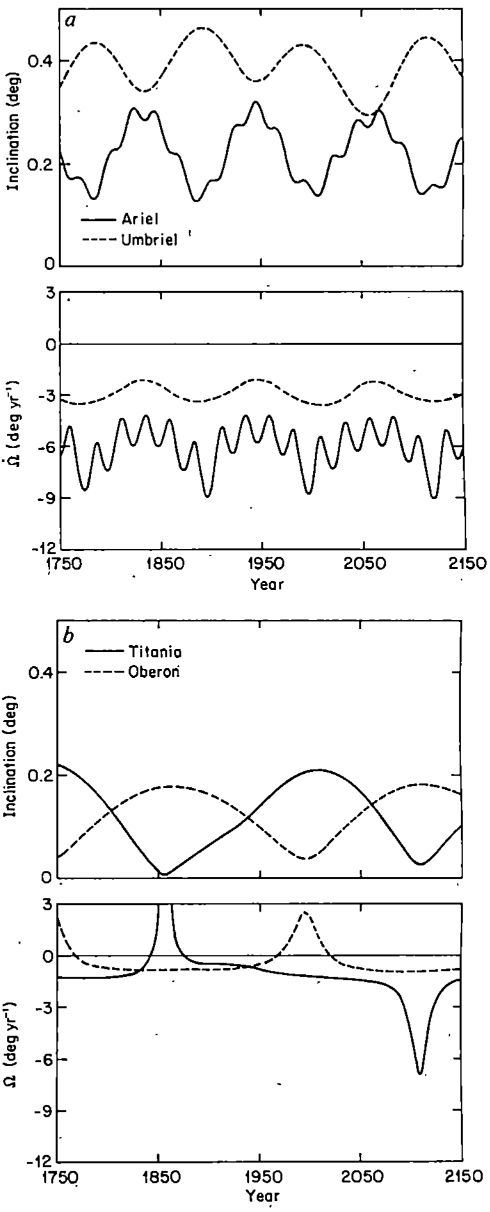

Fig. 3 Possible variations of the inclinations and the nodal precession rates of Ariel and Umbriel (*a*) and Titania and Oberon (*b*). We assume that the uranian satellites have a common density of 1.3 g cm^{-3}. The initial conditions are the orbital elements listed by Veillet[4], for the epoch 1950.0 (see Table 2).

Using masses for a nominal common satellite density of 1.3 g cm^{-3} (see Table 1), we have also calculated the normalized eccentricity and inclination eigenvectors shown in Table 3. These quantities together with the orbital elements determined by Veillet for epoch 1950.0 (see Table 2), which we use as a set of initial conditions, enable us to determine the amplitudes and the phases of the 10 eigenmodes and hence the variations of the orbital elements with time. Our results are shown in Figs 2–4. These should not be taken literally as representing 'the' variation of the uranian satellites' orbital elements, but rather as a typical example of many possible solutions. Not only is our assumption of a uniform density of 1.3 g cm^{-3} completely arbitrary (although plausible), but Veillet's elements were derived on the incorrect assumption that e and I are independent of time.

In all of these calculations, we have used the best values currently available[18] for Uranus' J_2 and J_4, adjusted to Veillet's determination of M. The semimajor axes of the satellites were re-calculated from the observed orbital periods, using the same values for M, J_2, and J_4.

Density of Ariel

Veillet[4] reports that the orbital inclination of Miranda is 4.22° ± 0.16°, in good agreement with the value of 4.0° ± 0.3° obtained by Greenberg and Whitaker[19,20]. The forced inclination components are negligible compared with this anomalously high value and Ω is, therefore, effectively constant, as shown in Fig. 4. This fact, combined with the near-equality of f_1 and B_{11} (compare with g_1 in Fig. 1), implies that the difference between the observed value of Miranda's nodal precession rate, $\dot{\Omega}_1$, and that due to the planetary oblateness alone, $\dot{\Omega}_P$ is related to the masses of the other satellites by

$$\dot{\Omega}_1 - \dot{\Omega}_P \simeq f_1 - \dot{\Omega}_P \simeq -\frac{1}{4} n_1 \sum_{k=2}^{5} \frac{m_k}{M} \alpha_{jk}\bar{\alpha}_{jk} b_{3/2}^{(1)}(\alpha_{jk}) \qquad (15)$$

Using the radii of Brown[2,3] and assuming that the four satellites ave a common density, ρ_A g cm^{-3}, this difference can be written

$$\dot{\Omega}_1 - \dot{\Omega}_p = -1.20\,\rho_A \text{ deg yr}^{-1} \qquad (16)$$

ince Ariel accounts for ~80% of the above nodal rate ifference, ρ_A is effectively the density of Ariel. $\dot{\Omega}_P = -18.99$ deg yr^{-1}, allowing for Miranda's inclination of 4.2° (ref.). If $\dot{\Omega}_1 = -19.76 \pm 0.22$ deg yr^{-1}, as reported by Veillet[4], then, llowing for the uncertainties in the satellite radii, we obtain:

$$\rho_A = 0.64 \pm 0.26 \text{ g cm}^{-3} \qquad (17)$$

his value is quite different from that calculated by Veillet[21], argely because he used an inappropriate value for the radius f Uranus (it is only the product R^2J_2 that is accurately known rom studies of the rings). If the densities of the outer satellites re greater than that of Ariel, or if unseen satellites of significant ass exist anywhere in the uranian system, then the density of riel must be even less than the remarkably low value given bove. This low density is inconsistent with that of a satellite ith a composition of rock and water-ice.

Greenberg and Whitaker[19], on the other hand, obtained a odal precession rate for Miranda of -21.6 ± 0.7 deg yr^{-1}, implyng a value for ρ_A of 2.2 ± 0.9 g cm^{-3}. These apparently inconistent results are disturbing, given the expected constancy of $_1$ and $\dot{\Omega}_1$, but the greatly enlarged data set used by Veillet hould lead to his value being preferred at present. At any rate, t is apparent that an accurate future determination of Miranda's odal precession rate would yield an important constraint on riel's density.

orced eccentricities

idal dissipation due to the tide raised by a planet on a satellite ends to circularize the satellite's orbit, while heating the satellite[8]. In the absence of eccentricity forcing, the orbital eccentricities of Miranda and Ariel would probably decay on timesales significantly less than the age of the Solar System (see able 2). Secular perturbations, on the other hand, result in an xchange of angular momentum between the inner and outer atellites on much shorter timescales (10–1,000 yr), and are thus ikely to considerably extend the eccentricity-decay times calcuated in Table 2. Essentially, the process of tidal dissipation ust now be thought of as damping entire eigenmodes, rather han individual satellite eccentricities. Naturally, those modes hich have their largest amplitudes for the inner satellites, that s modes 1 and 2 in Table 3*a*, will be damped most rapidly, hile modes 4 and 5, involving principally Titania and Oberon, ill be damped much more slowly.

An examination of the observed eccentricities of Miranda and riel, however, suggests that even modes 1 and 2 have not yet een completely damped. Based on the eigenmode solution in able 3, we find the 'forced' component of Miranda's eccentricity (due principally to Ariel) to be ~0.0003, or only about 0% of the observed value, while the forced component of riel's eccentricity (due principally to Umbriel) is ≈0.0008, ~25% of the observed value. (The term 'forced' is used loosely o refer to that component of the eccentricity which is not due o the eigenmode most closely associated with the satellite in uestion). This conclusion is supported by the observation that iranda and Ariel exhibit pericentre precession rates close to he calculated eigenfrequencies for modes 1 and 2, respectively see Tables 2, 3 and Fig. 1).

Thus, we cannot account for the observed eccentricities of iranda and Ariel purely in terms of forcing by the outer atellites. However, since Veillet's observational data need to e re-reduced in the light of our findings on the variability of e orbital elements, the latter conclusion may be premature. e note that the osculating elements of Miranda obtained by eillet from data taken on eight nearly consecutive nights in pril 1981 give an eccentricity of 0.0007 ± 0.0004 (ref. 21). This w value is consistent with what we would expect if tidal dissipation had entirely damped out the first eccentricity eigenmode, but not the second.

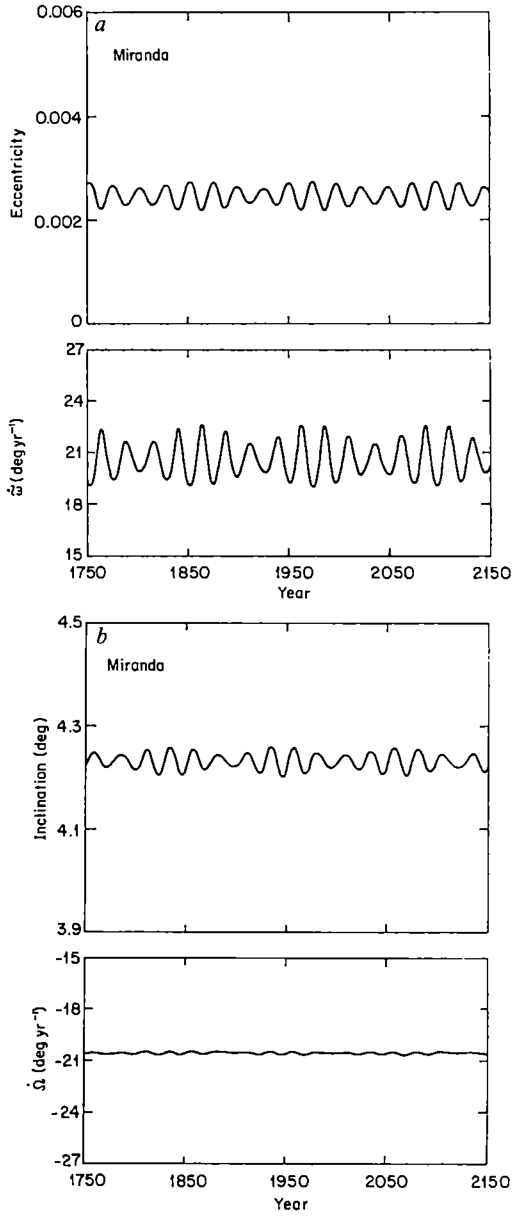

Fig. 4 Possible variations of the eccentricity (*a*) and the inclination (*b*) of Miranda and the corresponding variations in the precession rates, $\dot{\tilde{\omega}}$ and $\dot{\Omega}$. We assume that the uranian satellites have a common density of 1.3 g cm^{-3}. The initial conditions are the orbital elements listed by Veillet[4] for the epoch 1950.0 (see Table 2).

If the large amplitudes of the first two eigenmodes are confirmed by subsequent studies, then maintenance mechanisms outside those provided by low-order secular perturbation theory must be sought. Perturbation terms of second-order in the masses will produce variations in e and I on timescales $\Gamma \sim T/(m/M)^2$, where T is the characteristic orbital period. For the uranian satellites, $\Gamma \sim 10^8$ yr. If Γ is less than the eccentricity damping timescales, it is conceivable that these second-order perturbations may result in an exchange of angular momentum between the inner and the outer satellites sufficient to maintain the eccentricities of the inner satellites. This possibility will be investigated in the near future, by means of very long-term numerical integrations of test satellite systems (A. Milani and A. M. Nobili, personal communication). Another possibility is that an expansion of the orbits of Miranda and Ariel due to tidal dissipation in the planet has resulted in the comparatively

Table 3 Eccentricity and inclination eigenvectors for a common satellite density of 1.3 g cm^{-3}

a Normalized eccentricity eigenvectors						
Satellite	*j*	Mode 1	Mode 2	Mode 3	Mode 4	Mode 5
Miranda	1	0.9999	0.0674	0.0146	0.0036	0.0026
Ariel	2	−0.0031	0.9678	0.1688	0.0347	0.0216
Umbriel	3	−0.0002	−0.2424	0.9841	0.1744	0.0955
Titania	4	0.0000	−0.0024	−0.0521	0.8287	0.6098
Oberon	5	0.0000	−0.0004	0.0060	−0.5307	0.7865
Eigenfrequency (deg yr^{-1})		20.612	5.951	2.878	1.610	0.352
b Normalized inclination eigenvectors						
Satellite	*j*	Mode 1	Mode 2	Mode 3	Mode 4	Mode 5
Miranda	1	0.9999	0.0836	0.0225	0.0082	0.0070
Ariel	2	−0.0039	0.9553	0.1979	0.0599	0.0413
Umbriel	3	−0.0003	−0.2837	0.9769	0.2488	0.1423
Titania	4	0.0000	−0.0053	−0.0770	0.7972	0.6278
Oberon	5	0.0000	−0.0013	0.0097	−0.5468	0.7641
Eigenfrequency (deg yr^{-1})		−20.560	−6.005	−2.840	−1.696	−0.249

recent passage of these satellites through orbit-orbit resonances[14]. Passage through resonance may have resulted in the excitation of both a high eccentricity and a high inclination, but whereas the eccentricity would subsequently be damped by tidal dissipation, the high inclination would remain and would testify to the resonance passage.

Discussion

Because of the neglect of secular variations in all published analyses of the orbits and masses of the uranian satellites, including that of Veillet[4], the results obtained from these investigations must be treated with caution. The masses in particular, derived from an inappropriate expression for pericentre precession, may well be considerably in error. Unfortunately, it does not appear possible to correct these omissions and re-derive better values for the satellite masses without a reconsideration of all the available data. Such an investigation is beyond the scope of this paper. A thorough re-analysis of the uranian satellites' orbital elements, taking into account the present results, would probably start with the establishment of osculating elements from short ($\leq$5 yr) spans of data, and then attempt to model the longer-term variations in these osculating elements in terms of the theory of secular perturbations. Hints of such variations are already present in the large differences between some of the orbital elements derived by Harris in 1950, Dunham in 1970 and Veillet in 1983. Apart from yielding an improved set of masses, such an investigation may be expected to shed light on several other outstanding problems. These include: (1) a discrepancy of ~0.2° between the pole direction of Uranus deduced from stellar occultation studies of the rings[18,22] and that obtained by Veillet[4]; (2) a discrepancy between the observed period of the Miranda-Ariel-Umbriel longitude variation and that deduced from Veillet's masses[23]; and (3) the question of whether any 'secular librations' exist among the satellites, as suggested by Greenberg[17]. The results shown in Figs 2 and 3 and Table 3 indicate that Titania and Oberon could well be involved in such a libration, involving the arguments $\tilde{\omega}_4$-$\tilde{\omega}_5$ and/or Ω_4-Ω_5.

Although it does not seem possible, at present, to ascribe the apparently undamped eccentricities of Miranda and Ariel to secular perturbations alone, it is clear that a more realistic estimate of tidal damping timescales for the uranian satellites must take such perturbations into account. An investigation of this matter will form the subject of a future paper.

Finally, we note that the encounter with Uranus of the Voyager 2 spacecraft on 24 January 1986 should provide several pieces of information relevant to uranian satellite dynamics. Most important would be direct measurements of the satellite masses, which now must be considered as unknown. Only Miranda is to be approached relatively closely by the spacecraft, but all necessary steps should be taken to maximize the chances of successful mass determinations for the other four satellites, especially Ariel. Of secondary importance, but also valuable, would be the determination of a complete set of osculating orbital elements for the satellites, based on far-encounter and near-encounter imaging. In particular, an accurate Voyager determination of Miranda's node, combined with extensive ground-based observations of this satellite carried out over the past 9 yr (refs 21, 24, 25) should lead to an independent estimate of Ariel's density through equation (15).

We thank D. J. Stevenson, R. Hamilton Brown and W. Reid Thompson for useful discussions. This research was supported by NASA grants.

Received 29 July; accepted 31 October 1985.

1. Cruikshank, D. P. in *Uranus and the Outer Planets* (ed. Hunt, G.) 193-210 (Cambridge University Press, 1982).
2. Brown, R. H., Cruikshank, D. P. & Morrison, D. *Nature* **300**, 423-425 (1983).
3. Brown, R. H. & Clark, R. N. *Icarus* (in the press).
4. Veillet, C. thesis Univ. Paris 6 (1983).
5. Harris, D. L. thesis, Univ. Chicago (1949).
6. Dunham, D. W. thesis, Yale Univ. (1971).
7. Brown R. H. in *Uranus and Neptune* (ed. Bergstralh, J. T.) 437-461 (NASA Con. Pub. 2330, 1984).
8. Peale, S. J. Cassen, P. & Reynolds, R. T. *Science* **203**, 892-894 (1979).
9. Morabito, J., Synnott, S. D., Kupferman, P. W. & Collins, S. A. *Science* **204**, 972 (1979).
10. Cassen, P., Peale, S. J. & Reynolds, R. T. *Geophys. Res. Lett.* **7**, 963-970 (1980).
11. Cassen, P., Peale, S. J. & Reynolds, R. T. *Geophys. Res. Lett.* **6**, 731-734 (1979).
12. Squyres, S. W., Reynolds, R. T., Cassen, P. & Peale, S. J. *Nature* **301**, 225-226 (1983).
13. Squyres, S. W., Reynolds, R. T., Cassen, P. & Peale, S. J. *Icarus* **53**, 319-331 (1983).
14. Dermott, S. F. in *Uranus and Neptune* (ed. Bergstralh, J. T.) 377-404 (NASA Conf. Publ. 2330, 1984).
15. Squyres, S. W., Reynolds, R. T. & Lissauer, J. J. *Icarus* **61**, 218-223 (1985).
16. Brouwer, D. & Clemence, G. M. *Methods of Celestial Mechanics* (Academic, New York, 1961).
17. Greenberg, R. *Mon. Not. R. astr. Soc.* **170**, 295-303 (1975); in *Uranus and Neptune* (ed. Bergstralh, J. T.) 463-480 (NASA Conf. Publ. 2330, 1984).
18. French, R. G., Elliot, J. L. & Levine, S. E. *Icarus* (submitted).
19. Greenberg, R. & Whitaker, E. A. *Bull. Am. astr. Soc.* **6**, 207 (1974).
20. Whitaker, E. A. & Greenberg, R. *Mon. Not. R. astr. Soc.* **165**, 15p-18p (1973).
21. Veillet, C. *Astr. Astrophys.* **118**, 211-216 (1983).
22. Elliot, J. L. & Nicholson, P. D. in *Planetary Rings* (eds Greenberg, R. & Brahic, A.) 25-72 (University of Arizona Press, Tucson, 1984).
23. Lazzaro, D., Ferraz-Mello, S. & Veillet, C. *Astr. Astrophys.* **140**, 33-38 (1984).
24. Veillet, C., & Ratier, G. *Astr. Astrophys.* **89**, 342-344 (1980).
25. Veillet, C. *Astr. Astrophys.* **98**, 218-222 (1981).
26. Peale, S. J., Cassen, P. & Reynolds, R. T. *Icarus* **43**, 65-72 (1980).

Requirement of stereospecific alignments for initiation from the simian virus 40 early promoter

Keikichi Takahashi*, Marc Vigneron*, Hans Matthes, Alan Wildeman*, M. Zenke* & Pierre Chambon

Laboratoire de Génétique Moléculaire des Eucaryotes, CNRS, Unité 184 de Biologie Moléculaire et de Génie Génétique, INSERM, Institut de Chimie Biologique, Faculté de Médecine, Strasbourg 67085 Cédex, France

The distance between the simian virus 40 early promoter elements has been altered by inserting either odd or even multiples of half a DNA turn. There are marked differences in the in vivo *effects of these two types of insertions on initiation of transcription from this promoter.*

DISSECTION *in vivo* and *in vitro* of the simian virus 40 (SV40) early promoter region (see Fig. 1) has shown that it contains two overlapping promoters for RNA polymerase B (II), the early-early (EE) and late-early (LE) promoters (see refs 1-5 and refs therein). Accurate initiation of RNA synthesis at the early-early start sites (EES) requires the TATA box element, whereas the 21-base pair (bp) repeat region and the enhancer are both essential for efficient transcription. Efficient initiation of transcription from the late-early start sites (LES) also requires the presence of the 21-bp repeat region and of the enhancer, and occurs in the apparent absence of a TATA box. Six G·C motifs (Fig. 1; I-VI) are involved in the function of the 21-bp repeat region, but they do not contribute equally to stimulation of transcription from the EES and LES, G·C motifs I-III being the most important for initiation from EES, whereas initiation from LES is more dependent on G·C motifs IV-VI[4,5]. A systematic mutational dissection of the enhancer region has revealed that several sequence motifs are indispensable to its function, and that the same sequences are reponsible for enhancement of transcription from both the EES and the LES[6].

In vitro transcription studies have shown that different *trans*-acting factors bind specifically to these *cis*-acting regulatory sequences. The TATA box factor binds to the TATA box to form a stable complex; this is a prerequisite for specific initiation of transcription[7,8]. The transcription factor Sp1 binds specifically to the 21-bp repeat region and stimulates transcription from the EES and LES[4,9-11]. Different *trans*-acting factor(s) bind(s) to the enhancer and stimulate(s) transcription from both the SV40 early and heterologous promoter elements[12-15]. Moreover, footprinting experiments have shown that binding *in vitro* of the Sp1 factor[4,10,11] and enhancer[16] factor(s) to the 21-bp repeat and the enhancer regions, respectively, is severely impaired by mutations known to be detrimental to the *in vivo* function of these promoter elements.

Therefore, at least three different proteins (or sets of proteins), interacting with three different promoter elements, are required to allow RNA polymerase B to initiate transcription from the SV40 early promoter. However, both the 21-bp repeat element and the enhancer can operate when in an inverted orientation (refs 4-6 and refs therein), although they do not exhibit any obvious symmetry in their DNA sequence. In addition, the enhancer can stimulate transcription to some extent when inserted some distance away[17-19]. Thus, rather than stimulating transcription by interacting with each other and/or with RNA polymerase, the factors that bind to the 21-bp repeat and enhancer regions could induce a local perturbation in the structure of the DNA helix, which could be propagated close to the start sites, where it would facilitate initiation of transcription by RNA polymerase B. We have altered the distance between the three SV40 early promoter elements by inserting either odd or even multiples of half a turn of the DNA helix (DNA turn), and demonstrate here that there are marked differences in the *in vivo* effects of these two types of insertions on initiation from this promoter, which strongly suggests that protein-protein interactions are involved in activation of transcription initiation from an RNA polymerase B promoter.

Construction and assay of spacing mutants

All spacing mutant recombinants are similar to pDHB3.SV1 (ref. 5) and pSEGO (ref. 4) in that they contain the SV40 early promoter region (from *Hpa*II to *Hin*dIII; Fig. 1) inserted upstream from a promoter-less rabbit β-globin gene (position −9 to +1,650) and a complete rabbit β-globin gene (including its promoter region), acting as an internal 'reference' gene. The pS series contains 4-29-bp inserts at the *Sal*I site (position 32) between the 21-bp repeat and the TATA box region of pSO. The pSE series harbours 5-25-bp inserts at the *Bam*HI site (position 101) between the enhancer and 21-bp repeat region of pSEGO (similar to pSO, but containing a single 72-bp sequence). In the pSR series, inserts of 4-21 bp are introduced between the TATA box and the inverted 21-bp repeat region (from position 40 to 103) of pSRO (otherwise identical to pSO). The pSR series also contains 4-7-bp deletion mutants (Fig. 1). For most spacer lengths, we constructed two recombinants, A and B, with different inserted sequences (usually the same sequence in both orientations).

After transfection of the recombinants into HeLa cells, RNA initiated from the SV40 early promoter was measured by quantitative S_1 nuclease mapping using two probes as described previously[4,5]. The amount of RNA initiated from the reference β-globin gene (GLOB band in Figs 2-4) and the total amount of RNA initiated from the SV40 early promoter region (EP band in Figs 2-4) was determined with probe A. Probe B was used to accurately map and quantitate RNA initiated from the EES and LES of the SV40 early promoter (Figs 1-4; under the present stringent S_1 nuclease conditions, the bands corresponding to LES2 and LES3 were not resolved and no attempt was made to measure initiation from LES1—see refs 1 and 5 for a discussion of these points).

DNA turn-dependent insertions

Between the enhancer and 21-bp repeat region. Introduction of 10 bp and 21 bp, both near-integral multiples of the 10.5 bp per turn of B-DNA *in vitro*[20], between the 21-bp repeat region and the enhancer of pSEGO, causes an ~50% decrease in RNA

---

[*] Present addresses: Medical Institute for Bioregulation, Kyushu University, Maedashi 3-1-1, Higashi-ku, Fukuoka 812, Japan (K.T.); Department of Virology, The Weizmann Institute for Science, Rehovot, Israel (M.V.); Department of Molecular Biology and Genetics, University of Guelph, Guelph, Ontario, Canada NIG 2W1 (A.W.); European Molecular Biology Laboratory, Postfach 102209, D-6900 Heidelberg, FRG (M.Z.).

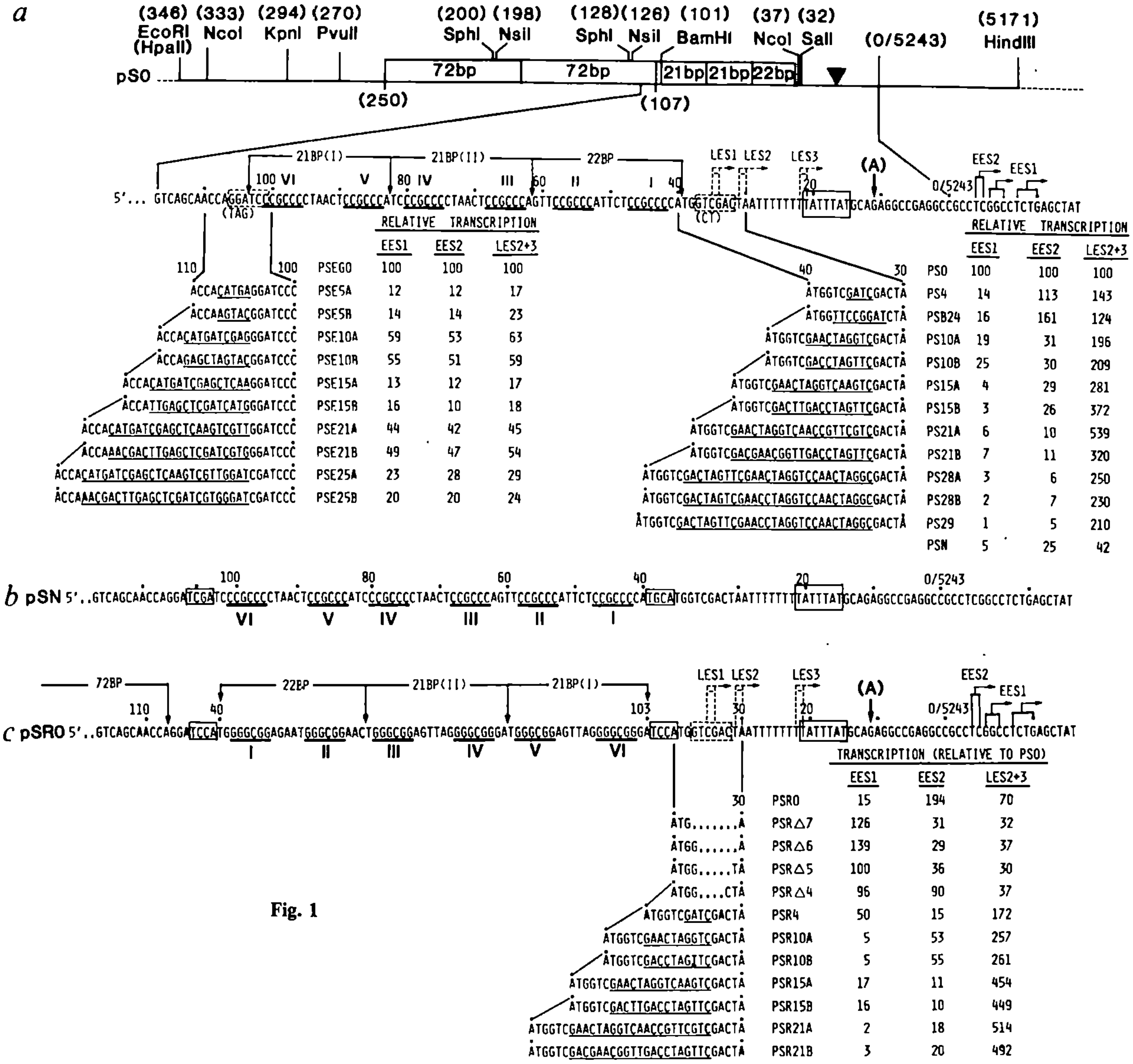
a
(346) EcoRI (HpaII)
(333) NcoI
(294) KpnI
(270) PvuII
(200) SphI
(198) NsiI
(128) SphI
(126) NsiI
(101) BamHI
(37) NcoI
(32) SalI
(0/5243)
(5171) HindIII
pSO
72bp
72bp
21bp 21bp 22bp
(250)
(107)
21BP(I)
21BP(II)
22BP
100 VI V 80 IV III 60 II I 40
LES1 LES2 LES3
(A)
EES2 EES1
0/5243
20
5'... GTCAGCAACCAGGATCCCGCCCCTAACTCCGCCCATCCCGCCCCTAACTCCGCCCAGTTCCGCCCATTCTCCGCCCCATGGTCGAGTAATTTTTTTTATTTATGCAGAGGCCGAGGCCGCCTCGGCCTCTGAGCTAT
(TAG)
(CT)
110
100
40
30
b pSN 5'..GTCAGCAACCAGGATCGATCCCGCCCCTAACTCCGCCCATCCCGCCCCTAACTCCGCCCAGTTCCGCCCATTCTCCGCCCCATGCATGGTCGACTAATTTTTTTTATTTATGCAGAGGCCGAGGCCGCCTCGGCCTCTGAGCTAT
100 80 60 40 20 0/5243
VI V IV III II I
72BP
22BP
21BP(II)
21BP(I)
110 40 103 30 20
LES1 LES2 LES3
(A)
EES2 EES1
0/5243
c pSRO 5'..GTCAGCAACCAGGATCCATGGGGCGGAGAATGGGCGGAACTGGGCGGAGTTAGGGGCGGGATGGGCGGAGTTAGGGGCGGGATCCATGGTCGACTAATTTTTTTTATTTATGCAGAGGCCGAGGCCGCCTCGGCCTCTGAGCTAT
I II III IV V VI
30

Fig. 1

RELATIVE TRANSCRIPTION

		EES1	EES2	LES2+3
	PSEG0	100	100	100
ACCACATGAGGATCCC	PSE5A	12	12	17
ACCAAGTACGGATCCC	PSE5B	14	14	23
ACCACATGATCGAGGGATCCC	PSE10A	59	53	63
ACCAGAGCTAGTACGGATCCC	PSE10B	55	51	59
ACCACATGATCGAGCTCAAGGATCCC	PSE15A	13	12	17
ACCATTGAGCTCGATCATGGGATCCC	PSE15B	16	10	18
ACCACATGATCGAGCTCAAGTCGTTGGATCCC	PSE21A	44	42	45
ACCAAACGACTTGAGCTCGATCGTGGGATCCC	PSE21B	49	47	54
ACCACATGATCGAGCTCAAGTCGTTGGATCGATCCC	PSE25A	23	28	29
ACCAAACGACTTGAGCTCGATCGTGGGATCGATCCC	PSE25B	20	20	24

RELATIVE TRANSCRIPTION

		EES1	EES2	LES2+3
	PS0	100	100	100
ATGGTCGATCGACTA	PS4	14	113	143
ATGGTTCCGGATCTA	PSB24	16	161	124
ATGGTCGAACTAGGTCGACTA	PS10A	19	31	196
ATGGTCGACCTAGTTCGACTA	PS10B	25	30	209
ATGGTCGAACTAGGTCAAGTCGACTA	PS15A	4	29	281
ATGGTCGACTTGACCTAGTTCGACTA	PS15B	3	26	372
ATGGTCGAACTAGGTCAACCGTTCGTCGACTA	PS21A	6	10	539
ATGGTCGACGAACGGTTGACCTAGTTCGACTA	PS21B	7	11	320
ATGGTCGACTAGTTCGAACTAGGTCCAACTAGGCGACTA	PS28A	3	6	250
ATGGTCGACTAGTCGAACCTAGGTCCAACTAGGCGACTA	PS28B	2	7	230
ATGGTCGACTAGTTCGAACCTAGGTCCAACTAGGCGACTA	PS29	1	5	210
	PSN	5	25	42

TRANSCRIPTION (RELATIVE TO PSO)

		EES1	EES2	LES2+3
	PSR0	15	194	70
ATG.......A	PSRΔ7	126	31	32
ATGG......A	PSRΔ6	139	29	37
ATGG.....TA	PSRΔ5	100	36	30
ATGG....CTA	PSRΔ4	96	90	37
ATGGTCGATCGACTA	PSR4	50	15	172
ATGGTCGAACTAGGTCGACTA	PSR10A	5	53	257
ATGGTCGACCTAGTTCGACTA	PSR10B	5	55	261
ATGGTCGAACTAGGTCAAGTCGACTA	PSR15A	17	11	454
ATGGTCGACTTGACCTAGTTCGACTA	PSR15B	16	10	449
ATGGTCGAACTAGGTCAACCGTTCGTCGACTA	PSR21A	2	18	514
ATGGTCGACGAACGGTTGACCTAGTTCGACTA	PSR21B	3	20	492

initiated from all EES and LES (pSE10 and 21 mutants; Figs 1, 2, 5). In marked contrast, alterations of the distance between these two promoter elements by odd multiples of half a DNA turn result in dramatic 80–90% decreases in transcription initiated from all start sites (pSE5, 15 and 25 mutants; Figs 1, 2, 5). This is well illustrated by the 'cyclic' variations in the total amount of RNA initiated from the SV40 early promoter region estimated from the intensity of the band EP in Fig. 2. As the EE and LE promoters share a common element—the 21-bp repeat region—these results indicate that efficient transcription from both the EES and LES requires stereospecific alignments between some elements of the enhancer and of the 21-bp repeat region (see below for further discussion). The present results also confirm our previous conclusion[1] that the enhancer is required for activating transcription from both the SV40 EE and LE promoters.

Several lines of evidence support the conclusion that the observed variations reflect modifications of the effect of the enhancer and not of the activity of a putative upstream element similar to the 21-bp repeat region, which would also be contained in the enhancer sequence. First, no mutations within the enhancer have been found that affect its activity specifically when it is in close apposition to the 21-bp repeat region, but not when it is moved far away[6]. Second, the level of all RNA species initiated downstream from the enhancer varies in parallel, which is in marked contrast to the differential variations observed with insertions between the 21-bp repeat region and the TATA box (see below). Third, there is no rapid overall decrease of RNA synthesis as the length of the 'even inserts' is increased and no decrease at all with 'odd inserts', which again is in marked contrast to the variations observed in either the pS or pSR series (see below). The last observation probably reflects the increasing possibility of achieving a proper alignment as the length of the odd inserts increases.

The sequence element(s) which, within the enhancer domains, is (are) responsible for this DNA turn-dependence of activation of transcription is (are) unknown. The SV40 enhancer is composed of at least two domains, A and B, which are very inefficient by themselves but, when juxtaposed, stimulate transcription from the early promoter by three orders of magnitude[6]. In an enhancer containing a single 72-bp sequence, domain A, which is centred on the *Sph*I site, spans the 3′ moiety of the 72-bp sequence, whereas domain B roughly spans the 5′ moiety of the 72-bp sequence and sequences located further upstream up to approximately the *Pvu*II site (ref. 6; see also Fig. 1). Inserting fragments of various lengths (4–50 bp) between domains A and B does not markedly affect the enhancer activity[6], indicating that there is apparently no stringent position requirement between the two domains nor between domain B and the 21-bp repeat region. (However, longer insertions result in a strong decrease of enhancer activity; see ref. 6.) It appears, therefore, that the cyclic variations in RNA synthesis observed in the pSE

Fig. 1 (Opposite) General organization and sequences of the SV40 early promoter region and the pS, pSE and pSR mutant series. *a*, Organization of SV40 early promoter region in recombinant pSO. Some key natural or engineered (*Bam*HI, *Sal*I) restriction sites are indicated with their position (BBB system; see ref 29) in parentheses. ▼, Location of the TATA box; the sequence of pSO (noncoding early strand) between coordinates 5,227 and 117 is shown. The SV40 wild-type bases mutated during the creation of the *Bam*HI (101) and *Sal*I (32) sites (dashed boxes; see ref. 4), are indicated in parentheses below the main sequence. The TATA sequence is boxed. The position of the early-early start sites (EES1 and EES2, arrows) and late-early start sites (LES1, LES2 and LES3, dashed arrows) are indicated (see ref. 1 and text). The position of start site (A) corresponding to the G residue at position 11 is indicated (see Fig. 3 and text). The directly repeated 21-bp sequences (I and II), and the 22-bp sequences are delimited by vertical, downward-pointing arrows. The six G·C motifs 5′ CCGCCC 3′ are underlined and identified by roman numerals[4]. The sequences inserted (underlined) in the pSE and pS mutant series are represented on the left- and right-hand sides below the pSO sequence, respectively. The pSE mutant series is derived from pSEGO (ref. 4), which contains a single 72-bp sequence, whereas the pS mutant series is derived from pSO which contains a complete 72-bp repeat (see below). Sequences of pSN (*b*) and pSRO (*c*), in which the 21-bp repeat region is in the natural and reverse orientation, are shown. Boxed sequences at the borders of the 21-bp repeat region correspond to the 4-bp inserts generated during the construction of these recombinants. pSN and pSRO have a complete 72-bp repeat. The sequences deleted or inserted (underlined) in the pSR mutant series are indicated below the pSRO sequence. The relative amount of RNA initiated at EES1, EES2 and LES2+3 after transfection of the various recombinants into HeLa cells was estimated by scanning autoradiograms (similar to those shown in Figs 2-4) from at least three different quantitative S_1 nuclease mapping experiments using different plasmid preparations. After correction for transcription from the reference β-globin gene[4,5] the results were expressed relative to pSO (for the pS and pSR series) or pSEGO (for the pSE series), taken as 100%.

Methods. Construction of pSO, pSRO and pSN. pSO, which is identical to pSEGO[4] but contains a complete 72-bp repeat, was constructed by ligating the *Hin*dIII/*Bam*HI fragment (position 5,171–101, BBB numbering system[29]) of pSEGO into the equivalent position of pSVTK2 (ref. 4). pSRO and pSN were constructed as follows: pTK4 is similar to pHB4 (ref. 4), but contains a complete 72-bp repeat, a *Sal*I site at position 32 (by exchange of the *Hin*dIII (5,171)/*Nco*I(37) fragment with that of pSEGO), and lacks the *Sal*I and *Sph*I sites in the pBR322 sequence (destroyed by repairing with Klenow DNA polymerase and blunt-end ligation). pTK4 was digested with *Nco*I (position 37) and *Bam*HI (position 101), and treated with Klenow DNA polymerase in the presence of all four dNTPs. The fragments were ligated back to yield two recombinants (pTK421N and pTK421R) containing the 21-bp region in either orientation between the repaired *Nco*I and *Bam*HI sites. The *Sal*I/*Kpn*I fragments (positions 32 and 294) of these two recombinants were isolated and ligated to pSO digested by *Sal*I and *Kpn*I to yield pSN and pSRO. Construction of mutants with insertions and deletions between the 21-bp repeat region and the TATA box region: Three sets of two overlapping complementary oligonucleotides (10-, 15-, 21-mers) with *Sal*I protruding 5′ ends were synthesized by the phosphotriester method as described previously[30]. The oligonucleotides were phosphorylated, mixed, heated to 60 °C for 30 min and then hybridized at room temperature for 1 h. pSO and pSR DNAs were digested with *Sal*I and ligated to the oligonucleotides to yield the pS (pS10, 15, 21) and pSR (pSR10, 15 and 21) mutant series, respectively, with inserts in either orientation (A and B). pS4 and pSR4 were constructed by blunt-end ligation of pSO and pSR cleaved with *Sal*I and repaired with Klenow DNA polymerase. pSB24 containing a different 4-bp insert was constructed by replacing the *Hin*dIII/*Nco*I (5,171–37) fragment of pSO with that of pDB3.B24[5]. pS28A, pS28B and pS29 were obtained during the cloning of pS10 (see Fig. 1). Deletion mutants of pSR were prepared as follows: 30 µg of pSRO was digested with *Sal*I, phenol–chloroform-extracted, precipitated with ethanol, and suspended in 400 µl S_1 nuclease mixture (30 mM NaoAc *p*H 4.5, 3 mM $ZnSO_4$, 400 mM NaCl). 250 units of S_1 nuclease were added, and after 10 min at 25 °C the reaction was stopped by adding 70 µl of 2 M Tris-HCl *p*H 8.0, 0.2 M EDTA. After phenol-chloroform extraction, the DNA was precipitated with ethanol and suspended in 30 µl 10 mM Tris-HCl *p*H 8.0, 1 mM EDTA. DNA (1 µg) was treated with Klenow DNA polymerase in the presence of all four dNTPs, then ligated to yield pSRΔ7–pSRΔ4 deletion mutants . Construction of mutants with insertions between the 21-bp repeat and the enhancer: The pSE mutant series was constructed by shot-gun ligation of synthetic oligonucleotides[31]. Briefly, eight sets of different overlapping oligonucleotides corresponding to the sequence between the *Bam*HI and *Nsi*I sites (positions 101 and 126) plus additional sequences of 5, 10, 15 and 21 bp at the *Bam*HI extremity were chemically synthesized. The oligonucleotides were phosphorylated at their 5′ ends, mixed and hybridized as above, and ligated directly into pSEGO (ref. 4) digested with *Nsi*I and *Bam*HI to yield the pSE mutant series. pSE25 (A and B) were constructed by cleaving pSE21 with *Bam*HI, followed by blunt-end ligation after reparation with Klenow DNA polymerase. Recombinant DNAs were grown and prepared as described previously[4] and monitored for possible rearrangements by restriction enzyme analysis. Sequence and orientation of the DNA inserts were determined by dideoxynucleotide sequencing of both strands using double-stranded plasmid DNAs as template, and synthetic oligonucleotide primers[32].

series reflect the necessity of a stereo-alignment between some elements contained in enhancer domain A and the G·C motifs of the 21-bp repeat region.

Between the 21-bp repeat and TATA box regions. In agreement with our previous results[4,5], insertion of DNA segments of increasing length between the 21-bp repeat and the TATA box regions leads to a rapid and drastic decrease in RNA initiated at the major early-early start sites, EES1 (Figs 1, 3, 5). It is, however, remarkable that 10- (pS10A and B) and 21-bp (pS21A and B) inserts are consistently less detrimental to transcription than 4- (pS4 and pSB24) and 15-bp (pS15A and B) inserts, respectively. It is particularly striking that the intensity of the two bands labelled EES2 in Fig. 3 varies in exactly the opposite way (see also Figs 1, 5). These two bands correspond to minor start sites which, contrary to EES1, do not disappear when the TATA box is mutated[1], but are absent when the row of Ts located immediately upstream from the TATA box is mutated (M. Pauly, M. Wintzerith, H.M. and P.C., unpublished results). It is probable, therefore, that this row of Ts acts as a substitute TATA box to direct initiation of transcription at EES2.

We conclude that some upstream elements must be located stereospecifically with respect to a given TATA box for initiation of transcription under its control to occur. To characterize these elements further, we constructed plasmid pSN (Figs 1, 4), which contains a 4-bp insertion at both ends of the 21-bp repeat region, so as to maintain the TATA box and enhancer elements close to their natural steric relationship. The pattern of initiation in pSN (EES2 favoured compared with EES1; Figs 1, 4) is very similar to those of pS4 and pSB24, which possess a single 4-bp insertion between the TATA box and the 21-bp repeat region. This result indicates that it is the steric location, relative to the TATA box, of the 21-bp repeat region rather than that of the enhancer which is responsible for the occurrence of initiation preferentially at EES1 or EES2. However, as expected from the results obtained with the pSE5 mutants, there was a general decrease in transcription from pSN compared with pS4 and pSB24.

Several lines of evidence support the conclusion that the region at which transcription initiation occurs is primarily determined by the location of the 21-bp repeat region, and that the TATA box element selects the precise site of initiation. Moving the 21-bp repeat region away from the TATA box region by >20 bp results in a dramatic decrease of transcription from both EES1 and EES2 start sites, whereas initiation from the LES is concomitantly increased, indicating that the location of the 21-bp repeat region is not optimal for initiation from LES. Using longer DNA inserts, we found that initiation at LES disappears, whereas new start sites located within a 30-50-bp region downstream from the 21-bp repeat region appear[4]. Note that with insertions of ≤21 bp there is very little initiation of transcription within the inserted sequence, as the band corresponding to the endpoint of homology between the wild-type probe and RNA transcribed from the spacing mutants is very weak, with the exception of mutants pS28A and B (not shown) and pS29 (Fig. 3, right-hand arrow). Whether the same late-early start sites were used in all insertion mutants cannot be determined from the present experiments, as all start sites in the A+T-rich region (positions 14–31) yield the same LES2+3 bands under the S_1 nuclease conditions used in this study (see above; there is, however, an additional start site A (Fig. 3) which appears to be preferentially used in some mutants). Thus, it is not possible from the present study to determine whether initiation of transcription from the various LES is also DNA turn-dependent.

Insertions and deletions between the inverted 21-bp repeat and TATA box regions. The 21-bp repeat region can stimulate initiation of transcription from the EES and LES, even when inserted in the reverse orientation in the SV40 early promoter region[2,4,5,21]. The pSR mutant series (Fig. 1) was constructed to determine whether altering the distance between the inverted 21-bp repeat region and the TATA box region would result in

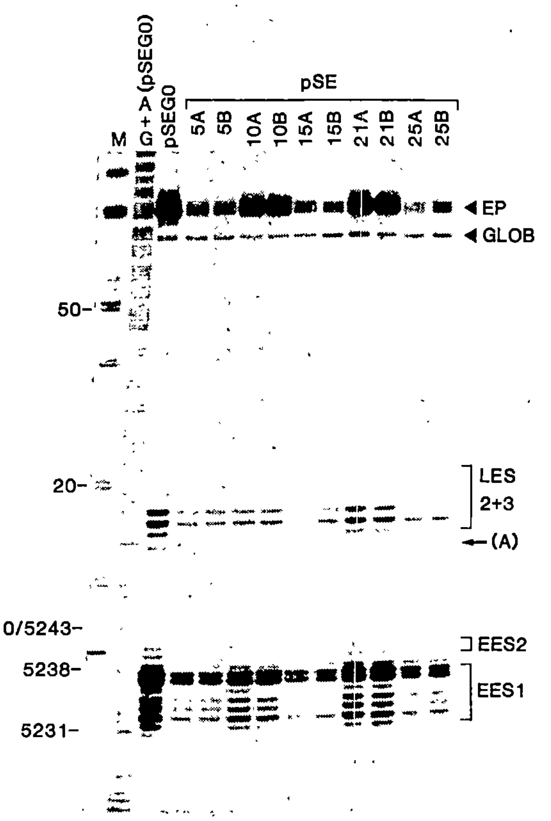

Fig. 2 Effect of insertions between the 21-bp repeat region and the enhancer on transcription initiated *in vivo* from the SV40 early-early and late-early start sites. HeLa cells were transfected with the pSE mutant series (as indicated at the top of each lane) and cytoplasmic RNA was analysed by quantitative S_1 nuclease mapping as described previously[4,5], using probes A and B which correspond to the [^{32}P]5'-end-labelled coding strand of the *Bst*NI fragment of the rabbit β-globin gene (position +138 to −84) and the [^{32}P]5'-end-labelled SV40 early coding strand of the *Hin*dIII to *Cla*I fragment of pSEGO, respectively. EP indicates the S_1 nuclease-resistant DNA fragment that arises from the homology between probe A and the SV40-globin hybrid transcripts. GLOB corresponds to the S_1 nuclease-resistant DNA fragment of probe A expected for RNA initiated at the start site of the reference β-globin gene contained in these recombinants. The S_1 nuclease-resistant bands EES1, EES2 and LES2+3 correspond to RNA initiated from the early-early and the late-early promoters, respectively, as described previously[1,5] and in the text. The arrow labelled A points to a resistant band corresponding to start site A indicated in Fig. 1. Numbers on the left-hand side pointing to the A+G sequence ladder of probe B indicate the SV40 nucleotide positions using the BBB numbering system. Lane M, size markers ([^{32}P]5'-end-labelled *Msp*I digest of pBR322).

the same critical DNA turn-dependence as that observed with the 21-bp repeat region in its natural orientation. In mutant pSRO, initiation is low from EES1 and high from EES2 compared with the wild-type early promoter in pSO, and similar to that of mutants pS4 and pSB24 containing a 4-bp insertion between the 21-bp repeat region and the TATA box (Figs 3-5). This observation is particularly striking because the first G·C motif (VI) in pSRO is at the same distance from the TATA box as the first G·C motif (I) in pS4 or pSB24, that is, approximately half a turn off from the natural configuration. Introducing deletions (pSRΔ4, pSRΔ5, pSRΔ6 and pSRΔ7) or an insertion of approximately one-half a DNA turn (pSR4) in pSRO, thereby rebuilding a wild-type architecture, resulted in a pattern of initiation from EES1 and EES2 that is very similar (EES1 much higher than EES2) to that observed with the naturally spaced promoter of pSO (Figs 1, 4, 5). Initiation from EES1 is the highest in the deletion mutant pSRΔ6, whereas it is concomitantly the lowest from EES2 (Figs 1, 4). A drastic decrease in RNA initiated at both EES1 and EES2 is observed with inserts of increasing length, but the pattern of initiation from these start sites shows the same dependence on DNA turn as in the pS series (compare pSRO, pSR10A and B and pSR21A and B with pSR4, pSR15A and B. We conclude that, even when inverted, the 21-bp repeat region has to be correctly aligned with the TATA box element to preferentially activate initiation of transcription from the EES1, and similarly will preferentially stimulate initiation from the EES2 when aligned with the T-rich substitute TATA box.

As in the case of the pS spacing mutant series, in which the 21-bp repeat region is in the normal orientation, initiation from the late-early start sites, LES2+3, of the pSR series increased with the length of the inserts. Finally, it should be stressed that all pSR recombinants contain a 4-bp insertion between the 21-bp repeat region and the enhancer. As introducing one-half a DNA turn between the enhancer and the 21-bp repeat region in its natural orientation results in a striking decrease of intiation from all start sites (pSE5 in Figs 2, 5), it is likely that these additional 4 bp are required to stereo-align some elements of the enhancer and the inverted 21-bp repeat region. In fact, the additional insertion of 5 bp between the 21-bp repeat region and the enhancer of pSRΔ4 results in a strong decrease in initiation from all start sites (data not shown).

A role for protein-protein interactions

Our results are most easily interpreted along the lines that protein-protein interactions are involved in activation of transcription initiation. An alternative possibility, that factors bound to the 21-bp repeat region and the enhancer induce stereospecifically related local perturbations in the DNA helix that are recognized by the rest of the transcription machinery, appears less likely in the light of our present knowledge.

The results obtained by inserting odd and even multiples of half a DNA turn between the 21-bp repeat region and the normal or substitute TATA box regions demonstrate clearly that efficient activation of initiation of transcription requires a stereospecific alignment between these elements, and that the region at which initiation of transcription occurs is determined primarily by the position of the 21-bp repeat region. Studies *in vivo* (refs 3-5, 21 and refs therein) and *in vitro* (refs 2, 4, 22 and refs therein) have shown that the first three G·C motifs (most notably GC-I) of the 21-bp repeat region (Fig. 1) are essential elements of the SV40 early promoter. *In vitro*, the transcription factor Spl contacts several G residues (underlined) of the 3' $G\underline{G}C\underline{GGG}$ 5' motif (refs 10, 11 and our unpublished results). A different factor binds to the TATA box (refs 7-9, 23; and our unpublished results). Thus, initiation of transcription appears to require a stereospecific alignment between the Spl and TATA box factors, which led us to propose the following model.

The transcription machinery (presumably RNA polymerase B) interacts primarily with at least the first of the three Spl factor molecules (bound to G·C motifs I-III) which are all located on one side of the DNA helix. The TATA box factor, when correctly positioned by a properly aligned TATA box, interacts with the polymerase and directs it to initiate principally at the corresponding start site(s) (EES1 in the wild type; mutating the TATA box results in the disappearance of RNA initiated at the EES1 both *in vivo* and *in vitro*[1]). Misalignment caused by inserting half a DNA turn leads to the preferential use of the T-rich substitute TATA box which is located on the other side of the helix and controls initiation at the EES2. Spl factors bound to G·C motifs II and III may either interact directly with the trancription machinery or interact with each other and their effect be mediated by the Spl factor bound to G·C-I. Whether this Spl factor and the TATA box factor interact directly with each other as well as with RNA polymerase, for instance to stabilize their respective interactions with their cognate binding sites, cannot be predicted from our present study. However, stable binding of Spl factor to the 21-bp repeat region *in vitro*

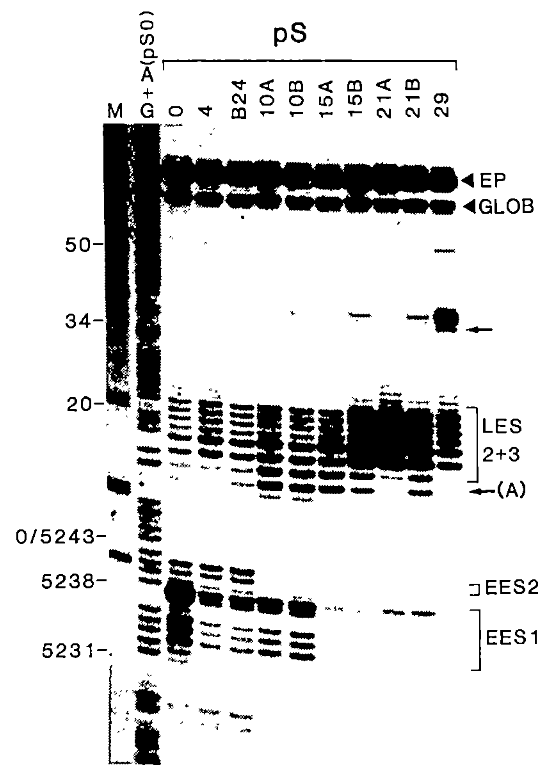

Fig. 3 Effect of insertions between the 21-bp repeat and the TATA box regions on trancription initiated *in vivo* from the SV40 early-early and late-early start sites. HeLa cells were transfected with the pS mutant series (as indicated) and cytoplasmic RNA was analysed by quantitative S_1 mapping using a probe B prepared from pSO. Symbols are as described in Fig. 2 legend. The arrow on the right-hand side indicates the beginning of all insertions (SV40 coordinate 34). Start site A corresponds to position 11.

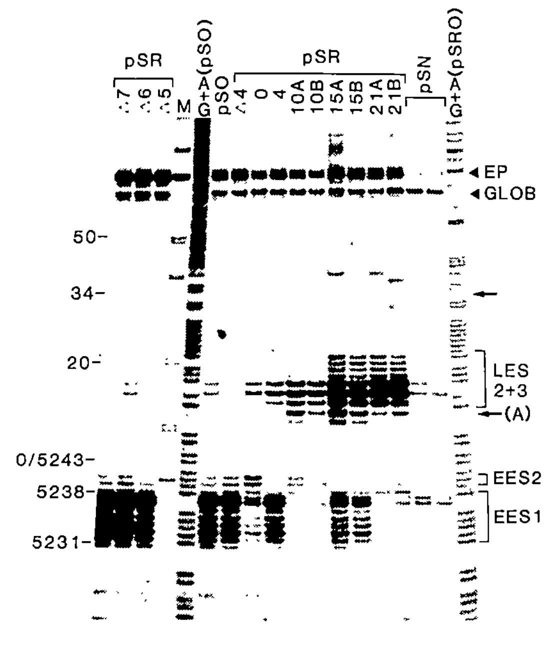

Fig. 4 Effect of deletion and insertion between the inverted 21-bp repeat region and the TATA box region on transcription *in vivo* from SV40 early-early and late-early start sites. Cytoplasmic RNA extracted from HeLa cells transfected with the pSR series mutants (as indicated) was analysed by quantitative S_1 nuclease mapping using a probe B prepared from pSO. Symbols are as described in the legends to Figs 2, 3. The arrow on the right-hand side of the figure indicates the beginning of all insertions (position 34). Start site A corresponds to position 11.

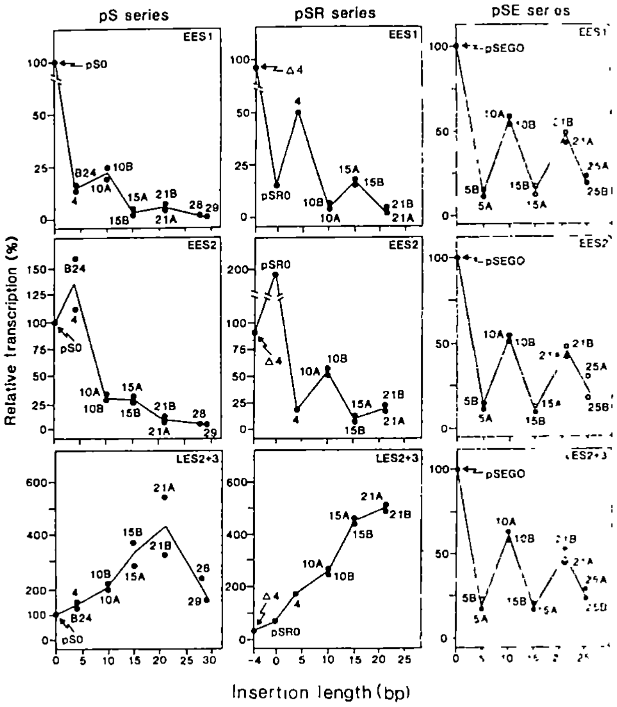

Fig. 5 Diagramatic comparison of the results obtained with the various insertion mutants. The length of the insertions (or deletion, pSR series) between the 21-bp repeat region and the TATA box region or the enhancer is indicated on the abscissa and the relative efficiency of transcription is given on the ordinate. The left-hand panels represent the results of the pS mutant series for transcription starting at EES1, EES2 and LES2+3, whereas the right-hand and centre panels show the results for the pSE (insertions between the TATA box and the 21-bp repeat region) and pSR (insertions between the TATA box and inverted 21-bp repeat region) mutant series, respectively. The values which are taken from Fig. 1 are expressed relative to EES1, EES2 and LES2+3 of pSO (for the pS and pSR series) and pSEGO (for the pSE series).

does not require the presence of the TATA box region[23]. Increasing the distance between the 21-bp repeat region and the TATA box (or its substitute) either prevents the transcription machinery from interacting efficiently with the bound TATA box factor (even when properly aligned) or prevents the TATA box factor from binding efficiently to the TATA box, and results in the observed rapid decrease in initiation from the EES1 and EES2. Weak substitute TATA box elements will then direct the transcription machinery to preferentially initiate at the various LES. With longer inserts, similar weak multiple substitute TATA box elements (see ref. 24) will direct the transcription machinery to initiate at multiple sites in the 30–50-bp region located immediately downstream from the 21-bp repeat region. Alternatively, RNA polymerase bound to the 21-bp repeat region may initiate at multiple sites without the help of the TATA box factor. Such a model readily accounts for the observation that there is no marked overall decrease in RNA initiated from the SV40 early promoter region in the insertion mutants (see band EP in Fig. 3, whose intensity reflects the total amount of RNA initiated from the SV40 early promoter region).

The study of the pSR series shows clearly that the 21-bp repeat region, even when inverted, has to be stereo-aligned with the TATA box or the substitute T-rich TATA box to preferentially stimulate initiation at the EES1 or EES2, respectively. It is particularly striking that the pattern of initiation of the wild-type naturally spaced pSO recombinant (EES1 much higher than EES2) is best reproduced with the inverted 21-bp repeat region recombinants pSR4 and pSRΔ6, whose position of the corresponding G·C-rich motifs is separated by 10 bp when their

TATA boxes are aligned. Thus, our results suggest strongly that equivalent protein–protein contacts can be established between the transcription machinery and the factor(s) bound to the G·C motifs, irrespective of the orientation of the 21-bp repeat region. This is very surprising because there is no apparent symmetry in the sequence of these motifs. Several explanations can be proposed to account for this paradox: (1) symmetry may be present in the G·C motif, even though it is not readily apparent; (2) Sp1 factor could be an asymmetrical molecule with equivalent protein interaction sites at either end; (3) the protein with which Sp1 factor interacts (for instance, RNA polymerase which has multiple subunits) may possess symmetrical protein interaction sites; (4) Sp1 factor may be composed of two functional domains linked by a flexible stem: one DNA-binding domain which would specifically recognize the G·C motifs, and one protein-interacting domain which would interact with some component of the transcription machinery. We find the two-domain hypothesis attractive because such separate domains for DNA binding and activation of transcription by protein interaction with RNA polymerase are known to exist in repressor proteins of *Escherichia coli* λ phages[25-27]. In this respect, we note that in the two inverted 21-bp region recombinants pSR4 and pSRΔ6 (see above) and in the wild-type recombinant pSO (which exhibit the same patterns of initiation at the EES1 and EES2), the N-7 of the G residues in the G·C motifs, which are protected by Sp1 factor from methylation by dimethylsulphate[11], are located on the same side of the DNA helix when their TATA box sequences are aligned (data not shown).

Our present results and those reported elsewhere[6] demonstrate that efficient initiation of transcription from the entire SV40 early promoter region requires a stereospecific alignment between some element(s) contained in domain A of the enhancer and the 21-bp repeat region. Transcriptional factors are known to bind *in vitro* to domain A[13,14,16]. Thus, it is likely that they have to be stereo-aligned with Sp1 factors for the enhancer to efficiently stimulate transcription. Note that the Sph motifs present in domain A, known to be important for enhancer activity[6], are separated by approximately one helical turn from one another and by a multiple of 10 bp from the G·C motifs. Thus, protein(s) bound to these Sph motifs and to the G·C motifs may be on the same side of the helix, and may specifically interact with each other and/or independently with some element(s) of the transcription machinery (for example, RNA polymerase; see above). Note that Sp1 factor can bind to the 21-bp repeat region *in vitro* in the absence of the enhancer sequence[10,23], whereas proteins appear to be less stably bound to the enhancer in the absence of the 21-bp repeat region[16], and that transcription can occur *in vitro* (but not *in vivo*) from an enhancer-less early promoter, although at a reduced rate[2,14].

It appears, therefore, that the assembly of proteins bound to the various elements of the SV40 early promoter could constitute a broad protein interaction region located mainly on one side of the DNA helix, where it could act as a specific recognition region for RNA polymerase B, which itself is composed of multiple subunits[28]. The part played by the transcriptional factors bound to the 21-bp repeat and the TATA box region would be to anchor stably RNA polymerase to enable it to initiate at the start sites, and perhaps also to have a role in its activation. The protein(s) bound to enhancer domain A would participate in activation of transcription initiation, either directly by interacting with RNA polymerase, or indirectly through contacts with the protein(s) bound to the 21-bp repeat region. All these interactions contribute to increase the transcription machinery concentration at a given promoter region which has to compete successfully with the rest of the very large genomic DNA for efficient initiation of transcription to occur. A DNA looping mechanism may account for the persistence of some enhancer activity (see refs 1, 19) as it is moved away from the other promoter elements. That the enhancer, and not only the 21-bp repeat region, can activate transcription irrespective of its orientation, can be explained by the hypothesis that proteins bound to it are composed of two distinct functional domains linked by a flexible stem (see above). The fact that enhancer domain B (essential for enhancer activity) apparently does not need to be stereospecifically aligned makes it unlikely that proteins bound to that domain belong to the broad RNA polymerase B binding and activation complex discussed above. However, *in vitro* studies[13,14] indicate that proteins bound to domain B are involved in the stimulation of transcription observed *in vitro* with templates that contain enhancers, suggesting that, nevertheless, these proteins interact in some way with the transcription machinery.

In conclusion, our results clearly support the view that multiple protein–protein interactions have a key role in the generation of an active transcriptional initiation complex at a promoter, which is a very large specific nucleoprotein structure composed of multiple sequence elements recognized by different cooperating factors. It is likely that this concept can be generalized to other class B(II) promoters, as the same DNA turn dependence has been observed when the SV40 enhancer activates transcription from the adenovirus-2 major late promoter (our unpublished results). *In vitro* studies aimed at reconstructing transcription initiation complexes from purified factors and RNA polymerase are in progress to investigate the validity of our model.

We thank J. Wang and M. Lewitt for helpful discussions; R. Breathnach, B. Wasylyk, G. Albrecht and I. Davidson for critical reading of the manuscript; our colleagues for generous gifts of recombinants; M. Acker for growing cells; A. Staub for synthesizing oligonucleotides; C. Werlé and B. Boulay for illustrations; and the secretarial staff for typing the manuscript. This work was supported by CNRS (ATP 3582), INSERM (PRC 124026), the Fondation pour la Recherche Médicale, the Ministère de la Recherche et de la Technologie (82V1283) and the Association pour le Développement de la Recherche sur le Cancer. K.T., A.W. and M.Z. were recipients of fellowships from INSERM/JSPS and CNRS, Natural Sciences and Engineering Research Council of Canada and the CNRS/Deutsche Forschungsgemeinschaft, respectively.

Received 3 September; accepted 15 November 1985.

1. Wasylyk, B., Wasylyk, C., Matthes, H., Wintzerith, M. & Chambon, P. *EMBO J.* **2**, 1605-1611 (1983).
2. Vigneron, M., Barrera-Saldana, H. A., Baty, D., Everett, R. E. & Chambon, P. *EMBO J.* **3**, 2373–2382 (1984).
3. Buchman, A. R., Fromm, M. & Berg, P. *Molec. cell. Biol.* **4**, 1900–1914 (1984).
4. Barrera-Saldana, H. A. *et al. EMBO J.* (in the press).
5. Baty, D., Barrera-Saldana, H. A., Everett, R. D., Vigneron, M. & Chambon, P. *Nucleic Acids Res.* **12**, 915–932 (1984).
6. Zenke, M. *et al. EMBO J.* (in the press).
7. Davison, B. L., Egly, J. M., Mulvihill, E. R. & Chambon, P. *Nature* **301**, 680–686 (1983).
8. Parker, C. S. & Topol, J. *Cell* **37**, 273–283 (1984).
9. Dynan, W. S. & Tjian, R. *Cell* **32**, 669–680 (1983).
10. Dynan, W. S. & Tjian, R. *Cell* **35**, 79–87 (1983).
11. Gidoni, D., Dynan, W. S. & Tjian, R. *Nature* **312**, 409–413 (1984).
12. Sassone-Corsi, P., Dougherty, J. P., Wasylyk, B. & Chambon, P. *Proc. natn. Acad. Sci. U.S.A.* **81**, 308–312 (1984).
13. Sassone-Corsi, P., Wildeman, A. G. & Chambon, P. *Nature* **313**, 458–463 (1985).
14. Wildeman, A. G., Sassone-Corsi, P., Grundström, T., Zenke, M. & Chambon, P. *EMBO J.* **3**, 3129–3133 (1984).
15. Sergeant, A., Bohmann, D., Zentgraf, H., Weiher, H. & Keller, W. *J. molec. Biol.* **180**, 577–600 (1984).
16. Wildeman, A. G. *et al Molec. cell. Biol.* (submitted).
17. Moreau, P. *et al. Nucleic Acids Res.* **9**, 6047–6068 (1981).
18. Banerji, J., Rusconi, S. & Schaffner, W. *Cell* **27**, 299–308 (1981).
19. Wasylyk, B., Wasylyk, C. & Chambon, P. *Nucleic Acids Res.* **12**, 5589–5608 (1984).
20. Wang, J. *Proc. natn. Acad. Sci. U.S.A.* **76**, 200–203 (1979).
21. Everett, R. D., Baty, D. & Chambon, P. *Nucleic Acids Res.* **11**, 2447–2464 (1983).
22. Hansen, U. & Sharp, P. A. *EMBO J.* **2**, 2293–2303 (1983).
23. Miyamoto, N. G., Moncollin, V., Egly, J. M. & Chambon, P. *Nucleic Acids Res.* **12**, 8779–8799 (1984).
24. Wasylyk, B., Wasylyk, C., Augereau, P. & Chambon, P. *Cell* **32**, 503–514 (1983).
25. Hochschild, A., Irwin, N. & Ptashne, M. *Cell* **32**, 319–325 (1983).
26. Wharton, R. P., Brown, E. L. & Ptashne, M. *Cell* **38**, 361–369 (1984).
27. Ptashne, M. *Trends biochem. Sci.* **9**, 142–145 (1984).
28. Kedinger, C., Gissinger, F. & Chambon, P. *Eur. J. Biochem.* **44**, 421–436 (1974).
29. Tooze, J. (ed.) *DNA Tumor Viruses* (Cold Spring Harbor Laboratory, New York, 1982).
30. Matthes, H. W. D. *et al. EMBO J.* **3**, 801–805 (1984).
31. Grundström, T. *et al. Nucleic Acids Res.* **13**, 3305–3316 (1985).
32. Wallace, R. B. *et al. Gene* **16**, 21–38 (1981).

A very high energy γ-ray burst from the Crab pulsar

P. N. Bhat, P. V. Ramanamurthy, B. V. Sreekantan & P. R. Vishwanath

Tata Institute of Fundamental Research, Homi Bhabha Marg,
Bombay 400005, India

The Crab pulsar, a source of pulsed photons over a wide range of energies, has been observed in the TeV energy range by several groups using the Atmospheric Cerenkov technique[1]. Time-averaged phasograms have shown signals on only a few occasions. The Durham University group[2] detected pulsed TeV γ-rays during two transients lasting 15 min, each in October, 1981, while the Ooty group[3,4] has shown that the transient duration could be on time scales of minutes or even seconds. In our recent observations, we identified a 15-min interval on 23 January 1985 during which pulsed TeV γ-rays were detected at a 5.1 sigma level at the same phase as the radio main pulse. Our inference of transient pulsed emission is strengthened by the absence of a signal in a nearby control telescope tilted 8° away from the pulsar and evidence for signal in another telescope 11 km away. We present here an analysis of the data from our 1984–1985 observations.

The Ooty array (for details, see refs 3 and 5), normally operated with 18 mirrors, was split up and operated at two sites, site A and site B, 11 km apart. At site A, eight large mirrors, with a diameter of 1.5 m, were used and at site B, 10 small mirrors, with a diameter 0.9 m were used. For some of the runs at site A, the eight large mirror array was further split into two halves with one half of the array (A1) pointing at Crab and the other half (A2) at a point 8° south of Crab. The trigger was derived from a three-out-of-four majority logic at site A and a coincidence of four mirror banks (at least two mirrors in each bank) at site B. The chance coincidence rates of the arrays were also monitored. The arrival time of the event was recorded to an accuracy of 0.1 ms at both the sites. In addition, the pulse from the photomultiplier on each mirror at site A was digitized with a LeCroy ADC (analog digital converter). The time keeping accuracy was 0.03 ms which was achieved with a NNSS (Navy Navigation Satellite System) satellite timing receiver. The average trigger rate at site A was 500 per min when the array was not split and about 300 per min for each of the half arrays (A1 and A2) when it was split. The average rate at site B was about 120 per min. Such high rates resulted from several factors: large mirror areas, majority logic and 4° apertures employed in the experiment. These rates convert to a threshold of 800 GeV for the full array at site A and 1.2 TeV for arrays A1 and A2. The energy threshold at site B was 2.2 TeV.

Data were taken during December 1984 and January and February 1985. The February runs were rejected because of persistent lightning. Data on Crab pulsar were taken on nine nights at site A, out of which the two array (A1 and A2) mode was used on four nights. At site B, there were 11 nights of observation, out of which there was overlap with observations at site A during six nights only. Total observation times at sites A and B were 1,436 and 1,908 min respectively. The total time of simultaneous observations at the two sites was 1,004 min, out of which the array at site A was operated in the two half array mode for 540 min.

The analysis of the data was carried out using the pulsar elements applicable to the epoch of our observations obtained from contemporaneous radio observations (by A. G. Lyne). A barycentric time reduction programme and related ephemeris (due to D. Richards and I. Shapiro respectively) were used to compute the number of Crab pulsar cycles at the barycentre for every half hour at the observation site. The pulsar phase for each event was then computed by interpolation (checked to be accurate to better than 0.0016%) and folded to obtain the phasogram for the pulsar. The number of bins used for the phasogram is 20.

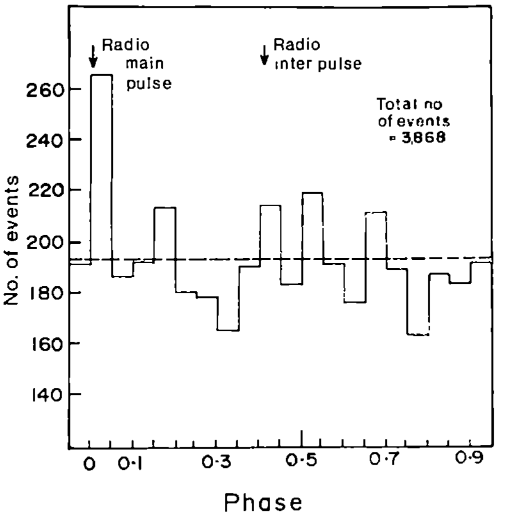

Fig. 1 The phasogram of events from array A1 looking at the Crab pulsar during the 15-min duration 1711 to 1726 h on 23 January 1985. Each bin has a width of 1.65 ms. The average for the whole phasogram is shown by the horizontal dashed line.

The data were split into mini-runs of duration five minutes each and a phasogram was constructed for each mini-run. Phasograms from three consecutive mini-runs were added to get one 15-min phasogram. There were such 116 independent 15-min phasograms from data at site B and 90 from site A, giving a total of 206 phasograms. When these phasograms were inspected for significant peaks, we found one 15-min interval during the night of 23 January 1985 from the half array A1 (looking at the Crab pulsar) at site A showing a 5.1 sigma peak at the position of the radio main pulse. In the phasogram, which is shown in Fig. 1, there are 72 excess events during the 15-min interval in the first phase bin when the average was 193 events. There is a minor (1.5σ) peak at the position of the radio inter-pulse. Figure 2*a*, *b* shows the observed number of events in the first phase bin and the average per-bin from the entire phasogram for all the three mini-runs from arrays A1 and A2 looking at and away from the pulsar respectively. While A1 has shown excess of $>2\sigma$ in all the three mini-runs, there is a non-significant excess only in the first mini-run in A2. The total number of excess events in the first phase bin from data at A2 is only seven when the average was 182 events per phase bin.

The array at site B had a higher energy threshold and since the photomultiplier pulses at site A were digitized, one can check whether the response at site B is commensurate with the energy spectrum of events at site A. From matching the ADC response with the number of events from site B, one can pick out the higher energy events. Figs 2*c* and 2*d* show the behaviour of higher energy events in the array A1 at site A and of all events at site B. In the first two mini-runs, the response of the two arrays is quite similar: 79 events were observed in the first phase bin at each of the two arrays when the average number of events per phase bin is 64. However, the array at site B seems to be deficient in the third mini-run. Therefore, we can only say that the two arrays have behaved similarly for at least 2/3 of the duration. We note that the trigger rates and chance coincidence rates at the two arrays did not show any significant increase during these 15 min.

The Poissonian probability that an excess of 72 or more events is seen when the average is 193, amounts to 6.1×10^{-7}. However, there were 206 independent 15-min intervals and each one was made up of three mini-runs of five minutes. Therefore, the probability has to be multiplied by 618, which is the total number of ways in which the 15 min intervals could be formed. Thus,

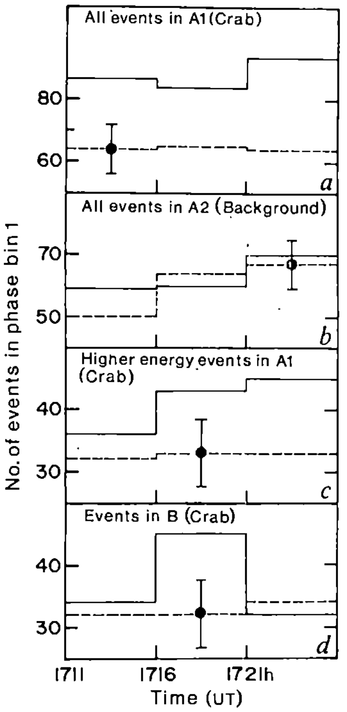

Fig. 2 Solid lines are the observed number of events in the phase bin 1 (0. to 0.05 in phase) during a 15 m interval 1711 to 1726 h (UT) on 23 January 1985 and the broken lines are the average per bin based on the full phasogram. Typical 1σ error bars are shown in each case. *a* Events in the array looking at Crab at site A. *b* Events in the array looking at a point 8°, south of Crab. *c* Higher energy events in the array looking at Crab at site A—the cut was made on energy such that the event rate matches with the one at site B. *d* All events in the array looking at Crab at site B.

the Poissonian probability that the peak is at the position of the radio main pulse due to chance turns out to be 3.8×10^{-4}. A more, conservative estimate for the same is obtained by O'Mongain's likelihood analysis[6] which is 4.2×10^{-3}. At this juncture, one has to ask about the similarity of VHE γ-ray phenomena with those seen by the COS-B (7) group at lower energies from the Crab pulsar. As some of the analyses of the VHE γ-ray observations did not have absolute phase information, it is not possible to say at what phase the signal was seen whenever a claim was made. In some cases, absolute phase information was available (for example, see ref. 1), but the phase of the VHE gamma ray signal did not coincide with that of the signal at lower energies. Therefore, if we accept that there could be phase differences between γ-ray emissions at different energies, one has to multiply the above probabilities by the number of bins which is 20. Therefore, the probability that the signal could appear in any bin due to chance is 7.6×10^{-3} (Poissonian). Thus, the confidence level for a VHE γ-ray signal in our data is 92% (O'Mongain) and 99.2% (Poissonian).

We have tried to verify the authenticity of the signal seen by us by changing the true Crab pulsar period in steps of $\Delta P = 10^{-7}$ s and computing the phasograms for each period. The step size of ΔP is chosen such that the neighbouring trials are independent of each other. 10,000 different periods were tried with 5,000 on either side of the true period; there was not even one trial in which a signal $>5\sigma$ was seen. The probability of seeing a $>5\sigma$ signal in any phase bin is therefore $<6.9/10{,}000 = 6.9\times10^{-4}$ with 99.9% confidence level which is much higher than the value of 92% derived from the likelihood analysis of O'Mongain. The latter may therefore be considered very conservative.

As noted earlier, two such 15-min bursts were seen by Gibson *et al.* in October 1981. The similarities between those and the present burst are that the duration is 15 min and the excess number of events is 70. Whereas the Durham observations did not have absolute phase information and the pulse had a long duration of 6 ms FWHM (full width at half maximum), the peak seen by us coincides with the radio main pulse. The pulse width of the peak in our data is <2 ms consistent with lower energy signals[7]. Finally, Gibson *et al.* saw a $18\pm7\%$ increase in the trigger rate during a 15-min interval on 23 October 1981. The increase in trigger rate of our array A1 was $5\pm4\%$, consistent with no increase. This particular burst seen by us was potentially observable only in those experiments operating from sites in the longitude range 30° E to 105° E during the time 1711 h to 1726 h on 23 January 1985. The time-averaged flux of γ-rays in the burst at site A over its duration of 15 min is calculated to be $(2.5\pm0.6)\times10^{-10}$ γ per cm^2 s^{-1} at $E_\gamma > 1.2$ TeV. The Durham group[2] reported a flux of $(2.0\pm0.3)\times10^{-10}$ γ per cm^2 s^{-1} at $E_\gamma >$ 3 TeV. They considered 34% of their events to be periodic. It appears that the phenomenon of transient pulsed emission occurs only very rarely. Neither Dowthwaite *et al.*[8] nor ourselves saw any more occurrences in observation times of 100 h each. There may also be a persistent weak pulsed emission from the Crab pulsar at the radio main phase[8].

Our conclusion that we are seeing a genuine pulsed emission from the Crab pulsar lasting for 15 min during the night of 23 January 1985 is strongly supported by the presence of a 5.1σ signal in one of the phase bins of the data from an array looking at the Crab pulsar; the absence of any signal in the data from an array looking simultaneously at background; the simultaneous presence of a signal in the same phase bin from an array situated 11 km away and looking at the pulsar; and the failure to obtain a 5σ peak in any phase bin when the same data were analysed in an identical fashion using 10,000 wrong periods. The fact that the signal is seen at the radio main phase shows that at least some of the VHE γ-ray phenomena stem from the same hot spot governing the lower energy processes.

We thank A. R. Apte, N. V. Gopalakrishnan, R. Mahalingam, S. Swaminathan and M. Venkateshwarlu for help in running the experiment; S. C. Tonwar for assistance with data at site B and A. G. Lyne for supplying pulsar elements.

Received 2 August; accepted 24 October 1985.

1. Porter, N. A. & Weekes, T. C. *Smithson. astrophys. Obs. spec. Rep. 381* (1978).
2. Gibson, A. I. *et al. Nature* **296**, 833-835 (1982).
3. Vishwanath, P. R. *Proc. International Workshop on Very High Energy Gamma Ray Astronomy* (Ootacamund, India), (eds P. V. Ramanamuthy & T. C. Weekes) 21-42 (1982).
4. Bhat, P. N. *et al. Adv. Space Res.* **3**, 135-138 (1982).
5. Ramanamurthy, P. V. *Non Solar Gamma Rays*, 71-84 (Oxford, Pergamon, 1979).
6. O'Mongain, E. *Nature* **241**, 376-379 (1973).
7. Wills, R. D. *et al. Nature* **296**, 723-746 (1982).
8. Dowthwaite, J. C. *et al. Astrophys. J.* **286**, L35-L38 (1984).

Solar ellipticity fluctuations yield no evidence of *g*-modes

J. R. Kuhn*, K. G. Libbrecht† & R. H. Dicke*

* Joseph Henry Laboratories, Princeton University, Princeton, New Jersey 08544, USA
† Solar Astronomy 264-33, California Institute of Technology, Pasadena, California 91125, USA

Although there have been several claims for the detection of solar *g*-modes with periods between 2 and 10 hours[1-3] and although the present sensitivity of the Princeton Solar Distortion Telescope should allow these low frequency modes to be observed, solar oblateness data from the summers of 1983 and 1984 show no evidence of such oscillations with periods between 1 and 5 hours. In about 250 days (nearly 1,000 hours) of observations, we find no evidence for significant spectral power associated with *g*-modes. In particular, there is no evidence of a 160.01-min period solar oscillation.

The surface velocity amplitudes of solar *g*-modes appear to be between 0.1 and 1 m s^{-1}, but there is little agreement between

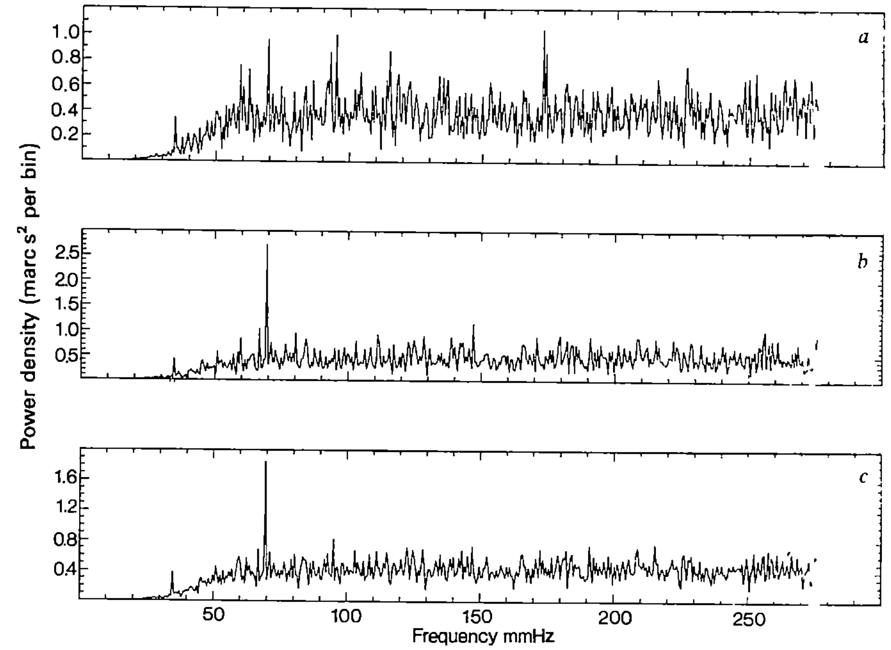

Fig. 1 *a*, Average of the least-squares spectra from the six 1983 data sets. *b*, Same as *a* but for 1984 datasets. *c*, All 12 spectra averaged from 1983 and 1984.

different observers on the excitation spectrum. Several groups have, however, claimed detection of a 160.01-min period solar oscillation[4,5] also with a velocity amplitude that seems to vary between 0.17 and near 1 m s^{-1}. All of these modes have been observed with low spatial resolution and are most probably of low spherical harmonic degree ($l \leq 2$).

It is notable that the surface amplitudes of these oscillations are comparable to 5-min *p*-mode amplitudes of about 15 cm s^{-1} (ref. 6). If the observations are correct, the energy per *g*-mode is roughly 10^8 times larger than typical *p*-mode energies, and is thus of considerable interest.

Except for the ACRIM data[3] and Hill's data[7] most of the low frequency data are due to Doppler velocity observations. Since the period of the modes discussed in this paper are long compared to a radiative relaxation time at the photosphere ($\sim 10^3$ s) the pressure density perturbations due to the oscillation will be nearly isothermal. It is therefore reasonable to calculate the shape change by following photospheric brightness contours as they move due to mass motion of the oscillation displacement field below the photosphere.

The distortion telescope and oblateness data have been described in detail elsewhere[8-10]. In brief, measurements of the deviation from a circular solar limb shape are obtained by measuring the flux from a solar image occulted by a slightly undersize circular occulting disk. The solar flux is measured in two broadband colours (0.5 μm and 0.8 μm) and at 256 positions around the limb. Between 9 and 20 arc seconds of the limb extends beyond the occulting disk. The data are obtained with a specialized telescope now operating at the Mount Wilson Observatory.

A data set at one of three possible limb exposures and two simultaneous colours is obtained approximately once every 5 min. The flux measurements in 128 distinct position angles (only symmetric distortions about the image centre may be observed) around the image are reduced to a displacement in arcseconds using a geometrical calibration. Corrections for optical imperfections of the telescope, mirror distortions, atmospheric transparancy and refraction and facular contamination are applied to the data before obtaining the two coefficients that describe the oblateness of the solar image. For the discussion below the oblateness is described by the coefficients *D* and *V* of a fit of $D \sin 2\theta + V \cos 2\theta$ to the binned shape data. Here θ measures the angle from the solar rotation axis projected onto the image plane (and the *V* and *D* coefficients determine the shape and orientation of the solar oblateness in a frame fixed with respect to the telescope). Thus each observation at a given limb exposure yields four coefficients—a *V* and *D* term for each of the two colour bands. Except for additional atmospheric corrections described by Dicke *et al.*[11] the analysis sketched above essentially follows the description in the references.

The two summers of observations yielded about 254 useful days of data, amounting to about 11,000 5-min observations distributed between the three possible limb exposures. After subtracting least-squares fitted daily quadratic polynomials, to remove daily trends, the standard deviation of the residuals was approximately 24 milliarcseconds in *D* or *V*. The oblateness data will not be sensitive to $l = 0$ or 1 oscillations, but *g*-modes with $l = 2, 3, \ldots$ will contribute to the observed power in the *V* or *D* coefficients. If the 160 min mode is, for example, an $l = 2$ *g*-mode, it will also contribute to the shape data.

For definiteness we will estimate the expected shape signal amplitude from the assumption that the 160 min mode is an $n = 9$, $l = 2$ *g*-mode (the closest predicted frequency for low order modes). The velocity amplitude of an $m = 0$ mode can be written

$$\vec{V}_n(r, \theta) = V_n(r) P_2(\cos\theta)\hat{r} + \frac{U_r(r)}{r}\frac{\partial P_2(\cos\theta)}{\partial\theta}\hat{\theta} \qquad (1)$$

A model calculation[12] gives for the $n = 9$ mode $V_9(R_{\text{sun}})/U_9(R_{\text{sun}}) = 1.14$. The line-of-sight velocity V_{0n} can be related to the modal amplitude V_n from

$$V_{0n} = S_n \cdot V_n \qquad (2)$$

where V_{0n} is the intensity weighted line-of-sight velocity, $\vec{V}_n \cdot \hat{z}$, integrated over the solar disk. The factor S_n is easily evaluated for full disk observations and has been tabulated[13]. For example, $S_9 = 1.3$ for the radial-transverse velocity ratio given above for the $n = 9$, $l = 2$ mode. Other long period $l = 2$ modes have values of S_n within about 50% of this value. Projecting the P_2 (cos θ) term against sin 2θ or cos 2θ gives an approximate relation between the coefficient *V* and the observed full disk velocity amplitude, V_0 of a *g*-mode of frequency ω,

$$V \cong 1.3\ V_0/\omega \qquad (3)$$

Thus, from the 160 min mode with an observed amplitude of about 1 m s^{-1} we expect an oblateness coefficient of $V \sim 2 \times 10^3\ m = 2.7$ milliarcsec. If the oblateness residials were uncorrelated such an oscillating shape signal would be observable with high signal-to-noise.

Below we address two questions: is there evidence of a 160.01-

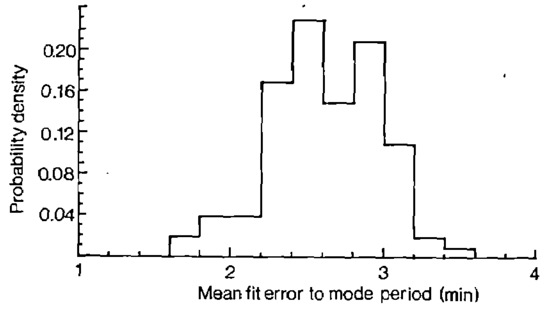

Fig. 2 Distribution of the mean fit errors to the g-mode asymptotic period relation from 100 synthetic peak lists.

min solar oscillation in these data? and is there evidence of any other solar oscillating power in the oblateness residuals? These questions are complicated by the very uneven sampling in time of the data. For example, in 1984 there were about 5,500 observations between day number 107 and 274, spaced at about 5-min intervals. Any mode structure will be aliased in the observed power estimates.

Data from the two colour channels are obtained simultaneously and are highly correlated. Thus to reduce the noise the colours are averaged before computing power spectra. By averaging the power spectrum from three possible limb exposures and both *V* and *D* coefficients we may hope to find a 160-min signal. This has been done in Fig. 1 for 1983 and 1984 data separately, and combined. 'Power spectra' are computed from the summed squared amplitude of least-squares fits of sin ωt and cos ωt to the colour averaged residuals.

Figure 1*c* is an average of 12 'pseudo-spectra' and is our first approximation to the actual mean power spectrum. We note that at frequencies near 104.16 μHz ($T = 160.01$ min) all peaks are smaller than twice the mean power level. To the extent that this approximates the actual mean spectrum the probability distributions of signal in the presence of noise calculated by Groth[14] are applicable here. We find that there is less than a 1% chance that the signal power at $f = 104.16$ μHz is larger than the mean noise power of about 0.4 milliarc². It is notable that there are prominent peaks in the averaged and yearly spectra at periods of 1/10, 1/9, 1/6, 1/5 and 1/3 days. Some 1 per day frequency sidelobes of the stronger peaks are also prominent.

Since we know the frequency and phase of the 160.01-min signal we can also fit for it directly in the data. To simplify the analysis the data were again averaged by colour and limb exposure and binned in half-hour intervals to obtain a single time series for each *V* and *D* coefficient for each year. phase and period described by Grec *et al.*[15] have been usec find the 160-min amplitude and fit error for 1983, 1984 combined datasets, displayed in Table 1. The results of a n linear fit with frequency treated as an adjustable parameter also displayed.

Only the *V* coefficient of the 1984 data shows a statistic significant amplitude at about the 2σ level, but even thi probably due to the nearby strong peak at a period of 159.90 n The results in Table 1 provide no evidence for the 160.01- oscillation with an amplitude greater than, approximately, fit uncertainty of 0.4 milliarcsec.

Several approaches have been considered to look for ot discrete frequency power contributions to the data. (The f technique we examined was used originally by Scherrer[1] finding *g*-modes, and as we will show below is not effective

Scherrer[1] claimed detection of *g*-modes by searching for pe in the Stanford data using an iterative least-squares fitting te nique (the 'clean' algorithm) and then noted that the peaks the asymptotic expression for the mode periods, $T(n, l)$:

$$T = T_0(n + l/2 - 1/4)\sqrt{l(l+1)}$$

where *n* and *l* are chosen separately for each mode to best the observed periods using a single value of T_0. With 14 po spectrum peaks with periods between 172 and 329 min Scher found a good fit with $T_0 = 38.6$ min and *l* and *n* values betwe 1 and 2, and 6 and 20. As a test of the uniquess of such a we have simulated this procedure on 100 sets of random numb evenly distributed in frequency between the corresponding lin ing periods in Scherrer's data. Each set of 14 'peaks' is used estimate a value of T_0 which minimizes the summed squa deviation of the period calculated from equation (4) and rand peaks. The integer *n* and *l* values are constrained to be less th or equal to 25 and 2 respectively and are adjusted to minim the error for each trial T_0 value. A 1% resolution search betwe 30 and 50 minutes finds a value of T_0 which minimizes t summed error. The 100 trials yielded the mean error distributio shown in Fig. 2. Notice that such a fit is not very conclusi since an r.m.s. error of about 3 min is often possible given t range of available parameters. From Scherrer's *n*, *l* and T_0 valu we calculated an r.m.s. value of 3.0 min from his data. Thus fit for T_0 provides no supporting evidence that the power sp trum peaks are of solar origin.

The second approach we tried for finding discrete po contributions was to reduce the aliased structure in the spectr by deconvolving the window function from the observed pow spectra. For this purpose the data were averaged over the thr

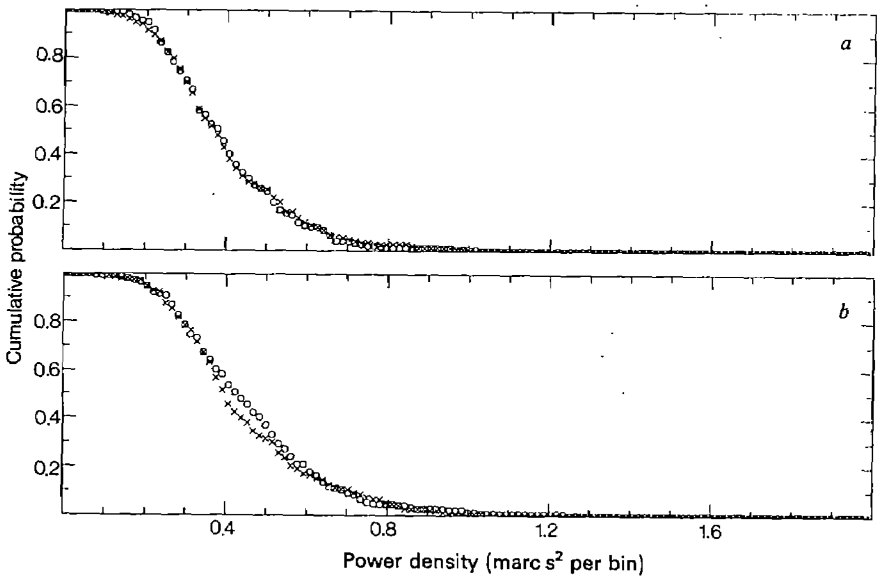

Fig. 3 *a*, Cumulative power distribution of the data in Fig. 1*a* (crosses) and the spectra of normally distributed white noise (circles). *b*, Same as *a*, except for 1984 data and time domain.

Table 1 Least-squares fit for 160.01-min oscillation

		1983	1984	Combined
$f = 104.16\ \mu$Hz				
amplitude	V	0.4 ± 0.5	1.7 ± 0.8	0.3 ± 0.4
(marc s)	D	0.3 ± 0.5	0.6 ± 0.8	0.3 ± 0.4
Frequency (μHz)	V	103.92 ± 0.02	104.23 ± 0.03	104.235 ± 0.003
	D	104.18 ± 0.01	104.00 ± 0.05	104.171 ± 0.003
Amplitude	V	1.3 ± 1.3	2.1 ± 2.0	1.7 ± 0.8
(marc s)	D	1.8 ± 1.3	1.3 ± 1.9	1.4 ± 0.8

limb exposures and two colours and binned in half-hour intervals. Under these conditions the 'filling factor' on the evenly spaced half-hour domain increases to 23% in 1983 and somewhat less in 1984. The technique we applied to work around the gaps is described by Kuhn[16,17]. By choosing a particular set of evenly spaced frequencies the window function effects can be minimized (the 'swap' technique). Unfortunately, numerical experiments on synthetic data with this domain could not be completely 'dealiased' and we've concluded that the domain is too sparse for this method (and probably any other). We finally settled on the statistical approach, described below, to search for g-modes.

We take as a null hypothesis that the 1983 and 1984 power spectra (Fig. 1) are the result of random uncorrelated normally distributed noise. If this is correct then the distribution of power from both years should be consistent with the power distribution generated from noise analysed in the same way as the data. Thus we generate fake data sets on the same domain as the actual data. The values are distributed normally from a distribution whose variance is scaled so that the mean fake power and actual power agree. The resulting cumulative power probability distributions are plotted in Fig. 3. The agreement is quite good if the anamolous peak at 1/6 day period in the 1984 data is ignored. The Kolmogorov-Smirnov test yields a useful quantitative description of the probability that both samples came from the same parent distribution. The K-S test is essentially a measure of the largest deviation between the two distributions[18]. Applying the test to the 1983 and 1984 data separately yields statistic values of 0.34 and 0.86 respectively, indicating that we should accept the null hypothesis. In short, we find no evidence of solar g-modes in oblateness power spectra of mean noise 0.4 milliarcsec^2.

Further, if the previously detected 160.01-min periodic signal is interpreted as evidence of an $l = 2$ g-mode then its amplitude has decreased from near 1 to 0.1 m s^{-1} since its detection in 1974. Unless a hitherto unknown damping mechanism is postulated this is inconsistent with the expected mode damping time of ~40,000 yr[12]. We believe it is more likely that the 160.01-min signal is not due to a solar g-mode.

This research was supported in part by the AFGL under contract number F19628-84-K-0024, and in part by the National Science Foundation.

Received 22 July; accepted 22 October 1985.

1. Scherrer, P. H. *Mem. Soc. astr. ital.* **55**, 83–89 (1984).
2. Isaak, G. R., Van der Raay, H. B., Palk, P. L., Roca Cortes, T. & Delache, P. *Mem. Soc. astr. ital.* **55**, 91–97 (1984).
3. Frolich, C. & Delache, P. *Mem. Soc. astr. ital.* **55**, 99–106 (1984).
4. Kotov, V. A., Severny, A. B. & Tsap, T. T. *Mem. Soc. astr. ital.* **55**, 117–122 (1984).
5. Scherrer, P. H. & Wilcox, J. M. *Sol. Phys.* **82**, 37–42 (1983).
6. Kuhn, J. R *Mem. Soc. astr. ital.* **55**, 69–74 (1984).
7. Hill, H. A., Bos, R. J. & Goode, P. R. *Phys. Rev. Lett.* **49**, 1794–1797 (1982).
8. Kuhn, J. R., Libbrecht, K. G. & Dicke, R. H. *Astrophys. J.* **290**, 758–764 (1985).
9. Libbrecht, K. G. & Kuhn, J. R. *Astrophys. J.* **277**, 889–895 (1984).
10. Dicke, R. H. & Goldenberg, H. M. *Astrophys. J. Supp.* **27**, 131–182 (1974).
11. Dicke, R. H., Kuhn, J. R. & Libbrecht, K. G. *Nature* **316**, 687–690 (1985).
12. Kuhn, J. R. & Boughn, S. P. *Nature* **308**, 164–165 (1984).
13. Christensen-Dalsgard, C. D. & Gough, D. O. *Mon. Not. R. astr. Soc.* **198**, 141–171 (1982).
14. Groth, E. J. *Astrophys. J. Supp.* **29**, 285–302 (1975).
15. Grec, C., Fossat, E. & Pomeratz, M. *Nature* **288**, 541–543 (1980).
16. Kuhn, J. R. *Astr. J.* **87**, 196–201 (1982).
17. Kuhn, J. R. *Solar Seismology from Space* (ed. Ulrich, R. K.) 283–289 (JPL, Pasadena, 1984).
18. Hollander, M. & Wolfe, D. *Non-parametric Statistical Methods*, 219–228 (J. Wiley, New York, 1973).

Are the Falkland Islands a rotated microplate?

C. Mitchell*, G. K. Taylor†‡, K. G. Cox* & J. Shaw†

* Department of Earth Sciences, University of Oxford, Parks Road, Oxford OX1 3PR, UK
† Department of Geology, University College, PO Box 78, Cardiff CF1 1XL, UK
‡ Present address: Department of Geology and Physical Sciences, Oxford Polytechnic, Headington, Oxford OX3 0BP, UK

Here we report preliminary palaeomagnetic evidence from dolerite dykes on West Falkland which suggests that the Falkland Islands were rotated through ~120° during the early stages of the break-up and dispersal of the southern part of Gondwanaland. The rotation itself, and evidence of palaeolatitude, confirm the proposal made by Adie[1] in 1952 that the islands were formerly situated adjacent to the Transkei area of South Africa, where they formed the south-east corner of the Karoo basin with its adjoining Palaeozoic fold belts. The first stage of continental drift probably took place during the Jurassic, as Antarctica separated from southern Africa, the islands moving as a microplate to a position approximately 500 km south-east of present-day Cape Town. Subsequently, during the opening of the South Atlantic, the islands and the Falklands Plateau have drifted to their present position and undergone a further rotation of ~60°.

Figure 1 outlines the geology of the Falkland Islands, and the inset shows the position they occupied before the opening of the South Atlantic in the Lower Cretaceous. This position is obtained by closing the South Atlantic by an anticlockwise rotation of the South American plate through 56.40° about a Euler pole at 46.75° N, 32.65° W, keeping the African plate fixed[2]. This is one of the more straightforward plate tectonic reconstructions which is constrained by a wealth of geophysical and bathymetric data, seafloor magnetic anomalies, the orientation of transform faults and the geometrical fit of the opposing continental shelves of South America and Africa[3,4].

Table 1 Palaeomagnetic results

Sample code	Dyke	n	R	k	α_{95}	Dec.	Inc.
F30	A	6	5.62	12.2	19.9	16.0	61.0
F29	A	5	4.86	91.6	8.0	335.4	63.4
F38	A	6	5.97	203.5	4.7	323.1	53.8
F23	B	6	5.92	62.9	8.5	332.1	65.8
F32	A	4	3.70	14.4	25.0	21.8	70.7
F24	B	6	5.93	78.6	7.6	300.5	69.3
F36	C	7	6.79	28.6	11.5	336.3	39.0
F25	B	6	5.94	79.1	7.6	349.2	55.9
F41	D	6	5.89	46.2	10.0	159.5	−24.5*
F31	A	5	4.97	128.9	6.8	7.4	8.6*
F46	E	4	3.94	48.2	13.4	174.9	−54.7
F47	E	6	5.13	5.7	30.6	357.8	−81.5*
F45	E	7	6.10	6.8	25.6	246.1	−24.5*
F6	E	4	—	—	—	—	—*
	Mean	9	8.73	29.5	9.6	342.8	61.1

Palaeomagnetic South Pole = 5.3 °S, 287.2° E. dp/dm = 11.3/14.8, where dp and dm are the semi-axes of the oval of 95% confidence about the palaeomagnetic pole. n, The number of specimens; k, Fisher's precison parameter; α_{95}, the radius of the 95% confidence cone about the mean direction; dec. and inc., the declination and inclination, respectively. Positive (negative) inclinations indicate reverse (normal) polarity in the Southern Hemisphere. Samples F45 and F47 are total NRM only. The first 10 samples in the table are from four different north-south dykes designated A–D. The last four samples are baked sediments from the contact of an east-west dyke, E.

* Sample direction not included in the calculation of the mean.

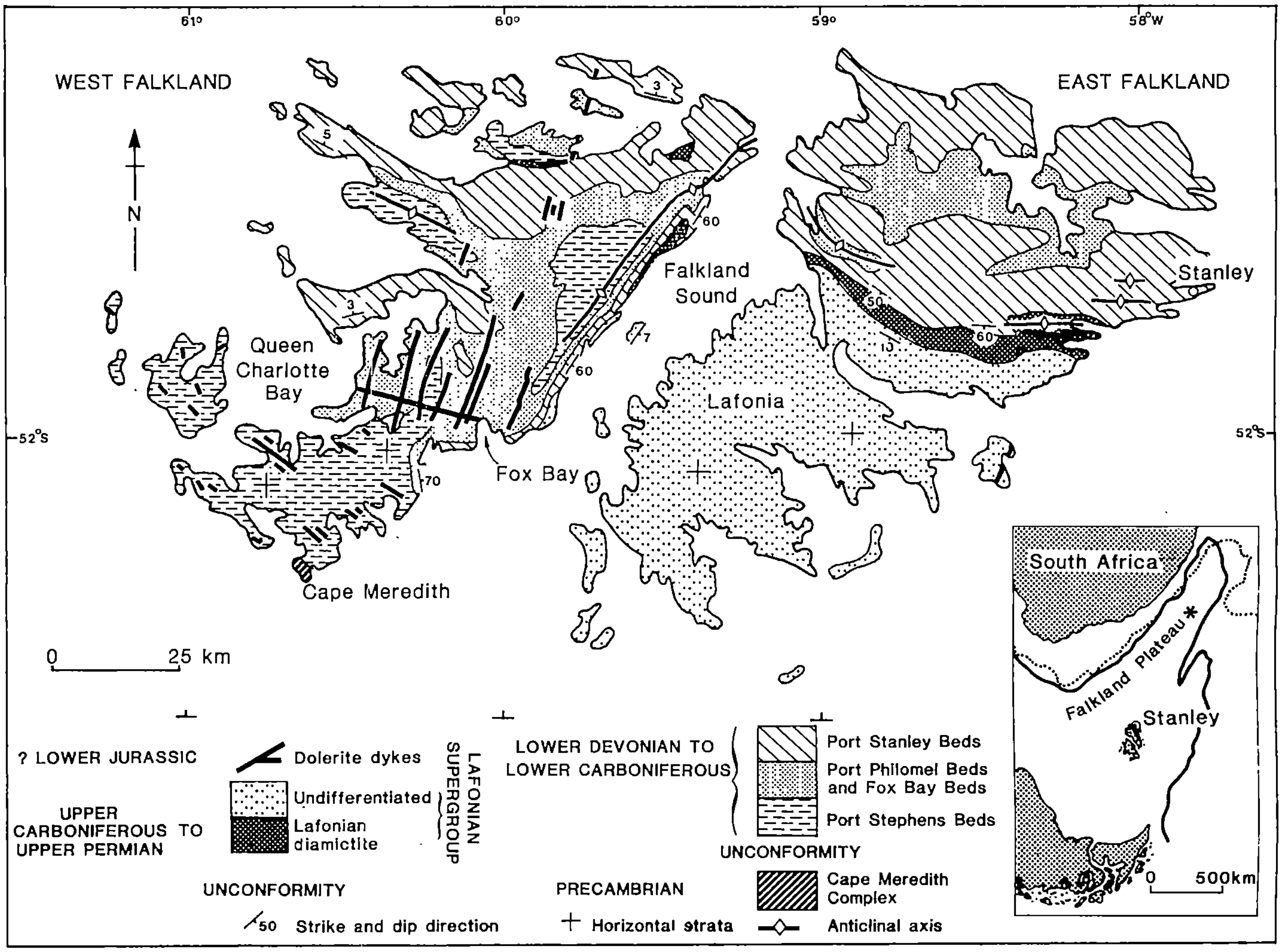
61°
60°
59°
58°W
WEST FALKLAND
EAST FALKLAND
N
Queen Charlotte Bay
Falkland Sound
Stanley
Lafonia
Fox Bay
Cape Meredith
52°S
0 25 km
? LOWER JURASSIC
Dolerite dykes
UPPER CARBONIFEROUS TO UPPER PERMIAN
Undifferentiated
Lafonian diamictite
LAFONIAN SUPERGROUP
UNCONFORMITY
LOWER DEVONIAN TO LOWER CARBONIFEROUS
Port Stanley Beds
Port Philomel Beds and Fox Bay Beds
Port Stephens Beds
UNCONFORMITY
PRECAMBRIAN
Cape Meredith Complex
50 Strike and dip direction
Horizontal strata
Anticlinal axis
South Africa
Falkland Plateau
Stanley
0 500km

Fig. 1 Geological map of the Falkland Island, after Greenway[17]. For purposes of comparison with South African geology, note that the Lafonian Supergroup correlates broadly with the Karoo, while the Port Stanley Beds, Fox Bay Beds and Port Stephens Beds correlate broadly with the South African units Witteberg, Bokkeveld and Table Mountain sandstone of the Cape Supergroup. Inset, position of the Falkland Islands and Falkland Plateau before the opening of the South Atlantic (Lower Cretaceous) (based mainly on Martin *et al.*[2]). The solid line marks the edge of the south American continental shelf; the dotted line marks that of South Africa. Asterisk shows the position of DSDP site 330 (ref. 14).

Nevertheless, before the development of plate tectonic theory, geologists sought to position the islands in reconstructions of Gondwanaland so that the main geological features matched those of neighbouring continents. For example, du Toit[5] placed the islands to the west of Cape Town, in order to achieve continuity of the east-west fold belts of the Cape, Port Stanley and northern West Falkland in the Falklands and of the Sierra de la Ventana in Argentina. Adie's suggestion[1] that the islands had previously been situated at the east end of the Cape fold belt (the Zwartberg fold belt), offshore from present-day Transkei (Fig. 2), provided near-perfect correlation of Falklands and South African geological features by rotating the islands through 180° from north to south; he cited transport directions in the Dwyka and Lafonian diamictites (with movement from south to north in the Falklands) in support of the postulated rotation. Adie's reconstruction juxtaposes the 1,000-Myr-Natal basement[6] and the Cape Meredith Complex in the Falkland Islands, which is of a similar age[7]; it also removes a problem inherent in the du Toit reconstruction by achieving continuity of the Karoo strata. The Adie reconstruction is much favoured by geological correlations but its validity depends on whether a substantial rotation of the Falkland Islands can be demonstrated.

During a field study in January 1985, C.M. and K.G.C. collected a number of magnetically orientated samples, which comprised 10 hypersthene-bearing dolerites from four different north-south-trending dykes and four baked shales adjacent to a large olivine-bearing east-west dyke, of which, however, no *in situ* exposures were found. All specimens were collected in the area between Fox Bay and Queen Charlotte Bay in West Falkland (Fig. 1). The dykes have usually been assumed to be of the same age as the Karoo dolerites of South Africa; the one published age-determination[8], from a dyke near Cape Meredith, yields a typical Karoo age (Lower Jurassic) of 192±10 Myr by the K-Ar method. Each of our specimens provided a minimum of five 9-mm cylindrical samples for measurement, using the automated SQUID magnetometer at Cardiff[9].

Most samples were demagnetized using alternating fields (AF), but a few were subjected to thermal demagnetization. The results were analysed by means of orthogonal and stereonet plots combined with principal-component analysis[10]. All 10 dolerite samples yielded stable coherent within-sample directions, but two samples (F41 and F31) clearly deviate from the mean of the others (Table 1). These two anomalous results may represent either poor orientation of the samples or the genuine recording of an intermediate geomagnetic field direction. The characteristic direction is generally stable in the range 15-70 mT, with randomly directed low-coercivity components removed on treatment to 15-20 mT, except samples F30 and F32 which were relatively unstable to both AF and thermal demagnetization, compared with the other samples. The AF demagnetization

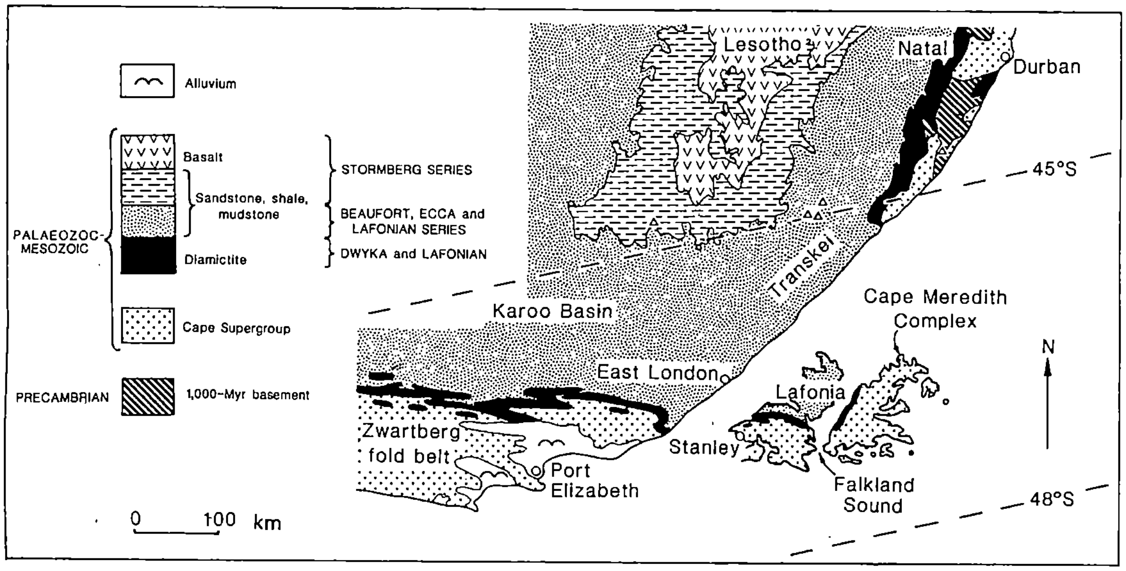
Alluvium
Basalt
Sandstone, shale, mudstone
Diamictite
Cape Supergroup
1,000-Myr basement
PALAEOZOC-MESOZOIC
PRECAMBRIAN
STORMBERG SERIES
BEAUFORT, ECCA and LAFONIAN SERIES
DWYKA and LAFONIAN
0 100 km
Lesotho
Natal
Durban
45°S
Transkei
Karoo Basin
Cape Meredith Complex
N
East London
Lafonia
Zwartberg fold belt
Stanley
Port Elizabeth
Falkland Sound
48°S

Fig. 2 Proposed reconstruction of the Falkland Islands relative to South Africa in the Lower Jurassic. This reconstruction is essentially similar to that of Aidie (see Fig. 2 of ref. 1). Palaeolatitude lines are based on McElhinny *et al.*[11]. △, Sites from which palaeomagnetic data for Karoo dolerites were obtained.

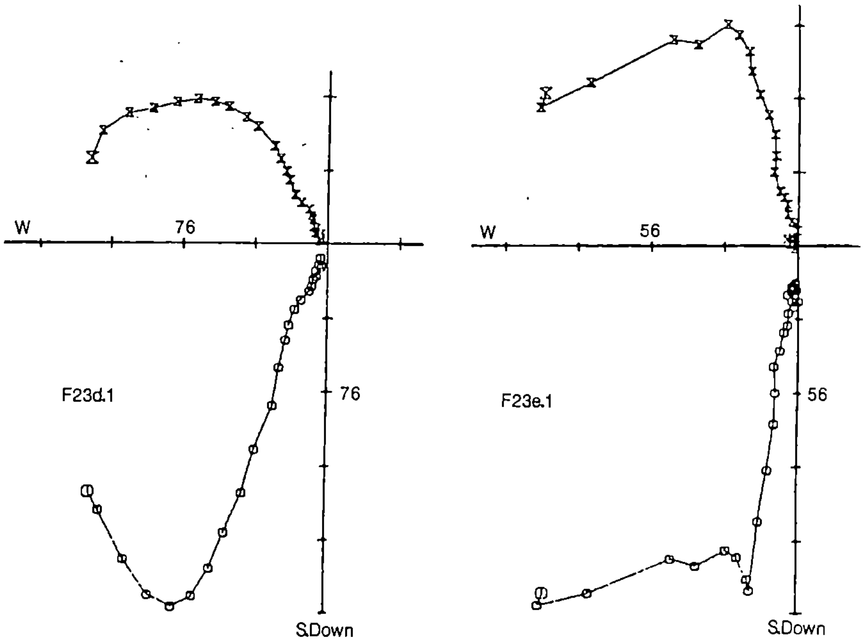

Fig. 3 Orthogonal demagnetization diagrams for two specimens from sample F23. Units for the axes are 10^{-3} Am^{-1}. ×, Horizontal projection; ○, Vertical up-down/east-west projection. Demagnetization steps are in 2.5 mT. See text for discussion.

ehaviour of two specimens from sample F23, a hypersthene-earing north-south dyke, is illustrated in Fig. 3. These two pecimens demonstrate the normal range of within-sample variaility; in specimen F23d.1 there is overlap of the low-coercivity omponents, typical of most specimens, while in F23e.1 these omponents are discrete. In both cases the characteristic direcion of the high-coercivity component is readily isolated.

Three of the four baked sediment samples have specimen otal NRM (natural remanent magnetism) intensities of $<1.5\times$ 0^{-9} A m^{2} kg^{-1} which are unstable to demagnetization, although amples F47 and F45 do yield poorly defined total NRM directions. Sample F46, however, has specimen total NRM intensities f 2-5 × 10^{-8} A m^{2} kg^{-1} which are stable to AF demagnetization. he AF demagnetization characteristics and thermal stability p to 550-580 °C suggest titanomagnetite as the main magnetic hase present in all samples.

The antiparallel nature of the directions for the dolerites ersus the baked sediments (F46, supported by F47 and F45) s indicative of a polarity change between emplacement of the orth-south and east-west dykes. The sample mean direction yields an *equatorial* pole position, and this is inconsistent with any data from southern Gondwanaland in Jurassic times. A rotation by a total of 180 ± 10° is needed to produce a palaeo-pole in the expected near-polar position. Further, the palaeolatitude derived from the inclination is 42 ± 6° S, precluding the conventional reconstruction position south of the Cape, which demands a palaeolatitude of ~55 °S. On the other hand, palaeolatitudes derived for southern Africa from Karoo dolerites, admittedly from old and limited data[11] (Fig. 2), suggest a palaeolatitude for the preferred reconstruction position of the Falklands at 47 ± 5° S, which is consistent with our results. However, because of the small number of samples involved, our results are of a provisional nature and will require confirmation by more detailed studies of both Falklands and Transkei dolerites.

Perhaps the most obvious problem with our proposed reconstruction is the mechanism by which the islands have travelled to their present location. All reconstructions of southern Gondwanaland are problematical and authors differ widely in their opinions as to the precise fit. Recent studies[12,13] have indicated that there are several microplates in the area, some of which have experienced complex movements, for example the Ellsworth Mountains in Antarctica. We tentatively suggest that the Falkland Islands formed one such microplate which was rotated through 180° and moved south and west as Antarctica moved southward and away from Africa during the Jurassic. The islands were then carried to their present location by the opening of the South Atlantic from the Lower Cretaceous onwards. However, drilling at site 330 (see Fig. 1) on the Maurice Ewing Bank[14] shows that the easternmost segment of the Falkland Plateau is composed of continental crust. Furthermore, Tarney[14] thought it likely that the whole of the Falkland Plateau was composed of similar continental crust because of petrographical and geochemical similarities to the Cape Meredith Complex. However, the crust drilled at site 330 yields an age of 535 Myr[15] hence cannot be correlated with the 1,000-Myr-old gneisses of the Cape Meredith Complex. Also, more recent geophysical surveys[16] of the Falkland Plateau revealed that the Falkland Plateau Basin, which separates the Maurice Ewing Bank from the main plateau, is floored by oceanic or highly thinned continental crust. Ludwig[16] aligned Mesozoic magnetic anomalies off South Africa with their equivalents just off the Maurice Ewing Bank and found that the bank probably occupied a position closer to the plateau than it does at present. He went on to suggest that the Falkland Plateau Basin may represent a zone of seafloor spreading or stretching and subsidence of continental crust during early rifting of the continents. Therefore, it now seems unlikely that the Falkland Plateau is a simple extension of the South American and South African continental crust, and we suggest that it may be a collage of microplates. If, as might be expected, all the microplates recognized in this area experienced complex motions during the break-up and dispersal of southern Gondwanaland, this may explain why reconstructions of southern Gondwanaland are so problematical.

We thank Dr C. W. M. Swithinbank (British Antarctic Survey) for drawing our attention to the existence of the Falklands dolerites. Thanks are also due to Mr and Mrs A. McMullen for their hospitality at Fox Bay West. Field and laboratory work in Oxford were supported by NERC research grant GR3/5350 and by a travel grant from the Royal Society. NERC grant GR3/3901 supported the development of the super conducting magnetometer used for this work at Cardiff.

Received 12 July; accepted 28 October 1985.

1. Adie, R. J. *Geol. Mag.* **89**, 401-410 (1952).
2. Martin, K. A., Hartnady, C. J. & Goodlad, S. W. *Earth planet. Sci. Lett.* **54**, 293-305 (1981).
3. Bullard, E. C., Everett, J. E. & Smith, A. G. *Phil. Trans. R. Soc.* **A1088**, 41-51 (1965).
4. Le Pichon, X & Hayes, D. E. *J. geophys. Res.* **76**, 6283-6293 (1971).
5. du Toit, A. L. *Publs Carnegie Instn* **381** (1927); *Our Wandering Continents* (Oliver & Boyd, Edinburgh, 1937).
6. Nicolaysen, L. O. & Burger, A. J. *Sci. Terre.* **10**, 497-516 (1965).
7. Rex, D. C. & Tanner, P. W. G. in *Antarctic Geoscience* (ed. Craddock, C.) 107-110 (University of Wisconsin Press, 1982).
8. Cingolani,, C. A. & Varela, R. in *Actas 6° Congreso Geologico Argentino* Vol. 1 (Congreso Gelogico Argentino, Buenos Aires, 1976).
9. Shaw, J., Share, J. A. & Rogers, J. *Geophys. J.R. astr. Soc.* **78**, 209-218 (1984).
10. Kent, J. T., Briden, J. C. & Mardia, K. V. *Geophys. J.R. astr. Soc.* **75**, 593-622 (1983).
11. McElhinny, M. W., Briden, J. C., Jones, D. L. & Brock, A. *Rev. Geophys.* **6**, 201-238 (1968).
12. Watts, D. R. & Bramall, A. M. *Nature* **293**, 638-640 (1981).
13. Longshaw, S. K. & Griffiths, D. H. *J. geol. Soc. Lond.* **140**, 945-954 (1983).
14. Tarney, J. *Init. Rep. DSDP* **36**, 893-921 (1977).
15. Beckinsale, R. D., Tarney, J., Darbyshire, D. P. F. & Humm, M. J. *Init. Rep. DSDP* **36**, 923-927 (1977).
16. Ludwig, W. J. *Init, Rep. DSDP* **71**, 281-293 (1983).
17. Greenwway, M. E. *Br. Antarctic Surv. Sci. Rep.* No. 76 (1972).

Production of ^{10}Be and ^{26}Al by cosmic rays in terrestrial quartz *in situ* and implications for erosion rates

K. Nishiizumi*, D. Lal†, J. Klein‡, R. Middleton‡ & J. R. Arnold*

*Department of Chemistry, B-017, and †Scripps Institute of Oceanography, A-020, University of California, San Diego, La Jolla, California 92093, USA
‡Tandem Accelerator Laboratory, Department of Physics, University of Pennsylvania, Philadelphia, Pennsylvania 19104, USA

We present results of determinations of ^{10}Be (half life = 1.6 Myr) and ^{26}Al (half-life = 0.705 Myr) produced by cosmic rays *in situ* in several terrestrial rock samples exposed at altitudes of 1–4 km. These experiments were designed to determine the feasibility of using quartz extracted from natural surfaces for studying continental weathering/erosion processes[1]. Quartz is attractive as a target material for several reasons. Its low aluminium concentration allows measurement of ^{26}Al after exposures as short as 10^3 yr; its integrity minimizes the possibility of contamination by rain with ^{10}Be produced in the atmosphere; and its ubiquity ensures that it is found in a wide variety of geological settings. However, the cosmic-ray production rates of ^{26}Al and ^{10}Be even at mountain altitudes are low[2,3], only 10–100 atoms g^{-1} yr^{-1}, with the consequence that earlier attempts[4,5] to determine *in situ* produced ^{36}Cl and ^{26}Al in rocks were not continued. Recent development of accelerator mass spectrometry (AMS) however, has made the measurement of 10–20g samples feasible. The results presented here demonstrate the feasibility of quantitatively measuring ^{10}Be and ^{26}Al produced *in situ* by cosmic rays in quartz and the possible applications of ^{10}Be and ^{26}Al as a pair for studying continental weathering/erosion processes.

Table 1 Sample description

Sample	Site	Elevation (m)	Weight of quartz analysed (g)	Al content of quartz (p.p.m.)	Be carrier added (mg)
ALH	Allan Hills, Antarctica	2,050	13.09	467	1.49
Q-1	Anza Borrego, California	1,140	20.22	4.9×10^4	1.37
Q-L	Anza Borrego California	1,200	22.18	100	1.50
KKS-1	Leh, Ladakh	4,000	17.29	52*	1.50
KKS-3	Kinnaur, Himachal Pradesh	3,400	16.39	289	1.50

* Intrinsic Al content of the purified quartz grains; an amount equivalent to 0.53 mg Al was added for AMS measurement.

The rock samples analysed are listed in Table 1. Sample ALH, which is quartzite (determined by thin section), was collected at the peak of Allan Hills, Antarctica (76°42′ S, 150°31′ E), elevation 2,050 m, by one of us (K.N.) during the 1983–84 field season of Antarctic search for meteorites. Allan Hills are located about 230 km north-west of McMurdo station. The large blue ice area (Allan Hills ice field) is stagnated by the Allan Hills. More than 2,000 meteorites have been found on the ice field and contiguous areas during the past 10 yr. At present, the Allan Hills are not covered with ice because of strong winds which prevent net snow accumulation in winter; in summer there is no precipitation. It would be useful to determine when Allan Hills lost their ice sheets. The sample was collected from the surface of a flat-top area, ~200 m north of the glaciological survey station[6]. The Q-1 and Q-L samples were collected from Anza Borrego, California (33°12′ N, 116°27′ W), ~100 km east of San Diego by A. E. Engel and us. The samples were collected from the flat tops of large rocks (~5 m in diameter) located at elevations of 1,140 m (Q-1) and 1,200 m (Q-L). The ^{40}K-^{40}Ar age of the Borrego rocks is ~90 Myr. Sample KKS-1 was collected from a quartz vein intruding Indus Flysch near Kiari, Kashmir, India (34° N, 78° E), at an elevation of 4,000 m. KKS-3 was collected from quartz-kyanite veins intruding Kyanitesillimanite schists, Himachal Pradesh, India (32° N, 78° E), elevation 3,400 m.

Quartz was extracted from the rocks primarily by using the higher reactivity of feldspars with HF (details will be presented elsewhere). The chemical procedure used for extraction of Be and Al was essentially the same as in previous experiments for meteoritic and lunar samples[7]. The ^{10}Be and ^{26}Al measurements were performed on the University of Pennsylvania FN Tandem Van de Graaff accelerator[8,9].

As the ratio $^{10}Be/^{9}Be$ in commercially available beryllium[10] is $\sim 1\times 10^{-14}$, we prepared a ^{9}Be carrier from a beryl (supplied by B. Dassanacharya). The measured $^{10}Be/^{9}Be$ and $^{26}Al/^{27}Al$ ratios and the ^{10}Be and ^{26}Al concentrations in the quartz samples are shown in Table 2. The $^{10}Be/^{9}Be$ and $^{26}Al/^{27}Al$ ratios of the samples were normalized to standards[7] after blank corrections. Our beryl derived Be carrier has a $^{10}Be/^{9}Be$ ratio $<3\times 10^{-15}$, corresponding to $<2\times 10^{5}$ atoms ^{10}Be/mg Be.

Table 2 shows that the ^{10}Be and ^{26}Al produced *in situ* by cosmic rays can be measured easily in natural quartz samples of 10-20 g size. And, in fact, measurement of ^{26}Al produced *in situ* on Earth is as easy as in extraterrestrial samples if the ^{27}Al concentration is <300 p.p.m.

Figure 1 shows the theoretical saturation values[1] plotted for ^{10}Be and ^{26}Al produced in quartz at the Earth's surface. The ^{10}Be is caused by nuclear spallation of Si and O, and the ^{26}Al is caused by nuclear spallation of ^{28}Si and negative mu-meson capture in ^{28}Si. Other contributions to the production of ^{26}Al and ^{10}Be from *in situ* radioactivity are negligible. The samples KKS-1 and KKS-3 are not surface samples; they were collected from quartz veins to obtain samples with low Al content. Figure 1 shows the ^{10}Be data for the three surface samples. These samples have concentrations lower than secular equilibrium values, corresponding to 2×10^{4}–1.5×10^{6} yr of effective irradiation. As the samples are not at the surface secular-equilibrium concentration value, they must have been shielded by some overburden of material for an appreciable fraction of the flux-integrating period of these isotopes, $\sim 10^{7}$ yr. This overlying material could have been removed either all at once or gradually. If the samples had been covered by a thick ice sheet, a sedimentary deposit, or a layer of rock which was removed during the retreat of a glacier, the time needed to remove this cover could have been short ($<10^{4}$ yr). If the overburden was removed by erosional weathering, the process could have been continuous, and the shielding of these samples could have been reduced gradually. The result is that the concentration of these radionuclides can be used to place upper limits on the rate of erosion (weathering) and lower limits on the amount of time that the samples have not been covered with an appreciable layer of either rock or ice. Such estimates depend on a knowledge of the rates of production of these isotopes, and on the model adopted to explain the exposure history of the samples.

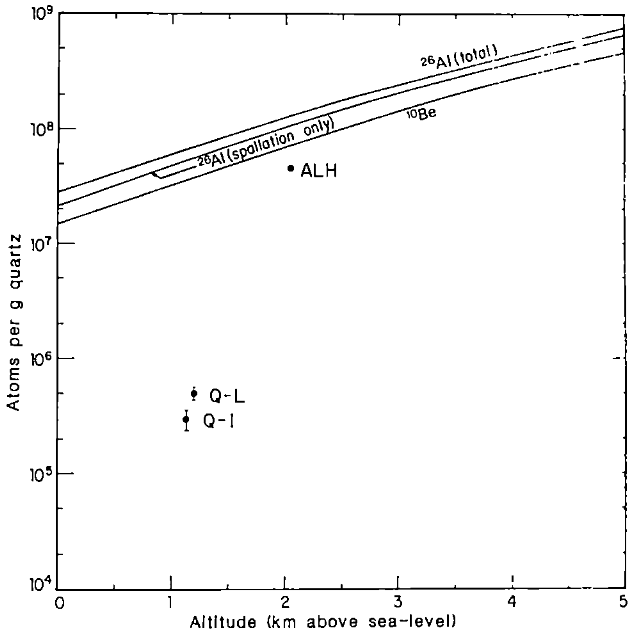

Fig. 1 Theoretically estimated *in situ* saturation values of ^{10}Be and ^{26}Al in quartz, based on production rates in ref. 1. Values are shown as a function of altitude for geomagnetic latitude (50–90°). ^{10}Be is produced in nuclear spallation of Si and O, and ^{26}Al from spallation of Si and negative mu-meson capture of ^{28}Si. The total production rate of ^{26}Al (spallation + capture) is shown as is the measured concentrations of ^{10}Be in three surface exposed rocks.

Next, we briefly consider the expected isotope concentrations in terms of a simple exposure history model which occurs without change in the altitude of the sample. The production rate in the rock, $P(t)$ is time dependent because of change in the rock geometry caused by erosion of overlying ice/sediment. If the production rate of an isotope at the surface of a flat rock is P_0, then the expected production rate $P(x)$ at x cm depth is:

$$P(x) = P_0\, e^{-\rho x/\Lambda} \qquad (1)$$

where Λ is the absorption mean-free-path ($\sim 150\ \mathrm{g\,cm^{-2}}$) and ρ is the density of the rock. If the variation in x with time is known, the production rate at the test point ($x = 0$) for all past times can be calculated. The expected concentration of an isotope C, at the present rock surface is given by:

$$C_{s(x=0)} = \int_0^\infty P(t)\, e^{-\lambda t}\, dt \qquad (2)$$

where λ is the disintegration constant of the isotope; and time, t, is reckoned backwards. For the simple case of a constant

Table 2 Measured ^{10}Be and ^{26}Al concentrations in quartz samples

Sample	$^{10}Be/^{9}Be$ ($\times 10^{-15}$)	^{10}Be (10^{6} atoms g^{-1})	$^{26}Al/^{27}Al$ ($\times 10^{-15}$)	^{26}Al (10^{6} atoms g^{-1})	$^{10}Be/^{26}Al$ (atom ratio)
ALH	$(6.00\pm 0.24)\times 10^{3}$	45.0 ± 1.8	$(1.93\pm 0.19)\times 10^{4}$	201 ± 20	0.224 ± 0.024
Q-1*	65 ± 14	0.29 ± 0.06	—	—	—
Q-L	110 ± 11	0.497 ± 0.050	$(1.48\pm 0.16)\times 10^{3}$	3.31 ± 0.36	0.150 ± 0.022
KKS-1†	14.2 ± 1.7	0.082 ± 0.010	107 ± 19	0.207 ± 0.037	0.396 ± 0.086
KKS-3†‡	4.8 ± 1.9	0.028 ± 0.011	$8.2^{+7.0}_{-4.4}$	$0.054^{+0.052}_{-0.029}$	(0.03–1.0)

* ^{26}Al could not be measured in this sample because of the high intrinsic aluminium content of the sample (see Table 1).

† These are not surface samples (see text); no estimates can be made on their shielding.

‡ The errors cited in the ^{26}Al values are the inverse Poisson estimates for three counts.

erosion ($dx/dt = \varepsilon$) the steady-state isotope concentration is given by:

$$C_{s(x=0)} = P_0/(\lambda + \rho\varepsilon/\Lambda) \qquad (3)$$

Inversion of equation (3) allows the deduction of the model erosion rates assuming that the sample is in secular equilibrium. An estimate based on another isotope of different half-life can be used to validate the erosion model adopted. In favourable cases, the ratio of concentrations of two isotopes can be used to determine the erosion rate, but if $\rho\varepsilon/\Lambda$ is $\leq\lambda$, the ratio can lead to erroneous estimates due to uncertainties in isotope production rates. If ε is too large, then isotopic concentrations are too low to measure. In practice, erosion rates $<10^{-2}$ cm yr^{-1} are easily measurable.

There are several advantages of using ^{10}Be and ^{26}Al, as opposed to ^{36}Cl, in this application. The production of ^{26}Al and ^{10}Be results from spallation of Si and O, the principal constituents of quartz. The production of ^{36}Cl is the result of spallation of several minor constituents, such as Ca, Ti, and the capture of thermal neutrons by ^{35}Cl. Furthermore, some of the chlorine in the rock is in a mobile form and can be exchanged in interactions with seepage water. Consequently, the ^{36}Cl production rates have to be determined for each rock studied. It is unlikely that the mineral phases which are best for the measurement of ^{36}Cl will also be suitable for measurements of ^{26}Al or ^{10}Be. In particular, minerals with sufficient concentration of target materials for the production of ^{36}Cl are unlikely to be low enough in ^{27}Al for ^{26}Al measurement. In addition, minerals with enough Ca and Ti for ^{36}Cl production are often easily altered during weathering, increasing the possibility of contamination from atmospheric sources of ^{10}Be and ^{36}Cl (from the bomb pulse).

We will discuss the implications of the results in Table 2 in view of the above simple steady-state erosional model and the theoretical ^{10}Be, ^{26}Al production rates in quartz, for samples ALH, Q-1 and Q-L only; the shielding depths of the two KKS samples are unknown, so that the absolute concentrations of ^{10}Be and ^{26}Al in terms of erosion rates cannot be considered.

The ^{10}Be/^{26}Al production ratios for 1-5 km altitude lie in the range 0.24-0.28 (Fig. 1); the atom ratios ^{10}Be/^{26}Al in rock samples should, therefore, be between 0.25 and 0.5, that is between the ratio at inception of production and the ratio at secular equilibrium. The measured values of the ratio do fall within this range for all samples except Q-L, which is lower than the lowest expected, by a factor of 1.7. The measured ratio in ALH is close to theoretical ratio at production which is surprising considering that the ^{10}Be concentration is high, corresponding to an effective period of irradiation (concentration/production rate at surface) of ~1.5 Myr, and one would expect a value of ~1.3 times the production ratio. The results of ALH and Q samples can be made consistent if one assumes a value for the ^{10}Be/^{26}Al ratio at production of ~0.15-0.17. This would imply either that we[1] overestimated the ^{10}Be production rate or that we underestimated ^{26}Al production by a factor of ~1.5. As the ^{26}Al concentration of the ALH sample is higher than the theoretical value, we probably underestimated the ^{26}Al production. Uncertainties in the estimation of production rates of ^{10}Be and ^{26}Al are at least ±20% and ±30% on the ratio. The disagreement is, therefore, not surprising.

Despite the uncertaintites in production rates, we can obtain fairly meaningful model values of erosion rates, based on the observed concentrations of one of the isotopes. By partial differentiation of equation (3), we obtain:

$$(d\varepsilon/\varepsilon)/(dP_0/P_0) = 1/(1 - \lambda T) \qquad (4)$$

where T is the effective irradiation period, $C_{x=0}/P_0$. Equation (4) shows that estimated rates of erosion are less sensitive to uncertainties in production rates for longer-lived isotopes, that is smaller λT. The effective irradiation periods (T) based on the ^{10}Be concentration for samples Q-1, Q-L and ALH are 1.75×10^4, 2.8×10^4 and 1.3×10^6 yr, respectively. These values correspond to erosion rates of 2.8×10^{-3}, 1.7×10^{-3} and 1.7×10^{-5} cm yr^{-1}. From equation (4), we deduce that a ±30% uncertainty in ^{10}Be production rate will lead to uncertainties of ±30, ±30 and ±68% in the erosion rates in these three cases.

Our results clearly demonstrate the feasibility of measuring ^{10}Be and ^{26}Al in quartz. ^{26}Al determinations require mineral phases low in Al so that the ^{26}Al/^{27}Al ratio is high enough to measure. ^{10}Be studies can be made in any mineral as long as it can be established that it does not absorb rainwater-scavenged atmospheric ^{10}Be, which we designate as the 'garden-variety' ^{10}Be to distinguish it from that produced *in situ*. Once erosional models have been checked by studies of several isotopes (for example, ^{14}C, ^{36}Cl, ^{26}Al, ^{10}Be) measured in the same sample, large-scale synoptic erosional studies of land masses can be made based on ^{10}Be concentrations in abundant suitable rock minerals. These techniques can also be used to measure exposure times in surfaces in which the erosion rate is sufficiently low, or even to date volcanic flows, if suitable mineral phases can be isolated. This approach may therefore be a method of obtaining quantitative data on denudation of rock surfaces, for which no techniques are available.

Our present results show the potential of using ^{10}Be and ^{26}Al produced *in situ* by cosmic rays for quantifying continental erosion rates and other processes; erosion rates are primarily based on estimates of the transport of detrital sediments and dissolved elements to oceans from continental runoff. It is clear that better estimates of the isotope-production rates are needed and checks of erosional history with other isotopes produced by cosmic rays (stable and radioactive) would be helpful.

We thank A. L. Engel and E. L. Winterer for discussions and K. K. Sharma for providing the high-purity quartz samples KKS-1 and KKS-3. We thank F. Kirchner for typing the manuscript. This work was supported by NASA grant NAG 9-33; NSF grant Phy 82-13598, and Cal Space grant CS-04-85.

Received 2 July; accepted 11 October 1985.

1. Lal, D. & Arnold, J. R. *Proc. Ind. Acad. Sci.* **94,** 1-5 (1985).
2. Lal, D & Peters, B. *Handbuch der Physik, XLVI/2,* 551-612 (Springer, Berlin, 1967).
3. Jha, R. & Lal, D. *Proc. 2nd Symp. on Natural Radiation Environment* (eds Vohra, K. G., Pillai, K. C., Mishra, U. C. & Sadasivan, S), 629-635 (Wiley Eastern Press, New Dehli, 1981).
4. Davis, R. & Schaeffer, O. A. *Annls N.Y. Acad. Sci.* **61,** 107-121 (1955).
5. Hampel, W. *et al. J. geophys. Res.* **80,** 3757-3760 (1975).
6. Nishio, F. & Annexstad, J. O. *Mem. Natn. Inst. Polar Res., Spec. Iss.* **15,** 13-23 (1979).
7. Nishiizumi, K. *et al. Earth planet Sci. Lett.* **70,** 157-163; 164-168 (1984).
8. Klein, J. *et al. Nucl. Instrum. Meth.* **193,** 601-616 (1982).
9. Middleton, R. *et al. Nucl. Instrum. Meth.* **218,** 430-438 (1983).
10. Middleton, R. *et al. Nucl. Instrum. Meth.* **B5,** 511-513 (1984).

Thermal erosion by komatiites at Kambalda, Western Australia and the genesis of nickel ores

D. I. Groves*, E. A. Korkiakoski*, N. J. McNaughton*, C. M. Lesher† & A. Cowden‡

* Department of Geology, University of Western Australia, Nedlands 6009, Australia
† Department of Geology, The University of Alabama, University, Alabama 35486, USA
‡ Kambalda Nickel Operations, Western Mining Corporation Ltd, Kambalda 6442, Australia

Huppert *et al.*[1] calculated that komatiites flow turbulently, transfer heat efficiently to their substrate, and thus potentially produce thermal-erosion channels in sequences onto which they were erupted. Their suggestion that komatiite-hosted (Kambalda-type[2]) nickel ores reside in such channels has led to resurgence of interest in volcanic models for ore emplacement[3-5] and caused controversy[6,7]. Such models have important implications, not only to ore-genetic studies but also to interpretation of the geochemistry

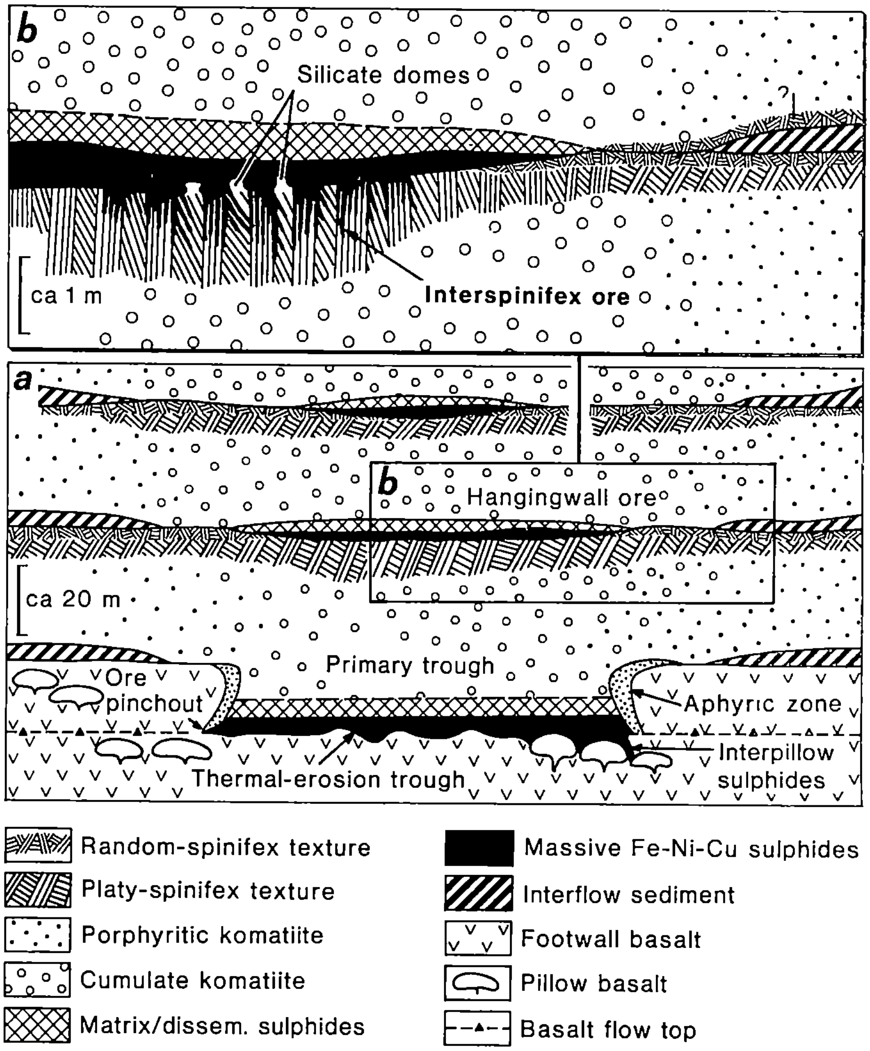

Fig. 1 Schematic representation (not to scale) of: *a*, Relationships in the lower part of the Kambalda komatiite pile emphasizing embayment (trough) structures and showing hangingwall ores (adapted from ref. 23); and *b*, relationships between massive ores, interspinifex ores and komatiite flow-tops at Lunnon Shoot.

of komatiites[8] and their Sm–Nd systematics[9,10]. Here we demonstrate that interspinifex Fe–Ni–Cu sulphide ores, which underlie some hanging wall massive sulphide ores at Kambalda the site of one of the world's major nickel deposits, formed through thermal erosion of underlying komatiite flows and possibly also sediments, providing proof of thermal erosion. However, we caution against the general application of thermal-erosion models to the eruption of komatiites. It seems that significant thermal erosion occurred rarely, and only where basal concentrations of highly thermally conductive sulphide liquid were present at the base of localized lava channels. Isotope data[11,12] and theoretical considerations[13] suggest that the komatiites were contaminated by crustal rocks before eruption, although there is limited evidence that localized contamination, including sulphide assimilation[4], may also have occurred below lava channels localized in pre-existing embayments or troughs.

Despite recent predictions that komatiites cause significant thermal erosion of their substrates[1], there has been no unequivocal supporting field evidence. This has led to suggestions that real komatiites may be less voracious than mathematical counterparts[6]. Therefore, we have tested the models using the well-documented Kambalda nickel deposits[2,3,5]. First, we present evidence for the role of thermal erosion in the formation of very localized interspinifex ores, and then we discuss its wider relevance.

Interspinifex ore is a very minor component of hanging wall ores at Lunnon, Fisher and Hunt Shoots, Kambalda[2]; its situation is shown schematically in Fig. 1. Basically, it comprises Fe–Ni–Cu sulphides interstitial to pseudomorphs after platey olivine spinifex. This ore type occupies shallow depressions in the top of the lowermost flow and is physically contiguous with overlying sulphide ore, which forms the base of the second flow in the komatiite pile. Replacement of original interstitial glass and/or pyroxene by Fe–Ni–Cu sulphides is required by (1) the almost perfect preservation of spinifex texture, and (2) transitions from sulphides to the mesostasis adjacent to pseudomorphs after olivine plates. The best interpretation is that glass and pyroxene in the spinifex-textured top of the lower flow were selectively melted by the overlying sulphide-bearing komatiite flow, and the generated silicate liquid was displaced upwards by the denser sulphide liquid. The critical evidence for such an origin includes: (1) the similarity of chemical compositions (Ni, Cu, Co, PGE) of spinifex-textured ore and overlying massive ore[14]; (2) the occurrence of magmatic ferrochromites in the spinifex-textured ores, and chromite zones on silicate-sulphide interfaces as in magmatic ores[15], (3) the presence of randomly buckled olivine blades, consistent with emplacement of hot sulphide liquid between them, and (4) the occurrence of small chromite-rimmed, silicate-rich domes, consistent with the composition of interpreted segregations of displaced silicate liquid, at the base of overlying massive ore. None of these features is consistent with metamorphic-hydrothermal replacement, the only alternative origin.

Interspinifex ore was formed at temperatures below the olivine liquidus[16] but above the sulphide liquidus[17]. The fact that virtually all interspinifex ore has platy-spinifex texture rather than random-spinifex texture, which typically occurs at the top of komatiite flows at Kambalda[18], suggests thermal erosion of the uppermost part of the underlying flow before formation of the interspinifex ore. Stratigraphical correlations with komatiite-komatiite contacts along strike, combined with measurements of the shallow depressions occupied by interspinifex ore, suggest a maximum of 1 m of erosion of komatiite before formation of that ore (Fig. 1*b*). Thus, a *prima facie* case for thermal erosion is established. The interflow sediment, present along strike, may also have been eroded but there is no direct evidence.

The significance of these observations to the applicability of thermal-erosion models, in general[1,6,7], can be assessed through (1) relationships along strike and down dip from interspinifex ores, and (2) consideration of observational data for more typical basal (contact) ores[2] in combination with accumulated petrological, geochemical and isotopic data from Kambalda komatiites.

Relationships in localized interspinifex ore environments indicate that thermal erosion is virtually restricted to some portions of the contact occupied by massive sulphide ores (Fig. 1). Normally, the upper komatiite flow conformably overlies interflow sulphidic sediments with little evidence for interaction, or directly overlies fine-grained random spinifex-textured komatiite. Thin amphibole-chlorite rich assemblages occur at the base of the upper flow in places[19], and probably represent former chilled margins[18]. Thus field evidence from hanging wall ore-environments at Kambalda indicates that thermal erosion of komatiite occurred locally only where pools of sulphide liquid had already accumulated, presumably caused by the order-of-magnitude higher thermal conductivity of the sulphide liquid[20] relative to komatiite liquid[21,22], and its lower liquidus temperature[17]. There is no definitive evidence to indicate whether the massive sulphides were purely magmatic liquids, or whether their occurrence marks the position of lava channels[4], in which more prolonged throughput of lava was capable of assimilating sulphide sediments and generating sulphide liquid below which thermal erosion of komatiite continued.

Observations on basal ore environments at Kambalda favour a primary volcanic/topographical control on embayments and localized lava channels[23] rather than initial formation by thermal erosion. Interpretation is hindered by subsequent, commonly severe, metamorphic alteration of the ultramafic rocks combined with structural modification[2,23]. Despite this, the komatiites within the lava channels are texturally and geochemically distinct from flanking flows[23], which have conformable contacts with underlying sulphide sediments over >90% of the total contact surface. Komatiites within the lava channels show evidence for prolonged flow-through of magma, not shown by flanking flows. Evidence from Kambalda that confining embayments were primary volcanic features before komatiite eruption includes: (1) stratigraphical control of some embayments whose base (the base of the initial komatiite flow) coincides with the flow top of the penultimate basalt flow[23], (2) the presence of probable aphyric margins on komatiites around some embayments[23], and (3) the elongated form of most major embayments parallel to the interpreted fault-bounded margins of the volcanic basin[24]. The presence of unassimilated or partly assimilated sediments in the similar embayments at Scotia and at Wannaway[3] indicate that those embayments also predate sulphide ore and komatiite emplacement.

Structural and metamorphic modification of ore environments inhibits unequivocal interpretation. However, there are second-order irregularities within major embayments that could possibly be formed by thermal erosion. These include: (1) spaced 1-2 m convex-upward, projections of basalt into massive ore (such as Long and Durkin Shoots)[23]; (2) small elliptical depressions confining Fe-Ni-Cu ores (such as Ken Far East, Juan East); (3) widespread, structurally modified, lateral tongues of massive sulphide in basalts in ore pinchouts (Fig. 1*a*); and (4) interpillow Fe-Ni-Cu sulphides which may well be representative of thermal erosion. The unusual silicate gangue mineralogy of massive ore[25,26] could also be partly caused by melting of basal chills and/or basalt, and preservation of so-formed immiscible silicate melt in sulphides below overlying crystallized olivine cumulates (compare with silicate domes associated with interspinifex ores). These features indicate the possibility that localization of lava channels and basal sulphide liquids in original volcanic/topographical embayments focused thermal erosion and modified the original embayments.

Several lines of evidence suggest that Kambalda komatiites are contaminated; (1) Sm-Nd (refs 9, 10) and Pb-Pb (ref. 12) or U-Pb (ref. 11) isotope studies indicate that Sm-Nd 'isochrons' are mixing lines between komatiites and older crustal components; (2) Pb-Pb studies of iron sulphides from nickel ores and adjacent sulphide sediments suggest mixing of mantle and older crustal lead[27]; (3) the similarity of S/Se ratios and $\delta^{34}S$ values of nickel ores and sulphide sediments[4,25] and anomalously high Zn chromites in mineralized komatiites[15,27]. Several of these geochemical parameters indicate that contamination affected both the basal mineralized komatiite(s) and the entire komatiite pile. These include: (1) the tight grouping of both komatiites and basalts on Sm-Nd mixing lines[6,9]; (2) the occurrence of >3,000 Myr xenocrystic zircons in overlying komatiitic basalts[11]; and (3) chalcophile-element depletion[28] and occurrence of Zn-rich chromites[15] throughout the Kambalda komatiite pile. Collectively, these data suggest that sulphide liquids separated from komatiites that were contaminated during ascent through older continental crust, as predicted theoretically[13]. However, the similarity of S/Se ratios and $\delta^{34}S$ values of nickel ores and adjacent sulphide sediments[4,25] plus the fact that lead isotope compositions of iron-sulphides from nickel ore could represent mixtures of mantle lead and lead from the sulphide sediments[27], suggests that assimilation of sulphide sediments contributed to sulphide liquids in at least some komatiites.

There is unequivocal evidence from hanging wall ore environments at Kambalda for localized, shallow thermal erosion channels in early komatiites (and possibly sediments) underlying subsequent komatiite flows containing basal sulphide liquid pools. Conduction of heat from the overlying turbulently convecting komatiite through the highly thermally conductive sulphides seems to have been the controlling process. In the major basal (contact) ore environments, however, primary major embayments were volcanic/topographical features. There is some evidence for melting of the basalt substrate by thermal erosion only beneath sulphide-liquid pools at the base of lava channels confined by the embayments. Some sulphide liquid probably formed as a result of initial thermal erosion of sulphidic sediments. Such assimilation can explain some of the contamination shown by komatiites, but other parameters suggest contamination during magma ascent. Our study suggests that komatiites were erosive, but were more lethargic than previously suggested. It stresses the role of highly conductive sulphides, associated with lava channels, in thermal erosion of komatiitic and basaltic substrates by komatiite lavas.

We thank J. J. Gresham of Kambalda Nickel Operations for access to the Kambalda deposits, and several other Kambalda geologists for documentation and discussions of Kambalda geology. We also acknowledge UWA colleagues, particularly N. Dahl and P. Parker, and CSIRO staff, especially R. E. T. Hill, for useful discussions. E.K. was sponsored by the Australia-European Awards Programme and partly funded by Kambalda Nickel Operations.

Received 7 August; accepted 21 October 1985.

1. Huppert, H. E., Sparks, R. S. J., Turner, J. S. & Arndt, N. T. *Nature* **309**, 19-22 (1984).
2. Gresham, J. J. & Loftus-Hills, G. D. *Econ. Geol.* **76**, 1373-1416 (1981).
3. Lesher, C. M., Arndt, N. T. & Groves, D. I. *Sulphide Deposits in Mafic and Ultramafic Rocks* (eds Buchanan, D. L. & Jones, M. J.) 70-80 (Institution of Mining and Metallurgy, London, 1984).
4. Lesher, C. M. & Groves, D. I. *Geology and Formation Conditions of Copper Deposits* (eds Naldrett, A. J., Ridge, J. D., Vokes, F. M., Genkin, A. D. & Sillitoe, R. H.) (Springer, Berlin, in the press).
5. Gresham, J. J. *Geology and Formation Conditions of Copper Deposits* (eds Naldrett, A. J., Ridge, J. D., Vokes, F. M., Genkin, A. D. & Sillitoe, R. H.) (Springer, Berlin, in the press).

6. Claoue-Long, J. C. & Nesbitt, R. W. *Nature* **313**, 247 (1985).
7. Huppert, H. E., Sparks, R. S. J. & Arndt, N. T. *Nature* **13**, 247-248 (1985).
8. Nisbet, E. G. *Nature* **309**, 14-15 (1984).
9. Claoue-Long, J. C., Thirlwall, M. F. & Nesbitt, R. W. *Nature* **307**, 697-701 (1984).
10. Bickle, M. J. *Nature* **312**, 702-703 (1984).
11. Compston, W., Williams, I. S., Campbell, I. H. & Gresham, J. J. *Earth planet. Sci. Lett.* (in the press).
12. Chauvel, C., Dupre, B. & Jenner, G. A. *Earth planet. Sci. Lett.* **74**, 315-324 (1985).
13. Huppert, H. E. & Sparks, R. S. J. *Earth planet. Sci. Lett.* **74**, 371-386 (1985).
14. Woolrich, P., Cowden, A. & Giorgetta, N. E. *Econ. Geol.* **76**, 1629-1644 (1981).
15. Groves, D. I., Barrett, F. N., Binns, R. A. & McQueen, K. G. *Econ. Geol.* **72**, 1224-1244 (1977).
16. Arndt, N. T. *Yb. Carnegie Instn. Wash* **75**, 555-562 (1976).
17. Craig, J. R. & Kullerud, G. *Econ. Geol. Monogr.* **4**, 344-358 (1969).
18. Ross, J. R. & Hopkins, G. M. F. *Economic Geology of Australia and Papua New Guinea, I. Metals* (ed. Knight, C. L.) 100-121 (Australian Institute of Mining and Metallurgy, Melbourne, 1975).
19. Bavinton, O. A. thesis, Australian National Univ. (1979).
20. Williams, R. K., Veeraburns, M. & Philbrook, W. O. *AIME Metall. Trans.* **3**, 255-260 (1972).
21. Jaeger, J. C. *Basalts: The Poldervaart Treatise on Rocks of Basaltic Composition* (eds Hess, H. H. & Poldervaart, A.) 503-536 (Wiley, New York, 1968).
22. Bickle, M. J. *Komatiites* (eds Arndt, N. T. & Nisbett, E. G.) 479-494 (Allen and Unwin, London, 1982).
23. Lesher, C. M. thesis, Univ. Western Australia (1983).
24. Groves, D. I., Lesher, C. M. & Gee, R. D. *Sulphide Deposits in Mafic and Ultramafic Rocks* (eds Buchannan, D. L. & Jones, M. J.) 1-13 (Institution of Mining and Metallurgy, London, 1984).
25. Groves, D. I., Barrett, F. M. & McQueen, K. G. *Can. Miner.* **17**, 319-336 (1979).
26. Ewers, W. E. & Hudson, D. R. *Econ. Geol.* **67**, 1075-1092 (1972).
27. Parker, P. thesis, Univ. Western Australia (1984).
28. Lesher, C. M., Lee, R. F., Groves, D. I., Bickle, M. J. & Donaldson, M. J. *Econ. Geol.* **76**, 1714-1728 (1981).

Estimating the error of age interpolation in sedimentary rocks

Catherine Badgley*, Lisa Tauxe† & Fred L. Bookstein‡

* Museum of Paleontology and ‡ Center for Human Growth and Development, University of Michigan, Ann Arbor, Michigan 48109, USA
† Scripps Institution of Oceanography, La Jolla, California 92093, USA

Magnetostratigraphic data can provide information on rates of sediment accumulation within a single sedimentation system over time spans from 10^4 to 10^6 yr. The short-term rate of sediment deposition varies with time; the apparent average rate over any longer interval also depends on the relative durations of periods of deposition, stasis (non-deposition), and erosion. While the average rate can be used to infer the time of occurrence of an event from its stratigraphical position, the inferred age has an uncertainty deriving from the variability in rate of sediment accumulation over all shorter timescales. We analyse here variability in sediment accumulation rates provided by the magnetostratigraphy of Miocene, Siwalik sediments from Pakistan. For long periods ($>10^6$ yr), sediment accumulation is approximately linear through time. Over short intervals (10^4–10^5 yr), however, there is considerable variability. To provide an error term for an absolute age interpolated between boundaries of polarity units, we use a resampling technique similar to the statistician's 'bootstrapping'. We illustrate this approach by estimating a standard error for the interpolated age of a biostratigraphical datum: the first appearance of hipparionine equids in the Siwalik sequence near the town of Khaur. The first appearance of "*Hipparion*" in the Khaur sequence is 9.22 ± 0.09 Myr.

The assignment of absolute age estimates to sedimentary rocks requires either horizons susceptible to radiometric dating or access to the geomagnetic reversal timescale (GRTS). Fossils may indicate relative chronology in sedimentary rocks but do not convey information about absolute age. Thus, stratigraphical sections usually contain an arbitrary scatter of levels from which age information is available. Ages of all other levels are estimated indirectly by linear interpolation between levels of more accurately known age.

Linear interpolation of an estimated age within a stratigraphical section assumes that the sediment accumulation rate calculated for the longer, dated portion of the sequence also applies to much shorter time intervals. This is rarely the case. Unless sediment accumulates continuously and without erosion, sediment accumulation rate decreases as the time span of measurement is increased[1-3]. Thus it is necessary to consider when linear interpolation of an age estimate is justified, and how to assess the accuracy of the age estimate. Sadler[2] proposed replacing an interpolated age value by an age range based on an estimated incompleteness of the section. The completeness estimates[2,4] are based on the pattern of sediment accumulation rate versus time span for a large compilation of data from one class of sedimentary environments, such as fluvial systems. There is, however, no particular reason why any such variance should usefully model the variance within a sedimentation system.

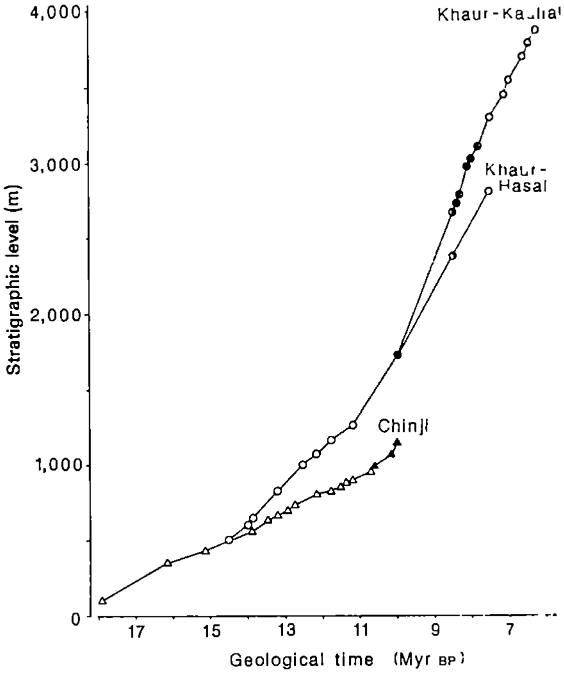

Fig. 1 Cumulative stratigraphic thickness over time in Siwalik sediments of northern Pakistan. Chinji and Khaur are two geographical areas in the same depositional system; Kaulial and Hasal are local section names[5]. Each data point demarcates a reversal of magnetic polarity. Triangles represent data from the Chinji area and circles data from the Khaur area. Solid symbols, strata older than 11 Myr; open symbols, strata younger than 11 Myr. A change in sediment accumulation rate occurred between 10 and 11 Myr, as indicated by the change in slope. Net sediment accumulation appears to be linear through time for the Chinji data older than 11 Myr and for the Khaur data younger than 11 Myr.

A more direct approach is to exploit observable variability of sediment accumulation rates within a sedimentation system to build a statistical description of the relationship between sediment accumulation and time. The problem in age interpolation is how to estimate the proportion of time span present in a known proportion of sediment thickness from the interval of interpolation. One way to assess the standard error of such ages is to document this variability using intervals of a similar length for which age is not interpolated but is rather observed. Long magnetostratigraphic sections provide independent measurements of sediment accumulation rate for every discernible magnetic polarity interval. We demonstrate a method of 'resampling' a magnetostratigraphic section to generate multiple intervals that can be divided into shorter intervals of known time span and thickness. The original and resampled data together provide an estimate of the standard error about an interpolated age.

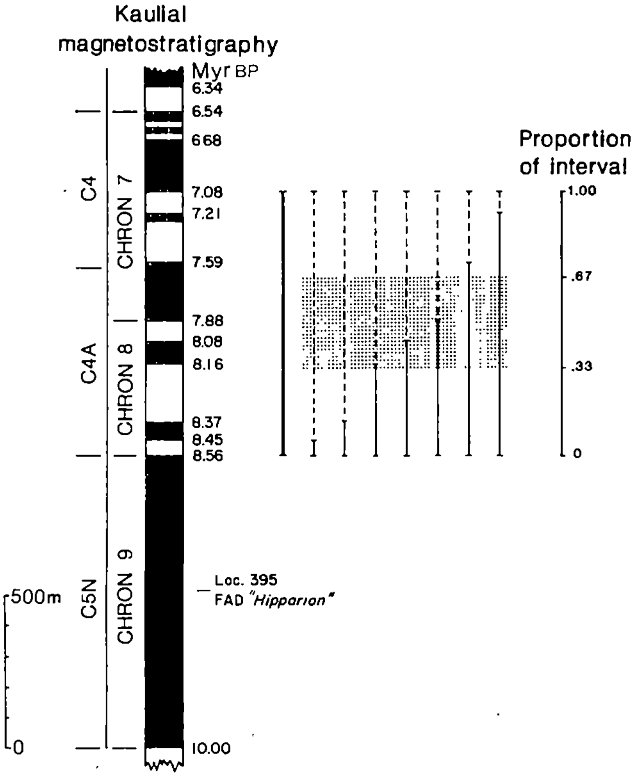

Fig. 2 Magnetostratigraphy from the Kaulial section in the Khaur area[5] illustrating the resampling method discussed. Absolute ages are indicated from the geomagnetic reversal timescale whenever a polarity interval is represented by at least three palaeomagnetic samples. Two timescales are used: that of Mankinen and Dalrymple[9] (right) and the new chron names (left) of Berggren *et al.*[8] given in the text. The first appearance datum (FAD) of "*Hipparion*" occurs within the long normal interval of Chron C5N. On the right, an interval is extracted from the left-hand record that is of about the same duration as Chron C5N. This long interval can be subdivided in seven different ways into complementary segment pairs of known thickness and time span; there result 14 calculations of proportion of sediment thickness and of time span. Of these segment pairs, three divide the long interval into segments between 33 and 67% (stippled band) of the whole. Ten intervals of durations between 1.2 and 1.8 Myr were located in Chrons C4 and C4A; the 104 segment pairs that can be formed within them provide the data in Fig. 3.

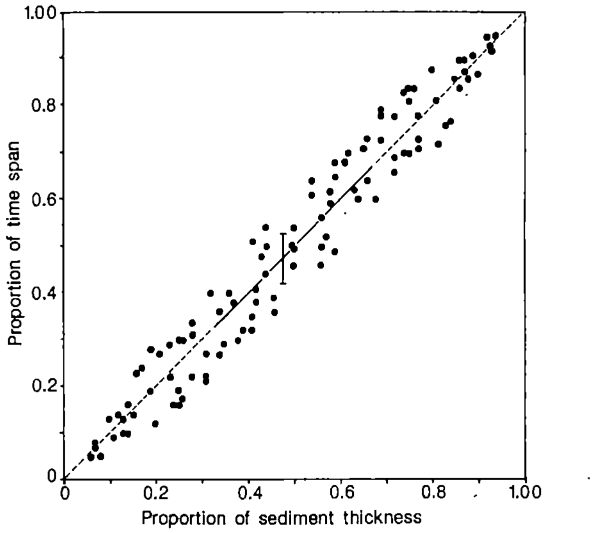

Fig. 3 Variability in proportion of time span in relation to proportion of sediment thickness from subsamples of 10 long intervals in the Kaulial palaeomagnetic section (Fig. 2). Five intervals are longer than the interval of interpolation (1.44 Myr) and five are shorter. Each subsample of a long interval gives rise to two complementary data points whose proportions along either axis sum to 100%. For this reason, the graph is unchanged by a 180° rotation about its centre. The standard error (vertical bar) of 0.06 (6%) was calculated for data in the region of the solid line ($n=40$), corresponding to subsamples of 50±17% of the whole interval. The value of ±6% appears characteristic of a considerably wider range of sediment proportions, perhaps 18–82%.

The data for demonstrating our approach are contained in two magnetostratigraphic studies of Siwalik sediments from Pakistan[5,6]. Siwalik rocks are a Neogene molassic sequence representing multiple fluvial systems on the southern margin of the Himalayas[7]. The pattern of Siwalik sediment accumulation through the middle to late Miocene in northern Pakistan is illustrated in Fig. 1. The Khaur sections exhibit higher sediment accumulation rates because they were closer than the Chinji sections to the inferred source area. In both areas, a change in sediment accumulation rate occurred between 10 and 11 Myr in response to an episode of Himalayan uplift[6]. This event, the major secular trend, constitutes a change in the controls of the sedimentation system. In each geographical location, sediment accumulation appears stationary on either side of this event. For the remainder of the discussion, we focus on a portion of the Khaur data.

Magnetostratigraphic data from the Khaur area are documented in 14 measured stratigraphic sections[5], each spanning part of a 2,100-m interval over a lateral extent of ~25 km. (Only two of these sections are shown in Fig. 1.) The sections are correlated by lithological marker horizons and magnetic polarity stratigraphy; sampling densities ranged from 1 in 3 m to 1 in 23 m. Altogether, the composite Khaur section represents 6.5–10.0 Myr, Chrons C4–C5N (terminology of Berggren *et al.*[8]). (We indicate also the GRTS of Mankinen and Dalrymple[9] in Fig. 2, for consistency with earlier studies. The choice of timescale does not affect the results of the technique presented here.) The longest continuous magnetostratigraphic section in deposits younger than 11 Myr, from Kaulial Kas (a local valley name), serves as the basis for the example discussed below (Fig. 2). The sampling density for this section ranged from 1 in 19 m to 1 in 23 m.

Siwalik sediments, rich in mammalian fossil remains, constitute the standard for South Asian, Neogene mammalian biostratigraphy[10,11]. The first appearance of the three-toed horse "*Hipparion*" in the Khaur Siwalik sequence is significant, both because it marks a rapid faunal turnover within the Siwalik mammalian fauna[10] and because it is used to link Miocene mammalian sites in the Old World[12]. "*Hipparion*" includes several hipparionine taxa not always represented by fossils diagnostic to the species level.) Since the first appearance of "*Hipparion*" in the Siwaliks occurs >2 Myr later than its first appearance in European and African sites[12–15], this event is also controversial. But it lies in the middle of the long normal interval of Chron C5N, thus being a genuine problem in age interpolation.

In the Kaulial section, the lowest occurrence of "*Hipparion*" is at the Harvard-Geological Survey of Pakistan Locality 395 (J. Barry, personal communication). Stratigraphically, Locality 395 lies 510 m above the base of the long normal unit, which is 940 m thick in Kaulial Kas (Fig. 2)[5]. A linear interpolation estimates this event to be 0.78 Myr younger than the age at the base of the long normal unit, or 9.22 Myr in absolute time. The "*Hipparion*" datum is near the middle of the long normal unit. To assess the expected error of this age estimate, we must know how the proportion of time span varies in relation to about half the sediment thickness for time intervals about the same length as the long normal period. Within the combined sequence of

Chrons C4-C4A, it is possible to delimit various intervals of durations between 1.2 and 1.8 Myr. These intervals can be subdivided into complementary pairs of segments, some representing about half of the full interval. For each segment, the discrepancy between proportion of time span and proportion of sediment thickness is directly observable. Thus, we use the pattern of sediment accumulation for a younger portion of the sediment regime to estimate the variance in an older part of the regime; the implied assumption of stationarity is justified by the linear pattern of cumulative stratigraphic thickness over the entire Kaulial sequence.

The resampling technique is illustrated in Fig. 2. The long interval shown as an example is 1.48 Myr in duration according to palaeomagnetic correlation. This interval contains nine short polarity intervals, of which the smallest, at 7.21 Myr, was represented by less than three samples. It was grouped with the next interval below it. (The same criterion was used to group together the four short intervals from 6.54 to 6.68 Myr in other samples.) The long interval may thus be broken into two pieces of known age in seven different ways. For each division, we calculated the proportion of total sediment thickness and proportion of total time span represented in each segment. In all, 10 long intervals, ranging from 1.25 to 1.77 Myr, were identified and subdivided in a similar fashion: these produced 104 segments, represented in Fig. 3.

For the "*Hipparion*" problem, the variance we need should correspond to a thickness proportion of ~0.50. We computed the mean sqaure

$$\frac{\Sigma\ (\text{time proportion} - \text{thickness proportion})^2}{n}$$

of time proportion about thickness proportion for thickness proportions between 0.33 and 0.67 (the solid line in Fig. 3). This quantity is equivalent to the variance in time proportion around a regression line on thickness proportion forced to have a slope of 1 and forced, also, to pass through the origin. For $n = 40$, within the central third of the range, the standard error of this discrepancy is 0.06. Thus, the standard error of the age estimate for the "*Hipparion*" datum should be taken as 6% of 1.44 Myr. By this approach, the age of the first appearance of "*Hipparion*" in the Khaur Siwalik sequence is 9.22 ± 0.09 Myr.

This method of generating a standard error is similar to bootstrapping, jackknifing, and other resampling techniques of modern statistical data analysis. One sample is used to generate many others through intensive resampling of the same data set[16,17]. The data of Fig. 3 are not statistically independent, even though that was assumed for the data of the original sample. In these circumstances, the computed value of 0.06 is a point estimate only, having no standard error itself.

The value 0.06 pertains to this particular situation, that is, the proportion of time span represented by 33-67% of sediment thickness for intervals of 1.2-1.8 Myr duration in Chrons C4 and C4A in the Kaulial section. The same standard error would apply to an interpolation problem concerning 55% of a polarity interval of 1.7-Myr duration, but not to 55% of an interval of 0.5-Myr duration. For this second case, it would be necessary to generate another sampling distribution. It is ultimately the pattern of the observed palaeomagnetic data which determines how the resampling technique can be applied. It would not be possible, in our example, to determine a standard error for intervals of 0.08 Myr duration, this being the shortest interval represented.

This standard error is not the only source of uncertainty in an interpolated age. Palaeomagnetic dates bear the limitations in time resolution of the GRTS, and the stratigraphic placement of reversal boundaries is partly a function of sample spacing. These factors contribute additional uncertainty to any palaeomagnetic age estimate (including age interpolations), although the error should not be a systematic one. The standard error calculated by this resampling method can be considered a minimum value attributable to variability in sediment accumulation rate.

Variation in sediment accumulation rates can be attributed to variation in instantaneous sedimentation rates and in completeness of stratigraphic sections. In a complete stratigraphic section with low variability of instantaneous sedimentation rates, linear interpolation provides the best estimate of age. But most stratigraphic sections cannot be considered complete. Even in systems such as lakes or deep ocean basins where deposition is virtually continuous, sediment is reworked by deep currents, turbidite processes, or dissolution. In fluvial systems, such as the Siwaliks, deposition in any one location is markedly discontinuous, even though deposition may occur most of the time somewhere in the system.

In incomplete sections, the results of linear interpolation are most plausible when gaps are relatively short and evenly distributed throughout the sedimentary record. But such convenient models cannot be assumed in general. The distribution of gaps relative to record must be interpreted in part by stratigraphic information from the section(s) under investigation. Fifty meters of laminated silt imply a markedly different distribution of gaps than 50 m of cross-bedded sandstone. When a pattern of sediment accumulation contains long, unevenly distributed discontinuities, linear age interpolation may be very prone to error; and whenever the magnitude of depositional and erosional events varies widely, the record is likely to be dominated by rare events of high magnitude[18].

These considerations argue against the computation of age-estimate errors according to any general stochastic model. In contrast, the resampling technique demonstrated here indicates the root-mean-square amount by which the interpolated age estimate differs from a 'known' value as a result of the variability in sediment accumulation rates specific to the particular sequence within which the interpolation is taking place. In this way, each system is characterized by its own pattern of variation in sediment accumulation rates, reflecting its own external factors, such as source-area uplift, or internal factors, such as local reworking of sediment.

We thank Gerald Smith, Jennifer Kitchell and Beth Dawson for constructive discussions. Karen Klitz drew Figs 1 and 2. This work was supported in part by NSF grant EAR 8305931 to C.B. and NSF grant OCE83-17546 to L.T.

Received 5 July; accepted 8 October 1985.

1. Schindel, D. E. *Palaeobiology* **6**, 408-426 (1980).
2. Sadler, P. M. *J. Geol.* **89**, 569-584 (1981).
3. Tipper, J. C. *Nature* **302**, 696-698 (1983).
4. Sadler, P. M. & Dingus, L. W. *Proc. 3rd N. Am. Paleontol. Conv.* **2**, 461-464 (1982).
5. Tauxe, L. & Opdyke, N. D. *Palaeogeogr. Palaeoclimatol., Palaeoecol.* 37, 43-61 (1982).
6. Johnson, N. M., Stix, J., Tauxe, L., Cerveny, P. F. & Tahirkheli, R. A. K. *J. Geol.* 93, 27-40 (1985).
7. Behrensmeyer, A. K. & Tauxe, L. *Sedimentology* **29**, 331-352 (1982).
8. Berggren, W. A., Kent, D. V., Flynn, J. & Van Couvering, J. A. in *Geochronology and the Geological Record* (ed. Snelling, N. J.) (Spec. Pap. Geological Society, London, in the press).
9. Mankinen, E. A. & Dalrymple, G. B. *J. geophys. Res.* **84**, 615-626 (1979).
10. Barry, J. C., Lindsay, E. H. & Jacobs, L. L. *Palaeogeogr. Palaeoclimatol. Palaeoecol.* 37, 95-130 (1982).
11. Barry, J. C., Johnson, N. M., Raza, S. M. & Jacobs, L. L. *Geology* (in the press)
12. Bernor, R. L., Woodburne, M. O. & Van Couvering, J. A. *Geobios* **13**, 705-739 (1980)
13. Ginsburg, L., Janvier, P., Mornand, J. & Pouit, D. *C. r. Somm. Séanc. Soc. Géol. Fr.* 223-227 (1979).
14. Tiercelin, J.-J., Michaux, J. & Bandet, Y. *Bull. Soc. Géol. Fr.* **21**, 255-258 (1979)
15. Hussain, S. T. & Bernor, R. L. *Himalay. Geol.* **11**, 35-42 (1983).
16. Diaconis, P. & Efron, B. *Scient. Am.* **248** (5), 116-130 (1983)
17. Efron, B. & Tibshirani, R. *Tech. Rep.* **101** (Division of Biostatistics, Stanford University, 1985).
18. Crowley, K. D. *J. sedim. Petrol.* **54**, 127-136 (1984).

Light quality and oceanic ultraphytoplankters

Hilary E. Glover, Maureen D. Keller & Robert R. L. Guillard

Bigelow Laboratory for Ocean Sciences, McKown Point,
West Boothbay Harbor, Maine 04575, USA

Photosynthetic prokaryotic picoplankters (<2 μm), *Synechococcus* spp.[1,2], provide a significant fraction of oceanic primary production[3,4]. The significance of similarly sized eukaryotic algae has not been fully appreciated until recently, as they are difficult to isolate in culture and many become distorted or disintegrate in preservatives[5,6]. Yet these eukaryotes, in the size range of *Synechococcus*, to perhaps 10 μm (refs 7–10), often numerically dominate ultraphytoplankton (<10 μm) at deep chlorophyll maxima[5,6,11–13]. Because temporal variability in oceanic productivity seems to be caused by changes at the bottom of the euphotic layer[14], the composition and activity of communities at chlorophyll maxima are of interest. Here we present evidence that eukaryotic ultraplankters have greater photosynthetic and growth efficiencies than *Synechococcus* in the dim blue–violet light occurring at the bottom of the euphotic zone. Our experiments at least partially explain the large numbers of eukaryotic ultraplankters in the open ocean at the 0.5% light level, below the population peak of *Synechococcus spp.*

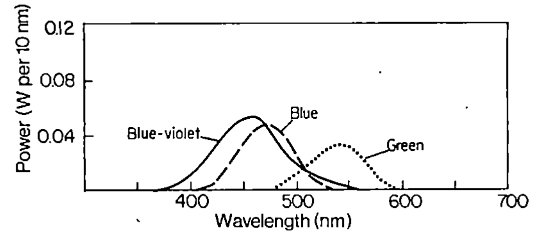

Fig. 1 Spectral quality of plastic filters used in physiological experiments: blue-violet filter (——), maximum transmittance 455 nm; blue filter (- - -), maximum transmittance 470 nm; green filter (· · · ·), maximum transmittance 542 nm.

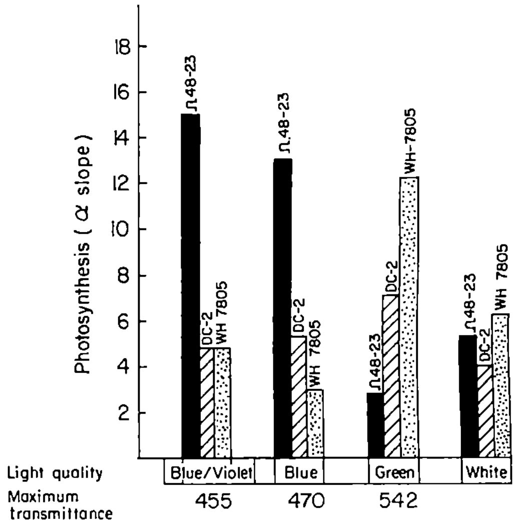

Fig. 2 Photosynthetic efficiencies in different light qualities for an ultraplanktonic prasinophyte clone Ω48-23 (■), *Synechococcus* clone DC-2 (▨) and *Synechococcus* clone WH 7805 (▩). Batch cultures were grown at 20 °C, in 14/10 h light/dark cycles in blue-violet light at 1.6×10^{15} quanta $cm^{-2}\,s^{-1}$. In 'log-phase', we determined chlorophyll *a* concentrations[24] and photosynthetic rates[25] at four rate-limiting fluxes of blue-violet, blue, green or white light, and determined the α slope as a measure of phytosynthetic efficiency[22]. α slope = photosynthesis (mg carbon per mg chlorophyll *a* per h)/irradiance (quanta $\times10^{-16}$ $cm^{-2}\,s^{-1}$).

We compared the performances in culture of oceanic clones of *Synechococcus* and eukaryotic algae from different classes in conditions of nutrient abundance but variable light intensity and quality. We also compared attenuation spectra and fluorescence emission spectra.

All eukaryotic phytoplankters have chlorophyll *a* as their major light-harvesting pigment. Large eukaryotic diatoms and dinoflagellates, which numerically dominate shallow neritic chlorophyll maxima, contain carotenoid pigments (fucoxanthin and peridinin, respectively), which absorb the available green light[15]. In contrast, eukaryotic ultraplankton species do not contain these carotenoids but have chlorophyll *b* or *c* as major accessory pigments[16]. While oceanic *Synechococcus* spp. contains chlorophyll *a*, phycoerythrin is the major light-harvesting pigment[17–20].

Excitation of *Synechococcus* clones with green (530 nm) light produced a much larger fluorescence emission than with blue (470 nm) light. Conversely, ultraplanktonic eukaryotic clones exhibited greater fluorescence emission with blue (470 nm) light than with green (530 nm) light. The ratio of fluorescence emission produced by excitation at 530 nm (green) to that produced by excitation at 470 nm (blue) was calculated for each clone. Except for large diatoms and dinoflagellates, ratios did not exceed 0.7 for eukaryotic algae (0.3–0.4 for ultraplanktonic prasinophytes, 0.4–0.7 for prymnesiophytes and chrysophytes). Highest ratios, 5.2 and 5.4, respectively, were observed for *Synechococcus* clones WH 8018 and WH 7805. These clones contain only phycoerythrobilin (PEB) chromophores in their phycoerythrin[18]. *Synechococcus* clones DC-2 and Syn-48 contain phycourobilin (PUB) in addition to PEB chromophores[18], which shift the excitation wavelength from 530 nm to 510 nm; for these two clones, ratios of fluorescence emission were 2.6 and 2.5 (at 510:470 nm excitation).

We performed photosynthesis and growth experiments in conditions of nutrient abundance but variable light intensity and quality. 'Daylite' fluorescent bulbs in conjunction with coloured filters (Fig. 1) were used to simulate two types of oceanic water[21]—blue-violet (maximum transmittance 455 nm) and blue (maximum transmittance 470 nm)—and coastal water[21]—green (maximum transmittance 542 nm). 'Vitalite' fluorescent bulbs were used to simulate daylight (white light). Photosynthetic efficiences were determined as light-limited α slopes[22] in white, green, blue and blue-violet light. All eukaryotic ultraplankton clones used blue-violet light most efficiently for photosynthesis, while phycoerythrin-rich *Synechococcus* clones photosynthesized most efficiently in green light. An example of this is shown in Fig. 2. *Synechococcus* clone DC-2, containing PUB chromophores, was able to use low fluxes of blue light more efficiently for photosynthesis than could *Synechococcus* clone WH 7805, which lacks PUB chromophores. Extending these studies to include growth experiments, we found that eukaryotic ultraplankton clones grew fastest in low fluxes of blue-violet light. In contrast, *Synechococcus* clones grew best in green light (see, for example, Fig. 3).

Even though larger eukaryotic algal clones could effectively use blue-violet light, they could not utilize very low photon flux densities as efficiently as could eukaryotic ultraplankters. This may be partly due to a more efficient absorption of light with decreasing cell size[23]. Thus, the bottom of the euphotic zone in the open ocean may provide insufficient photon flux densities for efficient photosynthesis and growth of larger forms.

Our experiments suggest that *Synechococcus* clones containing PUB chromophores should out-compete other *Synechococcus* clones at depth. Moreover, oceanic eukaryotic ultraplankters should have a competitive advantage over *Synechococcus* at the base of the euphotic zone in dim blue-violet light because of

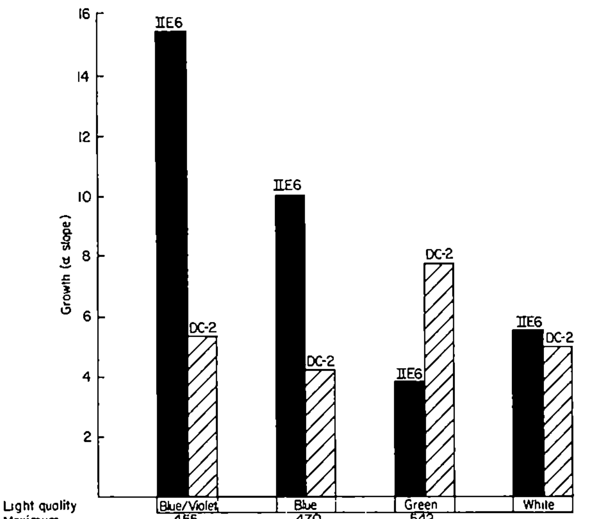

Fig. 3 Growth efficiencies in different light qualities for ultraplanktonic prymnesiophyte clone II E6 (■) and *Synechococcus* clone DC-2 (▨). We determined the daily increase in fluorescence[26] and cell numbers in batch cultures at 20 °C, in 14/10 h light/dark cycles at four rate-limiting fluxes of blue-violet, blue, green and white light, and determined the α slope as a measure of growth efficiency. The α slope = specific growth rate (h^{-1})/irradiance $(\text{quanta} \times 10^{-16}\ \text{cm}^{-2}\ \text{s}^{-1})$.

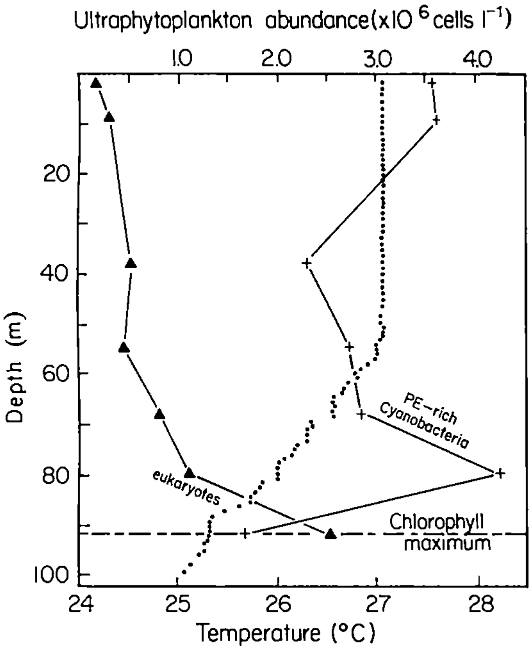

Fig. 4 Depth profiles of phycoerythrin(PE)-rich *Synechococcus* (+), eukaryotic ultraplankters (▲) and temperature (●). Data were collected from the Sargasso Sea at 34°49′ N, 66°20.6′ W in August 1983. Pump water was immediately filtered at <125 mm Hg through a 3-μm Nuclepore filter. The filtrate was passed through a 0.2-μm Nuclepore filter and cells were classified as either *Synechococcus* or eukaryotes[6].

functional differences in their pigment compositions. Recent field experiments support this hypothesis[20]. Ultraplankters sink at negligible rates[12], thus biomass peaks below the surface mixed layer[6,13] in the open ocean may be attributed to *in situ* growth. One advantage of inhabiting this dimly illuminated environment is the proximity to richer nutrient levels from upward advection across the thermocline. This enrichment enables cells to synthesize additional pigments for photoadaptation. Below the upper isothermal layer in the Sargasso Sea (Fig. 4), we found the maximum numbers of *Synechococcus* occurring at about 1% of surface irradiance, while the maximum abundance of eukaryotic ultraplankters occurred below this, constituting a chlorophyll maximum. This agrees with previous data from the central gyre of the North Atlantic[6].

It should also be noted that photosynthetic studies in deck-incubators, under natural light modulated in intensity but not quality, will underestimate the contribution of eukaryotic ultraplankters to the *in situ* rate of oceanic primary production.

We thank E. M. Haugen, A. E. Smith and R. Spinard for assistance with this research and C. S. Yentsch and L. A. Codispoti for reviewing this manuscript. The work was supported by NSF grants OCE-84-05299 and OCE-82-08626. This is Bigelow contribution 84034.

Received 30 April; accepted 24 December 1985.

1. Waterbury, J. B., Watson, S. W., Guillard, R. R. L. & Brand, L. E. *Nature* **277**, 293–294 (1979)
2. Johnson, P. W. & McN. Sieburth, J. *Limnol. Oceanogr.* **24**, 928–935 (1979)
3. Li, W. K. W. *et al. Science* **219**, 292–295 (1983).
4. Platt, T., Subba-Rao, D. V. & Irwin, B. *Nature* **301**, 702–704 (1983)
5. Furuya, K. & Marumo, R. *J. Plankton Res.* **5**, 393–406 (1983).
6. Murphy, L. S. & Haugen, E. M. *Limnol. Oceanogr.* **30**, 47–58 (1985)
7. Throndsen, J. *Sarsia* **63**, 273–284 (1978).
8. Throndsen, J. *Norw. J. Bot.* **23**, 269–293 (1976).
9. Johnson, P. W. & McN. Sieburth, J. *J. Phycol.* **8**, 318–327 (1982).
10. Yentsch, C. S. *Limnol. Oceanogr.* **28**, 597–599 (1983).
11. Takahashi, M. & Hori, T. *Mar. Biol.* **79**, 177–186 (1984).
12. Takahashi, M. & Bienfang, P. K. *Mar. Biol.* **76**, 203–211 (1983).
13. Glover, H. E., Smith, A. E. & Shapiro, L. *J. Plankton Res.* **7**, 519–535 (1985)
14. Bienfang, P. K., Szyper, J. P., Okamoto, M. Y. & Noda, E. K. *Limnol. Oceanogr.* **29**, 527–539 (1984).
15. Yentsch, C. S. & Yentsch, C. M. *J. mar. Res.* **37**, 471–483 (1979).
16. Foss, P., Guillard, R. R. L. & Liaaen-Jensen, S. *Phytochemistry* **23**, 1629–1633 (1984)
17. Kursar, T. A., Swift, H. & Alberte, R. S. *Proc. natn. Acad. Sci. U.S.A.* **11**, 6888–6892 (1981)
18. Alberte, R. S., Wood, A. M., Kusar, T. A. & Guillard, R. R. L. *Pl. Physiol.* **75**, 732–739 (1984)
19. Ong, L. J., Glazer, A. N. & Waterbury, J. B. *Science* **224**, 80–83 (1984)
20. Wood, A. M. *Nature* **316**, 253–255 (1985).
21. Jerlov, N. G. *Optical Oceanography*, 127 (Elsevier, Amsterdam, 1968)
22. Platt, T. & Gallegos, C. L. in *Primary Productivity in the Sea* (ed. Falkowski, P. G.) 339 (Plenum, New York, 1980).
23. Morel, A. & Bricaud, A. *Deep-Sea Res.* **11**, 1375–1393 (1981).
24. Yentsch, C. S. & Menzel, D. W. *Deep-Sea Res.* **10**, 443–448 (1963)
25. Morris, I. & Glover, H. E. *Mar. Biol.* **24**, 147–154 (1974).
26. Brand, L. E., Guillard, R. R. L. & Murphy, L. S. *J. Plankton Res.* **3**, 193–207 (1981).

Birds that 'cry wolf'

Charles A. Munn

Wildlife Conservation International, New York Zoological Society,
The Bronx Zoo, Bronx, New York 10460, USA

Reports of animals using alarm calls deceptively are rare (refs 1–3 and R. Cheney and D. Seyfarth, personal communication in ref. 4). Here I have studied two species of flycatching birds in Amazonia, *Lanio versicolor* and *Thamnomanes schistogynus*, which lead flocks of mixed species in the canopy and understorey of the forest, respectively, and act as sentinels, giving alarm calls at the approach of bird-eating hawks. These two species feed to a large extent on the insects flushed out by the foraging of the rest of the flock. My observations suggest that *L. versicolor* and *T. schistogynus* use the predator alarm call deceptively to distract other birds, thereby increasing their own chances of capturing arthropods. This result suggests that deception among animals may be more widespread than is generally assumed.

The mixed-species bird flocks of the Amazon forest are the most diverse multi-species associations described for any organisms[5–8]. At Cocha Cashu, Manu National Park, south-east Peru (71° 19′ W, 11° 51′ S, elevation ~400 m), the white-winged shrike-tanager (*L. versicolor*, Thraupinae) leads permanent mixed-species flocks in the canopy of the forest and helps maintain flock cohesion by means of loud vocalizations throughout the day[6–8]. At the same site, the bluish-slate antshrike (*T. schistogynus*, Formicariidae) performs the same role in permanent mixed-species flocks in the understorey[5–8].

In addition to their roles as flock leaders, these two species are also flock sentinels, as they are virtually always the first

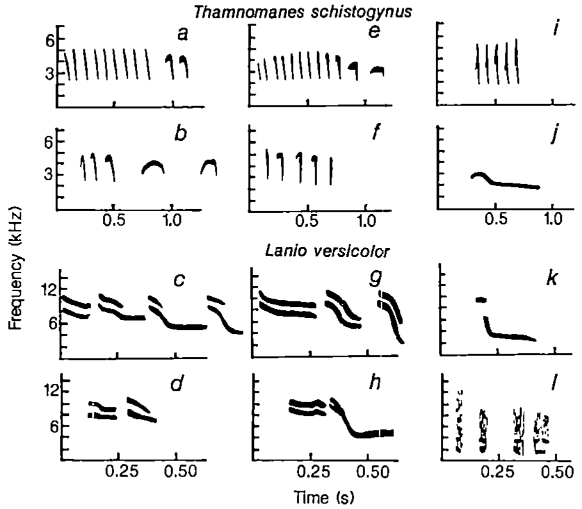

Fig. 1 Tracings of spectrograms of true alarm calls (*a–d*), false alarm calls (*e–h*), and other (non-alarm) calls (*i–l*) of *T. schistogynus* and *L. versicolor.* True alarms are given in response to real danger; false during a chase after arthropods; and other calls in entirely different contexts. The non-alarm rattle (*i*) was used as a control in the experiment. True and false alarms of *T. schistogynus* are characterized by repeated staccato notes of narrower bandwidth than the notes of the non-alarm rattle (*i*), which apparently is given to promote flock cohesion[4-6]. The true and false alarms of *L. versicolor* are characterized by descending notes with simple, strong harmonic structure; both characteristics are not found in other calls. Note that for *L. versicolor*, the timespan is halved, while the frequency range is doubled compared with the results for *T. schistogynus.* Spectrograms were made on a Kay Elemetrics 6061B machine with wide-band filter.

Table 1 Response of other understorey flock species to playback of true and false alarms and rattle (control) of *T. schistogynus*

	Bird reacts	Bird does not react	
Rattle (control) (*i* in Fig. 1)	0	15	
True alarm call (*a* in Fig. 1)	13	0	$P > 0.153$
False alarm call (*e* in Fig. 1)	13	3	
			$P < 0.001$

Other birds are equally startled by the true and false alarms of *T. schistogynus*, while they are not startled by the rattle. Fisher exact tests were used to calculate the probabilities associated with the two comparisons. Recordings and playback were via a Panasonic RQ 356 cassette recorder, JVC shotgun microphone, and a modified Olympus SMW SP5 field speaker.

species to give loud alarm calls at the approach of bird-eating hawks of the genera *Micrastur*, *Accipiter* and *Leucopternis*[5,6,8]; they are also the first to give short alarm calls when harmless hawk-sized birds fly by[6]. Finally, they are also the first species to sound an alarm when hawk models are shot past them[6]. Other species of flock birds look up, freeze, dive or jump into cover when a sentinel sounds the alarm.

The sentinel role has enabled *T. schistogynus* and *L. versicolor* to establish a novel symbiotic relationship with other flock members. Both sentinel species rely on the insect-flushing abilities of other flock species for ≥85% of their food[6]. Rarely do they steal arthropods directly from the bills of other birds. Rather, they sit in the centre or beneath a group of actively foraging flock species and fly out or dive down after dropping arthropods flushed from hiding by the more active species. When a bird of another species begins to chase an arthropod that it has flushed out, the faster-flying, more aerobatic sentinel often catches the arthropod first. It is during these multi-bird aerial tumbles after arthropods that both species of sentinel give the same alarm call used when a hawk attacks or flies by. I interpret these calls as false alarm calls, presumably used by the sentinel to distract other birds and thereby to increase its own chance of capturing the arthropod. These aerial contests are over in less than a second, so even a slight hesitation by other birds increases the likelihood that the sentinel will reach the arthropod first.

Using the following criteria, I classified 106 of 718 alarm calls as true or false: true if simultaneously I saw a hawk-like object fly by or if other flock species subsequently alarmed and froze for several minutes, and false if the sentinel flew into the open after a falling arthropod while I simultaneously had a clear view of the entire region within 20 m of the bird and could thus eliminate the possibility of a passing hawk. Sentinels remained motionless on partially concealed perches when giving true alarms, whereas when giving false alarms, they flew with other birds into the open in pursuit of flushed arthropods. Flying into the open is inappropriate for escape from fast-flying bird hawks. Furthermore, the probability is vanishingly small that hawk-like birds repeatedly flew by at the same instant that sentinels were competing with other birds for falling arthropods, as neither type of incident occurred more than three times per hour.

The context of the false alarms further strengthens my interpretation. *L. versicolor* sounded the alarm significantly less often when it alone was chasing an arthropod than when another bird was involved also (19 instances out of 131 versus 34 out of 56, $\chi^2 = 39.0$, $P < 0.001$). Furthermore, the rate of sounding of alarms increased dramatically when either sentinel species was feeding its young. As most of these additional alarms were given during multi-bird chases after flushed arthropods, and the young were often too far from the adults to hear the calls, I classified most of these additional alarms as false. Thus, the rate of sounding of alarm calls was higher when the opportunity for obtaining more food was greater and when the need for that food was more pressing.

Known true and false alarms are strikingly similar in outline and frequency on spectrograms, whereas both true and false alarms are very different from other calls in the repertoire of the two sentinel species (Fig. 1). Although alarm calls can vary from one or two notes to a whole series of sharp notes, only the first one or two are needed to trigger a startle or escape reaction from individuals of other species.

The postulated effect of the alarm calls, indeed the effect of only hearing the calls, was confirmed by an experiment in which I played back cassette recordings of a non-alarm rattle call, a known true alarm, and a known false alarm of *T. schistogynus* to understorey flock species. The birds treated both the true and the false alarms as true alarms, while they ignored the rattle (control) (Table 1). The canopy flocks foraged too high to permit the same experiment, but observation of natural true and false alarms of *L. versicolor* supported the interpretation of deceptive alarm calls. Even though about half of all *L. versicolor* alarm calls are false (56 out of 104 categorizable alarm calls), canopy flock birds reacted positively to 31 of 41 alarm calls of unknown context, which is significantly greater than the percentage of true alarms (46%; $\chi^2 = 9.14$, $P < 0.01$). On two of these 31 occasions, I saw another bird react to the call as if it were a true alarm call and then saw the *Lanio* fly out after an insect. In the 10 cases in which a bird showed no reaction to a sentinel alarm call, the bird was already in the open and was thus able to scan for hawks without moving. In contrast, birds with their heads inside leaves, or under their wings, bathing, or in other vulnerable positions, typically showed the most dramatic escape responses by diving for cover when any alarm call was given.

Theoretically, as in the story of the boy who cried "Wolf!" (ref. 9), there should be an upper limit to the proportion of false alarms that can be supported by a given rate of occurrence of true alarms. The potential penalty, however, for ignoring even one alarm call might be death; so it is not surprising that flock birds seem to take all alarm calls seriously, whether true or false. Presumably, the cost to the beater species of reacting to false alarms is the occasional loss of an arthropod to the sentinel, while the only cost to the sentinel is the energy used in producing the call. The possible benefit to the sentinel of sounding a false alarm could be a substantial increase in its daily intake of arthropods. Unfortunately, the outcomes of most of the multi-bird scrambles for arthropods were concealed by vegetation, so I cannot compare the rate of prey capture by sentinels when silent with their capture rates when giving false alarms.

In general, an animal competing with others for a resource might use deceptive alarm calls in contests of predictably short duration in which rivals who check for danger automatically lose.

I thank the Frank M. Chapman Fund of the American Museum of Natural History for support; W. J. Smith for use of his sonograph machine; J. Gould, D. Griffin, H. Horn and F. Nottebohm for constructive criticism; and the Ministry of Agriculture of Peru for permission to work in Manu National Park.

Received 29 May; accepted 5 November 1985.

1. Ruppell, G. Z. *Tierpsychol.* 26, 371-374 (1969).
2. Wilson, E. O. *The Insect Societies* (Harvard University Press, 1971).
3. Matsuoka, S. *Tori* 29, 87-90 (1980).
4. Dennett, D. *The Behavioural and Brain Sciences* Vol. 6, 343-355 (1983).
5. Munn, C. A. & Terborgh, J. W. *Condor* 81, 338-347 (1979).
6. Munn, C. A. thesis, Princeton Univ. (1984).
7. Munn, C. A. in *Neotropical Ornithology* (eds Buckley, P. A., Foster, M. S., Morton, E. S., Ridgely, R. S. & Buckley, F. G.) (American Ornithological Union, Washington DC, 1985).
8. Wiley, R. H. *J. Zool.* 191, 127-145 (1980).
9. Davis, R. H. *Boy Scout and Other Stories for Boys* (Scribner's, New York, 1917).

Synapsin I is a microtubule-bundling protein

Anthony J. Baines* & Vann Bennett

Department of Cell Biology and Anatomy,
Johns Hopkins University School of Medicine,
725 North Wolfe Street, Baltimore, Maryland 21205, USA

Synapsin I, a synaptic vesicle protein, is thought to be involved in the regulation of neurotransmission through its phosphorylation by the cyclic AMP-dependent and Ca^{2+}/calmodulin-dependent protein kinases which become activated upon depolarization of nerve endings[1-3]. However, despite its recent characterization[4] as a spectrin-binding protein immunologically related to erythrocyte protein 4.1, other interactions of synapsin I with structural proteins remain unknown. We report here that synapsin I can co-cycle with microtubules through three cycles of warm polymerization and cold depolymerization. Synapsin I binds saturably to microtubules stabilized by taxol, with an estimated dissociation constant (K_d) of 4.5 μM and a stoichiometry of 1.2 mol of synapsin binding sites per mol tubulin dimer. Synapsin I also increases the turbidity of tubulin solutions at 37 °C, but without causing detectable alterations in the critical concentration required for polymerization. Mixtures of synapsin I and tubulin observed by negative stain electron microscopy contain bundles of microtubules, accounting for the effect of synapsin I on tubulin turbidity. Synapsin I is thus a candidate to mediate or regulate the interaction of synaptic vesicles with microtubules.

Synapsin I was prepared from calf brains, as described in Fig. 1, by modifications of our previous procedure[4]. Tubulin was prepared from three-times-cycled microtubule protein from calf brain by chromatography on Whatman DE53 cellulose[5]. In preliminary experiments, synapsin I (0.5–5 μm) co-sedimented with microtubules after incubation with tubulin (10–50 μM, with reference to dimer) at 37 °C for 30 min, in a buffer optimal for microtubule assembly (0.1 M Na-PIPES, 1 mM MgCl$_2$, 1 mM GTP, 1 mM dithiothreitol (DTT), 1 mM EGTA, 1 mM NaN$_3$ *p*H 6.6: PMGDE buffer) (data not shown). However, an interaction between synapsin I and tubulin dimer was not detectable by sedimentation of mixtures of synapsin I and tubulin through linear sucrose gradients at 4 °C, suggesting that synapsin I will interact strongly only with tubulin in polymeric form.

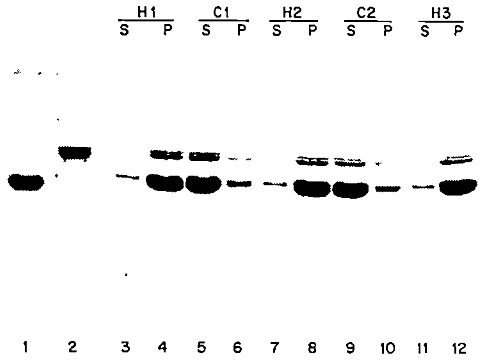

Fig. 1 Synapsin I co-cycles with tubulin during three cycles of warm polymerization and cold depolymerization. Supernatants (S) and pellets (P) from the first, second and third warm centrifugation steps (H1, H2 and H3), as well as those for cold centrifugation (C1 and C2) were analysed on an SDS-polyacrylamide gel. Lane 1, DEAE-purified tubulin (30 μg); 2, synapsin I (15 μg); 3, H1S; 4, H1P; 5, C1S; 6, C1P; 7, H2S; 8, H2P; 9, C2S; 10, C2P; 11, H3S; 12, H3P.

Methods. Synapsin was purified by modifications of our previous procedure[4]. Briefly, synapsin I was extracted from demyelinated brain membranes in the presence of 0.15 M NaCl, 1% Triton X-100 *p*H 7.1, and purified by chromatography on hydroxylapatite and carboxymethyl cellulose (A.J.B. and V.B., manuscript in preparation). Synapsins 1a and b were more than 90% of the protein in the final preparation, with a further 6–8% being proteolytic degradation products of relative molecular mass (M_r) > 50,000 (see lane 2, above). Tubulin was purified from three-times-cycled microtubules by DEAE chromatography[5]. Tubulin was about 98% of the final preparation, the major contaminant being MAP-1, which constituted no more than 1% of the total protein (see gel lane 1, above). For the experiments shown in Figs 2, 3 and 4, the tubulin was completely freed of MAP-1 by centrifugation of microtubules in the presence of 0.5 M NaCl: the microtubule pellet formed under these conditions contains no detectable MAP-1. Tubulin was stored as a microtubule pellet at −80 °C, and was cycled once prior to use. In the cycling experiment shown, synapsin I (7 μM) was combined with tubulin (66 μM) at 0 °C in PMGDE buffer (see text for buffer composition). Glycerol was added to give a final concentration of 20% (v/v) and the mixture was brought to 37 °C for 30 min. The microtubules that formed during the incubation were collected by centrifugation for 25 min at 150,000*g*, and were depolymerized in one-third of the initial volume of ice-cold PMGDE. After incubation for 30 min on ice, with intermittent shearing through a 26-gauge needle, the mixture was clarified by centrifugation at 150,000*g* for 25 min at 0 °C. Glycerol was added to the supernatant after this spin, the mixture brought to 37 °C, and the cycle repeated twice more. Samples were withdrawn from all supernatants and resuspended pellets produced for SDS-polyacrylamide gel electrophoresis. The pellets from C1 and C2 were resuspended in 1% SDS. Concentrations of synapsin I were estimated spectrophotometrically, assuming $E^{1\%}_{1\,\mathrm{cm}} = 6.74$ at 277 nm (ref. 12). Synapsin was assumed to be a monomer of M_r 75,000. Tubulin concentrations were estimated by a dye-binding assay[25] using bovine serum albumin as standard: molar concentrations were calculated assuming a tubulin dimer of M_r 100,000.

One characteristic of many microtubule-associated proteins (MAPs) is that they co-cycle with tubulin during repeated cycles of warm polymerization and cold depolymerization. When mixtures of synapsin I and tubulin were subjected to repeated

---

* Present address: University of Kent, Canterbury, UK.

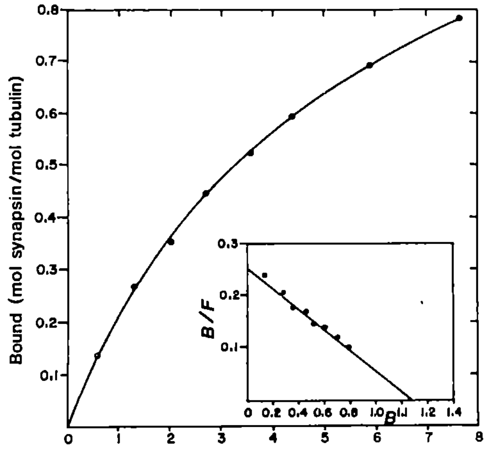

Fig. 2 Binding of ^{125}I-synapsin I to taxol-stabilized microtubules. *a*, Association of various concentrations of ^{125}I-synapsin I with 1.0 μM taxol-tubulin. Binding is expressed as mol synapsin I bound per mol tubulin (dimer), after subtraction of blank values. *b*, Data plotted according to the Scatchard equation, $B/F = N/K - B/K$ (ref. 9), where B is moles of synapsin bound per mole of tubulin (dimer), F is the concentration of unbound synapsin (μM), N is the number of binding sites (mol mol^{-1}) and K is the dissociation constant. The line shown is a calculated best fit for a single class of sites, which yields $K = 5$ μM and $N = 1.2$.
Methods. Synapsin I was labelled with ^{125}I-labelled Bolton Hunter reagent and diluted with unlabelled synapsin I to give 8.76×10^5 c.p.m. nmol^{-1}. DEAE-purified tubulin (52 μM dimer) was polymerized in PMGDE buffer without glycerol, and taxol was added from a 10 mM solution at 37 °C for 20 min. The resulting microtubules were resistant to cold depolymerization, and >98% of the tubulin was pelletable during centrifugation at 100,000*g* for 25 min. In the binding assay, taxol-tubulin was diluted to a final concentration of 1.0 μM (relative to dimer), with various concentrations of ^{125}I-synapsin I in PMGDE buffer, to give a volume of 100 μl, and allowed to stand for 1 h at 23 °C. Samples of 90 μl were layered over 100 μl of 20% sucrose, 20 μM taxol in PMGDE, in Beckman airfuge tubes. Taxol-stabilized microtubules, with bound ^{125}I-synapsin, were pelleted during centrifugation at 100,000*g* for 30 min in the airfuge. Aliquots of 50 μl supernatant were withdrawn from the meniscus, and the remaining supernatant aspirated. Supernatants and pellets were counted for ^{125}I in a γ-counter. Blanks, from which tubulin was omitted, were included in the assay. All points were determined in duplicate, the means of which are shown.

cycles of warm polymerization and cold depolymerization, synapsin I co-cycled with microtubules (Fig. 1). (Synapsin I alone showed no tendency to polymerize in the warm.) The ratio of synapsin I to tubulin in the experiment shown decreased by only 5% during three cycles (as judged by elution of dye from Coomassie blue-stained SDS-polyacrylamide gels of the pellets, followed by reading absorbance at 605 nm)[6], and we conclude that co-cycling reflects a stable interaction between tubulin polymer and synapsin I.

To quantitate such an interaction, the association of ^{125}I-synapsin with taxol-stabilized microtubules was measured. Taxol is an antimitotic drug[7] which virtually eliminates the critical concentration required for tubulin polymerization[8], allowing the use of very dilute tubulin polymers for saturation binding analysis. Binding of 0–7.5 μM ^{125}I-synapsin was examined at both 1.0 μM (Fig. 2) and 1.2 μM (not shown) tubulin (concentrations being expressed relative to dimer). When the data were plotted according to the Scatchard equation[9], a single class of binding sites (1.2 mol binding sites per mol tubulin dimer) was revealed, with a K_d of 4.5 μM. Experimental limitations on the concentration of synapsin prevented more than about 60% saturation of tubulin; thus additional lower-affinity classes of binding sites or negative cooperativity may become apparent at higher concentrations of synapsin (4.5 μM may be a minimum estimate for the K_d as drug-treated tubulin may not be as active as native tubulin). Synapsin I may also undergo limited self-association in the assay conditions used (see below), which may affect the apparent stoichiometry of the reaction.

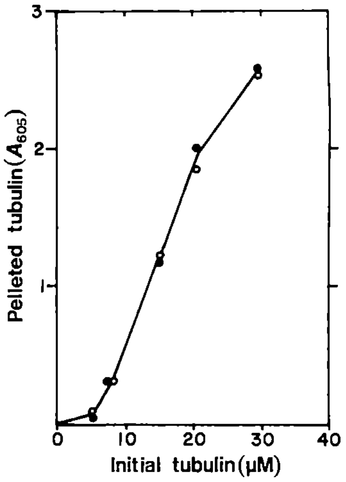

Fig. 3 Synapsin I does not alter the critical concentration for polymerization of tubulin. Various concentrations of tubulin (4.9–29.4 μM) were incubated with (●) or without (○) 5 μM synapsin I in PMGDE buffer containing 5% glycerol. After 30 min at 37 °C, the mixtures were centrifuged for 25 min at 100,000*g*, and samples of supernatants and pellets analysed by gel electrophoresis: tubulin was quantitated by dye elution from Coomassie-stained gels[6]. Data are plotted as total tubulin (μM) against tubulin pelleted (expressed as A_{605} of dye eluted from stained gels). The critical concentration is assumed to be represented by the point at which the linear portion of the curve intercepts with the *x*-axis. A critical concentration of 4–5 μM tubulin is estimated in the presence and absence of synapsin I.

Synapsin I increases the turbidity of tubulin solutions when incubated at 37 °C (not shown). Microtubule-associated proteins also do this, seemingly by reducing the critical concentration required for polymerization (see for instance refs 10, 11). That synapsin I might act similarly was examined in Fig. 3. Various concentrations of tubulin were incubated in PMGDE buffer containing 5% glycerol, in the presence or absence of 5 μM synapsin I. After 30 min at 37 °C, microtubules were collected by centrifugation. Pelleted tubulin was separated from bound synapsin by electrophoresis on SDS-polyacrylamide gels, and quantitated by dye elution from Coomassie blue-stained gels[6]. Synapsin I had no detectable effect on the final extent of tubulin polymerization, and a critical concentration of 4–5 μM is estimated both in the presence and absence of synapsin I (Fig. 3). By contrast, the addition of MAP-2 to tubulin in our assay conditions greatly reduces the critical concentration.

Since the increase in turbidity of tubulin solutions could not be accounted for by lowering of the critical concentration, synapsin I/tubulin mixtures were examined by negative stain electron microscopy (Fig. 4). While control tubulin formed single microtubules of normal appearance, randomly arranged on electron microscope grids, mixtures of synapsin I and tubulin revealed bundles of microtubules in tightly packed arrays. The extent of bundling was dependent on the amounts of synapsin I and tubulin in the incubation mixtures: at high concentrations of synapsin I and tubulin (for example 5 μM and 25 μM respectively), the bundles were sufficiently large to be easily distinguished in the light microscope.

Cross-linking of microtubules by synapsin implies that either synapsin has two or more binding sites for microtubules, or that synapsin has one tubulin binding site and achieves cross-linking by self-association. Synapsin is monomeric in dilute solution[4,12]; however, in concentrated solutions of synapsin (1.5 mg ml^{-1}),

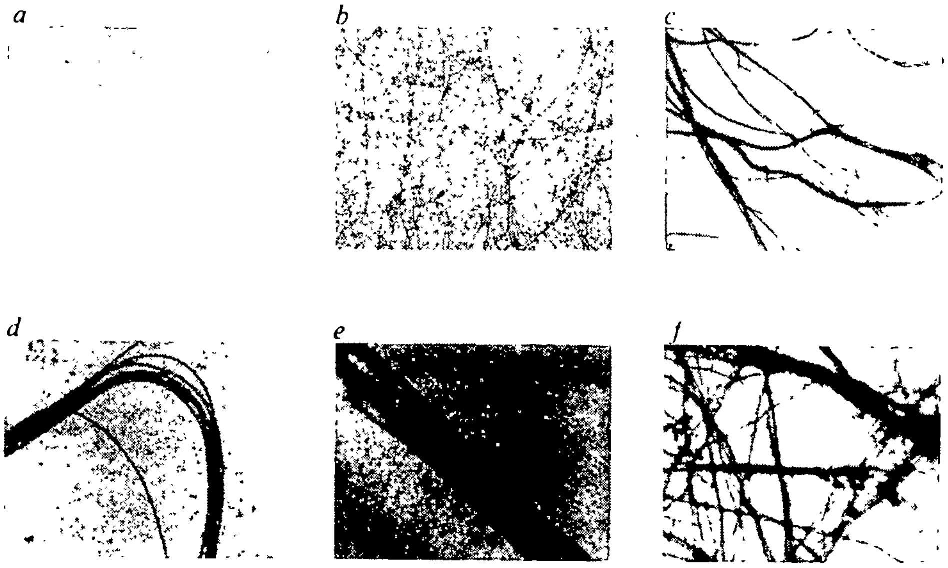

Fig. 4 Electron microscopy of synapsin I, tubulin and synapsin I/tubulin mixtures. Synapsin I (5 μM) and tubulin (10 μM or 25 μM) were incubated separately or together at 37 °C in PMGDE buffer in the absence of glycerol. After 30 min, samples were applied to Formvar carbon films on 400-mesh grids. The samples were rinsed with buffer, stained with 1% unbuffered uranyl acetate and examined in the electron microscope. *a*, Synapsin I alone; *b*, tubulin (10 μM) alone; *c*, *d*, *e*, synapsin I plus tubulin (10 μM); *f*, synapsin I plus tubulin (25 μM). The scale bar (lower right) represents 4.7 μm in *a*, *b*, *c* and *f*, 1.2 μm in *d* and 0.6 μm in *e*.

oligomers of synapsin up to tetramer in size are revealed by HPLC gel filtration or by chemical cross-linking (A.J.B. and V.B., unpublished data, but see also ref. 12). Therefore, it is possible that bundling of microtubules is dependent on self-association of synapsin into multivalent complexes. In future work it will be important to investigate the factors that regulate self-association, and the self-association state of synapsin in its vesicle-bound form.

In spite of repeated reports, based on electron microscopy, that synaptic vesicles might be attached to microtubules[13-16], the cytoskeletal interactions of synaptic vesicles are still very unclear (compare refs 14 and 17 but see also ref. 18). However, interactions between secretory vesicles and microtubules have been detected in reconstitution experiments[19,20] and, more recently, in taxol-stabilized complexes of microtubules and secretory granules isolated from exocrine pancreas[21]. Our observations suggest that synapsin I might act to link or regulate the linkage of microtubules to synaptic vesicles. The role of such a linkage is open to speculation, but it might play a part in axonal transport of vesicles, or in the placement of synaptic vesicles in the presynaptic active zones. The association of synaptic vesicles with microtubules is likely to be transient *in vivo*, as it is known that the interaction of synapsin I with its membrane binding site is weakened upon phosphorylation by Ca^{2+}/calmodulin-dependent protein kinase[2]. Furthermore, in view of alterations in the activities of MAP-2[22,23] and tau[24] in response to their phosphorylation, it is possible that the tubulin binding activity of synapsin will be altered by its phosphorylation. It is not yet known how the spectrin-binding activity of synapsin I relates to its tubulin-binding activity.

This work was supported by a Damon Runyon-Walter Winchell Cancer Fund Fellowship FRG700 and by NIH grants AM29808, RO 1 GM33996 and RCDA KO4 AM00926. We thank Arlene Daniel for preparation of the manuscript.

Received 19 June; accepted 14 November 1985.

1. Nestler, E. J. & Greengard, P. *Proc. natn. Acad. Sci. U.S.A.* **77**, 7479-7483 (1980); *Nature* **296**, 452-454 (1982).
2. Hutner, W. B., Schiebler, W., Greengard, P & DeCamilli, P. *J. Cell Biol.* **96**, 1374-1388 (1983).
3. Llinas, R., McGuinness, T. L., Sugimori, M & Greengard, P. *Proc. natn. Acad. Sci. U.S.A.* **82**, 3035-3039 (1985).
4. Baines, A. J. & Bennett, V. *Nature* **315**, 410-413 (1985).
5. Murphy, D. B. *Meth. Cell Biol.* **24**, 31-49 (1982).
6. Fenner, C., Traut, R. R., Mason, D. T. & Wikman-Coffelt, J. *Analyt. Biochem.* **63**, 603-606 (1975).
7. Wani, M. C., Taylor, H. L., Hall, M. E., Coggon, P. & McPhail, A. T. *J. Am. chem. Soc.* **93**, 2325-2327 (1971).
8. Schiff, P. B., Fant, J. & Horwitz, S. B. *Nature* **277**, 665-667 (1979).
9. Scatchard, G. *Ann. N.Y. Acad. Sci.* **57**, 660-672 (1949).
10. Murphy, D. B., Vallee, R. B. & Borisy, G. G. *Biochemistry* **16**, 2593-2605 (1977).
11. Kim, H., Binder, L. I. & Rosenbaum, J. L. *J. Cell Biol.* **80**, 266-276 (1979).
12. Ueda, T. & Greengard, P. *J. biol. Chem.* **252**, 5155-5163 (1977).
13. Jarlfors, U. & Smith, D. S. *Nature* **224**, 710-711 (1969).
14. Smith, D. S. *Phil. Trans. R. Soc.* B**261**, 395-405 (1971).
15. Bird, M. M. *Cell Tissue Res.* **168**, 101-115 (1976).
16. Gray, E. G. *Proc. R. Soc.* B**218**, 253-258 (1983).
17. Wickelgren, W. O., Leonard, J. P., Grimes, M. J. & Clark, R. D. *J. Neurosci.* **5**, 1185-1201 (1985).
18. Llinas, R. R. & Heuser, J. E. *Neurosci. Res. Prog. Bull.* **15**, 557-687 (1977).
19. Sherline, P., Lee, Y. C. & Jacobs, L. S. *J. Cell Biol.* **72**, 380-389 (1977).
20. Suprenant, K. A. & Dentler, W. L. *J. Cell Biol.* **93**, 164-174 (1982).
21. Dentler, W. L. & Suprenant, K. L. *J. Cell Biol.* **99**, 193a (1984).
22. Murthy, A. S. N. & Flavin, M. *Eur. J. Biochem.* **137**, 37-46 (1983).
23. Burns, R. G., Islam, K. & Chapman, R. *Eur. J. Biochem.* **141**, 609-615 (1984).
24. Lindwall, G. & Cole, R. D. *J. biol. Chem.* **259**, 5301-5306 (1984).
25. Flores, R. *Analyt. Biochem.* **88**, 605-611 (1978).

Functional corticotropin releasing factor receptors in the primate peripheral sympathetic nervous system

Robert Udelsman*, James P. Harwood, Monica A. Millan, George P. Chrousos†, David S. Goldstein‡, Reuven Zimlichman‡, Kevin J. Catt & Greti Aguilera

Endocrinology and Reproduction Research Branch, NICHD; * Surgery Branch, NCI; † Developmental Endocrinology Branch, NICHD; and ‡Hypertension-Endocrine Branch, NHLBI, National Institutes of Health, Bethesda, Maryland 20892, USA

Corticotropin releasing factor (CRF) is a key hormone in the integrated response to stress, acting both as the major regulator of pituitary adrenocorticotropic hormone (ACTH) release and as a neuropeptide in the brain[1,2]. The actions of CRF are mediated by specific plasma membrane receptors in the anterior pituitary gland[3] and in discrete brain areas including the cerebral cortex and several regions related to the limbic system[4,5]. In addition to the pituitary and central actions of CRF, systemic administration of the peptide in the rat[6], dog[7,8], monkey[9] and man[10-12] causes hypotension and tachycardia because of a decrease in peripheral vascular resistance. These observations, in conjunction with the finding of immunoreactive[13-17] and bioactive[14,18] CRF in peripheral tissues, suggest that the peptide is locally released in tissues to act as a neurotransmitter or paracrine hormone. As CRF is present in the adrenal medulla[13,14] and the peptide is known to modulate

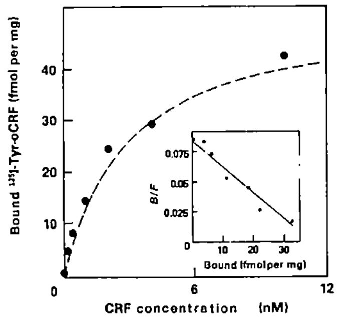

Fig. 1 Saturation curve and Scatchard analysis (inset) of ^{125}I-Tyr-ovine CRF binding to adrenal medulla membrane particles in the rhesus monkey. Each point represents the mean of duplicate incubations from a representative experiment.

Methods. Tissue was minced and homogenized in a 50 mM-Tris-HCl buffer (*p*H 7.4) containing 5 mM $MgCl_2$ and 2 mM EGTA, by six strokes on a mechanical homogenizer (Techmar). Homogenates were filtered through nylon gauze and centrifuged at 30,000*g* for 30 min at 5 °C. The membrane-rich pellet was resuspended in the same buffer to give a protein concentration of 2-8 mg ml^{-1}. Aliquots of 100 μl of membrane suspension were incubated with 100,000 c.p.m. of ^{125}I-Tyr-ovine CRF (0.1 nM) in a total volume of 300 μl of 50 mM Tris-HCl buffer containing 5 mM $MgCl_2$, 2 mM EGTA, 0.1% bovine serum albumin (BSA) and 100 kIU ml^{-1} of aprotinin (Sigma). After incubation for 30 min at 22 °C, bound radioactivity was separated from free tracer by centrifugation at 1,000*g* for 3 min at 4 °C following addition of 7.5% polyethylene glycol (PEG) in 50 mM Tris-HCl, *p*H 7.4. The precipitate was washed again with PEG, and the tips of the tubes were removed and analysed for radioactivity in a Beckman γ-spectrometer. Tracer degradation after 60 min incubation was <10% as evaluated by rebinding to rat pituitary membranes. Receptor concentration and affinity were estimated by computer analysis of the binding data[35], and protein concentration was measured[36] with BSA as a standard.

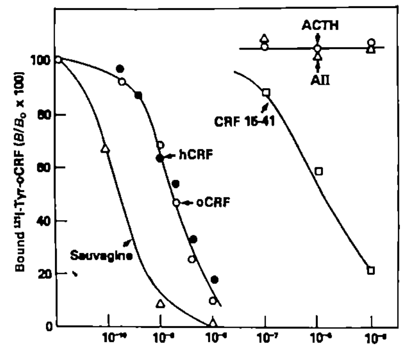

Fig. 2 Ligand specificity of medullary CRF sites in the rhesus monkey. Each point is the mean of duplicate incubations in a representative experiment, performed by the addition of increasing concentrations of CRF and other peptides to adrenal medulla particles incubated with ^{125}I-Tyr-ovine CRF.

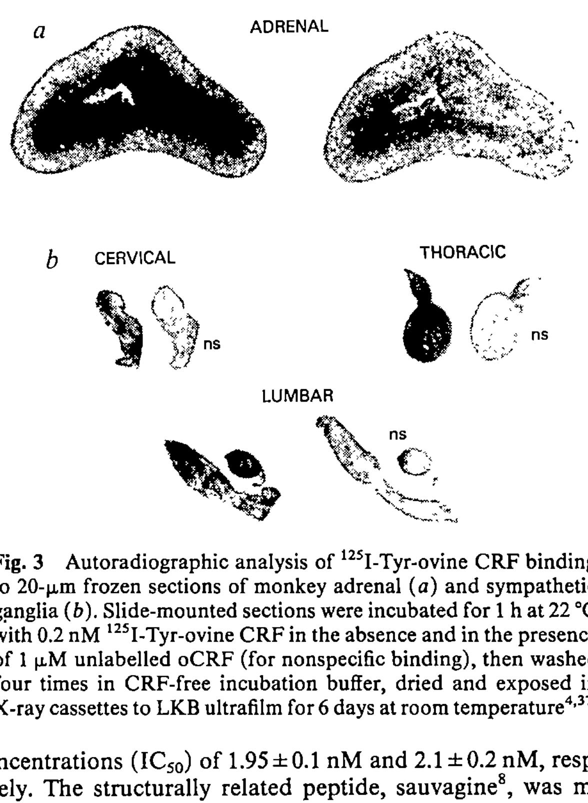

Fig. 3 Autoradiographic analysis of ^{125}I-Tyr-ovine CRF binding to 20-μm frozen sections of monkey adrenal (*a*) and sympathetic ganglia (*b*). Slide-mounted sections were incubated for 1 h at 22 °C with 0.2 nM ^{125}I-Tyr-ovine CRF in the absence and in the presence of 1 μM unlabelled oCRF (for nonspecific binding), then washed four times in CRF-free incubation buffer, dried and exposed in X-ray cassettes to LKB ultrafilm for 6 days at room temperature[4,37].

the central activity of the autonomic nervous system[1], we investigated the possibility that CRF is involved in the regulation of the peripheral autonomic nervous system. Such an action of CRF is supported by our demonstration of specific CRF receptors in the monkey adrenal medulla and sympathetic ganglia. In the adrenal medulla, these receptors are coupled to adenylate cyclase and can stimulate the secretion of catecholamines and Met-enkephalin.

Adrenal glands and lumbar, coeliac, thoracic and cervical sympathetic ganglia were obtained from cynomolgus and rhesus monkeys within 5 min of killing them with an overdose of pentobarbital. The adrenals were cleaned of connective tissue and dissected into three zones; medulla, zona glomerulosa and the inner zones of the cortex. CRF receptors were measured by binding of ^{125}I-Tyr-ovine CRF to the 30,000*g* membrane-rich fractions of tissue homogenates as described previously[3]. No CRF binding was found in either zona glomerulosa or inner zones of the cortex, but saturable, high-affinity binding was present in the adrenal medulla (Fig. 1). Specific binding of CRF in the adrenal medulla was linear up to 800 μg of membrane protein and reached equilibrium between 30 and 60 min at 22 °C with a half-maximum association time of 16 min. Addition of unlabelled oCRF at equilibrium resulted in rapid dissociation of the bound radioactivity with a half-time of 25 min. Scatchard analysis of the binding data revealed a single class of receptors with dissociation constant (K_d) of 5×10^{-9} and 2.3×10^{-9} M in cynomolgus and rhesus monkeys, respectively. The mean value of three experiments including both species was $3.2\pm1.0\times10^{-9}$ M. The binding capacity was also similar in both species, with values of 47 fmol mg^{-1} for cynomolgus and 39.2 ± 4.2 fmol mg^{-1} for the rhesus. This binding capacity of the adrenal medulla membrane fraction was similar to that observed in rat brain[4] and much less than that found in the rat pituitary gland[2].

The ligand specificity of the medullary binding sites for ^{125}I-Tyr-oCRF is shown in Fig. 2. The native peptides oCRF and human CRF were equipotent, with half-maximum inhibitory concentrations (IC_{50}) of 1.95 ± 0.1 nM and 2.1 ± 0.2 nM, respectively. The structurally related peptide, sauvagine[8], was more potent than CRF, whereas the CRF(15-41) fragment was 1,000 times less potent with an IC_{50} of 1.1 μM. The structurally unrelated peptides, ACTH and angiotensin II, showed no binding-inhibition activity at concentrations up to 10^{-5} M. This specificity is similar to that described for CRF receptors in the anterior pituitary gland[3] and in the brain[4]. Similarly, the relative affinities of CRF-related peptides to the adrenal receptor are consistent with the potencies of these peptides to stimulate ACTH release *in vivo*[1,19] and *in vitro*[20,21], and to decrease blood pressure following intravenous administration[6-9].

Binding sites for ^{125}I-Tyr-oCRF in the adrenal medulla were also evident on autoradiographic analysis of the binding in slide-mounted frozen sections of rhesus monkey adrenal glands. Consistent with the results in adrenal membranes, CRF receptors were confined to the adrenal medulla, with no specific autoradiographic staining in the adrenal cortex (Fig. 3*a*). Autoradiographic analysis also demonstrated specific CRF binding in several sympathetic ganglia including lumbar, thoracic, cervical (Fig. 3*b*), and coeliac (not shown). Analysis of the autoradiograms by computerized densitometry indicate optical densities of 0.69 ± 0.05 and 0.23 ± 0.03, respectively, in the

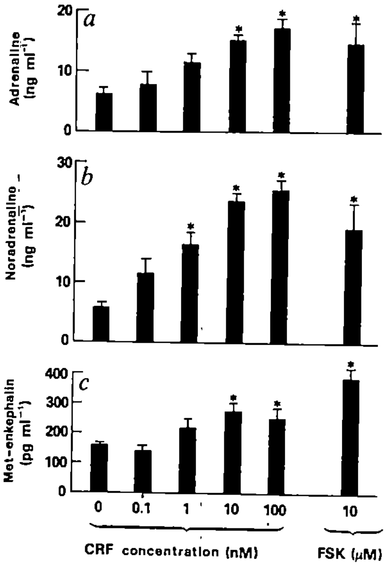

Fig. 4 Adrenaline, noradrenaline and Met-enkephalin production by bovine chromaffin cells during 24 h incubation with corticotropin releasing factor (CRF) or forskolin (FSK). Each bar indicates the mean±s.e. from triplicate incubations. Asterisks indicate significant differences ($P<.05$) as determined by Duncan's multiple range test[38].

Methods. Chromaffin cells were isolated from bovine adrenal glands after retrograde adrenal vein perfusion and collagenase treatment[39] and cultured in 24-well plates (Falcon) containing 1.5 ml per well of basal Eagle's medium with Earle's salts and 25 mM HEPES buffer (Gibco), 5% heat inactivated fetal calf serum, glutamine, penicillin and streptomycin. After incubation for 3 days at 37 °C the media was replaced and either CRF or FSK was added. After an additional 24 h incubation in the presence of CRF or FSK the media were acidified with 150 μl of 1 N HCl and frozen for subsequent assays. Catecholamine levels were determined by HPLC with electrochemical detection[40]. Met-enkephalin levels were determined by radioimmunoassay[41] after ODS-silica column extraction (ImmunoNuclear Corp.).

absence or presence of excess unlabelled CRF. In all sympathetic ganglia, complete inhibition of the specific binding was observed with 10 nM CRF, indicating the high affinity of the binding sites.

As the actions of CRF in well-recognized target tissues such as the pituitary[1,21] and brain[4] are accompanied by stimulation of adenylate cyclase, we determined whether CRF binding sites are associated with a similar function in the adrenal medulla by examining the ability of the peptide to stimulate the conversion of ^{32}P-ATP to cyclic AMP[21]. CRF caused a small but significant and dose-dependent stimulation of adenylate cyclase activity in the adrenal medulla. In three experiments, incubation of membrane-rich particles with ovine CRF increased the enzyme activity by 31±5%, from a basal value of 35.2±1.8 pmol mg^{-1} min^{-1} to a maximum of 46.2±3.2 pmol mg^{-1} min^{-1}, with an ED_{50} of $7.2\pm1.9\times10^{-8}$ M CRF. Stimulation of denylate cyclase was consistently observed with nanomolar oncentrations of CRF, although the ED_{50} for enzyme activation vas higher than the CRF receptor affinity, as frequently observed n broken cell preparations[4,21-24]. The relatively small degree of timulation over basal probably reflects the multiplicity of cell ypes in the adrenal medulla, of which only a small proportion ontain CRF receptors.

To determine whether activation of adrenal medullary CRF eceptors causes changes in secretory activity, the effect of CRF n catecholamine release was analysed in cultured bovine hromaffin cells. During short-term incubation (10–30 min), RF had no effect on catecholamine secretion, whereas nicotine aused a 30-fold stimulation over the basal value for both drenaline and noradrenaline. However, after culture of the hromaffin cells in the presence of CRF for 24 h there was a ignificant increase ($P<0.05$) in catecholamine release, to a maximum of threefold of the basal values for adrenaline (Fig. 4*a*) and fourfold for noradrenaline (Fig. 4*b*) with 10 mM CRF. A further increase in catecholamine release was observed at longer times of culture with 10 nM CRF (eightfold at 48 h and tenfold at 72 h), whereas nicotine-stimulated values remained at a plateau (5-fold). After incubation with nicotine for 72 h, the level of adrenaline increased from 5±1 to 25±1 ng ml^{-1} and that of noradrenaline from 7.1 to 37±3 ng ml^{-1}. A much greater stimulation to 52±1 ng ml^{-1} adrenaline and 69±1 ng ml^{-1} for noradrenaline was observed after incubation with CRF for the same period. The concentrations of CRF required to stimulate catecholamine release were consistent with the K_d of the CRF receptor in the monkey adrenal medulla.

Several peptide hormones have been associated with the function of the adrenal medulla. Vasoactive intestinal peptide (VIP), somatostatin, and many of the proopiomelanocortin derivatives including enkephalin, β-endorphin, ACTH and α-MSH have been identified by radioimmunoassay in normal adrenal medulla and pheochromocytomas[15,25-28]. Several of these peptides are concomitantly released with catecholamines during stimulation of chromaffin cells with carbachol, nicotine or high potassium, suggesting that they are also involved in the stress response[25-27]. Studies with cultured bovine chromaffin cells have shown stimulation of VIP and Met-enkephalin synthesis and release, and an increase in proenkephalin messenger RNA in cultures exposed to high levels of cyclic AMP or forskolin[30,31].

The ability of CRF to stimulate adenylate cyclase activity in the adrenal medulla suggested that the peptide could also modulate the secretion of enkephalin in chromaffin cells. As shown in Fig. 4*c*, addition of CRF to cultured bovine chromaffin cells for 24 h caused a significant increase in Met-enkephalin release, to a maximum of twice the basal value ($P<0.05$) with 10 nM CRF. Forskolin, a known stimulator of adenylate cyclase[32], also enhanced Met-enkephalin and catecholamine release.

The properties of the binding sites for CRF in the adrenal medulla, with specificity for CRF-related peptides, high affinity and the ability to stimulate adenylate cyclase and the secretion of catecholamines and Met-enkephalin, indicate that they represent functional receptors through which CRF modulates adrenal medullary function. The presence of similar binding sites in sympathetic ganglia suggests that CRF is also involved in the extra-adrenal peripheral autonomic nervous system. Both CRF and its receptors are present in the central nervous system at sites where the peptide is known to modify the activity of the autonomic nervous system. The CRF that is present in normal adrenal medulla and pheochromocytomas[13-15] could be locally released to serve as a paracrine or autocrine regulator of the secretion of other stress hormones. Such cyclic AMP-mediated effects of CRF could be particularly relevant during prolonged activation of the medulla, as suggested by the latency of the effect of CRF on catecholamine release, and may be important in long-term adaptation to stress.

A still unresolved question is the functional interaction between the adrenal medulla and cortex. As the circulation within the adrenal gland appears to flow from the cortex to the medulla[33,34], it is difficult to propose a mechanism by which peptides and/or catecholamines released from the medulla could have a direct effect in the cortical zones. However, it is possible that secretory products of the medulla can reach the cortex via local circulatory shunts or simple diffusion. Although the physiological role of CRF in the peripheral autonomic nervous system will require further study, the presence of the peptide and its functional receptors in the adrenal medulla and sympathetic ganglia suggest that CRF regulates the activity of the peripheral autonomic nervous system. These findings are consistent with the notion that CRF has a major role in the integrated response of the organism to stress, with actions at all levels of the neuroendocrine effector system.

We thank Robin W. Stull, Charles Grewe and Thomas P. Tomai for technical assistance.

Received 3 June; accepted 14 November 1985.

1. Vale, W., Spiess, J., Rivier, C. & Rivier, J. *Science* **213**, 1394–1397 (1981).
2. Aguilera, G. *et al. J. Neuroendocr.* (in the press).
3. Wynn, P. C., Aguilera, G., Morell, J. & Catt, K. J. *Biochem. biophys. Res. Commun.* **110**, 602–609 (1983).
4. Wynn, P. C. *et al. Peptides* **5**, 1077–1084 (1984).
5. De Souza, E. B. *et al. Science* **224**, 1449–1450 (1984).
6. Fisher, L. A., Brown, M. R. in *Current Topics in Neuroendocrinology* (eds Ganten, D. & Pfaff, D) 87 (Springer, Berlin, 1983).
7. MacCannell, K. L., Lederis, K., Hamilton, P. L. & Rivier, J. *Pharmacology* **25**, 116–120 (1982).
8. Brown, M. R. *et al. Regulat. Peptides* **4**, 107–114 (1982).
9. Udelsman, R. *et al.* in *The Adrenal Gland and Hypertension* (eds Mantero, F. & Biglieri, E.) (Raven, New York, in the press).
10. Orth, D. N. *et al. J. clin. Invest.* **71**, 587–595 (1983).
11. Hermus, A. *et al. Lancet* **i**, 776 (1983).
12. Schurmeyer, T. H. *et al. J. clin. endocr. Metab.* **59**, 1103–1108 (1984).
13. Suda, T. *et al. J. clin. endocr. Metab.* **58**, 919–924 (1984).
14. Hashimoto, K. *et al. Peptides* **5**, 707–711 (1984).
15. De Cherney, G. S., Nicholson, W. E., Jackson, R. V. & Orth, D. N. *Clin. Res.* **32**, 264A (1984).
16. Petrusz, P., Merchenthaler, I., Maderdrut, J. L., Vigh, S. & Schally, A. V. *Proc. natn. Acad. Sci.* U.S.A. **80**, 1721–1725 (1983).
17. Nieuwenhuijzen Kruseman, A. C., Linton, E. A., Lowry, P. J., Rees, L. H. & Besser, G. M. *Lancet* **ii**, 1245–1246 (1982).
18. Carey, R. M. *et al. New Engl. J. Med.* **311**, 13–20 (1984).
19. Schurmeyer, T. H. *et al. Endocrinology* **117**, 300–302 (1985).
20. Vale, W. *et al. Endocrinology* **113**, 1121–1131 (1983).
21. Aguilera, G. *et al. J. biol. Chem.* **258**, 8039–8045 (1983).
22. Mukherjee, C., Caron, M. C. & Lefkowitz, R. J. *Endocrinology* **99**, 347–357 (1976).
23. Lin, M. C., Lin, C.-S. & Whitlock, J. P. *J. biol. Chem.* **254**, 4684–4688 (1979).
24. Harwood, J. P., Reichert, N. D., Dufau, M. L. & Catt, K. J. *Endocrinology* **106**, 280–28 (1980).
25. Corder, R. *et al. Neuropeptides* **3**, 9–17 (1982).
26. Eiden, L. E., Eskay, R. L., Scott, J., Pollard, H. & Hotchkiss, A. J. *Life Sci.* **33**, 687–693 (1983
27. Evans, C. J., Erdelyi, E., Weber, E. & Barchas, J. D. *Science* **221**, 957–960 (1983).
28. Berenyi, M. R., Singh, G., Gloster, E. S., Davidson, M. I., Woldenberg, D. H. *Archs Patl* **101**, 31–35 (1977).
29. Wilson, S. P., Chang, K. J. & Viveros, O. H. *J. Neurosci.* **2**, 1150–1156 (1982).
30. Eiden, L. E. & Hotchkiss, A. J. *Neuropeptides* **4**, 1–9 (1983).
31. Quack, T. T. *et al. Molec. Pharmac.* **26**, 255–260 (1984).
32. Seamon, K. B., Padgett, W. & Daly, J. W. *Proc. natn. Acad. Sci. U.S.A.* **78**, 3363–3367 (1981
33. Sjostrand, T. *Skand. Archs Physiol.* **71**, 85–122 (1934).
34. Hamaji, M. & Harrison, T. S. in *Blood Vessels and Lymphatics in Organ Systems* (ec Abramson, D. I. & Dobrin, P. B.) 280–295 (Academic, New York, 1984).
35. Ketelslegers, J. M., Knott, G. D. & Catt, K. J. *Biochemistry* **14**, 3075–3083 (1975).
36. Lowry, O. H., Rosebrough, N. J., Farr, A. L. & Randall, R. J. *J. biol. Chem.* **193**, 265–27 (1951).
37. Quirion, R., Hammer, R. P., Herkenman, M. & Pert, C. *Proc. natn. Acad. Sci. U.S.A.* **7** 5581–5585 (1981).
38. Duncan, D. B. *Biometrics* **11**, 1–42 (1955).
39. Greenberg, A. & Zinder, O. *Cell Tissue Res.* **226**, 655–656 (1982).
40. Goldstein, D. S., Feuerstein, G., Izzo, J. L. Jr, Kopin, I. J. & Keiser, H. R. *Life Sci.* **2** 467–475 (1981).
41. Miller, R. J., Chang, K. J., Cooper, B. & Cuatrecasas, P. *J. biol. Chem.* **253**, 531–53 (1978).

IgE-mediated degranulation of mast cells does not require opening of ion channels

M. Lindau* & J. M. Fernandez

Department of Membrane Biophysics, Max-Planck-Institut für biophysikalische Chemie, D-3400 Göttingen, FRG

Rat peritoneal mast cells respond to antigenic stimulation by releasing histamine through exocytosis. The dynamics of exocytosis can be investigated by dialysing single cells with patch pipettes using the whole-cell recording configuration of the patch-clamp technique[1,2]. However, dialysed cells fail to respond to external stimuli such as compound 48/80 or antigens, suggesting that essential cytoplasmic components have been washed out. We have developed a new patch-clamp configuration in which the patch under the pipette tip is not disrupted but instead permeabilized, preventing the diffusion of large molecules out of the cell. In this configuration the cell responds to external stimulation, and the capacitance as well as the conductance of the cell membrane can be recorded during degranulation. On antigenic stimulation, the cell capacitance (proportional to plasma membrane area), after an initial delay, increases by a factor of about 3. This increase in capacitance is often preceded by a transient increase in conductance. Agents that block Ca-activated channels inhibit this conductance change without affecting the amplitude and time course of degranulation. We therefore conclude that, in contrast to excitable secretory cells such as chromaffin cells[2], mast cells do not use ion channels in stimulus–secretion coupling.

When antigens were added to cells passively sensitized with immunoglobulin E (IgE), the cell being dialysed with the patch pipette did not respond and no inward currents were detected (less than 1 pA at +5 mV), whereas the surrounding cells degranulated within a few minutes (Fig. 1). This suggests that essential components had been washed out or inactivated by the pipette solution (Fig. 2*a*), breaking the chain between stimulus and exocytosis. The idea underlying the present work was to make the interior of the cell accessible not by disrupting the patch under the pipette by means of suction, but by permeabilizing it so as to create small pores. This would prevent the rapid diffusion of large molecules out of the cell (Fig. 2*b*) so that it would remain responsive to external stimuli.

Mast cells are permeabilized if the extracellular side of th plasma membrane is exposed to ATP^{4-} (ref. 3). When a pipett containing ATP, no calcium and a calcium chelator (EGT or bis(*O*-aminophenoxy)ethane *N*,*N*,*N'*,*N'*-tetraacetic acid BAPTA) was sealed against the surface of a mast cell, th membrane patch under the pipette became permeable and capacitive current transient could be measured in response t a voltage pulse (Fig. 1*c*, inset). As in the whole-cell configuratio the membrane capacitance (C_m) and conductance (G_m) of th cell as well as the access resistance (R_a) were derived from th transient. Typical values obtained were 200–5,000 MΩ for th patch access resistance (corresponding to ~200 Ω cm²) and plasma membrane resistance (R_m) of 20–100 GΩ (~20,000 cm²). The values for R_m and C_m (5–10 pF) agree very closel with the corresponding results obtained in the whole-ce configuration[1,4]. In a few cells the patch was disrupted, an measurements confirmed the previously obtained values. As th main difference between the standard whole-cell mode[5] and ou method is the time constant of the capacitive transient, w propose the name 'slow whole-cell' (C_mR_a ~10 ms) for this ne method, as opposed to the 'fast whole-cell' (C_mR_a ~100 µs obtained by patch disruption.

In the slow whole-cell configuration, mast cells degranula together with the neighbouring cells in response to extracellul stimuli such as compound 48/80 or multivalent antigens. Figu 1*c* shows a group of mast cells that had been passively sensitize with IgE. Recordings were made from one cell of the group i the slow whole-cell mode (capacitive transient shown in t inset). On stimulation with dinitrophenyl linked to bovine seru albumin (DNP$_{43}$–BSA), all the mast cells degranulated simu taneously (Fig. 1*d*). The capacitive transient did not change i amplitude but became about three times slower, indicating th the capacitance of the cell had increased about threefold witho a significant change in access resistance. A small increase i membrane conductance also occurred after degranulatio (increased steady-state current in inset of Fig. 1*d*). The resu shown in Fig. 1*c*,*d* supports the idea of a wash-out of essenti cellular components by the fast whole-cell method (Fig. 2*a*).

Permeabilization of the patch provides a new method f monitoring exocytosis in undisturbed, intact mast cells. W anticipate that this method will be applicable to other cell typ by the use of pore-forming substances, thus enabling t monitoring of events that require an intact cytosol. The slo whole-cell method is similar to microelectrode recording bu unlike the latter technique, causes little damage to the cells.

Figure 3*a* shows typical time courses of changes in the ce membrane capacitance and conductance following stimulatio with DNP$_{43}$–BSA. In the slow whole-cell mode, capacitan

---

* Present address: Biophysics Group, Department of Physics, Freie Universität Berlin, D-1000 Berlin 33, FRG.

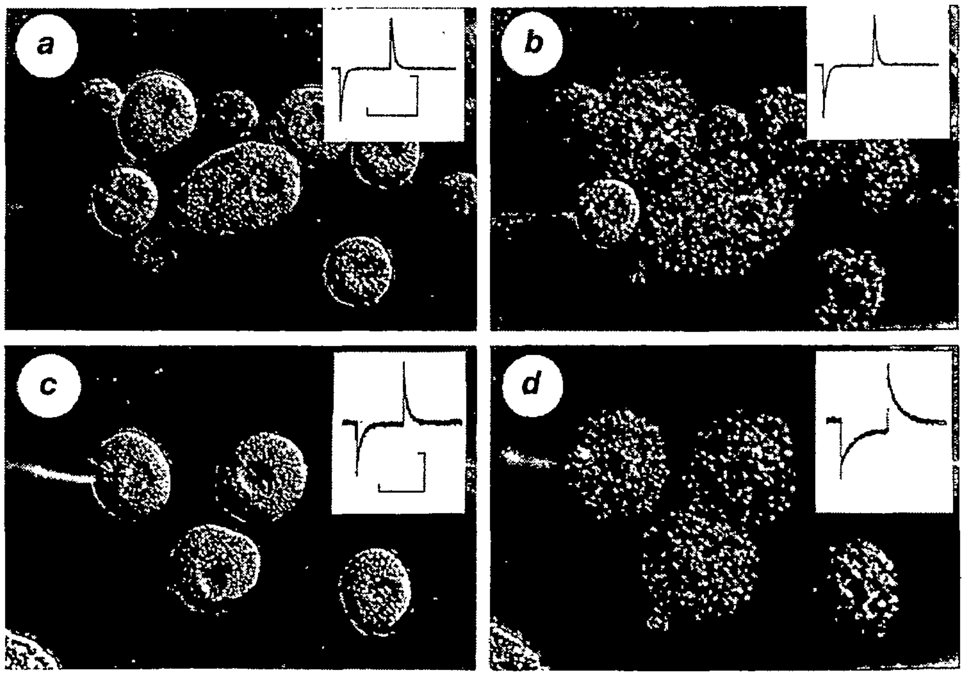

Fig. 1 Typical dispersions of cells from a rat peritoneal lavage. Mast cells are easily recognized by their large nucleus and granular appearance. The cells shown here were passively sensitized with monoclonal IgE before the experiment. *a*, A single mast cell in this group has been dialysed with our standard intracellular solution. Dialysis is accomplished in the whole-cell mode of the patch-clamp technique. In this configuration, a −20-mV voltage pulse (from 0 mV) induces a transient current (inset, calibration bars 1 ms, 2 nA), which corresponds to the charging of the cell membrane capacitance. The steady-state current is negligible due to the absence of ionic conductances in the mast cell membrane. *b*, On addition of DNP_{43}-BSA to the bath, all the mast cells except for the dialysed cell degranulate. The capacitive transient is also unmodified, implying that the membrane area, membrane conductance and pipette access resistance have not changed. Dialysis of rat peritoneal mast cells in these conditions thus renders the cells refractory to external stimulation, which suggests the loss of cytoplasmic components essential for stimulus-secretion coupling. *c*, A patch pipette containing a solution including 400 μM ATP and 400 μM BAPTA is sealed against one mast cell of the group. The membrane patch is permeabilized by this solution, allowing electrical measurements of the cell capacitance and conductance The inset shows the current transient in response to a −20-mV pulse (inset, calibration bars 100 ms, 10 pA). This transient is similar to the one obtained in the fast whole-cell configuration (*a*), but is about 100 times smaller and slower, as expected from the large access resistance R_a (see Fig. 2*c*). The resting cell parameters as determined from this transient are: $R_a = 1.9$ GΩ, $C_m = 6.3$ pF, $R_m = 34$ GΩ (29 pS). *d*, The same group of cells 5 min after addition of DNP_{43}-BSA to the bath. All the cells, including the one in slow whole-cell mode, degranulate simultaneously. The time constant of the capacitive transient (inset) is increased about threefold, but the amplitude is the same as in *c*, indicating an increase in the cell membrane capacitance by a factor of ~3, as expected from a degranulated cell. The steady-state current at the end of the pulse is also larger than before stimulation, indicating that the membrane conductance increased slightly. Cell parameters: $R_a = 1.9$ GΩ, $C_m = 18$ pF, $R_m = 7$ GΩ (140 pS).

Methods. The cells were incubated for more than 1 h with monoclonal IgE (1 μg ml^{-1}) at 37 °C before use. The chamber with the cells was mounted in the patch-clamp set-up and perfused with extracellular saline to wash off the unbound IgE. The external solution was then exchanged for a medium containing 145 mM NaCl, 2.8 mM KCl, 1 mM $MgCl_2$, 2 mM $CaCl_2$, 10 mM HEPES, 25 mM glucose, 100 μM phosphatidylserine. The pipette solution contained 150 mM K-glutamate, 10 mM HEPES, 7 mM $MgCl_2$, 200 μM Na_2ATP, 200 μM BAPTA. All solutions were adjusted to *p*H 7.2 with NaOH. A 20-μl aliquot of a solution of DNP_{43}-BSA in phosphate-buffered saline (100 μg ml^{-1}) was added in the vicinity of the observed cells to stimulate degranulation.

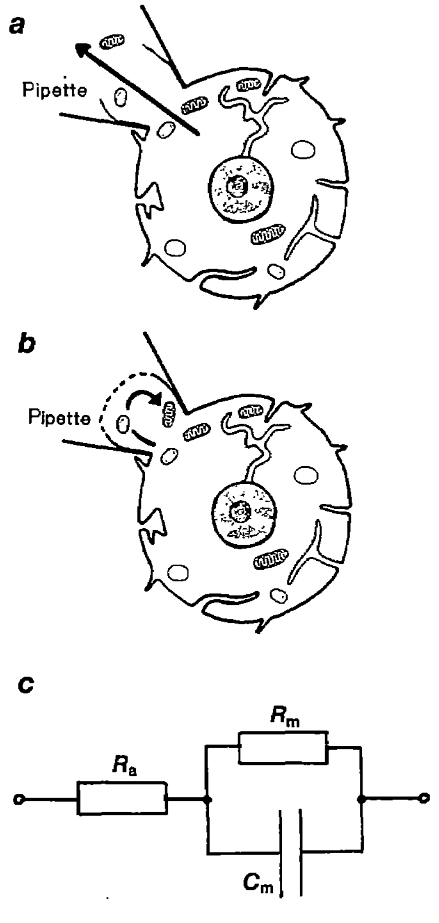

Fig. 2 Schematic representation of the fast and slow whole-cell configurations. *a*, Fast whole-cell configuration. The patch under the pipette has been disrupted by suction after seal formation. The diameter of the tip can be larger than 2 μm, allowing the diffusion of cytoplasmic components out of the cell volume (<1 pl) into the large volume of the pipette (~25 μl). *b*, Slow whole-cell configuration. The patch under the pipette is not disrupted but permeabilized, preventing the rapid loss of large cytoplasmic molecules and allowing the permeation of small ions. *c*, Equivalent circuit for both whole-cell configurations. The seal resistance between the interior of the pipette and the bath has been neglected. If a voltage pulse is applied, a capacitive transient is evoked which can be fitted by a single exponential. From the current response, C_m, R_m and R_a can be calculated. For mast cells, typical values are 5–10 pF for C_m and 20–100 GΩ for R_m, corresponding to a whole-cell conductance of 10–50 pS for a resting cell. The range of access resistance (R_a) is 1–20 MΩ in the fast whole-cell mode (*a*) and 100–5,000 MΩ in the slow whole-cell mode (*b*). If the current transient is recorded both in the slow whole-cell configuration and after patch disruption in the fast whole-cell mode, it is possible to determine the seal conductance. In these experiments the seal conductance was usually less than 15 pS.

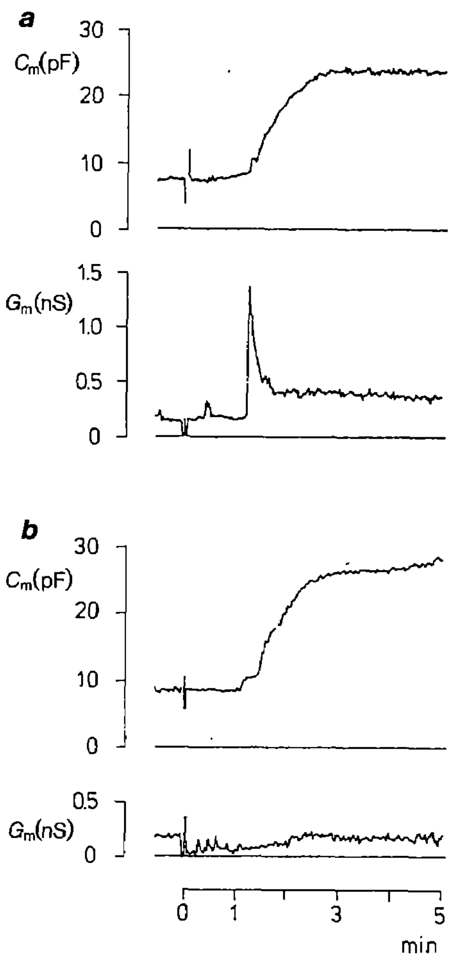

Fig. 3 Time course of capacitance and conductance of the mast cell membrane during IgE-mediated degranulation, recorded in the slow whole-cell configuration. *a*, Typical degranulation under normal conditions. Extracellular medium as in Fig. 1. DNP_{43}-BSA was added to the bath at time zero, causing the artefacts in the traces. The capacitance increased by a factor of ~3 after an initial delay of ~80 s (upper trace). The capacitance increase was preceded by a conductance transient of ~1.3 nS (lower trace). It probably corresponds to the opening of Ca-activated ion channels induced by a transient rise in the intracellular free calcium concentration. However, such transients were not observed in all cells. *b*, Degranulation in the presence of 10 μM pimozide (a gift from Janssen Pharmaceuticals). External solution as in Fig. 1, but containing 10 mM $CaCl_2$ and 10 μM pimozide. Pimozide was added from a 10 mM stock solution in ethanol. The time course and amplitude of the capacitance increase (upper trace) were similar to those shown in *a*. However, no significant conductance change was observed before degranulation. The addition of DNP_{43} was accompanied by a conductance decrease from 180 to ~50 pS in this experiment, probably due to an accidental improvement in the seal resistance. The following slow conductance increase is superimposable on the capacitance change, suggesting that the conductance increase simply reflects the increase of membrane area with a constant conductance per unit area. These results provide strong evidence that conductance changes are not necessary to activate exocytosis in these cells.

Methods. The increase of the membrane area during degranulation was monitored by measuring the membrane capacitance using the synthetic pseudo-random binary sequence (PRBS) method[6]. An 18-mV PRBS (128 bits long, 69 Hz bandwidth) was applied to the stimulus input of an EPC 7 patch-clamp amplifier (List electronics) operating in the voltage-clamp mode at a holding potential of 0 mV. The whole-cell current in response to the PRBS stimulus was sampled and stored by a PDP-11/23 minicomputer (Digital Equipment Corporation). The real part of the admittance was used to determine the capacitance C_m, the conductance $1/R_m$ of the plasma membrane, and the access resistance R_a. The d.c. conductance in *a* and *b* was determined by a fit of a quadratic function to the first eight data points at the low-frequency end of the admittance. After subtraction of this value, the frequency dependence can be linearized and C_m, G_m and R_a were then obtained by a linear least-squares fit. This procedure was carried out for each record (a record was taken every 1.8 s), giving the data points shown. The parameters obtained gave a good fit to the frequency dependence of the real and imaginary part of the admittance. All experiments were done at room temperature.

and conductance were determined every 1.8 s using a very low-frequency pseudo-random binary sequence technique (refs 1, 6; see Fig. 3 legend for details). After addition of DNP_{43}-BSA, the capacitance increased reproducibly by a factor of about 3 after a delay of 80±20 s (Fig. 3*a*). The half-time for the rising phase was 20–60 s. In most, but not all, cases, the capacitance increase was preceded by a transient conductance increase in the nanosiemens range (Fig. 3*a*, lower trace). At 0 mV holding potential, this conductance change was associated with only a slight shift of the current in the outward direction. We suspected that this conductance increase resulted from the elevation of the intracellular free calcium concentration, which could lead to the opening of Ca-activated channels that have been observed in the mast cell membrane[4]. This transient conductance increase was not always seen, but on the other hand, Ca-activated channels were not observed in all cells[4]. In the presence of either quinidine (500 μM) or pimozide (10 μM), which have been reported to block Ca-activated channels in other cell types[7,8], the extent and time course of degranulation were unchanged, as shown by the measurement of the cell capacitance (Fig. 3*b*, upper trace), but no significant conductance changes were observed before the onset of degranulation (Fig. 3*b*, lower trace). In these experiments the membrane conductance averaged 95± 75 pS ($n=4$) before degranulation started. The large scatter is probably due to different seal conductances. A small increase in the membrane conductance (from ~80 pS in the resting cell to 200 pS after degranulation; Fig. 3*b*) typically observed in parallel with the increase in capacitance, probably reflects the increase in membrane area. This suggests that the specific conductance of the granule membrane is not very different from that of the plasma membrane.

It is generally believed that the opening of Ca-selective ion channels is an essential step in stimulus-secretion coupling. For example, conductance changes in the range 800–2,000 pS are required for exocytosis in adrenal chromaffin cells[2], the increase in conductance resulting from the opening of Ca-selective ion channels. Accordingly, Ca channels might open in response to the crosslinking of the IgE receptors in mast cells[9,10]. In contrast to these expectations, our results show that rat peritoneal mast cells degranulate in response to antigenic stimulation without significant changes in membrane conductance.

Evidence for the entry of Ca as the main step in mast cell activation has been obtained from experiments showing that labelled Ca is taken up by degranulating mast cells[11], and that removal of extracellular Ca blocks antigen-induced degranulation[12]. However, the large increase in membrane area that occurs during degranulation can provide new binding sites for the labelled Ca, which may account for the Ca uptake observed[13] In our hands, the effect of removing Ca from the extracellular medium is time-dependent. If the cells are stimulated within 1 min of changing to a Ca-free extracellular solution, degranulation still occurs. Independence from extracellular Ca was also observed in experiments using intracellular Ca indicators which showed that mast cells stimulated 1 min after removal of extracellular Ca produced a significant intracellular Ca transient in response to antigens[14]. The long-term effects of the removal of extracellular Ca probably result from the unbinding of Ca from plasma membrane sites, which could damage the membrane components involved in stimulus-secretion coupling.

The results presented here, and the lack of effect of calcium antagonists[15] and of the removal of extracellular Ca at short times (ref. 14, also see above) argue against Ca entry as an obligatory event leading to exocytosis in mast cells.

We thank Dr H. Metzger for the gift of monoclonal IgE and its antigen, also Drs E. Neher, B. Sackmann, R. Eckert, M. Primke, A. Fahr and Mr J. Schroeder for discussions and comments on the manuscript. J.M.F. is an Alexander von Humboldt fellow.

Received 30 July; accepted 1 November 1985.

1. Fernandez, J. M., Neher, E. & Gomperts, B. D. *Nature* **312**, 453–455 (1984).
2. Neher, E. & Marty, A. *Proc. natn. Acad. Sci. U.S.A.* **79**, 6712–6716 (1982).
3. Bennet, J. P., Cockcroft, S. & Gomperts, B. D. *J. Physiol., Lond.* **317**, 335–345 (1981).
4. Lindau, M. & Fernandez, J. M. *J. gen. Physiol.* (submitted).
5. Hamill, O. P., Marty, A., Neher, E., Sakmann, B. & Sigworth, F. J. *Pflügers Arch. ges. Physiol.* **391**, 85–100 (1981).
6. Fernandez, J. M., Bezanilla, F. & Taylor, R. E. *J. gen. Physiol.* **79**, 41–67 (1982).
7. Fishman, M. C. & Spector, I. *Proc. natn. Acad. Sci. U.S.A.* **78**, 5245–5249 (1981).
8. Hoffman, E. K., Simonsen, L. O. & Lambert, I. H. *J. Membrane Biol.* **78**, 211–222 (1984).
9. Gomperts, B. D. *Nature* **306**, 64–66 (1983).
10. Mazurek, N., Schindler, H., Schuerholz, T. H. & Pecht, I. *Proc. natn. Acad. Sci. U.S.A.* **81**, 6841–6845 (1984).
11. Foreman, J. C., Hallet, M. B. & Mongar, J. I. *J. Physiol., Lond.* **271**, 193–214 (1977).
12. Foreman, J. C.& Mongar, J. L. *J. Physiol., Lond.* **224**, 753–769 (1972).
13. Grosman, N. & Diamant, B. *Trends Pharmac. Sci.* **5**, 183–184 (1984).
14. White, J. R., Ishizaka, T., Ishizaka, K. & Sha'afi, R. *Proc. natn. Acad. Sci. U.S.A.* **81**, 3978–3982 (1984).
15. Ennis, M., Ind, P. W., Pearce, F. L. & Dollery, C. T. *Ag. Actions* **13**, 144–148 (1983).

Murine cells expressing an HLA molecule re specifically lysed by HLA-restricted antiviral human T cells

. Gomard*, B. Begue*, S. Sodoyer†, J. L. Maryanski‡,
. R. Jordan† & J. P. Levy*

INSERM, U 152, Bâtiment Gustave Roussy, Hôpital Cochin,
7 rue du Faubourg Saint-Jacques, 75014 Paris, France
Centre d'Immunologie, INSERM-CNRS de Marseille-Luminy,
ase 906, Marseille Cedex 9, France
Ludwig Institute for Cancer Research, Brussels Branch,
4 Avenue Hippocrate, UCL 7459, B-1200, Brussels, Belgium

lass I HLA (histocompatibility locus antigen) molecules are the argets of allospecific cytolytic T lymphocytes (CTL) in graft ejection, and constitute the restricting elements necessary for the nteraction between antiviral CTL and virus-infected cells. Cells xpressing only one HLA in the absence of other human molecules ould provide a remarkable model for studying the function of hese molecules. However, HLA^{+} murine cells transfected with uman genes[1–5] are generally not lysed by allospecific human TL[5–8], and this is ascribed to insufficient HLA expression, lack f human β_2-microglobulin, alteration of HLA molecules or bsence of receptors for human T8 or LFA1 molecules in murine ells[6–8]. Here we report, for the first time, the specific lysis of irus-infected HLA^{+} murine cells by HLA-restricted antiviral uman CTL. Therefore, these murine cells constitute an excellent odel for studying the role of HLA molecules.

Murine cells expressing HLA-A2 or HLA-A11 molecules have een obtained by transfection of P815-HTR cells[9] with genomic lones of well-established HLA specificities described preiously[10,11]. These cells were infected with the A/Texas (AT) uman influenza A virus and successful infection was ascerined in a control experiment in which the cells were specifically lysed by syngeneic anti-influenza murine CTL (data not shown). Uninfected HLA-A2^{+} and HLA-A11^{+} P815-HTR cells or untransfected P815-HTR cells were used as controls. Human anti-influenza A CTL of high efficiency were obtained from blood lymphocytes of donors after several *in vitro* stimulations with the virus, as described previously[12]. CTL from donor HC12 lysed the autologous infected cells (HC12-EBV-AT) and similar degrees of lysis were found with other infected HLA-A2 target cells, as illustrated here by one example (M17-EBV-AT). HLA-incompatible infected target cells (M10-EBV-AT) were not lysed, as determined in several control experiments. As shown in Fig. 1 (and confirmed in five different experiments), the same CTL lysed with high efficiency the murine HLA-A2^{+} cells (P815-A2-AT) infected with influenza A virus. In fact, a similar level of lysis was observed with both human and murine HLA-A2^{+} target cells. Uninfected HLA-A2^{+} control P815 cells (P815-A2) were not lysed, confirming the viral specificity of the cytolysis. Furthermore, P815-A2 cells infected with influenza B Singapore virus were not lysed (data not shown).

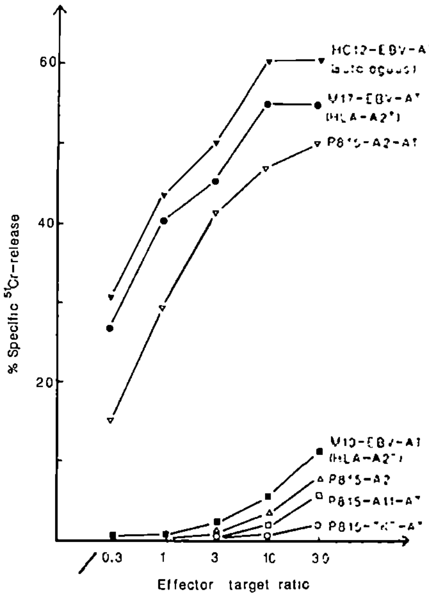

Fig. 1 Cytolytic activity of HLA-A2-restricted anti-influenza A human CTL on human or murine target cells. P815-HTR cells were transfected with either an HLA-A2 genomic clone[10] by the calcium phosphate DNA precipitation method[18], or an HLA-A11 clone[11] by the method of protoplast fusion in suspension[19]. HLA expression was ascertained by immunofluorescence using a monomorphic HLA-specific monoclonal antibody (B9.12.1). Lymphoblastoid cell lines were used as human target cells, as they are suitable targets and are easily infected with influenza virus[12]. The target cells were autologous (HC12), HLA-A2-compatible (M17) or HLA-incompatible (M10) with the effector cells. Effector cells were obtained from an HLA-A2 donor (HC12) whose peripheral blood lymphocytes had been stimulated three times *in vitro* with influenza AT-infected autologous lymphocytes in the presence of interleukin-2, as described previously[12]. The background lysis of target cells alone was between 20 and 24% for P815 cells whether infected or not, and between 15 and 26% for the human LCL target cells. The ^{51}Cr-release test was performed after incubation at 37 °C for 4 h.

To examine whether the lysis was HLA-restricted, untransfected infected P815-HTR cells (P815-AT) and HLA-A11^{+} infected P815-HTR cells (P815-A11-AT) were tested with human HLA-A2-restricted virus-specific CTL. These cells showed no lysis (Fig. 1). However, aliquots of P815-AT and P815-A11-AT cells were lysed very specifically by either murine anti-influenza CTL or murine anti-H-2^{d} CTL (not shown), confirming that these targets were virus-infected and lysable. Unfortunately, it was not possible to test HLA-A11-restricted human CTL, as HLA-A11 is a poor restricting element of anti-influenza responses in

Table 1 Treatment of effector cells with anti-T3, anti-T4 or anti-T8 monoclonal antibody (MAb) plus complement (C)

Treatment of effector cells	% Specific ^{51}Cr-release by: M17-EBV-AT	P815-A2-AT
—	37	41
Anti-T3 MAb+C	<2	2
Anti-T4 MAb+C	36	40
Anti-T8 MAb+C	<2	<2

HC12 anti-influenza AT effector cells were incubated for 30 min at 4 °C with OKT3, OKT4 or OKT8 monoclonal antibody (Ortho) diluted 1:100, then rabbit complement (Behring Institut) diluted 1:20 was added and the mixture incubated for 45 min at 37 °C, after which the cells were washed and resuspended in test medium. The effector/target cell ratio (calculated for effector cells before treatment) was 0.5:1.

man[13]. However, we have demonstrated that an influenza A-specific human CTL clone from the same donor but restricted by HLA-DRw8 (ref. 14) did not lyse P815-A2-AT cells. Furthermore, uncloned anti-influenza CTL restricted by HLA-B27 did not lyse P815-A2-AT (not shown). These results show that the human CTL used here lysed the P815 target cells not only in a virus-specific but also in an HLA-restricted manner, and similar results have been found with different batches of human effector cells, including CTL obtained after secondary stimulation *in vitro* and before their establishment as a permanent cell line.

The T4$^-$T8$^+$ phenotype of the human anti-influenza A CTL has been well established. To further confirm this identity for the present study, the effector cells were treated with anti-T3, anti-T4 or anti-T8 monoclonal antibody plus complement just before the chromium release test. Treatment with anti-T3 or anti-T8 antibody plus complement either abolished or strongly decreased the cytolysis of P815-A2-AT by human CTL, while anti-T4 had no effect (Table 1).

The present results show that murine cells infected with influenza A virus and expressing the HLA-A2 heavy chain can be lysed by HLA-A2-restricted anti-influenza A CTL of human origin as efficiently as the relevant human targets. The interaction is clearly virus-specific and HLA-A2-restricted, and the effector cells belong to the T8 subset of T cells. These results are in contrast to the negative or marginally positive results of experiments reported recently by several groups, including ourselves, in which anti-HLA human CTL were tested on HLA-transfected murine L-cells[6-8]. The discrepancies between these results may be caused by a number of factors. First, P815 cells are intrinsically better targets than L-cells when tested with murine CTL and, more significantly, with human allospecific CTL directed against an HLA molecule expressed on the (transfected) P815 target; this has been observed with P815-HLA-A24 cells[15] and we have found that P815-A2 and P815-A11 cells are lysed quite specifically by human anti-A2 or anti-A11 CTL, respectively[16]. However, a good degree of lysis has been observed recently with L-cells expressing a high concentration of a variant HLA-A3 antigen[17], which suggests that quantitative rather than qualitative factors may limit the interaction of human CTL with murine target cells. Another point to consider is that antiviral responses have been studied in the present experiments. In such reactions, the HLA epitope involved may be different from the epitopes recognized in anti-HLA responses. Moreover, simultaneous recognition of both HLA (restricting element) and viral protein by the T-cell receptor(s) may result in higher affinity. On the whole, and in contrast to previous suggestions[6-8], it is clear that murine cells transfected with human *HLA* genes provide a suitable model for the study of the relationship between the structure and function of human HLA molecules.

We thank Drs H. Orr and P. Paul for providing HLA-A2 and HLA-A11 genomic clones, Dr A. Van Pel for the gift of P815-HTR cells, and Mrs J. Debie for secretarial help.

Received 16 July; accepted 23 October 1985.

1. Lemonnier, F. A. *et al. Immunogenetics* **16,** 355-362 (1982).
2. Barbosa, J. A. *et al. Proc. natn. Acad. Sci. U.S.A.* **79,** 6327-6331 (1982).
3. Kavathas, P. & Herzenberg, L. A. *Proc. natn. Acad. Sci. U.S.A.* **80,** 524-528 (1983).
4. Herman, A., Parham, P., Weissman, S. M. & Engelhard, V. H. *Proc. natn. Acad. Sci. U.S.A.* **80,** 5056-5060 (1983).
5. Berbabeu, C. *et al. J. Immun.* **131,** 2032-2037 (1983).
6. Barbosa, J. A. *et al. Proc. natn. Acad. Scci. U.S.A.* **81,** 7549-7553 (1984).
7. Van de Rijn, M. *et al. Science* **226,** 1083-1085 (1984).
8. Bernabeu, C. *et al. J. Immun.* **133,** 3188-3196 (1984).
9. Van Pel, A., De Plaen, E. & Boon, T. *Somat. Cell molec. Genet.* (in the press).
10. Koller, B. H. & Orr, H. T. *J. Immun.* **134,** 2727-2733 (1985).
11. Paul, P. *et al. Immunogenetics* (in the press).
12. Toubert, A. *et al. Immunogenetics* **20,** 513-525 (1984).
13. Gomard, E., Witbon, M., Toubert, A., Begue, B. & Lévy, J. F. *Immunogenetics* **20,** 197-204 (1984).
14. Henin, Y. *et al. Immunogenetics* (in the press).
15. Maryanski, J. L. *et al. Eur. J. Immun.* (in the press).
16. Achour, A. *et al. Eur. J. Immun.* (submitted).
17. Cowan, E. P., Coligan, J. E. & Biddison, W. E. *Proc. natn. Acad. Sci. U.S.A.* (in the press).
18. Wigier, M., Pellicer, A., Silverstein, S. & Axel, R. *Cell* **14,** 725-731 (1978).
19. Litzkas, P., Jha, K. K. & Ozez, H. L. *Molec. cell. Biol.* **4,** 2549-2552 (1984).

A nuclear factor that binds to a conserved sequence motif in transcriptional control elements of immunoglobulin genes

Harinder Singh*, Ranjan Sen†, David Baltimore*† & Phillip A. Sharp*

* Center for Cancer Research and Department of Biology,
Massachusetts Institute of Technology, Cambridge,
Massachusetts 02139, USA
† Whitehead Institute for Biomedical Research, Cambridge,
Massachusetts 02142, USA

***Trans*-acting factors that mediate B-cell specific transcription of immunoglobulin genes have been postulated based on an analysis of the expression of exogenously introduced immunoglobulin gene recombinants in lymphoid and non-lymphoid cells. Two B-cell-specific, *cis*-acting transcriptional regulatory elements have been identified. One element is located in the intron between the variable (*V*) and constant (*C*) regions of both heavy and κ light-chain genes and acts as a transcriptional enhancer[1-6]. The second element is found upstream of both heavy and κ light-chain gene promoters. This element directs lymphoid-specific transcription even in the presence of viral enhancers[7-10]. We have sought nuclear factors that might bind specifically to these two regulatory elements by application of a modified gel electrophoresis DNA binding assay[11-13]. We report here the identification of a human B-cell nuclear factor (IgNF-A) that binds to DNA sequences in the upstream regions of both the mouse heavy and κ light-chain gene promoters and also to the mouse heavy-chain gene enhancer. This sequence-specific binding is probably mediated by a highly conserved sequence motif, ATTTGCAT, present in all three transcriptional elements. Interestingly, a factor showing similar binding specificity to IgNF-A is also present in human HeLa cells.**

Mouse and human light-chain promoters contain the octamer sequence ATTTGCAT approximately 70 base pairs (bp) upstream from the site of initiation[14,15]. Heavy-chain gene promoters contain the identical sequence in inverted orientation, ATGCAAAT, at the same position. This element seems to be essential for the efficient use of immunoglobulin promoters in B cells[5,7,15]. The high degree of sequence and positional conservation of this element as well as its apparent functional requirement suggests its interaction with a sequence-specific transcription factor. We have searched for such a factor in a B-cell nuclear extract by using a gel electrophoresis DNA binding assay with enhanced sensitivity. This assay, which is based on the altered mobility of protein-DNA complexes during gel electrophoresis, has been extensively used in equilibrium and kinetic analyses of purified prokaryotic gene regulatory proteins[11,12,16,17] and more recently to identify and isolate a protein

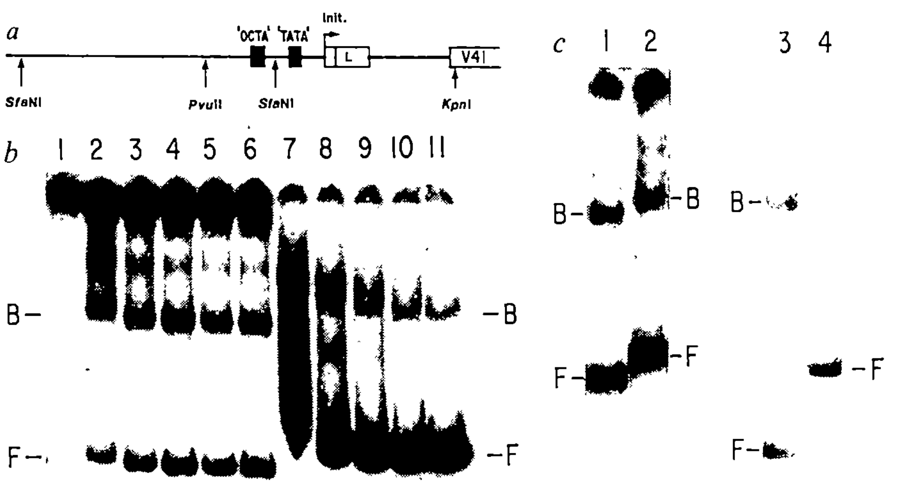

Fig. 1 Binding of a nuclear factor to the MOPC-41 κ promoter region. *a*, 5' region of the MOPC-41 V_κ gene segment. The 'OCTA' and 'TATA' elements start at positions −66 and −28, respectively. *b*, Gel electrophoresis DNA binding assays with the *Sfa*NI/*Sfa*NI κ promoter fragment (~300 bp). The *Sfa*NI fragment was subcloned into the *Sma*I site of pSP64 (pSPIgV$_\kappa$, provided by N. Speck). For binding analysis, this fragment was excised from pSPIgV$_\kappa$ by digesting with *Hin*dIII and *Eco*RI. These latter sites flank the *Sma*I site in the polylinker of pSP64. After end-labelling with [α-^{32}P]dATP and the large fragment of *E. coli* DNA polymerase I, the radiolabelled fragment was isolated by polyacrylamide gel electrophoresis. The ^{32}P-labelled fragment (~0.5 ng, 10,000 c.p.m.) was incubated with a nuclear extract[36] of a human B lymphoma cell line (EW[32]) in the absence (lane 1) or presence of two different non-specific competitor DNAs (lanes 2–11). Binding reactions (25 µl) contained 10 mM Tris-HCl (*p*H 7.5), 50 mM NaCl, 1 mM dithiothreitol, 1 mM EDTA, 5% glycerol and 8 µg EW nuclear extract protein. Reactions 2–6 also contained 800, 1,600, 2,400, 3,200 and 4,000 ng, respectively, of poly(dI-dC)·poly(dI-dC). Reactions 7–11 contained 300, 600, 900, 1,200 and 1,500 ng, respectively, of *Hin*fI-digested *E. coli* chromosomal DNA. After 30 min incubation at room temperature, the resulting complexes were resolved in a low-ionic-strength 4% polyacrylamide gel (acrylamide : bisacrylamide weight ratio of 30 : 1) containing 6.7 mM Tris-HCl (*p*H 7.5), 3.3 mM Na-acetate and 1 mM Na-EDTA[13]. The gel was pre-electrophoresed for 30 min at ~11 V cm^{-1}. Electrophoresis was carried out at the same voltage gradient for 90 min at room temperature with buffer recirculation. The gel was then dried and autoradiographed at −70 °C with a screen. F and B indicate positions of free and bound fragments, respectively. *c*, Binding assays as detailed in *b* using 2,400 ng poly(dI-dC)·poly(dI-dC) and the following DNA fragments: κ *Sfa*NI/*Sfa*NI (~0.5 ng, 10,000 c.p.m., lane 1), κ *Pvu*II/*Kpn*I (~0.5 ng/10,000 c.p.m., lane 2), κ *Pvu*II/*Sfa*NI (~0.1 ng, 5,000 c.p.m., lane 3) and pSP64 *Pvu*II/*Eco*RI (~0.2 ng, 5,000 c.p.m., lane 4). The κ *Pvu*II/*Sfa*NI fragment was derived from the plasmid pSPIgV$_\kappa$ by digesting with *Pvu*II and *Eco*RI. The *Eco*RI site is in the polylinker and therefore this fragment contains 16 bp of polylinker sequence.

that binds to satellite DNA from a nuclear extract of monkey cells[13]. In the latter study an excess of heterologous competitor DNA (*Escherichia coli*) was included with the specific probe fragment to bind the more abundant nonspecific DNA binding proteins in the extract. To minimize the binding of sequence-specific proteins to such heterologous sequence competitor DNA, we tested as a replacement the simple alternating co-polymer duplex poly(dI-dC)·poly(dI-dC).

A radiolabelled *Sfa*NI/*Sfa*NI DNA fragment derived from the upstream region of the MOPC 41 κ light-chain gene (Fig. 1*a*) was incubated with a nuclear extract of a human B-cell line in the absence or presence of two competitor DNAs. The resulting complexes were resolved from the free fragment by electrophoresis through a low-ionic strength, non-denaturing polyacrylamide gel and visualized by autoradiography (Fig. 1*b*). In the absence of competitor DNA, all of the labelled fragment was retained at the top of the gel (Fig. 1*b*, lane 1), probably due to the binding of an excess of non-sequence-specific proteins. With addition of increasing amounts of either poly(dI-dC)·poly(dI-dC) (Fig. 1*b*, lanes 2–6) or *E. coli* chromosomal DNA (lanes 7–11) as competitors, putative protein–DNA complexes which migrated more slowly than the free fragment were detected. The relative abundance of the major species of complex (B) as well as that of minor species was significantly greater in the presence of the alternating co-polymer competitor DNA. Because substitution of the simple co-polymer considerably increased the sensitivity of the assay, it has been used in all subsequent binding analyses.

To test the sequence specificity of the major species detected in the binding assay, a set of mutually overlapping κ promoter fragments (Fig. 1*a*, *Sfa*NI/*Sfa*NI, *Pvu*II/*Kpn*I and *Pvu*II/*Sfa*NI) and a similar-length fragment derived from the bacterial plasmid SP64 (*Eco*RI/*Pvu*II) were individually assayed (Fig. 1*c*). Whereas the bacterial DNA fragment showed no appreciable binding (Fig. 1*c*, lane 4), all of the κ promoter fragments yielded major discrete complexes of similar mobilities (lanes 1–3). We have found that the mobilities of a series of complexes formed with different-length fragment probes (75–300 bp) are approximately the same (data not shown). These data therefore suggested the binding of a specific nuclear factor within the region of overlap of the κ promoter fragments. This region includes the conserved octameric sequence but not the TATA element. Note that with the smallest 75-bp κ promoter fragment (Fig. 1*c*, lane 3), no appreciable label was retained at the top of the gel. Thus, as has been noted recently, the use of small probe fragments further enhances the sensitivity of detection of specific protein–DNA complexes[18].

The sensitivity gained by using both the co-polymer and a small fragment probe permitted the detection of two complexes, B1 and B2 (Fig. 2*a*, lane 1). The major species, B1, corresponds to complex B in Fig. 1. The relative affinity of the factor(s) for κ promoter DNA was estimated by a competition assay (Fig. 2*a*). Whereas a control plasmid (pSP64), when added in the above incubation, failed to compete for binding in the concentration range tested (Fig. 2*a*, lanes 2–4), the recombinant plasmid (pSPIgV$_\kappa$) effectively reduced the formation of both B1 and B2 in the same range (lanes 5–7). The latter plasmid was constructed by insertion of the upstream region of the κ promoter into pSP64. Assuming that the pSPIgV$_\kappa$ plasmid contains a single high-affinity binding site, these results suggest that the nuclear factor(s) responsible for B1 and B2 has at least a 10^4-fold higher affinity for its cognate sequence than for heterologous plasmid DNA (see Fig. 2*a* legend).

To determine if the factor(s) responsible for the formation of B1 and B2 is specific to B lymphocytes, a nuclear extract derived from human HeLa cells was assayed for binding to the κ promoter probe (Fig. 2*b*). Both B1 and B2 were generated at similar levels by the HeLa extract to those observed with B-cell extracts (Fig. 2*b*, lane 1); furthermore, both were specifically competed for by the pSPIgV$_\kappa$ plasmid (lane 2). Thus, HeLa cells also contain a factor(s) which binds specifically to the κ promoter upstream region.

DNase I footprint analysis was used to delineate at a higher resolution the binding domain(s) of factor(s) present in complexes B1 and B2[19,20]. To facilitate these studies, the binding factor(s) from B cells was partially purified by chromatography of nuclear extract protein on a heparin-Sepharose column. Most of the binding activity eluted in a 0.25 M KCl step fraction, giving an approximately fivefold purification (data not shown; see Fig. 3 legend). For footprint analysis, after incubation of the partially purified factor(s) with the κ promoter probe, sufficient DNase I was added to produce a partial digestion of the DNA. The B1 and B2 species were then resolved from free fragment by polyacrylamide gel electrophoresis. Bound DNA was eluted from both B1 and B2 bands and examined by denaturing polyacrylamide gel electrophoresis (Fig. 3, lanes 2, 3 and 2',

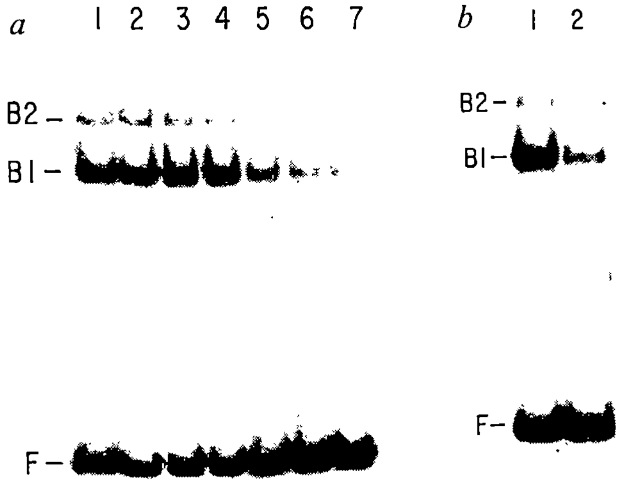

Fig. 2 Binding competition analysis in nuclear extracts of human EW and HeLa cells. ***a***, EW nuclear extract. Binding assays as detailed in Fig. 1*b* legend using radiolabelled κ *Pvu*II/*Sfa*NI fragment (~0.1 ng, 5,000 c.p.m.) and 2,400 ng poly(dI-dC)·poly(dI-dC). Reactions 2-4 additionally contained 50, 100 and 200 ng, respectively, of the bacterial plasmid pSP64 whereas reactions 5-7 contained 50, 100 and 200 ng, respectively, of the recombinant plasmid pSPIgV$_\kappa$. Assuming that a molecule of pSPIgV$_\kappa$ contains a single high-affinity site whereas a molecule of pSP64 (3,000 bp) contains 3,000 nonspecific sites, the apparent affinity ratio of the factor for these two types of sites is greater than $3{,}000\times200/50=1.2\times10^4$. ***b***, HeLa nuclear extract. Binding assays as detailed in Fig. 1*b* legend using radiolabelled κ *Pvu*II/*Sfa*NI fragment (~0.1 ng, 5,000 c.p.m.), 2,400 ng poly(dI-dC)·poly(dI-dC) and 6 μg HeLa nuclear extract protein[30] (provided by P. Grabowski). Reactions 1 and 2 additionally contained 100 ng of pSP64 and pSPIgV$_\kappa$, respectively.

3′). DNase I digests of the κ promoter probe in the absence of B-cell protein (Fig. 3, lanes 1 and 1′) and A+G chemical cleavage ladders were co-electrophoresed to map the binding domain. Factor(s) in the B1 complexes (Fig. 3, lanes 2 and 2′) appeared to protect a 19-nucleotide region on the coding strand. The 5′ and 3′ boundaries of the protected region map to positions −72 and −52, respectively, from the site of transcriptional initiation[3]. The region of DNase I protection was centred about the conserved octanucleotide sequence ATTTGCAT, suggesting its importance in the recognition of the immunoglobulin promoter by the nuclear factor. B2 complexes showed a virtually identical DNase I protection pattern to B1 complexes and therefore do not appear to involve additional DNA contacts (Fig. 3, lanes 3 and 3′). The simplest interpretation of this observation is that the B2 complex is generated by dimerization through protein-protein interactions of the factor responsible for the B1 complex. Alternatively, the B2 complex could be formed either by the binding of another protein to the factor responsible for the B1 complex or by recognition of the same set of sequences by a distinct DNA binding protein.

As the octamer sequence motif is present in both light- and heavy-chain gene promoters as well as in the enhancer elements of both mouse and human heavy-chain genes[15,21], we assayed for a factor binding to fragments from a mouse heavy-chain promoter (V_H) and the mouse heavy-chain enhancer. The V_H promoter fragment was derived from the 5′ region of the *V*17.2.25 gene and included nucleotides between positions −154 and +57 relative to the transcriptional start site[8]. In this promoter the conserved octanucleotide spans positions −57 to −50 (Fig. 4*a*). The heavy-chain enhancer fragment was derived from the germline joining-constant (J_H–C_μ) region and spanned positions 81–251 within a 313-bp region implicated in enhancer function[1]. The conserved octanucleotide is positioned between coordinates 166 to 173 in the above fragment (Fig. 4*a*). The B-cell heparin–Sepharose fraction (purified on the basis of binding to the κ promoter sequence; Fig. 4*b*, lane 1) produced a complex with both the V_H promoter fragment (lane 4) and the

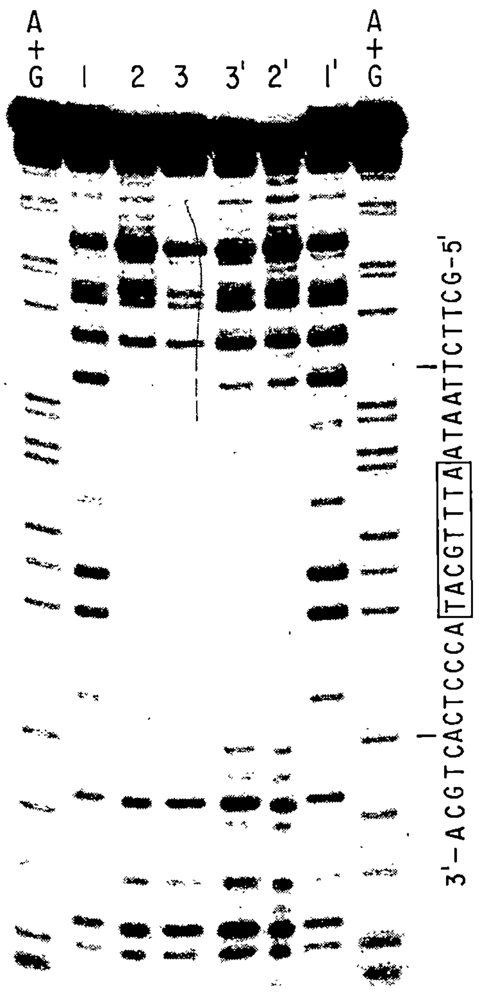

Fig. 3 DNase I footprinting of factor-DNA complexes. The B-cell nuclear extract was applied to a heparin–Sepharose column equilibrated with 20 mM HEPES *p*H 7.9, 20% glycerol, 1 mM dithiothreitol, 1 mM EDTA, 5 mM MgCl$_2$ and 0.1 M KCl. The κ-promoter binding factor was eluted with a 0.25 M KCl step. Binding reactions with this fraction (30 μl) contained 2.5 mM MgCl$_2$, κ *Pvu*II/*Sfa*NI (~1 ng, 100,000 c.p.m.) and 4,800 ng poly(dI-dC)·poly(dI-dC) in addition to components detailed in Fig. 1*b* legend. The coding strand of the κ promoter probe was 3′ end-labelled (*Eco*RI site) with [α-^{32}P]dATP using the large fragment of *E. coli* DNA polymerase. Reaction 1 was digested with DNase I (5 μg ml^{-1}) for 2.5 min at room temperature in the absence of B-cell nuclear protein. Reaction 2 was initially incubated with the heparin–Sepharose fraction of the EW nuclear factor (14 μg protein) for 15 min at room temperature and then digested with DNase I as above. Each reaction was stopped with EDTA (5 mM) and the products separated by native polyacrylamide gel electrophoresis as detailed for Fig. 1*b*. After autoradiography to visualize the various species, DNA was eluted from the free (reaction 1) and bound (B1 and B2, reaction 2) fragment bands by incubating gel slices in 0.5 M ammonium acetate (*p*H 7.5), 0.1% SDS and 1 mM EDTA with shaking at 37 °C overnight. The supernatants were extracted sequentially with phenol/chloroform/isoamylalcholol (25:24:1 v/v) and chloroform/isoamylalcohol (24:1 v/v) and precipitated with 2 vol ethanol in the presence of carrier transfer RNA. After a re-precipitation step, the products were analysed by separation in a 10% polyacrylamide gel (20:1) in the presence of 8 M urea followed by autoradiography at −70 °C with a screen. Lane 1 contains products of free fragment digestion from reaction 1. Lanes 2 and 3 contain digestion products eluted from bound fragment bands B1 and B2, respectively, from reaction 2. Lanes 1′, 2′ and 3′ correspond to 1, 2 and 3, respectively, except that the former set was digested with DNase I for 5 min. A+G chemical cleavage ladders[31] of the κ promoter probe were co-electrophoresed to map the binding domain.

a

V_L coding strand (-66) TC*TTAATA ATTTGCAT ACCCTC*AC

V_H non-coding strand (-50) CGCACATG ATTTGCAT ACTCATGA

J_H -C_μ coding strand (166) CCTGGGTA ATTTGCAT TTCTAAAA

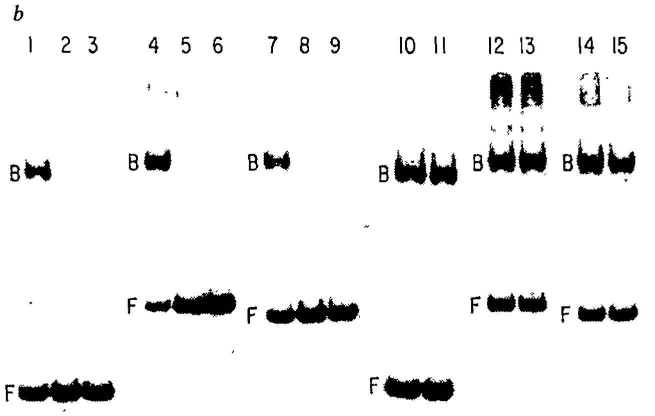

Fig. 4 Binding of a common nuclear factor to three immunoglobulin transcriptional control elements. *a*, Nucleotide sequences of actual and putative binding sites. The V_L binding site is defined by the DNase I protection assay (* indicates boundaries of the protected region). The V_H and J_H-C_μ sequence are putative binding sites in the *V*17.2.25 promoter[8] and the mouse heavy-chain enhancer[1], respectively. Numbers in parentheses indicate start coordinates of octamer motif. *b*, Binding competitions. Binding assays (10 μl) as detailed in Fig. 1*b* legend using 1,600 ng poly(dI-dC)·poly(dI-dC) and the heparin-Sepharose fraction of the EW nuclear factor (1.5 μg protein). V_L probe (~0.1 ng, 5,000 c.p.m.), lanes 1-3, 10, 11. V_H probe (~0.2 ng, 5,000 c.p.m.), lanes 4-6, 12, 13. J_H-C_μ probe (~0.2 ng, 5,000 c.p.m.), lanes 7-9, 14, 15. Lanes 2, 5, 8 additionally contained 5 ng of a V_L promoter oligomer (36 bp, spanning positions −81 to −44 of the MOPC-41 V_κ gene segment[3]) whereas lanes 3, 6, 9 contained 50 ng of the same oligomer. Lanes 11, 13, 15 additionally contained 50 ng of a J_H-C_μ oligomer that lacks the octamer motif (41 bp, spanning positions −1 to 40 of the heavy-chain enhancer[1,2]). Complementary single-stranded synthetic oligonucleotides were kindly made by Dr Ronald Mertz, Genzentrum der Universität München and Dr E.-L. Winnacker, Institut für Biochemie der Universität München. They were annealed before use as competition substrates in the binding assay.

enhancer fragment (lane 7). The mobilities of the complexes formed with the three fragments were very similar, consistent with the binding of a common factor. Furthermore, binding to these fragments was specifically competed for by a synthetic duplex 40-mer (Fig. 4*b* legend) that spanned the octanucleotide motif of the MOPC 41κ light-chain gene promoter (lanes 1-9). An oligomer of equivalent size containing a sequence from a region of the mouse heavy-chain enhancer lacking the octanucleotide motif (Fig. 4*b* legend) failed to compete for binding in the same concentration range (lanes 10-15). This competition analysis further strengthens the suggestion that a common nuclear factor (IgNF-A) binds to all three immunoglobulin transcriptional elements. As mentioned above these three transcriptional elements share an identical sequence motif, ATTTGCAT (Fig. 4*a*). Thus, the binding of a common nuclear factor is almost certainly mediated by this motif.

The use of a sensitive gel electrophoresis DNA binding assay in conjunction with the co-polymer competitor poly(dI-dC)·poly(dI-dC) has facilitated the identification of a putative mammalian gene regulatory factor. The simple alternating co-polymer probably competes less effectively than heterologous sequence DNA for binding of a sequence-specific factor, thereby significantly increasing the sensitivity of the assay. The synthetic co-polymer has proved similarly useful in the identification of other immunoglobulin enhancer binding factors (R.S. *et al.*, in preparation) and also a transcription factor that binds to an upstream sequence in the adenovirus major late promoter[22]. A further increase in sensitivity in this assay is obtained by the use of small DNA probes (<100 bp) which minimize nonspecific binding interactions in a crude extract[18]. Binding competitions and DNase I footprinting analysis can be used to test the affinity and sequence specificity of the protein-DNA complexes. In the future, relevant factors can be purified using this assay for structure-function analyses. Such an approach will greatly facilitate the elucidation of the set of DNA binding mammalian gene regulatory proteins.

The biological function(s) of IgNF-A and its biochemical mode(s) of action remain unknown. Since deletion or disruption of the IgNF-A binding site in immunoglobulin promoters significantly reduces the level of accurately initiated transcripts *in vivo*[5,7,15] and *in vitro* (R.S. *et al.*, in preparation), we propose that IgNF-A is a sequence-specific positive *trans*-acting factor. Its mode of action may be similar to the eukaryotic promoter-specific transcription factors Spl (refs 23) and heat-shock transcription factor (HSTF)[24].

The IgNF-A binding site seems to be a functional component of the B lymphocyte-specific immunoglobulin promoter[7]. For example, sequences from this promoter containing the IgNF-A binding site specify accurate transcription in B cells but not in HeLa cells. The role of IgNF-A in this B-cell specificity is unclear, since point mutations in the IgNF-A binding site have not been tested *in vivo* to determine whether this sequence is responsible for such specificity. IgNF-A may not be restricted to B cells, as a factor has been detected in HeLa cell extracts which generates complexes with similar mobilities and sequence specificity (as tested by competition analysis). However, further experiments will be necessary to show whether the factor in HeLa extracts is similar or identical to IgNF-A. Interestingly, the immunoglobulin octamer motif in the IgNF-A binding site has recently been shown to be present in the upstream region (about −225 bp) of vertebrate U1 and U2 small nuclear RNA genes[25-28]. More importantly, this element dramatically stimulates (20-50-fold) transcription of U2 snRNA genes in *Xenopus* oocytes[27,28]. Therefore, IgNF-A may be a constitutive activator protein that also functions in the high-level expression of U1 and U2 snRNA genes in vertebrate cells.

The presence of an IgNF-A binding site in the mouse heavy-chain enhancer is intriguing. It suggests the additional involvement of IgNF-A in enhancer function. Deletion of an 80-bp region of the enhancer containing the putative binding site reduces enhancer activity ~10-fold[1]. The occupation of this binding site, *in vivo*, has been inferred from the fact that the G residue in the enhancer octamer is protected from dimethyl sulphate modification only in cells of the B lineage[29]. Furthermore, IgNF-A also binds in a sequence-specific manner to the simian virus 40 enhancer (J. Weinberger, personal communication), which contains the immunoglobulin octamer motif[15], thereby strengthening the notion that the factor participates in enhancer function.

This work was supported by grants from NIH (R01-GM32467, R01-CA38660), partially from an NCI Cancer Center Support (core) (P30-CA14051), from NSF (PCM-8200309) to P.A.S. and by a grant from the American Cancer Society (IM-355Q) to D.B. H.S. is a fellow of the Jane Coffin Childs Memorial Fund for Medical Research. R.S. is a fellow of the Damon Runyon-Walter Winchell Cancer Fund. We thank Drs J. Weinberger and J. Lebowitz for helpful discussions and a critical reading of the manuscript.

Received 16 September; accepted 5 November 1985.

1. Banerji, T., Olson, L. & Schaffner, W. *Cell* **33**, 729-740 (1983).
2. Gillies, S. D., Morrison, S. L., Oi, V. T. & Tonegawa, S. *Cell* **33**, 717-728 (1983).
3. Queen, C. & Baltimore, D. *Cell* **33**, 741-748 (1983).
4. Picard, D. & Schaffner, W. *Nature* **307**, 80-82 (1984).
5. Bergman, Y., Rice, D., Grosschedl, R. & Baltimore, D. *Proc. natn. Acad. Sci. U.S.A.* **81**, 7041-7045 (1984).

6. Potter, H., Weir, L. & Leder, P. *Proc. natn. Acad. Sci. U.S.A.* **81,** 7161-7165 (1984).
7. Mason, J. O., Williams, G. T. & Neuberger, M. S. *Cell* **41,** 479-487 (1985).
8. Grosschedl, R. & Baltimore, D. *Cell* **41,** 885-897 (1985).
9. Falkner, F. G., Neumann, E. & Zachau, H. *Hoppe-Seyler's Z. physiol. Chem.* **365,** 1331-1334 (1984).
10. Foster, J., Stafford, J. & Queen, C. *Nature* **315,** 423-425 (1985).
11. Fried, M. & Crothers, D. M. *Nucleic Acids Res.* **9,** 6505-6525 (1981).
12. Garner, M. M. & Revzin, A. *Nucleic Acids Res.* **9,** 3047-3060 (1981).
13. Strauss, F. & Varshavsky, A. *Cell* **37,** 889-901 (1984).
14. Parslow, T. G., Blair, D. L., Murphy, W. J. & Granner, D. K. *Proc. natn. Acad. Sci. U.S.A.* **81,** 2650-2654 (1984).
15. Falkner, F. G. & Zachau, H. G. *Nature* **310,** 71-74 (1984).
16. Fried, M. G. & Crothers, D. M. *J. molec. Biol.* **172,** 241-262, 263-282 (1984).
17. Hendrickson, W. & Schleif, R. F. *J. molec. Biol.* **174,** 611-628 (1984).
18. Schneider, R., Dörper, Th., Gander, I., Mertz, R. & Winnacker, B.-L. *EMBO J.* (in the press).
19. Galas, D. & Schmitz, A. *Nucleic Acids Res.* **5,** 3157-3170 (1978).
20. Topol, J., Ruden, D. N. & Parker, C. S. *Cell,* **42,** 527-537 (1985).
21. Hayday, A. C. *et al. Nature* **307,** 334-340 (1984).
22. Carthew, R. W., Chodosh, L. A. & Sharp, P. A. *Cell* **43,** 439-448 (1985).
23. Dynan, W. S. & Tjian, R. *Cell* **32,** 669-680 (1983); **35,** 79-87 (1983).
24. Parker, C. S. & Topol, J. *Cell* **37,** 273-283 (1984).
25. Krol, A., Lund, E. & Dahlberg, J. E. *EMBO J.* **6,** 1529-1535 (1985).
26. Ciliberto, G., Buckland, R., Cortese, R. & Philipson, L. *EMBO J.* **6,** 1537-1543 (1985).
27. Ares, M. Jr, Mangin, M. & Weiner, A. M. *Molec. cell. Biol.* **5,** 1560-1570 (1985).
28. Mattaj, I. W., Leinherd, S., Jiricny, J. & DeRobertis, E. M. *Nature* **316,** 163-167 (1985).
29. Ephrussi, A., Church, G. M., Tonegawa, S. & Gilbert, W. *Science* **227,** 134-140 (1985).
30. Dignam, J. D., Lebovitz, R. M. & Roeder, R. G. *Nucleic Acids Res.* **11,** 1475-1489 (1983).
31. Maxam, A. & Gilbert, W. *Meth. Enzym.* **65,** 499-525 (1980).
32. Magrath, I. T. *et al. J. natn. Cancer Inst.* **64,** 465-476 (1980).

Activated human monocytes express the c-*sis* proto-oncogene and release a mediator showing PDGF-like activity

Yves Martinet, Peter B. Bitterman*, Jean-Francois Mornex*, Gary R. Grotendorst*, George R. Martin & Ronald G. Crystal

Pulmonary Branch, National Heart, Lung, and Blood Institute, and
Laboratory of Developmental Biology and Anomalies, National
Institute of Dental Research, National Institutes of Health, Bethesda,
Maryland 20892, USA

Current ideas about the mechanism of wound healing and the pathogenesis of atherosclerosis, pulmonary fibrosis and hepatic fibrosis suggest a central role for the mononuclear phagocyte in attracting and/or stimulating the proliferation of mesenchymal cells[1-5]. We demonstrate here that activated human blood monocytes, but not resting monocytes, release a mediator that attracts smooth muscle cells and cooperates with other mediators to stimulate fibroblast proliferation. This mediator is very similar to platelet-derived growth factor (PDGF): its chromatographic properties and chemical stability are similar to those of PDGF[6,7], it competes with ^{125}I-PDGF for binding to fibroblasts and it immunoprecipitates with anti-PDGF antibodies. In parallel, stimulated monocytes, but not resting monocytes, express the c-*sis* proto-oncogene, a gene coding for one of the PDGF chains[8,9], consistent with the concept that expression of the c-*sis* proto-oncogene may be involved in the ability of mononuclear phagocytes to modulate the accumulation of mesenchymal cells.

The idea that activated human blood monocytes release a mediator possessing PDGF-like activity evolved from the demonstration that blood monocytes can release a mediator that attracts smooth muscle cells (SMC) and cooperates with other mediators in stimulating fibroblasts to proliferate (Fig. 1). When activated, monocytes released into the media a mediator that attracted SMC in a concentration-gradient-dependent fashion. This was observed independently of the stimulus used; opsonized zymosan, immune complexes and lipopolysaccharide all activated monocytes to release this mediator in a time-dependent fashion, the activity increasing up to 4 h and then levelling off. In contrast, the release of SMC chemotactic activity by unstimulated cells was minimal. The release of the SMC chemotactic signal by stimulated monocytes was completely inhibited by cycloheximide (not shown), suggesting it was synthesized by monocytes in response to the activation stimulus. Following partial purification by carboxymethyl-cellulose and blue-Sepharose chromatography, the monocyte mediator with SMC chemotactic activity was also demonstrated to have growth activity for human diploid lung fibroblasts and BALB/c-3T3 fibroblasts. Importantly, the growth factor activity had characteristics of a competence factor, that is, although it did not by itself stimulate the growth of fibroblasts, it did so in the presence of the progression factor insulin. Furthermore, in all samples, this paralleled the chemotactic activity for SMC.

Table 1 Biochemical characteristics of the mediator released by activated monocytes

Conditions	% Activity
Heat (100 °C, 10 min)	80 ± 4
Acid (*p*H 2.5, 22 °C, 30 min)	63 ± 5
Reduction (2 mM 2-mercaptoethanol, 22 °C, 30 min)	0
Trypsin (5×10^{-6} M, 37 °C, 30 min)	24 ± 2

Monocytes were cultured with lipopolysaccharide B (LPS) for 24 h at 37 °C, and the supernatant was tested for SMC chemotactic activity as indicated in Fig. 1*a*. Before exposure to various treatments, the supernatant chemotactic activity was equal to 290 ± 37 chemotactic units. Aliquots (1 ml) were exposed to various experimental conditions and the chemotactic activity was quantified as the per cent activity before any treatment. Heat stability was evaluated by boiling the monocyte supernatant for 10 min, cooling to 23 °C and then testing for chemotactic activity. Acid stability was determined by dialysing 1 ml of the monocyte supernatant overnight against 0.5 M acetic acid, lyophilizing and redissolving it with HCl (to a final molarity of 10 mM) before diluting in culture media for testing for chemotactic activity. Sensitivity to reduction was evaluated by dialysing the monocyte supernatant overnight against 100 mM Tris-HCl *p*H 8.0; 2-mercaptoethanol was then added and the supernatant incubated for 30 min. The supernatant was then dialysed against culture medium overnight and tested for chemotactic activity. Sensitivity to trypsin was evaluated by adding trypsin (100 μg, Worthington) to 1 ml of monocyte supernatant. After 30 min at 37 °C, soybean trypsin inhibitor (200 μg, Worthington) was added and the supernatant tested for chemotactic activity. At the concentration used, the soybean trypsin inhibitor mixture with or without trypsin did not alter the activity of the original monocyte supernatant. All studies were performed in triplicate and the data are presented as mean ± s.d.

Although several biological compounds are known to be chemotactic for mesenchymal cells[10], only two, PDGF[11] and fibronectin[12], are known also to have growth-competence activity for fibroblasts. Mononuclear phagocytes produce fibronectin, but when the supernatant from activated monocytes was chromatographed on gelatin-Sepharose to remove fibronectin, none of the SMC chemotactic activity was removed. Furthermore, the chemotactic activity present in conditioned media was not inhibited by the addition of antibodies to fibronectin (not shown). Finally, the conclusion that this monocyte mediator possessing SMC chemotactic activity and growth-competence activity was not fibronectin is consistent with the finding that activated human blood monocytes release maximal amounts of the PDGF-like molecule within 4 h of culture but release significant amounts of fibronectin only after 48 h of culture[13].

Further evidence that this monocyte mediator is PDGF-like came from: (1) its behaviour following exposure to various conditions (Table 1); it was resistant to heat and acid, but was sensitive to proteolysis and its activity was completely abolished by reduction, suggesting that it required disulphide bonding for biological activity. (2) It displaced PDGF from its receptors on fibroblasts (Fig. 2). (3) When added to an anti-PDGF antibody, supernatant from activated monocytes as well as the partially purified factor displaced ^{125}I-PDGF from the antibody in a similar pattern to PDGF (undiluted supernatant from activated

---

* Present addresses: University of Minnesota, Minneapolis, Minnesota 55455, USA (P.B.B.); Hôpital Louis Pradel, 69394 Cedex 3, Lyon, France (J.-F.M.); Medical University of South Carolina, Charleston, South Carolina 29425, USA (G.R.G.).

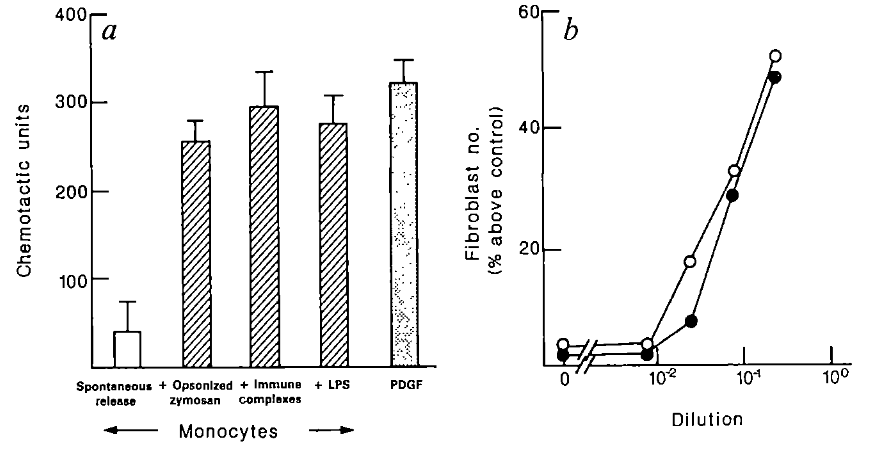

Fig. 1 Release of a mediator showing PDGF-like activity by activated human blood monocytes. *a*, Activated monocytes release a mediator possessing chemotactic activity for smooth muscle cells (SMC). *b*, Demonstration that the mediator with chemotactic activity for smooth muscle cells also exhibits PDGF-like growth activity for fibroblasts. The figure shows the number of fibroblasts (as % above the control of DMEM alone) with dilutions of the partially purified monocyte mediator (●) (starting concentration 50 μg protein per ml) or with dilutions of PDGF (○; starting concentration 25 ng ml^{-1}). Culture with the monocyte mediator alone, insulin alone or PDGF alone yielded no growth. All data points represent duplicates. Confirmation of the PDGF-like growth activity of the monocyte mediator was obtained by autoradiographic demonstration of ^3H-thymidine incorporation into nuclei of confluent BALB/c-3T3 (clone A-31; American Type Culture Collection CCL 163) in the presence of partially purified monocyte mediator and 50 μg ml^{-1} insulin (not shown).

Methods. ***a***, Monocytes were obtained by plating (plastic dish, 30 min, 37 °C) mononuclear cells isolated from blood by Hypaque–Ficoll centrifugation. Adherent cells (99% mononuclear cells, >87% monocytes) were cultured (4×10^6 cells ml^{-1}, 24 h, 37 °C) in Dulbecco's modified Eagle's medium (DMEM). In parallel cultures various stimuli were added: opsonized zymosan (zymosan A particles, Sigma; 10 particles per cell), immune complexes (human and rabbit anti-human albumin, Cappel; final protein concentration of 20 μg ml^{-1}) 1 LPS (*Escherichia coli* 0127; B8, Difco; 10 μg ml^{-1}). After culture (24 h, 37 °C), supernatants were collected and tested for chemotactic activity for SMC using a modified Boyden chamber[32]. SMC grown from explants of the medial layer of fetal bovine aortas[33] were suspended (4×10^5 cells ml^{-1}) in DMEM and placed in the upper wells; lower wells contained the supernatants to be tested. The filters (polycarbonate, 8 μm diameter pore size, Neuro Probe) were coated (72 h, 22 °C) with type V collagen obtained from human placental membranes. After incubation (4 h, 37 °C), the filters were removed, the cells were fixed and stained with Diff-Quik (American Scientific Products) and numbers of migrating SMC were determined[32] Each sample was tested in duplicate. The results (mean ± s.d. for 3 experiments) represent the value for each condition minus the chemotactic activity in response to DMEM alone. None of the stimuli by themselves had chemotactic activity. The attraction of the SMC by monocyte supernatants was demonstrated by checkerboard analysis to be concentration-gradient dependent, that is, chemotactic. Purified PDGF (5 ng ml^{-1})[34–37] was used as a positive control. For the monocyte supernatants, the data are presented as chemotactic units present in supernatant of 10^6 monocytes cultured for 24 h. ***b***, Monocyte supernatant obtained by culture of blood monocytes with LPS was dialysed for 48 h against 10 mM NaCl, 35 mM Na citrate, *p*H 7.0, and mixed overnight with carboxymethyl-cellulose (CMC, CM 52, Whatman). The CMC was then packed in a column, washed and eluted with a linear gradient (10 mM–1 M NaCl). The SMC chemotactic activity eluted with the front of the protein peak at 0.35 M NaCl. All active fractions were pooled and applied on a blue-Sepharose column (Affi-Gel Blue; Bio-Rad) which was eluted with 1 M NaCl, 35 mM Na citrate, *p*H 7.0, v/v ethylene glycol/H_2O. In parallel with SMC chemotactic activity, the growth activity for fibroblasts in this eluate was evaluated by a complementation test[11] using diploid human lung fibroblasts (HFL-1, American Type Culture Collection CCL 153)[38]. Non-cycling fibroblasts (culture in DMEM plus 0.4% calf serum for 4 days with an additional day in DMEM) were placed in DMEM with progressive dilutions of the blue-Sepharose eluate or PDGF in the presence of insulin (50 μg ml^{-1}; Collaborative Research). The fibroblasts were incubated for 3 days and then counted.

monocytes contained 10 ng ml^{-1} of the PDGF-like mediator; not shown).

The concept that activated monocytes release a PDGF-like mediator corresponds with the observation by Shimokado *et al.*[14] that activated macrophages secrete a PDGF-like molecule. Furthermore, it is consistent with various observations concerning the role of monocytes and their progeny in certain physiological and pathological situations. First, the classical description of wound healing includes the recruitment of monocytes to the wound, followed by the local accumulation and proliferation of mesenchymal cells. Consistent with the view that monocytes are central to this process, Leibovich and Ross[1] observed marked suppression of wound healing in animals depleted of mononuclear phagocytes. Second, in human fibrotic disorders, the accumulation and proliferation of mesenchymal cells and the subsequent formation of scar are invariably preceded by the accumulation of mononuclear phagocytes[4,5]. Third, animal models of atherosclerosis demonstrate the subendothelial accumulation of monocytes, followed by the recruitment of SMC and the development of the atherosclerotic plaque[2,3]. Finally, *in vitro* studies have shown that activated monocytes release 'monocyte-derived growth factor'[15], which possesses growth-competence activity for fibroblasts.

Since one of the PDGF chains (PDGF-2, B chain or peptide I) is encoded by the c-*sis* proto-oncogene (a gene on chromosome 22)[8,9], the fact that activated monocytes release a PDGF-like molecule suggests that monocyte activation is associated with the expression of c-*sis*. Consistent with this, we found that hybridization of monocyte poly$(A)^+$ RNA with a ^{32}P-labelled probe containing exons 6 and 7 of c-*sis* revealed the presence of a 4.2-kilobase (kb) c-*sis* messenger RNA transcript in activated but not in resting monocytes (Fig. 3). In contrast, using a probe for the γ-actin gene, we found that both resting and activated monocytes express the γ-actin gene 2.0-kb mRNA transcript, consistent with the knowledge that the γ-actin gene is expressed in all cell types[16].

The fact that human monocytes, when activated, express the

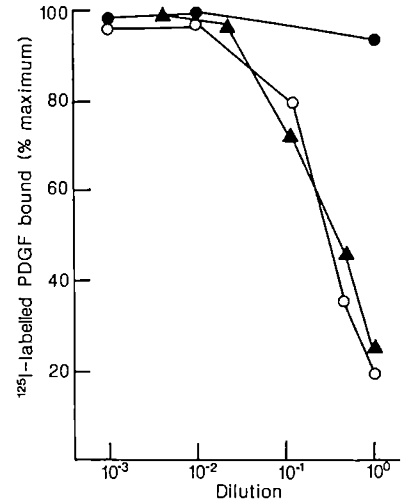

Fig. 2 Competition of the partially purified monocyte-derived factor with ^{125}I-labelled PDGF for binding to fibroblasts. Pure PDGF (1 μg) was labelled with ^{125}I using the chloramine-T procedure of Hunter *et al.*[39] and separated from free iodine by gel filtration on a PD-10 column (Pharmacia) previously equilibrated with 1 M acetic acid (titrated to *p*H 3.5 with NH_4OH) containing 1 mg ml^{-1} bovine serum albumin (BSA). The ^{125}I-labelled PDGF has a specific activity of 2×10^4 d.p.m. per ng. Receptor binding studies were performed as described by Heldin *et al.*[40]. BALB/c-3T3 fibroblasts (clone A-31; American Type Culture Collection CCL 163) were cultured for 5 days in DMEM with 10% calf serum in 24-well Falcon dishes (Becton-Dickinson) at which time they exhibited density arrest of growth. The cells were washed twice with binding medium (2 mM $CaCl_2$, 1 mM $MgSO_4$, 1 mg ml^{-1} BSA in phosphate-buffered saline (PBS)) and incubated with 5 ng (10^5 d.p.m.) of ^{125}I-PDGF containing: (1) progressive dilutions of non-labelled PDGF (○, starting concentration 1 μg ml^{-1}); (2) partially purified monocyte-derived factor (CMC, followed by blue-Sepharose, see Fig. 1*b* legend) (▲, starting concentration 400 μg ml^{-1}); (3) fibroblast growth factor (●, starting concentration 1 μg ml^{-1}, Collaborative Research) as a control After incubation (90 min, 22 °C) the cells were washed four times with washing media (2 mM $CaCl_2$, 1 mM $MgSO_4$, 1% calf serum in PBS) and lysed with lysing media (1% Triton X-100, 10% glycerol, 1 mg ml^{-1} BSA in 20 mM HEPES, *p*H 7.4). The bound ^{125}I-labelled PDGF activity was then quantified using a γ counter. All binding assays were done in duplicate; the data shown represent the mean values for three experiments.

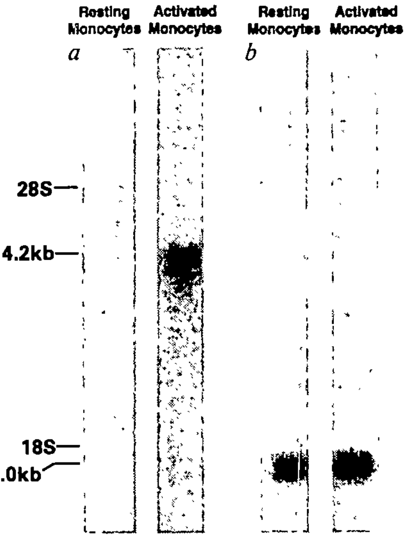

Fig. 3 Expression of the c-*sis* proto-oncogene in human monocytes. *a*, Presence of c-*sis* transcripts in activated monocytes; *b*, presence of γ-actin mRNA transcripts in both resting and activated monocytes.
Methods. Blood monocytes were cultured for 24 h with or without LPS (see Fig. 1*a* legend). After incubation, the cells were washed three times at 4 °C in PBS, *p*H 7.4, collected with a rubber policeman and pelleted by centrifugation (2,000*g*, 5 min). The cell pellet was homogenized in guanidine hydrochloride and subjected to ultracentrifugation through a caesium chloride cushion[41]. Total RNA was enriched for poly(A)$^+$ RNA by one cycle of oligo(dT)-cellulose affinity chromatography[42]. The poly(A)$^+$ RNA (5 μg each lane) samples were subjected to electrophoresis in a 1.1% agarose formaldehyde gel[43] and transferred to a nitrocellulose filter. The filter was hybridized with probes radioactively labelled with ^{32}P by nick-translation[44]. Hybridization and washing conditions were as described by Thomas[45]. RNA sizes were determined by comparison with human (28S, 18S) ribosomal RNA. The c-*sis* probe was clone pL335, a subclone of λ-L33 containing exons 6 and 7 of the human c-*sis* locus[17] kindly provided by E. Gelmann (NCI). The autoradiogram was exposed for 72 h. For *b*, the same filter as in *a* was used. After being allowed to undergo several half-lives of ^{32}P decay of the c-*sis* probe, the filter was hybridized to a human fibroblast cytoplasmic γ-actin cDNA (plasmid pHFγA-1)[46] kindly provided by L. Kedes (Stanford University). The autoradiogram was exposed for 8 h.

c-*sis* proto-oncogene in parallel with the release of a molecule showing PDGF-like activity is of interest in view of the known relationship of c-*sis* to the v-*sis* homologous sequences in the simian sarcoma transforming retrovirus[17], which induces NIH 3T3 fibroblasts and normal rat kidney cells to produce p28$^{v\text{-}sis}$ (ref. 18), a protein of relative molecular mass 28,000 showing close homology to one of the PDGF chains[19–21]. Since PDGF is a growth factor that induces its target cells to enter the G$_1$ phase of the cell cycle[11], the finding that a transforming virus contains sequences encoding a protein similar to one of the PDGF chains, and that the normal human genome contains sequences with >90% homology with p28$^{v\text{-}sis}$, has important implications for the initial events leading to malignancy. Consistent with these observations, a PDGF-like molecule has been detected in the culture media of human sarcoma[22] and glioma[23] and these cells express c-*sis* mRNA transcripts[24,25].

In addition to implications of the activation of c-*sis* for malignant growth, there is preliminary evidence that this proto-oncogene is involved in normal cell growth. In this context, cultured human and bovine endothelial cells express c-*sis*[26,27] and release a PDGF-like molecule[28], while rat arterial SMC release a PDGF-like protein[29]. Furthermore, using *in situ* hybridization, Goustin *et al.*[30] have recently demonstrated the presence of c-*sis* transcript in the cytotrophoblast of first-trimester human placenta in parallel with the release of a PDGF-like growth activity in the culture media. The present study extends these findings by demonstrating that c-*sis* proto-oncogene expression and release of a PDGF-like molecule occur in the activated human monocyte, a cell of major importance in scar formation and human fibrotic disorders as well as the early development of atherosclerotic plaque. These observations support the theory that common mechanisms are involved in the 'controlled' proliferation of cells involved in normal growth, the 'semi-controlled' proliferation of cells involved in the chronic inflammatory disorders, and the 'uncontrolled' proliferation of malignant cells.

We thank E. Gelmann, G. Wilding, N. Davidson and C. Agnor for help in carrying out this project and la Fondation pour la Recherche Médicale (for Y.M.) and Ministère des Relations Exterieures, France (for J.-F.M.) for partial financial support. *Note added in proof*: Since submission of this manuscript, Shimokado *et al.*[31] have also demonstrated that macrophages express c-*sis* and produce PDGF.

Received 25 July; accepted 18 October 1985.

1. Leibovich, S. J. & Ross, R. *Am. J. Path.* **78,** 71–100 (1975).
2. Gerrity, R. G. *Am. J. Path.* **103,** 181–190 (1981).
3. Faggiotto, A., Ross, R. & Harker, L. *Arteriosclerosis* **4,** 323–340 (1984).
4. Crystal, R. G., Bitterman, P. B., Rennard, S. I., Hance, A. J. & Keogh, B. A. *New Engl. J. Med.* **310,** 154–166; 235–244 (1984).
5. Kent, G. *et al. Proc. natn. Acad. Sci. U.S.A.* **73,** 3719–3722 (1976).
6. Westermark, B. *et al.* in *Growth and Maturation Factors* Vol. 1 (ed. Guroff, G.) 73–115 (Wiley, New York, 1983).
7. Deuel, T. F. & Huang, J. S. *J. clin. Invest.* **74,** 669–676 (1984).
8. Johnsson, A. *et al. EMBO J.* **3,** 921–928 (1984).
9. Chiu, I. M. *et al. Cell* **37,** 123–129 (1984).
10. Grotendorst, G. R., Pencev, D., Martin, G. R. & Sodek, J. in *Soft and Hard Tissue Repair* (eds Hunt, T. K., Heppenstall, R. B., Pines, E. & Rovee, D.) 20–40 (Praeger, New York, 1984).
11. Pledger, W. J., Stiles, C. D., Antoniades, H. N. & Scher, C. D. *Proc. natn. Acad. Sci. U.S.A.* **74,** 4481–4485 (1977).
12. Bitterman, P. B., Rennard, S. I., Adelberg, S. & Crystal, R. G. *J. Cell Biol.* **97,** 1925–1932 (1983).
13. Alitalo, K., Hovi, T. & Vaheri, A. *J. exp. Med.* **151,** 602–613 (1980).
14. Shimokado, K., Raines, E. W., Madtes, D. K. & Ross, R. *J. Leukocyte Biol.* **37,** 742–743 (1985).
15. Leibovich, S. J. & Ross, R. *Am. J. Path.* **84,** 501–514 (1976).
16 Firtel, R. A. *Cell* **24,** 6–7 (1981).
17 Dalla Favera, R., Gelmann, E. P., Gallo, R. C. & Wong-Staal, F. *Nature* **292,** 31–35 (1981).
18. Devare, S. G., Reddy, E. P., Law, J. D., Robbins, K. C. & Aaronson, S. A. *Proc. natn. Acad. Sci. U.S.A.* **80,** 731–735 (1983).
19. Doolittle, R. F. *Science* **221,** 275–277 (1983).
20. Waterfield, M. D. *et al. Nature* **304,** 35–39 (1983).
21. Robbins, K. C., Antoniades, H. N., Devare, S. G., Hunkapiller, M. W. & Aaronson , S. A. *Nature* **305,** 605–608 (1983).
22. Heldin, C. H., Westermark, B. & Wasteson, Å. *J. cell. Physiol.* **105,** 235–246 (1980).
23. Nistér, M., Heldin, C. H., Wasteson, Å. & Westermark, B. *Ann. N.Y. Acad. Sci.* **397,** 25–33 (1982).
24. Eva, A. *et al. Nature* **295,** 116–119 (1982).
25. Graves, D. T. *et al. Science* **226,** 972–974 (1984).
26. Barrett, T. B., Gajdusek, C. M., Schwartz, S. M., McDougall, J. K. & Benditt, E. P. *Proc. natn. Acad. Sci. U.S.A.* **81,** 6772–6774 (1984).
27. Jaye, M. *et al. Science* **228,** 882–885 (1985).
28. DiCorleto, P. E. & Bowen-Pope, D. F. *Proc. natn. Acad. Sci. U.S.A.* **80,** 1919–1923 (1983).
29. Nilsson, J., Sjölund, M., Palmberg, L., Thyberg, J. & Heldin, C. H. *Proc. natn. Acad. Sci. U.S.A.* **82,** 4418–4422 (1985).
30. Goustin, A. S. *et al. Cell* **41,** 301–312 (1985).
31. Shimokado, K. *et al. Cell* **43,** 277–286 (1985).
32. Bleiberg, I., Harvey, A. K., Smale, G. & Grotendorst, G. R. *J. cell. Physiol.* **123,** 161–166 (1985).
33. Ross, R. *J. Cell Biol.* **50,** 172–186 (1971).
34. Antoniades, H. N., Scher, C. D. & Stiles, C. D. *Proc. natn. Acad. Sci. U.S.A.* **76,** 1809–1813 (1979).
35. Deuel, T. F. *et al. J. biol. Chem.* **256,** 8896–8899 (1981).
36. Heldin, C. H., Westermark, B. & Wasteson, Å. *Biochem. J.* **193,** 907–913 (1981).
37. Raines, E. W. & Ross, R. *J. biol. Chem.* **257,** 5154–5160 (1982).
38. Bitterman, P. B., Rennard, S. I., Hunninghake, G. W. & Crystal, R. G. *J. clin. Invest.* **70,** 806–822 (1982).
39. Hunter, W. M. & Greenwood, F. C. *Nature* **194,** 495–496 (1962).
40. Heldin, C. H., Westermark, B. & Wasteson, Å. *Proc. natn. Acad. Sci. U.S.A.* **78,** 3664–3668 (1981).
41. Glisin, V., Crkvenjakov, R. & Byus, C. *Biochemistry* **13,** 2633–2637 (1974).
42. Aviv, H. & Leder, P. *Proc. natn. Acad. Sci. U.S.A.* **69,** 1408–1412 (1972).
43. Lehrach, H., Diamond, D., Wozney, J. M. & Boedtker, H. *Biochemistry* **16,** 4743–4751 (1977).
44. Rigby, P. W. J., Dieckmann, M., Rhodes, C. & Berg, P. *J. molec. Biol.* **113,** 237–251 (1977).
45. Thomas, P. S. *Proc. natn. Acad. Sci. U.S.A.* **77,** 5201–5205 (1980).
46. Gunning, P. *et al. Molec. cell. Biol.* **3,** 787–795 (1983).

Erratum

A closely linked genetic marker for cystic fibrosis

Ray White, Scott Woodward, Mark Leppert, Peter O'Connell, Yusuke Nakamura, Mark Hoff*, John Herbst†, Jean-Marc Lalouel, Michael Dean & George Vande Woude

Nature **318,** 382–384 (1985).

IN this letter, one of the authors' names was omitted (Y.N.). Yusuke Nakamura is at the Howard Hughes Medical Institute.

BOOKS RECEIVED

Mathematics

Analytical and Numerical Methods for Volterra Equations. By PETER LINZ. *Wiley: 1985. Pp.227. ISBN 0-89871-198-3. £28.25.*

Applied Linear Regression, 2nd Edition. By SANFORD WEISBERG. *Wiley: 1985. Pp.324. Hbk ISBN 0-471-87957-6. £35.75.*

The Beauty of Doing Mathematics: Three Public Dialogues. By SERGE LANG. *Springer-Verlag: 1985. Pp.127. Pbk ISBN 3-540-96149-6. DM 66.*

Computational Methods for Integral Equations. By L.M. DELVES and J.L. MOHAMED. *Cambridge University Press: 1985. Pp.376. Hbk ISBN 0-521-26629-7. £35, $69.50.*

Dynamical Problems in Soliton Systems. S. TAKENO (ed.). *Springer-Verlag: 1985. Pp.281. ISBN 3-540-15372-1/0-387-15372-1. DM 89.*

The Elements of Graphic Data. By WILLIAM S. CLEVELAND. *Wadsworth: 1985. Pp.323. Pbk ISBN 0-534-03730-5. Hbk $27.95; pbk £18.95.*

Encyclopedia of Statistical Sciences. Vol. 6 Multivariate Analysis — Plackett and Burman Designs. S. KOTZ, N.L. JOHNSON AND C.B. READ (eds). *Wiley: 1985. Pp.758. ISBN 0-471-05553-0. £74.*

Parallel Sorting Algorithms. By SELIM G. AKL. *Academic: 1985. Pp.229. Hbk ISBN 0-12-047680-0. £43.50, $49.50.*

Recursive Estimation and Control for Stochastic Systems. By HANS-FU CHEN. *Wiley: 1985. Pp.378. ISBN 0-471-81566-7. £46.20.*

Solving Equations with Physical Understanding. By J.R. ACTON and P.T. SQUIRE. *Adam Hilger: 1985. Pp.219. Hbk ISBN 0-85274-757-8; pbk ISBN 0-85274-789-5. Hbk £24, $36; pbk £12.95, $19.*

Statcalc. By T.J. BROWNE and R.B.G. WILLIAMS. *Macmillan: 1985. BBC Model B 40 Track. ISBN 0-333-39598-0. £26.50.*

Astronomy

Astronomy From Space. G.G FAZIO, J.A.M. BLEEKER, P.A.J. DE KORTE and J.J. CALDWELL (eds). *Pergamon Press:1985. Pp.212. Pbk ISBN 0-08-033192-0. Pbk £31, $49.50.*

Astronomy with a Small Telescope. By JAMES MUIRDEN. *George Philip, 12–14 Long Acre, London WC2E, UK:1985. Pp.224. Hbk ISBN 0-540-01088-X. £9.95.*

The Case for Mars II. Vol. 62, Science and Technology Series. CHRISTOPHER P. MCKAY (ed.). *Published for the American T Astronautical Society by Univelt, Inc., P.O. Box 28130, San Diego, California, USA:1985. Pbk ISBN 0-87703-220-3. Np.*

Europe/United States Space Activities, 23rd Goddard Memorial Symposium, 19th European Space Symposium. PETER M. BAINUM and FRIEDRICH VON BUN (eds). *Published for the American Astronautical Society by Univelt, Incorp., P.O. Box 28130, San Diego, California, USA: 1985. Np.*

Guidance and Control 1985. Vol. 57 Advances in the Astronautical Sciences. ROBERT D. CULP, EDWARD J. BAUMAN and CHARLES A. CULLIAN (eds). *American Astronautical Society:1985. Pp.601. ISBN Hbk 0-87703-211-4; pbk ISBN 0-87703-212-2. Hbk $65; pbk $50.*

Space Debris, Asteroids and Satellite Orbits. D.J. KESSLER, E. GRUN and L. SEHNAL (eds). *Pergamon: 1985. Pp.229. Pbk ISBN 0-08-033189-0. Pbk £31, $49.50.*

A Spacefaring People: Perspectives on Early Spaceflight. By ALEX ROLAND. *Scientific and Technical Information Branch, National Aeronautics nd Space Administration, Washington, USA: 1985. Pp.156. Pbk. Np.*

Spherical Astronomy. By ROBIN M. GREEN. *Cambridge University Press:1985. Pp.520. Hbk ISBN 0-521-23988-5; pbk ISBN 0-521-31779-7. Hbk £40, $69.50; pbk £15, $27.95.*

The Universe. By IAIN NICOLSON and PATRICK MOORE. *Collins:1985. Pp.248. Hbk ISBN 0-00-217397-2. £15.*

Vistas in Astronomy: An International Review ournal. Vol. 28, Parts 1,2. P. BEER, A.J. MEADOWS and A.E. ROY (eds). *Pergamon:1985. Pp.404. £50, $81.*

Physics

Clustering Aspects of Nuclear Structure. J.S. LILLEY and M.A. NAGARAJAN (eds). *Reidel, The Netherlands:1985. Pp.420. Hbk ISBN 90-277-2002-9. Dfl. 160, £44.50, $54.*

Electronic Properties of Polymers and Related Compounds. H. KUZMANY, M. MEHRING and S. ROTH (eds). *Springer-Verlag:1985. Pp.354. ISBN 3-540-15722-0/0-387-15722-0. DM 89.*

Groups Theory in Physics. By WU-KI TUNG. *Wiley:1985. Pp.344. Pbk ISBN 9971-966-57-3. £17.45.*

Highlights of Condensed-Matter Theory. F. BASSANI, F.G. FUMI and M.I. TOSI (eds). *North-Holland Physics Publishing, P.O. Box 103, 1000 AC Amsterdam, The Netherlands:1985. Pp.916. Hbk ISBN 0-444-86976-X. Dfl. 340.*

High-Power Laser Radiation in Atmospheric Aerosols. By V.E. ZUEV, A.A. ZEMLYANOV, YU. D. KOPYTIN and A.V. KUZIKOVSKII. *Reidel:1985. Pp.291. Hbk ISBN 90-277-1736-2. Np.*

High-Resolution Spectroscopy of Transient Molecules. By EIZI HIROTA. *Springer-Verlag:1985. Pp.233. ISBN 3-540-15302-0. DM 125.*

Large-Scale Computations in Fluid Mechanics. BJORN E. ENGQUIST, STANLEY OSHER and RICHARD C.J. SOMERVILLE (eds). *American Mathematical Society:1985. Pp.409. ISBN 0-8218-1122-3. $110.*

Microcomputer Quantum Mechanics, 2nd Edn. By J.P. KILLINGBECK. *Adam Hilger:1985. Pp.187. ISBN 0-85274-803-5. £12.95, $20.*

Modern Electronics and Integrated Circuits. By B.J. STANIER. *Adam Hilger:1985. Pp.152. Hbk ISBN 0-85274-550-8; pbk ISBN 0-85274-552-4. Hbk £20, $32; pbk £10, $15.*

Optical Bistability: Controlling Light with Light. By HYATT M. GIBBS. *Academic:1985. Pp.471. Hbk ISBN 0-12-281940-3. £47.50, $54.50.*

Physics and Contemporary Needs, Vol. 7. M.N. QAZI (ed.). *Wiley:1985. Pp.296. Hbk ISBN 9971-966-83-2. £42.30.*

Physics of Dense Matter. By Y.C. LEUNG. *Wiley: 1985. Pp.268. ISBN 9971-978-10-5. £38.10.*

Plasma Physics. By R.A. CAIRNS. *Blackie:1985. Pp.193. Hbk ISBN 0-216-91779-4; pbk ISBN 0-216-91783-2. Hbk £19.95; pbk £9.95.*

Plasma Polymerization. By H. YASUDA. *Academic:1985. Pp.432. ISBN 0-12-768760-2. $62, £62.*

Polarized Electrons at Surfaces. By J. KIRSCHNER. *Springer-Verlag:1985. Pp.158. ISBN 3-540-15003-X/0-387-15003-X. DM 69.*

Polarized Light in Nature. By G.P. KÖNNEN. *Cambridge University Press:1985. Pp.172. ISBN 0-521-25862-6. £19.50, $32.50.*

Problems in Perturbation. By ALI HASAN NAYFEH. *Wiley:1985. Pp.556. ISBN 0-471-82292-2. £40.85.*

Pseudopotential Theory of Atoms and Molecules. By LEVENTE SZASZ. *Wiley:1985. Pp.309. Hbk ISBN 0-471-82417-8. £56.20.*

Response and Stability. An Introduction to the Physical Theory. By A.B. PIPPARD. *Cambridge University Press:1985. Pp.228. Hbk ISBN 0-521-26673-4; pbk ISBN 0-521-31994-3. Hbk $49.50, £27.50. Pbk $17.95. £9.95.*

Solar Radiophysics. D.J. McLEAN and N.R. LABRUM. *Cambridge University Press:1985. Pp.516. ISBN 0-521-25409-4. £35, $59.50.*

Solid State Physics, 2nd Edn. By J.S. BLACKMORE. *Cambridge University Press:1985. Pp.506. Hbk ISBN 0-521-30932-8; pbk ISBN 0-521-31391-0. Hbk £27.95, $40.00; pbk £9.95.*

A Survey of the Spherical Space Form Problem. By J.F. DAVIS and R.J. MILGRAM. *Harwood:1985. Pp.283. Pbk ISBN 3-7186-0250-4. Pbk $19.*

The Theory of Constancy Through Relativity by Means of Light Dynamics. By SHRI RAM SAGAR. *Shri Ram Sagar, Balajipura, Amalner-425 401, Dist-Jalgaoner (M.S.), India:1985. Pp.125. Rs 30.*

Thermal Conductivity 18. T. ASHWORTH and DAVID R. SMITH (eds). *Plenum:1985. Pp.764. ISBN 0-306-41918-1. Np.*

Underwater Acoustics: A Linear Systems Theory Approach. By L.J. ZIOMEK. *Academic:1985. Pp.290. ISBN 0-12-781720-4. $45, £45.*

VLSI Electronics: Microstructure Science. NORMAN G. EINSPRUCH and ROBERT S BAUER (eds). *Academic:1985. Pp.383. ISBN 0-12 234110-4. $65, £65.*

White Light: Optical Signal Processing. By FRANCIS T.S. YU. *Wiley:1985. Pp.316. Hbk ISBN 0-471-80954-3. £46.00.*

Chemistry

Catalysis and Surface Science. HEINZ HEINEMANN and GABOR A. SOMORJAI (eds). *Marcel Dekker:1985. Pp.456. ISBN 0-8247-7328-4. $75.*

The Chemistry of the Metal–Carbon Bond. Vol. 3 Carbon–Carbon Bond Formation Using Organometallic Compounds. FRANK R. HARTLEY and SAUL PATAI (eds). *Wiley:1985. Pp.489. ISBN 0-471-90557-7. £98.*

Formaldehyde: Analytical Chemistry and Toxicology. VICTOR TUROSKI (ed.). *Advances in Chemistry Series, American Chemical Society:1985. Pp.393. Hbk ISBN 0-8412-0903-0. (US and Canada) $89.95, (Export) $107.95.*

Gas-Phase Chemiluminescence and Chemi-Ionization. ARTHUR FONTIJN (ed.). *North-Holland:1985. Pp.372. Hbk ISBN 0-444-86950-6 Dfl.110.*

General Chemistry: Principles and Modern Applications 4th Edn. By RALPH H. PETRUCCI. *Collier Macmillan:1985. Pp.131. Pbk ISBN 0-02-946550-8 Pbk £17.95.*

Higher Excited States of Polyatomic Molecules, Vol. III. By MELVIN B. ROBIN. *Academic.1985 Pp.465. ISBN 0-12-589903-3. $49.50, £49.50*

Introducing Organic Chemistry, 3rd Edn. By ANDREW STREITWIESSER and CLAYTON H. HEATHCOCK. *Collier Macmillan:1985. Pp.1197. Pbk ISBN 0-02-946720-9. Pbk £17.95.*

Mass Spectrometry of Heterocyclic Compounds, 2nd Edn. By Q.N. PORTER. *Wiley:1985. Pp.966. ISBN 0-471-09901-5. £289.15.*

Mechanisms of Inorganic and Organometallic Reactions. M.V. TWIGG (ed.). *Plenum:1985. Pp.519. Hbk ISBN 0-306-41960-2. Np.*

Methods for the Oxidation of Organic Compounds; Alkanes, Akenes, Alkynes, and Arenes. By ALAN H. HAINES. *Academic:1985. Pp.388. Hbk ISBN 0-12-315501-0. £75, $83.*

Organic Photochemistry. A. PADWA (ed.). *Marcel Dekker:1985. Pp.504. ISBN 0-8247-7421-3. $89.75.*

Oxidative Stress. HELMUT SIES (ed.). *Academic: 1985. Pp.507. ISBN 0-12-642760-7. $79, £72.*

Polyimides: Synthesis, Characterization, and Applications. K.L. MITTAL (ed.). *Plenum:1984. Pp.1182. ISBN 0-306-41673-5. $89.50.*

Process Systems Engineering PSE '85: The Use of Computers in Chemical Engineering. INSTITUTION OF CHEMICAL ENGINEERS. *Pergamon:1985. Pp.684. ISBN 0-08-031417-1. £53, $63.*

The Proton: Applications to Organic Chemistry. By ROSS STEWART. *Academic:1985. Hbk ISBN 0-12-670370-1. $65, £56.50.*

The Structure of Volatile Sulphur Compounds. By ISTVÁN HARGITTAI. *Reidel:1985. Pp.316. ISBN 90-277-1395-2. $49, £34.50.*

Synthetic Polymeric Membranes: A Structure Perspective, 2nd Edn. By ROBERT E. KESTING. *Wiley:1985. Pp.348. Hbk ISBN 0-471-80717-6. £55.75.*

Technology

Fiber Optics: Technology and Applications. By STEWART D. PERSONICK. *Plenum:1985. Pp.257 Hbk ISBN 0-306-42079-1. Np.*

Powtech '85: Particle Technology. INSTITUTION OF CHEMICAL ENGINEERS. *Pergamon:1985 Pp.294. ISBN 0-08-031443-0. £20, $24.*

The Social Shaping of Technology. DONALD MACKENZIE and JUDY WAJCMAN (eds). *Open University Press:1985. Pp.327. Pbk ISBN 0-335-15026-8. Pbk. Np.*

Solvent Extraction and Ion Exchange in the Nuclear Fuel Cycle. D.H. LOGSDAIL and A.J. MILLS (eds). *Wiley:1985. Pp.223. ISBN 0-85312-12-842-1. £28.50.*

Total Pressure Measurements in Vacuum Technology. By A. BERMAN. *Academic:1985. Pp.396. Hbk ISBN 0-12-092440-4. £52, $59.50.*

Computer Science

Algorithmically Specialized Parallel Computers. LAWRENCE SNYDER *et al.* (eds). *Academic: 1985. Pp.252. ISBN 0-12-654130-2. $26.50, £24.*

The Computer Culture: A Symposium to Explore the Computer's Impact on Society. DENIS P. DONNELLY (ed.). *Fairleigh Dickinson University Press, Cranbury, New Jersey, USA: 1985. Pp.176. Hbk ISBN 0-8386-3220-3. £24.50.*

Computer Speech Processing. FRANK FALLSIDE and WILLIAM A. WOODS (eds). *Prentice-Hall: 1985. Pp.506. ISBN 0-13-163841-6. £39.95.*

Fortran Optimization. By M. METCALF. *Academic: 1985. Pp.251. ISBN 0-12-492482-4. $26, £20.*

Foundations of Programming. By JACQUES ARSAC. *Academic: 1985. Pp.265. ISBN 0-12-064460-6. $29.50, £23.*

Getting Computers to Talk Like You and Me. By RACHEL REICHMAN. *MIT Press: 1985. Pp.221. ISBN 0-262-18118-5. $20.*

An Introduction to Linear Programming, 2nd Edn. By G.R. WALSH. *Wiley: 1985. Pp.240. Pbk ISBN 0-471-90719-7. Pbk £13.95.*

Prolog for Programmers. By FELIKS KLUZNIAK and STANISLAW SZPAKOWICZ. *Academic: 1985. Pp.400. ISBN 0-12-416520-6. $47.50.*

Stiff Computation. R.C. AIKEN (ed.). *Oxford University Press: 1985. Pp.462. ISBN 0-19-503453-8. £72.*

Earth Sciences

Dynamic Meteorology. By S. PANCHEV. *D. Reidel:1985. Pp.360. Hbk ISBN 90-277-1744-3. Dfl 200, £50.95, $74.00.*

The Earth's Surface Studied from Space. S.G. UNGAR (ed.). *Pergamon:1985. Pp.117. Pbk ISBN 0-08-033194-7. Pbk £31, $49.50.*

Explanatory Notes for the Geodynamic Map of the Circum Pacific Region. By GEORGE W. MOORE. *American Association of Petroleum Geologists, PO Box 979, Tulsa, OK 74101:1985. $15.*

Geomorphology and Soils. K.S. RICHARDS, R.R. ARNETT and S. ELLIS (eds). *George Allen & Unwin:1985. Pp.441. ISBN 0-04-551093-8. £35, $60.*

Groundwater Contamination. Studies in Geophysics. J. BREDEHOEFT *et al.* (eds). *National Academy Press:1984. Pp.179. Pbk ISBN 0-309-03441-8. Np.*

Journal of Atmospheric Chemistry, Vol. 3, No.1, June 1985. Scientific Application of Baseline Observations of Atmospheric Composition (SABOAC). Part 1. PAUL J. CRUTZEN and DIETER H EHHALT (eds). *Reidel, Holland and USA:1985. Pp.201. Pbk ISBN 0167-7764. Dfl.100, $38.00.*

Migmatites. J.R. ASHWORTH (ed.). *Blackie:1985. Pp.302. ISBN 0-412-00841-6. £27.50.*

The Weather Book. By RALPH HARDY, PETER WRIGHT, JOHN GRIBBON and JOHN KINGTON, *Mermaid Books:1985. Pp.224. Pbk ISBN 0-7181-2639-4. £8.95.*

Environmental Sciences

Chemical Water and Wastewater Treatment. A. GROHMANN, H.H. HAHN and R. KLUTE (eds). *Gustav Fischer Verlag:1985. Pp.310. ISBN 3-437-30503-4. Np.*

Estuarine Management and Quality Assessment. J.G. WILSON and W. HALCROW (eds). *Plenum:1985. Pp.225. ISBN 0-306-41911-4. Np.*

Ground Water Quality. C.H. WARD and P.L. McCARTY (eds). *Wiley:1985. Pp.545. ISBN 0-471-81597-7. £66.45.*

Laboratory Decontamination and Destruction of Carcinogens in Laboratory Wastes: Some Aromatic Amines and 4-Nitrobiphenyl. M. CASTEGNARO *et al.* (eds). *Oxford University Press:1985. Pp.85. Pbk ISBN 0-19-723064-4. Pbk £6.95.*

Occupational Hazards of Pesticide Use. G.J. TURNBULL (ed.). *Taylor & Francis:1985. Pp.184. ISBN 0-85066-325-3. £19.*

Troubled Skies, Troubled Waters: The Story of Acid Rain. By JON R. LUOMA. *Penguin:1985. Pp.178. Pbk ISBN 0-1400-8094-5. Pbk $5.95.*

Wastes in the Ocean, Vol. 4. Energy Wastes in the Ocean. IVER W. DUEDALL, DANA R. KESTER, P. KILHO PARK and BOSTWICK H. KETCHUM (eds). *Wiley:1985. Pp.818. Hbk ISBN 0-471-89332-3. £97.20.*

Biological Sciences

Action Systems. An Introduction to the Analysis of Complex Behaviour. By DAVID D. CLARKE and JILL CROSSLAND. *Methuen:1985. Pp.157. Pbk ISBN 0-416-36130-7. £14.95.*

The Alkaloids. A. BROSSI (ed.). *Academic:1985. Pp.357. ISBN 0-12-469524-8. $85, £85.*

Anales del Jardin Botanico de Madrid (Anales del Instituto Botanico, Tomo 41–II.) A.J. CAVANILLES. *2 Plaza de Murillo, 28014 Madrid, Spain:1985. Pp.483. Pbk ISBN 0211-1322. Np.*

Animal Thought. By STEPHEN WALKER. *Routledge & Kegan Paul:1985. Pp.437. Pbk ISBN 0-7102-0707-7. £6.95.*

Annals of Child Development, Vol.2. GROVER J. WHITEHURST (ed.). *JAI Press, 36 Sherwood Place, Greenwich, Connecticut, USA:1985. Pp.297. Hbk ISBN 0-89232-546-1. Np.*

The Aquarium Fish Survival Manual: A Comprehensive Guide to Keeping Freshwater and Marine Fish. By BRIAN WARD. *Macdonald & Co.:1985. Pp.176. Hbk ISBN 0-356-10792-2. £11.95.*

Atherosclerosis. Annals of the New York Academy of Sciences, Vol. 454. K.T. LEE (ed.). *The New York Academy of Sciences:1985. Hbk ISBN 0-89766-303-9; pbk ISBN 0-89766-304-7. Np.*

Atlas of Human Anatomy. By J.A. GOSLING, P.F. HARRIS, J.R. HUMPHERSON, I. WHITMORE and P.L.T. WILLAN. *Gower Medical Publishing:1985. Hbk ISBN 0-443-02913-X. £19.50.*

Avian Biology, Vol. VIII. DONALD S. FARNER, JAMES R. KING and KENNETH C. PARKES (eds). *Academic:1985. Pp.256. ISBN 0-12-249408-3. $49.50, £43.50.*

Bacterial Adhesion: Mechanisms and Physiological Significance. DWAYNE C. SAVAGE and MADILYN FLETCHER (eds). *Plenum:1985. Pp.476. ISBN 0-306-41941-6. Np.*

Bee Orchids. By STEPHEN BLACKMORE. *Shire Natural History:1985. Pp.24. Pbk ISBN 0-85263-745-4. Pbk £1.25.*

Biochemistry of Dioxygen. By LLOYD L. INGRAHAM and DAMON L. MEYER. *Plenum:1985. Pp.287. Hbk ISBN 0-306-41948-3. Np.*

Biochemistry and Function of Vacuolar Adenosine-Triphosphatase in Fungi and Plants. BERNARD P. MARIN (ed.). *Springer-Verlag:1985. Pp.259. ISBN 3-540-15267-9/0-387-15267-9. DM 84.*

Biology of Acanthocephala. D. CROMPTON and B. NICKOL (eds). *Cambridge University Press:1985. Pp.519. Hbk ISBN 0-521-24674-1. £60, $89.50.*

Biology of the Reptilia. Vol. 15. CARL GANS and FRANK BILLET (eds). *Wiley:1985. Pp.731. Hbk ISBN 0-471-81204-8. £81.80.*

Biophysical Control of Microfibril Orientation in Plant Cell Walls: Aquatic and Terrestrial Plants including Trees. By J.D. BOYD. *Dr W Junk:1985. Pp.200. ISBN 90-247-3101-1. $42, £30.50.*

Biotin. KRISHNAMURTI DAKSHINAMURTI and HEMMIGE N. BHAGAVAN (eds). *New York Academy of Sciences:1985. Pp.441. Pbk ISBN 0-89766-289-X. Np.*

British Warblers. By ERIC SIMMS. *Collins:1985. Pp.432. Pbk ISBN 0-00-219404-X. Np.*

Buttercups. By STEPHEN BLACKMORE. *Shire Natural History. Cromwell House, Church Street, Princes Risborough, Bucks HP17 9AJ:1985. Pp.24. Pbk ISBN 0-85263-763-2. Pbk £1.25.*

Cellular and Molecular Aspects of Aging: The Red Cell as a Model. JOHN W. EATON, DIANE K. KONZEN and JAMES G. WHITE (eds). *Alan R. Liss:1985. Pp.464. Hbk ISBN 0-8451-5045-6. £52.*

Cellular and Molecular Biology of Lymphokines CLEMENS SORG and ANNELIESE SCHIMP (eds). *Academic:1985. Pp.845. Hbk ISBN 0-12 656160-5. £60, $69.*

Central and Peripheral Mechanisms of Colour Vision. D. OTTOSON and SEMIR ZEKI (eds) *Macmillan:1985. Pp.239. Hbk ISBN 0-333-39321-X £60.*

The Cereal Rusts: Vol II, Diseases, Distribution Epidemiology and Control. ALAN P. ROELFS and WILLIAM R. BUSHNELL (eds). *Academic:1985 Pp.606. Hbk ISBN 0-12-148402-5. £64.50, $74.50.*

Cerebral Cortex, Vol. 3: Visual Cortex. ALAN PETERS and EDWARD G. JONES (eds) *Plenum:1985. Pp.424. Hbk ISBN 0-306-42025-2. Np.*

Cerebral Lateralization in Nonhuman Species STANLEY D. GLICK (ed.). *Academic:1985 Pp.288. ISBN 0-12-286480. $49.50. £49.50.*

Chemically Mediated Interactions Between Plants and Other Organisms. GILLIAM A. COOPER DRIVER, TONY SWAIN and ERIC E. CONN (eds). *Plenum:1985. Pp.246. ISBN 0-306-42006-6 Np.*

The Chemistry and Biology of Isoquinoline Alkaloids. J.D. PHILLIPSON, M.F. ROBERTS and M.H. ZENK (eds). *Springer-Verlag:1985. Pp.304 ISBN 3-540-13980-X/0-387-13980-X. DM 108.*

Communication and Noncommunication by Cephalopods. By MARTIN MOYNIHAM. *Indiana University Press:1985. Pp.141. ISBN 0-253-31382-1 $32.50.*

Contemporary Nephrology, Vol. 3. SAUL G KLAHR and SHAUL G. MASSRY (eds) *Plenum:1985. Pp.768. Hbk ISBN 0-306-41984-X. Np.*

Continuous Arteriovenous Hemofiltration (CAVH) H.G. SIEBERTH and H. MANN (eds). *Karger:1985 Pp.247. ISBN 3-8055-4077-9. DM 78, $27.75.*

Current Topics in Cellular Regulation. BERNARD L. HORECKER and EARL R. STADTMAN (eds) *Academic:1985. Pp.183. ISBN 0-12-152825-1. $45 £45.*

Earthworms. By R.W. SIMS and B.M. GERARD *The Linnean Society/E.J. Brill, Plantijnstraat 2, 232 JC Leiden, Belgium:1985. Pp.171. Pbk ISBN 90-04 07582-8. £12.50.*

Ecological Interactions in Soil: Plants, Microbes and Animals. A.H. FITTER *et al.* (eds). *Blackwel Scientific:1985. Pp.451. ISBN 0-632-01386-9. £34.50.*

Ecology and Genetics of Host–Parasite Interactions Papers presented at an International Symposium organized by the Linnean Society of London and the British Society for Parasitology. Linnean Society Symposium Series No.11. D. ROLLINSON and R.M ANDERSON (eds). *Published for the Linnean Society of London by the Academic Press:1985. Pp.266 Hbk ISBN 0-12-593690-7. £35, $45.*

The Encyclopaedia of Underwater Life. Dr KEITH BANISTER and Dr ANDREW CAMPBELL (eds) *George Allen and Unwin:1985. Pp.287. Hbk ISBN 0-04-500035-2. £25.*

The Enzymes of Biological Membranes, 2nd Edn ANTHONY N. MARTONOSI (ed.). Plenum:1985 Pp.586. ISBN 0-306-41454-6. Np.

The Evolution of Genome Size. T. CAVALIER SMITH (ed.). *Wiley:1985. Pp.523. Hbk ISBN 0-471 10272-5. £38.50.*

Flora of Kuwait. By HAZIN S. DAOUD. *KPI, 1 Leicester Square, London WC2H 7PH England:1985. Pp.224. ISBN 0-7103-0075-1. £45.*

Frontiers in Histamine Research: A Tribute to Hein Schild. C.R. GANELLIN and J.C. SCHWART (eds). *Pergamon:1985. Pp.442. ISBN 0-08-031989-0 £50, $80.*

Functions of the Brain. CLIVE WARWICK COE (ed.). *Oxford University Press:1985. Pp.209. Hb ISBN 0-19-857212-3. £15.*

Fungi. By P. FOREY. *Shire Natural History:1985 Pp.24. Pbk ISBN 0-85263-746-2. Pbk £1.25.*

Gene Expression During Normal and Malignant Differentiation. LEIF C. ANDERSSON, C.G. GAHMBERG and P. EKBLOM (eds). *Academic:1985 Pp.257. ISBN 0-12-059490-0. $30, £26.50.*

God's Acres: The Flowers and Animals of the Parish Churchyard. By FRANCESCA GREENOAK. *Orbi Publishing, 20-22 Bedfordbury, London WC2N 4BT UK:1985. Pp.192. ISBN 0-85613-800-2. £12.95.*

nature

British research scrutinized again

The House of Lords is to look again at the organization of British science. It could do worse than reprint its proposals on the same subject five years ago.

THE frequent complaint that the British parliament knows nothing of the conduct of science is a lie. Although the House of Commons is no better endowed with technical people than other elected legislatures, the House of Lords, for a quarter of a century dominated by people with only a life tenancy of a title, is a different kettle of fish. Five years ago, the Lords Select Committee on Science and Technology undertook an important study of how the British government runs research and concluded that affairs were badly managed. Now, with further experience bearing out that general conclusion, the same committee (with different people) is about to embark on essentially the same task, and is asking for opinions by 14 February (in writing) on the questions it has posed for itself. Here are shortened forms of the questions: the accompanying telegraphic answers are included for the convenience of readers too occupied with more urgent tasks (rewriting research grant applications, for example).

Q. *How far should public support for science and technology be an objective of national policy?* **A.** As far as a piece of string is long. All governments agree that there must be some public support; most know that an arbitrary degree of support will be justified by its consequences. The governments of France (see p. 165), Japan, West Germany and the United States, after five years of generous support for science and technology, are able to point to progress of the kind they promised; the British government, starting from the proposition that British science used to be a profligate business, can now claim as justification the fact that previously academic researchers have commonly become suppliants to industry for research funds.

Q. *Could the present division of responsibility between the research councils be improved?* **A.** What responsibility? The theory, at the time of the Rothschild report in 1971, was that the Science and Engineering Research Council (SERC, then significantly only SRC), is alone exclusively concerned with the welfare of academic research; the three other science research councils (the Economic and Social Research Council is in a dog-house all of its own) had specific remits for research in agriculture, medicine and the natural environment. They are goal-directed organizations, but their programmes range from basic research to some operational activity (geological survey, for example).

Much has changed in the past five years. Under financial pressure, the three operational research councils have been cutting back on their in-house research. (University people are also cheaper.) These councils appear also to have been genuinely moved by the condition into which British academic research has sunk, and are doing what they can to divert resources from their own establishments towards universities. When applied projects can usefully be carried out by academics, there is no complaint. One danger, probably not yet serious, is that there will be an awkward overlapping of criteria applied to basic academic research. Another, more immediate, is that the Agricultural and Food Research Council has probably now been weakened to the point at which it cannot do its job.

The Natural Environment Research Council (NERC) is in a different kind of trouble, never having been given a coherent job to do. The result is that it has a ragbag of functions, ranging from the support of academic earth science to the running of the British Geological Survey. The case for NERC's separate continued existence has vanished. (Lazy readers wishing to make the same point without being identified with the repetitious source of this opinion should either skip this question or say that the answer is "self-evident".)

Q. *What organizational changes are needed?* **A.** The fewest compatible with the survival of British research. There have been so many organizational changes so recently that stability would be welcome. Changes of substance are now more necessary than changes of form. But there is a need that some disinterested cabinet minister other than Mrs Margaret Thatcher should be asked to keep a watching brief on science, which is what the House of Lords committee recommended five years ago. Since then, the lack of political interest in science has patently allowed a once flourishing enterprise to be damaged, perhaps beyond repair.

If the case for a minister to look after science was strong five years ago, the intervening experience has only reinforced it. A strictly organizational benefit would be that the Advisory Board for the Research Councils, which exists merely to recommend a division of the annual science budget, would have a more pointed focus for its work. Subsuming NERC in other agencies would, by comparison, be a minor blessing.

Discerning readers will at this point recognize this question to be a trap. For all the constitutional importance of the House of Lords, it is not on this occasion bent on defending the entitlement of researchers in British laboratories to decent (let alone internationally competitive) salaries and other terms of service, but the personal penury that goes with a career in basic research will have to be tackled at some stage. What may worry the House of Lords (and should be keeping British researchers awake at nights) is the whiff of scandal that attends the quasi-autonomous conduct by British scientists of their own affairs.

Scandal? Nobody suggests that people have been stuffing public money into their pockets. The scandals that matter, and that damage science as well as the public purse, are more often errors of omission than of commission. There is, for example, the case of SERC's attempt, over four agonizing years, to reduce its spending on the infrastructure of astronomy: the committee charged with finding a solution, with the previous chairman of SERC at its head, has now apparently repeated the customary recommendation that nothing can be done. It seems not to be appreciated that indecisiveness on this scale plays into the hands of those in the British government, the Prime Minister in particular, who complain that basic research is effete. Maybe the new chairman of SERC, Professor Bill Mitchell, will be able to grasp the nettle that his predecessor has shrunk from, but the general question of how the research councils are managed needs attention. Professor Ralph Slatyer's argument (see *Nature* **319**, 3; 1986) in comparable Australian circumstances, that the chief executive should be the appointed servant of the policy-making council, should be compulsory reading for the House of Lords committee.

Q. *Are there other sources of funds than government for applied* *research?* **A.** Yes, but the question is badly put. Government spending on applied research is already substantial, chiefly through the government's own laboratories, especially defence laboratories; more should be spent by means of contracts with industrial and research organizations. What the House of Lords appears to have in mind is the possibility that industrial money from applied research might be used to prop up the research enterprise as a whole. Many universities have increased their incomes substantially by industrial contracts; the cost, in the diversion of creative people's interests, is not yet known. The chance that research council institutes may be able to save themselves by similar means is, however, much smaller.

Q. *How is the Rothschild principle working?* **A.** Not well at all, partly because the government that in 1971 enthusiastically welcomed the doctrine that applied research should be carried out by research councils, acting as contractors for customers identified as government departments, never gave the doctrine a chance. The notion that 10 per cent of the funds transferred in this way should be for basic research was never tried. Government departments have not been provided with chief scientists capable of operating the system, and have been free to renege on their commitments when it suited their convenience, causing mayhem in the research laboratories concerned.

Q. *Can defence research help civil research?* **A.** Yes, but only if the system is reorganized. The Prime Minister, Mrs Margaret Thatcher, and her now departed Defence Secretary, have never adequately delivered their promise, two years ago, to make defence research more open to British civil industry. Secrecy is only part of the problem. Lack of interest is a more serious obstacle. This is yet another reason why there should be a minister not merely to coordinate the government's spending on research but to develop a coherent policy on the subject.

The benefits of such a role are wider than mere coordination, although the value of a means of getting important questions decided cannot be underestimated. SERC may have procrastinated over the organization of astronomy, keeping those working at its establishments on tenterhooks, but the government is worse. Nothing has been heard of the proposal that Britain should bargain a reduced contribution to, or withdraw from, the European high-energy physics organization (CERN) since the government assumed responsibility from the Advisory Board for the Research Councils. Does anybody care what the consequences are for British academics, graduate students and potential graduate students who are vitally interested parties? On a smaller scale, but one not less vital for those whose careers are affected, the Ministry of Agriculture, Fisheries and Food has been brooding since last summer on an intelligent proposal that the Plant Breeding Institute, which develops new cereal varieties (among other things) should be joined in some manner to the National Seed Development Organization (which makes a profit for the Treasury by exploiting the same varieties. It is simply maladministration that these questions are neglected.

The question of money is important. The British government's policy for six years has been to keep the cost of civil science static. The enforced premature closure of once productive enterprises may have helped to balance the Treasury's books, but has otherwise been a diseconomy. It can only be a matter of time before the government (or its successor) has to change tack, and to behave like a spendthrift to undo some of the damage that has been done.

There is also the matter of people's morale to be considered. There is something in the belief that what is wrong with the British research enterprise is not the lack of money, serious though that may be, but the way in which continuing uncertainty has sapped people's belief that the research they do will be a foundation for even better things. In basic research, the time has gone, in Britain, when there was reasonable hope that modest beginnings could, if successful, grow into bigger enterprises. That is the sense that needs to be restored, more quickly than the supply of mere money. ☐

Agenda for Geneva

The resumption this week of the superpower talks is a time to ask what they can achieve.

As the Reagan–Gorbachev summit recedes in time, so do its problems. This week, the reassembly of the bilateral arms control negotiations at Geneva should bring them back abruptly. The US Strategic Defense Initiative (SDI) is bound to be high on the agenda; the summit participants agreed only to disagree about it. The first objective should be to prevent this divisive issue from wrecking the hard work that must be done on the control of strategic missiles. The second should be to confine the bargaining within the framework of what is realistically possible. Then, this year may even yield some tangible agreements.

This time, optimism is in order. That the summit happened, and did not finish up as a shouting match, is one good sign. That there is to be a second meeting later this year is another; the temptation to sign an agreement with some substance will be irresistible (especially with the mid-term elections in the United States just a few months off). But there is also a good chance that there will be progress in the multilateral talks at Stockholm; if some sting can be taken from the fear of a war in Europe, it should be possible for the stragetic negotiations to be flexible.

Finding a realistic framework for a year's work at Geneva will nevertheless be difficult. The Soviet Union and the United States, in the weeks before the summit, were talking about schemes for reducing strategic missile forces by about a half, but in terms that make each side's proposals unacceptable to the other. The Soviet plan has the added complication of counting as strategic missiles the French and British nuclear forces, over which the United States has no control. Attempting from Geneva to legislate for these missiles would be fruitless, at least in the immediate future. So the best strategy for the negotiators will be to adopt the goal of a 50 per cent reduction as one for 1987, and, during 1986, to aim at the more modest but attainable goal of putting the existing unratified agreement on strategic arms, SALT II, on a permanent basis that the US Congress will accept. Especially if there is some movement at the Stockholm negotiations, it should also be possible to deal with intermediate missiles by freezing them (with the proviso that the planned US deployment in Western Europe should be completed).

But why such a modest goal? Chiefly because a more ambitious agreement could not possibly be completed in the time available, but also because an agreement to make SALT II stick (it lapses in 1991) would force on the two governments concerned experience of the practical operation of arms control agreements which they at present lack. The idea that there should be regular meetings to discuss what missiles are where, and formal attempts to construct inventories of hostile forces, is unfamiliar. Operating such a system at strategic levels much like the present is a necessary preliminary. Aiming for a comprehensive test-ban now is similarly unrealistic. That is a task for 1988.

The complication of SDI should not be the obstacle public rhetoric suggests. The US administration insists that SDI is a means of making the world safe from the threat of nuclear weapons, the Soviet Union that it is a trick to make the United States alone immune from nuclear retaliation and therefore a provocation. If SDI is technically feasible, both views are tenable. But nobody can tell whether SDI is a realistic development programme or simply a technological mirage. The only reasonable technical prospect is that SDI will spawn, as a minor by-product, a satellite-borne warning system based on infrared detectors. So the Soviet interest would be met by an arrangement that the general character of SDI experiments beyond the atmosphere should be disclosed by a formal agreement to ban the development and testing of anti-satellite weapons and by the clarification and reaffirmation of the Anti-Ballistic Missile treaty. So much could be accomplished by the autumn of this year. ☐

French research strategy

CNRS embraces plans for research networks

THE French multidisciplinary research council, the Centre National de la Recherche Scientifique (CRNS), is learning to live on a static budget after a rapid period of expansion, its director-general Pierre Papon implied this week. This year's budget of FF8,000 million (roughly £800 million), although up by 8 per cent, will not be enough to cover the rising costs of keeping productively at work the 10,000 of France's most able researchers (10 per cent of whom are foreign) and the 15,000 technicians, engineers and administrators on CNRS's books. But CNRS does not intend to stagnate. Papon says that it will continue to move into new fields of research by adopting new methods of management and organization.

Papon's intentions make an interesting contrast with those of research organizations elsewhere, in Britain for example, similarly constrained by static budgets. Science minister Hubert Curien has effectively ruled out increased concentration of research resources on centres of excellence, saying that would be an unforgivable waste of research talent. This position is supported by Professor Frederick Joliot, science adviser to the prime minister, who argues that the US model for research support entails "excessive" competition, and that the French alternative, based on protected careers in research, allows greater freedom for the pursuit of long-term and speculative projects.

The key word in French science planning now is neither "selectivity" nor "concentration" but "networks", a term once fashionable at the European Commission in Brussels, but introduced in the context of CNRS by M. Curien just before Christmas. The intention is to link existing laboratories and their staffs into new projects, each lasting perhaps only a few years, to share staff and and equipment without a concomitant increase of costs.

So Papon and Curien intend that researchers should be more willing to change disciplines and that laboratories should be more open to others, both in France and elsewhere in Europe. Papon, for example, wants to create networks for the study and development of new materials, an approach that contrasts with the decision last year to set up a special laboratory devoted to one of the most fashionable of these, gallium arsenide.

Since 1981, CNRS has been creating new laboratories, usually linked with universities, at the rate of 20 a year, but last year there were only 10 and, during 1986, there will only "a few" additions to the present roster of 750 CNRS laboratories.

Even so, expansion will not be entirely halted. In what may turn out to be a last gesture towards expansionism, CNRS will build a dozen laboratories in the general field of information technology by the end of the decade at Marne la Vallée, a new town still under construction.

Growth will also be sustained by cooperation with regional governments, which now spend up to 3 per cent of their total budgets on research, and with industry. Thus, 1986 will see the beginning of a new metallurgy laboratory in cooperation with the company St Gobain and an inorganic polymer laboratory founded in conjunction with Rhone-Poulenc. But Papon insists that the work at the new laboratories will be basic and strategic — St Gobain, for example, is interested in metallic glasses — and that CNRS will not slip into the role of an applied research agency.

CNRS also intends in 1986 to create several "national laboratories" at which equipment and technicians will be provided only on condition that they are made available for use by other groups for a proportion of the time. An experiment on these lines in engineering science during 1985 is seen as a success and other disciplines are likely to follow in 1986.

During the year ahead, CNRS will have to find FF50 million for projects under the banner of Eureka, the European collaboration in high technology, out of the 8 per cent budget increase of FF700 million, but even so it will be able to increase spending on medium-scale equipment by 24 per cent, on minicomputers by a third and on large-scale equipment by 13 per cent. Spending on basic research materials will increase by 10 per cent in the life sciences, by 12 per cent in engineering and by 7 per cent overall.

CNRS intends to deal generously with some of its special programmes. Thus the budget of an interdisciplinary programme of materials research begun four years ago will increase by 58 per cent (to FF9.5 million), while there is to be a grand new programme (with a budget of FF11 million in the first year) to bring organic chemists and molecular biologists together.

CNRS will expand by a quarter its department concerned with the application of research, funds allocated to international cooperation are to increase by 13 per cent (international subscriptions are not included) and, in the scientific programme, there is to be more emphasis on the Earth sciences and oceanography (probably at the expense of astronomy); there is, for example, to be a new oceanography laboratory at Toulouse using remote-sensing data, particularly those from the SPOT series of satellites, not to mention a new programme of "cheap" communications research involving neurobiology, cognitive science, linguistics and artificial intelligence. Stasis does not mean to CNRS what it means to other people. **Robert Walgate**

Nuclear winter

Soviet researcher's part hyped

VLADIMIR Valentinovich Aleksandrov, the Soviet computer programmer who disappeared in Spain last March, was an "irreplaceable" Soviet scientist whose disappearance put an immediate end to East–West cooperation in the "mathematical modelling of global biosphere processes", in other words, research into nuclear winter, according to the Soviet weekly, *Literaturnaya Gazeta*. After a belated announcement by the Academy of Sciences (his employers) in December, which said little more than that he had disappeared, and a subsequent polemic in *Izvestiya* accusing the Central Intelligence Agency of having kidnapped him, *Literaturnaya Gazeta* devoted a full page to Aleksandrov and "nuclear winter".

By this account, Aleksandrov "is one of the scientists who have made the weightiest contribution to this field of research, thanks to which the consequences of a nuclear war have been placed before the entire world in an entirely new light, even more terrible than before". (He was in fact never more than a junior member of the Soviet teams to ENUWAR symposia discussing nuclear winter.) In the light of his lack of a doctoral degree, some Westerners have suggested that his place in the delegations may have been dictated by political rather than scientific motives; it is now claimed that he was too busy campaigning about nuclear winter, and that he was due to defend his doctoral thesis on 20 April.

According to his superior at the Computer Centre of the Academy of Sciences, Nikita Moiseev, despite his "comparative youth" (47), his election as a Corresponding Member of the Soviet Academy of Sciences was a foregone conclusion, although he has not been elected *in absentia*.

In one respect the paper is incorrect — international cooperation in "nuclear winter" studies was not "instantly broken" by Aleksandrov's disappearance. An ENUWAR symposium took place in June at the University of Essex, with a Soviet delegation clearly embarrassed by Aleksandrov's absence, to which it referred as a "tragedy". **Vera Rich**

German research agency

Ethologist takes the helm

Hamburg

PROFESSOR Hubert Markl, the distinguished ethologist from the University of Konstanz, is at 47 the youngest-ever president of the Deutsche Forschungsgemeinschaft (DFG), West Germany's principal agency for the support of basic research with federal government funds. Markl succeeded Professor Eugen Seibold, the geophysicist, at the beginning of the year. He has been elected as president for a period of three years in the first instance, having served as Seibold's vice-president.

Markl says that the appointment of one as young as he is "an experiment". On the telephone last week, he said that he regretted having to give up his university tasks and his scientific work for science administration, but that he was eager to fall in with the wishes of the members of DFG that he should be their president.

In his own way, Markl is somehow the representative of a new generation of scientists, and is endowed with remarkable optimism, dynamism and farsightedness. He says his most important tasks are "the justification of science to the public" and "the defence of the autonomy of science from which scientists cannot retreat".

Markl has strong views about the development of the university system in West Germany. On the contentious issue of the role of elite universities, Markl says that "one cannot simply copy systems that work well in other countries".

He sees no place in Germany for private elite universities, but instead looks for more competition between universities for good students. This, he believes, could lead to a system in which universities are distinguished by the fields in which they excel, with one being "top in agriculture, for example, another standing out for its chemistry". In this way, Markl says, "our scientific productivity will be used more effectively".

With the reduction of demand for student places now in prospect on demographic grounds, Markl believes that changes of the kind that he would welcome will come about automatically, especially as universities have more resources to devote to graduate education. He acknowledges that the age structure of university staffs in Germany is at present unsuitable, but hopes that DFG, with its annual budget of DM1,000 million, will be able to provide some relief. He is not especially alarmed at the risk that younger scientists will be sucked away to posts abroad, believes scientific exchange to be an important element of personal development, but says he would act to counter any threat of substantial loss of able people.

Markl has strong views on the social responsibility of science, which he says belongs not to "science as such, but to the individual scientist. Moral precepts never apply to abstract systems, but to the particular people who work for them."

He knows what he is talking about from his eventful life so far. Markl completed his doctorate (in Martin Lindauer's group at Munich) at the early age (by West German standards) of 24, and afterwards spent a year in the United States (at Harvard and the Rockefeller Universities). At the age of 29, then at Frankfurt, he completed his *Habilitation* (the formal qualification to hold a university professorship) as a zoologist, moving in turn to Darmstadt and Konstanz (in 1974).

Markl is likely to enjoy his spell as president of DFG, although his habit of saying what he thinks directly, even bluntly, could cause trouble from time to time. Markl recognizes the danger, saying that the years ahead will give him "a practical training in the applied ethology of science politics" and that "if I choose to walk through fire, I cannot complain of the heat". **Jürgen Neffe**

Seibold in Europe

Hamburg

PROFESSOR Eugen Seibold, who retired as president of DFG at the end of 1985, after serving two successive three-year terms, has been for many years one of the chief advocates in West Germany of international collaboration in research. A geologist by training, he was largely responsible for the development of the Geological Institute at the University of Kiel in the 1960s and 1970s.

Since the appointment last year of M. Hubert Curien as a minister in the French government, Seibold has been president of the European Science Foundation. In that role, he says, he will encourage the more rapid completion of the European Geotraverse, the deep seismic sounding of a dog-leg North–South section from Scandinavia to North Africa that is one of the foundation's chief projects. Jürgen Neffe

Antarctic treaty

Argentina expands research effort

ARGENTINA is to support its territorial claims in Antarctica by means of a major programme of research and geological exploration. According to the journal *Noticias Argentinas* last month, Argentina may also agree to an international system for the control of Antarctic mineral resources, but this, the paper said, would not prejudice Argentina's "reservations" about its sovereignty rights and maritime jurisdiction.

Argentina is alone among the seven countries that had laid territorial claims to the Antarctic continent before the 1959 Antarctic Treaty in still maintaining the apparatus of statehood there (including passport control). (It was partly the overlapping territorial claims of Britain, Chile and Argentina that led to the formulation of the treaty by which all claims to sovereignty were "frozen" until 1991.) Since the signing of the treaty, mineral wealth in the sector claimed by Argentina has been found to include chromium, nickel, cobalt, copper, gold, silver and iron.

Argentina maintains 16 bases on the Antarctic continent, including six permanent establishments, but only one of these has been engaged on scientific work. One result is that Argentina has carried out less scientific research than the other signatories of the treaty.

During 1985, Argentina sent 33 scientists, mainly geologists, to the Antarctic. In 1986, this number will be increased to 107 "scientists and technicians"; the possibility of opening a further base with a major airstrip is under serious consideration. The new emphasis on science is being presented as a "demilitarization" of Argentine Antarctic policy, although it is officially admitted that this will not mean a reduction in the logistic support provided by the Argentine armed forces. The (military) Argentine involvement in the Antarctic is said to cost some US $3 million a year. Partial "demilitarization" could make the effort partly self-financing, if Argentina sell equipment and services for Antarctic research and rents out its naval icebreakers for transporting scientific expeditions.

Official Argentine sources explain the need for the new policy by claims that New Zealand's "anti-nuclear" policy could lead to that country being used as a starting point for expeditions sponsored by the socialist bloc. There have also been unofficial indications that Argentina (and also its main Antarctic "rival" Chile) has been perturbed by the new "third world" interest in the Antarctic, demonstrated by the major expeditions by India and China which, it is considered, are operating far outside their own bailiwick.

The Indian position on this issue is, however, explicit; Antarctica is the southern boundary of the Indian Ocean, and may have an important influence on the monsoon and on the climate of India in general. China and Brazil, the two other recent recruits to the Antarctic Treaty, have less specific interests. **Vera Rich**

Nuclear safety

Opposition to relaxing standards

Washington

A ROW is brewing about the official calculations of the amounts of radioactivity likely to be released in nuclear accidents. The Union of Concerned Scientists (UCS) has added its criticisms to the reservations expressed last month by an advisory committee to the Nuclear Regulatory Commission (NRC) about the commission's proposed revision of "source terms" for nuclear power plants. These quantities refer to the probable amount and chemical form of radioactive releases to the environment in the event of a severe accident. UCS says the new source terms "deliberately" omit plausible accident sequences, including some that have actually occurred.

The new source terms are derived in a NRC draft report, NUREG-0956, and are inspired by research in the wake of the accident at Three Mile Island, some of which suggested that releases of radioactivity had been overestimated.

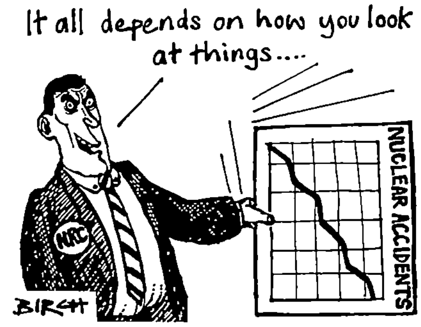
It all depends on how you look at things....
NRC
NUCLEAR ACCIDENTS
BIRCH

NRC's draft was criticized last month by its own Advisory Committee on Reactor Safeguards, which expressed "reservations" about the document and said the new source terms should "not be given much weight". Containment failure, an important factor in an accident, is treated, in a "rather preliminary fashion".

The NRC draft acknowledges the many uncertainties surrounding its estimates, and admits that the results depend critically on the design of particular plants. But externally initiated events, such as earthquakes, are not considered at all, according to UCS.

Although only five plants are modelled in the draft, NRC says it intends to go ahead and use the new source terms to re-evaluate and revise regulations governing power plant safety, from siting requirements to the design of safety systems. According to UCS, the revisions will in almost every case result in safety requirements being relaxed.

NCR's approach relies heavily on probabilistic risk assessment, which requires analysts to specify all possible routes to failure. Rupture of steam generator tubes, which has led to accidents in the past, is one omission cited by UCS, which has compiled a lengthy list of similar examples.

The UCS criticism comes at a bad time for NRC, which is investigating several accidents at nuclear plants that, according to Robert Pollard, UCS's nuclear safety expert and a former NRC official, occurred because NRC had not enforced its own requirements. The Toledo Edison Company may be fined $900,000 because of violations that led to an incident on 9 June last year, at its Davis–Besse plant in Ohio, when both main and auxiliary feedwater were lost. NRC has also upgraded its investigation of an accident in December at the Rancho Seco plant in California in which 450 gallons of contaminated water were spilled in an auxiliary building, leading to a small release of radioactive steam.

NRC says the UCS critique will be considered as a "comment" in its revision of NUREG-0956: a definitive report will be issued later this year. But Pollard doubts whether NRC will take notice "until we get them in court". How soon that will be depends of to what uses NRC puts its new source terms; but if the two do meet in court it will not be for the first time. Last time, UCS challenged NRC's right to restrict public comment on NRC rule-making. It won.

Tim Beardsley

Neutron research sources

US ambitions for new machine

Washington

COMPETITIVE juices are already rising in US laboratories hoping to capture a new advanced neutron source that they hope will be built during the first half of the next decade. Development funds for the instrument, which is seen as essential if the United States is to catch up with Europe on uses of slow neutrons, will be included in the Department of Energy (DoE)'s research budget for 1987, to be presented by the President to Congress next month.

Several recent studies requested by DoE have emphasized the European lead, which is ascribed largely to the success of the British/French/German collaboration at Institute Laue–Langevin in Grenoble in developing instrumentation for use in cold-neutron experiments. (Little account has yet been taken in the United States of the new British machine, the Neutron Spallation Source, commissioned last year by the UK Science and Engineering Research Council.) There is agreement that the immediate need is for a steady-state source producing up to 10^{16} neutrons $\mathrm{cm}^{-2}\mathrm{s}^{-1}$ (although the project would just get by with half-flux). Design concepts described at a recent workshop in Gaithersburg, Maryland, imply a facility costing about $300 million with running costs of about $25 million a year, although part of this could be saved by closing down one of the older sources when the new machine came on-line, according to Dr Donald Stephens, associate director of basic energy sciences at DoE.

Researchers are expecting about $6 million of development funds for the new machine in 1987. The most popular approach seems to be a 2–300 MW reactor source; Brookhaven National Laboratory is backing a design using small uranium oxide pellets, while Dr Ralph Moon of Oak Ridge National Laboratory wants a reactor with high-density uranium silicide fuel. A design suggested by Argonne National Laboratory, and disparaged as too preliminary by Moon, has rotating overlapping rings of fuel that would generate high flux densities near their point of contact and cool down during the rest of a revolution.

The chief technical problem foreseen for heavy water-cooled reactors operating at high power densities is in the formation of insulating aluminium oxide on fuel supports. Dr Robert Burke, of DoE's Hanford Engineering Laboratory in Washington state, favours instead a spallation design using a proton accelerator operating at a steady current of 100 mA. Burke says this approach would be more flexible than a reactor (because the protons could be used for other purposes) and that the less onerous safety requirements of an accelerator design mean that siting would be less critical. (He did point out that low electricity costs in the north-west Pacific would make this area attractive.)

The Hanford proposal would cost $300–450 million, according to Burke (although Moon says that $800–1,100 million would be nearer the mark), and he claims that the 100 mA proton-beam current required is feasible without extensive research. As a bonus, the Hanford design would allow the source to be upgraded easily should this be thought desirable.

For all the sparring over the design approaches, persuading Congress to build, or even to study, a new facility is not likely to be easy. But DoE's Energy Research Advisory Board has pointed out that existing major US neutron research facilities will be 30 years old by the time a replacement can be built, and the principal use of the new machine — neutron scattering — is the sort of research that can often bring immediate and tangible benefits. That might give it a better chance on Capitol Hill than the much more expensive facilities required for, say, high-energy physics.

Tim Beardsley

US/Canada acid rain

Envoys' compromise in dispute

Washington

A JOINT report on acid rain by US and Canadian special envoys met mixed reactions when it was delivered to the two governments last week. In Canada, there was a cautious welcome for the recognition that acid rain is a serious problem and that scientific knowledge is adequate to assess the effects of control strategies, but disappointment that no specific programme to reduce acid emissions was recommended. In the United States, President Reagan called the report a "step forward" and undertook to study it "carefully", but he avoided endorsing the principal recommendation that the US government should support half the cost of a $5,000 million programme to demonstrate new coal-burning technologies that minimize acidic emissions.

A Canadian government spokesman said that the report had "brought the acid rain question into the political arena, where it will be solved". Canada, whose tourism and fishing industries stand to lose from damage to lakes and forests, has long held that the scientific evidence justifies measures to reduce emissions from the tall stacks which are the principal sources of long-range pollution. Provincial governments in eastern Canada last year agreed with the national government that they will be responsible for reducing emissions of sulphur dioxide by 50 per cent by 1994. Automobile emissions of nitrogen oxides have also recently been brought into line with the more strigent US standard of 1 gram per mile. The US government, in contrast, has so far refused to acknowledge a link between acid emissions and environmental damage.

Richard Ayers, a lawyer for the Natural Resources Defense Council, says the report is a political compromise which nevertheless allows the utilities to delay action for another five years — well worth $2,500 million. But a more pessimistic view was offered by Adele Hurley of the Canadian Coalition on Acid Rain, who does "not expect to see the money".

The two special envoys, Drew Lewis (United States) and William Davis (Canada) were appointed last March to try to avoid a political impasse over the issue. There is no question that far more acid emissions find their way from the United States to Canada than in the opposite direction. The envoys say in their report that "it is very clear there is a solid link" between acid precipitation and emissions of acidic gases. Although clean-air legislation enacted in the United States in the early 1970s has improved ambient concentrations, long-distance transport (a result of tall smokestacks) has not improved.

The most widely used method of reducing emissions from existing plants, the scrubbing of flue gases, is expensive and produces enough waste to be a problem in its own right. New technologies that burn coal with increased efficiency and remove sulphur during combustion rather than afterwards, such as combined cycle gasification and fluidization bed combustion, offer a cheaper way to remove pollutants, but utilities say that they cannot be expected (because their tariffs are regulated) to risk huge sums on unproven technologies.

Meanwhile, the electricity utilities welcome the contention of the Lewis/Davis report that present scientific evidence is unsufficient to justify "punitive control". Industry spokesmen point out that utilities have already voluntarily spent $500 million on research into clean coal technology over the past 5 years, to be followed by another $500 million over the next 5 years.

The utilities' support for the envoys' recommendations is not altogether surprising because, if adopted, the recommendations would ensure that the US government pays half the cost of technology demonstration projects. The US Congress at the end of last year put $400 million into clean coal technology, but the industry has undertaken to spend up to $2,100 million if it gets a promise of support.

Some who have studied acid rain are less happy about the Lewis/Davis assessment that technology demonstrations are what is called for. David Schindler, who chaired a study on acid rain for the National Academy of Sciences in 1981, said he was "disappointed" that immediate control measures were not recommended and that the report concealed its true purpose of delaying action. Schindler said the evidence implicating sulphur dioxide in the acidification of lakes was "clearly strong enough" to support immediate action and stronger than the evidence on which the use of phosphorus in detergents was banned in the 1970s because of its effects on the Great Lakes.

Jack Calvert, of the National Center for Atmospheric Research, who chaired another National Academy study, said he had hoped the Lewis/Davis report would recommend a reduction in emissions from some of the major polluters in Pennsylvania, West Virginia or Ohio, so that actual effects could be observed and an informed decision taken on whether further controls are likely to be effective. Calvert applauded the report's support for greater efforts to monitor acid deposition, especially dry deposition, which is still not monitored systematically.

Whether the special envoys' work will lead to an easing of tensions between the United States and Canada over acid rain will now depend on the US administration's response to their recommendations, which include the setting up of a joint committee with a US cabinet-level representative.

The issue will be a "priority topic" at a meeting to be held in Washington in March between President Reagan and Canadian Prime Minister Brian Mulroney.

Tim Beardsley

Fusion research

US, Europe, Japan collaborate

IN an agreement signed yesterday (15 January), the United States, Europe and Japan, traditionally rivals in the search for economic energy from nuclear fusion, formalized a programme of enhanced cooperation in this direction. The agreement, signed at the Max-Planck-Institut für Plasmaphysik at Garching, Munich, commits scientists from the three programmes to hold regular trilateral workshops, to exchange basic data and experimental plans, and also personnel and equipment.

All three programmes are tokamak machines in which ionized hydrogen trapped in a toroidal container by magnetic fields may be heated to temperatures and densities sufficient for fusion reactions to occur. Basic heating is provided by passing a current through the torus, treating the plasma as a secondary winding in a transformer. But supplementary heating is required and, at all three tokamaks, is provided by a combination of high intensity radio waves generated from antennae in the torus walls and the injection of neutral atoms at high energy.

Present interest at all three tokamaks is in the development of the supplementary heating sytems; the problems of magnetic confinement and heating seem to have been solved. The heating system for Japan's JT–60 tokamak is expected to be working by next December, while at the Joint European Torus (JET) at Culham in Britain, the first stage of radio heating has been tested and neutral beam injection is about to be installed. Princeton's Tokamak Fusion Test Reactor (TFTR) is to embark this week on a lengthy experimental run.

According to Donald Grove of TFTR, the new agreement should make the three programmes more productive. "From now until the international fusion conference in Kyoto next November, the three tokamaks are on essentially the same footing", he says. It is hoped TFTR will achieve break-even in energy production, by means of deuterium fusion, by 1987.

Philip Campbell

British science

Researchers find a voice

British scientists, traditionally quiet and uncomplaining, have expressed their anger, in the form of Save British Science (SBS), an "appeal to public and Parliament to call on the Government to reverse the decline in support for scientific research", which was launched in London this week. Four Members of Parliament (MPs) are proposing a debate in the House of Commons, and will ask the government to spend £100 million this year on basic science research — enough to keep Britain level with other European countries.

Professor Denis Noble, one of the scientists launching the appeal, said this week that "a few years ago it would have been unthinkable that someone in my position would speak out publicly" about the state of science spending in Britain. The decline in real terms (see graph) at a time when France, West Germany, Italy and Japan are increasing research spending, means that "selectivity is becoming a polite word for retreat, which is now in danger of becoming a debacle", according to Dr J. Mulvey, secretary of SBS. Noble described examples of scientists leaving to work abroad, obsolete equipment and occasions where scientists who had written successful grant proposals did not receive enough money for their own salaries, but only enough for the project itself.

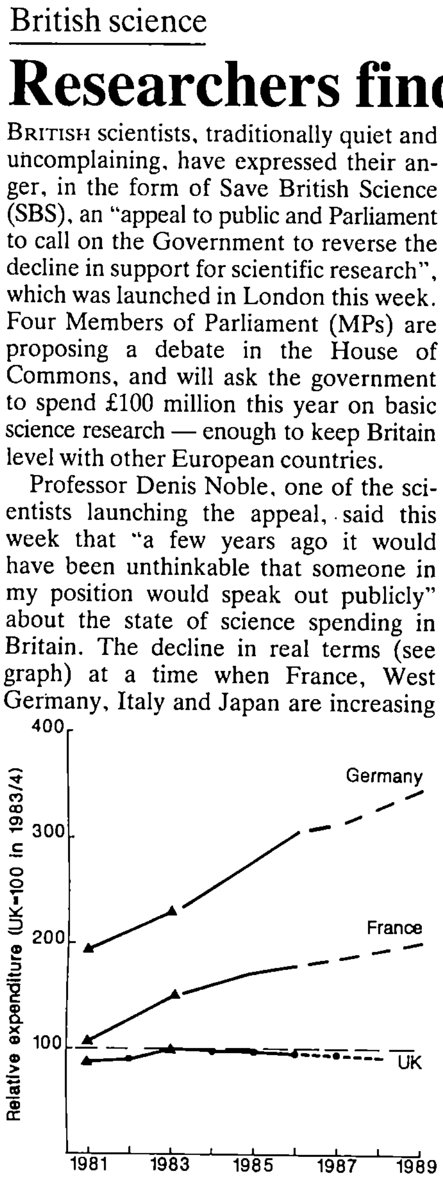

Government funding of basic research in the United Kingdon, France and West Germany. Triangles, data from the *Annual Review of Government Funded R & D 1984* and *1985*. Dotted lines, policies based on recent ministerial reports.

SBS has collected more than 1,500 contributions since it was formed last November, and claims that grassroots support is "snowballing". But, apart from an advertisement in *The Times* about the predicament of British science, no coherent policy has yet emerged. Others have already pointed out the dangers of failing adequately to support basic science research to the government, with little success. The group must turn into efficient lobbyers for parliamentary support, and, as suggested by the MPs present at its launch, be both apolitical and efficient in communicating with the Government. SBS should have a formal membership so that it can genuinely reflect the wishes of its supporters and become an effective force in popularizing the need for research. It wants to obtain more support for research from industry, and thinks that government-induced collaborations between industry and academics are unlikely to produce more money for basic research whereas a tax-credit system for industries that fund this type of research is more likely to achieve the aim.

In Parliament, SBS could investigate the setting up of a body like the US Office of Technical Assessment, to advise MPs on scientific issue and to contribute to informed debate and wider general acceptance of the importance of science. A policy must also be formulated on whether or not Britain should have a representative at cabinet level specifically for science, or how seriously to take the Prime Minister's contention that she represents the interests of scientists.

Maxine Clarke

Refusnik scientists

Dissenting dissidents agree

Learned societies campaigning for oppressed scientists in the Soviet Union should avoid mentioning "human rights" in letters to the Soviet scientific establishment, Dr Alexander Voronel of Tel Aviv University told a seminar in Oxford this week. The seminar, for representatives of national academies of science and learned societies, had met to discuss what such bodies can do to help Jewish *refusnik* scientists. Although there were some vehement objections to Dr Voronel's view, notably from a delegate from the United States who described himself as an "academic lawyer", Dr Voronel's record as founder and first convener of the original Moscow Sunday seminar for *refusniks* gave his views considerable weight.

Dr Voronel's contention is that any mention of "human rights" is an automatic irritant to Soviet officialdom, which counters by alleging that the West is trying to interfere in internal Soviet policy. One should rather campaign, he said, for Soviet scientists to be allowed to exercise their professional rights of appropriate employment, unrestricted professional correspondence, participation in scientific gatherings both at home and abroad, and — the particular issues in the case of *refusniks* — the right to emigrate. This "right", incidentally, is now of paramount importance to the *refusniks;* a message to the seminar from three leading refusnik scientists, Victor Brailovskii, Mark Freidlin and Aleksandr Ioffe, urged all well-wishers "in view of the extreme urgency of our problem, [to] put aside all other aspects of our being here, and the difficulties encountered in our daily lives" and campaign only on the emigration issue.

Mr Fabian Kolker, the US philanthropist, who two years ago founded a scholarship for ex-*refusniks* at Tel Aviv University, summed up the views of both Voronel and the *refusniks'* letter. "Our goal should be success in unlocking the gates of the Soviet Union", he said, "and we must therefore use language that the Soviets will accept."

How to put more leverage behind such "language" was the main point of discussion. The chairman, Dr Inga Fischer-Hjalmars of the University of Stockholm presented an 11-point programme of suggested action, particularly slanted towards making intervention by Western colleagues a "professional" and not merely a humanitarian matter. Thus *refusniks* can be elected to the appropriate learned societies, or asked to join editorial boards of scientific journals, giving such societies or boards a valid interest in the welfare of and continuous contacts with their fellow members. (A suggestion from the floor extended this to asking *refusniks* to review books, which would have the additional bonus of supplying them with works in their field.)

If learned societies are to help, however, they must concern themselves, the consensus of the seminar agreed, not just with *refusniks* but with the whole range of breaches of human rights under all forms of repressive regime. This has always been a divisive issue, with Israeli scientists maintaining that one must not confuse *refusniks* and dissidents, while their foreign colleagues pointed out that it was impossible to ask a fellow faculty member to sign a petition on behalf of Brailovskii or Shcharanskii, and they refuse to sign the petition he was organizing on behalf of oppressed scientists in Turkey or South Africa. This time, however, there was little contention. It is now accepted, even by the Israelis, that learned societies and academics have human rights committees that campaign across the political board for scientists victimized for their convictions. Nevertheless, as Dr Kristoffer Gjotterud of Oslo pointed out, the distinction is a real one, and in campaigning for Soviet scientists in trouble, he stressed that one should never confuse the dissidents who wish to change what they see as inherent injustices in the Soviet system and the Jewish *refusniks* who are penalized for wishing to leave the Soviet Union altogether.

Vera Rich

Viral cancers

AIDS virus at the centre

Los Trois Ilets, Martinique

"RESEARCH in viral-associated cancers has come of age", said Peter Fischinger, deputy director of the National Cancer Institute (NCI) at a three-day conference here co-sponsored by the National Institutes of Health (NIH) and the Association pour la Recherche sur le Cancer (ARC).

Initial enthusiasm for the possible role of viruses in cancer accompanied the discovery in the 1960s that Epstein–Barr virus is associated with Burkitt's lymphoma. But that enthusiasm abated when little evidence was found to implicate other viruses with human cancers.

Today, the enthusiasm has returned. Nasopharyngeal cancer, a much more significant worldwide health problem than Burkitt's lymphoma, has also been linked to Epstein–Barr virus. Hepatitis-B virus DNA has been found in hepatocellular carcinomas. Different variations of human papilloma virus have been identified in 80 per cent of human papillomas, and, according to Harald zur Hausen of the Deutsches Krebsforschungszentrum at Heidelberg, it is likely that some form of human papilloma virus will be found in all forms of human cervical cancer.

Probably the most significant reinforcement of interest in cancers associated with virus comes from the discovery that a human retrovirus, HTLV-I, causes adult T-cell leukaemia, and that another human retrovirus, HTLV-III/LAV, causes acquired immune deficiency syndrome (AIDS).

In 1985, NCI spent $135 million on viral cancer research, approximately 12 per cent of its budget. Whether that level of support will continue is unknown. Both NCI director Vincent DeVita and NIH director James Wyngaarden were forced to bow out of this conference at the last minute to devise a new budget for NIH under the guidelines set forth in the recently passed Gramm–Rudman legislation (see *Nature*, **318**, 495; 1985).

Although HTLV-III/LAV has not been directly associated with cancer, the explanation may be that patients are killed by opportunistic infections seen in AIDS before cancers can develop. According to Max Essex of the Harvard School of Public Health, many more cats die from opportunistic infection associated with feline leukaemia virus than die from leukaemia.

A possible human parallel is seen in Japan; Isao Miyoshi of the Kochi Medical School reports seeing infections similar to those seen in AIDS patients in individuals infected with HTLV-I. There may be more of these patients, but so far no one has thought to look for them. Ironically, it may yet turn out that HTLV-III/LAV will cause cancer if AIDS patients can be kept alive long enough to exhibit it.

The explosion in AIDS research has produced several interesting and potentially important discoveries. Evidence for heterosexual transmission of HTLV-III/LAV continues to grow. In 1979, 12 per cent of AIDS patients in Haiti were female; now, the number has grown to 30 per cent, and is expected to grow to 40 per cent in the next two years.

Conflict continues about what constitutes an effective therapy for AIDS. Research at the Pasteur Institute in Paris has focused on HPA-23, a compound that can block HTLV-III/LAV production *in vitro* and apparently *in vivo*. Sam Brower of NCI believes that a therapy that blocks viral replication is insufficient, and that the need is for an agent that will restore the helper/inducer T cells destroyed by HTLV-III/LAV infection. One such compound appears to be 3′ azido-3′-deoxythymidine (AZT), now in clinical trials at NIH. A major advantage of AZT is it can be taken orally, an important consideration as it will have to be taken for life.

There are also indications that a new generation of assays for HTLV-III/LAV is not too far off. An important first step achieved in a preliminary form by Biotech Research Laboratories in Rockville, Maryland, is the purification of viral coat proteins, which may also play an important role in vaccine development.

There was some tension at the meeting between NCI and Pasteur Institute researchers over the recent lawsuit by the French over the granting of a patent for an HTV-III/LAV antibody test (see *Nature* **318**, 595; 1985). Both Luc Montagnier, the Pasteur researcher who first reported the association of a retrovirus with AIDS, and Robert Gallo, the NCI researcher whose work led to the US patent, attended the meeting. Nomenclature became somewhat confusing as the virus was alternately referred to as "HTLV-III/LAV", "LAV/HTLV-III", "LAV" or "HTLV-III" depending on the nationality and affiliation of the speaker. Future collaborations are not likely to suffer because of the current contretemps.

But Gallo complains of one unpleasant side effect of the lawsuit; he has been ordered to make photocopies of all notes and data relating to his work by US government lawyers acting in the lawsuit; this, Gallo maintains, will set back his research schedule.

ARC, the French co-sponsors of the meeting, have taken an active interest in viral associated cancers, especially in their relevance to health issues in underdeveloped countries. They also pride themselves on bringing together researchers around the world to tackle problems of mutual interest. In March 1984, a conference in Marseilles on cancers of the Mediterranean included Arab and Israeli researchers.

Says Gerard Milhaud, a member of ARC's scientific advisory board, "We got the Israelis and the Arabs together for a meeting. Bringing Montagnier and Gallo together was easy." **Joseph Palca**

Infection mechanism?

NCI's Robert Gallo now believes that transmission of HTLV-III/LAV infection is through cells, not virus particles. His scenario for spread of infection suggests that when a donor cell is recognized by a recipient cell, there is a mixed lymphocyte reaction. This in turn releases lymphokines which activate the initiating sequences of the viral genes, including the transactivating transcription gene (*tat*), which in turn causes viral expression in the newly infected host. This mechanism would explain why HTLV-III/LAV is not highly contagious, requiring some transmission of body fluid containing lymphocytes.

Gallo also reported five new cases of HTLV-II infection, and suggested there is some evidence that this virus is also spreading.

Although evidence for brain infection by HTLV-III/LAV is now undisputed, the exact target for infection is still in doubt. Luc Montagnier of the Pasteur Institute believes glial cells are infected directly, and has *in vitro* evidence to support this. Gallo, however, believes that brain involvement comes from monocyte macrophages migrating to the brain, possibly turning into microglial cells. Joseph Palca

Polish astronomers

THREE **Polish astronomers from the Copernicus Astronomical Centre in Torun are expected to go on trial this week for possession of an illegal radio transmitter. Drs Jan Hanasz, Zygmunt Turlo and Leszek Zaleski, all members of the Polish Astronomical Society, were arrested on 26 September, together with Mr Piotr Lukaszewski, a technician from a local factory, charged with an offence against public order and possessing the transmitter.**

They had used it to put out a television broadcast calling for a boycott of the forthcoming general elections, which they categorized as "undemocratic".

The astronomers last weekend called on Western colleagues to take note of their case, urging that, under prevailing conditions in Poland, the normal methods of making one's viewpoint felt were not available. Vera Rich

British veterinarians

Pressures for collaboration

The six British universities providing courses in veterinary medicine are in the throes of deciding how to meet the demand that they should teach fewer students and, at the same time, cost the central budget less. At a meeting on Wednesday this week, heads of the six schools and officials of the Royal College of Veterinary Surgeons will have tried to put a plan together. The University Grants Committee (UGC) is looking for a firm proposal by 28 January, and will otherwise draw up a scheme of its own.

The six British veterinary schools (at Bristol, Cambridge, Edinburgh, Glasgow, Liverpool and London) are all having to adjust to smaller student numbers in the wake of the third quinquennial report on veterinary manpower, commissioned by the Ministry of Agriculture, Fisheries and Food, which recommended a reduction of 10 per cent in the numbers of students recruited into veterinary medicine, from a total of 335 a year to just 300. These reductions will take effect from the beginning of the next academic year.

Pressure from UGC arises from the high cost of teaching veterinarians in Britain. Courses last five years, following the pattern of medical education, with three "undergraduate" years of biological science and two years of clinical study, including a compulsory 26 weeks of on-the-job training. Professor E.J.L. Soulsby (Cambridge), last year's president of the Royal College and thus the initiator of the present reform, points out that the teaching of veterinarians and physicians differs in that part of the cost of medical teaching is provided indirectly by the public health services, which keep the teaching hospitals full of patients and provide for their care. Many veterinary schools have to rely on private practitioners to supply sick animals, which must then be treated and cared for out of university funds.

Several alternative proposals for reorganization are being considered, among them a plan to allow the six schools to continue in their slimmed-down form for the first three years of the standard course, but to concentrate resources required for the succeeding years at different schools, with the understanding that students would move from one place to another.

Professor I.A. Silver (Bristol) says that if the six schools have not agreed on a plan this week, it will fall to the college (of which he is president this year) to put forward a scheme acceptable to UGC. He is heartened that UGC says it will pay close attention to the quality and the amount of research in deciding which schools should be favoured.

Not all veterinarians are reconciled to the conclusion that student numbers should fall by 10 per cent. Professor A. Iggo (Edinburgh) points to the potential value of novel biological techniques in the future treatment and management of domestic animals and thinks that the manpower estimates may take too little account of research needs. He reckons that a third of the income of his own department may arise from research grants and contracts.

Most British schools appear, however to accept that the overseas demand for veterinarians has shrunk substantially, even though there is still a buoyant demand from overseas schools from students with a first degree seeking graduate training and experience.

DNA fingerprinting

DNA probes control immigration

One of the first uses of the technique developed at the University of Leicester by Dr Alec Jeffreys for telling the genetic identity of individuals by the use of gene probes is likely to be in the control of immigration into Britain. But the Foreign Office denied last week reports from Dacca, Bangladesh, attributing to Mr Timothy Eggar, Under-Secretary of State, the announcement of the introduction of an operational scheme by April this year.

The issue is potentially contentious between Britain and Bangladesh, and between the British government and its immigrant population, because of the requirements of the now strict immigration law distinguishing between blood relatives of different affinity. What appears to have happened so far is that the Home Office and the Foreign Office are jointly sponsoring a pilot study at Leicester, but have not yet decided whether to mount an operational scheme for verifying claims of kinship.

Jeffreys says, however, that the technique has already been used successfully in a number of disputed immigration cases, the first of them on the initiative of a solicitor (attorney) acting for the father of an immigrant boy whose kinship had been disputed. The solicitor had been alerted to the usefulness of the techniques by publicity following the publication of a paper last March (Jeffreys, A.L., Wilson, V. & Thein, S.L., *Nature* **314,** 67; 1985: see also News and Views **318,** 507; 1985). The first analysis proved the claim of kinship, but the Home Office withdrew from the case so that there is as yet no legal precedent in Britain for the use of evidence of this kind.

Jeffreys says that the use of DNA fingerprinting in immigration cases is likely to be more complicated than in common paternity cases because disputed kinships may centre on suspicions that an adult is seeking to pass off a nephew as a son. Because of the high frequency of common genes among siblings, it is therefore necessary to test for a greater number of restriction polymorphisms. Even so, he estimates that it should be possible in routine cases to attain a precision of more than 99 per cent in cases of disputed kinship.

The Home Office emphasizes that even if the technique is introduced on a regular basis in considering applications for immigration to Britain, this will be offered only on a voluntary basis. (Nothing is said of the fate of those who decline a blood sample.)

Whatever happens to the immigration project, the forensic use of the technique is likely to be widespread. The commercialization of Jeffrey's version of DNA fingerprinting is being exploited by the Lister Institute.

Romanian mathematics

Absent guest at Princeton

Dr Radu Rosu, a Romanian mathematician invited to the Princeton Institute of Advanced Studies, last week began a 12-day fast to mark the beginning of the second term in which he has not been able to take up his invitation. Rosu, who was due to begin work at Princeton last September, claims that his application for a passport is blocked by the Communist Party organization of the University of Bucharest.

Dr Rosu, a geometer, began his research career at the Institute of Mathematics of the Romanian Academy of Sciences. When the academy was stripped of its institutes in the mid-1970s, and pure mathematics was virtually eliminated on utilitarian grounds, Rosu became a programmer at the computer centre of the Research Institute for the Energy Network.

In 1979, he transferred to the Institute of Mathematics at the university, where, in 1983, he successfully defended his doctoral thesis. The invitation to Princeton seems to have been inspired by a paper with Soviet mathematician I.M. Gel'fand.

Dr Rosu is not the only Romanian mathematician resisting his government's repressive policy. Last week, Dr Mihai Botez gave an interview on French television drawing attention to (and defying), the ban on unauthorized contacts with foreigners.

Vera Rich

Division of Japanese psychiatry

SIR—As the visiting scientist who drew the attention of *Nature* to the events surrounding the seventh congress of the Japanese Society of Biological Psychiatry in April 1985 (see *Nature* **315**, 361; 1985), I was interested to read the contribution of Dr K Moriyama (*Nature* **318**, 308; 1985) to the debate. As I understood the situation (from psychiatrists attending the meeting in Nagoya), it was indeed threats from the group with which Dr Moriyama is associated that led to the abandonment of the seventh congress, a satellite symposium on schizophrenia to be held in Gifu and then the *ad hoc* meeting organized in a hotel in Nagoya.

Two issues have emerged. Undoubtedly there are aspects of the Japanese mental health care system that are at variance with practice in other advanced nations. The report of the fact-finding mission of the International Commission of Jurists and International Commission of Health Professionals (see *Nature* **316**, 571; 1985) highlights a number of problems. One would expect that these would be the subject of discussion within and outside the psychiatric community in Japan and that someone of Dr Moriyama's declared interests would be working within a professional and political context (for example through a body such as MIND) for legal changes.

The second issue relates to freedom of exchange of scientific information. Dr Moriyama writes of "protest action taken against the seventh congress". Undoubtedly he and his followers have created a situation in which organizers feel obliged to cancel meetings rather than face confrontation. I understood from the psychiatrists to whom I spoke at the aborted meeting in Nagoya that previous "protest action" had ended in physical violence with the possibility of serious injury to meeting participants. A visitor to Japan has difficulty in understanding how Dr Moriyama and his colleagues justify adopting tactics that presumably are illegal, and finds it equally perplexing that the congress organizers did not consider the protection of the law adequate to allow the congress to continue.

Dr Moriyama alleges that the papers to be presented at the seventh congress reveal "evidence of many unethical experiments". I have a copy of the volume of 114 numbered abstracts that were to have been presented. These are mostly in Japanese, although the sections that are not indicate that the topics include many that were discussed at the recent World Congress of Biological Psychiatry in Philadelphia. I invite Dr Moriyama to indicate which abstracts he considers raise particular ethical issues. I will then arrange for these abstracts to be translated and submitted to a United Kingdom ethical committee (see for example Denham *et al.* 'Work of a district ethical committee', *Br. Med. J.* **ii**, 1042–1045; 1979) or to a comparable American institutional review board. It will then be possible to assess whether there is independent support for the views expressed by Dr Moriyama.

T.J. CROW

Clinical Research Centre,
Division of Psychiatry,
Watford Road,
Harrow, Middlesex HA1 3UJ, UK

Animal intelligence

SIR—I should like to add to J.H. Fremlim's letter on animal intelligence (*Nature* **316**, 760; 1985). Human intelligence is not only quantitatively but also qualitatively different from animal intelligence because it recognizes time as a dimension. Man knows that there is a future in addition to the past and the present.

The awareness that a future exists gives man the incentive to plan, and to ensure that the plan succeeds. He therefore prepares weapons for the hunt and containers for the foraging expedition. This culminates in the discovery of agriculture, in the knowledge that seed planted in the spring will bring in a rich harvest in the fall, enabling him to survive the winter in comfort.

ANDREJS BAIDINS

1104 Windon Drive,
Wilmington, Delaware 19803, USA

Aleksandrov

SIR—Vera Rich writes (*Nature* **318**, 592; 1985) of "rumours circulating in the West" that Academician Vladimir Aleksandrov, who disappeared in Madrid last April, had been intending to defect, but was prevented by Soviet security men.

We no longer live in a time when every member of a Soviet delegation abroad is shadowed by another. Vladimir Aleksandrov, like many of his compatriots travelling in the West, had countless opportunities to defect. At a conference in Helsinki in 1984 I met him early one morning jogging in some woods — with nobody on his heels. And Western embassies in many capitals would surely be glad to give asylum to a leading Soviet mathematician and computer scientist.

It is also simply speculation to suppose that Soviet official silence on Academician Aleksandrov's disappearance indicates sinister goings-on. It is not Soviet policy to utter publicly on events that are bad news, unless it is to prevent their recurrence. Of course these rumours may be right, but where is the evidence?

STEWART BRITTEN

9d Stanhope Road,
London N6 5NE, UK

Creationism

SIR—In his Commentary on the unreasonable claims of scientific creationists, Michael Cavanaugh (*Nature* **315**, 185; 1985) seems to ignore the boundaries in biology that separate some observations from their causes and which are the basis for appealing to history, whether traditional or conjectured. Scientists have deciphered the genetic code, but chemical genetics has not supplied a theory for its origin. The stability of nuclear DNA has frustrated understanding how and from where organisms might acquire the enormous amount of genetic information needed to leap the persisting gaps in the fossil record — and on so grand a scale to bring whole populations into existence suddenly and worldwide. Cosmologists, too, recognize that the equations of the big bang theory are not capable of describing conditions before the big bang.

To assert in the absence of scientific theory that the origin of the genetic code and acquisition of new genetic information by organisms nevertheless occurred spontaneously is clearly a matter of faith. Evolutionists and creationists are therefore epistemological equals who are free to choose which history provides more meaning for life.

Creationists are indebted to evolutionists for having put the history of *Genesis 1* to the test. Practice of the scientific method has established boundary conditions concerning origins that are evidence for a creator. Along with evolutionists, creationists predict that these boundaries one day will open to rational thought.

D.H. KOOBS

Box 543, Loma Linda,
California 92354, USA

Is anyone there?

SIR—There must surely be *something* magical about the "magic frequencies" at which, you report (*Nature* **317**, 275; 1985), yet another project is searching for extraterrestrial signals. But the magic is that anyone should waste their time, and our money, searching the bands where interference and attenuation of any such signals is at a maximum.

Any rational ET communication engineer would transmit at frequencies where these are at a minimum. Is anyone looking in the right place?

M.H. MACDONALD

8 Wilton Street,
Brighouse, Yorkshire, UK

WHAT IMPACT ARE NEW BIOTECHNOLOGY TECHNIQUES HAVING ON MEDICINE WORLDWIDE TODAY?

Come to Nature's 7th International Conference in London on Molecular Biology in Medicine 1986 for all the up to date facts — and a look into the near future.

NEW TECHNOLOGY in BIOTECHNOLOGY

MOLECULAR BIOLOGY IN MEDICINE

a survey of its achievements and its potential

JUNE 18-20 1986 — LONDON

It is clear that the modern techniques of biotechnology are set to have a major impact on medicine. Over the next few years many new opportunities will emerge. This important conference will provide a wide-ranging survey of the most recent research in the fast changing field of molecular biology in medicine, and a look into the future. If you want an opportunity to see and hear for yourself what leading exponents have achieved in recent years — and to learn what new opportunities are on the horizon, come and join us. You'll find a booking form below.

JUST SOME OF THE NEW OPPORTUNITIES YOU CAN FIND OUT ABOUT FIRST HAND AT NATURE'S 7TH INTERNATIONAL CONFERENCE.

DIAGNOSTICS

Monoclonal antibodies to speed up and simplify laborious tests.

engineered antibodies to provide further sophistication.

gene probes to allow the detection of mutations that are linked to cancer.

THERAPEUTICS

the discovery of new families of proteins and peptides with potential clinical value.

the means to engineer proteins so as to improve their therapeutic value.

the use of monoclonal antibodies to target drugs to tissues.

PREVENTION

the first potential vaccines against several infectious diseases, such as malaria.

the refinement of existing vaccines.

the detection of genetic defects with sufficient confidence and speed to prevent or limit their damage.

AMONG THE LIST OF TOP CALIBRE INTERNATIONAL SPEAKERS WILL BE

G. Schild, National Institute for Biological Standards and Control, UK
A. Capron, Institut Pasteur, Lille, France
S. Gillis, Immunex, US
M. Neuberger, LMB, Cambridge, UK
L. Montagnier, Institut Pasteur, France
K. Sikora, Ludwig Institute, Cambridge, UK
R. Gerety, Merck Sharp & Dohme, US
T. Waldmann, NIH, US
R. Baldwin, Nottingham, UK
E. Tuddenham, Royal Free Hospital, UK
D. Weatherall, Oxford, UK
W.F. Anderson, NIH, US

OUR THREE DAY PROGRAMME ENABLES YOU TO ASSESS IMPORTANT NEW BIOTECHNOLOGY TECHNIQUES IN MEDICINE, MEET INTERNATIONAL RESEARCH SPECIALISTS, AND DISCUSS WHAT YOU LEARN WITH NEW CONTACTS FROM AROUND THE WORLD.

JOIN US AT NATURE'S 7TH INTERNATIONAL CONFERENCE, TO BE HELD AT THE LONDON WEST HOTEL, JUNE 18-20 1986.

REGISTER NOW TO ENSURE YOUR PLACE — SPACE IS LIMITED.

The **CONFERENCE FEE** is just £189 plus VAT for the three days of the conference. This includes entrance to all sessions, mid-morning coffee, afternoon tea and reading material. Group discounts are available on application to Janine Slipman, Macmillan Conferences and Exhibitions, 4 Little Essex Street, London WC2R 3LF, UK, Telephone (01) 836 6633.

Book before January 31st and we'll send you Nature's 1986 calendar FREE!

ACCOMMODATION has been reserved in the London West Hotel for conference participants. A booking form will be sent to you as soon as we receive your registration.

TECHNICAL SEMINARS and **POSTER SESSIONS** will be held each day.

CONFERENCE BOOKING FORM

NEW TECHNOLOGY in BIOTECHNOLOGY
MOLECULAR BIOLOGY IN MEDICINE

To register for the conference, please return to Macmillan Conferences and Exhibitions, 4 Little Essex Street, London WC2R 3LF, UK

Full name ____________________
Full job title ____________________
Address ____________________
____
____
____
____
Tel no: work __________ home __________

Please tick appropriate boxes

☐ I wish to make a firm reservation for the full duration of the conference, at £217.35 (£189 + VAT)

☐ I enclose a cheque made payable to Macmillan Journals

☐ Please charge my ☐ Visa ☐ Mastercard
account no. ____________________
expiry date ____________________
signature ____________________

☐ Please bill my organisation (please attach address and contact name if different from above)

☐ I am interested in attending the conference, please send me full programme details as soon as they are available.

☐ Please send me details of your group discounts.

NOTES: Please complete one form per person. Extra booking forms can be obtained from the address above or by telephoning Janine Slipman on (01) 836 6633

BOOK NOW AND RECEIVE NATURE'S 1986 CALENDAR FREE!

NATURE'S GUIDE TO

HOW BRITAIN RUNS ITS SCIENCE

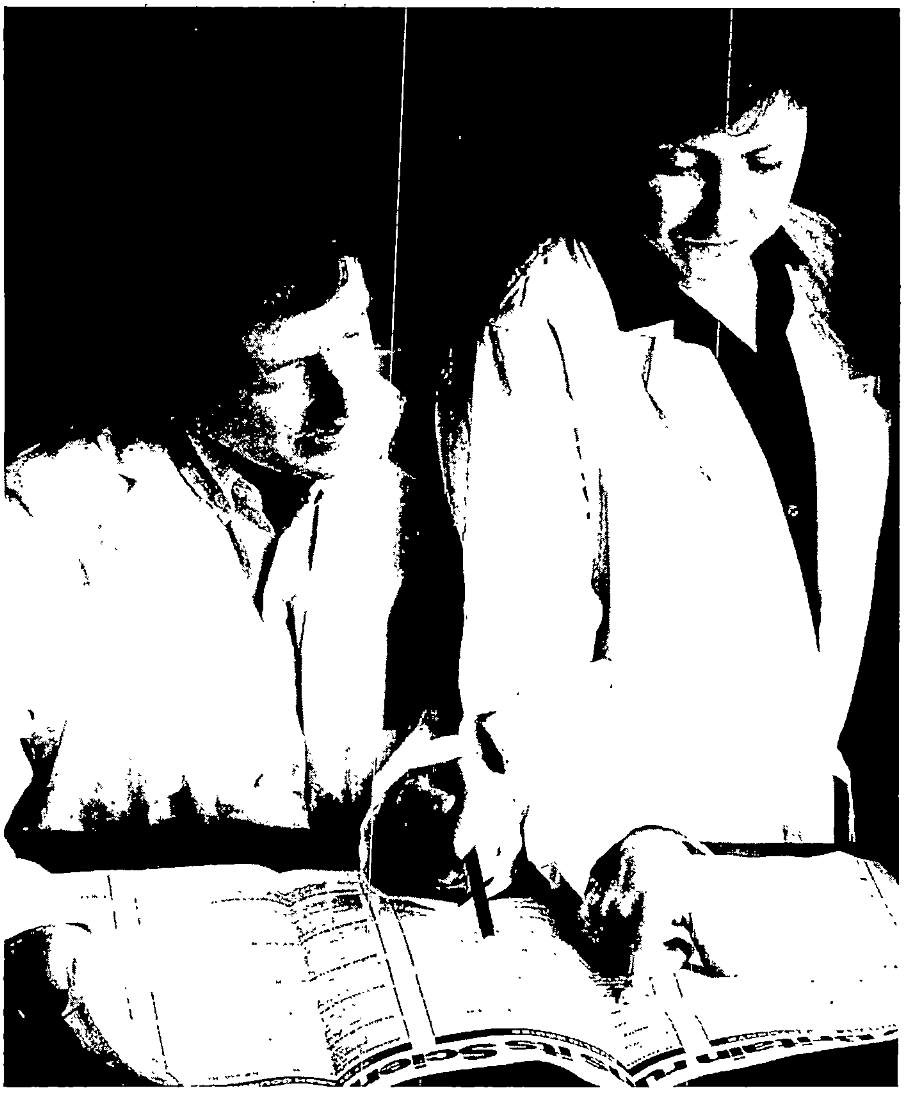

This highly successful wallchart has now been redesigned and updated to take account of changes in structure and personnel since the previous edition was published in 1983.

Compiled in Nature's editorial office, the guide provides a comprehensive survey of the administration of British science, showing at a glance the functions, key personnel and finance of government departments, public and independent bodies and the research councils.

Designed as a fold-out sheet, in red, blue, black and white, the 60 × 90cm chart can be carried easily to meetings or hung as a wall poster for permanent reference.

Copies are available from: Nature, Brunel Road, Houndmills, Basingstoke, Hants, RG21 2XS, UK. Prices: (including postage and packing) £4.75 (UK), US$8.50 (USA and Canada), £5.75 (all other countries).

nature

INTERNATIONAL WEEKLY JOURNAL OF SCIENCE

Name ____________________

Address ____________________

____

____

____

Please send me ____ Chart(s) of Nature's Guide to How Britain Runs its Science

Airmail despatch outside the UK

Payment with order please

Newtonian gravitation corrected

Suspicions that the inverse square law for the gravitational force between two objects may be incorrect at short distances appear to have been confirmed. Better measurements are required.

NEWTON's inverse square law of gravitation may, after all, be incorrect. That is the strange and somewhat mystifying conclusion of the latest investigation of the value of the universal constant of gravitation (G). For although there have been many recent suggestions, theoretical and otherwise, that the strength of the gravitational coupling between massive objects may be a function of distance at small distances, the surprise is that it has now been established by a re-examination of the results of the Eötvös measurements, widely accepted for more than half a century as a proof that gravitational interactions depend only on the mass of the objects involved.

The new development (*Phys. Rev. Lett.* **56**, 3; 1986) is the work of Ephraim Fischbach of the University of Washington, St Louis, Daniel Sudarsky, Aaron Szafer and Carrick Talmadge of Purdue University and S.H. Aranson of the Brookhaven National Laboratory. The essence of their conclusion is that G, the 'constant' in Newton's inverse square law, is in reality a function of the distance separating interacting masses, and is less by a few parts in a thousand at distances of the order of 200 m.

The reasons why G may not be constant have been widely canvassed, and follow naturally from the now common assumption that the four natural forces (gravitation, electromagnetism, the weak and the strong nuclear interaction) are, at some level of abstraction, aspects of one general interaction. Field theorists who have set their sights on the 'grand unification' of the elementary forces have long anticipated this conclusion. In such a scheme, the gravitational interaction between two masses is mostly explained by the exchange of hypothetical field particles ('gravitons'), just as the electromagnetic interaction is accounted for by the exchange of photons between interacting electric charges, but grand unification allows other field particles to chip in, modifying Newton's inverse square law.

The expectations have been nicely put by G.W. Gibbons and B.F. Whiting (*Nature* **291**, 636; 1981) for example, who argued for departures from Newton's inverse square law represented by a G which is a function of the distance r between interacting masses with the form $G = G_o\ (1 + \alpha e^{-r/\lambda})$ where G_o is the value of G at large distances; α and λ are constants, the second of which is determined by the mass of the extra field particle mediating the gravitational interaction and provides a scale of lengths at which departures from the inverse square law should be apparent.

Geophysical data provide supporting evidence. If G varies with distance, and if the characteristic length scale is of the order of metres, the acceleration of a satellite in orbit about the Earth should differ from that expected from the measured acceleration of a mass near the surface of the Earth and from a direct measurement of the force between two masses separated by a few centimetres, as in the measurements of Cavendish a century ago.

Geophysics should yield information on departures from Newton's law a little more directly, as F.D. Stacey and G.J. Tuck have clearly argued (*Nature* **292**, 230; 1981). They showed that it should be possible to use measurements of gravitational acceleration ('little g') in boreholes in the Earth's crust, together with measurements of the density of the rock strata they traverse, to estimate the possibility that G varies with distance. Two years ago (S.C. Holding and C.J. Tuck, *Nature* **307**, 714; 1984), results of gravity measurements in two mineshafts at the Mount Isa mine in Australia were held to be consistent with a variable G, although everybody seems to agree that measurements in mineshafts, especially in metalliferous regions, are far from ideal. Stacey seems to have been the first to press for measurements of g as a function of depth in the deep oceans, where inhomogeneity and uncertainty about the density of the surrounding material would be less serious complications.

Fischbach *et al.* take a different tack, going back to the classical measurements in which Eötvös sought to demonstrate that the gravitational attraction between two objects is simply a function of the product of their masses (and the distance between them). Several pairs of different materials were evaluated against each other — water, copper sulphate, platinum and even tallow against copper, for example. Fischbach *et al.* rightly say that the measurements have been taken as a proof that the mass, and not its constitution, is all that matters.

Their own starting point is more complicated. What if departures from newtonian gravitation are brought about by the exchange of massive photons such as might be associated with the non-conservation of charge and parity (*CP*-non-conservation, as it was called by Lee and Yang in the 1950s)? Then the extra force should be repulsive, and should be determined not by the masses of the gravitationally interacting objects but by their baryon numbers (or, more accurately, by their hypercharges).

But surely the baryon number of one gram of platinum will be the same as the baryon number of a gram of copper sulphate, and simply determined by the number of nucleons it contains? This is the simple explanation. But allowing both for the contribution of electron masses to the total mass of a material, and for nuclear packing fractions, it turns out that there are more baryons per unit mass in the middle of the periodic table (around Fe) than at either end.

All this is beyond dispute. The surprise is that Fischbach *et al.* have been able to find in the original Eötvös measurements evidence of departures from newtonian behaviour that correlate strikingly with the specific baryon number (the number of baryons per unit mass). Naturally, they go on to plead that the experiments should be repeated, but they also go on to say that their conclusion is sustained by measurements of anomalous properties of K mesons (kaons) at high energy.

What is to be made of the conclusion? The claim in the *New York Times* last week that Fischbach *et al.* have discovered a 'fifth force' is a little strong; if there are measurable departures from newtonian gravitation, those described are much what would be expected. That there is a significant difference between laboratory and geophysical measures of G seems now also well attested. The fact that the scale length calculated for the departure from the inverse square law is of the order of 200 m is consistent with that, but should suggest many novel ways of designing critical tests of the gravitational law now put forward.

That, in the end, is how the matter will have to be settled, for it is unthinkable that such an important issue as the behaviour of newtonian gravitation at short distances could for long be allowed to rest on a series of experiments carried out more than 60 years ago. But Fischbach *et al.* have provided an incentive for the design of better measurements by showing what kind of irregularity it will be sensible to look for.

John Maddox

Space physics

Does Uranus have a magnetic field?

from A.J. Dessler

In just a matter of days, Voyager 2, now nearly 8.4 years into its grand tour of the Solar System, will sweep past Uranus. The prospect has inspired discussion of the strength of the planet's magnetic field, published estimates of which at cloudtop level range from tens of gauss down to zero. This fascinating state of confusion is the result of recent data from Voyager which do not confirm past observations of Uranus from Earth orbit.

In 1982, John Clarke, using the Earth-orbiting International Ultraviolet Explorer (IUE), reported that Uranus is a bright scource of ultraviolet light[1]. Clarke's interpretation of these observations, which was immediately and widely accepted, was that the ultraviolet emission from Uranus is radiating from a bright aurora, which would be caused by the bombardment of the upper atmosphere by energetic electrons or ions. It is these and subsequent IUE observations, plus the specific hypothesis of an aurora on Uranus, that led to the estimates of a strong planetary field. To extract power either from the solar wind or from the rotation of the planet so as to drive an aurora that can produce the observed 10^{10} watts of ultraviolet emission, the planetary magnetic field has to create a magnetosphere large enough to engage the power source. Because of our experience with aurora on Earth, Jupiter and Saturn, quantitative models are at hand. Application of these models to Uranus results in a most probable value of the magnetic field at cloudtop level of 4–13 gauss, with 0.6 gauss as the minimum value[2].

Until a few months ago, Uranus was, in a sense, an astrophysical object. It can be seen well enough from Earth (and from Earth orbit) to learn a few facts and to develop some nice stories. Because there are few facts, simple ideas tend to fit them and they become a consensus rather quickly. Uncertainty and debate have been rare. But we are now witnessing a transition of Uranus from an astrophysical object to a space-physics object; facts provided by Voyager are about to overwhelm the theories. The impending encounter has made the theoretical community both humble and open-minded.

The problem is that if the IUE-detected ultraviolet light is indeed from an aurora created inside an enormous magnetosphere, then our experience with Earth, Jupiter and Saturn would lead us to expect Uranus to be a significant source of radio noise. Consequently, it was predicted that Voyager's first detection of magnetospheric radio emission would occur early last year and no later than August[2,3]. The failure of Voyager to pick up any radio signals from Uranus so far suggests that the ultraviolet emission is not generated by an aurora and that a strong (or even a weak) planetary magnetic field may not exist. Alternative explanations for the ultraviolet emission are therefore being put forward.

Shemansky, in the January issue of *Geophysical Research Letters*, and Ip, in next week's *Nature*, agree that the mysterious mechanism that produces bright ultraviolet glow from the sunlit hemispheres of Jupiter and Saturn also operates at Uranus. This glow is not auroral in nature — it occurs at lower and mid-latitudes, stops suddenly in the absence of sunlight and is clearly a separate phenomenon from the standard high-altitude aurora. Shemansky further suggests that Uranus has a negligible planetary magnetic field, while Ip argues that the strength of the magnetic field is immaterial, but it could be quite weak.

The lack of the expected radio emission has inspired yet another argument for a weak magnetic field. Curtis and Mess[4] note that the blackness of the rings and satellites of Uranus could be explained if there were no magnetosphere to shield them from the solar wind. Particle bombardment by the solar wind would remove surface ices, leaving dark, possibly carbonaceous, materials on the surface. They propose a cloudtop magnetic field of no more than 4×10^{-5} gauss.

Another proposal for a weak field will be put forward by Axford and Vasyliunas in next week's *Nature*. They argue that the magnetic field of Uranus originates in an

---

Jacques Oudin 1908–1985

With the death of Jacques Oudin on 15 October 1985, the international community of immunologists has lost one of its uncontested pioneers. From 1937, after completing his medical studies, Oudin spent his entire scientific career at the Pasteur Institute in Paris. From 1959 onwards he headed the laboratory of Immunochimie Analytique which was especially created for him. In 1979, the year after his retirement, a symposium at the Pasteur celebrated his exceptional career, highlighted by three major discoveries.

Some time after joining the Pasteur, while working in the laboratory of Chimie Microbienne, Jacques Oudin attempted to devise a one-step method to count the diverse antigen–antibody systems involved in the reaction of an appropriate antiserum and a complex mixture of antigens. He came up with the remarkable idea of using a gelled medium for the antigen–antibody precipitation reaction designing, in 1946, the method of immunochemical analysis. For a long time thereafter this was the only method for the enumeration and identification of antigens as well as the quantification of antigens and antibodies. Oudin formulated the quantitative laws and the general rules of the method, one of them — for which he had so often to fight — being that an antigen molecule gives only one precipitation zone with the corresponding antibodies.

It was while using antigen–antibody precipitates as immunizing material to elicit production of antibodies unispecific to the antigen present in the complex, that Jacques Oudin observed the first manifestation of what he defined in 1956 as allotypy of proteins, namely their property of exhibiting variations of antigenic specificities among individuals of an animal species. Before the multichain structure of immunoglobulins was known, he showed the presence on the same rabbit immunoglobulin molecule of allotypic specificities governed by genes at two different and independent loci, which he had just identified. The discovery of allotypy opened the fertile field of immunogenetics and the fascinating area of immune-system manipulations.

Working along the same lines, Oudin found in 1963 that rabbit antibodies possessed additional antigenic specificities which seemed unique to antibodies to a given antigen in one individual or a group of individuals. He proposed the term idiotypy to designate them. This observation (made independently in 1963 for human antibodies by Kunkel, Mannik and Williams at the Rockfeller Institute) led to experiments which were crucial to our appreciation of both the potential repertoire of antibody diversity and the regulation of its expression. It also provided the basic material for Jerne's theory of the network of antibody variable-domain interactions and of the dynamic equilibrium of the immune system.

It is worth pointing out how far and wide the words coined by Oudin have spread: isotypy and isotype, allotypy and allotype, and particularly idiotypy and idiotype. But it would be presumptuous to try to capture with mere words the rigour of Jacques Oudin's scientific thinking, the peculiarity of his solitary creativeness, his talent in identifying important facts in unexpected findings that would have disconcerted less discerning minds, his intransigent empiricism, his perfectionism and the extreme care he took over all his writing. We have been priviledged to benefit from such an exemplary mind.

Guy Bordenave

Earth-sized core, and they assume that the magnetic field from a body of this size must be about the same as the Earth's at the surface of the core. Thus, they conclude that the magnetic-field strength at cloudtop levels is about 10^{-2} gauss.

The proponents of a strong cloudtop magnetic field ($\geqslant 0.6$ gauss) for Uranus have become quiet apologists for the radio noise that has not been detected by Voyager: the radio emissions might be beamed away from the spacecraft; the aural electrons may be too low in energy (<1 keV) to support the excitation of radio emissions; there may not be enough background thermal plasma for the auroral beams to become unstable to radiofrequency oscillations; the magnetic field of Uranus may be so strong that the radio emissions are above the sensitive range of the Voyager radio receivers; the magnetosphere may be rather quiescent so that energetic particles that lose their energy through synchrotron radiation are not quickly replaced; and so forth.

Vociferous arguments in either side are lacking. The reason is plain — some of us are going to be embarrassed. Also, we have learned from other planetary encounters that nature is so clever at putting things together in completely unexpected ways that we now almost count on being astounded by what we find.

One cannot but wonder how, in a distant future, a community of, say, pulsar theorists will behave when an interstellar probe is about to fly by a pulsar for the first time. Rotating neutron star indeed! ☐

1. Clarke, J.T. *Astrophys. J.* **263**, L105 (1982).
2. Hill, T.W. & Dessler, A.J. *Science* **227**, 1466 (1985).
3. Desch, M.D. & Kaiser, M.L. *Nature* **310**, 755 (1984).
4. Curtis, S.A. & Ness, N.F. *Geophys. Res. Lett.* **12**, 855 (1985).

A.J. Dessler is Director of the Space Science Laboratory (ES01), NASA Marshall Space Flight Center, Huntsville, Alabama 35812, USA.

Earth sciences

Perovskites and plate tectonics

from Geoffrey D. Price

OUR ignorance of the dynamics of the Earth's mantle is such that it is still considered debatable whether the mantle convects as a whole, or in layers, divided one from another by a phase change or chemical boundary at the 670-km seismic discontinuity that separates the upper and lower mantle. Even though magnesium silicate perovskite probably makes up the vast majority of the lower mantle, and perhaps up to 40 per cent by volume of the entire Earth, little is known about its phase relations, its flow characteristics or its physical properties, all of which will critically influence the rheology and convective behaviour of the mantle. It is therefore essential to have a full knowledge of the nature of silicate perovskites if we are to understand the thermomechanical and chemical evolution of the Earth. The paper by Knittle *et al.* on page 214 of this issue attempts to provide the first data needed to begin such a task.

The lack of data on silicate perovskites is quite understandable, as it is not yet technically possible to measure the structural and physical properties of materials at the high pressures (>200,000 atm) and temperatures (>2,000 K) thought to characterize the lower mantle. To date, therefore, most of the theories concerning the behaviour of mantle-forming perovskite have have been derived from the study of the behaviour of non-silicate perovsites. For example, O'Keeffe and Bovin (*Science* **206**, 599; 1979) as well as Poirier *et al.* (*Phys. Earth planet. Inter.* **32**, 273; 1983) have suggested that magnesium silicate perovskite may behave like $NaMgF_3$ or $KZnF_3$, which are solid electrolytes at high temperatures.

Until now, work on magnesium silicate perovskite itself has been confined to its synthesis, its structure determination and the study of its phase relations in the $MgO{-}FeO{-}SiO_2$ system. The study of the thermal expansion of magnesium silicate perovskite by Knittle *et al.* is therefore to be welcomed as the first direct determination of any physical property of this mineral, and assumes particular significance when it is realized how difficult it is to use the diamond anvil cell to synthesize the quantity of perovskite that was needed for the thermal expansion study. Such cells are notorious for producing impurities, because of the heterogeneous nature of the pressure and temperature distribution within the cell, but Knittle *et al.* have obviously overcome these problems to the extent that they have produced material which behaves in a systematic and reproducible fashion.

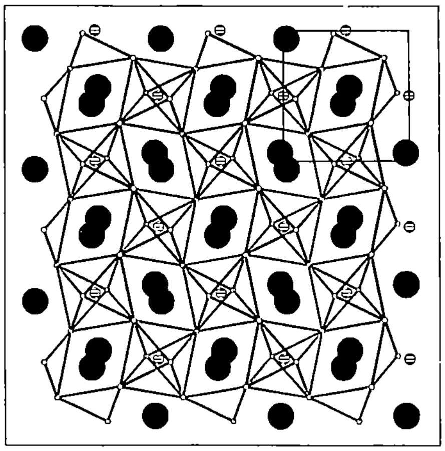

A polyhedral projection of the orthorhombically distorted perovskite structure adopted by magnesium silicate perovskite under ambient conditions. Magnesium ions (large filled circles) sit in the distorted cages formed by the outlined corner-sharing SiO_6 octahedra.

Because of the metastability of magnesium silicate perovskite under ambient pressure conditions, when studying its thermal expansion behaviour Knittle *et al* were restricted to temperatures below 840 K. To address questions concerning mantle processes, they were therefore forced to extrapolate from their data to the pressures and temperatures found in the lower mantle. They are on relatively firm ground in doing this when discussing the variation in the physical properties of perovskites with changing environment. But, unfortunately, crystal chemical models are less robust to extrapolation than are equations of state, and consequently their conclusions concerning the possible changes in the structure of perovskite with increasing depth within the mantle are conjectural in the extreme. Silicate perovskites develop an orthorhombic distortion (see figure) under ambient conditions, but the nature of possible changes in the perovskite structure at high pressures and temperatures has excited considerable debate (for example, O'Keeffe, M. *et al. Phys. Chem. Minerals* **4**, 299; 1979), and Knittle *et al.* cannot really shed light on this aspect of perovskite behaviour.

From their analysis of the thermal expansion behaviour of silicate perovskite, Knittle *et al.* infer that the lower mantle must be enriched in iron or silica relative to the upper mantle, and reasonably conclude that the upper and lower mantle must convect separately, and that mantle-wide chemical mixing is impeded. The experimental difficulties involved in studying these high-density silicates are such, however, that the uncertainty in their measurements are large: indeed the results are compatible with perovskite thermal expansion coefficents that range from 2×10^{-5} to 6×10^{-5} K^{-1}. Although not discussed in detail, it is to be expected that such uncertainties are too large to enable the conclusions drawn by Knittle *et al.* to be considered definitive. Nevertheless, their approach must be pursued, as it will only be from such investigations that we will be able to determine the true nature of mantle behaviour and thereby understand the fundamental processes involved in plate tectonics and the evolution of the Earth. ☐

Geoffrey D. Price is a Royal Society 1983 University Research Fellow in the Department of Geological Sciences, University College London, London WC1E 6BT, UK.

Inositol phosphates

Profusion and confusion

from Bob Michell

AFTER many years of argument, the past two years have brought agreement that receptor-stimulated hydrolysis of inositol phospholipids is a common mechanism for transmembrane signalling when cells respond to external stimuli such as hormones, neurotransmitters, antigens, light and some growth factors (reviewed in refs 1–3). But just as a slide depicting the simultaneous formation of two 'second messengers' within the cell by hydrolysis of phosphatidylinositol 4,5-bisphosphate (PtdIns(4,5)P_2) seems to have become a standard part of the travelling baggage of any scientist with an appreciable interest in cell responses to external stimuli, results from several laboratories suggest that this picture is greatly oversimplified. An up-to-date version of the formation and metabolism of inositol polyphosphate 'messengers' would need, unfortunately, to look something like that shown here.

The second messengers produced by the phosphoinositidase C (PIC)-catalysed hydrolysis of PtdIns(4,5)P_2 are *sn*-1,2-diacylglycerol and D-inositol-1,4,5-trisphosphate (Ins(1,4,5)P_3). The latter exerts its intracellular actions by releasing Ca^{2+} from an intracellular store, maybe in a compartment of the endoplasmic reticulum that is close to the plasma membrane[2], through interaction with an 'IP_3 receptor' that has now been detected by direct binding studies using liver microsomal membranes[4]. In solution at neutral *p*H, Ins(1,4,5)P_3 adopts the 'chair' configuration, with three phosphate groups lying around the periphery of the inositol ring[5], and this may be the configuration recognized by its receptor. The major mechanism for terminating Ins(1,4,5)P_3 action is thought to be removal of the 5-phosphate by a family of specific phosphatases, present both in the plasma membranes and cytosol of stimulated cells. Although this picture of the formation, second messenger action and inactivation of the released inositol trisphosphate headgroup is almost certainly correct, it is now clear that several additional inositol polyphosphates, with as yet unknown functions, are produced in stimulated cells.

The first hint of this unexpected complexity came last year when Robin Irvine and Peter Downes discovered that much of the $InsP_3$ that accumulates in cholinergically stimulated parotid glands is the 1,3,4-isomer rather than the expected 1,4,5-isomer[6]; although the Ins(1,4,5)P_3 formation is immediate, that of the Ins(1,3,4)P_3 is delayed as is its decline on removal of the stimulus[7,8]. The origin of Ins(1,3,4)P_3 was a mystery until the recent evidence for its formation by dephosphorylation at the 5-position of D-inositol 1,3,4,5-tetrakisphosphate (Ins(1,3,4,5)P_4)[11], probably by what had been characterized as an Ins(1,4,5)$P_3$5-phosphatase[9,10].

Ins(1,3,4,5)P_4 is formed as rapidly as Ins(1,4,5)P_3 in various stimulated tissues and cells[11,12] and at a recent meeting on inositol lipids in Germany*, Irvine and Michael Berridge presented evidence for a novel ATP-dependent kinase that converts Ins(1,4,5)P_3 to Ins(1,3,4,5)P_4. Because the absolute rates of synthesis and degradation of Ins(1,4,5)P_3 and of Ins(1,3,4)P_3 in stimulated cells appear to be of the same order, at least in the parotid gland[7], the pathway for metabolism of Ins(1,4,5)P_3 through Ins(1,3,4,5)P_4 to Ins(1,3,4)P_3, and hence for its inactivation as a Ca^{2+}-mobilizing ligand, may be quantitatively as important as its dephosphorylation to Ins(1,4)P_2. Although it seems quite likely that Ins(1,3,4)P_3 and/or Ins(1,3,4,5)P_4 will turn out to have intracellular messenger functions of their own, this idea remains to be tested because so far the compounds have only been obtained in trace quantities.

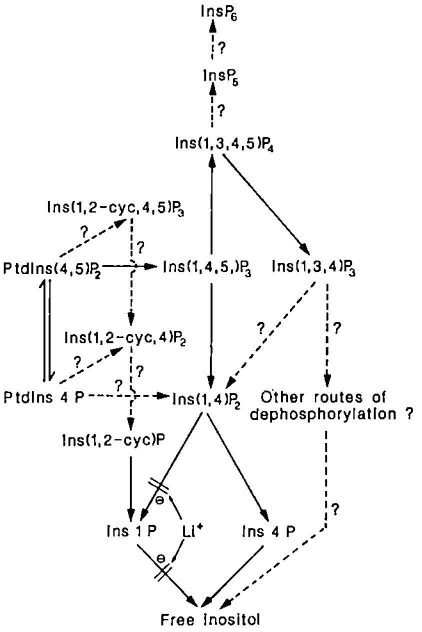

Some known (→) and probable ($\overset{?}{\dashrightarrow}$) interconversions of inositol lipids and inositol phosphates in stimulated cells.

Having found these unexpected inositol polyphosphates, the Cambridge groups looked further, and found that GH4 cells contain both an inositol pentaphosphate ($InsP_5$) and an inositol hexaphosphate ($InsP_6$), although their concentrations do not change dramatically on stimulation of cells[12]. There seem to be no previous reports of such highly phosphorylated inositol derivatives in mammalian cells, and their function and metabolism are unknown. However, $InsP_6$, better known as phytate, is a major phosphate store in some seeds, and the 1,3,4,5,6-isomer of $InsP_5$ is an allosteric regulator of oxygen binding to haemoglobin in avian erythrocytes.

Almost 15 years ago, it was discovered that a major product of PIC hydrolysis of phosphatidylinositol in cytosolic and plasma membrane fractions from brain is inositol 1,2-cyclic monophosphate[13–15] and that there is a widespread and specific phosphodiesterase that opens the 1,2-cyclic phosphate ring of this compound at the 2-position[16,17]. As a result, inositol 1,2-cyclic phosphate was briefly considered as a possible intracellular messenger compound[15]. Philip Majerus and his colleagues in St Louis have now found that 1,2-cyclic derivatives can also be produced from PtdIns(4,5)P_2 and PtdIns4P by two PICs isolated from sheep seminal vesicles, although in smaller quantities than the non-cyclic alternatives[18,19]. D-inositol-(1,2-cyc,4,5)trisphosphate (Ins(1,2-cyc,4,5)P_3) is less potent than Ins(1,4,5)P_3 in mobilizing Ca^{2+} in permeabilized platelets but more so in depolarizing intact *Limulus* photoreceptors[19]. Although these observations show that Ins(1,2-cyc,4,5)P_3 can mobilize Ca^{2+}, we do not yet know whether it is among the products of receptor-stimulated PIC activity in stimulated cells, because it would not survive the acidity of the media that are used for the efficient extraction of inositol trisphosphates from stimulated cells. If the 1,2-cyclic derivatives are formed in stimulated cells, it seems likely that they will be degraded, albeit more slowly, by the phosphatases that degrade Ins(1,4,5)P_3 and Ins(1,4)P_2, with the 1,2-cyclic ring being opened only after dephosphorylation to inositol 1,2-cyclic monophosphate[20]. Ins(1,2-cyc,4,5)P_3 may also be a substrate for Ins(1,4,5)P_3 3-kinase, so giving rise to Ins(1,2-cyc,3,4,5)P_4 and other cyclic phosphates derived therefrom.

A feature of the metabolism of receptor-generated inositol phosphates that has caused particular interest is its inhibition by Li^+ ions at extracellular concentrations similar to those that are effective in suppressing manic depressive symptoms. The dominant idea is that Li^+ inhibits Ins1p phosphatase[21] and thus may limit the supply of free inositol for inositol lipid synthesis (see ref. 2) and limit a cell's signalling capacity. Recent studies both *in vivo*[22] and *in vitro*[23,24] have, however, shown that Ins(1,4)P_2 can be degraded to inositol via inositol 4-phosphate as well as via inositol 1-phosphate. At least in liver, degradation via the 4-phosphate is Li^+-insensitive, whereas both steps in degradation via inositol 1-phosphate are equally Li^+-sensitive[24]. The relative rates of Ins(1,4)P_2 degradation by these two routes are not known for any intact cells, but it seems probable that variations in this ratio will render signalling more sensitive to Li^+ in some cells than in others.

---

*Inositol lipids and signal transduction, the 4th Ernst Klenk Foundation Conference, was held in Koln, FRG on 27–30 October 1985.

The point that emerges particularly forcefully from all of these recent findings is that the metabolism of inositol phosphates in stimulated cells is startlingly complex. It is clear that the very simple anion-exchange chromatographic methods that have been widely used for separating various inositol phosphate 'fractions' in recent years are quite unsuitable for analysing the complex mixtures of inositol phosphates present in stimulated cells. At present, the preferred method for more stringent analyses of the inositol metabolites present in stimulated cells is undoubtedly high-pressure liquid chromatography on anion-exchange resins. Three published methods[7,19,25] each have some desirable features, but we can look forward to refinement of such methods and to the development of selective and sensitive assays for individual inositol phosphates. ☐

1. Nishizuka, Y. *Nature* **308**, 693 (1984).
2. Berridge, M.J. & Irvine, R.F. *Nature* **312**, 315 (1984).
3. Downes, C.P. & Michell, R.H. in *Molecular Mechanisms of Transmembrane Signalling* (eds Cohen, P. & Houslay, M.D.) 3 (Elsevier, Amsterdam, 1985).
4. Spat, A., Fabiato, A. & Rubin, R.P. *Biochem. J.* **233**, 929 (1986).
5. Lindon, J.C., Baker, D.J., Farrant, R.D. & Williams, J.M. *Biochem. J.* **233**, 275 (1986).
6. Irvine, R.F., Letcher, A.J., Lander, A.J. & Downes, C.P. *Biochem. J.* **223**, 237 (1984).
7. Irvine, R.F., Anggard, E.E., Letcher, A.J. & Downes, C.P. *Biochem. J.* **229**, 505 (1985).
8. Burgess, G.M., McKinney, J.S., Irvine, R.F. & Putney, J.W. *Biochem. J.* **232**, 237 (1985).
9. Downes, C.P., Mussat, M.C. & Michell, R.H. *Biochem. J.* **203**, 169 (1982).
10. Hawkins, P.T., Michell, R.H. & Kirk, C.J. *Biochem. J.* **218**, 785 (1984).
11. Batty, I.R., Nahorski, S.R. & Irvine, R.F. *Biochem. J.* **232**, 211 (1985).
12. Heslop, J.P., Irvine, R.F., Tashjian, A.T. & Berridge, M.J. *J. exp. Biol.* (in the press).
13. Jungawala, F.B., Freinkel, N. & Dawson, R.M.C. *Biochem. J.* **123**, 19 (1971).
14. Lapetina, E.G. & Michell, R.H. *Biochem. J.* **131**, 433 (1973).
15. Michell, R.H. & Lapetina, E.G. *Nature* **240**, 258 (1972).
16. Dawson, R.M.C. & Clarke, N. *Biochem. J.* **127**, 113 (1972).
17. Clarke, N. & Dawson, R.M.C. *Biochem. J.* **130**, 229 (1972).
18. Wilson, D.B., Bross, T.E., Sherman, W.R., Berger, R.A. & Majerus, P.W. *Proc. natn. Acad. Sci. U.S.A.* **82**, 4013 (1985).
19. Wilson, D.B. *et al. J. biol. Chem.* (in the press).
20. Connolly, T.M., Wilson, D.B., Bross, T.E. & Majerus, P.W. *J. biol. Chem.* (in the press).
21. Hallcher, L.M. & Sherman, W.R. *J. biol. Chem* **255**, 10896 (1980).
22. Sherman, W.R., Honchar, M.P. & Munsell, L.Y. in *Cyclitols and Phosphoinositides* (eds Bleasdale, J.E., Eichberg, J. & Hauser, G.) 49 (Humana, New York, 1985).
23. Storey, D.J., Shears, S.B., Kirk, C.J. & Michell, R.H. *Nature* **312**, 374 (1984).
24. Michell, R.H. *et al.* in *Hormones and Cell Regulation* Vol. 10 (eds Dumont, J. & Nunez, J.) (Elsevier, Amsterdam, in the press).
25. Binder, H., Weber, P.C. & Siess, W. *Analyt. Biochem.* **148**, 220 (1985).

Bob Michell is Reader in Biochemistry at the Department of Biochemistry, University of Birmingham, PO Box 363, Birmingham B15 2TT, UK.

100 years ago from *Nature* **33** 252, 14 January 1886.

SOLAR SPOTS, MAGNETIC DECLINATION, AND AURORAL DISPLAYS.

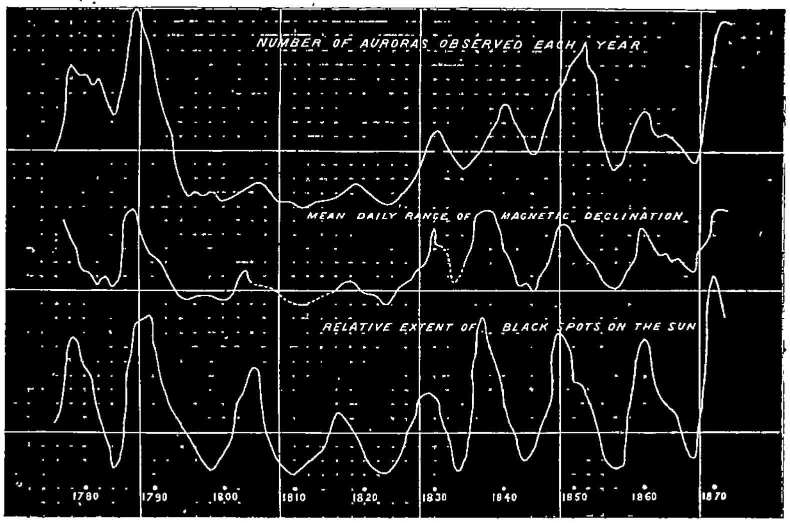

Materials science

Limits to Coulomb's law

from Robert W. Cahn

MANY of the scientific laws that the readers of this journal absorbed in their youth are more than a century old and a surprising number go back more than two centuries — but which of them can still claim exact congruence with experimental facts? Some continue in daily use as sound approximations, for example, Boyle's, Hooke's and Ohm's laws, but lose their applicability in specific contexts, such as the behaviour of supercritical steam, 'potty putty' or semiconductor resistivity. Others, such as Newton's laws of motion, remain very close approximations to the behaviour of the real world until extreme conditions (for example, velocities) are attained. On page 203 of this issue, K. Kendall challenges another venerable law — Coulomb's law, formulated in 1773, which describes the frictional behaviour of a bed of power.

According to Coulomb's law, the frictional force between a particle and a smooth plane pressed together by a normal force w is expressed as $f = k + \mu w$, where μ is the friction coefficient and k is a constant representing the intrinsic interaction — the van der Waals' attraction — between the mating surfaces. Coulomb's law has been used for a long time in engineering calculations, particularly in soil mechanics. Kendall now reports on experiments with wet sand confined between two silica plates and finds that the friction coefficient varies substantially, both with normal load and particle size.

The new findings imply that the van der Waals' interaction between, for example, two equal spheres depends on their diameters and on the force pressing them together; this was first established by K.L. Johnson, K. Kendall and A.D. Roberts (*Proc. R. Soc.* **A324**, 301; 1971). If other factors are constant, the friction in a powder bed will rise rapidly as finer particles are used. In view of the widespread use of ultrafine powders in advanced ceramics, this finding has considerable practical importance. As with other named laws, Coulomb's law will presumably remain an adequate approximation under the normal circumstances of coarse powders and soil mechanics, but not under extreme conditions.

Coulomb's law is just one small feature of the varied, untidy but widely useful field of powder mechanics, a term not commonly used, but one that collectively covers dynamics, statics and thermodynamics. Consider some of the ways a powder can behave. When dry and in a still atmosphere, a powder has a 'flowability' that depends on particle mean size, size distribution, mean shape and shape distribution and on intrinsic frictional properties. An assembly of needles may stick obstinately, whereas dry uniformly-sized sand flows easily. The capillary effect of moisture is crucial: common salt needs a hygroscopic additive to keep it free-running; dry powder snow responds to pressure quite differently from wet snow, as any skier knows. If the proportion of water becomes too high, the result may be an avalanche or a quicksand.

A dry powder can be made fluid by blowing air or some other gas through it. Such a 'fluidized' bed has much lower friction than a normal powder bed and resembles a highly mobile liquid. The theory of fluidized bed mechanics and heat transfer is important in chemical engineering, because such beds are commonly used for reacting solids with hot gases. When the gas pressure becomes too high, the agitation of the powder leads to erosion of the container. Such erosion has implications ranging from particle impact on the windscreens of supersonic aircraft to the sandblasting of castings or spark plugs. The abrasive wear of surfaces by powders has also become a large field of study.

The optimum feasible irregular packing of powders leads to complex statistical issues, which have been treated by J.D. Bernal and J.L. Finney (*Nature* **213**, 1079; 1967 and *Proc. R. Soc.* **A319**, 479; 1970). Their concept of dense random packing of equal-sized spheres, originally conceived as a model for monatomic liquids, has been extremely influential in guiding the modelling of metallic glasses. Surprisingly, a randomly packed assembly of monosized spheres can be within about five per cent of the density of a regular close-packed array. Dense random-packed arrays can be further densified by sintering, a technique that goes back to prehistoric practice in the baking of pottery. The stereology of solid-state sintering — the developing relation between packing fraction, porosity, permeability and specific surface area — has become a major field of scientific enquiry with relevance to metallurgy, ceramics and catalysis, and several novel experimental and conceptual tools have evolved with it. The mechanics of sintering — notably the crucial role of the curvatures of internal free surfaces and of intercrystalline boundaries — are now well understood. Through doping, subtle control of the motion of such boundaries has been achieved, making it possible to sinter to full denstiy; the absence of scattering from pores has enabled the creation of translucent or transparent polycrystalline ceramics, now used in very efficient high-temperature lamps.

The ubiquity of powders in applied science indicates that Kendall's discovery of a major departure from a long-accepted powder law is of wider import than might at first appear. We still have to see how representative the circumstances of Kendall's experiments are. He used a wet load and the moisture fraction is not stated; presumably dry sand would behave quite differently. The plastic domain, as in hot isostatic pressing of metallic powder compacts, must entail frictional regimes quite different from those in the elastic regime treated by Kendall. Even so, his work has reopened a field that has been hemmed in by orthodoxy and neglected because ultrafine powders have only recently become commercially important. ☐

Robert W. Cahn is currently Fairchild Distinguished Scholar in the Keck Engineering Laboratories, California Institute of Technology, Pasadena, California 91125, USA.

Cosmic rays

Where do antiprotons come from?

from Andrew Buffington

IT IS usually believed that the antiprotons ($\bar{p}$) in cosmic rays result from collisions between high-energy protons (p) and ambient interstellar gas. Recent measurements of $\bar{p}$ cosmic-ray fluxes between 0.1 and 10 GeV are, however, inconsistent with such a secondary source, if the observed p fluxes are assumed to illuminate the 5 – 7 gm cm^{-2} of interstellar material that has been deduced from studying heavier cosmic rays. Moreover, there is a kinematic cutoff for the reaction threshold of interstellar gas 'target-at-rest' interactions that predicts a dramatic drop in the $\bar{p}/p$ ratio below a few GeV, but the measurements show a practically constant ratio of 3×10^{-4}. The discrepancy factor at higher energy is about 5 but grows to about 100 close to 0.1 GeV. On page 205 of this issue C.D. Dermer and R. Ramaty[1] cite the recent $\bar{p}$ flux measurements and present a possible explanation for the reported similarity in $\bar{p}$ and p spectra.

Dermer and Ramaty suggest that the target material that is illuminated by high energy p to produce the $\bar{p}$ could be a relativistic plasma instead of cool interstellar gas. Such a plasma might be found in the vicinity of neutron stars or black holes. They then calculate that target particle motion is sufficient to remove most of the suppression of low energy $\bar{p}$ and show that production rate is significant for plasma temperatures above about 0.2 M_pc^2. They discuss constraints put on the model by γ-ray measurements and suggest that many of the observed antiprotons were originally created as antineutrons, whose charge neutrality helped them to escape confinement in the ambient plasma magnetic field.

Many authors have already advanced a variety of explanations for the $\bar{p}$ anomaly with models that range from those invoking primary antimatter to those that adopt closed-galaxy cosmic-ray propagation or various types of shells around some of the cosmic-ray sources. Some of these are cited by Dermer and Ramaty, to which might be added an important calculation of secondary $\bar{p}$ production by Protheroe[2], models by Kiraly *et al.*[3], Eichler[4], and Lagage and Cesarsky[5], and neutron oscillation as a possible separate source of low energy $\bar{p}$[6,7]. I consider that the recent $\bar{p}$ flux measurements have stimulated significantly revised calculations of $\bar{p}$ production in thick targets. In these, the effect of further $\bar{p}$ collisions has been included, particularly because these can 'fill in' the kinematic suppression of the $\bar{p}/p$ ratio at low energy. Tau and Ng[8] and Protheroe[2] have shown that the observed $\bar{p}$ spectrum can be matched, provided the $\bar{p}$ were produced in material with a thickness of about 30 gm cm^{-2}. In the case where all the $\bar{p}$ are secondary, the question becomes where might reside such a thickness for cosmic-ray protons to pass through and to what extent the heavier cosmic rays may also have passed through it. If the $\bar{p}$ are considered as secondary, our understanding of galactic cosmic rays stands at a major crossroads because $\bar{p}$ provide a unique tracer for the interactions of the primary p. (The spectrum of positrons, the other possible interaction-daughter candidate, are altered too much by photon interactions subsequent to their production to be useful.) The question is: should we adopt a different history for the plentiful cosmic-ray p, compared with that for the heavy cosmic rays?

We do not at present know what measurements could provide a definitive answer to this question but helium isotope spectra may be important as the next step. Because the helium-interaction mean free path is comparable to the 30 gm cm^{-2} of material indicated for parent-proton cosmic rays, considerable helium should survive the passage through even this thickness of material. As ^{3}He is expected to be rare in the cosmic-ray sources, the ^{3}He/^{4}He ratio shows whether helium cosmic rays have passed through a large amount of material, as some of the above models would predict. Recently, Jordan and Meyer[9] reported the first measurement of ^{3}He/^{4}He near 6 GeV per nucleon, an energy high enough that little correction is needed for solar modulation. They report a ratio of 0.24, which requires about 15 gm cm^{-2} of interstellar material. On the other hand, measurements of this ratio below a few hundred MeV per nucleon are consistent with the 5 – 7 gm cm^{-2} indicated by heavier cosmic rays, but in an energy range strongly affected by solar modulation. This discrepancy was the subject of lively discussion at a recent conference[10,11], so clearly Jordan and Meyer's result is not yet generally accepted.

These experiments are technically difficult, so that confirming and expanding experiments have been slow in coming, but this wave of new ideas about cosmic-ray origin and propagation needs new and better data to carry it along. It will be particularly important to have improved $\bar{p}$ data below 2 GeV, where the spectrum carries much information about re-interaction of the secondary $\bar{p}$; confirmation and extension of the high-energy helium isotope data is also needed. The group led by R. Golden at New Mexico State University has reconfigured their magnetic spectrometer, now ready for a new balloon flight, for $\bar{p}$ measurements to a lower energy range than they used previously; they have also made significant improvements in their trajectory measuring apparatus. New $\bar{p}$ instruments are also being planned by Goret[12] and by groups at Berkeley and Goddard[13,14]. Although no high-energy ^{3}He/^{4}He experiments seem to be planned, the stimulating and exciting new results underscore their need. ☐

Andrew Buffington is at the Center for Astrophysics and Space Sciences, University of California, San Diego, California 92093, USA.

1. Dermer, C.D. & Ramaty, R. *Nature* **319**, 205 (1986).
2. Protheroe, R.J. *Astrophys. J.* **251**, 387 (1981).
3. Kiraly, P. *et al. Nature* **293**, 120 (1981).
4. Eichler, D. *Nature* **295**, 391 (1982).
5. Lagage, P.O. & Cesarsky, C.J. *Astron. Astrophys.* **147**, 127 (1985).
6. Sawada, O. *et al. Astrophys. J.* **248**, 1162 (1981).
7. Sivaran, C. & Krishan, V. *Nature* **299**, 427 (1982).
8. Tau, L.C. & Ng, L.K. *J. Phys.* G9 227 (1983).
9. Jordan, S.P. & Meyer, P. *Phys. Rev. Lett.* **53**, 505 (1984).
10. Evanson, P. *et al. Proc. 19th Int. Cosmic Ray Conf.* **2**, 60 (1985).
11. Mewaldt, R.A. *Proc. 19th Int. Cosmic Ray Conf.* **2**, 69 (1985).
12. Goret, P. *Moriond Astrophys. Meeting, Cosmic Rays and Elementary Particles* (eds Audouze, J. & Tran Thanh Van, J.) 227 (1984).
13. Lloyd-Evans, J. *et al. Proc. 19th Int. Cosmic Ray Conf.* **3**, 254 (1985).
14. Solomon, M.H. *et al. Proc 19th Int. Cosmic Ray Conf.* **3**, 258 (1985).

Marine reptiles

Lifestyle of plesiosaurs

from Michael A. Taylor

THE plesiosaurs, large extinct carnivorous marine reptiles of the Mesozoic period, have always excited dispute over how they swam[1] and reproduced. Did they swim like marine turtles, 'flying' with winglike, hydrofoil limbs, or did they row by moving their limbs back and forth (Fig. 1*a*, *b*)? And did they come on shore to lay eggs, or give birth in the water to live young? Recent research provides a new animal model that might answer these questions.

In 1975, Jane Ann Robinson argued that the plesiosaurs must have flown underwater, like turtles and penguins, because this movement was the most efficient use of their long hydrofoil-like limbs[2]. If the plesiosaurs had rowed, they should have had webbed folding feet like those of ducks. She suggested that they swam by flapping both pairs of limbs up and down, producing lift force that propelled the animal forwards.

Seven years later Samuel Tarsitano and Jürgen Riess suggested a modification to Robinson's analysis[3]. Although agreeing that plesiosaurs must have used their limbs to fly underwater, they noted that the simplest — and apparently most effective — up-and-down action was anatomically impossible because the bones of the shoulder joints would block the appropriate operation of the forelimbs above the horizontal. Moreover, plesiosaurs do not seem to have had the large dorsal muscles needed to lift the wings powerfully upwards. Dino Frey and Jürgen Riess[4] then suggested that the 'wings' had an active downstroke, and a comparatively passive upstroke as they were returned to the starting point. They suggested that the two pairs of limbs beat out of phase: one pair propelling the animal during its downstroke while the other was being brought back to the start of its own active stroke. This limb action would still be relatively inefficient compared with that of modern animals such as penguins, whose wings produce propulsive force throughout virtually the whole of the upstroke and downstroke.

Stephen Godfrey has now suggested a different living model for comparison[5]. The sealion swims by beating its forelimbs forcefully downwards and then relatively passively upwards, while always moving them backwards. Once fully backwards, the limbs can then be feathered and brought forwards during the recovery stroke. Evidence points to the plesiosaurian shoulder and hip girdles having the massive muscles needed for such limb action (Fig. 1c). Ironically, sealion swimming combines elements of underwater flight — up-and-down action — with rowing — backwards movement. The new model thus combines both the old theories

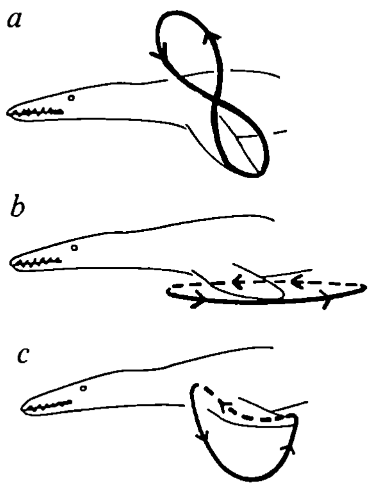

Fig 1. Possible mechanisms for swimming in plesiosaurs. The lines indicate the movement of the wingtip. *a*, Flying underwater like a penguin, with an up-and-down beat of the limbs; this movement would have been ideal for the limb shape but only the downstroke could have been really powerful. *b*, Rowing underwater like a duck, with an active power stroke backwards (bold line) then a recovery stroke forwards (dotted line). The plesiosaur's limb shape is particularly unsuited to such a movement. *c*, Swimming like a sealion, with a backwards power stroke and forwards recovery stroke, a movement combining elements of *a* and *b*.

If the plesiosaur had a swimming movement similar to that of the sealion, with a powerful downwards and backwards thrust, it is slightly easier to imagine how it pushed itself along a beach. However, the plesiosaurs with their rigid bodies could not have humped themselves along as sealions do but must have dragged themselves along, belly to sand, much as sea turtles now do. Whether they also laid eggs in the sand like turtles, or gave birth to live young in the water, as sea snakes do and ichthyosaurs are known to have done, is still unresolved.

The discovery of a pregnant female plesiosaur would settle the question, but none has yet been found. Perhaps we have not looked inside the bodies of enough plesiosaurs or perhaps the embryos decomposed before they could become fossilized. Two early reports of relevant fossils have recently been discounted. In the 1880s H. G. Seeley described an intriguing clutch of diminutive plesiosaur embryos from Whitby, Yorkshire, a discovery forgotten until R. A. Thulborn re-examined it[6]. The find turned out to be a forgery, an unusually shaped nodule (originally, he suggests, shrimp burrows) which had been 'improved' to strengthen resemblance to a clump of plesiosaur embryos, each several inches long. And a reported 'plesiosaur egg'[7] is now thought to be an inorganic concretion[8]; even if it was an egg, it would probably be crocodilian, because crocodiles were much more common than plesiosaurs in the Upper Lias of Whitby.

Tantalizingly, one clutch of eggs — but no young reptiles — was long ago reported from marine beach (or close inshore) deposits from the Middle Jurassic near Cirencester, England[9]. Again these were described as crocodilian rather than belonging to the much rarer plesiosaurs. What is needed, of course, is a clutch of eggs *in situ*, complete with tiny plesiosaurs; but such finds are exceedingly rare even for land animals such as dinosaurs[10] and are even more unlikely to have been preserved on a wave-washed beach. ☐

1. Taylor, M.A. *Nature* **290**, 628 (1981).
2. Robinson, J.A. *N. Jb. Geol. Paläont. Abh* **149** 286 (1975); **153**, 86 (1977).
3. Tarsitano, S. & Riess, J. *N. Jb. Geol. Palaont. Abh* **164** 188 (1982).
4. Frey, E. & Riess, J. *N. Jb. Geol. Paläont. Abh* **164** 193 (1982).
5. *Godfrey, S.J. N. Jb. Geol. Paläont. Mh.* **for 1984**, 661 (1984).
6. Thulborn, R.A. *Palaeontology* **25** 351 (1982)
7. Melmore, S. *Proc. Yorks. phils. Soc.* **for 1930**, 3 (1931)
8. Benton, M.J. & Taylor, M.A. *Proc. Yorks. geol Soc.* **44** 299 (1984).
9. Buckman, J. *Q.J. geol. Soc. Lond.* **16**, 107 (1860)
10. Horner, J.R. & Makela, R. *Nature* **282**, 296 (1982).

Michael A. Taylor works for the Area Museum Council for South-West England and is based at the City of Bristol Museum and Art Gallery, Queens Road, Bristol BS8 1RL, UK.

Neuroendocrinology

Molecular approach appraised

from Stafford Lightman

The mechanisms controlling neuroendocrine regulation can be modulated by a variety of hormones, neurotransmitters and neuromodulators both *in vivo* and *in vitro*. As these systems have been well characterized by physiologists, they clearly offer an extremely attractive model in which to study the control of gene expression. The benefits and problems of the application of molecular genetics to neuroendocrine models were brought up to date at a recent meeting*.

Characterization of the precursors of hormones continues to be an important step in understanding the regulation of hormone production and in the discovery of new candidate hormones. A good example is the recent description of the precursor to gonadotropin-releasing hormone (GnRH) with its carboxy-terminal sequence GAP, which itself inhibits prolactin and stimulates gonadotropin secretion (Nikolics *et al. Nature* **316,** 511; 1985). Further studies (P. Seeburg, Genentech) confirm that GAP coexists with GnRH in hypothalamic cells, but also show that it is present in portal blood and even in the ovary and testis where GnRH has previously been demonstrated.

Except in frog skin, where it is found in abundance (Richter, D. *et al. EMBO J.* **3,** 617; 1984), the precursor to the tripeptide (Gln–His–Pro) releasing hormone, TRH, has been particularly difficult to identify. The problem has now been circumvented with antibodies to a synthetic peptide (Cys–Lys–Arg–Gln–His–Pro–Gly–Lys–Arg–Cys) presumed to represent a portion of the TRH precursor (R. Goodman, New England Medical Center, Boston). The antibodies were used to screen a DNA library from rat hypothalami, which yielded a cDNA clone that encodes a protein containing five copies of the sequence Gln–His–Pro–Gly, flanked by pairs of basic amino acids. In support of the view that this protein is a TRH precursor, *in situ* hybridization with the cDNA was shown to detect neurones in those regions of the hypothalamus that are known to produce TRH. Thus, as with enkephalin, TRH has a precursor from which multiple copies of the biologically active peptide can be produced. Oddly, there is no homology between the frog-skin and rat hypothalamic precursors except for the TRH units themselves.

Defining the mechanisms of gene regulation is a major challenge to the molecular neuroendocrinologist. Quantitation of changes in pro-opiomelanocortin (POMC) mRNA in the anterior pituitary in response to corticotropin releasing factor and dexamethasone, or in the pars intermedia in response to bromocriptine, provide evidence of control at the level of gene transcription (J. Roberts, Columbia University, New York). The situation is more complex, however, in sex-hormone mediated changes in the arcuate nucleus of the hypothalamus. Treatment of a two-week ovariectomized adult rat with oestradiol results in a slow decline in the concentration of POMC mRNA in the arcuate nucleus and the expected corollary, a rapid decline in POMC transcription, which remains suppressed for days.

On the other hand, events controlling dopamine synthesis in the same system are not so clear. Oestradiol administration results within one hour in a fall of the transcription of the gene for tyrosine hydroxylase (TH) — the rate-limiting enzyme in catecholamine synthesis — with a gradual return to normal over 4 days, whereas the amount of TH mRNA begins to increase after 20 minutes and continues to rise for 4 days. This dissociation of the quantity of TH mRNA from the level of transcription of its gene implies that mRNA stabilization may be responsible for some of the quantitative changes in TH mRNA. Clearly, turnover of TH mRNA is the variable that we should like to measure, but the techniques are not available and, in particular, we have no idea how to study the rate of specific mRNA degradation.

Similar problems apply to the interpretation of *in situ* hybridization studies, in which the hybridization of intracellular mRNA with specific DNA probes is used to locate sites of gene expression in tissue sections. This technique cannot provide any measure of RNA turnover and suffers from a lack of sensitivity which still limits its application to quantifying intracellular mRNAs. Nevertheless, it is finding many applications. For example, POMC mRNA can be detected in the pars intermedia of the rat pituitary, but in the anterior pituitary it is only found after adrenalectomy (J. Coghlan, University of Melbourne). Atrial natriuretic peptide mRNA could not be detected in the hypothalamus but has been found in the cardiac atria; renin mRNA has been detected for the first time in the arcuate nucleus. Vasopressin and oxytocin cDNA probes have now been used to measure mRNA responses to different physiological conditions (J. McCabe, Rockefeller University). Rats whose drinking water has been substituted with two per cent saline have an increased proportion of hypothalamic magnocellular cells heavily labelled by vasopressin cDNA, and magnocellular cells from 15-day pregnant rats show an increase both in the number of heavily labelled cells and in the number of cells with any autoradiographic grains. Further experiments are needed to show whether this represents two different groups of responding cells within the magnocellular paraventricular nucleus.

Novel techniques to measure gene expression and post-translational processing are exciting considerable attention. One method of incorporating mRNA into cells is by the use of a vaccinia virus (VV) vector (G. Thomas, Oregon Health Sciences University). The infection cycle of VV, unlike that of other DNA viruses, occurs solely in the cytoplasm of the host cell. Insertion of a cDNA downstream from an early VV promoter leads to transcription of the cDNA in the host cell within minutes of infection and to efficient production of protein from the mRNA. The potential of the technique is illustrated by the infection of different cell lines with recombinant VV containing the cDNA for human proenkephalin. Infected BSC-40 cells contain 2 main peaks of enkephalin immunoreactivity of which only the larger precursor is secreted into the medium. Infected AtT-20 cells, however, contain five peaks of immunoreactivity, with met-enkephalin as the major secreted form. This is a good example of tissue-specific processing. The considerable versatility of the VV system will doubtless provide much further information on this and other processing systems. ☐

Stafford Lightman is Reader in Medicine at the Charing Cross and Westminster Medical School, London SW1P 2AP, UK.

---

*Neuroendocrine Molecular Biology, 13th annual meeting of the International Foundation for Biochemical Endocrinology, Edinburgh, 16–20 September, 1985.

Stamps of approval for Halley's comet

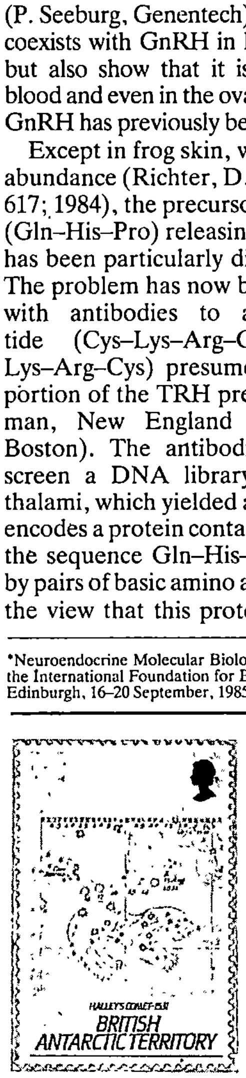

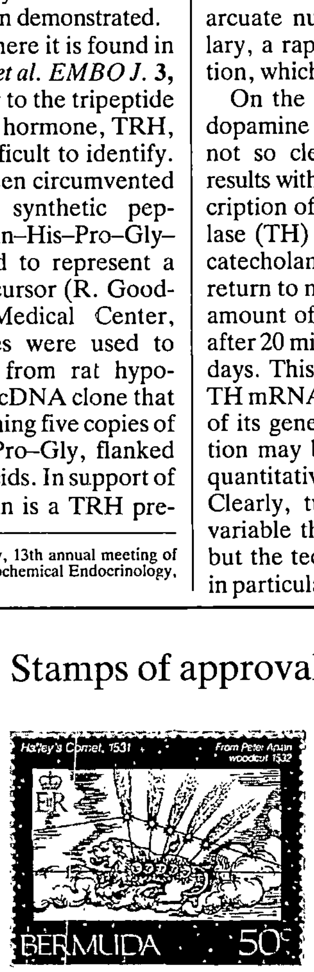

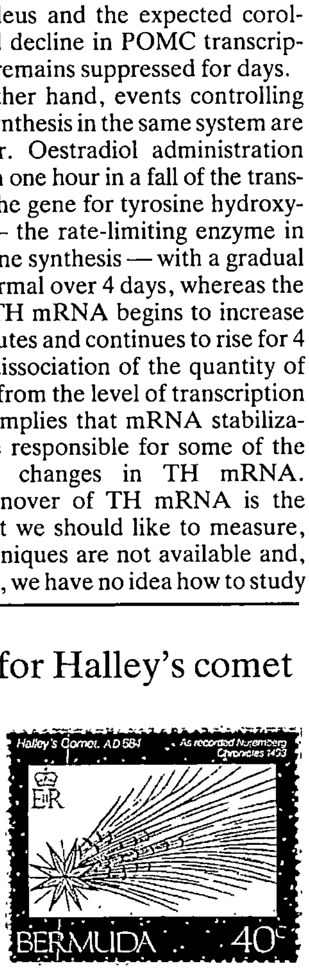

Carbon cycle

Photosynthesis seen from above

from R.A. Warrick

ONE of the latest developments in remote sensing, reported by Tucker *et al.* on page 195 of this issue[1], is the capacity to estimate green-leaf biomass of plant canopies and, presumably, terrestrial photosynthesis and primary production, on a global scale with fine temporal and spatial resolution. This development has the potential to sharpen our understanding of the role of terrestrial biota in the carbon cycle and could allow the monitoring of important changes in global vegetation and productivity resulting from increasing atmospheric CO_2 and climatic changes.

As a result of fossil fuel burning, deforestation and other changes in land use, the atmospheric concentrations of CO_2 have risen from a pre-industrial (mid-nineteenth century) level of 275±10 to 343±1 parts per million by volume in 1984 (ref. 2). With a doubling of the pre-industrial CO_2 level the world could become considerably warmer, by 1.5–5.5°C according to climate modellers[3] — the much-debated greenhouse effect. A major issue is when will this happen. The answer depends largely on future rates of energy consumption and CO_2 emissions, together with the sources and sinks of CO_2 and the fluxes between the various carbon reservoirs, which are the subjects of global carbon-cycle modelling. The terrestrial biota is a major component of such models.

In the presence of light, atmospheric CO_2 is assimilated by plants and transformed into carbohydrates — the process of primary production. Through respiration and the decay of organic matter, CO_2 is released back into the atmosphere. Because the rates of assimilation and release are dependent on solar radiation and temperature, and because the distribution of the terrestrial biota is lop-sided in favour of the northern hemisphere, the atmospheric CO_2 concentration has a strong seasonal cycle whose amplitude varies spatially. It has long been suspected that global-scale CO_2 variations are due to variations in primary production of the terrestrial biota, but the empirical demonstration and quantification of this has been hindered by insufficient data coverage, in terms of both time and space.

The remote-sensing techniques discussed by Tucker and his colleagues[1] take a large step towards remedying this problem. Their method involves advanced very high-resolution radiometer (AVHRR) sensors carried by the National Oceanic and Atmospheric Administration's polar orbiting meterological satellites. The sensors collect radiance data daily, at 4 km spatial resolution with global coverage. Daily collection is important, as it allows for selection of data for cloud-free days to minimize the effects of cloud cover. Tucker *et al.* have used these data to estimate the amount of intercepted photosynthetically active radiation (IPAR), the radiation in the spectral range that is strongly absorbed by leaves for driving photosynthesis. From this they estimate the green-leaf densities of plant canopies. If these factors provide an accurate measure of terrestrial photosynthesis, and if the annual CO_2 cycle is due mainly to photosynthesis variations, the satellite data should correlate well with atmospheric CO_2 variations.

The monthly, latitudinally-averaged values of a vegetation index derived from the data for the period 1982–84 have been compared with atmospheric CO_2 concentrations by Tucker *et al.* The patterns match well and show the expected inverse relationship: the higher the vegetation index, the lower the CO_2 concentration with a 1–2-month lag.

These remote-sensing techniques could potentially contribute to our understanding of the greenhouse problem in at least two ways. First, they could help in refining and validating global carbon-cycle models[4-6]. There is considerable uncertainty about how well the terrestrial biota is represented by these models; few detailed validations have been performed[2]. The global-wide data from the AVHRR sensors could provide an additional, independent data source against which CO_2 assimilation and release could be compared.

Second, they could be valuable for monitoring long-term effects of higher CO_2 concentrations and climatic change on the global vegetation. It is very uncertain whether and how the productivity of global ecosystems will be affected directly by higher CO_2 levels[7] — the CO_2-fertilization effect. In carbon-cycle models this effect is often represented by a simple one-parameter equation in which the assumed value of the biotic growth factor is estimated from results of greenhouse experiments. But scaling up the controlled experimental results from leaf or plant level to the real world of highly dynamic, interactive plant communities and ecosystems is fraught with difficulties[8]. The technique for monitoring changes in the productivity of global ecosystems could provide the empirical data with which to test the assumption of CO_2 fertilization.

Change in species composition or areal distribution of ecosystems could also be caused directly by increasing CO_2 levels and by climatic change. Such vegetation changes have obvious feedbacks to carbon reservoirs and fluxes as well. Again, the satellite data could prove useful for detecting any such shifts.

But the state-of-the-art in using the remote-sensing methods for relating reflected radiation, green-leaf biomass, primary production and atmospheric CO_2 levels is still immature. Tucker *et al.* note that unexplained variance and uncertainty exist at each link of this chain of relationships. How much confidence can we place in the approach? How much of an improvement over existing methods of measurement does it actually represent? Its biggest advantage is the global coverage, with fine resolution. But the sceptic must be convinced that we are not being sold sophisticated technology to address questions for which we largely know the answers.

Further careful comparisons of the satellite data with model results and ground-based data would help to establish the validity of the approach. Nevertheless, we have been given an enticing glimpse of a method with potentially far-reaching applications to the important global problems of the greenhouse effect and climatic change. □

1. Tucker, C.J., Fung, I.Y., Keeling, C.D. & Gammon, R.H. *Nature* **319**, 195 (1986).
2. Bolin, B. in *The Greenhouse Effect, Climatic Change and Ecosystems* (eds Bolin, B., Döös, B.R., Jager, J. & Warrick, R.A.) (Wiley, Chichester, in the press).
3. Dickinson, R.E. in *The Greenhouse Effect, Climatic Change and Ecosystems* (eds Bolin, B., Döös, B.R., Jager, J. & Warrick, R.A.) (Wiley, Chichester, in the press)
4. Björkström, A. in *The Global Carbon Cycle* (eds Bolin, B., Degens, E., Kempe, S. & Ketner, P.) 403 (Wiley, Chichester, 1979).
5. Emanuel, R.E., Killough, G.G., Post, W.M. & Shugart, H.H. *Ecology* **65**, 970 (1984).
6. Goudriaan, J. & Ketner, P. *Climatic Change* **6**, 167 (1984).
7. Wigley, T.M.L., Briffa, K.R. & Jones, P.D. *Nature* **312**, 102 (1984).
8. Shugart, H.H., Antonovsky, M.Ja., Jarvis, P.G. & Sandford, A.P. in *The Greenhouse Effect, Climatic Change and Ecosystems* (eds Bolin, B., Döös, B.R., Jager, J. & Warrick, R.A.) (Wiley, Chichester, in the press).

R.A. Warrick is in the Climatic Research Unit, School of Environmental Sciences, University of East Anglia, Norwich NR4 7TJ, UK.

Indo–Pacific sailfish

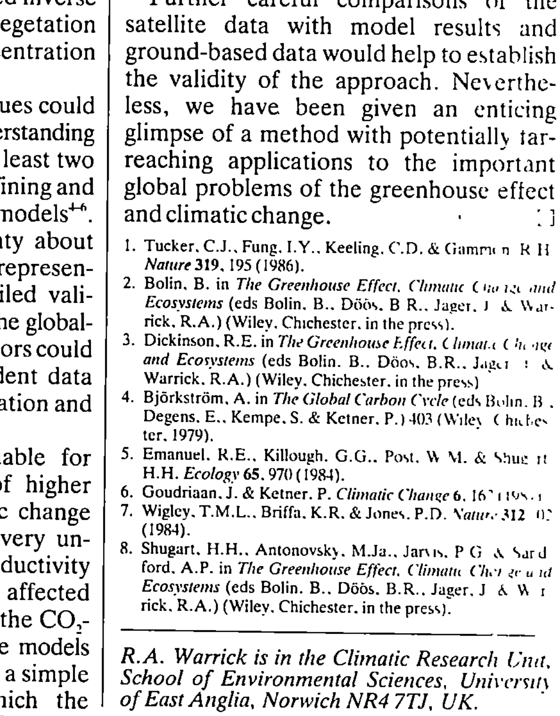

From *Billfishes of the World: An Annotated and Illustrated Catalogue of Marlins, Sailfishes and Swordfishes Known to Date* by Izumi Nakamura (FAO Fisheries Synopsis, No. 125, Vol. 5; 1985).

Hydrogenases

From chemistry to legume growth

from R. Cammack and M.G. Yates

Hydrogenases are enzymes used by bacteria and algae either to produce hydrogen or to consume it as a fuel. They are of interest not only as natural organometallic catalysts and because of the possibility of their application to biotechnological hydrogen production but also because hydrogenase genes may be used to increase agricultural productivity by improving the efficiency of nitrogen fixation. A recent symposium in Hungary* illustrated how the study of these fascinating enzymes has progressed.

It is now clear that there are two types of hydrogenase. The first contains iron, is extremely active and occurs in anaerobic bacteria such as *Clostridium*, which produce H_2 as an electron sink during their metabolism. The second type, one of the few enzymes known to require nickel, is more widely distributed and is used principally for H_2 uptake. It is less active in H_2 production than the Fe-hydrogenase, but from the biotechnological point of view it has the advantage of being much less sensitive to oxygen.

The structural genes of the Fe-hydrogenase of *Desulfovibrio vulgaris* have been sequenced (C. Veeger, Agricultural University, Wageninen). They encode a polypeptide of relative molecular mass (M_r) 46,000 and a hitherto undetected small subunit of M_r 13,500. The sequence indicates that two of the iron–sulphur clusters in this enzyme are of the conventional [4Fe–4S] kind and similar to those in bacterial ferredoxins; the third cluster is probably involved in catalysis.

The probable catalytic site of the Fe-hydrogenase from *Clostridium pasteurianum* has been scrutinized by Mössbauer spectroscopy and magnetic circular dichroism spectroscopy (L.E. Mortenson and M.W.W. Adams, Exxon Research, New Jersey; B.H. Huynh, Emory University, Atlanta; M.K. Johnson, Louisiana State University). It seems to be a unique type of four-iron cluster in which one iron atom is in a different environment but coupled to the other three.

The mechanism of action of the Ni-hydrogenases of *Desulfovibrio* species has been studied by electron-spin resonance and other spectroscopic techniques (J.J.G. Moura, Centro de Quimica Estrutural, Lisbon; J. LeGall, CEN Cadarache, France; R. C.). The nickel centre, which from EXAFS measurements seems to be surrounded by sulphur ligands, can take up several oxidation levels including Ni (III) at an extraordinarily low redox potential. A hydride seems to be involved in the hydrogenase reaction mechanisms but its structure is not yet known.

What seems to be the commonest type of hydrogenase contains two subunits of M_rs about 30,000 and 60,000. Important examples are the membrane-bound Ni-hydrogenases, which have been isolated from the hydrogen-oxidizing bacterium *Alcaligenes eutrophus* (K. Schneider and H.G. Schlegel, University of Göttingen), the aerobic nitrogen-fixing soil bacterium *Azotobacter vinelandii* and the symbiotic nitrogen-fixing organism *Rhizobium japonicum* (D.J. Arp, University of California, Riverside). These enzymes prove to be similar in structure and antigenic characteristics, as well as in regulatory factors (O_2, H_2 and carbon substrates) and genetic determinants.

The genetics of hydrogenase has developed only recently. In *Escherichia coli* there are probably three different hydrogenases (D. Boxer, University of Dundee). Mutants in the structural genes have not been identified because a deficiency in one is masked by the presence of another, but several mutants in which the hydrogenase activity is affected have been isolated. Lee *et al.* have evidence of two classes of mutants, one of which contains *hydA* and *hydB* genes[1,2]. The *hydB* gene is probably in a single operon with a gene encoding formate dehydrogenase and another for an electron-transport protein that couples formate dehydrogenase to hydrogenase. Of two newly discovered genes, *hydC* and *hydD* (L.F. Wu and M.A. Mandran-Berthelot, CNRS, Villeurbanne), the former may be involved in Ni processing.

The *hup* genes of *R. japonicum* Ni-hydrogenase have been isolated[3]. Plasmids containing these genes complement Hup$^-$ mutants of *Azobacter chroococcum* and the arrangements of the *hup* genes in the genomes of these two species are similar[4]. The *hup* genes of *R. japonicum* are probably contiguous and comprise 15.5–21 kilobases divided into at least three transcriptional units[5]. The *hox* (hydrogen oxidation) genes of *Alcaligenes eutrophus* are plasmid-borne, encode both the membrane-bound and a soluble, NAD-linked hydrogenase and contain the structural and regulatory genes in a 50-kilobase sequence. However, an additional chromosomal function is necessary to express the Hox activity. This function may be part of a general regulatory mechanism analogous to the *fnr* system of *E. coli* (B. Friedrich, Freie Universität, Berlin). The *hup* genes of *Rhizobium leguminosarum* are also plasmid-borne, those of *R. japonicum* may be, but those of *A. chroococcum* and one *Alcaligenes* strain are not; *hup* genes have also been isolated from the purple photosynthetic bacterium *Rhodopseudomonas capsulata* (A. Colbeau, A. Godfroy and P.M. Vignais, Centre d'Etudes Nucleaires, Grenoble).

Interest in hydrogenase genes is stimulated by the possibility that hydrogenase might improve the efficiency of biological nitrogen fixation by symbiotic rhizobia in leguminous plants, such as soybeans; many strains of rhizobia are naturally Hup$^-$ or express low activity in legume nodules. The energy-intensive reaction of the enzyme nitrogenase produces hydrogen gas as an apparently inevitable by-product. If it builds up inside the soybean nodule, the hydrogen may inhibit the nitrogenase and it certainly represents a waste of energy resources. Hydrogenase, by recycling the hydrogen, could in principle alleviate these problems. But do *hup* genes produce bigger plants?

H.J. Evans and co-workers have investigated this question by comparing yields of soybean plants inoculated with Hup$^+$ or Hup$^-$ strains of *R. japonicum*. Both naturally occurring and genetically engineered Hup$^+$ and Hup$^-$ strains were used[6]. A range of responses was obtained with statistically significant higher yields in the *hup*$^+$ series in most cases. Parallel work on free-living *A. chroococcum* (M.G.Y.) shows that its hydrogenase aids growth under selective conditions; these are carbon-limited, nitrogen-fixing continuous cultures at high dilution rates, or growth intiation in batch culture under air, together with low levels of carbon substrates.

The complexity of the *hup* operon appears to be comparable with that of the nitrogen-fixing *nif* operons. The fact that they have common regulatory factors (O_2, fixed nitrogen and temperature) is probably coincidental, although Hup$^-$ Nif$^-$ mutants of *R. japonicum* are known[7]. Both the biochemistry and genetics of hydrogenase are important areas for continued research. ☐

---

*Molecular Biology of Hydrogenases, Biological Research Centre, Hungarian Academy of Sciences, Szeged, 15–21 September, 1985

1. Lee, J.H., Patel, P., Sankar, P. & Shanmugam, K.T. *J. Bact.* **162**, 344 (1985).
2. Sankar, P., Lee J.H. & Shanmugam, K.T. *J. Bact* **162**, 353 (1985).
3. Lambert, G.R. *et al. Proc. natn. Acad. Sci. U.S.A.* **82**, 3232 (1985).
4. Tibelius, K.H. & Yates M.G. in *Nitrogen Fixation Research Progress* (eds Evans, H.J., Bottomley, P.J. & Newton, W.E.) 536 (Nijhoff, Doredecht, 1985).
5. Haugland, R.A. *et al. J. Bact.* **159**, 1006 (1984).
6. Evans, H.J. *et al.* in *Nitrogen Fixation and CO_2 Metabolism* (eds Ludden & Burris) 3 (Elsevier, Amsterdam, 1984).
7. Horn, S.S.M., Graham, L.A. & Maier, R.J. *J. Bact.* **161**, 882 (1985).

R. Cammack is in the Department of Biochemistry, King's College, (KQC), Campden Hill Road, London W8 7AH, UK; M.G. Yates is in the AFRC Unit of Nitrogen Fixation, University of Sussex, Brighton, BN1 9QJ, UK.

The real cause of Ethiopia's problems

SIR—Constructive analysis and critical review by the scientific community of possible interventions to avoid future disasters in the drought-stricken African Sahel is the least that can be asked. John R. Krebs and Malcolm J. Coe[1] have certainly made a positive contribution to this process by assessing recent reports of the causes of the disaster, paying particular attention to the impressive argument of A.R.E. Sinclair and J.M. Fryxell[2] who proposed that the contesting causes are the weather and man. Krebs and Coe single out man and his recent efforts to develop sedentary agriculture as drawing the largest portion of the blame, but I suggest that much of their argument is not appropriate to the highland areas of Ethiopia so severely affected by the recent famine. Furthermore, the suggestion that a return to migratory lifestyle is the most viable option is unlikely to be considered feasible in those areas of Ethiopia.

Drought is not new to Ethiopia. However, Sinclair and Fryxell[2] argue that previous years of below-average rainfall did not result in the extreme mortality seen in the past 10 years. This is not the case. Ethiopia's chronicles and other historical sources reveal 23 major famines between 1540 and 1800, with those of 1540 and 1702 receiving particular comment as to their severity[3]. The famine of 1828–29 resulted in severe loss of life, and was complicated by an epidemic of cholera. The most devastating and well-described famine of 1888–92 reputedly killed one-third of the Ethiopian population[4] and was complicated by a plague of locusts and an epidemic of rinderpest in cattle which almost destroyed the cattle population.

In many of the northern areas prone to cyclical drought, there is either no tradition of migration in search of pastures, water and cultivable soils or the migrations are distinct from the pastoral migrations more characteristic of other areas of Sahelian Africa. Sedentary agriculture in this area was established in the tropical highlands long before the advent of aid programmes which, along with colonization, have been proposed as major causes of the Sahelian famines[1,2]. Ethiopia was never colonized, with the exception of a five-year occupation by Mussolini's forces. Extensive agricultural aid programmes are a relatively recent introduction and, judging from my three years' experience in Ethiopia a decade ago, have not had the impact, penetration and conequently destruction of the environment nd the ecological balance that have ocurred in many other parts of Sahelian frica. Environmental destruction has of urse occurred, as a result of high popution density, overgrazing, denuding of vegetation and soil erosion, but this has generally been self-inflicted and has occurred over a long time. The northern highland region of the country, also the most severely affected in the drought and famine of 1972–73, is relatively densely populated (more than double the average population density of sub-Saharan Africa), and much of it is characterized by plateaus at an altitude of 2,500– 3,000m, gorges, mountain peaks and deep chasms. The peasant inhabitants are engaged in sedentary subsistence farming[5], cultivating small plots of land, which as a result of centuries of feudal land tenure system and the traditional bequests of land, have become smaller with time. The farmers are hampered by the terrain and soil erosion occurs on an immense scale. Severe transport and communication problems associated with the rugged landscape compound their difficulties. They live, therefore, on the edge of survival.

The rainfall of the region is largely dependent on the movement of the Intertropical Convergence Zone (ITCZ) and its relation to pressure changes in the surrounding regions. Annual rainfall figures show very pronounced fluctuation from year to year, with variations of 56–140% of the mean figure reported during a 70-year period[2]. Failure of the rains is therefore inseparable from the man-made components of this disaster. Furthermore, whereas overgrazing in highland Ethiopia is undeniably part of the man-made contribution to the cause, it is not the result of recent settlement near waterholes as suggested by Sinclair and Fryxell[2].

I submit therefore that in Ethiopia it is impossible to label the drought hypothesis as a misconception and to separate it from the alternative settlement-overgrazing hypothesis in discussion of the cause of the secular famines in that country. Furthermore, I think that broad generalizations of the Sahel which include Ethiopia should consider the geographical, historical, sociological and political factors which render it distinct from many other countries of the region.

Nevertheless, full support should be given to the recommendation of Sinclair and Fryxell that the improvement of the environment over several decades must be addressed by both developed and developing countries. The specific suggestions will require unprecedented collaboration between donor agencies and a close coordination between these agencies and the appropriate government departments in individual countries which, if to include such measures as cattle depopulation, will require a heavy hand to counteract traditional customs and practices relating to cattle keeping[6]. (For years veterinary services have contributed to the improvement of cattle production efficiency by reducing the prevalance of many major infectious diseases but this has not been matched by corresponding improvement in livestock offtake and marketing.) But most important, the environmental improvement projects should be tailored to fit the individual countries, or in the case of Ethiopia, regions within the country, to avoid the undesirable effects of yet further inappropriate development aid such as that we are currently criticizing.

BRIAN D. PERRY
Virginia-Maryland Regional College
of Veterinary Medicine,
Blacksburg, Virginia 24061, USA

1. Krebs, J.R. & Coe, M.J. *Nature* **317**, 13–14 (1985).
2. Sinclair, A.R.E. & Fryxell, J.M. *Can J Zool* 63, 987–994 (1985).
3. Pankhurst, R. *J. Hist. Med.* **21**, 95–124 (1966)
4. Pankhurst, R. *J. Hist. Med.* **21**, 271–294 (1966)
5. Gryseels, G. & Anderson, F.M. *ILCA Res Rep* No 4, (International Livestock Centre for Africa, Addis Ababa 1983).
6. Perry, B.D., Mwanaumo, B., Schels, H.F. Eicher, F & Zaman, M.R. *Prev. Vet. Med.* **2**, 633–653 (1984)

Major groove or minor groove?

SIR—After Matthews first proposed that cro protein has an α-helix that contacts the major groove of a right-handed B-DNA[1], it was soon realized[2] that the helix-major groove interaction might be a common feature by which many gene regulatory proteins recognize a particular sequence of DNA. Now we have the first crystallographic picture for this kind of binding in the studies on the phage 434 repressor–operator complex[3]. Although different in overall structure, endonuclease *Eco*RI has also been shown to have an α-helix contacting the major groove of its substrate[4]. I have suggested[5] that stereochemically the major groove of B-DNA does provide the best place for a sequence-specific DNA-binding protein to make extensive contact with a 'recognition helix' as the main determinant of specificity[6]. The argument is as follows[5]. First, the diameter of an α-helix is at least 10.7Å. Among common DNA structures, only the major groove of B-DNA is both broad and deep enough (about 11.7Å and 8.5Å) to accommodate an α-helix. Second, the major groove is much more specific than the minor groove for protein binding. This is because any type of mutation (A-T → T-A, A-T → G-C, A-T → C-G and C-G → G-C) changes the potential hydrogen bonding pattern much less in the minor groove compared to its effect on the pattern in the major groove. An extreme example is the A-T → T-A mutation, which keeps almost the same two H-donor positions in the minor groove but exerts a totally different hydrogen bonding pattern in the major groove. As for hydrophobic interaction, another important source of specificity, the main hydrophobic side chain (methyl thymine) of DNA lies in the ma- ove as well.

jor groove contact is not universal, however. If the the protein in question is not a sequence-specific one, the minor groove can also be its binding site, as reported by Klug and his colleagues in the histone core-DNA structure[8]. Also, proteins involved in transcription, reverse transcription and in the priming of DNA replication have a DNA-RNA hybrid as the binding partner. The hybrid molecule has been shown to assume A-form conformation[9]. Yet in A-conformation only the minor groove is open to proteins, while the major groove is too narrow and deep (2.7Å in width and 13.5Å in depth). Moreover, the two edges of the major groove are laced together by a continuous network of water molecules, making the major groove harder to access. It is then conceivable that the minor groove turns out to be the better binding site for those proteins. Since these DNA-binding proteins are not sequence-specific ones, the less specific minor groove is just good enough.

Wang Jia-huai

Biophysics Institute,
Academia Sinica, Beijing, China

1. Anderson, W.F., Ohlendorf, D.H., Takeda, Y. & Matthews, B.W. *Nature* **290**, 754-758 (1981).
2. Sauer, R.T., Yocum, R.R., Doolittle, R.F., Lewis, M. & Pabo, C.O. *Nature* **298**, 449-451 (1982).
3. Anderson, J.E., Ptashne, M. & Harrison, S.C. *Nature* **316**, 596-601 (1985).
4. Frederick, C.A., *et al. Nature* **309**, 327-331 (1984).
5. Wang, J-H., in *The China-Japan bilateral symposium on biophysics* 142 (ed. Biophysics Society of China). (China Academic Publisher, 1985).
6. Wharton, R.P., & Ptashne, M. *Nature* **316**, 602-605 (1985).
7. Conner, B.N. *et al. Nature* **295**, 294-299 (1982).
8. Richmond, T.J. *et al. Nature* **311**, 532-537 (1984).
9. Wang, A. H.J. *et al. Nature* **299**, 601-604 (1982).

The facts on cystic fibrosis testing

Sir—The *News and Views* item[1] on a series of papers[2-5] reporting DNA probes showing linkage to the cystic fibrosis (CF) gene observes "a start has at least been made on the development of the prenatal test for cystic fibrosis". It continues "the new data offer immediate prospects for the prenatal testing of cystic fibrosis". The reader would be entitled to conclude first that no prenatal test for CF currently exists and second that advances in molecular biology have radically altered this situation. Neither conclusion is correct.

Two years ago we reported that measurement of microvillar enzymes in amniotic fluid supernatant could be used as an *in utero* test for CF[6,7]. Our data have been confirmed in many other laboratories and a special issue of the journal *Prenatal Diagnosis*[8] was devoted to this subject. Although the test is not perfect, it has a very adequate detection rate of 95% at 18 weeks of pregnancy and a false positive rate of 5%. In the past two years more than 450 at-risk pregnancies have been prospectively screened by our procedures, and the birth of over 100 children with CF prevented. With the possible exception of Tay–Sachs disease and β-thalassaemia, no other mendelian disorder has been as successfully tackled.

At first sight, it might seem that a restriction fragment length polymorphism (RFLP) tightly linked to the CF gene could improve prenatal testing by moving it from amniotic fluid samples in the second trimester of pregnancy to chorionic villus samples in the first trimester. However, this ignores a cardinal requirement of prenatal testing, namely that some method of confirmation of diagnosis on the abortus be available. This problem has been solved for the second-trimester fetus, first by the observation that most CF fetuses have the macroscopic appearance of meconium ileus[8], and second by protein and enzyme analysis of meconium samples scraped from the fetal ileum[9]. These anatomical and biochemical changes are probably specific to the second trimester and observable only on an intact fetus. If they existed in the first-trimester fetus (which we doubt) they could not be assessed in materials removed by vacuum aspiration, the procedure for termination at this stage of pregnancy.

It is difficult to see how CF-linked RFLPs make reliable prenatal diagnosis 'a reality'. The critical question of the possible genetic heterogeneity of the disease has yet to be addressed. There are suggestions in two of the papers reviewed[3,4] that the CF linkage relationship in the Amish may be different from that in other populations. Even if CF turns out to be a genetically homogeneous entity, much work needs to be done on producing highly informative flanking RFLPs, and on defining the extent of recombination expected with different types of multi-point analysis. But until the CF gene or its protein product is identified, the use of RFLPs on chorionic villus samples will lead to a form of prenatal testing without the benefits of confirmation of diagnosis. It must be emphasized that this is a radical departure from accepted norms of *in utero* testing.

We also have doubts about the value of RFLP-based heterozygote testing in CF. Here the need is for population-wide screening, so that heterozygous couples could be identified before the birth of the first affected child. Programmes of prenatal screening for Tay–Sachs disease and for β-thalassaemia have been effective, largely because heterozygosity tests have been simple, cheap and rapid. The current state of DNA technology is not yet suitable for this type of application.

There has been a tendency recently to exaggerate the immediate clinical benefits of advances in molecular biology. Careful assessment of the potential of RFLP-based diagnosis of genetic disease suggests that its role is likely to be drastically limited by a number of factors such as genetic heterogeneity, the need to have information on whole families rather than individual patients, and expense. Although localization of a mutant gene on a particular chromosome will undoubtedly assist attempts at cloning that gene and identification of its protein product, it must be noted that this is yet to be achieved for any unsolved mendelian disorder, and may well prove more difficult than has been anticipated.

David J.H. Brock
Veronica van Heyningen

University of Edinburgh,
MRC Clinical and Population
Cytogenetics Unit,
Western General Hospital,
Edinburgh EH4 2XUf, UK

1 Newmark, P. *Nature* **318**, 309 (1985).
2 Knowlton, R.G. *et al. Nature* **318**, 380-382 (1985).
3 White, R. *et al. Nature* **318**, 382-384 (1985).
4 Wainwright, B.J. *et al. Nature* **318**, 384-385 (1985).
5 Tsui, L–C. *et al. Science* **230**, 1054-1057 (1985).
6 Carbarns, N.J.B., Gosden, C. & Brock, D.J.H. *Lancet* **i**, 329-331 (1983).
7 Brock, D.J.H. *Lancet* **ii**, 941-943 (1983).
8 *Prenatal Diagnosis* **5**, 93-148 (1985).
9 Brock, D.J.H. *et al. Lancet* **i**, 1175-1178 (1985).

Long-running experiments

Sir—Your coverage of long-running experiments (*Nature* **318**, 310; 408 (1985)) brings to mind an experiment that although begun in this century will probably not be complete for millennia.

In 1918 Howard and Daniels[1] devised the simple but ingenious idea of sealing nitric oxide in glass tubes, some of which contained potential catalysts. Nitric oxide is thermodynamically unstable ($\Delta G^{\circ}_{f\,298} = 86.6\,\mathrm{kJ\,mol^{-1}}$) and any decomposition resulting from $2NO \rightarrow N_2 + O_2$ would be followed by $2NO + O_2 \rightarrow 2NO_2$ and the brown nitrogen dioxide produced would be easily detectable. When the tubes were examined 40 years later, decomposition was found neither in tubes containing pure NO nor in tubes containing NO plus catalyst.

The result was no surprise because an extrapolation of their higher temperature work in the presence of a calcium oxide catalyst indicated that 70,000 years would be required for 2% decomposition (the minimum they could detect) at room temperature. Howard and Daniels gave some of their tubes to the Smithsonian Institution, Washington DC, for future examination. In the case of the homogeneous gas phase decomposition o NO at room temperature, even if w assume a detection system sensitive to 10 molecules of NO_2, it would still take ~10 years for any decomposition to be noticed

Sidney To

Physical Chemistry Laboratory,
South Parks Road, Oxford, UK

1. Howard, C.S. & Daniels, F. *J. phys. Chem.* **62**, 360 (1958).

health care venture capital

S/L HEALTH CARE VENTURES is the leading health care venture capital fund in the world that has the scientific, business and capital resources to form new health care companies of substantial size. The General Partners of the fund are all scientists who have significant corporate business experience with major health care companies and who have successfully founded and built over twenty companies in the health care field. We will be pleased to consider either business plans or research support that can be built into major businesses. Capitalization for any situation ranges between $250,000 and $1 million.

S/L HEALTH CARE VENTURES
1250 BROADWAY, NEW YORK, NY 10001

Reader Service No.14

Copies of articles from this publication are now available from the UMI Article Clearinghouse.

For more information about the Clearinghouse, please fill out and mail back the coupon below.

UMI Article Clearinghouse

Yes! I would like to know more about UMI Article Clearinghouse
I am interested in electronic ordering through the following system(s).

☐ DIALOG/Dialorder ☐ ITT Dialcom
☐ OnTyme ☐ OCLC ILL Subsystem
☐ Other (please specify)__________
☐ I am interested in sending my order by mail.
☐ Please send me your current catalog and user instructions for the system(s) I checked above.

Name__________
Title__________
Institution/Company__________
Department__________
Address__________
City__________State______Zip______
Phone (_____)__________

Mail to: University Microfilms International
300 North Zeeb Road, Box 91 Ann Arbor, MI 48106

MACMILLAN 1985/6 ACADEMIC BOOK SALE

The following selection of books at greatly reduced prices may now be ordered from all major bookstores. This offer is open until 28th February 1986 only. Order now using the spaces provided below.

_____**International Mortality Statistics** P. Alderson 23969 5 (£47.00) £14.95
_____**Biochemistry of Parasitic Helminths** John Barrett 25669 7 (£12.95) £3.95 (paperback)
_____**Urban Air-Pollution Modelling** Michael M. Benarie 23391 3 £35.00 £17.50
_____**Birth Defects Compendium** Daniel Bergsma (ed.) 27876 3 (£50.00) £25.00
_____**Polar Dielectrics and Their Applications** Jack C. Burfoot and George W. Taylor 17958 7 (£20.00) £6.95
_____**The Ultimate Software Selector** Federation of Micro System Centres 37556 4 (£9.95) £2.95
_____**Environmental Factors in Mammal Reproduction** Desmond Gilmore and Brian Cook (eds.) 24150 9 (£25.00) £8.95
_____**X-Ray Microanalysis** M. A. Hayat 32355 6 (£30.00) £9.95
_____**Horticultural Reviews Volume 4** Jules Janick (ed.) 34192 9 (£25.00) £8.95
_____**The RAE Table of Earth Satellites, 1959-1982, 2nd Ed.** D. G. King-Hele, J. A. Pilkington, D. M. C. Walker, H. Hillier and A. N. Winterbottom 35374 9 (£50.00) £25.00
_____**Hydrogen and Energy** Charles A. McAuliffe (ed.) 18432 7 (£12.00) £4.95
_____**Plant Galls of India** M. S. Mani 18067 4 (£12.50) £3.95
_____**The Design of Air Quality Monitoring Networks** R. E. Munn 30460 8 (£20.00) £6.95
_____**Growth Without Ecodisasters?** Nicholas Polunin (ed.) 23521 5 (£22.50) £5.95
_____**The Arctic Ocean: The Hydrographic Environment and the Fate of Pollutants** Louis Rey (ed.) 31017 9 (£45 00) £12 50
_____**Developmental Psychology and Society** John Sants (ed) 21340 8 (£20 00) £6 95
_____**Cancer and the Environment** L. A. Sobel (ed.) 28591 3 (£15 00) £4 95
_____**The Fast Breeder Reactor – Need? Cost? Risk?** Colin Sweet (ed) 27973 5 (£20.00) £6 95

Please complete and return this form to your bookseller, or in case of difficulty to: **Macmillan Distribution Ltd, Houndmills, Basingstoke, Hampshire RG21 2XS, UK.**

Please supply ______ titles as indicated

☐ Please invoice me. Postage and packing £1.00 per title.

☐ I enclose a cheque for £__________

☐ Charge £______ to my credit card as shown. Access/Visa/Amex/Diners Club

Card No.__________Expiry Date______
Signature__________
Name (capitals)__________
Address (capitals)__________

This offer is not applicable in USA

M MACMILLAN PRESS LTD.
Houndmills, Basingstoke, Hants RG21 2XS, UK. M

Current Topics in Microbiology and Immunology

Volume 122

The BALB/c Mouse

Genetics and Immunology

Editor: **M. Potter,** Bethesda
1985. 85 figures. XVI, 253 pages. Hard cover DM 126,-
ISBN 3-540-15834-0

Contents: History of the BALB/c Family. - Genetic Differences in BALB/c Sublines. - Differences in Response to Infections. - Immune Response Differences. - Plasmacytomagenesis and Response to Mineral Oils.

Volume 121

Bacteria and Complement

Editor: **M. Loos,** University of Mainz
1985. 76 figures. IX, 191 pages. Hard cover
DM 136,-. ISBN 3-540-15877-4

This volume contains the first synopsis of important aspects of host defence and how this system effectively acts against infectious micro-organisms. Its purpose is to bring together in one volume separate up-to-date reviews on the activation and effector phases of the complement system and the way these proteins are triggered off by the envelope structures of gram-negative and gram-positive bacteria.

Volume 120

Parasite Antigens in Protection, Diagnosis and Escape

Editor: **R. M. E. Parkhouse,** London
1985. 17 figures. 260 pages. Hard cover DM 168,-
ISBN 3-540-15859-6

Contents: Introduction. - The *Eimeria*. - *Entamoeba Histolytica,* Antigens and Amoebiasis. - Parasite Antigens, Their Role in Protection, Diagnosis and Escape: The Leishmaniases. - Parasite Antigens in Protection, Diagnosis and Escape: *Plasmodium*. - Toxoplasmosis: The Need for Improved Diagnostic Techniques and Accurate Risk Assessment. - Antigens of African Trypanosomes. - Antigens of Taeniid Cestodes in Protection Diagnosis and Escape. - Nematode Antigens. - Schistosomes: Surface, Egg, and Circulating Antigens. - Trematodes, Excluding Schistosomes, With Special Emphasis on *Fasciola.*

Volume 119

Images of Biologically Active Structures in the Immune System

Their Use in Biology and Medicine

Editors: **H. Koprowski,** Philadelphia; **F. Melchers,** Basel
1985. 22 figures. XI, 142 pages. Hard cover DM 96,-
ISBN 3-540-15760-3

The articles assembled in this volume offer new information on the potential practical applications of the network theory of the immune system. They report on the search for molecules and their biological functions and for the regulation of the immune response itself in autoimmunity and vaccination.

Volume 123

Retroviruses 4

new

Editors: **P. K. Vogt,** Los Angeles, **H. Koprowski,** Philadelphia
1986. 23 figures. VII, 98 pages. Hard cover DM 86,-. ISBN 3-540-15947-9

Contents: Interaction of the Rous Sarcoma Virus Protein pp60^{src} with the Cellular Proteins pp50 and pp90. - Microinjection Studies of Retroviral Polynucleotides. - The Viral Tyrosine Protein Kinases. - Homology Among Oncogenes.

By the same editors:

Volume 112

Retroviruses 3

1984. 19 figures. VII, 115 pages. Hard cover DM 72,-. ISBN 3-540-13307-0

Contents: Bovine Leukemia Virus. - Spleen Focus Forming Virus: Relationship of an Altered Envelope Gene to the Development of a Rapid Erythroleukemia. - The Genetics of Murine Leukemia Viruses. - Expression of Cellular Oncogenes.

Volume 107

Retroviruses 2

1983. 26 figures. VII, 180 pages. Hard cover DM 124,-. ISBN 3-540-12384-9

Contents: Acute Transforming Feline Retroviruses. - Asymmetric Chromosomal Distribution of Endogenous Retrovirus Loci in Chickens and Mice. - Subcellular Localization of pp60^{src} in RSV-Transformed Cells. - Regulation of Cell Growth and Transformation by Tyrosine-Specific Protein Kinases: The Search for Important Cellular Substrate Proteins. - Phosphotyrosyl-Protein Phosphatases.

Volume 103

Retroviruses 1

1983. 16 figures. V, 146 pages. Hard cover DM 104,-. ISBN 3-540-12167-6

Contents: Avian Endogenous Viral Genes. - Synthesis, Integration, and Transcription of the Retroviral Provirus. - Defective Avian Sarcoma Viruses. - Murine Leukemia Viruses with Recombinant env Genes: A Discussion of Their Role in Leukemogenesis. - Avian Acute Leukemia Viruses. - Molecular and Cellular Biology of Abelson Virus Transformation.

Volume 118

Genetic Approaches to Microbial Pathogenicity

Editor: **W. Goebel,** University of Würzburg
1985. 47 figures. XI, 283 pages. Hard cover DM 160,-
ISBN 3-540-15597-X

Volume 117

The Biology of Trypanosomes

Editor: **L. Hudson,** London
1985. 25 figures. X, 183 pages. Hard cover DM 124,-
ISBN 3-540-15512-0

3180/4/1

Prices are subject to change without notice

Springer-Verlag Berlin Heidelberg New York Tokyo
Heidelberger Platz 3, D-1000 Berlin 33
175 Fifth Ave., New York, NY 10010, USA
37-3, Hongo 3-chome, Bunkyo-ku, Tokyo 113, Japan

Springer

Reader Service No. 2

What's in the name?

John A. Campbell

Artificial Intelligence: The Very Idea. By John Haugeland.
MIT Press:1985. Pp.289. $14.95, £14.95.

AMONG scientific subjects, artificial intelligence has one unique distinction: it has been the victim of its own name. Because the name comes straight from everyday language, too many people have found futuristic messages in it merely through the associations that occur when "intelligence" and "artificial" are coupled together. The results have included science-fiction interpretations and unreasonable expectations of the subject, and confusion of what has been achieved with what has not. Quite rightly, some of the founding fathers have conceded, at least in private, that not enough care was taken 30 years ago to find a label free of loaded words.

But is there any future in Artificial Intelligence, Baron Frankenstein?

Among specialists, there are at least three different definitions of what artificial intelligence involves. One is the study of human intelligence through the use of methods and metaphors depending essentially on computers and computation; this admits both a middle-of-the-road view, in which the definition means neither more nor less than what it says, and a man-in-the-black-box view, whose meaning is self-evident. A second definition is subtly different on paper but very different in practice: the computational study of tasks and processes which have previously been observed only in association with human intelligence. The third has arisen as a result of the subject's actual successes, and the observation that some concepts and techniques have recurred in many of the best pieces of work. By this modest operational definition, a project is an example of artificial intelligence if it relies mainly on those concepts or techniques. (A collection of this information, deliberately expressed in English rather than some high-level programming language, is given by P.H. Winston in the second edition of *Artificial Intelligence*, published by Addison-Wesley in 1984.)

The first definition is closest to the popular impression of what artificial intelligence is. It may even be a surprise to non-specialists to learn that the other two exist, the main reason being that books intended for a general audience and taking either of them as their starting-point have not been very visible in the past. Haugeland's book does not fill this gap. Instead, it joins the queue (or, rather, the unruly crowd) attached to the first and most adventurous definition. It is, nevertheless, a welcome newcomer, because of its relative moderation and avoidance of science fiction.

As no exploration of the consequences of the definition can go far without touching on questions which were once regarded as lying exclusively within philosophical territory, it is an advantage that Haugeland's background is that of a philosopher. On previous evidence, such a vantage point has been no guarantee of successful writing on artificial intelligence — indeed, it seems rather to have guaranteed frequent encounters with the technical and even philosophical banana-skins that litter the field — but Haugeland arrives almost undamaged at the finishing line in this obstacle course.

His central concern is to explore the connection between intelligence and the idea of thought as a formal or at least rational manipulation of symbols. A first chapter on the evolution of philosophical views of "mind" is therefore followed by straightforward description of some of the symbol-manipulating systems, such as Turing machines, that have had the most influence on theoretical computer science and computability. There is also a simple account of models of computation, which makes the point that today's standard computer architecture, not well adapted to any of the definitions of artificial intelligence, is easy to replace with alternative designs that perform better in simulations. This is not news to specialists in advanced computing and to people familiar with the Japanese Fifth Generation plan, but it deserves repetition for a general audience.

As a basis for his substantive arguments, Haugeland's tour of the history of theoretical computer science is less satisfactory than his discussion of issues where he is surer of his philosophical ground. In the historical sections, for example, Alonzo Church is short-changed (by omission) on two counts and possibly three, with partial compensation for this Churchless picture only in the footnotes (where there is still confusion about the difference between Turing's "thesis" and Church's thesis, among other lesser things). Computer scientists may have the sense of seeing their subject through frosted glass here, but at least the author's heart is in the right place. And there is plenty of nourishment in the footnotes in general, collected conveniently at the end of the book, they can be sampled like a chariot of desserts.

The main value of the book to both specialists and non-specialists lies in the attention given to the two principal difficulties of current research in artificial intelligence. These are the frame problem, which is the problem of knowing how to link an item of information efficiently with all the other items that may be needed to establish the context in which its meaning may be determined properly, and the problem of how to assign and manipulate meanings (semantics) of expressions whose rules for structural (syntax) transformations are spelled out in formal symbol-manipulating systems. The problems themselves are well described, so that a general reader can appreciate the irritation that they cause to researchers, especially in speculation on how the human brain solves or avoids them. Haugeland weighs the balance of impressions justly: he is a pessimist rather than an optimist, but admits that, on the evidence, the basic questions of the achievability of "artificial intelligence" remain open.

While contexts and meanings may complicate work in artificial intelligence, there are both possible and desirable ways of reducing the complexity. On the "possible" level, problems of how to represent meaning may become much more tractable if the basic semantic operation used in a formal computational system, or even a brain, is nothing more than a two-way choice or distinction between alternatives or stimuli. And artificial-intelligence research can desire nothing better of its spectators than that they agree to replace the subject's label with one that calls up no wild associations. "AI" for "artificial intelligence", say? The very idea! □

John A. Campbell is Professor in the Department of Computer Science, University of Exeter, Exeter EX4 4PT, UK.

Two brains but of a single mind

John C. Marshall

The Duality of the Mind. By A.L. Wigan. Foreword by Joseph Bogen. *Joseph Simon, PO Box 4071, Malibu, California 90265, USA: 1985. Pp.346. $35.*

THE question of how many angels can dance on the head of a pin has long since ceased to exercise our finest scholars. Yet if one wanted a contemporary analogue the following might suffice: how many minds may a man (or woman) manifest? "One", said René Descartes; "Two", said Arthur Wigan and Roger Sperry; "Forty-two", said Franz-Joseph Gall.

The answer "Two" was sanctified by the award of the 1981 Nobel Prize in Medicine and Physiology to Sperry for the work that he and his colleagues had undertaken on commissurotomized patients. Some 20 years earlier, the eminent Los Angeles neurosurgeon Joseph Bogen had succeeded in reducing the incidence of major convulsive seizures in a small group of severely epileptic patients by sectioning the main cortical fibre tracts (commissures) that connect the two hemispheres of the brain. Sperry's intensive testing of the cognitive functions of these patients' now-disconnected cortices sparked a veritable explosion of interest in the differential psychological capacities of the left and right cerebral hemispheres. On one account of the results, Bogen's operation did not *create* two minds within a single body but rather revealed that we are all dual creatures, deluded in our belief that each of us is an indivisible self.

Bogen's (or Bogens') own interest in these issues has extended beyond the investigation and interpretation of his "split-brain" patients to include the history of neurological speculation about cerebral duality. One fruit of his delving into the past is this splendidly handsome reprint of Arthur Wigan's Victorian epic of 1844, the scope and character of which is best shown by its full title: *A New View of Insanity: The Duality of the Mind Proved by the Structure, Functions, and Diseases of the Brain and by the Phenomena of Mental Derangement, and Shown to be Essential to Moral Responsibility.* Indeed, Wigan's version of the "two-brain" theory is sufficiently close to some modern accounts for Bogen to name his own position "neowiganism".

Who might want to read the book today? To begin with, anyone who is concerned with the relationship between the neurosciences and society will be fascinated to see Wigan struggling to resolve the tension between biological determinism, educability and moral choice. Wigan's phraseology, and the certainty of his Victorian belief in scientific and ethical progress, may seem quaint to our more cynical ears:

> The only limit to our researches on the nature of the mind, will ultimately be the boundary fixed by the Almighty to the powers of the human intellect — a point from which we are yet immeasurably distant. When we shall have cultivated all the faculties which He has bestowed upon us, to their full extent and perfection, then indeed will come the Millennium — an issue towards which we are steadily and rapidly advancing. . . . ;

yet his discussion of the potential conflicts between humanistic and scientific approaches to psychiatry and neurology is a good deal more honest and open than many current positions.

Second, the book *should* be read by all students of neuropsychology. Wigan is a pre-modern in that his work pre-dates the discovery of complementary hemispheric specialization that became (and remains) the central dogma of human neuropsychology. Thus the notion that the left hemisphere is primarily implicated in language functions and the right in visuospatial functions is quite alien to Wigan's time. For Wigan, the hemispheres are full duplicates with respect to their intrinsic cognitive capacities; it is solely "slight inequalities" of "form, energy, and function" that suffice "to produce all the varieties of character which are to be found in the world". Accordingly, many of the case reports that Wigan describes are directed towards showing that "One cerebrum may be destroyed, yet the mind remain entire". The contemporary student would benefit greatly from the exercise of contemplating whether Wigan's conclusion derives merely from inadequate testing of non-verbal skills or rather contains an important truth that has been buried under our own obsession with complementary specialization. □

John C. Marshall is in the Neuropsychology Unit, part of the Neuroscience Group at the Radcliffe Infirmary, Oxford OX2 6HE, UK.

A southern man

Derek Fordham

Shackleton. By Roland Huntford. *Hodder & Stoughton/Atheneum: 1985. Pp.774. £19.95, $29.95.*

"MEN wanted for hazardous journey. Small wages, bitter cold, long months of complete darkness, constant danger. Safe return doubtful. Honour and recognition in case of success." Thus Sir Ernest Shackleton chose to launch his 1915 Imperial Trans-Antarctic Expedition and was overwhelmed by thousands who wanted to join.

Years earlier, in 1900, Shackleton had been in the Antarctic for the first time and Roland Huntford spares no one in setting out the dreadful deficiencies and incompetence of that *Discovery* expedition under the leadership of Commander Robert Falcon Scott. During the expedition Shackleton came close to death and subsequently suffered the ignominy of being invalided home on Scott's orders. Scott's action was undeniably motivated by his dislike of Shackleton, who had shown himself to be a natural leader, in which respect Scott rightly doubted his own abilities.

In a spirit of defiant rivalry, heavily in debt and with a suspected weak heart, Shackleton set about organizing his own expedition, which sailed south in 1907. Shackleton and his team, poorly equipped and ill-prepared, penetrated to within 97 miles of the Pole before he decided to turn back, the hardest decision he ever had to make, but inescapable if he was to bring his team back alive. In so doing he laid bare the geography of the polar plateau and opened the route to the Pole for Scott and Amundsen to follow in 1911. His hero's return was marred by financial difficulties and the scandal of an errant brother, suspected of stealing the Irish crown jewels.

His resources in the face of failure were taxed again in October 1915 at the start of The Imperial Trans-Antarctic Expedition, when his ship, *Endurance*, having drifted helpless for 1,500 miles trapped in the pack-ice, was crushed and sunk in the Weddell Sea. For 600 miles Shackleton led his men over shifting, breaking ice to the floe edge and then across the storm-swept open sea to the desolation of Elephant Island. Having established his men in a primitive camp he set off a few days later with five companions on a further 700 mile open boat journey across the Southern Ocean to South Georgia. A final desperate traverse of a range of unmapped icy mountains led to the whaling station from which the rescue of his expedition was mounted. Shackleton the survivor had once again brought his men back from the prospect of certain death.

But a world on the brink of war failed to recognize the staggering accomplishment of this impetuous man and he had to struggle to raise further funds for his last expedition, during which the misfortunes encountered on his earlier Antarctic forays took their toll. He died as his ship reached South Georgia, ironically the scene of his return from the dead in 1916.

This is Roland Huntford's second polar book — the first, published in 1979, having left the schoolboy image of Captain Robert Falcon Scott somewhat mangled and the subject of much controversy — and deals with the very different but no less intriguing figure of a man who mixed Irish dreaming and poetry with the power to inspire those who worked with and for him in a manner previously unknown in polar exploration. The differences between Shackleton and Scott are developed and the author sees the comparison between the upright, unsure naval officer and the breezy, extrovert Irish poet as illustrating how, in an age before technology came to dominate polar exploration, Shackleton's great achievement was to break by sheer power of leadership and commitment to his objectives the mediocrity that had until then laid its dead hand over much British polar activity. It was not without reason his men called him simply, "Boss".

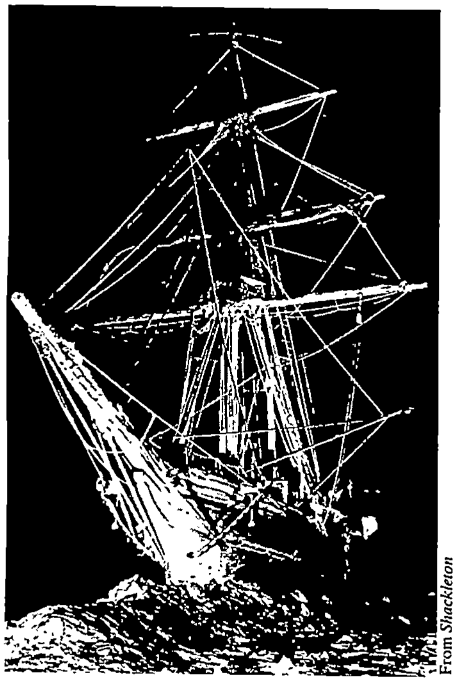

From Shackleton

Ice-bound: Endurance *trapped by pack-ice in the Weddell Sea.*

This is an impressive work and will surely stimulate new interest in a man whose achievements in the field of polar exploration have down the years been largely overshadowed by the tragic nature of his former leader's death.

On the crossing of South Georgia, which ended the journey for which above all else the world should remember Shackleton, he and his two companions felt they were accompanied by an extra person. This is a not uncommon experience for explorers under stress, and Shackleton's account of this phenomenon inspired a haunting reference in T.S. Eliot's poem, *The Wasteland*, "Who is the third who walks always behind you?".

Perhaps for "The Boss" it was the embodiment of the conventional hero, which his enigmatic spirit never quite embraced. □

Derek Fordham, 66 Ashburnham Grove, Greenwich, London SE10 8UJ, UK, is Secretary of the Arctic Club.

States of alteration

C. Ladd Prosser

Changes in Eukaryotic Gene Expression in Response to Environmental Stress. Edited by B.G. Atkinson and D.B. Walden. *Academic: 1985. Pp.378. $71.50, £60.*

The Adaptive Role of Lipids in Biological Systems. By Neil Hadley. *Wiley: 1985. Pp.319. $39.95, £41.40.*

ATKINSON and Walden are concerned with the control of protein synthesis and, as the basis for discussion, the contributors to their book have focused on proteins made in response to stress. It was observed 30 years ago that brief exposure to heat brings about puffs on salivary chromosomes of *Drosophila* and leads to the synthesis of several proteins in large quantity — the so-called heat-shock proteins. In *Drosophila*, seven proteins of different molecular weights have been identified and several have now been cloned. Although most information on heat-shock proteins is available for *Drosophila*, and this is reflected in the book, other chapters describe heat-shock proteins in a slime mould, sea urchin tissues, amphibians, birds and mammals, and in plants.

The heat-shock proteins in different organisms are of various sizes but the most prevalent one is of 70 K molecular weight. They are highly conserved and can be induced by heat exposure of isolated cells as well as of intact organisms. Control has implicated both translation and transcription but evidence from inhibitors emphasizes the increase in transcription of specific mRNAs as most critical. It appears that heat exposure turns on certain genes and one effect of the synthesis of heat-shock proteins is to repress action of mRNAs for other proteins. The chapter by Lindquist and Didomerico on gene expression in *Drosophila* uses synthesis of the mRNA for the 70 K protein as a model for gene regulation in general. The *in vitro* induction of heat-shock proteins in avian red blood cells is covered in chapter by Atkinson and Dean. In mammals, a fever of only 2°C is sufficient to induce heat-shock proteins in the brain.

Synthesis of these proteins is stimulated by other stresses, particularly toxins and drugs, hence the term stress proteins may be more appropriate than heat-shock proteins. Less is known of their synthesis in plants than in other organisms, but maize seedlings and soybean embryos do produce them. There seems no doubt that synthesis of heat-shock proteins is associated with increased resistance to heat stress. Although much is known of the sequence of specific gene activation and protein synthesis, the mechanisms by which heat-shock proteins protect against the lethal action of heat remain mostly speculative. But Atkinson and Walden have succeeded well in integrating the groundwork essential for a final answer to the question of mechanism within the seventeen chapters of the book.

Adaptation in a different system is the topic of the volume by Hadley. He has considered the adaptive function of lipids in a number of biological roles. The book could serve well for one part of a course in comparative physiology. The treatment of biochemistry of lipids is adequate for physiology students but probably not sufficient for lipid chemists. Lipids, predominantly phospholipids, constitute 25–75% of cell membranes by weight. The lipid composition of plasma and organelle membranes can be altered by nutrition and by temperature, but the way in which membrane lipids modify the functioning of membrane proteins remains an unsolved problem

A useful chapter on surface waxes precedes a detailed discussion of the role of waxes in the water relations of terrestrial plants and animals. Their protective role against evaporative loss of water is made clear, but the significance of the diversity in composition of surface waxes — hydrocarbons, ketones, esters, alcohols, sterole and triterpenes — is not explained.

Lipids, especially triglycerols, are stored as fuel that can be accumulated at certain times, for example at the pre-migration stage in insects and birds. Several roles for fat tissue are further described. Brown fat is a ready source of heat, present in most mammalian neonates and hibernants. Because fat has low thermal conductivity it is an insulator, especially in aquatic and cold-dwelling mammals. Some marine plants and animals are neutrally buoyant because of low-density fats. Buoyancy is implemented by an increase in total body lipids and by deposit of lipids of low density. A use of lipids not often considered is in chemical communication, especially in pheromones; some esters of plants are insect repellents. A final chapter deals with medical aspects — pulmonary surfactants, bile salts, fat absorption.

The overall impression to be gained from this book is of the extreme diversity of structure and function of biolipids. Clearly, this is a field of research in which comparative biochemists and ecophysiologists can profitably cooperate. □

C. Ladd Prosser is Emeritus Professor of Physiology in the Department of Physiology and Biophysics, University of Illinois at Urbana-Champaign, 524 Burrill Hall, 407 South Goodwin Avenue, Urbana, Illinois 61801, USA.

• *Ancestors: The Hard Evidence*, the proceedings of a symposium held in April 1984, has been published by Alan R. Liss/Wiley. The meeting was attended by leading workers in palaeoanthropology and was reported in *Nature* 208, **309** (1984). Editor of the book is Eric Delson, price is $49.50, £38.

Talking of muscles and motion

R.M. Simmons

Design and Performance of Muscular Systems. Edited by C.R. Taylor, E. Weibel and L. Bolis. *The Company of Biologists Limited: 1985. Pp.412. £25, $60. Available from the Biochemical Society Book Depot, PO Box 32, Commerce Way, Colchester CO2 2HP, UK.*

One of the main themes of this book, which is based on papers presented at the Seventh International Conference on Comparative Physiology in June 1984, concerns problems of gait during locomotion, such as why animals adopt narrow ranges of speed for particular gaits and why they change from one gait to another (Cavagna, Hedlund, McMahon and Taylor). Some of the illustrations are drawn from unusual human gaits such as hopping, Groucho running (that is, with very bent knees like Groucho Marx) and running on very compliant surfaces.

One idea, now 10 years old, is that an animal can be considered during locomotion as a multi-jointed mass-spring system with a characteristic resonant frequency, and thus a preferred stride rate. As speed increases, say in walking, the ride becomes uncomfortable and less economical because of the stiffness of the spring arrangement and running is more comfortable as the ride is softer and it is less costly in energy consumption. Maximum speed might be determined by maximum stress and this varies with body size much as expected (Alexander). Under the mass-spring model, unusual gaits extend the range of observations.

In locomotion on a flat surface the net external work done is small, but groups of muscles alternately shorten and are stretched thus performing positive and negative work respectively. The tuned-spring model implies that energy imparted to muscles by stretch is recovered when they shorten; indeed, this was first demonstrated in Margaria's laboratory 20 years ago. The positive work phase can thus appear surprisingly efficient, up to 70% in large animals, though much lower in smaller animals for reasons that are not entirely clear. More details of the process of energy storage come from experiments on isolated muscles (by Cavagna and his colleagues), showing increased energy output when an actively contracting muscle is first stretched before being allowed to shorten, some of the power coming from elastic energy stored in the tendons and some apparently stored in the cross-bridges.

Another theme in the book concerns the properties and determinants of the two main muscle fibre types in mammals, the fast-twitch fibres whose mechanical properties are fast and whose metabolism is mainly glycolytic, and the slow-twitch fibres which are slower and are mainly oxidative. The current state of knowledge about structural protein isoforms is given by Perry and Whalen, but most of the new findings about the proteins in mammalian muscle are concerned with mitochondrial enzymes: in separate studies Pette and Edgerton agree that the heterogeneity found in a given fibre type implies a different mode of specification than for the structural proteins, but disagree about whether fibres innervated by branches of the same nerve show heterogeneity. Kushmerick presents his now completed study of the energetics of isometric contractions in two muscles from the mouse, one predominantly slow and the other fast.

A third theme concerns the malleability of the system. Muscles predominantly of one fibre type can be converted into the other by cross-innervation or by changing the pattern of muscle activation artificially: continuous low-frequency stimulation yields slow-twitch charateristics, whereas occasional bursts of stimulation make for fast-twitch fibres. The major determinant of muscle speed is the myosin isoform, while the duration and rapidity of response to a stimulus is probably determined by the membrane systems.

From painstaking stereological measurements it appears that the membrane systems change before the structural proteins (Eisenberg): this can induce an abnormally high mitochondrial content in a fast to slow transformation, the muscle's response to the energetic demands caused by more frequent stimulation and longer response times while fast-cycling myosin is still present. A similar type of mismatch arises during early postnatal development in the rat if a nerve is crushed and then allowed to re-innervate a muscle (Vrobova). The pattern of motorneurone activity is changing during this period, so that by the time re-innervation is complete the immature muscle encounters a mature rate of stimulation and partial atrophy results. In the adult, complete recovery results, the reverse of what might be expected intuitively of variation in plasticity with age.

The sequence of appearance of myosin isoforms during development now seems well established (Whalen). Development from embryonic through neonatal to fast myosin occurs whether or not the muscle is innervated, but induction of slow myosin is nerve-driven. However, thyroid hormone is needed for the transition from neonatal to adult fast myosin. A recent report (discussed here both by Howald and Goldspink) describes changes in myosin isoform from slow to fast as a consequence of training in the rat, but changes in man seem to be less pronounced. Successful athletes in endurance events, such as long-distance runners, have a preponderance of slow twitch fibres and sprinters have more fast twitch fibres. Training in man can induce selective fibre type hypertrophy and an increase in mitochondrial content (Gollnick, Hoppeler), but it is still not clear whether an athlete's fibre typology selects the best event for him or the athlete selects the typology for his chosen event by training.

Other aspects of muscle performance such as whole body response and the control of movement are also covered by appropriate experts. There are in all 34 articles, mostly by different authors, and although the introductory chapters (by H. Huxley, Peachey and Wilkie as well as those by Perry and Whalen already mentioned) are good, I think the novice might find it hard to follow the threads of some of the arguments. For the professional and others with some background in the fundamental properties of muscle, however, this book offers some valuable insights into the design and performance of muscular systems. ☐

R.M. Simmons is Head of the Department of Biophysics, Cell and Molecular Biology at King's College London (KQC), 26–29 Drury Lane, London, WC2B 5RL, UK.

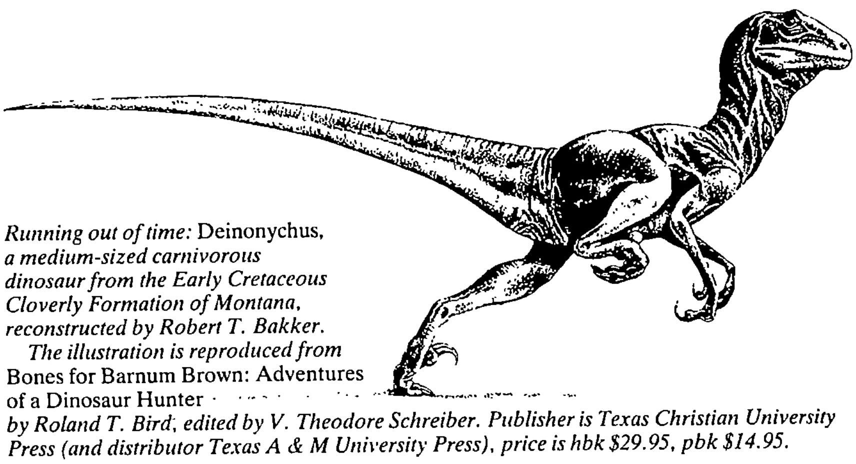

Running out of time: Deinonychus, *a medium-sized carnivorous dinosaur from the Early Cretaceous Cloverly Formation of Montana, reconstructed by Robert T. Bakker. The illustration is reproduced from* Bones for Barnum Brown: Adventures of a Dinosaur Hunter *by Roland T. Bird; edited by V. Theodore Schreiber. Publisher is Texas Christian University Press (and distributor Texas A & M University Press), price is hbk $29.95, pbk $14.95.*

Edwin Hubble: legal eagle

from N. Hetherington

Edwin Hubble skilfully employed trial tactics and techniques to attain favourable verdicts from the court of science.

THERE is more to the advance of science than new observations and new theories. Ultimately, people must be persuaded.

Galileo, a master polemicist, appealed skillfully and effectively to a public forum when science, yet to be differentiated from philosophy, was still accessible to most educated people. An explosion of knowledge and specialization has since narrowed the body from which competent jurors can be drawn for the trial of a scientific idea. Yet, whether before the public or before a jury of their peers, scientists are still concerned with persuasive presentation.

The twentieth-century astronomer Edwin Hubble well appreciated the advocative aspect of science and was a skilled practitioner. Reading Roman law at Oxford and practising as an attorney in the United States were good preparation for a subsequent career in science. Trial tactics and techniques gained for Hubble favourable verdicts more quickly than might otherwise have been attained.

Independent witnesses

Hubble's bold extrapolations from near to distant galaxies presumed uniformity within the universe, a uniformity somewhat supported by Hubble's own studies at the Mount Wilson Observatory of the distribution of absolute magnitudes among isolated nebulae. Harlow Shapley at Harvard, however, had reasonable doubts. Hubble, attempting to persuade doubters with independent corroboration, emphasized, perhaps even exaggerated, the independence of Nick Mayall's study at the Lick Observatory.

Hubble had supported Mayall's dissertation proposal, and Mayall's analysis of nebular counts turned out to agree reasonably well with Hubble's own data[1]. When it came to publishing Mayall's results, though, Hubble contrived to have the study appear as a completely independent body of work. Thus it might more strongly persuade astronomers in the eastern United States, including Shapley. Hubble wrote to Mayall[2]:

> your investigation should be considered as absolutely independent of our work here. Actually it would have greater influence on the eastern gang if there were a note of challenge.

Thus was Mayall's evidence presented in court, to Hubble's satisfaction[3]:

> I am glad to hear that the thesis will be in print soon and thoroughly agree with the committee that it should be published without reference to my paper. Actually I have a personal interest in this decision for I am eager to have as much independent investigation as possible so that the accumulating evidence will eventually convince the eastern group of the importance of careful work. It was partly for this reason that I suggested so pointedly that you keep a skeptical point of view and look for discrepancies rather than consistency.

Mayall's corroborative evidence, independent in appearance, would weigh more favourably with the jury.

Cross-examination

Another of Hubble's discoveries to face trial was his calculation of great distances to spiral nebulae using the period–magnitude relationship for Cepheid stars. This was a major scientific revolution. Shapley, receiving the news in a letter from Hubble, said "here is the letter that has destroyed my universe"[4]. The focus of research at Harvard and elsewhere abruptly shifted from the local area to distant galaxies. The only evidence against Hubble's great distances was van Maanen's asserted detection of motions in spiral nebulae[5]. "So a consistent picture of the spiral is built on the basis of the Cepheid criterion ... save for a disturbing shadow cast by the measures of Mr van Maanen", wrote Hubble in notes for a talk before colleagues at Mount Wilson.

The shadow could be shortened, by stripping away the corroboration claimed by van Maanen[6]. Hubble found only one of the corroborations deserving of consideration, and in it the probable error exceeded the mean motion measured. Another study was vitiated by internal inconsistencies and in two others measured motion was in the opposite direction to that reported by van Maanen. Hubble later wrote, in a manuscript never published, that "reference to these [claimed corroborations] as 'similar motions', implying corroborative evidence, indicates an uncritical imagination"[7].

Edwin Hubble, photographed by Jay Barrie, from the posthumous The Nature of Science and Other Lectures *(Huntington Library, San Marino, 1954).*

Additionally, van Maanen claimed corroboration by Seth Nicholson, a colleague at Mount Wilson who had checked some of van Maanen's measurements. Hubble, though, observed that Nicholson's measures gave "results within the uncertainties of the material and hence do not themselves definitely indicate rotation"[7].

Van Maanen took Hubble's criticism "in a wildly personal manner"[8]. Shapley, a friend of van Maanen, was also disturbed, and felt that Hubble could afford to be less openly critical[9]. At first, Hubble was. Mrs Hubble later remembered that[10]:

> It was, the contradiction, not very important in the long run. The work had become so obvious and so extensive that van Maanen's measurements could be ignored ... Van Maanen had refused to discuss the subject or to re-examine his work. Edwin had decided to ignore the discrepancy for the time and go on with his work. A friend of his told me years afterwards that he [Hubble] said to him 'They asked me to give him [van Maanen] time. Well, I gave him time, I gave him ten years.' He [Hubble] knew the measurements were wrong, his close colleagues knew. To him that would be enough. To publish would be to expose van Maanen to public humiliation

But the ten years passed and van Maanen's measurements remained. Indeed, they may have begun to draw support once again. As Hubble explained:

> When a speaker at the RAS [Royal Astronomical Society] announced, if it were not for van Maanen's measurements, Hubble's results might be accepted, I decided to make the measurements.

Hubble had come to fear loss of support for his work unless van Maanen's contradictory evidence were challenged. Another potential loser was the Mount Wilson Observatory if Hubble and van Maanen were to engage in an unseemly public quarrel. Frederick Seares, editor of Mount Wilson publications, ruled Hubble's prosecution of van Maanen out of order[11]:

> For two men in the same institution there is opportunity for personal contact and for direct examination of each other's results, and hence for the private adjustment of differences in opinion. The institution itself it seems to me, is under obligation to see that all adjustment possible be made in advance of publication. If agreement cannot be attained it may be necessary for the institution to specify how results shall be presented to the public. In that event, however, there must be opportunity for the expression

> of individual opinion, but any such expression should be concerned only with the scientific aspects of the question at issue.

It seems Hubble was not completely happy with the decision, as Seares added[11]:

> The institution has, I think, the right to enforce this procedure; but in certain cases it may be wiser to waive its technical right and say to a dissatisfied individual, 'Print what you like, but print it elsewhere'.

Hubble needed to rephrase his questions of van Maanen, at least in Seares' courtroom.

Faced with the choice between leaving van Maanen's work unchallenged or challenging it directly in an ungentlemanly manner, Hubble found an ingenious solution. He made new measures and included Nicholson in the effort[12]. Thus a former witness for the defence was to give testimony favourable to the prosecution. Nicholson did not explicitly recant his earlier evidence or van Maanen's claimed corroboration, but jurors could easily have formed that impression. Hubble may have hoped they would. And, by using indirect implication rather than direct criticism, Hubble avoided alienating the jury of scientific peers with an explicit attack on a colleague.

In a brief paper immediately following Hubble's, van Maanen in a face-saving gesture presented new measures in partial confirmation of his own while conceeding that "it is desirable to view the motions with reserve"[13]. It was more a plea of *nolo contendere* than of innocent or guilty. Obviously the revised pleading had been negotiated with Hubble.

Innocent by implication

In another case Hubble also encouraged jurors to hear more than the witness said, and less. The otherwise puzzling appearance of colleagues ostensibly to verify a calculation scarcely requiring verification becomes understandable as a bit of legalistic legerdemain in aid of the establishment of the velocity-distance relation.

An increase in the red shift or velocity of extragalactic nebulae proportional to their distances from the Solar System had been discussed by the Dutch astronomer Willen de Sitter as early as 1917[14,15], and in 1924 Ludvik Silberstein at Rochester had attempted to establish de Sitter's predicted velocity-distance relation using globular clusters[16,17]. Silberstein, however, had not used all the data available and he had excluded three clusters with velocities not consonant with the theory he was attempting to prove. Strömberg[18] and Lundmark[19] at Mount Wilson found no correlation between the radial velocities and the distances of globular clusters.

They carefully distinguished Silberstein's discredited work from the general hypothesis of a velocity-distance relation. A conclusive test of de Sitter's hypothesis would have to wait a determination of distances of spiral nebulae because globular clusters might not be distant enough to have a measurable velocity-distance relation. Nevertheless, theoretical preconception such as had influenced Silberstein's analysis was suspect.

Motivated by de Sitter's theory, Hubble had Humason at Mount Wilson systematically observe faint and more distant nebulae to see if they had larger velocities than closer nebulae. Yet in 1929, in the resulting report, Hubble emphasized empirical aspects of his work[20]. Humason published his measures separately[21], so Hubble could refer to them as independent evidence. Not until the final paragraph did Hubble mention de Sitter or theory, then noting that the velocity-distance relation might represent the de Sitter effect and might be of interest for cosmological discussion. An understated introduction to the key to the scientific exploration of the universe!

Hubble did emphasize from the beginning paragraph a connection between his velocity-distance relation and earlier determinations of the motion of the Sun with respect to the extragalactic nebulae involving a velocity factor, the *K* term, apparently varying with distance. The *K* term now was largely irrelevant, because Hubble's new data indicated a linear correlation between velocity and distance regardless of whether the velocities were corrected for the solar motion. Intended or not, the *K* term served as a red herring, diverting attention from suspect theoretical considerations. It also provided an opportunity to introduce Strömberg and Lundmark as witnesses.

Hubble used the assumption of a velocity-distance relation to determine the solar motion relative to two groupings of nebulae. The two calculations produced approximately the same result, thus tending to confirm the assumption. Hubble mentioned that Strömberg had checked the general order of the values using different groupings of nebulae. Hubble did not state explicitly that Strömberg accepted the assumption of the velocity-distance relation, though readers could easily have leapt to that implication.

Lundmark could not be brought into court as readily, since he had by now returned to Sweden. But Hubble could cite Lundmark's solution for the solar motion. No matter that it differed from Hubble's solution, or that Lundmark had used a velocity-distance relation different from Hubble's simple linear proportionality. Hubble did not emphasize these differences to the jurors. Nor did Hubble reveal that he generally distrusted Lundmark's work[22]. What Hubble wanted was Lundmark's appearance on the stand as a friendly witness, not any actual testimony.

Certainly Hubble required neither Strömberg's nor Lundmark's assistance to check the straightforward calculation of the solar motion. The testimony c Strömberg and Lundmark was nc necessary. The presence of Silberstein' critics, though, implied that Hubble' work did not suffer from the same fault:

Hubble's establishment of an empirica velocity-distance relation, although begu in a climate of scepticism and suspicior proceeded smoothly and quickly. Withi two years, Hubble had decisively won ove the jury of scientific opinion. The scientifi case was outstanding, and it did not hu to have it argued by a skilled barrister.

Hubble later described modern scienc in the language of law, writing that scienc deals "with judgments on which it is poss ible to obtain universal agreement" an "agreement is secured by observation an experiment—impartial courts c appeal"[23]. He made the observations an experiments necessary to win his case: and skillfully argued the cases.

If Hubble's orchestration of evidenc appears unusual, it is because of the cor ductor's skill and the audience's incom plete view of science. No doubt man scientists orchestrate their evidence Hubble's orchestration is unusual in th degree to which it has been analysed.

It is not a matter of the fabrication c falsification of data, nor the use of fudg factors. Hubble's data was honest. And he tilted the playing field upon which h interpretations of data battled others, often was to restore a balance, to overcom prejudice against his ideas or in favour c others and to attain a fair hearing.

The propriety of any particula orchestration of evidence may be que: tioned. Perhaps a heroic image of pristin science excludes all orchestration c evidence. But advocacy is an integral pa of real science, not to be judged good c bad but to be recognized and studied.

1. Hubble, E. to J. Moore, 23 Oct. 1932 and to N. Mayall, 3 Oct. 1933; Hubble Collection, Huntington Library.
2. Hubble, E. to N. Mayall, 23 Feb. 1934; quoted in N Hetherington, *Hist. Stud. Phys. Sci.* **13**, 41-67 (1982).
3. Hubble, E. to N. Mayall, 23 Feb. 1934.
4. Payne-Gaposchkin, C. *An Autobiography and other Reco lections* 209 (Cambridge University Press, 1984).
5. Hetherington, N. *Nature* **306**, 727-730 (1983); *Q. Jl R. as Soc.* **13**, 25-39 (1972).
6. van Maanen, A. *Astrophys. J.* **57**, 264-278 (1923).
7. Hubble, E. Manuscript, Hubble Collection.
8. Hubble, E. to H. Shapley, 11 March 1925; quoted in Smit R. *The Expanding Universe* (Cambridge University Pres 1982).
9. Shapley, H. to F. Seares, 12 May 1925, *ibid.*.
10. Hubble, Mrs E. to Michael Hoskin, 7 March 1968, Hubb Collection.
11. Seares, F. to G. Hale, 24 Jan. 1935; quoted in Smith, *The Expanding Universe* 136 (Cambridge Universi Press, 1982).
12. Hubble, E. *Astrophys. J.* **81**, 334-335 (1935).
13. van Maanen, A. *Astrophys. J.* **81**, 336-337 (1935).
14. de Sitter, W. *Mon. Not. R. astr. Soc.* **78**, 3-28 (1917).
15. Hetherington, N. *Isis* **62**, 309-313 (1971).
16. Silberstein, L. *Phil. Mag.* **47**, 907-917; **48**, 619-628 (192 *Mon. Not. R. astr. Soc.* **84**, 363-366 (1924).
17. Hetherington, N. thesis, Indiana Univ. (1970).
18. Strömberg, G. *Astrophys. J.* **61**, 353-362 (1925).
19. Lundmark, K. *Mon. Not. R. astr. Soc.* **84**, 747-769 (192
20. Hubble, E. *Proc. natn. Acad. Sci. U.S.A.* **15**, 168-173 (192
21. Humason, M. *Proc. natn. Acad. Sci. U.S.A.* **15**, 167-1 (1929).
22. Smith, R. *The Expanding Universe*, 183 (Cambridge Unive sity Press, 1982).
23. Hubble, E. *The Nature of Science and Other Lectur* (Huntington Library, San Marino, California, 1954).

Is the galactic centre black hole a dwarf?

David A. Allen* & Robert H. Sanders†

* Anglo-Australian Observatory, PO Box 296, Epping, New South Wales 2121, Australia
† Kapteyn Astronomical Institute, Postbus 800, 9700 AV Groningen, The Netherlands

A 2.2-μm image of IRS 16, the relatively blue infrared source near the galactic centre, is presented at the highest spatial resolution yet reported. It comprises several discrete, extended sources. By intercomparison of radio and infrared images of the region, the non-thermal radio source Sgr A can be located relative to IRS 16 without the uncertainty of intermediate astrometric frames. No component of IRS 16 is coincident with Sgr A*. These data preclude the presence of a massive ($>10^6\ M_\odot$) black hole at the galactic centre. Any black hole present has a mass nearer to $100\ M_\odot$.*

EVIDENCE for a black hole at the galactic centre has been discussed by Brown and Liszt[1] and is summarized here. The primary evidence is the presence of a compact radio source, Sgr A*, first described by Balick and Brown[2]. Its linear size is <20 AU (ref. 3) whilst its radio luminosity, 2×10^{34} erg s^{-1}, is many orders of magnitude greater than that of any pulsar. Within the Galaxy, Sgr A* is unique. Probably coincident with it is a soft X-ray source similar to those in active galactic nuclei but emitting only 10^{35} erg s^{-1}. Moreover, within 4° of the centre is an extraordinary, variable source emitting the positronium annihilation line at 0.5 MeV (ref. 4).

Around Sgr A* is a striking radio continuum structure—the 'mini-spiral' of Ekers *et al.*[5]—which suggests special kinematic activity, either mass ejection[1] or accretion of small clouds onto a compact mass[6]. The inner region is largely free from dust, but far-infrared maps[7] indicate a ring of dust of inner radius about 1 pc which may coincide with portions of the mini-spiral. This dust is heated by a central source of radiation with a total optical/ultraviolet luminosity $\sim10^{40}$ erg s^{-1} and a temperature <35,000 K (ref. 8).

At spatial resolutions of 1-2 arc s, attention is focused on the near-infrared source IRS 16 (ref. 9), which lies very close to Sgr A*. Near IRS 16, emission lines of H and He I include a broad component[10,11] of velocity width 1,500 km s^{-1}. Assuming virial equilibrium, the dynamical mass near IRS 16 is thus $10^7\ M_\odot$. IRS 16 has been resolved[12] into three merged components aligned roughly along the galactic equator.

It has been recognized for many years[13] that the near-infrared emission from the central region of the Galaxy traces the stellar density distribution. The implied distribution approximates $r^{-1.8}$ over the range $0.1<r<40$ pc (refs 14, 15). Because the exponent is tantalizingly close to that predicted for the cusp around a black hole, it is tempting to identify IRS 16 with the bright central region of the cusp. If a massive black hole is present, we therefore expect a spatial coincidence between Sgr A* and one component of IRS 16.

As a test of the coincidence, astrometry of IRS 16 has been performed relative to a system of optical standard stars. Sgr A* is also located relative to the same reference frame of standard stars through a number of compact radio sources with optical counterparts. The accumulated uncertainty in the infrared-radio astrometry is estimated to be 0.5 arc s. The two determinations[12,16] suggest that IRS 16 centre coincides with Sgr A*, although the radio source appears displaced westwards according to the data of ref. 12.

A second, potentially more accurate, technique is that of directly comparing the radio and infrared maps and positioning them by common features. The first such comparison was made

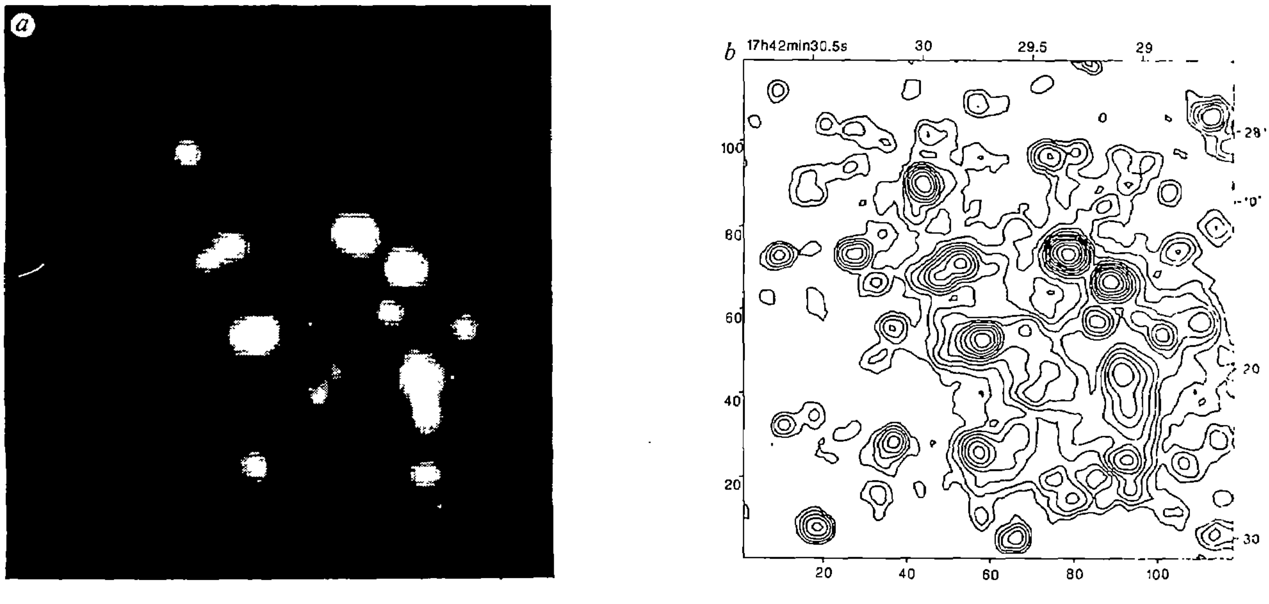

Fig. 1 *a*, The galactic centre at 3.8 μm; image made on 11 July 1984. The image measures 29.5 arc s on a side. IRS numbers are given for some sources. North is up and east to the left on this and all subsequent images. IRS 16 is the complex of sources to the west of IRS 1W. *b*, The same image in contour form. Contours are separated by 0.5 stellar magnitudes. A point source of 3.8 μm (L') magnitude 4.5 will just reach the highest contour; one of magnitude 9.5 the lowest plotted.

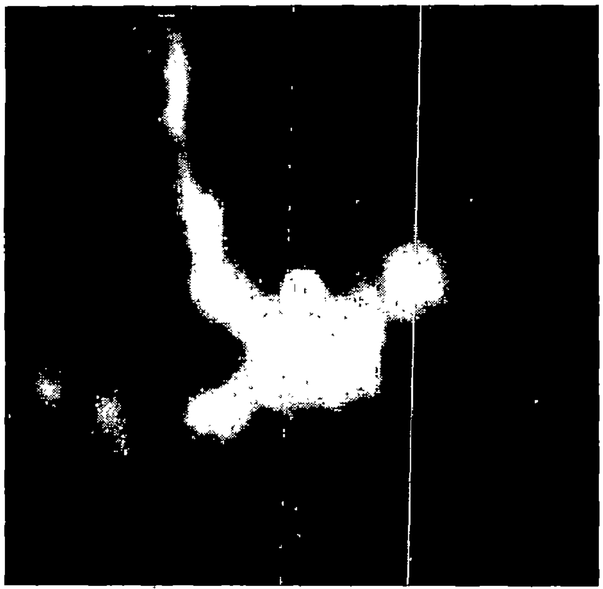

Fig. 2 A reproduction of the 6-cm data of Lo and Claussen[6]. Crosses mark the centres of the compact infrared sources as found by the best fit of the infrared data.

by Ekers[17], who used a published map of Br γ emission[12] to conclude that Sgr A* lies about 1 arc s west of every component of IRS 16.

We present an improved comparison of the radio and infrared maps of the galactic centre using new data at 3.8 and 4.8 μm. In agreement with Ekers, we find that Sgr A* does not correspond to the bright components of IRS 16.

Infrared data and radio structure

At short wavelengths, the galactic centre region is dominated by highly reddened stars and IRS 16 is a prominent object[9,18]. At longer wavelengths the pattern of radiation approaches that of the thermal radio, but IRS 16 cannot be detected. To make a direct comparison with the radio, we made a deep image of the region at 3.8 μm. Data described by Storey and Allen[12] have demonstrated that IRS 16 has identical structure at 1.6, 2.2 and 3.8 μm (a colour composite of the three was constructed and reproduced in ref. 19).The new image is reproduced in Fig. 1. We used the 3.9-m Anglo-Australian Telescope, with the infrared photometer-spectrometer operated in its imaging mode. At the focal plane a 1-arc s circular aperture was used; the seeing did not appreciably degrade the resolution. The image was sampled every 0.5 arc s, and in constructing Fig. 1 we have expanded the data to 0.25 arc s pixels by linear interpolation. Four separate images were combined into Fig. 1, allowing us to assess the internal positional accuracy as better than 0.15 arc s.

For the comparison with the radio data, we used the image at 6 cm made by Lo and Claussen[6]. This image (Fig. 2) also has a spatial resolution of about 1 arc s. It was sent in digital form to permit manipulations of the two images using Starlink software on the AAO VAX 11/780.

On the 3.8-μm image, the density of point sources is high. Some of them have not been recorded at other wavelengths. Most lack radio counterparts, but several diffuse patches of emission do correspond well with the radio map, and there is undoubtedly a strong correlation in the vicinity of IRS 2/13, on which we place much reliance. Nonetheless, before a secure fit of the two images could be made, a map at a longer wavelength was necessary to locate the compact sources IRS 1W, 5 and 10 relative to the northeasterly arm of radio emission.

An image at 4.8 μm was secured at a later date. The observational configuration duplicated that of the 3.8-μm map, but poorer seeing degraded the spatial resolution. Figure 3 reproduces this image. The details resemble more closely those at 6 cm, but with local enhancements of intensity. IRS 2/13 remains prominent. IRS 1W, 5 and 10 are now seen to lie east of the radio structure. IRS 1W and 10 have weak counterparts in the radio, whilst IRS 5 barely contacts the radio contours. Their locations strongly suggest a relationship with the mini-spiral. Presumably, they are single or multiple stars close enough to the gas clouds to cause local heating of the dust. Their displacement from the ionized gas is itself an interesting matter not addressed here.

With the help of the 4.8-μm image we located the 3.8-μm and 6-cm images with a relative uncertainty little more than 1 pixel or 0.25 arc s. Sgr A* was then found to lie significantly to the west of all components of IRS 16. Attempts to overlay the images with Sgr A* superimposed on any component of IRS 16 do not permit satisfactory registration of the infrared and radio sources.

IRS 16 in detail

Our attention turned to the region west of IRS 16. A small strip image was made at 2.2 μm (K) using a focal-plane diaphragm of 0.7 arc s diameter. Seeing at that wavelength was mostly below 0.5 arc s at the time. Several images were made, but only those with consistently good seeing were combined to create Fig. 4, which has almost double the spatial resolution of previous data[12]. The strip map includes IRS 7, and some faint point sources to the south. IRS 16 NE is bisected at the left edge of the image.

IRS 16 SW and centre are now seen to be discrete sources extended on the scale of about 1 arc s. A previously ignored component, IRS 16 NW, is unresolved, and for this reason appears as intense as the peak of SW and centre. Faint emission is seen west of IRS 16 centre, at the location of Sgr A*. Adopting $K=6.7$ for IRS 7, the various components of IRS 16 peak at about 10.0 mag in the 0.7-arc s beam. The sources at the location of Sgr A* has $K=11.4$. Both of these numbers have been corrected from the raw data for the fact that the darkest part of Fig. 4 (relative to which the photometry is performed) lie above the dark sky level on the data of ref. 12.

We now examine the impact of these observations on models invoking a massive black hole at the site of Sgr A*.

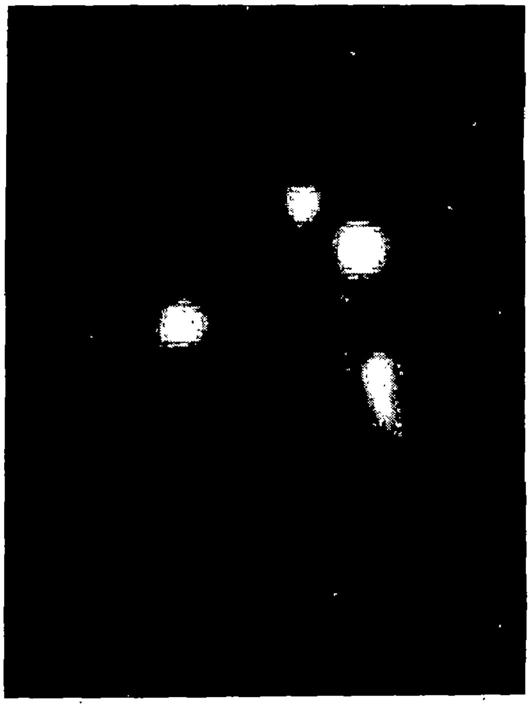

Fig. 3 4.8-μm image (8 November 1984). Although inferior to Figs 1 and 2, features of both these images can be seen.

IRS 16 as the cusp core

We adopt the popular assumption that Sgr A* is a 10^6–10^7 $M_\odot$ black hole. We first ask whether the observed structure of IRS 16 is consistent with this complex source being the core of a cusp around the black hole.

A point mass in an extended distribution of stars dominates the gravitational potential within the classical accretion radius (r_a):

$$r_a = \frac{2GM_h}{v_s^2} = \frac{M_h}{5\times10^6\,M_\odot}\left[\frac{225\text{ km s}^{-1}}{v_s}\right)^2 \text{pc} \sim 20\text{ arc s} \qquad (1)$$

where M_h is the mass of the object, and v_s is the stellar velocity dispersion. Due to energy diffusion, a cusp in the stellar density distribution of the form $\rho \propto r^{-1.75}$ will develop[20,21] within r_a on a timescale longer than the initial two-body relaxation time[22]:

$$t_R = \frac{\sqrt{2}\,v_s^3}{\pi G^2 M_*^2 n \ln(0.5N)} \qquad (2)$$

in a stellar system with a mean stellar mass M_*, a stellar density of n, and a total number of stars N. The inferred properties of the inner 1 pc of the galactic nucleus ($n \sim 4\times10^5\text{ pc}^{-3}$, $v_s \sim$ 200–300 km s^{-1})[14] imply that $t_R \sim 10^{11}$ yr at the present epoch. However, even without energy diffusion, the adiabatic growth of a black hole produces a cusp in the stellar density[23] of the form $r^{-1.5}$. Therefore, the formation of a cusp around such a hypothetical black hole in the galactic centre would seem inevitable.

The observed density index in the central parsec of the Galaxy is −1.8, consistent with that of an energy diffusion cusp. Using existing data[14,15], the integrated magnitude at K within a circular aperture of radius r is $m(r) = 8.5 - 3\log(r)$. Within the 0.7-arc s aperture of the present observation, we should therefore expect $K = 9.9$, consistent with any of the IRS 16 components, but 1.5 mag brighter than found at the location of Sgr A*.

Can the hole migrate away from the centre of its cusp due to interactions with cusp stars[24]? Although the hole may deviate from the centre-of-mass of the hole-cusp system, it cannot deviate significantly from the position of maximum brightness of the cusp. The innermost, tightly bound stars will follow the hole on its brownian motion resulting from interactions with more distant cusp stars. The only possible deviation of the hole from the point of maximum brightness can be due to statistical fluctuations in the space density of cusp stars, and this does not become significant except at radii within which there are only about 10 cusp stars, in this case 10^{-5} pc. We find a displacement of Sgr A* from the IRS 16 components of >1,000 times this limit, implying that none of the bright IRS 16 components can be the core of a hypothetical cusp.

Association of young stars

The fact that Sgr A* does not coincide with any of the bright components of IRS 16 implies that a possible black hole associated with this object does not emit significantly at 2.2 μm. If we characterize the radiation from the hole's accretion disk by a black body, we have an upper limit to its temperature of 35,000 K from the presence of Ne II (ref. 8). To provide the optical and ultraviolet energy seen to be heating the dust requires a K magnitude of about 8, which is clearly precluded. This is a lower bound to K for any reasonable energy distribution other than line emission. Thus no object associated with Sgr A* provides the bulk of the luminosity of the galactic centre. The observed K magnitude of 11.4 implies an upper limit to the luminosity of about 10^{39} erg s^{-1}, which is compatible with the low level of radio and X-ray activity, and with the presence of an inactive, massive black hole there. But then, what is the source of ionizing radiation at the galactic centre?

There are many discrete sources in the galactic centre region which must contain stars of significant luminosity. The differences between the infrared and radio continua alone indicate this fact. The discrete infrared sources can be interpreted either as local centres of heating[25] or as external heating of local density enhancements[26]. Most of these sources appear to suffer local extinction from the dust that re-radiates at long wavelength; they cannot illuminate the dust ring 2 pc from the centre because it is transparent to their radiation. We should seek the required luminosity in the bluer infrared sources. IRS 16 is the brightest of these.

Geballe *et al.*[11] demonstrated that IRS 16 (loosely defined within a 4-arc s beam) is responsible for most of the ionization within the central parsec. Its integrated K magnitude is about 8, so if the constituent stars approach 35,000 K in temperature, they alone can account for the required luminosity. The concentration of M supergiants near the galactic centre may be explained by a burst of star formation which occurred in the nuclear region $\sim10^7$ yr ago[27,28]. Such a burst would leave at least one concentration of B stars now. We therefore regard all the components of IRS 16 as clusters of hot stars, remnants of the last starburst. If their mean spectral type is B0, about 100 are required, or roughly 25 in each of the four major components. The clumpy, irregular appearance of these components is better explained in this way than as the more symmetrical cusp or compact accretion disk associated with an active black hole.

However, the proximity of these objects to the point radio source severely constrains the mass of the black hole. If, as we suggest, the sources are unbound clumps of B stars, then they will disperse on a timescale roughly comparable to the orbit time about the black hole, or

$$t_D \sim 2\left(\frac{GM_h}{r_0^3}\right)^{-1/2} \sim 500\left(\frac{M_h}{5\times10^6\,M_\odot}\right)^{-1/2} \text{yr} \qquad (3)$$

where $r_0 \sim 0.1$ pc is the typical projected distance of the clumps from the hole. The probability of observing two or three such

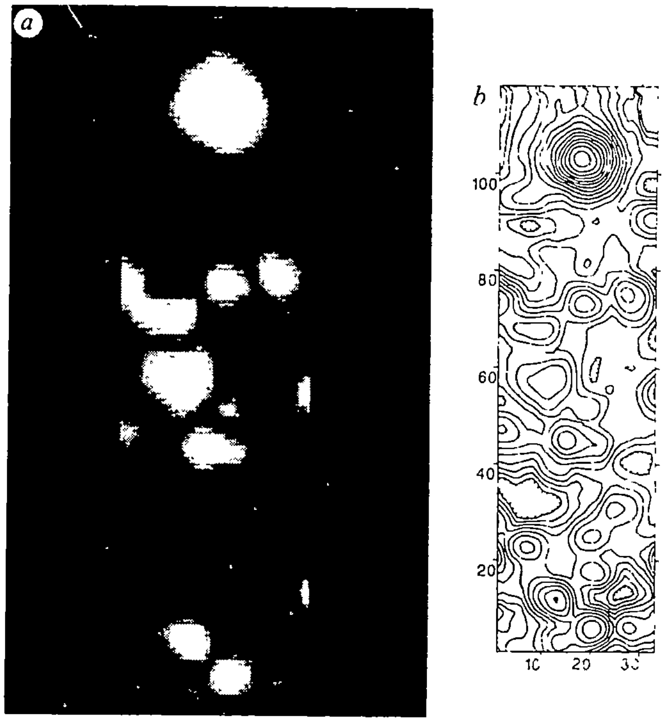

Fig. 4 *a*, Strip image at 2.2 μm through IRS 7 and 16. The image measures 5.0 × 17.7 arc s and the pixels are 0.15 arc s square. The spatial resolution, about 0.8 arc s, is a factor of two higher than any previous data. The IRS sources are identified and Sgr A* is marked by a cross of dimension 0.5 arc s^{-1}, the 2σ uncertainty in its position. *b*, The same image in contour form. The contours are separated by 0.5 stellar magnitude and range between 6.5 and 14.0 in K magnitude.

clumps in the central 0.1 pc is extremely low unless star formation is occurring continuously. For any likely initial mass function, this is precluded by the cool radiation field of the region. Moreover, the tidal field of a massive black hole would require implausibly dense protostellar clouds:

$$\rho > \frac{6M_h}{r_0^3} \sim 7\times10^{-13}\frac{M_h}{5\times10^6\,M_\odot}\,\mathrm{g\,cm^{-3}} \qquad (4)$$

What alternative interpretations of the IRS 16 sources are possible?

(1) They are background or foreground sources seen in projection within 2 arc s of the black hole. Not only would it be highly fortuitous that the only blue objects seen in the inner 2 pc apparently lie so close to the centre, but we should have to find another source of luminosity to power the far-infrared emission.

(2) The clumps are dense gravitationally bound subclusters. It has been suggested[29] that globular clusters will be dragged into the centre of a galaxy by dynamical friction. Again, to prevent tidal disruption, their mean density must be given by equation (4). This corresponds to a stellar density in the subcluster of almost $10^{10}\,M_\odot\,\mathrm{pc}^{-3}$ within 0.02 pc. Certainly, no presently observed globular cluster cores have these properties; in the most dense globulars $n \sim 10^5\,M_\odot\,\mathrm{pc}^{-3}$ (ref. 30).

The clumps could be the highly evolved cores of old, massive globular clusters. But the present stellar relaxation time in such systems is only $\sim10^7$ yr. Because the lifetime of such a cluster is no more than 30 t_R (ref. 31), to see several of them they would have to be replaced or reformed every 10^8 yr. External replacement over 10^{10} yr would have produced an unacceptably large mass in the central 0.1 pc of the Galaxy, exceeding $3\times10^7\,M_\odot$.

(3) Several massive black holes occupy the central regions, each with its own cusp of bound stars. Such a configuration is dynamically unstable[32], leading to the formation of at most a binary system. Nor does it explain the uniqueness of Sgr A*.

(4) The bright components are one or more background stars in the Galaxy which have been gravitationally imaged by the massive black hole. The required amplification factor, 10^5–10^6, implies that the star lies within 4×10^{-5} arc s of the direction of the black hole. Given the mean density of stars along a line-of-sight through the Galactic plane, the probability of this is $\sim10^{-7}$.

A low-mass black hole

We have attempted to reconcile the observations with the existence of a black hole coincident with Sgr A* and of mass exceeding $10^6\,M_\odot$ and have failed to do so. Our conclusion, which we now justify, is that the black hole within Sgr A* is no more massive than about 100 $M_\odot$.

This alternative does not contradict the great body of observational material. None of the phenomena noted above requires a black hole more massive than 100 $M_\odot$. Suggestions[33] that the kinematic evidence requires a point mass $>10^6\,M_\odot$ assume that the gas motions within 0.5 pc of the centre are virialized and thus trace the gravitational potential. This need not be the case; indeed, the broad emission lines seen in the direction of IRS 16 may be high-velocity outflow from the region of a low-mass black hole (as suggested in ref. 11). The fact that the central ionization source can be attributed to the clumps of B0 stars identified with IRS 16 removes the justification for a more bizarre source. Moreover, the most straightforward interpretation[34] of the positronium annihilation line implies a black hole of mass no more than a few hundred $M_\odot$.

The similarity of the stellar density distribution in the inner parsec to that in a cusp around a massive black hole is not compelling: the density law also resembles an isothermal sphere (r^{-2}) with a small (0.1 pc) core and a central density $>10^7\,M_\odot\,\mathrm{pc}^{-3}$. The two-body relaxation time in that core would be 2×10^9 yr and the stellar collision time would be 9×10^9 yr. As the timescale for dynamical evolution is the smaller of t_{coll} and 20–30 t_R, the structure need change very little over the age of the Universe.

The dispersal of unbound groups of young stars would be considerably less rapid in this case. In a constant-density or 'harmonic' case, where all orbit periods are equal, structure would never disappear. It is unrealistic to assume that the IRS 16 associations lie in a pure harmonic oscillator potential; a 5–10% variation in the density of the underlying isothermal core would cause dispersal by phase mixing in 10–20 orbit times, or about 10^4 yr. Moreover, if $M_h < 5\times10^4\,M_\odot$, the Roche limit constraint (equation (4)) is relaxed and the associations could be gravitationally bound subclusters of no more than 1,000 $M_\odot$. Thus the existence of associations or clusters of young stars, as evidenced by the structure in IRS 16, is only plausible if the mass of the hole is considerably less than the mass of the isothermal core, that is, $M_h < 10^5\,M_\odot$.

Determination of the velocities of the IRS 16 components would verify (or falsify) our claim that the black hole is much less massive than $10^6\,M_\odot$. For a massive black hole, the IRS 16 components should have a velocity $>450\,\mathrm{km\,s^{-1}}$. This could be detected in the radial velocity of the associated Br γ line.

The arguments we have given do not tightly constrain the mass of the black hole. However, consideration of the growth rate of a black hole in the stellar density of the galactic centre make it unlikely that the mass is as high as 1,000 $M_\odot$; such a black hole would consume the galactic core, thus growing to a mass of 10^6–$10^7\,M_\odot$ in 10^9 yr (refs 35, 36). The upper bound to the luminosity of Sgr A* is about that of a 100 $M_\odot$ black hole accreting at the Eddington luminosity. Therefore, we conclude that the central parsec of the Galaxy comprises an isothermal sphere of stars having a core radius ~0.1 pc and central density $>10^7\,M_\odot\,\mathrm{pc}^{-3}$, a few small associations or clusters of newly formed B stars within that core, and an accreting black hole of mass $\leq 100\,M_\odot$.

Received 29 July; accepted 21 October 1985.

1. Brown, R. L. & Liszt, H. L. *A. Rev. Astr. Astrophys.* **22**, 223–265 (1984).
2. Balick, B. & Brown, R. L. *Astrophys. J.* **194**, 265–270 (1974).
3. Lo, K. Y. *et al. Nature* **315**, 124–126 (1985).
4. Riegler, G. R. *et al. Astrophys. J. Lett.* **248**, L13–L16 (1981).
5. Ekers, R. D., van Gorkom, J. H., Schwartz, U. J. & Goss, W. M. *Astr. Astrophys.* **122**, 143–150 (1983).
6. Lo, K. Y. & Claussen, M. J. *Nature* **306**, 647–651 (1983).
7. Becklin, E. E., Gatley, I. & Werner, M. W. *Astrophys. J.* **258**, 135–142 (1982).
8. Lacy, J. H., Townes, C. H., Geballe, T. R. & Hollenbach, D. J. *Astrophys. J.* **241**, 132–146 (1982).
9. Becklin, E. E. & Neugebauer, G. *Astrophys. J. Lett.* **200**, L71–L74 (1975).
10. Hall, D. N. B., Kleinmann, S. G. & Scoville, N. Z. *Astrophys. J. Lett.* **260**, L53–L57 (1982).
11. Geballe, T. R. *et al. Astrophys. J.* **284**, 118–125 (1984).
12. Storey, J. M. V. & Allen, D. A. *Mon. Not. R. astr. Soc.* **204**, 1153–1161(1983).
13. Becklin, E. E. & Neugebauer, G. *Astrophys. J.* **151**, 145–161 (1968).
14. Bailey, M. E. *Mon. Not. R. astr. Soc.* **190**, 217–225 (1980).
15. Allen, D. A., Hyland, A. R. & Jones, T. J. *Mon. Not. R. astr. Soc.* **204**, 1145–1152 (1983).
16. Henry, J. P., De Poy, D. L. & Becklin, E. E. *Astrophys. J. Lett.* **285**, L27–L30 (1984).
17. Ekers, R. D. *Pap. at Workshop Galactic Centre* (California Institute of Technology, city? 1984).
18. Bailey, J., Hough, J. H. & Axon, D. J. *Mon. Not. R. astr. Soc.* **208**, 661–671 (1984).
19. Henbest, N. *New Scient.* **97**, 460-461 (1983).
20. Bahcall, J. N. & Wolf, R. A. *Astrophys. J.* **209**, 214–232 (1976).
21. Duncan, M. J. & Shapiro, S. L. *Astrophys. J.* **268**, 565–581 (1983).
22. Spitzer, L. & Harm, R. *Astrophys. J.* **127**, 544–550 (1958).
23. Young, P. J. *Astrophys. J.* **217**, 287–295 (1977).
24. Lin, D. N. C. & Tremaine, S. *Astrophys. J.* **242**, 789–798 (1980).
25. Lebofsky, M. J., Rieke, G. R., Deshpande, M. R. & Kemp, J. C. *Astrophy. J.* **163**, 672–676 (1982).
26. Gezari, D. Y. *et al. NASA techn. Mem.* 86225 (1985); *Astrophys. J.* (in the press).
27. Lebofsky, M. J., Rieke, G. R. & Tokunaga, A. T. *Astrophys J.* **263**, 736–740 (1982).
28. Lacy, J. H., Townes, C. H. & Hollenbach, D. J. *Astrophys. J.* **262**, 120–134 (1982).
29. Tremaine, S. D., Ostriker, J. P. & Spitzer, L. *Astrophys. J.* **196**, 407–411 (1975).
30. Peterson, C. J. & King, I. R. *Astr. J.* **80**, 427–436 (1975).
31. Lightman, A. P. & Shapiro, S. L. *Rev. mod. Phys.* **50**, 437–481 (1978).
32. Saslaw, W. C., Valtonen, M. J. & Aarseth, S. J. *Astrophys. J.* **190**, 253–270 (1974).
33. Crawford, M. K. *et al. Nature* **315**, 467–470 (1985).
34. Lingenfelter, R. E. & Ramaty, R. *The Galactic Center* 148–159 (American Institute of Physics, New York, 1982).
35. Hills, J. G. *Nature* **254**, 295–298 (1975).
36. Ozernoy, L. M. *IAU Colloq.* **45**, 121–124 (1977).

Relationship between atmospheric CO_2 variations and a satellite-derived vegetation index

C. J. Tucker*, I. Y. Fung†, C. D. Keeling‡ & R. H. Gammon§

* NASA/Goddard Space Flight Center, Code 623, Greenbelt, Maryland 20771, USA
† NASA/Goddard Institute for Space Studies, New York, New York 10025, USA and Lamont-Doherty Geological Observatory of Columbia University, Palisades, New York, New York 10964, USA
‡ Scripps Institution of Oceanography, La Jolla, California 92093, USA
§ NOAA/GMCC, Boulder, Colorado 80302, USA

Estimates derived from satellite data of photosynthetically active radiation absorbed by terrestrial vegetation correlate with atmospheric carbon dioxide concentrations measured at surface recording stations, suggesting that satellite data can be used to estimate terrestrial photosynthesis.

TERRESTRIAL photosynthesis is inversely related to atmospheric carbon dioxide concentrations and is an important component of the global carbon cycle. The lack of temporal resolution and global data has prevented comparisons between estimates of terrestrial photosynthesis and measurements of atmospheric CO_2 concentrations from remote maritime monitoring stations. This is now possible using data derived from meteorological satellites.

Primary production

The biosphere absorbs CO_2 from the atmosphere through photosynthesis which incorporates absorbed carbon into carbohydrates, giving off O_2. In the terrestrial biosphere, CO_2 absorption occurs in the green leaves of plants, where intercepted photosynthetically active radiation (IPAR) (0.4–0.7 μm) is absorbed by the photosynthetic pigments. The energy of the absorbed photons is used to drive the reaction of photosynthesis, yielding carbohydrates through primary production. Incident radiation in the 0.4–0.7-μm region is strongly absorbed by green leaves (by scattering and absorption by photosynthetic pigments), and radiation in the 0.7–1.1-μm region is strongly backscattered or reflected (by scattering in the absence of absorption)[1-5]. Thus, reflected radiance from the red and near-infrared spectral regions can be used to estimate the green-leaf biomass of plant canopies[6,7], are directly be related to the IPAR[8-13], the photosynthetic capacity and the resistance to water-vapour transfer of plant canopies[13].

Atmospheric CO_2

Measurements of atmospheric CO_2 concentrations at monitoring stations have a seasonal oscillation superimposed on an annually increasing trend. The annual amplitude of this oscillation is ~15 parts per 10^6 (p.p.m.) at Point Barrow, Alaska, and decreases southward to ~6 p.p.m. at Mauna Loa, Hawaii, and to ~1–2 p.p.m. in the Southern Hemisphere. The annual maximum atmospheric CO_2 concentration in the Northern Hemisphere occurs in the late spring or early summer and the annual minimum concentration occurs in the autumn[14,15]. The annual oscillation of atmospheric CO_2 is due primarily to seasonal exchange of CO_2 with the terrestrial biosphere[14,16,17]; in contrast, there is little seasonal exchange of CO_2 with the upper ocean[18,19]. The CO_2 exchange with the biosphere has been simulated using diffusion, advection-diffusion, three-dimensional tracer models[20-22] and biospheric-exchange functions. Bolin and Keeling[23] and Pearman and Hyson[24] derived CO_2 sources and sinks consistent with atmospheric CO_2 observations, while Azevedo[25] constructed simple biospheric-exchange functions based on assumed vegetation seasonality and geographical location. However, the biospheric CO_2 drawdown and release functions that correlated best with measured CO_2 concentrations showed differences by at least a factor of 2 (refs 20–25). The release of CO_2 from terrestrial vegetation can be approximated if primary production and the temperature regime are known; the drawdown of CO_2 by terrestrial vegetation can be determined if primary production is known. Thus, elucidation of the role of the terrestrial biota in the gobal carbon cycle requires an estimate of the terrestrial primary production; this can be achieved through remote sensing by satellite.

Remote sensing

By monitoring global changes in the IPAR of the terrestrial biota, an estimate of CO_2 drawdown and primary production can be obtained through the relationships between leaf structure, leaf density and light in plant canopies, and that between IPAR and photosynthetic capacity[13].

The CO_2 cycle involves not only photosynthesis and respiration, but also decomposition of carbon compounds, uptake and release by oceans, combustion of fossil fuels, and fires involving vegetation. Deforestation contributes towards atmospheric CO_2 through burning and/or subsequent decomposition of phytomass, litter and associated carbon concentrations in the soil, although the magnitude of this contribution is uncertain[26,27]. Remote sensing by satellite enables the temporal and spatial variations in the IPAR of the terrestrial biota to be quantified.

Remote-sensing studies of the biota have used Landsat and meteorological satellites data. Landsat multispectral scanner (MSS) data, with a spatial resolution of 80 m, are not appropriate for the study of seasonal changes in the terrestrial biota, because ~5,000 Landat MSS scenes would be required to cover the world's surface. The polar-orbiting meteorological satellites of the National Oceanic and Atmospheric Administration (NOAA) are suitable for observing terrestrial IPAR dynamics. The advanced very-high-resolution radiometer (AVHRR) sensor on board these polar-orbiting satellites daily collects global radiance data at a 4-km spatial resolution. Combinations of channel 1 (0.55–0.68 μm) and channel 2 (0.73–1.1 μm) data from the NOAA satellites' AVHRR have been used to study continental land cover, global vegetation phenology and net primary production by grasslands using data from 1 to 4-yr periods[28-31].

Data methods and use

Data on monthly atmospheric CO_2 concentrations for 1982–84 were obtained for Point Barrow, Alaska (147° W, 71° N), and

---

§ Present address: NOAA/PMEL, Seattle, Washington 98115, USA.

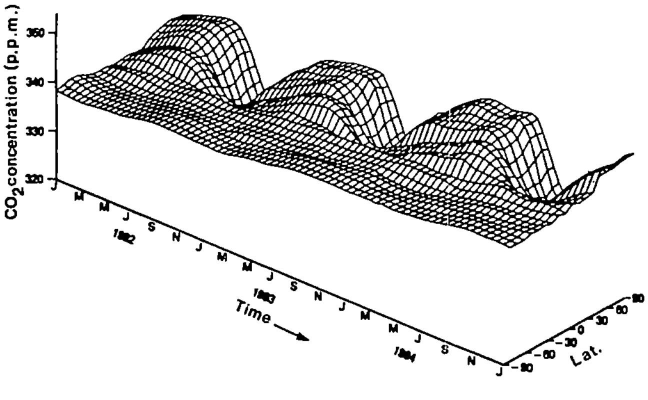

Fig. 1 Variation of global atmospheric CO_2 concentrations with latitude and time based on the NOAA/GMCC flask measurements for 1982–84.

Mauna Loa, Hawaii (156° W, 20° N); and from January 1982 to September 1984 for the South Pole (90° S). Stations there are operated by the NOAA Geophysical Monitoring for Climatic Change (GMCC) programme, and the CO_2 flask samples are analysed at the Scripps Institute of Oceanography. CO_2 concentrations for 20 globally dispersed monitoring sites operated and analysed by NOAA/GMCC for 1982–84 were also obtained.

The atmospheric CO_2 concentration is the combined response to terrestrial biospheric, oceanic and anthropogenic sources and sinks, convolved with long-range transport. Figure 1 shows the total CO_2 signal from January 1982 to December 1984 measured at the 20 global monitoring stations. An annually increasing trend of ~1.5 p.p.m. yr^{-1} from anthropogenic sources, and an annual cycle, with an amplitude greatest around 50°–70° N, is evident. To extract the seasonal variation from the CO_2 records, we computed the 12-month running means for each station and subtracted these from the CO_2 record (see ref. 15).

Global weekly data from NOAA-7's AVHRR were obtained for the period from 12 April 1982 to 28 October 1984 (ref. 32). These data were re-mapped from a polar stereographic projection to a Mercator projection so that the world could be represented in a single image. The normalized difference vegetation index (NDVI) $[(C_2-C_1)/(C_2+C_1)]$ was calculated[6,7], and the highest monthly NDVI value was selected from the weekly data for each month between April 1982 and October 1984 (Table 1). This procedure minimizes the effects of Sun angle, off-nadir viewing, atmospheric pathlength and aerosols, and clouds, all of which decrease the NDVI[33]. In winter conditions, spurious NDVI values result from a combination of low solar illumination levels, differing dark-current levels in channels 1 and 2, and pathlength-associated variation in atmospheric effects. These effects are apparent not only during the respective hemisphere winters, but also if the NDVI is calculated from AVHRR data acquired during the night. To compensate for these spurious values, mean monthly surface temperature data were acquired[34], and areas within the 0 °C or colder regions were assigned NDVI values of 0.00 because physiological evidence suggests that the rate of photosynthesis at 0 °C is close to zero[35].

The monthly NDVI data, which have an average grid-cell size of ~40 km, were used to compute average values for global latitude zones. The zonal averages were multiplied by the land area within each zone (to weight the averages by the land area involved) and summed for various latitude zones; the sum for each larger zone was then divided by the total land area in that zone. The NDVI for a latitude zone represents the potential IPAR; hence, we have assumed that the NDVI is directly related

Table 1 Weekly data used for monthly NDVI composite images

Month	Year	Weeks used	Comments
April	1982	12–18, 19–25, 26–30 April; 1–2 May	Includes 1–2 May
May	1982	3–9, 10–16, 17–23, 24–30 May	
June	1982	31 May; 1–6, 7–13, 14–20, 21–27 June	Includes 31 May
July	1982	5–11, 12–18, 19–25, 26–31 July; 1 August	Includes 1 August
August	1982	2–8, 9–15, 16–22, 23–29 August	
September	1982	30–31 August; 1–5, 6–12, 13–19, 20–26 September	Includes 30 and 31 August
October	1982	4–10, 11–17, 18–24, 25–31 October	
November	1982	1–7, 8–14, 15–21, 22–28 November	
December	1982	29–30 November; 1–5, 6–12, 13–19, 20–26 December	Includes 29 and 30 November
January	1983	3–9, 10–16, 17–23, 24–30 January	
February	1983	31 January; 1–6, 7–13, 14–20, 21–27 February	Includes 31 January
March	1983	28 February; 1–6, 7–13, 14–20, 21–27 March	Includes 28 February
April	1983	4–10, 11–17, 18–24, 25–30 April; 1 May	Includes 1 May
May	1983	2–8, 9–15, 16–22, 23–29 May	
June	1983	30–31 May; 1–5, 6–12, 13–19, 20–26 June	Includes 30 and 31 May
July	1983	4–10, 11–17, 18–24, 25–31 July	
August	1983	8–14, 15–21, 22–28 August	No data 1–7 August
September	1983	5–11, 12–18, 19–25, 26–30 September; 1–2 October	Includes 1 and 2 October
October	1983	3–9, 10–16, 17–23, 24–30 October	
November	1983	31 October; 1–6, 7–13, 14–20, 21–27 November	Includes 31 October
December	1983	5–11, 12–18, 19–25, 26–31 December; 1 January	Includes 1 January
January	1984	2–8, 9–12, 16–22, 23–29 January	No data 13–15 January
February	1984	30–31 January; 1–5, 6–12, 27–28 February; 1–4 March	Includes 30–31 January and 1–4 March; no data 13–26 February
March	1984	5–11, 12–14, 19–25 March	No data 14–18, 26–31 March
April	1984	2–8, 9–14, 16–21, 23–29 April	No data 15 and 22 April
May	1984	30 April; 1–6, 7–13, 14–20, 21–27 May	Includes 30 April
June	1984	4–10, 11–17, 18–24, 25–30 June; 1 July	Includes 1 July
July	1984	2–8, 9–15, 16–22, 23–29 July	
August	1984	30–31 July; 1–5, 6–12, 13–19, 20–26 August	Includes 30 and 31 July
September	1984	3–9, 10–16, 17–23, 24–30 September	
October	1984	1–7, 8–14, 15–21, 22–28 October	

The maximum monthly value was selected from the weekly data.

Fig. 2 Weighted NDVI data plotted against time and latitude zone. Note the highly seasonal effects in the northern latitudes, the influence of deserts in the 20°-30° N latitude zone, the generally constant response in equatorial areas, and the influence of the low proportion of land area south of 30° S. See also Fig. 1. The average NDVI value for each 5° latitude zone has been multiplied by the land area in the zone to compensate for global variations in land area.

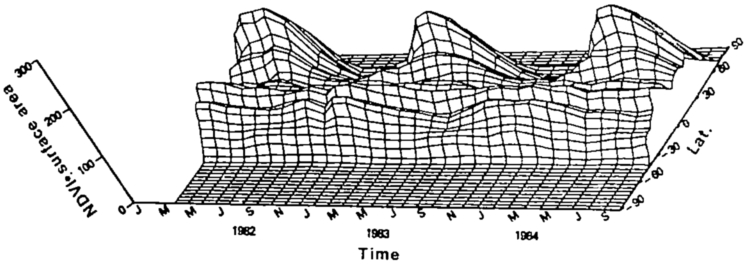

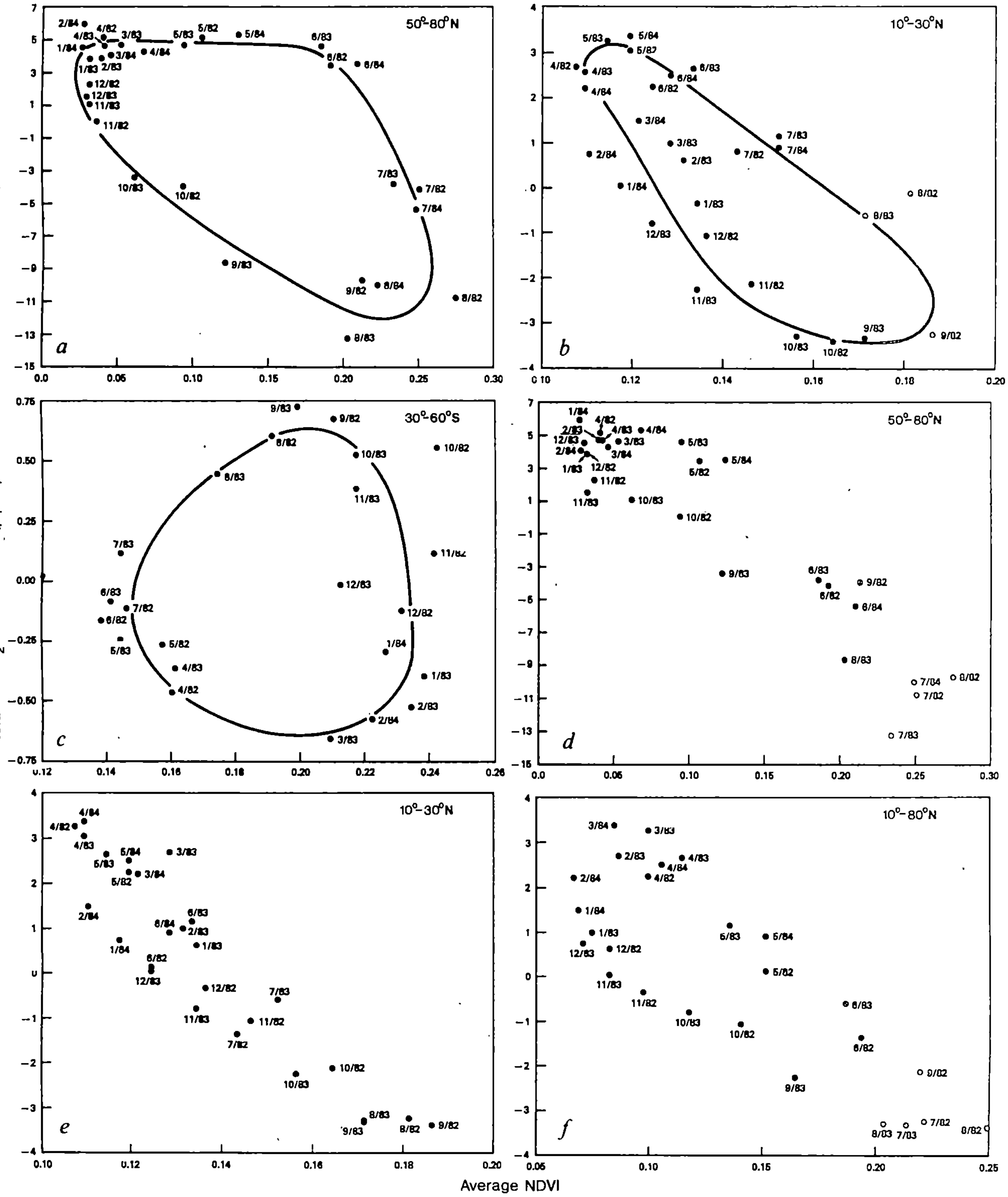

Fig. 3 Relationships between atmospheric CO_2 concentrations and NDVI averages with and without time lags between NDVI measurements and CO_2 measurements. The CO_2 data are from stations at Point Barrow, Alaska: *a*, no time lag; *d*, 1-month lag; Mauna Loa, Hawaii: *b*, no time lag; *e*, 1-month lag; *f*, 2-month lag; South Pole: *c*, no time lag. The corresponding NDVI averages are from 50° to 80° N for Point Barrow, 10° to 30° N and 10° to 80° N for Mauna Loa, and 30° to 60° S for the South Pole.

to the photosynthetic capacity[13] of the terrestrial surface in that zone and should be inversely related to atmospheric CO_2 concentrations. Figure 2 shows the latitudinal and temporal variation of the zonally averaged NDVI (weighted by land area) from April 1982 to October 1984. Consistent with considerations of growing seasons, the maximum zonally averaged and weighted NDVI occurs in summer at middle to high latitudes in the Northern Hemisphere. This pattern is a consequence both of the large proportion of land area and the highly seasonal behaviour of vegetation at these latitudes. The Southern Hemisphere south of 30° S has a low weighted NDVI because its vegetation is not as seasonal and the proportion of land area is less than in latitude zones north of 30° S. The weighted NDVI in equatorial areas is high throughout the year, and a desert belt is apparent as a depressed weighted NDVI from ~20° N to ~30° N. Figure 2 also shows differences in the weighted NDVI from 1982 to 1984. The 1982 global peak occurred in August, whereas the 1983 and 1984 global peaks occurred in July.

Results

The data presented in Figs 1 and 2 reveal an inverse relationship between the NDVI and the seasonal variations in atmospheric CO_2: in the Northern Hemisphere, the NDVI increased in spring to summer as the atmospheric CO_2 concentration decreased.

The NDVI data were plotted against the atmospheric CO_2 data from the Point Barrow, Mauna Loa and South Pole stations (Fig. 3). The South Pole data (Fig. 3*c*) showed no relationship between NDVI and CO_2: south of 30° S, the oceanic area is greater than land area which leads to smaller land/sea contrasts in air temperature. Consequently, seasonal behaviour of both the NDVI and the atmospheric CO_2 concentrations is less marked than in corresponding latitudes of the Northern Hemisphere (Figs 1, 2). Remote sources of CO_2 may also dominate or obscure local sources of CO_2 through atmospheric circulation and mixing in this region.

In contrast, the CO_2 data from Point Barrow and Mauna Loa and the NDVI data from 50 to 80° N and from 10 to 30° N, respectively (Figs 3*a*, *b*), showed a circular/elliptical relationship. At Point Barrow, the data showed no change in relative CO_2 concentration from April to June of 1982, 1983 and 1984, while the NDVI from 50 to 80° N increased (Fig. 3*a*). At Mauna Loa, however, the data showed a decrease in relative CO_2 concentration from May to June of 1982 and 1983, while the NDVI from 10 to 30° N again increased (Fig. 3*b*).

The Point Barrow results are consistent with heterotrophic respiration rates reported for soil and litter in the tundra and taiga zones between April and June[36,37]. As soon as the ground thaws, soil and litter respiration releases a burst of CO_2 and this could explain the April to June displacement of the relative CO_2-NDVI relationship in Fig. 3*a*.

Atmospheric circulation and boundary-level mixing effects would be expected to delay equilibration of CO_2 concentrations by several weeks. A time lag between the NDVI and the measured atmospheric CO_2 concentrations would be expected because of the distance between the Point Barrow and Mauna Loa stations and mid-latitude forest sites which have maximum seasonality in photosynthesis. When the NDVI for month n was plotted against the atmospheric CO_2 concentration for month $n+1$, approximately linear relationships were found with the Point Barrow and Mauna Loa data (Fig. 3*d*, *e*). The negative slopes in Fig. 3*d* and *e* indicate the increased absorption of CO_2 by increased amounts of terrestrial photosynthetic activity.

Inverse linear relationships, found between the Mauna Loa CO_2 concentrations, lagged by 2 months, and the NDVI for 10–80° N (Fig. 3*f*) showed that CO_2 oscillations at Mauna Loa represented the CO_2 response to the seasonal vegetation dynamics of the Northern Hemisphere and were not dominated by proximate sources and sinks. In addition, the globally averaged CO_2 cycle has a peak-to-peak amplitude of 4–5 p.p.m., about 75% of that at Mauna Loa, and is nearly in phase with the cycle there. The annual cycle at Mauna Loa is thus characteristic of the globally averaged cycle.

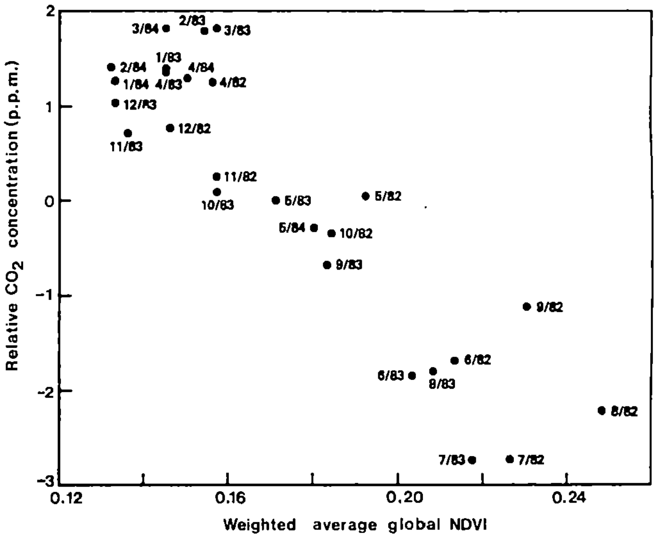

Fig. 4 The globally averaged atmospheric CO_2 concentration plotted against the globally averaged NDVI with a time lag of 1 month. The CO_2 data are from the global network of 20 NOAA/GMCC stations.

Figure 4 shows the globally averaged CO_2 measurements from the 20 stations plotted against the globally averaged NDVI. When a lag of 1 month was introduced into the CO_2 data, an inverse linear relationship was found, suggesting that the global NDVI represents the photosynthetic capacity of the terrestrial biosphere.

Conclusions

Our data show the relationship between monthly variations in atmospheric CO_2 concentrations and terrestrial NDVI dynamics, which are, in turn, estimates of IPAR and photosynthetic capacity. Note that we have not considered factors such as respiration, decomposition, consumption of fossil fuels, oceanic processes and burning of vegetation, all of which influence atmospheric CO_2 concentrations. Our analysis demonstrates the measurable link between atmospheric CO_2 drawdown and terrestrial NDVI dynamics and suggests that there may be quantitative relationships between multi-temporal satellite data and atmospheric CO_2 drawdown. The inclusion of oceanic CO_2 uptake and release, respiration and decomposition processes, fossil fuel contributions and other CO_2 sources and sinks can be used to advance our quantitative understanding of the global CO_2 cycle.

We thank T. Goff, B. Rank, E. Matthews, K. Prentice and J. Lerner for assistance, T. J. Conway for the 1984 NOAA/GMCC flask data, and A. M. Heasty for comments. This research was supported in part by NASA Life Sciences Division, by NASA Earth Observation Division, and by NASA cooperative agreement NCC5-29 with Columbia University, as well as by the Carbon Dioxide Research Division, Office of Energy Research, US Department of Energy, under contract 19X-2229C with the Lamont-Doherty Geological Observatory of Columbia University with Martin Marietta Energy Systems, Inc., under contract DE-AC05-840R21400.

Received 6 February; accepted 31 October 1985.

1. Gates, D. M., Keegan, H. J., Schleter, J. C. & Weidner, V. P. *Appl. Opt.* **4**, 11–20 (1965).
2. Knipling, E. B. *Remote Sens. Envir.* **1**, 115–119 (1970).
3. Woolley, J. T. *Pl. Physiol.* **47**, 656–662 (1971).
4. Kumar, R. & Silva, L. *Appl. Opt.* **12**, 2950–2954 (1973).
5. Tucker, C. J. & Garratt, M. W. *Appl. Opt.* **16**, 635–642 (1977).
6. Tucker, C. J. *Grass Forage Sci.* **35**, 177–182 (1980).
7. Curran, P. J. *Phil. Trans. R. Soc.* **A309**, 257–270 (1983).

8. Kumar, M. & Monteith, J. L. in *Plants and the Daylight Spectrum* (ed. Smith, H.) 133–144 (Academic, London, 1982).
9. Daughtry, C. S. T., Galio, K. P. & Bauer, M. E. *Agron. J.* **75**, 527–531 (1983).
10. Hatfield, J. L., Asrar, G. & Kanemasu, E. T. *Remote Sens. Envir.* **14**, 65–76 (1984).
11. Wiegand, C. L. & Richardson, A. J. *Agron. J.* **76**, 543–548 (1984).
12. Asrar, G., Fuchs, M., Kanemasu, E. T. & Hatfield, J. L. *Agron. J.* **76**, 300–306 (1984).
13. Sellers, P. J. *Int. J. Remote Sens.* **6**, 1335–1372 (1985).
14. Keeling, C. D. *Proc. Carbon Dioxide Research Conference: Carbon Dioxide, Science and Consensus* 2.1–2.62 (Department of Energy Conf.-82097, 1982).
15. Komhyr, W. D. *et al. J. geophys. Res.* **90**, 5567–5596 (1985).
16. Machta, L., Hansen, K. & Keeling, C. D. in *The Fate of Fossil Fuel CO_2 in the Oceans* (eds Anderson, N. R. & Malahoff, A.) 131–144 (Plenum, New York, 1977).
17. Woodwell, G. M., Houghton, R. A. & Tempel, N. R. *J. geophys. Res.* **78**, 932–940 (1973).
18. Fung, I. Y. in *Proc. 6th Oak Ridge natn. Lab. Life Sci. Symp. on the Global Carbon Cycle* (ed. Jacobs, V.) (US Department of Energy, Oak Ridge, in the press).
19. Heimann, M. M., Keeling, C. D. & Fung, I. Y. in *Proc. 6th Oak Ridge natn. Lab. Life Sci. Symp. on the Global Carbon Cycle* (ed. Jacobs, V.) (US Department of Energy, Oak Ridge, in the press).
20. Junge, C. E. & Czeplak, G. *Tellus* **20**, 422–434 (1968).
21. Machta, L. *Bull. Am. met. Soc.* **53**, 402–420 (1972).
22. Fung, I. Y., Prentice, K., Mathews, E., Lerner, J. & Russel, G. *J. geophys. Res.* **88**, 1281–1294 (1983).
23. Bolin, B. & Keeling, C. D. *J. geophys. Res.* **68**, 3899–3920 (1963)
24. Pearman, G. I. & Hyson, P. *J. geophys. Res.* **85**, 4457–4467 (1980)
25. Azevedo, A. E. thesis, Columbia University (1982).
26. Woodwell, G. M. *et al. Science* **222**, 1081–1086 (1984)
27. Woodwell, G. M. in *The Role of Terrestrial Vegetation in the Global Carbon Cycle Measurement by Remote Sensing* (ed. Woodwell, G. M.) 1–17 (SCOPE 23, Wiley, New York, 1984)
28. Tucker, C. J., Townshend, J. R. G. & Goff, T. E. *Science* **227**, 369–375 (1985)
29. Justice, C. O., Townshend, J. R. G., Holben, B. N. & Tucker, C. J. *Int. J. Remote Sens.* **6**, 1278–1318 (1985).
30. Goward, S. N., Tucker, C. J. & Dye, D. G. *Vegetacio* (in the press)
31. Tucker, C. J., Vanpraet, C. L., Sharman, M. J. & Van Ittersum, G. *Remote Sens. Envir.* **17**, 233–249 (1985).
32. Tarpley, J. D., Schneider, S. R. & Money, R. L. *J. Climate appl. Met.* **23**, 491–493 (1984)
33. Holben, B. N. & Fraser, R. S. *Int. J. Remote Sens.* **5**, 145–160 (1984)
34. Schutz, C. & Gates, W. L. Preprint (Rand Corporation, R-1029-ARPA, Santa Monica, 1972)
35. Larcher, W. & Bauer, H. in *Physiological Plant Ecology* (eds Lange, O. L., Nobel, P. S., Osmond, C. B. & Ziegler, H.) 403–437 (Springer, Berlin, 1981)
36. Swift, M. J., Heal, O. W. & Anderson, J. M. *Decomposition in Terrestrial Ecosystems*, [illegible] (Blackwell, Oxford, 1979).
37. Linkins, A. E., Melillo, J. M. & Sinsabaugh, R. L. *Current Perspectives in Microbial Ecology* (eds Klug, M. J. & Reddy, C. A.) 572–579 (American Society of Microbiology, Washington, DC, 1984).

Solvation energy in protein folding and binding

David Eisenberg & Andrew D. McLachlan*

Molecular Biology Institute and Department of Chemistry and Biochemistry, University of California at Los Angeles,
Los Angeles, California 90024, USA
* MRC Laboratory of Molecular Biology, Hills Road, Cambridge CB2 2QH, UK

We have developed a method for calculating the stability in water of protein structures, starting from their atomic coordinates. The contribution of each protein atom to the solvation free energy is estimated as the product of the accessibility of the atom to solvent and its atomic solvation parameter. Applications of the method include estimates of the relative stability of different protein conformations, estimates of the free energy of binding of ligands to proteins and atomic-level descriptions of hydrophobicity and amphiphilicity.

OF the forces that guide a polypeptide chain to its folded form in water, solvent interactions, including the hydrophobic interaction, are thought to be among the most important[1–4]. Yet these interactions are currently evaluated by relatively primitive methods. This is in contrast to the other component energies that stabilize proteins, such as hydrogen bonds, for which atom-atom potential functions have been devised[5–7]. Present methods for estimating the contribution of solvation energy to protein stability include the assumption that the hydrophobic character of each amino-acid residue can be summarized by a single number, the amino-acid hydrophobicity[8–12]. This is an oversimplification for amino acids such as Trp, Tyr, Glu, Gln, Lys and Arg which have both polar and apolar parts. Some authors have tried to overcome this limitation by devising more elaborate residue hydrophobicities to improve the description[8,13,14]. Also an oversimplification is the commonly used approximation that the hydrophobic energy of a folded protein molecule is proportional to the total protein surface that is accessible to water, regardless of whether the exposed surface is apolar, polar or charged[15].

To develop an explicitly atomic description of the interaction of water with a protein, we extend the ideas of Langmuir[16], Cohn and Edsall[17], and others[18,19]. The basic assumption is that the free energy of interaction of a solute with water can be considered as a sum of energies of atomic groups. We follow Langmuir in using the exposed surface areas of a group as a measure of its interaction with solvent. In practice we use the solvent-accessible surface area of Lee and Richards[20] and other recent workers[21–24]. This is defined as the area over which the centre of a water molecule of radius 1.4 Å can move while maintaining unobstructed contact with the group. In our method, the sign and strength of the water-solvent interaction are specified by the atomic solvation parameter (ASP) of each atom accessible to water. These values are determined, as described below, from free energies of transfer[8–12]. Thus, our method effectively combines two common approaches for evaluating hydrophobic forces: computation of solvent-accessible surface areas; and estimating energies from free energies of transfer. Our method, however, extends the first approach by weighting the effect of each atom by its polar or apolar character, and extends the second in permitting calculation of the solvation energy from the coordinates of individual atoms in each residue. It advances both methods in permitting estimates of the free energy of transfer of small molecules and of the contribution of solvation to the free energy of binding of small molecules to proteins.

Atomic contributions

Here we express the contribution of protein-solvent interactions to the free energy of protein folding as a sum over all atoms of the structure (except hydrogen atoms, which are not treated explicitly). The term for each atom is the product of its solvent-accessible area[20] and its ASP for transfer from the interior of a protein to aqueous solution. The transfer to solution of a single atom, i, immersed in protein is depicted in Fig. 1*a*. Let the accessible surface area of the atom be given by A_i, and its atomic solvation parameter be given by $\Delta\sigma_i$. Then the free energy of transfer (ΔG) is

$$\Delta G_i = \Delta\sigma_i A_i \qquad (1)$$

Now consider the transfer to water of amino-acid residue R immersed in protein (Fig. 1*a*). We assume that the change in free energy for this process can be approximated as a sum of atomic terms, each like that of equation (2)

$$\Delta G_R = \sum_{\text{atoms i}} \Delta\sigma_i A_i \qquad (2)$$

Note that the areas A_i now depend on the conformation of the amino acid, and that some atoms will be obscured by their

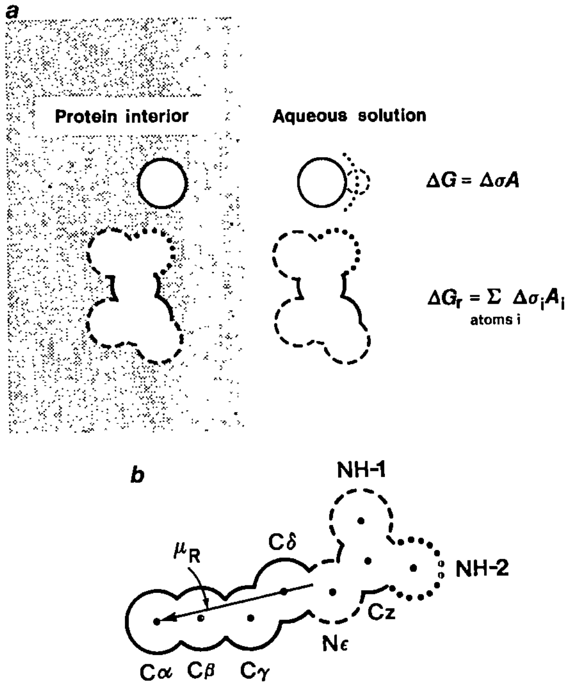

Fig. 1 *a*, Transfer of an atom and a molecule immersed in protein to water. The molecule contains three different types of atoms, represented by solid, dashed and dotted outlines. The definition of accessible surface area is illustrated for the atom at the right, where the centre of a sphere of radius 1.4 Å, tangent to the atom, sweeps out the accessible area. *b*, The atomic hydrophobic moment for the Arg side chain, shown as a vector running from the side-chain centre to the α-carbon atom. The chain takes the conformation specified in the CORELS[40] computer program dictionary. The dotted NH-2 atom is the most exposed nitrogen and is accordingly treated as the charged nitrogen.

neighbours. We assume that conformation is not significantly changed during transfer.

The validity of equation (2) can be tested by a fit to experimental free energies of transfer. For proteins the fit is carried out by considering atoms in five classes: carbon, neutral oxygen and nitrogen (N/O), charged oxygen (O^-), charged nitrogen (N^+) and sulphur. Then the free energies of the common amino acids can be represented by equations of the type

$$\begin{aligned}\Delta G_R = {} & \Delta\sigma(\mathrm{C}) \sum_{\mathrm{C\ atoms\ i}} A(\mathrm{C_i}, \mathrm{R}) \\ & + \Delta\sigma(\mathrm{N/O}) \sum_{\mathrm{N,\ O\ atoms\ i}} A(\mathrm{N/O_i}, \mathrm{R}) \\ & + \Delta\sigma(\mathrm{O^-}) \sum_{\mathrm{O^-\ atoms\ i}} A(\mathrm{O_i^-}, \mathrm{R}) \\ & + \Delta\sigma(\mathrm{N^+}) \sum_{\mathrm{N^+\ atoms\ i}} A(\mathrm{N_i^+}, \mathrm{R}) \\ & + \Delta\sigma(\mathrm{S}) \sum_{\mathrm{S\ atoms\ i}} A(\mathrm{S_i}, \mathrm{R}) \qquad (3)\end{aligned}$$

in which $\Delta\sigma(\mathrm{C})$ is the ASP for carbon and $A(C_i, \mathrm{R})$ is the solvent-accessible surface area of carbon atom i in a standard conformation[21] of residue R, and so forth for the other terms. The O^- term describes the charged oxygen atoms in Glu and Asp; the N^+ term describes the charged nitrogen atoms in Lys, Arg and His residues; the N/O term describes all uncharged N and O atoms. In Asp, Glu and Arg the most exposed N or O atom is taken to be the atom on which the charge is concentrated. Only certain terms of equation (3) are needed to describe any given residue. For example, Asn requires only C and N/O terms. The *p*H dependence of charges is ignored, an assumption that might be thought to be poor for His, but the solvent-accessible areas of the N atoms are not large.

Table 1 Amino-acid sovation free energies and group moments

Amino-acid residue	ΔG_{OBS}*	ΔG_R†	ΔG_{TAN}‡	μ_a§	cos θ
Gly	(0)	(0)	(0)	(0)	—
Ala	0.42	0.67	0.50	0	—
Val	1.66	1.5	1.50	0.48	0.84
Leu	2.32	1.9	1.80	1.0	0.89
Ile	2.46	1.9	—	1.2	0.99
Pro	0.98	1.2	—	0.18	0.22
Cys¶	1.34	0.38	—	0.17	0.76
Met	1.68	2.4	1.30	1.9	0.94
Thr	0.35	0.52	0.40	1.5	0.09
Ser	−0.05	0.01	−0.30	0.73	−0.67
Phe	2.44	2.3	2.50	1.1	0.92
Trp	3.07	2.6	3.40	1.6	0.67
Tyr	1.31	1.6	2.30	1.8	−0.93
Asn	−0.82	−0.60	—	1.3	−0.86
Gln	−0.30	−0.22	—	1.9	−1.0
Asp	−1.05	−1.2	—	1.9	−0.98
Glu	−0.87	−0.76	—	3.0	−0.89
His	0.18	0.64	0.50	0.99	−0.75
Lys	−1.35	−0.57	—	5.7	−0.99
Arg	−1.37	−2.1	—	10.0	−0.96
Group		ΔG_{OBS}‖ (ref. 17)		ΔG_R# (equation (3))	
$-CH_2-$		0.67		0.56	
$-C_6H_5$		1.90		1.6	
-OH		−0.76		−0.66	
$-CH_2-CONH-$		−1.14		0.66	
Gly ionization		−3.7		−2.6	

Observed and calculated free energies of transfer are given in units of kcal mol^{-1}, calculated residue hydrophobic moments μ_a are given in kcal mol^{-1} Å. ΔG_{OBS} and ΔG_{TAN} are experimental free energies of transfer relative to glycine. ΔG_R is the calculated value; μ_a is the calculated residue hydrophobic moment; and θ is the angle between the direction of the residue hydrophobic moment and a line from the α-carbon nucleus to the geometric centre of each side chain.

* ΔG_{OBS} is the observed value of π reported by Fauchere and Pliska[25] multiplied by $2.30\,RT = 1.36$ kcal mol^{-1}; π(side chain) is defined as log *D*(acetyl amino-acid amide) − log *D*(acetyl glycine amide), where *D* is the distribution coefficient for octanol/water.

† Calculated from equation (3).

‡ Observed values for transfer from ethanol to water from ref. 9.

§ Atom-based hydrophobic moment, defined in equation (5), below, using solvent-accessible surface areas from ref. 21 and atomic coordinates from ref. 39. These moments depend on the detailed conformation of the side chain, but not sensitively, because the corresponding values based on the coordinate dictionary supplied with the computer program CORELS[40] differ by an average of only 3%.

‖ Experimental values from ref. 17 (from p. 212 except for the value for the -OH group which is from p. 206). Gly ionization is for the process: $NH_2\text{-}CH_2\text{-}COOH \rightarrow {}^+NH_3\text{-}CH_2\text{-}COO^-$.

# Calculated from equation (3) as follows: $-CH_2-$, using the average accessible are of 8 $-CH_2$ groups in 5 residues; Gly ionization from tabulated areas[21]; and the -OH group as $\Delta G_R(\mathrm{Ser}) - \Delta G_R(\mathrm{Ala})$ and $-C_6H_5-$ as $\Delta G_R(\mathrm{Phe})\text{-}G_R(\mathrm{Ala})$, corresponding to the experimental values[17].

¶ Both ΔG_{OBS} and ΔG_R refer to half-cystine. We were unable to derive a reliable value for -SH.

The assumption in equation (3) is that 20 residue hydrophobicities (ΔG_R) can be represented by five ASPs ($\Delta\sigma$s), provided that suitable values of $\Delta\sigma$ can be found. We now show that a consistent set of $\Delta\sigma$s can be derived from experimental data on free energies of transfer. The accessible areas A_i of residues in standard conformations can be calculated from known structures; we have adopted the areas calculated by Shrake and Rupley[21], which are close to those found by C. Chothia (personal communication); they are for the amino acid X in a Gly-X-Gly sequence in a typical extended conformation. The values of the $\Delta\sigma$s were determined by a linear least-squares fit of equations (3) to observed values for the free energy of transfer, ΔG_R, of the amino-acid side chains. The measured ΔGs were those determined by Fauchere and Pliska[25] from transfer free energies of amino-acid residue analogues from n-octanol to water. Our estimated ASP values (with their standard deviations) are:

$$\Delta\sigma(\mathrm{C}) = \ 16 \pm 2 \ \mathrm{cal\ \AA^{-2}\ mol^{-1}}$$

$$\Delta\sigma(\mathrm{N/O}) = \ -6 \pm 4$$

$$\Delta\sigma(\mathrm{O^-}) = -24 \pm 10$$

$$\Delta\sigma(\mathrm{N^+}) = -50 \pm 9$$

$$\Delta\sigma(\mathrm{S}) = \ 21 \pm 10$$

The quality of the fit is illustrated in Fig. 2, and the observed and calculated values are given in Table 1. The fit is generally good except for Lys and Cys. Note that the non-polar atoms C and S increase the free energy of the system as they are transferred from the interior of the protein to water. Polar atoms decrease the free energy in the same process; charged atoms cause a much larger decrease.

Solvation contribution

With $\Delta\sigma$ values, it is possible to estimate the solvation contribution to the free energy of protein folding, ΔG_s. This energy with respect to a reference state r is given by

$$\begin{aligned}\Delta G_s = {} & \Delta\sigma(\mathrm{C}) \sum_{\mathrm{C\ atoms\ i}} (A_i - A_i^r) \\ & + \Delta\sigma(\mathrm{N/O}) \sum_{\mathrm{N,\ O\ atoms\ i}} (A_i - A_i^r) \\ & + \Delta\sigma(\mathrm{O^-}) \sum_{\mathrm{O^-\ atoms\ i}} (A_i - A_i^r) \\ & + \Delta\sigma(\mathrm{N^+}) \sum_{\mathrm{N^+\ atoms\ i}} (A_i - A_i^r) \\ & + \Delta\sigma(\mathrm{S}) \sum_{\mathrm{S\ atoms\ i}} (A_i - A_i^r) \qquad (4)\end{aligned}$$

in which A is the solvent-accessible surface area of an atom in the folded state and A^r is that in the reference state[21]. In the usual way in which equation (4) is used, the reference state does not matter because the energies of the same polypeptide chain are compared in two conformations having a common reference state. This is true for the application described below.

Improperly folded structures

One potential use of equation (4) is to assess the stabilities of modified or redesigned proteins. To illustrate such a calculation, the models of Novotný *et al.*[1] for incorrectly folded proteins are useful. These models were generated by exchanging the 113 side chains on the correctly folded α-carbon backbone of haemerythrin[26] from *T. dyscritum* with those from the correctly folded, β-sheet backbone of an immunoglobulin variable light-chain (V_L) domain[27] having the same number of residues. Novotný *et al.* used an energy-minimizing computer program to make small annealing adjustments in coordinates, and to reduce the potential energies of the two incorrectly folded structures to local minima. These annealed structures then had satisfactory van der Waals contacts, with normal valence angles and bond lengths, but no explicit account had been taken of solvation effects. Novotný *et al.*[1] noted that there is greater exposure of apolar residues in the misfolded structures. To these model misfolded structures, as well as to their energy-annealed, correctly folded analogues, we have applied equation (4) to estimate the solvation contribution to the free energy of folding. Our procedure consists simply of: first, computing[22] solvent-accessible atomic areas of the four structures from atomic coordinates; and second, weighting each atomic area by its ASP, and summing.

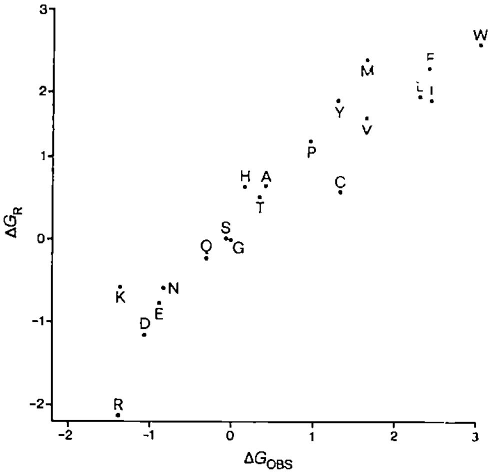

Fig. 2 Comparison of experimental values ΔG_{OBS} for free energies of transfer for amino-acid residues with the values of ΔG_R calculated from equation (3), using ASPs determined by linear least squares. The details of the least-squares fit are as follows. Fauchere and Pliska[25] deduced the hydrophobic parameter π for 19 amino-acid side chains as the difference between the logarithm of the measured distribution coefficients of the acetyl amino-acid amides and acetyl-glycine amide. Equation (3) was fitted to the free energies of transfer, $2.303\ RT\pi = \Delta G_{OBS}$, with the aid of NAG library routines G02BFF and G02CHF (Numerical Algorithms Group Ltd, Mayfield House, 256 Banbury Road, Oxford OX2 7DE, UK). In this fitting procedure, the difference between ΔG_R and ΔG_{OBS} is minimized by least-squares determination of the ASP values. The values of A for the appropriate atoms in each side chain are taken from ref. 21. For all residues, only the differences in area with the Gly residue are considered. Thus backbone atoms are ignored, except for the difference in exposed area for the α-carbon atom of glycine and of the other side chains. The deviation of points of the figure from a straight line can be explained by any of: (1) errors in measurements of ΔG_{OBS}; (2) inappropriate areas in equation (3); or (3) faulty assumptions in the formulation of equation (3) (see below). The multiple correlation coefficient R is 0.95, and the value of its square corrected for the number of parameters (ASPs), R^2_{COR}, is 0.88. The R^2_{COR} suggests that the separate ASPs for O^- and N^+ are justified, as is the sulphur ASP: with only a single type of charged atom, R^2_{COR} falls to 0.85 and R to 0.93; for only C/S and N/O ASPs, R^2_{COR} falls to 0.11 and R to 0.45. Fits to other hydrophobicity scales give different values for the ASPs. For example, the consensus scale of Eisenberg *et al.*[12], an average of five scales, yields $R = 0.97$ for a five-term fit. The ASP values for the consensus fit are similar to those reported here, but the O^- and N^+ ASPs have larger values. Despite the better fit to the consensus scale, the ASPs based on the data of Fauchere and Pliska[25] have been used in our calculations, in part because the absolute level of the consensus scale is unknown and in part because the new ASPs for the charged atoms seem more reasonable.

The solvation free energy is lower for the correct structures (Table 2). Both real structures have solvation free energies lower than the hypothetical, unfolded reference state by some 100 kcal $\mathrm{mol^{-1}}$, ~1 kcal per residue. Moreover, the solvation free energies for the real structures are markedly lower than for the incorrectly folded ones. Not only does each correctly folded structure have lower solvation free energy than the same polypeptide sequence folded improperly, but also each correct structure has lower free energy than the other sequence folded with the same backbone pattern. These results can be contrasted with the behaviour of traditional energy terms[1], which are not significantly different in the folded and misfolded structures.

When contributions to the solvation energy of folding for the natural structures are examined, interesting details emerge. For example, in the haemerythrin structure, 95 of the 113 side chains stabilize the solvation energy. Only one side chain, Asp 11, is destabilizing by so much as 1 kcal $\mathrm{mol^{-1}}$. For this side chain, both oxygen atoms are somewhat shielded from solvent relative to the extended reference structure. But for the protein as a whole, the process of folding from the extended reference state

Table 2 Solvation free energies of folding ΔG_s for an immunoglobulin V_L domain and haemerythrin

	V_L immunoglobulin domain	Haemerythrin
Correct fold	−106	−113
Incorrect fold (with the same sequence)	−72	−96
Net stabilization of correct structure	−34	−17

Values are calculated for the natural structures and the incorrectly folded structures (with exchanged amino-acid sequences) constructed by Novotný *et al.* Energies are given in kcal mol^{-1}. Equation (4) is used, with areas determined by the program ACCESS[22]. The uncertainty in the net stabilization of the correct structure was estimated from the standard deviations in the ASPs and by assuming that the fractional uncertainty in the sums of the atomic areas of each type is 0.05; this results in an overall uncertainty of ~10 kcal mol^{-1}.

yields −159 kcal for sequestering the 606 C and 3 S atoms away from the solvent (the sum of the first and last terms of equation (4)), while the partial covering of the 297 N/O, 17 O^-, and 21 N^+ atoms consumed only 25, 12 and 11 kcal mol^{-1}, respectively. Significant contributions to the stability of the folded state come from the apolar carbon atoms of the 29 Lys, Arg, Asp and Glu residues (a total of 41 kcal mol^{-1}). These contributions would be obscured or neglected in energetic models that are cast in terms of whole residue hydrophobicities; clearly, whole-residue hydrophobicities cannot account adequately for the folding energies of proteins.

Agreement with experimental data

Although it is reassuring that the estimated free energy of folding is lower for the real protein structures than for the incorrectly folded chains, this result falls well short of experimental verification of the method proposed here. Here we examine its assumptions and compare its predictions with experiment.

The principal assumption in the use of equation (3) to derive the ASPs is that the free energy of transfer is a linear function of the accessible areas of the constitutent atoms of the transferred molecule. This assumption is supported indirectly by the observed linearity of free energy with surface area for the transfer of many compounds from various non-aqueous liquids into water[15,28–31]. Of more direct bearing on the assumption is the accumulated evidence that molecular free energies of transfer can often be reckoned as a sum of energies for atomic groups[19]. This is not a new idea. Cohn and Edsall[17] made a critical analysis of evidence which suggested that the free energy of transfer of a chemical group such as $-CH_2-$, from ethanol and other apolar solvents to water is often independent of the molecule in which it is found. Some values for the free energy of transfer for various groups as compiled by Cohn and Edsall are given in Table 1, where they are compared with our new values calculated from equation (3). Generally, the computed values agree well in sign and magnitude with the experimental values, especially considering the diversity of the groups considered. The calculated values for side-chain transfers are also in reasonable agreement with the well-known measured values of Nozaki and Tanford[9] (Table 1). An exception to agreement in Table 1 is the free energy of transfer of the glycyl residue, for which equation (3) gives the wrong sign. This is probably because our model takes virtually no account of the partial charges on the amide N and O atoms. The reason is that the backbone atoms are omitted in the fitting procedure used to determine the ASPs, because the data being fitted are all differences between acetyl glycyl amide and the corresponding derivative of other amino acids. From the value in Table 2 for the free energy of transfer of the glycyl residue from ethanol to water, it is possible to estimate a crude value for the ASP for the amide N and O atoms at ~ −50 cal Å^{-2} mol^{-1}. If this value is qualitatively correct, then our solvation energies of folding are somewhat overestimated. To resolve this uncertainty, it will be necessary to fit a larger database of comparable free energies of transfer, which is not yet available.

An additional assumption in the use of equation (4) is that a non-polar liquid is an adequate model for the interior of a protein, as the ASPs derived from transfers between liquids are applied by equation (4) to transfer from liquid to protein interior. This assumption has been examined by Richards[24], who also considered amino-acid crystals as models for the protein interior. Richards concluded that an ASP somewhere in the range of 13–26 cal Å^{-2} mol^{-1} is appropriate for the transfer of apolar atoms. Our $\Delta\sigma(C)$ and $\Delta\sigma(S)$ values of 16 and 21 cal Å^{-2} mol^{-1} lie in this range, but may deserve revision as further free-energy data become available. The value for $\Delta\sigma(S)$, resting on only two measurements, is particularly subject to revision.

Atomic hydrophobic moments

In earlier work we described the amphiphilicity (asymmetry of hydrophobicity) of segments of regular protein secondary structure in terms of hydrophobic moments[32]. It was found that the hydrophobic dipole moments of neighbouring segments of secondary structure tend to oppose each other in correctly folded proteins[12], but not in incorrectly folded ones[33], and that hydrophobic moments can be used to classify helices on the basis of amino-acid sequences[34,35] and to detect periodicities[36,37]. These applications of hydrophobic moments were all formulated in terms of residue moments and can perhaps be made more precise with atomic-level moments.

The hydrophobic moment can be defined as an atomic property using the ASP values determined here. The hydrophobic dipole moment of a group of atoms is given by a sum over atoms i

$$\boldsymbol{\mu}_a = \sum_{\text{atoms i}} \Delta\sigma_i A_i \boldsymbol{r}_i - \langle \Delta\sigma A \rangle \sum_{\text{atoms i}} \boldsymbol{r}_i \qquad (5)$$

in which $\boldsymbol{r}_i$ is a vector from any origin to the position of atom i, and where the brackets indicate the mean value for all atoms of the group. The second term ensures that the value of $\boldsymbol{\mu}_a$ is independent of the choice of origin. When the sum in equation (5) is restricted to the atoms in a single side chain, a residue hydrophobic dipole moment is defined. This quantity is a measure of the amphiphilicity of the side chain, as distinct from its hydrophobicity. The values of these moments are tabulated in Table 1.

From these values it is apparent that the residues of greatest intrinsic amphiphilicity are Arg, Lys and Glu. In contrast, the most hydrophobic residues, Trp, Phe, Leu and Ile, all have small amphiphilicities. The direction of the hydrophobic moment is also defined by equation (5). This is expressed in Table 1 as the cosine of the angle between the direction of the moment and the direction of the vector from the α carbon to the side-chain centre. For the highly amphiphilic residues, the direction of the moment is nearly antiparallel to the α-carbon side-chain vector (cos θ near to −1). This is illustrated in Fig. 1*b* for Arg. Some of the most hydrophobic side chains (for example, Ile, Met and Phe) have moments nearly parallel to the α-carbon-centre vector (cos θ near to +1). Note that when the phenolic oxygen (with negative $\Delta\sigma$) is added to Phe to form Tyr, it reverses the direction of the moment (from +0.92 to −0.93).

Implications and extensions

How does the solvation free energy defined in equation (4) correspond to the component of the free energy of protein folding first described by Kauzmann as hydrophobic[3]? Kauzmann suggested that exposed apolar side chains increase the free energy of the system because they decrease the entropy of water. This effect on the free energy is described in equation (4) by the terms $\Delta\sigma(C)$ and $\Delta\sigma(S)$. Kauzmann's approach is extended in equation (4) by including the terms $\Delta\sigma(N/O)$,

$\Delta\sigma(O^-)$ and $\Delta\sigma(N^+)$. This has been done to introduce information from empirical free-energy measurements in a self-consistent way, and to impose a penalty in free energy for burial of charged and polar groups with a magnitude determined from experiments. These terms probably include contributions from electrostatic[38] and hydrogen-bonding effects as well. A full understanding of these contributions would require a knowledge of the structure of the molecules used to derive the ASPs, including states of protonation and hydration in both solvents. In short, ΔG_s includes contributions to the free energy of folding that go beyond the entropy change of the solvent. For this reason we call this energy the solvation free energy, rather than the hydrophobic free energy.

One use of equation (4) is in assessing the stability of proposed new proteins. These can either be genetically redesigned proteins or proteins designed for peptide synthesis. The energy of any model described in atomic coordinates can be tested against equation (4), although it may be necessary to supplement this equation with terms for other components of the folding energy. Another use is in energy-coupled X-ray phase refinement of protein structures[39-42]. In existing procedures, a model is determined that is the best compromise between the potential energy of the structure and the fit to the X-ray data. These methods do not go far enough in that it is the free energy, including solvation effects, that determines the structure. These effects could be incorporated by using ASPs as suggested here, along with the analytical method of Richmond[23], for computing accessible surface areas and their spatial derivatives. Similarly, the addition of a solvation energy term of the form of equation (4) could be made to molecular dynamics calculations. Finally, we note that the general method of computing solvation energy expressed in equation (4) could be developed further to compute the solvation contribution to the free energy for association of proteins with membranes or nucleic acids.

We thank Drs Novotný, Brucolleri and Karplus for making available the coordinates of the incorrectly and correctly folded protein structures described in ref. 1; Dr C. Chothia for his values of accessible surface areas of amino acids in extended polypeptide chains; Dr Richmond for use of his computer program ACCESS; and Drs D. Abrahams, F. R. Salemme and C. Schutt for discussions. D.E. acknowledges a Guggenheim fellowship and support from NIH and NSF. A computer program to calculate solvation energy according to equation (4) is available from the authors.

Received 19 July; accepted 30 October 1985.

1. Novotný, J., Bruccoleri, R. & Karplus, M. *J. molec. Biol.* **177**, 787-818 (1984).
2. Kauzmann, W. *Adv. Protein Chem.* **14**, 1-63 (1959).
3. Creighton, T. E. *Proteins* (Freeman, San Francisco, 1984).
4. Tanford, C. *The Hydrophobic Effect* 2nd edn (Wiley, New York, 1980).
5. Karplus, M. & McCammon, A. *A. Rev. Biochem.* **52**, 263-300 (1983).
6. Nemethy, G. & Scheraga, H. A. *Q. Rev. Biophys.* **10**, 239-352 (1977).
7. Levitt, M. & Warshel, A. *Nature* **253**, 694-698 (1975).
8. Rose, G. D., Geselowitz, A. R., Lesser, G. J., Lee, R. H. & Zehfus, M. H. *Science* **229**, 834-838 (1985).
9. Nozaki, Y. & Tanford, C. *J. biol. Chem.* **246**, 2211-2217 (1971).
10. Janin, J. *Nature* **277**, 491-492 (1979).
11. Wolfenden, R., Anderson, L., Cullis, P. M. & Southgate, C. C. B. *Biochemistry* **20**, 849-855 (1981).
12. Eisenberg, D., Weiss, R. M., Terwilliger, T. C. & Wilcox, W. *Faraday Symp. chem. Soc.* **17**, 109-120 (1982).
13. Guy, H. R. *Biophys. J.* **47**, 61-70 (1985).
14. Frommel, C. *J. theor. Biol.* **111**, 247-260 (1984).
15. Chothia, C. *Nature* **248**, 338-339 (1974).
16. Langmuir, I. *Colloid Symp. Monogr.* **3**, 48-75 (1925).
17. Cohn, E. J. & Edsall, J. T. in *Proteins, Amino Acids and Peptides as Ions and Dipolar Ions*, Ch. 9 (ACS Monograph Series, Reinhold, New York, 1943).
18. Tanford, C. *J. Am. chem. Soc.* **84**, 4240-4247 (1962).
19. Hansch, C. & Leo, A. in *Substitution Constants for Correlation Analysis in Chemistry and Biology* (Wiley, New York, 1979).
20. Lee, B. & Richards, F. M. *J. molec. Biol.* **55**, 379-400 (1971)
21. Shrake, A. & Rupley, J. A. *J. molec. Biol.* **79**, 351-371 (1973)
22. Richmond, T. J. & Richards, F. M. *J. molec. Biol.* **119**, 537-555 (1978)
23. Richmond, T. J. *J. molec. Biol.* **178**, 63-89 (1984).
24. Richards, F. M. *A. Rev. Biophys. Bioengng* **6**, 151-176 (1977)
25. Fauchere, J.-L. & Pliska, V. *Eur. J. med. Chem.-Chim. ther.* **18**, 369-375 (1983)
26. Stenkamp, R. E., Sieker, L. C. & Jensen, L. H. *Acta crystallogr* **B38**, 784-792 (1978)
27. Segal, D. M. *et al. Proc. natn. Acad. Sci. U.S.A.* **71**, 4298-4302 (1974)
28. Hermann, R. B. *J. phys. Chem.* **76**, 2754-2759 (1972).
29. Nandi, P. K. *Int. J. Peptide Protein Res.* **8**, 253-264 (1976).
30. Gelles, J. & Klapper, M. H. *Biochim. biophys. Acta* **533**, 465-477 (1978)
31. Creighton, T. E. *J. molec. Biol.* **129**, 235-264 (1979).
32. Eisenberg, D., Weiss, R. M. & Terwilliger, T. C. *Nature* **299**, 371-374 (1982)
33. Eisenberg, D., Wilcox, W. & McLachlan, A. D. *Proc. UCLA Symp. Protein Structure, Folding and Design* (in the press).
34. Eisenberg, D., Schwarz, E., Komaromy, M. & Wall, R. *J. molec. Biol.* **179**, 125-142 (1984).
35. Pownall, H. J., Knapp, R. D., Gotto, A. M. Jr & Massey, J. B. *FEBS Lett.* **159**, 17-23 (1983)
36. Eisenberg, D., Weiss, R. M. & Terwilliger, T. C. *Proc. natn. Acad. Sci. U.S.A.* **81**, 140-144 (1984).
37. Finer-Moore, J. & Stroud, R. M. *Proc. natn. Acad. Sci. U.S.A.* **81**, 155-159 (1984)
38. Warshel, A. & Russell, S. T. *Q. Rev. Biophys.* **17**, 283-422 (1984)
39. Diamond, R. *J. molec. Biol.* **82**, 371-391 (1974).
40. Susman, J. L., Holbrook, S. R., Church, G. M. & Kim, S.-H. *Acta crystallogr* **A33**, 800-804 (1977).
41. Levitt, M. *J. molec. Biol.* **82**, 393-420 (1974).
42. Konnert, J. H. *Acta crystallogr.* **A32**, 614-617 (1976).

LETTERS TO NATURE

Inadequacy of Coulomb's friction law for particle assemblies

K. Kendall

ICI New Science Group, PO Box 11, The Heath, Runcorn,
Cheshire WA7 4QE, UK

Wherever powders are manipulated by mechanical means, adhesive and frictional forces act between the solid grains. For two centuries, these forces have been described by Coulomb's law[1], a law which originally proved useful in designing civil engineering structures, and which has since been profitably extended to the understanding of the powder flows in chemical plants[2]. However, we have now found that Coulomb's law is not adequate to explain the compaction of fine powders in the manufacture of ceramic articles, where it has been observed that friction appears to increase for smaller particles. This apparent increase in friction is explained by considering in detail the contact of loaded, adhesive, elastic spheres.

Consider the ideal experiment (Fig. 1*a*) in which a bed of particles is loaded onto and sheared along a polished plate of the same material[3]. The nominal shear stress F/A (where F is force and A is area) required to slide the powder across the plate under the normal stress W/A (where W is normal load) has usually been interpreted by Coulomb's law:

$$F/A = K + \mu W/A \tag{1}$$

where K represents the cohesive shear strength of the particle/plate assembly (that is, the shear stress experienced at zero normal load) and μ is the coefficient of friction between the surfaces[4]. This law, in combination with the geometrical constraints on powder motion first mentioned by Reynolds in 1885, has been much used to describe the deformation of powders and soils in complex stress states[5-7]. Here we demonstrate that equation (1) does not follow the experimental results satisfactorily, and we propose a new argument which provides an improved fit to the observed behaviour.

The problem of applying Coulomb's law to assemblies of fine particles is that the friction coefficient calculated from equation (1) does not generally match that measured in a standard friction test between macroscopic blocks of material. First, the calculated μ is often higher than expected: for example, sand particles of diameter 0.5 mm in water give $\mu = 0.45$ whereas two large quartz blocks give $\mu = 0.3$ (Fig. 1*b*). A second difficulty is that the friction coefficient increases as the grains are made smaller,

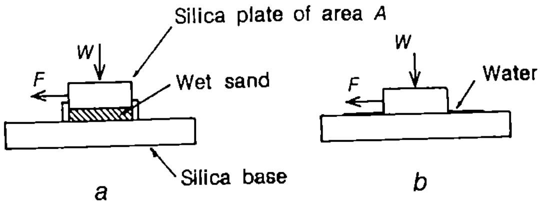

Fig. 1 *a*, Experimental set-up for measuring friction of wet sand particles pressed against a smooth silica plate. *b*, Friction measurement on macroscopic silica plates.

rising to $\mu = 0.6$ for wet sand of 0.01 mm diameter. Finally, the friction of powders does not remain constant as the normal pressure is increased, but falls substantially at high loads, in conflict with Coulomb's law. Therefore, a new theory is required to account for these curious effects.

The fundamental origin of Coulomb's law may be seen by considering a spherical particle in frictional contact with a smooth plane under normal load w and shear force f (Fig. 2). Because the particle experiences a surface attraction towards the plane as a result of van der Waals' force w_s, the total load on the contact is $w_s + w$ and the frictional force is thus

$$f = \mu(w_s + w) = k + \mu w \qquad (2)$$

which is the form of equation (1). Thus, Coulomb's law is the simplest expression for frictional resistance, taking into account both the external load and the interfacial attraction between the particle and the plane.

Equation (2) has been predominant in describing soil behaviour[8]; it has been re-derived by Derjaguin[9], and verified by Lazarev[10] for flat surfaces in extended molecular contact. It is used to this day to account for the friction of powders[11,12] and fibres[13] although it does not follow the results satisfactorily.

The difficulty with the simple Coulomb model is the assumption that the external load and the interfacial force are independent. This assumption is wrong, as indicated by recent studies on the contact of elastic spheres exhibiting surface attractions[14]. For a sphere of diameter D resting on a plane surface of the same material with interface energy Γ (the energy required to break unit area of contact) and normal load w, the effective load pressing the sphere onto the plane has been shown to be[14]

$$\frac{3\pi D\Gamma}{2} + w + \left[3\pi D w\Gamma + \left(\frac{3\pi D\Gamma}{2}\right)^2\right]^{1/2} \qquad (3)$$

so that the equation for shear force becomes

$$f = \frac{\mu 3\pi D\Gamma}{2} + \mu w + \mu\left[3\pi D w\Gamma + \left(\frac{3\pi D\Gamma}{2}\right)^2\right]^{1/2} \qquad (4)$$

This equation is similar to the Coulomb form of equation (2) in that the first term stems from surface attraction and the second term is due to the external load; it differs, however, from the Coulomb model in the extra term which gives the interdependence of the molecular forces and the applied load. It also differs from the recent theory for the sliding of adhesive spheres suggested by Savkoor and Briggs[15].

Equation (4) is useful in describing some of the anomalies reported previously. For example, it explains the nonlinearity of plots of friction force against normal load noted by Briscoe and Kremnitzer on polyethylene terephthalate fibres[13]. Figure 2 shows how the new theory follows the experimental data. The spread of friction results suggested a value of interface energy Γ of $\sim$0.01–0.04 J m^{-2}, in fair agreement with the value calculated from direct adhesion tests. Note that the apparent friction coefficient (the slope of the curve) is twice the true μ near zero load, but decreases to the correct value at high loads, or for large particles.

The predictions of equation (4) were tested experimentally, using the apparatus of Fig. 1*a* to determine the friction of wet silica powder. Sand was sieved into fractions and was loaded between smooth silica sheets, then sheared to measure the friction force. This friction force remained constant over many traversals of the silica, suggesting that the deformation was largely elastic, as assumed in the theory. Various loads were used, giving normal pressures close to 100 kPa, and the slope of the friction force/normal force curve was calculated. This slope was the apparent friction coefficient, μ_{app}, which was then compared with the theoretical value computed by differentiation of equation (4):

$$\mu_{app} = \frac{df}{dw} = \mu\left[1 + \left(1 + \frac{4PD}{3\pi\Gamma}\right)^{-1/2}\right] \qquad (5)$$

where $P \approx w/D^2$ is the normal applied pressure.

Figure 3 shows the experimental results for μ_{app} as a function of the particle size at a normal pressure of 100 kPa. The apparent friction coefficient achieved a maximum of 0.63 for the smallest grains, falling steadily for larger particles, and reaching a value of 0.34 for the macroscopic plates. The theoretical curve plotted from equation (5) gave a remarkably good fit to the data when the interface energy Γ was taken to be 2 J m^{-2} and the true friction coefficient was $\mu = 0.332$. Although this value of interface energy seems somewhat high for wet silica, a similar discrepancy has been noted in electron microscope studies of

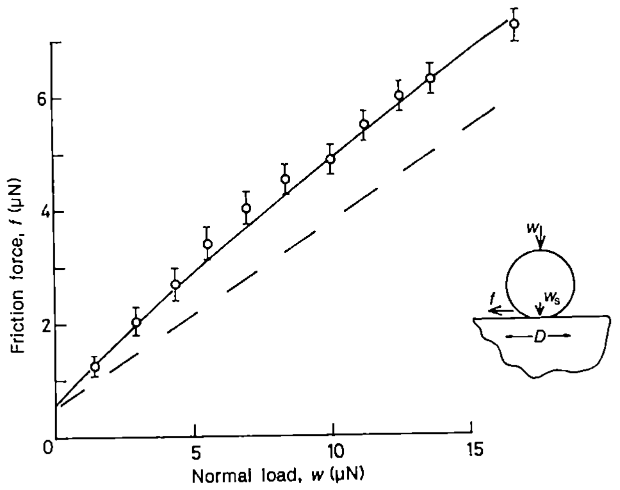

Fig. 2 Contact between a particle and a plate exhibiting interfacial attractive energy Γ under a normal load w and shear force f. The surface attraction between the spheres leads to a nonlinear relation between f and w [equation (4)] which differs from Coulomb's law at low loads but approaches Coulomb behaviour at high loads. ——, Curve derived from equation (4) with $\mu = 0.33$, $\Gamma = 0.01$ J m^{-2}; - - -, curve derived from Coulomb's law, $\mu = 0.33$; ○, results from ref. 13.

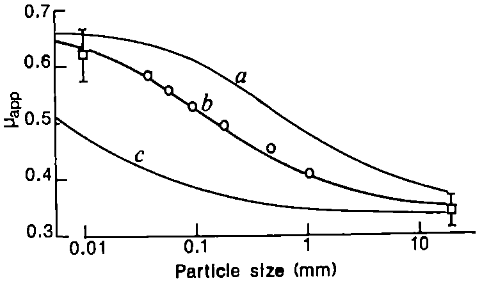

Fig. 3 Plot of μ_{app} against particle size derived from equation (5) for comparison with experimental results on wet sand. A good fit with the experimental results was obtained when the true friction coefficient was assumed to be 0.332 and the interface energy 2 J m^{-2}. *a–c*, Curves derived from equation (5) with $\Gamma = 10$, 2 and 0.1 J m^{-2}, respectively. □, Our results; ○, those of Rowe[3].

adhering metal particles, probably owing to the nonspherical nature of the grains[16].

It seems likely, therefore, that the new theory presented here offers the correct explanation for the failure of Coulomb's law in describing the odd frictional behaviour of fine powders, particularly those materials of high surface area which are used in the field of modern ceramics.

Received 13 August; accepted 31 October 1985.

1. Coulomb, C. A. *Mém Acad. Sci. Savants Étrangers* **7**, 343-382 (1773).
2. *Proc. IUTAM Symp. on Deformation and Failure of Granular Materials*, (Balkema, Delft, 1982).
3. Rowe, P. W. *Proc. R. Soc.* **A269**, 500-527 (1962).
4. Bowden, F. P. & Tabor, D. *Friction and Lubrication of Solids* Pts I and II (Clarendon, Oxford, 1950 and 1964).
5. Reynolds, O. *Phil. Mag.* **20**, 468-481 (1885).
6. Bolton, M. *A guide to Soil Mechanics* Ch. 4 (Macmillan, London, 1979).
7. Thornton C. & Barnes, D. J. *Proc. IUTAM Symp. on Deformation and Failure of Granular Materials*, 69-77 (Balkema, Delft, 1982).
8. Terzhagi, K. *Theoretical Soil Mechanics*, **7**, (Wiley, New York, 1943).
9. Derjaguin, B. V. *Phis. Khim.* **5**, 1163 (1934).
10. Derjaguin, B. V. & Lazarev, V. P. *Kolloid. Zh.* **1**, 293 (1935).
11. Chappuis, J., Hoeppner, D. W. & Neumann, A. W. *Tribology Ser.* **7**, 71-80 (Elsevier, Oxford, 1982).
12. Omenyi, S. N., Chappuis, J. & Neumann, A. W. *J. Adhesion* **13**, 131-139 (1981).
13. B. J. Briscoe, & Kremnitzer, S. L. *J. Phys. D* **12**, 505-516 (1979).
14. Johnson, K. L., Kendall, K. & Roberts, A. D. *Proc. R. Soc.* **A324**, 301-313 (1971).
15. Savkoor, A. R. & Briggs, G. A. D. *Proc. R. Soc.* **A356**, 103-114 (1977).
16. Tholen, A. R. *Tribology Ser.* **7** 263-277 (Elsevier, Oxford, 1982).

Secondary antiproton production in relativistic plasmas

C. D. Dermer & R. Ramaty

Laboratory for High Energy Astrophysics, NASA/Goddard Space Flight Center, Greenbelt, Maryland 20771, USA

Recent measurements[1-3] of the low-energy flux of antiprotons ($\bar{p}$) in cosmic rays give ratios of $\bar{p}/p$ which are greater by a factor of 3-5 than predicted by the simple 'leaky box' model of cosmic-ray propagation. Here we report on an investigation of the possibility that the low-energy $\bar{p}$ excess reflects an origin in p-p collisions in relativistic plasmas. Because of both target and projectile motion in such plasmas, the antiproton production threshold in the frame of the plasma is much lower than the threshold of antiproton production in cosmic ray interactions with ambient matter. The spectrum of the resultant antiprotons therefore extends to much lower energy than in the cosmic ray case. Sites at which matter is accreted by compact objects could be sources of the low energy antiprotons. Escape of the antiprotons could be mediated by antineutron production.

Golden *et al.*[1] have reported an antiproton to proton ($\bar{p}$/p) ratio of $5.2(\pm 1.5)\times 10^{-4}$ in the cosmic radiation in the energy range 4.7-11.6 GeV. Bogomolov *et al.*[2], on the basis of only two events, report a $\bar{p}$/p ratio of $6(\pm 4)\times 10^{-4}$ at energies between 2 and 5 GeV. Buffington *et al.*[3] report a $\bar{p}$/p ratio of $2.2(\pm 0.6)\times 10^{-4}$ between 130 and 320 MeV, and also determine that the antihelium to helium ratio $\bar{\alpha}/\alpha < 2.2\times 10^{-5}$ in the energy range 130-370 MeV per nucleon. Upper limits on previous antinucleus searches are also given here.

The simple 'leaky box' model of cosmic-ray propagation predicts a $\bar{p}$/p ratio smaller by a factor of 3-5 than the values measured in the Golden and Bogomolov experiments. Because of the kinematic cutoff associated with the high $\bar{p}$ production threshold in p-p collisions when one of the protons is at rest, the $\bar{p}$/p ratio predicted by this model is about two orders of magnitude lower than the value reported by Buffington *et al.*, even after the effects of solar modulation are taken into account[4]. The low $\bar{\alpha}/\alpha$ ratio, in comparison with the $\bar{p}$/p ratios, suggests a secondary origin of the $\bar{p}$, although primary cosmic-ray antiproton theories, with subsequent breakdown of the $A > 1$ antinuclei, have been proposed (see ref. 5).

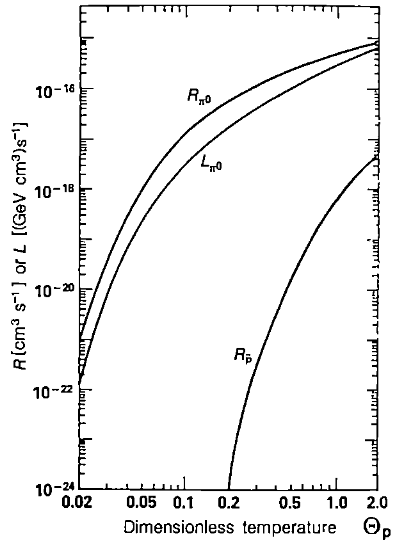

Fig. 1 The rate coefficients for secondary π^0 and $\bar{p}$ production from p-p collisions in a relativistic plasma at temperature $\Theta_p = kT/m_pc^2$. Also shown is the π^0 luminosity coefficient giving the total energy in secondary π^0 γ-rays produced at temperature Θ_p.

Theories of secondary $\bar{p}$ production in p-p collisions in the Galaxy are constrained by the observed galactic γ-ray luminosity. The observed antiproton flux $\phi_{\bar{p}}(E)$ implies a total galactic $\bar{p}$ production rate

$$Q(\bar{p}) \sim \frac{4\pi V}{c}\int_0^\infty dE \frac{\phi_{\bar{p}}(E)}{\beta\tau(E)} \sim (3.5\times 10^{-14} V/\tau)\bar{p}\,s^{-1}$$

where V is the galactic confinement volume and τ is the average galactic $\bar{p}$ residence time. Taking $V \sim \pi(15\,\text{kpc})^2\,(1\,\text{kpc}) \sim 1.2\times 10^{67}\,\text{cm}^3$ and $\tau \sim 10^7$ yr gives $Q(\bar{p}) \sim 2.1\times 10^{39}\bar{p}\,s^{-1}$. If the production of a secondary $\bar{p}$ is accompanied by the production of $\langle n \rangle$ π^0-decay γ-rays, the resultant γ-ray luminosity of the galaxy $Q(\gamma) \sim \langle n \rangle Q(\bar{p})$. In the case of the production of > 100 MeV photons in cosmic-ray interactions, $\langle n \rangle_{cr} \sim 2.7\times 10^3$, from the calculations of Stephens and Badhwar[6] and Tan and Ng[4]. If the $\bar{p}$ in the cosmic radiation are entirely cosmic-ray secondaries, the > 100 MeV luminosity of the Galaxy should, therefore, be at least $5.7\times 10^{42}\,\gamma\,s^{-1}$, in contrast to the value of $\sim 2.5\times 10^{42}\,\gamma\,s^{-1}$ deduced from the COS-B γ-ray observations[7]. This latter number is an upper limit, since it includes a significant contribution from bremsstrahlung and inverse Compton γ-rays.

Various models have been designed to either increase the $\bar{p}$ lifetime τ, incorporate additional $\bar{p}$ sources, or conceal the π^0 γ-rays. Although the integral production rate of $\bar{p}$ can then be made to agree with observations, most models still fail to predict a substantial low-energy $\bar{p}$ flux because of the low energy cutoff that results from secondary interactions with stationary targets, in disagreement with the observation[3]. Models that provide deceleration of the $\bar{p}$ after production or require that the Solar System occupies a special position in the Galaxy have also been proposed[8,9].

We examine the possibility that the low-energy antiprotons observed in the cosmic radiation are produced through secondary p-p interactions in relativistic plasmas in the vicinity of neutron stars or black holes. At proton temperatures $\theta_p = kT/m_pc^2 \gtrsim 0.2$ ($\theta_p = 1$ corresponds to $\sim 10^{13}$ K), a significant number of secondary $\bar{p}$ can be produced. We have calculated the rate coefficients and production spectra[10,11] for secondary $\bar{p}$ using the invariant cross-section of Tan and Ng[12] and the results are shown in Figs 1 and 2. We have also calculated the rate and luminosity coefficients from secondary π^0 production data. From Fig. 1 we find that the efficiency for $\bar{p}$ production compared with π^0 production is greater than in the cosmic-ray case for $\theta_p \gtrsim 0.5$, so the total π^0-decay γ-ray luminosity will not

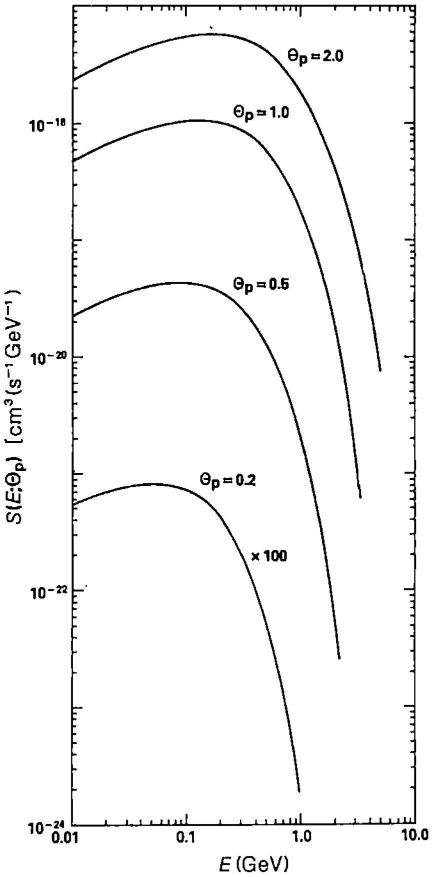

Fig. 2 Secondary $\bar{p}$ production spectra at various temperatures $\Theta_p = kT/m_pc^2$ are given as a function of kinetic energy E.

exceed limits implied by γ-ray observations of the Galaxy. In addition, several absorption processes likely to occur near compact objects, such as photon-photon or magnetic pair production, can further reduce the π^0 γ-ray luminosity.

The $\bar{p}$ spectra shown in Fig. 2 for a variety of temperatures extend to low energies without the appearance of the kinematic cutoff found in the cosmic-ray problem. The spectra peak at higher energies with increasing temperature, and exhibit an exponential decline above the peak temperature. But in all cases a very low-energy secondary $\bar{p}$ component is calculated, which could explain the low-energy $\bar{p}$ observation[3].

Possible production sites of the $\bar{p}$ include the galactic bulge binary X-ray sources or the objects associated with the γ-ray point sources (for example, CygX-3). Models for disk accretion[13] and spherical accretion incorporating shocks[14] could yield proton temperatures as high as $\Theta_p \sim 1$. Although the establishment of a thermal distribution of protons may not be possible at these temperatures, this assumption affords the simplest calculations. Preliminary estimates employing nonthermal proton spectra in relativistic plasmas suggest low-energy $\bar{p}$ spectra similar in form to the results of Fig. 2.

Transport of the secondary $\bar{p}$ from the production site can occur because antineutrons $\bar{n}$, produced in equal numbers as the $\bar{p}$ (ref. 15), are not confined by the ambient plasma magnetic field. The $\bar{n}$ will escape to the interstellar medium and subsequently decay into $\bar{p}$ (the calculations of Figs 1 and 2 refer only to these particles). Because of the finite lifetime of the $\bar{n}$, an upper limit can be placed on the mass of black holes that serve as production sites for the $\bar{p}$. Requiring that the marginally relativistic $\bar{n}$ escape to ~10 Schwarzschild radii implies a maximum black hole mass of $<10^7 M_0$. Past activity around such a massive black hole at the galactic centre could have produced the antiprotons without a large contemporaneous γ emission. A detailed comparison of $\bar{p}$ production in relativistic plasma with observations must also include distortions of the emergent $\bar{n}$ due to the intense gravitational field of the compact object, reacceleration and energy losses of the source spectrum in the galactic environment, and modulation in interplanetary space.

We have presented a model that can produce low-energy antiprotons through secondary p-p interactions in relativistic plasmas. Such a model is in agreement with the observation of low-energy antiprotons in the cosmic radiation and the observed γ-ray luminosity of the galaxy. Moreover, it agrees with the present lack of observations of antinuclei in the cosmic radiation, whose formation by secondary production processes is entirely negligible.

C.D.D. is a NAS/NRC resident research associate.

Received 27 September; accepted 5 November 1985.

1. Golden, R. L. *et al. Phys. Rev. Lett.* **43**, 1196-1199 (1979).
2. Bogomolov, E. A. *et al. Proc. 16th int. Cosmic Ray Conf.* **1**, 330-335 (1979).
3. Buffington, A. *et al. Astrophys. J.* **248**, 1179-1193 (1981).
4. Tan, L. C. & Ng, L. K. *J. Phys.* G **9**, 227-242 (1983).
5. Stecker, F. W. *et al. Astrophys. Space Sci.* **96**, 171-177 (1983).
6. Stephens, S. A. & Badhwar, G. D. *Astrophys. Space Sci.* **76**, 213-233 (1981).
7. Bloemen, J. B. G. M. *et al. Astrophys. J.* **279**, 136-143 (1984).
8. Stephens, S. A. & Mauger, B. G. in *Proc. 19th Recontre de Moriond Astrophysics Meet.*, 217-225 (1984).
9. Tan, L. C. & Ng, L. K. *Astrophys. J.* **269**, 751-764 (1983).
10. Weaver, T. A. *Phys. Rev.* A**13**, 1563-1569 (1976).
11. Dermer, C. D. *Astrophys. J.* **280**, 328-333 (1984).
12. Tan, L. C. & Ng, L. K. *Phys. Rev.* D **26**, 1179-1182 (1982).
13. Eilek, J. A. *Astrophys. J.* **236**, 664-673 (1980).
14. Meszaros, P. & Ostriker, J. P. *Astrophys. J.* **273**, L59-L63 (1983).
15. Gaisser, T. K. & Maurer, R. H. *Phys. Rev. Lett.* **30**, 1264-1267 (1973).

Specific role of transient O^-(s) at Mg(0001) surfaces in activation of ammonia by dioxygen and nitrous oxide

C. T. Au & M. W. Roberts

Department of Chemistry, University College, Cardiff CF1 1XL, UK

It has been established[1–3] that oxygen chemisorbed at a metal surface can activate an otherwise unreactive molecule, as in the activation of S—H, N—H, O—H and C—H bonds. We have now extended these studies to more complex systems involving co-adsorbed molecules in the hope of throwing some light on the mechanisms of heterogeneous catalysts. We have previously established the mechanisms by which unreactive molecular water, adsorbed on a Zn(0001) surface, is activated when co-adsorbed with nitric oxide[4], and have demonstrated N—H activation in ammonia co-adsorbed with nitric oxide at an atomically clean Mg(0001) surface at 295 K (Fig. 1*a* and ref. 5). Activation was attributed to surface oxygen generated in the dissociative chemisorption of nitric oxide. Here we establish the nature of the 'oxygen' species involved and reveal details of the molecular steps.

It is important to establish whether the 'oxygen' generated in the act of dissociative chemisorption of nitric oxide, that is, a short-lived species O^-(s), has any specific chemical reactivity that distinguishes it from the thermodynamically more stable surface 'oxide' species, O^{2-}(a), which was observed in the post-reaction XPS (X-ray photo-electron spectroscopy) study. Dynamic XPS over a wide temperature range is used to obtain information concerning the individual molecular steps.

We established first that a pre-oxidized Mg(0001) surface did not chemisorb ammonia at 295 K. Bulk MgO is also known to be unreactive to ammonia as judged by infrared spectroscopy[6,7]. The active oxygen species is clearly not the thermodynamically stable O^{2-}(a) species formed in the dissociative chemisorption of nitric oxide. However, dioxygen-ammonia mixtures also generate stable NH_2(a) species[8], which raises the issue of the possible steps that occur during the dissociative chemisorption of

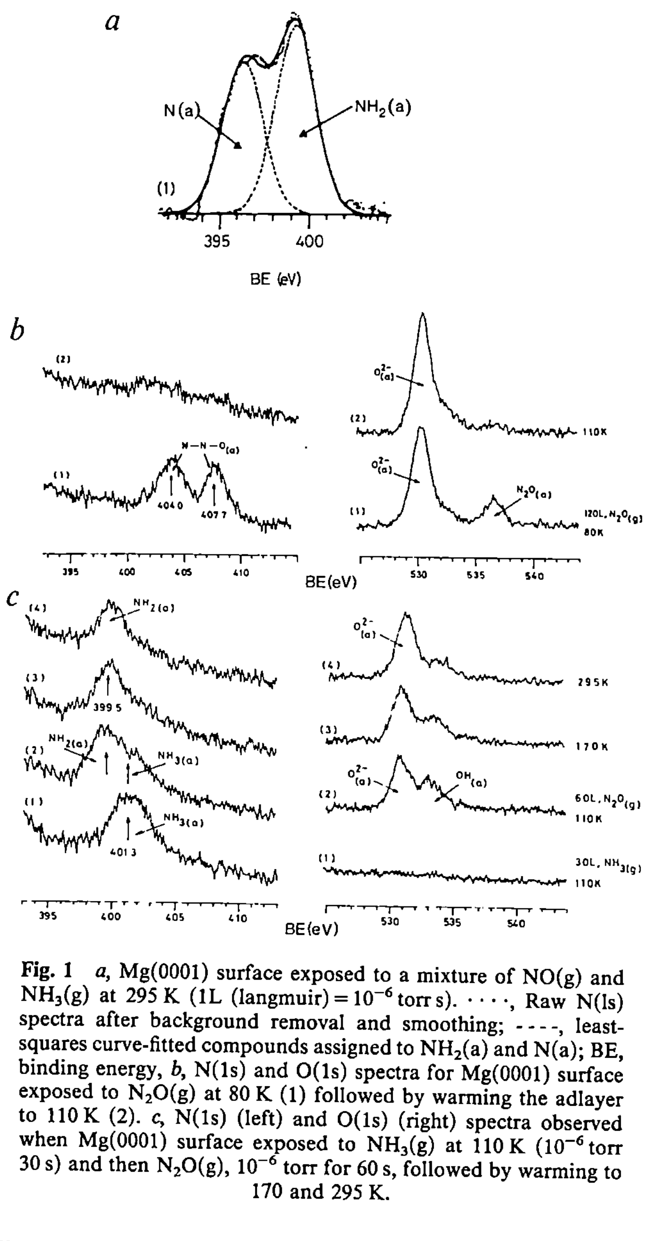

Fig. 1 *a*, Mg(0001) surface exposed to a mixture of NO(g) and $NH_3(g)$ at 295 K (1L (langmuir) = 10^{-6} torr s). · · · ·, Raw N(1s) spectra after background removal and smoothing; - - - -, least-squares curve-fitted compounds assigned to $NH_2(a)$ and N(a); BE, binding energy, *b*, N(1s) and O(1s) spectra for Mg(0001) surface exposed to $N_2O(g)$ at 80 K (1) followed by warming the adlayer to 110 K (2). *c*, N(1s) (left) and O(1s) (right) spectra observed when Mg(0001) surface exposed to $NH_3(g)$ at 110 K (10^{-6} torr 30 s) and then $N_2O(g)$, 10^{-6} torr for 60 s, followed by warming to 170 and 295 K.

dioxygen at a metal surface and leading to oxidation. As kinetic (XPS) data have established the existence of a molecularly adsorbed oxygen precursor in the oxidation of aluminium at low temperatures (77 K) and both XPS and ultraviolet photoelectron spectroscopy have established[4] the presence of $O^-(a)$ species during oxygen interaction with Zn(0001) surfaces, the following steps can be delineated for the dissociative chemisorption of oxygen at a metal surface

$$O_2(g) \rightarrow O_2(a) \rightarrow O^-(a) \rightarrow O^{2-}(a)$$

The step $O^-(a) \rightarrow O^{2-}(a)$ is initially kinetically fast at a Zn(0001) surface even at 77 K but with increasing $O^{2-}(a)$ concentration the process becomes activated so that at 77 K the $O^-(a)$ species represent a substantial (~60%) fraction of the $O^{2-}(a)$ concentration[4]. As the $O^-(a)$ species have been shown to abstract hydrogen from molecularly adsorbed water a mechanism of NH_3 activation could involve the intermediate $O^-(s)$. Note that there is no *a priori* reason why the above scheme for the dissociative chemisorption of dioxygen should not also include the $O_2^-(s)$ species and present at the surface as a transient. By studying the co-adsorption of ammonia with nitrous oxide starting at low temperature (110 K), this point can be resolved because N_2O is anticipated and shown to chemisorb (Fig. 1*b*) as indicated below. We use $O^-(s)$ to represent a surface transient and to

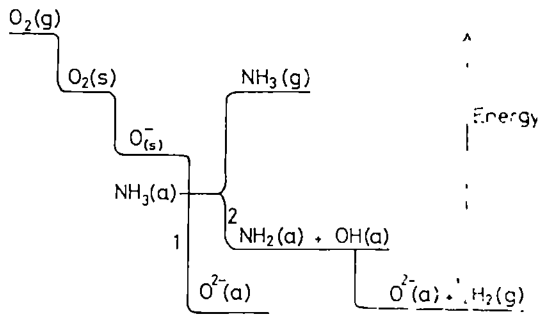

Fig. 2 Reaction scheme. Schematic representation of reaction pathways in the co-adsorption of 'oxygen' (N_2O, NO or O_2) and ammonia at 295 K; the ammonia diverts the 'oxygen' away from pathway 1(the oxide route) and along pathway 2 (the amide route) in spite of its very weak interaction with Mg(0001), ammonia desorbs at 170 K. Also an oxide overlayer, $O^{2-}(a)$, is, like bulk MgO, unreactive to ammonia under these conditions.

distinguish it from the more stable $O^-(a)$ and $O^{2-}(a)$ species for which direct XPS evidences is available,

$$N_2O(g) \rightarrow N_2O(a) \rightarrow N_2(g) + O^-(s) \rightarrow O^{2-}(a)$$

Figure 1*c* shows the N(1s) and O(1s) spectra observed when N_2O and NH_3 co-adsorbed at 110 K at a Mg(0001) surface was warmed to 295 K. Ammonia is physically adsorbed at 110 K and characterized by a single N(1s) peak at a binding energy of 401.3 eV. The calculated[2,9] surface concentration is 0.4×10^{15} cm^{-2}. When this adlayer is exposed to $N_2O(g)$, the N(1s) peak develops a second component at 399.5 eV. This is assigned[9] to the $NH_2(a)$ species. The O(1s) spectrum indicates surface oxide, $O^{2-}(a)$, and hydroxyl species with binding energies of 530.5 and 533.0 eV, respectively. On increasing the temperature first to 170 and then to 295 K, ammonia desorbs and intensity is lost from the 533.0-eV component to the 530.5-eV peak. The steps involved are as follows

$$NH_3(g) \xrightarrow{110K} NH_3(a)$$

$$N_2O(g) \xrightarrow{110K} N_2(g) + O^-(s)$$

$$O^-(s) \xrightarrow{110K} O^{2-}(a)$$

$$O^-(s) + NH_3(a) \xrightarrow{110K} OH(a) + NH_2(a)$$

$$OH(a) \xrightarrow{>110K} O^{2-}(a) + \tfrac{1}{2}H_2(g)$$

There is, therefore, good experimental evidence that the oxygen species participating in the activation of ammonia is a transient, $O^-(s)$, formed during the oxidation of Mg(0001) by dioxygen, nitrous oxide and nitric oxide. We emphasize that the surface amide species $NH_2(a)$ are strongly chemisorbed and could not have been anticipated on the basis of the lack of reactivity of NH_3 with both atomically clean Mg(0001) and with the 'bulk' MgO. Oxygen is, therefore, both a promoter and a poison for the activation; in its thermodynamically stable oxide state $O^{2-}(a)$, it is unreactive. We can envisage ammonia as an 'interceptor' molecule in that it influences the particular reaction pathway chosen by the co-adsorbed system. It is the efficiency of the NH_3—$O^-(s)$ step, that is, the ability of the ammonia to re-route the 'oxygen' along pathway 2 and away from pathway 1, that is crucial. This step can only be properly understood when knowledge of the surface lifetime of $O^-(s)$ becomes available. There may be alternative methods of generating the active oxygen species (such as lasers and discharges) so that unlikely reaction pathways, with (relatively) unfavourable thermodynamics can compete successfully with routes which at first sight, that is, with no knowledge of the details of the molecular events involved, would be considered most probable.

There are also important analogies to be drawn between our results and those reported recently[10,11] by Lunsford's group and commented on by Thomas[12] where activation of the C—H bond in methane by oxygen led to the formation of methyl radicals and surface hydroxyls. This was observed at high temperature (500 °C) with lithium-doped MgO where the active oxygen species was suggested to be O^-(s). The NH_2 species generated by hydrogen abstraction from ammonia at low temperature (Fig. 1) are also free radicals but, rather than desorb, are rapidly chemisorbed at the 'free' magnesium sites. Depending on the precise conditions at the surface, they may react with other species (if the number of Mg^0 sites is limited), including each other, and desorb as hydrazine. By changing the 'oxygen'-to-ammonia ratio, evidence for this alternative possibility has been obtained[8]. Note that in Lunsford's work the addition of water vapour to the oxidant was beneficial[10]. We have established elsewhere[9,13,15] that water vapour can enhance the presence of surface defects such as O^-(a) and OH(a) and which we have suggested[9] accounts for some oxides such as NiO · OH exhibiting specific oxidation behaviour to organic molecules.

We thank SERC for support.

Received 19 August; accepted 4 November 1985.

1. Au, C. T. & Roberts, M. W. *Chem. phys. Lett.* **74,** 472-474 (1980).
2. Roberts, M. W. *Adv. Catalysis* **29,** 51-95 (1980).
3. Roberts, M. W. *Proc. Indian natn. Sci. Acad.* **51A,** 165-179 (1985).
4. Au, C. T. & Roberts, M. W. *Proc. R. Soc.* **A396,** 165-181 (1984).
5. Au, C. T. Carley, A. F. & Roberts, M. W. *Phil. Trans. R. Soc.* (in the press).
6. Tench, A. J. & Giles, D. *JCS Faraday Trans. I* **68,** 193-196; 197-201 (1972).
7. Coluccia, S. Garrone, E. & Borello, E. *JCS Faraday Trans. 1* **79,** 607-613 (1983).
8. Au, C. T. & Roberts, M. W. (in preparation).
9. Au, C. T., Carley, A. F. & Roberts, M. W. *Int. Rev. phys. Chem.* (in the press).
10. Driscoll, D. J., Martir, W., Wang, Ji-Xiang & Lunsford, J. H. *J. Am. chem. Soc.* **107,** 58-63 (1985).
11. Ito, T. & Lunsford, J. H. *Nature* **314,** 721-722 (1985).
12. Thomas, J. M. *Nature* **314,** 669-670 (1985).
13. Carley, A. F., Grubb, S. & Roberts, M. W. *JCS chem. Commun.* 459-460 (1984).
14. Moroney, L., Roberts, M. W. & Smart, R. *JCS Faraday Trans. I* **79,** 1769-1778 (1983).
15. Carley, A. F., Rassias, S. & Roberts, M. W. *Surface Sci.* **135,** 35-51 (1983).

A new method for measuring palaeomagnetic intensities

Mark Boyd

Department of Earth Sciences, University of Cambridge,
Madingley Road, Cambridge CB3 0EZ, UK

Because measurements of palaeomagnetic intensities (henceforth palaeointensities) are usually time-consuming and the success rate only poor, say, 30–50%, many palaeointensity values are based on as few as three experimental results. In an attempt to improve on this, a technique has been developed using automated equipment which is faster, and which can detect alteration of a sample during measurement, allowing the experiment to be terminated and another sample to be tried. The technique, described here, has been used on a collection of ancient bricks, and the results show the palaeofield at Cambridge (England) to have decreased from about 49 μT in AD 1511 to 42 μT in AD 1758, in good agreement with results using Shaw's method.

A SQUID (superconducting quantum interference device) magnetometer is used to measure the magnetic moment of a 4 mm diameter sample held at an elevated temperature within a compact non-magnetic oven that can be heated and cooled rapidly because of its low thermal capacity. Because the magnetometer is totally automated and the sample does not have to be repeatedly cooled to room temperature, as in the Thellier[1] and similar methods, palaeointensities can be obtained in 75 min; Shaw's method[2], by contrast, takes at least 140 min and the Thellier method can take anything from 3 h to several days.

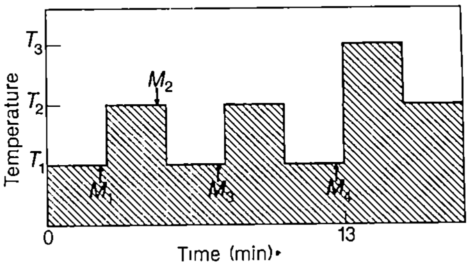

Fig. 1 Sequence of steps for one palaeointensity measurement typically a sample spends 130 s at equilibrium at each temperature.

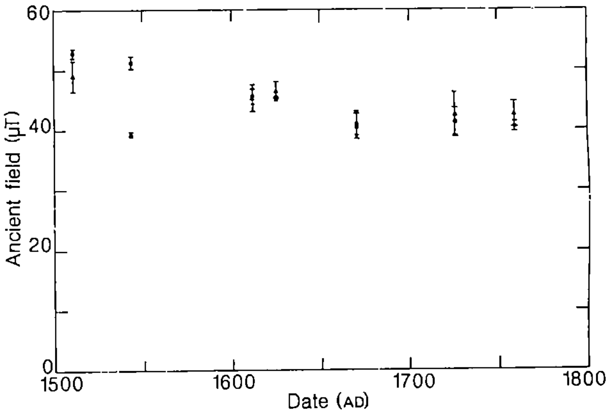

Fig. 2 Intensity of the geomagnetic field at Cambridge since AD 1500. ● Results from Shaw method; ▲, results from the present thermal method. Each point is the average result from three samples and the error bars one standard deviation. Only the AD 1543 bricks show significant disagreement.

The measurement sequence which allows the calculation of a palaeointensity (Fig. 1) begins by heating the sample to a base temperature T_1 and taking the first measurement of its magnetic moment M_1. Raising the temperature to T_2, a second measurement, M_2, is made before the sample is cooled back to the base temperature for the M_3 measurement, thermally demagnetizing the sample. At this point in the sequence, a magnetic field of known strength and direction is applied to the sample and maintained while the sample is again cycled to temperature T_2 and cooled to T_1, giving the sample a partial thermal remanent magnetization (PTRM). After removing the magnetic field the final measurement of the sequence M_4 is made.

This procedure effectively selects the magnetic grains which have blocking temperatures between T_1 and T_2. The natural remanent magnetization (NRM) preserved in this group of grains is the difference between M_1 and M_3 whereas the difference between M_4 and M_3 is the magnitude of the PTRM that these grains have acquired in the laboratory field. The ratio of these values combined with the laboratory field strength F_L gives the ancient field intensity, F_A

$$F_A = F_L \times \frac{M_1 - M_3}{M_4 - M_3}$$

To examine the grains with blocking temperatures between T_2 and T_3 the measurement cycle is repeated raising the base temperature to T_2. Because the M_2 measurement from the previous cycle is identical to M_1 for the present one, the initial measurement can be omitted from all subsequent cycles. Thus, six or seven cycles can be made before the Curie temperature of the sample is reached.

Although the sample quickly reaches thermal equilibrium after each heating and cooling phase, its magnetic moment is

Table 1 Two complete sets of experimental results

Temperature	M_1	M_3	M_4	M_2'	Ratio $\frac{M_1-M_3}{M_4-M_3}$	Alteration estimate $\frac{(M_2'-M_2)}{M_1-M_3}\times\frac{M_1}{M_2}$
No alteration						
110	11,546	10,918	11,669		0.84	-1.8
165	10,219	8,951	10,289	10,208	0.95	0.8
230	8,169	7,235	8,349	8,178	0.84	-1.2
310	6,348	5,202	6,434	6,337	0.93	1.3
375	4,356	3,252	4,554	4,369	0.85	3.0
440	2,502			2,528		
Alteration >7%						
110	3,922	3,658	4,013		0.74	6.6
165	3,459	3,308	3,671	3,476	0.42	20.4
230	3,137	3,054	3,337	3,166	0.29	0.4
310	2,829	2,672	3,039	2,830	0.43	30.9
375	2,413	2,195	2,612	2,457	0.52	−20.4
440	1,930			1,890		

The top set is from a sample which suffers no alteration. The ancient field intensities predicted at each temperature step are consistent. The lower set of results have values of >7% alteration effect, consequently this sample was rejected.

far from stable. Viscosity effects, the relaxation of grains with blocking temperatures higher than the sample temperature, mean that its magnetic moment is constantly changing. However, these viscous changes of moment can be allowed for and good results obtained provided. (1) each phase of the experiment, after the sample has reached a new thermal equilibrium, lasts the same length of time, typically 130 s; and (2) all measurements of the moment are taken at exactly the same length of time after thermal equilibrium is achieved. Usually the moment is averaged over the period 100-130 s.

Care must be taken that chemical or physical alteration of the magnetic carriers during measurement does not produce apparently acceptable, yet erroneous, results. This method provides several independent tests for such alteration. (1) The ratios obtained from each temperature step should be the same—this is equivalent to the linearity test used by the Thellier method. (2) Measurements of the samples' susceptibility are repeated at each base temperature which may show up any alteration. (3) The difference between M_2 and M_3 is caused by the increase in spontaneous magnetization of the oriented grains with blocking temperature above the temperature at which M_2 was taken. If an additional cooling step is included at the end of each cycle the saturation magnetization change can again be measured, checking for alteration that may occur during the heating phases between the two measurements. (4) A final heating step can be added to each cycle to repeat the M_2 measurement and monitor[3] any alteration that may occur during the cycle. This will not show any alteration that has occurred during heating immediately before M_2. However, it is unlikely that this alteration will have saturated; it will continue while the sample is held at this temperature. The repeat measurement M_2' should record the resultant change of moment which is expressed as a percentage of NRM lost in this single temperature cycle. Table 1 shows two sets of experimental data, the first sample did not suffer alteration but the second had to be discarded. An alteration effect of >7% is considered unacceptable.

Tests (3) and (4) show up alteration occurring only in the magnetic grains whose moment is actually contributing to the estimate of the ancient magnetic field. Alteration of the other magnetic grains is tolerable as they do not influence the ancient field estimate. Such alteration may be detected by conventional tests and cast unnecessary doubts on the results.

Four test samples were laboratory fired in a known field, using the above procedure in an attempt to recover the TRM field strength. The field strengths predicted ranged between +3.7 and −3.4% of the actual TRM field strength (Table 2).

Table 2 Results from four samples fired in a known magnetic field in the laboratory

Sample	TRM field (μT)	Field during experiment (μT)	Calculated cooling field (μT)	Age error (%)
1	67.56	61.93	67.32 ± 0.83	−0.4
2	33.78	39.41	32.63 ± 1.19	−3.4
2	33.78	33.78	33.68 ± 0.74	−0.3
3	36.60	33.78	35.60 ± 0.64	−2.7
4	59.38	53.73	61.60 ± 1.58	+3.7
4	50.86	48.03	52.35 ± 1.17	+2.9

The method has recovered these fields to within an average of 2%

To test this method, it was used on a collection of dated bricks taken from Colleges in the Cambridge area. These samples were also measured in the Cardiff laboratory[4] using the modified Shaw method[5]. Figure 2 shows that, except for one brick both sets of results were in good agreement. The average error between the two sets is 3.4%, four results being higher with the thermal method and two lower. These indicate that the geomagnetic field intensity at Cambridge has decreased smoothly from ~49 μT in AD 1511 to 42 μT in AD 1758. The original brick collection contained samples dated up to 1979, but all the bricks younger than 1758 exhibited unacceptable alteration and produced no results.

The major advantage of the thermal palaeointensity method described here is that its speed allows more samples to be measured so that the high failure rate, common to all thermal methods, becomes more tolerable. More results allow more accurate determinations of the ancient field. In addition, this experimental procedure automatically gives information on the spontaneous magnetization curve of the sample and a measurement of its d.c. susceptibility at each base temperature. This information in surplus to that required to produce an estimate of the ancient magnetic field but may give an indication of the magnetic carriers present in the sample.

This work was funded by N.E.R.C. grant GR3/4670 and the Northern Ireland Education Board.

Received 5 August; accepted 30 October 1985.

1. Thellier, E. & Thellier, O. *Annls Geophys.* **15,** 285-376 (1959).
2. Shaw, J. *J. Geophys. J.R. astr. Soc.* **39,** 133-144 (1974).
3. Walton, D. *Nature* **310,** 740-743 (1984).
4. Shaw, J., Share, J. A. & Rogers, *J. Geophys. J.R. astr. Soc.* **78,** 209-217 (1984).
5. Rolph, T. C. & Shaw, *J. Geophys. J.R. astr. Soc.* **80,** 773-781 (1985).

Seismic reflection imaging of the subducting Juan de Fuca plate

A. G. Green*, R. M. Clowes†, C. J. Yorath‡, C. Spencer*, E. R. Kanasewich§, M. T. Brandon‡ & A. Sutherland Brown‡

* Division of Seismology and Geomagnetism, Department of Energy, Mines and Resources, 1 Observatory Crescent, Ottawa, Ontario, Canada K1A 0Y3
† Department of Geophysics and Astronomy, University of British Columbia, Vancouver, British Columbia, Canada V6T 1W5
‡ Pacific Geoscience Centre, Department of Energy, Mines and Resources, Sidney, British Columbia, Canada V8L 4B2
§ Department of Physics, University of Alberta, Edmonton, Alberta, Canada T6G 2E1

McKenzie and Parker's early suggestion[1] that the Juan de Fuca plate is underthrusting North America has since been confirmed by numerous studies. Evidence for plate convergence along this junction includes: a sediment-filled trench[2–7], intense compressional deformation of the continental slope and shelf sediments[2–7], seafloor magnetic anomalies that extend beneath the continental slope[2,4], inland andesitic volcanoes[8], paired low/high heat flow and gravity anomalies[9,10], active onshore deformation[11,12], onshore crustal earthquakes with compressional axes parallel to the direction of plate convergence[13], sinistral strike-slip earthquakes along the Nootka Fault (Fig. 1)[14], and a well-defined Benioff–Wadati zone[6,15,16]. Here we report the results of a seismic reflection survey that has delineated two slabs of oceanic lithosphere underlying Vancouver Island, one that is currently being subducted and one that is underplated. These findings lead us to speculate that successive underplating of oceanic lithosphere may be an important process in the evolution and growth of continents.

A total of 205 km of deep seismic reflection data have been collected along the four profiles shown in the simplified geological map of southeastern Vancouver Island (Fig. 1). The VISP1 line crosses the width of the island and is almost coincident with one of the gravity profiles studied by Riddihough[10] and with the combined onshore/offshore seismic refraction line of Spence *et al.*[17]. Some three-dimensional control on the interpretation of VISP1 is available from the VISP3 line located 15–20 km to the east and from a short test line described by Clowes *et al.*[18]. The two southeasterly lines, VISP2 and VISP4, were designed to determine the attitudes and significance of the San Juan, Survey Mountain and Leech River faults.

Line drawings of the reflections are shown in Fig. 2 and a typical example of the data, with an accompanying simplified interpretation, is shown in Fig. 3. Two very prominent reflection zones, C and E in Figs 2 and 3, are observed on all seismic sections. They underlie most of southeastern Vancouver Island including the youngest allochthonous terrains along the southeastern tip of the island. Both reflection zones dip to the north-east, parallel to the direction of convergence between the Juan de Fuca and North American plates (Fig. 1).

Reflection zone E probably originates from the boundary region between the descending Juan de Fuca plate and the overriding North American plate. It lies at a depth of only ~23 km beneath the southern end of VISP1, based on migrated travel-times and velocities from Spence *et al.*'s[17] seismic refraction model, and is deepest at ~34 km beneath the north-central region of the island. Its overall dip in the vicinity of VISP1 is to the north-east at an angle of 9–13°. From Fig. 2, the average

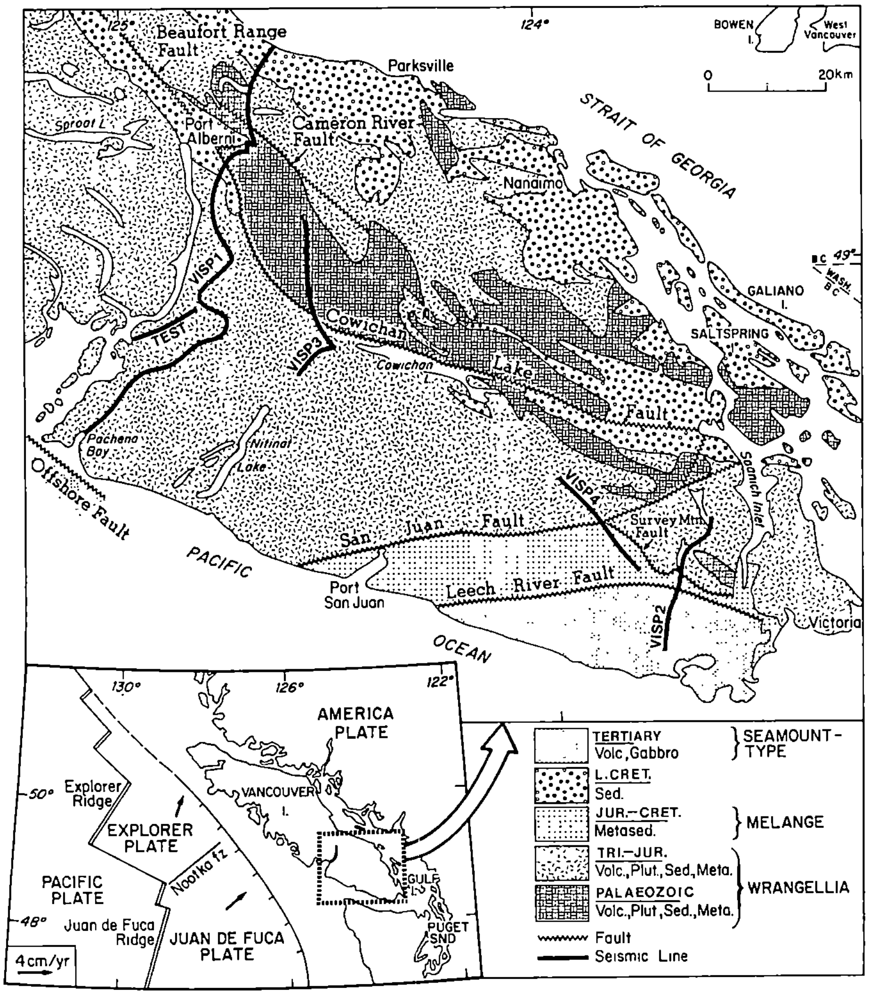
125°
Beaufort Range Fault
124°
Parksville
Sproat L.
Port Alberni
Cameron River Fault
STRAIT OF GEORGIA
Nanaimo
BOWEN I.
West Vancouver
0
20km
49°
BC
WASH.
GALIANO I.
SALTSPRING
VISP1
TEST
VISP3
Cowichan Lake
Cowichan Lake Fault
Pachena Bay
Nitinat Lake
Offshore Fault
San Juan Fault
Survey Mtn Fault
VISP4
Saanich Inlet
Leech River Fault
Port San Juan
PACIFIC OCEAN
VISP2
Victoria
130°
126°
122°
AMERICA PLATE
50°
Explorer Ridge
EXPLORER PLATE
VANCOUVER I.
PACIFIC PLATE
Nootka f.z.
48°
Juan de Fuca Ridge
JUAN DE FUCA PLATE
GULF I.S
PUGET SND
4cm/yr
TERTIARY Volc, Gabbro
SEAMOUNT-TYPE
L.CRET. Sed.
JUR.–CRET. Metased.
MELANGE
TRI.–JUR. Volc., Plut., Sed., Meta.
PALAEOZOIC Volc., Plut, Sed., Meta.
WRANGELLIA
Fault
Seismic Line

Fig. 1 Simplified geological map of southeastern Vancouver Island showing the locations of the four seismic reflection profiles, VISP1 to VISP4, and the short seismic reflection profile, TEST, of Clowes *et al.*[18]. Geology is mostly from Muller[44], with minor modifications based on recent mapping programmes. The region to the north of the San Juan Fault is part of the exotic Wrangellia terrain of Palaeozoic and Mesozoic age. Between the San Juan and Leech River faults is an allochthonous mélange of Mesozoic metasediments and to the south of the Leech River Fault lies a volcanic terrain that may have been part of a Cenozoic seamount chain. The inset shows the location of the geological map with respect to the major plate boundaries.

depth to zone E is shown to be somewhat less than the depth to the active subduction zone of the seismic refraction model. However, Spence *et al.*[17] have demonstrated that the depth and structure of the subducting plate beneath Vancouver Island are only weakly constrained by the onshore/offshore seismic data. The location and attitude of zone E match well Riddihough's[10] estimates for the top of the subduction zone based on a variety of seismic and gravity data, and the northeasterly dip of 9-13° is in excellent accord with the $\sim$9° value obtained from an onshore/offshore seismic refraction study of the Washington continental margin[19] and the 11-15° dip of the Benioff-Wadati zone below southern Vancouver Island, Puget Sound and western Washington[6,15,16]. The shallow dip estimates are also consistent with the pattern of recent onshore deformation in this region[11] and with teleseismic waveforms recorded at seismographic stations on Vancouver Island and in western Oregon[20].

Towards the northern end of VISP1 there is some evidence for an increase in the dip of reflection zone E (Fig. 2). It is near to this location that the subducting plate in Riddihough's density models[10] begins to plunge more steeply into the mantle. Such a feature is common in other subduction zones[21] and is generally consistent with the steeply dipping slab of high-velocity material required to explain the pattern of travel-time anomalies to the north-east of Puget Sound[22]. The apparent absence of the deepest reflections beneath the northernmost region of VISP1 has at least two possible explanations. This part of the profile traverses the nose of a NW-SE-trending anticlinal ridge that exposes the oldest rocks on the island before crossing an escarpment onto a late Cretaceous sedimentary basin (Fig. 1), so the absence of deep reflections here may be related to geological and topographic complexities. Alternatively, if the dip of the subducting plate increases to a value in excess of $\sim$45°, as shown in some of Riddihough's density models[10] and as required by McKenzie and Julian's travel-time analysis[22], the relatively conventional data processing that we have applied would have effectively filtered out any reflections from this zone.

Figure 4 shows a contour map of two-way travel-times to the top of reflection zone E. Particularly noteworthy is the structure that is required to explain the variations in depth and attitude of the reflection zone between the western pair of seismic profiles (1 and 3) and the eastern pair (2 and 4). Of course, the dashed parts of the contour diagram are speculative; a major fault anywhere between the two pairs of profiles would allow an equally valid interpretation of existing data. Warping and frac-

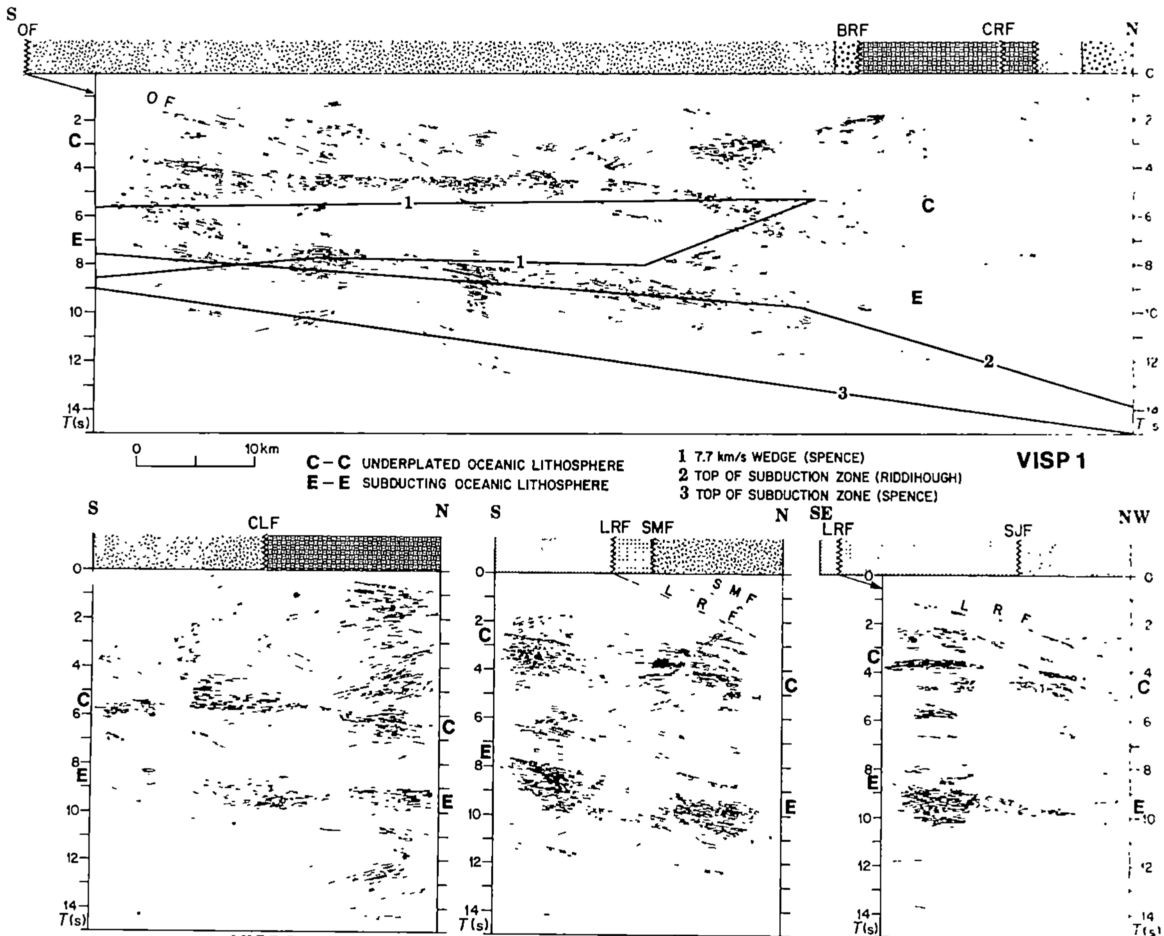
S
OF
BRF
CRF
N
C
E
1
2
3
T(s)
0
10km
C–C UNDERPLATED OCEANIC LITHOSPHERE
E–E SUBDUCTING OCEANIC LITHOSPHERE
1 7.7 km/s WEDGE (SPENCE)
2 TOP OF SUBDUCTION ZONE (RIDDIHOUGH)
3 TOP OF SUBDUCTION ZONE (SPENCE)
VISP 1
CLF
LRF
SMF
SE
SJF
NW
VISP3
VISP2
VISP4

Fig. 2 Line drawings showing the unmigrated reflections recorded on the four seismic reflection profiles. Vertical scale is two-way travel-time in seconds (T). All lines were recorded to 16 s with 30-fold coverage. Acquisition methods were similar to those used in the US by the COCORP group[45]. Final processing included single-fold trace editing, crooked line geometry and elevation corrections, automatic gain control, normal move-out corrections, trim statics using a correlation window of $T = 1$-12 s, common reflection point stacking, bandpass filtering of 8-40 Hz and trace-to-trace amplitude equalization using a $T = 4$-8 s window. Patterns at the top of each section show the surface geology crossed; an explanation of the various patterns is given in Fig. 1. On the VISP1 section the -1- border delineates the high-velocity (7.7 km s^{-1}), high-density (3.3 g ml^{-1}) block proposed by Spence *et al.*[17], and the -2- and -3- boundaries show, respectively, the Riddihough[10] and Spence *et al.*[17] estimates for the top of the actively subducting Juan de Fuca plate. C-C and E-E are prominent reflection zones that delineate the upper boundary of the high-velocity, high-density block (the underplated oceanic lithosphere) and the top of the actively subducting Juan de Fuca plate respectively. OF, Offshore (or Tofino[46]) Fault; BRF, Beaufort Range Fault; CRF, Cameron River Fault; CLF, Cowichan Lake Fault; LRF, Leech River Fault; SMF, Survey Mountain Fault; SJF, San Juan Fault (locations of faults are shown in Fig. 1). A typical example of the seismic reflection data is shown in Fig. 3.

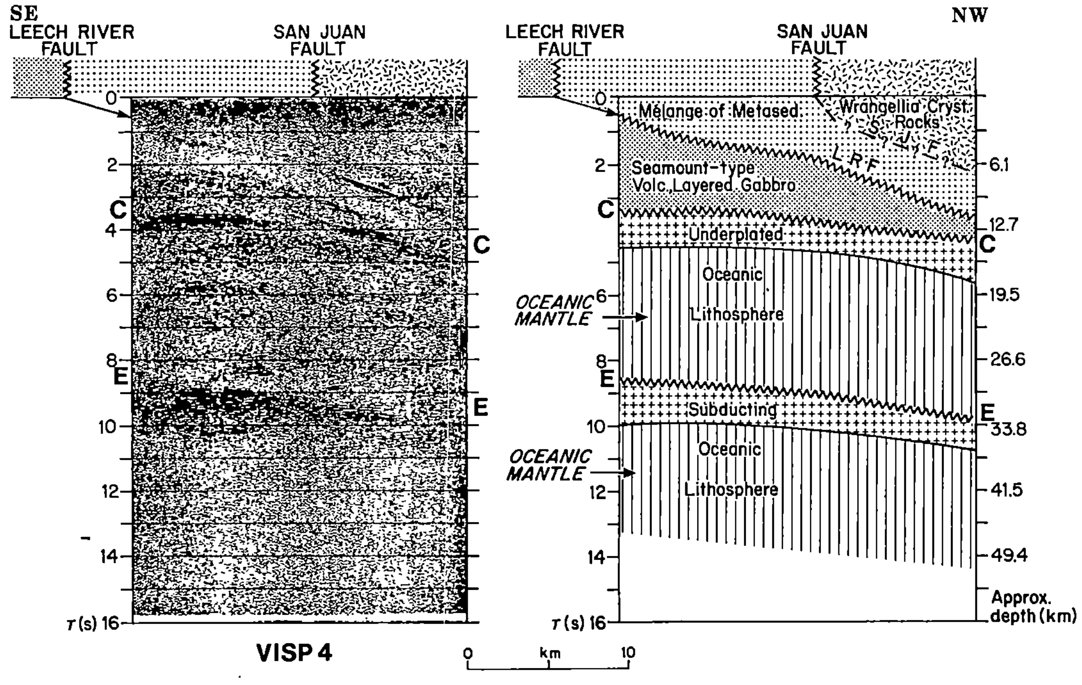

Fig. 3 A typical unmigrated seismic reflection section and simplified interpretation obtained from data recorded on Vancouver Island. Figure 1 shows the location of the profile and Fig. 2 (bottom right) shows a line diagram of the individual reflections recorded on the section. Patterns at the top of both the section and the interpretation diagram show the surface geology; an explanation of the various patterns is given in Fig. 1. The regions of + signs correspond to the reflection zones C and E. Approximate depths shown are based on the seismic refraction model of Spence *et al.*[17]. The seismic reflection data were recorded by Veritas Geophysical Ltd and processed by Veritas Seismic Ltd.

turing of the subducting plate in this general region have been predicted by Rogers[15] and by Keen and Hyndman[9] on the basis of seismicity patterns, fault plane solutions and the geometry of the Juan de Fuca–North American plate interactions. Some relatively deep strike-slip earthquakes in western Washington suggest that intra-plate faulting or segmentation may be a common feature of the downgoing Juan de Fuca plate[16].

The nature of the E reflection zone requires some discussion. On the migrated sections it is 3–5 km thick (1–1.5 s two-way travel-time) and has a strongly laminated character that could result from layered sediments, intercalated volcanics and sediments, layered igneous rocks or tectonic structures induced by underthrusting. Undeformed sediments are known to have been subducted to considerable depths beneath the forearc basins of several island arcs, including those of Japan[23,24], the Aleutians[25,26] and the Caribbean[27,28]. However, in the general region of Vancouver Island there are numerous single- and multi-fold seismic reflection profiles which show that the majority of sediments have been scraped off the descending oceanic plate to form the accretionary wedge that now constitutes the continental margin[2–7]. Reflection zone E is therefore unlikely to have originated from a simple stack of sedimentary layers riding on top of the descending oceanic plate. Nevertheless, it is feasible that the lowermost layers of lithified sediments have been taken down into the subduction zone and that these sediments and possibly the upper crystalline layers have been transferred or underplated to the base of the overriding plate. Successive underplating of this type would result in the formation of a thick layered sequence between the descending Juan de Fuca slab and the overriding North American plate. This particular process of accretion, termed subcretion by Karig and Kay[29], has been invoked by Von Heune[25] to explain some multi-fold seismic reflection data collected across the Aleutian trench and forearc basin.

Episodic and rapid sedimentation from the North American continent[2–7], combined with episodic volcanism involving extensive lava flows from the nearby oceanic spreading centres[30], have probably resulted in the widespread interlayering of oceanic basalts and sediments on the Juan de Fuca plate. Comprehensive studies across the northern parts of the Explorer plate (Fig. 1) and adjacent ridge segments have revealed ubiquitous interfingering of basaltic lavas and turbidites[3,30–33], and similar features are shown on the generalized geological cross-section of the central Oregon continental margin[34].

Based on the results of multi-fold seismic reflection surveys, high-quality seismic refraction surveys and deep-sea drilling, Talwani *et al.*[27] have proposed that interlayered extrusive and intrusive (mostly sills) rocks are the source of some laterally extensive reflections from within the acoustic basement of the small Caribbean plate. As similar lava flows and sills are expected to occur in the upper regions of the Juan de Fuca plate, some of the reflections in the E zone, particularly those near to the base of the zone, could have originated from structures within the descending oceanic crust.

Finally, at some subduction zones, notably those off the coasts of Java and Ecuador[24], there is a hint that layered reflections along the boundary of the descending plate only become pronounced landward of the trench. Layering of this nature could either be produced by the selective slicing away of sedimentary rocks from the underside of the accretionary wedge or it could result from brittle and/or ductile deformation induced by the relative motion between the two plates.

We interpret the region between reflection zones C and E as a tectonically underplated slab of older oceanic lithosphere, which was accreted to the base of Vancouver Island after the westward jump in the locus of subduction in Eocene times[35,36]. As shown in Fig. 2, our interpretation is supported by the gravity and seismic refraction models which require high-density (3.3 g ml^{-1}) and high-velocity (7.7 km s^{-1}) mantle-type material and velocity discontinuities at the appropriate shallow depths. The upper boundary of the high-velocity material at ~18 km depth is well-delineated from interpretations of the combined onshore/offshore seismic refraction line[17] and an intersecting refraction line that was recorded along the length of the island[37], so its coincidence with the base of reflection zone C is significant. On the seismic reflection lines the thickness of the interval between zones C and E varies from 9 to 18 km, which is comparable to the 17–20 km range that Spence *et al.*[17] derived for the thickness of the high-velocity mantle material in the descending Juan de Fuca plate.

Reflection zone C is strikingly similar to reflection zone E. It has a similar laminated character, an average thickness of 3–5 km and an overall dip to the north-east of 5–8°. It seems to have acted as a decollement zone to a number of major northeasterly-dipping structures, most of which can be projected to the surface where they coincide with mapped faults or plutonic contacts.

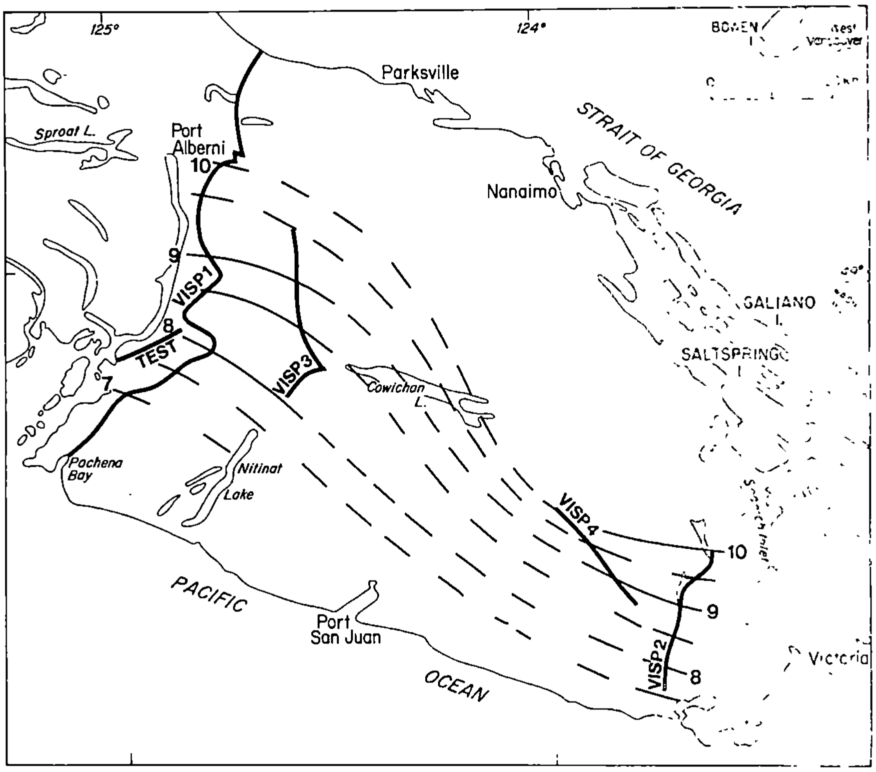

Fig. 4 Contours are two-way travel-times (unmigrated) (in s) to the top of reflection zone E. The curvature of the dashed contours between the western pair of seismic profiles (VISP1 and VISP3) and the eastern pair (VISP2 and VISP4) is speculative; a major fault anywhere between the two pairs of profiles would be an equally valid interpretation of the travel-time information.

Relative motion during the waning stages of this earlier phase of plate convergence would have occurred along these moderately dipping structures and along the decollement zone. A necessary consequence of our tectonic model is the removal of the lower lithosphere of the overriding plate during Eocene and earlier times.

It seems to us that under favourable but frequently occurring conditions, tectonic underplating of oceanic lithosphere at the base of convergent margins is a rapid means of adding large volumes of material to terrains that eventually become continental. This process is capable of creating root zones beneath the mountain ranges of active continental margins and of substantially increasing the crustal thicknesses of island arc-trench systems. In addition to our Vancouver Island example, thin slabs of underplated oceanic lithosphere have been proposed to underlie parts of Java[38], the Aleutians[25] and southern Alaska[39]. The underplated oceanic lithosphere would generally be of higher density, higher velocity and more basic than the overlying material. Across such terrains now interior to the continents, seismic refraction methods would resolve a broad-scale subhorizontal layering of the crust (including zones of high and low velocity), whereas seismic reflection techniques would see the pronounced reflection zones. Although many regions do not reveal such a simple image of the continental crust, a two- to four-layered crustal section with laminated reflections in the mid- to lower regions is a common feature on most continents[40]. Of course, we do not claim that underplating is the only or the dominant means of crustal thickening, but it is an important process that requires further investigation. In particular, the new mechanism could help to explain the anomalously high continental growth rates obtained for Precambrian shields[41,42]. Tectonic processes in Archaean times were probably dominated by the rapid movements of small, short-lived oceanic plates[41,43] and, like the present situation along the west coast of North America, subduction of the young and buoyant oceanic lithosphere would have occurred at relatively shallow angles.

We thank Drs J. Adams, M. Berry and R. Kurtz for critical reviews of the first draft of this manuscript and Dr E. Irving for pointing out the significance of Reymer and Schubert's work. This work was conducted as part of the LITHOPROBE program to study the three-dimensional structure of key geological targets on the Canadian landmass and adjacent offshore margins. We are grateful to Veritas Geophysical Ltd and Veritas Seismic Ltd for collecting and processing our data. This is LITHOPROBE paper 7; Earth Physics Branch contribution 1202.

Received 5 July; accepted 21 October 1985

1. McKenzie, D. P. & Parker, R. L. *Nature* **216**, 1276-1280 (1967)
2. Silver, E. A. *Mar. Geol.* **13**, 239-249 (1972).
3. Tiffin, D. L., Cameron, B. E. B. & Murray, J. W. *Can. J. Earth Sci.* **9**, 280-296 (1972)
4. Barr, S. M. *Can. J. Earth Sci.* **11**, 1187-1199 (1974).
5. Ellis, R. M. *et al. Can. J. Earth Sci.* **20**, 719-741 (1983).
6. Kulm, L. D. *et al. Atlas 1 Ocean Margin Drilling Program* (Marine Science International Regional Atlas Ser., 1984).
7. Clowes, R. M. *et al. J. Can. Soc. exp. Geophys.* **20**, 23-39 (1984)
8. Dickinson, W. R. *Rev. Geophys.* **8**, 813-860 (1970).
9. Keen, C. E. & Hyndman, R. D. *Can. J. Earth Sci.* **16**, 712-747 (1979)
10. Riddihough, R. P. *Can. J. Earth Sci.* **16**, 350-361 (1979).
11. Savage, J. C., Lisowski, M. & Prescott, W. H. *J. geophys. Res.* **86**, 4929-4940 (1981)
12. Adams, J. *Tectonics* **3**, 449-472 (1984).
13. Weaver, C. S. & Smith, S. W. *J. geophys. Res.* **88**, 10371-10383 (1983)
14. Rogers, G. C. *Can. J. Earth Sci.* **16**, 523-531 (1979).
15. Rogers, G. C. *U.S. geol. Surv. Open File Rep.* **83-19**, 19-39 (1983)
16. Taber, J. J. & Smith S. W. *Bull. seism. Soc. Am.* **75**, 237-249 (1985)
17. Spence, G. D., Clowes, R. M. & Ellis, R. M. *J. geophys. Res.* **90**, 6754-6772 (1985)
18. Clowes, R. M. *et al. Nature* **303**, 668-670 (1983).
19. Taber, J. J. thesis, Univ. Washington, Seattle (1983).
20. Langston, C. A. *J. geophys. Res.* **86**, 3857-3866 (1981).
21. Pennington, W. D. *Science* **220**, 1045-1047 (1983).
22. McKenzie, D. P. & Julian, B. *Bull. geol. Soc. Am.* **82**, 3519-3524 (1971)
23. Aoki, Y., Tamano, T. & Kato, S. *Mem. Am. Ass. Petrol. Geologists* **34**, 309-322 (1982)
24. Lehner, P. *et al. Am. Ass. Petrol. geol. Stud. Geol. Ser. 15* Vol. 3, 3.4.2 1-3.4.2 12 (1983)
25. Von Heune, R. *Mem. Am. Ass. Petrol. Geologists* **29**, 261-272 (1979)
26. Von Heune, R. *et al. Am. Ass. Petrol. Geol. Stud. Geol. Ser. 15* Vol 3, 3.4.2 135-3.4.2 139 (1983).
27. Talwani, M. *et al. Am. Geophys. Un., M. Ewing Ser.* **1**, 83-98 (1977)
28. Westbrook, G. K. *et al. Nature* **300**, 625-628 (1982).
29. Karig, D. E. & Kay, R. W. *Phil. Trans. R. Soc.* **A303**, 233-251 (1981).
30. Davis, E. E. *Bull. geol. Soc. Am.* **93**, 1023-1029 (1982).
31. Clowes, R. N. & Knize, S. *Can. J. Earth Sci.* **16**, 1265-1280 (1979)
32. Riddihough, R. P., Currie, R. G. & Hyndman, R. D. *Can. J. Earth Sci.* **17**, 577-593 (1980)
33. Davis, E. E. & Riddihough, R. P. *Can. J. Earth Sci.* **19**, 767-788 (1982)
34. Snavely, P. D., Wagner, H. C. & Lander, D. L. *Bull. geol. Soc. Am.* **91**, 143-146 (1980)
35. Dickinson, W. R. *Can. J. Earth Sci.* **13**, 1268-1287 (1976).
36. Muller, J. F. *Can. J. Earth Sci.* **9**, 2062-2085 (1977).
37. McMechan, G. A. & Spence, G. D. *Can. J. Earth Sci.* **20**, 742-752 (1983)
38. Hamilton, W. *U.S. Geol. Surv. Prof. Pap.* 1078 (1979).
39. Ambos, E. L. *et al. EOS* **66**, 301 (1985).
40. Oliver, J. E., Cook, F. & Brown, L. *J. geophys. Res.* **88**, 3329-3347 (1983)
41. Dewey, J. F. & Windley, B. F. *Phil. Trans. R. Soc.* **A303**, 189-206 (1981)
42. Reymer, A. & Schubert, G. *Tectonics* **3**, 63-77 (1984).
43. Abbot, D. H. & Hoffman, S. E. *Tectonics* **3**, 429-448 (1984)
44. Muller, J. E. *Geol. Surv. Can. Open File Map* 463 (1977).
45. Schilt, S. *et al. Rev. Geophys. Space Phys.* **17**, 354-368 (1979).
46. Brandon, M. T. *Geol. Soc. Am. Cord. Sect. Mtg*, Vancouver, BC, 7.1-7.2 8 (1985).

Thermal expansion of silicate perovskite and stratification of the Earth's mantle

Elise Knittle*, Raymond Jeanloz* & Gordon L. Smith†

* Department of Geology and Geophysics, University of California, Berkeley, California 94720, USA
† Lawrence Livermore National Laboratory, Livermore, California 94550, USA

A pressure of 24 GPa and temperatures of about 2,000–3,000 K correspond to the observed 670-km seismic discontinuity which separates the upper and lower mantle. In such conditions the major minerals of the Earth's upper mantle, olivine ((Mg, Fe)$_2$SiO$_4$), pyroxene ((Mg, Fe)SiO$_3$) and garnet ((Mg, Fe, Ca)$_3$Al$_2$Si$_3$O$_{12}$) transform to a distorted (orthorhombic) perovskite-structured mineral ((Mg, Fe)SiO$_3$), or to a perovskite-dominated assemblage (refs 1–4). Because silicate perovskite is stable to at least 70 GPa, it is thought to be the most abundant mineral in the lower mantle and, possibly, in the entire Earth. Despite its importance, silicate perovskite was only discovered in 1976, and little is known about its physical properties because of the difficulty in achieving the conditions of pressure and temperature required for the synthesis of this phase. For example, the value of the thermal expansion coefficient of perovskite provides an important constraint on possible compositional models for the lower mantle[5–7]. We have recently produced sufficient amounts of (Mg$_{0.9}$, Fe$_{0.1}$)SiO$_3$ perovskite to measure its zero-pressure thermal expansion to 840 K by X-ray diffraction. At high temperatures, the average thermal expansion coefficient is 4×10^{-5} K^{-1}. Such a large value for the thermal expansion coefficient implies that standard models of upper mantle composition, such as pyrolite or garnet peridotite (Mg value ≈ 0.89), yield zero-pressure densities that are about 2% lower than that of the density of the lower mantle extrapolated to zero pressure conditions. This result suggests that the upper and lower mantle are chemically distinct, in accord with layered models of the thermal and convective state of the mantle.

We have measured the thermal expansion coefficient of (Mg$_{0.9}$, Fe$_{0.1}$)SiO$_3$ perovskite using a high-temperature Guinier X-ray diffraction camera, and diffraction patterns at room and higher temperature were collected on film. The perovskite was synthesized from a natural orthopyroxene ((Mg$_{0.88}$, Fe$_{0.12}$)SiO$_3$) above 35 GPa (350 kbar) and 2,000 K using laser heating through a Mao-Bell type diamond-anvil cell[8]. No pressure medium was used in the synthesis, and no ruby was used for pressure calibration, to prevent contamination of the perovskite. The sample pressure for the synthesis runs was determined from the force applied to the diamonds, which was independently calibrated as a function of pressure by the ruby fluorescence technique[9,10]. Lattice parameters of the quenched perovskite at ambient conditions were determined from the (002), (110), (111), (020), (112), (200), (210) and (211) diffraction lines, and gave lattice parameters of $a=478.3$ (±0.7) pm, $b=495.3$ (±0.8) pm, $c=688.6$ (±0.7) pm and a density $\rho=4.216$ (±0.004) Mg m^{-3}, in good agreement with previous results[11–13]. The high-temperature experiments were performed on quenched perovskite samples at zero pressure to temperatures exceeding 900 K (630 °C). Each high-temperature run required 35–50 diamond cell samples, which were loaded into a 200-μm fused-quartz capillary tube. NaCl was mixed with the perovskite to act as a temperature calibrant. At high temperatures, the lattice parameters and, therefore, the high-temperature volumes were determined from the (110), (020), (112), (200) and (211) diffraction lines. The perovskite, which is metastable at room temperature and pressure, reverted to enstatite between 840 and 875 K (567–602 °C) as evidenced from a rapid change in the X-ray diffraction pattern between these temperatures. Figure 1 shows the increase in volume (decrease in density) with temperature for perovskite at zero pressure. The b/a and c/a lattice-parameter ratios of the perovskite remained constant within the error bars to 840 K indicating no further distortion in the perovskite structure at high temperature. Similarly, Yagi *et al.*[14] found no conclusive evidence for a change in structural disrtortion with hydrostatic pressure to 8.4 GPa. From these two lines of evidence, we conclude that silicate perovskite does not undergo significant distortion from its zero-pressure orthorhombic structure at high pressure and temperature. Therefore, the physical properties of the quenched perovskite measured in the laboratory are relevant to silicate perovskite which exists at high pressure and temperature in the Earth's mantle.

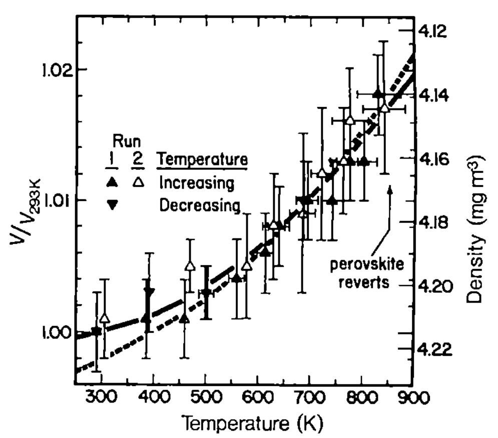

Fig. 1 The volume expansion of (Mg$_{0.9}$Fe$_{0.1}$)SiO$_3$ perovskite at zero pressure as measured by X-ray diffraction from room temperature to 840 K. Above 840 K the high-pressure perovskite structure reverts to the low-pressure structure of orthopyroxene. The curves through the data represent two fits to the measurements using the Suzuki formalism for Gruneisen's theory of thermal expansion. The solid line is the best fit to all of the data and is used to obtain the thermal expansion coefficient from 0 to 2,500 K. The dashed line is a fit to the high-temperature data only. Note that in the high-temperature region, between 450 and 850 K, the volume increases by 1.6%, which corresponds to an average thermal expansion coefficient of 4×10^{-5} K^{-1}.

Because the thermal expansion of perovskite cannot be measured above 840 K at zero pressure, our data must be extrapolated to temperatures for the Earth's mantle. We calculated the high-temperature thermal expansion coefficients using Gruneisen's theory of thermal expansion as formulated by Suzuki *et al.*[15,16]. In this procedure, we fit the measured data to obtain values for the Gruneisen parameter γ, the Debye temperature θ, the pressure derivative of the bulk modulus K_0' and the zero-temperature molar volume for perovskite (Table 1). Two acceptable fits to the data were obtained as indicated in Fig. 1.

Comparison of the high-temperature, zero-pressure perovskite densities can be made with the density and temperature of the decompressed lower mantle. Based on seismic observations, the bulk of the lower mantle appears to be homogeneous and adiabatic[17–19], and an Eulerian finite strain formalism can be used to extrapolate the density of the lower mantle adiabatically to zero-pressure, high-temperature conditions as was first done by Birch[19–22]. These calculations give a decompressed value of 4.00±0.01 Mg m^{-3} for the zero-pressure, high-temperature density of the high-pressure mineral assemblage comprising the lower mantle.

The temperature of the lower mantle on adiabatic decompression is uncertain. However, an estimated lower bound for this temperature, 1,700 (±250) K (~1,400 °C), is based on the phase equilibria of the olivine-spinel phase transitions which are thought to occur at 400 km depth[20,23–25]. If the mantle is stratified and the 670-km discontinuity is a thermal as well as a chemical boundary layer, the zero-pressure temperature of the lower mantle adiabat may exceed 2,000 K (ref. 25).

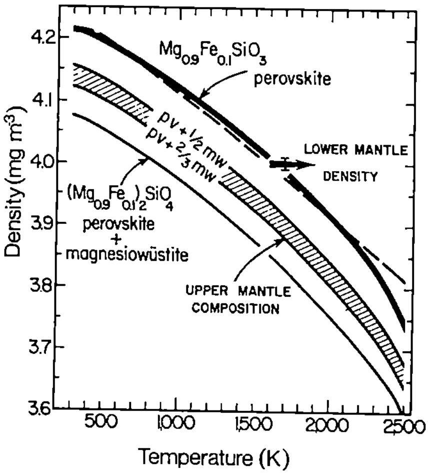

Fig. 2 Densities of proposed lower mantle assemblages (curves) are compared with the adiabatically decompressed values of density and temperature for the lower mantle (bold arrow). The zero-pressure value of the lower mantle density is well constrained (4.00±0.01 Mg m^{-3}), but only a minimum value for the lower mantle adiabat (zero-pressure temperature of 1,700 K) is known with confidence: the bold arrow illustrates that higher temperatures are possible. The zero-pressure density of (Mg, Fe)SiO$_3$ perovskite was extrapolated to high temperatures using the thermal expansion coefficient measured in this study (the solid and dashed bold curves correspond to the best fit and the high-temperature fit, respectively, shown in Fig. 1). A mineralogical model that satisfies the observed lower-mantle density consists of (Mg, Fe)SiO$_3$ pyroxene alone, in its high pressure perovskite phase. Lower-mantle assemblages consistent with a uniform mantle composition are indicated by the shaded band labelled 'upper mantle composition' (bounded by compositions between 1:1 and 2:1 olivine:pyroxene ratios, with pv and mw referring to perovskite and magnesiowüstite phases). All the models are based on $X_{Mg}=0.89$ (refs 27, 28) and the measured pv-mw partition coefficients[29,30]. None of the proposed upper mantle compositions or olivine alone (1:1 pv:mw) satisfy the observed lower mantle density at the appropriate conditions.

Table 1 Thermal expansion parameters for (Mg, Fe)SiO$_3$ perovskite

	γ	Θ(K)	K_0'	Molar volume at 0 K (V(0 K), cm^3 mol^{-1})
Best fit	1.77	525	7	24.46
High-temperature fit	2.20	825	4	24.39

Equation for volume at temperature T (see refs 15, 16):

$$V(T)=\frac{V(0\,\text{K})}{2k}\left[1+2k-((1-4kE)/Q)^{1/2}\right]$$

where $k=(K_0-1)/2$; $E(T,\Theta)=45\,RT(T/\Theta)^3\int_0^{\Theta/T} z^3/(e^z-1)\,dz$, $Q=K_0V(0\,\text{K})/\gamma$; $K_0=260(\pm 20)$ GPa (ref. 14).

Figure 2 shows the effect of temperature on the densities of perovskite (pv) and several perovskite-magnesiowüstite (pv-mw) assemblages compared at zero pressure with the density and temperature inferred for the lower mantle. The thermal expansion of perovskite is extrapolated to high temperatures using the data summarized in Table 1, whereas that of magnesiowüstite has been measured to 1,300 K (the mean thermal expansion coefficient from 300 to 1,300 K is 4.8×10^{-5} K^{-1})[15,26]. The region labelled upper mantle composition on Fig. 2 is bounded by the high-pressure phases which would result from a composition of olivine:pyroxene ratio between 1:1 and 2:1 (refs 27, 28). In each case, the upper mantle minerals are assumed to contain a ratio of magnesium to iron plus magnesium endmember components (X_{Mg}) of 0.89. The partitioning of iron between the resulting high-pressure phases was calculated using the partition coefficients determined by Bell *et al.*[29] and Ito and Yamada[30]. Also included in Fig. 2 is the change in density with temperature for an olivine-only composition (1 pv: 1 mw). It can be seen that the olivine-rich representative upper mantle compositions do not coincide with current estimates of the zero-pressure density and minimum adiabat temperature of the lower mantle (bold arrow).

To match the observed density of the lower mantle, a small but apparently significant enrichment of iron or silica (or both) is required relative to the composition of the upper mantle. If only iron enrichment is considered (upper mantle olivine:pyroxene ratio of 1:1 to 2:1) a value $X_{Mg}\leq 0.84$ (±0.02) is required to match the zero-pressure density of the lower mantle (4.00 (±0.01) Mg m^{-3} at 1,700 K). In contrast, current estimates of the average upper mantle composition yield $X_{Mg}=0.89$ (±0.02) (refs 6, 7, 27, 28). Our results are unlikely to be sensitive to the presence of minor components such as aluminium or calcium[7,20]. Nevertheless, we cannot uniquely determine the composition that is required to satisfy the observed properties of the lower mantle because of the tradeoff between the effects of iron content, silica content and temperature. For example, a pure perovskite composition with $X_{Mg}=0.87$ (±0.01) coincides with the lower mantle density at 2,000 K, an adiabat temperature consistent with the presence of a thermal boundary layer associated with a compositional change at 670-km depth[35].

The idea that the upper and lower mantle are chemically distinct has been previously suggested from geophysical, petrological and geochemical arguments[31-34]. Based on our new data on the high-temperature properties of perovskite we also find that the conventional model of upper mantle composition (such as peridotite with $X_{Mg}=0.89$ or pyrolite[27,28] seems not to be consistent with the observed lower mantle density. We cannot distinguish between possible iron enrichment or silica enrichment of the lower mantle, but are led to conclude that the 670-km discontinuity represents a change in average chemical composition of the Earth's mantle. Compositional stratification at this depth, in turn, suggests that the convection pattern within the mantle is predominantly two-layered, and that the timescale for the thermal evolution of the Earth's interior is considerably longer than the 1,000–2,000 Myr expected with unlayered, whole-mantle convection[35]. The presence of chemical stratification in the mantle depends on a delicate balance between the compositionally-induced density change and the Raleigh number for lower mantle convection, because at sufficiently large Raleigh number, convection would destroy any chemical layering (see refs 36–38). Although some leakage may occur between the upper and lower mantle[19,39], our data suggest that the intrinsically higher density of the lower (relative to the upper) mantle impedes mantle-wide mixing and results in a chemical and thermal boundary layer at 670-km depth.

We thank M. H. Manghnani, S. Akimoto and T. J. Ahrens for helpful comments. Work supported by the University of California Institute for Geophysics and Planetary Physics (L.L.N.L. branch).

Received 22 April; accepted 24 October 1985.

1. Akaogi, M. & Akimoto, S. *Phys. Earth planet. Inter.* **15**, 90–106 (1977).
2. Akimoto, S., Yagi, T. & Inoue, K. in *High-Pressure Research* (eds Manghnani, M. H. & Akimoto, S.) 585–692 (Academic, New York, 1977).
3. Liu, L. in *The Earth: Its Origin Structure and Evolution* (ed. McElhinny, M. W.) 177–202 (Academic, New York, 1979).
4. Yagi, T., Bell, P. M. & Mao, H.-K. *Yb. Carnegie Instn Wash.* **78**, 614–615 (1979).
5. Liu, L. *Earth planet. Sci. Lett.* **42**, 202–208 (1979).
6. Jackson, I. *Earth planet. Sci. Lett.* **62**, 91–103 (1983).
7. Jeanloz, R. & Thompson, A. B. *Rev. Geophys. Space Phys.* **21**, 51–74 (1983).
8. Mao, H.-K., Bell, P. M., Dunn, K. J., Chrenko, R. M. & Devries, R. C. *Rev. Scient. Instrum.* **50**, 1002–1009 (1979).
9. Barnett, J. D., Block, S. & Piermarini, G. J. *Refv. Scient. Instrum.* **44**, 1–9 (1973).
10. Mao, H.-K., Bell, P. M., Shaner, J. W. & Steinberg, D. J. *J. appl. Phys.* **49**, 3276–3283 (1978).
11. Liu, L. *Phys. Earth. planet. Inter.* **11**, 289–298 (1976).
12. Ito, E. & Matsui, Y. *Earth planet. Sci. Lett.* **38**, 435–443 (1978).
13. Yagi, T., Mao, H.-K. & Bell, P. M. *Phys. Chem. Miner.* **3**, 97–103 (1978).

14. Yagi, T., Mao, H.-K. & Bell, P. M. *Physical Geochemistry* (ed. Saxena, S. K.) 317-325 (Springer, New York, 1982).
15. Suzuki, I. *J. Phys. Earth* **23**, 145-159 (1975).
16. Suzuki, I., Okajima, S. & Seya, K. *J. Phys. Earth* **27**, 63-69 (1979).
17. Masters, G. *Geophys. J.R. astr. Soc.* **57**, 507-534 (1979).
18. Dziewonski, A. M. & Anderson, D. L. *Phys. Earth planet. Inter.* **25**, 297-357 (1981).
19. Birch, F. *J. geophys. Res.* **69**, 4377-4388 (1964).
20. Jeanloz, R. in *Convection in the Earth's Mantle* (ed. Peltier, W. R.) (Gordon and Breach, New York, in the press).
21. Davies, G. F. & Dziewonski, A. M. *Phys. Earth planet. Inter.* **10**, 336-343 (1975).
22. Dziewonski, A. M., Hales, A. L. & Lapwood, E. R. *Phys. Earth planet. Inter.* **10**, 12-48 (1975).
23. Akimoto, S., Akaogi, M., Kawada, K. & Nishizawa, O. in *The Geophysics of the Pacific Ocean Basin and Its Margin* (eds Sutton, G. H., Manghnani, M. H. & Moberly, R.) 399-405 (AGU, Washington DC, 1976).
24. Anderson, D. L. *Science* **157**, 1165-1173 (1967).
25. Jeanloz, R. & Richter, F. M. *J. geophys. Res.* **84**, 5497-5504 (1979).
26. Touloukian, Y. S., Kirby, R. K., Taylor, R. E. & Lee, T. Y. R. in *Thermal Expansion, Non-metallic Solids* (TPRC 13) 1658 (IFI/Plenum, New York, 1977).
27. Ringwood, A. E. *Composition and Petrology of the Earth's Mantle* (McGraw-Hill, New York, 1975).
28. Yoder, H. S. Jr *Generation of Basaltic Magmas* (National Academy of Sciences, Washington DC, 1976).
29. Bell, P. M., Yagi, T. & Mao, H.-K. *Yb. Carnegie Instn Wash.* **78**, 618-619 (1979).
30. Ito, E. & Yamada, H. in *High Pressure Research in Geophysics* (eds Akimoto, S. & Manghnani, M. H.) 405-419 (Center for Academic Publishing, Tokyo, 1982).
31. Lees, A. C., Bukowinski, M. S. T. & Jeanloz, R. *J. geophys. Res.* **88**, 8145-8159 (1983).
32. Anderson, D. L. *A. Rev. Earth planet. Sci.* **5**, 179-202 (1977).
33. O'Nions, R. K., Eversen, N. M. & Hamilton, P. J. *J. geophys. Res.* **84**, 6091-6101 (1979).
34. Jacobsen, S. B. & Wasserburg, G. J. *J. geophys. Res.* **84**, 7411-7427 (1979).
35. McKenzie, D. & Richter, F. M. *J. geophys. Res.* **86**, 11667-11680 (1981).
36. Richter, F. M. & Johnson, C. E. *J. geophys. Res.* **79**, 1635-1639 (1974).
37. Olson, P. *J. geophys. Res.* **89**, 11293-11301 (1984).
38. Hoffman, N. R. A. & McKenzie, D. P. *Geophys. J.R. astr. Soc.* **82**, 163-206 (1985).
39. Creager, K. C. & Jordan, T. H. *J. geophys. Res.* **89**, 3031-3050 (1984).

^{187}Os/^{186}Os in marine manganese nodules and the constraints on the crustal geochemistries of rhenium and osmium

Martin R. Palmer* & Karl K. Turekian

Department of Geology and Geophysics, Yale University, Box 6666,
New Haven, Connecticut 06511, USA

During their formation, marine manganese (or more properly ferromanganese oxide) nodules include and commonly concentrate elements dissolved in seawater. This attribute makes them especially valuable recorders of the isotopic composition of elements supplied to the oceans having radiogenic isotopes, for these can be used in exploring crustal composition and evolution[1-5]. From measurements of ^{187}Os/^{186}Os ratios in marine manganese nodules and comparison with the ^{143}Nd/^{144}Nd ratios of the same nodules, we have calculated the Os isotopic composition and the osmium and rhenium concentrations of the weatherable portion of the continental crust, together with the proportions of 'ultramafic' and 'granitic' rock that constitute this crustal mass.

Our earlier studies in this laboratory[5,6] sought to relate the Os isotopic composition of marine manganese nodules to the sources of Os in the oceans. ^{187}Re decays ($\lambda = 1.52 \times 10^{-11}$ yr^{-1}) to form ^{187}Os. Variations in the ^{187}Os content of Os are commonly reported as the ^{187}Os/^{186}Os ratio since ^{186}Os is not radiogenic and is approximately equal in abundance to ^{187}Os in primitive materials such as meteorites[7]. The ^{187}Os/^{186}Os ratio depends on the age of the system and its ^{187}Re/^{186}Os ratio. The ^{187}Os/^{186}Os in manganese nodules records the mixing in the oceans of Os from systems with different ages and ^{187}Re/^{186}Os.

To unravel these sources and their properties, additional information is required. ^{87}Sr/^{86}Sr is a possible aid, but it depends mainly on temporal changes rather than regional diversity to recover such information[5]. Lead isotopes are complex and show perhaps too high a sensitivity to their sources[1] for our purposes. Variations in the ^{143}Nd/^{144}Nd ratio in manganese nodules have been well established and appear to provide the necessary constraint to the understanding of the ^{187}Os/^{186}Os texture of the oceans. Turekian and Luck[6] made an initial attempt at coupling the ^{187}Os/^{186}Os and ^{143}Nd/^{144}Nd systems to decipher sources of Os to the oceans. We now report additional Os isotopic data on nodules previously analysed for Nd isotopes and refine the interpretations made earlier.

The experimental procedures for measuring Os isotope ratios in manganese nodules have been discussed elsewhere[5,8]. Briefly, the technique consists of dissolving 10 g of the sample in a warm oxalic acid solution followed by distillation to extract the volatile OsO_4. This is then converted to $OsCl_6^{2-}$, purified on an ion-exchange column and plated on a silicon chip. The chloride salt is converted to the metal in a vacuum furnace. The actual Os isotopic composition is determined by secondary-ion microprobe mass spectrometry using the MIT-Brown-Harvard consortium Cameca IMS-3f ion microprobe. Osmium concentrations were determined in a few samples by isotope dilution.

The ^{187}Os/^{186}Os ratios measured in this study are listed in Table 1, together with those determined by Luck and Turekian[5]. All errors are 2σ of the mean. The data set is too small to provide an unambiguous judgement about details of the regional differences in ^{187}Os/^{186}Os, but the following observations can be made: (1) the mean values of the Atlantic, Pacific and Indian oceans are indistinguishable; (2) the largest range in ^{187}Os/^{186}Os of these basins occurs in the Atlantic (5.2-10.9); (3) some areas of an ocean basin have relatively homogeneous values, whereas others (such as, the eastern North Atlantic) show large differences within relatively small distances (see Fig. 1).

Turekian and Luck[6] have demonstrated that the Os extracted from manganese nodules, using the techniques discussed above, is virtually free of ^{187}Os produced *in situ* from the decay of ^{187}Re or Os associated with meteoritic debris trapped in the nodule. Although they addressed the problem of the contribution of magnetic spherules of meteoritic origin included in nodules, they assumed that all meteoritic debris is deposited on the ocean floor as particles. However, if all the meteoritic debris did go into solution, the meteoritic flux of osmium to seawater could be three times the riverine flux[9]. This would virtually homogenize the ^{187}Os/^{186}Os of the oceans. Clearly, this is not the case. Brownlee *et al.*[10] have recently demonstrated that Os and Ir occur as metallic 'nuggets' of ~10-μm diameter within magnetic spherules produced by the oxidation of meteoritic iron grains, probably during passage through the atmosphere. Therefore, because Os and Ir remain as refractory metals, they are less likely to be dissolved than some other elements of meteoritic origin. Hence, the measured ^{187}Os/^{186}Os ratios are the result of the integration of sources of dissolved Os with different isotopic compositions supplied to the oceans, primarily from terrestrial sources, and deposited in the nodule.

The strong differences in ^{187}Os/^{186}Os within ocean basins, and in some cases between nodules in close proximity, indicate that Os has a short mean oceanic residence time (~10^2 yr). For this reason, the relative input rates of Os of different isotopic compositions to each basin will be imprinted in the manganese nodules forming there.

We now characterize the potential sources of Os to the major ocean basins by coupling measurements of ^{143}Nd/^{144}Nd and ^{187}Os/^{186}Os in manganese nodules. The result of these calculations yields the ^{187}Os/^{186}Os ratio of the continental crust. This will provide constraints on the average Re/Os ratio of the crust and point to directions for verification. It will also provide information concerning the sources of mantle-derived Os to the different ocean basins. We draw on a model previously described[6] but with some modifications. Whereas before regional ^{143}Nd/^{144}Nd values were used, in the present study both Os and Nd isotopic measurements are available for each nodule.

We treat each of the major oceans separately, starting with the Pacific because of its size, relatively simple water structure compared with the Atlantic and the greater homogeneity of the ^{187}Os/^{186}Os ratios there.

To determine the ^{187}Os/^{186}Os ratio of the continental crust

---

* Present address: Department of Earth, Atmospheric and Planetary Sciences, Massachusetts Institute of Technology, Cambridge, Massachusetts 02139, USA.

Table 1 Os concentration, $^{187}Os/^{186}Os$ and $\varepsilon_{Nd}(O)$ of marine manganese nodules

Sample	Location		[Os] (p.p.b.)	$^{187}Os/^{186}Os$		$\varepsilon_{Nd}(O)$†
Atlantic						
V19 D11	38°04′ N	60°13′ W		8.09±0.06*		(−12.0)
V27 D11	42°20′ N	27°0′ W		7.97±0.11*		(−11.6)
V27 133	45°05′ N	7°56′ W		10.96±0.40		(−11.5)
VEMA FZ	10°54′ N	45°18′ W	2.39±0.02	8.11±0.18	8.01±0.08	−10.6
RC 16 D10	28°25′ S	40°45′ W		6.68±0.10*		(−14.0)
V16 SBT3	13°04′ S	24°41′ W		7.44±0.20		−10.9
V26 57	20°46′ S	24°08′ W		6.66±0.19		(−10.8)
V15 138	49°35′ S	48°05′ W		7.56±0.26		−8.4
CHN115 146	30°13′ S	39°4′ W	1.59±0.13	7.68±0.19	7.23±0.20	−14.0
V27 D5	56° N	21° W		5.27±0.19	5.13±0.22	−10.3
BP 2381	31°4′ N	78°9′ W		8.49±0.13		−11.0
KNR42-166	35°36′ N	58°41′ W		8.30±0.09	8.41±0.07	−11.4
V27 58	75°32′ N	2°40′ E		7.03±0.18		−10.0
Indian						
RC14 D3	34°45′ S	44°46′ E	0.82±0.09	8.00±0.19	7.39±0.07	−9.7
RC14 D5	19°2′ S	61°1′ E		8.33±0.09*		(−8.4)
DODO 232D	5°23′ S	97°29′ E	0.84±0.02	7.02±0.18	7.20±0.11	−7.3
DODO 127D	6°40′ S	51°54′ E		8.10±0.17		−7.8
DODO 62D	16°18′ S	104°16′ E		7.37±0.16		−7.3
Pacific						
MN 139	20°01′ N	136°36′ E	0.87±0.02	8.27±0.15	8.07±0.08	−3.6
A47 16	9°02′ N	151°11′ W		7.65±0.07*		(−3.9)
Challenger 276	13°28′ S	149°30′ W		5.95±0.18*		(−3.4)
A50 D	32°42′ N	158°15′ E		8.91±0.26		−3.7
V28 D8	0° N	179° W		7.50±0.26		−3.4
Antp 580	18°57′ N	135°48′ W	1.95±0.07	7.80±0.12	7.84±0.06	−4.3
E11 USC 887	56°54′ S	115°13′ W		8.38±0.19*		(−6.6)
SCAN 35D	20°55′ N	142°22′ E		8.23±0.09		−3.5
MN 171 DJ25	9°22′ N	151°12′ W		7.00±0.16		(−3.9)
MN 196 DJ52	9°20′ N	151°27′ W		7.20±0.22		(−3.9)
MN 203 DJ59	9°18′ N	151°32′ W		7.06±0.31		(−3.9)

$\varepsilon_{Nd}(O)$ value in parentheses indicates that a value is not available for that nodule and Nd isotopic data from the nearest available nodule are given.
* From ref. 5; † refs 2–4.

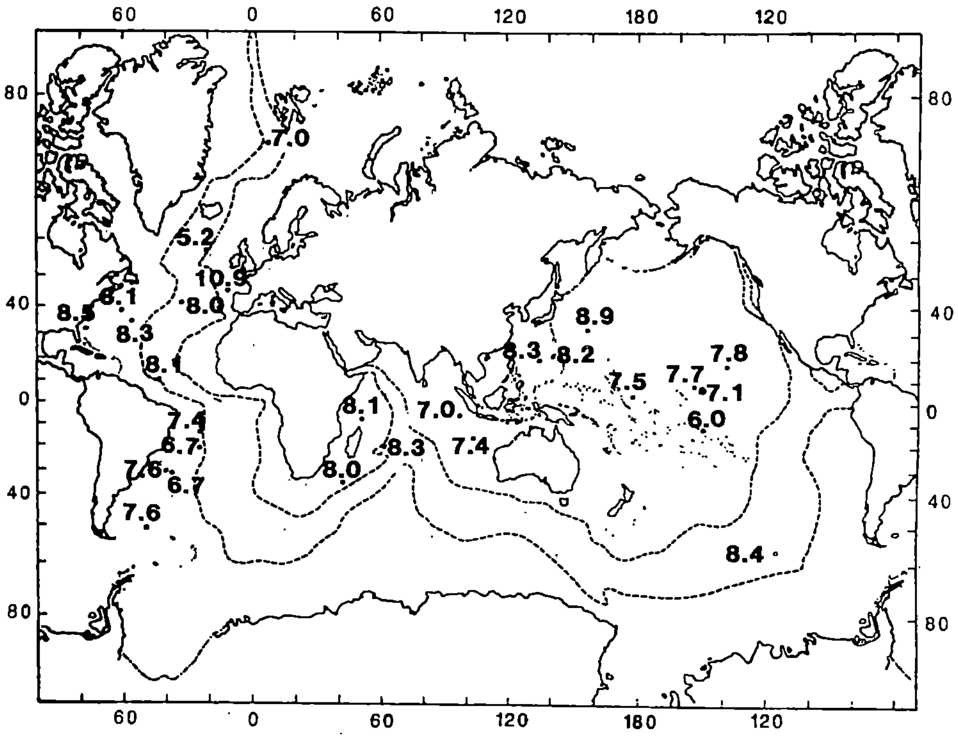

Fig. 1 $^{187}Os/^{186}Os$ ratios in marine manganese nodules.

Table 2 Ir (Os) and Nd concentrations and $^{187}Os/^{186}Os$ and $\varepsilon_{Nd}(O)$ values of sources to the oceans

Source	[Ir] (p.p.b.)*	[Nd] (p.p.m.)	[Ir]/[Nd]	$^{187}Os/^{186}Os$	$\varepsilon_{Nd}(O)$
Continental crust					
Precambrian shield composite[26]	0.05	19.4	2.58×10^{-6}	—	—
Mississippi suspended particulates[27]	0.056	28.9	1.94×10^{-6}	—	—
Mississippi sediment† (corrected for authigenic component)[12,27]	0.081	32.6	2.48×10^{-6}	—	—
Ocean island basalt[28-30]†	0.44	35	12.6×10^{-6}	1	+6
Peridotite[7,20]†	5	0.5	10.6×10^{-3}	1	+10

* [Ir]≅[Os].

† Values used for calculations in text.

Table 3 $^{187}Os/^{186}Os$ of continental crust

Sample	$\varepsilon_{Nd}(O)$ nodule*	$^{187}Os/^{186}Os$ Nodule	$^{187}Os/^{186}Os$ Continental crust
MN 139	−3.6	8.27	35.5
A47 16	(−3.9)	7.65	30.7
Challenger 276	(−3.4)	5.95	25.4
A50 D	−3.7	8.91	37.8
V28 D8	−3.4	7.50	33.0
Antp 580	−4.3	7.80	29.2
E11 USC 887	(−6.6)	8.38	20.5
SCAN 35D	−3.5	8.23	35.9
MN 171 DJ25	(−3.9)	7.00	27.8
MN 196 DJ52	(−3.9)	7.06	28.1
MN 203 DJ59	(−3.9)	7.20	28.7
Mean			30.2

$\varepsilon_{Nd}(O)$ value in parenthesis indicates that a value is not available for that nodule and Nd isotopic data from the nearest available nodule is given.

* From refs 2–4.

that is recorded by the Pacific nodules, we make the following assumptions, most of which are reasonable in the face of our current ignorance: (1) the present-day $^{187}Os/^{186}Os$ ratio of mantle-derived material is 1 (ref. 7); (2) the dominant source of mantle-derived Nd and Os in the Pacific is the alteration (low temperature and hydrothermal) of ocean island basalt (OIB) represented by Hawaii and other 'hotspot' islands and seamounts; (3) the supply of Os and Nd from tholeiitic mid-ocean ridge hydrothermal vent systems is negligible[11]; (4) Nd and Os are released congruently during weathering and alteration; (5) the continental $^{143}Nd/^{144}Nd$ ratio supplied to the Pacific Ocean is the average of values for the major rivers flowing into the Pacific Ocean basin[12]; (6) the mean oceanic residence times of Os and Nd are short relative to the mixing times of the oceans (see above); (7) Nd and Os in labile sites in deep sea deposits define the isotopic composition of provinces within the ocean basins; (8) in the absence of a significant amount of reliable crustal Os concentration data, we assume the Os/Ir ratio is approximately 1, as determined in meteorites and ultramafic rocks[13-15]. This ratio refers to the component of Os having a mantle isotopic imprint.

The continental crustal $^{187}Os/^{186}Os$ ratio can then be obtained from[6]:

$$R_c = \frac{\dfrac{[Os]_c}{[Nd]_c}\cdot\dfrac{\varepsilon_b-\varepsilon_s}{\varepsilon_s-\varepsilon_c}R_s+\dfrac{[Os]_b}{[Nd]_b}(R_s-R_b)}{\dfrac{[Os]_c}{[Nd]_c}\times\dfrac{\varepsilon_b-\varepsilon_s}{\varepsilon_s-\varepsilon_c}}$$

where R_c is the $^{187}Os/^{186}Os$ ratio of the continental crust; R_s is the $^{187}Os/^{186}Os$ ratio of the sample; $R_b = 1$, $^{187}Os/^{186}Os$ ratio of the 'mantle' source (OIB); $\varepsilon_c = -10.7$, ε_{Nd} (O) of the continental crust supplying the Pacific Ocean; ε_s is the ε_{Nd} (O) of the sample; $\varepsilon_b = +6$, ε_{Nd} (O) of the 'mantle' source (OIB); $[Nd]_c = 32.6$, Nd concentration (p.p.m., parts per 10^6) of the crust; $[Nd]_b = 35$, Nd concentration (p.p.m.) of the 'mantle' source (OIB); $[Os]_c = 0.081$, the Os concentration (p.p.b., parts per 10^9) of the crust; $[Os]_b = 0.44$, the Os concentration (p.p.b.) of the 'mantle' source (OIB).

The sources of the data are listed in Table 2. Note that the absolute concentrations of Os and Nd are not required, but rather their ratios in the major rock types are used in the calulations. In crustal rocks, the Ir/Nd ratio is fairly constant (see Table 2). A sensitivity test conducted for reasonable variations in the parameters used in the equation above demonstrated that the calculated continental crustal $^{187}Os/^{186}Os$ ratio does not vary enough to alter significantly the conclusions presented below. (Hydrothermal ferromanganese deposits are not considered here.)

This calculation has been performed for all the Pacific nodules and the results are summarized in Table 3. The average $^{187}Os/^{186}Os$ ratio for the continental crust is 30. Thus ~25% of the Os found in Pacific manganese nodules is from continental crustal sources and the remaining 75% is from OIB alteration.

If we assume that the average age of the continental crust being drained by the major rivers flowing into the Pacific is equal to that of the continental crust being drained by Atlantic rivers[12], ~25% of the Os in the Atlantic manganese nodules is also derived from the continental crust, because the mean $^{187}Os/^{186}Os$ of both oceans is approximately the same. (Actually the average $^{143}Nd/^{144}Nd$ of the Atlantic feeding rivers is slightly lower than those for the Pacific[12], but the differences are too small to be of significance.) Atlantic manganese nodules, however, unlike those from the Pacific, have $\varepsilon_{Nd}(O)$ values that fall within the range for the average continental crustal value of -11.4 ± 4.0 (ref. 12). The source of the mantle-derived Os cannot, therefore, be the alteration of high Nd rocks such as OIB that are so abundant in the Pacific. We believe that these high Os, low Nd sources in the Atlantic are ultramafic rocks. Specifically, we identify them as the commonly serpentinized ultramafic rocks associated with the fracture zones along the mid-Atlantic ridge.

The Os concentration of peridotites is approximately two orders of magnitude higher than that of the continental crust and one order higher than OIB. Because ocean floor peridotites are virtually all strongly altered to serpentinite[16], the Os in peridotites is probably available for release to the oceans at the time of alteration. These aspects of the process have still to be investigated. Ocean floor peridotites are generally restricted to the walls of fracture zones associated, with the relatively slow spreading mid-Atlantic and the Atlantic–Indian ridges[16-19] (see Fig. 2). Very few peridotites have been recovered from the Pacific fracture zones. The low concentration of Nd in peridotites[20], relative to other mantle oceanic rocks indicates that they are not a significant source of Nd during submarine weathering or hydrothermal alteration.

From the continental crustal $^{187}Os/^{186}Os$ ratio of 30 we can determine the average Re/Os ratio by assuming a mean continental crust age of 2×10^9 yr (ref. 12, for example) and the establishment of the crust 4×10^9 yr ago. Assuming a constant rate of continental growth and equal availability to weathering of all age rocks, a $^{187}Os/^{186}Os$ ratio would correspond to a $^{187}Re/^{186}Os$ of ~1000, that is, an elemental Re/Os ratio of ~25. Thus the continental crustal Os concentration (Table 2) yields a Re concentration range between 1.25 and 2 ng Re g^{-1}.

An independent estimate of the Re concentration of the continental crust can be obtained by using its close relationship to Mo in crustal rocks. This is most obviously seen in the high concentrations of Re in molybdenites[21]. Newsom and Palme[22] have estimated that the Mo concentration of the upper mantle is 0.059 μg Mo g^{-1}. Chou *et al.*[15], using a slightly different

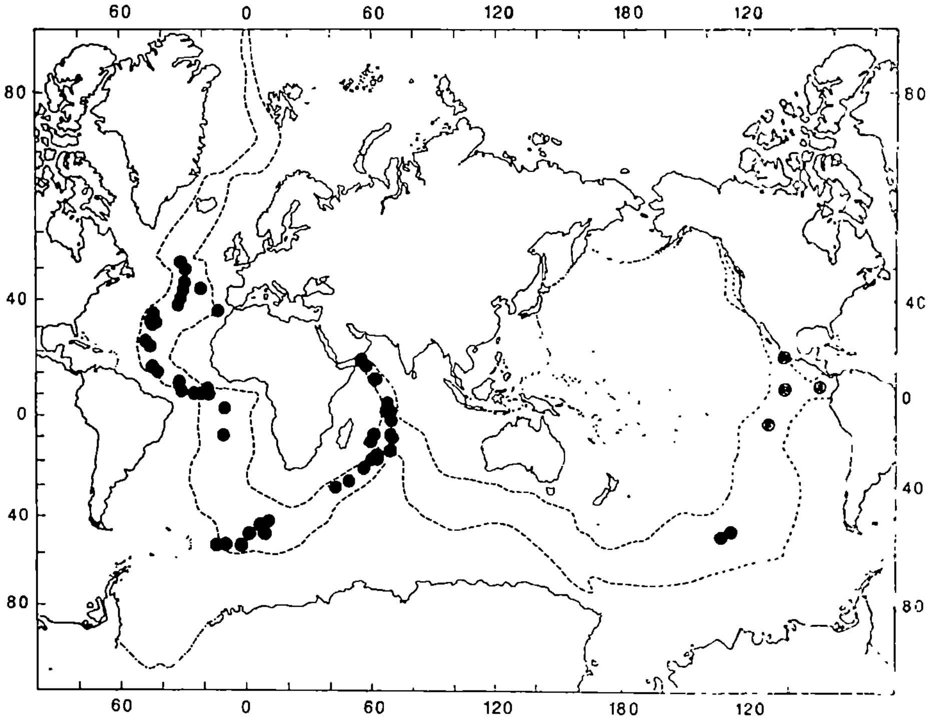

Fig. 2 Distribution of peridotites recovered from fracture zones at mid-ocean ridges[16-19].

method arrive at a Re concentration in the upper mantle of 0.25 ng Re g^{-1}. This yields a Re/Mo ratio of 0.0042. Estimates of the Mo concentrations of the continental crust range between 1 and 1.5 μg Mo g^{-1} (see ref. 23 for a summary). An average value of 1.3 μg Mo g^{-1} gives a continental crustal Re concentration of 5.5 ng Re g^{-1}, assuming no fractionation between mantle and crust. If this is correct, then the Os concentration of the continental crust, based on a $^{187}Os/^{186}Os$ ratio of 30 and a Re/Os ratio of 25 (see above), would be 0.22 ng Os g^{-1}. This value is much higher than the value of 0.08 based on the Ir concentrations discussed above.

Assuming the Re/Mo ratio of the mantle determined from the data of Chou *et al.*[15] and Newsom and Palme[22] is correct, it is more likely that fractionation of Re and Mo during the formation of the crust from the mantle has resulted in a crustal Re/Mo ratio that is one-third that of the mantle.

Turekian and Luck[6] used a simple model of weathering to explain the crustal $^{187}Os/^{186}Os$ ratio calculated for the Atlantic and Pacific basins. The difference between the Atlantic and Pacific Os and Nd isotopic signatures requires an ultramafic source to contribute Os more efficiently to the Atlantic Ocean than the Pacific Ocean. We have reaffirmed that the differences are due to the alteration of ultramafic rocks uniquely present within the Atlantic Ocean basin. We have assumed that all the continents yield the same $^{187}Os/^{186}Os$ ratio. Turekian and Luck[6] allowed for the possibility that the 'ultramafic' to 'granite' ratio could vary between the continents and, therefore, the $^{187}Os/^{186}Os$ ratio of the continents could differ. This mechanism is not required if, as has been demonstrated here, the internal ocean basin imprints are significant and vary between the Atlantic and Pacific.

We can continue to use their model to calculate the relative proportions of 'ultramafic' and 'granitic' rocks that are undergoing weathering worldwide. The model partitions the continental crust into an 'ultramafic' component with $^{187}Os/^{186}Os = 1$ and a purely radiogenic ^{187}Os component associated with high Re-bearing mineral phases of 'granitic' rocks. These Re-bearing minerals are probably those rich in Mo, most notably molybdenite[21].

The amounts of 'granitic' and 'ultramafic' rocks undergoing weathering are designated A_G and A_U, respectively; the continental crustal $^{187}Os/^{186}Os = 30$ and ultramafic rock $^{187}Os/^{186}Os = 1$; the Os concentration of ultramafic rock is 5 ng Os g^{-1} (refs 7, 15); the mean age of the continents is 2×10^9 yr; $[^{187}Os]_G = [^{187}Re]_G \lambda t$. With these parameters we can determine the relationship between the concentration of Re in the 'granitic' crust and the ratio of 'ultramafic' to 'granitic' rocks being weathered (A_U/A_G). For the 'ultramafic' contribution we get:

$$[^{187}Os]_U = 0.016[Os]_U = 0.016 \times 5 \text{ ng } ^{187}Os \text{ g}^{-1}$$
$$= 0.08 \text{ ng } ^{187}Os \text{ g}^{-1}$$

and for the 'granitic' contribution we get:

$$[^{187}Os]_G = 0.63[Re]_G \lambda t$$
$$= [Re]_G \times 0.63 \times 1.52 \times 10^{-11} \text{ yr}^{-1} \times 2 \times 10^9 \text{ yr}$$

(0.016 and 0.63 are the fractions of ^{186}Os and ^{186}Re in Os and Re respectively).

The relationship between $[Re]_G$ and A_U/A_G in these conditions (assuming total dissolution during weathering) is:

$$[Re]_G = 121.4 \, A_U/A_G$$

If $[Re]_G = 2.0$ then $A_U/A_G = 0.0165$, a value close to Daly's[24] estimate of the relative proportions of 'ultramafic' and 'granitic' rocks in the continental crust. To obtain A_U/A_G close to Knopf's[25] estimate (0.0025) requires $[Re]_G$ to be an order of magnitude lower than the value used here.

We thank J. M. Luck and N. Shimizu for technical help, D. J. Piepgras, S. L. Goldstein and S. E. Calvert for donating samples, and S. R. Hart for permission to use the SIMS ion probe at MIT. M. Lindner of the Lawrence Livermore National Laboratory made and provided us with ^{185}Os tracer. This research was funded by NSF grant OCE-8414753. M.R.P. acknowledges the partial support of a NATO fellowship. We thank R. K. O'Nions for comments.

Received 14 June; accepted 14 October 1985.

1. Chow, T. J. & Patterson, C. C. *Geochim. cosmochim. Acta* **26**, 263-308 (1962).
2. O'Nions, R. K., Carter, S. R., Cohen, R. S., Evenson, N. M. & Hamilton, P. J. *Nature* **273**, 435-438 (1978).
3. Piepgras, D. J., Wasserburg, G. J. & Dasch, E. J. *Earth planet. Sci. Lett.* **45**, 223-236 (1979).
4. Goldstein, S. L. & O'Nions, R. K. *Nature* **292**, 324-327 (1981).
5. Luck, J. M. & Turekian, K. K. *Science* **222**, 613-615 (1983).
6. Turekian, K. K. & Luck, J. M. *Proc. natn. Acad. Sci. U.S.A.* **81**, 8032-8034 (1984).
7. Allegre, C. J. & Luck, J. M. *Earth planet. Sci. Lett.* **48**, 148-154 (1980).

8. Luck, J. M. thesis, Univ. Paris 7 (1982).
9. Turekian, K. K. *Geol. Soc. Am. Spec. Pap.* **190,** 243-247 (1981).
10. Brownlee, D. E., Bates, B. A. & Wheelock, M. M. *Nature* **309,** 693-695 (1984).
11. Piepgras, D. J. & Wasserburg, G. J. *Earth planet. Sci. Lett.* **72,** 341-356 (1985).
12. Goldstein, S. L., O'Nions, R. K. & Hamilton, P. J. *Earth planet. Sci. Lett.* **70,** 221-236 (1984).
13. Barker, J. L. & Anders, E. *Geochim. cosmochim. Acta* **32,** 627-645 (1968).
14. Hertogen, J., Janssens, M. J. & Palmė, H. *Geochim. cosmochim. Acta* **44,** 2125-2143 (1980).
15. Chou, C. L., Shaw, D. M. & Crocket, J. H. *J. geophys. Res.* Vol. 88 Suppl., A507-A518 (1983).
16. Bonatti, E. & Hamlyn, P. R. in *The Sea* Vol. 4 (ed. Emiliani, C.) (Wiley, New York, 1981).
17. Udintsev, G. B. & Dmitriev, L. V. in *The Sea* Vol. 4 (ed. Maxwell, A. E.) (Wiley, New York, 1971).
18. Hebert, R., Bideau, D. & Hekinian, R. *Earth planet. Sci. Lett.* **65,** 107-125 (1983).
19. Dick, H. J. W., Fisher, R. L. & Bryan, W. B. *Earth planet. Sci. Lett.* **69,** 88-106 (1984).
20. Frey, F. A. in *Rare Earth Element Geochemistry* (ed. Henderson, P.) (Elsevier, Amsterdam, 1984).
21. Luck, J. M. & Allègre, C. J. *Earth planet. Sci. Lett.* **61,** 291-296 (1982).
22. Newsom, H. E. & Palme, H. *Earth planet. Sci. Lett.* **69,** 354-364 (1984).
23. Manheim, F. T. in *Handbook of Geochemistry* II-4 (ed. Wedepohl, K. H.) (Springer, Berlin, 1969).
24. Daly, R. A. *Igneous Rocks and the Depths of the Earth* (McGraw-Hill, New York, 1933).
25. Knopf, A. *J. Geol.* **24,** 620-622 (1916).
26. Shaw, D. M., Dostal, J. & Keays, R. D. *Geochim. cosmochim. Acta* **40,** 73-83 (1976).
27. Fenner, F. D. & Presley, B. J. *Nature* **312,** 260-262 (1984).
28. White, W. H. & Hoffman, A. W. *Nature* **296,** 821-825 (1982).
29. Zoller, W. H., Parington, J. R. & Phelan Kotra, J. M. *Science* **222,** 1118-1121 (1983).
30. Sun, S. S. *Phil. Trans. R. Soc. Lond.* **297A,** 409-445 (1980).

Protein kinase C activation induces conductance changes in *Hermissenda* photoreceptors like those seen in associative learning

J. Farley* & S. Auerbach†

* Program in Neuroscience and Behavior, Department of Psychology, Princeton University, Princeton, New Jersey 08540, USA
† Department of Biological Sciences, Rutgers University, Piscataway, New Jersey 08854, USA

Phosphorylation of ion channels has been suggested as one molecular mechanism responsible for learning-produced long-term changes in neuronal excitability[1]. Persistent training-produced changes in two distinct K$^+$ currents (I_A (ref. 2), $I_{K\text{-}Ca}$ (refs 3, 4)) and a voltage-dependent calcium current (I_{Ca}; refs 3, 4) have previously been shown to occur in type B photoreceptors of *Hermissenda*, as a result of associative learning. But the identity of the phosphorylation pathway(s) responsible for these changes has not as yet been determined. Injections of cyclic AMP-dependent protein kinase[5] reduce a K$^+$ current (I_K) in B cells which is different from those changed by training, but fails to reduce I_A and $I_{K\text{-}Ca}$. Phosphorylase *b* kinase (an exogenous calcium/calmodulin-dependent kinase) reduces I_A[6], but whether $I_{K\text{-}Ca}$ and I_{Ca} are changed in the manner of associative training is not yet known. Another protein kinase present in high concentrations in both mammalian brain and molluscan nervous systems is protein kinase C[7,8], which is both calcium- and phospholipid-sensitive[9,10]. We now present evidence that activation of protein kinase C by the tumour promoter phorbol ester (PDB) and intracellular injection of the enzyme induce conductance changes similar to those caused by associative training in *Hermissenda* B cells (that is a reduction of I_A and $I_{K\text{-}Ca}$, and enhancement of I_{Ca}). These results represent the first direct demonstration that protein kinase C affects membrane K$^+$ ion conductance mechanisms.

Hermissenda's phototaxic behaviour is suppressed when light stimuli are presented in association with rotation (an unconditioned noxious stimulus)[11,12]. Long-lasting changes in the neural excitability of the B photoreceptors underlie this associative learning[13,14]. The persistent changes in B photoreceptor excitability include an enhancement of the cells' steady-state depolarizing light response and a decrease in resting membrane conductance[14,15]. These, in turn, arise from training-produced reductions in a transient voltage-dependent K$^+$ current (I_A[2]), a delayed calcium-activated K$^+$ current ($I_{K\text{-}Ca}$[3,4,16]) and enhancement of a slow voltage-dependent calcium current (I_{Ca}[3,4]). Previously, it was suggested that the long-term K$^+$ current changes were due to a calcium/calmodulin-mediated phosphorylation process[6], stimulated by pairing-specific increases in intracellular calcium levels arising from enhanced calcium influx during the acquisition phase of associative learning[17]. No mechanism for training-produced changes in I_{Ca} in B cells has been previously proposed or demonstrated.

In B cells, exogenous application of serotonin (10^{-5} M), an endogenous neurotransmitter present within the optic ganglia near photoreceptor fine processes and released during associative training[18], produces the same changes of conductance and of light response as associative training[19].

The membrane-soluble tumour promoter 4β-phorbol 12β,13α-dibutyrate ester (PDB), an activator of protein kinase C[20], consistently enhanced the steady-state depolarizing response of type B photoreceptors produced by light when present in concentrations of 1-10 nM (Fig. 1) and decreased the resting membrane conductance (Table 1). These effects were observed within 1-2 min in every cell examined ($n = 23$) and persisted for the duration of recording (~1 h) even when followed by extensive washing. Inactive forms of the ester (4α-phorbol) as well as solvent application (10^{-6}% acetone, v/v) had no effect. Pretreatment of B cells with 10^{-5} M serotonin enhanced the steady-state light response and decreased the resting membrane conductance, as reported previously[19], and diminished the effect of PDB on B cells (Table 1).

Iontophoretic injections of protein kinase C (PKC) mimicked the effects of PDB, serotonin and associative training. PKC enhanced the magnitude of the light response and decreased net membrane conductance in all 13 B cells tested (Fig. 1, Table 1). As was the case for PDB, these effects were extremely persistent, lasting for the duration of recording (~1 h). Iontophoretic injections of heat-inactivated PKC ($n = 10$), buffer ($n = 5$), or material from a non-PKC peak eluting from the DEAE-cellulose column ($n = 3$) were all without effect.

Previous research has determined that the light response of the type B photoreceptor arises from the combined effects of light-, voltage- and calcium-activated ionic currents. Two distinct light-gated currents have been identified: (1) a transient, inward Na$^+$ current[21] ($I_{Na\text{-}light}$), which is tetrodotoxin-insensitive, voltage-independent, and underlies the rapid depolarizing limb of the light-induced generator potential and (2) a slower inward current which reflects both a cation-nonspecific conductance increase (J.F., unpublished observations) as well as a light-mediated reduction in a resting K$^+$ conductance[22]. Three voltage-dependent currents have been described: (1) I_A[23], a transient, rapidly inactivating, 4-aminopyridine (4-AP)-sensitive K$^+$ current which is reduced by both associative training[2] and intracellular calcium load[24]. In contrast to 'A' currents seen in other gastropod neurones[25,26], I_A in *Hermissenda* B cells is activated at membrane potentials near the resting potential of the cell (−50 to −60 mV) and is half-inactivated at a steady-state membrane potential of ~ −45 mV[23]. In contrast, half-maximal inactivation in both dorid[25] and *Tritonia*[26] neurones occurs at a considerably more negative membrane potential (−70 to −75 mV). (2) I_K, a delayed, sustained, tetraethylammonium (TEA)-sensitive outward K$^+$ current observed in many neurone somata[27], and (3) I_{Ca}, a small voltage-sensitive inward calcium current[28]. Also present in B cells is a calcium-activated K$^+$ current ($I_{K\text{-}Ca}$)[3,4,28] which resists block by extracellular TEA and 4-AP, contributes to the steady-state depolarizing light response, and is reduced by associative training[3,4]. We have examined each of these currents to determine which are affected by PDB and PKC.

Under voltage-clamp control, nanomolar concentrations of PDB reduced the fast, rapidly inactivating K$^+$ current (I_A) in each of 12 B cells (Fig. 2, Table 1). In eight of these cells PDB application also resulted in a hyperpolarizing shift in the voltage-dependence of inactivation of ~6-8 mV and a more modest shift of 3-4 mV in the voltage-dependence of activation. Because

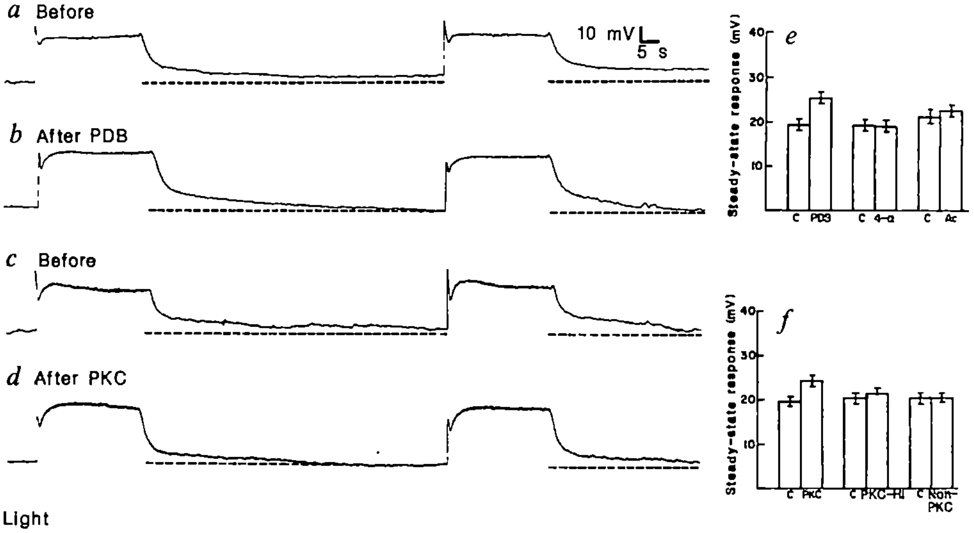

Fig. 1 PDB and PKC enhance the steady-state depolarizing light response of type B photoreceptors. Type B cells were prepared for recording as in previous studies[2-6] and were ligated so as to remove action- and synaptic-potential-generating areas of the cell. Intracellular recordings were made with a single glass microelectrode (10–30 MΩ, 3 M KCl) connected to a bridge circuit for current injection. Light-evoked depolarizing generator potentials were elicited by 30-s presentations of a 4.0×10^{-4} W cm^{-2} (at 510 nM) light step every 2 min. ***a***, Light-induced B-cell response before PDB, in standard artificial sea water (ASW). ***b***, Effect of PDB (2 min after bath application). PDB (Sigma) was diluted with acetone to make a 5 mg ml^{-1} stock which was stored frozen at −20 °C. The stock was diluted with ASW on the day of the experiment. Final concentrations of PDB and acetone in the bath were $1\text{–}10\times10^{-9}$ M and 10^{-6}% (v/v), respectively. Application of solvent alone, or inactive forms of the phorbol ester (4α-phorbol) had no effect. PDB enhanced the steady-state component of the light response. ***c***, Light-induced B-cell response in ASW, prior to PKC injection. ***d***, Effect of PKC (2 min post-injection). A single 30-s injection of PKC enhanced the steady-state light response of the B cells; a modest reduction of the initial transient depolarizing limb of the generator potential was also often observed. ***e***, Summary of data obtained from 23 cells exposed to PDB, 5 cells exposed to acetone solvent (Ac), and 11 cells exposed to 4α-phorbol (4-α) (C = control). Measurements of the steady-state light-response amplitude were taken at 25 s after light onset and are averages from the three light presentations prior to, and 2 min after, application. ***f***, Summary of data from 13 cells exposed to PKC injections, 10 cells exposed to heat-inactivated PKC injections (PKC-HI), and 8 cells exposed to either buffer alone ($n = 5$; not shown) or injections of a non-PKC peak eluting from the DEAE-cellulose column ($n = 3$, non-PKC). Only PKC injections produced an enhancement of the B cells' light response. All other treatments had no effect. Protein kinase C was partially purified from rat brain using the procedure of Niedel *et al.*[35], by ammonium sulphate precipitation and chromatography on a DEAE-cellulose column. The DEAE-cellulose column was washed with 10 ml of the equilibration buffer (20 mM Tris-HCl, *p*H 7.5/50 mM 2-mercaptoethanol), then a 60-ml linear gradient of 0–0.6 M NaCl in equilibration buffer was applied. The protein peak eluting at 0.3–0.4 M NaCl contained protein kinase C activity, as demonstrated by incorporation of ^{32}P from [γ-^{32}P]ATP into histone type III-S and ^{3}H-phorbol diester binding. With incubation conditions as described previously[36], in the presence of both Ca^{2+} and phospholipids, enzyme activity resulted in transfer of 54 pM of phosphate per min per mg protein. In the absence of either Ca^{2+} or diacylglycerol, no activity could be detected. Thus, the enzyme was injected in a largely inactive form. The electrode tip was filled via capillary action with PKC in a 20 mM Tris-HCl/350 mM NaCl solution (*p*H = 7.5). Protein kinase C was iontophoresed as an anion using 1–3 consecutive 15–30-s pulses of anodal (1.0–3.0 nA) current, resulting in the ejection of PKC quantities capable of producing 5×10^{-8} units of activity[9]. A small constant (+0.05 nA) cathodal brake current was applied to prevent leakage of PKC before and after each injection.

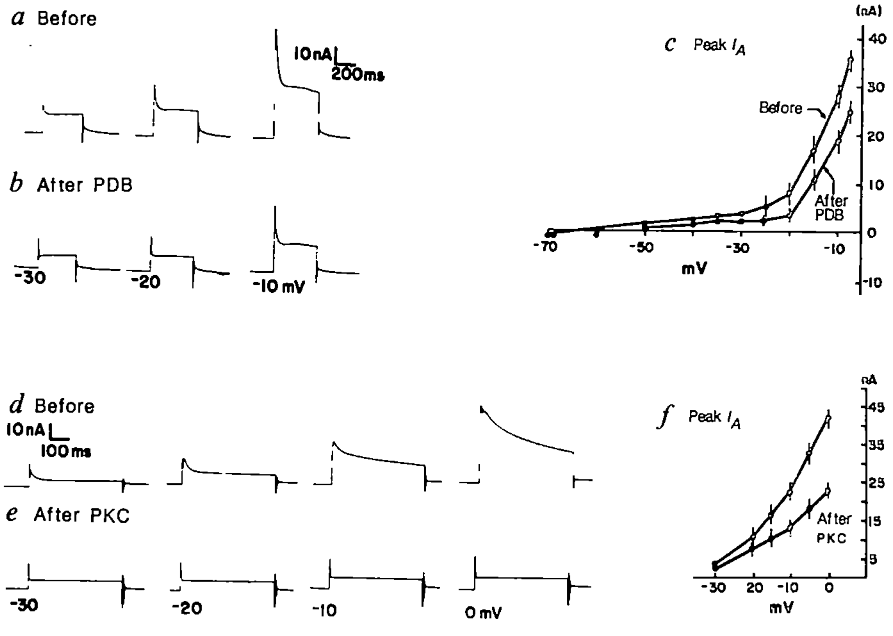

Fig. 2 PDB and PKC reduce I_A. ***a***, Outward current records elicited by command steps to potentials more positive than −30 mV in standard ASW exhibit an early (20–50 ms) transient peak (I_A) which then decays to a smaller sustained level of current (comprised of both I_K and $I_{K\text{-Ca}}$). Holding potential (V_h) was −60 mV. Records were obtained before addition of PDB. ***b***, Transient peak A current amplitude was reduced by 10^{-9} M bath-applied PDB, as was the steady-state outward current. Records obtained 2 min after PDB application. ***c***, Effects of PDB on I_A, averaged for 12 cells. Each data point in the *I–V* plot represents the average of four or five measurements of transient peak current (absolute amplitude corrected for leakage) at the indicated membrane potentials. Steps were presented at frequencies sufficiently low to preclude any slow-inactivation[37] contamination (once per 30 s). ***d***, Fast, rapidly inactivating K^{+} currents elicited in ASW from a holding potential of −60 mV before PKC injections. ***e***, A currents were reduced by a single 30-s (−3.0-nA anodal current) injection of PKC. Records obtained 5 min after PKC injection. ***f***, Average effect of PKC on I_A currents for 10 cells. Error bars represent 1 s.e.m.

Methods. Single synaptically isolated medial and intermediate type B photoreceptors were obtained from the eyes of adult untrained *Hermissenda* by enzymatic treatment with protease (Sigma Type VII) and ligature effected by a razor lesion of the optic nerve. In intracellular microelectrode (3 M KCl, 10–20 MΩ) recording studies (Fig. 1), B cells were characterized by resting potentials > −45 mV, membrane resistance >25 MΩ, peak and steady-state light-induced (4×10^{-4} W cm^{-2} at 510 nM) generator potentials of >25 and >20 mV, respectively, after 6 min of dark adaptation. Two-electrode voltage-clamp methods for the B-cell soma have been extensively described elsewhere[2-6] (3 M KCl electrodes, ~6 MΩ for current electrode; 10–20 MΩ for the voltage electrode). Space-clamp control was more than adequate, as judged by the ability to clamp the light-induced generator currents arising on the rhabdomere. In three experiments the cell's isopotentiality was confirmed by inserting a third electrode some distance away from the voltage-recording and current-passing electrode. Membrane potential settling time was 0.2–1.0 ms for all experiments reported. When impaled with two electrodes, cells either satisfied the following criteria or were discarded: (1) resting potential (V_m) > −40 mV; (2) equivalent resting (±2 mV) and light-induced (peak) generator potentials (>20 mV) as recorded through current and voltage electrodes; (3) holding currents in ASW ($V_h = -60$ mV) < −2.0 nA. The standard bathing fluid (ASW), unless otherwise noted, was (in mM): 430 Na^{+}, 10 K^{+}, 10 Ca^{2+}, 50 Mg^{2+}, 10 Tris, 570 Cl^{-} (*p*H = 7.6). All experiments were done at room temperature (20 °C). All reported current values for Figs 1–3 were corrected for leakage current by extrapolation from a linear portion of the current–voltage relation (10, 20-mV steps from $V_h = -60$ mV).

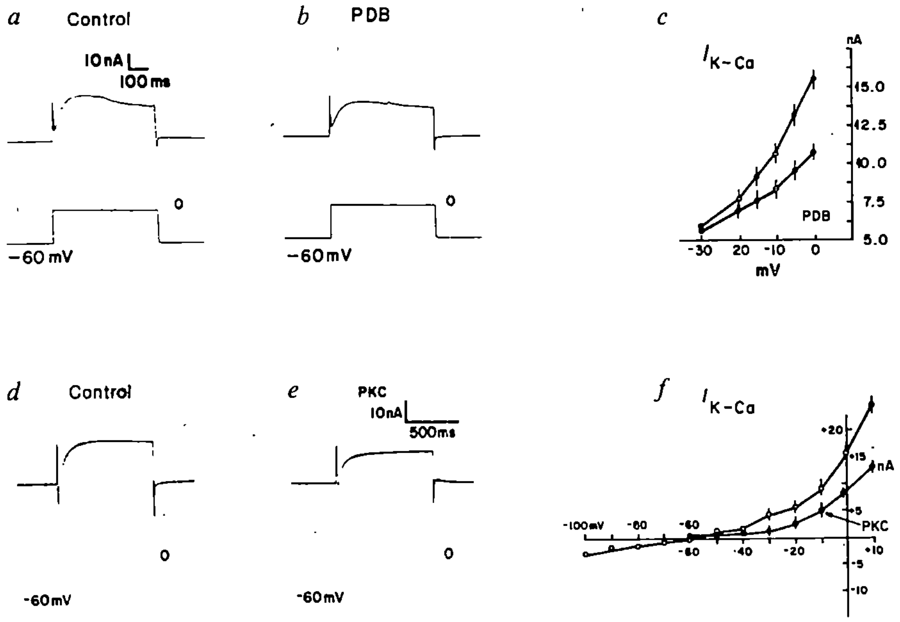

Fig. 3 PDB and PKC reduce $I_{K\text{-}Ca}$. *a*, $I_{K\text{-}Ca}$ measured at 0 mV before PDB application. $I_{K\text{-}Ca}$ was isolated using 5 mM 4-AP (Sigma) and 100 mM TEA (Aldrich) to block other voltage-dependent K^+ currents[28]. *b*, PDB reduces $I_{K\text{-}Ca}$. Measurements taken 5 min after bath application of PDB (1×10^{-9} M). Initially, PDB resulted in a slight enhancement of $I_{K\text{-}Ca}$ which lasted for 0.5–1.5 min (not shown). *c*, Average PDB effects for 10 cells, 5 min post-PDB (see also Table 1). *d*, $I_{K\text{-}Ca}$ measured before PKC injection. *e*, PKC injection reduced $I_{K\text{-}Ca}$; measurements taken 1.5 min after the PKC injection. *f*, Average results for 8 cells (see also Table 1), 1.5 min post-PKC injection. Error bars, 1 s.e.m.

reduction of I_A by PDB was near-maximal (>90%) in the remaining four preparations, and could not be overcome by steps to more positive potentials or by holding at more negative potentials, it is unlikely that the changes in voltage-dependence account completely for the reduction in the macroscopic current but rather appear to be an additional effect. Bath application of PDB also resulted in a biphasic modulation of $I_{K\text{-}Ca}$. The initial effect (1–3 min) was to enhance $I_{K\text{-}Ca}$; this was followed, however, by persistent reductions of 20–63% in the current (Fig. 3, Table 1).

The sole voltage-dependent inward current (I_{Ca}) present in B cells is carried by calcium ions[28]. I_{Ca} is increased by serotonin[19] as well as by associative training[3,4]. PDB application increased I_{Ca} in the nine cells examined (Fig. 4, Table 1), without obvious effect on the kinetics or voltage-dependence of activation or inactivation. Similar effects on I_{Ca} of *Aplysia* bag-cell neurones by a phorbol ester (tetradecanoyl phorbol 13-acetate) and protein kinase C were described recently by DeRiemer *et al.*[29].

Under voltage-clamp control, iontophoretic injections of PKC reduced I_A (Fig. 2, Table 1) and $I_{K\text{-}Ca}$ (Fig. 3, Table 1), and enhanced I_{Ca} (Fig. 4, Table 1). Pretreatment of B cells with serotonin reduced these effects of PKC (Table 1). At bath concentration of 1–10 nM, imipramine, which has been reported to inhibit PKC activation[30], blocked the enhancement of the B

Table 1 Effects of serotonin, phorbol ester (PDB) and protein kinase C (PKC) on *Hermissenda* type B photoreceptor light response, resting membrane conductance and ionic currents

	Steady-state light response (mV)		Net input resistance (MΩ)		I_A (nA)†		$I_{K\text{-}Ca}$ (nA)†		I_{Ca} (nA)‡	
Agent tested	Before	After	Before	After	Before	After	Before	After	Before	After
Serotonin (10^{-5} M)	18.7 ±1.2	23.7* ±0.8 ($n=9$)	45.3 ±3.4	71.4* ±2.9 ($n=9$)	31.2 ±1.4	16.3* ±1.2 ($n=9$)	12.3 ±0.6	2.1* ±0.9 ($n=10$)	3.5 ±0.4	5.9* ±0.4 ($n=8$)
PDB (10^{-9} M)	19.1 ±1.3	25.0* ±1.3 ($n=23$)	42.4 ±2.8	67.9* ±2.7 ($n=23$)	33.3 ±2.0	15.7* ±2.1 ($n=12$)	17.2 ±2.4	9.4* ±1.8 ($n=10$)	3.1 ±0.5	6.3* ±0.9 ($n=9$)
PDB(serotonin-pretreated) (10^{-9} M, 10^{-5} M)	24.2 ±1.6	23.9 ±1.4 ($n=9$)	63.8 ±5.3	66.1 ±5.2 ($n=9$)	20.7 ±2.5	18.7 ±2.3 ($n=12$)	3.7 ±1.9	2.9 ±2.1 ($n=9$)	2.5 ±0.6	3.1 ±0.7 ($n=8$)
4α-phorbol (10^{-9} M)	19.3 ±0.9	19.2 ±1.3 ($n=5$)	41.9 ±2.7	39.2 ±2.3 ($n=5$)	35.3 ±2.2	32.9 ±1.4 ($n=4$)	15.7 ±1.3	14.3 ±1.9 ($n=4$)	2.9 ±1.0	2.7 ±0.9 ($n=4$)
Acetone (10^{-6}%)	21.1 ±1.7	21.9 ±1.8 ($n=11$)	40.3 ±2.2	38.7 ±2.3 ($n=11$)	30.0 ±1.8	28.5 ±1.5 ($n=4$)	18.0 ±1.2	16.7 ±1.9 ($n=4$)	3.1 ±0.7	2.9 ±0.8 ($n=3$)
PKC	19.6 ±0.9	23.5* ±0.7 ($n=13$)	39.3 ±1.9	57.6* ±2.1 ($n=13$)	31.7 ±1.8	10.2* ±0.8 ($n=10$)	16.3 ±1.2	8.7* ±0.9 ($n=8$)	2.9 ±1.2	5.8* ±0.9 ($n=7$)
PKC(serotonin-pretreated)	23.9 ±1.3	24.2 ±1.5 ($n=7$)	52.3 ±4.2	50.9 ±3.7 ($n=7$)	13.0 ±0.9	12.8 ±0.7 ($n=5$)	4.2 ±1.2	3.9 ±0.9 ($n=4$)	5.1 ±0.5	4.9 ±0.6 ($n=4$)
PKC, heat-inactivated	20.1 ±0.8	21.1 ±1.2 ($n=10$)	37.4 ±1.2	39.1 ±2.0 ($n=8$)	29.7 ±1.7	26.4 ±1.2 ($n=5$)	14.7 ±1.0	11.1 ±1.2 ($n=4$)	3.4 ±1.5	3.2 2.4 ($n=3$)

Values are means ± s.e.m. All current values are leak-corrected.

* $P<0.05$, two-tailed *t*-test; before versus after.

† Peak outward current measured at −10 mV, from $V_h=-60$ mV, 5-min post-treatment.

‡ Steady-state – inward current, measured at 0 mV, 5 min post-treatment.

cell's light response and the decrease in conductance caused by PDB and PKC.

These data indicate that activation of protein kinase C in *Hermissenda* B cells can lead to reductions in both voltage- and calcium-activated potassium currents, and enhancement of a voltage-dependent calcium current. The net effect of these conductance changes is an enhancement of the B cell's depolarizing light response and a decrease in resting membrane conductance. Because these effects of PKC are essentially identical to those produced by associative training of the animal, which in turn are mimicked by serotonin application, it is attractive to suppose that serotonin-induced PKC activation is one mechanism by which long-term excitability changes in B cells arise from associative training. It is a mechanism which may be distinct from the previously proposed calcium/calmodulin-dependent phosphorylation pathway. Although PKC does require calcium for full activity, data from cell-free enzymatic reaction systems indicate this requirement to be a biochemical rather than a physiological one[8]. In blood platelets 10^{-7} M free calcium has a maximal and saturating effect on PKC activity[9]. Free calcium levels in nerve and neurones are typically already 10^{-7} M[11], which would be expected to confer a relative independence of PKC from physiological changes in intracellular calcium levels.

Although molecularly distinct, calcium-calmodulin-dependent and PKC-dependent phosphorylation may act in a synergistic fashion to effect long-term current changes in B cells. I_A[24] and $I_{K\text{-}Ca}$[22] in *Hermissenda* B cells are reduced by large increases in the intracellular calcium concentration. Illumination of B cells leads to the release of calcium from intracellular stores in B cells[17,22], and may thereby transiently reduce I_A and $I_{K\text{-}Ca}$. In other tissues[32], serotonin can lead to mobilization of intracellular calcium, mediated by inositol trisphosphate[33], in addition to its activation of PKC. Thus, it is possible that light and serotonin may act in a synergistic manner in their activation of both protein kinase C and calcium-calmodulin-dependent protein kinase in the B cell. In future studies it will be important to determine whether the effects of PDB and PKC on the ionic conductances are direct, representing PKC-dependent phosphorylation of ionic channels, or indirect, perhaps through an interaction with calcium/calmodulin or cyclic nucleotide pathways (as has been demonstrated in oocytes[34]).

This research was supported by NSF grant BNS-8316707 (J.F.).

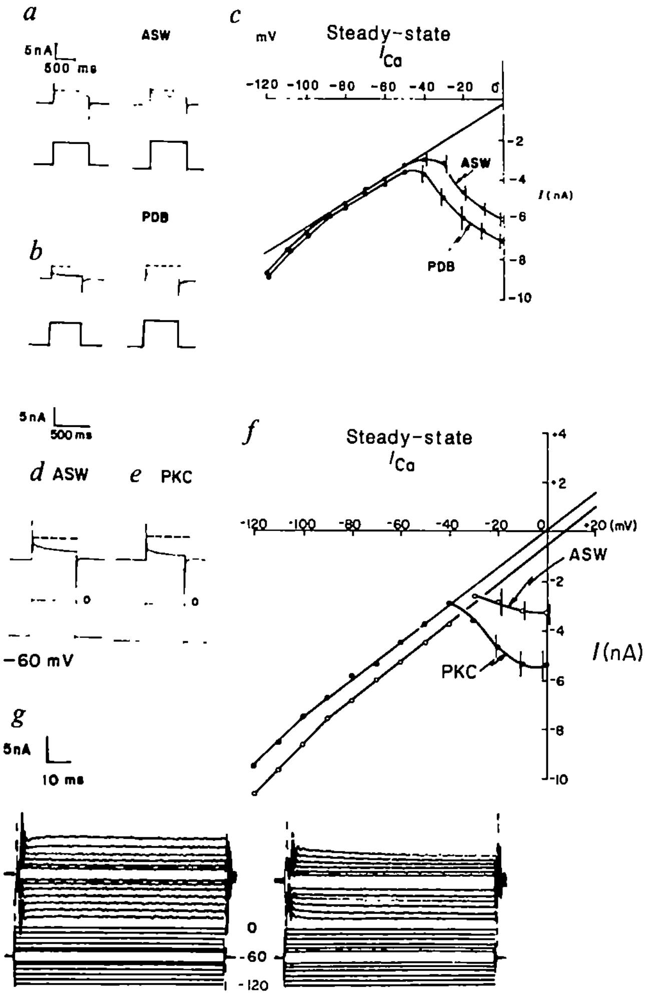

Fig. 4 PDB and PKC enhance I_{Ca}. ***a***, I_{Ca} measured at −10 and 0 mV, respectively, before PDB application. I_{Ca} was isolated using 5 mM 4-AP, 100 mM TEA, 10 mM Ba_0^{2+} for Ca_0^{2+}, and 300 mM K_0^+. In these conditions[28], $E_K = \pm 2$ mV. Thus, measurements of the inward current at 0 mV are uncontaminated by any residual K^+ conductance[28]. Extrapolated leak-current values are denoted by the dotted line. ***b***, I_{Ca} measured 2 min after application of 10^{-9} M PDB. I_{Ca} was enhanced. PDB did not result in any change in holding current, however, indicating that it largely affected the voltage-dependent conductance. Leak currents were unaffected. ***c***, Average results for nine cells (see also Table 1). Values are for total membrane current. ***d***, I_{Ca} measured at 0 mV prior to PKC injection. ***e***, PKC injection enhanced I_{Ca} (record obtained 2 min after injection). ***f***, Average results for 7 cells (see also Table 1). Values are for total membrane current. PKC injections enhanced I_{Ca} at all potentials more positive than −30 mV. Error bars, 1 s.e.m. ***g***, Enhanced inward current is not sodium-dependent. In previous work[28], the possibility that Na^+ influx might contribute to the inward current was not directly addressed. Consequently, in further experiments sodium chloride was replaced in Na-free saline by substituting tetramethylammonium chloride (TMA, $n = 6$) or trizma base ($n = 3$) in equimolar concentrations. These substitutions had no effect on the magnitude or kinetics of the inward current, measured in either the presence or absence of PKC injections, except that with prolonged exposure to 0 Na saline, the cells became rather leaky. Shown here is the inward current measured in TMA-ASW before (left) and after (right) PKC injection.

Received 3 June; accepted 15 November 1985.

1. Nestler, E. J. & Greengard, P. *Nature* **305**, 583–588 (1983).
2. Alkon, D., Lederhendler, I. & Shoukimas, J. *Science* **215**, 693–695 (1982)
3. Farley, J. & Alkon, D. L. *Soc. Neurosci. Abstr.* **9**, 167 (1983).
4. Farley, J., Sakakibara, M. & Alkon, D. L. *Soc. Neurosci. Abstr.* **10**, 270 (1984).
5. Alkon, D. L., Acosta-Urquidi, J., Olds, J., Kuzma, G. & Neary, J. T. *Science* **219**, 303–305 (1983).
6. Acosta-Urquidi, J., Alkon, D. L. & Neary, J. T. *Science* **224**, 1254–1257 (1984)
7. Minakuchi, R., Takai, Y., Yu, B. & Nishizuka, Y. *J. Biochem., Tokyo* **89**, 1651–1654 (1981)
8. Nishizuka, Y. *Science* **225**, 1365–1370 (1984).
9. Kishimoto, A., Takai, Y., Mori, T., Kikkawa, W. & Nishizuka, Y. *J. biol. Chem.* **255**, 2273–2276 (1980).
10. Berridge, M. J. *Molec. cell. Endocr.* **24**, 115–140 (1981).
11. Crow, T. & Alkon, D. L. *Science* **201**, 1239–1241 (1978).
12. Farley, J. & Alkon, D. L. *Science* **209**, 412–414 (1980).
13. Farley, J., Richards, W., Ling, L., Liman, E. & Alkon, D. L. *Science* **221**, 1201–1203 (1983)
14. Farley, J. & Alkon, D. L. *J. Neurophys.* **48**, 785–807 (1982).
15. West, A., Barnes, E. & Alkon, D. L. *J. Neurophys.* **48**, 1243–1255 (1982)
16. Grover, L. & Farley, J. *Soc. Neurosci. Abstr.* **11**, 788 (1985).
17. Connor, J. & Alkon, D. L. *J. Neurophys.* **51**, 745–752 (1984).
18. Auerbach, S., Grover, L. & Farley, J. *Soc. Neurosci. Abstr.* **11**, 481 (1985)
19. Wu, R. & Farley, J. *Soc. Neurosci. Abstr.* **10**, 620 (1984).
20. Castagna, M. *et al. J. biol. Chem.* **257**, 7847–7851 (1979).
21. Alkon, D. L. *Science* **205**, 810–816 (1979).
22. Alkon, D. L. & Sakakibara, M. *Soc. Neurosci. Abstr.* **10**, 10 (1984)
23. Shoukimas, J. J. & Alkon, D. L. *Soc. Neurosci. Abstr.* **6**, 17 (1980).
24. Alkon, D. L., Shoukimas, J. J. & Heldman, E. *Biophys. J.* **40**, 245–250 (1982)
25. Connor, J. A. & Stevens, C. F. *J. Physiol., Lond.* **213**, 21–30 (1971)
26. Thompson, S. *J. Physiol., Lond.* **265**, 465–488 (1977).
27. Adams, D. J., Smith, S. J. & Thompson, S. H. *A. Rev. Neurosci.* **3**, 141–167 (1980)
28. Alkon, D. L., Farley, J., Sakakibara, M. & Hay, B. *Biophys. J.* **46**, 605–614 (1984)
29. DeRiemer, S. A., Strong, J. A., Albert, K. A., Greengard, P. & Kaczmarek, L. K. *Nature* **313**, 313–316 (1985).
30. Mori, T., Takai, Y., Minakuchi, R., Yu, B. & Nishizuka, Y. *J. biol. Chem.* **255**, 8378–8380 (1980).
31. Baker, P. F. *Prog. biophys. molec. Biol.* **24**, 177–223 (1972).
32. Berridge, M. J. *Biochem. J.* **212**, 849–858 (1983).
33. Berridge, M. J. & Irvine, R. F. *Nature* **312**, 315–321 (1984).
34. Dascal, N., Lotan, I., Gillo, B., Lester, H. A. & Lass, Y. *Proc. natn. Acad. Sci. U.S.A.* **82**, 6001–6005 (1985).
35. Niedel, J. E., Kuhn, L. J. & Vandenbark, G. R. *Proc. natn. Acad. Sci. U.S.A.* **80**, 36–40 (1983)
36. Wise, B. C., Raynor, R. L. & Kuo, J. F. *J. biol. Chem.* **257**, 8481–8488 (1982)
37. Aldrich, R. W. Jr, Getting, P. A. & Thompson, S. H. *J. Physiol., Lond.* **291**, 531–544 (1979)

Differential expression of α-fetoprotein genes on the inactive X chromosome in extraembryonic and somatic tissues of a transgenic mouse line

R. Krumlauf*, V. M. Chapman†, R. E. Hammer‡, R. Brinster‡ & S. M. Tilghman*

* Institute for Cancer Research, 7701 Burholme Ave, Philadelphia, Pennsylvania 19111, USA
† Roswell Park Memorial Institute, 666 Elm St, Buffalo, New York 14263, USA
‡ Laboratory of Reproductive Physiology, School of Veterinary Medicine, University of Pennsylvania, Philadelphia, Pennsylvania 19104, USA

During development of the female mouse embryo, one of the two X chromosomes is inactivated in a random manner in most cell lineages[1]. However, in the extraembryonic trophectoderm and primary endoderm lineages there is preferential inactivation of the paternally derived X chromosome[2–4]. The inactivated X chromosomes of the extraembryonic and somatic tissues appear equally inactive at the level of the expression of X-linked genes[2–7]. However, there are differences in the timing of their replication[8–10] and the extent of DNA modification as determined by gene transfer[11–15]. The identification of transgenic animals carrying X-linked modified α-fetoprotein (AFP) genes allowed us to examine whether the inactivation process extends to an autosomal gene which is normally expressed at high levels in specific extraembryonic and somatic cells, and if so, whether the inactivation process is different in these two tissues. Our results demonstrate that the X-linked AFP genes were expressed on the inactive X chromosome in the visceral endoderm of the yolk sac but not in fetal liver. Thus, the transcriptional activity of the AFP minigene on the inactive X chromosome is dependent on the tissue in which it resides, and most probably reflects differences in the nature of the maintenance of the inactive state of the extraembryonic and embryonic X chromosomes.

We have shown previously that transgenic mice carrying exogenous AFP genes express these genes in a tissue-specific and temporally appropriate manner in the visceral endoderm of the yolk sac, the fetal liver and the fetal gastrointestinal tract[16]. During breeeding experiments with one line derived from a male F_1 of the founder mouse, 47-3, we observed that the two to three tandem copies of the AFP minigene were segregating with the X chromosome. In analysing more than 1,200 progeny derived from five F_1 transgenic males, all females and no males carried the AFP minigenes. In contrast, females were able to transmit the genes equally to females and males. A partial pedigree is shown in Fig. 1.

To determine whether the AFP minigenes on the paternally derived X chromosome were preferentially inactivated in the visceral endoderm of the yolk sac, a tissue in which AFP messenger RNA constitutes 20% of the mRNA pool, animals were obtained by caesarean section at 14–16 days of fetal development from matings between $(C57Bl/6\times SJL)F_1$ mice with either male or female transgenic mice. Transgenic fetuses were identified by hybridizing fetal liver genomic DNA to a first exon-specific AFP probe able to detect both the endogenous and the introduced AFP genes[16,17]. The sex of the fetuses was determined by hybridization of genomic DNA to a retroviral probe (M270) that can detect sequences on the Y chromosome[18] (data not shown).

Total yolk sac poly(A)$^+$ RNA from female transgenic progeny was isolated, fractionated by electrophoresis and hybridized to an AFP probe. The introduced AFP minigene is an internally deleted AFP gene[16,17] that generates a correctly initiated and processed 600-nucleotide poly(A)$^+$ RNA readily distinguished

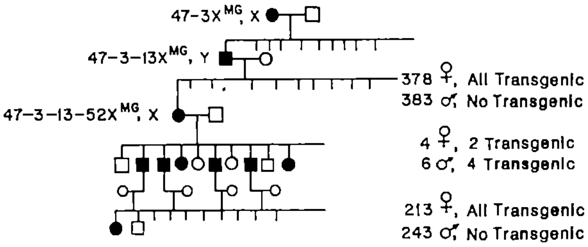

Fig. 1 Simplified pedigree of the 47-3-13 line showing segregation of the X-linked AFP minigenes. The founder mouse (47-3) was mated to $(C57BL/6\times SJL)F_1$ males and one of her male progeny (47-3-13) was mated to BALB/cJ mice. The sex of all subsequent progeny was determined by external genitalia and/or tail DNA analysis[16] using the retroviral probe (M720) which is able to detect sequences on the Y chromosome[18]. Males are indicated by squares and females by circles. Transgenic animals (closed symbols) were identified with an AFP hybridization probe in the manner shown in Fig. 4*b*. MG refers to the AFP minigene.

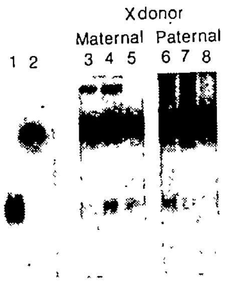

Fig. 2 Expression in yolk sac of the AFP minigenes located on the inactive paternal or active maternal X chromosome. Lanes 1 and 2 are control RNAs denoting the migration of AFP minigene (lane 1) and authentic AFP mRNA (lane 2). Transgenic females or males were mated to $(C57BL/6\times SJL)F_1$ animals, and transgenic female progeny were identified on days 14–16 post-fertilization by hybridization of fetal liver and yolk sac DNAs, isolated according to published procedures[16], to AFP- and Y-chromosome[18]-specific sequences. Poly(A)$^+$ RNA was isolated from individual yolk sacs of progeny derived from transgenic females (lanes 3–5) and males (lanes 6–8), fractionated on denaturing formaldehyde 1.7% agarose gels and transferred to nitrocellulose. The RNAs were hybridized to an AFP-specific single-stranded RNA probe as detailed previously[16].

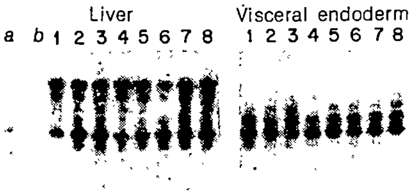

Fig. 3 Differential expression of HPRT isozymes in the yolk sac and liver of transgenic females. The pattern of expression of HPRT isozymes in eight transgenic female livers (lanes 1–8, left) and visceral endoderms (right) was determined. Lanes *a* and *b* are control samples for the HPRT-A and HPRT-B isozymes, respectively. Male transgenic animals carrying the *pgk*-1^b and *hprt*^{b} alleles were mated to C3H/He female congenic mice heterozygous for the *pgk*-$1^{a/b}$ and *hprt*$^{a/b}$ alleles. Fetuses were obtained by caesarian section at 14–16 days' gestation and the livers and yolk sacs removed. The visceral endoderm of the yolk sac was separated from the mesodermal layer by incubating the tissue in an enzyme mixture (2.5% pancreatin, 0.5% trypsin, 1 × pucks saline A) at 4 °C for 1 h as described previously[5–7,9,15,28]. The tissue was transferred to phosphate-buffered saline at 4 °C and the layers were separated with forceps under a dissecting microscope. In some cases DNA and RNA were isolated from the tissues and analysed, and in others HPRT and PGK isozyme analysis was performed as described previously[12,15,19,20]. Only progeny which exhibited the informative *hprt*$^{a/b}$ and *pgk*-$1^{a/b}$ genotype (16/97) are shown.

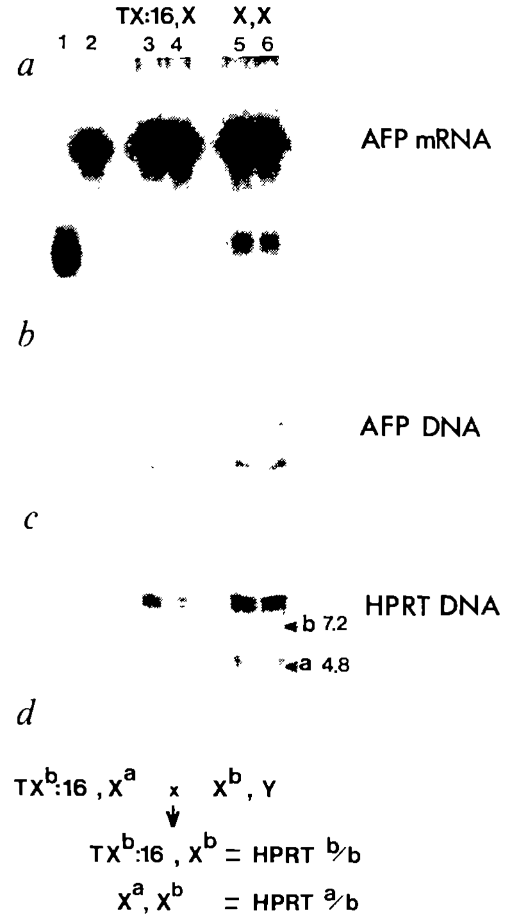

Fig. 4 Expression of the X-linked AFP minigenes in the livers of animals bearing the Searle's translocation. *a*, Poly(A)$^+$ RNA was isolated from day 1 neonatal animals and analysed after gel electrophoresis by hybridization to an AFP-specific probe. Lane 1 is a control for the migration of the minigene mRNA and lane 2 is a control RNA isolated from a non-transgenic animal. Lanes 3 and 4 are from two transgenic animals carrying the Searle's translocation and lanes 5 and 6 from two normal XX transgenic littermates. *b*, Hybridization of genomic DNA isolated from livers of the same animals as in *a* to an AFP-specific probe. The faster-migrating band indicates the presence of the X-linked minigene in lanes 3–6. *c*, Hybridization of the same genomic DNA in lanes 3–6 with an *hprt* cDNA probe that distinguishes between the *hprt*^{a} and *hprt*^{b} alleles. *d*, A diagramamatic representation of the mating and predicted genotypes of the female offspring.

Methods. Female mice carrying Searle's translocation[21] have the *pgk*-1^b and *hprt*^{b} alleles on the translocated portion of the X chromosome, and the *pgk*-1^a and *hprt*^{a} alleles on the normal X chromosome. These animals were mated to transgenic males carrying the X-linked *hprt*^{b} and *pgk*-1^b alleles and the AFP minigenes. Progeny were killed on day 1 of neonatal life and RNA and DNA were isolated from the liver as described previously[16]. The DNA samples (10 μg) were restricted with *Hin*dIII, electrophoresed through a 1% agarose gel, transferred to nitrocellulose and hybridized with either a nick-translated AFP probe or an *hprt* cDNA probe as described elsewhere[16]. The 4.8-kb *Hin*dIII fragment is a restriction fragment length polymorphism associated with the *hprt*^{a} allele used in this cross (F. Berger and V.M.C., unpublished results). It is present on the intact X chromosome of the t(X; 16H) dam of these offspring. Thus *hprt*$^{a/b}$ progeny are X/X while *hprt*^{b} progeny are probably t(X; 16H) since *hprt* maps within 5 centimorgans of the translocation breakpoint. The poly(A)$^+$ RNA samples (~1 μg) were fractionated by electrophoresis through a denaturing formaldehyde agarose gel, transferred to nitrocellulose and hybridized with a single-stranded AFP probe as described previously[16].

from the 2.2-kilobase (kb) endogenous mRNA. Figure 2 shows that the AFP minigenes were expressed in the extraembryonic yolk sac, irrespective of whether they derived from the paternal (inactive) or maternal (active) X chromosome. Partial paternal X inactivation was suggested by a general two- to three-fold higher level of expression from the AFP minigenes when they were present on the maternally derived X chromosome.

To ensure that the paternal X chromosome was actually inactivated, male transgenic animals carrying the X-linked phosphoglycerate kinase-B (*pgk*-1^b) and hypoxanthine phosphoribosyl transerase-B (*hprt*^{b}) alleles were mated to C3H/He female congenic mice carrying the *pgk*-1^a and *hprt*^{a} alleles derived from wild mice[19,20]. Fetuses were collected at 14–16 days of gestation and the visceral endoderm of the yolk sac was isolated by dissection following enzymatic digestion[5,7,9,15]. Assays to distinguish the PGK and HPRT isoenzyme[15,19,20] and to quantitate AFP minigene mRNA were performed on both fetal liver and visceral endoderm samples. For eight of the appropriate females, both the A and B isozymes of HPRT were expressed in liver, whereas only the A isozyme from the maternally derived X chromosome was expressed in the visceral endoderm of the same animals (Fig. 3). Similar results were obtained for PGK (data not shown). However, as before, the AFP minigenes were expressed irrespective of their origin. Therefore, the ability of the minigenes to escape X-chromosome inactivation cannot be attributed to their presence interfering with the inactivation of the entire chromosome.

This experiment does not exclude the possibility that the AFP minigenes have integrated into a region of the X chromosome which normally escapes inactivation. On the other hand, the activity of X-linked AFP genes in the extraembryonic lineage could be a unique property of the X chromosome of that tissue. One way to distinguish between these possibilities is to examine the activity of the AFP minigenes on the inactive X chromosome in a somatic tissue, such as fetal liver. To do this we took advantage of a strain of mice carrying one copy of a balanced X: autosome translocation (t(X; 16H)) termed Searle's translocation[21]. In all females that carry the translocated X, the normal X chromosome donated by the male is inactive[5,7,10,12,15,22], presumably to prevent the partial monosomy of chromosome 16 that would otherwise occur. Thus, by crossing a transgenic male to a Searle's female, we will generate female progeny in which the X chromosome bearing the AFP minigene is inactive in all tissues. Normal XX females which will also result from this cross display random X inactivation and serve as controls. A diagrammatic representation of the mating and expected genotypes is shown in Fig. 4*d*.

Progeny were killed on day 1 of neonatal life and DNA and RNA were isolated from the liver, a tissue where AFP mRNA levels are ~10% of total poly(A)$^+$ mRNA. Transgenic animals were identified by DNA hybridization to an AFP probe (Fig. 4*b*) and normal XX females were distinguished from translocation-bearing females by using a restriction fragment length polymorphism that distinguishes between the *hprt*^{a} and *hprt*^{b} alleles (Fig. 4*c*). Analyses of AFP minigene expression in representative transgenic females are shown in Fig. 4*a*. The AFP minigenes were not expressed in liver on the inactive X of the females bearing the translocation, although expression was observed in normal XX littermates. Therefore, the transcriptional activity of the AFP minigenes on the inactive X chromosome is dependent on the tissue in which the chromosome resides.

The lack of expression of the minigenes on the inactive X chromosome in liver could be anticipated from studies on X chromosome: autosome translocations, where the inactive state extended past the breakpoint into the autosomal genes[23–25]. The surprising result is the continued expression in the visceral endoderm, which suggests that the inactivation mechanism can discriminate between an X-linked gene and an autosomal gene. This difference may not be a property of the X chromosome, but rather reflects differences in the modes of regulation of the

AFP gene itself in these tissues; for example, the concentration of critical transcription factors may be high enough in the visceral endoderm to gain access to the gene even on the inactive X.

Alternatively and more likely, these findings can be interpreted as support for the notion that there are functional differences between the inactive X chromosome in extraembryonic versus embryonic tissues. It has been argued that these differences reside at the level of the maintenance[12,15] rather than the establishment of inactivation, as by the criteria of gene activity both chromosomes are equally inactive. The X-linked AFP genes were partially inactivated (two–three-fold) on the paternal X in visceral endoderm, which is consistent with this idea.

One candidate to explain the differences between the two inactive chromosomes is differences in DNA modification, particularly methylation. This argument is based on gene transfer experiments which demonstrated that the activity of the *hprt* gene can be transferred to a recipient cell from the inactive X chromosome of embryonic origin after treatment of the cell with 5-azacytidine, unlike the extraembryonic derived *hprt* gene, which can be transferred without drug treatment. The genomes of the extraembryonic lineages in general are undermethylated relative to other somatic tissues[26,27], a condition that extends from structural genes independently of whether they are expressed to satellite DNA. Using the isoschizomers *Msp*I and *Hpa*II, which monitor the methylation status of a subset of CpG sites in the AFP minigene integration site, we have not detected any significant differences between the degrees of methylation of the locus on the inactive X in visceral endoderm and liver (data not shown). These experiments argue against global methylation differences as an explanation for continued expression of the minigenes on the visceral endoderm-derived inactive X chromosome.

In conclusion, the differential expression of the AFP minigenes on the inactive X chromosome in the visceral endoderm and liver suggests that the mechanism of maintenance of the inactive state is discriminating between normally X-linked genes and an autosomal gene in the former tissue but not in the latter.

We thank E. Eicher for providing the M720 probe, T. Caskey for the *hprt* cDNA probe, A. McLaren, M. Monk, B. Hogan and T. Vogt for valuable discussions and Marie Estes for the preparation of the manuscript. R.K. and R.E.H. were supported by NIH postdoctoral training grants CA09035 and HD07155, respectively. This work was also supported by NIH grants HD17321, GM24125, CA06927, CA28050 and RR05539 and an appropriation from the Commonwelath of Pennsylvania.

Received 19 September; accepted 31 October 1985.

1. Lyon, M. F. *Nature* **190**, 372–373 (1961).
2. Takagi, N. & Sasaki, M. *Nature* **256**, 640–642 (1975).
3. West, J. D., Frels, W. I., Chapman, V. M. & Papaioannou, V. E. *Cell* **12**, 873–882 (1977).
4. Papaioannou, V. E. & West, J. D. *Genet. Res. Camb.* **37**, 183–197 (1981).
5. McMahon, A., Forsten, M. & Monk, M. *J. Embryol. exp. Morph.* **64**, 251–258 (1981).
6. McMahon, A., Forsten, M. & Monk, M. *J. Embryol. exp. Morph.* **74**, 207–220 (1983).
7. McMahon, A. & Monk, M. *Genet. Res. Camb.* **41**, 69–83 (1983).
8. Takagi, N. *Expl Cell Res.* **86**, 127–135 (1974).
9. Sugawara, O., Takagi, N. & Sasaki, M. *Chromosoma* **88**, 133–138 (1983).
10. Disteche, C. M., Eicher, E. M. & Latt, S. A. *Expl Cell Res.* **133**, 357–362 (1981).
11. Liskay, R. M. & Evans, R. J. *Proc. natn. Acad. Sci. U.S.A.* **77**, 4895–4898 (1980).
12. Chapman, V. M. *et al. Proc. natn. Acad. Sci. U.S.A.* **79**, 5357–5361 (1982).
13. Lester, S. C., Korn, N. J. & DeMars, R. *Somatic Cell Genet.* **8**, 265–284 (1982).
14. Venolia, L. *et al. Proc. natn. Acad. Sci. U.S.A.* **79**, 2352–2354 (1982).
15. Kratzer, P. G., Chapman, V. M., Lambert, H., Evans, R. E. & Liskay, R. M. *Cell* **33**, 37–42 (1983).
16. Krumlauf, R., Hammer, R. E., Tilghman, S. M. & Brinster, R. L. *Molec. cell. Biol.* **5**, 1639–1648 (1985).
17. Scott, R. W., Vogt, T. F., Croke, M. E. & Tilghman, S. M. *Nature* **310**, 562–567 (1984).
18. Phillips, S. J., Birkenmeier, E. H., Callahan, R. & Eicher, E. M. *Nature* **297**, 241–242 (1982).
19. Nielsen, J. T. & Chapman, V. M. *Genetics* **87**, 319–325 (1977).
20. Chapman, V. M., Kratzer, P. G. & Quarantillo, B. A. *Genetics* **103**, 785–795 (1983).
21. Lyon, M. F., Searle, A. G., Ford, C. E. & Ohno, S. *Cytogenetics* **3**, 306–323 (1964).
22. Takagi, N. *Chromosoma* **81**, 439–445 (1980).
23. Russell, L. B. & Montgomery, C. S. *Genetics* **64**, 281–312 (1970).
24. Russell, L. B. *Science* **140**, 976–978 (1963).
25. Ohno, S. & Lyon, M. F. *Chromosoma* **16**, 90–100 (1965).
26. Young, P. R. & Tilghman, S. M. *Molec. Cell Biol.* **4**, 898–907 (1984).
27. Sanford, J. P., Chapman, V. M. & Rossant, J. *Trends Genet.* **1**, 89–93 (1985).
28. Levak-Svajger, B., Svajger, A. & Skreb, N. *Experientia* **25**, 1311–1312 (1969).

The *neu* oncogene encodes an epidermal growth factor receptor-related protein

Cornelia I. Bargmann, Mien-Chie Hung & Robert A. Weinberg

Whitehead Institute for Biomedical Research, 9 Cambridge Center,
Cambridge, Massachusetts 02142 and Department of Biology,
Massachusetts Institute of Technology, Cambridge,
Massachusetts 02139, USA

The *neu* oncogene is repeatedly activated in neuro- and glioblastomas derived by transplacental mutagenesis of the BDIX strain of rat with ethylnitrosourea[1]. Foci induced by the DNAs from such tumours on NIH 3T3 cells contain the *neu* oncogene and an associated phosphoprotein of relative molecular mass 185,000 (p185)[2]. Previous work has shown that the *neu* gene is related to, but distinct from, the gene encoding the EGF receptor (c-*erb-B*)[3,4]. Here we decribe a *neu* complementary DNA clone isolated from a cell line transformed by this oncogene; the clone has biological activity in a focus-forming assay. The nucleotide sequence of this clone predicts a 1,260-amino-acid transmembrane protein product similar in overall structure to the EGF receptor. We found that 50% of the predicted amino acids of *neu* and the EGF receptor are identical; >80% of the amino acids in the tyrosine kinase domain are identical. Our results suggest strongly that the *neu* gene encodes the receptor for an as yet unidentified growth factor.

Transcripts of the *neu* gene were identified in NIH 3T3 cells transformed by *neu*. Polyadenylated RNA was isolated from B104-1-1, an NIH 3T3-derived cell line transformed by DNA from the B104 rat neuroblastoma cell line and known to express a high level of p185 (ref. 2). RNA was also isolated from NIH 3T3 cells transformed by a *ras* oncogene and from Rat-1 cells, a rat fibroblast line which expresses a protein immunologically related to p185 (ref. 3). This protein, which is also of $M_r \sim$ 185,000, is probably the product of the normal allele of the *neu* gene. A Northern blot of these RNAs was probed with R4E, a 4-kilobase (kb) *Bam*HI clone isolated from a genomic rat liver library by hybridization with part of the v-*erb-B* oncogene. This clone corresponds to the putative kinase domain of the rat *neu* gene (data not shown).

Under stringent conditions, this probe hybridized with RNAs of 4.4, 5.0 and 9 kb present in the *neu*-transformed NIH 3T3 cell line that were not present in the *ras*-transformed cell line (Fig. 1*a*,*b*). The smaller of these RNAs appeared also to be present in Rat-1 cells (Fig. 1*c*). These data strongly suggest that these messenger RNAs are the transcripts derived from the rat *neu* gene present in B104-1-1 cells and not the endogenous mouse gene. Quantitation of RNA levels by hybridization with a single-stranded RNA probe specific for *neu* indicated that these *neu* transcripts represent between 0.01 and 0.05% of the polyadenylated RNA in B104-1-1 cells.

A cDNA library was prepared from B104-1-1 polyadenylated RNA using standard S_1 snapback techniques[5]. Nine recombinant plasmids reactive with a *neu* probe were isolated, eight of which were derived from the same family of mRNAs as determined by restriction mapping. The largest of these, designated neuc(t)34, had an insert of 4.8 kb and was used for all subsequent studies.

In Northern analysis this cDNA clone reacted with all three of the mRNAs detected by the genomic clone (data not shown) and with no additional transcripts. A 400-base pair (bp) fragment from the extreme 3′ end of neuc(t)34 was used as a probe on an identical Northern filter and, as shown in Fig. 1*d*–*f*, it preferentially detected the 5.0- and 9-kb mRNAs in these cell lines. This suggests that the difference between the 4.4- and the 5.0-kb mRNAs resides at the 3′ end of the gene and that the neuc(t)34 cDNA is derived from the 5.0-kb mRNA.

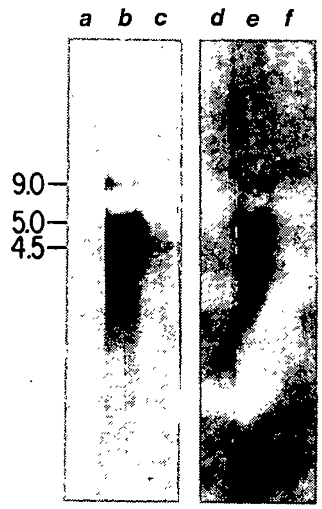

Fig. 1 Northern blot analysis of *neu*-related RNAs. Poly(A)$^+$ RNA (10 μg per lane) was hybridized with radiolabelled DNA from a genomic rat *neu* clone (*a–c*) or from the extreme 3′ end of the cDNA clone neuc(t)34 (*d–f*). RNA was extracted from Ki-*ras*-transformed NIH 3T3 cell line A5-2 (*a*, *d*), *neu*-transformed NIH 3T3 cell line B104-1-1 (*b*, *e*), or the Rat-1 fibroblast line (*c*, *f*) by standard methods[7], followed by oligo(dT) selection and separated on a formaldehyde-containing 1% agarose gel. *Hin*dIII-cleaved λ DNA was run as a marker. The RNA was transferred to nitrocellulose and hybridized in 50% formamide, $5\times$SSCPE, $1\times$ Denhardt's, 100 μg ml^{-1} boiled DNA and 10% dextran sulphate containing 5×10^6 c.p.m. of either a 500-bp *Bgl*I–*Stu*I fragment of genomic clone R4E (described in the text) or a 1.5-kb *Bam*HI fragment of neuc(t)34 nick-translated to a specific activity of 10^9 c.p.m. μg^{-1}; the nitrocellulose filters were washed at 65 °C in $2\times$SSCPE, 0.1% SDS and exposed to Kodak X-omat R film for 3 days at −70 °C using an intensifying screen.

The 4.8-kb insert of neuc(t)34 was introduced into the expression vector pSV2 (ref. 6) and tested for biological activity by transfection into NIH 3T3 cells. This clone was highly active in causing focus formation, yielding ~1,000 foci per μg of transfected DNA. Cell lines isolated from such foci contain a protein that is immunologically related to and co-migrates with the authentic p185 of B104-1-1 cells (data not shown). We conclude that neuc(t)34 is a biologically active clone of the *neu* gene present in B104-1-1 cells and encodes a full-length (or nearly full-length) p185 gene product.

Both strands of the coding region of neuc(t)34 were sequenced. Most parts of the gene were sequenced at least once each by the dideoxy and Maxam–Gilbert methods[7–9]. Figure 2 shows the DNA sequence of the *neu* cDNA and the predicted amino-acid sequence of its protein product; this predicted protein sequence is compared with that of the human EGF receptor in Fig. 3.

Neuc(t)34 has an open reading frame of 3,780 nucleotides and encodes a putative primary translation product of 1,260 amino acids that has a total M_r of 139,221, significantly smaller than the observed size of the *neu* gene product (M_r = 185,000). Glycosylation accounts for 15,000 daltons of the discrepancy (D. Stern and R.A.W., in preparation), and other post-translational modifications have not been excluded.

Sixteen of the 19 amino acids following the first ATG in the sequence are hydrophobic residues, consistent with the formation of a signal sequence for insertion into the membrane[10]. Residues 658–680 of the sequence are also highly hydrophobic, which suggests that this region represents a transmembrane domain. The location of these sequences and their similarity to sequences in the evolutionarily related EGF receptor[11] lead us to propose that p185 is organized similarly to the EGF receptor. Thus, the first few amino-acid residues of p185 would represent a cleaved signal sequence, the next 640 residues would include

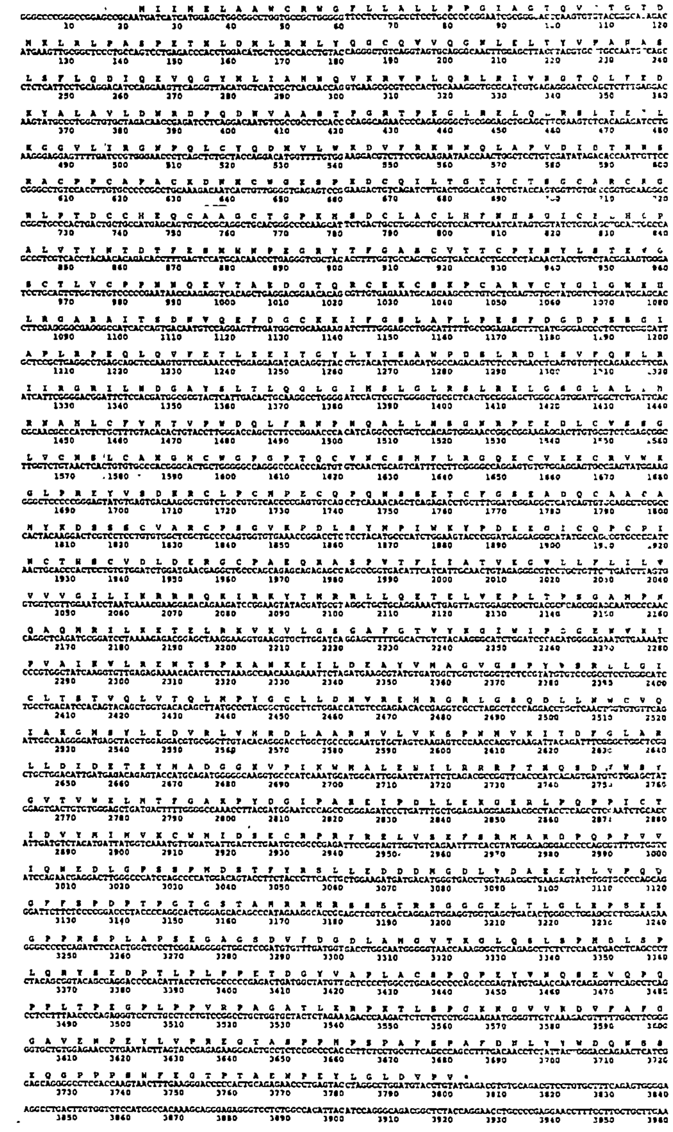

Fig. 2 DNA sequence of *neu*. Maxam–Gilbert sequencing[9] and M13 chain-termination sequencing[10,11] have been described elsewhere. Nucleotides 1–5 were generated by the tailing of the cDNA and do not represent sequences present in the RNA.

Methods. Poly(A)$^+$ RNA (5 μg) isolated as described in Fig. 1 legend was denatured in 12.5 mM methyl mercury hydroxide and reverse-transcribed in 50 mM Tris-HCl *p*H 8.3, 100 mM KCl, 10 mM $MgCl_2$, 5 mM dithiothreitol (DTT) and 0.5 mM of each dNTP with 50 μg ml^{-1} oligo(dT) (Collaborative Research), 120 U RNase (Promega Biotech) and 150 U reverse transcriptase (Boehringer-Mannheim) for 90 min at 42 °C. Nucleic acids were precipitated and the second-strand polymerization carried out in 50 mM KCl, 10 mM $MgCl_2$, 50 mM Tris *p*H 7.5, 1 mM DTT and 0.5 mM of each dNTP with 50 U DNA polymerase I large fragment (New England Biolabs) for 12 h at 16 °C after a second methyl mercury hydroxide denaturation. Hairpin loops were nicked with S_1 nuclease (600 U; Sigma) in 50 mM NaOAc *p*H 4.5, 0.2 M NaCl and 2 mM $ZnSO_4$ for 20 min at 37 °C. Double-stranded cDNA was size-selected over a BioGel A15 column (BioRad) and tailed using 30 U terminal transferase (BRL) in 200 mM potassium cacodylate, 2 mM DTT, 0.5 mM $CoCl_2$, 20 mM Tris *p*H 6.9, 600 μg ml^{-1} bovine serum albumin, and 0.1 mM dCTP for 2 min at 30 °C, phenol-extracted, ethanol-precipitated and annealed into dG-tailed *Pst*-cut pBR322 (BRL). 50,000 independent colonies were derived after transformation of cDNA into competent *Escherichia coli* and plating onto tetracycline-containing plates; these colonies were screened with a nick-translated fragment of a genomic clone of rat *neu* consisting of a 500-bp *Bgl*I to *Stu*I fragment which encompasses two exons of the *neu* tyrosine kinase domain. Nine recombinant plasmids reactive with this probe were purified; neuc(t)34, the largest, was sequenced.

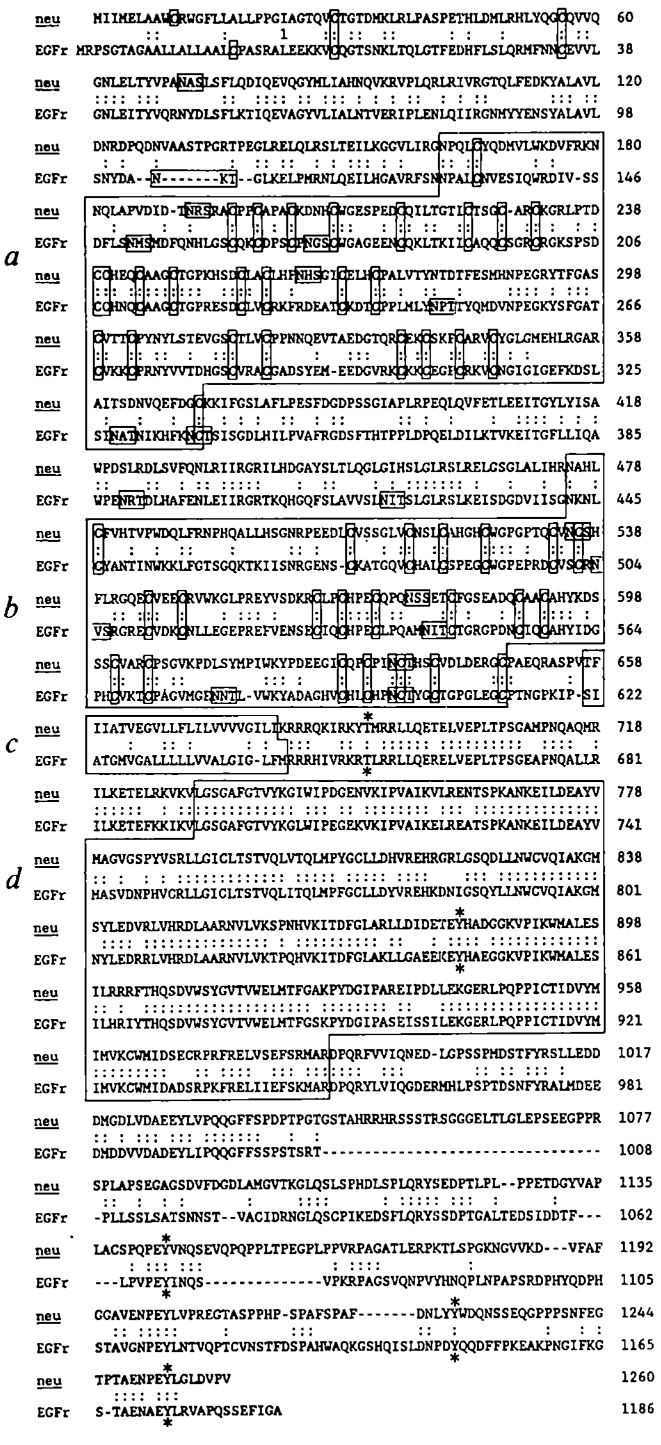

Fig. 3 Comparison of predicted amino-acid sequences of the *neu* gene product and the EGF receptor. Identities in sequence are marked by two dots between the conserved residues. All cysteine residues in the extracellular regions are boxed. Consensus sequences for *N*-linked glycosylation are marked by horizontal boxes. Asterisks denote residues which may be modified by phosphorylation. Boxed areas *a* and *b* represent the cysteine-rich domains of the extracellular part of the protein. *c*, Putative transmembrane domain; *d*, region homologous with the conserved region of the tyrosine kinase gene family. The first amino acid (leucine) of the mature EGF receptor protein is numbered (1).

an extracellular ligand-binding domain, and the 580 amino acids lying after the second hydrophobic (presumably transmembrane) domain would constitute cytoplasmic effector determinants of p185.

The putative extracellular domain of p185 contains two cysteine-rich areas between amino acids 162–372 and 475–649; these stretches contain 26 and 22 cysteines, respectively. This organization is strikingly similar to that of the comparable region of the EGF receptor[11]. As shown in Fig. 3, the two proteins show 43% identity of amino-acid residues in the extracellular portions. Note, however, that the positions of cysteines are highly conserved. All 50 cysteines predicted in the two extracellular domains are in equivalent positions in the two proteins.

These cysteine residues are also 80–90% conserved between these proteins and the insulin receptor[12,13]. As the peptide ligands of the insulin receptor and the EGF receptor are clearly unrelated, and as p185 does not bind either of these ligands (D. Stern and R.A.W., unpublished data), it seems that these residues must play a part other than forming the specific ligand-binding domain. They may constitute the structural scaffolding of the receptor or act to facilitate signal transduction after the receptor recognizes its ligand.

The two cysteine-rich regions of the EGF receptor bear homology with one another[11]. Similarly, the two cysteine-rich areas of *neu* are homologous. Comparison of the two EGF receptor domains, the two *neu* domains and the insulin receptor domain reveals that 15 residues out of ~180 appear to be conserved in this family of receptors (Fig. 4*a*). These residues include 11 cysteines as well as several other invariant residues. There are six predicted *N*-linked glycosylation sites in *neu*. Only one corresponds precisely in position to a glycosylation site in the EGF receptor.

A stretch of 25 hydrophobic amino acids followed by a lysine and three arginines appears to separate the extracellular from the cytoplasmic determinants of *neu*. The most obvious characteristic of the cytoplasmic region is the stretch of 250 amino acids homologous with the conserved region present in all tyrosine kinases[14]. Previous evidence indicated that the p185 protein has such an associated enzyme activity (D. Stern and R.A.W., in preparation); the sequence strongly suggests that this activity is intrinsic to the p185 protein itself.

Figure 4*b* compares this kinase domain with that of several other known tyrosine kinases and the cyclic AMP-dependent protein kinase. *neu* is more closely related to the EGF receptor gene than to all other members of this gene family; 82% of the amino-acid residues in this region of the EGF receptor and p185 are identical. The *neu* gene encodes the residues conserved among the proteins specified by the tyrosine kinase gene family (25% of the total residues in this domain), including the tyrosine residue that acts as an autophosphorylation site in pp60^{src} (residue 882 in the *neu* protein product).

After the kinase domain there are 60 amino acids that are 55% identical between the EGF receptor and *neu*. These residues are followed by a stretch of 198 amino acids in *neu* that are only distantly related to the last 172 amino acids of the EGF receptor; even when many gaps are inserted, only 58 residues (~30%) are comparable. This region of the protein consists of 20% proline residues and 10% each of glycine and serine residues, with only 25% of the residues being hydrophobic. Such hydrophilicity is characteristic of comparable regions of the EGF and insulin receptors.

Three tyrosine residues have been identified in the EGF receptor that serve as acceptor sites for *in vitro* autophosphorylation; these three and a fourth, as yet unlocalized, tyrosine are present in EGF receptor labelled *in vivo*[15]. The major site of phosphorylation of the EGF receptor *in vivo* is Tyr 1,173, 14 residues from the carboxy terminus of the EGF receptor. A similar tyrosine seems to exist eight residues from the carboxy terminus of p185 (Tyr 1,253). Tyrosine residues in homologous positions with the other two EGF receptor phosphotyrosine sites

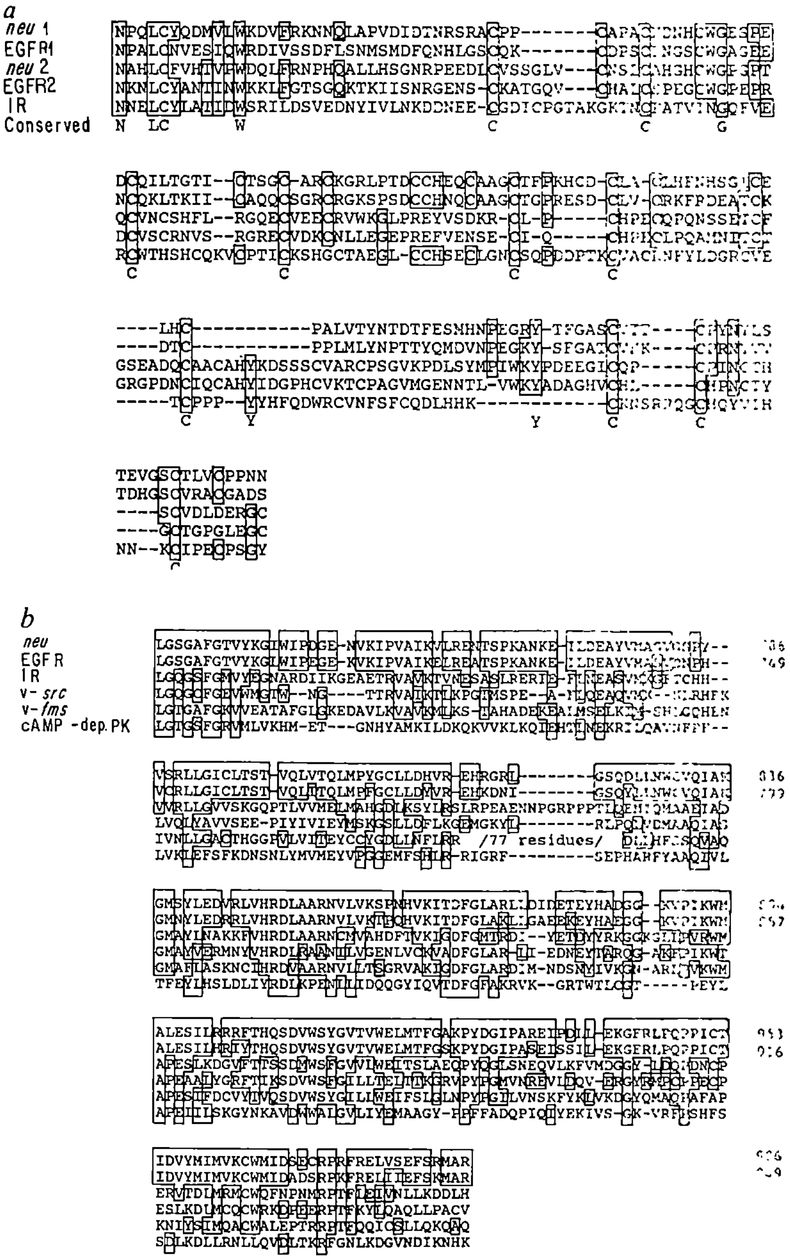

Fig. 4 *a*, Comparison of the cysteine-rich external domains of *neu*, the EGF receptor (EGFR) and the insulin receptor (IR). EGFR1 and *neu*1 are the more amino-terminal of the cysteine-rich domains found in these two proteins; *neu*2 and EGFR2 are the more carboxy-terminal of the domains found in the respective proteins. The following amino acids of the predicted protein sequences make up the domains shown: *neu*1, residues 162–323; *neu*2, 475–647; EGFR1, 129–291; EGFR2, 442–612, and IR, 122–292. Residues conserved in three or more of the five domains are boxed; residues present in all five are denoted underneath the sequences. *b*, Comparison of the putative tyrosine kinase domain of the *neu* gene product with the corresponding domains of the EGF receptor, the insulin receptor (IR), the products of the v-*src* and v-*fms* genes and the bovine cyclic AMP-dependent protein kinase. All residues shared between *neu* and one or more of the other kinases are boxed. The residues shown consist of amino acids 731–986 in the *neu* protein.

can also be found in *neu*. The tyrosine residues at EGF receptor position 1,068 and *neu* 1,144 are surrounded by similar residues in both proteins. The third tyrosine (EGF receptor, position 1,148) lies in a position homologous with a tyrosine residue in p185 (residue 1,227), but the residues surrounding it are not as similar.

Some or all of these tyrosines may act as regulatory sites for the *neu* gene product, but there are no data suggesting that they are phosphorylated. Another regulatory site may exist close to the membrane at position 691, 12 amino acids carboxy-terminal to the transmembrane domain. Exactly 12 amino acids from the transmembrane domain in the EGF receptor lies a threonine site that is phosphorylated by protein kinase C in response to the tumour promoter tetradecanoyl phorbol 13-acetate[16]. Phosphorylation at this site seems to cause the disappearance of a high-affinity class of EGF receptors from the cell surface[17,18]. The identically situated threonine in p185 could serve as such a site for negative regulation of receptor activity. Like Thr 654 of the EGF receptor and other known protein kinase C acceptor sites, it is surrounded by several basic residues[16].

Several oncogenes are mutated versions of cellular growth factors or their receptors[19], including v-*sis* (platelet-derived growth factor[20,21]), v-*erb-B* (truncated EGF receptor[22]), v-*fms* (slightly altered colony-stimulating factor (CSF)-1 receptor[23])) and v-*ros* (insulin receptor-related[12,13,24]). Various features of the deduced amino-acid sequence of p185 suggest that it is also a growth factor receptor, although the nature of its ligand is not yet known. Most suggestive is the colinearity and homology between *neu* and the gene for the EGF receptor. The extracellular cysteine-rich domains present in *neu* are characteristic of the EGF receptor, the insulin receptor and the low-density lipoprotein receptor[25]. An intracellular tyrosine kinase domain is also present on several growth factor receptors.

The accompanying report by Yamamoto *et al.*[26] describes the human homologue of the *neu* gene, which was isolated by virtue of its hybridization with the *erb-B* gene. Comparison of the human and rat sequences presented here reveals strong similarity between the two and demonstrates that they are in fact the same gene.

We thank Snezna Rogelj for assistance and advice on cDNA cloning techniques and Alan Schechter and David Stern for discussion and critical reading of the manuscript. We also thank T. Yamamoto for communicating his sequence before publication. This work was supported by Program Project Grant CA

17537-10 from the NCI and by a grant from the American Business Cancer Research Foundation. M.-C.H. was supported by a postdoctoral fellowship from the Cancer Research Institute. R.A.W. is an American Cancer Society Research Professor.

Received 30 August; accepted 15 November 1985.

1. Schubert, D. *et al. Nature* **249**, 224-227 (1974).
2. Padhy, L. C. *et al. Cell* **28**, 865-871 (1982).
3. Schechter, A. L. *et al. Nature* **312**, 513-516 (1984).
4. Schechter, A. L. *et al. Science* **229**, 976-978 (1985).
5. Maniatis, T., Fritsch, E. F. & Sambrook, J. *Molecular Cloning* (Cold Spring Harbor Laboratory, New York, 1982).
6. Mulligan, R. C. & Berg, P. *Science* **209**, 1422-1427 (1980).
7. Maxam, A. M. & Gilbert, W. *Meth. Enzym.* **65**, 499-580 (1980).
8. Sanger, F., Nicklen, S. & Coulson, A. R. *Proc. natn. Acad. Sci. U.S.A.* **74**, 5463-5467 (1977).
9. Biggin, M. D., Gibson, T. J. & Hong, G. F. *Proc. natn. Acad. Sci. U.S.A.* **80**, 3963-3965 (1983).
10. Blobel, G. *et al. Symp. Soc. exp. Biol.* **33**, 9-36 (1979).
11. Ullrich, A. *et al. Nature* **309**, 418-425 (1984).
12. Ullrich, A. *et al. Nature* **313**, 756-761 (1985).
13. Ebina, Y. *et al. Cell* **40**, 747-758 (1985).
14. Bishop, J. M. *A. Rev. Biochem.* **52**, 301-354 (1983).
15. Downward, J., Parker, P. & Waterfield, M. D. *Nature* **311**, 483-485 (1984).
16. Hunter, T., Ling, N. & Cooper, J. A. *Nature* **311**, 480-483 (1984).
17. Friedman, B. *et al. Proc. natn. Acad. Sci. U.S.A.* 3034-3038 (1984).
18. Davis, R. J. & Czech, M. P. *Proc. natn. Acad. Sci. U.S.A.* **82**, 4080-4084 (1985).
19. Hunter, T. *Trends biochem. Sci.* **10**, 275-280 (1985).
20. Doolittle, R. F. *et al. Science* **221**, 275-277 (1983).
21. Waterfield, M. D. *et al. Nature* **304**, 35-39 (1983).
22. Downward, J. *et al. Nature* **307**, 521-527 (1984).
23. Scherr, C. J. *et al. Cell* **41**, 665-676 (1985).
24. Neckameyer, W. S. & Wang, L. H. *J. Virol.* **53**, 879-884 (1985).
25. Yamamoto, T. *et al. Cell* **39**, 27-38 (1984).
26. Yamamoto, T. *et al. Nature* **319**, 230-234 (1986).

Similarity of protein encoded by the human c-*erb-B*-2 gene to epidermal growth factor receptor

Tadashi Yamamoto, Shuntaro Ikawa, Tetsu Akiyama*, Kentaro Semba, Nobuo Nomura†, Nobuyuki Miyajima, Toshiyuki Saito & Kumao Toyoshima

Institute of Medical Science, University of Tokyo, 4-6-1, Shirokanedai, Minato-ku, Tokyo 108, Japan
* Meiji College of Pharmacy, 1-35-23, Nozawa, Setagaya-ku, Tokyo 154, Japan
† Nippon Medical School at Sakuragi, 1-10-19, Uenosakuragi, Taito-ku, Tokyo 110, Japan

A novel v-*erb-B*-related gene, c-*erb-B*-2, which has been identified in the human genome[1,2], maps to human chromosome 17 at q21 (ref. 40), and seems to encode a polypeptide with a kinase domain that is highly homologous with, but distinct from, that of the epidermal growth factor (EGF) receptor[1]. The c-*erb-B*-2 gene is conserved in vertebrates and it has been suggested[1] that the *neu* gene, detected in a series of rat neuro/glioblastomas[3], is, in fact, the rat c-*erb-B*-2 gene. Amplification of the c-*erb-B*-2 gene in a salivary adenocarcinoma and a gastric cancer cell line MKN-7 suggests that its over-expression is sometimes involved in the neoplastic process. To determine the nature of the c-*erb-B*-2 protein, we have now molecularly cloned complementary DNA for c-*erb-B*-2 messenger RNA prepared from MKN-7 cells. Its sequence shows that the c-*erb-B*-2 gene encodes a possible receptor protein and allows an analysis of the similarity of the protein to the EGF receptor and the *neu* product. As a consequence of chromosomal aberration in MKN-7 cells, a 4.6-kilobase (kb) normal transcript and a truncated 2.3-kb transcript of c-*erb-B*-2 are synthesized at elevated levels. The latter transcript presumably encodes only the extracellular domain of the putative receptor.

Poly(A)$^+$ RNA was prepared from MKN-7 cells, a gastric cancer cell line in which the c-*erb-B*-2 gene is amplified[40] and over-expressed (see below). A cDNA library constructed from the MKN-7 mRNA was screened initially with a 440-base pair (bp) KX DNA fragment prepared from a c-*erb-B*-2 genomic clone and then with cDNA probes as described in Fig. 1 legend. Among 113 positive clones, pCER204 carried the longest insert of 4.0 kb, whereas the c-*erb-B*-2 mRNA is 4.6 kb long. Restriction mapping of the positive clones having an insert of >1.5 kb led to the identification of two distinct classes of clones (Fig. 1*A*),

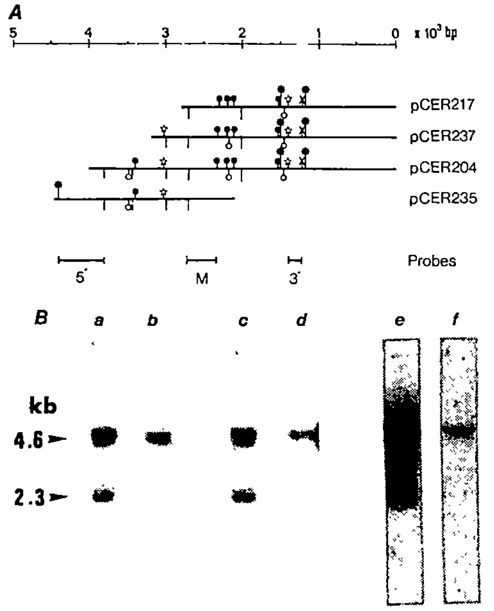

Fig. 1 Analysis of c-*erb-B*-2 clones. *A*, Restriction maps of c-*erb-B*-2 clones; *B*, Northern analysis of MKN-7 and placental mRNAs. *A*, Maps were constructed by the standard procedure for restriction digestion analysis of plasmid DNA[41]. Single or double digestion with restriction endonucleases *Kpn*I(×), *Eco*RI(☆), *Bam*HI (●), *Pvu*II (|), *Sma*I (*) and *Acc*I (○) was performed. The *Acc*I site at position 2.2 kb in this map is absent from the pCER217 insert but pCER237 and pCER204 were cleaved with the enzyme at this position. Sequence data reveal that pCER217 carries a deletion of 42 bp in this region (see Fig. 2 legend). The exon sequence of the 440-bp KX DNA prepared from the genomic clone λ107 (ref. 1) corresponds to a 150-bp *Eco*RI–*Kpn*I fragment of pCER217 (3' probe). A 450-bp *Pvu*II–*Bam*HI fragment of pCER217 (middle probe) and a 650-bp *Sma*I–*Pvu*II fragment of pCER235 (5' probe) were used for the second and third screenings, respectively, of the MKN-7 cDNA library. Total RNA was prepared from MKN-7 cells by the guanidine isothiocyanate–caesium chloride method[28]. Poly(A)$^+$ RNA was selected by two cycles of oligo(dT)–cellulose column chromatography[29]. A cDNA library was constructed by the method of Okayama and Berg[30], using 5.4 μg poly(A)$^-$RNA and 2.8 μg vector-primer DNA. (Avian myeloblastosis virus reverse transcriptase was from Dr J. W. Beard.) *Escherichia coli* MC1061 (ref. 31) was used for transformation[32]. Ampicillin-resistant transformants (60,000 independent clones) were first screened by hybridization at 60 °C for 16 h in the solution described previously[33] with the 440-bp KX DNA fragment. Among 21 distinctive positive clones, pCER217 carried the longest insert of 2.8 kb. To obtain clones harbouring cDNA for further upstream sequence, 50,000 independent clones of the same library were screened with the 450-bp *Pvu*II–*Bam*HI fragment mapped in the 5' portion of the pCER217 insert. Of 44 positive clones, plasmid pCER237 carried the longest insert (3.2 kb). A plasmid pCER235 was assumed to be derived from an aberrant c-*erb-B*-2 mRNA which shared 5' sequence with normal 4.6-kb mRNA, as described in the text. The MKN-7 cDNA library (100,000 clones) was again screened with a 650-bp *Sma*I–*Pvu*II restriction fragment derived from pCER235; 48 positive clones were obtained, one of which, designated pCER204, contained the longest insert (4.0 kb) and the restriction maps of its 5' one-third and 3' two-thirds were identical to those of pCER235 and pCER217, respectively. *B*, Nitrocellulose filters containing poly(A)$^+$ RNAs from MKN-7 (lanes *a*, *c*, *e*) and human placenta (lanes *b*, *d*, *f*) were hybridized with the 5' (lanes *a*, *b*), middle (lanes *c*, *d*) and 3' probes (lanes *e*, *f*) shown in *A*. Lanes *b* and *d* are photographs obtained after longer exposure of the film (overnight exposure for lanes *a*, *c*; 2 weeks exposure for lanes *b*, *d*). Poly(A)$^+$ RNA (2 μg) from MKN-7 cells was denatured with 50% formamide and 2.2 M formaldehyde and applied to a 1% agarose gel containing 2.2 M formaldehyde[34]. RNAs on the gel were transferred to a nitrocellulose filter[35], which was then hybridized for 16 h under stringent conditions (50% formamide, 4×SSC, 42 °C) with the DNA probes. After hybridization, the filter was washed under stringent conditions as described elsewhere[1]. Under the hybridization conditions used, no hybridization of the DNA probes with the EGF receptor mRNA was observed. The DNA probes were labelled with [α-^{32}P]dCTP (3,000 Ci mmol^{-1}; Amersham) by nick-translation[36].

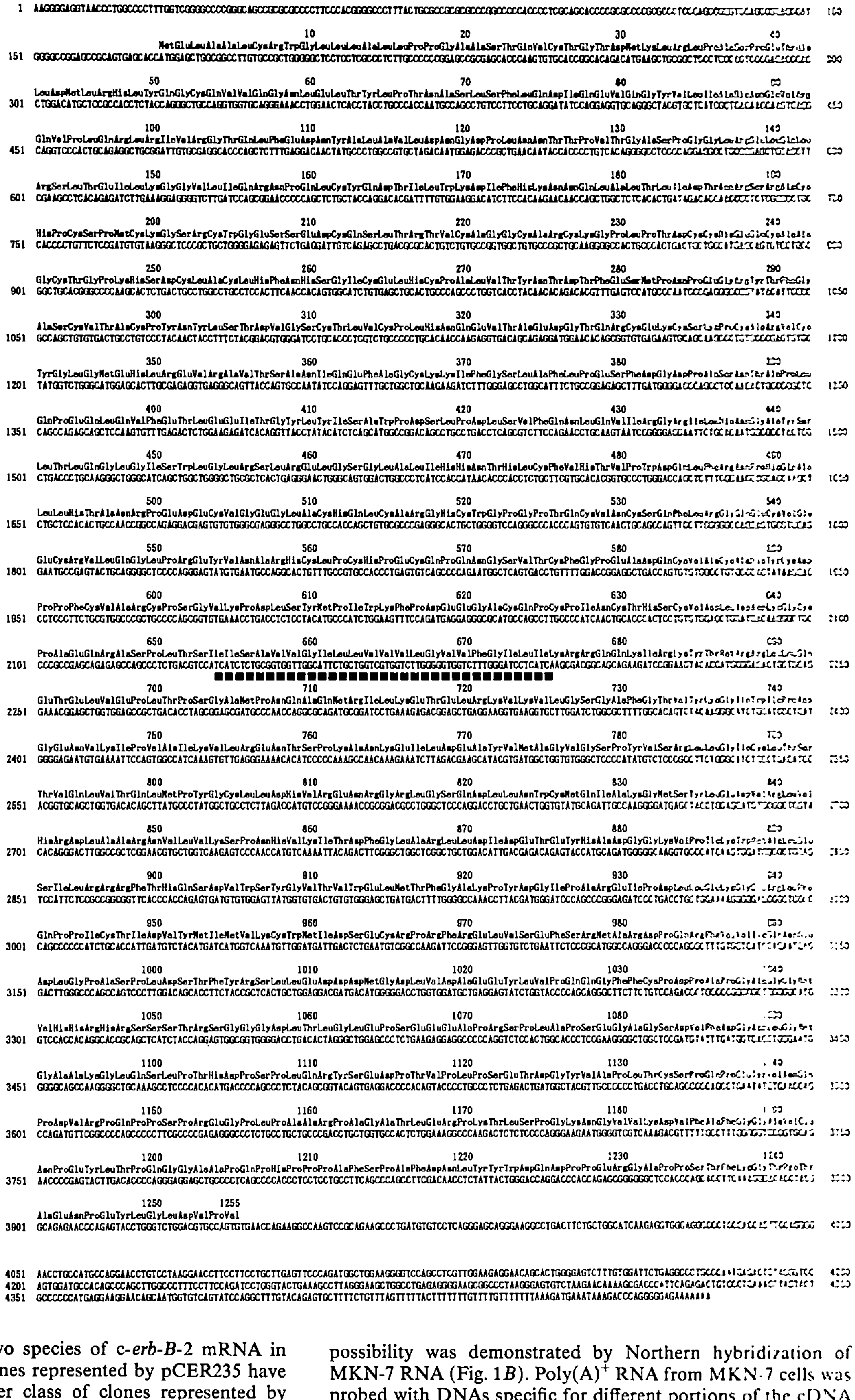

Fig. 2 The c-*erb-B*-2 cDNA nucleotide sequence and predicted amino-acid sequence. Nucleotides are numbered at both sides. Amino-acid sequence is numbered from the putative signal peptide above the sequence. Black dotted bars indicate the putative transmembrane region. The AATAAA box is followed (14 bp downstream) by the polyadenylated 3′ end of the mRNA. The nucleotide sequence from residues 1 to 1,810 was from pCER235 and that from residues 1,583 to the extreme 3′ end was from pCER217, except that the sequence of the 77-bp *Bam*HI fragment (2,314–2,390) was from pCER237, as a sequence of 42 bp was apparently deleted in pCER217 (see Fig. 1 legend). The overlapping nucleotide sequences (1,583–1,810) of pCER217 and pCER235 match. The extreme 3′ sequence of pCER235, which was derived from a sequence of unknown origin caused by chromosomal translocation is not shown here. The nucleotide sequence was determined by the Maxam-Gilbert[37] procedure and the dideoxy chain termination method in conjunction with bacteriophage M13mp19 (refs 38, 39).

suggesting that there are two species of c-*erb-B*-2 mRNA in MKN-7 cells. As cDNA clones represented by pCER235 have inserts of ≤2.3 kb, the other class of clones represented by pCER204 (or 217 and 237) was thought to be derived from the 4.6-kb mRNA. The pCER235 insert has a sequence that corresponds to the 5′ half, but not the 3′ half, of the pCER204 insert, suggesting that pCER235 was derived from mRNA which shares its sequence with the 5′ portion of normal 4.6-kb mRNA. This possibility was demonstrated by Northern hybridization of MKN-7 RNA (Fig. 1*B*). Poly(A)$^+$ RNA from MKN-7 cells was probed with DNAs specific for different portions of the cDNA clones. Using the 3′ probe, equivalent to the KX DNA probe[1], we observed a single species of 4.6-kb mRNA, which is expressed at an elevated level in MKN-7 cells (50-fold relative to placenta). However, both the *Pvu*II-*Bam*HI fragment (middle probe) and the *Sma*I-*Pvu*II fragment (5′ probe) reacted with a 2.3-kb

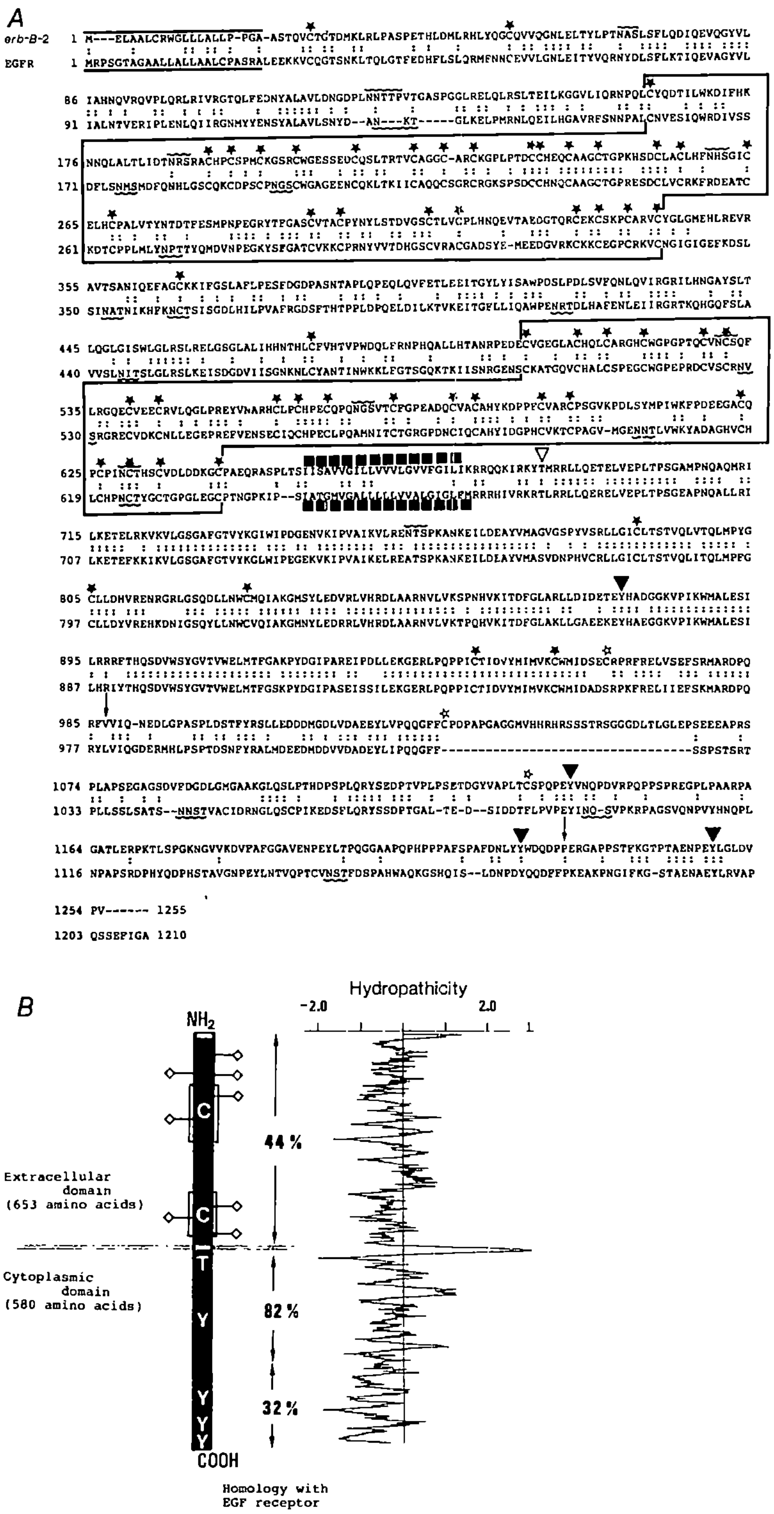
A
erb-B-2
EGFR
B
NH2
C
C
T
Y
Y
Y
Y
COOH
44 %
82 %
32 %
Extracellular domain (653 amino acids)
Cytoplasmic domain (580 amino acids)
Hydropathicity
-2.0
2.0
Homology with EGF receptor

Fig. 3 Amino-acid sequence of c-*erb-B*-2. ***A***, Alignment of the amino-acid sequences of c-*erb-B*-2 and EGF receptor (EGFR). Amino acids of the two proteins are numbered on the left. Identities in the sequences are marked by two dots between the two lines; predicted transmembrane regions are represented by dotted black bars; the possible *N*-linked glycosylation sites by wavy lines; horizontal lines indicate signal peptides (putative for c-*erb-B*-2); stars indicate cysteine residues in the sequence: solid stars are common to the two proteins and the open stars are specific to c-*erb-B*-2. The major sites of threonine and tyrosine phosphorylation of the EGF receptor or pp60^{src} are conserved in c-*erb-B*-2 and are shown by open and closed triangles, respectively. The amino-acid residues corresponding to the extreme carboxy terminus of pp60^{src} and v-*erb-B* protein are indicated by vertical arrows at positions 986 and 1,228, respectively. Boxed sequences show the cysteine clusters. ***B***, Schematic illustration of the c-*erb-B*-2 protein. Amino-acid sequence homologies of the c-*erb-B*-2 protein and the EGF receptor are shown. T, threonine and Y, tyrosine are possible phosphorylation sites. C, cysteine clusters (also boxed). —◇, Possible glycosylation sites. An open box at the amino terminus shows the putative signal peptide and that in the middle shows possible transmembrane sequence. The hydropathicity of the c-*erb-B*-2 sequence is also shown.

mRNA in addition to the 4.6-kb mRNA in MKN-7 cells, but with the 4.6-kb mRNA alone in placenta. The 2.3-kb mRNA was over-produced to about the same extent as the 4.6-kb mRNA.

Thus, the nucleotide sequences of the cloned inserts of pCER235 and pCER217 (237 or 204) were assumed to represent the overall sequence of the c-*erb-B*-2 gene product. The entire nucleotide sequence of 4,480 bp obtained from pCER235, pCER237 and pCER217 is shown in Fig. 2. The longest open reading frame is composed of 3,765 nucleotides, whose translated amino-acid sequence of 1,255 residues is also shown. The predicted initiation codon ATG is flanked by nucleotides that match Kozak's criteria[4] for a translation initiation site. A primary translation product of the c-*erb-B*-2 gene was calculated to have a relative molecular mass (M_r) of 137,895.

Previous analysis of the c-*erb-B*-2 genomic clone λ107 showed that the c-*erb-B*-2 gene product has a kinase domain that is highly homologous with that of EGF receptor/v-*erb-B*[1]. As shown in Fig. 3*A*, the entire amino-acid sequences of the two proteins are extremely similar and the hydrophilicity profiles[5] (Fig. 3*B*) and secondary structure[6] (data not shown) predicted from the amino-acid sequence of the c-*erb-B*-2 protein are also similar to those predicted for the EGF receptor. A sequence of 22 amino-acid residues (654–675) is strongly hydrophobic and

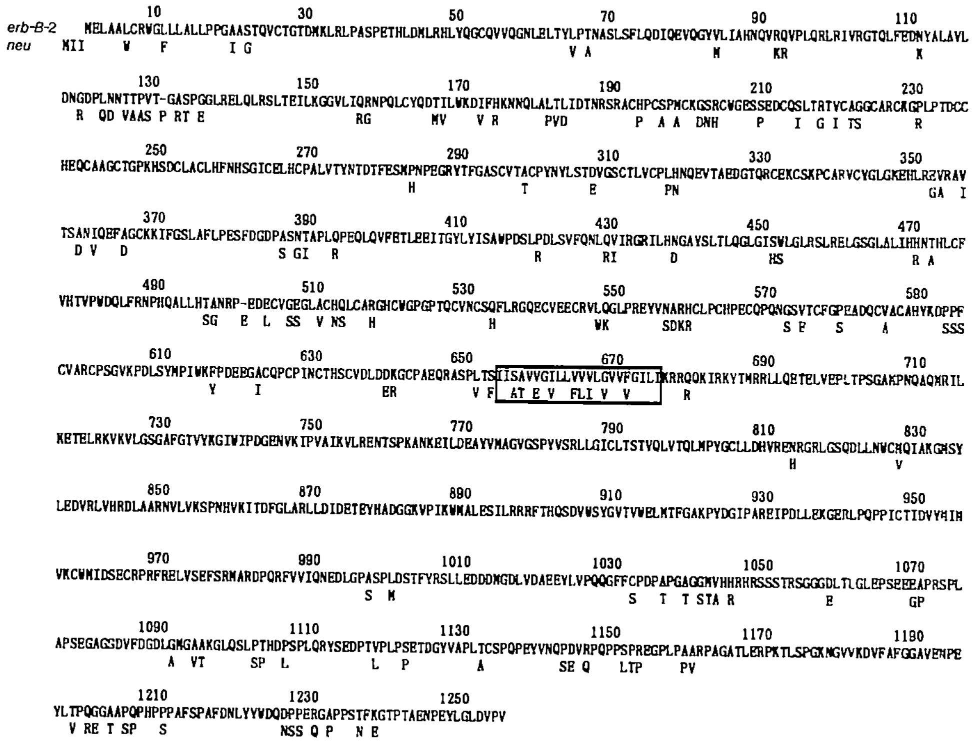

Fig. 4 Comparison of rat *neu* and human c-*erb-B*-2. The amino-acid sequence of c-*erb-B*-2 is compared with that of *neu* (kindly communicated by Dr R. A. Weinberg). Only non-identical amino acids are shown for *neu*. The amino acids for c-*erb-B*-2 are numbered above the sequence. The boxed sequence indicates the transmembrane domain.

could serve as a membrane-anchoring domain. This sequence, like those of other receptors[7-10], is followed immediately by basic amino acids (Lys-Arg-Arg), which helps in the correct allocation of the protein at the cell surface. The first 21 amino-acid residues are also highly hydrophobic, which suggests that they represent a signal sequence for membrane glycoprotein. Eight possible sites of *N*-linked glycosylation were identified in the amino-terminal moiety of the c-*erb-B*-2 protein. These data indicate that the two proteins with similar sizes have transmembrane topologies that resemble each other. Therefore, we tentatively conclude that the c-*erb-B*-2 protein is a receptor for an unknown growth factor.

The sequence of the putative extracellular domain shows 44% homology with the ligand binding domain of the EGF receptor. A striking similarity is the presence of two cysteine-rich regions, in which the spatial distribution of cysteine residues is virtually identical with that in the EGF receptor. The sequences of cysteine clusters are rather hydrophilic (Fig. 3*B*) and would facilitate the generation of a specific conformation for signal transmission through intramolecular or intermolecular S–S bridges, as is suggested for other receptors for growth factors[8-10]. These findings also suggest that the extracellular domains of the c-*erb-B*-2 protein and EGF receptor form similar configurations and bind to structurally related ligands. However, not only EGF but ligands such as tumour growth factor (TGF)-β, TGF-γ, fibroblast growth factor, erythropoietin, nerve growth factor, insulin and platelet-derived growth factor all failed to activate the kinase activity that is presumably intrinsic to the c-*erb-B*-2 protein (data not shown).

The sequence of 260 amino acids (residues 727–986), including the postulated ATP-binding site[11] of the cytoplasmic domain of the c-*erb-B*-2 protein, is homologous with the kinase domain of the EGF receptor (82% homology) and with retroviral oncogene products of the *src* family (25–40% homology[1]). Therefore, the c-*erb-B*-2 protein seems to have tyrosine kinase activity. Preliminary experiments using antiserum raised against a synthetic peptide of 14 amino-acid residues at the carboxy terminus of c-*erb-B*-2 show that the c-*erb-B*-2 protein gp185 exhibits tyrosine kinase activity (T.A. *et al.*, in preparation). The homology between the two proteins decreases to 32% in the 269 amino-acid residues at the carboxyl end. However, three major *in vitro* phosphorylation sites of the EGF receptor[12] are also conserved (tyrosine residues at 1,139, 1,222 and 1,248 of c-*erb-B*-2), indicating that the c-*erb-B*-2 protein could also be autophosphorylated.

Another interesting feature of the c-*erb-B*-2 protein is the presence of a threonine residue at position 686, surrounded by basic amino-acid residues, which is equivalent to threonine 654 of the EGF receptor on which protein kinase C-mediated phosphorylation occurs[13]. Therefore, the c-*erb-B*-2 protein may be phosphorylated by protein kinase C, which would play an important role in signal transmission as suggested for the EGF receptor.

Comparison of the nucleotide sequences and deduced amino-acid sequences of the recently characterized rat *neu* (see accompanying paper[14]) and human c-*erb-B*-2 (our present results) reveal that the *neu* gene is the rat counterpart of the c-*erb-B*-2 gene (see Fig. 4 for the amino-acid sequences). Surprisingly, only two amino acids in the kinase domain (residues 813 and 817) differ between the two proteins, although we do not know whether the c-*erb-B*-2 gene of MKN-7 cells can transform NIH 3T3 cells. The possible glycosylation sites of the *neu* product are located at positions corresponding to those of the c-*erb-B*-2 product, except that no sequence corresponding to Asn-Asn-Thr-Thr (positions 124–127 of c-*erb-B*-2) is found in *neu*, suggesting that the mature c-*erb-B*-2 protein is as large as the *neu* gene product gp185.

Evidence is accumulating that amplification and overexpression of a proto-oncogene can cause cell transformation *in vitro* and can play a part in the neoplastic process of human tumours[15-20]. Amplification and elevated expression of the EGF receptor gene have been observed in glioblastomas and in squamous carcinoma cell lines[21-24]. In contrast, amplification of the c-*erb-B*-2 gene has been seen in three human adenocarcinomas: one salivary adenocarcinoma[1], one mammary carcinoma[2] and one MKN-7 gastric cancer cell line, suggesting that increased expression of the c-*erb-B*-2 gene provides a selective advantage in the formation or the progress of tumours of epithelial cells.

Because the cDNA clone pCER235 derived from the 2.3-kb mRNA does not contain a signal for membrane anchoring of the predicted polypeptide (data not shown), the translation product of the 2.3-kb mRNA, corresponding to the sequence of the c-*erb-B*-2 ligand-binding domain, should be secreted by MKN-7 cells. Similarly, a truncated EGF receptor sequence has been reported to be over-expressed concomitantly with the EGF receptor in A431 cells[7,25,26], as a consequence of a strong aberration of the chromosomes[27]. Production of the truncated receptor in MKN-7 cells may also be caused by chromosomal aberration[40]. We cannot exclude the possibility that extracellular accumulation of truncated growth factor receptors is associated with the appearance of the transformed phenotype. It is also possible that they provide a growth advantage to the cells in culture, in which the growth factor receptors are over-expressed.

We thank N. Kitamura, H. Okubo and S. Nakanishi for help in constructing the MKN-7 cDNA library, H. Kawano for technical assistance and S. Sasaki for help in preparing the manuscript. We also thank Y. Kaziro for critical reading of the manuscript.

Received 28 August; accepted 27 November 1985.

1. Semba, K., Kamata, N., Toyoshima, K. & Yamamoto, T. *Proc. natn. Acad. Sci. U.S.A.* **82,** 6497-6501 (1985).
2. King, C. R., Kraus, M. H. & Aaronson, S. A. *Science* **229,** 974-976 (1985).
3. Schubert, D. *et al. Nature* **249,** 224-227 (1974).
4. Kozak, M. *Nucleic Acids Res.* **9,** 5233-5252 (1981).
5. Kyte, J. & Doolittle, R. F. *J molec. Biol.* **157,** 105--132 (1982).
6. Chou, P. Y. & Fasman, G. D. *A. Rev. Biochem.* **47,** 251-276 (1978).
7. Ullrich, A. *et al. Nature* **309,** 418-425 (1984).
8. Ebina, Y. *et al. Cell* **40,** 747-758 (1985).
9. Ullrich, A. *et al. Nature* **313,** 756-761 (1985).
10. Yamamoto, T. *et al. Cell* **39,** 27-38 (1984).
11. Kamps, M. P., Taylor, S. S. & Sefton, B. M. *Nature* **310,** 589-592 (1984).
12. Downward, J., Parker, P. & Waterfield, M. D. *Nature* **311,** 483-485 (1984).
13. Hunter, T., Ling, N. & Cooper, J. A. *Nature* **311,** 480-483 (1984).
14. Bargmann, C. I., Hung, M.-C. & Weinberg, R. A. *Nature* **319,** 226-230 (1986).
15. Chang, E. H., Furth, M. E., Scolnick, E. M. & Lowy, D. R. *Nature* **297,** 479-483 (1982).
16. Gazit, A. *et al. Cell* **39,** 89-97 (1984).
17. Clarke, M. F. *et al. Nature* **308,** 464-467 (1984).
18. Schwab, M. *et al. Nature* **305,** 245-248 (1983).
19. Kohl,, N. E. *et al. Cell* **35,** 359-367 (1983).
20. Schwab, M. *et al. Proc. natn. Acad. Sci. U.S.A.* **81,** 4940-4944 (1984).
21. Libermann, T. A. *et al. Cancer Res.* **44,** 753-760 (1984).
22. Libermann, T. A. *et al. Nature* **313,** 144-147 (1984).
23. Cowley, G., Smith, J. A., Gusterson, B., Hendler, F. & Ozanne, B. in *Cancer Cell I* (eds Levine, A. J., VandeWoude, G. F., Topp, W. C. & Watson, J. D.) 5-10 (Cold Spring Harbor Laboratory, New York, 1984).
24. Yamamoto, T. *et al. Cancer Res.* (in the press).
25. Merlino, G. T. *et al. Science* **224,** 417-419 (1984).
26. Weber, W., Gill, G. N. & Spiess, J. *Science* **224,** 294-297 (1984).
27. Merlino, G. T. *et al. Molec. cell. Biol.* **5,** 1722-1734 (1985).
28. Chirgwin, J. M., Przybyla, A. E., MacDonald, R. J. & Ruffer, W. J. *Biochemistry* **18,** 5294-5299 (1979).
29. Aviv, H. & Leader, P. *Proc. natn. Acad. Sci. U.S.A.* **69,** 1408--1412 (1972).
30. Okayama, H. & Berg, P. *Molec. cell. Biol.* **2,** 161-170 (1982).
31. Casadaban, M. & Cohen, S. N. *J. molec. Biol.* **138,** 179-207 (1980).
32. Hanahan, D. & Meselson, M. *Meth. Enzym.* **100,** 333-342 (1983).
33. Iwai, T. *et al. Proc. natn. Acad. Sci. U.S.A.* **80,** 7405-7409 (1983).
34. Lehrach, H., Diamond, K., Wozney, J. M. & Boedtker, H. *Biochemistry* **16,** 4743-4751 (1977).
35. Thomas, P. S. *Proc. natn. Acad. Sci. U.S.A.* **77,** 5201-5205 (1980).
36. Maniatis, T., Jeffery, A. & Kleid, D. *Proc. natn. Acad. Sci. U.S.A.* **12,** 1184-1188 (1975).
37. Maxam, A. M. & Gilbert, W. *Meth. Enzym.* **65,** 109-111 (1979).
38. Sanger, F., Nicklen, S. & Coulson, A. R. *Proc. natn. Acad. Sci. U.S.A.* **74,** 5463-5467 (1977).
39. Messing, J. *Meth. Enzym.* **101,** 20-77 (1983).
40. Fukushige, S. *et al. Molec. cell. Biol.* (in the press).
41. Maniatis, T., Fritsch, E. & Sambrook, J. in *Molecular Cloning: A Laboratory Manual* (Cold Spring Harbor Laboratory, New York, 1982).

Primate η-globin DNA sequences and man's place among the great apes

Ben F. Koop*, Morris Goodman*§, Peilin Xu†, Keith Chan† & Jerry L. Slightom†‡

*Department of Anatomy, Wayne State University School of Medicine, Detroit, Michigan 48201, USA
†Laboratory of Genetics, University of Wisconsin, Madison, Wisconsin 53706, USA
‡Upjohn Company, Kalamazoo, Michigan 49001, USA

Molecular studies indicate that chimpanzee and gorilla are the closest relatives of man (refs 1–7 and refs therein). The small molecular distances found point to late ancestral separations[2,4,7], with the most recent being between chimpanzee and man, as judged by DNA hybridization[3,8]. Kluge[9] and Schwartz[10] contest these conclusions: morphological characters group a chimpanzee–gorilla clade with the Asian ape orang-utan in Kluge's cladistic study and with an orang-utan–human clade in Schwartz's study. Clearly, extensive sequencing of nuclear DNA is needed to resolve by cladistic analysis the branching order within Hominoidea[11]. Towards this goal, we are sequencing orthologues of the primate ψη-globin locus[12,13]. Here, we compare the newly completed sequences of orang-utan and rhesus monkey with human, chimpanzee, gorilla, owl monkey, lemur and goat orthologues. Our findings substantially increase the evidence indicative of a human–chimpanzee–gorilla clade with ancestral separations around 8 to 6 Myr ago. We also verify that neutral hominoid DNA evolved at markedly retarded rates.

The η locus is one of five ancient β-related globin genes linked in a cluster 5′-ε-γ-η-δ-β-3′ that arose from tandem duplications (200-100 Myr)[12,13]. This ancient η gene was embryonically expressed in early eutherians and persisted as a functional gene in artiodactyls, but became a pseudogene in proto-primates and was lost from rodents and lagomorphs. Previous work from this laboratory[13] established that the goat η gene sequence

Fig. 1 (Opposite) Aligned nuceotide sequences of seven primate ψη-globin genes and the active goat η-globin gene. Total DNA was isolated from orang-utan (*Pongo pygmaeus*) no. 1 liver (Yerkes Primate Center) and from a rhesus monkey (*Macaca mulatta*) blood sample (California Primate Center). DNAs were subjected to a series of limited *Eco*RI digestions and size-selected fragments, 15-25 kilobases (kb), were cloned into the λ vector Charon 32[33] by the procedure described by Slightom *et al.*[34]. Recombinant phage DNAs were packaged into phage capsids using the *in vitro* phage packaging procedure[35]. Charon 32 phage were plated on the recA⁻ *Escherichia coli* host ED8767[36] and screened using a ^{32}P-labelled 245-base-pair (bp) *Ava*II–*Eco*RI fragment isolated from the γ-globin cDNA clone pJW151[37]. The ψη-containing *Eco*RI fragments were subcloned into pBR322 (orang 7.0 kb, rhesus 10.0 kb). DNA sequencing was done using the chemical procedure described by Maxam and Gilbert[38]. The nucleotide sequences fo human, chimpanzee and gorilla are from Chang and Slightom[16], an owl monkey and lemur are from Harris *et al.*[12]. Only the 5′-flanking t exon 2 of the lemur sequence is orthologous to the η gene[12,15]; therefor only this part of the sequence is used in our analyses. The goat η-globi gene (goat ε^{II} gene) nucleotide sequence is from Shapiro *et al.*[14]. Th nucleotide sequencing numbering system is based on the overall alignment among these sequences. The complete nucleotide sequence for th human ψη-globin gene (HUMA) is presented on the top line an differences are given for the remaining sequences. Asterisks indicate th presence of gaps placed to minimize the number of geneic change during descent[13,39]. The simian ψη genes are divided into three exon separated by two introns each obeying the GT–AG splicing rule[40]. Lemu ψη[12,15] extends only to the 3′ end of exon 2 and has a defective intro 1 splice site. Intron 1 sequences are all 121 bp in length, while intron lengths vary between 841 to 877 bp. The 5′-flanking region of the oran ψη gene contains a 38-bp direct repeat (positions 205–244 and 245–282 common to hominoid ψη genes. Each repeat contains a CCAAT typ promoter element. The RNA polymerase II binding site (TATAA) ha diverged in the ψη genes from that found in normal β-type globi genes[41] (note positions 299–304). As in the other primate ψη genes th initiation codon (INT positions 384–386) of orang and rhesus sho defects that prohibit translation. All of the primate ψη genes share terminator sequence TGA (positions 1,885–1,888) and have the canon cal poly(A) addition signal[42]. With regard to the direct repeat at position 1,895–1,914 and 1,915–1,940, the 22-base gap (positions 1,895–1,914 in orang and rhesus could be the result of either two independen deletions or a deletion of the 5′ direct repeat in the stem catarrhine followed by a reduplication in the stem hominines. Exons terminate the ---→ sites.

---

§To whom correspondence should be addressed.

```
HUMA GAAGTCCTTGAGAAATAAACTGCACACTGGATGGTGGGGG*TAGTGTAGGAAAA*TGGAGGGGAAGGAAGTAAAGTTTCAAATTAAGCCTGAACAGCAAAGTTCCCCTGAGAAGGCCACC
CHIM  AAGT C      A     C  C   CTGGATT C GGGG*   T T GG    *TG  GG    G    TA A   TC     A G    A CA   A   TC C    GAAGGCC  C
GORI  AAGT C      A     C  C   CTGGACG T GGGA*   C T GG    *TG  GG    G    TA A   CC     A G    A CA   A   TC C    GAAGGCC  C
ORAN  GACT C      A     C  C   CTGGATG T GGAG*   T T GG    *TG  GC    G    TA A   TC     A G    A CA   A   TC C    GAAGGCC  C
RHES  AAGA T      A     C  C   CTGGATG T GGGG*   T T GG    *TG  GG    A    TA A   TC     A G    A CA   A   TC C    GAAGCCC  C
OWLM  AAGA C      T     C  T   *****TG T GAGG*   T G GA    *TA  TG    A    AG A   TC     A G    A CA   A   CC T    GTGGG*A  A
LEMU  GGGC C      A     T  C   CTTGATG T AGGGA   T T CC    AAA  GG    A    TG G   TA     G T    A TG   G   CC *    GGGGGCC  C
GOAT                                                                                            > CT   G   AT C    TAGAGCC  C
     ---------+---------+---------+---------+---------+---------+---------+---------+---------+---------+---------+---------+ 120

                                                                                          CCAAT
HUMA TGGATTCTATCAGAAACTCGAATGTCCATCTTGCAAAACTTCC*TTGCCCAAACCCCACCCCTGG*AGTCACAACCCACCCTTGACCAATAGATTCATTTCACTGAGGGAGGCAAA*GGG
CHIM TGGATTCTAT A  A  TCG   G       TGCAA A TT C*     C  ACC     CC  G* G CA A   CAC C    C      AT      C C GA AG GGC  A*GGG
GORI TGGATTCTAT A  A  TCG   G       TGCAA A TT C*     C  ACC     CC  G* G CA A   CAC C    C      AT      C C AA AG AGC  A*GGG
ORAN CGGATTCTAT A  A  TCG   G       TGCAA A TT C*     C  ACC     CC  G* G CA A   CAC C    C      AT      C C GG AA GGC  A*GCG
RHES CGGATTCTAT A  A  TTG   G       TGCAA A TT CC     C  ACC     CC  A* G CG A   CAC C    C      AT      C C GA AC GGC  AAGGG
OWLM CAGATGCTAT A  A  TCG   G       TGCAA A TT TT     T  ACC     TT  G* G CA A   CAC C    C      AT      C C GG AG GGC  A*GGG
LEMU ********** T  G  ACA   A       CATAA G CT CC     C  ACT     CT  GG * CA A   CGC C    A      CC      C T AG AG GAC  A*CGG
GOAT AACA**CTAT A  G  ACA   G       TGCTG C CA CC     C  GTT     CC  GC G GA C   TAG T    C      TC      T T GG GG AGG  G*GGC
     ---------+---------+---------+---------+---------+---------+---------+---------+---------+---------+---------+---------+ 240

                                                              AATAAAA                        CAP
HUMA CTGGTCAATAGATTCATTTCACTGGGAGAGGCAAAGGGCTGGGGGCCAG*AGAGGAGAAGTAAAAAGCCACACA*TGAAGCAGCAATGCAGGCATGCTTCTGGCTCATCTGT*GATCACC
CHIM C   TCAATAGATTCATTTCACTGGGAGAGACAAAGGGCTGG  GC AG*   G  GA GTA  GA    CAC *T       CGATG   GCAT C    GG T   CTGT* A  A
GORI C   TCAATGGATTCATTTCACTGGGAGAGGCAAAGGGCTGG  GC AG*   G  GA GTA  AA    CAC *T       CAATG   GCAT T    GG T   CTGT* A  A
ORAN T   TCAACAGATTCATTTCACTGGGAGAGGCAAAGGGCTGG  GC AG*   G  GA ATG  AA    CAC *T       CAGTG   GCAT C    GG T   CTGT* A  A
RHES C   **************************************  GC GG*   G  GA ACA  *A    CAC *A       AAGTA   GTAT C    GG T   CTAC* A  G
OWLM C   **************************************  AT AA*   G  GA GTA  AA    CAC *T       CAGTG   ACAT C    GG T   CTGT* A  A
LEMU C   **************************************  GC AG*   T  AG ATA  AG    TGG GA       CAGTA   GTGA C    AA T   CCGT* G  A
GOAT C   **************************************  ** AGC   T  GG ATA  AG    TGC GT       CGGCA   ACTT C    GG C   *TATG A  A
     ---------+---------+---------+---------+---------+---------+---------+---------+---------+---------+---------+---------+ 360

                            INTEXON 1 ----                                                                         --- >/
HUMA AGGAAACTCCCAGATCTGACACTGTAGTGCATTTCACTGCTGACAAGAAGGCTGCTGCCACCAGCCTGTGAAGCAAGGTTAAGGTG*AGAAGGCTGGAGGTGAGATTCTGGCAGGTAGG
CHIM A G AAC  C    TCTGA A TGTA        C   G T  CAAG A    G   CCACC  C  GTGAAG A GG TA G * AA  CT   A TG    TT   G GC    T GG
GORI A G AAC  C    TCTGA A TGTA        C   G T  CAAG A    G   CCACC  C  GTGAAG A GG TA G * AA  CT   A TG    TT   G GC    T GG
ORAN G G AAA  C    TCTGA A TGTA        C   G T  CAAG A    G   CCAAT  C  GTGAAG A GG TA G * AA  CT   A TG    CT   G GC    T GG
RHES A G AAC  C    TCTGA A CGTG        C   G T  CGAG A    G   CCACT  C  GTGAAG A GT T* G * AA  CT   A TG    TT   G GT    T GG
OWLM A G AAC  C    CCTGA A CGCG        C   G C  CGAA G    G   CCACT  C  ATGGAG T GG TG T * AA  CT   A TG    TT   G GC    T GC
LEMU A C GAC  G    CCTGA G TGTG        C   G A  GGCA A    *   CGGCT  C  GCCAGG A CA GA T G GA  CT   A CA    TC   G GC    C GG
GOAT A T AGC  C    ***** A CATG        T   A C  GGAG A    G   TTGCT  T  GTGGGC A AG GA T G GT  TC   C TG    GC   A CA    T AG
     ---------+---------+---------+---------+---------+---------+---------+---------+---------+---------+---------+---------+ 480

HUMA TACTGGAAGCC***GGGACAAG*GTGCAGAAAGGCAGAAAGTGTTTCTG*AAAGAGGGATTAGCCCGTTGTCTTACATAGTCTGACTTTGCACCTGCTCTGTGATTATGACTATCCCACA
CHIM T CTG  AG C***G GGCAA * T C G      A   A     T T *        AT A CCCGT G  T  C T G C      TGC C   C C G   TTATG CTAT C  AC
GORI T CTG  AG C***G GGCAA * T C G      A   A     T T *        AT A CCCAT G  T  C T G C      TGC C   C C G   TTATG CTAT C  AC
ORAN T CCG  AG C***G GGCAA * T C G      A   A     T T *        AT A CCCGT G  T  C T G C      TGC C   C C G   TTATT CTAT A  AC
RHES T CTG  AG C***A GGCGA * T C G      A   T     T T *        AC A CCCAT G  T  C T G C      TGC T   C C G   TTATG CTGT C  TC
OWLM T CTA  AG C***A AGCAA * T C G      A   A     C T *        AT A CCAGT G  T  C T T C      TGC T   C C T   TTATG TTAT C  AC
LEMU C CTG  GG C***A GGTCA * A C G      A   A     C T *        GA A CCAGT A  C  T C G A      TGC T   T T G   C***G CTGC C  AT
GOAT C GTG  CA AGGTA GAGAG A T T C      T   A     C A A        AC G TTAGG T  T  C T C C      CTT T   T C G   CTATG TCAT C  AT
     ---------+---------+---------+---------+---------+---------+---------+---------+---------+---------+---------+---------+ 600

     EXON 2 ----
HUMA GTCTCCTGGTT****GTCTACCCATGGACCTAGAGGTACTTTGAAAGTTTTGGA*TATCTGGGCTCTGACTGTGCAATAATGGGCAACCCCAAAGTCAAGGCACATGGCAAGAAGGTGCT
CHIM  TC  C  G T****     CC    AAC T   G TAC  TGAA G T    A*T TC GGGC    AC G  CAA     G     CC A       G AC T GC A     GTG
GORI  TC  C  G T****     CC    GAC T   G TAC  TGAA G T    A*T TC GGGC    AC G  CAA     G     CC A       G AC T GC A     GTG
ORAN  TC  C  G T****     CC    GAC C   G CAG  TGAA G T    C*T TC GGGT    AC G  CAA     G     CT A       G AC T GC A     GTG
RHES  TC  C  G T****     CC    GAC C   G TAC  TGAA C T    C*T TC GGGC    AC G  CAA     G     TC A       G AC T GA A     GTG
OWLM  TC  C  G T****     CC    GAT C   A TAC  *GAA G C    C*A TC GGGC    AC G  TAA     *     CC A       G AC T *C A     GTG
LEMU  GT  T  C TGTTT     TT    TTC C   A TTC  CAGT A T    GGA TT GTCC    GC C  TGC     C     CC G       T TT T GC A     CAA
GOAT  GC  T  A C****     CC    GAC C   G TTC  TGAC G T    T*A CT ATGC    AG C  CCA     G     CC G       G CC C GC G     GTG
     ---------+---------+---------+---------+---------+---------+---------+---------+---------+---------+---------+---------+ 720

                                                                                                                 ---->/
HUMA GATCTCCTTCGGAAAAGCTGTTATGCTCACGGATGACCTCA***AAGGCACCTTTGCTACACTGAGTGACCTGCACTGTAACAAGCTGCACGTGGACCCTGAGAACTTCCTGGTGAGTAG
CHIM   T  C TTTGG   A CTG   T CT  CG    AC TC *** A    C      TACA  G  T  C G C     A     C G TG     C   GA     T CTGGT  G AC
GORI   T  C TTCGG   A CTG   T CT  CG    AC TC *** A    C      TACG  G  T  C T C     A     C G CG     C   GA     T CTGGT  G AC
ORAN   T  T ***GG   A CTG   T CT  TG    AC TC *** A    C      TACA  G  T  C T C     A     C G CG     C   GA     T CTGGT  G GC
RHES   T  C TTCGA   A CTG   T CT  TG    AC TC *** A    C      TATG  G  T  C T T     A     C G CG     C   GA     T CTGGT  G AC
OWLM   T  C TTCAG   A CTG   T CT  TG    CT AT GTA A    C      TATA  G  T  C T C     G     C A CA     C   GA     T CTTGA  A TC
LEMU   C  * TTTGG   A ATG   C TG  CT    AT TC *** A    A      TGAG  G  T  G T C     G     T G TG     T   GA     G AGG<
GOAT   A  C TTTGG   T CCA   A CA  TG    AT TC *** G    C      AGAT  A  C  G T C     G     T G CG     T   CC     T AGGGT  G TC
     ---------+---------+---------+---------+---------+---------+---------+---------+---------+---------+---------+---------+ 840

HUMA TAAGTACACTCACGCTTTCTTCTTTACCCTTAGATATTTGCACTATGGGTACTTTTGAAAGCAGA**GGTGGCT*TTCTCTTGTGTTA*TG*AGTCAGCTATGGGATATGATATTTCAGC
CHIM  AA T CA TCACG    C   T  ACC TT GA A TT CA TA   GTAC  T G A  C   **GG  GC *TTC    GT T A*  *   C GC A G   TA G         C
GORI  AA T CA TCACA    C   T  ACC TT GA A TT CA TA   GCAC  T G A  C   **GG  GC *TTC    GT T A*  *   C GC G G   TA A         C
ORAN  AA T CA TCACG    C   T  ACC TT GA A TT CA TA   GTAC  T G A  C   **GG  GC *TTC    GT T A*  *   C GC A G   TA G         C
RHES  AA T TA TCATG    C   T  ACC TT GC A TT CA CA   GTAC  T G A  C   **GG  GG *TTC    GT C A*  *   C GC A G   TA G         C
OWLM  AA C CA TCATG    C   C  CCC TT AA A TT CA GA   CTAC  T G A  C   **GG  GC *TTC    GT C A*  *   C GC G G   TA G         *
GOAT  GG T TG CTGTG    G   T  CAT *C GG T CA TG TG   ****  A A T  *   ACAC  AC CAAG    AA C GT  A   * TT T T   GG A         *
     ---------+---------+---------+---------+---------+---------+---------+---------+---------+---------+---------+---------+ 960

HUMA AGTGG*****GATTTTGAGAGTTATGTT***GCTGTAAATAACATA*ACTAA**AATTTGGTAGAGCAAGGACTATGAATAATGGAAGGCCACTTACCATTTGATAGCTCTGAAAAACAC
CHIM A TGG***** A T   AG  T A    *** CTGTA  T ACA A*A TA **A   TGGTAGAGCA GGA   T  AT A    AG C    TAC   T     GC         CAC
GORI A TGG***** A T   AG  T A    *** CTGTA  T ACA A*A TA **A   TGGTAGAGCA GGA   C  AT A    AG C    TAC   T     GC         CAC
ORAN A TGG***** A T   AG  T A    *** TTGTA  T ACA A*A TA **A   TGGTGGAGCA GGA   T  AT A    GG C    TAC   T     GC         C*C
RHES A T*GGGATC T T   AG  T A    *** CTCTA  T ACA A*A TG **T   TGGTAGAGCA GGA   T  AT A    AA G    TAC   T     GC         CAC
OWLM T TTGGGATA A T   AG  T A    *** GTCCA  T GCA G*C TA **A   TGGTAGAGTA GGA   C  AT G    AG C    TAC   T     GC         CAC
GOAT A AAAGGCTT A C   GT  G *    CCA AGGTC  * GGT AGA CA GTA   ********** CTC   T  CC G    *G T    GGT   C     AT         ***
     ---------+---------+---------+---------+---------+---------+---------+---------+---------+---------+---------+---------+ 1080

HUMA ATCTTATAAAAAAT*TCTGG**CCAAAATCAAA*CTGAG***TGTTTTT*GG*ATGAGGGAACAGAAGTTGAGATAGAGAAAATAACATCTTTCCTTTGGTCAGCGAAATTTTCTATAAA
CHIM ATCTTAT A     * CTG ** CAA  TCA  *C    ***   T T *  *A  A G   CAG  GTT   ATAG GAA  T   C    T      G C GC      TT   A AA
GORI ATCTTAT A     * CTG ** CAA  TCAA *C    ***   T T *  *A  A G   CAG  GTT   ATAG GAA  T   C    T      G C GC      TT   A AA
ORAN ATCTTGT A     * CTG ** CAA  TCGG *C    ***   T T *  *A  A G   CAG  GTT   ATAG GAA  T   C    T      G C GT      TT   A GA
RHES GTCTTAT C     * CTG ** CAA  TTAA *C    ***   T T *  *A  A G   TGG  GTT   ATGG GGA  T   C    T      G C TT      TT   G AA
OWLM ATCTTAT A     * CTG ** CAG  TTGA *A    ***   T G *  *A  A G   CAA  GTT   GTAG GAA  T   C    G      G C CT      TT   G GA
GOAT *****AG A     G GAA AA ACC  CCAA CC    CTA   G T C  CC  * A   TAC  ACC   GCAT CAG  G   T    G      A A CT      CC   A GG
     ---------+---------+---------+---------+---------+---------+---------+---------+---------+---------+---------+---------+ 1200

HUMA AATTAAT****AGTCACTTTTCTGCATAGTCCTGGAGGTTAGAAAAAGA*TCAACT*GAACAAAGTAGTGGGAAGCTGTTAAAAA***GAGGATTGT**TTCCCTCC*GAATGATGATGG
CHIM   TT   ****AGTCA T   C GCAT G CT  GAGG T A AA A  * C A T*GAGC A G  GT G A G  G  A A* *** AAGG  G TT TC C  C*G ATG      G
GORI   TT   ****AGTCA T   C TCAT G CC  GAGG T G AA A  * C A T*GAAC A G  GT G A G  G  A AA *** AGGA  G ** TC C  C*T ATG      G
ORAN   TT   ****AGACA T   C GCAT G CC  GAGG T G AA A  * C A T*GAAC G G  GT G A A  G  A AA *** AGGA  G ** TC C  T*G ATG      G
RHES   TT   ****GGACA T   C GCAT G CC  GAAG C G AA C  * C A T*AGAA G T  AT G A G  T  C AA *** AGGA  G ** TC T  T*G ATG      G
OWLM   TT   ****AGACA T   C GCCT G CC  GAGG T G AA A  * A C TAGAAC G G  AT G A G  T  A AA *** AAGA  G ** TC C  T*G ATG      A
GOAT   CC   GAATATATT C   A G*** T TT  AGTT T A GG G  C A A A*GGGC A A  A* A C A  T  C CA TGT TGCC  C TC CT A  TCT GCA      A
     ---------+---------+---------+---------+---------+---------+---------+---------+---------+---------+---------+---------+ 1320

HUMA TATACTTTTGTACGCATGGTACAGGATTCTTTGTTATGAGTGTTTGGGAAAATTGTATGTATGTATGTA*TGTATGTGATGACTGGGGACTTATCCTATCCATTACTGTTCCTTGAAGTA
CHIM T  AC     CACG  T G A A     CTT  TTATG G  TT  GGA   TTG A  TA   ATGTA*T****GT  TG  TGGGG CT  T C    CAT  CTGTT     GA T
GORI T  AC     TACG  T G A A     CTT  TTATG G  TT  GGA   TTG A  TA   ATGTA*T****GT  TG  TGGGG CT  T C    CAT  CTGTT     GA T
ORAN T  AC     TACG  T G A A     CTT  TTATG G  TT  GGA   TTG A  TG   *************  TG  TGGGG CT  T C    CAT  CTGTT     GA T
RHES T  AC     TGCA  T G A A     CTT  TTATG G  TT  GGA   TTG A  TG   *************  TG  TGGGG CT  T C    CCT  CGGTT     GA T
OWLM T  GC     TACA  T T A A     TTT  TTATG G  TT  CAA   TTG G  TG   ***********GT  TA  TGGGA CT  T C    CCT  CTGTT     GA T
GOAT A  GT     TATA  A G G T     CC*  CGTCA A  GA  TCC   CAA C  AA   ATGTAATATCAG*  GA  ****A TA  * A    ***  GTCC*     TC C
     ---------+---------+---------+---------+---------+---------+---------+---------+---------+---------+---------+---------+ 1440

HUMA CTATTATCCTACTTTTTAAAAGGACGAAGTCTCTAAAAAAAAAATGAAAC****AATCACAATATGTTGGGG*TAGTGAGTTGGCATAGCAAGTAAGAGAAGGATAGGACACAATGGGAG
CHIM   A T TCC  C    T   AGG CGA  TCTCT*AAAAAA AAT AAA ****AA C CAATAT C GG  * AGTGA T G   T  C  G AAGA       AGG     A   GA
GORI   A T TCC  C    T   AGG CGA  TCTCT**AAAAA AAT AAA AATTAA C CAATAT C GG  * AGTGA T G   T  C  G AAGA       AGG     A   GA
ORAN   A T TCC  C    T   AGG CGG  TCTCT***AAAA AGT AAA AATTAA C CAATAT C GG  * AGTGA T G   T  C  G AAGA       AGG     A   GA
RHES   G T TCC  T    A   AGG CAG  TCTCT***AAAA AGT AAA AATTAA C CACTGT C GG  * AGTGA T G   T  C  G AAAG       AGG     A   GA
OWLM   A T TCC  C    T   AGG TGG  CCTTT***AAAA GGT AAA AATTAG C CAATGT C GT  * AATGA T G   T  C  G AAGA       AGG     A   AA
GOAT   A A GTT  C    *   GTA TGG  ************ GCG *** AATCCA G GCA*AT C CA  C TGAAC C A   G  A  A GGGA       GTA     G   G*
     ---------+---------+---------+---------+---------+---------+---------+---------+---------+---------+---------+---------+ 1560

HUMA GTGCAGGGCTGCCAGTCATATTGAAGCTGATATCTAGCCCATAATGGTG****************************AGAGTTGCTCAAACTCTGGTCAAAAAGGATGTAAGTGTTATAT
CHIM   GG  GG   CC     TAT  G TA  AT TAGC CA          **************************** G  T      AA    GG C  A A GATGTA G    A
GORI   TG  GG   CC     TAT  G TG  AT TAGC CA          **************************** G  T      AA    GG C  A A GATGTA G    A
ORAN   TG  GG   CC     TAT  G TC  GT TAGC CA          **************************** G  T      AA    GG C  A A GATGTA G    G
RHES   TG  GC   CC     TAT  G TG  GT TATC CA          AACTTACCTTTGTGAGAATAAGAC**TG G  T      AA    GG C  A A GAAGTA G    G
OWLM   TG  GG   GC     TAT  G TG  GT TAGC CA          TACTTACCTTTGTGAGAATAAGACTCTG G  T      AA    TG C  A A AAAATA G    G
GOAT   TT  *G   GG     **C  T CA  GC AGGT TC          CACTT****TTGTGGGAACATGGCCATG A  C      CC    TA G  G G ACCGGC *    G
     ---------+---------+---------+---------+---------+---------+---------+---------+---------+---------+---------+---------+ 1680

                                                                                   EXON 3 ----
HUMA CTATTTAC*TGCAAGTCCAGCTTGAGGCCTTCTATTCACTATGTACCATTTTCTTTTTTATCTTCACTCCCTCCCCAGCTCTTAGGCAACGTGATATTGATTGTTTTGGCAACCCACTTC
CHIM C   T AC*  C   TC  G T    G   TC A    C       CA T T      T  CTTCACTCCCTC     C  T  G C  CG          TG T      A
GORI C   T AC*  C   TC  G T    G   TC A    C       CA T T      *  CTTCACTCCCTC     C  T  G C  CG          TG T      A
ORAN C   T AC*  C   TC  G T    G   TC A    C       CA T T      *  CTTCACTCCCTC     C  T  G C  CG          TG T      A
RHES C   G AT*  C   TC  A T    G   TC A    C       CA T T      *  CTTCACTCCCTC     C  T  A C  CG          TA T      A
OWLM T   T AT*  C   TC  G T    G   GT A    C       CA T C      *  CTTCACTCCCTC     T  T  G C  TG          GG T      G
GOAT C   T GCT  G   GG  G C    A   TC C    T       TG C T      *  T***********     C  C  G A  CA          TG C      A
     ---------+---------+---------+---------+---------+---------+---------+---------+---------+---------+---------+---------+ 1800

                                                                                    ---->/TER
HUMA AGCGAGGATTTTACCCTACAGATACAGGCTTCTTGGCAGTAACTAACAAATGCTGTGGTTAATGCTGTAGCCCACAAG*ACCACTGAGTTCCCTGTCC*ACTATGTTTGTACCTA*TGGT
CHIM   CG G G        TA  C  A      T TT    GTAA TA CA  TGCTGTGGTTAA   TG A    A   G* C  C G  TTC  TGTCC*ACTATGTTTGTACCTA*TGGT
GORI   CG G G        TA  G  A      T CT    GTAA TA CA  TGCTGTGGTTAA   TG A    A   G* C  C G  TCC  TGTCC*ACTATGTTTGTACCTACTGGT
ORAN   CG G G        TA  G  A      T TT    GGAA TA CA  TGCTGTGGTTAA   TG A    A   GG C  C G  TTC  C************************GT
RHES   *A A G        TA  G  A      T TT    GGAA CC CA  TGCTGTGGCTAA   TG A    T   GG C  T G  TTC  T************************GT
OWLM   CG G G        TA  G  A      T CG    AAGA CA TA  ************   CA G    A   TT T  C G  CTC  GGTCC*ACTGTGTGTGTACCTACTGGT
GOAT   CA G A        CG  G  G      G TT    GAAG TG CC  CGCTGTGGCTAA   TC G    A   GT C  C *  TTG  TGGCCTACCATGCTGGTGCCTA*****
     ---------+---------+---------+---------+---------+---------+---------+---------+---------+---------+---------+---------+ 1920

                                                                                                                 /POLYA/
HUMA CCACTATGTTTGTACCTATGTCCCAAAATCTCATCTCCTTTAGATGGGGAGGTTGGGGAGAAGAGCAGTATCCTGCCTGCTGATTCAGTTCCTGCATGATAAAAATAGAATAAAGAAAT
CHIM CCACTA  TTT**A  TA G   CGA  TC    C    TT   TG GGGAGGTTGG      A   AGTA C    CTG TG   TC GT C TGC  G   A    AA      GA A
GORI CCACTA  TTTGTA  TA G   CCA  TC    C    TT   TG GGGAGGTTGG      A   AGTA C    CTG TG   TC GT C TGC  G   A    AA      GA A
ORAN CCACTA  TTTGTA  TA G   CAA  TC    C    TT   TG GGGAGGTTGG      A   AGTA C    CTG TG   TT GT A TGC  G   A    AA      GA A
RHES CCACTA  TTTGTA  TA G   CAA  GC    T    TT   CG GGGACACTGA      A   AGTA C    CTG AG   TC GT C TGC  G   A    AA      GA A
OWLM CCGCCA  TTTGTA  CA A   TAA  GC    C    TT   TG AGGATGTTGG      A   AATA C    CTG AG   TC GC C TGC  G   A    AA      GA A
GOAT ****TC  AAGGC*  AG G   CAG  GT    C    GA   CA A********G      *   ***T T    AGA AT   ** AC C AAT  A   C    GA      ** G
     ---------+---------+---------+---------+---------+---------+---------+---------+---------+---------+---------+---------+ 2040

HUMA *ATGCTCTCTAAGAAATATCATTGTACTCTTTTTCTGTCTTTATATTTACCCTGATTCAGCCAAAAGGACGCACTATTTCTGATGGAAATGAGAATGTTGGAGAATGGGAGTTTAAGGA
CHIM *A  C CTCT  GA   ATCAT G  TTC T T C   C   A A     CCC                 CG   C          G     AG TGT          G   T     GA
GORI *A  C CTCT  GA   ATCAT G  TTC T T C   C   A A     CCC                 CG   C          G     AG TGT          G   C     GA
ORAN *A  C ****  GA   ATCAT G  TTC T T C   C   A A     CCC                 CA   C          G     AG TGT          G   T     GA
RHES *C  C CTCT  GA   ATTAT G  TTC T T C   C   A A     CAT                 CC   C          A     AA CAT          G   T     GG
OWLM *G  C GTTA  GA   ATCAG A  TAT T T C   C   A G     TGT                 TG   C          G     GG CAC          A   T     AA
GOAT CA  G CTAT  TG   GCCCT G  TTT C C T   T   G A     <
     ---------+---------+---------+---------+---------+---------+---------+---------+---------+---------+---------+---------+ 2160

HUMA CAGAGAAGATACTTTCTTGCAATCCTGCAAGAAAAGAGAGAACTCGTGGGTGGATTTAGTGGGTAGTTACTCCTAGGAAGGGGAAATCGT
CHIM C        T       C    T    C    A           TA    G AA        G    T       AGA    GG AA  G
GORI C        T       T    T    C    A           TG    T AA        G    T       AGA    GG AA  G
ORAN C        T       T    T    C    A           TG    G GC        G    T       AGG    CA AA  G
RHES T        T       T    A    A    T           TG    G GC        A    T       AGG    GG AA  G
OWLM T        G       T    T    A    T           TG    G GA        G    C       GCA    GG GG  A
     ---------+---------+---------+---------+---------+---------+---------+---------+---------+- 2251
```

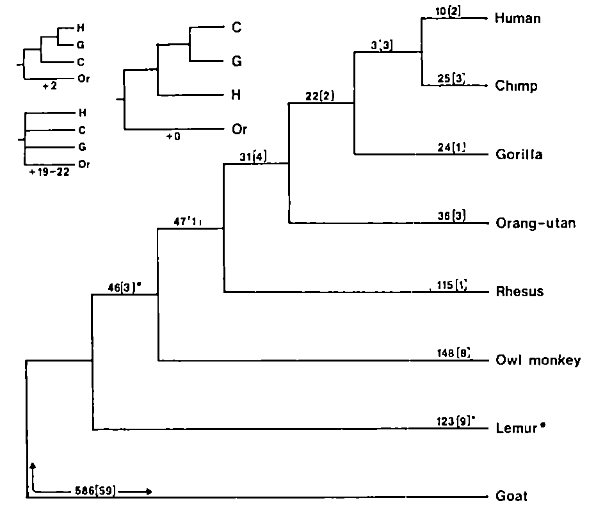

Fig. 2 Species relationship as indicated by a parsimony analysis[43,44] of the aligned sequences in Fig. 1. The upper right tree required 1,075 mutation events (1,218 after correction[31,32] for multiple substitutions occurring at the same site). Alternative trees (upper left) required 0, +2, +19-22 additional events. The 12 trees requiring +19-22 additional events resulted from breaking up a monophyletic African ape-human clade by introduction of orang. Branch lengths include both the corrected number of substitutions and the number of insertion/deletion events (the number of insertion/deletion events alone are given in brackets). The asterisk indicates the branches and corresponding link lengths in which geneic events were recorded only over those alignment positions that the much shorter lemur $\psi\eta$ sequence shared with other sequences. Normalization of the starred values requires multiplication by approximately 2.6. Ancestral sequences for the nodes of the upper right tree were deduced by our maximum parisomony method; from 548 ancestral-to-descendant substitutions occurring within the primate $\psi\eta$ gene region, the calculated[45] relative frequencies of the 12 types of substitutions were 20.5% G→A, 20.3% C→T, 14.3% A→G, 12.3% T→C, 5.9% G→C, 5.7% G→T, 4.7% C→A, 4.0% T→G, 3.3% A→T, 3.1% C→G, 2.8% T→A. The expected base composition at equilibrium (19% G, 29% A, 31% T and 21% C), calculated[46,47] from the above relative frequencies, was found to approximate to that of the large introns of β-globin-related genes (21% G, 29% A, 33% T and 17% C, averaged over 33 such introns) which are thought to represent selectively neutral DNA. Within the primate $\psi\eta$ gene regions the distribution of relative frequencies of substitutions was not found to differ significantly between exon and non-exon regions, nor did the exon and non-exon regions differ in overall substitution rates. Compared with the base composition of the exons of goat η and other functional globin genes (28% G, 22% A, 23% T and 27% C, averaged over 72 globin genes), the base composition of primate $\psi\eta$ exons (26% G, 26% A, 25% T and 23% C) is clearly evolving towards the equilibrium composition of neutral DNA.

(originally named ε^{11})[14] and primate η pseudogene sequences (each originally named either $\psi\beta^{15,16}$ or $\psi\beta1^{12,17}$) are orthologues. With addition of rhesus and orang orthologues (shown in Fig. 1 aligned against other η sequences), the seven primate pseudogenes represent most major taxonomic groups within primates. The rhesus and orang sequences prove to be typical representatives of this $\psi\eta$ locus; they contain mutations which inactivate functional genes (defective initiation codon at position 384-386, a stop codon at position 429-431, and frameshift deletions at orang position 447 and rhesus positions 441, 447 and 1,803; Fig. 1). The defective A→G substitution in the initiation codon is shared by all primate sequences, thereby supporting the deduction that the η-globin locus became nonfunctional in proto-primates to the primate radiation (approximately 60 Myr).

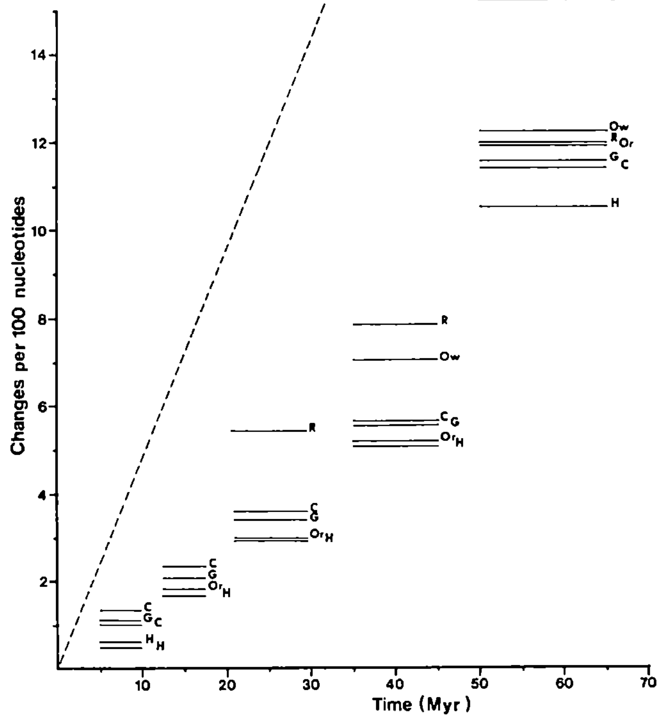

Fig. 3 The number of changes per 100 nucleotides from ancestral nodes to extant species plotted against a range of palaeontological time estimates[11,23-28]. The dashed line represents 5×10^{-9} substitutions per site per yr. 50-65 Myr is suggested as the divergence time of the prosimian and simian lineages, 35-45 Myr indicates Platyrrhini-Catarrhini divergence, 20-30 Myr indicates cercopithecoid-hominoid divergence, 13-18 Myr indicates *Pongo*-Hominine divergence and 5-10 Myr indicates human-chimpanzee-gorilla divergence plus human-chimpanzee (chimpanzee-gorilla) divergence times. The following labels for species are used: L, lemur; Ow, owl monkey; R, rhesus; Or, orang-utan; G, gorilla; C, chimpanzee; H, human. The slope of the dashed line represents the substitution values determined for mammalian pseudogenes other than the $\psi\eta$ genes and has been equated to the neutral mutation rate[18,19].

Trees describing the genealogical relationships of the η-globin sequences were constructed by the most parsimonious placement of nucleotide substitutions. This cladistic procedure does not require clock-like behaviour in rates of change but only that matches in nucleotide sequence among taxa result more often from shared common ancestry than from convergencies, reversals or parallelisms. The two most parsimonious trees found (Fig. 2) required 1,075 independent genetic events to explain the pattern of variation among the eight η-globin sequences. One of these two trees, after separation of *Gorilla*, places only three derived mutations on the common stem of a *Homo*(human)-*Pan*(chimpanzee) branch: a deletion at position 1,491-1,494, an insertion at position 1,739 and a deletion at position 1,916. The last event is equivocal because an alternative parsimony solution redistributes the duplication and deletion events that occur in that region (positions 1,895-1,941). In the other most parsimonious tree, *Homo* separates from the common stem of a *Pan-Gorilla* branch; this latter grouping is obtained by two transitional substitutions (G→A) at positions 2,213 and 2,238. No events uniquely support a human-gorilla branch. As evident from Fig. 2, a Homininae branch of *Homo-Pan-Gorilla* is strongly supported; there are 22 derived mutations on its common stem: an insertion at positions 1,385-1,391, a deletion at position 1,879 and 20 nucleotide substitutions of which 17 are unequivocal (positions 121, 300, 326, 422, 631, 654, 750, 1,185, 1,214, 1,263, 1,307, 1,381, 1,467, 1,484, 1,592, 1,677, 1,840).

Table 1 Inter-taxonomic DNA divergences from DNA hybridization and η nucleotide sequence data

Species comparisons	DNA hybrids		ETA gene	
	TMH	TMH-C	Dist.	Dist.-C
Huma.-Chim.	1.9*	1.9	1.7	1.7
Huma.-Gori.	2.4*	2.4	1.7	1.7
Huma.-Oran.	3.6*	3.7	3.4	3.4
Chim.-Gori.	2.2*	2.2	2.2	2.3
Chim.-Oran.	3.7*	3.8	4.0	4.1
Gori.-Oran.	3.8*	3.9	3.9	4.0
Homi.-Cerc.	7.7*	8.1	8.0	8.5
Homi.-Cebo.	12.2†‡	13.3	11.6	12.6
Homi.-Pros.	22.8†‡	27.2	23.9	28.8
Homi.-Euth.	31.6‡§	41.0	30.9	39.8
Cerc.-Cebo.	13.5†	14.9	12.9	14.1
Cerc.-Pros.	23.5†¶	28.2	24.3	29.4
Cerc.-Euth.	—	—	32.6	42.9
Cebo.-Pros.	24.0†¶	28.9	25.5	31.1
Cebo.-Euth.	—	—	32.8	43.1
Pros.-Euth.	29.3‡§	37.2	27.4	34.1

TMH indicates median sequence divergence determined from thermal stability measurements[8,29,30]. Dist. indicates divergence determined from nucleotide sequences. TMH-C or Dist.-C indicates divergence after correction for multiple substitutions[31,32]. For taxonomic comparisons the following abbreviations are used: Huma., human; Chim., chimpanzee; Oran., orang-utan; Homi., homininae; Cerc. Cercopithecoidea; Cebo., Cebroidea; Pros., lemurs (or galago); Euth., goat (or tree shrew). Note that comparisons involving the goat η sequence are underestimates due to the inclusion of conserved functional exon regions in these comparisons. This is particularly true in the lemur-goat η comparison in which the shortened lemur sequence corresponds to the most conserved region (exons 1 and 2) of the functional goat η gene.

*Values from ref. 8.

†Values from ref. 29.

‡Values from ref. 30.

§Divergence from tree shrew rather than goat.

¶Divergence from galago rather than lemur.

The genealogical family Hominidae (Homininae plus *Pongo*) is also very strongly supported; it is defined by three deletions (at positions 164, 966-970, 1,610-1,637), an insertion (positions 245-282) and 27 separate substitutions of which 24 are unequivocal (positions 5, 66, 383, 405, 495, 573, 780, 853, 926, 1,268, 1,278, 1,334, 1,422, 1,667, 1,859, 1,949, 2,002, 2,093, 2,137, 2,138, 2,161, 2,188, 2,193, 2,213). A total of 47 shared derived mutations define infraorder Catarrhini and another 46 define suborder Anthropoidea.

Rates of $\psi\eta$ sequence evolution were calculated from the number of events on the branches of our genealogical reconstruction (Fig. 2). It is apparent from Fig. 3 that marked variations in lineage rates exist. The fastest rates are shown by lemur (2.7×10^{-9}) and in the early common simian stem (2.9×10^{-9}), intermediate rates by owl monkey and rhesus monkey and the slowest rates by hominoids (averaging 1.3×10^{-9} in descent from the catarrhine branchpoint). All primate rates are less than the average mammalian neutral rate[18,19] and the two slowest rates, those of human and orang lineages, are only one-fifth this average neutral rate.

It follows from the close correspondence of interspecies DNA divergence estimated by DNA hybridization and $\psi\eta$ sequence results (Table 1) that the retardation of primate rates evident in the $\psi\eta$ sequences applies to total single-copy DNA. This supports Britten's analysis[20], which demonstrated that rates of neutral DNA sequence evolution vary by as much as a factor of five, with hominoids and some bird taxa showing the slowest rates and rodents, *Drosophila* and sea urchins showing the fastest rates. Explanations for the retarded hominoid rate invoke lengthening generation times, improved DNA repair mechanisms and combinations of both factors[20-22].

Clearly varying rates of evolution in different lineages affect the ability of a global molecular clock to predict specific divergence times. An alternative approach is to focus on a more localized set of branchpoints within a particular lineage and to use one or more well-established palaeontological time points within that lineage to calibrate a local clock. We have carried out such local clock calculations for Catarrhini, Hominidae and Homininae using the Anthropoidea branchpoint as an outside reference on assigning a palaeontological time of 35-45 Myr[23,24] to this reference. The date found for the Catarrhini branchpoint is 22.2-28.2 Myr, the Hominidae (*Pongo*-Homininae) branchpoint is 12.7-16.4 Myr and the Homininae branchpoint is 6.3-8.1 Myr. These local clock dates correspond well with assessments of the hominoid fossil record[11,25-28]. However, applying the local clock calibration to simian-lemur, primate-nonprimate and *Mus-Rattus* DNA hybridization distances results in dates that are too ancient (72-92 Myr, 98-125 Myr and 52-68 Myr).

In conclusion, to a high degree of certainty, the DNA sequence data have established the genealogical validity of grouping *Homo*, *Pan* and *Gorilla* and excluding *Pongo* in a monophyletic subfamily Homininae. However, within Homininae the relationships remain unclear, perhaps due to relative close divergence points. Our analysis of the primate $\psi\eta$ globin genealogy also raises questions concerning the validity of using global clocks to estimate divergence times. Because of variability in rates of divergence in different lineages, we suggest that local clocks in some cases yield more accurate divergence times.

We thank Dr E. A. Zimmer for the gift of orang-utan No. 1 DNA, Dr S. Martin for rhesus DNA, J. Reneke and J. Bliska for help in isolating phage and Dr N. Maeda for communicating restriction enzyme map data of the rhesus β-globin gene cluster before publication. J.L.S. thanks Drs Frederick R. Blattner and Oliver Smithies for the use of shared laboratory space and equipment in the Department of Genetics, University of Wisconsin. We also thank Wen-Hsiung Li, Roy J. Britten and Raoul E. Benveniste for providing us with pre-publication manuscripts. This study was supported by grants from NIH, HD16595 (J.L.S.), NSF, BSR82-07336 (M.G.) and Alfred P. Sloan Foundation (M.G.).

Received 12 August; accepted 13 November 1985.

1. Goodman, M. *Ann. N.Y. Acad. Sci.* **102**, 219-234 (1962); in *Classification and Human Evolution* (ed. Washburn, S. L.) 204-234 (Aldine, Chicago, 1963).
2. Sarich, V. M. & Wilson, A. C. *Science* **158**, 1200-1203 (1967).
3. Hoyer, B. H., van de Velde, N. W., Goodman, M. & Roberts, R. B. *J. hum. Evol.* **1**, 645-649 (1972).
4. Sarich, V. M. & Cronin, J. E. in *Molecular Anthropology* (eds Goodman, M. & Tashian, R E.) 141-170 (Plenum, New York, 1976).
5. Brown, W. M., Prager, E. M., Wong, A. & Wilson, A. C. *J. molec. Evol.* **18**, 225-239 (1982).
6. Tashian, R. E., Hewett-Emmett, D. & Goodman, M. in *Isozymes* Vol. 7 (eds Rattozzi, M. C., Sandalias, J. G., Siciliano, M. Y. & Whitt, G. S.) 79-100 (Liss, New York, 1983)
7. Goodman, M., Braunitzer, G., Stangl, A. & Schrank, B. *Nature* **303**, 546-548 (1983).
8. Sibley, C. G. & Ahlquist, J. E. *J. molec. Evol.* **20**, 2-15 (1984).
9. Kluge, A. G. in *New Interpretations of Ape and Human Ancestry* (eds Ciochon, R. L. & Corruccini, R. S.) 151-177 (Plenum, New York, 1983).
10. Schwartz, J. H. *Nature* **308**, 501-505 (1984).
11. Andrews, P. *Nature* **314**, 498-499 (1985).
12. Harris, S., Barrie, P. A., Weiss, M. L. & Jeffreys, A. J. *J. molec. Biol.* **180**, 784-802 (1984).
13. Goodman, M., Koop, B. F., Czelusniak, J., Weiss, M. L. & Slightom, J. L. *J. molec. Biol.* **180**, 803-823 (1984).
14. Shapiro, S. G., Schön, E. A., Townes, T. M. & Lingrel, J. B. *J. molec. Biol.* **169**, 31-52 (1983).
15. Jeffreys, A. J. *et al. J. molec. Biol.* **156**, 487-503 (1982).
16. Chang, L.-Y.E. & Slightom, J. L. *J. molec. Biol.* **180**, 767-783 (1984)
17. Jagadeeswaran, P., Pan, J., Forget, B. G. & Weisman, S. M. *Cold Spring Harb. Symp. quant. Biol.* **47**, 1079-1086 (1983).
18. Hayashida, H. & Miyota, T. *Proc. natn. Acad. Sci. U.S.A.* **80**, 2671-2675 (1983).
19. Li, W-H., Luo, C-C. & Wu, C-I. in *Molecular Evolutionary Genetics* (ed. MacIntyre, R.) (Plenum, New York, in the press).
20. Britten, R. J. *Science* (in the press).
21. Neel, J. V. *J. Heredity* **74**, 2-15 (1983).
22. Goodman, M. *BioEssays* **3**, 9-14 (1985).
23. Rosenberger, A. L. *J. hum. Evol.* **13**, 737-742 (1984).
24. Gingerich, P. D. *Ybk phys. Anthrop.* **27**, 57-72 (1984).
25. Andrews, P. J. in *New Interpretations of Ape and Human Ancestry* (eds Ciochon, R. L. & Corruccini, R. S.) 440-463 (Plenum, New York, 1983).
26. Ciochon, R. L. in *New Interpretations of Ape and Human Ancestry* (eds Ciochon, R. L. & Corruccini, R. S.) 783-843 (Plenum, New York, 1983).
27. Pilbeam, D. *Scient. Am.* **250** (3), 84-97 (1984).
28. Hill, A. *Nature* **315**, 222-224 (1985).

29. Benveniste, R. E. in *Molecular Evolutionary Genetics* (ed. MacIntyre, R.) (Plenum, New York, in the press).
30. Bonner, T. I., Heinemann, R. & Todaro, G. J. *Nature* **286**, 420-423 (1980).
31. Jukes, T. H. & Cantor, C. R. in *Mammalian Protein Metabolism* (ed. Munro, H. N.) 21-123 (Academic, New York, 1969).
32. Gojobori, T., Ishii, K. & Nei, M. *J. molec. Evol.* **18**, 414-423 (1982).
33. Loenen, W. A. M. & Blattner, F. R. *Gene* **26**, 171-179 (1983).
34. Slightom, J. L., Blechl, A. E. & Smithies, O. *Cell* **21**, 627-638 (1980).
35. Hohn, B. *Meth. Enzym.* **68**, 299-309 (1979).
36. Murray, N. E., Brammer, W. J. & Murray, K. *Molec. gen. Genet.* **150**, 53-61 (1977).
37. Wilson, J. T. *et al. Nucleic Acids Res.* **5**, 563-581 (1978).
38. Maxam, A. M. & Gilbert, W. *Meth. Enzym.* **65**, 400-560 (1980).
39. Smith, F. & Waterman, M. S. *J. molec. Biol.* **147**, 195-197 (1981).
40. Breathnack, R., Benoist, C., O'Hare, K., Gannon, F. & Chambon, P. *Proc. natn. Acad. Sci. U.S.A.* **75**, 4853-4857 (1978).
41. Efstratiadis, A. *et al. Cell* **21**, 653-668 (1980).
42. Proudfoot, N. J. & Brownlee, G. G. *Nature* **263**, 211-214 (1976).
43. Goodman, M. *Prog. biophys. molec. Biol.* **38**, 105-164 (1981).
44. Czelusniak, J. *et al. Nature* **298**, 297-300 (1982).
45. Gojobori, T., Li, W-H. & Graur, D. *J. molec. Evol.* **18**, 360-369 (1982).
46. Wright S. *Evolution and the Genetics of Populations* Vol. 2 (University of Chicago Press, 1969).
47. Tajima, F. & Nei, M. *J. molec. Evol.* **18**, 115-120 (1982).

---

fgr proto-oncogene mRNA induced in B lymphocytes by Epstein–Barr virus infection

Marc S. C. Cheah*, Timothy J. Ley†, Steven R. Tronick* & Keith C. Robbins*

* Laboratory of Cellular and Molecular Biology, National Cancer Institute and
†Clinical Hematology Branch, National Heart, Lung and Blood Institute, Bethesda, Maryland 20205, USA

Several acute transforming retroviruses encode tyrosine-specific protein kinases which possess structural and functional relationships to cell-surface receptors for certain growth factors[1,2]. One such tyrosine kinase is encoded by the *onc* gene, v-*fgr*, of Gardner–Rasheed feline sarcoma virus (GR-FeSV)[3–6]. Recently, we have isolated and characterized the human gene, c-*fgr*, corresponding to the viral *onc* sequence and have shown that c-*fgr* is a unique gene located on the short arm of chromosome 1 (ref. 7). Here we report that certain lymphomas (but not sarcomas or carcinomas) express *fgr*-related messenger RNA. This transcript is detected in Burkitt's lymphoma cell lines naturally infected with Epstein–Barr virus (EBV), but not in EBV-negative Burkitt's lymphoma cells. Normal umbilical cord or peripheral blood lymphocyte lines established *in vitro* by EBV infection also contain detectable c-*fgr* mRNA. Moreover, a 50-fold increase of the steady-state c-*fgr* mRNA concentration is observed when uninfected Burkitt's lymphoma cell lines are deliberately infected with EBV. These findings demonstrate for the first time the induction of a proto-oncogene in response to infection by a DNA tumour virus.

To investigate whether the *fgr* proto-oncogene was expressed in human tumour cells, RNAs were prepared from selected cell lines representing a diverse spectrum of human cancers. After selection on oligo(dT) columns, poly(A)$^+$ RNAs were examined for the presence of v-*fgr*-related mRNA by Northern blotting. c-*fgr* transcripts were detected in 6 of 11 cell lines derived from myelo- or lymphoproliferative disorders, but not in any of the 9 carcinoma or 6 sarcoma cell lines examined. In a representative experiment (Fig. 1) the *fgr*-related mRNA detected was 3 kilobases (kb) long, which is in close agreement with the length of the transcript detected in normal human lung tissue[7].

Because our initial survey had indicated the presence of the c-*fgr* transcript in cell lines derived from lymphoproliferative disorders, our analysis was extended to include various B-cell lines derived from African and American undifferentiated lymphomas of the Burkitt and non-Burkitt types. As summarized in Table 1, the c-*fgr* transcript was detected in approximately half of the lymphoma cell lines tested. All cell lines infected with EBV expressed detectable *fgr* mRNA. One non-Burkitt's

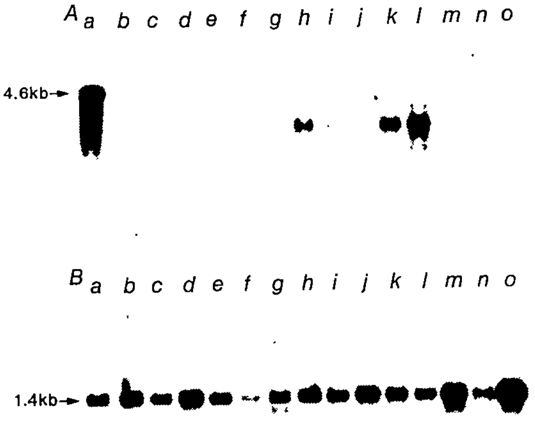

Fig. 1 *A*, Survey of human tumour cell lines for expression of c-*fgr*-related RNA. Poly(A)$^+$-containing RNA was prepared, as described elsewhere[22], from human tumour cell lines and examined by the Northern technique using a v-*fgr*-specific DNA fragment as probe[7]. Carcinoma-derived cell lines A2054, A549, A2182, A431, A1847 and A2199 (ref. 23 and S. A. Aaronson and N. Ellmore, unpublished) (lanes *b*–*g*, respectively), lymphoma-derived cell lines JI, MC116, JD38, Raji and Namalwa (lanes *h*–*l*, respectively), as well as sarcoma-derived cell lines A375, A1632 and A2984 (ref. 23 and S. A. Aaronson and N. Ellmore, unpublished) (lanes *m*–*o*, respectively), were examined. RNA from GR-FeSV-infected mink cells (lane *a*) was used as a control. The relative amounts of hybridizable RNA transferred to nitrocellulose filters were shown to be similar by rehybridization with a GR-FeSV-derived, actin-specific probe (*B*).

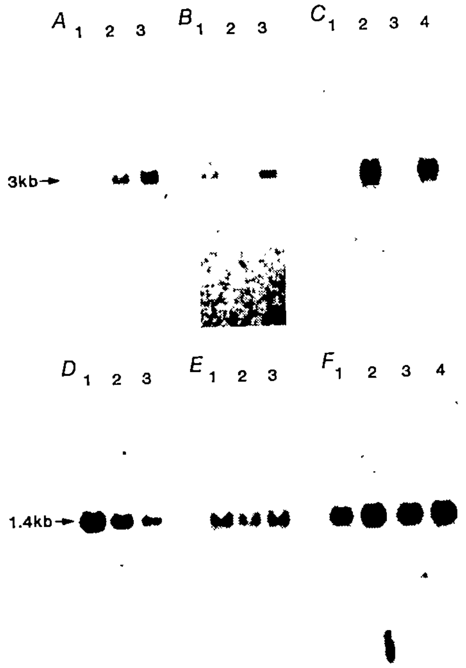

Fig. 2 Expression of *fgr*-related mRNA in cells infected with EBV *in vitro*. Poly(A)$^+$-containing RNAs prepared from EBV-infected normal peripheral (*A*) or umbilical cord (*B*) blood lymphocytes, as well as uninfected (*C*, lanes 1, 3) or EBV-infected (*C*, lanes 2, 4) BJAB (lanes 1, 2) or Ramos (lanes 3, 4) Burkitt's lymphoma cell lines[24,25], were analysed as described in Fig. 1 legend. Relative amounts of hybridizable RNA transferred to nitrocellulose filters were shown to be similar by rehybridization with a GR-FeSV-derived actin-specific probe (*D*–*F*).

lymphoma cell line that expressed detectable c-*fgr* mRNA was not nuclear antigen(EBNA)-positive. These results revealed an association of *fgr* proto-oncogene mRNA with Burkitt's lymphoma cells which had been naturally infected with EBV.

To further assess the association between expression of the *fgr* proto-oncogene and EBV infection, we examined RNAs prepared from normal umbilical cord or peripheral blood lymphocyte cell lines established as a result of EBV infection. Figure 2 shows that the *fgr* proto-oncogene transcript was expressed at detectable levels in each of these cell lines, providing further evidence that EBV infection was responsible for the increased concentration of *fgr* proto-oncogene transcripts detected in the lymphoid cells. Preliminary efforts to determine whether normal B lymphocytes express c-*fgr* mRNA have revealed that normal peripheral blood mononuclear cells contain this transcript. However, such preparations consist of a variety of cells, of which only about 10% are B lymphocytes. Thus, further studies will be required to identify the source of c-*fgr* mRNA in peripheral blood (see note added in proof). In any case, the fact that normal lymphocytes become immortalized as stable cell lines in response to EBV infection, but do not acquire fully neoplastic properties, suggests that expression of c-*fgr* RNA alone is not sufficient to induce the neoplastic state.

We extended our analysis to EBV-negative Burkitt's lymphoma cells which are susceptible to EBV infection. BJAB cells infected with a prototype EBV, B95-8, which is capable of immortalizing normal B lymphocytes[8,9], or Ramos cells infected with a nontransforming derivative, P3HR-1 (ref. 10), were examined for the presence of *fgr* proto-oncogene transcripts. These converted cell lines are known to closely resemble their parental lines in morphology and with regard to karyotype and HLA- and B-antigen typing[11]. As shown in Fig. 2*C*, uninfected BJAB or Ramos cell lines expressed little or no detectable c-*fgr* mRNA, whereas cells infected with either of the two EBV strains expressed the c-*fgr* transcript. We conclude from these results that the increase in c-*fgr* RNA concentration was a specific event associated with EBV infection. Moreover, as infection with either an immortalizing or a non-immortalizing EBV strain led to an increase in the steady-state concentration of *fgr* mRNA, we suggest that altered c-*fgr* expression alone is insufficient for lymphocyte immortalization.

To assess the level of c-*fgr* transcript induction in response to EBV infection, DNA fragments containing a dihydrofolate reductase exon (*dhfr*)[12] or human c-*fgr* sequences[7] were used as probes in quantitative S_1 nuclease protection experiments. As a positive control for each probe, RNA prepared from normal human peripheral blood mononuclear cells was examined (Fig. 3). As expected, a major band of 144 nucleotides was protected with the *dhfr* probe in the cell lines that were in cycle[12]. The c-*fgr* DNA probe detected sequences of 165 and 120 nucleotides, sizes which were consistent with those of v-*fgr*-related stretches present in the DNA fragment used as a probe (data not shown). The intensity of bands detected with each DNA probe increased as a function of RNA concentration, making it possible to quantitate the level of c-*fgr* mRNA induction. RNAs from uninfected or EBV-infected cell lines contained similar amounts of *dhfr* mRNA, as indicated by the intensity of the 144-nucleotide *dhfr* probe fragment (Fig. 3*B*). In contrast, c-*fgr* sequences of 165 and 120 nucleotides were protected by RNA from EBV-infected but not uninfected BJAB or Ramos cells. By varying the exposure times, we calculated that the steady-state concentration of c-*fgr* mRNA increased by at least 50-fold in response to EBV infection. Based on other data obtained with probes of similar specific activity[13], we estimate that the EBV-infected lines contain <20 copies of c-*fgr* mRNA per cell.

The correlation of increased *fgr* proto-oncogene expression with EBV infection of transformed lymphocytes was nearly absolute. Increased concentrations of c-*fgr* mRNA were detected in Burkitt's lymphoma cells whether infected naturally or deliberately in tissue culture. In addition, each of the umbilical cord or peripheral blood lymphocyte cell lines established by EBV infection expressed c-*fgr* mRNA. Increases in the levels of transcripts related to other mammalian tyrosine kinase-coding *onc* genes (v-*fms* and v-*fes*) were also detected in some EBV-infected Burkitt's lymphoma cell lines (data not shown), but these RNAs were not consistently detected in EBV-infected lines and were, in some cases, detectable in uninfected cell lines. Taken together, these results establish a specific relationship between EBV infection and expression of the *fgr* proto-oncogene, which suggests that EBV infection results in transcriptional activation of c-*fgr*. Further studies will be required to show whether increased transcription rates alone are responsible for the increase in steady-state concentration c-*fgr* mRNA.

Integration of EBV into host chromosomal DNA of Namalwa and IB4 cell lines has been described elsewhere[14]. In Namalwa cells, the site of integration is close to the *fgr* proto-oncogene locus on chromosome 1 (refs 7, 14), whereas in IB4 cells the

Table 1 Detection of *fgr* proto-oncogene mRNA in cell lines derived from Burkitt's and non-Burkitt's undifferentiated lymphomas

Histopathology	Cell line	EBNA status	Chromosome translocation	Geographical origin	Expression of v-*fgr*-related transcript*
Burkitt's lymphoma	Namalwa	+	8; 14	Africa	+++
	Keeper	+	8; 14	S. America	+++
	AG876	+	8; 14	Africa	++
	JI	+	2; 8	Europe	++
	Raji	+	8; 14	Africa	++
	LY47	+	8; 22	Africa	+
	BL2	−	8; 22	Europe	−
	ST486	−	8; 14	USA	−
	MC116	−	8; 14	USA	−
	CA46	−	8; 14	S. America	−
Non-Burkitt's lymphoma	EW36	−	8; 14	USA	−
	DS179	−	8; 14	USA	+
	JD38	−	8; 14	USA	-
	JLPC119	−	8; 14	USA	

The characteristics of the cell lines examined have been described previously[19,20]. The concentration of 3-kb *fgr*-related mRNA was determined by analysing 10 μg of poly(A)$^+$ RNA in formamide-formaldehyde agarose gels as described[21]. The relative amounts of hybridizable RNA transferred to nitrocellulose filters were determined by rehybridization with a GR-FeSV-derived actin-specific probe.

* Detectable levels were graded by exposing hybridized nitrocellulose filters for various times as follows: +++, detected after overnight exposure; ++, detected after 2 days of exposure; +, detected after 5 days of exposure; −, not detectable after 5 days of exposure.

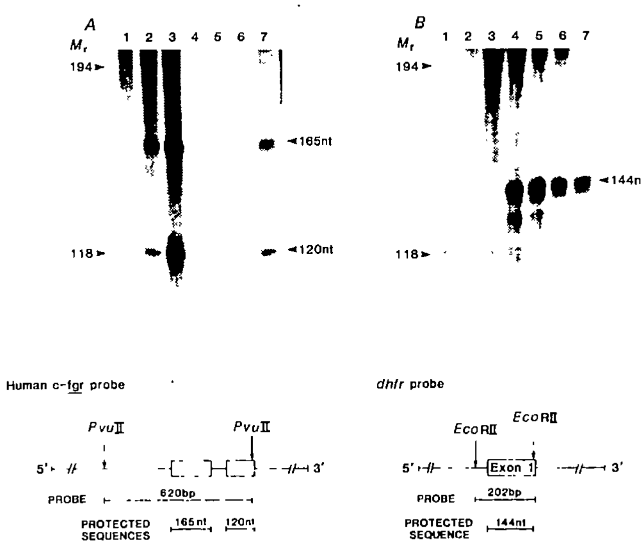

Fig. 3 Quantitation of *fgr* proto-oncogene mRNA induction in response to EBV infection. DNA fragments derived from the region 6.0-6.62 kb of the human *fgr* proto-oncogene[7] (*A*) or the 5′ end of the dihydrofolate reductase gene[12] (*B*), were cloned into M13 phage vectors and used as templates for the synthesis of uniformly labelled anti-sense DNA probes. Conditions for hybridization of total cellular RNA with the DNA probe, S_1 nuclease digestion and polyacrylamide gel electrophoretic analysis of protected sequences were as described elsewhere[26,27]. Samples tested included 5 μg (lanes 2) or 20 μg (lanes 3) total cellular RNA from normal human peripheral blood mononuclear cells, 20 μg RNA from uninfected Ramos (lanes 4) or BJAB (lanes 6) cells, as well as P3HR1-infected Ramos (lanes 5) or B95-8-infected BJAB (lanes 7) cell lines. Negative controls consisted of labelled probe hybridized in the absence of RNA and treated with S_1 nuclease (lanes 1). As expected, no *dhfr* mRNA was detected in peripheral blood mononuclear cells as these cells were not in cycle. The diagrams at the bottom of the figure show human c-*fgr* and *dhfr* exons and their protected sequences. The extent and locations of the human c-*fgr* exons shown were confirmed by nucleotide sequence analysis.

EBV genome integrates into chromosome 4. In the case of the Namalwa cell line, EBV may have a *cis*-acting effect on the expression of the *fgr* proto-oncogene. However, in most cases the influence of EBV on c-*fgr* is more likely to be *trans* as the EBV genome typically exists in the host as an episome. Thus, the isolation of EBV genes having specific functions may make it possible to identify the region of the EBV genome responsible for the increase in *fgr* proto-oncogene mRNA.

Several lines of evidence suggest that Burkitt's lymphoma results from a multi-step process involving the alteration of several genetic elements[15]. Epidemiological data suggest that EBV has an important role in the aetiology of African Burkitt's lymphoma[16]. Molecular studies have strongly implicated alterations of *myc* proto-oncogene expression in the process leading to American as well as African Burkitt's malignancies[17,18]. However, there is no evidence to indicate that such genetic alterations are the only changes required to achieve lymphoid cell transformation. From the results of the present study we conclude that increased concentrations of c-*fgr* mRNA alone are not sufficient to induce malignant transformation of normal lymphocytes or even to immortalize them as continuous cell lines. Moreover, we have no direct evidence that EBV-induced immortalization involves c-*fgr*. Nevertheless, our results are consistent with the possibility that one step in EBV-induced B-cell immortalization involves transcriptional activation of the *fgr* proto-oncogene in response to an EBV-encoded function.

We thank N. Ellmore, L. Mickley and C. Lengel for technical assistance; N. Raab-Traub, I. T. Magrath and D. Ablashi for providing cell lines; T. Kawakami for making unpublished nucleotide sequence data available to us; T. Shimada and A. Nienhuis for the *dhfr* probe; and S. Aaronson for helpful discussions.

Note added in proof: Recent experiments have revealed that c-*fgr* mRNA is not expressed in normal resting or activated B lymphocytes.

Received 8 July; accepted 24 October 1985.

1. Downward, J. *et al. Nature* **307**, 521-527 (1984).
2. Ullrich, A. *et al. Nature* **313**, 756-761 (1985).
3. Rasheed, S., Barbacid, M., Aaronson, S. A. & Gardner, M. B. *Virology* **117**, 238-244 (1982).
4. Naharro, G., Dunn, C. Y. & Robbins, K. C. *Virology* **125**, 502-507 (1983).
5. Naharro, G. *et al. J. Virol.* **47**, 611-619 (1983).
6. Naharro, G., Robbins, K. C. & Reddy, E. P. *Science* **223**, 63-66 (1984).
7. Tronick, S. R. *et al. Proc. natn. Acad. Sci. U.S.A.* **82**, 6595-6599 (1985).
8. Henle, W. *et al. Science* **157**, 1064-1065 (1967).
9. Pope, J. H., Horne, M. K. & Scott, W. *Int. J. Cancer* **3**, 857-866 (1968).
10. Miller, G., Robinson, J., Heston, L. & Lipman, M. *Proc. natn. Acad. Sci. U.S.A.* **71**, 4006-4010 (1974).
11. Klein, G. *et al. Int. J. Cancer* **18**, 639-652 (1976).
12. Chen, M.-J. *et al. J. biol. Chem.* **259**, 3933-3943 (1984).
13. Ley, T. *et al. Proc. natn. Acad. Sci. U.S.A.* **81**, 6618-6622 (1984).
14. Henderson, A., Ripley, S., Heller, M. & Kieff, E. *Proc. natn. Acad. Sci. U.S.A.* **80**, 1987-1991 (1983).
15. Klein, G. & Klein, E. *Nature* **315**, 190-195 (1985).
16. Geser, A. *et al. Int. J. Cancer* **29**, 397-400 (1982).
17. Dalla Favera, R. *et al. Proc. natn. Acad. Sci. U.S.A.* **79**, 7824-7827 (1982).
18. Taub, R. *et al. Proc. natn. Acad. Sci. U.S.A.* **79**, 7837-7841 (1982).
19. Lenoir, G. M., Preud Homme, J. L., Bernheim, A. & Berger, R. *Nature* **298**, 474-476 (1982).
20. Benjamin, D. *et al. J. Immun.* **129**, 1336-1342 (1982).
21. Lehrach, H., Diamond, D., Wozney, J. M. & Bodtker, H. *Biochemistry* **16**, 4743-4751 (1977).
22. Adams, S. L. *et al. Proc. natn. Acad. Sci. U.S.A.* **74**, 3399-3403 (1977).
23. Giard, D. J. *et al. J. natn. Cancer Inst.* **51**, 1417-1423 (1973).
24. Clements, G. B., Klein, G. & Povey, S. *Int. J. Cancer* **16**, 125-133 (1975).
25. Klein, G. *et al. Intervirology* **5**, 319-334 (1975).
26. Berk, A. J. & Sharp, P. A. *Cell* **12**, 721-732 (1977).
27. Ley, T. J., Anagnou, N. P., Pepe, G. & Niehuis, A. W. *Proc. natn. Acad. Sci. U.S.A.* **79**, 4774-4779 (1982).

Expression of cauliflower mosaic virus reverse transcriptase in yeast

Hiroshi Takatsuji, Hirohiko Hirochika, Takao Fukushi* & Joh-E Ikeda

Laboratory of Molecular Genetics, National Institute of
Agrobiological Resources, Tsukuba Science City, Yatabe,
Ibaraki 305, Japan
* Institute of Applied Biochemistry, Tsukuba University,
Tsukuba Science City, Ibaraki 305, Japan

Cauliflower mosaic virus (CaMV) is a double-stranded DNA plant virus[1-3] for which evidence has been presented that its replicative cycle involves a reverse transcription step[4-14]. Until now, however, there has been no direct evidence for such a step. The sequence of the CaMV genome contains a number of open reading frames, one of which (ORF V) encodes a protein of predicted sequence homologous to retroviral reverse transcriptases[10]. We have cloned this gene, and expressed it in the yeast *Saccharomyces cerevisiae*. We report here that yeast expressing this gene accumulate significant levels of reverse transcriptase activity. This provides strong evidence that CaMV really does replicate through an RNA intermediate, converted to DNA by reverse transcriptase.

To obtain the direct expression of the ORF V gene in yeast cells, we constructed the plasmid pAM.ORFV in which the entire ORF V gene is inserted immediately downstream from the acid phosphatase (APase) promoter of the yeast expression vector pAM82 (ref. 15) (Fig. 1*b*). The resulting Leu^+ yeast transformant AH22/pAM.ORFV was obtained. The integrity of the ORF V gene in pAM.ORFV was confirmed by fine restriction mapping of a rescued pAM.ORFV from AH22/pAM.ORFV cells (Fig. 1*b*).

AH22/pAM.ORFV and AH22/pAM82 cells were grown in a liquid medium and then induced in phosphate-deprived medium. The extract from AH22/pAM.ORFV cells, but not

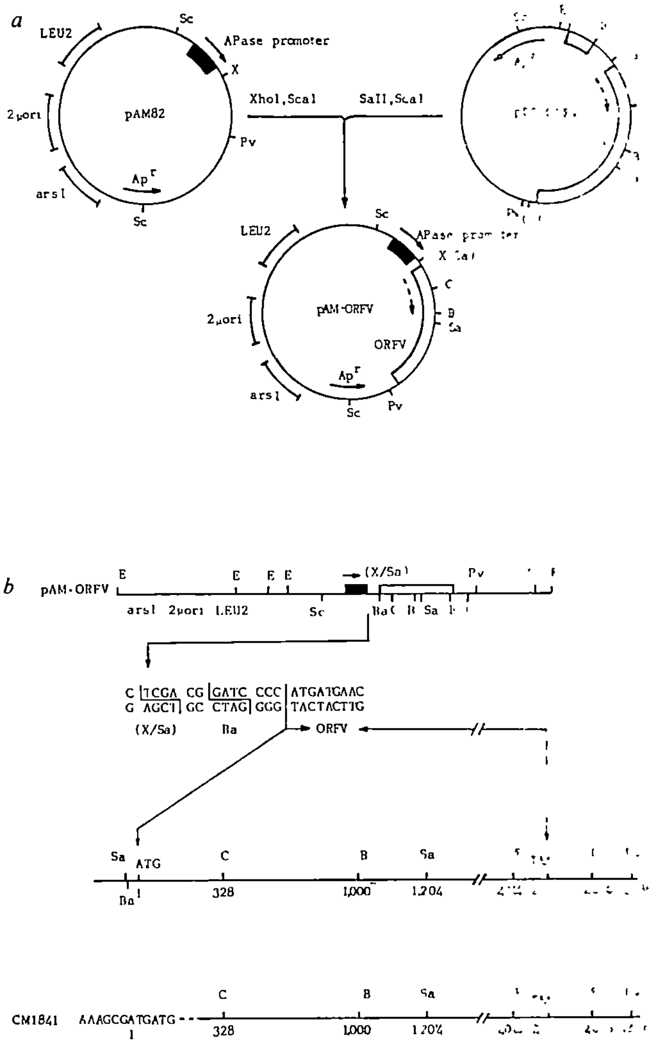

Fig. 1 *a*, Construction of yeast expression plasmid pAM.ORFV. Restriction sites for the enzymes *Bam*HI (Ba), *Bgl*II (B), *Cla*I (C), *Eco*RI (E), *Pvu*II (Pv), *Sal*I (Sa), *Sca*I (Sc) and *Xho*I (X) are indicated. The fusion junction of *Xho*I and *Sal*I sites is shown as (X/Sa). Solid boxes represent the APase promoter region; open boxes represent the ORF V sequence. An arrow above the APase promoter region shows the direction of transcription started from the APase promoter. A broken arrow shows the direction of translation started from the ATG initiator codon of the ORF V gene. Ap^r represents the ampicillin resistance gene. *b*, Fine restriction map of pAM.ORFV rescued from AH22/pAM.ORFV cells. All symbols represented are the same as indicated in *a*.

Methods. *a*, ORF V gene was recovered from pCaMV10 (ref. 29), which contains a full-length copy of CaMV strain CM1841 cloned at the *Sal*I site of pBR322. In the plasmid, the ORF V gene was contained in a form interrupted at the *Sal*I site by pBR322 sequences. The *Cla*I/*Sal*I fragment containing the 5′ half of ORF V and the *Pvu*II/*Sal*I fragment containing the whole 3′ half of ORF V were excised from pCaMV10, re-ligated at the *Sal*I site and cloned into the *Cla*I/*Pvu*II site of pBR322 (pBR.ORFV-D). The *Pst*I fragment containing the whole 5′ half of ORF V was excised from pCaMV10 and 'nibbled' with *Bal*31 to the nucleotide next to the first ATG in two adjacent putative initiation codons, followed by *Bgl*II digestion. This fragment and the *Eco*RI/*Bgl*II fragment, which contains the 3′ half of ORF V from pBR.ORFV-D, were inserted together into the *Sma*I/*Eco*RI site of M13mp8. pBR.ORFV, which contains the entire ORF V gene in correct orientation, was obtained by the insertion of the *Bgl*II fragment of the recombinant of mp8 and ORF V into the *Bgl*II site of pBR.ORFV-D. The *Sal*I/*Sca*I fragment of pBR.ORFV, containing the entire ORF V gene, was inserted into the *Xho*I/*Sca*I site of pAM82. The *Sal*I terminus of the former fragment was joined to the *Xho*I site of pAM82 at a position downstream from the APase promoter. The resultant plasmid, pAM.ORFV, was directly transformed into yeast AH22 cells. Transformation of yeast was performed by the modified method of Beggs[30] as described by Sherman *et al.*[31]. Leu$^+$ transformants were selected on high-P_i medium containing 2% agar. *b*, *E. coli* C600 (M^-, R^-) was transformed with the plasmid DNA fraction which was prepared from spheroplasted AH22/pAM.ORFV cells (2×10^7 cells). The rescued pAM.ORFV DNAs were prepared from eight clones out of the ampicillin-resistant transformants (1×10^3 per μg DNA) and subjected to fine restriction mapping.

from AH22/pAM82 cells, revealed an inducible RNA-dependent DNA polymerase activity which could use poly(rC)-oligo(dG) as well as poly(rA)-oligo(dT) as template-primer (Table 1). Eukaryotic DNA polymerases β and γ are known to use poly(rA)-oligo(dT), but not poly(rC)-oligo(dG)[16]. The low levels of activity observed with the extract from non-induced AH22/pAM82 cells could be explained by the presence of a β-type DNA polymerase observed previously in yeast[17]. The activity seen on poly(rC)-oligo(dG) with the extract from induced AH22/pAM.ORFV cells corresponds to the distinctive template specificity of a retroviral reverse transcriptase[18]. Negligible amounts of ^{3}H-dGMP were incorporated using poly(rA)-oligo(dT) as a template, eliminating the possible presence or induction of terminal deoxynucleotidyl transferase. Our experiments also ruled out either induction or activation of a reverse transcriptase encoded by the host. An RNA-dependent DNA polymerase activity induced specifically in AH22/pAM.ORFV cells was therefore identified as the ORF V-encoded reverse transcriptase.

The specific activity of the ORF V protein produced in yeast by AH22/pAM.ORFV was purified about 4,000-fold over crude extracts, with a yield of 20% (Table 2*a*). During glycerol gradient centrifugation, the enzyme activity sedimented as a single peak of apparent relative molecular mass (M_r) ~70,000 (Fig. 2); this is consistent with the ORF V coding capacity of 78,000. Pfeiffer and Hohn[19] have found that a 79,000-M_r polypeptide in organelles extracted from CaMV-infected turnips showed reverse transcriptase-like activity. The molecular size of our purified ORF V-encoded polymerase in its native condition is similar to that found in the virus-infected turnips. Therefore, CaMV-encoded reverse transcriptase can be active as a monomeric polypeptide, as is murine leukaemia virus (MuLV)-encoded reverse transcriptase (reviewed in ref. 20). However, in contrast to the findings of Pfeiffer and Hohn[19], the purified ORF V-encoded polymerase (glycerol gradient fraction) failed to show any activity on SDS-polyacrylamide gel electrophoresis. Furthermore, because of the very small yield of the purified ORF V-encoded polymerase, it is hard to estimate the size of the polymerase by SDS-polyacrylamide gel electrophoresis.

The purification of the CaMV reverse transcriptase was also monitored by examining the template specificity of the enzyme fraction at each purification step (Table 2*b*). Regardless of the step of purification, substantial activity was obtained by poly(rC)-oligo(dG) as well as with poly(rA)-oligo(dT). CaMV reverse transcriptase was also characterized as a MuLV-type reverse transcriptase by virtue of its activity on poly(rCm)-oligo(dG) and its divalent metal ion requirements[21]. CaMV reverse transcriptase requires 2 mM MnCl$_2$ (instead of 5 mM MgCl$_2$) for maximum polymerization activity, and the reaction proceeds linearly for 2 h at an optimum temperature of 20 °C (data not shown). For reverse transcription with native RNA, for example, human liver messenger RNAs primed with oligo(dT) and tobacco mosaic virus RNA primed with synthetic DNA (25 bases), which is complementary to a 3′ end of the viral RNA, Mn^{2+} was more effective than Mg^{2+} in promoting the synthesis of longer complementary DNA (in preparation), and also for promoting DNA-dependent DNA polymerase activity with native DNA such as single-stranded mp8 DNA primed with synthetic sequencing primer (in preparation). Neither endo- nor exodeoxyribonuclease activity other than

Table 1 RNA-dependent DNA polymerase activity in crude extracts of yeast AH22/pAM.ORFV and AH22/pAM82

		dNMP incorporation using different template-primers (pmol per mg protein)		
Transformant	Induction	poly(rA)-oligo(dT) ^{3}H-dTMP	poly(rC)-oligo(dG) ^{3}H-dGMP	poly(rA)-oligo(dT) ^{3}H-dGMP
AH22/pAM82	−	60.2	14.3	ND
AH22/pAM82	+	12.2	11.1	10.8
AH22/pAM.ORFV	−	34.6	14.2	ND
AH22/pAM.ORFV	+	486.0	191.0	13.0

The growth of yeast cells and induction were performed as described elsewhere[15]. Yeast cells were grown in high-inorganic phosphate (P_i) medium at 30 °C with aeration. When the cell density reached $\sim 1\text{–}2 \times 10^6$ cells ml^{-1}, the cells were centrifuged and resuspended in low-P_i medium for induction. Control samples were treated similarly, with the exception that high-P_i medium was used. When the density reached $2\text{–}3 \times 10^7$ cells ml^{-1}, 50-ml samples of induced (+) and non-induced (−) cultures were centrifuged. The cells were suspended in a 15-ml solution of Zymolyase (200 $\mu g\ ml^{-1}$), 1.2 M sorbitol, 50 mM Tris-HCl (*p*H 7.5), 14 mM 2-mercaptoethanol and incubated for 30 min at 30 °C. The spheroplasts were collected by centrifugation and lysed in 2 ml of 50 mM Tris-HCl (*p*H 7.5), 0,1% Triton X-100, 1 mM dithiothreitol. The lysate was clarified by centrifugation at 10,000*g* for 10 min. Protein concentration was measured by the modified Bradford method[26] using a Bio-Rad protein assay kit. RNA-dependent DNA polymerase activity was assayed as described by Marcus *et al.*[27] and Dion *et al.*[28] with modifications. Unless otherwise stated, the reaction mixture (0.05 ml) contained 50 mM Tris-HCl (*p*H 7.5), 50 mM KCl, 2 mM $MnCl_2$, 80 $\mu g\ ml^{-1}$ poly(rA), 10 $\mu g\ ml^{-1}$ oligo(dT), 4 μM ^{3}H-dTTP (3,000–4,000 c.p.m. $pmol^{-1}$), 5 mM dithiothreitol, 0.01% Nonidet P-40 (NP40), 0.1 mg ml^{-1} bovine serum albumin and 9 μg protein of the crude extracts, and was incubated for 30 min at 30 °C. When indicated, poly(rC)-oligo(dG) (90 $\mu g\ ml^{-1}$) or poly(rCm)-oligo(dG) (90 $\mu g\ ml^{-1}$) was substituted for poly(rA)-oligo(dT) and ^{3}H-dGTP (2,000 c.p.m. $pmol^{-1}$) was substituted for ^{3}H-dTTP. Reactions were halted by the addition of 0.1 ml of herring sperm DNA (1 mg ml^{-1}), 0.1 ml of 0.1 M sodium pyrophosphate and 3 ml of 10% (w/v) trichloroacetic acid and kept on ice for 10 min. Radioactivities incorporated into acid-insoluble fractions were counted. ND, not done.

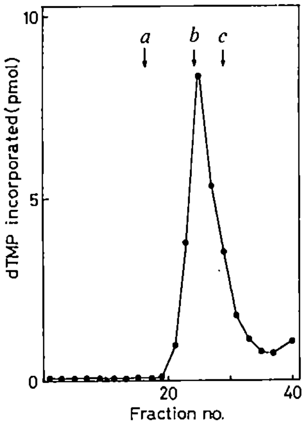

Fig. 2 Glycerol gradient centrifugation of CaMV reverse transcriptase. The enzyme fraction of step III was sedimented through a glycerol gradient as described in Table 2 legend. Aliquots (0.12 ml) of the fractions were collected from the bottom of the tube and 2-μl aliquots assayed for RNA-dependent DNA polymerase activity using poly(rA)-olido(dT) as template-primer. The positions of the marker proteins phosphorylase *b* (M_r 92,500) (*a*), bovine serum albumin (68,000) (*b*) and ovalbumin (43,000) (*c*) in a parallel gradient are indicated.

ribonuclease activities, which seriously affected cDNA synthesis with native RNAs, was associated with reverse transcriptase in a glycerol gradient fraction. This finding might be expected in view of the absence of a putative endonuclease coding domain in CaMV ORF V[22].

We have also attempted to express the CaMV ORF V gene in *Escherichia coli*. The entire ORF V gene, which lacks the first of two adjacent putative initiation codons, was inserted immediately downstream from the initiation codon of the *tac* promoter in the *E. coli* expression vector ptac12. The recombinant plasmid was transformed into *E. coli* NK5830 cells and the resulting transformant, NK5830/ptac.ORFV, was treated with 1 mM isopropyl β-D-thiogalactoside to induce the ORF V product under control of the *tac* promoter. The induction-specific polypeptide with an apparent M_r of 70,000 was found in SDS-polyacrylamide gels (data not shown). The polypeptide was accumulated as 1–3% of the total protein in *E. coli* during an induction of 2 h. The M_r of the polypeptide induced in *E. coli* was nearly the same as that of a native CaMV reverse transcriptase produced in yeast cells. However, in *E. coli*, no reverse transcriptase-like activity was detected, even in the partially purified fractions.

Some other foreign proteins, such as the human hepatitis B surface antigen gene[15,23], have been difficult to express in active form in *E. coli*. It is conceivable that post-translational modification and/or slight processing which is not sufficient to affect the apparent size of the polymerase could be required to produce CaMV reverse transcriptase in active form. For example, a putative protease-coding domain has also been predicted in the CaMV ORF V gene by Toh *et al.*[22]. This putative protease may be required to process a reverse transcriptase to active form in yeast cells. Recently, MuLV reverse transcriptase, of which the NH_2 and COOH termini approximate the correct termini of the authentic protein, has been expressed in active form in *E. coli* cells[24,25]. In the case of our cloning of CaMV reverse transcriptase, we did not leave any coding sequences

Table 2 Purification of ORF V gene product induced in yeast cells (*a*) and template specificity of enzyme fraction in each purification step (*b*)

a

Fractionation procedure	Total protein (mg)	Total units	Specific activity
I Crude extract	90	105.3	1.18
II Phosphocellulose	2.52	37.1	15.1
III Denatured-DNA cellulose	0.41	23.4	74.9
IV Glycerol gradient	<0.005	20.2	>4,032.0

b

	Specific activity		
Fractionation procedure	poly(rA)-oligo(dT)	poly(rC)-oligo(dG)	poly(rCm)-oligo(dG)
I Crude extract	1.21	0.418	ND
II Phosphocellulose	20.1	2.82	1.41
III Denatured-DNA cellulose	87.7	13.7	9.23
IV Glycerol gradient	4,050.1	1,030.0	1,050.3

a, CaMV reverse transcriptase was purified from 50 ml of crude extract (step I, 90 mg total protein). The crude extract was prepared from the spheroplasts obtained from 1.5 l culture of induced yeast AH22/pAM.ORFV cells, as described in Table 1 legend. Step I product was applied to a phosphocellulose column (2 cm × 3 cm) equilibrated with buffer A (50 mM Tris-HCl (*p*H 7.5), 2 mM 2-mercaptoethanol, 0.2 mM EDTA, 0.01% NP40, 20% (v/v) glycerol) containing 50 mM KCl. The column was washed with 30 ml of the same buffer and the enzyme was eluted with a 100-ml linear gradient of 0.05–0.8 M KCl in buffer A. RNA-dependent DNA polymerase fractions (0.4–0.55 M KCl) were pooled and dialysed against buffer A containing 20 mM KCl (step II). Step II product (2.5 mg protein) was applied to a denatured DNA cellulose column (1.2 × 2.5 cm) equilibrated with buffer A containing 20 mM KCl. The column was washed with 5 ml of the same buffer and the enzyme was eluted with a 30-ml linear gradient of 0.02–1.0 M KCl in buffer A. The enzyme fractions (0.26–0.38 M KCl) were pooled (step III). Step III product (0.41 mg protein) was diluted with two volumes of buffer A and applied to a small phosphocellulose column (1.2 × 1 cm) equilibrated with buffer A. The concentration of the enzyme was carried out by stepwise elution with buffer B (50 mM Tris-HCl (*p*H 7.5), 2 mM 2-mercaptoethanol, 0.01% NP40, 0.2 mM EDTA, 10% (v/v) glycerol, 1.0 M KCl). The concentrated enzyme fraction was applied to a 5-ml glycerol gradient (15–30%) in buffer B. Centrifugation was for 20 h at 48,000 r.p.m. in an RPS-50-2 Hitachi rotor at 4 °C. Active fractions were pooled and dialysed against buffer A containing 50% (v/v) glycerol and 1.0 M KCl, and stored at −20 °C (step IV, 0.005 mg protein). After this step, no detectable loss of activity occurred over 3 months at −20 °C. Aliquots of 5 ng–9 μg protein from each step of enzyme fraction were used for the RNA-dependent DNA polymerase assay with poly(rA)-oligo(dT), as described in Table 1 legend. One unit of the enzyme catalysed the incorporation of 1 nmol of dTMP in 60 min at 20 °C. *b*, Each step of enzyme fraction (5 ng–9 μg protein) was assayed for RNA-dependent DNA polymerase using poly(rA)-oligo(dT), poly(rC)-oligo(dG) and poly(rCm)-oligo(dG) as described in Table 1 legend. The incubation time at 20 °C was the same as above except that step I was for 15 min.

between the APase or *tac* promoter and the initiation codon of the ORF V gene in the expression plasmids, and so the products should be a non-fused, complete ORF V polypeptide. This has yet to be confirmed by amino-acid sequence studies.

We thank Dr R. J. Shepherd for pCaMV10, Dr K. Matsubara for the yeast expression vector pAM82 and yeast AH22, Mr T. Noguchi for his help in restriction mapping, and Dr T. R. Broker for his reading of the manuscript. This work is supported in part by Funds for Promoting Science and Technology from the Science and Technology Agency of Japan, and Grants-in-Aid for Cancer Research and for Cooperative Research from the Ministry of Education, Science and Culture of Japan.

Received 8 August; accepted 30 October 1985.

1. Shepherd, R. J. *A. Rev. Pl. Physiol.* **30,** 405-423 (1974).
2. Hohn, T., Richards, K. & Lebeurier, G. *Curr. Topics Microbiol. Immun.* **96,** 194-236 (1982).
3. Howell, S. H. *A. Rev. Pl. Physiol.* **33,** 609-650 (1982).
4. Varmus, H. E. *Nature* **304,** 116-117 (1983).
5. Pfeiffer, P. & Hohn, T. *Cell* **33,** 781-789 (1983).
6. Hull, R. & Covey, S. N. *Trends biochem. Sci.* **8,** 119-123 (1983).
7. Thomas, C. M., Hull, R., Bryant, J. A. & Maule, A. J. *Nucleic Acids Res.* **13,** 4557-4576 (1985).
8. Boeke, J. D., Garfinkel, D. J., Styles, C. A. & Fink, G. R. *Cell* **40,** 491-500 (1985).
9. Shibata, T. & Saigo, K. *Nature* **302,** 119-124 (1983).
10. Toh, H., Hayashida, H. & Miyata, T. *Nature* **305,** 827-829 (1983).
11. Flavell, A. J. *Nature* **310,** 514-516 (1984).
12. Saigo, K. *et al. Nature* **312,** 659-661 (1984).
13. Summers, J. & Mason, W. S. *Cell* **29,** 403-415 (1982).
14. Hirochika, H., Takatsuji, H., Ubasawa, A. & Ikeda, J.-E. *EMBO J.* **4,** 1673-1680 (1985).
15. Miyanohara, A. *et al. Proc. natn. Acad. Sci. U.S.A.* **80,** 1-5 (1983).
16. Gerald, G. F., Rottman, F. & Green, M. *Biochemistry* **13,** 1632-1641 (1974).
17. Chang, L. S. *J. biol. Chem.* **252,** 1873-1880 (1977).
18. Verma, I. M. *Biochim. biophys. Acta* **473,** 1-38 (1977).
19. Hohn, T., Hohn, B. & Pfeiffer, P. *Trends biochem. Sci.* **10,** 205-209 (1985).
20. Dickson, C., Eisenman, R., Fan, H., Hunter, E. & Teich, N. in *Molecular Biology of Tumor Viruses* (eds Weiss, R. A., Teich, N., Varmus, H. E. & Coffin, J. M.) 513-648 (Cold Spring Harbor Laboratory, New York, 1982).
21. Kohno, M. & Ishihama, A. *Eur. J. Biochem.* **97,** 257-266 (1978).
22. Toh, H. *et al. EMBO J.* **4,** 1267-1272 (1985).
23. Valenzuela, P., Mediana, A., Rutter, W. J., Ammerer, G. & Hall, B. D. *Nature* **298,** 347-350 (1982).
24. Tanase, N., Roth, M. & Goff, S. P. *Proc. natn. Acad. Sci. U.S.A.* **82,** 4944-4948 (1985).
25. Kotewicz, M. L., D'Alessio, J. M., Driftmier, K. M., Blodgett, K. P. & Gerard, G. F. *Gene* **35,** 249-258 (1985).
26. Bradford, M. M. *Analyt. Biochem.* **72,** 248-254 (1976).
27. Marcus, S. L., Modak, M. J. & Cavalieli, L. F. *J. Virol.* **14,** 853-859 (1974).
28. Dion, A. S., Vaidya, A. B., Fout, G. S. & Moore, D. H. *J. Virol.* **14,** 40-46 (1974).
29. Gardner, R. C. *et al. Nucleic Acids Res.* **9,** 2871-2888 (1981).
30. Beggs, J. D. *Nature* **275,** 104-109 (1978).
31. Sherman, F., Fink, G. R. & Hicks, J. B. *Methods in Yeast Genetics,* 112-115 (Cold Spring Harbor Laboratory, New York, 1982).

Detection of cytosine methylation in the maize alcohol dehydrogenase gene by genomic sequencing

Harry Nick*, Barbara Bowen*, Robert J. Ferl† & Walter Gilbert*

Biogen Research Corporation, Cambridge, Massachusetts 02142, USA
† Department of Botany, University of Florida, Gainesville, Florida 32611, USA

DNA methylation is believed to be involved in the control of gene expression[1,2]. In higher plants, up to 30% of the cytosine residues can be methylated—at C-X-G trinucleotides as well as C-G dinucleotides—compared with only 2–8% of total cytosines appearing exclusively as 5-methyl-C-5-methylcytosine in higher animals[1–4]. We have used the genomic sequencing technique of Church and Gilbert[5] to study the methylation of an alcohol dehydrogenase gene, *Adhl*, from maize. *Adhl* is one of two unlinked maize alcohol dehydrogenase genes[6,7] and appears in several tissues, including the scutellum of the kernel and the primary root of the seedling. It is further induced in primary roots subjected to anaerobiosis[8–10]. However, this gene is totally repressed in maize leaves[11]. Nonetheless, we have now found that a 900-base-pair (bp) region 5′ to the ATG is not methylated in leaves, even though it is rich in potential methylation sites. The first methylations occur 965 bp 5′ to the ATG. Thus, methylation does not appear to be involved in repressing this plant gene.

Restriction endonucleases whose activity is blocked when their recognition site is methylated have been used to detect modified C-G sites in the genome[12,13]. However, even with the ability to use additional enzymes such as *Pst*I and *Pvu*II (ref. 14) for methylation analysis in plants, restriction sites represent a small percentage of potential methylation sites. To demonstrate the applicability of genomic sequencing to the maize genome, which, at $\sim 7\times10^9$ bp, is two to three times larger than the mammalian genome[15,16], we analysed the methylation levels of cytosine residues in the 5′-flanking region of *Adhl*.

Figure 1 illustrates the genomic sequencing strategy. After cutting genomic DNA with a restriction enzyme that acts near a region of interest, the DNA was reacted with hydrazine and piperidine to liberate fragments terminating at cytosine

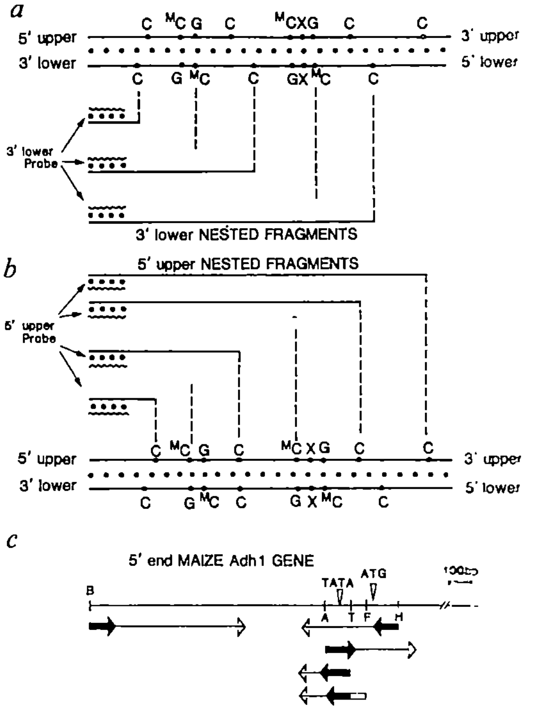

Fig. 1 ***a,*** A double-stranded genomic restriction fragment showing upper and lower strands in a 5′ to 3′ convention. A collection of nested fragments are generated by a partial cleavage with hydrazine and piperidine specific for cytosine residues. Methylation of cytosine prevents reaction with hydrazine so that no fragment is generated which terminates at this residue and thus the corresponding band on a sequencing gel is absent. Four possible strand-specific end-labelled sequences may be displayed. A 3′ lower probe illustrates the detection of the 3′ lower nested fragments. ***b,*** The detection of the opposite strand sequence originating from the same genomic restriction fragment. The hybridization with a 5′ upper probe displays the collection of 5′ upper nested fragments terminating in cytosine residues. Similarly, sequence originating from either the 3′ upper or 5′ lower strands may be displayed with the corresponding 3′ upper and 5′ lower probes. ***c,*** The region at the 5′ end of maize *Adhl* gene probed for cytosine methylation using genomic sequencing. The ATG codon and TATA box are shown by open arrows. The five vertical lines illustrate the position of the genomic restriction sites (*Bam*HI (B), *Hae*III (A), *Taq*I (T), *Hin*fI (F) and *Hin*dIII (H)), from which genomic sequence (thin lined arrow) was derived using the corresponding 100-bp single-strand DNA probes (thick darkened arrows). The open portion of one arrow shows how a probe starting from the *Taq*I site was used to probe *Hin*fI-cut chemically treated genomic fragments.

---

* Present addresses: Department of Biochemistry and Molecular Biology, College of Medicine, University of Florida, Gainesville, Florida 32610, USA (H.N.); Biological Laboratories, Harvard University, 16 Divinity Avenue, Cambridge, Massachusetts 02138, USA (B.B., W.G.).

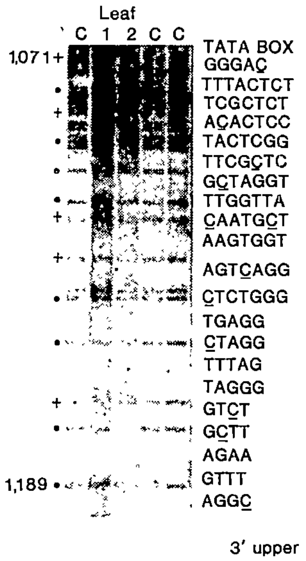

Fig. 2 Genomic sequence originating from the *Hin*dIII site extending towards the TATA box. Lane 1, 50 μg leaf genomic DNA; lane 2, 25 μg DNA. The lanes labelled C are hydrazine reactions on cloned plasmid DNA restricted with *Hin*dIII to illustrate the position of each cytosine residue. The sequence begins at position 1,189 (numbering scheme in Fig. 4) and proceeds 5′ to the TATA box near position 1,071. The dots and crosses denote the positions of cytosines in C-G dinucleotides and C-X-G trinucleotides, respectively.

Methods. DNA was isolated from maize leaves by a modification of published procedures[27]; the nucleus isolation buffer was 0.3 M sucrose, 50 mM Tris-HCl *p*H 8.0, 5 mM $MgCl_2$, 15 mM NaCl; 0.1 mM phenylmethylsulphonyl fluoride, 0.1 mM EGTA and 0.5 mM 2-mercaptoethanol. The crude nuclear pellet was lysed in 50 mM Tris-HCl *p*H 8.0, 20 mM EDTA, 1% sarkosyl and the DNA purified by equilibrium density centrifugation in CsCl. Leaf genomic DNA was digested to completion with *Hin*dIII, reacted with hydrazine and piperidine[17], applied to a denaturing gel, electrotransferred and the nylon ultraviolet irradiated as described elsewhere[5]. The 3′ upper strand sequence is displayed by hybridization with a 3′ upper single-strand DNA probe[5]. We have noted that identical single-copy maize signals may be obtained, with a corresponding lower noise level, when 0.25 mCi of label, rather than 1 mCi, is used. The hybridizations were performed at 65 °C as described above except that some of the filters were hybridized in a lexan tube submerged in water at 65 °C in a new rotating device, which will be described elsewhere (R. Tizard and H.N., manuscript in preparation). Washes were performed as described previously[28]. The membranes were autoradiographed with an intensifying screen for 2.5 days to 2 weeks.

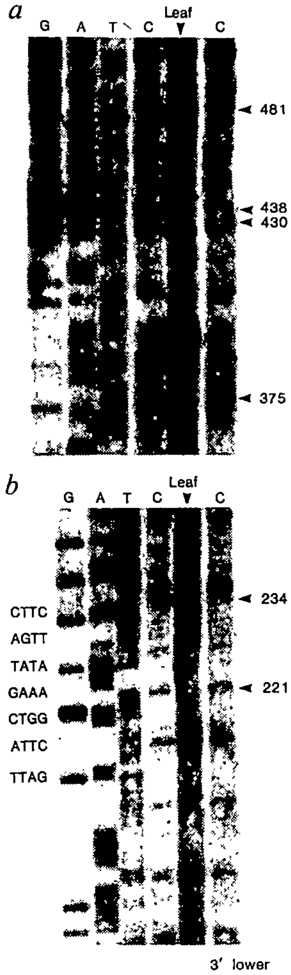

Fig. 3 Genomic sequence originating from the *Bam*HI site 1,200 bp 5′ to the ATG codon. Parts *a* and *b* are from the same autoradiogram. Leaf genomic DNA (30 μg) was digested to completion with *Bam*HI and treated as in Fig. 2. A 3′ lower probe was hybridized with this membrane to display 3′ lower strand sequence, which begins at position 192 and extends 3′ towards position 481 at the top of *a*. *a*, The positions of four potential methylation sites (481, 438, 430 and 375) are shown by the arrows. All of these bands are detectable, as compared with the G, A, T and C reactions on the cloned plasmid DNA. *b*, The next two potential methylation sites (234 and 221) as indicated by the arrows are absent due to cytosine methylation at a C-A-G and C-T-G trinucleotide.

residues[17]. The fragments were then separated on a denaturing gel, electrotransferred to a non-charged nylon membrane and photo-crosslinked to the nylon. Hybridization with an end-specific, strand-specific DNA probe displayed the sequence of the desired genomic restriction fragment (the 5′ upper or 3′ lower probe in Fig. 1[5]). Because 5-methylcytosine does not react with hydrazine, no fragment was generated from this site[18]. In plants, this will result from methylation of either the sequence C-X-G or C-G (refs 3, 4 and Fig. 1*a*, *b*).

Figure 1*c* summarizes the probes used and the region studied. Hybridization with a 3′ upper probe originating from a *Hin*dIII site in the first intron produced the sequence of the 3′ upper strand from a *Hin*dIII digest of leaf genomic DNA. Figure 2 displays sequence from 25 and 50 μg of leaf DNA, flanked by control cytosine reactions from cloned plasmid DNA. The sequence runs out 100 bases to the TATA box and covers 13 potential methylation sites. All of the bands corresponding to C-G to C-X-G sites are present in the genomic DNA, which demonstrates that the 5′ end of *Adhl* is hypomethylated in leaves. Further data (Fig. 4) show that at least 350 bp in the 5′ region are hypomethylated in leaves.

We searched for methylation in an area further 5′ to the gene by probing from a *Bam*HI site 1,200 bp from the gene's ATG codon. Figure 3*a* depicts the 3′ lower strand sequence and the four potential methylation sites; these sites are also hypomethylated. However, Fig. 3*b* from the same autoradiogram reveals two methylated sites 950 bp upstream of the start site, at positions 234 and 221 in the trinucleotide sequences C-T-G and C-A-G. This experiment thus defines a transition in the state of methylation at the 5′ end of the maize *Adhl* gene.

Figure 4 summarizes our data and gives the number of potential methylation sites per 100 bp. We have probed 61 out of 107 of the C-G and C-X-G sites within 1,400 bp surrounding the 5′ end of *Adhl.* For 950 bp flanking the ATG codon, the *Adhl* gene is completely hypomethylated in leaves (with a single gap in our data at position 650–900; Fig. 4). We were unable to find probes that would yield clean sequence across the 650–900-bp region. We attribute this either to the fact that this region and its immediate vicinity are repetitious or that there is a universal nicking of the DNA strands in this region in the nuclear prepar-

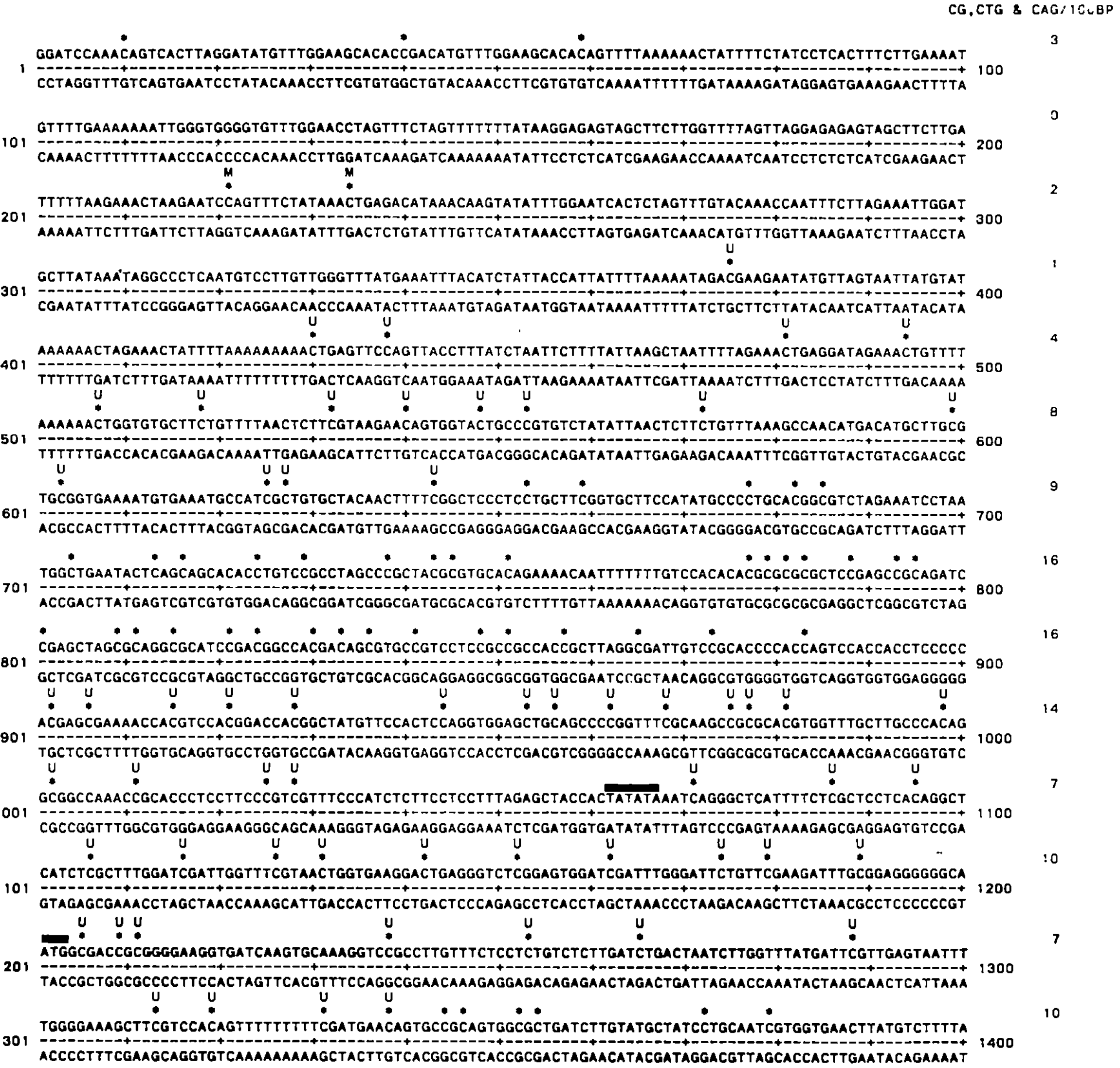

Fig. 4 Summary of cytosine methylation at the 5′ end of the maize *Adhl* gene. An asterisk appears above each potential methylation site in the 1,400 bp of 5′-flanking sequence. Only three types of sites, C-G, C-A-G and C-T-G, are indicated. The TATA box is centred at position 1,065 and the ATG codon at position 1,201, each denoted by a dark line. The U designates sites which are unmethylated and the M sites which have been found to be methylated. A gap exists in our data between sites 650 and 900. Only a small amount of the primary data have been shown; all of the data are illustrated on the top strand for simplicity. The numbers in the column on the right give the number of C-G, C-A-G and C-T-G sites per 100 bp.

ations. We expect this 'gap' to be hypomethylated, since the flanking sequences are uniformly hypomethylated. At 130 bases further 5′, we detect the first cytosine methylation; positions 234 and 221 are completely methylated.

The frequency of potential methylation sites in the first 300 bp of Fig. 4, the methylated region, is 1.3 sites per 100 bp. This is very low compared with the average of 9.3 sites per 100 bp in the next 1,100 bases, which is the statistical expectation and suggests that this last region is never methylated in any tissue and therefore never subjected to the pressures of transition mutagenesis through spontaneous deamination[19-21].

Considerable data have been accumulated using modification-sensitive restriction endonucleases, predominantly with animal genes[1,2]. The major implication of such data is that actively transcribed genes are hypomethylated relative to inactive genes—specifically, C-G sites at the 5′ end of genes[22,23]. The application of methylation-sensitive restriction enzymes in plants has previously been limited to studies of the T-DNA of crown gall tumours, repetitive sequences and 5S RNA genes[14,24-26]. Our results are the first extensive methylation study in plants correlated to a unique gene sequence, *Adhl*, as well as the application of genomic sequencing to a genome as large as that of maize.

Because the 950 bases in front of the gene, in a tissue in which this gene is completely repressed, are hypomethylated, we do not see any role for methylation in the control of expression of *Adhl*. If methylation were to function in repression here, it would do so from a distance of 1,000 bp.

We thank Marty Sachs and W. J. Peacock for sequence data before publication, M. Freeling for the genomic clone and Anna-Lisa Paul for technical assistance. This research was supported by USADA/CARGO grant 83-CRCR-1-1271 and Biogen Research Corporation.

Received 31 July; accepted 11 October 1985.

1. Cooper, D. N. *Hum. Genet.* **64**, 315-333 (1983).
2. Doefler, W. *A. Rev. Biochem.* **52**, 93-124 (1983).
3. Gruenbaum, Y., Naveh-Many, T., Cedar, H. & Razin, A. *Nature* **292**, 860-862 (1981).
4. Vanyushin, B. F. *Curr. Topics Microbiol. Immun.* **108**, 99-114 (1984).
5. Church, G. M. & Gilbert, W. *Proc. natn. Acad. Sci. U.S.A.* **81**, 1991-1995 (1984)
6. Schwartz, D. *Proc. natn. Acad. Sci. U.S.A.* **56**, 1431-1436 (1966).
7. Dennis, E. S. *et al. Nucleic Acids Res.* **12**, 3983-4000 (1984).
8. Ferl, R. J., Dlouhy, S. R. & Schwartz, D. *Molec. gen. Genet.* **169**, 7-12 (1979)
9. Freeling, M. *Molec. gen. Genet.* **127**, 215-227 (1973).

10. Sachs, M. M., Freeling, M. & Okimoto, R. *Cell* **20**, 761-767 (1980).
11. Okimoto, R., Sachs, M. M. & Freeling, M. *Planta* **150**, 89-94 (1980).
12. Bird, A. & Southern, E. M. *J. molec. Biol.* **118**, 27-47 (1978).
13. Waalwijk, C. & Flavell, R. A. *Nucleic Acids Res.* **5**, 4631-4641 (1978).
14. Hepburn, A. G., Clarke, L. E., Pearson, L. & White, J. *J. molec. appl. Genet.* **2**, 315-329 (1983).
15. Fasman, G. D. (ed.) *Handbook of Biochemistry and Molecular Biology* 3rd edn, Vol. 2, 284-306 (1983).
16. Bennett, M. D. & Smith, J. B. *Phil. Trans. R. Soc.* **B274**, 227-274 (1976).
17. Maxam, A. & Gilbert, W. *Meth. Enzym.* **65**, 499-560 (1980).
18. Ohmori, H., Tomizawa, J. & Maxam, A. M. *Nucleic Acids Res.* **5**, 1479-1486 (1978).
19. Coulondre, C., Miller, J. H., Farabaugh, P. J. & Gilbert, W. *Nature* **274**, 775-780 (1978).
20. Bird, A. *Nucleic Acids Res.* **8**, 1499-1504 (1980).
21. Barker, D., Schafer, M. & White, R. *Cell* **36**, 131-138 (1984).
22. Busslinger, M., Hurst, J. & Flavell, R. A. *Cell* **34**, 197-206 (1983).
23. Ott, M. *et al. Cell* **30**, 825-833 (1982).
24. Gelvin, S. B., Karcher, S. J. & DiRita, V. J. *Nucleic Acids Res.* **11**, 159-174 (1983).
25. Deumling, B. *Proc. natn. Acad. Sci. U.S.A.* **78**, 338-342 (1981).
26. Goldsbrough, P. B., Ellis, T. H. N. & Lomonossoff, G. P. *Nucleic Acids Res.* **10**, 4501-4514 (1982).
27. Rivin, C., Zimmer, E. & Walbot, V. *Maize for Biological Research* (ed. Sheridan, W.) (University of North Dakota Press, Grand Forks, 1982).
28. Ephrussi, A., Church, G. M., Tonegawa, S. & Gilbert, W. *Science* **227**, 134-146 (1985).

Transcription factor Sp1 recognizes a DNA sequence in the mouse dihydrofolate reductase promoter

William S. Dynan*‡, Shelley Sazer†, Robert Tjian* & Robert T. Schimke†

* Department of Biochemistry, University of California, Berkeley, California 94720, USA
† Department of Biological Sciences, Stanford University, Stanford, California 94305, USA

Human (HeLa) cells contain a host-cell-encoded transcription factor, Sp1, which is required for transcription of simian virus 40 (SV40) promoters[1,2]. Since the discovery of Sp1 we have been interested in learning what role this factor plays in uninfected cells. A monkey cellular gene promoter interacts with Sp1[3], but no gene products linked to this promoter have yet been identified. The finding that the sequence of the 5′-flanking DNA[4] of the mouse dihydrofolate reductase (DHFR) gene contains several regions showing strong homology to the Sp1 binding region of simian virus 40 (SV40) prompted us to undertake experiments with *dhfr*. We report here that Sp1 binds to these regions in the *dhfr* promoter, and that Sp1-containing preparations stimulate transcription from the *dhfr* promoter in an *in vitro* reaction. Our results suggest that in addition to its interactions with the SV40 viral promoter, one function of Sp1 is to direct the expression of the cellular DHFR gene.

DHFR catalyses the production of tetrahydrofolate, which is required for *de novo* synthesis of thymidylate, purines and glycine. The level of *dhfr* RNA varies during the cell cycle, being maximal at the onset of DNA synthesis[5]. Recent studies indicate that the 5′ end of the major *dhfr* messenger RNA lies 55 base pairs (bp) 5′ of the translation start[25] while the previously described −115 terminus[4,5] is a minor species in exponentially growing cells. As with SV40[6] and the monkey cellular gene promoter[7], transcription from the *dhfr* promoter region is bidirectional, with a transcript of unknown function synthesized from the opposite strand[8].

Deletion analysis of the *dhfr* promoter has been used to localize sequences showing promoter activity. DNA sequences within 300 bp of the *dhfr* initiation codon direct sufficient expression for cell survival in selective medium[4]. When partially purified Sp1 from human (HeLa) cell extracts was incubated with an end-labelled *dhfr* fragment containing this promoter region, four discrete regions were protected from DNase I in a footprinting assay (Fig. 1). Each footprint covered 20 bp on each strand of the DNA and included one 'GC box', a decanucleotide homologous to the consensus Sp1 binding sequence (Fig. 1*a*, *b*). To show that Sp1 was specifically responsible for the observed protection, the binding assay was carried out in the presence of several competitor DNAs (Fig. 2). The unlabelled *dhfr* fragment competed for protein bound to the *dhfr* promoter region, and almost eliminated the protection (Fig. 2*a*). A fragment containing the Sp1 binding region of the SV40 gene also reduced protection to a similar extent (Fig. 2*b*), suggesting that the same protein binds to the promoter regions of the SV40 gene and *dhfr*. By contrast, a fragment of similar size containing the adenovirus-2 (Ad-2) major late promoter, which has no Sp1 binding site, had no effect on the pattern of protection (Fig. 2*c*). The reciprocal experiment, where the various fragments were added to a binding reaction containing labelled SV40 probe, gave similar results (not shown).

In vitro transcription of *dhfr* directed by a HeLa nuclear extract was mapped in a runoff assay (Fig. 3*a*). Using two different templates, we saw transcripts (Fig. 3*a*, lanes 1, 3, arrows) of roughly the size expected for RNA initiating at −55, relative to the translational start codon. The position of the 5′ end, 40 bp downstream from the most proximal Sp1 site, corresponds to the pattern seen in SV40 and herpesvirus transcription units (refs 2, 9, 10 and K. Jones, K. Yamamoto and R. T., unpublished; for review, see ref. 11). α-Amanitin (1 μg ml^{-1}) inhibited synthesis, as expected for products of RNA polymerase II. When the *in vitro* RNA was analysed by primer extension (Fig. 3*b*, lane 1), one major group of bands was again seen, corresponding to initiation on the *dhfr* coding strand near −55 (Fig. 3*b*, large arrow); a less intense band was also visible, corresponding to initiation at −115 (small arrow). Several bands of smaller size, present in variable amounts, could represent either RNA initiating downstream of −55, or incomplete complementary DNA products synthesized from the major *dhfr* transcript. A similar primer extension analysis carried out using *in vivo* RNA (Fig. 3*b*, lane 2) produced essentially identical results, showing that the *in vitro* transcription system faithfully reproduced the *in vivo* pattern of RNA synthesis.

These experiments were then extended to a more highly purified transcription system, where Sp1 had been separated from the other enzymatic components required for transcription initiation. Without Sp1, *dhfr*-specific transcription was not detected (Fig. 4). Addition of partially purified Sp1 resulted in a significant activation of transcription. The pattern of Sp1-dependent transcripts was similar to that seen using the unfractionated extract, with a prominent start at the −55 site. As expected, Sp1 similarly stimulated the SV40 gene early promoter, but had no effect on the Ad-2 major late promoter. The *dhfr* template in this experiment was cleaved at −406, indicating that sequences upstream of this position are not required for Sp1-responsive transcription. Preliminary results, however, indicate the presence of additional Sp1 binding sequences in this upstream region. Moreover, in some experiments where sequences upstream to −900 were present, a higher basal level of transcription was seen in the absence of Sp1, reducing the net Sp1 stimulation. These results indicate that additional Sp1-dependent and independent transcription control elements are probably present in the region upstream of −406, and agree with earlier studies showing that this upstream region has promoter activity *in vivo* when fused to the DHFR structural gene[4].

All mammalian *dhfr* genes so far examined contain potential Sp1 binding sites. The mouse[4], human[12] and hamster (P. Mitchell and L. Chasin, personal communication) *dhfr* genes each have at least 5 GC box decanucleotide sequences within the 700 nucleotides upstream of the 5′ end of the mRNA. Although interaction with Sp1 has been confirmed experimentally only for the mouse *dhfr* promoter, the apparent conservation of Sp1 sites provides additional evidence that the binding of this factor has a functional role.

Recent reports indicate the presence of potential Sp1 binding sites in the 5′-flanking regions of cellular genes in addition to

---

‡ Present address: Department of Chemistry and Biochemistry, University of Colorado, Boulder, Colorado 80309, USA.

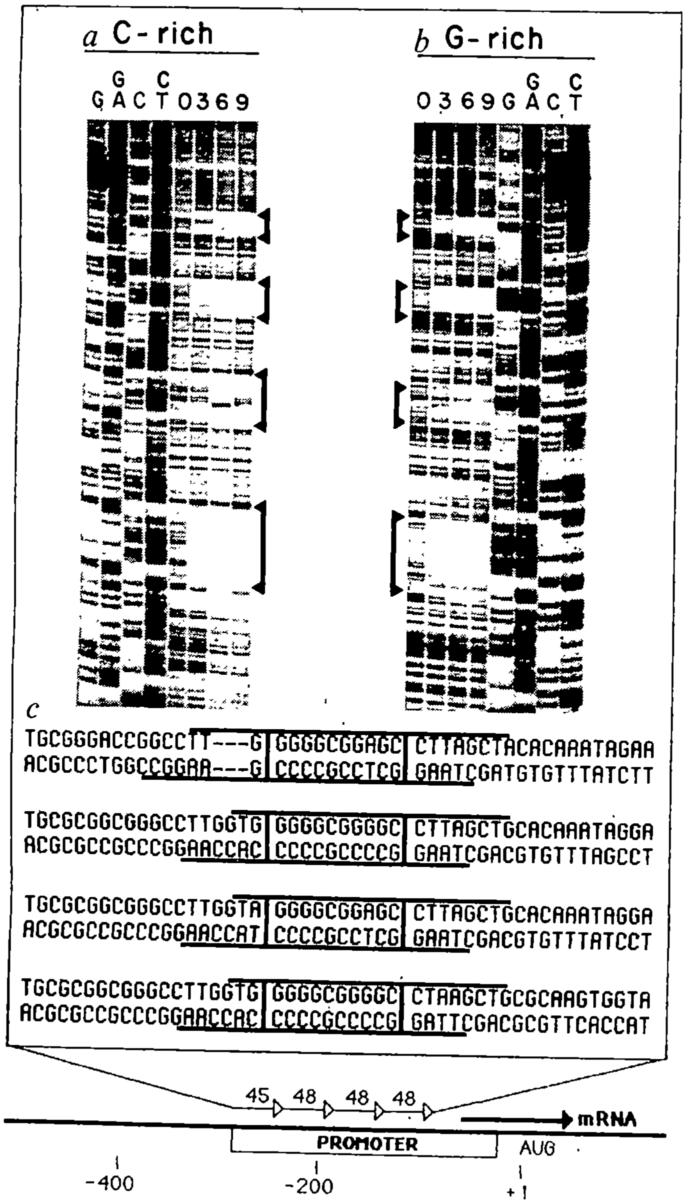
a C-rich
G C
G A C T 0 3 6 9
b G-rich
G C
0 3 6 9 G A C T
c
TGCGGGACCGGCCTT---G GGGGCGGAGC CTTAGCTACACAAATAGAA
ACGCCCTGGCCGGAA---G CCCCGCCTCG GAATCGATGTGTTTATCTT
TGCGCGGCGGGCCTTGGTG GGGGCGGGGC CTTAGCTGCACAAATAGGA
ACGCGCCGCCCGGAACCAC CCCCGCCCCG GAATCGACGTGTTTAGCCT
TGCGCGGCGGGCCTTGGTA GGGGCGGAGC CTTAGCTGCACAAATAGGA
ACGCGCCGCCCGGAACCAT CCCCGCCTCG GAATCGACGTGTTTATCCT
TGCGCGGCGGGCCTTGGTG GGGGCGGGGC CTAAGCTGCGCAAGTGGTA
ACGCGCCGCCCGGAACCAC CCCCGCCCCG GATTCGACGCGTTCACCAT
45
48
48
48
mRNA
PROMOTER
AUG
-400
-200
+1

Fig. 1 Binding of Spl to a double-stranded DNA fragment containing the proximal portion of the *dhfr* promoter. *a*, 5′ End of the C-rich strand labelled downstream of +6. DNA sequence markers were prepared by chemical cleavage[21] (far left). Binding reactions contained 0, 3, 6 or 9 μl of Spl as indicated above the lanes. Four discrete regions of protection are marked by vertical brackets on the right. *b*, Same fragment with 3′ end of the G-rich strand labelled downstream of +6. DNA sequence markers and binding reactions are as shown on the left. The promoter region contains four 45–48-bp imperfect tandem repeats; the sequence is written at the bottom (*c*), aligned for maximum homology. Bars indicate areas protected from DNase and boxes enclose GC box decanucleotides. The consensus Spl binding decanucleotide derived from analysis of a number of viral and cellular promoters[22] is:

$$\overset{G}{\underset{T}{}}\text{GGGCGG}\overset{GGC}{\underset{AAT}{}}$$

The map indicates the position of the major mRNA initiation site relative to 45–48-bp repeats; the area marked as promoter is sufficient for *in vivo dhfr* expression. Numbering is relative to the *dhfr* initiation codon at +1.

Methods. DNA was labelled at a linker downstream of position +6, using polynucleotide kinase and [γ-^{32}P]ATP to label the 5′ end of the C-rich strand, or reverse transcriptase and [α-^{32}P]-deoxynucleotide triphosphates to label the 3′ end of the G-rich strand. DNA was cut with a second restriction enzyme in a linker upstream of −406, and the resulting fragment isolated. Pooled Spl fractions from the Sephacryl S-300 column[1] were used in DNase footprinting reactions[2,9]. Binding incubation was at 0 °C, with reactions warmed to room temperature immediately before DNase addition. Reactions contained 18 fmol of labelled probe and 1 μg of native calf thymus DNA carrier.

Fig. 2 Binding of Spl to *dhfr* in the presence of competitor DNA. Three competitor DNA fragments were prepared: *dhfr*, a 412-bp fragment extending from −406 to +6; SV40, a 311-bp fragment (the *Eco*RII 'G' fragment) containing the functional early promoter and Spl binding sites; and Ad-2 P_L, a 290-bp fragment extending from 280 bp upstream of the adenovirus-2 major late initiation site to 10 bp downstream. The competitor fragment and native calf thymus DNA (0.5 μg) were incubated with 0, 3 or 6 μl of Spl for 10 min at 0 °C, then 18 fmol of labelled *dhfr* fragment ('C-rich'; see Fig. 1) was added. The incubation was continued for a further 10 min at 0 °C, then DNase was added and the products were analysed as described[2,9]. The competitor fragment, when present, was in 5-, 10- or 20-fold molar excess over the labelled fragment, as indicated above each lane.

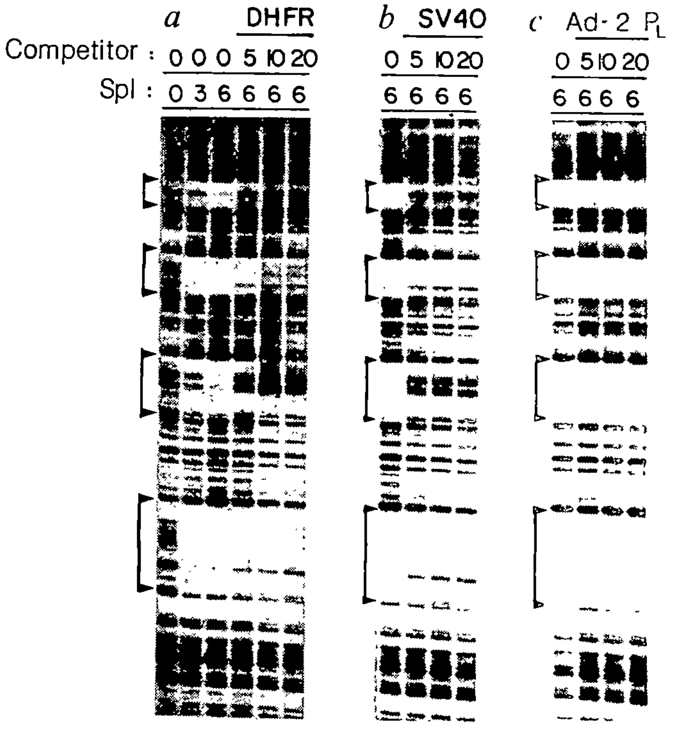
a DHFR
Competitor : 0 0 0 5 10 20
Spl : 0 3 6 6 6 6
b SV40
0 5 10 20
6 6 6 6
c Ad-2 P_L
0 5 10 20
6 6 6 6

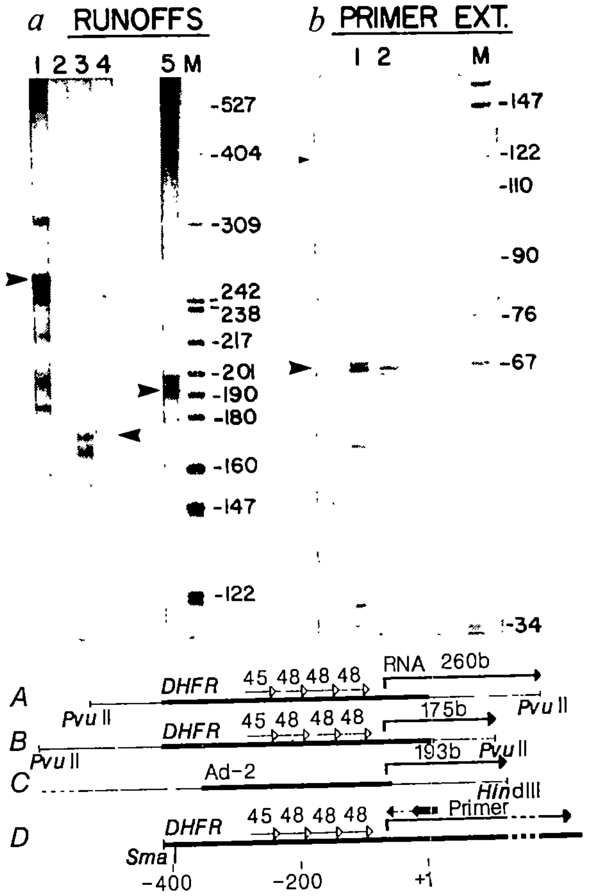

Fig. 3 Transcription of *dhfr*. *a*, *In vitro* runoff transcription. Lane 1, transcription directed by the *dhfr* promoter, template *A* in the diagram at the bottom. The arrow marks the major transcript migrating at 260 bases, relative to DNA size markers. Lane 2, as lane 1 with $1\ \mu g\ ml^{-1}$ α-amanitin. Lane 3, transcription directed by the *dhfr* promoter, template *B*. The arrow marks the transcript at 175 bases. Lane 4, same with $1\ \mu g\ ml^{-1}$ α-amanitin. Lane 5, transcription directed by adenovirus major late promoter, template *C*. The arrow marks the transcript at 195 bases. Lane M, pBR322/*Hpa*II size markers. *b*, Analysis by primer extension. Labelled 24-base synthetic primer has its 5′ end at +11 in the *dhfr* coding region. Lane 1, *in vitro* transcription directed by the *dhfr* promoter, template *D*. The large arrow marks the major extension product, the small arrow the minor product. Lane 2, *in vivo* RNA from nuclei of *dhfr*-amplified cells. Lane M, pBR322/*Hpa*II size marker fragments. *c*, Diagram showing template DNAs. Thick lines, eukaryotic inserts; thin lines, attached vector sequences. **Methods.** Transcription reactions ($50\ \mu l$) contained $15\ \mu l$ of a nuclear extract prepared from human (HeLa) cells[23] and 500 ng of isolated *dhfr* promoter fragment (lanes 1–4) or 1,000 ng of plasmid containing the adenovirus major late promoter (lane 5). Reactions were run as described elsewhere[1]. Runoff reactions contained $50\ \mu Ci$ $[\alpha\text{-}^{32}P]$ CTP and $5\ \mu M$ unlabelled CTP, and were incubated for 60 min. Products were analysed on a thin 5% polyacrylamide-urea gel. Reactions for primer extension contained $250\ \mu M$ nonradioactive CTP and were incubated for 30 min. *In vivo* RNA was isolated from nuclei of *dhfr*-amplified cell line 3T6R50 (ref. 24) as described elsewhere[5]. Hybridization and cDNA synthesis were as described previously[2], and products were analysed on a thin 8% polyacrylamide-urea gel.

dhfr. Several other genes involved in purine metabolism have sequences homologous to the consensus GC box decanucleotides, including those for mouse hypoxanthine phosphoribosyltransferase[13], mouse adenine phosphoribosyltransferase[14] and human adenosine deaminase[15]. Other genes with potential binding sites include rat type II procollagen[16], several members of the human metallothionein family[17,18], human urokinase-plasminogen activator[19] and hamster hydroxymethyl glutaryl CoA reductase[20]. Because there is no known common pattern of regulation for this diverse group of genes, the possible role of Sp1 in their regulation is not immediately apparent. Perhaps the regulatory consequences of Sp1 binding depend on sequences adjacent to the Sp1 sites in a particular promoter, or are the result of interactions between Sp1 and other, as yet unidentified, factors. Further genetic analysis will help to elucidate the physiological role of Sp1 in the regulation of *dhfr* and other cellular genes.

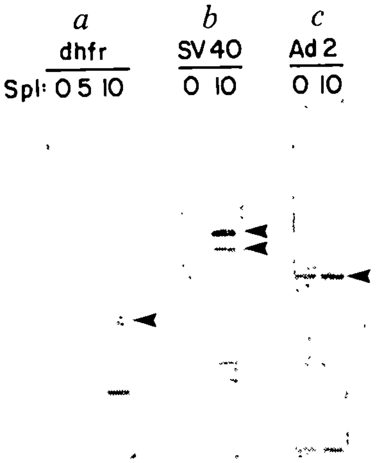

Fig. 4 Sp1-dependent *in vitro* transcription. Reactions contained 250 ng of promoter-containing linearized plasmid DNA, and 0, 5 or $10\ \mu l$ of Sp1, as indicated. Separate complementary oligonucleotide primers were used for each template. Arrow in *a* marks the *dhfr* transcript initiating at about −55. Arrows in SV40 (*b*) and Ad-2 (*c*) mark transcripts initiating at the expected positions. **Methods.** Reactions contained $9\ \mu l$ of endogenous RNA polymerase II fraction and $3\ \mu l$ of transcription factor Sp2, prepared from a whole-cell extract described previously[1]. Sp1 was prepared by a new method (M. Briggs and R.T., unpublished) in which a nuclear extract was passed directly over an S-300 gel filtration column. Pooled fractions had approximately the same specific activity as those pooled from the S-300 column in the previous scheme. Similar stimulation of *dhfr* transcription has been seen with Sp1 fractions prepared by our previous method (not shown)[1].

We thank Pam Mitchell and Larry Chasin for providing the sequence of the 5′-flanking region of hamster *dhfr*. This research was funded by NIH grants to R.T. (CA25417) and R.T.S. (CA16318). W.S.D. was a Senior Postdoctoral Fellow of the American Cancer Society, California Division, Inc. S.S. was a predoctoral trainee supported by USPHS NIH grant GM07276.

Received 19 August; accepted 11 October 1985.

1. Dynan, W. S. & Tjian, R. *Cell* **32**, 669–680 (1983).
2. Dynan, W. S. & Tjian, R. *Cell* **35**, 79–87 (1983).
3. Dynan, W. S., Saffer, J., Lee, W. S. & Tjian, R. T. *Proc. natn. Acad. Sci. U.S.A.* (in the press).
4. McGrogan, M. M., Simonsen, C. C., Smouse, D. T., Farnham, P. J. & Schimke, R. T. *J. biol. Chem.* **260**, 2307–2314 (1985).
5. Farnham, P. J. & Schimke, R. T. *J. biol. Chem.* **260**, 7675–7680 (1985).
6. Tooze, J. *Molecular Biology of Tumor Viruses* 2nd edn, Pt 2, revised (Cold Spring Harbor Laboratory, New York, 1981).
7. Saffer, J. & Singer, M. *Nucleic Acids Res.* **12**, 4769–4788 (1984).
8. Farnham, P. J., Abrams, J. M. & Schimke, R. T. *Proc. natn. Acad. Sci. U.S.A.* **82**, 3978–3982 (1985).
9. Gidoni, D., Dynan, W. S. & Tjian, R. *Nature* **312**, 409–413 (1984).
10. Jones, K. & Tjian, R. *Nature* **317**, 179–182 (1985).
11. Dynan, W. S. & Tjian, R. *Nature* **316**, 774–778 (1985).
12. Chen, M. J. *et al. J. biol. Chem.* **259**, 3933–3943 (1984).
13. Melton, D. W., Konecki, D. S., Brennand, J. & Caskey, C. T. *Proc. natn. Acad. Sci. U.S.A.* **81**, 2147–2151 (1984).
14. Dush, M. K., Sikela, J. M., Khan, S. A., Tischfield, J. A. & Stambrook, P. J. *Proc. natn. Acad. Sci. U.S.A.* **82**, 2731–2735 (1985).
15. Valerio, D. *et al. EMBO J.* **4**, 437–443 (1985).
16. Khono, K., Sullivan, M. & Yamada, Y. *J. biol. Chem.* **260**, 4441–4447 (1985).
17. Karin, M. & Richards, R. I. *Nature* **299**, 797–802 (1982).
18. Richards, R. I., Heguy, A. & Karin, M. *Cell* **37**, 263–272 (1984).
19. Riccio, A. *et al. Nucleic Acids Res.* **13**, 2759–2771 (1985).
20. Reynolds, A. B. *et al. Cell* **38**, 275–285 (1984).
21. Maxam, A. & Gilbert, W. *Meth. Enzym.* **65**, 499–560 (1980).
22. Kadonaga, J., Jones, K. & Tjian, R. *Trends biochem. Sci.* (in the press).
23. Dignam, J. D., Lebovitz, R. M. & Roeder, R. G. *Nucleic Acids Res.* **11**, 1475–1489 (1983).
24. Brown, P. C., Beverley, S. M. & Schimke, R. T. *Molec. cell. Biol.* **1**, 1077–1083 (1981).
25. Sazer, S. & Schimke, R. T. *J. biol. Chem.* (in the press).

nature

NATURE VOL. 319 23 JANUARY 1986

Europe still unsure of itself

The past few weeks have produced yet more evidence that European states are unsure where Europe as a whole is heading. They should make up their minds.

THE great excitement in Britain in the past two weeks about the fate of a small and unsuccessful helicopter company has been presented as part of the struggle for a United States of Europe (see *Nature* **319**, 86; 1986). Mr Michael Heseltine, Secretary of State for Defence two weeks ago, walked out of the British Cabinet for all kinds of reasons, some of which may have been strictly personal, but ostensibly because he said his colleagues in the government were less than fair towards his scheme for letting control of the helicopter company pass to a European rather than to a US-Italian consortium. The general assumption seems to be that those who favour the European bid are true Europeans, and that the supporters of the Sikorsky–Fiat deal, by contrast, are lukewarm or even hostile to Europe. Everybody seems to have overlooked the truth, that the notion that Westland helicopters should be "saved" for Europe by a hastily constructed financial bid is a measure, rather, of the stark inadequancy of Europe's economic integration so far. For in a rational Europe, tears might be shed about the disappearance of a single helicopter manufacturer, but potential purchasers of these machines (of which there are few) would know that there are other companies to which they could turn for supplies.

Much the same applies to the announcement on Monday this (see p.251) week of the agreement between France and Britain that there should be a fixed link across the strip of water that divides them. Officials in Paris have made heavy weather, in the past few weeks, of their attempt to choose one from among the several competing schemes for forging such a link. Because civil servants are not renowned as engineers, it is not surprising that their technical appraisal has been tortuous and that its outcome commands very little confidence. The mere fact that the two governments have been drawn into the adjudication is, however, a confession of the incompleteness of the European programme. In a properly organized Europe, the question of whether private capital should be used to build a bridge, a tunnel or some hybrid of the two would no doubt have been the subject of a public administrative inquiry (since local interest in both countries will be affected), but the technical feasibility of the scheme would have been left to a decision by the markets in which the builders will have to raise the money.

The account on p.255 of the surplus of teachers in West Germany points from a different angle towards the conclusion that Europe is still an awkward compromise between the ideal and the politically possible. For a variety of reasons, West Germany seems to have continued training teachers, many of them specialists who would have taught in high schools, for longer than could be justified by the decline of the birth-rate that seems to have been general in Western Europe during the 1970s. But elsewhere within the European Communities, there are shortages of teachers. Even in Britain, where successive governments have acted vigorously to save public money by cutting back on teacher training and have created a climate in which recruitment to the teaching profession is difficult, there is now the prospect that the acute shortage of science teachers of the past few years will become chronic. Why do not out-of-work West German teachers move to Britain to fill these empty posts? Language difficulties are not a sufficient explanation. Only the general sense that Europe is still an entity largely in name, which affects both individuals and institutions, can explain this immobility in the face of strictly parochial misfortune.

What is to be done? Last week, the European Parliament in Strasbourg gave its blessing to the moderate programme of reform of European institutions that has been negotiated over the past nine months between the governments of the European Communities. The effect will be to remove some of the impediments that now exist to the free movement of goods and services throughout Europe. But the reform is far less radical than some governments (that of France especially) had been crying for last year. It is far less than that required to make Europe an integrated economic unit — yet, even so, there is a chance that Denmark, which is committed to holding a referendum on the issue, will be found blocking this modest programme when it comes for decision in the Council of Ministers later in the year.

If these prevarications and inconsistencies persist, Europe's bluff that it is a continent will soon be called. When the Treaty of Rome that created the European Communities was negotiated in the early 1950s, everybody acknowledged that the new Europe would not spring into being overnight. Now, with more than a third of a century gone, the every-day spectacle of quarrels about the retention of customs posts (one of the matters glossed over in last week's Strasbourg vote) squares badly with proposals such as that of Mr Heseltine that European taxpayers should dig into their pockets to keep a helicopter manufacturer artificially in business for fear of undermining a purportedly integrated European defence industry. United Europe is now not much more than a collection of separate nations agreed to conceal their differences from each other beneath a cloak of even more dedicated extra-European chauvinism. That a united Europe would be an inward-looking Europe has always been a danger; the reality of a disunited xenophobic Europe is an even meaner outcome.

Mercifully, the other side of the coin is now wholly blank. Some European schemes have worked reasonably well. Participants in the Esprit programme for collaborative information technology, for example, say they have won benefits from joint support from Brussels that would not otherwise have arisen. They seem either not to know or not to care that they echo the public statements of participants in the early Euratom programmes of the 1950s, who were invariably well disposed towards unearned income. On this occasion, of course, things may turn out differently. Technological Europeans, in other words, should acknowledge that nothing much has yet been accomplished but that something may be. In other fields, much the same is true; even the freedom of people to move from one place to another only half restores *de jure* what was *de facto* commonplace two centuries ago (when "Europe" was twice as big).

The effective remedy therefore may be the calling of the European bluff. What can Europe do for European voters that national governments do not at present accomplish? The simplest answer is that intra-European trade has increased in the past 30 years, but this makes little sense because it came at a time when world trade as a whole was growing; since the faltering of world trade a decade ago, crises like that at Westland Helicopters have become two a penny. That is why Mr Heseltine's supporters should tell him that while his heart is in the right place, his head is in the clouds; that battling for a united Europe with Westland Helicopters as a slogan is fruitless. Mr Heseltine's local difficulty is that his supporters are not, like him, Europeans by instinct but rather xenophobes. He will not be the first to find himself caught out like that. □

No more numbers game

Last week's Soviet arms control proposals are the best yet, perhaps the best for forty years.

WASHINGTON is still forgivably hesitant and uncertain about last week's proposals on strategic arms control, which are breathtaking in their radicalism. Such a break with the recent past is bound to catch people off guard, which is as it should be. But it would be a great mistake to write off Mr Mikhail Gorbachev's suggestions for what should happen next at Geneva as yet another proposal which, when picked apart, will be found to contain little of substance, or be otherwise objectionable. For the novelty in what Mr Gorbachev had to say last week is his explicit acknowledgement that substantial controls on strategic weapons will not be reached quickly, and that it may take until the end of the century for the abolition of nuclear weapons to be feasible. Previous Soviet leaders have so often impeded rational discussion with impatient demands for "general and comprehensive disarmament" the day after tomorrow that the influence of a pragmatist should be generally welcomed.

The further merit of the Gorbachev plan, with several independent components such as the withdrawal of Soviet and US missiles from the European theatre, a reduction by a half of strategic arms and so on, is that the scheme is plainly not meant as a package but as a negotiating framework. If it is the will of the superpowers to reduce the numbers of strategic weapons they deploy against each other, for their mutual benefit and that of bystanders, it is clear that progress can be made only step by step, and that the first steps must be taken before even the character of later steps is known. The trick is to ensure that none of the intermediate steps will be obstacles to those certain to follow. The negotiators at Geneva are hardly in a position to take such a grand view, which is why there is a need for a response from none other than President Reagan himself.

There are two snags, of which the first is the obvious danger that the future ideal may undermine what is feasible now. It is clearly essential that the goal of abolishing nuclear weapons by the end of the century should not distract attention from tangible steps that could be taken now. The Geneva negotiators who reassembled last week could do worse than settle for a tidying up of the agreements to which they are already parties, SALT II and the Anti-Ballistic Missile Treaty in particular (see *Nature* **319**, 164; 1986), which would seem far from an empty achievement if there is a firm promise of better things to come.

But does the world, or anybody, wish to see the back of nuclear weapons altogether? That is the second snag that everybody must face. The immediate reaction to the Gorbachev proposals from Mr Zbigniew Brzezinski, President Carter's National Security Advisor, that the scheme is a recipe to "make the world safe for conventional war", points to the nub of the difficulty. Nuclear weapons have become so much an aid to the preservation of the *status quo* that even the most farsighted statesmen will think twice before suggesting their abolition. Only the most idealistic or naive believe that the abolition of nuclear weapons could be finally accomplished without agreement on the uses to which conventional forces would be put. But issues like that even touch the degree to which national sovereignty is an autonomous force in international relations. Perhaps it is not too soon to begin asking questions like these, but their difficulty should warn even the optimists that Mr Gorbachev's timetable, worthy though it is, will be much delayed. □

Scribes in space

The US government plans to put a journalist in space later in the year. Is it wise?

SOME years ago, US journalism was enlived by a stocky character with a Brooklyn accent whose career had been transformed by a single assignment, that of being the first journalist to witness in that capacity the explosion of a nuclear weapon at a Pacific atoll. William L. Lawrence by birth, he was known to everybody as "Atomic Bill", and required by the expectations of his companions and editors to fill the role, whatever his inclinations may have been. For decades afterwards, no nuclear reactor could go critical, no diplomatic conference on the future of nuclear energy could take place, without his presence. Only when he retired from the *New York Times* to a Mediterranean island was Atomic Bill able to follow his chief interest, pre-nucleic acid biochemistry. But now, with characteristic indifference to the lessons of history, the National Aeronautics and Space Administration (NASA) is about to wish a similar fate on another unsuspecting journalist, the first ever to be sent up by shuttle.

By the closing date for applications last Thursday, the US Association of Schools of Journalism and Mass Communication, rising to the only occasion in its history likely to be remembered generally, was said to be swimming in a large proportion of the 4,000 application forms requested by aspiring Orbit Micks (or Megs, as the case may be), many of them turned in, in the best traditions, right on deadline. It is hoped that not too many readers will cancel their subscriptions because none of the members of *Nature*'s staff who satisfies the condition of being a US citizen will also meet the requirement of having been in journalism for five years. But there are more onerous conditions.

The worst is that the unlucky winner of the competition will have to work as a one-person "pool", a kind of communal resource to be exploited by all his or her natural competitors, who will be free to demand answers to whatever questions come into their heads. ("Say, *that* nausea, is it worse when you move about?") With NASA in charge of all communications, the pool reporter's traditional ingenuity in keeping the best scraps of information for his own employers will be fully tested. NASA's demand that the reporter should "not intrude on the private lives" of his companions "without their express permission" will not easily be satisfied. It will be irksome that personal equipment that cannot be "flight-qualified" will have to be replaced by what NASA thinks best. The summer in Houston is not everybody's idea of bliss.

Who will be chosen? This is where the fun will start. The medical examination seems not much of a hurdle. The need for a security clearance may be a more serious obstacle even though NASA promises that recruitment will not be based on "political associations or beliefs". But the real fun starts with the two "essay questions" that applicants must answer. One whole sheet of blank paper awaits the response to "How will you attempt to fulfill" the purpose of communicating the "unique experience of space travel"? Maybe the selection panels, representing as they do the schools of journalism and mass communication, have ways of telling when people who fill this sheet with phrases like "mankind liberated from tedious Earth" will lapse, in the event, into phrases like "I can see Paris, France!" But the trick question is the second, which asks that the chosen journalist should speculate, "looking 10 or 20 years into the future", about the value to journalism of the facility "to report regularly from space". It is as if a restaurant were to offer free dinners to those with interesting opinions on the value of dining out. Cruelly, NASA retains the right to publish these essay questions, ensuring that it can ruin not just the career of its equivalent of Atomic Bill, but all those who answer this question with a straight face. □

Archaeologists

World congress quits Southampton for Mainz

The University of Mainz (West Germany), rather than Southampton (England), will host the 11th World Archaeology Congress in September 1986. The executive committee of the International Union of Prehistoric Sciences (IUPPS), at an extraordinary meeting in Paris last week, took the unprecedented step of "withdrawing recognition" of the congress from the University of Southampton.

Professor John Evans, chairman of the executive committee and president of IUPPS, resigned his position during the Paris meeting, but is to stay on as an ordinary member of the executive. Professor Peter Ucko, organizer of the Southampton congress, ceased to be a member of the executive after the decision to remove the congress from Southampton and left the Paris meeting before it ended.

IUPPS's decision resolves the bitter dispute caused by the banning of South African delegates, including scientists of other nationalities who work in South Africa, from the Southampton meeting (see *Nature* **317**, 754; 1985). The ban resulted from pressure by Southampton's city council and university teachers' and students' trades unions, although Ucko argued strongly against it.

More than 200 participants from the United States, as well as the delegations from France, West Germany, The Netherlands, Belgium, Switzerland and Spain, would have boycotted the meeting had the ban been upheld, whereas many African delegates would not have attended had the ban not been introduced. The IUPPS executive took its action because the organizing committee of the Southampton meeting had departed from IUPPS's statutes and longstanding policy to keep all its activities open to all "*bona fide* scholars". For more than 50 years, the 10 congresses sponsored by IUPPS have been organized on this basis and scholars have been admitted irrespective of race, nationality, religion or political convictions.

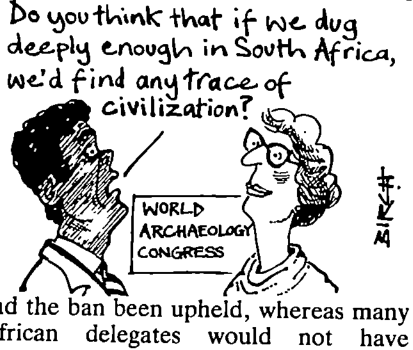
Do you think that if we dug deeply enough in South Africa, we'd find any trace of civilization?
WORLD ARCHAEOLOGY CONGRESS

The new president of IUPPS and chairman of the executive committee is Professor K. Böhner of Mainz, and Dr K. Weidermann is the organizing secretary. Notice of the decision to move the congress is to be sent to the members of the permanent council of IUPPS for approval by postal vote.

Professor Phillip Tobias, a member of the council, said in Paris this week that the action "constitutes a landmark decision in the history of the struggle for the freedom of science and for the free circulation of scientists. . . .The IUPPS resolutions constitute a striking reaffirmation of the need to keep scientific intercourse and the access to knowledge free from political, racial or geographical limitations."

Maxine Clarke

Searle's UK research lab closes

G.D. Searle, the US drug company, is to end its pre-clinical research programme in the United Kingdom by closing its High Wycombe laboratories with the loss of 300 jobs. The decision was made largely to avoid a "duplication of effort" in company laboratories in other countries and is part of a worldwide reorganization of the company in the wake of Searle's recent merger with the giant US chemical company Monsanto. At that time, Searle said that the research enterprises of the two companies would reinforce each other.

Much of Searle's UK research effort will be absorbed by Monsanto's directly comparable biotechnology research institute in St Louis, Missouri; the rest will go to Searle laboratories in Belgium and France. Staff will be offered transfers on an "individual basis".

Searle's decision to stop its UK programme stems partly from its disillusionment with the British government's recent regulations designed to save money on National Health Service drugs prescriptions. British-owned companies get a better price for drugs than foreign companies. But a company spokesman stressed last week that Searle will spend more this year on research and development worldwide than ever before; $160–170 million in 1986 compared with $130–140 million in 1985. And individual projects in universities, for example a £1 million project at the University of Oxford, will continue. Searle is now looking for a new site in High Wycombe for its business operations — the present laboratories are considered "unsuitable" for that purpose. Maxine Clarke

---

Channel tunnel

Rail plan gets go-ahead

After nearly two centuries of talking, Britain and France are to be linked by a tunnel under the English Channel (*La Manche,* the "sleeve", to the French). A historic moment? Not to judge by the French media, which have taken very little interest in the prospect of getting from Paris to London in three and a half hours rather than five.

This is understandable. Through the tunnel, Britain sees the whole of Europe: France sees only Britain. And what do the French think of Britain? In a recent poll by a French science magazine, readers were asked with which country they would like to see French industry and scientists cooperating in high technology. Nearly 30 per cent said West Germany. Only 1 (yes, 1) per cent said Britain.

But, notwithstanding popular French indifference, Prime Minister Margaret Thatcher and President François Mitterrand announced on Monday that construction can now begin of a twin-bore rail tunnel, though which trains will carry freight direct and cars piggy-back. The rail tunnel should be open by 1993. This looks like defeat for the "road" lobby, Mrs Thatcher included, although the winning consortium, the Channel Tunnel Group (CTG), will be asked to prepare plans for a twin road tunnel to be built within fifteen years — if it appears economic.

The decision has not pleased those placed either side of the tunnel. The mayor of Calais, the principal French ferry port, has said that within a few years of the opening of the tunnel Calais would become "a ghost town". That might be true, and the same for Dover, if the rail tunnel provides transit at costs much lower than the ferries, as predicted by CTG's chairman, Sir Nicholas Henderson. A spokesman for the now-defunct "Euroroute" bridge scheme, however, claims that drilling problems and heating and ventilation of a tunnel will force up costs far beyond those now predicted.

A more optimistic scenario, however, has it that the "chunnel" will indeed reduce transit costs, and thus encourage new industries to set up near the tunnel entrances. However, the zone south of the tunnel (in north-east France) may well prove more attractive than that north of it (in Kent and Sussex), as the former will also provide a crossroads for traffic moving east and west across Europe.

French rail interests are also keen on the prospect of running the advanced French high-speed train, TGV (*Train Grand Vitesse*) to London. In many ways, it seems, Monday's decision looks like a French success. **Robert Walgate**

Japanese science budget

Some gains, some losses

Tokyo

BESIDES some big funding increases for a handful of key projects, there is little good news for scientists in the 1986 budgets of two of Japan's major science ministries, the Science and Technology Agency (STA) and the Ministry of International Trade and Industry (MITI).

This year, as for the past few years, the government has done everything it can to cut the size of the budget. What makes this necessary is the enormous fiscal deficit, proportionately just as big as that of the United States. And despite Japan's booming economy, the alternative of raising taxes is no more popular in Japan than in the United States. All ministries are under pressure to make cutbacks and the fact that there have been small increases for science reflects its high priority. The small gains in research and development budgets are in fact scarcely enough to cover inflation. But that has not stopped the launching of new projects and the concentration of funds in key areas.

Within STA's budget, the biggest leap of all (a 750 per cent increase) is seen for the construction of a bathyscaphe capable of diving to perhaps 6,500 m. The plan to build such a vessel — at present only France and the United States have a bathyscaphe capable of going that deep — has been around for many years. With the succesful completion in 1981 of Shinkai 2000, which can reach 2,000 m, it has become a logical step. The new vessel will allow direct observation of the deep troughs off Japan where many earthquakes originate.

Another major budget increase is for planning of a module to be attached to the US space station. The budget is still not large in real terms, however, and if the project is delayed by the United States it may not prove too unwelcome to the government. If the module is built, a major use will be the manufacture of new materials in a gravity-free environment. MITI has launched a new project on this subject with an initial budget of 200 million yen. Interest from industry is strong enough that it may find it has a commercial competitor one day: the Taisei construction company is thinking of building a gravity-free environment on Earth. The trick is to carry out the manufacturing process in a capsule in free-fall down a deep mine, or from the top of a tall building.

Japan's science budget

	Yen (thousand million)	Percentage increase or decrease
Science and Technology Agency		
Research and development budget	427.8	+1.6
Special promotion funds	7.9	+8.2
Space	94.5	+3.3
Nuclear Energy	277.7	+4.2
Ocean Research	7.4	+7.3
ERATO	2.8	+4.6
Ministry of International Trade and Industry		
Research and development budget	197.0	+4.4
Agency of Industrial Science and Technology	113.4	+0.2
Basic technologies for future industries	6.5	+0.1
Large-scale industry	15.2	+3.4
Sunshine project	43.0	−1.9
Moonlight project	12.3	+10.8
Fifth-generation computer project	4.5	−6.3

Another area of space research where Japan is aiming to acquire expertise is the construction of the H-II rocket. Although Japan's large launch vehicles have so far been mainly built under licence, STA's H-II is seen as competing with Ariane and the space shuttle for commercial satellite launches towards the end of the century. This year its budget has leapt by nearly 300 per cent.

Another growth area for STA is in a project to build a heavy-ion accelerator to treat cancer. Funds available for basic research grants are also up, although not by such a huge percentage, and some new funds are available for "frontier research". These confirm STA's role as a supporter of small-scale basic research — a position traditionally held by the Ministry of Education, Culture and Science — as well as a supporter of "big science", space, nuclear energy and the like.

MITI's budget shows continuing support for its large-scale projects — the Sunshine project to develop new energy sources, the Moonlight project to cut energy waste, particularly in large-scale manufacturing, and the set of industrial technology projects. A new theme to be added to the "Basic technologies for future industry project" is that for bioelectronics. Although application is a long way in the future, there has been considerable interest from several large companies, including NEC. Interest stems from twin beliefs that computer manufacturers can learn from the structue of the nervous system, which is why MITI's industrial research agency supports physiology research, and that biological systems might be worth studying as the ultimate in miniaturization.

One project that is not growing as originally planned is the Fifth Generation Computer Project. The belief seems to be that the project's limits are not being set by financial resources but by human ones — there is not enough expertise available to justify further massive spending at present.

Alun Anderson

Space research

Texas A & M fly space-grant kite

Washington

TEXAS A & M University, in an attempt to fill what it sees as a vacuum, is pushing for the creation of a space-grant programme, modelled on the concept of the land-grant and sea-grant programmes. If Texas A & M has its way, it will add space-grant to its land-grant and sea-grant designations.

The sea-grant programme, started in the late 1960s, is a cooperative effort between universities, industry and government to provide financial support for research and public information. The space-grant programme would extend this to include space-based research, as well as research performed on Earth to support long-term projects in space.

Frank Vandiver, president of Texas A & M, sees the space-grant programme as "a good way for government to maximize research dollars". Federal dollars should encourage participation by private industry in university projects, and the financial benefits of the collaboration should be shared by all. That, at least, is the idea.

The land-grant concept has had a profound effect on US higher education. In 1862, the Morrill Act provided federal lands to the states as an endowment for colleges teaching the mechanical and agricultural sciences. The emphasis on applied sciences was reinforced by later legislation providing for research activities and extension services for the dissemination of newly gained knowledge. The triad of teaching, research and public education forms the basis for most modern universities. The original land endowments now amount to less than $3 million in university support, but the research and extension services are supported at levels reckoned in thousands of millions of dollars.

Whether space grant is a truly practical idea is unclear. The sea-grant programme's annual appropriation, this year $37 million, is routinely eliminated from the budget by the Reagan administration, only to be restored by congressional supporters such as Senator Lowell Weicker (Republican, Connecticut). A space-grant programme would be yet another financial burden. Vandiver insists that the initial burden would be more than paid off by applications of sponsored research. He has persuaded Senator Lloyd Bensten (Democrat, Texas) to introduce legislaon establishing a space-grant programme, although the Gramm–Rudman Act (see p.254) makes new spending programmes unattractive.

Some see the space-grant idea as a ploy to increase visibility in an era of tight budgets. But Vandiver insists "it is no flight of fancy with me".

Joseph Palca

Television

Defence of the realm

If further proof were needed that the British establishment is very cool to the idea of Europe, it came last week in the House of Lords report on international television. In answer to the European Commission's proposal to remove some of the restrictions on the flow of television across international barriers, the Select Committee on the European Communities responded with a disdain that can only keep the barriers up.

Not that the lords object to the objectives behind the European Economic Community's green paper of May 1984: *Television Without Frontiers*. Those are unimpeachable: to create a common market in television programmes and to create a sense of European identity. Nor would the subcommittee on energy and technology which took evidence for the report and included Lord Swann (former chairman of the British Broadcasting Corporation) and Lord Zuckerman wish to be seen to oppose the principle of free flow of information, still less to be trying to stop the advance of technology. The report recognizes the inevitable: broadband cable networks and direct-to-home satellite broadcasting will eventually blanket Europe. But the report's conclusions boil down to delaying tactics — not now, not here, not that way.

In fact, the Commission's own proposals to which the lords were objecting are quite modest: that members of the European Community countries come to an agreement on some common advertising standards (to remove such absurdities and barriers to television exchange as the ban on petfood advertising in Italy and on contact lens commercials in Britain). They would also impose a quite relaxed limit on the total amount of programming time (20 per cent) that might, within the Community, be devoted to advertising. They also proposed a possible way through the copyright thicket. As copyright agreements are bound by national borders, it is nightmarish for writers, producers, musicians to try to negotiate the rights for their programmes to be shown in another country or, in the case of Britain, on the mainland of Europe at all. US experience suggests that the new approach to the problem can only come through blanket licensing arrangements; the days of negotiating for each individual transaction disappeared with the arrival of the audio and video tape.

The lords committee, however, firmly rejected every proposal. Rejected in turn were: restricting television advertising time (that could inhibit new kinds of advertising channels); adopting a blanket copyright procedure (that would deprive copyright holders of their freedom). The lords even rejected as unacceptable or unworkable two things the green paper did not propose: a total ban on alcohol advertising and a statutory right to reply for aggrieved parties. In sum, they found the Community the wrong body to regulate and said, contradictorily, that its proposed regulations were both premature and unnecessary as "viewers' freedom to choose will inevitably take the place of regulation".

The committee's strongest point was to argue that the Community is too small (even with 12 members) to adopt such regulations. If the new television environment has satellite signals disregarding all national boundaries, certainly wafting all across Europe, any code that ignores Austria, Norway and Switzerland will not mean very much.

In its confident nationalism, the lords' report sounds remarkably similar to the view of the BBC, the Independent Broadcasting Authority and the European Braodcasting Union. It has fallen victim to the besetting European sin of thinking that in really vital areas (telecommunications procurement is another) national is best — particularly in broadcasting.

But the report, with the notable exception of its evidence, (one of the best summaries available of the hard-to-get information on the status of cable and satellite television in Europe) smacks of Little Englander thinking. The new standards would be minimum, not mandatory. If Britain wanted to restrict its own broadcast television to seven minutes an hour, it could still do so.

British broadcasting is probably the best in the world and regulation of the domestic product can keep it that way. But outsiders' television is crowding in. The Community's proposals are a step toward accepting that fact, and the even more uncomfortable one that if Europe is to become a real community, television programmes should be as free to travel as are workers. **Brenda Maddox**

Television Without Frontiers (HL 43). House of Lords Select Committee on the European Communities: 4th Report 1985 86 HMSO, £12.

UK public spending

No pre-election sweetener

Hopes that the restraints on British research and education spending might be relaxed with the approach of the next general election (due no later than mid-1988) were dashed last week, with the publication of the government's estimates for public spending in the next three years (to April 1989).

The cash value of the science budget, mostly spent by the research councils, estimated at £585 million in the current year and due to rise by £15 million in real terms in the next year, will reach a total of £650 million in 1988–89, an increase that will be eaten away by an inflation rate of 3.5 per cent a year. The cash value of the government subvention of the universities over the same period similarly increases by just 10 per cent.

In spite of the pressures of the past few years, the British system of higher education is not yet actually shrinking, but has stabilized at a total of 484,000 students. Within this total, a decline in university student numbers of roughly 5 per cent (to a total of 256,000) has been offset by the steady growth of the polytechnic system. The government's white paper says that the "participation rate" (the proportion of the annual age group entering higher education) has risen to 14 per cent and will continue to increase for the remainder of the decade.

On research, the government says that its aim is "to maintain and enhance the strength and quality of the science base". The document says the government believes there is further scope for "greater concentration and selectivity", with more emphasis on value for money. The document includes a number of examples of British inventions that have been commercialized successfully, including the synthetic pyrethroids and the cephalosporins. The details of how funds will be distributed among the research councils will be settled, year by year, by the Advisory Board for the Research Councils.

Meanwhile, it seems plain that the squeeze on research will continue in those departments of state that have it within their control. Last year's decision by the Ministry of Agriculture, Fisheries and Food (MAFF) to cut back on research is the chief reason why agricultural research has been forced to continue cutting back on the work at its institutes; last week's document makes it plain that there will be no reprieve, for total spending is to be reduced to £90 million three years from now from the present £95 million, inflation notwithstanding.

Even defence research, the British government's chief outlet for research money in the past, will not be immune. Last week's statement shows that defence research and development spending will have fallen from 13.4 per cent of the total in 1979–80 to 12.8 per cent in the current year (when total UK defence spending is estimated at £18,222 million). □

The Government's Expenditure Plans 1986 – 87 to 1988 89 (House of Commons 9702 – I & II, HMSO, Vol. I £4.80. Vol. II £20.)

Gramm–Rudman Act

Automatic cuts threatened

Washington

WASHINGTON bureaucrats are slowly waking up to the uncomfortable realities of the Gramm–Rudman deficit reduction act approved by Congress at the end of last year. A comparatively modest 4.3 per cent across-the-board cut in non-defence spending for the current fiscal year will, barring some extraordinary legislative contortions, take effect on 1 March, together with a 4.9 per cent cut in defence spending, the saving will be $11,700 million. But that is only a foretaste of the act's potential to wreak havoc. In order to avoid much larger cuts in future, totalling more than $60,000 million in 1987, Congress is steeling itself for some uncharacteristic self-discipline.

The Gramm–Rudman Act seeks to eliminate the federal budget deficit, which was to amount to $220,000 million this year, in five equal annual steps. If the President and Congress can agree each year on a budget that meets that year's target, all well and good. If not, the act mandates "sequestrations" to bring the deficit into line with the target. Defence spending has to carry half of the cuts, and there are exemptions for social security and welfare programmes.

The legislation has fundamentally changed the nature of the political game in Washington. Before, interest groups within the government could try to use their influence to secure their desired level of funding without much fear of adverse consequences. Now, they are having to learn that failure to agree would take the matter out of their hands. The first taste of serious deficit cutting will come next month when President Reagan delivers to Congress his proposed budget for 1987, which will attempt to meet Gramm–Rudman's $144,000 million deficit target and so avoid automatic cuts.

Dr John McTague, acting director of the White House's Office of Science and Technology Policy, was nevertheless taking an optimistic view last week of the prospects for research. McTague pointed out that this year's 4.3 per cent "cut" was on a base already 7 per cent above last year's. As for future years, McTague said basic research had always been one of President Reagan's top priorities and observed that "we have a remarkably consistent President". McTague justified the President's decision to exempt the Strategic Defense Initiative (SDI) from cuts this year on the grounds that SDI "serves a different purpose" from other research.

National Science Foundation (NSF) officials are similarly cheerful, with good reason. The President's 1987 budget request includes a healthy 9 per cent increase for the foundation over last year's total of $1,524 million, which is likely to cause envy among less fortunate agencies. NSF is praying that Congress will manage to pass a budget that avoids the need for Gramm–Rudman's across-the-board cuts next year, which could at a stroke change a 9 per cent increase to an estimated 10 per cent decrease. Erich Bloch, NSF's director, last week termed the automatic cuts provision an "unintelligent" approach to budget planning.

The National Aeronautics and Space Administration (NASA) is in a much less comfortable position. This year's 4.3 per cent cut could lead to lay-offs and even the postponement of shuttle missions unless Congress passes legislation allowing NASA to transfer funds between its four main accounts, research, flight operations, salaries and facilities.

Looking to the future, the brunt of the savings being sought will fall on the space station, leading to a delay of 2–3 years for the project. NASA officials do not deny reports that despite an original 1987 budget request of $580 million, the Office of Management and Budget is unwilling to countenance anything above $100 million.

The National Institutes of Health (NIH) are as yet undecided about how they will cope with this year's cut. But it seems likely that they will try to avoid cutting back on numbers of grants, and instead reduce the size of the cheques.

Each of the various institutes will have to reduce its budget by 4.3 per cent in total, but directors will have discretion to redistribute funds within their own budgets to minimize disruption. NIH officials seem not to have thought seriously about what they would do if faced with large cutbacks next year; NIH usually end up with far more than the administration requests anyway.

Non-nuclear research at the Department of Energy (DoE) will be hit hard, with cuts in 1987 of more than 50 per cent from this year's total of $700 million.

The Department of Agriculture says it will not have much difficulty in achieving 4.3 per cent cuts in the Agricultural Research Service this year, and that savings from vacant posts will probably account for many of them. But if across-the-board cuts are required in 1987 the results will be "too horrible to contemplate".

Many officials and congressional staff admit privately to doubts about whether Gramm–Rudman can survive for long: the savings sought are unprecedented in recent history. But while it may at some point be struck down on constitutional grounds, or simply eroded away by exemptions until it becomes meaningless, in the short term its effects will be real enough. **Tim Beardsley**

Genetic engineering

Frost damage tests blocked

Washington

A NEW set of regulatory hurdles is impeding plans by Applied Genetic Sciences (AGS) of Oakland, California, to release bacteria, genetically altered to protect strawberry plants from frost damage, into the environment.

The problem now lies with the local government in Monterey County, California, where AGS plans to conduct its field trial. Sam Karas, chairman of the Monterey County Board of Supervisors, says residents are unhappy that the first trial is being conducted in a densely populated region. Local citizens are also upset at having no say in the matter. The board is seeking ways to block the trial until local concerns can be dealt with.

In addition, the Monterey Bay Unified Air Pollution Control District wants to see a detailed environmental impact statement before allowing the test to proceed, and has threatened legal action to block the trial if the information is not forthcoming.

The local furore has taken AGS by surprise. Despite the difficulty in obtaining federal approval, Douglas Sarojak, AGS director of product development and marketing, maintains that his company "did not realize the sensitivity to the issue". He adds, "We're scientists, not public relations experts."

AGS won an experimental use permit for its new strain of *Pseudomonas syringae* from the Environmental Protection Agency (EPA) on 14 November after a long struggle (see *Nature* **318**, 96; 1985). The genetically altered bacteria lack a segment of the genome coding for an ice-nucleation protein responsible for frost damage to plants. The new strain will protect plants for competing with wild-type bacteria for positions on leaves.

The local controversy has taken on an international flavour. Karas reports that members of the board of supervisors have received telegrams from members of the Green Party in the West German Parliament as well as from members of the European Parliament urging them to oppose the tests. The board plans to hold a public hearing on 27 January to give all sides a chance to air their views.

Even if AGS receives permission from the local authorities, it may still not be able to proceed. The Foundation on Economic Trends in Washington led by Jeremy Rifkin has a suit pending in federal court seeking to overrule EPA approval of the experimental use permit for *P. syringae*, and Rifkin has gone to court to seek a temporary restraining order to prevent the field trial from starting before the lawsuit is settled. **Joseph Palca**

Soviet Union

Scientists facing redundancy

Most Soviet scientists will henceforth be paid in accordance with their job and performance. A recent joint decision of the Central Committee of the Communist Party of the Soviet Union, the Council of Ministers and the All-Union Central Council of Trade Unions approved new procedures and pay scales that will apply to more than half of all scientists and over 90 per cent of designers and technicians.

Although the new scheme has been presented as part of the Gorbachev package of reforms aimed at streamlining the economy, criticism in the Soviet media of the old system goes back a number of years. Under a set-up in which jobs and salaries depended strictly on academic qualifications and length of service, many scientists in the 35–45 age group, holding the degree of Candidate of Science (roughly equivalent to PhD), were actively or passively discouraged from improving their qualifications by taking a doctorate of sciences. In many cases, acquiring a doctorate would mean seeking work in another town, with consequent disruption to spouse's career and children's education. Scientists who wished, for their own personal satisfaction, to take a higher degree, and who were in some cases willing to continue temporarily in their old jobs and at their old salaries, were told that this would be detrimental to work discipline.

Under the new system, a degree or engineering diploma will be merely one of several criteria determining job and pay scales. From now on a scientist's pay will depend on the effectiveness of his or her research, its scientific and economic importance, and what Valentin Kharin, a senior official of the State Committee for Labour and Social Problems, described in an interview with the Moscow weekly *Literaturnaya Gazeta* as "personal impact" in getting concepts implemented in the economy. (The gap between research and implementation is a longstanding problem to the Soviet planners.) In particular, technicians and engineers without an academic degree seem likely to benefit. According to Mr Kharin, the new scheme will allow them to earn up to 350 rubles monthly, instead of the present maximum of 190 (the national average is around 170 rubles a month).

The new scheme makes likely the redundancy of up to 10 per cent of the present scientific work-force, with, Mr Kharin admits, some difficulty in finding new jobs for those who are dismissed. People who do not work, or who work badly, are liable to find themselves out of a scientific post, regardless of their length of service, he said. This is a remarkable development in Soviet terms. Unemployment was officially abolished in the Soviet Union more than 50 years ago, and people without work are liable to find themselves facing prosecution for "parasitism" — being without visible means of support.

Compulsory retirement of senior scientists may be one way of weeding out the superfluous work force. Already, in Uzbekistan, the President of the local Academy of Sciences, Dr Abid S. Sadykov, has been eased out of his post. According to the Uzbek republic daily *Pravda Vostoka* (22 November 1985), by continuing in office for several years after health and age (he is 72) made him unfit for duty, Sadykov had, by default, allowed corruption, nepotism and general slackness to creep into his academy. *Pravda Vostoka* noted disapprovingly that the average age of Uzbek academicians (75) is far too high and that more room should be made for younger talent. If this trend spreads, it could have important consequences for Soviet participation in world science. Attendance at foreign conferences has until now been viewed by the Soviets principally as a reward for long and faithful service. The Gorbachev efficiency drive could therefore produce a more flexible approach to foreign travel for younger scientists.

Vera Rich

West German schools

Teachers swell dole queues

Hamburg

Unemployment among West Germany's schoolteachers has become a scandal. The number has now reached 100,000, and is continuing to rise. The social cost is very large, given that a qualified teacher will have spent an average of six years at university, as well as perhaps two years at school practice (Referendariat).

Because of the waiting period of a year to eighteen months between university and Referendariat, the average age of qualifying teachers is as high as 30. Yet teachers are almost completely dependent on the state for jobs, in the person of the Kulturministers (the ministers for culture, education and church affairs) of the *Länder*. Fewer than one per cent of all teaching positions in West Germany are in private schools.

Several attempts are being made to solve the problems, but they are too late to help most teachers. Yet the present situation could have been foreseen many years ago from the crudest statistics. The Kulturministers had themselves published several documents giving calculations and predictions for the trends in supply and need of teachers, but nothing was done to prevent catastrophe. Until 1980, every newly qualifying teacher was assured of a post almost automatically. As civil servants, West German teachers are promised lifelong tenure.

The overproduction of teachers resulted from a campaign during the early 1970s when a shortage of schoolteachers of every type was emphasized. Too many students elected to become teachers, even when it became obvious that the shortages no longer existed. Even now, there are still too few teachers in some subjects, but the *Länder* do not want to spend more money in schools at which the numbers of pupils are decreasing sharply.

There have been protests from the teachers' professional organizations, chiefly the Gewerkschaft Erziehung und Wissenschaft (Union for Education and Sciences) and the Deutscher Philologenverband (German Philologists' Society), but they represent only the employed teachers and there is little solidarity.

The ministers meet regularly, but they usually postpone discussion of this issue to their next meeting. They have not managed to answer even the most pressing question: how can the reduction of working hours — agreed for all civil servants during the union negotiations in 1984 — be applied to teachers? The absurd situation exists where one fewer teaching hour each week for all 590,000 teachers in post would provide jobs for 22,400 of their unemployed colleagues: education experts in both the Social Demorcatic and the Christian Democratic parties recommend such a reduction, but the civil servants have so far been successful in their opposition. They themselves are asking for more jobs to be created before they will agree to any kind of compromise.

The ministers, however, know that something must be done, even at this late stage. In Bavaria, all teachers over the age of 55 are to have their working week reduced by two hours. Nordrhein-Westfalia has given some applicants jobs for three-quarters of the time, but only on a three-year basis. Many unemployed teachers are, however, unwilling to give up jobs as taxi drivers, innkeepers, clerks or sales representatives only to face even bigger problems in three years' time.

At present, almost 5 per cent of West Germany's unemployed are teachers, but the proportion is growing dramatically. The vice-president of Munich University, Otto Speck, predicts an increase of 72,000 in 1986. The schools are facing "Vergreisung" (a growing percentage of older teachers), but the finance ministers of the *Länder* contine to argue that "teachers cannot be a privileged group among the unemployed".

Jürgen Neffe

West German universities

SIR—Your article on West German universities (*Nature* **316**, 96; 1985) only reflects part of the actual situation.

The concept of "shifting balance within the university committees to a wider group" was indeed an integral part of the university reform that was rushed through some *Länder* parliaments in the early 1970s, without consulting academic staff. The anti-industry attitude then prevailing also led to the institutionalization of rigorous limitations on *Drittmittelforschung*, that is, industry-supported research. The idea was to reduce if not abolish access of individual staff members to research funds, and to ensure control of all departmental activities by "democratic" committees that were usually dominated by extreme left-wing activists.

The new legislation required all decisions concerning such divergent matters as professional appointments, finance, extension of contracts of laboratory assistants or undergraduate courses to be arrived at by majority vote in "democratic" committees. The resulting meetings occupied a considerable part of the staff's time — up to 90 hours per month was not unusual. Plans to abolish individual examinations as relics of capitalist exploitation and to accept examination papers produced by teams of comrades, so that the strong could support the weak, have been seriously discussed in this context.

This led to a decrease in research activities and further weakened the potential of German universities which had suffered from the exodus during the early years of Nazism, from twelve years of dictatorial rule and persecution and from the war. It is no accident that research papers from German universities are only rarely found in the pages of *Nature*, while the independent Max-Planck Institutes (MPIs) are now the main source of internationally recognized research in Germany. The same applies to the job situation — openings advertised in *Nature* are usually in MPIs and not in universities.

You refer to professorships that "were distributed too readily during the years of expansion"; the years of expansion were the 1960s, when common sense still prevailed; ready distribution of professorships took place under the new university regulations when pressure from the non-professional majorities on committees resulted, for instance, in the University of Hamburg elevating 400 lecturers to professors (not on merit!) by a single decree.

This is why prospects for promotion in universities are now discouraging and why the scientific standard of professors in "reformed" German universities does not compare favourably with the United Kingdom.

Let me conclude by saying that my friends in British universities are invariably horrified when they learn about the new German "system", which, in recent years, has also been adopted in my native Austria. A head of department is now a mere figurehead who has to maintain the goodwill of the powerful departmental committee by populist measures or by bowing to the majority of the less-qualified. A more appropriate title for your article would thus have been "Is there still hope for German universities?" — by dropping the unrealistic and unproductive "plans for change" before it is too late. Isolation from the international scientific community and lowering of standards in teaching and research would otherwise be inevitable.

E.F. STUMPFL

Institute of Mineralogy
and Petrology,
Mining University,
A-8700 Leoben, Austria

Prizes for Germany

SIR—When Klaus von Klitzing said (see *Nature* **317**, 667; 1985) that he hoped it would not be another 22 years before a West German won a Nobel prize (for physics), he was *not* referring to the prize awarded that long ago to the Munich physicist Mössbauer, but to the Heidelberg physicist J. Hans Jensen (1907 – 1973), who shared the Nobel prize for physics in 1963 with Maria Goeppert-Mayer, La Jolla (one half of the prize, the other half was awarded to Eugen Wigner, Princeton). Rudolf Mössbauer, München, shared the Nobel prize for physics 1961 with Robert Hofstadter, Stanford.

ROSWITHA SCHMID

Naturwissenschaftliche Rundschau,
Postfach 40,
D-7000 Stuttgart 1, FRG

UK physics

SIR—I read "Sociological problems of high-energy physics" (*Nature* **318**, 243; 1985) with interest but with some dismay, as I did not entirely recognize the field in which I work from the text. The article indulges happily in unsupported generalizations, and hypotheses based on speculations by the gurus of long ago. Perhaps from their American viewpoint they do not see the vitality and innovation of the field over here. Nobody looking at the L3 and DELPHI experiments at LEP could consider them as conservative. Even a project such as OPAL, founded on the premise that it must work reliably from turn-on, is benefiting every day from the individual initiative and innovation of its younger members.

The "10–25 per cent heterodox research" advocated in the article is thriving in the United Kingdom (see the 1984 Rutherford Annual Report for a full list) but will have to diminish if the cuts recommended in the Kendrew report are inflicted.

There is a sociological problem in high-energy physics, certainly in the United Kingdom, forced on us by the persistent negativism of our paymasters. First-rate researchers leave the field, for lack of career advancement, and young people are discouraged fron entering as the number of posts is whittled down. (The breathing space afforded by the Science and Engineering Council's New Blood schemes is now over.) This is occurring at a time when the country desperately needs scientists who have been trained in making their mark in a European environment. British industry is not going to be helped by seeking artificially sheltered conditions in which to train our best researchers.

It is fashionable to decry high-energy physics now. Let us not be misled. In spite of official discouragement, the field remains a vital and exciting one in which to work.

D.H. SAXON

16 Membury Way,
Grove, Wantage,
Oxfordshire OX12 0RP, UK

AFRC cuts

SIR—Over the past few years you have given detailed consideration to the financial problems of the Agricultural and Food Research Council (AFRC), culminating in your report of the severity of the latest cuts at this institute (*Nature* **317**, 663; 1985).

It is not, however, generally appreciated that the extensive cuts at the Institute for Research on Animal Diseases include the savaging of the molecular biology department, which was set up some four years ago to introduce genetic manipulation and allied techniques to the institute's research programme. In view of the stated commitment of AFRC to a programme of modern biology, one would have expected maintenance or even expansion of this programme.

On the contrary, the number of permanent scientific staff in the department has declined at a faster rate than that of the institute staff as a whole. At a time when molecular biology has expanded elsewhere, it is strange that the opposite should be true of AFRC's restructuring plans at this institute.

G. D. HUNTER

(Chairman, AFRC Higher Grades Panel,
Institute of Professional Civil Servants)
ARC Institute for Research
on Animal Diseases, Compton,
near Newbury, Berkshire RG21 0NN, UK

Growth by cannibalization

A new calculation of the process of condensation suggests that more attention should be paid to the correlations between neighbouring droplets.

HERE is as neat a piece of classical physics as one could hope to find. The problem is the apparently simple one of predicting the behaviour of an assembly of droplets such as might be found in a condensing cloud in the atmosphere. Large drops will grow at the expense of smaller drops. The classical problem, of obvious importance in meteorology, is to know how the size distribution changes with time. It is now thirty years since the essentials of the problem were stated and solved by two Soviet physicists, I.M. Lifshitz and V.V. Slyozov. The nub of their result is that, where large droplets grow at the expense of small, the average radius increases with time (t) in proportion to the cube root, $t^{1/3}$.

This cube-root dependence on time of the average radius of the droplets in a cloud seems to be borne out by observation, not merely of the sizes of droplets in an atmospheric water cloud but in other comparable situations, the radii of particles crystallizing from a molten metal, for example. But the other features of the size distribution predicted by Lifshitz and Slyozov are not nearly as well established. And now Dr M. Marder from the University of California at Santa Barbara has been able to correct the older arguments in a particularly interesting way (*Phys. Rev. Lett.* **55**, 2953; 1985).

Because the vapour pressure of a small droplet varies inversely with its radius, small droplets are unstable, and will evaporate rather than grow unless the vapour pressure in the immediate environment is greater than that corresponding to equilibrium. This is why cloud formation requires some mechanism of nucleation, and why the environment of a cloud usually manifests a degree of supersaturation with respect to the equilibrium vapour pressure of bulk water at the temperature of cloud formation. But if those conditions are met, it also follows that large droplets will grow at the expense of smaller droplets.

The practical need is to derive quantitative estimates of the preferential growth of larger particles. The process is dominated by diffusion; a shrinking small drop will not be able to continue shrinking if evaporated water vapour accumulates near the drop, increasing the local vapour pressure above equilibrium value. Similarly, a large drop will not be able to continue growing if it should so denude the local environment of water that the vapour pressure is less than the equilibrium value. So the rate of growth of a particular droplet may be determined by its immediate past history (which determines whether the immediate neighbourhood is enriched by or depleted of water vapour), as well as by the behaviour of nearby droplets which, by shrinking or growing, may add or subtract water vapour from the environment.

The problem is therefore one in kinetic theory, but with the proviso that equilibrium does not apply. The first successful treatment seems to have been given by the two Soviet physicists. Their argument may be summarized as follows. The simplest case is that in which the medium in which the droplets grow is so massively supersaturated that neighbouring drops have no influence on each other and even the effects of surface tension can be neglected. Then, the rate of growth of a particular drop will be determined by the rate at which water vapour can diffuse to reach its surface. In terms of the radius, R, the rate of change will be the simple function $(D/R).\,Q^\circ$, where D is the molecular diffusion constant, Q° is the mixing ratio of the water vapour expressed as the ratio of the volume of the water if it were totally condensed to that of the total space occupied and R enters the equation reciprocally because of the geometry of diffusion onto a small supposedly spherical droplet through the surrounding medium.

A missing ingredient from this extreme approximation has the effect of subtracting from Q° an amount d/R, where d is some quantity proportional to surface tension and the reciprocal of R, appearing as a factor. This accords physically with the circumstance that the effect of surface tension is to reduce the rate of growth of drops, the smaller the droplet the more markedly.

The other obviously missing ingredient is some allowance for the extent to which one drop influences its neighbours. First, it is necessary to adjust Q° (by subtraction), the volume fraction of the water already condensed, and then to allow for the way in which the growth of a particular droplet is affected by all the behaviour of all the other droplets in the system, by a separate adjustment representing the influence of each of them. Shrinking droplets will add to the availability of material elsewhere, which explains why the rate of change enters linearly in each adjusting term, adding to the availability of material (and thus Q° when it is negative). The radius of every other drop, or rather its square, also enters, but the distant effect of each droplet is attenuated in the same way as diffusive effects are invariably attenuated by gaussian factors in respect of both distance and time; in short, the growth of a particular droplet will be more affected by the recent behaviour of other nearby droplets than by the remote (in time) behaviour of distant droplets. The result is a horrid set of nonlinear interlocking equations that nobody would think of solving directly, not merely because solution would be impossible but because the problem is in any case statistical.

Lifshitz and Slyozov dealt with the problem by averaging, on the specific assumption that drops of different random sizes are randomly distributed through the available space. Apart from their conclusion about the average size r, they also concluded that the size distribution of growing droplets, strictly a function both of radius and of time, should ultimately be given by a calculable function only of the ratio R/r, which of course involves the time as a variable because the average radius r grows with time. Marder's point is that while the cube-root dependence of r has been well confirmed by observation, the size distribution of particles that grow partly by the remote cannibalization of each other usually turns out to be much broader than that calculated.

What can have gone wrong? Marder's answer is simple; Lifshitz and Slyozov had no business to determine the average behaviour of a droplet by assuming that droplets of different sizes may be randomly distributed. On the contrary, Marder says, precisely because a shrinking drop will add preferentially to the growth of its immediate neighbours rather than more distant drops, there will be a tendency for large and small drops to be paired together statistically. By good fortune, the more exact correlation is calculable. The proof of the conclusion is that the calculated size distribution agrees well with data previously gathered for the particle-size distribution in slowly solidifying alloys of Fe-Si-Ti and Ni-Si, both of which are broader than predicted by Lifshitz and Slyozov. More detailed calculations of the evolution of a system of mutually cannibalizing particles can pass through a stage in which there is a distinctly bimodal distribution of size, with one group of smallish particles and another which is much larger.

John Maddox

Sex chromosomes

Mammalian X and Y crossover

from Paul S. Burgoyne

HYPOTHESIS and fact, although semantically distinct, are less easy to separate in the real world. Scientific concepts often seem to weave to and fro across this semantic divide before eventually being universally accepted or rejected. A paper by F. Rouyer *et al.*[1] on page 291 of this issue, together with three others recently published in *Nature*[2–4], present incontrovertible evidence for regular exchange (crossing over) between X and Y chromosomes in both mouse and man. This finally validates the concept of X–Y crossing over which dates back to Darlington in 1934, and must surely persuade even the most persistent doubters[5,6].

In 1982, two papers[7,8] appeared that reiterated the case for genetic homology and crossing over within the X–Y pairing segment in man and other mammals. In my paper[7], I chose to emphasize a conclusion, derived from the unusual inheritance of the sex-reversed factor (*Sxr*) in the mouse, that a single 'obligatory' crossover occurred in the X–Y pairing segment. To describe genes that are exchanged between the X and Y by this crossover and therefore misleadingly seem to be linked to an autosome rather than the X or Y chromosome, I suggested the term 'pseudoasutosomal'. Polani[8] had the foresight to see how molecular genetic approaches could be used to provide the definitive evidence and a search for DNA sequences shared by human X and Y chromosomes ensued. Such sequences were found but, obtusely, they were not located in the X–Y pairing segment. A substantial amount of the X–Y sequence homology proved to be the result of an evolutionarily recent transposition of X-chromosomal material to the Y chromosome[9].

A non-molecular approach provided the first genetic evidence that crossing over is a regular feature of normal X and Y chromosomes: Keitges *et al.*[4] demonstrated that a mouse steroid sulphatase (*STS*) variant, which had seemed to be inherited autosomally, was in fact transmitted to XO offspring via the X chromosome. This observation, together with the existing pedigree data, proved that the mouse *STS* gene was present and expressed on the X and Y chromosomes and that there must be an obligatory crossover proximal to the *STS* locus to account for the absence of either X or Y linkage of *STS*. This pseudautosomal mode of inheritance of the mouse *STS* gene contrasts with that in the human, where the *STS* gene is X-linked, although close to the pseudoautosomal region.

The molecular approach has now also borne fruit with the description of pseudoautosomally inherited human DNA sequences[2,3], culminating in the elegant linkage analysis of three pseudoautosomal loci reported by Rouyer *et al.*[1]. The features of the obligatory X–Y crossover model[7], incorporating the most recent findings, are illustrated for the human X–Y pair in the figure. The existence of an obligatory X–Y crossover, at least in those spermatocytes generating functional sperm, is clearly confirmed by X–Y recombination data[1,4]. This brings the X–Y pair in line with the autosomes, where there is a minimum of one chiasma, the morphological manifestation of crossing over, for each meiotic chromosome pair (bivalent), irrespective of the size of the chromosome.

Although in most mammals no obvious X–Y chiasma can be seen by light microscopy, chiasmate X–Y associations have been demonstrated with the electron microscope[10]. They have not been found in all X–Y bivalents but this could be due to technical difficulties. In some instances the absence of an X–Y chiasma may result from inadequate X–Y pairing. In XY *Sxr* mice there is a high incidence of X–Y separation at pachytene, presumably because the presence of *Sxr* distal to the pairing segment sometimes interferes with the pairing process. Nevertheless, the recombination data for *Sxr* confirm that all functional sperm are derived from spermatocytes that had an X–Y chiasma, adding weight to the view that there is a meiotic 'quality-control' mechanism that prevents primary spermatocytes with unpaired chromosomes from forming viable sperm[11].

I find that it helps to think of the pseudoautosomal segment of the X–Y bivalent as a very small extra pair of autosomes. Rouyer *et al.*[1] estimate that the human pseudoautosomal segment contains 2,000–5,000 kilobases, which would make it about one-tenth the size of the smallest human autosomal bivalent. An obligatory crossover in such a short length inevitably results in a high recombination frequency per unit length[1]. In the X bivalent of females, the obligatory crossover is not constrained within the pseudoautosomal region, so recombination in this region is reduced almost tenfold[1].

What determines the limits of the pseudoautosomal segment? As originally defined[7], it is that part of the X–Y bivalent where there is exchange by crossing over, a definition that includes genes showing partial sex linkage — those with less than 50 but greater than 0 per cent X–Y recombination.

In practice it may be necessary to set an abitrary minimum of say 1 per cent recombinants as defining a pseudoautosomal locus, as it is important to exclude those X-linked (for example, *Xg*) or Y-linked (for example, *TDF*) genes that are occasionally exchanged between the X and Y chromosomes[12] by unknown mechanisms

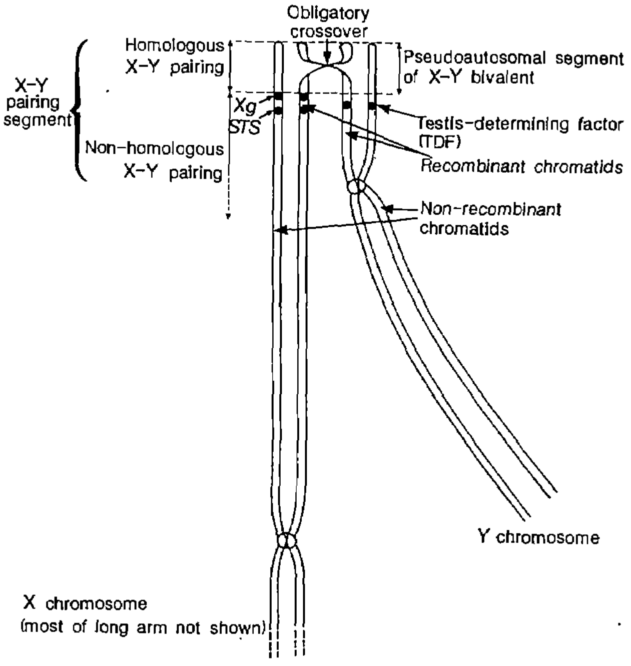
Obligatory crossover
Homologous X-Y pairing
X-Y pairing segment
Non-homologous X-Y pairing
Pseudoautosomal segment of X-Y bivalent
Xg
STS
Testis-determining factor (TDF)
Recombinant chromatids
Non-recombinant chromatids
Y chromosome
X chromosome (most of long arm not shown)

Crossing over between the human X and Y chromosome. The pseudoautosomal segment is that part of the X–Y bivalent where there can be X–Y exchange by crossing over. X–Y homology in this segment is maintained by, and may be necessary for, this crossing over. There is always one 'obligatory' X–Y crossover but, because its position varies, only the more distal pseudoautosomal loci show 50% X–Y recombination. More proximal loci show a hierarchy of partial sex linkage (<50% but >0% X–Y recombination), reflecting their order within the pseudoautosomal segment[1]. X-dosage compensation is unnecessary for pseudoautosomal genes and they are expressed in double dose in both males and females. X-linked genes bordering the pseudoautosomal segment (*Xg*, *STS*) are also at least partially expressed on the 'inactive' X of females. The length of the X–Y pairing segment varies with meiotic stage and can extend well beyond the pseudoautosomal segment into the Y long arm. Much (perhaps all) of the synaptonemal complex formed outside the pseudoautosomal segment represents non-homologous pairing. (Modified from ref. 7.)

that are not formally distinguishable from crossing over.

These problems of definition apart, what is it that constrains the obligatory crossover to occur in the pseudoautosomal segment of the X–Y bivalent? The constraint is certainly not the length of the pairing segment — in man, X–Y pairing, as defined by the formation of a synaptonemal complex, includes most of the Y short arm and can extend into the long arm, much longer than the pseudoautosomal segment. More probably it is the extent of X–Y homology in the pairing segment.

In other situations where stretches of synaptonemal complex are formed between non-homologous chromosome segments, crossing over is excluded from these non-homologous regions. Because there are degrees of homology, the pseudoautosomal segment may end in a zone where the likelihood of a crossover rapidly decreases in conjunction with a decrease in homology, rather than having a discrete boundary.

It is generally agreed that the heteromorphic mammalian X–Y pair must have evolved from a pair of homologous chromosomes. The pseudoautosomal segment might therefore represent a region of the original homologous pair that has been retained to ensure chiasma formation and orderly X–Y separation at meiotic metaphase I. Although gene-dosage considerations do not preclude the pseudoautosomal segment from exchanging material with the autosomes[7], it may nonetheless be a conserved linkage group with significant homology between mammalian species. If so, with relaxed hybridization conditions it should be possible to use human pseudoautosomal DNA probes to pull out related pseudoautososmal sequences from the mouse genome.

Combining the flexibility of mouse breeding with the exceptionally high recombination frequency in the pseudoautosomal segment should allow a rapid and detailed genetic analysis of this region. Now the molecular geneticists have stuck in their thumbs, I am sure that they will pull out some plums. 1986 promises to be a good year. □

1. Rouyer, F. *et al. Nature* **319**, 291 (1986).
2. Cooke, H.J. *et al. Nature* **317**, 687 (1985).
3. Simmler, M.-C. *et al. Nature* **317**, 692 (1985).
4. Keitges, E. *et al. Nature* **315**, 226 (1985).
5. Ashley, T. *Hum. Genet.* **67**, 372 (1984).
6. Ashley, T. *Genetica* **66**, 161 (1985).
7. Burgoyne, P.S. *Hum. Genet.* **61**, 856 (1982).
8. Polani, P.E. *Hum. Genet.* **60**, 207 (1982).
9. Page, D.C. *et al. Nature* **311**, 119 (1984).
10. Holm, P.B. & Rasmussen, S.W. *Carlsberg Res. Commun.* **48**, 415 (1983).
11. Burgoyne, P.S. & Baker, T.G. in *Controlling Events in Meiosis* (eds Evans, C.W. & Dickenson, H.G.) 349 (Company of Biologists, Cambridge, 1984).
12. De la Chapelle, A. *et al. Nature* **307**, 172 (1983).

Paul S. Burgoyne is in the Medical Research Council Mammalian Development Unit, University College London, 4 Stephenson Way, London NW1 2HE, UK.

Nuclear winter

Towards a scientific exercise

from K.A. Emanuel

THE detonation of the first atomic bomb on 16 July 1945 changed the world in many ways, not least of which is the view some scientists have taken towards their profession. Many have come to feel that resposibility for the influence of their achievements rests partially with them and should not reside solely with politicians. While imparting certain benefits to political decision making, this attitude has at times tainted the objectivity that is crucial to scientific endeavour. Nowhere is this more apparent than in the recent literature on 'nuclear winter' research, which has become notorious for its lack of scientific integrity. Among the most serious criticisms levelled at this work has been the failure to quantify the large uncertainties associated with estimates of the war-initiated fires and their combustion products, the highly approximate nature of the global circulation models used in the calculations, and the appearance of the results in popular literature before being exposed to the rigours of peer review.

Although controversy continues to surround this work, serious research is beginning to qualify the earlier bold assertions. A good example appears on page 301 of this issue in the paper by B.W. Golding, O. Goldsmith, N.A. Machin and A. Slingo, which attempts to examine the physical factors affecting the disposition of a smoke plume shortly after its inception. These authors point out that previous estimates of the nuclear winter effect have relied either on one-dimensional models, which must assume a uniform distribution of smoke, or on three-dimensional models with grid intervals too large to resolve mesoscale (medium-scale) circulations very near recently initiated plumes. Yet it is likely that such circulations would result from the horizontal temperature gradients produced by radiative heating of the smoke.

Using a mesoscale numerical model, Golding *et al.* show that mesoscale ascent rates of 20 cm s^{-} are possible 12 h after plume initiation; such rates will rapidly lead to condensation of water vapour even in circumstances where the air is initially quite dry. Subsequent scavenging of the smoke by precipitation could substantially alter the characteristics of the plume before it diffuses into the continental-scale pall which is the starting point of most nuclear winter calculations.

The calculations presented by Golding *et al.* are themselves dependent on assumptions concerning the concentration, geometry and radiative characteristics of the smoke plume and the large-scale meteorological conditions in which it is released, and the model does not explicitly deal with the interaction of condensed water and snoke particles. The results do strongly suggest, however, that more attention must be paid to the mesoscale characteristics of the plume in the first day or so of its lifetime. The paper is a welcome step in transforming nuclear winter research from a means of political advocacy to a scientific exercise. □

K.A. Emanuel is at the Center for Meterology and Physical Oceanology, Massachusetts Institute of Technology, Cambridge, Massachusetts 02139, USA.

Archaeology

Reconstructing ancient diets

from Richard Burleigh

A PAPER published recently (*Nature* **317**, 806; 1985) and one on page 321 of this issue make significant new contributions to the investigation of ancient human diets by the analysis of stable isotopes in skeletal remains. In the first, M.J. DeNiro is concerned with the detection of changes in the composition of sub-fossil bone (diagenesis) that might lead to false results. The other, by S.H. Ambrose and M.J. DeNiro, deals with reconstruction of patterns of diet in humans who are known from historic records or presumed from archaeological evidence to have followed particular modes of subsistence. Both papers help to provide a firmer basis for possible investigation of human diet in the much more remote past.

Measurement of the ratios of stable carbon isotopes ($^{13}C/^{12}C$) in collagen from skeletal remains has been used successfully in recent years to establish prehistoric human diets and hence, somewhat more inferentially, patterns of subsistence in the past, for example, in parts of North America, Africa and north-west Europe. The basis of this method is that the carbon-isotope composition of collagen in bone reflects the isotopic composition of the plants that form the base of the food web, isotope ratios being expressed as $\delta^{13}C$ values, or the difference in parts per thousand from a standard, as measured by mass spectrometry. Thus, the relative importance in the diet of C_3 and C_4 plants, which have different photosynthetic pathways characterized by distinct $\delta^{13}C$ values, can be determined. Marine sources of food can confuse this picture but more recently it has been found that, by simultaneous measurement of stable nitrogen ratios ($^{15}N/^{14}N$), the respective contribution of marine and terrestrial sources of food can be distinguished from the differences in $\delta^{15}N$. Because there is a small incremental enrichment of ^{13}C and ^{15}N as these isotopes are moved up the food chain, the $\delta^{15}N$ values in particular also give an indication of the relative importance in the diet of animal products compared with more direct exploitation of plant foods.

Ambrose and DeNiro have investigated the $\delta^{13}C$ and $\delta^{15}N$ values of collagen recovered from the bones of about 100 individuals representative of particular groups of hunter–gatherers, pastoralists and agriculturalists both from the historic period and from archaeological sites in Kenya, Tanzania and South Africa. The bones of wild mammalian species representing browsers feeding mainly on C_3 trees, of grazers feeding mainly on C_4 grasses and of carnivores, also analysed, showed isotopic differences clearly reflecting these animals' diets (with an apparent preference by carnivores for preying on grazers). These results provide a convincing demonstration that in the same biome in Africa, human diets based variously on C_3 and C_4 plants, meat of grazing and browsing animals, and other animal products such as milk and blood, should be distinguishable by a combination of the $\delta^{13}C$ and $\delta^{15}N$ values.

The diets of the historic populations investigated were known from ethnographic records, and Ambrose and DeNiro found very close agreement of the isotope values with this evidence. This in turn gives confidence that their reconstruction of the diets of the prehistoric groups from isotope analyses is essentially correct, as direct archaeological evidence of food resources in the form of animal and plant remains is inevitably incomplete and may sometimes be misleading.

A logical step from this is, the authors suggest, the intriguing possibility of reconstructing the diets of much earlier human ancestors. The living primates most closely related to *Homo sapiens* are predominately C_3 plant feeders. Australopithecines probably were as well, but there is evidence to suggest that the true hominids, *H. habilis* and *H. erectus*, were more dependent on meat. Independent validation of this could have great importance for the study of human evolution, but depends entirely on the isotope record being preserved in bones of Pliocene–Pleistocene age, that is, at least 4 million years old. This may be unattainable in practice, though the photosynthetic pathways with their isotopic differences were certainly established well before then.

A more immediate question is raised by DeNiro, who examines the assumption, implicit in most previous studies, that the isotopic composition of collagen in the bones has not subsequently been adversely altered. Inevitably sub-fossil bone will have undergone physical and chemical changes, which may have resulted in the addition or removal of organic components; much therefore depends on the extent to which the organic fraction used for analysis represents the original collagen. To test this, he analysed bones of marine carnivores and terrestrial herbivores from archaeological sites varying in age from hundreds to thousands of years, and from various depositional environments ranging from arid desert conditions to peat bogs. These species were chosen because the feeding patterns and isotope values of their modern counterparts have previously been well established.

DeNiro finds that, independent of age, those sub-fossil bones with C/N ratios in the range 2.9 to 3.6, characteristic of fresh modern bone, have $\delta^{13}C$ and $\delta^{15}N$ values consistent with expectation. In contrast, burnt bones, where the C/N ratios are outside the normal range, have isotope values that are shifted erratically. It is a reasonable assumption that at least some of the other, often individually indeterminate, diagenetic processes to which sub-fossil bone is subjected might produce similar isotopic shifts. A sensitive criterion, representing the sum of these processes, that allows altered material to be easily recognized and rejected in advance is therefore of the greatest value, although it cannot be applied retrospectively to previous studies without published C/N ratios.

The determination of stable carbon and nitrogen isotope ratios also has purely biological applications, for example, to the investigation of the differential feeding patterns of closely related animal species living in restricted environments, such as those found on remote oceanic islands. These two new papers not only add rigour to a scientific method that is beginning to give results of real importance to archaeologists and anthropologists but are also highly relevant to the refinement of other applications of the method. □

Richard Burleigh was at the Research Laboratory, The British Museum, London WC1B 3DG, and is now at the Museum of Mankind, 6 Burlington Gardens, London WC1X 2EX, UK.

Ecology

Tundra river transformation

from S.I. Heaney

THE past quarter century has seen a great interest and concern over anthropogenic phosphorus loading of lakes and reservoirs. Such enrichments of standing waters often lead to the formation of troublesome surface blooms of algae and deoxygenation of the colder lower layers (Edmondson, W.T. & Lehman, J.T. *Limnol. Oceanogr.* **26**, 1; 1981). Much less attention has been paid to the role of phosphorus in running waters. So the report by B.J. Peterson *et al.* (*Science* **229**, 1383; 1985) on the effects of experimental addition of phosphorus to a nutrient-impoverished arctic river is both important and surprisingly overdue.

Peterson's group added phosphorus to a portion of the Kuparuk River in the Alaskan tundra, raising the concentration of PO_4-P from ambient levels of $< 1-4\ \mu g\ l^{-1}$ to $10\ \mu g\ l^{-1}$, and then monitored the river upstream and downstream of the site of addition. Within six weeks the biomass of the algae (measured as µg chlorophyll *a* per cm^2) attached to the stones on the river bottom had increased tenfold within a kilometre of the site of phosphorus addition. This increased biomass was sustained for several kilometres downstream but there was a negligible change of biomass upstream. The result is probably to have been expected considering the concentrations of other dissolved plant nutrients (carbon, nitrogen) in the stream water. However, the strength and originality of the work lies just as much in the efforts made to separate and quantify the microbial metabolism into heterotrophic (bacterial) and autotrophic (algal) processes and to attempt to see how these induced microbial changes influenced the higher tropic levels (dominant aquatic insects) of the ecosystem.

No less than eleven authors from four institutions were involved in the study, which involved several disciplines and techniques and made possible a holistic approach to this relatively simple ecosystem. Although the results are necessarily restricted they appear convincing enough to support the conclusions: first, photosynthesis and biomass production in the river are limited by phosphorus concentration. Second, on the addition of phosphorus, photosynthetically fixed energy replaced organic matter entering the stream as the major energy source. Third, as a result of increased photosynthesis, algal activity increased on rocks of the river bottom. And fourth, as illustrated by the increase in the size and developmental stage of some aquatic insects, there was food limitation at higher trophic levels in this nutrient-poor environment.

This innovative experiment provokes further questions. Phosphorus was added only during July and August when water temperatures were between 7 and 14°C. As some freshwater algae, including diatoms, can grow at temperatures down to freezing with enough light and nutrients, what would be the effect on the community if phosphorus were added throughout the ice-free period? With continuously elevated phosphorus concentrations, what would be the long-term consequences on the abundance and periodicity of algae other than diatoms? Is the timing of the spring algal growth period significant in relation to the emergence and growth of dominant insect grazers? What is the relationship between suspended phytoplankton and attached algae?

Answers to some of these questions can be sought from studies of phosphorus-enriched rivers. Nevertheless, the experimental work of Peterson's group, earlier pioneer work in experimentally increasing heterotrophic microbial production in trout streams in Oregon (Warren C.E., Wales, J.H., Davis, G.E. & Doudoroff, P. *J. wildl. Mgmt.* **28**, 617; 1964) and that of the Freshwater Biological Association using its experimental circulating channels (Marker, A.F.H. & Casey, H. *Phil. Trans. R. Soc.* **B298**, 265; 1982) will be vital for a fuller understanding of the processes controlling production in rivers. ☐

S.I. Heaney is at the Freshwater Biological Association Windermere Laboratory, Ambleside, Cumbria LA22 0LP, UK.

Developmental biology

Unscrambling egg structure

from Hugh Woodland and Elizabeth Jones

In these columns, we recently reviewed the evidence for the suggestion that the complexity of the amphibian embryo is generated by progressively more complex interactions between a few cell types in the early embryo[1]. These cell types, possibly just the ectoderm and endoderm, probably arise by the partitioning of different cytoplasmic constituents from the egg. What could these differences be?

In the amphibian, one of the few ways to identify them is to pick a molecule and look for its uneven distribution in the egg. There is some evidence from other organisms, particularly insects, that RNA which specifies future cell types is distributed in this way. Several groups have now looked to see if particular messenger RNAs show differences along the animal–vegetal axis of *Xenopus* eggs. *In vitro* translation has shown that at least 17 mRNA species are asymmetrically distributed, which is 4 per cent of the total translatable RNA[2].

The logical extension of this approach is to clone such mRNAs; this has now been achieved for four mRNAs which are concentrated in either the animal hemisphere (An1–3) or in the vegetal hemisphere (Veg1)[3]. All these RNAs are accumulated steadily during oogenesis and two of them, An1 and Veg1, are synthesized only during oogenesis and disappear during gastrulation. The behaviour of these transcripts, especially An1 and Veg1, suggests that they have an interesting role in development.

The ease with which antibodies, as well as sense and anti-sense RNA, can be injected into specific cells in the cleaving embryo suggests obvious approaches to finding their function. Sequencing the clones also suggests a function for the mRNAs; it would be particularly interesting to find hints of activities that could set up positional information (such as gradients of small molecules) to provide the spatial coordinates by which developing cells sense their position and respond accordingly.

Drosophila

If one employs genetics to approach this same subject, one can at least start with a knowledge of what the genes do in the developing animal, because they will have been identified by virtue of some interesting, probably dramatic, effect on the developing embryo. This is why current intense activity in *Drosophila* developmental genetics is so exciting for embryologists of all kinds. Most such work recently published in these pages has been concerned with homoeotic genes, like those of the antennapedia complex, or the segmentation genes, for example, *fushi tarazu* and *engrailed*. These genes are expressed after fertilization and interpret spatial cues established at earlier stages. The latter are produced by other genes transcribed during oogenesis, that is, they are 'maternal effect' genes. These genes do not affect the maternal carrier, but their malfunctions are revealed as abnormalities in all eggs produced by females carrying any copies of the mutant gene in the case of dominant genes, or lacking wild-type genes in recessives. Such genes have global effects on the major body axes of the embryo, to be expected if they set up some kind of network of positional information, such as gradients.

Judging by the major classes of maternal mutants discovered, there seems to be two kinds of positional information in the early insect embryo, that for the antero-posterior axis and that for the dorso-ventral axis. These two sets of information would be sufficient to make every point in the left or right halves of the embryo unique. Our knowledge of the dorsal group of genes has mainly derived from the work in Christiane Nüsslein-Volhard's laboratory[4-6]. At least 10 separate loci are involved in establishing the dorso-ventral axis, all manifesting themselves as recessive mutations in which the developing embryo lacks cells of the ventral type. Because a recessive mutation usually results in the loss of function of a gene (for example, its deletion, or encoding of a non-functional protein) this indicates that the products of these genes are necessary to form ventral structures (their confusing name of 'dorsal-type' is because genes are typically named after the observed effect of their malfunction, and not that of their normal function). A particularly important feature of most of these genes is that they can be rescued by injecting cytoplasm into the eggs of mutant females, thus restoring the normal phenotype at least to some extent. In all cases where this can be achieved except one (*dorsal*), pure RNA is also effective (see table).

Two recent reports[7,8] indicate that one of these maternal effect genes, *Toll*, is particularly interesting. *Toll* is unique among such genes because it not only has recesive, lack-of-function dorsalizing alleles, but also has dominant gain-of-function ventralizing alleles. Perhaps the most immediately striking observation about all the dorsal-type mutants is that among the mutants rescuable by injection with RNA, it is only in *Toll*$^-$ embryos (those laid by females homozygous for *Toll*$^-$ recessive mutations) that it matters where the cytoplasm or RNA is injected[4]. The point of injection marks the future ventral region of the rescued embryo. In the other dorsal-type mutants, the ventral region is always in the usual place, recognizable by the asymmetrical shape of the egg. This indicates that the dorso-ventral polarity still exists in some form in these embryos,

Maternal effect loci affecting the dorso-ventral axis (from refs. 6 and 7).

			+ type Rescue	
			Cyto-plasm	RNA
Gastrulation defective	Recessive	Dorsalized	–	ND
Pipe	Recessive	Dorsalized	–	ND
Dorsal	Recessive	Dorsalized	+	–
Nudel	Recessive	Dorsalized	–	ND
Tube	Recessive	Dorsalized	+	+
Snake	Recessive	Dorsalized	+	+
Easter	Recessive	Dorsalized	+	+
Toll	Recessive	Dorsal	+	+
	Dominant	Lateralized or ventralized	ND	ND
Spätzle	Recessive	Dorsalized	+	+
Pelle	Recessive	Dorsalized	+	+

but needs the expression of the non-*Toll* dorsal-group genes to be interpreted. *Toll*$^-$ embryos must have no inherent dorso-ventral axis, and at least a partial axis is organized at the position where normal cytoplasm is injected.

Anderson, Jürgens and Nüsslein Volhard have conducted an intensive genetic analysis of *Toll*, which has led them to postulate that the *Toll*$^+$ product is immediately involved in setting up the hypothetical morphogen gradient that establishes the dorso-ventral axis[7]. It cannot be the morphogen itself because rescue of the eggs of *Toll*$^-$ females can be achieved with cytoplasm taken from anywhere in the wild-type egg (see figure).

Although the *Toll*$^+$ product is evenly distributed throughout the embryo, it is presumably only active in the ventral region. Hence it may be present as a precursor which is activated only in this region (1 in the figure). The 'precursor' could be mRNA, in which case 'activation' is its controlled translation. Because *Toll*$^+$ RNA produces a ventral region where it is injected into an egg lacking the *Toll*$^+$ product, they propose that the precursor self-activates in the absence of other *Toll*$^+$ products, although this explanation is not very satisfactory without further evidence.

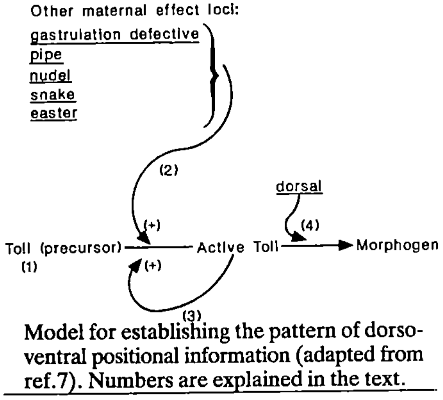

Model for establishing the pattern of dorso-ventral positional information (adapted from ref.7). Numbers are explained in the text.

There are four dominant alleles of *Toll*, divided into two groups. In eggs from heterozygous females carrying all these mutations, only ventral structures are present. When one of the pair of alleles *Tl*^{5B} and *Tl*^{84C} is present together with any homozygous dorsal-type recessive mutation from those listed in Table 1, the resulting embryos have only dorsal structures. Thus, *Toll* requires each one of these dorsal-type gene products for its activity (2 in the figure). Furthermore, these dominant alleles *Tl*^{5B}and *Tl*^{84C} only produce their totally ventral phenotype when there is also a copy of *Toll*$^+$ present, that is, in the absence of normal *Toll*$^+$ product they produce the totally dorsalized phenotype characteristic of no *Toll* activity, as seen in the recessive *Toll* mutants. This could mean that *Toll* produces a multisubunit protein, which needs some normal subunits for these dominant alleles to exert their effect. However, the authors favour the possibility that the active form of the product stimulates its own synthesis, *Tl*^{5B} and *Tl*^{84C} having lost this function.

The other two dominant alleles of *Toll* (*Tl*^{I} and *Tl*^{9Q}) will at least partially override all of the dorsal-type genes, except *dorsal* itself, to produce intermediate lateralized embryos. In addition, these alleles do not need the presence of a normal *Toll* gene for their expression. It is therefore assumed that *Tl*^{I} and *Tl*^{9Q} bypass the precursor activation step by making an altered *Toll* product that is active or self-activating, hence uncoupling the dependence of *Toll* on the other dorsal-type genes and eliminating the positive-feedback loop (3 in the figure). The role of the dominant alleles of *Toll* in interactions with other dorsal-type genes has also been investigated by cytoplasmic rescue experiments[8]. The cases of *gastrulation defective* and *pipe* are especially interesting, because eggs affected by mutations in these genes cannot be rescued by the injection of normal cytoplasm. This can perhaps be explained for *gastrulation defective* as it has a temperature-sensitive period (time of activity) from before to a little after fertilization, earlier than the other genes tested. Thus, cytoplasm is injected into these eggs too late to effect rescue. However, cytoplasm from the *Tl*^{9Q} dominant eggs will rescue them, emphasizing the escape of the *Tl*^{9Q} product from control by the other genes.

All the *Toll* dominant alleles require the presence of an active *dorsal* gene in the female to produce their ventralizing effect (4 in the figure). This suggests a special position for the *dorsal*$^+$ product. It is put later in the chain of events because rescue by *dorsal*$^+$ cytoplasm requires the injection to be ventral, that is, into the area where the hypothetical *Toll* product is activated. *Dorsal*$^+$ has an early time of action, overlapping but extending longer than *gastrulation defective*. It can only be rescued by cytoplasm and not by RNA, suggesting that it is translated early on. However, it is a puzzle that the *dorsal* RNA is actually present throughout early development[10]. Validation of this interesting model will require the cloning of the genes concerned, which is no small task.

It is intriguing that a new example of a maternal effect gene has been isolated by virtue of its containing a homoeo box sequence[11]. This gene, *caudal*, is unknown genetically but is expressed in oogenesis and its product becomes localized to a band at the posterior tip of the embryo at the cellular blastoderm stage. This gene may be a relative of the bithorax complex controlling the development of the partially suppressed ninth abdominal segment. The most interesting feature of *caudal* is that it is the first maternally expressed *Drosophila* gene with a homoeo box, although one such *Xenopus* gene also has this sequence[12]. This suggests a new way to obtain genes that control patterns of vertebrate development, and re-emphasizes the considerable general impact of *Drosophila* genetics.

100 years ago

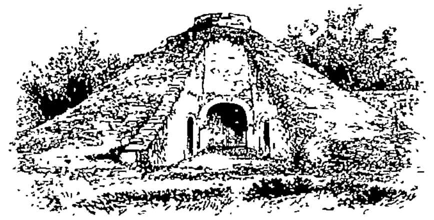

THE Lions' House in the grounds of John Hunter's house at Earl's Court. It was "a raised mound of earth. The earth rests upon an arched structure, which, at the time of my visit, was in excellent condition." The sketch was one of a series of homes and birthplaces of illustrious men drawn by Bertram Richardson.
from *Nature* **33** 275, 21 January 1886.

Finally, there are two parallels which may be drawn between the establishment of the dorso-ventral axis in insects and vertebrates. First, the key area in the dorso-ventral positional field of insects is the ventral part of the embryo. This is where the mesoderm develops, and the region is supposed to organize the dorso-ventrally graded ectoderm dorsal to it by some kind of long-range interaction. In vertebrates, the central nervous system (the most dorsal ectoderm) is also generated by a signal from the mesoderm, the phenomenon called neural induction[1]. Second, in insects the ventral *Toll*$^+$ component may be generated by activation of an inactive precursor (or translation of an RNA). It is proposed that the amphibian dorso-ventral axis is also generated by the unmasking of a ubiquitous component, although here it marks the dorsal limit of the dorso-ventral axis and the response is polarized by a cytoplasmic movement, usually in response to sperm entry[13]. The parallels are certainly intriguing and it will be fascinating to see how real they are. ☐

1. Woodland, H.R. & Jones, E.A. *Nature News and Views* **318**, 102 (1985).
2. King, M.-L. & Barklis, E. *Devl Biol.* **112**, 203 (1985).
3. Rabagliati, M.R., Weeks, D.L., Harvey, R.P. & Melton, D.A. *Cell* **42**, 769 (1985).
4. Nüsslein-Volhard, C. in *Determinants of Spatial Organisation* (eds Subtelney, S. & Konigsberg, I.R.) 185 (Academic, New York, 1979).
5. Anderson, K.V. & Nüsslein-Volhard, C. *Nature* **311**, 223 (1984).
6. Anderson, K.V. & Nüsslein-Volhard, C. in *Pattern Formation* (eds Malacinski, G.M. & Bryant, S) 269 (Macmillan, New York, 1984).
7. Anderson, K.V., Jürgens, G. & Nüsslein-Volhard, C. *Cell* **42**, 779 (1985).
8. Anderson, K.V., Bokla, L. & Nüsslein-Volhard, C. *Cell* **42**, 791 (1985).
9. Santamaria, P. & Nüsslein-Volhard, C. *EMBO J.* **2**, 1695 (1983).
10. Steward, R., McNally, F.J. & Schedl, P. *Nature* **311**, 262 (1984).
11. Meodzik, M., Anders, F. & Gehring, W.J. *EMBO J.* **4**, 2961 (1985).
12. Müller, M.M., Carrasco, A.E. & DeRobertis, E.M. *Cell* **39**, 157 (1984).
13. Gerhart, J.C. *et al. Proc. R. Soc.* **B307**, 319 (1984).

Hugh Woodland and Elizabeth Jones are in the MRC Developmental Biology Group, Department of Biological Sciences, Warwick University, Coventry CV4 7AL, UK.

Solar physics

What causes the solar cycle?

from Douglas Gough

THE dynamics of the solar cycle are not understood. The main obstacle to progress is the paucity of data in a form that is immediately pertinent to the alternative theories that have been put forward to account for the cycle. That situation is bound to be improved by the interesting new analysis of solar magnetic fields reported by J. O. Stenflo and M. Vogel on page 285 of this issue[1].

The most popular theories presume that the cycle results either from a coherent magnetically controlled global oscillation of the Sun, or from some dynamo process that is essentially confined to the turbulent convection zone and possibly its immediate environs. The first alternative is perhaps the more obviously appealing, for it yields the observed 22-year period in a quite natural way, requiring simply that there is a large-scale internal magnetic field whose intensity is comparable to that observed in sunspots. Dynamo theories are less transparent, but they can rationalize the observed period by adjusting the quite uncertain statistical properties of the turbulence. They have been more highly developed, and consequently have gathered a larger following. But their failure to explain, in particular, the migration towards the equator of the sunspot belts has cast doubts even in the minds of some of their most ardent supporters. There is also evidence that the mechanism of the cycle extends well beneath the base of the convection zone.

One of the first hints that the solar cycle is not confined to the convection zone came from a dendrochronological analysis by Stockton *et al.*[2] of drought in North America. It was anticipated there would be a correlation with the solar cycle, with a period of 11 years. If contemporary dynamo models were correct, the entire magnetic field would be the same every half-cycle. Because the structure of the Sun cannot depend on the polarity of the field, any solar variation that might influence the climate should therefore have the 11-year period.

But to everyone's surprise, the drought period was found to be 22 years. Therefore the Sun can sense the difference between its north and its south, which can be so only if there is a nonreversing field, presumably in the radiative interior, that is strongly coupled to the oscillating field outside. It has been claimed that the Princeton oblateness measurements[3] and the fine structure in the power spectrum of low-degree acoustic oscillations[4] also show indirect evidence for a deep-seated magnetic field. Moreover, the existence of widely spaced stable longitudes of magnetic activity seems to be more readily comprehensible if there is a coherent field that extends into the radiative interior.

The climatic record could be regarded as no more than a clue, for perhaps the solar–terrestrial connection filtered the 22-year period: if climatic variation results from the modulation of the Earth's ionosphere by charged particles from the Sun, it could be that the geomagnetic field determines the invariant direction. However, corroborating evidence that the direction is determined in the Sun was provided by Sonnet[5], who pointed out a systematic difference between odd and even sunspot cycles. And more recently, Eddy and Fröhlich[6] have found decade timescale variations in 17-year records of solar constant and diameter measurements that seem to be consistent with a 22- but not a 11-year periodicity.

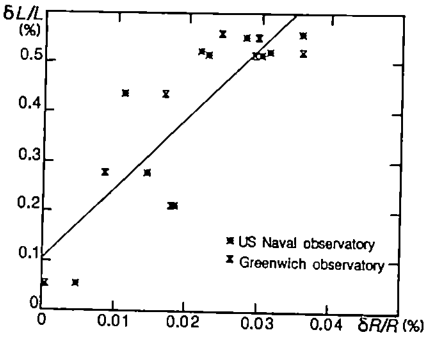

Relation between relative radius ($\delta R/R$) and solar luminosity ($\delta L/L$) variations in the period 1967–1982 (after ref. 6).

Another interesting result that emerged from the analysis by Eddy and Fröhlich is the ratio, W, of the infrared relative radius and solar luminosity variations (see figure). It had previously been shown that the value of W is an indicator of the depth, d, in the Sun at which the variations are produced[7] and it had also been conjectured that W is an increasing function of d. Eddy and Fröhlich obtained a value for W ($\simeq 0.078 \pm 0.026$) which points to a disturbance near the base of the Sun's convection zone, a natural location for the alternating external field and the direct internal field to meet, rather than in the superficial layers or the energy-generating core. One is reminded of the proposal by Spiegel and Weiss[8] that the main role of the turbulence in the convection zone is to concentrate the field at its base until instability causes the field to erupt into the start of a new sunspot cycle.

This argument too must be viewed with caution. Variations in the Sun's diameter are notoriously difficult to measure. On timescales of centuries widely divergent results have been reported. Much of the discrepancy has been attributed to errors introduced by changes in the observing conditions. The data analysed by Eddy and Fröhlich[9] seem to have been obtained under relatively uniform conditions, so perhaps their variation is a more reliable indicator of a corresponding solar variation. But, they may not reflect gross compressions and rarefactions of the Sun; superficial changes in the scale of solar granulation and in the structure of the solar atmosphere that have been reported to be correlated with the 11-year sunspot cycle may have 22-year counterparts that influence the size of the solar image.

Even if the diameter measurements have been correctly interpreted, one cannot be sure that a process concentrated near the base of the convection zone is responsible for the variations. First, recent calculations[9,10] have shown that W is not a function solely of d. Second, the seat of the cycle may not be localized near a particular depth; perhaps the value of 0.078 for W is an average response to a mechanism acting throughout the interior of the Sun. Indeed, R. Davis (personal communication), among others, has noticed a correlation between a decade timescale variation in the neutrino flux and sunspot numbers. The result is barely significant but if it does reflect a causal connection, one would surely be compelled to conclude that the core partakes in the cycle. In this connection it is worth noting recent evidence that the core is rotating more rapidly than the rest of the Sun[11]; the angular velocity variation is unstable, and one might conjecture that the ensuing motion, which is predominantly on spherical surfaces, oscillates with the solar cycle. If there were also a radial advection of material, the variation of chemical composition in the core would modify the neutrino production rate.

Until now there has been only meagre evidence on which to base conjecture but the analysis by Stenflo and Vogel of the Mount Wilson / Kitt Peak magnetic-field measurement might be the start of a new era in solar-cycle diagnosis. Inspired by studies of five-minute oscillations, they projected the signal at each moment on to (axisymmetrical) spherical harmonics and Fourier analysed the resulting time series. Several remarkable properties are revealed, the most surprising of which is that harmonics of odd and even degree, l, behave quite differently.

All odd harmonics with $l < 14$ exhibit the 22-year periodicity. That is to be expected, for it is well known that the oscillating magnetic field is dominated by a component that is antisymmetrical about the equatorial plane; the field is unlikely to be spherically harmonic, so the periodicity should be present in all odd-degree projections. And as the cycle is commonly considered to be a nonlinear phenomenon, it should not be surprising that no other incommensurable period is present. But it was not anticipated that the coherent variation would be almost sinusoidal, as indicated by the lack of the temporal harmonics of 22 years.

The power spectrum of the even-degree components with $l \leq 14$ is quite startling for, as Stenflo and Vogel point out, it looks superficially like a branch of the spectrum of the five-minute oscillations. Is it a magnetic analogue of linear *p* modes, as Stenflo and Vogel suggest? If so, why should the spatial structure of the oscillating field be spherically harmonic, for the basic state cannot be spherically symmetrical? Why does there appear to be just one branch of the dispersion relation? Is it only that one branch which has a positive growth rate in linear theory, or do nonlinearities suppress the other modes? And why do only the $l=10$ (and possibly the $l=14$) even-degree modes show power near 22 years? One is reminded of the apparently anomalous rotational splitting of the (neibouring) $l=11$ acoustic modes reported by Duvall and Harvey[12].

Perhaps the most exciting prospect offered by Stenflo and Vogel's *p*-mode analogy is the possibility of a seismological inversion to determine the magnetic field inside the Sun. If that prospect becomes reality, many questions about the nature of the solar cycle might be answered. But first we must understand the nature of the magnetic oscillations, and learn how to compute their frequencies. Since, unlike the five-minute modes, the eigenfunctions are not obviously separable, that is likely to be a formidable task, even if linerarized theory is adequate. Simple plane-wave analysis such as that presented by Gilman[13] may provide insight, if not quantitatively correct results. Indeed, such analysis suggests that there are three obvious long timescales that are relevant to the problem: the rotation period P, a characteristic Alfvén time T_A, and the time $\tau = T_A^2/P$. It is interesting that if $\tau=22$ years, then $T_A =$ (22 years×25 days)$^{1/2} \simeq$ 1.2 years, which is close to the period at which the curve in Stenflo and Vogel's Fig. 2 flattens. We must await further research to know whether that correspondence is causal or accidental.

We also eagerly await the analysis of the nonaxisymmetrical modes that Stenflo and Vogel promise. If their *p*-mode analogy is reliable, these modes will surely provide much more detailed information about the structure of the magnetic field, just as Brown's observations[14] of nonaxisymmetrical *p* modes can yield the latitudinal variation of the Sun's internal angular velocity. There is, however, an obvious aspect of the subject where the analogy does not hold: when Deubner first unambiguously resolved the five-minute oscillations there was a theory of acoustic modes with which to compare the results; for Stenflo and Vogel there is no such theory. □

Douglas Gough is visiting the Tata Institute of Fundamental Research, Homi Bhabha Road, Bombay, India, on leave from the Institute of Astronomy, Madingley Road, Cambridge, UK.

---

1. Stenflo, J.O. & Vogel, M. *Nature* **319**, 285 (1986)
2. Mitchell, J.M. Jr, Stockton, C.W. & Meko, D.M. in *Solar-Terrestrial Influences on Weather and Climate* (eds McCormac, B.M. & Seliga, T.A.) 125 (Reidel, Dordrecht, 1979)
3. Dicke, R.H. *Solar Phys.* **78**, 3 (1982).
4. Isaak, G.R. *Nature* **296**, 130 (1982).
5. Sonnet, C.P. *Nature* **306**, 670 (1983).
6. Eddy, J.A. & Fröhlich, C. *Adv. Space Res.* **4**(8), 121 (1984).
7. Gough, D.O. *Variations of the Solar Constant* (ed. Sofia, S.) 185 (NASA conf. publ. 2191, Washington DC, 1981).
8. Spiegel, E.A. & Weiss, N.O. *Nature* **287**, 616 (1980).
9. Däppen, W. *Astron. Astrophys.* **124**, 11 (1983).
10. Endal, A.S., Sofia, S. & Twigg, L.W. *Astrophys. J.* **290**, 748 (1985).
11. Duvall, T.L. Jr *et al. Nature* **310**, 22 (1984).
12. Duvall, T.L. Jr & Harvey, J.W. *Nature* **310**, 19 (1984).
13. Gilman, P.A. *Astrophys. J.* **162**, 1019 (1970).
14. Brown, T.M. *Nature* **317**, 591 (1985).

Nucleic acid-binding proteins

More metal-binding fingers

from Jeremy M. Berg

WHEN Miller *et al.*[1] analysed the sequence of TFIIIA, a protein involved in the control of transcription of the 5S RNA gene of *Xenopus*, they identified repeated metal-binding domains (fingers) which they suggested bind to the nucleic acid. Recent reports of the primary structures of several other regulatory proteins, including that of the *Krüppel* segmentation gene of *Drosophila* described by Rosenberg *et al.* on page 336 of this issue[2], reveal the presence of repeated fingers closely homologous to those of TFIIIA. It seems likely that metal-binding domains are frequently used as structural units in nucleic acid-binding proteins.

Nucleic acid-binding proteins are involved in the positive and negative control of gene transcription. By recognizing specific nucleic acid sequences such proteins play crucial roles in development and gene expression. The determination of the three-dimensional structures of several prokaryotic DNA-binding proteins led to the discovery of a common structural motif used in DNA recognition, consisting of an alpha helix, a short turn and a second alpha helix[3]. The structurally characterized proteins form dimers such that the two helix–turn–helix units are related by a two-fold axis as shown on the left hand side of the figure. Based largely on the presence of relatively invariant hydrophobic residues that are involved in stabilizing the bihelical structure, similar structures were recognized in several phage and bacterial proteins (see ref.3) as well as certain yeast mating factors and eukaryotic homeo-box proteins[4,5]. The helix–turn–helix unit became recognized as one frequently used motif for DNA binding.

The newly emerging alternative motif of metal-binding domains began with the recognition of nine tandem copies of an imperfectly repeated sequence of about 30 amino acids, including two cysteines and two histidines in essentially conserved positions, with a consensus sequence: (Tyr-Phe)-X-Cys-X_4-Cys-X_3-Phe-X_5-Leu-X_2-His-X_3-His-X_{2-6}, where X is any amino acid. The underlined Cys and His residues are thought to bind Zn^{2+} ions — the ribonucleoprotein particle containing TFIIIA binds 7–11 Zn^{2+} ions per polypeptide chain — the Tyr, Phe and Leu residues may form a hydrophobic core within each domain, and the domains may bind to nucleic acids by means of hydrophilic amino acid side chains[1]. A possible structure is shown on the right hand side of the figure.

Four tandem repeats with a consensus sequence (Phe, Tyr) - X - Cys - X_2 - Cys - X_3 - Phe-X_5-Leu-X_2-His-X_3-His-X_5, nearly identical to that of TFIIIA, are revealed in the sequence of *Krüppel*[2] and similar units have also been discovered in the sequence of the *Serendipity* locus of *Drosphila*[6]. Here, the beta protein-coding region has five tandem repeats with sequences very similar to those of the *Krüppel* and TFIIIA repeats immediately preceeded by a similar sequence of the form Cys-X_2-Cys-X_3-Phe-X_5-Leu-X_2-His-X_5-Cys-X_5. The homologous delta region sequence has six tandem repeats followed by a non-homologous sequence of about 40 amino acids and then one final repeat. Another example of a protein containing repeated metal-binding domains is ADRI (ref. 7), a positive regulatory protein from yeast. This protein has two tandem repeats homologous to those from TFIIIA.

A variety of other regulatory and nucleic acid-binding proteins contain sequences which, while not closely homologous to the TFIIIA-like sequences, are nevertheless highly suggestive of metal-binding domains. One example is found in the recently reported sequence of the human glucocorticoid receptor[8] which has a basis region of about 60 amino acids that contains several Cys-X_2-Cys units and additional Cys residues. Another set of examples is provided by some retroviral nucleic acid-binding proteins[9,10] that contain either one or two sequences of the form Cys-X_2-Cys-X_4-His-X_4-Cys. Several other proteins contain single copies of sequences with four Cys and/or His residues spaced in a manner suggestive of a metal-binding domain[7,10].

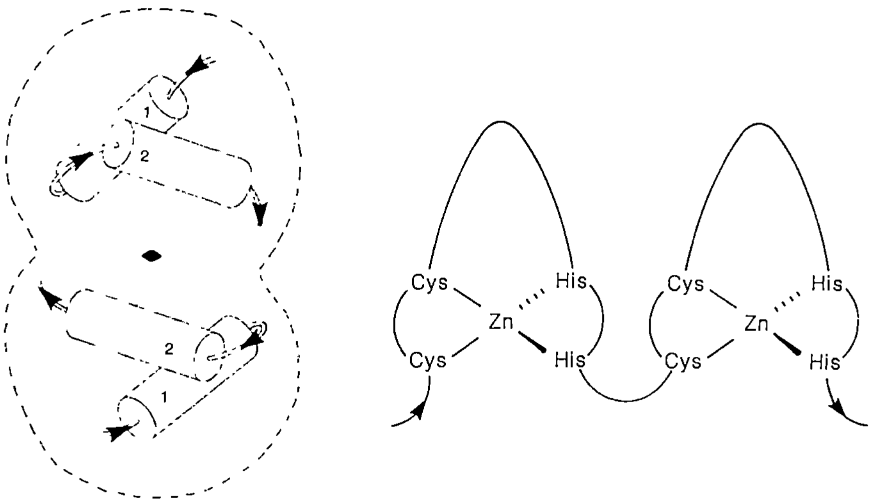

Left, schematic structure of a dimeric protein containing the helix–turn–helix motif; such proteins bind DNA with the first helix of each unit interacting with the DNA backbone and the second helix lying in the major groove. Right, a possible structure for the repeated domains from a TFIIIA-like protein. Nucleic acids might bind to such a structure by interacting with the end of each domain or, perhaps, by lying in the clefts between adjacent domains.

The discovery of internally-repeated sequences in TFIIIA and of its high Zn^{2+} content led to the proposal of a novel structure based on tandemly repeated domains, each of which is structurally based on a tetrahedrally coordinated Zn^{2+} ion. The conserved hydrophobic residues must play a role in stabilizing the precise polypeptide conformation. One known example of a protein that is built up from small domains is wheat-germ agglutinin[11]. Its structure consists of four 41 amino-acid domains each of which is stabilized by four disulphide bridges. Given the rapid rate at which proteins are currently characterized, particularly with respect to sequence, more examples of small metal-binding domains can certainly be expected soon. Many exciting results will follow from studies of the structures, functions and mechanisms of action of these proteins. ☐

1. Miller, J., McLachlan, A.D. & Klug, A. *EMBO J.* 4, 1609 (1985).
2. Rosenburg, U.B. *et al. Nature* 319, 336 (1986).
3. Pabo, C.O. & Sauer, R.T. *A. Rev. Biochem.* 53, 293 (1984).
4. Shepherd, J.C.W. *et al. Nature* 310, 70 (1984).
5. Laughon, A. & Scott, M.P. *Nature* 310, 25 (1984).
6. Vincent, A. *et al. J. molec. Biol.* 186, 149 (1985).
7. Hartshorne, T.A., Blumberg, H. & Young, E.T. *Nature* (in the press).
8. Weinburger, C. *et al. Nature* 318, 670 (1985).
9. Copeland, T.D. *et al. FEBS Lett.* 162, 390 (1983).
10. Berg, J.M. *Science* (in the press).
11. Wright, C.S. *J. molec. Biol.* 111, 439 (1977).

Jeremy M. Berg is a Jane Coffin Childs Postdoctoral Fellow in the Biophysics Department of the Johns Hopkins University School of Medicine, Baltimore, Maryland 21205, USA.

Extinct animals

The mammoths' last migration

from Jared Diamond

MAMMOTH madness reigned in Helsinki last summer when the Soviet Academy of Sciences loaned Finland a unique and comprehensive collection of Russian mammoth memorabilia, including the baby mammoth named Dima and two adults, preserved hair and all in the Siberian permafrost. Thanks to such finds, more is known about the biology of mammoths than about most extinct animals and many extant ones, and the Great Mammoth Exhibit illuminated questions of the distribution, foraging ecology and eventual end of the beasts. The exhibition was, however, the last migration for the Russian mammoths. The Soviet Academy has reluctantly decided not to expose this unique collection to another trip abroad.

Pleistocene mammoths of various species occupied cold tundra habitats of Eurasia from Britain east to the Pacific and south to the Mediterranean and China, as well as western parts of North America and south into Central America[1,2]. To judge from the quantities of mammoth bones littering Siberia, the animals must once have been widespread but became extinct about 11,000 years ago[1-4].

Because of the excellent preservation of mammoth soft tissue in the permafrost, Soviet scientists have been able to reconstruct the diet of mammoths from gallons of frozen stomach contents: grasses, sedges and shoots of willows, birch and alder predominate. How did they reach plants through the snow cover during the long Siberian winter? The shapes of the tusks provide a clue. In young mammoths, the tusks pointed forwards but they became increasingly curved with age until the terminal parts were horizontal and almost perpendicular to the head-to-tail axis. Although ill-suited for defence they would have been well adapted for use as ploughs to clear snow from ground vegetation mammoths may have wintered in groups in which older members functioned as snow ploughs.

Upper Palaeolithic hunters often killed mammoths and may have been decisive in exterminating them. All North American sites associated with Clovis hunters (the first widespread big-game hunters of the New World, about 11,000 years ago) that contain animal bones also contain mammoth bones: the Escapule mammoth skeleton had two Clovis projectile points among its ribs, the Naco mammoth eight (ref. 5). How were mammoths hunted? Standing beneath the two preserved adult mammoths in the exhibition created gives a vivid impression of the suicidal insanity of attacking such an animal. The question is as difficult to solve as it would be for archaeologists contemplating butchered whale bones in Eskimo middens to deduce whale-hunting techniques without the benefit of present-day observations.

The conventional view, reconstructed in familiar paintings, of near-naked ape-like brutes brandishing boulders and crude clubs at an enraged mammoth cannot be accurate. Men could hardly have survived naked on the Siberian winter tundra, let alone subdued a mammoth with such crude weapons. Nor could they have afforded to run serious risks to themselves in mammoth hunts. Assuming a human band size of 50 with 10 adult male hunters, 10 reproductive-age women, live births spaced at 4 years and one mammoth hunt per month, then no more than 10 per cent of mammoth hunts could have led to a hunter's death, otherwise the death rate would have exceeded the male birth rate and humans would have become extinct rather than mammoths.

Evidently, palaeolithic hunters evolved much more efficient, risk-free methods. Anatomically, they were fully modern and since Clovis hunters specialized in mammoths they were presumably as, or more, skilled than people who now successfully hunt elephants on a casual basis without firearms. Modern Africans and Asians use a great variety of low-risk methods to disable elephants: traps (stockades, pitfalls, footsnares, trunk snares or weighted hanging spears), poisoned arrows, encircling with fire and even spearing or hamstringing after a stealthy approach on foot[6]. These methods exploit detailed knowledge of behaviour of elephants, such as their vulnerability while bathing, fear of fire, use of regular paths and waterholes and reliance on smell to detect danger. Palaeolithic hunters probably exploited similarly detailed knowledge of mammoth behaviour — cave paintings in France and Spain depict traps and pitfalls;

the Lehner and Murray Springs mammoth-kill sites were apparently ambushes at streams. A realistic painting of mammoth hunting should show warmly clad professionals calmly spearing a mammoth already crippled by a trap or ambush.

Did hunting really exterminate mammoths or did they die out solely because of late-Pleistocene climatic changes and retreat of tundra? These alternatives have been much debated, not only for mammoths but also for other large extinct Pleistocene mammals[4]. The accurate radiocarbon dating of very small fossil samples by tandem accelerator mass spectrometry[7] may provide some of the answers. With this technique, Mead *et al.* have just shown that a species derived from cold climates, Harrington's mountain goat, and a species derived from warm climates, the Shasta ground sloth, both disappeared in Arizona at essentially the same time — 11,160 ± 125 and 11,018 ± 50 years BP, respectively[8]. This pairing does not fit a climatic extinction hypothesis but coincides suspiciously with the period of the Clovis hunters. It is also suspicious that the abundant mammoths and many other large New World mammals survived at least 22 Pleistocene glacial cycles, to disappear about the time that Clovis hunters arrived. Using tandem accelerator mass spectroscopy to date more precisely the last mammoths will provide a test of this suspicion. ☐

1. Agenbroad, L.D. in *Quaternary Extinctions* (eds Martin, P.S. & Klein, R.G.) 113 (University of Arizona Press, Tucson, 1984).
2. Vereshchagin, N.K. & Baryshnikov, G.F. in *Quaternary Extinctions* (eds Martin, P.S. & Klein, R.G.) 438 (University of Arizona Press, Tucson, 1984).
3. Vereshchagin, N.K. *Vestnik zoologii* 3, 32 (1982).
4. Martin, P.S. & Klein, R.G., *Quaternary Extinctions* (University of Arizona Press, Tucson, 1984).
5. Haynes, C.V. *Can, J. Anthrop.* 1, 115 (1980).
6. Johnson, D.L. *et al. Can. J. Anthrop.* **1,** 107 (1980).
7. Haynes, C.V. *et al. Archaeol. Eastern North. Am.* **12,** 184 (1984).
8. Mead, J. *et al. Proc. natn. Acad. Sci. U.S.A.* (in the press).

Jared Diamond is Professor of Physiology at the University of California Medical School, Los Angeles, California 90024, USA.

Planetary meteorology

Is there lightning on Venus?

Janet G. Luhmann and Andrew F. Nagy

Is lightning unique to Earth, or does the phenomenon occur on other planets? The answer to this question will have implications for matters ranging from the nature of the atmospheric chemistry and the meteorology of the planets[1] to the existence of life. Because aerosols of volcanic origin enhance lightning production, geological processes must also be involved in this familiar phenomenon[2].

Venus is particularly fascinating, both because of its proximity and because of its permanent obscuring cloud layers. Because lightning on the Earth is associated with the generation of electrical charges in convective clouds, there seems a good chance that Venus is also a candidate for this type of meteorological activity. But the dynamic and thermal conditions in the venusian atmosphere are probably quite different from those on Earth; the clouds, for example, are composed of sulphuric acid instead of water vapour. If the necessary ingredient of strong convection is absent, and the electrical properties of the cloud constituents or other environmental conditions are not appropriate, venusian clouds should never be brightened by the types of discharges found on Earth. Yet there have been inferences that lightning does occur on Venus.

The Soviet space probes Venera 11 and 12 first detected impulsive very low frequency electric fields below the cloud tops which resemble the lightning-generated 'sferics' seen in terrestrial data[3]. A more recent reanalysis of Venera 9 spectrometer measurements[4] found supporting optical data, although a search with the star tracker on the US spacecraft Pioneer Venus Orbiter had failed to show any evidence for lightning[5]. However, the plasma-wave experiment on that spacecraft, showing a whistler-type electric field noise in the 100-Hz channel in the nightside ionosphere[6-8], reinforced the Venera results. (Whistlers are a well known electromagnetic signature of lightning discharges on Earth.)

Scarf and Russell[9] have extended the interpretation of the electric field observations of lightning by demonstrating that well-ordered magnetic fields with approximately vertical orientation 'duct' the whistlers from the lower nightside atmosphere to the spacecraft located at altitudes above 150 km. Moreover, these ducts, when traced along straight lines in the direction along the magnetic field towards the planet, all appear to intersect the ground near regions identified as volcanic highlands by radar experiments[10]. On this basis, Scarf and Russell concluded that the lightning sources on Venus are clustered near specific topographical features where aerosols, such as those associated with active volcanism, may be present.

Taylor and coworkers[11] have now suggested that Scarf and Russell's results are simply a coincidence arising from the combination of the sampling bias imposed by the spacecraft orbit, planetary rotation and the magnetic field geometry at Venus. Their main arguments stem from the observation that depletions or troughs in the observed ionospheric ion densities occur in conjunction with the vertical magnetic field present during the 100-Hz bursts, but that the vertical fields associated with the longer duration troughs do not map preferentially to the highlands. They point out that several other studies show that the vertical magnetic fields are related to the solar wind interaction with the planetary ionosphere causing the interplanetary field to become 'hung up' in the ionosphere[12,13], and that it is unlikely that these fields penetrate to the ground. Moreover, the ion-density depletions must also result from the interaction between the solar wind and the ionosphere[14]. Similar ion troughs occur in the Earth's ionosphere at mid- and high latitudes in response to magnetosphere – ionosphere coupling. As plasma instabilities can result from gradients in the plasma properties, it is not surprising that plasma waves occur in conjunction with the ionospheric density gradients on Venus. Lightning need not be invoked; therefore the argument for volcanism is moot.

Indeed, evidence continues to accumulate showing that the vertical magnetic fields in the nightside ionosphere of Venus are the result of the solar wind interaction. The ion-density depletions and density gradients are associated with the vertical fields[11] but this does not mean that the vertical fields and ionosphere troughs produced by the solar wind interaction cannot duct lightning-induced whistlers to the spacecraft when there is a favourable connection to the highlands.

Because the Pioneer Venus mission has continued to accumulate data, Scarf and coworkers can look for further support for their claims as new areas of venusian topography rotate into the nightside region of vertical magnetic fields. Meanwhile, theoretical investigations of the nature of the alleged plasma instabilities in the ion troughs may help finally to resolve the question. ☐

1. Rinnert, K. *J. geophys. Res.* **90,** 6225 (1985).
2. Veimeister, .P.E. *The Lightning Book* (MIT, Boston, 1961).
3. Ksanfomality, L.V. *et al. Pisma Astron. Zh.* **5,** 229 (1979).
4. Krasnopolsky, V.A. *Cosmic Research* **18,** 429 (1980).
5. Borucki, W.J. *Icarus* **52,** 354 (1982).
6. Taylor, W.W.L., Scarf, F.L., Russell, C.T. & Brace, L.H. *Nature* **279,** 614 (1979).
7. Scarf, F.L., Taylor, W.W.L., Russell, C.T. & Brace, L.H. *J. geophys. Res.* **85,** 8158 (1980).
8. Ksanfomality, L.V., Scarf, F.L. & Taylor, W.W.L. in *Venus* (ed. Hunten, D.) 565 (Univ. Arizona Press, 1983).
9. Scarf, F.L. & Russell, C.T. *Geophys. Res. Lett.* **10,** 1192 (1983).
10. Mazursky, H. *Lunar and Planetary Science XIV* part 2, 466 (LPI/USRA, Houston, 1983).
11. Taylor, H.A., Jr, Grabowsky, J.M. & Cloutier, P.A. *J. geophys. Res.* **90,** 7415 (1985).
12. Luhmann, J.G. & Russell, C.T. *Geophys. Res. Lett.* **10,** 409 (1983).
13. Marubashi, K. *et al. J. geophys. Res.* **90,** 1385 (1985).
14. Brace, L.H., Theis, R.F., Mayr, H.G., Curtis S.A. & Luhmann, J.G., *J. geophys. Res.* **87,** 199 (1982).

Janet G. Luhmann is at the Institute of Geophysics and Planetary Physics, University of California, Los Angeles, California 90024; Andrew F. Nagy is in the Department of Atmospheric and Oceanic Science, University of Michigan, Ann Arbor, Michigan 48109, USA.

Cerebral damage and functional localization

SIR—H. Stowell's[1] response to my *News and Views* comment[2] on the paper by Hart *et al.*[3] raises more problems than it solves. I, of course, agree that the brain damage sustained by Hart *et al.*'s patient was indeed global by the criteria of those who work with surgical ablations in animals (not to speak of single cell recordings). But by the standards of human neuropsychology, the infarct was relatively focal; we work with the lesions that nature, sadly, gives us.

Like Stowell, I too have my doubts about direct mappings between categories of cognitive impairment and lesion sites and find no difficulty in providing Stowell with further ammunition for his position. For example: in 1925, Vendryes[4] wrote that "it is wrong to think of the brain as if it were built on the plan of a grammar, cut into sections for the different parts of speech." Yet in 1985, McCarthy and Warrington[5] could report a case of severe agrammatism, consequent upon diffuse cortical atrophy, in which a specific disorder of verb use was the most outstanding symptom. If it is any consolation to Stowell, I lie awake at nights worrying about how such phenomena are possible.

Finally, I have the greatest respect for Maxwell, Einstein, Pellionisz, and Llinás, and would much appreciate hearing from Stowell about exactly how we could apply their insights to the interpretation of the highly constrained linguistic deficits seen after (not so focal) brain damage.

JOHN C. MARSHALL
Neuropsychology Unit,
The Radcliffe Infirmary,
Oxford OX2 6HE, UK

1. Stowell, H. *Nature* **318**, 414 (1985).
2. Marshall, J.C. *Nature* **316**, 388 (1985).
3. Hart, J., Berndt, R.S. & Caramazza, A. *Nature* **316**, 439 (1985).
4. Vendryes, J. *Language: A Linguistic Introduction to History* (Routledge and Kegan Paul, London, 1925).
5. McCarthy, R. & Warrington, E.K. *Neuropsychologia* **23**, 709 (1985).

The magnetic field of Uranus

SIR—Reports that the Planetary Radio Astronomy experiment (PRA) on Voyager 2 has not so far detected radio emissions from Uranus, particularly in the previously reported[1] 0.5 MHz region, do not necessarily imply that Uranus has no magnetic field. On the contrary, we think it likely that Uranus will be found to have a polar magnetic field strength of 0.01 to 0.1 gauss, which would imply a magnetosphere extending out to 8 to 16 planetary radii (R_U). But such field strengths would be unlikely to lead to radio emissions detectable by PRA and also imply that the observed[2,3] Lyman-α emission from Uranus may only in part be caused by the interaction of the solar wind with the magnetosphere.

The presence of a magnetic field, however small, is suggested by estimates of the internal composition of Uranus leading to the conclusion that the planet has a core constituted of refractory elements (Si, Mg, Fe, Ni,...) with a radius of 0.3 R_U and a mass four times that of the Earth[4-7]. Such a core would contain about 10% Fe and Ni oxides and, if some of the SiO_2 were in the liquid metal form, there would be a liquid core similar in size to that of the Earth. On this basis, one might assume a molten core with a magnetic moment not very different from that of the Earth, which would in turn imply a field strength at the surface equal to that of the Earth at a distance of R_U, whence the estimate of a polar field strength of 0.01 gauss.

The corresponding distance to the magnetopause on the upstream side, assuming a modified Chapman–Ferraro estimate of the maximum magnetic pressure, is in the range 8–16 R_U, in which case the magnetosphere may extend as far as the orbit of the satellite Umbriel or, at the strong-field end of the range, at least to that of Oberon. A complication, at the present heliocentric phase of Uranus, is that the magnetic axis should be approximately aligned with the solar wind; the funnel, however, should end about two-thirds of the distance to the magnetopause[8], while the penetration of the solar wind plasma will be determined primarily by the reconnection of the magnetic field lines. Accordingly, we expect that Voyager 2 will enter the magnetosphere at 8–16 R_u, some 2–3 hours before closest approach, that it will miss the dayside funnel or polar cusp and remain in the magnetotail for about 12–24 hours after closest approach.

Using these estimates and the calculations of Siscoe[9] (modified by a planetary rotation period of 16.3 hours), we conclude that the plasmasphere will extend essentially to the magnetopause with a convection timescale of 14 to 29 hours.

We estimate that the power supplied to the system by the magnetohydrodynamic dynamo driven by the solar wind will be in the range 2–9 × 10^9 W, greater than the power supplied by a disk-driven dynamo of the kind considered by Hill and Dessler[10], which, with our parameters, would lie between 1 × 10^8 and 2 × 10^9 W. The magnetic field-strength in the tail will range from 1.5 nanotesla near the planet to 0.5 nanotesla at greater distances.

It is also possible to predict the geometry of the auroral emissions on the planet's disk if the magnetosphere is taken to be Earth-like with due allowance for the pole-on orientation of Uranus. On the night side of the planet, hard plasma-sheet precipitation should produce a crescent-shaped auroral band on one side of the polar cap, while soft polar-cusp precipitation should produce another band on the other side. The same configuration is expected on the day-side on Uranus, but with the difference that the plasma-sheet aurora will be thin and that the polar-cusp aurora will fill a substantial part of the polar cap.

The failure of the Voyager PRA experiment to detect radio emission early in the approach to Uranus is explicable if the planet has a comparatively weak magnetic field. Radio emission will be confined[11] to those regions in which the ratio of the electron-plasma and gyro-frequencies is less than unity, which implies that for B = 0.01 to 0.1 gauss, there will be no wave generation even at the ionospheric electron densities of about 10^4 cm^{-3} typical of those in the terrestrial ionosphere.

Two other arguments lead to the conclusion that radio emission from the magnetosphere of Uranus may have been too weak to be detected in the early stages of the approach of Voyager 2. The observed radio emissions from the Earth, Jupiter and Saturn, when scaled empirically, suggest that the total power radiated is approximately 5 × 10^{-6} of the energy flux of the incident solar wind, which implies that if there is any dayside emission from Uranus, the flux would be 1–5 × 10^9 W, corresponding to 4–20 × 10^{-18} W m^{-2} at a distance of 1 astronomical unit, which is considerably less than the radio power from the three other sources. Further support for the view that the radio emission from Uranus would not have been detected early in the encounter comes from the assumption that it may be permissible to scale the frequency-peak of the emission from a planet with the strength of the magnetic field, in which case the frequency maximum at Uranus should appear at 0.3 to 3.0 kHz, 0.5–5.0 kHz and 5.0–50.0 kHz if scaled from Earth, Jupiter and Saturn, respectively[12]. But the lowest frequency channel of the PRA experiment at 0.7–1.7 kHz is below the plasma frequency of the solar wind plasma behind the bow shock, while the next channel (19.9–20.9 kHz) is well above the position of the peak unless the magnetic field at the surface of Uranus is greater than about 0.04 gauss.

For these reasons, we believe that the absence of radio emissions in the early records of the PRA experiment does not imply that Uranus does not have a significant magnetic dipole moment and a magnetosphere of considerable extent.

W.I. AXFORD
V.M. VASYLIUNAS

Max-Planck-Institut für Aeronomie,
D-3411 Katlenburg-Lindau,
FRG

1. Brown, W.L. *Astrophys. J.* **207**, L209 (1976).
2. Durrance, S.T. & Moos, H.W. *Nature* **299**, 426 (1982).
3. Clarke, J.T. *Astrophys. J.* **263**, L105 (1982).
4. Reynolds, R.T. & Summers, A.L. *J. geophys. Res.* **70**, 199 (1965).
5. Hubbard, W.B. & MacFarlane, J.J. *J. geophys. Res.* **85**, 225 (1980).
6. Podolak, M. & Reynolds, R.T. *Icarus* **46**, 40 (1981).
7. Stevenson, D.J. *A. Rev. Earth planet. Sci.* **10**, 257 (1982).
8. Midgley, J.E. & Davis, L. Jr *J geophys. Res.* **67**, 499 (1962).
9. Siscoe, G.L. *Icarus* **24**, 311 (1975).
10. Hill, T.E. & Dessler, A.J. *Science* **227**, 1466 (1985).
11. Curtis, S.A. *Nature* **318**, 47 (1985).
12. Kaiser, M.L. & Desch, M.D. *Rev. Geophys. Space Phys.* **22**, 373 (1984).

Solar wind interaction with Uranus' atmosphere

SIR—The failure of Voyager 2 to detect radio emission from Uranus even from within 1 astronomical unit may be explained along the lines suggested by Axford and Vasyliunas (preceding letter) by supposing that the surface magnetic field is approximately 0.01 to 0.1 gauss, but it is also possible that Uranus simply has no intrinsic magnetic field. In that case, the solar wind may impinge directly on the neutral upper atmosphere, as it does on Venus. I shall explore briefly the consequences of this assumption for the forthcoming encounter between Voyager 2 and Uranus.

Figure 1 shows the circumstances likely to be encountered by Voyager 2. The scavenging effect of the solar wind should produce a wake of exospheric ions (H_2^+, He, H_3^+, CH_4^+ and so on) converging behind the planet[1,2]. As well as this trail of atmospheric ions, Voyager 2 must be expected to measure a flux of heavy ions sputtered from the particles of which the rings are made. There is thus a chance that some information on the surface composition of these narrow rings may be obtained, while the total area of the optically opaque ring system (approximately 4×10^{17} cm^2, or more than three times the projected area of Uranus itself) may constitute a detectable obstacle to the flow of the solar wind.

Even if Uranus itself has no magnetic field, it is to be expected that there will be a certain degree of amplification of the interplanetary field in the neighbourhood of the planet, as there is in the neighbourhood of Venus; we estimate[3,4] that a peak field of 4 nanotesla in the sub-solar regions may be induced in this way. Moreover, the interplanetary field lines will be expected to be draped around Uranus, forming a downstream magnetotail, as at Venus and as observed by Voyager 1 during its close encounter with the Saturn satellite Titan.

The intense ultraviolet emission from Uranus must be explained within the same framework. The total energy flux of the solar wind at the projected cross section of Uranus is of the order of 5×10^9 W, which is several orders of magnitude less than the flux required if the observed Lyman-α emission is to be excited directly by charged particle impact. This is the argument by which Hill and Dessler concluded that a mechanism based on auroral excitation would require a sizeable magnetosphere with a surface magnetic field of a few gauss, but if the function of the charged particle impact is to fragment H_2 molecules, which then give rise to ultraviolet emission by the resonant scattering of solar radiation, the energy requirements are less critical. Even so, the upper limit of 5×10^9 W in the case of a Venus-like interaction is a stringent condition on the energy deliverable to the atmosphere of Uranus by the solar wind.

Support for the view that the Lyman-α flux may arise from processes other than the direct impact of magnetospheric electrons has been provided by the earlier encounters of Voyager spacecraft with Titan and by investigations of the surroundings of Venus, chiefly by means of Soviet spacecraft. One idea is that the effect of the enhanced curvature of the magnetic field lines around Titan is to increase the flux of suprathermal magnetospheric electrons on the atmosphere of the satellite, which is apparent both in the increased flux of ultraviolet radiation from N_2 molecules and in the depletion of the flux of magnetospheric electrons above 700 eV.

It is important that atmospheric precipitation of charged particles may not be a sufficient explanation. N_2 emission has been observed on the dayside disc of Titan and attributed to the effect of solar radiation on the interaction between the magnetospheric plasma and the atmosphere[4,6]. Another possibility is that the circumstances around Titan may resemble those around Venus, and also Uranus, in allowing the enhanced ionization of atmospheric constituents (see refs 7–11).

W.-H. IP

Max-Planck-Institute für Aeronomie,
D-3411 Katlenburg-Lindau, FRG

1. Ip, W.-H. in *Future Missions in Solar, Heliospheric and Space Plasma Physics* (Proc. ESA workshop Garmisch-Partenkirch) 65 (ESA SP-235, 1985).
2. Gringauz, K.I. in *Venus* (eds Hunten, D.M. *et al.*) 779 (University of Arizona Press, Tucson, 1983).
3. Smith, G.R. *et al. J. geophys. Res.* **87**, 1351 (1982).
4. Neubauer, F.M. *et al.* in *Saturn* (eds Gehrels, T. & Matthews, M.S.) 760 (University of Arizona Press, Tucson, 1984).
5. Russell, C.T. & Vaisberg, O.L. in *Venus*, (eds Hunten, D.M. *et al.*) 873 (University of Arizona Press, Tucson, 1983).
6 Hartle, R.E. *Adv. Space Res.* **5**, 321 (1984).
7. Alfvén, H. *Rev. mod. Phys.* **37**, 652 (1985).
8. Danielsson, L. *Phys. Fluids* **13**, 2288 (1970).
9. Raadu, M.A. *Astrophys. Space Sci.* **55**, 125 (1978).
10. Formisano, V., Galeev, A.A. & Sagdeev, R.Z. *Planet. Space Sci.* **30**, 491 (1982).
11. Vaisberg, O.L. & Zeleny, L.M. *Icarus* **58**, 412 (1984).

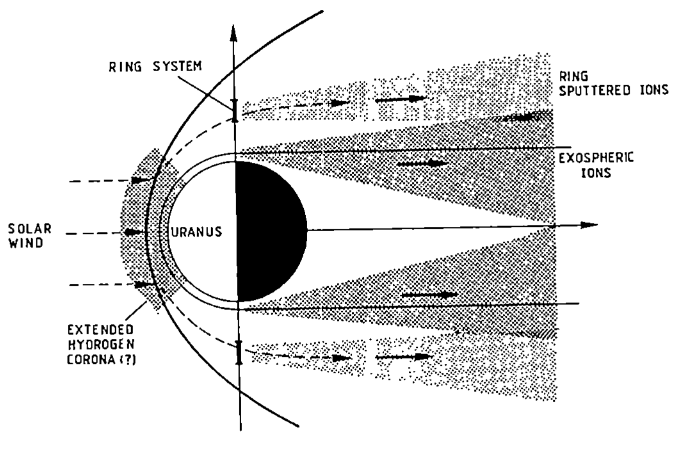

Fig. 1 A schematic view of possible direct solar wind interaction with the neutral atmosphere of Uranus. Points of interest are the upstream ionization interaction with the (putative) extended corona of H atoms; the plasma mantle formed by pickup of the exospheric ions; and the cylindrical sheath of sputtered ions from the rings.

Archaebacterial terminator

SIR—In his *News and Views* article on "The uniqueness of archaebacteria" (*Nature* **318**, 234; 1985) Roger A. Garrett quotes me as having suggested "that five consecutive thymidines might be sufficient for ending the methyl-CoM-reductase gene of *Methanococcus voltae*". That is, in fact, not true. Our findings on the terminator structure in *Methanococcus* have since been published (*Nucleic Acids Res.* **13**, 6439-6445; 1985). The terminator strongly resembles a eubacterial terminator.

ALBRECHT KLEIN

Philipps Universität Marburg,
Fachbereich Biologie,
Molekulargenetik,
Karl-von-Frisch-Strasse,
3550 Marburg, FRG

R.A. GARRETT REPLIES—This archaebacterial terminator was selected from several reported that appeared non-eubacterial in character. Other putative terminators, including those for the ribosomal RNA genes of the extreme halophile *Halococcus morrhuae* and the thermoproteale *Desulfurococcus mobilis*, remain exceptional. ☐

How to test special relativity

SIR—In the light of the recent debate in *Nature* about possible tests of special relativity[1-3], we wish to direct attention to a relevant question posed in *Nature* in 1968 by A.C.W.V. Clarke[4]: "What preference is to be given or denied to [the Earth's reference] frame?"

To the best of our knowledge, no subsequent paper in *Nature* has addressed this simple question. We submit that the physical significance of this neglected problem is of a fundamental character, and we briefly explain below how the quest for the answer points to new important tests of special relativity.

The latter theory was built largely on the basis of the following ideas: Owing to the Earth's known orbital motion, the terrestrial laboratory was considered to be a moving frame of reference. Moreover, owing to the continuous change in direction of the Earth's velocity, it was tacitly assumed that the terrestrial laboratory constitutes different reference frames in different seasons (assumption A).

So when the velocity of light was measured (in the terrestrial laboratory), and its value c was discovered to be paradoxically the same in every direction and in every season, Einstein drew his well known conclusions: first, that c may be referred to any and every reference frame; and second, that all frames are therefore equivalent.

If assumption A is granted, this is sound reasoning. Now in kinematics assumption A is quite obviously true indeed. However, despite its apparent plausibility, there is considerable evidence[5-10] casting doubt on its general validity in many aspects of dynamics, electromagnetics, and optics. In these fields there is some cause to resort to assumption B, that the terrestrial laboratory constitutes at all times one and only one reference frame, namely the unique Earth's frame.

When c is measured in the terrestrial laboratory, the terrestrial environment (atmosphere, gravitational and electromagnetic fields and so on) remains practically unaltered in every season, despite the Earth's orbital and other motions. Because of its size, the Earth exerts autonomy over its domain of influence, and there is no gravitational or electromagnetic field wind, nor a wind of any other kind. So in considerations of this kind, assumption A fails and assumption B seems to be valid.

For these and other reasons, it has been suggested[9] that the correct interpretation of Maxwell's electromagnetic theory of light might be to postulate that the velocity c of light (Maxwell's electromagnetic waves) has to be referred to the rest frame of the ambient electromagnetic field (Maxwell's electromagnetic ether) through which the light is propagated, and to this frame only.

In the light of this analysis, all known tests of the special relativistic postulates are rendered inconclusive, for the experiments which led to the inception and testing of the theory of relatively moving frames were all performed in a single stationary frame, the terrestrial laboratory.

Thus from an historical viewpoint, the answer to Clarke's question is that the Earth's frame was unduly given an exclusive preference. From a physical viewpoint, however, the question still remains to be answered. It could not be answered experimentally in 1905 when Einstein published his postulates — he could then perform only *gedanken* experiments.

The advent of the space age, however, has given rise to new possibilities. All sorts of experiments have already been conducted in space. But the few experiments which might have truly tested the perhaps most fundamental and controversial hypotheses in twentieth century physics — Einstein's postulates — have curiously not been done.

The best known, most accurate, and often repeated experiment which led to the genesis of special relativity was first carried out by Michelson and Morley in 1887, and repeated many times thereafter with ever greater precision. Would it not be fitting for a space agency to repeat it for the first time in space during its hundredth anniversary in 1987?

M. PSIMOPOULOS
T. THEOCHARIS

Physics Department,
Imperial College,
The Blackett Laboratory,
Prince Consort Road,
London SW7 2BZ, UK

1. Maddox, J. *Nature* **316**, 209 (1985).
2. Tiomno, J. *Nature* **317**, 772 (1985).
3. Aspden, H. *Nature* **318**, 317–318 (1985).
4. Clarke, A.C.W.V. *Nature* **217**, 20 (1968).
5. Essen, L. *Nature* **199**, 684 (1963).
6. Bourdikis, Z.L. *Proc. IREE Australia* **29**, 343–358 (1968).
7. Zappfe, C.A. *Speculations Sci. Technol.* **2**, 439–459 (1979); **8**, 61–72 (1985).
8. Aspden, H. *Physics Unified*, 47–69 (Sabberton Publications, Southampton, 1980).
9. Theocharis, T. *Lett. Nuovo Cimento* **36**, 325–332 (1983).
10. Hodges, R. *Electronics Wireless World* **90**, 23–24 (December 1984).

Ontogeny of natural killer cells

SIR—We disagree with the *News and Views* article "Ontogeny of natural killing", in which it was proposed that natural killer (NK) cells are simply immature T lymphocytes, "whose recognition mechanisms never grew up"[1]. This is an over-simplification, not substantiated by the present data.

Specifically, we challenge the following statements:

(1) "The (T cell antigen) receptor-positive cells, however, represent only something like 5 per cent of NK cells: in the rest, although the β-chain genes are rearranged and transcribed[34], they give rise only to truncated RNA that cannot participate in the formation of a functional receptor." The data in ref. 34 (Reynolds, C.W. *et al.*, *J. exp. Med.* **161**, 1249; 1985) were misquoted. In fact, the title of the article is "Lack of gene rearrangement and mRNA expression of the β-chain of the T cell receptor in spontaneous rat large granular lymphocyte leukemia lines." Furthermore, Ritz *et al.*[2] have demonstrated that human CD3- NK clones do not rearrange the β-chain genes. Recently, we isolated CD3-, CD16+ NK cells directly from peripheral blood and have proven that this population does not rearrange the β-chain genes[3]. Although a truncated β-chain mRNA may be present in CD3- NK cells, B cell lines also produce abortive β-chain transcripts[4].

(2) It is implied that CD3- NK cells are simply stage I thymocytes, based on the observation that NK cells express CD2, but usually lack CD4 and CD8. By extrapolation, should the reader also conclude that monocytes and a subset of T cells are ontogenetically related, since both express the CD4 antigen? There is no experimental evidence indicating that a CD3- peripheral blood NK cell can be induced to rearrange T-cell antigen receptor genes or differentiate into CD3+ T lymphocytes. Although NK cells and T cells may share a common bone marrow precursor cell, there is no evidence to suggest that NK cells arise from the thymus.

(3) "A careful analysis of T-cell receptor gene expression in parallel with physiological studies on NK cells has now confirmed their membership of the T-cell lineage, but seriously damaged their credibility as a legitimate T-cell subset." Since CD3- NK cells do not rearrange T-cell antigen receptor β-chain genes, and cannot be induced to differentiate into CD3+ cells, what is the basis for concluding that they have been definitively assigned to the T-cell lineage? Moreover, the small CD3+ T cell subpopulation that does mediate non-MHC restricted cytotoxicity, productively rearranges and transcribes the T-cell antigen receptor genes, and recognizes antigen via the CD3/Ti complex[3]. We propose that these non-MHC restricted cytotoxic T lymphocytes do in fact constitute a legitimate T-cell subset, and should be referred to as "non-MHC restricted CTL", rather than NK cells.

Perhaps the underlying cause for this confusion is that there has been no precise definition for an NK cell. Unfortunately, any lymphoid population killing K562 or YAC has been called an "NK cell" or "NK-like" cell. However, the functional, antigenic, and molecular genetic studies on both freshly isolated lymphocytes and

IL-2 dependent clones clearly indicate that both a CD3+ T cell population, and a distinct CD3- NK cell population mediate non-MHC restricted cytotoxicity[2,3]. There is no evidence to suggest that CD3- NK cells, a population comprising ~ 10% of peripheral blood lymphocytes, are an immature member of the T cell lineage. Hopefully, the relationship of NK cells and T cells will be clarified by the discovery of the NK cell target recognition receptor.

Lewis L. Lanier
Joseph H. Phillips

Becton Dickinson Immunocytometry Systems,
PO Box 7375, Mountain View,
California 94039, USA

1. Robertson, M. *Nature* **317**, 768–771 (1985).
2. Ritz, J. *et al. Science* **228**, 1540–1543 (1985).
3. Lanier, L.L., Cwirla, S., Federspiel, N. & Phillips, J.H *J. exp. Med.* (in the press).
4. Calman, A.F. & Peterlin, B.M. *Fed. Proc.* **44**, 1319 (1985).

Miranda Robertson replies—My remark on the possibility that NK cells might be arrested T cells was intended only as speculation: I was explicit about this. Ritz *et al.*[1] did not address the question of rearrangement but state that truncated beta transcripts are made from $T3^-$ NK cells; Reynolds *et al.* (my ref. 34) state that beta genes are transcribed at low levels in LGL cells and "the size of the mRNA from the LGL leukaemias is restricted to be 1.0 kb size. A beta chain message of this size is probably transcribed from an unrearranged or simple DJ rearrangement" (*sic*). So it is true that I overstated the data in those two papers: in fact the only claim for rearrangement was by Yanagi *et al.* (*Nature* **314**, 631; 1985; my ref. 33). I also accept that it does not necessarily follow from the data of Siliciano *et al.* (*Nature* **317**, 428; 1985; my ref. 35) that NK cells belong to the T lineage, and my wording was incautious. Finally I heartily agree on the need for a precise definition of an NK cell and the identification of its receptor.□

The search for extraterrestrials

Sir—I welcomed the review article by M.D. Papagiannis on the Search for extraterrestrial intelligence (SETI) (*Nature* **318**, 13; 1985) which, I am sure, gives an accurate view of the global programme.

Faced with the cosmic haystack, I could not help thinking that the approach to SETI so far was somewhere between that of the drunk in the dark who searched for the lost diamond ring under the lamppost, and the rich father-in-law who brought in a bulldozer to do the job properly. The lamppost approach is to some extent inevitable: we have to search in spectral regimes that are technically open to us. But faced with a dauntingly wide spectrum there is opportunity to use a bit more intelligence and a bit less bulldozer when it comes to constructing vast capacity multichannel spectrum analysers.

First, the microwave window (Fig. 2 of Papagiannis) has a fairly well defined minimum arising from the cosmic background, the galactic non-thermal background and the quantum limit. This will be apparent to any galactic civilization capable of interstellar communications and occurs between 4 and 6 GHz.

Second, the so called magic frequencies of H and OH, while they are most important as absolute standards, are contaminated by natural backgrounds and they do not occur at the optimum frequency in the microwave window.

What SETI needs is a "search filter" which it can apply to the cosmic haystack so as to assign search priorities on the basis of the rational choice of transmission frequency. This choice should combine a physical constraint such as the energy constraint which defines the minimum in the microwave window, an absolute frequency standard such as the H line, and a civilization signature constant (CSC): some absolute number by which the frequency standard can be multiplied or divided to obtain the final transmission frequency.

The most obvious choice for the CSC is π or e, and using the H line we arrive at 4.468 GHz and 3.863 GHz as most likely communication frequencies. Since it is difficult to determine the cultural bias in choosing the CSC, care should be taken in investigating such CSCs as $(e\pi)^4$, π^2 and dimensionless physical constants.

If the systematic searches of the microwave spectrum first concentrate on a narrow frequency band that encompasses the Doppler broadening about the above absolutely defined frequencies, they will increase their chance of early success, without prejudicing the rest of the search.

Unimagined technologies could radically alter the physical constraints. The physical constraint would be quite different for a civilization which is in close proximity to an old and permanently nulled pulsar. In this case the pulsar could very effectively be used as a broad band transmitter of radio pulses, by firing projectiles at it with the appropriate modulation. Since a significant fraction of the projectile rest mass would be converted to radiation, this would provide a powerful means of interstellar communications, with a range of several kiloparsecs. It might be worth examining known pulsars for signs of amplitude or phase modulation.

Papagiannis is right that the answer can only come through "scientific searches . . . pursued vigorously", but we should give "them" credit for some rationality when we devise the search. If they do not want to communicate, and if we are simply eavesdropping, the bulldozer approach may be the only way, but the chance of early success will then probably be limited.

D.G. Blair

Department of Physics,
Nedlands, Western Australia 6009

Clone controversy at Immunex

Sir—At the Fourth International Lymphokine Workshop in West Germany on 17–21 October 1984, an executive of the company Immunex challenged our claim to have cloned the complementary DNA for interleukin–1 (IL–1) and informed the workshop that we had instead cloned some other monocyte product produced in response to lipopolysaccharide stimulation. Although not willing to present any scientific data to validate his claim at the time, he then added that Immunex had obtained a similar clone to ours several months previously, but had discounted it as being that of IL–1. A full account of this public outburst is now available[1].

We therefore read with great interest the recent article[2] entitled "Cloning, sequence and expression of two distinct human interleukin–1 complementary DNAs" from Immunex Corporation, of which the same executive is an author. Immunex now obviously feels confident about the fidelity of our human IL–1 cDNA clone since they confirm our work on the molecular cloning of the predominant (pI 7) form of monocyte-derived human interleukin–1 which is now published[3].

In addition Immunex has added unnecessary confusion to the field by assigning an 'α–β' nomenclature to the IL–1 sequences. We take issue with this action on two counts. First, we feel that the establishment of such classification is premature when based solely on characterization of cDNA clones. A meaningful classification can only be established when information is available on complexities of genomic organization, post-transcriptional and/or translational processing and the relationship to the multiple forms of IL–1 protein which have been described. Second, in the event that the 'α–β' system were to be adopted, we suggest that it would be more appropriate to call the pI 7 form 'α' and the pI 5 'β' rather than the reverse which was proposed by Immunex. This suggestion is based upon criteria of prevalence of the molecule (50-fold more pI 7 than pI 5) and the chronology of the cloning in the human.

Sheldon M. Wolff
Philip E. Auron
Charles A. Dinarello
Lanny J. Rosenwasser

New England Medical Center,
Boston, Massachusetts 02111, USA

Andrew C Webb

Wellesley College,
Wellesley, Massachusetts 02181, USA

Alexander Rich

Massachusetts Institute of Technology,
Cambridge Massachusetts 02139, USA

1. *Lymphokine Res.* 4, 51 (1985).
2. March, C.J. *et al. Nature* **315**, 641–647 (1985).
3. Auron, P.E. *et al Proc. natn. Acad. Sci. U.S.A.* **81**, 7907–791 (1984).

Between men and women

Robert Attenborough

The Descent of Woman: A New Edition. By Elaine Morgan.
Souvenir Press: 1985. Pp.288. Hbk £8.95; pbk £5.95.
Myths of Gender: Biological Theories About Women and Men.
By Anne Fausto-Sterling. *Basic Books: 1986. Pp.258. $18.95.*

THERE are some books which a male reviewer takes on at his peril. These two come into that category. Both authors are female and feminist, and both write about human evolution and biology with a particular interest in the female side (or, to put it more even-handedly, in sex and gender). But there, on the whole, the resemblances end. Elaine Morgan is a Welsh freelance writer, and her speculative evolutionary history, of woman as well as man, dates back to 1972. Anne Fausto-Sterling is an American academic (a developmental geneticist), and her new book surveys a series of controversies about the biology of sex differences and roles.

Elaine Morgan's publishers puff up her book as "the classic study of evolution — a new edition". Certainly it was enjoyed by many, was welcomed as a breath of fresh air by feminists and was found stimulating by at least some evolutionary biologists. If the books of Robert Ardrey, Konrad Lorenz and Desmond Morris (in order of chronology, not merit) represented the first generation of the speculative human ethology which began in the 1960s, Elaine Morgan's belonged to the second. She had read the earlier books, and to some extent the academic literature beyond them, and wrote a riposte in a similar style giving her version of the human evolutionary scenario in the manner that Stephen Gould calls "adaptive storytelling". Her particular theme was a dual one: that evolutionary views of "man the hunter" and so on were too male-centred, not just in using "man" and "he" for the species but in paying too little attention to female roles and selection pressures; and that a better scenario for human evolution could be based on the "aquatic ape" hypothesis — the idea, proposed by Sir Alister Hardy and outlined to a wider public by Desmond Morris, that there was an aquatic (perhaps better, littoral) phase in human evolution during the Pliocene which influenced our adaptations then and since.

Morgan wrote with an engaging panache, and while not all her arguments and criticisms hit their target effectively, some certainly did. That she was right to focus more attention on the female part in human evolution is clear, and other books such as Nancy Tanner's *On Becoming Human* (Cambridge University Press, 1981) and Sarah Hrdy's *The Woman That Never Evolved* (Harvard University Press, 1981) have since made the same point in different and more scholarly ways. Not so many authors have followed Morgan in the aquatic hypothesis, but she herself wrote a second book, *The Aquatic Ape* (Souvenir Press, 1982), designed, with some success, to win from academics a more serious hearing for the idea. In both its main themes, then, *The Descent of Woman* is now largely superseded. In not revising the book beyond deleting one chapter and adding a 15-page postscript, Elaine Morgan herself seems to admit to a view of the book as more a period piece than an essay to be taken at face value today for its substantive content.

By contrast, *Myths of Gender* certainly does ask, and deserve, to be taken seriously. Rather than tracing an evolutionary sequence or developing a cumulative argument, Anne Fausto-Sterling devotes the core of her book to examining a set of controversial propositions which have in common simply that they attribute some aspect of females, males or the differences between them to biology. Principally, these propositions concern intellectual differences between the sexes, the development of sex roles in society; the behavioural impact of female hormones in menstruation and menopause; the relationship between male hormones and aggression; and evolutionary (especially sociobiological, needless to say) theories of the behaviour and relationships of the sexes. These are the "myths" of the title, and although that does not strictly imply that they are untrue, the burden of the book is that the propositions in question need sceptical examination, and are often wrong or unsubstantiated.

Fausto-Sterling makes this argument in each case in a way that is in some respects conventionally academic. She herself says that in this politically sensitive area she applies especially high scientific standards, but that is not just an excuse to dismiss unpalatable findings: on the contrary, the book is closely and intelligently argued, well documented factually and carefully referenced (albeit by the irritating end-note method). There are, throughout, interpretations one might argue with, and on occasion there are factual errors (for example that "humans are the only primates exhibiting handedness or hemispheric specialization"). Perhaps, too, the coverage would have been strengthened by greater input from the social sciences.

For whom the book is intended is not entirely evident. Fausto-Sterling can write quite well and clearly, and the book demands little prior knowledge. In some ways, it reads as if designed for a first-year undergraduate audience, perhaps even as

TO CRYSTALLIZATION

The atom is a crystal
of a sort; the lattices
its interlockings form
lend a planarity most pleasing
to the abysses and cliffs, much magnified,
of (for example) salt and tourmaline.
Arise, order,
out of necessity!
Mock, you crystals,
with all appearance of chiselled design,
our hope of a Grand Artificer.
The graceful layered frost-ferns the midnight elves
left on the Shillington windowpanes
for my morning astonishment were misinformation,
as is
the glittering explosion of tinted quartz
discovered in earth like a heart of thought,
buried evidence
crying out for release to the workman's pick,
tangled hexagonal hair of an angel interred
where it fell, our earth still molten, in the Fall.

When, on those anvils at the center of stars
and those even more furious anvils
of the exploding supernovae,
the heavy elements were beaten together
to the atomic number of 94
and the crystalline metals with their easily lost
valence electrons arose,
their malleability and conductivity
made Assyrian goldsmithing possible,
and most of New York City

Stendhal thought that love
should be likened to a bare branch crystallized
by a winter in the depths of the salt mines of Hallein
"the tiniest twigs, no bigger
than a tomtit's claws, are spangled with an infinite
number of shimmering, glistening crystals."
Our mathematics and hope of Heaven
alike look to crystals;
their arising, the mounting
of molecules one upon the other, suggests
that inner freezing whereby inchoate
innocence compresses a phrase of art
Music rises in its fixed lattices
and its cries of aspiration chill our veins
with snowflakes of blood,
the mind grapples up an inflexible relation
and the stiff spheres chime --
themselves, the ancients thought, all crystal
In this seethe of hot muck there is *something else*
the ribs of an old dory emerge from the sand,
the words set their bevelled bite on the page,
the loved one's pale iris flares in silent assent,
the electrons leap, leaving positive ions
as the fish-scales of moonlight show us water's perfect dance
Steno's Law, crystallography's first
the form of crystal admits no angle but its own.

(*Reproduced from* Facing Nature, *a collection of poems by John Updike published today in Britain by André Deutsch £9.95. Publisher in the United States is Alfred A. Knopf, price $13.95.*)

if the topics were selected more to spark an immediate response in that audience than out of the author's own intellectual interest in them. The way topics are presented, too, suggests an anxiety to keep courting the reader's flagging attention: though the academic content is substantial, it is larded at frequent intervals with turns of phrase that are highly coloured or seek a (contrived) intimacy with the reader — "like the merits of Mom and apple pie . . . ", "hormonal hurricanes", "math and sex is a hot topic" and so on. If it is a university audience that Fausto-Sterling has in mind, this surely implies a depressing (but accurate?) estimation of students' stamina for unalloyed academic argument.

What is clear about the intended audience is that it is American. That emerges from the style, the references to "this country" (the United States) and the overwhelmingly American literature that Fausto-Sterling draws on. Indeed, in one sense her book is more revealing about the state of contemporary American society than about the fundamental biology of the sexes, especially in focusing critical attention on some strongly hereditarian and perhaps even social-Darwinist (if that misnomer may be excused) strands surviving in American political life. Fausto-Sterling is greatly and understandably concerned about the presentation of biological theories in the media, and about the tenor of public debates on their social implications, for example on whether arguments about the biological basis of female or male actions should be accepted in the courts as diminishing responsibility for them. This results in frequent references to what *Time, Newsweek, Mainliner* (apparently an American in-flight magazine) and many others have to say. Up to a point, this is right and proper, since a socially responsible scientist should undoubtedly take notice of what the public at large is reading about science: but it seems to me that some overly superficial treatments are here allowed to determine the agenda and set the tone of the debate.

In short, Elaine Morgan is the more natural and more successful writer of the two, and what she has to say commands attention if not conviction. Stimulating though it was at first publication, however, *The Descent of Woman* is outdated. Anne Fausto-Sterling's *Myths of Gender* is substantial and useful, and has considerable intellectual merits: but, for my money, the author (not uniquely) strives too hard for commercial appeal, and might have been more successful had she had more confidence in the intrinsic interest of her material. ☐

Robert Attenborough is a Lecturer in Biological Anthropology in the Department of Prehistory and Anthropology, A.D. Hope Building, Australian National University, GPO Box 4, Canberra, ACT 2601, Australia.

At the information exchange

Eugene Garfield, Henry Small and George Vladutz

Scientific Communications and Informatics. By A. I. Mikhailov, A. I. Chernyi and R. S. Giliarevskii. Translated by Robert H. Burger. *Information Resources Press, Suite 700, 1700 North Moore Street, Arlington, Virginia 22209, USA: 1984. Pp.402. $55.50.*

THE East Europeans have often excelled as theoreticians out of necessity. Lacking a technological infrastructure that allows them the luxury of developing practical solutions to many problems, they lag in applied science but have the time to view developments from the outside. While there are many good theoreticians in the Western world, the distractions of applied research are frequent and often compelling.

The re-publication in English of a leading Soviet book, about eight years after its appearance in Russian, speaks of some strange priorities in the Soviet Union. There the scientist is deprived of the immediacy and convenience of personal access to foreign journals and books; nor are the authorities willing to truly join in international communication by allowing their own journals and books to be published first in English — the lingua franca of international science. Without this misplaced linguistic pride, the seminal research of such as the biochemist Shemyakin would have been known to the rest of the world much earlier. Instead, dozens of notable works by Soviet scientists are doomed to delayed recognition.

How does one properly appraise the translation of a book that itself was not very current? Ten years ago we would have had to say it is a very important work, remarkable as a thorough compilation and analysis of materials on information science (or informatics, as Mikhailov named it many years ago). Today it is still interesting for some of its statistical tables, but there is little in it that is new to the serious student of the subject.

One of the book's most appealing features (although others may find it annoying) is the frequent allusion to historical, sociological and philosophical work which serves to place the field of information science historically and intellectually in the social sciences. Much of what the authors say on the topic of contrasting national styles in information science remains valid, showing how little the field has progressed on the international front. Also, even now the succinct discussion of refereeing — the subject of a vast literature — makes interesting reading. Here the authors quote John Ziman; it will amuse him to learn that he is an American.

One wonders if the book review editor of *Nature* wasn't a bit mischievous in asking staff of the Institute for Scientific Information to review a work by leaders of its Soviet counterpart. There is, for instance, only a cursory remark (p. 159) about ISI's *Science Citation Index*, in connection with Derek de Solla Price's "half-life" index for literature obsolescence. Price leaned heavily on the *Index* for support for his theoretical notions — as, incidentally, did V. V. Nalimov, who coined the term "scientometrics" ("naukometriia") for the "science of science". But although the ageing effect is illustrated by the interesting discussion on pp. 152–153 of "low-calibre" articles, and Price is quoted, the term "uncited" has been ignored. Similarly, had the book been translated by an information scientist, the term "substantive" might have been replaced by "citation classic". The translator, the authors and Norbert Wiener, whom they quote on the cumulative effects of scientific work, all seem to have been unaware of Ortega y Gasset or the so-called Ortega hypothesis.

More generally, the authors' claim that our failure in the West to read Russian puts us at a disadvantage. This is no more significant than our inability to read Japanese or Chinese; the importance of each "exotic" language varies from field to field and from time to time. The unfortunate effect of the language barrier in the past was in delayed recognition. In the case of Shemyakin we could only have known about his work a year earlier, because it was abstracted. But its publication in Russian, rather than in English, was the principal factor in its relatively low citation compared to the work of David E. Metzler.

There can be little doubt that this book should be in every school of library or information science, though the publisher would have been wiser to urge (or allow) the authors to provide an up-to-date bibliography and a decent index, especially to cited authors. Writing a completely revised second edition will be a considerable task, but no doubt it will occur. We must hope that when it does, the English version will appear simultaneously with the Russian. The publication delay for the translation of the present book, which is by no means uncommon, makes communicating with our Soviet colleagues much like communicating with Mars. ☐

Eugene Garfield, Henry Small and George Vladutz are at the Institute for Scientific Information, 3501 Market Street, Philadelphia, Pennsylvania 19104, USA.

• Springer-Verlag has published Part I in Series A (original scientific publications) of *Heisenberg: Collected Works*. Price is DM 180. Part IB was reviewed by Nicholas Kemmer in *Nature* **313**, 826 (1985).

The bacteria with a difference

D.B. Nedwell

Archaebacteria. The Bacteria: A Treatise on Structure and Function, Vol. VIII. Edited by Carl R. Woese and Ralph S. Wolfe. *Academic: 1985. Pp.582. $85, £85.*

THE aim of this series of books, of which this volume is the eighth, is a comprehensive review of the structure and function of bacteria. Previous volumes have been concerned with structure, metabolism, biosynthesis, etc., but this latest volume is rather different in not being orientated towards a topic but dealing in depth with a specific group of microorganisms.

Archaebacteria are the group considered, despite accumulating evidence that they are quite distinct from most prokaryotic bacteria. The editors' introduction emphasizes this point, and that the degree of difference between prokaryotic bacteria and archaebacteria justifies their placement in distinct kingdoms. The inclusion of a volume on the archaebacteria in a series on bacteria is, therefore, a contradiction, but nonetheless justified as they have in the past been considered as prokaryotic bacteria, which they superficially resemble. Comparison of information in this volume with that on prokaryotes in preceding volumes indicates the basis upon which this fundamental division has been established.

The book is divided into three sections: biochemical diversity and ecology; RNA translation apparatus; and general molecular characteristics. Chapters in the first section deal specifically with each of the major groups of archaebacteria: the methanogens and extreme halophiles, together with the thermoacidophiles (sulphur-dependent archaebacteria). Each chapter succinctly reviews the taxonomy, ecology and biochemistry of the group, as far as it is known, and an interesting fourth chapter in this section deals with the geochemical evidence of archaebacterial evolution from the sedimentary record, including abundance and distribution of archaebacterial biomarkers.

The second section has four chapters dealing with archaebacterial ribosomes, nucleic acids and elongation factors: while in the third section, five chapters cover, amongst other topics, cell envelopes, lipids, antibiotic sensitivity and genome structure. This last section tends to be rather a catch-all without the cohesion found between chapters in the first two sections, but this is probably inevitable given the large gaps in current knowledge of the group.

The book is well produced. The standard of writing is uniformly lucid and comprehensive, and the text is well illustrated with photographic plates at relevant points. The high standard set by the preceding volumes in this series has been maintained. It pulls together and presents the overall evidence for the distinct nature of archaebacteria, which should be extremely useful for teachers having to adjust their undergraduate lectures to reflect the many recent developments in the knowledge about these organisms. At its price I doubt whether it will find many private purchasers, but it is predominantly a reference text which, in institutional libraries, will be particularly useful at the postgraduate level. □

D.B. Nedwell is a Lecturer in the Department of Biology, University of Essex, Colchester CO4 3SQ, UK.

Living in the past

Paul G. Bahn

On the Track of Ice Age Mammals. By Antony J. Sutcliffe. *British Museum (Natural History): 1985. Pp.224. £12.95. To be published in the United States later this year by Harvard University Press, $25.*

ANTONY Sutcliffe has produced a book which is, presumably, aimed at the kind of interested laymen who visit the Natural History Museum in London. Scholars in the several disciplines on which he draws will merely pick up some new information here and there, but the general public will find a well-produced guide to many aspects of the Ice Age — easy to read, wide-ranging and profusely illustrated (the five colour reconstructions of fauna in landscapes are particularly fine).

The author stresses that he has not written the book as a comprehensive treatise on Ice Age fauna. Instead he has wisely concentrated on a selection of subjects, sites and parts of the world. Inevitably, perhaps, there is an imbalance caused by emphasis on areas with which Sutcliffe himself is most familiar. Thus readers are presented with rather more information on British quaternary deposits and terraces than they might welcome; the East African evidence and the work of the Leakeys is covered in far more detail than South African material; and while early man looms large in the African chapter, he is barely mentioned in chapters on other parts of the world. This is regrettable since the thorny question of when man entered the New World and Australia has much relevance to the problem of animal extinctions, covered in the final chapter.

The chapter on dating explains some methods and their applications with great clarity, but one wonders why terms such as "isotope" and "amino acid racemization" are left unexplained. Part of the author's task was to show how a specialist in one field needs to draw on researches in others. He has generally succeeded in this, but the difficulty of coping with such a wide range of topics shows through at times, especially in the chapter on palaeolithic art which contains several elementary mistakes: there is no salmon engraving in the floor of Bédeilhac cave (it is in Niaux); Kesslerloch cave is in Switzerland; and there was never a continuous barrier of ice from the Atlantic to the Mediterranean along the Pyrenees — Spain was never cut off completely from France.

The fact remains that it is notoriously difficult to write a serious but accessible account of any part of science. Future visitors to the Natural History Museum, and like-minded people elsewhere, should be grateful to the author for providing them with such an elegant and informative book. □

Paul G. Bahn is currently a J. Paul Getty Post-doctoral Fellow in the History of Art and the Humanities, and can be contacted c/o the School of Archaeology, University of Liverpool, PO Box 147, Liverpool L69 3BX, UK.

Frozen find: the carcass of a 6–7-month-old woolly mammoth, discovered near the River Kirgilyakh, Siberia, in 1977. The animal died some 40,000 years ago, and was 115 cm long, 104 cm high and had a trunk 57 cm in length. In life it had a hairy coat, some of which is still visible around the feet. (Reproduced from On the Track of Ice Age Mammals, *courtesy USSR Academy of Sciences.)*

Genius in a bottle

Augustine Brannigan

Changing Order: Replication and Induction in Scientific Practice. By H.M. Collins. *Sage: 1985. Pp.187. Hbk £20, $25; pbk £9.95, $12.50.*

COLLINS argues that facts are like model ships in glass bottles: the ships are bits of knowledge and the bottles are truth, and once the ships have been assembled, they look like they've always been there and could never come out again. His task has been to study how shipbuilders — the scientists — construct and deconstruct what goes in and out of science. He focuses on the reconstruction of the TEA laser, the gravity waves controversy and disputes over the claims of paranormal phenomena. The work is based on interviews and observations of researchers in each of these areas over the past decade or so, and most of it has already appeared elsewhere. This volume highlights the similar patterns of reality construction and the way conceptual order has been achieved in these areas.

Like most British social studies of science, Collins's approach is brazenly relativist. Order is achieved not because nature dictates what theories work and which do not, but because the language, models and concepts of science shape how we investigate and experience the world. While this is not new, Collins's work is attractive because he focuses on one of the cornerstones of objectivism: the actual process of replication in science. This is crucial since it is argued that the replication of an effect recommends the independence, the objectivity of the finding. For Collins, what is intriguing is what *counts* as a replication (or falsification) can be very controversial. Generally, unless one is attempting to disconfirm a hypothesis, there is little incentive in exact or identical replication. Also, since publications never spell out (and arguably cannot spell out) all the contingencies in experimental research, replication failures are open to challenge for not being identical. This raises the experimenter's regress:

> What the correct outcome is depends upon whether there are gravity waves hitting the earth in detectable fluxes. To find this out we must build a good gravity wave detector. . . . But we don't know that we have built a good detector until we have tried it and obtained the correct outcome! But we don't know what the correct outcome is until . . . and so on *ad infinitum* [p.84].

The most compelling chapter describes the replication of the TEA laser by Robert Harrison (then at the University of Bath) with, we gather, the amateur assistance of Collins. It demonstrates that the replication did not follow an algorithm of inference (nor does induction generally); that the expertise acquired in creating something the first time through is largely tacit and marked by trial and error; that knowledge transfer in publications is quite incomplete; and, finally, that when the procedure works or the model crystallizes the previous sequence appears immediately to be forgotten and the account of how the discovery was made is reconstructed as if it followed an algorithm or recipe, with the experience of contingency and trial and error written off as "human" error. Induction becomes idealized like the ship in the bottle. Science education fosters this picture by directing attention exclusively to completed ships, and ignoring the first-time-through experience.

Change occurs in the relativist world by the construction of novel conceptual systems. These must have an empirical basis, and a conceptual plausibility, yet for Collins what could count as proof is not dictated by a direct grasp of nature, but the negotiation of claims in the institutional or conventional framework. "What counts" is mediated by preferences for different methodologies, different procedures for data analysis and the reaction of the "core set", the cluster of relevant experts. The credibility of a candidate discovery is negotiated through various replications and the scientific community's use of the innovation. Nature does not limit unambiguously what counts as fact, for the relevance of empirical observation is already imbued with constructs from previous theories. Even the checks on experimenter regress are problematic. For example, the calibration of the sensitivity of gravity wave detectors by introducing electrostatic stimuli to measure their responsiveness entails *a priori* assumptions about the properties of the waves which equate them with other forms of electromagnetic radiation, which, for Collins, puts "constraints on [Weber's] freedom to interpret results" (p.105). However, I think it must be conceded that the acceptance of some such conventions provides positively for the accreditation of evidence, even for, and perhaps especially for, the relativist. The suggestion that gravity waves could have survived beyond their demise in 1975 by use of *ad hoc* hypothesis, and that this would be consistent with the spirit of science, while the destruction of them by failures to replicate was somehow motivated by non-scientific intrigues is not a proposition that is likely to receive much sympathy.

The book gives a vivid sense of the contingent nature of research and is generally a good read, though Collins frequently has a penchant for irreverence and seems to be writing for an introductory audience. My main misgiving surrounds his view of the extra-scientific factors which influence change in science:

> For scientific culture, the mediating role of the core set, its laundering of 'illegitimate social interest', and its transubstantiation of social contingency into methodological propriety, along with its privacy, explain the paradox of reification [p.145].

In my view, the core set of experts is unfairly cast as a sort of irrational masonic lodge. No particularly strong evidence is advanced to support this view (though I fear we are into the experimenter's regress?) Also, the idea that illegitimate factors influence the adoption of innovations is not established by discussion of the attribution of character, competence and credibility in the weighing of evidence.

Finally, it seems odd for a relativist to complain that some fact is a reification. This appears to betray a subterranean objectivism, for whatever else could facts be for relativists but reifications? Though the first five chapters are at times brilliant, the final chapter, which deals with the theoretical crux of the matter, how change is accomplished, does not quite get all the pieces into the bottle. ☐

Augustine Brannigan is Associate Professor in the Department of Sociology, University of Calgary, Alberta T2N 1N4, Canada.

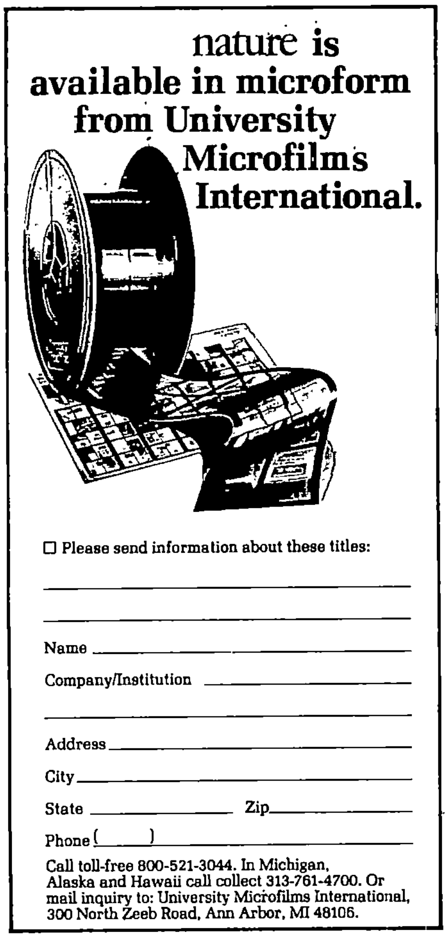

nature is available in microform from University Microfilms International.

☐ Please send information about these titles:

Name

Company/Institution

Address

City

State Zip

Phone ( )

Call toll-free 800-521-3044. In Michigan, Alaska and Hawaii call collect 313-761-4700. Or mail inquiry to: University Microfilms International, 300 North Zeeb Road, Ann Arbor, MI 48106.

New in paperback

Time's Arrows: Scientific Attitudes Toward Time, by Richard Morris. Publisher is Touchstone, New York (an imprint of Simon and Schuster), price is $8.95. The book was reviewed by David Park in *Nature* **314**, 687 (1985).

Uncertainty and the Strategic Defense Initiative

from John Wright

The latest developments in strategic thinking in the US administration make it necessary to restate classical nuclear strategy.

THERE comes a stage in any debate when it helps to restate basic principles. For nuclear weapons, these were arrived at when the need for some consensus first emerged in the late 1950s and early 1960s. It is because the fundamental facts have not changed but are in danger of being overlaid or overlooked that some restatement is needed now, when we see the possibility of some further agreement emerging between the United States and the Soviet Union and when the view is being put forward that the classic theories are outmoded by new technical possibilities, of which the most important is the 'Star Wars' anti-ballistic missile Strategic Defense Initiative (SDI). The debate itself, both now and twenty-five years ago, often strikes the participant and the observer as both deadly and unreal. The potential for disaster requires the most careful analysis; yet we have so little to work on apart from basic beliefs and aspirations about human behaviour, plus an all-too-detailed knowledge of the capabilities of the weapons themselves. This has always been so and is unlikely to change.

Basic nuclear strategy

In terms of what we can properly call the classical analysis there is little being said now which was not said a generation ago. The nature of that debate is worth remembering. The problem then, as now, was the role of nuclear weapons in achieving some durable strategic military stability. No more was expected or hoped for. The bulk of the work was undertaken in the United States, with much of it being conducted in the Rand Corporation. The conclusion come to then was that stability would be achieved by the possession of an invulnerable retaliatory force capable at all times and in all circumstances of reaching vital targets in enemy territory. The technical implications for command and control, penetration of defensive systems and so on, were worked out in some detail. For such a system to be strategically stable it had to present the same characteristics to the Soviet Union as to the United States. Unfortunately for the subsequent history of the deployment of nuclear weapons, the implications of this analysis could not at the time be accepted and acted upon by either the US or Soviet governments.

The realization that stability depended on at least a measure of mutual understanding with the Soviet government, if not outright collaboration, came at the wrong time politically. The United States had for the first time been put on the defensive technically—and, it was held, militarily—by the 1957 Sputnik satellite. The emotional impact was reinforced by the realization that the continental United States could, for the first time, be vulnerable to attack by thermonuclear warheads carried on a rocket of a size and power that the United States could not hope to match for many years. Only the unique prestige of President Eisenhower prevented the immediate outbreak of an arms race. But the attempt to come to an understanding with the Soviet government was aborted in the May 1960 summit; the fiction of the missile gap became established and became an element in the 1960 presidential election. The Kennedy administration was committed to correcting it by installing a thousand Minuteman missiles, plus the Polaris programme, as well as retaining the land and seaborne bomber forces of Strategic Air Command (SAC) and the US Navy.

It was at this stage that things started to go wrong. The United States did not wish to give up what many of them saw as a still persisting or recoverable strategic superiority. That this was a dubious concept when the opponent possessed an invulnerable second strike capability was discounted. World peace had been assured by the United States' conscientious policies when they held a nuclear monopoly and this remained a desirable objective, albeit with monopoly diluted to superiority.

This might have been how it appeared to the United States, but the Russians were no more disposed to rely on the US conscience for their continued existence than they are today. Indeed, the Soviet objective throughout seems to be consistent. There is one theme which is never changed: the need to ensure that the United States (or NATO) does not achieve a strategic superiority which would once again require the Soviet Union to rely on United States restraint for her security. Of equal, if not greater importance is the Soviet government's insistence that the United States admit openly that this is indeed the case. Here we enter into the uncertainties of national psychologies. For whatever reason, be it some ingrained insecurity stemming understandably enough from their own history, or some feeling of continuing inferiority faced with western technical prowess, the Russians do not content themselves with basing their security on the objective reality itself but require this reality to be acknowledged by all.

Faced with the original US monopoly of nuclear weapons, albeit initially in small numbers, they developed their own weapons quickly; they combined this with an army capable of inflicting devastation on western Europe, which to the recipients might not appear all that different from a nuclear strike. The first Soviet missile force developed in strength consisted of 750 medium-range ballistic missiles (MRBMs) capable of reaching all of Germany and most of Europe. The British built up their V-bomber force to about 100 aircraft and the French took the decision under the Fourth Republic to use their existing atomic installations to build weapons.

Although the picture in western Europe must have been satisfactory to the Soviet government—there was no shortage of authoritative spokesmen saying that the Soviet MRBM force could devastate western Europe several times over—this was not the case for them *vis à vis* the

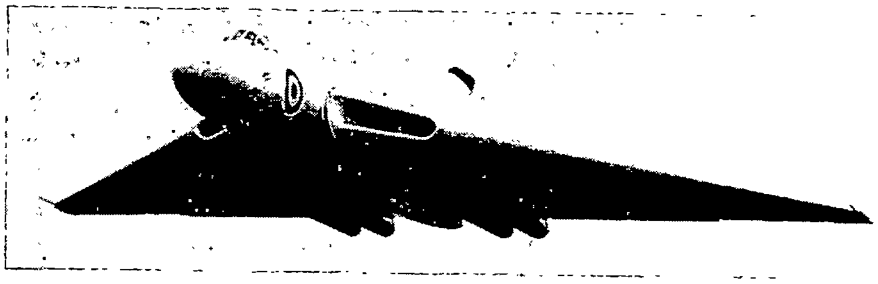

The British 'deterrent' in the form of the Avro Vulcan, as seen at the 1957 Farnborough air display (Photos: Popperfoto.)

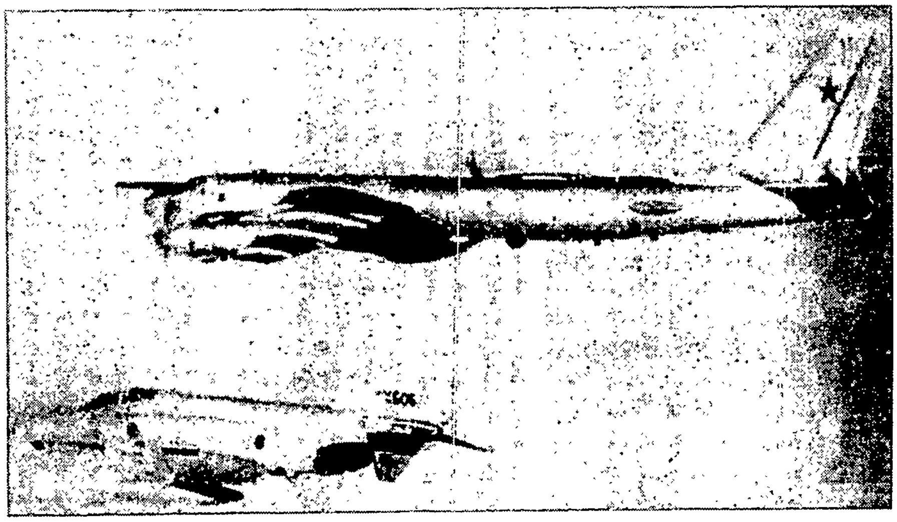

A South Korean airforce Phantom escorting a Soviet TU-95 ('Bear') in international air space over the Yellow Sea between China and Korea in 1985.

United States, which was beyond their range.

The first attempt to rectify this situation consisted in the construction of a small number of four-engined turbo-prop 'Bear' bombers. They were capable of reaching the continental United States, carrying a thermonuclear device. With this capability Kruschev, for one, believed that he had what we have come rather loosely to call a deterrent. For reasons we shall come to, he was of course quite right. But in the circumstances of the Sputnik and the alleged missile gap, this was an admission which the US government could not make; their public stance was that they were threatened by missiles measured in hundreds, not by subsonic bombers measured in tens. The United States had to catch up. With the announcement of the Minuteman programme of just over one thousand solid-fuelled missiles in hardened silos, the Russians in their turn had to catch up. (In terms of the classical analysis, the possession of a nuclear striking force more powerful than that needed to ensure an invulnerable retaliatory capability did not make strategic sense. Only if one believed that it was possible to eliminate the other side's nuclear forces, thus taking away his second-strike capacity, were there targets to aim at; and those days were over.)

Not long after the Kennedy inauguration, the deployment by the Soviet Union of long range liquid-fuelled intercontinental ballistic missiles (ICBM) in unprotected launch sites had started. Kruschev too thought he was or could soon be facing a missile gap and attempted in Cuba to reproduce in North America some of the characteristics of the situation in western Europe. What happened showed, amongst other things, the limitations in practice of the military effectiveness of nuclear weapons. Kruschev was deterred but the outcome was determined by the local application of a superior US conventional force in the established way.

The Cuban missile crisis brought home the need to establish some understanding between the nuclear powers on the role of nuclear weapons in order to avoid war by miscalculation or by accident. The partial nuclear test ban treaty was signed within a year and a secure 'hot-line' set up between Moscow and Washington. But still there was no formal admission of stalemate or of nuclear parity. Instead we saw the development of McNamara's strategy of 'flexible response'. This permitted the Americans, but obviously not the British or the French, to choose to hit only military targets in a retaliatory or second strike, while still keeping in being sufficient weapons to strike at civilian targets later if need be. This strategy was designed in McNamara's words to give 'a possible opponent the strongest imaginable incentive to refrain from striking our own cities'. In part, this approach was held to be an attempt to answer the question of what happened if deterrence were to fail. This has never been answered satisfactorily and probably never will be.

Unfortunately, and indeed understandably, it is unlikely that the Russians saw the resultant increase in weapon numbers in the same way. In their eyes the force being assembled could, with at least equal plausibility, be construed as an attempt to recreate that strategic superiority which the Soviet government still asserts to be the fundamental objective of US policy. Their reaction was to continue to increase their missile numbers until what they, themselves, would recognise as objective parity had been achieved. But one man's parity is to his opponent a threat of superiority. It is not surprising that the ageing lessons of the classical analysis—especially the sufficiency of an invulnerable second-strike capability for strategic stability—were deemed less relevant.

Successive attempts to achieve some stable and fixed level of nuclear weapons at above the tactical have by and large failed. How can one equate such technically diverse elements? Still more difficult, how does one secure the political reassurance needed when, in order to do so, one has to take into account such a wholly different mix of past history. Thus, technically the best invulnerable second strike platform is the submarine. To British and to American readers with a history frequently reaffirmed of naval success, this is an idea easy to assimilate and to act on. But to the Russians? A history of naval defeat and a geography of confined access to the open sea has made such a policy difficult to believe in the past, despite the technical arguments. By now of course the Soviet submarine-based missile force is established to a degree which many thought unlikely twenty years ago. Technically, the position becomes more difficult every day. At one stage it might have been possible to reach agreement on a limit on 'throw-weight' or the weight each side's striking force could deliver on to the other's territory. The concept had the advantage of flexibility; numbers of missiles alone did not determine the balance; national preferences could be taken into account, in for example the mix between, say, warheads and penetration aids. We have to face what would seem to be an intractable problem if we are still to attempt to define nuclear strike capacity in discrete numerical terms; some strategic delivery vehicles now have a dual role, with interchangeable nuclear and conventional war-heads. The latest is the Tomahawk submarine-launched cruise missile. Again the problem is not new; aircraft have always had a dual capacity and the attempt to verify the stockpile of aircraft-launchable nuclear weapons has always faced difficulties which have proved insurmountable.

Importance of uncertainty

It is at this stage that another look at one fundamental of the classical analysis is useful. In the discussions now in train we hear much less of an idea which was basic to it: the importance of uncertainty.

To the military, as well as in science, the one thing that can be counted on in the real world is uncertainty. The elder von Moltke told his sovereign that he should be reluctant to embark upon any military operation, even after the most careful calculation, because no one knew what might result. Science is full of uncertainty; the examples are endless. One hesitates also to advance the philosophical objections to certainty in the world of events, though one cannot help feeling that a reading of David Hume would reinforce further the experience of the military and the scientists, should that be necessary.

The fundamental point in the elaboration of any strategy or consistent body of ideas concerning the role of nuclear weapons is that it is uncertainty which, by inhibiting action, provides us with that stability we seek. In the language of classical nuclear deterrence, we can say that a government is deterred from an action if it cannot be certain that an opponent in possession of nuclear weapons cannot use them to inflict unacceptable damage. The crucial distinction is between those who seek the certain ability to inflict unacceptable damage and those who say that, given the power of the weapons in question, it is sufficient if the government contemplating military action cannot be certain that they cannot be used effectively against it. Returning to Kruschev and his free-fall thermonuclear weapons carried by aircraft, he was right to believe that a United States government, knowing that he controlled such a weapons system, would not use nuclear weapons against the Soviet Union.

What constitutes unacceptable damage has always been a matter of nice debate; it varies with circumstances and by being itself uncertain adds further to the basic stability of the nuclear situation. It is generally accepted that the loss of, say, twenty or fifty major cities in the United States or the Soviet Union in a bilateral exchange would qualify as unacceptable damage in any conceivable set of circumstances; arguably the largest number of nuclear strikes which would make strategic sense was calculated in the Pentagon in Mr McNamara's day to be four hundred of one megaton each. Above this level the incremental increase in effectiveness measured by the number of deaths likely to ensue falls away rapidly. For lesser military powers the objective can be more modest—their ability to destroy one major city in, say, the Soviet Union is likely to constitute unacceptable damage given that the nuclear striking power of the US would remain intact. China has sometimes been held to be a different case; at one stage the leadership apparently believed that alone of the major powers, China could survive an all-out nuclear attack in sufficient numbers to ensure that they won the ensuing war. This view did not long survive the Chinese construction of their own nuclear weapons. It might not have survived an examination of the results of the largest nuclear test ever conducted—the explosion in the atmosphere by the Soviet Union in 1961 of a clean thermonuclear device with a yield in excess of 50 megatons. If the device had been provided with a surrounding layer of natural uranium the yield would have been substantially increased, but more importantly so would the radioactive fallout. Such a weapon could conceivably just make sense if designed for use against a rural population; relatively few would be needed to produce so much fallout as to kill the bulk of the population in the rice-growing areas of China as well as their major cities.

The principle of uncertainty can be extended further. Much effort has been spent on trying to establish what it is that the possession of nuclear weapons with a delivery mechanism capable of reaching an opponent's homeland in fact deters him from doing. Clearly, there is a high probability that it deters him from using nuclear weapons against one's own homeland. But what else? McNamara has said recently that they are 'totally useless—except only to deter one's opponent from using them'. Given the implications of uncertainty, this could be too restrictive a view.

While it is logically possible that, despite its declared policy of doing so, NATO forces might not use nuclear weapons in defence of western Europe against a conventional attack, no certain reliance could be placed upon such an outcome. The posed threat of escalation is effective because no one can risk basing a course of military action on any *expectation* that escalation will not in the event happen; only certainty would do and that is not attainable. The uncertainty is increased when an evident mechanism for escalation is in place and is known to form part of the training of the armed forces stationed in the areas concerned. The Russians appear to share at least part of this view when they say that any conflict in western Europe is bound to become a nuclear conflict, and nuclear conflict is indivisible. Clear statements from the Soviet side are not all that easy to find, especially in the lucid and, we hope, logical form we like to expect in the West. Perhaps Kruschev said it all when he said in 1964: "Nuclear war is stupid, stupid, stupid! If you reach for the push button, you reach for suicide". Nevertheless, in 1969 the Soviet negotiators to the treaty banning unlimited antiballistic missile (ABM) deployment underwrote the principle of deterrence when they said: "Even in the event that one of the sides were the first to be subjected to attack, it would undoubtedly retain the ability to inflict a retaliatory strike of crushing power".

While their daunting power and uncertainty as to whether they might or might not be used makes military leaders pause as never before, they also find themselves faced with a situation on the ground that no responsible military commander can tolerate. Hitherto in war the prudent general has always had in his mind some way of recovering a situation should his well-laid plans go wrong. Nuclear weapons make such prudence untenable; once embarked upon, recovery is impossible. In more general terms we are justified in believing that a proper fear of the unknown future inhibits the possessors of nuclear weapons across a whole range of circumstances in their dealings with opponents who also possess these weapons.

The importance of uncertainty extends too to defensive systems, in particular to the point-defence systems subject to the control of the 1972 Anti-Ballistic Missile agreement between the USA and the Soviet Union, and now to the more ambitious proposals for the interception and destruction of incoming missiles by a system some of whose components would be stationed in outer space.

Relevance to SDI

The 1972 ABM Treaty and the associated SALT I agreements were made possible when both the US and Soviet governments became convinced that the defensive measures available to them, if deployed, would not alter the strategic balance but would accelerate the arms race. The agreement prohibited all but a limited deployment but permitted research. (The authors of the Treaty understood that research could not be restricted by agreement, the crucial difference here being between research designed to protect against one's opponent stealing a damaging march and research designed to lead to a forbidden deployment. The former used to be US policy in the ABM field; it is in danger with SDI of changing to the latter and, in the course of doing, so generating its own momentum towards deployment).

The issues posed by the SDI are similar in most respects to those posed by the ABM. The debate which led to the 1972 ABM Treaty limiting deployment of defensive systems and to the first agreement to place a limit on some strategic nuclear weapons established that the latter was not feasible without the former, and that any significant deployment of defensive systems would most probably have as its consequence an increase in the opposing side's offensive missiles. As it was then deemed that the cost of providing a quantum of defence was higher than the cost of providing the increase in striking force needed to render it strategically nugatory, it was concluded sensibly enough that everyone would be better off if any defensive deployment were to be strictly limited. At no stage did anyone advance any plausible argument to suggest that anything other than a point, as opposed to an area, defence was feasible. Technically the argument was—and is—that discrimination between incoming objects becomes sufficiently easy to permit the operation of some practical intercepting mechanism only when they re-enter the atmosphere. Outside the atmosphere, the argument goes, plastic balloon decoys behave in much the same way as warheads—and even more like warheads enclosed in plastic balloons. Thus an attack could be attenuated but not eliminated. While this could be held to be of some strategic value in protecting the fixed land-based missiles, it provided no solution to the problem of protecting populations. The one major respect in which the SDI differs from the

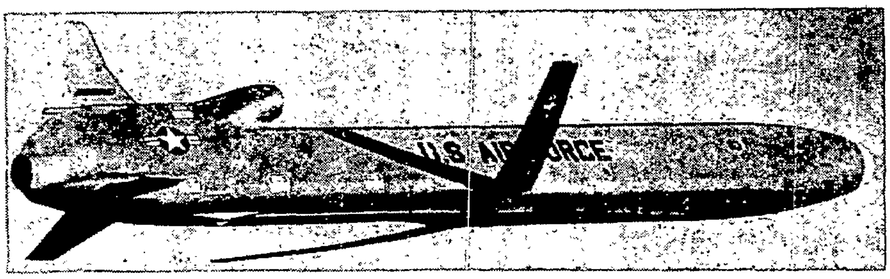

The US Navy's Tomahawk cruise missile under test at Dugway Proving Ground, Utah.

earlier ABM proposals lies in its emphasis on the attempt to destroy missiles in the boost phase, and thus offer some prospect of area defence. The technical arguments cannot be resolved on the basis of present knowledge but the relevance of uncertainty reasserts itself.

The crucial point in judging the relevance of SDI to the strategic situation we all now face is that any government seeking to base its policy on a defensive system and to discard retaliatory weapons must be certain amongst other things that at all times (including the most difficult—the first time) all incoming nuclear warheads directed at its cities will be destroyed. In an alliance it could be that the same criteria must be made to apply convincingly to its allies also.

Leaving aside the technical difficulties of believing this could ever be the case, we need to recall the possibility of countermeasures. Again we do not know on the basis of present knowledge how effective such measures might be; but they are unlikely all to be completely ineffective. It is calculated, for example, that the burn time for an MX type missile could be reduced from its present 120 seconds to some 60 seconds at a sacrifice of about 18 per cent of payload; there is the possibility of armouring or rotating to protect against beam attack; decoy 'boosters' might be ignited; and of course all equipment in space is easy to find and is vulnerable. Be that as it may, for as long as it is the case that the cost of overcoming a defence remains less than the cost of erecting one—and there is no evidence that the present relationship might be reversed—then the appropriate response to the SDI would not be to construct another SDI, but to increase the power of the offense. This would appear to be the policy of the Soviet government; the only unfamiliar component would be space-stationed weapons designed to destroy the spaceborne element of SDI. It is worth recording a Soviet statement made soon after President Reagan's announcement of the SDI. The following is an extract from an interview which Mr Andropov gave to Pravda on 27 March 1983.

> President Reagan has announced the beginning of work on a wide-scale and highly efficient anti-missile defence system. At first [illegible] this might sound attractive to the ill- [illegible] the President spoke only of what seemed to be defensive systems. This would, however, be a superficial impression emanating from those unfamiliar with these matters. In fact, the US would continue to develop its offensive strategic forces rapidly and with one end in view, that of acquiring a first strike nuclear capability. In such a situation, the intention of being able to destroy the other side's weapons by means of an anti-missile defence, and thus deprive it of its ability to make a retaliatory strike, is designed to disarm the Soviet Union in the face of an American nuclear threat. (Reprinted in translation in the *Speeches and Writings of Y. V. Andropov*, Pergamon, Oxford, 1983, p. 302).

Mr Gorbachev's views appear to be similar. Indeed immediately after the Geneva summit he made a point of saying that in the event of any likely deployment of space defence systems by the United States, the Soviet response would be effective, cheaper and quicker. He might have had in mind the updating of what many consider to have been the first fully effective Soviet weapons system capable of landing nuclear warheads on the continental United States, namely the placing of two short-range surface-to-surface missiles each armed with a 440 kiloton warhead on a diesel powered submarine capable of reaching the eastern US seaboard. There are other possibilities.

One of the many difficulties in dealing clearly with the arguments for the SDI is that they tend to change according to the proponent and the audience. President Reagan states that the objective of his SDI is indeed to render nuclear weapons impotent and obsolete by providing a perfect defence for the inhabitants of the territories of the United States and its allies. (Nuclear weapons cannot of course be eliminated; both because of the impossibility of accounting for and verifying existing stockpiles and because of the relative ease with which they may be manufactured by any nation with the necessary knowledge and skills at its command.) Others who share the doubts that such an objective is attainable, whether they argue in terms of uncertainty or otherwise, will speak in favour of the system on the grounds that it will produce some useful measure of additional protection for land-based missiles. Others who might well regard the fate of land-based missiles as being largely irrelevant to maintaining strategic stability, tend to be heard less.

Discussion in terms of only land-based missiles can obscure important issues. It permits one to talk of a 'window of vulnerability' which, starting from a consideration of US land-based missiles alone, is applied by extension to the strategic situation of the NATO alliance as a whole; the fact that for evident reasons the majority of NATO strategic weapons are seaborne tends to be overlooked. So too is the still formidable penetration power of a conventional manned bomber force, whether or not enhanced by the supersonic bomber or by aircraft designed to diminish their detection by radar. Neglected too in this equation is the ability of relatively cheap cruise missiles whether land or sea based to penetrate any foreseeable defences, let alone the existence of clandestinely delivered nuclear weapons strategy which even now probably cannot be proved not to be in place. Secretary of Defense Weinberger has put in a logically irrefutable bid for a massive anti-bomber defence system on the grounds that the SDI is effective only against a certain range of weapons. One awaits the bid for an expanded programme designed to offer assured defence against the cruise missile, land or sea based.

Be that as it may, if we believe that a government is deterred as long as it cannot be certain that its opponent's thermonuclear weapons cannot be delivered, it is not possible today to conceive of a situation where mutual nuclear deterrence can fail for technical reasons, and the margins of safety are considerable.

The political arguments

It would be wrong though to leave the analysis at the technical/strategic stage. The point of strategic stability can only be political. Fortunately, political considerations reinforce the stability created by the nature of nuclear weapons and the military immobility they induce. Instead of considering matters such as second strike capability and unacceptable damage and so on we have to face the more fundamental question of whether there can be any circumstances in which a government could believe that it would be better off as a result of initiating the use of nuclear weapons (or indeed other forms of military action) against a nuclear power or its allies. Given the risks involved, which stem from the power of the weapons themselves, it is difficult, indeed probably impossible, to devise such a political set of circumstances. To put the extreme case, what possibility of uncertain political gain could make a government believe it would be better off if, as a result of seeking to achieve that gain, it brought about the destruction of its own largest city? Or indeed even its own probable destruction? In practice no nuclear power would allow its ability to strike to be so limited; not one, but many cities would be at risk. The political arguments reinforce the military and technical ones to induce that state of paralysis which has helped preserve the peace for the last forty years.

Implications for allies

Although the basis of mutual nuclear deterrence between the United States and the Soviet Union will not be disturbed by the SDI the matter does not end there. The security of other nations is involved also. The debate is only now beginning, but two distinct though complementary points have emerged: the first suggests that any increase in protection that defensive systems could supply would also increase the probability that the United States would risk nuclear war in the nuclear defence of Europe. The second states that if both the US and the USSR were to be in a position to disregard one another's nuclear weapons as they affected their national territories, then this would increase, not diminish, the probability of a 'tactical' nuclear war in Europe, whose effects could hardly be distinguished by its inhabitants from all-out nuclear war. Using Soviet terminology, nuclear war would no longer be indivisible—and hence would be more likely. Europe would, it is argued, become a bull-ring for the superpowers. It is difficult to see how either argument can stand up to precise examination; although the hope has been held out that one day in some way the US, which must be taken to mean US cities, might be made invulnerable to a Soviet attack, this must remain a dubious proposition for the reasons gone into. These arguments too fall down on the impossibility ever of being able to remove the last element of uncertainty in any calculation as to whether the Russian nuclear force could, and in the event would penetrate US defences, and vice versa. Military planners in Europe and Japan and their political masters are, however, unlikely to see their problems so simply in this light. Any such development would be likely to lead to pressure towards a strengthening of national nuclear forces where they exist and to increasing pressures to create them where they do not. The more the Americans appeared to believe in the effectiveness of their defensive systems and thus tended to withdraw from a commitment to the nuclear defence of Europe, the greater the pressures for more and better national systems in Europe. The implications are incalculable but almost uniformly unpleasant.

Although unrealistic, the declared intention of the US President to render nuclear weapons impotent and obsolete, without, it would seem, thinking through the implications of achieving such a state of affairs, is not reassuring to Europe—strong though its appeal must be to American isolationists. Any move to restore the worlds of 1870, 1914, 1940 and 1941, when state power meant mass armies and where attacking first was held to be a basic rule of military prudence, would be deemed correctly to be reducing European security. It would, by opening the way again to blitzkrieg as a rational military option, mean replacing the present stalemate by one of a conflict in which for reasons of space as well as strength the Soviet Union would have the overwhelming advantage.

Neither are they likely to be reassured by undertakings to consult before deployment when they remember that they were not asked for their views on the proposal before it was first made public; or by any offer to use some of the best of their own scarce scientific resources on a project which for them is militarily useless and where any other advantage is likely to be slight—if only because of the US record and legislation on the sharing of technology.

Fortunately few of these are much more than debating points; they do not touch the vital issues of strategic stability, which will remain unaffected by SDI. However, unless there are agreements to limit the deployment of new and even more ingenious nuclear delivery systems and their defensive counterparts, we might well have to face up to further substantial expenditures which will nevertheless leave us strategically where we are now. Some might argue that it is this bringing to bear on the Soviet Union of further economic pressure and an increasing demand for scarce skills which forms the true basis of US policy; it is of evident concern to the Soviet government who can ill afford seeing these resources used in this way when there are so many other pressing demands upon them.

Whether that is the case or not, the fundamental facts remain the same now as they were at the time when classical nuclear strategy was first formulated; first, the most important characteristic of a nuclear weapon is its unprecedented power to destroy; and, second, no government can ever be sure that nuclear weapons cannot be exploded on its territory. As a consequence, governments are deterred from a whole range of military actions. We sit on our hands and call it peace—which indeed it is. □

John Wright, formerly on the staff of the Chief Scientific Adviser at the Ministry of Defence, is at 47 Brunswick Gardens, London W8.

REVIEW ARTICLE

Ocean variability in relation to living resources during the 1982–83 El Niño

Richard T. Barber & Francisco P. Chávez

Duke University, Beaufort, North Carolina 28516-9721, USA

Ocean/atmosphere perturbations that generate large-scale thermal anomalies in the Pacific are natural processes that cause significant variability in living resources. Analysis of the 1982–83 El Niño indicates that depression of the nutricline set in motion a decrease in productivity that eventually affected survival and reproduction at higher trophic levels. This impact, together with large-scale southward redistributions, accounted for most of the observed changes in the abundance of living resources.

EL NIÑO is the name given to a series of ocean and atmosphere changes that spread across the Pacific from Australia and Asia to South America, then move to the north and south so that the Americas are affected from Alaska to the tip of Chile[1,2]. Although El Niño originally referred to a warm surface current that flows southwards along the coast of Ecuador and northern Peru[1], the term El Niño is now applied to interannual episodes of anomalously warm water, high sea level, depressed thermocline and greatly increased rainfall that extend over most of eastern tropical Pacific Ocean. El Niño is one facet of a global process that is called the El Niño Southern Oscillation (ENSO) phenomenon. Philander[1] and Gill and Rasmusson[2] have recently described ENSO phenomenon paying particular attention to the severe 1982-83 El Niño. Here, we shall use their descriptions as a basis for understanding the effects of the 1982-83 anomaly on living resources of the eastern tropical Pacific Ocean. El Niño, through its impact on the global atmosphere and the low- and mid-latitude ocean, is a major natural process causing variability of living resources in the ocean. Some biological and economic consequences of the 1982-83 El Niño are well documented[3], but the widespread ecological impacts of this phenomenon are still not fully understood. When considering El Niño it is customary to refer to 'low latitude' effects, but reports of significant ecological changes in the high-latitude Southern Ocean indicate that ecological effects may extend far beyond the tropical ocean[4-6].

The coastal ocean off the west coast of South America is the most productive region of the world ocean[7]; this richness depends on coastal upwelling. Coastal upwelling is a circulation pattern that overrides both the nutrient limitation characteristic of warm, permanently-stratified waters, and the light limitation characteristic of deeply-mixed waters[8]. Coastal upwelling is set in motion by equatorwards winds that transport water offshore, resulting in water flowing up close to the coast to replace the water moved offshore. The subsurface waters of the ocean are cool and separated from the surface layer by a thermal gradient, or thermocline, below which the cool water is rich in inorganic plant nutrients such as nitrate, phosphate and silicate. Vertical transport of subsurface water provides continuous injection of new nutrients to the surface and the formation of a shallow wind-driven surface layer, which is vertically stabilized by a thermal gradient, provides optimal light conditions for primary production[9]. Productivity enhancement continues as long as winds are upwelling-favourable, so the annual primary production is much higher in low-latitude upwelling than it is in temperate or high-latitude ecosystems. Abundant phytoplankton are eaten by herbivores and, through grazing and predation, the abundant organic matter passes to zooplankton, fish, benthic animals, birds and marine mammals[9].

Among ocean phenomena affecting man, coastal upwelling has a relatively direct impact on the social fabric. Traditionally, it is stated[7] that upwelling regions, while comprising <1% of the ocean's surface, provide more than one-half of the protein collected from the sea. Whatever the proportion, a significant part of the world's fish catch is directly dependent on the physical processes of upwelling. This relationship is illustrated by comparison of the annual temperature anomaly off Peru with the annual catch of anchovy and sardine (Fig. 1). When the ocean is warmer than average the catch is reduced, indicating that warm anomalies such as El Niño are associated with reductions in the abundance of fish and other living resources. Using observations (Fig. 2) from the 1982-83 El Niño, we describe how this reduction takes place and speculate on the speed and nature of the ecosystem recovery.

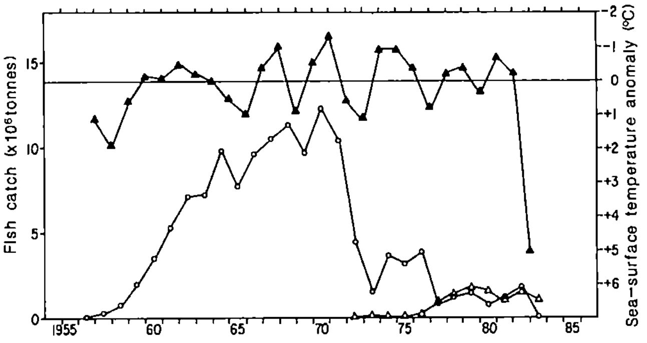

Fig. 1 Physical and biological coupling in the eastern tropical Pacific shown by the relationship between the annual anomaly of surface temperature and the annual catch of anchovy and sardine of Peru. The anomaly temperature scale is inverted: upwards indicates cooler temperatures; downwards indicates warmer temperatures (El Niño). The annual temperature anomaly is relative to the 26-yr mean temperature of 16.9 °C at Chicama. The anomaly is calculated for the Southern Hemisphere thermal year from July to June spanning half of 2 calendar years; the value is plotted in the middle of the thermal year at January. The fish catch for each calendar year is plotted in the middle of the calendar year at July. ▲, Anomaly; ○, anchovy; △, sardine. Updated from ref. 8.

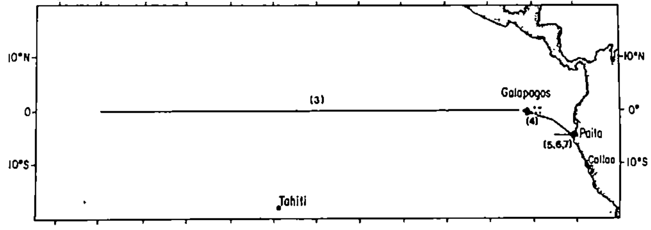

Fig. 2 Chart of the equatorial Pacific Ocean showing the transects and locations that provided our observations. The numbers in parentheses next to the transect or location show the results from that transect or location. Note that the equatorial transect leaves the Equator west of the Galapagos Islands and passes through 2° S and 85° W and ends at the coast of Peru at 5° S and 82° W.

Environmental setting

Coastal upwelling is a response of the ocean to local winds; in actual dimensions the winds at a specific site affect the ocean for a region as small as 50 km around that point[9]. However, the winds along the west coast of South America are part of the trade-wind system of the Pacific, so variations in coastal winds are related to changes in large-scale winds. Barnett[10] has shown that sea-surface temperature off the west coast of South America is best predicted by variations in the trade winds in the western Pacific, not from wind variations in the eastern Pacific where the upwelling actually takes place. The mechanism responsible for this dependence of temperature on remote winds is that the trade winds set up a basinwide east/west slope in sea level[11] and the thermal structure of the Pacific[12-14]. During normal conditions the persistent easterly trades exert a westwards frictional drag on the ocean resulting in the piling up of warm water in the western Pacific[11]. This dynamic accumulation of mass in the west produces a sea-level slope of ~0.5 m higher in the west and a thermocline slope of the order of 100 m with the west being deeper[12] (Fig. 3). This condition stores the potential energy to drive a rapid redistribution across the Pacific if the trade winds weaken or reverse.

The east/west slope that exists during normal trade-wind conditions brings the thermocline close to the surface of the ocean off the west coast of South America (Fig. 3). By controlling the depth of the thermocline, large-scale winds control the temperature of the water that feeds into the upwelling circulation because coastal upwelling entrains water from a relatively shallow depth of 40-80 m (ref. 9). The gradient separating nutrient-rich subsurface waters from nutrient-depleted surface waters is called the nutricline. The thermocline and nutricline in the eastern portion of the Pacific (Fig. 3) are much shallower than they are in the central or western Pacific because of the basinwide slope. Thus winds have two relatively separate connections to the coastal upwelling ecosystem: (1) they provide the local driving force for vertical transport; and (2) they set up the basinwide thermocline and nutricline slope that determines the temperature and nutrient content of the water that is entrained into the upwelling circulation. Obviously both local and large-scale winds of the Pacific must be favourable to provide the climatological mean conditions of high nutrient levels and high rates of biological productivity.

Analyses of coastal wind measurements in the past 5 yr have indicated that in previous El Niño events[15] and in the 1982-83

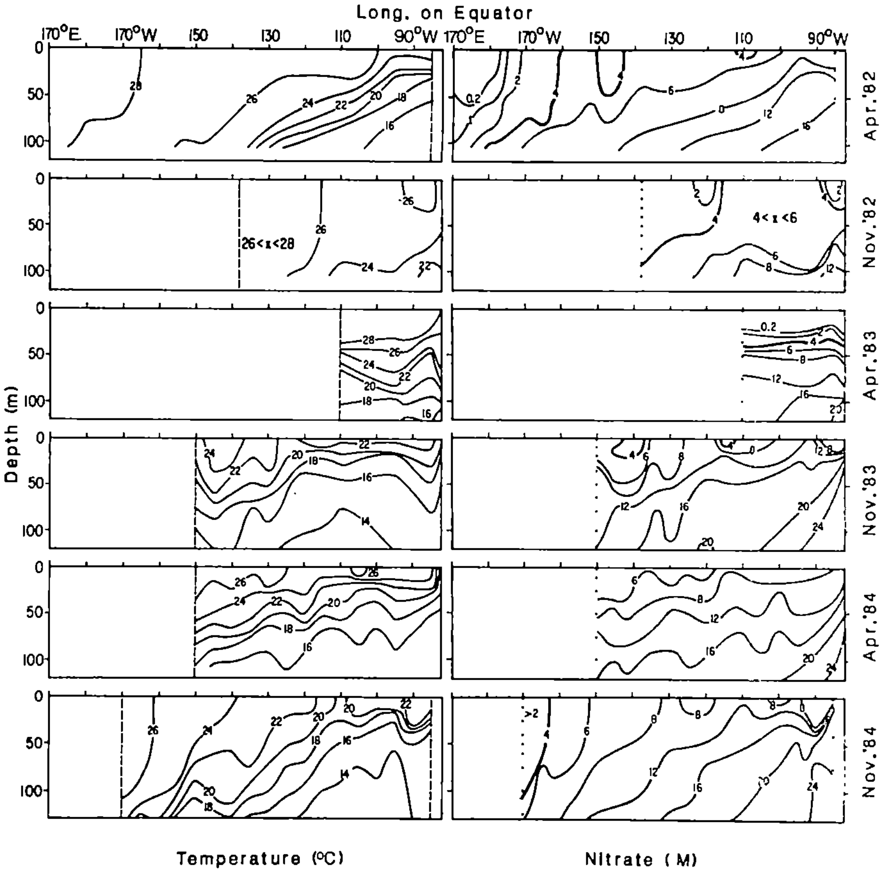

Fig. 3 Nitrate and temperature profiles on the equatorial transect (Fig. 1) showing changes in thermocline and nutricline tilt before, during and after the 1982-83 El Niño. Nitrate is presented as an indicator of the nutrient condition; parallel observations are available for phosphate, silicate and nitrite. Updated from ref. 14.

El Niño[16,17], the equatorwards winds driving coastal upwelling did not weaken. During the 1982-83 El Niño, coastal winds and locally forced upwelling appeared to continue through March 1983, but after November 1982 the surface waters had significantly reduced nutrients and increased temperature (Fig. 4). The explanation of these changes that occurred during local upwelling was that the thermocline and nutricline were progressively depressed below the depth where source water was entrained into the upwelling circulation (40-80 m). Figure 3 shows the large-scale thermocline and nutricline topography for April and November of 1982, 1983 and 1984. In November 1982, the thermocline and nutricline were clearly depressed and by April 1983 the characteristic east/west slope had gone[18]. Figure 4 shows day-by-day changes in temperature and nitrate at an ocean station in the Galapagos Islands (at ~ long. 90° W in Fig. 4) in late 1982 and 1983. The elevated ocean temperatures that delineate El Niño are clearly associated with a reduction in surface nitrate. The surprising conclusion from these observations is that nutricline depression, not cessation of upwelling, is the process that initially reduces the nutrient supply to the surface layer. This reduction caused primary production to decrease and eventually affected the higher trophic levels of the equatorial and coastal upwelling ecosystems. Upwelling ecosystems are therefore vulnerable to remote ocean/atmosphere perturbations such as the trade-wind anomalies that characterize El Niño Southern Oscillation phenomena[1-3].

Progression of the 1982-83 event

The 1982-83 El Niño reached the Galapagos Islands in August 1982 (ref. 19) and the coast of Peru at 5° S in late September 1982 (ref. 20). Figure 4 shows the progression of changes in temperature and nitrate at the surface and at 60-m at an ocean station in the Galapagos Islands. The transition phases of onset in September 1982 and recovery in June 1983 are best delineated in the temperature changes at 60-m. The variation in nitrate (Fig. 4) shows that El Niño enormously reduced the surface nutrient concentration. At the beginning and end of the time series shown in Fig. 4, surface nitrate values were 4-6 μM. The large-scale zonal profiles of nitrate shown in Fig. 3 show that this concentration range is the mean condition for the region during normal or non-El Niño conditions.

The relationship between phytoplankton growth and ambient nutrient concentration is complex[21,22], but for understanding the ecological impact of El Niño it is adequate to know that

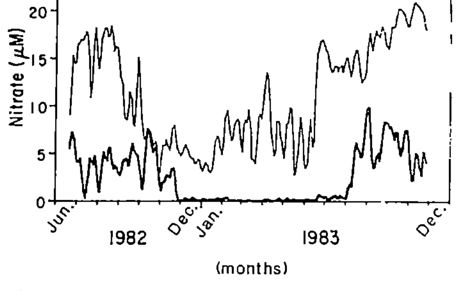

Fig. 4 Time series of triweekly observations of *a*, temperature and *b*, nitrate made during the 1982-83 El Niño on Santa Cruz Island in the Galapagos Islands. Bold line, 0 m; lighter line, 60 m.

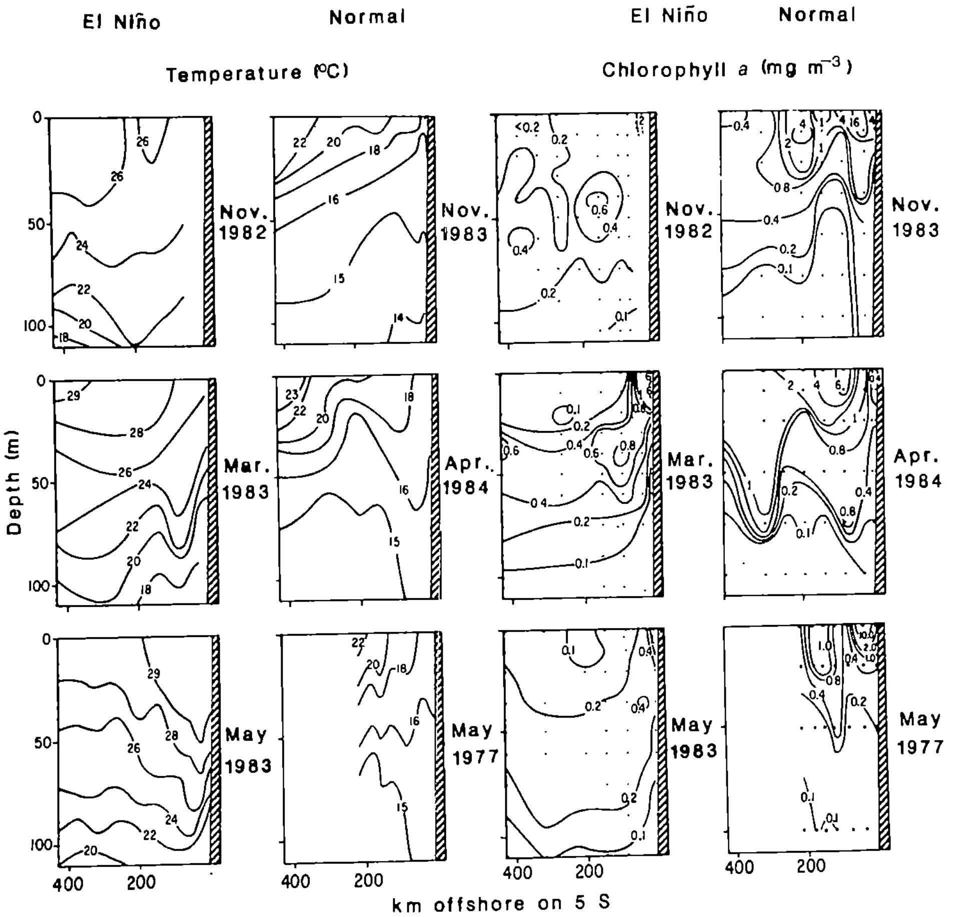

Fig. 5 Cross-shelf profiles of temperature and chlorophyll along a transect at 5° S from 85° W to the coast of Peru. The sequence shows conditions during onset (November 1982); maturation (March 1983) and the peak (May 1983) of the 1982-83 El Niño and compares the anomalous conditions with observations made during November 1983, April 1984 and May 1977 when no thermal anomaly was present. Modified from ref. 8.

nitrate concentrations of ≥2 μM constitute favourable nutrient conditions where the uptake versus concentration relationship is saturated. Figures 3 and 4 show that, in the absence of El Niño, the equatorial and coastal waters of the eastern tropical Pacific are nutrient rich; that is, they contain saturating concentrations of nitrate in the surface layer. In contrast, during the 1982-83 El Niño the surface concentration of nitrate for six and a half months, from December 1982 to mid-June 1983, was very low, often below the detection limit of 0.02 μM. Such concentrations are clearly nutrient-poor and will decrease the rate and quantity of new primary production by phytoplankton[23]. The progression of changes in nitrate is parallelled by changes in phosphate and silicate; see ref. 18.

The November 1982 section at 5° S on the coast of Peru was sampled during onset of El Niño (Fig. 5), but the temperature anomaly had already reached 5 °C by this time and thermocline and nutricline depression were evident. The 20 °C isotherm, which is the middle of the thermocline, is depressed over 100 m close to the coast when compared with the section made in November 1983 (Fig. 5). Comparison of the surface temperature along the 5° S transect during November 1982 and November 1983 (Fig. 6) shows that the offshore to inshore temperature gradient was similar in magnitude even though the entire section is 5 °C warmer during November 1982. The persistence of this onshore/offshore gradient indicates that upwelling continued close to the coast supplying the inshore waters band next to the coast with nutrients. During November 1982 the high phytoplankton biomass zone, defined by the 1 mg m^{-3} chlorophyll contour extended only ~30 km out from the coast; after recovery in November 1983 the high chlorophyll zone extended ~150 km from the coast (Fig. 5). There was an inshore productivity maximum present in November 1982, but productivity integrated across the 5° S transect from the coast to 85° W was much reduced (Fig. 6). The mean surface productivity along the transect during November 1982 was 51 mgC m^{-3} day^{-1}, whereas during November 1983 the average was 192 mgC m^{-3} day^{-1}, or 3.8 times higher.

In March 1983, the thermocline was slightly shallower along the 5° S transect than it was during onset phase (Fig. 5) and coastal upwelling continued as shown by the upward tilt in the isotherms close to the coast and the continued presence of the offshore-to-inshore temperature gradient of ~3 °C (Fig. 6). High chlorophyll concentrations in March 1983 were restricted to a 30-km wide zone next to the coast; after recovery in April 1984 the zone of high chlorophyll and high primary productivity extended 400 km from the coast. In March 1983, the mean surface primary productivity along the 5° S transect was reduced to 27 mgC m^{-3} day^{-1}, or 9.2 times higher than the El Niño conditions.

May 1983 showed maximum expression of the biological and physical anomalies of the 1982-83 El Niño (Fig. 7). The surface temperature anomalies reached 10 °C and the middle of the thermocline was depressed below 100 m (Fig. 5). During May 1983 the isotherms tilted downwards towards the coast, indicating onshore and poleward flow in the eastern boundary region rather than coastal upwelling. A comparable section in May 1977 showed the upward tilt typical of coastal upwelling with offshore and equatorwards flow. The chlorophyll distribution in May 1983 shows that the normally rich coastal ocean has changed to a relatively barren condition characteristic of a low latitude gyre, including even the narrow 30-km inshore zone of high chlorophyll water. However, by July 1983 (Fig. 6) a rapid recovery of normal upwelling resulted in the return of high phytoplankton productivity and biomass in the nearshore zone along the entire coast of Peru. During May 1983, the mean surface primary productivity along 5° S dropped to 10 mgC m^{-3} day^{-1}, during July 1983 it was 219 mgC m^{-3} day^{-1}, a value 21.3 × higher than the El Niño condition. At the peak of the anomaly primary production in coastal waters was reduced to 5% of the quantity observed during non-El Niño conditions.

Effects on living resources

Large-scale and persistent changes in sea-surface temperature along the coast of Peru are well known because the warm anomalies have been associated with changes in the abundance of the Peruvian anchovy (Fig. 1). Early workers studying the effects of El Niño on fish and sea birds, particularly the Peruvian scientists who are most familiar with the phenomenon[24,25], believed that reductions were caused by reproductive failures resulting from disruption of the normal upwelling food chain; observations of nutrients and primary production during the 1982-83 El Niño confirm this connection. It seems logical that 4-20-fold reduction in productivity and biomass of phytoplankton would decrease the growth, survival and reproductive success of these organisms, but there are opposing views on the effect of El Niño on living resources. A decade ago it was suggested[26] that anchovies simply swam away to deeper, cooler water during the anomaly, and it was predicted in 1972 that the fish would return to the Peruvian coastal waters when the thermal anomaly ended; Fig. 1 shows that this prediction was not correct. After the warm anomalies of 1972 and 1976 anchovies did not return to their previous level of abundance and the catch became lower and lower.

These observations suggest that for some of the commercially important species of the upwelling ecosystem a major effect of El Niño is an absolute decrease in growth and reproduction; that is, the total productivity of the region was reduced, not simply rearranged in space along the coast. However, some dramatic large-scale redistributions of certain species of invertebrates and fish were observed during the 1982-83 event and it is important to consider both processes.

Redistribution is an accurate description of the response of hake (*Merluccius gayi*) to the 1982-83 El Niño. Fishermen report that the relatively large and motile bottom-dwelling hake moved down the continental slope, staying with the cool water to which it is adapted. Comparison of Fig. 5 with Fig. 7 shows that when the 16 °C isotherm was depressed to a depth of several hundred metres (November 1982), hake disappeared from the catch off northern Peru. The fishermen also indicate that in addition to going deeper hake moved or were transported southward[27]. The stronger than average polewards flow of the Peru/Chile undercurrent[16] may have been involved in this movement. It is not clear whether there was a temperature-mediated migration by hake southwards in response to the warm water or whether this and other species were passively transported by the strong southward flows in both surface[28] and subsurface currents[16]. Hake were the first fish to leave the northern Peru region but the last to return. In this context, it is clear that hake did not return as soon as the physical conditions in their habitat returned to normal. By November 1983 temperature conditions in the shelf and shelf-break environment had returned to normal (Fig. 5), but despite continued fishing effort, significant catches of hake did not resume until January 1984 (Fig. 7). The hake yield in late 1984 at northern Peru was high[27], suggesting that the fish returned in both large numbers and relatively good physiological condition.

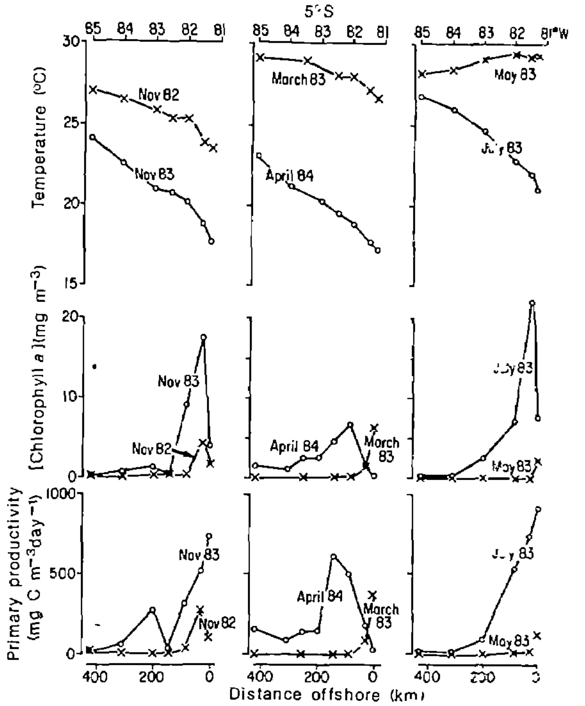

Fig. 6 Surface temperature, chlorophyll and primary production along 5° S from 85° W to the coast of Peru showing the comparison between El Niño (November 1982, March 1983 and May 1983) conditions and conditions during November 1983, April 1984 and July 1983 when no thermal anomaly was present.

The increase in shrimp catches at Paita (Fig. 7) is an accurate index of changes in abundance that occurred throughout the region from Colombia to Peru[29]. The catch of the three major species of shrimp (*Xiphopenaeus riueti, Penaeus occidentalis* and *Trachypenaeus byesi*) did not change on the Pacific coast of Colombia from January to September 1982 but decreased in the last three months of that year. The shrimp harvest along the coast of Ecuador increased greatly during the first half of 1983 (ref. 29) and the catch in northern Peru, which is usually very low[30], began to increase as the temperature increased from November 1982 to February 1983 (Fig. 7). The southwards progression of shrimp abundance probably resulted from their partially planktonic character. That is, shrimp may have been carried southward by the nearshore current that is historically associated with El Niño[31]. It is unlikely that the southwards redistribution was the result of an organized behavioural migration because penaeid shrimp are relatively weak swimmers.

The scallop *Argopecten purpuratus* underwent a rapid increase in abundance during the anomaly; in 1983 the harvest of scallops increased 40-fold to ~20,000 tonnes (ref. 32). By January 1984, the population increase was over and the abundance had returned to its previous level[32]. Scallops are common permanent residents in the inshore waters of Peru, so the increase did not necessarily result from migration or transport. Adult scallops are sessile and their planktonic larvae are not thought to survive long distance transport, so it is hypothesized that the extraordinary population increase resulted from *in situ* increases in growth and reproduction. Positive effects from the elevated temperatures that may have contributed to the population increase are: (1) faster maturation of the adults; (2) faster larval development causing reduced dispersion of the planktonic stages; (3) reduction of predators; and (4) faster maturation of the juvenile scallops after they settle out of the plankton. Because a generation of scallops requires from 4 to 8 months in most favourable conditions this increase was apparently the result of one or two generations of scallops that enjoyed extremely high reproductive success and then found excellent growing conditions. Although there was a general decrease in the abundance of phytoplankton food in the region (Fig. 6), the quantity of phytoplankton available during the anomaly must have been adequate for rapid growth and successful reproduction. An inshore maximum of chlorophyll and primary production persisted along the Peru coast even at the peak of the anomaly in May 1983 (see Fig. 6). Another species of the genus *Argopecten*[11] showed a saturation in the growth rate at 28 °C requiring a chlorophyll concentration of 2.4 mg m^{-3}; the Peruvian scallop beds contained chlorophyll concentrations in this range in February 1983[34]. Although the phytoplankton biomass was reduced from the climatological mean, it remained high enough in the nearshore waters to support a dramatic, but very shortlived, population increase in this species.

Jack mackerel (*Trachurus symmetricus*) disappeared from the catch in the Paita region in December 1982 (Fig. 7) between the periods that hake and sardine disappeared from the catch.

This timing is closely connected to the progression of physical changes in the habitats of these three species. Jack mackerel normally occupy the offshore half of the coastal upwelling ecosystem where their euphausid food is most abundant[8]. The warm (>26 °C) water present in the outer 300 km during November 1982 (Fig. 5) concentrated jack mackerel in the inner 100 km even during onset. Oceanic predators in the form of bonito (*Sarda chiliensis*), dorado (*Coryphaena hippurus*) and yellowfin tuna (*Thunnus albacores*) became much more abundant during onset of the 1982-83 El Niño[30]. Increased predation on the concentrated jack mackerel by both man and natural predators must have contributed to the reduction in abundance December 1982 in northern Peru, but this species also apparently widened its latitudinal distribution to both the north and the south. The catch of jack mackerel off Chile decreased from 1.5 million tonnes in 1982 to 0.8 million tonnes in 1983. In late 1983, jack mackerel returned in relatively large number to the northern Peru region (Fig. 7) and in 1984 catch off Peru and Chile returned to the pre-Niño level[35]. The fish were reported to have relatively normal length-weight relationships indicating that jack mackerel dispersed to areas of favourable food conditions. Clearly, this species has a remarkable ability to survive even a very severe El Niño.

In 1983, the sardine (*Sardinops sagax*) decreased almost to zero in the Ecuadorian catch, decreased slightly in the Peruvian catch (Fig. 1) and increased in the Chilean catch, indicating a southwards shift of the population[35,36]. Despite this large-scale southward shift, the maintenance of relatively high levels of sardine abundance off northern Peru throughout March 1983 (Fig. 7) was consistent with environmental conditions revealed by cross-shelf profiles (Fig. 5). During the November 1982 to March 1983 period sardines remained in the narrowing band along the coast where chlorophyll concentrations were $>1\ \mathrm{mg\,m^{-3}}$. Chlorophyll is an index of phytoplankton abundance, but because phytoplankton are the major food of zooplankton, chlorophyll concentration can also delimit habitat where both zooplankton and phytoplankton are abundant. In addition, stomach content analyses carried out in Paita in 1983 showed that 47% of the material in sardine stomachs was phytoplankton and 40% was zooplankton. These observations suggest that chlorophyll concentration is an approximate index of habitats that are favourable to sardines.

As adult sardines concentrated in the nearshore region they were easily caught, but reduction of their oil content to <1% by weight and reduction in individual body weight by 20% (ref. 36) indicated that their nutritional condition was decreasing. By April 1983 (Fig. 7), sardines disappeared from the Paita region and the May 1983 profiles show that water with $>1\ \mathrm{mg\,m^{-3}}$ chlorophyll was virtually eliminated from the region and primary production was reduced 20-fold (Fig. 6). The reduction in sardine catch at Paita in May 1983 was indicative of the reduction that occurred along the entire coast of Peru[36] during that period and Fig. 1 shows that the catch for all of 1983 was also reduced.

The most dramatic biological effect of the 1982-83 El Niño was on the Peruvian anchovy (*Engraulis ringens*), once the basis of the world's largest fishery[24,25]. Figure 1 shows the covariation of thermal anomalies and anchovy catch; we suggest that this correlation reflects a causal relationship that depends on changes in the large-scale thermal and nutrient dynamics that take place during El Niño in the Pacific. Depressing the nutricline (Fig. 3) makes nutrient conditions less favourable (Fig. 4) for phytoplankton primary production. The 20-fold decrease in phytoplankton production that occurred during the peak of the anomaly in 1983 necessarily decreased growth, survival and reproductive success of the anchovy. Growth and survival were affected because adult anchovy feed, in part, directly on phytoplankton[38]. Because larval survival is a function of the abundance and type of phytoplankton food[37], reproductive success was especially reduced in the 1982-83 event[36]. Taken together,

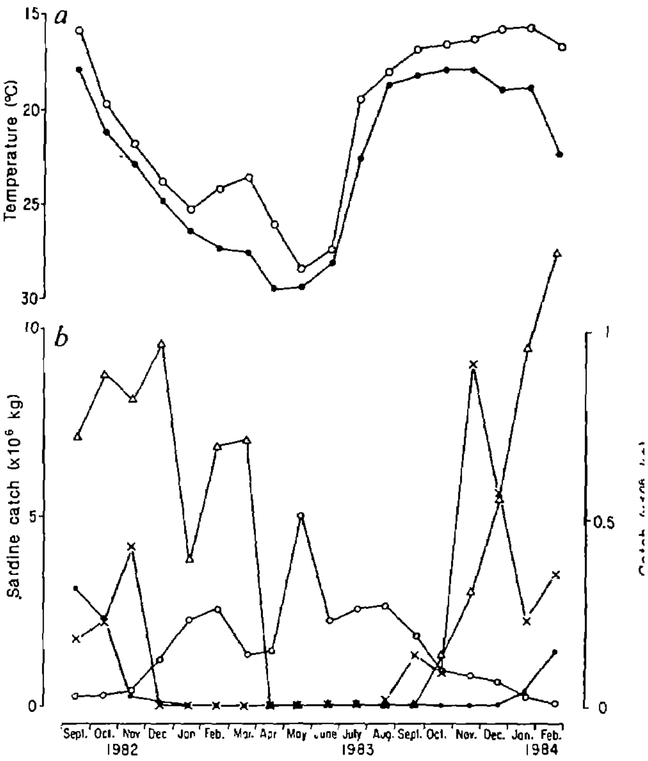

Fig. 7 *a*, Monthly mean surface (●) and 60-m (○) temperatures at an ocean station off Paita, Peru (5° S). *b*, Monthly landings of sardine (△), jack mackerel (×), hake (●) and shrimp (○) at Paita. Updated from ref. 8.

these larval and adult processes reduced the anchovy stock t record low levels during the 1982-83 El Niño. The catch in 198 was 118,000 tonnes <1% of the catch of a decade ago (Fig. 1)

Of the important fish stocks in this region (hake, mackerel jack mackerel, sardine and anchovy), anchovy experienced th greatest mortality during the 1982-83 El Niño. This vulnerabilit can be explained in general terms if the anchovy is the specie best adapted to the high biological productivity of coastal upwel ling. Being best adapted to high productivity, it is the specie most affected by a reduction in the productivity. The vulnerabil ity can also be explained in terms of a specific behavioura mechanism of anchovy. Anchovy seek out and remain in rela tively cool water of 16-18 °C (ref. 38). During normal condition this behaviour leads anchovy to the portion of the coasta upwelling ecosystem where phytoplankton are most abundan (see the location of the chlorophyll maximum in Fig. 6). Durin onset of El Niño this behaviour causes anchovy to concentrat in the persistent inshore upwelling; the distribution of thes relatively cooler centres along the coast as late as February an March 1983 was shown by Smith and Huyer[16]. Concentratio in these upwelling centres is adaptive behaviour if the El Niñ is weak or does not fully develop, as was the case in 1975 (ref 39); but during a very strong El Niño this behaviour makes th persistent upwelling centres traps for anchovy. As the 1982-8 event progressed, anchovy that concentrated[36] in the upwellin centres were surrounded by warmer water on three sides an land on the fourth side. At this stage in the development of th anomaly, temperature-mediated behaviour was unable to lea the fish out of the upwelling pockets to more favourable habita When the cool pockets were eliminated by alongshore or onshor flow large numbers of anchovies perished[8].

An indication of the severity of nutritional stress on th Peruvian anchovy was seen in the effects of the 1982-83 El Niñ on the northern anchovy (*Engraulis mordax*) off Californi where expression of the anomaly was similar to that off Sout America, but considerably weaker. Off California, there wer thermocline anomalies[40], reversal of flow to a poleward direction[41] and reduced phytoplankton and primary production[42,43]. Analysis of the response of northern anchovy[44] to the anomaly showed that: (1) body weight of spawning females was very low in 1983-84; (2) spawning occurred at smaller sizes than ever before observed; (3) growth of juveniles was 36% less than previous years; and (4) the spawning biomass was the lowest since 1962. Because the reduction in plankton biomass and productivity was proportionally much greater in the habitat of the Peruvian anchovy, the increased reproductive failure and adult mortality off America is not surprising.

Abrupt changes in the dominance of pelagic fish stocks after decades of apparent stability have long been unexplained[46]. Steele and Henderson[47] explained such changes by using a population model with multiple equilibrium states and subjecting the model to environmental variability that increased in variance per unit frequency as periodicity increased from years to decades. The extreme variance of 1982-83 El Niño is a classic example of the reality of the environmental assumption used by Steele and Henderson[47], but El Niño and longer-term climate anomalies have always been part of anchovy's environment. A dominance shift as a result of the 1982-83 El Niño would provide evidence that fish stocks are more vulnerable to environmental variability when they are heavily exploited.

Since the end of the 1982-83 event, environmental conditions in the coastal upwelling ecosystem and phytoplankton productivity have returned to normal (Fig. 6). Indeed, the levels of primary production observed in July 1983, November 1983 and April 1984 were among the highest observed in 19 yr along the Peru coast[9]. The resilience of the species that are major living resources in the region affected by the 1982-83 El Niño is made more interesting by the rapid return of very high levels of phytoplankton productivity. Visual observations made on a March 1985 cruise and reports from fishermen indicate that relatively large adult anchovies are once again abundant in certain locations along the coast. These reports suggest anchovy possess considerable resilience to El Niño even when heavily exploited. In this context, anchovy appears to be the species best adapted to the alternating El Niño/upwelling cycle; the enormous reproductive capacity of this species[24,25,38] enables it to recolonize the upwelling ecosystem faster than other pelagic fish after a very severe anomaly. Although the evidence is incomplete, there are indications that the living resources along the west coast of South America are in the process of rapidly recovering from the 1982-83 El Niño.

This research was supported in part by NSF grant OCE-8110702. Information on monthly fish catch at Paita was provided by Instituto del Mar del Peru. We thank colleagues in Peru, Ecuador and Chile for providing data.

1. Philander, S. G. H. *Nature* **302**, 295-301 (1983).
2. Gill, A. E. & Rasmusson, E. M. *Nature* **306**, 229-234 (1983).
3. Rasmusson, E. M. *Am. Scient.* **73**, 168-177 (1985).
4. Wormuth, J. H. & Berkowitz, S. P. *Eos* **65**, 922 (1984).
5. Shulenberger, E. & Loeb, V. J. *Eos* **65**, 922 (1984).
6. Heywood, R. B., Everson I. & Pridle, J. *Deep-Sea Res.* **32**, 369-378 (1985).
7. Ryther, J. H. *Science* **166**, 72-76 (1969).
8. Barber, R. T. & Chavez, F. P. *Science* **222**, 1203-1210 (1983).
9. Barber, R. T. & Smith, R. L. in *Analysis of Marine Ecosystems* (ed. Longhurst, A. R.) 31-68 (Academic, New York, 1981).
10. Barnett, T. P. *J. phys. Oceanogr.* **11**, 1043-1058 (1981).
11. Wyrtki, K. J. *J. phys. Oceanogr.* **5**, 572-584 (1975); *J. geophys. Res.* **89**, 10419-10424 (1984).
12. Mangum, L. J. & Hayes, S. P. *J. geophys. Res.* **89**, 10441-10449 (1984).
13. Cane, M. A. *Science* **222**, 1189-1195 (1983).
14. Rasmusson, E. M. & Wallace, *J. M. Science* **222**, 1195-1202 (1983).
15. Enfleld, D. B. *J. geophys. Res.* **86**, 2005-2016 (1981).
16. Smith, R. L. *Science* **221**, 1397-1399 (1983).
17. Smith, R. L. & Huyer, A. *Trop. Ocean-Atmos. Newslett.* **21**, 28-29 (1983).
18. Barber, R. T., Kogelschatz, J. E., Chavez, F. P. & Thayer, V. G. in *El Nino Atlas 1982-1983* (eds Leetma, A. & Witte, J.) 149-155 (US Government Printing Office, Atlanta, 1984).
19. Lukas, R., Hayes, S. P. & Wyrtki, K. *J. geophys. Res.* **89**, 10425-10430 (1984).
20. Chavez, F. P., Barber, R. T. & Soldi S., H. *Nature* **309**, 47-49 (1984).
21. Dugdale, R. C. Jones, B. H., Jr, MacIsaac, J. J. & Goering, J. J. *Can. Bull. Fish. Aquat. Sci.* **210**, 234-250 (1981).
22. Eppley, R. W. *Can. Bull. Fish. aquat. Sci.* **210**, 251-263 (1981).
23. Dugdale, R. C. *Limnol. Oceanogr.* **12**, 685-695 (1967).
24. Guillen, O., Calienes, R. & Izaguirre de Rondan, R. *Bol. Inst. Mar Peru* **2**, 49-76 (1969).
25. Valdiva G., J. E. *Rapp. P. V. Reun. Cons. int. Explor. Mer* **173**, 196-202 (1978)
26. Murphy, G. T. *Geoforum* **11**, 63-71 (1972).
27. Arntz, W. E. *Oceanus* **27**, 36-39 (1984).
28. Castillo, R. *Estudio Regl Fenummon El Niño Bol.* **12**, 3-5 (1985).
28. Halpern, D., Leetma, A., Hansen, D. & Philander, G. *Science* **221**, 1173 1174 (1983)
29. Herdson, D. *Trop. Ocean-Atmos. Newslett.* **28**, 14-16 (1984).
30. Velez, J., Zeballos, J. & Mendez, M. *Trop. Ocean-Atmos. Newslett* **28**, 10-12 (1984)
31. Eguiguren, V. *Bol. Soc. Geogr. Lima* **4**, 241-258 (1894).
32. Wolff, M. *Trop. Ocean-Atmos. Newslett.* **28**, 8-9 (1984).
33. Kirby-Smith, W. W. & Barber, R. T. *Aquaculture* **3**, 135-145 (1974).
34. Barber, R. T. & Kogelschatz, J. E. *Data Rep. of WECOMA Cruises WFLOC 83-2 and 83 3* (Duke University, Beaufort, USA)
35. Avaria, S. *Estudio Regl Fenummon El Niño Bol.* **13**, 17-25 (1985).
36. Santander, H. & Zuzunaga, J. *Trop. Ocean-Atmos. Newslett.* **28**, 9-10 (1984)
37. Lasker, R. *Fish. Bull.* **73**, 453-462 (1975).
38. Jordan, R. *Invest. Pesq.* **35**, 113-126 (1971).
39. Cowles, T. J., Barber, R. T. & Guillen, O. *Science* **195**, 285-287 (1977).
40. Simpson, J. J. *Geophys. Res. Lett.* **10**, 937-940 (1983).
41. Lynn, R. *J. geophys. Res. Lett.* **10**, 1093-1095 (1983).
42. Fieldler, P. C. *Science* **224**, 1251-1254 (1984).
43. McGowan, J. A. *Trop. Ocean-Atmos. Newslett.* **21**, 23 (1983).
44. Fiedler, P. C. *CalCOFI Rep.* **25**, 53-58 (1984).
45. Fiedler, P. C. & Hewitt, R. P. *Eos* **65**, 910 (1984).
46. Steele, J. H. *Nature* **313**, 355-358 (1985).
47. Steele, J. H. & Henderson, E. W. *Science* **224**, 985-987 (1984).

ARTICLES

Global resonances in the evolution of solar magnetic fields

J. O. Stenflo & M. Vogel

Institute of Astronomy, ETH-Zentrum, CH-8092 Zurich, Switzerland

Decomposition of the pattern of solar magnetic fields in spherical harmonics for a data set of 25 years and power spectrum analysis of the harmonic coefficients reveals a strikingly resonant modal structure. The resonance frequencies contain information on the structure of the magnetic fields in the Sun's interior.

THE remarkably rich spectrum of acoustic global oscillations of the Sun with periods around 5 min (refs 1, 2) demonstrates how an apparently chaotic body in a highly turbulent state can exhibit extremely well-defined resonant behaviour. Exploration of the resonance frequencies allows a determination of the internal structure of the Sun[2].

Such resonances naturally result in any closed system, when perturbations around an equilibrium can be described by a wave equation. A spherical system like a star or an atom forms closed cavities in which the waves can interfere constructively or destructively. This leads in the case of the de Broglie waves in the atoms to the resonant structure exhibited by atomic spectra. Analysis of such spectra allows the internal structure of matter to be determined. Analogously, the acoustic waves in the Sun give rise to the p-mode oscillation spectrum. Because the orthogonal functions used to describe the eigenmodes in spherical geometry are the spherical harmonics, characterized by the n, l and m quantum numbers, the classification of both stellar and atomic modes is in terms of these numbers.

In the case of the Sun, the wave equation describes how the perturbation of the equilibrium state tends to be restored under the action of a force. When the restoring force is the pressure force, the spectrum of p-mode oscillations results. When the restoration is done by the gravity force, another spectrum is obtained. Attempts have been made to observe this g-mode spectrum[3-5], which has oscillation periods of the order of 1 h or longer, but the g modes have not yet been definitely identified empirically.

There is a third force on the Sun that has not yet been invoked in this connection: the electromagnetic force. If, for instance, waves of hydromagnetic nature (such as dynamo waves) could interfere constructively and destructively globally in the Sun, a third type of resonant spectrum could result. The expected resonance periods depend on the strength and depth distribution of the magnetic fields inside the Sun, but, as we shall see, crude estimates indicate periods much longer than those of the p or g modes, typically in the range of years.

Sunspot magnetic polarities vary with a magnetic cycle of 22 yr, a cycle that the polarities of the polar magnetic fields on the Sun also seem to follow, although the north and south heliographic poles do not reverse polarity in synchrony[6]. The whole solar surface is, however, covered by a complex magnetic field pattern, which is highly structured from the largest to the smallest (sub-arc second) scales, and which evolves all the time. Although this evolution is very complicated, it seems to proceed in an orderly manner, as though globally regulated.

Attempts have been made to explain the 22-yr magnetic cycle and the migration of the sunspot latitude zones in terms of dynamo theory[7-9], but this approach has recently encountered difficulties. No attempt has been made to see if the evolution of the global magnetic-field pattern can be explained in terms of constructive and destructive interference of waves.

We demonstrate here that the magnetic-field pattern, in fact, has a modal structure characterized by sharp global resonances. Furthermore, the resonances for the modes of odd and even parity are decoupled from each other, indicating an underlying selection rule. This new 'emission-line' spectrum of solar magnetic fields does not seem to be explicable within the framework of current concepts such as dynamo theory, but should contain potentially powerful diagnostic information on the interior magnetic structure of the Sun and on the origins of solar activity.

Data set and reduction procedure

To explore whether there are global resonances in the Sun's magnetic field, we have to decompose the field pattern in its spherical harmonic coefficients and then perform a power spectrum analysis of each coefficient, showing the results in frequency (ν)-l space (as for the p-mode oscillations). As the expected periods are very long (years), we need synoptic observations of the magnetic field over all heliographic latitudes and longitudes, over a time span of many years, if possible longer than the 22-yr magnetic cycle. Thanks to the synoptic magnetogram programme started at the Mount Wilson Observatory in 1959 and at the Kitt Peak National Observatory (KPNO) in 1975, such a data set is available. The combined data set that we have used thus covers 25 yr.

Each synoptic map of the magnetic field, giving the average field strength as a function of heliographic latitude and longitude, has been pieced together from daily magnetograms obtained over one rotation period (about 27 days) of the Sun. Normally, the field observed around the central meridian in each magnetogram is used to provide the data for the various longitude bands. When some days of observations are missing, magnetogram data away from the central meridian are used to fill in the various longitudes. The longitudes are assigned according to the system introduced by R. Carrington, based on a rotation period of 27.2753 days. This period may seem somewhat arbitrary, since the Sun rotates differentially, but the precise choice of longitude system does not affect the type of analysis that we performed. By convention, the Carrington periods are numbered with the first period starting 9 November 1853. Our full data set covers rotations 1,417–1,751, corresponding to August 1959–July 1984.

The data from Mt Wilson cover rotations 1,417–1,648 (August 1959–December 1976), the Kitt Peak data rotations 1,622–1,751 (January 1975–July 1984). The major data gaps are for Mt Wilson rotations 1,462–1,468 (January–June 1963), for Kitt Peak rotations 1,640–1,644 (April–July 1976) and 1,647–1,648. As the latter data gaps are covered by the Mt Wilson data, we use the Kitt Peak data only from rotation 1,649 when both data sets are connected together as a continuous, 25-yr time series. When, on the other hand, the Kitt Peak data are used by themselves (as when we want to exploit their higher spatial resolution), the full series starting with rotation 1,622 is used. Each synoptic map is a matrix of values of the line-of-sight component of the field strength averaged over intervals in latitude and longitude. The divisions are equidistant in longitude and in the sine of the latitude. The Mt Wilson data that we have obtained were transformed into the synoptic format largely by Altschuler *et al.*[10] at the High Altitude Observatory, and have 30 zones in sine(latitude) and 36 sectors (10° each) in longitude. The Kitt Peak data compiled by J. W. Harvey has the higher-resolution format of 180 zones and 360 sectors.

The raw synoptic maps are uncorrected for actual inclination of the field vector, Zeeman saturation and temperature weakening of the spectral line used for the observations, and magnetogram cutoff for strong sunspot magnetic fluxes. The correction for these effects of the Mt Wilson data has been detailed elsewhere[11], so we will only summarize the procedure here.

To correct for the inclination of the magnetic field to the line-of-sight, we have to assume what the true field direction is. A good approximation should be to assume that the magnetic field in the photospheric layers, where it is observed, is, on average, along the radial direction; the reason for this is that the large-scale magnetic flux is made up of very small-scale, discrete flux tubes, and that buoyancy forces acting on each of them tend to make them as vertical as possible.

In their computations of the extrapolated coronal magnetic fields, Altschuler and Newkirk[12] postulated that the direction of the photospheric magnetic fields is determined by the solution of Laplace's equation for the assumed vacuum field in the solar corona, with the observed photospheric line-of-sight component as a lower boundary condition. This assumption, however, cannot be valid, since the force-free approximation is not applicable in the photosphere, where the field is measured. Instead, the photospheric field consists of highly intermittent flux tubes, which are not affected by the global topology of the coronal field because very local pressure and gravity forces exceed magnetic tension forces. Higher in the atmosphere the field must adjust to the force-free state, but that is not where the field is measured.

Accordingly, assuming that the photospheric field is radial on average, we have transformed all the synoptic charts into maps of the radial magnetic flux. As the Mt Wilson synoptic maps become saturated at about 100 G, flux densities in sunspots will be greatly underestimated unless this effect is corrected for. Therefore, for each synoptic map, a set of sunspot corrections has been applied[11]. The Kitt Peak measurements do not contain this type of saturation, so the sunspot fluxes measured are less distorted. Accordingly, no sunspot correction has been applied to the Kitt Peak data.

The Mt Wilson magnetograph recordings have been made with the spectral line Fe I λ5,250.22 Å, which has considerable Zeeman saturation (nonlinearity in the polarization signal when the Zeeman splitting is large) and temperature sensitivity (weakening of the line in magnetic regions). These effects and

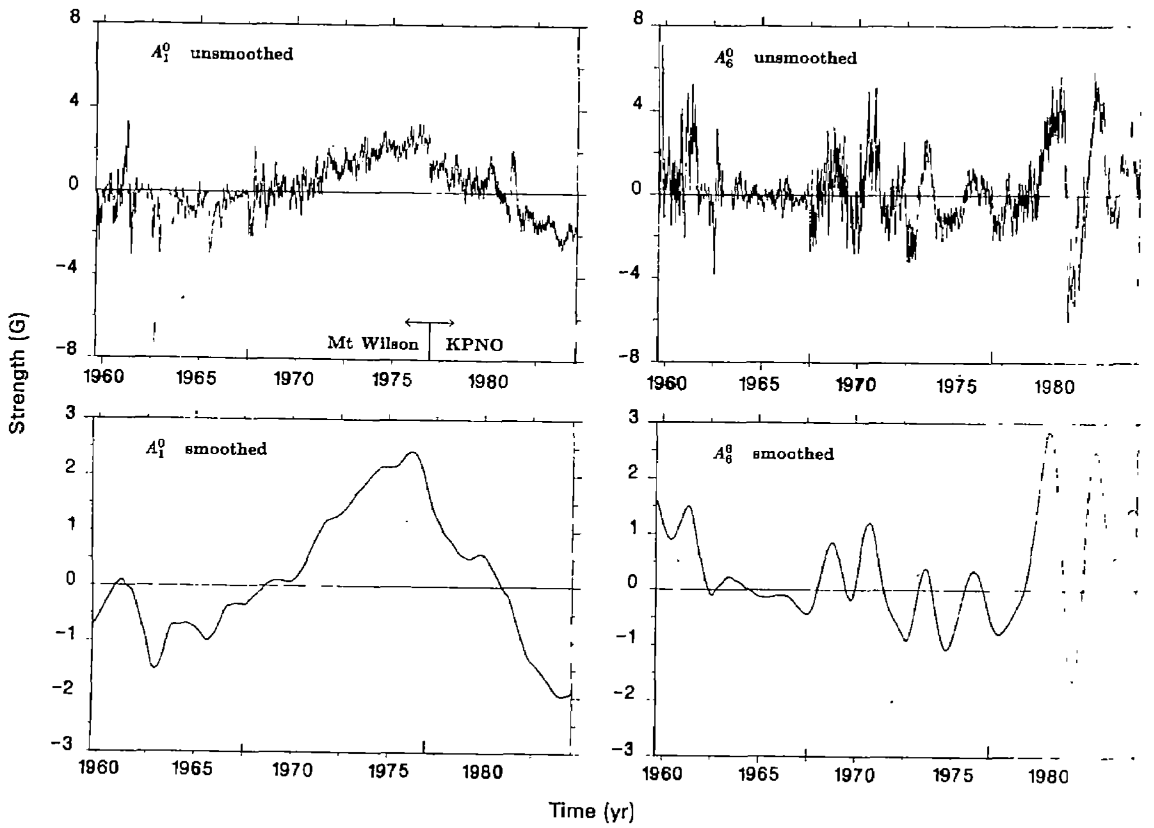

Fig. 1 Time series of spherical harmonic coefficients A_1^0 and A_6^0. The upper diagrams show the unsmoothed data, the lower diagrams the curves when smoothed with a triangular window of total half-width 1 yr.

their centre-to-limb variations have been calibrated[13], so we have been able to correct all the Mt Wilson synoptic charts for them. The Kitt Peak observations, on the other hand, are based on the spectral line Fe I λ8,688.64Å, which has much less temperature sensitivity and Zeeman saturation. As in addition, no calibrated correction factors for this line are available, the Kitt Peak data have not been corrected for these spectral effects, which should in any case be small.

Expanding the radial field B_r in spherical harmonics, and redefining the coefficients to make them real and to absorb in them time-invariant factors, we obtain

$$B_r(\vartheta,\varphi,t)=\sum_{l=0}^{\infty}\sum_{m=0}^{l}[A_l^m(t)\cos m\varphi + B_l^m(t)\sin m\varphi]P_l^m(\cos\vartheta) \qquad (1)$$

where P_l^m are the associated Legendre polynomials, ϑ is the co-latitude, φ the longitude and t the time. The coefficients can be obtained from the observed B_r through

$$A_l^0(t)=\frac{2l+1}{4\pi}\int B_r(\vartheta,\varphi,t)P_l(\cos\vartheta)\,d\Omega,$$

$$\begin{Bmatrix}A_l^m(t)\\B_l^m(t)\end{Bmatrix}=\frac{2l+1}{2\pi}\frac{(l-m)!}{(l+m)!}\times\int B_r(\vartheta,\varphi,t)P_l^m(\cos\vartheta)\begin{Bmatrix}\cos m\varphi\\ \sin m\varphi\end{Bmatrix}d\Omega \qquad (2)$$

where the integrations are to be made over all solid angles. In practice, the integrals are, of course, replaced by sums over the discrete matrix representing the synoptic chart.

In the reduction, the small unphysical magnetic monopole contribution is calculated by

$$A_0^0=\frac{1}{4\pi}\int B_r\,d\Omega \qquad (3)$$

and subtracted from the original B_r values. These corrected B_r values are used in equation (2) to compute the A_l^m and B_l^m coefficients.

Legendre polynomial coefficients of the Sun's magnetic field have been derived previously by others[10,12,14-16] by fitting a solution of the Laplace equation for the coronal field to the observed photospheric line-of-sight field. This procedure is not used here, for three reasons: (1) It is physically incorrect (the Laplace equation has no relevance to the photosphere, as pointed out above). (2) All the coefficients become coupled to each other, so the values of the low-degree coefficients depend on the cutoff of the expansion, with poor convergence properties. (3) The computational speed of our method is of the order of 1,000 times faster.

To obtain a practically continuous time series for each of the coefficients, the consecutive synoptic charts have been shifted relative to each other not by one solar rotation, but by 10° in longitude. The time step in the series is thus 27.2753/36 ≈ 0.76 days. We recall that the observational sampling was made at daily intervals, but that a synoptic chart is composed of observations collected over 27 days. The exploration of evolutionary effects is thus limited to longer periods.

A 25-yr time series thus consists of about 12,000 data points. The next step is to compute power spectra $PA_l^m(\nu)$ and $PB_l^m(\nu)$ of $A_l^m(t)$ and $B_l^m(t)$, where ν is the frequency. To obtain a smoother representation of the power spectra when examining the low-frequency domain, the time series were extended with zeroes before computing the fast Fourier transforms, thereby reducing the spacing between the discrete ν values in the power spectra.

The spatial resolution determined by the discretization in latitude and longitude of the synoptic charts allows the coefficients to be calculated up to l-values of 14 in the case of the Mt Wilson data and 89 in the case of the Kitt Peak data. All our computations have been made with a VAX 11/780 and an image processing system De Anza IP-8500 at the Institute of Astronomy in Zurich.

Resonant structure of zonal modes

We will limit ourselves here to a discussion of the results for the zonal modes, those with spherical harmonic order $m=0$, which are symmetrical around the rotational axis. The properties of the other modes will be considered elsewhere.

A hint at the resonant structure of the magnetic-field pattern is obtained from the time series of the harmonic coefficients. Figure 1 illustrates the time variation of coefficients A_1^0 (the north-south magnetic dipole) and A_6^0. The portions of the time axis covered by the Mt Wilson and Kitt Peak data are indicated. In June 1967, a significant improvement of the Mt Wilson magnetograph system was introduced[10,17,18] (as marked by an upward-directed tick mark in Fig. 1). Before then, the quality of the data was poorer. The smoothing in the lower half of Fig. 1 has been done using a triangular window with a total half-width of 1.0 yr, to bring out the evolutionary characteristics.

Hoeksema[16] calculated the A_1^0 coefficient for the time span 1976–83 using a different method, but with results in qualitative agreement with ours.

The dominating feature of the north-south dipole is its expected variation with a 22-yr period, with sign reversals near the times of maximum solar activity. The behaviour of the coefficient A_6^0 is, however, qualitatively entirely different. The 22- or 11-yr cycles cannot be seen, but instead there is a very pronounced cyclic variation with a period of 2 yr. Inspection of the time series of other coefficients with even l values shows a similar cyclic behaviour, but the periods depend on l, whereas coefficients with odd l only show the 22-yr cycle (when $l \leqslant 14$).

Only a power spectrum analysis, however, can properly bring out the remarkable resonant structure of the magnetic-field pattern in an objective way. Figure 2 plots the power $PA_l^0(\nu)$ against frequency ν and harmonic degree l, for $l \leqslant 14$ and $\nu \leqslant 30$ nHz. Since the modal structure is found to be entirely different for odd and even l, we have plotted the results for the odd and even modes separately. The open box to the right of the diagrams gives the resolution in ν-l space. The frequency resolution is given by $1/T$, where T is the length of the time series, in our case 25 yr.

The modes with odd l are antisymmetrical, those with even l symmetrical, with respect to reflections in the plane of the equator. They therefore represent modes of odd and even parity in the magnetic-field pattern.

Figure 2 represents the combined 25-yr data set Mt Wilson-Kitt Peak. To form a homogeneous set, the higher spatial resolution in the Kitt Peak data has been degraded by averaging over the latitude bins defining the resolution elements in the Mt Wilson synoptic maps. We have further normalized the power to its maximum value separately for each value of l. This normalization, which also applies to Figs 3 and 4, shows more clearly the frequency structure in the grey-scale diagrams.

The most striking feature of Fig. 2 is that the power is concentrated at discrete frequencies, with the modes of odd and even parities forming two decoupled systems. The power for the odd modes is concentrated around a sharp resonance with a period of 22 yr, independent of the value of l. This corresponds to the well-known 22-yr cycle of sunspot polarities (twice the cycle of the sunspot number). It is, however, remarkable that no overtones (such as the 11-yr period) are present.

With the exception of $l=10$ and possibly $l=14$, the 22-yr cycle is absent in the even-parity modes. Instead, there is another well-defined resonance for each value of l. The resonance frequency increases in a systematic way with l, as we have emphasized by drawing a smooth curve through the maxima in Fig. 2*b*. Thus the resonant period is about 14 yr for $l=2$ and 1.4 yr for $l=14$. This ν-l relation for the even-parity modes is qualitatively similar to the ν-l diagram for the p-mode oscillations, suggesting that the underlying mechanism is a system of standing waves in the Sun's interior, although other interpretations might be possible. Whatever the cause, this new 'emission-line' spectrum is likely to contain information on the magnetic field distribution inside the Sun.

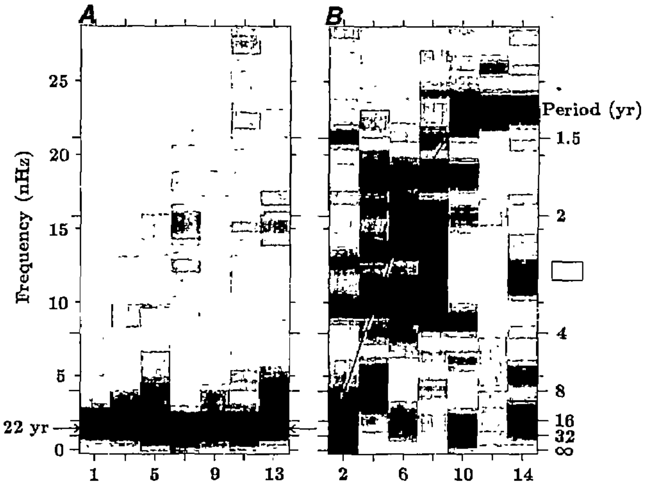

Fig. 2 Power spectra of the harmonic coefficients A_l^0, as a function of frequency in nHz and spherical harmonic degree l, for $l \leqslant 14$. *A*, Odd values of l; *B*, even values. A smooth curve has been drawn in the diagram for even l to indicate the l dependence of the resonance frequencies. The resolution is shown by the open box to the right.

The resolution box to the right in Fig. 2 indicates that the frequency widths of the resonances are still unresolved. The coherent time of the standing waves thus seems to be longer than 25 yr.

Let us next consider the reliability of these results and how they are influenced by various spurious effects. To do this, we use the data in Fig. 3 to address the following questions. (1) Does the limited spatial resolution of the Mt Wilson data lead to aliases from higher spatial frequencies, which are undersampled? (2) Do the Mt Wilson and Kitt Peak data, when treated separately, give the same results, although the time periods and instrumentation are different? (3) How stable are the results with respect to the length of the time series?

Figure 3 compares the ν-l diagrams of three data sets for $l \leqslant 24$: *a*, the Kitt Peak data, using their full spatial resolution of 180 latitude zones; *b*, the Kitt Peak data, spatially degraded to the Mt Wilson format by averaging over the 30 latitude bins (as was done when they were combined with the Mt Wilson data in Fig. 2); *c*, the Mt Wilson data. The resolution for the respective data sets is given in Fig. 3*A* for the Kitt Peak data (open box in Fig. 3*A b*) and the Mt Wilson data (Fig. 3*A c*).

Let us first consider the problem of aliasing. For a given harmonic component, there are $l-m+1$ latitude zones, that is, $l+1$ zones in our case (since $m=0$). To avoid aliasing, one needs to sample twice per zone. Thus, with 30 latitude bins as in the Mt Wilson format, one would expect to be able to determine modes up to $l=14$ without aliasing, if the zones were equidistant in the sine of the latitude (as our bins are). Since, however, the zones are not spaced this way, aliasing may also result for $l \leqslant 14$, depending on the importance of the high-latitude magnetic fields, for which undersampling due to the difference between the bin and zone divisions becomes significant. On the other hand, the averaging of the magnetic field over each bin in sine latitude acts as a spatial filter, suppressing the high-frequency components, which could be potentially responsible for aliasing.

Figure 3 shows that the aliasing and averaging effects are insignificant in the region $l \leqslant 14$, where the degraded and undegraded Kitt Peak data give practically identical results. This gives us confidence that Fig. 2 (which contains the results for $l \leqslant 14$) is free from limited spatial resolution effects. For $l > 14$,

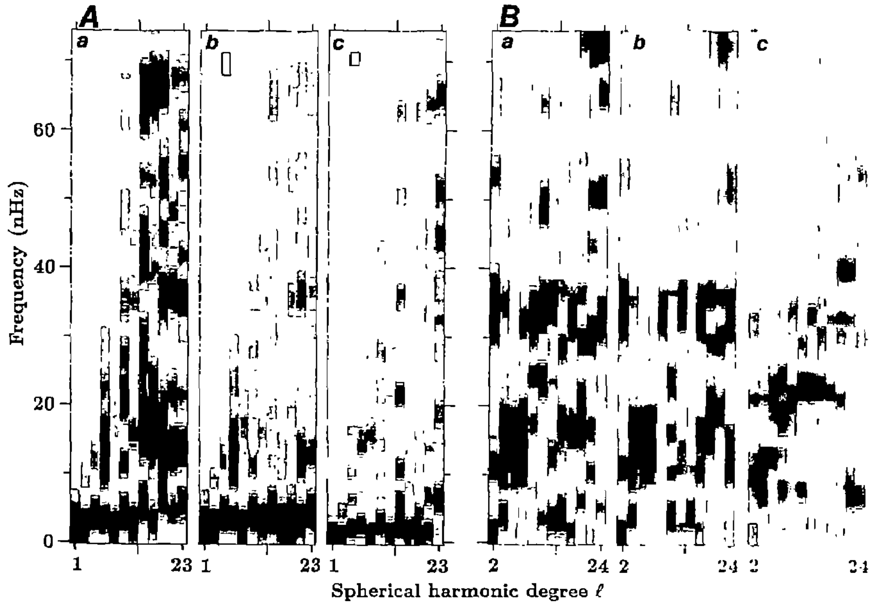

Fig. 3 Comparison of the modal structures for $l \leq 24$ in the power spectra of the harmonic coefficients calculated from: *a*, the Kitt Peak data (using the full latitude resolution); *b*, the Kitt Peak data after spatial degrading by averaging over the 30 bins in sine (latitude) used for the Mt Wilson data format; *c*, the Mt Wilson data. The boundary of the region ($l \leq 14$) free from spatial-resolution effects (when the Mt Wilson format is used) is indicated by a long tick mark. *A*, Odd values of *l*; *B*, even values.

however, the effects are quite large, particularly in the odd-parity diagrams.

Next let us compare the Mt Wilson data with the Kitt Peak data, spatially degraded to the Mt Wilson format. The results are consistent with each other in the following sense. (1) Both data sets show that the odd- and even-parity modes form two decoupled systems. (2) Since the Mt Wilson time series (17.2 yr) is about twice as long as that of Kitt Peak (9.6 yr), the power estimates of the Kitt Peak data are much less stable. (3) Even though the Kitt Peak time series is much shorter than the 22-yr period, this resonance of the odd-parity modes is revealed in the Kitt Peak data, although the power tends to be shifted to higher frequencies. This shift is, however, entirely a consequence of the shortness of the time series. (4) Within the statistical fluctuations, the Kitt Peak and Mt Wilson data sets separately both show the ν-l behaviour for the even-parity modes given by Fig. 2. (5) In addition, the Kitt Peak data for the even-parity modes show some higher-frequency peaks, the statistical significance of which is uncertain.

The comparisons that we have made in Fig. 3 show that we can have confidence in the general results of Fig. 2, but that the length of the time series is critical to obtaining statistically stable results. This stability is more important than the frequency resolution provided by a long time series. The combined series of 25 yr seems to give us the needed stability.

It should be possible to calculate the harmonic coefficients up to an *l* value equal to half the number of sine (latitude) bins in the synoptic chart minus one, without running into spatial resolution problems. As the Kitt Peak synoptic maps contain 180 sine (latitude) bins between the north and south heliographic poles, it should thus be useful to consider modes up to $l = 89$ in the case of the Kitt Peak data. The results of such calculations are shown in Fig. 4.

For Fig. 4, the combined Mt Wilson-Kitt Peak data set has been used for $l \leq 14$, the Kitt Peak data alone for larger values of *l*. The resolution for the Kitt Peak data is shown by the open box to the right. The frequency resolution for the combined Mt Wilson-Kitt Peak data is better by almost a factor of three, which is also evident from the sharpness of the power peaks for $l \leq 14$.

The difference in statistical stability between the regions with *l* below and above 14 is also striking. In the region of the combined data set, not only is the frequency location of the resonances more well defined, but the noise in the form of the background 'continuous' spectrum is much reduced. The dependence of the background on the length of the time series suggests that the intrinsic solar continuous background is weak, and that the 'true' spectrum may be a typical 'emission-line' spectrum.

In spite of the considerable stochastic noise fluctuations in Fig. 4, some general conclusions are possible. (1) The ν-l pattern contains discrete bands all the way up to $l = 89$. With increased resolution and stability, these bands might well narrow down to sharply defined resonances of large coherence length. (2) The diagrams of odd and even parity tend to be more similar to each other for $l > 15$ than in the case of Fig. 2 (for $l \leq 14$), although many apparently significant differences occur. (3) The 22-yr cycle is absent for all modes with $l \geq 15$ (see also Fig. 3), but is dominant for smaller odd *l* values. The 22-yr resonance

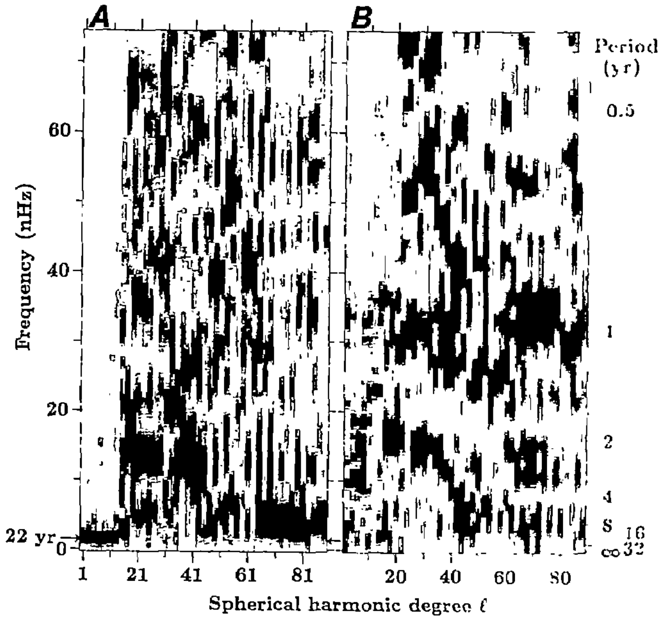

Fig. 4 Power spectra of the harmonic coefficients for $l \leq 89$. The combined Mt Wilson-Kitt Peak data set has been used for $l \leq 14$, the Kitt Peak data set alone for larger values of *l*. The resolution is indicated by the open box to the right. *A*, Odd values of *l*, *B*, even values.

may be related to the parity symmetry-breaking mechanism, since the decoupling between odd and even parity appears to be complete only where the 22-yr cycle is present. The qualitative change occurring at $l \approx 15$ has nothing to do with the choice of the Mt Wilson data format of 30 sine (latitude) bins, as it is seen independently in the Kitt Peak data alone (Fig. 3), which have a much higher resolution (180 bins). (4) There is substantial power for odd l at periods of 2-3 yr when $17 \leq l \leq 39$, and around 6-9 yr for $l \geq 65$, which warns us not to carry the analogy with p-mode oscillations too far.

Only with an extended Kitt Peak time series can the noise be sufficiently suppressed to allow more definite quantitative statements to be made. The presence of structures at all l values up to 89 emphasizes the need for a very long continuous database of synoptic magnetic-field observations of highest possible spatial resolution, as carried out in the Kitt Peak programme. At the same time, it is important that the Mt Wilson programme should also continue, since these synoptic observations started 17 years before the corresponding Kitt Peak programme, and thus provide the best information for modes with $l < 15$.

Discussion

The present analysis has revealed a complex resonant modal structure in the evolution of the pattern of solar magnetic fields. The coherence length of these resonances appears to be greater than the length of the time series used, which is 25 yr for the combined Mt Wilson–Kitt Peak data. A parity selection rule, which is particularly striking for spherical harmonic degree $l < 15$, determines the pattern in ν–l space. Thus, for $l < 15$, the 22-yr cycle is the only feature of the odd-parity modes, whereas the modes of even parity show a ν–l dependence reminiscent of global standing waves in the solar interior. For $l \geq 15$ the parity symmetry breaking is a much less dominant feature, and the 22-yr periodicity is absent. The complex resonant pattern in ν–l space continues until the highest-order modes resolved, with $l = 89$.

The next question that arises concerns the nature of the discrete modes of even partity for $l \leq 14$. The periods of years are clearly too long for the pressure or the gravity force to have a dominant role. As the resonances occur in the magnetic-field pattern, it is natural to imagine that the electromagnetic force plays a central role. Let us now examine whether an interpretation in terms of internal waves makes sense.

The relation between angular frequency ω, wavenumber κ, and wave speed c is

$$\omega = kc \tag{4}$$

In analogy with the treatment of p-mode oscillations[19], we assume that the wavenumber vector becomes horizontal at some radial distance r_t from the centre of the Sun, so that

$$k = \sqrt{l(l+1)}/r_t \tag{5}$$

there. The nature of the waves is not known, but possible candidates are dynamo waves and hydromagnetic waves. For any mechanism involving hydromagnetic waves it is natural to identify c with the speed of Alfvén waves (in a compressible medium hydromagnetic waves will not be pure Alfvén waves, but the use of the Alfvén speed is appropriate for our purpose of obtaining an order-of-magnitude estimate):

$$c = B/\sqrt{4\pi\rho} \tag{6}$$

B being the magnetic field strength and ρ the gas density. We further use

$$\omega = 2\pi/P \tag{7}$$

P being the wave period. Then, we obtain an expression for the field strength required:

$$B = 4\pi^{3/2}\frac{r_t\sqrt{\rho}}{P\sqrt{l(l+1)}} \tag{8}$$

As we have no developed theory for these waves, and as we do not know the internal magnetic-field distribution in the Sun, we do not know at what distance r_t to apply equation (8). Thus, we will only select some values representative of the convection zone to indicate the order of magnitude of the magnetic field required. Let us as an example take the magnetic mode with $l = 6$, which according to Fig. 2 has a period P of 2 yr. Inserting this in equation (8), and taking ρ from a convection-zone model[20], we obtain $B = 1{,}200$ G if the data for the bottom of the convection zone are used ($r_t/R_\odot = 0.72$), whereas $B = 740$ G at the middle of the convection zone ($r_t/R_\odot = 0.86$). These values of B seem reasonable, because they are similar to the values we observe directly on the solar surface, in sunspots, faculae, or the quiet network. Our estimates and method of calculation are similar to that used to determine the possible torsional oscillations of the Sun[21].

Most previous attempts to explain the evolution of solar magnetic fields have almost exclusively been made in terms of dynamo theory[7-9]. It seems doubtful, however, that current dynamo theories provide a good theoretical framework for the explanation of the resonant structure of the even-parity modes. Although the kinematic dynamo equations decouple for the odd- and even-parity modes[22,23], both categories of modes are excited with about equal ease, and no variation of cycle frequency with l number or parity is predicted.

The symmetry breaking between odd and even parity is, however, entirely consistent with Hale's polarity law, which states that the orientation of the plus and minus magnetic polarities in sunspot groups is opposite in the two hemispheres, and reverses sign with the beginning of a new 11-yr sunspot cycle. This rule is strictly obeyed on the Sun and implies that the toroidal flux system giving rise to the sunspots is purely antisymmetric with respect to the equator (odd parity), and varies with a 22-yr cycle. A recent attempt to explain this polarity law in terms of dynamo theory has been made[24], invoking anisotropic diffusivity to generate a difference in growth rates between odd and even modes.

We thank Gordon Newkirk for providing us with the Mt Wilson data compiled and digitized in the 'Boulder format' (30×36 matrix per synoptic chart, with data on corrections for sunspot saturation) at the High Altitude Observatory. The Mt Wilson synoptic programme was set up and directed by Robert Howard. We also thank J. W. Harvey for providing the full Kitt Peak data set of high-resolution synoptic maps of the magnetic field.

Received 14 July; accepted 14 October 1985.

1. Duvall, T. R. Jr *Trans. IAU* (Rep. IAU Commission 12, in the press).
2. Deubner, F. L. & Gough, D. *A. Rev. Astr. Astrophys.* **22**, 593–619 (1984).
3. Delache, P. & Scherrer, P. H. *Nature* **306**, 651–653 (1983).
4. Scherrer, P. H. in *Solar Seismology from Space* (eds Ulrich, R. K. *et al.*) 173–182 (JPL Publ. 84–84, Pasadena, 1984).
5. Fröhlich, C. & Delache, P. in *Solar Seismology from Space* (eds Ulrich, R. K. *et al.*) 183–193 (JPL Publ. 84–84, Pasadena, 1984).
6. Stenflo, J. O. *Proc. 3rd Eur. Solar Meet.*, Oxford 11–34 (1981).
7. Schüssler, M. *IAU Symp.* No. 102, 213–236 (1983).
8. Gilman, P. A. *IAU Symp.* No. 102, 247–270 (1983).
9. Yoshimura, H. *Astrophys. J. Suppl.* **52**, 363–385 (1983).
10. Altschuler, M. D., Trotter, D. E., Newkirk, G. N. Jr & Howard, R. *Sol. Phys.* **39**, 3–17 (1974).
11. Stenflo, J. O. *Sol. Phys.* **23**, 307–339 (1972).
12. Altschuler, M. D. & Newkirk, G. N. Jr *Sol. Phys.* **9**, 131–149 (1969).
13. Howard, R. & Stenflo, J. O. *Sol. Phys.* **22**, 402–417 (1972).
14. Levine, R. H. *Sol. Phys.* **54**, 327–341 (1977).
15. Altschuler, M. D., Levine, R. H., Stix, M. & Harvey, J. *Sol. Phys.* **51**, 345–375 (1977).
16. Hoeksema, J. T. thesis. Stanford Univ. (1984).
17. Howard, R., Tanenbaum, A. S. & Wilcox, J. M. *Sol. Phys.* **4**, 286–299 (1968).
18. Howard, R., Boyden, J. E., Bruning, D. H., Clark, M. K., Christ, H. W. & Labonte, B. J. *Sol. Phys.* **87**, 195–203 (1983).
19. Christensen-Dalsgaard, J., Duvall, T. L. Jr, Gough, D. O., Harvey, J. W. & Rhodes, E. J. Jr *Nature* **315**, 378–382 (1985).
20. Spruit, H. C. *Sol. Phys.* **34**, 277–290 (1974).
21. Layzer, D., Rosner, R. & Doyle, H. T. *Astrophys. J.* **229**, 1126–1137 (1979).
22. Steenbeck, M. & Krause, F. *Astr. Nachr.* **291**, 49–84 (1969).
23. Deinzer, W. & Stix, M. *Astr. Astrophys.* **12**, 111–119 (1971).
24. Yoshimura, H., Wu, F. & Wang, Z. *Astrophys. J.* **285**, 325–338 (1984).

A gradient of sex linkage in the pseudoautosomal region of the human sex chromosomes

François Rouyer, Marie-Christine Simmler, Christophe Johnsson, Gilles Vergnaud, Howard J. Cooke* & Jean Weissenbach

Unité de Recombinaison et Expression Génétique, INSERM U163, CNRS UA271, Institut Pasteur, 28 rue du Dr Roux, 75724 Paris Cedex, France
* MRC Mammalian Genome Unit, King's Buildings, West Mains Road, Edinburgh EH9 3JT, UK

Three independent pseudoautosomal loci are linked to sex determination at frequencies which define a gradient of linkage. The segregation patterns of these loci indicate that X / Y recombination results from a single obligatory meiotic crossing-over in the pseudoautosomal region. Recombination in male germ cells in the terminal regions of the short arms of the X and Y chromosomes is 10-fold greater than between the same regions of the X chromosomes in female germ cells.

THE distal parts of the short arms of the human X and Y chromosomes contain homologous sequences[1,2] and have identical telomeres.[3] Alleles of some of these homologous sequences undergo reciprocal interchange between the X and Y chromosomes[1,3]. Thus, the distal short arms of the human sex chromosomes probably consist of a pseudoautosomal region[4] characterized by the genetic identity[5] of loci undergoing recombination. To test whether these exchanges result from gene conversion or cross-over, we followed segregation of three independent polymorphic pseudoautosomal DNA loci in eight large families. Results of this analysis give a picture of the genetic properties of the human X/Y pseudoautosomal region.

Extensive variability

Two of the pseudoautosomal loci studied have been described previously[1,3]. Hybridization patterns of probe 29Cl (ref. 3), which detects an extremely polymorphic DNA locus, *DXYS14* (refs 6, 7), located close to the telomere of the sex chromosomes, and of probe 113D, which defines another highly polymorphic pseudoautosomal DNA locus, *DXYS15* (refs 1, 6, 7), are shown in Figs 1 and 2. The third probe (601) used in this study originates from a complementary DNA library (see Fig. 1 legend) and defines an additional pseudoautosomal locus, *DXYS17* (refs 6, 7), mapping to Xp22.3 and Yp. Probe 601 detects many restriction-fragment length polymorphisms (RFLPs) in different restriction enzymes digests. Not all these RFLPs co-segregate and their molecular basis is not yet fully determined. Two of them are illustrated in Figs 1*c*, *d* and 2*c*.

The *DXYS17 Taq*I RFLP consists of a series of at least eight allelic fragments ranging from 1.9 to 1.1 kilobases (kb) (alleles *DXYS17 T1-DXYS17 T8*). The size variations of the *Taq*I RFLP can be observed with other restriction digests and may therefore be ascribed to an insertion/deletion process. The segregation of three allelic *Taq*I fragments (*T3, T4* and *T6*) is shown in Fig. 1*d*. The *DXYS17 Eco*RI RFLP (Fig. 1*c*) consists of two allelic fragments of 17 kb (*DXYS17 R1*) and ~7 kb (*DXYS17 R2*) which occur in the population with a frequency of 30 and 70%, respectively. This size difference has not been found in the other RFLPs detected by 601, indicating that the *Eco*RI RFLP probably originated from a point mutation with loss or gain of *Eco*RI site. In addition, *DXYS17 R2* is stable in a single family, but can fluctuate among unrelated individuals from ~6.5 to 7.5 kb. In some of the individuals homozygous for the *DXYS17 R2* allele, it is possible to distinguish the two forms of this allele. This is consistent with the superimposition of a second type of variation possibly related to the *DXYS17 Taq*I polymorphism. Probably the same variations occur in the *DXYS17 R1* allele, but without detectable effect on its electrophoretic mobility. Both the *DXYS17 Eco*RI and *Taq*I alleles are inherited in a Mendelian fashion and their combinations define several haplotypes (see Fig. 1 legend).

*Taq*I and *Eco*RI DNA digests of 12 unrelated individuals have been hybridized to probe 601 (not shown) and 11 different haplotypes can be deduced from the different allelic combinations. Strikingly, the *DXYS17 R1* and *DXYS17 R2* alleles can both be associated with alleles *DXYS17 T3, DXYS17 T5, DXYS17 T6* and *DXYS17 T8.* Assuming that a single allele can only exceptionally arise twice independently, it is highly unlikely that the two *DXYS17 R* alleles can be associated with more than one common *DXYS17 T* allele. This strongly suggests that several recombination events have occurred between both polymorphic sites and have generated new haplotypes in which both *DXYS17 R* alleles have been reassorted with new *DXYS17 T* alleles.

Thus, all three probes used in this study detect highly polymorphic DNA sequences. Similarly, pseudoautosomal loci such as *DXYS20* (refs 6, 7) and others (G.V., unpublished data) also exhibit highly polymorphic restriction fragments. In general, isolation of probes detecting highly polymorphic sequences is rare. As only very few additional pseudoautosomal probes have been reported[1], this region appears to be very diverse. With the exception of the *DXYS17 Eco*RI polymorphism, RFLPs associated to these three probes have not been ascribed to point mutations. It is not clear yet whether these polymorphisms have originated through unequal recombination events, as proposed recently for minisatellite sequences[8], or by some other mechanism.

Recombination of pseudoautosomal loci

To determine recombination frequency, DNA samples from large families were analysed for the RFLPs detected by pseudoautosomal probes 29Cl, 113D and 601. *Taq*I or *Eco*RI Southern blots of the available samples of the paternal grandparents, parents and children from eight families were probed with all three pseudoautosomal sequences. As a control, the sex of each individual has been reconfirmed using probe 49f which detects multiple Yq-specific *Taq*I fragments, some of which are polymorphic. Many haplotypes of the human Y chromosome can be defined from the different existing combinations of the polymorphic 49f *Taq*I fragments[9]. All males of a family showed the same 49f haplotype (data not shown). Segregation of alleles from the different pseudoautosomal loci in paternal and maternal meiosis is analysed for two families in Figs 1 and 2 legends. Recombination for all three loci occurs in at least one of these families, as shown in Figs 1 and 2. Segregation of *DXYS14, DXYS15* and *DXYS17* with respect to sexual phenotype has been analysed for the eight families and recombination events are indicated in Table 1. The overall results obtained for segregation between sex and loci *DXYS14, DXYS15* and *DXYS17* are also summarized in Table 1. These family studies show that three pseudoautosomal loci, detected by randomly derived DNA probes, can be transferred from one sex chromosome to the

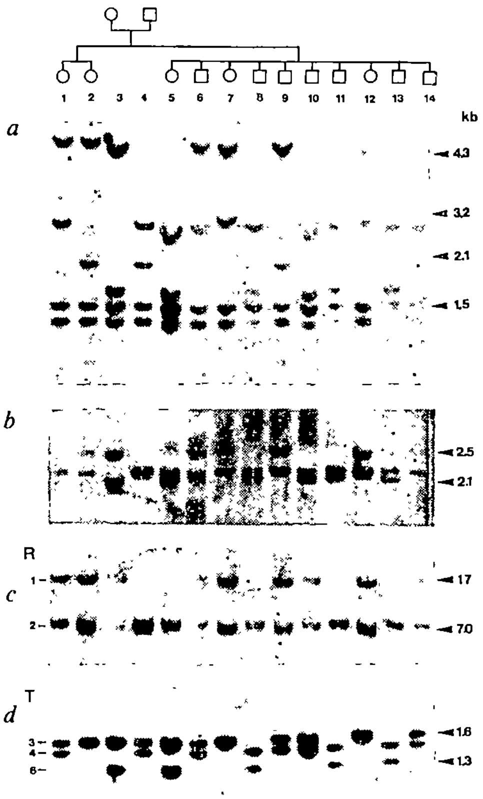

Fig. 1 Pedigree of family PO and hybridization patterns to Southern blots of restriction digests of DNAs from the family. Circles, females; squares, males. *a*, *Taq*I digests probed with 29Cl (ref. 3); *b*, *Taq*I digests probed with 113D (ref. 1); *c*, *d*, *Eco*RI and *Taq*I digests, respectively, probed with 601.

Methods. DNA (5–12 μg) was completely digested with an excess of restriction endonuclease, electrophoresed on a 1% agarose gel, transferred to nylon membranes and irradiated with a standard ultraviolet transilluminator for 5 min. After prehybridization at 42 °C for 4 h in 50% formamide, 5 × SSX (1 × SSC: 0.15 M NaCl, 15 mM Na-citrate *p*H 7), 5 × Denhardt's solution (Denhardt's solution: 0.02% Ficoll 400, 0.02% polyvinylpyrrolidone, 0.02% bovine serum albumin), 20 mM Na-phosphate *p*H 6.6 and 50 $\mu g\,ml^{-1}$ denatured sonicated salmon-sperm DNA, filters were hybridized overnight at 42 °C in the same solution with addition of 10% dextran sulphate and $10–30\times10^6$ c.p.m. of ^{32}P-labelled DNA probe. Probes used were DNA inserts nick-translated to a specific activity $>10^8$ c.p.m. μg^{-1}. After washing, the filters were autoradiographed with Kodak XAR5 films backed with one or two intensifying screens for 1–4 days at −70 °C. Probe 601 is isolated from a cDNA library derived from the 3E7 hybrid cell line (C.J., manuscript in preparation), a mouse-human somatic hybrid containing Y as the only recognized human chromosome. After hybridization, the filters were washed in 2 × SSC. Segregation analysis: definition of haplotypes: In this family, the higher maternal *Taq*I *DXYS17* fragment of 1.6 kb (*DXYS17 T3*) (*d*) and *Eco*RI *DXYS17 R1* allele (*c*) are strictly linked and hence define a first haplotype (*DXYS17 T3–R1*), whereas the second maternal haplotype (*DXYS17 T6–R2*) consists of the lower 1.3-kb *Taq*I allele (*DXYS17 T6*) associated with the lower *Eco*RI fragment *DXYS17 R2*. Combinations of paternal alleles define two other haplotypes which consist of the lower *Eco*RI *DXYS17 R2* allele associated either with the higher *Taq*I *DXYS17 T3* fragment (haplotype *DXYS*17 *T*3–*R*2) or with the intermediate one of 1.5 kb (*DXYS17 T4*) (haplotype *DXYS17 T4–R2*). Maternal meiosis: Maternal heterozygosity for all four RFLPs (*DXYS14*, *DXYS15*, *DXYS17 T* and *DXYS17 R*) and a difference among parents for at least one allele, makes family PO informative for recombination in maternal meiosis. Maternal haplotype *DXYS17 T3–R1* segregates with the higher *DXYS15* allelic fragment of 2.5 kb in cases 1, 2, 6, 7, 9, 12 and 14 and haplotype *DXYS17 T6–R2* with the lower *DXYS15* allelic fragment of 2.1 kb in cases 5, 8, 11 and 13. This association is not observed in case 10 where the lower *DXYS15* allele co-segregates with haplotype *DXYS17 T3–R1*. The maternal X chromosome of individual 10 therefore results from a recombination between *DXYS15* and *DXYS17*. Paternal meiosis: The phase of paternal alleles of pseudoautosomal loci of the family has been determined from a study of the grandparents (not shown). The *DXYS14* paternal Y allele is found in daughters 1, 5, 7 and 12. Conversely the paternal X allele is found in son 9. These five children thus carry a recombined paternal sex chromosome and the seven remaining children carry the same *DXYS14* allele as their father on their paternal X or Y chromosome. As the father is homozygous for locus *DXYS15* the family is not informative for segregation of this locus. All seven sons inherit paternal Y haplotype *DXYS17 R2–T4*, whereas one daughter (number 1) out of five inherits this haplotype as well and is the only child showing recombination for *DXYS17*.

other. Assuming that the interchange event is strictly reciprocal, recombination should occur in both male and female progeny with the same probability. For *DXYS14* where there are sufficient data, this expectation is fulfilled.

According to the segregation analysis of family PO (Fig. 1), the maternal X chromosome of individual 10 results from a recombination between *DXYS15* and *DXYS17*, indicating that these loci are not tightly linked. A similar conclusion can be drawn for *DXYS14*, which recombines with *DXYS17* in this individual. The recombination data for the pseudoautosomal loci in female meiosis are given in Table 2. No recombination between *DXYS14* and *DXYS15* has been observed in female meiosis.

A single obligatory X–Y crossover

All the families presented in Table 1 are informative for three-point linkage analysis (sexual phenotype and two pseudoautosomal loci) (see Table 3 for summary). The assumption that each pseudoautosomal locus may reassort independently in male meiosis predicts a frequency for each of the different possible combinations, but the less frequently recombined locus *DXYS17* never segregated independently from either *DXYS14* or *DXYS15* (Tables 1, 3). Similarly, a recombination of locus *DXYS15* always involved the most frequently recombined locus *DXYS14* (Table 1, 3). In addition, some of the frequencies predicted if in equilibrium are in total discrepancy with the observed values: in type *a* crosses (Table 3) we would expect, respectively, 16% of double recombinants (0.5×0.315), 34% of single recombinants with *DXYS14* $[0.5\times(1-0.315)]$, 16% of single recombinants with *DXYS15* $[(1-0.5)\times0.315]$ and 34% of non-recombined paternal sex chromosomes $[(1-0.5)\times(1-0.315)]$. However, we observe 34% of double recombinants, 14% of recombinants mobilizing *DXYS14* exclusively, no recombinants with *DXYS15* exclusively and 51% non-recombinants. In type *c* crosses (Table 3) an independent reassortment of pseudoautosomal loci in male meiosis also predicts, that *DXYS17* co-segregates with *DXYS15* in 31% of the *DXYS17* recombinants, whereas in the other 69% *DXYS17* should recombine without *DXYS15*. Instead we observe co-segregation of both loci in all *DXYS17* recombinants (Table 3). These three-point analyses eliminate the possibility of an independent reassortment of pseudoautosomal loci in male meiosis. Recombination frequencies between pseudoautosomal loci range between 14.5 and 36% (Table 2), indicating an obvious linkage between them. Co-segregation of three independent pseudoautosomal loci is not consistent with recombination via gene conversion which is supposed to take place on short stretches of DNA and should result in an independent segregation of each locus. On the contrary, linkage of the three loci and absence of independent segregation of the less frequently recombining ones demonstrate the occurrence of crossing-over events in the pseudoautosomal regions of the X and Y chromosomes.

As inferred from Table 1, pseudoautosomal loci display either partial linkage to their paternal sex chromosomes with recombination rates <50% for *DXYS15* and *DXYS17* or no sex linkage with a recombination frequency of ~50% for *DXYS14*. As we have established that sex chromosomes recombine through crossing-over, partial sex linkage can be interpreted in several ways: (1) X/Y crossing-over occurs occasionally during meiosis; (2) an obligatory X/Y crossing-over takes place at different locations from one meiosis to another and thus does not always mobilize the same loci; and (3) a few X/Y crossovers occur during a single meiosis. If X/Y crossing-over is occasional, frequencies of 50% would not be observed with the telomeric locus *DXYS14*. Nor are frequencies of 50% consistent with the occurrence of several crossovers involving the same chromatids during a single meiosis. In addition, if a single X/Y pair underwent multiple recombinations, there should be examples of independent segregation of each of the studied loci. The two

Table 1 Segregation of loci *DXYS14*, *DXYS15* and *DXYS17* with respect to sexual phenotype in male meiosis

Family	Proband	Sex	Recombination with *DXYS14*	Recombination with *DXYS15*	Recombination with *DXYS17*
NG	42	M	+	NI	−
	35	F	−	NI	−
	36	F	+	NI	−
	37	M	−	NI	−
	43	F	+	NI	+
	26	M	−	NI	−
PO	01	F	+	NI	+
	02	F	−	NI	−
	05	F	+	NI	−
	06	M	−	NI	−
	07	F	+	NI	−
	08	M	−	NI	−
	09	M	+	NI	−
	10	M	−	NI	−
	11	M	−	NI	−
	11	F	+	NI	−
	13	M	−	NI	−
	14	M	−	NI	−
66	6603	M	+	+	−
	6609	M	+	+	−
	6606	M	−	−	−
	6607	F	−	−	−
	6604	F	−	−	−
K1332	8252	F	+	+	NI
	8265	F	−	−	NI
	8261	M	+	−	NI
	8256	F	−	−	NI
	8255	F	−	−	NI
	8259	F	−	−	NI
	8253	M	+	−	NI
	8254	M	−	−	NI
K1346	8364	F	−	−	−
	8362	M	−	−	ND
	8357	M	+	+	+
	8603	M	−	−	−
	8359	M	+	−	−
	1370	M	−	−	−
K1413	1085	M	+	NI	−
	1084	M	+	NI	+
	1072	M	+	NI	+
	1092	F	+	NI	−
	1091	M	−	NI	−
	1279	M	−	NI	−
	1081	M	−	NI	−
	1078	M	−	NI	−
	1079	F	+	NI	−
	1080	M	−	NI	−
	1076	M	+	NI	−
	1087	M	+	NI	−
	1088	F	+	NI	−
	1090	M	+	NI	−
K1418	1262	F	−	−	NI
	1267	F	+	+	NI
	1260	F	+	−	NI
	1261	F	+	−	NI
	1256	F	−	−	NI
	1263	F	−	−	NI
	1258	M	+	+	NI
	1259	M	+	+	NI
K1421	1309	F	+	+	−
	1326	F	+	+	+
	1308	F	−	−	−
	1306	F	−	−	−
	1307	F	+	+	+
	1560	M	−	−	−
	1543	M	−	−	−
	1304	M	+	+	−
Total recombined X chromosomes			15	5	4
Total recombined Y chromosomes			18	6	3
Total recombined sex chromosomes			33	11	7
Total meioses with X			30	19	19
Total meioses with Y			37	16	31
Total meioses			67	35	50
Recombined X chromosomes (%)			50	26.5	21
Recombined Y chromosomes (%)			48.5	37.5	9.5
Recombined sex chromosomes (%)			49.5	31.5	14

(+), Involvement of a pseudoautosomal locus in a recombination affecting a paternal sex chromosome; (−), absence of recombination between a pseudoautosomal locus and sexual phenotype; NI, non-informative paternal phenotype; ND, not determined. Segregation of pseudoautosomal loci has been analysed on Southern blots with probe 29Cl for locus *DXYS14*, probe 113D for locus *DXYS15* and probe 601 for locus *DXYS17*. DNA from each individual was digested with *Taq*I and with *Eco*RI for DNAs from families PO, K1346 and K1421. Chromosomal assignment for the paternal alleles is deduced from an analysis of the paternal grandparents. DNA samples from families 28, 66, K1332, K1346, K1413, K1418 and K1421 were provided by CEPH. Family 28 was only informative for female meiosis and is not shown here.

most widely separated loci, *DXYS14* and *DXYS17*, are 36 recombination units apart. In *DXYS17* recombinants, a second crossing-over proximal to the telomeric locus *DXYS14* is theoretically possible in such a recombination interval. No example of double recombination has been found in any of the seven *DXYS17* recombinants analysed here (Table 3). Similarly, no second event is found in the smaller *DXYS14*/*DXYS15* interval (14.5 units) in the 12 *DXYS15* recombinants. However, the small size of the sampling may be at the limit of statistical significance. Nonetheless a frequency of 50% for the telomere would otherwise require during each meiosis the occurrence of many recombination events which should be observed even in small samples. Furthermore, as shown below, in the pseudoautosomal region recombination frequencies can be added up to 50% without any distortion, again reflecting the existence of a single crossover event. Therefore, taken together, our results strongly support hypothesis (2) in which a single obligatory crossover accounts for a recombination frequency of 50% of the telomeric region and for co-segregation of the more distal loci in recombinations affecting the proximal ones.

Recombinational hotspot

The extent of the pseudoautosomal region remains unknown. According to cytogenetic measurements, the size of the Y chromosomal short arm is generally estimated to range from 5,000 to 10,000 kb whereas the size of the pairing region is

Table 2 Recombination between pseudoautosomal loci

Recombination between	*DXYS14/DXYS15*	*DXYS15/DXYS17*	*DXYS14/DXYS17*
Female meiosis			
Recombined loci	0	2	2
Meioses	48	40	52
Recombination rate (%)	0	5	4
Male meiosis			
Recombined loci	5	4	18
Meioses	35	18	50
Recombination rate (%)	14.5	22	36

Results for female meiosis are as follows: (1) Recombination between loci *DXYS14* and *DXYS15* was not observed in families PO, 28 (children 2803, 2804, 2805, 2806, 2807, 2808, 2809), 66 K1332, K1418 and K1421, other families being non-informative. (2) Recombination between loci *DXYS14* and *DXYS17* was observed in case 10 from family PO and in case 1304 from family K1421 whereas no recombination was observed in the rest of those two families as well as in familes 28, 66, K1332 and K1346. The other families were not informative. (3) Recombination between loci *DXYS15* and *DXYS17* was again observed in case 10 from family PO and in case 1304 from family K1421, whereas the rest of these families and families 28, 66, and K1332 did not display recombination. Other families were not informative for these two loci. Results for male meiosis are derived from Table 1.

Table 3 Non-occurrence of double recombination events in male meiosis examined in three-point analyses

Three-point analysis	Type *a*	Type *b*	Type *c*
Pesudoautosomal loci involved in recombination			
DXYS14 exclusively	5	18	—
DXYS15 exclusively	0	—	4
DXYS17 exclusively	—	0	0
Both pseudoautosomal loci	12	7	3
Nonrecombinants	18	25	11
Total meioses	35	50	18

Type *a* analysis considers segregation of *DXYS14, DXYS15* and sexual phenotype; *b* segregation of *DXYS14, DXYS17* and sexual phenotype; and *c* segregation of *DXYS15, DXYS17* and sexual phenotype.

variable and can even stretch beyond Yp (ref. 10). As many Yp-specific DNA sequences have no homologous counterparts on Xp (refs 11-13) and our unpublished results) it follows that X/Y synapsis is partly non-homologous and no accurate correlation between X/Y pairing and sequence homologies can be drawn. More than 90% of the Yp-specific DNA probes we have isolated to date are not pseudoautosomal (refs 11, 12 and our unpublished results). If our Yp-specific DNA probes and those obtained at random by the different laboratories are representative of the DNA composition of the chromosome short arm, it seems unlikely that the maximum size of the pseudoautosomal region is >5,000 kb.

The recombination frequency between *DXYS14* and *DXYS17* (Table 2) in male meiosis (36%) is ninefold higher than that obtained from female meiosis (4%) and contrasts with a significant general increase reported for the autosomal frequency in female meiosis as compared with that in male meiosis[14,15]. In the human, 1% recombination (1 centimorgan) is generally taken to represent a chromosomal distance of 1,000 kb (ref. 16) and accordingly, loci *DXYS14* and *DXYS17* should be located 36,000 kb apart. The actual size of this interval is probably one order of magnitude lower as reflected by the recombination frequency observed in female meiosis (4%). It thus appears that the pseudoautosomal region is a recombinational hotspot in male meiosis. Such an overestimation is consistent with the view that a single crossover between the X and Y chromosomes is an obligatory step in male meiosis. It has been proposed that chiasmata play a part in the disjunction of chromosomes[17] during the first meiotic division and that at least one chiasma takes place in each bivalent to ensure proper segregation. This view could apply to the pseudoautosomal region of the X/Y pair. The apparent 10 fold increase in recombination frequency in males compared with females is then a direct consequence of a chiasma having to be formed between each chromosomal pair in this limited region.

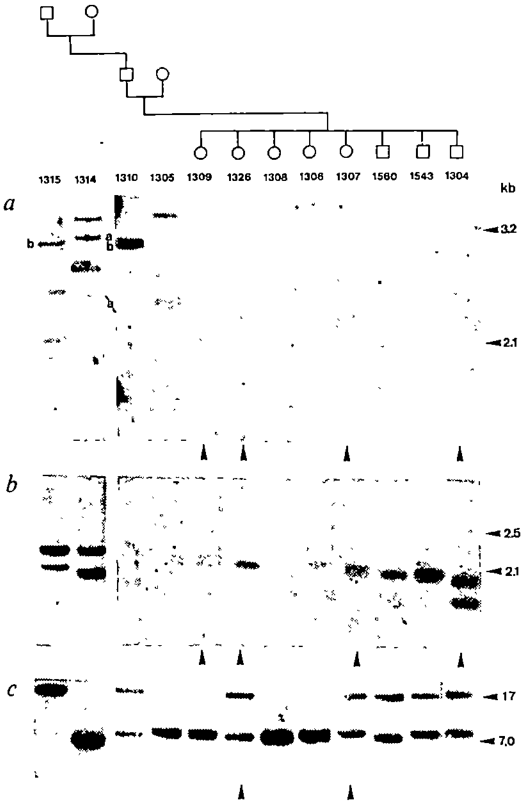

Fig. 2 Pedigree of CEPH family K1421 and hybridization patterns to Southern blots of restriction digests of the family. DNA digestions, blotting, hybridizations and washings were as described in Fig. 1. *a*, *Taq*I digestions probed with 29C1 (ref. 3); *b*, *Taq*I digestions probed with 113D (ref. 1); *c*, *Eco*RI digestions probed with 601. Segregation analysis: genotypes of grandparents have been determined independently and are displayed in the left part of the figure. In this family the father (1310) has inherited the *DXYS14* a allele (represented by two fragments) from his mother (1314), a is thus X-located whereas the b allele, originating from his father (1315), must be Y-located (*a*). Daughters 1309, 1326 and 1307 carry the paternal Y allele b. As the X-located paternal allele a is not found in these three daughters the paternal b allele must now be carried by their X chromosome. Conversely the paternal X allele a must be carried on the paternal Y chromosome in son 1304. There is no recombination of a or b alleles with sex phenotype in children 1308, 1306, 1560, 1543. Paternal X and Y alleles of locus *DXYS15* co-segregate strictly with paternal X and Y alleles of locus *DXYS14* (*b*). The paternal Y allele of locus *DXYS17* is only found in daughters 1326 and 1307 whereas daughter 1309 and son 1304, like the other children, show no recombination for this locus (*c*).

Genetic map

As the recombination frequency is extremely high in male meiosis, a detailed genetic map of the pseudoautosomal region can be constructed. Genetic distances between the pseudoautosomal loci are given in Table 2. According to these values *DXYS15* is located within the *DXYS14*/*DXYS17* interval (Fig. 3). Strikingly, the sum of the distances between *DXYS14* and *DXYS15* and between *DXYS15* and *DXYS17* is almost equal

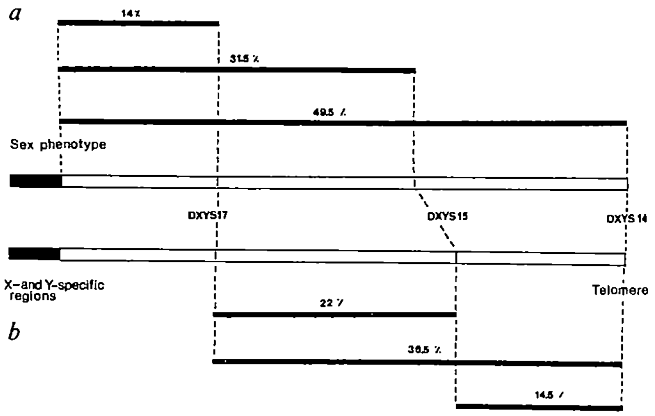

Fig. 3 Correlation of two genetic maps of the human pseudoautosomal region. *a*, Map derived from the recombination frequencies of pseudoautosomal loci with sexual phenotype; *b*, map derived from the recombination frequencies between pseudoautosomal loci in male meiosis.

to the value of the *DXYS14*/*DXYS17* interval. It appears that the recombination frequency additivity rule applies to the pseudoautosomal region for values of up to 36%. It may even apply to the entire pseudoautosomal region, as the distance between sex and *DXYS17* (14%) is again extremely close to the value obtained by subtracting the *DXYS14*/*DXYS17* distance from the distance between *DXYS14* and sex (49.5 − 36%). Despite a slight discrepancy between maps *a* and *b* in the position of *DXYS15* (Fig. 3) which remains to be investigated, these results demonstrate the occurrence of a single crossing-over in the pseudoautosomal region. Thus, a gradient of sex linkage can be correlated with the linear order of the pseudoautosomal loci. In other words, the recombination frequency directly reflects the position of the locus with respect to the regions specific to one of the sex chromosomes. The telomere is being exchanged at a rate of 50% whereas the more proximal loci are mobilized less frequently.

To date, construction of a deletion map of the human Y chromosome has been achieved using non-pseudoautosomal probes[11] and the testis-determining factor has been definitely assigned to Yp (refs 11, 18). Recombination mapping of the Y chromosome pseudoautosomal region represents a new method of approaching the sex determination region. Highly polymorphic pseudoautosomal probes also provide a supplementary tool for the analysis of the aetiology of XX maleness by allowing assessment of the paternal origin of the pseudoautosomal region.

The elevated recombination frequency in the human pseudoautosomal region provides a valuable opportunity to correlate experimental values and physical distances as chromosome walking can be performed over distances of several hundred kilobases of DNA. Alternatively, the physical distance between two loci may be amenable to determination by pulse-field electrophoresis, and a size estimation of the whole pseudoautosomal region could be drawn from measurements of recombination frequency. The human pseudoautosomal region also presents an opportunity to investigate chromosomal recombination by both molecular and genetic methods. A molecular analysis of the highly polymorphic pseudoautosomal loci could reveal new structural features directly related to the crossing-over mechanism.

Conclusions

Several characteristics of pseudoautosomal sequences have been demonstrated in this report: (1) they can be exchanged between the X and Y chromosomes by a crossing-over mechanism; (2) they can exhibit partial sex linkage, the extent of the linkage being different for three independent pseudoautosomal loci; and (3) the pseudoautosomal region is characterized by a high recombinational activity and thus lends itself to extensive mapping. This mapping is even facilitated by occurrence of a single crossing-over per meiosis taking place at varying locations in the region.

Crossing-over between the mammalian sex chromosomes was proposed many years ago[19]. Recombination nodules have even been observed within the distal short arms of the human X/Y pair[20]. The present data validate these earlier statements and confirm the view that the mammalian sex chromosomes originated from an ancestral pair of homologues. Indirect genetic evidence has shown the existence of crossing-over in mouse[21-24]. However in this species, both the steroid sulphatase (*STS*) gene[24] and the sex-reversing (*Sxr*) mutation[21-23] seem to recombine with a 50% frequency, whereas in humans frequencies specific for each pseudoautosomal locus have been observed. The *Sxr* mutation is probably distal to the mouse pseudoautosomal region[22,23] and a frequency of 50% (ref. 24) should be expected. A frequency of 50% observed with the *STS* gene indicates that crossing-over is obligate for this locus either because it is very distal in mouse or because there is only one or a cluster of very few crossover points in the mouse X/Y pair. A small number of crossover points in the pseudoautosomal region indicates that this region is rather small in the mouse and contains only a few genes. This could explain why the lack of a set of these few genes in 39,X mouse is considerably less harmful[25] than the absence of one copy of the pseudoautosomal region in human 45,X Turner females[26].

Differences in genetic behaviour of pseudoautosomal regions between species may reflect a continuing process of sex-chromosome differentiation. Perhaps the size of the pseudoautosomal region is reduced by divergence of the most proximal areas which recombine at the lowest frequencies. We do not know if a reduction in recombination is a cause or a consequence of divergence, or if there is a discrete boundary to the pseudoautosomal region.

We thank the Centre d'Etude du Polymorphisme Humain (CEPH) for the family DNA samples; the CEPH staff for its kindness; Pierre Tiollais for encouragement; and Colin Bishop, Adrian Bird and William Brown for reading this manuscript. G.V. is a member of Délégation générale de l'Armement.

Received 23 September; accepted 12 November 1985.

1. Simmler, M. C. *et al. Nature* **317**, 692-697 (1985).
2. Buckle, V., Mondello, C., Darling, S., Craig, I. W. & Goodfellow, P. N. *Nature* **317**, 739-741 (1985).
3. Cooke, H. J., Brown, W. A. & Rappold, G. A. *Nature* **317**, 687-692 (1985).
4. Burgoyne, P. S. *Hum. Genet.* **61**, 85-90 (1982).
5. Polani, P. E. *Hum. Genet.* **60**, 207-211 (1982).
6. Willard, H. F. & Skolnick, M. H. *Cytogenet. Cell Genet.* (in the press).
7. Goodfellow, P. N., Davies, K. E. & Ropers, H. H. *Cytogenet. Cell Genet.* (in the press).
8. Jeffreys, A. C., Wilson, V. & Thein, S. L. *Nature* **314**, 67-73 (1985).
9. Ngo, K. Y., Vergnaud, G., Johnsson, C., Lucotte, G. & Weissenbach, J. *Am. J. hum. Genet.* (in the press).
10. Chandley, A. C., Goetz, P., Hargreave, T. B., Joseph, A. M. & Speed, R. M. *Cytogenet. Cell Genet.* **38**, 241-247 (1984).
11. Vergnaud, G. *et al. Am. J. hum. Genet* (in the press).
12. Geldwerth, D. *et al. EMBO J.* **4**, 1739-1743 (1985).
13. Page, D. C., Harper, M. E., Love, J. & Botstein, D. *Nature* **311**, 119-123 (1984)
14. Cook, P. J. L. *Am. J. hum. Genet.* **28**, 393-401 (1965).
15. Renwick, J. H. *Bull. Eur. Soc. hum. Genet.* **2**, 7 (1968).
16. Renwick, J. H. *Br. med. Bull.* **25**, 65-73 (1969).
17. Darlington, C. D. *Recent Advances in Cytology* (Churchill, London, 1937)
18. Casanova, M. *et al. Proc. natn. Acad. Sci. U.S.A.* (submitted).
19. Koller, P. C. & Darlington, C. D. *J. Genet.* **29**, 159-173 (1934).
20. Solari, A. J. *Chromosoma* **81**, 315-337 (1980).
21. Cattanach, B. M., Pollard, C. E. & Hawkes, S. G. *Cytogenetics* **10**, 318-337 (1971)
22. Singh, L. & Jones, K. W. *Cell* **28**, 205-216 (1982).
23. Evans, E. P., Burtenshaw, M. D. & Cattanach, B. M. *Nature* **300**, 443-445 (1982)
24. Keitges, E., Rivest, M. Siniscalco, M. & Gartler, S. M. *Nature* **315**, 226-227 (1985)
25. Russel, W. L., Brauch Ressel, L. & Gower, J. S. *Proc. Natn. Acad. Sci. U.S.A.* **45**, 544-560 (1959).
26. Ford, C. E., Jones, K. W., Polani, P. E., de Almeida, J. C. & Briggs, J. H *Lancet* i, 711-713 (1959).

Large-scale dissociation of molecular gas in galaxies by newly formed stars

R. J. Allen*†, P. D. Atherton*‡ & R. P. J. Tilanus*

* Kapteyn Astronomical Institute, University of Groningen,
Postbus 800, 9700 AV Groningen, The Netherlands
† Department of Astronomy, University of Illinois,
1011 West Springfield Avenue, Urbana, Illinois 61801, USA
‡ Queensgate Instruments Ltd., 112 Windmill Road,
Sudbury-on-Thames, Middlesex TW16 7HB, UK

Molecular hydrogen is thought to form from atomic hydrogen on the surface of dust grains in the interstellar medium, and to be dissociated primarily by ultraviolet radiation from hot stars[1]. This process has been modelled on the 1 pc length scale for the case of dense interstellar clouds[2] and near newly formed ionizing stars[3]. Observational evidence that molecular hydrogen is indeed dissociated in shells around young OB stars in the Galaxy has been presented recently[4–6]. We suggest here that the same dissociation process occurs on the kpc scale in active star-forming regions of some galaxies, and that this dissociation may strongly affect the observed morphology of atomic hydrogen in spiral arms.

The large-scale distribution of molecular gas in galaxies is poorly known, not only because of the limited availability of observable tracers and the low angular resolution and sensitivity of the instrumentation but also because of the difficulties of interpreting the observed surface brightness of molecular lines as column densities of H_2. Observations of the CO molecule in several galaxies do, however, indicate that the general distributions of molecular and atomic gas appear to be different. In particular, the central H I depressions observed at radii ≤ 5 kpc in several prominent bright late-type spiral galaxies may be filled in with molecular gas[7,8]. One such galaxy is M83 (NGC5236) and, although the angular resolution of the CO observations which are available at millimetre wavelengths is insufficient to discern details on the scale of a spiral arm, the ^{12}CO is concentrated in the central regions within a radius of ~1 arc min (ref. 9). Recent observations of several galaxies in ^{12}CO and ^{13}CO with a resolution of 65 arc s confirm that molecular gas is present over the whole disk of M83, although the quantitative interpretation in terms of H_2 column density is uncertain[10].

More detailed pictures of nearby galaxies can be made of the distribution of atomic H I using centimetre-wavelength aperture synthesis radio telescopes. Contrary to the situation with the molecular gas, the conversion of an observed surface brightness in the 21-cm line to a column density of H I atoms is straightforward and independent of the excitation temperature, provided the latter is substantially higher than the temperature of the cosmic microwave background radiation. Over a wide range of conditions relevant to the present case, the excitation temperature of H I is equal to the kinetic temperature of the interstellar gas[21], and this is much higher than 3K. It is highly unlikely that substantial quantities of H I remain undetected in the nearby galaxies.

We have observed M83 in H I with a maximum resolution of 10 arc s using the Very Large Array (VLA), and combined the data with lower resolution VLA observations by M. Ondrechen and J. M. van der Hulst (personal communication) to produce the final maps. Figure 1 shows the distribution of H I at 25 arc s resolution after subtraction of the continuum, along with a sketch of several prominent dust lanes. The warped outer H I 'ring' described by Rogstad *et al.*[14] lies outside the frame of Fig. 1. Although the contour map does not show it very clearly, other methods of displaying this data indicate that the central region with diameter 2 arc min is essentially devoid of H I. In the following discussion, we argue that, independent of the controversy surrounding the interpretation of the CO observations, it is likely that the H I void in M83 is filled with molecular gas in quantities similar to the H I found at slightly larger radii.

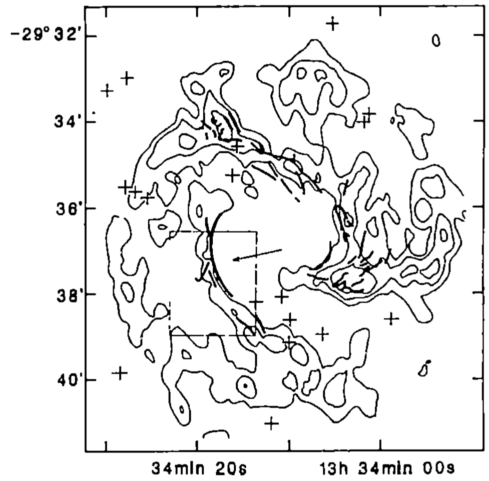

Fig. 1 The distribution of atomic hydrogen and dust lanes in M83. Contours are taken from VLA-H I synthesis observations at 25 arc s resolution. The dust lanes have been drawn from inspection of an optical photograph. The crosses refer to a set of secondary standard stars. The arrow indicates the inner eastern arm; the frame drawn corresponds approximately with the frames of Fig. 2.

As part of a project to study the temporal sequence of star formation in spiral arms, we have been examining in detail a portion of M83 which includes the boundary zone at the edge of the H I void. This region is indicated by the small frame and the arrow in Fig. 1. As a tracer for the young stars, we have mapped the galaxy in the optical H β emission line using the Taurus imaging Fabry-Pérot spectrometer[11] attached to the Anglo-Australian Telescope. In the region indicated by the small frame in Fig. 1, the distribution of H β emission is shown in Fig. 2*a* after subtraction of the continuum and smoothing to a resolution of 5 arc s. For comparison, Fig. 2*b* shows the H I distribution with a resolution of 10 arc s. The prominent dust lanes are indicated by the thick lines and the dashed line shows roughly the ridge of the H I emission from the 25 arc s map of Fig. 1. Finally, the main features of the H β (dashed contours) and the H I (solid contours) along with the dust lanes (thin and thick lines) are summarized in Fig. 2*c*.

Figure 2*a* shows that the H β emission (and thus the young, massive stars which ionize the gas) appears along a locus roughly parallel to the dust lane, but shifted about 15 arc s to the east of it. This shift corresponds to a radial displacement of 700 pc in the plane of the galaxy for an assumed distance of 8.9 Mpc and inclination of 24°.

Figure 2*b* shows that the H I ridge is also displaced to the east of the dust lane, and the approximate coincidence of the dashed line (the 25 arc s H I ridge) with the peaks of H I in Fig. 2*b* (10 arc s resolution) confirms that this shift is not a consequence of beam-smoothing.

Fig. 2*c* shows that, while the ridge line of the H I (solid contour) corresponds closely with that of the H β (dashed contours), there is no detailed coincidence between the individual bright peaks of atomic and ionized hydrogen.

In the framework of the picture (summarized in ref. 12) in which a passing density wave in the underlying stellar disk induces shocks in the gas followed by cloud collapse and star formation, several inferences concerning changes in the state of the interstellar gas in M83 can now be made. In this theoretical picture, the position of the shock front is given by the dust lane, and the typical gas streaming into and out of this region is indicated by the numbered arrows 1 and 2 in Fig. 2*a* (the observed structure of the velocity field[13] indicates that the south-

29. Marsh, H. & Rand, B. in *3rd Conf. Industrial Carbon and Graphite*, 93 (Academic, London, 1970).
30. Seiber, B. A., Wood, B. E. & Smith, A. M. *Science* **170**, 652-654 (1970).
31. Ghormley, J. A. & Hochanadel, C. J. *Science* **171**, 62-64 (1971).
32. Sceats, M. G. & Rice, S. A. in *Water, a Comprehensive Treatise* Vol. 7 (ed. Franks, F.) Ch. 2 (Plenum, New York, 1982).
33. Narten, A. H., Venkatesh, C. G. & Rice, S. A. *J. chem. Phys.* **64**, 1106-1121 (1976).
34. Temkin, R. J., Paul, W. & Connell, G. A. *Adv. Phys.* **22**, 581-641 (1973).
35. Ehrenreich, H. & Turnbull, D. *J. Non-Crystalline Solids* **8-10**, 19-35 (1972).
36. Bienenstock, A. *Amorphous Liquid Semiconductors, Proc. 5th int. Conf.* (Taylor & Francis, London, 1974).
37. Alben, R. & Boutron, P. *Science* **187**, 430-432 (1975).
38. Mayer, E. & Pletzer, R. *J. chem. Phys.* (in the press).
39. Aharoni, C. & Suzin, Y. in *Characterization of Porous Solids* (eds Gregg, S. J., Sing, K. S. W. & Stoeckli, H. F.) 173-180 (Society of Chemical Industry, London, 1979).
40. Hollenbach, D. & Salpeter, E. E. *J. chem. Phys.* **53**, 79-86 (1970).
41. Hollenbach, D. & Salpeter, E. E. *Astrophys. J.* **163**, 155-164 (1971).
42. Ponec, V., Knor, Z. & Černý, S. *Adsorption on Solids*, 373 (Butterworths, London, 1974).
43. Brackmann, R. T. & Fite, W. L. *J. chem. Phys.* **34**, 1572-1579 (1961).
44. Govers, T. R., Mattera, L. & Scoles, G. *J. chem. Phys.* **72**, 5446-5455 (1980).
45. Schutte, A., Bassi, D., Tommasini, F. & Turelli, A. *J. chem. Phys.* **64**, 4135-4142 (1976).
46. Whipple, F. L. *Astrophys. J.* **111**, 375-394 (1950), **113**, 464-474 (1951).
47. Delsemme, A. H. & Swings, P. *Ann. Astrophys.* **15**, 1-6 (1952).
48. Miller, S. L. *Proc. natn. Acad. Sci. U.S.A.* **47**, 1798-1808 (1961).
49. Delsemme, A. H. & Wenger, A. *Planet. Space Sci.* **18**, 709-715 (1970).
50. Barrer, R. M. & Edge, A. V. *Proc. R. Soc.* **A300**, 1-24 (1967).

Importance of local mesoscale factors in any assessment of nuclear winter

B. W. Golding, P. Goldsmith*, N. A. Machin & A. Slingo

Meteorological Office, London Road, Bracknell,
Berkshire RG12 2SZ, UK

There is a possibility that severe climate perturbations would follow a major nuclear war (the 'nuclear winter') due to the injection of large amounts of smoke into the atmosphere[1-6]. Given assumptions about the amount of smoke generated, its carbon content, the size of the particles and their optical properties, calculations of the subsequent cooling of the surface air temperatures have been made with a variety of atmospheric models. It has not been possible in these models, however, to represent any effects due to the initially patchy nature of the smoke. We investigate here whether such effects could be important by using a 15-km resolution atmospheric model to simulate the mesoscale response to a single smoke plume. Our results show that vertical circulations created by the radiative heating of the smoke may be sufficiently intense to lead to cloud formation and hence to scavenging of the smoke.

Simulations of the cooling of the surface following a nuclear war have been based on either one-dimensional models[1] or versions of coarse three-dimensional global atmospheric circulation models originally designed to study global climate variability. The one-dimensional models have to assume a uniform smoke distribution while the three-dimensional models[6] have a resolution of no better than about 5° latitude which prevents the representation of mesoscale processes. Given the local nature of the initial smoke intrusions, and the strong temperature gradients that their radiative characteristics would create, it is reasonable to suppose that mesoscale atmospheric circulations would be set up, especially near the edges of the plumes. This is in addition to any circulations that might be expected locally at the source of the smoke due to the heat and moisture which inevitably must be associated with the smoke generation. If such circulations were to produce cloud, it would be expected to increase either the scavenging rate or the rate at which smoke particles coagulate. For a given mass of smoke the radiative effects change significantly as the size of the particles increases[7].

To test the possibility that such mesoscale circulations might occur, a case study has been completed using a numerical mesoscale model currently under development in the Meteorological Office for improving short-period weather forecasting. Briefly, it is a non-hydrostatic, compressible model using a semi-implicit time-stepping scheme to ensure numerical stability[8]. The vertical coordinate is height above orography[9], and in the study, 16 levels were used with 5 in the lowest 1 km of the atmosphere and the highest at 12 km. The domain used covered the British Isles with a 15-km grid mesh. The model has an explicit representation of grid-scale clouds[10] and uses a one-dimensional steady-state cloud model to parameterize deep convection. A $1\frac{1}{2}$-order closure diffusion scheme models sub-grid-scale turbulence. In normal use, radiative effects are calculated only for computing the surface heat balance. A detailed radiation scheme[11] was therefore used to develop a parameterization of short-wave heating by smoke which could easily be added to the model. The scheme has 24 spectral bands from 0.2 to 4 μm and treats Rayleigh and multiple scattering, and absorption by smoke, water vapour and ozone. The smoke properties were taken from the baseline calculations in the US National Academy of Sciences[5]. Vertical profiles of the heating rates for various aerosol loadings in a cloudless mid-latitude summer atmosphere, a surface albedo of 0.2 and 60° solar zenith angle

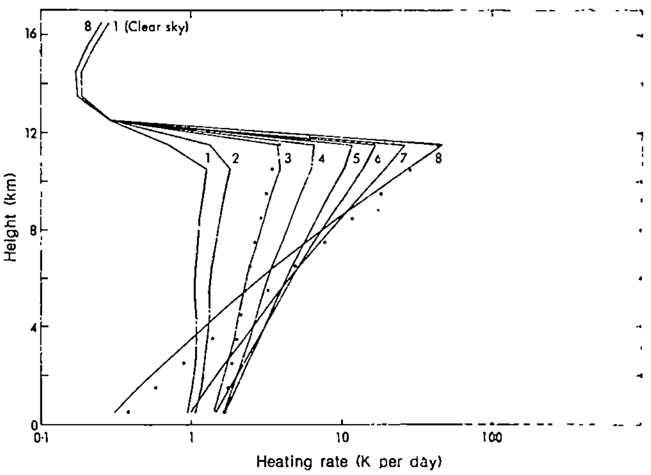

Fig. 1 Vertical profiles of the short-wave heating in an atmosphere containing various loadings of soot aerosols (solid lines). Numbers refer to values given in Table 1. ●, The heating rate profiles obtained with the simple parameterization indicated in Table 1 for curves 3 and 8.

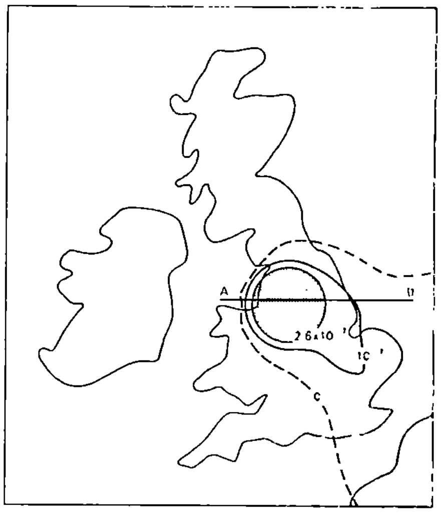

Fig. 2 Smoke concentration in kg per kg at 9 km altitude (~300 mbar) after 12 h integration. The stippled area shows the source region.

---

* Present address: European Space Agency, Paris, France.

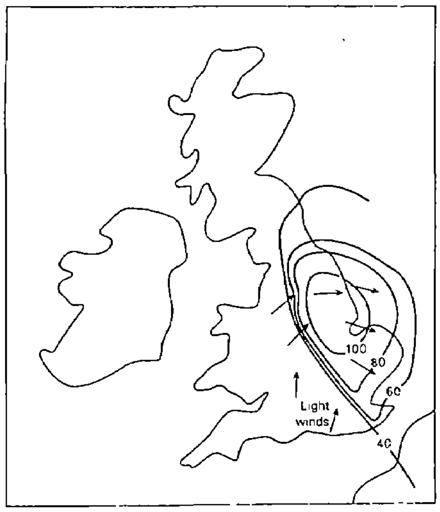

Fig. 3 Air flow and relative humidity (%) at 10.5 km altitude near the smoke plume after 12 h integration.

are plotted in Fig. 1. Downward fluxes at the surface are listed 'exact' in Table 1. In all cases, the heating profile is well approximated by exponential attenuation of the incident flux. It was found that an effective attenuation coefficient of 1.5 $m^2 g^{-1}$ gave a reasonable fit both to the surface flux (last entry in Table 1) and to the heating rates (filled dots) and this was used in the model integration.

In the study, a smoke source was inserted in a column of radius 75 km near the centre of the model grid (see Fig. 2). The vertical profile of the smoke was chosen to be consistent with the published data and to have a concentration of 6.1×10^{-4} kg m^{-2} over the model depth and a peak at 9 km of 1.1×10^{-7} kg m^{-3}. This profile was artificially constrained to be constant in the source area. The smoke was transported from this source by the model winds but was not affected by any other model variables. The model evolution was affected by the internal radiative heating of the smoke and by the reduction in solar radiation at the ground. Using the absorption coefficient quoted above, we obtained an optical depth of 0.91 for the source region at normal incidence or transmission of 20% of the incoming flux at 53° elevation. This depletion of the solar beam is modest compared with previous studies.

The day chosen for the study was 15 June 1984, when an anticyclone covered England and Wales and skies were generally clear. Initial actual data for 0600 GMT were used. A weak northwesterly wind at upper levels resulted in the main plume spreading to cover much of northern England, the East Midlands and East Anglia (see Fig. 2) by 1800 GMT. Solar absorption early in the forecast period quickly resulted in a 5 °C temperature excess at about 300 mbar near the centre of the plume compared with a control run for the same occasion but without the smoke plume. This excess produced a vertical circulation of air with maximum upward motion of 0.2 m s^{-1} in the smoke and weaker subsidence around it. One effect of this circulation was to limit the temperature rise through adiabatic cooling, and after sunset to remove it. Another was to increase the humidity as illustrated in Fig. 3, where the air blowing through the source region has been lifted, with the result that its associated water vapour condensed to produce cloud. This cloud was absent in the control run and has a water content sufficient to produce precipitation which, in turn, would evaporate in the dry air below cloud base. The relationship of this cloud to the smoke is shown in the cross-section (Fig. 4) along the line A–B of Fig. 2. Associated with the thickest smoke, upward motion has been much enhanced and, in the indicated regions, cloud has formed. The model does not attempt to represent the physics of the interaction between water and smoke; however, the results confirm that local circulations, capable of producing cloud formations that otherwise would not occur, can be set up by the local smoke plume.

Table 1 Details of vertical profile curves in Fig. 1

Curve in Fig. 1	Column density ($g m^{-2}$)	Hemispheric loading (Mtonnes)	Total downward flux at the surface ($W m^{-2}$) Exact	Parameterization
1	0	0	509.2	509.2
2	0.0125	3.2	482.5	490.4
3	0.0625	15.9	393.1	422.1
4	0.125	31.9	307.4	349.9
5	0.250	63.8	192.7	240.5
6	0.375	95.6	124.4	165.3
7	0.625	159.4	56.0	78.1
8	1.25	318.8	11.0	12.0

The column densities which were assumed and the corresponding hemispheric loadings, followed by the total (direct plus diffuse) downward broad-band solar flux at the surface (exact) and the value given by a simple parameterization (see text).

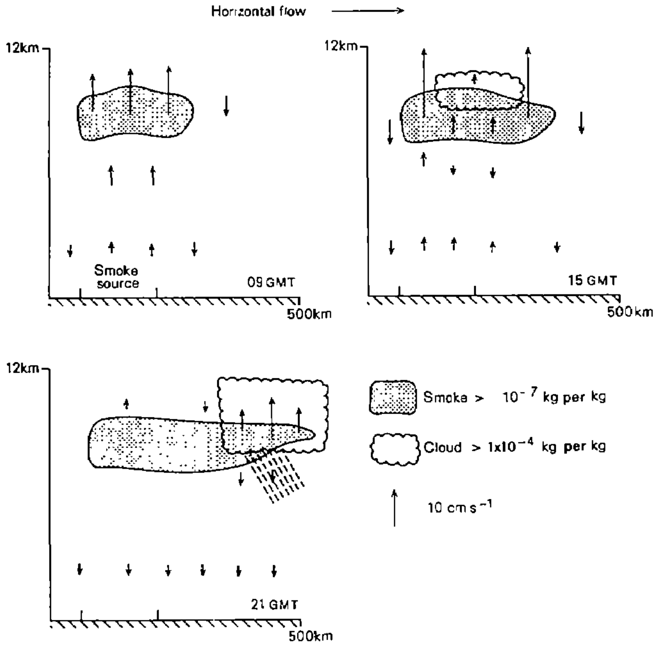

Fig. 4 Schematic representation of the development of a vertical circulation about the smoke and the subsequent formation of cloud seen in the cross-section A–B in Fig. 2.

These results suggest that smoke plumes associated with individual targets could have fairly immediate consequences on the local meteorology, with the result that the characteristics of the smoke may be modified before it has been diffused into the continental-scale smoke pall which has been the starting point of 'nuclear winter' calculations in the past. Further work is needed to establish how sensitive this result is to the approximations made in the modelling process, to the weather situation selected, and to the mode of insertion of the smoke, including the interaction of several plumes. The realism of the experiment could be improved, in particular, by a more detailed treatment of the source region, including the concomitant sources of heat and moisture, and also by including the physics of interactions between water and smoke.

In conclusion we emphasize that, in the case described, fairly dry anticyclonic conditions prevailed and so washout of smoke would be expected to be minimal. It has been demonstrated that heating of the smoke could lead to condensation and hence to interaction between cloud water and smoke particles.

Received 5 August; accepted 31 October 1985.

1. Turco, R. P., Toon, O. B., Ackerman, T. P., Pollack, J. B. & Sagan, C. *Science* **222**, 1283-1292 (1983).
2. Crutzen, P. J., Galbally, I. E. & Bruhl, C. *Climatic Change* **6**, 323-634 (1984).
3. Covey, C., Schneider, S. H. & Thompson, S. L. *Nature* **308**, 21-25 (1984).
4. Alexandrov, V. V. & Stenchikov, G. L. in *Proc. Appl. Math.*, Moscow (1983).
5. *The Effects on the Atmosphere of a Major Nuclear Exchange* (National Academy Press, Washington, 1985).
6. Thompson, S. L. *Nature* **317**, 35-39 (1985).
7. Ramaswamy, V. & Kiehl, J. T. *J. geophys. Res.* **90**, 5597-5613 (1985).
8. Tapp, M. C. & White, P. W. *Q. Jl R. met. Soc.* **102**, 277-296 (1976).
9. Carpenter, K. M. *Q. Jl R. met. Soc.* **105**, 629-688 (1979).
10. Golding, B. W. & Machin, N. A. *Proc. Nowcasting-II Symp.*, Norrkoping (ESA-SP 208, 1984).
11. Slingo, A. & Schrecker, H. M. *Q. Jl R. met. Soc.* **108**, 407-426 (1982).
12. McClatchey, R. A., Fenn, R. W., Selby, J. E. A., Volz, F. E. & Garing, J. S. *Envir. Res. Pap.* No. 411 (Air Force Cambridge Research Laboratories, Massachusetts, 1972).

Evolution of an impact-induced atmosphere and magma ocean on the accreting Earth

Takafumi Matsui & Yutaka Abe

Geophysical Institute, Faculty of Science, University of Tokyo, Bunkyo-ku, Tokyo 113, Japan

Early rapid formation of the atmosphere and hydrosphere on the terrestrial planets has recently been proposed[1,2]. Here we present a quantitative study of this process during accretion by planetesimal impacts. These impacts increase the surface temperature and thus affect the formation of either a proto-atmosphere or a proto-hydrosphere by degassing of volatiles. We show that an impact-induced H_2O atmosphere increases the surface temperature of the Earth to a stage where a magma ocean is possible, with the total amount of H_2O in the proto-atmosphere clustering around 10^{21} kg, this number is rather insensitive to variations in the input data. We suggest that the apparent coincidence of the H_2O abundance in the proto-atmosphere with the present mass ($\sim 1.4\times10^{21}$ kg) of the ocean is evidence for an impact origin for the atmosphere and hydrosphere.

Planets were formed by accretion of planetesimals in heliocentric orbits[3]. High-velocity planetesimal impacts produce craters on the surface of a growing planet. Cratering includes not only the formation of a cavity and the release of impact energy but also the ejection of dust and the shock-heated volatile gases, such as H_2O and CO_2, retained in planetesimals and the surface layer. The frequency of high-velocity collisions during planetary accretion results in an impact-induced atmosphere surrounding the entire surface of a growing planet. The existence of such an atmosphere affects the energy balance between the impact energy released in the surface layer, radiative heat transfer from the surface to interplanetary space, and heating of the surface layer. Previous studies have ignored this effect and assumed a fixed surface temperature[4,5]. A more complete description of the early thermal history of a planet needs to include simultaneous growth by planetesimal impacts and the evolution of an impact-generated atmosphere. As H_2O is the most abundant volatile on the Earth, we consider an evolution of the atmosphere consisting only of H_2O in the following analysis.

The formation of an H_2O atmosphere depends on the surface temperature T_s. When $T_s \leq 900$K, impact dehydration is a promising source mechanism to produce such an atmosphere. According to Lange and Ahrens[6], serpentine loses its structural water when peak impact pressure exceeds the critical impact pressure required for the dehydration reaction of serpentine. The critical impact pressure is estimated to be $P_{cr} = 6\times10^{10}$ Pa when the surface layer and planetesimals have zero porosity[6]. P_{cr} is a function of the porosity; P_{cr} reduces to 2.28×10^{10} Pa for a porosity of 17%. Because the surface of the growing Earth was heavily bombarded by high-velocity planetesimal impacts, we used $P_{cr} = 2.28\times10^{10}$ Pa in our model. The peak impact pressure is given by $P_{imp} = \rho[C_0 + (K'+1)V_i/8]V_i/2$, where ρ, C_0 and K' are density, bulk sound velocity and partial derivative of incompressibility with respect to pressure. The impact velocity is given by $V_i^2 = (2GM/R) + u^2$, where G, M, R and u are the gravitational constant, mass and radius of a growing Earth, and velocity of planetesimals relative to a growing Earth at very great distance ($u = (GM/R\theta)^{1/2}$, where θ is the Safronov number). We used $\rho = 4{,}200$ kg m^{-3}, $C_0 = 3{,}000$ m s^{-1}, $K' = 5$ and $\theta = 4$ for the standard model.

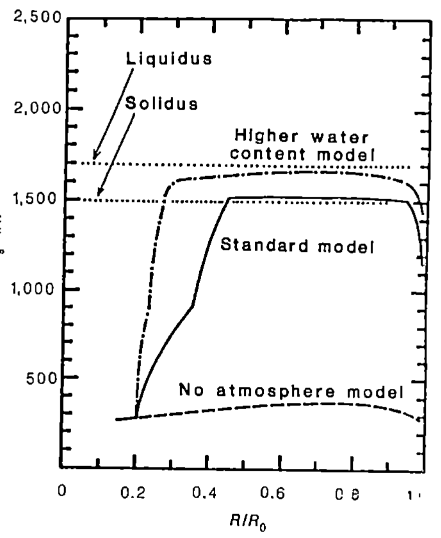

Fig. 1 The evolution of surface temperature during accretion for the standard Earth and higher W_{prj} models. The radius is normalized by the final value. The broken line traces the surface temperature of the model without an impact-generated atmosphere ($\tau_{acc} = 5\times10^7$ yr). The surface temperature begins to increase once the impact velocity exceeds a critical value. The rapid rise in the surface temperature after the Earth grows to $\sim 0.3\ R_0$ is due to an increase in the total mass of the atmosphere because of initiation of the complete dehydration reaction of the surface layer. Once the surface temperature reaches the melting temperature, it becomes constant.

Once the peak pressure exceeds the critical impact pressure, the dehydration reaction is assumed to proceed completely. Then the growth of the impact-generated H_2O atmosphere during the Earth's accretion from M to $M+\Delta M$ can be expressed by

$$\Delta M_a = \Delta M W_{prj} f$$

where ΔM_a is the increase in mass of the H_2O atmosphere, W_{prj} is the water content of the planetesimals and f = (amount of the water added to the atmosphere)/(amount of the water released by shock heating). If all the water added to the Earth is now in the hydrosphere, $W_{prj} = 0.027\%$. This is a minimum estimate of W_{prj} and we used $W_{prj} = 0.1\%$ in our standard model. It is, however, difficult to estimate both W_{prj} and f, the latter ratio primarily expressing the loss mechanism of H_2O. The water vapour may be removed from the atmosphere by the following processes: (1) dissociation of H_2O into hydrogen and oxygen by photochemical reactions, with subsequent escape of hydrogen into space; (2) thermal escape of water vapour into interplanetary space without dissociation; (3) oxidation of the surface aided by photostimulation; (4) re-hydration with the surface minerals; (5) oxidation of Fe metal; and (6) dissociation of water into silicate melt. Processes (1)-(3) are not important because the accretion time required for the growth of ΔM is much shorter than the characteristic decay time of those mechanisms[6,7]. Mechanism (5) is also not important[7]. Therefore, the hydration reaction may be the most dominant loss mechanism in this temperature range. As the reaction rate of the hydration reaction is fast compared with the accretion time, the loss of H_2O may be limited by the amount of available reactants: that is, the thickness of the layer wherein the hydration reaction can occur determines the loss of H_2O. Shock dehydration occurs even in relatively deep regions, but dehydration reactions occur only in the uppermost layer which is in contact with the atmosphere for a long time. The amount of released water is qualitatively larger than that of rehydrated water, and hence an atmosphere may be formed. We adopted $f = 0.2$ as the standard model. In fact, the choice of f does not affect the evolution of the atmosphere because the surface temperature reaches 900 K even for a very small value.

When T_s is >900 K and less than the melting temperature T_m, hydrous minerals become unstable. Then, instead of a hydration reaction, a dehydration reaction occurs even without impact heating. Therefore, we can consider that $f = 1$ in this temperature range.

When $T_s \geq T_m$, the sixth mechanism dominates the loss mechanism for H_2O because H_2O dissolves into a silicate melt under high atmospheric pressure. According to Fricker and Reynolds[8], the amount X_w (in weight %) of water dissolved into silicate melt at pressure, P_a (in pascal), is approximately given by

$$X_w = 2.08 \times 10^{-6} P_a^{0.54}$$

Assuming a plane-parallel atmosphere, $P_a = M_a g / 4\pi R^2$, where M_a and g are the total mass of the H_2O atmosphere and the gravity at the surface of a growing Earth, respectively. The growth of the atmosphere in this temperature range can be simply calculated by

$$\Delta M_a = \Delta M (W_{prj} - \alpha X_w)$$

where α is the degree of melt determined from the distribution of the latent heat between the solidus and liquidus. The solidus and liquidus temperatures are assumed to be $T_{sol} = 1{,}500$ K and $T_{liq} = T_{sol} + 200$, respectively. The latent heat (400 kJ kg^{-1} K^{-1}) is assumed to be uniformly distributed between solidus and liquidus temperatures.

Next, we estimated the effect of the H_2O atmosphere on the surface temperature of the Earth growing by planetesimal impacts. The energy balance equation at the surface layer of a growing Earth is given approximately by

$$h \Delta M V_i^2 / 2 = 4\pi R^2 F_{atm} \Delta t + C_p \Delta M (T_s - T_p)$$

where h, Δt, C_p, T_s and T_p are the fraction of the released impact energy retained in the surface layer, the time interval required for the growth from M to $M + \Delta M$, the specific heat of the surface layer, the temperature of the surface layer and the original temperature of the accreting planetesimal[7]. To derive this equation, for simplicity, we assumed impact energy as the primary heat source and a δ-function-like size-distribution of planetesimals. The quantity h is, in fact, close to but not exactly 1, which means that some fraction of impact energy was imparted into the sub-surface layers; for simplicity, however, we take $h = 1$. However, this assumption does not affect the estimate of the surface temperature because $T_s \propto h^{1/4}$. We used $C_p = 10^3$ J kg^{-1} K^{-1}, and $T_p = 250$ K as the standard model. F_{atm} is the energy flux escaping from the surface into interplanetary space through the atmosphere:

$$F_{atm} = 2\sigma (T_s^4 - T_0^4) / (\tau_s^* + 2)$$

where σ and T_0 are the Stefan-Boltzmann constant and the black body equilibrium temperature of the proto-Earth heated only by solar irradiation, and τ_s^* corresponds approximately to an optical depth for the optically thin atmosphere. We assumed that the atmosphere is gray, plane-parallel and radiatively equilibriated. Then, τ_s^* can be defined by $\tau_s^* = (3/2) \int_0^\infty \kappa \rho_a \, dz = (3\kappa M_a)/(8\pi R^2)$, where κ is the coefficient of absorption[7].

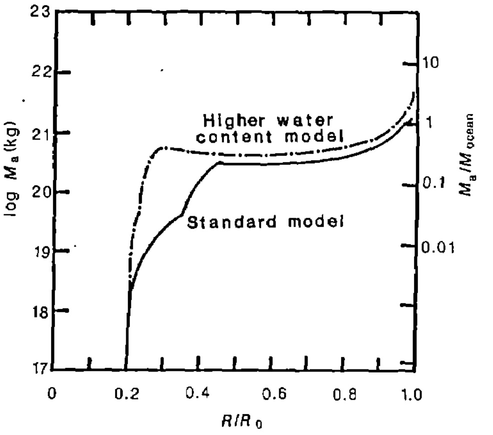

Fig. 2 The total mass of the impact-generated H_2O atmosphere is plotted against the normalized radius for the standard ($W_{prj} = 0.1\%$) Earth and higher water-content ($W_{prj} = 1\%$) models. Note that the total mass remains nearly constant after the Earth grows to 0.4 R_0 and is very close to the present mass of the Earth's oceans ($\sim 1.4 \times 10^{21}$ kg).

Assuming hydrostatic equilibrium and direct proportion of κ to pressure, κ is given by $\kappa = (\kappa_0 g / 3 P_0)^{1/2}$, where κ_0 is the coefficient of absorption at pressure P_0 (ref. 7). We should use an absorption coefficient averaged over a wide range of wavelengths because we assumed a gray atmosphere. We adopted a value of the smoothed absorption coefficient around the window region ($\sim$1,000 cm^{-1}) as κ_0: $\kappa_0 = 0.01$ m^2 kg^{-1} and $P_0 = 101{,}325$ Pa (ref. 9). Note that the κ_0 value thus determined is a minimum. As the mass of the atmosphere increases, the lower atmosphere becomes optically thick and equilibrates convectively. A straightforward estimate of the surface temperature follows from assuming that $T_s = (P_s / P_{eff})^{(\gamma-1)/\gamma} T_{eff} = (\tau_s^*)^{(\gamma^{-1}/\gamma)} T_{eff}$, where T_{eff} is the effective temperature given by $T_{eff} = (F_{atm}/\sigma + T_0^4)^{1/4}$, P_{eff} and P_s are the atmospheric pressure at the tropopause and the base of the atmosphere, and γ is the ratio between the specific heat with constant pressure and the specific heat with constant volume ($= C_p / C_v$). In this case, $F_{atm} = (T_s^4 / \tau_s^* - T_0^4)$. This gives an energy flux that is lower than the flux given for the radiative case, thereby resulting in a higher surface temperature. However, the difference is small. For simplicity, we use the energy flux equation for the radiative case to calculate the surface temperature even for an optically thick atmosphere.

We need an accretion model to solve the energy balance equation. According to Safronov[3], the accretion rate of the Earth is given by

$$\Delta M / \Delta t = 4\pi R^2 (1 + 2\theta) \sigma_p / P_k$$

where P_k is the period of Kepler motion of the accreting Earth and σ_p is the surface density. We simply assumed $\sigma_p = (M_0 - M)/S$, where M_0 and S are the final mass of the Earth and the area from which the Earth collects planetesimals. We used $M_0 = 6.0 \times 10^{24}$ kg and $S = 4.08 \times 10^{22}$ m^2, which gives an accretion time for the Earth of about 5×10^7 yr.

By integrating numerically the above equations with respect to time we determine the evolution of the surface temperature and impact-generated H_2O atmosphere. Figure 1 shows a trace of the surface temperature of the standard Earth and higher W_{prj} (1%) model. The surface temperature increases due to the blanketing effect of the atmosphere, and the surface of the accreting Earth begins to melt once the radius exceeds 0.4 R_0, where R_0 is the final radius ($R_0 = (3M_0/4\pi\rho)^{1/3} = 6{,}987$ km). After the surface temperature reaches the melting temperature, it becomes nearly fixed at about the melting temperature. This is because an increase in the surface temperature increases the degree of melting, which causes efficient absorption of H_2O

molecules from the atmosphere. A decrease in the H_2O content of the atmosphere results in decreasing the efficiency of the blanketing effect, thereby decreasing the surface temperature. A decrease in the surface temperature allows the surface to resolidify, but this increases the H_2O in the atmosphere. The surface temperature decreases rapidly at the final stage of growth. This is because the accretion rate assumed in this study decreases rapidly as the final radius is approached. The surface temperature, however, may not decrease in the final stages when the effect of solar irradiation on the atmosphere (the so-called greenhouse effect) is taken into account. The evolution of the atmosphere after solar irradiation becomes a primary heat source (replacing impact energy) is one of the most important problems for future study.

Figure 2 shows the evolution of the H_2O atmosphere for the standard Earth model and for a model with higher water content ($W_{\mathrm{prj}} = 1\%$, with other parameters the same as the standard model). The amount of the H_2O atmosphere becomes nearly constant once the radius exceeds about 0.4 R_0, at which point the surface temperature reaches the melting temperature (see Fig. 1). This confirms the above interpretation concerning the constant surface temperature, where the solubility of water into silicate melt controls the amount of water in the atmosphere. The atmospheric pressure and τ_s^* also become nearly constant (at $\sim 10^7$ Pa and 10^3, respectively). It is shown elsewhere[10] that melting the surface layer requires an atmosphere whose τ_s^* is 10^3. At the final stages of growth the total mass of the atmosphere increases gradually. This is caused by resolidification of the surface layer.

Comparison of the standard Earth and higher water-content models reveals that the final mass of H_2O atmosphere does not differ significantly between these models even though the time at which the mass of the atmosphere reaches this value differs. This suggests that the amount of H_2O in the atmosphere does not depend on the water content of the raw materials; rather it depends on the surface temperature during accretion. The total interior water content, however, is plainly dependent on the original water content. The surface temperature history for the higher water-content model also resembles that shown in Fig. 1. The initial thermal profile is shown not to depend heavily on the water content. It is very interesting to note that the final mass of the H_2O atmosphere is fairly close to the present mass of the oceans ($\sim 1.4 \times 10^{21}$ kg). The level at which the mass of the H_2O atmosphere becomes nearly constant is only weakly dependent on the accretion time and absorption coefficient. The depth of a magma ocean and degree of partial melt also depend on these parameters. For W_{prj} greater than 1%, the level of constant mass of the H_2O atmosphere depends weakly on this quantity. This is because the solubility of water in silicate melt at $\sim 10^7$ Pa is $\sim 1\%$. A choice of reasonable values for these and other parameters, as shown here, leads to an apparent coincidence of the H_2O abundance in the proto-atmosphere with the present mass of the oceans. This suggests that an impact origin for the atmosphere and hydrosphere is feasible. Incorporating CO_2 would increase the optical depth by several hundred, but this increase does not significantly change the conclusion derived in this study. The oldest rock ($\sim 3.8 \times 10^{-1}$ yr) known so far is of sedimentary origin, which suggests that an extensive hydrosphere was already formed at that time. We conclude that the present mass of the oceans provides evidence for their impact origin and for the past existence of a magma ocean on the proto-Earth.

We thank P. H. Schultz, T. J. Ahrens, and S. C. Solomon for their critical comments on an earlier draft of this paper. This research was partially supported by grants-in-aid for Scientific Research (Nos 60540247 and 59390007) sponsored by the Ministry of Education, Science, and Culture of Japan. The final stage of preparation of this work was carried out while T.M. was on leave at the Department of Earth, Atmospheric and Planetary Sciences, Massachusetts Institute of Technology.

Received 3 June; accepted 20 November 1985.

1. Fanale, F. P. *Chem. Geol.* **8**, 79–105 (1971).
2. Cogley, J. G. & Henderson-Sellers, A. *Rev. Geophys. space Phys.* **22**, 131-175 (1984).
3. Safronov, V. S. NASA Techn. Transl., TTF-677, p. 206 (1972).
4. Safronov, V. S. *Icarus* **33**, 3–12 (1978).
5. Kaula, W. M. *J. geophys. Res.* **84**, 999–1088 1979).
6. Lange, M. A. & Ahrens, T. J. *Icarus* **51**, 96–120 (1982).
7. Abe, Y. & Matsui, T. J. geophys. Res. **89**, C323–C328 (1984).
8. Fricker, P. E. & Reynolds, R. T. *Icarus* **9**, 221–230 (1968).
9. Yamamoto, G. *Sci. Rep. Tohoku Univ. Ser. 5* **4**, 9–23 (1952).
10. Matsui, T. & Abe, Y. *Earth, Moon Planets* (in the press).

Chemical effects of large impacts on the Earth's primitive atmosphere

Bruce Fegley Jr, Ronald G. Prinn, Hyman Hartman & G. Hampton Watkins*

Department of Earth, Atmospheric, and Planetary Sciences,
Massachusetts Institute of Technology, Cambridge,
Massachusetts 02139, USA

Intense bombardment of the moon and terrestrial planets ~3.9–4.0 × 10^9 years ago[1,2] could have caused the chemical reprocessing of the Earth's primitive atmosphere[3]. In particular, the shock heating and rapid quenching caused by the impact of large bodies into the atmosphere could produce molecules such as HCN and H_2CO[4] which are important precursors for the abiotic synthesis of complex organic molecules[5–7]. Here we model the production of HCN and H_2CO by thermochemical equilibrium and chemical kinetic calculations of the composition of shocked air parcels for a wide range of temperatures, pressures and initial compositions. For atmospheres with C/O ≥ 1, our results suggest that bolide impacts cause HCN volume mixing ratios of approximately 10^{-3} to 10^{-5} in the impact region and global average ratios of 10^{-5} to 10^{-12}. The corresponding H_2CO mixing ratios in the impact region are 10^{-7} to 10^{-9}; no-global mixing can occur, however, as H_2CO is rapidly destroyed or rained out of the atmosphere within days to hours. Rainout to the oceans of 3–15% of the HCN produced can provide ~(3–14) × 10^{11} mol HCN per year. This is somewhat larger than other predicted sources of HCN[8] and H_2CO[9] on the primitive Earth.

The atmosphere appeared on Earth very early in its history. Argon and xenon isotope geochemistry[10,11] indicate that the mean age of the atmosphere is 4.4×10^9 yr. The carbonate-bearing sedimentary rocks in the Isua, Greenland supracrustal rocks further suggest the presence of an atmosphere-ocean system 3.8×10^9 yr ago[12]. To evaluate the effects of impacts on this early atmosphere we consider a suite of more than 100 pressure (P) and temperature (T) composition points in the H-C-N-O tetrahedron ranging from chemically reducing to chemically neutral atmospheres, shock pressures from 10^{-3} to 10^3 bar, and shock temperatures from 500 to 5,000 K. Although precise knowledge of the composition of the pre-Archean atmosphere is unavailable, a plausible range of primitive atmosphere compositions can be defined by considering the oxidation states and compositions of present-day volcanic gases, of volcanic gases in equilibrium with metallic iron and of the outgassing from chondritic planets[12–15]. Plausible atmospheres all contain N_2 and small amounts of H_2O in equilibrium with liquid water. Carbon may occur predominantly as CH_4, CO, or CO_2 depending on the assumed oxidation state and H_2 may be present in small amounts conversant with its rapid atmospheric escape.

Thermochemical equilibrium calculations were done using a Gibbs free energy minimization code[16]; thermodynamic data for more than 50 compounds in the H-C-N-O system were taken from standard sources[17,18]. The quenched abundances of HCN

---

* Present address: J. S. Lewis Associates Inc., Tucson, Arizona 85745, USA.

Table 1 Reactions and rate constants used to estimate t_{chem} values for HCN and H_2CO

Reaction	Rate constant	Source
(1) $CHO+H \rightarrow CO+H_2$	$6\times10^{13}\exp(-2{,}500/T)$	19
(2) $CHO+M \rightarrow CO+H+M$	$7\times10^{13}\exp(-7{,}550/T)$	19*
	$2\times10^{13}\,T^{1/2}\exp(-14{,}000/T)$	
(3) $CHO+O \rightarrow CO+OH$	3×10^{13}	19
(4) $CHO+O \rightarrow CO_2+H$	3×10^{13}	19
(5) $CHO+OH \rightarrow CO+H_2O$	6×10^{12}	19*
	3×10^{13}	
(6) $CHO+O_2 \rightarrow CO+HO_2$	3×10^{13}	19*
	$6\times10^{12}\exp(-3{,}650/T)$	
(7) $H_2CO+H_2 \rightarrow OH+CH_3$	$1.4\times10^{14}\exp(-36{,}200/T)$	21
(8) $H_2CO+M \rightarrow HCO+H+M$	$4\times10^{12}\exp(-18{,}500/T)$	22†
(9) $CN+NO \rightarrow CO+N_2$	8.9×10^{12}	20‡
(10) $CN+NO \rightarrow NCO+N$	$1.0\times10^{14}\exp(-21{,}190/T)$	23
(11) $CN+CN \rightarrow C_2+N_2$	$2.5\times10^{17}\exp(-48{,}000/T)$	20*
	$1.6\times10^{15}\exp(-21{,}700/T)$	
(12) $CN+O \rightarrow CO+N$	1.0×10^{13}	20
(13) $CN+O_2 \rightarrow CNO+O$	$2.4\times10^{13}\exp(-450/T)$	20
(14) $CN+C \rightarrow N+C_2$	$3.0\times10^{14}\exp(-18{,}000/T)$	20
(15) $CN+N \rightarrow C+N_2$	$4.4\times10^{14}\exp(-4{,}600/T)$	20
(16) $HCN+H_2 \rightarrow CH_2+NH$	$6.5\times10^{15}\exp(-70{,}456/T)$	24
(17) $HCN+M \rightarrow H+CN+M$	$1.0\times10^{16}\exp(-54{,}650/T)$	25
(18) $HCN+O \rightarrow NCO+H$	$7.2\times10^{13}\exp(-7505/T)$	26

Units for two-body rate constants are $cm^3\ mol^{-1}\ s^{-1}$.

* Calculations done with both expressions.

† Also see Bowman[27] for a similar expression.

‡ Average of values given by Baulch *et al.*[20].

and H_2CO in the shock wave were estimated using the relationship

$$t_{chem}(T_Q) \simeq t_{cool}(T_Q) \qquad (1)$$

where t_{chem} is the chemical lifetime of HCN or H_2CO; t_{cool} is the characteristic cooling time of the shock wave and T_Q is the quench temperature. The t_{chem} values for HCN and H_2CO were estimated using kinetic data for the relevant destruction reactions of CN and HCO (see Table 1)[19–27]. This treatment is valid when HCN and CN, and H_2CO and HCO remain in equilibrium (which we verified). Analogous calculations have also been done by previous investigators estimating NO_x production from high temperature shock phenomena (such as nuclear explosions[28–32], lightning discharges[8,33] and large impacts in the atmosphere[34,35]).

The calculated thermochemical equilibrium mixing ratios of important species in the shocked air parcels are illustrated in Fig. 1. These profiles are representative of those obtained by shocking atmospheric compositions which are chemically neutral (Fig. 1*a*) or chemically reducing (Fig. 1*b*). The major species produced from a CO_2-rich atmosphere are CO, O_2, H_2 and NO; CO-rich atmospheres yield primarily CO_2, H_2, CH_4, HCN, NH_3 and H_2CO. Graphite precipitation is also possible in CO-rich systems but may be kinetically inhibited if nucleation is slow relative to t_{cool}.

Calculations over a wide range of assumed atmospheric compositions show that the C/O atomic ratio strongly influences the yields of the shock products (see Table 2). Our calculated HCN and NO abundances follow the same pattern first noted by Chameides and Walker[8]. We find that the interconversions between HCN and NO for different major carbon-bearing species are described by the reversible equilibrium reactions:

$$2NO+2C(gr)+3H_2 \rightleftharpoons 2HCN+2H_2O \qquad (2)$$

$$2NO+2CH_4 \rightleftharpoons 2HCN+2H_2O+H_2 \qquad (3)$$

$$2NO+2CO+5H_2 \rightleftharpoons 2HCN+4H_2O \qquad (4)$$

$$2NO+2CO_2+7H_2 \rightleftharpoons 2HCN+6H_2O \qquad (5)$$

The thermochemical equilibrium calculations also show that the HCN volume mixing ratio near T_Q is not sensitive to large changes in the total pressure. It decreases by only two orders of magnitude as P varies from 10^3 to 10^{-3} bar. However, the H_2CO mixing ratio varies as P above the graphite condensation temperature and is pressure independent below this point.

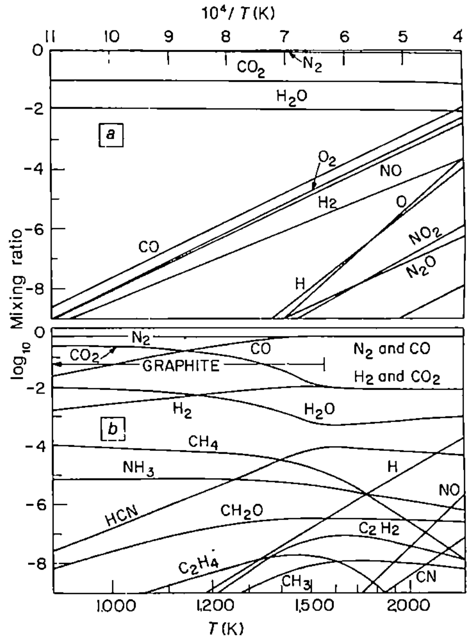

Fig. 1 Equilibrium abundances of important species in a cooling parcel of shocked air. *a*, Neutral atmosphere of 90% N_2, 9% CO_2, 1% H_2O at a shock pressure of 10 bar. HCN, H_2CO, NH_3 and many other species with mixing ratios $<10^{-9}$ are not shown here. *b*, Reducing atmosphere of 49.5% N_2, 49.5% CO, 1% H_2O at a shock pressure of 100 bar. Graphite precipitation occurs at 1,556 K; it is a major carbon sink by 1,000 K. All hydrocarbons (except C_2H_2 and C_2H_4) have mixing ratios $<10^{-9}$. In both cases increasing dissociation of molecules to radicals, atoms, and ions occurs with increasing temperature.

Calculated chemical lifetimes for HCN and H_2CO are compared with the radiative cooling time for the shocked air column in Fig. 2. The HCN quench temperatures vary from 1,560 to 2,100 K depending on the specific HCN destruction reactions. The H_2CO quench temperatures are in contrast <1,110 K. If reaction (2) in Table 1 is relatively fast, H_2CO may remain in equilibrium below 650 K. The corresponding mixing ratios for HCN ($T_Q \approx 1{,}600$ K) and for H_2CO ($T_Q \approx 1{,}000$ K) from Fig. 1*b* are 10^{-4} and 10^{-8}, respectively. For the range of reducing atmospheres studied we calculate HCN mixing ratios of 10^{-3} to 10^{-5} at T_Q and H_2CO mixing ratios of $\sim10^{-7}$ to 10^{-9} at T_Q in the impact region.

Globally averaged HCN mixing ratios were estimated using a simple model developed to describe NO_x production by the putative Cretaceous/Tertiary impactor[34]. We take the HCN production efficiency as 10^7 molecules erg^{-1} (for a $CO+N_2$ atmosphere) from Chameides and Walker[8]. This efficiency is strongly composition-dependent ranging from $\sim10^{10}$ molecules erg^{-1} (CH_4+N_2) to $\sim10^3$ molecules erg^{-1} ($CO_2+N_2+H_2O$)[8]. From Lewis *et al.*[34] we take the energy deposited in the atmosphere by a 10^{17} g metal-rich impactor (vertical entry angle $\sim12\ km\ s^{-1}$) as $\sim10^{25.8}$ erg and the energy deposition by a 10^{18} g cometary impactor (grazing entry angle $\sim65\ km\ s^{-1}$) as $\sim10^{30.3}$ erg. The estimated HCN yields are in the range of 10^{33}–10^{37} molecules per impact and the fraction of the atmosphere shocked per impact is in the range 10^{-8}–10^{-3} (assuming HCN mixing ratios of $\sim10^{-3}$ to 10^{-5} at T_Q and the present atmospheric mass of 5.1×10^{21} g). Corresponding globally-averaged HCN and H_2CO mixing ratios would be from 10^{-5} to 10^{-12} and from 10^{-10} to 10^{-16}, respectively. However, these globally-averaged values are relevant only if the chemical lifetimes of the species are longer than the global atmospheric mixing time of 1-3 yr.

Several potential loss mechanisms for HCN and H_2CO are

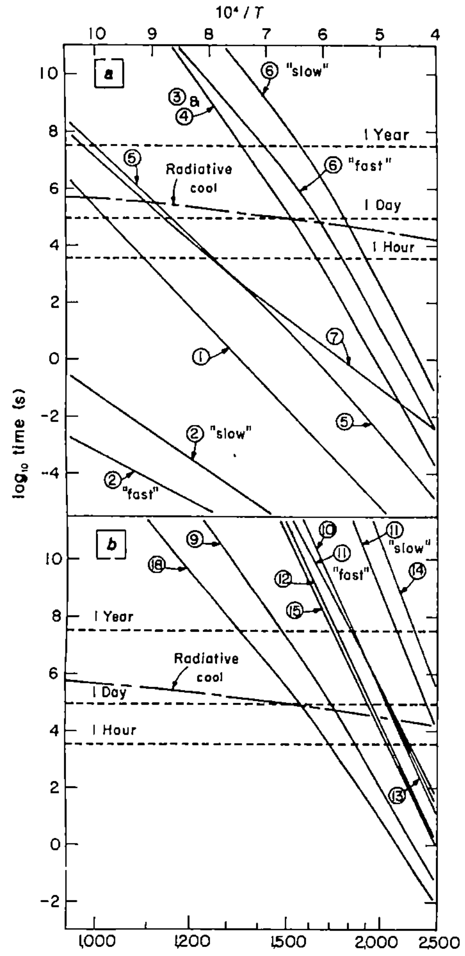

Fig. 2 Calculated chemical lifetimes for H_2CO (*a*) and HCN (*b*) for the reducing atmosphere shown in Fig. 1*b*. The numbers refer to the reactions in Table 1; reaction 16 has a t_{chem} very similar to those for reactions 12, 13, 15 and is not shown. The radiative cooling time is calculated from the Stefan-Boltzman law. For $T > T_Q$, $t_{chem} < t_{cool}$ and the HCN and H_2CO remain in equilibrium, while for $T < T_Q$, $t_{chem} > t_{cool}$ and the HCN and H_2CO are quenched at their mixing ratios established at $T = T_Q$ where $t_{chem} = t_{cool}$. The T_Q values used for HCN and H_2CO in our discussion are 1,600 K and 1,000 K respectively. However, H_2CO may remain in equilibrium below ~650 K if reaction (2) is fast.

possible; we qualitatively discuss these by analogy with these processes in the present-day terrestrial atmosphere. Precipitation can transport HCN and H_2CO to the primitive oceans where abiotic syntheses of complex organic molecules may occur[5-7,12]. Cicerone and Zellner[36] deduced that HCN has a long rainout lifetime of about 34 yr; H_2CO is much more soluble (it polymerizes in aqueous solution) and has a rainout lifetime[37] of about 10 days. Both species are also destroyed by solar ultraviolet photolysis and by reaction with OH. The HCN and H_2CO chemical lifetimes in the present day atmosphere are ~1-5 years[37] and ~3 hours[38], respectively. However, the latter value refers to the sunlit troposphere at 30° N and at noon; a diurnal average is probably 3-4 times longer. These general considerations suggest that isolated impacts are a negligible global H_2CO source relative to possible photolytic sources[9]; only small, temporally and spatially localized production may occur. However, these considerations are consistent with a significant global source of HCN from isolated impacts.

To a first order, 1/34 to 5/34 of the HCN produced in a single impact event will be rained out of the atmosphere based on the lifetimes quoted above. Taking the present globally averaged rainfall rate[37] of 3.3×10^{-6} g cm^{-2} s^{-1}, a Henry's law constant[36] of 4×10^3 and a HCN global mixing ratio of 10^{-6} we derive a HCN rainout rate of 3 to 14×10^{11} mol yr^{-1}. This is somewhat larger than predicted H_2CO (from photolysis)[9] and HCN (from lightning)[8] rainout rates on the primitive Earth of ~10^{11} mol yr^{-1}.

Table 2 Equilibrium mixing ratios of HCN, NO and H_2CO for different assumed atmosphere compositions at 2,000 K and shock pressures of 10 and 100 bar

$p = 10$ bar Starting composition	log$_{10}$ mixing ratios HCN	 NO	 H_2CO
44.4% N_2, 44.4% CO, 11.1% H_2*†	−2.6	−9.3	−6.6
14.3% N_2, 57.1% CO, 22.6% CH_4†	−2.6	−9.6	−6.0
9% N_2, 90.1% CO, 1% H_2O	−5.0	−7.5	−7.2
49.5% N_2, 49.5% CO, 1% H_2O	−5.2	−7.0	−7.5
1% N_2, 98% CO, 1% H_2O	−5.4	−8.1	−7.2
70% N_2, 26.4% CO_2, 2.6% CO, 1% H_2O	−9.9	−4.1	−10.4
80% N_2, 17.3% CO_2, 1.7% CO, 1% H_2O	−10.0	−4.1	−10.6
80% N_2, 19% CO_2, 1% H_2O	−12.2	−3.2	−12.3
$p = 100$ bar Starting composition	**log$_{10}$ mixing ratios** HCN	 NO	 H_2CO
10% N_2, 80% CO, 10% H_2 *	−3.2	−8.8	−6.3
9% N_2, 90% CO, 1% H_2O	−4.0	−8.0	−6.2
49.5% N_2, 49.5% CO, 1% H_2O	−4.1	−7.4	−6.5
1% N_2, 98% CO, 1% H_2O	−4.4	−8.5	−6.2
70% N_2, 26.4% CO_2, 2.6% CO, 1% H_2O	−8.9	−4.6	−9.4
80% N_2, 17.3% CO_2, 1.7% CO, 1% H_2O	−9.0	−4.6	−9.6
80% N_2, 19% CO_2, 1% H_2O	−12.0	−3.4	−11.9

* High H_2 mixing ratio cannot be sustained for long periods. This case is shown for illustrative purposes only.

† Graphite saturated system. This case is shown for illustrative purposes only

Impactor fluxes on the primitive Earth are not well constrained. However, a few large impacts every 1-5 yr will maintain the globally averaged HCN mixing ratios and rainout rates calculated above. More frequent impacts will lead to increasing HCN abundances.

Preliminary stages of this work were supported by NASA grant NGR-22-007-269 to Harvard University. The final part was supported by NSF grants ATM-84-01232, NAG9-108 and NAGW-114 to MIT.

Received 23 September; accepted 29 November 1985.

1. Tera, F., Papanastassiou, D. A. & Wasserburg, G. J. *Earth planet. Sci. Lett.* **22**, 1-21 (1974).
2. Wetherill, G. W. *Proc. 6th lunar Sci. Conf.* 1539–1561 (1975).
3. Hochstim, A. R. *Proc. natn. Acad. Sci. U.S.A.* **50**, 200–208 (1963), in *Chemical Evolution and the Origin of Life* (eds Buvet, R. & Ponnamperuma, C.) 96-113 (North-Holland, New York, 1971).
4. Fegley, B., Hartman, H. & Prinn, R. G. *EOS* **63**, 1018 (1982).
5. Oro, J. & Kimball, A. P. *Archs biochem. Biophys.* **94**, 217–227 (1961)
6. Cairns-Smith, A. G. *Genetic Takeover and the Mineral Origins of Life*, 21-31 (Cambridge University Press, 1982).
7. Abelson, P. H. *Proc. natn. Acad. Sci. U.S.A.* 1365–1372 (1966).
8. Chameides, W. L. & Walker, J. C. G. *Origins Life* **11**, 291–302 (1981)
9. Pinto, J. P., Gladstone, G. R. & Yung, Y. L. *Science* **210**, 183–185 (1980).
10. Sarda, P., Staudacher, Th. & Allegre, C. J. *Earth planet. Sci. Lett.* **72**, 357–375 (1985)
11. Staudacher, Th. & Allegre, C. J. *Earth planet. Sci. Lett.* **60**, 389–406 (1982).
12. Holland, H. D. *The Chemical Evolution of the Atmosphere and Oceans* (Princeton University Press, 1984).
13. Holland, H. D. in *Petrologic Studies: A Volume to Honor A. F. Buddington* (ed Engel, A. E. J., *et al.*) 447–477 (Geological Society of America, Boulder, 1962)
14. Gerlach, T. M. & Nordlie, B. E. *Am. J. Sci.* **275**, 353–410 (1975).
15. Lewis, J. S. & Prinn, R. G. *Planets and their Atmospheres Origin and Evolution*, 225-233 (Academic, New York, 1984).
16. Gordon, S. & McBride, B. J. *NASA SP273* (1976).
17. *JANAF Thermochemical Tables* (eds Stull, D. R. & Prophet, H.) NSRDS-NBS 37 (US Government Printing Office, Washington, 1971).
18. Glushko, V. P. *et al.* (eds) *Thermodynamic Properties of Individual Substances* Vols 1-4 (High-Temperature Institute, Moscow, 1978–1982).
19. Baulch, D. L., Drysdale, D. D., Duxbury, J. & Grant, S. J. *Evaluated Kinetic Data for High Temperature Reactions* Vol. 3, 337–361 (Butterworths, London, 1976).
20. Baulch, D. L., Duxbury, J., Grant, S. J., Montague, D. C. *Evaluated Kinetic Data for High Temperature Reactions* Vol. 4, 576–635 (*J. phys. Chem. Ref. Data* **10**, Suppl 1, 1981)
21. Prinn, R. G. & Barshay, S. S. *Science* **198**, 1031–1034 (1977).
22. Chen, C. J. & McKenney, D. J. *Can. J. Chem.* **50**, 992–998 (1972)
23. Colket, M. B. *Int. J. Chem. Kinet.* **16**, 353-369.
24. Prinn, R. G. & Fegley B. Jr. *Astrophys. J.* **249**, 308–317 (1981).
25. Szekely, A., Hanson, R. K., and Bowman, C. T. *J. phys. Chem.* **88**, 666-668 (1984).
26. Higashihara, T., Salto, K. & Murakami, I. *J. phys. Chem.* **87**, 3707–3712 (1983)
27. Bowman, C. T. *Symp. 15th Int. Combust. Proc.* 869-882 (Combustion Institute, Pittsburgh, 1974).
28. Foley, H. M. & Ruderman, M. A. *J. geophys. Res.* **78**, 4441–4450 (1973).
29. Gilmore, F. R. *J. geophys. Res.* **80**, 4553–4554 (1975).
30. Goldsmith, P., Tuck, H. F. Foot, J. S., Simmons, E. L. & Newson, R. L. *Nature* **244**, 545-551 (1973).

31. Johnston, H., Whitten, G. & Birks, J. *J. geophys. Res.* **78**, 6107-6135 (1973).
32. Zeldovich, Ya. B. & Raizer, Ya. *Physics of Shock Waves and High Temperature Phenomena* Vol. 2, 566-571 (Academic, New York, 1967).
33. Chameides, W. L. *Nature* **277**, 123-125 (1977).
34. Lewis, J. S., Watkins, G. H., Hartman, H. & Prinn, R. G. *Geol. Soc. Am. Spec. Pap.* **190**, 215-221 (1982).
35. Park, C. *Acta astronautica* **5**, 523-542 (1978).
36. Cicerone, R. J. & Zellner, R. *J. geophys. Res.* **88**, 10, 689-10, 696 (1983).
37. Giorgi, F. & Chameides, W. L. *J. geophys. Res.* **90**, 7872-7880 (1985).
38. Lowe, D. C. & Schmidt, U. *J. geophys. Res.* **88**, 10, 844-10, 858 (1983).

Direct conversion of methane to methanol, chloromethane and dichloromethane at room temperature

Kotaro Ogura & Kenji Takamagari

Department of Applied Chemistry, Yamaguchi University,
Ube 755, Japan

As methane is extremely inert, its conversion into a form suitable for chemical use has been achieved by an indirect process in which methane is first converted to synthesis gas and then to methanol and to ethylene glycol[1]. One disadvantage of this route of conversion is that it requires conditions of high temperature and pressure[2]. Here we report the direct conversion of methane to methanol, chloromethane and dichloromethane at the three-phase interface (gas/solution/electrode) on illumination at room temperature. The key steps in this process are: (1) electrochemical oxidation of the chloride ion; (2) generation of the chlorine radical under illumination; and (3) formation of the methyl radical by the reaction of methane with the chlorine radical.

In the present study, we attempted the combined photochemical and electrochemical oxidation of methane at room temperature. A conventional two-compartment glass electrolysis cell was used, with the anode compartment separated from the cathode compartment by a fritted-glass partition. A water-sealed stopcock and a Luggin capillary provided contact between the anode and the reference electrode. The anode compartment incorporated a flat quartz window through which we illuminated the cell, using as a light source a 4-W low-pressure mercury lamp (Hamamatsu TV, L937-04). The wavelength of the illumination was 254 nm. The anode comprised a platinum plate partially immersed in the anolyte, and methane was introduced above the level of the solution. Only the surface of the platinum exposed to the gas phase was illuminated. To collect volatile products, the effluent gas was passed through a trap (25 cm^3) containing 20% KOH by weight. Both the electrolytic solution and the trap were kept at 25 ± 1 °C. Various strengths of KCl solution were used as electrolytes; the results presented here are for a 0.6 M KCl solution of *p*H 11.0.

We determined the oxidation products present in both the electrolyte and residues in the trap by steam chromatography using an Ohkura Model SSC-1 which uses steam as the carrier gas and incorporates a flame ionization detector (FID) and a Poropak R column. This equipment is capable of detecting directly organic substances dissolved in an aqueous solution, without any pretreatment[3].

The steam chromatograms of the solution after electrolysis at potentials more positive than +1.3 V (compared with the standard calomel electrode, SCE) showed four peaks at 2.0, 3.3, 10.0 and 26.1 min corresponding to chloromethane, methanol, dichloromethane and trichloromethane, respectively. However, the peak due to trichloromethane was very small compared with the other three peaks. No such peaks were observed for the solution electrolysed in the dark.

Table 1 Yield of chloromethane, methanol, dichloromethane and trichloromethane in a 0.6 M KCl solution at *p*H 11.0

V_e (V)	CH_3Cl	CH_3OH	CH_2Cl_2	$CHCl_3$
1.1	0.4	0.2	0.0	0.0
1.2	15.3	0.8	0.0	0.0
1.3	24.9	6.1	9.6	0.3
1.4	164.3	6.3	16.7	0.3
1.5	239.9	10.5	17.9	0.9
1.6	18.1	1.1	0.2	0.0
1.7	29.3	1.9	0.4	0.0
1.8	59.6	2.9	1.6	0.1
1.9	95.1	6.6	6.4	0.3
2.0	95.8	7.4	8.6	0.7

V_e, electrolysis potential compared with the saturated calomel electrode. Values shown are the quantities (in μmol) of electrolysis products. Electrolysis time was 3 h; volume of electrolyte 20 cm^3; the anode comprised a platinum plate of area 6 cm^2.

Table 1 shows the amounts of CH_3Cl, CH_3OH, CH_2Cl_2 and $CHCl_3$ produced in the 0.6 M KCl solution at *p*H 11.0 for various anodizing potentials. At potentials more negative than +1.0 V, there was no oxidation of methane. Conversion to $CHCl_3$ and CH_3OH commenced at +1.1 V, and further conversion to CH_2Cl_2 and $CHCl_3$ began at +1.3 V. At +1.5 V, the formation of these compounds was at a maximum, the current efficiencies being 12.8% (CH_3Cl), 0.38% (CH_3OH) and 2.05% (CH_2Cl_2) where the electric charge passed was 361.7 C. Chemical and gas-chromatographic analyses were done to detect other species such as HCHO or CO_2; however, the results were negative.

The results presented here indicate that the electrochemical evolution of the chlorine molecule and the formation of its radical on illumination are prerequisites for triggering the activation of methane. The photochemical chlorination of methane is well understood. Mixtures of methane and chlorine react rapidly in the presence of light. However, for this reaction to occur, the two gases must be mixed at an appropriate ratio, and the reaction is difficult to control as hydrogen atoms are replaced by chlorine atoms almost at random. In the combined photochemical/electrochemical method described here, the chlorination can be stopped after the initial stage because the formation of the products is a function of the electrode potential. Another feature of this method is that methane is converted directly to methanol. The formation of methanol may be explained in two ways. First, by the further oxidation of the methyl radical by electrolytic catalysis:

$$\mathrm{M(electrode)} + H_2O \rightarrow MOH + H^+ + e^- \qquad (1)$$

$$MOH + \cdot CH_3 \rightarrow CH_3OH + M \qquad (2)$$

where MOH is the intermediate species in the electrochemical evolution of oxygen[4]. The second explanation involves hydrolysis of CH_3Cl:

$$CH_3Cl + OH^- \rightleftharpoons CH_3OH + Cl^- \qquad (3)$$

Reaction (1) is endoergic, and reaction (3) seems to predominate. In fact, the formation of methanol was more favourable at higher *p*H. However, reactions (1) and (2) must occur because methanol was produced even in strongly acidic solution (*p*H 1). We are presently studying the mechanism in detail. The rather complicated effect of the anodizing potential on the formation of the electrolytic products may be related to the evolution of oxygen—that is, an oxygen or hydroxyl radical generated during anodization could act as a scavenger for chlorine and methyl radicals. That the most important step in this conversion process is the radical reaction in the gas phase is demonstrated by the very small amounts of the products yielded when a methane-saturated solution was used, but the electrode was completely immersed (the light then passing through the solution).

Received 12 August; accepted 7 November 1985.

1. Hatch, L. F. & Matar, S. *From Hydrocarbons to Petrochemicals* 58-61 (Gulf Publishing Company, Houston, 1981).
2. Kuhre, C. J. & Shearer, C. J. *Oil Gas J.* 85-90 (1971).
3. Nonaka, A. *Analyt. Chem.* **44**, 271-276 (1972).
4. Bockris, J. O'M. *J. chem. Phys.* **24**, 817-825 (1956).

Does partial melting reduce the creep strength of the upper mantle?

S. Karato

Ocean Research Institute, University of Tokyo, Minamidai,
Nakano, Tokyo 164, Japan

The seismic low-velocity zone has been thought to correspond to a zone of partial melting that significantly reduces the creep strength, making it possible for the plates to decouple from the underlying mantle[1,2]. This view is examined here in light of recent experimental results which show that water has more effect on the creep strength of olivine[3–6] than does partial melting[7,8] and that the former depends on the fugacity of water[5,6]. When there is a limited amount of water, partial melting will result in depletion of water from olivine, and therefore have a hardening, rather than a softening, effect.

Recent experimental studies on olivines containing a small amount (a few per cent) of partial melt have demonstrated that it has only a minor effect on creep strength (enhancement of creep rate by a factor of ≤2-5) both in water-free[7] and water-saturated[8] conditions. Water, however, has a more drastic effect (enhancement of creep rate by a factor of ≥20-50) both on the disolcation creep[3-6] and on the grain size sensitive (diffusion) creep regime[5]. The water effect has been shown to depend on the fugacity of the water (concentration of water in olivine)[5,6].

These observations suggest that the fugacity of water should have an important role in the rheology of the upper mantle. The fugacity of water, and, therefore, water content in olivine, depends on the amount of water present and the number of phases which can incorporate water. Silicate melts significant amounts of water[9] so partial melting will reduce both the fugacity of water and its content in olivine if the melt fraction exceeds a certain value.

At the pressure and the temperature conditions in the low-velocity and high-conductivity zone, most hydrous phases are unstable and water can therefore exist either free and/or dissolved in melt and/or nominally anhydrous solid phase (olivine). Recent experimental work[6] indicates that the solubility of water in olivine is $\sim 5\times10^{-5}$ mol per mol (or 10^{-3} wt%) at the confining pressure of 300 MPa. The solubility of water in the basaltic melts is quite large, ~0.5 mol per mol (or ~6 wt%) at the same pressure[9]. These results indicate that when the basaltic melt coexists with olivine, water will be concentrated in the melt phase with a partition coefficient $K = c_{w,m}/c_{w,s} \sim 10^4$ (at 300 MPa) where $c_{w,m}$ and $c_{w,s}$ are the solubility of water in the melt and that in the solid phase (olivine) respectively. Here we assumed that the partition of water between the melt and the olivine is independent of the fugacity of water and of the melt fraction. The actual value of K in the mantle may depend on the fugacity of water because of the possible difference in the dependence of water solubility in the melt ($c_{w,m} \sim f^{1/2}_{H_2O}$) (ref. 9) and in the olivine ($c_{w,s} \sim f^{m}_{H_2O}$, $m = 1/3$-$1/5$) (refs 5, 6) on the water fugacity. However, this possible dependence of K on water fugacity is small in the present context and will not be used in the following argument.

When the melt fraction is small, a partially-melted rock will be saturated with water. The amount of water in olivine is equal to the solubility (limit) $c^0_{w,s}$. Undersaturation of a rock with water occurs when the melt fraction exceeds a critical value $f_c = c_t/c^0_{w,m} - K^{-1}$, where c_t is the water content of a rock and $c^0_{w,m}$ is the solubility (limit) of water in the melt. The concentration of water in olivine in this case $c_{w,s}$ is given by

$$c_{w,s}/c^0_{w,s} = (1+f_c(K-1))/(1+f(K-1))$$

where f is the melt fraction, here the dependence of K on the fugacity of water is neglected. $c_{w,s}/c^0_{w,s}$ represents the ratio of the water content in olivine at an undersaturated condition to that at saturated (or melt-free) condition, and is termed a water-depletion factor. Figure 1 shows the water depletion factor as a function of melt fraction for several values of the total water content. Significant depletion of water from olivine will occur when the melt fraction exceeds a critical value. In the simplest model, where the creep rate is proportional to the concentration of water (or water-related species[10]), the magnitude of water depletion is proportional to the magnitude of reduction of creep rate. Therefore, partial melting will result in hardening, when the melt fraction is significantly larger than the critical value, but does not exceed the value above which the direct weakening effect of partial melting (the effect at constant water fugacity) becomes important.

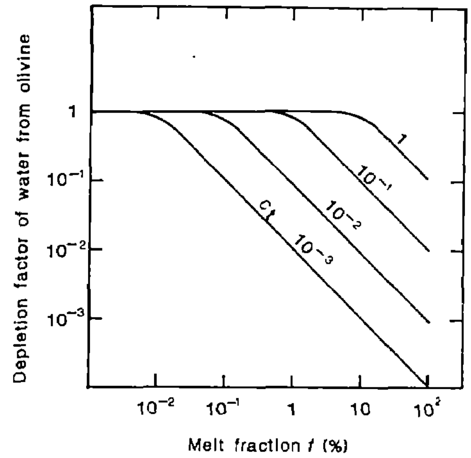

Fig. 1 Depletion factor of water in olivine due to partial melting as a function of melt fraction f for several values of total water content c_t (wt%). The water content of the source region of MORB is estimated to be $\sim 10^{-2}$ wt% based on the measured value of water content of MORB[12]. Significant depletion of water and resultant hardening will occur when the melt fraction greatly exceeds the critical value, but remains less than the larger amounts (~20%) of melt needed to weaken the rocks[18] directly.

The relevance of these results to the Earth depends on the water content and the melt fraction in the Earth, quantities which may vary according to the variation of the tectonic setting[11,12]. For the source region of mid-ocean ridge basalts (MORB), the low-velocity and high-conductivity zone under the oceanic plates, the water content of the mantle (c_t) is $\sim 10^{-2}$ wt% based on the measured water content of MORB[12], assuming that MORB is formed by ~20% partial melting[13]. This gives $f_c = 10^{-1}$% a value significantly smaller than the estimated degree of partial melting in the low-velocity and high-conductivity zone[14], although this estimation contains a large uncertainty. We suggest, therefore, that this hardening effect is likely to occur in the low-velocity and high-conductivity zone under the oceanic plates.

The weakening effect of partial melting observed in the laboratory is likely to depend on the grain-size sensitivity. In the Earth, the grain-size insensitive dislocation creep may also have to be considered in which the effect of partial melting will be much smaller. Therefore, the experimentally-observed weakening effect of partial melting must be regarded as the upper limit to the realistic value.

The above argument also assumes that laboratory data on the creep strength of the olivine+basalt system is applicable to the Earth. Although the melt fraction (several per cent) in these experiments[7,8] probably represents the typical value of degree of partial melting in the Earth, the effect of other minerals must be examined before the results can be applied. Recent experiments[15] on the melt-solid geometry of a partially melted peridotite indicates that the olivine-basalt-olivine boundary has the smallest dihedral angle. This suggests that the experimental results on the olivine+basalt system give the lower limit of the creep strength of the realistic partially-melted system.

Note that so far we have considered the effect of changing the melt fraction and kept the other variables unchanged. This is certainly not realistic. An increase in the melt fraction in the Earth is nearly always associated with increase in temperature and/or in water content (or water fugacity). Both of these effects will tend to reduce the creep strength and will, therefore, partially offset the present argument. Even in these cases, the proposed mechanism will counteract to the softening effects due to the increase in temperature and/or in water content and must be regarded as a relative hardening effect.

I conclude that partial melting reduces the creep strength only in restricted conditions. The reduction in water content in olivine can be associated with partial melting in the low-velocity and high-conductivity zone under the oceanic plates, which may increase the creep strength compared with a (hypothetical) melt-free situation. Therefore, creep strengths of the low-velocity and high-conductivity zone may be significantly larger than in the case where no partial melting occurs.

This mechanism may explain the puzzling observation that the extrapolation of experimental results on water-saturated ('wet') olivine rheology predicts an embarrassingly weak creep strength of the upper mantle[16,17].

I thank David Kohlstedt and Prame Chopra for helpful comments, Toshitsugu Fujii for discussions on the petrological aspects, and Mitsuhiro Toriumi for stimulating discussions.

Received 2 July; accepted 25 September 1985.

1. Ringwood, A. E., in *The Earth's Crust and Upper Mantle* (ed. Hart, P. J.) 1-17 (American Geophysics Union, Washington DC, 1969).
2. Anderson, D. L. & Sammis, C. *Phys. Earth planet. Inter.* **3**, 41-50 (1970).
3. Chopra, P. N. & Paterson, M. S. *Tectonophysics* **78**, 453-473 (1981).
4. Chopra, P. N. & Paterson, M. S. *J. geophys. Res.* **89**, 7861-7876 (1984).
5. Karato, S., Paterson, M. S. & FitzGerald, J. D. *J. geophys. Res.* (in the press).
6. Mackwell, S. J., Kohlstedt, D. L. & Paterson, M. S. *J. geophys. Res.* (in the press).
7. Cooper, R. F. & Kohlstedt, D. L. *Tectonophysics* **107**, 207-233 (1984).
8. Chopra, P. N. & Kohlstedt, D. L. *EOS* **64**, 323 (1983).
9. Burnham, C. W. in *The Evolution of the Igneous Rocks* (ed. Yoder, H. S. Jr) 439-482 (Princeton University Press, 1979).
10. Hobbs, B. E. *J. geophys. Res* **89**, 4026-4038 (1984).
11. Ito, E., Harris, D. M. & Anderson, A. T. Jr *Geochim. cosmochim. Acta* **47**, 1613-1624 (1983).
12. Moore, J. G. *Contr. Miner. Petrol.* **28**, 272-279 (1970).
13. Ringwood, A. E. *Composition and Petrology of the Earth's Mantle* (McGraw-Hill, New York, 1975).
14. Shankland, T. J., O'Connell, R. J. & Waff, H. S. *Rev. Geophys. Space Phys.* **29**, 394-406 (1981).
15. Toramaru, A. & Fujii, N. *J. geophys. Res.* (submitted).
16. Goetze, C. in *High Pressure Research, Application in Geophysics* (eds Manghnani, M. H. & Akimoto, S.) 3-23 (Academic, New York, 1977).
17. Karato, S. *Tectonophysics* **104**, 155-176 (1984).
18. van der Molen, I. & Paterson, M. S. *Contr. Miner. Petrol.* **70**, 299-318 (1979).

Partial melting zones in the crust in southern Tibet from magnetotelluric results

Van Ngoc Pham*, Danièle Boyer*, Pierre Therme*, Xue Cheng Yuan†, Li Li† & Guo Yuan Jin†

* Laboratoire de Géophysique Appliquée et Structurale (LA 235), Ecole Nationale Supérieure de Géologie, BP 40, 54501 Vandoeuvre Cedex, France
† Bureau of Geophysical and Geochemical Exploration, Ministry of Geology and Mineral Resources, Xi Si, Beijing, China

Magnetotelluric studies in southern Tibet along a north–south traverse, 200 km long, crossing the Yarlung–Zangbo suture zone near Lhasa, have enabled us to construct a two-dimensional model in which layers of anomalously high conductivity exist at depths shallower than 33 km. The electrical properties of these layers are different on the two sides of the suture zone. We show here that the most plausible explanation of the high conductivity is the existence of partial melting zones in the upper part rather than the lower part of a crust ~70 km thick. This represents a powerful constraint for thermo-mechanical models of continental collisions.

The Tibetan Plateau is the largest topographical mass on the Earth, with an unusually high average elevation (5 km above sea level). Although its uplift must be related to the Himalayan continental collision and penetration of India into Asia[1], there is considerable debate over its present structure and mode of formation[2]. The chief aim of the 3-year programme of French-Chinese cooperation for the study of Tibet and the northern Himalayas, which began in 1980, was to improve the understanding of the local geology by using new techniques and observations. The programme involved magnetotelluric (MT) exploration in southern Tibet, in the area around the Yarlung-Zangbo suture (YZS) zone which marks the boundary between the Indian continent to the south and the Lhasa Block to the north[3] (Fig. 1).

MT studies provide information about the electrical properties of the crust and upper mantle, and may have an important role in characterizing contemporary tectonic activity in a continent-continent collision zone since, at different levels of the crust and upper mantle, the electrical resistivity will reflect several thermally related processes. Indeed the Tibetan Plateau is characterized by strong geothermal activity[4] with more than 600 hydrothermal areas, of which 70% are concentrated in southern Tibet in the so-called 'Himalayan geothermal belt' (HGB) along both sides of the YZS zone[5]. So far, 11 hydrothermal explosions, 3 geysers and 42 boiling springs have been discovered. The temperature of the hot springs varies from 35 °C to 100 °C[6].

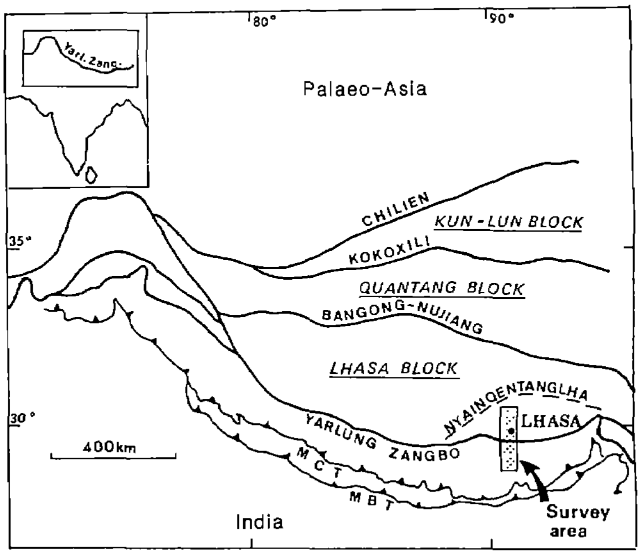

Fig. 1 Schematic tectonic map of the Tibetan Plateau and the North Indian Margin showing several independent tectonic blocks (underlined) separated by suture zones (heavy lines). Dashed line, Nyainqentanglha Range, barbed lines indicate continental underthrusting within the Indian continent. MCT, Main Central Thrust; MBT, Main Boundary Thrust. Shading marks the location of the MT survey area (from ref. 3).

Neogene calc-alkaline volcanic rocks have been found over much of Tibet[7]. Potassic lavas (tephrites, trachytes) located at Machiang, just north of the YZS[8], have been recently dated by $^{39}Ar/^{40}Ar$ methods at 10-15 Myr (C. Coulon, personal communication), while a granite outcrop west of Kangmar area, ~80 km south of the YZS, has an age of 6-8 Myr (ref. 9).

The geothermal activity in southern Tibet is closely related to recent magmatic activity and contemporary tectonic movements. Consequently, the thermal structure of Tibet is a very important parameter for understanding the active processes in

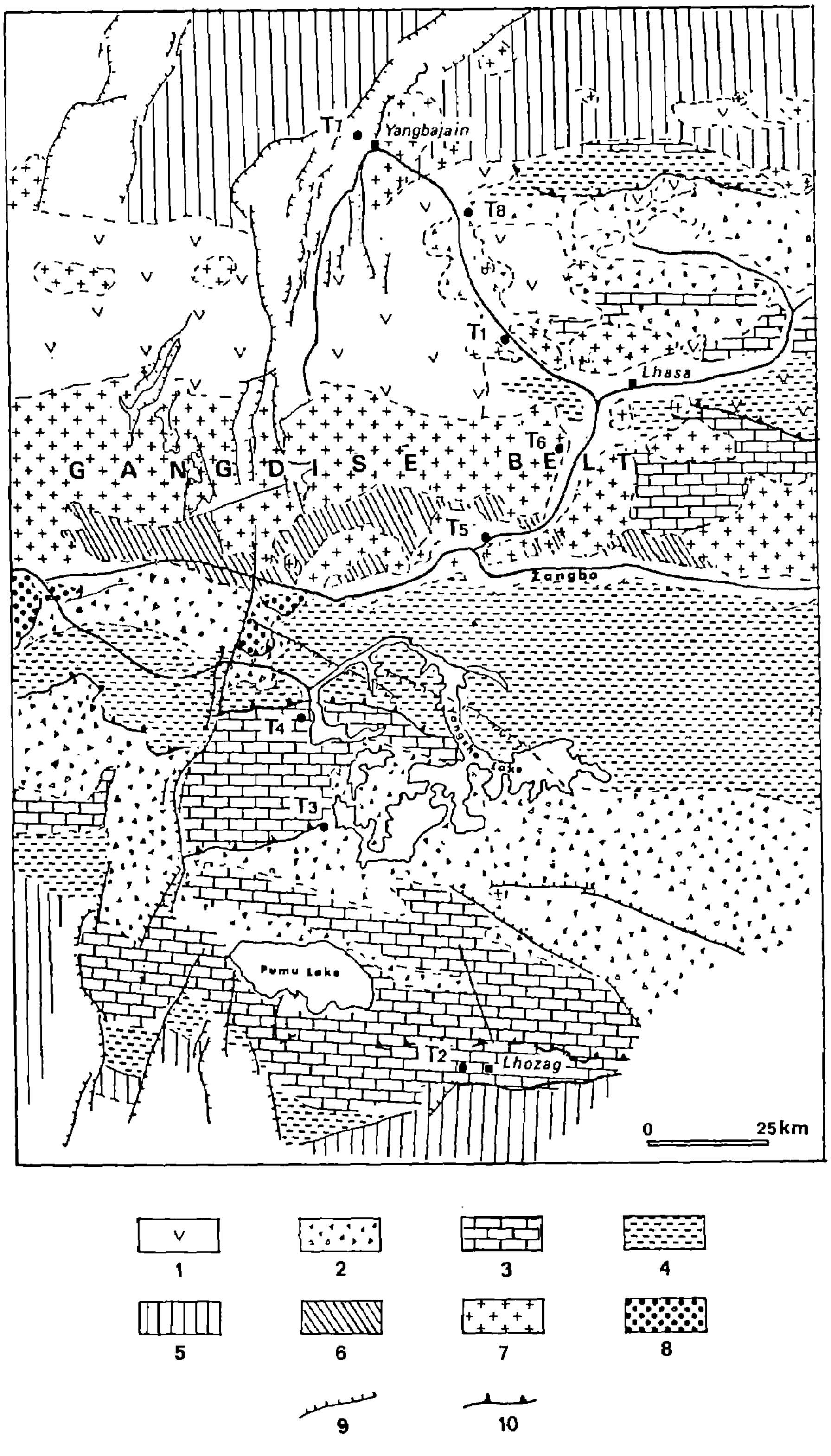

Fig. 2 Location of MT stations on the simplified geological map of the survey area. 1, Cenozoïc volcanic series; 2, Cretaceous; 3, Jurassic; 4, Trias-Liassic; 5, Palaeozoïc, gneiss; 6, amphibolite; 7, calc-alkaline and granite plutons; 8, ophiolites; 9, Quaternary normal fault; 10, major thrust (redrawn from ref. 14).

a continent-continent collision zone. One explanation of the geothermal activity is the existence of a partial melting zone in the crust[4,5,6,10], which should be detectable by MT studies because the electrical resistivity of rocks decreases as the temperature increases and falls dramatically at the melting point.

The Tibetan Plateau results from the juxtaposition of small continental blocks against Palaeo-Asia during the Mesozoic[3] (Fig. 1). These are now separated from each other by ophiolitic sutures. The southernmost block, the Lhasa Block, is bounded to the north by the Bangong-Nujiang suture (BNS) and to the south by the YZS which corresponds to the last collision with the Indian continent and seems to be the most important one. The geology (stratigraphy and tectonics) of the surrounding area of the YZS zone has been well studied during the French-Chinese joint programme (see refs 2, 3, 11-14).

The main tectonic feature of the Lhasa Block is a major strike-slip fault associated with the Nyainquentanglha range crossing near Yangbajain (Fig. 1) which divides the Lhasa Block into two parts with different tectonic histories[15,16]. In the southern part, where half of the surveyed area is located, Cretaceous to Palaeocene volcanism, which volumetrically is more important than in northern parts is typical of an active continental margin. It reflects the northward subduction of the Indian oceanic crust beneath the Lhasa Block[8].

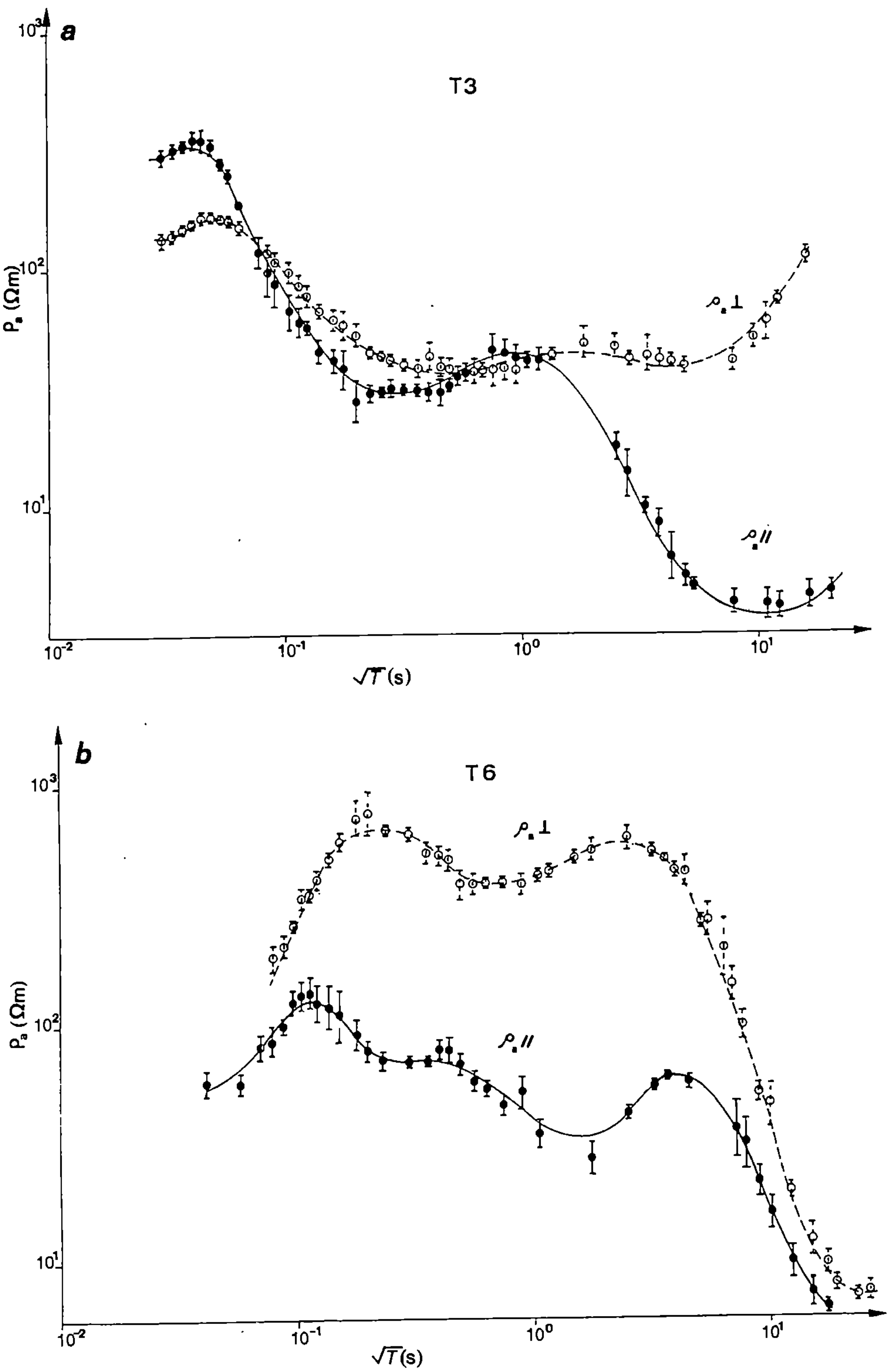

Fig. 3 MT sounding curve showing parallel and perpendicular apparent resistivities against square root of period for: *a*, station T_3; *b*, station T_6.

Following the mechanism proposed by Mattauer[17,18], the crust of the North Indian Margin has doubled in thickness (~70 km) through the formation of a crustal stacking wedge. This necessitates crust-mantle decoupling with very flat-lying thrusts. Moreover, seismic results indicate that decoupling and thrusting separate lower and upper crustal layers[19,20].

Along a north-south traverse over ~200 km passing near Lhasa and running on both sides of the YZS, eight deep MT soundings were carried out from Yangbajain to the north, to Lhozag to the South (Fig. 2). Three stations, T_2, T_3 and T_4, are located to the south of Zangbo in the Jurassic and Cretaceous series, and two stations, T_5 and T_6, lie must north of Zangbo in the Gangdise granitoid belt. Farther north, T_1 is located in the Lhasa granite pluton, T_8 in the Cretaceous and Cenozoic volcanic series and T_7 in the Quaternary Yangbajain graben.

MT soundings consist of studying the variation of apparent resistivity ρ_a with the period T (or square root of period) of the natural electromagnetic field. At each station, MT signals were recorded over several ranges of periods, thereby covering more than six orders of magnitude, from 10^{-3} s to 10^3 s. Furthermore, recordings were carried out simultaneously along two perpendicular directions (east-west and north-south) to study how the electrical anisotropy was related to the micro- or macro-anisotropy and to the heterogeneity of the structure. The digital

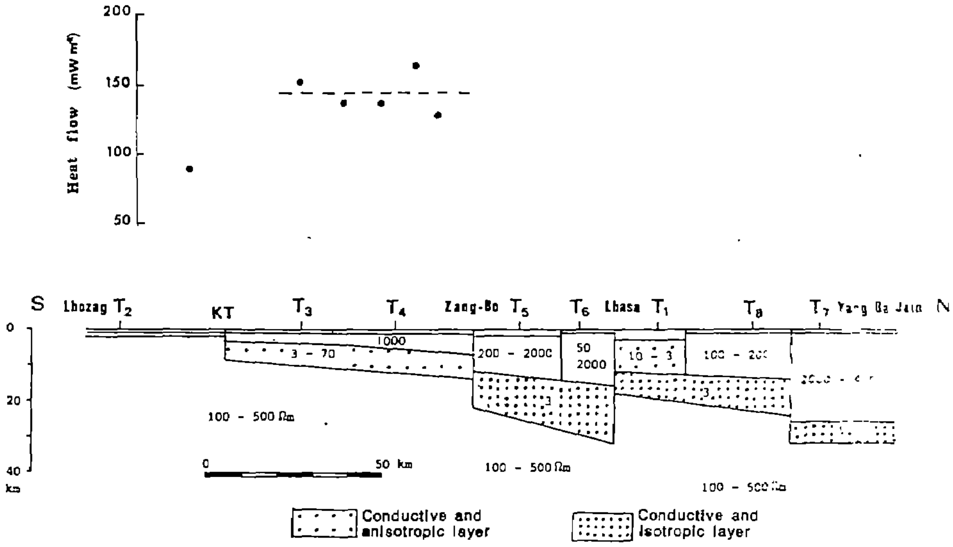

Fig. 4 Geo-electrical section along the traverse obtained from MT two-dimensional modelling (no vertical exaggeration). In each layer, the values indicate the resistivities in Ωm. In the case of anisotropic layer, the first value corresponds to ρ'' and the second value to $\rho^{\perp}$. The upper part shows the heat flow values at their respective locations (after ref. 32).

data were analysed to estimate MT impedance tensor elements[21] and apparent resistivities along two principal directions in the case of two-dimensional earth. Apparent resistivities parallel (ρ_a'') and perpendicular ($\rho_a^{\perp}$)[22] to the tectonic strike correspond respectively to the E and H polarization cases[22] in the two-dimensional modelling described below. The geological map (Fig. 2) of the area surveyed shows that the direction of the tectonic strike is near east-west and the structure is mostly two-dimensional. Table 1 summarizes information regarding the angle θ of the strike direction from the north[23] and the two-dimensionality indicator, the 'skew' index[22,23]. These data confirm that the strike direction is near east-west at all stations except at station T_7 located in the Quaternary Yangbajain graben, striking along a north-east direction. The relatively low skew index confirms the two-dimensionality of the geological structure.

Although MT sounding curves were anisotropic at all stations, this depends on the range of periods and varies from one zone to the other along the traverse. For example, Fig. 3 shows two typical MT sounding curves corresponding to two stations, T_3 and T_6, located respectively south and north of the YZS zone.

At station T_3 (Fig. 3*a*), apparent resistivities are low and probably isotropic for short periods below 1 s and become strongly anisotropic for long periods above, with a minimum ρ_a'' of about 4 Ωm. This indicates the existence of a deep conductive and anisotropic zone to the south of the YZS. At station T_6 (Fig. 3*b*), apparent resistivities are highly anisotropic in the range of periods between 10^{-2} and 10^2 s, with ρ_a'' very low and $\rho_a^{\perp}$ very high. This anisotropy may be related to the micro- or macro-anisotropy provoked by the schistosity and foliation of the compressed Gangdise granitoid belt. Above a period of 100 s both ρ_a'' and $\rho_a^{\perp}$ decrease dramatically by several orders of magnitude, indicating the presence of a strongly conductive zone at depth.

Two-dimensional modelling of the geoelectric structure was carried out to explain the resulting MT response along the traverse, allowing for both heterogeneous and anisotropic features of the structures. The best fitting model is given in Fig. 4. A full description of the modelling procedure[24,25] and details of these geoelectrical studies will be published elsewhere. We focus here on the origin of the highly conductive zones in the crust.

The most outstanding feature observed on the geoelectrical section (Fig. 4) is the existence of layers of very low resistivity in the upper crust, between 3 and 33 km depth. To the south of the YZS zone, a conductive and anisotropic layer is observed between 3 and 14 km depth, with parallel resistivity $\rho'' = 3$ Ωm and perpendicular resistivity $\rho^{\perp} = 70$ Ωm. This layer dips slightly to the north and is bounded laterally by the YZS and the Kangmar thrust (KT). To the north of the YZS zone, a strangely conductive and isotropic zone is observed between 12 and 33 km depth. This zone is divided into several compartments bounded by three major discontinuities located at the central zone between two stations, bracketing each of them respectively around YZS, Lhasa and Yangbajain. Just to the north of Lhasa, and under station T_1, a more localized conductive but anisotropic zone is observed between the 3 and 13 km which overlays the conductive and isotropic zone.

Explanations for conductive zones in the Earth's crust include: (1) solid conduction through the bulk silicate material at high temperatures; (2) electrolytic conduction through fluids contained in cracks and pores; (3) conduction through a melt fraction.

Solid conduction in the bulk silicate phase due to increased temperature alone seems to be ruled out because temperatures would have to be extremely high at shallow levels in the crust, >1,000 °C to decrease the resistivity below 10 Ωm[26] (ref. 26).

In considering the contribution of the electrolytic conduction, the critical factor is the porosity. Often only a few kilometres of depth are sufficient for continuing pressures to close cracks and pores. Nevertheless, even at greater depth, free water can be released from hydrated minerals during metamorphism[27]. There are persistent fluids having water pressure almost equal to lithostatic pressure, particularly in metamorphic regions. In crustal conditions, low porosity (0.01-0.1%) may exist within fractures rather than on a grain boundary scale and would be kept open by the low effective pressure[28]. Laboratory measurements indicate that only a little water is required to decrease

Table 1 Characteristics of the two-dimensionality of the structures in the range of periods 1-1,000 s

Station	θ* (deg)	Skew†
T_1	+100±4	0.4±0.2
T_2	+90±5	0.2±0.2
T_3	+102±5	0.4±0.2
T_4	+98±4	0.4±0.1
T_5	+91±4	0.3±0.2
T_6	+100±3	0.4±0.2
T_7	+40±5	0.4±0.1
T_8	+78±4	0.4±0.2

* Mean value of the angle of structural strike clockwise from the north and r.m.s. error.

† Mean value of the skew index and r.m.s. error.

resistivity by many orders of magnitude[29]. Consequently, low resistivity values could be produced by such environments.

However, in active tectonic regions characterized by strong geothermal activity, the main contribution to lowered resistivities may be the partial melting of rock components, especially if the conductive zone has a very low resistivity, below 10 Ωm. This seems to apply to the area surveyed in southern Tibet[30].

The electrical characteristics of the conductive zones are quite different in the southern and northern parts of the YZS zone. To the south, the conductive zone is located at a relatively shallow depth (3–14 km) under stations T_3 and T_4 and is anisotropic. Although the presence of water-rich fluid with a strong content of conducting solutes could explain its high conductivity, because of the very low value of the parallel resistivity ($\rho'' = 3\ \Omega\mathrm{m}$), there must be another contributory factor. Recent heat flow measurements carried out in the same area show that heat flow rises sharply from 91 to 146 mW m^{-2} precisely above the southern boundary of the conductive zone (between stations T_2 and T_3), and remains approximately constant over a distance >40 km towards the YZS zone[31] (Fig. 4). This suggests that the heat source has large horizontal dimensions. A model using both the amplitude and the spatial characteristics of the thermal anomaly shows that the heat source must be younger than 1 Myr and shallower than 10 km (ref. 32). This agrees well with the spatial characteristics of the conductive zone outlined by MT results. This anomalous source of heat could be a hot intrusive body[31]; however, the anisotropic character of the conductive zone makes it more likely that the interstitial melt was acting in series with host rocks, intruding along fractures parallel to the tectonic strike in an east-west direction, and producing the 'macro-anisotropy' observed from MT results in this area.

To the north of the YZS zone, the most plausible explanation for the strongly conductive and isotropic zones between 12 and 33 km depth is the existence of a large melt fraction concentrated along intergranular boundaries. With the onset of melting there is a dramatic increase in the electrical conductivity[33]. The degree to which partial melt increases the total conductivity of a material depends on the geometry of the melt distribution, particularly on the connectivity of the fluid phase throughout the solid matrix[34,35], and on the presence of water[29,33]. In the presence of excess water, granite melts in the crust[36] at a temperature between 600 and 650 °C. Either these temperatures exist under the northern part of the YZS zone at the levels of the conductive zones, where a large amount of free water was released by different processes of metamorphism, or the primary melt was formed at greater depth and migrated vertically over a large distance. In any case, a resistivity as low as 3–5 Ωm and the isotropic character of these conductive zones imply the existence of a large melt fraction. Another interesting observation on the geoelectrical section of Fig. 4 is the existence of a conductive and anisotropic zone overlying the conductive and isotropic zone under station T_1. Again, one must invoke the interstitial melt which produces the observed macro-anisotropy. But here, the perpendicular resistivity is slightly lower than the parallel resistivity, contrary to what occurs in the southern part of the YZS zone. This feature can be explained by the intrusion of melt along recent north-south normal faults observed around Lhasa[37,38] resulting from a dominant tectonic process of east-west extension during the Quaternary[2,11].

The MT results reported here suggest that regional melting conditions are reached at relatively shallow crustal depths in southern Tibet, contrary to previous reports; in particular, the study of long-period seismic wave propagation[10,39] suggested a possible partial melting zone in the lowermost part of the crust, that is >40–50 km depth in the case of a 70-km thick crust. The actual MT results show that partial melting exists only in the upper crust. No conductivity anomaly has been detected in the lower crust or the upper mantle. The excellent agreement with heat flow measurements in the southern part of the YZS zone strengthens our hypothesis for the origin of conductive zones.

The existence of partial melting zones at relatively shallow depth is evidently related to the recent magmatic and geothermal activities in southern Tibet. Its localization in the upper rather than the lower crust represents a powerful constraint for thermomechanical models of continental collisions.

This work is sponsored by INAG and CNRS (France) and the Ministry of Geology and the Academia Sinica of China. We thank all Chinese colleagues of the Ministry of Geology who participated in the fieldwork during two missions in Tibet.

Received 18 July; accepted 28 October 1985.

1. Molnar, P. & Tapponnier, P. *Science* **189,** 419–426 (1975).
2. Tapponnier, P. *et al. Nature* **294,** 405–410 (1981).
3. Allègre, C. J. *et al. Nature* **307,** 17–22 (1984).
4. Wang, J. Y. *et al. J. Volcanal. geotherm. Res.* **9,** 57–76 (1981).
5. Tong W. & Zhang, M. T. *Proc. Symp. Qinghai-Xizang (Tibet) Plateau,* 841–846 (Science Press Beijing, 1981).
6. Wei, S. Y. *et al. Proc. Symp. Qinghai-Xizang (Tibet) Plateau,* 865–874 (Science Press Beijing, 1981).
7. Kidd, W. S. F. *EOS* **56,** 453 (1975).
8. Coulon, C., Maluski, H. & Wang, S. C. *Int. Symp. Himalayan Geol. Abstr.,* Cheng Du (Chinese Academy for Geological Sciences Beijing, 1984).
9. Maluski, H. *Int. Symp. Himalayan Geol. Abstr.,* Cheng Du (1984).
9. Maluski, H. *Int. Symp. Himalayan Geol. Abstr.,* Cheng Du (1984).
10. Toksöz, M. N., Buck, W. R. & Hsui, A. T. *Proc. Symp. Qinghai-Xizang (Tibet) Plateau,* 847–857 (Science Press Beijing, 1981).
11. Tapponnier, P., Mercier, J. L., Armijo, R., Tonghin, H. & Ji, Z. *Nature* **294,** 410–414 (1981).
12. Nicolas, A. *et al. Nature* **294,** 414–417 (1981).
13. Burg, J. P. & Chen, G. M. *Nature* **311,** 219–223 (1984).
14. Burg, J. P. thesis, Univ. Montpellier (1983).
15. Achache, J., Courtillot, V. & Zhou, Y. X. *J. geophys. Res.* **89,** 10311–10339 (1984).
16. Tapponnier, P., Peltzer, G. & Armijo, R. in *Collision Tectonics* (eds Ries, A. & Coward, M.) (Geological Society, London, in the press).
17. Mattauer, M. *Collision Tectonics* (Spec. Pap. Geological Society London, 1985).
18. Mattauer, M. *C. r. hebd. Séanc. Acad. Sci., Paris* **296,** 481–486 (1983).
19. Hirn, A. *et al. Nature* **307,** 23–25 (1984).
20. Hirn, A. *et al. Nature* **307,** 25–27 (1984).
21. Sims, W. E., Bostick, F. X. & Smith, H. W. *Geophysics* **36,** 938–942 (1971).
22. Vozoff, K. *Geophysics* **37,** 98–141 (1972).
23. Swift, C. M. Jr thesis, Massachusetts Inst Technol. (1967).
24. Doucet, D. & Pham, V. N. *Geophys. Prosp.* **32,** 292–316 (1984).
25. Chung, S. G. thesis, INPL, Nancy (1984).
26. Stanley, W. D. *et al. J. geophys. Res.* **82,** 2501–2514 (1977).
27. Berdichevsky, M. N. *et al. Beitr. Geophys.* **81,** 187–196 (1972).
28. Shanland, T. J. & Ander, M. E. *J. geophys. Res.* **88,** 9475–9484 (1983).
29. Olhoef, G. R. *J. geophys. Res.* **86,** 931–936 (1981).
30. Pham, V. N., Boyer, D. & Therme, P. *Terra Cognita* **3,** 270 (1983).
31. Francheteau, J. *et al. Nature* **307,** 32–36 (1984).
32. Jaupart, C., Francheteau, J & Shen, X. J. *Geophys. J. R. astr. Soc.* **81,** 131–155 (1985).
33. Lebedev, E. B. & Khitarov, N. I. *Geokhimiya* **3,** 195–201 (1964).
34. Waff, H. S. *J. geophys. Res.* **79,** 4003–4010 (1974).
35. Hermance, J. F. *Geophys. Res. Lett.* **6,** 613–616 (1979).
36. Wyllie, P. J. *Geophys. Monogr.* **14,** 279–301 (1971).
37. Chen, G. M. & Li, T. D. *Mission franco-chinoise 1980,* 357–383 (CNRS, France, 1984).
38. Armijo, R. *et al. EOS* **63,** 1093 (1982).
39. Bird, P. & Toksöz, M. N. *Nature* **266,** 161–163 (1977).

Isoleucine stereoisomers on the Earth

Jeffrey L. Bada*, Meixun Zhao*, Spencer Steinberg† & Edward Ruth†

* Amino Acid Dating Laboratory (A-012B),
Scripps Institution of Oceanography, University of California,
San Diego, La Jolla, California 92093, USA
† Institute of Geophysics and Planetary Physics,
University of California, Los Angeles, California 90024, USA

The amino acid L-isoleucine (L-Ile) undergoes epimerization at the α-carbon producing D-*allo*-isoleucine (D-*a*Ile), an amino acid not generally found in living organisms. In fossils and oceanic sediments, this reaction has a half-life, that is, the time required to reach D-*a*Ile/L-Ile ~0.4, of 10^5–10^7 yr (ref. 1). Two other possible isoleucine stereoisomers, D-isoleucine (D-Ile) and L-*allo*-isoleucine (L-*a*Ile), have not been previously detected in fossils or sediments. These amino acids could be produced by epimerization of L-Ile and D-*a*Ile at the β-carbon[2]. However, the β-carbon is insulated from the amino and carboxy groups which by electron-withdrawing effects and resonance stabilization promote epimeriz-

ation at the α-position[3]. Thus, the β-epimerization rates of the isoleucine stereoisomers are predicted to be extremely slow in comparison to their α-epimerization rates. However, no kinetic studies have been conducted. To assess whether the D-Ile and L-*a*Ile could be produced on the Earth from β-epimerization of L-Ile and D-*a*Ile, we have measured the β-epimerization rate at 250 °C in aqueous solution, and determined the isoleucine stereoisomeric composition in fossil molluscs of various geological ages.

The four isoleucine stereoisomers are shown in Fig. 1 as are their interconversion pathways by epimerization at the α- and β-carbons. The α-epimerization rates of D-Ile and L-*a*Ile would be expected to be similar to those of the diastereomeric pair L-Ile and D-*a*Ile. Interconversion of the enantiomers L-Ile and D-Ile, and D-*a*Ile and L-*a*Ile, should not occur as this would require simultaneous inversion at two chiral centres.

Aliquots of L-Ile in phosphate buffer (*p*H 7.4 at 25 °C) were sealed in Teflon-lined steel reaction vessels and heated at 250 °C for periods ranging from 5 h to 3 days. The *p*H of the solution after heating was identical to the initial *p*H. Based on the extrapolation of the *p*H versus temperature equations[4] for phosphate buffers determined from measurements between 0 and 90 °C, we estimate that the *p*H of our solution at 250 °C was ~8.4. The heated solutions were desalted using cation exchange chromatography and then analysed using the TPC (trifluoroacetyl-L-prolyl chloride) gas-chromatography method[5]. The results of the 250 °C experiment are shown in Fig. 2. The estimated half-life at 250 °C and *p*H ~ 8.4 for the β-epimerization of L-Ile is ~11 days, whereas that for D-*a*Ile is ~25 days. The isoleucine decomposition rate was found greatly to exceed the rate of β-epimerization. In the sample heated for 70 h, only 2% of the initial isoleucine remained. Epimerization at the α-carbon is rapid at 250 °C. After only 5 h, D-*a*Ile/L-Ile = 1.3, the approximate equilibrium ratio of these two diastereomers[3]. The half-life at neutral *p*H for α-epimerization of L-Ile estimated by extrapolation of measurements[6-8] made between 90 and 180° is ~3-6 min at 250 °C. The aqueous solution measurements indicate that the ratio of the α- to β-epimerization rates of isoleucine is 10^3–10^4 in the neutral *p*H region at 250 °C. If this ratio is also applicable to geochemical systems, then the isoleucine β-epimerization rate should have a half-life of ~10^8–10^{11} yr on the Earth's surface. This half-life implies that little if any β-epimerization of L-Ile and D-*a*Ile would occur even over the entire age of the Earth. Because the isoleucine decomposition rate is greater than β-epimerization, isoleucine would also decompose faster than D-Ile and L-*a*Ile would be produced through β-epimerization. The slow isoleucine β-epimerization rate and the rare occurrence of D-Ile and L-*a*Ile in the biota[9,10] suggest that L-Ile and D-*a*Ile should be the only isoleucine stereoisomers in the Earth's amino-acid reservoir. In contrast, all four isoleucine stereoisomers are present in approximately equal amounts in amino-acid rich meteorites[11], which is expected since the meteoritic amino acids are produced by abiotic processes[12].

For a better evaluation of the isoleucine geochemical β-epimerization rate we analysed fossil molluscs with ages of ~50,000 and ~1 Myr (Table 1). Both D-Ile and L-*a*Ile were detected in the oldest sample and these isoleucine stereoisomers seem to increase in abundance with increasing geological age. The β-epimerization rate of L-Ile is ~2-3 times that of D-*a*Ile, which is consistent with the rates determined in our 250 °C experiment. Using the data in Table 1, we calculate that the ratio of the α- to β-epimerization rates in these calcareous fossils is ~10-50. The rate of isoleucine epimerization at the β-carbon in the fossil mollusks therefore appears to be substantially enhanced compared with the aqueous solution measurements at 250 °C and neutral *p*H.

The apparent enhanced rate of isoleucine β-epimerization in the carbonate fossils may be due to several factors. The *p*H dependence of the α/β-epimerization rate ratio has not been

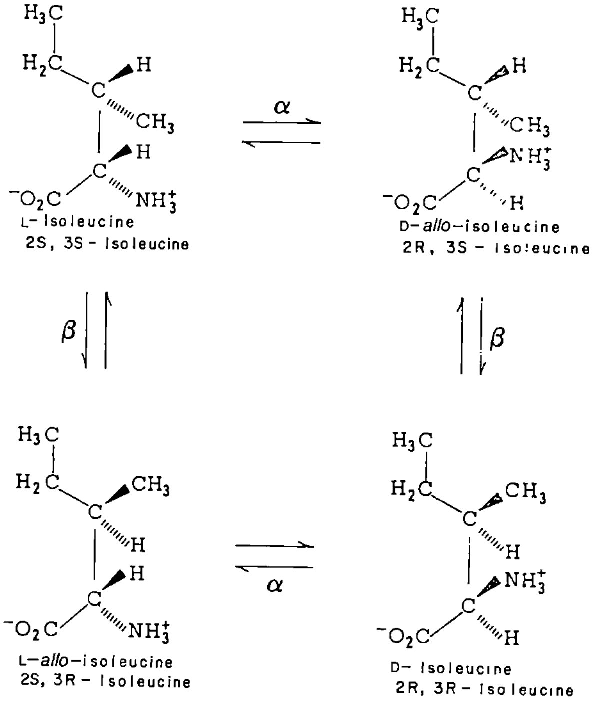

Fig. 1 Structures of the various isoleucine stereoisomers[18]. Both the common and R-S system names are given. Interconversion pathways at the chiral centres are indicated by α and β.

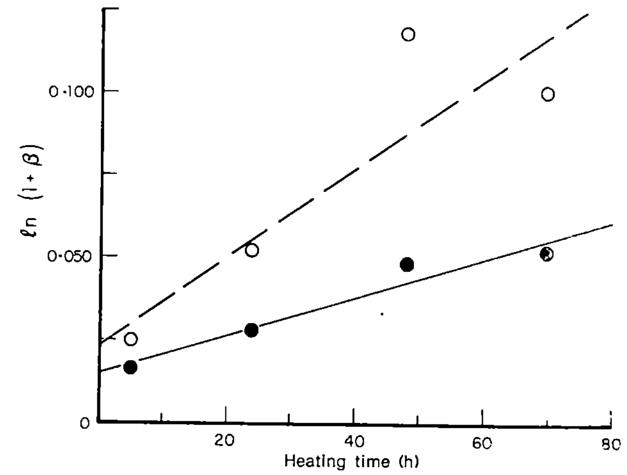

Fig. 2 An irreversible first-order kinetic plot[3] for β-epimerization of L-Ile and D-*a*Ile at 250 °C and *p*H ~ 8.4. Although the starting solutions contained only L-Ile, D-*a*Ile was rapidly produced through α-epimerization of L-Ile; the estimated half-life for α-epimerization at 250 °C, *p*H 7.6 is ~3-6 min (see text). The β term in the log function equals either D-Ile/D-*a*Ile (●) or L-*a*Ile/L-Ile (○). The slopes of the lines equal k_β, the respective β-epimerization rates of L-Ile and D-*a*Ile. The half-life for β-epimerization ~ln 2/2 k_β. The stereoisomeric ratios were determined by synthesizing the TPC amino-acid methyl esters[6]. Separations were performed using the gas chromatographic system and conditions described elsewhere[19]. All four isoleucine stereoisomers are baseline separated by this analytical method. Stereoisomeric ratios were calculated from peak heights. The detailed analytical procedures and representative gas chromatographic results will be published elsewhere.

Table 1 Isoleucine stereoisomers in fossil molluscs

Sample	Approximate age (yr)	Total *a*Ile/Ile*	D-Ile/D-*a*Ile†	L-*a*Ile/L-Ile†
Saxidomas‡ Cape Blanco, Oregon	50,000	0.19 (0.18)	0.00§	0.00§
Mercenaria‡ Calabash, North Carolina	Early Pleistocene 10^6	1.12 (1.10)	0.06	0.16

* The total ratio, (D-*a*Ile+L-*a*Ile)/(D-Ile+L-Ile) was determined on a Beckman 119 amino-acid analyser. The number in parentheses is the average ratio determined by ion-exchange chromatography (see ref. 20).

† Computerized gas chromatography/mass spectrometry with specific ion monitoring and peak-area integration was used to determine the stereoisomeric ratios. Gas chromatography methodology is the same as that used in the 250 °C experiment shown in Fig. 2. We estimate that these ratios have an uncertainty of ~±10%.

‡ Specimens used in the interlaboratory comparison study of Wehmiller[20]. We also analysed the third sample in the Wehmiller study, such as, the 100,000–250,000-yr old *Mercenaria* (clam) shell from Charleston, South Carolina. Although we were able to detect trace quantities of D-Ile and L-*a*Ile in this sample by gas chromatography using flame ionization detection, we were unable to confirm their presence by specific ion monitoring because of the small quantities.

§ Neither D-Ile or L-*a*Ile were detectable in this sample.

determined. The effective *p*H of the carbonate matrix could result in a α/β epimerization rate ratio which is less than we measured in our 250 °C, *p*H ~ 8.4 experiment. In addition, because the temperature dependence of β-epimerization is unknown, the α/β rate ratio could be substantially different at environmental temperatures compared with that at 250 °C. Another factor could be catalysis by mineral surfaces. Catalysts are apparently important in epimerization reactions at hydrophobic chiral centres[13,14], and thus carbonate may selectively catalyse epimerization at the β-position. Finally, D-Ile and L-*a*Ile in fossils might be produced from β-methyl-α-ketovaleric acid, the α-keto acid analogue of isoleucine, rather than through β-epimerization. This α-keto acid undergoes rapid enolization at slightly basic *p*H values, resulting in racemization at the β position[15]. If L-β-methyl-α-ketovaleric acid was present initially in small quantities in the carbonate matrix, its racemization and subsequent transamination could result in the production of the D-Ile and L-*a*Ile over geological time. However, β-methyl-α-ketovaleric acid has not been reported in carbonate fossils, although several simpler α-keto acids have been detected[16].

Our fossil data suggest that all four isoleucine stereoisomers are present in ancient biogenic carbonates. We estimate that the half-life for β-epimerization in the calcareous matrix is ~5–10 Myr in temperate climatic environments. In ocean sediments, the half-lives could be of the order of 100 Myr assuming that the Arrhenius activation energy E_a for β-epimerization is similar to that at the α-position[6,8], for example, $E_a \cong 30$ kcal mol^{-1}. The β-epimerization reaction of isoleucine has important geochemical implications. It could provide an index of the degree of preservation of isoleucine in ancient fossils and sediments. For example, syngenetic isoleucine in Precambrian carbonaceous sedimentary rocks should exist as an equilibrium mixture containing all four isoleucine stereoisomers. The β-epimerization of isoleucine could also be useful in dating fossils and sediments in which the other amino acids have been completely racemized. The geological interval where β-epimerization of isoleucine could be used as a geochronological method would greatly exceed that generally applicable to amino acid racemization dating which at present is limited to Pleistocene, and perhaps Pliocene, samples[1,17].

We thank the donors of the Petroleum Research Fund, administered by the American Chemical Society, for partial support of this research. Research at UCLA was supported by a grant from the Department of Energy (award DE-AT03-76EV70134).

Received 23 July; accepted 17 October 1985.

1. Bada, J. L. *A. Rev. Earth planet. Sci.* **13,** 241–268 (1985).
2. Kvenvolden, K. A. *A. Rev. Earth planet. Sci.* **3,** 183–212 (1975).
3. Bada, J. L. in *Chemistry and Biochemistry of the Amino Acids* (ed. Barrett, G. C.) 399–414 (Chapman and Hall, London, 1985).
4. Bates, R. G. *Determination of pH* 76 (Wiley, New York, 1964).
5. Hoopes, E. H., Peltzer, E. T. & Bada, J. L. *J. chromatogr. Sci.* **16,** 556–560 (1978).
6. Bada, J. L. *Adv. Chem. Ser.* No. **106,** 309–331 (1971).
7. Dungworth, G., Vincken, N. J. & Schwartz, A. W. *Adv. org. Geochim.* **1973,** 689 (1974).
8. Smith, G. G., Williams, K. M. & Wonnacott, D. M. *J. org. Chem.* **43,** 1–5 (1978).
9. Bodansky, M. & Perlman, D. *Nature* **218,** 291–292 (1968).
10. Yajima, T., Grigg, M. A. & Katz, E. *Archs biochem. Biophys.* **151,** 565–575 (1972).
11. Cronin, J. R., Gandy, W. E. & Pizzarello, S. *J. molec. Evolut.* **17,** 265–272 (1981).
12. Wolman, Y., Haverland, W. J. & Miller, S. L. *Proc. natn. Acad. Sci. U.S.A.* **69,** 809–811 (1972).
13. Ensminger, A. *et al. Adv. org. Geochim.* **1973,** 245–260 (1974).
14. Sieskind, O., Joly, G. & Albreicht, P. *Geochim. cosmochim. Acta* **43,** 1675–1679 (1979).
15. Meister, A. *J. biol. Chem.* **190,** 269–276 (1951).
16. Steinberg, S. M. & Bada, J. L. *Geochim. cosmochim. Acta* **47,** 1481–1486 (1983).
17. Wehmiller, J. F. in *Quaternary Dating Methods* (ed. Mahaney, W. C.) 171–193 (Elsevier, Amsterdam, 1984).
18. Cohn, W. E. *Meth. Enzymol.* **106,** 3–17 (1984).
19. Boehm, M. F. & Bada, J. L. *Proc. natn. Acad. Sci. U.S.A.* **81,** 5263–5266 (1984).
20. Wehmiller, J. F. *Quat. Res.* **22,** 109–120 (1984).

Bicadinane, a C_{30} pentacyclic isoprenoid hydrocarbon found in crude oil

H. C. Cox*‖, J. W. de Leeuw*, P. A. Schenck*, H. van Koningsveld*, J. C. Jansen*, B. van de Graaf*, V. J. van Geerestein†, J. A. Kanters†, C. Kruk‡ & A. W. H. Jans§

* Department of Chemistry and Chemical Engineering, Delft University of Technology, Delft, The Netherlands
† Laboratory of Crystal and Structural Chemistry, Utrecht State University, Utrecht, The Netherlands
‡ Laboratory of Organic Chemistry, University of Amsterdam, Amsterdam, The Netherlands
§ Free University, Brussels, Belgium

It is generally accepted that saturated polycyclic hydrocarbons such as steranes and triterpanes, present in crude oils and sediments, originate from naturally occurring steroids and triterpenoids. The occurrence of individual steranes and triterpanes can be used to relate the oil or sediment sample to the biological material from which it is derived. All previously known saturated C_{30} pentacyclic hydrocarbons could be related to a naturally occurring triterpenoid. Here we report that the structure of a novel $C_{30}H_{52}$ pentacyclic isoprenoid hydrocarbon present in some Far Eastern crude oils has been established as 2,6a,12-trimethyl-4,9-diisopropyl-perhydrobenzo[de]naphthacene by joint application of chromatographic methods, mass spectrometry (MS), nuclear magnetic resonance (NMR), molecular mechanics and X-ray diffraction. As far as we know, this is the first report of the occurrence in nature of a pentacyclic C_{30} isoprenoid compound with a perhydrobenzo[de]naphthacene skeleton. It can be considered as a dimer of the sesquiterpane cadinane. A biosynthesis of the skeleton by direct cyclization of squalene seems impossible in this case.

‖ To whom correspondence should be addressed at: Organic Geochemistry Unit, De Vries van Heystplantsoen 2, 2628 RZ Delft, The Netherlands.

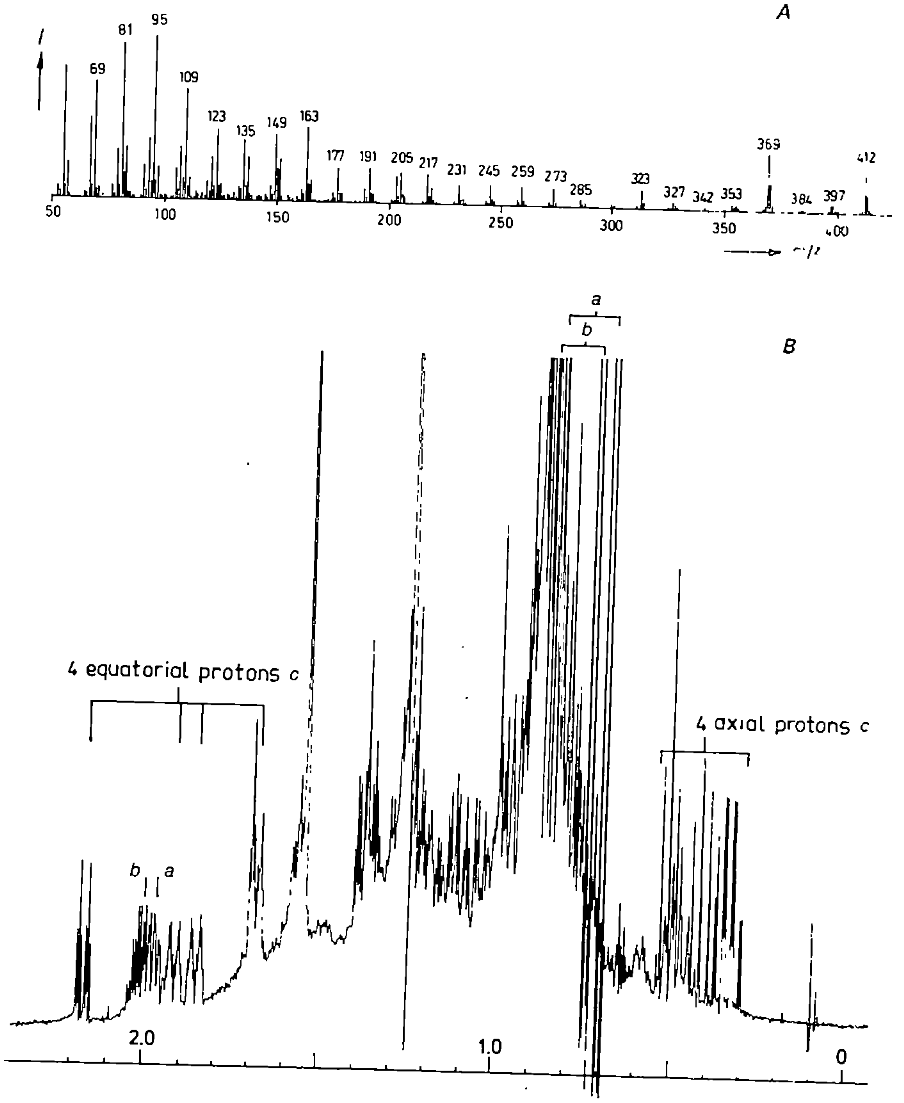

Fig. 1 *A*, Mass spectrum of compound T from crude oil from well W. Prabumulih-3; *B*, 500 MHz ^{1}H-NMR spectrum of compound T. Isopropyl group *a*, $\delta CH_3 = 0.68$ and 0.83, δtert H = 1.96, $J = 6.9$ Hz. Isopropyl group *b*, $\delta CH_3 = 0.72$ and 0.84, δtert H = 2.10, $J = 6.9$ Hz. Four high-field protons *c*, $\delta = 0.3$–0.5, each coupled to a geminal equatorial proton in the region δ1.7–2.2.

In 1982, Grantham *et al.*[1] reported the occurrence of three new compounds relatively abundantly present in the saturated hydrocarbon fractions of several Far Eastern crude oils. Based on gas chromatographic/low resolution mass spectrometric (GC/LRMS) data, they preliminarily characterized these compounds (labelled W, T and R) as C_{30} pentacyclic hydrocarbons, presumably originating from Tertiary land-plant resins. Because of their selective occurrence in these oils, these components are thought to be important biological markers with a potential use in oil/oil and oil/source rock correlation studies. Therefore, we have undertaken the structural identification of one of these compounds, T.

Very small amounts of spontaneously formed crystals, present n molecular distillation fractions of saturated hydrocarbons solated from a South Sumatra crude oil, were analysed by GC nd GC/LRMS. GC-retention time and mass spectral data of his crystalline compound were the same as those obtained for ompound T present in a crude oil from the W. Prabumulih-3 vell. The crystals were carefully rinsed with *n*-hexane and a ingle crystal was subjected to X-ray diffraction analysis using n Enraf-Nonius CAD-4 single-crystal diffractometer. For 7,114 ndependent reflections the intensities were collected using raphite-monochromatized MoKα radiation. The space group vas established as $P2_12_12_1$ with $a = 10.106(1)$, $b = 17.831(3)$, $= 29.666(5)$ Å, with two independent molecules in the asymmetric unit. An additional translational pseudosymmetry eriously hampered a straightforward determination of the structure by conventional direct methods. To overcome these difficulties, more structural information was necessary to limit the number of search models for the application of a recently developed Patterson search program[2]. Therefore, larger amounts of pure compound T were required. Following the procedure for the isolation of triterpanes previously described by Hills and Whitehead[3], 4 mg of almost pure compound T was isolated from 100 cm^3 of crude oil from the well W. Prabumulih-3. Compound T was obtained from the appropriate molecular distillation fraction (checked by GC analysis) by column chromatography on SiO_2 and Al_2O_3, treatment with 5-Å molecular sieves, repeated column chromatography on Al_2O_3 with *n*-hexane as an eluent and urea clathration. Resulting crystalline material was purified by recrystallization from *n*-heptane. Some 2.5 mg of compound T, isolated and purified in this way, was used for NMR analyses. Another aliquot was investigated by MS. The mass spectrum is shown in Fig. 1*A*. Exact mass measurements of the molecular ion at 412 daltons yielded a value of 412.405, which corresponds to a calculated value of 412.406 for $C_{30}H_{52}$. A linked scan with B^2/E constant, performed for $m/z = 313$, showed that the principal mother ions of this fragment are $m/z = 369$ ($M^{+} - 43$) and $m/z = 412$ (M^{+}). The mass spectral data suggest the presence of at least one isopropyl group. The loss of 99 daltons as indicated by the relative abundance of $m/z = 313$ probably reflects a two-stage fragmentation process, thus making the presence of a C_7H_{15} side chain less likely (compare with ref. 1).

Figure 1*B* shows the 500-MHz ^{1}H-NMR spectrum. Double-resonance experiments and ^{1}H shift-correlated two-dimensional

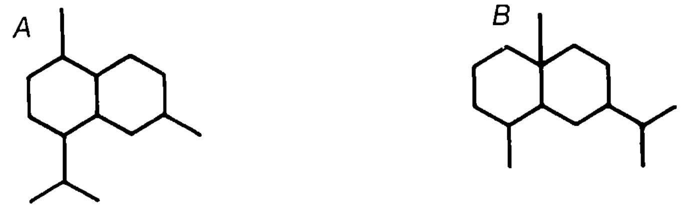

Fig. 2 *A*, Cadinane; *B*, eudesmane.

NMR (COSY)[4,5] showed the presence of two non-equivalent isopropyl groups and four CH_2 groups in the 2-position of a 1,3-di-equatorially substituted cyclohexane ring[6]. Analysis of 62.8-MHz proton-decoupled ^{13}C-NMR spectra indicated that all 30 carbons have sp^3 hybridization. Information about the multiplicity of the carbons could be obtained by using the APT[7] and DEPT[8] pulse sequences. A combination of these experiments with a 125-MHz $^{13}C-^{1}H$ shift-correlated two-dimensional NMR spectrum[9] revealed the presence of 7 CH_3-, 9 CH_2-, 13 CH-groups and 1 quaternary carbon atom. The NMR techniques used are described in detail elsewhere[4,5,7-9].

From these NMR data it became clear that the $C_{30}H_{52}$ compound T is not a triterpane in the usual sense because only one quaternary carbon atom is present in the structure. The elemental formula and the presence of two isopropyl groups and three additional methyl groups indicate that the skeleton is pentacyclic and consists of 21 carbon atoms. A literature search for natural compounds with structural features as revealed by the NMR and MS data (high-field protons, isopropyl substituents, only one quaternary carbon atom) led us to consider saturated sesquiterpenoid hydrocarbons, especially cadinane and eudesmane[10] (Fig. 2). These compounds, although containing only 15 carbon atoms, possess an isopropyl group, one or no quaternary carbon atom and the characteristic CH_2 group with a high-field proton. Moreover, the mass spectra of these compounds are very similar to the lower part of the mass spectrum of compound T. Further circumstantial evidence for the presence of these sesquiterpenoid moieties in compound T was obtained from the relative abundance of cadinane in the crude oil as revealed by GC/MS analysis. Additional information resulted from Curie point pyrolysis/GC/MS[11] of the Lumapas resin, shown to be a source of components R, T and W on heating[1]. Many sesquiterpenoid hydrocarbons with at least one isopropyl group were encountered in the pyrolysate. These additional data suggested that compound T could be considered as a 'dimer' of cadinane or eudesmane. Coupling of two decalines through a methene group structured in a cyclopentane or cyclohexane ring indeed yields a pentacyclic skeleton of 21 carbon atoms. A pentacyclic structure with five six-membered rings was preferred, as the 125-MHz proton-coupled ^{13}C-spectrum did not reveal $^{1}J_{C-H}$ values greater than 126 Hz. The Patterson map calculated from the X-ray data precluded structures with a central cyclopentane ring. Only six skeletons containing 21 carbon atoms and consisting of five six-membered rings exist (Fig. 3*A*–*F*). Structures *D*, *E* and *F* in Fig. 3 are less likely because they cannot be constructed from two decaline systems. Molecular mechanical calculations using the MM2 force field[12] revealed steric energies for the all-*trans* structures *A*, *B* and *C* of 26, 28 and 36 kcal mol^{-1} respectively. Therefore, only structures *A* and *B* were considered to be promising search models. After Patterson searches with the Patsee program, skeleton *B* appeared to be the correct one. Structure expansion revealed the complete structure, which refined to a final *R* of 0.056. From this result the structure was unequivocally established as 2,6a,12-trimethyl-4,9-diisopropyl-perhydro-benzo[de]naphthacene (Fig. 4).

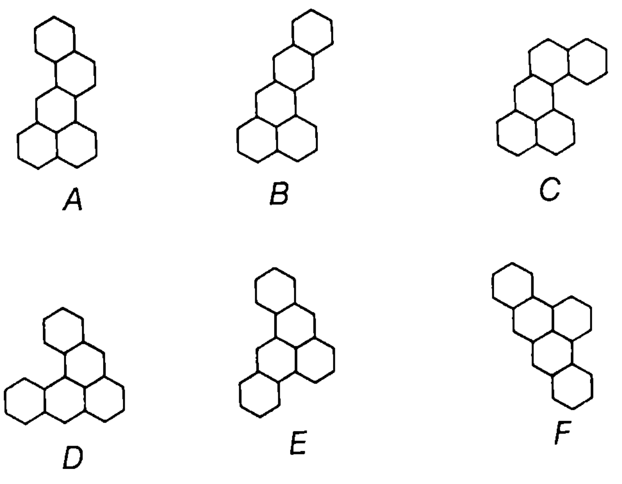

Fig. 3 Pentacyclic skeletons possible which contain 21 carbon atoms.

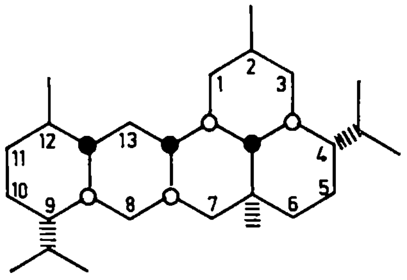

Fig. 4 Structure of compound T.

This structure indeed consists of two cadinane units; the four high-field protons observed in the ^{1}H-NMR spectrum are located at positions 1, 3, 8 and 13. Based on this identification and the similarity of the mass spectra of compounds W, R and T, we believe that compounds W and R may be stereoisomers of the compound identified. Further research is necessary to confirm this hypothesis.

We have encountered only one natural compound containing a dimeric cadinane skeleton; this is gossypol, a toxic yellow pigment from cotton seed oil[13]. However, its structure is completely different from that described above.

Several possibilities for the origin of this novel pentacyclic compound can be considered. The hydrocarbon could be derived from a functionalized precursor of biosynthetic origin. The biosynthesis could involve a cyclization of an acyclic C_{30} isoprenoid compound or a dimerization of cadinene, known to occur in several plants. We emphasize, however, that biosynthesis by direct cyclization of squalene seems impossible in this case. A dimerization as the result of a purely chemical process in the geosphere cannot be ruled out completely at this stage

We thank the Koninklijke/Shell Exploratie en Produkti Laboratorium (Shell Research BV) for providing samples and for some financial support. We acknowledge the technical assistance of Mrs J. K. C. Hessels and Mrs E. H. Nieberg-van Velze in isolating the compound.

Received 22 July; accepted 28 October 1985.

1. Grantham, P. J., Posthuma, J. & Baak, A. in *Advances in Organic Geochemistry 1981* (ed Bjorøy, M. *et al.*) 675-683 (Wiley, New York, 1983).
2. Egert, E. & Sheldrick, G. M. *Acta crystallogr.* **A41**, 262-268 (1985).
3. Hills, I. R. & Whitehead, E. V. in *Advances in Organic Geochemistry 1966* (eds Hobso G. D. & Speers, G. C.) 89-110 (Pergamon, Oxford, 1970).
4. Aue, W. P., Bartholdi, E. & Ernst, R. R. *J. chem. Phys.* **64**, 2229 (1976).
5. Nagayama, K., Kumar, A., Wüthrick, K. & Ernst, R. R. *J. magn. Res.* **40**, 321 (1980).
6. Daneels, D. & Anteunis, M. *Org. magn. Reson.* **6**, 617-621 (1974).
7. Patt, S. L. *J. magn. Res.* **46**, 535 (1982).
8. Doddrel, D. M., Pegg, D. T. & Bendall, M. R. *J. magn. Res.* **48**, 323 (1982).
9. Bax, A. & Morris, G. *J. magn. Res.* **42**, 501 (1981).
10. Moshonas, M. G. & Lund, E. D. *Flavour Ind.* **1**, 375-378 (1970).
11. Van de Meent, D., Brown, S. C., Philp, R. P. & Simoneit, B. R. T. *Geochim. cosmochi Acta* **44**, 999-1013 (1980).
12. Allinger, N. I. *J. Am. chem. Soc.* **99**, 8127-8134 (1977).
13. Adams, R., Morris, R. C., Geissman, T. A., Bufferbough, D. J. & Kirkpatrick, E. C. *J. A chem. Soc.* **60**, 2193-2204 (1938).

Early Eocene *Cantius torresi*— oldest primate of modern aspect from North America

Philip D. Gingerich

Museum of Paleontology, University of Michigan, Ann Arbor, Michigan 48109, USA

The oldest primates of modern aspect (primates of prosimian tarsiiform–lemuriform or higher grade) are known from Lower Eocene strata of Sparnacian age in Europe[1,2], Bumbanian age in Asia[3,4], and Wasatchian age in North America[5]. These first appearances coincide on all three northern continents with initial records of Artiodactyla, Perissodactyla and other modern mammalian groups appearing approximately 53 Myr BP[6,7]. Here I report that a newly discovered basal Wasatchian faunal assemblage older than any known previously includes the well-preserved dental remains of a new species of *Cantius*, the earliest representative of Eocene Adapidae and the oldest evidence of primates of modern aspect known from North America. This new *Cantius* is possibly ancestral to all later adapids, including the European *Donrussellia* and North American *Pelycodus*. *Cantius torresi* has premolars reminiscent of those in Omomyidae, suggesting that earlier lemuriform and tarsiiform primates were closely related and little differentiated at the beginning of the Eocene.

Two major groups of primates of modern aspect, tarsiiform Omomyidae and lemuriform Adapidae, are represented in the early Eocene of Europe[8-12], Asia[3,4,13] and North America[14-20]. Both groups appeared suddenly on northern continents during an interval of climatic warming[21]. No plausible ancestors of the two groups are present in known European, Asian or North American faunas of late Palaeocene age, suggesting their immigration from equatorial areas. The oldest North American omomyid, *Teilhardina americana*, is similar to the European *Teilhardina belgica*[15,19]. The oldest North American adapid known previously, *Cantius ralstoni*, is likewise similar to the European *Cantius eppsi*[17,18]. The discovery of a new North American *Cantius* demonstrably older than *C. ralstoni* is important in clarifying the dental morphology of primitive Adapidae.

Cantius torresi n. sp.

Holotype. University of Michigan [UM] 83470, left dentary vith P_3–M_1 collected by Victor Torres from locality SC-67 in he Willwood Formation at the south end of Polecat Bench, ark County, Wyoming.

Age and distribution. Earliest Wasatchian Land-Mammal Age early Eocene) of the Clark's Fork Basin, Wyoming, western North America. This species is known from two adjacent ocalities (SC-67 and 69) in a restricted 10-m stratigraphic interal within the Clarkforkian–Wasatchian boundary sandstone of Kraus[22].

Referred specimens. Holotype; UM 83467, left dentary with M_2; and Um 83475, right maxilla with M^{1-3} from the type ocality. Um 66143, right dentary with M_{2-3} from SC-69.

Diagnosis. Differs from *C. ralstoni*, *C. eppsi* and all other ecies of *Cantius* in being smaller, having relatively square pper molars, and having shorter, relatively broader lower preolars and molars. P_4 is distinctive in having a broad trigonid nd talonid. The paracristid connecting the paraconid and proconid on P_4 forms a right-angle with the metacristid connecting e metaconid and protoconid.

Description. The holotype dentary (Fig. 1*a*) preserves matrixled alveoli for the lower canine, a single-rooted P_1 and a uble-rooted P_2. The crown of P_3 is simple with a single central otoconid cusp, no accessory paraconid or metaconid, and tle more than a trace of a talonid. P_3 is 2.4 mm long and 1.8 mm in maximum breadth. The crown of P_4 is more complex, with a well-developed paraconid and metaconid in addition to the central protoconid. The metaconid is medial to the protoconid, making the trigonid unusually broad. The talonid on P_4 is also broad, with a prominent central cristid obliqua and shallowly basined posteromedial corner. P_4 is 2.8 mm long and 2.4 mm in maximum breadth. The crown of M_1 is tritubercular with three distinct trigonid cusps and a broadly basined talonid. M_1 is 3.3 mm long and 2.9 mm in maximum breadth. The crown of M_2 is partially preserved in two specimens (UM 66143 and 83467), both are small, measuring 3.4×3.2 mm and 3.2 × 3.1 mm in length and width, respectively. The crown of M_3 preserved in UM 66143 has a short trigonid, with paraconid and metaconid cusps closely appressed (Fig. 1*c*). M_3 is 4.3 mm long and 2.7 mm in maximum breadth. The talonid of M_3 resembles that in other early *Cantius* species in having a very narrow hypoconulid lobe (1.5 mm broad).

Upper molars are preserved intact in one specimen (UM 83475; Fig. 1*d*). The crowns of both M^1 and M^2 are relatively square by comparison with later species of *Cantius*; both have prominent protocones, distinct paracones and metacones, and small but distinct paraconules and metaconules. There is a crest behind the protocrista representing a '*Nannopithex* fold' or partially developed postprotocingulum as in other primitive adapids and omomyids. In later Adapidae this crest is either reduced and lost (*Donrussellia*, *Protoadapis*) or it is expanded

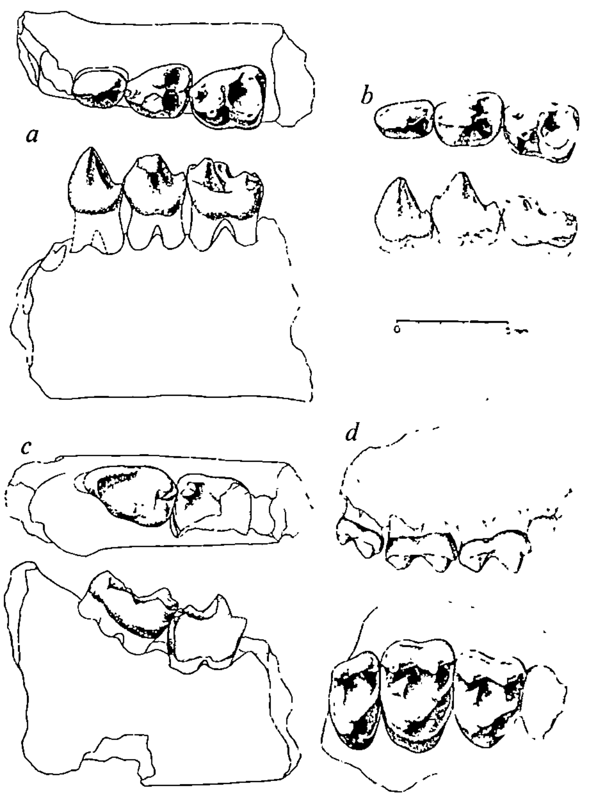

Fig. 1 Dentition of *Cantius torresi*, from the earliest Wasatchian of western North America, and *Cantius eppsi*, from the Sparnacian of UK. *a*, Left dentary of *C. torresi* [UM 83470, holotype] with P_3–M_1 in occlusal (top) and lateral (bottom) view. Partial alveoli for the single-rooted P_1 and double-rooted P_2 are shown in outline The remains of the alveolus for the larger lower canine are obscured in these views. *b*, Right P_3–M_1 (reversed for comparison) of *C. eppsi* [Br. Mus. (Nat. Hist.) 15773, holotype] in occlusal and lateral view. *c*, Right dentary of *C. torresi* [UM 66143] with M_{2-3} in occlusal and lateral view. *d*, Right maxilla of *C. torresi* with M^{1-3} in lateral and occlusal view. Note the short *Nannopithex* fold of enamel running up the posterior surface of the protocone in occlusal view. This enamel fold does not join the postcingulum, and the earliest *Cantius* lacks a fully developed postprotocingulum.

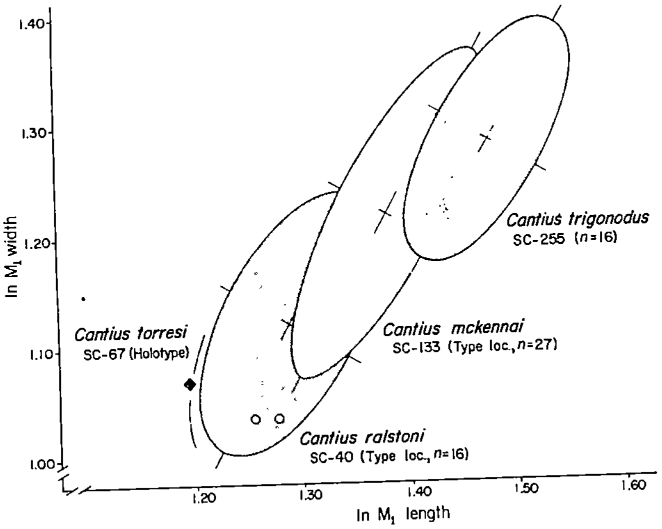

Fig. 2 Comparison of the sizes of the first lower molars in four species of *Cantius* from successive stratigraphically superposed intervals of the early and middle Wasatchian, Clark's Fork Basin, Wyoming. Equiprobability ellipses enclose 90% of the observed variation in early Wasatchian *C. ralstoni* (type sample), *C. mckennai* (type sample), and the later *C. trigonodus*. The holotype of *C. torresi* is just outside the 95% equiprobability contour for *C. ralstoni*. Open circles within the distribution of *C. ralstoni* represent the type sample of *C. eppsi* from Abbey Wood, Kent. Note that *C. torresi* differs from *C. ralstoni* and *C. eppsi* in shape as well as size, having a shorter and relatively broader M_1.

into a full postprotocingulum (later *Cantius*, *Pelycodus*). There is a complete lingual cingulum on M^2. M^1 is 3.3 mm long and 4.5 mm in maximum breadth. M^2 is 3.3 mm long and 5.3 mm in maximum breadth. The crown of M^3 is shorter and consequently relatively broader than those of M^1 and M^2; it is 2.5 mm long and 4.3 mm in maximum breadth.

Judging from the available evidence, *C. torresi* is the smallest and most generalized species of *Cantius* known anywhere. It is similar in size to *C. eppsi* from the Sparnacian Blackheath Beds of the United Kingdom (Abbey Wood, Kent), with a body weight estimated[23] from tooth size to be 1,100–1,200 g. *C. torresi* differs from *C. eppsi* in having shorter and broader premolars (Fig. 1*a*, *b*) and molars (Fig. 2). The type sample of *C. torresi* comes from the Clark's Fork Basin of northwestern Wyoming where more than 760 specimens of *Cantius*, including the type sample of *C. ralstoni* and the type sample of *Cantius mckennai*, are linked in one evolving lineage. As the oldest member of this lineage, *C. torresi* effectively defines the morphology of primitive North American *Cantius*.

Comparing the European *C. eppsi* from the type locality, Abbey Wood, with the North American sequence of *Cantius* species in the Clark's Fork Basin, the size and proportions of upper and lower cheek teeth agree most closely with *C. ralstoni* (Fig. 2), which suggests that *C. eppsi* and *C. ralstoni* represent equivalent grades of evolution and, further, that *C. eppsi* and *C. ralstoni* may be approximately equivalent in age. Radiometric dating and correlation based on palaeomagnetic stratigraphy are insufficiently precise to resolve time on this scale, but comparison of the fauna from SC-67, the type locality of *C. torresi*, with that from Abbey Wood substantiates an older age for *C. torresi*. Perissodactyls are particularly useful here, *Hyracotherium* from SC-67 being smaller and notably less lophodont than any European specimens (including problematical remains from the French locality of Meudon).

Donrussellia provincalis, a European contemporary of *C. eppsi*[1,12], differs from *C. torresi* in being smaller and having the anteroposteriorly elongated P_4 characteristic of *Protoadapis* and later Adapidae, but it could be derived from a generalized *C. torresi* or a similar structural ancestor. *C. torresi* has relatively square upper molars like those of the later North American *Pelycodus jarrovii*[18,24] and, if intermediates were known connecting them through time, *C. torresi* could easily be regarded as an early species of *Pelycodus*.

Of greater interest and importance is the fact that the form of P_4 in *C. torresi* is as similar to the fourth premolars of early tarsiiform Omomyidae as it is to those of later lemuriform Adapidae, suggesting that Omomyidae and Adapidae (and the prosimian infra-orders that they represent) were probably still little differentiated at the beginning of the Eocene. This premolar conformation linking Omomyidae and Adapidae serves, at the same time, to distinguish them from all archaic Palaeocene pleisiadapiform primates of more primitive 'praesimian' grade[25]. Similarly, the presence of a limited *Nannopithex* fold, rather than a full postprotocingulum connecting the protocone to the posterior cingulum, is another feature distinguishing primitive Adapidae and Omomyidae from earlier plesiadapiform primates with a fully developed postprotocingulum. This weakens earlier dental evidence suggesting close linkage of *Plesiadapis* and its allies in the order Primates[26]. While I would still classify *Plesiadapis* as a primate[27], new evidence and interpretations presented here and elsewhere[11,16,25,27,28] indicate that Plesiadapiformes represent an evolutionary radiation distinct from primates of modern aspect.

Previous comparisons of European Sparnacian mammalian faunas with known North American early Wasatchian faunas indicated that *C. eppsi* and contemporary European mammals of other orders were more primitive and therefore probably older than *C. ralstoni* and its North American contemporaries[12,29], suggesting that primates of modern aspect, Artiodactyla, hyaenodontid Credonta, Perissodactyla and other Wasatchian groups reached North America by dispersal from Europe. The discovery of a new and distinctive mammalian assemblage at the base of the North American Wasatchian, including a primate *C. torresi* that is more primitive than any known European adapid, complicates this interpretation. Based on present evidence, it seems that Sparnacian primates of modern aspect and at least some representatives of other modern mammalian orders reached Europe by dispersal through North America.

The geographic area of origin of primates of modern aspec is as yet unknown, but the presence of Lemuroidea on Madagas car today, Lorisoidea in Africa since the early Miocene[30], possible Oligocene adapid (*Oligopithecus*) in Africa[31], and th recent discovery of Oligocene Tarsioidea in Africa[32] make likely that primates of prosimian grade originated on the Africa continent. Africa and Europe were separated by the Tethys Se and Obik Sea throughout the Palaeocene and most of th Eocene[33]. However, Africa may have been connected to centr Asia by way of the Arabian peninsula and Indo-Pakistan subcon tinent[34]. Climatic warming in the late Palaeocene and earlie Eocene[21] undoubtedly facilitated poleward dispersal of endem equatorial African mammals. Thus, one may reasonably speci late that the earliest primates of modern aspect evolved equatorial Africa during the late Palaeocene and disperse rapidly through Arabia, South Asia, Central Asia and Nor America to reach Europe as part of a broader pattern of faun interchange on northern continents leading to the holarct cosmopolitanism evident in the early Eocene.

I thank T. M. Bown and R. D. Martin for reviewing t manuscript, and J. J. Hooker for casts and discussion. Specime were prepared by W. Ryan, figures by K. Klitz. This resear was supported by NSF grants BNS 80-16742, DEB 82-062 and EAR 84-08647.

Received 10 May; accepted 1 November 1985.

1. Godinot, M. *C. r. hebd. Séanc. Acad. Sci., Paris* **D286**, 1869–1872 (1978).
2. Hooker, J. J. & Insole, A. N. *Tertiary Res., Rotterdam* **3**, 31–45 (1980).
3. Dashzeveg, D. & McKenna, M. C. *Acta palaeont. pol.* **22**, 119–137 (1977).

4. Dashzeveg, D. *Bull. Soc. géol. Fr. Sér.* 7 **24**, 275-281 (1982).
5. Rose, K. D. *Science* **208**, 744-746 (1980).
6. Berggren, W. A., McKenna, M. C., Hardenbol, J. & Obradovich, J. D. *J. Geol.* **86**, 67-81 (1978).
7. Harland, W. B. *et al. A Geologic Time Scale* (Cambridge University Press, 1982).
8. Simons, E. L. *Bull. Br. Must. nat. Hist., Geol.* **7**, 1-36 (1962).
9. Russell, D. E., Louis, P. & Savage, D. E. *Univ. Calif. Publs geol. Sci.* **73**, 1-46 (1967).
10. Szalay, F. S. *Folia Primatol.* **22**, 116-133 (1974).
11. Gingerich, P. D. *Folia Primatol.* **28**, 60-80; 144-153 (1977); *J. hum. Evol.* **10**, 345-374 (1981).
12. Godinot, M. *Palaeovertebrata* **10**, 43-126 (1981); *Geobios, Mém. Spéc.* **6**, 403-412 (1982).
13. Rose, K. D. & Krause, D. W. *J. Mammal.* **65**, 721-726 (1984).
14. Russell, D. E. & Gingerich, P. D. *C. r. hebd. Séanc. Acad. Sci., Paris* **D291**, 621-624 (1980).
15. Bown, T. M. *Folia Primatol.* **25**, 62-72 (1976).
16. Szalay, F. S. *Bull. Am. Mus. nat. Hist.* **156**, 157-450 (1976).
17. Gingerich, P. D. & Simons, E. L. *Contr. Mus. Paleont. Univ. Mich.* **22**, 245-279 (1977).
18. Gingerich, P. D. & Haskin, R. A. *Contr. Mus. Paleont. Univ. Mich.* **25**, 327-337 (1981).
19. Rose, K. D. & Bown, T. M. *Nature* **309**, 250-252 (1984).
20. Bown, T. M. & Rose, K. D. *Folia Primatol.* **43**, 97-112 (1984).
21. Buchardt, B. *Nature* **275**, 121-123 (1978).
22. Kraus, M. J. in *Early Cenozoic Paleontology and Stratigraphy of the Bighorn Basin, Wyoming* (ed. Gingerich, P. D.) 87-94 (University of Michigan Museum of Paleontology, Ann Arbor, 1980).
23. Gingerich, P. D., Smith, B. H. & Rosenberg, K. *Am. J. phys. Anthrop.* **58**, 81-100 (1982).
24. Rose, K. D. & Bown, T. M. *J. Paleont.* **58**, 1532-1535 (1984).
25. Gingerich, P. D. *Yb. phys. Anthrop.* **27**, 57-72 (1984).
26. Gingerich, P. D. in *Prosimian Biology* (eds Martin, R. D., Doyle, G. A. & Walker, A. C.) 531-541 (Duckworth, London, 1980).
27. Gingerich, P. D. in *Major Topics in Primate and Human Evolution* (eds Wood, B. A., Martin, L. B. & Andrews, P.) (Cambridge University Press, in the press).
28. MacPhee, R. D. E., Cartmill, M. & Gingerich, P. D. *Nature* **301**, 509-511 (1983).
29. Gingerich, P. D. *A. Rev. Earth planet. Sci.* **8**, 407-424 (1980).
30. Walker, A. C. in *Prosimian Biology* (eds Martin, R. D., Doyle, G. A. & Walker, A. C.) 435-447 (Duckworth, London, 1980).
31. Gingerich, P. D. *Geobios, Mém. Spéc.* **1**, 165-182 (1977).
32. Simons, E. L. & Bown, T. M. *Nature* **313**, 475-477 (1984).
33. McKenna, M. C. *Ann. M. bot. Gdn* **62**, 335-353 (1975).
34. Smith, A. G. & Briden, J. C. *Mesozoic and Cenozoic Paleocontinental Maps* (Cambridge University Press, 1977).

Reconstruction of African human diet using bone collagen carbon and nitrogen isotope ratios

Stanley H. Ambrose* & Michael J. DeNiro†

Department of Earth and Space Sciences, and †Archaeology Program, University of California, Los Angeles, California 90024, USA

Behavioural modifications associated with the exploitation of new food resources have been linked to major steps in hominid evolution and in subsequent human cultural development[1,2]. Testing of specific hypotheses concerning the influence of dietary change on these processes would be facilitated by quantitative estimates of early hominid and human diets. Although most methods of obtaining such evidence provide only qualitative information[2], the stable carbon and nitrogen isotope ratios of animal tissues, and in particular, bone collagen, can be used to quantify the consumption of foods having different isotopic compositions[3–5]. As reported here, analysis of the collagen of historic and prehistoric African human populations from Kenya, Tanzania and South Africa that have reasonably well-known diets shows that stable carbon and nitrogen isotope ratios in bone collagen can distinguish marine foragers from populations consuming terrestrial resources, pastoralists from farmers, farmers consuming grains from those consuming non-grain crops, and camel pastoralists from capri-bovine pastoralists.

Several major classes of food resources can be distinguished on the basis of their isotopic composition. Among terrestrial plants, carbon isotope ratios differentiate between C_3 plants and C_4 and CAM (crassulacean acid metabolism) plants[6]. C_4 plants include maize, sorghum, African millets and tropical pasture grasses. Most succulents such as cacti are CAM plants. Other staple foods, including wheat, rice, nuts and most vegetables and fruits, are C_3 plants[6]. The average $\delta^{13}C$ values (see Table 1 for an explanation of δ values) for C_3, C_4 and CAM, and marine plants, are −26.5, −12.0, and −19.0‰, respectively Nitrogen isotope ratios distinguish marine from terrestrial plants and nitrogen-fixers from other plants. The $\delta^{15}N$ values of marine plants are ~4‰ higher than those of terrestrial plants that use soil nitrogen[5]. Plants that use fixed atmospheric nitrogen (for example, legumes) have lower $\delta^{15}N$ values than other plants The isotopic compositions of animal tissues reflect the isotope ratios of the plants at the bases of food chains[3,4]. However, there is a small stepwise enrichment of ^{13}C and a larger one of ^{15}N as carbon and nitrogen move to higher trophic levels[3]. In fact, enrichment in ^{15}N is large enough to serve as an indicator of trophic level[5].

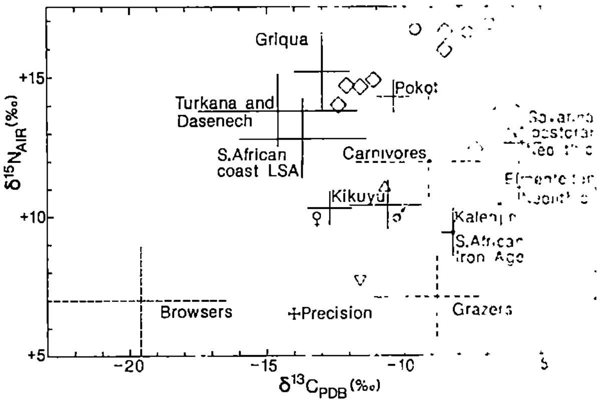

Fig. 1 $\delta^{15}N$ and $\delta^{13}C$ values of bone collagen from African human and non-human mammal populations and individuals. The means (±1 s.d.) are indicated by symbols or solid lines for human groups and by broken lines for modern non-human East African mammals. The symbols represent individual determinations for the following human groups and individuals: △, proto-historic Kikuyu from site GsJj31, Naivasha, Kenya; ∇, proto-historic Luyia from site GnJc51, Bungoma, Kenya; ⊙ and ◇, prehistoric individuals from Sechikuencho Cairns and from Gishimangeda Cave respectively, Lake Eyasi, northern Tanzania.

Given these basic differences in the isotopic composition of food resources, it should be possible to use $\delta^{13}C$ and $\delta^{15}N$ values to distinguish between human populations relying mainly on animal products as opposed to plant foods, the meat of grazing animals as opposed to that of browsing animals, or C_3 as opposed to C_4 plants. These expectations are fulfilled for modern non-human mammals collected in Kenya and Tanzania (see Fig. 1). These results, based on the analysis of 15 carnivores, 111 grazers and 82 browsers (10, 13 and 18 species, respectively) serve as a standard against which isotopic data for humans presented in this study can be evaluated.

Bones of historic, proto-historic (Table 1) and prehistoric (Table 2) humans were obtained from museum collections in Kenya, Tanzania and South Africa. Bone collagen was purified and its $\delta^{13}C$ and $\delta^{15}N$ values determined by mass spectrometry, as described elsewhere[3–5].

Table 1 lists, in rank order of importance, the major components of the diets of Kikuyu farmers of central Kenya[9], Luyia farmers of western Kenya[10], Turkana and Dasenech pastoralists of northern Kenya[11,12], highland and lowland Pokot of north west Kenya[13,14], Nandi and Kipsigis (Kalenjin) farmers and pastoralists of highland western Kenya[13], and Griqua pastoralists and farmers of the Orange Free State, South Africa[15].

The diets of the prehistoric populations are less well understood because of food preservation biases inherent in the archaeological record. The diet of Elmenteitan Neolithic and Iron Age peoples of highland western Kenya is considered to have been similar to that of the historic Kalenjin[16]. The diet of Savanna Pastoral Neolithic (SPN) peoples appears to have been dominated by cattle and caprine pastoralism but their degree of dependence on agriculture is under debate[16,17]. There is inadequate information regarding the diets, ages and cultural

---

* Present address: Department of Anthropology, University of Illinois, Urbana, Illinois 61801, USA.

Table 1 $\delta^{15}N$ and $\delta^{13}C$ values (‰) of bone collagen from historic and proto-historic human populations from Kenya, Tanzania and South Africa

	$\delta^{15}N$				$\delta^{13}C$						
Population	$\bar{x}$	s.d.	Min.	Max.	$\bar{x}$	s.d.	Min.	Max.	No. of individuals	Diet	Ref.
Kenya											
Kikuyu (♂)	+10.4	0.9	+9.3	+12.3	−10.6	1.4	−13.1	−7.3	12	C_3/C_4 agriculture, with small amounts of cattle and caprines	11
Kikuyu (♀)	+10.3	0.6	+9.6	+11.2	−12.7	0.8	−13.9	−11.6	5		
Kikuyu, 19th century (GsJj31, Naivasha)	+11.1				−10.7				1		
Turkana/Dasenech	+13.8	1.3	+12.1	+16.0	−14.6	2.9	−18.0	−10.4	7	Camel, cattle, caprine pastoralism, some C_4 grains and wild C_3 plants	13, 14
Pokot	+14.2		+13.4	+14.9	−10.4		−11.2	−9.7	2	Cattle, caprine and camel pastoralism and C_4 grains	15, 16
Kalenjin	+10.4		+10.3	+10.5	−6.5		−6.7	−6.3	2	C_4 grains, and cattle and caprine pastoralism	15
Luyia, 19th century (GnJc51, Bungoma)	+7.7				−11.6				1	C_3/C_4 agriculture with small amounts of cattle and caprines	12
South Africa											
Griqua, 19th century	+15.2	1.4	+13.5	+17.7	−13.0	1.0	−14.7	−11.4	12	Cattle and caprine pastoralism and C_3 agriculture	17

Major classes of food resources are listed in rank order of importance in the diet of the populations. Isotope ratios are expressed as δ values, where $\delta^{*}X = [[(^{*}X/X)_{\text{sample}}/(^{*}X/X)_{\text{standard}}] - 1] \times 1{,}000‰$. For carbon, $^{*}X/X$ is $^{13}C/^{12}C$ and the standard is the PDB carbonate. For nitrogen, $^{*}X/X$ is $^{15}N/^{14}N$ and the standard is atmospheric (Ambient Inhalable Reservoir, AIR) nitrogen.

affiliations of the individuals from the Eyasi Basin, Northern Tanzania[18]. The cultural and economic history of this region is among the most complex in Africa[18], so it is possible that not all the prehistoric individuals had the same diets. The diet of the Later Iron Age peoples of the Northern Transvaal, South Africa, is considered to have been similar to that of the historic Pedi, who depend mainly on C_4 grains, supplemented by wild and domestic C_3 plants; cattle, caprines and wild animals contribute little to their diet[19]. The Later Stone Age hunter-gatherers of the South African Cape coast between Port Elizabeth and Hermanus subsisted on marine vertebrates and invertebrates, terrestrial C_3 plants and the flesh of herbivores[20].

The results of the isotopic analyses of the historic populations can be compared with published descriptions of their diets (Table 1, Fig. 1). Those groups described as being most dependent on plant foods (Luyia, Kikuyu and Kalenjin) have $\delta^{15}N$ values between +8 and +12‰, while those most dependent on the milk, meat and blood of domestic animals (Turkana, Dasenech, Pokot and Griqua) have $\delta^{15}N$ values between +12 and +18‰. The Kalenjin, who consume mostly C_4 plants and animals that grazed on C_4 grasses, have a mean $\delta^{13}C$ value of −6.5‰. Those populations depending on a mix of C_3 and C_4 plants and/or a mix of products from C_4-grazing and C_3-browsing animals (Luyia, Kikuyu, Pokot, Turkana, Dasenech and Griqua) have mean $\delta^{13}C$ values ranging from −10 to −15‰.

The pastoral/agricultural and C_3/C_4 distinctions are also apparent among the prehistoric populations (Table 2, Fig. 1). The mean $\delta^{15}N$ values for the South African Later Iron Age, Elmenteitan and SPN populations are +9.4, +11.0 and +12.7‰, respectively. This ranking by $\delta^{15}N$ values is consistent with archaeological evidence for their degree of dependence on animal as opposed to plant products. The Elmenteitan and SPN groups have virtually identical mean $\delta^{13}C$ values, indicating nearly exclusive use of C_4-based resources; however, $\delta^{15}N$ values indicate that they fed at different trophic levels. The mean $\delta^{13}C$ value of −8.2‰ for the South African Later Iron Age population indicates their relatively greater dependence on C_3 plant foods relative to East African Neolithic populations.

The prehistoric southern Cape coastal forager sample set (Table 2) has a mean $\delta^{15}N$ value of +12.8‰, which is within the range of previously analysed populations from other coastal regions[21]. Their $\delta^{13}C$ values, with one exception, reflect a diet of no more than 50% terrestrial resources[21]. As in the western Cape[22], our isotopic evidence seems inconsistent with a model of seasonal transhumance between coastal and montane environments[20]. However, this region is transitional between winter and summer rainfall regions so the grass flora at different locations within the region contains from 0 to 75% C_4 grasses[23]. Therefore, skeletons from montane environments need to be analysed in order to confirm this conclusion.

The $\delta^{13}C$ and $\delta^{15}N$ values of the 15 prehistoric individuals from Tanzania[18] form three discrete clusters (Fig. 1). Six individuals are within the range of the Kenyan SPN. The second cluster has mean $\delta^{15}N$ and $\delta^{13}C$ values of +14.6 and −11.8‰, respectively, indicating a diet dominated by animal resources that included some browsing animals, supplemented by wild plant foods and/or C_3 crops. The third cluster has the highest average $\delta^{15}N$ value in the sample set and must reflect a diet dominated by the protein of grazing animals. The $\delta^{13}C$ values for this cluster indicate that small amounts of C_3 plants and/or browsing animals were eaten.

The agreement between the isotopic composition of bone collagen from the populations analysed and their diets as inferred from ethnographic and archaeological evidence is remarkably close in almost every case. Those groups depending largely on the milk, meat and blood of domestic animals have the highest $\delta^{15}N$ values, while those that subsist mainly on plants have the lowest ones. Groups subsisting mainly on C_4 plants or the protein of grazing herbivores have higher $\delta^{13}C$ values than those depending on a mix of C_3 and C_4 plants and grazing and browsing animals.

There is also close agreement between the isotopic compositions of prehistoric and historic members of the same ethnic groups. The nineteenth-century Kikuyu individual has an isotopic composition that is within the range determined for twentieth-century Kikuyu males (Table 1, Fig. 1). It has been proposed that the Kalenjin are the descendants of Elmenteitan Neolithic peoples[16,24] and the similarity in the isotopic compositions suggests similar diets.

The isotopic composition of the Kenyan Neolithic groups helps us to resolve the current controversy over their dietary adaptations[16,17]. Evidence from linguistic studies suggests that

Table 2 $\delta^{15}N$ and $\delta^{13}C$ values (‰) of bone collagen from humans recovered from archaeological sites in Kenya, Tanzania and South Africa

Group and location	Site	$\delta^{15}N$	$\delta^{13}C$	Ref.
Elmenteitan Neolithic and Iron Age, Kenya	Deloraine Farm (GqJh6)	+10.6	−4.8	24
	Rigo Cave (GrJh3/44)	+11.8	−5.4	32
	Rigo Cave (GrJh3/32)	+10.3	−6.0	32
	Rigo Cave (GrJh3/33)	+10.9	−5.0	32
	Rigo Cave (GrJh3/6)	+11.7	−7.3	32
	Egerton Cave (GrJh10/2)	+11.4	−5.1	33
	Egerton Cave (GrJh10/3)	+12.2	−5.8	33
	Egerton Cave (GrJh10/4)	+10.9	−5.8	33
	Egerton Cave (GrJh10)	+8.6	−6.1	33
	Keringet Caves	+11.3	−6.4	34
Savanna Pastoral Neolithic (SPN), Kenya	Marula rockshelter (GSJj24)	+12.9	−6.5	35
	Cole's Farm (GrJj5a)	+11.4	−5.0	16
	Cole's Farm (GrJj5a/132)	+12.4	−4.8	16
	Lukenya Hill (GvJm202/541)	+12.0	−6.2	35
	Lukenya Hill (GvJm202/785)	+11.6	−5.1	35
	Lukenya Hill (GvJm202/513)	+13.1	−4.5	35
	Mt Suswa (GuJj14)	+13.1	−6.5	35
	Naivasha Burial Site (KNM-NV43)	+12.6	−6.9	36
	Kisima Farm (KFR-A5, no. 11)	+13.9	−5.9	37
	Makalia Burial Site (II)	+13.0	−5.9	37
Prehistoric burials, Lake Eyasi, Tanzania	Gishimangeda Cave	+12.9	−6.2	18
	Gishimangeda Cave	+16.6	−8.5	18
	Gishimangeda Cave	+11.8	−5.3	18
	Gishimangeda Cave	+12.4	−7.4	18
	Gishimangeda Cave (A)	+12.9	−5.7	18
	Gishimangeda Cave (B)	+15.9	−8.5	18
	Gishimangeda Cave (C)	+14.7	−11.6	18
	Gishimangeda Cave (D)	+14.0	−12.4	18
	Gishimangeda Cave (E)	+13.7	−5.9	18
	Gishimangeda Cave (F)	+14.7	−12.2	18
	Gishimangeda Cave (G)	+14.9	−11.2	18
	Gishimangeda Cave	+13.6	−6.6	18
	Sechikuencho Cairns	+16.9	−6.9	18
	Sechikuencho Cairns	+16.6	−7.7	18
	Sechikuencho Cairns	+16.7	−9.6	18
Later Iron Age, northern Transvaal, South Africa	Makapan (2429AA4)	+9.7	−7.9	38
	Maxonwa Maone (2329CD12)	+9.1	−8.3	38
	Bambo (2329CD9C)	+11.1	−8.6	38
	Tauhatswana (2329BB2A, no. 1)	+8.0	−7.8	38
	Tauhatswana (2329BB2A, no. 2)	+8.3	−7.8	38
	Bambo (2329CD9A, no. 3)	+9.4	−9.3	38
	Bambo (2329CD9A, no. 1)	+9.7	−8.0	38
	Nylsvley (2248DA)	+10.2	−7.8	38
Later Stone Age, southern Cape coast, South Africa	Knysna Strandlooper (A1070A)	+11.9	−14.5	39
	Knysna Strandlooper (A1070B)	+15.7	−11.2	39
	Schoenmakaskop (A1116)	+12.4	−13.2	39
	Loeritank (A1117)	+14.0	−12.0	39
	Sunday's River (A1118)	+14.0	−13.6	39
	Sea View (A1138)	+11.8	−11.0	39
	Zitzikama (A1155)	+13.2	−19.2	39
	Zitzikama Rock Shelters (A1112)	+13.3	−12.5	40
	Zitzikama Rock Shelters (A1112, ZA2)	+12.9	−15.5	40
	Byneskranskop 3 (no. 10)	+10.2	−14.6	41
	Byneskranskop 3 (no. 3)	+13.3	−11.4	41
	Byneskranskop 3 (no. 4)	+11.6	−15.4	41

both groups were familiar with C_4 grain crops[25], but archaeological evidence suggests that SPN populations were pastoralists rather than farmers[16]. The mean $\delta^{15}N$ values of the Elmenteitan and SPN groups are significantly different ($P < 0.01$), but both are intermediate between historic pastoral and agricultural groups. Lower $\delta^{15}N$ values for the Elmenteitan suggest an even mix of plant and animal resources whereas higher values for the SPN suggest a greater reliance on animal products. High $\delta^{13}C$ values indicate that the plant and animal components of the diets of both groups were almost entirely C_4 grains and grazing animals.

The $\delta^{15}N$ values of the pastoral populations are significantly higher than those of the East African carnivores (Fig. 1). This unexpected result suggests that the former populations consumed resources having $\delta^{15}N$ values higher than those eaten by the carnivores. Milk and blood appear to be enriched in ^{15}N relative to the flesh of animals[26], which could account for this observation.

Our results suggest that it should be possible to use stable isotopes to test models of prehistoric hunter-gatherer diets. For example, most modern hunter-gatherers in the tropics live in marginal environments and are heavily dependent on plant foods[27]. However, before the advent of food production they inhabited non-marginal environments and may have exploited fewer plant foods[28]. If this dietary shift can be demonstrated isotopically, widely held concepts of tropical hunter-gatherer adaptations, and of the relative significance of hunting versus gathering in human evolution, would require revision.

We can also speculate on the expected isotopic composition of different Plio-Pleistocene hominids. Australopithecine diets are considered to have been predominantly vegetarian[29]. As virtually all wild plant foods now eaten by African humans and primates[30] are C_3 and the consumption of C_4 grasses can be ruled out on the basis of dental microwear evidence[2], we would expect Australopithecines to have low $\delta^{13}C$ and $\delta^{15}N$ values. Archaeological evidence suggests that *Homo habilis* and *Homo erectus* consumed the meat of grazing animals[31], so we would expect them to have higher $\delta^{15}N$ and $\delta^{13}C$ values than the Australopithecines. However, before early hominids are analysed it will be necessary to demonstrate that organic fractions retaining their *in vivo* isotopic record exist in samples of Plio-Pleistocene age and that stable isotopes can distinguish among grazers, browsers and carnivores contemporary with the early hominids.

We thank the National Museums of Kenya and Tanzania, the South African Museum and the Departments of Archaeology and Anatomy, University of Witwatersrand, and numerous individuals for providing human bone samples. Support was provided by the L.S.B. Leakey Foundation, The Foundation for Research into the Origin of Man, and NSF grants BNS79-24756, BNS81-18026 and BNS84-18280.

Note added in proof: All prehistoric samples discussed here had atomic carbon-to-nitrogen ratios in the range 3.0-3.5 and thus retain their *in vivo* isotopic signatures, according to the criterion proposed by DeNiro[42].

Received 26 July; accepted 24 October 1985.

1. Isaac, G. L. In *Evolution from Molecules to Men* (ed. Bendall, D. S.) 509-543 (Cambridge University Press, 1983).
2. Walker, A. *Phil. Trans. R. Soc.* B292, 57-64 (1981).
3. DeNiro, M. J. & Epstein, S. *Geochim. cosmochim. Acta* 42, 495-506 (1978).
4. DeNiro, M. J. & Epstein, S. *Geochim. cosmochim. Acta* 45, 341-351 (1981).
5. Schoeninger, M. J. & DeNiro, M. J. *Geochim. cosmochim. Acta* 48, 625-639 (1984).
6. Smith, B. N. *BioScience* 22, 226-231 (1972).
7. Delwiche, C. C., Zinke, P., Johnson, C. M. & Virginia, R. A. *Bot. Gaz.* 140 (Suppl.), S65-S69 (1979).
8. Ambrose, S. H. & DeNiro, M. J. *Oecologia* (submitted).
9. Leakey, L. S. B. *The Southern Kikuyu Before 1903* Vol. 1 (Academic, London, 1977).
10. Wagner, G. *The Bantu of North Kavirondo* Vol. 2 (International African Institute, London, 1956).
11. Gulliver, P. & Gulliver, P. H. *The Central Nilo-Hamites* (International African Institute, London, 1953).
12. Carr, C. J. *Pastoralism in Crisis: The Dasenech and their Ethiopian Lands* (Univ. Chicago Dep. Geogr. Res. Pap. 180, 1977).
13. Huntingford, G. W. B. *The Southern Nilo-Hamites* (International African Institute, London, 1953).
14. Conant, F. P. *Am. Anthrop.* 67, 429-434 (1965).
15. Morrison, A. thesis, Univ. Witwatersrand, Johannesburg (1984).
16. Ambrose, S. H. in *From Hunters to Farmers* (eds Clark, J. D. & Brandt, S. A.) 212-239 (University of California Press, 1984).
17. Robertshaw, P. T. & Collett, D. P. *Wld Archaeol.* 15, 67-78 (1983).
18. Ikeda, J. & Hayama, S. *Afr. Stud. Monogr.* 2, 1-26 (1982).
19. Mõnnig, H. O. *The Pedi* (Van Schaik, Pretoria, 1967).
20. Deacon, H. J. *S. Afr. archaeol. Soc. Goodwin Ser.* 1, 26-45 (1972).
21. Schoeninger, M. J., DeNiro, M. J. & Tauber, H. *Science* 220, 1381-1383 (1983).
22. Sealy, J. C. & van der Merwe, N. J. *Nature* 315, 138-140 (1985).
23. Vogel, J. C., Fuls, A. & Ellis, R. P. *S. Afr. J. Sci.* 74, 209-215 (1978).
24. Ambrose, S. H. *Azania* 19, 79-104 (1984).

25. Ehret, C. *Ethiopians and East Africans: The Problem of Contacts* (East African Publishing House, Nairobi, 1974).
26. Steele, K. W. & Daniel, R. M. *J. agric. Sci.* **90,** 7-9 (1978).
27. Lee, R. B. in *Man the Hunter* (eds Lee, R. B. & DeVore, I.) 30-48 (Aldine, Chicago, 1968).
28. Ambrose, S. H. *Sugia* (*Sprache und Geschichte in Afrika*) **7** (in the press).
29. Pilbeam, D. & Gould, S. J. *Science* **186,** 892-901 (1974).
30. Peters, C. R. & O'Brien, E. M. *Curr. Anthrop.* **22,** 127-140 (1981).
31. Isaac, G. L. *Adv. Wld Archaeol.* **3,** 1-87 (1984).
32. Wandibba, S. *Azania* **18,** 81-92 (1983).
33. Faugust, P. M. & Sutton, J. E. G. *Azania* **1,** 149-175 (1966).
34. Cohen, M. *Azania* **5,** 27-38 (1970).
35. Ambrose, S. H. thesis, Univ. California, Berkeley (1984).
36. Leakey, L. S. B. *The Stone Age Races of Kenya* (Oxford University Press, London, 1935).
37. Siriäinen, A. *Azania* **12,** 161-186 (1977).
38. Moore, M. J. thesis, Univ. Witwatersrand, Johannesburg (1981).
39. Fitzsimmons, F. W. S. *S. Afr. J. Sci.* **25,** 448-450 (1928).
40. Laing, G. D. & Gear, H. S. *S. Afr. J. Sci.* **26,** 575-601 (1929).
41. DeVilliers, H. & Wilson, M. L. *Ann. S. Afr. Mus.* **88,** 205-248 (1982).
42. DeNiro, M. J. *Nature* **317,** 806-809 (1985).

Blue light-dependent proton extrusion by guard-cell protoplasts of *Vicia faba*

K. Shimazaki*†, M. Iino*‡ & E. Zeiger†

† Department of Biological Sciences, Stanford University, Stanford, California 94305, USA
‡ Carnegie Institution of Washington, Department of Plant Biology, 290 Panama Street, Stanford, California 94305, USA

In plant leaves, light regulation of stomatal movement, and hence of gas exchange[1], involves a non-photosynthetic photosensory system sensitive to blue light[2–6], which transduces many other plant movement responses. The exact nature of the primary photoreactions of this system is still not known[7]. Stomatal opening is, in general, based on swelling of the guard cells driven by ion uptake[1], and it has been suggested that energy for such uptake may be provided by a chemi-osmotic extrusion of protons across the plasmalemma[1,8,9]. We report here that guard-cell protoplasts from *Vicia faba*, irradiated continuously with photosynthetically saturating, high-fluence-rate red light, extrude H^+ ions in response to a short pulse (30 s) of blue light. The response is relatively long-lived, such that a high rate of H^+ extrusion continues for several minutes after the pulse stimulation, indicating that continuous input of blue light energy is not required for a sustained response. The kinetic relation between pulse input and response output matched closely that found for the stomatal response in intact leaves[6]. In agreement with the chemi-osmotic hypothesis, activation of an electrogenic plasmalemma H^+-ATPase is postulated as the cause of blue light-induced H^+ extrusion.

Proton transport in guard cells can be studied most effectively by using protoplasts because they can be obtained free of other contaminating cell types[3,10,11] and because no highly buffering cell wall is present[12]. The blue light-sensitive system can be effectively isolated for study with a dual-beam protocol in which a blue light pulse is applied during a continuous, background irradiation with high-fluence-rate red light. This method has been used successfully to study the stomatal opening transduced by the blue light-sensitive photosystem, without additional photosynthesis-related stomatal respones[6].

In dark-adapted preparations, red light irradiation caused an alkalinization of the medium (Fig. 1*A*) which lasted for about 1 h. (This response, frequently observed with photosynthetically competent cell preparations, is usually a consequence of CO_2 fixation[13].) A 30-s pulse of blue light, given after medium *p*H reached a steady state under red light, caused an acidification that continued for about 10 min (Fig. 1*B*). Although the magni-

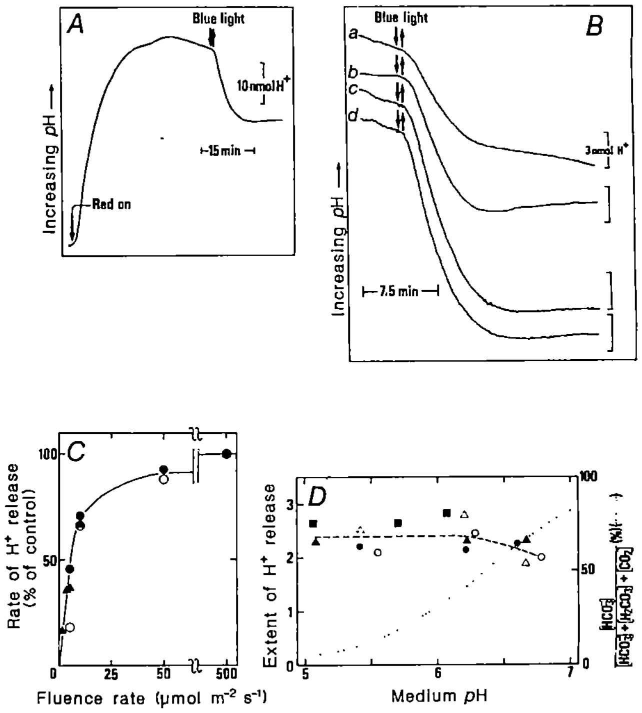

Fig. 1 Blue light-induced medium acidification by *Vicia* guard-cell protoplasts. *A*, Medium alkalinization in response to continuous red light (fluence rate, 800 μmol m^{-2} s^{-1}) and acidification in response to a subsequent blue light pulse (30 s, indicated by arrows; fluence rate, 500 μmol m^{-2} s^{-1}). Without a blue light pulse, the red light-induced alkalinization was followed by a nearly steady *p*H level. *B*, Typical acidification profiles in response to different fluences of blue light (pulse duration, 30 s), applied about 1 h after the onset of red light irradiation. *a*, 150; *b*, 300; *c*, 1,500; and *d*, 15,000 μmol m^{-2} of blue light. Fluence rate was adjusted with neutral density filters. *C*, Rate of H^+ release as a function of fluence rate of blue light (pulse duration, 30 s) in three different experiments. Rates were normalized relative to those measured in response to 500 μmol m^{-2} s^{-1} blue light. Identical symbols correspond to the same protoplast batch. *D*, Blue light-induced acidification as a function of medium *p*H, expressed as μmol H^+ released per mg chlorophyll per pulse. Identical symbols indicate measurements with the same protoplast batch. Dotted line is the percentage of HCO_3- concentration in the total concentration of HCO_3-, CO_2 and H_2CO_3 in water, calculated from the Henderson-Hasselbach equation ($pK_1 = 6.35$, 25 °C).

Methods. Guard-cell protoplasts were isolated enzymatically from abaxial epidermis of 4- to 5-week-old leaves of *Vicia faba* L. (cv. Long Pod) as described previously[11]. Suspension of isolated protoplasts (about 10^6 cells) in 1.2 ml of 0.5 mM methane ethane sulphonate-NaOH buffer (*p*H 6.2, unless otherwise stated) containing 0.35 M mannitol, 1 mM $CaCl_2$ and 10 mM KCl, was continuously stirred in an open glass vessel enclosed in a Plexiglas water jacket filled with circulating water at 25 °C. Medium *p*H was measured with a *p*H glass electrode (Beckmann 39522) connected to a *p*H meter (Radiometer 26) and a chart recorder. An intrinsic response of the *p*H electrode was eliminated by shielding it with a piece of Cinemoid 5A film. Amounts of acid equivalents were determined by a calibration caused by the addition of 10 nmol H^+ at the end of each experiment. (Blue light-induced acidification occurred within 0.05 *p*H units.) The chlorophyll concentration in each protoplast preparation was determined by the method of Arnon[22]. Rates of H^+ release were calculated per unit weight of chlorophyll. Rates of H^+ release per unit area of plasmalemma were estimated given an average cell chlorophyll content[21] of 2 pg and an average protoplast diameter of 16 μm. Red light was obtained by passing light from a 500-W Sylvania tungsten lamp through a Corning 2-61 red filter and a layer of Cinemoid 5A; blue light, by passing light from a Kodak Carousel 4200 projector (300-W EXR lamp) through a Corning 5-60 filter and a 4-cm layer of a 0.2% copper sulphate solution. Fluence rates were measured with a Li-Cor quantum sensor.

---

* Present addresses: Division of Environmental Biology, National Institute for Environmental Studies, Yatabe-machi, Ibaraki 305, Japan (K.S.); Department of Biology, Tokyo Metropolitan University, Fukazawa, Tokyo 158, Japan (M.I.).

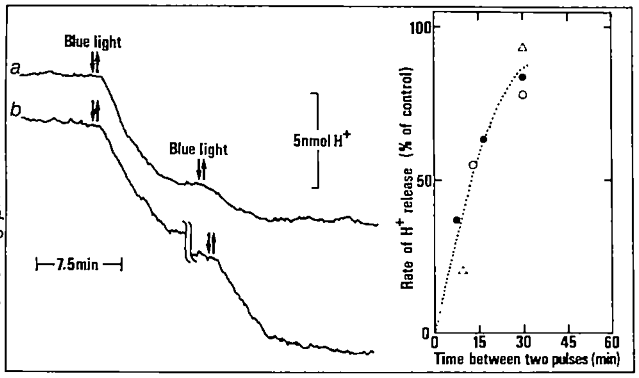

Fig. 2 H^+ release in response to two consecutive, saturating pulses (each pulse: 30 s with 50 μmol m^{-2} s^{-1}). Traces *a* and *b*, two pulses given 7.5 and 30 min apart, respectively. Inset: rates of H^+ release in response to a second pulse, as a function of the time between two pulses. The rate of H^+ release in response to a second pulse is expressed as a percentage of that obtained with the first pulse. Background red light irradiation and other experimental details are as in Fig. 1. Identical symbols correspond to the same protoplast batch.

tude of the response was fluence-dependent, the relative time courses obtained with different fluences were nearly congruent (Fig. 1*B*), with maximal rates of acidification observed within 2 min after pulse stimulation. A pulse of red light (30 s with 500 μmol m^{-1} s^{-1}) superimposed on background red irradiation, induced no detectable *p*H change, demonstrating that the acidification was a specific response to blue light.

The pulse-induced response described above was saturable (Fig. 1*C*), with half-saturations at about 180 μmol m^{-2} (30 s with 6 μmol m^{-2} s^{-1}). The protoplasts once saturated by a single pulse, however, became responsive to another saturating pulse. This was indicated by an additional acidification caused by a second pulse given with sufficient delay (Fig. 2). These properties of the acidification response agree very well with pulse-induced stomatal opening seen in intact leaves[6]. It is noteworthy that with both phenomena, responsiveness to a second pulse progressed with nearly identical kinetics, with half-maximal response occurring at a 10-min interval between pulses (Fig. 2 and ref. 6). The similarity indicates that the cellular events underlying the blue light-induced acidification in protoplasts are components of the sensory transduction process mediating the blue light-dependent stomatal movement. This view was further supported by the finding that blue light-induced medium acidification was inhibited, though partially, by the phytohormone abscisic acid (Fig. 3), an important mediator of the closure response of stomata to water stress[8,14].

Medium acidification could be a result of cellular H^+ extrusion or of increased respiration rates[15] and concomitant CO_2 evolution. CO_2 in solution equilibrates with HCO_3^- through the reaction $CO_2 + H_2O \rightleftharpoons HCO_3^- + H^+$. Thus, an acidification caused by CO_2 release should be markedly dependent on medium *p*H (dotted line in Fig. 1*D*). Data presented in Fig. 1*D* show that the blue light-induced acidification was independent of medium *p*H from 5 to 7, ruling out a significant contribution to the measurements from CO_2 evolution. Further evidence against respiration as a primary cause of the acidification was obtained with measurements of O_2 tension in the suspension medium, by using a Clark-type O_2 microelectrode. The measurements failed to show any detectable change in O_2 levels during blue light-induced acidification (not shown). These data indicate that the observed acidification was primarily a result of H^+ extrusion by guard-cell protoplasts.

In recent work with the electrophysiological technique of patch clamping, *Vicia* guard cell protoplasts clamped at a constant current showed a membrane hyperpolarization in response to a blue-light pulse under a background of red light[16]. Under constant voltage, blue light pulses elicited a transient outward current, with both the hyperpolarization and current measurements[16] showing time courses similar to those seen with the blue light-induced acidification reported here. Maximal rates of H^+ extrusion per plasmalemma unit area, estimated from results of many experiments, ranged between 2 and 6 pmol H^+ cm^{-2} s^{-1}. These values agree closely with the measured outward current density of 0.88 μA cm^{-2} (ref. 16). The temporal homology between acidification and hyperpolarization responses, and the quantitative agreement between the measured current density and H^+ release rate strongly indicate that the blue light-depen-

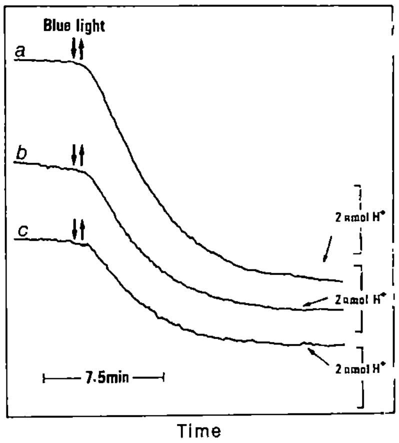

Fig. 3 Effect of abscisic acid on the blue light-induced acidification by guard-cell protoplasts. The extent of acidification induced by a saturating pulse of blue light (trace *a*) was reduced by 40% by an addition of 5 μM abscisic acid (trace *b*). A higher concentration of abscisic (50 μM) increased the inhibition only slightly (trace *c*). Abscisic acid was added to the protoplast suspension 20 min before the blue light treatment (30 s with 50 μmol m^{-2} s^{-1}). Experiments repeated three times on different occasions showed similar results. Other details as in Fig. 1.

Table 1 Effects of vanadate, diethylstilboestrol and CCCP on the proton extrusion induced by a blue light pulse and fusicoccin

Inhibitor	Concentration	Rate of proton release (% of control) Blue light pulse	Fusicoccin
Diethylstilboestrol	50 μM	0	0
CCCP	10 μM	0	0
Vanadate (*p*H 6.2)	0.16 mM	ND	119
	0.83 mM	113	ND
	1.0 mM	98	ND
	1.67 mM	ND	106
Vanadate (*p*H 7.0)	2.5 mM	108	ND

Fusicoccin (Farmoplant) was applied at 15 μM to a 1.2-ml suspension of guard-cell protoplasts kept under continuous red light (800 μmol m^{-2} s^{-1}). Proton extrusion started immediately after addition of fusicoccin, at rates ranging between 9.4 and 12.8 pmol cm^{-2} s^{-1} and continued for at least 15 min. Control rates for the blue light-induced proton extrusion (30-s pulse at 50 μmol m^{-2} s^{-1}) ranged between 2.4 and 5.6 pmol cm^{-2} s^{-1}. Rates of proton extrusion in the presence of inhibitors were given as percentage of control values. Rates of H^+ extrusion were calculated as in Fig. 1. CCCP, diethylstilboestrol and vanadate were added to the suspension medium from stock solutions, 30 min before the application of a blue light pulse or the addition of fusicoccin. The vanadate solution at 20 μM, *p*H 7.0, inhibited a *Neurospora* plasmalemma ATPase preparation by 90% (C. Borgeson, personal communication). 'Zero' indicates no detectable change in *p*H baseline levels throughout the time course of the observed response in the presence of inhibitor; ND, no determined. In all cases, the blue light pulse was given on a background of continuous red light.

dent, electrogenic ion pump resolved in the path-clamp experiments[16] is a H^+ pump. The results support a chemi-osmotic mechanism as the basis of ion uptake by guard cells[1].

Proton pumping in plant cells is usually attributed to the activity of a plasmalemma ATPase[17], with its activity reported to be inhibited by vanadate[18]. However, vanadate failed to affect the blue light-induced acidification, even at 2.5 mM (Table 1). Because this finding could imply that blue light-activated H^+ extrusion is mechanistically different from other H^+-pump systems previously described[17], we tested the vanadate sensitivity of the fusicoccin-induced H^+ extrusion, which is known to be mediated by a plasmalemma ATPase[19]. The high rate of H^+ extrusion elicited by fusicoccin in guard-cell protoplasts was also not affected by vanadate (Table 1). Inability of guard-cell protoplasts to take up vanadate could explain the results[18]. On the other hand, blue light-induced acidification was abolished by diethylstilboestrol, a putative inhibitor of plasmalemma ATPase[20] (Table 1). Carbonyl cyanide-*m*-chlorophenylhydrazone (CCCP) also completely suppressed both the blue light- and fusicoccin-dependent acidification (Table 1). CCCP is a protonophore that disipates H^+ gradients; it can also suppress ATPase activity by reducing ATP levels in guard-cell protoplasts[21]. Although the results from the inhibitor experiments described above are in accord with the possible mediation of blue light-induced H^+ extrusion by a plasmalemma ATPase, conclusive demonstration awaits further investigation.

The acidification response to blue-light pulses has further implications for the role of blue light in the activation of the H^+ pump. The observed high rates of H^+ release for minutes after pulse application argues against a direct energetic contribution by blue light for H^+ extrusion. Furthermore, conservatively assuming a H^+/ATP ratio of 2 (ref. 17), a calculation of the maximal efficiency of light quanta for H^+ extrusion, estimated from the initial slope of the data shown in Fig. 1*C*, indicates that this blue light response is about 15-fold more efficient, based on a unit chlorophyll weight, than the ATP formation from non-cyclic photophosphorylation, measured in *Vicia* guard-cell chloroplasts[10]. Thus, the activated, blue light receptor probably functions as a modulator of H^+-pumping activity, and not as a source of energy for the pump. Further characterization of sensory transduction in guard cells should increase our understanding of the photobiological and bioenergetic properties of the blue light response[7].

We thank Dr B. B. Jørgensen (Aarhus University, Denmark) for the O_2 microelectrode methodology and equipment. This research was supported by the NSF, the US Department of Energy and the Department of Agriculture. K.S. gratefully acknowledges a McKnight postodoctral fellowship. M.I. thanks Dr W.R. Briggs for generous encouragement during this work. Publication no. 903 of the Carnegie Institution of Washington, Department of Plant Biology.

Received 24 June; accepted 7 November, 1985.

1. Zeiger, E. *A. Rev. Pl. Physiol.* **34,** 441-475 (1983).
2. Hsiao, T. C., Allaway, W. E. & Evans, L. T. *Pl. Physiol.* **51**, 82-88 (1973).
3. Zeiger, E. & Hepler, P. K. *Science* **196,** 887-889 (1977).
4. Ogawa, T., Ishikawa, H. Shimada, K. & Shibata, K. *Planta* **142,** 61-65 (1978).
5. Schwartz, A. & Zeiger, E. *Planta* **161,** 129-136 (1984).
6. Iino, M., Ogawa, T. & Zeiger, E. *Proc. natn. Acad. Sci. U.S.A.* **82,** 8019-8023 (1985).
7. Senger, H (ed.) *Blue Light Effects in Biological Systems* (Springer, Berlin, 1984).
8. Gepstein, S., Jacobs, M. & Taiz, L. *Pl. Sci. Lett.* **28,** 63-72 (1982).
9. Zeiger, E., Moody, W., Hepler, P. K. & Varela, F. *Nature* **270,** 270-271 (1977).
10. Shimazaki, K. & Zeiger, E. *Pl. Physiol.* **78,** 211-214 (1985).
11. Shimazaki, K., Gotow, K. & Kondo, N. *Pl. Cell Physiol.* **23**, 871-879 (1982).
12. Raschke, K. & Humble, G. D. *Planta* **115,** 47-57 (1973).
13. Neumann, J. & Levine, R. P. *Pl. Physiol.* **47,** 700-704 (1971).
14. Hornberg, C. & Weiler, E. W. *Nature* **310,** 321-324 (1984).
15. Kowallik, W. *A. Rev. Pl. Physiol* **33,** 51-72 (1982).
16. Assmann, S. M., Simoncini, L. & Schroeder, J. I. *Nature* **318,** 285-287 (1985).
17. Spanswick, R. M. *A. Rev. Pl. Physiol.* **32,** 267-289 (1981).
18. Lew, R. R. & Spanswick, R. M. *Pl. Physiol* **75,** 1-6 (1984).
19. Marré, E. *A. Rev. Pl. Physiol.* **30,** 273-288 (1979).
20. Balke, N. E. & Hodges, T. K. *Pl. Sci. Lett* **10,** 319-325 (1977).
21. Shimazaki, K., Gotow, K., Sakaki, T. & Kondo, N. *Pl. Cell Physiol.* **24,** 1049-1056 (1983).
22. Arnon, D. *Pl. Physiol* **24,** 1-15 (1949).

Magnocellular axons in passage through the median eminence release vasopressin

Megan C. Holmes*, Ferenc A. Antoni*†‡, Greti Aguilera* & Kevin J. Catt*

* Endocrinology and Reproduction Research Branch,
National Institute of Child Health and Development, and
†Laboratory of Cell Biology, National Institute of Mental Health,
National Institutes of Health, Bethesda, Maryland 20892, USA

Vasopressin (arginine vasopressin, AVP) is present in two types of nerve fibres in the median eminence (ME)[1–3]. First, it is found in nerve terminals that originate in the parvicellular neurones of the hypothalamic paraventricular nucleus (PVN) and abut on the pericapillary space surrounding the fenestrated capillaries of the primary pituitary portal plexus in the external zone (EZ) of the ME. These neurones also synthesize corticotropin-releasing factor (CRF)[4–6], which acts synergetically with vasopressin to stimulate release of adrenocorticotropin (ACTH) from the pituitary gland (see ref. 7). Second, vasopressinergic axons of the magnocellular neurosecretory system pass through the internal zone (IZ) of the ME to terminate in the neurohaemal contact zone of the neurohypophysis. The involvement of vasopressinergic magnocellular neurones in the control of ACTH secretion is much debated[7]. Of particular interest in this context is the origin of the vasopressin found in pituitary portal blood[1,8,9]. Although it has been demonstrated that vasopressin and CRF are present in the same neurosecretory granules of EZ fibres[3], parallel determinations of vasopressin and CRF in pituitary portal blood have shown alterations of the concentration of vasopressin without a concomitant change in that of CRF[8,9]. Such a dissociation suggests that either differential release of vasopressin and CRF can occur from a single population of nerve endings, or there are fibres in the pituitary-stalk ME which release vasopressin but not CRF. Here we present evidence for the latter. Our results indicate that stimuli causing depolarization of the axonal membrane *in vitro* elicit release of vasopressin from nerve fibres in the external and internal zones of the ME.

We have reported that K^+ ions and veratridine stimulate secretion of CRF and vasopressin from the ME *in vitro* in a dose-dependent manner, and that this process depends on extracellular Ca^{2+} (ref. 10). Immunocytochemical and radioimmunoassay studies have shown that the amount of CRF in the magnocellular fibre system of the ME is at least one order of magnitude lower than that in the EZ parvicellular fibres (see ref. 7). Hence, the release of CRF appears to be an appropriate marker for the secretory activity of the CRF/AVP nerve endings of the EZ; we have used this to analyse the possible compartments of vasopressin release by the ME *in vitro*, after impairing the function of the fibres in the EZ by various experimental manipulations.

First, rats were pretreated with reserpine, which activates the hypothalamo-pituitary-adrenocortical system by inducing hypersecretion of CRF[11]. As a result, the peptide content of the CRF/AVP terminals in the EZ is dramatically decreased but there is no apparent change in the vasopressin content of the IZ magnocellular fibres[12,13]. In our hands, pretreatment with reserpine decreased the CRF content of the ME by 64% but had no effect on the amounts of vasopressin in either the ME or the neutrointermediate lobe of the pituitary (Fig. 1). The latter result suggests that the quantity of vasopressin in the EZ system is close to that of CRF, that is, small compared with the total ME vasopressin content, and hence minor changes of EZ

---

‡ Present address: Department of Human Anatomy, University of Oxford, Oxford OX1 2JD, UK.

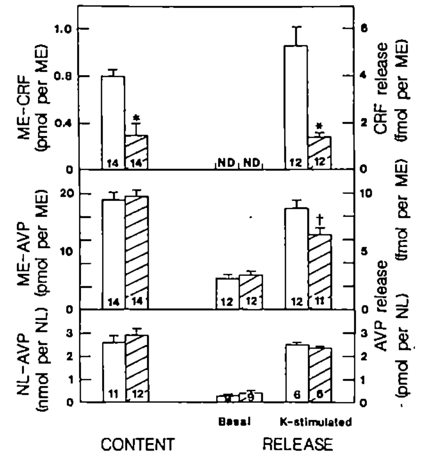

Fig. 1 Effects of pretreatment with reserpine on the content (left) and *in vitro* release (right) of vasopressin and CRF in ME or neurointermediate lobes of the pituitary gland (NL). Tissues were obtained from male Sprague-Dawley albino rats (200-300 g body weight) injected s.c. with either 10 mg per kg reserpine dissolved in dimethyl sulphoxide (DMSO) (hatched columns) or 2 ml per kg of the vehicle alone (open columns) 24 h before killing by decapitation. The columns represent the mean ± s.e.m., and the numbers of observations are shown at the bottom of each column. The piece of tissue referred to as median eminence also contained variable portions of the pituitary stalk but never any part of the neural lobe of the pituitary gland. The relative amounts of vasopressin released from the two pools of vasopressin in the ME may be estimated as follows: assuming that a proportionate amount of vasopressin is co-released with CRF from a population of parvicellular nerve endings[3], the secretion of vasopressin from these fibres should decrease to the same extent as the release of CRF, that is, by 75%. Hence, 75% of AVP released from the CRF/AVP compartment is equivalent to the 44% decrease in the total K^+-stimulated release of AVP (release in the presence of K^+ minus basal release) provided that reserpine does not affect the release of vasopressin from a second compartment that has no CRF. From this, the amount of vasopressin released by the CRF/AVP compartment in untreated rats can be estimated as 44/75, which is ~60% of the total release of vasopressin. The remaining 40% of the vasopressin secreted would originate from the reserpine-insensitive compartment.

Methods. The incubations were performed in 350 μl of Krebs-Ringer-bicarbonate (KRBG) medium, containing 11.1 mM D-glucose 0.1 mM L-ascorbate and bovine serum albumin (1 g l^{-1}), at 37 °C in an atmosphere of O_2/CO_2(95 : 5). After dissection from the brain, the median eminences (6-7 per tube) were preincubated for 30-45 min, after which the medium was carefully removed and changed every 10 min during the period of the experiment for any one of the following: fresh KRBG, KRBG with 48 mM K^+, from which an appropriate amount of NaCl was omitted to maintain iso-osmotic conditions; KRBG with 10 μM veratridine (supplied by Dr G. Brown, University of Alabama, Birmingham); KRBG containing 1 mM EGTA and no added calcium; KRBG containing 1 μM tetrodotoxin. The concentrations of CRF and vasopressin in the incubation medium were determined by specific radioimmunoassays as described elsewhere[10]. After the incubation, the tissues were homogenized in 100 μl of 0.1 M HCl containing 1 mM ascorbate, and after appropriate dilution in 0.05 M sodium phosphate buffer containing 0.1% Triton X-100 (v/v), the peptide content was determined by radioimmunoassay. * $P < 0.01$; † $P < 0.05$ by Student's *t*-test in comparison with the group treated with vehicle alone.

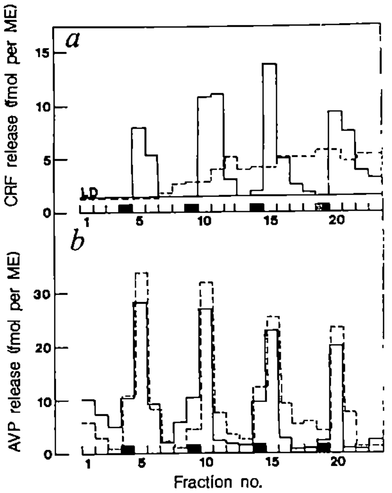

Fig. 2 Potassium-evoked release of CRF (*a*) and vasopressin (*b*) by median eminences obtained from sham-operated (solid line) or 7-day PVN-lesioned (broken line) rats. The solid bars indicate the application of KRBG containing 48 mM KCl. The abscissa shows the number of 10-min fractions collected. In *a*, the continuous line at the bottom of the figure, labelled LD, indicates the limit of detection in the radioimmunoassay. Data are representative of six pairs of similar experiments.

Methods. Lesioning of the PVN was performed in rats anaesthetized with chloral hydrate (4 g per kg body weight) using a specially designed microknife[15]. After killing by decapitation on post-operative day 7, the site of the lesion in each brain was examined in serial coronal sections (300-400 μm thick)[15] prepared during the period of preincubation of the median eminences in individual wells of a 24-well polystyrene tissue-culture plate. Subsequently, the tissues from sham-operated rats or those with complete lesions of the PVN were pooled (6-7 per tube) and incubated as described in Fig. 1 legend. The CRF content of each ME was measured after the incubation as an additional indicator of the completeness of the lesion.

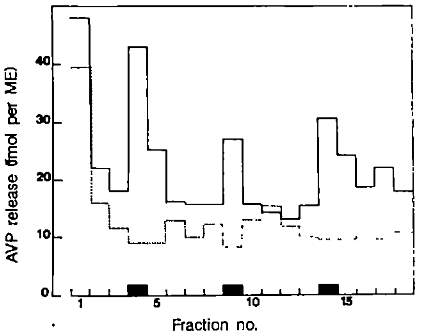

Fig. 3 Potassium-evoked release of vasopressin by median eminences obtained from sham-operated rats (solid line) or from animals subjected to anterolateral transection of the hypothalamus 7 days before the experiment (dotted line). Solid bars indicate the application of KRBG containing 48 mM KCl. The abscissa shows the number of 10-min fractions collected. The data are representative of three pairs of similar experiments. Three ME were incubated per tube as described in Fig 1 legend. Anterolateral cuts were made with a bayonet-shaped knife, in rats anaesthetized with chloral hydrate as described previously[18]. Each brain was examined to determine the site of the cut as described in Fig 2 legend.

vasopressin content are unlikely to be detected. In parallel with the decrease of CRF content, the K^+-stimulated release of CRF was reduced by 75% in rats treated with reserpine (Fig. 1). Pretreatment with reserpine also diminished the K^+-evoked release of vasopressin from the ME, but to a lesser extent (44%) than that of CRF. In contrast, no change of the K^+-induced release of vasopressin from neurointermediate lobes was found (Fig. 1). These findings are consistent with the suggestion that secretion of vasopressin occurs from two compartments in the ME. One of these compartments also releases CRF and is depleted of peptides by reserpine, whereas the other is not affected by the drug and neither contains nor releases CRF. Neuroanatomical evidence[1-7,12,13] indicates that the CRF/AVP fibre compartment is present in the EZ, whereas the compartment containing only vasopressin and which is not affected by reserpine is localized in the IZ of the ME.

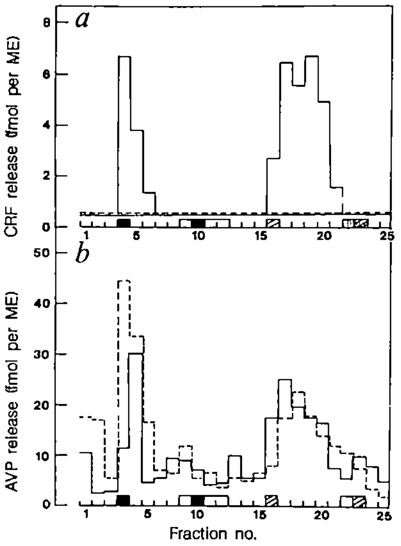

Fig. 4 Release of CRF (*a*) and vasopressin (*b*) *in vitro* by median eminences of PVN-lesioned (broken line) and sham-operated (solid line) rats. The abscissa indicates the number of 10-min fractions collected. Solid bars indicate the application of 48 mM KCl; open bars, Ca^{2+}-free medium; hatched bars, 10 μM veratridine; stippled bars, 1 μM tetrodotoxin. Data are representative of four pairs of similar incubations.

To obtain further evidence for the release of vasopressin from magnocellular axons in the IZ, we examined the secretion of vasopressin and CRF by ME obtained from rats which had been subjected to surgical ablation of the PVN. It has been shown previously that such lesions decrease drastically the CRF content of the ME, as well as the numbers of the nerve fibres that are immunoreactive for CRF and vasopressin in the EZ (see, for example, refs 1, 7). In contrast, the magnocellular neurones of the supraoptic nucleus and the supraoptico-hypophysial tract remain intact after PVN lesions. In agreement with these findings, we observed a marked decrease in the CRF content of the ME 7 days after hypothalamic surgery: from 848 ± 88 fmol in sham-operated controls to 75 ± 16 fmol in lesioned animals (mean ± s.e.m., $n = 11$ in both groups). The vasopressin content of the ME was also decreased, from 22.9 ± 2.9 pmol in controls to 12.0 ± 0.8 pmol in lesioned rats (mean ± s.e.m., $n = 10$ and 11, respectively). These results are consistent with the neuroanatomical observation that ~40% of the vasopressinergic magnocellular neurones lie in the region destroyed by the PVN lesion[14]. There was no release of CRF in response to K^+ in ME obtained from PVN-lesioned rats (Fig. 2). In contrast, K^+ released substantial amounts of vasopressin from the same segments of tissue that showed no CRF response. In three series of experiments, the average amounts of vasopressin released by a 10-min exposure to high-K^+ medium were similar in sham-operated and PVN-lesioned rats (15.0 ± 2.2 and 16.0 ± 3.0 fmol per ME; mean ± s.e.m., $n = 15$ and 13, respectively). This finding contrasts with the 40% decrease of vasopressin content mentioned above, and suggests that a compensatory increase of releasable vasopressin occurs in the ME after PVN lesions. The nature of this apparently compensatory response is not clear, however it was not inhibited by dexamethasone (250 μg per kg given to PVN-lesioned rats subcutaneously (s.c.) for 7 days; data not shown), making it unlikely that the build-up of vasopressin occurs in surviving cells of the parvicellular CRF/AVP system, which are strongly inhibited by glucocorticoid hormones[1,15]. Moreover, to compensate for the loss of 90% of the CRF/AVP neurones, the cells spared by the lesion would have to increase their ability to secrete vasopressin by 900% in 7 days; this is also improbable, as in the absence of glucocorticoid feedback following bilateral adrenalectomy, it takes 3-4 weeks for ME vasopressin release to increase by 500%[10]. Moreover, PVN-lesioned rats have high concentrations of circulating corticosterone (~40% of controls)[16,17], and circadian rhythms of corticosterone are also apparent[16].

To demonstrate that degenerating magnocellular fibres cannot be the source of the vasopressin release in response to depolarization, ME obtained from rats with anterolateral hypothalamic transections[18] were tested for their ability to release the peptide (these lesions transect all vasopressinergic axons, including those in the supraoptico-hypophysial tract, that project to the ME). Seven days after the lesion, the vasopressin content of the ME was decreased by ~90% (2 ± 0.6 pmol per ME, $n = 9$ compared with 18 ± 3, $n = 9$ in controls; mean ± s.e.m.) and there was no detectable release of vasopressin in response to a high K^+ concentration (Fig. 3).

The release of AVP from the ME of sham-operated or PVN-lesioned rats had similar properties (Fig. 4): the release evoked by K^+ was calcium-dependent, and that elicited by veratridine was blocked by tetrodotoxin. The activity of the cytoplasmic enzyme lactate dehydrogenase[19] (EC 1.1.1.27) was not above background (0.001 extinction units per 120 s) in high-K^+ medium bathing ME from PVN-lesioned rats, but on addition of 0.1% Triton X-100, enzyme activity increased 14-fold, indicating leakage of the enzyme from the cytoplasm. Taken together, these data suggest that the release of vasopressin from the ME of PVN-lesioned rats occurs from magnocellular fibres of the supraoptico-hypophysial tract in the IZ of the ME, via a physiologically relevant exocytotic process.

The magnocellular axons in passage through the IZ are varicose unmyelinated fibres with distinct swellings, called Herring bodies, in which mitochondria and neurosecretory vesicles containing immunoreactive vasopressin are abundant[20,21]. It appears that the cellular machinery necessary for neurotransmitter release is present along the entire length of the axon, albeit at lower density than at nerve terminals (compare with refs 22, 23), and it is well documented that most of the vasopressin found in the ME is in the biologically active form (see refs 24, 25). Hence, a small but significant fraction of the peptide present in IZ fibres may be released in response to depolarizing stimuli, perhaps preferentially at Herring bodies. The released peptide could gain access to the pituitary portal circulation via the extensive network of fenestrated primary portal capillaries which penetrates the IZ[20,21] and is not separated by any morphologically evident diffusion barrier from the fibres in passage[21,22]. Because the amount of vasopressin in the IZ fibre system is about 10-20-fold higher than in the EZ, release from the IZ neurites may account for a substantial proportion (~40%; see Fig. 1 legend) of the vasopressin in pituitary portal blood.

Although we have no direct evidence that the release process described above operates *in vivo*, a considerable amount of functional data favours the existence of two independent sources of ME vasopressin secretion. It has been noted that the concentrations of vasopressin and CRF may vary independently in pituitary portal blood (see refs 8, 9). Furthermore, PVN lesions prevent the increase of plasma ACTH after adrenalectomy, a manoeuvre that stimulates parvicellular CRF/AVP neurones, but not, or only slightly, the magnocellular system[1,25,26]. In contrast, PVN lesions merely attenuate the pituitary-adrenocortical response to stressful stimuli such as ether-venesection and ether-laparatomy[16,17], which are known to activate the parvicellular CRF/AVP system[7] as well as the magnocellular vasopressinergic neurones[8,27]. Anterolateral hypothalamic transections that destroy all vasopressinergic fibres (parvicellular as well as magnocellular) reaching the ME completely block the ACTH response to adrenalectomy or the stressful stimuli mentioned above[7,17].

Intriguingly, these functional findings are paralleled by studies on the release of vasopressin from the ME *in vitro*, in which lesions of the PVN abolished the enhancement by bilateral adrenalectomy of the depolarization-induced release of vasopressin[26]. Here we have reported that lesioning of the PVN in otherwise intact rats did not diminish substantially the release of vasopressin from the ME, whereas anterolateral cuts abolished the vasopressin response to depolarization.

Thus, our data suggest that the original, and now largely rejected, proposal that magnocellular neurones contribute to the regulation of anterior pituitary hormone secretion by releasing neurohormones in the ME[28], should be reconsidered with respect to the control of ACTH secretion.

We thank Drs M. H. Whitnall, E. Mezey and H. Gainer for communicating their findings to us before publication.

Received 27 August; accepted 21 November 1985.

1. Zimmerman, E. A. *et al. Ann. N.Y. Acad. Sci.* **297,** 405-417 (1977).
2. Burlet, A., Chateau-Chapler, M. & Dreyfuss, F. *Neuroendocrinology of Vasopressin, Corticoliberin and Opiomelanocortins* (eds Baertschi, A. J. & Dreyfuss, J. J.) 95-106 (Academic, London, 1982).
3. Whitnall, M. H., Mezey, E. & Gainer, H. *Nature* **317,** 248-250 (1985).
4. Kiss, J. Z., Mezey, E. & Skirboll, L. *Proc. natn. Acad. Sci. U.S.A.* **81,** 1854-1858 (1984).
5. Sawchenko, P. E., Swanson, L. W. & Vale, W. W. *Proc. natn. Acad. Sci. U S A* **81,** 1883-1887 (1984).
6. Tramu, G., Croix, G. & Pillez, A. *Neuroendocrinology* **37,** 467-469 (1983)
7. Makara, G. B., Antoni, F. A., Stark, E. & Karteszi, M. *Perspectives in Neuroendocrinology* Vol. 3 (eds Müller, E. E. & McLeod, R. M.) 71-119 (Elsevier, Amsterdam, 1984)
8. Gibbs, D. M. *Fedn Proc.* **44,** 203-206 (1985).
9. Plotsky, P. M. *Fedn Proc.* **44,** 207-213 (1985).
10. Holmes, M. C., Antoni, F. A., Catt, K. J. & Aguilera, G. *Neuroendocrinology* (in the press)
11. Bhattacharya, A. N. & Marks, B. H. *J. Pharmac. exp. Ther.* **165,** 108-116 (1969).
12. Seybold, V., Elde, R. & Hokfelt, T. *Endocrinology* **108,** 1803-1809 (1981)
13. Bugnon, C. *et al. J. Steroid Biochem.* **20,** 183-195 (1984).
14. Rhodes, C. H., Morrell, J. L. & Pfaff, D. W. *J. comp. Neurol.* **198,** 45-64 (1984)
15. Antoni, F. A., Holmes, M. C. & Kiss, J. Z. *Endocrinology* **117,** 1293-1299 (1985)
16. Ixart, G. *et al. Neuroendocrinology* **35,** 270-276 (1982).
17. Makara, G. B. *Adv. physiol. Sci.* **14,** 31-44 (1981).
18. Antoni, F. A., Makara, G. B. & Rappay, Gy. *J. Endocr.* **91,** 415-423 (1981)
19. Marchbanks, R. M. *Biochem. J.* **104,** 148-157 (1967).
20. Seitz, H. M. *Z. Zellforsch. Mikrosk. Anat.* **67,** 351-366 (1965).
21. Page, R. B. & Dovey-Hartman, J. *J. comp. Neurol.* **226,** 274-288 (1984)
22. Grafstein, B. & Forman, D. S. *Physiol. Rev.* **60,** 1167-1283 (1980).
23. Reichardt, L. F. & Kelly, R. B. *A. Rev. Biochem.* **52,** 871-926 (1983).
24. Gillies, G. & Lowry, P. J. *Frontiers in Neuroendocrinology* Vol. 7 (eds Ganong, W. F. & Martini, L.) 45-75 (Raven, New York, 1981).
25. Russell, J. T., Brownstein, M. J. & Gainer, H. *Brain Res.* **201,** 227-232 (198[illegible])
26. Knepel, W., Nutto, D., Meyer, D. K. & Vlaskovska, M. *Neurosci. Lett.* **48,** 321-326 (1984)
27. Andersson, E. *Science* **152,** 379-380 (1966).
28. Green, J. D. & Harris, G. W. *J. Endocr.* **5,** 136-145 (1947).

Excitatory amino acids inhibit stimulation of phosphatidylinositol metabolism by aminergic agonists in hippocampus

Michel Baudry, Jim Evans & Gary Lynch

Department of Psychobiology and Center for the Neurobiology of
Learning and Memory, University of California, Irvine,
California 92717, USA

Since the initial observations in the 1950s[1,2] a large number of neurotransmitters and hormones have been shown to influence phosphatidylinositol (PI) metabolism in brain and peripheral ganglia (see ref. 3 for review). This has led to the suggestion that PI is part of an intracellular second messenger system for some types of diffusible chemical factors[4,5]. Consistent with this are recent reports that one of the products of PI turnover (diacylglycerol) stimulates the Ca-dependent phospholipid-dependent protein kinase (kinase C) while a second (inositol trisphosphate) causes the release of calcium from intracellular stores[6,7]. Thus it is possible that at least some brain neurotransmitters utilize the PI system to produce functional effects that are in addition to and which outlast the very brief physiological responses they elicit. Although it had been anticipated that another class of receptors might inhibit receptor-mediated stimulation of PI breakdown, no clear examples of such effects have been described. We now report that acidic amino acids, which are thought to be excitatory neurotransmitters at the majority of brain synapses[8], strongly inhibit the stimulation of PI metabolism elicited by carbachol, histamine, or by potassium-induced depolarization, without changing the response to noradrenaline. As well as indicating a novel function for the excitatory amino acids, these results suggest that the central nervous system possesses cell–cell interactions of a previously unsuspected type.

The experiments were performed on transverse rat hippocampal slices prepared as described previously[9]. Following preincubation for 1 h at 33 °C in Krebs-bicarbonate medium under a constant stream of O_2/CO_2 (95:5), the slices were further preincubated for 1 h at 33 °C in the presence of ^{3}H-*myo*-inositol (NEN, 15-20 Ci mmol^{-1}). The accumulation of ^{3}H-inositol phosphate derivatives (^{3}H-InsP) induced by various agonists was then determined in the presence of 5 mM lithium chloride as described by Brown *et al.*[10] (see Fig. 1). The elution profile of the ^{3}H-inositol phosphates obtained by stepwise addition of formate solutions of increasing strength indicated that more than 90% of these derivatives corresponded to *myo*-inositol-1-phosphate, a result in good agreement with that of Brown *et al.*[10]. Figure 1 indicates that two different excitatory amino acids, *N*-methylaspartic acid (NMA) and kainic acid (KA) had a small although not statistically significant inhibitory effect on basal accumulation of ^{3}H-InsP. As previously reported by various groups[10,11], carbachol caused a large and concentration-dependent stimulation of ^{3}H-InsP accumulation. Both NMA (50 μM)

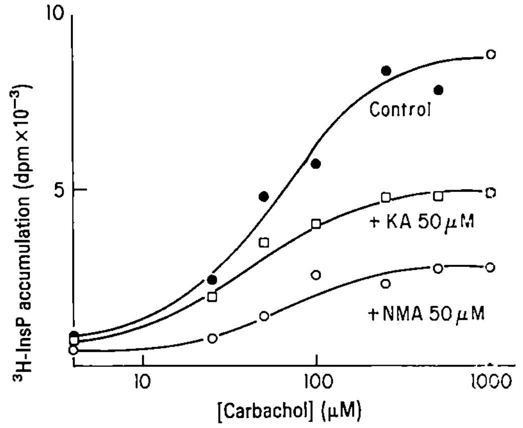

Fig. 1 Effects of *N*-methylaspartic acid (NMA) and kainic acid (KA) on basal and carbachol-stimulated accumulation of ^{3}H-InsP in rat hippocampal slices. Transverse hippocampal slices (0.4 mm thick) were cut with a McIlwain tissue chopper and preincubated for 60 min at 33 °C in Krebs–Ringer bicarbonate medium containing (final concentration in mM): NaCl 124, KCl 3.33, Mg_2SO_4 2.42, $CaCl_2$ 3.1, KH_2PO_4 1.25, $NaHCO_3$ 25, D-glucose 10, urea 2 and ascorbic acid 2, under a constant stream of O_2/CO_2 (95:5). After three washes with freshly oxygenated medium, slices were further incubated for 60 min at 33 °C in the same medium containing ^{3}H-*myo*-inositol (NEN, 15.8 Ci mmol^{-1}, 5 μCi ml^{-1}). Slices were washed again three times with freshly oxygenated medium and were distributed in incubation vials (two or three slices per vial) and incubated for 10 min at 33 °C in the presence of 5 mM LiCl and various concentrations of carbachol and excitatory amino acids (final volume 0.25 ml). At the end of the incubation 940 μl of a mixture of chloroform/methanol (1:2) were added, slices were sonicated briefly and 310 μl of chloroform and 310 μl of H_2O were added to separate the phases. Aliquots of the upper aqueous phase (0.75 ml) were transferred to a column containing ~175 mg of an anion-exchange resin (Bio-Rad AG 1X-8, 100-200 mesh, formate form). The columns were washed with 10 ml of H_2O to remove ^{3}H-*myo*-inositol. Labelled ^{3}H-inositol phosphate derivatives (^{3}H-InsP) were eluted with 5 ml of 200 mM ammonium formate/100 mM formic acid and counted in a liquid scintillation counter, and are expressed as d.p.m. of ^{3}H-InsP accumulated and represent means of 4–6 experiments with s.e.m. less than 10% of the means.

and kainic acid (50 μM) markedly inhibited this latter effect, apparently by decreasing the maximal response to carbachol without significantly changing its apparent EC_{50} (50% effective concentration) (Fig. 1); this inhibition, as well as that produced by two other excitatory amino acids, was found to be concentration-dependent (Fig. 2; NMA, IC_{50} (50% inhibitory concentration) of 20 μM; D, L-homocysteic acid, IC_{50} of 40 μM; kainic acid, IC_{50} of 50 μM; and L-glutamic acid, IC_{50} of 1.5 mM). The inhibitory action of NMA was blocked by two specific antagonists of the NMA receptors, D, L-aminophosphonovaleric acid (APV) and D-α-aminoadipate (D-AA) (80±5% inhibition by 400 μM APV, 50±5% inhibition by 2 mM D-AA), while the response to kainic acid was not changed by these compounds. NMA action (but not KA) was also antagonized by ketamine, again suggesting that NMA acts by stimulating a physiological receptor, since it has been shown that dissociative anaesthetics act as NMA antagonists[12]. The effect of the excitatory amino acids was not due simply to the depolarization they produce as potassium-induced depolarization increased ^{3}H-InsP accumulation and left the carbachol response unchanged (data not shown). Calcium did not appear to be involved since the amino acids blocked the stimulation of PI breakdown elicited by carbachol in calcium-free medium containing 0.1 mM (Table 1) or 0.5 mM EGTA (data not shown). Note that Kendall and Nahorski[13] found the PI response to carbachol to be markedly reduced in tissue sections preincubated in the absence of calcium while, as shown in Table 1, we did not obtain this result in brain slices preincubated in normal media and then tested without calcium. Preincubation presumably results in extremely low levels of extracellular calcium as well as changes in the intracellular distribution of the cation—thus stimulation of the PI system may have an absolute requirement for calcium. But the occurrence of typical cholinergic and amino-acid responses in calcium-free medium supplemented with high concentrations of EGTA (Table 1) indicates that the effects reported here are not due to physiological fluxes of calcium. In contrast, removal of sodium from the incubation medium reduced carbachol-induced ^{3}H-InsP accumulation and virtually eliminated the inhibitory effects of the amino acids (Table 1); moreover, high concentrations of veratridine, which result in the opening of sodium channels[14], also reduced the stimulation by carbachol of PI metabolism (60% reduction at 100 μg ml^{-1} veratridine). To assess the specificity of the inhibition produced by excitatory amino acids, we tested NMA with non-cholinergic agents known to stimulate PI breakdown (Table 2). While 100 μM NMA almost totally blocked the stimulation induced by K^+(50 mM) or histamine (100 μM) it did not detectably alter the response to noradrenaline (100 μM).

Table 1 Effects of NMA and KA on carbachol stimulation of PI turnover in Na^+- or Ca^{2+}-free medium

	Basal	Carbachol (0.5 mM)	Carbachol + NMA (50 μM)	Carbachol + KA (50 μM)
Normal medium (6)				
^{3}H-InsP (d.p.m.)	850±80	8,280±485	2,355±600	3,980±210
% Basal		974±57	277±71	468±25
Na^+-free medium (4)				
^{3}H-InsP	2,123±175	4,931±302	4,595±430	4,838±276
% Basal		232±14	216±23	272±16
Ca^{2+}-free medium (4)				
^{3}H-InsP	670±134	9,045±905	2,438±138	2,648±440
% Basal		1,350±135	364±21	395±66

Results are expressed as d.p.m. ^{3}H-InsP accumulated in the presence of various effectors as well as in percentage of basal values; they represent means ±s.e.m. of the indicated number of experiments (in parentheses). Hippocampal slices (0.4 mm thick) were preincubated for 60 min at 33° C in normal Krebs–Ringer bicarbonate buffer under a constant stream of O_2/CO_2 (95 : 5). After washing with fresh medium they were further incubated for 60 min at 33 °C in the same medium in the presence of ^{3}H-*myo*-inositol (5 μCi ml^{-1}). They were then washed with either normal Krebs–Ringer medium (normal medium) or with a medium in which NaCl and $NaHCO_3$ were substituted with Tris (the *p*H being adjusted with HCl) (Na^+-free medium) or with a medium in which $CaCl_2$ was substituted with $MgCl_2$ and supplemented with 0.1 mM EGTA (Ca^{2+}-free medium). Slices were then incubated for 10 min at 33 °C in the presence of 5 mM LiCl with or without carbachol (0.5 mM), NMA (50 μM), KA (50 μM) and combinations of these agonists. ^{3}H-InsP accumulation was determined as described in Fig. 1 legend.

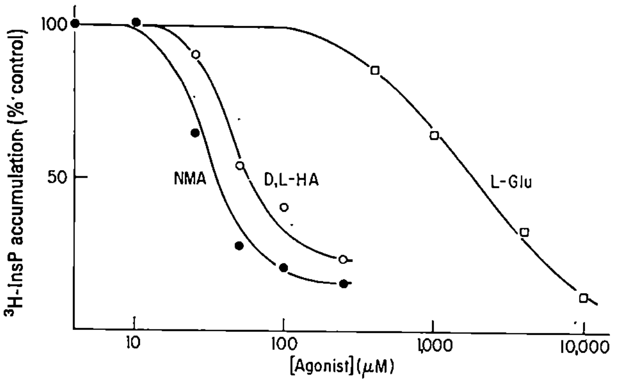

Fig. 2 Effects of various excitatory amino acids on the carbachol-stimulated accumulation of ^{3}H-InsP in rat hippocampal slices. The effects of various concentrations of different excitatory amino acids—*N*-methylaspartic acid (NMA), D,L-homocysteic acid (D, L-HA) and L-glutamic acid (L-Glu)—on the carbachol-stimulated accumulation of ^{3}H-InsP in rat hippocampal slices were determined as described in Fig. 1 legend. Results are expressed as a percentage of the accumulation elicited by carbachol (0.5 mM) in the presence of the indicated concentrations of excitatory amino acids and are means of 4 experiments, with s.e.m. representing less than 10% of the means.

The present results indicate clearly that activation of excitatory amino-acid receptors suppresses receptor-activated phosphoinositol breakdown. This is evidenced by the fact that the apparent IC_{50} values of various excitatory amino acids in inhibiting the carbachol response are identical to their apparent EC_{50} values for stimulation of receptor-activated sodium fluxes measured under the same conditions[15]. Moreover, selective antagonists of certain classes of glutamate receptors[16] block the negative actions of some agonists. There are several routes through which the suppressive effects of the amino acids might be mediated. First, these compounds interact with receptors to open membrane channels for various ion species that might then act on the stimulation of PI metabolism via other receptors. Extracellular calcium is not likely to be involved since both carbachol and the amino acids were effective in calcium-free medium. However, certain of our results point to a build-up of intracellular sodium as a triggering mechanism. As mentioned above, there is a striking correspondence between the concentrations of different amino acids needed for suppression of the response of the PI system to carbachol and those required to promote sodium fluxes; moreover, removal of sodium ions eliminates the effect of the amino acids. While potassium-induced depolarization, which would be expected to cause substantial fluxes of several ion species including sodium, stimulates PI metabolism and does not detectably influence the carbachol-elicited response, the many effects produced by release of neurotransmitters and modulators make the interpretation of

Table 2 Effect of NMA on ^{2}H-InsP accumulation elicited by potassium, noradrenaline and histamine in rat hippocampal slices

Agonists	Control	+ NMA (100 μM)
None	1,253±110	800±70
K^+ (50 mM)	4,441±590	1,747±225*
NA (100 μM)	2,947±265	2,647±224
Histamine (100 μM)	2,252±379	1,286±125*

Details as for Table 1, except that slices were incubated for 30 min at 33 °C in the presence of the various effectors. Results are expressed as d.p.m. ^{3}H-InsP accumulated and are means±s.e.m. of 6–10 experiments.

* $P < 0.01$ (Student's *t*-test).

the results obtained with this procedure quite difficult. Given the links between intracellular sodium and calcium[17], it is conceivable that the large sodium fluxes elicited by excitatory amino acids alter intracellular levels of calcium which could then be responsible for the suppressive effects on PI metabolism.

Receptor–receptor interactions offer a second means through which the excitatory amino acids might block carbachol-induced ^{3}H-InsP accumulation. There is some evidence that receptor-mediated stimulation of PI turnover involves an interaction with a GTP-binding protein in a manner analogous to the coupling of the adrenergic receptor with adenylate cyclase[6]. Processes such as these might prove to be susceptible to lateral effects set up in the membranes by the binding of ligands to neighbouring non-cholinergic receptors. However, the absence of an NMA effect on stimulation of PI metabolism by noradrenaline would argue against such a mechanism unless the adrenergic and excitatory amino-acid receptors were located in different parts of the cells and/or in different types of cells. There is indeed some evidence for the existence of different pools of inositol phospholipids associated with different receptors and possibly at different cellular locations[13].

Finally, the excitatory amino-acid receptors could be associated with second messenger systems of their own that, among other things, inhibit the hydrolysis of phosphatidylinositol. Recent studies have shown that phorbol esters inhibit carbachol-induced stimulation of PI metabolism, possibly by activating protein kinase C, suggesting the existence of a negative feedback between kinase C activation and PI metabolism[18].

Whatever mechanism is involved, the results reported here indicate that the large number of transmitter or hormone receptors positively linked to PI metabolism are to some degree balanced by other receptors that suppress the activation of this second messenger system. This offers the potential for interaction between chemical messengers at the level of intracellular transducer systems and strengthens the idea that neurones integrate chemical as well as electrical signals.

This research was supported by grant BNS 8112156 to M.B. and AFOSR 82-0116 B to G.L. We thank Jackie Porter for secretarial assistance.

Received 24 July; accepted 8 November 1985.

1. Hokin, L. E. & Hokin, M. R. *Biochim. biophys. Acta* **16**, 229; **18**, 102 (1955)
2. Larrabee, M. G. *J. Neurochem.* **15**, 803–808 (1968).
3. Michell, R. H. *Biochim. biophys. Acta* **415**, 81-147 (1975)
4. Michell, R. H. *Neurosci. Res. Prog. Bull.* **20**, 338–350 (1981).
5. Downes, C. P. *Trends Neurosci.* **6**, 313-316 (1983).
6. Berridge, M. J. & Irvine, R. F. *Nature* **312**, 315–321 (1984)
7. Nishizuka, Y. *Science* **225**, 1365-1370 (1984).
8. Roberts, P. J., Storm-Mathisen, J. Jr & Johnston, G. (eds) *Glutamate as a Transmitter* (Wiley, New York, 1980).
9. Baudry, M., Siman, R., Smith, E. K. & Lynch, G. *Eur. J. Pharmac.* **90**, 161-163 (1983)
10. Brown, E., Kendall, D. A. & Nahorski, S. R. *J. Neurochem.* **42**, 1379-1387 (1984)
11. Janowsky, A., Labarca, R. & Paul, S. M. *Life Sci.* **35**, 1953-1961 (1984)
12. Thomson, A., West, D. C. & Lodge, D. *Nature* **313**, 479–481 (1985)
13. Kendall, D. A. & Nahorski, S. R. *J. Neurochem.* **42**, 1388-1394 (1984)
14. Narahashi, T. *Physiol. Rev.* **54**, 813–889 (1974).
15. Baudry, M., Kramer, K., Fagni, L., Recasens, M. & Lynch, G. *Molec. Pharmac.* **24**, 222-223 (1983).
16. Foster, A. C. & Fagg, G. E. *Brain Res. Rev.* **7**, 103–164 (1984)
17. Erulkar, S. D. & Fine, A. *Rev. Neurosci.* **4**, 179–323 (1979)
18. Labarca, R., Janowsky, A., Patel, J. & Paul, S. M. *Biochem. biophys. Res. Commun.* **123**, 703–709 (1984).

Expression of a translocated c-*abl* gene in hybrids of mouse fibroblasts and chronic myelogenous leukaemia cells

Danuta Kozbor*, Agata Giallongo*†, Michael E. Sierzega*, James B. Konopka‡, Owen N. Witte‡, Louise C. Showe* & Carlo M. Croce*

* Wistar Institute of Anatomy and Biology, 36th Street at Spruce,
Philadelphia, Pennsylvania 19104, USA
‡ Department of Microbiology and Molecular Biology Institute,
University of California, Los Angeles, Los Angeles,
California 90024, USA

Chronic myelogenous leukaemia (CML) is a clonal disease arising from malignant transformation of pluripotent hematopoietic stem cells. In most cases, it is characterized by the presence of the Philadelphia (Ph^1) chromosome (22q−) which results from a reciprocal translocation between chromosomes 9 and 22 (refs 1–3). In this translocation, the human homologue of the Abelson virus oncogene, c-*abl*, normally on chromosome 9, is moved to chromosome 22, while c-*sis*, the cellular homologue of the simian sarcoma virus oncogene, is moved from chromosome 22 to chromosome 9 (refs 4–6). CML cells carrying the t(9; 22) chromosomal translocation are known to produce an 8-kilobase (kb) c-*abl* transcript in addition to the normal 6- and 7-kb transcripts[6–9] and to express the normal p145 *abl* protein and a p210 c-*abl* protein possessing a tyrosine kinase activity not detected in the p145 species[10–12]. Results of our analyses using somatic cell hybrids between a mouse fibroblast line and two human CML-derived cell lines which carry the Ph^1 chromosome and are phenotypically identical to the fibroblast parent indicate that only the hybrid cells containing Ph^1 chromosome express both the 8-kb c-*abl* RNA and the p210 protein. Thus, expression of the altered c-*abl* transcripts and protein depends on the presence of the Ph^1 chromosome and is not myeloid-specific.

To establish whether the 8.0-kb c-*abl* aberrant transcript and the p210 protein are derived solely from the translocated c-*abl* oncogene on the Ph^1 chromosome, we constructed somatic cell hybrids between LM-TK$^-$ mouse fibroblasts[13] and K562 (ref. 14) or Bv173 (ref. 15) cells and followed the segregation of the Ph^1 chromosome and the normal chromosome 9 from these hybrids. Because the hybrids are phenotypically indistinguishable from the rodent parental cells, it is also possible to determine whether the expression of the altered c-*abl* transcript requires a myeloid cellular background.

The DNA of both human and mouse parents and of hybrid clones containing different complements of human chromosomes were screened by Southern blot analysis using c-*sis*, constant-region light-chain (C_λ) and v-*abl* probes to select hybrids containing either the 9q+ or the 22q− (Ph^1) chromosome (Fig. 1). The v-*abl* probe used was the 1.6-kb *Bgl*II/*Bgl*II fragment from 2.5 to 4.1 kb on the Abelson oncogene map[16]. The C_λ probe was a genomic clone (Chr22λ5) of the C_λ gene in λWes (ref. 17). This clone contains an 8.5-kb *Eco*RI fragment that includes *Ke*$^-$*Oz*$^-$ and *Ke*$^-$*Oz*$^+$ (refs 17, 18). The c-*sis* probe was constructed by subcloning a 1.7-kb *Bam*HI restriction fragment into the plasmid pBR322; this fragment comprises the 3′ exon of the human c-*sis* homologue[5]. With these probes, three hybrid clones (clone 260-3-1-3 from the Bv173 × LM-TK hybrids and clones KL-17-9-1 and KL-17-9-3 from the K562 × LM-TK$^-$ hybrids) were identified which contained the Ph^1 chromosome. All three hybrids (Fig. 1*a*, *b*, lanes 4-6) were positive for human c-*abl* (17.0 kb), C_λ (17.0, 11.2 and 10 kb) and mouse c-*abl* (7.7 and 3.7 kb) sequences. Only 10-20% of the cells in the KL-17-9-3 clone contained the human c-*abl* oncogene, indicating that the 17.0-kb c-*abl* signal in this clone is very weak (Fig. 1*a*, lane 5). The human C_λ probe did not cross-hybridize with mouse DNA. The variable-region light-chain (V_λ), C_λ and c-*abl* genes were amplified five- to ninefold in K562 cells[19–21]. The V_λ, C_λ and c-*abl* sequences were on the same aberrant chromosome derived from the Ph^1 chromosome of K562 cells[20]. DNA of hybrids KL-17-9-1 and KL-17-9-3 (Fig. 1*c*, lanes 4, 5) hybridized with both human (19 kb) and

---

† Present address: Istituto di Biologia dello Suiluppo, Via Archirafi 20, 90100 Palermo, Italy

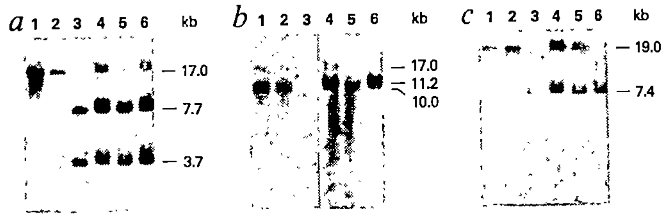

Fig. 1 Southern blot analysis of *Hin*dIII-digested cellular DNA using v-*abl* (*a*), C_λ (*b*) and c-*sis* (*c*) probes. Lane 1, K562 DNA; lane 2, Bv173 DNA; lane 3, LM-TK$^-$ DNA; lanes 4 and 5, hybrids KL-17-9-1 and KL-17-9-3 DNA, respectively; lane 6, hybrid 260-3-1-3 DNA. 10 μg of DNA was loaded in lanes 1–3 and 20 μg in lanes 4–6, exposure time was 42 h. Number on the right of each panel indicate size markers.

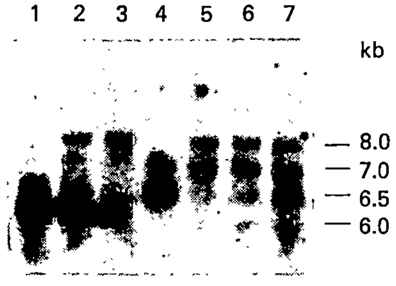

Fig. 2 c-*abl*-related RNA transcripts in PAF (lane 1), K562 (lane 2), Bv173 (lane 3), LM-TK$^-$ (lane 4) cells and Ph^1-positive hybrids of K562 and Bv173 with LM-TK$^-$ (lanes 5 and 6, hybrids KL-17-9-1 and KL-17-9-3, respectively; lane 7, hybrid 260-3-13). Cytoplasmic RNA was extracted by the caesium chloride method[22]. Total RNA was enriched for poly(A)-containing RNA by one cycle of oligo(dT)-cellulose affinity chromatography[3]. RNA was denatured in 1 M glyoxal in 10 mM sodium phosphate buffer, *p*H 7.0, at 50 °C for 1 h, electrophoresed in 1% agarose gel, transferred to nitrocellulose, prehybridized and hybridized to 0.2 μg of the v-*abl* probe according to the method of Thomas[24]. 10 μg of RNA was loaded in lanes 1–4 and 20 μg in lanes 5–7. Exposure time was 42 h.

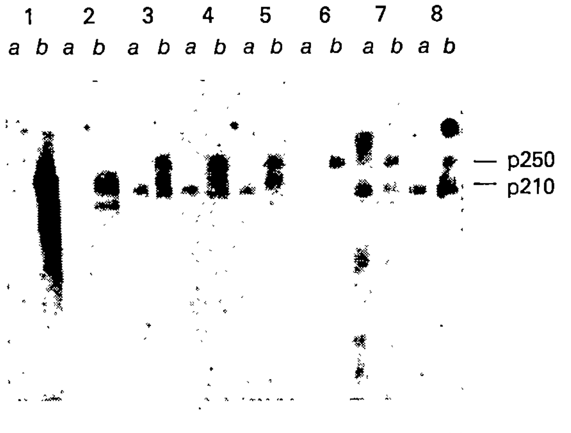

Fig. 3 *In vitro* phosphorylation of altered p210 c-*abl*. For *in vitro* phosphorylation assays, cell extracts were immunoprecipitated with 5 μl of normal rabbit serum(*a*) or pEX-5 antiserum (*b*). Lane 1, K562; lane 2, Bv173; lane 3, KL-17-9-1; lane 4 4, KL-17-9-3; lane 5, 260-3-1-3; lane 6, Ph^1-negative hybrid 260-3-12-3; lane 7, LM-TK$^-$; lane 8, IT-22. Immunoprecipitates were washed and incubated in 20 mM PIPES (*p*H 7.0) containing 10 mM $MnCl_2$, 10 μM NaF and 5 μCi [γ-^{32}P]ATP for 5 min at 30 °C. Samples were washed and analysed by SDS-polyacrylamide gel electrophoresis and autoradiography for 2 days.

mouse (7.4 kb) c-*sis*, indicating that these hybrids contain either both the normal chromosome 22 (C_λ- and c-*sis*-positive) and normal chromsome 9 (c-*abl*-positive) alternatively the 9q+ chromsome (c-*sis*-positive) and the Ph^1 chromosome. Isoenzyme analysis for adenylate kinase (AK)-1 and -3, chromosome 9 markers (AK-3 is a marker for region 9p13–p24; AK-1 is a marker for region 9q33–qter)[22], revealed that neither the normal chromosome 9 nor the 9q+ chromosome is present in the hybrids. Only hybrid 260-3-1-3 (Fig. 1*c*, lane 6), which is negative for c-*sis* but positive for C_λ and c-*abl*, contains only the Ph^1 chromosome, while the other two contain the the Ph^1 chromosome and the normal chromosome 22 (Table 1).

To analyse expression of the altered 8-kb c-*abl* transcript further, as well as the p210 protein with its associated tyrosine kinase activity, we performed Northern blot analysis of poly(A)-containing RNA extracted from parental and hybrid cells (Fig. 2). Two major transcripts of 6 and 7 kb were detected in simian virus 40-transformed Ph^1-negative human fibroblast (PAF) control cells (lane 1). The levels of the normal transcripts in K562 and the PAF control cells were equivalent, whereas in BV173 cells they were three- to fivefold less, as estimated by densitometry. A faint band of 6.5 kb was also observed in RNA from PAF cells. In addition to the normal transcripts, both K562 (lane 2) and Bv173 (lane 3) expressed the 8-kb aberrant transcript. Two major bands of 6.5 and 7 kb were detected in the mouse LM-TK– RNA (lane 4), while the K562 and Bv173 hybrids contained the human as well as the mouse c-*abl* transcripts. The 8-kb transcript was also present in all three hybrids containing the Ph^1 chromosome. Hybrids that were negative for the Ph^1 chromosome but which contained either the normal chromosome 22 or 9q+ did not express the 8-kb transcript (data not shown). The expression of the 8-kb transcripts does not require the presence of any other human chromosome, because the only common denominator of all the hybrids expressing the 8-kb transcript was the presence of the Ph^1 chromosome or the Ph^1 chromosome derivative in K562 hybrids. However, we were unable to isolate hybrids containing the normal chromosome 9, as this chromosome is preferentially lost from mouse and human hybrids[23]. In addition, little or none of the normal 6-kb c-*abl* transcript was detected in these hybrids, suggesting that these transcripts initiate only from the normal chromosome 9 and not from the c-*abl* locus involved in the translocation.

To correlate the presence of the p210 protein with the 8-kb *abl* RNA in Ph^1 chromosome-positive cells, we assayed hybrid cell extracts for *in vitro* kinase activity. Figure 3*b* shows the electrophoretic profile of cell extracts immunoprecipitated with the *abl*-specific antiserum pEX-5 and then incubated with [γ-^{32}P]ATP in conditions allowing autophosphorylation. The pEX-5 antiserum was obtained from a rabbit immunized with a v-*abl* polypeptide prepared in a bacterial expression system and has been shown to precipitate the phosphorylated p210 protein in K562 cells[10–12]. The p210 protein possessing phosphokinase activity was present in Ph^1-positive K562 (Fig. 3, lane 1) and Bv173 (lane 2) cells, whereas the normal p145 protein was present at equivalent levels in K562 and Ph^1-negative control HL60 cells, but was not detected in Bv173 cells in the same conditions[12]. The latter finding is consistent with the lower levels of normal c-*abl* RNA observed in the BV173 cells. In all hybrids and in parental LM-TK$^-$ mouse cells, an additional protein of relative molecular mass 250,000 (p250) was detected. This protein is also present in another mouse fibroblast cell line, IT 22, which is derived from 3T3 cells[24]. The reaction with this protein suggests that some anti-*abl* sera recognize antigenic determinants unique to p250 but that others do not, as it is only detected with certain anti-*abl* sera (J.B.K. and O.N.W., unpublished results). No p210 was precipitated by normal rabbit serum (Fig. 3*a*).

We have used somatic cell hybrids between LM-TK– mouse fibroblasts and cell lines K562 and Bv173 derived from CML patients to study the effect of the t(9 ; 22) translocation on the

Table 1 Characterization of hybrid clones

Hybrid clones	Oncogene present c-*abl*	c-*sis*	C_λ	Relevant chromosomes*
KL-17-9-1	+	+	+	Ph^1, 22
KL-17-9-3	+	+	+	Ph^1, 22
260-3-1-3	+	−	+	Ph^1

The DNA of hybrid clones was screened by Southern blot analysis using the v-*abl*, C_λ and c-*sis* probes. Cells that were positive for c-*abl* and C_λ and negative for c-*sis* contained the Ph^1 chromosome. Hybridization with c-*sis* indicated the presence of either normal chromosomes 22 and 9, or chromosomes 9q+ and Ph^1. Isoenzyme analysis for AK-1 and AK-3, markers for the long and short arms of chromosome 9, respectively revealed no normal chromosome 9 or 9q+ chromosome present in the hybrids.

* Data are based on Southern blot and isoenzyme analyses.

regulation of c-*abl* expression. As the altered c-*abl* RNA and protein are present in hybrid cells which contain only the Ph^1 chromosome and not other relevant chromosomes, we conclude that they must be derived from the c-*abl* locus on the Ph^1 chromosome. The results of the analysis of c-*abl* protein expression in these hybrids are consistent with the proposed relationship between the transcript and the p210 c-*abl* protein[11].

We have reported previously that there is a marked reduction in the levels of human c-*myc* transcripts in hybrid cells of mouse fibroblasts and Burkitt's lymphoma cells possessing the 8 ; 14 translocation[25-27]. Thus, although the translocated c-*myc* oncogene is expressed at elevated levels in the B-cell background, it is clearly repressed in cells of other differentiation lineages (for example, fibroblasts)[25-27]. In contrast, the expression of the c-*abl* 8-kb transcripts and p210 in the fibroblast hybrids indicates that the activation of the c-*abl* oncogene as a result of the chromosomal translocation is not myeloid-specific. Furthermore, the presence of the Ph^1 chromosome in haematopoietic lineages other than myeloid[28,29] raises the possibility that the effect of the altered c-*abl* protein differs for different cell types. This possibility is also supported by the observation that Epstein-Barr virus-transformed lymphoblastoid cell lines derived from Ph^1-positive CML patients express the 8-kb aberrant c-*abl* transcripts and the p210 protein (O.N.W., unpublished results).

We thank Ms Marina Hoffman for editorial assistance. This work was supported by NCI grants CA-16685, CA-36521, CA-23568, CA-25875 to C.M.C., NIH grant GM-32583 to L.C.S., and by a Faculty Scholar Award from the American Cancer Society and by NIH research grants CA-27505, CA-32737 to O.N.W. D.K. is a postdoctoral fellow of the National Cancer Institute of Canada. J.B.K. is supported by USPHS National Service Award GM-07185.

Received 25 March; accepted 23 October 1985.

1. Nowell, P. C. & Hungerford, D. A. *J. natn. Cancer Inst.* **25**, 85-109 (1960).
2. Rowley, J. D. *Nature* **243**, 290-291 (1979).
3. Rowley, J. D. *Science* **216**, 749-751 (1982).
4. de Klein, A. *et al. Nature* **300**, 765-767 (1982).
5. Dalla-Favera, R., Gallo, R. C., Giallongo, A. & Croce, C. M. *Science* **218**, 686-688 (1982).
6. Groffen, J. *et al. J. exp. Med.* **158**, 9-15 (1983).
7. Cannani, E. *et al. Lancet* **i**, 593-595 (1984).
8. Collins, S. J., Kubonishi, I., Miyoshi, I. & Groudine, M. T. *Science* **225**, 72-74 (1984).
9. Gale, R. P. & Canaani, E. *Proc. natn. Acad. Sci. U.S.A.* **81**, 5648-5652 (1984).
10. Konopka, J. B., Watanabe, S. M. & Witte, O. N *Cell* **37**, 1035-1042 (1984).
11. Davis, R. L., Konopka, J. B. & Witte, O. N. *Molec. cell. Biol.* **5**, 204 (1985).
12. Konopka, J. B., Watanabe, S. M., Singer, J. W., Collens, S. J. & Witte, O. N. *Proc. natn. Acad. Sci. U.S.A.* **82**, 1810-1814 (1985).
13. Dubbs, D. R. & Kit, S. *Expl Cell Res.* **33**, 19-28 (1964).
14. Lozzio, C. B. & Lozzio, B. B. *Blood* **45**, 321-334 (1975).
15. Pegararo, L. *et al. J. natn. Cancer Inst.* **70**, 447-453 (1983).
16. Srinivasan, A., Reddy, E. P. & Aaronson, S. A. *Proc. natn. Acad. Sci. U.S.A.* **78**, 2077-2081 (1981).
17. Croce, C. M. *et al. Proc. natn. Acad. Sci. U.S.A.* **80**, 6922-6926 (1983).
18. Heiter, P. A., Hollis, G. F., Korsmeyer, S. J., Waldman, T. A. & Leder, P. *Nature* **296**, 536-560 (1981).
19. Collins, S. J. & Groudine, M. T. *Proc. natn. Acad. Sci. U.S.A.* **80**, 4813-4817 (1983).
20. Selden, J. R. *et al. Proc. natn. Acad. Sci. U.S.A.* **80**, 7289-7292 (1983).
21. Tsujimoto, Y. & Croce, C. M. *Nucleic Acids Res.* **12**(22), 8407-8414 (1984).
22. McKusick, V. A. *Cytogenet. Cell Genet.* **32**, 7 (1982).
23. Ruddle, R. & Creagan, R. *A. Rev. Genet.* **9**, 407-486 (1975).
24. Croce, C. M., Barrick, J., Linnenbach & Koprowski, H. *J. cell. Physiol.* **99**, 279-284 (1979).
25. Nishikura, K. *et al. Proc. natn. Acad. Sci. U.S.A.* **80**, 4822-4826 (1983).
26. Nishikura, K. *et al. Science* **224**, 399-402 (1984).
27. Croce, C. M., Erikson, J., ar-Rushdi, A., Aden, D. & Nishikura, K. *Proc. natn. Acad. Sci. U.S.A.* **81**, 3170-3174 (1984).
28. Karpas, A., Fischer, P. & Swirsky, D. *Lancet* **i**, 931-933 (1982).
29. Minowada, J., Tsubota, T., Greaves, M. F. & Walters, T. R. *J. natn. Cancer Inst.* **70**, 447-453 (1983).

Disease-specific and tissue-specific production of unintegrated feline leukaemia virus variant DNA in feline AIDS

James I. Mullins*, Carol S. Chen*
& Edward A. Hoover†

* Department of Cancer Biology, Harvard School of Public Health, Boston, Massachusetts 02115, USA
† Department of Pathology, College of Veterinary Medicine, Colorado State University, Ft Collins, Colorado 80523, USA

Feline leukaemia viruses (FeLVs) have long been known to be associated with induction of proliferative and anti-proliferative diseases of domestic cats[1]. Strains of FeLV have been recognized which specifically induce lymphosarcoma[2,3], aplastic anaemia[4-6], myelodysplastic anaemia[6], and, recently, feline AIDS (acquired immune deficiency syndrome), a naturally occurring immunosuppressive syndrome[7] strikingly similar to human AIDS which is lethal in 100% of inoculated and viraemic specific-pathogen-free (SPF) cats[8]. Here, we have analysed FeLV DNA in tissues of 22 SPF cats that had been inoculated with the feline AIDS strain (FeLV-FAIDS) and we find two classes of viral DNA—a monotypic common form which is detectable in bone marrow regardless of disease state, and variant forms, recognizable by restriction site differences, whose appearance correlates with onset of disease symptoms and persists throughout the course of the disease. FeLV-FAIDS variant DNA is detected at high concentration (10–50 copies per cell) and principally as unintegrated viral DNA (UVD) in bone marrow of cats with feline AIDS. In marked contrast, high levels of UVD were not present in cats in the terminal-stages of T-cell lymphosarcoma, aplastic anaemia, or myelodysplastic anaemia induced by other FeLV strains. These results parallel recent observations in humans, where high levels of UVD were sometimes found in cells derived from AIDS patients infected with human T-lymphotropic virus type III (HTLV-III)/lymphadenopathy-associated virus (LAV), and suggest that persistence of unintegrated variant viral DNA is a crucial indicator of retrovirus-induced cytopathic disease syndromes such as AIDS.

DNA from the tissue samples described below was extracted and analysed for the presence of exogenous FeLV sequences after digestion with the restriction endonuclease *Kpn*I, agarose gel electrophoresis, Southern transfer and hybridization using the exogenous FeLV long terminal repeat (LTR)-specific hybridization probe exU3 as described previously[9]. In this analysis, viral DNA produces two bands which hybridize to the exU3 probe: an internal virus band derived from the 3′ end of the viral genome and a band derived from LTR sequences at the 5′ end of the genome, which, if linked to adjacent cellular DNA, is referred to as a host-virus junction band. The intensity of the internal band reflects the average provirus copy number per cell in the tissue examined. The DNA in Fig. 1, lane 1, was derived from RD-FeLV-2, a single cell clone of human RD cells infected with the Gardner–Arnstein subgroup B strain of FeLV (FeLV-B-GA)[10]. A 3.65-kilobase (kb) internal virus band with an intensity representing ~22 copies was detected, as well as an equivalent number of single-copy bands derived from host-virus junction fragments. DNA derived from a field case of T-cell lymphosarcoma (animal DQ; Fig. 1, lane 2) gave a similar

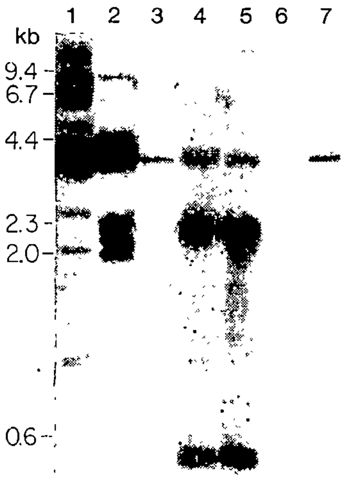

Fig. 1 Exogenous FeLV sequences in animals infected with FeLV-FAIDS. The DNA samples analysed were the RD-FeLV-2[10] cloned cell line (lane 1), thymic tumour from animal DQ (lane 2), spleen (lane 3) and bone marrow (lane 4) from animal 1082 with experimentally induced feline AIDS, bone marrow (lane 5) and lymph node (lane 6) from animal 1220 with experimentally induced feline AIDS, and bone marrow (lane 7) from animal 1044, an asymptomatic animal inoculated with FeLV-FAIDS. Relative molecular mass (M_r) markers are shown in kilobase pairs (kb).

Methods. Total cellular DNA (7.5 μg) was purified, digested with *Kpn*I, electrophoresed in 1.2% agarose gel, transferred to nitrocellulose and hybridized in the presence of 10% dextran sulphate and 50% formamide as described previously[9]. The probe, derived by gel purification[23] of the insert in plasmid pexU3 (J.I.M. *et al.*, in preparation), was ^{32}P-nick-translated[24] to a specific activity of 8×10^8 d.p.m. μg^{-1} and was used at a concentration of 10^6 c.p.m. ml^{-1}. After hybridization at 42 °C, for 36 h, the filter was incubated in five changes of 2×SSC (0.3 M NaCl, 0.03 M sodium citrate), 0.05% sodium pyrophosphate and 0.1% sodium lauryl sarkosine at 50 °C, dried and exposed to X-ray film at −70 °C with an intensifying screen for 6 h prior to development. Mean virus copy numbers (per cell) were estimated from densitometer scans of the exposed films.

pattern, with a single prominent 3.65-kb internal virus band and ~12 single-copy host-virus junction bands, indicating that the tumour is a clonal cell outgrowth of FeLV-infected cells.

In the present study, cell-free tumour extract from DQ was used as a source of the feline AIDS virus[8] and was inoculated into newborn, weanling and adult cats. Two cats (1220, 1082) that developed acute feline AIDS following inoculation were killed and their tissue DNA prepared for analysis. Spleen DNA from cat 1082 showed a non-clonal pattern of virus integration, with a single copy of the internal virus band of 3.65 kb, the same length as the prominent provirus in the DQ tumour (Fig. 1, lane 3). The bone marrow of both diseased cats contained ~2 copies per cell of this provirus (Fig. 1, lanes 4 and 5) but in addition contained two bands of intensity ~15 copies per cell, one at 2.1 kb and the other at 0.4 kb. No viral DNA was detected in the lymph node of cat 1220 (Fig. 1, lane 6), who had severe lymphoid cell depletion in that organ. Bone marrow from an adult cat (1044) that was asymptomatic when the sample was taken, contained only the form of virus giving the 3.65-kb *Kpn*I band (Fig. 1, lane 7).

The state of viral DNA integration was examined by Southern blot analysis without prior restriction enzyme digestion (Fig. 2). A prominent band at 8.7 kb was detected in each feline AIDS bone marrow sample (Fig. 2, lanes 3, 5), co-migrating with unintegrated lines FeLV DNA derived from RD cells freshly infected with FeLV-B-GA (Fig. 2, lane 4)[10]. A deleted 7.5-kb form of unintegrated viral DNA and a small amount of relaxed circular viral DNA migrating with 18-kb linear DNA[10,11] were detected in both the RD infected (FeLV-B-GA) cell preparation and the feline AIDS bone marrow samples. Evidently, over 90% of viral sequences in these cells are present as UVD and it is unclear whether any bone marrow-specific viral sequences are integrated into cell DNA. As it is unlikely that all cells within the bone marrow are infected and/or have the same amount of unintegrated DNA, we suspect that the concentration of UVD in some infected cells is much higher than the average of 15 variant molecules per cell noted above.

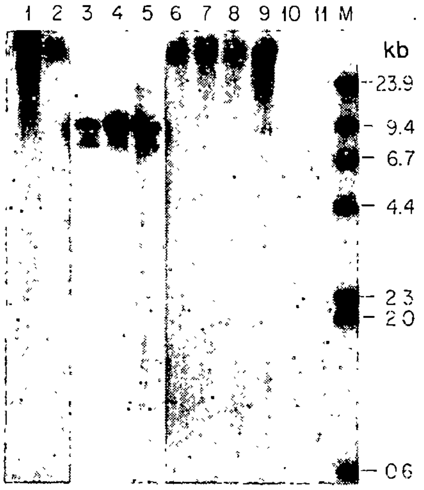

Fig. 2 Exogenous FeLV in undigested cat cellular DNAs. Total cellular DNA was purified and analysed as described in Fig. 1 legend, except that samples were examined without restriction enzyme digestion and a 0.8% agarose gel was used. DNA samples analysed were: lane 1, thymic tumour from animal DQ; lane 2, spleen from animal 1082; lane 4, the extrachromosomal, Hirt-supernatant fraction[25] of RD cell DNA taken 24 h after infection with FeLV-B-GA at a multiplicity of infection ~1.0 ref. 10); lanes 3 and 5, bone marrow samples from animals 1082 and 1220, respectively, lanes 6, 7, two animals with aplastic anaemia; lane 8, animal 1044; lane 9, an animal with a thymic tumour; lanes 10, 11, two animals with myelodysplastic anaemia. Lanes 3–6 were exposed to X-ray film for 6 h before development; the remaining lanes were exposed for 16 h. Lane M, M_r markers.

A similar analysis was performed 'blindly' on bone marrow samples taken from 19 additional animals inoculated with FeLV-FAIDS and a sample from animal 1044 following the development of symptoms of feline AIDS. Representative examples of this survey are shown in Fig. 3. In the bone marrow from animal 1044 and from an additional animal (1161) with overt disease, we detected ~50 copies per cell of unintegrated FeLV-variant DNA. We found a low level of integrated variant DNA in animal 1276, which developed clinical signs of acute disease within a week after the bone marrow sample was extracted for analysis. Terminal tissue samples from this animal revealed a high level of variant UVD in bone marrow and common as well as variant proviral DNA in other tissues (data not shown).

Unintegrated viral DNA is an obligatory intermediate in the life cycle of retroviruses[12], it is detected *in vitro* usually only for a few days following synchronous infection of cells at high virus multiplicity, as shown in Fig. 2 for FeLV-B-GA-infected RD cells. UVD is rarely detected *in vivo* as few cells in a tissue are likely to have been infected immediately before tissue sampling. Known exceptions to this include a recent report of persistent UVD in the bone of avian leukosis virus-infected osteopetrotic chickens[13] and following generation of MCF recombinant viruses in pre-leukaemic AKR mice[14]. Interestingly, transient production of a high level of UVD folowing *in vitro* infection with certain avian retroviruses correlates with viral cytopathicity[15,16], and infection of sheep chloroid plexus cells with the cytopathic ovine visna lentivirus results in persistent synthesis of UVD[17]. Therefore, we sought to determine whether

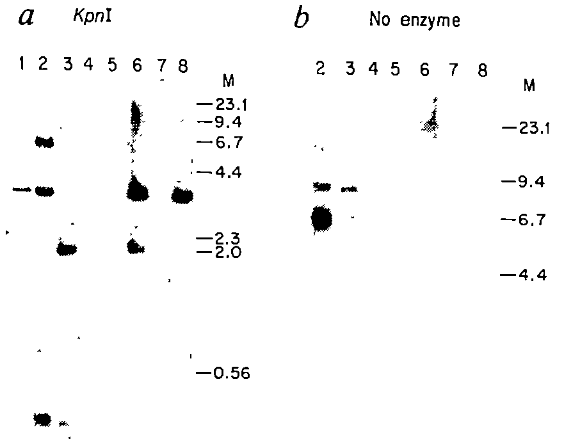

Fig. 3 Exogenous FeLV in animals inoculated with FeLV-FAIDS. DNA samples derived from bone marrow of 19 animals were analysed as described in Fig. 1 legend (*a*, *Kpn*I digests) and as described in Fig. 2 legend (*b*, undigested DNA). Samples from seven animals and RD-FELd-2 cells (lane 1) are shown: those in lanes 2 and 3 are from animals (1044 and 1161, respectively) with feline AIDS. Animal 1276 (lane 6) developed symptoms of feline AIDS within 1 week after the bone marrow sample was taken. Samples in lanes 4 (1237), 5 (1238) and 8 (1283) are from viraemic, asymptomatic animals. The sample in lane 7 (1282) is from an asymptomatic animal in which viral infection regressed.

detection of UVD in cats was specific to feline AIDS and not found in the bone marrow of cats with other diseases induced by defined strains of FeLV (Fig. 2). DNAs from the following sources were analysed for the presence of UVD: terminal-stage thymic lymphosarcoma tissue from cat DQ (Fig. 2, lane 1); spleen from cat 1082 with feline AIDS (lane 2); bone marrow from two SPF cats with terminal-stage aplastic anaemia induced experimentally by the molecularly cloned subgroup C, Sarma strain of FeLV (FeLV-C-S)[6] (lanes 6, 7); bone marrow from a viraemic, asymptomatic cat inoculated with FeLV-FAIDS (cat 1044, lane 8; 17 more cats in this category were examined with identical results); bone marrow from a tumour-bearing cat inoculated with the T-cell lymphosarcoma-inducing Rickard strain of FeLV[2] (lane 9); and bone marrow from two SPF cats with terminal-stage myelodysplastic anaemia induced by inoculation of molecularly cloned B-FeLV-GA (J.I.M. *et al.*, in preparation) (lanes 10, 11). We detected no UVD in the DQ tumour or bone marrow of any other animal, except at a low concentration in the marrow from the cat with lymphosarcoma induced by FeLV-Rickard (less than one copy per cell in this clonal cell population).

Because of the striking similarity between the pathology of human and feline AIDS, we sought to determine whether HTLV-III/LAV, the aetiological agent of human AIDS[18], could be detected as unintegrated viral DNA. We (N. Riedel *et al.*, in preparation) and others[19] found that 25% of the HTLV-III/LAV DNA present in the established cell line HT/H9 was present as unintegrated linear viral DNA. Shaw *et al.*[18] also reported detection of UVD in a few fresh tissues from AIDS patients, whereas we detected no UVD in any of four HTLV-III/LAV DNA-positive fresh tissue samples.

We detect three features in the behaviour of FeLV-FAIDS which distinguish it from all previously recognized FeLV strains: (1) marked tissue-specific replication of a variant form of virus; (2) distinct disease-specific association with synthesis of variant FeLV DNA; and (3) high concentrations of unintegrated viral DNA *in vivo* at terminal stages of the disease. The possibility that feline AIDS variant FeLVs possess a cell-specific tropism is supported by our finding of high concentrations of variant viral DNA in bone marrow but not at detectable levels in other tissues in two out of three cats examined. It is unclear at present whether cell- or tissue-selective replication, *de novo* recombination or mutation accounts for the detection of the bone marrow-specific feline AIDS variant. As every cat that became viraemic after inoculation with the DQ tissue-derived stock of FeLV-FAIDS developed severe immunosuppression and clinical feline AIDS[8] and four of five variants detected had the same 2.1 kb internal *Kpn*I fragment, it is possible that variant viruses were present but did not replicate efficiently in the initial lymphosarcoma tissue. The correlation between the production of variant UVD and the appearance of disease is particularly striking. Each of five cats with overt disease had high levels of variant UVD in the bone marrow, whereas none of 17 FeLV-FAIDS viraemic but asymptomatic cats had detectable levels of variant or UVD in their bone marrow.

The FeLV-FAIDS preparation contains viruses which fall within the A and B interference subgoups (ref. 20 and O. Jarrett, personal communication). Subgroup A viruses are generally considered to be minimally pathogenic but able to establish viraemia in a high proportion of infected cats[20,21]. Subgroup B viruses are less capable of establishing viraemia in other than newborn animals without concurrent infection with subgroup A FeLV[21]. The appearance of FeLV-B in the blood of cats infected with both subgroups has been associatd with onset of other FeLV-associated diseases[21], and at least one strain of molecularly cloned FeLV-B is pathogenic when inoculated into newborn SPF cats (J.I.M. *et al.*, in preparation). Since the bone marrow-specific form of FeLV-FAIDS was detected as unintegrated linear viral DNA and because persistence of high levels of UVD is associated with retrovirus cytopathicity, we suggest that the bone marrow-specific component is likely to be the cytopathic component of the strain mixture (possibly the subgroup B component, by analogy with the work of Jarrett and co-workers[21]) while the subgroup A component is probably the highly replicative, helper-like, common form virus.

The striking similarity between the clinico-pathological features of human and feline AIDS[8], the apparent cytopathic effect of both viruses on selected T-cell populations[6], and the detection of persistent unintegrated viral DNA in both disease processes suggest that experimentally induced feline AIDS will serve as a useful model in which to: (1) investigate the pathogenetic mechanisms of AIDS; (2) delineate the viral genomic component(s) responsible for lymphocytopathicity, and (3) evaluate the efficacy of antiviral compounds or viral vaccines in the treatment or prevention of retrovirus-mediated acquired immune deficiency in humans as well as animals. Unlike LAV/HTLV-III, which is not closely related to HTLV-I and -II[22], the feline AIDS virus is closely related to other FeLVs (for example, detection of virus using the exU3 hybridization probe indicates strong conservation of LTR-enhancer sequences). The relatedness of apathogenic FeLVs and FeLV-FAIDS strains should facilitate elucidation of the viral determinants critical to immunosuppressive cytopathicity.

We thank Dr M. O. Nicolson for providing Hirt-supernatant FeLV DNA. This work was supported by grants to J.I.M. from the NIH (CA34975) and the Massachusetts AIDS Research Council, and by a scholar award from the American Cancer Society, Massachusetts Division, and by grants to E.A.H. from the NIH (CA32552 and CA32563).

Received 21 June; accepted 1 November 1985.

1. Hardy, W. D. Jr. in *Feline Leukemia Virus* (eds Hardy, W. D. Jr, McClelland, A. J. & Essex, M.) 3-78 (Elsevier, New York, 1980).
2. Rickard, C. G., Post, J. E., de Noronha, F. & Barry, L. M. *J. natn. Cancer Inst.* 42, 987-1014 (1969).
3. Hoover, E. A., Perryman, L. E. & Kociba, G. J. *Cancer Res* 33, 145-152 (1973)
4. Hoover, E. A. *et al. J. natn. Cancer Inst.* **53**, 1271-1276 (1974)
5. Mackey, L., Jarrett, W., Jarrett, O. & Laird, H. *J. natn. Cancer Inst.* **54**, 209-217 (1975)
6. Riedel, N., Hoover, E. A., Gasper, P. W., Nicolson, M. O. & Mullins, J. I. *J. Virol.* (submitted)
7. Hardy, W. D. in *Human T-Cell Leukemia/Lymphoma Virus* (eds Gallo, R. C., Essex, M. E. & Gross, L.) 35-43 (Cold Spring Harbor Laboratory, New York, 1984)
8. Hoover, E. A., Mullins, J. I., Gasper, P. W. & Quackenbush, S. L. *Science* (submitted)
9. Mullins, J. I., Brody, D. S., Binari, R. C. Jr & Cotter, S. M. *Nature* **308**, 856-858 (1984)
10. Mullins, J. I. *et al. Nucleic Acids Res.* **8**, 3287-3305 (1980)
11. Sherr, C. J. *et al.* in *Feline Leukemia Virus* (eds Hardy, W. D. Jr, McClelland, A. J. & Essex, M.) 293-307 (Elsevier, New York, 1980).
12. Varmus, H. & Swanstrom, R. in *RNA Tumour Viruses* (eds Weiss, R., Teich, N., Varmus, H. & Coffin, J.) 369-512 (Cold Spring Harbor Laboratory, New York, 1982)

13. Robinson, H. L. & Miles, B. D. *Virology* **141**, 130-143 (1985).
14. Herr, W. & Gilbert, W. *J. Virol.* **50**, 155-162 (1984).
15. Keshet, E. & Temin, H. M. *J. Virol.* **31**, 376-388.
16. Weller, S. K. & Temin, H. M. *J. Virol.* **39**, 713-721 (1981).
17. Harris, J. D. *et al. Proc. natn. Acad. Sci. U.S.A.* **81**, 7212-7215 (1984).
18. Gallo, R. C. *et al. Science* **224**, 500-503 (1984).
19. Shaw, G. M. *et al. Science* **226**, 1165-1171 (1984).
20. Sarma, P. S. *et al. Proc. Soc. exp. Biol. Med.* **14**, 757-762 (1974).
21. Jarrett, O. in *Feline Leukemia Virus* (eds Hardy, W. D. Jr, McClelland, A. J. & Essex, M.) 473-479 (Elsevier, New York, 1980).
22. Gonda, M. A. *et al. Science* **227**, 173-177 (1985).
23. Waalwijk, C. & Flavell, R. A. *Nucleic Acids. Res.* **5**, 3231-3236 (1978).
24. Mullins, J. I. *et al. J. Virol.* **38**, 688-703 (1981).
25. Hirt, B. *J. molec. Biol.* **26**, 365-369 (1967).

Structural homology of the product of the *Drosophila Krüppel* gene with *Xenopus* transcription factor IIIA

Urs B. Rosenberg, Christian Schröder, Anette Preiss, Andrea Kienlin, Serge Côté, Isolde Riede* & Herbert Jäckle

Max-Planck-Institut für Entwicklungsbiologie, Abteilung Biochemie II, Spemannstrasse 35, D-7400 Tübingen, FRG
* Max-Planck-Institut für Biologie, Abteilung Henning, Corrensstrasse 38, D-7400 Tübingen, FRG

Segmentation of the *Drosophila* embryo is established at around the blastoderm stage[1-3] and requires both maternal information in the egg cytoplasm[4,5] and expression of the zygotic genome. Zygotic genes involved in segmentation have been defined by mutations that affect the segmental pattern of the embryo[6-10], and these fall into several different classes, such as the 'gap' genes, mutations of which cause the loss of contiguous segments[6]. *Krüppel* (*Kr*) is an example of a *Drosophila* gap gene, strong *Kr* mutant embryos lacking all thoracic and five anterior abdominal segments, with part of the remaining posterior abdominal segments being present as a mirror-image duplication (weaker alleles cause shorter deletions[11,12]). *Kr* has been cloned[12] and shown to encode a blastoderm-gastrulation stage-specific transcript expressed in regions of the embryo affected by *Kr* mutants[13]. We report here that the protein product of the *Kr* gene predicted from DNA sequences is structurally homologous to the transcription factor TFIIIA which regulates 5S gene expression in *Xenopus*. Like TFIIIA, the predicted *Kr* protein has an internally repetitious sequence, and as has been suggested for TFIIIA, the repeat units may form DNA-binding domains.

Different DNA fragments from the 18-kilobase (kb) DNA segment containing essential Kr^+ sequences (−5.1 to +12.7; for details see Fig. 3 in ref. 12) were used to analyse Northern blots loaded with RNA from different stages of *Drosophila* development (Fig. 1). None of the fragments hybridized to poly$(A)^-$ RNA (data not shown) and only one, the 5.4-kb fragment (+1.5 to +6.9), hybridized to poly$(A)^+$ RNA in a broad 2.5-kb band, as seen earlier with an overlapping 9.5-kb *Eco*RI fragment[12]. A series of corresponding complementary DNA clones were isolated from several libraries prepared from poly$(A)^+$ RNA of 2-5-h-old embryos (blastoderm to gastrula). All of them map within a 2.5-kb segment of genomic DNA (Fig. 1*a*,*b*).

Different fragments from two almost full-size cDNA clones (see Fig. 1*b*) were probed to developmental Northern blots. Each of the fragments hybridized to the broad 2.5-kb band of poly$(A)^+$ RNA seen with the genomic DNA fragment (see above). Using higher-resolution agarose gels (Fig. 1*c*,*h*), this band could be resolved as a doublet of transcripts lying about 350 base pairs (bp) apart. Both transcripts were expressed in 2-5-h-old embryos (blastoderm-gastrula). Extended exposure of the Northern blots revealed that Kr^+ transcripts are present up until larval stages, being about two orders of magnitude below their abundance at blastoderm-gastrulation stages (data not shown).

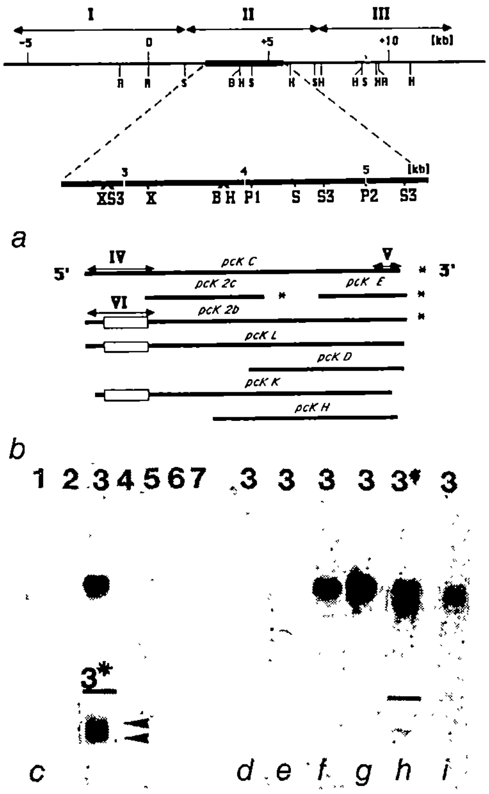

Fig. 1 *Kr* transcript analysis. *a*, Restriction map of the *Kr* region (for details see Fig. 3 in ref. 12) and its enlarged core (below). Restriction enzymes used are *Eco*RI (R), *Sal*I (S), *Bam*HI (B), *Hin*dIII (H), *Pvu*I and *Pvu*II (P1, P2), *Xba*I (X) and *Sau*3A (S3). Fragments I, II and III, which originate from the ER3 clone[12], were used as probes for Northern analysis (lanes *c*–*e*). *b*, Alignment of *Kr* cDNA clones relative to the restriction map of genomic DNA shown above. Boxes indicate an intron (see Fig. 2) that is absent from the respective clones. The 5′ to 3′ orientation was established by single-strand cDNA mapping[31] and confirmed by sequencing (see Fig. 2) of genomic DNA and the cDNA clones marked with an asterisk. Note the location of fragments IV, V and VI used for Northern analysis. Lanes *c*–*i*, localization of *Kr* transcripts within cloned DNA and the developmental profile of *Kr* transcript accumulation. Numbers over the lanes designate the developmental stages at which the poly$(A)^+$ RNA was extracted: 1, unstaged ovaries; 2, 0-1-h-old embryos; 3 and 3*, 2-5-h-old embryos; 4, 8-24-h-old embryos; 5, larvae; 6, pupae; 7, adults. *c*, Developmental Northern profile of *Kr* transcripts. Note that the broad 2.5-kb poly$(A)^+$ RNA band (lanes 3) is actually a doublet of bands (lane 3*) which differ in ~350 bp. The Northern blot was probed with fragment II. The same Northern blot (only lanes 3 shown) was probed with fragments I (lane *d*) or fragment III (lane *e*). In both cases, extended exposure revealed no signal. Parallel Northern blots were probed with pcK2b (lane *f*) and pcKC (lane *g*). Lane *h*, Northern blots probed with intron containing (probe IV, upper portion) and intron lacking (probe VI, lower portion) sequences prepared from cDNA clones. Note the similar intensities of the doublets with probe VI and a stronger signal of the longer band with probe IV. Lane *i*, Northern blot probed with the 3′ end of one cDNA clone (probe V). Note the low level of background smear due to poly(A) tail homologies.

Methods. cDNA clones were isolated from libraries prepared from 2-4-h and 2-5-h embryos. pcK2b and pcK2c were found in the Goldschmidt-Clermonts library (unpublished); the other clones were from a freshly prepared library (U.B.R., unpublished). Preparation of poly$(A)^+$ RNA, nick-translation of the probes and Northern blot analysis have been described earlier[12]. Gels for Northern blots were loaded with 10 μg poly$(A)^+$ RNA per lane using 1.0% agarose gels (lanes without asterisks) or 2 μg poly$(A)^+$ RNA using 0.7% agarose gels and prolonged separation (lanes with asterisks).

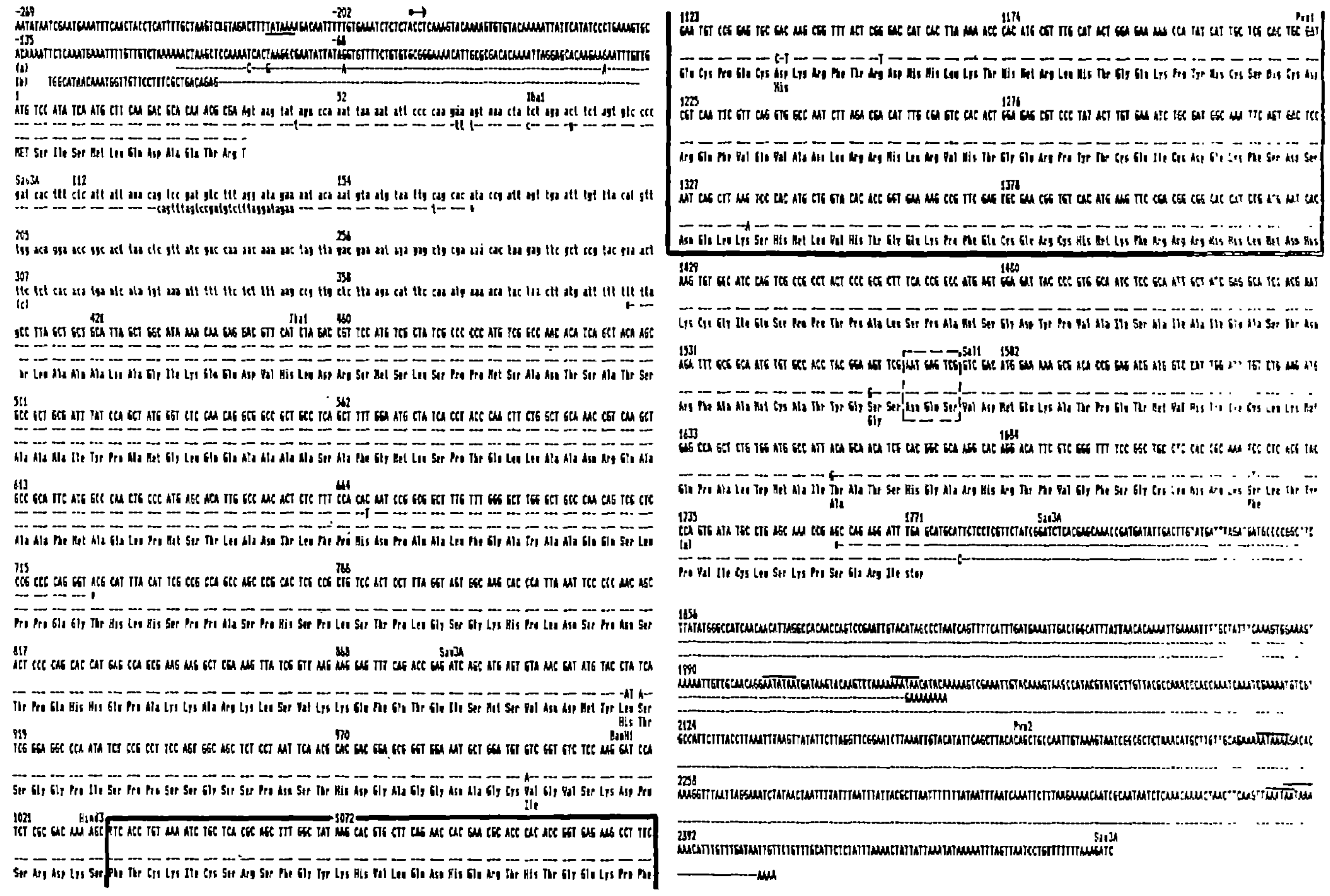

Fig. 2 Sequence of the *Kr* gene and presumptive amino-acid sequence of the *Kr* protein. Sequence of *Kr* genomic DNA, cDNA sequences (pcKC, pcK2b and pcK2c designated (a), (b) and (c) below the genomic sequence and the only open reading frame amino-acid sequence below. Asterisks indicate that cDNA clone pcKC is not sequenced completely; the intron acceptor site was sequenced in pcKC (sequence identical to genomic DNA) and in pcK2c (between the second and third asterisks in the cDNA pcKC sequence). Note the TATA box (underlined), the cap site (arrow), the exon/intron/exon borders in positions 37 and 409, a presumptive glycosylation site at position 1,564-1,572, the translation stop in position 1,771-1,774 followed by a series of five polyadenylation signals (overlined). Note that at least two of them are used in pcK2b and pcKC. The heavily boxed sequence (position 1,036-1,371) contains the domain of the four complete 28-amino-acid repeat sequences followed by a fifth incomplete repeat unit (see text and Fig. 3 for details). For sequencing, genomic DNA clones and the cDNA clones (see Fig. 1*b*, labelled by asterisks) were subcloned into pUC 18/19 or mp 18/19 using a single restriction enzyme (*Xba*I or *Sau*3A) or a combination of the others (see Fig. 1*a*) to produce subclone fragments in overlapping orientations. Dideoxy sequencing was carried out as described previously[15], using both sequencing of both strands and verification of the sequence in cDNA clones as a strategy. In this way, each part was confirmed in a minimum of two independent sequencing reactions.

The *Kr* gene contains a 1,398-bp open reading frame which is split by a 372-bp intron (Fig. 2). Transcription starts at position −185, consistent with both primer extension studies (data not shown) and the structure of the cDNA clones (see below). Two 'TATA' boxes occur 86 and 26 bp upstream from this transcriptional start; the latter (underlined in Fig. 2) is the more conventional spacing. A series of five polyadenylation signals are found downstream from the translated sequence. The first Met codon in our sequence starts with residue 184 downstream from the transcription start. However, neither this nor a second Met codon upstream from the intron border fits the consensus sequence (CCG/ACCATGG) for eukaryotic translation initiation sites[14] and, therefore, initiation of translation at the first conventional Met codon (in position 466-469) cannot be positively ruled out.

One *Kr* cDNA clone (pcK2b) was sequenced completely, others were partly sequenced (Fig. 2). The cDNA clones pcK2b and pcKC terminate at different positions, suggesting that more than one of the five potential polyadenylation sites are used. The 5′ end of the pcKC cDNA sequence starts at position −101, indicating that this clone is close to full size. In contrast, the 5′ end of the pcK2b cDNA clone does not correspond to the genomic sequence, suggesting an artefact during cDNA synthesis (as observed earlier in other cDNAs of the same library; for details see refs 15, 16). The major difference between the two cDNA clones, aside from using a different polyadenylation site (see above), is that the intron is spliced in pcK2b but present in pcKC and several other cDNA clones (Fig. 1*b*). Nucleotide differences, including a polymorphic *Xba*I site (position 82-87), a small duplicated segment in the intron and a few base pair changes, reflect minor differences in various wild-type strains (data not shown) and mismatch reading by the reverse transcriptase during cDNA construction.

Translation initiation at the first ATG in the *Kr* transcript (position 1) results in a small 19-amino-acid peptide which is interrupted by a stop codon inside the intron present in clone pckC. However, initiation at the same position results in a readthrough equivalent to a 466-amino-acid protein (Fig. 2) in spliced *Kr* messenger RNA represented by clone pck2b. Alternatively, translation could be initiated at the 'conventional' ATG codon in position 484 (ref. 14), leaving an unusually long 5′-untranslated sequence in both transcripts for possible regulation at the translational level.

The *Kr* protein deduced from the 1,398-bp open reading frame seems to be divided into three domains. The amino-terminal region up to position 1,035 is extremely rich in Ala, Ser and Pro (>30%) and folds into a globular structure. The carboxy-terminal region (after position 1,480) shows similar features, including a putative glycosylation site[17]. In contrast to

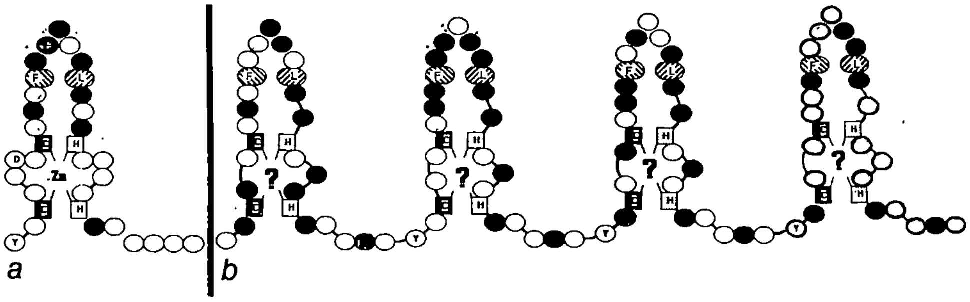

Fig. 3 Folding scheme for a linear arrangement of a TFIIIA repeated domain and *Kr* protein. *a*, TFIIIA 'finger structure' as described in detail in ref. 18. Each of the nine repeated domains is centred on a tetrahedral arrangement of zinc (Zn) ligands. Marked amino-acid residues are conserved. They include Tyr (Y), the Cys (C) and His (H) zinc ligands and the hydrophobic Phe (F) and Leu (L). Black circles mark the position of DNA-binding amino acids[21]. The folding scheme shows that zinc draws the ends of each unit together, leaving the central residues to form a potential DNA-binding loop (finger). *b*, *Kr* protein folding structure. Note the structural homology to the proposed TFIIIA structure, leaving the Cys–His arrangement and central residues to form a potential DNA-binding finger. Note that His 23 is followed by an invariant stretch of amino acids (position 24–28), and the variable positions of DNA-binding amino acids (black circles) in the finger loop (position 8–19). For the amino-acid sequence see the boxed area in Fig. 2. Orientation of the protein domain is amino (left) to carboxy terminus (right). Since the fifth, incomplete repeat unit lacks His 23, it may not fold into a finger and is therefore not included in the scheme.

the central portion (see below), the amino and carboxyl ends are relatively neutral (10% basic). At position 1,036, the *Kr* protein starts an internal 28-amino-acid repeat unit consisting of the following motif: Phe 1 (or Tyr 1), Cys 3, Cys 6, Phe 10, Leu 16, His 19, His 23 followed by Thr, Gly, Glu, Lys or Arg (position 24–27) and Pro 28 (see Figs 2, 3). Four such complete units are arranged tandemly, ending with Pro 28 in position 1,372, and they are followed by a fifth incomplete repeat which shares most of the above structural motif. This portion of the *Kr* protein domain may fold into a structure similar to that proposed by Klug and co-workers[18] for TFIIIA (see Fig. 3); TFIIIA is needed for transcription by polymerase III, which acts on a limited number of genes including those coding for 5S RNA of *Xenopus laevis*. The TFIIIA protein was shown to bind both 5S RNA and its cognate DNA and represents a key element in the autoregulation of 5S gene transcription[19,20]. In analogy to TFIIIA, the *Kr* repeat unit may fold into four potential DNA-binding loops ('fingers'), each centred on invariant pairs of Cys and His (compare Fig. 3*a* and *b*). Each finger consists of two hydrophobic amino acids (Phe 10, Leu 16) surrounded by non-conserved, mostly basic or positively charged amino acids, followed by a stretch of five conserved amino acids (position 24–28). The 'fingertip' is rich in positively charged 'DNA-binding'[21] amino acids, representing the potential DNA-binding region of the *Kr* protein. The specificity of DNA binding would be provided by the side groups of Lys, His, Asn, Gln and Thr (interacting with the phosphate backbone of DNA) and Arg (forming hydrogen bonds to the base pairs)[21]. The conserved stretch of amino acids following His 23 suggests that each repeat represents an extended DNA-binding finger domain linked by invariant joints. Each finger possibly interacts with about six nucleotides—half a DNA period (for details see ref. 18).

This structural feature of the *Kr* protein makes it different from the other segmentation and homoeotic gene products so far analysed. More importantly, it demonstrates a connection between a segmentation gene and a transcription factor known to bind to DNA (see Fig. 3), which suggests that DNA binding may be an important feature of *Kr* function, as proposed for other segmentation and homoeotic genes of *Drosophila* which contain the conserved 'homoeo-box' domain[15,16,22–27]. However, in view of the unrelated protein structure, the interaction of the *Kr* protein with DNA should be different from that of the homoeo-box domain proteins[15]. Whereas the latter domain provides general DNA-binding features that may become specific through variability in the adjacent sequences, as found in all genes so far analysed[15,16,22–27], the *Kr* finger motif could possibly specify directly for the DNA-binding site. In analogy to TFIIIA and 5S RNA regulation during *Xenopus* development (see refs 19, 20 for details), the *Kr* finger domain could then bind to specific DNA sequences to form stable transcriptional complexes which act on few other (sets of) specific genes, and it might also be involved in autoregulation as outlined in Meinhard's model of pattern formation[28,29]. In addition, the *Kr* protein may bind to RNA (see below).

In looking for possible DNA-binding sites on the *Kr* gene, it was interesting to note a six-nucleotide repeat (ACAAAA) (see Fig. 4) that could be a target for maternal factors which are expected to initiate and regulate *Kr* gene expression[11,13] and/or a target for the *Kr* protein for autoregulation processes (see above). The 'ACAAAA box' is repeated eight times (on both DNA strands and in both orientations) within 180 bp downstream from the *Kr* TATA box and five times downstream from the TGA stop codon (Fig. 4*a*), forming part of the non-translated sequences. This hexanucleotide repeat and its location within the transcribed region of the *Kr* gene are reminiscent of the multiple contact binding of other transcription factors[30], including a single finger loop of TFIIIA[18], thus, as a multiple-finger protein, *Kr* (in analogy to TFIIIA) may bind many such recognition sites within the transcribed region of genes. As there is no need for multiple fingers merely to bind DNA, it would be reasonable to speculate that the targets for the *Kr* protein binding might be internal (see the above ACAAAA box) and/or that its multiple fingers allow binding during the rapid DNA replication that occurs at the time *Kr* is first expressed[12,13]. In addition, as the ACAAAA box occurs three times in a hypothetical secondary structure of *Kr* mRNA (Fig. 4*b*) and twice in mRNA of the pair-rule segmentation gene[31] *fushi tarazu* (*ftz*; Fig. 4*c*), it could allow the *Kr* protein to interact with its own gene and/or the derived mRNA (for autoregulation at the transcriptional and/or translational level) and to regulate *ftz* gene expression in the *Kr* domain of the embryo defined by *Kr* mutants. The latter proposal is based on changes in the *ftz* expression pattern in Kr^- embryos which suggest that Kr^+ activity is required for normal *ftz* gene expression (S. Carroll and M. Scott; P. Ingham; W. J. Gehring, personal communications).

In *Drosophila*, the finger motif is seen in several proteins encoded by the *serendipity* (*sry*) locus[32,33]. This observation and the structural homology to the frog TFIIIA suggest conservation of the finger motif. We suspect an ancestral single functional unit that binds to a half-turn of DNA[18]. During evolution, the finger unit may have multiplied by sequence duplication or gene conversion[34] and adjusted to more subtle and specialized sequences by joining several similar units in series. In this way, the many-fingered protein offers an ideal way of recognizing specific DNA sequences through changing the amino acids at the fingertips and, therefore, modulating the DNA binding. This allows a huge number of combinatorial possibilities for specific DNA binding, all based on this structural scheme. This combinatorial aspect resembles protein recognition and protein binding by antibodies, and in view of this, it is not surprising

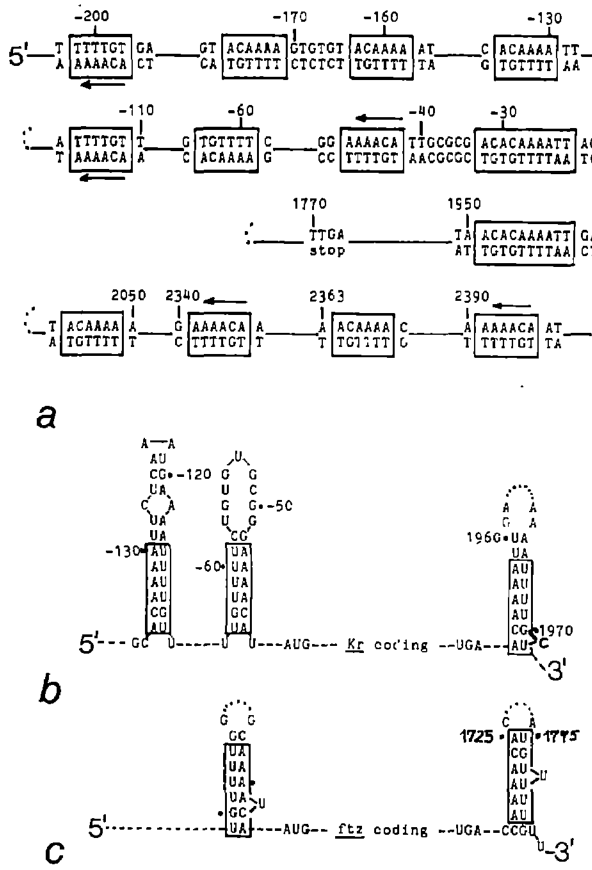

Fig. 4 Distribution of small repeated sequences in *Kr* genomic DNA and in a presumptive secondary structure of *Kr* and *ftz* mRNA. *a*, Nucleotide sequence of *Kr* untranslated 5′ and 3′ sequences. Nucleotide numbers refer to positions in Fig. 2. Note the eight repeats of the ACAAAA sequence (orientation indicated by arrows) within 180 bp at the 5′ end, the five repeats at the 3′ end and an extended 10-bp repeat (large boxes) at both the 5′ and 3′ end. A hypothetical palindrome structure of *Kr* (*b*) and *ftz* (*c*) mRNA leaving two and one ACAAAA palindrome at the 5′ and 3′ end of *Kr* mRNA, respectively, and one each at the 5′ and 3′ end of *ftz* mRNA. Note that the 5′ palindrome was recovered in *ftz* cDNA (for details and discussion see ref. 15, Fig. 4) and in *Kr* pcK2b cDNA (see Fig. 2), being part of the hairpin structure which possibly serves as primer for the synthesis of the second cDNA strand. The numbering of nucleotides refers to Fig. 2.

to detect, under conditions of reduced stringency, *Kr*-homologous sequences (S.C. *et al.*, in preparation) which may reflect *Kr*-related members of the 'finger protein gene family' in addition to TFIIIA, *sry* and *Kr*.

We thank M. Rosbash and A. Vincent for pointing out the Klug paper to us and for sharing unpublished data, and M. Goldschmidt-Clermont, David Marcey, P. Ekblom, Ch. Nüsslein-Volhard, A. Gierer, R. Lehmann, H. Saumweber, U. Schwarz, D. Marcey, T. Berleth, U. Nauber, I. Baxivanelis and R. Groemke-Lutz for their many and various contributions. S.C. was supported by a NSERC of Canada postdoctoral fellowship.

Note added in proof: The TFIIIA structure has also been described by Brown *et al.*[35].

Received 9 October; accepted 19 November 1985.

1. Wieschaus, E. & Gehring, W. *Devl Biol.* **50**, 249–263 (1976).
2. Szabad, J., Schüpbach, T. & Wieschaus, E. *Devl Biol.* **73**, 265–271 (1979).
3. Simcox, A. A. & Sang, J. H. *Devl Biol.* **97**, 212–221 (1983).
4. Nüsslein-Volhard, C. in *Determinants of Spatial Organisation* (eds Subtelney, S. & Konigsberg, I. R.) 185–211 (Academic, New York, 1979).
5. Schubiger, G., Moseley, R. C. & Wood, W. J. *Proc. natn. Acad. Sci. U.S.A.* **74**, 2050–2053 (1977).
6. Nüsslein-Volhard, C. & Wieschaus, E. *Nature* **287**, 283–295 (1980).
7. Wieschaus, E., Nüsslein-Volhard, C. & Jürgens, G. *Wilhelm Roux Arch. dev. Biol.* **193**, 296–307 (1984).
8. Nüsslein-Volhard, C., Wieschaus, E. & Kluding, H. *Wilhelm Roux Arch. dev. Biol.* **193**, 267–282 (1984).
9. Jürgens, G., Kluding, H., Nüsslein-Volhard, C. & Wieschaus, E. *Wilhelm Roux Arch. dev. Biol.* **193**, 283–295 (1984).
10. Nüsslein-Volhard, C., Wieschaus, E. & Jürgens, G. *Verh. dt. zool. Ges.*, 91–104 (1982).
11. Wieschaus, E., Nüsslein-Volhard, C. & Kluding, G. *Devl Biol.* **104**, 172–186 (1984).
12. Preiss, A., Rosenberg, U. B., Kienlin, A., Seifert, E. & Jäckle, H. *Nature* **313**, 27–32 (1985).
13. Knipple, D. C. *et al. Nature* **317**, 40–44 (1985).
14. Kozak, M. *Nucleic Acids Res.* **12**, 857–872 (1984).
15. Laughton, A. & Scott, M. P. *Nature* **310**, 25–31 (1984).
16. Poole, S., Kauvar, L. M., Drees, B. & Kornberg, T. *Cell* **40**, 37–43 (1985).
17. Marshall, R. D. *A. Rev. Biochem.* **41**, 673–702 (1972).
18. Miller, J., McLachlan, A. D. & Klug, A. *EMBO J.* **4**, 1609–1614 (1985).
19. Pelham, H. R. B. & Brown, D. D. *Proc. natn. Acad. Sci. U.S.A.* **77**, 4170–4174 (1980).
20. Hoda, B. W. & Roeder, R. G. *Cell* **22**, 119–126 (1980).
21. Ohlendorf, D. H. & Matthews, B. W. *A. Rev. Biophys. Bioengng* **12**, 259–284 (1983).
22. McGinnis, W., Levine, M., Hafen, E., Kuroiwa, A. & Gehring, W. J. *Nature* **308**, 428–433 (1984).
23. McGinnis, W., Garber, R. L., Wirz, J., Kuroiwa, A. & Gehring, W. J. *Cell* **37**, 403–408 (1984).
24. Carrasco, A. E., McGinnis, W., Gehring, W. J. & De Robertis, E. M. *Cell* **37**, 409–414 (1984).
25. Shepherd, J. C. W., McGinnis, W., Carrasco, A. E., De Robertis, E. M. & Gehring, W. J. *Nature* **310**, 70–71 (1984).
26. Levine, M., Rubin, G. & Tjian, R. *Cell* **38**, 667–673 (1984).
27. Fjose, A., McGinnis, W. J. & Gehring, W. J. *Nature* **313**, 284–289 (1985).
28. Meinhard, H. *Ber. Bunsenges. phys. Chem.* **89**, 691–699 (1985).
29. Meinhard, H. *J. Cell Sci.* (in the press).
30. Dyan, W. S. & Tjian, R. *Nature* **316**, 774–777 (1985).
31. Kuroiwa, A., Hafen, E. & Gehring, W. J. *Cell* **37**, 825–831 (1984).
32. Vincent, A., O'Connell, P., Gray, M. R. & Rosbash, M. *EMBO J.* **3**, 1003–1013 (1984).
33. Vincent, A., Colot, H. V. & Rosbash, M. *J. molec. Biol.* **186**, 149–166 (1985).
34. Hood, L. M., Campbell, J. H. & Elgin, S. C. R. *A. Rev. Genet.* **9**, 305–334 (1975).
35. Brown, R. S., Sander, C. & Argos, P. *FEBS Lett.* **186**, 271–274 (1985).

Induction of yeast Ty element transcription by ultraviolet light

Mark Rolfe, Ad Spanos & Geoffrey Banks

Genetics Division, National Institute for Medical Research,
The Ridgeway, Mill Hill, London NW7 1AA, UK

Gene expression induced in response to DNA damage is now well characterized in *Escherichia coli* (reviewed in ref. 1), and the functions of the proteins encoded by some of these genes are also understood. Physiological evidence has implicated similar responses in eukaryotes[2–9], and recently DNA sequences whose transcription can be induced by ultraviolet (UV) irradiation have been identified and cloned from the yeast *Saccharomyces cerevisiae*[10–12]. With the exception of the *Ustilago maydis* Rec1 protein, however[13], no inducible eukaryotic proteins have been characterized with respect to their role in post-irradiation DNA metabolism. Using differential colony hybridization methods, we have described the cloning of four *S. cerevisiae* DNA sequences whose transcript levels increase ~10-fold after a dose of UV irradiation which was previously shown to induce two novel proteins in yeast[12,14]. Although they possess different restriction enzyme maps, these sequences did share elements of homology as defined by cross-hybridization experiments. We show here that all four sequences possess homology with yeast Ty elements. These elements comprise a family of heterogeneous, dispersed and moderately repetitive transposable DNA sequences which are present as ~30 copies per haploid genome in laboratory strains and whose archetypal structure is shown in Fig. 1 (refs 15, 16 and reviewed in ref. 17). We also show directly that the 5.7-kilobase (kb) major Ty transcript, initiated in one terminal direct repeat sequence (δ) and terminated in the other[18], is induced by UV irradiation.

To confirm that the cloned yeast DNA in plasmids pMR1, pUV1, pUV2 and pUV3 (ref. 12) contained Ty element sequences, chromosomal DNA was cleaved by the *Xho*I restriction enzyme and hybridized to each labelled plasmid and to an intact Ty*1-15* element in turn. Most Ty elements contain a *Xho*I cleavage site in each δ sequence, but none in the intervening sequences, and so genomic cleavage generates characteristic 5.7-kb Ty fragments (see Fig. 1). Figure 2 shows that each plasmid hybridized to such a 5.7-kb *Xho*I chromosomal DNA

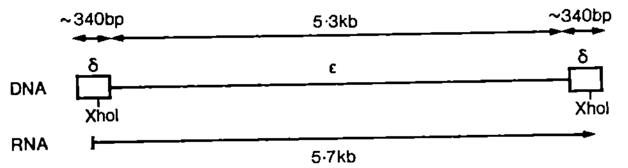

Fig. 1 Generalized Ty element structure. Delta (δ) sequences of ~0.34 kb, usually containing *Xho*I restriction enzyme sites, are separated by ~5.3 kb of epsilon (ε) sequence. Transcription is initiated in one δ, extends through the ε sequence and terminates in the other δ, producing a 5.7-kb RNA transcript[15,16,18].

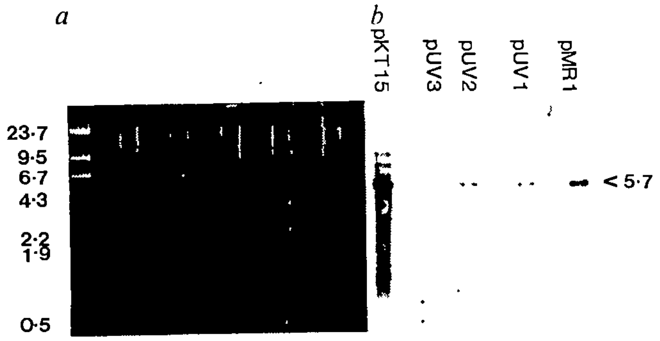

Fig. 2 Hybridization of chromosomal Ty elements to the four cloned inducible yeast DNA sequences[12]. Total *S. cerevisiae* YNN27 DNA was digested with *Xho*I enzyme, electrophoresed and transferred to nitrocellulose[25]. Plasmids pKT15, pMR1, pUV1, pUV2 and pUV3 were labelled by nick-translation[26] and hybridized to the immobilized *Xho*I fragments[27]. The 5.7-kb *Xho*I fragment characteristic of Ty elements is arrowed. *Hin*dIII-digested λ DNA was run as a size marker (left-hand lane, with fragment sizes in kb). *a*, Ethidium bromide fluorescence of DNA digests after electrophoresis. *b*, Hybridizations to the DNA probes (shown above the lanes) after transfer of the digests to nitrocellulose.

fragment, indistinguishable from that to which the Ty*1-15* sequence hybridized. Specific plasmid to plasmid hybridization experiments with Ty and δ probes also confirmed this conclusion (data not shown).

We have previously shown that sequences in all four of the cloned yeast DNA fragments hybridize to yeast transcripts of identical size whose abundances increase ~10-fold after UV irradiation[12]. To identify these transcripts more definitively, equal amounts of total RNA from UV-irradiated and from unirradiated yeast cells were probed with labelled pMR1 and with pKT1-15 (containing the Ty*1-15* element) DNA after electrophoretic separation and Northern transfer of the RNA. Figure 3*a* shows that both probe sequences hybridized to transcripts of identical size (5.7 kb) whose abundance after UV irradiation increased about 10-fold. Hybridization of these RNAs with a labelled plasmid encoding the non-inducible yeast proteins H2A and Protein 1 demonstrated the specificity of the induction of the Ty element transcription (Fig. 3*b*).

The evidence presented above demonstrates that transcription of yeast transposable Ty elements is strongly stimulated by UV irradiation and identifies the δ sequence promoter as being UV-inducible. Because our experiments measured steady-state messenger RNA levels, it is possible that an increase in mRNA stability contributes to the observed increase in transcript levels after UV irradiation. It has also been established recently that the transcription of the *Drosophila melanogaster copia* element is induced by environmental stress such as elevated temperature and exposure to certain chemicals[19]. The elegant experiments of Boeke and co-workers have established that increased levels of Ty transcripts are correlated with increased transposition of marked Ty elements to a target plasmid and to chromosomal locations[20]. Their experiments also implicate an RNA intermediate in the pathway of transposition, thereby inviting comparison with the structure and mode of integration of retroviruses into a host chromosome (refs 20-22 and reviewed in refs 23, 24). We are now investigating whether the increased Ty element transcription induced by UV irradiation of yeast cells is accompanied by Ty transposition events. Such a process may well contribute to the induction of mutations and other chromosomal aberrations by UV irradiation.

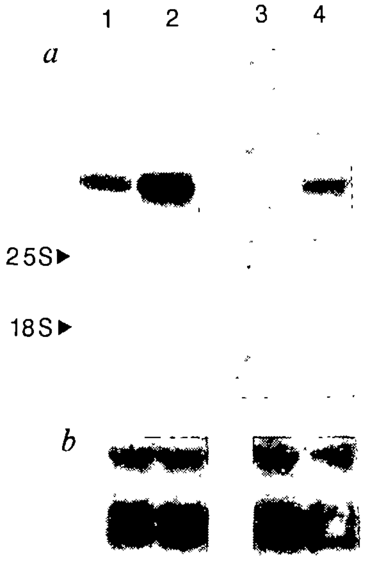

Fig. 3 *a*, Hybridization of pKT15 (lanes 1, 2) and pMR1 (lanes 3, 4) DNAs to RNA from unirradiated (lanes 1, 3) or UV-irradiated (lanes 2, 4) *S. cerevisiae* YNN27 cells. The cells were irradiated and total RNA extracted as described previously[12]. The resulting RNA was denatured by glyoxal and dimethyl sulphoxide, electrophoresed through a 1% agarose gel[28] and transferred to Gene Screen Plus membranes before hybridization. The mobilities of the two largest ribosomal RNAs are indicated. *b*, Control hybridization of the RNAs with a plasmid pMH501 probe. pMH501 contains an *Sst*I fragment of TRT-1 DNA in the vector pEMBL18 and thus carries the yeast H2A and Protein 1 genes[29]. The upper band is an uncharacterized, strain-dependent hybridization (L. Capsey, personal communication).

We thank Drs Alan Kingsman, Peter Phillipsen and Ron Davis for gifts of plasmids used in this work, and Steven Sedgwick and Robin Holliday for discussions.

Received 16 May; accepted 3 December 1985.

1. Walker, G. C. *Microbiol. Rev.* **48,** 60–93 (1984).
2. Holliday, R. *Mutat. Res* **29,** 149–153 (1975).
3. Moore, P. D. *Mutat. Res.* **28,** 367–380 (1975).
4. Fabre, F. & Roman, H L. *Proc. natn. Acad. Sci. U.S.A.* **74,** 1667–1671 (1977).
5. Leaper, S., Resnick, M. A. & Holliday, R. *Genet. Res. Camb.* **35,** 291–307 (1980)
6. Stadler, D. & Moyer, R *Genetics* **98,** 763–774 (1981).
7. Lee, M. G. & Yarranton, G. T. *Molec. gen. Genet.* **185,** 245–250 (1982).
8. Baker, T. I. *Molec. gen. Genet.* **190,** 295–299 (1983).
9. Siede, W., Eckardt, F. & Brendel, M. *Molec. gen. Genet.* **190,** 406–412 (1983).
10. McClanahan, T. & McEntee, K. *Molec. cell. Biol.* **4,** 2356–2363 (1984).
11. Ruby, S. W. & Szostak, J. W *Molec. cell. Biol.* **5,** 75–84 (1985).
12. Rolfe, M. *Curr. Genet.* **9,** 533–538 (1985).
13. Kmiec, E., Brougham, M., Yarnall, M., Kroeger, P. E. & Holloman, W. K. *UCLA Symp. molec. cell. Biol.* **10,** 753-760 (1983).
14. Rolfe, M. *Curr. Genet.* **9,** 529–532 (1985).
15. Cameron, J. R., Loh, E. Y. & Davis, R. *Cell* **16,** 739–751 (1979).
16. Kingsman, A. J , Gimlich, R. L., Clarke, L., Chinault, A. C. & Carbon, J. *J. molec. Biol.* **145,** 619-632 (1981)
17. Williamson, V. M *Int. Rev. Cytol.* **83,** 1-25 (1983).
18. Elder, R. T., St John, T. P., Stinchcomb, D. T. & Davis, R. W. *Cold Spring Harb. Symp. quant. Biol.* **45,** 581-584 (1981).
19. Strand, D. J. & McDonald, J. F. *Nucleic Acids Res.* **13,** 4401–4410 (1985).
20. Boeke, J. D., Garfinkel, D. J., Styles, C. A. & Fink, G. R. *Cell* **40,** 491–500 (1985).
21. Mellor, J. *et al. Nature* **313,** 243–246 (1985).
22. Hauber, J , Nelbock-Hochstatter, P. & Feldmann, H. *Nucleic Acids Res.* **13,** 2745–2758 (1985).
23. Baltimore, D. *Cell* **40,** 481–482 (1985).
24. Varmus, H. E. *Nature* **314,** 583–584 (1985).
25. Southern, E. M. *J molec. Biol.* **98,** 503–517 (1975).
26. Rigby, P. W. J., Dieckmann, M., Rhodes, C. & Berg, P. *J. molec. Biol.* **113,** 737–751 (1977).
27. Maniatis, T., Fritsch, E. F. & Sambrook, J. in *Molecular Cloning,* 124 (Cold Spring Harbor Laboratory, New York, 1982).
28. Thomas, P. S. *Proc. natn. Acad. Sci. U.S.A.* **77,** 5201–5205 (1980).
29. Hereford, L., Fahrner, K , Woolford, J. Jr, Rosbash, M. & Kaback, D. B. *Cell* **18,** 1261–1271 (1979).

BOOKS RECEIVED

Physics

Aspects of Matter in Science Today: Discussion with Emile Noël. W.J. DUFFIN (ed.). *W.J. Duffin, 14 Orchard Croft, Cottingham, North Humberside HU16 4HG, England: 1985. Pp.196. Pbk ISBN 0-9510438-0-3. Pbk £3.95.*

Classical and Quantum Field Theory of Exactly Soluble Nonlinear Systems. By PIOTR GARBACZEWSKI. *Wiley: 1985. Pp.244. ISBN 9971-966-55-7. £33.85.*

Collisions of Fast Charged Particles in Solids. By N.P. KALASHNIKOV, V.S. REMIZOVICH and M.I. RYAZANOV. KONSTANTIN ERASTOV (trans.). *Gordon & Breach: 1985. Pp.438. Hbk ISBN 2-88124-039-9. $145.00*

Einstein's Relativity The Greatest Fallacy in the Twentieth Century. By SHARAD TIPNIS. *Madhav Publications, 40/1 Dattakrupa, Adarshnagar, Pune-Satara Road, Pune-411 037, India: 1985. Pp.199. Rs.90.*

Electroweak Effects at High Energies. HARVEY B. NEWMAN (ed.). *Plenum: 1985. Pp.866. ISBN 0-306-41904-1. Np.*

Entropy, Large Deviations, and Statistical Mechanics. By RICHARD S. ELLIS. *Springer-Verlag: 1985. Pp.364. Hbk ISBN 3-540-96052-X. DM 184.*

Fourier Transforms in Physics. By D.C. CHAMPENEY. *Adam Hilger: 1985. Pp.64. Pbk ISBN 0-85274-794-2. Pbk £2.95.*

Fundamentals of Laser Interactions. F. EHLOTZKY (ed.). *Springer-Verlag: 1985. Pp.314. Pbk ISBN 3-540-15640-2/0-387-15640-2. Np.*

Large-scale Computations in Fluid Mechanics. BJORN E. ENGQUIST, STANLEY OSHER and RICHARD C.J. SOMERVILLE (eds). *American Mathematical Society, Providence, Rhode Island: 1985. Pp.370. Hbk ISBN 0-8218-1122-3. Np.*

Lecture Notes In Physics. Hadrons and Heavy Ions, Proceedings, Cape Town, South Africa 1984. W.D. HEISS (ed.). *Springer-Verlag: 1985. Pp.458. Pbk ISBN 3-540-15653-4. DM 73.*

Macroscopic Modelling of Turbulent Flows. U. FRISCH *et al.* (eds). *Springer-Verlag: 1985. Pp.360. Pbk ISBN 3-540-15644-5/0-387-15644-5. Pbk DM 45.*

Magnetospheric and Ionospheric Plasmas. E.R. SCHMERLING, S.W.H. COWLEY and P.H. REIFF (eds). *Pergamon: 1985. Pp.426. Pbk ISBN 0-08-033193-9. Pbk $49.50, £31.*

Maxwell's Equations and their Applications. By E.G. THOMAS and A.J. MEADOWS. *Adam Hilger: 1985. Pp.54. Pbk ISBN 0-85274-778-0. Pbk £2.95.*

Mechanics of Continua and Wave Dynamics. By L. BRETHOVSKIKH and V. GONCHAROV. *Springer-Verlag: 1985. Pp.342. ISBN 3-540-13765-3. DM 139.*

Muon Spin Rotation Spectroscopy: Principles and Applications in Solid State Physics. By A. SCHENCK. *Adam Hilger: 1985. Pp.325. ISBN 0-85274-551-6. £39, $58.*

Oscillations and Waves. By R. BUCKLEY. *Adam Hilger: 1985. Pp.64. Pbk ISBN 0-85274-793-4. Pbk £2.95.*

Physics of Magnetic Materials, Jadwisin '84 (Poland). J. RAULUSZKIEWICZ, H. SZYMCZAK and H.K. LACHOWICZ (eds). *Wiley: 1985. Pp.580. ISBN 9971-978-34-2. £57.15.*

Quantum Reality: Beyond the New Physics. By NICK HERBERT. *Anchor/Doubleday: 1985. Pp.268. ISBN 0-385-18704-1. $16.95.*

Quarks, Leptons, and Beyond. H. FRITZSCH, R.D. PECCEI, H. SALLER and F. WAGNER (eds). *Plenum: 1985. Pp.555. ISBN 0-306-41925-4. Np.*

Roundabout: The Physics of Rotation in the Everyday World. Readings from Scientific American. By JEARL WALKER. *W.H. Freeman: 1985. Pp.70. Hbk ISBN 0-7167-1724-7; pbk ISBN 0-7167-1725-5. Hbk $19.95; pbk $11.95.*

Spectrometric Techniques, Vol.4. GEORGE A. VANASSE (ed.). *Academic: 1985. Pp.262. Hbk ISBN 0-12-710404-6. $75.50, £65.50.*

Springer Series in Chemical Physics, Vol.41: High Resolution Spectral Atlas of Nitrogen Dioxide 559 – 597 nm. By K. UEHARA and H. SASADA. *Springer-Verlag: 1985. Pp.226. ISBN 3-540-15027-7, 0-387-15027-7. DM 99.*

Biological Sciences

The Grizzlies of Mount McKinley. By ADOLPH MURIE. *University of Washington Press:1985. Pp.270. Pbk ISBN 0-295-96204-6. Pbk $9.95.*

Growth, Health and Fitness of Teenager. H.C.G. KEMPER (ed.). *Karger:1985. Pp.202. ISBN 3-8055-4042-6. DM 139, $49.50.*

Habitat Selection in Birds. MARTIN L. CODY (ed.). *Academic:1985. Pp.558. ISBN 0-12-178080-5. $69.50, £69.50.*

Hawk-Moths of the British Isles. By MICHAEL EASTERBROOK. *Shire Natural History:1985. Pp.24. Pbk ISBN 0-85263-743-8. Pbk £1.25.*

Hormones: The Messengers of Life. By LAWRENCE CRAPO. *Freeman:1985. Pp.194. Hbk ISBN 0-7167-1757-3; pbk ISBN 0-7167-1753-0. Hbk $19.95; pbk $11.95.*

Human Nature: Darwin's View. By ALEXANDER ALLAND Jr. *Columbia University Press:1985. Pp.242. Hbk ISBN 0-231-05898-5. $25.*

Immune Recognition of Protein Antigens. Current Communications in Molecular Biology. W. GRAEME LAVER and GILLIAN M. AIR. *Cold Spring Harbor Laboratory, P.O. Box 100, Cold Spring Harbor, New York 11724, USA:1985. Pp.197. Pbk ISBN 87969-185-9. $30.*

Immunology of the Bacterial Cell Envelope. D.E.S. STEWART-TULL and M. DAVIES (eds). *Wiley:1985. Pp.391. ISBN 0-471-90551-6. £40.*

Interface between Neurology and Psychiatry. M.R. TRIMBLE (ed.). *Karger:1985. Pp.190. ISBN 3-8055-4023-X. DM 137, $48.50.*

International Review of Cytology. G.H. BOURNE and J.F. DANIELLI (eds). *Academic:1985. Pp.306. ISBN 0-12-364494-1. $49.50, £49.50.*

International Review of Neurobiology, Vol. 26. JOHN R. SMYTHIES and RONALD J. BRADLEY (eds). *Academic:1985. Pp.342. ISBN 0-12-366826-3. $65, £65,*

Intrinsic Motivation and Self-Determination in Human Behaviour. By EDWARD L. DECI and RICHARD M. RYAN. *Plenum:1985. Pp.371. Hbk ISBN 0-306-42022-8. Np.*

Mamiferos Silvestres de la Cuenca de Mexico. By GERARDO CEBALLOS GONZALEZ and CARLOS GALINDO LEAL. *Instituto de Ecologia, A.C., Apartado Postal 18–845, Delef Migual Hidalgo, 11800 Mexico, DF:1985. Pp.299. ISBN 968-18-1700-1. $15.*

Mechanisms of Cell-Mediated Cytotoxicity II. PIERRE HENKART and ERIC MARTZ (eds). *Plenum:1985. Pp.568. ISBN 0-306-42009-0. Np.*

Mechanisms of Cytotoxicity by NK Cells. RONALD B. HERBERMAN and D.M. CALLEWAERT (eds). *Academic:1985. Pp.669. Hbk 0-12-341370-2. £49.50, $57.*

Modification of Proteins During Aging. RICHARD C. ADELMAN and EUGENE E. DEKKER (eds). *Alan R. Liss.:1985. Pp.122. Hbk ISBN 0-8451-2307-6. £25.*

The Modulation of Immunity. M.S. MITCHELL (ed.). *Pergamon:1985. Pp.478. ISBN 0-08-031977-7. £80, $130.*

Molecular Basis of Nerve Activity. J.-P. CHANGEUX, F. HUCHO, A. MAELICKE and E. NEUMANN (eds). *Walter de Gruyter & Co., 13 Genthiner Str., 1000 Berlin 30, FRG:1985. Pp.784. Hbk ISBN 311-010345-1. DM 260.*

The Molecular Biology of the Bacilli. DAVID A. DUBNAU (ed.). *Academic:1985. Pp.259. ISBN 0-12-2227702-6. $49, £49.*

Molecular Structure of the Number 21 Chromosome and Down's Syndrome. GEORGE F. SMITH (ed.). *New York Academy of Sciences:1985. Pp.250. Pbk ISBN 0-89766-295-4. Np.*

Molecule, Nerve and Embryo. By RICHARD R. RIBCHESTER. *Blackie:1985. Pp.204. Hbk ISBN 0-216-91800-6. £14.95.*

Neuroendocrine Perspectives. EUGENIO E. MULLER, ROBERT U.M. MACLEOD and LAWRENCE A. FROHMAN (eds). *Elsevier Biomedical Press:1985. Pp.301. Hbk ISBN 0-444-80665-2. Dfl 216, $65.*

Neuro-Oncology. F.CLIFFORD ROSE and W.S. FIELDS (eds). *Karger:1985. Pp.274. Hbk ISBN 3-8055-4050-X. SwFr. 230, DM 276, £71.90, $98.*

Organized Multienzyme Systems Catalytic Properties. G. RICKEY WELCH (ed.). *Academic:1985. Pp.458. Hbk ISBN 0-12-744040-2. £65, $75.*

The Origin and Evolution of Sex. MBL Lectures in Biology, Vol. 7. HARLYN O. HALVORSON and ALBERTO MONROY (eds). *Alan R Liss:1985. Pp.350. Hbk ISBN 0-8451-2206-1. £52.*

Oro-Facial Pain and Neuromuscular Dysfunction: Mechanisms and Clinical Correlates. I. KLINBERG and B. SESSLE (eds). *Pergamon:1985 Pp.229. ISBN 0-08-032001-5. £48, $82.*

Parasitic Worms. By JIM FLEGG *Shire Natural History:1985. Pp.24. Pbk ISBN 0-85263-761-6 Pbk £1.25.*

The Peccaries. By LYLE K. SOWLS. *University of Arizona Press:1984. Pp.251. ISBN 0-8165-0822-4. $22.50.*

Pelargonium Family. By WILLIAM J. WEBB. *Croom Helm:1984. Pp.104. ISBN 0-7099-2737-7 £19.95.*

Physiological Strategies in Avian Biology. By J.G PHILLIPS, P.J. BUTLER and P.J. SHARP *Blackie:1985. Pp.218. Hbk ISBN 0-412-00921-8; pbk ISBN 0-412-00931-5. Hbk £19.95; pbk £9.95.*

The Pineal Gland: Endocrine Aspects. G.M BROWN and S.D. WAINWRIGHT (eds) *Pergamon:1985. Pp.367. Pbk ISBN 0-08-031991-2 Pbk £31.*

Protein and Nucleic Acid Structure and Dynamics. JONATHAN KING (ed.). *Addison-Wesley, Wokingham, Berkshire, UK:1985. Pp.587. Hbk ISBN 0-8053-5403-4. £29.95.*

Proteinuria. M.M. AVRAM (ed.) *Plenum:1985. Pp.232. ISBN 0-306-41956-4. Np.*

The Puffin. By JIM FLEGG. *Shire Natural History:1985. Pp.24. Pbk ISBN 0-85263-744-6. Pbk £1.25.*

The Pulmonary Circulation and Acute Lung Injury. SAMI I. SAID (ed.). *Futural Publishing, 295 Main Street, Mount Kisco, New York 10549:1985. Pp.472. ISBN 0-87993-249-X. $65.*

The Receptor, Vol. 2. P. MICHAEL CONN (ed.). *Academic:1985. Pp.436. Hbk ISBN 0-12-185202-4. £56.50, $65.*

Regulation of Pituitary Function. Tj.B VAN WIMERSMA GREIDANUS and S.W.J. LAMBERTS (eds). *Karger:1985. Pp.218. Hbk ISBN 3-8055-4061-2. SwFr. 179, DM 214, £56, $76.25.*

Sharks of the World. By RODNEY STEEL *Blandford Press, Link House, West Street, Poole, Dorset BH15 1LL, UK:1985. Pp.192. Hbk ISBN 0-7137-1425-5. £10.95.*

Sleep: Neurotransmitters and Neuromodulators. A. WAUGUIER *et al.* (eds). *Raven:1985. Pp.344. ISBN 0-88167-102-9. $63.*

Snail. By JENS OLESEN. *A. and C. Black:1985. Pp.25. Hbk ISBN 0-7136-2708-5. £3.95.*

Spectroscopy and the Dynamics of Molecular Biological Systems. PETER M. BAYLEY and ROBERT E. DALE (eds). *Academic:1985. Pp.406. ISBN 0-12-083240-2. $42.50, £38.50.*

Spectroscopy of Biological Molecules. A.J.P. ALIX, L. BERNARD and M. MANFAIT (eds), *Wiley:1985. Pp.465. ISBN 0-471-90883-5. £28.*

The Starling. By C.J. FEARE. *Shire Natural History:1985. Pp.24. Pbk ISBN 0-85263-764-0. Pbk £1.25.*

Statistics in Ornithology. B.J.T. MORGAN and P.M. NORTH (eds). *Springer-Verlag:1985 Pp.418. Pbk ISBN 3-540-96189-5. DM 65.*

The Status of Ecological Reserves in Canada. By P.M. TASCHEREAU. *Institute for Resource and Environmental Studies:1985. Pp.120. Pbk ISBN 0-7703-0462-1. Pbk $8.*

Structure and Function of Sarcoplasmic Reticulum. SIDNEY FLEISCHER and YUJI TONOMURA (eds). *Academic:1985. Pp.597. ISBN 0-12-260380-X. $49, £49.*

Tidal Flat Ecology; An Experimental Approach to Species Interactions. By KARSTEN REISE. *Springer-Verlag:1985. Pp.191. Hbk ISBN 3-540-15447-7. DM 98.*

Viral Haemorrhagic Fevers: Report of a WHO Expert Committee. Technical Report Series 721. *World Health Organization:1985. Pp.126. Pbk ISBN 92-4-120721-3. SwFr. 10.*

Whales, Dolphins and Seals and their Kin. *Longman Nature Library, Longman:1985. Pp.130. Hbk ISBN 0-582-89262-7. Np.*

Willows of the British Isles. By THERESA BRENDELL. *Shire Natural History:1985. Pp.24. Pbk ISBN 0-85263-765-9. Pbk £1.25.*

The Wolves of Mount McKinley. By ADOLPH MURIE. *University of Washington Press:1985. Pp.258. Pbk ISBN 0-295-96203-8. Pbk $9.95.*

The Year in Immunology 1984–85. J.M. CRUSE and R.E. LEWIS, Jr. (eds). *Karger:1985. Pp.234. ISBN 3-8055-4025-6. DM 189, $67.25.*

Yeast Identification Program. By J.A. BARNETT, R.W. PAYNE and D. YARROW. *Cambridge Micro Software (Cambridge University Press):1985. For DEC Rainbow using MS-DOS. ISBN 0-521-30918-2. £85.*

Applied Biological Sciences

Advances in Enzyme Regulation 23. By GEORGE WEBER. *Pergamon:1985. Pp.463. ISBN 0-08-032727-3. £99, $160.*

Advances in Parasitology. Vol. 23. J.R. BAKER and R. MULLER (eds). *Academic:1984. Pp.255. ISBN 0-12-031723-0. $40, £27.*

Animal Cell Biotechnology, Vol. 2. R.E. SPIER and J.B. GRIFFITHS (eds). *Academic:1985. Pp.475. Hbk ISBN 0-12-657552-5. £59, $66.*

Approaches to Antiviral Agents. MICHAEL R. HARNDEN (ed.). *Macmillan Press:1985. Pp.350. Hbk ISBN 0-333-35928-3. £45.*

Autoimmunity and Endocrine Disease. ROBERT VOLPÉ (ed.). *Marcel Dekker:1985. Pp.488. ISBN 0-8247-7311-X. $75.*

Bacterial Endotoxins: Structure, Biomedical Significance, and Detection with the Limulus Amebocyte Lysate Test. JAN W. ten CATE, HARRY R. BULLER, AUGUESTE STURK and JACK LEVIN (eds). *Alan R. Liss:1985. Pp.466. Hbk ISBN 0-8451-5039-1. £52.*

Biochemical Pharmacology and Toxicology. Vol. 1, Methodological Aspects of Drug Metabolizing Enzymes. D. ZAKIM and D.A. VESSEY (eds). *Wiley: 1985. Pp.372. Hbk ISBN 0-471-86793-4. £66.50.*

Bone Resorption, Metastasis, and Diphosphonates. SILVIO GARATTINI (ed.). *Raven Press:1985. Pp.221. Hbk ISBN 0-88167-137-1. $43.50.*

Burkitt's Lymphoma: A Human Cancer Model. G. LENOIR, G. O'CONOR and C.L.M. OLWENY (eds). *International Agency for Research on Cancer, Lyon:1985. Pp.484. Hbk ISBN 0-19-723057-1. £20.*

Carcinoma of the Large Bowel and its Precursors. J.R.F. INGALL and A.J. MASTROMARINA (eds). *Alan R. Liss:1985. Pp.305. ISBN 0-8451-5036-7. £37.*

Cardiovascular Shunts: Phylogenetic, Ontogenetic and Clinical Aspects. KJELL JOHANSEN and WARREN BURGGREN (eds). *Munksgaard:1985. Pp.492. ISBN 87-16-09822-6. D.Kr.350.*

Care of the Burn Wound: Wound Healing, Grafts and Transplantation, Synthetic Skin Substitutes. S. RANDOLPH MAY and GIOVANNI DOGO (eds). *Karger:1985. Pp.246. ISBN 3-8055-3991-6. DM264, $93.75.*

Chemically Induced Birth Defects. By JAMES L. SCHARDEIN. *Dekker:1985. Pp.904. ISBN 0-8247-7247-4. $125.*

Chemotherapy of Gastro-Intestinal Helminths. H. VANDEN BOSSCHE, D. THIENPONT and P.G. JANSSENS (eds). *Springer-Verlag:1985. Pp.719. ISBN 3-540-13111-6/0-387-13111-6. DM660.*

Clinical Oncology and Cancer Nursing. F.J. CLETON *et al.* (eds). *Pergamon:1985. Pp.125. Pbk ISBN 0-08-030786-8. Pbk £21, $34.*

Cooperative Approaches to Research and Development of Orphan Drugs. MELVIN H. VAN WOERT and EUNYONG CHUNG (eds). *Alan R. Liss:1985. Pp.210. Hbk ISBN 0-8451-5047-2. $36.*

The Cytobiology of Leukaemias and Lymphomas. D. QUAGLINO and F.G.J. HAYHOE (eds). *Raven Press:1985. Pp.524. Hbk ISBN 0-88167-091-X. $65.50.*

Diagnosis and Treatment of Erectile Disturbances: A Guide for Clinicians. R. TAYLOR SEGRAVES and HARRY W. SHEONBERG (eds). *Plenum:1985. Pp.253. ISBN 0-306-41871-1. Np.*

Diagnostic Accuracy: Effect on Treatment Planning. ROBERT J. SHPRINTZEN and NATALIE W. PAUL (eds). *Alan R. Liss:1985. Pp.151. ISBN 0-8451-1059-4. £28.*

Drugs Affecting Lipid Metabolism VIII. DAVID KRITCHESVKY, WILLIAM L. HOLMES and RODOLFO PAOLETTI (eds). *Plenum:1985. Pp.502. ISBN 0-306-41914-9. Np.*

Environmental Carcinogens: Selected Methods of Analysis. Vol. 7: Some Volatile Halogenated Hydrocarbons. L. FISHBEIN and I.K. O'NEILL (eds). *Oxford University Press:1985. Pp.479. Hbk ISBN 92-832-1168-5. £20.*

Enzyme-Mediated Immunoassay. T.T. NGO and H.M. LENHOFF (eds). *Plenum:1985. Pp.489. Hbk ISBN 0-306-42085-6. Np.*

Experimental Assessments and Clinical Applications of Conditioned Food Aversions. NORMAN S. BRAVEMAN and PAUL BRONSTEIN (eds). *New York Academy of Sciences:1985. Pp.441. Pbk ISBN 0-89766-281-4. Np.*

Experiments in Plant Tissue Culture, 2nd Edn. By JOHN H. DODDS and LORIN W. ROBERTS. *Cambridge University Press:1985. Pp.232. Hbk ISBN 0-521-30478-4; pbk ISBN 0-521-31516-6. Hbk £25, $44.50; pbk £8.95, $14.95.*

Fish Aquaculture: Technology and Experiments. By CHRISTOPH MESKE. *Pergamon:1985. Pp.237. Pbk ISBN 0-08-024191. Hbk £30, $48; pbk £19, $30.*

Growth Factors and Transformation, Cancer Cells 3. J. FERAMISCO, B. OZANNE and C. STILES (eds). *Cold Spring Harbor Laboratory, P.O. Box 100, Cold Spring Harbor, New York 11724, USA:1985. Pp.450. Pbk ISBN 0-87969-178-6. $70.*

A Guide to Medical Endocrinology. By TAREK HASSAN. *Macmillan:1985. Pp.269. Hbk ISBN 0-333-32027-1; pbk ISBN 0-333-32029-8. Hbk £17; pbk £8.95.*

Human Prenatal Diagnosis. KAREN FILKINS and JOSEPH F. RUSSO (eds.) *Dekker:1985. Pp.424. Hbk ISBN 0-8247-7368-3. $75 (US and Canada), $90 (all other countries).*

Human Sexuality: Psychosexual Effects of Disease. MARTIN FARBER (ed.). *Collier Macmillan:1985. Pp.335. ISBN 0-0-02-336190-5. Hbk £35; pbk £25.*

Infection, Immunity, and Blood Transfusion. R.Y. DODD and L.F. BARKER (eds). *Alan R. Liss:1985. Pp.464. ISBN 0-8451-5032-4. £52.*

The Inflammatory Reaction. By HENRY ZOLTAN MOVAT. *Elseview:1985. Pp.365. ISBN 0-444-80662-8. $96.25.*

Inherited Disorders of Vitamins and Cofactors. G.M. ADDISON, K. BARTLETT, R.A. HARKNESS and R.J.POLLITT (eds). *MTP Press, Falcon House, Queen Sq., Lancaster, UK:1985. Pp.154. Hbk ISBN 0-85200-914-3. £29.95.*

Integrated Mosquito Control Methodologies, Vol. 2. MARSHALL LAIRD and JAMES W. MILES (eds). *Academic:1985. Pp.444. ISBN 0-12-434002-4. $85, £65.50.*

International Review of Experimental Pathology, Vol. 27. G.W. RICHTER and M.A. EPSTEIN (eds). *Academic:1985. Pp.246. ISBN 0-12-364927-7. $59, £59.*

Introduction to Wildlife Management. By JAMES SHAW. *McGraw-Hill:1985. Pp.316. ISBN 0-07-056481-7. £28.75.*

***In Vitro* Fertilization and Embryo Transfer.** MARKKU SEPPÄLÄ and R.G. EDWARDS (eds). *New York Academy of Sciences:1985. Pp.619. Pbk ISBN 0-89766-279-4. Pbk np.*

Issues and Reviews in Teratology, Vol. 3. HAROLD KALTER (ed.). *Plenum:1985. Pp.299. Hbk ISBN 0-306-41988-2. Np.*

Laser Application to Occlusive Vascular Disease. By MICHAEL W. BERNS and MAHMOOD MIROSEINI (eds). *Alan R. Liss:1985. Pp.344. ISBN 0-8451-0246-X. £22.*

Ligand-Binder Assays: Labels and Analytical Strategies. By LARRY J. KRICKA. *Dekker:1985. Pp.336. ISBN 0-8247-7420-5. $65.*

Macromolecules as Drugs and as Carriers for Biologically Active Materials. DAVID A. TIRRELL, L. GUY DONARUMA and ANNE B. TUREK (eds). *New York Academy of Sciences:1985. Pp.458. Pbk ISBN 0-89766-287-3. Np.*

Management of Arterial Hypertension: A Practical Guide for the Physician and Allied Health Workers. By F. GROSS, Z. PISA, T. STRASSER and A. ZANCHETTI. *World Health Organization:1985. Pp.72. Pbk ISBN 92-4-154197-0. SwFr.11.*

Memory Dysfunctions: An Integration of Animal and Human Research From Preclinical and Clinical Perspectives. DAVID S. OLTON, ELKAN GAMZU and SUSANNE CORKIN (eds). *New York Academy of Sciences:1985. Pp.553. Pbk ISBN 0-89766-283-0. Np.*

Modern Approaches to the Dementias. Part I Etiology and Pathophysiology. Part II Clinical and Therapeutic Aspects. F. CLIFFORD ROSE (ed.). *Karger:1985. Part I ISBN 3-8055-3980-0. Part II ISBN 3-8055-3981-9. Np.*

No Magic Bullet: A Social History of Venereal Disease in the United States Since 1880. By ALLAN M. BRANDT. *Oxford University Press:1985. Pp.245. ISBN 0-19-503469-4. £18.50.*

Osteoporosis. 2 Vols. C. CHRISTIANSEN *et al.* (eds). *Copenhagen International Symposium on Osteoprosis, Glostrup Hospital, University of Copenhagen, 2600 Glostrup, Denmark:1984. Vol. 1 Pp.536. Vol. 2 Pp.842. Np.*

Pathophysiological Aspects of Cancer Epidemiology. G. MATHE and R. REIZENSTEIN (eds). *Pergamon:1985. Pp.264. ISBN 0-08-030780-9. £50, $81.50.*

Patty's Industrial Hygiene and Toxicology, Vol. 3B 2nd Edn. Theory and Rationale of Industrial Hygiene Practice: Biological Responses. LEWIS J. CRALLEY and LESTER V. CRALLEY (eds). *Wiley:1985. Pp.753. ISBN 0-471-82333-3. £92.*

Pediatric Thyroidology. F. DELANGE *et al.* (eds). *Karger:1985. Pp.412. ISBN 3-8055-3777-8. DM330, $117.25.*

Peptide Hormones as Mediators in Immunology and Oncology. R.D. HESCH (ed.). *Raven Press:1985. Pp.254. Hbk ISBN 0-89004-609-3. $46.50.*

The Pharmacological Basis of Therapeutics. ALFRED GOODMAN GILMAN, LOUIS S. GOODMAN, THEODORE W. RALL and FERID MURAD (eds). *Collier Macmillan, New York:1985. Pp.1839. Hbk ISBN 0-02344710-9. £65.*

Psychophysiology of Cardiovascular Control: Models, Methods and Data. J.F. ORLEBEKE, G. MULDER and L.J.P. VAN DOORNEN (eds). *Plenum:1985. Pp.959. ISBN 0-306-42007-4. Np.*

Pulmonary Circulation in Chronic Lung Diseases: Experimental and Clinical Approach. J. WIDIMSKÝ, J. HERGET and J. MICZOCH (eds). *Karger:1985. Pp.192. ISBN 3-8055-3961-4. Np.*

Reproductive Toxicology. ROBERT L. DIXON (ed.). *Raven:1985. Pp.368. ISBN 0-89004-474-0. $76.50.*

Retinal Degeneration. Experimental and Clinical Studies. MATTHEW M. LAVAIL, JOE G. HOLLYFIELD and ROBERT E. ANDERSON (eds). *Alan R. Liss:1985. Pp.485. Hbk ISBN 0-8451-4200-3. £53.*

Soil Fertility and Fertilizers, 4th Edn. By SAMUEL L. TISDALE, WERNER L. NELSON and JAMES D. BEATON. *Macmillan, NY:1985. Pp.754. Pbk ISBN 0-02-946760-8. Pbk £14.95.*

Testicular Cancer and Other Tumors of the Genitourinary Tract. M. PAVONE-MACALUSO, P.H. SMITH and M.A. BAGSHAW (eds). *Plenum:1985. Pp.537. ISBN 0-306-41906-8. Np.*

Third European Congress on Biotechnology. Proceedings Vol. IV. EUROPEAN FEDERATION OF BIOTECHNOLOGY. *VCH Publishers:1985. Pp.592. ISBN 0-89573-524-5. Np.*

Toxicology of the Eye, Ear, and Other Special Senses. A. WALLACE HAYES (ed.). *Raven Press:1985. Pp.254. Hbk ISBN 0-89004-840-1. Np.*

Triangle. Sandoz Journal of Medical Science. Vol. 24, No. 1/2: Obstructive Lung Disease, Hypertension, Geriatric Endocrinology. *Sandoz Pharmaceuticals: 1985. Pp.70. Pbk np.*

Understanding Dental Caries: Prevention. By GORDON NIKIFORUK. *Karger:1985. Pp.288. ISBN 3-8055-3905-3. DM69, $24.75.*

Urolithiasis and Related Clinical Research. PAUL O. SCHWILLE *et al.* (eds). *Plenum:1985. Pp.997. ISBN 0-306-41931-9. Np.*

nature

How governments should be run

The latest twist in the British government's newest political crisis is less a sign that some people have behaved badly than a proof (if one were needed) that the British constitution needs changing.

WHO would have guessed, two months ago, that the fate of an unsuccessful helicopter manufacturer called Westland (see *Nature* **319**, 86; 1986) would have led to the resignation of two senior cabinet ministers and raised serious questions about the survival of the Prime Minister herself? Mr Michael Heseltine, previously Secretary of State for Defence, stormed out of a cabinet meeting on 9 January, complaining that he would be muzzled in his attempts to persuade a European consortium to rescue the nearly bankrupt helicopter company if he were compelled to check his public statements with his colleagues. Now the Secretary of State for Trade and Industry, Mr Leon Brittan, among other things the minister for helicopters, has been compelled to quit the government because of two successive blunders: concealing his knowledge of a letter bearing on the Westland issue from a commercial company (British Aerospace) because it had been marked "confidential" and, then, having taken the initiative, at an earlier stage, in leaking to the press an extract from an indubitably confidential letter, from another of his colleagues to Mr Heseltine, in a way that was bound to seem to damage the Heseltine cause. The Prime Minister, Mrs Margaret Thatcher, has been put in political jeopardy, now or later, because it is not clear whether she conspired in the decision to leak the crucial section of the confidential letter (the rest of which had not been published until Monday).

Few in Britain seem to recognize that this heady scandal, like many others in recent decades, is a predictable consequence of the way the British government runs its affairs. The principle, told at length and usually with boastful pride in British high-school textbooks, is that the government should consist only of people who are members of the British Parliament and that it governs only with the consent of the Parliament or, in this context, of the House of Commons. That, the argument goes, is how it should be. All members of the government are personally answerable to one or other of the two legislative chambers, while it makes sense that the House of Commons should have the dominant role in deciding what political party shall form a government, given that it consists of people who have run for public office and who have been democratically elected. The government, like executive branches everywhere, must then administer affairs, seeking legislative authority from the Parliament whenever necessary. The British conceit is that the system of cabinet government is uniquely virtuous. The theory is that all decisions, small as well as large, are made collectively by a group of senior ministers who are the sole repositories of executive power.

There are some obvious and long-recognized defects of this system. The convention that governments may govern only with the consent of the House of Commons does not make Members of Parliament individually powerful. On the contrary, political party discipline usually ensures that they toe the party line. The result is that they are mostly impotent fellows, with very little influence even on the details of legislation, although they have during the past decade won the right to question government departments about their policies and even to complain about them. But even this right is proscribed; it will be virtually impossible for the House of Commons defence committee to get to the bottom of the Westland affair, as it intends, if the government insists on its right not to make documents available or to allow civil servants to be questioned. But the same convention of government by parliamentary consent, coupled with the practice of fierce party discipline, means that governments are rarely changed except at general elections. This is the origin of one of the most disconcerting features of British politics since the Second World War, the sharp swings of policy that occur when one government succeeds another.

The convention that only the cabinet collectively can make decisions is similarly crippling of intelligent public discussion. Mr Heseltine's views about the manufacture of helicopters were at odds with the cabinet decision that the British government as such should have no opinion about the future of the Westland company, but this decision appears to have been reached not in a general discussion of the issue, but by a small subcommittee whose conclusion was then rubber-stamped by the rest of the cabinet. British academics and researchers, smarting from the way in which they are unable to perform their own jobs well for lack of funds, will now be asking whether the twenty-three members of the British cabinet have all deliberately decided that this is the fate the basic research enterprise in Britain deserves, or whether that too is the opinion of a few which has been given the appearance of consensus by the convention of collective responsibility.

There is worse to be said, bearing more directly on the Westland affair. The convention of collective responsibility means that only members of the cabinet can be seen to have taken decisions. Even if a minister has merely followed the recommendation of his civil servants, the convention is that the decision is his alone. Moreover, there is nothing in the British system that compels him or her to explain how the decision has been reached, while the documents preparatory to important decisions remain secret for thirty years unless the government decides they should be published. (Fair play, the present government has been more liberal, if selectively, in this respect than most of its recent predecessors.) Indeed, there is an Act of Parliament that makes it an offence for people other than ministers to release such information; it is even a criminal offence to be the recipient of such information. This is why Mr Heseltine, now an ex-minister, could make public the unpublished part of the letter he was sent by his erstwhile colleague in the government, the Solicitor-General, or a second letter that would have undone some of its damage; for that, he had to wait on the Prime Minister's pleasure, until Monday.

None of this implies that information bearing on what the government has decided or intends never finds its way into the public domain. The British newspapers are full of it. But much of the most important information is made public only by means of deliberate leaks, either by ministers or civil servants sympathetic to their cause (as with Mr Brittan's leak of the Solicitor-General's letter) or, about as commonly, by civil servants who believe their minister is wrong to (as when, at the end of 1984, Mr Clive Ponting, then a civil servant, sent anonymously to a newspaper a document prepared by Mr Heseltine about British public opinion on cruise missiles and, more recently, some civil servants sought to dissociate themselves from Sir Keith Joseph's disastrous green paper on higher education). The manipulation of information in this way is bound in the long run to undermine public understanding of what the government is doing even if, in the short run, it renders ministers more powerful and relatively immune from criticism.

Britain's complacent tolerance of these ways of doing government business probably implies that there is little hope of change. Yet, the Westland affair is merely the most spectacular of the ways in which even governments are caught out by their own malpractices. Why should not Mr Brittan have denied receiving a letter from British Aerospace (it had been sent to the Prime Minister) when he had no reason to fear that it would be made public? And why should he not have leaked another knowing that such things go on all the time?

The less spectacular damage done to British public life by this seamy side of the British constitution is even more serious. The violent swings of policy on important issues such as education and the management of the economy have done great damage, wasting time and resources and creating a general sense of uncertainty within Britain and outside. The convention that only ministers matter is not only bad for their opinions of themselves (and their manners) but means that government policy is often no more convincing than the person who happens for the time being to be its personal embodiment. Legalized secrecy modified by vicarious and selective leaking, which may be as damaging to governments (as the past few weeks have shown) as to their electors, saps people's confidence in the process of government. And the personality traits which this poisonous combination of malpractices engenders are infectious. All the way down the hierarchy of government, there are civil servants and the chairmen of public corporations who enjoy the power of keeping secrets — and of letting some of them slip. The folly of the second part of the Official Secrets Act was acknowledged almost a decade ago (and Mrs Thatcher's predecessor promised at one stage to get rid of it). Might not she start where he gave up, and offer some such reform as expiation in the trouble she has stumbled into? □

Max-Planck survives

The 75th anniversary of the Max-Planck-Gesellschaft is a time for celebration.

THE Max-Planck-Gesellschaft is celebrating its seventy-fifth anniversary this year with a greater sense of security than would have been possible at any previous time since its formation, as the Kaiser-Wilhelm Gesellschaft, in the deceptively secure days just before the First World War. Originally the vision of the theologian Adolf Harnack (who was the society's president until 1930), the first two institutes had hardly been founded on the plot of ground donated by the Kaiser at Berlin-Dahlem before the Great War began. In what must have seemed bewilderingly quick succession, there followed the financial storm of the 1920s, the Nazi government and the Second World War. Only since the society was allowed to begin again, temporarily at Gottingen, in 1946, can it have seemed as if the stability promised by the founding fathers might yet materialize. In the event, the society was formally reconstituted, with its present name (wished on it by the British army then in occupation of Lower Saxony), only in February 1948.

Among publicly supported research organizations, the Max-Planck or MPG is distinctive and may even be unique. The original conception, that of a network of free-standing research institutes devoted largely to basic research, was not merely in 1911 quite different from anything elsewhere, but was a break with the traditions of German scholarship which, throughout the nineteenth century, had turned around the doctrine of Wilhelm von Humbolt that teaching and research are inseparable. Part of Harnack's ambition was that German science (which, in the old tradition, covers the humanities as well) should secure a measure of independence that the German universities could not then aspire to. This was to be secured by setting up the society with a generous endowment, and 10 million marks of the day were indeed collected in the three months before the Kaiser-Wilhelm Gesellschaft came into being at 11.00 a.m. on 11 January 1911. At the outset, the society was responsible for its own running costs and capital works, although the government paid the salaries of institute directors, but the inflation of the 1920s quickly put paid to that, even though the society was still clever enough to recruit Einstein from Switzerland. Mercifully, the doctrine of independence survived, at least until the National Socialists took office in 1933.

There followed the society's most difficult period. The edict that Jews were unwelcome became the law. Fritz Haber resigned because two of his division heads had to be expelled for being Jewish. Carl Neuberg, director of the institute for biochemistry, was forced into early retirement and eventually, in 1939, forced to leave Germany altogether. Between 1933 and 1938, nearly a third of all the scientific members of the society were forced out, mostly on racial grounds. Max Planck himself, who had succeeded Harnack as president and who believed that the Nazis would disappear as quickly as they had arrived, resigned once the twenty-fifth anniversary had passed.

It says much for the strength of the network of the 1930s that it was somehow able to survive the Second World War. The British insistence that the name should be changed was natural in the circumstances. The remarkable feature of the post-war reconstitution is that nobody thought it feasible to change the constitution that, among other things, gives the members of the society the right to elect their president. The result, in the circumstances of post-war West Germany, is that the government of the Federal German Republic naturally regarded MPG as a means by which West German science could be rapidly strengthened. Especially during the 1960s and 1970s, the network of research institutes grew quickly. Now there are sixty of them, with a total strength of 10,000 people of whom 4,000 are scientists. They range in size and scope from huge research establishments such as that for plasma physics at Garching near Munich to small informal places, hardly distinguishable from university departments, such as that for mathematics at Bonn. MPG has an annual budget of DM 1,000 million, which is a mere 2.2 per cent of what West Germany spends on research each year. Its influence inside and outside West Germany is disproportionately great.

Why has the organization succeeded so well? Part of the explanation is that the institutes have indeed allowed people to get on with research, free from teaching and administrative duties. But the network has cleverly done its best to avoid the obvious danger that it will become ingrown by insisting on its right to hire people from outside West Germany, both as investigators and as advisers. MPG has also been able to insulate its people from the social upheaval in the universities that has occupied much of the past twenty years. In many ways, it has had an easier task than its publicly supported partner in research support, the Deutscheforschungsgemeinschaft (DFG), with a budget of roughly the same size and a remit to support basic research in the universities.

Not everything is cheerful, however. Self-consciously though it has tried, MPG has not preserved all its institutes from inwardness. Now, with a static budget, the going may be harder; starting a new institute seems to require that one already in being should be closed. Moreover, the days when MPG seemed the best way to strengthen West German science have gone. The universities are stronger now, as is West German science as a whole. The obvious need is to forge better links between the universities and the sometimes still too-independent research institutes. It is good news that MPG appears to recognize the need; something like ten per cent of its scientific staff now double as university teachers. But there is still some way to go. □

Solar System

Voyager passes Uranus, Giotto rescued

Washington

VOYAGER project scientists are ecstatic about the first flood of data sent back by the Voyager 2 spacecraft during its closest encounter with Uranus.

By Monday, the total number of moons around Uranus had risen to 15, only five of which were known before the Voyager mission. A tenth ring was also discovered just inside the brightest and outermost ring around the planet, and there is evidence for ten additional faint rings. Voyager's telemetry also indicates the presence of high-energy radiation belts similar to those around Saturn, Jupiter and Earth.

The debate over the strength of Uranus' magnetic field has been resolved by Voyager. According to Dr Ellis Miner, deputy Voyager project manager at the Jet Propulsion Laboratory (JPL) in Pasadena, California, the magnetic field strength is 0.25 gauss at the cloud top. The field has a peculiar orientation, tilted 55 degrees from the rotational axis, so that one of the polar regions is pointing towards the Sun.

According to A.J. Dessler, director of the Space Science Laboratory at Marshall Space Flight Center, there is "hardly any glory for anybody" in the 0.25 gauss figure. The proponents of a strong cloud top magnetic field were expecting a figure greater than 0.6 gauss and the weak magnetic field proponents were looking for something in the range of 4×10^{-5} gauss. Dessler believes that the 0.25 figure may be revised upwards when the data from Voyager are further analysed.

Pictures sent back by Voyager 2 of Miranda, a 310-mile-wide satellite closest to the planet's surface of the five major moons, were causing wonderment among members of the photographic interpretation team.

"If you took all the bizarre geology in the Solar System and put it back into one object, that would be Miranda", Dr Laurence Soderblom of the US Geological Survey was quoted as saying.

Miranda's surface appears to be a hodgepodge of valleys, cliffs, fault zones, craters and broad terraces. The peculiar mix of features was so startling, mission scientists were loath to speculate whether external or internal forces were involved in creating the formations.

An unexpected event of Friday in the midst of the Voyager flyby gave the National Aeronautics and Space Administration (NASA) and the European Space Agency (ESA) a chance to show how well they can cooperate.

ESA ground controllers were experiencing communications problems with Giotto because of a pointing problem with one of the spacecraft's antenna systems. As it happened, a large number of the Giotto team were at JPL for meetings, and after a brief consultation, NASA turned over a portion of the Deep Space Network of tracking stations to ESA. The Giotto scientists at JPL established a direct link with Giotto mission control in Darmstadt, West Germany, and the problem was resolved within hours with no loss of data from either mission. **Joseph Palca**

Asbestos ban?

Washington

THE US Environmental Protection Agency (EPA) has succumbed to growing pressure to ban all uses of asbestos. The agency last week formally proposed a regulation that would place an immediate ban on asbestos in five use categories, and phase out all other uses within 10 years. All forms of asbestos are treated similarly by the proposed regulation.

Regulations to ban the use of asbestos, based on studies by the Consumer Product Safety Commission and the National Academy of Sciences, were first drafted two years ago. Both studies essentially concluded that no safe lower limit for exposure could be established and led EPA to decide that asbestos should be banned where substitutes are available. But the regulations were held up by objections on cost grounds from the Office of Management and Budget; EPA's administrator, Lee Thomas, said last week that the new proposal had resolved the budget difficulties.

A final decision on whether to go ahead with the ban will be taken after a 90-day comment period. A spokesman for the Asbestos Information Association said a ban would be "totally unjustified and out of step with the international consensus on current use". The association points out that the estimated 3,300–12,000 deaths each year in the United States that can be attributed to asbestos are the result of exposures of 20 years ago and more. Nevertheless, EPA estimates that the ban will save 1,000 lives before the end of the century, and officials say the ban now has a lot of momentum. The EPA proposal would ban immediately manufacturing importing and end-processing of asbestos roofing felt, flooring felts and tiles, asbestos cement pipe and fittings, and asbestos clothing. Other uses would be phased out over 10 years. Tim Beardsley

---

SDI

Software rows

Washington

THE difficulty of developing reliable software for the Strategic Defense Initiative (SDI) has surfaced once again. An SDI advisory panel had concluded that contractors working on preliminary design concepts for a space-based shield against nuclear weapons have not paid sufficient attention to the problem. The SDI organization appears to have taken the panel's criticism seriously; officials have been quoted as saying that the amount spent on software problems will be increased.

Critics of SDI hold that contractors have failed to address the issue adequately because the job simply cannot be done. The advisory panel, known as the Eastport Group, does however maintain (on the basis of qualitative argument) that reliable software can be tested and developed within the next several years.

SDI software must keep track of possibly thousands of warheads and many more decoys, coordinating multiple layers of weapons systems and sensors in real time to stop as many missiles as possible from reaching their target. Those convinced that the problem cannot be solved argue that the system cannot be tested under real conditions and that it must work first time. Analogies are made with the software failures that have often delayed space shuttle launches, for example. David Parnas, of the University of Victoria in British Columbia, resigned from the Eastport Group last year on just these grounds. Parnas now says that the group has not refuted his arguments and that he is "amazed at how little thought" has been given to his publicly stated criticisms; he accuses administrators at the SDI organization of incompetence.

One central issue is the extent to which the system functions as a single coordinated whole rather than as several functionally-autonomous subunits with built-in redundancy. A distributed system would be less vulnerable to the inevitable software errors. The Eastport Group favours a distributed system because it would make the software problem more tractable; the contractors' ideas so far, however, are based on more tightly coordinated systems.

Parnas believes the contractors chose a coordinated system because they realized SDI would not work otherwise, whereas the Eastport Group went for a distributed system because the software development would otherwise be too difficult; "they're both right". The Eastport Group says that contractors have too closely followed model system descriptions intended only for illustrative purposes that were included in the two-year-old Fletcher report on the feasibility of SDI. **Tim Beardsley**

US research costs

Government to turn screws

Washington

A long-simmering controversy over how the federal government should compensate universities for the facilities and services they provide to researchers is threatening to return to the boil, fuelled by rumours of major changes in the compensation rules by the White House Office of Management and Budget (OMB). Adding to the cauldron of controversy are two reports apparently guiding OMB in formulating new policies, one by the White House Science Council and the other by the Department of Health and Human Services. Both point to significant changes of practice in reimbursing universities and other institutions for the so-called indirect costs of research.

Indirect costs can be broken down into administrative and non-administrative categories. OMB is considering fixing administrative cost reimbursement in this fiscal year at 26 per cent of the total direct costs of research carried out under federal contracts and grants, which is the national average at present. That figure would drop to 20 per cent in 1987. OMB is also giving serious consideration to capping the portion of administrative cost reimbursement specifically related to departmental administration at 7 per cent, a figure that would further decrease the recovery of indirect costs allowed.

Particularly upsetting to universities is the widely held belief that OMB will shortly publish sweeping changes in circular A-21, the blueprint for indirect cost reimbursement, with an extremely short comment period and without prior consultation with the universities affected.

"We are accustomed to being dealt with in a fair and reasoned way", says Janet Sweet, assistant controller responsible for indirect cost control at Stanford University. If OMB proceeds as expected, it would be a "dramatic change from the reasoned approach the government has been taking", says Sweet.

The issue of indirect costs has long been divisive for university faculties and administrations. Researchers have seen the dollar amounts of their grants grow but the money available for research shrink as an ever larger portion is devoured by indirect costs.

The Health and Human Services report (*The Impact of Indirect Costs on Research Sponsored by the Federal Government at Universities and Colleges*) takes universities to task for charging faculty salaries and other departmental overhead costs to research grants as indirect costs.

Data from 13 universities show that indirect cost payments rose from $900 million in 1978 to $1,700 million in 1984, an increase from 36 per cent to 45 per cent of direct cost.

According to the report, departmental administrative costs now account for a third of all indirect costs. By capping allowable departmental administrative costs at 7 per cent, the Inspector General estimates that between $225 million and $375 million can be saved per year.

Critics of the report argue that the 7 per cent figure is unreasonable and that departmental costs vary widely, depending on the administrative structure of a university. For some, departmental costs are insignificant, but for others departments are a major part of the total university structure.

The report also suggests that many costs now charged indirectly should more properly be charged as direct costs, a version of robbing Peter to pay Paul, according to critics.

Dr Alan Barber, vice-chancellor for research programmes at the University of California, Los Angeles, says the arbitrary assignment of 7 per cent for allowable departmental administrative costs "makes a sham" of years of trust between universities and government auditors.

Others are not convinced that attacking administrative costs will solve the problem of rising indirect costs. Dr David Blake, associate dean for research at the Johns Hopkins School of Medicine, points to a study by Hopkins and Stanford University showing that non-administrative costs rise nearly ten times faster than administrative costs at Hopkins, but only three times faster at Stanford.

"It's clear to me", says Blake, "that all of the real increase in indirect cost has been in facilities."

The White House Science Council report (*A Renewed Partnership*. White House Science Panel on the Health of US Universities and Colleges) is less distressing for universities, although it also advocates that the growth of indirect costs should be contained by limiting administrative cost reimbursement, in this case by establishing over a two-year period a fixed level for reimbursement for indirect costs as a percentage of direct costs.

The report contains several suggestions that will clearly please universities, among which are less paperwork and, specifically, the removal of the hated "effort reporting" instituted by auditors to force faculty to say how their time is divided between administration, research and teaching. Accelerated depreciation of equipment and facilities and tax credits as a way of encouraging industry participation in capital expenditures are also suggested by the report.

But the White House Science Council's recommendations would cost money. The report says that "the source of such funding in these times of fiscal stringency is not obvious". **Joseph Palca**

Panel's prescription

Washington

The White House Science Council report, released in draft form on 17 January, raises doubts about the preparedness of US universities to face the coming decades.

The doubts are engendered both by the government and the universities, according to a special panel on the health of US universities and colleges chaired by David Packard, chairman of the board of Hewlett-Packard Company. On the one hand, the panel says, federal support has not allowed universities to meet the demands for new talent and new knowledge, while variable levels of federal support have prevented universities from making the most efficient use of their resources.

On the other hand, the report chastises universities for "attempting to ride out what were hoped to be temporary budget shortfalls" by mortgaging their research futures to "maintain research personnel rather than investing in needed instrumentation and facilities". Researchers themselves are criticized for being too conservative in their research goals.

As well as the specific recommendations relating to reimbursements, the report urges the federal government to help restore university infrastructures by forging stronger ties between industry, universities and the federal government. It also advocates that the durations of research grants should be longer and that investigators should have more flexibility in distributing grant monies and altering research goals. Joseph Palca

---

Poles sentenced

The three Polish scientists from Torun accused of illegal possession and use of a television transmitter (see *Nature* 319, 170; 1986) were last week each sentenced to 18 months imprisonment while the electronics specialist in whose apartment they were arrested was sentenced to a year in prison. All sentences were suspended, however, on condition of good behaviour for three years, so that Professor Jan Hanasz and Dr Zygmunt Turlo were able to return at once to their work at the Copernicus Astronomical Centre. (The third scientist, Dr Leszek Zaleski, is a pensioner.)

Colleagues of the accused had been campaigning throughout the past four months for their release from pre-trial custody. The presence of Dr Hanasz, in particular, they explained, was essential for many important astrophysical experiments, including joint research with the Soviet Union and France. Vera Rich

Japanese education

Uncertain future for reform

Tokyo

JAPAN's special Council on Education Reform, personally set up by the Prime Minister in 1984, delivered its draft recommendations last week. "Diversity, flexibility and decentralization" are seen as the keys to transforming the present rigid, hierarchical education system. But vigorous opposition to the plans, especially from the Teachers' Union, must put their implementation in doubt.

The 25-member council has looked at everything from kindergarten education to the support of university research. At the top, the council proposals are conventional: extension of the postdoctoral system, begun in Japan only last year with just 160 fellowships, and funds to bring more foreign researchers to Japan. It is also suggested that the minimum length of study prescribed for masters' and doctoral courses be reduced to allow talented researchers to get ahead quickly.

Reform of the universities is more controversial for it is here that the root of the education system's problems lies. It is not average standards of education that worry the Japanese; 35 per cent of all 18-year-olds already attend university and 95 per cent of children pass through senior high school. The problems are excessive uniformity and competition.

The two problems are inextricably entwined. Top universities can provide a passport to top jobs so it is little surprise that there is severe competition to enter Tokyo University, for example. What is surprising is that all Japan's universities, and even faculties, can be finely ranked according to how difficult they are to enter. That is possible only because of uniformity: the Ministry of Education closely controls school curricula and textbooks, there are selective courses at high school and university entrance examinations are of the multiple-choice type that produces scores on a single scale. That scale both defines a student's place, and by the score at which a university will accept students, a university's place, in the hierarchy.

The good side of the system is that it is completely open and fair; the bad side is that it ignores individual vocation and often tests abilities of little real use. In the English examination, for example, subtle grammatical points are tested in multiple-choice questions but not the ability to write or speak English, which would be impossible to quantify accurately.

The reforms are intended to loosen up this system. It is proposed that it should be made easier for students to transfer from one university to another through a "credit" system recognized by all universities or by a new degree-conferring body. Diversity in the universities themselves is to be encountered by loosening the Ministry of Education's strict rules for the establishment of new universities and by granting freedom to put together new faculties without ministerial interference. The establishment of a "university council" responsible for both public and private universities that can make recommendations direct to the minister is also proposed. Further possibilities include allowing students to graduate in three years instead of four and lowering the university entrance age — at present the talented cannot move ahead of others.

These changes, although they scarcely seem revolutionary, all have their critics. One of the chief objections is that the system is indeed being redesigned to help the talented and does nothing for the great mass of ordinary students. But really fierce criticism is reserved for the proposed reforms of pre-university education.

Just like universities, high schools are graded. The ten or so schools in a typical catchment area are ranked according to how many students they send to which universities and their entrance examinations, taken on completion of junior high school, are correspondingly severe. Once entrance has been achieved, however, there is no streaming by ability nor much choice over what is studied. Thus two Japanese desires are satisfied: educational competition is free, fair and measurable while there is no discrimination among members of the same group.

The council's reforms, however, mostly centre on improving the quality of teachers by extending probation periods, reviewing teacher performance and removing those found wanting, and bringing in older and retired teachers to train newcomers. These proposals are seen by the left-wing Teachers' Union as a direct attack on the union and an attempt to increase government control over education. The union's counter-proposals are more practical: reduce class sizes to a maximum of 35 students, eliminate huge schools, increase the number of public high schools and eliminate the high-school entrance examinations.

The total opposition of the teachers makes it hard to see how reforms will ever be enacted. What will happen in the future is strongly linked to the fate of the Prime Minister, who has taken a personal interest in the reform council. Under party rules, his term of office expires in October and cannot be extended. If he retires then, little more may be heard of the education council. But there is still a chance that he will call a snap election to prove his personal popularity and then force a change in the party rules so as to stay on.

Alun Anderson

US animal drugs

FDA chastised by Congress

Washington

THE US Food and Drug Administration (FDA) has denied charges by a congressional committee that it has "consistently disregarded its responsibility" for assuring the safety of drugs used in food-producing animals. Following publication of a scathing report by the House of Representatives' Committee on Government Operations which details several failures by FDA to meet its legal obligation, FDA felt obliged to issue a statement claiming that "the US food supply is the safest in the world". But FDA admitted that the committee had found "deficiencies", many of which have already been repaired.

The government operations committee, chaired by Representative Ted Weiss (Democrat, New York), is an oversight committee: it has little power to enforce. But it has succeeded in its objective of drawing the issue to public attention.

The major charge is that 90 per cent or more of the 20,000 to 30,000 "new" animal drugs on the market have not been certified by FDA as "safe and effective", thus violating the Food, Drug and Cosmetic Act. FDA does not dispute the finding, but points out that 90 per cent of the animal drugs actually used — by volume — have in fact been approved; many of the rest are vitamins, mineral supplements and liniments that are exceedingly unlikely candidates for causing harmful effects in people. And in reply to a charge that only 7 per cent of new drugs on the market have even been catalogued, FDA says a new data-handling system should ensure that the backlog is cleared by September 1986.

Weiss's committee goes on to list "potentially unsafe" animal drugs that, it says, FDA knew presented carcinogenic risk but for which there are no adequate methods for detection of residues, as required by law: dimetridazole, ipronidazole and carbadox. And the committee quotes FDA's own investigators' conclusion that veterinary prescription drugs are widely and illegally available.

The fairest judgement seems to be that FDA's Center for Veterinary Medicine, which has responsibility for the area, lacked adequate resources to follow the letter of the law and so concentrated resources in areas where they would do most good.

While the legal failings are not easily dismissed, the extent of any actual risk to public health arising from drug residues is unclear; the extreme difficulty of extrapolating from animal carcinogenicity tests to human carcinogenesis makes attempts to quantify risk almost meaningless. But in such a cancer-conscious country, nearly is not good enough.

Tim Beardsley

British universities

Academic leaders answer back

BRITISH university vice-chancellors have made a stinging reply to the government's discussion paper on its future policy on higher education, saying that the policy document published last May is "blinkered". This strong language appears in the formal response to the policy document by the Committee of Vice-Chancellors and Principles (CVCP), the representative body of British university heads.

The document is chiefly significant for its directness, and for the bluntness of its language. On many occasions, CVCP has been able to make only a muffled response to statements of government policy because of differences of opinion among vice-chancellors, who are in any case unable to speak for their universities.

CVCP now says that last year's policy statement, technically a green (discussion) paper (see *Nature* 315, 265; 1985), "failed to address itself adequately to the problems which we face". "Nor did it display any sense of the way in which education is both necessity and catalyst in a modern society."

The CVCP response does not set out to be a full reply to all the points raised by the government, saying that its views may be taken as identical with those of the University Grants Committee (UGC) on matters not explicitly dealt with. The committee deals with the chief questions raised as follows.

Student numbers. CVCP disagrees with government projections that the numbers of university students can be allowed to fall between now and 1995 (when the present demographic decline of the entry age-groups will begin to be reversed). Its report says flatly that there will be no decline in the demand for higher education, and points to the conflict between government statements about the importance of skill in a modern economy and its plans that the output of graduates from the universities should be reduced by 14 per cent by the end of the next decade. CVCP remarks that the proportion of people with first degrees in the British labour force was only 6 per cent in 1980, compared with 19 per cent in the United States, 13 per cent in Japan and 8 per cent in West Germany.

Tartly, CVCP also draws attention to the conflict between present policies and the green paper's own calculation of the "social rate of return" on funds spent on higher education, which concluded that the "gains from higher education overall are satisfactory even when these are limited to a purely financial calculation". If allowance were made for the benefits of personal development and other intangible consequences of higher education, CVCP says that investment in higher education might well yield returns twice as great as "from any comparable investment".

CVCP also points to the way in which the government's ambitions for an improvement in the quality of high-school education will be jeopardized by the decline in the numbers of graduates, noting that, in 1984, 30 per cent of physics teachers and 26 per cent of mathematics teachers had no qualifications in those subjects. In contrast, CVCP notes the conflict between the government's belief that the quality of school education can be improved and its assumption that this will not increase the demand for higher education.

Students' affairs. CVCP complains that the government has allowed the value of students' maintenance awards to decline by 12 per cent since the beginning of the decade, and has shifted an increasing proportion of the cost of higher education onto parents. It remarks that the government has failed to fulfill its promise to introduce a more rational system of student support, and says that if the government will not introduce an equitable system of student maintenance grants, it should devise a loan scheme instead. CVCP says that there should be more support for the European scheme to encourage the international movement of students, and that the government has "misjudged" the importance of "cultural diplomacy" in charging full fees to students from overseas.

Continuing education. The vice-chancellors accept that universities have a fuller part to play in the provision of post-experience education, but their document dissents from the government's view that the costs should mostly be borne either by industry or the individuals concerned. Noting that this policy ignores the national benefits of continuing education, the CVCP document insists that there should be at least two changes in the present arrangements; government help with the initial costs of post-experience courses and an understanding that fees paid by individuals for continuing education should be tax-deductible.

Research. CVCP notes the common misuse of the term "research" and suggests that part of the reason why technology transfer in Britain may have been laggard is the relatively small proportion of 1.6 per cent of Gross Domestic Product (GDP) spent on civil research, compared with 2 per cent in the United States and 2.5 per cent in West Germany and Japan.

The document goes on to plead for a continuation of the practice by which research councils and UGC have jointly supported academic research, the latter by means of the annual subvention of universities. On links between academic and industrial research, CVCP says the reduction of the numbers of graduate students by about 10 per cent in the past decade works against the government's ambitions that universities should do more to help industry, that the potential usefulness of universities to help British industry by the publication of new knowledge has been impeded by the relative neglect of the scientific literature by the putative beneficiaries and that the government should set up a fund to assist with the direct exploitation of academic innovations.

Salaries. The CVCP response to last year's green paper is most scathing in what it has to say about the conditions under which university teachers work. It says that declining salaries have created "grievance and distrust" whose effects, by way of recruitment, will have the effect of making universities less efficient and effective. The present age-structure of British academic staff is such that too few vacancies will arise in each of the next ten years to allow for the replacement of 3.5 per cent of the teaching force each year, even if British universities had the funds to fill all vacant posts, which seems unlikely.

In sum, CVCP conveys an air of exasperation with the government's demands on British universities. "The government asks for more and thinks that it can provide less and less without adulterating the quality of what is produced. The response to the green paper concludes by pleading that "the people of this country" should take "a political decision" about the resources to be devoted to higher education. □

SFC defies Congress

Washington

JUST weeks before its own demise, the Synthetic Fuels Corporation (SFC) has given a new lease on life to the Union Oil Shale Project in Parachute Creek, Colorado.

In its final scheduled meeting, the SFC board signed a contract for $327 million in loan guarantees for the Parachute Creek project. The contract must still be approved by the Treasury Department before the funds will be released.

Congress voted at the end of last year to terminate SFC, and specifically prohibited it from spending any more money (see *Nature* 319, 89; 1986). SFC, however, unilaterally decided that the loan deal was not a new expenditure, but instead a formalization of a part of a larger price support agreement reached last October.

Opponents of the synthetic fuels programme are incensed by this latest move, but they admit that if the Treasury Department approves SFC's action, the government will probably be stuck with the obligation. Joseph Palca

IVF

Another bill bites the dust

The medical research councils of nine European countries have agreed on a policy about *in vitro* fertilization (IVF). Recognizing the need for "informed public debate", the councils last week sent British Members of Parliament (MPs) copies of a statement detailing their conclusions. The statement reached MPs in time for a proposed debate in the House of Commons in which Mr Ken Hargreaves was reintroducing a bill to ban the creation or use of human embryos except for "enabling a child to be borne by a specified woman", a re-run of Mr Enoch Powell's bill which did not succeed in the last parliamentary session. In the event, the bill was not debated because of lack of time; it is unlikely to be revived.

The nine research councils (Denmark, Finland, West Germany, Italy, Sweden, the Netherlands, United Kingdom, Austria and Belgium) agree that IVF research should be restricted to the "pre-embryo", the collection of dividing cells before the appearance of the primitive streak, and should have the aims only of reducing infertility, of reducing congenital and hereditary disorders and of the development of safer contraceptive methods. Cloning of pre-embryos, manipulation of the genome to alter characteristics, growing pre-embryos beyond 14 days and the production of hybrids are all banned. Each country is urged to set up an ethical committee "to advise doctors and scientists and to inform and reassure the public". The committee should also contain "substantial lay membership".

The British Medical Research Council has given a £400,000 grant to the University of Edinburgh for IVF research. The programme will first develop a test to identify accurately healthy pre-embryos. The identification of gross embryo abnormalities in the laboratory will lead to a better chance of live births from replaced embryos, fewer multiple births and reduction in the risk of genetic disease, according to Professor David Baird, leader of the project. **Maxine Clarke**

Academic redundancies

Committee retires in confusion

A House of Commons inquiry into the circumstances under which British academics have been prematurely pensioned off collapsed last week when it seemed to the committee concerned, the powerful Public Accounts Committee, that the National Audit Office (NAO) and the Department of Education and Science (DES) could not agree about the consequences of the rapid contraction of the university system begun in 1981.

The committee had met to consider a report on the contraction of the British university system prepared by NAO which dealt with the question whether the cost of retiring academics early, estimated at £238 million, had been a sensible use of public money. The report (HC 598) is still available from Her Majesty's Stationery Office at £2.80 even though the Public Accounts Committee, on the showing of last week, plainly considers it valueless.

The committee first looked into the effects of government policy towards the universities before the first cuts took effect in August 1981, and was then told that some 3,000 academics and 4,000 non-academic people would have to leave the universities. In the event, by September 1984, a total of 4,400 academics, but only 2,800 non-academics, had left. In retrospect, NAO estimates that the extra cost of the compensation paid to those leaving early consists of £153 million paid directly by the University Grants Committee together with an estimated £85 million universities will have to contribute towards pensions schemes (out of their recurrent grants) in the years ahead.

Last week's fiasco seems to have arisen because the permanent secretary at DES, Sir David Hancock, drew into the discussion matters outside the period covered by the NAO review, which was exclusively concerned with the redundancy of university staff members up to September 1984. Thus he drew attention, for example, to the scheme for the appointment of "new blood" lectureships at the universities, offering this as one of the ways in which DES had helped to undo some of the damage done in the universities.

This is where the parliamentary system comes up against a brick wall. It is accepted that civil servants cannot criticize the policies of the governments for which they work, but if unpleasant things occur as a result of those policies, when does the cataloguing of those events add up to criticism?

The result, last week, was that the parliamentary committee became too confused to carry on. Believing that NAO and DES were somehow in disagreement, it sent them away with instructions to produce an agreed report. But DES said earlier this week that the existing document had been agreed between the two parties. Could last week's abortive committee hearing have been a clever ploy to postpone discussion of an embarrassing report? **Charles Wenz**

US research grants

Experiment in informality

Washington

A unique experiment intended to cut down the time spent by researchers on tedious form-filling is due to start next month in Florida. Officials of five federal agencies have agreed that, for the next two years, they will use a single simplified form of research grant in the hope of reducing the administrative burdens of most principal investigators.

The Florida Demonstration Project arose out of discussions organized last summer by the National Academy of Sciences' government/university/industry research roundtable. In contrast with many similar past discussions, this led directly to a decision by officials to devise a test of how proposed improvements might work. Remarkably, the scheme has been set in place in just eight months.

The basic problem, the group agreed, is that existing federal accounting procedures tend to work best for projects with specific goals, rather than for research, which is by its nature unpredictable. Futhermore, as things are, accounting procedures are often duplicated at institutional and state levels. The end result, for the principal investigator, is that there are several forms to fill in, while Washington must be consulted in writing whenever funds allocated for foreign travel are used for buying a new piece of laboratory equipment, for example.

The new standard grant removes many of the cumbersome restrictions on normal grants, leaving the institution to which a grant is made responsible for accountability. Explicit prior approval would, for example, no longer be necessary should an institution choose to risk spending grant money before its award is confirmed.

Another irritation is the need to keep accounts from different grants separate, even when the work being supported may be hard to distinguish. Under the simplified grant, only the requirement that the scope of the research or the principal investigator should not be changed are retained. Dr Thomas Walsh of the University of Florida at Gainesville estimates that principal investigators might save up to 15 per cent of their time under the new rules.

The five research agencies that have agreed to participate in the scheme are the National Institutes of Health, the Department of Energy, the Department of Agriculture, the National Science Foundation and the Office of Naval Research. Nine institutions of higher education in Florida have agreed to be guinea pigs. Enthusiasts hope that all federal research grants in universities will eventually be modelled on the new grant. **Tim Beardsley**

French nuclear power

Problems of plenty and success

NUCLEAR power provided more than two-thirds of French electricity in 1985. With six more 1,300-MW reactors coming on line in 1986, more later, and four more ordered by the government from the national constructor, Framatome, could there soon be too much? That now seems the view of Marcel Boiteux, director-general of the national utility, Electricité de France (EdF), in an astoundingly open interview with *Le Monde,* France's leading daily, earlier this month. Boiteux has thus brought into the open a festering conflict between the utility and ministry of energy about the number of nuclear reactors France actually requires.

According to Boiteux, there are two major issues. First, EdF is now in debt to the tune of FF216,000 million (£20,000 million) due to its long period of investment in nuclear construction — but the government's policy of low pricing for electricity means that EdF cannot pay off the debt (a large fraction of which is in dollars) but can only cover the interest on its borrowing.

Second, although French electricity demand grew more than 7 per cent last year, EdF's need for new power sources is slight. Framatome has been required to develop and introduce a so-called "grey mode" technology, which allows a reactor to be switched from full power production to just 30 per cent within minutes, to cope with sudden falls in demand. If EdF had had its way, there would have been only one order for a reactor in 1984 (there were two), and none in 1985–87.

But EdF's overcapacity may be relatively shortlived. Orders would have had to begin again in 1988, Boiteux said, to start replacing earlier reactors coming to the end of their life. And, apart from the debt question, nuclear power had kept French electricity prices 30–50 per cent lower than they would have been if the utility had had to rely on coal or oil-fired power stations. The reactors will also "remain profitable" even if they are run at only 30 per cent of capacity, the EdF director insisted.

Meanwhile, Framatome, which is geared up to produce not one reactor a year as is now ordered by the government to 1989, but four, will be covering the gap with a recent order for two reactors from China (though these are rumoured to have been offered at below cost), and by a new strategy of shifting heavily towards after-sales service, concentrating on robotic aids for maintenance of reactor cores and steam generators. Those services will not be limited to Framatome reactors in France, but will be offered throughout the world to all reactor owners, including those in the United States.

One area of French business is nevertheless booming — the nuclear fuel cycle, where the national nuclear fuel company, Cogema, has announced that its revamped reprocessing plan at La Hague near Cherbourg on the Channel coast has worked so well over the past year that it can now reduce reprocessing charges. Previously, La Hague had been plagued by inefficiency and shutdowns, but last year its UP II plant was able to reprocess 418 tons of spent fuel from pressurized water reactors, compared with its nominal 400 tons. Cogema plans to quadruple that capacity to 1,600 tons a year by 1992, which will further reduce costs, and claims that it is already 11 per cent cheaper to reprocess fuel through La Hague than to deal with it in any other way (such as stockpiling).

Superphénix, the world's first commercial-scale fast breeder reactor, has also just delivered the first tentative fraction of its full 1,200 MW of power to the French grid at Creys-Malville in the south of France, in what has been a busy few weeks for the French nuclear industry. The reactor, which is 51 per cent French, a third Italian, and 16 per cent German, Dutch and Belgian, is functioning as expected. But according to Boiteux, there is no hope for the moment of a "series" of reactors based on the Superphénix design being profitable, or competitive with the (oversupplied) EdF pressurized water reactors. The last thing EdF would want at present is another fast breeder — as is being planned by the national nuclear agencies of Europe. But, said Boiteux, anxious not to be too much of a thorn in the nuclear flesh, it would not be unreasonable to expect fast breeders to be profitable by the end of the century — and it is certainly necessary, in the meantime, to maintain the viability of the existing fast breeder design teams.

Robert Walgate

Nuclear power

Yugoslav plans approved

THE Yugoslav federal government is now accepting tenders for the construction of two nuclear power stations by the end of the century. According to present plans, a further two will be started in the year 2000. During the past few weeks, however, there has been a wave of opposition to the whole concept of nuclear power, on both economic and safety grounds. The situation is further complicated by Yugoslavia's federal structure. The Yugoslav constitution put considerable decision-making power in the hands of the governments of the six constituent republics, but foreign currency controls mean that a major contract with the hard-currency area must be decided at federal level.

The arguments advanced for and against atomic power during the past few weeks have been fairly predictable. A typical headline in the Belgrade daily *Politika* was "100 years of risk" above a photograph of the Three Mile Island power station. Yugoslavia has coal reserves for at least 100 years, say the opponents of nuclear power, so why not at least proclaim a 25-year moratorium as the Scandinavian countries have done? Moreover, although Yugoslavia does have some uranium of its own, if this runs out, the country might become dependent on one of the major powers for fuel supplies, which would imperil its non-aligned stance. It would be far better, therefore, to devote the huge sums of money that would otherwise be spent on nuclear power stations to better exploitation of Yugoslavia's potential water-power, developing energy-saving technologies and investigating unconventional energy sources, including solar energy and biomass. The pro-nuclear lobby, on the other hand, maintains that a nuclear power programme would create jobs in the construction sector and provide a boost for Yugoslav science and technology generally.

So far, Yugoslavia has one nuclear power station, at Krsko on the Slovene–Croatian border. A second nuclear station was proposed at the end of the 1970s, was eventually shelved due to the policy of economic "consolidation" (retrenchment) introduced at the beginning of the 1980s.

The new plans so far have proposed only one site, Prevlak, also on the Slovene–Croatian border. The Slovenes, however, are not particularly enthusiastic about another joint project. The construction of Krsko was fraught with difficulties and delays, which not only greatly increased the costs, but also caused friction with the US supplier (Westinghouse); the Slovene government began to import more and more electricity from Austria which it now considers a cost-effective alternative. Croatia has considerable energy problems, but cannot afford to construct a nuclear power station on its own. Other countries either lack the necessary infrastructure, or are unsuitable geographically. Serbia proper would be possible from the point of view of infrastructure, but so far no site in the Serbian republic has been seriously mooted. It may be significant, therefore, that during his visit to Italy last week, the Croatian premier Ante Markovic was reported to be seeking long-term credits from the Italians to help finance construction of a nuclear station.

Vera Rich

French science

New role for academy?

The French Académie des Sciences, which began as an informal club for such *savants* as Descartes and Pascal (and was formalized by the Sun King, Louis XIV), is stuck: stuck in ancient rules which forbid it to increase its tiny membership of 130 full fellows. Compared, for example, with the Royal Society of London, with over a thousand fellows for a similar national population, the French academy is both small and powerless. Compared with the US National Academy of Sciences, it is almost non-existent, and yet there are plenty of highly motivated French scientists who believe that the academy could and should play a larger role. And this new role may be on its way, to judge by a speech made by the academy's new president, M. André Blanc-Lapierre, earlier this month.

M. Blanc-Lapierre is the energetic ex-president of one of France's élite engineering schools, the Ivy League of French education, which provides the cream of management, the civil service and the political parties, and must be well aware of the nature of power and influence in French society. He says there has been a "certain decline" in the influence of the few reports that the academy produces and wants a rapid increase in membership.

The Académie des Sciences is one of five academies that together form the illustrious Institut National des Sciences et des Arts, which was formed from existing institutions shortly after the French Revolution of 1789. At the tôp of the "Institut" comes the Académie Française, with its 40 leading French writers and intellectuals — and these and the other academies of the "Institut" are not inclined to let the wayward, new-fangled Académie des Sciences actually grow, or influence government.

Under the present constitution, the only way open to increase membership would be the "infiltration" of outside talent. This, it seems, is just what M. Blanc-Lapierre has in mind. Beside the 130 full fellows, there are 80 foreign fellows and 160 "correspondents". These have no voting power in the election of fellows, but are not subject to the same restrictions in numbers as the full fellows; so Blanc-Lapierre's intention is to increase the number of correspondents by some 90 active scientists, who though unable to vote could play their full part on committees.

Blanc-Pierre would also like to see an increase in the size of what is effectively a small academy for engineering within the Académie des Sciences, a body called CADAS (the Comité Académique des Applications de la Science) which was created in 1982. CADAS was a compromise over the establishment of a true engineering academy within the Institut: The Académie des Sciences was to nurse it, inviting a membership half of outsiders (mostly engineers) and half of existing members of the Académie des Sciences. It now has nine academicians and ten outsiders but its size must be doubled, Blanc-Lapierre says, thus increasing the competence of the academy in relating science to the economy, the key political issue at present, and, incidentally, increasing the likelihood that a true engineering academy will one day be cloned from CADAS.

Whether finally the academy will really add to what is at present its principal duty, the publishing of the major French scientific journal, the *Compte Rendu* of the academy, and truly gain more influence over government through the changes foreseen may, however, be doubted. As the chairman of CODER, the Académie's Comité des Études et Rapports (reports and studies committee) said rather sadly last week, "our object has been to issue reports, but unfortunately the government hasn't asked us many questions . . . Advisory committees in France are rarely consulted". Such a situation would continue even if the academy were reformed.

Robert Walgate

Hungarian dam

HUNGARIAN opponents of the controversial Gabcikovo-Nagymaros hydroelectric project (see *Nature* 313, 615; 1985) have condemned the recent decision of the Austrian government to lend Hungary more than US$500 million to complete the dam. The loan will be repaid in electricity once the project is completed, thereby enabling the Austrians to cancel their own plans for a similar scheme at Hainburg. This, the Hungarian statement says, is equivalent to Austria exporting its environmental problems downstream to Hungary.

However, for some years, the Hungarian government has been stalling on its part of the project — the downstream installations at Nagymaros — ostensibly due to lack of funds, but almost certainly also as a result of the increasing pressure from environmentalists. They maintain that building the three dams involved (at Dunakiliti, Gabcikovo and Nagymaros) and the diversion of the flow of the Danube through a concrete channel, will put at risk the ecology of the river, destroy the wetlands of north-west Hungary, and affect the water-table of the riparian countries, making it necessary to pipe in drinking water at a cost that will largely consume the expected economic benefit of the power produced.

Vera Rich

Marine science

Proposal for British overseer

THE proposal that British marine science should be safeguarded by a separately constituted research board is the nub of a report by the House of Lords Select Committee on Science and Technology, published this week. The committee says that such a body is needed to develop a strategy for the exploitation of the British exclusive economic zone, the 200-km offshore area that Britain has not yet formally declared. The committee says that fragmentation and the lack of funds endanger Britain's international standing.

The Natural Environment Research Council (NERC), every committee's whipping-boy these days, is criticized for its management, which the select committee describes as "the way of most resistance". Specifically, the committee says that NERC's plan that a centrally located director of marine science should superintend its own research institutes, confusing relationships between the people concerned, should be replaced by a supervisory board of which the institute directors would be members.

According to the House of Lords committee, the Marine Science Board itself should not be a part of NERC but of the Science and Engineering Research Council, although it does not follow that the research institutes should similarly be transferred.

The committee is also concerned at the budget for marine research, which amounted to £70 million for civil research in 1983-84, compared with military spending on marine research of £122 million. The committee says that two research vessels were laid up during 1985 for lack of funds (and a third was in dry dock being fitted with a new engine). Invidiously, the committee compares British spending with that in the United States and France. The Woods Hole Oceanographic Institution has a budget of $52 million a year, while spending by the French marine research agency Ifremer exceeds the total of all British research spending from public funds in the civil sector.

The House of Lords committee also complains of the lack of coordination between the nine government departments and two research councils with a hand in British marine science. The committee argues that only a single board can be expected to take a broad strategic view in these circumstances, especially because the problems that arise are often literally global. It says that funds must also be provided by the government (although industry has, in fact, agreed to pay up to half the cost of British participation in the Ocean Drilling Project).

Peter Gambles

Free will and determinism

SIR—With reference to the letter from S.J. Starkie (*Nature* **318**, 406; 1985), it is clear that freedom of will must be narrowly limited by our bodily structure and experience, but complete determinism is not credible. I can easily decide that I am so bad at guessing the interest of letters in *Nature* by reading their titles that I would do better to find a method of making a genuinely chance selection. For example, I could set up a Geiger counter in a background giving an average of 20 counts a minute. Then, starting from an arbitrary time, I could record the times of occurrence of the next ten clicks. If the first occurred after 2 seconds I would read the first letter starting after 2 pages from the last Article: if the next click occurs at 7 seconds I would read the first letter starting after page 7, and so on. I would have surrendered any possible freedom of will in exchange for a programme based on a series of fundamentally indeterminate events. A newly qualified doctor could use an exactly similar method to decide in which continent he would look for his first job.

Even without such an unlikely way of making decisions,it is oversimplifying to say that either our thoughts or our actions are directly determined in any simple way by our structure and experience. Experiences are inaccurately and incompletely recorded, and the older records must have been damaged by the destruction of critical parts of cells by unpredictable fast electrons or alpha particles from randomly occurring radioactive decays from our natural radioactive background. And of course our thoughts and decisions can be affected only by what remains of the records, not by the experiences themselves.

This is a triviality; however much damaged the records are, they could still determine our thinking.

Like most people, I *feel* that I have some freedom of will, but this feeling itself could have been programmed into me by the records of past events. While I may be programmed to think erroneously that I have some degree of free will, many of those who have thought deeply on the subject believe — or perhaps I should say are programmed to believe — that they have not. They may of course be right; but I find it difficult to accept that a rigidly determined belief in rigid determination can be a valid proof that this is how the world actually is; the argument has an undesirably circular smell.

What I am quite certain of is that we cannot get any further by talking about the problem, any more than we could have foretold the production of monoclonal antibodies by talking about heredity and immunity.

Any experimental investigation must start with a detailed study of our conscious awareness. Our consciousness is, in biological terms, very expensive. The temperature and concentrations of a great variety of substances in our brains have to be controlled far more closely than they need to be to keep the body and most of the nervous system fully operational. We should not have evolved the necessary high quality stabilization systems if consciousness were unimportant to our survival. The survival can have depended only on what we *did*, not on what we thought about what we did, so our consciousnesses cannot have been simply epiphenomena without practical influence. During the long and climatically uniform period of the Cretaceous, there could have been little advantage to an individual in diverging from the built-in instinctive behaviour that had been optimized by selection over several million years.

The sudden and permanent change of environment hypothesized to have resulted from the impact of an asteroidal body at the end of the Cretaceous period would, however, have made much of the built-in programmes inappropriate to the new conditions, and individual or group experience could often have offered a better guide to action. For this to be useful, it would have been essential to have a mechanism for deciding whether to follow the inherited programme or a new programme based on experience. I believe that our conscious awareness, useless to a creature whose behaviour was hereditarily determined, developed as the organ of choice.

When we have gained a full understanding of the way in which some ten thousand million cells, with their complex multiple interconnections, can support a single apparently unitary conscious awareness, and when we have learned how the brain so promptly finds and presents the relevant memories to the consciousness to make optimum choices possible, we can begin again seriously to discuss free will.

I expect that we shall find that our decisions are largely determined by the records of our experiences, together with a sizeable contribution from hereditarily built-in motivations, and with a random element arising from the fact that all of the records are fuzzy round the edges. When all of these components have been recognized and allowed for, we can usefully re-examine the nature, if any, of our "freedom".

J.H. FREMLIN

46 Vernon Road,
Edgbaston,
Birmingham B16 9SH, UK

SIR—Apparently one of the most deterministic aspects of human neural functioning is a compulsion to argue about free will. The recent letter by D.H. Evans (*Nature* **317**, 762; 1985) claims that because the synaptic interactions among an array of neurones is far from thermodynamic equilibrium, "entropy production makes it impossible for the brain function of free will to be determined" since "causes are lost in this increase of entropy . . . as far as predicting the future is concerned". On the contrary, much behaviour is predictable despite mediation through non-equilibrium neural interactions: a host of perceptual, motor and reflex actions can be reproducibly elicited by peripheral and central stimulation.

More to the point is recognition that free will does not reflect the absence of a causal network, from increasing entropy or quantum indeterminacy of synaptic contacts or whatever. Free will implies that our volitions (a wish to argue neuroscience, to write a letter to *Nature*) causally determine certain of our actions (arguing, writing). Indeed, if such actions are not strictly determined, having these volitions would be futile. And insofar as non-equilibrium neural arrays must translate these volitions, they too must be deterministic.

The question remains, of course, as to how our volitions arise. Introspection suggests that these do not arise randomly, but that they too have causes. Free will does not imply an indeterminate or probabilistic selection, but a causally-determined choice.

JOSEPH D. ROBINSON

Department of Pharmacology,
SUNY Upstate Medical Center,
Syracuse, New York 13210, USA

If (1986)...

SIR—
If you concede that *something* in the Cosmos
Determines every move you make on Earth,
And not resist its force but match its purpose
And tread the path laid down for you from birth;
If you are true to Self (as Jung and Shakespeare
And sundry other schools, I think, agree)
Instead of to some norm of "right" behaviour
Or someone else you think you'd rather be;
If you will grant your favourite conviction
Will only take you far away from home
And, though it send you in the same direction,
Can only land you back where you ran from;
If you allow that, solid as you stand there,
You are no more than a character in a tale,
Of the same stuff as fantasy and dreams are,
Enacted on a universal scale,
Then you will unequivocally see
That Entropy and Order are all One,
And know how good it feels to live life free
And, which is more.....
.....you will be a *god*, my son.

KEITH DIXON

Bankside,
Clapham Station,
via Lancaster, UK

Molecular biology in Tokyo

The widespread influence of molecular biology on the biological sciences was well illustrated at Nature*'s first conference in Japan on 20–22 January.*

THOSE who think of molecular biology as a field of study, much as is botany or immunology, and that it occupies a disproportionate amount of space in many journals, this included, might have modified their views had they attended *Nature*'s first conference in Japan. Held in Tokyo last week, the conference demonstrated unambiguously that molecular biology is not a subject but a tool, and one that can advance botany or immunology as well as numerous other fields of study.

To start with botany, Jim Peacock (CSIRO, Canberra) described experiments aimed at establishing the means by which certain plants respond to a lack of oxygen by inducing a set of enzymes, including alcohol dehydrogenase. A cell biologist might look to see if the oxygen-depleted cells change shape, a physiologist might measure changes in the ion concentration or *p*H of the cells, a biochemist would probably establish the kinetics of appearance of the new enzymes, but a molecular biologist heads for the genes. For Peacock, that meant in the first place trying to establish which DNA sequences, flanking the alcohol dehydrogenase coding sequences, are responsible for mediating the gene's induction following oxygen depletion.

The hunt, so far, has been narrowed to a stretch of about 20 base pairs, which are shared by pea and maize alcohol dehydrogenase genes. Transferred to tobacco cells, the 20-base-pair maize sequence will confer responsiveness to oxygen depletion upon tobacco but only if an 'enhancer' sequence from a gene that is active in tobacco is also added.

It will, of course, be necessary to work "upwards" from this information to find out how the 20-base-pair stretch is activated — no doubt by a protein — how the protein is produced in response to oxygen depletion, and so forth. But at the very least, the molecular biological approach will have opened up a new way to study an old problem.

Peacock also mentioned a contribution of the molecular biological approach to plant pathology; a DNA probe for the barley yellow dwarf virus can diagnose in hours the presence of the virus in the leaf sap of plants suspected of being infected by the virus, replacing a cumbersome test that took weeks or months. And for Australian farmers, molecular plant breeders hope to be able to engineer the genes of alfalfa so that a protein of high sulphur content is produced in the plant's leaves; sheep that graze on this alfalfa might yield 30 per cent more wool than at present.

Professor Setsuro Ebashi

The opening ceremony

Immunology

Having, in essence, solved the problem of the generation of vast numbers of antibodies from a limited number of genes, molecular immunologists have turned their attention to other phenomena. Susumu Tonegawa (Massachusetts Institute of Technology, but a graduate of Kyoto University) is concentrating on the T-cell receptor for antigen. Since it faces the same need as antibody to bind antigen, and faces the same multitude of antigens, it is not altogether surprising that it too is encoded by a limited number of genes that are able by combinatorial means to produce a much larger number of proteins. The receptor on mature T cells consists of a dimer of α and β proteins but there is also a γ chain looking for a function (to be more accurate, there is a γ gene for certain and a candidate protein). Tonegawa reported that whereas the β gene is transcribed into RNA at the same rate throughout development, the γ gene is transcribed at early stages to be replaced by transcription of the α-chain gene at a later stage. He suggested that a receptor comprising β and γ chains on the early T cell is involved in the process of learning by the cell to recognize 'self', and that the switch to an $\alpha\beta$ dimer on the mature cell enables the cell to fulfill its role of recognizing antigen in the context of 'self' molecules without being 'self' aggressive.

Tasuku Honjo (Kyoto University) and Tadatsugu Taniguchi (Osaka University) share an interest in the secreted proteins by which different cells of the immune system can speak to each other, and the cell-surface receptors for such proteins. Both have developed a system for obtaining functional receptors for one such protein, interleukin-2, from cloned DNA for the receptor, enabling structure/function studies to be started. Honjo reported that removal of most of the cytoplasmic tail of the receptor does not affect its binding capabilities for interleukin-2, and Taniguchi presented evidence that the high and low affinity receptors for interleukin-2 are products of the same gene.

Honjo's new interest is in the so-called B-cell differentiating factors, a group of ill-defined substances. Honjo's group has succeeded in cloning the DNA corresponding to B-cell growth factor 1, as defined by its behaviour in bioassays. Since the substance stimulates T cells and macrophages as well as B cells, Honjo is inclined to rename it interleukin-4 (a proposal that will no doubt be pondered upon by a worthy committee long after the matter has been decided by popular acclaim).

Chemistry

Richard Lerner (Scripps Clinic, La Jolla) described how molecular immunology has led him to the iconoclastic view that many peptides adopt a preferred structure in solution. His starting point was the question of why monoclonal antibodies to a short peptide corresponding to a segment of a protein can also react with the protein. At first he favoured the idea that the antigenic sites on proteins correspond to segments on the surface that have the most atomic mobility and therefore are the most likely to be able to 'match' whatever peptide structure the antibody can see. Now, however, nuclear magnetic resonance spectroscopy is providing evidence that peptides corresponding to an antigenic site on a protein adopt a structure in solution that resembles that in the protein. For example, the immunodominant peptide of the haemagglutinin of influenza virus adopts a reverse-turn conformation in solution and a peptide from myohaemerythrin has helical structure in solution.

Tasuku Honjo and Hal Weintraub

Lerner also described how technical advances now allow methodical analysis of the contribution of each amino acid in a peptide to the antigenicity of the peptide. A set of peptides is made in which every one of the amino acids is in turn replaced by each of the 19 other possible amino acids, and monoclonal antibodies to each of these peptides are tested on the protein of which the original peptide is a part.

The information so obtained can pinpoint the crucial amino acid in a peptide and the essential parts of that amino acid; for example must it be charged? And that information can then be fed back into what is known about the structure of the protein to obtain, in favourable cases, a very detailed picture of what constitutes the precise antigenic site on the protein.

Hisayuki Matsuo (Miyazaki Medical College) has a different interest in peptides, to find and characterize new peptides from biological material. He has identified a family of neuromedins and is now pursuing the family of atrial natriuretic peptides. These peptides are secreted by the atrium of the heart and are thought to play an important role in the regulation of kidney function and blood pressure. Matsuo and others have identified three basic peptides in the family; the γ peptide is an extended form of the α, and the β is an antiparallel dimer of the α. Much effort is going into trying to establish exactly which peptides are active where, and why.

Sydney Brenner

What monoclonal antibodies are to Ler-

Problems of polyglot participation

Tokyo

WHEN 'Molecular Biology Becomes Biotechnology', *Nature's* first conference in Japan, was opened by Prince Hitachi on 20 January, it became the first 'foreign' conference to be opened by a member of the Imperial family. Prince Hitachi, second son of the Emperor, is a full-time cancer researcher in Tokyo. Professor Setsuro Ebashi of the National Institute for Physiological Sciences in Okazaki and Professor Toshitsugu Oda of the National Medical Centre, both of whom were on the advisory board for the conference, also participated in the formal opening.

The three-day conference, held in the Keio Plaza Intercontinental Hotel in Tokyo, was addressed by eighteen scientists from Japan, the United States, England, Switzerland and Australia. One of the speakers, Dr James Watson, had to cancel his appearance at the last minute but, with the help of two of *Nature's* staff in Washington, recorded a 20-minute video film that was shown to the audience.

More than 500 scientists attended the conference, including a sprinkling from overseas: China, the Soviet Union, Korea, Thailand, India, the United States and some European countries were all represeted, but perhaps inevitably the great majority of the audience came from research laboratories in Japanese universities and industry.

Because of the inevitably high cost of mounting such a conference with many overseas speakers, the registration fee was clearly going to be beyond the reach of younger academic students. But, in the end, more than 200 of the audience were Japanese students and younger academics whose presence was made possible by a scholarship scheme financed by 25 companies*. This was the first foreign conference to be supported by Japanese industry and also the first to be endorsed by the Japanese Ministry of International Trade and Industry.

To judge by the proportion of the audience who made use of the simultaneous translation system, at least half of them were happy to listen to presentations in English, the language used by all overseas speakers with the exception of Professor Thomas Blundell of Birkbeck College, London, who made a brief excursion into Japanese. There was much discussion among the Japanese speakers as to which language to use. In part because they felt that English is the international language of science and that all Japanese scientists need to be familiar with it, Professor Shosaku Numa and Professor Tasuku Honjo of Kyoto University, as well as Professor Tadatsugu Taniguchi of Osaka University, chose to speak in English. So too did Professor Susumu Tonegawa of Massachusetts Institute of Technology, who claimed that after many years out of Japan it was easier to cope with phrases such as 'haemopoietic stem cells' in English than in Japanese. □

*Ajinomoto Co. Inc., Asahi Chemical Industry Co. Ltd, Chugai Pharmaceutical Co. Ltd, Daiichi Seiyaku Co. Ltd, Dainippon Pharmaceutical Co. Ltd. Eisai Co. Ltd, Fujisawa Pharmaceutical Co. Ltd, Kanebo Ltd, Kureha Chemical Industry Co. Ltd, Kyowa Hakko Kogyo Co. Ltd, Meiji Milk Products Co. Ltd, Mitsubishi Chemical Industries, Ltd, Nippon Kayaku Co. Ltd, Nitto Chemical Industry Co. Ltd, Sankyo Co. Ltd, Shionogi & Co. Ltd, Sumitomo Chemical Co. Ltd, Suntory, Ltd, Taisho Pharmaceutical Co. Ltd, Takeda Chemical Industries, Ltd, Teijin Ltd, Toray Industries Inc., Wakunaga Pharmaceutical Co. Ltd, Yakult Honsha Co. Ltd, Yamanouchi Pharmaceutical Co. Ltd.

Shosaku Numa and Hisayuki Maisuo

ner, databases are to Tom Blundell (Birkbeck College, London). Because of the problems of determining crystal structures of proteins, he is trying to derive empirical rules of three-dimensional structure on the basis of the amino-acid sequences of proteins. He is optimistic that, with the aid of computer graphics, it will be increasingly possible to recognize sequence motifs that correspond to folded structures, thus leading to improved prediction of structure from sequence.

His group's model of the structure of renin based on its amino-acid sequence and the crystal structure of homologous proteins is still being refined, partly in the interests of being able to suggest how to design better drugs to control blood pressure, but more as an acid test of the predictive techniques when the day comes that the crystal structure of renin is determined.

Development

It is clear from the events of the past year or two that molecular biology can contribute in important ways to the understanding of development. The fruitfly, *Drosophila melanogaster*, and the nematode, *Caenorhabditis elegans*, are two favoured organisms in which to carry out the studies and were accounted for in Tokyo by Walter Gehring (Biozentrum, University of Basel) and Sydney Brenner (Laboratory of Molecular Biology, Cambridge), respectively.

Gehring described some of the latest experiments on the genes that control *Drosophila* development, in particular *fushi tarazu*, which is Japanese for "not enough segments" and which is indeed a gene whose inactivation results in the loss of alternate segments in the embryo. The gene is normally expressed in stripes of activity across the embryo corresponding to the segments that form thereafter. The effects of inactivating the gene can be reversed by incorporating the cloned normal gene into the mutant embryo. And experimental manipulation of the extensive (6,000 bases) non-coding sequences upstream of the coding sequence for *fushi tarazu* has shown that separate sequences are responsible for the correct formation of stripes of activity and the pattern of activity in the nervous system.

An intriguing new result from *Caenorhabditis* is the sequence of *lin 12*, a gene that is necessary for the correct course of development. It has a sequence that is clearly related to that of the precursor of epidermal growth factor, which suggests that its product is probably involved in a cell-signalling process of some sort.

Thomas Blundell, Yoshiki Hotta and Charles Weissmann

Brenner described why and how he and his colleagues have undertaken to produce a complete genetic map of *Caenorhabditis* and reported that about two-thirds of the genome has already been covered but that some of the gaps will be difficult to close.

Gene expression

The study of gene expression is the heart of current molecular biology, or molecular genetics as this pursuit is more accurately termed. Hal Weintraub (Fred Hutchinson Cancer Center, Seattle) outlined the possibilities and problems of using 'antisense' RNA to inactivate the specific gene that is producing the corresponding 'sense RNA'. In his experience, the method can be made to work for almost any gene but it is probable that it works through more than one mechanism Antisense RNA is likely to be an increasingly important tool in identifying the function of genes and their products

No such help is needed by T.S Okada (National Institute of Basic Biology, Okazaki) as his studies concern the genes for crystallin, the major protein of the lens

His problem is to understand how the expression of the gene is normally confined to the lens when it can be experimentally expressed in other cell types. Experimental systems are proving to be a problem: only two transgenic mice have been obtained and they both expressed the crystallin gene in the brain's pyramidal neurones rather than the lens; transgenic fish were much more readily obtained but gene expression was not confined to the lens; tumours developed from teratocarcinoma cells into which a crystallin gene had been inserted expressed the gene regardless of cell type; but, more promisingly, when the teratocarcinoma cells were fused with mouse blastocysts, expression of the crystallin genes was confined to the lines of chimaeric mice that developed.

Whereas most studies of gene expression are concerned with 'front-end control', that is by the upstream noncoding sequences of a gene, Stanley Cohen (Stanford University) has concentrated on 'back-end control', determined by the stability of messenger RNA. He described experiments that establish that mRNA (from bacteria at least) is degraded from the 3′ end and that the half-life of different mRNAs can vary from 2 to 20 minutes or so. By making a variety of hybrid mRNAs between parts of molecules with very different half-lives, Cohen has shown that the 5′ end of one mRNA can impose its rate of degradation upon the 3′ end of another mRNA attached to it. In *Rhodopseudomonas capsulata*, he has found an example of a single mRNA (for light harvesting and reaction centre proteins involved in photosynthesis) that is degraded differentially on either side of a 'barrier', with the result that 20 times as much of one protein is produced as of the other.

Virology

One virus per speaker was the order of the day. Kenichi Matsubara (Osaka University) presented his latest data on the integration of the hepatitis B virus into the genome of human hepatoma cells. No consistent picture emerges. On the contrary, apart from the fact that in no case is the complete viral genome integrated, in no case is the same pattern of integration observed. In half the cases, the integration is complex with a variety of discontinuities and rearrangements.

Question .... time

The latest information to emerge from Mitsuaki Yoshida's continuing studies of the human T-cell leukaemia virus, which causes adult T-cell leukaemia, shows that the *pX* gene encodes two proteins in addition to the protein that is responsible for the transactivation of transcription. Yoshida does not yet know the function of these two new proteins, which are encoded in a different reading frame and are mainly to be found in the nucleus.

Charles Weissmann (University of Zurich) is more concerned with the mechanism of interferon-mediated resistance to viral infection than in the viruses themselves. He has recently identified a protein that is induced by interferon and seems to be responsible for the specific resistance of Mx^+ strains of mice to influenza virus. The protein is localized to the nucleus of cells, consistent with the large number of basic amino acids revealed by cDNA sequencing. Incorporation of the DNA into Mx^- cells confers upon them resistance to influenza virus. Weissmann suggested that resistance to the virus might therefore be transgenically conferable upon Mx^- animals but that the results might not be altogether beneficial because why otherwise should the majority of laboratory strains of mice and even a sizeable proportion of wild mice be Mx^-?

Evolution

Walter Gilbert (Harvard University) described the technique of direct genomic sequencing and some of its applications. It enables the direct sequencing of gene fragments in a mixture of low complexity without the need first to purify the fragment. The essential requirement is enough knowledge of the sequence to make probes that are used to 'hook' the fragment.

From a knowledge of the coding sequence for triose phosphate isomerase of corn, that technique was used to identify the gene's intron/exon boundaries. A comparison of the location of the eight introns so found with the six in the chicken's gene, five in *Aspergillus* and the absence of any introns in yeast's gene, provided Gilbert with a strong argument in favour of the primitive origin of introns — that is to say, the ancestral triose phosphate isomerase gene would have contained all the introns represented in contemporary genes, and perhaps even more, and that introns have been lost in the course of evolution. That conclusion and recent evidence of certain introns with a phosphodiesterase activity led Gilbert to put forward an RNA view of the origin of life in which RNA with enzymatic and transpositional activities emerged before proteins. Proteinaceous enzymes evolved later because of their superior enzymatic function. And DNA evolved last as a means of perpetuating information.

Peter Newmark

Stanley Cohen and Shosaku Numa

Vision

Shortcomings of an eagle's eye

from Graham R. Martin

EXCEPTIONAL sensory capacity has often been invoked as an explanation of apparently unusual behavioural performance. For example, superiority of visual resolution over that of other animals is often cited to explain the hunting prowess of diurnal birds of prey: modern ornithology texts quote estimates of maximum visual resolution in the larger eagles of up to ten times that of man. However, as knowledge has increased of the physical and physiological factors that ultimately limit the visual resolution of vertebrate eyes[1], visual scientists have come to question the possibility that visual performance in these birds can attain the high levels claimed. The first evidence that visual performance in a raptorial bird does not outstrip that of man came three years ago when maximum spatial visual acuity in a small falcon, the American kestrel, *Falco sparverius*, was shown just to equal that of man[2]. Now, the first measurement of the spatial visual acuity of an eagle's eye shows that its resolution out-performs that of man by a factor of two at best[3].

Working with a wedge-tailed eagle, *Aquila audax*, Liz Reymond of the Australian National University trained the bird to learn a two-choice simultaneous discrimination task. The bird viewed the stimulus panels from six metres and expressed its choice by flying to one of two perches placed in front of the stimuli. With this arrangement it was possible to measure how the bird's visual resolution varied with both the contrast and luminance of the stimuli; Reymond was also able to test human subjects in the same apparatus to provide direct comparisons.

Reymond's findings are important since they show that the maximum performance of this eagle's eye can be predicted in a straightforward manner from knowledge of the focal length of the eye and the dimensions of the cone photoreceptors in the central fovea of the retina. Thus they provide a confident base for the prediction of visual resolution in other raptors and also demonstrate that there is no need to invoke a special role for the fovea in providing some sort of local magnification of the retinal image to enhance acuity, an idea which has been presented a number of times[4]. It may simply be that the eagle's fovea is no more than an area where the neural layers have been radially displaced so that light scattering is reduced before it reaches the cone photoreceptors.

The dimensions and packing density of the retinal cone cells in the eagle's fovea were found to be very close to the ultimate limit predicted by the waveguide properties of photoreceptors[5]. It should be a simple matter to predict the maximum spatial resolution to be found in the eye of other eagles as long as the size of the eye, or preferably the focal length of the eye, is known. (The focal length of the wedge-tailed eagle's eye is about 22 mm; that of the human is about 17 mm.) In absolute terms the eye of the wedge-tailed eagle is among the largest known and so it is unlikely that maximum spatial resolution in any other bird eye will be greater.

Reymond's study also shows that the eagle's eye is specialized for vision at the highest light levels that occur naturally. This has definite penalties once light levels start to fall and, in the eagle, spatial resolution deteriorates more rapidly with reducing light levels than in the case of man. Again this is in line with predictions based on the physical factors that limit the ways in which information can be extracted from an image by an array of receptors[6]. It also explains why raptors rarely hunt at or after twilight.

Ornithologists, falconers and the casual bird watcher may have difficulty in reconciling these findings with their field observations of the hunting performance of the eagle. They might, however, find comfort in the fact that the eagle's eye seems to obey in a straightforward manner the predictions of optical physics. □

1. Barlow, H.B. *Proc. R. Soc.* **B212**, 1 (1981)
2. Hirsch, J. *Nature* **300**, 57 (1982).
3. Reymond, L. *Vision Res.* **25**, 1477 (1985)
4. Martin, G.R. in *Form and Function in Bird.* Vol.3 311 (Academic, London, 1985)
5. Enoch, J.M. & Tobey, F.L. *Vertebrate Photoreceptor Optics* (Springer, Berlin, 1981).
6. Snyder, A.W., Laughlin, S.B. & Stavenga, D.G. *Vision Res.* **17**, 1163 (1977).

Graham R. Martin is a lecturer in the Department of Zoology and Comparative Physiology, University of Birmingham, Birmingham B15 2TT, UK.

Meteorites

Unexpected Antarctic chemistry

from George W. Wetherill

THE meteorites found in Antarctica during the past 16 years are clearly different from those found elsewhere in several well-understood ways. Approximately 7,000 have been collected — they are on average much smaller than other meteorites, because it is easier to identify a small black fragment on a glacier; and they have been on Earth much longer, because they have been relatively protected against weathering by being encased in glacial ice. On page 390 of this issue, J.E. Dennison and colleagues report another difference that is both surprising and less easy to explain[1]. They find that the concentrations of a number of trace elements in a sample of Antarctic meteorites is different from the concentrations in a similar-sized sample of non-Antarctic meteorites. Several explanations can be suggested but various reasons make all of them difficult to believe.

The great importance of Antarctica for the recovery of meteorites was accidentally discovered by Japanese glaciologists in 1969. Since then, frequent expeditions from several nations have collected thousands of meteorites, probably representing more than 1,000 separate events. Dennison *et al.*[1] report neutron activation measurements on 23 stony meteorites from Victoria Land, near the Ross Sea and McMurdo Sound, all of the same chemical class and metamorphic grade (H5 ordinary chondrites). The analyses were compared with a sample of 20 non-Antarctic meteorites of the same type.

For 8 of the 13 elements studied, the differences in mean concentrations of the two samples were judged to be statistically significant. Plausible reasons are presented for believing that these differences are not laboratory artefacts or sampling bias and the authors conclude that two distinguishable populations are being sampled. They also give reasons for rejecting the hypothesis that the differences are attributable to weathering of the Antarctic samples during the approximately 3×10^5 years since they fell to Earth, so they propose that the differences must be extraterrestrial in origin. They suggest that the differences result from variation with time of the asteroidal source regions from which meteorites of this kind are derived and present a scenario in which such a change in population would result from a single burst in ejection occurring after the fall of the Antarctic meteorites. They also propose that such differences may be caused by decay of meteorite fluxes with time, caused by discrete bursts at different times before the fall of the Antarctic meteorites.

No timescale is given for this scenario — the authors note that serious difficulties arise with attempts to be more quantitative. For example, an event occurring since the fall of the Antarctic samples would result in an abundance of cosmic-ray exposure ages of less than 3×10^5 years in non-Antarctic samples, but such young ages are rare for meteorites of this kind. Explanations based on temporal decay of flux components are equally difficult to accept. Theoretical, analytical and numerical studies by a number of authors[2-4] present excellent reasons for believing that the natural timescales for decay of such populations is about 10^7 years, primarily through collisions with small debris as the meteorites pass through the asteroid belt when near their aphelion. This collision timescale is consistent with observed cosmic-ray exposure ages. Not much decay would therefore be expected in 3×10^5 years.

It might be thought that 'meteorite streams' exist, analogous to the well-recognized meteor streams of cometary origin. Coherent changes in the orbits of the stream members might lead to intersection with the orbit of the Earth of one stream at one time, and with another at a different time. This analogy is not valid, however, because these cometary streams remain in coherent orbits only for about 10^4 years. They are easily observed above the sporadic background only because these small meteoroids are removed on a timescale much shorter than that appropriate to meteorites. In agreement with this, the orbits of large meteors identified as stony meteorites that have been photographed by the Smithsonian's Prairie Network[5] are not clustered into streams[6]. It is, therefore, difficult to believe that such rapid temporal variations in the chemical composition of the terrestrial meteorite flux are any more plausible than the alternative hypotheses that were rejected by the authors. On the other hand, if the differences are real, they must have some explanation, possibly one that has not yet been considered. If it does turn out that some apparently well-established earlier conclusion has to be rejected, this would represent an important discovery.

How can this interesting suggestion be pursued? Probably the most fruitful approach would be to convince sceptics that the distinction reported is as real as the authors claim, thereby enlisting the considerable effort that will be required to understand it. All the differences in the mean concentrations for individual elements are within the overlap of the stated 1σ uncertainties. It is not unusual for authors to use such data as evidence against a difference. Dennison *et al.* are to be commended for not taking the easy route, as data can only be expected to reveal small but important differences when pressed to the limits. One approach that would probably satisfy many would be a hypothesis that such specific differences exist between meteorites of about 3×10^5 years old and present-day ones of this kind. This hypothesis would predict that a second investigation with a new sample of meteorites would lead to similar differences in the mean concentrations of the same elements. ☐

1. Dennison, J.E., Lingner, D.W. & Lipschutz, M.E. *Nature* **319**, 390 (1986).
2. Öpik, E.J. *Interplanetary Encounters* (Elsevier, Amsterdam, 1976).
3. Arnold, J.R. *Astrophys. J.* **141**, 1536 (1965).
4. Wetherill, G.W. *A. Rev. Earth planet. Sci.* **2**, 303 (1974).
5. Ceplecha, Z. & McCrosky, R.E. *J. geophys. Res.* **81**, 6257 (1976).
6. Wetherill, G.W. & ReVelle, D.O. *Icarus* **48**, 308 (1981).

George W. Wetherill is Director of the Department of Terrestrial Magnetism, The Carnegie Institution, Washington, DC 20015, USA.

Neuropharmacology

Acetylcholine and brain cells

from David Brown

ACETYLCHOLINE has been recognized as a major neurotransmitter in the mammalian brain for more than 40 years. Our knowledge of how it works at the level of the individual brain cell is still, however, rather sparse, largely because the brain is complicated and difficult to study. Over the past few years some of the difficulties have been circumvented by the development of methods for intracellular recording from single cells in isolated slices of brain tissue maintained in *in vitro*. Two papers in this issue[1,2] illustrate how such methods can be used to provide new information about the ionic conductance changes that acetylcholine produces in brain cells, and the way these changes affect neuronal excitability. They also help to provide a clearer pharmacological definition of the receptors involved.

It is known from experiments on intact brains that acetylcholine may either accelerate or retard the firing rate of individual neurones — that is, it may either excite or inhibit them, or sometimes it does both[3]. Three mechanisms for excitation have so far been identified: inhibition of a slow voltage-dependent K^+ current[4]; inhibition of a slow Ca^{2+}-activated K^+ conductance[5,6]; and activation of a cation (presumed Na^+) conductance (T.M. Egan and R.A. North, unpublished data). Hitherto, the mechanism of inhibition has not been ascertained, although experiments on the analagous responses of peripheral ganglion cells suggested that the activation of a K^+ conductance was the probable cause. Such an effect has now been demonstrated in cells in two areas of brain studied *in vitro* — the parabrachial nucleus[1] and the nucleus reticularis of the thalamus[2]. The latter can be directly inhibited through this mechanism by cholinergic afferents from the brainstem reticular formation; the parabrachial neurones, on the other hand, are themselves cholinergic and so it is argued that the increase in K^+ conductance might subserve a form of auto-inhibition at their axon terminals.

One of the central points arising from these and other studies is that, in the brain, acetylcholine does not simply act as a 'turn-on / turn-off' switch to initiate or stop activity, but works more like a tuning device by modifying the frequency and pattern of cell firing. Brain cells, like heart cells, show complex electrical 'behaviour patterns', determined by the subtle interplay of various time- and voltage-dependent membrane currents. Thus, K^+-current inhibition by acetylcholine eliminates an important component of spike frequency adaptation, thereby converting the response of the neurone from phasic to tonic firing in the face of sustained excitation[6,7]; it also promotes burst firing[8], by releasing the cell from the braking effect of endogenous K^+ currents. It is particularly interesting that the hyperpolarization induced by acetylcholine in the reticular neurones also modifies the firing pattern of the cells, favouring a form of burst firing[2]. It does this by driving the membrane potential into a range where a normally inactivated transient Ca^{2+} current is primed and capable of generating a burst of spikes when activated by a brief depolarization. The old classification of acetylcholine actions into excitatory and inhibitory is clearly an oversimplification.

All of these effects of acetylcholine conform to those originally described by Dale in 1914 as 'muscarine-like' in that they are imitated by the alkaloid muscarine and are antagonized by atropine — in modern parlance, they are mediated by muscarinic receptors. This contrasts with the well-known action of acetylcholine on skeletal muscle, which is mediated by nicotinic receptors. Muscarininc receptors have been isolated and purified to homogeneity as a single protein of relative molecular mass 80,000 but, unlike the nicotinic receptor, its amino-acid sequence is not yet known. Characterization therefore depends on traditional pharmacological approaches, which have revealed subtle heterogeneity in their recognition site, at least for antagonists. Although the receptors show a constant affinity for the classical antagonists atropine and scopolamine, there is a substantial difference in the apparent affinities of receptors from different loci for the antagonist pirenzepine, which has led to a provisional sub-classification into M_1 and M_2 receptors[9]. By this criterion of pirenzepine affinity, the receptors mediating the increased K^+ conductance in brain cells conform to the M_2 type[1], whereas those inhibiting K^+ conductances probably fall into the M_1 category.

Whether this apparent correlation between receptor subtype and ionic conductance is other than coincidental remains to be determined. One facet of muscarinic action which distinguishes it from nicotinic receptor activation is that the transduction between receptor activation and membrane conductance change is less direct, probably being mediated by a linkage of the activated receptor to a GTP-binding protein (G protein)[10]. This may directly close or open K^+ channels, as in the heart[11,12], or it may activate a polyphosphatidylinositol phosphomonoesterase or inhibit adenylate cyclase, both of which have been detected following activation of neural muscarinic receptors (see, for example, refs 13, 14), thereby indirectly changing ionic permeability of the membrane through channel phosphorylation or dephosphorylation. Given the widespread occurrence of these enzymes and of G proteins, preservation of a rigid link between receptor subtype and ion channel might depend on selective coupling to the appropriate G protein. Further studies using reconstituted systems[10] may assist in unravelling these linkages. ☐

1. Egan, T.M. & North, R.A. *Nature* **319**, 405 (1986).
2. McCormick, D A. & Prince, D A. *Nature* **319**, 402 (1986).
3. Krnjevic, K. *Physiol. Rev.* **54**, 418 (1974).
4. Krnjevic, K., Pumain, R. & Renaud, L. *J. Physiol., Lond.* **215**, 247 (1971).
5. Halliwell, J.V. & Adams, P.R. *Brain Res.* **250**, 71 (1982).
6. Cole, A.E. & Nicoll, R.A. *Science* **221**, 1299 (1983).
7. Brown, D.A. *Trends Neurosci.* **6**, 302 (1983).
8. Bernado, L.S. & Prince, D.A. *Brain Res.* **211**, 227 (1981).
9. Hammer, R. & Giachetti, A. *Life Sci.* **31**, 2991 (1982).
10. Haga, K. *et al. Nature* **316**, 731 (1985).
11. Pfaffinger, P.J., Martin, J.M., Hunter, D.D., Nathanson, N.M. & Hillie, B. *Nature* **317**, 536 (1985).
12. Bretweiser, G.E. & Szabo, G. *Nature* **317**, 538 (1985).
13. Fisher, S.K., Klinger, P.D. & Agranoff, B.W. *J. biol. Chem.* **258**, 7358 (1983).
14. Olianos, M.C., Onali, P., Neff, N H. & Costa, E. *Molec. Pharmac.* **23**, 393 (1983).

David Brown is Professor of Pharmacology at the School of Pharmacy, 29/39 Brunswick Square, London WC1N 1AX, UK.

Celestial mechanics

Testing Solar System stability

from P.J. Message

The stability of the Solar System has proved a very fruitful question for stimulating the invention of mathematical tools in the two centuries since the powerfully illuminating researches of Laplace and Lagrange[1]. We now know that the successive approximations of perturbation theory indicate stability, in the framework of mutual gravitational attractions of the planets, to whatever finite order of the perturbations we press the calculations. The convergence of the infinite series thus derived is, however, not straightforward and we do not yet know the limits of validity of the expressions obtained. Consequently, tests by numerical experiments using computer integrations of the equations of motion over long spans of time are of considerable importance. The LONGSTOP project, some early results of which are reported elsewhere in this issue[2] has now provided an integration of the four outer major planets over 9.3 million years, revealing long-period variations in the major semi-axes of the planets' orbits. Such oscillations support the indications of long-term stability predicted by analytical perturbation theory.

The question of Solar System stability has very often been interpreted as whether the mutual gravitational attractions of the planets will leave the principal characteristics of their orbital motions unaltered. These characteristics are generally taken to be that the orbits are nearly circular, nearly coplanar, spaced well apart so that there are no very close approaches between two planets, and of approximately their present sizes. In the real Solar System, there are also non-gravitational forces on the planets, albeit very small, some of which are dissipative in effect and will, after a very long time, ultimately disrupt the present form of the system.

The question posed for the purely gravitational system is especially challenging mathematically and the answers obtained over the past two centuries have reflected the increasing rigour and precision of mathematical techniques and understanding. Laplace and Lagrange[1] first found parameters describing the shapes and orientations of the orbits in terms of which the differential equations for the long-term changes in the orbits are approximately linear. They showed that the approximate linear equations indicate stability and the changes in the parameters are the superpositions of periodic oscillations with periods of up to about two million years, termed secular variations.

Laplace also showed that the sizes of the orbits, as measured by their major semi-axes, are subject only to periodic oscillations, to the first order in the perturbations. In an appropriate formulation, this is also true to the second order, as announced initially by Poisson[3,4], but, using the method generally employed in the nineteenth century to construct theories of planetary perturbations, not to the third order[5,6]. This indicated possible underlying steady changes (secular terms) in the sizes of the orbits, suggesting a possible threat to the ultimate stability of the Solar System from gravitational interactions alone.

A series of more recent investigations, using methods originated by Poincaré[7,10], has made it clear that the variations are all periodic, if appropriate parameters and method of proceeding to successive orders of the perturbations are chosen, to whatever order of the perturbations we work Some of the periods are very long, as already found in the theory of the secular variations. It is now clear that the secular terms in the major semi-axes shown by earlier methods are simply the start of such oscillations of very long period, appearing as power series in the time. But because of the convergence problems and the consequent difficulty in determining for what sets of parameters and time span these results are valid, stability is not yet proven by these methods.

It is clear that error bounds found by straightforward applications of the ordinary processes of mathematical analysis are much too pessimistic and grossly underestimate the true scope of validity of these expressions. Experiments by numerical integration have, however, been made in systems that do not share all of the well-ordered characteristics of the real Solar System mentioned above or in which the planetary masses have been artificially augmented. These show departures from well-ordered stable behaviour, sometimes referred to as wildness[11,14]. But, to be relevant to the actual Solar System, numerical experiments must not use fictitiously augmented values of the planetary masses and instabilities are not expected to manifest themselves before the elapse of a very long time, if at all.

The integrations performed by Hubbard and Oesterwinter[15] covered one million years and verified that the shape and orientation parameters showed only the superposition of long-period oscillations predicted by the secular variation theory over that interval. A more recent integration, made by Kinoshita and Nakai, covering five million years, has also led to the identification of a significant interchange of angular momenum between the orbital motions of Jupiter and Uranus with a period of just over 1.1 million years[16]. This is a manifestation of a beat frequency between two of the fundamental oscillations of the secular variations.

1. Laplace, P.-S. & Lagrange, J L. *Nouv. Mém Acad r Sci Belles-Lett. Berlin* (1781); Oeuvres de J L. Lagrange, Vol.5, 123 (Gauthier-Villars, Paris, 1870)
2. Milani, A., Nobili, A.M , Fox, K. & Carpino, M *Nature* **319**, 386 (1986).
3. Poisson, S.D. *J. Éc. polytech.* **15**, 1 (1809)
4. Duriez, L. *Astr. Astrophys.* **68**, 199 (1978)
5. Haretu, S.C. thesis, Univ. Paris (1878)
6. Eginitis, M.D. *Annls Obs. Paris, Mém* **19**, H1 (1889)
7. Poincaré, H. *Méthodes Nouvelles de la Mécanique Céleste*, Chs 9, 10, 21 (Gauthier-Villars, Paris, 1893)
8. Newcomb, S. *Smithson. Contr. Know* No 281 (1874)
9. Duriex, L. thesis, Univ. Sciences Techniques, Lille (1979). *Astr. Astrophys.* **54**, 93 (1977).
10. Message, P.J. *Celest. Mech.* **26**, 25 (1982)
11. Hénon, M. & Heiles, C. *Astr. J.* **69**, 73 (1964)
12. Hills, J.G. *Nature* **225**, 840 (1970)
13. Birn, J. *Astr. Astrophys.* **24**, 283 (1974)
14. Nacozy, P. *Astr. J.* **81**, 787 (1976).
15. Cohen, C.J., Hubbard, E.C. & Oesterwinter, C *Astr Pap. Am. Ephem. Wash.* **22**, Pt 1 (1972)
16. Milani, A. & Nobili, A.M. *Nature* **310**, 753 (1984)

Now the LONGSTOP project, the long-term gravitational study of the outer planets begun under Professor Archie Roy of Glasgow University, has covered 9.3 million years and hopes ultimately to cover up to ten times this span. Analysis of results[2] has shown long-period oscillations in the major semi-axes of the individual orbits, or in their energies, which are functions of the major semi-axes. In particular, they find an energy exchange between Uranus and Neptune with the same period as that previously found between Jupiter and Uranus[16]. Although 9.3 million years is still a small fraction of the history of the Solar System, the LONGSTOP integrations show no evidence for gradual secular changes and thus they validate, over this period, the results of analytical perturbation theory. ☐

P.J. Message is in the Department of Applied Mathematics and Theoretical Physics, University of Liverpool, Liverpool L69 3BX, UK.

Ocean Drilling Program

Formation of the Norwegian Sea

*from the Leg 104 shipboard scientific party**

A MAJOR objective of the Ocean Drilling Program is to increase our understanding of the formation of a deep ocean basin and its subsequent development through time. The early history of such events is hidden beneath the Earth's passive continental margins, where thick covers of sediment often make detailed studies difficult. The continental margin off Norway, however, is a relatively young geological feature, and thus is particularly well suited for studying problems of this kind. Although systematic geophysical surveys off Norway have revealed buried features on the lower continental slope that seem to be closely related to the break-up of a continent and the earliest history of sea-floor spreading, no consensus as to the nature and crustal composition of these features had been reached before ODP Leg 104 drilling of a transect across the Vøring Plateau off northern Norway.

The primary features revealed by past surveys in this region are structural highs delimiting sedimentary basins. The formation of these basins off the Norwegian coast culminated in the late Jurassic, considerably pre-dating the time of initiation of sea-floor spreading in the Norwegian Sea estimated at 56–58 Myr ago. Beneath a cover of sediment, the tops of the highs are characterized by a pronounced seismic marker of basaltic origin. Below the basalt are zones of seaward-dipping reflector sequences resting on an acoustically homogenous basement complex. Similar seismic features have been reported at many other passive margins where there is little evidence for extensional faulting before spreading.

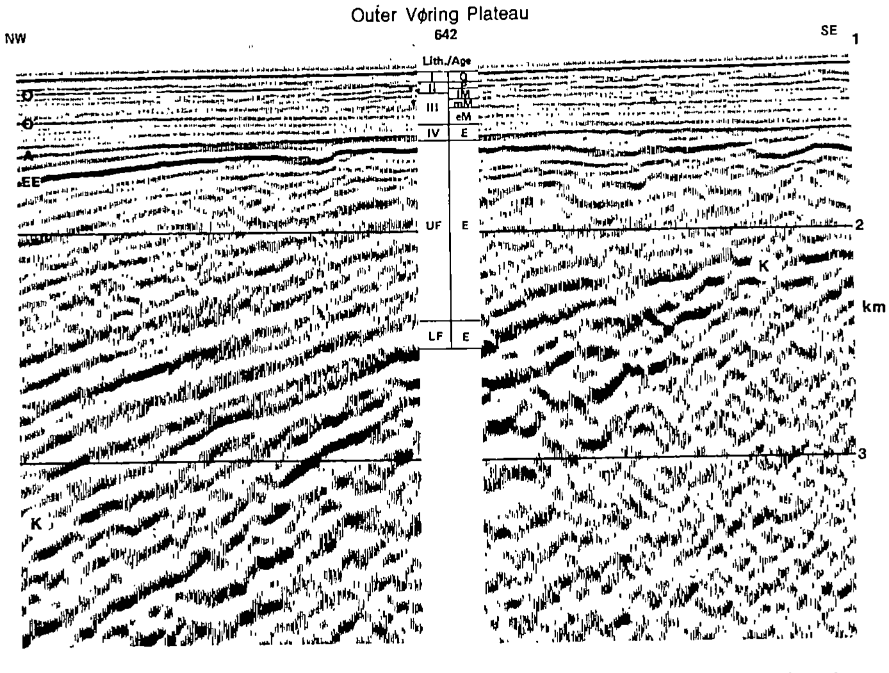

Fig. 2 Depth-migrated seismic section across the Outer Vøring Plateau, showing the sediment cover, dipping reflector sequence, reflector K and the location of Site 642. Q, Quaternary; P, Pliocene; lM, late Miocene; mM, middle Miocene; eM, early Miocene; E, Eocene; UF, upper volcanic flow series; LF, lower volcanic flow series.

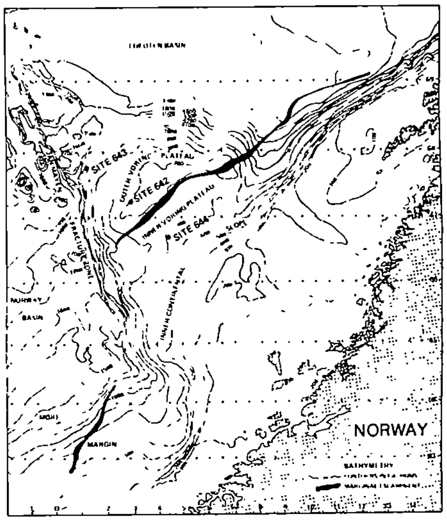

Fig. 1 Location of ODP Leg 104 drill sites in the Norwegian Sea.

During Leg 104, eight holes were drilled at three sites. A deep drill hole (site 642) was located at the inner part of a prominent wedge of dipping reflectors on the Outer Vøring Plateau (see figures). Coring at site 642, in a water depth of 1,290 m, recovered a 914-m-thick volcanic sequence below a 315-m-thick cover of predominantly pelagic to hemipelagic Cenozoic sediments. The entire volcanic section is Eocene in age and contains 121 volcanic flows, 49 volcaniclastic sediment layers and 7 shallow-level dikes. The volcanic sequence can be divided into an upper and a lower series that are distinctive in the textural, mineralogical and structural characteristics of the flows, as well as in the compositions of interlayered volcaniclastic sediments. The upper series is both subaerial and subaqueous in origin, whereas the lower series is entirely subaqueous. Thus the seaward-dipping reflector sequence is now proven to consist of cyclic tholeiitic basalt flows and interbedded volcaniclastic sediments that form the upper volcanic series.

Coring at site 642 also penetrated the underlying rock unit, which is separated from the dipping sequence by a distinct reflector, K, in the seismic record. Reflector K seems to originate from a distinct volcaniclastic unit that defines the transition between the upper and lower volcanic series. Preliminary shipboard petrographic studies indicate a distinct boundary at this level. The proposed lithologic contact is supported by measurements of physical properties, the magnetic character of the rocks and a vertical seismic profiling experiment. We note that the volcanic series boundary is associated with a rapid decrease in both density and seismic velocity, giving rise to a large negative reflection coefficient.

Existing models proposed to account for reflector K have not gained support from Leg 104 drilling. Two significant observations are that the lower volcanic-flow series is apparently andesitic in nature and that interbedded volcaniclastics of the lower series contain mica, quartz and lithic fragments of continental origin. While awaiting additional chemical analyses, we tentatively suggest that the lower series is related to the transition between rift and drift phase, whereas the upper series was emplaced later, probably at the time of the North Atlantic Thulean volcanic surge in the lower Eocene (approximately 53–56 Myr ago).

A palaeoenvironmental drill-site transect combining site 642 with site 643 near the foot of the Voring Plateau and site 644 in the inner Voring Basin was used to study the evolution and variability of the Norwegian current. This current, a continuation of the Gulf Stream, transports temperate North Atlantic water along the Norwegian margin to the Arctic Ocean and provides northwestern Europe with warm climates. The Vøring Plateau is well suited to study this palaeoceanographic problem because of its regular blanket of pelagic and hemipelagic sediments. The transect recovered material from environments varying from the deep ocean basin to the central continental slope, and will allow detailed studies of horizontal and vertical temporal gradients associated with the current system. The two innermost sites document only the Neogene and Quaternary history of the ocean basin (the last 24 Myr) but the sedimentary record of site 643 extends back into the early Eocene (about 53 Myr).

All sites yielded sediment sections with high-resolution Neogene and Quaternary magnetostratigraphic and biostratigraphic records, allowing detailed reconstructions of the palaeoceanography of the Norwegian–Greenland Sea and of northern hemisphere palaeoclimate. A temperate Norwegian current was long-lived during the Neogene but began to deteriorate at 2.8–2.9 Myr (possibly as early as 4.5 Myr), being replaced by intermittent cold ice-covered polar water masses. Layers of dark, carbonate-poor glacial muds, interbedded with light-coloured interglacial sediments, constitute the most conspicuous evidence that glacial climates existed in the Norwegian Sea during the past 3 Myr. At that same time, cold-water planktonic faunas and floras begin to appear in the surface water masses. In the mid-Quaternary (0.73 Myr), the intermittently occurring high abundances of biogenic opal disappear from the sediments, suggesting a dramatic drop in surface water productivity. Calcareous nannoplankton and planktonic foraminifers, however, persist in abundance until 0.4 Myr, producing enough particles to form calcareous muds and marly oozes interbedded with the glacial layers. Around 0.4–0.5 Myr the Norwegian Sea depositional environments become almost exclusively dominated by the glacial mode.

The transition from the pre-glacial to glacial palaeoenvironment occurs 0.5 Myr earlier in the Norwegian Sea than in the North Atlantic Ocean to the south of the Greenland–Scotland Ridge, but it is preceded by the 4–6 Myr glacial record of the Arctic Ocean. We also note that the cessation of pre-glacial conditions occurred almost simultaneously with a similar major northwards expansion of Antarctic polar water. □

Prehistoric ecology

Clues from the pollen record

from Peter D. Moore

For many years palaeobotanists and archaeologists have used pollen analyses of peats and lake sediments as a guide to the use of land by prehistoric communities. Certain characteristic pollen types and particular changes in pollen frequency are now accepted as evidence for the involvement of prehistoric man in the modification of vegetation. But many of these conventional interpretations have developed mainly as a consequence of informed speculation; there has been very little empirical analysis of the man – vegetation–pollen relationship. The International Geological Correlation Programme has set up a working group to consider the value of 'anthropogenic indicators' in pollen diagrams; the first meeting was in Wilhemshaven, West Germany, on 3–8 October 1985.

Some of the most significant research has been carried out by K.-E. Behre (Wilhemshaven), whose group has been excavating Iron Age and later settlements in the marshes and sandy heaths of north Germany. In the low-lying lands around the mouth of the Weser River, the waterlogged soils are valuable to archaeobotanists because of the excellent preservation of the remains of wooden artefacts, fragments of textiles and crop plants. In Iron Age and Roman times, settlements were established on *Wurten*, artifically constructed mounds of earth that elevated their populations above the level of the floods. The soils for cultivation (plaggen soils) had to be imported from the higher sandy ground; the remains of these soils and the Celtic fields of Iron Age times are still abundant in the area.

Well-documented, extensively excavated archaeological remains in close proximity to wet, peat-forming habitats, both on the ill-drained plains and in kettle-holes within the sandy uplands, have permitted close comparison of the historical and prehistorical records with the evidence from stratified pollen in the peats. In particular, the frequency of peat deposits allows the study of lateral spatial variation on the registration of cultivation events in pollen diagrams. There are also bogs of different sizes, allowing local and regional events to be differentiated.

Kettle-hole bogs in the sandy areas are particularly interesting because cultivation took place in the immediate catchment of their basins. The site of Schwienskuhle, for instance, now lies within dense beech forest, parts of which still have the distinctive marks of an Iron Age field system. The bog is only about 30 metres in diameter, so is likely to contain a record of events that were mainly local. It is in a site like this, therefore, that one might expect to find the most marked development of anthropogenic-indicator pollen. This has proved to be the case — high pollen levels of cultivated plants such as rye (*Secale cereale*) are found, together with their associated weed flora, particularly the cornflower (*Centaurea cyanus*) which seems to be strongly associated with winter cereals. Also found are indirect indicators, such as the sorrel (*Rumex acetosella*) and heather (*Calluna vulgaris*), which owe their presence to the general disturbance of the sandy soils and the opening up of woodland canopies. During the Middle Ages cultivation reached its peak, with rye attaining 55 per cent (expressed as a percentage of tree pollen), corn spurrey (*Spergula arvensis*) 36 per cent and ribwort plantain (*Plantago lanceolata*) 60 per cent.

But one of the most interesting features of Behre's analyses from this site is not a maximum, but a 'settlement gap' in the cereal and weed record, which occurs in the Iron Age/Roman cultivation episodes at about AD 500 and may have lasted for as long as 200 years. This gap has posed a fresh problem — identifying the cause of the decline. So far, theories include plague and a mass emigration of population, perhaps to the British Isles.

Another area in which some progress is being made is the detection of associations between supposed anthropogenic indicators in pollen diagrams. Can one detect specific weed or crop assemblages and interpret them precisely in terms of the land use? J. Turner (Durham, UK) has tackled this question by using multivariate analyses on several published pollen diagrams from different parts of Europe. Using principal components analysis (PCA) she looked for species clusters and found that some pollen types do tend to behave in similar ways.

---

*Co-chief scientists, O. Eldholm (Univ. Oslo) and J. Thiede (Universität Kiel, FRG); ODP staff representatives, E. Taylor (Texas A&M Univ.), C. Barton, U. Bleil, K. Bjorklund, P. Ciesielski, A. Desprairies, D. Donally, C. Froget, R. Goll, R. Henrich, E. Jansen, L. Krissek, K. Kvenvolden, A. LeHuray, D. Love, P. Lysne, T. McDonald, P. Mudie, L. Osterman, L. Parson, J. Phillips, A. Pittenger, G. Qvale, G. Schoenharting and L. Viereck.

In one site in East Anglia, for example, wheat (*Triticum*) is closely associated with Compositae (Tubuliflorae) pollen types at certain levels — perhaps the latter were the weed flora of the wheat crop. At the same site, *Secale* is found close to flax (*Linum usitatissimum*) on the PCA plots. It is unlikely that the two crops were grown together but it is possible that they were grown sequentially in a form of rotation. Not surprisingly, patterns vary in different parts of Europe. The strong correlation between rye and cornflower in northern Germany, for example, is not seen in pollen diagrams from Czechoslovakia, whereas in Central Europe cornflowers seem to be associated with buckwheat (*Fagopyrum esculentum*) in the fossil pollen record.

In the far north of Europe, the whole problem of detecting the past influences of man is compounded by the general paucity of the flora. In the region of Bergen, Norway, P.E. Kaland has concentrated largely on the history of heathland, where it is possible to detect the effects of such land-use practices as burning, grazing and scything for fodder. The northern limit of heathland in Norway coincides with the 0°C isotherm for the coldest month — under colder conditions animals cannot be kept outside in winter, hence heathland is never developed.

Even further north, in the Tromsø region, K.-D. Vorren has met with more problems. Here, the effects of grazing encourage plants such as *Botrychium*, *Polemonium* and *Trollius*, natural components of the Arctic grassland. No longer can one rely on the standard anthropogenic indicators of the south; subtle variations in the proportions of certain meadow species must be sought. The Arctic may prove as enigmatic as the arid zone in the quest for pollen indicators of man's former activities. □

Peter D. Moore is Reader in Ecology in the Department of Biology, King's College (KQC), 68 Half Moon Lane, London SE24 9JF, UK.

Physics of liquids

Are diameters rectilinear?

from J.S. Rowlinson

FORMULATED a hundred years ago[1], the law of rectilinear diameters has become one of the classic laws of the physics of liquids. In the past fifteen years, however, doubts have been raised about the validity of the 'law' on several occasions. The latest and most serious challenge comes from S. Jüngst, B. Knuth and F. Hensel[2].

The law describes the change with temperature of the mean density of a liquid, ϱ_l, and of the vapour in equilibrium with it, ϱ_g. The law states that $\bar{\varrho}=\frac{1}{2}(\varrho_l+\varrho_g)$ is a linear function of temperature, T. Since both ϱ_l and ϱ_g approach the limiting density, ϱ_c, at the gas–liquid critical point, the law can be written

$$\bar{\varrho}-\varrho_c=D_1\tau \tag{1}$$

where $\tau=(T_c-T)/T_c$ and D_1 is a constant. Each density separately approaches ϱ_c as τ^β, where the index β is about 0.32 (see figure)

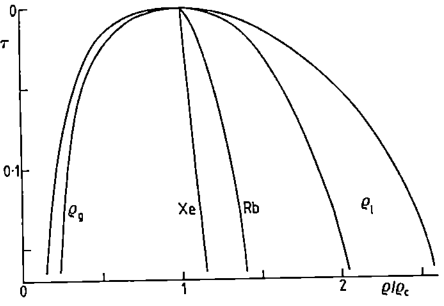

The reduced densities of gaseous and liquid xenon (inner curves) and rubidium (outer curves). Central lines are the mean densities, $\bar{\varrho}$.

$$\varrho_l-\varrho_c=B_0\tau^\beta;\ \varrho_g-\varrho_c=-B_0\tau^\beta \tag{2}$$

Is the law true? Experiments seemed to confirm it. But serious doubts were first raised when it was found to be false for a theoretical model of a liquid[3], which had instead the expansion

$$\bar{\varrho}-\varrho_c=D_0\tau^{1-\alpha}+D_1\tau+\;-- \tag{3}$$

where the index $\alpha=0.11$ is that which describes the well-known singularity in the heat capacity, C_V. A term in $\tau^{0.89}$ might be difficult to distinguish experimentally from one in τ, but interest was excited by the possible existence of a singularity in a function that had been thought to be well-behaved and the theoretical and experimental hunt was on.

A second model[4] was soon found that also has a singular diameter, although this result was complicated by the fact that here $\alpha=\frac{1}{2}$ and $\beta=\frac{1}{4}$, so that $1-\alpha=2\beta$, and a term in $\tau^{2\beta}$ is known to designate the 'wrong' choice of order parameter. Suppose ϱ_l and ϱ_g conform strictly to equations (1) and (2) but, to distinguish liquid from vapour, we choose instead a variable that is an analytic function of ϱ, for example the molar volume ϱ^{-1}. It would follow that for the mean of this function there is a term in $\tau^{2\beta}$ on the right-hand side of equation (1) or (3) which is an even stronger singularity than that in $\tau^{1-\alpha}$ because, for real liquids, 2β is about 0.65. There is no *a priori* reason why ϱ should be chosen, but it certainly seems to be the best function in practice as, with this choice, no term in $\tau^{2\beta}$ has ever been detected.

There were soon other theoretical models[5,6] for which it could be shown rigorously that there was a term in $\tau^{1-\alpha}$, but the size of the coefficient D_0 was unknown. Belief in the existence of this term was strengthened by arguments based on the renormalization group[7,8]. Meanwhile, despite much effort, the experimentalists failed to find convincing evidence: the figure shows the results for xenon[9]. The only simple liquid for which there is good evidence[10] of a singularity is SF_6, but even here it has been suggested[11] that the measured density of the vapour might be too high because of a wetting layer on the inside of the cell.

The whole subject has been re-opened with some difficult, but apparently accurate, measurements of the liquid and vapour densities of the two alkali metals, rubidium and caesium, by Hensel and his colleagues at Marburg[2]. Their results for rubidium are included in the figure and the contrast with those for xenon is clear; near T_c, $\bar{\varrho}$ is not a linear function of T. Their analysis suggests that a term in $\tau^{2\beta}$, if present, is at least 30 times smaller than that in $\tau^{1-\alpha}$ for $10^{-1}>\tau>10^{-3}$. Their values of $1-\alpha$ are 0.86 for Rb and 0.87 for Cs, which are close to the value of 0.89 found for simple liquids from the singularity in the heat capacity.

If the long-predicted singularity has at last been unambiguously detected it is important to know why it is seen only for liquid metals and not for conventional liquids. Liquid metals conduct electricity but their vapours do not. The metal–insulator transition is at a density about that of the critical point, so Goldstein and Ashcroft[12] have argued that it is the strong dependence on density, near ϱ_c, of the screened-ion interaction that is responsible for the strength of the singular term. This argument looks convincing and leads to the interesting suggestion that a similar effect might be found in the coexistence curves of metal–ammonia solutions. □

1. Cailletet, L. & Mathias, E. *C.r. hebd. Séanc. Acad. Sci., Paris,* **102**, 1202, (1886); **104**, 1563 (1887).
2. Jüngst, S., Knuth, B. & Hensel, F. *Phys. Rev. Lett.* **55**, 2160 (1985).
3. Widom, B. & Rowlinson, J.S. *J. chem. Phys.* **52**, 1670 (1970).
4. Hemmer, P.C. & Stell, G. *Phys. Rev. Lett.* **24**, 1284 (1970).
5. Mermin, N.D. *Phys. Rev. Lett.* **26**, 169 (1971); **26**, 169, 957 (1971).
6. Mulholland, G.W., Zollweg, J.A. & Levelt Sengers, J.M.H. *J. chem. Phys.* **62**, 2535 (1975).
7. Nicoll, J.F. *Phys. Rev.* A**24**, 2203 (1981).
8. Nicoll, J.F. & Zia, R.K.P. *Phys. Rev.* B**23**, 6157 (1981).
9. Cornfeld, A.B. & Carr, H.Y. *Phys. Rev. Lett.* **29**, 28 (1972).
10. Weiner, J., Langley, K.H. & Ford, N.C. *Phys. Rev. Lett.* **32**, 879 (1974).
11. Moldover, M.R. & Gammon, R.W. *J. chem. Phys.* **80**, 528 (1984).
12. Goldstein, R.E. & Ashcroft, N.W. *Phys. Rev. Lett.* **55**, 2164 (1985).

J.S. Rowlinson is Dr Lee's Professor of Chemistry, Physical Chemistry Laboratory, South Parks Road, Oxford OX1 3QZ, UK.

JOURNAL OF MOLECULAR BIOLOGY

Editors in Chief: J. Kendrew and S. Brenner

Publication: Bi-weekly.

Subscription: Volumes 187-192, 1986. £576.00 (U.K.)/$1250.00 (Overseas)

The journal continues to provide up-to-date and comprehensive coverage of the entire rapidly expanding field. The journal publishes papers on molecular genetics, mechanisms of replication and translation, and biological structures. There has been increased coverage of those areas of cell biology in which the molecular approach is now achieving substantial results. To give the reader rapid access to papers of special interest, but to avoid dividing the journal into separate sections, papers in each issue are organised by subject area.

MOLECULAR BIOLOGY & MEDICINE

Editors in Chief: J. Sambrook and S. Brenner

Publication: Bi-monthly.

Subscription: Volume 3, 1986. £60.00 (U.K.)/$100.00 (Overseas)

Molecular Biology & Medicine takes as its main task the provision of a meeting ground between the basic scientist and the clinician, and to build up connections between molecular biology and clinical medicine.

Recent rapid developments in biological sciences draw together many areas of biology and have made possible the study of aspects of human biology which only a few years ago would have been considered intractable.

Molecular Biology & Medicine publishes papers in molecular biology, cell biology, biochemistry, biophysics. Preference is given to articles on human material or other material with implications for the human. From the clinical side, work is reported that offers the basic scientist opportunities in new areas for the application of modern concepts and new methods.

Reader Service No.67

Theory and Methods in the Biochemical Sciences

ANALYTICAL BIOCHEMISTRY

Editorial Committee Chairmen: N.O. Kaplan and W.D. McElroy

Volumes 152–159 (1986), 16 issues (including annual subject index)

In the U.S.A. and Canada: $792.00. All other countries $899.00. In the U.K.: £666.00

Analytical Biochemistry, an international journal of analytical and preparative methods, presents original articles on methods of interest to the biochemical sciences and to all fields that impinge on biochemical investigation.

ARCHIVES OF BIOCHEMISTRY AND BIOPHYSICS

Co-Chairmen of Editorial Committee: R. W. Estabrook and S. Udenfriend

Volumes 244–251 (1986), 16 issues (including annual subject index)

In the U.S.A. and Canada: $792.00. All other countries: $905.00. In the U.K.: £670.50

Archives of Biochemistry and Biophysics presents articles in the developing areas of biochemistry and biophysics, especially those related to molecular biology, cell biology, and developmental biology.

BIOCHEMICAL AND BIOPHYSICAL RESEARCH COMMUNICATIONS

Editors: E. Carafoli, P. Cuatrecasas, I. C. Gunsalus, O. Hayaishi, B. L. Horecker, M. D. Lane, W. J. Lennarz, W. D. McElroy, F. C. Neidhardt, C. Paoletti, W. D. Phillips, A. Sols

Volumes 134–141 (1986), 24 issues plus annual index issue

In the U.S.A. and Canada: $596.00. All other countries: $684.00. In the U.K.: £507.00

Biochemical and Biophysical Research Communications is an international journal devoted to the rapid dissemination of timely and significant experimental results in the diverse fields of modern biology. Articles in this journal emphasize the innovative aspects of the research reports.

For more information or free sample copies, please write or call:

Academic Press, Inc., Journal Promotion Dept., 1250 Sixth Avenue, San Diego, CA 92101, U.S.A. Tel: (619) 230-1840.

Academic Press, Inc., (London) Ltd., Journal Marketing Dept., 24-28 Oval Road, London NW1 7DX, England. Tel: 01-267 4466

(Please specify journal title)

Reader Service No.68

ACADEMIC PRESS

AP

A MAJOR NEW JOURNAL

PROTEINS

Structure, Function, and Genetics

Important advances are being made in all aspects of the research on protein molecules and the genes that encode them. Recent developments are having a major impact on the rate and ease with which the three-dimensional structure of proteins and protein complexes can be determined. There are new molecular genetic methods for introducing site-specific mutations and for obtaining high-level expression of proteins. New insights into the relationships between protein structure and function are being provided by the increased power of computational analysis and advances in the understanding of the physical chemistry involved. Developing knowledge of primary and secondary structure of nucleic acids and the proteins which interact with them is yielding a new understanding of the ways in which gene expression is controlled.

To keep readers abreast of significant advances and offer investigators a vehicle to report their important new work, a new journal, **PROTEINS: Structure, Function, and Genetics,** is being launched.

PROTEINS: Structure, Function, and Genetics concentrates on advances in all areas of protein research—structure, function, genetics, computation, and design.

Specific areas covered include:

- structure-function relationships of proteins and inhibitors
- structure determination including discussions of new techniques
- designing of new proteins and small molecules that can interact with them
- studies of the interactions between proteins and nucleic acids
- modifications of proteins by altering the genes which encode them
- modifications of proteins by chemical means
- results and methods of computational analysis for protein structures and function

PROTEINS: Structure, Function, and Genetics welcomes full-length articles reporting new experimental and theoretical results. In addition, each issue will include review articles. Those wishing to make contributions should contact: Cyrus Levinthal, Editor-in-Chief • **PROTEINS: Structure, Function, and Genetics** • c/o Alan R. Liss, Inc. • 41 East 11th Street • New York, New York 10003 • (212) 475-7700.

INFORMATION/SAMPLE COPY REQUEST FORM

☐ Please send me additional information on **PROTEINS: Structure, Function, and Genetics,** Volume 1, 1986, four issues, September, October, November, December.

☐ Please send me instructions for contributors.

☐ Please send me a sample copy of the first issue.

Please return this form to the publisher.

PLEASE PRINT

Name ____________________

Address ____________________

____

City State Zip

Country ____________________

1/86 SA-ABAE

Alan R. Liss, Inc. • 41 East 11th Street • New York, NY 10003

EDITOR-IN-CHIEF

Cyrus Levinthal
Department of Biological Sciences
Columbia University
New York, New York

EDITORIAL BOARD

John Abelson
Robert L. Baldwin
Herman Berendsen
David Botstein
Jean-Michel Claverie
David Davies
William F. DeGrado
Richard E. Dickerson
David Eisenberg
Robert Fletterick
Walter Gilbert
Nobuhiro Go
Arnold Hagler
Steven C. Harrison
Jan Hermans
Barry Honig
Michael James
Emil T. Kaiser
Arthur Karlin
William Konigsberg
Joseph Kraut
Robert Langridge
Dale L. Oxender
Alexander Rich
Jane Richardson
Chris Sanders
Robert Sauer
Robert Schleif
David Shortle
Paul Sigler
Thomas Steitz
Lubert Stryer
Don Wiley
Kurt Wüthrich

Additional editorial board members to be named shortly.

PAPERS ARE NOW BEING ACCEPTED FOR PUBLICATION

Reader Service No.190

Thunder in the air

Gwyn Macfarlane

The Life of Ernst Chain: Penicillin and Beyond. By Ronald W. Clark. *Weidenfeld & Nicolson: 1985. Pp.217. £14.95. To be published in the United States by St Martin's Press at the end of March, $25.*

Ernst Chain (1906–1979), the third man in the trio of penicillin Nobel Laureates, has a distinguished biographer in Ronald Clark. Much has been written about Fleming, less about Florey and — apart from E.P. Abraham's admirable Biographical Memoir for the Royal Society — virtually nothing about Chain. This, the first full-length biography, is a factual account of a gifted, highly temperamental and provocative scientist.

Clark devotes only six pages to Chain's early life, and we miss the personal details that might have explained the moulding of his extraordinary character. His parents were Jewish, his father a Russian chemist who had established a chemical works in Berlin, his mother German. The death of the father and the failure of his business left the family impoverished, but Ernst's education at school and university did not suffer. He loved music, becoming a fine concert pianist and music critic for a Berlin newspaper. A career in music was considered, but he also loved science, graduating in chemistry and physiology and then studying chemical pathology at the Charité Hospital. He was, we are told, liable to "violent outbursts with shouting and throwing things about".

Ernst Chain: *"It seems to be my destiny to be involved in fights. . .".*

From *The Life of Ernst Chain*

Under this excitability there was a native shrewdness and, alarmed by the growing antisemitism in Germany, he left in April 1933 to seek refuge in England. In London he was befriended by J.B.S. Haldane who found a post for him with C.R. Harington at University College Hospital Medical School. It was an unhappy arrangement. Chain complained about the lack of equipment, quarrelled with Harington and left within a few months "after a row". Haldane rescued him and settled him with Gowland Hopkins in Cambridge. Here he was happy, finding Hopkins "one of the most considerate and kindest of human beings". Working for a PhD, he studied enzyme chemistry and showed that the neurotoxin of a snake venom was an enzyme that destroyed a component of the respiratory chain, thus explaining (for the first time, he claimed) the biochemical action of a natural toxin.

In 1935, Howard Florey, newly-appointed professor of pathology in Oxford, was looking for a young biochemist. Hopkins recommended Chain, and Florey appointed him. For the first few years all was well between them, and Chain's work went brilliantly. Florey had asked him to study lysozyme, the natural bacteriolytic agent discovered by Fleming in 1921. Chain, with L.A. Epstein, showed that it was an enzyme and identified its substrate as a component of bacterial cell walls, thus explaining its lytic action. He then proposed a joint investigation, with Florey, of other natural antibacterial agents, including penicillin, discovered by Fleming in 1928.

Clark gives a lucid and impartial account of the now-familiar Oxford penicillin story. Chain had his own version with considerable differences in emphasis, like a photographic print and its negative. Clark has achieved a synthesis by quoting Chain with qualifications. For example, Chain used to assert that it was he who introduced Florey to penicillin after reading Fleming's original paper. But Clark quotes an earlier conversation in which Florey described penicillin and the failure of Raistrick — a famous biochemist — to obtain a stable extract. "He can't have been such a very good chemist" remarked Chain. But it was, it seems, Chain's enthusiasm that set practical work in motion. The biochemical problem challenged him, and Florey's interest was in the action of penicillin on virulent staphylococci.

Chain and Epstein started work in 1938 and Clark quotes the latter as saying that "results were unimpressive". Then N.G. Heatley joined in, and his innovative mechanical genius increased the production of crude penicillin so that Chain was able to obtain active extracts. He asked Florey to test the toxicity of these, and was annoyed when he delayed. So Chain asked J.M. Barnes to inject a mouse, and when this seemed none the worse, claimed exultantly that "this was the crucial day in the whole development of pencillin". As Clark points out, the non-toxicity of penicillin had, in fact, already been shown (by Fleming). However, Chain's impatience stimulated a rather aggrieved Florey to take active control of the whole project.

The really crucial day was 25 May 1940, when the first animal protection test proved the immense therapeutic possibilities of penicillin. The story then moves on two fronts, the drama of the first clinical trials in man and the biochemical triumphs of Abraham and Chain in purifying penicillin and discovering its β-lactam structure. But, as success mounted, personal rifts opened between Chain and Florey. One concerned patents. Chain, the son of an industrial chemist, knew their importance, and urged protection for the Oxford processes. He was over-ruled by Edward Mellanby, of the Medical Research Council, who found the very idea unethical, and by Florey. Bitter arguments ensued and Chain's resentment was increased when, a few years later, events proved him to have been, in principle, right.

The second breach was more personally wounding. In 1941, it was agreed with Mellanby that Florey should go to the United States to seek commercial help in producing penicillin. Chain had expected to go with him, but Florey decided to take Heatley, the production expert, and the first that Chain knew of this was the sight of the packed bags in Florey's room. "I left the room silently", he wrote years later, "but shattered by the experience of this underhand trick and act of bad faith". Thereafter, as the fame of penicillin grew, Chain came to fear that he would be cheated of the credit he believed to be due to him. In 1944, premature rumours that a Nobel prize would be awarded to Fleming and possibly Florey increased Chain's agitation and he considered pressing his own claim. In fact, in 1945, the prize was equally divided between Fleming, Florey and himself.

A Nobel prize and international renown only increased Chain's sense of grievance in Oxford. He considered his colleagues' account of the penicillin work for a joint book on antibiotics "a travesty of the true facts", and his own 19 pages of amendments seriously delayed publication. In particular, he objected to the concept of an Oxford team led by Florey. He was frustrated, too, by the rejection of his proposals for a fermentation plant in Oxford, and a national penicillin factory. He began to establish outside links, becoming a consultant to various pharmaceutical firms and foreign government agencies, and to the Weizmann Institute in Israel, where a tempting position was on offer. Finally, in 1948, he agreed to direct the new biochemistry department of the Istituto Superiore di Sanità in Rome, where Marotta, the head of the Institute, could satisfy his demands for space and funds.

Chain's new department produced important work, the most significant arising from the idea of modifying the penicillin molecule to produce more effective compounds. He was a consultant to the Beecham Group, who took up the idea, sending biochemists to work with him in Rome. They isolated the nucleus of penicillin and, on returning to England, produced semi-synthetic derivatives of great therapeutic (and commercial) value. In 1964, trouble struck the Rome Institute. In an incomprehensible political vendetta, Marotta and several staff members were charged with the alleged misuse of government funds, and sentenced to long terms of imprisonment. Chain was not on trial, though the prosecution claimed that the Italian government had a right to the Beecham patents. Meanwhile, he had left Rome to become professor of biochemistry at Imperial College, London.

MONOGRAPHS TEXTBOOKS...

and other technical publications on Nuclear Energy

write for free publications and services catalog

American Nuclear Society
555 N. Kensington Ave.
La Grange Park, IL 60525
(312) 352-6611

Reader Service No.14

Chain's plans for his (second) new department were so grand that the cost was far beyond the available College or University funds. But he refused to modify them, and himself raised over £600,000 from various sources, including the Wolfson Foundation and Lord Rank. The new buildings housed a fermentation plant, spacious laboratories and a luxurious penthouse apartment for the professor and his family. As in Rome, Chain's years there were fruitful and happy up to a stormy finale. A knighthood in 1969 had removed a growing sense of injustice. Then, in 1973, when he was due to retire, he insisted on the right to nominate his successor under the terms of the Rank gift. He was over-ruled and then fought legal battles with great tenacity but with ultimate defeat and much bitterness.

Chain's remaining years were filled by ceaseless activity. He retained many commercial consultancies and travelled incessantly, lecturing in any one of his five fluent languages, lobbying for his pet causes or against those he disliked. He was seldom for long either in his Wimbledon home, or his house in the West of Ireland, where he died after a heart attack in 1979.

Ronald Clark has produced a readable, lucid but unduly deferential book on a difficult subject. For technical matters he has evidently (and wisely) drawn heavily on Abraham's Memoir. While he faithfully recounts the facts of Chain's highly coloured career and achievements, and quotes extensively from his writings, he makes little attempt to analyse motives and character. In consequence, the book seems remote and bloodless. It is difficult, perhaps, to present a clear picture of someone in constant — almost frantic — movement, and whose violent emotional drives could change course almost overnight.

There were steadier drifts in Chain's life. Between youth and age he moved from the political left to the right, and became more firmly attached to his Jewish faith. The sense of personal injustice was a constant companion, unresolved by great scientific and material success. He never learned that too much shouting for what you want makes people deaf and then hostile. "It seems to be my destiny to be involved in fights throughout my career" he wrote (to Sir Robert Robinson) during the Imperial College affair. In truth, his destiny was simply to be himself. ☐

Gwyn Macfarlane, Mallie's Cottage, Opinan, Laide, Ross-shire IV22 2NU, UK, is Emeritus Professor of Clinical Pathology at the University of Oxford. He is author of Howard Florey: The Making of a Great Scientist *(Oxford University Press, 1979) and* Alexander Fleming: The Man and the Myth *(Chatto & Windus/Harvard University Press, 1984).*

All about being an amphibian

Tim Halliday

Biology of Amphibians. By William E. Duellman and Linda Trueb. *McGraw-Hill: 1985. Pp. 670. $40, £40.*

AMPHIBIANS are of increasing importance in several areas of biology, including ethology, physiology and embryology, and a new textbook that presents an up-to-date and interdisciplinary account of the group is extremely welcome. The last such textbook was G.K. Noble's classic *Biology of the Amphibia,* published in 1931. This is, inevitably, a very different book. Apart from being much larger, it is much more densely packed with the detailed and quantitative information that is nowadays considered essential in scientific texts. Sadly, the chatty and discursive style used by Noble is no longer appropriate in such a book.

Duellman and Trueb intend that their book should be used either as an advanced course textbook or as a general reference book on all aspects of amphibian biology. They have deliberately adopted a functional and evolutionary approach, dividing the 19 chapters into four parts which deal with life history, ecology, morphology and evolution. They have relied heavily on review articles, rather than primary research papers; even so, the bibliography contains some 2,500 references, of which about a third have been published since 1980.

Individual chapters deal with topics that have a biological coherence and do not necessarily reflect divisions between academic disciplines. Thus, behaviour and locomotion are not treated as separate topics but are discussed as and when they are relevant in chapters on, for example, mating and courtship, feeding and defence. This is a particular strength of the book as it allows the biology of the animals themselves to emerge more clearly than it otherwise would.

The balance of subject matter is also good. Most fields of amphibian research are covered in some detail so that, with its bibliography, the book provides an excellent starting point for anyone wishing to study a particular aspect in detail. One area that receives less than adequate coverage is endocrinology, despite the fact that it has been the subject of a lot of recent research. It is surprising, for example, to find no mention of the hormone prolactin, given its importance in the control of fluid balance in a group of animals whose lives are so dependent on water. In selecting their examples, Duellman and Trueb set out to include animals from all parts of the world. They have been more successful in this than in providing a geographically comprehensive coverage of the literature to amphibian research — the references to the work of continental Europeans, particularly the Italians, are very sparse.

Perhaps the most valuable part of the book is that dealing with evolution and taxonomy. Since Noble's day, many new species have been described and the classification of amphibians has undergone radical changes. Duellman and Trueb draw on data from a variety of sources, including cytogenetics, molecular biology and biogeography, to present a coherent and up-to-date account of amphibian phylogeny.

The text is clear and concise and richly illustrated with diagrams and numerous photographs, though some of these are too indistinct to be very informative. Amphibians and their fascinating and varied habits have long deserved a major textbook. This book goes some way towards being all one could wish for and is likely to be an important source of reference for several years. □

Tim Halliday is a Reader in the Department of Biology, Open University, Walton Hall, Milton Keynes MK7 6AA, UK.

A sense of the past

Patrick Rabbitt

Neuropsychology of Memory. Edited by Larry R. Squire and Nelson Butters. *Guilford Press: 1985. Pp.655. $75, £62.50.*

At first sight this is yet another bulky, and startlingly expensive, compendium of articles. It consists of 54 review and experimental papers, loosely organized under three headings: "Studies of Normal and Abnormal Memory in Humans", "Studies of Memory in Non-Human Primates" and "Studies of Memory in Non-primates: Physiology, Pharmacology and Behaviour". On closer reading one finds that it is brilliantly edited. The contributors have not merely been selected for eminence, but because they have something important to say — and they have been disciplined to say it very concisely. In total, however, the book reads like a collection of reports by members of an irreconciliable committee, but this perhaps is the most honest and useful reflection of our current knowledge of the nature and pathology of memory.

Mayes and Meudell capture some of the main tensions in their insightful and critical review. Experts disagree whether "amnesia" is a unitary, or a multiple condition; as to which precise locus of damage to a human or animal brain produces the condition; and as to precisely what disabilities distinguish the "amnesic syndrome" from non-pathological "poor memory" and whether this syndrome is produced by damage to a single critical area or varies with idiosyncratic patterns of multiple lesions. But possibly the most important contribution of this book is that it forces us to recognize an even more fundamental weakness in memory studies: the functional descriptive framework in which all theories have been cast, all experiments designed and all results interpreted over the past 30 years is becoming increasingly unsatisfactory, but no useful alternative has yet been worked out.

This tacit framework has been that "information" from sense organs is "filtered" by a process known as "selective attention". It is then (or later) "encoded" and then (or later) "stored" as an "engram" which is later "retrieved" when required. Studies of memory have attempted to reveal the characteristics of each of these three hypothetical "information processing stages". A tape recorder can be an apt metaphor for this framework as Rose points out in his review, but he goes on further to describe its weakness.

A good example of this weakness is to be found in the paper by Hall and Loftus who consider the case where people experience a particular event and then, subsequently, receive further information which bears upon it and which, apparently, makes them misreport the original details in good faith. The "tape and tape recorder" metaphor rigidly restricts alternative explanations to "overwriting", but the main trouble with this simple underlying model is that it is hard to disprove in specific cases. Even results discrepant from Loftus's, such as those of Bowers and Bekerian, can be re-cast in the same context.

To escape the pervasive assumptions of this framework we must consider how inadequate they are to interpret the more subtle phenomena of memory loss. For example Cermak, greatly extending observations by Kinsbourne, points out that early "memories" produced by amnesics have the characteristic of inferential reconstructions. When pressed, a patient may admit that he cannot recollect any specific episode in his life when he went sailing, but can nevertheless well recall the nature of the sport and, from other incidental evidence, can specify a period of his life when he frequently sailed. Thus the interesting thing about memory is that "retrieval" of information is not simple "reading" of passive "records" by a "tape head", but rather a process of inferential reconstruction — at least as complex as that which occurs in the perceptual interpretation of sensory events. Why has the Lockian associationist fallacy, so long dismissed from perception, persistently lingered in memory studies?

It has been inevitable that rival theories of amnesia should also have been proposed in terms of loci of deficit within this three-stage model. Since it is logically impossible to demonstrate that a given piece of information is *not* held, albeit incommunicado, in "memory store", the trichotomy becomes a dichotomy — disturbances of encoding of relevant information (e.g. Butters and Cermak) or disturbances of "automatic" encoding (e.g. Hirst) as against disturbances of retrieval processes (e.g. Weiskrantz and Warrington). Once again, the model carries restrictive conviction, and even encourages very useful applied work — such as Mathis and Korner's demonstration, in this book, that, like normal people, amnesic patients are helped to learn word lists by a variety of mnemonic techniques.

Thus, though the book will be very helpful to all trying to find their bearings in a complex literature, perhaps its main contribution is to force on us the embarrassment of recognizing that we know that the models of memory we still use are inadequate, but that we do not know how to do better. Perhaps one way out of this is to try and define clearly what *kind* of model we now need. Perhaps, to shake us loose from our restrictive assumptions, we need a few Zen koans to meditate? In his excellent initial chapter, Craik, who gets nearer to the heart of these issues than any commentators before him, seems to attempt just this useful provocation:

> if memory is like perceiving, then it is perhaps no more likely that memory traces exist in the absence of remembering than it is that percepts exist in the absence of perceiving . . .

and

> Good memory for an event is associated with situations in which the event is related to the subject's past knowledge in a meaningful way yet is also treated in a way that is distinctive from this past knowledge . . .

and

> students of memory should not be striving to model the system "at rest" or in isolation – that is, as some entity with an existence separate from its activities. Rather our goal should be to model the interactions themselves — the interactions among tasks, environmental events, and mental representations of past knowledge.

Sensai! □

Patrick Rabbitt is Director of the Age and Cognitive Performance Research Centre, University of Manchester, Manchester M13 9PL, UK

New in paperback

- *The Great Mental Calculators: The Psychology, Methods, and Lives of Calculating Prodigies, Past and Present* by Steven B. Smith. Publisher is Columbia University Press, price is $15. For review see *Nature* **310,** 79 (1984).
- *Glimpsing an Invisible Universe: The Emergence of X-ray Astronomy* by Richard F. Hirsh. Publisher is Cambridge University Press, price is £8.95, $17.95. For review see *Nature* **306,** 508 (1983).

Putting the protists in their place

F.E.G. Cox

An Illustrated Guide to the Protozoa. Edited by John J. Lee, Seymour H. Hutner and Eugene C. Bovee. *Society of Protozoologists, PO Box 368, Lawrence, Kansas 66044, USA: 1985. Pp.629. $80 (non-members of the Society), $60 (members).*

ONLY after a long gestation period has this mammoth publication finally appeared. It comes in large format, printed on glossy paper, and is illustrated with over 3,000 line drawings, photographs, and transmission and scanning electron micrographs. The stated objective was to produce a book "which would enable scientists and students working with protists to place them in an up to date taxonomic scheme". Certainly, every protozoologist should have a copy (or access to one) but whether it will be used as a continual source of reference is debatable.

In general, the 1980 Society of Protozoologists classification (the Levine scheme) has been used, with minor modifications to the phyla Sarcomastigophora, Labyrinthomorpha, Apicomplexa and Myxozoa, major changes to the Microspora and a completely new classification of the Ciliophora. In other respects, the 23 authors have adopted different approaches. For some groups, particularly among the Phytomastigophorea, the reader is taken to species, in others, for example the Ciliophora, the genus, and for some, including the Foraminifera, the family. For the Ciliophora, there is an overall dichotomous key that leads to the order followed by subsequent keys to family. Other groups have keys starting with higher taxa and some, notably the Apicomplexa, have none.

Who is this book for? Certainly not the novice. I had difficulty in following some of the keys and had to resort to the well-tried technique of finding a suitable picture and working backwards. The editors point out that the original literature will have to be consulted, and most protozoologists concerned with taxonomic problems will do this automatically. But those who are not experts, or do not have access to library facilities, might be tempted to use the book as a substitute for the original literature.

Parasitologists, too, may find it a bit disappointing. Those interested in trypanosomes will be alarmed to read on p.9 that *Trypanosoma gambiense* is a parasite of rodents, and on p.142 that the flagellum does not arise from a flagellar pocket (thus distorting the whole of the key), and will be dismayed by the diagram of "*Trypanosoma congolense*" (p.151) which is actually *Cryptobia vaginalis*. Unfortunately, this cannot be checked because the reference given is not actually cited in full and is in fact wrong. Other such errors limit the book's value considerably.

Overall, this guide represents a heroic effort which does not quite come off; in retrospect, a series of specialist keys, which could be revised easily, might have been better. Treated with caution, however, this is a nice book to have around and we shall never see its like again. □

F.E.G. Cox is a Professor in theDepartment of Biophysics, Cell and Molecular Biology, King's College London (KQC), London WC2R 2LS, UK.

Threads of insight

John J. O'Reilly

Fiber Optics: Technology and Applications. By Stewart D. Personick. *Plenum:1985. Pp.257. $45, £38.03.*

STEWART Personick has been a leading figure in optical fibre research for some 15 years, and his early papers on receiver design for digital fibre optic systems are still the key references in this area. A new work by such an eminent author is thus well deserving of special attention. The book is an outgrowth of an introductory course on the subject and, consequently, the author does not go into much detail. Rather, he presents first, in Part I, an overview of components and subsystems with a view to providing a basis upon which the reader can build an understanding of the practical applications and limitations surveyed in Part II.

In addition to the usual material on principles, sources and detectors, Part I includes helpful discussions of practical transmitter drive circuits, receiver design and optical components. System impairments arising from interactions between the source and the fibre, such as modal noise, mode partition, modal distortion and laser noise induced by reflections, are also outlined.

The applications considered in Part II range widely, encompassing telecommunications trunk transmission systems, data links, local area networks, and analogue and broadband networks. Sensing systems are covered briefly, as are system measurements. There is, too, a very brief account of emerging technologies such as integrated optoelectronics, coherent systems and optical switching.

The book is well provided with diagrams and photographs which should enhance its usefulness for the novice. In some instances, though, the reproduction process has resulted in an unfortunate lack of detail (and on one or two occasions the author refers to the colours in monochrome photographs!). The text is largely non-mathematical in nature and there is little in the way of fundamental analysis. For all that, this is not a lightweight book; what it lacks in rigour it makes up for in practical insight and experience.

The descriptions are clear, concise and simple, enabling the underlying principles to be readily appreciated, while references are provided to enable the reader to follow up on the details. The book does not, however, offer us anything new; indeed, several sections of the early chapters seem to have much in common with the author's previous book, *Optical Fiber Transmission Systems*, which was published in 1981 as a volume in the same series.

All in all, this is an interesting collection of topics, pitched at a level which will allow a newcomer to the subject to get to grips with the basic ideas and gain some insight into industrial practice. But, for me, it lacks the style and flair which characterize so much of Dr Personick's output in the technical journals. □

John J. O'Reilly is Professor in the School of Electronic Engineering Science, University College of North Wales, Bangor, Gwynedd LL57 1UT, UK.

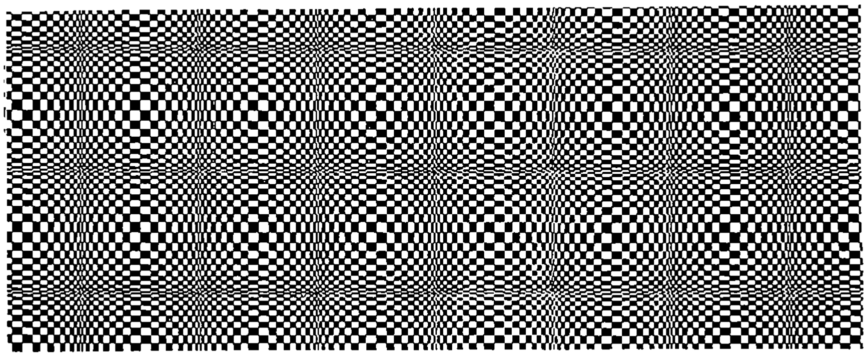

Fechner's colours: as the eye scans across the diagram, the spatial pattern is translated into a temporal pattern of stimulation. Because the different cones and chromatic channels respond at different rates, unsaturated colours may be seen. The illustration is taken from a new textbook published by Harper & Row, Seeing the Light: Optics in Nature, Photography, Color, Vision, and Holography, *by David Falk, Dieter Brill and David Stork. Price is $35.50, £31.95.*

The fight for science textbooks

from Thomas H. Jukes

Many scientists have deplored the success of creationists in expunging evolution from school science textbooks. A sustained and arduous effort is necessary for a reversal of this process.

California in the past year has been the scene of a sustained struggle between creationists and science. For those involved, it was necessary to work with committees of educators who use a specialized language unfamiliar to scientists, with the State Board of Education, with textbook publishers and with the media. Our best results were with the media.

Led by State Superintendent of Public Instruction Bill Honig, the California State Board of Education ("the board") had started a programme to improve the quality of education. Among other things, the State Department of Education seeks to improve school science textbooks. These have long been inadequate, especially in their treatment of evolution. Genetics is described forthrightly without being termed, let us say, "Beliefs of the possibility of inheritance", but the word "evolution" is usually not mentioned for fear of reprisals by creationists[1,2]. As a consequence, the meagre and muted descriptions of evolution in such textbooks appear under chapter headings such as "Changes over Time", or "Evidence of Change".

A Curriculum Commission, reporting to the board, supervises the steps needed for official adoption of the school science textbooks. The first step in the current round, on 24 July 1985, was a hearing, in Costa Mesa, California, on 7th and 8th grade science textbooks, conducted by the commission. Several scientists, including William Bennetta, John A. Moore and Kevin Padian, urged more and better treatment of evolution. The usual litany of objections was presented by a chorus of creationists. Following the hearings, the commission recommended that none of the books be adopted until they were revised to comply with an official publication, the *Science Framework Addendum* of 1984[3]. Revisions, said the commission, were needed in treatment of four topics: cell biology, genetics and evolution; earth science; human reproduction; ethical considerations. Inclusion of the magic word "evolution" alerted veterans of the perennial controversy.

On 12 September, the board met at the headquarters of the Department of Education, Sacramento, to consider the rejection of the books by the commission. Again, several scientists spoke, also three clergymen, urging revision of the textbooks, and again a number of creationists opposed this. Next day, the board voted unanimously for revision of the books as recommended by the commission.

During the hearings, a board member, Angie Papadakis, said she was not convinced about evolution because she could not imagine that primitive creatures could have given rise to males and females, but she was in favour of science because it had produced cosmetics and emollients.

In the next few weeks, deliberations took place involving the commission's Science Subject Matter Committee (SSMC) and the textbook publishers. The chairman of both the commission and SSMC is Robert Douglas, a professional educator who is director of special services for Plumas School District, Quincy, California. SSMC had no biologist as a member, and did not seek advice from any professional biologist. (Two scientists were on the committee that prepared the 1978 Framework and wrote Appendix A.) SSMC stated on 31 October that haste was needed because revisions had to be presented to the board by 13 December for a vote on adoption of the revised books. SSMC met again on 13 November, and set a deadline of 21 November for submission of revisions by publishers. (The books and their publishers were: Heath *Life Science* and *Earth Science*; Holt *Science*; Macmillan *Life Science, Earth Science* and *Physical Science*; Merrill *Focus on Life Science* and *Principles of Science*; Prentice-Hall *General Science* and *Life Science*; Scott Foreman *Life Science*.)

This left twelve working days for public inspection and comment on revisions. Only one copy of the revisions was made available for inspection, because of a weird excuse that they had not been copyrighted, therefore no copying of revisions would be permitted. Viewing would be permitted only in Sacramento.

Copies of the revisions were obtained by Bennetta, however. They were perfunctory and inadequate; and in some cases actually weakened the original text. For example, the phrase "still holds true", in the sentence "Although . . . [Lamarck's] idea that animals that have homologous structures are closely related still holds true" was changed to "is still accepted by scientists". Many obviously erroneous statments remained unrevised and uncorrected. Such qualifying phrases as "some scientists think" were widely used in descriptions of evolutionary processes, though not for other scientific phenomena. Obviously, these servilities were intended to appease creationists.

In our criticisms, we had to avoid antagonizing members of the board, or they might have second thoughts about improving the books. Also, four positions on the board would soon be scheduled for replacements, to be appointed by Governor Deukmejian. We were in a dilemma: we wanted to support Bill Honig's intent to improve the teaching of evolution, but the books were just as bad as before revision. One book said that "some scientists believe" that dinosaurs roamed the Earth millions of years ago.

Nevertheless, we could not condone the impending travesty, and Bill Bennetta lambasted the books and revisions in a widely distributed 19-page letter (2 December). This produced responses, quoting his criticisms, by newspapers, radio and television. We converged on Sacramento for the public hearings on 12 December to learn that individual statements would be limited to 3 minutes.

Douglas presented his committee report containing the clause "The antidogmatism guidelines were considered throughout this revision process" but not mentioning the fact that these guidelines refer to "discussing origins of life and Earth", not to evolution. He recommended adoption, without change, of all revisions dealing with evolution.

About 20 pro-evolution speakers then made statements, including two Roman Catholic priests, a rabbi, various biologists on the faculties of the University of California, Berkeley, San Jose State University, San Diego State University, and scientists from the California Academy of Sciences. Each of these speakers severely criticized a single textbook and its revisions in detail, and furnished a copy of his or her statement (unabbreviated to the 3-minute limit) to each board member at the hearing. However, the vote of the committee took place during the hearings, so the copies of our statements were not perused by its members.

Kelly Segraves and his mother Nell[1], who are creationists, made their usual protest about violation of the rights of Christian children by the teaching of evolution, violations of the antidogmatism policy, and so on.

The chairman, Mr Romero, then called on Douglas for a summary, which was mainly a rebuttal of pro-evolution statements. Douglas said he knew of no biology textbook at this level (7th and 8th grades) that used evolution as the central theme. He said our objection to the incessant caveat "some scientists believe . . ." should be ignored, because *National Geographic* magazine used this phrase in November 1985, and this august publication "is not subjected to pressures". He said that, in deference to us, he had persuaded Merrill to remove a paragraph recommending readers to arrange for a pupil to discuss creationism in science class, and that he had persuaded Heath to change "many scientists think that dinosaurs were the ancestors of modern reptiles" to "scientists classify dinosaurs as the ancestors of modern reptiles". This announcement was greeted with guffaws by the audience. Superintendent Bill Honig said that the publishers had complied with the request for more examples of evolution, including fossils, blood comparisons and description of embryos.

Discussion by board members followed. Board member Angie Papadakis said she could not understand why scientists claimed that the North and South poles had changed places several times. Why couldn't scientists make up their minds? Board member John Ward said that he had "suddenly become aware [*sic*] that large numbers of people believe in divine creation, that probably there is something other than evolution", and that we should "leave a window where students could have some belief other than evolution" to account for their existence, "perhaps divine creation".

The committee voted unanimously to approve the Douglas report. Next day, the full board voted 7 to 2 to accept the report.

The "Antidogmatism Policy", The Science Framework for 1978 (6), Appendix A, included statements on evolution including:

> "The process [evolution] has been going on so long that it has produced all the groups and kinds of plants and animals now living as well as others that have become extinct. . . Another characteristic of life is change in its genetic material with passage of time. This process, termed evolution. . . indicates that all living organisms on Earth have a common ancestor from which they have diverged by evolution during about three billion years. . ."

These statements were contested in court by Segraves *et al.* in 1981[1]. Judge Irving Perluss refused to change them and "found, that in discussing evolution, Appendix A of the Science Framework, along with an antidogmatism policy adopted by the State Board of Education in 1972, fully accommodates plaintiffs' religious views". The "antidogmatism policy" refers only to "discussing origins of life and Earth in public schools"[3].

The *Science Framework Addendum* (1984) seems to have lost track of Appendix A, and has diluted and abbreviated the 1978 Framework's description of evolution. The Addendum assures its readers that "*all science materials* [emphasis added] on the State Board of Education's approved list have been measured against the Board's antidogmatism policy. . ." These warnings evidently cowed publishers, and inhibited them in revising their books, or even, in the case of Prentice-Hall, led to weakening of the original text.

We were permitted one small postlude. The board said that a final check of the books for factual errors, but not for method of presentation, could be made within the next week. Four of us went again to Sacramento, and gave lists of such errors to the Department of Education, and we were told that our lists would be sent to the publishers.

None of the books that we saw describes evolution as well as *The Young Scientist Book of EVOLUTION* (yes, in huge block capitals), 32 pages (Usborne Publishing Ltd, 20 Garrick St, London WC2E 9BJ). But, after all, England is the home of evolution.

Thomas H. Jukes is at the Department of Biophysics and Medical Physics, University of California at Berkeley, Berkeley, California 94720, USA.

1. Jukes, T.H. *Perspect. Biol. Med.* 25, 207 (1982).
2. Bennetta, W. *Pacific Discovery* (California Academy of Sciences, Golden Gate Park, San Francisco, California), January–March 1985.
3. *Science Framework Addendum for California Public Schools* (California State Department of Education, Sacramento, 1984).

ARTICLES

Isolation of a cDNA clone coding for a possible neural nicotinic acetylcholine receptor α-subunit

Jim Boulter, Karen Evans, Dan Goldman, Gary Martin, Doug Treco, Steve Heinemann & Jim Patrick

Molecular Neurobiology Laboratory, Salk Institute, PO Box 85800, San Diego, California 92138, USA

We have isolated a complementary DNA clone containing sequences homologous to those encoding the α-subunit of a mouse muscle nicotinic acetylcholine receptor. Based on the structural similarities between the encoded protein and the muscle acetylcholine receptor α-subunit, and the presence of hybridizing RNA species in the brain, we propose that this clone codes for a neural nicotinic acetylcholine receptor α-subunit.

NICOTINIC acetylcholine receptors are present at the vertebrate neuromuscular junction, in vertebrate sympathetic ganglia and in the vertebrate central nervous system. These receptors can be distinguished on the basis of the spectrum of ligands that open or block ligand-induced opening of the ion channel. For example, the elapid α-neurotoxins that block activation of nicotinic acetylcholine receptors at the neuromuscular junction fail to block the activation of nicotinic acetylcholine receptors found on several different cell types including PC12 (a chromaffin-cell-derived rat cell line)[1], chick sympathetic ganglia[2], chromaffin cells[3] and Renshaw cells[4]. It seems likely, however, that the nicotinic acetylcholine receptors at the neuromuscular junction are structurally related to the neural nicotinic acetylcholine receptors because antibodies directed against the muscle-type receptor will block ligand-induced activation of an α-neurotoxin-resistant acetylcholine receptor[5]. To gain access to this different class of acetylcholine receptors, we used a complementary DNA clone coding for the mouse muscle acetylcholine receptor α-subunit to find, by low-stringency DNA/DNA hybridization, related sequences expressed in the PC12 cell line. We describe here the isolation and properties of a cDNA clone encoding a protein homologous to the muscle

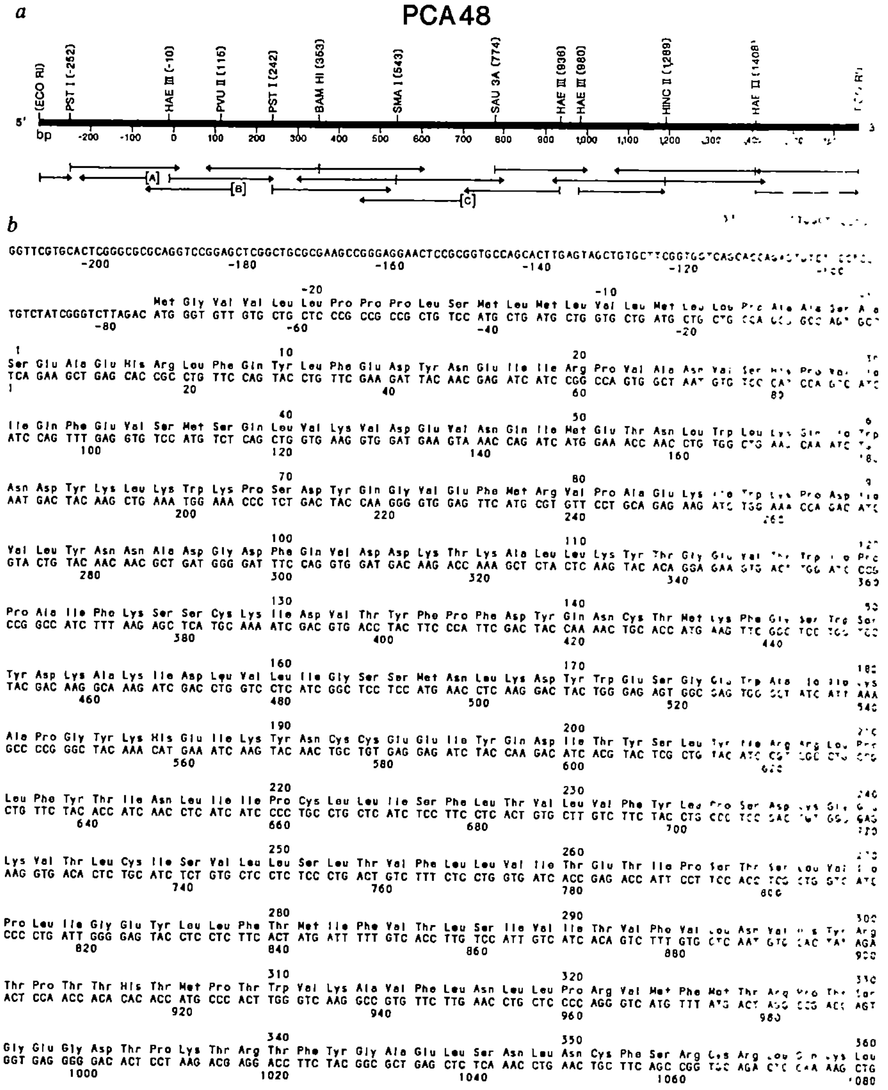

Fig. 1 *a*, Partial restriction endonuclease map and nucleotide sequencing strategy for the λPCA48 cDNA clone. Relevant restriction endonuclease sites are identified by numbers in parentheses which correspond to the 5'-terminal nucleotide in the recognition sequence. The bracketed *Eco*RI sites at the ends of the clone were inserted as linkers during the construction of the cDNA library. The extent and direction of sequence determinations are indicated by horizontal arrows. In some cases, synthetic oligonucleotide primers were used instead of the M13 universal primer for sequence determinations and these are designated by letters in brackets:

[A], 3'-AGGGGAGGGACAGATAGCCC-5';

[B], 3'-CAGTGGAAGAGGGGTGTCAG-5';

and

[C], 3'-GTCACCTTCTCCCCACAGTC-5'.

b, The nucleotide and deduced amino-acid sequence of clone λPCA48. The nucleotides are numbered in the 5' to 3' direction, starting with the first nucleotide in the codon corresponding to the putative amino-terminal residue in the mature protein. Nucleotides extending 5' of base 1 are designated with negative numbers and include residues encoding the putative signal peptide and the 5'-untranslated region. The 5'-untranslated nucleotide sequence presented does not extend to the end of the cDNA in λPCA48; approximately 110 nucleotides from the *Eco*RI linker at the 5' terminus of the cloned DNA extending 3' to nucleotide −225 have been omitted. Nucleotide sequence data in this region show it to be a cloning artefact (see text); furthermore, S_1 nuclease experiments demonstrate that PC12 mRNA will only protect 5'-untranslated sequences up to approximately residue −225 (see Fig. 3). There are 281 nucleotides in the 3'-untranslated region. The λPCA48 sequence includes residues −225 to 1,655 (the clone ends here with an *Eco*RI linker). The sequence in this region is extended 3' with clone λPCA44, which contributes nucleotides 1,656–1,707. The deduced amino-acid sequence for the λPCA48 clone is shown above the nucleotide sequence, with the first amino acid representing the putative amino terminus of the mature peptide.

Methods. A cDNA library was constructed using poly(A)$^+$ RNA isolated from the rat phaeochromocytoma cell line PC12[6]. Size-fractionated double-stranded cDNA was prepared using the method of Gubler and Hoffman[8], ligated to phosphorylated *Eco*RI linkers (10-mer, 5'-CCGAATTCGG-3') and cloned into the *Eco*RI site of bacteriophage λgt10 (ref. 9). The library base was 5×10^6 plaques. Approximately 1×10^6 plaques were screened with a radiolabelled 540-bp *Pvu*II/*Hin*cII fragment derived from the plasmid pMARα15 which contains coding sequences for the mouse muscle acetylcholine receptor α-subunit[17]. This cDNA fragment (nucleotides 132–672) codes for a part of the amino-terminal extracytoplasmic portion of the mature α-subunit as well as the putative acetylcholine binding site and the beginning of the first membrane-spanning region (amino acids 37–216). Three independent clones were isolated, λPCA44, λPCA48 and λPCA54. Partial restriction endonuclease mapping (data not shown) revealed common fragment lengths for the three clones. The longest clone, λPCA48, was ~2 kb and was selected for sequence analysis. DNA sequencing was performed using the dideoxynucleotide chain-termination method of Sanger[10] and M13 bacteriophage vectors mp18 and mp19 (ref. 11).

receptor α-subunit. Based on this homology and on the distribution of homologous RNA species in the rat brain, we propose that the protein encoded by this cDNA clone is an α-subunit of a neural nicotinic acetylcholine receptor.

Isolation and sequencing

The rat phaeochromocytoma cell line PC12[6] expresses a neural nicotinic acetylcholine receptor that is pharmacologically similar to that found on sympathetic postganglionic neurones[1]. We used a radioactive probe prepared from a cDNA clone (pMARα15) coding for the α-subunit of mouse muscle nicotinic acetylcholine receptor[7] to detect hybridizing RNA species present in poly(A)$^+$ RNA prepared from this cell line. At low stringency (5×SSPE, 50% formamide, 42 °C), we found two sizes of RNA hybridizing to this probe, one species of about 2 kilobases (kb) and the other of about 3.5 kb (data not shown).

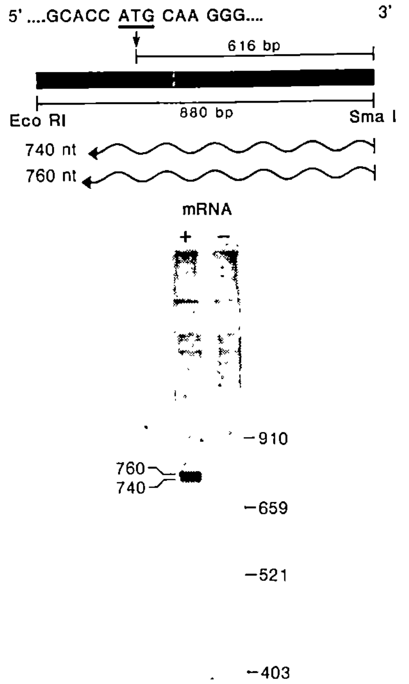

Fig. 2 S$_1$ nuclease analysis of the 5' end of the λPCA48 cDNA clone, performed as described previously[16]. Appropriate single-stranded M13 phage harbouring the 5' *Eco*RI (nucleotide 1) to *Sma*I (nucleotide 880) fragment from λPCA48 was annealed with or without 10 μg poly(A)$^+$ RNA purified from PC12. The sample was digested with 400 units ml^{-1} S$_1$ nuclease for 40 min at 40 °C, extracted with phenol/chloroform/isoamyl alcohol, precipitated with ethanol and resuspended in formamide. Samples were electrophoresed on a 3% acrylamide, 8 M urea gel and electroblotted to Gene Screen Plus. The blot was probed using the nick-translated *Eco*RI/*Sma*I fragment from λPCA48 with prehybridization, hybridization, washing and autoradiography conditions as described earlier[16]. Exposure time was 16 h at −70 °C. The numbers to the right of the figure are the number of nucleotides in relative molecular mass (M_r) standards electrophoresed in adjacent lanes; the estimated sizes of the two protected fragments, 740 and 760 nucleotides, are shown on the left of the figure.

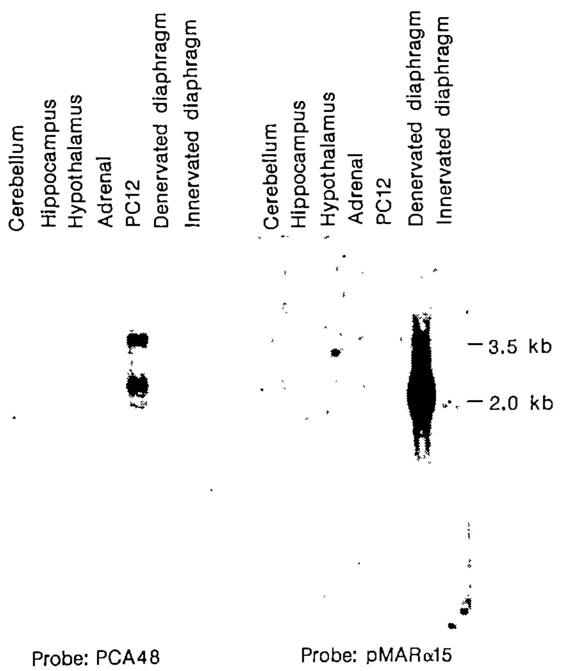

Fig. 3 Northern blot analysis of RNA isolated from Sprague-Dawley rats. Indicated regions of brain or muscle tissue were dissected, poly(A)$^+$ RNA was prepared, resolved on 1.4% agarose gels and transferred to Gene Screen Plus. Filters were hybridized to probes prepared by nick-translation of λPCA48 or pMARα15. Hybridization was carried out in 5×SSPE, 50% formamide at 42 °C and the filters were washed in 0.2×SSPE at 65 °C.

The 2-kb species was always present in poly(A)$^+$ RNA prepared from PC12, but the 3.5-kb species was detected only occasionally. Hybridization was not detected under conditions of higher stringency (0.2×SSPE, 65 °C), suggesting that the hybridizing species were homologous but not identical to the cDNA coding for the muscle nicotinic receptor α-subunit.

We prepared a cDNA library using as template poly(A)$^+$ RNA isolated from PC12 cells. Double-stranded cDNA was made using a modification of the Gubler and Hoffman procedure[8] and ligated into λgt10 (ref. 9) using *Eco*RI linkers. The library had a base of 5×10^6 and was screened at low stringency (5×SSPE, 50 °C) without amplification using a probe prepared from pMARα15. This screening revealed three positive overlapping clones out of the 10^6 examined. One of these positive clones, λPCA48, was chosen for further study.

The nucleotide sequence of λPCA48 was determined using the dideoxy-sequencing reactions developed by Sanger[10] in conjunction with the M13 strains developed by Messing[11]. λPCA48 was subcloned into the vector pSP65 (ref. 12) and the locations of various restriction endonuclease sites were determined. Purified restriction fragments were subcloned into M13mp18 and M13mp19 and their sequences determined. Regions not covered by restriction fragments were sequenced using oligonucleotide primers corresponding to portions of the sequence already determined. A partial restriction map of λPCA48 and a description of the sequencing strategy are shown in Fig. 1*a*.

λPCA48

The nucleotide sequence of λPCA48 was determined over both strands. Figure 1*b* shows the sequence from nucleotide −225 to the 3' end together with the deduced amino-acid sequence. The sequence includes an open reading frame of 1,497 nucleotides beginning at position −75 and extending to position 1,422. This open reading frame codes for a protein that is 47% homologous to the α-subunit of the mouse muscle-type nicotinic acetylcholine receptor (see Discussion and Fig. 6). Based on an alignment of these α-subunit sequences, we identified the amino terminus of the mature protein and a leader sequence of 25 residues beginning with the methionine encoded by the ATG at nucleotide position −75. The sequence around this ATG corresponds to a favoured canonical sequence for translation initiation sites[13] and initiation at the methionine encoded by the ATG at position −75 would produce a leader of similar length to the leaders found in other muscle acetylcholine receptor α-subunits.

Analysis of the sequence of clone λPCA48 revealed that the 5' end of the clone is derived partly from the 5'-untranslated portion of the messenger RNA and partly from an internal sequence. The first 99 nucleotides (nucleotides −324 to −225) of the clone are the reverse and complement of the sequence beginning at nucleotide 456 and extending to nucleotide 554 in the coding portion of λPCA48. The presence of internal sequences at the 5' end of a cDNA has been seen in other cDNA clones (unpublished observation) and probably represents a cloning artefact.

To test whether the remaining nucleotides between nucleotide −225 and the ATG at position −75 were colinear with the mRNA, the 5' *Eco*RI/*Sma*I fragment (nucleotides 1–880) was subcloned into M13mp19 and single-strand DNA prepared. This DNA was incubated with and without poly(A)$^+$ RNA isolated from PC12 cells and the heteroduplexes were digested with endonuclease S$_1$. The resulting fragments were denatured, fractionated on acrylamide/urea gels and electroblotted to Gene

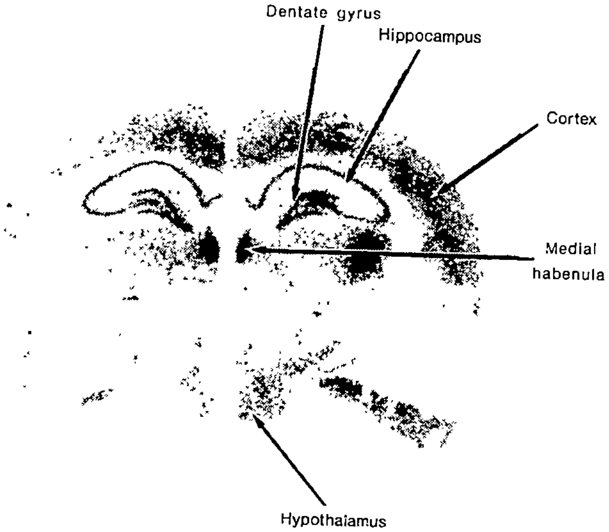

Fig. 4 Autoradiograph of *in situ* hybridization in a coronal section of a rat brain. Tissue was fixed as described by Swanson *et al.*[32] and hybridization was performed using a procedure based on that described by Cox *et al.*[33]. Briefly, sections (20 μm) were mounted on polylysine-coated slides, air-dried, digested with proteinase K, acetylated with 0.25% acetic anhydride, dehydrated and hybridized with ^{32}P-radiolabelled single-stranded RNA probe prepared from an SP6 vector containing λPCA48 cDNA insert. After hybridization, sections were treated with RNase A and washed at a final stringency of 0.5×SSC, 42 °C. Dehydrated slides were exposed to X-ray film for 4 days.

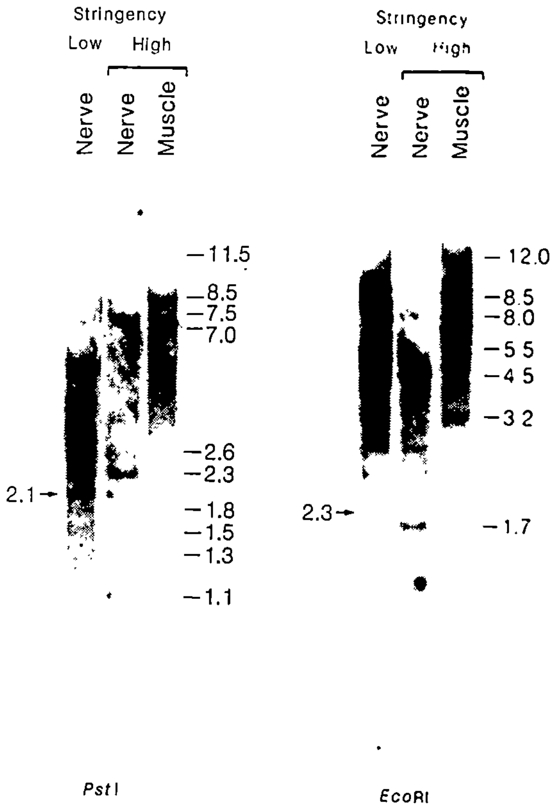

Fig. 5 Mouse genomic restriction fragments hybridizing to λPCA48 or pMARα15. Genomic DNA was purified from liver of adult female C3H mice and digested with *Eco*RI or *Pst*I. The digestion products were resolved on 1.4% agarose gels, transferred to nitrocellulose and hybridized to probes prepared by nick-translation of λPCA48 or pMARα15. Hybridization was carried out in 3×SSC, 1×Denhardt's, and 100 μg ml^{-1} carrier DNA at 65 °C. The filters were washed at 65 °C in 5×SSC (low stringency) or 0.1×SSC (high stringency). The size of the hybridizing fragments (M_r×10^{-3}) was determined from the sizes of known restriction fragments prepared from λ DNA.

Screen Plus. The bands in Fig. 2 were revealed by hybridization to the radiolabelled *Eco*RI/*Sma*I restriction fragment. Two DNA fragments were protected, one of which was 120 bases smaller and one which was 140 bases smaller. We conclude that there are two mRNA species homologous to λPCA48 and that these species differ by about 20 bases at their 5′ ends. Furthermore, the untranslated sequences between nucleotide −220 and the ATG at position −75 are derived from the 5′-untranslated portion of the mRNA as they are protected from endonuclease S_1 by the mRNA.

The open reading frame beginning at position −75 and ending at position 1,422 encodes a protein of 499 amino acids. We compared the sequence of the encoded protein with the α-subunit of the mouse muscle acetylcholine receptor (see Discussion and Fig. 6) and found considerable sequence homology. Based on this homology and the known amino terminus of the *Torpedo californica* acetylcholine receptor α-subunit[14], we have placed the amino terminus of the mature protein as indicated in Fig. 1*b*. This results in a leader sequence of 25 amino acids and a mature protein of 474 amino acids. All the reported muscle-type acetylcholine receptor α-subunit sequences are comprised of 437 amino acids and are therefore smaller by 37 amino acids and 5,500 daltons than the 54,780-dalton protein encoded by λPCA48. As discussed below, this additional mass is found in the proposed cytoplasmic domain located between the third membrane-spanning region and the amphipathic helix.

Although the protein encoded by λPCA48 is homologous to the α-subunits of muscle-type nicotinic acetylcholine receptors from a variety of species, it could be a rat muscle acetylcholine receptor α-subunit, a rat neural acetylcholine receptor α-subunit or a rat bungarotoxin-binding component. We tested the first alternative by preparing poly(A)$^+$ RNA from both innervated and denervated rat diaphragm muscle, size-fractionated it on agarose gels, transferred it to Gene Screen Plus and hybridized it with probes made from either λPCA48 or pMARα15. Denervation of skeletal muscle has been shown to result in an increase in the abundance of acetylcholine receptors and RNA coding for the α-subunit[15,16]. pMARα15, the mouse muscle acetylcholine receptor α-subunit clone, hybridized to a 2-kb mRNA in rat muscle that increased in abundance following denervation (Fig. 3). In contrast, a probe made from λPCA48 failed to hybridize to this mRNA species after medium-stringency washes (2X SSPE, 65 °C). In addition, poly(A)$^+$ RNA from PC12 protected λPCA48 from digestion with endonuclease S_1 while poly(A)$^+$ RNA from rat diaphragm muscle failed to protect λPCA48, but did protect portions of pMARα15 (data not shown). Therefore, the λPCA48 corresponds to a mRNA which is different from the mRNA coding for the muscle α-subunit. We conclude that λPCA48 does not encode the α-subunit of rat muscle nicotinic acetylcholine receptor.

If the protein encoded in λPCA48 is a neural nicotinic acetylcholine receptor α-subunit, it should be present in neural tissue known to contain nicotinic acetylcholine receptors. Poly(A)$^+$ RNA was prepared from a rat hypothalamus punch, and hippocampus, cerebellum, adrenal gland, innervated and denervated muscle, and the PC12 cell line. The RNA was fractionated on agarose gels, transferred to Gene Screen Plus and hybridized with probes prepared from either λPCA48 or pMARα15. The results (Fig. 3) show that the λPCA48 hybridizes to RNA species in all the tissues except muscle. Other experiments demonstrated that λPCA48 hybridizes to RNA prepared from cow adrenal medulla, but not the adrenal cortex, consistent with the idea that the λPCA48 encodes a receptor expressed in chromaffin cells (data not shown).

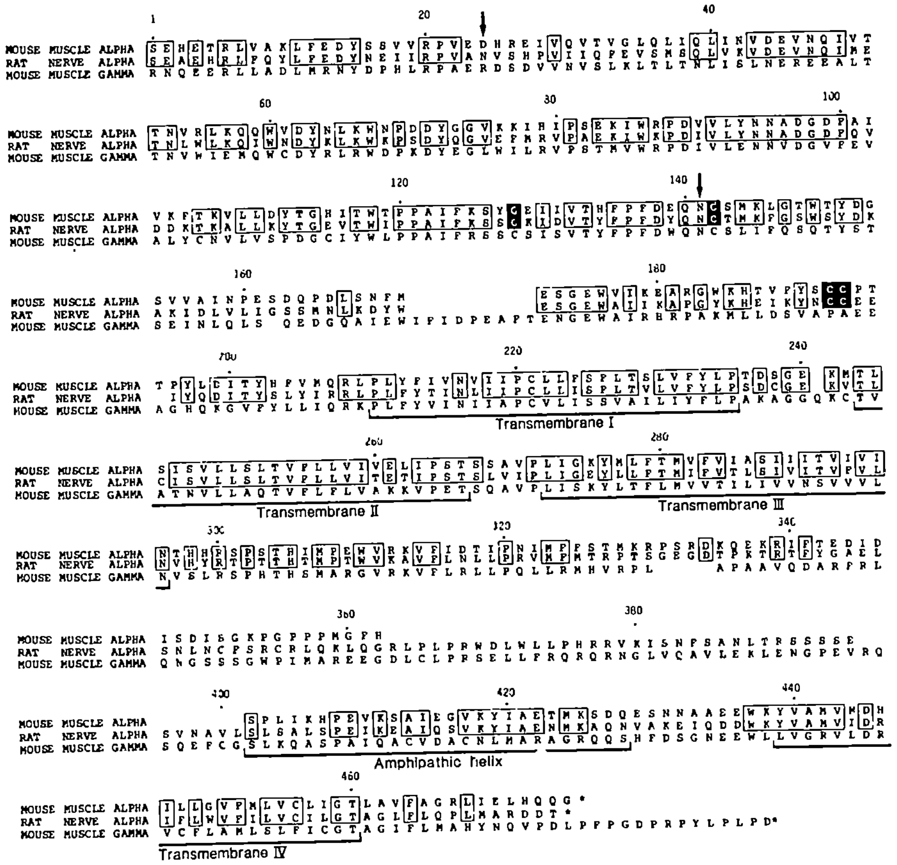

Fig. 6 Comparison of the sequences of the mouse muscle acetylcholine receptor α-subunit[17] and γ-subunit[18] with the rat neuronal α-subunit encoded by λPCA48. Putative transmembrane regions and the proposed amphipathic helix are indicated. The four extracellular cysteine residues characteristic of muscle α-subunits and found in the λPCA48 protein are shown on a black background. The arrows indicate canonical glycosylation sites. Gaps were inserted in sequences to achieve maximum alignment. The overall homology between the amino-acid sequences of the mouse muscle α-subunit and the λPCA48 protein is 47%. At the nucleotide level the homology is 58%. Specific regions within the protein exhibit greater homology; for example, the sequences from the amino terminus to the first transmembrane region are 52% homologous (nucleotide homology, 59%), the sequences in transmembrane 1 are 73% (nucleotide, 75%), those in transmembrane II are 87% (74%), those in transmembrane III are 72% (67%), those in transmembrane IV are 68% (69%) and those in the amphipathic helix are 47% homologous (58%).

The regional distribution of RNA species hybridizing to λPCA48 was also determined by *in situ* hybridization. Figure 4 shows an autoradiogram of a coronal section of a rat brain following hybridization to a probe prepared from λPCA48. Labelling is seen in the hippocampus, the dentate gyrus and, most heavily, in the medial habenula. No such labelling is seen with probes prepared from vector sequences. This pattern of labelling is consistent with the data obtained by Northern blot analysis. In addition, the strong labelling to the medial habenula is consistent with the idea that λPCA48 encodes the α-subunit of a neural nicotinic acetylcholine receptor, as this region of the brain binds cholinergic ligands and does not bind α-bungarotoxin[17].

The above experiments demonstrate that there are RNA species homologous to the λPCA48 clone expressed in the central nervous system. To test the possibility that RNA species homologous to the muscle-type pMARα15 clone also exists in the nervous system, we screened a series of tissues for homologous sequences. Northern blot analysis (Fig. 3) shows that pMARα15 hybridizes to RNA species extracted from the cerebellum, hippocampus, hypothalmus and adrenal gland. The size of the RNA species homologous to the pMARα15 probe varies in different tissues and is clearly different from the RNA species that are homologous to the λPCA48 probe. These results suggest that genes coding for peptides homologous to the muscle-type α-subunit are expressed in the adrenal gland and the central nervous system.

Genomic sequences hybridizing to λPCA48

The mouse muscle α-subunit and the mouse homologue of the rat nerve-type α-subunit are encoded by different genes in the mouse. Figure 5 shows a Southern blot of mouse (BALB/c) genomic DNA digested with endonucleases *Pst*I and *Eco*RI. The transferred DNA was hybridized with probes prepared using pMARα15 and λPCA48 at low stringency (3 × SSC, 65 °C) and at high stringency (0.1 × SSC, 65 °C). At high stringency the two probes hybridized to DNA fragments of different lengths, arguing that the two clones correspond to mRNAs that are the products of different genes. At low stringency the probe prepared from λPCA48 hybridized to a number of additional restriction fragments, for example, the 2.1-kb *Pst*I fragment and the 2.3-kb *Eco*RI fragment (Fig. 6), which were not seen at high stringency in blots probed with either λPCA48 or pMARα15. This suggests additional genes coding for nicotinic acetylcholine receptors exist in the mouse genome.

Discussion

Clone λPCA48 is derived from RNA synthesized by the PC12 phaeochromocytoma cell line and encodes a protein homologous to the α-subunit of muscle nicotinic acetylcholine receptor. We have shown that this clone does not encode the rat muscle nicotinic acetylcholine receptor α-subunit. The PC12 cell line expresses both a neural nicotinic acetylcholine receptor and an α-bungarotoxin binding component, either of which may be encoded by λPCA48. The evidence that best allows us to distinguish between these alternatives comes from *in situ* hybridization data in which λPCA48 hybridizes most consistently to brain regions known to contain cell bodies possessing dendritic processes which bind cholinergic agonists and do not bind α-bungarotoxin. These data are consistent with the idea that λPCA48 codes for the α-subunit of a neural receptor. Furthermore, as the mRNA was derived from a cell line of probable neural crest origin, the encoded protein is likely to be an α-subunit of a ganglionic-type neural nicotinic acetylcholine receptor.

The amino-acid sequences of the mouse muscle α-subunit[7], the rat neural α-subunit and the mouse muscle γ-subunit[18] are aligned in Fig. 6. The amino acids are numbered with respect to their position in the neural α-subunit sequence. The muscle acetylcholine receptor α-subunits have four hydrophobic sequences which are thought to form four transmembrane regions. The protein encoded by λPCA48 also has four hydrophobic sequences and in this respect is structurally similar to the muscle acetylcholine receptor α-subunits.

Finer-Moore[19] and Guy[20] have proposed a fifth membrane-spanning region which may contribute to the ion channel in the receptor. This region is identified in Fig. 6 as the amphipathic helix. This helix partitions charged and hydrophobic amino acids such that the hydrophobic side of the helix could interact with the interior of the membrane or with hydrophobic membrane-spanning regions. The face of the helix containing the charged residues might then, through juxtaposition with homologous sequences in the other subunits, form an ion channel. The distribution of charged residues through the channel alternates with a ring of cationic residues followed by a ring of anionic residues. The protein encoded by λPCA48 contains a sequence homologous to the amphipathic helix found in the α-subunits of the muscle nicotinic acetylcholine receptor. Although the sequence homology is not as great as is seen in the hydrophobic membrane-spanning regions, the distribution of charged and uncharged residues about the helix is similar. The conservation of this sequence between muscle and neural α-subunits supports the idea that the amphipathic helix forms a functionally important receptor domain. In fact, the single-channel conductances of rat ganglionic (44 pS)[21] and bovine chromaffin (31 pS)[22] nicotinic acetylcholine receptors are similar to the single-channel conductance of nicotinic acetylcholine receptor at the motor endplate (31 pS)[23].

All four subunits of muscle nicotinic receptor sequenced to date have a potential asparagine-linked glycosylation site at Asp 141. This site is also found in the protein encoded by λPCA48. An additional glycosylation site occurs at Asp 24 which is not seen in the muscle α-subunit.

There is considerable evidence that both α-neurotoxins and various cholinergic agonists bind to the α-subunit of muscle acetylcholine receptor. The binding site for agonists is probably near a disulphide bond[24]. The extracellular portion of the muscle α-subunit contains four cysteines at positions 128, 142, 192 and 193. Numa *et al.*[25] proposed that there is a disulphide bond between Cys 128 and Cys 142 and that the loop formed by this disulphide constitutes the acetylcholine binding site. It was subsequently proposed[26] that the disulphide bond is not between 128 and 142 but that there is a double disulphide bond between 128 and 192 and between 142 and 193, thus bringing into close proximity two regions of the extracellular α-subunit sequence. Kao *et al.*[27] have shown that an affinity labelling reagent reacts with Cys 192 and Cys 193, placing these residues in the vicinity of the acetylcholine binding site. The protein encoded by λPCA48 also contains the four cysteines found in all the α-subunits of the muscle-type nicotinic receptor, reinforcing the idea that these residues are essential to the function of this subunit.

Although the four cysteine residues are conserved, the sequences that surround them are not. The λPCA48-encoded protein differs from the mouse skeletal muscle receptor at 4 of the 13 residues between Cys 128 and Cys 142. Two of these substitutions, a lysine for a glutamate at position 129 and an aspartate for an isoleucine at position 130, are not conservative changes. The amino acids at these positions are conserved in all the reported muscle-type α-subunit sequences[7]. The other two substitutions are at positions which are not conserved among the α-subunits of the muscle-type receptor. If this sequence forms all or part of the acetylcholine binding site, the substitution at positions which are conserved in the muscle-type α-subunits may account for the pharmacological differences between the neural and muscle-type nicotinic acetylcholine receptors.

The sequence between Cys 142 and Cys 192 might reasonably be involved in ligand or α-neurotoxin binding, as it is contiguous with the cysteines labelled by affinity-labelling reagents. Interestingly, this sequence is one of the least conserved in the λPCA48 protein. Specifically, the 19-residue amino-acid sequence between residues 153 and 172 has only one residue in common with the mouse muscle α-subunit sequence. Furthermore, 8 out of the 19 residues exhibit non-conservative substitutions, replacing uncharged residues with charged residues. If this sequence is involved in ligand or toxin binding, the differences we see between the neural and muscle α-subunits could account for the fact that α-neurotoxins bind and block the muscle acetylcholine receptor but often have no effect on the neural nicotinic acetylcholine receptors. On the other hand, the region 143–191 has been proposed to form two additional membrane-spanning sequences, an extended chain membrane-spanning sequence followed by an amphipathic helix membrane-spanning region[28]. Two observations argue against this last proposal. First, a peptide corresponding to the sequence between 173 and 204 has been synthesized and shown to bind α-bungarotoxin, suggesting that this region of the protein contributes to an α-bungarotoxin binding site[29]. Second, the residues between 144 and 190 in the neural α-subunit are neither hydrophobic nor conserved, as are the other membrane-spanning regions in the acetylcholine receptor subunits.

The alignment of sequences seen in Fig. 6 shows an additional difference between the neural type α-subunit and the muscle-type α-subunits. In the muscle nicotinic acetylcholine receptor, the cytoplasmic domain, that is the region between the third hydrophobic membrane-spanning region and the amphipathic helix, is shorter in the α-subunit than in the β-, γ or δ-subunits. The neural-type α-subunit, however, is 37 amino acids longer than the muscle-type α-subunit and the alignment shown in Fig. 6 places these residues in the cytoplasmic domain. In this respect, the neural-type α-subunit resembles the β-, γ- and δ-subunits of muscle receptor.

Conclusions

The protein encoded by the cDNA clone λPCA48 has a sequence that is homologous to the α-subunit of the muscle-type nicotinic acetylcholine receptor α-subunits, but differs extensively from them in two regions, one of which falls in the cytoplasmic domain of the protein while the other joins the two pairs of cysteine residues in the extracellular domain. This clone hybridizes to RNA species in neural tissue that are different from those recognized by a clone encoding the muscle-type α-subunit. The genomic restriction fragments that hybridize to the clone encoding the muscle-type α-subunit differ in size from those that hybridize to λPCA48. In addition, at low stringency, additional restriction fragments hybridize to λPCA48, suggesting that there are several related coding sequences in the mouse genome. A similar situation occurs in the chicken, where genomic clones have been found that code for two different α-subunits[30]. In addition, an α-bungarotoxin binding site has been isolated from chicken brain and shown to contain a peptide with an N-terminal sequence showing both similarities to and differences from the muscle α-subunit[31]. We have made cDNA libraries from mRNA isolated from various rat brain regions and have found clones that hybridize at low stringency to probes prepared either from λPCA48 or from pMARα15. This approach allows us to identify in the central nervous system a family of acetylcholine receptor molecules that are expressed in different regions of the brain. The availability of cDNA clones and the amino-acid sequence of the encoded proteins makes it possible to study these receptors in detail for the first time.

This work was supported by grants from the Amoco Foundation, the Keck Foundation, the Army Medical Research and Development Command (contract DAMD17-85-C-5198), the NIH and the Muscular Dystrophy Association. D.G. is supported by an NIH postdoctoral fellowship and D.T. is a fellow of the Muscular Dystrophy Association. We thank Donna Simmons and Larry Swanson for providing tissue sections and for help with the analysis of the *in situ* hybridization data, W. Luyten for helpful discussions during this project, and B. Cessna for her help in preparing the manuscript.

Received 25 September; accepted 15 November 1985.

1. Patrick, J. & Stallcup, W. *Proc. natn. Acad. Sci. U.S.A.* **74,** 4689-4692 (1977).
2. Carbonetto, S. T., Fambrough, D. M. & Moller, K. J. *Proc. natn. Acad. Sci. U.S.A.* **72,** 1016-1028 (1978).
3. Wilson, S. P. & Kirshner, N. *J. Neurochem.* **28,** 687-695 (1977).
4. Duggan, A. W., Hall, J. G. & Lee, C. Y. *Brain Res.* **107,** 166-170 (1976).
5. Patrick, J. & Stallcup, W. *J. biol. Chem.* **252,** 8629 (1977).
6. Greene, L. A. & Tischler, A. S. *Proc. natn. Acad. Sci. U.S.A.* **73,** 2424-2428 (1976).
7. Boulter, J. *et al. J. Neurosci.* **5,** 2545-2552 (1985).
8. Gubler, U. & Hoffman, B. J. *Gene* **25,** 263-269 (1983).
9. Huynn, T. V. Young, R. A. & Davis, R. W. in *gt10 and gt11 in DNA Cloning Techniques: A Practical Approach* (ed. Glover, D.) (IRL Press, Oxford, 1984).
10. Sanger, F., Nicklen, S. & Coulson, A. R. *Proc. natn. Acad. Sci. U.S.A.* **74,** 5463-5467 (1977).
11. Messing, J., Gronenborn, B., Muller-Hill, B. & Hofschneider, P. H. *Proc. natn. Acad. Sci. U.S.A.* **74,** 3642-3646 (1977).
12. Melton, D. A., Krieg, P. & Green, M. R. *Nucleic Acids Res.* **12,** 7035 (1984).
13. Kozak, M. *Nucleic Acids Res.* **9,** 5233-5252 (1981).
14. Raftery, M. A., Hunkapiller, M. W., Strader, C. D. & Hood, L. E. *Science* **208,** 1454-1457 (1980).
15. Merlie, J. P., Isenberg, K. E., Russell, S. D. & Sanes, J. R. *J. Cell Biol.* **99,** 332-335 (1984).
16. Goldman, D., Boulter, J., Heinemann, S. & Patrick, J. *J. Neurosci.* **5,** 2553-2558 (1985).
17. Clarke, P. B. S., Schwartz, R. D., Paul, S. M., Pert, C. B. & Pert, A. *J. Neurosci.* **5,** 1307-1315 (1985).
18. Boulter, J. B. *et al. J. biol. Chem.* (submitted).
19. Finer-Moore, J. & Stroud, R. M. *Proc. natn. Acad. Sci. U.S.A.* **81,** 155-159 (1984).
20. Guy, H. R. *Biophys. J.* **45,** 249-261 (1984).
21. Rang, H. P. *J. Physiol., Lond.* **311,** 23-55 (1981).
22. Fenwick, E. M., Marty, A. & Neher, E. *J. Physiol. Lond.* **331,** 577-597 (1982).
23. Colquhoun, D. in *The Receptors: A Comprehensive Treatise* Vol. 1 (ed. O'Brien, R. D.) 93-142 (Plenum, New York, 1979).
24. Karlin, A. & Cowburn, D. A. *Proc. natn. Acad. Sci. U.S.A.* **70,** 3636-3640 (1973).
25. Numa, S. *et al. Cold Spring Harb. Symp. quant. Biol.* **48,** 57-70 (1983).
26. Luyten, W., Kellaris, K., Kyte, J., Heinemann, S. & Patrick, J. *Neurosci. Abstr.* **10,** 734 (1983).
27. Kao, P. N. *et al. J. biol. Chem.* **259,** 1162-1165 (1984).
28. Criado, M., Hochschwender, S., Virender, S., Fox, J. L. & Lindstrom, J. *Proc. natn. Acad. Sci. U.S.A.* **82,** 2004-2008 (1985).
29. Wilson, P. T., Lentz, T. L. & Hawrot, E. *Proc. natn. Acad. Sci. U.S.A.* (in the press).
30. Mauron, A. *et al. Neurosci. Abstr.* **11,** 171 (1985).
31. Conti-Tronconi, *et al. Proc. natn. Acad. Sci. U.S.A.* **82,** 5208-5212 (1985).
32. Swanson, L. W., Sawchenko, P. E., Rivier, J. & Vale, W. W. *Neuroendocrinology* **36,** 165-186 (1983).
33. Cox, K. H., DeLeon, D. V., Angerer, L. M. & Angerer, R. C. *Devl Biol.* **101,** 485-502 (1984).

Expression of the c-*myb* proto-oncogene during cellular proliferation

Craig B. Thompson*, Peter B. Challoner, Paul E. Neiman* & Mark Groudine†

Fred Hutchinson Cancer Research Center, 1124 Columbia Street, Seattle, Washington 98104, USA
Departments of * Medicine and † Radiation Oncology, University of Washington, Seattle, Washington 98195, USA

In several cell types, messenger RNA levels of the nuclear proto-oncogene c-myb *vary as a function of cellular proliferation; a transient increase in* c-myb *steady-state mRNA, mediated by post-transcriptional mechanisms, occurs during cell-cycle progression. In contrast, both quiescent and proliferating immature thymocytes contain exceptionally high levels of* c-myb *mRNA as a consequence of increased* c-myb *transcription.*

ALTHOUGH there is increasing evidence that cellular proliferation is controlled, at least in part, by extracellular growth factors, relatively little is known about how this control is mediated within the cell (see refs 1, 2 for reviews). The characterization of several genetic lesions resulting in arrest at specific points of the cell cycle in both yeast and several cell lines implies that there are specific regulatory (restriction) points in the growth cycle of the cell[3,4]. A gene that exhibits a transient increase in expression during the cell cycle could, therefore, either be a regulator of a restriction point, or be responding to a cell-cycle-specific regulatory signal. Several genes involved in DNA synthesis, including dihydrofolate reductase (*dhfr*)[5,6], thymidine kinase (*tk*)[7,8] and thymidylate synthetase (*ts*)[9], undergo transient expression in the cell cycle.

Several lines of evidence suggest that proto-oncogenes are involved in the intracellular events that govern cellular proliferation[1]. As many of the changes required for cell replication occur within the nucleus, one or all of the nuclear proto-oncogenes c-*myc*[10], c-*fos*[11] and c-*myb*[12,13] may play a regulatory role. Both c-*myc* and c-*fos* expression increase transiently following the stimulation of quiescent cells to proliferate[14-17]. However, neither of these genes shows any variation in expression within the cell cycle itself[8,18,19]. It has not been determined if the third nuclear proto-oncogene c-*myb*, the cellular homologue of the transforming gene (v-*myb*) of the avian myeloblastosis virus, is involved either in the activation or in the subsequent proliferation of quiescent cells. As both the messenger RNA and protein products of c-*myb* have short half-lives[13,20], it is possible that changes in the expression of this gene could occur within the time-frame of these events. Here we demonstrate that c-*myb* is expressed in association with cell proliferation in various cell types. Unlike c-*myc* and c-*fos*, c-*myb* is not involved in the immediate response to serum growth factors, but does undergo a transient increase in expression that appears to correlate with cell-cycle progression in chicken embryo fibroblasts (CEF). In at least some cell types, such as MSB-1 cells (a chicken T-cell line), c-*myb* appears to undergo a transient increase in expression in each cell cycle during exponential growth. The changes observed in c-*myb* expression during cell proliferation in both CEF and MSB-1 cells appear to be regulated primarily by post-transcriptional mechanisms. In contrast to these results, we find that the high level of expression of c-*myb* reported in immature thymic cells[21-25] is not cell-cycle-dependent and instead correlates with the increased transcription of c-*myb* in these cells.

c-*myb* expression

To examine whether the expression of c-*myb* varies with the proliferative state of the cell, we determined the amount of c-*myb* mRNA as cells in mass culture were shifted between exponential growth and growth arrest. Two types of avian cells were analysed in this way (Fig. 1): MSB-1, a transformed chicken T-cell line grown in suspension culture; and CEF. MSB-1 cells were stimulated to proliferate by diluting the cells to 2×10^5 cells per ml in fresh media. Following an initial period of exponential growth, the number of cells proliferating in culture declined until the culture entered growth arrest. The cells were then returned to exponential growth by redilution in fresh media. Total cell RNA was isolated from cells at the indicated time-points using guanidinium isothiocyanate[26]. Northern blots were prepared from RNA samples equalized as described previously[8] and hybridized sequentially with probes specific for the c-*myb*[27] and glyceraldehyde 3-phosphate dehydrogenase (*gpd*)[28] genes. The levels of *gpd* mRNA, a ubiquitously expressed 'housekeeping' gene, varied little. In contrast, the level of c-*myb* mRNA was highest during the period of exponential growth and decreased as the percentage of cells in the cell cycle declined in the culture over time. When the cells were restimulated to enter the cell cycle by redilution, levels of c-*myb* mRNA characteristic of exponentially growing cells were again observed. To confirm these results in a non-transformed cell type, CEF were made quiescent by density arrest. The cells were then replated at low density and cultured through exponential growth until they again reached density arrest. The

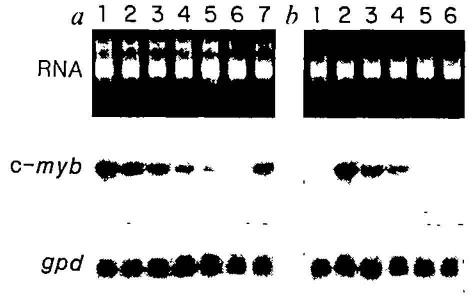

Fig. 1 c-*myb* mRNA levels in proliferating cells. *a*, MSB-1 cells; *b*, CEF cells. *a*, MSB-1 cells were cultured at 2.0×10^5 cells per ml and entered exponential growth (lane 1). They were then maintained in culture until no further increase in cell number was observed (lanes 2–6), and finally recultured at 2.0×10^5 per ml. Following reculture, the cells resumed exponential growth in 24 h (lane 7). At daily intervals as the cells went from exponential growth to saturation arrest, an aliquot was removed and total cell RNA extracted using guanidinium isothiocyanate[26]. The samples were equalized for rRNA, and the equalization confirmed by ethidium bromide staining of equal amounts of the RNA samples separated on a non-denaturing 1% agarose gel (upper panel). These equalized RNA samples (2–10 μg) were separated on 1% agarose/formaldehyde gels and transferred to nitrocellulose. The filters were hybridized sequentially with a ^{32}P-labelled 1.0-kilobase (kb) *Bam*HI fragment containing a portion of the v-*myb* gene from avian myeloblastosis virus[27] (a gift from M. A. Baluda) and a 1.2-kb *Pst*I fragment containing a portion of the *gpd* gene[28]. Autoradiograms were exposed for 2–48 h and equivalent exposures compared. Relative molecular masses of the mRNAs that hybridized to each of the probes agreed with previously published values[23,28]. Quantitation was performed by densitometry. *b*, CEF cells were recultured at a density of 1×10^6 cells per 150 mm plate and maintained until confluent (lane 1). At daily intervals, as cells went from exponential growth to density arrest, an aliquot was removed and total cell RNA extracted (lanes 2–6). Samples were equalized for rRNA and Northern blots were prepared and hybridized with v-*myb* and *gpd* probes as described above. In *a* and *b*, cell viabilities as measured by trypan blue exclusion were >95%. In both cell types, >40% of the cells were in S or G_2/M phase during exponential growth and <5% had $>2N$ DNA content during growth arrest as measured by propidium iodide staining of isolated nuclei[8].

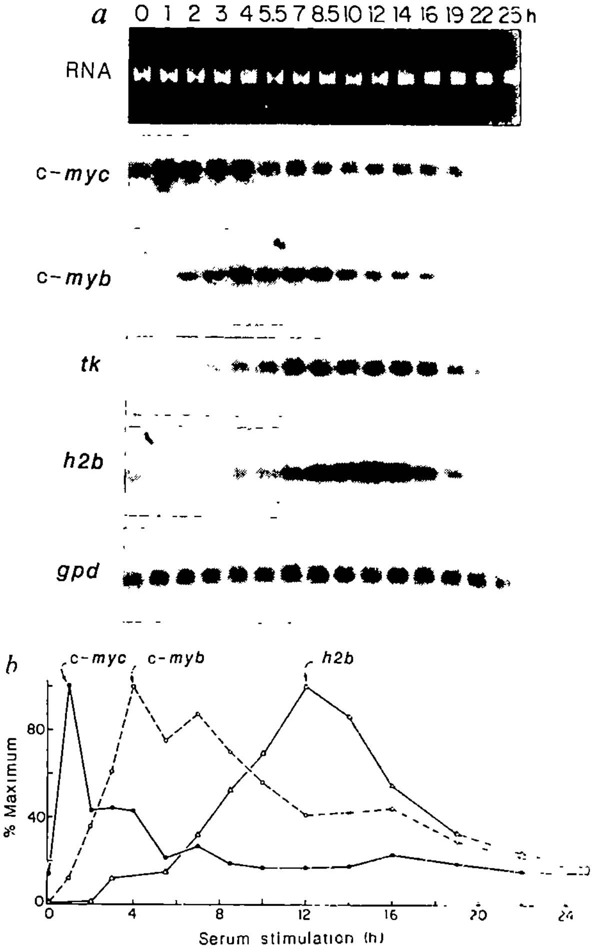

Fig. 2 *a*, The c-*myb*, c-*myc*, *tk*, *h2b* and *gpd* steady-state mRNA levels of CEF following serum deprivation and subsequent restimulation. Confluent CEF were serum deprived for 12 h (lane 1) and then stimulated to proliferate by the addition of fresh media containing 6% serum (lanes 2–15). RNA was extracted at each of the indicated time points, equalized for RNA (upper panel) and Northern blots were prepared as described in Fig. 1 legend. Filters were hybridized sequentially with nick-translated probes for v-*myb*, c-*myc*, *tk*, *h2b* and *gpd*. The c-*myc* probe was a 3.2-kb *Sst*I fragment containing the chicken c-*myc* gene[7]; the *tk* probe was a 2.9-kb *Hin*dIII fragment containing a portion of the *tk* gene[7] (a gift of M. Wigler); and the *h2b* probe was a 1.1-kb *Xho*I/*Sac*II fragment containing the *h2b* gene[34] (a gift of P. A. Krieg). Numbers at the top of the lanes represent the time (h) after serum stimulation that RNA was extracted. *b*, Changes in c-*myb*, c-*myc* and *h2b* mRNA levels as measured by scanning densitometry and expressed as a percent of the maximal level obtained are plotted against time for the experiment described in *a*. The *gpd* levels underwent a steady increase of just under twofold through the fractions.

c-*myb* mRNA levels were low in quiescent cultures, increased as the cells entered exponential growth and declined as the percentage of cycling cells decreased. Again, the mRNA levels of *gpd* were relatively constant throughout.

To examine more closely the relationship between c-*myb* expression and cellular proliferation, we next analysed c-*myb* expression in serum-deprived CEF that were stimulated to proliferate by the addition of serum (Fig. 2). Under these conditions, ~80% of CEF cells will be stimulated synchronously to enter and traverse one cell cycle. After stimulation, the cells reach S phase in 10–14 h and mitosis in 20–25 h[8]. Total cell RNA was extracted after serum stimulation and Northern blots of equalized RNA were prepared and hybridized sequentially with probes specific for c-*myb*, c-*myc*[7], histone 2B (*h2b*)[8], *tk*[7] and *gpd* genes. c-*myb* mRNA was first detected 2 h after serum stimulation, reached a maximum level between 4 and 8 h after stimulation, and then declined. In contrast, levels of an S-phase-expressed gene, *h2b*, did not increase until 7 h after stimulation and reached a maximum 12 h following serum addition. The *tk* mRNA is expressed with kinetics similar to *h2b*. As previously reported[15], c-*myc* underwent transient induction 1 h after stimulation and then remained relatively constant over the time course of the experiment. The levels of c-*myc*, c-*myb* and *h2b* mRNA are plotted against time in Fig. 2*b*.

As an alternative approach to examining the relationship of c-*myb* expression to cell proliferation, levels of c-*myb* mRNA isolated during specific stages of the cell cycle were also examined. Exponentially growing MSB-1 cells were separated by centrifugal elutriation to enrich for populations of cells at different stages of the cell cycle (Fig. 3). Centrifugal elutriation is a counterflow centrifugation method which separates cells on the basis of volume, a parameter which correlates well with progression through the cell cycle in MSB-1 cells[8,19]. Total RNA from each cell-cycle-dependent subpopulation was isolated and the levels of ribosomal RNA equalized to avoid the measurement of mRNA variations attributable only to increases in cell volume during growth. Northern blots of these RNAs were hybridized sequentially with the c-*myb*, c-*myc*, *h2b*, *tk* and β-actin probes. As measured by scanning densitometry, the amount of c-*myb* transcripts varied 5–10-fold through the cell cycle, with the highest levels occurring in the subpopulation most enriched in

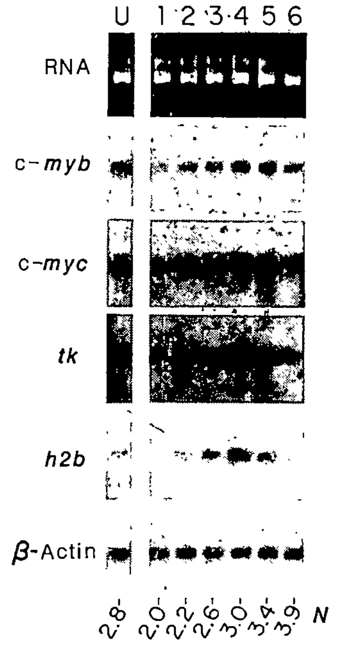

Fig. 3 The c-*myb* mRNA levels in the cell cycle. Exponentially growing MSB-1 cells were separated by counterflow centrifugation according to size[8]. Fluorescence analysis of nuclear DNA content following propidium iodide staining of cells from each fraction confirmed that an effective cell-cycle separation had occurred, cells in the first fraction had a $2n$ DNA content and cells in the last fraction had a predominantly $4n$ DNA content. RNA was extracted and equalized for rRNA levels (upper panel). A Northern blot was prepared with equal amounts of RNA from each fraction and hybridized sequentially with nick-translated probes for v-*myb*, c-*myc*, *tk*, *h2b* and the β-actin gene as described in Fig. 1 legend. Fraction numbers of the subpopulations, with the smallest cells in fraction 1 and the largest in fraction 6, are shown above the autoradiograms. The percentages of cells in each fraction were as follows: 1, 9%; 2, 21%; 3, 24%; 4, 22%; 5, 13%; 6, 11%. The β-actin probe was a 0.59-kb *Hin*dIII fragment containing the 3′-untranslated region of the β-actin gene[8] (a gift from D. W. Cleveland). Lane U, unfractionated population before separation. Numbers below the autoradiograms represent average haploid DNA content (n) of the cells in each fraction.

S-phase cells. In contrast, the levels of c-*myc* and β-actin mRNA varied <20% throughout the cell cycle. *h2b* appeared to be expressed only in populations of cells containing S-phase cells and *tk* underwent a variation in expression within the cell cycle similar in pattern and magnitude to that of c-*myb*. These observations represent consistent findings from several experiments involving MSB-1 cells. Using the same methods, we have also observed an increased level of c-*myb* mRNA in subpopulations enriched for S phase cells from CEF and HL-60, a human promyelocytic cell line[22]. In these cell types, the increase in c-*myb* mRNA is 2–3-fold rather than the 5–10-fold increase observed in MSB-1 cells. However, the level of change in c-*myb* mRNA during the cell cycle in all cell types is proportional to the cell-cycle variations observed in *tk* mRNA.

Control of c-*myb* expression

These results suggest that c-*myb* mRNA levels undergo significant variations during proliferation, either by an increase in transcription or by a stabilization of c-*myb* mRNA. To distinguish between these possibilities, the transcriptional activity of c-*myb* was examined in exponentially growing CEF, quiescent serum-deprived CEF and CEF at various times following serum stimulation of quiescent cells. From each population, nuclei were isolated and assayed by runoff transcription (Fig. 4*a*). No significant variation in transcriptional activity of either c-*myb* or c-*myc* was observed irrespective of the growth state of the cells. In contrast, the transcriptional activity of *h2b* was several-fold higher in exponentially growing cells than in the serum-

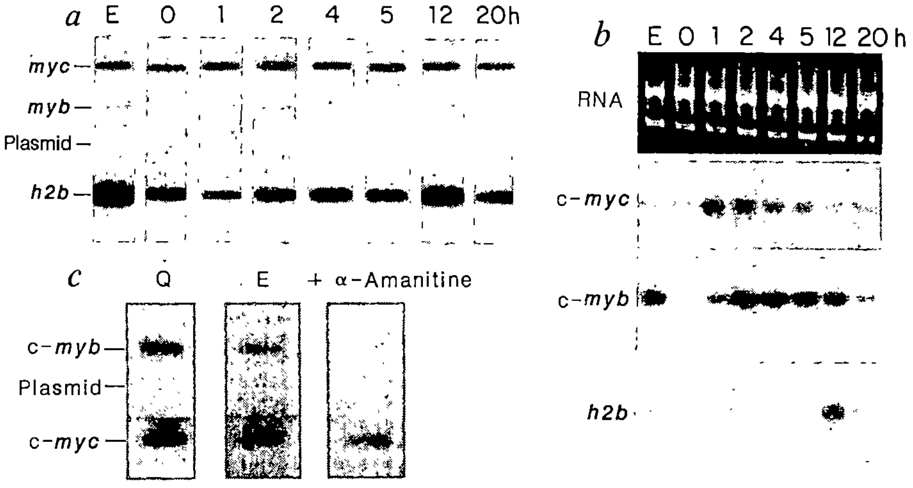

Fig. 4 *a*, The transcription rate of c-*myb*, c-*myc* and *h2b* in CEF following serum deprivation and subsequent stimulation; *b*, Northern blots; *c*, transcription rate of c-*myb* and c-*myc* in MSB-1 cells during saturation arrest (Q) and exponential growth (E). **Methods.** *a*, CEF were serum-deprived as described in Fig. 3 legend and then stimulated to proliferate by the addition of 6% serum. At various time-points, cells in several 150-nm plates were washed with ice-cold phosphate-buffered saline and trypsinized to remove them from the plate. Nuclei were isolated and frozen at −70 °C as described previously[35]. Nuclei from different time-points were thawed simultaneously and assayed by runoff transcription as described by Groudine *et al.*[35] using the modifications described by Linial *et al.*[33]. Equal c.p.m. of the ^{32}P-labelled transcription products were diluted in 2.25 ml high-stringency hybridization buffer[16] and used to hybridize filters containing 5 μg each of indicated plasmids for 36 h at 65 °C. The filters were prepared and processed after hybridization as described elsewhere[16] using the following plasmids: pCM1, an Sp65 plasmid containing a 2.4-kb *Sst*I/*Eco*RI genomic fragment of c-*myc*; pHAX4, a pBR322 plasmid containing a 1.0-kb *Hae*II/*Xba*I fragment of v-*myb*[27]; pSp65 as a plasmid control; and pH2bD1, a pSp62 plasmid including a 1.1-kb *Xho*I/*Sac*II genomic fragment including a chicken *h2b* gene[34]. As measured by scanning densitometry, a less than twofold variation in the hybridization of either c-*myb* and c-*myc* was found between any of the time-points. *b*, Northern blots were prepared and hybridized as described in Fig. 3 using RNA from cells isolated at the same time as those used for the runoff transcription assay. The numbers above the autoradiograms refer to the time following serum stimulation, except that the first lane (E) was isolated from an exponentially growing control population. *c*, Cells in both saturation arrest and exponential growth were obtained as described in Fig. 1 legend. Nuclei were isolated and assayed by runoff transcription as described above. Addition of 2 μg ml^{-1} of α-amanitine to the runoff reaction for MSB-1 cells eliminated hybridization to the v-*myb*-containing plasmid. The small residual hybridization to the c-*myc*-containing plasmid is probably the result of nonspecific hybridization of 28S rRNA.

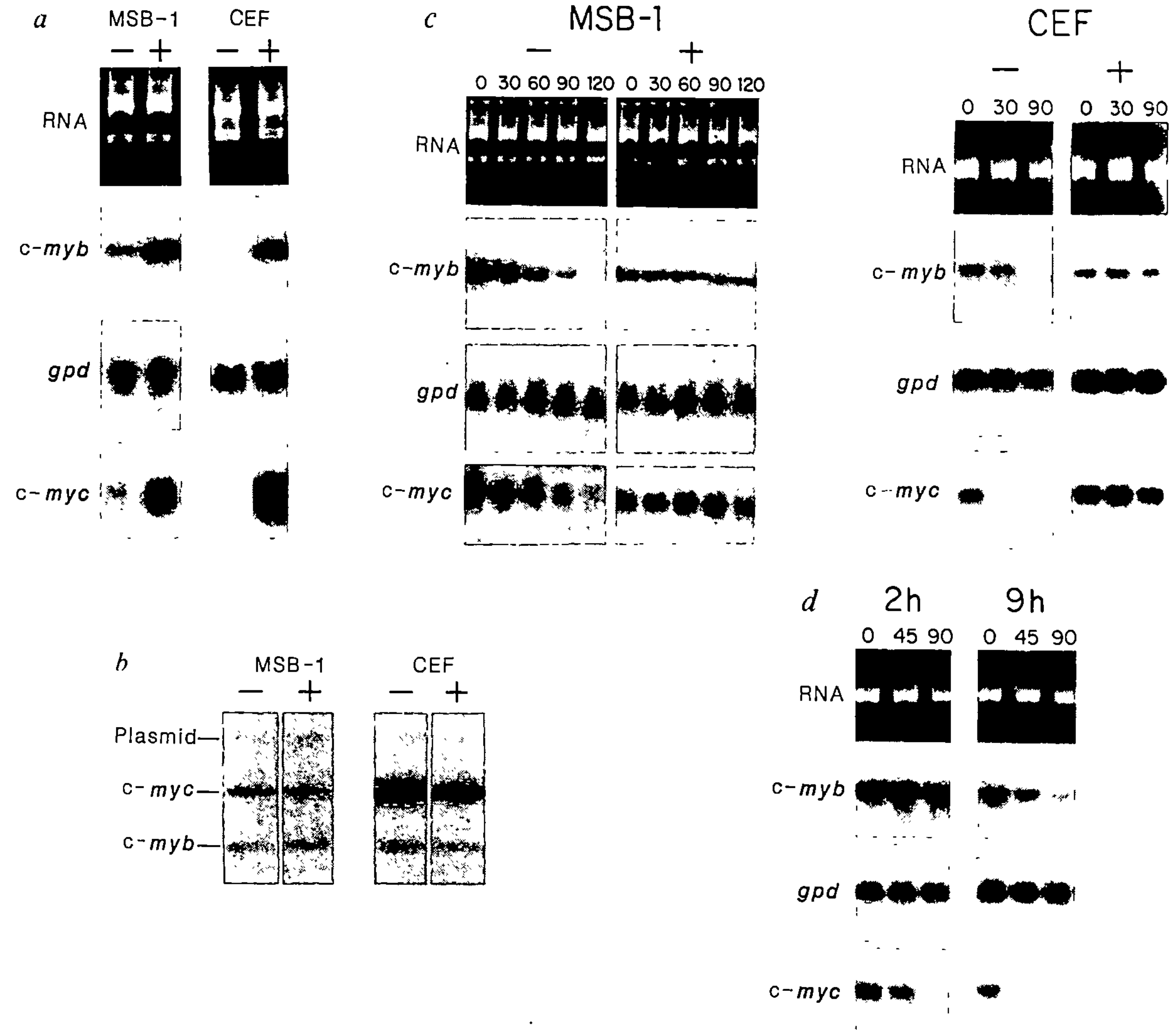

Fig. 5 *a*, The effect of cycloheximide on steady-state c-*myb* mRNA levels in CEF and MSB-1 cells. Upper panels, equalized rRNA levels; lower three panels, result of hybridizations with c-*myb*, *gpd* and c-*myc*. *b*, The effect of cycloheximide on the transcriptional rate of c-*myb* in CEF and MSB-1 cells. *c*, Effect of cycloheximide on the half-life of c-*myb* mRNA in CEF and MSB-1 cells. Upper panels, RNA equalization gels; lower three panels, hybridization with c-*myb*, *gpd* and c-*myc*. *d*, Half-life of c-*myb* mRNA 2 and 9 h after serum stimulation of serum-deprived CEF. Upper panels, RNA equalization gels; lower three panels, hybridization with c-*myb*, *gpd* and c-*myc*.

Methods. *a*, Quiescent CEF and MSB-1 cells were cultured for 3 h in the presence or absence of 10 μg ml^{-1} cycloheximide. RNA was isolated from the cells and Northern blots prepared and hybridized as described in Fig. 1 legend. *b*, Nuclei were prepared from cells treated for 3 h in the presence or absence of cycloheximide and runoff transcription assays performed as described in Fig. 4. The ^{32}P-labelled RNAs were hybridized to filters with 5 μg each of the v-*myb*, c-*myb* and plasmid control DNAs as described in Fig. 4 legend. *c*, The half-life of c-*myb* mRNA was measured by determining the relative amounts of steady-state mRNA following treatment of the cells with 5 μg ml^{-1} actinomycin D. To examine the effect of cycloheximide on message stability, the cells were pretreated for 30 min with 10 μg ml^{-1} cycloheximide before the addition of actinomycin D. At the indicated times following the introduction of actinomycin D, total cell RNA was extracted, the rRNA levels were equalized, and Northern blots were prepared and hybridized as described in Fig. 1 legend. Half-lives were estimated by scanning densitometry and obtaining a best linear fit for the data after log conversion of the hybridization intensity. *d*, Quiescent cells were stimulated by the addition of serum as described in Fig. 2 and 5 μg ml^{-1} of actinomycin D added at 2 and 9 h after stimulation. RNA was isolated from the cells by the guanidinium isothiocyanate method, 15 min after the addition of actinomycin D (time 0) and 45 and 90 min thereafter. The rRNAs from these samples were equalized and Northern blots prepared and hybridized as described in Fig. 1 legend.

deprived cells, increased three- to fivefold as the cells traversed S phase 12 h after serum stimulation and then decreased at 20 h as the cells entered mitosis. The total RNA isolated from the same cells confirmed that the changes in steady-state mRNA levels shown in Fig. 2 also occurred in this experiment (Fig. 4*b*). These results suggest that variation in c-*myb* (and c-*myc*) mRNA levels during changes in the proliferation of CEF are governed primarily by post-transcriptional mechanisms. Figure 4*c* shows the transcriptional activity of c-*myb* in exponentially growing and saturation-arrested MSB-1 cells. Despite the large differences in c-*myb* mRNA levels under these conditions (Fig. 1), no significant difference in transcription was observed.

Inhibition of protein synthesis by cycloheximide results in the stabilization of c-*myc* mRNA and thus causes a substantial increase of steady-state c-*myc* mRNA[15]. As in our experiments both c-*myc* and c-*myb* appeared to be post-transcriptionally regulated, we next determined if cycloheximide treatment had a similar effect on c-*myb* mRNA levels. When quiescent CEF or MSB-1 cells were cultured for 3 h (Fig. 5*a*) a 5-10-fold increase in c-*myb* mRNA was observed in cycloheximide-treated cells. As the *gpd* mRNA levels were unchanged in this experiment, cycloheximide induction of c-*myb* mRNA cannot be the result of a nonspecific increase in total mRNA. Also, the transcriptional activity of the c-*myb* and c-*myc* genes in the presence

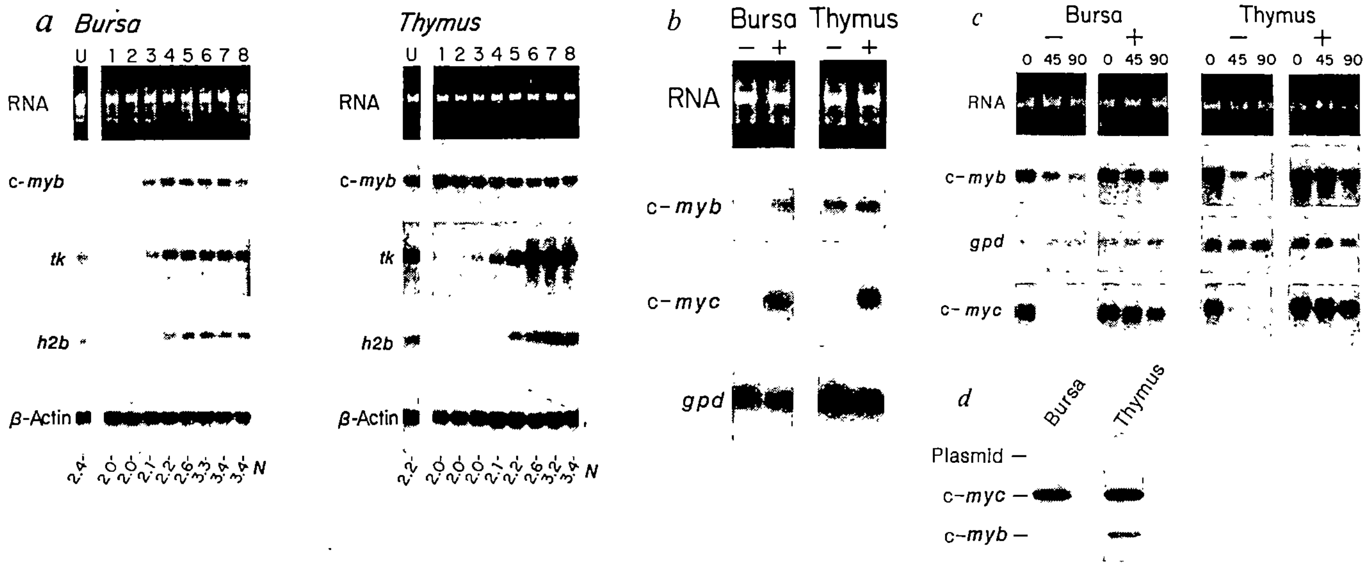

Fig. 6 *a*, The c-*myb* mRNA levels of cell-cycle-separated chicken bursal and thymus cells. Numbers at the bottom of the lanes represent the average DNA content per cell (*n*). Total RNA was prepared from the unfractionated thymocytes (lane U) and each of the subpopulations (lanes 1–8). The rRNA concentrations in all fractions were equalized (upper panel) and Northern blots prepared from the equalized samples as described in Fig. 1 legend. Autoradiograms of sequential hybridizations with c-*myb*, *tk*, *h2b* and β-actin are shown. *b*, Effect of cycloheximide on c-*myb* mRNA levels in bursal cells and thymocytes. *c*, Estimates of the half-life of c-*myb* in the presence or absence of 10 μg ml^{-1} cycloheximide for both bursal and thymic cells. Upper panels. RNA equalization gels; lower panels, hybridizations to c-*myb*, c-*myc* and *gpd*. *d*, Transcriptional rate of c-*myb* in bursal cells and thymocytes.

Methods. *a*, Single-cell suspensions were prepared by gently teasing apart the organs of a 6-week-old chicken and filtering the cells thrugh nylon mesh to remove clumps. Contaminating non-lymphoid cells were removed by centrifuging the cell suspension over Ficoll-Hypaque; >95% of cells prepared from either organ in this manner stained positively with monoclonal antibodies specific for cells of the respective organ. In both organs >50% of the cells were isolated in the first three fractions, which consisted predominantly of cells with 2*n* DNA content. The average DNA content increased through the following fractions, confirming that a cell-cycle-dependent separation had occurred. *b*, Single-cell suspensions of both organs were cultured in Ham's F-10 medium containing folic acid, multivitamins and 12% serum for 3 h in the presence or absence of 10 μg ml^{-1} cycloheximide. RNA was then extracted and equalized (upper panel). Northern blots were prepared from the equalized samples and hybridized sequentially with c-*myb*, c-*myc* and *gpd* probes. *c*, Estimates were obtained using actinomycin D as described in Fig. 5*c* legend. At the indicated times following the addition of 5 μg ml^{-1} of actinomycin D, total cell RNA was extracted, rRNA levels were equalized, and Northern blots were prepared and hybridized as described in Fig. 1 legend. Estimates of the half-lives were obtained as described in Fig. 5 legend. *d*, Nuclei were prepared and runoff transcription assays performed as described in Fig. 4 legend. The ^{32}P-labelled RNA was hybridized to filters containing c-*myb*, c-*myc* and plasmid control DNAs.

or absence of cycloheximide was determined directly by nuclear runoff (Fig. 5*b*). No change in the transcriptional activity of either gene was detected following cycloheximide treatment, again suggesting that the primary control of these genes is post-transcriptional.

The simplest way to account for the observed increase in c-*myb* steady-state mRNA in the absence of a change in transcription is by stabilization of the mRNA. To investigate this possibility, the half-life of c-*myb* mRNA was determined in exponentially growing CEF and MSB-1 cells in the presence or absence of cycloheximide (Fig. 5*c*). Cells were treated with 5 μg ml^{-1} actinomycin D to inhibit transcription and the rate of mRNA decay was measured. Although the half-life of c-*myb* was significantly longer in CEF than in MSB-1 cells (31 min compared with 22 min), in both cell types the mRNA half-life of c-*myb* was prolonged to >200 min in the presence of cycloheximide. As reported by others[29], cycloheximide also significantly prolongs the half-life of c-*myc* mRNA. In contrast, cycloheximide treatment has little effect on the half-life of *gpd* mRNA. Therefore, the cycloheximide-induced increase in both c-*myb* and c-*myc* mRNA levels is caused by the stabilization of the mRNAs.

As c-*myb* levels can be significantly altered by changes in their half-life, we next determined whether or not there were differences in the half-life of c-*myb* during the accumulation and decline of c-*myb* following serum stimulation of CEF (Fig. 5*d*). Serum-deprived cells were stimulated by the addition of serum and the half-life of c-*myb* measured at 2 h when c-*myb* mRNA levels are rising, and at 9 h when c-*myb* mRNA levels are declining (see Fig. 2). The half-life of c-*myb* is significantly prolonged at 2 h (246 min) compared with 9 h (28 min). The half-life of c-*myc* is also longer at 2 h (44 min) than at 9 h (18 min). This is not surprising, as the peak of c-*myc* expression following serum stimulation often does not occur until 2 h post-stimulation (see Fig. 4*b*; ref. 14) and also appears to be controlled by post-transcriptional mechanisms. The *gpd* mRNA half-life did not change significantly between the two time periods. At present we do not know whether the prolongation of c-*myb* and c-*myc* mRNA half-lives found 2 h after serum stimulation is specific for these genes or reflects a general prolongation of the half-lives of short-lived mRNA species. However, these results do support the conclusion that post-transcriptional regulation plays an important role in controlling c-*myb* mRNA levels during the response to proliferation.

In vivo expression of c-*myb*

To ensure that the variations in c-*myb* expression observed *in vitro* during proliferation also occur *in vivo*, we examined cell-cycle-dependent subpopulations of cells isolated from either the bursa of Fabricius or the thymus (Fig. 6). Cells from both organs were isolated as single-cell suspensions and then separated by counterflow centrifugation into size-dependent subpopulations. Total RNA was isolated from each subpopulation and used to measure steady-state mRNA levels as described for the CEF and MSB-1 experiments. In the bursa, c-*myb* mRNA levels in subpopulations containing late G_1, S and G_2 cells were >10 times greater than in subpopulations containing the smaller G_0 and early G_1 cells. The pattern of c-*myb* expression in the bursa is similar to that of the cell-cycle-regulated genes *h2b* and *tk* (Fig. 6*a*).

In the thymus, c-*myb* expression did not correlate with position in the cell cycle. The level of c-*myb* mRNA was greatest in the subpopulations containing the smaller G_0 and early G_1 cells and decreased progressively in the subpopulations containing the larger cells in later stages of the cell cycle. Despite this, the patterns of expression of both *tk* and *h2b* mRNAs in the thymus were nearly identical to those found in the bursa, and the progressive increase in DNA content per cell through the fractions also confirmed that an effective cell-cycle-dependent separation of the thymus cells had occurred. β-Actin mRNA was present at similar levels in all fractions. As reported by others[21–23], we found the steady-state level of c-*myb* mRNA in the thymus to be ~10-fold greater than in any of the other cell types examined.

A qualitative difference in the regulation of c-*myb* expression between the bursa and the thymus is also shown by the effect of cycloheximide treatment on the steady-state level of c-*myb* mRNA. Bursal cells undergo a 10-fold increase in c-*myb* levels after 3 h in cycloheximide, whereas c-*myb* mRNA levels increase less than twofold in cycloheximide-treated thymocytes (Fig. 6*b*). In contrast to these results, the levels of c-*myc* mRNA increased more than 10-fold in both cell types. These differences in c-*myb* regulation between bursal and thymic cells do not appear to be controlled by differences in mRNA stability in the two cell types as the mRNA half-life of c-*myb* is similar in each one (30 min and 25 min, respectively), and the half-life of c-*myb* is prolonged more than sixfold in both tissues in the presence of cycloheximide (Fig. 6*c*). The major difference in c-*myb* regulation between bursal and thymic cells is that thymocytes have a higher absolute rate of c-*myb* transcription as assayed by nuclear runoff (Fig. 6*d*).

Conclusions

Our data indicate that c-*myb* is expressed during proliferation in several cell types, including CEF, MSB-1 cells and B cells from the bursa of Fabricius. In MSB-1 cells, the induction of c-*myb* expression occurs not only during the initial activation of cells to proliferate, but also in subsequent cell cycles during exponential growth. The amount of variation in c-*myb* mRNA in the cell cycle of MSB-1 cells is similar to the variations in mRNA levels reported for several other cell-cyle-regulated genes: *tk*[7,30], *ts*[9] and *dhfr*[5]. For these genes, changes in mRNA levels are paralleled by variations in enzymatic activity. In addition, the expression of c-*myb* in CEF during proliferation demonstrates that c-*myb* mRNA expression is not confined to haematopoietic cells[24]. Thus, the low levels of c-*myb* found in various tissues most likely reflects the presence of few actively proliferating cells, rather than contamination of haematopoietic cells.

The precise relationship of changes in steady-state c-*myb* mRNA levels to the cell cycle is difficult to determine. In exponentially growing MSB-1 cells, the peak of c-*myb* expression correlates well with S phase. In contrast, the increase in c-*myb* mRNA following serum stimulation of quiescent CEF occurs in late G_1, and high levels of c-*myb* mRNA persist throughout S phase. This could reflect the difficulty in distinguishing between events in late G_1 and early S phase in exponentially growing cells separated on the basis of size. Alternatively, c-*myb* mRNA may peak during S phase, but this could be obscured in serum-deprived CEF by an earlier increase in c-*myb* mRNA levels caused by recovery from the artificial state of serum deprivation.

Regardless of the precise relationship of c-*myb* expression to position in the cell cycle, variations in c-*myb* mRNA levels during cellular activation and proliferation seem to be predominantly the result of post-transcriptional control. There is little or no change in c-*myb* transcription between exponentially growing and quiescent CEF or MSB-1 cells measured by nuclear runoff, despite the significant differences in steady-state c-*myb* mRNA levels in these conditions. Also, there is no change in the transcription rate of c-*myb* observed in CEF following serum stimulation. In contrast, increases in c-*myb* mRNA can be induced in various cell types by cycloheximide treatment through an increase in c-*myb* mRNA stability. Changes in mRNA stability also occur following serum stimulation of quiescent CEF. The half-life of c-*myb* mRNA during the period in which c-*myb* mRNA is accumulating in the cells is significantly longer than during the period in which c-*myb* mRNA is declining (246 versus 28 min). Alteration of mRNA stability as a mechanism of gene regulation is not unique to this system. In prokaryotic cells, the level of several growth rate-dependent genes are controlled by the selective modulation of mRNA stability[31]. Two other cell-cycle-dependent eukaryotic genes, *tk* and *dhfr*, are regulated by post-transcriptional mechanisms[5,7]. Histone genes also display a cell-cycle-dependent pattern of expression that is controlled by both changes in the rate of histone mRNA degradation and changes in the transcriptional rate during S phase[32].

Previous reports concerning c-*myb* expression have described a high level of c-*myb* mRNA found in thymic lymphocytes and immature haematopoietic cells[20–25]. When immature myeloid cells are induced to differentiate, c-*myb* expression stops[20,25]. As these cells stop proliferating during differentiation, decline in c-*myb* expression may simply reflect a decrease in the proliferation of these cells. Similarly, the expression of c-*myb* is high in immature thymocytes and decreases during T-cell differentiation *in vivo*[24]. We observed levels of c-*myb* mRNA in the thymus that are at least 10-fold greater than in other lymphoid organs. Our results also suggest that the high levels of c-*myb* mRNA in the thymus are not linked to proliferation or regulated in a cell-cycle dependent manner. Thymocytes have higher levels of c-*myb* transcription than other lymphoid cells and thymic c-*myb* mRNA levels increase less than twofold following cycloheximide treatment. Thus, unlike the post-transcriptional regulation of c-*myb* expression in the cell cycle, the increased expression of c-*myb* in the thymus appears to be transcriptionally regulated. One intriguing and testable possibility is that the c-*myb* gene contains an enhancer element that responds to tissue-specific regulatory factors in the thymus. A preliminary result that supports this hypothesis is that c-*myb* transcription in the thymus decreases in response to cycloheximide treatment, suggesting that a labile protein is involved in the increased thymic transcription of c-*myb*. This could explain why cycloheximide fails to increase significantly the levels of c-*myb* mRNA in the thymus despite the observed increase in the half-life of c-*myb* mRNA following cycloheximide treatment. A precedent for this form of transcriptional regulation has been reported for the retroviral long terminal repeat enhancement of c-*myc* expression in bursal lymphoma cells[33].

We suggest that c-*myb* has both a specific function in thymic differentiation, as revealed by the high level of tissue-specific expression in the thymus, and a more general function in cellular proliferation, as characterized by the proliferation-associated expression of c-*myb* in other cells. Thus, the c-*myb* gene may have more than one role in the regulation of cellular proliferation and differentiation.

We thank our colleagues Kathleen Conklin, Robert Eisenman, William Forrester, Stephen Hann, Kate Levine, Maxine Linial, Robert E. Steele and Hal Weintraub for discussions and Hal Hendron and Angela Hein for technical asisistance. This investigation was supported by NCI grant CA 20068 and NSF grant PCM 82-04696. P.C. is supported by NIH fellowship F32 HD06583-02. C.T. is a lieutenant-commander in the U.S. Navy attached to the Naval Medical Research Institute. M.G. is a scholar of the Leukemia Society of America.

Received 11 July; accepted 18 November 1985.

1. Heldin, C.-H. & Westermark, B. *Cell* 37, 9–20 (1984).
2. Pardee, A. B., Campisi, J. & Croy, R. G. in *Cancer Cells* Vol. 3 (eds Feramisco, J., Ozanne B. & Stiles, C.) 389–392 (Cold Spring Harbor Laboratory, New York, 1985).

3. Hartwell, L. H., Culotti, J., Pringle, J. & Reid, B. *Science* **183**, 46-51 (1974).
4. Siminovitch, L. & Thompson, L. H. *J. cell Physiol.* **95**, 361-366 (1978).
5. Leys, E. J. & Kellems, R. E. *Molec. cell. Biol.* **1**, 961-971 (1981).
6. Farnham, P. J. & Schimke, R. T. *J. biol. Chem.* **260**, 7675-7680 (1985).
7. Groudine, M. & Casimir, C. *Nucleic Acids Res.* **12**, 1427-1446 (1984).
8. Thompson, C. B., Challoner, P. B., Neiman, P. E. & Groudine, M. *Nature* **314**, 363-366 (1985).
9. Storms, R. *et al. Molec. cell. Biol.* **4**, 2858-2864 (1984).
10. Eisenman, R. N., Tachibana, C. Y., Abrams, H. D. & Hann, S. *Molec. cell. Biol.* **5**, 114-126 (1985).
11. Curran, T., Miller, A. D., Zokas, L. & Verma, I. M. *Cell* **36**, 259-268 (1984).
12. Klempnauer, K.-H., Symonds, G., Evan, G. I. & Bishop, J. M. *Cell* **37**, 537-547 (1984).
13. Boyle, W. J., Lampert, M. A., Lipsick, J. S. & Baluda, M. A. *Proc. natn. Acad. Sci. U.S.A.* **81**, 4265-4269 (1984).
14. Kelly, K., Cochran, B. H., Stiles, C. D. & Leder, P. *Cell* **35**, 603-610 (1983).
15. Greenberg, M. E. & Ziff, E. B. *Nature* **311**, 433-438 (1984).
16. Muller, R., Bravo, R., Burckhardt, J. & Curran, T. *Nature* **312**, 716-720 (1984).
17. Kruijer, W., Cooper, J. A., Hunter, T. & Verma, I. M. *Nature* **312**, 711-716 (1984).
18. Muller, R., Curran, T., Muller, D. & Guilbert, L. *Nature* **314**, 546-548 (1985).
19. Hann, S. R., Thompson, C. B. & Eisenman, R. N. *Nature* **314**, 366-369 (1985).
20. Craig, R. W. & Bloch, A. *Cancer Res.* **44**, 442-446 (1984).
21. Gonda, T. J., Sheiness, D. K. & Bishop, J. M. *Molec. cell. Biol.* **2**, 617-624 (1982).
22. Westin, E. H. *et al. Proc. natn. Acad. Sci. U.S.A.* **79**, 2194-2198 (1982).
23. Coll, J. *et al. Expl. Cell Res.* **149**, 151-162 (1983).
24. Sheiness, D. & Gardinier, M. *Molec. cell. Biol.* **4**, 1206-1212 (1984).
25. Gonda, T. J. & Metcalf, D. *Nature* **310**, 249-251 (1984).
26. Chirgwin, J. M., Przbyla, A. E., MacDonald, R. J. & Rutter, W. J. *Biochemistry* **18**, 5294-5299 (1979).
27. Perbal, B. & Baluda, M. A. *J. Virol.* **41**, 250-257 (1982).
28. Dugaiczyk, A. *et al. Biochemistry* **22**, 1605-1613 (1983).
29. Dani, C. *et al. Proc. natn. Acad. Sci. U.S.A.* **81**, 7046-7050 (1984).
30. Stuart, P., Ito, M., Stewart, C. & Conrad, S. E. *Molec. cell. Biol.* **5**, 1490-1497 (1985).
31. Nilsson, G., Belasco, J. G., Cohen., S. N. & von Gabain, A. *Nature* **312**, 75-77 (1984).
32. Sittman, D. B., Graves, R. A. & Marzluff, W. F. *Proc. natn. Acad. Sci. U.S.A.* **80**, 1849-1853 (1983).
33. Linial, M., Gunderson, N. & Groudine, M. *Science* **230**, 1126-1132, 1985.
34. Krieg, P. A. & Melton, D. A. *Nature* **308**, 203-206 (1984).
35. Groudine, M., Peretz, M. & Weintraub, H. *Molec. cell. Biol.* **1**, 281-288 (1981).

LETTERS TO NATURE

Origin of ultra-high-energy γ-rays from Cygnus X-3 and related sources

Demosthenes Kazanas & Donald C. Ellison

Laboratory for High Energy Astrophysics, Code 665,
NASA/Goddard Space Flight Center, Greenbelt, Maryland 20771,
USA and Astronomy Program, University of Maryland, College Park,
Maryland 20742, USA

Ultra-high-energy (UHE) γ-ray emission from Cygnus X-3 (refs 1, 2) and the several other binary X-ray sources has been observed at γ-ray energies $\geq 10^{15}$ eV (refs 3–5). Also, collisionless shocks are expected to form in accretion flows onto neutron stars or black holes[6]. Here, therefore, we consider the diffusive shock acceleration of ions as the mechanism responsible for the γ-ray emission observed. The shock acceleration time can under reasonable assumptions be sufficiently short to allow acceleration of ions to energies near 10^{16} eV. We propose that the subsequent proton–proton (p–p) collisions and photodissociation of ^{4}He can produce a flux of neutrons that escapes from the acceleration site despite the high magnetic fields ($\sim 10^8$ G). These neutrons, by interacting with the binary companion[7,8], produce the observed UHE radiation. Radiation at such energies might be a common property of accreting binaries.

An important feature of Cyg X-3 (as well as the other sources) is that the power of the UHE emission is a sizeable fraction of the power emitted at much lower energies, that is, in X rays, indicating that the emission in the $>10^{12}$ eV range is an integral part of the radiation-emitting mechanism. At X-ray energies, the emission almost surely originates from accretion onto a compact object. This suggests that the origin of the UHE emission may also be sought in the accretion, although alternatives such as the rotational energy of the underlying compact object[9] or the accretion disk[10] (coupled with the exisiting magnetic fields to produce large electrostatic potential drops) have been suggested.

Our model uses accretion as the energy source and first-order Fermi (or diffusive) shock acceleration of ions[11-14] as the mechanism responsible for the production of the high-energy particles required to produce the observed radiation. We favour this mechanism because it is conceptually well understood, has been studied theoretically in detail, has been experimentally tested in the heliosphere[15-17] and in galactic cosmic rays[18,19], it can convert a large fraction of the incoming energy flux into relativistic particles, and because shocks are ubiquitous in astrophysical environments. In particular, shocks should readily form when plasma accretes onto compact objects because the accretion velocities (of the order of the speed of light for neutron stars and black holes) are much higher than the thermal velocities of the accreting matter.

We consider that material accretes at a rate $\dot{M} = \mathrm{d}M/\mathrm{d}t$ onto a compact object of mass M, and that a collisionless shock (one in which the dissipation results from the elastic scattering of particles off magnetic field inhomogeneities rather than from particle–particle collisions) forms at a radius R. In normalized units we have $\dot{m} = \dot{M}/(M_\odot\,\mathrm{yr}^{-1})$, $M_1 = M/(10\,M_\odot)$, and the shock position, $x = R/R_\mathrm{S} = R/(3\times 10^6\,M_1)$, where $M_\odot$ is the solar mass and R_S is the Schwarzschild radius. We also assume that the accretion is spherically symmetric so that the number density and ram pressure of the accreting plasma are given by

$$n \simeq 10^{25}\,x^{-3/2}\,\frac{\dot{m}}{M_1^2}\,\mathrm{cm}^{-3} \qquad (1)$$

$$\rho v^2 \simeq 1.7\times 10^{22}\,x^{-5/2}\,\frac{\dot{m}}{M_1^2}\,\mathrm{erg\,cm}^{-3} \qquad (2)$$

respectively, where ρ is the density, v is the free-fall velocity, that is, $(v/c)^2 = R_\mathrm{s}/R = x^{-1}$, and c is the speed of light.

The diffusive shock mechanism accelerates ions to a maximum energy such that either the acceleration time equals the energy loss time, or the particles escape from the accelerating region. These accelerated ions will produce neutrons: by high-energy proton–proton collisions ($\mathrm{p}+\mathrm{p}\rightarrow \mathrm{n}+\mathrm{X}$); and by the photodissociation of the UHE nuclei (mainly ^{4}He). We suggest that these neutrons can then, by interaction with the stellar companion of the compact object, produce the observed narrow (in-phase) UHE γ-ray pulse[7,8]. The production of neutrons is crucial because it allows the transport of energy away from the acceleration site without invoking special magnetic field configurations (see also ref. 20). The escape of charged particles would be greatly inhibited by the presence of the strong ($\sim 10^8$ G) magnetic field inferred in our model. Furthermore, it is difficult to see how the escape of charged particles by diffusion could produce the observed narrow pulse profile. Also photons of $\sim 10^{16}$ eV produced at the acceleration site would pair produce in magnetic fields larger than $\sim 10^3$ G and would not escape either (ref. 21 and D.K., unpublished calculations). (Actually, in the $\simeq 10^8$ G fields considered here, photons of energy $E \gtrsim 10^{11}$ eV would be subject to this constraint. This argument, along with future observations in the 1 GeV–1 TeV range, might provide an estimate of the magnetic field strength.)

In high-energy p–p collisions, because of resonance formation, there is an $\sim 25\%$ probability for transforming the incoming high-energy proton into a neutron with roughly one-half the energy. (The inclusive cross-section for neutron formation in the reaction $\mathrm{pp}\rightarrow \mathrm{nX}$ is 50% of the total inelastic cross-section; there is also an additional 50% probability that the incoming high-energy proton will be the one to be converted into a neutron; low-energy neutrons decay *in situ* and do not contribute to the UHE flux.) Neutrons can also be produced efficiently by the photodissociation of high-energy ^{4}He nuclei. This process, taking into account the cosmic ^{4}He abundance (~one out of 10 nuclei is ^{4}He), has an efficiency of ~20%. Therefore, ~50% of the high-energy protons can transform into high-energy neutrons, producing a nearly isotropic neutron source. These neutrons can then, by impinging on the companion star, produce the observed radiation.

The acceleration time, τ_a, of particles to a Lorentz factor γ in diffusive shock acceleration is approximately[18]

$$\tau_a \simeq 2.2 \times 10^{-4} \frac{Af x \gamma}{ZB} \text{ s} \qquad (3)$$

where B is the magnetic field in G, f is a numerical factor (of the order 1–10) giving a measure of the particle's mean free path in gyroradii, A and Z are the ion mass and charge number, respectively, and we have used $(v/c)^2 = x^{-1}$, where v is the accretion velocity (assumed to be equal to the shock velocity).

The magnetic field B is unknown, but it can be expressed in terms of accretion quantities and the β of the accreting plasma, where $\beta = 8\pi\rho v^2/B^2$ ($\beta = 1$ for equipartition between the magnetic and particle energy densities). Assuming further that the accretion energy flux, $\frac{1}{2}\rho v^3$, is converted into radiation at the shock radius, x, we have (from equation (2))

$$\dot{m} \simeq 3.5 \times 10^{-9} x L_{38} \qquad (4)$$

where $L_{38} = L/10^{38}$ is the luminosity in units of 10^{38} erg s^{-1}. Therefore,

$$B \simeq 3.9 \times 10^7 x^{-3/4} M_1^{-1} (L_{38}/\beta)^{1/2} \text{ G} \qquad (5)$$

The maximum Lorentz factor achievable, γ_{max}, can then be estimated by setting the acceleration time equal to the loss time. In the conditions presently considered, the most significant ion energy loss mechanisms are: ion synchrotron; particle diffusion away from the shock; photo-pion production; and photodissociation. For shock acceleration, which demands that ions be scattered by the magnetic field, the ion synchrotron losses determine the maximum possible energy[22] independent of the restrictions imposed by the other loss mechanisms.

The synchrotron loss time is

$$\begin{aligned}\tau_s &\simeq 3 \frac{A^3}{Z^4} \frac{m_p^3 c^5}{e^4 B^2 \gamma} \\ &\simeq 6 \times 10^{18} \frac{A^3}{Z^4} \frac{1}{B^2 \gamma} \text{ s}\end{aligned} \qquad (6)$$

where m_p is the proton mass and e is the electronic charge.

Setting $\tau_a = \tau_s$ yields

$$\gamma_{max} \lesssim 1.7 \times 10^{11} (fxB)^{-1/2} \frac{A}{Z^{3/2}} \qquad (7)$$

and substituting the value for the magnetic field in equation (5) gives

$$\gamma_{max} \lesssim 3 \times 10^7 M_1^{1/2} (\beta/L_{38})^{1/4} x^{-1/8} f^{-1/2} AZ^{-3/2} \qquad (8)$$

Particle loss may produce a more restrictive condition if cross-field diffusion allows particles to diffuse away from the shock in a time less than the acceleration time. Using this condition, Eichler and Vestrand[23] find

$$\gamma_{max} \lesssim 7.1 \times 10^6 x^{-1/4} (L_{38}/\beta)^{1/2} \left(\frac{Z}{A}\right) \qquad (9)$$

If synchrotron losses predominate, the maximum energy per nucleon is a few 10^{16} eV for protons and for ^{4}He nuclei ($A = 4$, $Z = 2$) with $\beta = 10$ (magnetic field a factor of 3 less than equipartititon), could reach ~10^{17} eV. The secondary neutrons will be about a factor two lower in energy and can then (in identical fashion to protons as discussed by Hillas[8]) produce the observed ~10^{15} eV γ-rays through hadronic collisions in the atmosphere of the companion star and subsequent π^0 production and decay.

Considering the simplicity of the arguments involved, the predicted maximum energy is in good agreement with the observations. This agreement becomes more significant considering the weak dependence of equation (8) on the unknown parameters of the problem. Even values of $L_{38} = 10^3$, required to account for the tentative observations of neutrino-produced muons in the IMB detector[24], would only change γ_{max} by a factor of ~5, provided that the other parameters remain the same. The weak dependence on these parameters also implies that other X-ray binary sources would produce γ-rays of similar energies. If instead, equation (9) determines γ_{max}, this model may not generate nucleons with sufficient energy to explain the ~10^{16}-eV γ rays observed from Cyg X-3.

In both of the alternative energy loss mechanisms (photo-pion production and photodissociation, the photons of the ambient radiation field when viewed from the frame of the high-energy proton or nucleus, appear as γ-rays. These γ-rays can, in turn, either produce pions in p–γ collisions, or photodissociate the nucleus, thereby limiting the maximum attainable energy. To estimate the timescales for these processes, one needs to know the photon field of the source. The spectrum of Cyg X-3 peaks at an energy ε_m ~3 keV, and is well fit by a black body of temperature T ~1 keV (ref. 25). The cross-sections for both the above processes also peak at an energy we denote as E_i ($E_i = E_\pi \simeq 300$ MeV for photo-pion production and $E_i = E_d \simeq 30$ MeV for ^{4}He photodissociation). Because of the peaked form of the target photon density, one need only calculate the timescales for a particular Lorentz factor, namely that for which $\gamma\varepsilon_m \simeq E_i$. Higher or lower energies would result in longer timescales. One should then compare τ_a to $\tau_{p\gamma}$ ($\gamma = E_\pi/\varepsilon_m$) for photo-pion production and to τ_{dis} ($\gamma = E_d/\varepsilon_m$) for photodissociation. If $\tau_a < \tau_{p\gamma}$ or τ_{dis} for the specific value of the Lorentz factor corresponding to each process, then these processes should not play a part in determining the maximum energy, which should then be given by equation (8) or (9).

For photo-pion production the energy loss rate is

$$m_p \frac{d\gamma}{dt} = \frac{L}{\pi R^2 \varepsilon_m c} c (K_p \sigma)_{max} \gamma m_\pi \text{ erg s}^{-1} \qquad (10)$$

where $(K_p\sigma)_{max}$ is the maximum value of the cross-section, σ, multiplied by the inelasticity, K_p, of the process[26], m_π is the mass of the pion, and $L/(\pi R^2 \varepsilon_m c)$ is the photon number density at the peak energy, ε_m, of their distribution. The photo-pion production timescale is, therefore, given by

$$\tau_{p\gamma} = \frac{\gamma}{d\gamma/dt} \simeq \frac{5\pi R^2 \varepsilon_m}{L(K_p\sigma)_{max}} \text{ s} \qquad (11)$$

Substituting the values of $\varepsilon_m \sim 3$ keV, $R = xR_s$, and $(K_p\sigma)_{max} \sim 8 \times 10^{-29}$ cm^2, one obtains

$$\tau_{p\gamma} \simeq 8.5 \times 10^{-5} \frac{x^2 M_1^2}{L_{38}} \text{ s} \qquad (12)$$

This value agrees very well with that obtained by scaling (to a black body of temperature ~1 keV) the results of Protheroe[27], who has numerically integrated the cross-section over the photon distribution.

This timescale has to be compared with the acceleration timescale

$$\tau_a \simeq 5.7 \times 10^{-12} \frac{A}{Z} \frac{f x^{7/4} M_1 \beta^{1/2}}{L_{38}^{1/2}} \gamma \text{ s} \qquad (13)$$

for $\gamma \sim 10^5$. It can be seen that $\tau_a \ll \tau_{p\gamma}$ for reasonable values of the parameters. At high energies, $K_p\sigma$ levels off to $\sim 5 \times 10^{-29}$ cm^2 (ref. 26) and this process will ultimately become important. Its magnitude, though, depends very sensitively on the photon number density in the acceleration region. Assuming the latter to be that of a $T \sim 1$ keV black body, the constraint imposed by this process is less restrictive than that of equation (8).

The same calculation can be performed for the photodissociation of ^{4}He by using the cross-section appropriate for this process, $\sigma_{\text{dis}} \simeq 2 \times 10^{-27}$ cm^{-2} (ref. 28); since the peak of the cross-section is at $E_m \sim 30$ MeV, the value of γ considered here should be $\gamma \sim 10^4$. Hence,

$$\tau_{\text{dis}} = \frac{\pi R^2 \varepsilon_m}{L\sigma_{\text{dis}}} \simeq 6.8 \times 10^{-7} \frac{x^2 M_1^2}{L_{38}} \text{ s} \qquad (14)$$

This value is still larger than that of equation (13) for $\gamma = 10^4$, however the available margin is less and it may be possible that for certain parameters, $\tau_{\text{dis}} < \tau_a$. In this case, the efficiency of the source should be cut in half as those neutrons originating from the dissociation of ^{4}He would not be available at the highest energies.

Somewhat larger $\gamma_{\max}$ might be possible if the acceleration time is shorter then that given by equation (3). The latter result was derived assuming a single-plane parallel shock. Multiple shocks or converging magnetic fields which would reflect the particles back towards the shock might result in shorter acceleration times and thus larger maximum Lorentz factors. However, the constraint given by equation (9) must still be obeyed.

The observed photon spectrum from Cyg X-3 ($\propto E^{-2}$ photons erg^{-1}) can be obtained either by an E^{-2} input neutron spectrum extending to $\sim 10^{17}$ eV, or by an electromagnetic cascade of a high-energy ($\sim 10^{17}$ eV) monoenergetic beam as suggested by Hillas[8]. Shock acceleration can accommodate both cases. Strong classical hydrodynamic shocks have a compression ratio $r \sim 4$ and produce $E^{-(r+2)/(r-1)} \sim E^{-2}$ power law spectra[18]. Nonlinear shock acceleration, however, which allows for the fact that the accelerated particles may be dynamicallly significant, allows compression ratios larger than 4 and can produce very flat spectra at high energy[19,29].

Independent of the acceleration mechanism, the observation of 10^{16}-eV photons implies the existence of $\sim 10^{17}$-eV hadrons and hence, as argued above, the existence of neutrons of approximately the same energy. It is intriguing to examine the possibility of directly observing these 10^{17}-eV neutrons. Hillas[8] has estimated that the luminosity in the hadronic component (neutrons in our model) needed to account for the γ-ray observations is

$$L \simeq 1.4 \times 10^{39} \left(\frac{\Omega}{4\pi}\right)\left(\frac{0.05}{\Delta}\right)\left(\frac{d}{10\,kpc}\right)^2 \text{erg s}^{-1} \qquad (15)$$

where Ω is the solid angle of (neutron) emission by the compact object ($\Omega = 4\pi$ in our model) and Δ is the duty cycle of the source (which could be as small as 0.02). Therefore, assuming a distance d of 10 kpc and a neutron e-folding lifetime $\tau \simeq 10^3$ s, the flux of 10^{17}-eV neutrons at the Earth, F_{17}, will be

$$F_{17} = \frac{L}{4\pi d^2 E_n} \exp\left(-\frac{m_n c d}{E_n \tau}\right) \simeq 3.5 \times 10^{-17} \text{ neutrons cm}^{-2}\text{ s}^{-1} \qquad (16)$$

where E_n and m_n are, respectively, the energy and mass of the neutron. This value should be compared with the cosmic ray flux above 10^{17} eV (ref. 30), that is, $F_{cr}(>10^{17}\text{ eV}) \simeq 10^{-6}\text{ m}^{-2}\text{ h}^{-1}\text{ sr}^{-1} \simeq 8.5 \times 10^{-18}\text{ cm}^{-2}\text{ s}^{-1}\text{ deg}^{-2}$. From this comparison it becomes apparent that an air shower array with angular resolution better than $\sim 2 \times 2$ (and with sufficient area) should be able to distinguish Cyg X-3 above the cosmic ray background at $\sim 10^{17}$ eV.

If the high-energy particle spectrum cuts off exponentially above 10^{17} eV like $E^{-2} \exp(-E/E_o)$ with $E_0 \simeq 10^{17}$ eV, then at energies up to 10^{18} eV the cut-off of the particle flux is offset by the corresponding increase in the neutron lifetime to give a flux $\propto E^{-2}$. As this slope is flatter than that of the background cosmic ray flux, one should be able to improve the signal to background ratio by looking for air showers at energies near 10^{18} eV. Unfortunately, the angular resolution of these extensive air shower arrays decreases with energy and may offset this gain. The importance of such observations may warrant improving the angular resolution of high-energy arrays.

Note that even if the primary beam of particles were protons of $E \sim 10^{17}$ eV, neutrons of the same energy could still be produced when the protons interact with the atmosphere of the companion star (R. Ramaty, personal communication). The pulse profile of these nuetrons should be narrow and similar to that of the 10^{16}-eV γ-rays. In contrast, the neutrons originating directly from the acceleration site near the compact object, as proposed here, should have a light curve similar to that of the X rays. The ratio of intensities in the two cases should be $\sim 1/4$ (only one out of four high-energy protons is converted into a high-energy neutron).

The neutron-initiated air showers are muon-rich and hence potentially observable with detectors sensitive to muons such as the proton decay detectors. However, the recently reported muon observations from the direction of Cyg X-3 in two of these detectors[31,32] imply primary neutron fluxes well in excess of equation (15) and, therefore, cannot account for these observations.

We thank J. Lloyd-Evans for numerous discussions, comments, and information concerning UHE γ-ray sources, also J. Barnard, C. Dermer, D. Eichler, T. Gaisser, A. Harding, J. Ormes, R. Ramaty and F. Stecker for helpful discussions. This work was supported in part by NSF grant AST-83-17755 and NASA grant NGR 21-002-316.

Received 1 July; accepted 26 September 1985.

1. Samorski, M. & Stamm, W. *Astrophys. J. Lett.* **268**, L17–L21 (1983).
2. Lloyd-Evans, J. *et al. Nature* **305**, 784–787 (1983).
3. Baltrusaitis, R. M. *et al. Astrophys. J. Lett.* **293**, L69–L72 (1985).
4. Protheroe, R. J., Clay, R. W. & Gerhardy, P. R. *Astrophys. J. Lett.* **280**, L47–L50 (1984).
5. Protheroe, R. J. & Clay, R. W. *Nature* **315**, 205–207 (1985).
6. Hawley, J. F., Smarr, L. L. & Wilson, J. R. *Astrophys. J. Suppl.* **55**, 211–246 (1984).
7. Vestrand, W. T. & Eichler, D. *Astrophys. J.* **261**, 251–258 (1982).
8. Hillas, A. M. *Nature* **312**, 50–51 (1984).
9. Eichler, D. & Vestrand, W. T. *Nature* **307**, 613–614 (1984).
10. Chanmugam, G. & Brecher, K. *Nature* **313**, 767–768 (1985).
11. Krymsky, G. F. *Dokl. Akad. Nauk SSSR* **234**, 1306–1308 [*Soviet Phys. Dokl. Engl. transl.* **22**, 327–328 (1977)].
12. Axford, W. I., Leer, E. & Skadron, G. *Proc. 15th int. Cosmic Ray Conf., Plovdiv* **11**, 132–137 (1977).
13. Bell, A. R. *Mon. Not. R. astr. Soc.* **182**, 147–156 (1978).
14. Blandford, R. D. & Ostriker, J. P. *Astrophys. J. Lett.* **221**, L29–L32 (1978).
15. Lee, M. A. *Rev. Geophys. Space Phys.* **21**, 324–338 (1983).
16. Ellison, D. C. *J. geophys. Res.* **90**, 29–38 (1985).
17. Ellison, D. C. & Ramaty, R. *Astrophys. J.* **298**, 400–408 (1985).
18. Axford, W. I. *Proc. 17th int. Cosmic Ray Conf.*, Paris **12**, 155–203 (1981).
19. Ellison, D. C. & Eichler, D. *Phys. Rev. Lett.* **55**, 2735–2738 (1985).
20. Eichler, D. & Wiita, P. J. *Nature* **274**, 38–39 (1978).
21. Stephens. S. A. & Verma, R. P. *Nature* **308**, 828–830 (1984).
22. Hillas, A. M. *A. Rev. Astr. Astrophys.* **22**, 425–444 (1984).
23. Eichler, D. & Vestrand, W. T. *Proc. 19th int. Cosmic Ray Conf.*, La Jolla **1**, 115–118 (1985).
24. Stecker, F. W., Harding, A. K. & Barnard, J. J. *Nature* **316**, 418–420 (1985).
25. White, N. E. & Holt, S. S. *Astrophys. J.* **257**, 318–337 (1982).
26. Stecker, F. W. *Phys. Rev. Lett.* **21**, 1016–1018 (1968).
27. Protheroe, R. J. *Nature* **310**, 296–298 (1984).
28. Kinsey, J. H. *Astrophys. J.* **158**, 295–302 (1969).
29. Ellison, D. C. & Eichler, D. *Astrophys. J.* **286**, 691–701 (1984).
30. Gaisser, T. K. & Yodh, G. B. *A. Rev. nucl. part. Sci.* **30**, 475–542 (1980).
31. Marshak, M. L. *et al. Phys. Rev. Lett.* **54**, 2079–2082 (1985).
32. Battistoni, G. *et al. Phys. Lett.* **155B**, 465–468 (1985).

NATO International Scientific Exchange Programmes

Advanced Study Institutes ASIs

60 tutorial meetings a year on advanced topics not in regular university course. International faculty. Two weeks' duration.

Advanced Research Workshops ARWs

30 working meetings a year for intense exchanges between senior scientists to review progress in a given field and recommend future research

Research Fellowships

1000 fellowships per year at post-graduate level and higher in support of research and study abroad.

Collaborative Research Grants

400 awards each year in support of cooperation on specific projects carried out jointly by research teams in different countries.

Double-Jump

Fellowships, collaborative research grants, ASIs, ARWs on projects of industrial interest, to promote closer international cooperation between universities and industry.

Special Programmes

Intense international cooperation in a few innovative fields at the frontier of disciplines

Advanced Study Institutes

1986

Advanced Research Workshops

The Advanced Study Institutes and Advanced Research Workshops to be held in 1986 are given in the following pages. The two distinct types of meeting are described briefly below.

Participation or tuition fees are not usually requested from participants, some of whom may obtain small grants from the meeting director to assist with travel and living expenses. The meetings marked ● are of particular industrial interest. Locations and dates may change. Titles and addresses have been abridged. Many meetings are of an interdisciplinary nature : please check all subject areas. **Each meeting is held under the responsibility of its director, to whom all requests for information, attendance or support should be addressed.**

The meetings are supported under either the general NATO Advanced Study Institutes/Advanced Research Workshops Programme, or the Special Programmes on Global Transport Mechanisms (GTM), Selective Activation of Molecules (SAM), Cell to Cell Signals in Plants and Animals (C-CS), Sensory Systems for Robotic Control (Rob), and Condensed Systems of Low Dimensionality (CSLD).

PUBLICATION : The papers and discussions are published in the NATO ASI Series by :
Plenum - Reidel -Nijhoff - Springer Verlag.

ADVANCED STUDY INSTITUTES

ASIs are tutorial courses of two weeks' duration on new, important topics for up to 100 scientists and research students. They aim at the dissemination of advanced scientific knowledge and the promotion of international contacts among scientists. Attendance is by application to course director.

ADVANCED RESEARCH WORKSHOPS

ARWs are working meetings which enable leading researchers scientists and engineers to review the state-of-the-art in specific topics in fast moving fields and to formulate recommendations for the future. They are of about five days' duration. Attendance is limited and usually by invitation only.

NATO Scientific Affairs Division, B-1110 Brussels, Belgium. Tel. (02)241.44.00

1986

Advanced Study Institutes

LIFE SCIENCES *SCIENCES DE LA VIE*

BIOSTATISTICS FOR EXPERIMENTAL AND CLINICAL ATHEROSCLEROSIS RESEARCH
BIOSTATISTIQUES DANS LA RECHERCHE CLINIQUE EXPERIMENTALE SUR L'ATHEROSCLEROSE
Dr. PL DUCIMETIERE, Unité INSERM d Epidémiol. cardiovasc., 15 rue de l'Ecole de Médecine, 75006 Paris, France
31 August - 12 September 1986 Les Arcs, France 546/84

DNA-LIGAND INTERACTIONS : FROM DRUGS TO PROTEINS
INTERACTION ADN-LIGANDS : DES DROGUES AUX PROTEINES
Dr. W GUSCHLBAUER, Dépt. de Biologie, CEN-Saclay, Bât. 142, 91191 Gif-Sur-Yvette Cedex, France
1 - 12 September 1986 Fontevraud (Saumur), France 020/85

MEMBRANE RECEPTORS, DYNAMICS AND ENERGETICS
Prof KWA WIRTZ, Biochemistry Lab., Rijksuniversiteit, Postbus 80.054, 3584 CH Utrecht, Netherlands
17 - 30 August 1986 : Spetsai, Greece 308/85

BIOPOLYMERS
Prof. CA NICOLINI, Biophysics, Faculty of Medicine, Viale Benedetto XV, 2, Genova, Italy
22 June - 5 July 1986 : Erice, Italy 315/85

MOLECULAR GENETICS OF MICROORGANISMS, BIOTECHNOLOGICAL APPLICATIONS
GENETIQUE MOLECULAIRE DES MICROORGANISMES, APPLICATIONS EN BIOTECHNOLOGIE
Dr. M GRUNBERG-MANAGO, Inst. Biologie Physico Chimique, 13 rue P&M Curie, 75005 Paris, France
31 August - 13 September 1986 . Spetsai, Greece 453/85

RADIOLABELED MONOCLONAL ANTIBODIES FOR IMAGING AND THERAPY : POTENTIAL, PROBLEMS AND PROSPECTS
Dr. SC SRIVASTAVA, Medical Dept., Bldg. 801, Brookhaven National Laboratory, Upton, NY 11973, USA
20 July - 1 August 1986 . Il Ciocco, Italy 553/85

NERVOUS SYSTEMS IN INVERTEBRATES/*LES SYSTEMES NERVEUX DES INVERTEBRES*
Prof. MA ALI, Dépt. de Biologie, Université, CP 6128, Succ. A, Montreal, PQ H3C 3J7, Canada
20 July - 2 August 1986 Lennoxville, Québec, Canada 625/85

MOLECULAR BIOLOGY OF THE ARTERIAL WALL
Prof. G SCHETTLER, Universität, Medizinische Klinik, Bergheimerstr. 58, 6900 Heidelberg, Germany
22 September - 3 October 1986 Heidelberg, Germany 454/85

ANIMAL SONAR SYSTEMS
Dr. PE NACHTIGALL, Research Br., Naval Ocean Syst. Ctr., P.O.B. 997, Kailua, Hawaii 96734-0997, USA
10 - 19 September 1986 : Denmark 622/85

MOLECULAR BASIS OF VIRAL REPLICATION
Dr. R PEREZ-BERCOFF, 11A Catt di Virologia, V. di Porta Tiburtine 28, 00185 Rome, Italy
26 August - 6 September 1986 · Maratea, Italy 785/85

PRINCIPLES AND CLINICAL IMPLICATIONS OF NEURORECEPTOR MODULATION
Dr. B WEISS, Dept. Pharmacology, Med. College of PA, 3300 Henry Avenue, Philadelphia, PA 19129, USA
16 - 27 June 1986 : Corfu, Greece 818/85

ECOLOGY *ECOLOGIE*

TOXICOLOGY OF PESTICIDES - EXPERIMENTAL, CLINICAL AND REGULATORY PERSPECTIVES
Prof. Corrado GALLI, Inst. Pharmacol. & Pharmacognosy, Univ. of Milan, V. Balzaretti 9, 20133 Milan, Italy
6 - 15 October 1986 : Limone sul Garda, Italy 652/85

SOCIAL, BEHAVIOURAL AND POLITICAL SCIENCES
SC. SOCIALES, POLITIQUES ET DU COMPORTEMENT

KINDLING - A MODEL FOR BEHAVIORAL NEUROSCIENCE
Dr. DI MOSTOFSKY, Dept. of Psychology, Boston Univ., 64 Cummington Street, Boston, MA 02215, USA
18 - 29 May 1986 . Maratea, Italy 283/85

THE EVOLUTIONARY BIOLOGY OF INTELLIGENCE
Prof. HJ JERISON, Dept. of Psychiatry & Biobehavioural Sc., UCLA Med. Sch., Los Angeles, CA 90024, USA
7 - 18 July 1986 : Poppi, Perugia, Italy 567/85

BIOLOGICAL BASES OF ANTISOCIAL BEHAVIOR
Dr SA MEDNICK, U of Sthn Cal., Denney Res., University Park-MC-1111, Los Angeles, CA 90089, USA
15 - 28 September 1986 · Skiathos, Greece 620/85

MULTIPLE CRITERIA DECISION MAKING AND RISK ANALYSIS USING MICROCOMPUTERS
Dr. B KARPAK, Fac. Business Administration, Istanbul Univ., Rumelihisariustu, Istanbul, Turkey
5 - 15 August 1986 . Istanbul, Turkey 671/85

PHYSICS AND CHEMISTRY *PHYSIQUE ET CHIMIE*

GIANT RESONANCES IN ATOMS, MOLECULES AND SOLIDS
LES RESONANCES GEANTES DANS LES ATOMES, LES MOLECULES ET LES SOLIDES
Prof. JP CONNERADE, Blackett Lab., Imperial College, London SW7 2AZ, UK
16 - 26 June 1986 Les Houches, France 098/85

PHYSICS OF STRONG FIELDS
Prof. W GREINER, Theoretische Phys., Univ., Robert-Mayer-Str. 10, 6000 Frankfurt am Main, Germany
1 - 14 June 1986 : Maratea, Italy 267/85

AQUEOUS IONIC SOLUTIONS
SOLUTIONS AQUEUSES IONIQUES
Dr. MC BELLISSENT-FUNEL, L.L.B., CEN-Saclay, 91191 Gif-Sur-Yvette Cedex, France
22 June - 6 July 1986 : Cargèse, Corsica, France 273/85

LOW DIMENSIONAL CONDUCTORS AND SUPERCONDUCTORS
CONDUCTEURS ET SUPRACONDUCTEURS DE BASSE DIMENSIONNALITE
Dr. D JEROME, Lab. de Physique des Solides, Univ. Paris Sud, 91405 Orsay, France
24 August - 6 September 1986 . Magog, Quebec, Canada 277/85

CHANCE AND MATTER/*LE HASARD ET LA MATIERE*
Mr. R STORA, Division Théorique, CERN, 1211 Geneva 23, Switzerland
30 June - 1 August 1986 : Les Houches, France 284/85

PHYSICOCHEMICAL HYDRODYNAMICS - INTERFACIAL PHENOMA
Prof. MG VELARDE, U.N.E.D -Facultad Ciencias, Apartado 50.487, Madrid, Spain
1 - 11 July 1986 : La Rabida (Huelva), Spain 285/85

SYNCHROTRON RADIATION FOR X-RAY CRYSTALLOGRAPHY
Prof. M HART, Department of Physics, The University, Manchester M13 9PL, UK
10 - 19 June 1986 : Erice, Italy 538/85

LOCALIZATION AND INTERACTION IN DISORDERED METALS AND DOPED SEMICONDUCTORS
Dr. DP TUNSTALL, Physics Dept., The University, North Haugh, St. Andrews, Fife, KY16 9SS, UK
21 July - 8 August 1986 : St. Andrews, Scotland 541/85

CARBON DIOXIDE : CHEMICAL AND BIOCHEMICAL USES AS A SOURCE OF CARBON
Prof. M ARESTA, Dept. of Chemistry, University of Bari, 173 Via Amendola, 70126 Bari, Italy
22 June - 3 July 1986 : Pugnochiuso (Vieste), Italy 543/85

TECHNIQUES AND CONCEPTS OF HIGH ENERGY PHYSICS
Prof. T FERBEL, Dept. of Physics, University of Rochester, Rochester NY 14627, USA
19 - 30 June 1986 : St. Croix, Virgin Islands, USA 544/85

HIGH BRIGHTNESS PARTICLE ACCELERATORS
Dr. AH GUENTHER, Air Force Weapons Lab/CCN, Kirtland Air Force Base, New Mexico 87117-6008, USA
21 July - 1 August 1986 . Italy or Portugal 552/85

MOLTEN SALT CHEMISTRY ●
Dr. G MAMANTOV, Dept. of Chemistry, University of Tennessee, Knoxville, TN 37996-1600, USA
3 - 15 August 1986 : Camenno, Italy 565/85

STRUCTURE/REACTIVITY AND THERMOCHEMISTRY OF IONS
Dr. P AUSLOOS, Ctr. for Chemical Physics, Nat Bureau of Standards, Gaithersburg, MD 20899, USA
30 June - 11 July 1986 . Les Arcs, France 566/85

PHYSICS AND CHEMISTRY OF INTERFACES UNDER LASER IRRADIATION ●
PHYSIQUE ET CHIMIE DES INTERFACES SOUS IRRADIATION LASER
Prof. LD LAUDE, Lab. de Phys. de l'état solide, Université, Av. Maistriau 23, 7000 Mons, Belgium
14 - 25 July 1986 · Maratea, Italy 570/85

GRAVITATION
Prof. M LEVY, Musée Nat. des Sc., des Techn. et des Industries, 211 Av. J. Jaurès, 75019 Paris, France
14 - 31 July 1986 : Cargèse, France 539/85

PHYSICS OF THE TWO-DIMENSIONAL ELECTRON GAS
Prof. JT DEVREESE, Dep. Natuurkunde, Univ. Antwerp, Univ. plein 1, 2610 Wilrijk-Antwerpen, Belgium
2 - 14 June 1986 : Corsendonk, Belgium 710/85

ADVANCES IN HIGH PRESSURE STUDIES OF CHEMICAL AND BIOCHEMICAL SYSTEMS
Dr. R VAN ELDIK, Physical Chemistry Univ. of Frankfurt, Niederurseler Hang, 6000 Frankfurt/Main, Germany
28 September - 11 October 1986 : Corfu, Greece 793/85

CHEMICAL DYNAMICS OF SEASONAL SNOWCOVERS
Prof. HG JONES, INRS-EAU, Univ. du Québec, 2700 Einstein, Ste-Foy, Québec G1V 4C7, Canada
13 - 27 July 1986 : Les Arcs, France 807/85

THE LIMITS OF NUCLEAR STABILITY
LES LIMITES DE LA STABILITE NUCLEAIRE
Mr. R STORA, Division Théorique, CERN, 1211 Geneva 23, Switzerland
5 - 30 August 1986 : Les Houches, France 815/85

MICROELECTRONIC MATERIALS AND PROCESSES ●
Dr. RA LEVY, AT&T Bell Laboratories, Murray Hill, NJ 07974, USA
30 June - 11 July 1986 : Il Ciocco, Italy 827/85

GEOPHYSICS AND ASTROPHYSICS
GEOPHYSIQUE ET ASTROPHYSIQUE

STATISTICAL TREATMENTS FOR ESTIMATION OF MINERAL AND ENERGY RESOURCES
Dr AG FABBRI, Ist. di Geologia Marina del C.N.R., Via Zamboni 65, 40127 Bologna, Italy
22 June - 4 July 1986 : Il Ciocco, Italy 413/85

GENESIS AND PROPAGATION OF COSMIC RAYS
Prof. MM SHAPIRO, 205 Yoakum Pkwy., 2-1720, Alexandria, VA 22304, USA
1 - 9 June 1986 : Erice, Italy 571/85

PHYSICAL PROCESSES IN ASTROPHYSICS
Dr. G MORFILL, MPI für Physik und Astrophysik, Inst. f. extraterrestrische Physik, 8046 Garching, Germany
August 1986 : Europe 573/85

THE GALAXY
Dr. G GILMORE, Inst. of Astronomy, University of Cambridge, Madingley Road, Cambridge CB3 0HA, UK
4 - 15 August 1986 : Cambridge, UK 806/85

THE EARLY UNIVERSE
Prof. WG UNRUH, Dept. Physics, Univ. of B. C., 6224 Agriculture Rd, Vancouver, BC V6T 2A7, Canada
17 - 30 August 1986 Vancouver Island, Canada 816/85

NEUTRON STARS, AGN, AND JETS - NATURE OF THE ENGINES AND THEIR JETS
Prof. W KUNDT, Inst. F. Astrophysik, Univ. Bonn, Auf dem Hügel 71, 53 Bonn, Germany
17-25 September 1986 : Erice, Italy 830/85

PHYSICALLY-BASED MODELLING AND SIMULATION OF CLIMATE AND CLIMATIC CHANGE
Prof. ME SCHLESINGER, Dept. of Atmospheric Sc., Oregon State University, Corvallis, OR 97331, USA
11-23 May 1986 : Erice, Italy (GTM) 598/84

MATHEMATICS *MATHEMATIQUES*

DEFORMATION THEORY OF ALGEBRAS AND APPLICATIONS
Prof. M HAZEWINKEL, CWI, P.O.B. 4079, 1009 AB Amsterdam, Netherlands
1-14 June 1986 : Il Ciocco, Italy 347/85

VARIATIONAL METHODS IN NONLINEAR PROBLEMS
METHODES VARIATIONNELLES DANS LES PROBLEMES NON LINEAIRES
Prof. A DAIGNEAULT, Dépt. de Math. et de Stat., Univ., CP 6128, Succ. A, Montreal, PQ HBC 3J7, Canada
7-25 July 1986 : Montreal, Canada 569/85

INFORMATICS *INFORMATIQUE*

LOGIC OF PROGRAMMING AND CALCULI OF DISCRETE DESIGN ●
Prof. FL BAUER, Inst. für Informatik, Technische Univ., Postfach 20 2420, 8000 Munchen 2, Germany
29 July-10 August 1986 : Marktoberdorf, Nr. Munich, Germany 321/85

PERFORMANCE LIMITS IN COMMUNICATION, THEORY AND PRACTICE ●
Dr. JK SKWIRZYNSKI, Marconi Res. Ctr., Hanningfield Rd., Great Baddow, Chelmsford Essex CM2 8HN, UK
7-19 July 1986 : Il Ciocco, Italy 568/85

LOGIC SYNTHESIS AND SILICON COMPILATION FOR VLSI DESIGN ●
Prof P ANTOGNETTI, Dept. of Electronics (DIBE), Univ. of Genova, V. Causa 13, 16145 Genova, Italy
7 June-18 July 1986 : L'Aquila, Italy 572/85

DISTRIBUTED OPERATING SYSTEMS - THEORY AND PRACTICE ●
Prof. Y PAKER, Polytechnic Central London, 115 New Cavendish St., London W1M 8JS, UK
18-29 August 1986 : Cesme, Izmir, Turkey 651/85

GAUGE THEORY AND THE EARLY UNIVERSE
Prof. DN SCHRAMM, Astron. & Astroph. Ctr., Univ. of Chicago, 5640 So. Ellis Ave., Chicago, IL 60637, USA
20-30 May 1986 : Erice, Italy 657/85

PATTERN RECOGNITION THEORY AND APPLICATIONS ●
Dr. P DEVIJVER, Philips Res. Labs., Av. Van Becelaere, 2, Box 8, 1170 Brussels, Belgium
9-20 June 1986 : Spa, Belgium 831/85

MATHEMATICS AND COMPUTER SCIENCE IN MEDICAL IMAGING
Dr. MA VIERGEVER, Dept of Math. & Inform., Delft Univ of Techn., P.O.B. 356 2600 AJ Delft, Netherlands
21 September-4 October 1986 : Il Ciocco, Italy 842/85

APPLIED SCIENCES AND ENGINEERING *SCIENCES APPLIQUEES ET INGENIERIE*

MINERAL PROCESSING AT A CROSSROADS - PROBLEMS AND PROSPECTS ●
Dr. BA WILLS, Camborne School of Mines, Pool, Redruth, Cornwall, UK
24 March-4 April 1986 : Falmouth, Cornwall, UK 251/85

SOLAR ENERGY UTILIZATION FUNDAMENTALS AND APPLICATIONS
Dr. HY YUNCU, Dept. of Mechanical Engineering, Middle East Techn. University Ankara Turkey
23 June-4 July 1986 : Cesme, Turkey 257/85

COMPUTER AIDED OPTIMAL DESIGN - STRUCTURAL AND MECHANICAL SYSTEMS ●
Prof. CA MOTA SOARES, CEMUL/IST, Technical Univ., Av Rovisco Pais, P-1096 Lisboa Codex Portugal
29 June-11 July 1986 : Troia, Portugal 274/85

CEREBRAL BLOOD FLOW - MATHEMATICAL MODELS, INSTRUMENTATION, AND IMAGING TECHNIQUES
Dr. CC DUNCAN, Neurosurgery, Yale Univ. School of Medicine, 333 Cedar Str New Haven CT 06510 USA
2-13 June 1986 : L'Aquila, Italy 299/85

PHYSICS AND TECHNOLOGY OF HYPERTHERMIA
Prof. C FRANCONI, Medical Physics Inst., II University of Rome, Via O. Raimundo 00173 Rome Italy
25 July-9 August 1986 : Urbino, Italy 542/85

OPTICAL FIBER SENSORS ●
Prof. S MARTELLUCCI, Mechanical Eng. Dept., 2nd Univ. of Rome, Via O Raimondo 00173 Rome Italy
2-10 May 1986 . Erice, Italy 594/85

REMOTE SENSING APPLICATIONS IN METEOROLOGY AND CLIMATOLOGY
Prof. AP CRACKNELL, Carnegie Lab. of Physics, The University, Dundee DD1 4HN UK
17 August-6 September 1986 : Dundee, UK (GTM) 1023/83

1986

Advanced Research Workshops

LIFE SCIENCES *SCIENCES DE LA VIE*

AUDITORY FREQUENCY SELECTIVITY
Dr. BCJ MOORE, Dept. of Experim. Psychology, The University, Downing St., Cambridge CB2 3EB, UK
23-27 June 1986 : Cambridge, UK 574/84

ADVANCED DRUG DELIVERY SYSTEMS FOR PEPTIDES AND PROTEINS ●
Prof. SS DAVIS, Dept. of Pharmacy, The University, University Park, Nottingham NG7 2RD, UK
28 May-1 June 1986 : Copenhagen, Denmark 678/84

CEREBELLUM AND BEHAVIOURAL PLASTICITY
Prof. M GLICKSTEIN, Neural Mechanisms of Behav., Univ. College, 3 Malet Place, London WC1E 7JG, UK
7-9 April 1986 : Oxford, UK 295/85

ADVANCED TECHNOLOGIES & THEIR NUTRITIONAL IMPLICATIONS IN THE PRODUCTION OF EDIBLE FAT ●
Prof. Claudio GALLI, Ist. di Farmacologie e di Farmacognosia, Via A. Del Sarto 21, 20129 Milan, Italy
17-20 March 1986 : Milan, Italy 591/85

BIOMECHANICS OF CELL DIVISION
Dr. N AKKAS, Graduate Sch. of Natural and Applied Sc., Ankara Univ., F.K. 39, Altindag, Ankara, Turkey
1-31 October 1986 : Istanbul, Turkey 412/85

SOMITE DEVELOPMENT
Prof. R BELLAIRS, Anatomy and Embryology Dept., Univ. College, Gower Street, London WC1E 6BT, UK
6-9 April 1986 : Glasgow, Scotland, UK 563/85

LIPID MEDIATORS, IMMUNOLOGY AND SHOCK ●
MEDIATEURS LIPIDIQUES ET IMMUNOLOGIE DANS LE CHOC SEPTIQUE ASSOCIE AUX LESIONS THERMIQUES ●
Dr. PG BRAQUET, Inst. Henri Beaufour, 17 Av. Descartes, F-92350 Le Plessis Robinson, France
10-15 August 1986 : Copenhagen, Denmark 589/85

CELLULAR AND HUMORAL COMPONENTS OF CEREBROSPINAL FLUID IN MULTIPLE SCLEROSIS
Prof. A LOWENTHAL, Dept. Neurochem., Borne-Bunge Found. Un. Antwerp, Univ. plein 1, 2610 Wilrijk, Belgium
20-24 April 1986 : Hengelhoef, Houthalen, Limburg, Belgium 794/85

BIOLOGY OF ICOSANOIDS AND RELATED SUBSTANCES IN BLOOD AND VASCULAR CELLS
BIOLOGIE DES ICOSANOIDES ET DES SUBSTANCES VOISINES DANS LES CELLULES SANGUINES ET VASCULAIRES
Dr. M LAGARDE, U63, Lab. d'Hémobiologie, Inst. Pasteur, Fac. A. Carrel, 69372 Lyon Cédex 08, France
Septembre 1986 : Lyon, France 801/85

THE BIOLOGICAL SIGNIFICANCE OF THE MAJOR HISTOCOMPATIBILITY COMPLEX
Dr. AJ MUNRO, Dept. of Pathology, Cambridge University, Tennis Court Rd., Cambridge, CB2 1QP, UK
16-28 April 1986 : Sorrento, Italy 821/85

RECOGNITION IN MICROBE-PLANT SYMBIOTIC AND PATHOGENIC SYSTEMS
Prof. EJJ LUGTENBERG, The University, Botanical Lab., Nonnensteeg 3, 2311 VJ Leiden, Netherlands
11-16 May 1986 : Dronten, Netherlands (C-CS) 703/84

MESENCHYMAL-EPITHELIAL INTERACTIONS IN NEURAL DEVELOPMENT
Prof. JR WOLFF, Zentrum Anatomie der Universität, Kreuzbergring 36, 3400 Göttingen, Germany
17-21 March 1986 : Berlin, Germany (C-CS) 815/84

MOLECULAR AND CELLULAR PROCESSES UNDERLYING DESENSITIZATION AND ADAPTATION TO SIGNAL MOLECULES
Prof. TM KONIJN, Zoological Lab., The University, Kaiserstraat 63, 2311 GP Leiden, Netherlands
29-31 May 1986 : Noordwijkerhout, Netherlands (C-CS) 824/84

PLANT HORMONE RECEPTORS
Dr. D KLAMBT, Dept. of Botany, University of Bonn, Meckenheimer Allee 170, 5300 Bonn 1 Germany
18-22 August 1986 : Bonn, Germany (C-CS) 837/84

MECHANISM OF FUNCTION OF THE ACETYLCHOLINE RECEPTOR
Prof. A MAELICKE, MPI für Ernahrungsphys., Rheinlanddamm 201, 4600 Dortmund 1, Germany
12-17 May 1986 : Santorin (Thira), Greece (C-CS) 767/84

HOST-PARASITE RECOGNITION AND INTERACTION IN PROTOZOAN DISEASES OF MAN
Prof. KP CHANG, Univ. of Health Sciences, 333 Green Bay Rd., N. Chicago, IL 60064, USA
28 September-1 October 1986 : Maratea, Italy (C-CS) 769/84

MODIFICATION OF CELL TO CELL SIGNALS DURING NORMAL AND PATHOLOGICAL AGEING
Dr. S GOVONI, Inst. of Pharmacology & Pharmacognosy, Via A. del Sarto 21, 20129 Milan, Italy
11-17 May 1986 : Limone, Italy (C-CS) 476/85

GANGLIOSIDES AND MODULATION OF NEURONAL FUNCTIONS
Prof. DH RAHMANN, Zoological Inst., Univ. Stuttgart-Hohenheim, 7000 Stuttgart 70, Germany
19-24 October 1986 : Stuttgart, Germany (C-CS) 809/85

THE SEMIOTICS OF CELLULAR COMMUNICATION IN THE IMMUNE SYSTEM
Dr. EE SERCARZ, Dept. of Microbiology, Univ of California, Los Angeles, CA 90024, USA
5-10 May 1986 : Bellagio, Italy (C-CS) 837/85

ECOLOGY *ECOLOGIE*

NUMERICAL ECOLOGY
Prof. P LEGENDRE, Dépt. de Sc. Biologiques, Université, CP 6128, Succ. A, Montreal H3C 3J7, Canada
3-11 June 1986 : Roscoff, Brittany, France 590/85

TAXONOMY OF PORIFERA FROM NE ATLANTIC AND MEDITERRANEAN SEA
TAXONOMIE DES PORIFERES DANS LE N-E ATLANTIQUE ET LA MEDITERRANEE
Dr. J VACELET, Ctre d'Océanol., Station Marine d'Endoume, r. Batterie des Lions, 13007 Marseille France
22-27 September 1986 : Marseille, France 820/85

POPULATION DYNAMICS AND CONSERVATION OF SEABIRDS
DYNAMIQUE DE LA POPULATION ET PRESERVATION DES OISEAUX DE MER
Dr. X MONBAILLIU, MEDMARAVIS, 20 rue St. Martin, 75004 Paris, France
26-31 March 1986 : Alghero, Sardinia, Italy 850/85

SOCIAL, BEHAVIOURAL AND POLITICAL SCIENCES
SC. SOCIALES, POLITIQUES ET DU COMPORTEMENT

INDIGENOUS COGNITION AND MODELS OF INFORMATION PROCESSING
Dr. JW BERRY, Psychology Dept., Queens University, Kingston, Ontario, Canada
16-20 June 1986 : Kingston, Ontario, Canada 546/85

THE PSYCHOPHYSICS OF SPEECH PERCEPTION
Dr. MEH SCHOUTEN, Inst. of Phonetics, Rijksuniversiteit, Trans 14, 3512 JK Utrecht, Netherlands
30 June-4 July 1986 : Utrecht, Netherlands 549/85

MATHEMATICAL ECONOMICS
Prof. P DEHEZ, European University Institute, 50016 San Domenicodi Fiesole, Italy
8-20 September 1986 : Florence, Italy 558//85

CRIME AND ITS VICTIMS - INTERNATIONAL RESEARCH & PUBLIC POLICY ISSUES
Prof. E VIANO, The American University, School of Justice, Washington, DC 20016, USA
May 1986 : Bari, Italy 670//85

SOCIAL AND ENVIRONMENTAL PSYCHOLOGY AND EUROPEAN INTEGRATION
Prof. JC JESUINO, ISC do Trabalho e da Empresa, Av. das Forces Armadas, 1600 Lisbon, Portugal
1-5 April 1986 : Lisbon, Portugal 798/85

LANGUAGE GENERATION ●
Prof. GAM KEMPEN, Psychol. Lab., Univ. of Nijmegen, Montessoril. 3, 6525 HR Nijmegen, Netherlands
19-23 August 1986 : Nijmegen, Netherlands 844/85

PHYSICS AND CHEMISTRY *PHYSIQUE ET CHIMIE*

CHEMISTRY AND PHYSICS OF FRACTURE ●
Dr. RM LATANISION, Materials Sc. & Eng., MIT, 77 Mass. Ave. 8-202, Cambridge, MA 02139, USA
23 June-1 July 1986 : Bad Reichenhall, Germany 255/85

RELATIVISTIC PARTICLE CHANNELING
Prof. JA ELLISON, Dept. of Math. & Stat., University of New Mexico, Albuquerque, NM 87131, USA
31 March-4 April1986 : Maratea, Italy 294/85

IONOMERS/*IONOMERES*
Dr. M PINERI, Ctre d'études Nucléaires, DRF/SHP/PCM, 85 X, 38041 Grenoble Cedex, France
15-21 June 1986 : Villard de Lans, Isère, France 370/85

STRUCTURE AND DYNAMICS OF WEAKLY BOUND MOLECULAR COMPLEXES
Dr. A WEBER, Molecular Spectr. Div., Nat. Bureau of Standards, Gaithersburg, MD 20899, USA
22-26 September 1986 : Maratea, Italy 583/85

PATTERNS, DEFECTS AND MICROSTRUCTURES IN NONEQUILIBRIUM SYSTEMS ●
Prof. I PRIGOGINE, Serv. Chimie Phys. II, CP 231, Campus Pl. ULB, Bld. du Triomphe, 1050 Bruxelles, Belgium
24-28 March 1986 : Austin, Texas, USA 559/85

STOCHASTICITY AND INTRAMOLECULAR REDISTRIBUTION OF VIBRATIONAL ENERGY
ASPECTS STOCHASTIQUES ET REDISTRIBUTION INTRAMOLECULAIRE DE L'ENERGIE DE VIBRATION
Prof. R LEFEBVRE, Lab. de Photophysique Moléc., Campus d'Orsay, 91405 Orsay, France
2-12 June 1986 : Orsay, France 627/85

QUANTUM VIOLATIONS, RECENT AND FUTURE EXPERIMENTS AND INTERPRETATIONS
Dr. WM HONIG, Div. of Sc. & Eng., W. Australian Inst. of Techn., Perth, Sth Bentley, 6102 W. Australia
July 1986 : USA 686/85

NON-STOICHIOMETRIC COMPOUNDS ●
Dr. CRA CATLOW, Dept. of Chemistry, Keele University, Keele, Staffs ST5 5BG, UK
31 August-6 September 1986 : Keele, Staffordshire, UK 796/85

SUPER FIELD THEORIES
Dr. HC LEE, Theoretical Physics Br., Chalk River Nuclear Labs., Chalk River, Ont. KOJ 1J0, Canada
25-30 July 1986 : Vancouver, Canada 811/85

POLYMER COLLOIDS ●
Prof. MS EL-ASSER, Emul. Polymers Inst., 226 Sinclair Lab. No. 7, Lehigh Univ., Bethlehem, PA 18015, USA
30 June-5 July 1986 : Wingspread, Racine, Wisconsin, USA 834/85

OPTICAL PROPERTIES OF NARROW GAP LOW DIMENSIONAL STRUCTURES
Prof. RA STRADLING, Dept. of Phys., Blackett Lab., Imperial College, Prince Consort Rd., London SW7 2BZ, UK
29 July-1 August 1986 : St. Andrews, Scotland, UK (CSLD) 810/85

THIN FILM GROWTH TECHNIQUES FOR LOW DIMENSIONAL STRUCTURES
Dr. RFC FARROW, IBM Research Lab., 5600 Cottle Road K32/281, San Jose, CA 95193, USA
15-19 September 1986 : Brighton, Sussex, UK (CSLD) 845/85

THE STRUCTURE AND DYNAMICS OF PARTIALLY SOLIDIFIED SYSTEMS
Prof. D LOPER, Geophysical Fluid Dynamics Inst., Florida State University, Tallahassee, FL 32306, USA
12-16 May 1986 : Tahoe, California, USA (GTM) 785/84

SUBSTITUENT EFFECTS IN RADICAL CHEMISTRY
EFFETS DE SUBSTITUTION EN CHIMIE DES RADICAUX
Prof. HG VIEHE, Lab. of Organic Chem., UCL, Place Louis Pasteur, 1, 1348 Louvain-La-Neuve, Belgium
20-24 January 1986 : Louvain-la-Neuve, Belgium (SAM) 832/84

SURFACE ORGANOMETALLIC CHEMISTRY -
MOLECULAR APPROACH TO SURFACE SCIENCE AND CATALYSIS
CHIMIE ORGANOMETALLIQUE DES SURFACES -
APPROCHE MOLECULAIRE DES SURFACES ET CATALYSE
Dr. JM BASSET, CNRS Inst. de Rech. sur la Catalyse, 2 Av. A. Einstein, 69626 Villeurbanne Cédex, France
25-30 May 1986 : Grospierres, France (SAM) 814/85

THE DESIGN, ACTIVATION AND TRANSFORMATION OF ORGANOMETALLICS INTO COMMON & EXOTIC MATERIALS
Dr. RM LAINE, Chem. Program, SRI International, 333 Ravenswood Ave., Menlo Park, CA 94025, USA
Date and Place to be announced (SAM) 865/85

GEOPHYSICS AND ASTROPHYSICS
GEOPHYSIQUE ET ASTROPHYSIQUE

GALAXY DISTANCES AND DEVIATIONS FROM THE UNIVERSAL EXPANSION
Dr. RB TULLY, Inst. for Astronomy, 2680 Woodlawn Drive, Honolulu, HI 96822, USA
13-17 January 1986 : Kona, Hawaii, USA 293/85

POLYCYCLIC AROMATIC HYDROCARBONS AND ASTROPHYSICS
HYDROCARBURES POLYCYLIQUES AROMATIQUES, ET ASTROPHYSIQUE
Dr. A LEGER, Grpe Phys. des solides de l'ENS, Univ. Paris 7-Tr. 23, 2 Pl. Jussieu, 75251 Paris Cedex 05, France
17-22 February 1986 : Les Houches, France 687//85

HIGH ENERGY GAMMA RAY ASTRONOMY
Dr. KE TURVER, Dept. of Physics, Univ. Science Labs., South Rd., Durham DH1 3LE, UK
11-15 August 1986 : Durham, UK 825/85

ORIGINS OF IGNEOUS LAYERING
Dr. I PARSONS, Dept. of Geology and Mineralogy, Marischal College, Aberdeen AB9 1AS, UK
1-14 August 1986 : Narssarssuaq, Greenland (GTM) 802/85

MATHEMATICS *MATHEMATIQUES*

DYNAMICS OF INFINITE DIMENSIONAL SYSTEMS
Prof. JK HALE, Div. of Applied Maths., Brown University, Providence, RI 02912, USA
19-24 May 1986 : Lisbon, Portugal 296/85

PERIODIC SOLUTIONS OF HAMILTONIAN SYSTEMS
Prof. PH RABINOWITZ, Dept. of Mathematics, Univ. of Wisconsin-Madison, Madison, WI 53706, USA
October 1986 : Il Ciocco, Italy 372/85

GEOMETRIES AND GROUPS, FINITE AND ALGEBRAIC
Dr. AM COHEN, CWI-Ctr. for Math. & Computer Sc., 1098 SJ Amsterdam, Netherlands
24-28 March 1986 : Amsterdam, Netherlands 592/85

MATHEMATICAL ASPECTS OF GRAVITY AND SUPERGRAVITY
Prof. A ROSENBLUM, Dept. of Physics, Utah State University, Logan, Utah 84322, USA
21-25 July 1986 : Logan, Utah, USA 788/85

NUMERICAL INTEGRATION - RECENT DEVELOPMENTS, SOFTWARE AND APPLICATIONS
Dr. P KEAST, Dept. of Maths. Statistics & Computing Sc., Dalhousie Univ., Halifax, NS B3H 4H8, Canada
18-22 August 1986 : Halifax, Nova Scotia, Canada 800/85

INFORMATICS *INFORMATIQUE*

INFORMATION SYSTEMS - A METHOD OF FAILURE ANALYSIS
Prof. A DEBONS, Information Sc. Dept., Univ. of Pittsburgh, 730 Lis Building, Pittsburgh, PA 15260, USA
18-22 August 1986 : Tournai, Belgium 823/85

EXPERT JUDGMENT AND EXPERT SYSTEMS ●
Dr. J MUMPOWER, Rockefeller Coll. Public Affairs and Policy, Milne 103, SUNY, Albany, NY 12222, USA
August 1986 : Porto, Portugal 838/85

MACHINE INTELLIGENCE AND KNOWLEDGE ENGINEERING FOR ROBOTIC APPLICATIONS
De. AKC WONG, Dept. of Systems Design Eng., University of Waterloo, Waterloo, Ontario N2L 3G1, Canada
May 1986 : Maratea, Italy (Rob) 018/85

PYRAMIDAL SYSTEMS FOR IMAGE PROCESSING AND COMPUTER VISION
Dr. V CANTONI, Dip. Informatica e Sistemistica, Strada Nuova 106/C, 27100 Pavia, Italy
6-9 May 1986 : Maratea, Italy (Rob) 170/85

APPLIED SCIENCES AND ENGINEERING
SCIENCES APPLIQUEES ET INGENIERIE

HALIDE GLASSES FOR INFRARED FIBEROPTICS
Dr. RMA ALMEIDA, Ctr. De Fisica Molec., Inst. Sup. Tecn., Av. Rovisco Pais, 1000 Lisboa Codex, Portugal
31 March-4 April 1986 : Vilamoura (Algarve), Portugal 292/85

MECHANICAL VIBRATIONS AND AUDIBLE NOISE IN ALTERNATING CURRENT MACHINES ●
Mr. R BELMANS, Dept. of Electrical Engineering, Kard. Mercierlaan 94, B-3030 Leuven-Heverlee, Belgium
4-8 August 1986 : Leuven, Belgium 15/85

FUNDAMENTALS OF PHYSICAL-CHEMISTRY OF PULVERIZED COAL COMBUSTION ●
ASPECTS FONDAMENTAUX DE LA CHIMIE-PHYSIQUE DE LA COMBUSTION DU CHARBON PULVERISE ●
Dr. J LAHAYE, Ctre de Rech. sur la Phys.-Chim. des surf. solides, 24 Av. Prés. Kennedy, 68200 Mulhouse, France
11-15 August 1986 : Le Bischenberg, France 584/85

INTERACTIONS AT THE SOIL COLLOID - SOIL SOLUTION INTERFACE
Prof. MFL DE BOODT, Fakulteit Landbouw, RUG, Coupure Links 533, 9000 Gent, Belgium
3-9 August 1986 : Gent, Belgium 797/85

SENSORS AND SENSORY SYSTEMS FOR ADVANCED ROBOTS
Dr. P DARIO, Centro "E. Piaggio", University of Pisa, Via Diotisalvi 2, 56100 Pisa, Italy
28 April-3 May 1986 : Maratea, Italy (Rob) 623/85

LANGUAGES FOR SENSOR-BASED CONTROL IN ROBOTICS
Prof. U REMBOLD, Universität Karlsruhe, Inst. f. Informatik III, Postfach 6380, 7500 Karlsruhe 1, Germany
September 1986 : Limone sul Garda, Italy (Rob) 871/85

KINEMATIC AND DYNAMIC ISSUES IN SENSING-BASED CONTROL
PROBLEMES CINETIQUES ET DYNAMIQUES DANS LE CONTROLE A BASE DE SENSEURS
Dr. B ESPIAU, IRISA, Campus de Beaulieu, 35042 Rennes Cédex, France
October 1986 : Limone sul Garda, Italy (Rob) 872/85

Further information on a particular meeting should be obtained from the meeting Director named above. Reader Service No.27

Further information on the NATO Science Programmes may be obtained from : NATO Scientific Affairs Division, B-1110 Brussels, Belgium.

Period derivative and orbital eccentricity of binary pulsar 1953+29

L. A. Rawley*, J. H. Taylor* & M. M. Davis†

* Joseph Henry Laboratories and Physics Department,
Princeton University, Princeton, New Jersey 08544, USA
† Arecibo Observatory, Arecibo, Puerto Rico 00613, USA

PSR1953+29, the second fastest of more than 400 known pulsars[1], has a period of 6.133 ms and is a member of a binary system with an orbital period of 117.35 days. The system is of great interest because of what it can reveal about the evolution of pulsars and close binary stars[2–4]. Recently we have carried out observations to determine two of the most important parameters of the system, the pulsar period derivative $\dot{P}$ and the orbital eccentricity e. We find a small but non-zero eccentricity, $e=(330.3\pm 0.4)\times 10^{-6}$, and a spindown rate of $\dot{P}=(1\pm 6)\times 10^{-20}$ s s^{-1}, smaller than that measured for any other pulsar. These values are consistent with an evolutionary history involving spin-up during a mass accretion phase, but are difficult to reconcile with a recent report of periodically pulsed γ rays from this object[5].

Observations were made with the 305-m telescopes of the Arecibo observatory on 26 different days between 16 February and 10 October 1985, during which time the pulsar completed almost exactly two orbits. At an observing frequency of 430 MHz, the Arecibo system provides a system noise temperature of 140 K and an antenna sensitivity of 14 K Jy^{-1} in each sense of circular polarization. (These figures include an allowance for 70 K of sky background noise in the direction of PSR1953+29 and for the degradation of sensitivity and increase in system noise at zenith angles near 12°.) Data acquisition is accomplished with a system built at Princeton especially for timing measurements of fast pulsars. This equipment makes use of a $2\times 32\times 30$-kHz filter-bank spectrometer which provides the sums of detected, orthogonally polarized signals in each of 32 channels covering a total bandwidth of 960 kHz. Each of the 32 total-power signals is sent to a hard-wired digital signal averager which samples the intensity 128 times per period and produces an integrated pulse profile for every 1 or 2 min of observing time.

The profiles are stored on magnetic tape together with the universal time of the first sample taken in a period near the midpoint of the integration. In the first stage of data analysis, each profile is corrected to a reference frequency of 430.0 MHz, using the value of dispersion measure (DM) from Table 1, and the sets of 32 simultaneoulsy recorded profiles are then summed. The summed profiles are cross-correlated with a standard profile, obtained by averaging many of the 2-min integrations. The observed phase delays are added to the start times of the integrations to obtain effective pulse arrival times at Arecibo. Measured pulse arrival times have uncertainties in the range 25–50 μs, depending on signal strength and zenith angle.

Table 1 Parameters of the PSR1953+29 system

Right ascension (1950.0)	$\alpha=19$ h 53 min 26.731 s $\pm$ 0.003 s
Declination (1950.0)	$\delta=29°\,00'\,43.68''\pm 0.17''$
Pulsar period	$P=6133166488.9\pm 0.6$ ps
Period derivative	$\dot{P}=(1\pm 6)\times 10^{-20}\ s\,s^{-1}$
Epoch of period	$t_0=2446113.13$ JED
Projected semi-major axis	$a_1\sin i=31.41269\pm 0.00002$ light s
Eccentricity	$e=(330.3\pm 0.4)\times 10^{-6}$
Orbital period	$P_b=10138963\pm 2$ s
Longitude of periastron	$\omega=29.5474\pm 0.08$ deg
Time of periastron	$T_0=2446113.0009\pm 0.03$ JED
Dispersion measure	DM $=104.58\pm 0.05$ cm^{-3} pc

In the table we quote uncertainties equal to three times the formal standard errors, our caution based mostly on the large covariances between P, $\dot{P}$ and δ, because our data span is shorter than a year, and between ω and T_0, because the eccentricity is so small. DM is measurable because we included in the data set 3 days of observations made at 1,408 MHz, using a $2\times 32\times 250$ kHz filter bank. The error quoted for DM reflects the uncertainty in finding a reference point on a pulse profile that changes shape dramatically between 430 and 1,408 MHz[7]. The post-fit weighted r.m.s. residual for our solution is 35 μs, fully consistent with the measurement uncertainties, and there is no evidence for significant non-random behavior of the residuals.

JED = Julian Ephemeris Date.

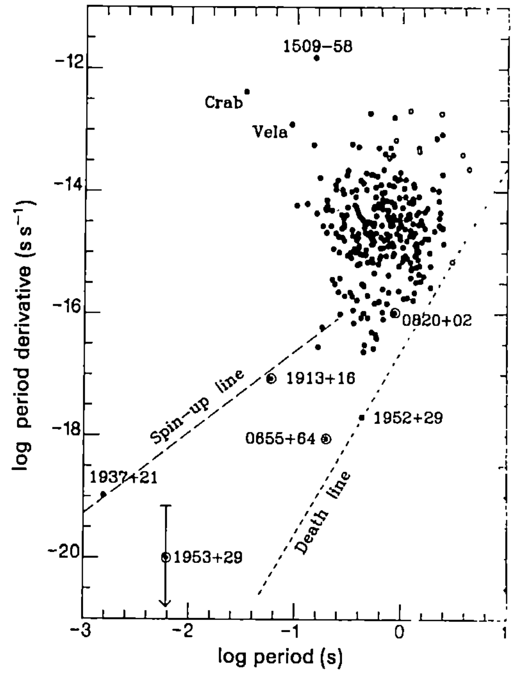

Fig. 1 Distribution of periods and period derivatives for 305 pulsars. Several pulsars of particular interest are identified, and four of the five known binary pulsars are indicated by circles around the dots. (No estimate of period derivative is yet available for the fifth binary, PSR2303+46.) The spin-up line and death line are described in the text, and original references for most of the period derivatives can be found in ref. 9. (A few measurements of $\dot{P}$ are unpublished results obtained by the Princeton University pulsar group.)

Subsequent analysis of the pulse times proceeded as follows. Data obtained on a given day, usually covering 20–60 min, were reduced to equivalent Solar System barycentric times with the aid of a numerical ephemeris of the Earth's motion[6]. As a first approximation we assumed the celestial coordinates of the pulsar to be those determined with the Very Large Array (VLA) telescope[7]. Because the orbital period of the system is so long, changes in orbital motion cause negligible period variations over ~1 h. Therefore, we obtained a best-fit pulsar period for each day's data in the reference frame of the Solar System barycentre, and used these values to carry out a least-squares solution for the binary orbital period, P_t, the time of passage through the ascending node, T_0, the projected semimajor axis, $a_p \sin i$ (where i is the angle between the plane of the orbit and the plane of the sky) and the pulsar period in its own rest frame, P. At this stage of the analysis we could determine only an upper limit to e.

With the resulting parameters as starting values we were able to assign unambiguous pulse numbers to all the measured arrival times and thus to carry out a phase-coherent analysis of the entire data set[8]. This procedure was considerably more difficult than it has been for the other four known binary pulsars, largely because the ratio of orbit size (in light seconds) to pulsar period is much larger for PSR1953+29 than for the other pulsars. A linearized least-squares fit to the topocentric arrival times yielded the parameter values listed in Table 1.

For comparison purposes, the values of P and $\dot{P}$ measured for PSR1953+29 are illustrated in Fig. 1, together with corresponding values for 304 other pulsars[9]. Although our measurement of $\dot{P}$ is only an upper limit, it is already the smallest known period derivative of any pulsar. Our values for the celestial coordinates are consistent with those obtained with the VLA[7], but more accurate by factors of 20 and 4 in α (right ascension) and δ (declination), respectively. The position is consistent (at the 2σ level) with that of the candidate companion star observed by Loredo *et al.*[10], although the star field is so crowded that the probability of a chance superposition within $\sim0.3''$ is at least a few per cent.

We next summarize some astrophysical implications of the newly determined parameters of PSR1953+29. For radio pulsars, the braking torque is thought to be dominated by magnetic dipole radiation at the rotation frequency[8], or possibly by the effects of longitudinal current flow along the open magnetic-field lines of the pulsar[11]. Under either assumption, pulsars are expected to evolve downwards and to the right in Fig. 1, initially along lines of slope between 0 and −1. Within a few million years, the evolutionary tracks steepen because of magnetic-field decay[12] or a tendency towards counter-alignment of the magnetic and spin axes[11]. At the same time the radio luminosity begins to decrease[13], and, for electrodynamical reaons[14], the pulsar will probably cease to function when it reaches a 'deathline' with a form like $\dot{P} \propto P^3$, beyond which the induced potential differences in the polar-cap region are insufficient to support electron-positron pair production. Thus, most features of the distribution of points in Fig. 1 can be understood if pulsars are born with short-to-moderate periods and large period derivatives; as they age, pulsars evolve through the general clump of points in the figure and die near the death line within $\lesssim 10^7$ yr.

The surface magnetic-field strength of a pulsar, if dipole radiation is the braking mechanism, is related to P and $\dot{P}$ by

$$B = 3.2\times10^{19}\, I_{45}^{1/2}\, R_6^{-3}\, (\dot{P}P)^{1/2}$$

where B is the field strength in gauss, I_{45} the moment of inertia in units of 10^{45} g cm^2 and R_6 the radius in units of 10^6 cm. With $I_{45} = R_6 = 1$, PSR1953+29 has field $<7\times10^8$ G, close to the value obtained for PSR1937+21, 4×10^8 G. Such small magnetic fields imply that these objects, and others with small values of both P and $\dot{P}$, are much older than ordinary pulsars, their fields presumably having decayed from typical pulsar values of $\approx10^{12}$ G.

Several studies have emphasized that unusually old pulsars can be accommodated in this evolutionary picture with one additional hypothesis: those born in undisrupted binary systems can be spun up by the accretion of mass and angular momentum from their companion stars (see refs 15–18 and refs therein). The angular velocity of the pulsar asymptotically approaches that of the accretion disk at its boundary with the magnetosphere. When accretion ends, the pulsar will begin to slow down according to

$$\dot{P} \approx 3\times10^{-20}\, I_{45}^{-1}\, (10^3\, P)^{4/3}\, M^{5/3}\, \dot{m}_{17}$$

where M is the pulsar mass in solar units and $\dot{m}_{17}$ the accretion rate in untits of 10^{17} g s^{-1} (see ref. 18 for details). The spin-up line at the left of Fig. 1 illustrates this relation for $I_{45} = \dot{m}_{17} = 1$ and $M = 1.4$

Our observations of PSR1953+29 suggest that it was 'reborn' by accreting matter from its companion. The small orbital eccentricity observed for the system implies a protracted phase of accretion accompanied by non-conservative viscous forces. Because our value of $\dot{P}$ places PSR1953+29 well below the spin-up line, it seems likely that this pulsar, like PSR0655+64, had a smaller accretion rate (or smaller mass, larger moment of inertia or some combination of these factors) than PSR1913+16. It is also possible that PSR0655+64 and PSR1953+29 are extremely old objects that have spun down to their present P and $\dot{P}$ from initial values much closer to the spin-up line.

If the period derivative of PSR1953+29 is positive and equal to the upper limit consistent with our data, the rate of rotational energy loss is $\dot{E} = 1.3\times10^{34}\, I_{45}$ erg s^{-1}. For $I_{45} \approx 1$, and an assumed distance of 2.7 kpc, this rate is 20-fold less than the luminosity reported[5] for the nearby γ-ray source 2CG065+0. Therefore, physical association of the pulsar with the γ-ray source seems unlikely. Although the gain of angular momentum from infalling matter could account for the very small (and possibly negative) period derivative of the pulsar an accretion powered γ-ray mechanism is inconsistent with the observed very high rotational stability. Note that our improved orbital elements can now be used to re-analyse the γ-ray data for modulation at the pulsar period without having to search over a range of possibilities.

We thank Angel Vazquez and Reinaldo Velez for performing some of the observations, other members of the Arecibo observatory staff for their support, and the NSF for financial support.

Note added in proof: Data obtained up to 6 December 1985 now yield a period derivative $\dot{P} = (3.2\pm1.4)\times10^{-20}$ s s^{-1}, which replaces the upper limit given in Table 1 and Fig. 1.

Received 23 October; accepted 27 November 1985.

1. Boriakoff, V., Buccheri, R. & Facui, F. *Nature* **304**, 417–418 (1983).
2. Paczynski, B. *Nature* **304**, 421–422 (1983).
3. van den Heuvel, E. P. J. in *Millisecond Pulsars* (eds Reynolds, S. P. & Stinebring, D. R.) 86–103 (National Radio Astronomy Observatory, Green Bank, 1984).
4. Joss, P. C., & Rappaport, S. A. *Nature* **304**, 419–421 (1983).
5. Chadwick, P. M. *et al. Nature* **317**, 236–238 (1985).
6. Chandler, J. F., Babcock, R. W., Reasenberg, R. D. & Shapiro, I. I. Preprint PEP-740R (1984).
7. Boriakoff, V., Buccheri, R., Fauci, F., Turner, K. & Davis, M. M. in *Millisecond Pulsars* (eds Reynolds, S. P. & Stinebring, D. R.) 24–29 (National Radio Astronomy Observatory, Green Bank, 1984).
8. Manchester, R. N. & Taylor, J. H. *Pulsars* (Freeman, San Francisco, 1977).
9. Manchester, R. N. & Taylor, J. H. *Astr. J.* **86**, 1953–1973 (1981).
10. Loredo, T. J., Ricker, G. R., Rappaport, S. A. & Middleditch, J. in *Millisecond Pulsars* (eds Reynolds, S. P. & Stinebring, D. R.) 48–57 (National Radio Astronomy Observatory, Green Bank, 1984).
11. Beskin, V. S., Gurevich, A. V. & Istomin, Ya. N. *Astrophys. Space Sci.* **102**, 301–326 (1984).
12. Lyne, A. G., Ritchings, R. T. & Smith, F. G. *Mon. Not. R. astr. Soc.* **171**, 579–597 (1975).
13. Lyne, A. G., Manchester, R. N. & Taylor, J. H. *Mon. Not. R. astr. Soc.* **213**, 613–639 (1985).
14. Ruderman, M. A. & Sutherland, P. G. *Astrophys. J.* **196**, 51–72 (1975).
15. Smarr, L. L. & Blandford, R. *Astrophys. J.* **207**, 574–588 (1976).
16. Blandford, R. D. & DeCampli, W. M. *IAU Symp.* No. 95 (eds Wielebinski, R. & Sieber, W.) 371–377 (Reidel, Dordrecht, 1981).
17. Backus, P. R., Taylor, J. H. & Damashek, M. *Astrophys. J. Lett.* **255**, L63–L67 (1982).
18. Alpar, M. A., Cheng, A. F., Ruderman, M. A. & Shaham, J. *Nature* **300**, 728–730 (1982).

Feasibility of a low-mass binary source progenitor for PSR1937+214

L. C. Jeffrey

Department of Physics, Princeton University,
Princeton, New Jersey 08544, USA

One suggested progenitor system for the 1.5-ms pulsar PSR1937+214 is a close binary containing, in the late stages of its evolution, a neutron star and a very-low-mass ($\lesssim 0.1\, M_\odot$) degenerate dwarf helium star[1,2]. The two main questions that affect the plausibility of this scenario are: (1) whether the system's evolution would in fact leave the neutron star at the observed high spin rate; and (2) whether the secondary could be disrupted, leaving a single pulsar. Here, we have analysed such a system using the predictions of Ghosh and Lamb[3], and find that the equilibrium rotation period predicted for the neutron star immediately before the disruption of the secondary is so large that matter accreted from a disk after disruption would be unlikely to spin the pulsar up to the observed period. Furthermore, our estimate for the magnitude of tidal torques that transfer rotational angular momentum from an accretion disk back into the orbital motion may give values substantially higher than the previous estimate[1]. It is thus unlikely that PSR1937+214 originated in a binary system in which the companion had an extremely low mass at disruption.

Among the proposed progenitors for PSR1937+214 are two involving low-mass binaries. In one version proposed by Ruderman and Shaham[1,2,4], a neutron star accretes matter from a low-mass companion and may be spun up to a 1.56-ms period; the companion, which becomes rich in helium during its evolution, continues to lose mass until it reaches a sufficiently low mass ($\sim 0.0053\ M_\odot$)[2,5] that it disrupts. This can only happen if the system enters a regime where angular momentum accumulates in the accretion disk around the primary. Bonsema and van den Heuvel[5,6], on the other hand, have proposed that the pulsar might have evolved from a neutron star binary system in which the secondary is a massive white dwarf ($\geqslant 0.65\ M_\odot$). For a secondary mass $\geqslant 0.655\ M_\odot$, the secondary will be disrupted regardless of whether tidal forces act to prevent angular momentum from accreting in the disk. In the first scenario, over the long time before disruption ($\sim 10^{10}$ yr), the mass transfer rate may decay by several orders of magnitude. Li *et al.*[7] have shown that if the companion is described by the $n=\frac{3}{2}$ polytropic equation of state, and if the only angular momentum loss from the system is that due to gravitational radiation, then for a secondary of initial mass $M_2(0)$, mass fraction of hydrogen X and total system mass M (assumed conserved), we have

$$\frac{\dot{M}_2(t)}{\dot{M}_2(0)}=\left(\frac{M_2(t)}{M_2(0)}\right)^{14/3}=\frac{1}{(1+t/\tau)^{14/11}}$$

$$\tau=(1.3\times10^2\ \text{yr})(1+X)^{20/3}\left(\frac{M}{M_\odot}\right)^{-2/3}\left(\frac{M_2(0)}{M_\odot}\right)^{-11/3} \qquad (1)$$

$$|\dot{M}_2|=(2.1\times10^{-3}\ M_\odot\,\text{yr}^{-1})\left(\frac{M}{M_\odot}\right)^{2/3}\left(\frac{M_2}{M_\odot}\right)^{14/3}\times(1+X)^{-20/3}$$

If the primary has mass $1.4\ M_\odot$, the mass transfer rate corresponding to a pure-helium 0.01-$M_\odot$ secondary, twice the mass necessary for disruption, is $1.2\times10^{-12}\ M_\odot\,\text{yr}^{-1}$, four orders of magnitude less than the Eddington rate. Vila's more accurate calculations based on the Zapolsky-Salpeter model[6] show the same behaviour. The calculation of Li *et al.* assumes that no mass or angular momentum accumulates in the disk or is lost from the system over its long-timescale steady-state evolution; however, Taam and Wade[9], who consider systems which lose mass and angular momentum by material outflow, find a similar decay unless all the angular momentum that flows into the disk is lost from the system. The equilibrium period (P_{eq}) for a spun-up neutron star is[4,10]

$$P_{eq}=(1.57\times10^{-3}\ \text{s})\left(\frac{M_1}{M_\odot}\right)^{-5/7}(B_8R_6^3)^{6/7}(\dot{M}_{-9})^{-3/7} \qquad (2)$$

where B_8 is the neutron star surface magnetic field in units of 10^8 G, R_6 the neutron star radius in units of 10^6 cm, M_1 the neutron star mass and $\dot{M}_{-9}$ the mass transfer rate in units of $10^{-9}\ M_\odot\,\text{yr}^{-1}$. The minimum neutron star radius permitted by most equations of state is ~ 7.5 km, which occurs for a neutron star mass no greater than $1.6\ M_\odot$ (ref. 11). For a magnetic field of 5×10^8 G (the current estimate on the basis of measurements of P and $\dot{P}$), the equilibrium period corresponding to $1.2\times10^{-12}\ M_\odot\,\text{yr}^{-1}$ must then be greater than ~ 35 ms.

The theory of Ghosh and Lamb[3,10] treats the spin-down mechanism. The equilibrium period is achieved at a particular value of the ratio of the magnetosphere radius to the corotation radius, r_m/r_{co}. Outside r_{co} the accretion disk around the neutron star rotates more slowly than the magnetic field lines, so the magnetic coupling to the disk in this region tends to slow the neutron star down. Inside r_{co} the disk rotates more rapidly than the field lines, tending to spin the star up. A decrease in the mass transfer rate increases r_m so that more magnetic flux threads the region outside r_{co} and the star spins down. The magnetic coupling that facilitates this spin-down transfers angular momentum into the disk, from which it can be removed via tidal torques into the orbital motion. The equation governing the angular velocity Ω is[3]

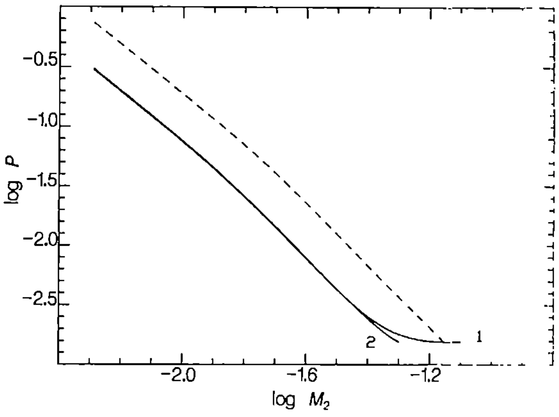

Fig. 1 Solid lines show the evolution of the period (in s) versus the secondary mass (in $M_\odot$) from integration of equation (3) using equation (1), for $B_8=5$, $I_{45}=1$, $R_6=1$ and $M_1\approx1.4$. The initial value of P is 1.56 ms, and the initial values of M_2 are 0.08 $M_\odot$ (curve 1) and 0.05 $M_\odot$ (curve 2). For comparison, the broken line shows the result for $M_2(0)=0.07$ if $B_8=14.1$, $I_{45}=2$ and $R_6=1$. (This corresponds to increasing I by a factor of 2 and also increasing the constant k in the equation $BR^3I^{-1/2}=k(P\dot{P})^{1/2}$ by a factor of 2.)

$$\dot{\Omega}=(6.16\times10^{-3}\ \text{s}^{-2})(B_8R_6^3)^{2/7}\left(\frac{M_1}{M_\odot}\right)^{3/7}\times I_{45}^{-1}(\dot{M}_{-9})^{6/7}n(\omega_s) \qquad (3)$$

where I_{45} is the neutron star moment of inertia in units of 10^{45} g cm^2, $\omega_s=0.35\ \Omega/\Omega_{eq}$ is the fastness parameter [Ω_{eq} is the equilibrium angular velocity given by equation (2)] and $n(\omega_s)$ is a dimensionless torque given approximately for $0<\omega_s<0.9$ by[3]

$$n(\omega_s)=\frac{1.39}{(1-\omega_s)}\{1-\omega_s[4.03(1-\omega_s)^{0.173}-0.878]\} \qquad (4)$$

The theory is not valid for $\omega_s\geqslant0.95$. We have integrated this equation for an initial period of 1.56 ms, and find that for $B_8=5$, $I_{45}=1$ and $R_6=1$, if the mass of the helium secondary is greater than $\sim 0.05\ M_\odot$, the system evolves to a final period at disruption that is much greater than 1.56 ms (see Fig. 1); throughout this evolution the fastness parameter remains less than 0.95. The timescale for approaching the equilibrium period, given a constant mass transfer rate[10],

$$\tau_\Omega=(1.2\times10^8\ \text{yr})(B_8)^{-8/7}(R_6)^{-24/7}(\dot{M}_{-9})^{-3/7}I_{45}\left(\frac{M_1}{M_\odot}\right)^{2/7} \qquad (5)$$

goes like $(1+t/\tau)^{6/11}$, while for the polytropic equation of state the timescale for change in the mass transfer rate is $\tau_{ev}=\dot{M}/\ddot{M}=11/14(t+\tau)$. Thus, for large times $\tau_\Omega\ll\tau_{ev}$, and we indeed expect to observe the equilibrium period associated with the current mass transfer rate, which, as shown above, must be much larger than the initial period.

After the secondary disrupts, it will form a disk around the neutron star, some of which may be accreted and spin the neutron star up. This does not alter the above conclusions: if matter accretes from the magnetosphere boundary with the usual keplerian specific angular momentum, as several authors have established[4,12], $\sim 0.1\ M_\odot$ would need to be transferred from the disk onto the neutron star to spin it up to 1.56 ms from a spin rate substantially below that, for the standard parameters assumed for PSR1937+214. (In Bonsema and van den Heuvel's scenario, on the other hand, the disk that results after disruption is massive enough[6] that sufficient angular momentum can accrete from it onto the neutron star to spin the neutron star up to

1.5 ms, so that such a progenitor is feasible regardless of the behaviour of the mass transfer rate before disruption.)

We now consider the second question. The condition for the disruption of the secondary via runaway mass transfer is

$$\left|\frac{\mathrm{d}\ln R_2}{\mathrm{d}\ln M_2}\right| > \left|\frac{\mathrm{d}\ln R_\mathrm{L}}{\mathrm{d}\ln M_2}\right| \tag{6}$$

where R_2 is the radius of the secondary and R_L the equi-volume radius of its Roche Lobe. This condition is never satisfied[5,13,14] for $M_2 \leqslant 0.1\,M_\odot$ unless angular momentum accumulates in the accretion disk rather than being transferred back into the orbital motion via tidal torques, in which case it is satisfied for very low masses ($\leqslant 0.0053\,M_\odot$)[2,5]. Ruderman and Shaham[1] have estimated that for $M_2 \ll M_1$, the tidal interaction between the disk and the secondary contributes a term of order $(M_2/M_1)^2$ to $\mathrm{d}\ln R_\mathrm{L}/\mathrm{d}\ln M_2 = 1/3 - 4(M_2/3M_1)^{1/3}$ and is hence negligible. They do not present a derivation for this estimate. We have estimated the torque using equation (46) from Goldreich and Tremaine's paper on two-dimensional gas disks[15]. We find that the contribution to $\mathrm{d}\ln R_\mathrm{L}/\mathrm{d}\ln M_2$ is of order $(M_2/M_1)^2(M_\mathrm{d}/\dot{M}_2 T)$ where T is the orbital period and M_d the disk mass. If, in order to produce an instability, mass must accumulate in the disk, the disk mass may come to greatly exceed the amount of matter transferred into the disk in one orbital period unless the timescale for the evolution of the instability is of the order of the orbital period. One may then not be able to discount the tidal interaction.

It is not clear how to construct a binary-origin scenario with a very-low-mass secondary in the late stages of evolution that avoids the problems of spin-down due to mass transfer rate decay over the long time before disruption of the secondary, and of angular momentum being transferred out of the disk via tidal torques. It would seem that to prevent mass transfer rate decay, angular momentum must be lost from the system or accumulate in the disk during the long time necessary to reach the disruption mass, a rather strong condition. We suggest that without such a condition, mass transfer rate decay may render a scenario of this type unworkable. The progenitor in which the secondary is a massive white dwarf, which avoids these difficulties, may offer a better solution.

I thank B. Paczynski and J. H. Taylor for helpful discussions. This project was partly supported by NSF grant AST-8317116 to B. Paczynski.

Received 4 June; accepted 13 November 1985.

1. Ruderman, M. A. & Shaham, J. *Nature* **304**, 425–427 (1983).
2. Ruderman, M. A. & Shaham, J. *Astrophys. J.* **289**, 244–246 (1985).
3. Ghosh, P. & Lamb, F. K. *Astrophys. J.* **234**, 296–316 (1979).
4. Alpar, M. A., Cheng, A. F., Ruderman, M. A. & Shaham, J. *Nature* **300**, 728–730 (1982).
5. Bonsema, P. F. J. & van den Heuvel, E. P. J. *Astr. Astrophys.* **146**, L3–L5 (1985).
6. van den Heuvel, E. P. J. & Bonsema, P. T. J. *Astr. Astrophys.* **139**, L16–L18 (1984).
7 Li, F. K., Joss, P. C., McClintock, J. E., Rappaport, S. & Wright, E. L. *Astrophys. J.* **240**, 628–635 (1980).
8. Vila, S. C. *Astrophys. J.* **168**, 217–223 (1971).
9. Taam, R. E. & Wade, R. A. *Astrophys. J.* **293**, 504–507 (1985).
10. Henrichs, H. F. in *Accretion-Driven Stellar X-ray Sources* (eds Lewin, W. H. G. & van den Heuvel, E. P. J.) 393 (Cambridge University Press, 1983).
11. Shapiro, S. L. & Teukolsky, S. A. *Black Holes, White Dwarfs and Neutron Stars* (Wiley, New York, 1983).
12. Henrichs, H. F. & van den Heuvel, E. P. J. *Nature* **303**, 213–215 (1983).
13. Hut, P. & Paczynski, B. *Astrophys. J.* **284**, 675–684 (1984).
14. van den Heuvel, E. P. J. in *Proc. Green Bank Workshop on Millisecond Pulsars* (eds Reynolds, S. & Stinebring, D.) 86–103 (National Radio Astronomy Observatory, Green Bank, West Virginia, 1984).
15. Goldreich, P. & Tremaine, S. *Astrophys. J.* **233**, 857–871 (1979).

Long-term changes in the semimajor axes of the outer planets

A. Milani*†, A. M. Nobili*†, K. Fox* & M. Carpino‡

* Theoretical Astronomy Unit, School of Mathematical Sciences, Queen Mary College, Mile End Road, London E1 4NS, UK
† Dipartimento di Matematica, Universitá di Pisa, I-56100 Pisa, Italy
‡ Centro Nazionale Univeritario di Calcolo Elettronico, I-56100 Pisa, Italy

One of the oldest problems of celestial mechanics is that of the long-term behaviour of the semimajor axes a of the planetary orbits. Analytical theories[1,2] predict periodic variations in a, some of which may have very long periods, but these terms have never been computed. We have now performed a 9.3-Myr numerical integration of the orbits of the outer planets, using a pure newtonian point mass model. An accurate integrator and an effective low-pass filtering of the output allow us to detect high-order variations in the energies, and hence also in a, with periods ranging from tens of thousand to millions of years. The most interesting feature is an energy exchange between Uranus and Neptune with a period of 1,119,000 years, the same as the period of the libration between the perihelia of Jupiter and Uranus[3,4]. The mechanism involves Jupiter and also Saturn; moreover, their energy shows puzzling longer-term trends. The energy of Pluto changes mostly with periods close to that of the 3:2 libration in mean motion with Neptune. Its spectrum in this region shows a very complicated structure; however, we have found no indication of chaotic behaviour.

Two centuries ago, Lagrange showed that to a first order in the masses μ of the perturbing planets (in units of the mass of the Sun; $M_\odot = 10^{-3}$ at most, in the case of Jupiter), the semimajor axes are subject only to short periodic changes whose frequencies are linear combinations of the mean motions and which show neither secular nor long-period changes. Message[1,2], following Poincaré[5], showed that to any order in μ the semimajor axes have periodic changes only, some with the very long periods of the quantities e, i, $\bar{\omega}$, Ω (eccentricity, inclination, longitude of the pericentre and longitude of the mode respectively) which describe the shape and orientation of the orbit. On the other hand, according to Poisson, the time derivative of a has neither secular nor long-period terms to the order μ^2. We conclude that the largest long-period variations in a must be of the order of μ^3 divided by a 'small divisor' which is the frequency of the quantities e, i, $\bar{\omega}$, Ω. These frequencies are zero in the degenerate problem in which the pericentres and the nodes are not perturbed by the neighbouring planets, and are of the order of μ in the real problem. Therefore, we searched for long-period variations in a of the order of μ^2, that is, of relative amplitude 10^{-6} or smaller.

Within the Longstop project, we performed a numerical integration of the five outer planets for 9.3 Myr on the Cray 1S at the University of London Computer Centre. We used a new numerical integrator (Encke's method with non-restarting rectification; A.M., N.M.N and M.C., manuscript in preparation); the relative variation of the total energy at the end of the integration is only $\simeq 3\times 10^{-10}$. Because the energies of the planets have short-period variations of the order of μ, they must be filtered out so that long-period variations can be detected. We designed an *ad hoc* low-pass filter with a pass band for periods $>$10,000 yr, a dark band between 11 and 5,000 yr, and a gap (where the performance of the filter is poor) between 5,000 and 10,000 yr, where it is known that the spectrum of the Solar System is devoid of lines. The attenuation factor in the dark band is 10^{-4}, smaller than μ, so we can be sure that the short-period terms become smaller than the long-period ones. The filter was applied concurrently with the integration, and the initial conditions were fitted to the Nautical Almanac ephemerides (A. T. Sinclair, personal communication). The effect of the inner planets was taken into account only by adding their mass to that of the Sun. Details will be presented elsewhere (A.M., A.M.N. and M.C., manuscript in preparation).

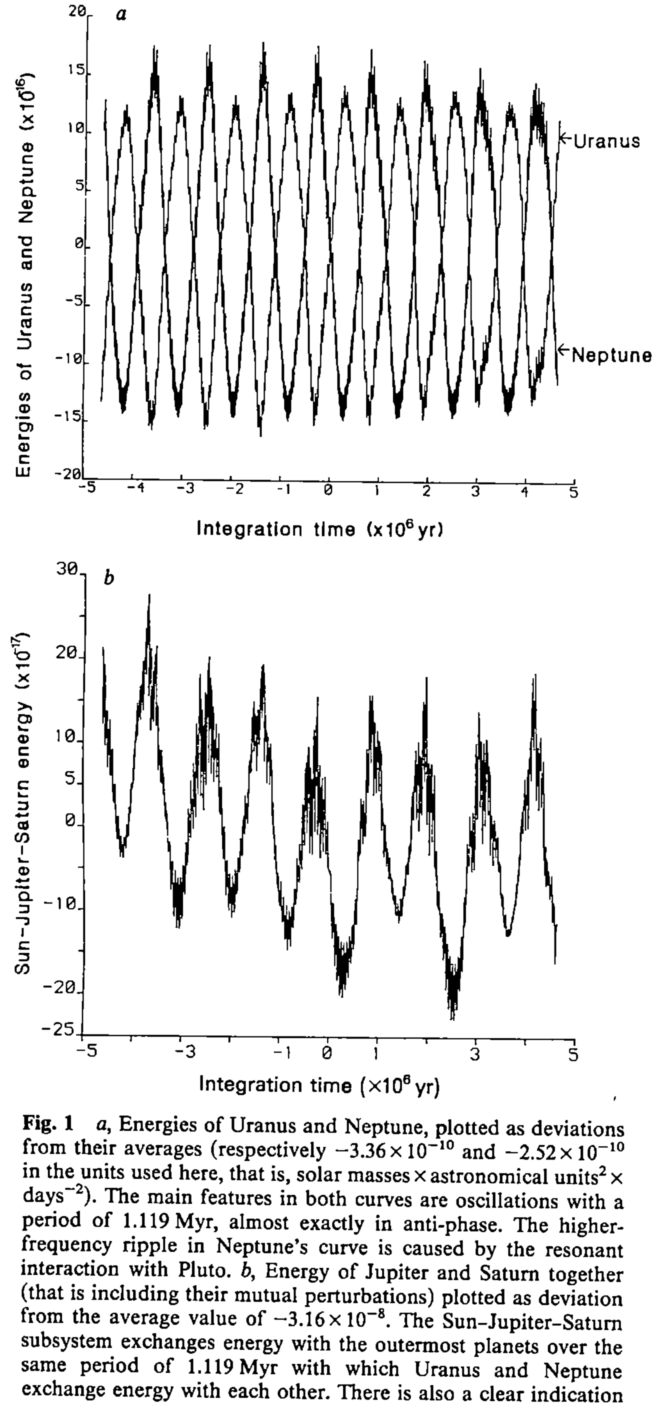

Fig. 1 *a*, Energies of Uranus and Neptune, plotted as deviations from their averages (respectively -3.36×10^{-10} and -2.52×10^{-10} in the units used here, that is, solar masses × astronomical units^2 × days^{-2}). The main features in both curves are oscillations with a period of 1.119 Myr, almost exactly in anti-phase. The higher-frequency ripple in Neptune's curve is caused by the resonant interaction with Pluto. *b*, Energy of Jupiter and Saturn together (that is including their mutual perturbations) plotted as deviation from the average value of -3.16×10^{-8}. The Sun-Jupiter-Saturn subsystem exchanges energy with the outermost planets over the same period of 1.119 Myr with which Uranus and Neptune exchange energy with each other. There is also a clear indication of a longer-period term.

The most interesting result is shown in Fig. 1, where the energies of Uranus and Neptune are plotted as functions of time (4.6 Myr forwards and 4.6 Myr backwards from the present). There is an exchange of energy (relative energy exchanged $\simeq 5\times10^{-6}$) with a period of 1.119 Myr; this is also the period over which Jupiter and Uranus exchange angular momentum and it is known to be essential for maintaining the stability of the system[3,4]. The energy of Jupiter shows a dominant variation with period 54,000 yr (the mutual period of the perihelia of Jupiter and Saturn) modulated over 1.119 Myr. The same is true for Saturn. However, the energy of the Sun-Jupiter-Saturn three-body subsystem[4] (including their mutual perturbations) shows a dominant 1.119-Myr oscillation, in phase with that of Neptune, with an indication of a longer-period term (Fig. 2*a*). Figure 2*b* plots the total energy of the system, showing the round-off error, and we can see that the long-term trend apparent in Fig. 2*a* is not caused by the numerical error, because the latter is roughly 10 times smaller.

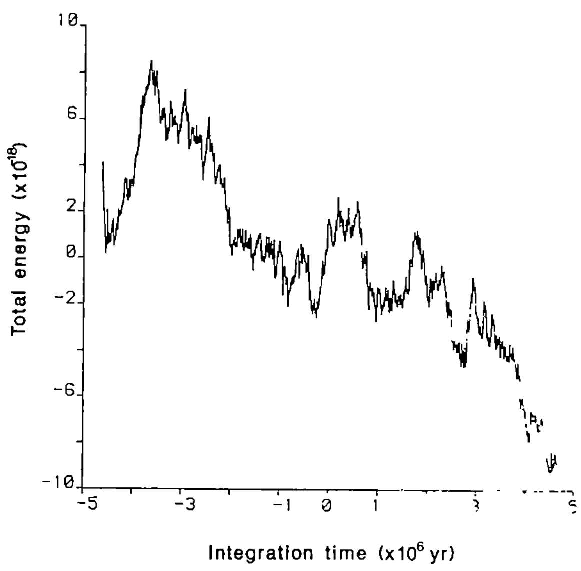

Fig. 2 The total energy as a function of time computed from the output of our numerical integration (deviations from the average value of -3.22×10^{-8}). The rounding-off error is mostly responsible for the slow pseudo-random drift of this function, which would be constant along the exact solution. The ostensibly linear trend (of $\sim10^{-17}$ over 9.3 Myr) is, however, smaller than all the features shown in the other figures.

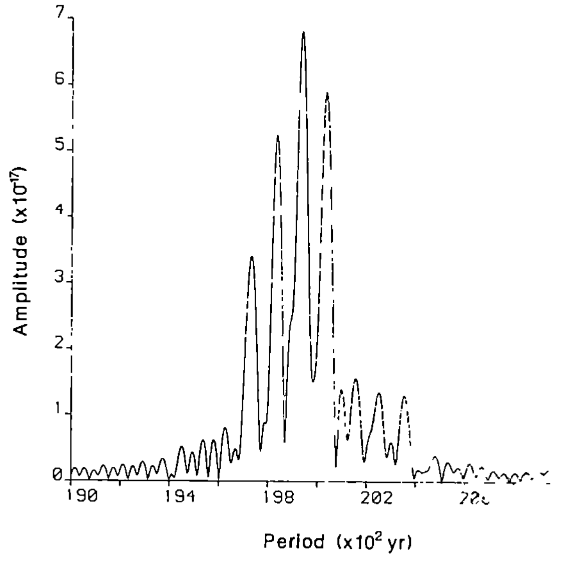

Fig. 3 An enlarged view from the spectrum of the energy of Pluto. The main lines are separated in frequency by multiples of the frequency of libration of Pluto's argument of perihelion[8].

Figure 3 shows the spectrum of Pluto's energy around the 19,900-yr period of the 3:2 resonance in the mean motion with Neptune. The finding that the spectral line corresponding to the critical argument of this resonance is split into several evenly spaced lines suggests the possible existence of a 'modulational layer'[6] where resonances overlap. If this is the case, a slow diffusive change in the orbital elements could occur and a chaotic behaviour could appear in the long term. However, the integration time is too short to distinguish between a continuous and a discrete spectrum. Pluto's dynamical behaviour seems to be regular in 9.3 Myr and the usual test of the divergence of nearby orbits[7] also shows no indication of instability.

Our analysis, using the same methods, of a previous 5-Myr integration[8] gives consistent results. At present there is no explicit analytical theory on the long-term behaviour of the semimajor axes with which these results can be compared. A comparison is possible for the quantities e, i, $\tilde{\omega}$ and Ω and shows quite good agreement for first-order terms, although serious differences arise for the higher-order ones.

A time of 9.3 Myr is still very short compared with the age of the Solar System, and longer numerical integrations are needed; we and others[9] are working in this direction. For longer integrations to be significant, the round-off error must be carefully controlled to ensure that it will not mask important dynamical features; furthermore, a better physical model must be used to represent the real problem. We are about to start a 100-Myr integration of the outer planets using the same numerical method but improving the physical model. The secular perturbations caused by the inner planets on the perihelia and the nodes of the outer planets are significant over such timescales (for example, the effect of the Earth on the perihelion of Jupiter in 50 Myr is ~88°). General relativistic corrections are small but not negligible[10]. Moreover, the relative mass loss of the Sun through electromagnetic emission only produces a relative semimajor axis increase of $6.6\times10^{-14}\ \mathrm{yr}^{-1}$. In our integration this effect is already three orders of magnitude larger than the round-off error. However, one might argue that the mass loss of the Sun will simply rescale the orbits and the periods of the planets and therefore is not likely to have any significant effect on the dynamical structure of the whole system, whereas the numerical errors act in different ways on the different planets and therefore in the long run will affect the dynamical structure. We conclude that the control of the numerical errors, especially the round-off, is at present our most serious problem in elucidating the stability of the Solar System.

We thank our colleagues in the Longstop project, partiularly Professor A. E. Roy who inspired it. This work has been supported by SERC, NATO and CNR.

Received 9 September; accepted 13 November 1985.

1. Message, P. J. in *Long-Time Predictions in Dynamics* (eds Szebehely, V. & Tapley, B.) 279-293 (Reidel, Dordrecht, 1976).
2. Message, P. J. *Celestial Mech.* **26**, 25-39 (1982).
3. Milani, A. & Nobili, A. M. *Nature* **310**, 753-755 (1984).
4. Milani, A. & Nobili, A. M. *Celestial Mech.* **35**, 269-287 (1985).
5. Poincaré, H. *Methodes Nouvelle de la Mechanique Celeste* Vol. 2 (Gauthier-Villars, Paris, 1893).
6. Vivaldi, F. *Rev. mod. Phys.* **96**, 737-754 (1984).
7. Benettin, G., Galgani, L. & Strelcyn, J. M. *Physical Review A* **14**, 2338-2345 (1976).
8. Kinoshita, H. & Nakai, H. *Celestial Mech.* **34**, 203-217 (1984).
9. Applegate, J. F. *et al. IEEE Trans. Computers* **c34**, 822-831 (1985).
10. Nobili, A. M. & Roxburgh, I. W. *Proc. IAU Symp.* **114** (in the press).

D to H ratio and the origin and evolution of Titan's atmosphere

Joseph P. Pinto*, Jonathan I. Lunine†, Sang-Joon Kim‡ & Yuk L. Yung§

* Hoffman Laboratory, Department of Geological Sciences, Harvard University, Cambridge, Massachusetts 02138, USA
† Lunar and Planetary Laboratory, University of Arizona, Tucson, Arizona 85721, USA
‡ NASA/Goddard Space Flight Center, Greenbelt, Maryland 20771, USA
§ Division of Geological and Planetary Sciences, California Institute of Technology, Pasadena, California 91125, USA

A value of 1.7×10^{-3} has been reported[1] for the ratio of CH_3D to CH_4 in the stratosphere of the saturnian moon Titan. A lower value of 6×10^{-4} for this ratio in the deeper part of Titan's atmosphere was reported by de Bergh *et al.*[2]. For comparison[3-11] we note that the CH_3D to CH_4 ratio on Saturn and Jupiter is 8.7×10^{-5} and 6.7×10^{-5}, respectively (see Table 1). We estimate the uncertainties in all these observations and data reduction to be about a factor of 2. Despite these uncertainties it appears that Titan's atmosphere is enriched in deuterium by a factor of $\geqslant 3$ relative to Jupiter and Saturn. Potential causative factors examined here for this enrichment are condensation to form tropospheric methane clouds, fractionation occurring over a hypothetical CH_4–C_2H_6 ocean and between the ocean and the clathrate crust beneath, fractionation which occurred during the formation of Titan and fractionation occurring as a result of the evolution of Titan's atmosphere. We conclude that the greater part of the observed fractionation is probably derived from the formation of Titan and the subsequent evolution of Titan's atmosphere driven by photochemistry.

We first consider possible fractionation that occurs during formation of tropospheric methane clouds. Data in ref. 12 indicate the CH_4-CH_3D liquid solution to be ideal in the sense that the ratio of components in the gas phase is equal to that in the liquid, multiplied by the saturation vapour pressure ratio. As the saturation vapour pressures of CH_4 and CH_3D are within 2% of the temperature range of Titan's tropopause, we conclude that no fractionation effects greater than a few per cent can occur with cloud formation.

Of greater concern are the relative solubilities of CH_4 and CH_3D in the postulated ethane-methane ocean[13]. In the limit that the CH_3D-CH_4 solution is considered as a single component of the ethane-methane system, the CH_3D/CH_4 ratio in the ocean would be within several per cent of that in the corresponding vapour, based on the preceeding argument. Alternatively, the deuterated methane could be regarded as a distinct dilute component in the ocean, and its solubility computed from data on binary mixtures. Using data on CH_4-C_2H_6 mixtures[14-16] extrapolated to extreme dilution, and assuming the solubility of CH_3D in C_2H_6 is the same for a fixed composition as that of CH_4 in C_2H_6, we find $(CH_3D/CH_4)_{\mathrm{atmosphere}}/(CH_3D/CH_4)_{\mathrm{ocean}}\approx 1.3$. We cannot rule out either limiting estimate in the absence of experimental data, and hence conclude that the enrichment factor is in the range 1.0–1.3.

The ocean is likely to be underlain by a water-ice crust[17]; hence, clathrate formation should occur at the interface. The relative extent of incorporation of molecules of similar shape in the clathrate structure tends to follow their vapour pressure[18]; since these are nearly identical for CH_3D and CH_4 no partitioning is expected. In any event, the mass of the clathrate layer in contact with the ocean is estimated to be small compared with that of the ocean[17].

Little is known about the D/H ratio in the primordial gaseous nebula from which satellites formed, because this ratio is sensitive to physical and chemical processes involved in satellite formation which are not well quantified. In a gas containing cosmic abundances of H, O, C and N molecular species, the substitution of a deuterium for a hydrogen in heavier molecules leads to an increase in the binding energy, which becomes increasingly important as the thermal energy per molecule decreases. According to Hubbard and MacFarlane[19] the D/H enhancement for methane in equilibrium with H_2 is about 2 at 500 K and can be as large as 7 at 200 K. Opposing such enhancements are the rather long equilibration times required in the gas phase. Estimates by Beer and Taylor[20] suggest that for $\tau \leqslant 500$ K the equilibration time would exceed 10^8 yr, which is considerably longer than the timescale for satellite formation[21,22]. Catalysis on the surface of metal rich grains may lower the equilibration times[23-27]. Recent calculations of D. H. Grinspoon and J. S. Lewis (personal communication) suggest that surface catalysis

Table 1 Observations of the relative abundances of deuterium and hydrogen in planetary atmospheres

Planetary body	Relevant physical quantity	Notes
Titan	$CH_3D/CH_4 = 1.7\times10^{-3}$	Ref. 1, based on ν_6 band of CH_3D at 8.6 μm; Voyager IRIS data[3]
	$CH_3D/CH_4 = 6\times10^{-4}$	Ref. 2, personal communication based on 6,425 cm^{-1} band of CH_3D; ground-based data; result probably more certain than that using ν_6 emission feature
Saturn	$CH_3D/CH_4 = 8.7\times10^{-5}$	Ref. 5, based on ν_6 band of CH_3D; Voyager IRIS data
Jupiter	$CH_3D/CH_4 = 6.7\times10^{-5}$	Refs 4 and 5, based on ν_6 band of CH_3D; Voyager IRIS data; ref. 11
Earth	$4\times(D/H) = 6.2\times10^{-4}$	Ref. 8, based on standard mean ocean water (SMOW); for juvenile water see ref. 9
Venus	$4\times(D/H) = 6.4\times10^{-2}$	Refs 6 and 7, based on D^+ and HDO measurements on Pioneer Venus
Mars	$4\times(D/H) = 6.2\times10^{-4}$	Ref. 10, based on $\delta D \sim -80$ to 52% in Shergotty meteorite; connection with the martian atmosphere controversial

on micrometre-sized nickel grains at 500 K can lead to equilibration times for exchange of deuterium between H_2O and H_2 of 3×10^5 yr, which is roughly the dynamic timescale for the saturnian nebula[21]. The dynamic timescale gives a crude upper limit to the lifetime of material in the saturnian nebula; hence, equilibration times longer than 10^5 yr for the exchange reaction are not plausible. This limits the exchange to high temperatures (>500 K, achievable in the innermost regions of the nebula with gas then being mixed outward to the cooler regions), and the resulting deuterium enrichment in H_2O to at most a factor of 2. We conclude by analogy that an enhancement factor in deuterated methane of 2 is possible in the primordial saturnian nebula out of which Titan formed. This value may be an upper limit because water could dominate the adsorption sites on the grains. Furthermore, once accretion had started the rates of these reactions would have slowed dramatically because the metallic grains would combine chemically to form minerals with a markedly lower catalytic ability[24].

Geiss and Reeves[28] examined a variety of mechanisms to explain the deuterium enrichment in terrestrial planets and meteorites, and concluded that exchange mechanisms in the solar nebula were probably less important than earlier enhancement processes in interstellar clouds out of which the solar nebula presumably formed. It is possible that some interstellar grains, greatly enriched in deuterium, retained the enrichment during heating processes accompanying the formation of the solar nebula and/or passage through the accretion shock at the solar nebula/interstellar medium boundary. However, such grains, accreting onto Titan during or shortly after its formation could have been subjected to temperatures in excess of 500 K for perhaps as long as 10^8 yr after the accretion of Titan, based on detailed models by one of us (J.I.L.)[36]. If the highly deuterated grain material was in thermodynamic contact with a substantial reservoir of non-enriched hydrogen in the primordial atmosphere during this time, dilution of the enrichment could have occurred. This possibility is admittedly very speculative and requires modelling beyond the scope of the present effort. Exchange reactions in the Saturn nebula, therefore, probably produced at most a factor of 2 deuterium enrichment in methane incorporated into Titan from the nebular gas; we acknowledge, however, that highly deuterated material in interstellar grains could have been incorporated in Titan, avoided reprocessing and possibly increased the enhancement of deuterated methane.

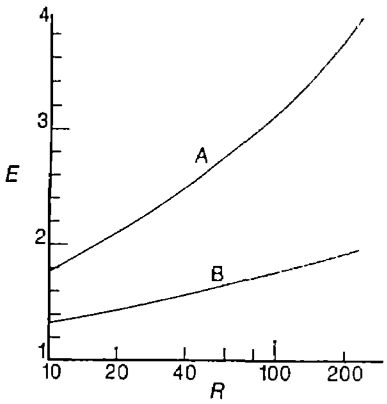

Fig. 1 Enrichment factor E as defined in the text versus R, the ratio of total initial CH_4 reservoir to the total present CH_4 reservoir.

In the atmosphere of Titan, CH_4 is the major observed hydrogen reservoir. Recent photochemical modelling[29,30] suggests that a large quantity of CH_4 has been converted into heavier hydrocarbons. The destruction of CH_4 occurs mainly through the catalytic cycle

$$\begin{array}{l} C_2H+CH_4\to C_2H_2+CH_3 \\ C_2H_2+h\nu\to C_2H+H \\ \hline \text{net } CH_4\to CH_3+H \end{array} \qquad (1)$$

Following the escape of hydrogen from Titan's atmosphere, CH_3 radicals combine irreversibly to form C_2H_6. Subsequent reactions lead to the production of smaller amounts of other hydrocarbons. The current rate of destruction of CH_4 (referred to the surface) is $\phi = 1.5\times10^{10}\ cm^{-2}\ s^{-1}$. Rate coefficients for reactions of deuterated molecules are usually much smaller than the corresponding value for the molecule composed of the lighter isotope[31-34]. The rate coefficient for

$$C_2H+CH_3D\to \text{products} \qquad (2)$$

has not been measured. Because of the greater binding energy of D compared with H, the rate coefficient for reaction (2) may only be a fraction of that for (reaction 1), that is, $k_2 = rk_1$ where $r<1$. We adopt two values for r, 0.75 (case A) and 0.875 (case B), the former being the preferred value (A. H. Laufer, personal communication). We assume that reactions (1) and (2) are the primary cause of isotopic enrichment in the photochemical model.

The theory of isotopic enrichment in a planetary atmosphere due to photochemical processes has been worked out by McElroy and Yung[35], whose methodology and notation we follow. Let $N_1(t)$ and $N_2(t)$ be the total column abundance of CH_4 and CH_3D, respectively, on Titan at time t. The evolution of $N_1(t)$ and $N_2(t)$ is given by

$$\frac{dN_1(t)}{dt} = -\phi, \quad \frac{dN_2(t)}{dt} = -rf(t)\phi, \quad f(t) = \frac{N_2(t)}{N_1(t)}$$

where ϕ is the column integrated destruction rate of CH_4 (assumed to be constant with time) defined earlier, $f(t)$ is CH_3D to CH_4 ratio, and time is defined so that $t=0$ refers to the time of formation of Titan and $t=\tau=4.5\times10^9$ yr corresponds to the present. We solve this set of equations by using the observed present value $f(\tau)$ and integrating the equations backwards to $t=0$ for a range of assumptions for $N_1(t)$. The most interesting results in this computation are the ratio of the initial reservoir

Table 2 Enrichment factors for deuterium on Titan

Process	Enrichment factor	Remarks
(1) Cloud formation	1	See text
(2) C_2H_6-CH_4 ocean	1–1.3	Assuming 20% CH_4, 80% C_2H_6 ocean
(3) Ocean-ice crust formation	1	See text
(4) Equilibrium between CH_4 and H_2 in the saturian nebula	1–2	Assuming 500 K nebula tempfeature; isotopic exchange catalysed by metal grains
(5) Atmospheric evolution	1.7	Based on curve A in Fig. 1 and $R=10$
Total	1.7–4.4	Products of all enrichment factors (1)–(5)

of CH_4 to the present reservoir which is $R=N_1(0)/N_1(\tau)$, and the enrichment factor due to atmospheric evolution which is $E=f(\tau)/f(0)$.

A simple analytical solution exists, which relates E and R, $E=R^{1-r}$. The numerical results are summarized in Fig. 1. The enrichment factor E is plotted against R, which is a measure of the extent of atmospheric evolution. For both case A ($r=0.75$) and case B ($r=0.875$), E increases with R, and could become very large if $R\gg 100$. For an ocean composition of 20% CH_4 and 80% C_2H_6 (ref. 13), the value for R is 9 and the enrichment factor based on our preferred case A is 1.7. It can be shown that isotopic exchanges such as $H+CH_3D \rightleftharpoons HD+CH_3$ and recombination reactions such as $H+CH_2D+M \rightarrow CH_3D+M$ are of relatively minor importance on Titan. Isotopic re-equilibration could also occur either in the ocean or deeper in Titan's interior. However, temperatures in the ocean are much too low (~90 K) to permit appreciable thermal decomposition of either CH_4 or C_2H_6 to form radicals which mediate the isotopic exchange. In addition, since the reactions involve neutral species in an ocean of non-polar molecules CH_4 and C_2H_6, we also would not expect solvent interactions to affect reaction rates. While any treatment of chemical processes in the interior of Titan is necessarily speculative, we would not expect significant re-equilibration to occur at greater depths. This inference is based on current theories of the internal structure of Titan, which propose an icy mantle with a maximum temperature at the core-mantle boundary of $\leqslant$400 K. The first condition implies greatly restricted mobility of reactants and the second, that temperatures are still too low for thermally-driven reactions to occur.

The relative abundance of deuterium to hydrogen in a planetary atmosphere is one readily available measure of the origin and evolution of the hydrogen bearing volatiles on the planet (see Table 1). If we take the de Bergh *et al.*[2] value 6×10^{-4} for the ratio CH_3D/CH_4 on Titan, and the Voyager value of 8.7×10^{-5} for Saturn, we note that deuterated methane is enriched 6.9-fold on Titan. The uncertainty associated with the derivation of this number is about a factor of 2–3. Note that the uncertainty must include not only the errors in measurement, but also the plausible range in the fractionation factor between CH_3D and HD within the atmosphere of Saturn[20], since the ratio of interest refers to the bulk saturnian value. The physical and chemical enrichment factors considered in this paper are summarized in Table 2. The cumulative enrichment factor is 2–4, which is below the observed value but within the estimated uncertainties of the observations. It is more difficult to interpret the observed value of CH_3D/CH_4 obtained by Kim and Caldwell[1]. We have neglected early evolution of Titan's atmosphere driven by planetesimal impacts and early solar extreme ultraviolet which could have increased the atmospheric D/H ratio, allowed some reequilibration between deuterated species, or provided an era of enhanced photodissociation of methane. Future observations of deuterated species on Titan and the giant planets are obviously needed to remove the large uncertainties in the D/H measurements. For a more realistic treatment of the photochemically-driven evolution of D/H on Titan, we recommend a laboratory experiment to measure the relative rate constants of the reaction C_2H with CH_3D and CH_4.

We thank Mark Allen, Larry Nyquist, Al Laufer, Ray Reynolds and Dave Stevenson for useful discussions and Catherine de Bergh, Barry Lutz, Tobias Owen, Sam Epstein and Jongmann Yang for communication of their results before publication. This research was supported by NASA grants NAGW-254 and NSG 7376 to the California Institute of Technology. Contribution no. 4164 of the Division of Geological and Planetary Sciences, California Institute of Technology.

Received 20 May; accepted 14 October 1985.

1. Kim, S.-J. & Caldwell, J. *Icarus* **52**, 473–482 (1982).
2. de Bergh, C. *et al. Bull. Am. astr. Soc.* **13**, 703 (1981).
3. Hanel, R. *et al. Science* **212**, 192–200 (1981).
4. Kunde, V. *et al. Astrophys. J.* **263**, 443–467 (1982).
5. Courtin, R. *et al. Astrophys. J.* **287**, 899–916 (1984).
6. McElroy, M. B., Prather, M. J. & Rodriguez, J. M. *Science* **215**, 1614–1615 (1982).
7. Donahue, T. M. *et al. Science* **216**, 630–633 (1982).
8. Craig, H. *Science* **133**, 1833–1834 (1961).
9. Craig, H. & Lupton, J. E. *Earth planet. Sci. Lett.* **31**, 369–385 (1976).
10. Fallick, A. E. *et al. Lunar planet. Sci. Abstr.* **XIV**, 183–184 (1983).
11. Bjoraker, G. L. thesis, Univ. Arizona (1985).
12. Armstrong, G. T., Brickwedde, F. G. & Scott, R. B. *J. Res. natn. Bur. Stand.* **55**, 39–52 (1955).
13. Lunine, J. I., Stevenson, D. J. & Yung, Y. L. *Science* **222**, 1229–1230 (1983).
14. Miller, R. C. & Staveley, L. A. K. *Adv. Cryog. Eng.* **21**, 493–500 (1976).
15. Cheung, H. & Wang, D. I.-J. *I. E. C. Fund.* **3**, 355–361 (1964).
16. Parrish, W. R. & Hiza, M. J. *Adv. Cryog. Eng.* **21**, 485–492 (1976).
17. Lunine, J. I. & Stevenson, D. J. in *Proc. NATO Conf. Ices in the Solar System* (ed. Klinger, J.) (Reidel, Dordrecht, 1985).
18. Lunine, J. I. & Stevenson, D. J. *Astrophys. J. Suppl. Ser.* (in the press).
19. Hubbard, W. B. & MacFarlane, J. J. *Icarus* **44**, 676–682 (1980).
20. Beer, R. & Taylor, F. W. *Astrophys. J.* **179**, 309–327 (1973).
21. Stevenson, D. J. *Planet. Space Sci.* **30**, 755–764 (1982).
22. Prinn, R. G. & Fegley, B. Jr *Astrophys. J.* **249**, 308–317 (1981).
23. Solomon, P. M. & Woolf, N. J. *Astrophys. J. Lett.* **180**, L89–L92 (1973).
24. Anders, E., Hayatsu, R. & Studier, M. H. *Science* **182**, 781–790 (1973).
25. Lewis, J. S. & Prinn, R. G. *Astrophys. J.* **238**, 357–364 (1980).
26. McKee, D. W. & Norton, F. J. *J. phys. Chem.* **68**, 481–489 (1964).
27. McKee, D. W, *J. phys. Chem.* **70**, 525–530 (1966).
28. Geiss, J. & Reeves, H. *Astr. Astrophys.* **93**, 189–199 (1981).
29. Strobel, D. F. *Icarus* **21**, 466–470 (1974).
30. Yung, Y. L., Allen, M. & Pinto, J. P. *Astrophys. J. Suppl. Ser.* **55**, 465–506 (1984).
31. Wiberg, K. B. & Motell, E. L. *Tetrahedron* **19**, 2009–2023 (1963).
32. Husain, D. *et al. JCS Faraday Trans. II*, **80**, 713–728 (1984).
33. Pasteris, L. *et al. Ber. Buns. Phys. Chem.* **88**, 568–571 (1984).
34. Tschuikow-Roux, E. & Niedzielski, J. *J. Photochem.* **27**, 141–150 (1984).
35. McElroy, M. B. & Yung, Y. L. *Planet. Space Sci.* **24**, 1107–1113 (1976).
36. Lunine, J. I. thesis, California Institute of Technology (1985).

Antarctic and non-Antarctic meteorites form different populations

Jane E. Dennison, David W. Lingner*
& Michael E. Lipschutz†

Department of Chemistry, Purdue University, West Lafayette,
Indiana 47907, USA

Compared with non-Antarctic falls, Antarctic meteorites include many of hitherto rare, unique or unknown type[1], such as lunar and putative martian samples[2–4]. Attention has not previously been paid to the more common sorts of Antarctic meteorites and here we focus on the most frequently encountered, H5 chondrites. We find that compositional differences between Antarctic and non-Antarctic specimens of this class, especially those involving thermally sensitive trace and ultra-trace elements, are so substantial that it seems extremely doubtful that the two sample populations are derived from the same parent population. This implies that

---

* Present address: Scripps Institute of Oceanography, La Jolla, California 92023, USA.
† To whom correspondence should be addressed.

the contemporary falls (less than 200 years old) and the substantially older (on average, 300,000 years for Victoria Land) Antarctic meteorites either differ in genetic history or sample different extraterrestrial parent populations, or both.

At present, over 7,000 meteorites have been recovered from opposite ends of Antarctica, mainly from Queen Maud Land[5], and from Victoria Land in East Antarctica and Marie Byrd Land in West Antarctica[6]. Some samples can confidently be shown to be fragments of the same meteorite, while others are unique. Taking the estimate that Antarctic meteorite impacts yielded, on average, 2-6 fragments per impact[7], the recovered meteorite population represents 1,200-3,500 separate events. This is comparable to the 2,611 meteorites[8] recovered elsewhere on the Earth during the past few centuries, despite the fact that the Antarctic sample essentially represents only 15 years of collection.

The contents of selected trace elements in Antarctic and non-Antarctic congeners of rare type often differ, seemingly reflecting actual source variations[9-13] rather than weathering of Antarctic meteorites since their arrival on Earth (typically $\geq 10^5$ yr[1]). These differences for uncommon meteorites suggested to us that common meteorites might also show inherent differences. Indeed, merely considering the grossest classification (Table 1), the Antarctic Search for Meteorites (ANSMET) sample contains proportionally fewer stony-irons and irons than do non-Antarctic falls. Ordinary chondrites (H, L, LL for high, low or very low total Fe contents) from Victoria Land (Table 1) and Queen Maud Land[14] also differ strikingly: LL chondrites are deficient and the H/L chondrite ratio is triple the value for non-Antarctic falls (and finds)[8].

To look for differences on a finer scale, we analysed H5 chondrites for trace elements (Co, Au, Sb, Se, Rb, Cs, Te, Bi, Ag, In, Tl, Zn and Cd) that vary widely in meteorites and yield important genetic information. These elements represent a variety of geochemical behaviours and span broad volatility and/or mobility ranges. This and their trace concentration (levels of parts per million (p.p.m.) to parts per trillion (p.p.t.)), which amplify small absolute variations into large relative ones, make these elements especially useful for this study. We chose H chondrites not only because they form the majority of Antarctic meteorites but also because concentrations of many trace elements in non-Antarctic L4-6 chondrites are reduced by extended heating from collisional break-up of their parent body 5×10^8-6×10^8 yr ago[15-17]. Hence, for a complete comparison, shock histories of Antarctic L chondrites must also be determined, a time-consuming task. (Preliminary data indicate that, on average, ordinary chondrites from Antarctica differ in shock histories from their non-Antarctic brethren.) In non-Antarctic H4-6 chondrites, volatile/mobile trace-element contents reflect early heating[18], making later shock history irrelevant. (This trace-element difference parallels major element and thermoluminescence trends[16,19].) Although mobile trace-element contents vary little with petrological type in type 4-6 L and H chondrites[15-18], we minimized variables by studying type 5, the most common sort of H chondrite. Since Queen Maud Land and Victoria Land meteorites differ in mean terrestrial age[1], we studied samples only from the latter and non-Antarctic falls. The meteorites were analysed by neutron activation analysis with radiochemical separation.

To assess accuracy and experimental precision, we analysed Allende standard reference meteorite powder before beginning the actual study. Allende results of analysts whose H5 chondrite data are involved in this study are listed in Table 2; none differs significantly from previous data (Student's *t*-test at the 5% level), other than Co which differs at the 10% test level. With 13 elements, this seems fortuitous and we do not suspect systematic analytical bias. From these homogeneous replicates, we estimate relative experimental precisions of 4-10% for all elements. Replicate analyses of 0.2-0.3-g chips of the same ordinary chondrite[15-17] reveal slightly poorer but comparable precision. This should not affect our conclusions here because all samples studied were chips of comparable mass and experimental uncertainties should cloud, not simulate, compositional differences. Even severe Antarctic weathering has only a minor role in perturbing trace-element contents in H5 chondrites: Bi and Cs are significantly higher and Co, Sb and Tl possibly so in types A and B samples than in severely (C) weathered ones. We have thus calculated means for these elements using only samples of weathering types A and B.

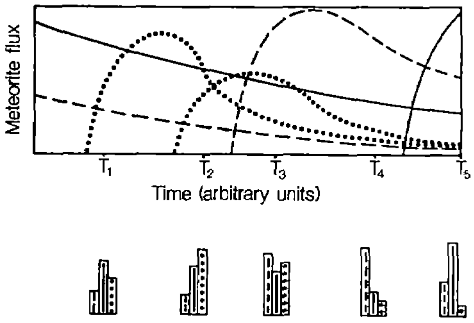

Fig. 1 Temporal variation of meteorite flux. Three sources are represented. Sources A (solid lines) and B (dashed lines) each represent a burst of meteoritic material ejected from an extraterrestrial source by a large impact in the same parent region that produced the smoothly decaying flux, generated by continuous impacts decreasing in frequency with time. Source C (dotted lines) represents meteoritic material ejected from a source region in bursts from two major impacts. Relative proportions at five different times are indicated by histograms at the bottom; these differ with time.

Most statistical tests implicitly assume that sample populations follow either normal or log-normal gaussian compositional distributions[20]. Our Co, Au, Se and Zn data follow a normal gaussian better than a log-normal one while Sb, Rb, Cs, Te, Ag, In, Bi, Tl and Cd better follow a log-normal distribution. The choice of a particular distribution may slightly decrease or increase the strength of a given difference, but should not affect overall trends or conclusions.

Eight of 13 elements compared in Antarctic and non-Antarctic samples differ using a single-tailed *t*-test (Table 3); we consider differences at the 5% level to be significant, those at the 10% level as possibly so. (If the eight weathering-type C chondrites are included, Sb and Tl differences become possibly significant; the Bi difference is no longer statistically significant. Hence, 7 of 13 elements differ—still an impressive proportion. Essentially the same differences hold if the Antarctic population is divided into two randomly chosen, equal subsets and compared with the non-Antarctic population.) These data provide strong reason to doubt that both sample populations were drawn from the same parent population. If this is so, the simplest and most direct conclusion is that H5 chondrites that fell in Victoria Land 1×10^5-7×10^5 (average 3×10^5) yr ago include a substantial

Table 1 Comparative numbers of selected meteorite types found in Victoria Land and falling in non-Antarctic regions

Meteorite type	Victoria Land* No.	Victoria Land* %	Non-Antarctic[8] No.	Non-Antarctic[8] %
Chondrites	756	92.4	784	86.6
H	542	66.3	276	30.5
L	167	20.4	319	35.2
LL	24	2.9	66	7.3
Achondrites	45	5.5	69	7.6
Irons	14	1.7	42	4.6
Stony-Irons	3	0.4	10	1.1
Total	818	100.0	905	100.0

* Data corrected for known pairing. More work needs to be done on pairing in equilibrated ordinary chondrites.

component deriving from parent regions different from those yielding contemporary (0–200-yr-old) non-Antarctic falls.

It is unlikely that these compositional differences are related to Antarctic weathering, since the compositions of Antarctic and non-Antarctic meteorites of rare types are strongly correlated[10,11], there is no evidence in Antarctic H5 chondrite interiors for loss of trace elements known to be leached from meteorite exteriors during Antarctic weathering[9] and no significant compositional difference exists between H5 chondrite interiors and weathering rinds beyond that attributable to chance. Furthermore, differences in direction of trace-element enrichments exist in H5 and L6 chondrites[21] and, in general, variances for Antarctic chondrite distributions are lower than for non-Antarctic ones (see Table 3), probably because of shock-induced trace-element loss; weathering should broaden, not narrow, innate distributions[21].

The *t*-test implicitly assumes equal population variances, but the Levene test[22] for elements in Table 3 reveals that Se, Rb, Zn and Cd variances in Antarctic and non-Antarctic sample populations differ at the 10% test level. However, for 13 elements, 1 or 2 may differ at the 10% test level purely by chance. The Welch or Brown-Forsythe test for populations with unequal variances[22] indicates virtually no change in significance levels for differences in means. This subtlety may be ignored in comparing sample populations.

Table 2 Trace-element data for homogenized Allende standard reference meteorite powder

Element	This work* D.W.L.	This work* J.E.D.	Purdue mean*†	Ref. 26*‡
Ag (p.p.b.)	105±8 (5)	95.2±9.5 (6)	98.4±9.3 (53)	
As (p.p.m.)	1.62±0.11 (5)		1.50±0.21 (27)	
Au (p.p.b.)		145±14 (5)	145±10 (16)	
Bi (p.p.b.)	49.6±3.5 (7)	44.9±4.2 (5)	48.6±3.3 (36)	
Cd (p.p.b.)	525±47 (14)	463±45 (6)	508±58 (50)	
Co (p.p.m.)	554±53 (10)	665±37 (6)	612±44 (60)	600±100
Cs (p.p.b.)	86.2±7.5 (8)	87.1±3.8 (6)	87.2±5.2 (54)	100
In (p.p.b.)	29.4±3.6 (11)	29.6±2.9 (6)	30.7±3.3 (46)	29±1
Rb (p.p.m.)	1.24±0.15 (4)	1.08±0.07 (6)	1.11±0.14 (48)	1.2±0.1
Sb (p.p.b.)	89.8±4.2 (5)	92.6±4.2 (5)	84.0±13.8 (33)	
Se (p.p.m.)	8.83±0.70 (5)	9.19±0.38 (6)	8.77±1.17 (38)	
Te (p.p.m.)	1.02±0.09 (14)	0.95±0.08 (6)	1.02±0.10 (59)	
Tl (p.p.b.)	62.2±5.3 (7)	59.7±6.8 (6)	61.2±4.5 (62)	
Zn (p.p.m.)	119±9 (11)	111±11 (6)	116±8 (59)	110±5

* Uncertainties are one sample standard deviation; numbers in parentheses are number of replicates. p.p.b., parts per 10^9.

† All previous analyses were performed at Purdue (see ref. 25 and references therein).

‡ Recommended values in ref. 26 are from far fewer data than those included in the Purdue mean.

A conceivable source of systematic bias is that different analysts in our group measured non-Antarctic and Antarctic H5 chondrites. Hence, we normalized the data of an analyst (Table 2) to the Allende mean determined by that analyst and used these ratios to assess sample population compositional differences. This implicitly treats analytical bias as multiplicative rather than additive, a gross overcorrection. Even with this over-conservative approach, 8 of 13 elements differ, Sb, Tl and Zn being possibly significant (10% level) and Co, Se, In, Bi and Cd differing at the 5% level. The non-Antarctic H4–6 chondrites we studied have lowered K/Ar age[18]. As radiogenic gas data are rare for Antarctic samples, this could have introduced a sample selection bias. However, when the 3 H5 chondrites with K/Ar ages ≤3.1 Gyr in the non-Antarctic population are ignored, 8 of 13 elements still differ, 6 at the 5% confidence level (Table 3). Hence, such bias cannot explain the compositional differences between the two populations. Finally, we used the Mann-Whitney non-parametric test to compare Antarctic and non-Antarctic sample populations[23]. Once again, differences are common (Sb, Se, Rb, Bi, In, Tl and Cd being significant and Zn possibly so); therefore, elemental distribution modelling is not biasing our results.

Having eliminated these possibilities, we conclude that only extraterrestrial causes can account for the observed compositional variations between Antarctic and non-Antarctic congeners. Possibilities include differences in sample population physical properties, orbital characteristics and meteoroid flux with time; each of these is problematic.

Any difference in physical properties (such as crushing strength) that might generate a difference between the contemporary flux and the Antarctic population would imply a chemical subdivision of H5 chondrites. Qualitatively, the unusual nature of the numerous Antarctic meteorites could be accounted for if they are derived from parent bodies in highly inclined orbits. However, at 1 AU, this could account for a fall frequency enhancement of only a few per cent and would also imply fundamentally different parent regions.

As the mean terrestrial ages of the two groups differ by about 10^5 yr[1], a change in meteoroid flux with time could be invoked. Figure 1 illustrates a change in the relative proportions of three sorts of samples, which represent different meteorite types or different parent body regions of the same meteorite type. Differences in number and kind of meteorites of rare or unique type in non-Antarctic falls and Antarctic finds[1–4] illustrate the former, differences among H5 chondrites (Table 3), the latter. However, current dynamic models imply chondritic flux averaging over their 10^6–10^7-yr cosmic-ray exposure age timescale[24].

Table 3 Comparison of significant differences in mean trace-element contents in Antarctic and non-Antarctic H5 chondrites

Element	Antarctic*	Non-Antarctic* All	Significance level	>40% ^{40}Ar retention	Significance level
Sb (p.p.b.)	83^{+24}_{-19} (14)†	69^{+21}_{-16} (18)	>97	69^{+22}_{-16} (16)	>90
Se (p.p.m.)	9.0±1.1 (22)	8.2±1.2 (20)	>99	8.1±1.0 (17)	>99
Rb (p.p.m.)	$2.0^{+0.5}_{-0.4}$ (22)	$2.5^{+1.8}_{-1.0}$ (20)	>97	$2.5^{+1.9}_{-1.1}$ (17)	>95
Bi (p.p.b.)	$2.8^{+7.1}_{-2.0}$ (14)†	$1.14^{+2.4}_{-0.37}$ (20)	>98	$1.05^{+2.3}_{-0.72}$ (17)	>99
In (p.p.b.)	$0.21^{+0.78}_{-0.16}$ (22)	$0.49^{+1.5}_{-0.37}$ (20)	>97	$0.57^{+1.8}_{-0.43}$ (17)	>99
Tl (p.p.b.)	$0.81^{+2.7}_{-0.62}$ (14)†	$0.24^{+1.7}_{-0.21}$ (20)	>96	$0.28^{+2.1}_{-0.25}$ (17)	>90
Zn (p.p.m.)	42.8±8.8 (22)	53.1±24.0 (20)	>96	53.3±25.1 (17)	>96
Cd (p.p.b.)	$0.72^{+2.0}_{-0.53}$ (23)	$3.7^{+16}_{-3.0}$ (20)	>99	$3.8^{+13}_{-2.8}$ (17)	>99

Samples weighed 0.2–0.3 g. Potentially contaminated surfaces were removed from all samples, which were analysed as chips. All elements were measured in each sample to minimize heterogeneity effects. To exclude paired samples (that is, different specimens from the same Antarctic meteorite impact), we selected H5 chondrites from widely dispersed parts of Victoria Land whenever possible. When selecting samples from nearby regions, we used field data and/or contents of cosmogenic ^{26}Al to choose unpaired ones. We omitted regolith breccias from consideration since compositionally they reflect peculiar individual histories[27]. To minimize systematic analytical bias, we ignored compositional data by others for non-Antarctic H5 chondrites (no previous Antarctic results exist). Elsewhere, we report our H4–6 chondrite data and compare these with others; agreement is as usual[15–17].

* Uncertainties listed are 1σ values for normal (Se, Zn) or log-normal distributions. Numbers in each sample population are listed in parentheses.

† Mean for weathering types A and B only. Raw data can be obtained from the authors.

While a gross error in the dynamic arguments may be unlikely, this possibility should be checked in the absence of a viable alternative explanation.

If there are compositional differences between Victoria Land and non-Antarctic meteorites, they should not be confined to rare or unique types and H5 chondrites; indeed, H4-6 and L4-6 chondrites differ compositionally[21]. Whether Queen Maud Land meteorites constitute a subpopulation is a possibility we are now investigating.

We thank W. A. Cassidy, R. T. Dodd, J. E. Evans, R. Score and D. W. Sears for access to data in advance of publication, J. O. Annexstad, W. A. Cassidy, R. Hutchinson, L. A. Rancitelli and G. W. Wetherill for valuable discussions, and also D. D. Bogard, C. B. Moore, R. Hutchison, E. Olsen, P. Signer, F. Wlotzka, T. Kirsten, R. Clarke, the Meteorite Working Group, and staffs of the NASA Johnson Space Center's Planetary Materials Branch and the University of Missouri Research Reactor. This study is in partial fulfilment of PhD degree requirements for J.E.D. and D.W.L. and was supported by DOE grant DEFG 0280 ER 10725, NASA grant NAG 9-48 and NSF grants DPP-8111513 and DPP-8415061.

Received 19 August; accepted 25 November 1985.

1. Bull, C. B. B. & Lipschutz, M. E. *Lunar planet. Inst. (Houston) tech. Rep.* 82-03 (1982).
2. Marvin, U. B. *Geophys. Res. Lett.* 10, 775 (1983).
3. Yanai, K., Kojima, H. & Katsushima, T. *Meteoritics* 19, 342-343 (1984).
4. Bogard, D. D., Nyquist, L. E. & Johnson, P. *Geochim. cosmochim. Acta* 48, 1723-1739 (1984).
5. Yanai, K. & Kojima, H. *Proc. 9th Symp. Antarctic Meteorites* (ed. Nagata, T.) 18-34 (National Institute of Polar Research, Tokyo, 1984).
6. Antarctic Meteorite Working Group *Antarctic Meteorite Newsl.* NASA Johnson Space Center, Houston, (1978-85).
7. Scott, E. R. D. *Proc. 9th Symp. Antarctic Meteorites* (ed. Nagata, T.) 102-125 (National Institute of Polar Research, Tokyo, 1985).
8. Graham, A. L., Bevan, A. W. R. & Hutchison, R. *Catalogue of Meteorites* 4th edn (British Museum (Natural History), London, 1985).
9. Biswas, S., Ngo, H. T. & Lipschutz, M. E. *Z. Naturforsch.* 35a, 191-196 (1980).
10. McSween, H. Y. Jr *et al. Earth planet. Sci. Lett.* 45, 275-284 (1979).
11. Biswas, S., Walsh, T. M., Ngo, H. T. & Lipschutz, M. E. *Proc. 6th Symp. Antarctic Meteorites* (ed. Nagata, T.) 221-228 (National Institute of Polar Research, Tokyo, 198).
12. Verkouteren, R. M., Dennison, J. E. & Lipschutz, M. E. *Geophys. Res. Lett.* 10, 821-824 (1983).
13. Smith, M. R. *et al. J. geophys. Res.* 81 *Suppl.*, B216-B630 (1984).
14. Mason, B. & Yanai, K. *Proc. 8th Symp. Antarctic Meteorites* (ed. Nagata, T.) 7-23 (National Institute of Polar Research, Tokyo, 1983).
15. Huston, T. J. & Lipschutz, M. E. *Geochim. cosmochim. Acta* 48, 1319-1329 (1984).
16. Neal, C. W., Dodd, R. T., Jarosewich, E. & Lipschutz, M. E. *Geochim. cosmochim. Acta* 45, 891-898 (1981).
17. Walsh, T. M. & Lipschutz, M. E. *Geochim. cosmochim. Acta* 46, 2491-2500 (1982).
18. Lingner, D. W., Huston, T. J. & Lipschutz, M. E. *Meteoritics* 19, 261-262 (1984).
19. Sears, D. W. G., Bakhtiar, N., Keck, B. D. & Weeks, K. S. *Geochim. cosmochim. Acta* 48, 2265-2272 (1984).
20. Sacks, L. *Applied Statistics A Handbook of Techniques* (transl. Regnarowich, Z.) (Springer, New York, 1982).
21. Kaczaral, P. W., Dennison, J. E., Lingner, D. W. & Lipschutz, M. E. *Lunar planet. Sci.* 16, 418-419 (1985).
22. Dixon, W. J. & Brown, M. B. (eds) *BMDP Biomedical Computer Programs, P-Ser.* (University of California Press, Berkeley, 1979).
23. Neter, J., Wasserman, W. & Whitmore, G. A. *Appl. Statist.*, 370-376 (Allyn & Bacon, Boston, 1978).
24. Wetherill, G. W. *Ann. Rev. Earth planet. Sci.* 2, 303-331 (1974).
25. Verkouteren, R. M. & Lipschutz, M. E. *Geochim. cosmochim. Acta* 47, 1625-1633 (1983).
26. Jarosewich, E., Clarke, R. S. Jr. & Barrows, J. N. (eds.) preprint, US National Museum (1985).
27. Lipschutz, M. E., Biswas, S. & McSween, H. Y. Jr *Geochim. cosmochim. Acta* 47, 169-179 (1983).

A new optical photochemical memory device in a light-sensitive chemical active medium

L. Kuhnert

Zentralinstitut für physikalische Chemie der Akademie der
Wissenschaften der DDR, 1199 Berlin-Adlershof,
Rudower Chaussee 5, Berlin, DDR

Active media are physical, chemical or biological systems which can compensate their internal energy dissipation by a continuous power input. In homogeneous well stirred chemical systems, self-sustained oscillations can occur. However, in distributed systems which provide spatially distributed energy sources, propagation effects—including waves—can be observed. The most extensively studied example of such a system model is the Belousov–Zhabotinsky reaction[1,2]. This reaction shows a range of unusual kinetic phenomena, especially in the distributed system, where trigger waves and phase waves can be observed[3]. By using $Ru(bpy)_3^{2+}$ as catalyst for the Belousov-Zhabotinsky reaction we obtained a light-sensitive chemical active medium and had been able to manipulate the character of wave phenomena by photochemical action[4]. Here we suggest a new kind of optical photochemical memory-device based on photoinduced phase shift in a distributed chemical oscillating medium.

The Belousov–Zhabotinsky reaction is an extremely complex system[5], but the most important reaction steps can be represented:

$$BrO_3^- + Br^- + 2H^+ \rightarrow HBrO_2 + HOBr \qquad (1)$$

$$HBrO_2 + Br^- + H^+ \rightarrow 2HOBr \qquad (2)$$

$$BrO_3^- + HBrO_2 + 3H^+ + 2Ru(\text{II}) \rightarrow 2Ru(\text{III}) + 2HBrO_2 + H_2O$$
$$Ru(\text{II}) = Ru(bpy)_3^{2+} \qquad (3)$$

$$4Ru(\text{III}) + BrCH(COOH)_2 + 2H_2O \rightarrow$$
$$4Ru(\text{II}) + HCOOH + 2CO_2 + 5H^+ + Br^- \qquad (4)$$

$$2HBrO_2 \rightarrow HOBr + BrO_3^- + H^+ \qquad (5)$$

By reducing the mechanism to such simple skeleton the Oregonator[6] and other models[7] were developed, which give a satisfying qualitative (and, in some respects, quantitative) account of the complex behaviour of the reaction including the wave phenomena.

For the occurrence of oscillations, the autocatalytic oxidation of the catalyst, reaction (3), is crucial. Bromide ions are the counterpart of the autocatalysis. Via reaction (2) they may inhibit the autocatalytic oxidation. The source for bromide is reaction (4) the reduction of the oxidized catalyst by brominated organic species like bromomalonic acid. For oscillations to occur it is important that the bromide production, reaction (4) is coupled with reaction (3) as a delayed inhibitor production. This means that bromide ions are the most important control intermediate of the system.

In continuous stirred tank reactor (CSTR) experiments we can realize bifurcations between several types of reactions regimes (oscillating to nonoscillating) by varying the bromide input stream. If the system is in the oscillating regime and we chose the bromide concentration is varied only within a narrow range, only the parameters of the oscillations (frequency and amplitude) will be changed[8].

The light-sensitive Ru-catalysed system offers the possibility of selecting the rate of bromide production by photochemical action. The absorption of light induces a dramatic change in the redox properties of Ru(II).

$$\left.\begin{array}{ll} Ru(\text{III}) + e^- \rightarrow Ru(\text{II}) & E_0 = 1.26\,\text{V} \\ Ru(\text{III}) + e^+ \rightarrow {}^*Ru(\text{II}) & E_0 = -0.84\,\text{V} \end{array}\right\} \quad \text{(ref. 9)}$$

In contrast to the ground state it is evident that the excited molecule is expected to be a very strong reducing agent. *Ru(II) in the excited state is able to reduce bromate to the inhibitor bromide directly via:

$$6{}^*Ru(\text{II}) + BrO_3^- + 6H^+ \rightarrow 6Ru(\text{III}) + 3H_2O + Br^- \qquad (6)$$

By illuminating the Ru-catalysed Belousov-Zhabotinsky reaction in the distributed system we can control the propagating effects and manipulate the character of wave phenomena.

In the present work a distributed oscillating system was used. The reaction medium changes colour periodically. Practically, in the absence of stirring, this colour change does not take place

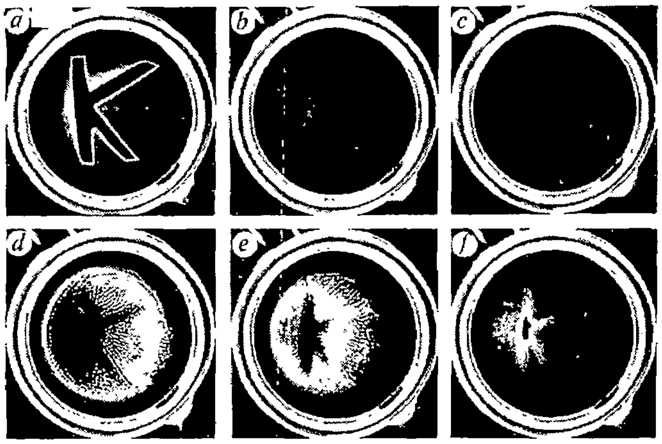

Fig. 1 A new optical photochemical memory-device in a light-sensitive chemical active medium. Initial concentrations were: $NaBrO_3 = 0.31$; $H_2SO_4 = 0.135$; Malonic acid = 0.045; Bromomalonic acid = 0.105; $Ru(bpy)_3SO_4 = 0.004$ M. The Petri dish was thermostatted at 25 °C. Diameter was 7 cm and depth of the reaction layer 1.3 mm. Illumination was for 15 s from a 25-W tungsten-lamp. Photographs were taken at the following times after illumination through a blue filter: *a*, 5 s; *b*, 15 s; *c*, 20 s; *d*, 30 s; e, 35 s; *f*, 45 s.

simultaneously in the whole medium. Spatial inhomogeneities may induce a phase shift in the oscillating reaction. The wall of the reaction vessel is especially a source for such inhomogeneities, due to influence of oxygen. So the oscillating reaction starts at the wall of a Petri dish, moves as a phase wave to the middle point and then vanishes. This phenomenon proceeds with a well defined constant frequency. By taking advantage of the action of light, we can change the conditions spatially; for example, we can induce a phase shift in the illuminating region. This phase shift forms a pattern which is 'frozen' in the oscillating medium and will have reproduced as a positive-negative image several times.

Considering the complex kinetics in the chemical active medium, when contrasted to normal simple chemical or photochemical reactions, new possibilities for storage and processing of information impressed by a photoreaction will be opened. For instance, we may construct a new type of an optical photochemical memory device as is demonstrated in Fig. 1*a–f*.

In Fig. 1*a*, the medium is illuminated from above by focusing light through a template in the shape of the letter K. The original state of the medium is coloured. Black areas in the figure correspond to the reduced orange state (Ru(II)) and white areas to the blueish fluorescent oxidized (Ru(III)) state of the system. Under the influence of light (Fig. 1*a*), the reduced state is stabilized. A phase shift on the oscillating medium between illuminated and nonilluminated areas occurs. In Fig. 1*b–f* the successive stages in the dark reaction are shown. The medium has stored the photochemically impressed information as a phase shift and can process this information. If we called the first picture (Fig. 1*a*) a positive image, then after one oscillating cycle this positive is converted into a negative (Fig. 1*b*). The area that was formerly reduced is now oxidized and the surrounding area is reduced. In an intermediate range, the picture may also be invisible (Fig. 1*c*). The whole system is in the reduced state.

In Fig. 1*d*, the letter is in the reduced state and the surrounding area in the oxidized state. In Fig. 1*e*, the changeover to the reduced state has been completed and a further change to the oxidized state has begun. The change to the oxidized state is hardly complete in Fig. 1*f*. After some further cycles the contrast will progressively vanish and finally disappear.

This new photochemical system is able to store time-impressed optical information and to process this information in some oscillating cycles, as a dynamically working memory device.

Received 17 June; accepted 6 November 1985.

1. Belousov, B. P. *Sb. Ref. Radiats Med. Moscow* **1958**, 145–147 (1959).
2. Zhabotinsky, A. M. *Dokl. Akad. Nauk SSR* **157**, 392–395 (1964).
3. Zaikin, A. N. & Zhabotinsky, A. M., *Nature* **225**, 535–537 (1970).
4. Kuhnert, L., *Naturwiss.* (submitted).
5. Field, R. J., Körös, E. & Noyes, R. M. *J. Am. Chem. Soc.* **94**, 8649–8664 (1972).
6. Field, R. J. & Noyes, R. M. *J. Chem. Phys.* **60**, 1877–1884 (1974).
7. Rovinsky, A. B. & Zhabotinsky, A. M. *J. Phys. Chem.* **88**, 6081–6084 (1984).
8. De Kepper, P. & Boissonade, J. in *Oscillations and Travelling Waves in Chemical Systems* (eds R. J. Field & M. Burger) (Wiley-Interscience, New York, 1984).
9. Sutin, N. & Creutz, C., Adv. in *Chemistry Series No. 168, Inorganic and Organometallic Photochemistry* 1–27 (1978).

A plate tectonic model of the eastern Indonesia collision zone

T. R. Charlton

Department of Geology, Royal Holloway and Bedford New College,
Egham Hill, Egham, Surrey TW20 0EX, UK

Eastern Indonesia is unique in the present global plate configuration, being situated at the T-junction between the world's two main active orogenic belts—the Alpine-Himalayan and Circum-Pacific belts. Consequently the tectonics of this region must be understood as a zone of interaction between three major plates, whereas most other orogenic areas can be modelled as deformation between just two major plates with numerous intervening microplates or terranes. Previous models to explain the tectonics of eastern Indonesia have generally started from small-scale geological observations and attempted to work upwards to an overall plate synthesis. In this paper I reverse the process, suggesting what might be expected from one particular collision model in a three-plate system and comparing this with what is actually seen in the region's geological record.

Consider a hypothetical three-plate indenter model (Fig. 1*a*). The body to be indented comprises two plates: a continental plate (A) in the west and an oceanic plate (B) to the east. Continent A is constrained on its western and northern margins, but unconstrained on its other two sides. This continent will be taken as fixed, with other plate movements described relative to it. Oceanic plate B is converging upon continent A, moving due westwards. Convergence between the two is taken up by simple subduction beneath A. The indenter comprises a second continent (C) initially surrounded by passive margins. Continent C is asymmetrical with a large oceanic embayment on its western side. The indenter is required to move northward at a constant speed, but is unconstrained on its sides, and so is free to have an eastward or westward component of movement if the forces acting on it so dictate. The boundary between plates A and C is a simple northward subduction of oceanic plate C below continental plate A. The boundary between plates B and C is a combination of normal subduction of C under B, and sinistral strike-slip parallel to the plate margin taken up within the overriding plate.

The model is arranged so that the indenter collides with the easternmost edge of continent A and the westernmost part of ocean B (Fig. 1*b*). Upon collision, subduction reversal takes place in the eastern part of the collision zone, with ocean B now subducting beneath continent C. In the western part, continent-continent collision occurs and subduction ceases. Instead a conjugate set of fractures develop in continent A (compare with actual indenter models, for example, in refs 1–3). Because continent A has an unconstrained eastern margin, and because the indenter can have an eastward component of movement, the sinistral set of fractures is preferentially developed. In particular, one fracture originating near the northwest corner of the indenter will take up the bulk of the compensational deformation within continent A, becoming a trench–trench transform[4]

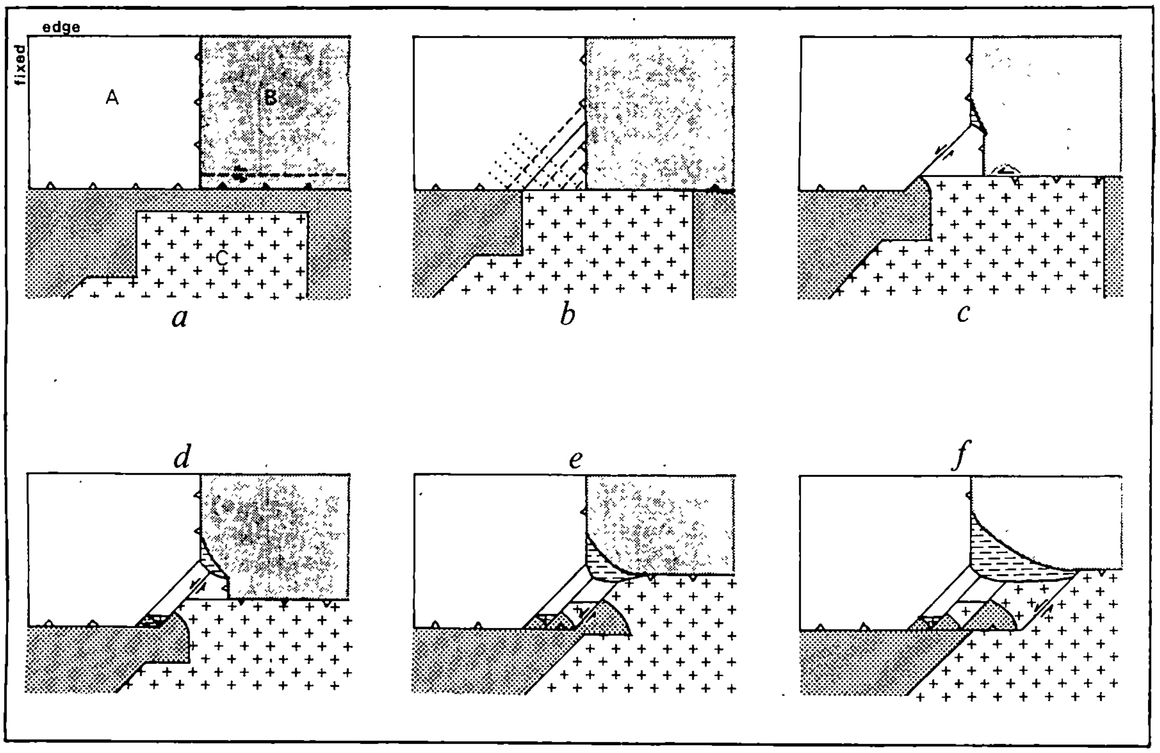

Fig. 1 Hypothetical indentation model to explain the tectonics of eastern Indonesia. *a*, 'Australia' (continent C) moves north to collide with 'Southeast Asia' (continent A). Oceanic areas are stippled. Toothed lines are subduction zones with the teeth on the overriding plate. Half arrows represent strike-slip components. *b*, Upon collision, conjugate fractures develop in Southeast Asia. *c*–*e*, Development of a series of trench-trench transforms segmenting the former Australia-Asia collision zone. Dashed area is the region of New Guinea-Pacific displaced terranes. *f*, Position immediately prior to second collision of 'Australia' (Timor region) with 'Banda arc'.

Fig. 2 Interpretation of the present configuration of eastern Indonesia in terms of the model developed in the text and in Fig. 1. Crosses: Australian crust. Blank: Asian crust. Dots: Asia-Australia collision zone. Fine stipple: Pacific-related oceanic crust. Heavy stipple: Indian Ocean crust. Cross-hatching: Local seafloor spreading associated with transtension. Irregular dashes: current volcanic arc. Triangles: early Neogene volcanic arc. Toothed lines: subduction zones. Vertical hatching: current forearc. Paired solid and dashed line: southwestern limit of New Guinea-Pacific displaced terranes. Trench-trench transforms are numbered consecutively. Note that division of forearc and Australian crust around the Banda arc is somewhat arbitrary.

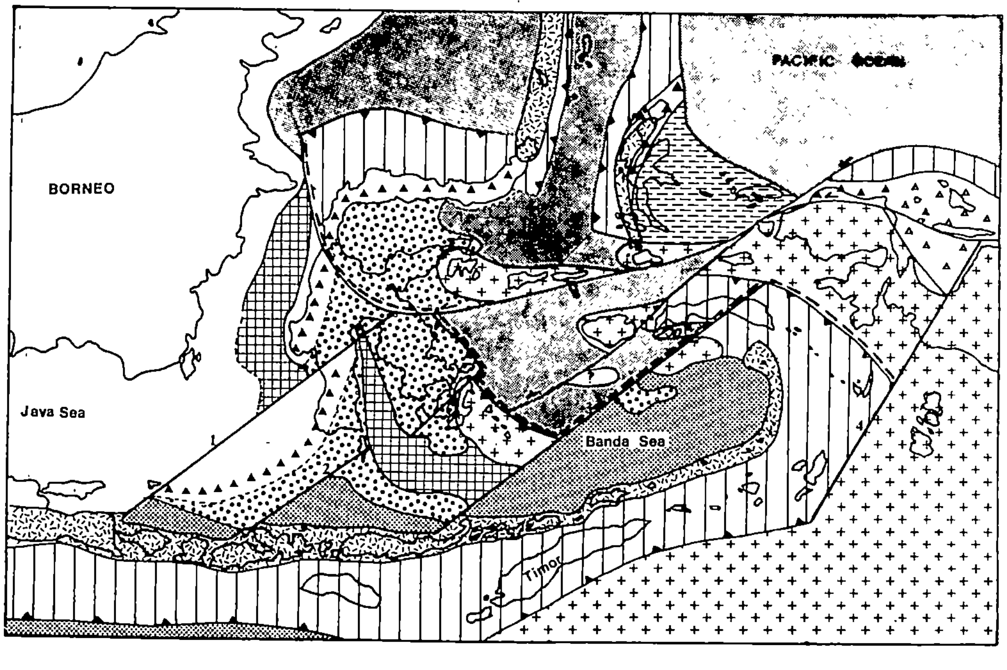

(Fig. 1*c*). This transform is terminated at its northeastern end by a trench-trench-transform triple junction[4].

At the same time as the trench-trench transform is developing between ocean B and the oceanic part of plate C, the leading edge of the indenter is experiencing a combination of pure and simple shear. The compressive pure shear is produced by the northward movement of the indenter; the simple shear, sinistral in sense, results from the westward movement of plate B and the eastward component of movement of plate C relative to the fixed continent A. The northeastern margin of the indenter thus experiences transpression[5,6], with anticlockwise block rotation[7] and sinistral displacement of terranes. Consequently, a neck of deformed crust develops between continent A and the indenter, while displaced terranes accumulate in the corner formed by the trench-trench-transform triple junction, hindering the development of the transform (Fig. 1*c*). Eventually, it becomes easier to initiate a new transform than to rejuvenate the older one. A new transform will be initiated to the southeast of the original one where the neck between the two oceans is narrowest. Once this develops, subduction must commence to the south of the transform-bounded sliver (Fig. 1*d*). The pattern of dynamics will then be similar to that after the initial rupture, and after some time the same inhibition of the second transform by displaced terranes will occur, followed by another southwestward jump to a new transform. However, the time between the first and second jump will be greater than the time from initiation of the original transform to the first jump because the new zone of terrane accretion has first to infill the gap between the rigid edge of continent A and the new triple junction (Fig. 1*d*).

This repetitive initiation of new transforms after increasingly long periods will continue until the indenter has moved sufficiently far eastward to resume purely northward movement. Progressively larger portions of the oceanic part of plate C will become trapped behind an island arc migrating eastward in steps as successive transforms become inactive (Fig. 1*e*). Interspersed between these trapped oceanic fragments will be slivers of continental crust derived from both continental masses.

This simple three-plate model can be used as a basis for interpreting the tectonics of eastern Indonesia (Fig. 2). However, the plate convergence vector of the Indo-Australian plate relative to the Southeast Asian plate is not due north, but 20° east of north[8]. Similarly the Pacific plate convergence vector is about 20° north of west. Thus to be more closely comparable with eastern Indonesia, the model outlined above must be rotated 20° clockwise.

If the model is applicable to the tectonic evolution of eastern Indonesia, it implies that the main collision between the Australian and Southeast Asian continents has already taken place. Numerous lines of geological evidence point to a major tectonic reorientation in Southeast Asia during mid Miocene times. This is here interpreted as the time when indentation was initiated following the main collision orogeny.

The post-collisional offset of Australia relative to Southeast Asia has been taken up on four main transform faults. The first (Fig. 2) accommodated about 300 km offset. The second accommodated about 350 km offset, and the third about 600 km. The sequentially increasing offsets on the transforms explained by the model can be seen from the relative sizes of the portions of Indian Ocean crust trapped in the southern Banda Sea. The eastward younging of volcanic initiation in the Sunda/Banda arc is seen in the decrease in size of the volcanic edifices from west to east.

The final transform may have had more than 400 km of offset. However, with this final transform the simplicity that had previously existed broke down as a result of a second collisional phase (Fig. 1*f*). The collision of Australian crust with the Banda arc in the vicinity of Timor occurred after the inactivation of the third transform, and after the Banda arc had completed its eastward migration. Analogous indentation processes are now occurring on a smaller scale in the Timor region (T. R. Charlton and A. J. Barber, manuscript in preparation).

Received 1 October; accepted 21 November 1985.

1. Molnar, P. & Tapponnier, P. *Science* **189**, 419-426 (1975).
2. Tapponnier, P. & Molnar, P. *Nature* **264**, 319-324 (1976).
3. Tapponnier, P., Peltzer, G., Le Dain, A. Y., Armijo, R. & Cobbold, P. *Geology* **10**, 611-616 (1982).
4. McKenzie, D. P. & Morgan, W. J. *Nature* **244**, 125-133 (1969).
5. Harland, W. B. *Geol. Mag.* **108**, 27-42 (1971).
6. Sanderson, D. J. & Marchini, W. R. D. *J. struct. Geol.* **6**, 449-458 (1984).
7. McKenzie, D. & Jackson, J. *Earth planet. Sci. Lett.* **65**, 182-202 (1983).
8. Minster, J. B. & Jordan, T. H. *J. geophys. Res.* **83**, 5331-5345 (1978).

Tectonics of the westernmost Gulf of Aden and the Gulf of Tadjoura from submersible observations

Cyaden Scientific Team: P. Choukroune*, B. Auvray*, J. Francheteau†, J. C. Lepine†, F. Arthaud‡, J. P. Brun§, J. M. Auzende||, B. Sichler|| & Y. Khobar

* University of Rennes, 35042 Rennes Cedex, France
† IPG, Paris, University of Paris. 7, 75230 Paris Cedex 05, France
‡ University of Montpellier, 34060 Montpellier Cedex, France
§ University of Paris 7, 75230 Paris Cedex 05, France
|| IFREMER, 29273 Brest Cedex, France
ISERT, Djibuti, Republic of Djibuti

The Gulf of Tadjoura, separating the Danakil and Somalia plates[1], represents the western extension of the Sheba Ridge between Arabia and Somalia in the Gulf of Aden (Fig. 1). It has been assumed that a simple plate-tectonic scheme could be applied to the area with NE–SW transform faults offsetting roughly east–west zones of accretion represented by the major bathymetric troughs[1–8] (Fig. 1*c*). More recently this boundary has been interpreted as a westward-propagating rift with its present-day tip on land in the region of the Asal Lake[9,10]. Here we present data from dives with the submersible *Cyana* which show that there have been two episodes of extensional faulting, an older inactive phase parallel to the general ENE–WSW direction of the gulf and a younger fault set along discontinuous zones striking 140°. There is no surface evidence for any transform fault zone in the area covered and the incipient spreading segments whose geometry implies extension on 050° do not define a plate boundary. The faulting observed is at odds with that predicted by orthodox plate tectonics.

The seismicity recorded locally since 1972 in the Republic of Djibuti shows a marked contrast between a concentrated zone of earthquakes in the Gulf of Tadjoura and Ghoubbet al Kharab and a diffuse zone of seismicity west of the Ardoukoba Rift[6,11] (Fig. 1*a*). In November and December 1978, a seismic and volcanic event occurred in the western part of the Gulf of Tadjoura with a prominent break marked by a line of aftershocks striking 140° in the area of 42°50′ E (Fig. 1*b*). This fault line remained unexplained in the plate tectonic framework accepted by most investigators (Fig. 1*c*).

An extensive aeromagnetic survey[9] of the Republic of Djibuti and the Gulf of Tadjoura up to 44° E shows that the linear, approximately east–west, magnetic anomalies of oceanic character are found only in the eastern part of the Gulf of Tadjoura. West of 43°20′ E, the magnetic anomalies are less linear and can often be attributed to point sources. The propagating rift model was partially based on this data set, which used the boundary of the oceanic and continental-like anomalies.

In December 1984, 26 dives were conducted by the French submersible *Cyana* at the axis of the westernmost Gulf of Aden and Gulf of Tadjoura in order to make field observations of a nascent zone of accretion between the Danakil and Somalia plates. The diving programme was designed to scan the geometry of the plate boundary in order to test current plate tectonic models which predict a series of short east–west spreading segments bounded by closely spaced NE–SW transform faults (Fig. 1*c*). The dives were also designed to complement both previous submersible investigations at the axis of steady-state mid-ocean ridges (12 to 17) and previous extensive land investigations conducted in the Republic of Djibuti around the Gulf of Tadjoura (see ref. 18 for a recent synthesis).

The bathymetry of the western part of the Gulf of Aden and of the Gulf of Tadjoura has been established, following earlier work by Peter and de Wald[12] and Backer *et al.*[13], using data from the 1977 Sumerouad cruise of the NO *Le Suroit*, and the 1983 Precyad cruise of the NO *Jean Charcot*, which used the Seabeam bathymetric swath system. The maximum depth at the axis of the gulf increases from west to east from 200 m in the Goubbet al Kharab, to 800 m in the Tadjoura Trough (area III in Fig. 2*a*), to 1,000 m in the Maskali Trough (west portion of

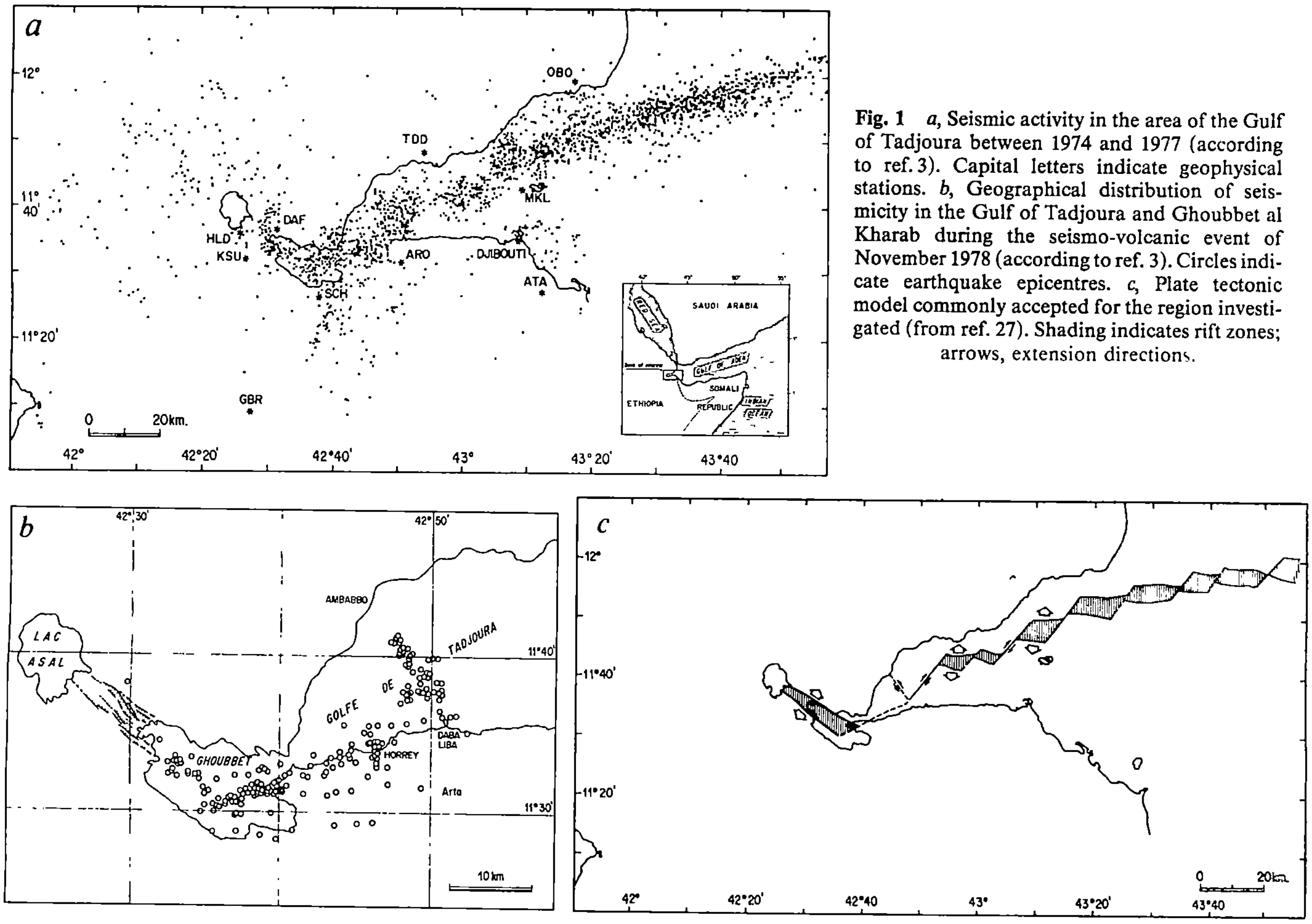

Fig. 1 *a*, Seismic activity in the area of the Gulf of Tadjoura between 1974 and 1977 (according to ref. 3). Capital letters indicate geophysical stations. *b*, Geographical distribution of seismicity in the Gulf of Tadjoura and Ghoubbet al Kharab during the seismo-volcanic event of November 1978 (according to ref. 3). Circles indicate earthquake epicentres. *c*, Plate tectonic model commonly accepted for the region investigated (from ref. 27). Shading indicates rift zones; arrows, extension directions.

area II in Fig. 2*a*). In plan shape the troughs are aligned on a mean 070° direction and are interrupted approximately every 30 km by bathymetric highs (sills) trending NW-SE. Three detailed areas were mapped (zones I, II and III in Fig. 2*a*). The dives were conducted in three additional areas (IV-VI in Fig. 2*a*) to cover the principal supposed transform zones linking the main troughs.

During the *Cyaden* cruise, a total bottom coverage of 118 km was achieved; there were nine dives in zone I (Fig. 2*a*), eight in zone II, four in zone III, two in the area between 42°50' and 43° (zones IV and V) and three in the Ghoubbet al Kharab (zone VI). More than 100 samples were collected *in situ* by the submersible. In addition, three piston cores were taken (one in zone I, one in zone III and one in the Ghoubbet (zone VI)) and two dredge hauls were made (one each in zones I and II). All dive data were positioned using acoustic navigation. The Seabeam maps were constructed using satellite navigation, radar fixes and dead-reckoning. Registration of the Seabeam map with respect to the dive data was made by performing additional bathymetric surveys between the diving periods.

The diving programme has yielded information on volcanism, sedimentation, faulting and hydrothermal activity:

Volcanism. Recent volcanism was found in the two eastern areas and in zone IV. In zone I, the zone of recent flows is very narrow and restricted to a NW-SE 2-km-wide volcanic ridge linking the two main walls of the depression. The flows are glassy pillow lavas sticking out of a heavily sedimented terrane. In zone II, the region of fresh flows is limited to a 5-km-wide NW-SE volcanic ridge. In zone IV, the dive was conducted on a young linear seamount parallel to a NW-SE direction. The older flows are characterized by weathered pillow lavas and occupy the walls of the main depression. Most basaltic samples are aphyric and highly vesicular.

Note that the main bathymetric highs segmenting the depression are to constructional volcanic highs in areas I and II. In areas III and V, the highs correspond to horsts made of corolline (madreporia) material.

Sedimentation. All troughs in the depression are heavily sedimented. A 3.5-kHz seismic survey conducted in zone I showed that the western trough includes at least 60 m of locally faulted hemipelagic sediments, in contrast to the eastern trough which exhibits a quiet regime of sedimentation: the very high rate of sedimentation ($100\,\mathrm{m\,Myr^{-1}}$) determined by Olauson and Olsson[14] in varved sediments nearby 44°18' E seems to be confirmed by our observations and particularly by a large amount of sediment cover on parts of volcanic ridges which are known to be recent because they are covered by fresh glass when exposed.

The second type of sediment which has been encountered and sampled during the dives consists of biogenic sediments which are presently being studied to assess vertical movements.

Faulting. Throughout the study area, two main fault directions are found, 060° and 140° (Fig. 2*c*). In zones I-VI, the active tectonic zones in sediments and recent flows are very localized and along 140. In zones IV-VI, no 060 faults have been observed. In zones II and III, the 060 faults are clearly older and at present inactive: this is shown by the occurrence of smoothed scarps covered by undisturbed sediment or scarps abutting a flat undisturbed beach-like sediment cover. In contrast, along the 140 fault scarps, reworked sediment and rubble attest to the recent activity. The rim of these fault scarps are generally sharp.

Lastly, in zones I and II, the 060 faults are locally clearly buried by recent lava flows which are cut by the 140 faulting. In these zones, the active 140 faults cut through both lavas and indurated sediments or volcano-sedimentary rocks in which spectacular high pitch striae have been observed on scarps. In

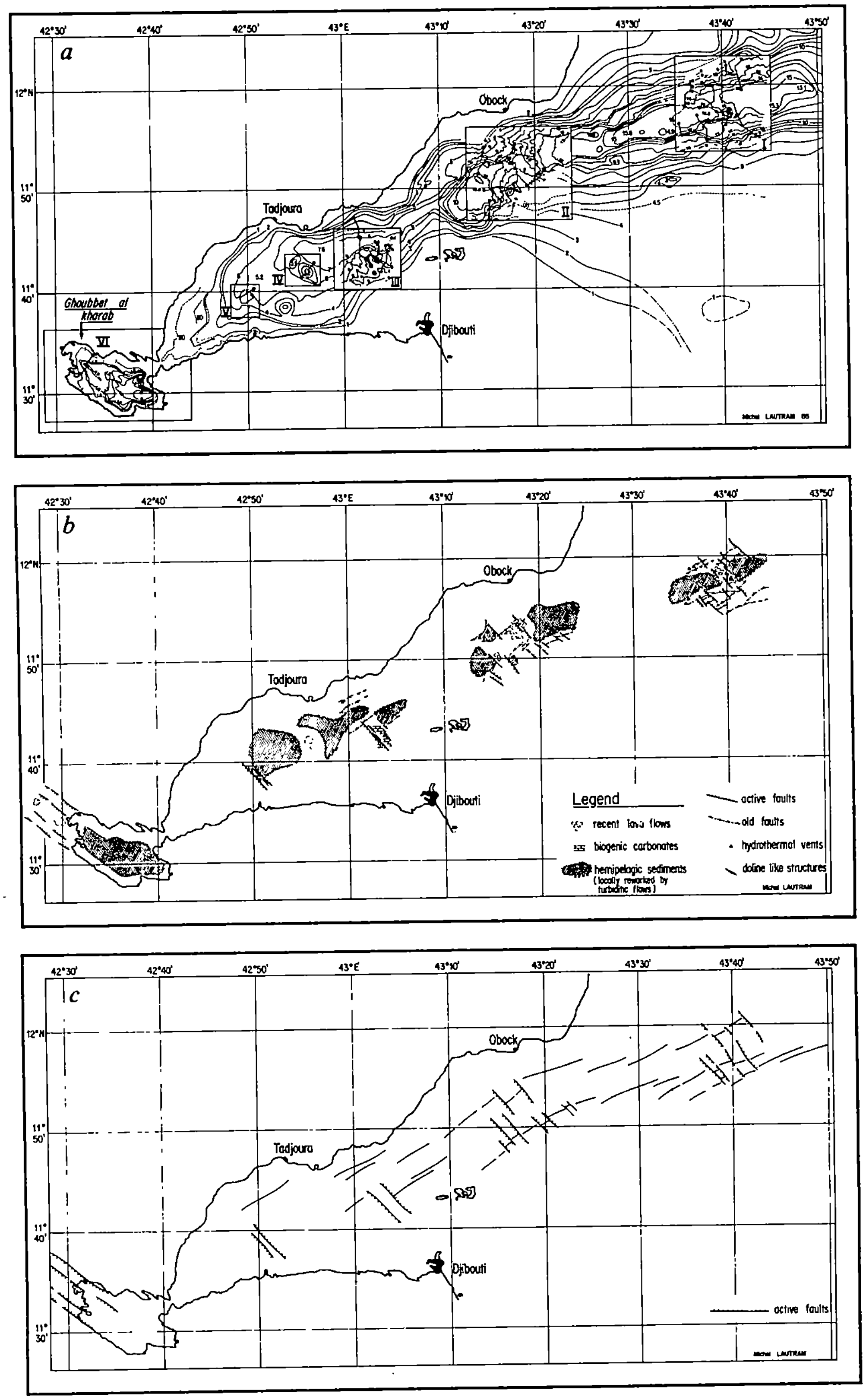
a
b
c
42°30'
42°40'
42°50'
43°E
43°10'
43°20'
43°30'
43°40'
43°50'
12°N
11° 50'
11° 40'
11° 30'
Obock
Tadjoura
Djibouti
Ghoubbet al kharab
I
II
III
IV
V
VI
Legend
recent lava flows
biogenic carbonates
hemipelagic sediments (locally reworked by turbidic flows)
active faults
old faults
hydrothermal vents
doline like structures
Michel LAUTRAM

Fig. 2 *a*, Bathymetry of the Gulf of Tadjoura and Ghoubbet al Kharab including details covered by Seabeam (zones I–III). The six dive areas explored during the *Cyaden* programme in December 1984 are marked (contour intervals every 100 m). *b*, Outline of the main geological features directly observed during the *Cyaden* programme. *c*, The two main directions (060° and 140°) of faulting observed in the Gulf of Tadjoura area. Note the absence of NE–SW (010°–020°) faults corresponding to transform direction as proposed by previous tectonic interpretation of this region (to be compared with Fig. 1*c*).

zone I, however, faulting interference 060 and 140 is pronounced at the outcrop scale and elsewhere. Some 060 faults have been slightly reactivated, as shown by a light-coloured strip of disturbed sediment at the foot of scarps. Low pitch striae were never observed and the vertical component of displacement along the two sets of faults was the only one which could be assessed.

In the western areas (zones III–VI), alignment of doline-like collapse in sediments is common along 140 in active tectonic zones. A spectacular example of this was recognized and followed in area V along the line of aftershocks during the seismic crisis of 1978[3]. It is clear from the observations that: (1) a major change has occurred in the direction of extensional faulting from 060 to 140; as the faulting is not synchronous, none of the two trends can represent a possible transform direction; (2) no typical rift topography has been produced; at the map scale, the active 140 volcanic and tectonic zones constituting discrete

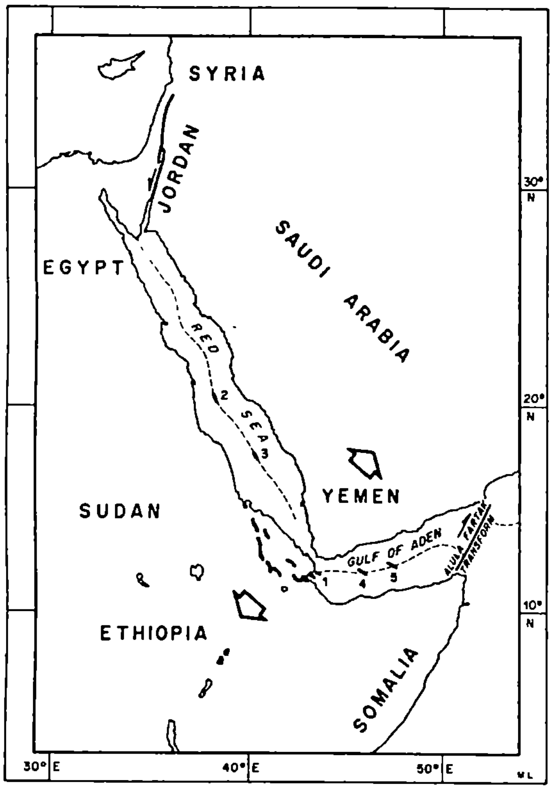

Fig. 3 Active tectonic zones of the Gulf of Aden–Afar–Red Sea–Levant area. The axis of maximum depth of the Gulf of Aden–Gulf of Tadjoura and Red Sea has been marked by a thin dotted line. The zones of recent generation of oceanic (or oceanic-like in the case of Afar) crust have been marked by black lenses with their elongation parallel to that of graben and axial volcanoes. These lenses can be thought of as magma fissures in the crust and lithosphere. The numbered zones of extension represent detailed study areas by *Cyaden* (zone 1), *Discovery* and *Chain Deeps* (zone 2), Monin *et al.* (zone 3)[20], Zonenshain *et al.* (zone 4)[18] and Laughton *et al.* (zone 5)[7]. The entire tectonic system is compatible with rigid motion of Saudi Arabia away from Africa between the transform faults represented by the Alula-Fartak and Levant faults. This motion is indicated by the two wide arrows. In this model, the African Rift system is inactive and the opening of the Gulf of Aden–Red Sea between the transform faults results in only a few discontinuous loci of emplacement of new oceanic crust in a predominantly continental region.

topographic highs are built on the bottom of the main 060 older sedimented trough.

Hydrothermal activity. Three types of hot water venting have been seen: a linear field of diffuse hydroxide gel-producing warm water on the south wall of zone I along 140° trending faults; an isolated vent with concentrated jetting of hot water in a canyon on the north wall of the main depression in area II; and a field of varicoloured patches of hydrothermal material covering sediments, in area III. No evidence of black or white smoker-type vents or any sulphide deposits was found.

It is clear that the widely accepted plate boundary geometry, as presented in Fig. 1*c*, is not compatible with the field observations. First, the zones of active extension strike normal to the main elongation of the gulf. Second, these zones are discrete and there is no continuous zone of deformation. Third, there is no evidence of transform fault zones. The existence of poorly developed and discrete accreting zones strongly suggests that the present system is in a nascent and non-steady-state mode.

The overall status of faulting shows that there have been at least two successive stages of extensional faulting, running almost at right angles, the first one probably being responsible for the creation of the gulf. The present direction of rifting oblique to the elongation at the gulf appears to be consistent throughout, both on land (Ardoukoba Rift) and in the gulf. This extension direction also coincides with the fault breaks outlined during the 1978 seismic and volcanic event, which raises some doubt over the strike-slip earthquake first motion solution for the 1978 series of shocks[3]; the solution was, however, composite and may therefore be incorrect.

The precise timing of the deformation event characterized by north-west normal faults is not known. Nevertheless, one can argue on the basis of an age of 0.9 Myr[15] for the oceanic tholeites in the Ardoukoba rift and the homogeneity of the faulting direction that the north-west normal faulting has been initiated within the past million years.

The present faulting pattern in the Ardoukoba Rift—Gulf of Tadjoura region is homogeneous and can be extended to a much wider region (Fig. 3). In the Gulf of Aden, the present zones of accretion also strike NW–SE and appear, at least in the eastern half of the gulf, to be offset by well-defined NE–SW, nearly orthogonal transform faults (that is, the Alula-Fartak Transform Fault). The other recent volcanic zones in the Afar Triangle (Manda-Inakir, Manda Harraro, Erta Ale) are also aligned along a 130–140° direction, but there is no evidence for active transform faulting. The only transform fault (or zone) recognized in Afar is located on land on the south side of the Gulf of Tadjoura[16]. In the Red Sea, the direction of present rifting is also NW–SE[17,18]. It has been argued that, locally, transform faults exist at the axis of the gulf showing a NE–SW direction[16,17]. The overall pattern of the present extension is compatible with slight motion of only two main rigid plates, Arabia and Africa; the 'oceanic' zones of the Red Sea and Gulf of Aden are linked through the 'continental' region of Afar, including the Gulf of Tadjoura. The proposed interaction between only two plates implies negligible opening along the East African Rift. Our model is at variance with other plate tectonic models which involve at least three plates[1,2,7,8], even if the observed spreading direction is compatible with that predicted (035°) by Minster and Jordan[19]. In our model, the Afar Triangle could represent a diffuse but coherent relay zone between the Aden Rift and the Red Sea Rift. If this is the case, the notion of a propagating rift could be inappropriate for describing the structural evolution of this region. Indeed, the area between the southward-propagating Red Sea Rift and the westward-propagating Aden Rift is theoretically an area of no strain. In this case also, assuming that the lithospheric units are totally rigid, large true accretion in the wedge would fall to zero at the advancing tip. In contrast, the situation described here concerns a zone of distributed strain and motion between two incipient accreting zones. However, this implies that the lithosphere is not completely rigid.

The *Cyaden* cruise was sponsored by the PIROCEAN (CNRS-MEN) which we thank for its support. We also thank the captain, officers and crew of the NO *Le Suroit* and P. Plasseraud, engineers, pilots and divers for smooth and efficient *Cyana* dives. Funds for the cruise were provided by IFREMER and PIROCEAN.

Received 23 July; accepted 31 October 1985.

1. Le Pichon, X. & Francheteau, J. *Tectonophysics* **26**, 369–406 (1978).
2. Barberi, F. & Varet, J. *Bull. geol. Soc. Am.* **88**, 1251–1266 (1977).
3. Lepine, J. C., Ruegg, J. C. & Anis, A. M. *Bull. Soc. géol. Fr.* **22**, 809–816 (1980).
4. Arthaud, F., Choukroune, P. & Robineau, B. *Bull. Soc. géol. Fr.* **22**, 901, 908 (1980).
5. Arthaud, F., Choukroune, P. & Robineau, B. *Bull. Soc. géol. Fr.* **22**, 909–915 (1980).
6. Needham, H. D. *et al. Earth planet. Sci. Lett.* **28s**, 439–453 (1976).
7. Laughton, A. S., Whittmarsh, R. N. & Jones, M. T. *Phil. Trans. R. Soc.* **A267**, 227–266 (1970).
8. Girdler, R. W., Brown, C., Moy, D. J. M. & Styles, P. *Phil. Trans. R. Soc.* **A298**, 1–41 (1980).
9. Courtillot, V., Galdeano, A. & Le Mouel, J. L. *Earth planet. Sci. Lett.* **47**, 144–160 (1980).
10. Courtillot, V. *Phys. Earth planet. Inter.* **21**, 343–350 (1980).
11. Stieljes, L., Joron, J. L., Treuil, M. & Varet, J. *Bull. Soc. géol. Fr.* **17**, 851–862 (1976).
12. Peter, G. & de Wald, O. *Bull. geol. Soc. Am.* **80**, 2313–2316 (1969).
13. Backer, H., Clin, N. & Lange, K. *Mar. Geol.* **15**, 309–327 (1973).
14. Olausson, E. & Olson, I. U. *Palaeogr. Palaeoclimatol. Palaeocol.* **6**, 87–103 (1969).
15. Richard, O. thesis., Univ. Orsay (1979).
16. Lepine, J. C., Richard, O., Ruegg, J. C., Treuil, M. & Varet. J. *Cr. hebd. Séanc. Acad. Sci., Paris* **283**, 9–12 (1976).
17. Juteau, Th. *et al. Bull. Cent. Rech. expl. Prod. Elf-Aquitaine* **7**, 1, 217–231 (1980).
18. Zonenshain, L. P., Monin, A. S. & Sorokhtin, O. G. *Geotektonika* **2**, 3–22 (1981) (in Russian).
19. Minster, J. B. & Jordan, T. H. *J. geophys. Res.* **83**, 5331–5354 (1978).
20. Monin, A. S. *et al. Deep Sea Res.* **29**, 361–373 (1982).

Formation of cubic structures in microemulsions containing equal volumes of oil and water

J. Tabony

CEA-IRDI-DESICP, Département de Physico-Chimie,
Centre d'Études Nucléaires de Saclay, 91191 Gif-sur-Yvette Cedex,
France

Microemulsions are dispersions of oil and water stabilized by an interfacial film of surfactant and co-surfactant[1]. Frequently a short-chain alcohol, such as butanol or pentanol, is used as the co-surfactant. Stable dispersions can often be formulated over a wide range of oil and water volume fractions. In the regions of the phase diagram containing low concentrations of either oil or water, the structure has frequently been found to be one of oil droplets in water or water droplets in oil[2]. In many cases by simply changing the volume fractions of oil and water, it is possible to effect a gradual transition from an oil-in-water microemulsion to a water-in-oil microemulsion. This raises the question of the structure of the microemulsion in the intermediate region where there are approximately equal volumes of oil and water, and also that of the mechanism of the structural inversion. Microemulsions of such a type are frequently thought of as being constituted by ill-defined oil and water regions arranged with an almost total absence of long-range order[3]. However, I now report neutron small-angle scattering measurements[4] on one such microemulsion containing tetradecyl trimethylammonium bromide, butanol, octane and water which shows a well defined diffraction pattern consistent with a cubic arrangement of oil and water domains. This result shows that microemulsions of this type can be considerably more structured than presently thought and can sometimes resemble cubic liquid crystals.

Figure 1*a* shows the neutron small-angle scattering spectrum measured from a microemulsion containing approximately equal volumes of oil and water and having the following overall composition: tetradecyl trimethylammonium bromide (2.1 g), butanol (1.5 ml), octane (4 ml) and water (4 ml). The microemulsion is optically isotropic and of low viscosity. The spectrum shows a peak similar to that observed in other microemulsions of similar composition[4,5]. The radius of curvature of the spheroidal domains, as estimated from the scattering curve, is 50 Å. Consistent with its low viscosity, this microemulsion has little or no long-range order and individual Bragg peaks are not observed. A second system was therefore formulated whereby the extent of long-range order in the microemulsion was increased by decreasing the alcohol content. Addition of alcohol to surfactant-water lyotropic liquid crystals tends to destroy the long-range order in these mesophases. As there is a relatively large amount of alcohol (2.5 molecules of butanol for each molecule of surfactant) in the first mocroemulsion, one may expect the reverse process to occur—reducing the alcohol content could increase the long-range order in the system and lead to the appearance of resolved Bragg peaks in the neutron spectrum. This turns out to be the case. Figure 1*b* shows the neutron small-angle spectrum from a dispersion containing 30% less alcohol than before (1 ml of butanol instead of 1.5 ml). The microemulsion is now extremely viscous but remains optically isotropic. The broad envelope seen in Fig. 1*a* has split and at least five diffraction peaks are clearly resolved. The position of the most intense peak remains unchanged and this suggests that, apart from the extent of long-range order, the structure of the microemulsion is unaffected by reducing the alcohol content. The diffraction pattern shown in Fig. 1*b* indexes onto a cubic lattice. In cubic liquid crystals it is difficult to distinguish between primitive, face-centred, body-centred and diamond-like structures; however, the observed spectrum seems to be in better agreement with a diamond arrangement than with the others.

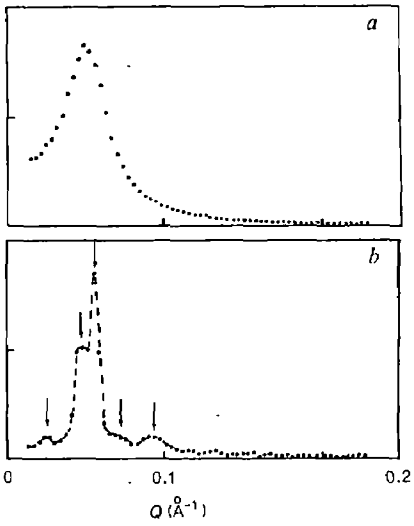

Fig. 1 Neutron small-angle scattering spectra from microemulsions containing equal volumes of oil and water (tetradecyl trimethylammonium bromide, 2.1 g; octane, 4 ml; and water, 4 ml) but having different butanol contents: *a*, 1.5 ml; *b*, 1.0 ml. The spectrum shown in *b* indexes onto a cubic structure. The spectra were measured using the D16 camera[10] at the Institut Laue-Langevin, Grenoble on samples containing D_2O as the only deuterated component.

In the phase diagram, the viscous isotropic phase borders onto a birefringent phase which may have a lamellar structure, while the fluid phase of higher alcohol content meets up at lower surfactant concentrations with microemulsions which show Winsor I-Winsor III-Winson II phase transitions with added salt[6]. A similar phase behaviour occurs for the SDS/butanol/toluene/water system. The viscous isotropic phase obtained in this system also shows a diffraction pattern similar to that shown in Fig. 1*b*, and such cubic structures may well be a general feature of this type of microemulsion.

Of the different possible cubic structures, the most likely appears to be the interwoven bicontinuous arrangement proposed by Scriven[7]. However, the possibility that the microemulsion is comprised of an organized dispersion of oil or water or droplets cannot, for the time being, be discounted. The latter type of structure would support the interpretation of Kotlarchyk *et al.*[5], whose results were obtained using a different type of surfactant.

The observation of cubic diffraction patterns from a microemulsion containing equal volumes of oil and water, shows not only that the oil and water domains are arranged on a cubic lattice, but also that under some circumstances considerable long-range order may exist. Rather than having ill-defined structures, some of these microemulsions show a strong resemblance to the cubic liquid crystalline mesophases[8,9] that occur in surfactant-water binary mixtures.

I thank the Institut Laue-Langevin for providing neutron beam time, and S. Wilson and L. Braganza for assistance with the D16 diffractometer.

Received 12 July; accepted 8 October 1985.

1. Prince, L. M. *Microemulsions. Theory and Practice* (Academic, New York, 1977).
2. Cebula, D. J., Harding, L., Ottewill, R. H. & Pusey, P. N. *Colloid Polym. Sci.* **258**, 973-97x (1980).
3. Talmon, Y. & Prager, S. *J. chem. Phys.* **69**, 2984 (1978).
4. de Geyer, A. & Tabony, J. *Chem. Phys. Lett.* **113**, 83 (1985).
5. Kotlarchyk, M., Chen, S. H., Huang, J. S. & Kim, M. W. *Phys. Rev. Lett.* **53**, 941 (1984).
6. Winsor, P. A. *Solvent Properties of Amphiphilic Compounds* (Butterworths, London, 1954).
7. Scriven, L. E. *Nature* **263**, 123 (1976).
8. Elkwall, P. in *Advances in Liquid Crystals* (ed. Brown, G. H.) Vol. 1, Ch. 1 (Academic, New York, 1971).
9. Tiddy, G. J. T. *Phys. Rep.* **59** (1980).
10. *Neutron Beam Facilities Available for Users* (Institut Laue-Langevin, Grenobles, 1981).

Electroreception and electrolocation in platypus

Henning Scheich*, Gerald Langner*, Chris Tidemann†, Roger B. Coles‡ & Anna Guppy‡

* Zoological Institute, Technical University Darmstadt,
Schnittspahnstrasse 3, 6100 Darmstadt, FRG
† Zoology Department and ‡ Research School of Biological Sciences,
Australian National University, PO Box 475, Canberra City,
ACT 2601, Australia

Electroreceptors with sensitivity in the microvolt range, which mainly function to detect live prey, are well known in phylogenetically old fishes and some amphibians[1–4]. In African mormyriform and South American gymnotiform fishes this sense has evolved to an active system using an electric organ as a source for impedance measurement of the environment and for communication[5,6]. Electroreception in higher vertebrates has not previously been reported. Here we establish that the platypus, the Australian nocturnal diving monotreme, can locate and avoid objects on the basis of d.c. fields. High-frequency sensitivity to a.c. could allow the detection of muscle activity of animals, such as crustaceans, which are preyed on by the platypus. Recordings of cortical evoked potentials showed that the bill of the platypus, previously considered to be exclusively mechanoreceptive[7–9], is also an electroreceptive organ with behavioural and electrophysiological sensitivity of ~50 μV cm^{-1}. Several lines of evidence suggest that electroreception has evolved independently in this monotreme.

One male and three female platypuses (*Ornithorhynchus anatinus*) were kept in a round pool filled with conditioned tap water (diameter 3 m, depth 40 cm, resistivity 14 kΩ cm). Hungry platypuses tended to circle the bottom of the pool, with eyes, ear canals and nares closed, keeping one forefoot in contact with the wall. The bill made 2–3 undulatory sweeps per second parallel to the bottom, which characterized the 'patrol' phase. This became the 'search' phase when the bill made contact with interesting objects, traces of food smell in the water (presumably mediated by the large vomero nasal organ) and weak electric dipole fields, whereas NaCl tablets did not elicit search behaviour. The search phase consisted of erratic movements of the bill over a restricted area of the bottom of the pool and resulted in the platypus homing-in on a freshly killed shrimp or an electric dipole. The sequence was completed by an 'attack' phase in which the object of interest was seized with rapid snaps of the bill.

We used the change from patrol to search phase as a quantitative measure of the ability of the platypus to localize a 1.5-V miniature alkaline battery with a measured dipole field placed on the bottom of the pool at different locations and at systematically varied radial distances from the pool wall. In 88 trials, one animal showed 100% success in the detection of a source 10 cm away with a gradient of 2 mV cm^{-1} (Fig. 1*d*). The working range extended down to 300 μV cm^{-1} at 30 cm, when search bouts were seen only occasionally. Successful detection of the battery was reinforced with a piece of shrimp after every fourth trial in which the battery was attacked. Control experiments offering a choice between a battery, a piece of shrimp tail or a dead battery placed 10 cm apart from each other established a clear preference for the active battery. The possibility that the battery was located chemically by the products of electrolysis near the battery terminals cannot be completely excluded but seems unlikely, especially in view of the experiments described below.

In a second experiment, two 40×40-cm aluminium plates were placed in the pool 3 m apart and connected to the 1.5-V

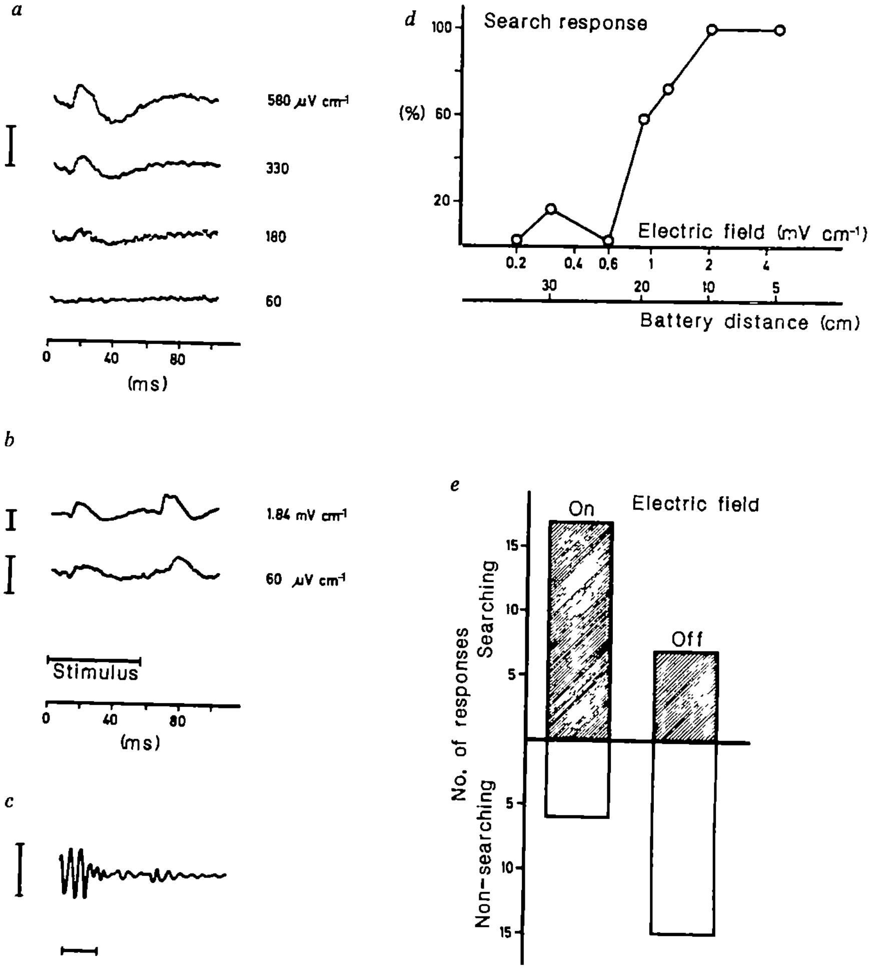

Fig. 1 *a*, Cortical evoked potentials in response to 1-ms rectangular pulse stimulation vertically across the bill of platypus. Series with decreasing voltage. Potentials represent the average response to 1,000 stimuli delivered at 6 s^{-1}. Scale bar, 300 μV. *b*, Stimulation with pulses of 55 ms duration. Scale bars, 300 μV. *c*, Compound action potentials recorded differentially with silver wires in the water during tail flicks of *M. australiense* at a distance of 5 cm. The peak power is close to 140 Hz = 1/(7 ms), that is, in the range of electrophysiological sensitivity shown in *a* and *b*. Scale bars: vertical, 1 mV; horizontal, 20 ms. *d*, Behavioural detection of the dipole field of a 1.5-v miniature battery as a function of distance. Note that once a search was elicited the battery was invariably found and attacked ($n = 88$). *e*, Search in a hollow brick when the platypus passed through a gradient of 330 μV cm^{-1} ($P < 0.01$, χ^2-test).

battery through an attenuator. The combined effects of circuit resistance and very large electrodes minimized the current density at the electrode surface, ensuring that electrode potentials and polarization were of negligible proportions. Switching of the field elicited reflex movements of the heads and tails of the animals. Threshold values, when the animals were in approximately the centre of the homogeneous field, were 500 μV cm^{-1} for the male and 500, 100 and 50 μV cm^{-1} for the females, respectively (50 μV cm$^{-1} \triangleq 4$ nA cm^{-2}). The switches include transients estimated by fast-sweep cathode-ray oscilloscope to be 25% of the plateau voltage.

In a third experiment, one animal learned to avoid a vertical plastic plate that had carbon electrodes attached at its end, carried a d.c. current and was 40 cm wide and as deep as the water. The plate was placed in the pathway during the patrol phase of the underwater search and no food reinforcement given. The animal detoured around the plate at a distance corresponding to a d.c. field gradient of <200 μV cm^{-1}, but regularly bumped into the plate when the field was switched off.

In a fourth experiment (Fig. 1*e*), we made use of the fact that platypuses investigate hollow bricks and sometimes turn them over, particularly when shrimps are hiding inside. The same behaviour was elicited by switching on a field between two carbon electrodes placed behind a brick ($30\times15\times10$ cm) near the wall of the pool. The search occurred in 74% of the trials, when the transients had a gradient of 330 μV cm^{-1}, measured in front of the brick, compared with 32% when there was no field.

As well as establishing thresholds for electroreception, these four experiments suggest that the platypus can make use of d.c. and a.c. fields in different behavioural contexts, such as object location and avoidance. Electric fields generated by live animals could be used to find food, as has previously been demonstrated for electrosensitive fishes and amphibians[3,4,10,11]. We have found that the tail flicks of a freshwater shrimp (*Macrobrachium australiense*), which formed the main diet of the platypus used in our study, produce compound action potentials that vary between 0.2 and 1 mV cm^{-1} at a distance of ~5 cm (Fig. 1*c*). Platypuses feed exclusively on live prey, including several species of decapod crustaceans, frogs and small fishes[12-14]. As the tail flick of the shrimp moves the animal only a few centimetres, the myogenic electric fields probably provide a guide to its position when it is disturbed by a platypus probing blindly in the mud or among stones.

Finally, the electrosensitivity of the bill was monitored using cortical evoked potentials (e.ps). A previous study[7] of somatosensory, visual and auditory e.ps provides a comprehensive frame of reference. Recordings were made from the exposed left posterior hemisphere of two animals under anaesthesia (Hypnodil 25 mg per kg body weight plus Ketanest 5 mg per kg per h). The dorsal and ventral surfaces of the upper bill were covered with a thick cushion of wet cotton, keeping the nostrils free for breathing. The side of the bill contralateral to the exposed cortex was stimulated dorsoventrally across the cotton layers with a pair of Ag/AgCl electrodes. The total resistance of the circuit was of the order of 100 kΩ. The maximal voltage gradient for transient-free rectangular pulses was calibrated with a pair of recording electrodes orientated vertically between the stimulating electrodes, using the same pulse-generating system. Applying a 1-ms pulse stimulation across the proximal third of the bill produced a focus of activity on the posterior-lateral hemisphere with a threshold <180 μV cm^{-1} and a maximum of 300 μV with a voltage gradient of 580 μV cm^{-1} (Fig. 1*a*). With a 55-ms pulse, on- and off-responses could be distinguished (Fig. 1*b*), with a threshold of 80 μV cm^{-1} in one animal and below 60 μV cm^{-1} in the other. To relate the electroreceptive cortical area to the sensory maps previously described[7], auditory e.p.s were recorded in one platypus in response to acoustic clicks (0.5 ms duration, 8 s^{-1}, 80 dB sound pressure level). Short-latency auditory e.p.s were recorded in an area of the dorsocaudal cortex corresponding to that of ref. 7. The largest electroreceptive e.p. was recorded 5 mm ventral to the largest auditory e.p. Rostrally, the electroreceptive e.p. decreased rapidly in amplitude when recording in what seemed to be the area receiving somatosensory inputs from the bill[7].

Although we identified the bill as the electroreceptive organ, the question of which type of receptor might be used to detect electrical currents remains open. However, recent electron microscope studies of receptor specializations in the bill of the platypus[15] have revealed gland duct receptors. These receptors are unique to platypuses but occur in a simpler form in the echidna. The receptors consist of small protoplasmatic protrusions from myelinated axons of trigeminal neurones, which form filamentous processes extending into the ducts of serous or mucous skin glands. This arrangement is ideal for electroreception in a semi-aquatic animal. Because the epidermis of the bill dries out when the platypus leaves the water, electroreceptors associated with a gland help to preserve conductivity and to prevent damage by desiccation.

All electroreceptors found in fishes and amphibians that do not have electric organs are of the ampullary receptor type[1,2,13,16] and probably derive from the acoustic-lateralis system[17,18]. The postulated electroreceptors in platypus belong to the trigeminal system, with a cortical representation next to the trigeminal map of the bill mechanoreceptors. Their sensitivity to 1-ms pulses contrasts with the d.c. or low-frequency responsiveness of ampullary receptors, which cannot detect muscle action potentials. Together with the unique morphology of the receptors, these features suggest that electroreception has evolved independently in this group of lower mammals.

This work was supported by SFB 45 German Science Foundation and a Heisenberg fellowship to G.L.

Received 29 May; accepted 10 December 1985.

1. Bullock, T. H. *A. Rev. Neurosci.* **5**, 121–170 (1982).
2. Fritzsch, B. & Wahnschaffe, U. *Cell Tissue Res.* **229**, 483–503 (1983).
3. Kalmijn, A. J. in *Handbook of Sensory Physiology* Vol. III/3, 147–200 (Springer, Berlin, 1974).
4. Scheich, H. in *Biophysics*, 764–776 (Springer, Berlin, 1983).
5. Heiligenberg, W. Principles of Electrolocation and Jamming Avoidance in Electric Fish (Springer, Berlin, 1977).
6. Scheich, H. & Bullock, T. H. in *Handbook of Sensory Physiology* Vol. III/3 201–256 (Springer, Berlin, 1974).
7. Bohringer, R. C. & Rowe, M. J. *J. comp. Neurol.* **174**, 1–14 (1977).
8. Poulton, E. B. *J. Physiol., Lond.* **5**, 15–16 (1885).
9. Wilson, J. T. & Martin, C. J. *Linn. Soc. NSW, Macleay mem. Vol.*, 190–200 (1893).
10. Digkgraaf, S. & Kalmijn, A. J. *Z. vergl. Physiol.* **47**, 438–456 (1963).
11. Himstedt, W., Kopp, J. & Schmidt, W. *Naturwissenschaftern* **69**, 552 (1982).
12. Crowther, A. B. *Pap. Proc. R. Soc. Tasm.*, 96–99 (1879).
13. Faragher, R. A., Grant, T. R. & Carrick, F. N. *Aust. J. Ecol.* **4**, 171–179 (1979).
14. Grant, T. R., Williams, R. & Carrick, F. N. *Aust. Zool.* **19**, 117–124 (1977).
15. Andres, K. H. & von Düring, M. in *Sensory Receptor Mechanisms* 81–89 (World Science, Singapore, 1984).
16. Münz, H., Claas, B. & Fritzsch, B. *J. comp. Physiol.* **A154**, 33–44 (1983).
17. Bennett, M. V. L. in *Fish Physiology*, 492–600 (Academic, London, 1971).
18. Szabo, T. in *Handbook of Sensory Physiology* Vol. III/3, 13–58 (Springer, Berlin, 1974).

Acetylcholine induces burst firing in thalamic reticular neurones by activating a potassium conductance

David A. McCormick & David A. Prince

Department of Neurology, Stanford University Medical Center,
Stanford, California 94305, USA

Recent studies have emphasized the role of acetylcholine (ACh) as an excitatory modulator of neuronal activity in mammalian cortex[1-5] and hippocampus[6-9]. Much less is known about the mechanism of direct cholinergic inhibition in the central nervous system or its role in regulating neuronal activities. Here we report that application of ACh to thalamic nucleus reticularis (nRt) neurones, which are known to receive a cholinergic input from the ascending reticular system of the brain stem[10,11], causes a hyper-

polarization due to a relatively small (1–4 nS) increase in membrane conductance to K^+. This cholinergic action appears to be mediated by the M_2 subclass of muscarinic receptors and acts in conjunction with the intrinsic membrane properties of nucleus reticularis neurones to inhibit single spike activity while promoting the occurrence of burst discharges. Thus, cholinergic inhibitory mechanisms may be important in controlling the firing pattern of this important group of thalamic neurones.

Application of ACh to thalamic nucleus reticularis neurones recorded intracellulary in thalamic slices maintained *in vitro*[12,13] resulted in a hyperpolarization with a minimum onset latency of approximately 80 ms and a duration of 5–20 s (Fig. 1*a*). The amplitude of the current induced by ACh and changes in the apparent input conductance (G_i) were estimated by manually clamping the membrane potential (V_m) at resting level while applying hyperpolarizing conductance test pulses (Fig. 1*b*). Using this approach we found that ACh caused an increase in G_i of 1–4 nS and an estimated outward current of 25–75 pA. This ACh-induced change in G_i was dose-dependent, but was less than 6 nS even with applications of large amounts of ACh (500–1,000 times the typical threshold dose).

To test whether the hyperpolarizing response to ACh was due to a direct action on the cell studied or was mediated through the release of another neurotransmitter[4-7], we blocked synaptic transmission by bathing the slices in solution containing low Ca^{2+} (0.5 mM) and Mn^{2+} (2 mM), or by local application of tetrodotoxin (10 μM). Neither of these manipulations blocked the ACh-induced inhibition ($n = 8$), although the response to an orthodromic stimulus was abolished completely. Therefore, this effect of ACh appears to be due to interaction with receptors located directly on the cell studied.

The results of previous extracellular studies indicate that the actions of ACh on nRt neurones are mediated by muscarinic receptors[14]. In support of this, we found that local applications (10 μm; $n = 3$) of the specific muscarinic antagonist scopolamine completely blocked the ACh-induced hyperpolarization and applications of the specific muscarinic agonist acetyl-β-methacholine (5 mM; $n = 4$) mimicked the actions of ACh (not shown). Furthermore, these responses appear to be mediated by the M_2 subclass of muscarinic receptors as we found that bath applications of the specific M_1 antagonist pirenzepine[15,16] in doses more than sufficient to block M_1-mediated responses in the cerebral cortex (10 and 100 μM; $n = 7$)[4] failed to block the ACh response of nRt neurones. This finding agrees with recent autoradiographic data which show that the nRt contains muscarinic receptors of the M_2 subtype[16,17].

The ACh-induced hyperpolarization could be due to an increase in membrane conductance to K^+ or Cl^- or a decrease in a voltage-dependent depolarizing current (that is, Na^+ or Ca^{2+}). To distinguish between these possibilities, the effect of changes in V_m on the ACh-induced hyperpolarization was assessed. Hyperpolarization of V_m produced by intracellular current injection decreased the amplitude of the hyperpolarizing response to ACh and revealed that the response had a mean reversal potential of −89 mV (±5.8 mV, s.d.; $n = 8$; Fig. 2) in 5.0 mM K. This effect of V_m on the ACh response indicates an increase in membrane conductance to either K^+ or Cl^-. If the change in membrane conductance induced by ACh was primarily to K^+, then changing the extracellular K^+ concentration ($[K^+]_o$) should effect the equilibrium potential of the ACh-induced response as predicted by the Nernst equation (61 mV shift in E_{ACh} per 10-fold change in $[K^+]_o$). The average reversal potential of the ACh-induced hyperpolarization was −104 mV (±4.8; $n = 4$) in 2.5 mM K^+ and −75 mV (±2.9; $n = 4$) in 7.5 mM K^+. By extrapolation, E_{ACh} was calculated to change by 58 mV for each 10-fold change in $[K^+]_o$ (Fig. 2*b*). In contrast, the average reversal potential of responses to γ-aminobutyric acid (GABA), another inhibitory neurotransmitter which typically increases membrane Cl^- conductance, ranged from −62 to −67 mV and varied by only 11 mV for each 10-fold change in $[K^+]_o$ (Fig. 2*b*), probably due to secondary shifts in Cl^- distribution[18]. These results suggest that the ACh-induced hyperpolarization is due to an increase in membrane K^+ conductance. To test this hypothesis further, neurones were impaled with KCl containing electrodes and Cl^- iontophoresed intracellularly by passing negative current (0.25–0.5 nA) through the electrode. Application of GABA to neurones under such circumstances resulted in large depolarizations that caused the generation of action potentials and had reversal potentials which were always well above firing threshold (that is positive to −50 mV; $n = 7$),

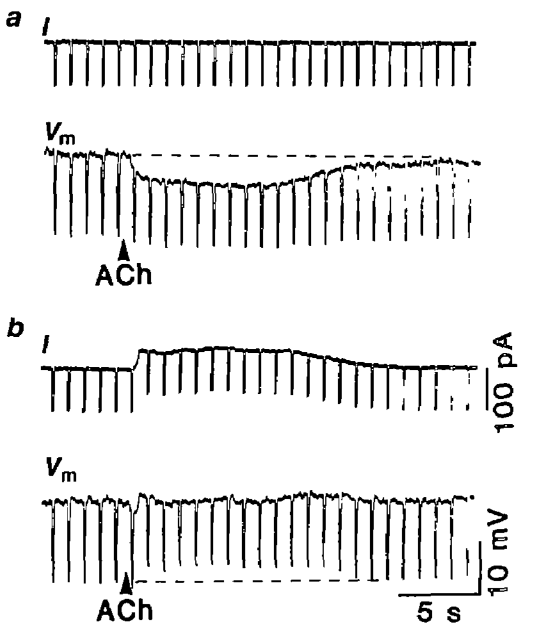

Fig. 1 Effect of ACh on membrane potential and apparent input conductance of nRt neurones. *a*, During constant current recordings, application of ACh resulted in a hyperpolarization. *b*, Manual compensation for the slow hyperpolarization using intracellular injection of depolarizing current during a second application of ACh to the neurone of *a*. Approximately 50 pA of compensating current was required and the response was associated with an apparent increase in input conductance of ~2 nS.

Methods. Intracellular recordings from nRt neurones were obtained using standard techniques[5,6]. Coronal thalamic slices, 500 μm thick, containing the anterior portions of the Rt nucleus were prepared on a Vibratome from tissue obtained from anaesthetized male or female guinea pigs. Slices were maintained in an interface type chamber at 36 ± 1 °C. Slice bathing solution contained (in mM): NaCl, 124; KCl, 5; $MgSO_4$, 2; $NaHCO_3$, 26; NaH_2PO_4, 1.25; $CaCl_2$, 2; glucose, 10 and was saturated with 95% O_2, 5% CO_2 to a final *p*H of 7.4. ACh (5 mM) and GABA (1 mM) were applied from a broken micropipette (2 μm tip diameter) by pressure pulses (typically 20 ms) in volumes of 1–10 pl, within 75 μm of the recorded neurone. Microelectrodes were filled with either 4 M KAc or 3 M KCl and bevelled to final resistances of 100–200 MΩ. Apparent input conductance was monitored with intracellular current pulses (typically 0.1 nA, 120 ms) delivered at a rate of 1 Hz. Extracellular single unit recordings were obtained with coated tungsten electrodes (Frederick–Haer). When testing the effects of ACh on neuronal responses to synaptic stimulation or applications of glutamate, these excitatory inputs were adjusted to yield only one or two spikes. Synaptic stimuli were delivered through a bipolar concentric stimulating electrode located in the white matter just lateral to the nRt. When Mn^{2+} was added to the bathing solution, sulphate and phosphate were omitted to prevent precipitation. When the concentration of K^+ was varied, the concentration of Na^+ was changed to maintain the same osmolarity. The nRt was identified in the guinea pig by immunohistochemical staining for glutamic acid decarboxylase (GAD)[19]. Neurones within this immunoreactive nucleus were readily distinguished from other thalamic neurones by their position within the slice and their distinctive electrophysiological properties which included action potentials of unusually brief duration (0.4–0.8 ms at base) and the ability to fire at high frequencies (>500 Hz).

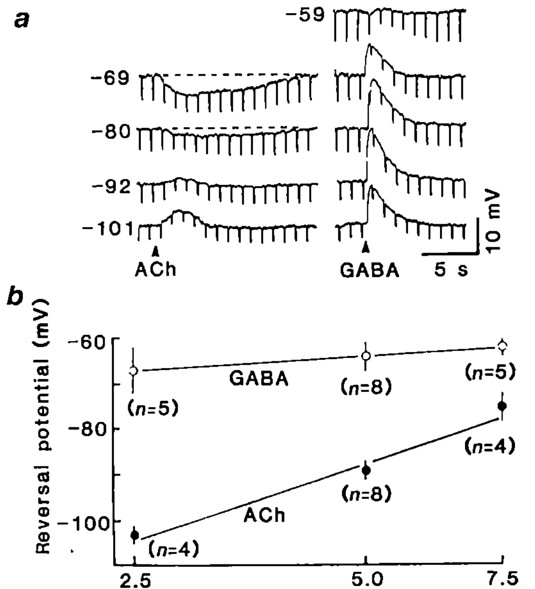

Fig. 2 Reversal potentials for responses to ACh and GABA and the effect of extracellular K^+ concentration on these. *a*, Application of ACh to this neurone in normal solution (5 mM K) caused a hyperpolarization which had a reversal potential of ~ −90 mV (*a*, left). The duration of the ACh response appeared to shorten during large current-induced hyperpolarizations (−92 and −101 mV). The ACh responses of −92 and −101 mV appear to be slightly biphasic, although this effect was small and inconsistent and therefore could not be investigated thoroughly. In contrast, applications of GABA to this same neurone caused a depolarization which had a reversal potential of ~ − 59 mV (*a*, right). The responses to ACh and GABA in this cell were obtained after blockade of Na^+-mediated action potentials with the local application of tetrodotoxin (10 μM). *b*, Group data illustrating the effect of varying the concentration of K^+ in the bathing medium on the reversal potentials of ACh- and GABA-induced responses. The reversal potential for ACh-induced responses changed by 58 mV for each 10-fold increase in $[K^+]_o$, while that for responses induced by GABA was shifted by only 11 mV, indicating that the ACh, but not the GABA, response was probably due primarily to an increase in conductance to K^+. The plotted data are mean ± s.e.m.

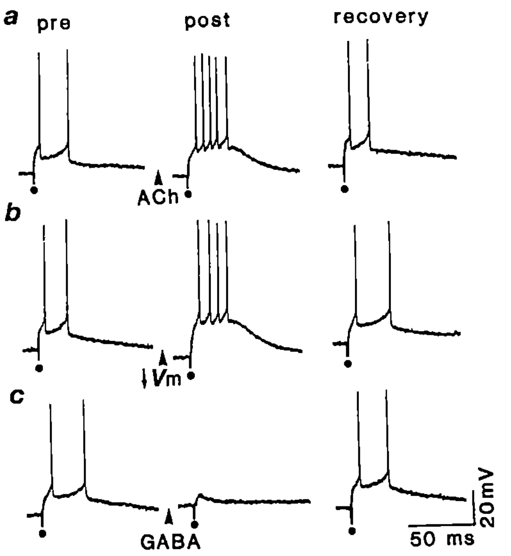

Fig. 3 Effect of ACh, GABA and change in membrane potential on the response of a nucleus reticularis neurone to orthodromic synaptic inputs. *a*, Application of ACh at upward-pointing arrow causes a membrane hyperpolarization, presumably through an increase in K^+ conductance, and changes the response of the neurone to the synaptic stimulus (dot) from two action potentials (pre) to a burst of five (post). After ~15 s, the response of the neurone returns to normal (recovery). *b*, Hyperpolarizing the membrane potential through the intracellular injection of current alone has a similar effect on the response of this neurone to the synaptic stimulus. *c*, In contrast, application of GABA, which presumably causes an increase in Cl^- conductance, depolarizes the membrane potential and inhibits all spike activity. Synaptic stimuli were of constant amplitude and delivered at 0.2 Hz. All records from the same nRt neurone.

indicating that a positive shift in E_{Cl} of at least 20 mV had occurred. In these conditions applications of ACh still caused hyperpolarizations when membrane potentials were manipulated between −65 and ~ −90 mV ($n = 7$), and the average E_{ACh} was −89 mV (±2.5; $n = 3$). These results confirm that the membrane conductance activated by ACh is predominantly for K^+ ions.

Although the above actions of ACh and GABA are, strictly speaking, both inhibitory in nature, the intrinsic properties of nRt neurones are such that the net effect on neuronal activity is quite different for these two agents. When compared with neurones of other thalamic nuclei (see also refs 12, 13), neurones of nRt display unique electrophysiological properties including high input resistance (typically 75-250 MΩ) and an apparent high specific membrane resistivity (as evidenced by relatively long membrane time constants of 20-50 ms). In addition, we found that, like other thalamic neurones[12,13], nRt cells can generate a low-threshold, tetrodotoxin-resistant, slow spike which underlies burst discharges. This potential is inactivated near or above firing threshold, but can be de-inactivated by hyperpolarization of V_m to 5-20 mV below firing threshold[12,13]. As a consequence of these intrinsic properties of nRt neurones, the relatively small K^+ current induced by ACh was effective in causing a substantial shift in V_m towards E_K and consequently deinactivating the low-threshold Ca^{2+} spike and associated burst discharges. Thus, application of ACh to single nRt neurones recorded extracellularily resulted in inhibition of spontaneous activity and, in some cells, an increased frequency of spike burst discharge, as has been reported previously *in vivo*[14]. Furthermore, if ACh was applied during orthodromic stimulation (Fig. 3*a*), during pressure pulse applications of glutamate (0.5 mM), or during intracellular depolarizing current pulses, the response of the neurones to these excitatory inputs would change from single spike activity to a burst response of 3-8 spikes. A similar effect occurred when V_m was hyperpolarized with the intracellular injection of current alone (Fig. 3*b*). In contrast, applications of GABA caused inhibition of all spike activity by evoking an increase in membrane conductance to Cl^-, which shifted V_m away from the potentials at which the burst mechanism is active (Fig. 3*c*).

Because of their widespread projection to thalamic relay and intralaminar nuclei and the presence of diverse inputs from corticothalamic and thalamocortical axons[20], the GABAergic neurones of the nRt[19] are ideally situated to influence excitability of both thalamus and cortex[20]. Our results, and others[14], indicate that the portion of the ascending brainstem reticular system which is cholinergic in nature may have a major role in these interactions by controlling the relative dominance of single spike versus burst firing patterns of activity of neurones in the nucleus reticularis of the thalamus.

We thank Dr B. W. Connors for comments on the manuscript, J. Kadis for technical assistance, and C. Joo for help in manuscript preparation. This study was supported by NIH grants NS 12151 (D.A.P.) and NS 07331 (D.A.M.) and by fellowships from the Huntington's Disease Foundation of America and the Giannini Foundation (D.A.M.).

Note added in proof: We have recently found that applications of ACh to neurones of the lateral and medial geniculate yield a hyperpolarization virtually identical to that reported here, indicating that ACh induced increases in K conductance may be a general mechanism for cholinergic inhibition in the thalamus.

Received 16 July; accepted 27 November 1985.

1. Constanti, A. & Galvan, M. *Neurosci. Lett.* **39**, 65-70 (1983).
2. ffrench-Mullen, J. M. H., Nori, H., Nakanishi, H., Slater, N. T. & Carpenter, D. O. *Cell. molec. Neurobiol.* **3**, 163-181 (1983).
3. Krnjevic, K., Pumain, R. & Renaud, L. *J. Physiol. Lond.* **215**, 447-465 (1971).
4. McCormick, D. A. & Prince, D. A. *Proc. natn. Acad. Sci. U.S.A.* **82**, 6344-6348 (1985).
5. McCormick, D. A. & Prince, D. A. *J. Physiol., Lond.* (in the press).
6. Bernardo, L. S. & Prince, D. A. *Brain Res.* **249**, 315-333 (1982).
7. Bernardo, L. S. & Prince, D. A. *Brain Res.* **249**, 334-344 (1982).
8. Cole, A. E. & Nicoll, R. A. *J. Physiol., Lond.* **352**, 173-188 (1984).
9. Halliwell, J. V. & Adams, P. R. *Brain Res.* **250**, 71-92 (1982).
10. Fibiger, H. C. *Brain Res. Rev.* **4**, 327-388 (1982).
11. Mesulam, M.-M., Mufson, E. J., Wainer, B. H. & Levey, A. I. *Neuroscience* **10**, 1185-1201 (1983).
12. Jahnsen, H. & Llinas, R. *J. Physiol., Lond.* **349**, 205-226 (1984).
13. Jahnsen, H. & Llinas, R. *J. Physiol., Lond.* **349**, 227-247 (1984).
14. Ben-Ari, Y., Dingledine, R., Kanazawa, I. & Kelly, J. S. *J. Physiol., Lond.* **261**, 647-671 (1976).
15. Hammer, R., Birdsall, N. J. M., Burgen, A. S. V. & Hulme, E. C. *Nature* **283**, 90-92 (1980).
16. Birdsall, N. J. M., Hulme, E. C. & Stockton, J. M. *Trends pharmac. Sci. Suppl.*, 4-8 (1983).
17. Wamsley, J. K., Zarbin, M. A. & Kuhar, M. J. *Brain Res. Bull.* **12**, 233-243 (1984).
18. Deisz, R. A. & Lux, H. D. *J. Physiol.* Lond. **326**, 123-138 (1982).
19. Houser, C. R., Vaughn, J. E., Barber, R. P. & Roberts, E. *Brain Res.* **200**, 341-354 (1980).
20. Steriade, M. & Deschenes, M. *Brain Res. Rev.* **8**, 1-63 (1984).

Acetylcholine hyperpolarizes central neurones by acting on an M_2 muscarinic receptor

Terry M. Egan & R. Alan North

Neuropharmacology Laboratory, 56-245 Massachusetts Institute of Technology, Cambridge, Massachusetts 02139, USA

Acetylcholine (ACh) is considered to act as a neurotransmitter in the mammalian brain by binding to membrane receptors and bringing about a change in neurone excitability. In the case of muscarinic receptors, cell excitability is usually increased[1]; this effect results from a closure of membrane potassium channels in cortical cells[2,3]. However, some central neurones are inhibited by ACh[1], and we hypothesized that these two opposite effects of ACh resulted from interactions with different subtypes of muscarinic receptor. We made intracellular recordings from neurones in the rat nucleus parabrachialis, a group of neurones in the upper pons some of which themselves synthesize ACh[4,5]. ACh and muscarine caused a membrane hyperpolarization which resulted from an increase in the membrane conductance to potassium ions. The muscarinic receptor subtype was characterized by determining the dissociation equilibrium constant (K_D) for pirenzepine during the intracellular recording; the value of ~600 nM indicates a receptor in the M_2 class. This muscarinic receptor is quite different from that which brings about a decrease in potassium conductance in other neurones, which has a pirenzepine K_D of ~10 nM (M_1 receptors)[6–8]. It is possible that antagonists selective for this kind of M_2 receptor would be useful in the management of conditions, such as Alzheimer's disease, which are associated with a reduced effectiveness of cholinergic neurones.

Intracellular recordings were made from neurones of the nucleus parabrachialis contained within a slice cut from the pons of a rat and superfused *in vitro* with a physiological saline solution (see Fig. 1 legend and ref. 9). The parabrachial neurones had resting membrane potentials of -65.6 ± 1.1 mV (mean ± s.e.m., $n = 17$) and apparent input resistances of 200-400 MΩ. Many neurones exhibited spontaneous depolarizations which were apparently synaptic potentials (they were blocked in calcium-free superfusion solutions) and these occasionally gave rise to action potentials.

ACh hyperpolarized the membrane when it was added to the superfusion solution, or when it was ejected from a pipette onto the surface of the tissue slice. The amplitude of the hyperpolarization depended on the concentration of ACh applied and readily attained 20-25 mV (Fig. 1*a*). The effective concentrations were 100 nM to 30 μM in the presence of neostigmine (1 μM), and 10-300 μM in the absence of neostigmine. This effect of neostigmine indicates that a substantial proportion of the added ACh is destroyed by cholinesterase in the brain slice before reaching the impaled neurone (Fig. 1*b*). Muscarine (1-100 μM) also hyperpolarized parabrachial neurones, the effect being observed in 21 of 32 cells. The muscarinic hyperpolarization persisted during superfusion with a solution which contained decreased calcium (0.6 mM) and increased magnesium (20 mM) concentrations. This implies that the effect of the ACh was not due to the liberation of other transmitters, because such solutions blocked the spontaneous synaptic potentials.

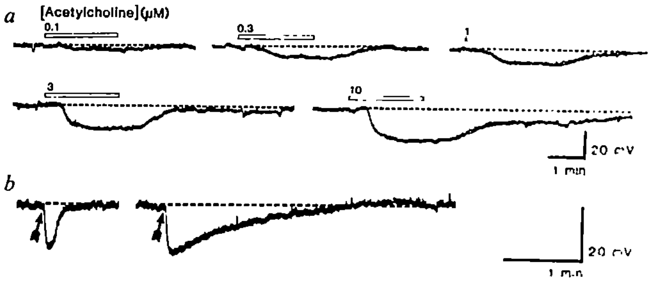

Fig. 1 Acetylcholine (ACh) hyperpolarizes neurones of rat nucleus parabrachialis. Records show membrane potential (resting level −60 mV). *a*, The bar above each trace indicates the period during which the superfusion solution contained ACh (concentration indicated); the solution also contained neostigmine (1 μM) throughout this experiment. Approximately 5 min elapsed between each of the traces shown. The neurones did not fire action potentials spontaneously during the hyperpolarization evoked by ACh, and it was difficult to evoke action potentials by passing depolarizing current pulses, presumably because of the increased membrane conductance (see Fig. 2). *b*, The arrows indicate the time of application of a pressure pulse (70 kPa, 10 ms) to a pipette that contained ACh chloride (1 mM), the tip of which (diameter 10 μm) was positioned beneath the surface of the superfusion solution. Left trace, control. Right trace, the same ACh application in the presence of neostigmine (1 μM).

Methods. Slices of rat pons containing the nucleus parabrachialis were obtained in a manner similar to that described for the locus coeruleus[9]. Male Sprague-Dawley rats were lightly anaesthetized with ether and killed by a blow to the chest; the brain was quickly removed and placed in physiological saline solution at ~4 °C. A slice of pons containing the nucleus parabrachialis close to its maximum lateral extent was cut with a Vibratome; the slice also usually contained the rostral pole of the locus coeruleus. The dorsal and ventral divisions of the nucleus could be seen on either side of the superior cerebellar peduncle. The slice was completely submerged in a chamber (capacity ~500 μl) through which flowed a solution, heated to 37 °C, of the following composition (mM): NaCl 126, KCl 2.5, NaH_2PO_4 1.2, $MgCl_2$ 1.3, $CaCl_2$ 2.5, $NaHCO_3$ 25, glucose 11, saturated with 95% O_2/5% CO_2. Intracellular recordings of membrane potential were made with electrodes containing potassium chloride or potassium acetate. In some experiments, membrane currents were measured directly with a single electrode amplifier which switched from voltage measuring to current-passing mode at a frequency of 3-6 kHz (Axoclamp II)

The muscarinic hyperpolarization resulted from an increase in the conductance of the cell membrane to potassium ions. In the first place, ACh caused a fall in the neurone input resistance measured by passing small hyperpolarizing currents (Fig. 2). Second, the hyperpolarization was associated with an outward current measured under voltage clamp. Both the muscarinic hyperpolarization and the current amplitude were linearly dependent on the membrane potential, having zero amplitude at a potential which changed with the logarithm of the potassium concentration in the superfusion solution ($[K^+]_o$) (Fig. 2). In control solutions ($[K^+]_o = 2.5$ mM), the reversal potential was -104.4 ± 1.1 mV ($n = 8$) (Fig. 2). Third, muscarinic hyperpolarizations were reproducible for several hours whether the recording electrode contained potassium chloride or potassium acetate. Fourth, the hyperpolarization was blocked by barium (4 mM). Muscarinic hyperpolarizations with similar characteristics have been described previously in peripheral autonomic neurones[10–12], but not in the central nervous system.

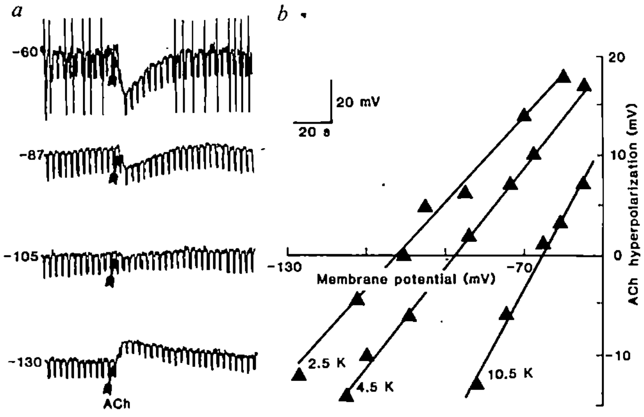

Fig. 2 Acetylcholine increases potassium conductance. *a*, Records of membrane potential; downward deflections are electrotonic potentials evoked by passing current pulses which were constant throughout. Action potentials and their afterhyperpolarizations are also seen in the top trace, but the full amplitude of the action potentials is not reproduced by the pen recorder. The arrows indicate the times of application of ACh. The ACh was ejected from a pipette containing ACh chloride (see Fig. 1 legend). The ACh hyperpolarization became smaller when the membrane was hyperpolarized and reversed polarity at about −105 mV. *b*, Complete results from the same neurone. The voltage dependence of the ACh response was determined first in control (2.5 mM) and then in solutions containing higher potassium concentrations as indicated (in mM).

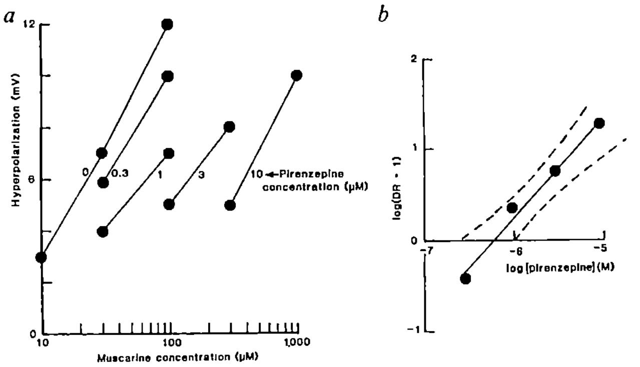

Fig. 3 The muscarinic receptor on parabrachial neurones is of an M_2 subtype. *a*, Hyperpolarizations were evoked by superfusion of various concentrations of muscarine, which was first applied alone and then in the presence of four different concentrations of pirenzepine. All records were obtained during recording from one neurone. *b*, Schild plot for the antagonism of muscarine by pirenzepine. The slope of the line (1.08) was not significantly different from 1. The pirenzepine K_D was 590 nM. Broken lines are the 95% confidence limits of the line. Two other experiments yielded similar results, with confidence limits of the estimates of the K_D of 200–1,100 nM.

The hyperpolarizations were completely blocked by atropine and hyoscine (3–100 nM, $n = 4$) but were unaffected by nicotine (50 μM) or hexamethonium (400 μM). Neurones located in the nearby locus coeruleus were never hyperpolarized by ACh or muscarinic agonists (see ref. 13); furthermore, noradrenaline and enkephalin, which hyperpolarize locus coeruleus neurones[14,15], had no effect on cells of the nucleus parabrachialis.

Pirenzepine is a muscarinic receptor antagonist that has different affinities for the two different subtypes of muscarinic receptors[16,17]. Pirenzepine did not affect the muscarinic hyperpolarizations in concentrations less than 300 nM ($n = 5$), but higher concentrations caused a parallel shift in the ACh dose-response curve. In three experiments, sufficient agonist and antagonist concentrations were applied for the results to be analysed by the Gaddum-Schild method[18]. This indicated that pirenzepine competitively blocked the effect of muscarine, with K_D values of 500, 590 and 725 nM (Fig. 3). The relatively low affinity of pirenzepine for this receptor indicates that it belongs to the M_2 category[14,15]. Estimates of the dissociation equilibrium constant of atropine were not made, because previous studies have shown that atropine has the same K_D for both the M_1 and M_2 receptors[19]. Our own experiments on single neurones support this. Cells of the rat locus coeruleus (part of which is contained within the same brain slice as the nucleus parabrachialis) are depolarized by muscarinic agonists; the receptors underlying this effect (M_2) have a K_D for atropine of ~680 pM and for pirenzepine of 230 nM (ref. 13). On the other hand, neurones in the guinea pig enteric nervous system are depolarized by muscarinic agonists through a different ionic mechanism[20]. On these cells the muscarinic receptor is the M_1 subtype, having a K_D for pirenzepine of ~3 nM, but the K_D for atropine is 1 nM, a value close to that found in the locus coeruleus[21]. In the present experiments we found that a concentration of atropine close to this K_D value (3 nM) prevented or reduced the muscarinic hyperpolarization, suggesting that atropine is not likely to be useful in further characterization of the receptor subtype involved.

ACh acts on muscarinic receptors in excitable tissues to bring about a variety of membrane conductance changes, some of which can now be ascribed to particular receptor subtypes. The decrease in potassium conductance[2,3,6,8,20] results from an action on M_1 receptors, which bind pirenzepine with a K_D of ~10 nM (refs 6, 17). The increase in potassium conductance reported here results from activation of an M_2 receptor having a pirenzepine K_D of 600 nM; the same value for the pirenzepine K_D has been reported for antagonism of muscarinic slowing of the guinea pig heart[22], which probably also results from an increase in potassium conductance of the atrial cells[23]. A third effect of muscarinic agonists is a reduction in a voltage-dependent calcium conductance[24-26]. There are no estimates of a pirenzepine K_D for block of this muscarinic action. However, the negative inotropic effect on the heart (which may correlate with a reduced calcium conductance) appears to involve an M_2 receptor having a pirenzepine K_D of 186 nM, a value which may be different from that obtained when cardiac slowing is measured[22]. This suggests that the M_2 receptors associated with potassium conductance increase and reduction in calcium conductance may be distinguishable. A fourth type of effect is an increase in membrane conductance, predominantly to sodium ions, which brings about a depolarization of some gland cells[27], neurones[13,28] and smooth muscle cells[29]. An M_2 receptor is also implicated in one of these effects[13]. It is likely that the further development of antagonists will allow the discrimination among the 'M_2' receptors responsible for these distinct effects on ion conductances.

There is considerable evidence for presynaptic location of M_2 receptors on peripheral cholinergic and adrenergic fibres[6,30,31] and binding sites believed to identify these receptors have been assigned a presynaptic location in the central nervous system[32,33]. Lesions that result in loss of neurones containing choline acetyltransferase (CAT) also lead to loss of cortical M_2 binding sites, implying that the latter may be 'autoreceptors'[33]. It is of interest, therefore, that the neurones hyperpolarized in the present study were in a part of the brain (nucleus parabrachialis) which contains CAT-immunoreactive cells[4], although it should be stressed that the individual cells from which the recordings were made have not been shown to contain CAT. The potassium conductance increase in the soma will result in strong inhibition of firing, and if a similar effect were to occur close to axon terminal release sites it would reduce the amount of transmitter released. A blockade of these actions of endogenous ACh by selective M_2 receptor antagonists might be useful in the treatment of those disorders, such as Alzheimer's disease, that involve a loss of cholinergic neurones bearing this muscarinic receptor subtype[33].

This work was supported by grants AM32979 and DA03161 from the US Department of Health and Human Services.

Received 15 July; accepted 21 November 1985.

1. Krnjevic, K. *Physiol. Rev.* **54**, 418–540 (1974).
2. Krnjevic, K., Pumain, R. & Renaud, L. *J. Physiol., Lond.* **215**, 247–268 (1971).
3. Halliwell, J. & Adams, P. R. *Brain Res.* **250**, 71–92 (1982).
4. Armstrong, D. M., Saper, C. B., Levey, A. I., Wainer, B. H. & Terry, R. D. *J. comp. Neurol.* **216**, 53–68 (1983).
5. McGeer, P. L., McGeer, E. G. & Peng, J. H. *Life Sci.* **34**, 2319–2338 (1984).
6. North, R. A. & Surprenant, A. *J. Physiol., Lond.* **368**, 435–452 (1985).
7. Brown, D. A., Forward, A. & Marsh, S. *Br. J. Pharmac.* **71**, 362–364 (1980).
8. Brown, D. A. & Constanti, A. *Br. J. Pharmac.* **70**, 593–608 (1980).
9. Williams, J. T., North, R. A., Shefner, S. A., Nishi, S. & Egan, T. M. *Neuroscience* **13**, 137–156 (1984).
10. Hartzell, H. C., Kuffler, S. W., Stickgold, R. & Yoshikami, D. *J. Physiol., Lond.* **271**, 817–846 (1977).
11. Dodd, J. & Horn, J. P. *J. Physiol., Lond.* **334**, 271–291 (1983).
12. Cole, A. E. & Shinnick-Gallagher, P. *Nature* **307**, 270–271 (1984).
13. Egan, T. M. & North, R. A. *Br. J. Pharmac.* **85**, 733–735 (1985).
14. Williams, J. T., Henderson, G. & North, R. A. *Neuroscience* **14**, 95–101 (1985).
15. Williams, J. T., Egan, T. M. & North, R. A. *Nature* **299**, 74–76 (1982).
16. Goyal, R. K. & Rattan, S. *Gastroenterology* **74**, 598–618 (1978).
17. Hammer, R., Berrie, C. P., Birdsall, N. J. M., Burgen, A. S. V. & Hulme, E. C. *Nature* **283**, 90–92 (1980).
18. Arunlakshana, O. & Schild, H. O. *Br. J. Pharmac.* **14**, 48–58 (1959).
19. Hirschowitz, B. I. *et al.* (eds) *Subtypes of Muscarinic Receptors* (Elsevier, Amsterdam, 1984).
20. Morita, K., North, R. A. & Tokimasa, T. *J. Physiol., Lond.* **333**, 125–139 (1982).
21. Surprenant, A. *Trends pharmac. Sci.* (in the press).
22. Chassaing, C., Dureng, G., Baissat, J. & Duchene-Marullaz, P. *Life Sci.* **35**, 1739–1745 (1984).
23. Brown, H. F. *Physiol. Rev.* **62**, 505–530 (1982).
24. Ijima, T., Irisawa, H. & Kameyama, M. *J. Physiol., Lond.* **359**, 485–501 (1985).
25. Belluzi, O., Sacchi, O. & Wanke, E. *J. Physiol., Lond.* **358**, 109–129 (1985).
26. Kuba, K. & Koketsu, K. *Jap. J. Physiol.* **26**, 703–716 (1976).
27. Iwatsuki, N. & Petersen, O. H. *J. Physiol., Lond.* **269**, 735–751 (1977).
28. Kuba, K. & Koketsu, K. *Prog. Neurobiol.* **11**, 77–169 (1977).
29. Bolton, T. B. *Physiol. Rev.* **59**, 606–718 (1979).
30. Kilbinger, H., Halim, S., Lambrecht, G., Weiler, W. & Wessler, I. *Eur. J. Pharmac.* **103**, 313–320 (1984).
31. Fuder, H., Rink, D. & Muscholl, E. *Naunyn-Schmiedebergs Archs Pharmak.* **318**, 210–219 (1982).
32. Raiterai, M., Leardi, R. & Marchi, M. *J. Pharmac. exp. Ther.* **228**, 209–214 (1984).
33. Mash, D. C., Flynn, D. D. & Potter, L. T. *Science* **228**, 1115–1117 (1985).

Primary structure of *Torpedo californica* acetylcholinesterase deduced from its cDNA sequence

Mark Schumacher*, Shelley Camp*, Yves Maulet*, Michael Newton*, Kathleen MacPhee-Quigley*‡, Susan S. Taylor‡, Theodore Friedmann† & Palmer Taylor*

* Division of Pharmacology, Department of Medicine, † Division of Molecular Genetics, Department of Pediatrics, and ‡ Department of Chemistry, University of California, San Diego, La Jolla, California 92093, USA

Acetylcholinesterase, an essential enzyme of the nervous system, rapidly terminates the action of acetylcholine released into the synapse. Acetylcholinesterase is also found (in lower abundance) in extrajunctional areas of muscle and nerve and on erythrocyte membranes[1,2]. Hydrodynamic analyses of the native enzyme[3] and characterization of its dissociated subunits have revealed multiple enzyme forms which can be divided into two classes: (1) dimensionally asymmetric forms which are usually found within the synapse and contain a collagen-like structural subunit disulphide-linked to the catalytic subunits; and (2) globular forms which appear to be widely distributed on the outer surface of cell membranes. Both forms have been characterized in the ray *Torpedo californica* and, although their catalytic behaviours seem to be identical, they differ slightly in amino-acid composition, peptide maps and reactivity with certain monoclonal antibodies[4–7]. Here, we report the complete amino-acid sequence of an acetylcholinesterase inferred from the sequence of a complementary DNA clone. The 575-residue protein shows significant homology with the C-terminal portion of thyroglobulin[8].

Five candidate cDNA clones remained after the sequential screening procedure described in Fig. 1*a*. To confirm that these cDNA clones encoded acetylcholinesterase, two of them (λACHE-1 [insert size 2.3 kilobases (kb)] and λACHE-5 [insert size 1.4 kb]) were selected for characterization. Poly(A)$^+$ RNA, selected by hybridization with clone λACHE-5, directed the translation of at least one peptide of relative molecular mass (M_r) ~62,000 (62K) in a rabbit reticulocyte translation system. The polypeptide was selectively immunoprecipitated with antibodies to *Torpedo* acetylcholinesterase and was enriched over total translation products after hybridization selection (not shown). The nucleotide sequence of λACHE-5 that is homologous to probes 1 and 2 corresponded exactly to the CNBr peptide used to design the oligonucleotides (Fig. 1*b*, residues 379–405) as well as to other overlapping tryptic and chymotryptic peptides (residues 358–386). Hybridization and sequence comparison showed that λACHE-5 is identical to the 1.4-kb *Eco*RI fragment of λACHE-1 (Fig. 1*a*). As λACHE-1 contained the largest insert (2.3 kb) and sequence coding for the amino-terminal region of the peptide, it was selected for complete sequence analysis.

When the amino acids inferred from the λACHE-1 sequence are aligned with the peptide sequences (Fig. 1*b*), the entire coding region for the processed enzyme is defined, starting at nucleotide 41 (residue 1), which corresponds exactly to the N-terminal peptide, and ending at residue 575, which corresponds to the candidate C-terminal tryptic peptide determined from amino-acid sequencing. This portion of the coding region has a calculated M_r of 65,612. The slight difference in size compared with the native catalytic subunits can be attributed to the presence of 7–8% carbohydrate. The amino-acid composition, inferred from the cDNA sequence, is in accord with compositions reported for the native enzyme[4,9]. The enzyme contains eight cysteines, at least one of which is involved in intersubunit crosslinking.

The region 5′ of the amino-terminal residue in the native enzyme (nucleotides 2–40) codes for 13 amino acids which form a portion of the leader peptide characteristic of membrane-associated and exported protein precursors[10]. Leader peptides are rich in hydrophobic amino acids and terminate with amino acids containing small neutral side chains[11]. These criteria are consistent with the sequence in this region, which has hydropathy values compatible with a membrane-spanning segment and ends with alanine. Analysis of the hydropathy[12] of acetylcholinesterase reveals a profile typical for a globular protein (data not shown). Hydrophilic regions were found between residues 39 and 93 and between residues 535 and 572. Long hydrophobic regions, which are candidates for membrane-spanning segments, were not found; this was expected as the asymmetric form is associated with the basal lamina of the synapse and the globular form contains a post-translational modification whose hydrophobicity probably accounts for its membrane association[5].

A serine hydroxyl serves as the esteric subsite of the active centre where breakdown of the acetyl-enzyme is rapid. The slower breakdown for phosphoryl esters accounts for their inhibitory properties and the active-site serine can be labelled with ^{3}H-diisopropylfluorophosphate. The position of the active-site serine (residue 200) was identified by aligning the active-centre peptide sequence[13] with the inferred amino-acid sequence (Fig. 1*b*, arrow). A search for internal homologies failed to show significant duplication within the amino-acid sequence, although two segments of short length with predominantly negative charges (residues 133–145 and 444–466) showed some similarity. Whether these regions contribute to the peripheral anionic site and the anionic subsite of the active centre must await their assignment by site-directed labelling and analysis of crystal structure.

The catalytic subunits of the asymmetric form of acetylcholinesterase migrate more slowly on SDS-gel electrophoresis

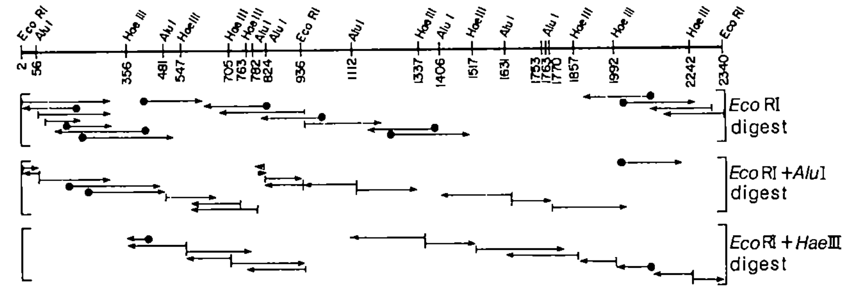

b

```
                16                  31                  46
G AAT TCC GTG CTT CTG CAC TTG GTC GTC CTG TGC CAG GCG GAC GAT CAC TCT
  Asn Ser Val Leu Leu His Leu Val Val Leu Cys Gln Ala Asp Asp His Ser
                                                       1
        61                  76                  91                  106
GAG CTC CTG GTC AAC ACC AAG TCG GGA AAA GTC ATG GGA ACA AGA GTC CCA GTC
Glu Leu Leu Val Asn Thr Lys Ser Gly Lys Val Met Gly Thr Arg Val Pro Val
 5
                121                 136                 151
CTC TCC AGC CAC ATC AGC GCT TTC CTG GGG ATT CCC TTT GCC GAG CCT CCA GTT
Leu Ser Ser His Ile Ser Ala Phe Leu Gly Ile Pro Phe Ala Glu Pro Pro Val
 23
    166                 181                 196                 211
GGG AAC ATG AGG TTC AGG AGA CCT GAG CCC AAG AAA CCG TGG TCG GGA GTC TGG
Gly Asn Met Arg Phe Arg Arg Pro Glu Pro Lys Lys Pro Trp Ser Gly Val Trp
 41
                226                 241                 256
AAC GCT TCC ACC TAT CCC AAC AAC TGC CAG CAG TAC GTT GAC GAG CAG TTC CCT
Asn Ala Ser Thr Tyr Pro Asn Asn Cys Gln Gln Tyr Val Asp Glu Gln Phe Pro
 59
271                     286                 301                 316
GGA TTT TCA GGT TCA GAG ATG TGG AAT CCG AAC AGA GAG ATG AGT GAG GAC TGT
Gly Phe Ser Gly Ser Glu Met Trp Asn Pro Asn Arg Glu Met Ser Glu Asp Cys
 77
        331                 346                 361                 376
TTG TAC CTC AAC ATT TGG GTG CCT TCT CCG AGG CCG AAG AGT ACA ACC GTC ATG
Leu Tyr Leu Asn Ile Trp Val Pro Ser Pro Arg Pro Lys Ser Thr Thr Val Met
 95
                391                 406                 421
GTG TGG ATC TAC GGA GGC GGT TTC TAC AGC GGG TCC TCG ACG TTG GAC GTC TAC
Val Trp Ile Tyr Gly Gly Gly Phe Tyr Ser Gly Ser Ser Thr Leu Asp Val Tyr
113
    436                 451                 466                 481
AAT GGG AAA TAC CTT GCC TAC ACC GAG GAG GTG GTG CTG GTC TCT CTG AGC TAC
Asn Gly Lys Tyr Leu Ala Tyr Thr Glu Glu Val Val Leu Val Ser Leu Ser Tyr
131
                496                 511                 526
CGG GTG GGC GCT TTT GGT TTT CTC GCC CTC CAC GGC AGC CAG GAG GCA CCA GGA
Arg Val Gly Ala Phe Gly Phe Leu Ala Leu His Gly Ser Gln Glu Ala Pro Gly
149
541                     556                 571                 586
AAT GTG GGC CTC CTG GAC CAG AGG ATG GCA CTG CAG TGG GTG CAC GAC AAC ATC
Asn Val Gly Leu Leu Asp Gln Arg Met Ala Leu Gln Trp Val His Asp Asn Ile
167
        601                 616                 631             ▼   646
CAG TTC TTC GGC GGG GAC CCC AAG ACG GTG ACC ATC TTC GGA GAG AGT GCC GGC
Gln Phe Phe Gly Gly Asp Pro Lys Thr Val Thr Ile Phe Gly Glu Ser Ala Gly
185
                661                 676                 691
GGC GCC TCT GTC GGC ATG CAC ATT CTC TCC CCG GGG AGC CGA GAC CTC TTC CGC
Gly Ala Ser Val Gly Met His Ile Leu Ser Pro Gly Ser Arg Asp Leu Phe Arg
203
    706                 721                 736                 751
CGG GCC ATC CTT CAG AGC GGC TCG CCC AAT TGC CCG TGG GCG TCT GTC TCT GTT
Arg Ala Ile Leu Gln Ser Gly Ser Pro Asn Cys Pro Trp Ala Ser Val Ser Val
221
                766                 781                 796
GCT GAA GGC CGC AGG AGG GCG GTC GAG CTG GGA AGA AAC CTC AAC TGT AAC CTC
Ala Glu Gly Arg Arg Arg Ala Val Glu Leu Gly Arg Asn Leu Asn Cys Asn Leu
239
811                     826                 841                 856
AAC AGC GAC GAA GAG CTC ATC CAC TGT CTG AGG GAA AAG AAG CCT CAG GAG TTG
Asn Ser Asp Glu Glu Leu Ile His Cys Leu Arg Glu Lys Lys Pro Gln Glu Leu
257
        871                 886                 901                 916
ATT GAC GTG GAG TGG AAT GTC CTT CCC TTT GAC AGT ATC TTC AGG TTC TCC TTC
Ile Asp Val Glu Trp Asn Val Leu Pro Phe Asp Ser Ile Phe Arg Phe Ser Phe
275
                931                 946                 961
GTT CCC GTC ATC GAT GGG GAA TTC TTC CCA ACC TCC CTG GAA TCT ATG TTG AAC
Val Pro Val Ile Asp Gly Glu Phe Phe Pro Thr Ser Leu Glu Ser Met Leu Asn
293
    976                 991                 1006                1021
TCT GGC AAC TTC AAG AAG ACT CAG ATC TTA CTG GGA GTC AAC AAG GAC GAG GGC
Ser Gly Asn Phe Lys Lys Thr Gln Ile Leu Leu Gly Val Asn Lys Asp Glu Gly
311
                1036                1051                1066
TCG TTT TTC CTC TTG TAC GGA GCG CCG GGT TTC AGC AAG GAC TCT GAA AGC AAA
Ser Phe Phe Leu Leu Tyr Gly Ala Pro Gly Phe Ser Lys Asp Ser Glu Ser Lys
329

1081                    1096                1111                1126
ATC TCT CGG GAA GAC TTC ATG TCA GGG GTC AAG CTA AGC GTT CCC CAC GCC AAT
Ile Ser Arg Glu Asp Phe Met Ser Gly Val Lys Leu Ser Val Pro His Ala Asn
347
        1141                1156                1171                1186
GAC TTA GGG TTG GAC GCT GTC ACG CTA CAG TAC ACA GAC TGG ATG GAT GAC AAC
Asp Leu Gly Leu Asp Ala Val Thr Leu Gln Tyr Thr Asp Trp Met Asp Asp Asn
365
                1201                1216                1231
AAT GGT ATA AAG AAC AGA GAT GGA TTG GAC GAC ATC GTA GGG GAC CAC AAC GTC
Asn Gly Ile Lys Asn Arg Asp Gly Leu Asp Asp Ile Val Gly Asp His Asn Val
383
    1246                1261                1276                1291
ATA TGC CCC TTG ATG CAC TTT GTT AAC AAG TAC ACC AAG TTT GGC AAT GGC ACC
Ile Cys Pro Leu Met His Phe Val Asn Lys Tyr Thr Lys Phe Gly Asn Gly Thr
401
                1306                1321                1336
TAC CTG TAC TTC TTC AAC CAC CGA GCC TCA AAC CTG GTG TGG CCG GAG TGG ATG
Tyr Leu Tyr Phe Phe Asn His Arg Ala Ser Asn Leu Val Trp Pro Glu Trp Met
419
1351                    1366                1381                1396
GGC GTC ATC CAC GGC TAT GAG ATT GAG TTC GTC TTC GGG CTG CCT CTG GTG AAG
Gly Val Ile His Gly Tyr Glu Ile Glu Phe Val Phe Gly Leu Pro Leu Val Lys
437
        1411                1426                1441                1456
GAG CTG AAC TAC ACA GCG GAG GAG GAA GCG CTG AGC CGG AGG ATA ATG CAT TAC
Glu Leu Asn Tyr Thr Ala Glu Glu Glu Ala Leu Ser Arg Arg Ile Met His Tyr
455
                1471                1486                1501
TGG GCG ACA TTC GCA AAG ACT GGA AAC CCA AAC GAA CCC CAC TCA CAG GAG AGC
Trp Ala Thr Phe Ala Lys Thr Gly Asn Pro Asn Glu Pro His Ser Gln Glu Ser
473
    1516                1531                1546                1561
AAA TGG CCT CTC TTC ACT ACC AAG GAG CAG AAA TTT ATT GAC CTC AAC ACA GAA
Lys Trp Pro Leu Phe Thr Thr Lys Glu Gln Lys Phe Ile Asp Leu Asn Thr Glu
491
                1576                1591                1606
CCC ATG AAA GTC CAC CAG CGA CTC CGA GTT CAG ATG TGC GTG TTC TGG AAC CAG
Pro Met Lys Val His Gln Arg Leu Arg Val Gln Met Cys Val Phe Trp Asn Gln
509
1621                    1636                1651                1666
TTC CTC CCC AAG CTC CTC AAC GCC ACA GAG ACC ATT GAT GAG GCA GAA CGC CAG
Phe Leu Pro Lys Leu Leu Asn Ala Thr Glu Thr Ile Asp Glu Ala Glu Arg Gln
527
        1681                1696                1711                1726
TGG AAG ACG GAG TTT CAT CGG TGG AGT TCC TAC ATG ATG CAC TGG AAG AAC CAA
Trp Lys Thr Glu Phe His Arg Trp Ser Ser Tyr Met Met His Trp Lys Asn Gln
545
                1741                1756                     1778       1788
TTT GAC CAC TAC AGC AGA CAC GAG AGC TGT GCT GAG CTG TGA GCTCTGCTCT GCAGGTCGCC
Phe Asp His Tyr Ser Arg His Glu Ser Cys Ala Glu Leu
563
       1798       1808       1818       1828       1838       1848       1858
TGGTGAAGCA GAGAGCAGAG TCCGATATTG ACCAGACACC CAGTCTAGTT CCTGGAGACC CTGCCTGGCC

       1868       1878       1888       1898       1908       1918       1928
CTCTGAGCCC CCCCCCCCCA CCCCGCCAAA CCTCGCCTTC GAGACTGCCT CCCTCCCATC CCTCCTCTAA

       1938       1948       1958       1968       1978       1988       1998
CCCCAGGCTG CCGACCTCGT CTCTCGCACC GTCACTCGTA AATCTGCGGC ACCAATCTTT CGGCCACCCA

       2008       2018       2028       2038       2048       2058       2068
CTCTCGCATC AGCCCAACTC TCTCCTTCCT CTTCCCCACC ACTACCCCCC TATTACCCAC TCTCCACCTG

       2078       2088       2098       2108       2118       2128       2138
CCGCACTCTC TCTCCCAATA CCGTCAGCAA CCATTCCAAT CCCCTAAATC TCTCTCCTGT CACCTATTGA

       2148       2158       2168       2178       2188       2198       2208
CGTTCTACCC CCCCCCCCTC ACTCTGTCTC CCCAAGTACT CCCTCCCCGT TCATCCCAGA GTTCCCAACT

       2218       2228       2238       2248       2258       2268       2278
CCCCAAAAGA CTTCTGGTCT CCTTCCTAAG TGGCCCTTCA CCTGTACAAA TCTGGGTGAG AGCCAATATG

       2288       2298       2308       2318       2328       2338
ATCCTGGCTG ATTCTCTGCT TTATCCAGTT TCCTTGCCCA ATCATTAGAT CCTCCAACTC GAATTC
```

Fig. 1 *a*, Sequencing strategy for cDNA clone λACHE-1 encoding acetylcholinesterase from the electric organ of *Torpedo californica*. Restriction endonuclease *Eco*RI fragments from a partial digest of λACHE-1 were isolated and either inserted into the sequencing verctor M13mP8 (ref. 30) or digested further with *Alu*I or *Hae*III and then cloned. DNA sequencing of the resulting M13-ACHE-1 recombinants was done by the dideoxynucleoside sequencing procedure[31]. Sequencing reactions were primed with either a 17-mer universal primer (Amersham N.4511) (indicated by a vertical line at the beginning of an arrow) or unique 17-mer primers chemically synthesized from a confirmed cDNA sequence (indicated by arrows beginning with a solid circle). Confirmed sequence was obtained from both strands of the cDNA as indicated by arrow length and direction. Sequence data were managed and fragment overlaps determined using computer programs developed by Staden[32]. Assignment of the correct open reading frame was determined by overlap with the sequence of ~80% of the tryptic peptides and 30% of the CNBr peptides. *b*, Primary structure of the *T. californica* acetylcholinesterase. The nucleotide sequence of the mRNA was deduced from the 2,344-base nucleotide sequence of cDNA clone λACHE-1. Nucleotides are numbered in the 5′ to 3′ direction. The predicted amino acids are shown below the corresponding nucleotide sequence, beginning with residue 1 (nucleotide 41), the first amino acid of the mature enzyme, and terminating at position 1,765 with the translation stop codon (TGA), followed by 579 nucleotides of untranslated sequence. Neither the 5′ nor the 3′ end of the mRNA sequence is complete, given the absence of the initiation codon AUG(Met) at the 5′ end, and the polyadenylation signal AATAAA and poly(dA) tract at the 3′ end of λACHE-1. Underlining indicates some of the peptides used to determine the correct reading frame including the N-terminal peptide, active-centre peptide (the arrow indicates the active-site Ser 200), overlapping tryptic and CNBr peptides used for probe design, and the carboxy-terminal tryptic peptide. A broken line indicates the location of the peptide sequence used for oligonucleotide construction. There are four potential sites of *N*-linked glycosylation (residues 59, 416, 457 and 533) predicted by the sequence Asn-X-Ser/Thr, where X represents any amino acid except proline[33].

Methods. *a*, A cDNA library (provided by Dr Toni Claudio of Yale University) was constructed from total poly(A)$^+$ RNA extracted from the electric organ of *T. californica* and was inserted into the *Eco*RI site of λgt10. The λgt10 library (2×10^5 plaque-forming units) was plated out, and nitrocellulose filter copies were prepared[34] and screened with two adjacent but not overlapping oligonucleotide probes based on the observed amino-acid sequence of a CNBr peptide isolated from the asymmetric form of the enzyme. Each probe was designed to complement the predicted mRNA sequence as follows. Probe 1, (Met)-Asp-Asp-Asn-Asn-Gly-Ile [5′-ATNCC(A,G)TT(A,G)TT(A,G)TC(A,G)TCCAT-3′], a 20-mer with 64-fold degeneracy; probe 2, Asp-Gly-Leu-Asp-Asp-Ile [5′-AT(A,G)-TC(A,G)TCNA(A,G)NCC(A,G)TC-3′], a 17-mer with 256-fold degeneracy (N = A, G, T or C). Oligonucleotides used for filter hybridization screening were synthesized on a Systec Microsyn-1450 automated DNA synthesizer using phosphoramidite chemistry[35]. After ultraviolet shadow-purification (M. Zoller, personal communication), oligonucleotides were 5′-end-labelled with [γ-^{32}P]ATP (>7,000 Ci mmol^{-1}, Biomedicals, Inc.) using polynucleotide kinase (Amersham). Unreacted [γ-^{32}P]ATP was removed using NACS prepack columns (BRL), resulting in specific activities of 1×10^8–10^9 c.p.m. μg^{-1}. Conditions of hybridization were essentially those of Wallace *et al.*[36], with the addition that the filter copies were washed at successively higher temperatures to optimize the signal-to-background ratio. When 24 candidates selected on the basis of hybridization were rescreened with probes 1 and 2, seven different plaques gave signals greater than the control. A final screening of these candidates provided five plaques which hybridized unambiguously to both probes on duplicate filters. λ DNA was prepared from the final candidate plaques by established methods[37]. After digestion of clones λ-ACHE-1-5 with *Eco*RI, insert sizes were found to range from 1.4 to 2.3 kb. Four inserts contained an internal *Eco*RI site generating a common 0.9-kb fragment plus a fragment in the range 1.2–1.4 kb. A fifth clone contained a single 1.4-kb fragment. Probe 1 hybridized to the 1.2–1.4-kb fragments whereas a probe derived from the amino-terminal protein sequence reacted only with the common 0.9-kb fragment of λACHE-1-4.

than the globular form, either as the mature protein or following deglycosylation. Electrophoretic analysis of *in vitro* translation products of *Torpedo* electric organ RNA showed two distinct immunoprecipitable products migrating just slower than the corresponding deglycosylated asymmetric and globular forms (ref. 14 and data not shown). These results indicate that the different forms of acetylcholinesterase may arise from different messenger RNAs. Northern blot hybridization of *Torpedo* electric organ RNA revealed multiple RNA species remaining after high-stringency washes (Fig. 2); identical results were found when either pACHE-1a or the C-terminal (1.4 kb) fragment of pACHE-5 was used as a probe. The multiple RNA species were enriched in the poly(A)$^+$-containing lane and ranged in size from 2.2 to nearly 20 kb. The larger of these species may be due to unprocessed RNA transcripts as both nuclear and cytoplasmic RNAs are present[15]. It is plausible that multiple mRNA species are formed, as when size-fractionated RNA from human brain is microinjected into *Xenopus* oocytes, three broadly distributed

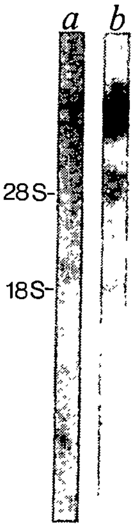

Fig. 2 Blot analysis of *T. californica* electric organ RNA using cDNA probes coding for acetylcholinesterase. Total RNA was prepared by the method of Chirgwin *et al.*[15]. Approximately 15 μg of both total (*a*) and poly(A)$^+$-selected (*b*) RNA were denatured with glyoxal, electrophoresed and transferred to nitrocellulose[38]. In addition, *Torpedo* ribosomal RNA and *Hin*dIII fragments of λ DNA were denatured identically and electrophoresed in parallel lanes as standards. Hybridization probes used were: *a*, pACHE-1a, the N-terminal *Eco*RI fragment of λACHE-1 (nucleotides 2-936) subcloned into the replicative form (RF) of M13mP8; and *b*, pACHE-5, the C-terminal *Eco*RI fragment (nucleotides 936-2,340) subcloned into M13mP8RF. Both probes were labelled with $[\alpha\text{-}^{32}\text{P}]$dATP (3,000 Ci mmol^{-1}; Amersham) by nick-translation, and used in hybridization at 5×10^6 c.p.m. per lane.

peaks of mRNA induce active cholinesterase[16]. Approximately 80% of the tryptic peptides obtained from the catalytic subunit of the asymmetric enzyme have been sequenced (K.MacP.-Q., unpublished results) and these peptides are all found within the sequence inferred from the cDNA clone λACHE-1. Furthermore, the first of two translation stop codons of ACHE-1 appears directly after the sequenced C-terminal tryptic peptide candidate. Hence, the sequence of λACHE-1 probably derives from a cDNA encoding the catalytic subunit of the asymmetric rather than the globular form of the enzyme, although a definitive assignment awaits sequencing of other cDNA clones.

A comparison of the sequence of acetylcholinesterase with proteins found in Newat[17], NBRF and Genbank (BIONET) revealed several interesting features. First, acetylcholinesterase shows neither significant sequence homology in local regions nor global homology with the four nicotinic acetylcholine receptor subunits[18-20], despite their similar specificity for inhibitory ligands[21] and a propensity for both molecules to localize in close apposition at the synapse[22]. The lack of homology is not unexpected as the dissociation constant (K_D) of acetylcholine for the desensitized state of the receptor is 1.0-3.0 nM[23,24], compared with a K_D for acetylcholinesterase of 0.1 mM[25]. These differences probably reflect receptor recognition of the acetylcholine molecule with its trigonal ester bond, whereas the active centre of acetylcholinesterase can better accommodate a tetrahedral transition state in catalysis[26].

Second, although *Torpedo* acetylcholinesterase and human butyrylcholinesterase are homologous in the active-centre region[13,27], the two cholinesterases show only limited homology around the active-centre serine with other serine hydrolases; the closest homology was found with aliesterases and carboxylesterases. However, no significant homology extending throughout the sequences was found with other serine hydrolases. The serine proteases confer nucleophilicity on the serine through a charge-relay system involving aspartate and histidine residues[28,29]. In most of these enzymes the positions of the three residues in the overall sequence are conserved. Although acetylcholinesterase contains the active-site serine (residue 200) in a similar position, we did not find a histidine within a potential cysteine loop near residue 57, as would be expected if acetylcholinesterase directly diverged from the pancreatic proteases.

There is a striking homology between acetylcholinesterase starting at residue 30 and the C-terminal domain of bovine thyroglobulin starting at residue 2,210 (ref. 8). Thyroglobulin is a high-M_r dimeric glycoprotein (2×330K) that serves as the iodinated precursor of the thyroid hormones thyroxine (T_4) and triiodothyronine (T_3). Alignment of the 546- and 540-residue segments on the two proteins shows 28% identity, with only 5 gaps in the two peptide sequences. Although the active-site serine at position 200 is not conserved, the region between residues 144 and 195 in acetylcholinesterase shows 60% residue identity with thyroglobulin. The positions of six of the eight cysteines in the homologous segments are also conserved, which suggests a similar folding pattern in the two proteins. Bovine thyroglobulin is a protein 2,750 amino acids long which contains a C-terminal domain not homologous with other portions of the peptide. As far as is known, acetylcholinesterase, being an enzyme of neurotransmitter degradation, and thyroglobulin, the precursor of T_4 and T_3, have in common only the functional property of being secreted from specialized cells.

Although the localization and abundance of acetylcholinesterase and the acetylcholine receptor are regulated by synapse formation and muscle activity, acetylcholinesterase alone exhibits extensive structural polymorphism and regulation of distribution of the individual species. The availability of cDNAs for the enzyme should now allow an examination of the regulation of the acetylcholinesterase species at the transcriptional and translational levels.

We thank Dr Toni Claudio for the cDNA library; Dr R. Doolittle for sequence analysis and for pointing out the homology with thyroglobulin; Ms Barbara Thompson for peptide isolation; Ms Patricia La Porte and Louise Schmidt for oligonucleotide synthesis; Dr M. Zoller for the oligonucleotide purification protocol; Ms D. David and Drs D. Jolly, J. Moores, J. Respess, J. Yee and S. Kim for helpful advice and support; Dr F. Esch of the Salk Institute for confirming the sequence of the CNBr peptide; and Ms S. Dutky and Ms J. Frink for preparation of the manuscript. This work was supported in part by USPHS grant GM 18360, DAMD 17-83-C-3202, and the Biomedical Research Technical Programme (BIONET) 1U41RR-01685-02. Y.M. and M.N. are recipients of Fogarty International Fellowship F05 2344 8 and USPHS Fellowship NS 07622.

Received 24 September; accepted 25 November 1985.

1. Massoulié, J. & Bon, S. *A. Rev. Neurosci.* **5**, 57-106 (1982).
2. Rosenberry, T. L. in *The Enzymes of Biological Membranes* 2nd edn, Vol. 4 (ed. Martonosi, A. N.) 403-429 (Plenum, New York, 1985).
3. Massoulié, J. *Eur. J. Biochem.* **11**, 441-455 (1969).
4. Lee, S. L., Camp, S. J. & Taylor, P. *J. biol. Chem.* **257**, 12302-12309 (1982).
5. Futerman, A. M., Fionini, R. M., Roth, E., Low, M. G. & Silman, I. *Biochem. J.* **226**, 369-377 (1985).
6. Lee, S. L., Heinemann, S. & Taylor, P. *J. biol. Chem.* **257**, 12283-12291 (1982).
7. Doctor, B. P., Camp, S., Gentry, M. K., Taylor, S. S. & Taylor, P. *Proc. natn. Acad. Sci. U.S.A.* **18**, 5767-5771 (1983).
8. Mercken, L., Simons, M. J., Swillens, S., Massaer, M. & Vassart, G. *Nature* **316**, 647-650 (1985).
9. Taylor, P. & Jacobs, N. M. *Molec. Pharmac.* **10**, 78-92 (1974).
10. Blobel, G. & Dobberstein, B. *J. Cell Biol.* **67**, 835-851 (1975).
11. Garnier, J., Gaye, P., Mercier, J. C. & Robson, B. *Biochimie* **62**, 231-239 (1980).
12. Kyte, J. & Doolittle, R. *J. molec. Biol.* **157**, 105-132 (1982).
13. MacPhee-Quigley, K., Taylor, P. & Taylor, S. S. *J. biol. Chem.* **260**, 12185-12189 (1985).
14. Sikorav, J. L., Grassi, J. & Bon, S. *Eur. J. Biochem.* **145**, 519-529 (1984).
15. Chirgwin, J. M., Przybyla, A. E., McDonald, R. J. & Rutter, W. J. *Biochemistry* **18**, 5294-5299 (1979).
16. Soreq, H., Zeyin-Sankin, D. & Razon, N. *EMBO J.* **3**, 1371-1375 (1984).
17. Doolittle, R. F. *Science* **214**, 149-159 (1981).
18. Claudio, T., Ballivet, M., Patrick, J. & Heinemann, S. *Proc. natn. Acad. Sci. U.S.A.* **80**, 1111-1115 (1983).
19. Noda, M. *et al. Nature* **299**, 793-797 (1982).
20. Noda, M. *et al. Nature* **301**, 251-255 (1983).
21. Changeux, J. P. *Molec. Pharmac.* **2**, 369-392 (1966).
22. Fallon, J. R., Nitkin, R. M., Reist, N. E., Wallace, B. G. & McMahan, U. J. *Nature* **315**, 571-574 (1985).
23. Taylor, P., Brown, R. D. & Johnson, D. A. *Curr. Topics Membranes Transport* **18**, 407-444 (1983).
24. Changeux, J.-P., Devilers-Thiery, A. & Chemouilli, P. *Science* **225**, 1335-1345 (1984).
25. Rosenberry, T. L. *Adv. Enzym. Relat. Areas molec. Biol.* **43**, 102-218 (1975).
26. Taylor, P. & Jacobs, N. M. *Molec. Pharmac.* **10**, 93-107 (1974).
27. Lockridge, O. in *Cholinesterases: Fundamental and Applied Aspects* (eds Brzin, M., Barnard, E. A. & Sket, D.) 5-11 (Walter de Gruyter, Berlin, 1984).
28. Hartley, B. S. *Phil. Trans. R. Soc.* **B257**, 77-87 (1970).
29. Davie, E. W., Fujikawa, K., Kurachi, K. & Kisiel, W. *Adv. Enzym.* **48**, 277-318 (1979)
30. Messing, J. *Meth. Enzym.* **101**, 20-78 (1983).
31. Sanger, F., Nicklen, S. & Coulson, A. R. *Proc. natn. Acad. Sci. U.S.A.* **74**, 5463-5467 (1977).
32. Staden, R. *Nucleic Acids Res.* **8**, 3673-3694 (1980).
33. Bause, E. *Biochem. J.* **209**, 331-336 (1983).
34. Benton, W. D. & Davis, R. W. *Science* **196**, 180-182 (1977).
35. Sinha, N. D., Biernat, J., McManus, J. & Koster, H. *Nucleic Acids Res.* **12**, 4539-4557 (1984).
36. Wallace, R. B. *et al. Nucleic Acids Res.* **9**, 879-894 (1981).
37. Davis, R. W., Botstein, D. & Roth, J. R. *Advanced Bacterial Genetics*, 70-82 (Cold Spring Harbor Laboratory, New York, 1980).
38. Thomas, P. S. *Meth. Enzym.* **100**, 255-266 (1983).

Single channels and ionic currents in peptidergic nerve terminals

José R. Lemos*, Jean J. Nordmann*, Ian M. Cooke & Edward L. Stuenkel*

Békésy Laboratory of Neurobiology, University of Hawaii,
1993 East-West Road, Honolulu, Hawaii 96822, USA

Control of secretion, by a mechanism in which membrane depolarization leads to Ca^{2+} entry[1], has been extensively studied. The small size and inaccessibility of most nerve terminals, however, have precluded direct analysis of membrane ionic currents and their influence on secretion (with some notable exceptions[2,3]). Recently, patch-clamp methods have been applied to several secretory systems[4–6] for both voltage-clamp and single-channel recordings. We now report the extension of this analysis to isolated peptidergic nerve terminals. We used terminals obtained from a crustacean neurohaemal organ, the sinus gland. Analyses of currents under whole-terminal voltage clamp showed inward currents carried by Na^+ and by Ca^{2+}, and outward currents carried predominantly by K^+. Furthermore, we have observed two types of single-channel currents that may be unique to nerve terminals. Both show little selectivity between Na^+ and K^+. The first channel is activated by intracellular Na^+ and the second by intracellular Ca^{2+}. These channels have conductances of 69 and 213 pS, respectively, in symmetrical 310 mM KCl. It should now be possible to compare electrical activity recorded intracellularly from intact nerve endings[7,8], with whole-cell and single-channel currents and with the release of peptide neurohormones from isolated neuronal terminals.

Sinus gland terminals from the land crab, *Cardisoma carnifex*, are easily isolated after treatment with collagenase (see Fig. 1). In electron micrographs the isolated nerve endings appear as circular profiles densely packed with neurosecretory granules (Fig. 1*C*). Dissociated neuronal terminals are morphologically very similar to non-dissociated nerve endings *in situ* (compare with Fig. 1*A*). The same morphologically distinguishable terminal types as those observed *in situ*[9] can be recognized among the isolated terminals (Fig. 1*C*). A single *C. carnifex* sinus gland yields hundreds of isolated terminals, many of diameter >10 μm (Fig. 1*B*). The terminals readily form seals of >10 GΩ with fire-polished electrodes, making feasible the application of patch-clamp techniques[10] in order to characterize the ionic currents and channels of the nerve terminal membrane. Dissociated nerve terminals exhibit resting potentials between −30 and −50 mV (intact nerve endings have values of −50 to −60 mV[8]) and spontaneous overshooting action potentials. These and other observations, reported below, show that the nerve terminals, after dissociation, are viable and comparable to nerve endings *in situ*.

Currents in isolated nerve terminals were recorded under voltage clamp by 'whole-terminal recording' in analogy with whole-cell recording[10]. In response to depolarizing voltage commands, the initial current was inward, followed by outward, maintained current (Fig. 2*A*). In some nerve terminals, the inward current has the properties expected of a Ca current[11]: it is not blocked by tetrodotoxin (TTX) [Fig. 2*A*(ii)], it is reduced by external application of Cd^{2+} [Fig. 2(iii)], and it begins to 'run down' after 30-40 min. The Ca current relaxes more slowly in certain terminals, which could explain observed differences in the release pattern. Release of red-pigment-concentrating hormone[12] is brief and is associated with a voltage-dependent Ca entry which inactivates[13], while the release of other peptides is more prolonged and is probably associated with non-inactivating Ca entry[8]. In some terminals a Cd^{2+}-resistant component [Fig. 2*B*(ii)] was blocked by TTX [Fig. 2*B*(iii)]. Thus, there are two inward currents: one carried by Na^+ and the other by Ca^{2+}. This was expected as previous studies showed that most crab nerve endings exhibit overshooting action potentials having both Na^+ and Ca^{2+} components[7,8,14]. Outward currents were partially reduced by the application of tetraethylammonium (TEA; Fig. 2*A*) (consistent with an increase by TEA of the duration of the action potential in intact terminals[14]) and totally blocked if the terminal was internally perfused with Cs^+ (Fig. 2*B*). These results indicate that the outward currents are carried by K^+.

Single-channel currents were recorded from terminals in cell-attached and inside-out patches with 310 mM KCl on both sides of the patch. Two types of ionic channels—possibly unique to nerve terminals—were observed: (1) the f channel (for 'first') shows brief (millisecond) transitions to the open state, sometimes occurring in bursts, with long (seconds) intervals between openings [Fig. 3*A*(i)]. This channel, in symmetrical K^+ (□), has a mean slope conductance of 69±3.6 pS ($n=6$) (Fig. 3*C*). The single-channel *I–V* curve is not changed by substitution of K_2SO_4 (data not shown) or Na_2SO_4 (▲) for KCl on the external (or internal) face of the patch, but shows rectification when CsCl (●) is substituted, indicating failure of the channel to pass Cs^+ or Cl^- (Fig. 3*C*). Channel currents in the presence of a salt gradient show nearly perfect selectivity for cations as opposed to anions (see, for example, Fig. 3*A*). With a fourfold salt gradient (external NaCl concentration = 310 mM, internal NaCl concentration = 78 mM; osmolarity preserved with sucrose) we found that these currents reversed at +35 mV, as would be expected for a perfectly cation-selective channel. These two observations argue against a significant anion permeability of the channels. Na^+ passes through the channel just as easily as K^+ because the reversal potential with equal concentrations of KCl externally and NaCl internally remained at 0 mV (data not shown). Furthermore, this (420 mM) and lower (for example, 78 mM) concentrations of Na^+ on the inside of the patch, caused this type of cation channel to remain open for longer periods [Fig. 3*A* (ii)] on depolarization. This channel can be observed in solutions having the internal Ca^{2+} concentration ($[Ca^{2+}]_i$) buffered to 10^{-8} M with EGTA.

(2) The other type of channel (s, for 'second') exhibits much longer (seconds) openings (Fig. 3*B*) and has a mean conductance (Fig. 3*D*) of 213±6.1 pS ($n=4$) in symmetrical K^+ (□). The openings seem to occur in bursts with rapid flickering back to the closed state. This channel type is rarely observed in solutions having low $[Ca^{2+}]_i$ (data not shown), except during large voltage steps (+80 mV), but is activated by increasing the internal free Ca^{2+} concentration to >1 μM (see Fig. 3*B*). Higher concentrations of Ca^{2+} cause a transient activation of channel activity. Ion substitution experiments indicate that this channel also has nearly equal permeabilities for Na^+ (△) and K^+(□), but, unlike the f channel, it allows Cs^+ (●) to pass through (Fig. 3*D*). Inward current events having the characteristics of this large channel can be observed in whole-terminal recordings, under voltage clamp, with crab saline[15] in the bath. The s channel, therefore, has the characteristics of a Ca-activated cation channel[16], but exhibits a much larger slope conductance than has been observed in other cells (22-38 pS[6,16,17]). This channel could be termed the 'maxi' Ca-activated cation channel, in analogy with Ca-activated K^+ channels[18]. The f channel is seen in almost every patch, but the other, larger s channel occurs less frequently; this could be caused by our use of low Ca^{2+} concentrations to achieve the inside-out configuration.

One could conceive of a scheme by which Na^+ and/or Ca^{2+} entry activates the channel(s), which then becomes inactivated by Ca^{2+} after a period of seconds. These channels could be responsible for the long-lasting plateau potentials which underlie bursting in these terminals[7,19]. Burst patterns lead to the potentiation of hormone release, for example, in the isolated

---

* Present addresses: Worcester Foundation for Experimental Biology, 222 Maple Avenue, Shrewsbury, Massachusetts 01545, USA (J.R.L.); Centre de Neurochimie, 67084 Strasbourg, France (J.J.N.); Department of Physiology, University of California, San Francisco, California 94143, USA (E.L.S.).

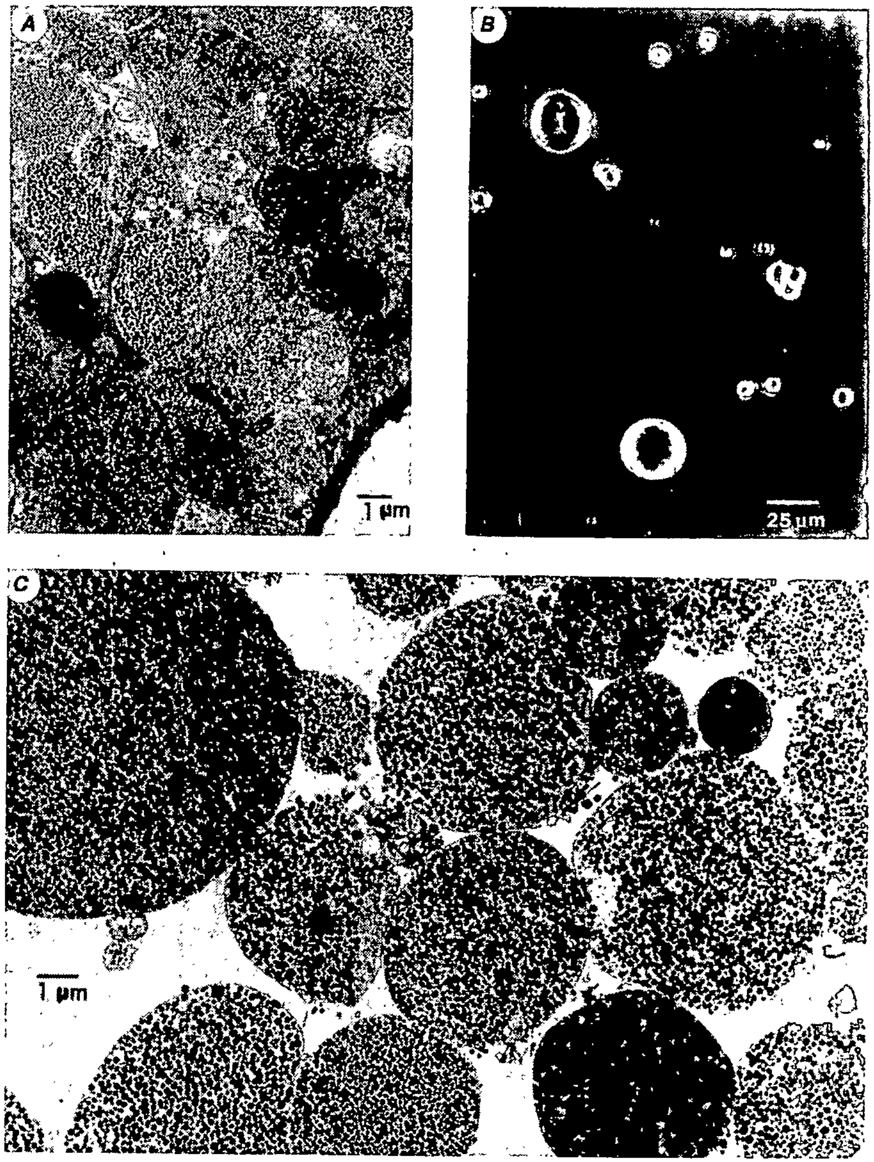

Fig. 1 *A*, Electron micrograph of intact sinus gland showing the dense aggregation of terminals and of neurosecretory granules within terminal profiles. Note the large size (5-30 µm diameter) of the terminals, the paucity of non-terminal structures, and the close apposition of the terminals to epineurium and blood sinus (where the scale bar = 1 µm) is located). *B*, Phase-contrast micrograph of dissociated nerve terminals after isolation for patch-clamping experiments. Two large terminals (~25 µm in diameter) can be seen in this field. Note the variety of sizes (corresponding to *in situ* distribution), paucity of non-terminal material, and abundance of terminal structures. *C*, Electron micrograph of isolated nerve endings. Note that the nerve terminals are membrane-delimited and still densely packed with neurosecretory granules; they are comparable to nerve endings in the intact sinus gland (see *A*).

Methods. Isolation of peptidergic neurosecretory terminals. The sinus gland was exposed to collagenase (1 mg ml^{-1}) for 30 min at 32 °C (this treatment does not affect channel activity, but does lead to better seals on the terminal membrane), rinsed, dissociated by drawing the gland in and out of a pipette tip in an 'intracellular-type' medium [(in mM): 300 KCl, 15 NaCl, 2 EGTA, 100 HEPES (*p*H 7.2), 2 $\mathrm{MgCl_2}$, 0.3 $\mathrm{CaCl_2}$, 2 ATP, 530 sucrose, giving a free $\mathrm{Ca^{2+}}$ concentration of 10 nM] and then returned to crab saline[15] containing 5 mM glucose. Care was taken when changing solutions so that the terminals were never exposed to conditions where release would occur (that is, elevated [$\mathrm{K^+}$] with [$\mathrm{Ca^{2+}}$] greater than 100 nM). The isolated nerve endings were then attached to the bottom of a plastic dish which had been treated previously with 1% protamine sulphate. For electron microscopy, the nerve terminals were centrifuged, fixed with 4% glutaraldehyde in 0.1 M cacodylate *p*H 7.0, containing 400 mM sucrose, and post-fixed with 1% $\mathrm{OsO_4}$.

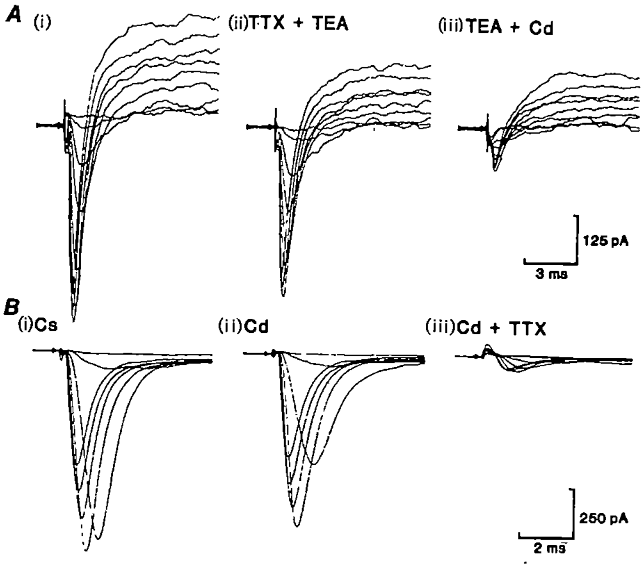

Fig. 2 Activation of whole-cell currents in dissociated sinus gland nerve terminal during depolarizing voltage steps from a holding potential equal to the normal resting potential (−50 mV). Note that the magnitude of the currents is directly related to the size of the terminal (compare *A* with *B*), as might be expected from differences in their membrane surface area. All records are leak-subtracted. *A*(i), Appearance of both inward and outward currents during clamp steps to membrane potentials of −25 mV to +15 mV, incremented by +5 mV each time; 10 s between steps. Isolated nerve ending of 10 µm diameter. (ii) Effect of TEA. Same protocol as for *A*(i). Note the partial reduction of the inward currents in 6×10^{-7} M TTX. (iii) Effect of $\mathrm{Cd^{2+}}$ on inward currents. Perfusion with 1 mM $\mathrm{Cd^{2+}}$ of the same terminal (but in 50 mM TEA) caused a marked reduction of the inward currents. *B*(i), Effect of $\mathrm{Cs^+}$ on outward currents in a different nerve terminal (15 µm diameter). Same protocol as in *A*, except that steps were from −25 mV to +35 mV in 10 mV increments, and $\mathrm{K^+}$ was replaced by $\mathrm{Cs^+}$ in the patch pipette, resulting in an absence of outward currents [compare with *A*(i)]. (ii) 1 mM $\mathrm{Cd^{2+}}$ had little effect on inward currents in this terminal. Same protocol as for *B*(i). (iii) Perfusion of 6×10^{-7} M TTX blocked residual inward current in this nerve ending.

Methods. Standard patch-clamp recording techniques[10] were used to attain whole-cell configurations with seal resistances of >10 GΩ from dissociated nerve terminals of the sinus gland. The nerve endings were perfused with crab saline[15] externally and the pipette contained 'intracellular-type' medium (see Fig. 1 legend). In *B*, 315 mM CsCl replaced both KCl and NaCl in the patch pipette. All solutions were made osmotically equivalent by either reducing the NaCl concentration or adding sucrose.

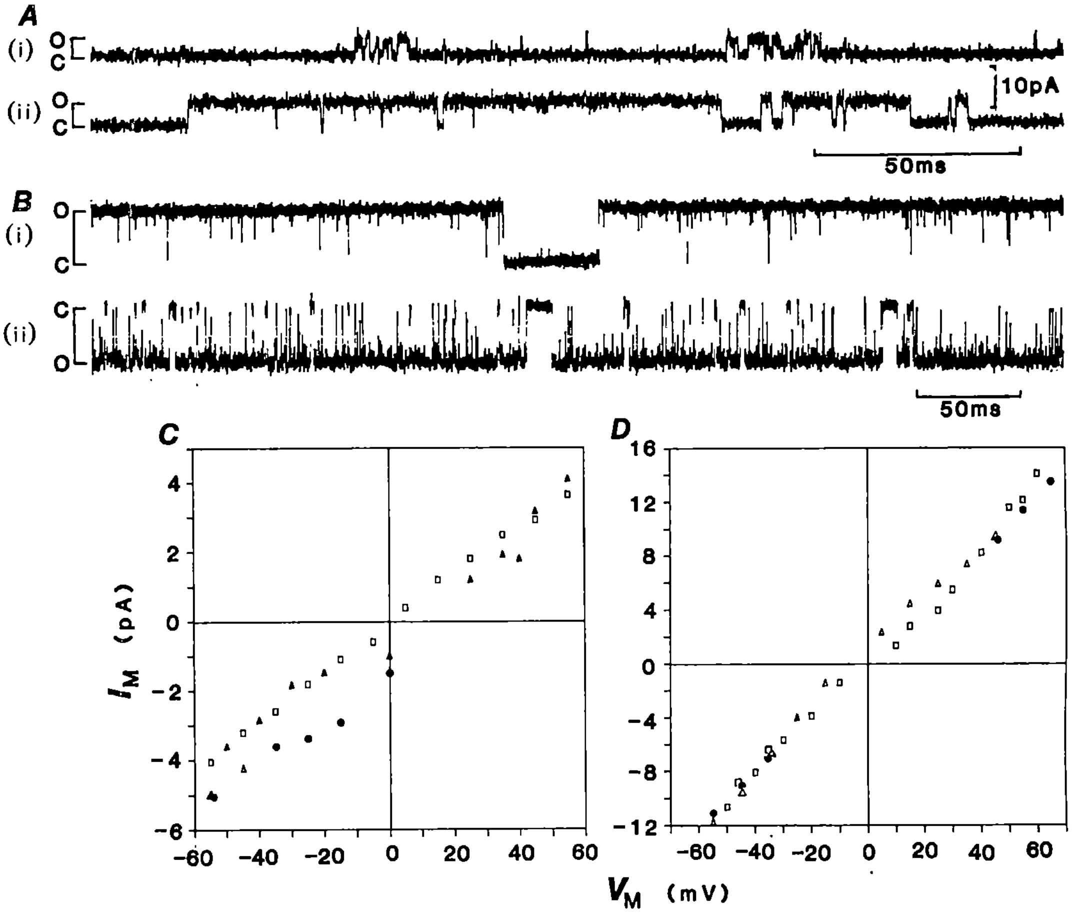

Fig. 3 Single-channel currents from inside-out patches showing two types of cation channels observed in isolated nerve terminals. *A*, First ('f') channel type: (i) patch held at +55 mV in symmetrical KCl. Note the bursts of channel openings. Upward openings (O) indicate outward current. (ii) Same patch held at +45 mV with 310 mM KCl outside and 210 mM Na_2SO_4 inside. Note the increased duration of the openings. Similar effects were seen with 78 mM NaCl (comparable to concentrations of Na^+ which activate a cardiac outward current[23]) on the inside of the patch. The similar amplitude as at +55 mV (i) is the result of a shift in the I-V relationship due to the assymetrical salt gradient and is in the direction predicted by the Nernst equation for a cation-selective channel. The increased duration of openings is not caused by a difference in holding potential. *B*, Second ('s') channel type: (i) patch held at +55 mV with 310 mM KCl inside and 210 mM Na_2SO_4 outside, and with 3 μM $[Ca^{2+}]_i$. (ii) Same patch as (i) but held at −40 mV. Note the similar amplitude as that obtained at +55 mV, resulting from a shift in the I-V relationship due to the asymmetrical salt gradient, again in the direction predicted for a cation-selective channel. Channel openings are rarely, if ever, seen at these potentials if the $[Ca^{2+}]_i$ is less than 10^{-6} M. Downward openings indicate inward current. All records are at the same gain to emphasize the difference in size of the two channel types. *C*, I-V relationship of the f channel. Channel openings of small amplitude (I_M) and short duration (see *A*) were plotted against patch potential (V_M). The calculated regression has a slope conductance of 69 pS ($r = 0.99$; $n = 6$) in symmetrical KCl (□). Note that there was little change in conductance when KCl in the external solution was replaced by 210 mM Na_2SO_4 (▲), but rectification occurred when it was replaced in the internal solution by 310 mM CsCl (●). *D*, I-V relationship of the s channel. Channel openings of larger amplitude and longer duration (see *B*) were plotted against patch potential. The calculated regression has a slope conductance of 213 pS ($r = 0.95$; $n = 4$) in symmetrical KCl (□). Note that there was little change in conductance when KCl in the internal solution was replaced by either 210 mM Na_2SO_4 (△) or 310 mM CsCl (●).

Methods. Standard patch-clamp recording techniques[10] were used to form 'inside-out' patches with seal resistances of >10 GΩ from dissociated nerve terminals of the sinus gland. Records in *A* and *B* were filtered at 4 kHz with 8-pole Bessel characteristics. In *C* and *D* mean channel current values, with symmetrical solutions (310 mM KCl, 2 mM $MgCl_2$, 2 mM ATP, 485 mM sucrose, 100 nM free Ca^{2+} buffered with 2 mM EGTA, 100 mM HEPES *p*H 7.2) on both sides of the patch (□) or substitutions as outlined above, are plotted.

neurohypophysis[20,21]. These two types of channels may also help to explain Na enhancement of transmitter release at crustacean neuromuscular junctions[22].

We thank Drs I. Levitan and S. Treistman for critical comments on the manuscript and Drs R. Latorre, C. Miller and G. Yellen for helpful discussions. This work was supported by grants NS15453 and BNS81-07289 to I.M.C., NATO and Fondation de la Recherche Médicale grants to J.J.N. and National Service Award NS07072 to J.R.L.

Received 22 August; accepted 22 November 1985.

1. Douglas, W. W. *Br. J. Pharmac.* **34**, 451-474 (1968).
2. Katz, B. & Miledi, F. *J. Physiol., Lond.* **192**, 407-436 (1967).
3. Llinas, R., Steinberg, I. Z. & Walton, K. *Biophys. J.* **33**, 289-322 (1981).
4. Fenwick, E. M., Marty, A. & Neher, E. *J. Physiol., Lond.* **331**, 557-597 (1982).
5. Kidokoro, Y. in *The Electrophysiology of the Secretory Cell* (eds Poisner, A. M. & Trifaro, J. M.) 195-218 (Elsevier, New York, 1985).
6. Maruyama, Y. & Petersen, O. H. *Nature* **299**, 159-161 (1982).
7. Cooke, I. M. *J. exp. Biol.* **118** (in the press).
8. Stuenkel, E. L. *J. Physiol., Lond.* **359**, 163-187 (1985).
9. Weatherby, T. M. *Cell Tissue Res.* **220**, 293-312 (1981).
10. Hamill, O. P., Marty, A., Neher, E., Sakmann, B. & Sigworth, F. J. *Pflügers Arch. ges. Physiol.* **391**, 85-100 (1981).
11. Hagiwara, S. & Byerly, L. *A. Rev. Neurosci.* **4**, 69-125 (1981).
12. Fernlung, P. & Josefsson, L. *Science* **177**, 173-175 (1972).
13. Cooke, I. M. & Haylett, B. A. *J. exp. Biol.* **113**, 289-321 (1984).
14. Nagano, M. & Cooke, I. M. in *Neurosecretion: Molecules, Cells, Systems* (eds Farner, D. & Lederis, K.) 501-502 (Plenum, New York, 1981).
15. Pantin, C. F. A. *Notes on Microscopical Technique for Zoologist* (Cambridge University Press, 1948).
16. Colqhoun, D., Neher, E., Reuter, H. & Stevens, C. F. *Nature* **294**, 752-754 (1981).
17. Yellen, G. *Nature* **296**, 357-359 (1982).
18. Latorre, R. & Miller, C. *J. Membrane Biol.* **71**, 11-30 (1983).
19. Cooke, I. M. & Stuenkel, E. L. in *The Electrophysiology of the Secretory Cell* (eds Poisner, A. M. & Trifaro, J. M.) 115-164 (Elsevier, New York, 1985).
20. Dutton, A. & Dyball, R. E. J. *J. Physiol., Lond.* **348**, 601-613 (1984).
21. Cazalis, M., Dayanithi, G. & Nordmann, J. J. *J. Physiol., Lond.* **369**, 45-60 (1985).
22. Atwood, H. L., Charlton, M. P. & Thompson, C. S. *J. Physiol., Lond.* **335**, 179-195 (1983).
23. Kameyama, M. *et al.* *Nature* **309**, 354-356 (1984).

Neonatal T-cell tolerance to minimal immunogenic peptides is caused by clonal inactivation

Guy Gammon, Karen Dunn, Nilabh Shastri, Alan Oki, Stanley Wilbur & Eli E. Sercarz

Department of Microbiology, University of California at Los Angeles, Los Angeles, California 90024, USA

The mechanisms underlying T-lymphocyte tolerance induced in neonatal mice are still unknown[1-3]. It is unclear whether the tolerant state is the result of inactivation of T cells on exposure to antigen during development or of active suppression by other T cells specific for the same antigen. To distinguish between these two hypotheses, we have analysed the specificity of tolerance to three cytochrome peptides which differ by only a single amino-acid substitution in the epitope recognized by proliferative T cells. The peptides stimulate proliferative responses which are highly specific with minimal cross-reactivity. As antigen-induced clonal inactivation would address the same cells normally activated by that antigen, the specificity of tolerance should exactly match that of the proliferative response to the antigen, and each cytochrome peptide should induce tolerance to itself alone. Conversely, as T-suppressor (T_s) and T-proliferative (T_p) cells almost invariably seem to recognize distinct, non-overlapping determinants on protein antigens (see, for example, refs 4–6), suppressor-mediated tolerance should not be affected by substitutions in the proliferative T-cell epitope. Tolerance would depend solely on the existence of a shared suppressor determinant, so each cytochrome peptide should induce cross-tolerance to the others. We found that the specificity of tolerance matched that of the proliferative response: each peptide induced tolerance for itself but the response to the variants was unaltered. This result strongly supports the hypothesis of clonal inactivation as an important mechanism in induction of neonatal tolerance.

Three peptides were used in this study: K99, which corresponds to amino acids 93-103 of moth cytochrome *c*, and two variants with glutamine or arginine substituted for lysine at residue 99 (Q99 and R99 respectively). These peptides are close to the minimal size for induction of a proliferative response[7]; further shortening of this 11-amino-acid C-terminal peptide of cytochrome *c* substantially reduces its ability to stimulate a response[8]. Furthermore, these peptides were chosen because amino-acid residue 99 has been shown to form a critical part of the major proliferative T-cell epitope on cytochrome *c*[8,9], and substitutions at this site radically alter the composition of the responding population. Thus, lymph node cells from adult B10.A mice which had been immunized with K99, R99 or Q99 gave *in vitro* proliferative responses that were highly specific with little cross-reactivity between the peptides (Fig. 1).

Tolerance to each peptide was induced in neonatal B10.A mice by two injections of peptide at 24 and 72 h after birth and the specificity of tolerance was tested in each group by challenge with the peptides at 8-10 weeks. Figure 2*a* shows the responses of K99-tolerant mice to K99, Q99 and R99. Neonatal administration of K99 induced essentially complete tolerance to itself with only a minimal response even at the highest *in vitro* concentration of the peptide. However, these K99-tolerant mice (broken lines in Fig. 2*a*) responded normally on immunization with the other peptides, Q99 and R99, compared with the control responses (solid lines). Figure 2*b, c* shows the results of reciprocal experiments in the Q99- and R99-tolerant groups. The results were comparable: tolerance was specific for the peptide used for its induction and the response to the other peptides was unaffected. Thus, the specificity of tolerance is dependent on substitutions in the proliferative T-cell epitope, and the absence of cross-tolerance between peptides matches the lack of cross-reactivity in the normal response. These data support the hypothesis of clonal inactivation, and exclude a mechanism of suppression by cells recognizing an epitope distinct from the proliferative epitope, which would cause tolerance to be cross-reactive.

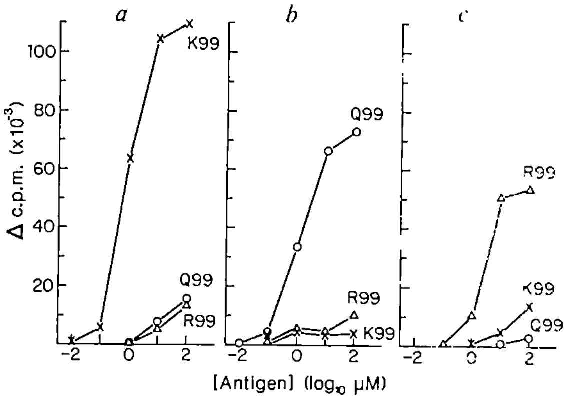

Fig. 1 Specificity profiles of T cells induced by synthetic cytochrome peptides in B10.A mice. The mice were immunized with K99 (*a*), Q99 (*b*) or R99 (*c*). The peptides were prepared by solid-phase peptide synthesis and purified by reverse-phase HPLC using a preparative C_8 column and a solvent system of 0.1% trifluoroacetic acid with an increasing gradient of acetonitrile. Peptide K99 corresponds to the 11 carboxy-terminal amino acids of moth cytochrome *c*, amino acids 93–103 (NH_2-ELIAYL*K*QATK-COOH). Q99 and R99 are variants with glutamine or arginine substituted for lysine at residue 99.

Methods. B10.A mice (8–10 weeks old) were immunized with 5 μg of peptide in saline in a 1:1 emulsion with complete Freund's adjuvant (CFA; Difco) in the hind footpads. After 10 days, popliteal and inguinal lymph nodes were removed and cells from each group (three mice) were pooled. The lymph node cells were washed twice in balanced salt solution and added to 96-well plates at 4×10^5 per well in Click's medium supplemented with penicillin/streptomycin, glutamine, sodium pyruvate, 2-mercaptoethanol and 0.5% normal mouse serum, as well as a range of *in vitro* antigen concentrations (0.01–100 μM). The cultures were incubated for 5 days in 2% CO_2, 98% air at 37°C and 1 μCi ^3H-thymidine (ICN 27 Ci $mmol^{-1}$) was added for the last 18 h The cells were collected onto glass fibre sheets and incorporation of labelled thymidine was measured by scintillation counting All cultures were performed in triplicate and the results shown are the arithmetic mean c.p.m. per culture with the background (medium alone) subtracted. The standard errors of the mean were all less than 10,000 c.p.m. and have been omitted for clarity. (27 Ci $mmol^{-1}$; International Chemical & Nuclear.)

Although, *a priori*, it may seem unlikely that a T_s-inducing and a T_p-inducing determinant would coexist on an 11-amino-acid peptide, the possibility of an overlapping suppressor cell epitope should be considered. As the tolerance we have described is peptide-specific, if T_s were involved, they too would have to be non-cross-reactive and recognize an epitope including the unique residue 99. Such suppressor cells could not interact with their targets directly via an antigen bridge but could act by secretion of nonspecific suppressor factors. Functionally, this suppression would be antigen-specific despite the nonspecific effector mechanism as, for example, K99-specific T_s would be activated only by K99 and not by Q99 or R99. This hypothesis was tested by co-immunization of tolerant mice with a mixture of two peptides, one of which had been used to induce tolerance. Clonal inactivation of the T cells specific to one peptide should not affect the response to a second peptide. However, suppression which was nonspecific in the effector phase would inhibit the response to both peptides equally. The experiment shown in Fig. 3 demonstrates that K99-tolerant mice that were co-immunized with a mixture of K99 and R99 gave a nearly normal response to R99. The difference between the normal R99 response and the R99 response in K99-tolerant mice can be

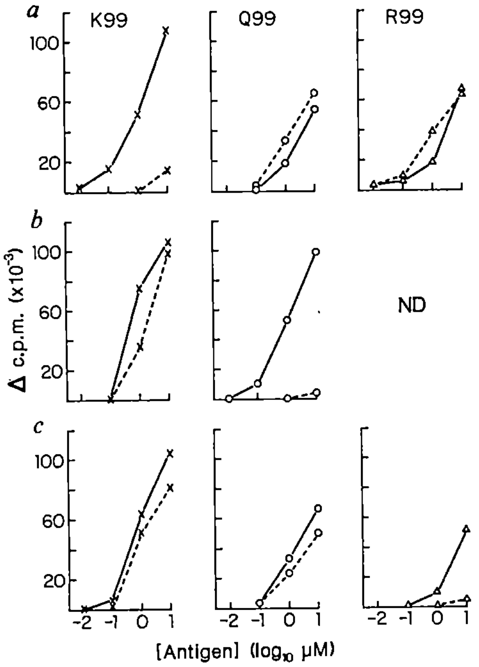

Fig. 2 The specificity of tolerance induced in neonatal mice. Tolerance was induced in neonatal B10.A mice by a method similar to that described previously[10]. Peptide (20 µg) in incomplete Freund's adjuvant (Gibco) was injected into the peritoneal cavity at 24 and 72 h after birth. The mice were immunized at 8–10 weeks of age and their responses measured in an *in vitro* proliferation assay as described in Fig. 1 legend. *a*, The proliferative response of K99-tolerant mice (broken line) compared with normal age- and sex-matched B10.A mice (solid line), and immunization with (from left to right) K99, Q99 or R99. The same peptide as used for immunization was added to the *in vitro* cultures at concentrations from 0.01 µM to 10 µM. *b*, *c*, The response of Q99- and R99-tolerant mice, respectively, compared with that of normal controls. ND, not determined.

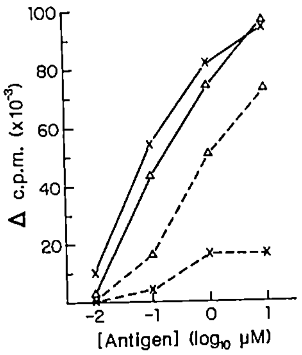

Fig. 3 The response of K99-tolerant mice after co-immunization with a mixture of K99 and R99 peptides. Tolerance was induced to K99 as described in Fig. 2 legend, and the mice were immunized at 8 weeks old with a mixture of K99 and R99 (5 µg of each) in CFA. The proliferative response of tolerant (broken lines) and age- and sex-matched normal mice (solid lines) to each peptide was assayed *in vitro*. Δ, Response to R99; ×, response to K99.

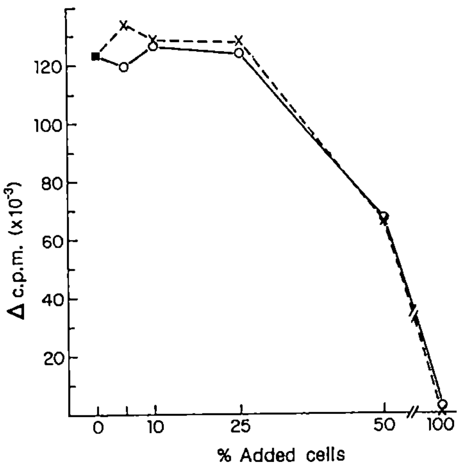

Fig. 4 Effect of the addition of lymph node cells from tolerant mice to normal primed cells, on the K99 proliferative response. K99-tolerant B10.A mice were challenged with K99 and the pooled unfractionated, tolerant lymph node cells (×---×) were added in increasing proportions to the cells from normal primed mice. The immunization and culture conditions were as described in Fig. 1 legend. The control wells contained equivalent numbers of lymph node cells from CFA/saline-primed B10.A mice added to the responsive cells (○—○). The number of cells per well was kept constant at 4×10^5, and the *in vitro* antigen used was K99 (10 µM).

explained by the loss of the small K99/R99 cross-reactive population seen in Fig. 1. These results exclude the possibility of T$_s$ cells acting by a nonspecific effector mechanism.

To obtain direct evidence for possible active suppression, tolerant cells were mixed *in vitro* with normal, primed cells. The ability of T$_s$ to prevent a proliferative response has been demonstrated in several systems[10-12]. Lymphocytes from tolerant mice or from complete Freund's adjuvant (CFA)/saline-primed mice were added to the responsive T cells (Fig. 4), but there was no difference between the groups. No indication of suppression was seen over a wide range of cell–cell ratios. Even when tolerant cells constituted a large proportion of the cells in culture, and the number of responsive proliferative cells was limiting, no suppression was observed. Previous work has shown in adult-induced tolerance to hen egg-white lysozyme (HEL), that *in vitro* suppression of the plaque-forming cell response can be masked by other regulatory T cells and can be revealed by removing Lyt 1$^+$2$^+$ cells from the tolerant lymph node population (A.O. and E.E.S., unpublished). However, treatment of lymphocytes from cytochrome *c*-tolerant mice, using the same protocol, failed to unmask suppression (data not shown).

The results presented here strongly support clonal inactivation as an important mechanism in induction of neonatal tolerance. In the case of tolerance to minimal immunogenic cytochrome peptides, it appears to be the only mechanism involved. Both antigen-bridging suppression, which is responsible for tolerance to native HEL in adult B10.A mice[13], and suppression by nonspecific suppressor factors, have been excluded in the present study. However, suppression by T$_s$ which directly recognize idiotopes on the proliferative T cells cannot be eliminated, although we consider this unlikely, especially as there was no evidence of suppression on mixing tolerant and normal responding cells. The failure to demonstrate suppression using these minimal immunogenic peptides is not inconsistent with reports of suppressor cell induction by neonatal administration of native proteins[3,14]; instead, it supports the concept that the T$_s$- and T$_p$-inducing determinants on proteins are inherently different and even in the neonatal milieu, T$_p$-inducing determinants do not activate T$_s$. One would expect that a small peptide which bears a suppressor determinant would induce T$_s$ in neonatal mice and subsequently suppress the response to the whole molecule. Thus, both mechanisms—clonal inactivation and suppression—could have a complementary role in induction and maintenance of tolerance. We propose that clonal inactivation is a primary mechanism of T-cell tolerance to proteins and the only mechanism involved in tolerance to minimal immunogenic peptides.

This work was supported by NSF grant PCM83-02679 and NIH grant AI-11183. We thank Lisa Yeaton for preparing the manuscript and Margaret Kowalczyk for preparing the figures.

Received 17 September; accepted 22 November 1985.

1. Nossal, G. J. V. *A. Rev. Immun.* **1**, 33–62 (1983).
2. Weigle, W. O. *Adv. Immun.* **30**, 159–273 (1980).
3. Loblay, R. H., Fazekas de St Groth, B., Pritchard-Briscoe, H. & Basten, A. *J. exp. Med.* **157**, 957–973 (1983).
4. Adorini, L., Harvey, M. A., Miller, A. & Sercarz, E. E. *J. exp. Med.* **150**, 293–306 (1979).
5. Kryzch, U., Fowler, A. & Sercarz, E. E. in *Protein Conformation as an Immunological Signal* (eds Celada, F., Schumaker, N. & Sercarz, E. E.) 395–408 (Plenum, London, 1983).
6. Swanborg, R. H. *J. Immun.* **114**, 191–194 (1975).
7. Thomas, D. W., Meltz, D. S. K. & Wilner, G. D. *J. Immun.* **123**, 759–764 (1979).
8. Hansburg, D., Fairwell, T., Schwartz, R. H. & Appella, E. *J. Immun.* **131**, 319–328 (1983).
9. Schwartz, R. H. *A. Rev. Immun.* **3**, 237–261 (1985).
10. Araneo, B. A. & Kapp, J. A. *J. Immun.* **125**, 118–128 (1980).
11. Yowell, R. L., Araneo, B. A., Miller, A. & Sercarz, E. E. *Nature* **279**, 70–71 (1979).
12. Ikezawa, Z. *et al. J. Immun.* **131**, 1646–1649 (1983).
13. Oki, A. N. & Sercarz, E. E. *J. exp. Med.* **161**, 897–911 (1985).
14. Waters, R. H., Pilarski, L. M., Wegmann, T. G. & Diener, E. *J. exp. Med.* **149**, 1134–1151 (1979).

Molecular cloning and expression of cDNA for human granulocyte colony-stimulating factor

Shigekazu Nagata, Masayuki Tsuchiya, Shigetaka Asano, Yoshito Kaziro, Tatsumi Yamazaki*, Osami Yamamoto*, Yuichi Hirata*, Naoki Kubota*, Masayoshi Oheda*, Hitoshi Nomura* & Masayoshi Ono*

Institute of Medical Science, University of Tokyo,
4-6-1 Shirokanedai, Minato-ku, Tokyo 108, Japan
* New Drug Research Laboratories, Chugai Pharmaceutical Co.,
3-41-8 Takada, Toshima-ku, Tokyo 171, Japan

Granulocyte colony-stimulating factor (G-CSF) is a member of the CSF family of hormone-like glycoproteins that regulate haematopoietic cell proliferation and differentiation[1,2], and G-CSF almost exclusively stimulates the colony formation of granulocytes from committed precursor cells in semi-solid agar culture[2]. Recently, Nomura *et al.*[3] have established a human squamous carcinoma cell line (designated CHU-2) from a human oral cavity tumour which produces large quantities of CSF constitutively, and the CSF produced by CHU-2 cells has been purified to homogeneity from the conditioned medium. We have now determined the partial amino-acid sequence of the purified G-CSF protein, and by using oligonucleotides as probes, have isolated several clones containing G-CSF complementary DNA from the cDNA library prepared with messenger RNA from CHU-2 cells. The complete nucleotide sequences of two of these cDNAs were determined and the expression of the cDNA in monkey COS cells gave rise to a protein showing authentic G-CSF activity. Furthermore, Southern hybridization analysis of DNA from normal leukocytes and CHU-2 cells suggests that the human genome contains only one gene for G-CSF and that some rearrangement has occurred within one of the alleles of the G-CSF gene in CHU-2 cells.

Human G-CSF was purified to homogeneity from the conditioned medium of the human squamous carcinoma cell line CHU-2 as described elsewhere[3], then the NH_2-terminal amino-acid sequences of several peptides obtained by tryptic digestion and two major peptides generated by chemical cleavage with cyanogen bromide were determined. One of the tryptic fragments showed an amino-acid sequence of Ile-Trp-Gln-Gln-Met-Glu-Glu-Leu-Gly-Met, and a 30-nucleotide oligonucleotide (IWQ probe, ATITGGCA$^{A}_{G}$CA$^{A}_{G}$ATGGA$^{A}_{G}$GA$^{A}_{G}$CTIGGIATG) was synthesized chemically. This oligonucleotide contained deoxyinosine at three positions[4] where three or four different nucleotides can be assigned due to codon degeneracy. G-CSF mRNA was prepared from the human CHU-2 cell line and two different cDNA libraries were constructed using either pBR322 as vector (library A) or the λgt10 vector[5] system (library B). The IWQ probe was labelled with ^{32}P, and library A was screened. One clone gave a positive result and was designated pHCS-1. This clone contained a 308-base-pair (bp) insert whose nucleotide sequence confirmed the presence of a homologous region with our probe and whose amino-acid sequence, deduced from the nucleotide sequence, was identical to that of homogeneous human G-CSF. The nucleotide sequence of pHCS-1 also revealed that it can code for 83 carboxy-terminal amino acids of G-CSF, which is about half the number of amino acids expected for G-CSF. Using the cDNA insert of pHCS-1 as probe, five clones were then isolated from cDNA library B and designated as λgt-1 to λgt-5. *Eco*RI restriction enzyme digestion of DNAs from these clones released inserts of 3.5, 1.3, 0.75, 1.6 and 1.5 kilobases (kb), respectively, and these were subcloned into the *Eco*RI site of pBR327 (denoted as pBRG-1 to pBRG-5). As 1.5 kb of cDNA is long enough to encode the G-CSF protein (relative molecular mass (M_r) 19,000)[3], two clones, pBRG-4 (~1.6 kb insert) and pBRG-5 (~1.5 kb insert), were further characterized by restriction enzyme analysis and nucleotide sequence determination.

Table 1 G-CSF activity in the culture medium of COS cells transfected with plasmid pHGA410

		Human bone marrow			Mouse bone marrow	
		(no. of colonies)				
Transfected with						
pdKCR	(*a*)	0	0	0	0	0
	(*b*)	0	0	0	NT	NT
pHGA410	(*a*)	104	128	128	51	42
	(*b*)	54	48	51	NT	NT
Purified G-CSF		72	50	97	47	53
Saline		0	0	0	0	0

COS cells (2×10^6) were seeded on a dish of 9 cm diameter with 10 ml of Dulbecco's minimal essential medium (Nissui) containing 10% fetal calf serum (Gibco). The cells were transfected with 20 μg of pHGA410 or pdKCR DNA using DEAE-dextran (Pharmacia) essentially as described elsewhere[10], and treated with 1 mM chloroquine (Sigma) for 2 h. After incubation for 72 h, the medium (40 ml) was collected and G-CSF was partially purified by various procedures, including reverse-phase HPLC essentially as described by Nomura *et al.*[3]. The eluate from the HPLC column was lyophilized and dissolved in 2 ml of Iscove's modified medium containing 10% fetal calf serum and assayed for CSF activity as described previously[25]. Briefly, for the human cell assay, 2×10^5 non-adherent bone marrow cells obtained from normal volunteers were added to 35-mm Petri dishes in a total volume of 1 ml of McCoy's 5A medium containing 15% fetal calf serum. 0.3% agar and 0.1 or 0.05 ml of the test sample. Cultures were incubated for 7 days at 37 °C, and colonies containing more than 50 cells were counted. For the mouse cell assay, 5×10^4 cells from a C3H/He mouse were incubated in 1 ml of McCoy's 5A medium containing 40% horse serum, 0.7% agar and 0.1 ml of the test sample. After incubation at 37 °C for 5 days, colonies consisting of more than 50 cells were counted. The assays were carried out in triplicate (for human cells) or duplicate (for mouse cells), and for the assay with human cells, 100 μl (*a*) or 50 μl (*b*) of CSF was tested. As a control, a homogeneous preparation of human G-CSF (20 ng) or saline was added to the incubation mixture instead of the test sample. NT, not tested.

Figure 1 shows the complete nucleotide sequence of the pBRG-4 insert (1,508 nucleotides long excluding the poly(A) tract). Apart from the fact that pBRG-5 insert is 8 nucleotides shorter at its 5′ terminus than the pBRG-4 insert, and the poly(A) tract of pBRG-4 at the 3′ terminus is about 80 bases long while that of pBRG-5 is 17 bases long, the nucleotide sequences of pBRG-5 and pBRG-4 are identical. Furthermore, comparison of the nucleotide sequences of pBRG-4 and pHCS-1 revealed a single difference at nucleotide position 586 (the third base in the Leu 155 codon), which does not change the amino-acid sequence. The cDNA in the pBRG-4 clone appeared to be of full length, as Northern hybridization analysis of CHU-2 mRNA with the cDNA of pBRG-4 revealed a band of ~1,600 nucleo-

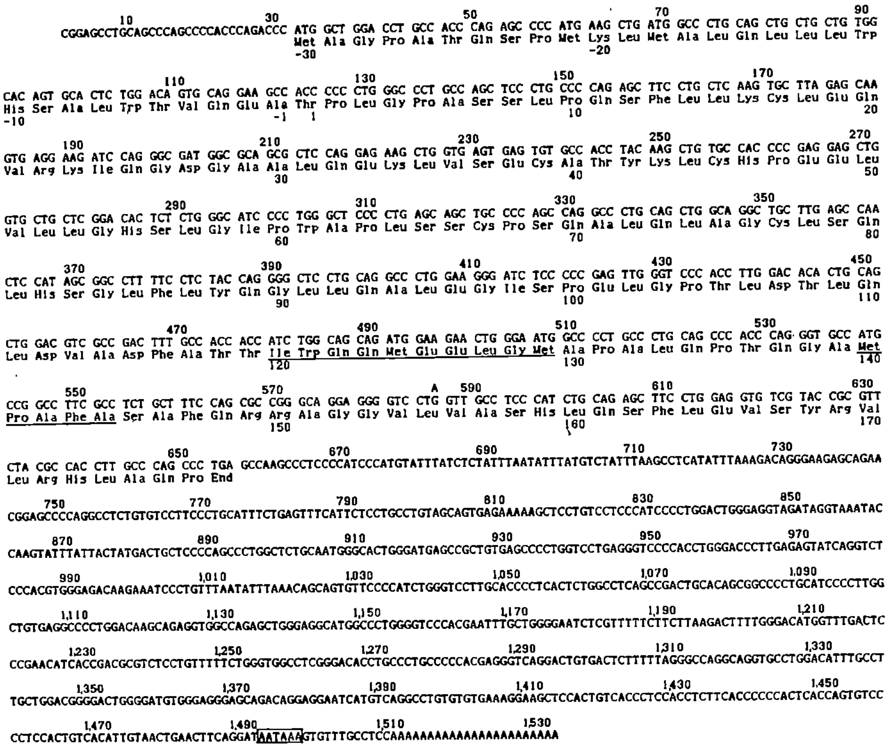

Fig. 1 Nucleotide sequence and deduced amino-acid sequence of human G-CSF cDNA. Numbers above and below each line refer respectively to nucleotide position and amino-acid position. Amino acids are numbered starting at Thr 1 of the mature G-CSF protein sequence; they are preceded by a 30-residue signal sequence. The peptides underlines are those used to design the synthetic oligonucleotide probes. The AATAAA polyadenylation signal close to the poly(A) tail is boxed. The nucleotide sequence of pHCS-1 differs from those of λgt-4 or λgt-5 at nucleotide position 586, where the nucleotide of pHCS-1 was A while that of λgt-4 and λgt-5 was G.

Methods. The IWQ probe was phosphorylated at the 5′ end with T4 polynucleotide kinase (Toyobo Co.) and [γ-^{32}P]ATP which was prepared as described elsewhere[29] using ^{32}P-phosphate (Amersham, carrier-free). To construct library A, double-stranded (ds) DNA was synthesized essentially as described elsewhere[30,31] using 42 μg of messenger RNA prepared from CHU-2 cells, and dsDNA > 500 bp was recovered after 1.2% agarose gel electrophoresis. The dsDNA was tailed with deoxy(C) and annealed with plasmid pBR322 which was tailed with deoxy(G) at the *Pst*I site. The annealed mixture was used to transform *E. coli* χ1776 and resultant tetracycline-resistant colonies were processed as described by Taub and Thompson[32]. Filters were hybridized with ^{32}P-labelled IWQ probe at 56 °C for 12 h in 6 × NET containing 1 × Denhardt's and 100 μg ml^{-1} denatured salmon sperm DNA[4]. Filters were then washed twice at room temperature in 6× SSC followed by a washing for 1.5 min at 56 °C in 6 × SSC. One clone out of about 30,000 clones gave a positive signal and was designated pHCS-1. The plasmid DNA of pHCS-1 was digested with *Eco*RI and *Sau*3AI and the ~600-bp DNA fragment was isolated by 1.0% agarose gel electrophoresis. This fragment was labelled with ^{32}P by nick-translation and used to screen library B, constructed according to Hall and Brown[33]. Briefly, dsDNA complementary to CHU-2 mRNA was synthesized using avian myeloblastrosis virus reverse transcriptase (Seikagaku Kogyo Co.) for the first strand and *E. coli* DNA polymerase I (New England Biolabs), RNase H (Takara Shuzo Co.) and *E. coli* DNA ligase (Takara Shuzo Co.) for the second strand. The dsDNA was methylated with *Eco*RI methylase (New England Biolabs) and ligated with *Eco*RI linker. The dsDNA was then digested with *Eco*RI, passed through Ultrogel AcA34 (LKB) to remove the excess linker, and ligated with the *Eco*RI-digested λgt10 vector DNA. Recombinant DNA was packaged *in vitro*[34] and ~100,000 phages were plated on *E. coli* C600 Hfl (ref. 5). This library was screened[35] with a ^{32}P-labelled ~600-bp DNA fragment of pHCS-1 in stringent conditions as described elsewhere[36]. Five phage clones were hybridized with the probe, plaque-purified [35] and the cDNA inserts of the five clones were subcloned into pBR327 at the *Eco*RI site. The nucleotide sequences of two of the cDNA clones (λgt-4 and λgt-5) were determined by the dideoxy chain termination method after subcloning into M13 phage derivatives[37].

tides (Fig. 3*a*). The NH$_2$-terminal amino acid of mature G-CSF was located at nucleotides 122-124, since the NH$_2$-terminal amino-acid sequence[3] of the intact G-CSF was Thr-Pro-Leu. There are three potential initiation codons AUG in the correct reading frame, at amino-acid positions −30, −21 and −18 (nucleotide positions 32-34, 59-61 and 68-70, respectively). Because the nucleotide sequence around these putative initiation codons agrees equally well with the consensus sequence (CC$^{\mathrm{A}}_{\mathrm{G}}$CCAUGG) characteristic of the initiation codon of many eukaryotic mRNAs[6], the first AUG codon from the 5′ terminus (at nucleotide positions 32-34) was tentatively assigned as the initiation codon for G-CSF, as it is for most eukaryotic mRNAs[7]. Consequently, G-CSF mRNA can code for a protein consisting of 207 amino acids of which 177 code for mature G-CSF while 30 hydrophobic amino acids encode the signal sequence. The M_r of the mature G-CSF protein was calculated to be 18,987, which agrees with that of the purified G-CSF (19,000 ± 1,000). Although no potential *N*-glycosylation sites (Asn-X-Ser or Asn-X-Thr)[8] were found in the G-CSF amino-acid sequence, some sugar moieties (Gal. GalNAc, NeuNAc) were found in the homogeneous preparation of human G-CSF[3], suggesting that human G-CSF may be *O*-glycosylated. Actually, the common sequences for galactosamine attachment[9] occur at several points (for example, amono acids 1, 7 and 8) on the human G-CSF sequence (Fig. 1).

Comparison of the structure of G-CSF protein with those of human granulocyte-macrophage colony-stimulating factor (GM-CSF)[10-11] and mouse interleukin-3 (IL-3)[12,13], which like G-CSF stimulate the growth of granulocyte and/or macrophage colonies, revealed little homology. This result is consistent with the recent observation[14] that mouse G-CSF does not share its receptor with GM-CSF, IL-3 or M-CSF. Furthermore, when the sequence of human G-CSF was compared with all the sequences in Genbank, using the SEQF program[15] in IDEAS[16], no significant homology was found.

To prove that the cloned cDNA of pBRG-4 actually encodes human G-CSF, used a mammalian cell system to express the cDNA. The 720-bp *Eco*RI/*Aha*III fragment containing the G-CSF coding sequence (Fig. 1) was recloned into the expression vector pdKCR (refs 17, 18), and the resultant plasmid (pHGA410), which contains the G-CSF cDNA in the same orientation relative to the simian virus 40 early promoter, was used to transfect COS cells[19]. After 72 h, the G-CSF secreted into the medium was assayed for CSF activity, either directly or after partial purification, using human or mouse bone marrow cells. As a control, the vector plasmid pdKCR, containing no cDNA insert, was transfected into COS cells and the COS cell supernatant was processed as described above. When the medium from pHGA410-transfected COS cells was assayed directly for CSF, no activity was detected. In contrast, the partially purified sample from the pHGA410-transfected COS cell supernatant showed CSF activity in both human and mouse bone marrow cells (Table 1). No CSF activity was detected in the sample purified from the medium of COS cells transfected with the pdKCR vector. To confirm that the colonies formed by the pHGA410-transfected COS cell supernatant are

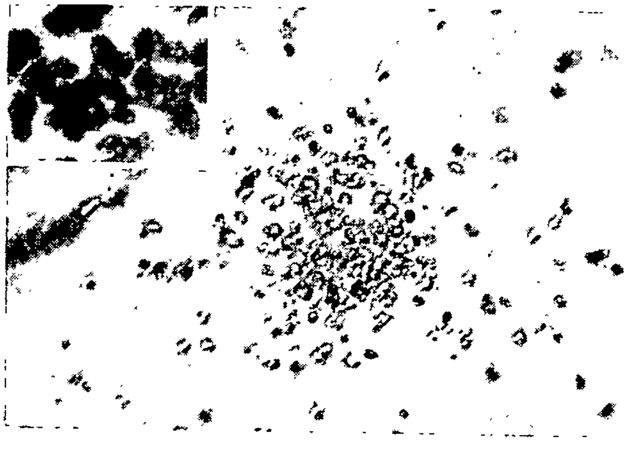

Fig. 2 Phase microscopic appearance of a human bone marrow colony stimulated by a cDNA-directed human G-CSF preparation. Inset, cells stained with Wright-Giemsa. Methods for the transfection of COS cells, purification of G-CSF from the medium conditioned with COS cells and assay for G-CSF using human bone marrow cells were as described in Table 1 legend. On day 7, several colonies were picked up on a glass plate and stained with Wright-Giemsa.

granulocyte colonies, the colonies from the human bone marrow CSF assay were examined by Wright-Giemsa and double esterase staining (Fig. 2). In most colonies, all the cells were positive for specific esterase, showing segmented or stubbed nuclei, and no colonies consisting of eosinophilic granulocytes were observed. These properties are similar to those of human CSF-β partially purified from medium conditioned with human placenta[20] or 5637 bladder carcinoma cells[21]. The failure to detect CSF activity directly in the transfected COS cell supernatant is probably due to a low specific activity of protein or a low expression of the protein in COS cells. In this regard, we have recently found[22] a second G-CSF cDNA which has a three-amino-acid deletion at around amino acid 35 compared with the cDNA described in Fig. 1. When this cDNA was expressed in COS cells, CSF activity was detected in the COS cell supernatant without purification.

Several tumours[23-25] are known to produce haematopoietic regulators which function within the granulocyte-macrophage pathway. The specific expression of G-CSF by these cells was investigated by preparing mRNAs from human lung carcinoma (OTUK)[25], human lower jaw carcinoma (LJC-1-JCK)[24] and CHU-2 cells, which produce proteins possessing CSF activity, and the human B-cell line Namalwa which does not produce CSF. Figure 3*a* shows the Northern hybridization analysis of the mRNAs using G-CSF cDNA as probe. About 1.6 kb of mRNA hybridized very strongly with mRNA from CHU-2 cells and weakly with mRNA from LJC-1-JCK cells, while no signal was detected with mRNA from OTUK and Namalwa cells. These results indicate that CHU-2 and LJC-1-JCK cells actually synthesize G-CSF mRNA. Furthermore, proteins showing CSF activity which are produced by OTUK cells are probably not G-CSF, but rather for example, GM-CSF[26], pluripotent-CSF[27] or haemopoietin-1[28], which act within the granulocyte-macrophage pathway.

To determine how many G-CSF genes exist in the human genome, and whether any amplification or rearrangement of the gene has occurred in CHU-2 cells producing G-CSF constitutively, DNAs from human normal leukocytes and CHU-2 cell were analysed by Southern hybridization. In DNA from leukocytes, a single DNA fragment was detected after digestion with any of four restriction enzymes used (Fig. 3*b*), which suggests that human G-CSF is encoded by a single gene; this has been confirmed by molecular cloning of the chromosomal gene for human G-CSF[22]. On the other hand, in DNA from CHU-2 cells, additional DNA fragments were observed after digestion with *Eco*RI (Fig. 3*b*, lane 2), *Hin*dIII (lane 6) or *Bam*HI (lane 8), which may indicate that some rearrangement but no amplification of the G-CSF gene had occurred in CHU-2 cells. Therefore, it is possible that alterations within one of the alleles of the G-CSF gene or its flanking regions led to the constitutive production of G-CSF in CHU-2 cells. Detailed analysis of the G-CSF chromosomal gene structure in normal and CHU-2 cells may reveal the mechanism of the constitutive synthesis of G-CSF in CHU-2 cells. The availability of human G-CSF cDNA should facilitate the production of large quantities of human G-CSF in appropriate host cells and study of the role of this factor in haematopoietic cell proliferation and differentiation.

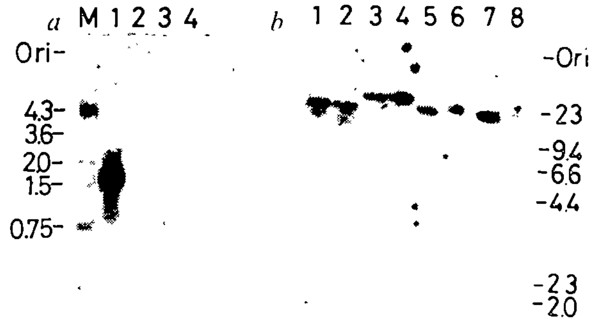

Fig. 3 Characterization of the mRNA and genomic gene coding for human G-CSF. *a*, Northern hybridization analysis of G-CSF mRNA. The following cells were used to prepare poly(A) RNA lane 1, human squamous carcinoma, CHU-2 cells; lane 2, human lung carcinoma, OTUK cells; lane 3, human lower jaw carcinoma, LJC-1-JCK; lane 4, human B-cell line, Namalwa, lane M, size marker, a mixture of 5'-^{32} P-labelled *Eco*RI, *Eco*RI/*Pst*I and *Eco*RI/*Pst*I/*Pvu*II-digested pBR322. The numbers are the sizes of the marker DNAs(in kb). *b*, Southern hybridization of the G-CSF gene. Sources of DNA are: lanes 1, 3, 5, 7, human normal leukocytes: lanes 2, 4, 6, 8, CHU-2 cells. Restriction enzymes used are: lanes 1, 2, *Eco*RI; lanes 3, 4, *Bgl*II; lanes 5, 6, *Hin*dIII, lanes 7, 8, *Bam*HI.

Methods. *a*, Poly(A) RNA was prepared from various cell lines[34] Poly(A) RNAs (5 μg) were electrophoresed through 1.2% agarose gel containing formaldehyde[34] and blotted onto a nitrocellulose filter. The ^{32}P-labelled EcoRI cDNA insert of pBRG-4 was used for hybridization in stringent conditions[36]. *b*, High-M_r DNAs were prepared from human leukocytes, or CHU-2 cells as described previously[34]. DNAs (10 μg) were digested with various restriction enzymes, electrophoresed on a 0.8% agarose gel and transferred to a nitrocellulose filter. The filter was hybridized with the ^{32}P-labelled *Eco*RI cDNA insert of pBRG-4 as described above

We thank Drs K. Oda and K. Matsubara for the protocols of the λgt10 vector system and hybridization with oligonucleotide-containing deoxyinosine, respectively, Dr M. Kanehisa for the "IDEAS" system, Mr I. Imazeki for technical assistance, and Drs S. Miwa, H. Ogawa, S. Hata, H. Okazaki and T. Hayashi for encouragement and support.

Received 7 October; accepted 12 December 1985.

1. Burgess, A. W. & Metcalf, D. *Blood* **56**, 947-958 (1980)
2. Metcalf, D. *Science* **229**, 16-22 (1985).
3. Nomura, H. *et al. EMBO J.* (submitted)
4. Takahashi, Y. et al. *Proc. natn. Acad. Sci. U.S.A.* **82**, 1931-1935 (1985)
5. Huynh, T., Young, R. A. & Davis, R. W. in *DNA Cloning Techniques, A Practical Approach* (ed. Glover, D. M.) 49-78 (IRL Press, Oxford, 1985)
6. Kozak, M. *Nucleic Acids Res.* **12**, 857-872 (1984)
7. Kozak, M. *Cell* **15**, 1109-1123 (1978).
8. Winzler, R. J. in *Hormonal Proteins and Peptides* (ed Li, C. H.) 1-15 (Academic, New York, 1973).
9. Takahashi, N., Takahashi, Y. & Putnam, F. W. *Proc. natn. Acad. Sci. U.S.A.* **81**, 2021-2025 (1984).
10. Lee, F. *et al. Proc. natn. Acad. Sci. U.S.A.* **82**, 4360-4364 (1985)
11. Wong, G. G. *et al. Science* **228**, 810-815 (1985)
12. Yokota, T. *et al. Proc. natn. Acad. Sci. U.S.A.* **81**, 1070-1074 (1984)
13. Fung, M. C. *et al. Nature* **307**, 233-237 (1984)
14. Nicola, N. A. & Metcalf, D. *Proc. natn. Acad. Sci. U.S.A.* **81**, 3765-3769 (1984).
15. Wilbur, W. J. & Lipman, D. J. *Proc. natn. Acad. Sci. U.S.A.* **80**, 726-730 (1983)
16. Kanehisa, M. *Nucleic Acids Res.* **10**, 183-196 (1982).

17. O'Hare, K., Benoist, C. & Breathnach, R. *Proc. natn. Acad. Sci. U.S.A.* **78**, 1527-1531 (1981).
18. Fukunaga, R., Sokawa, Y. & Nagata, S. *Proc. natn. Acad. Sci. U.S.A.* **81**, 5086-5090 (1984).
19. Gluzman, Y. *Cell* **23**, 175-182 (1981).
20. Nicola, N. A., Metcalf, D., Johnson, G. R. & Burgess, A. W. *Blood* **54**, 614-627 (1979).
21. Nicola, N. A., Begley, C. G. & Metcalf, D. *Nature* **314**, 625-628 (1985).
22. Nagata, S. *et al. EMBO J.* (submitted).
23. Asano, S. *et al. Br. J. Cancer* **41**, 689-694 (1980).
24. Sato, N. *et al. Cancer* **43**, 605-610 (1979).
25. Asano, S. *et al. Blood* **49**, 845-852 (1977).
26. Gasson, J. C. *et al. Science* **226**, 1339-1342 (1984).
27. Welte, K. *et al. Proc. natn. Acad. Sci. U.S.A.* **82**, 1526-1530 (1985).
28. Jubinsky, P. T. & Stanley, E. R. *Proc. natn. Acad. Sci. U.S.A.* **82**, 2764-2768 (1985).
29. Walseth, T. F. & Johnson, R. A. *Biochim. biophys. Acta* **562**, 11-31 (1979).
30. Land, H., Grez, N., Hansen, H., Lindermaier, W. & Schuetz, G. *Nucleic Acids Res.* **9**, 2251-2266 (1981).
31. Gubler, U. & Hoffman, B. J. *Gene* **25**, 263-269 (1983).
32. Taub, F. & Thompson, E. B. *Analyt. Biochem.* **126**, 222-230 (1982).
33. Hall, A. & Brown, R. *Nucleic Acids Res.* **13**, 5255-5268 (1985).
34. Maniatis, T., Fritsch, E. F. & Sambrook, J. *Molecular Cloning, A Laboratory Manual* (Cold Spring Harbor Laboratory, New York, 1982).
35. Benton, W. D. & Davis, R. W. *Science* **196**, 180-182 (1977).
36. Wahl, G. M., Stern, M. & Stark, G. R. *Proc. natn. Acad. Sci. U.S.A.* **76**, 3683-3687 (1979).
37. Messing, J. *Meth. Enzym.* **101**, 20-78 (1983).

'Brain-specific' transcription and evolution of the identifier sequence

Carmen Sapienza & Benoit St-Jacques

Department of Biology and Centre for Human Genetics,
McGill University, 1205 avenue Docteur Penfield,
Montreal, Quebec, Canada H3A 1B1

A recent model for the transcriptional control of gene expression in neural cells involves a dispersed repetitive DNA sequence termed the identifier (ID) sequence[1]. However, the model is based on circumstantial evidence from studies on rat brain gene expression[2-4]. Furthermore, available data are complicated by observations from several laboratories which suggest that the ID sequence is a family of mobile genetic elements[5-10]. Although this does not preclude a role for some family members in regulating gene expression, the contention that these sequences are transcribed tissue-specifically (refs 1-4, but see ref. 11) is not proof of such a role[12]. We have now measured the genomic copy number and tissue pattern of transcription of ID sequences in the rat, mouse and hamster, and have found that ID-homologous, BC1-like[2] RNAs are restricted to brain in all three species, but that ID-homologous transcripts occur in total cellular RNAs of brain, liver and kidney of all three organisms. The genomic copy number of the ID sequences varies over two orders of magnitude between these species. Our data suggest that most ID sequences in these genomes are dispersed at random with respect to transcription units. A *cis*-acting, transcriptional-level controlling role for the ID therefore seems unlikely.

The function of the ID sequence cannot be tested directly, but because the idea of multiple independent origins for the vertebrate brain seems improbable, a functional role for the ID sequence requires that at least two evolutionary criteria be fulfilled: (1) a homologous dispersed repetitive-sequence family which is transcribed neurone-specifically should be present in the genomes of related organisms and (2) that sequence family should contain enough members to be present in most neurone-specific genes. Our experiments assessed ID sequences for these characteristics.

We isolated total cellular RNA from the brain, liver and kidney of rat, mouse and hamster by guanidinium isothiocyanate/hot phenol extraction[13]. These RNAs were fractionated on a denaturing polyacrylamide gel, electroblotted and probed with the rat ID clone p2A120 (ref. 2) (Fig. 1). Both BC1 and BC2 RNAs were detected in the rat brain sample, as well as a previously unreported salt-soluble species of ~70 nucleotides. (Previous studies indicate that a substantial fraction of brain messenger RNAs are not polyadenylated[14-16]. These RNAs, as well as BC2 RNA[1], would be eliminated by oligo(dT)-cellulose chromatography. We fractionated BC1 and BC2 into the same compartment and enriched for larger RNA species by salt precipitation.) ID-homologous RNAs of similar mobility to BC1 and BC2 were found in total mouse brain RNA and a 135-nucleotide species was found in total hamster brain RNA. The level of hybridization to larger species (the smear which runs at the limiting mobility of the gel, presumed to be heterogeneous nuclear RNA[1,11]) was much greater in the rat than in the mouse or hamster. Under the hybridization and washing conditions used in Fig. 1, another RNA species that co-migrated with 7SL RNA was detected after prolonged autoradiographic exposure in all three tissues of all three organisms. We do not know whether this RNA is in fact 7SL RNA, but weak homology between *Alu* sequences and the ID sequence does exist (22 of the first 30 nucleotides of CHO *Alu* clone 49 (ref. 17) are homologous with the ID clone p2A120, and similar levels of homology occur with many published *Alu* sequences).

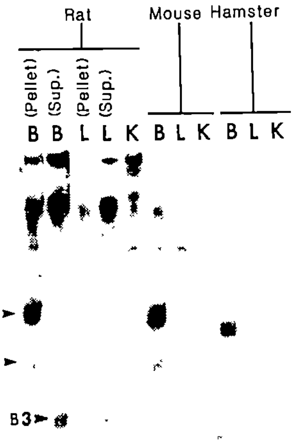

Fig. 1 Northern blot analysis of ID-homologous RNAs extracted from brain (B) liver (L) and kidney (K) of rat, mouse and hamster. Total cellular RNAs were isolated by guanidinium isothiocyanate/hot phenol extraction[13]. In some cases RNAs were fractionated by precipitation in 2.5 M NaCl at −8 °C for 6-10 h. Total cellular or salt precipitated RNAs (20 μg) were denatured at 67 °C in 30% dimethyl sulphoxide[4] and subjected to electrophoresis on denaturing 6% polyacrylamide gels[13]. The RNAs were then transferred to Zetabind nylon membrane (AMF Cuno, Meriden, Connecticut) by electroblotting[13]. The electrophoretically purified 580-bp *Pst*I fragment of p2A120[2] was labelled *in vitro* with [α-^{32}P]dCTP (3,000 Ci mmol^{-1}, Amersham) to specific activities of 5×10^7-2×10^8 c.p.m. μg^{-1} by nick translation[13]. Hybridization was done at 42 °C in 50% formamide/5×SET (0.75 M NaCl/0.15 M Tris-HCl *p*H 8/10 mM EDTA)/1×Denhardt's/50 μg ml^{-1} salmon-sperm DNA/0.5% SDS for 36-40 h. Four stringency washes (40 min each) were done in 2×SSC/0.1% SDS at 60-62 °C. Blots were then exposed to Kodak XAR-5 film with Dupont Lightning Plus intensifying screens at −80 °C for 15-48 h. The higher M_r smears hybridized in the salt supernatant fractions are probably due to DNA contamination, as samples in this figure were not treated with DNase I. Rats were Sprague-Dawley strain, mice were strain BALB/c ByJ and hamsters were Golden Syrian.

Having shown that the nucleotide sequence of the ID is at least partially conserved between the rat, mouse and hamster, we used dot-blot hybridization to examine the relative level of ID-homologous transcripts present in salt-precipitated RNA from brain, liver and kidney of each organism. Figure 2*a* shows that ID-homologous transcripts are present in liver and kidney samples of all three organisms. Densitometric tracing of lighter exposures of Fig. 2*a* indicated that there were approximately four and eight times as many ID-homologous transcripts in rat brain as in kidney and liver, respectively. To determine what fraction of ID-homologous brain RNA was caused by the presence of BC1 and BC2 RNAs in rat and the 135-nucleotide RNA

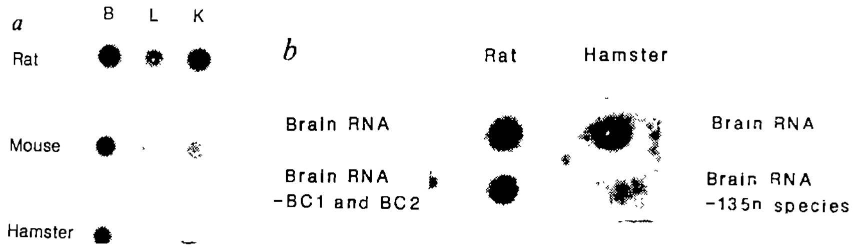

Fig. 2 *a*, Dot-blot hybridization assaying levels of ID-homologous transcripts in brain (B), liver (L) or kidney (K) RNAs from rat, mouse and hamster. *b*, ID-homologous transcripts of rat and hamster brain from which the BC1 and BC2 RNAs and the 135-nucleotide RNA respectively have been removed.

Methods. *a*, Salt-precipitated RNA samples were first treated with DNase I (50 μg ml^{-1}, Bohringer Mannheim) in the presence of 2,000 U ml^{-1} RNasin (Promega Biotec) for 30 min at 37 °C. After phenol/chloroform extraction and ethanol precipitation, the RNA was redissolved and the concentration estimated spectrophotometrically[13]. There was no apparent quantitative or qualitative difference in the ethidium bromide staining pattern of RNAs treated in this manner and run on denaturing 6% polyacrylamide gels, as compared with untreated samples (data not shown). All of the small RNAs normally present were clearly visible[4]. 8 μg of each RNA was denatured in 50% formamide at 75 °C for 10 min, cooled in ice H_2O, made 1 M in NH_4OAc and filtered onto a nylon membrane using a Hybri-Dot manifold (Bethesda Research Laboratories). The absence of contaminating DNA was confirmed by the complete lack of hybridization to NaOH-treated control samples in adjacent spots. Hybridization and washing were done as in Fig. 1 with *in vitro* labelled 580-bp *Pst*I fragment from p2A120. Probe was judged to be in effective excess by the linearity of autoradiographic response over 1, 2 and 4 μg of rat brain RNA treated as above and present on the same blot (data not shown). *b*, Salt-precipitated rat brain or hamster brain RNA was fractionated on denaturing 5% polyacrylamide gels. The RNA was extracted from the gel[13] either excluding or including regions of the gel containing BC1 and BC2 RNA in the case of rat or the 135-nucleotide species in the case of hamster. To ensure effective extraction of larger species, regions of the gel containing RNAs larger than 7SL RNA were treated with 10 mM NaOH for 15 min at room temperature. The final products of this extraction procedure ran as a smear between 80 and 500 nucleotides in length on denaturing 6% polyacrylamide gels; 5 μg of each RNA was treated as in *a*.

in hamster, we removed these species from samples of rat and hamster brain RNA by fractionation on a denaturing 5% polyacrylamide gel, followed by extraction of the RNA from the gel, either excluding or including species of these relative molecular masses (M_rs). Densitometric tracing of Fig. 2*b* indicates that >90% of the ID-homologous transcripts present in hamster brain RNA are caused by the 135-nucleotide species, whereas approximately half of ID-homologous rat brain RNAs result from BC1 and BC2 RNAs.

Using this estimate, we conclude that ID-homologous transcripts (other than BC1 and BC2) are two- to fourfold more prevalent in rat brain RNA than in liver or kidney RNA. Our results for the higher level of ID-homologous transcripts present in the rat brain agree qualitatively with those of Sutcliffe and co-workers, but the rather small quantitative differences and the fact that we observe similar differences between liver and kidney lead us to believe that these differences are artefactual[11].

We also measured the copy number of ID-homologous sequences in the genomes of rat, mouse, hamster, guinea pig and rabbit by several different methods. Figure 3*a* shows that, at the same hybridization stringency used to detect ID-homologous transcripts in Figs 1 and 2, the rat genome contains at least four times as many copies of the ID sequence as do the genomes of any of the other organisms. Prolonged exposure of this autoradiogram revealed a faint signal in the 50-ng mouse DNA spot which is ~1/10th as intense as the rat 50-ng spot.

Figure 3*b* shows an identical dot blot hybridized with a 900-base-pair (bp) *Sau*3A fragment containing the rat ID-homologous portion of a positive mouse library phage clone (designated pM3A-2, and which gives a pattern of hybridization on Northern blots identical to that obtained with p2A120; data not shown). The result is qualitatively the same; there are an order of magnitude more mouse-ID-homologous sequences in the rat genome than in the mouse, hamster, guinea pig or rabbit genomes.

Of 10^4 plaques of the Sargent and Bonner rat genomic library[18] screened with p2A120, 39% were positive and thus contained at least one copy of the ID sequence (Table 1), implying that there are ~135,000 copies per genome. This agrees well with the estimate of Sutcliffe *et al.* that 43% of randomly chosen rat clones contain at least one copy of the ID sequence[3]. Only 3.6% of 10^3 plaques of a mouse genomic library hybridized to either p2A120 or the mouse ID clone pM3A-2, implying ~12,000 copies of the ID sequence per mouse genome. We constructed a partial genomic library of hamster DNA *Sau*3A fragments in the plasmid vector pEMBL8$^+$ and screened 1,800 clones containing inserts averaging 600 bp in length (a significant fraction of recombinant plasmids contained more than one insert) with both the rat and mouse ID inserts of p2A120 and pM3A-2. We detected no homologous sequences with either clone, indicating a maximum of 4,700 copies of the ID per hamster genome. Comparable estimates were obtained by saturation hybridization with either p2A120 or pM3A-2 as driver (Table 1). Between 11 and 20% of the counts hybridized were released by treatment with S_1 nuclease, providing a rough estimate of between-member divergence of ID sequences present in each genome.

With regard to the model for control of gene expression proposed by Sutcliffe and co-workers[1], Owens *et al.*[11] have recently demonstrated that there are no differences in the level of ID-homologous transcripts in brain, liver or kidney hnRNA in either the rat or mouse. Their estimate of the relative difference in absolute amount of ID-homologus hnRNA between rat and mouse[11] is in good agreement with the difference we measure in ID copy number between these species. These observations

Table 1 Identifier sequence copy number

	Saturation hybridization		
	p2A120	pM3A-2	Library screen
Rat	133,000 (13)	120,000 (ND)	135,000 (39% of 10^4 plaques)
Mouse	19,500 (19)	15,800 (21)	12,500 (3.6% of 10^3 plaques)
Hamster	1,600 (20)	2,500 (11)	<4,700 (0 of 1,000 kb)

Saturation hybridizations were done with rat ID clone p2A120 or mouse ID clone pM3A-2 as driver. Samples of plasmid DNA were linearized by cleavage with *Eco*RI, denatured and fixed to 2.4-cm Zetabind' circles. Samples of each genomic DNA were cleaved with *Sau*3A (Boehringer Mannheim) to generate fragments averaging 300 bp in length (minimizing 'network' formation) and *in vitro* labelled with [α-^{32}P]dCTP and [α-^{32}P]dATP to specific activities of 9.4×10^7–1.2×10^8 c.p.m. μg^{-1}. Hybridizations were carried out for 39 h at 42 °C in 50% formamide/5 × SSC/20 mM Na-phosphate *p*H 6.7/1 × Denhardt's/50 μg salmon sperm DNA ml^{-1} and four stringency washes done at 60–62 °C in 2 × SSC/0.1% SDS. Filter-bound DNA was judged to be in excess because 1, 3.3 and 10 μg of each plasmid DNA bound the same fraction of input c.p.m. Filters containing 3.3 μg of plasmid DNA were then incubated with increasing amounts of labelled genomic DNA. The fraction of input c.p.m. bound was linear over the range tested. The c.p.m. bound were corrected for the efficiency of hybridization (as measured by hybridization of labelled p2A120 or pM3A-2 to homologous filter-bound DNA, 39% in the case of p2A120, 35% in the case of pM3A-2) and copy number was calculated as (corrected c.p.m. bound/input c.p.m.) × 2.5×10^9 bp (rodent genomic compexity) ÷ 82 bases (length of the ID sequence). Numbers in parentheses in the saturation hybridization columns represent the fraction of c.p.m bound released by S_1 nuclease treatment (ND, not determined). Phage and plasmid library screening were done as described elsewhere[13] and copy number calculated also as described previously[3]. The mouse genomic library was obtained from Y. Nishioka and constructed in the laboratory of S. Tonegawa by ligating partial *Eco*RI digests of mouse genomic DNA to λ Charon 4a arms.

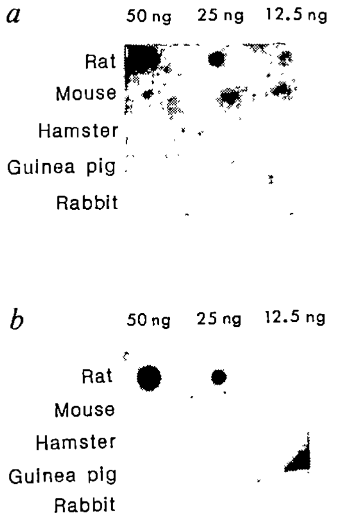

Fig. 3 Estimation of the relative copy number of ID-homologous sequences in the genomes of rat, mouse, hamster, guinea pig and rabbit. The hybridization probes are the *in vitro* labelled 580-bp *Pst*I fragment of p2A120 (*a*) and the *in vitro* labelled 900-bp *Sau*3A fragment from the mouse ID clone pM3A-2 (see test) (*b*). DNA prepared from the liver of each organism[20] was digested with *Eco*RI (Boehringer Mannheim) and fixed to a nylon membrane as described elsewhere[21].

suggest that the vast majority of ID sequences within these genomes are dispersed approximately at random with respect to transcription units. These data further suggest that the demonstrated brain specificity of 160- or 135-nucleotide BC1-like RNAs is not caused by the transcription of thousands of different 82-nucleotide IDs located in brain gene introns[1], but is more probably the result of transcription of a small subset of ID-homologous genes that specifically code for this RNA. Unequivocal data on the sequence diversity of BC1 RNA will help to determine whether the between-species differences in ID copy number reflect the generation of pseudogenes or transposition processes like those invoked for the derivation of *Alu* sequences from 7SL RNA[19].

We thank Jane Holbrook for assistance with many of the experiments, and Fran Langton for preparation of the manuscript, and W. E. Hahn and J. G. Sutcliffe for communication of results before publication. Identifier sequence clone p2A120 was graciously provided by J. G. Sutcliffe. This research was supported by the NSERC and MRC of Canada.

Received 13 August; accepted 18 November 1985.

1. Sutcliffe, J. G., Milner, R. J., Gottesfeld, J. M. & Reynolds, W. *Science* **225**, 1308–1315 (1984).
2. Sutcliffe, J. G., Miller, R. J., Bloom, F. E. & Lerner, R. A. *Proc. natn. Acad. Sci. U.S.A.* **79**, 4942–4946 (1982).
3. Milner, R. J., Bloom, F. E., Lai, C., Lerner, R. A. & Sutcliffe, J. G. *Proc. natn. Acad. Sci. U.S.A.* **81**, 713–717 (1984).
4. Sutcliffe, J. G., Milner, R. J., Gottesfeld, J. M. & Lerner, R. A. *Nature* **308**, 237–241 (1984).
5. Barta, A., Richards, R. I., Baxter, J. D. & Shine, J. *Proc. natn. Acad. Sci. U.S.A.* **78**, 4867–4871 (1981).
6. Schuler, R. A., Weber, J. L. & Gorski, J. *Nature* **305**, 159–160 (1983).
7. Lemischka, I. & Sharp, P. A. *Nature* **300**, 330–335 (1982).
8. Watanabe-Nagasu, N. *et al. Nucleic Acids Res.* **11**, 1791–1801 (1983).
9. Hastie, N. *Trends Genet.* **1**, 37 (1985).
10. Page, G. L., Smith, S. & Goodman, H. M. *Nucleic Acids Res.* **9**, 2087–2103 (1981).
11. Owens, G. P., Chaudhari, N. & Hahn, W. E. *Science* **229**, 1263–1265 (1985).
12. Davidson, E. H. & Posakony, J. W. *Nature* **297**, 633–635 (1982).
13. Maniatis, T., Fritsch, E. F. & Sambrook, J. *Molecular Cloning, a Laboratory Manual* (Cold Spring Harbor Laboratory, New York, 1982).
14. Chikaraishi, D., *Biochemistry* **18**, 3249–3258 (1979).
15. Van Ness, J. Maxwell, J. H. & Hahn, W. E. *Cell* **18**, 1341–1349 (1979).
16. Hahn, W. E., Chaudhari, N., Beck, L., Wilber, K. & Peffley, D. *Cold Spring Harb. Symp. quant. Biol.* **48**, 465–475 (1983).
17. Haynes, J. R. & Jelinek, W. R. *Proc. natn. Acad. Sci. U.S.A.* **78**, 6130–6134 (1981).
18. Sargeant, T. D. *et al. Proc. natn. Acad. Sci. U.S.A.* **76**, 3256–3260 (1979).
19. Ullu, E. & Tschudi, C. *Nature* **312**, 171–172 (1984).
20. Scott, M. P. *et al. Cell* **35**, 763–776 (1983).
21. Kafatos, F. C., Jones, C. W. & Efstratiadis, A. *Nucleic Acids Res.* **7**, 1541–1552 (1979).

Rearrangement of two distinct T-cell γ-chain variable-region genes in human DNA

M.-P. Lefranc*, A. Forster & T. H. Rabbitts

Medical Research Council Laboratory of Molecular Biology,
Hills Road, Cambridge CB2 2QH, UK

* Permanent address: Laboratoire d'Immunogénétique, Université des Sciences et Techniques du Languedoc, 34060 Montpellier Cedex, France.

Selective cloning procedures for T-cell-specific complementary DNAs have revealed the existence of a gene designated[1] γ as well as the main antigen receptor α- and β-chain genes[2–10]. The γ-chain genes undergo rearrangement during T-cell differentiation but the patterns and complexity of such rearrangements differ markedly in mouse[11–13] and human[14]. In mouse, a panel of cytotoxic T-lymphocyte clones exhibit the same rearrangement pattern with a γ-chain gene probe[11] and a set of three γ-chain variable (*V*) genes have been identified in the DNA[12]. Clonal diversity in mouse seems to be confined to *V–J* (joining) regions[11]. In contrast, human T-cell lines exhibit diverse rearrangements[14] suggestive of a family of differing V_γ genes variously rearranging to the two γ-chain constant (*C*) region genes[14,15]. Here we report the cloning of two very different V_γ genes rearranged to *J* segments upstream of the two human C_γ genes. Both V_γ genes are rearranged productively but nucleotide sequence comparison shows that they possess very little homology with each other. This shows that human T-cell V_γ genes exist which differ significantly from each other at the nucleotide level and that such diverse genes can be usefully rearranged in different T cells.

A further investigation of the diversity in the human T-cell γ-chain gene locus was carried out by cloning rearranged V_γ genes from λ phage libraries made from two different T-cell lines. We first determined the location of the J_γ segments. A probe from upstream of the $C_\gamma 1$ gene was previously used to detect rearrangement in various human T cells[14]. All such rearrangements were observed in a 2-kilobase (kb) *Hin*dIII fragment found next to each of the C_γ genes; therefore it seems likely that they include the J_γ segments. The nucleotide sequences of the 2.1-kb *Hin*dIII fragments from upstream of $C_\gamma 1$ and $C_\gamma 2$ were therefore determined. Each sequence was scanned for

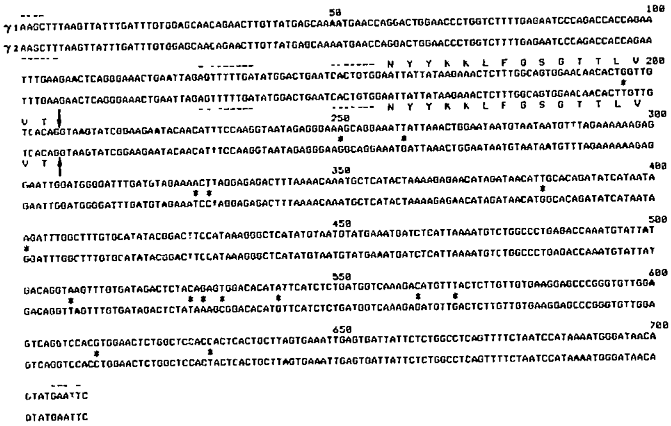

Fig. 1 Nucleotide sequence comparison of human $J_\gamma 1$ and $J_\gamma 2$ regions. Nucleotide sequences are shown extending from *Hin*dIII to *Eco*RI sites of M13H60 (ref. 14) and the equivalent fragment of the $\gamma 2$-chain gene, determined and aligned using random sequencing methods[18–20]. The relevant restriction sites are indicated at the start and end of the sequence and nucleotide differences are starred. The J_γ sequences are shown together with the conserved nanomer (AGTTTTGA) and heptamer sequences (CACTGTG) (lines above and below); the RNA splice donor sites are arrowed.

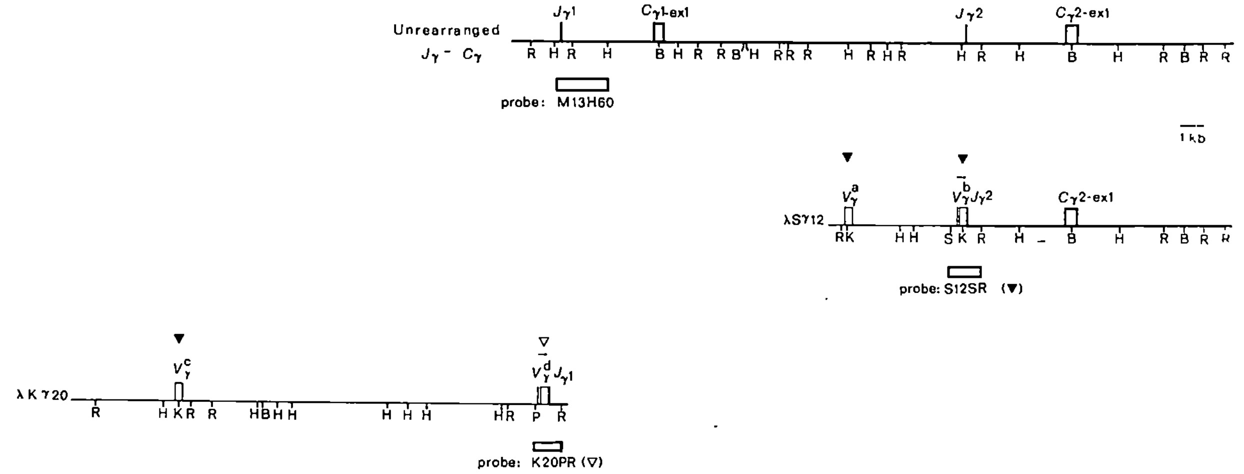

Fig. 2 Restriction maps of germline and rearranged γ-chain genes. λ phage clones were isolated from either a genomic library prepared from SUPT1 cells[16] (λSγ12) or from Karpas 1010 (λKγ20). Both libraries were prepared in λ2001 (ref. 21). Top line, unrearranged gene organization of J_γ-C_γ region[14,15] with only the first exon of C_γ genes indicated. Middle line, restriction map of λ clone Sγ12; bottom line, restriction map of the γ clone Kγ20. Horizontal arrows, known transcriptional orientations; ▽, V_γ genes that are cross-hybridizing species. Restriction sites indicated are: R, *Eco*RI; H, *Hin*dIII; B, *Bam*HI; S, *Sac*I; K, *Kpn*I and P, *Pst*I (not all S, K and P sites are given).

the presence of potential J segments and only one J segment was found in each case. The aligned nucleotide sequences, including the $J_\gamma 1$ and $J_\gamma 2$ segments, are shown in Fig. 1 from the upstream *Hin*dIII site to an *Eco*RI site 710 base pairs (bp) downstream. Conserved nanomer-heptamer sequences, implicated in the V-J joining process, occur immediately upstream of each J segment; the spacing of these nanomer-heptamer sequences is 12 bp. The protein coding sequences of the two J_γ segments are identical. In this respect the human and mouse γ-chain genes are similar because in mouse each C_γ gene has only one J segment[12]. There is considerable sequence homology between the two regions in the human DNA, but sufficient differences exist to allow unequivocal assignment of rearranged genes to $J_\gamma 1$ or $J_\gamma 2$ (see below).

The location of the two identified human J_γ segments relative to the first exon of each C_γ gene is shown in the restriction map at the top of Fig. 2 (unrearranged J_γ-C_γ). To study the diversity of V_γ genes, we screened genomic libraries made from two different human T-cell lines (both of which display rearranged γ-chain genes[14]) using the M13H60 (J_γ) probe (Fig. 2, top). The restriction maps of representative clones isolated from these two libraries appear in Fig. 2. One set of clones (derived from a library of DNA from the T-cell line Karpas 1010), represented by λKγ20, was found by nucleotide sequencing to have a V_γ gene segment (designated V^d_γ) joined to $J_\gamma 1$ (see below). The other set, represented by λSγ12, has a V_γ gene (designated V^b_γ) joined to $J_\gamma 2$ and was isolated from a phage library prepared from DNA[16] of the cell line *SUPT*1 (ref. 17). The nucleotide sequences of the rearranged V_γ genes showed that in both cases a productive rearrangement between V_γ and J_γ had occurred (Fig. 3). In common with other V genes, both the rearranged γ-chain genes have a short leader sequence split by an intron of ~120 bp. Comparison of the nucleotide sequences of the two rearranged V_γ genes showed very little homology. However, some degree of homology was observed between the potential protein products of the V_γ genes (Fig. 4*a*). Although the precise degree of homology is difficult to assess because of high divergernce, the two V_γ genes are estimated to be ~30% similar. Certain conserved residues are observed; for example, cysteine residues probably involved in the intra-chain disulphide bonds and the region near the J_γ segment (Tyr-Tyr-Cys-Ala). However, the two V_γ genes are clearly very different and represent two distinct V_γ families.

Two further V_γ genes were found in the human γ clones described here by cross-hybridization experiments using the probe S12RS (Fig. 2) which contains the rearranged V^b_γ gene (data not shown). One gene (designated V^c_γ; Fig. 2) occurs ~14 kb upstream of the rearranged V^d_γ gene in λKγ20 and the

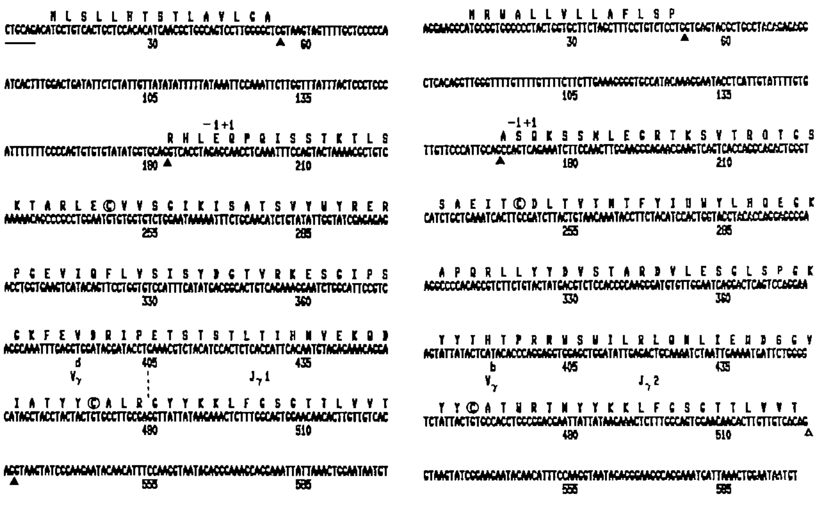
a
$V^d_\gamma J_\gamma 1$ (λKγ20)
b
$V^b_\gamma J_\gamma 2$ (λSγ12)

Fig. 3 Nucleotide sequences and derived protein sequences of rearranged V_γ genes. *a*, V-J junction in λKγ20: *b*, V-J junction in λSγ12.

Methods. *a*, The *Pst*I site underlined at the start of the sequence was used to prepare a 1-kb *Pst*I/*Eco*RI fragment from which the DNA sequence was obtained by the random procedure; only the relevant sequence region is shown. RNA splice sites are arrowed and cysteine residues involved in putative intra-chain disulphide bond are circled. The V-J junction is indicated by a vertical dotted line. *b*, The nucleotide sequence was obtained by the random cloning procedures from a 1.2-kb *Sac*I/*Eco*RI fragment (identical with S12SR; Fig. 2) containing $J_\gamma 2$. Annotations and symbols are as in *a*.

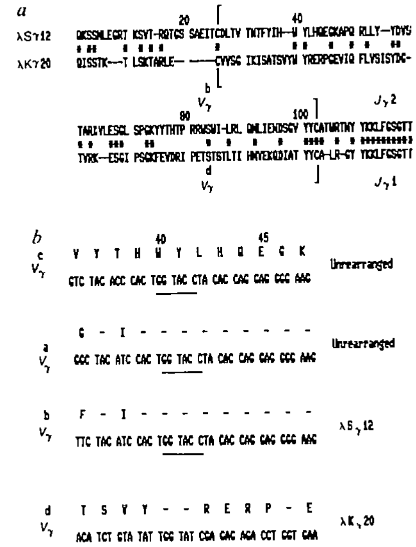
a
20
40
λSγ12
QKSSNLEGRT KSVT-RQTGS SAEITCDLTV TNTFYIH--W YLHQEGKAPQ RLLY--YDVS
λKγ20
QISSTK---T LSKTARLE-- -----CVVSG IKISATSVYW YRERPGEVIQ FLVSISYDG-
b
Vγ
80
100
Jγ2
TARLYLESGL SPGKYYTHTP RRWSWI-LRL QNLIENDSGV YYCATWRTNY YKKLFGSGTT
TVRK--ESGI PSGKFEVDRI PETSTSTLTI HNVEKQDIAT YYCA-LR-GY YKKLFGSGTT
d
Vγ
Jγ1
b
40
45
c
Vγ
V Y T H W Y L H Q E G K
GTC TAC ACC CAC TGG TAC CTA CAC CAG GAG GGC AAG
Unrearranged
G - I - - - - - - - - -
a
Vγ
GGC TAC ATC CAC TGG TAC CTA CAC CAG GAG GGC AAG
Unrearranged
b
Vγ
F - I - - - - - - - - -
TTC TAC ATC CAC TGG TAC CTA CAC CAG GAG GGC AAG
λSγ12
d
Vγ
T S V Y - - R E R P - E
ACA TCT GTA TAT TGG TAT CGA GAG AGA CCT GGT GAA
λKγ20

Fig. 4 Sequence comparisons of human V_γ genes, *a*, Alignment of rearranged V_γ protein sequences from λSγ12 and λKγ20. Sequences were aligned manually by inserting spaces as appropriate: the positions of Cys residues presumably involved in disulphide bond formation are shown. Stars represent sequence identity. *b*, Comparison of V_γ sequences around the Trp-Tyr codons 40 and 41. Dashes indicate amino-acid identity. The *Kpn*I restriction sites in V_γ^c, V_γ^a and V_γ^b are underlined. This site was used to obtain nucleotide sequence (in M13 vectors)[22] of the unrearranged genes.

other gene (designated V_γ^a; Fig. 2) occurs 4.5 kb upstream of V_γ^b in λSγ12. Both unrearranged *V* genes contain a site for the restriction enzyme *Kpn*I (GGTACC). An analogous restriction site occurs in the V_γ^b gene of λSγ12, part of which corresponds to the conserved codons Trp-Tyr (Fig. 4*a*). Confirmation that the hybridizing segments were V_γ genes is provided by partial nucleotide sequencing around the *Kpn*I site. These sequences are shown in Fig. 4*b* and compared with the corresponding regions of the V_γ^b and V_γ^d (that is, the two rearranged) genes. All the V_γ genes contain the conserved Trp-Tyr codons but V_γ^d does not retain the *Kpn*I restriction site. Figure 4*b* compares a short stretch of DNA sequence (around the Trp-Tyr codons) of V_γ^c with the other unrearranged V_γ^a gene and with the two rearranged genes. Both V_γ^a and V_γ^b (the latter rearranged in λSγ12) show a high degree of similarity with V_γ^c but both differ from it at two positions, resulting in amino-acid replacements (these replacements are at identical positions in V_γ^a and V_γ^b). In addition the unrearranged genes V_γ^a, V_γ^c and the rearranged V_γ^b cross-hybridize, and therefore the data are indicative of related but non-identical *V* genes. On the other hand, in the region compared here, the unrearranged V_γ^c gene and the rearranged V_γ^d differ at 9 codons out of 12. Further, the probe K20PR (Fig. 2), which contains the rearranged V_γ^d gene segment, hybridized to the homologous segment in λKγ20 but not the V_γ^c gene (data not shown), strengthening the view that the set of genes derive from two different V_γ families. Nucleotide sequencing shows that the V_γ genes are arranged in the same transcriptional orientation. This is different from to the situation found in mouse DNA where two of the three identified V_γ genes are separated by only 2.5 kb and are arranged in a head-to-head transcriptional orientation. This is different from the situation that the two human C_γ genes have an associated J_γ segment to which V_γ genes can productively join. The nanomer-heptamer conserved sequences are, like the equivalent mouse γ-chain system[12], separated by 12 bp. Four human V_γ genes have been identified thus far and the two rearranged V_γ genes are rather distinct from each other at both nucleotide and protein level (Fig. 4*a*). This is different from the situation in mouse where limited diversity[11] appears to be confined to three V_γ genes[12], although it now seems that a further mouse V_γ gene exists[13].

As far as the human γ-chain genes are concerned, our data show at least four different V_γ segments which fall into two distinct families based on the sequence homology described here. One V_γ gene family has a minimum of three members (here designated V_γ^a, V_γ^b and V_γ^c); the other family has only one member at present (designated V_γ^d). The possible existence of further members of these two families and even of further diverse human V_γ families must therefore be considered, particularly in the light of multiple rearrangements seen in human T-cell lines[14]. The function of the γ-chain gene product remains a matter of speculation because of the lack of data in protein expression. The apparent diversity of variable-region segments which can result from the two families of human V_γ genes identified preclude the formulation of simple models.

We thank Dr R. Baer for the SUPTI phage library and Drs Malik and Karpas for the 1010 phage library. M.P.L. is the recipient of an EMBO fellowship.

Received 11 October; accepted 9 December 1985.

1. Saito, H. *et al. Nature* **309**, 757-762 (1984).
2. Chien, Y.-H. *et al. Nature* **312**, 31-35 (1984).
3. Gascoigne, N. R. J., Chien, Y.-H., Becker, D. M., Kavaler, J. & Davis, M. M. *Nature* **310**, 387-391 (1984).
4. Hedrick, S. M., Nielsen, E. A., Kavaler, J., Cohen. D I & Davis, M. M. *Nature* **308**, 153-158 (1984).
5. Saito, H. *et al. Nature* **312**, 36-40 (1984).
6. Sim, G. K. *et al. Nature* **312**, 771-775 (1984).
7. Sims, J. E., Tunnacliffe, A., Smith, W. S. & Rabbitts, T. H. *Nature* **312**, 541-545 (1984).
8. Siu, G. *et al. Cell* **37**, 381-391 (1984).
9. Yanagi, Y. *et al. Nature* **308**, 145-149 (1984).
10. Yanagi, Y., Chan, A., Chin, B., Minden, M. & Mak, T. W. *Proc. natn. Acad. Sci. U.S.A.* **82**, 3430-3434 (1985).
11. Kranz, D. M. *et al. Nature* **313**, 752-755 (1985).
12. Hayday, A. C. *et al. Cell* **40**, 259-269 (1985).
13. Heilig, J. S. *et al. Nature* **317**, 68-70 (1985).
14. Lefranc, M.-P. & Rabbitts, T. H. *Nature* **316**, 464-466 (1985).
15. Murre, C. *et al. Nature* **316**, 549-552 (1985).
16. Baer, R., Chen, K. C., Smith, S. D. & Rabbitts, T. H. *Cell* **43**, 705-713 (1985).
17. Smith, S. D. *et al. Cancer Res.* **44**, 5657-5660 (1984).
18. Sanger, F., Coulson, A. R., Barrell, B. G., Smith, A. J. H. & Roe, B. A. *J. molec. Biol.* **143**, 161-178 (1980).
19. Staden, R. *Nucleic Acids Res.* **8**, 3673-3694 (1980).
20. Staden, R. *Nucleic Acids Res.* **12**, 521-538 (1984).
21. Karn, J., Matthes, H. W. D., Gait, M. J. & Brenner, S. *Gene* **32**, 217-224 (1984).
22. Vieira, J. & Messing, J. *Gene* **19**, 259-268 (1982).

An *Agrobacterium* transformation in the evolution of the genus *Nicotiana*

Ian J. Furner*, Gary A. Huffman*,
Richard M. Amasino*, David J. Garfinkel*,
Milton P. Gordon & Eugene W. Nester

Department of Microbiology and Immunology,
University of Washington, Seattle, Washington 98195, USA

***Agrobacterium rhizogenes* provokes neoplastic outgrowths on higher plants by transferring two small regions from the root-inducing (Ri) plasmid to the host genome[1–3]. Homology with the left transferred DNA (T_L DNA) was detected in uninfected *Nicotiana glauca*[1] and a molecular clone (λNg31) of this region was obtained from *N. glauca*[4]. We report here that the genome of *N. glauca* contains a large inverted repeat which is homologous with the single copy T_L DNA of *A. rhizogenes*. Related sequences are present in several *Nicotiana* species, but are absent in others. The DNA sequence of the centre of the inverted repeat has been compared with the corresponding region from the bacterium. Both contain open reading frames which could potentially produce similar polypeptides. The data strongly suggest that an *Agrobacterium* infection resulted in genetic transformation early in the evolution of the genus *Nicotiana*.**

---

* Present addresses: Department of Genetics, University of Cambridge, Cambridge CB2 3EH, UK (I.J.F.); Pioneer Hi-Bred, Johnston, Indiana 50131, USA (G.A.H.); Department of Biochemistry, University of Wisconsin, Madison, Wisconsin 53706, USA (R.M.A.); Biology Department, Massachusetts Institute of Technology 56-344, Cambridge, Massachusetts 02139, USA (D.J.G.).

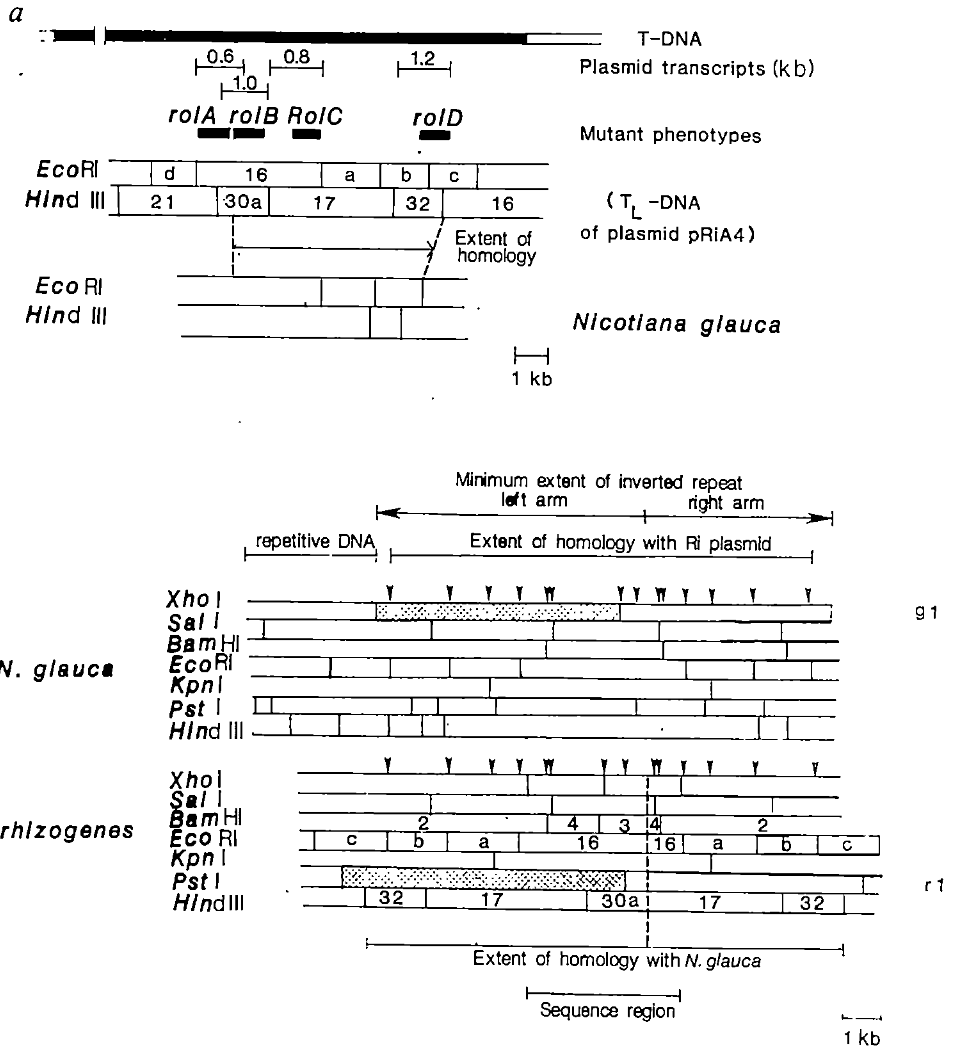
a
T-DNA
Plasmid transcripts (kb)
0.6
0.8
1.0
1.2
rolA rolB RolC
rolD
Mutant phenotypes
EcoRI
Hind III
d
16
a
b
c
21
30a
17
32
16
(T_L-DNA
of plasmid pRiA4)
Extent of homology
EcoRI
Hind III
Nicotiana glauca
1 kb
b
Minimum extent of inverted repeat
left arm
right arm
repetitive DNA
Extent of homology with Ri plasmid
XhoI
SalI
BamHI
EcoRI
KpnI
PstI
HindIII
N. glauca
g1
XhoI
SalI
BamHI
EcoRI
KpnI
PstI
HindIII
A.rhizogenes
2
4
3
4
2
c
b
a
16
16
a
b
c
32
17
30a
17
32
r1
Extent of homology with N. glauca
Sequence region
1 kb

Fig. 1 *a*, Organization of the left T-DNA of plasmid pRiA4b. Indicated are: The approximate extent of plasmid DNA found in tumours[3] (a break is indicated at the left end of the T-DNA as the left border varies but is usually left of this point). The positions and approximate sizes of transcripts are found in transformed *N. glauca* tissue[5]. The positions of the *rol* loci as defined by transposon mutagenesis[3]. These data are superimposed on an *Eco*RI and *Hin*dIII restriction map of this region. The extent of homology to the *N. glauca* genome and to λNg31 is indicated (region enclosed by broken lines). The *Eco*RI and *Hin*dIII map of the left arm of the *N. glauca* inverted repeat is shown at the bottom of the figure. In this presentation the left arm is shown in opposite orientation to *b*. *b*, A restriction map of the Ri-T_L homologous region of λNg31 compared with the left T-DNA of pRiA4b. The pRiA4b region is drawn as an imperfect inverted repeat with a breakpoint indicated by the dotted line. In the bacterium it is organized as *a*. Common restriction sites are shown above each map as arrows. Also indicated as hatched areas are the location of subcloned probes from these regions, g1 is from λNg31 and r1 from pFW94[2]. pFW94 is a cosmid clone including the left DNA of pRiA4b[2,3].

Methods. Restriction maps were made by single or multiple restriction enzyme digests of λNg31 or pFW94 or of subclones of these two. The alignment between the two maps was deduced from Southern blots of pFW94 probed with subclones of λNg31 and vice versa. Restriction digests were as manufacturer's instructions and Southern blots were as previously described[12]. The clone g1 was subcloned from λNg31 DNA digested with *Xho*I into the *Sal*I site of pUC8[13]. The clone r1 was subcloned from pFW94 as a *Pst*I fragment in pUC8.

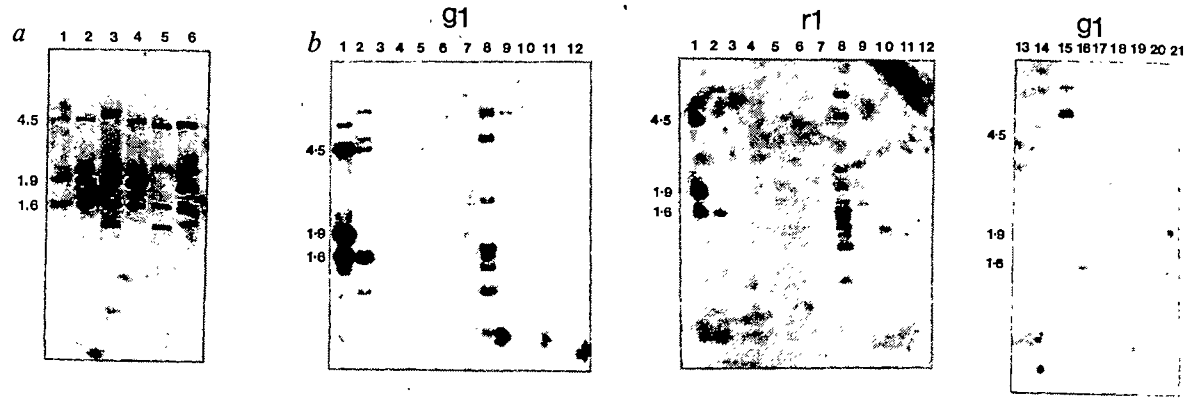
a
1 2 3 4 5 6
4.5
1.9
1.6
b
g1
1 2 3 4 5 6 7 8 9 10 11 12
4·5
1·9
1·6
r1
1 2 3 4 5 6 7 8 9 10 11 12
4·5
1·9
1·6
g1
13 14 15 16 17 18 19 20 21
4·5
1·9
1·6

Fig. 2 *a*, Genomic Southern blots of *Eco*RI digest total DNA of six varieties of *N. glauca* hybridized with probe g1 from the Ri-T_L homologous DNA of *N. glauca*. The position and extent of g1 is indicated on Fig. 1*b*. Samples: 1, our standard line from which λNg31 was obtained; 2, line 23; 3, line 23a; 4, line 23b; 5, line 23c; and 6, line 23d. *b*, Genomic Southern blots of a variety of species from the genus *Nicotiana* and the family *Solanaceae* hybridized with either the left arm of the *N. glauca* inverted repeat, g1, or the corresponding region from pRiA4b probe r1 (positions indicated in Fig. 1*b*). Species are: 1, *N. glauca*; 2, *N. tabacum*; 3, *N. benthamiana*; 4, *N. debneyi*; 5, *N. langsdorffii*; 6, *N. glutinosa*; 7, *Solanum americanum*; 8, *N. otophora*; 9, *Petunia hybridia*; 10, *N. rustica*; 11, *Datura stramonium*; 12, *Solanum melongena* (Eggplant); 13, *N. knightiana*; 14, *N. benavidesii*; 15, *N. tomentosa*; 16, *N. tomentosiformis*; 17, *N. solanifolia*; 18, *N. cordifolia*; 19, *N. setchellii*; 20, *N. paniculata*; 21, *N. raimondii*. Control blots probed with the vector, pUC8 with no insert, showed no hybridization (data not shown). The 23 numbered *N. glauca* lines and some of the other tobaccos were obtained from V. A. Sissons, USDA, Agricultural Research Service, Tobacco Research Laboratory, Route 2, Box 16G, Oxford, North Carolina 27565, USA.

Methods. Southern blots were prepared as previously described[13]. The blots presented in panels *b* were prepared with the following modifications. Hybridization was performed in 50% formamide with 5×SSC at 42 °C. The blots were washed three times, for 30 min each, at 67 °C in 1×SSC. The blots presented in panel *a* were prepared as described previously[13]. The final high stringency wash was omitted.

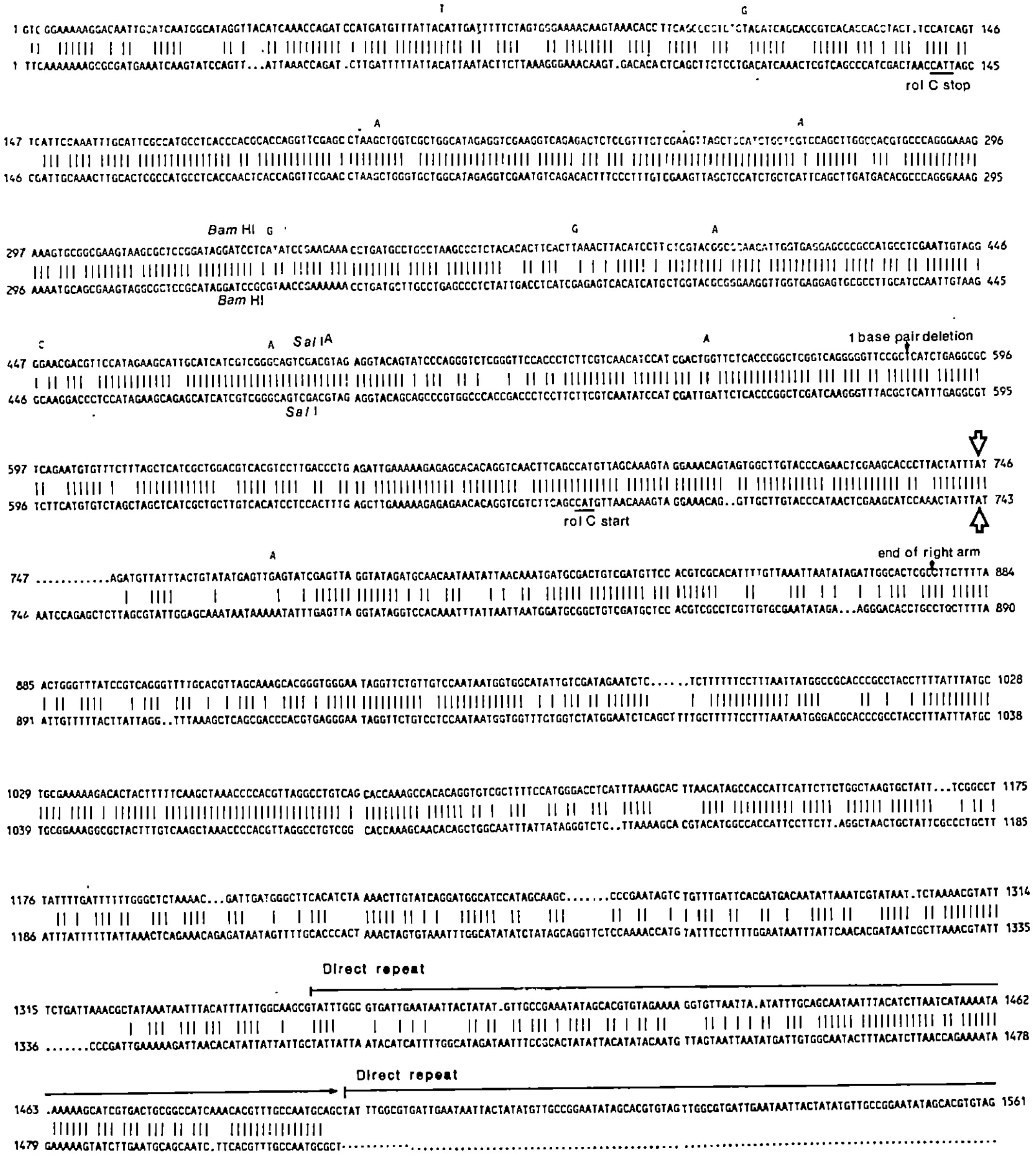

Fig. 3 Comparison of the nucleotide sequence of the *rolB-C* region of *N. glauca* (upper) and pRiA4b (lower). The upper strand is from the left arm of the *N. glauca* inverted repeat up to the break point. The right arm is fused to the left at nucleotide 875 and it is completely homologous with the left except at the positions indicated above the upper strand. Bars indicate homology. (Gaps were inserted on each strand to obtain alignment). *rolB* and *rolC* TATAA boxes are indicated by open arrows.

Methods. The dideoxy chain termination method was used to sequence deletions of M13 clones derived from either λNg31 or pFW94[14,15]. Both strands of both regions were sequenced.

The *A. rhizogenes* T_L DNA is dispensable for rhizogenesis on many species of plants. However, four *rol* loci affecting rhizogenesis on *Kalanchöe* have been described[3]. Figure 1*a* summarizes previously published data on the T_L DNA of pRiA4b[3,5]. The T_L DNA is compared with the extent of the homologous region from *N. glauca*, which is shorter than the T_L DNA (refs 3, 4; Fig. 4). This *N. glauca* region contains homology with *rolB*, *rolC* and *rolD*, but not with *rolA*. Restriction mapping of the region of λNg31 homologous with the T_L DNA showed that this region is organized an inverted repeat at least 13 kilobases (kb) in length (Fig. 1*b*). This repeat is imperfect at its centre such that the left arm is longer than the right. Also shown is the corresponding region from pRiA4b which is present as a single copy and for illustration is drawn as an imperfect inverted repeat. Comparison of the restriction sites between the two structures reveals that more than half of the sites examined are common to both. The fragment lengths are similar and within the region sequenced common sites are homologous (Fig. 4). Each arm of the *N. glauca* structure is approximately colinear with the T_L DNA (Ri-T_L) of pRiA4b. The structure and close correspondence of this region of the *N. glauca* genome to the Ri plasmid suggested it may be a result of a recent infection of *N. glauca* by an *A. rhizogenes* strain closely related to pRiA4b. Transformation by an *Agrobacterium* strain bearing the related Ti-plasmid can result is similar inverted repeat T-DNAs[6].

To examine the distribution of related sequences within the species *N. glauca*, the genomes of five varieties were analysed with Southern blots using a probe subcloned from λNg31 (Fig. 2*a*). Homology with the left arm of the inverted repeat was detected in all five varieties. Three of these varieties were collected from the wild in Peru, Bolivia and Paraguay, respectively. As the Ri-T_L homologous region was detected in all varieties of *N. glauca* tested, the evolution of these sequences in higher plants or introduction from *Agrobacterium* may have preceded the speciation of *N. glauca*.

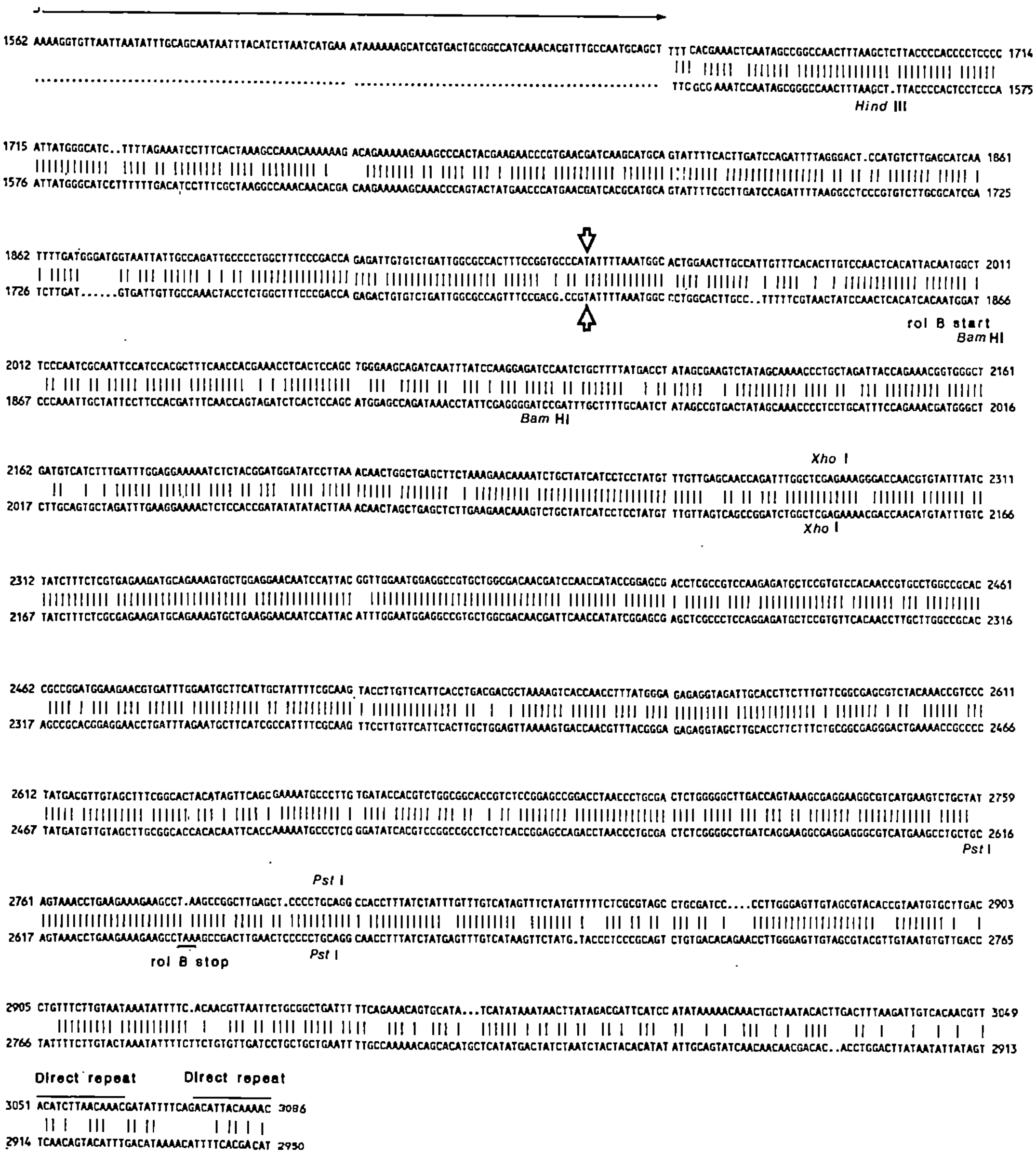
Hind III
rol B start
Bam HI
Bam HI
Xho I
Xho I
Pst I
Pst I
rol B stop
Pst I
Direct repeat
Direct repeat

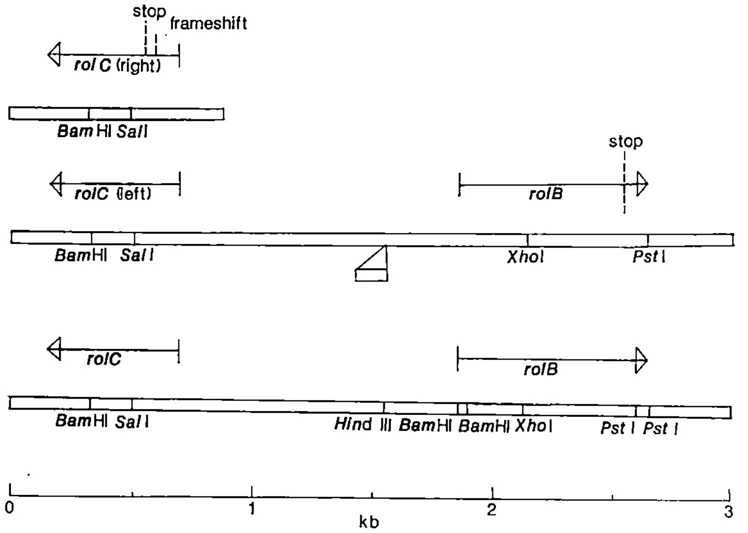
stop
frameshift
rol C (right)
Bam HI Sal I
N.glauca
stop
rolC (left)
rolB
BamHI Sal I
XhoI
PstI
rolC
rolB
A.rhizogenes
BamHI Sal I
Hind III BamHI BamHI XhoI
Pst I Pst I
0
1
2
3
kb

Fig. 4 Comparison of the *rolB-C* region of *N. glauca* (top) and pRiA4b (bottom), based on the sequence data presented in Fig. 5. The left arm of the *N. glauca* structure is shown, 875 bp of the right arm is shown inverted and above the corresponding region of the left. The reading frames of pRiA4b and the corresponding regions from *N. glauca* are drawn as arrows. Interruptions in the *N. glauca* reading frames are indicated (dashed lines).

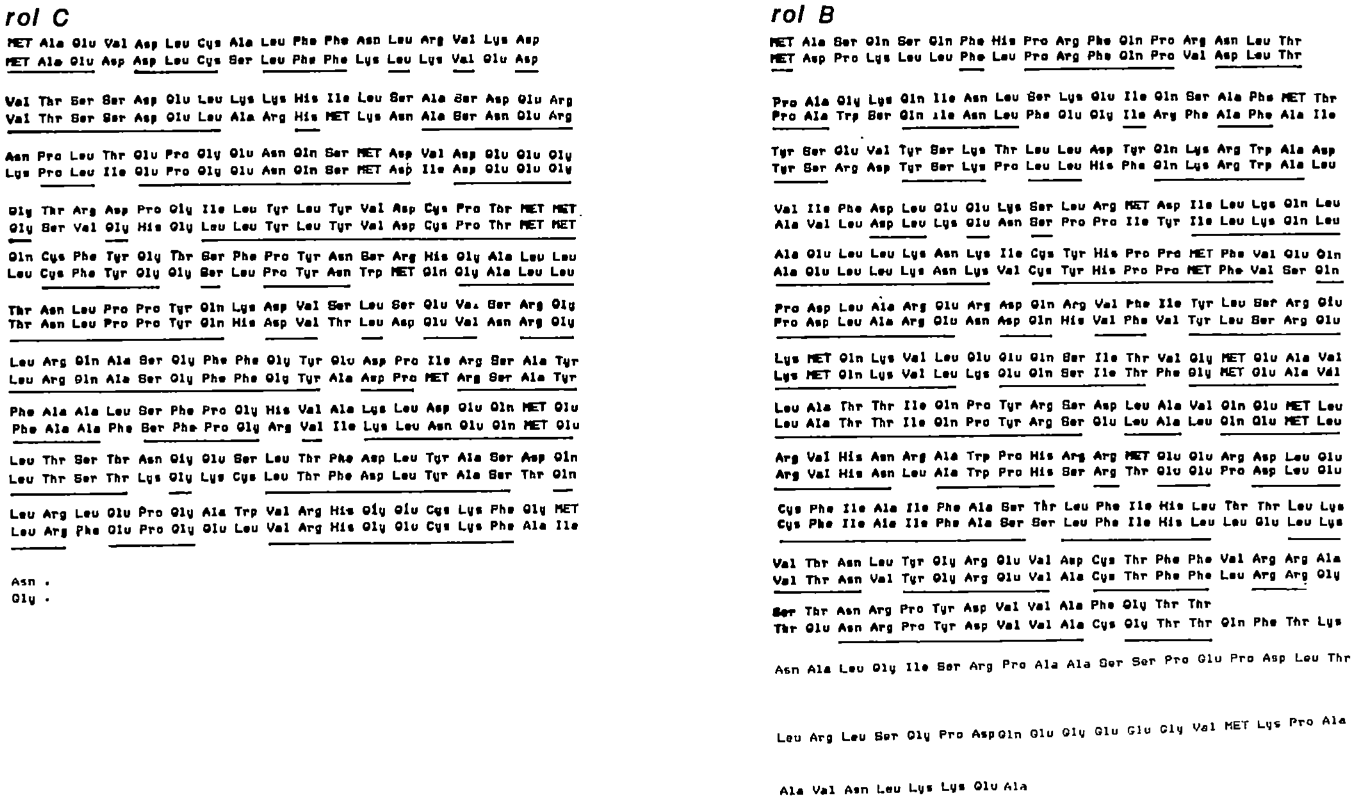

rol C

```
MET Ala Glu Val Asp Leu Cys Ala Leu Phe Phe Asn Leu Arg Val Lys Asp
MET Ala Glu Asp Asp Leu Cys Ser Leu Phe Phe Lys Leu Lys Val Glu Asp

Val Thr Ser Ser Asp Glu Leu Lys Lys His Ile Leu Ser Ala Ser Asp Glu Arg
Val Thr Ser Ser Asp Glu Leu Ala Arg His MET Lys Asn Ala Ser Asn Glu Arg

Asn Pro Leu Thr Glu Pro Gly Glu Asn Gln Ser MET Asp Val Asp Glu Glu Gly
Lys Pro Leu Ile Glu Pro Gly Glu Asn Gln Ser MET Asp Ile Asp Glu Glu Gly

Gly Thr Arg Asp Pro Gly Ile Leu Tyr Leu Tyr Val Asp Cys Pro Thr MET MET
Gly Ser Val Gly His Gly Leu Leu Tyr Leu Tyr Val Asp Cys Pro Thr MET MET

Gln Cys Phe Tyr Gly Thr Ser Phe Pro Tyr Asn Ser Arg His Gly Ala Leu Leu
Leu Cys Phe Tyr Gly Gly Ser Leu Pro Tyr Asn Trp MET Gln Gly Ala Leu Leu

Thr Asn Leu Pro Pro Tyr Gln Lys Asp Val Ser Leu Ser Glu Val Ser Arg Gly
Thr Asn Leu Pro Pro Tyr Gln His Asp Val Thr Leu Asp Glu Val Asn Arg Gly

Leu Arg Gln Ala Ser Gly Phe Phe Gly Tyr Glu Asp Pro Ile Arg Ser Ala Tyr
Leu Arg Gln Ala Ser Gly Phe Phe Gly Tyr Ala Asp Pro MET Arg Ser Ala Tyr

Phe Ala Ala Leu Ser Phe Pro Gly His Val Ala Lys Leu Asp Glu Gln MET Glu
Phe Ala Ala Phe Ser Phe Pro Gly Arg Val Ile Lys Leu Asn Glu Gln MET Glu

Leu Thr Ser Thr Asn Gly Glu Ser Leu Thr Phe Asp Leu Tyr Ala Ser Asp Gln
Leu Thr Ser Thr Lys Gly Lys Cys Leu Thr Phe Asp Leu Tyr Ala Ser Thr Gln

Leu Arg Leu Glu Pro Gly Ala Trp Val Arg His Gly Glu Cys Lys Phe Gly MET
Leu Arg Phe Glu Pro Gly Glu Leu Val Arg His Gly Glu Cys Lys Phe Ala Ile

Asn .
Gly .
```

rol B

```
MET Ala Ser Gln Ser Gln Phe His Pro Arg Phe Gln Pro Arg Asn Leu Thr
MET Asp Pro Lys Leu Leu Phe Leu Pro Arg Phe Gln Pro Val Asp Leu Thr

Pro Ala Gly Lys Gln Ile Asn Leu Ser Lys Glu Ile Gln Ser Ala Phe MET Thr
Pro Ala Trp Ser Gln Ile Asn Leu Phe Glu Gly Ile Arg Phe Ala Phe Ala Ile

Tyr Ser Glu Val Tyr Ser Lys Thr Leu Leu Asp Tyr Gln Lys Arg Trp Ala Asp
Tyr Ser Arg Asp Tyr Ser Lys Pro Leu Leu His Phe Gln Lys Arg Trp Ala Leu

Val Ile Phe Asp Leu Glu Glu Lys Ser Leu Arg MET Asp Ile Leu Lys Gln Leu
Ala Val Leu Asp Leu Lys Glu Asn Ser Pro Pro Ile Tyr Ile Leu Lys Gln Leu

Ala Glu Leu Leu Lys Asn Lys Ile Cys Tyr His Pro Pro MET Phe Val Glu Gln
Ala Glu Leu Leu Lys Asn Lys Val Cys Tyr His Pro Pro MET Phe Val Ser Gln

Pro Asp Leu Ala Arg Glu Arg Asp Gln Arg Val Phe Ile Tyr Leu Ser Arg Glu
Pro Asp Leu Ala Arg Glu Asn Asp Gln His Val Phe Val Tyr Leu Ser Arg Glu

Lys MET Gln Lys Val Leu Glu Glu Gln Ser Ile Thr Val Gly MET Glu Ala Val
Lys MET Gln Lys Val Leu Lys Glu Gln Ser Ile Thr Phe Gly MET Glu Ala Val

Leu Ala Thr Thr Ile Gln Pro Tyr Arg Ser Asp Leu Ala Val Gln Glu MET Leu
Leu Ala Thr Thr Ile Gln Pro Tyr Arg Ser Glu Leu Ala Leu Gln Glu MET Leu

Arg Val His Asn Arg Ala Trp Pro His Arg Arg MET Glu Glu Arg Asp Leu Glu
Arg Val His Asn Leu Ala Trp Pro His Ser Arg Thr Glu Glu Pro Asp Leu Glu

Cys Phe Ile Ala Ile Phe Ala Ser Thr Leu Phe Ile His Leu Thr Thr Leu Lys
Cys Phe Ile Ala Ile Phe Ala Ser Ser Leu Phe Ile His Leu Leu Glu Leu Lys

Val Thr Asn Leu Tyr Gly Arg Glu Val Asp Cys Thr Phe Phe Val Arg Arg Ala
Val Thr Asn Val Tyr Gly Arg Glu Val Ala Cys Thr Phe Phe Leu Arg Arg Gly

Ser Thr Asn Arg Pro Tyr Asp Val Val Ala Phe Gly Thr Thr
Thr Glu Asn Arg Pro Tyr Asp Val Val Ala Cys Gly Thr Thr Gln Phe Thr Lys

Asn Ala Leu Gly Ile Ser Arg Pro Ala Ala Ser Ser Pro Glu Pro Asp Leu Thr

Leu Arg Leu Ser Gly Pro AspGln Glu Gly Glu Glu Gly Val MET Lys Pro Ala

Ala Val Asn Leu Lys Lys Glu Ala
```

Fig. 5 Predicted amino-acid sequence of the *rol* gene products: left panel, Ng *rolC* left (upper) and Ri*rolC* (lower), right panel, Ng*rolB* (upper) and Ri*rolB* (lower). Identical amino acids are underlined.

To learn more of the origin of the region, we included other members of the genus *Nicotiana* and the family Solanaceae in the study (Fig. 2*b*). Homology with both the left arm of the *N. glauca* inverted repeat, gl, and the corresponding *A. rhizogenes* subclone, rl, is limited to species in the subgenera *rustica* and *tabacum*. However, not all species in these two subgenera showed homology. *Nicotiana otophora*, *N. tomentosiformis*, *N. tomentosa* and *N. benavesdesii* all show homology. Probes from both *A. rhizogenes* and *N. glauca* hybridized to similar bands in each species. No homology was detected in three members of the subgenus *petunioides*. Other members of the Solanaceae (Fig. 2*b*) and other higher plant genera (data not shown) did not hybridize to these probes. In at least one species, *N. tabacum*, a large region corresponding to the *rolB* and *rolC* loci, is absent (data not shown). The dispensability and limited distribution provide strong evidence for the hypothesis that the T_L-homologous region results from an *Agrobacterium* infection early in the evolution of the genus *Nicotiana*.

We propose that early in the evolution of the genus *Nicotiana* an infection by *Agrobacterium* resulted in the introduction of a T-DNA closely resembling T_L DNA of pRiA4b into the plant genome. This event may not have resulted in neoplastic growth because present-day Ri-T_L DNA is insufficient for rhizogenesis on any host tested[3]. However, even if neoplastic growth resulted, *A. rhizogenes*-transformed tissue can revert to normal growth both *in vitro* and *in vivo*[7,8]. We further propose that flowering shoots derived from the transformed tissue were fertile and gave rise to a transformed progeny. This mechanism is plausible as *A. rhizogenes*-transformed plants are fertile and transmit T_L DNA to their progeny[7,8]. Subsequent evolution of the transformed plants gave rise to the subgenera *rustica* and *tabacum*. The data suggest that this infection occurred in the species complex preceding the divergence of pre-*tabacum* and pre-*rustica* lines. Species lacking detectable homology may result from subsequent loss of these sequences. An alternative possibility is a later origin and lateral spread through these two subgenera by interspecific hybridization.

The sequence of the plant and plasmid copies of *rolB-C* region are presented and compared in Fig. 4. Only two open reading frames >300 base pairs (bp) were found in the 3-kb region of pRiA4b sequence. The positions correspond to the locations of *rolB* and *rolC* as identified by transposon mutagenesis and to the approximate position and sizes of messages (compare Figs 3 and 4 and Fig. 1*a*). We designate these *A. rhizogenes* reading frames as Ri*rolB* and Ri*rolC*, to distinguish them from the corresponding regions from *N. glauca*, Ng*rolB* and Ng*rolC*.

The corresponding region of the *N. glauca* T_L homologous region is the centre of the imperfect inverted repeat. In this presentation the sequence of the long left arm is shown up to the break point of the inversion (Fig. 4). We sequenced 875 bp of this right arm and compared it with the left (Fig. 4). Since the generation of the inverted repeat, the two arms have diverged by 1.5%. Within the sequenced regions each arm of the inverted repeat is approximately colinear with the corresponding *A. rhizogenes* sequence. We examined the *N. glauca* sequence for reading frames corresponding to those found in *A. rhizogenes*. Because of the imperfect inverted repeat, two regions corresponding to *rolC* are present in *N. glauca*. The *rolC* region of the right arm of the inverted repeat, Ng*rolC* right, is a pseudo-gene. The reading frame corresponding to Ri*rolC* is interrupted by a 1-bp pair deletion only 100 bp into the gene and 32 bp later a substitution generates a stop codon in the original reading frame. The Ng*rolC* left reading frame is intact and translation start and stop codons are present at the corresponding positions to Ri*rolC*. The Ng*rolB* reading frame starts at the corresponding base and continues for 633 bp, 144 bp shorter than Ri*rolB*. Ng*rolB* has an early stop codon compared with Ri*rolB* (Figs 4, 5). Thus, Ng*rolB* can potentially encode a polypeptide 48 amino acids shorter than Ri*rolB* (Fig. 5). The sequence of Ng*rolB* beyond the early stop is strongly homologous with Ri*rolB*. The above considerations reveal that *N. glauca rolB* and *rolC* genes are at least partially degenerate in that *rolB* is truncated and *rolC* right has both a frameshift and a stop codon. As Ng*rolC* left is intact and Ng*rolC* right is not, it is reasonable to assume their common ancestral sequence resembled Ng*rolC* left at these positions. All five reading frames are preceded by a sequence similar to a TATAA box and all show a concensus eukaryotic ribosome binding site of the form A/GXXATGG[9].

Since the divergence of these *A. rhizogenes* and *N. glauca* sequences, only a single frameshift has occurred in 1,857 bp of reading frame. In contrast, 25 frameshifts are evident in 1,240 bp of homologous intergenic DNA. This difference implies that selection has maintained the open reading frames in both sequences. The reading frames are 83% homologous in DNA sequence, whereas the homology in the intergenic regions averages only 75%, not counting frameshifts and not including obviously non-homologous regions. Comparing Ng*rolC* left and Ri*rolC*, the number of changes at the third base of the codon exceeds the sum of such changes at the first and second. The amino-acid sequences of the predicted polypeptides are 75% homologous (Fig. 5). Both sets of reading frames have been conserved in length and content for at least some of the period of time since their divergence.

The Ri-T_L homologous region found in *N. glauca* is a large, imperfect, inverted repeat. Similar structures can be generated on integration of T-DNAs[6]. None of the *A. rhizogenes* strains examined to date are duplicated in this region[2,3,10,11]. Therefore, the inverted repeat was probably generated in the genus *Nicotiana* either at integration or by a later duplication. The levels of sequence divergence between the left and the right arms can be used to set a minimum estimate on the divergence since the original integration event. The sequence divergence between the left and right arms is 1.5% and for the *rolC* region alone is 1.9%, whereas the divergence between Ri*rolC* and either Ng*rolC* is 17%. Most of the divergence preceded duplication of the *N. glauca* region and may have occurred in the *Agrobacterium* strain inciting the infection. If duplication occurred at infection, >85% of the divergence would have been in separate *Agrobacterium* strains. It seems possible that *A. rhizogenes* strains more related to the inciting bacterium than pRiA4b exist.

The left arm of the *N. glauca* inverted repeat contains an intact *rolC* reading frame and a *rolB* reading frame nearly 80% of the length of the *A. rhizogenes rolB* reading frame. The integrity of these reading frames might be taken as evidence for conservation,, and thus function, in the genus *Nicotiana*. However, most of the divergence preceded duplication of this region and may have occurred in *Agrobacterium* where selective pressure would maintain these reading frames. If this is true, the presence of these reading frames in *N. glauca* may merely reflect the passage of insufficient time to allow them to become obviously degenerate.

We have presented evidence for a lateral interkingdom transfer of DNA from *Agrobacterium* to *Nicotiana* and its subsequent passage in evolutionary time. Plants transformed with the T_L DNA of present-day strains of *A. rhizogenes* show various developmental changes, including reduced apical dominance, wrinkled leaves and an increased width-to-length ratio in leaves[8]. These phenotypes are presumably caused by the expression of the integrated *rol* genes. The presence of comparable reading frames in the genome of *N. glauca* may have in evolution and may now significantly contribute to phenotype of plants containing them.

We thank Alice Montoya and Al Legro for help and advice, and Donna Akyioshi, Toby Bradshaw, Anath Das, Dean Rigeur and Steve Zeigler for critical reading of the manuscript. I.J.F. was supported initially by a Damon-Runyon postdoctoral fellowship and subsequently by an SERC (UK) postdoctoral fellowship.

Received 12 July; accepted 30 October 1985.

1. White, F. F., Ghidossi, G., Gordon, M. P. & Nester, E. W. *Proc. natn. Acad. Sci. U.S.A.* **79**, 3193–3197 (1982).
2. Huffman, G. A., White, F. F., Gordon, M. P. & Nester, E. W. *J. Bact.* **157**, 269–276 (1984).
3. White, F. F., Taylor, B. H., Huffman, G. A., Gordon, M. P. & Nester, E. W. *J. Bact.* **164**, 33–44 (1985).
4. White, F. F., Garfinkel, D. J., Huffman, G. A., Gordon, M. P. & Nester, E. W. *Nature* **310**, 348–350 (1983).
5. Taylor, B. H., White, F. F., Nester, E. W. & Gordon, M. P. *Molec. gen. Genet.* (in the press).
6. Kwok, W. W., Nester, E. W. & Gordon, M. P. *Nucleic Acids Res.* **13**, 459–471 (1985).
7. Costantino, P., Spano, Pomponi, M., Benvenuto, E. & Ancora, G. *J. Molec. appl. Genet.* **2**, 465–470 (1984).
8. Tepfer, D. *Cell* **37**, 959–967 (1984).
9. Barker, R. F., Idler, K. B., Thompson, D. V. & Kemp, J. D. *Pl. molec. Biol.* **2**, 335–350 (1983).
10. Lahners, K., Byrne, M. C. & Chilton, M.-D. *Plasmid* **11**, 130–140 (1984).
11. Spano, L., Pomponi, M., Costantino, P., Van Slogteren, G. M. S. & Tempe, J. *Pl. molec. Biol.* **1**, 291–300 (1982).
12. Thomashow, M. F., Nutter, R., Montoya, A. L., Gordon, M. P. & Nester, E. W. *Cell* **19**, 729–739 (1980).
13. Vieira, J. & Messing, J. *Gene* **19**, 259–268 (1982).
14. Sanger, F., Nicklen, S. & Coulson, A. R. *Proc. natn. Acad. Sci. U.S.A.* **74**, 5463–5467 (1977).
15. Guo, L.-H. & Wu, R. *Nucleic Acids Res.* **10**, 2065–2084 (1982).

Erratum

Mycobacterium leprae-specific protein antigens defined by cloned human helper T cells

T. H. M. Ottenhoff, P. R. Klatser, J. Ivani, D. G. Elferink, M. Y. L. de Wit & R. R. P. de Vries

Nature **319**, 66-68 (1986).

In this letter there were errors in the Note Added in Proof, which which should read: Recent experiments show that also on the recombinant 36K *M. leprae*-specific protein, expressed in *Escherichia coli*, different *M. leprae*-specific protein determinants are detected by these *M. leprae*-specific TLC.

Corrigendum

Efficiency of petroleum expulsion from shale source rocks

D. Leythaeuser, M. Radke & R. G. Schaefer

Nature **311**, 745-748 (1984).

As discovered only recently, the squalane product which we used as internal standard for quantitation of the gas chromatography data was contaminated by 5.4% pristane. Therefore, the data based on pristane concentrations shown in Figs 2 and 3, respectively, are in error. Values were corrected accordingly and selected rock samples re-analysed for verification. Listed are sample depth (m); the corrected pristane/*n*-heptadecane ratio; and, in parentheses, the pristane/phytane ratio: 1,126.7 = 0.60 (3.21); 1,131.3 = 0.44 (2.95); 1,132.6 = 0.58 (2.65); 1,133.1 = 0.48 (2.50); 1,135.3 = 0.29 (1.60); 1,142.8 = 0.21 (1.96); 1,148.1 = 0.14 (1.82); 1,152.65 = 0.19 (1.96); 1,155.5 = 0.11 (1.58); 1,159.5 = 0.06 (2.14); 1,161.0 = 0.06 (1.26); 1,162.5 = 0.05 (1.16).

As seen from these corrected data, our earlier conclusion of an increasing fractionation between pristane and *n*-heptadecane (expressed by the increase of the ratio between both compounds) with increasing degree of hydrocarbon expulsion from shale source rocks remains valid. However, the magnitude of this fractionation and the corresponding ratio changes are considerably less than we previously thought.

Palaeontological and molecular views of panda phylogeny

THE recent valuable contribution to panda phylogeny by O'Brien *et al.*[1] corroborates quite well the existing palaeontological information.

Ailuropoda, the giant panda, has distinctive teeth and skull. It was a major and widespread element in the early Pleistocene fauna of southeast Asia, and its ancestors occurred much farther afield. Thenius[2,3] has shown that it originated from the poorly known late Miocene bear *Agriarctos*, which has not yet been found outside Europe. *Agriarctos* had a separate origin from the modern bears in the earlier Miocene genus *Ursavus*. Thenius put the divergence time of *Ailuropoda* between 15 and 20 Myr, as does an average of the molecular chronologies of O'Brien *et al.*, although neither approach can as yet be very accurate here.

Thenius[2] and others[4,5] have also contributed to the fossil history of *Ailurus*, the lesser panda. The Holarctic Pliocene genus *Parailurus* is a collateral relative, and both came from the Eurasian genus *Sivanasua* of the early and middle Miocene. *Sivanasua* is a good if primitive procyonid, branching between the divergence of modern mustelids and procyonids. The Procyonidae would perhaps be polyphyletic if the ancestral musteloids are excluded from this family; even *Ailurus* retains some basicranial and other features changed in other modern procyonids but also retained by bears. The relevant late Eocene and Oligocene genera of the Amphicyonidae, in a broad sense, have not yet been studied adequately by current methods and so the time of divergence of Procyonidae and Ursidae within that interval is unclear. I agree[1,6] that subfamilial distinction of each panda, with its relatives, from the rest of the members of their respective families is appropriate.

LEIGH M. VAN VALEN
Biology Department (Whitman),
University of Chicago,
915 East 57th Street,
Chicago, Illinois 60637 USA

1. O'Brien, S. J., Nash, W. G., Wildt, D. E., Bush, M. E. & Benveniste, R. E. *Nature* **317**, 140-144 (1985).
2. Thenius, E. *Z. Säugetierk.* **44**, 286-305 (1979).
3. Thenius, E. *Z. Geol. Wiss.* **10**, 1029-1042 (1982).
4. Pilgrim, G. E. *Palaeont. Indica, New Ser.* **18**, 1-232 (1932).
5. Tedford, R. H. & Gustafson, E. P. *Nature* **265**, 621-623 (1977).
6. Stains, H. J. in *Orders and Families of Recent Mammals of the World* (eds Anderson, S. & Jones, J. K., Jr) 491-521 (Wiley, New York, 1984).

O'BRIEN *ET AL.* REPLY—We are pleased indeed to have our molecular phylogeny corroborated by the palaeontological record as pointed out by such eminent authorities as Professors Kurtén (*Nature* **318**, 487; 1985) and Van Valen (above). It is reassuring to find that the molecular topology we have constructed can be consistently interpreted by the limited, but informative fossil record of the ursid and procyonid progenitors. Because of inherent limitations in any individual approach, synthetic analysis of multiple methods of phylogenic inference is particularly important in the resolution of evolutionary relationship. Derivation of a consensus molecular / cytogenetic / palaeontological story for the pandas is a persuasive example of how a long debated puzzle can be correctly resolved and the bases for the controversies themselves ultimately interpreted. I hope that our agreement concerning the assignment of subfamily status of the giant panda in the Ursidae will be adopted by students of mammalian taxonomy.

STEPHEN J. O'BRIEN*
WILLIAM G. NASH*
RAOUL E. BENVENISTE*
DAVID E. WILDT†
MITCH E. BUSH†
**Laboratory of Viral Carcinogenesis,*
National Cancer Institute,
Frederick, Maryland 21701, USA
† *Department of Animal Health,*
National Zoological Park,
3000 Connecticut Avenue,
Washington, DC, USA

Oncofetal antigens

IN the review article by Feizi[1] the term 'oncofetal' antigen (OFA) is used to describe those determinants that are expressed in fetal, tumour and specific adult tissues in modified or quantitatively varying levels. This misnomer has become a common problem to many tumour biologists. Many view the oncofetal antigen prototype as carcinoembryonic antigen (CEA) or α-fetoprotein (AFP). This is incorrect. Although these antigens were first considered as examples of re-expressed fetal gene products that were proposed to be tumour-specific in adults, the subsequent discovery of their presence in diseased, non-tumour tissue as well as some limited expression in normal adult tissues should have caused them to be classified as differentiation antigens. The purpose of this response is to implore tumour biologists to use the correct nomeclature.

For clarification, the original definition of the term oncofetal antigen, put into contemporary use in the early 1970s by Alexander, Medawar and my group after CEA and AFP were found not to be tumour-specific markers, was as follows: OFAs are antigen substances expressed exclusively as phase-specific autoantigens in developing embryo or fetal tissues of metazoans and in their tumours[2]. The important criteria that must be fulfilled if an epitope is to be classed as an OFA are: (1) The expression of the OFA epitope must be restricted to embryo, fetal and tumour tissue and not be found in any adult, normal tissue; (2) The OFA epitope must be autoantigenic in the pregnant female carrying the embryo or fetus and in the tumour-bearing host.

Epitopes not fulfilling these criteria are differentiation antigens if they are transiently or permanently expressed in adult as well as fetal and/or tumour tissue with or without autoimmunogenicity and reflect various stages of cellular differentiation.

Adherence to this simple set of distinguishing criteria in naming tissue-associated antigens will greatly avoid confusion. Examples of possible true OFAs are the polypeptides of relative molecular mass 44,000 and 200,000 recently described in fetal and tumour cells of rodents and man[3] and possibly certain phosphorylated or truncated forms of the protein p53.

I further recommend that antigens similar to those described in ref. 1 be designated embryo/fetal/tumour (EFT) differentiation antigens. Such EFT differentiation determinants would conventionally be detected with xenogeneically derived antibody or monoclonal antibody as epitopes that appear in greater concentration in embryo-fetal and tumour tissue than in normal, fully differentiated, adult tissue. The term oncodevelopmental antigen should be discontinued as it has never been formally defined.

JOSEPH H. COGGIN JR
Department of Microbiology
and Immunology,
University of South Alabama
College of Medicine, Mobile,
Alabama 36688, USA

1. Feizi, T. *Nature* **314**, 53-57 (1985).
2. Ambrose, K., Andersson, N. & Coggin, J. *Nature* **233**, 194-195 (1971).
3. Payne, W. & Coggin, J. H. *J. natn. Cancer Inst.* **75**, 527-544 (1985).

FEIZI REPLIES—My article[1] was based on information available on the precise antigenic determinants expressed on the surface of cells and recognized by monoclonal antibodies as tumour-associated, developmentally regulated or other differentiation antigens. At the time (and to my knowledge even now) the only characterized determinants have been carbohydrate sequences. Clearly it will be desirable to classify properly the various antigens in their biological context when their structures and distributions in diverse tissues have been thoroughly evaluated. Nomenclature can then be rationalized.

TEN FEIZI
Applied Immunochemistry Research Group,
Clinical Research Centre,
Watford Road, Harrow,
Middlesex HA1 3UJ, UK

Automated continuous flow peptide synthesis

From R.P. Andrews

As peptide-based drugs and reagents become a reality, a new method of peptide synthesis is beginning to come into its own.

THE chemical synthesis of peptides is a rapidly expanding feature of biotechnology, urged on by the two areas of research that stand to benefit from it. In immunolo-ology, detailed antigen–antibody studies consume large numbers of peptides, and analogues of a single parent sequence are often needed in smaller quantities. In pharmaceutical research, short peptide fragments mimicking fragments of viral protein are the key components of synthetic vaccines[1].

Synthetic peptides can be genetically engineered, but this process involves a large initial capital outlay and is generally unsuitable for producing small amounts of short (less than 30 amino acids) peptides for research use. Attention has therefore focused on ways of improving the chemical methods for peptide synthesis. Within the past few years, a novel and superior chemistry has emerged.

Tradition

Merrifield first introduced the solid-phase method of peptide synthesis in 1962[2]. Initially, an ester linkage attaches the C-terminal amino acid to a polystyrene support. Subsequent amino acids are added by a repetitive protocol of: (1) amino protecting group cleavage by trifluoroacetic acid (TFA); (2) neutralization using triethylamine/dichloromethane (DCM); and (3) acylation/amino-acid addition, usually using *t*-butoxycarbonyl (Boc) amino acids in the presence of dicyclohexylcarbodiimide (DCCI) and DCM.

Anhydrous hydrogen fluoride breaks the ester linkage to the polystyrene support and removes the side-chain protecting groups from those amino acids with reactive side chains.

Although the Merrifield chemistry has been used successfully for 20 years, it does have drawbacks. The use of TFA at every addition cycle and the use of hydrogen fluoride for removing the peptide from the resin can cause side reactions with many amino acids that are unstable in vigorous acidic treatment[3-6]. The products of acid-catalysed cleavage reactions can cause additional problems; for instance, benzyl cations can react with the nucleophilic sulphur atom of methionine or modify tyrosine's phenolic ring. The repeated use of strong acids can also cause selective peptide bond cleavage — aspartyl-prolyl bonds are particularly susceptible[7].

Overall, the Merrifield method often achieves high levels of protein purity after a final purification by HPLC. Purification of the final synthesis product, however, still poses difficulties, as even the most sophisticated HPLC systems may not separate peptide impurities that are of marginally different length and composition.

Polyamide method

At the Medical Research Council (MRC) in Cambridge, England, workers have devised a new method of peptide synthesis that eliminates many of the customary problems and could eventually allow full control of the synthesis reaction[8-10]. Based on polyamide resin rather than polystyrene, this solid-phase system conducts all the chemical operations under mild and substantially optimized reaction conditions. The method still adheres to the basic principles laid down by Merrifield, but differs from the established technique in several ways.

First, the substituting of polystyrene with polar polyamide gel supports enables polar aprotic solvents such as dimethylformamide (DMF) to freely permeate the gel media. Second, the use of fluorenylmethoxycarbonyl (Fmoc) amino-acid derivatives[11], rather than Boc derivatives, removes the requirement for repeated acid treatments at each deprotection reaction. Third, instead of a simple benzyl ester agent for peptide–resin linkage, the polyamide method uses a range of substituted benzyl alcohol derivatives that can be cleaved under either strong acid (TFA), dilute acid or basic conditions[12].

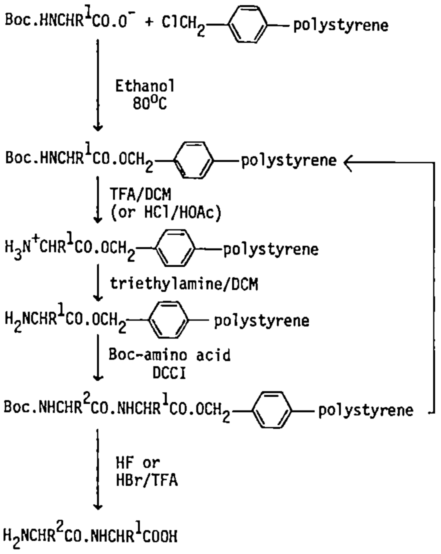

Boc.HNCHR^{1}CO.O$^-$ + ClCH$_2$ polystyrene
Ethanol 80°C
Boc.HNCHR^{1}CO.OCH$_2$ polystyrene
TFA/DCM (or HCl/HOAc)
H$_3$N$^+$CHR^{1}CO.OCH$_2$ polystyrene
triethylamine/DCM
H$_2$NCHR^{1}CO.OCH$_2$ polystyrene
Boc-amino acid DCCI
Boc.NHCHR^{2}CO.NHCHR^{1}CO.OCH$_2$ polystyrene
HF or HBr/TFA
H$_2$NCHR^{2}CO.NHCHR^{1}COOH

Fig. 1 Protocol for peptide synthesis using the polyamide method and Fmoc amino-acid PFP esters. Norleucine (Nle) is permanently bound to the polymer and acts as an internal reference.

Perhaps the main advantage of the polyamide method is its suitability for use in a continuous flow system. The introduction of a composite resin[11] is the key to this method's success. In this resin, the dimethylacrylamide-based monomer mixture is polymerized within the pores of a rigid, macroporous, kieselguhr matrix. Reactant diffusion into and out of this matrix is rapid and pressure evolution is negligible under normal flow conditions. Of equal importance, flow systems are more amenable to analytical control. Continuous spectrophotometric effluent monitoring is easily achieved and raises the possibilty of automated feedback control of each synthesis cycle.

The chemical character of the amino-acid derivatives figures importantly in schemes for true synthesis automation. For polyamide chemistry, Fmoc amino-acid symmetric anhydrides have been the derivatives of choice, but these unstable compounds must be formed immediately prior to synthesis. The introduction of Fmoc amino-acid pentafluorophenyl (PFP) active esters combines the high reaction rates and freedom from side reactions achievable with Fmoc amino-acid anhydrides with the crystallinity and stability of active esters[13]. Full automation of the Fmoc polyamide method is then relatively simple.

The synthesis protocol in conjunction with Fmoc amino-acid PFP esters is shown in Fig. 1. The first amino-acid derivative is secured with the formation of an ester bond using 4-dimethylaminopyridine (DMAP) in DMF. Deprotection of the N-terminal amino-acid group is rapidly achieved using 20 per cent piperidine in DMF. Subsequent amino-acid derivatives are then added in DMF with 1-hydroxybenzotriazole (HOBT) acting as a catalyst, and each N-terminal amino-acid group must be deprotected before the next amino-acid is added. The protocol shown in Fig. 1 incorporates an acid–labile peptide–resin linkage agent which is finally removed in 95 per cent TFA.

In 1983, Sheppard described a semi-automated instument for peptide synthesis using the polyamide protocol[9]. In collaboration with the MRC in Cambridge, LKB Biochrom has now developed a fully automated system.

The commercial instrument closely follows the original design[9]. A single amino-acid addition (except for the C-terminal residue) follows the sequence:

(1) The autoinjector draws a mixture of

amino-acid derivative and HOBT catalyst dissolved in DMF and the mixture is delivered to the column via the spectrophotometer. The instrument then enters a recirculation mode. During the first pass of the amino-acid derivative through the column, 90 to 95 per cent of the amino groups available are acylated[9]. Subsequent passes usually complete acylation in 30 min.

(2) Unreacted Fmoc amino-acid PFP ester is pumped to waste and the column is washed with DMF.

(3) To deprotect the N-terminal amino-acid, 20 per cent piperidine in DMF is pumped through the column.

(4) All traces of piperidine are removed from the column with a DMF wash cycle, which prepares the column for the next amino-acid addition. A complete cycle takes approximately one hour.

Cycle control must be accurate and flexible, a personal computer is required to store and execute synthesis protocols. The computer enables the user to change synthesis parameters such as acylation or deprotection times.

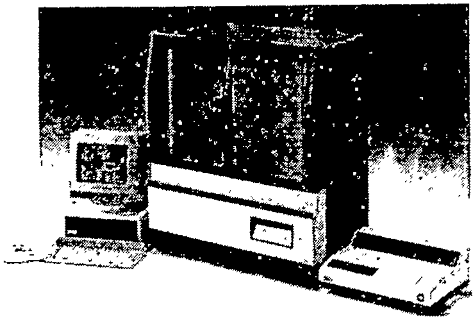

Fig. 2 LKB's fully automated continuous-flow peptide synthesizer

The complete peptide synthesis system is shown in Fig. 2. HPLC data from unpurified cleaved peptides have revealed excellent purity levels[14], indicating that once continous-flow polyamide synthesis has been fully developed the purification step may become unnecessary. ☐

R.P. Andrews is at LKB Biochrom Limited, Science Park, Milton Road, Cambridge CB4 4FJ, UK

1. Audibert, F. *et al. Proc. natn. Acad. Sci. U.S.A.* **79**, 5042 (1982).
2. Merrifield, R.B. *Fedn Proc.* **21**, 41 (1962): *J Am. chem. Soc.* **85**, 2149 (1963).
3. Sano, S., & Kawanishi, S. *Am. chem. Soc.* **97**, 3480 (1975).
4. Feinberg, R.S. & Merrifield, R.B. *J. Am. chem Soc.* **97**, 3485 (1975).
5. Brandt, W.F., Henschen, A. & Van Holt, C. in *Methods in Protein Sequence Analysis* (ed. Elzinga, M.) 101-109 (Humana Clifton, New Jersey, 1982).
6. Ondetti, M.A., Deer, A., Sheenan, J.T., Pluscic, J. & Kocy, O. *Biochemistry* **7**, 4069 (1968).
7. Wade, J.D., Fitzgerald, S.P., McDonald, M.R., McDougall, J.G. & Treger, G.W. *Biopolymers* (in press).
8. Atherton, E., Gait, M.J., Sheppard, R.C. & Williams, B.J. *Bioorgan. Chem.* **8**, 351-370 (1979).
9. Sheppard, R.C. *Chem. Brit.* **19**, 402-414 (1983).
10. Atherton, E., Clive, D.L.J. & Sheppard, R.C. *J.C.S. Perkin* 529-537 (1981).
11. Atherton, E., Logan, C.J. & Sheppard, R.C *J.C.S. Perkin I* 529-537 (1981).
12. Sheppard, R.C. & Williams, B.J. *Int. J. Peptide Protein Res.* **20**, 451-454 (1982).
13. Atherton, E., Brown, E. & Sheppard, R.C. *JCS Chem Commun.*, 1151-1152 (1981).
14. Auffret, A.D. & Meade, L.G. *Proc. Synth. Peptides Biol. Med.*, Hämeenlinna, Finland 6-8 June 1985 (in press).

A separation sampler

Innovations in separation methods dominate the new products for peptide and DNA research. Machery Nagel has introduced a new series of **anion-exchange HPLC columns** that will separate compounds ranging from oligonucleotides to very large DNA molecules. (Reader Service No. 100). The Nucleogen stationary phase series consists of three groups of columns based on silica gel with pore sizes of 60 Å, 500 Å and 4,000 Å. The Nucleogen DEAE 60-7 column is designed for the isolation of short nucleic acid chains (MW 25,000 to 1,000,000), while the DEAE 4000-10 performs separations of high-molecular weight nucleic acids. The columns operate at high flow rates and high pressures (up to 300 bar) and will survive 1,000 repetitions without loss of resolution. In the United Kingdom these new columns are available from Technicol Ltd.

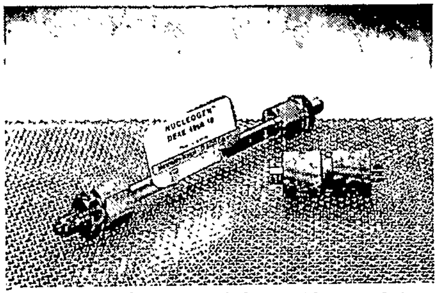

Nucleogen columns work from pH *2.5 to 8.0*

The Separations Group is offering a high-efficiency **HPLC column for rapid nucleotide analysis** (Reader Service No. 101). Using a low-capacity ion-exchange material on a protected silica substrate, the Vydac nucleotide analysis column can resolve the twelve major mono-, di- and triphosphonucleotides completely in 10 minutes. It measures 5 cm in length with a 4.6 mm internal diameter, and supports a flow rate of 2.0 ml per minute.

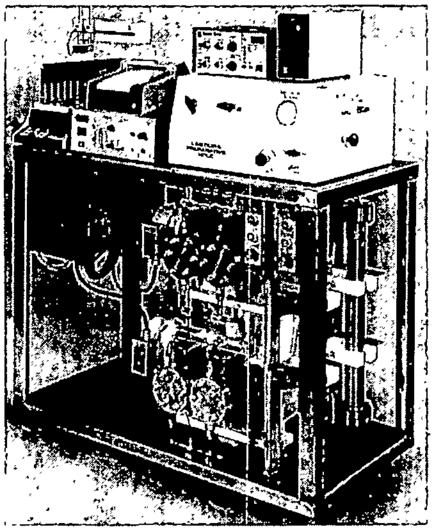

The Vydac improves upon traditional HPLC

For **preparative and process HPLC**, Separations Technology Inc. has produced three new instruments able to provide both isocratic and continuous gradient solvent delivery (Reader Service No. 102). Because all three systems feature hydraulic dual-head pumps for high-pressure operation, they can be packed with particles as small as 10 μm in diameter to achieve optimum resolution. The versatile ST/LAB 800 utilizes 1- to 4-inch diameter columns and performs at pressures up to 1,800 p.s.i. It accommodates a sample load of up to 250 g and has a maximum flow rate of 1,600 ml per minute. The ST/LAB 2000 provides pilot-plant level HPLC for sample loads ranging from 50 to 1,000 g per minute. The unit has a throughput of up to 3,000 ml per minute on 1- to 6-inch diameter columns. Completely explosion-proof, the ST/LAB 2000 and the process-scale ST/Process 2000 systems operate at pressures up to 2,000 p.s.i. The ST/Process 2000 will separate kilogram-size sample loads on 4- to 10-inch diameter columns with a maximum throughput of 8,500 ml per minute.

For high-pressure separation of active proteins and peptides, Pharmacia Inc. makes fully **biocompatible FPLC systems** supplemented by a new line of components (Reader Service No. 103). The new FPLC instruments extend the system's solvent delivery capacity to 5,100 p.s.i. and can construct configurations for both isocratic and gradient separations. The centre of the expanded solvent delivery system, the high performance pump P-3500, produces highly consistent flow rates with low pulsation. The low dead volume mixer, model 35 MPa, and the PV-7 valve or PMV-7 motor valve comprise the remainder of the new system. The 7-port valves enable manual or automatic sample injection, respectively. The tubing kit, P-3500, connects the instruments with tubings, fittings and unions made from inert materials.

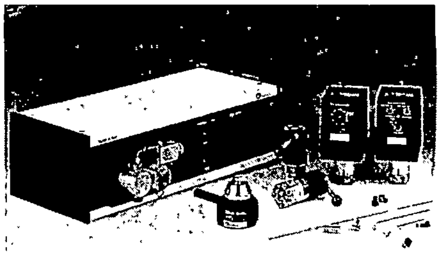

Pharmacia's system preserves bioactivity

The first **phenyl-bonded reversed-phase column** of polymer base gel comes from Kratos Analytical (Reader Service No. 104). Highly concentrated phenyl groups

These notes are based on information provided by the manufacturers. To obtain further details about these products use the reader service card bound inside the journal.

give this new column the capacity to separate proteins and biological polymers. The average pore size of the Toyo Soda TSKgel Phenyl-5PW RP is about 100 nm.

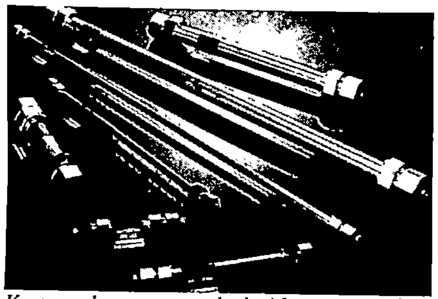

Kratos columns are packed with two new gels

It boasts outstanding chemical stability and separation of high-molecular-weight proteins over a wide pH and solvent range. Kratos also supplies a **silanol-free stationary phase column** that performs separations not previously possible with reversed-phase columns with a minimal amount of organic solvent. The C_1-bonded silica gel gives a high recovery rate and low adsorptivity, and the TSKgel TMS-250 is best suited to analytical and preparative chromatographic resolution.

Interaction Chemicals Inc. has developed **a novel material for reversed-phase liquid chromatography** applications. The ACT-1 column contains Macrophase-1, a polymer that has been covalently bonded with $-(CH_2)_{17}CH_3$, or 'C18', functional groups (Reader Service No. 105). Because only carbon–carbon and carbon–hydrogen bonds exist in the polymer matrix, the material remains stable from pH 0 to 14. The C18 groups reduce capacity factors dramatically, allowing separation of aliphatic and heterocyclic amines. The ACT-1's rigid structure (80 Å pore size) holds up under normal HPLC conditions, and its pH stability facilitates the separation of nitrogen-containing compounds.

For fast protein profiling, the Bio-Rad Quick Check analyser gives **HPLC results in 15 to 20 minutes** (Reader Service No. 106). The instrument can monitor protein purification steps or enzymatic reactions, and check the purity of individual proteins. It separates proteins by size with an efficiency and gentleness comparable to that of classical gel filtration chromatography. The analyser's buffers will not denature samples, so fragile molecules can be recovered intact for further analysis and characterization.

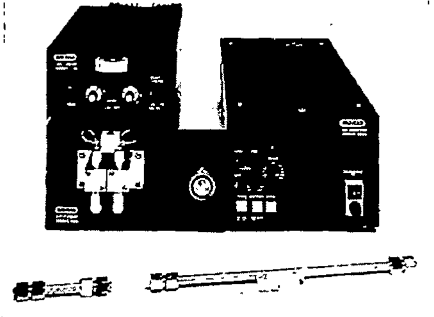

The Quick Check gives optimum results between pH 2.0 and 7.0

Du Pont has introduced a new addition to its **gel filtration** family for separating proteins by size. The Zorbax GF-450 Bio Series column performs separations of biomolecules with molecular weights from 17,500 to 900,000 with high resolution, outstanding reproducibility and durability over a broad pH range (Reader Service No. 107). As with other Bio Series columns, the typical protein recovery rate of the GF-450 is 95% or greater, and biological activity is generally maintained. The column will carry out lengthy separations in aqueous mobile phases having pH values up to 8.5. The GF-450 is 25 cm long and has an inner diameter of 9.4 mm.

Electrophoresis extras

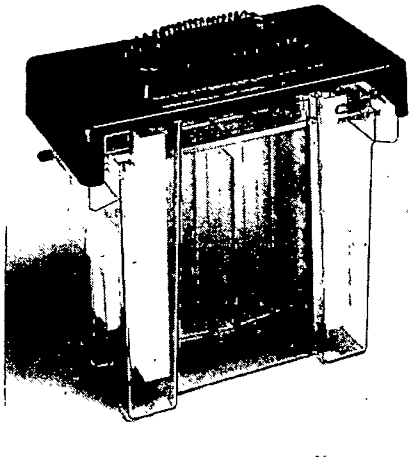

Bio-Rad's Protean II is a snap to assemble

Several manufacturers offer other **improvements in electrophoresis equipment.** Bio Rad's versatile Protean II slab cell (Reader Service No. 108) can accommodate most common electrophoretic techniques, including SDS, two-dimensional, native and agarose gel electrophoresis. Supplemented with various combs, spacers and accessories, the Protean II can run up to four slab gels or 16 tube gels simultaneously. The basic unit handles gels 16 or 20 cm long, and requires only 1.5 litres of buffer. The central cooling core of the Protean II cell assures even heat distribution over the entire gel length, and single-screw sandwich clamps provide even pressure distribution.

For electrophoretic separation of DNA and RNA fragments in horizontal agarose gels, LKB-Produkter AB now produces **complete agarose submarine systems** based on the new Miniphor and Maxiphor units (Reader Service No. 109). The Maxiphor system is intended for preparative and analytical separations and is compatible with any gel not greater than 10 mm thick, 15 cm wide and 25 cm long. The Miniphor system performs rapid analytical separations. Both units include the MacroDrive I power supply and are accompanied by a MacroVue ultraviolet transilluminator for visualizing fragments stained with ethidium bromide.

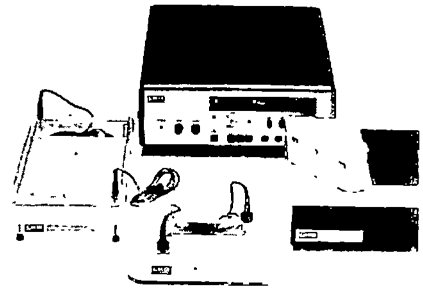

LKB designed two new agaroses for these submarine units

Four **calibration protein kits** are now available from Boehringer Mannheim Biochemicals (Reader Service No. 110). The kits supply individually packaged, highly purified and carefully selected proteins for even band distribution and equal band intensity. Two of the kits are applicable for molecular sieve gel chromatography, the other two for SDS gel electrophoresis.

Gradients, home-made or ready-made

As an accessory to the Mighty Small I and II vertical slab gel units, Hoefer Scientific Instruments now offers a Mighty Small **dual gel caster,** SE 265 (Reader Service No. 111). Included in the Mighty Small package are 10 glass plates, two alumina plates, an acrylic stand, 100 sheets of waxed paper and four of Hoefer's T-shaped spacers.

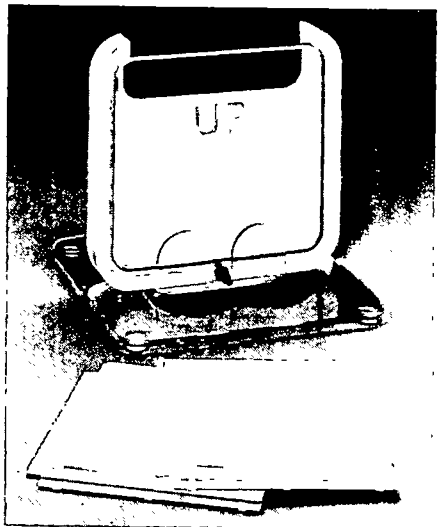

Hoefer's gel caster sets two 7 × 8 cm gels

Integrated Separation Systems details their line of pre-cast, ready-to-use 1.5 mm thick **gradient polyacrylamide gels** in their Sepragels brochure (Reader Service No. 112). The gels are ideal for silver staining and two-dimensional analysis. Sepragels come in heavy-metal-free glass cassettes with glass spacers, and fit all large-gel Hoefer, Bio-Rad, LKB and Pharmacia vertical devices using cassettes in which both glass plates are flush across the top.

A new arrival in **HPLC gradient systems,** Life Science Laboratories Ltd's low-pressure gradient module S8110 can produce binary and ternary gradients with a reproducibility at least as good as that achieved by high-pressure methods (Reader Service No. 113). Gradient profiles made up of two or three solvents can be mixed with 1% accuracy. Interfaced to the S2000 microprocessor-based controller, the S8110 creates a gradient by the selective switching of two-way solenoid valves attached to pressurized reagent bottles. The valves and mixing chambers are designed to eliminate temperature effects, and all components that come into contact with the solvents are composed of inert materials.

Quick and easy cartridges

Romicon, Inc. is ushering in a **new series of disposable cartridges** under the Romisorb title (Reader Service No. 114). The Romisorb SP cartridge comes prepacked with Rohm and Haas's macroreticular copolymer resin, Amberlite XAD-4. This non-ionic resin is suitable for sorbate with MW below 1,000. It adsorbs via van der Waals' interactions, so lends itself to the adsorption of molecules with aromatic rings or aliphatic tails.

ROMISORB
LOT
romicon
SP

The Romisorb resin features 780 square metres of surface area

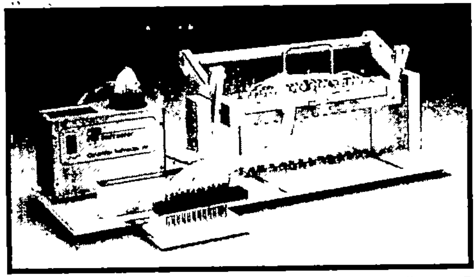
ADVERTISEMENT.

PHD™ Cell Harvesters

Fast error-free results or your money back.

- Deposits 24 samples per operation directly into ANY type of small scintillation vials.
- Tray holds vials in the same orientation as original plate.
- Saves labor and tedium. Mix-ups are impossible.
- Deposits samples into vials at time of harvesting or, optionally, later if desired.
- Rugged and easy-to-use stainless-steel and aluminum mechanism. Lasts a lifetime.
- Unique 24-port wash valve makes flooding impossible and allows use as an EIA/ELISA plate washer.
- Many options and low-cost disposables available:
  - —supernatant collection systems,
  - —harvest-heads and trays for test tubes,
  - —multiple-wash manifolds, hot/cold valves,
  - —harvest-heads for any kind of plate,
  - —harvest-head quick-disconnects, & more.

PHD™ Cell Harvesters cost less than units with fewer features: $2985. We provide a 60-day trial. Complete satisfaction guaranteed or your money back.

Cambridge Technology, Inc.

2464 MASSACHUSETTS AVE., CAMBRIDGE, MA 02140 U.S.A. (617)876-0891

Reader Service No.4

Du Pont has developed an **extraction cartridge for rapid and reliable purification** of nucleic acids. The Nensorb 20 cartridges can purify samples of single- or double-stranded DNA or RNA in a single step taking 15 minutes or less (Reader Service No. 115). Sample size can range from 1 ng to 20 μg with recovery rates of 60 to 90%. Whereas most other solid-phase extraction cartridges are based on ion-exchange resins, the Nensorb 20 contains a proprietary packing material that allows recovery of DNA/RNA in a salt-free water–ethanol solution.

The pick of the literature

Several **new catalogues** have been compiled to tempt the peptide or olignucleotide researcher. Vega Biotechnologies, Inc. is offering three free chemical catalogues: the *Peptide Synthesis Reagent Catalog*, the *DNA Synthesis Reagent Catalog* and *Bioactive Peptides/Enzymes Substrates/General Biochemicals* (Reader Service No. 116). Sigma Chemical Company offers two new product brochures highlighting their lectins and peptides (Reader Service No. 117). *Lectins from Sigma* describes more than 180 lectins and conjugates with a table on lectin properties and a section on raw material sources. Sigma's new *Bioactive Peptides Catalog* lists over 400 chemicals both by alphabetical order and according to their categories. Amersham International has lumped over 90 of its peptide research products into one listing which groups the products into areas of interest (Reader Service No. 118). A batch-specific analytical data sheet comes free with any order for a Novabiochem catalogue (Reader Service No. 119). This year's updated editions include *Amino Acid Derivatives and Reagents for Peptide Synthesis, Biologically Active Peptides, ^{125}I-Labelled Peptides, Enzymes* and *Enzyme Substrates and Enzyme Inhibitors.*

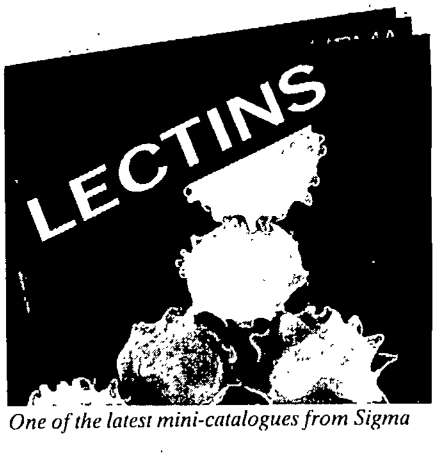

One of the latest mini-catalogues from Sigma

An **applications data sheet** from Beckman Instruments, Inc. describes a gene construction strategy geared to the Beckman System I DNA synthesizer and the yeast copper-metallothionein (Cu-MT) gene (Reader Service No. 120). Data sheet DS-671, entitled *Construction of New Genes and Functional DNA Elements Using System 1 DNA Synthesizer*, gives details on selecting sequences for creating sticky ends, unique restriction sites, phosphorylation of the 5′ ends and annealing of the DNA fragments to assemble a 105-base-pair portion of the gene.

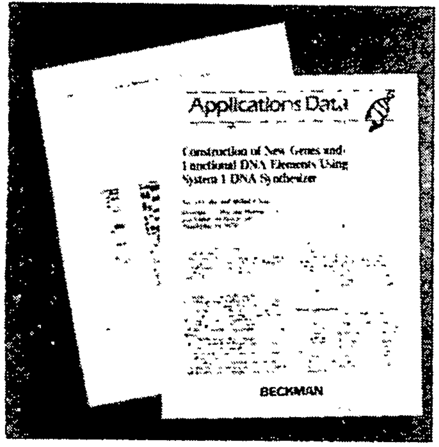
Applications Data
Construction of New Genes and Functional DNA Elements Using System 1 DNA Synthesizer
BECKMAN

The story of one gene's synthesis

Analysis...

A new **amino acid analysis system** for HPLC has arrived from Pickering Laboratories (Reader Service No. 121). The system can be adjusted for either protein/collagen hydrolysates or physiologic fluids and other biological samples. It can be coupled with both integrated liquid chromatographs and component equipment. The product features ion-exchange columns for sodium or lithium chemistries, optimized for regular or high-speed analysis. Two types of guard columns maximize column life. Options available for Pickering Labs' assembly include the CRX390 Post-Column Reactor for high-efficiency ninhydrin development, the FC4870A Flow Conditioner for reagent pump pulse dampening and the CRX650 Column Temperature Controller. Pickering also supplies OPA and TRIONE reagents and sodium and lithium eluents.

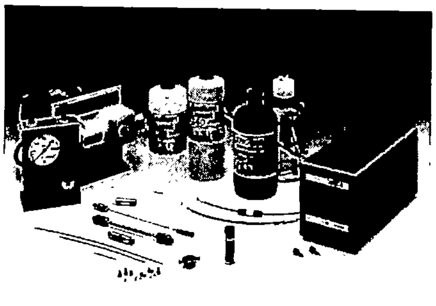

Peptide unpacking gear from Pickering

DNA fragments that resist sequencing by DNA polymerase I Klenow fragment may prove more cooperative when subjected to Bio-Rad's M13 Sequencing Kit-RTase (Reader Service No. 122). The new technique uses **AMV reverse transcriptase for sequencing** by the dideoxy-chain termination method. Bio-Rad's kit also includes deoxy and dideoxy nucleotides, primer No. 1, single-strand sequencing control DNA, reaction buffer, chase solution, stop/load solution, a comprehensive manual and a short protocol. One kit's contents will supply at least 50 sequences.

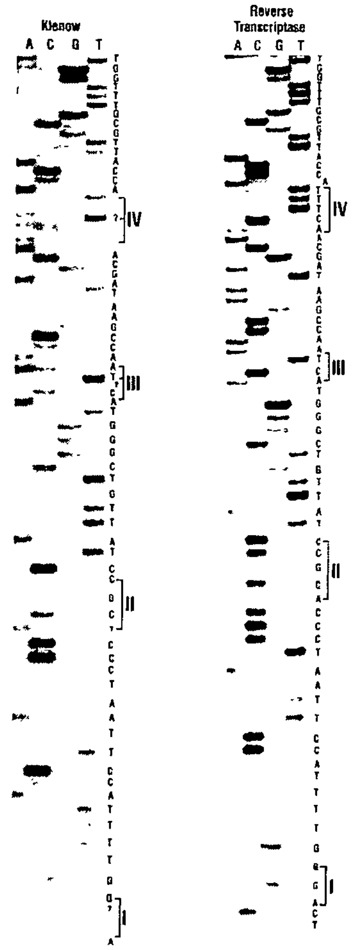

A Bio-Rad alternative for DNA sequencing

...and synthesis

Vega Biotechnologies, Inc. has devised amino acid-substituted PAM (0CH2-phenylacetamidomethyl) resins well-suited to automated or manual solid-phase **synthesis of short or long peptide chains** (Reader Service No. 123). Vega determines the substitution of each lot analytically; values usually lie between 0.3 and 0.5 mmole per gram. Vega also confirms particle size, which usually falls between 200 and 400 mesh (polystyrene resin 1% divinylbenzene crosslinked).

Beckman Ltd., Cruachem Inc. and New Brunswick Scientific (U.K.) Ltd. are promoting their **latest in DNA synthesizers.** Beckman's System 1 Plus incorporates the IBM-PC as its interactive graphic controller, using the computer keyboard or a light pen to enter sequences in the 5′ to 3′ direction (Reader Service No. 124) Selected bases then appear on the screen, colour-coded and with proper codon breaks. Up to 102 bases can be programmed, and a screen indicates which reagent reservoirs will need refilling before the sequence can be completed. Deviations from the standard program, such as altered pump flow rates or synthesis steps, are effected using a programme adjust.

New Brunswick's model 8600 synthesizer uses both β-cyanoethyl amidite and phosphotriester chemistries for **customizing synthesis cycles** (Reader Service No 125). With cyanoethyl amidite, fragments in excess of 150 bases with OD 250 or more of product can be produced with cycle time of less than 6 minutes per coupling. Phosphotriester chemistry is appropriate for rapid, economical short-chain synthesis, such as oligonucleotide fragments up to 50 bases long. The phosphotriester cycle time is less than 7 minutes. With both methods the 8600 offers automated mixed probe-syntheses, automatic de-protection and cleavage and simultaneous four-column synthesis.

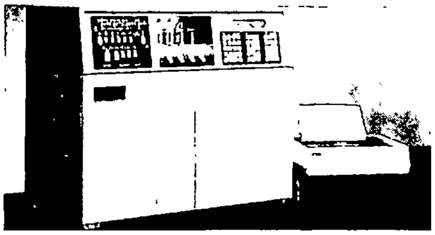

The New Brunswick synthesizer is fully programmable

The PS 200 from Cruachem Inc. utilizes phosphotriester or phosphoamidite protocols in **an interactive four-column synthesis system** (Reader Service No 126). Its programmable software issues status reports and directs the operator with screen prompts. A single module houses the valves, controllers and reaction columns An optional enclosed carousel accommodates up to eight solvent reservoirs.

Schleicher and Schuell have developed four **high-purity grades of blotting paper** as an alternative to the chromatographic grades originally employed in blot transfer techniques (Reader Service No. 127). GB 001, the thinnest blotting paper featured, is intended for protecting gels or cellulose nitrate. GB 004, the thickest paper, has a high absorption capacity to facilitate rapid and complete transfer as required, for example, with the Southern blot method. ☐

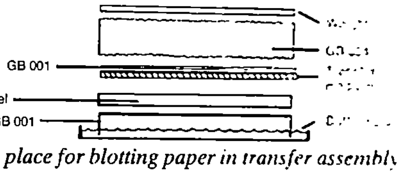

A place for blotting paper in transfer assembly

BOOKS RECEIVED

Astronomy

New Aspects of Galaxy Photometry. J.L. NIETO (ed.). *Springer-Verlag:1985. Pp.350. ISBN 0-387-15657-7. Pbk DM 52.*

The Sky at Night. By PATRICK MOORE. *Patrick Stephens, Wellingborough, UK:1985. Pp.192. Pbk ISBN 0-85059-753-6. £6.99.*

Venus, Mars and Satellites of the Outer Planets. R.W. SHORTHILL and A.T. BASILEVŠKY (eds). *Pergamon:1985. Pp.124. Pbk ISBN 0-08-033197-1. Np.*

Psychology

Critical Issues in American Psychiatry and the Law, Vol.2. RICHARD ROSNER (ed.). *Plenum: 1985. Pp.307. Hbk ISBN 0-306-41954-8. Np.*

The Hands of the Living God: An Account of a Psycho-analytic Treatment. By MARION MILNER. *Chatto & Windus: 1985. Pp.444. ISBN 0-7012-0299-8. £17.50.*

Psychology. By DIANE E. PAPALIA and SALLY WENDKOS OLDS. *McGraw-Hill: 1985. Pp.658. ISBN 0-07-048401-5. £26.25.*

When Children Don't Learn; Understanding the Biology and Psychology of Learning Disabilities. By DAVE DIANE MCGUINNESS. *Basic Books Inc, New York: 1985. Pp.310 Hbk ISBN 0-465-09178-4. $19.95.*

Sociology

The Custody of Children: A Behavioural Assessment Model. By RICHARD A. MARAFIOTE. *Plenum: 1985. Pp.277. Hbk ISBN 0-306-41874-6. Np.*

Early Identification of Children at Risk: An International Perspective. WILLIAM K FRANKENBURG, ROBERT N EMDE and JOSEPH W SULLIVAN (eds). *Plenum: 1985. Pp.393. Hbk ISBN 0-306-41946-7. Np.*

History of Science

From Maxwell to Microphysics: Aspects of Electromagnetic Theory in the Last Quarter of the Nineteenth Century. By JED Z. BUCHWALD. *University of Chicago Press: 1985. Pp.339. Hbk ISBN 0-226-07882-5. Np.*

The Papers of Joseph Henry, Vol.5, January 1841–December 1843. NATHAN REINGOLD (ed.). *Smithsonian Institution Press: 1985. Pp.506. Hbk ISBN 0-87474-793-7. $45.*

The Prehistory of Flight. By CLIVE HART. *University of California Press: 1985. Pp.279. ISBN 0-520-05213-7. £29.75, $40.25.*

General

About Science. By BARRY BARNES. *Basil Blackwell: 1985. Pp.163. Pbk ISBN 0-631-14158-8. Hbk £16.50; pbk £5.95.*

Alternative Therapies. G.T. LEWITH (ed.). *Heinemann: 1985. Pp.223. Pbk ISBN 0-433-19270-4. £9.95.*

Anticipatory Systems: Philosophical, Mathematical and Methodological Foundations. By ROBERT ROSEN. *Pergamon: 1985. Pp.436. ISBN 0-08-031158-X. $35.*

The Art of Planning: Selected Essays of Harvey S. Perloff. LELAND S. BURNS and JOHN FRIEDMANN (eds). *Plenum: 1985. Pp.364. Hbk ISBN 0-306-42030-9. Np.*

Beningfield's English Landscape. By GORDON BENINGFIELD. *Viking: 1985. Pp.140. Hbk ISBN 0-670-80202-6. £14.95.*

Benzene: Scientific Update. MYRON A. MEHLMAN (ed.). *Alan R. Liss: 1985. Pp.499. ISBN 0-8451-0245-1. £19.*

Bergson. By LESZEK KOLAKOWSKI. *Oxford University Press: 1985. Pp.115. Hbk ISBN 0-19-287645-7; pbk ISBN 0-19-287644-9. Hbk £8.95; pbk £2.25.*

Cambridge and Clare. By HARRY GODWIN. *Cambridge University Press: 1985. Pp.230. ISBN 0-521-30765-1. £19.50. $42.50.*

A Century of Controversy: Ethnological Issues from 1860 to 1960. By ELMAN R. SERVICE. *Academic: 1985. Pp.351. ISBN 0-12-637380-9. $48, £42.*

Chemie und Gesellschaft: Herausforderung an Eine Welt im Wandel. By G. BOCHE. *Pp.215. ISBN 3-921324-01-7. DM 68.*

Computational Methods for the Determination of Formation Constants. DAVID J. LEGGETT (ed.). *Plenum: 1985. Pp.478. Hbk ISBN 0-306-41957-2. Np.*

Creativity in Science — A Symposium Organized by the Fellows of the Los Alamos National Laboratory. MUDUNDI R. RAJU. JAMES A. PHILLIPS and FRANCIS HARLOW (eds). *Los Almos National Laboratory, New Mexico: 1985. Np.*

Cultural Imperialism and Exact Sciences. German Expansion Overrseas 1900–1930. By LEWIS PYENSON. *Peter Lang: 1985. Pp.342. Hbk ISBN 0-8204-0159-5. SWFr 80.*

The Cultural-Bound Syndromes: Folk Illnesses of Psychiatric and Anthropological Interest. RONALD C. SIMONS and CHARLES C. HUGHES (eds). *D. Reidel: 1985. Pp.516. Hbk ISBN 90-277-1858-X. Dfl.195, £54.25, $69.00.*

Curious Encounters: Phantom Trains, Spooky Spots, and Other Mysterious Wonders. By LOREN COLEMAN. *Faber and Faber: 1985. Pp.176. Pbk ISBN 0-571-12542-5. $11.95.*

Current Concepts in Surfactant Research. P. VON WICHERT (ed.). *Karger: 1984. Pp.310. ISBN 3-8055-3916-9. DM 269, $148.*

Ethics and Nuclear Arms; European and American Perspectives. RAYMOND ENGLISH (ed.). *Ethics and Public Policy Centre, Washington, D.C.: 1985. Pp.144. Pbk ISBN 0-89633-095-8. $7.*

Explosive Remnants of War: Mitigating the Environmental Effects. ARTHUR H. WESTING (ed.). *Published for the Stockholm International Peace Research Institute by Taylor & Francis: 1985. Pp.120. Hbk ISBN 0-85066-298-2. £4.95, $9.*

Family and Individual Development. J.A. MEACHAM (ed.). *Karger: 1985. Pp.114. Hbk ISBN 3-8055-4037-X. SFr.73, DM 87, $31.25.*

Fluidization, 2nd Edn. J.F. DAVIDSON, R. CLIFT and D. HARRISON (eds). *Academic: 1985. Pp.733. ISBN 0-12-205552-7. $96.50, £75.*

Forestry Sciences. Winch and Cable Systems. By IVAR SAMSET. *Martinus Nijhoff/Dr W Junk Publishers: 1985. Pp.539. Hbk ISBN 90-247-3205-0. Dfl.175, £60, $48.50.*

Foundations of Business Information Systems. By ANDREW DOSWELL. *Plenum: 1985. Pp.221. Pbk ISBN 0-306-41796-0. Np.*

A Future for Game? By COLIN MCKELVIE. *George Allen & Unwin: 1985. Pp.228. Hbk ISBN 0-04-799030-9. £10.95.*

The Future of Piagetian Theory: The Neo-Piagetians. VALERIE L. SHULMAN, LILLIAN C.R. RESTAINO-BAUMANN and LORETTA BUTLER (eds). *Plenum: 1985. Pp.222. ISBN 0-306-41940-8. Np.*

Gesundheit und Tierschutz. Wissenschaftler melden-sich zu Wort. By K.J. ULLRICH and O.D. CREUTZFELDT. *ECON Verlag, Dusseldorf, Vienna: 1985. Pp.300. Hbk ISBN 3-430-19229-3. Np.*

Glowing Birds: Stories from the Edge of Science. By PATRICK HUYGHE. *Faber: 1985. Pp.241. Pbk ISBN 0-571-12533-6. Pbk $9.95, £5.25.*

The Great American Biotic Interchange. FRANCIS G. STEHLI and S. DAVID WEBB (eds). *Plenum: 1985. Pp.532. Hbk ISBN 0-306-42021-X. Np.*

Handbook of Discourse Analysis. Vol. 3: Discourse and Dialogue. TEUN A. VAN DIJK (ed.). *Academic: 1985. Pp.251. ISBN 0-12-712003-3. $49.50, £40.*

Handbook of Discourse Analysis. TUEN A. VAN DIJK (ed.). *Academic: 1985. Pp.228. ISBN 0-12-712004-1. $45.50, £40.*

Innovation Policy for Small Farmers in the Tropics: The Economics of Technical Innovations for Agricultural Development. By HANS RUTHERNBERG. *Oxford University Press: 1985. Pp.176. ISBN 0-19-859487-9. £17.50.*

Localization and Metal–Insulator Transitions. HELLMUT FRITZCHIE and DAVID ADLER (eds). *Plenum: 1985. Pp.533. Hbk ISBN 0-306-42077-5. Np.*

Portrait of a Country Artist. By C.F. TUNNICLIFFE. *Gollancz: 1985. Pp.160. Pbk ISBN 0-575-03694-X. Pbk £6.95.*

Positive Operators. By CHARALAMBOS D. ALIPRANTIS and OWEN BURKINSHAW. *Academic: 1985. Pp.367. Hbk ISBN 0-12-050260-7. £51.50, $59.*

Pulse: An Ada-Based Distributed Operating System. By D. KEEFFE, G.M. TOMLINSON, I.C. WAND and A.J. WELLINGS. *Academic: 1985. Pp.244. Hbk ISBN 0-12-402970-1. £15.50, $18.50.*

Representation and Responsibility: Exploring Legislative Ethics. BRUCE JENNINGS and DANIEL CALLAHAN (eds). *Plenum: 1985. Pp.332. Hbk ISBN 0-306-41994-7. Np.*

Return from Death: An Exploration of the Near-Death Experience. By MARGOT GREY. *Arkana: 1985. Pp.206. Pbk ISBN 1-85063-019-4. Pbk £4.95.*

Reversal Theory: Applications and Developments. M.J. APTER, D. FONTANA and S. MURGATROYD (eds). *University College Cardiff Press: 1985. Pp.203. ISBN 0-906449-74-X. £17.50.*

Self-Organization: Autowaves and Structures Far from Equilibrium. V.I. KRINSKY (ed.). *Springer-Verlag: 1985. Pp.263. ISBN 3-540-15080-3/0-387-15080-3. DM 98.*

Shackleton. By RONALD HUNTFORD. *Hodder and Stoughton: 1985. Pp.774. Hbk ISBN 0-340-25007-0. £19.95.*

The Skywatcher's Handbook: Night and Day. By COLIN A. RONAN. *Corgi: 1985. Hbk ISBN 0-552-99196-1; pbk ISBN 0-552-99146-5. Pbk £6.95.*

The Structure of Moral Action: A Hermeneutic Study of Moral Conflict. By M.J. PACKER. *Karger: 1985. Pp.158. ISBN 3-8055-3999-1. Np.*

The Structure of Surfaces. M.A. VAN HOVE and S.Y. TONG (eds). *Springer-Verlag: 1985. Pp.435. ISBN 3-540-15410-8/0-387-15410-8. DM 138.*

Uranium and Nuclear Energy:1984. PROCEEDINGS OF THE NINTH INTERNATIONAL SYMPOSIUM HELD BY THE URANIUM INSTITUTE. *The Uranium Institute:1984. Pp.395. ISBN 0-946777-047. £45.*

Victimization in Schools. By GARY D. GOTTFREDSON and DENISE C. GOTTFREDSON. *Plenum: 1985. Pp.250. Hbk ISBN 0-306-42023-6. Np.*

A Victorian World of Science. By ALAN SUTTON. *Adam Hilger, Techno House, Redcliffe Way, Bristol: 1985. Pp.227. Hbk ISBN 0-85274-559-1. £12.50, $20.*

Vietnam Veterans: The Road to Recovery. By JOEL OSLER BRENDE and ERWIN RANDOLPH PARSON. *Plenum:1985. Pp.270. ISBN 0-306-41966-1. Np.*

Le Vipere d'Italia e d'Europa. By SILVIO BRUNO. *Calderini: 1985. Pp.269. Pbk ISBN 88-206-2500-8. Np.*

Visions of Apocalypse: End or Rebirth? SAUL FRIEDLANDER, GERALD HOLTON, LEO MARX AND EUGENE SKOLNIKOFF (eds). *Holmes & Meier, New York: 1985. Pp.268. Hbk ISBN 0-8419-0673-4; pbk ISBN 0-8419-0755-2. Hbk $28.50; pbk $15.*

Water, Earth, and Fire: Land Use and Environmental Planning in the New Jersey Pine Barrens. By JONATHAN BERGER and JOHN W. SINTON. *The Johns Hopkins University Press: 1985. Pp.228. ISBN 0-8018-2398-6. £24.*

Women, Drinking and Pregnancy. By MOIRA PLANT. *Tavistock: 1985. Pp.168. ISBN 0-422-7810-1. £16.*

World Nutritional Determinants. G.H. BOURNE (ed.). *Karger: 1985. Pp.225. ISBN 3-8055-3948-7. DM 237, $118.75.*

Archaeology

Ancient Sedimentary Environments (3rd edn.). By R.C. SELLEY. *Chapman & Hall: 1985. Pp.317. Pbk ISBN 0-412-25730-0. £10.95.*

Beringia in the Cenozoic Era. V.L. KONTRIMACICHUS (Editor-in-Chief). *Balkema: 1985. Pp.724. ISBN 90-6191-445-0. Dfl.120, $38.50, £30.*

South Atlantic Paleoceanography. K.J. HSU and H.S. WEISSERT (eds). *Cambridge University Press: 1985. Hbk ISBN 0-521-26609-2. £40, $69.50.*

nature

Why did Challenger matter?

The loss last week of the US shuttle Challenger has in some sense shocked the world. It would be good if it helped the United States to a better programme.

THE anguish in the United States and around the world about last week's shuttle accident requires explanation. Why was this accident so much more compelling of public grief than, say, the loss of more than 200 US servicemen in an aircraft accident in Newfoundland just before Christmas or the other even more horrific accidents that studded 1985? There are two threads in any account of how last week's tragedy gripped the sombre imagination of the whole world, of which the first is the proof that Challenger provided that Marshall McLuhan's "global village" is now indeed a reality. The television cameras that recorded both the destruction of the spacecraft and the personal grief of the relatives of its occupants made personal tragedies general. The same television cameras brought the Vietnam war into the living rooms of the United States just over a decade ago, with awesome consequences. Last year, there was the famine in Ethiopia. Nobody will or should complain at the discovery, now, that the global village will increasingly haunt us.

The second reason for the sense of national tragedy in the United States last week is that Challenger carried with it into the Atlantic some of the sense of hope that the United States has cherished for its space programme. The competition in technology from Japan may have turned from an irritation to a cause for dismay, international problems that once seemed small, as in Central America, the Middle East and Central Europe, have turned out to be devilishly complicated, but there seemed, until last week, a high chance that the United States would win a new set of spurs for having made space travel by people into a routine happening. That there might nevertheless be an accident was always on the cards; reason says that the only question to answer was not "whether" but "when". But it is natural, and understandable, that people's pride should have given way to profound disappointment. Mourning is an appropriate mechanism of catharsis. That there has been, with the State of the Union message postponed a week, and the government's tight timetable with it. So what will happen now?

Future

President Reagan says the shuttle programme will continue, and his decision has been echoed, mostly with enthusiasm, throughout the United States. That, no doubt, is what the seven brave men and women who died with Challenger would have wished. Any other decision would turn the present sense of disappointment into one of outright failure. And, for strictly practical reasons, there is no choice. The Pentagon has been anxious about the reliability of the shuttle, and its turn-round time, for years, and is refurbishing some Titan rockets as satellite launchers until a batch of ten specialized rockets are delivered in 1988 or so; but, for some time, the three surviving models of the shuttle have a crucial job to do. The queue of commercial satellites waiting to be put in orbit is also long, and lengthening; and delay means more than mere cost. But this year was also intended to be a good year for launching scientific satellites, of which the Hubble Space Telescope (originially due to go up in August) is by far the most important. The scientific community, of which an influential part is fond of saying that the objectives of the space programme could all more surely and safely be attained with unmanned rockets, should remember that this important instrument will require repeated visits by a shuttle crew during the fifteen years of its intended life.

So what lessons are to be learned? The hardest is that there are no simple lessons. No doubt the National Aeronautics and Space Adminstration will soon find the cause of last week's accident, modify the remaining spacecraft accordingly and restart the programme. In its short time at work, the shuttle has in any case amply demonstrated its usefulness, if not its effectiveness in economic terms. But one of the lasting casualties of last week's accident will be the administration's ambition to put the operation of the shuttle on a commercial footing. Another will be the notion that the entire ambition of the United States in space can be sustained by one chief launching instrument. It would be safer and probably also cheaper to keep the shuttle for the jobs that only the shuttle can carry out, using some other rocket to put everyday satellites into orbits. The obvious difficulty, in the year when the Gramm–Rudman Act will be playing havoc with the federal budget, is that there is no obvious place from which the extra funds can come. But it will be a great misfortune if last week's mood of resolution is too quickly lost in squabbling about budgets.

Plans

That is why it is sensible that the White House is taking a wider look at the future of the space programme as a whole. There are too many anomalies for comfort built into plans for the immediate future. Even Spacelab is an embarrassment, with its complicated arrangements for anticipating what the future could hold by running electrophoresis experiments whose time has not yet come. But the United States is more ambitiously committed to the concept of building a space station somewhere up there. Would it not make sense to let that plan lapse? Certainly the lobby that has been building up to send some kind of mission to Mars had better go into hiding for a while. None of this implies that the successes of the past few years now count for nothing; it is merely that they have enjoyed a run of luck, statistical in nature, that could not have been anticipated. To succeed with the help of luck is no shame, of course, but to expect that the luck will never run out is unwise.

There was particular sadness last week about the death of Christa McAuliffe, the New Hampshire schoolteacher on the shuttle. She had responded to President Reagan's offer, during the 1984 election campaign, to send a schoolteacher into space as an inspiration to students and, perhaps, also to the National Education Association, which seemed to be on the point of endorsing Mr Walter Mondale, Mr Reagan's chief opponent for the presidency. The unpalatable truth is that the venture was a publicity stunt of a kind too often foisted on the US space programme in the past, sometimes by its own managers. What last week's tragedy shows is that there is now no case for carrying on shuttle flights passengers whose presence is not essential. There should be no more schoolteachers, congressmen or even journalists (see *Nature* **319**, 250; 1986) until experience has shown shuttle flights to be mere routine. On the sad showing of last week, that will take some time. □

End of the road?

The British seem to be retreating from the plan to form a strong centre of clinical research.

Nearly a quarter of a century ago, after the first post-war generation of westward transatlantic travellers had returned from Europe with tales of what they had seen, the National Institutes of Health at Bethesda was almost always spoken of with that mixture of admiration and envy that presages imitation. In Britain, by a slow process, the result was eventually a decision to found a clinical research centre, under the aegis of the Medical Research Council (MRC). Now, after fifteen years, the council has been told in clear language (see p.442) that the time has come to call a halt to the venture. The Clinical Research Centre (as the institution is indeed called) has not lived up to expectations. So there are two choices: either merge it with another institution (the Royal Postgraduate Medical School, integrally part of the University of London for sure, possibly the council's own National Institute for Medical Research for another) or, the unpalatable course, close it. How can it be that a scheme that seemed a central part of Britain's research strategy a mere fifteen years ago should now be faced with the prospect of going out of business?

Nobody is particularly to blame, although it remains a fact that the centre has never functioned as what it was intended to be, a national centre of excellence in clinical research. Some of the reasons are peculiarly British. Thus, as it now emerges, those who in 1959 were envious of what was happening at Bethesda, Maryland, also took the view that "in this country the idea of a hospital purely for research is unlikely to acceptable". Thus was born the homespun notion that the new British centre would attempt to weld an excellent research enterprise onto a general hospital, one serving the needs of a local community even if built from scratch for demographic reasons. The expectation that such a hospital could nevertheless become the focus for referrals from the rest of Britain has not been fulfilled; the London teaching hospitals are fierce competitors for patients, teaching hospitals elsewhere especially so. The result, it now appears, is that a third of the special allocation of beds and the general hospital to the centre are, in practice, in the gift of the local public health authority, not the researchers. So perhaps nobody is much to blame for the lacklustre quality of the centre's achievements over the past fifteen years. Even in its own field, other clinical centres increasingly call the shots.

In the circumstances, radical change is obviously desirable. MRC and its advisers appear to agree on that. Indeed, the report which the council has now endorsed describes the outcome of the proposed merger in glowing terms. From the ashes of past disappointment, the story goes, will rise the centre of excellence that people dreamed of decades ago. What are the chances? There are two serious impediments to the proposed recreation of the ideal of the clinical centre, of which the most immediate is boringly administrative. The past few years in Britain have shown how notoriously unwilling are institutions to give up automony. Medical institutions seem especially obdurate in resisting change, at least when it is imposed from outside. Forcing even two of the three institutions now canvassed into one will be an uphill task, likely to be accomplished only if some institution can bless the merger with funds on a scale no longer available. The research council is powerfully placed, knowing that all those concerned are in one way or another in its pay. But it will make no sense to create another organization to pursue excellence in clinical research on a shoestring. Better to close down the Clinical Research Centre than to force it into an impoverished marriage the outcome of which will be yet more disappointment.

The second impediment to the changes now canvassed is qualitatively different and much more serious. Those who recommend change at the Clinical Research Centre skirt around the question why it is so difficult, not merely in Britain but in much of the rest of Europe, to persuade physicians to take research more seriously. This is not to say that there is no worthwhile activity in the field, nor centres of some distinction. But it appears to be a sad property of European medicine that the generality of physicians are more concerned with practising their craft than with turning it into a science. Even the physicians working for the health services alongside the staff of the clinical centre appear not to have been enthused, which is another proof of the disappointment of the past 15 years. Off and on, universities, sometimes with the help of charitable foundations, have sought to tempt physicians into science by one means or another, but without much success. It could be that MRC would more easily attain the objective it has been nursing all these years if it spent some of its resources on tackling the problem at source. Making clinical research worthwhile would be a start. ☐

Giving bugs the vote

The row about the use of genetically engineered bacteria should be stopped.

THE public inquiry (see p.441) about the proposed trial of the efficacy of *Pseudomonas* bacteria in protecting plants against frost damage has become a kind of pantomime. The idea, now well understood, spring from the knowledge that the naturally occurring bacteria are of two kinds, one of which, lacking a protein that provides a nucleating centre for water vapour, can safeguard plant cells from damage caused by ice crystals forming within them. In the wild, the proportions of the two strains of the effective species vary naturally, although there remains some doubt about the reasons why this should be so, which amounts to saying that it is not fully clear what benefits the bacteria derive from their presumably symbiotic relationship with plants. The scheme for protecting plants against frost entails the release of bacteria in which the proportions of protective strains have been artificially increased. This is the prospect described to the Monterey inquiry last month, by the ubiquitious Mr Jeremy Rifkin, as the latter-day equivalent of the first explosion of a nuclear weapons in the atmosphere.

Mr Rifkin must know that he has fertile soil to work. It is, perhaps, a pity that this first case (which, in one form or another, has dragged on for the best part of two years) did not first arise in Iowa, or Texas, where the democratic tendency to accord every possible opinion a semblance of equal time is less well developed. The difficulty in California, which the Monterey inquiry seems to have illustrated, is that freedom of expression has been extended so far that, occasionally, Mr Rifkin appears to be speaking for bacteria, not people. Cleverly he seems to have succeeded in making it possible for ordinary grown-ups to identify with micro-organisms.

The trouble, as with most of the events with which Mr Rifkin is concerned, is that the consequences of the continuation of the pantomime are potentially serious. How so? The economic case for protecting plants from frost cannot easily be denied, but is not as strong as would be, for example, a piece of genetic engineering providing all plants with a means of fixing nitrogen, even in temperate climates. (Monterey enters not because it is prone to frost, but because it is a good site for testing bacterial survival.) But the trouble with what has been happening at Monterey is that Mr Rifkin and his friends may be able to win their point by appealing to simple unreason. Although there is no basis of any kind to suspect that the end point (after a few weeks) of the bacterial populations to be released in the trials would be any different from the naturally varying populations, the doctrine of the equality of all possible opinions, which is too often mistaken for a restatement of the Bill of Rights, may carry the day. It is high time that the seriousness of the threat, no from Mr Rifkin but from the infection of the imagination that h seems bent on producing, is recognized and countered. ☐

US space research

Nobody knows what will happen next

Washington

THE destruction last week of the Challenger space shuttle and the subsequent suspension of the whole US shuttle flight programme has thrown into disarray what was to have been the most ambitious year yet for space science. The thirteen shuttle flights planned for the rest of 1986, including four military missions, now face an indefinite delay. Some will miss launch windows that will not recur for more than a year.

The National Aeronautics and Space Administration (NASA) is setting up an exhaustive accident investigation in order to discover what caused the explosion; with hundreds of photographs and abundant wreckage being discovered, as well as telemetry data intact on the ground, there seems to be a good chance that a definite cause will be found.

NASA personnel are avoiding public speculation about the cause of the accident, but it is most likely that something caused a failure of the hydrogen containment. Photographs released by NASA last weekend appear to show that the right solid-fuel booster rocket burnt through its casing about one quarter of the way up from the nozzle at least 14 seconds before the final explosion. Flames from the breach may well have played on the large external fuel tank containing liquid hydrogen and oxygen, causing it to explode.

How long the remaining three orbiters will remain grounded is anybody's guess. While some communications satellites might conceivably be switched to the European Ariane launcher (although Arianespace has full order books for the next two years), the scientific missions are designed in such a way that they have to be flown on the shuttle.

When it exploded, Challenger was carrying in its payload bay a low-cost satellite called Spartan–Halley that was to have observed ultraviolet emissions from comet Halley at its closest approach to the Sun, and a tracking and data relay satellite (TDRS) that was to be the second of what will eventually be four NASA satellites in geosynchronous network for low Earth orbital operations. The first TDRS was launched in April 1983, and a third was to have been launched next July. The TDRS system will eventually replace NASA's network of groundstations throughout the world, some of which have already been transferred to deep space uses.

The TDRS system was to have been used (though incomplete) for several planned space science missions during the year. An ultraviolet observatory known as Astro was to have been flown by the orbiter Columbia in March, with one of its principal objectives being to observe Halley at the same time as the European Giotto and Soviet Vega spacecraft intercept the comet. Dr Arthur Davidsen of Johns Hopkins University, principal investigator of one of the Astro instruments, said last week that he had not given up hope that Astro might fly in time to make observations of Halley — any time before the start of May — but admitted that the chances were slim.

Davidsen said it was particularly unfortunate that the accident had occurred just before the first ever shuttle flight devoted exclusively to scientific observations, rather than to engineering demonstrations relating to science. The loss of one TDRS would not have affected Astro, but NASA officials said there is “no chance” of Astro flying in time to see Halley anyway.

The loss of one of the TDRS system satellites will have important consequences for the Hubble Space Telescope, if it is now launched before the system has two functioning satellites. The telescope had already slipped from its scheduled August launch spot to October before last week's accident, in order to give increased “contingency time” for its journey by sea from California to Florida through the Panama canal. When it will now be launched is unknown, but an incomplete TDRS system would limit data flow rates significantly, if not enough to be a “major deterrent”, according to NASA.

Two major science missions that are certain to be affected are the joint NASA/European Space Agency solar polar Ulysses mission, and NASA's Galileo Jupiter probe. Both were to have been launched in May, by Challenger and Atlantis respectively, and both have a launch window that will not recur for 13 months. If neither is flown in May 1986, as now appears quite likely, then both may be competing for the same launch window 13 months later. The maximum separation of the two launches is about five weeks, which is not enough time for one orbiter to be refurbished for a second flight, and with one less orbiter in the fleet, either Ulysses or Galileo may have to wait for more than two years.

The list of space science missions that might be affected depends on how long the shuttle fleet is out of service and how NASA rearranges flight priorities. The Earth Observation Mission scheduled for launch in August must now also be in jeopardy; NASA programme managers at Marshall Space Flight Center are putting all their effort into the investigation of the Challenger explosion and have not yet studied its effects on science missions.

The Department of Defense will also have its nose put out of joint by a long grounding of the shuttle fleet; three classified payloads were to have been flown this year, in addition to a July flight including Teal Ruby, an infrared tracking experiment with applications to the Strategic Defense Initiative (SDI), and Cirrus, a US Air Force Geophysical Laboratory experiment on infrared emissions from Earth's aurora.

Further SDI experiments had been expected in 1987, and pressure from the Pentagon for shuttle payloads to make up for lost time once the fleet is back in operation will doubtless be intense; the Pentagon can “bump” civilian payloads if it chooses.

Tim Beardsley

SDI on campus

Washington

A NEW study of research contracts let by the Strategic Defense Initiative (SDI) organization highlights the Pentagon's growing influence on basic research at US universities. The Department of Defense (DoD) now supports 16 per cent of all federally funded research, up from 10 per cent in 1980. DoD represents the fastest-growing source of research support and now exceeds support from the National Science Foundation, if off-campus research is included.

The new study, by the New York-based Council on Economic Priorities, shows that more than half of federally funded work in mathematics and computer sciences is supported by DoD, as is 82 per cent of astronautical engineering and 56 per cent of electrical engineering.

The trend is likely to continue, according to the study. The SDI organization's innovative science and technology office, which targets university research, is planned to account for 5 per cent of the SDI budget; its 1986 budget is $100 million but could expand to $300 million by 1988. The study voices concern that, despite the SDI office's insistence that basic research will remain unclassified, secrecy clauses will be invoked as soon as the research starts to yield results of military significance.

Of SDI contracts let to universities, the great majority by value have been to Massachusetts Institute of Technology (MIT). Including the off-campus Lincoln Laboratories, MIT has so far received over $59 million from SDI. Other major university recipients of SDI contracts are the University of Texas ($5.6 million), Georgia Tech Research Company (4.5 million) and Johns Hopkins University ($2.9 million).

Tim Beardsley

Ariane

France waits in the wings

THE loss of the space shuttle Challenger last week has caused some heart-searching in France about the future of Hermes, the French-inspired project for a miniature space-plane to sit atop a magnified version of the European space launcher, Ariane. But according to Frédéric d'Allest, director-general of the French space agency CNES, man's presence in space is essential, so the development of Hermes will certainly continue.

The French plan has not yet been approved by the other European partners in Ariane, notably West Germany, Britain and Italy. Hermes would carry mainly people, with a small amount of cargo (4,500 kg compared with the shuttle's 20,000 kg). Heavier cargo would be carried separately, but both would be lifted into space by Ariane-5, a liquid hydrogen-fuelled version of Ariane now under development. Although safety has of course been a major consideration, critics now point out that Hermes could be more dangerous than the shuttle, because it would have only one engine.

Nevertheless, given enough warning, Hermes could use an auxiliary escape rocket to fire the space-plane upwards and out of danger more quickly than could the shuttle sitting astride its main fuel tank.

In fact, more than two years ago, Hermes designers at Aerospatiale, one of the principal French aerospace companies, were designing the escape rocket for Hermes so that it functions in what seems to be an exact analogue of last week's accident, the explosion of the second stage at the moment of maximum dynamic pressure. The designers concluded that a small rocket under the body of Hermes, capable of giving it an 8 g vertical accelaration, could save it.

This week, French space specialists would draw no firm conclusions from the shuttle disaster. On present plans, Hermes' first manned launch will take place in 1995, on what will be only the third test flight of Ariane 5, a prospect that might now appear foolhardy. According to d'Allest, the dangers of entering space can be compared with those of entering a radiation zone in a nuclear reactor. The comparison may be more than apt, as increased public pressure for radiation protection has led to improved safety systems and correspondingly increased nuclear construction costs; similarly, the public unacceptability of an accident like last week's may well do the same for Hermes and other planned space-planes.

In the now long-running competition between the shuttle and present versions of Ariane, the commercializer of the European launcher, Arianespace, was not prepared last week to comment on the impact of the shuttle disaster. On the face of it, it would seem that satellite companies might now favour unmanned launchers, particularly as there is now a long queue of satellites waiting to be launched in what was to be the shuttle's busiest-ever year. But satellites that have been prepared for the shuttle would have to be modified to make them suitable for launching on Ariane or similar vehicles. In any case, capacity on Ariane is almost entirely taken up with a £1,000 million backlog of contracts. Although a second launch site is being opened at Kourou, French Guiana, next month, Arianespace foresees no more flight opportunities in 1986, just one in 1987 and three in 1988.

Moreover, Ariane has its own difficulties. The last flight (V15) led to destruction as the result of a leaking fuel valve. With that problem now supposed solved after a slight design modification, Ariane V16 is sitting on site in Kourou awaiting a replacement for a water cooling tank, which was found to be cracked and leaking just before the planned launch on 11 January. V16 should now fly, carrying the first French Earth observation satellite SPOT and a Swedish scientific satellite Viking, on 21 February. **Robert Walgate**

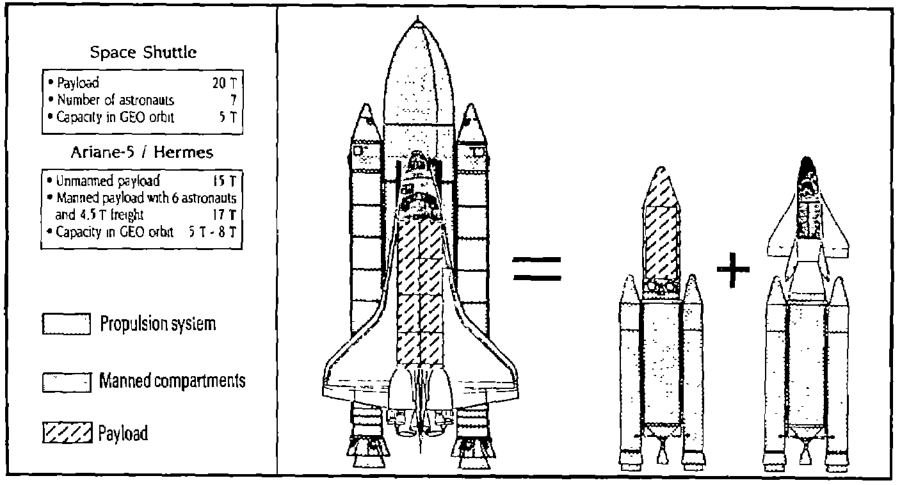

Marine satellites

Japan offers free data

Tokyo

DATA from Japan's marine observatio satellite MOS-1, due to be launched nex year, are available for anyone willing an able to participate in the verification programme for the satellite. Japan's Nationa Space Development Agency (NASDA will supply MOS-1 data free of charge provided the data are used only for peacefu purposes, are valuable from scientific and technical viewpoint and ar "useful to NASDA", which means helping in evaluation of the radiometric an geometric performance of the satellite Such is the gist of a guideline distribute by NASDA to organizations in 11 countries, including the European Spac Agency (ESA). The deadline for proposals to NASDA is the end of February.

MOS-1 will view the whole surface o the Earth every 17 days and, with its thre scanners and data-collection system is theoretically, capable of transmittin more information than the Landsat satellites now in use. But coverage will be restricted by the availability of suitabl equipped monitoring stations and the battery power of the satellite. Apart fro NASDA's Earth Observation Center i Japan, which can monitor the satellite over north-east China, Taiwan, Korea, Japan and the eastern Soviet Union, agreement has just been reached wit Thailand to build a monitoring station o the outskirts of Bangkok at a cost to Japan of 800 million yen (about £3 million). This station will cover the Philippines, Indonesia, east India and western China.

NASDA also hopes that ESA's statio at Las Palmas in the Canary Islands wil monitor the satellite and that Australia may upgrade its satellite stations to receive MOS data. But NASDA official stress that MOS-1 is only experimental, with limited power. The satellite's powe should be adequate if data are transmitted only during the day, but night-scanning will drain its batteries, according t Yasushi Horikawa, director of NASDA's Earth Observation Satellite Program.

MOS-1 scanners will be trained largely on the sea where its high resolution (50 m) multi-spectrum electronic self-scanning radiometer and visible and thermal infrared radiometer will provide information on ocean currents, red tides, pollution and volcanic eruptions, while its microwave scanning radiometer will monito atmospheric water vapour content, sea ice and snow distribution.

By the time it is launched early in 1987, MOS-1 will have run up a bill of Y56,000 million (£200 million). Its expected mission life is two years. **David Swinbanks**

Voyager 2

Uranus is something else again

Washington

A new kind of atmospheric emission that has been called "electroglow" was one of the most striking results of the Voyager 2 flyby of Uranus, according to Dr Ed Stone, project leader. Electroglow, observed by Lyle Broadfoot, head of the ultraviolet spectrometry team, is believed to result from a different process than either aurora or airglow. Aurorae are caused by the precipitations of charged particles in the polar atmosphere. Airglow is the result of high-frequency solar photons in the atmosphere. Electroglow also needs solar photons to ionize constituents of the atmosphere, but thereafter some unknown mechanism seems to provide energy to the electrons to cause the glow. The glow is observed only on the dayside of Uranus, in the ultraviolet; it had been observed before on Saturn and Jupiter, but only at Uranus did it "become clear that this was a totally new phenomenon", according to Stone. In comparison with aurorae, electroglow is caused by very-low-energy electrons very high in the atmosphere.

The uranian magnetosphere contains mainly protons, rather than helium nuclei, for which the uranian atmosphere is the most likely source, according to S.M. Krimigis. There is in addition a warm plasma of a hundred thousand degrees and a very hot plasma of ten million degrees, reported by Fran Bagenal. Explanations for these observation have yet to be made.

The rotation period of the planet has been measured and is close to 17 hours, not too different from estimates made on the basis of the rate of precession of the rings. The magnetic field of about 0.25 gauss, with its peculiar 55 degree inclination from the rotational axis, will doubtless provide fodder for theorists for years to come.

Most of the moons are greyish in colour, suggesting that meteoritic material (together with water ice) is their main constituent. A reddish coloration would have argued for more hydrocarbons resulting from irradiation of methane.

Sizes and densities of the moons have been established; the densities of the four for which data are so far available are about 1.6, suggesting a composition of 50 per cent water ice and 50 per cent rocky material.

The uranian atmosphere was found by radiooccultation and other techniques to consist of about 12 per cent helium (plus or minus four per cent); the remainder is mostly hydrogen. This result, reported by Len Tyler, is consistent with solar composition and in accordance with expectations. A methane cloud layer at about 1.6 bars was detected; water and ammonia were not detected directly but are presumed to exist at much greater depths.

It is clear that Uranus does have an internal heat source, but no estimate has yet been made of its size. Part of the evidence for this is that the poles are not warmer that the equator, as expected in a planet whose axis of rotation is in the plane of its orbit around the Sun. Winds on Uranus rotate in the same direction as the planet itself, also unexpected for the same reason.

New rings around the planet were discovered, but attempts to number them give rise to problems of definition, according to Jeff Cuzzi. In any event, material was found orbiting the planet both inside and outside the previously known rings. One of the surprises of the mission is that there are few particles smaller than about a metre in diameter, in contrast with the rings of Saturn and Jupiter. One possible explanation is that if the uranian magnetic field wobbles, small particles might become magnetized and get swept out the ring; atmospheric drag might also provide an answer. Of the ten new moons discovered, at least two appear to be shepherd moons for rings.

Many of the questions raised by these preliminary results will be stated more carefully, or even partly answered, by the time the 30-day post-encounter report is completed, according to Stone. Now, the hundreds of visiting scientists who have been working at the Jet Propulsion Laboratory in Pasadena, California, for the past several weeks in preparation for the encounter have started to head for home. But the new data gathered should keep many of them busy for years.

Tim Beardsley

Soviet environment

Now pollution on television

The new Soviet television series, "Problems, Searches and Solutions", in which experts discuss viewers' questions on key issues of the national economy, dealt on 24 January with environmental protection and natural resources. Since the programme was launched last November (see *Nature* **318**, 593; 1985) the format has been changed; no attempt is made to create the illusion of off-the-cuff replies to telephone questions. Nevertheless, the pre-selected questions dealt with by the panel not only reflected a growing public interest in environmental matters, but also pinpoint a number of areas where Soviet policy needs to be strengthened.

The most striking feature of the programme is the large number of experts empanelled. Apart from Dr Yurii Izrael, chairman of the State Committee for Hydrometeorology and Environmental Control, it included a minister, a deputy minister, a vice-president of the Soviet Academy of Sciences and representatives of two other state committees and a government commission.

The discussion showed only too clearly that many of the most serious issues, such as the protection of small rivers, come under the jurisdiction of at least three of these bodies (State Committee for Forestry, Ministry of Land Reclamation and the Commission of the Presidium of the USSR Council of Ministers for the Protection of the Environment and natural resources), to say nothing of bodies involved in the long-term Food Programme.

Similarly, the drainage of forest marshland in Lithuania and Byelorussia turns out to involve not only the same three governmental bodies, but also a Byelorussian research institute working on the culture of heavy-fruiting cranberries in natural marshland or industrial plantations. Environment could well benefit from the kind of superministry recently established for agriculture, as part of Mr Mikhail Gorbachev's drive to streamline the economy.

The Gorbachev reforms have undoubtedly made it easier to discuss past mistakes in environmental planning. Both *Pravda* and *Izvestiya* have given extensive coverage, in the past few weeks, to the environmental threat from the two cellulose combines on Lake Baikal which, in spite of expensive purification installations, still continue to endanger the lake.

Dr Aleksandr Yanshin, vice president of the Soviet Academy of Sciences, pointed out in the television programme that the pollutants discharged by these combines are incorporated in the shells of the minute crustacean, *Epischura baikalensis* which, when it dies, carries the shell to the bed of the lake. But the life-cycle of *E. Baikalinsis* is short, and the bed conditions of the lake play an important part in maintaining the exceptional purity of the lake water under natural conditions; even a relatively small discharge of pollutant is a considerable threat.

The chairman of the Committee for Forestry admitted that, although over-felling had been reduced by some 80 per cent over the past fifteen years, some 12 million m^3 of wood is still being over-felled every year, thus violating "the basic principle of timber use". But only a few years ago, over-fulfilment of targets was urged in every sector of the Soviet economy, including forestry. Some officials may not yet have made the necessary mental adjustment to the new circumstances.

Vera Rich

Animal welfare

OTA squares circle of dissent

Washington

THE Office of Technology Assessment (OTA) has weighed in to the debate over the use of animals in research with a report that even critics regard as comprehensive, and which will have to be reckoned with in any future debates on the subject.

More than two years in the making, at a cost of $425,000, the report (*Alternatives to Animal Use in Research, Testing and Education*) looks into alternatives to the use of animals, not just in research, but in education and testing as well, judging them by the extent to which they replace, reduce and refine present techniques.

While acknowledging that "some biological research requires — and in the foreseeable future will continue to require — the use of live animals", the report notes that the alternatives to tests such as the LD_{50} test that are now more widely adopted in industry, and looks for potential parallels elsewhere in testing and research. To reduce the use of animals in science, the role of computers can be expanded beyond that of a tool for modelling animal behaviour. Using computers to improve information exchange about data already collected can eliminate redundancies in research. But the report acknowledges that the United States lags behind European countries and Japan in the protection of laboratory animals.

Difficulty in estimating the numbers of animals bedevils attempts to evaluate current usage. The best data come from the Animal and Plant Health Inspection Service (APHIS) of the US Department of Agriculture, which collects records on the use of dogs, cats, hamsters, rabbits, guinea pigs and non-human primates. This group of animals represents only about 10 per cent of animal use; reporting on rats, mice and birds is not required. Extrapolating from these numbers, OTA estimates that between 17 and 22 million animals were used during 1983 in research and testing.

Even before the report was officially released, some groups were rejecting it. The People for Ethical Treatment of Animals calls the report biased, saying that it does not reflect the views of the animal rights movement. Connie Kagan of the Animal Political Action Committee calls it "disappointing", and doubts if it will have much impact on Congress.

But most observers agree that the report is as comprehensive as could be reasonably expected, and Barbara Orlans of the Scientists' Center for Animal Welfare, believes it will be "recognized as a bible".

Sensitivity about the use of animals in science has been growing recently in the United States. The Animal Welfare Act was amended last year, strengthening its provisions, and the Health Research Extension Act of 1985 puts the force of law behind some parts of the current Public Health Service guidelines on animal use. These changes in federal law have shifted much of the responsibility for oversight of animal use onto institutional review committees, and OTA estimates that "the overwhelming majority of experimental-animal users in the United States" now come under the oversight of a "structured, local review committee".

Perhaps the single greatest accomplishment of the report is that it seems to have generated surprisingly little acrimony. According to Arthur Caplan, chairman of the OTA advisory panel, the report transcends "the name calling, finger pointing and hair pulling that normally accompanies the discussion of animal use in science".

Joseph Palca

Guidelines off

Washington

THE new guidelines adopted by the National Science Teachers Association (NSTA) for animal use in US elementary and secondary schools will not be endorsed by the National Academy of Sciences.

While the Office of Technology Assessment (OTA) report indicates that the "overwhelming majority" of animals used in research and testing are governed by some sort of institutional review process, the same cannot be said for the use of animals in education, especially at the elementary and secondary school levels.

What guidance there is comes primarily from guidelines established by NSTA and the National Association of Biology Teachers (NABT).

In 1981, NSTA submitted its guidelines to the National Academy of Sciences, and they were eventually endorsed by the National Research Council. The guidelines prohibit "experimental procedures on mammals, birds, reptiles, amphibians or fish that cause the animal pain". The 1981 guidelines also state that "students shall not perform surgery".

But not all members of NSTA and NABT were content with these restrictions. Many felt that they would hamper the education of outstanding students. Moreover, the guidelines were more restrictive than those accepted by the International Science and Engineering Fair, which sets standards for many school science fairs.

So in 1985, NSTA rewrote the guidelines. The language was altered to read that no experiment causing "unnecessary pain" should be performed, and surgery was permitted, so long as it was supervised.

In December, NSTA resubmitted their guidelines to the academy, hoping for endorsement. But the academy declined, although it has yet to issue a public statement on the matter. One possibility is that the academy will issue its own guidelines later this year, and these are likely to conform more closely to the 1981 NSTA guidelines.

Joseph Palca

Preaching to converts

Washington

GROWING awareness may have inspired the report of the Office of Technology Assessment (OTA) on alternatives to animal use, but in the commercial field, business savvy may provide its own reasons for abandoning animal resources. So Charles River Biotechnical Services (CRBS) joined the industry-wide shift from *in vivo* to *in vitro* monoclonal antibody production with last month's purchase of the Opticell branch of KC Biologicals. Executive vice-president Melvin Balk says the acquisition will expand the Massachusetts company's bioprocessing services to include vaccines and recombinant proteins, while Opticell's culture system will gradually usurp the mouse as CRBS's antibody factory.

Balk also served on the advisory panel for OTA's project, as much, he says, to scout for alternatives that make "economic sense" as to further OTA's evaluation. In the case of cell culture methods for monoclonal antibody production, economic sense and ethical sensitivities coincide. Balk says the techniques avoid costly problems associated with, for example, varability and contamination of mouse monoclonals. But the success of these methods is still contingent on improvements in product yield and the stability of large-scale markets. Although *in vitro* products such as human chorionic gonadotropin are aimed at high-demand diagnostic or therapeutic markets, most *in vitro* methods cannot yet equal the milligram per millilitre harvest that mice supply.

Echoing OTA's conclusion, Balk insists that mice will always be necessary for monoclonal production because some hybridomas simply will not thrive elsewhere. Other industry experts paint a more optimistic picture for the future of cell culture. Allan Jarvis at Damon Biotech anticipates a time when *in vivo* production may be superfluous and outdated; Damon has survived five years without it. At Becton-Dickson in California, the mood is more cautious. Before launching an *in vitro* programme, the company's attempts to evaluate different culture systems have been frustrated because these systems are still in their largely untried infancy. The venture will probably be risky and, as one manager remarks, a half-million-dollar mistake is not a welcome alternative to animal use.

Karen Wright

Pacific volcano

Transient Iwojima calf

Tokyo

THE Japanese islands burst into life last month when a submarine volcano south of Iwojima broke surface, sending a plume of smoke and ash billowing skywards. Within a day, a crescent-shaped island almost 1 km in length had formed around the volcanic vent, but, as with previous attempts to join the Japanese archipelago, the island will probably disappear again.

The submarine volcano Fukutokuokanoba lies 1,300 km south of Tokyo at a point 5 km north-east of Minami (south) Iwojima (24° 17′ N, 141° 29′ E). Its first recorded eruption began on 14 November 1904. By 1 February 1905, an island 5 km in circumference and 150 m high had formed and was named Shin (new) Minami Iwojima. But by June of that year, it was reduced to a shoal 150 m in circumference and, by 1910, the point where the island had been was 424 m deep.

Infrared satellite images indicate that the present eruption began on the night of 18 January. Activity peaked on 20 January when a column of smoke 50 m wide rose to 3,000 m, blocks of volcanic rock up to 10 m in diameter were hurled hundreds of metres into the air and a plume of discoloured water spread for about 20 km in a south-easterly direction. The island was reported to be 700 m long from east to west, 500 m wide and 15 m high, but a week later it was 500 m in length and showed signs of rapid erosion.

The little island's big brother, Minami Iwojima, is a 3.5 km^2 uninhabited jungle-capped cone of basalt. It lies at the southern end of a 1,250-km-long strip of active volcanoes that starts at Mount Fuji and then runs along the edge of the Philippine plate through the Izu Seven Islands (Shichito).

While most of the islands of the Shichito–Iwojima chain are composed of tholeitic basalt typical of the front of volcanic island arcs, the rocks of Minami Iwojima and Iwojima (also known as Naka (middle) Iwojima) belong to the alkali suite usually found at the backside of island arcs. Rock collected from the temporary islands formed in 1904 and 1914 and from the top of Fukutokuokanoba in 1982 were all olivine-augite trachyandesite with high alkali contents. The new volcanic island is thus probably closer in composition to Naka Iwojima 50 km to the north-west than to nearby Minamai Iwojima which is composed of alkali baslats, according to Shigeo Aramaki of Tokyo University's Earthquake Research Institute.

In contrast, Kita (north) Iwojima, about 70 km north of Naka Iwojima, is a tholeitic basalt volcano. The abrupt change to alkali volcanics at the southern end of the Shichito–Iwojima ridge is puzzling. Alkali-rich magmas are thought to form at high pressures at the lower end of the plate subducting beneath the volcanic island arc. Thus, according to Teruaki Ishii of Tokyo University's Ocean Research Institute, the occurrence of alkali volcanics in the southern half of the group of islands may be related to the steep dip of the subducting Pacific plate as the Ogasawara Plateau, a large guyot riding on the Pacific plate, plunges into the Izu-Bonin trench immediately opposite the islands. Ishii points out, however, that this explanation fails to account for the lack of tholeitic basalt volcanoes between Iwojima and the trench. **David Swinbanks**

Trials on ice

Washington

AFTER a lively public hearing last week at Salinas, California, Advanced Genetic Sciences (AGS) announced that it will postpone for thirty days the environmental release of its gentically altered bacteria designed to protect plants from frost damage (see *Nature* 319, 254; 1986).

Monterey County Supervisors scheduled the hearing to air questions about the safety of the release. Sam Karas, chairman of the board of supervisors, said some of the most influential evidence came from Dr Lee Cavalieri, retired member of the Sloan Kettering Institute for Cancer Research. Karas left the meeting with the understanding that Cavalieri was suggesting there is evidence that the experiment may pose some cancer risk, but Cavalieri emphatically denies making any such statement.

AGS has already won approval from the Environmental Protection Agency and the California Department of Food and Agriculture to proceed with the test on a farm near Salinas, but local opposition brought its plans up short. Despite vocal opposition, AGS plans to proceed with the trial, but not before it has satisfied the local authorities that the bacteria poses no threat to residents. A compromise may be to move the site of the trial to a less populous part of the region. Joseph Palca

---

AIDS

Academy looks for strategy

Washington

A NATIONAL agenda on research and health care for acquired immune deficiency syndrome (AIDS) is the objective of a six-month project of the National Academy of Sciences and the Institute of Medicine (IOM) in the United States, the approach so far is considered to have been random and uncoordinated.

A single report will be generated from the work of two panels, one on research and development, the other on health care and public health. According to Sam Thier, president of IOM, the report is not to be a definitive treatise on AIDS, but rather part of "a continuum of effecting national action".

The panel on research and development will examine current research efforts to determine if they are properly organized and sufficiently well supported IOM hopes to weigh up whether a programme on the scale of the Manhattan Project or Project Apollo is justified by the size of the current health problem, and whether such a large-scale programme would provide a return commensurate with its costs.

"It is critical to be sure that for an area as important as this that the research agenda and strategy is as well crafted as we can have it", says Thier. "We have to be sure that all segments of the research community are integrated into the effort, and if necessary recruited into it where they are not as actively involved."

The other panel will investigate the social and public policy questions raised by AIDS. It is still unclear how the health-care delivery system can most effectively cope with a disease for which there is as yet no cure. Some rational strategy that takes into account the needs of the AIDS patient and the needs of society must be developed.

Almost any active steps to control the AIDS epidemic will of course cost money, a conclusion that troubles law makers in these days of the Gramm–Rudman Act and it will force budget reductions. While Thier acknowledges these financial problems, he considers the IOM effort should not have to be sidetracked by the uncertainties of funding.

"It's all well and good to say we have Gramm–Rudman, and there are cutbacks and so on", says Thier. "But that is not going to stop the progress of this disease"

The IOM report is being put on a fast track. Thier is anxious to see this and other IOM projects completed faster than the 18 months typical for reports in the past. IOM could then play a larger role in affecting national policy on the critical health issues. **Joseph Palca**

British clinical research

Shotgun merger proposed

A SINGLE centre of excellence is the only solution to Britain's national "crisis in clinical research", according to a committee reporting last week to the Medical Research Council (MRC). Although set up to advise MRC on the future of its Clinical Research Centre (CRC), the most costly of its research establishments, the committee strongly urges a merger of CRC with the Royal Postgraduate Medical School (RPMS), an entity under the wing of the University of London. Ideally, it says, the National Institute for Medical Research (NIMR) should also be merged with CRC and RPMS. And if it is not possible to combine CRC with RPMS, CRC should be disbanded.

Indications of the poor state of UK clinical research include the particularly marked fall in grant applications to MRC from clinical scientists, according to the committee. This reflects a situation where young doctors are increasingly unprepared to obtain delayed professional accreditation by undertaking research training. And established clinical academic staff are too beset by administrative problems brought about by financial constraints to apply for grants and hold together a research team.

Chaired by Sir Michael Stoker, and taking over where his previous committee left off (see *Nature* **314**, 487; 1985), the new committee reports that "CRC has not developed the national role envisaged when it was first established" fifteen years ago. While offering faint praise for CRC's director, Sir Christopher Booth, for bringing together basic medical and clinical science, the committee's report says that yet more basic science is needed, whence its suggestion that NIMR should be party to the merger.

Stoker's committee identifies as one of CRC's chief problems its attachment to a hospital that has developed no specializations on which the research could be focused. Blaming this on a failure to develop an appropriate administration of the hospital, with a greater role for the director of CRC, at Northwick Park in North London, the committee concludes that "there is a growing divergence of the two populations of clinical staff on the site"; it sees little prospect of the necessary unity of purpose emerging, and that CRC suffers from the lack of a graduate programme.

Sir Christopher Booth acknowledges both failings, but says that the report overstates the lack of unity between the hospital and the centre, and that it is misguided in its implied criticism of a programme of research based on "common" diseases — those that predominate at a general hospital — rather than the more rare disorders by which researchers are attracted.

Reactions to the suggested merger are generally favourable, at least in principle. MRC has endorsed the report, Booth strongly supports the idea of a single centre of clinical research and Sir Frederick Dainton, chairman of the council of RPMS, has said that the suggested merger is an exciting prospect.

For RPMS, the most tangible gain would be greater financial security. Cutbacks in university funds and a fall in the number of overseas students following the British government's withdrawal of subsidy for them mean that RPMS now exists on more "soft" than "hard" money according to its dean, Dr D.N.S. Kerr. CRC, by contrast, has an enviable number of established MRC posts. A merger of the best of the two institutes would make sense in those terms, particularly since MRC spends £6.3 million a year at RPMS and just over £10 million at CRC.

Doubts at RPMS focus on two points. The first is the extent to which the school's ambition for more and better basic research would be met by a merger with CRC, which itself is lacking in that respect. Second, and perhaps inevitably, there would be no enthusiasm for moving to CRC, which has more space but not as good a relationship with Northwick Park Hospital as RPMS has built up with Hammersmith Hospital in West London. But in principle CRC has 160 beds at Northwick Park at its disposal, while RPMS has none reserved for its use.

Sir James Gowans, secretary of MRC, believes that "the barometer is set fair" for a merger of CRC and RPMS, that the merger has to be on one site and that the exercise would cost rather than save money in the short term. If no merger could be agreed, the council would "return to the recommendation" that CRC be disbanded, a view MRC has not endorsed.

As to the possibility of NIMR joining CRC and RPMS, the prospects seem remote. The original intention of MRC had been to merge CRC and NIMR, but the idea was set aside in 1980 and NIMR has since set off on a different course under a new director. Moreover, NIMR does not have access to a hospital and so would have to move to one of the other two sites at enormous cost. **Peter Newmark**

MRC attacked

THE British Medical Research Council (MRC) is under attack in the pages of the *British Medical Journal* for its lack of support of overtly medical research.

The correspondence was started by Professor Miles Irving of Hope Hospital in Salford who criticized the council's intention to close down its trauma unit in Manchester. He implies that MRC's failure to find a suitable replacement for the retiring director reflects the council's lack of understanding of the importance of such research. "To many surgeons and anaesthetists the council appears to be out of touch with everyday clinical practice".

Support for this view comes from Professor John Dobbing of the University of Manchester, who claims that his own research on the effects of social and nutritional adversity on the development of brain and behaviour was denied further support by MRC at the same time as being praised in its annual report.

In replying to Irving, Sir James Gowans, secretary of MRC, denies any bias against surgical disciplines, a view in which he is supported by a member of one of MRC's boards, Professor David Hamblen of the Department of Orthopaedic Surgery at the Western Infirmary in Glasgow. "Until surgeons regard research as providing a scientific basis for all surgery and not just occupational therapy for academic departments", he writes, "the situation is unlikely to improve."

Peter Newmark

Budget of INSERM grows

THE French medical research council INSERM, whose generous budget has always been the envy of biologists supported by the larger but multidisciplinary research council, the Centre National de la Recherche Scientifique (CNRS), will have four per cent more in real terms to distribute in 1986 than in 1985.

The new money will be spent, INSERM says, on fifteen new laboratories, on improved support of existing laboratories, a doubling of the budget for large laboratory equipment and on 70 new research posts, a four per cent increase on the present INSERM research staff of 1,700. There will also be 20 new temporary posts for foreign researchers.

The new research groups mostly fall in the "priority research areas" identified by INSERM. Grants to extramural groups in university, CNRS, hospital and other laboratories will also increase this year, by a sustantial 19 per cent. But the FF50 million (£10 million) spent outside INSERM's walls is less that a tenth of the FF519 million (excluding salaries) that will be spent in the council's own laboratories in 1986. Including salaries and overheads, INSERM's gross budget for the year will be some FF1,650 million for 1,700 scientists. By comparison, the budget of the CNRS life sciences department is similar, at around FF1,800 million, but it must support some 2,700 researchers, whence the envy INSERM excites. Robert Walgate

Bulgar identity

Proofs of ethnic purity advanced

A MAJOR research project into the present state and future prospects of Bulgarian brain and intellect, carried out at the Institute of Brain Research of the Bulgarian Academy of Sciences, suggests that the modern Bulgarian has a very flexible intellect, but fails to use it to its full potential. According to Dr Ana Vrbanova, the director of the institute, this unsatisfactory situation is caused by poor use and organization of Bulgarian culture and traditions.

Reporting on the preliminary results of what is admitted to be a far from complete study, the Bulgarian media have stressed the declaration of a recent Central Committee plenary meeting that "the construction of a developed socialist society not only asks for but also demands the activation of the brain cells".

This premature media coverage is not simply a way of urging Bulgarians in the learned professions to work harder during the new five-year plan, but seems to be related to current political and ethnographic claims of the purity of the Bulgarian nation and, in particular, of the absence of a Turkish ethnic minority.

This emphasis on Bulgarian specificity accords well with the current official Bulgarian view of its Turkish minority. During the past few years, large numbers of Bulgarians of Islamic descent have ("voluntarily", it is claimed) changed their Turkish-sounding given names and surnames to Slavonic names. Protests from Turkey that the changes were being carried out under pressure brought a rejoinder from Sofia that the people concerned were not Turkish at all, but ethnic Bulgarians whose ancestors had been converted to Islam under the Ottoman Empire.

Now the Bulgarian Academy of Sciences has published a monograph, *Anthropology of the Bulgarian Nation*, said to be based on more than 30 years work by the Institute of Morphology of the Bulgarian Academy of Sciences, using, in particular, anthropometric measurements carried out in areas hitherto thought to contain members of Bulgaria's Turkish and Greek "minorities".

According to a review in the daily *Otechestven Front* (1 January 1986), the studies revealed so high a degree of homogeneity that the experts conclude that the fusion of Slavonic, Thracian and Asiatic ethnic elements that gave rise to the Bulgarian nation was complete by the end of the tenth century, and that the past 1,000 years of foreign incursions, including centuries of Ottoman rule, have left no ethnic trace whatsoever. Bulgaria's Turkish minority, the reader is left to deduce, does not exist.

This remarkable piece of dialectic is not Bulgaria's first effort in political anthropology. In 1978, the Bulgarian Academy produced a monograph *Macedonia*, which set out to prove that the Macedonian nation did not exist.

The international repercussions of the academy's new monograph too are likely to be acrimonious, particularly in Greece and Turkey. The study of Bulgarian brainpower, although clearly part of the same political stance, will probably have its greatest effect at home, and may possibly engender conflict within the Bulgarian scientific establishment. For, according to Dr Vrbanova, the main purpose in studying Bulgarian brain-power is to activate sociologists, psychologists and doctors into finding and developing techniques to expand the potential of "Bulgarian's nine million brains". **Vera Rich**

EPA expansion urged

Washington

AN advisory panel to the US Environmental Protection Agency (EPA) has concluded that EPA needs to expand its research programme in order to cope with the expected influx of requests to release genetically altered organisms into the environment. The panel says it is impressed with what EPA has done, given the resources at its disposal, but says the agency should do more to establish test protocols for considering environmental releases.

The Study Group on Biotechnology, set up under EPA's congressionally established Science Advisory Board, is a public group intended to provide external review of the agency's actions. The study group was chaired by Martin Alexander, a microbiologist at Cornell University. EPA has not officially responded to the report, but its scientists say they broadly concur with its conclusions. EPA recently approved the first environmental release of genetically engineered microorganisms into the environment, and ran straight into a controversy (see *Nature* 319, 254; 1986). The agency will shortly be publishing general terms and conditions that it will use for considering such applications.

The study group says an adequate research programme for environmental releases should address survival, growth, genetic tranfer *in situ*, dispersal, environmental effects, health effects, remedial action and use of biotechnology for destroying pollutants. So far, EPA has examined applications on a case-by-case basis but the study panel says the "absence of generally accepted tests and test methods . . . is cause for concern". The panel observes that EPA has "essentially no program" of research into environmental effects, and says EPA needs increased resources to conduct "innovative research" that will lead to definitive generally accepted test protocols. It also recommends that another special panel be established to provide peer review of EPA's risk-assessment efforts. Tim Beardsley

---

Marine science

Changes afoot

PLANS are afoot for changes in the style of British marine research. Even as the House of Lords Select Committee on Science and Technology finished its report (see *Nature* **319,** 351; 1986), the Science and Engineering Research Council (SERC) was preparing to divest itself of its Marine Technology Directorate (MTD). With a 1984–85 budget of more than £5 million, it was established over nine years ago to develop academic involvement in marine matters. It achieved this by a system of grants to seven centres mainly in British universities. Within the next few months, the directorate is to be replaced by a separate corporate entity, MTD Ltd, under the aegis of the Fellowship of Engineering (the engineers' equivalent of the Royal Society). SERC will for the next three years provide only one-third of the £300,000 operating costs, with the balance being raised by subscription by industry and government departments. SERC will also cut its research contribution and hope that industry will plug the gap.

SERC policy is that directorates should be discontinued as in-house activities after a formative period. A.M. Adye, director of MTD, said that he was not aware of any change in SERC plans in response to the House of Lords committee recommendation that an overseeing Marine Board be established within SERC. But he agreed with the main thrust of the report -- that there is too much fragmentation of interests and an overview is needed.

Hugh Fish, chairman of the Natural Environment Research Council, supporting his council against the attacks contained in the report, also agreed that greater co-ordination was necessary. But he felt that a better solution could be found than "the bolting-on of a Marine Board . . . to the existing organizations".

Another spoke in the wheel is the Department of Trade and Industry's Marine Technology Committee, which handles the department's marine research budget. This body is just starting the ball rolling in an effort to develop a co-ordinated national programme for ocean resources such as metallic nodules and "soft" energy (excluding hydrocarbons). The main aim is to encourage industrial interest in both these resources and the technological infrastructures needed for their exploitation.

Peter Gambles

Remote viewing exposed

Sir—Some years ago, we challenged experiments on remote viewing conducted by Targ and Puthoff[1] on the grounds that sensory cues were available to the judges, enabling correct matching of the subjects' descriptions against the target locations[2]. This objection was countered when another investigator, Tart, attempted to remove all the cues and organized a rejudging that yielded results as significant as those originally obtained[3]. At this stage, we asked for access to the data, and we are now pleased to acknowledge that, after a three-year interval, Puthoff has released the relevant data from the first experimental series with the subject Price. Having examined both the edited and unedited transcripts, we note that Tart failed to remove a number of potentially useful cues from the transcripts given to his judge. This bias in Tart's editing, as was suspected earlier[4], invalidates the judging exercise.

The Price series of remote viewings consisted of nine experiments. Eight of the allegedly edited transcripts (all except the one from Experiment 2) retain information concerning the subject's location. These were a park in Experiments 1 and 2, an office in Experiment 5, and a shielded room in the remainder of the experiments. The transcript for Experiment 1 also retains the passage at the very beginning where Price expresses apprehension about being able to perform the task: "the feeling that one can't or won't be able to do it and shouldn't even try it". The transcript from Experiment 3, the first to be conducted inside the shielded room, quotes a question from Targ as to whether the subject noticed "any difference in being in a shielded room compared to being in the park".

Targ and Puthoff's publication *Mind-Reach*[5] contains extracts from the transcripts for Experiments 1, 4 and 9 and publishes in full the transcript for Experiment 7. *Mind-Reach* also lists the correct order of target sites and the subject's location during each of the experiments. Given the public availability of *Mind-Reach* at the time when the rejudging was conducted, it was not a valid procedure to include all nine of the transcripts, as the judge could easily look up the relevant information or recall it using memory based upon earlier reading of the material. Only the five targets not cued by the information in *Mind-Reach* should have been employed (Experiments 2, 3, 5, 6 and 8) as in the case of the unsuccessful rejudging reported by Marks and Kammann[2] which used transcripts with all cues deleted. Furthermore, the cues contained in the transcripts associated with Experiments 1 and 3 invalidate the inclusion of Experiments 1, 2 and 3 as the transcripts for all three of these experiments can be readily matched using the available cues. Experiment 5 is also invalidated because its transcript contains the uniquely diagnostic cue of the subject's location (an office) used only on this occasion. Hence only Experiments 6 and 8 remain potentially uncued in the rejudging exercise.

Considering the importance for the remote viewing hypothesis of adequate cue removal, Tart's failure to perform this basic task seems beyond comprehension. As previously concluded[2], remote viewing has not been demonstrated in the experiments conducted by Puthoff and Targ, only the repeated failure of the investigators to remove sensory cues.

David Marks

Department of Psychology,
University of Otago,
Dunedin, New Zealand

Christopher Scott

60 Highgate Hill,
London N19, UK

1. Targ, R. & Puthoff, H. *Nature* **251**, 602–607 (1974).
2. Marks, D. & Kammann, R. *Nature* **274**, 680–681 (1978).
3. Tart, C.T., Puthoff, H. & Targ, R. *Nature* **284**, 191 (1980).
4. Marks, D. *Nature* **292**, 177 (1981).
5. Targ, R. & Puthoff, H. *Mind-Reach* (Delacorte, New York, 1977).

No sexism please

Sir—Gerald Weissmann, in his zeal to defend the University of Texas Health Services Center (*Nature* **318**, 308; 1985), appears to have committed a gaffe of his own. Presumably "daughters" as well as "sons" of the university will be future Nobel laureates, assuming that the university employs both male and female scientists.

Ann S. Hobbs

Department of Physiology,
University of Maryland,
School of Medicine,
660 West Redwood Street,
Baltimore, Maryland 21201, USA

Future UNESCO

Sir—Whatever the reasons for the withdrawal of the United States and Britain from UNESCO, such drastic action is needed in my opinion to dismantle an institution that has sunk into a vicious circle of rot. UNESCO is not the only UN agency that needs stripping; others also suffer innumerable faults in their operation. The United Nations embodies the highest ideals of mankind and if its scientific agencies are to function with minimum errors and deviations, then they should be serviced by the highest calibre of scientists, not by those whose prime motives are in financial reward and political glory.

Your leading article (**318**, 397; 1985) omits a dire consequence that may result from the departure of Britain from UNESCO — the export of inferior value in science and education to the English speaking developing countries in Afric by those who are probably eager to ste into the niche left by the departing British Modest but good and useful science wa established by the British in their forme colonies. The high quality of relevant environmental sciences in East Africa befor and for about a decade after the independence of these countries is one such example. Subsequently, scientific research i these countries declined. Now, I canno help thinking of the possible infiltratio into these countries of what I see as "science without its scientific ethics", and th threat that this would pose to the furthe decay and distortion of the image of science in these countries.

W. Oker

43 Margaret Street,
Walkerville,
South Australia 5081

Catastrophism

Sir—I refer to Paul R. Weissman's lette (*Nature* **316**, 572; 1985) "Catastrophism still unexplained", and the 1978 and 197 references.

The suggestion that the Sun's motion i the Galaxy might be a possible cause o terrestrial extinctions was made by J Steiner as early as 1967[1] and again, independently, by A.A. Meyerhoff in 1973[2] though these references suggest the Sun's intragalatic orbit as the cause of the 250-million-year cycle if it exists.

W. Stannage

5 Coastguard Station,
Robin Hood Bay,
North Yorkshire YO22 4SY, UK

1. Steiner, J. *J. geol. Soc. Aust.* **14** (1), 99 (1967).
2. Meyerhoff, A.A. *Can. Soc. Petrol. Geol. Memoir* **2**, 74 (1973).

Eureka!

Sir—Buckminsterfullerene is not only a clumsy name for an outstandingly beautiful molecule (*Nature* **318**, 162–164; 1985); it is also historically inappropriate. The truncated icosahedron was known to the First Century Alexandrian mathematicians Heron and Pappos, who refer to a text on this and a dozen other such solids by Archimedes. The original treatise has since been lost, but it would be a fitting tribute to call the new substance Archimedene. This could be abbreviated to Archene (particularly suitable if this should indeed turn out to be one of the oldest molecules in the Universe — Greek *arkhe* 'origin'), or ARCH (all-round carbohedron).

Philip J. Stewart

University of Oxford,
Pauling Human Sciences Centre,
58 Banbury Road,
Oxford OX2 6QS, UK

Galactic voids may be statistical

Excitement in the past few years about the apparent clumpiness of galactic clusters, leaving empty spaces in between, may be misplaced.

When is a void real and not just a statistical artefact? The question has become topical and important because of recent reports that the Universe, statistically homogeneous though it may be, is also clumpy. There is no preferred direction in space, at least within the limits of experimental errors as they are, but nevertheless the visible matter is not merely collected into galaxies but the galaxies themselves appear to occur as clusters. More than that, as well as clusters there appear also to be voids, patches on the sky where there are no recognizable clusters of galaxies. Is this a phenomenon requiring a physical explanation? Or may the appearance of the voids be a statistical illusion which does not contradict the notion that galaxies and clusters thereof are distributed at random?

The circumstances are, or should be, familiar to cosmologists and astrophysicists. Observational bias is a recurring trouble. Whenever new techniques are used to search the sky, there is obviously a risk that the first novel objects to be found will have declared their presence only because they are exceptional. The only remedy is patience, but that is not as simple as it sounds. In spite of all the energy expended on the observation and interpretation of quasars in the past quarter of a century, for example, it is still not certain whether the apparent scarcity of quasars at a distance greater than that corresponding to a redshift parameter $z=3.5$ or thereabout implies either that quasars do not often form in more distant or younger galaxies or that there is an observational bias against the detection of more distant objects. The quasars are also the cause of a running battle between the US observer Arp and most other quasar watchers about his assertion that these objects turn out to be more often geometrically related to each other, in straight lines for example, than chance would allow.

The treatment of the problem of voids by David H. Politzer and John P. Preskill of the California Institute of Technology (*Phys. Rev. Lett.* **56**, 99; 1986) should be read by all those embroiled in arguments like these. Briefly, the conclusion is that the voids so far described on the surface of the sky are almost as likely to be consistent with randomness as with some physical process for concentrating galaxy clusters elsewhere, away from the voids. The curious feature of this article is that the underlying problem is so important and general, and the solution so simple, that one is bound to wonder why it has not been dealt with in a quite different context. At the very least, it will have cropped up as a problem for students to solve in a final examination at one of the better Victorian universities.

At first sight, indeed, there seems to be no problem. For the sake of definiteness, the case of the two-dimensional observable surface of the sky is a good place to start. The objects observed may be galaxies, or galaxies brighter than some arbitrary limit, or clusters, or clusters with redshifts between arbitrary limits. "Voids" will be only relatively empty; a patch of sky of area S will not be entirely devoid of objects, but, rather have fewer, perhaps many fewer, than most other patches of the same size. So the problem seems tractable by the elementary application of Poisson statistics. The chance that a patch of area S will contain k objects will be given by $(1/k)\ (nS)^k e^{-nS}$, where n is the average density of objects, just as it is the statistical distribution of the numbers of soldiers in the old Prussian army killed each year by being kicked by a horse. A void corresponds to the cases in which k is less than the average number in a patch of area S, given by nS.

The snag, unfortunately, is that a calculation that a specified patch in the sky will be a void, however defined, does not directly correspond to what people with telescopes actually observe. Physically, what matters is not that a specified patch on the sky should contain a void, but that the sky as a whole should contain some such patch. So the problem that matters is to calculate the probability that a void with predetermined shape and content will appear somewhere in the sky from the assumption that the objects being observed are distributed randomly. The trick, perhaps not surprisingly, has something in common with the process of swinging a telescope across the sky, searching for a void with characteristics specified in advance.

The principle is simple even if the algebra may be tedious. If a void is defined in advance as a circular patch that must contain no more than, say, k objects, the sensible course to follow is to cover the sky with a regular array of overlapping patches of that size, calculating the chance that one or more of them may correspond to a void, and then to allow the density of the overlapping patches to increase indefinitely. Technically, this is done by centring circles on the intersections of some kind of lattice structure whose spacings are then made indefinitely to shrink. The same kind of calculation can be carried through with other shapes of voids than circles.

Not surprisingly, the chance of finding a specified void somewhere in the sky turns out to be greater than that a particular patch will contain such a void. More significantly, numerical factors apart, the chances of finding predetermined voids are related to the Poisson distribution by factors of the form (nS) raised to the power two in the case of circular patches on a two-dimensional sky, but which may be raised to a higher power if the voids are elliptical in shape and allowed to assume any orientation. What this implies is that the presence of voids in the distribution of objects in the sky is certain to be much more common than has been assumed.

The argument applies directly to one of the first claims of the presence of a void in the distribution of rich galaxy clusters (Bachall, N. and Soneira, R. *Astrophys. J.* **262**, 419; 1982), which has been the stimulus for other such claims in the more recent literature. As Politzer and Preskill argue, the chance that the observed distribution has arisen from a random distribution of galaxies is something like 30 per cent, which goes to show that the occurrence, dramatic though it may appear, is nowhere out of the ordinary.

There is, of course, no reason why anybody should be upset by this turn of events. What stands out a mile is that simple expectations of the consequences of the random distribution of objects on the sky are unreliable. The surprise is that the accurate calculation has not been made before this. And even if it should be that voids are less remarkable than they have seemed in the past few years, that does not imply that they are entirely without interest.

For galaxies are not distributed at random. Large clusters are gravitationally bound and presumably collapsing. Much of the immediate interest in this field is that of measuring the dynamics of the clusters, which may throw light on their origin. This why Politzer and Preskill want to turn their problem around, and use the measured distribution of voids as a way of inferring something of non-random distribution of galaxies and of clusters of galaxies.

John Maddox

Palaeontology

New fossil finds in old rocks

from S. M. Awramik

THE well-preserved stromatolites from 3,300–3,500-Myr-old rocks in South Africa described on page 489 of this issue[1] are not the first report of stromatolites from the Early Archaean, but these structures are by far the best preserved and morphologically convincing examples of such stromatolites that can be interpreted as microbial in origin. This discovery reinforces the notion[2,3] that the Earth's earliest biota was much more advanced morphologically, and presumably metabolically, than has previously been thought.

Dealing with Archaean fossils is a tricky business. First, you have to convince the scientific community that the objects in question are really fossils; then demonstrate that the rocks in which the fossils were found are of the proposed Archaean age; and finally show that the fossils were coeval with the rocks. With almost every claim for the discovery of an Archaean fossil there are counterclaims proposing alternative non-biological origins, or that the rock or fossil in question is not of Archaean age[4]. Such prudence is justifiable because, in addition to extending the known record of life, Archaean fossils provide information on the diversity and relative abundance of early life, and lead to interpretations of metabolic characteristics and affinities of the microbes concerned. They also have significant bearing on evolutionary models that include the origins of life, its early diversification, phylogenetic relationships, rates of evolution and evolutionary events leading to the appearance of eukaryotes, animals and plants.

The general model for the early history of life used to be one of sluggishly evolving prokaryotes that took some 2,000 Myr to reach the eukaryotic grade and another 800 Myr before the animal level of organization evolved. The picture of life on the early Earth has become sharper in recent years as a result of important discoveries of fossils in the Early Archaean, 3,800–3,400 Myr ago. These discoveries have been made mainly in two regions: the Pilbara Block in Western Australia; and the Barberton Mountain Land in South Africa, areas that have excellent exposures of the oldest known relatively unmetamorphosed sedimentary rocks.

In rocks from the Swaziland Supergroup in the Barberton Mountain Land, solitary spheroidal microfossils, several micrometres across, that are interpreted as bacteria, have been detected in chert[5,6]. Although these are currently regarded as 'dubiofossils', because there are doubts about their cellular microbial origin[7], they were headline news in the 1960s as they extended the first appearance of life by more than 1,000 Myr. Such small roundish microfossils were what most scientists would have predicted the Earth's oldest cells should have looked like. More convincing reports of spheroidal microfossils[8] and the discovery of paired cells in the South African rocks soon followed[9]. The dyads suggested that these prokaryotes reproduced by binary fission and they made a stronger case for the biogenicity of the microfossils.

In 1980, two reports appeared[10,11] on the discovery of stromatolites in the 3,400–3,500-Myr-old Warrawoona Group sediments from the Pilbara Block. Stromatolites present a very different picture when reconstructing the Early Archaean biosphere. They suggest more advanced microbial life. Stromatolites are conventionally viewed as biosedimentary structures produced by communities of photoresponsive microbes that trap and bind sediment. At times, these microbes can generate layered domed and columnar structures centimetres to metres in size. Cyanobacteria (in particular filamentous cyanobacteria) and microbes that behave like cyanobacteria, are the dominant stromatolite builders today and were probably responsible for most fossil stromatolites. We do not know whether cyanobacteria existed in the Early Archaean but the stromatolites imply that proto-cyanobacteria, cyanobacteria-like microbes or some other prokaryote with stromatolite-building capabilities had already evolved the ability to live in shallow, agitated waters and cope with sediment and sunlight.

It is not surprising that the biological nature of the Warrawoona stromatolites has been questioned[12,13]. Their morphology is simple, evaporites are associated with them and no microbial fossils were detected in their laminae. The growth of the evaporite minerals could have produced the simple doming. But this also occurs in modern evaporitic mat environments, where the shape of microbial mats (incipient stromatolites) is modified by the growth of evaporites.

Independent support for a microbial origin comes from the discovery of filamentous microbial fossils in Warrawoona chert[3]. Tubular fossil filaments suggest that the sheathed filamentous habit of prokaryotes, a highly successful stromatolite-building characteristic, has already evolved by the latter part of the Early Archaean. Unfortunately, these microfossils were not found in domed stromatolites. In summary, although the evidence is strong, the jury is still out on the biogenicity of the Warrawoona stromatolites.

The focus for the oldest remains of life on Earth now returns to South Africa, to the Swaziland Supergroup, where the lowest part, the Onverwacht Group, is approximately the same age as the Warrawoona Group. Members of the research team at Louisiana State University that discovered stromatolites in the Warrawoona[10] and microfossils in the Onverwacht[14] now describe morphologically complex, biogenically convincing stromatolites from the Fig Tree Group, another part of the Swaziland Supergroup[1]. These stromatolites are significant partly because their morphology is much more complex than the simple dome shapes found in the Warrawoona. The complex pseudocolumnar shape, good preservation, mode of occurrence, well-defined laminae and laminar microstructure are a combination of features that are difficult to explain by abiogenic processes. The closest abiogenic analogue would be geyserite. Furthermore, they are strikingly similar to other less ancient stromatolites, including early Proterozoic (2,500–1,600 Myr) biogenic stromatolites from the Gunflint Iron Formation and superficially similar to some modern non-marine cyanobacterial stromatolites. Combined with all the microbial fossil and organic geochemical data from the Early Archaean, the discovery adds to an impressive array of palaeobiological information on the biosphere of the early Earth.

It is unfortunate that stromatolites have played a relatively minor part in unravelling the early history of life. In many ways, the presence of stromatolites in such ancient rocks as the Swaziland Supergroup can reveal more about the degree of microbial evolution than microbial fossils preserved in chert, the common palaeobiological standard for the level of evolution in the Precambrian. Early Archaean stromatolites have interesting, if highly speculative, implications for the microorganisms that built them. First, as early as 3,500 Myr ago, microbes must have evolved that were benthic through-

---

1. Byerly, G.R., Lowe, D.R. & Walsh, M.M. *Nature* **319**, 489 (1986).
2. Knoll, A.H. *Paleobiology* **11**, 53 (1985).
3. Awramik, S.M., Schopf, J.W. & Walter, M.R. *Precambrian Res.* **20**, 357 (1983).
4. Cloud, P. & Morrison, K. *Precambiran Res.* **9**, 81 (1979).
5. Pflug, H.D. *Univ. Witwatersrand Econ. Geol. Res. Unit Info. Circ.* **28**, 1 (1966).
6. Schopf, J.W. & Barghoorn, E.S. *Science* **156**, 508 (1967).
7. Schopf, J.W. & Walter, M.R. in *Earth's Earliest Biosphere* (ed. Schopf, J.W.) 214 (Princeton University Press, 1983).
8. Muir, M.D. & Grant, P.R. in *The Early History of the Earth* (ed. Windley, B.F.) 595 (Wiley, London, 1976).
9. Knoll, A.H. & Barghoorn, E.S. *Science* **198**, 396 (1977).
10. Lowe, D.R. *Nature* **284**, 441 (1980).
11. Walter M.R., Buick, R. & Dunlop, J.S.R. *Nature* **284**, 443 (1980).
12. Buick, R., Dunlop, J.S.R. & Groves, D.I. *Alcheringa* **5**, 161 (1981).
13. Cloud, P. *Proc. 27th Int. Geol. Congr. (Moscow)* **5**, 173 (1984).
14. Walsh, M.M. & Lowe, D.R. *Nature* **314**, 530 (1985).

out most or all of their life cycle and were either fast-growing or motile — otherwise they could not have maintained their position at or near the sediment/fluid interface and would have been buried. A positive photoresponsive behaviour would enhance this ability, and presumably the microbes were photoautotrophic. Second, because the stromatolites formed in very shallow waters, they must have had some minimum resistance to high-energy solar radiation and finally, it is probable that some of the builders were filamentous forms with sheaths around the trichomes.

No longer can the evolutionary history of Precambrian life be viewed as slowly changing microbial biota that gradually increased in diversity and complexity until the appearance of eukaryotes. The Swaziland stromatolites and the other Archaean fossil data indicate that by 3,300–3,500 Myr ago, diverse microbial life existed on Earth, some of which was organized into microbial ecosystems. Once life appeared on the early Earth, it diversified rapidly and in all probability explored and occupied most if not all habitable ecological zones. ☐

S.M. Awramik is in the Department of Geological Sciences, University of California, Santa Barbara, California 93106, USA.

Developmental genes

Mediators of cell communication?

from Michael Akam

THE control of development operates at many different levels. In recent months this has become easy to forget, with the nucleus the focus of attention and the DNA-binding properties of the homoeo box taking much of the limelight. Now the sequencing of two other 'controlling' genes, one from insects and the other from nematodes, has revealed homology with mammalian proteins of very different function. The *lin-12* gene of *Caenorhabditis*, which controls patterns of cell lineage[1], and the *Notch* gene of *Drosophila*, which plays a role in the early development of the nervous system[2], both encode proteins homologous with epidermal growth factor (EGF) and the structurally related family of mammalian proteins. Other members of this family are all membrane-bound or secreted proteins, suggesting that *Notch* and *lin-12* act at or beyond the cell membrane, perhaps to mediate cell communication.

The family of EGF-related proteins all share a characteristic cysteine-rich peptide of 40 – 50 amino acids. This sequence occurs nine times in the membrane-bound precursor of EGF; the terminal copy of the repeat, cleaved from the precursor, is the EGF peptide itself[3]. The *Notch* and *lin-12* genes also encode multiple copies of this peptide motif. The complete structure of the lin-12 protein is not yet clear, but I. Greenwald[1] finds eleven copies of the EGF motif within the four exons that have been sequenced. *Notch* seems to encode an enormous protein of some 2,700 amino acids in a 10.5-kilobase-long transcript. K. Wharton and colleagues[2] have sequenced all but a few hundred bases of this transcript from overlapping complementary DNA clones. In the amino-terminal half of the derived protein they predict 36 tandem repeats of a 40-amino-acid motif that shares the conserved cysteine spacing of EGF, and shows limited homology at other sites within the repeat. This region is followed by a putative transmembrane sequence of hydrophobic amino acids, followed by a large carboxy-terminal region which, except for a polyglutamine stretch, bears no close homology with other known proteins.

The structure of the Notch protein predicted by this sequence, which includes an extracellular EGF-like domain, resembles that of the membrane-bound protein in the EGF family, for example, the low-density lipoprotein (LDL) receptor and the precursors of several growth hormones (EGF, tumour growth factor and vaccinia virus growth factor). But the EGF family also includes secreted proteins with diverse functions, including the blood-clotting factors urokinase and plasminogen activator. The role of the EGF domain within these secreted proteins is not known.

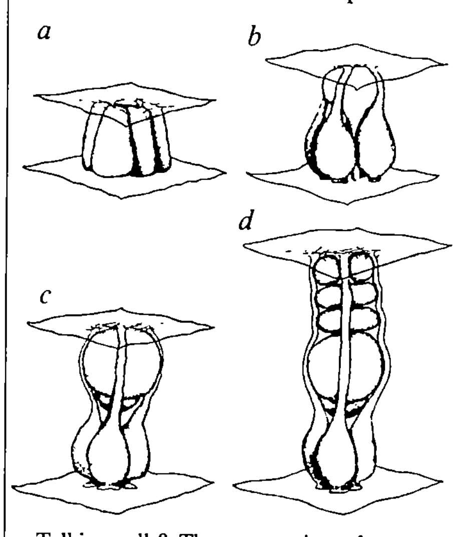

Talking cells? The segregation of neuroblasts is an early step in the formation of the insect nervous system, in this case the grasshopper, and one which requires adjacent cells to communicate. The *Notch* mutations of *Drosophila* disrupt this process (see text). In insects, neuroblasts segregate from a sheet of apparently equivalent cells in the embryonic ectoderm (*a*). The first sign that a cell will become a neuroblast is the dorsal shift of its nucleus and cell body towards the interior of the embryo (*b*). Several cells in each region may initiate this process but only a single cell completes it. This cell will undergo the characterisitic pattern of divisions which generate neurones (*c*,*d*). (Redrawn from ref. 9.)

At first sight, the effects of *lin-12* and *Notch* mutations have little in common with one another or with the functions of the EGF protein family. The *lin-12* mutations cause losses and duplications of a range of structures in the animal, which result from alterations in the normally precise control of cell lineage during embryogenesis[4]. Recessive lethal *Notch* mutations (which cause notching in the adult wing when heterozygous) result in overgrowth of the nervous system in embryos[5]. There are, however, close parallels in the cellular phenomena underlying these different phenotypes. Both mutations alter the way in which equivalent cells choose between alternative developmental pathways. In both cases the decisions affected may depend on local interactions between neighbouring cells.

A functioning *lin-12* gene is needed for the normal development of several groups of cells during embryogenesis and maturation of *Caenorhabditis*. Cells of each affected group are characterized by analogous positions in the cell-lineage tree. In normal development, cells within each of these groups adopt two or more different fates (say A and B), each fate being defined by subsequent patterns of cell division and differentiation. When the *lin-12* gene does not function, all cells within a group are forced to adopt the same fate (fate A), or a subset of their normal fates. However, when mutation results in overexpression of the *lin-12* gene, all cells of the group are forced to adopt the alternative fate (B). Thus mutations that modulate *lin-12* activity switch the development of cells in a way that parallels the choices made during normal development. This suggested that the role of the *lin-12* gene in normal development was analogous to that of the homoeotic selector genes in *Drosophila*[6].

Several experiments where individual cells are killed show that the groups of cells affected by *lin-12* have the special properties of 'equivalence groups'[7]. In such a group, all cells seem to have the same intrinsic developmental potential; the fate adopted by each cell is specified by its location and by the interactions it makes with neighbours. One of the possible fates of a cell in an equivalence group is usually dominant; when a cell that will fulfill the dominant fate is killed, another member of the group alters its own behaviour to replace the dead cell.

Notch mutations seem to have a primary effect on neuroblast segregation. Recent descriptions of this process in insects[8,9], and of the effect that killing a single neuroblast has on the final pattern[10], suggest that the determination of neuroblasts is in many ways analogous to the determination of cells within an equivalence group. In this case the neuroectoderm seems to comprise a sheet of equivalent cells, although the probability of neuroblasts forming is particularly high in certain regions of the sheet. In each of these regions, several cells may initiate the morphological changes leading to neuroblast formation (see figure), but one will come to dominate and inhibit its neighbours. In normal *Drosophila* embryos, about a quarter of the cells in the neuroectoderm become neuroblasts; the remainder make the larval epidermis. In *Notch* mutant embryos, it seems that the mechanism of domination and inhibition fails; all cells of the neuroectoderm become neuroblasts and no cells are left to form the epidermis.

The effects of *Notch* and of *lin-12* mutations could result from a failure at one of the many levels in the hierarchy of control but, because of the homologies with EGF, it seems most likely that the defect lies in the ability of cells to sense or influence their environment. The gene product, at least in the case of *Notch*, is unlikely to be a hormone, because the effects of *Notch* mutations in genetic mosaics are expressed even in small regions of mutant tissue. The most attractive possibility is that Notch and lin-12 are membrane proteins which transmit developmental signals between adjacent cells. ☐

1. Greenwald, I. *Cell* **43**, 583 (1985).
2. Wharton, K., Johansen, T.X. & Artavanis-Tsakonas, S. *Cell* **43**, 567 (1985).
3. Scott, J. *et al. Science* **221**, 236 (1983).
4. Greenwald, I., Sternberg, P.W. & Horvitz, R. *Cell* **34**, 435 (1983).
5. Lehman, R. Jimenez, F., Dietrich, W. & Campos-Ortega, J.A. *Wilhelm Roux Arch. dev. Biol.* **192**, 62 (1983).
6. Lawrence, P.A. *Nature* **306**, 643 (1983).
7. Kimble, J. *Devl Biol.* **87**, 286 (1981).
8. Hartenstein V. & Campos-Ortega, J.A. *Wilhelm Roux Arch. dev. Biol.* **193**, 308–325 (1984).
9. Doe, C.Q. & Goodman, C.S. *Devl Biol.* **111**, 93 (1985).
10. Doe, C.Q. & Goodman, C.S. *Devl Biol.* **111**, 206 (1985).

Michael Akam is a Medical Research Council Senior Fellow in the Department of Genetics, University of Cambridge, Downing Street, Cambridge CB2 3EH, UK.

Earth sciences

Sources of basic magmas

from R.N. Thompson

WHERE do basic magmas come from? Although more than 20 years have passed since it was generally agreed that the answer to this question is the Earth's mantle, there is still much debate and no unanimity as to the precise sites of basic magma genesis in the upper mantle. The source regions that are candidates for this role are the convecting asthenosphere and rigid lithosphere. The latter is absent immediately beneath mid-ocean ridges and can therefore be excluded as a source of erupted magmas at spreading centres. In contrast, both sources occur in the older parts of ocean basins, near subduction zones and throughout the continents. The problem is that it is relatively easy to produce element and isotope analyses of basic rocks consistent with the genesis of their parental magmas by melting either a hypothetical lithosphere or asthenosphere mantle source, but it is extremely difficult to devise a real test between these alternatives. J.G. Fitton and H.M. Dunlop have recently devised such a test for a major group of basic magmas[1], consisting of basalts, with subordinate basanites and olivine tholeiites.

As a group these rocks are chemically indistinguishable from the basalts of ocean islands such as Hawaii and Iceland. Fitton and Dunlop's samples are from the Cameroon line, a 1,600-km chain of volcanoes. This immense igneous province runs from the oceanic islands of Pagalu, Sao Tômé and Principe, in the Gulf of Guinea, across Cameroon to the Biu Plateau in north-east Nigeria, and straddles a continental boundary. The volcanoes of both the oceanic and the continental sectors of the line have been intermittently active throughout the past 25 Myr; most of them have erupted most recently within the past 1 Myr[1]. Therefore, despite its suggestive appearance on the map, the line cannot represent the surface trace of an upwelling mantle plume beneath the African lithospheric plate, but rather it must be the locus of upward leakage from a long zone of basic magma generation in the upper mantle. The test presented by this zone is therefore a simple one. If lithospheric mantle does provide the source of magmas along the line, basalts from the oceanic and continental segments should be very different in their element and isotope composition because the sub-oceanic lithospheric in the Gulf of Guinea was formed at a spreading centre no more than about 125 Myr ago[2], whereas the sub-continental lithosphere beneath Cameroon is Precambrian. Fitton and Dunlop examined many trace elements and strontium isotopes, and showed that the average compositions of the basic magmas from the oceanic and continental segments of the Cameroon line are identical and therefore that the magmas must have originated in the convecting upper mantle and cannot have interacted to any significant extent with lithosphere mantle[1].

The importance of this study lies in the ordinariness of the Cameroon-line lavas, which are typical ocean-island basalts, supporting earlier suggestions that these basalts contribute to continental magmatism[3] and consistent with models that require the source mantle of ocean-island basalts to be continuous beneath the continents[4-6]. Does this mean that oceanic and continental basalt magmatism (away from subduction zones) are the same phenomenon? Far from it: most continental basalts — especially those of the great lava floods — contain abundances of elements and isotopes from the oceanic compositional range. Explanations for these differences are usually either that the magmas originated from the same asthenospheric sources as oceanic basalts and reacted with continental crust on their way to the surface[7], or that the magmas were formed by melting of subcontinental lithospheric mantle which had developed a distinctive composition during prolonged isolation from the convecting asthenosphere[8].

Mafic magmas are hundreds of degrees hotter than the liquidi of the most fusible parts of continental crusts, which makes it difficult to understand why evidence for

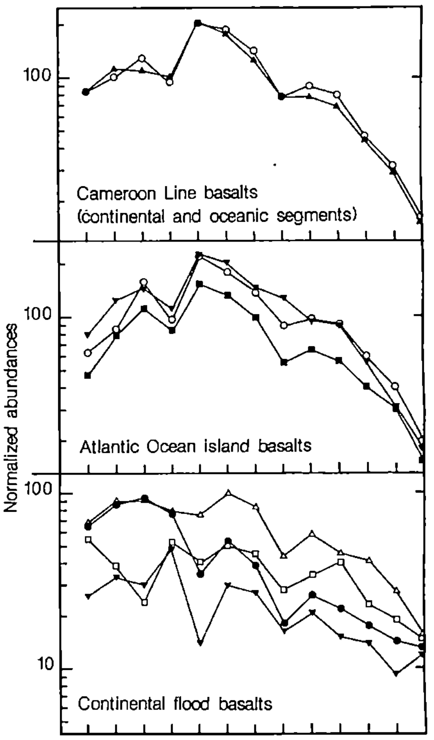

Abundance of a range of elements in basalts from the Cameroon line and elsewhere, normalized to facilitate synoptic comparisons. The Atlantic Ocean island samples are from Tenerife, Madeira and St Helena, the continental flood basalt samples from the Columbia River Plateau and Snake River Plain, USA, the Parana Basin, Brazil, and Karoo, South Africa.

crustal contamination of the liquids during magma upwelling is not found more often. H.E. Huppert and R.S.J. Sparks[9] have recently provided one solution to this problem by investigating the fluid dynamics of subterranean magma migration in regions of volcanism associated with lithospheric extension, such as the Cameroon line, where the magmas probably rise in dykes. They calculate that the rheology of the upwelling liquids varies from laminar to turbulent within the geologically relevant range, turbulent behaviour occurring mainly at the high flow rates associated with the large eruptions that characterize flood basalts. Huppert and Sparks point out that a basic magma moving in a laminar manner through a conduit forms a chilled skin along the contact which tends to prevent incorporation of potentially fusible wall-rock into the fluid. In contrast, a turbulent magma will actively erode any patches or layers of fusible material along the margins of its conduit.

This argument does not apply only to magma–crust interaction. The Mg-rich, low-viscosity ultramafic magmas, which are identified by phase-equilibria studies to be the parents of flood basalts[10–11], are also likely to behave turbulently as they rise through the subcontinental lithosphere. They are hot enough to melt and incorporate selectively the relatively fusible 'metasomatic' veins and patches that characterize subcontinental lithospheric mantle[8]. It therefore seems possible that fluid dynamics holds the key both to the eruption of unmistakably oceanic asthenosphere-source basic magmas along the continental segment of the Cameroon line (small magma batches traverse the lithosphere by laminar flow, with minimal interaction), and to the contrasting compositions of almost all flood basalts (large and fast-moving magma batches rise turbulently through the subcontinental lithosphere and incorporate sufficient of its most fusible constituents to emerge with compositions suggesting an ancient lithospheric source). ☐

1. Fitton, J.G. & Dunlop, H.M. *Earth planet. Sci. Lett.* **72**, 23 (1985).
2. Le Pichon, X. & Huchon, P. *Earth planet. Sci. Lett.* **67**, 123 (1984).
3. Allègre, C.J., Dupré, B. Lambret, B. & Richard, P. *Earth planet. Sci. Lett.* **52**, 85 (1981).
4. McKenzie, D.P. & O'Nions, R.K. *Nature* **301**, 229 (1983).
5. Thompson, R.N., Morrison, M.A., Hendry, G.L. & Parry, S.J. *Phil. Trans. R. Soc.* **A310**, 549 (1984).
6. Allègre, C.J. & Turcotte, D.L. *Geophys. Res. Lett.* **12**, 207 (1985).
7. Carlson, R.W., Lugmair, G.W. & MacDougall, J.D. *Geochim. cosmochim. Acta* **45**, 2483 (1981).
8. Hawkesworth, C.J., Rogers, N.W., Van Calsteren, P.W.C. & Menzies, M.A. *Nature* **311**, 331 (1984).
9. Huppert, H.E. & Sparks, R.S.J. *Earth planet. Sci. Lett.* **74**, 371 (1985).
10. Cox, K.G. *J. Petrol.* **21**, 629 (1980).
11. Thompson, R.N., Morrison, M.A., Dickin, A.P. & Hendry, G.L. in *Continental Basalts and Mantle Xenoliths* (eds Hawkesworth, C.J. & Norry, M.J.) 158 (Shiva, Nantwich, 1983).

R.N. Thompson is at the Department of Geology, Imperial College, London SW7 2BP, UK.

The sand-bubbler crab *Scopimera intermedia*, showing the unique air-breathing structures, called gas windows, on the legs. In this species the gas windows are red. Each leg membrane (there are two per leg) is very thin (0.6 μm) and covers a large area (up to 25 mm^2). A complex capillary-like network of blood vessels lies beneath. See p. 493 for a complete description. (Photograph by David P. Maitland.)

Human evolution

How small was the bottleneck?

from J. S. Jones and S. Rouhani

THE human fossil record is no exception to the general rule that the main lesson to be learned from palaeontology is that evolution always takes place somewhere else. Even the best fossil beds preserve evidence of about one skeleton per million[1], and this, combined with problems of dating, means that the pattern of origin of modern *Homo sapiens* remained obscure until recently. It is not surprising that palaeontologists have at different times hailed Europe, Africa, Asia and even the Americas as the birthplace of modern man[2]. Mankind, however, retains a more complete record of history in its genes, and a paper on page 495 of this issue[3] provides new evidence that the origin of modern man lies in Africa.

In their study, Wainscoat *et al.*[3] examine the patterns of relatedness of a small segment of nuclear DNA from five closely linked restriction sites in the β-globin gene cluster from Europeans, Indians, Asiatics and Africans. A total of 32 haplotypes (combinations of alternative sites) can be generated from these 5 variants; but in the event only 14 are found among the 601 chromosomes studied, and only 5 of these are common. There is a striking geographical pattern in their distribution. Three β-globin haplotypes are widespread in all non-African populations (and are rare in Africa) whereas the African population is characterized by a high frequency of two haplotypes, one of which is rare and the other absent from the rest of the world. For this segment of DNA, mankind can be divided into an African and a non-African lineage.

The replacement of Neanderthal man by anatomically modern *H. sapiens* in a few thousand years in Europe (about 30,000 years ago) and fossils similar to modern humans have been found in Asian beds which may be as much as 50,000 years old[2,4]. It is sometimes suggested that the relatively sudden appearance of widespread populations of modern man means that evolution of the species occurred independently in different parts of the world[2]. This does not agree with modern theories of speciation: the probability of a single transition between the adaptive peaks that represent species is low, and the chance of a simultaneous peak shift in an evolving lineage is small[5,6]. The replacement of Neanderthals and other archaic humans by modern man in most parts of the world is much more likely to have resulted from the extinction of the older population by new hominids spreading from a single centre of origin. Expanding human populations did spread remarkably quickly. Most palaeontologists agree that the Americas were devoid of mankind until about 12,000 years ago, but once man had entered the empty New World he reached the southern tip of the continent in less than 1,000 years[7]. The wave of advance of early farmers in Europe, measured by the appearance of their artefacts and by the gradients in gene frequency which persist in modern populations[8], occurred at about 1 km a year across Europe from 6,000 BC — an advance sufficiently fast to pass from Greece to England in two millennia.

Wainscoat *et al.*[3] suggest that the pattern of distribution of β-globin haplotypes is consistent with the rapid spread of modern man from a centre of origin in Africa, and that the spread of the species to the rest of the world led to a drastic shift in haplotype frequencies because of a population bottleneck and sampling drift in the emigrant population. New fossil evidence strongly supports the view that man's origin was indeed Africa. Anatomically modern human fossils from 100,000 years ago have been found at the mouth of the Klasies River in South Africa and modern man was widespread in Africa by 50,000 years BP (ref. 9), at a time when Europe was populated by Neanderthals. Studies of blood group and enzyme alleles in Africa and of DNA sequences associated with the sickle-cell mutants suggest that African populations are genetically more subdivided than are those from other parts of the world[10,11]. This again suggests a longer history of evolution *in situ* in Africa than anywhere else.

When did modern man leave Africa and how small a population emigrated? Although the evidence from fossils is sparse, their distribution suggests that the first emigrants had left their continent of birth by 50,000 BP and were widespread by 30,000 BP. The social structure of modern African hunter–gatherers does predispose them to rapid genetic changes resulting from sampling drift[12]. However, the global extent of β-globin divergence has at first sight some startling demographic implications because the hunter–gatherers who migrated from Africa. Europe and Asia have rather similar haplotype frequencies. Hence, the emigrants must have undergone the major change in haplotype frequency in the interval between leaving Africa and dispersing throughout the rest of the world. Assuming — and this is little more than an informed guess — that this interval was 20,000 years, population-genetics theory tells us that the mean effective size of the ancestral population for all non-Africans throughout this period must have been 600 individuals; or alternatively that the bottleneck was 6 individuals for 200 years, or even a single couple for 60 years. (The expected time for the loss of a neutral gene present in the population at frequency p is $\mathrm{E}(T) = -4\mathrm{N}\ p\ln p/1-p$, where N is the population size[13]. We assume a generation interval of 20 years and that the 4 common haplotypes were present at equal frequencies in the ancestral African population.) If this is the case, much of mankind was an endangered species during an important part of its evolution.

Population bottlenecks of this severity in modern human populations can have untoward genetic consequences. Afrikaners returned to the land of their African ancestors about 300 years ago, and most of them can trace their families to one of a few Dutch founders. One partner of a couple who married in 1688 carried an allele for the recessive disease porphyria variegata. This allele is now carried by many of their descendents and is hundreds of times more common among white South Africans than elsewhere[14]. If the distribution of β-globin haplotypes is typical of those in the human genome, founding populations of non-African man may have suffered a considerable genetic load because of inbreeding. There are some puzzling inconsistencies when the global patterns of these haplotypes are compared with those of other human polymorphisms. These can give widely different estimates of the size of the human population during its flight from Africa.

Sequence data for mitochondrial DNA (which is maternally inherited) suggest that African populations are ancestral to others[15]. Casanova *et al.* have found analogous differences between African and European peoples in a Y chromosome-linked DNA polymorphism (which is paternally transmitted and hence may be useful in studying gene flow through males[16]). Calculations of the size of the bottleneck that can explain the relatively lower mitochondrial diversity of non-African populations compared with Africans suggest a population of 4,000 individuals for 20,000 years, or 40 individuals for two centuries. Mitochondrial divergence therefore implies that mankind underwent less of a bottleneck on emigration from Africa than the estimate derived from β-globins. Global patterns of blood group and enzyme diversity are on the average much more uniform geographically than are those of either β-globin or mitochondrial DNA sequences: the mean difference between Africa and Europe is not much greater than that which exists between two Africa tribal groups or two European countries[17]. For these genes there is no need to postulate a bottleneck during the emergence from Africa very different from those which have occurred in man's immediate past.

Why should different genes produce such different estimates of the size of the founding non-African population? Mitochondria have peculiarities in their mode of transmission and mutation rate which limit their value as indicators of evolutionary relatedness[18], and natural selection on some enzymes and blood groups may obscure their demographic history[19]. Most important, statistical problems mean that estimates of the time and pattern of divergence and of the size of evolving populations based on individual DNA sequences have large systematic errors[20,21]. Such estimates depend greatly on the number of unlinked loci surveyed, so that single short sequences of closely linked markers may be misleading indicators of population history. These uncertainties can be seen in a recent study of 43 sequence variants in a 2,400 base pair region of the alcohol dehydrogenase locus of the fruitfly *Drosophila melanogaster*[22]. Although the genetic information available for *Drosophila* is much greater than is that for human β-globin, it makes it possible to estimate the date of origin of the enzyme polymorphism only to within a range of 0·6–3.5 Myr BP.

These statistical problems mean that the phylogeny of individuals genes may be a misleading indicator of the phylogeny of the populations from which they come. Quite often two alleles will diverge before the date of splitting of an ancestral population[23]. This is already clear from studies of human populations: nobody claims that the common high frequency of the B blood group (an allele that is absent from many human populations) which is found in Russians and chimpanzees is a reliable indicator of a shared evolutionary history! The same caution must be observed when reconstructing human evolution from other individual genes or DNA sequences.

It is thus possible that future sequence studies of the human genome will cast a different light on population bottlenecks during the spread of modern man. However, unlike students of the human fossil record, molecular biologists know that the information they need to reconstruct human evolution is easily available and merely awaits their attention. ☐

1. Cronin, J.E. *et al. Nature* **292**, 113 (1981).
2. Howell, F.C. in *The Origins of Modern Humans* (eds Smith, F.H. & Spencer F.) xiii (Liss, New York, 1984).
3. Wainscoat, J.S. *et al. Nature* **319**, 495 (1986).
4. Stringer, C.B. *et al.* in *The Origins of Modern Humans* (eds Smith, F.H. & Spencer, F.) 51 (Liss, New York).
5. Barton, N. & Charlesworth, B. *A. Rev. Ecol. Syst.* **15**, 133 (1984).
6. Lande, R. *Proc. natn. Acad. Sci. U.S.A.* **82**, 7641 (1985).
7. Owen, R.C. in *The Origins of Modern Humans* (eds Smith, F.H. & Spencer, F.) 517 (Liss, New York, 1984).
8. Ammerman, A.J. & Cavalli-Sforza, L.L. *The Neolithic Transition and the Genetics of Populations in Europe* (Princeton University Press, 1984).
9. Brauer, G. in *The Origins of Modern Humans* (eds Smith F.H. & Spencer, F.) 327 (Liss, New York, 1984).
10. Nei, M. & Roychoudhury, A.K. *Evol. Biol.* **14**, 1 (1982).
11. Pagnier, J. *et al. Proc. natn Acad. Sci. U.S.A.* **81**, 1771 (1984).
12. Harpending, H. & Wandsnider, L. in *Curr. Dev. Anthr. Genet.* **2**, 29 (1982).
13. Kimura, M. & Ohta, T. *Genetics* **61**, 893 (1969).
14. Dean, G. *The Porphyrias: a Study of Inheritance and Environment* 2nd edn (Pitman Medical, London, 1971).
15. Johnson, M.J. *et al. J. molec. Evol.* **19**, 255 (1983).
16. Casanova, M. *et al. Science* **230**, 1403 (1985).
17. Latter, B.D.H. *Am. Nat.* **116**, 220 (1980).
18. Wilson, A.C. *et al. Biol. J. Linn. Soc., Lond.* **26**, 375 (1985).
19. Piazza, A.A. *et al. Proc. natn. Acad. Sci. U.S.A.* **78**, 2638 (1981).
20. Tajima, F. *Genetics* **105**, 437 (1983).
21. Takahata, N. & Nei, M. *Genetics* **110**, 323 (1985).
22. Stephens, J.C. & Nei, M. *J. molec. Evol.* **22**, 289 (1985).
23. Hudson, R.R. *Evolution* **37**, 203 (1983).

J.S. Jones and S. Rouhani are in the Department of Genetics and Biometry, University College London, London NW1 2HE, UK.

X-ray astronomy

New results from Exosat

from A.C. Fabian

THE European X-ray astronomy satellite Exosat has been in orbit for more than two years. Its orbital period of almost 100 h allows a long uninterrupted view of X-ray sources to an extent that was impossible with earlier satellites in near-Earth orbits under the radiation belts, and has led to the many discoveries discussed at a recent meeting*. X-ray astronomers are used to each successive satellite probing deeper in a discovery space that has coordinate axes in spatial, spectral and temporal resolution, together with sky and time coverage. Exosat excels in this last respect, with further advances made possible by its good response to very soft X-rays and the high spectral resolution to photons at the energy of the iron line.

The recently discovered narrow galactic ridge (Warwick, R. *et al. Nature* **317**, 218; 1985) has been studied in more detail (R. Warwick, University of Leicester). Some bright spots on the ridge are supernova remnants, but these cannot explain all of the ridge. The spectrum of the 'diffuse' emission is consistent with that of gas at $kT=8$ keV, as found independently by observers using the Japanese satellite Tenma. There are many point sources that are probably X-ray binaries, some of which are new. One such transient X-ray source, EXO0748-676, discovered while the satellite was slewing between targets, was discussed by A. Parmar and M. Gottwald (European Space Operations Centre, ESOC). The source is a member of the class of 'dipping' X-ray sources which display recurrent shallow dips in their light curves. The source also shows X-ray bursts, the recurrence time of which correlates strikingly with the persistent source luminosity in a manner opposite to that suggested by current theories. Several bursts were followed by a second burst within 20 min or less.

Exosat monitoring of the well-known jet emitter SS 433 was reported by G. Stewart (University of Leicester). A strong iron-emission line at about 7 keV was Doppler-shifted in phase with the 164-day precession cycle of the jets. As only one line is observed, that caused by the approaching jet, instead of two lines as seen at optical wavelengths, Stewart concludes that the iron emission originates from close to the central object. The other jet is presumed to be obscured by an accretion disk.

Most excitement was centred on the discovery of quasi-periodic oscillations (QPOs) in several low-mass X-ray binaries. These were first reported by M. van der Klis and colleagues (*Nature* **316**, 225; 1985) from the source GX5-1. Power spectra of the light curve show a low-Q peak that shifts according to the apparent luminosity. There are now about seven sources that display this phenomenon, which in many respects resembles the behaviour of some cataclysmic variables observed at optical wavelengths. S. Ilovaisky (University of Besançon) pointed out that QPOs are also observed in the candidate black hole GX339-4. They are found optically when the source is either very bright or faint, but not when it is in any intermediate state. G. Hasinger (Max Planck Institute for Extraterrestrial Physics) summarized the X-ray QPOs from CygX-2 which are at about 40 Hz, a much higher frequency than any yet observed optically.

Light (X-ray) curves of NGC4051, showing rapid movements (K. Pounds).

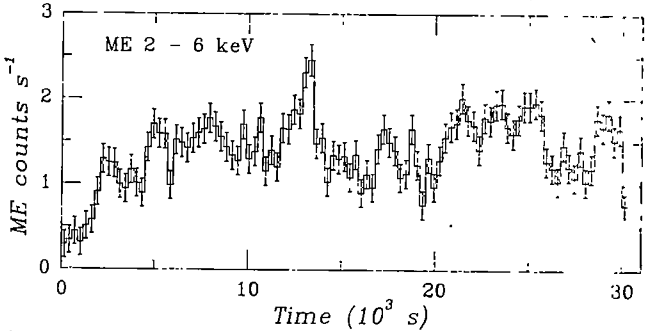

It is not known why QPOs were not observed by previous X-ray satellites, although they were detected in 1982 during some flat-topped bursts of the rapid burster with the satellite Hakucho. J. Swank (NASA Goddard Space Flight Center) has analysed Einstein satellite data and found no QPOs. Her limit for CygX-2 is about 3 per cent, whereas reports from Exosat give 7 per cent. The long-duration Exosat observations produce clean power spectra that must contribute to the detection of a weak, fluctuating signal. W. Priedhorsky (Los Alamos) found QPOs in the brightest continuous X-ray source in the sky, SCOX-1, which has been extensively studied; the QPOs are only seen when the source is not flaring. His data and the new results of van der Klis show that the source behaviour in the QPO frequency–intensity plane is no simple correlation but may show complete open loops.

Stella (ESOC) reported on QPOs in GX17+2 and the rapid burster, where the frequency behaviour is again complex. The limits on regular pulsations in all these objects is often better than 1 per cent and makes demands on some of the models for QPOs (Lamb, F.K. *et al. Nature* **317**, 681; 1985) that rely on magnetic effects, as stressed by J. van Paradijs (University of Amsterdam). To have a sufficiently strong magnetic field to cause QPOs from the difference between the magnetosphere and disk rotation rates, he argues that the neutron stars must be young ($<5\times10^7$ yr). The stars then need evolved companions so that a high rate of mass transfer could have pushed their progenitor white dwarf over the Chandrasekhar limit. We are likely to hear a lot more about QPOs as they are one of the few observational handles that we have on low-mass X-ray binaries.

The more detailed studies of X-ray bursts made possible by Exosat have revealed unusual events. A. Tennant (University of Cambridge) reported on a train of bursts observed from CirX-1, a source previously thought to be a candidate black hole. As all bursts yet seen appear to originate from neutron stars, we must reassign CirX-1. The bursts observed by Tennant have a short recurrence time of about 40 min and occur half-way between the characteristic 16.6-day outbursts.

Short recurrence times were also found in MXB1705-44 by M. Sztajno (Max Planck Institute for Extraterrestrial Physics). There, small bursts occurred only a few minutes after several larger bursts. The generally accepted model for the Type I X-ray bursts, which show a rapid rise followed by a cooling decay, invokes a thermonuclear flash of the accreted helium. This may also trigger off rapid hydrogen burning, which at lower temperatures is restricted to a slow rate by β-decays in the CNO cycle. The spectrum of the emission is usually fitted to that of a black body from which source size and luminosity can be estimated as long as the distance is known.

This approach has often led to problems with source radii smaller than that of theoretical neutron stars computed using current equations of state and bursts that seem to exceed the Eddington limit. The problems can in part be resolved by a correct model atmosphere calculation for the spectrum rather than a simple black body. A. Foster (University of Cambridge) has fitted the spectra to bursts from MXB1728-34 and obtained luminosities at sub-Eddington limits for a sensible radius and acceptable source distance.

Exosat has also been used to monitor active galactic nuclei (AGN). The extra-soft response of the low-energy telescopes over that of the Einstein observatory has paid off with the discovery of soft X-ray excesses in the spectra of several AGN. G. Branduardi-Raymont (Mullard Space Science Laboratory), in spectra of NGC5548, and K. Pounds (University of Leicester), in a survey of 27 galaxies, find such excesses; 18 of the 27 AGN show a typical power-law spectrum with a photon slope of 1.71±0.11 (see figure). Line-of-sight absorption above that expected from within our Galaxy has been detected in 10 objects. None of this X-ray absorption has yet been observed to vary. Several AGN sources vary on timescales of hours and days, the most rapid variability being reserved for the lowest luminosity sources such as NGC4051. A. Lawrence (Queen Mary College, London) saw this source vary by factors of around two on a timescale of 1,000 s and P. Barr (ESOC) saw similar amplitude changes in the nucleus of M81 in 10 min. His work suggests that there is a good correlation between the fastest time-resolved variation timescale of an AGN and its luminosity.

---

*Cambridge Exosat discussion meeting, Institute of Astronomy, Cambridge, UK; 5 – 6 November 1985.

The rate of change of the luminosity of Seyfert galaxies indicates that electron – positron pairs are common. A. Treves (Milan) has found an extreme change in the BL Lac object PKS 2155-304 where the X-ray luminosity increased from 1.5×10^{45} to 10^{46} erg s^{-1} in about 3×10^{3} s. Unless relativistic effects are present, the mass-to-energy conversion efficiency exceeds 50 per cent.

The high observing efficiency of Exosat, which is not affected by the South Atlantic anomaly and only rarely by Earth occultation, has produced an enormous quantity of data that would have taken about five years to collect from a near-Earth orbit. So far, the main results have arisen from the exploitation of light curves and power spectra. The spectral results will follow when the detailed calibrations are made. P. Giommi (ESOC) has compiled a database of serendipitous sources that has barely been investigated. And yet more new discoveries can be expected from the remaining year of Exosat's life (assuming successful perigee boosts next January) both from the satellite itself and from the databank. □

A.C. Fabian is at the Institute of Astronomy, The Observatories, Madingley Road, Cambridge CB3 0HA, UK.

Neurobiology

Microcircuits to see by

from Gordon M. Shepherd

It has been known for 20 years, from work in the retina[1] and olfactory bulb[2], that neuronal dendrites can send synaptic signals as well as receive them and can take part in microcircuits for local information processing. In virtually every vertebrate species studied it has been established that all but one of the main cell types in the retina have axons and/or dendrites that are both presynaptic and postsynaptic (*a* in the figure). The conspicuous exception has been the ganglion cell, the long-axon projection neurone that sends the retinal output to the lateral geniculate nucleus, the next station in the visual pathway. The report on p.495 of this issue by Sakai, Naka and Dowling[3] brings the ganglion cell in out of the cold and shows that its dendrites can be presynaptic as well as postsynaptic.

Working with the catfish retina, Sakai *et al.* labelled ganglion cells with horseradish peroxidase (HRP) so that ganglion cell bodies and dendrites containing HRP reaction product could be identified in electron micrographs. Using serial sections the authors could distinguish between proximal and distal dendrites, and were able to characterize the types of synaptic connections. Intracellular recordings of the ganglion cell responses to light stimuli before HRP injection permitted correlations between physiological properties, dendritic branching pattern and synaptic organization.

The analysis confirmed the previously accepted pattern of synaptic connections on ganglion cells, as shown on the right in *a*. They also found the connections shown on the left of *a*; distal dendrites of large-field ganglion cells making synapses on vesicle-containing processes (amacrine or ganglion cell dendrites) and ribbon-containing processes (bipolar cell axon terminals). The bipolar and amacrine cell terminals receiving these synapses were grouped in clusters around the distal dendrites. But these patterns of synaptic connections were found only on large-field ganglion cells with varying properties (on-off, on-centre, off-centre) — by contrast, no presynaptic dendrites or distal terminal clusters were seen around small-field ganglion cells.

An interesting parallel to this work is a recent study by Fahrenbach[4] of the synaptic organization of the compound eye of *Limulus*, the horseshoe crab. The classical work of Hartline and collaborators showed that the eccentric cells in *Limulus* eye are involved in lateral inhibitory interactions with each other, taking place through synaptic connections made by eccentric cell neurites in the neural plexus that lies just below the eye. Using serial sections through the plexus Gur *et al.*[5] demonstrated both single and reciprocal synapses that could mediate the lateral inhibition; they believed that these connections were made at or near the site of impulse initiation in the axon.

Fahrenbach has examined a series of more than 1,000 sections with loss of only 1 section, covering an area of 22 ommatidia and extending from the eccentric cell bodies to the base of the neural plexus. From this he was able to reconstruct the complete synaptic connectivity of all the neurites from 54 eccentric cells that branched within one small knot (microglomerulus) of neuropile in the plexus. He found no synapses on the axon itself, but collaterals close to the point where they branched from their axons of origin had a high synaptic density and a predominance of input synapses; terminals of branches far from the axon had a low synaptic density and a predominance of output synapses. Up to 50 per cent of the synapses were arranged in reciprocal pairs (*b* in the figure). Many terminals appeared to be grouped in clusters.

The single-cell analyses in the retina are technically demanding and the exhaustive reconstruction in *Limulus* even more so: are such herculean efforts worth it? The answer lies in the insights gained about the relationships between structure and function and the principles they suggest. In vertebrates, the retinal ganglion cell can now be classed with the olfactory mitral cell[2] as a long-axon neurone with dendrites that are both presynaptic and postsynaptic. The findings of Sakai *et al.* add to the evidence that synaptic triads (tight pattens of connections between afferent terminals, relay neurones and interneurones) involving presynaptic dendrites are a dominant theme of the synaptic organization of the visual pathway at every level up to the cortex. For example, this type of organization has been further documented in the lateral geniculate nucleus by Hamos *et al.*[6]. In arthropods, several neurones with long axons connecting intersegmentally[7] or to muscles[8] have branches that are both presynaptic and postsynaptic; some patterns of synaptic connections of the branches resemble those seen in the eccentric cell. Integration of synaptic inputs and outputs within

---

1. Dowling, J.E. & Boycott, B.B. *Proc. R. Soc.* **B166**, 80 (1966).
2. Rall, W., Shepherd, G.M., Reese, T.S. & Brightman, M.W. *Expl Neurol.* **14**, 44 (1966).
3. Sakai, M.S., Naka, K.-I. & Dowling, J.E. *Nature* **319**, 495 (1986).
4. Fahrenbach, W.H. *Proc. R. Soc.* **B225**, 219 (1985).
5. Gur, M., Purple, R.L. & Whitehead, R. *J. gen. Physiol.* **59**, 285 (1972).
6. Hamos, J.E., van Horn, S.C., Raczkowski, D., Ulrich, D.J. & Sherman, S.M. *Nature* **317**, 618 (1985).
7. Watson, A.H.D. & Burrows, M. *J. comp. Neurol.* **205**, 383 (1982).
8. Selverston, A.I., Russell, D.F., Miller, J.P. & King, D.G. *Prog. Neurobiol.* **7**, 215 (1976).
9. Ralston, H.J. III *Nature* **230**, 585 (1971).
10. Koch, C., Poggio, T. & Torre, V. *Phil. Trans. R. Soc.* **B298**, 227 (1982).
11. Peters, B.H., Altman, J.S. & Tyrer, N.M. *J. comp. Neurol.* **233**, 269 (1985).
12. Nishimura, Y. & Rakic, P. *J. comp. Neurol.* **241**, 420 (1985).

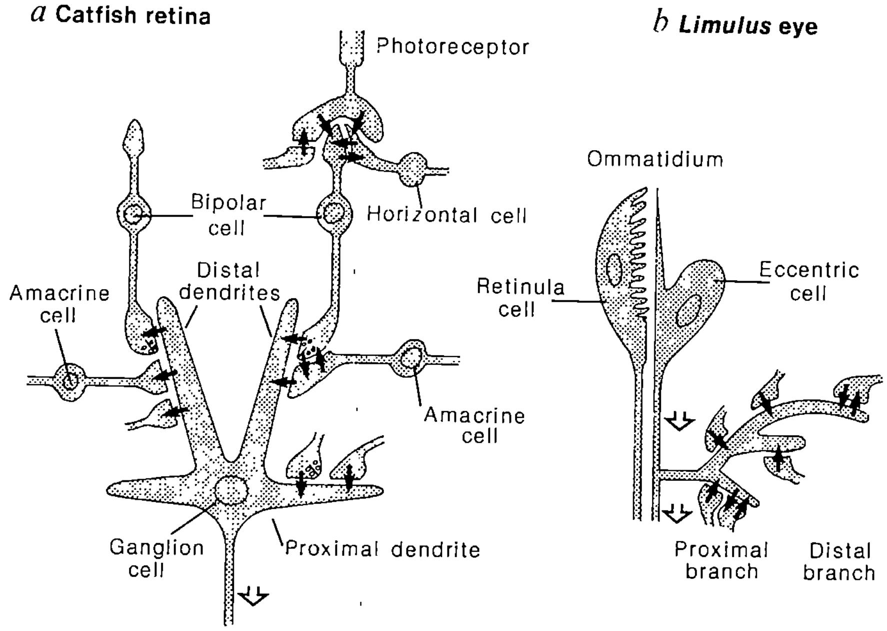

Aspects of the organization of presynaptic dendrites and microcircuits in vertebrate and invertebrate eyes. The sites and polarities of individual chemical synapses are indicated by solid arrows, the direction of spike conduction by open-headed arrows. *a*, Catfish retina: the main types of retinal cells are shown, with some of the main synaptic connections. The connections shown on the right of the ganglion cell are the well-established inputs; on the left, the newly described ganglion cell output synapses on to bipolar cell processes and amacrine or ganglion cell processes[3], found on distal dendrites of ganglion cells (see text). *b*, Compound eye of *Limulus*: schematic representation of an ommatidium containing retinular cells and an eccentric cell. The eccentric cell is analogous to the ganglion cell in having a long axon that projects to higher visual centres. The synaptic connections made by a branch in the neural plexus are indicated. There is a predominance of input synapses on proximal branches and a relatively larger proportion of output synapses distally[4]. The significance of this distribution is discussed in the text.

neuronal branches thus seems to be a common mechanism in arthropods.

The ganglion cell is known to lack recurrent axon collaterals and has been believed to function entirely as a follower cell, driven by its inputs from bipolar and amacrine cells. The new evidence[3] indicates that at least some of the ganglion cells can take part in shaping their own response properties through the microcircuits formed by their presynaptic dendrites. Sakai *et al.* point out that the synaptic clusters around distal dendrites can function as relatively independent sites for local signal processing, which also seems to apply to the clusters in *Limulus*. Individual or clustered synapses functioning as integrative units are becoming familiar in many systems[9-11]. The degree to which the relative independence of such units is influenced by passive membrane properties and by active dendritic sites is under investigation in several laboratories.

How are dendritic input and output synapses laid down during ontogeny? This is the subject of recent work by Nishimura and Rakic[12] in the inner plexiform layer of the primate. In work in progress, they find a sequence in which single ganglion cell synapses appear first, followed by single amacrine – amacrine synapses, bipolar ribbon synapses on ganglion cells and finally, bipolar ribbon synapses on amacrine cells. This sequence appears to be genetically determined, because it is not correlated with birth or exposure to light. Ganglion cell dendrites have not been observed to be presynaptic in this study but it will be interesting to use the HRP labelling technique of Sakai *et al.* to pursue this point.

In *Limulus*, Fahrenbach speculates that the relatively uniform distribution of output synapses on proximal and distal branches would be determined by the genome during synaptogenesis; by contrast, the distribution of input synapses, heavily skewed toward the proximal branches, might be determined by a gradient of impulse activity spreading decrementally from the axon into the arborization. In this scheme of activity-generated synaptogenesis, "any branch would in effect provide the signal to generate its own inhibitory input, graded with distance from the parent axon"[4]. This would account for the gradation of inhibitory interactions.

How gene expression is synchronized in two or more sets of neurones to bring about the coordinated assembly of synaptic circuits, shaped by concurrent or subsequent functonal activity, is one of the most challenging problems in neurobiology. Microcircuits make excellent test systems for pursuing this problem. □

Gordon M. Shepherd is Professor in the Section of Neuroanatomy, Yale University School of Medicine, New Haven, Connecticut 06510, USA.

Rings and a moon of the planet Uranus

On the right are the ten rings of Uranus, photographed from a distance of 1,120,000 km on 23 January 1986. This is among the first of the pictures produced by Voyager 2. The newly discovered tenth ring is barely visible about midway between the bright, outermost epsilon ring and the next ring down, called delta. The tenth ring orbits Uranus at a radius of about 50,000 km. On the left is a full-disk view of the moon Titania, taken early in the morning of 24 January 1986 from a distance of 500,000 km. The many cicular depressions are probably impact craters and the bright linear troughs right of the picture are probably canyons. The troughs break the crust in two directions, indicating that the icy satellite has a dynamic, active interior. Photographs courtesy of NASA/Jet Propulsion Laboratory.

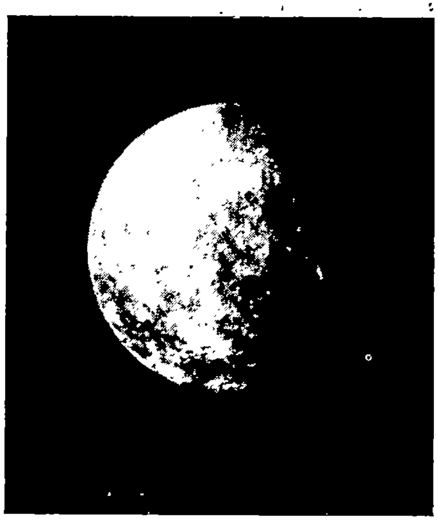

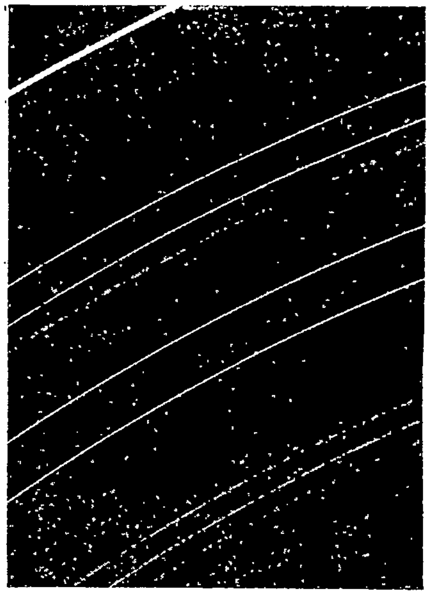

Large computers key to aggregation phenomena

SIR—We thank you for devoting a part of a *News and Views* editorial[1] to one of our recent papers[2]. Our paper describes a reversible process of particle–cluster aggregation–disaggregation in which particles at the periphery of a cluster may escape and come back again after undergoing a random walk in space. We agree with your argument that this does not truly represent aggregation at equilibrium, but the motivation behind our work was somewhat different. We aimed to describe more exactly some kind of dynamic equilibrium or steady state in which a flux of incoming diffusing particles strictly compensates a flux of outgoing diffusing particles.

In this spirit, our work was and attempt to include restructuring processes in the existing models of aggregation (other attempts are by Meakin and Jullien[3] as you quoted, but also P. Meakin[4]). This was a first step before studying cluster–cluster aggregation–disaggregation processes, where bonds can be annealed randomly all along the diffusion-sticking mechanism. This last model was recently studied by Kolb[5].

We agree that our main result (our clusters have apparently the same fractal dimension as animals) is quite intricate. When describing our model to several colleagues, we got a large range of guesses and speculations; they predicted either DLA, or Eden, or animals and so on. This is why our paper included a detailed discussion explaining that it was none of those. However, since we found a fractal dimension close to the one for animals, we insisted on the comparison with this at-equilibrium model.

Interestingly, however, cluster–cluster aggregation–disaggregation, as demonstrated by Kolb, also yields the same fractal dimension. Moreover, in the past[6], Stauffer used a process very similar to ours (but without any diffusion) in which particles are randomly released from the perimeter and then put back randomly on it (this is a "chemical" version of our aggregation–disaggregation model). Stauffer claimed that his objects were in the same universality class as animals.

It is very surprising that these three aggregation–disaggregation models all share the same fractal dimension, since different rules might be expected to induce different statistics. The cluster statistics for small clusters are clearly not the same as for large clusters, so why do they peak to an average configuration in the thermodynamic limit of very large clusters?

To conclude, we think that as long as there is no analytical progress in these fields, large size computer simulations will be the *only* tool enabling us to understand and classify the models. Moreover, they can define the basis for a search for analytical solutions. In the case of aggregation phenomena the two basic models (particle–cluster and cluster–cluster aggregation) are now well characterized and they must be modified and extended to better apply to experiments (compare for example the recent attempt to take into account cluster polarizability[7], to explain the experiment by Hurd and Schaefer[8]). It is however essential that in the course of these improvements, the models do not lose their high degree of simplicity and generality.

R. BOTET
R. JULLIEN

Université de Paris-Sud,
Centre d'Orsay,
Laboratoire de Physique des Solides,
91405 Orsay, Paris, France

1. Maddox, J. *Nature* **318**, 229 (1985).
2. Botet, R. & Jullien, R. *Phys. Rev. Lett.* **55**, 1943–1946 (1985).
3. Meakin, P. & Jullien, R. *J. Physique* **46**, 1543–1552 (1985).
4. Meakin, P. *J. chem. Phys.* **83**, 3645–3649 (1985).
5. Kolb, M. *J. Phys.* A, (in the Press).
6. Stauffer, D. *Phys. Rep.* **54**, 1–74 (1979).
7. Jullien, R. *Phys. Rev. Lett.* **55**, 1692–1697 (1985).
8. Hurd, A. & Schaefer, D. *Phys. Rev. Lett.* **54**, 1043–1046 (1985).

Minimum energy configurations

SIR—Berezin[1] has recently pointed out that the minimum energy configuration for a system of m identical point charges interacting via the Coulomb potential $1/r$ and confined to a circular region in a plane has all the charges on the circumference only if $m \leq 11$. For $m > 11$ some of the charges are in the interior. (Specifically, Berezin showed that the energy of configuration B ($m-1$ charges uniformly distributed around the circumference plus one charge at the centre) is lower than that of configuration A (m charges uniformly distributed around the circumference) for $m > 11$. We have extended Berezin's work and have shown that at $m = 17$ it is advantageous to have two particles in the interior. Note also that for $m \to \infty$ the problem becomes that of the conducting disk.) He conjectured that a similar result might obtain in three dimensions. Unfortunately one can show, using the fact that the Coulomb potential is harmonic in three dimensions[2], that the minimum energy configuration for a system of m identical point charges confined to a region of space has all the charges on the surface of the region, independent of the number of particles m. If, however, we change Berezin's conjecture slightly, the problem again becomes interesting.

We ask: what is the minimum energy configuration for a system of m identical particles interacting via a non-harmonic potential $1/r^n$, $n > 1$, and confined to a spherical volume? (This is why Berezin's two dimensional system has charge in the interior — the potential $1/r$ is not harmonic in two dimensions. If, as MacGowan[3] suggests, one uses the potential $\ln(r)$, harmonic in two dimensions, the charge all lies on the circumference.) Clearly, for $m = 2,3,4$, the particles will lie on the surface of the sphere independent of n. For higher m the problem becomes more difficult.

Melnyk *et al.*[4] have studied in detail the problem of the minimum energy configuration for systems of particles constrained to the surface of a sphere. Calculations based on their configurations lead us to conjecture that the minimum energy configuration has all the particles on the surface for $m \leq 12$, independent of the power n of the potential. For $m = 13$ and higher, however, the situation is different. This can be seen most easily in the short range limit $n \to \infty$. In this limit the energy is dominated by nearest neighbour interactions. At $m = 13$ the nearest neighbour distance becomes less than 1 (in units of the sphere radius) and it becomes advantageous to remove one particle from the surface and place it at the centre of the sphere (leading to a minimum energy configuration of icosahedron plus one at the centre). We have shown that this situation persists if the power of the interaction n is as small as approximately 6.3.

For $n < 6.3$ the minimum energy configuration has all the particles on the surface in the configuration described by Melnyk *et al.*[4]. It seems likely that a similar situation will persist for still larger numbers of particles: for low powers of the interaction all the particles will be on the surface; for higher powers some particles will be in the interior. A complete mapping of the "$m-n$ phase plane", will, however, involve much detailed study.

M.G. CALKIN
D. KIANG
D.A. TINDALL

Department of Physics,
Dalhousie University,
Halifax, Nova Scotia,
Canada B3H 3J5

1. Berezin, A.A. *Nature* **315**, 104 (1985).
2. Kellog, O.D. *Foundations of Potential Theory* 223 (Springer, Berlin, 1929).
3. MacGowen, D. *Nature* **315**, 635 (1985).
4. Melnyk, T.W., Knop, O & Smith, W.R. *Can. J. Chem.* **55**, 1745-1761 (1977).

Scientific Correspondence

Scientific Correspondence is intended to provide a forum in which readers may raise points of a rather technical character which are not provoked by articles or letters previously published (where the Matters Arising section remains appropriate).

Copies of articles from this publication are now available from the UMI Article Clearinghouse.

For more information about the Clearinghouse, please fill out and mail back the coupon below.

UMI Article Clearinghouse

Yes! I would like to know more about UMI Article Clearinghouse.
I am interested in electronic ordering through the following system(s):

☐ DIALOG/Dialorder ☐ ITT Dialcom
☐ OnTyme ☐ OCLC ILL Subsystem
☐ Other (please specify)________________
☐ I am interested in sending my order by mail.
☐ Please send me your current catalog and user instructions for the system(s) I checked above.

Name________________
Title________________
Institution/Company________________
Department________________
Address________________
City____________State________Zip________
Phone (______)________________

Mail to: University Microfilms International
300 North Zeeb Road, Box 91 Ann Arbor, MI 48106

Oxford University Press for Freeman, Cooper and Co.

Oxford University Press is pleased to announce that it is now distributing geology titles from Freeman, Cooper and Co. outside the USA.

Igneous Petrology

Alexander R. McBirney

This up-to-date and attractively written textbook combines lucidity of description with a thought-provoking approach to igneous petrology. The author presents the principles of the subject, not as fixed dogma, but as ideas that evolve with new information and fresh insights. The object throughout is to lead the student through the kinds of logic speculation, and intuitive reasoning that are central to petrological thinking.

0 19 857810 5, 448 pp., illus., OUP/Freeman, Cooper and Co. £37

Backlist titles are also available; a full list is obtainable from OUP

Oxford University Press

Reader Service No.1

MACMILLAN 1985/6 ACADEMIC BOOK SALE

The following selection of books at greatly reduced prices may now be ordered from all major bookstores. This offer is open until 28th February 1986 only. Order now using the spaces provided below.

____**International Mortality Statistics** P. Alderson 23969 5 (£47.00) £14.95
____**Biochemistry of Parasitic Helminths** John Barrett 25669 7 (£12.95) £3.95 (paperback)
____**Urban Air-Pollution Modelling** Michael M. Benarie 23391 3 £35.00 £17.50
____**Birth Defects Compendium** Daniel Bergsma (ed.) 27876 3 (£50.00) £25.00
____**Polar Dielectrics and Their Applications** Jack C. Burfoot and George W. Taylor 17958 7 (£20.00) £6.95
____**The Ultimate Software Selector** Federation of Micro System Centres 37556 4 (£9.95) £2.95
____**Environmental Factors in Mammal Reproduction** Desmond Gilmore and Brian Cook (eds.) 24150 9 (£25.00) £8.95
____**X-Ray Microanalysis** M. A. Hayat 32355 6 (£30.00) £9.95
____**Horticultural Reviews Volume 4** Jules Janick (ed.) 34192 9 (£25.00) £8.95
____**The RAE Table of Earth Satellites, 1959-1982, 2nd Ed.** D. G. King-Hele, J. A. Pilkington, D. M. C. Walker, H. Hillier and A. N. Winterbottom 35374 9 (£50.00) £25.00
____**Hydrogen and Energy** Charles A. McAuliffe (ed.) 18432 7 (£12.00) £4.95
____**Plant Galls of India** M. S. Mani 18067 4 (£12.50) £3.95
____**The Design of Air Quality Monitoring Networks** R. E. Munn 30460 8 (£20.00) £6.95
____**Growth Without Ecodisasters?** Nicholas Polunin (ed.) 23521 5 (£22.50) £5.95
____**The Arctic Ocean: The Hydrographic Environment and the Fate of Pollutants** Louis Rey (ed.) 31017 9 (£45.00) £12.50
____**Developmental Psychology and Society** John Sants (ed.) 21340 8 (£20.00) £6.95
____**Cancer and the Environment** L. A. Sobel (ed.) 28591 3 (£15.00) £4.95
____**The Fast Breeder Reactor – Need? Cost? Risk?** Colin Sweet (ed.) 27973 5 (£20.00) £6.95

Please complete and return this form to your bookseller, or in case of difficulty to: **Macmillan Distribution Ltd, Houndmills, Basingstoke, Hampshire RG21 2XS, UK.**

Please supply ______ titles as indicated

☐ Please invoice me. Postage and packing £1.00 per title.

☐ I enclose a cheque for £________________

☐ Charge £______ to my credit card as shown. Access/Visa/Amex/Diners Club

Card No.________________Expiry Date ______
Signature________________
Name (capitals)________________
Address (capitals)________________

This offer is not applicable in USA.

M MACMILLAN PRESS LTD.
Houndmills, Basingstoke, Hants RG21 2XS, UK. M

Two Springer Series sponsored by the International Life Sciences Institute (ILSI)

The International Life Sciences Institute (ILSI) is a scientific foundation which addresses critical health and safety issues of national and international concern. ILSI promotes international cooperation by providing the mechanism for scientists from government, industry, and universities to work together on cooperative programs to generate and disseminate scientific data. The members and trustees of the Institute believe that questions regarding health and safety are best resolved when scientists can examine and discuss issues as an independent body, separate from the political pressures of individual countries and the economic concerns of individual companies.

Monographs on Pathology of Laboratory Animals

The monographs provide authoritative microscopic and ultrastructural descriptions of naturally occuring or experimentally induced neoplastic and nonneoplastic lesions in several species of laboratory animals. The indentifying pathologic features are correlated with toxicologic, biologic and behavioral data as well as with data from other species including man. An internationally accepted nomenclature is used in order to facilitate worldwide communication among scientists, industries and governmental agencies investigating the safety of foods, drugs and chemicals subject to animal tests.

Series Editor: **T. C. Jones,** Harvard Medical School

Digestive System

Editors: **T. C. Jones, U. Mohr, R. D. Hunt**

1985. 352 figures, 24 tables. XVIII, 386 pages
Hard cover DM 292,-. ISBN 3-540-15815-4

Respiratory System

Editors: **T. C. Jones, U. Mohr, R. D. Hunt**

1985. 279 figures, 20 tables. XV, 240 pages
Hard cover DM 245,-. ISBN 3-540-13521-9

Endocrine System

Editors: **T. C. Jones, U. Mohr, R. D. Hunt**

Consultant on Comparative Endocrinology: **C. C. Capen**

1983. 346 figures, 26 tables. XV, 366 pages
Hard cover DM 220,-. ISBN 3-540-11677-X

Current Issues in Toxicology

This series not only attempts to examine the factors which influence the evaluation of the safety of chemicals, but also to develop principles, recommend guidelines, and define areas requiring additional research. Each volume consists of two or three articles in which renowned scientists examine specific aspects of toxicologic research.

Series Editor: **H. C. Grice,** Scientific Coordinator, International Life Sciences Institute, Nepean, Ontario

Interpretation and Extrapolation of Chemical and Biological Carcinogenicity Data to Establish Human Safety Standards

The Use of Short-Term Tests for Mutagenicity and Carcinogenicity in Chemical Hazard Evaluation

Editor: **H. C. Grice**

1984. IX, 197 pages
Soft cover DM 55,-. ISBN 3-540-13696-7

The Selection of Doses in Chronic Toxicity/Carcinogenicity Studies

Age-Associated (Geriatric) Pathology: Its Impact on Long-Term Toxicity Studies

Editor: **H. C. Grice**

1984. 3 figures. VII, 114 pages
Soft cover DM 38,-. ISBN 3-540-12845-X

Prices are subject to change without notice

Springer-Verlag Berlin Heidelberg New York Tokyo

Heidelberger Platz 3, D-1000 Berlin 33
175 Fifth Ave., New York, NY 10010, USA
37-3, Hongo 3-chome, Bunkyo-ku, Tokyo 113, Japan

Springer

Reader Service No. 2

BOOK REVIEWS

All change for the RI

Roy Porter

The Royal Institution: An Informal History. By Gwendy Caroe.
John Murray: 1985. Pp.180. £13.95.

WHEN insiders write institutional history, all too often they serve up an official version for public consumption; conversely, outsiders generally lack a feel for the place. Who better, then, for avoiding both of these shortcomings in tracing the story of the Royal Institution than the late Gwendy Caroe? As the daughter of Sir William Bragg, and the sister of Sir Lawrence, she was steeped in the atmosphere of Albemarle Street. From the time of her mother's early death, Gwendy was hostess at her father's weekly scientific dinner parties there (she tells a hair-raising story against herself, of when she flipped a glass of claret over H.G. Wells's shirt just before he was due to lecture). Yet, never having been on the establishment, she can look at its august, if somewhat chequered, history with proper detachment.

As all who have read her biography of her father will know, Gwendy Caroe wrote with rare grace, lucidity and a vivid turn of phrase. In this new book those assets are again matched with an eye for telling detail and a wise gift for getting to the heart of people — Faraday, whose science was animated by profound religious humility and a dread of worldly clamour; Tyndall who sought society because he was essentially lonely; Davy who craved it, because his vanity couldn't bear not being fêted. The chapter on Sir James Dewar in particular brings a neglected yet fascinating character to life.

It would be wrong to assume that just because the book is subtitled *An Informal History*, and is not weighed down by footnotes and graphs, it is merely a piece of light reading. Far from it. Not only is this the only account we have of the RI from its foundation in 1799 to the present, but it is a penetrating and original interpretation at that, the fruit of much delving in the archives. Not least, Gwendy Caroe shows how the RI's fortunes are a story of permanent change.

Amongst institutions, the RI has always been something of a curiosity, being neither fish, flesh nor fowl; neither simply a learned society, nor a specialist research agency, nor chiefly a centre of scientific training, nor an organ of state. It has carried its essentially protean nature right from its first foundation, when, as Gwendy Caroe stresses, one of its key aspirations was to bring together the worlds of science and fashion. As science has marched on, and fashions have come and gone, so the RI has changed with them.

The initial idea was that, through promoting applied science, the RI could help the rich do their bit for the poor. Its early patrons — the benevolent but ambitious Count Rumford, the evangelical Thomas Bernard, the autocratic president of the Royal Society, Sir Joseph Banks — and the grandees whose subscriptions made them Managers saw the Institution as a philanthropic laboratory. It would develop technologies to better the condition of lower orders in that age of French Revolutionary turmoil: improved kitchen utensils, fuel economies, dietary innovations, simpler soap-boiling and the like. Meantime, lecture courses teaching trades to artisans would foster independence and self-improvement. And all of these good causes would be financed via scientific lectures delivered to High Society.

The fashionable lectures throve — Davy in particular dazzled the duchesses — but the philanthropy was soon dropped. Instead, the RI took on an important function as a centre of scientific analysis for aiding farmers and manufacturers. At the Managers' behest, Davy and then Faraday devoted themselves to long years of practical investigation into tanning, dyeing, soil science, miners' safety lamps, optical glasses and scores of other utilitarian subjects, to show how science could be the willing servant of an industrializing society. Yet eventually the professors dug in their heels. First Faraday, and then more particularly John Tyndall, insisted that the best return for the Institution would come through the pursuit of what Faraday called "the advancement of science for its own sake". Faraday's great electro-magnetical discoveries, Tyndall's explorations of heat, pressure and gaseous radiation, and Sir James Dewar's achievements in the liquefaction of gases were some of the fruits.

Yet the move in the latter part of Victoria's reign towards pure science, allowing the professors to get on with their own private research interests and consultancy work, left the Institution as such in the doldrums. It ceased to lead society, state and even fashion. Its subscriptions dropped off. By the time of the First World War, even its splendid new research laboratory (the Davy–Faraday), so handsomely financed by Ludwig Mond, was gathering dust.

New directions were needed. They came from the Braggs. In turn, in the 1920s and the 1950s, they brought fresh collective purpose. Sir William pioneered group research at the RI, developing his own X-ray crystallography research school. Father and son both revitalized the "club" functions and the public lecturing programme, pioneered contacts with the BBC and put School Science Lectures on the footing that does so much to keep the RI in the public eye today. Not least, under their guidance, the old shoe-string private experimentation gave way to research more adequately funded from government sources. Over the past 20 years with Sir George Porter at the helm, the RI has continued to branch out in new directions. What has been demonstrated is that though the RI cannot pretend to fulfil all the functions of the Royal Society, university science institutes, the research councils and the like, there continues to be a need for a popular forum for science.

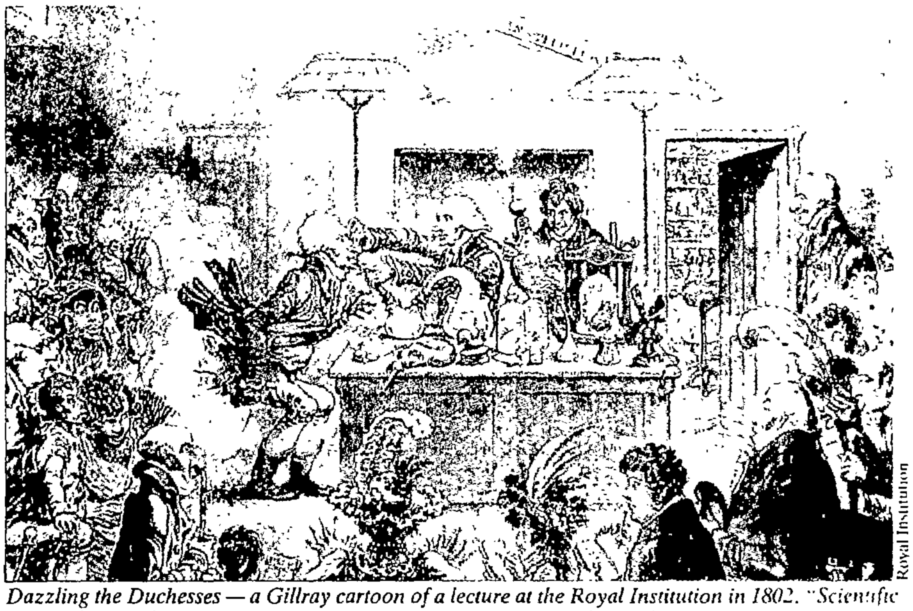

Royal Institution

Dazzling the Duchesses — a Gillray cartoon of a lecture at the Royal Institution in 1802. "Scientific Researches — New Discoveries in PNEUMATICKS!". Davy holds the bellows.

which the RI is uniquely equipped to provide.

It has always been easy to be somewhat snooty about the RI. Fellows of the Royal Society have often found it vulgar (William Buckland spoke sneeringly of "a sort of Albemarle Street dilettante meeting"); and today, a school of radical historians decries it for having been a "tool of capitalism". Yet, as Gwendy Caroe shows, the RI has played a crucial role in English science: it created an open forum for science, amateur and professional, in contrast to the Royal Society's oligarchy and subsequent elitism; it supported an industrial laboratory in days when manufacturers were still poo-pooing science; it offered a refuge for religious Dissenters such as Faraday long before they could gain admission to English universities, and a livelihood for promising young talent — Davy was 23 and Faraday 21 when they came to the RI — before science had evolved a regular professional career structure; and not least, it provided a bridge between the "two cultures", and between experts and the public. Science and fashion have truly met at the RI. For an institution so often capable of meeting the challenge of the new, the future surely holds exciting prospects. ☐

Roy Porter is at The Wellcome Institute for the History of Medicine, 183 Euston Road, London NW1 2BP, UK.

MAJOR NEW JOURNAL
Alimentary Pharmacology & Therapeutics
Editors:
Dr. R.E. Pounder, *Royal Free Hospital, London*
Professor M.J.S. Langman, *University Hospital, Nottingham*
To be published bi-monthly from January 1987
Further details can be obtained from Allen Stevens, Journal Marketing Manager, Blackwell Scientific Publications, Oxford OX2 0EL, UK
Reader Service No.4

Looking beyond Bohr

Philip Pearle

Quantum Fluctuations. By Edward Nelson. *Princeton University Press:1985. Pp.146. Hbk $32, £21.50; pbk $12.95, £9.40.*

It was Niels Bohr who gave quantum theory the closest of possible shaves with Occam's razor, in declaring that comprehension of quantum phenomena with classical ideas was impossible, and that we must never never never try to understand what goes on in nature in between measurements. How well it speaks for the vigour of physics, just over 100 years after the birth of Bohr*, that a book should appear attempting all that he told us not to do.

In Nelson's picture of nature, classical point particles moving under classical forces are jostled by a fluctuating hypothetical "background field". This requires a statistical description of the motion. Such a description inevitably entails two equations: one deals with the ensemble of particles, ensuring that none of them get lost ("conservation of probability"); the other is an equation of motion for each individual particle. These two equations are shown to be precisely equivalent to the imaginary and real parts, respectively, of the Schrödinger equation.

Nelson, more than anyone else who has worked with such ideas, has made the equation of motion plausible. The difficulty is that plausibility often means analogy, and there is none. A speedily moving jostled particle (such as a mote of dust battered by air molecules) will not maintain that velocity, not even on the average the way a quantum particle will, but will slow down and come to thermal equilibrium with its environment. Such a classical motion is called a *dissipative* (because the particle loses energy) *Markovian* (meaning that the present, and not past history, determines the future) *diffusion* (referring to the dispersal of particles with initially identical position and velocity).

Lacking an analogy, Nelson has invented "stochastic mechanics", a non-dissipative (conservative) Markovian diffusion process, in which particles do *not* lose their energy on the average. The first half of the book is a masterly instruction in diffusive motion on manifolds (curved spaces), with particular attention to elucidation of the time-reversal-symmetric description. It culminates in a very natural variational principle (largely due to Guerra and co-workers), the minimization of the expectation value of the action, which gives the desired equation of motion. This is equivalent to, but more elegant than, an earlier (1966) formulation of Nelson's, in which he wrote down Newton's second law of motion but with the acceleration of the particle defined in a particular time-symmetric way.

Next come examples of things that quantum theory never talks about. We learn that particles never cross the nodes of wavefunctions. We see the electron jiggling in hydrogen, drifting towards the Bohr radius in the ground state, and rotating about the nucleus on the average in a non-zero angular momentum eigenstate. There are explanations of half-integer spin, of statistics, and of the quantum theory expression for the momentum probability distribution.

It is in the discussions of locality and of two-slit interference that challenges to stochastic mechanics emerge. Nelson shows that, in this theory, disturbance of one of two widely separated particles instantly disturbs the diffusion of the other particle, which is a non-local behaviour, and poignantly writes: "I have loved and nurtured Markovian stochastic mechanics for 17 years, and it is painful to abandon it. But its whole point was to construct a physically realistic picture of microprocesses, and a theory that violates locality is untenable". (He then argues that non-Markovian motion may not have this defect.) It is interesting that upon encountering this difficulty, David Bohm, the author of a similar theory (differing from Nelson's in that the equation of motion is deterministic), has embraced it, delighting in the principle that everything is connected to everything else.

I believe it is two-slit interference that best illustrates a difficulty many physicists have with this theory. Nelson clearly shows how particles go through either one slit or the other and then diffuse to form the interference pattern (" . . . this is a misnomer: nothing is interfering with anything"). But such diffusion is effectively determined by the wavefunction of quantum theory, and it is hard to see how a "background field" can give rise to the effects of the wavefunction. Examples of a background field causing conservative diffusion are needed.

Nelson himself appreciates the point: he is probably his own theory's severest critic. He writes: "Stochastic mechanics is quantum mechanics made difficult". Physicists may well ask why they should consider the complications that stochastic mechanics brings to quantum theory. The answer is that it is worth the difficulty of opening our minds, to see what may be revealed if we attempt to peer past the curtain erected by Bohr. ☐

Philip Pearle is Chairman of the Department of Physics, Hamilton College, Clinton, New York 13323, USA.

---

* A celebration of Bohr and his achievements, *Niels Bohr: A Centenary Volume,* edited by A.P. French and P.J. Kennedy, will be reviewed in *Nature* of 20 March.

What is theoretical biology?

Lee A. Segel

Theoretical Biology and Complexity: Three Essays on the Natural Philosophy of Complex Systems. Edited by Robert Rosen. *Academic: 1985. Pp.210. $57, £48.*

In his preface, Robert Rosen states that the three scientists whose essays make up this book

> . . . each began with a conviction that contemporary physics already contained the necessary universals with which to cope with the phenomena of life and that therefore only a clever rearrangement and redeployment of these universals would suffice to bring them to bear effectively on biology. . . . we each came separately, and with great reluctance, to admit the possibility that this conviction might not be true and hence that a true theory of the organism required new physics and new epistemology. And again separately, we realized that the measurement process, which lies at the very heart of every mode of system description, provides perhaps the only safe and fundamental point of departure for building a comprehensive theory, not only of organisms, but of natural systems in general.

I believe that most workers in theoretical biology are indifferent to, or disagree with, the main points just cited. But as I have no brief to speak for others, let me give my own views.

It is inappropriate to try to build comprehensive theories at this early stage in the modern study of biology. Rather, it is better to tackle particular phenomena and to try to generalize from the results. Although there is probably need to redress a present-day over-confidence in the comprehensiveness of conclusions that can be reached by molecular biology, the remedy is not to concentrate upon epistemology.

Certainly, an eventual aim should be to understand "the organism"; that is, answer the question "What is life?". But there are other, equally important and more approachable questions to be asked, such as "How does a baby develop from a fertilized egg?" or "How does the brain process, store and retrieve information?". Of course, new physics is needed for this enterprise—for example, even recent extensions of thermodynamics apply only to situations that are close to equilibrium. The major province of present-day theoretical biologists is to extend old concepts and introduce new ones in phenomenological fashion, at appropriately selected levels in the hierarchy of biological organization.

To my mind, saying that the measurement process is central to biology is to relapse into the sin of adopting too uncritically the ideas of physics. An example of a more successful point of departure is the stress on computation in the study of vision by D. Marr and his associates.

The authors are of course entitled to have their say. In an extension of classical formulations of mechanics and thermodynamics, I.W. Richardson discusses the interaction between particles and the consequent observable manifestations thereof. (There is no explicit mention of biology in his essay.) A.H. Louie tries to deal with problems of measurement, interaction and representation using category theory, a relatively recent branch of abstract algebra. (More than one hundred special symbols are listed at the beginning of the essay, signalling the fact that it will be comprehensible to few apart from mathematicians.) Here, too, there is little specific contact with biology.

Rosen's article does contain quite a bit about biology and is relatively accessible. But for two reasons I doubt the need for his urgings to go beyond the evolving state description that has been so successful in particle physics — such descriptions have in fact proved valuable in large areas of biology (for example in biochemical theories that exploit the law of mass action), and alternative formalisms have frequently been employed (for example graph theory in ecology).

The authors' point of view is best summed up by Dr Louie, who states that "I have always been more interested in 'conceptual' biomathematics than in looking at specific models of a biological process. In other words, my interest is oriented more toward the *logic* of mathematical biology". Those who share this attitude and who have a good mathematical background will find food for thought in this book. Those who are more pragmatically inclined should peruse the *Journal of Theoretical Biology, Biophysical Journal*, the "Models and Hypotheses" section of *Differentiation* or some of the more than 60 volumes in Springer-Verlag's series *Lecture Notes in Biomathematics*. Included in such publications, albeit embedded in inescapable chaff, are many specific kernels of understanding that theorists have brought to biology. □

Lee A. Segel is a Professor in the Department of Applied Mathematics, Weizmann Institute of Science, Rehovot 76100, Israel.

On the track of an epidemic

Richard S. Tedder

Understanding AIDS: A Comprehensive Guide. Edited by Victor Gong. *Rutgers University Press/Cambridge University Press:1985. Pp.240. Hbk $20, £17.50; pbk $9.95.*

AIDS: The Acquired Immune Deficiency Syndrome. By Victor G. Daniels. *MTP Press:1985. Pp.155. £9.95, $16.25.*

AIDS: Etiology, Diagnosis, Treatment and Prevention. By Vincent DeVita, Jr., Samuel Hellman and Steven Rosenberg. *Lippincott/Harper & Row:1985. Pp.352. $38, £41.95.*

To call Acquired Immune Deficiency Syndrome the infectious disease of the 1980s may unhappily be wishful thinking — although this decade has seen the emergence of AIDS, it is most unlikely to see its departure. Initially thought to be limited to homosexual men, there is no doubt that the causative virus, HTLV III/LAV, is becoming widely established in the human population. It is especially unfortunate that the homosexual man bears the brunt of infection, since this has engendered both a moralistic and a narrow view of the disease. Moralistic, in the sense that people who do not have homosexual lovers can underline their disapproval by invoking Divine Retribution; narrow, in that a belief that the virus is confined to gay men encourages complacency about public health.

It is the speed with which HTLV III/LAV has established itself as an *endemic* infection within the human race that should be the main cause for concern, and not merely the increasing numbers of patients with AIDS. Taken alone, the figure for cases of AIDS is a gross underestimation of the prevalence of infection and the true size of the problem for the future. Early in any epidemic the initial cases of disease will be those with a short incubation and will underrepresent the clinical attack rate. There is now clear evidence that the virus may be transmitted by heterosexual intercourse and is not only passed on by homosexual activity. This is particularly true of the African epidemic which is itself of recent origin; moreover, women may transmit the disease to the next generation, either *in utero* or possibly through breast milk. The human race is facing a microbial threat which, rightly or wrongly, must call into question current attitudes to all sexual practices. It is surely not sufficiently comforting to remark that AIDS is essentially a disease of certain limited segments of the population when we know that infected persons may be both infectious and themselves subject to illness of diverse forms for an entire lifetime.

Set against this background, any book called *Understanding AIDS: A Comprehensive Guide* is in for a certain amount of scepticism. Where knowledge is accruing so fast, any book on the subject will be out of date as soon as it is published. However in this instance it may never have been "in date". Although the editorial preface was written in February 1985, the book itself appears to have been written largely before HTLV III/LAV was acknowledged as the causative agent. The various contributions are generally adequate but read in a very disjointed manner. Though understandable this is annoying — it is as if the galley proofs were returned with a request to mention HTLV III/LAV "since it might be relevant". Perhaps the publishers would have been wise to ask for a full revision. There are no illustrations or figures and the bibliography is rather sparse.

The two other books are different from each other and from the previous one. They serve different functions and will be of value to different readers. *AIDS* by Victor Daniels is a concise book, "in English", and in the first 100 pages provides an up-to-date compilation of current knowledge about AIDS and its relation to infection by HTLV III/LAV. The remaining 50 pages include a glossary, and appendices on blood donors, immunology, viruses, definitions and a useful list of contact addresses of support groups in Britain. This is not a scientific textbook, but it will be invaluable to any non-specialist or lay person and of particular use to those involved in counselling of infected and affected patients.

The last book comes with a picture of the HTLV III retrovirus (with all credits) on the cover, so its pedigree cannot be called into question. Scientifically it is the most robust of the three, and is a well-rounded collection of review articles, each fully referenced and well illustrated. In particular it is a pleasure to see good colour prints of both the clinical lesions and the histology of Kaposi's sarcoma including patients with classical non-epidemic disease — an illness only rarely encountered outside Africa. One feels mild irritation in certain chapters at the parochially American view point — for example reference to European work, such as that of the Pasteur group, is minimal. The chapter on diagnostic tests is disappointing, with Western blotting still firmly placed as the gold standard, and the molecular virology is sketchy. However these are small quibbles and it remains a book to be recommended for workers in the field or the technically inclined non-specialist.

What none of these books does is to speculate on the origin of HTLV III/LAV and question the established dogma that Africa is the source of the infection; nor does any of them give an indication of possible future courses of the epidemic. On these topics, perhaps, too many reputations are at stake. Only time will tell. □

Richard S. Tedder is Senior Lecturer and Head of the Virology Section in the Department of Medical Microbiology, School of Pathology, Middlesex Hospital Medical School, Riding House Street, London W1P 7PN, UK.

Current prospects

Daniel D. Eley

Molecular Semiconductors: Photoelectrical Properties and Solar Cells. By J. Simon and J.-J. André. *Springer-Verlag: 1985. Pp.288. DM174, $72.50.*

In this book, consideration of molecular semiconductors is restricted to organic semiconductors, apart from brief sections on two types of inorganic conductors (tetracyanoplatinates and sulphur-nitride polymers). The last comprehensive account of the subject as a whole appeared in 1974, and even then a list of 2,579 references was included. It seems logical, therefore, that Simon and André should now concentrate on one section of the field currently of great interest. There is at present little indication that an organic photovoltaic cell will be able to compete with amorphous silicon in solar applications, but all the more reason for the publication of a book such as this to help stimulate research in the area.

After a short introduction to basic notions in solid state physics, the authors set out in a second longer chapter their approach to photoelectric phenomena in molecular photocells. They characterize their treatment as involving localized-states; it might also be called quasi-chemical. A fairly full account of Schottky junctions is included, stating further that the various characteristics of these contacts are quite easily obtained from alternating current studies. I would dispute this, since hopping mechanisms within the bulk of the organic can also give rise to alternating current dispersions and so complicate the overall picture. Here, too, the authors could have said with advantage something about photocarrier lifetime and photoconduction gain, which must be important for a successful solar energy device.

The next chapter deals with metallophthalocyanines and Chapter 4 with polyacetylene. These are followed by a chapter giving brief accounts of some ten or so other systems, including the inorganics already referred to, and superconductors. The list of 1,191 references is a useful guide to the relevant literature.

In a one-page conclusion, the authors rightly point out that the low mobilities found in organic semiconductors limit their possible applications. One might add that not enough efforts have so far been made to measure mobilities in organics, and to establish mobility–structure relationships. The authors further conclude that "no physical or theoretical considerations limit the possibility of obtaining molecular semiconductors". Unfortunately chemical stability problems, such as those that bedevil linear polyene and especially iodine-doped systems, do limit useful applications. In this respect it is sensible that the longest chapter is concerned with phthalocyanines, renowned for their stability (although they are not completely free from such problems, and also the difficulties associated with purification).

This is a useful and well-written book, of reasonable length. It should attract attention from the solid-state community in general, but it will be of particular interest to chemists working on the conduction properties of molecular semiconductors. □

Daniel D. Eley is Emeritus Professor of Physical Chemistry at Nottingham University, University Park, Nottingham NG7 2RD, UK.

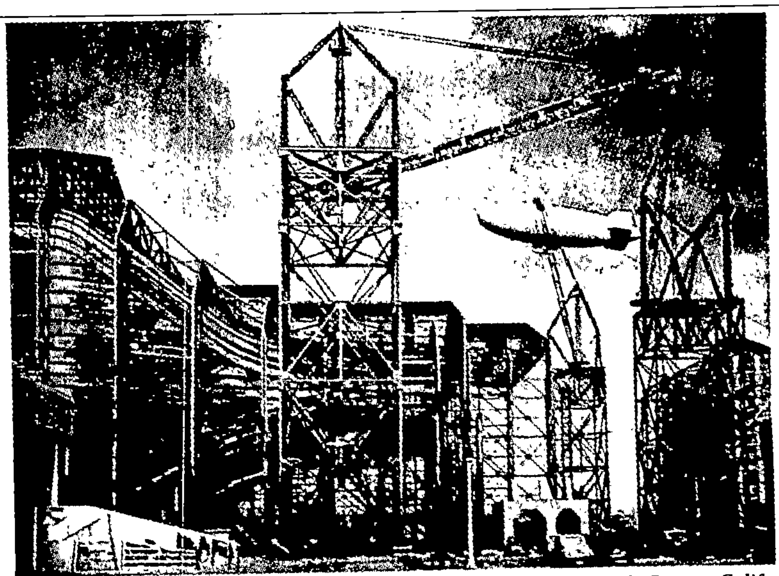

The largest wind-tunnel in the world under construction at Ames Research Center, California, in 1943. The picture is reproduced from Searching the Horizon, *by Elizabeth A. Muenger, a history of Ames from 1940 to 1976. The book is published by NASA as SP 4304 and is available from the US Government Printing Office, price pbk $13.*

Optical synchrotron emission in the southern lobe of 3C33

K. Meisenheimer* & **H.-J. Röser**

Max-Planck-Institut für Astronomie, Königstuhl, D-6900 Heidelberg 1, FRG

Charge coupled device polarimetry at a wavelength of 660 nm has detected a highly-polarized optical source, which is coincident with the radio hotspot at the leading edge of the southern lobe of 3C33. The optical polarization data perfectly match the high-frequency Very Large Array observations, thus providing the first direct evidence for optical synchrotron radiation from a classic double radio source. The extended structure of the emission region requires a huge particle accelerator boosting electrons to highly relativistic energies (up to 100 GeV) over a region several kiloparsecs in extent.

THE double radio source 3C33 consists of two extended lobes ~4 arc min apart from each other[1]. Coincident with the central D galaxy ($z = 0.0592$ (ref. 2)) there is a compact radio core[1]. Thus, 3C33 is a typical example of the powerful classic edge-brightened double radio sources, most commonly found in surveys at low frequencies (for example, 3C-, 4C-, Bologna-survey; extended radio sources are reviewed in ref. 3). At a resolution level of a few arc seconds high surface-brightness radio hotspots were detected in many extended radio lobes. For the radio hotspot located at the outer edge of the southern lobe of 3C33 (refs 4–6) a close association with a faint diffuse optical object has been reported[7].

The nature of such associations is unclear as there is little information about the optical emission processes involved. Furthermore, significant mismatches between the suggested optical counterparts and the radio maxima are frequently encountered[8], strongly enhancing the probability of chance coincidences with faint field objects.

The detection of optical synchrotron radiation from extended radio lobes would have special significance, since the path length of the highly relativistic electrons responsible for this radiation is short ($\lesssim 1$ arc s for redshifts $z \gtrsim 0.05$ and typical magnetic field strengths of ~10 nT).

Thus, optical synchrotron emission would directly map the regions where particle acceleration takes place. In addition, the overall nonthermal spectrum and the energy distribution of the relativistic electrons would be fixed over a much wider range, leading to more reliable estimates of the total emitted power and to details of the acceleration mechanism involved[3,9,10].

The most striking characteristic of synchrotron radiation is its high linear polarization. The detection of a highly polarized optical object in the vicinity of a radio lobe would, therefore, establish direct evidence for optical synchrotron emission. Here we present our first results of CCD polarimetry in the fields of extended radio lobes. The southern lobe of 3C33 was chosen to start with because of its bright and compact hotspot and the reported optical emission.

Observations

The optical field around the southern lobe of 3C33 was observed on 14, 15 and 16 November 1984 by the 2.2-m telescope on La Silla (Chile). Polarization analysis of all objects in the field was made possible by replacing one of the filter wheels in front of the direct imaging CCD camera (thinned RCA chip, 45 e$^-$ read-out-noise) by a rotatable plane parallel double calcite plate. It splits the light from each object in the field into two (perpendicularly) polarized images which are recorded simultaneously on the CCD detector (see Fig. 1, details of the method and the analysing procedure are given in ref. 11). The observations were made in a red bandpass ($\lambda_0 = 660$ nm, $\Delta\lambda = 150$ nm (full width at half maximum)).

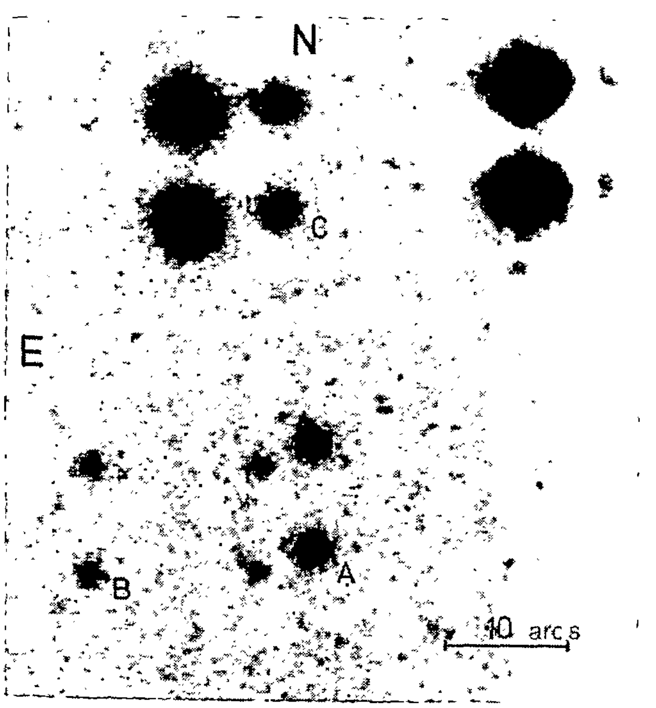

Fig. 1 Optical field around 3C33 south. This frame is a superposition of three CCD exposures (20 min each) taken through the double calcite plate in a red bandpass ($\lambda = 660$ nm). Each object in the field is split into two polarized images, separated in north-south direction. Southern images of reference stars are labelled A, B and C, respectively. The optical counterpart of the hotspot located 5 arc s south-east from star A is highly polarized as is obvious from the large brightness difference between the two images.

After the first 30-min exposure, a highly polarized optical object near the hotspot of 3C33 south was immediately conspicuous (see Fig. 1). Two subsequent exposures, taken with different position angles of the calcite plate, confirmed the detection. Three additional sets of frames with different orientations of the calcite plate were obtained in the following nights. Each set consists of three 20-min exposures with a fixed orientation of the calcite plate but slightly different pointing of the telescope.

For the detailed analysis of optical morphology and polarization of the hotspot counterpart each single CCD frame had to be corrected for sensitivity variations over the CCD detector and interference fringes. The appropriate flat field frames were generated by averaging all exposures of the same night which were taken through the same filter and at similar zenith distances. To avoid distortions of the flat field frames due to the astronomical objects present on each exposure, we employed a κ-σ test[12] among the (normalized) values of each pixel in different frames, which were exposed with different telescope pointing. Discrepant pixel values are subsequently ignored in calculating the average flat field frames.

---

* Present address: Royal Observatory, Blackford Hill, Edinburgh EH9 3HJ, UK.

After the flat field correction, all exposures taken with the same orientation of the calcite plate are collated. On the resulting fully corrected frames the remaining background variations do not exceed $\pm 0.3\%$ on scales $\geqslant 2$ arc s.

Optical counterpart of 3C33 south

The relative position of the highly polarized optical object and the radio hotspot in the southern lobe of 3C33 is determined with respect to the stars labelled A and C in Fig. 1, for which Rudnick *et al.*[6] measured coordinates. The radio hotspot position is taken from the 15-GHz map with 0.85 arc s resolution published by Dreher[5]. We find a positional offset (optical − radio) $\Delta\alpha = -0.03 \pm 0.02$ s and $\Delta\delta = +0.1 \pm 0.3$ arc s, so in what follows we assume a common radio and optical position of the hotspot maximum located at $\alpha_{1950} = 01$ h 06 min 12.10 s, $\delta_{1950} = +13°02'27.5''$.

As the extended structure of the optical counterpart is obvious, even on a single exposure, we superimpose all 18 images present on the three sets of CCD frames to obtain an image with optimum signal-to-noise ratio (Fig. 2*a*). The optical brightness distribution reproduces the four uppermost contours on the 5-GHz VLA (Very Large Array) map[6] very well (see Fig. 2*b*). The backward tail of the hotspot pointing towards the central galaxy as well as the roughly perpendicular wing towards the north-west are clearly detected at $\lambda = 660$ nm. The main difference with respect to the radio map is the longer backward tail observed on our red image. A careful comparison with the blue 200-in plate[7] indicates that this backward tail is of similar length in blue light, while hardly any blue radiation is detected from the hotspot itself (positional reference is based on the stars A and B, see Fig. 1).

Optical polarization

Since the optical counterpart of 3C33 south is clearly resolved, we attempt to obtain a polarization map. For this purpose, we select 11 different positions on the optical image at which we evaluate the optical polarization separately. The polarization analysis basically requires the comparison of the integrated counts within corresponding apertures on the two polarized images and is done in the same way as for the jet of 3C273 described elsewhere[11].

The optical polarization in 3C33 south, evaluated for an effective beamwidth of 2.0 arc s, is given in Table 1, columns 4 and 5. In addition, the polarization analysis was carried out for all other objects in the field and for about 50 (empty) positions around 3C33 south, producing a very reliable estimate of the actual measuring errors involved. For comparison, the apparent polarization values as obtained for two positions located in the extremely steep brightness gradient of star A are also included in Table 1 (labelled A-1 and A-2). They demonstrate the perfect matching of corresponding apertures and exclude any severe distortion of the polarization measurements in 3C33 south due to this nearby 20 mag star A.

The optical polarization map (Fig. 3) shows that the polarization position angle of the hotspot coincides with the direction of the backward tail, as observed at 6 and 2 cm (ref. 6). Crossing the hotspot and the adjacent wing from the south-east to the north-west, a rotation of the polarization angle by ~40° is observed at both optical and radio frequencies (see Table 1). The mean optical polarization of the hotspot (average over positions 1 to 5) is $P = (29.2 \pm 2.4)\%$ at a position angle of the E vector PA $= 54° \pm 4°$. In the backward tail, just inwards of the hotspot (position 10) the orientation of the E vectors seems to flip abruptly by about 90°. Although we failed to reach a 3-σ significance level in the amount of polarization at these faint brightness levels ($\geqslant 24$ mag/arc s^2, that is $\leqslant 2.5\%$ of the total background surface brightness which is doubled through use of the calcite plate), this 90° flip is in accordance with the magnetic field orientation inferred from the radio maps (compare with positions 10 and 11 in Table 1).

For a quantitative comparison with our optical results we measure the radio polarization at the 11 positions on enlarged copies of the maps published by Rudnick *et al.*[6] (6-cm data are given in columns 6–8 of Table 1). Using the six positions near the radio hotspot for which the optical polarization exceeds 3σ we find a mean rotation of the polarization angle $\Delta\chi$ (6 cm-opt.) = {PA (6 cm) − PA (opt.)} $= -7\overset{\circ}{.}2 \pm 2\overset{\circ}{.}8$, and $\Delta\chi$ (2 cm-opt.) $= -0\overset{\circ}{.} \pm 2\overset{\circ}{.}5$. Interpreting $\Delta\chi$ in terms of the Faraday rotation would result in a rotation measure (RM) of the hotspot RM $= (-35 \pm 13)$ rad m^{-2}, roughly consistent with the overall rotation measure of 3C33 south: RM $= -12$ rad m^{-2} (refs 13, 14). In addition, there seems to be depolarization at 6 cm: $P(6\text{ cm})/P(\text{opt.}) = 0.75 \pm 0.07$ which is not present in the 2-cm data: $P(2\text{ cm})/P(\text{opt.}) = 1.02 \pm 0.07$ (see ref. 6). This cannot be attributed to internal Faraday rotation alone, because even for a homogenous source (that is constant magnetic field and elec-

Table 1 Optical polarization in 3C33 (south) and comparison with radio data

		Optical (660 nm)			Radio (6 cm)		
Position	$\Delta\alpha$, $\Delta\delta$ (arc s)	Relative flux/beam†	P(%)	PA (deg)	Relative (flux/beam*)	P(%)	PA (deg)
1*	−0.3, −0.3	0.73	34±6	57±7	0.61	29	45
2*	0, 0	1.00	29±4	53±6	1.00	18	50
3*	0.3, 0.3	0.85	23±4	50±7	0.73	?	?
4*	0.4, −0.7	0.50	28±6	44±12	0.42	25	45
5*	−0.7, 0.3	0.72	39±7	63±5	0.24	36	54
6*	−0.7, 0.7	0.45	48±13	70±5	0.12	34	65
7	−1.4, 1.1	0.25	46±25	82±6	0.06	46	75
8	−1.1, 1.4	0.23	48±24	81±7	0.06	46	75
9	−0.7, 1.8	0.21	43±19	78±10	0.06	50	76
10	1.0, 1.1	0.22	27±11	128±23	0.30	20	120
11	1.6, 2.0	0.21	26±11	88±9	0.24	20	90
A-1	−1.5, 1.8	0.56	10±8	91±15	—	—	—
A-2	−2.2, 2.5	2.32	4.8±1.6	78±8	—	—	—

* Optical polarization exceeds 3σ.

† The optical data are integrated within an effective beamwidth of 2.0 arc s FWHM, the beamwidth of the radio data[6] is 0.85 arc s FWHM.

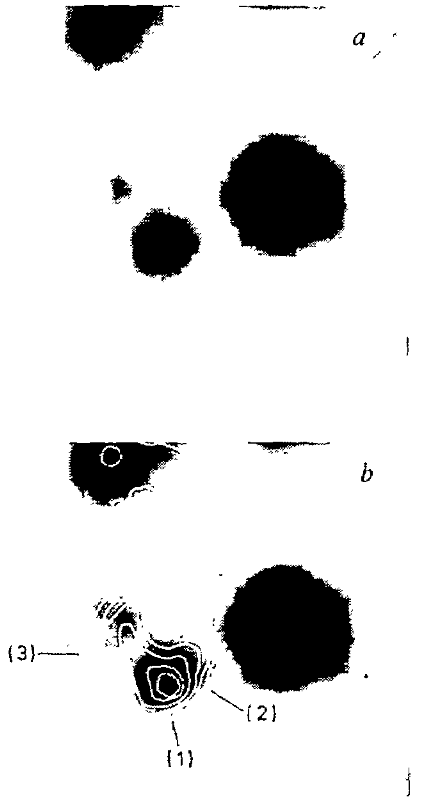

Fig. 2 High signal-to-noise image of 3C33 south at $\lambda = 660$ nm. *a*, Superposition of $3\times3\times2$ images from the three sets of CCD frames. The pixel size is 0.35×0.35 arc s; 1 arc s corresponds to a linear size of 1.05 kpc. (Secondary images of star A and the hotspot are present near the upper left edge of the field). *b*, As *a* with 5-GHz contours from ref. 6 superimposed. Individual regions are: 1, hotspot; 2, north-west wing; 3, backward tail. The direction towards the central galaxy is indicated by an arrow.

tron density along the line-of-sight) the above RM would yield a depolarization <1%.

Discussion and interpretation

The detection of a highly polarized optical counterpart for the hotspot in the southern lobe of 3C33 establishes a synchrotron origin for the radiation emitted at optical frequencies. Furthermore, the excellent agreement in both amount and orientation between optical and radio polarization strongly argues for a common emission region. Thus, for the first time, we can base the discussion of the overall nonthermal hotspot spectrum in a classical double radio source on the frequency range 10^9-10^{14} Hz.

Calibrating our data with reference to several standard stars observed with the same instrument yields a hotspot flux

$$F_\nu\ (\nu = 4.5\times10^{14}\ \mathrm{Hz}) = 4.2\pm0.8\ \mu\mathrm{Jy}$$

within an aperture of 2 arc s diameter. Based on the mean surface brightness of the diffuse patch as given by Simkin[7] a blue magnitude $B' = 25.0\pm0.5$ would result using the same aperture. Actually this value should be regarded as an upper limit because hardly any blue radiation is detected from the hotspot itself on Arp's 200-in plate (Fig. 1*c* in ref. 7) and the synchrotron origin of that radiation is not established. Therefore, we assume F_ν ($\nu = 6.8\times10^{14}$ Hz) $\leq 0.5\ \mu$Jy for the blue hotspot flux. A more recent flux measurement based on Arp's 200-in plate supports this value (S. M. Simkin, personal communication).

In Fig. 4, the optical flux values are compared with simple power law extrapolations $F_\nu \sim \nu^{-0.89\pm0.05}$ of the radio flux at 5 GHz (ref. 6). Obviously, a smooth link to the optical data requires a sharp spectral break around 10^{14} Hz.

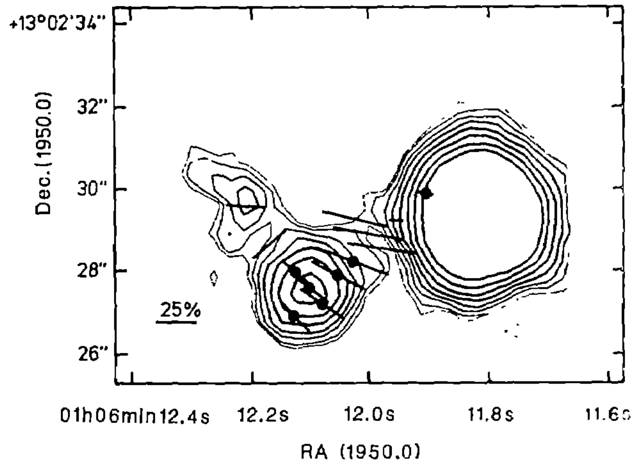

Fig. 3 Map of optical brightness and polarization within 3C33 south. The contours give 10%, 14%, 20%, ..., 80% of the peak flux at 660 nm (1.5 arc s resolution). The vectors superimposed show the fractional amount of linear polarization, integrated over an effective circular beam of 2.0 arc s FWHM. Positions where the amount of polarization exceeds 3σ are indicated by a central dot (see Table 1).

In fact, the synchrotron cutoff spectrum expected from a powerlaw electron energy distribution with a high-energy cutoff at $E_{\mathrm{max}} = \gamma_{\mathrm{max}}\, m_{\mathrm{e}}c^2$ and a corresponding cutoff frequency[10]

$$\nu_{\mathrm{c}} = 46\ \mathrm{Hz}\ \gamma^2_{\mathrm{max}} \frac{B_\perp}{1\ \mathrm{nT}} = (1.3\pm0.1)\times10^{14}\ \mathrm{Hz}$$

describes the data sufficiently well ($B_\perp$ = magnetic field perpendicular to the line-of-sight). A similar spectrum is observed from the hotspot at the outer end of 3C273A (ref. 11). Infrared photometry at 2.2 μm (expected flux: 50 up to 130 μJy) of the hotspot in 3C33 south would provide a crucial test for the cutoff spectrum which we will assume throughout the following discussion. So the power emitted by the hotspot between millimetre and infrared wavelengths is double that from the radio domain:

$$L_{\mathrm{mm\text{-}IR}} = 3.5\times10^{35}\ \mathrm{W}\ (\text{frequency range: } 10^{11}\text{-}10^{14}\ \mathrm{Hz})$$

$$L_{\mathrm{radio}} = 1.6\times10^{35}\ \mathrm{W}\ (\text{frequency range: } 10^{8}\text{-}10^{11}\ \mathrm{Hz})$$

Additional physical parameters estimated from the canonical formulae[3,9] for the hotspot and its adjacent regions (see Fig. 2) are summarized in Table 2. Note that only the total luminosity but not the minimum energy density and the corresponding magnetic field B_{me} ($\cong$ equipartition magnetic field) is affected by the detection of optical synchrotron radiation. Most strongly, however, the required maximum Lorentz factors γ_{max} of the relativistic electrons are increased. Within the hotspot, γ_{max} should be at least 2×10^5 (that is, $E_{\mathrm{max}} = 100$ GeV) or even higher if the magnetic field strength is overestimated by its equipartition value. Only lower limits to γ_{max} can be set in the backward tail and the north-west wing where our optical data are less stringent as regards the high-frequency cutoff. These high Lorentz factors yield very short synchrotron lifetimes of the order of 100 yr (see Table 2). Even if $B_\perp = 0.1\ B_{\mathrm{me}}$ the synchrotron lifetimes are too short for electrons accelerated in the hotspot to reach the backward tail or the north-west wing without losing about half of their energy. The cutoff frequency would then be shifted to $\nu_{\mathrm{c}} \leq 4\times10^{13}$ Hz, completely depressing the optical radiation. The observed optical brightness distribution, however, does not differ significantly from that found at 5 GHz (see Table 1).

On the other hand, much weaker fields (that is $B_\perp < 0.01\ B_{\mathrm{me}}$) are highly implausible, because an overwhelming fraction of the total energy would then be stored in relativistic particles. In this case, the highly ordered magnetic field, required for the observed radio-to-optical polarization and for fast electron drift velocities $v_{\mathrm{drift}} \cong c$, could not be maintained against destructive induction effects due to the tightly gyrating electrons (or positrons). Therefore, highly relativistic particles must be accelerated inside all the regions from where optical synchrotron radiation is observed. Furthermore, from the similarity between the optical and the 6-cm map (τ_{synch} (6 cm) $\gtrsim 140\tau_{\mathrm{synch}}$ (opt.)) we conclude that the drift velocities of the relativistic electrons through the hotspot region have to be much smaller than the speed of light.

Our observation of spatially resolved optical synchrotron emission demands an acceleration process which can boost electrons to highly relativistic energies and works efficiently over a region of >2 kpc in extent. Significant improvement of the angular resolution at optical frequencies (that is, Space Telescope resolution) should show whether this accelerator consists of several well separated substructures or smoothly fills the whole emission region.

With regard to the nature of the acceleration mechanism, several authors[16,17] have shown that diffuse shock acceleration (Fermi acceleration) at strong shocks would produce power law energy distributions of relativistic electrons with a high-energy cutoff if synchrotron losses are taken into account. Thus, Fermi acceleration at strong shocks, which may be very efficient due to 'bootstrapping' by nonlinear effects[18], seems to be a promising way of explaining the synchrotron spectrum observed from the hotspots in 3C33 south and 3C273A. Note, however, that such a high-energy cutoff is not a unique feature of diffuse shock acceleration but should occur in any process where the energy gain per duty cycle may eventually be balanced by the synchrotron losses (in practice this also limits the maximum energy in the case of man-made electron synchrotrons).

The presence of a strong shock within the hotspot fits well into the standard twin jet model for double radio sources[19,20] where hotspots represent the working surfaces of collimiated supersonic flows ramming into the intergalactic medium. Detailed hydrodynamic simulations of jets and their beam heads were presented by Smith *et al.*[21]. On first sight, there are obvious similarities between the observed morphology of the hotspot region in 3C33 south and the numerically-simulated structures of beam caps (compare our Figs 2 and 3 with Figs 4-8 in ref. 21). Within the framework of the gas dynamical jet models, the high linear polarization[22] and the sharp leading edge of the hotspot and the north-west wing (which has a less pronounced south-east correspondence) as well as the detection of a well separated precursor on Dreher's highly resolved 15-GHz map[5] would argue for inclination angles $30° < \theta_j < 70°$ between the jet axis and the line-of-sight. Such direct comparison betwee model jets and observations, however, may be greatly mis leading, since Smith *et al.*[21] did not take into account dissipativ losses and magnetic fields, which do have an important role i producing the observed radiation. In addition, their brightnes maps[21] were calculated under the assumption that the pat lengths of relativistic particles significantly exceed th dimensions of the beam caps. As discussed above, this assump tion is not valid in the case of 3C33 south.

Nevertheless, gas dynamic models of jets and hotspots ma have some physical significance, if the gas pressure dominate the total pressure within the jet. Then the jet speed v_j can b

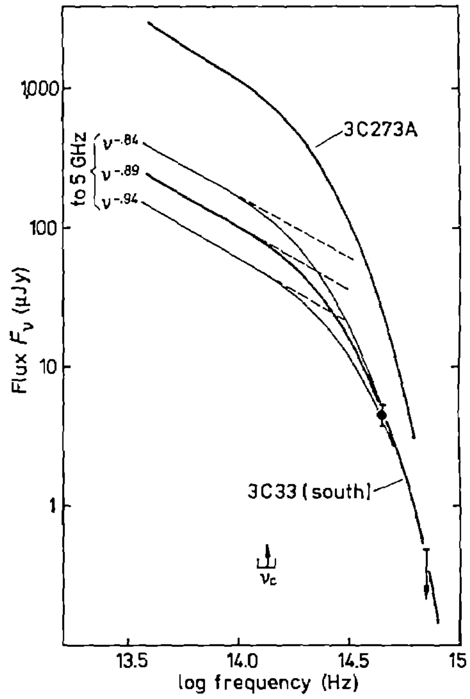

Fig. 4 Comparison between optical flux from the hotspot in 3C33 south (see text) and power law extrapolations $F_\nu \sim \nu^\alpha$ ($\alpha = -0.89 \pm 0.05$) of the flux density at 5 GHz (ref. 6). A synchrotron cutoff spectrum with cutoff frequency ν_c allows a smooth linking between radio spectrum and optical data. For comparison, the spectrum of 3C273 A (hotspot at the leading edge of the jet) is plotted, as it would be observed with the same redshift as 3C33 ($z = 0.06$).

Table 2 Physical parameters of the synchrotron-emitting regions

Region	Hotspot	NW wing	Backward tail
Positions (see Table 1)	1, 2, 3, 4, 5	7, 8	10, 11
Assumed: Volume (kpc^3)	1.0	2.0	1.6
Spectrum $F_\nu \sim \nu^\alpha$, $\alpha =$	−0.89	−0.8	−0.8
Calculated:			
Luminosity L_{synch} (10^{35} W)	5.5	2.4	4.1
Minimum energy density u_{me}(10^{-8} Jm^{-3})	3.8	1.1	1.6
Magnetic field B_{me} (nT)	64	34	42
Lorentz factor			
$\gamma_{\max}$ (B_{me}, 10^{14} Hz) (10^5)	1.9	>2.6†	>2.4†
$\gamma_{\max}$ (0.1 B_{me}, 10^{14} Hz) (10^5)	6.1	>8.4†	>7.5†
Synchrotron lifetime*			
τ_{synch} (B_{me}, 10^{14} Hz) (10^3 yr)	0.09	<0.23	<0.17
τ_{synch} (0.1 B_{me}, 10^{14} Hz) (10^3 yr)	2.8	<7.4	<5.4
Distance from hotspot d (kpc)	—	1.5	2.5
$d/c\tau_{\mathrm{synch}}$ (B_{me}, 10^{14} Hz)	18‡	>21	>48
$d/c\tau_{\mathrm{synch}}$ (B_{me}, 5 GHz)	0.12‡	>0.14	>0.34

* We assume $H_0 = 75$ km s^{-1} Mpc^{-1}, $q_0 = \phi$, $\nu_{\min} = 10^7$ Hz, $\nu_{\max} = 10^{14}$ Hz, relative amount of energy stored in protons: $k = 100$, see ref. 9.
† No evidence for a cutoff at $\nu_c = 10^{14}$ Hz.
‡ Calculated for $d = 0.5$ kpc (that is, HWHM of hotspot profile).

estimated from the requirement that the bulk kinetic energy supplied by the jet flow should at least balance the emitted power of the lobe. If we estimate the jet density from the rotation measure of the hotspot by assuming internal Faraday rotation in a magnetic field $B_{\|} = B_{\mathrm{me}}/\sqrt{3}$, we find $v_j \geqslant 0.14\,c$ (for a cold jet with radius $R_j = 0.5$ kpc, $L \geqslant 10^{36}$ W and $\varepsilon = 0.1$ see ref. 23). An alternative argument based on the momentum flux as calculated from the minimum pressure $p_{\mathrm{me}} = u_{\mathrm{me}}/3$ (Table 2) yields a similar lower limit for the jet speed[24]. So the power emitted from the southern hotspot and lobe of 3C33 could be supplied by a jet flow with mildly relativistic speeds as are directly observed in the galactic twin jet source SS433 (ref. 25). For comparison, we note that the momentum flux argument yields $v_j > 0.76\,c$ in the case of the more powerful double radio source Cygnus A (refs 24, 26).

CCD polarimetry, therefore, opens up a new frequency range for investigating the nonthermal radiation from radio lobes. Our results from 3C33 south point to several general conclusions.

First, optical synchrotron radiation from hotspots in extended radio lobes inevitably demands the presence of *in situ* acceleration processes. In 3C33 south, the synchrotron-emitting region is clearly extended, thus the acceleration process must occur within a large volume ($d \geqslant 2$ kpc). Space Telescope observations should allow us to decide whether the acceleration takes place within more compact substructures.

Second, our data on the hotspots in 3C33 south and 3C273A indicate synchrotron spectra with cutoffs at nearly identical frequencies $\nu_c = 10^{14}$ Hz. We note that very similar spectra are observed in some QSO cores[27,28]. Although Fermi acceleration at strong shocks could account for the cutoff, the intriguing fact of similar cutoff frequencies in compact cores ($d < 1$ pc) and extended sources ($d > 1$ kpc) still needs to be explained. Both hotspots emit a substantial fraction of their luminosity in the millimetre to infrared range. This makes observations with IR-arrays very promising.

Finally, any detailed comparison between observations and numerical simulations of jets and hotspots has to be treated with caution, as the processes which are responsible for the observed radiation are not considered in the model calculation (for example, dissipative losses, magnetic fields, and particle acceleration). It is necessary to investigate how these processes affect the hydrodynamic models. As we have found that optical (and possibly radio) maps mainly represent the accelerating regions, detailed models of Fermi acceleration or alternative mechanisms are urgently needed.

This work was based on observations made at the European Southern Observatory, La Silla (Chile) with the 2.2-m telescope of the Max Planck Society.

Received 30 July; accepted 24 October 1985.

1. Hargrave, P. J. & McEllin, M. *Mon. Not. R. astr. Soc.* **173,** 37–63 (1975).
2. Simkin, S. M. *Astrophys. J.* **234,** 56–67 (1979).
3. Miley, G. K. *A. Rev. Astr. Astrophys.* **18,** 165–218 (1980).
4. Gopal-Krishna, Joshi, M. N. & Ananthakrishnan, S. *Astrophys. Lett.* **17,** 11–14 (1976).
5. Dreher, J. W. *Astr. J.* **86,** 833–847 (1981).
6. Rudnick, L., Saslaw, W. C., Crane, P. & Tyson, J. A. *Astrophys. J.* **246,** 647–652 (1981).
7. Simkin, S. M. *Astrophys. J. Lett.* **222,** L55–L58 (1978).
8. Crane, P., Tyson, J. A. & Saslaw, W. C. *Astrophys. J.* **265,** 681–700 (1983).
9. Pacholczyk, A. G. *Radio Astrophysics* (Freeman, San Francisco, 1970).
10. Begelman, M. C., Blandford, R. D. & Rees, M. J. *Rev. Mod. Phys.* **56,** 255–351 (1984).
11. Röser, H.-J. & Meisenheimer, K. *Astr. Astrophys.* (in the press).
12. Newell, E. B. in *Image Processing in Astronomy* (eds Sedmark, G., Capaccioli, M., Allen, R. J.) (Osservatorio Astronomico di Trieste, 1979).
13. Haves, P. *Mon. Not. R. astr. Soc.* **173,** 553–568 (1975).
14. Vallée, P. J. & Kronberg, P. P. *Astrophys. J.* **193,** 303–308 (1974).
15. Ginzburg, V. L. & Syrovetskij, S. I. *The Origin of Cosmic Rays* (transl. Massey, H. S. H.) (Pergamon, Oxford 1964).
16. Webb, G. M., Drury, L. O'C. & Biermann, P. *Astr. Astrophys.* **137,** 185–201 (1984)
17. Bregman, J. N. Preprint (1984).
18. Völk, H. J. in *Trends in Physics* Vol. 1, 162–169 (European Physics Society 1985).
19. Rees, M. J. *Nature* **229,** 312–317 (errata p. 510) (1971).
20. Blandford, R. D. & Rees, M. J. *Mon. Not. R. astr. Soc.* **169,** 395–415 (1974).
21. Smith, M. D., Norman, M. L., Winkler, K.-H. A. & Smarr, L. *Mon. Not. R. astr. Soc.* **214,** 67–85 (1985).
22. Laing, R. A. *Mon. Not. R. astr. Soc.* **193,** 439–449 (1980).
23. Perley, R. A., Bridle, A. H. & Willis, A. G. *Astrophys. J. Suppl.* **54,** 291–334 (1984)
24. Dreher, J. W. in *Physics of Energy Transport on Extragalatic Radiosources* (eds Bridle, A. H. & Eilek, J. A.) 109–113 (NRAO Proc., Green Bank, 1984).
25. Margon, B. *A. Rev. Astr. Astrophys.* **22,** 507–536 (1984).
26. Perley, R. A., Dreher, J. W. & Cowan, J. J. *Astrophys. J. Lett.* **285,** L35–L38 (1984)
27. Bregman. J. N. *et al. Nature* **293,** 714–717 (1981).
28. Rieke, G. H., Lebofsky, M. J. & Wisniewsky, W. Z. *Astrophys. J.* **263,** 73–78 (1982)

Homologies in both primary and secondary structure between nuclear envelope and intermediate filament proteins

Frank D. McKeon*, Marc W. Kirschner* & Daniel Caput†‡

* Department of Biochemistry and Biophysics, University of California San Francisco, San Francisco, California 94143, USA
† Chiron Corporation, 4560 Horton St, Emeryville, California 94608, USA

The A, B and C lamins are the major proteins of the nuclear envelope. The complete nucleotide sequence of the coding region of the A and C lamins shows that these proteins are identical except for their carboxy termini. The most prominent structural feature of both lamins is an α-helical region of repeating heptads of amino acids that shows striking homology with the entire family of cytoplasmic intermediate filament proteins. These features suggest that the nuclear envelope is made up of a network of coiled-coil polymers.

THE eukaryotic nuclear envelope is responsible for segregating the cytoplasm from the nucleoplasm and thereby channelling all transport across the nuclear membrane through an array of specialized structures termed nuclear pores[1,2]. As the nuclear envelope is the site at which the very first events of chromosome condensation occur[3,4], it has also been suggested that it is involved in the maintenance of interphase chromosome organization[5]. Despite the fact that the nuclear envelope appears to be very stable in isolated nuclei, it can be very dynamic when it breaks down and rapidly reforms during mitosis[6,7].

Although the nuclear envelope is not completely defined biochemically, it is now known that its major structural component is the nuclear lamina, a durable, fibrous layer on the nucleoplasmic surface of nuclear membranes[8] which acts as a scaffold for the nuclear pores and may interact with interphase chromatin[9,10]. The structural integrity of the lamina is under strict cell-cycle control, as shown by its disintegration soon after chromosome condensation in prophase and its reappearance around telophase chromosomes[6,7].

---

‡ Present address: ELF Biorecherche, La bege-innopole, BP 137 31328, Castanet Tolosan Cedex, France.

In mammals the nuclear lamina is composed primarily of three proteins, lamins A, B and C, present in equal amounts in the interphase nuclear envelope[11]. Of these proteins, lamins A (relative molecular mass, $M_r = 70,000$) and C ($M_r = 60,000$) appear to be closely related on the basis of peptide maps and immunological cross-reactivity[11,12]. By these criteria, lamin B ($M_r = 68,000$) has a very different structure. Increased phosphorylation of the lamin proteins occurs before nuclear envelope disintegration in prophase and probably plays a crucial role in the regulation of associations between lamin proteins[11,13,14].

To understand better the structure of the nuclear envelope, we have examined in detail the structure of the lamin proteins. We wish to know whether these proteins interact directly with the chromatin or with the nuclear membrane, and also what accounts for the considerable stability of the nuclear envelope in interphase and yet allows for its complete disassembly and reassembly during mitosis. In addition there are questions of the individual role of the A, B and C lamins, their organization and their mechanism of assembly. As a first step in this analysis, we have isolated complementary DNAs containing the complete coding sequences of both the A and C lamins, screened using a high-titre anti-lamin serum obtained from a patient with the autoimmune disease linear scleroderma[15]. The predicted amino-acid sequences of the A and C lamins are indicative of unusual secondary structures and show a strong homology to all five classes of cytoplasmic intermediate filament proteins[16-18]. These structural features suggest that the nuclear envelope derives its structural integrity from coiled-coil interactions between lamin proteins in a manner similar to those in the intermediate filaments.

cDNAs encoding the A and C lamins

Human autoantibodies to the A and C lamins were used to screen a T-cell cDNA expression library. The auto-antiserum (LS-1) was derived from a patient with linear scleroderma[15] and shown to possess high-titre antibodies against conserved determinants of the A and C lamins. The cDNA library was constructed from human T-cell messenger RNA using the primer-adaptor method[19], which ensures that the cDNA is in the proper orientation for expression from the *lacZ* promoter on pUC9 (ref. 20) (Fig. 1*a*). Bacterial colonies expressing the *lacZ*-lamin fusion proteins were detected using the LS-1 serum, followed by ^{125}I-goat anti-human immunoglobulin G antibodies[21]. Although we expected only 1 of 3 cDNAs to be in the proper reading frame for expression, we found that 14 out of 15 of the A and C lamin cDNAs in the library could be detected using the antibodies. We suspect that the G-C tail between the *lacZ* gene and the cDNA coding sequence caused some frameshifting, resulting in this unusually high proportion of cDNAs expressing immunoreactive proteins.

The 15 putative lamin cDNAs obtained from this library fell into two groups, based on restriction mapping, distinguished by different 3′ ends. The longest cDNA from each group was expressed in *Escherichia coli* and the fusion proteins detected by Western blots[22] (Fig. 1*b*). The cDNA-7 expresses a protein with an apparent M_r of 72,000 whereas cDNA-13 yields a fusion protein of M_r ~84,000. As shown below, these two cDNAs show extensive homologies over most of their sequences. Although these apparent M_rs are considerably larger than the native lamin standards (Fig. 1*b*), we explain this by the presence of a 5′-untranslated sequence in-frame with the *lacZ* initiating methionine. To determine whether these immunoreactive proteins are indeed lamin proteins, we examined proteolytic digests of the fusion proteins produced in *E. coli* from the cDNAs together with the native lamin proteins derived from nuclear envelopes. The native lamin C and fusion protein from a putative lamin cDNA yield very similar peptide patterns after partial digestion with V8 protease (Fig. 2*a*). We obtained further evidence that these cDNAs encode nuclear lamins by observing the immune response in mice to the injected fusion proteins. Four weeks after immunization with the cDNA-7 fusion protein, we detected a strong immune response to the nuclear envelope in the serum using an immunofluorescence assay (Fig. 2*b*). Spleen cells from one mouse were fused with myeloma cells to produce monoclonal antibody-secreting hybridomas[23], of which several recognized the nuclear envelope in the same immunofluorescence assay (Fig. 2*b*). One of these hybridomas produced antibodies that reacted with A and C lamins in primates only, as shown in the Western blot against both Chinese hamster ovary cell and HeLa cell nuclear envelopes (Fig. 2*c*). The similarity of the peptide patterns and the highly specific immune response against primate lamins suggest that cDNA-7 and -13 encode the human lamin proteins.

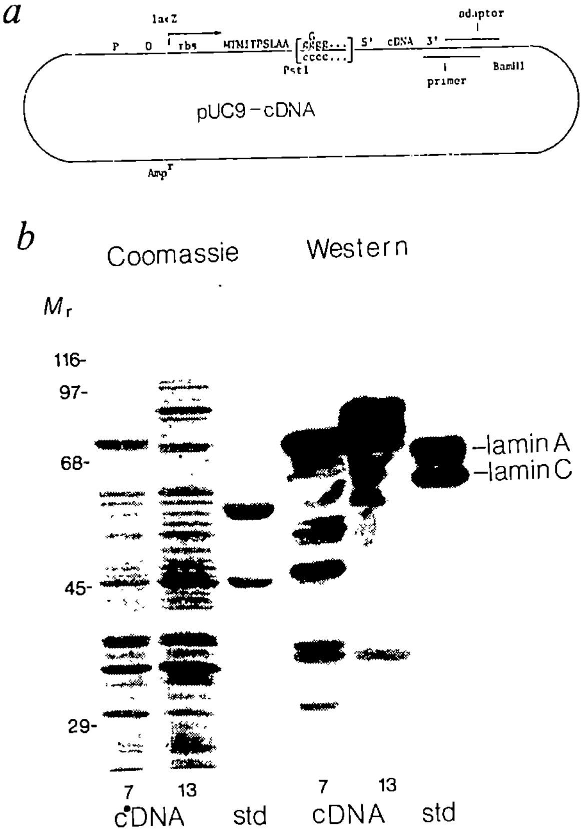

Fig. 1 Construction and expression of cDNAs. *a*, cDNA was synthesized from poly(A) RNA obtained from peripheral human lymphocytes using a primer-adaptor method[19]. This method constructs the recombinants such that the cDNA is in the proper orientation with respect to the *lacZ* start of transcription. The resulting fusion protein starts with the 10 amino acids of the β-galactosidase protein (MTMITPSLAA), continues with ~5 glycine residues translated from the G-C tail, and ends with the cDNA sequence. P, promoter; O, operator; rbs, ribosome binding sequence; adapter and primer are both synthetic oligonucleotides as described elsewhere[19]. *b*, Expression of cDNA proteins in *E. coli*. The figure shows a Coomassie blue-stained SDS-polyacrylamide gel[43] showing solubilized whole *E. coli* (D1210) harbouring cDNAs 7 and 13 after 10 h of induction with 2 mM isopropyl-β-D-thiogalactopyranoside (IPTG). A Western blot[22] identical to the stained gel was probed with the human autoantibody to the A and C lamins followed by ^{125}I-goat anti-human IgG. The fusion proteins have a higher M_r than those of the lamin standards derived from CHO interphase nuclear envelopes.

Relationship between A and C lamins

Evidence that cDNA-7 encodes lamin C and cDNA-13 lamin A is provided by Northern blots and DNA sequencing. Laliberté *et al.*[24] showed that a 3-kilobase (kb) mRNA encoded a precursor to lamin A of M_r 74,000, whereas a 2.2-kb species encoded lamin C. In agreement with these data, we found that DNA

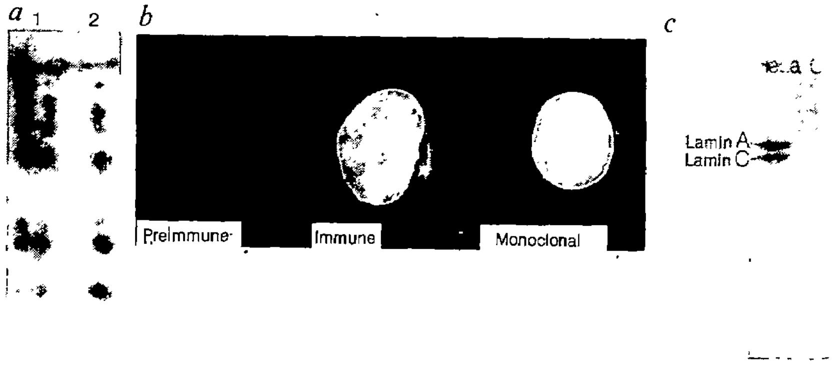

Fig. 2 Peptide mapping and immunological response to fusion proteins. ***a***, Peptide comparison between the cDNA-4 fusion protein and the CHO C lamins. *E. coli* harbouring cDNA-4 and nuclear envelopes from Chinese hamster ovary cells were fractionated on an SDS-polyacrylamide gel[43] (cDNA-4 encodes ~55K of lamin C and is identical in sequence to 1,800 nucleotides of cDNA-7. It is expressed at very high levels in *E. coli*, facilitating its use in peptide mapping.) Lamin and fusion proteins were excised and digested with V8 protease[44]. The peptides were then fractionated on an SDS-polyacrylamide gel and transferred electrophoretically to nitrocellulose[22]. The blot was probed with the LS-1 anti-lamin serum and then with ^{125}I-goat-anti-human IgG. Lane 1, lamin C peptides; lane 2, peptides from the cDNA-4 fusion protein. ***b***, Immunological response to lamin fusion proteins. D1210 *E. coli* (5 ml) harbouring cDNA-4 was grown overnight in Luria Broth media with 100 μg ml^{-1} carbenicillin and 2 mM IPTG, pelleted by centrifugation and lysed with 400 μl 6 M guanidine-HCl for 1 min. The lysate was diluted with 1.6 ml H_2O and precipitated by addition of 8 ml acetone. After centrifugation, the pellet was sonicated in an equal volume of Freund's incomplete adjuvant and 20 μl of the emulsion was injected into each footpad of a BALB/c female mouse on day 1, followed by 50-μl injections (interperitoneal) on days 12 and 21. The mice were bled on day 28 and the serum diluted 1:500 for indirect immunofluorescence against BSCl (African green monkey kidney) cells grown on coverslips and fixed with 1% formaldehyde for 5 min[15]. The preimmune serum shows low diffuse reactivity, whereas the immune serum yields a strong response to the nuclear envelope. Analysis of the hybridomas produced from the spleen cells of these mice revealed several that secreted antibodies to the nuclear envelope, at least one of which recognized primate A and C lamins exclusively, as shown by immunofluorescence and Western blotting. ***c***, Western blot of HeLa and CHO nuclear lamins probed with a monoclonal antibody to the lamin fusion proteins. Equal amounts of HeLa and CHO nuclear lamins were prepared as described elsewhere[15], fractionated on an SDS-polyacrylamide gel and transferred electrophoretically to nitrocellulose.

probes made from either cDNA-7 or cDNA-13 detect a 3- and 2.2-kb mRNA from human cells (Fig. 3). From the respective sizes of the cDNAs, cDNA-13 (2.7 kb) must encode lamin A and cDNA-7 (2.2 kb) lamin C; in fact, cDNA-13 encodes a polypeptide ~11,000 (11K) larger than the cDNA-7 peptide produced in *E. coli* (Fig. 1*b*). The sequences of the cDNA-7 and the cDNA-13 clones (Fig. 4) show that they are identical from the extreme 5′ end up to a position near the 3′ end. When translated, the pre-lamin A sequence of cDNA-13 encodes a protein 12.5K larger than the cDNA-7 sequence, in good agreement with the products observed in gels.

The exact sizes of the pre-A and C fusion products in *E. coli* (88,021 and 73,757, respectively, determined from the sequence) are larger than those expected for the pre-A and C lamin proteins. The reason for this was apparent from the sequence. Both cDNAs have 5′ noncoding regions in-phase with the initiating methionine of β-galactosidase. Therefore, ~9K of amino-acid sequence read from the noncoding 5′ end of the lamin mRNAs is present in the fusion products. In examining the sequences it was clear that the pre-A and C lamins must be initiated from a single in-frame methionine at the position shown in Fig. 4, which results in a M_r of 79,409 for the pre-A lamin and 65,145 for the C lamin. The pre-A lamin is further processed in the nucleus to give the mature A lamin[14,24]. It is not possible to determine the site of proteolytic cleavage from the nucleic acid sequence alone.

Homology to intermediate filaments

Over a large part of the amino-acid sequence, lamins A and C show strong homology with intermediate filament proteins. There are 111 identities out of 394 possible matches with only 2 gaps when lamins A and C are compared with vimentin using a sequence-matching computer program[25]. The sequence and the structural homologies between lamins and intermediate filaments are illustrated using the suggested secondary structure of lamin C (Fig. 5).

Intermediate filaments contain a ~310-residue stretch of amino acids which is thought to be α-helical and which has a distinctive structural feature suggesting that these helices can form coiled-coils with a similar α-helix[16-18]. This distinctive feature is the presence of repeats of seven amino acids, such that if the positions in these repeats are denoted a, b, c, d, e, f and g, residues a and d are generally hydrophobic and this sequence is repeated without gaps. This places the a and d residues next to each other on one side of the α-helix so that two helices can wind around each other, held together by hydrophobic interactions. Tropomyosin is the best-studied example of a protein with extensive helical domains capable of forming coiled-coils[26]. Intermediate filaments contain three or four major α-helical regions spaced by linkers which do not form these heptad repeats[16-18].

As shown in Fig. 5, a short stretch of amino acids, which has a high tendency to form an α-helix but does not have heptad repeats[18], precedes the first coil. Directly after this sequence is the coil 1A domain of 39 residues, in which all 11 a and d positions in the heptad repeats are hydrophobic. The heptad repeats are shown directly in Fig. 4 where the a and d positions are placed in the corresponding position used for intermediate filament proteins[16]. The coil 1A region and the preceding helix are not only structurally homologous but also closely related in sequence. In Fig. 5*b* the precoil helix and amino-terminus of

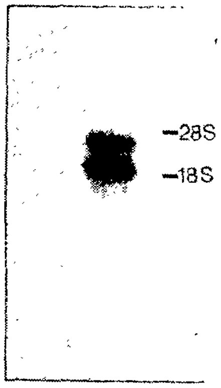

Fig. 3 The mRNA complexity of A and C lamins. Human poly(A) selected RNA was fractionated by electrophoresis through a 1% agarose gel containing formaldehyde and transferred to nitrocellulose[45]. This filter was probed with a nick-translated 1-kb *Hin*dIII–*Bam*HI fragment from the 3′ end of cDNA-7, yielding two bands migrating at 2.2 and 3.0 kb. The 28S and 18S rRNAs are 5.0 and 2.1 kb.

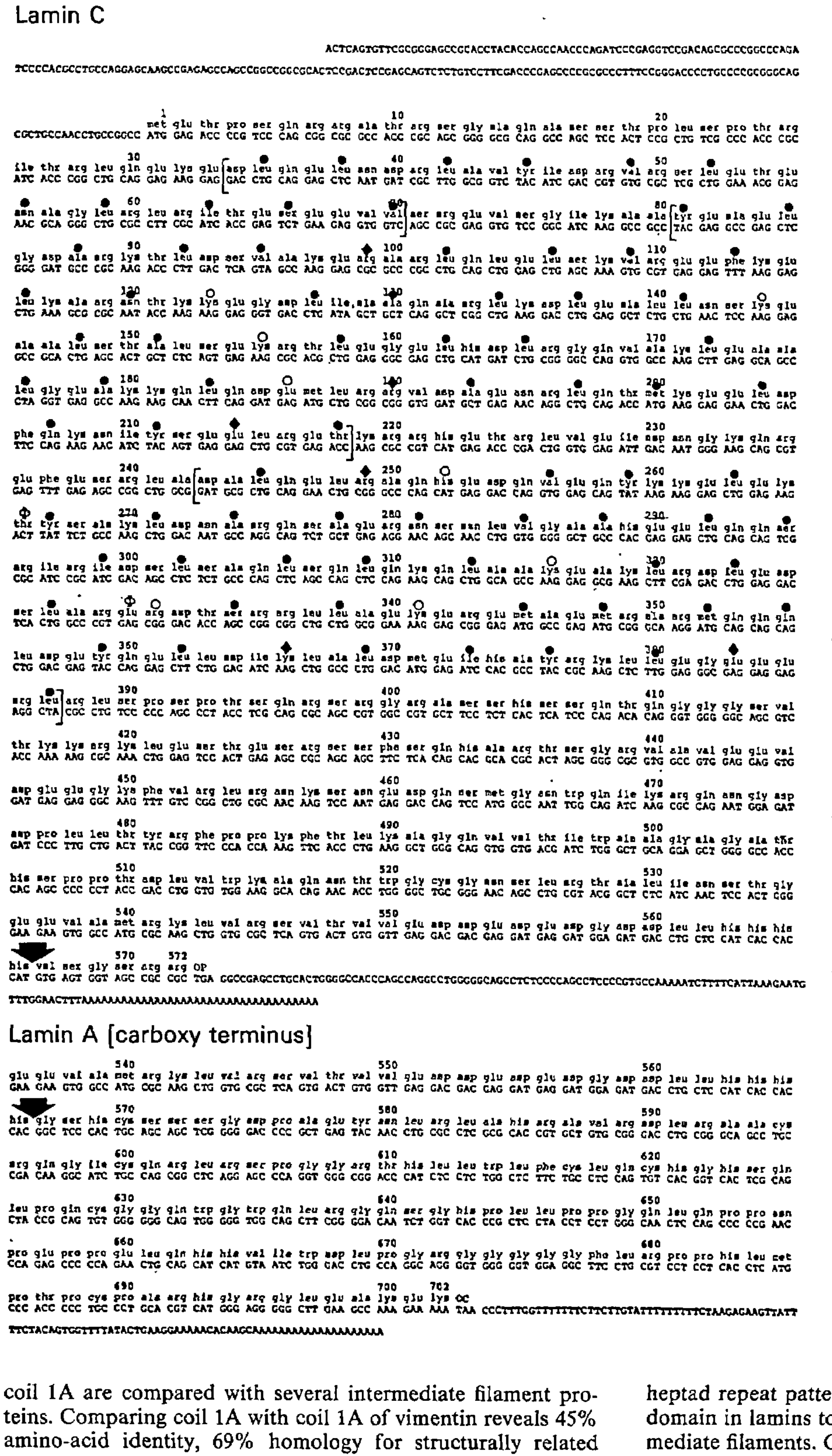

Fig. 4 The cDNA-7 (encoding lamin C) and cDNA-13 (encoding lamin A). Both cDNAs were sequenced completely from both strands using M13 dideoxy methods using several overlapping restriction fragments[46]. In addition, portions of three other lamin C clones and one other lamin A clone were also sequenced and did *not* disagree with our sequence. Translation of the sequence was started at the first in-phase methionine. The complete sequence of lamin A is identical to the lamin C sequence up to amino-acid position 566, denoted by arrows. Only the 3′ sequence of lamin A is shown. Note that although amino-acid residue 566 is the same in both sequences, the third base of its codon is different. The first set of brackets (residues 33–70) refers to the coil 1A region, the second set (residues 81–218) corresponds to coil 1B and the third set (residues 243–387) to coil 2. Filled circles, open circles and diamonds refer to the a and d positions of the heptad repeats corresponding to those found in all intermediate filaments[16]. Filled circles, hydrophobic amino acids; filled diamonds, polar amono acids conserved between lamin and vimentin; open circles, polar amino acids in lamins which do not correspond to polar amino acids in vimentin. The two Φ symbols at positions 266 and 330 are two phase changes in the heptad repeats, both of which are conserved between lamin and intermediate filaments.

coil 1A are compared with several intermediate filament proteins. Comparing coil 1A with coil 1A of vimentin reveals 45% amino-acid identity, 69% homology for structurally related amino acids and no gaps.

The heptad repeats end for coil 1A at the same place as in intermediate filaments at a 10-amino-acid-long linker, L1. This linker shows no obvious sequence relationship to the 8–14 amino acids in L1 of intermediate filaments[17]. Coil 1B has a lower overall sequence identity with vimentin but preserves the heptad repeat pattern and often has substituted polar amino acids in the a and d positions at the same place as the sites of insertion in intermediate filaments. Interestingly, coil 1B contains a 43-amino-acid-long insert (residues 120–162) which shows no homology with intermediate filaments but which continues the heptad repeat pattern in-phase. This causes the overall helica domain in lamins to be ~12% larger than the domain in inter mediate filaments. Coil 1B is separated from coil 2 by a secon linker of 24 amino acids which shows little homology wit intermediate filaments.

Coil 2 consists of 145 amino acids and shows a strong cor servation of heptad repeats. At two places in coil 2 the hepta repeats change phase (indicated at Φ in Fig. 4) and these occu in the same positions in intermediate filaments. However, in a intermediate filaments the first phase change occurs at a con served tryptophan, whereas in the A and C lamins it occurs a a threonine. The carboxy-terminal domain of coil 2 has a amino-acid sequence homologous with all intermediate filamen proteins (Fig. 5*c*). The homology with vimentin, the hepta

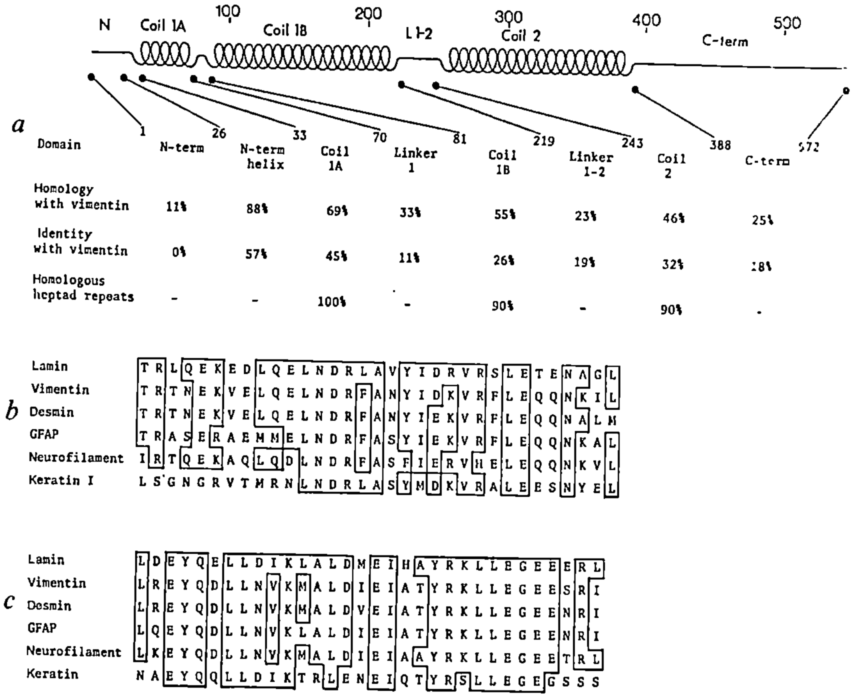
a
N
Coil 1A
100
Coil 1B
200
L1-2
300
Coil 2
400
C-term
500
1
26
33
70
81
219
243
388
572
Domain
N-term
N-term helix
Coil 1A
Linker 1
Coil 1B
Linker 1-2
Coil 2
C-term
Homology with vimentin
11%
88%
69%
33%
55%
23%
46%
25%
Identity with vimentin
0%
57%
45%
11%
26%
19%
32%
28%
Homologous heptad repeats
-
-
100%
-
90%
-
90%
-
b
Lamin T R L Q E K E D L Q E L N D R L A V Y I D R V R S L E T E N A G L
Vimentin T R T N E K V E L Q E L N D R F A N Y I D K V R F L E Q Q N K I L
Desmin T R T N E K V E L Q E L N D R F A N Y I E K V R F L E Q Q N A L M
GFAP T R A S E R A E M M E L N D R F A S Y I E K V R F L E Q Q N K A L
Neurofilament I R T Q E K A Q L Q D L N D R F A S F I E R V H E L E Q Q N K V L
Keratin I L S G N G R V T M R N L N D R L A S Y M D K V R A L E E S N Y E L
c
Lamin L D E Y Q E L L D I K L A L D M E I H A Y R K L L E G E E E R L
Vimentin L R E Y Q D L L N V K M A L D I E I A T Y R K L L E G E E S R I
Desmin L R E Y Q D L L N V K M A L D V E I A T Y R K L L E G E E N R I
GFAP L Q E Y Q D L L N V K L A L D I E I A T Y R K L L E G E E N R I
Neurofilament L K E Y Q D L L N V K M A L D I E I A A Y R K L L E G E E T R L
Keratin N A E Y Q Q L L D I K T R L E N E I Q T Y R S L L E G E G S S S

Fig. 5 *a*, Secondary structure and sequence homologies of lamins and intermediate filaments. The lengths of various coil, linker and non-helical domains are drawn to scale and aligned with intermediate filament structures[16]. The homology arises from using structurally related amino acids of the following families: A, I, L, V; Q, N; F, Y, W; P; E, D; H, R, K; S, T; G; C; M. Identities were from alignment matching[25]. Homologous heptad repeats refer to hydrophobic residues or polar substitutions conserved in vimentin and lamin C in the a and d positions of the heptads. *b*, Sequence comparison of the amino-terminal region of coil 1A of lamins A and C (residues 27–58) with those of hamster vimentin[37], chicken desmin[39], mouse GFAP, porcine neurofilament[38] and mouse epidermal keratin II (ref. 40). *c*, Sequence comparison of lamins A and C with the carboxy-terminal region of coil 2 (residues 355–387).

repeats and the α-helical structure of lamins A and C end abruptly at residue 387. In coils 1A, 1B and 2, the a and d positions contain 85% uncharged residues, whereas 48% of the remaining positions are uncharged. The corresponding values for mouse epidermal keratin are 81 and 61% (ref. 27).

We predict that the amino- and carboxy-terminal domains have mixed secondary structure. These domains show no overall homology with intermediate filaments. The very short amino-terminal non-helical region is strongly basic in lamins and in vimentin. The much larger carboxy-terminal region has clustered charged groups; in particular, 24% of the 50 amino acids next to coil 2 are basic, with an unusual stretch containing 30% serine residues. The extreme carboxy-terminus of the C lamins is highly charged.

To give some statistical picture of where the A and C lamins fit in the intermediate filament family, we have compared the sequences using a sequence-matching algorithm[25]. There is a very strong relationship of lamins to all intermediate filaments, except for the 68K neurofilament protein (Table 1). These relationships are weaker than the close relationship of vimentin, desmin and glial fibrillary acidic protein (GFAP) (three intermediate filament proteins considered to be members of a related superclass[17]) to each other. However, the relationship of the A and C lamins to the vimentin/desmin/GFAP group is much closer than the relationship of this superclass to the neurofilament proteins. To show that these relationships are not merely a consequence of the α-helical structure involved in coiled-coil interactions, we have compared all of these sequences with rabbit skeletal muscle tropomyosin and nematode myosin. The structural identity here, although possibly statistically significant, is much lower than the lamin–intermediate filament comparisons (Table 1).

Implications of lamin structure

Consideration of the A and C lamins as members of the intermediate filament protein family depends on their possession of several characteristic features of that family. The most striking structural features are: the long α-helical stretch with heptad repeats; the conserved position of the linkers; the conserved replacement of charged amino acids in the heptad repeats; the conserved position of the phase changes in coil 2; and, particularly, the strong regions of sequence identity in coils 1A and

Table 1 Alignment identities between amino-acid sequences of proteins capable of coiled-coil interactions

	Lamin C	Vimentin	GFAP	Desmin	Keratin II	Keratin I	Neurofilament (68K)	Myosin heavy chain
Vimentin	44	—	—	—	—	—	—	—
GFAP	43	201	—	—	—	—	—	—
Desmin	41	123	159	—	—	—	—	—
Keratin II	38	62	68	69	—	—	—	—
Keratin I	34	62	70	68	55	—	—	—
Neurofilament	18	29	33	36	33	33	—	—
Myosin heavy chain	9	4	6	6	4	12	3	—
Tropomyosin	5	5	2	5	2	8	3	17

Sequences were aligned using an alignment score program[25] based on the Needleman and Wunsch algorithm[36]. The alignment score is the number of standard deviations (s.d.) by which the best alignment score differs from the mean alignment score of the randomly permuted sequences, divided by the s.d. of the distribution. The sequence of lamin C is compared with that for hamster vimentin[37], mouse GFAP[38], chicken smooth muscle desmin[39], human type II epidermal keratin[28], mouse type I epidermal keratin[27], porcine 58K neurofilament protein[40], nematode myosin heavy chain[41], and rabbit skeletal muscle tropomyosin[42].

2. Although there is strong sequence divergence in the carboxy-terminus of lamins A and C, this is also a common feature of intermediate filaments, for example, the 50K and 56K keratins[27–29]. The fact that the A and C lamins share a 1,910-residue stretch of identical nucleotide sequence suggests strongly that these proteins arise from the same gene by differential processing. In support of this suggestion, we see only a single band in *Eco*RI and *Bam*HI digests of human genomic DNA (data not shown). A full understanding of how the mRNA sequences arise requires a study of genomic clones. There are no obvious sequence homologies with other known proteins in the carboxy-terminal and amino-terminal non-coil domains of the lamins. In particular, there is no extensive hydrophobic region characteristic of membrane-binding domains. The membrane anchorage sites may be a property of lamin B as suggested by biochemical studies[11].

In analysing lamin structure, we were fortunate that the proteins to which they are homologous have been studied so extensively. Despite considerable sequence divergence outside the central α-helical domain, all the intermediate filament proteins seem to be built on the same model. The basic substructure of intermediate filaments is a coiled-coil molecule thought to be composed of two chains[16–18]. Despite the presence of heterogeneous amino- and carboxy-terminal domains, all intermediate filament proteins assemble into the same fundamental 10-nm filament, but the assembly is thought to involve interactions in the non-coiled-coil regions. As non-helical domains in lamins are not related to those in intermediate filament proteins, we cannot be sure that the lamins will assemble into 10-nm filaments. Thus, nuclear lamins almost certainly form coiled-coil oligomers that probably assemble further into elongated molecules of as yet undetermined structure. (Note that Goldman and co-workers have reported that putative lamin-like proteins from BHK cells will form paracrystals with the same axial repeat as found in intermediate filaments[30]. This and other preliminary information suggested to these workers that lamins and intermediate filaments might share structural homologies[31].) Unfortunately, a definitive structure of the lamina has not been observed using the electron microscope: We could postulate that lamin filaments are arranged in long fibres or in a dense network similar to that of spectrin in the erythrocyte plasma membrane[32]. The 1 : 1 : 1 stoichiometry of the A, B and C lamins in the nuclear envelope suggests that lamin B also contains an extensive α-helical region capable of forming a coiled-coil with the lamin A or C. Thus, the nuclear lamina, like intermediate filaments, may comprise a heteropolymer (by analogy with the keratins and neurofilaments, where differences between the A/C and B lamins may be principally in the non-helical regions). As in neurofilaments, there may be some flexibility in the exact composition of these heteropolymers[33].

The recent demonstration that the nuclear envelope of *Xenopus* oocytes and early embryos is composed of only one form of nuclear lamin protein suggests that a homopolymer of lamin molecules is sufficient to provide the stability of the nuclear envelope[34,35]. The introduction of additional types of lamin proteins, which occurs at a specific developmental step (the mid-blastula transition in *Xenopus*), indicates that more complex functions of the envelope are required in nuclei undergoing active transcription[34,35].

It remains a fascinating structural question as to how such a stable and chemically resistant structure involving coiled-coil interactions over a distance of 350 amino acids could be destabilized by phosphorylation during mitosis[11,13,14]. It will be of interest to determine whether the phosphorylation sites affecting lamin stability are located in the coiled-coil domains or whether they are found in the amino or carboxy termini. Although the α-helical domains may, as in the intermediate filaments, form the basic structure of the nuclear envelope, it may be the non-α-helical domains on the amino and carboxy termini that are involved in supporting the nuclear pores and chromatin, and interacting with other nuclear proteins. An investigation of these functions should provide insights into various aspects of the structure and activity of the nucleus.

We thank Pablo Garcia, Fernando Bazan and Robert Fletterick for help with the sequence homology search and the secondary structure predictions, David Drechsel for the peptide mapping experiments and help in the early stages of this project; Sumire Kobayashi for technical assistance; Jeff Edman for instruction on M13 subcloning; Phil Barr and Guy Mullenbach for providing synthetic oligonucleotides; and Ray Sanchez for help with sequencing. We also thank David Gard and Peter Walter for helpful comments on the text; and Cynthia Hernandez for editing the manuscript. F.D.M. is a Giannini Fellow of the Bank of America. This work was supported by grants from the United Scleroderma Foundation, the NIH and the American Cancer Society.

Received 8 August; accepted 3 December 1985.

1. Franke, W. W., Scheer, U., Krohne, G. & Jarasch, E.-D. *J. Cell Biol.* **91**, 39s–50s (1981).
2. Maul, G. G. *Int. Rev. Cytol. Suppl.* **6**, 75–185 (1977).
3. Gurley, L. R., D'Anna, J. A., Barham, S. S., Deaven, L. L. & Tobey, R. A. *Eur. J. Biochem.* **84**, 1–15 (1978).
4. Foe, V. E. & Alberts, B. M. *J. Cell Sci.* **61**, 31–70 (1983).
5. Gerace, L. & Blobel, G. *Cold Spring Harb. Symp. quant. Biol.* **46**, 967–978 (1982).
6. Krohne, G., Franke, W. W., Ely, S., D'Arcy, A. & Jost, E. *Cytobiology* **18**, 22–38 (1978).
7. Gerace, L., Blum, A. & Blobel, G. *J. Cell Biol.* **79**, 546–566 (1978).
8. Fawcett, D. W. *Am. J. Anat.* **119**, 129–146 (1966).
9. Aaronson, R. P. & Blobel, G. *Proc. natn. Acad. Sci. U.S.A.* **72**, 1007–1011 (1975).
10. Dwyer, N. & Blobel, G. *J. Cell Biol.* **70**, 581–591 (1976).
11. Gerace, L. & Blobel, G. *Cell* **19**, 277–287 (1980).
12. Shelton, K., Higgins, D., Cochran, D., Ruffolo, D. J. & Egle, P. *J. biol. Chem.* **255**, 10976–10983 (1980).
13. Miake-Lye, R. & Kirschner, M. W. *Cell* **41**, 165–175 (1985).
14. Ottoviano, Y. & Gerace, L. *J. biol. Chem.* **260**, 624–632 (1985).
15. McKeon, F. D., Tuffanelli, D. L., Fukuyama, K. & Kirschner, M. W. *Proc. natn. Acad. Sci. U.S.A.* **80**, 4374–4378 (1983).
16. Weber, K. & Geisler, N. in *Cancer Cells 1, The Transformed Phenotype*, 153–159 (Cold Spring Harbor Laboratory, New York, 1984).
17. Steinert, P. M., Steven, A. C. & Roop, D. R. *Cell* **42**, 411–419 (1985).
18. Traub, P. *Intermediate Filaments* (Springer, Berlin, 1985).
19. Caput, D. *et al. DNA* (in the press).
20. Vieira, J. & Messing, J. *Gene* **19**, 259–268 (1982).
21. Helfman, D. M., Feamisco, J. R., Fiddes, J. C., Thomas, G. P. & Hughes, S. H. *Proc. natn. Acad. Sci. U.S.A.* **80**, 31–35 (1983).
22. Burnette, W. N. *Analyt. Biochem.* **112**, 195–203 (1981).
23. Kohler, G. & Milstein, C. *Eur. J. Immun.* **6**, 511–519 (1976).
24. Laliberte, J. F. *et al. J. Cell Biol.* **98**, 980–985 (1984).
25. Orcutt, B. C., Dayhoff, M. O. & Baker, W. C. *Protein Identification Resources* (National Biomedical Program, Washington, D.C., 1984).
26. McLachlan, A. D. & Stewart, M. *J. molec. Biol.* **98**, 293–304 (1975).
27. Steinert, P. M., Rice, R., Roop, D. R., Trus, B. L. & Steven, A. C. *Nature* **302**, 794–800 (1983).
28. Hanukoglu, I. & Fuchs, E. *Cell* **31**, 243–252 (1982).
29. Hanukoglu, I. & Fuchs, E. V. *Cell* **33**, 915–924 (1983).
30. Goldman, R. D. *et al. J. Cell Biol.* **97**, 221a (1983).
31. Zackroff, R. V., Goldman, A. E., Jones, G. R., Steinert, P. M. & Goldman, R. D. *J. Cel Biol.* **98**, 1231–1237 (1984).
32. Bennett, V. *A. Rev. Biochem.* **54**, 273–304 (1985).
33. Shaw, G. & Weber, K. *Expl Cell Res.* **136**, 119–125 (1981).
34. Benavente, R., Krohne, G. & Franke, W. W. *Cell* **41**, 177–190 (1985).
35. Strick, R. & Hausen, P. *Cell* **41**, 191–200 (1985).
36. Needleman, S. B. & Wunsch, G. D. *J. molec Biol.* **48**, 443–453 (1970).
37. Quax-Jenken, Y. E. F. M., Quax, W. J. & Bloemendal, H. *Proc. natn. Acad. Sci. U.S.A.* **80**, 3540–3552 (1983).
38. Lewis, S. A., Balcarek, J. M., Krek, V., Shelanski, M. L. & Cowan, N. J. *Proc. natn. Acad Sci. U.S.A.* **81**, 2743–2746 (1984).
39. Geilser, N. & Weber, K. *Proc. natn. Acad. Sci. U.S.A.* **78**, 4120–4123 (1981).
40. Geisler, N., Kaufmann, E., Fischer, S., Plessman, V. & Weber, K. *EMBO J.* **2**, 1295–130 (1983).
41. McLachlan, A. D. & Kairn, J. *Nature* **299**, 226–231 (1982).
42. Stone, D. & Smillie, L. B. *J. biol. Chem.* **253**, 1137–1148 (1978).
43. Laemmli, U. K. *Nature* **227**, 680–685 (1970).
44. Cleveland, D., Fischer, S., Kirschner, M. & Laemmli, U. *J. biol. Chem.* **252**, 1102–1106 (1977)
45. Thomas, P. S. *Proc. natn. Acad. Sci. U.S.A.* **77**, 5201–5205 (1980).
46. Sanger, F., Coulson, A. R., Barrell, B. G., Smith, A. J. H. & Roe, J. H. *J. molec. Biol.* **143** 161–178 (1980).

Quasi-periodic oscillations in the X-ray flux of Cyg X-2

G. Hasinger*, A. Langmeier*, M. Sztajno*, J. Trümper*, W. H. G. Lewin†§ & N. E. White‡

* Max-Planck-Institut für Extraterrestrische Physik,
8046 Garching, FRG
† Massachusetts Institute of Technology, Center for Space Research,
Cambridge, Massachusetts 02139, USA
‡ Exosat Observatory, Space Science Department of ESA, ESOC,
6100 Darmstadt, FRG

We have discovered quasi-periodic X-ray oscillations (QPOs) (30–45 Hz) and low-frequency noise (below 15 Hz) in Cyg X-2 (ref. 1). The centroid frequency of the oscillations is correlated with the source intensity in the same way as in GX 5-1 (refs 2, 3): the frequency increases when the source intensity goes up. Cyg X-2 differs, however, from GX 5-1 (refs 2, 3), where the amplitude of the oscillations and of the low-frequency noise go hand in hand, in that the amplitude of the QPOs decreases while that of the low-frequency noise increases with increasing source intensity. We describe here the spectrum of the persistent emission as the sum of a variable 1.2-keV black-body component, a more or less constant 7 keV thermal bremsstrahlung component and an iron emission line. This is the first report of spectral variations associated with QPOs[2–6], which could themselves reflect variations in either the black body or the thermal bremsstrahlung component.

Observations of Cyg X-2 (4U 2142+380) with the Exosat instruments termed the medium energy experiment[7] (ME) and gas scintillation proportional counter[8] (GSPC) were carried out during a 14 h period beginning at 02:07 UT on 23 July, 1984. One half of the ME monitored the background. ME data were telemetered with 0.3-s time resolution in 32 energy channels; for 12 of the 14 h high-time-resolution data (7.8 ms) with no spectral resolution were also transmitted. The source intensity varied between ~700 and 1,000 counts per s (c.p.s.) in the ME, corresponding to 1–20 keV luminosities of $(0.9\text{–}1.3)\times 10^{38}$ erg s^{-1}, respectively for a distance of 8 kpc (ref. 9).

We independently Fourier-analysed 2-s stretches of high-time-resolution data and averaged them to give mean power spectra for four intensity intervals (Table 1). Our normalization[10] was the same as that of Van der Klis *et al.*[3]. Analysis of shorter or longer stretches of data (0.25–8 s) give the same results. The mean power spectra (Fig. 1) show three components: (1) low-frequency noise (LFN) below 15 Hz; (2) a broad peak characteristic of quasi-periodic oscillations (QPO), whose centroid frequency rises from 30 to 45 Hz as the source intensity increases; and (3) white noise from poissonian counting statistics. The function[3]:

$$P(f)=2.0+A/B\exp(-f/B)+C/\pi E(1+((f-D)/E)^2)^{-1}$$

fits the power spectra (solid lines in Fig. 1). The first term, the white noise power, was held fixed at a value of 2.0, as justified by earlier Exosat results in the same mode[3,11]. The existence of QPOs in the highest intensity interval depends on this choice, that is, on the assumption that the source does not produce intrinsic white noise power. The second term, an exponential with integral A and e-folding frequency B, describes the LFN (power law fits to the LFN were not acceptable). The third term is a lorentzian peak profile with integral C, centroid frequency D, and half-width at half-maximum E. The results are summarized in Table 1. All errors are standard deviations (s.d.) $(\chi^2_{\min}+1)$ for one parameter of interest[12].

The spectral analysis was complete before the QPO discovery[13]. Energy spectra (1.6–20 keV) were derived for five intensity intervals (which are reasonably close to those used for the time series analysis). Statistically acceptable fits require at least three simple 'standard' components: (1) a black-body spectrum ($kT \sim 1.2$ keV); (2) a thermal bremsstrahlung spectrum ($kT \sim 7$ keV); and (3) a very weak iron emission line. GSPC data fixed the energy, FWHM and equivalent width of the iron line at 6.5±0.1 keV, 0.6±0.2 keV, and 41±10 eV, respectively. Spectra with fewer components and other combinations of three standard spectra, for example, including a 'multi-colour' disk black-body spectrum[14], gave unacceptable fits. It is not obvious that there is a physical mechanism which could lead to the optically thin thermal bremsstrahlung spectrum observed in this case[15–17], but it fits the second component well. For the lack of a better term we will call it the 'thermal component'. Unsaturated comptonized spectra for the thermal component[13–18] did not improve the fits significantly, but yielded an optical depth of ~9 and an electron temperature of ~4 keV (using a solution to the Komaneets equation by Sunyaev and Titarchuk[18]). Figure 2 shows the correlation of luminosity with temperature for the black-body and the thermal component. Plotted errors are s.d. $(\chi^2+5.9)$ for four parameters of interest[12]. The black-body component is always weaker than the thermal one. The thermal component is stable within 20%, whereas the black-body luminosity varies by a factor of 2.7 without a change in its temperature.

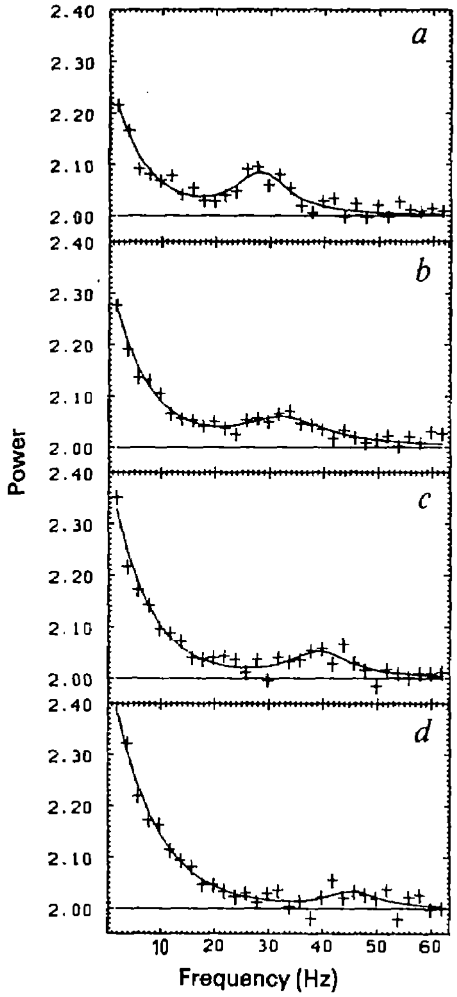

Fig. 1 Average power spectra of Cyg X-2 for four intensity intervals *a*, 800–850 c.p.s.; *b*, 850–900 c.p.s.; *c*, 900–1,000 c.p.s.; *d*, 1,000–1,200 c.p.s. Curved lines, functional least-square fits (see text). The power spectra would follow horizontal lines if there were no intrinsic source signal above counting statistics.

We related the centroid frequency of the QPO to the luminosity of the individual spectral components. A power-law dependence $f \sim L^{\alpha}$ between frequency and black-body-, thermal-, and

---

§ Present address: The Max-Planck-Institut für Extraterrestrische Physik, 8046 Garching, FRG.

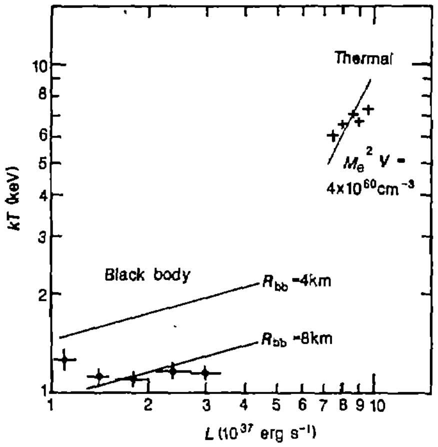

Fig. 2 X-ray luminosity (for a distance of 8 kpc (ref. 9), and assumed isotropic radiation) versus the temperature of the black-body and thermal components. Solid lines: lower left, tracks for constant black-body radii; upper right, the track of thermal bremsstrahlung with a constant emission measure. The luminosity of the thermal component remains approximately constant, but that of the black-body component changes by a factor of ~2.7 without a noticeable change in the black-body temperature. Consequently, the deduced black-body radius changes from ~6 to ~12 km.

total luminosity, yields $\alpha_{BB} = 0.59 \pm 0.05$, $\alpha_{Th} = 2.6 \pm 0.2$, and $\alpha_{tot} = 1.67 \pm 0.14$, respectively. Of course, other functional forms also fit the data.

QPOs with much longer periods and often with higher coherence, are common in cataclysmic variables (see for example, ref. 19). Although their detailed properties vary considerably even in the class of cataclysmic variables, some of them may share a similar origin with QPOs in the bright X-ray sources[1-6]. We restrict our discussion to models which assume a neutron star with considerable magnetic field. We do not imply, however, that non-magnetospheric models (reviewed in ref. 3) can be excluded.

In a model by Bath[20], the oscillations represent the keplerian frequency of plasma clumps (plasmoids) at the magnetospheric boundary. For details see ref. 3; our calculations are identical to theirs, except that we used the magnetospheric radius for disk accretion[21] instead of spherical accretion. For Cyg X-2 we find a magnetic field, B, of 5×10^{10} G, and a corresponding magnetospheric radius, r, of 150 km. The Van der Klis *et al.*[3] data imply very similar values for GX 5-1. The change of frequency with total luminosity is $\alpha_{tot} = 1.7$, also comparable to that for GX 5-1 (ref. 3); however, both are larger than the expected α of 3/7 (refs 3, 20). To explain this discrepancy, Alpar and Shaham[22,23] suggested that the observed frequency is a beat between the keplerian frequency and the neutron star rotation frequency (f_s). This idea was earlier suggested by Warner[24] for dwarf nova oscillations. For a harmonic number[25] $n = 1$ (one intensity maximum per beat cycle), we deduce $f_s = 108 \pm 15$ Hz, $B = (9.9 \pm 1.3)\times10^9$ G, and $r \sim 55$ km. Similar values are obtained for GX 5-1 (ref. 3), where $f_s = 95.2 \pm 3.6$ Hz, $B = 1.8\times10^{10}$ G (disk accretion), and $r \sim 60$ km. Morfill and Trümper[26] suggest a beat-frequency model in which a rotating non-spherically symmetric Alfvén shell excites two plasma density waves interacting with the plasmoids. Here, the harmonic number[25] $n = 2$, and we find $B = (2.2 \pm 0.3)\times10^{10}$ G and $f_s = 54 \pm 8$ Hz.

The relative amplitude (in terms of an r.m.s. equivalent sinusoidal modulation) of the low-frequency noise (LFN) is anticorrelated to that of the QPO. In GX 5-1, the QPO and LFN amplitudes are, however, proportional[3]. This is not the case here, and in Sco X-1, where the QPO can be strong and the LFN nearly absent[6]. In magnetospheric models invoking plasmoids[20,22-26], the LFN is a 'logical consequence' of QPO and its amplitude is in first order expected to follow that of the QPO (however, see ref. 26). For any magnetospheric model it is disturbing that coherent pulsations are not detected. Reasons why they may not be observable (for example, intrinsically weak beaming which is further isotropized in a scattering cloud) are discussed[3,25,27].

In Cyg X-2 and GX 5-1 (refs 2, 3), there is a strong correlation between the frequency of QPO and the total source flux. Recent spectral studies[13-17,28-33] show that many low-mass binaries (including Cyg X-2, GX 5-1, and Sco X-1) have two-component spectra. If the oscillations are of magnetospheric origin the mass accretion rate, $\dot{M}$, onto the magnetosphere (not the luminosity) determines the magnetospheric radius[21] and the oscillation frequency. $\dot{M}$ cannot be unambiguously deduced from the spectra; the results are model dependent. In interpreting the spectra, it is commonly assumed that the disk reaches the neutron star[13-17]. The highly variable black-body component is then attributed to the neutron star—as suggested by the derived black-body radii of order 10 km. The more stable, and more luminous, thermal component is assumed to come from the inner disk. It has been suggested that large variations in the black body component can be produced by small changes in $\dot{M}$ (refs 14-18); in this case the observed black-body flux is not a good measure for $\dot{M}$, but the thermal flux would be. For Cyg X-2, the dependence of frequency on accretion rate ($\alpha' = \mathrm{d}(\log f)/\mathrm{d}(\log \dot{M})$) is then $\alpha_{Th} = 2.6$ (see above).

Lewin and Van Paradijs[34] have pointed out that the above interpretation may be incorrect for low-mass binaries with an evolved companion such as Cyg X-2, where a moderate neutron star magnetic field is expected. For a magnetospheric radius of the order of 10^2 km, any disk component could only contribute a small fraction (~10%) to the total luminosity. An interpretation of the spectra not in conflict with the magnetospheric models assigns the thermal component to the neutron star, and the black-body component to the inner disk. When $\dot{M}$ increases, the neutron star may not be able to accept this increase, if it already radiates close to the Eddington limit. The excess mass would be blown off as an accretion driven wind. This could explain why the thermal flux changes less than the black-body

Table 1 Parameters of the power spectra in four intensity intervals

Interval j	I	II	III	IV
$M(j)$	6,565	5,698	4,951	4,761
I_{min}-I_{max} (c.p.s.)	800–850	850–900	900–1,000	1,000–1,200
I_{mean} (c.p.s.)	818	874	939	1,097
$A(P_{LFN})$	1.75 ± 0.11	2.33 ± 0.15	2.89 ± 0.12	3.96 ± 0.13
B (Hz)	6.3 ± 0.7	6.9 ± 0.6	6.9 ± 0.5	8.2 ± 0.5
$C(P_{QPO})$	1.58 ± 0.2	1.77 ± 0.35	1.13 ± 0.23	0.61 ± 0.20
D (Hz)	28.3 ± 0.6	32.4 ± 1.1	39.4 ± 1.2	45.3 ± 2.0
E (Hz)	6.0 ± 0.6	9.8 ± 1.3	6.9 ± 1.0	6.0 ± 1.8
χ^2/26d.f.	1.27	0.71	1.14	1.22
a_{LFN} (%)	4.63 ± 0.15	5.16 ± 0.17	5.55 ± 0.12	6.01 ± 0.10
a_{QPO} (%)	4.8 ± 0.3	5.0 ± 0.5	4.1 ± 0.4	2.9 ± 0.5
β_{QPO}	0.847	0.800	0.723	0.648
L_{BB} (erg s^{-1})	1.2×10^{37}	1.6×10^{37}	1.9×10^{37}	2.8×10^{37}
L_{Th} (erg s^{-1})	8.0×10^{37}	8.2×10^{37}	8.7×10^{37}	9.7×10^{37}

Parameters of functional fits to the average power spectra in Fig. 1. $M(j)$ is the number of power spectra averaged in the jth intensity interval. I_{min}, I_{max} and I_{mean} are the minimum, maximum and mean count rate (including a background of about 80 c.p.s.). The parameters are: A, integrated power in the LFN; B, e-folding frequency; C, integrated power in the QPO; D, centroid frequency; E, peak HWHM. The reduced χ^2 (26 d.f.) is also given. a_{LFN} and a_{QPO} give the r.m.s. amplitudes of an equivalent sinusoidal modulation of the power in the LFN, and the QPO, respectively: $a_{QPO} = (P_{QPO}/I_{mean} * \beta_{QPO})^{0.5}$; $a_{LFN} = (P_{LFN}/I_{mean})^{0.5}$; β_{QPO} is a window function introduced by the bin size[10]. These amplitudes correspond to those given by Van der Klis *et al.*[3] which should also be regarded as r.m.s. values. L_{BB}, and L_{Th} give the black body and the thermal luminosity (1–20 keV; for a distance of 8 kpc)[9] respectively, interpolated from the spectral fits.

flux, which presumably follows the $\dot{M}$ changes. The appropriate value of α' is then $\alpha_{BB} = 0.59$, in reasonable agreement with the value of 1/3 expected for radiation outside the magnetosphere[23]. A magnetospheric scenario[20] without a beat mechanism could, therefore, fit Cyg X-2.

Other interpretations of the two-component spectra are possible (see refs 27, 28), however, all are very speculative. We can not judge whether either of the two spectral components in Cyg X-2 reflects the mass flux through the magnetospheric boundary layer. The association of spectrally resolved QPO with either of the two components would be a great help in understanding the QPO, and could also give some insight into the physics underlying the two-component spectra.

We thank Jan van Paradijs, Fred Lamb and Bill Priedhorsky for comments on various versions of this manuscript. W.H.G.L. acknowledges a generous award from the Alexander von Humboldt Stiftung and support from the John Simon Guggenheim Foundation.

Note added in proof: Since this paper was submitted, we have observed Cyg X-2 again several times and found QPO in all observations. In the meantime, four more QPO sources have been discovered, so that a total of seven objects are known now. For details see IAU Circulars 4081, 4101, 4102, 4110, 4116, 4117, 4140, 4147 and 4153.

Received 17 July; accepted 13 November 1985.

1. Hasinger, G., Langmeier, A., Sztajno, M. & White, N. E. *IAU Circ.* No. 4070 (1985).
2. Van der Klis, M. *et al. IAU Circ.* No. 4043 (1985).
3. Van der Klis, M. *et al. Nature* **316**, 225 (1985).
4. Middleditch, J. & Priedhorsky, W. *IAU Circ.* No. 4060 (1985).
5. Van der Klis, M., Jansen, F., White, N., Stella, L. & Peacock, A. *IAU Circ.* No. 4063 (1985).
6. Van der Klis, M. *Pap. at NATO Workshop on the Evolution of Galactic X-Ray Binaries*, Schloss Ringberg (1985).
7. Turner, M. J. L., Smith, A. & Zimmermann, H. U. *Space Sci. Rev.* **30**, 513–524 (1981).
8. Peacock, A. *et al. Space Sci. Rev.* **30**, 525–534 (1981).
9. Cowley, A. P., Crampton, D. & Hutchings, J. B. *Astrophys. J.* **231**, 539–550 (1979).
10. Leahy, D. A. *et al. Astrophys. J.* **266**, 160–170 (1983).
11. Langmeier, A., Sztajno, M. & Trümper, J. *Adv. Space Res.* **5**, 121 (1985).
12. Avni, Y. *Astrophys. J.* **210**, 642–646 (1976).
13. Hasinger, G., Pietsch, W., Sztajno, M. & White, N. E. *Pap.* at *ESA Workshop on Cataclysmic Variables and Low-mass X-ray Binaries*, Bamberg (1985).
14. Mitsuda, K. *et al. Publ. astr. Soc. Jap.* **36**, 741–759 (1984).
15. Hasinger, G., Langmeier, A., Pietsch, W. & Sztajno, M. *Space Sci. Rev.* **40**, 233–238 (1985).
16. White, N. E., Peacock, A. & Taylor, B. G. *Astrophys. J.* (submitted).
17. White, N. E. *et al. Mon. Not. R. astr. Soc.* (submitted) (1985).
18. Sunyaev, R. A. & Titarchuk, L. G. *Astr. Astrophys.* **86**, 121–138 (1980).
19. Cordova, F. A. & Mason, K. O. in *Accretion Driven Stellar X-ray Sources* (eds Lewin, W. H. G. and Van den Heuvel, E. P. J.) 147–187 (Cambridge University Press, 1983).
20. Bath, G. T. *Nature phys. Sci.* **246**, 84–87 (1973).
21. Ghosh, P. & Lamb, F. K. *Astrophys. J.* **234**, 296–316 (1979).
22. Alpar, M. A. & Shaham, J. *IAU Circ.* No. 4046 (1985).
23. Alpar, M. A. & Shaham, J. *Nature* **316**, 239 (1985).
24. Warner, B. in *Cataclysmic Variables and related Objects* (eds Livio, M. & Shaviv, G.) 155–172 (Reidel, 1983).
25. Lamb, F. K., Shibazaki, N., Alpar, M. A. & Shaham, J. *Nature* (in the press).
26. Morfill, G. & Trümper, J. *Nature* (submitted).
27. Lamb, F. K. *Pap. at NATO Workshop on the Evolution of Galactic X-Ray Binaries*, Schloss Ringberg (1985).
28. Hirano, T. *et al. Publ. astr. Soc. Jap.* **36**, 769–784 (1984).
29. Kendziorra, E., Collmar, W., Brunner, H., Staubert, R. & Pietsch, W. *Space Sci. Rev.* **40**, 361–366 (1985).
30. Sztajno, M., Trümper, J., Hasinger, G. & Langmeier, A. *Space Sci. Rev.* **40**, 293–296 (1985).
31. Langmeier, A., Sztajno, M., Trümper, J. & Hasinger, G. *Space Sci. Rev.* **40**, 367–370 (1985).
32. Tanaka, Y. *Pap. at NATO Workshop on the Evolution of Galactic X-Ray Binaries*, Schloss Ringberg (1985).
33. Trümper, J. *et al. Space Sci. Rev.* **40**, 255–262 (1985).
34. Lewin, W. H. G. & van Paradijs, J. *Astr. Astrophys.* (in the press).

How old is Cygnus A?

M. J. Spinks, W. G. Rees & P. J. Duffett-Smith

Mullard Radio Astronomy Observatory, Cavendish Laboratory,
Madingley Road, Cambridge CB3 0HE, UK

We have mapped the extragalactic radio source Cygnus A at 81.5 MHz using a two-element interferometer with variable orientation and spacing (maximum 45 km). This is the lowest frequency at which the radio source has been mapped with sufficient resolution (16 arc s) to resolve the bridge of emission joining the two outer lobes, and our data provide new information about the radiation spectrum. By comparing our map with one made at 2.7 GHz, (ref. 1) we have measured the two-point spectral index as a function of distance along the source axis. We estimate the age of the radio source by using a model in which two oppositely directed beams ram their way out through the surrounding medium, depositing relativistic plasma as they do so[2,3]. Synchrotron radiation losses are more severe at high frequencies, causing a break in the spectrum which occurs at progressively lower frequencies as the plasma ages, and our analysis suggests that Cyg A is ~3 Myr old.

Our interferometer, which will be described in detail elsewhere, consisted of part of a large fixed antenna (effective collecting area ~200 m^2) at the observatory near Cambridge, together with a single Yagi antenna (~10 m^2) which we moved around to obtain the desired coverage of the projected aperture plane (the u-v plane). Tracking for a total of 6 h about meridian transit was possible, during which time the data were digitized (1-bit representation) at each antenna and recorded on video cassette tapes in eight contiguous frequency bands of 125 kHz each between 81 and 82 MHz. The signals were later processed using a purpose-built play-back terminal and correlator. We observed the radio source on each of 17 baselines for several consecutive days to check for repeatability and as an insurance against manmade interference. We found that the fringe amplitudes were reproducible to within 5% and that interference was never a serious problem, even when the portable array was set up in the centre of Cambridge itself. The coverage of the u-v plane is shown in Fig. 1.

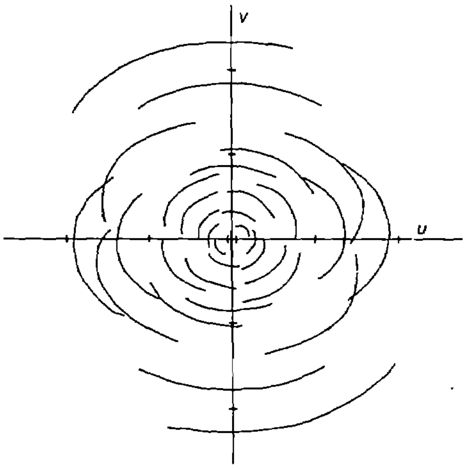

Fig. 1 Coverage of the u-v plane. The pips are at intervals of 5,000λ (18.4 km).

The local oscillators at each antenna were locked to rubidium frequency standards, themselves locked to the ground-wave component of the 100-kHz LORAN-C signals from Sylt (Frisian Islands), which were sufficiently stable to allow coherent integration of the data for periods of at least 45 min. We used an integration time of 1 min so that our fringe amplitudes were not significantly affected by phase drifting. However, we were unable to correct the interferometer fringe phase for the residual random drifting of the local oscillators and ionospheric propagation effects. We therefore used a symmetric double-lobe model of Cyg A and assigned a phase of 0° or 180° to the fringe amplitudes, switching the phase wherever an amplitude passed through a zero. The shapes and magnitudes of the measured amplitudes near zeroes suggested that the antisymmetric component of the radio emission was <20% of the whole at 81.5 MHz, insufficient to cause appreciable error in the calculation of the ages.

The raw map, resulting from Fourier inversion of the measured amplitudes and assigned phases, was processed using

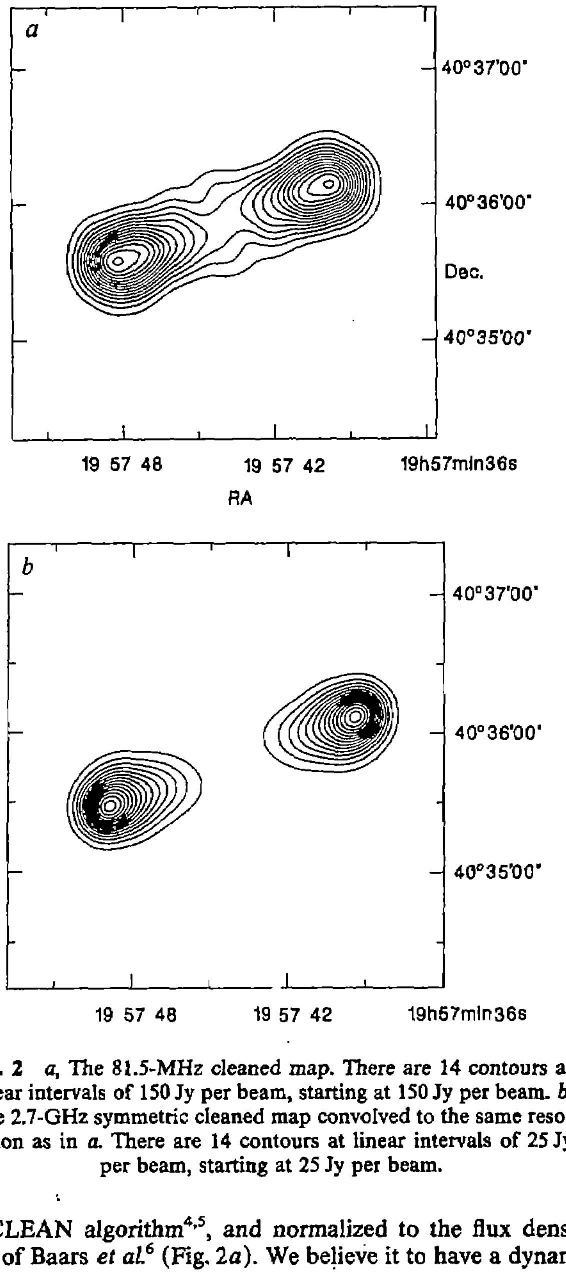

Fig. 2 *a*, The 81.5-MHz cleaned map. There are 14 contours at linear intervals of 150 Jy per beam, starting at 150 Jy per beam. *b*, The 2.7-GHz symmetric cleaned map convolved to the same resolution as in *a*. There are 14 contours at linear intervals of 25 Jy per beam, starting at 25 Jy per beam.

the CLEAN algorithm[4,5], and normalized to the flux density scale of Baars *et al.*[6] (Fig. 2*a*). We believe it to have a dynamic range of more than 15:1, so that the lowest contour drawn in Fig. 2*a* is significant. A 2.7-GHz map made by Alexander *et al.*[1] using the 5-km telescope was processed in a similar fashion and then convolved to the resolution of the low-frequency map (Fig. 2*b*). As expected from the model, the spectral index steepens markedly towards the centre of the radio source.

The age of the plasma, t, depends on the characteristic synchrotron break frequency, ν_T, and the magnetic flux density, B, and is given by[7]

$$t=1.06\times10^{6}(\nu_T B^{3})^{-0.5}\quad \mathrm{s}$$

The magnetic flux density can be estimated by requiring that the total energy within the plasma is a minimum, giving nearly equal partition between the magnetic field and the particles. This leads to the formula[7]

$$B=5.67\times10^{-9}\left[\frac{1+k}{\eta}(1+z)^{(3+\alpha)}\frac{F\nu^{\alpha}}{\theta\Phi S}\times\frac{\nu_2^{(1/2-\alpha)}-\nu_1^{(1/2-\alpha)}}{\frac{1}{2}-\alpha}\right]^{2/7}\quad \mathrm{T}$$

where k (assumed equal to 1) is the ratio of proton to electron energies, η (=1) is the filling factor, F (Jy) is the flux density at frequency ν(GHz) arising from an area of the plasma θ by Φ arc s in extent, S (kpc) is the depth of the region in the line-of-sight, α is the spectral index (flux density proportional to $\nu^{-\alpha}$), ν_1 and ν_2 are the lower and upper frequencies defining the range in which there is significant synchrotron emission (we take $\nu_1 = 10$ MHz and $\nu_2 = 100$ GHz), and z (=0.0574)[8] is the redshift. Our calculations are based on the further assumptions that the source is cylindrically symmetrical about its long axis and lies in the plane of the sky[9], that the injection energy spectrum of the particles is constant in time with the value required to give the observed radiation spectral index (0.6) at low frequencies, and that the Hubble constant $H_0 = 50$ km s^{-1} Mpc^{-1}. Note that the value of B is insensitive to errors in α because of the 2/7 exponent in the above equation; choosing $\alpha = 0.7$ changes the age of the source by ~10%.

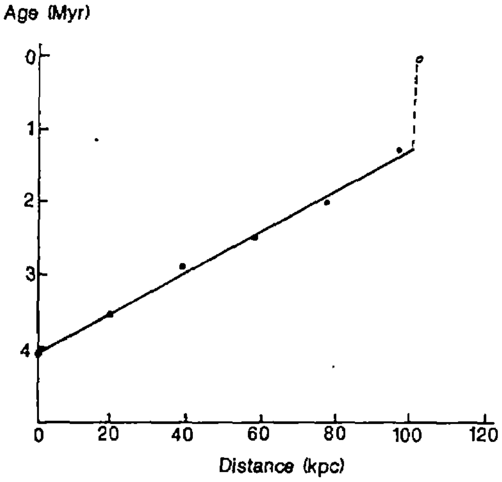

Fig 3 Spectral age versus distance along the axis from the centre of the source. The open circle indicates the positions of the hotspots seen in the full-resolution 2.7-GHz map.

Applying this analysis to our data gives a value of $B = 5.3$ nT, with about 1 nT variation leading to the ages shown in Fig. 3. We deduce that Cyg A itself is ~3 Myr old, on the assumption that the abrupt change in slope at the points where the beams impinge upon the external medium (the 'hotspots') is caused by rapid ageing of the plasma in strong local magnetic fields. Our value is significantly lower than the only previous estimate which was based on a map made at 151 MHz by Winter *et al.*[10], who obtained an age of 6 Myr with the same assumptions. However, their equivalent of Fig. 3 shows considerable curvature. When only the central part of their curve is considered, there is close agreement with our value. The slope of the line in Fig. 3 shows that the hotspots must be moving apart at ~0.11c (where c is the velocity of light) at constant speed over most of the age of the source. The same speed was obtained by Alexander *et al.*[1] by observing spectral ageing within the outer lobes themselves.

The age of the Universe depends on the value of the Hubble constant and cosmological model adopted. Popular values lie in the range 10,000–18,000 Myr. The central galaxy in Cyg A must have been around for a substantial fraction of this time. It seems, therefore, that the phenomenon of double radio emission in this radio source must be comparatively short-lived. The galaxy either erupts once and dies (in radio terms), or else undergoes repeated outbursts. However, we find no evidence of emission from previous recent eruptions which would be expected to show up in a low-frequency map.

We thank many land owners around Cambridge who allowed us to erect the portable outstation and P. Alexander for discussions. M.J.S. acknowledges the support of a studentship from the SERC, and W.G.R. the support of a Research Fellowship at Christ's College, Cambridge.

Received 20 September; accepted 10 December 1985.

1. Alexander, P., Brown, M. T. & Scott, P. F. *Mon. Not. R astr. Soc.* **209**, 851-868 (1984).
2. Rees, M. J. *Nature* **229**, 312-317 (1971).
3. Scheuer, P. A. G. *Mon. Not. R astr. Soc.* **166**, 513-528 (1974).
4. Hogbom, J. A. *Astr. Astrophys. Suppl.* **15**, 417-426 (1974).
5. Clark, B. G. *Astr. Astrophys.* **89**, 377-378 (1980).
6. Baars, J. W. M., Genzel, R., Pauliny-Toth, I. I. K. & Witzel, A. *Astr. Astrophys.* **61**, 99-106 (1977).
7. Pacholczyk, A. J. *Radio Astrophysics*, Ch. 6, 139-161 (Freeman, San Francisco, 1970).
8. Spinrad, H. & Stauffer, J. R. *Mon. Not. R astr. Soc.* **200**, 153-158 (1982).
9. Hargrave, P. J. & Ryle, M. *Mon Not. R astr. Soc.* **166**, 305-327 (1974).
10. Winter, A. J. B. *et al. Mon. Not. R astr. Soc.* **192**, 931-944 (1980).

Ionic origins of carbenes in space

Diethard K. Bohme

Department of Chemistry and Centre for Research in
Experimental Space Science, York University, Downsview,
Ontario, Canada M3J 1P3

Among the many molecules now known to enrich interstellar space are carbenes, molecules which have two electrons available on a carbon atom for chemical bonding. The dicarbenes :C=C: and :C=C=C: occur widely in the Universe, mainly in comets and the atmospheres of carbon stars[1]. Other carbenes, including: :C=S, :C=O, :C=C=C=O and :C=NH, have been identified in cool molecular gas clouds[1]. The origin of these molecules may involve ionizing radiation which, in these environments, can drive reactions between ions and molecules towards the formation of ionic carbene precursors. I now report experiments which suggest that a much higher proportion of the ion chemistry in partially ionized regions in space is directed towards the formation of carbene molecules than has previously been recognized. I identify plausible reaction paths which lead to both known and previously unknown carbenes, such as the cyclopropenylidene ring and long carbon-chain molecules. The cyclopropenylidene ring has recently been reported to be ubiquitous in the Galaxy[2,3], whereas long carbon-chain molecules have been implicated in the origin of diffuse interstellar lines[4].

The reaction paths reported here that lead towards ionic carbene precursors have been identified using the selected-ion flow tube (SIFT) apparatus which allows the measurement of specific reaction rates and product distributions of individual ion/molecule reactions[5,6] Each step in a path towards ionic growth has been studied in isolation. The ion/molecule reactions reported here have all been observed to proceed near the collision rate at room temperature and hence without activation energy. This allows the laboratory results at room-temperature to be applied to the much cooler conditions of interstellar environments.

The atomic carbon ion is fundamental to the proposed carbene ion chemistry. Measurements in our laboratory have shown that C^+ reacts quickly with acetylenes and substituted acetylenes to establish carbene cations. With acetylene for example, the $:C_3H^+$ carbene cation, a resonance hybrid of $HC^+{=}C{=}C:$ and $HC{\equiv}C{-}C:^+$, is established at the collision rate with a reaction rate constant, k, of 2.2×10^{-9} cm^3 molecule^{-1} s^{-1} (ref. 7). Carbene ions of this type are most suited to molecular growth in two important ways. First they may grow heteroatomic chain molecules because of their ability to coordinate to non-bonded electron pairs according to reaction (1), where X is the heteroatom,

$$H(C_2)_n{-}C:^+ + :XR \rightarrow H(C_2)_n^+{=}C{=}X + R \qquad (1)$$

Second, they may grow hydrocarbon-chain molecules because of their tendency for C—H bond insertion according to reaction (2):

$$R(C_2)_n{-}C:^+ + H{-}R' \rightarrow R(C_2)_n{-}CH^+{-}R' \qquad (2)$$

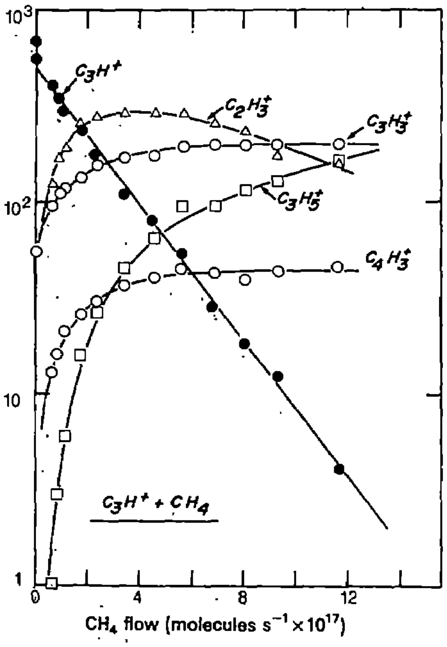

Fig. 1 Variations of ions observed with the addition of methane into the reaction region of a SIFT apparatus in which C_3H^+ has been established initially as the predominant ion[8]. The C_3H^+ is derived from propylene by electron impact at 45 eV. $P = 0.353$ torr, $\bar{v} = 7.4 \times 10^3$ cm s^{-1}, $L = 46$ cm, $T = 297$ K, where P, $\bar{v}$, L and T are the pressure, average flow velocity, reaction length and temperature.

The product ion in reaction (2) may dissociate or lose energy by radiative or collisional stabilization. Reactions of types (1) and (2) will produce unsaturated neutral carbenes in subsequent neutralization reactions. These may involve H atom loss by recombination with an electron or the transfer of a proton to a recipient molecule, M. The neutral carbenes produced in this manner are indicated in reactions (3) and (4)

$$H(C_2)_n^+{=}C{=}X + e(M) \rightarrow :(C{=}C)_n{=}C{=}X + H(MH^+) \qquad (3)$$

$$R(C_2){-}CH^+{-}R' + e(M) \rightarrow R(C{\equiv}C)_n{-}\ddot{C}{-}R' + H(MH^+) \qquad (4)$$

and involve either cumulative double bonds or conjugated triple bonds.

In reactions of type (1), $:C_3H^+$ has been shown to abstract an oxygen atom from various interstellar molecules to form an ion which may give tricarbon monoxide on neutralization[8]. There is also an analogous sulphur chemistry which leads to the prediction of the formation of tricarbon sulphide, $:C{=}C{=}C{=}S$, in the presence of H_2S in the interstellar medium. A higher multi-carbon monoxide ion was also observed to be formed in our laboratory by addition of $:CO$ to $:C_3H^+$, which suggests an analogous addition by radiative association and thus formation of $:C{=}C{=}C{=}C{=}O$ in interstellar regions rich in carbon monoxide. Of course, $:C_3H^+$ itself may neutralize by proton transfer or electron/ion recombination to form the dicarbene $:C{=}C{=}C:$.

Other reactions of C^+ are expected to lead to $:C_3H^+$ and higher members of the homologous $H(C_2)_n{-}C:^+$ series of carbene cations, as well as substituted carbene cations of the type $R(C_2)_n{-}C:^+$. For example, we have observed that C^+ reacts with cyanoacetylene to form $:C_3H^+$ and $:C_4N^+$ in a proportion of 4:1 with $k = 6.1 \times 10^{-9}$ cm^3 molecule^{-1} s^{-1}, and with diacetylene to produce $:C_5H^+$ and $:C_3H^+$ in a proportion of 10:1 with $k = 1.6 \times 10^{-9}$ cm^3 molecule^{-1} s^{-1} (refs 9, 10). Similar reactions with higher polyacetylenes and the known interstellar polycyanoacetylenes[1] should produce the corresponding higher carbene cations $:C_5H^+$, $:C_7H^+ \cdots :(C_2)_n{=}CH^+$ and $:C_6N^+$, $:C_8N^+ \cdots :C^+{-}(C_2)_n{-}CN$. The former groups of ions in turn should spawn the cumulative dicarbenes $:(C{=}C)_n{=}C:$ directly

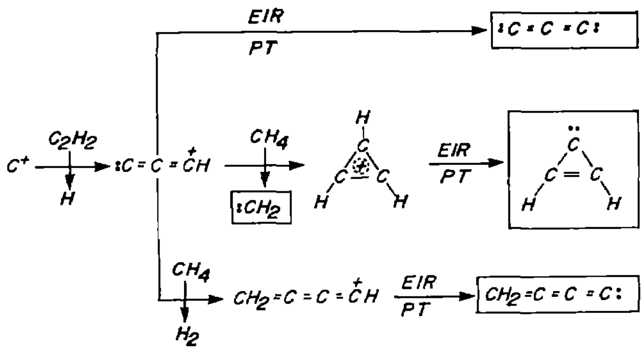

Fig. 2 Ion/molecule reactions which lead to the proposed formation of neutral carbenes from $:C_3H^+$. EIR, electron/ion recombination; PT, proton transfer.

by recombination with electrons or by proton transfer. Reactions with oxygen- or sulphur-bearing molecules will establish higher members of the unsaturated heteroatomic carbenes $:(C_2)_n{=}C{=}O$ and $:(C_2)_n{=}C{=}S$. The reactions of $:C^+{-}(C_2)_n{-}CN$ are uncertain but analogous reactions followed by neutralization by electron transfer could produce non-carbene chain radicals of the type $XC^{\cdot}{-}(C_2)_n{-}CN$, where X may be O or S.

The reaction of $:C_3H^+$ with methane is particularly noteworthy as it allows formation of the cyclopropenylidene ring carbene in only three steps. This reaction has been observed to be rapid, $k = 5.5\times10^{-10}$ cm^3 molecule^{-1} s^{-1}; $C_3H_3^+$ is one of the product ions (Fig. 1). Available thermochemical data dictate that only formation of the cyclopropenium ion is exothermic with methylene as the required neutral product[8]. Neutralization of this ion by electron/ion recombination or proton transfer can lead to cyclopropenylidene. We can therefore anticipate the formation of this ring carbene as well as methylene in ionized interstellar regions containing abundant acetylene and methane in the manner shown in Fig. 2. The formation of $C_3H_3^+$ from the reaction of $:C_3H^+$ with H_2, which has been proposed as an alternative intermediate step in the formation of $:C_3H_2$, is less definitive because both the cyclopropenium and the linear propargyl cations are possible products[11]. Figure 1 also demonstrates that another channel for the reaction of $:C_3H^+$ with CH_4 is the production of $C_4H_3^+$ which may neutralize to form the carbene $:C{=}C{=}C{=}CH_2$. The next member of the homologous series of these carbenes also appears to be accessible, in this case through the reaction of CH_3^+ with diacetylene, which has been seen to produce $C_3H_3^+$ in 1 of 10 reactive collisions with $k = 1.3\times10^{-9}$ cm^3 molecule^{-1} s^{-1} (ref. 10). The $C_5H_3^+$ cation may neutralize to form $:C{=}C{=}C{=}C{=}CH_2$ (or $:CH{-}C{\equiv}C{-}C{\equiv}CH$).

Reactions of type (2) were observed to predominate, with the carbene cations $:C_3H^+$ and $:C_4H^+$ in reactions with HCN, CH_3CN, and HC_2CN. Exclusive addition reactions were observed in our laboratory to proceed with unexpectedly high efficiency at the collision rate[8,9]. The high efficiencies suggest that analogous addition reactions proceed in the interstellar medium by radiative association as in reaction (5)[12].

$$R{-}C:^{+} + H{-}R' \rightarrow R{-}CH^{+}{-}R' + h\nu \qquad (5)$$

Neutralization according to reaction (4) will then produce the carbene. Reactions of type (2) were observed which correspond to the possible formation of the substituted carbenes $:C(C_2H)CN$, $:C(C_2H)CH_2CN$, $:C(C_2H)C_2CN$ and $:C(C_2CN)_2$.

In summary, the observed ion chemistry clearly points towards the formation of many carbenes including methylene, completely unsaturated chain-like carbenes (with some incorporating an oxygen, sulphur or nitrogen atom), slightly hydrogenated chain-like carbenes and one aromatic ring carbene. I have shown that formation of these carbenes can be initiated by rapid reactions of C^+ with simple interstellar molecules. Also, radiative association reactions are proposed which may lead to larger substituted carbene molecules. Formation of all these carbenes should provide further opportunities for molecular growth in the interstellar medium. This growth would not be restricted to reactions with ions but could involve reactions of carbenes with neutral molecules or other carbenes. In terrestrial organic chemistry, carbenes are among the most versatile and synthetically useful reactive intermediates, and they should have a similar function in extraterrestrial chemistry. For example, there are intriguing possibilities for the growth of graphite-like molecules from carbenes with either cumulative double bonds or conjugated triple bonds. Side-on interaction between two carbenes of one type or the other can lead to ring formation through cross-bonding, the inverse of the pyrolitic decomposition of graphite[13]. Alternatively, the long-chain carbenes may aggregate to form small interstellar grains, as suggested by Douglas[4].

I thank the Natural Sciences and Engineering Research Council of Canada for financial support and Mr A. Fox for helpful discussions.

Received 28 August; accepted 22 November 1985.

1. Irvine, W. M. & Hjalmarson, A. in *Cosmochemistry and the Origin of Life* (ed. Ponnamperuma, C.) 113-142 (Reidel, Dordecht, 1983).
2. Vrtilek, J. M., Thaddeus, P. & Gottlieb, G. A. *Bull. Am. astr. Soc.* 17, 568 (1985).
3. Matthews, H. E., Irvine, W. M., Madden, S. C. & Swade, D. A. *Bull. Am. astr. Soc.* 17, 568 (1985).
4. Douglas, A. E. *Nature* **269**, 130-132 (1977).
5. Mackay, G. I., Vlachos, G. D., Bohme, D. K. & Schiff, H. I. *Int. J. Mass Spectrom. Ion Phys.* **36**, 259-270 (1980).
6. Adams, N. G. & Smith, D. *J. Phys.* B9, 1439-1451 (1976).
7. Bohme, D. K., Raksit, A. B. & Schiff, H. I. *Chem. Phys. Lett.* **93**, 592-597 (1982).
8. Raksit, A. B. & Bohme, D. K. *Int. J. Mass Spectrom. Ion Processes* **55**, 69-82 (1984).
9. Raksit, A. B. & Bohme, D. K. *Can. J. Chem.* **63**, 854-861 (1985).
10. Dheandhanoo, S., Forte, L., Fox, A. & Bohme, D. K. *Can. J. Chem.* (in the press).
11. Herbst, E., Adams, N. G & Smith, D. *Astrophys. J.* **285**, 618-621 (1984).
12. Bates, D. R., *Astrophys. J.* **270**, 564-577 (1983).
13. Heimann, R. B., Kleiman, J. & Salansky, N. M. *Carbon* **22**, 147-156 (1984).

An intense cold core eddy in the North-East Atlantic

S. L. Kupferman*, G. A. Becker†, W. F. Simmons‡, U. Schauer†, M. G. Marietta* & H. Nies†

* Sandia National Laboratories, Albuquerque,
New Mexico 87185, USA
† Deutsches Hydrographisches Institut, Postfach 2 20,
2000 Hamburg 4, FRG
‡ Technadyne Engineering Consultants, Woods Hole,
Massachusetts 02543, USA

We describe here a large intense mesoscale feature in the North Atlantic (48° N, 22° W) observed in April 1985. From the thermal structure of this feature at a depth of 475 m (Fig. 1*a*) and from the pattern of larger scale flow (dominated by a nearly rectilinear thermal front (NE–SW), Fig. 1*b*) we conclude that the feature is the eastern basin counterpart of the Gulf Stream cold-core eddies often observed in the western basin[1,2]. To our knowledge, this is the most intense coherent cold-core eddy so far surveyed in this region, and the only such eddy for which data bearing on the mechanism of formation are available.

Western basin cold core eddies are spawned from Gulf Stream meanders that intensify, grow into loops, and pinch off from the main stream to form rings of current that wander independently in the waters to the south and south-east of the Gulf Stream[3]. They are readily distinguishable from other mesoscale features through their water mass properties, characterized by

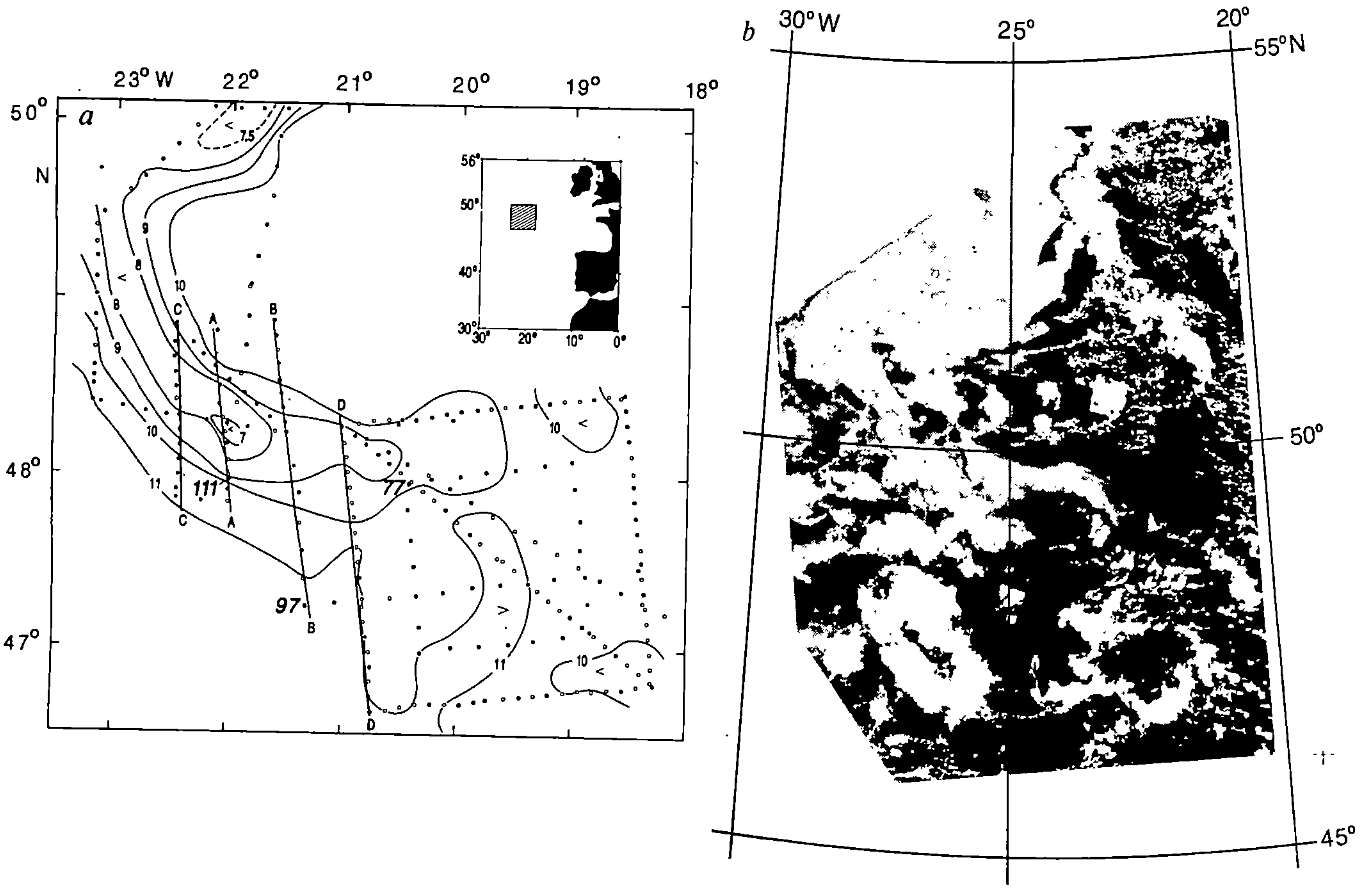

Fig. 1 *a*, Configuration of the cold-core eddy as defined by isotherm patterns at a depth of 475 m. The stations of the 185 km square and diagonal to the south-east were collected synoptically (3 days) at the outset of the cruise. They are primarily Sippican T-7 expendable bathythermographs (XBTs), plotted as open circles. The three north-south sections west of the square (A, B, C) were also synoptic and were occupied 10 days later. The irregular pentagon north and north-west of sections A, B and C was also synoptic and was occupied some 4 days after these sections. The 100-km box to the south-east (which is circumscribed by the 185-km box mentioned above) and the stations within it, were occupied during the 4 days after sections A, B and C were completed. They are mostly Neil Brown CTD stations, plotted as solid circles. *b*, Configuration of the surface temperature field in the neighbourhood of the eddy as defined by Advanced Very High Resolution Radiometric data from the NOAA 9 polar orbiter on 1 April 1985 (Ch. 4, 10.3-11.3 μm). Lighter areas are cooler, darker are warmer. Pure white areas are cloud tops. The NE-SW thermal front that dominates the field is identified as a downstream fragment of the Gulf Stream; that is, an element of the North Atlantic Current System[12]. The feature corresponding to the eddy shown in *a* is roughly centre field, but is well to the north of the position at depth.

otential temperature (θ) and salinity (S). Water interior to the ing is cooler and fresher, like slope water. Water towards the xterior is warmer and saltier, like Sargasso Sea water[3].

The eddy we observed is well-developed, but still attached to he parent current. Based on the 9 °C isotherm at 475 m (Fig. *a*), the eddy is tongue-like in shape, nearly 300 km long (NW-E) and as little as 40 km wide (NE-SW). The minimum bserved temperature at 475 m is 6.8 °C. It is found only 30 km outh-west of the 10 °C isotherm at the same depth.

The vertical structure of the eddy is shown in temperature ection A-A of Fig. 2. We chose this section because the feature as intense and the data were synoptic within the limitations f shipboard expendable bathythermograph/conductivity-emperature-depth (XBT/CTD) work. The temperature section learly shows isotherms rising and falling abruptly, characteristic f a cold-core eddy. The strongest gradients occur on the outhern flank, where the isotherms are regularly spaced. The orthern flank is somewhat gentler, with gradients strongest at epth and weakening toward the surface. Isotherm spacing is regular. We will show that intrusive interleaving of different ater masses occurs; it can cause such irregularities. The width f the feature, as measured by the 9 °C isotherm at 475 m, ppears to be 67 km, but as this section is skew to the eddy axis e actual width is closer to 47 km. The overall vertical isotherm xcursion is about 400 m in the 8-11 °C range. It is 450 m at 10.5 °C. The surface temperature variability across the eddy is about 1.5 °C (cooler in the interior). Therefore the eddy should be detectable by satellite radiometry given sufficient breaks in the clouds (Fig. 1*b*). Deep CTD data taken contemporaneously suggest the eddy structure persists to at least 2,500 m. The eddy signal may in fact penetrate to the bottom (4,400 m), but topography plays an important role in this region[4] and topographically induced signals are strong enough over the bottom 1,000 m to mask eddy signals which are weaker at depth.

Geostrophic shears were calculated from deep CTD stations along section B-B of Fig. 1*a*. The feature there is less intense than in section A-A, but section B-B is longer and its CTD data are more plentiful and better spaced, which is important given the abrupt transitions in water mass properties. Geostrophic shears, with respect to 3,000 m, are strongest above 700 m. The relative velocity at the surface reaches a maximum of 36 cm s^{-1} towards the east along the southern flank of the meander. Considering the coarse resolution, maxima are probably higher. The maximum at 700 m is 19 cm s^{-1}, and at 2,700 m is a few cm s^{-1}. Transports are all towards the east over the southern part of the section, totalling 14 sverdrups (1 Sv = 10^6 m^3 s^{-1}) above 1,200 m and 4 Sv between 1,200 m and 3,000 m for a total eastward transport of 18 Sv. Transports are to the west in the northern part of the section and are generally smaller. The maximum surface current there is 17 cm s^{-1} and the current

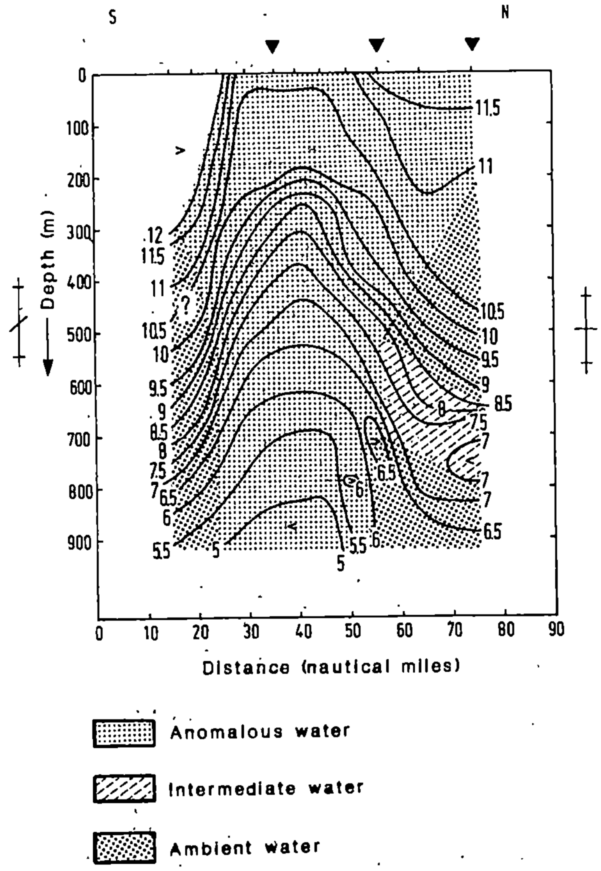

Fig. 2 A temperature section (A–A in Fig. 1*a*) through the eddy core. XBT stations are indicated by hatch-marks; three CTD stations are marked by triangles. The three principal water types, classified according to Fig. 3, are distinguished by stippling. The question mark on the southern flank connotes uncertainty due to the lack of CTD data.

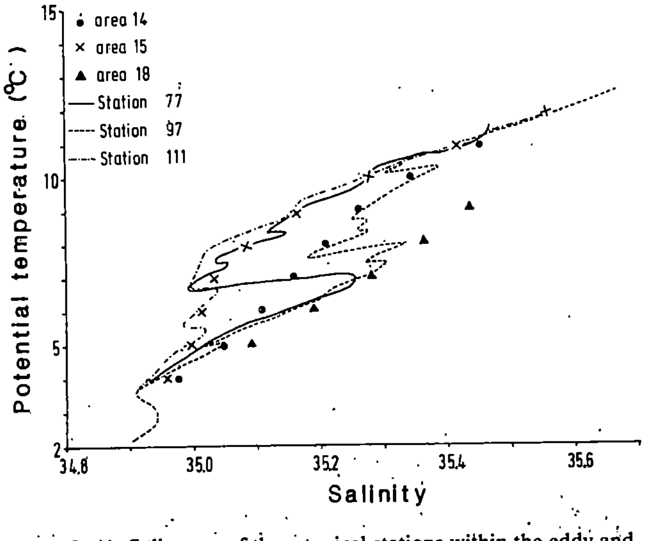

Fig. 3 θ–S diagram of three typical stations within the eddy and three reference θ–S relationships in the North Atlantic[15]. The three typical stations are: *a*, Station 97 (· · · · ·), characteristic of ambient type water; *b*, station 111 (–·–·–), characteristic of anomalous type water, and *c*, station 77 (——), characteristic of an abrupt shift between the two water types. The three reference stations are: *d*, Area 15 (×××), in the nomenclature of Emery and Dewar[15], which is typical of ambient conditions to the west (45° N, 32.5° W); *e*, area 14 (· · ·), typical of ambient conditions in the observed region[15], *f*, area 18 (▲▲▲), typical of ambient conditions northeast of the observed region[15].

at 700 m is 10 cm s^{-1}. Both of these values occur between the northernmost pair of stations. Above 1,200 m, the northernmost three stations show westward flow at 8 Sv whereas below 1,200 m only the northernmost two stations flow westward at 2 Sv. Thus, the eddy tends to lean somewhat to the south (see Fig. 2). The total westward transport observed on the northern flank is 10 Sv. Geostrophic shear calculations from other deep CTD stations give current patterns that are consistent with Fig. 1.

Current meter mooring data of 6 months duration 60 nautical miles to the south-east show brief bursts of speeds up to 20 cm s^{-1} at a depth of 377 m, with more frequent maxima of 10 cm s^{-1} (E. Mittelstaedt, unpublished data). An earlier current meter mooring of 8 months duration at 47° N, 15° W shows a month-long northward outbreak with speeds up to 22 cm s^{-1} at 400 m (ref. 5). It occurs in September, when the surface stratification, and therefore the width and range of influence of the average Subpolar Front, is at a maximum[6]. Thus, the instantaneous eddy kinetic energy associated with the cold-core feature reported here would have to be classified as generally higher than those previously reported[7], and feasible only in the context of a narrow intense branch of the North Atlantic Current System (NACS). On longer timescales, the occurrence of such an eddy once per year could measurably increase the local annual mean eddy kinetic energy.

The idea of eddies in the NACS is not wholly new. Dietrich[6] depicted two blister-like features in the summertime thermal structure of the Subpolar Front at 400 m just west of our survey. His station spacing, however, is not sufficiently dense to establish that the blisters are actually loops; that is, that water from the northwestern side has been drawn southeastwards and been encased in a circulating boundary of North Atlantic Central Water[8] from the southern side of the front. Dickson and Gurbutt saw a similarly sized feature in a temperature section some 300 km to the north[9] and Wegener reported a large-scale topographically induced feature to the west[10]; neither section included salinity. Howe and Tait[11] performed a CTD survey of the upper 500 m of a similarly sized feature about 600 km to the north in July. It too contained anomalous water. However, despite the stronger development of the seasonal thermocline at that time of year, their feature had no surface signature. Moreover, geostrophic shears increased with depth and were weaker than ours by a factor of roughly three. Using θ–S characteristics, they conjectured their feature had formed some 200 km to the west roughly 35 days before observation (based on an estimated migration speed of 0.08 m s^{-1}). A western basin eddy having these characteristics would have been thought of as older[2]. They speculated that their eddy might be attached to a front, but the data were inconclusive. Using satellite-tracked surface drifters, Krauss and Käse[12] have shown the North-West Atlantic to have an abundance of mesoscale features. However, without hydrographic or geochemical data, it is impossible to distinguish features with water property anomalies from those without. In the western North Atlantic, the latter far outnumber the former[13].

Figure 3 summarizes the observed water mass types and configurations based on the variation of their θ–S characteristics with depth; 'ambient water' is relatively warmer and has higher salinities due to the influence of Mediterranean Water. It is typical of the water in the North-East Atlantic[5,14]. Below 1,200 m, ambient water is composed of Subpolar Intermediate Water (SIW). In contrast, 'anomalous water' has θ–S values characteristic of the Newfoundland basin[14,15] to the west. Below 8 °C, anomalous water cools at roughly constant salinity (~35‰), until it too joins the SIW below 1,200 m.

Many of our stations are either wholly ambient or wholly anomalous water. However, most involve both types. Typically, a station will start as one type, then will shift abruptly to the other. Often it will shift back again in an interleaving pattern. There is rarely evidence of intermediate water types. When intermediate water types are suggested, they are limited to thin

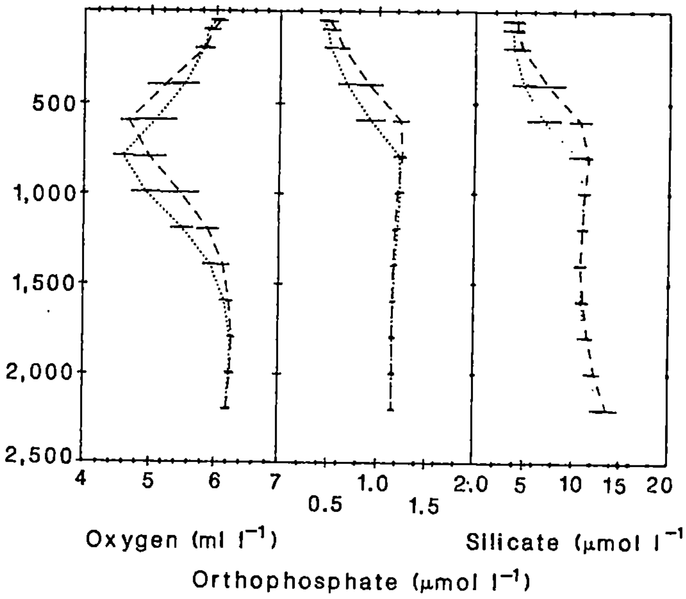

Fig. 4 Oxygen, orthophosphate and silicate profiles from the upper 13 of 24 samples taken throughout the water column. The values at each depth are averaged for ensembles of 39 ambient (···) and 23 anomalous (---) water stations as identified by θ-S characteristics (Fig. 3). The bars indicate one standard deviation.

bands of no more than 50–150 m in thickness. This, the relative intensity of the flow and its proximity to the rectilinear surface feature suggest that the feature is a newly forming cold-core eddy in the NACS.

Regions of ambient, anomalous and mixed water in the eddy are shown in Fig. 2. The pattern which emerges is that of a deep elongated lens of anomalous water riding along the centre and southern flank of the eddy feature, and surrounded on all sides by ambient water. We were unable to occupy a CTD station at the southern extreme of the section shown in Fig. 2, but other observations in the area during the same general time frame ndicate the presence of ambient water to the south of the eddy.

XBT data from a March 1985 cruise in the same area show hat the eddy feature was clearly present at that time on the ection nearest to 21° W (D–D in Fig. 1*b*). It was still present and intense during a mid-May 1985 cruise, although its surface emperature signal had weakened. Its surface salinity signal emained.

By analysing pattern shifts between cruises, it is possible to nfer that the feature as a whole moved to the north-east (~3 km er day) and that its principal axes rotated cyclonically ~0.5 deg per day). The eddy is better developed in mid-May n that more of the isotherms are closed (E. Mittelstaedt, peronal communication). On-board efforts to map the eddy objectively in April show it to be attached to a small current fragment n the north-west corner of the computational domain. Preiminary dynamical forecasts[16] lead to detachment, but the orecasted timescale for detachment is too short.

Analyses for levels of dissolved oxygen, orthophosphate and ilicate were carried out at each station. Compared with ambient water, anomalous water showed larger but similarly distributed oncentrations of phosphate and silicate from 0 to 800 m, with inks at the oxygen minimum that are ~200 m shallower (Fig.). Oxygen profiles were related oppositely down to the oxygen ninimum (~800 m). Below 800 m, anomalous water values are igher. Profile differences are discernible to roughly 1,600 m. herefore, nutrient-depth profiles may be helpful in the idenfication of water mass anomalies. However, when nutrients nd oxygen are plotted against temperature, water types can no nger be positively distinguished. Differences within water pes are about equal to differences between types. This characristic is also observed in western basin eddies[17] and may suggest that the decomposition of organic matter in the two water types is similar and possibly temperature-controlled.

There has recently been a sustained interest in the circulation and variability of the North-East Atlantic. It is an important region in terms of its unique flow characteristics, its position in the general circulation, its relationship to the European continent and the shallow northern seas, and to other applied and specific fields of study including fisheries and waste disposal research. We feel, therefore, that it is important to call attention to the existence of this intense eastern eddy feature with a view towards promoting awareness and stimulating additional hydrographic or other water-mass-sensitive observations in the region.

We acknowledge the support of the Bundesminister für Forschung und Technologie of the FRG and Sandia National Laboratories (SNL) through contract DE-AC04-76DP00789 from the US Department of Energy. We also thank the officers and crew of the RV *Meteor* for their support, the technicians and students of the Deutsches Hydrographisches Institut for analyses, and J. Garner of SNL for computer systems support. Satellite data were provided by M. Eckardt, image processing was performed by W. Tonn of the Freie Universität Berlin. E. Mittelstaedt discussed his May 1985 data with us before publication for which we thank him.

Received 8 July; accepted 30 October 1985.

1. Richardson, P. L. *J. phys. Oceanogr.* **10**, 90–104 (1980).
2. Joyce, T. & Weiler, P. *Oceans* **26**, 2, 34–44 (1983).
3. Richardson, P. L. in *Eddies in Marine Science* (ed. Robinson, A. R.), 17–45 (Springer, New York, 1983).
4. Becker, G. A., Bork, I. & Schauer, U. *Deutsches Hydrographisches Zeitung* **37** (Deutsches Hyrographisches Institut, Hamburg, 1984).
5. Groupe Tourbillon *Deep-Sea Res.* **30**, 475–511 (1983).
6. Dietrich, G. *Atlas of the Hydrography of the Northern North Atlantic Ocean* (Conseil Hydrographique Charlottenlund Slot, Copenhagen, 1969).
7. Dickson, R. R., in *Eddies in Marine Science* (ed. Robinson, A. R.), 278–328 (Springer, New York, 1983).
8. Sverdrup, H. U., Johnson, M. W. & Fleming, R. H. *The Oceans* (Prentice-Hall, Englewood Cliffs, 1942).
9. Dickson, R. & Gurbutt, P. *Polymode News* **74**, 1–9 (Woods Hole Oceanographic Institution, 1980).
10. Wegener, G. *Polymode News* **70**, 3–11 (Woods Hole Oceanographic Institution, 1979).
11. Howe, M. R. & Tait, R. I. *Deep-Sea Res.* **14**, 373–378 (1967).
12. Krauss, W. & Käse, R. H. *J. geophys. Res.* **89**, 3407–3415 (1984).
13. Robinson, A. R. (ed.) *Eddies in Marine Science* (Springer, New York, 1983).
14. Emery, W. J. & Dewar, J. S. *Prog. Oceanogr.* **11**, 219–305 (1982).
15. Wright, W. R. & Worthington, L. V. *Am. Geogr. Soc.* Folio 19 (1970).
16. Robinson, A. R. *et al. Nature* **309**, 781–783 (1984).
17. Wiebe, P. H. *et al. Deep-Sea Res.* **23**, 695–710 (1976).

Nd–Sr–Pb isotope constraints on the sources of West Maui volcano, Hawaii

E. Hegner*†, D. Unruh* & M. Tatsumoto*

* US Geological Survey, PO Box 25046, Denver Federal Center, Denver, Colorado 80225, USA
† Colorado School of Mines, Golden, Colorado 80401, USA

The origin of the Emperor–Hawaiian volcanic chain is attributed to the northwesterly movement of the Pacific plate over a stationary mantle plume (hotspot)[1]. There has been considerable controversy as to the nature and number of sources of Hawaiian hotspot volcanism. Thus far, most geochemical models have been based on rock suites that are not representative of fully developed volcanoes. Nd and Sr isotope ratios and trace element concentrations of volcanics from Haleakala (Maui), where all three volcanic stages are developed, have been interpreted as reflecting a mixing process of two isotopically distinct sources[2,3]. In an attempt to test our earlier multiple-source model[4], we have analysed Pb, Sr and Nd isotope ratios in volcanics from West Maui, the only other volcano with a complete volcanic record. Our results, presented here, indicate at least three isotopically distinct sources, one of which is heterogeneous with respect to Pb. Furthermore, the inferred depleted source for post-erosional volcanics has a Pb and Sr isotope composition intermediate between those of depleted and enriched mid-ocean ridge basalts (MORB, N-type and P-type), suggesting that this source is also heterogeneous.

Maui, located ~100 km north-west of Hawaii, comprises two volcanoes, Haleakala in the east and the smaller West Maui Volcano. All lavas are younger than 1.3 Myr and volcanism in the western part of Maui preceded that of Haleakala, which erupted last in AD 1790[5]. The evolution of fully developed Hawaiian volcanoes can be described by three main phases[6]: (1) the shield-building stage with voluminous tholeiitic basalts; (2) the caldera-filling or late-stage volcanism with both tholeiitic and alkalic rocks; and (3) the post-erosional stage with minor silica-undersaturated rocks (for example, basanites and nephelinites).

Pb, Sr and Nd isotope ratios for our samples from West Maui and Haleakala are listed in Table 1 and are shown in Figs 1-3. Sr and Nd isotope ratios vary inversely for lavas from West Maui, as do those from Haleakala and other Hawaiian volcanoes (Fig. 1). Shield-building tholeiites and caldera-filling alkalic lavas from West Maui volcano alone correlate negatively and plot at the upper end of the Hawaiian data array with indistinguishable Nd and Sr isotope ratios. A close genetic relationship of tholeiites and associated alkali basalts is also indicated for Waianae (Oahu)[4] and Mauna Kea (Hawaii)[7,8]. However, the isotopic dissimilarity of tholeiites and late-stage alkali basalts as seen at Haleakala[2], East Molokai[9] and Kohala[10] indicates a complex genetic relationship between these rock types. Where tholeiites are isotopically distinct from late-stage alkali basalts, they tend to have more enriched Nd and Sr compositions, as is well documented at Haleakala[2]. We regard this as reflecting decreased lithosphere contamination of the tholeiitic magmas due to earlier established conduit systems and thinned lithosphere caused by nearby volcanism. On Hawaii, with five closely spaced volcanoes, the youngest tholeiites are not more enriched isotopically than the older ones. $^{206}Pb/^{204}Pb$ ratios, however, increase progressively along the Kea lineament[7] from Kohala through Mauna Kea to Kilauea (Fig. 3). This indicates, in our opinion, increasing involvement of radiogenic Pb from old uppermost lithosphere (Kea component[7]) in the magma generation process and ongoing lithospheric thinning.

Post-erosional lavas from Maui have similar $^{143}Nd/^{144}Nd$ but lower $^{87}Sr/^{86}Sr$ ratios than the older volcanics, and they plot

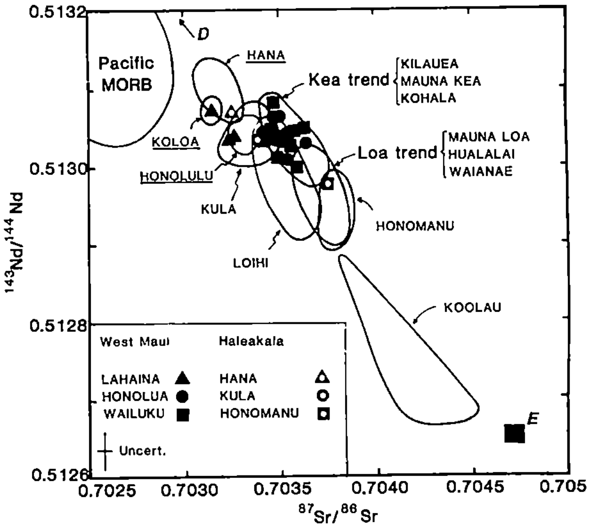

Fig. 1 Plot of $^{87}Sr/^{86}Sr$ versus $^{143}Nd/^{144}Nd$, showing the data from West Maui and other Hawaiian volcanic rocks. Data points for shield-building (Wailuku) and caldera-filling (Honolua) rocks from West Maui are indistinguishable and plot with low $^{87}Sr/^{86}Sr$ ratios at the upper end of the Hawaiian trend. Post-erosional volcanics (Lahaina) from West Maui possess distinctly lower $^{87}Sr/^{86}Sr$ ratios than the associated volcanics and plot like other Hawaiian post-erosional suites (Hana, Koloa, Honolulu, underlined) close to the Pacific MORB field. Also shown are the data for three samples from East Maui (Haleakala); symbols represent same volcanic stages as for West Maui. Inferred enriched (E) and depleted (D) sources are indicated. Data sources: refs 2, 4, 11, 14 and 16.

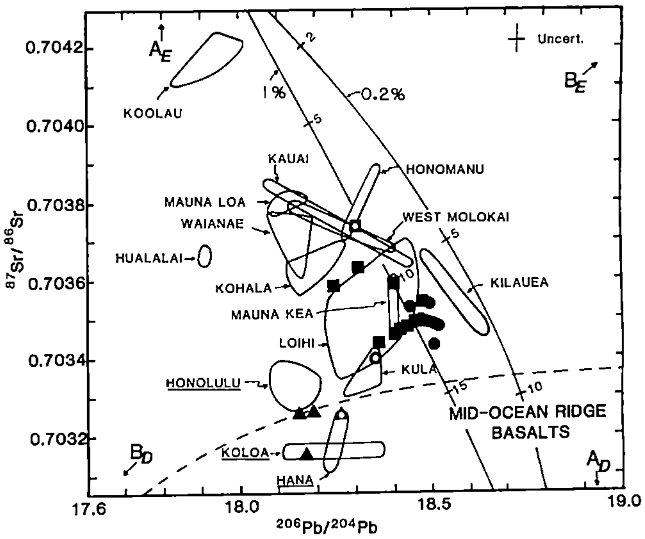

Fig. 2 Plot of $^{206}Pb/^{204}Pb$ versus $^{87}Sr/^{86}Sr$, showing the data of shield-building and caldera-filling samples from West Maui plotting close to the Kilauea apex. The younger post-erosional volcanics have less radiogenic Pb and Sr compositions, similar to other post-erosional rocks, and plot near or in the MORB field. Endmembers are indicated by arrows. Subscripts E and D refer to enriched and depleted sources, respectively. Mixing lines for melts produced by 1% (tholeiites) and 0.2% (post-erosional rocks) melting of a depleted source and 13% and 14% melting of an enriched source are shown. Ticks on mixing lines indicate the proportion of melt from the depleted source. Modelling parameters for tholeiites and post-erosional rocks, Sr concentrations in endmembers and mineral/melt partition coefficients were taken from ref. 2. The Pb mineral/melt partition coefficient was inferred to be 0.001 for all phases. Pb concentrations from ref. 13; the Pb concentration of the enriched source is that of 'mean mantle', which is compositionally similar to the enriched source used in the Haeakala model[2]. Data sources: refs 4, 11, 14, 24; MORB field from ref. 25.

Table 1 Isotope data for Maui volcanics

West Maui		^{143}Nd/^{144}Nd	^{87}Sr/^{86}Sr	^{206}Pb/^{204}Pb	^{207}Pb/^{204}Pb	^{208}Pb/^{204}Pb
Lahaina volcanics*						
C-130	basanite	0.51309±3 0.51311±1	0.70315±3	18.169	15.452	37.750
C-115	basanite	0.51303±2	0.70326±2	18.191	15.460	37.833
HMT 79-5	(C-115)	0.51303±2	0.70325±4 0.70327±3	18.155	15.432	37.735
Honolua volcanics						
C-155	mugearite	0.51304±1	0.70343±4	18.513	15.494	38.050
C-153	hawaiite	0.51304±1	0.70353±3	18.447	15.456	37.917
C-150	mugearite	0.51307±1	0.70349±3	18.502	15.483	38.033
C-149	mugearite	0.51304±6	0.70349±3	18.509	15.489	38.030
C-128	trachyte	0.51303±2	0.70347±3	18.492	15.476	38.003
C-116	trachyte	0.51306±1	0.70348±5	18.523	15.471	37.961
C-92	trachyte	0.51304±2	0.70349±3	18.482	15.466	37.956
HMT 79-1a	(C-92)	0.51303±2	0.70355±4	18.487	15.462	37.947
HMT 79-2b	alkali basalt†	0.51302±3	0.70354±3	18.506	15.560	38.040
Wailuku volcanics						
C-119	tholeiite	0.51304±3	0.70347±4	18.426	15.472	37.904
HMT 79-2a	(C-119)	0.51303±2	0.70356±3	18.462	15.454	37.899
C-118	alkali basalt	0.51305±1	0.70364±4	18.258	15.471	37.762
C-117	tholeiite	0.51301±2	0.70359±2‡ 0.70359±3 0.70361±2	18.404	15.492	37.940
C-114	alkali basalt	0.51303±2	0.70346±4	18.412	15.472	37.906
C-110	tholeiite	0.51305±1	0.70363±3 0.70365±3‡	18.309	15.476	37.874
C-107	tholeiite†	0.51307±1	0.70348±3	18.438	15.499	37.948
C-100	tholeiite	0.51303±1	0.70361±4 0.70344±3†	18.365	15.470	37.877
East Maui (Haleakala)						
Hana volcanics						
C-129	basanite	0.51307±1	0.70325±3	18.259	15.453	37.828
Kula volcanics						
C-127	hawaiite	0.51303±2	0.70339±4	18.351	15.468	37.938
Honomanu volcanics						
C-122	tholeiite	0.51298±2	0.70374±3 0.70374±4	18.303	15.452	37.924

Uncertainties are 2σ of the mean based on in-run statistics; repeated analyses of standards indicate an error of $\sim 2\times 10^{-5}$ in the ^{143}Nd/^{144}Nd ratio for reproduction of data. Ratios are normalized to ^{146}Nd/^{144}Nd = 0.7219 and ^{86}Sr/^{88}Sr = 0.1194. The following standard isotope ratios were measured: ^{143}Nd/^{144}Nd, 0.511856 ± 10 (La Jolla Nd Standard) and 0.512654 ± 20 (BCR-1); ^{87}Sr/^{86}Sr 0.710265 ± 15 (NBS Standard SRM-987), 0.705029 ($n = 2$, BCR-1). Pb isotope ratios are corrected for mass fractionation of 0.12 ± 0.03% per AMU based on analyses of NBS standard SRM-982 and are precise to 0.04% per AMU.

* Formerly designated 'Volcanic Series'. Sample numbers in parentheses indicate that rock types and sampling locations of HMT samples are the same as those of the corresponding C-sample. Sample locations are: C-149, Pohakupue Gulch; C-150, Honolulu Gulch; C-153, rock boulder from Kanaha Stream below Paupau Hill; C-155, Makamakaole Gulch; the remaining samples are from MacDonald's collection[6].

† Analyses from P. Stille *et al.* (personal communication).

‡ Leached samples (6M HCl for 10 h); more than one analysis indicates re-determined values.

lose to the MORB field (Fig. 1), as do other Hawaiian post-rosional volcanics. Chen and Frey[2,3] found that Sr and Nd sotope ratios and the concentrations of some incompatible lements could be reproduced by variable mixing of melts generted from a depleted (MORB-like) and an enriched mantle ource compositionally similar to inferred primitive mantle[11,12]. he high incompatible-element concentrations of the alkalic nd post-erosional volcanics could then be produced by a very w degree of melting of the MORB-like source. The Sr and Pb otope data from West Maui require more than two isotopically istinct sources, as will be shown.

The ^{206}Pb/^{204}Pb–^{87}Sr/^{86}Sr data for Hawaiian volcanics can e modelled with the two sets of endmembers shown in Fig. 2. oth endmember pairs yield analogous results in binary mixing alculations as established for Haleakala. Using endmember set , one can see in Fig. 2 that the data points of shield-building nd caldera-filling volcanics from West Maui and other awaiian islands require a swarm of mixing lines. Pb and Sr ata of shield-building rocks from West Maui can be explained y 9–13% mixing of a melt derived from a MORB-like source ith a melt from a reservoir with a 'mean mantle' composition[13], nce Sr and Pb concentrations are adjusted for crystal fractionion. Mixing calculations using the Haleakala model paraeters for post-erosional lavas indicate that the compositions the latter lie on mixing lines to the right of those for tholeiites d late-stage alkali basalts, in contrast to the situation depicted Fig. 2; this results from the higher incompatibility of Pb compared with Sr in mantle phases[14,15]. Lowering the degree of partial melting of the MORB-like source enriches the melt in MORB-Pb relative to MORB-Sr. Consequently, the melt mixtures have a pronounced MORB-Pb signature and a large variation in their ^{87}Sr/^{86}Sr ratios (Fig. 2). This evidence requires contributions from more than two isotopically distinct sources and requires a more complex magma generation model than that proposed for Haleakala post-erosional lavas. It has been suggested that Hawaiian post-erosional lavas, with their relatively nonradiogenic Pb, could have originated in the uppermost lithosphere[16]. After ~80 Myr (the age of the oceanic crust underlying Hawaii) a MORB-like ^{238}U/^{204}Pb ratio of 20–30 would cause a ^{206}Pb/^{204}Pb ratio of 18.1 to evolve to 18.6. The relatively little radiogenic Pb in post-erosional lavas thus argues against an origin in the uppermost lithosphere.

Figure 3 shows the Pb isotope ratios of West Maui and other Hawaiian volcanics. The data show a wide range and plot on the Hawaiian trend. The apparent Pb isochron with an age of ~950 Myr[7] must be interpreted as a mixing line because at least three components in Hawaiian volcanics are indicated. This conclusion is also supported by the Pb data in Fig. 3, which would lie on a straight mixing line in a two-endmember model. The highly fractionated caldera-filling rocks possess higher ^{206}Pb/^{204}Pb ratios than the shield-building volcanics. This is interpreted as reflecting contamination of the magmas by old oceanic crust with an evolved ^{206}Pb/^{204}Pb ratio during fractionation in shallow magma chambers.

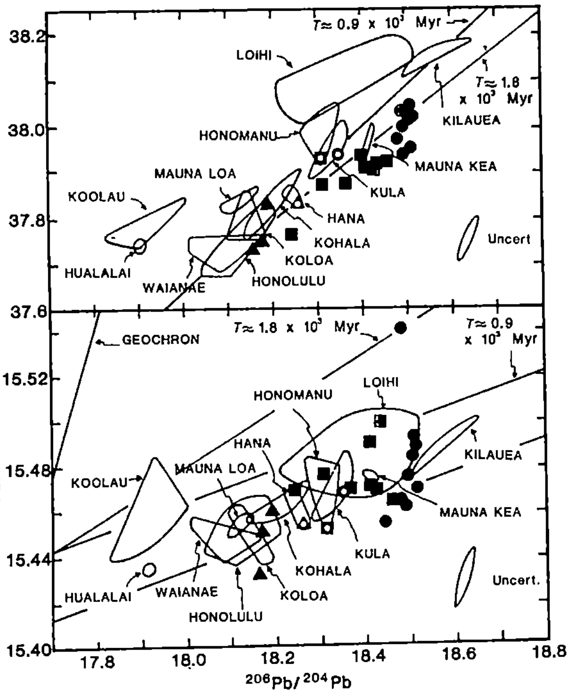

Fig. 3 Relationship of $^{208}Pb/^{204}Pb$ and $^{207}Pb/^{204}Pb$ to $^{206}Pb/^{204}Pb$ for Hawaiian lavas. Shield-building and caldera-filling volcanics from West Maui plot on the more radiogenic side of the Hawaiian trend. Fractionated caldera-filling rocks are slightly more radiogenic in Pb, while post-erosional lavas are less radiogenic in their Pb isotope composition than shield-building volcanics. *T*, Age calculated from the respective lines. Data sources: refs 4, 7, 14, 24.

Three major isotopically distinct sources are required to explain the sources of Hawaiian volcanism: Honolulu-Lahaina, Kilauea and Koolau, although the composition of the pure component will lie beyond the named endmembers (Fig. 2). Figures 1 and 2 show that Honolulu and Lahaina and other Hawaiian post-erosional volcanics plot with comparatively non-radiogenic Pb composition close to the MORB field, suggesting a depleted reservoir as their principal source[6,14,17]. The Pb-Sr relationship indicates that the depleted component in the post-erosional rocks is a mixture of N- and P-type MORB. This delineates the asthenosphere as the probable source region, as has been proposed on the basis of petrological evidence from xenoliths in post-erosional lavas[18].

Kilauea, the second component, is characterized by the most radiogenic Pb and moderately radiogenic Nd. Seismic data reveal that Kilauea and Mauna Loa share a common plumbing system at a depth of 30-50 km[19]. Therefore, their different Pb isotope compositions were probably created in the uppermost lithosphere or crust, our preferred Kilauea source.

Koolau data indicate a component less depleted than the other endmembers, with Sr and Nd ratios close to inferred primitive mantle values[11,12], and low $^{206}Pb/^{204}Pb$ ratios. On this basis we assign this component to the mantle plume fed by a primitive reservoir. He, Ar and Xe isotope ratios indicate the presence in some Hawaiian magmas of a component derived from a long-lived undegassed reservoir[20-22]. Similar analyses on Koolau volcanics would be a useful further test of our hypothesis. The fact that the Koolau component is least represented in Hawaiian volcanics also agrees with both He and Ar isotope evidence indicating a proportion of less than 30% of plume component in the magmas from Kilauea[23].

Our results demonstrate the need for comprehensive geochemical studies on systematically sampled rock suites to elucidate further the magma generation at the Hawaiian hotspot.

We thank P. Lipman and Z. Peterman for commenting on an earlier version of the manuscript, and F. A. Frey for his detailed and constructive criticism.

Received 24 July; accepted 26 November 1985.

1. Wilson, J. T. *Can. J. Phys.* **41**, 863-870 (1963).
2. Chen, C. Y. & Frey, F. A. *Nature* **302**, 785-789 (1983).
3. Chen, C. Y. & Frey, F. A. *J. geophys. Res.* **90**(B10), 8743-8768 (1985).
4. Stille, P., Unruh, D. & Tatsumoto, M. *Nature* **304**, 25-29 (1983).
5. McDougall, I. *Bull. geol. Soc. Am.* **75**, 107-128 (1964).
6. Macdonald, G. A. & Katsura, T. *J. Petrol.* **5**, 82-133 (1964).
7. Tatsumoto, M. *Earth planet. Sci. Lett.* **38**, 63-87 (1978).
8. Frey, F. A. *et al. EOS* **65**, 300 (1984).
9. Clague, D. H., Frey, F. A. & Beeson, M. H. *EOS* **64**(45), 902 (1983).
10. Hofmann, A. W., Raczek, I. & Feigenson, M. D. *Terra Cognita* 4(2), 189 (1984).
11. O'Nions, R. K., Hamilton, P. J. & Evenson, N. M. *Earth planet. Sci. Lett.* **39**, 13-22 (1977).
12. Jacobsen, S. B. & Wasserburg, G. J. *J. geophys. Res.* **84**, 7411-7422 (1979).
13. Davies, G. F. *J. geophys. Res.* **89**(37), 6017-6040 (1984).
14. Sun, S. S. *Phil. Trans. R. Soc.* **A297**, 409-445 (1980).
15. Watson, E. B., Ben Othman, D., Luck, J. M. & Hofmann, A. W. *Terra Cognita* **5**(1), 276 (1985).
16. Staudigel, H. *et al. Earth planet. Sci. Lett.* **69**, 13-29 (1984).
17. Feigenson, M. D., Knorr, R. & Raczek, I. *EOS* **65**(16), 301 (1984).
18. Sen, G. *Earth planet. Sci. Lett.* **66**, 215-228 (1983).
19. Klein, F. W. *J. geophys. Res.* **87**, 7719-7723 (1982).
20. Kaneoka, I. & Takaoka, N. *Earth planet. Sci. Lett.* **39**, 382-386 (1978).
21. Kurz, M. D., Jenkin, W. J. & Hart, S. R. *Nature* **297**, 43-47 (1982).
22. Allegre, C. J., Staudacher, T., Sarda, P. & Kurz, M. *Nature* **303**, 762-766 (1983).
23. Kaneoka, I. *Nature* **302**, 698-700 (1983).
24. Unruh, D., Stille, P. & Tatsumoto, M. *EOS* **64**(18), 347 (1983).
25. White, W. M. *Geology* **13**, 115-118 (1985).

Carbon and sulphur isotopic composition of Kilauea parental magma

Terrence M. Gerlach

Geochemistry Division, 1543, Sandia National Laboratories,
Albuquerque, New Mexico 87185, USA

Donald M. Thomas

Hawaii Institute of Geophysics, University of Hawaii,
2525 Correa Road, Honolulu, Hawaii 96822, USA

All the available data for the isotopic composition of carbon in gases emitted from summit fumaroles at Kilauea volcano, Hawaii, indicate that the carbon is enriched in ^{13}C compared with oceanic tholeiite and in contrast to most estimates for the isotopic composition of mantle carbon[1-6]. Several mechanisms proposed to explain this enrichment of ^{13}C have proved unsatisfactory[2]. We show here that recent models[7,8] for the volatile contents and degassing of Kilauea magma permit a satisfactory reinterpretation of carbon and sulphur isotope data[1-3,9,10] for Kilauea. The results indicate that Kilauea parental magma is significantly enriched in ^{13}C compared with mid-oceanic basalts and with inferred isotopic compositions for mantle carbon[3-6]. Hence, mantle sources of hotspot and mid-oceanic basalts may differ in $\delta^{13}C$. In contrast, the isotopic composition of sulphur in Kilauea parental magma is similar to that of mid-oceanic basalts[11].

Kilauea volcano is detached from the south-east shield of Mauna Loa volcano by east and south-west rifts (Fig. 1)[12]. The roof of the summit magma chamber is approximately 2 km under the caldera and 1 km under Halemaumau pit crater[13]. Mantle sources at 30-90 km depth supply parental magma to the chamber[14-16]. The chamber has been described as a dyke-and-sill complex with a floor at 6 km, a crown at 1-2 km, and an east-rift duct at 1-2 km connected to the east-rift magma reservoirs[12,17,18]. Communication between the summit and south-west rift reservoirs is poorly defined[19,20]. A relatively steady supply of magma inflates the summit chamber before being discharged to the surface or into the rifts[20,21].

According to a recent model[7], the melt fraction of the parenta magma contains approximately 0.30 wt% H_2O, 0.65 wt% CO_2 and 0.13 wt% S. Because parental melt saturates in CO_2 long before reaching the summit chamber, the processes of reservoir equilibration during residence at the summit include separation of excess volatiles in a chamber gas containing about 90 vol.% CO_2, 10 vol.% SO_2 and minor H_2O. Chamber-gas venting o

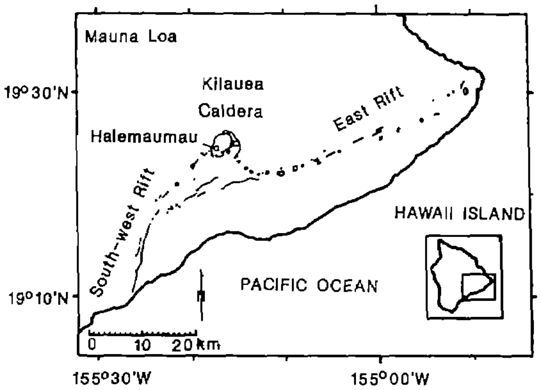

Fig. 1 Sketch map of Kilauea volcano, Hawaii. The east rift extends along its subaerial north-east trend for ~70 km under the sea.

CO_2 occurs at the impressive rate of 3,600 tons per day. The reservoir-equilibrated melt contains approximately 0.27 wt% H_2O, 0.07 wt% S and 0.02–0.10 wt% CO_2 (depending on the depth of equilibration). Thus, most of the parental CO_2 is degassed from the summit chamber. An alternative model[8], derived from different geochemical data, proposes similar volatile contents and reservoir equilibration processes for Kilauea magma. Reservoir-equilibrated magma is ultimately erupted in the summit region or injected into the rifts, from which it may subsequently be discharged during subaerial and submarine eruptions.

Three early CO_2 samples from Sulphur Bank fumarole just north-east of the caldera show a range of $\delta^{13}C$ values of −3.4 to −3.2‰ relative to the PDB standard (Table 1). D.M.T.[2] collected gas samples between 1975 and 1977 from Sulphur Bank and from the 1971 and 1974 fissure fumaroles formed during summit eruptions on the southern edge of the caldera, directly above the summit chamber. The temperature of the 1971 fissure fumarole was 140 °C and it emitted H_2O, CO_2 and SO_2 with small amounts of H_2S, N_2 and trace rare gases. The fumaroles sampled at Sulphur Bank and the 1974 fissure were at the local boiling point (96 °C) and emitted gases much poorer in sulphur. Sampling, extraction and analytical procedures have been described in detail elsewhere[2]. The results (Table 1) yield an average $\delta^{13}C$ of −3.2‰. Duplicate samples showing $\delta^{13}C$ differences as large as those between samples collected several months apart are apparently caused by Rayleigh distillation processes related to cyclic accumulation and flashing of water at shallow depths[2].

Table 1 $\delta^{13}C$ values for Kilauea summit fumaroles

Site	Ref.	Date	$\delta^{13}C$ (‰)
Sulphur Bank	1	Not given	−3.2, −3.3, −3.4
Sulphur Bank	2	5 Aug. 1975	−3.19, −2.62
		18 Aug. 1975	−3.43
		8 Nov. 1975	−2.29, −3.24
		Dec. 1975	−3.01, −2.54
		13 Aug. 1976	−3.42
		17 Aug. 1976	−3.37
		13 Oct. 1976	−3.61, −3.01
		1 Dec. 1976	−2.68
		28 Dec. 1976	−3.51
		28 Jan. 1977	−3.3
1971 fissure	2	13 Aug. 1975	−3.35
		19 Aug. 1975	−3.21
		8 Nov. 1975	−3.29
		1 Dec. 1975	−3.19, −3.31
		9 Aug. 1976	−3.18, −3.28
		26 Aug. 1976	−3.41
		13 Oct. 1976	−2.81, −3.50
		1 Dec. 1976	−3.19
		28 Dec. 1976	−4.16
		29 Dec. 1976	−3.57
		29 Jan. 1977	−3.4
1974 fissure	2	29 Jan. 1977	−3.13
		10 Feb. 1977	−2.95

Table 2 Estimated $\delta^{13}C$ values for Kilauea chamber gas and parental magma

$\Delta^{13}C_{g-m}$	$\delta^{13}C_{cg}$	$\delta^{13}C_{pm}$*	$\delta^{13}C_{pm}$†
3.8	−3.2	−3.5	−3.6
4.0	−3.0	−3.3	−3.4
4.3	−2.7	−3.0	−3.1

All units are ‰.
* $(wt\%\ CO_2)_{rem} = 0.049$, $(wt\%\ CO_2)_{pm} = 0.65$ (ref. 7).
† $(wt\%\ CO_2)_{rem} = 0.03$, $(wt\%\ CO_2)_{pm} = 0.32$ (ref. 8).

Because most parental CO_2 is vented from the summit chamber[7,8], the $\delta^{13}C$ of parental magma may be similar to the fumarole value. We have tested this hypothesis with simple equilibrium and mass-balance models based on the assumptions: (1) that Rayleigh fractionation by continual loss and isolation of carbon in exsolved CO_2 is minimal during transport from the mantle and (2) that carbon in the chamber gas approaches isotopic equilibrium with carbon in co-genetic reservoir-equilibrated melt. Recent work[3] has shown that Rayleigh fractionation effects on carbon isotopes are minimal during exsolution associated with the ascent and eruption of mid-oceanic basalt at seafloor depths >500 m. Thus, it is reasonable to assume that the same is true for the exsolution of CO_2 at considerably higher pressures from ascending Kilauea parental melt. Assumption (2) is supported by observations[3] that the distribution of carbon isotopes between CO_2 in vesicles and the glass of mid-oceanic basalts corresponds closely to the experimentally determined equilibrium fractionation[22].

For equilibrium fractionation of carbon isotopes between chamber gas and reservoir-equilibrated melt, the $\delta^{13}C$ for chamber gas ($\delta^{13}C_{cg}$) can be expressed as

$$\delta^{13}C_{cg} = \delta^{13}C_{rem} + \Delta^{13}C_{g-m} \qquad (1)$$

where $\delta^{13}C_{rem}$ is the $\delta^{13}C$ for reservoir-equilibrated melt and $\Delta^{13}C_{g-m}$ is an approximation to the ‰ fractionation factor (1,000 ln α_{g-m}) for carbon isotopes between CO_2 gas and basaltic melt. The value for $\Delta^{13}C_{g-m}$ has been determined from experimental products[22] and samples of seafloor basalt[3]. The experimental data[22] give a mean value of 4.3 for seven experiments over a temperature range of 1,120°–1,280 °C at 7–8.5 kbar; temperature dependence is insignificant at the 95% confidence level. The mean $\Delta^{13}C_{g-m}$ calculated from isotope data for four seafloor basalts[3] is 3.8. Therefore, we have used $\Delta^{13}C_{g-m} = 3.8$–4.3 in our calculations. Recent carbon isotope data for submarine lavas along the east rift[3] provide an estimate for $\delta^{13}C_{rem}$. The $\delta^{13}C$ values for these flows at depths >500 m vary from −9 to −5‰, with a mean value of −6.2‰. The data support the interpretation[3], however, that most of the lavas are derived from shallower portions of the rift storage system, which tend to accumulate CO_2-rich bubbles that are either carried into the rift from the summit chamber or exsolved during subsequent crystallization or depressurization associated with transport in the rift. As a result of ^{13}C-enrichment in CO_2 gas relative to melt, the mean $\delta^{13}C$ for these flows is thought to be too high to be characteristic of the bulk of the reservoir-equilibrated magma[3]. Therefore, in our calculations we have used the intermediate value of −7‰ for $\delta^{13}C_{rem}$.

Our results (Table 2) are similar to the $\delta^{13}C$ data for the summit fumaroles (Table 1), suggesting that CO_2 degassed from the summit chamber is the principal source of summit fumarole carbon. Moreover, they suggest that carbon isotopes in CO_2 vented from the summit chamber experience little fractionation in transit to the summit fumaroles, despite evidence for some carbonate alteration product formation in the hydrothermal system overlying the summit chamber[23].

The $\delta^{13}C$ for the parental magma ($\delta^{13}C_{pm}$) can be estimated from the conservation of CO_2 and carbon isotopes among parental magma, reservoir-equilibrated magma and chamber gas. This approach yields the mass-balance equation

$$\delta^{13}C_{pm} = \delta^{13}C_{cg} + \frac{(\text{wt\% } CO_2)_{rem}}{(\text{wt\% } CO_2)_{pm}}(\delta^{13}C_{rem} - \delta^{13}C_{cg}) \qquad (2)$$

We have evaluated equation (2) for the same set of data as was used to calculate $\delta^{13}C_{cg}$. The CO_2 concentrations are based on two models for the volatile contents and degassing of Kilauea magma[7,8]: one model[7] gives 0.65 wt% CO_2 for the parental melt and 0.049 wt% CO_2 for reservoir melt equilibrated at an average depth of 3 km; the other[8] gives corresponding values of 0.32 wt% CO_2 and 0.03 wt% CO_2. Because the concentration ratio in equation (2) is similar for each model, the estimates for $\delta^{13}C_{pm}$ summarized in Table 2 are in close agreement and lie in the range −3.6 to −3.0‰.

The $\delta^{13}C_{pm}$ values clearly support the hypothesis that carbon in parental magma isotopically resembles fumarole carbon and is similarly enriched in ^{13}C compared with mid-oceanic basalt ($\delta^{13}C = -4.5$ to -8‰)[3,4,6] and with recent estimates for mantle carbon ($\delta^{13}C = -5$ to -7‰)[3]. Performing the calculations for $\delta^{13}C_{rem} = -6.2$‰, the mean value for east-rift submarine basalts[3], gives even heavier parental carbon. If some Rayleigh fractionation is assumed during vapour exsolution, the estimated value for $\delta^{13}C_{pm}$ is also increased. Moreover, note that for $\delta^{13}C_{pm}$ to have a value in the range considered characteristic of mantle carbon, the parental CO_2 concentration would have to be reduced to ~0.07 wt%, which would imply summit CO_2 emissions of ~120 tons per day—that is, more than an order of magnitude lower than the observed rate[8]. Finally, fractionation and contamination mechanisms that may operate in the hydrothermal/fumarole system either are unable to transform carbon with $\delta^{13}C$ in the range considered characteristic of the mantle to that with $\delta^{13}C$ characteristic of the fumaroles, or they require removal of unrealistically large amounts of CO_2 as carbonate[2].

Turning to sulphur, recent work[9,10] provides $\delta^{34}S$ data for east-rift submarine basalts, subaerial Kilauea lava (flows, spatter tephra, bombs), shallow dykes and summit fumarole gases (the 96 °C Jaggar well fumarole at Sulphur Bank, a 128 °C 1971 fissure fumarole and a 145 °C 1974 fissure fumarole). $\delta^{34}S$ as used here refers to total sulphur (sulphide plus sulphate) in ‰ relative to the Canyon Diablo troilite standard. In reinterpreting these data, we assume Rayleigh fractionation during subaerial eruptive degassing, and estimate the fractionation factor ($\alpha_{g\text{-}m}$) for sulphur isotopes between gas and melt phases from the equation

$$\delta^{34}S_{rem} - \delta^{34}S_{rsd} = 1{,}000 \ln f^{\alpha-1}_{g\text{-}m} \qquad (3)$$

The weight fraction of sulphur remaining in lava after eruptive degassing ($f = 0.214$) is calculated from the residual sulphur content of glassy fountain spatter (150 parts per 10^6, p.p.m.)[24] and the sulphur content of the reservoir-equilibrated melt (700 p.p.m.)[7,9,10,25]. $\delta^{34}S_{rem}$ values fall in a narrow range around 0.7‰, based on data for east-rift submarine basalts[9,10]. $\delta^{34}S_{rsd}$, the analogous quantity for the residual sulphur, has a value of −0.4‰, based on the mean of data reported for spatter, bomb and shallow dyke samples[9]. The $\delta^{34}S_{rsd}$ value used here does not include data for lava flows, which can continue to degas during flow after release of eruptive gases[24]. The resulting value for $\alpha_{g\text{-}m}$ is 1.00075.

We used an equation analogous to equation (1), with $\Delta^{34}S_{g\text{-}m} = 1{,}000 \ln \alpha_{g\text{-}m} = 0.75$, to calculate $\delta^{34}S_{cg} = 1.5$‰. From an equation analogous to equation (2), we estimate that $\delta^{34}S_{pm} = 1.1$‰, in agreement with data for mid-oceanic basalts ($\delta^{34}S = -1$ to 2‰)[11,26-28]. The $\delta^{34}S_{cg}$ value is higher than that measured for the 1971 and 1974 fissure fumaroles (0.9‰)[9] but considerably lower than that observed for Sulphur Bank (8.0‰)[9]. The high value at the Sulphur Bank boiling-point fumarole is probably the result of fractionation associated with precipitation of sulphur by reaction of H_2S and SO_2 in the presence of liquid water. We attribute the difference in $\delta^{34}S$ values between the chamber gas and fissure fumaroles to loss of heavy sulphur during sulphate formation in hydrothermal processes adjacent to the summit chamber. Sulphate formation by disproportionation of chamber-gas SO_2 would produce fumarole gases relatively depleted in ^{34}S compared with the chamber gas[29]. Loss of chamber-gas SO_2 in this manner is consistent with the observations that measured abundances of SO_2 emitted in the summit region[30,31] are smaller than SO_2 discharges predicted for the summit chamber[7].

Thus, we conclude that Kilauea parental magma is significantly enriched in ^{13}C compared with mid-oceanic basalt and in contrast to previous estimates of the isotopic composition of mantle carbon, although it is similar to mid-oceanic basalt in sulphur isotope composition. Moreover, massive chamber degassing of CO_2 effectively buffers the isotopic composition of carbon in the summit hydrothermal system and the summit fumaroles at values close to that of the parental magma, while sulphur isotopes in the chamber-gas discharge are significantly fractionated by reactions in the hydrothermal system.

The simplest explanation for enrichment of heavy carbon in Kilauea parental magma is a mantle with isotopically heterogeneous carbon, thereby permitting sources of hotspot and mid-oceanic basalt to differ in $\delta^{13}C$. Most models for the petrogenesis of Hawaiian tholeiite infer volatile components to have a deep, undepleted mantle source[16,32]. The present results indicate that the source is enriched in heavy carbon, which in turn suggests an oxidized chemical form such as carbonate or CO_2. To render our results consistent with a mantle in which carbon is isotopically homogeneous[6], it is necessary to assume (1) that carbon in the mantle and in the parental magmas of mid-oceanic basalt is heavier than the carbon observed in the seafloor lavas and (2) that an early stage of degassing analogous to Kilauea summit-chamber degassing removes heavier carbon from mid-oceanic basalt before it is extruded on the sea floor.

This work was supported at Sandia National Laboratories by the Office of Basic Energy Research, US Department of Energy under contrast DE-AC04-76DP00789. We thank H. Craig, L. P. Greenland and T. J. Casadevall for stimulating discussions.

Received 19 July; accepted 31 October 1985.

1. Craig, H. in *Nuclear Geology on Geothermal Areas* (ed. Tongiorgi, E.) 17-53 (Consiglio Nazionale Della Ricerche, Laboratorio Di Geologia Nucleare, Pisa, 1963).
2. Thomas, D. M. thesis, Univ. Hawaii (1977).
3. Des Marais, D. J. & Moore, J. G. *Earth planet. Sci. Lett.* **69,** 43-57 (1984).
4. Pineau, F., Javoy, M. & Bottinga, Y. *Earth planet. Sci. Lett.* **29,** 413-421 (1976).
5. Deines, P. *Geochim. cosmochim. Acta* **44,** 943-961 (1980).
6. Pineau, F. & Javoy, M. *Earth planet. Sci. Lett.* **62,** 239-257 (1983).
7. Gerlach, T. M. & Graeber, E. J. *Nature* **313,** 273-277 (1985).
8. Greenland, L. P., Rose, W. I. & Stokes, J. B. *Geochim. cosmochim. Acta* **49,** 125-129 (1985).
9. Sakai, H., Casadevall, T. J. & Moore, J. G. *Geochim. cosmochim. Acta* **46,** 729-738 (1982).
10. Sakai, H., Des Marais, D. J., Ueda, A. & Moore, J. G. *Geochim. cosmochim. Acta* **48,** 2433-2441 (1984).
11. Puchelt, H. & Hubberten, H.-W. *Init. Rep. DSDP* **51, 52, 53, 54,** Pt 2, 1145-1148 (1980).
12. Swanson, D. A., Duffield, W. J. & Fiske, R. S. *U.S. geol. Surv. prof. Pap.* **963,** 1-39 (1976).
13. Ryan, M. P., Blevins, J. Y. K., Okamura, A. T. & Koyanagi, R. Y. *J. geophys. Res.* **88,** 4147-4181 (1983).
14. Eaton, J. P. in *The Crust of the Pacific Basin* (ed. Endo, E. T.) 13-29 (American Geophysical Union, 1962).
15. Ellsworth, W. L. & Koyanagi, R. Y. *J. geophys. Res.* **82,** 5379-5394 (1977).
16. Wright, T. L. *J. geophys. Res.* **89,** 3233-3252 (1984).
17. Ryan, M. P., Koyanagi, R. Y. & Fiske, R. S. *J. geophys. Res.* **86,** 7111-7129 (1981).
18. Wright, T. L. & Fiske, R. S. *J. Petrol.* **12,** 1-65 (1971).
19. Duffield, W. A., Christiansen, R. L., Koyanagi, R. Y. & Peterson, D. W. *J. Volcanol. geotherm Res.* **13,** 273-307 (1982).
20. Dzurison, D., Koyanagi, R. Y. & English, T. T. *J. Volcanol. geotherm. Res.* **21,** 177-206 (1984)
21. Macdonald, G. A. & Abbott, A. T. *Volcanos in the Sea* (University Press of Hawaii, 1974)
22. Javoy, M., Pineau, F. & Iiyama, L. *Contr. Miner. Petrol.* **67,** 35-39 (1978).
23. Keller, G. V., Grose, L. T., Murray, J. C. & Skokan, C. K. *J. Volcanol. geotherm. Res.* **5** 345-385 (1979).
24. Swanson, D. A. & Fabbi, B. P. *J. Res. U.S. Geol. Surv.* **1,** 649-658 (1973).
25. Moore, J. G. & Fabii, B. P. *Contr. Miner. Petrol.* **33,** 118-127 (1971).
26. Kanehira, K., Yui, S., Sakai, H. & Sasaki, A. *Geochemistry* **7,** 89-96 (1973).

27. Grinenko, V. A., Dmitriev, L. V., Migdisov, A. A. & Sharaskin, A. Ya. *Geochem. Int.* **1975**, 132-137 (1975).
28. Sakai, H., Ueda, A. & Field, C. W. in *Short Pap. 4th int. Conf. Geochronology, Cosmochronology and Isotope Geology* (ed. Zartman, R. E.) 372-374 (US Geological Survey Open-File Report 78-701, 1978).
29. Ohmoto, H. & Rye, R. O. in *Geochemistry of Hydrothermal Ore Deposits* (ed. Barnes, H. L.) 509-567 (Wiley, New York, 1979).
30. Stoiber, R. E. & Malone, G. B. *EOS* **56**, 461 (1975).
31. Casadevall, T. J. & Hazlett, R. W. *J. Volcanol. geotherm. Res.* **16**, 173-188 (1983).
32. Sen, G. *Earth planet. Sci. Lett.* **62**, 215-228 (1983).

Calcium anomalies in the mantle and a subducted metaserpentinite origin for diamonds

Daniel J. Schulze*

Geophysical Laboratory, Carnegie Institution of Washington,
Washington, DC 20008, USA

Most natural diamonds are thought to have formed within the upper mantle, before transport to the surface by kimberlites or lamproites, in a magnesian, calcium-poor, garnet-bearing harzburgite or dunite. Serpentinites, formed by hydration of oceanic lithosphere, are sufficiently poor in calcium and have high enough Mg/(Mg+Fe) values that, following subduction and prograde metamorphism to ~1, 100 °C, 55–60 kbar, they would equilibrate as such harzburgites and dunites. Diamonds may be the high-pressure equivalent of graphite produced, or introduced, during serpentinization. The apparent restriction of diamonds and low-Ca garnet xenocrysts to cratons may result from the fact that subducted metaserpentinites, lodged within the mantle beneath the cratons, have been effectively isolated from participation in subsequent tectonic and magmatic events that occurred outside the craton margins.

The most important constraint on the origin of diamonds is imposed by the composition of the minute syngenetic mineral inclusions that occur in some diamonds. These minerals are considered to have been in stable coexistence with their host diamond at the time of their inclusion[1,2], so their compositions can yield valuable information concerning the chemical environment and ambient pressure and temperature during diamond formation. The composition of these mineral inclusions has been well documented (see refs 1-4). Most syngenetic mineral inclusions belong to one of two suites, a peridotitic suite and an eclogitic suite, corresponding to the two most abundant types of ultramafic xenoliths found in kimberlites. Just as peridotite xenoliths are more abundant than eclogite xenoliths, the peridotitic inclusions in diamonds are more common than are eclogitic suite inclusions.

There are, however, distinct and important differences in paragenesis and chemical composition between the minerals included in diamonds and most of their xenolithic counterparts. Within the peridotite suite of diamond inclusion minerals diopside is rare. Most assemblages represent a garnet-bearing dunite or harzburgite paragenesis (olivine ± garnet ± orthopyroxene ± chromite), which is also reflected in the Mg-rich and Ca-poor mineral compositions. Most peridotitic garnets and orthopyroxenes found as inclusions in diamonds have calcium contents too low to have been in equilibrium with diopside[5]. This situation is in stark contrast to the fact that garnet lherzolites are the most abundant variety of upper mantle xenolith found in kimberlites[6]. Furthermore, peridotite minerals found as inclusions in diamonds are generally more magnesian than their counterparts in the common garnet peridotite xenoliths. For example, olivine inclusions in diamonds generally have Mg/(Mg+Fe) values of 0.92-0.95 (refs 2, 7), whereas olivines in garnet peridotites most often have values of 0.90-0.93 (see refs 8-10).

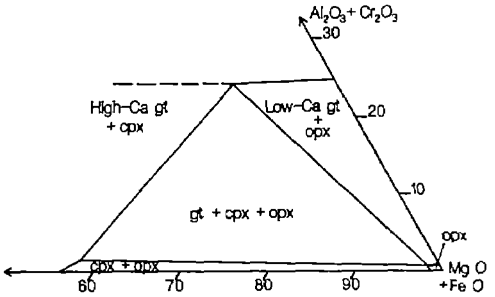

Fig. 1 Phase compatibility diagram (modified ACF plot) for ultrabasic compositions equilibrated near 1,100 °C, 55-60 kbar (mol %). Data used to construct this diagram were taken from the compositions of minerals associated with diamonds from the Finsch Mine in South Africa[2,4,13,44] and the experimental data of Lindsley and Dixon[45].

Diamond-bearing peridotites also occur, although only about 20 are known. Four of these are garnet lherzolite that are virtually indistinguishable in texture, mode and mineral chemistry from the abundant diamond-free garnet lherzolite xenoliths from kimberlites[11-13]. Most diamondiferous peridotites, however, are garnet- and chromite-bearing harzburgites, and dunites, the minerals of which have the same chemical characteristics as those that occur as inclusions in diamonds[12,14,15].

Thus, diamonds with peridotite affinity seem to occur almost exclusively in a magnesian, Ca-deficient peridotite source rock, a garnet harzburgite or garnet dunite that is chemically unlike most of the upper mantle. Two of the outstanding problems regarding the genesis of diamond are therefore: (1) how a calcium-deficient peridotite acquires such unusual chemical characteristics in a 'diopside-saturated' upper mantle; and (2) why diamonds are found almost exclusively in this rock type, and generally not in the more abundant garnet lherzolites.

Students of ultramafic rocks occurring in the Earth's crust are familiar with rocks of both anomalously low and high calcium contents. During serpentinization of peridotite, a process restricted to lower temperature crustal conditions, calcium is removed from pyroxenes and is deposited in associated non-peridotite lithologies—dykes, country rock or tectonic inclusions[16]. The rocks resulting from this process are serpentinite, with a very low calcium content, and related rodingite, with an anomalously high calcium content. It is proposed that subduction of serpentinites, formed by hydration of oceanic lithosphere, and subsequent metamorphism to garnet peridotite facies may be responsible for upper mantle garnet peridotites that are depleted in calcium relative to most of the upper mantle. Several other workers have previously suggested that certain upper mantle xenoliths in kimberlites formed from subducted oceanic crust[17-22]. These models are compared with the present one below.

To test the hypothesis that serpentinite could be the chemical equivalent of Ca-poor, garnet-bearing harzburgite in the upper mantle, a phase compatibility diagram has been constructed (Fig. 1), corresponding to natural peridotite at ~1,100 °C and 55-60 kbar, the approximate equilibration conditions of diamond inclusions and diamond-bearing peridotites from the Finsch kimberlite in South Africa[13]. By plotting serpentinite bulk chemical compositions, the serpentinites are effectively recast into approximate proportions of the various minerals that are stable in these conditions.

Most of the natural compositions used to construct Fig. 1 were taken from the data of Gurney and co-workers for the Finsch pipe in South Africa[2,4,13,44,45]. These were used because they represent the best documentation of diamond-related

---

[*] Present address: Department of Geological Sciences, Queen's University, Kingston, Ontario, Canada K7L 3N6.

minerals from a single pipe, and because two diamond-bearing garnet lherzolites have been described from this pipe[13].

Projected onto the CaO- and ($Al_2O_3+Cr_2O_3$)-poor area of this diagram, expanded in Fig. 2, are the bulk compositions of 57 serpentinites taken from the literature. Most are from Alpine-type serpentinites and abyssal serpentinites and are massive rocks, although some vein serpentinites have been included. Figure 2 shows that most (42) of these serpentinites are compositionally equivalent to harzburgites in which a low-calcium garnet is stable. The remainder of the compositions plot in the fields of garnet lherzolite and garnet-free harzburgite.

The Mg/(Mg+Fe) values of the 42 serpentinites that correspond to low-calcium, garnet-bearing peridotites on this diagram range from 0.88 to 0.98, although most of them have values between 0.92 and 0.95, with a mean value of 0.931. This value is well within the range of Mg/(Mg+Fe) values of olivines that occur as inclusions in diamonds.

On the basis of the similarities in chemical composition between the serpentinites and the minerals included in diamonds, it is concluded that serpentinite has the requisite bulk composition to be a suitable host rock for diamonds of peridotite affinity, if subducted under the continent and equilibrated at ~1,100 °C and 55–60 kbar. These pressure and temperature conditions correspond roughly to 180–200 km beneath a stable shield, on a continental geothermal gradient[13].

Several of the serpentinite analyses plot in the garnet lherzolite field of Fig. 2. Their relatively high calcium contents are probably due to the presence of relict diopside that was not completely replaced by serpentine. Such rocks could be protoliths of diamond-bearing garnet lherzolites.

Theories on the origin of diamonds, centred around the need to explain the calcium-poor nature of the included peridotite minerals, are (1) that diamonds are phenocrysts in an early stage of the kimberlite magma, and the Ca-poor nature of their associated minerals is due to complexing of the calcium in the diopside of a garnet lherzolite parent by partial melting in the presence of CO_2 (ref. 34), and (2) that the low-Ca garnet harzburgite is a residue remaining after extraction of komatiite liquids from parental garnet lherzolite in Archaean time[35]. Richardson *et al.*[36] have essentially combined both of these theories, although rejecting the hypothesis that the diamonds are actual phenocrysts in the same kimberlite that carried them to the surface, because of the age difference between the young kimberlites (~90 Myr, ref. 37) and the Archaean Sm–Nd model ages of garnet inclusions in diamonds[36].

The komatiite residue models are based on the apparent restriction of komatiites, diamonds and low-Ca garnets to stable Archaean cratons, and on the assumption that a garnet harzburgite or garnet dunite would remain as a residue of partial melting of peridotite to yield komatiite. Phase-equilibrium studies, however, have shown that during high degrees of partial melting of garnet peridotite, either garnet or diopside may be the first phase to be consumed, depending on the original bulk composition[38]. The spatial association of low-Ca garnets and komatiites[35] may, therefore, be coincidental.

In the serpentinite model for the origin of peridotite-suite diamonds, the apparent restriction of Ca-poor garnet harzburgites to stable cratons (such as Kaapvaal Craton in South Africa[35]) may be due to the fact that following serpentinite emplacement, perhaps through shallow subduction[39,40], the subcratonic mantle remained 'cool'. The upper mantle in adjacent mobile belts, however, has been remobilized and heated by tectonism and magma production during subsequent orogenesis. During such events, diamond-bearing metaserpentinites may lose both their diamonds and their low-Ca 'signature' through heating and hybridization (for example, ref. 41).

An origin involving a subducted protolith has previously been invoked for several types of xenoliths, including diamonds[17–22]. The model proposed here is similar in several respects to two of these earlier models, which are discussed below.

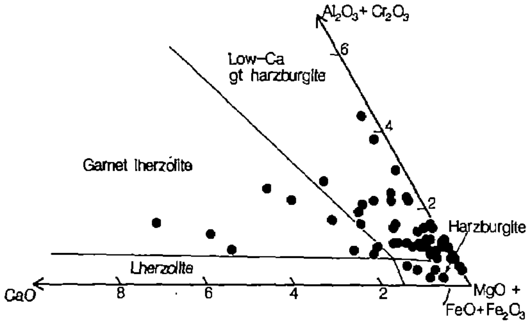

Fig. 2 Bulk serpentinite compositions, plotted in an expanded portion of the lower right-hand side of Fig. 1. Serpentinites taken from refs 16, 23–33.

Ringwood[19] proposed that diamonds originate in subducted oceanic spinel-bearing harzburgite cumulates. Although serpentinization is included in his model, its role is minor, and apparently was included only to facilitate partial melting during subduction, yielding the residual character of the subducted peridotite. The low-calcium nature of the harzburgite in Ringwood's model is attained through igneous processes, with no major role attached to the serpentinization. In the present model, the precise chemical nature of the peridotite protolith, especially its calcium content, before serpentinization, is unimportant. Thorough serpentinization removes Ca from the bulk rock so efficiently that even a lherzolite parent can yield a Ca-poor serpentinite product (see ref. 23). A cumulate harzburgite as proposed by Ringwood[19], therefore, is unnecessary.

Helmstaedt and co-workers[20,21] have proposed that grospydite xenoliths (grossular garnet, omphacitic clinopyroxene and kyanite) are the prograde products of metamorphosed subducted rodingites. This process is the complement of that proposed here. They also suggested that the serpentinites subducted together with rodingites would form garnet peridotites in the mantle, although they did not explore the possibility that serpentinites could be the chemical equivalents of the low-calcium garnet peridotites.

Although it is generally assumed that carbon is present in the mantle as graphite or diamond, graphite-bearing peridotites are even less abundant than are the very rare diamond-bearing samples (F. R. Boyd, personal communication). It appears, therefore, that the source of the carbon is linked with the processes that deplete peridotite in calcium, which in this model is serpentinization.

Pasteris[42] has shown that graphite can occur in serpentinized olivine. Whether it is formed from CO_2 inclusions in the preexisting olivine or from methane-bearing fluids in the reducing conditions that exist during serpentinization[43], or was present in the fresh olivine itself[44] and was only released as graphite during serpentinization, is not clear. It is possible, however, that the carbon that eventually formed as diamond originated in the process of serpentinization, as did the chemical signature of the calcium-deficient peridotite host rock.

I thank F. R. Boyd, H. Helmstaedt, B. O. Mysen and H. S. Yoder Jr, for helpful reviews and M. Imlay for technical assistance.

Received 19 June; accepted 15 October 1985.

1. Meyer, H. O. A. & Boyd, F. R. *Geochim. cosmochim. Acta* **36**, 1255–1273 (1972).
2. Gurney, J. J., Harris, J. W. & Rickard, R. S. in *Kimberlites, Diamonds and Diatremes: Their Geology, Petrology and Geochemistry* (eds Boyd, F. R. & Meyer, H. O. A.) 1–15 (American Geophysical Union. Washington DC, 1979).
3. Prinz, M., Manson, D. V., Hlava, P. F. & Keil, K. *Phys. Chem. Earth* **9**, 797–815 (1975).
4. Tsai, H. M., Meyer, H. O. A., Moreau, J. & Milledge, H. J. in *Kimberlites, Diamonds and Diatremes: Their Geology, Petrology and Geochemistry* (eds Boyd, F. R. & Meyer, H. O. A.) 16–26 (American Geophysical Union, Washington, DC, 1979).
5. Sobolev, N. V., Lavrent'ev, Y. G., Pokhilenko, N. P. & Usova, L. V. *Contr. Miner. Petrol.* **40**, 39–52 (1973).
6. Mathias, M., Siebert, J. C. & Rickwood, P. C. *Contr. Miner. Petrol.* **26**, 75–123 (1970).
7. Meyer, H. O. A. & Tsai, H. M. *Miner. Sci. Engng* **8**, 242–261 (1976).
8. Nixon, P. H. & Boyd, F. R. in *Lesotho Kimberlites* (ed. Nixon, P. H.) 48–56 (Cape and Transvaal, Capetown, 1973).

9. Boyd, F. R. & Nixon, P. H. *Phys. Chem. Earth* **9**, 431–454 (1975).
10. Danchin, R. V. in *The Mantle Sample: Inclusions in Kimberlites and Other Volcanics* (eds Boyd, F. R. & Meyer, H. O. A.) 104–126 (American Geophysical Union, Washington, DC, 1979).
11. Dawson, J. B. & Smith, J. V. *Nature* **254**, 580–581 (1975).
12. Pokhilenko, N. P., Sobolev, N. V. & Lavrent'ev, Yu. G. in *Extended Abstr. 2nd int. Kimberlite Conf.*, Santa Fe (American Geophysical Union, Washington, DC, 1977).
13. Shee, S. R., Gurney, J. J. & Robinson, D. N. *Contr. Miner. Petrol.* **81**, 79–87 (1983).
14. McCallum, M. E. & Eggler, D. H. *Science* **192**, 253–256 (1976).
15. Boyd, F. R. & Finnerty, A. A. *J. geophys. Res.* **85**, 6911–6918 (1980).
16. Coleman, R. G. *Bull. N.Z. geol. Surv.* **76**, 102 pp.
17. Sharp, W. E. *Earth planet. Sci. Lett.* **21**, 351–354 (1974).
18. Helmstaedt, H. & Doig, R. *Phys. Chem. Earth* **9**, 95–111 (1975).
19. Ringwood, A. E. *Earth planet. Sci. Lett.* **36**, 443–448 (1977).
20. Helmstaedt, H. *EOS* **59**, 392–393 (1978).
21. Helmstaedt, H., Carmichael, D. M. & Percival, J. A. *Abstr. Prog. geol. Soc. Am.* **11**, 442 (1979).
22. Exley, R. A., Smith, J. V. & Dawson, J. B. *Am. Miner.* **68**, 512–516 (1983).
23. Nicolas, A. *Bull. volcan.* **32**, 499–508 (1969).
24. Aumento, F. & Loubat, H. *Can. J. Earth Sci.* **8**, 631–663 (1971).
25. Chidester, A. H. *U.S. geol. Surv. prof. Pap.* **345** (1962).
26. Coleman, R. G. & Keith, T. E. *J. Petrol.* **12**, 311–328 (1971).
27. Francis, G. H. *Am. J. Sci.* **254**, 201–226 (1956).
28. Grubb, P. L. C. *Econ. Geol.* **57**, 1228–1246 (1962).
29. Hess, H. H., Smith, R. J. & Dengo, G. *Am. Miner.* **37**, 68–75 (1952).
30. Larrabee, D. M. *Bull. U.S. geol. Surv.* **1283** (1969).
31. Loferski, P. J. thesis. Virginia Polytechnic Inst. (1980).
32. Mumpton, F. A. & Thomspon, C. S. *Clays Clay Miner.* **23**, 131–143 (1975).
33. Prinz, M. *et al. J. geophys. Res.* **81**, 4087–4103 (1976).
34. Harte, B., Gurney, J. J. & Harris, J. W. *Contr. Miner. Petrol.* **72**, 181–190 (1980).
35. Boyd, F. R. & Gurney, J. J. *Yb. Carnegie Instn Wash.* **81**, 261–267 (1982).
36. Richardson, S. H., Gurney, J. J., Erlank, A. J. & Harris, J. W. *Nature* **310**, 198–202 (1984).
37. Davis, G. L. in *Extended Abstr. 2nd int. Kimberlite Conf., Santa Fe* (American Geophysical Union, Washington DC, 1977).
38. Davis, B. T. C. & Schairer, J. F. *Yb. Carnegie Instn Wash.* **64**, 123–126 (1965).
39. Vajner, V. J. *A. Rep. 1972–73, Precamb. Res. Unit, Univ. Cape Town*, 12–23 (University of Cape Town, 1974).
40. Helmstaedt, H. & Gurney, J. J. in *Kimberlites I: Kimberlites and Related Rocks* (ed. Kornprobst, J.) 425–434 (Elsevier, Amsterdam, 1984).
41. Wyllie, P. J. & Sekine, T. *Contr. Miner. Petrol.* **79**, 375–380 (1982).
42. Pasteris, J. D. *Geology* **9**, 356–359 (1981).
43. Freund, F., Kathrein, H., Wengeler, H., Knobel, R. & Heinen, H. J. *Geochim. cosmochim. Acta* **44**, 1319–1333 (1980).
44. Gurney, J. J. & Switzer, G. S. *Contr. Miner. Petrol.* **39**, 103–116 (1973).
45. Lindsley, D. H. & Dixon, S. A. *Am. J. Sci.* **276**, 1285–1301 (1976).

Mechanism of aqueous dissolution of silicate glasses yielded by fission tracks

J.-C. Dran*, J.-C. Petit† & C. Brousse†

* Laboratoire René Bernas, CNRS, BP 1, 91406 Orsay, France
† SESD/LECALT, CEA, CEN-FAR, BP 6,
92260 Fontenay-aux-Roses, France

Controversy continues over the mechanism of the aqueous corrosion of silicate glasses, largely because the processes by which the superficial hydrated layer is formed have not been clearly identified[1]. Two alternative models are current. One view[2–4] is that mobile ions in the glass network (such as Na^+, Li^+ and K^+) are exchanged with hydrogen ions (such as H^+ and H_3O^+) and even H_2O in the solution[5]; the other is that the hydrated layer results from the re-precipitation from solution of dissolved network material[6–12]. The first model is thought appropriate for simple man-made glasses and the second for more complex and natural glasses. We report here an optical and scanning electron microscope study of the corrosion of various borosilicate glasses irradiated by fission fragments. For all glass-solution combinations studied, we find that the hydrated layer embodies relics of the fission tracks, suggesting that this layer is mainly formed by *in situ* replacement, but in some cases a step re-precipitation is also apparent.

Our starting point was the assumption that it might be possible simply to discriminate between the two models by inducing structural microscale modifications of the glass surface and following their evolution during dissolution. We thought that these modifications could be introduced by external irradiation using low doses of fission fragments (FF) emitted by a ^{252}Cf source; these heavy ions are indeed able to produce in insulators very small linear zones of heavily damaged material known as latent tracks. If dissolution is selective, the hydrated layer is mainly formed by an *in situ* transformation of the glass, in which case it may be possible to observe specific track remnants by choosing convenient experimental conditions. In contrast, in the case of congruent dissolution at the reaction interface, the hydrated layer is a re-precipitated coating that should gradually fill and cover the tracks. This simple idea requires that the local modifications have small dimensions compared with the thickness of the hydrated layer implied by dissolution in convenient experimental conditions; this is the case for latent fission tracks (length~10 μm, diameter ~50–100 Å).

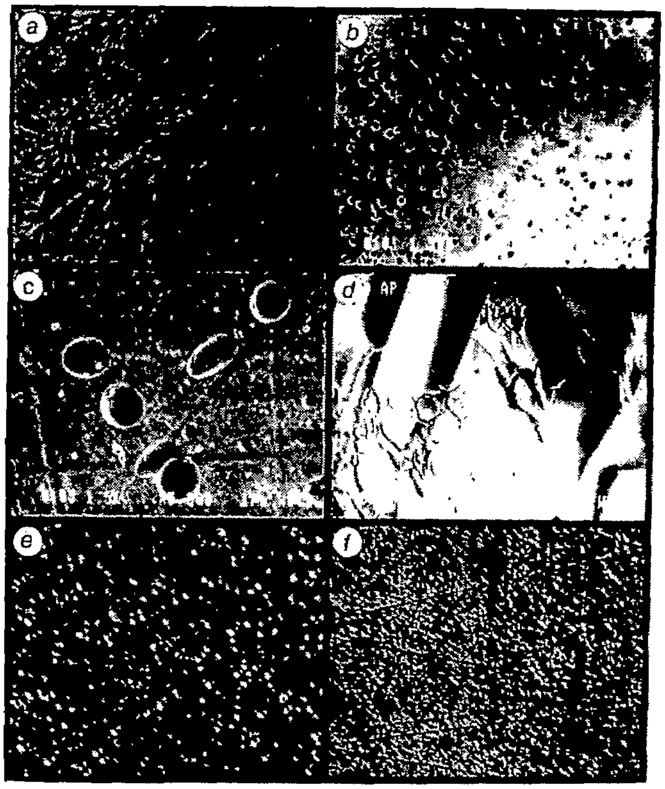

Fig. 1 *a–d*, Fission tracks in simple silicate glass 1 (SiO_2, 54.5%; B_2O_3, 29.2%; Na_2O, 10.3%; Li_2O, 4.9%), etched in deionized water. *a*, Transmission optical micrograph, 15 h at 50 °C (average track length 10 μm); *b*, *c*, SEM micrograph, 60 min at 100 °C; *d*, SEM micrograph of a grain leached for 5 days at 50 °C clearly showing the formation of the hydrated layer. Note the sharp smooth interface with the pristine glass, its fissuring as well as its peeling off. Completely similar results were also obtained with glass 2 (SiO_2, 64%; B_2O_3, 12%; Na_2O, 24%). H- and Na-depth profiling by means of specific resonant nuclear reactions, respectively $^1H(^{15}N, \alpha\gamma)^{12}C$ and $^{23}Na(p, \alpha\gamma)^{20}Ne$, allowed us[15] to demonstrate ion exchanges in sodium-containing glasses leached at low temperatures (<100 °C) for short periods of time and developing a thin (a few thousand Å) hydrated layer. Direct visual observations for samples leached at a higher temperature (160 °C) show that a 1-cm-thick layer can easily be formed[17]. *e*, *f*, Fission tracks in complex glass 3 (SiO_2, 54%; B_2O_3, 13.5%; Na_2O, 13%; CaO, 5%; various transition and heavy-element oxides, 14%) and complex glass 4 (SiO_2, 46.1%; Al_2O_3, 5%; B_2O_3, 14.2%; Na_2O, 12.5%; CaO, 4.1%; Li_2O, 2%; P_2O_5, 0.24%; various oxides, 15.9%) leached at 100 °C during 423 h in H_2O and 33 h in 250 g l^{-1} NaCl solution, respectively.

Methods. Polished sections of different borosilicate glasses were first irradiated with a ^{252}Cf source at total doses of 10^6–10^9 FF cm^{-2}, then placed in Teflon bottles and subjected to dissolution in deionized water, NaCl brine (250 g l^{-1}) or an HF solution (0.4 wt%) at temperatures of 20, 50 and 100 °C, and for times ranging from a few hours to several days. Observations were made on an optical microscope fitted with a Nomarski interference contrast device and on a Jeol JSM 840 scanning electron microscope, allowing a direct observation of samples at low accelerating voltage without any conducting surficial coating.

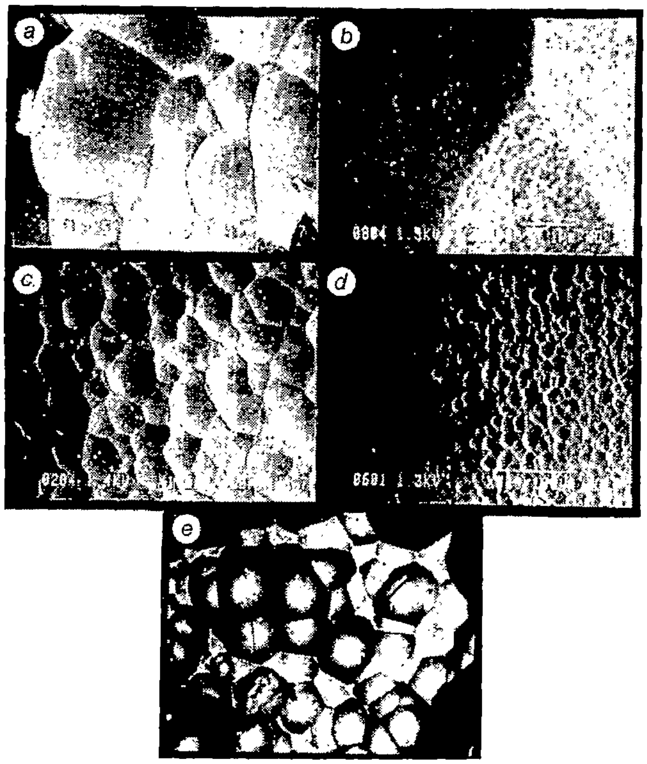

Fig. 2 *a*, *b*, SEM micrographs showing the cupule structure obtained in glass 1 after leaching for 5 days at 50 °C. *c*, *d*, A very similar surficial structure produced by prolonged dissolution of fission tracks in the same glass, 16 h at 100 °C (see text). Note in *d* the limit between irradiated (right) and unirradiated zones (left). *e*, Reflection optical micrograph of glass 3, leached for ~1 week at 100 °C in water at $pH \sim 5.3$, showing, after removal of the hydrated layer, a typical cupule structure.

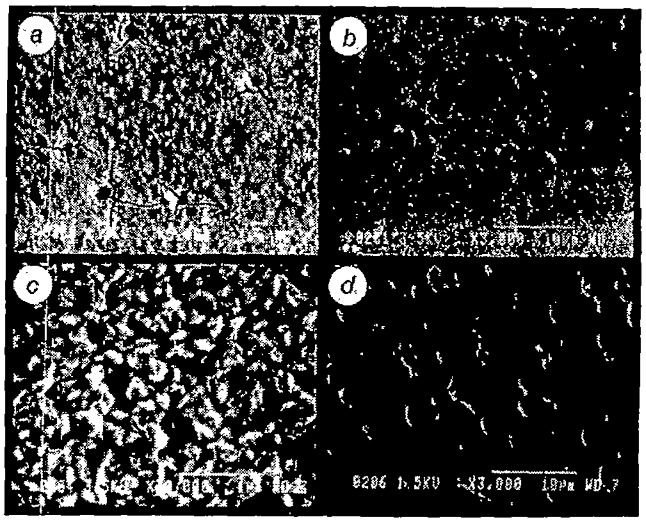

Fig. 3 Evolution during leaching in pure water of pre-etched fission tracks (5 min HF 1/100) in complex silicate glass 5 (SiO_2, 45.5%; Al_2O_3, 4.9%; B_2O_3, 14%; Na_2O, 9.9%; CaO, 4%; Fe_2O_3, 2.9%; ZnO, 2.5%; ZrO_2, 1%; Li_2O, 2%; P_2O_5, 0.28%; various transition and heavy-element oxides, 13%). *a*, SEM micrograph showing in the hydrated layer (leaching conditions, 69 h at 100 °C) remnants of FF tracks and their associated micro-cracks (see text); note the small granules on the surface. ×1,950. *b*, As in *a*, but after 240 h; the arrows indicate partially obstructed tracks and still open ones. Such a feature, combined with the absence of track-induced fracturing, argues strongly for a precipitated coating. ×1,170. *c*, Same field of view showing the granules at higher magnification. ×11,700. *d*, Track remnants in the inner hydrated layer after careful mechanical removal of the surficial sub-layer. ×1,170.

We found that in simple glasses, etched fission tracks are clearly seen in most glass/solution combinations, and particularly in deionized water (Fig. 1). This result is interesting because, in such detectors, tracks are usually revealed only when very strong etchants, such as acid or alkaline solutions[13], are used. Moreover, the scanning electron micrographs clearly show the presence of an apparently homogeneous hydrated layer ~1 μm thick; the fact that the ~10-μm-long tracks intersect this layer and keep perfect elliptical or circular openings argues strongly for the *in situ* formation of such a layer, and therefore for a selective dissolution. This conclusion agrees well with previous results obtained on this type of glass using various surface analytical techniques[3,14,15].

On continued etching, such that the thickness dissolved exceeds the range of the fission tracks, the etch pits develop a spherical shape, due to the isotropy of the etch rate in glasses, and begin to overlap. The resulting topography of the dissolution front (Fig. 2*c*, *d*), showing a typical cup-shaped ('cupule') structure, is very similar to that obtained during the normal dissolution of the same glass (Fig. 2*a*, *b*). The two hypotheses invoked to explain the formation of dissolution cupules are chemical/structural heterogeneities in the bulk of the glass and surficial defects, perhaps due to sample preparation techniques (sectioning and polishing). Clearly, the first hypothesis is the more interesting as, in this case, the cupule structure is related to the basic process of dissolution, which should therefore be congruent; the cupule should perpetuate itself as dissolution proceeds. In contrast, in the second hypothesis, cupules are merely artefacts, which should slowly disappear with sufficiently long dissolution times. Our results provide the first clear demonstration that surficial defects are indeed sufficient to propagate a structure of dissolution cupules at large depths. Therefore, cupules are probably artefacts produced by the surface state of the sample and are not necessarily linked to bulk microheterogeneities. An additional (and we think strong) argument is the absence of the 'cupule-within-cupule' structure which would occur when the dissolution front of one major cupule encounters new bulk heterogeneities. Moreover, although we agree that the spherical shape of the cupules implies a constant progression rate of the dissolution front, this is not necessarily indicative of a congruent dissolution. There are two arguments against this interpretation. First, high-resolution scanning electron micrographs (see Fig. 2*b*) show that the surface of the cupules is rough, rather like a hydrated silica gel, and not smooth as would be expected for a direct attack on the network. Second, both a constant progression rate and a sharp interface between the pristine glass and the hydrated layer can be simply explained by a marked increase of diffusivities of species in the layer relative to the glass (the hydrated layer is then almost 'transparent' for diffusion)[16,17]. This seems likely if one takes into account the high porosities of such layers. In this hypothesis, the selective processes occurring at the interface are limited to very small thicknesses (for example <100–1,000 Å); this is compatible with the sharpness of the interface reported by various investigators[6,8,9,11,12,18].

In contrast, in complex glasses, the observations are more difficult to interpret because etched fission tracks are seen in some glass/solution combinations but not in others (see Fig. 1*e*, *f*), and there seems to be no simple correlation with glass/solution composition. We have already reported that such complexity[19,20] exists in the behaviour of implanted surfaces with regard to aqueous corrosion and consider that this simply reflects our poor understanding of the dissolution processes in multicomponent glasses. However, our results prove that fission tracks can, in many cases, be preferentially etched in complex glasses by solutions such as those found in geological environments. This is the first report of such an observation, and its implications

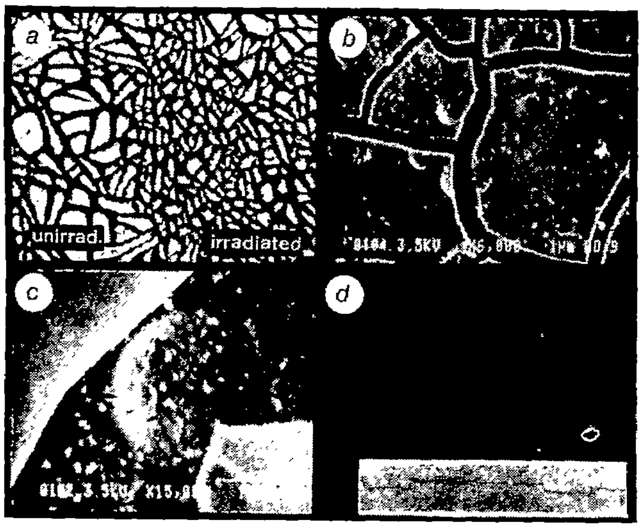

Fig. 4 Evolution during leaching in the NaCl brine of pre-etched fission tracks (5 min HF 1/100) in complex silicate glass 5. *a*, Reflection optical micrograph after 90 h at 100 °C (mean fracture width 1 μm); note the difference in fracture densities between irradiated and unirradiated areas (see text); the micro-cracking has often been reported in silica gel layers, but our observations show that for high doses of FF ($>10^7$ FF cm^{-2}), the density of this crack network, which mimics the image of the grid used as a mask during the irradiations, is markedly increased. As this phenomenon is probably an artefact of the observation technique, it may not affect the overall glass dissolution rate. *b*, *c*, SEM micrographs after 340 h at 100 °C showing track remnants in both sub-layers. This two-sub-layer structure has been described by others[6,8,11,18]. In the case of glass 5, for instance, the inner sub-layer tends to accumulate elements such as Si, P, Zr, U, Th, rare-earth elements, Cr and Mn, whereas the external one preferentially concentrates elements forming very insoluble compounds, such as Ni; Fe and Zn are present in both sub-layers. In contrast, Na, B, Mo, Cs, Ca and Al are strongly depleted in the hydrated layer. In addition, in such complex glasses the hydrated layer contains tiny crystalline phases[8,9,11]. *d*, The result of a complementary experiment in which a polished section of a glass had been implanted through an electron microscope grid with 207-keV lead ions (range ~500 Å) at a dose of 10^{13} ions cm^{-2} and then leached in the same NaCl solution. The example given is of glass 6 (SiO_2, 54%; Al_2O_3, 14%; B_2O_3, 9%; $Na_2O+K_2O+MgO+Fe_2O_3$, 2%; CaO, 21%), showing the formation of bumps ~200 Å high in the irradiated areas (width 100 μm), faithfully following the irradiation geometry (see corresponding step-height profile). This feature is explained by the preferential hydration and correlative swelling of the ~1,000-Å-thick implanted material[19] and not by a re-precipitated coating, which would not show the irradiation geometry so clearly.

for the resistance to aqueous corrosion of glasses containing fissionable elements (spontaneous or induced fission) should be carefully investigated.

In other experiments, we pre-etched the fission tracks in a dilute HF solution and further dissolved the samples in various mild solutions. Using the scanning electron microscope (SEM), we observe (see, for example, Figs 3 and 4 for glass 5) that the microstructure of the hydrated layer and therefore the evolution of the pre-etched holes strongly depend on the nature of the leachant. For example, in water, for leach times of ~69 h at 100 °C, the layer incorporates remnants of tracks, thereby confirming that it develops *in situ* and is not completely redeposited material. This conclusion is confirmed by the observation that stresses are induced inside the hydrated layer by each track and are seen as micro-cracks. These probably formed during the desiccation of the sample that was required for its observation in the vacuum chamber of the SEM. We think that the tracks can induce stresses in the hydrated layer only if it develops around them; if the overall hydrated layer was a redeposited coating, it could not be stressed by pre-existing etched tracks. However, we note that even after 69 h of leaching, the tracks are strongly obstructed, which indicates that transfer of matter over small distances (~5,000 Å) also occurs. For longer leach times (240 h), the tracks are slowly covered by small (~1,000 Å) particles of unidentified nature and crystallinity which finally form a uniform surficial coating of granular aspect. These aspects support the conclusion that the inner part of the layer is indeed mainly formed *in situ*, whereas the external one, which grows slowly over long leach times, is mostly constituted of re-precipitated particles. Indeed, for more extreme experimental conditions, the formation of analcime or tobermorite, which can only be precipitated from the solution, has been confirmed[8,11,18].

In NaCl brine (250 g l^{-1}, Fig. 4), the hydrated layer is also composed of two sub-layers, the inner one showing a high density of micro-cracks (0.1 μm × 1 μm) and a few very long fractures, and the external one being much smoother and highly fractured. In both sub-layers we observe clear remnants of the initial tracks, thus confirming that the hydrated layer is formed *in situ*. Moreover, the density of fractures in the external sub-layer, which are known to be due to the desiccation of silica gels, is directly related to the density of the tracks (Fig. 4*a*); indeed, most fractures are generated by the disruption of tracks (Fig. 4*b*).

We conclude that the hydrated layer is mostly formed *in situ* by a two-step mechanism and is not a purely re-precipitated coating. '*In situ*' here means that the basic architecture of the layer must be derived from that of the pristine glass (for instance by hydration) if it is to 'keep the memory' of the presence of pre-etched tracks. However, its chemical and structural characteristics could also involve other complex phenomena, such as ion exchange, precipitation of diffusing species and polymerization of silica, as long as they imply the transport of small quantities of matter and/or very small distances compared with the characteristic dimensions of the tracks. However, in the case of one complex glass dissolved in H_2O at 100 °C, we have observed a probable re-precipitation step which produces the granules of the external sub-layer, thus confirming the observations of Nogues[6].

We thank G. Baudin, M. Jorda and H. Bernas for their constant interest in this work, the French Atomic Energy Commission for financial support, N. Jacquet-Francillon for providing samples of complex glasses 3, 4 and 5, and M. Okuzumi (Jeol-France) for SEM micrographs.

Received 29 July; accepted 28 October 1985.

1. Scholtze, H. *J. non-cryst. Solids* **52**, 91–103 (1982).
2. Doremus, R. H. *J. non-cryst. Solids* **19**, 137–144 (1975).
3. Lanford, W. A., Davis, K., Lamarche, P., Laursen, T. & Groleau, R. *J. non-cryst. Solids* **33**, 249–266 (1979).
4. Smit, W., Stein, H. N. *J. non-cryst. Solids* **34**, 357–370 (1979).
5. Smets, B. M. J., Lommen, T. P. A. *Phys. Chem. Glasses* **24**, 35–36 (1983).
6. Nogues, J.-L. thesis, Univ. Montpellier (1984).
7. Crovisier, J.-L., Fritz, B., Grambow, B. & Eberhart, J.-P. *MRS Proc. Symp. Scientific Basis of Nuclear Waste Management, Stockholm, September 1985* (North-Holland, Amsterdam, in the press).
8. Lutze, W., Malow, G., Ewing, R. C., Jercinovic, M. J. & Keil, K. *Nature* **314**, 252–255 (1985).
9. Crovisier, J.-L., Thomassin, J.-H., Juteau, T. & Eberhart, J.-P. *Geochim. cosmochim. Acta* **47**, 377–387 (1983).
10. Grambow, B. *MRS Proc.* **11**, 93–102 (1983).
11. Bates, J. K., Jardine, L. J. & Steindler, M. J. *Science* **218**, 51–54 (1982).
12. Thomassin, J.-H. thesis, Univ. Orléans (1984).
13. Fleischer, R. L., Price, P. B. & Walker, R. M. *Nuclear Tracks in Solids* (University of California, 1975).
14. Smets, B. M. J., Lommen, T. P. A. *Phys. Chem. Glasses* **23**(3), 83–87 (1982).
15. Della Mea, G., Dran, J.-C., Petit, J.-C., Bezzon, G. & Rossi-Alvarez, C. *Nucl. Instrum. Meth.* **218**, 493–499 (1983).
16. Crank, F. *The Mathematics of Diffusion* (University of Oxford Press, 1978).
17. Petit, J.-C., Langevin, Y., Lameille, J.-M. & Dran, J.-C. *MRS Proc.* **5**, 203–210 (1982).
18. Lutze, W., Malow, G. & Rabe, H. *MRS Proc.* **15**, 37–45 (1983).
19. Petit, J.-C. thesis, Univ. Paris, Orsay (1982).
20. Arnold, G. W., Petit, J.-C. *Nucl. Instrum. Meth.* **209/210**, 1071–1077 (1983).

Pb–Pb systematics of Lewisian gneisses—implications for crustal differentiation

M. J. Whitehouse & S. Moorbath

Department of Earth Sciences, University of Oxford, Parks Road, Oxford OX1 3PR, UK

Combined use of Rb–Sr, U–Pb and Sm–Nd decay schemes in geochronology provides insights into the evolution of ancient continental crust[1] such as the Lewisian of north-west Scotland. We report here a Pb–Pb whole-rock isochron date of 2,950 ± 70 Myr on amphibolite-facies grey gneisses from the northern region of the Lewisian; this is essentially the same as a Sm–Nd whole-rock isochron date (2,920 ± 50 Myr) which was interpreted as the time of separation of igneous protoliths from the mantle[2]. A period of ~240 Myr separates this date from the Scourian peak of granulite-facies metamorphism. This result indicates, for the Lewisian, that high-grade metamorphism and crustal stabilization cannot have been the result solely of thermal equilibration. More generally, it suggests that tectonic thickening was an important process during Archaean crustal evolution[3] and that although whole-rock systems may remain open with respect to U–Pb until the termination of granulite-facies metamorphism, they may be closed during amphibolite-facies metamorphism.

The Lewisian Complex of mainland north-west Scotland is divided into three main regions which are considered to have originally occupied different crustal levels[4]. The central region, between Loch Laxford and Gruinard Bay, preserves granulite facies gneisses from the Scourian metamorphism which has been dated at 2,680 ± 60 Myr[5]. A recent estimate of metamorphic conditions indicates temperatures and pressures in excess of 1,000 °C and 8.5 kbar respectively[6]. Amphibolite facies gneisses are dominant in the northern and southern regions and previous isotopic work has shown that these record both the Scourian event with whole-rock Pb-Pb[7–10] and zircon U-Pb[11] dates in the range 2,900–2,600 Myr as well as the Proterozoic Laxfordian event with Rb-Sr[12] and K-Ar[13] dates in the range 1,880–1,550 Myr. Extensive granitic intrusions along the Laxford Front, the boundary between the northern and central regions, have been dated by Pb-Pb and Rb-Sr methods at ~1,700 Myr[14].

A period of 100–200 Myr between extraction of igneous precursors of crustal gneisses and their subsequent stabilization has been recognized in many Archaean regions from studies of initial $^{87}Sr/^{86}Sr$ ratios[1,15]. Stabilization is produced by high-grade metamorphism purging the lower crust of heat-producing elements (K, Rb, U and Th) and other large-ion lithophiles (LIL)[16]. The whole process from accretion to final differentiation has been termed a 'crustal accretion-differentiation superevent' (CADS)[1,15]. The Sm-Nd date of 2,920 ± 50 Myr reported by Hamilton *et al.*[2] was obtained on a lithologically diverse suite of gneiss samples, which are not necessarily co-genetic, from the northern and central regions. The difference of ~240 Myr between this and Scourian dates obtained by other methods was interpreted[2] as the approximate duration of the Scourian CADS

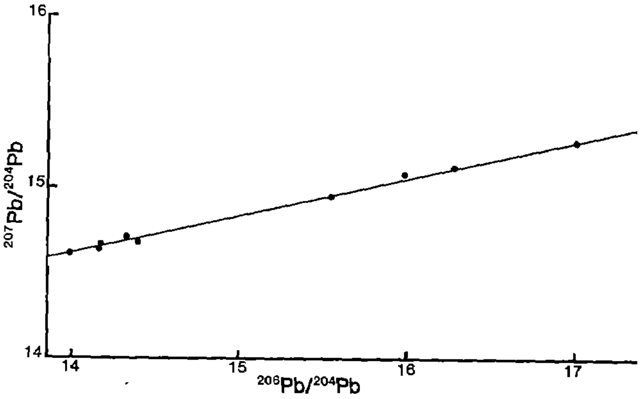

Fig. 1 $^{207}Pb/^{204}Pb$ versus $^{206}Pb/^{204}Pb$ isochron plot of the grey gneiss data. Age = 2,950 ± 70 Myr; $\mu_1 = 7.82$; MSWD = 1.94.

North of the Laxford Front the distribution of Laxfordian intrusions and migmatization becomes more localized, most of the region consisting of gneisses belonging to the three intergradational petrographic divisions recognized by the Geological Survey[17]—that is, 'grey gneiss', in which biotite is the principal ferromagnesian mineral, 'hornblende-biotite gneiss' and 'dark gneiss', in which ferromagnesian minerals predominate. Samples collected for the present study were chosen so as to minimize the effects of post-Scourian disturbance. Gneisses containing, or adjacent to, discordant granitic and pegmatitic intrusions, as well as finely banded gneisses, which may have been affected by fluid movement, were avoided. Sample localities are given in Table 1.

Pb was extracted using standard dissolution and ion-exchange techniques. Details of Pb mass spectrometry are given in ref. 14. Decay constants for ^{238}U and ^{235}U were taken as $1.55125 \times 10^{-10}\ yr^{-1}$ and $9.85484 \times 10^{-10}\ yr^{-1}$ respectively. All dates quoted here from early publications have been recalculated using these values, and are quoted with a 2σ error. The analyses are presented in Table 1 and $^{207}Pb/^{204}Pb$ and $^{206}Pb/^{204}Pb$ ratios are plotted in Fig. 1.

A 10-point isochron (MSWD = 1.94) yields a date of 2,950 ± 70 Myr (2σ). A model $^{238}U/^{204}Pb$ (μ_1) ratio of 7.82 for two-stage isotopic evolution is typical of late Archaean upper mantle source regions[1].

This result indicates that the whole-rock U–Pb system in the grey gneisses has remained undisturbed since late Archaean times despite significant Laxfordian reworking at ~1,700 Myr.

Table 1 Analytical data

Sample	Locality	Grid ref.	$^{206}Pb/^{204}Pb$	$^{207}Pb/^{204}Pb$	$^{208}Pb/^{204}Pb$
MJW192	Rhiconich	NC251534	14.399	14.676	36.578
MJW193	Rhiconich	NC251534	13.986	14.612	34.992
MJW220	Rhiconich	NC252538	14.328	14.711	36.372
MJW211	Kinlochbervie	NC230563	14.177	14.668	36.071
MJW241	Laxford	NC233485	14.171	14.641	34.799
MJW251	Rispond	NC449656	17.380	15.337	38.699
MJW252	Rispond	NC449656	16.285	15.117	36.533
MJW253	Rispond	NC449656	16.997	15.260	38.336
MJW254	Rispond	NC449656	15.983	15.075	35.396
MJW255	Rispond	NC445653	15.548	14.951	36.624

Within-run precision of Pb isotope ratios between 0.02 and 0.05% (2σ). Analyses are corrected for mass fractionation of −0.1 ± 0.03% per AMU. Overall analytical errors < 0.1%.

The measured date is similar to the Sm-Nd accretion date of 2,920±50 Myr[2] but outside the error of published Scourian Pb-Pb and Rb-Sr dates. This result indicates that closure of this whole-rock system in the northern region, shortly after crystallization, occurred over 200 Myr earlier than the peak of high-grade metamorphism in the central region. Any model for early evolution of the Lewisian crust must provide for granulite-facies conditions in the lower crust after this lengthy time interval. In addition, the preservation of an older date from amphibolite-facies gneisses suggests that although final closure of whole-rock U-Pb systems occurs only on cessation of granulite-facies metamorphism, these systems may remain closed during amphibolite-facies and lower grades of metamorphism.

The thermal history of magmatically accreted crust has been considered by Wells[18] for three accretion scenarios—under-accretion in which magma is plated onto the base of existing crust; over-accretion in which magma is emplaced at a high crustal level; and random accretion in which the level of emplacement within the crust varies randomly. The over-accretion and random-accretion models can produce temperature maxima in the lower crust after cessation of magma addition, though this occurs only for accretion events of less than ~35 Myr duration and cannot explain a time interval as long as 240 Myr. Under-accretion cannot produce a post-magmatic temperature maximum.

An alternative to thermal models which rely only on the conductive heating effect of newly emplaced intrusions as well as radioactive heating, is one involving tectonic thickening of unstable juvenile crust[3]. The thermal model considered by Hamilton *et al.*[2] to explain the length (~240 Myr) of the observed time interval assumed constant crustal thickness and implied granulite P-T conditions and extensive melting by ~2,820 Myr; unless the heat-producing and LIL elements migrated to higher structural levels before ~2,820 Myr. This is inconsistent with Sr-isotope data (M.J.W., unpublished) which indicate that the average ^{87}Rb/^{86}Sr ratio between crustal accretion at ~2,920 Myr and high-grade metamorphism at ~2,680 Myr was high and shows no evidence for Rb depletion. Oxburgh and Turcotte[19] have discussed the perturbation of the regional conductive geothermal gradient caused by overthrusting with specific reference to the Eastern Alps. Once an equilibrium gradient has been restored the overall effect is one of increased metamorphic grade in the lowermost tectonic units. The style of the predominantly flat-lying f_1 foliation in the Lewisian[20] is consistent with major horizontal movements associated with thrusting. This model could also account for occurrence of gneisses of supracrustal origin throughout the complex[21].

The juxtaposition of crustal levels across the Laxford Front as well as the geochronological data reported here require a major thermal event long after an equilibrium conductive geothermal gradient has been established. Large-scale intra-continental thrusting and associated crustal thickening is one mechanism for producing the requisite high-grade metamorphism which terminated the Scourian CADS at ~2,700 Myr.

We thank P. N. Taylor and R. St J. Lambert for constructive criticisms. M.J.W. acknowledges receipt of a NERC studentship.

Received 1 August; accepted 12 November 1985.

1. Moorbath, S. & Taylor, P. N. in *Precambrian Plate Tectonics* 491–525 (ed. Kröner, A.) (Elsevier, Amsterdam, 1981).
2. Hamilton, P. J., Evensen, N. M., O'Nions, R. K. & Tarney, J. *Nature* **277**, 25–28 (1979).
3. Kröner, A. *Rev. Bras. Geocienc.* **12**, 15 (1982).
4. Sheraton, J. W., Skinner, A. C. & Tarney, J. in *The Precambrian of Scotland and Related Rocks of Greenland* 13 (eds Park, R. G. & Tarney, J.) (Department of Geology, University of Keele, 1973).
5. Chapman, H. J. & Moorbath, S. *Nature* **268**, 41–42 (1978).
6. Barnicoat, A. C. *J. metamorphic Geol.* **1**, 163–182 (1983).
7. Moorbath, S. & Park, R. G. *Scott. J. Geol.* **8**, 51–74 (1972).
8. Moorbath, S., Powell, J. L. & Taylor, P. N. *J. geol. Soc.* **131**, 213–222 (1975).
9. Moorbath, S., Welke, H. & Gale, N. H. *Earth planet. Sci. Lett.* **6**, 245–256 (1969).
10. Holland, J. G. & Lambert, R. St J. *Precambr. Res.* **2**, 161–188 (1975).
11. Lyon, T. D. B. & Bowes, D. R. *Krystalinikum* **13**, 53–72 (1977).
12. Chapman, H. J. thesis, Univ. Oxford (1978).
13. Lambert, R. St J. & Holland, J. G. *J. geol. Soc.* **128**, 3–19 (1972).
14. Taylor, P. N., Jones, N. W. & Moorbath, S. *Phil. Trans. R. Soc.* A310, 605–625 (1984)
15. Moorbath, S. *Chem. Geol.* **20**, 151–187 (1977).
16. Tarney, J. & Windley, B. F. *J. geol. Soc.* **134**, 153–172 (1977).
17. Peach, B. N. *et al. Mem. geol. Surv. UK* 33–268 (1907).
18. Wells, P. R. A. *Earth planet. Sci. Lett.* **46**, 253–265 (1980).
19. Oxburgh, E. R. & Turcotte, D. L. *Schweiz. miner. petrogr. Mitt.* **54**, 641–662 (1974).
20. Sheraton, J. W., Tarney, J., Wheatley, T. J. & Wright, A. E. in *The Precambrian of Scotland and Related Rocks of Greenland*, 31 (eds Park, R. G. & Tarney, J.) (Department of Geology, University of Keele, 1973).
21. Watson, J. *Spec. Rep. geol. Soc. Lond.* **6**, 15–29 (1975).

Stromatolites from the 3,300–3,500-Myr Swaziland Supergroup, Barberton Mountain Land, South Africa

Gary R. Byerly, Donald R. Lower & Maud M. Walsh

Department of Geology, Louisiana State University, Baton Rouge, Louisiana 70803, USA

A morphologically variable assemblage of stromatolites has been discovered in thin chert layers within the Fig Tree Group of the Swaziland Supergroup, South Africa. They are commonly low-relief, nearly stratiform, laterally linked domes. Rarer forms include pseudocolumns and crinkly stratiform stromatolites. The stromatolites grew on a substrate of altered komatiitic lava and sediments deposited on the lava surface, and in most places are covered by later komatiitic flows. Abundant fine-grained tourmaline included within the stromatolite laminae suggests that stromatolites formed in an environment dominated by boron-rich hot-spring emissions and evaporitic brines.

The Swaziland Supergroup of the Barberton Mountain Land consists of a lower sequence (Onverwacht Group) of ultramafic and mafic lava flows containing thin interbedded cherty layers, an overlying sequence of chert, clastic sediments, and some interbedded volcanics (Fig Tree Group), and an uppermost unit of primarily conglomerate, sandstone and shale (Moodies Group). A minimum age of 3,300 Myr for the Fig Tree Group is provided by K-Ar dating of low-grade regional metamorphism[1], and the lower part of the Onverwacht is considered to have an age of 3,500 Myr based on Nd-Sm techniques[2]. Stromatolites occur in three separate areas (Fig. 1). The most extensive development is at locality A where they are found throughout an area roughly 1×2 km in an isoclinal antiform broken up by small throw, high-angle faults.

At localities A and B, the stromatolites overlie silicified komatiite flows showing well-developed spinifex and cumulus textures. The surfaces of the flows are irregular, however, and in places there is from 1 to 18 m of sedimentary rocks between the altered lava and the stromatolitic cherts. These associated sediments include banded ferruginous and carbonaceous chert; thin, graded layers of volcanic accretionary lapilli, ash and dust; and minor sandstones derived by erosion of the underlying volcanic rock. Also common are fine breccias containing debris eroded from the stromatolites. The stromatolites were covered by later komatiitic lava flows up to 20 m thick. Most are massive but some include pillowed or hyaclastite facies. Spinifex-textures are widely developed. The bases of these flows commonly form casts of the stromatolite surface. At least one other stromatolitic chert unit is interbedded with the later komatiitic lavas at locality A.

At locality B the stromatolites grew directly on the top of an irregular pinnacle of a silicified komatiitic flow rock. Laterally, banded chert, detrital sediments including stromatolitic debris, and volcaniclastic layers overlie the silicified volcanic basement. The stromatolitic zone is succeeded by >300 m of cherts and clastic sediments of the Fig Tree Group. At location C the stromatolites are in a tectonically isolated block that is surrounded by komatiites. The stromatolites are underlain by 1–2 m of

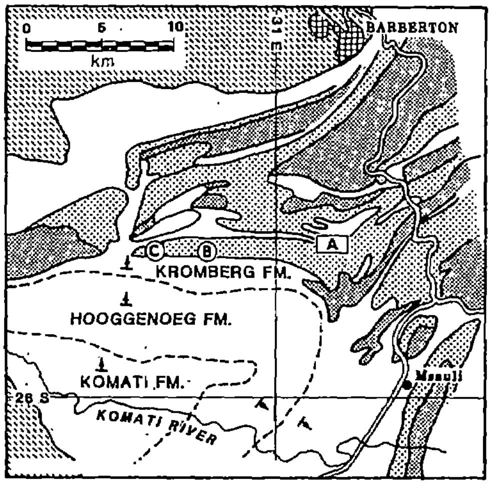

Fig. 1 Map of the Barberton Greenstone Belt with newly discovered stromatolite localities A, B and C in the Fig Tree Group. No pattern, Onverwacht Group; coarse stipple, Fig Tree Group; fine stipple, Moodies Group; and diagonal pattern, granitic rocks. Locality A is a prominent chert ridge on the south-east side of the narrow valley at 25°54'10.5" S and 31°02'41" E; locality B is a smaller outcrop on the south-facing ridge about 0.5 km north of the Msauli River at 25°54'28" S and 30°55'33" E; locality C is a very small outcrop at 25°54'15.5" S and 30°53'40.3" E along an old forestry road.

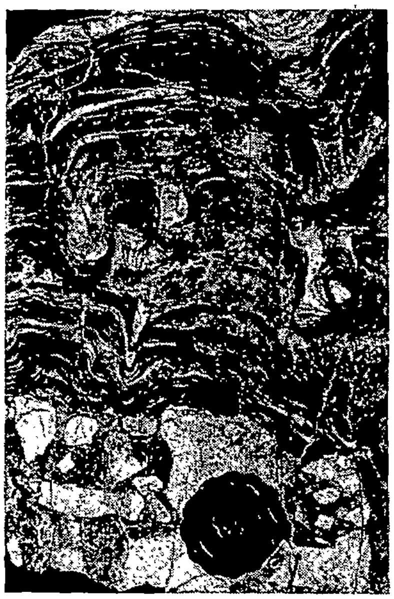

Fig. 2 Stromatolites directly overlying brecciated top of komatiitic lava flow. Small basal domes are covered by large, slightly asymmetrical domes or pseudocolumns. These are, in turn, overlain by very low-relief laminae with high inheritance. Note also the stromatolite flake breccia in the lower layer extending down into black chert surrounding komatiitic clasts. Samples have been slabbed and polished, then etched in hydrofluoric acid to bring out the fine detail of laminae. Coin diameter, 2.5 cm.

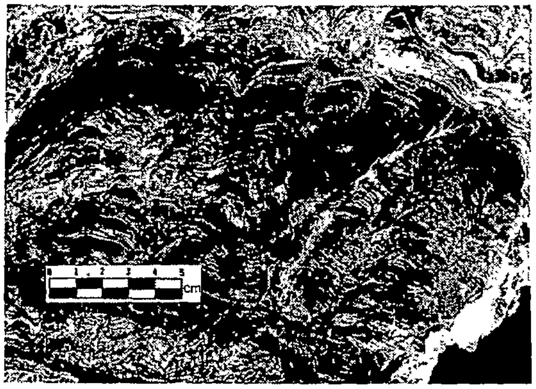

Fig. 3 Pseudocolumnar stromatolites in a thin (1-m) chert between komatiitic lava flows at locality C. Columns are inclined, and composed of wrinkled laminae with high inheritance.

banded black and white chert and may be overlain by lavas. At locality A, the only site where the stromatolites can be traced laterally, the stromatolitic layers are thin and laterally discontinuous, ranging from <1 to ~20 cm thick and typically extending for about 5 m along strike. They pinch out over highs on the underlying lavas. Individual chert units interbedded with komatiitic lava flows commonly include two or three stromatolite layers separated by 10-40 cm of non-stromatolitic sediment.

The most common stromatolites are low-relief domes ranging from ~1 cm wide and 0.5 cm high to ~3 cm wide and 3 cm high. In some places, the small domes have developed upwards into larger domes, compound domes, or pseudocolumns with heights up to 10 cm (Figs 2 and 3). The large domes generally have gently convex, almost flat crests, but some are concave. Both the large and small domes are slightly asymmetrical, and plan views show some elongation of domes. The domes are, in places, associated with stratiform stromatolites with fine crinkly laminae. Synoptic relief of laminae ranges from a few millimetres in the small domes to ~1.5 cm in the larger domes, with greater degrees of inheritance in the larger domes and pseudocolumns. In some places, laminae form bridges between adjacent domes (Fig. 2).

In all areas, the stromatolites are preserved within grey to black chert that shows fine laminae consisting mainly of microcrystalline quartz. Both light and dark laminae range in thickness from 50 to 100 μm and are made up primarily of microcrystalline quartz of 2-4 μm grain size. The darker laminae contain very fine, submicrometre-sized material that is possibly organic matter. In many samples, the dark laminae also include tourmaline crystals ranging from 25 to 200 μm, and 25 to 50 μm crystals of sericite, haematite and rutile. Individual laminae may be traced through single tourmaline crystals. Composite laminae commonly up to 500 μm in thickness can be recognized by their variable tourmaline or sericite contents. Some composite laminae contain up to 50% tourmaline. Fine sandy layers of stromatolite fragments occur between some laminae.

Stromatolites are 'organosedimentary structures produced by sediment trapping, binding and/or precipitation as a result of the growth and metabolic activity of microorganisms'[3]. The identification of the Fig Tree structures as stromatolites is based on their similarity to previously described stromatolites. Both the domal and pseudocolumnar macrostructures and the fine crinkly laminations argue for a biological influence on the sediment. The Fig Tree stromatolites most notably resemble both stratiform and columnar stromatolites of the Proterozoic Gunflint Iron Formation[4-6]. Stromatolite-like structures may be formed inorganically, but the structures reported here lack obvious features, such as cross-lamination or discordant relationship to other sediments, that would indicate an evaporitic or other non-biological origin[7].

It has been suggested that early Archaean stromatolite-building organisms were not unlike those of the Proterozoic and Phanerozoic: probably filamentous, but possibly coccoidal bacteria or cyanobacteria[8,9]. Microfossils have not been found within the stromatolitic rocks of the Fig Tree, but coccoidal microfossils have been described in black cherts of the lower Fig Tree[10] and filamentous microfossils found in the immediately underlying Kromberg Formation[11,12].

The morphological characteristics of stromatolites probably reflect both the type of organism that constructed the stromatolite and environmental factors[6]. Certain features of the Fig Tree stromatolites have environmental implications. The predominance of lateral linkage between both stromatolite domes and low-relief mounds suggests that wave or current action was slight enough that intermound growth was undisturbed[13]. The stromatolites formed mainly on basement highs, indicating that one or more of the following might have been required for stromatolite development: shallow water, availability of a hard substrate, or sparse to absent clastic sedimentation. The common occurrence of stromatolite flake breccias suggests that subaerial exposure and desiccation of stromatolites occurred, although storms might have eroded subaqueous stromatolites. In areas away from the actual growth sites, the presence of stromatolite flake debris may provide a useful indicator of the existence of stromatolites.

The tourmaline that is commonly found within the stromatolitic laminae suggests the influence of silica, magnesia, iron- and boron-enriched waters[14]. Tourmaline-rich sedimentary layers are associated with Proterozoic stratabound sulphide deposits considered to be of marine exhalative origin and from evaporitic environments where they are associated with carbonate sediments[14].

The stromatolites reported here are widespread, morphologically variable, and associated with lithologically diverse sedimentary units that include a possible evaporitic component. The other two occurrences of well-documented early Archaean stromatolites are in the Warrawoona Group of Western Australia. In this area, the regionally extensive Strelley Pool Chert[8] includes laterally linked conical pseudocolumnar stromatolites interbedded with silicified evaporites, and the Towers Formation locally contains stromatolites[9] similar to those described here, also interbedded with deposits interpreted to represent evaporites. The results of these studies suggest that early Archaean stromatolites may have been widely developed within a range of shallow-water settings, but may have been particularly favoured by conditions associated with near-evaporitic or evaporitic environments.

Field studies in the Barberton Mountain Land were supported by NSF grants EAR7919907 to G.R.B. and D.R.L., EAR7919908 and EAR8206015 to D.R.L., and an NSF Fellowship to M.M.W. The ARCO Foundation, Anglo-American Corporation, and the University of Cape Town Departments of Geochemistry and Geology provided additional support.

Received 19 April; accepted 11 October 1985.

1. deWit, M. J., Hart, R., Martin, A. & Abbot, P. *Econ. Geol.* **77**, 1783-1802 (1982).
2. Hamilton, P. J., Evensen, M. M., O'Nions, R. K., Smith, H. S. & Erlank, A. J. *Nature* **297**, 298-300 (1979).
3. Awramik, S. M. & Margulis, L. in *Stromatolites* (ed. Walter, M. R.) 1 (Elsevier, Amsterdam, 1976).
4. Awramik, S. M. in *Stromatolites* (ed. Walter, M. R.) 311-336 (Elsevier, Amsterdam, 1976).
5. Awramik, S. M. & Semikhatov, M. A. *Can. J. Earth Sci.* **16**, 484-495 (1979).
6. Semikhatov, M. A., Gebelein, C. D., Cloud, P., Awramik, S. M. & Benmoire, W. C. *Can. J. Earth Sci.* **16**, 992-1015 (1979).
7. Walter, M. R. in *Earth's Earliest Biosphere* (ed. Schopf, J. W.) 187-213 (Princeton University Press, 1983).
8. Lowe, D. R. *Nature* **284**, 441-443 (1980).
9. Walter, M. R., Buick, R. & Dunlop, J. S. R. *Nature* **284**, 443-445 (1980).
10. Knoll, A. H. & Barghoorn, E. S. *Science* **198**, 396-398 (1977).
11. Walsh, M. M. & Lowe, D. R. *Abstr. 14th lunar Planet. Sci. Conf.* **2**, 814 (1983)
12. Walsh, M. M. & Lowe, D. R. *Nature* **314**, 530-532 (1985).
13. Logan, B. W., Rezak, R. & Ginsburg, R. N. *J. Geol.* **72**, 68-83 (1964).
14. Slack, J. F., Herriman, N., Barnes, R. C. & Plimer, I. R. *Geology* **12**, 713-716 (1984).

Evolutionary relationships of human populations from an analysis of nuclear DNA polymorphisms

J. S. Wainscoat, A. V. S. Hill, A. L. Boyce*, J. Flint, M. Hernandez, S. L. Thein, J. M. Old, J. R. Lynch, A. G. Falusi†, D. J. Weatherall & J. B. Clegg

Medical Research Council Molecular Haematology Unit,
Nuffield Department of Clinical Medicine, University of Oxford,
John Radcliffe Hospital, Oxford OX3 9DU, UK
* Department of Biological Anthropology, University of Oxford,
Oxford OX2 6QS, UK
† Department of Haematology, University College Hospital,
Ibadan, Nigeria

The genetic relationships of human populations have been studied by comparing gene frequency data for protein and blood-group loci of different populations[1,2]. DNA analysis now promises to be more informative since not only do the DNA coding sequences have more variation than their corresponding proteins but, in addition, noncoding DNA sequences display more extensive polymorphism[3,4]. We have now studied the frequency of a group of closely linked nuclear DNA polymorphisms (haplotypes)[5] in the β-globin gene cluster of normal (β^A) chromosomes of individuals from eight diverse populations. We have found that all non-African populations share a limited number of common haplotypes whereas Africans have predominantly a different haplotype not found in other populations. Genetic distance analysis based on these nuclear DNA polymorphisms indicates a major division of human populations into an African and a Eurasian group.

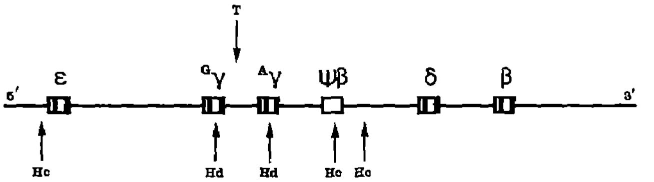

Fig. 1 Schematic representation of the β-globin gene cluster; the linkage of the five polymorphic restriction enzyme sites shown below the cluster constitutes the haplotype studied. Hc, *Hin*cII; Hd, *Hin*dIII. The polymorphic *Taq*I site (T) is shown above the cluster. DNA was recovered from peripheral blood by phenol-chloroform extraction, and restriction enzyme analysis performed as described in ref. 24. The haplotypes were determined from the *Hin*cII and *Hin*dIII digests as in ref. 5. The *Taq*I polymorphic restriction site is present in all of 100 representative non-African chromosomes studied, resulting in $^G\gamma$ restriction-fragment lengths of 1.7 and 2.5 kilobases. It is absent in 10 African − − − − + haplotypes, giving $^G\gamma$ restriction fragment lengths of 1.7 and 3.0 kilobases.

Genetic distance analysis for protein loci suggests that during human evolution the negroid group and the caucasoid-mongoloid group diverged first and that the caucasoid and mongoloid groups diverged from each other at a later date[2]. In contrast, phylogenetic trees of human races based on blood groups[6] and histocompatibility locus antigens[7] have their primary divisions between the mongoloid and the caucasoid-negroid groups. It has been considered that the protein data may be more reliable than blood-group results because they more closely reflect variation in DNA sequence. However, the best way to study population affinities is by comparing DNA sequences of individuals from different populations, since not only is DNA analysis more informative than analysis of proteins but it is also direct and unambiguous. Human restriction enzyme polymorphisms now provide a method of detecting DNA sequence changes and can be used to examine large numbers of individuals. A previous study of mitochondrial DNA polymorphisms in different populations indicated that the two African populations formed a distinct lineage from the others studied[8]. This observation was interpreted as being due to a higher mutation rate in the Bushman population, although there

Table 1 Numbers of chromosomes possessing the various haplotypes in each population

Haplotypes	British	Cypriot	Italian	Asian Indian	Thai	Melanesian A	Melanesian B	Polynesian	African A	African B
+−−−−	16	59	32	58	29	44	73	43	0	3
−+−++	15	14	15	28	0	10	19	6	2	4
−++−+	5	8	2	15	2	3	0	0	1	0
+−−++	0	0	0	0	0	3	8	0	0	0
−++−−	1	1	1	3	0	0	0	0	0	0
−++++	0	0	0	0	0	0	5	1	0	0
++−++	0	0	0	3	0	0	0	0	0	0
−−−−−	0	0	0	1	0	0	2	1	0	0
+++−+	0	0	0	1	0	0	0	0	0	0
−−−++	0	0	0	1	1	0	0	0	0	0
++−−−	0	0	0	1	0	0	0	0	0	0
−+−−−	0	0	0	0	0	0	0	0	1	1
−+−−+	0	0	0	0	0	4	0	4	6	6
−−−−+	0	0	0	0	0	2	0	0	16	21
Totals	37	82	50	111	32	66	107	55	26	35

The Italian, Cypriot and Asian Indians studied were parents of thalassaemic children referred for genetic analysis. The haplotypes of the norma (β^A) chromosomes were determined by family linkage studies. All the other population groups consisted of healthy individuals with norma haemoglobin electrophoresis results. The first group of Africans (African A) were university students originating from sub-Saharan countries Gambia, Kenya and Nigeria; the second group of Africans (African B) were Nigerians mainly from the Yoruba, Bendel and Ibo. The Melanesian and Polynesians studied were individuals showing normal haemoglobin electrophoresis results taken from a larger study of the incidence of th haemoglobinopathies in those populations. The first group of Melanesians was from the eastern and southern highlands of Papua New Guinea the second group was from north coastal Papua New Guinea and Vanuatu. The Thai individuals were from Bangkok and the British individual were from Oxford. All first-degree relatives have been excluded from the study. A polymorphic restriction site is denoted as being present in particular haplotype by a + symbol and absent by a − symbol.

is no direct evidence for this. Mitochondrial DNA has a maternal pattern of inheritance, which means that the dispersal rate of mitochondrial genes is that of females rather than being representative of both sexes. We have therefore sought to investigate human population relationships by analysing nuclear DNA polymorphisms and comparing these data with the mtDNA polymorphism results.

We have studied five linked polymorphic restriction enzyme sites in the β-globin gene cluster[5] (Fig. 1), the combination of the sites along one chromosome being referred to as a haplotype. The five sites show strong linkage disequilibrium and are 5′ to a recombination hotspot in the gene cluster[5]. Although these restriction sites are in a functional gene cluster, we have analysed only those chromosomes bearing normal β^A-globin genes on which there is no known selection pressure. The numbers of the haplotypes found are reported for eight population groups; British, Italian, Cypriot, Asian Indian, Melanesian, Polynesian, Thai and African. Analysis of 601 chromosomes revealed 14 of the 32 (2^5) possible haplotypes (Table 1). One haplotype (+−−−−) is the most common in all seven non-African populations and is found at similar frequencies in each of them. The second most common haplotype (−+−++) is found in all the non-African populations with the exception of the Thai population, although it has been observed previously in South-East Asia[9]. A third haplotype (−++−+) accounts for the majority of the remaining haplotypes found in the non-African populations. The two African populations have a common haplotyp (−−−−+) which is absent in all the non-African population with the exception of two individuals from the Papau Ne Guinea (PNG) highland population. However, even these tw exceptions may be distinguished from the common Africa haplotype by the presence of a *Taq*I restriction-site polymorphism 3′ to the $^G\gamma$ gene (Fig. 1). Hence it seems probable that thi PNG haplotype has an independent non-African origin throug recombination. Two other new haplotypes (+−−++ an −++++), presumably formed by recombination events, wer found in the Melanesian and Polynesian populations.

It is interesting that none of these four common haplotype can be derived from any of the other three by either a singl crossover or by a single-base mutation causing the loss or acqu sition of a restriction enzyme site. We suggest, therefore, th these four haplotypes predate the racial divergence and henc that these structures have been stable for long periods of tim of the order of 100,000 yr. For example, the highland Melanesia population has similar haplotype frequencies to the European from which they have been separated for 20,000-40,000 yr[1 Most of the rarer haplotypes may be derived from the fou common ones by single crossovers. Theoretically there are 1 haplotypes which may be accounted for in this way, and 8 hav been observed in our study, in contrast to only 3 of a possibl

Table 2 Genetic distances for the 10 populations

Balakrishnan-Sanghvi (G_c) distances

	British	Cypriot	Italian	Thai	Indian	Melanesian	Polynesian	African
British	–							
Cypriot	0.6908	–						
Italian	0.5363	0.4012	–					
Thai	1.3064	0.7366	0.9695	–				
Indian	0.6472	0.6533	0.6869	1.0734	–			
Melanesian	1.0239	0.6843	0.6977	0.9533	0.9872	–		
Polynesian	1.1368	0.6650	0.7323	0.8305	1.0360	0.5975	–	
African	2.8658	2.8399	2.8300	2.9619	2.8719	2.7742	2.7288	–

The haplotype data of the two Melanesian populations have been combined, as have the haplotype data of the two African populations.

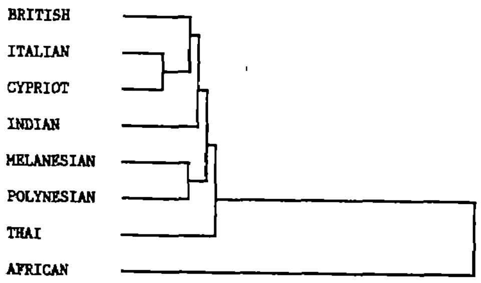

Fig. 2 Dendrogram for the eight population groups studied.

remaining 15 haplotypes which cannot be accounted for by single crossovers between the common haplotypes.

Genetic distance analysis of the populations was undertaken using the G_c distance measure of Balakrishnan and Sanghvi[11] (Table 2). The dendrogram based on these distances, using single-linkage cluster analysis[12], is shown in Fig. 2. Certain population groups which are close geographically are separated by small genetic distances, for example, the Cypriot and Italian, and the Polynesian and Melanesian populations. However, a striking finding is the large genetic distance observed between the African and non-African populations. Interestingly, among the known race-specific polymorphisms there does seem to be a predominance of unique alleles at both protein and blood-group loci in negroid populations[13]. Furthermore, several negroid-specific DNA polymorphisms have been described at well-characterized loci, for example, α-globin[14], β-globin[15,16], growth hormone[17], dihydrofolate reductase[18] and insulin[19]. Similarly, a negroid-specific haplotype has been described at the albumin locus[20]. These nuclear DNA data seem to support a primary division of human populations into an African and a Eurasian group. Thus, it may not be necessary to invoke a difference in mutation rate between populations to explain the genetic distance pattern observed by mtDNA analysis.

The earliest fossils of anatomically modern man (*Homo sapiens sapiens*) have been found in Africa at Omo in Ethiopia, Border Cave in South Africa and at Klasies River Mouth in South Africa[21]. The data from the last site suggest that *H. sapiens sapiens* was present in South Africa more than 100,000 yr ago[22], and an adult mandible from Border Cave has been dated to about 90,000 yr BP[23]. Hence, it has been argued that the evolution of modern man took place in Africa[21]. Our data are consistent with such a scheme, in which a founder population migrated from Africa and subsequently gave rise to all non-African populations. Such a group would appear to have lost the now predominant African haplotype (− − − − +), suggesting that the founder population was small. Comparative studies of other groups of nuclear DNA polymorphisms, particularly those which are population-specific, should provide further information on the prehistoric migrations and genetic affinities of human populations.

We thank Professors P. Wasi and G. J. F. Essan and Drs M. Sampietro, D. K. Bowden, S. J. Oppenheimer, R. J. Trent, K. Mickleson, K. Bhatia and B. Modell for help with the collection of samples for the original studies, and the Rockefeller Foundation for financial support.

Received 2 September; accepted 9 December 1985.

1. Nei, M. & Roychoudhury, A. K. *Science* **177**, 434–436 (1972).
2. Nei, M. & Roychoudhury, A. K. *Evol. Biol.* **14**, 1–59 (1982).
3. Jeffreys, A. J. *Cell* **18**, 1–10 (1979).
4. Cooper, D. N., Smith, B. A., Cooke, H. J., Niermann, S. & Schmidtke, J. *Hum. Genet.* **69**, 201–205 (1985).
5. Antonarakis, S. E., Boehm, C. D., Giardina, P. J. V. & Kazazian, H. H. *Proc. natn. Acad. Sci. U.S.A.* **79**, 137–141 (1982).
6. Cavalli-Sforza, L. L. & Edwards, A. W. F. *Genetics Today* (Pergamon, Oxford, 1964).
7. Piazza, A., Sgaramella-Zonta, L., Gluckman, P. & Cavalli-Sforza, L. L. *Tissue Antigens* **5**(5), 445–463 (1975).
8. Johnson, M. J., Wallace, D. C., Ferris, S. D., Rattazzi, M. C. & Cavalli-Sforza, L. L. *J. molec. Evol.* **19**, 255–271 (1983).
9. Cheng, T. *et al. Proc. natn. Acad. Sci. U.S.A.* **81**, 2821–2825 (1984).
10. Bellwood, P. *Man's Conquest of the Pacific* (Collins, London, 1978).
11. Balakrishnan, V. & Sanghvi, L. D. *Biometrics* **24**, 859–865 (1968).
12. Sneath, P. H. A. & Sokal, R. R. *Numerical Taxonomy* (Freeman, San Francisco, 1973).
13. Mourant, A. E. *Histocompatibility Testing*, 31–37 (1972).
14. Goodbourn, S. E. Y., Higgs, D. R., Clegg, J. B. & Weatherall, D. J. *Molec. Biol. Med.* **2**, 223–238 (1984).
15. Kan, Y. W. & Dozy, A. M. *Science* **209**, 492–493 (1980).
16. Orkin, S. H., Antonarakis, S. E. & Kazazian, H. H. *Prog. Haemat.* **13**, 49–73 (1983).
17. Chakravarti, A., Phillips, J. A., Mellits, K. H., Buetow, K. H. & Seeburg, P. H. *Proc. natn. Acad. Sci. U.S.A.* **81**, 6085–6089 (1984).
18. Anagnou, N. P. *et al. Proc. natn. Acad. Sci. U.S.A.* **81**, 5170–5174 (1984).
19. Bell, G. I. Horita, S. & Karam, J. H. *Diabetes* **33**, 176–183 (1984).
20. Murray, J. C., Mills, K. A., Demopulos, C. M., Hornung, S. & Motulsky, A. G *Proc. natn. Acad. Sci. U.S.A.* **81**, 3486–3490 (1984).
21. Stringer, C. in *Hominid Evolution* (ed. Foley, R.) 55–83 (Academic, New York, 1984).
22. Singer, R. & Wymer, J. *The Middle Stone Age at Klasies River Mouth in South Africa* (University of Chicago Press, 1982).
23. De Villiers, H. *S. Afr. J. Sci.* **72**, 213–215 (1976).
24. Old, J. M. & Higgs, D. R. *Meth. Haemat.* **6**, 74–102 (1982).

Crabs that breathe air with their legs—*Scopimera* and *Dotilla*

David P. Maitland

School of Zoology, University of New South Wales, PO Box 1,
Kensington, New South Wales, Australia 2033

Sand-bubbler crabs, *Scopimera* and *Dotilla* (Crustacea, Brachyura, Ocypodidae, Scopimerinae), are small (carapace width 1 cm) round-bodied crabs which occur in vast numbers throughout the Indo–Pacific on suitable tropical and sub-tropical sheltered sandy beaches. At high tide they are found in burrows that contain a trapped pocket of air in which the crabs are able to breathe until low tide. During low tide they become active and emerge from their burrows to feed on surface detritus and stranded plankton[1–3]. One of the most striking, and unique, features of these crabs is the presence of large membranous disks ('tympana') on the meral segments of the legs (Fig. 1) and sometimes (in *Dotilla*) on the thoracic sterna[3]. Although in 1893 Aurivillius suggested that the membranes might be used for hearing[4], their function has remained unknown. Here I present evidence which suggests that, rather than being auditory organs, the tympana are primarily respiratory structures used in aerial gas exchange. As the generic name *Scopimera* means "thighs with windows in them"[5], I have coined the term 'gas windows' for these membranes.

Scopimera inflata, which is endemic to Australia, is a typical scopimerine crab with slender legs and meri expanded and flattened in the vertical plane. On both sides of each merus (including the chelae) is a large oval membrane stretched across the curved frame of the leg—the gas window (see Fig. 2*A*). Immediately below the gas-window membrane lies a complex system of blood spaces (Fig. 2*B*–*D*). To visualize these spaces, autotomized legs were injected with Batson's No. 17 corrosion compound (Polysciences, Warrington, Pennsylvania) into the leg sinus between the dactylus and propodus joint (see ref. 6 for additional methods).

In general, a single artery supplies the legs of crabs with oxygenated blood and venous blood drains into the leg sinus which surrounds the muscles like a sleeve[7]. In *S. inflata* the venous blood flows relatively freely back up the leg sinus towards the body until it reaches the meral segment; here it is divided and collected in a complex series of large blood channels formed by a matrix of connective tissue sheets and partitions (Fig. 2*C*). The blood is directed towards the respiratory epithelium within branching channels of ever decreasing diameter (30 μm to 15 μm to 5 μm) until it is spread as a thin layer (3–5 μm) directly below the gas-window membrane (Fig. 2*D*) (compare with the lacunar beds of crab lungs[6,8]). The blood from the smaller spaces ('lacunae') is subsequently guided away from the membrane within a closely interdigitating series of larger, flattened channels

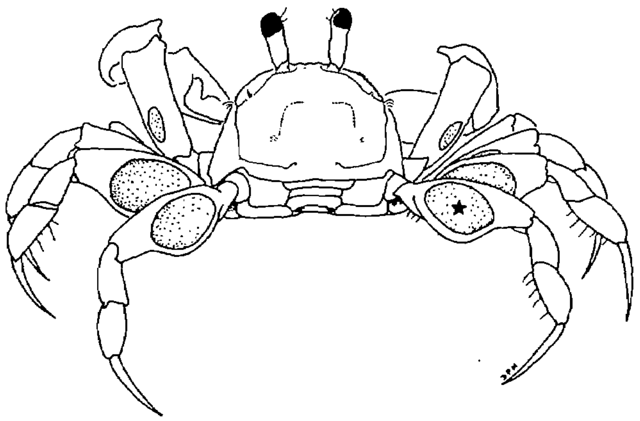

Fig. 1 The sand-bubbler crab *Scopimera inflata* is typical among scopimerine crabs in possessing a pair of membranous disks (gas windows) in each leg meral segment (indicated by a star). The crab measures 1 cm across the carapace.

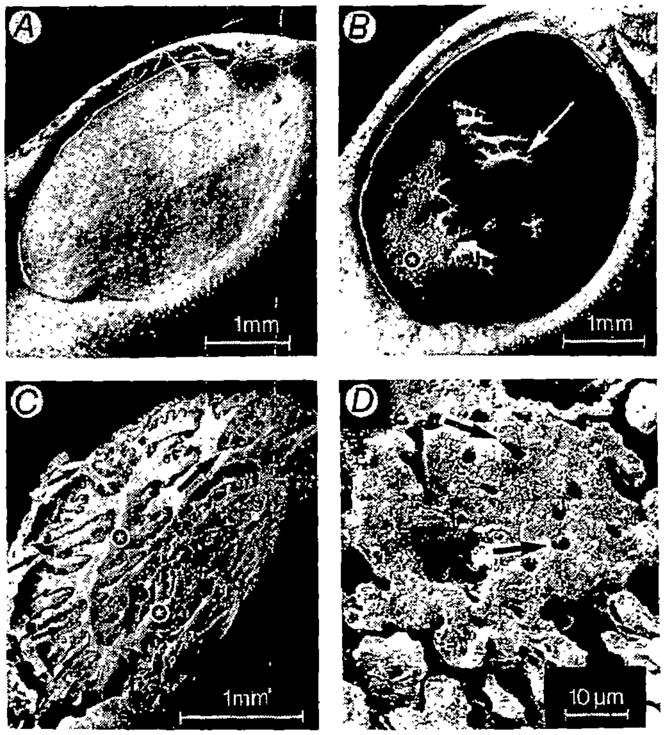

Fig. 2 *A*, Scanning electron micrograph (SEM) of the anterior gas window on the merus of the second right walking leg of *S. inflata* (dorsal is top left and proximal is top right). *B–D*, SEMs of plastic casts of gas-window blood channels in the legs of *S. inflata*. Blood flows towards the body from lower left to upper right in each case. *B*, A partial cast showing the organization of blood channels in relation to the merus of the second walking leg (anterior face). Large blood channels (located away from the membrane) supplying the posterior gas window (arrow) are visible behind the anterior gas-window blood system. Small blood channels (star) project towards the anterior gas-window membrane. Dorsal is top left, proximal top right. *C*, The internal surface of a complete cast. A distributing system (arrows, lower left) is linked to a collecting system (arrow, top right) via one or more 'portal' systems (stars). The blood is forced to pass from system to system through fine channels ('lacunae'; see *D*) in direct contact with the gas-window membrane. Same orientation as in *A* and *B*. *D*, The external surface of a cast showing the flat lacunar distribution of blood directly beneath the gas-window membrane. The small round holes (arrows) mark the positions of 'pillar cells'[8] which anchor the connective tissue matrix to the membrane and which have been removed during the casting procedure.

(100-200 μm wide and 40-70 μm deep) before being redirected towards a new patch of membrane through a new set of smaller channels. The process is repeated one or more times until the blood leaves the gas-window complex via a collecting system (Fig. 2*C*) (compare with the crab lung portal systems[9]). In *Scopimera* most, if not all, of the venous blood returning from the leg segments distal to the merus is forced to pass through the gas-window complex (D.P.M., unpublished). The cuticle covering the gas window is extremely thin (0.6 μm) (D.P.M., unpublished) and compares well with the ultra-thin lung cuticle (0.2 μm) of other air-breathing crabs[6,8,10].

The total surface area of the gas window in *S. inflata* is large (Fig. 3*A*) and greater than the predicted lung surface area in another air-breathing crab, *Holthuisana transversa*[11]. Some species of *Dotilla* (for example *Dotilla myctiroides*) also have gas windows on the sternal plates of the thorax[3]. Although *D. myctiroides* has consistently smaller leg gas windows and narrower meri than *S. inflata*, the total membrane area in *D. myctiroides* is greater because of the added area provided by the sternal gas windows (Fig. 3*A*).

On morphological grounds, therefore, the gas windows are well suited for aerial gas exchange. To obtain physiological evidence for such a function, the oxygen consumption of 11 male *S. inflata* was measured using Warburg respirometers[12] adapted to accommodate crabs. The gas windows were painted over with a coat of Humbrol (Hull, UK) non-toxic, oil-based enamel paint and the rate of oxygen consumption was compared with the rate before painting of the windows and with the rate after the paint had been removed (Fig. 3*B*). While in the flasks, the crabs were continually active, consuming large amounts of oxygen even when the flasks were kept in the dark. This response was consistent and prevented measurement of basal metabolic rates. Behavioural observations revealed that crabs always attempted to move off and away from non-sand substrates (for example, glass) or continually attempted to dig. However, when the gas windows were painted over, mean oxygen consumption (±s.d.) fell by 59.8±8.5% (range 40.9-69.9%); when the paint was removed the oxygen consumption rose significantly ($P>0.001$, paired Student's *t*-test). Although animals sometimes did not recover to 'pre-painted' levels, the effect was nonetheless dramatic and certainly indicates that gas windows are involved in aerial gas exchange. Indeed, the fall in oxygen consumption would have been more dramatic had the crabs not been able to remove some of the paint (before it dried) by scraping their legs together—a behaviour that was difficult to prevent. When another coat of paint was applied to the legs after the first had dried, the gas windows were completely sealed and these animals always died soon after. Crabs never died, however, when the two coats of paint were perforated, and in these cases the oxygen consumption was similar to that in crabs with one coat of paint. To a certain extent, this result excludes a possible toxic effect of the paint and confirms the importance of the gas windows in aerial gas exchange.

The most characteristic structural adaptation to air-breathing in crabs has been the expansion and vascularization of the branchiostegites forming an air cavity above the gills, and thus a lung[6,9,13]. *Scopimera* and *Dotilla* are most unusual among air-breathing crabs because they do not have a lung; the brachial chambers are small and are completely filled by the six gills which are continually bathed in water and are therefore not available for aerial gas exchange. The branchiostegites are poorly vascularized and are not expanded laterally. There is, therefore, no air cavity or vascular lining above the gills through which any significant aerial gas exchange might occur. Instead, these crabs have developed an alternative air-breathing structure—the unique, extra-branchial gas windows. These structures almost certainly serve to oxygenate venous blood returning from the leg sinuses.

Despite the obvious vulnerability of such thin and exposed membranes, gas windows have evolved in several genera of

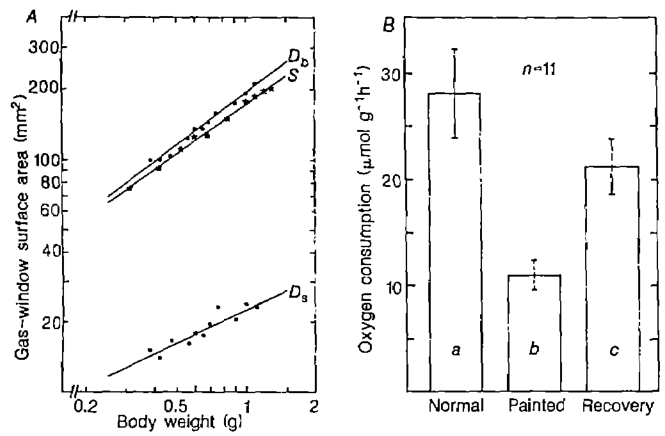

Fig. 3 *A*, Graphs showing the total surface area of gas-window membranes on legs of male *Scopimera inflata* of different body weights (S); and for *Dotilla myctiroides* the total surface area of both leg and sternal gas windows (D_b), and the area of sternal gas windows alone (D_s). Lines were fitted to the data by least-squares linear regression, $y = aM^b$ where y = the total surface area in mm^2, M = body wet weight (in g), a = value of y when $M = 1$ g and b = slope of regression of log y on log M: for S, $y = 172.2M^{0.699}$; for D_b, $y = 190.6M^{0.730}$; for D_s, $y = 22.8M^{0.476}$. The surface area of leg gas windows alone in *D. myctiroides* follows the relationship $y = 167.8M^{0.769}$ (not shown). Surface areas were calculated by cutting out camera lucida tracings of gas-window perimeters (drawn at ×25 or ×50 magnification) and their weights were compared with that of a similar piece of paper of known surface area. *B*, Histograms showing the rate of oxygen consumption of 11 male *S. inflata* ((0.78–1.12 g) before painting of the gas-window membrane (a); after painting (b); and after the paint has been removed by simply peeling it off (c). Mean oxygen consumption (±s.d.) was 27.8 ± 4.3 μmol g^{-1} h^{-1} in a, 10.8 ± 1.4 μmol g^{-1} h^{-1} in b, and 21.0 ± 2.7 μmol g^{-1} h^{-1} in c; b is significantly different from both a and c (paired t-test, $P > 0.001$). Warburg flasks of 60–62 cm^3 internal volume were used. Crabs were collected daily and rates of respiration were measured in air. Crabs and apparatus were equilibrated for 30 min and experiments were run for 2 h at 28 °C. Readings were taken every 10 min and the rate of oxygen consumption (per g wet weight per h) was calculated from the mean of these values and corrected to standard conditions of temperature and pressure, dry. Normal and painted crabs were run consecutively and recovery was checked the following morning.

ocypodid crabs[3]. To the researcher they present a unique expanse (up to 25 mm^2) of exposed, ultra-thin respiratory membrane which is readily accessible and easily manipulated. As the membranes are transparent, the mechanisms of blood flow through a capillary-like network can also be observed directly. Thus, they represent a useful experimental system.

I thank the Australian Institute of Marine Science, Townsville, for the use of facilities during oxygen consumption measurements; P. Ng and L. Tan at The Department of Zoology, National University of Singapore for their generous hospitality; J. Zeil, C. Farrelly, D. Sandeman and P. Greenaway for useful discussion; and R. Foertmeyer for translations from the German literature. This work was supported by an ARGS grant to D. C. Sandeman.

Received 16 September; accepted 15 November 1985.

1. McCulloch, A. R. & McNiell, F. A. *Rec. Aust. Mus.* **14**, 49–59 (1923–1926).
2. Hartnoll, R. G. *Estuar. coast. mar. Sci.* **1**, 137–152 (1973).
3. Kemp, S. *Rec. Indian Mus.* **16**, 305–348 (1919).
4. Aurivillius, C. W. S. *Nova Acta R. Soc. Scient. Upsal. Ser. 3)* **16**, 1–43 (1893).
5. de Haan, W. in *Fauna Japonica* (ed. de Siebold, Ph. Fr.) 24–25 (J. Muller & Sons, Amsterdam, 1833–1850).
6. Greenaway, P. & Farrelly, C. A. *J. Morph.* **181**, 133–142 (1984).
7. Maynard, D. M. *The Physiology of Crustacea* Vol. 1, 161–226 (Academic, London, 1960).
8. Storch, V. & Welsch, U. *Mar. Biol.* (*Berl.*) **29**, 363–371 (1975).
9. von Raben, K. *Z. wiss. Zool.* **145**, 425–461 (1934).
10. Taylor, H. H. & Greenaway, P. *J. Zool.* **189**, 359–384 (1979).
11. Greenaway, P. *Aust. J. Zool.* **32**, 1–6 (1984).
12. Umbreit, W. W., Burris, R. H. & Stauffer, J. F. *Manometric and Biochemical Techniques* 5th edn (Burgess, Minnesota, 1972).
13. Diaz, H. & Rodriguez, G. *Biol. Bull. mar biol. Lab., Woods Hole* **153**, 485–504 (1977).

Ganglion cell dendrites are presynaptic in catfish retina

Hiroko M. Sakai, Ken-Ichi Naka & John E. Dowling

National Institute for Basic Biology, Okazaki 444, Japan

The retinal ganglion cells are third-order, spike-generating neurones whose axons transmit the output of the retina to the rest of the brain. It has long been believed that the dendrites of the retinal ganglion cells, like the dendrites of most other Golgi type I neurones, are only postsynaptic. Here we have studied the synapses made onto the ganglion cells in the catfish (*Ictalurus punctatus*), and we report that the distal dendrites of large-field ganglion cells make conventional chemical synapses onto other inner plexiform layer processes. We have also found that, more than 100 μm away from the cell perikaryon, the synapses made onto and by these ganglion cell dendrites are often tightly clustered. These synaptic clusters appear to be quite regularly spaced along the dendrites. Our results have important implications for the identification of ganglion cell dendrites within the inner plexiform layer as well as for the understanding of the ganglion cell response and receptive field generation[1,2].

Ganglion cells in the catfish eyecup preparation were filled with horseradish peroxidase (HRP) either by intracellular injection following the recording of their physiological responses, or by back-filling by immersion of the cut optic nerve in Ringer's containing HRP for 3–5 h. Then, the eyecup was fixed in 4% paraformaldehyde and 1.25% glutaraldehyde in 0.1 M cacodylate buffer overnight. The retina was removed from the eyecup, reacted with diaminobenzidine, postfixed with 2% osmium tetroxide and embedded in Epon. The retina was sectioned tangentially, initially at a thickness of 30 μm, and stained ganglion cells were photographed and drawn. Sections containing one intracellularly stained ganglion cell, or several back-filled ganglion cells, were glued to blank Epon blocks, and thin (800 Å) serial sections were cut, mounted on Formvar-coated slot grids and stained with uranyl acetate and lead citrate for electron microscopy[3].

Figure 1A shows a photograph and a camera lucida drawing of a large-field ganglion cell injected with HRP. This cell fired spikes at both the onset and cessation of a step of light, that is, it was an 'on-off' ganglion cell[4,5]. Its perikaryon was located in the ganglion cell layer and its dendritic tree was bistratified, with processes running in both sublamina *a* and *b* of the inner plexiform layer[6]. The dendritic field of the cell was over 1 mm in diameter. An axon-like process was seen emerging from the perikaryon and running towards the optic nerve (not shown) The cell perikaryon and dendrites were examined by electron microscopy for evidence of synaptic junctions. The results (Fig. 1*A*) were typical of the large-field ganglion cells examined so far. The perikaryon and proximal dendrites were only postsynaptic. For the cell shown in Fig. 1*A*, all but one of the synapses made on the proximal dendrites were of the conventional type (solid arrowheads), indicating that these were likely to be amacrine cell synapses[1]. One synaptic junction was of the ribbon type (open arrowhead), indicating that it was a bipolar cell junction[1]. In other cells, a more even mix of bipolar and amacrine cell input was observed on the proximal dendrites, and synapses were also found on the cell perikaryon.

Beyond about 100 μm from the cell perikaryon, clusters of synaptic contacts were observed along the dendrites in sublamina *a* and *b*. These clusters consisted of 3–7 synaptic contacts spread along 10–30 μm of dendrite. Along one dendrite, which was followed for over 400 μm, three clusters were observed that were each separated by ~100 μm. We observed both amacrine (conventional) and bipolar (ribbon) synapses onto the ganglion cell dendrites in every cluster. In addition, synapses made by

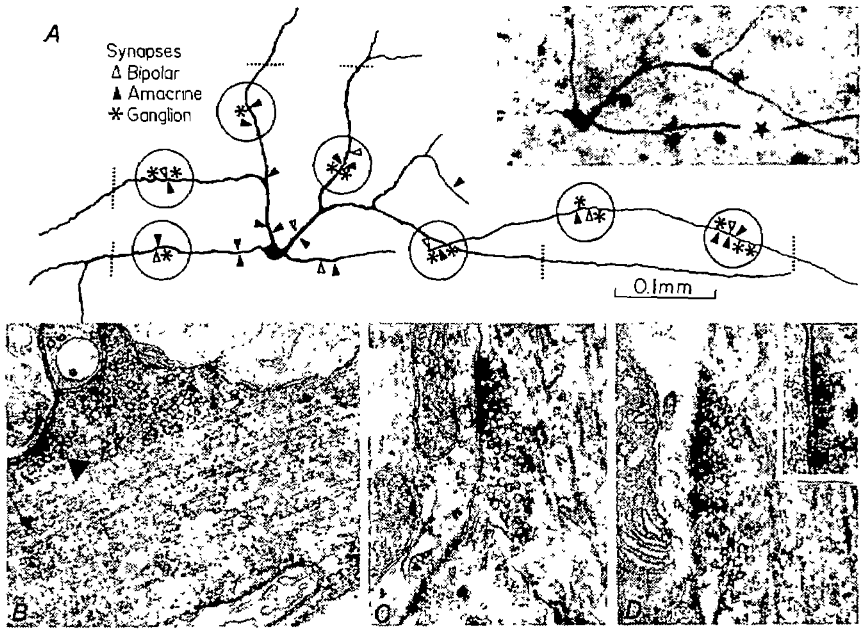

Fig. 1 *A*, Camera lucida drawing of an HRP-stained, large-field, on-off ganglion cell contained within a 30-μm tangential section of the catfish retina. One series of thin sections encompassed the entire cell perikaryon and the dendrites out to the dotted lines. Synapses made onto and by the cell are indicated approximately where they were observed on the cell. Each circled area represents a cluster of input and output synapses. Inset, a light micrograph showing part of the cell. The star indicates a small portion of the dendrite that was not included in the 30-μm-thick section of the cell. *B*, *C*, Electron micrographs showing synapses made by the ganglion cell in *A*. In *B* the synapse is marked by an arrowhead. *D*, Synapses observed in back-filled ganglion cell dendrites. Magnifications: *B*, ×23,000; *C*, ×21,000; *D*, +26,000; inset, ×32,000.

the ganglion cell dendrites were observed at these sites. As such synaptic junctions have not been seen previously, they will be described in detail.

Immediately adjacent to the synapses made by the ganglion cell dendrites, a dense aggregation of synaptic vesicles was typically observed. Often the dendrite bulged outwards slightly at such places (Fig. 1*B*), but this was not always the case (Fig. 1*C*). At the presumed site of synaptic contact, electron-dense material was usually observed in association with the membranes of the contacting elements and within the synaptic cleft (Fig. 1*B*–*D*). Synaptic vesicles were never observed in the ganglion cell dendrites away from the synaptic sites. The synapses made by the ganglion cell dendrites were often on processes that contained no synaptic vesicles. However, we have observed ganglion cell synapses on vesicle-containing (amacrine or ganglion cell) processes and on ribbon-containing (bipolar cell) processes. As yet, a ganglion cell synapse on a process that was itself synapsing on the dendrite (a reciprocal synapse) has not been observed. It was not possible to observe synapses made by the dendrites in every large-field HRP-stained ganglion cell. If the HRP stain was very dense, intracellular structures were obscured and it was impossible to observe the synapses. We have been successful, however, in identifying dendritic synapses in those large-field cells that were stained dark enough to be positively identified in the electron microscope, but light enough for the cell interior to be visualized. So far, we have observed synapses made by the distal dendrites of the following three large-field ganglion cells injected intracellularly with HRP: the bistratified 'on-off' cell shown in Fig. 1*A*; a monostratified, large-field, on-centre ganglion cell; and a monostratified, large-field, off-centre ganglion cell[7].

Figure 2 shows data recorded from the large-field, off-centre ganglion cell; this cell was spontaneously active and responded to full-field illumination with a sustained hyperpolarization followed by transient depolarizations on removal of the light (Fig. 2*A*). The cell perikaryon was located in the ganglion cell layer, and its dendrites were confined to sublamina *b* of the inner plexiform layer. The dendritic field of this cell also extended over 1 mm in diameter. Conventional (amacrine cell) synapses were seen on the cell perikaryon, while on the proximal dendrites both conventional and ribbon (bipolar cell) synapses were found. Beyond about 100 μm from the cell perikaryon, synapses made by the ganglion cell dendrites were observed and, as was the case for the on–off cell shown in Fig. 1, clusters of synapses were observed along the distal dendrites. Figure 2*C* shows an example of a synapse made by this cell which was found about 150 μm from the perikaryon (arrow in Fig. 2*B*).

Although each of the large-field ganglion cells studied so far gave typical ganglion cell responses, with spikes of amplitude 5–20 mV, an axon was positively identified only for the cell shown in Fig. 1*A*. To ensure that we had correctly identified these neurones as ganglion cells, we examined three series of sections containing back-filled ganglion cells. In each of these series, synapses made by stained dendrites, similar to those observed in the intracellularly stained cells, were seen. Figure 1*D* shows two such examples. The preservation of the back-filled ganglion cells was not usually as satisfactory as that of the intracellularly injected cells; nevertheless, the results were unequivocal in showing synaptic junctions made by the dendrites of back-filled ganglion cells.

We have also studied two small-field ganglion cells, filled intracellularly with HRP, whose dendritic fields were, respectively, ~200 and 350 μm in diameter. Synapses onto the perikarya and dendrites of these cells were readily observed, but the synapses did not appear to be clustered along the dendrites as was the case for the large-field cells. Furthermore, no synapses made by the dendrites of these ganglion cells have been observed. The HRP staining of these cells was denser than that of the large-field ganglion cells described above, and intracellular structures in some of the dendrites were obscured. However, about two-thirds of the dendrites were stained lightly enough for the synapses to have been observed if they were present. Thus, it seems likely that synapses are made only by the distal dendrites of the large-field ganglion cells in catfish.

It has long been recognized that the dendrites of many short-axon or axonless (Golgi type II) cells in the retina and elsewhere may be both pre- and postsynaptic[1,8–10]. Many of these cells have been shown to function mainly with sustained, graded potentials[11,12]. Only in a few instances have presynaptic dendrites been observed in long-axon cells[8,13], and there has been no evidence so far that any of the long-axon ganglion cells of the retina, which are typical Golgi type I cells, have dendrites which are presynaptic. An obvious and important question to ask is whether ganglion cells in other species, and other Golgi type I cells, make dendritic synapses. It is of interest to note in this regard that there is recent physiological evidence for direct interactions between ganglion cells in the cat retina[14]. These authors argued, however, that these interactions are more likely

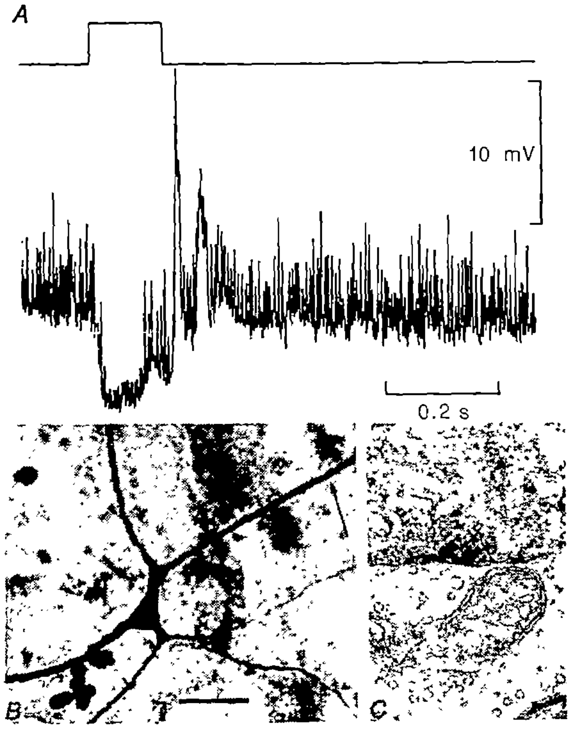

Fig. 2 *A*, Step-evoked response from a large-field, off-centre ganglion cell. The cell showed spontaneous activity which was depressed during the light-evoked hyperpolarization. The transient depolarizations that occurred during the sustained hyperpolarization are characteristic of off-centre ganglion cells in catfish. Two large sharp depolarizations occurred on removal of the light. The smaller amplitude of the spikes compared with the excitatory postsynaptic potentials seen in this cell suggests that the spikes must have been produced some distance away from the recording site. The light stimulus was 0.1 μW cm^{-2}. *B*, Light micrograph showing part of the large-field off-centre ganglion cell whose response to light is shown in *A*. Scale bar, 50 μm. *C*, An electron micrograph showing a synapse made by a dendrite of the ganglion cell shown in *B*. The site of the synapse is indicated by an arrow in *B*. ×26,000.

to be mediated by electrical junctions than by chemical synapses.

The clustering of synapses along the distal dendrites of the catfish large-field ganglion cells is a novel observation which has implications for the generation of ganglion cell responses and for inner plexiform layer information processing. Similar clustering of pre- and postsynaptic sites has been observed in certain leech and insect neurones[15-17]. That the clusters are separated by 100 μm or more along the ganglion cell dendrites suggests that these synaptic aggregations operate relatively independently of one another and may represent sites for local signal processing within the inner plexiform layer[2].

As noted above, the dendritic fields of many of the catfish ganglion cells extend well over 1 mm in diameter. It is unlikely that single synaptic inputs several hundred micrometres away from the cell perikaryon will significantly affect the spike output of the cell. Thus, the clusters of synapses observed along the distal dendrites may also serve as integrating centres such that, when acting in concert in a cluster, the distal synapses are capable of shaping the ganglion cell responses.

J.E.D. was on leave of absence from Harvard University and was supported by a grant from the Japanese Society for the Promotion of Science.

Received 16 September; accepted 21 November 1985.

1. Dowling, J. E. & Boycott, B. B. *Proc. R. Soc.* B166, 80-111 (1966).
2. Koch, C., Poggio, T. & Torre, V. *Phil. Trans. R. Soc.* B298, 227-264 (1982).
3. Sakai, H. & Naka, K.-I. *Vision Res.* 23, 339-351 (1983).
4. Hartline, H. K. *Am. J. Physiol.* **121**, 400-415 (1938).
5. Chan, R. Y. & Naka, K.-I. *Vision Res.* **16**, 1119-1129 (1976)
6. Nelson, R., Famiglietti, E. V. Jr & Kolb, H. *J. Neurophysiol.* **41**, 472-483 (1978)
7. Davis, G. W. & Naka, K.-I. *J. Neurophysiol.* **43**, 807-831 (1980)
8. Rall, W., Shepherd, G. M., Rees, T. S. & Brightman, M. W. *Expl Neurol.* **14**, 44-56 (1966)
9. Ralston, H. J. III *Nature* **230**, 585-587 (1971).
10. Ralston, H. J. III in *The Neurosciences: 4th Study Program* (eds Schmitt, F. O. & Worden, F. G.) 373-379 (MIT Press, 1979).
11. Werblin, F. S. & Dowling, J. E. *J. Neurophysiol.* **32**, 339-355 (1969)
12. Kaneko, A. *J. Physiol., Lond.* **207**, 623-633 (1970).
13. Hamos, J., Van Horn, S. C., Baczkowski, D., Uhlrich, D. J. & Sherman, S. M. *Nature* 317, 618-621 (1985).
14. Mastronarde, D. W. *J. Neurophysiol.* **49**, 350-365 (1983).
15. Muller, K. J. & McMahan, U. J. *Proc. R. Soc.* B194, 481-499 (1976)
16. Watson, A. H. D. & Burrows, M. *J. comp. Neurol.* **205**, 383-397 (1982)
17. Watson, A. H. D. *J. Neurocytol.* 13, 303-327 (1984).

Different factors from the central nervous system and periphery regulate the survival of sensory neurones

Alun M. Davies, Hans Thoenen & Yves-Alain Barde

Department of Anatomy, St George's Hospital Medical School,
Cranmer Terrace, London SW17 0RE, UK and Department of
Neurochemistry, Max Planck Institute for Psychiatry,
8033 Planegg-Martinsried, München, FRG.

Work on nerve growth factor has established that the survival of developing vertebrate neurones depends on the supply of a neurotrophic factor from their target field[1-5]. The discovery of several new neurotrophic factors[6] has raised the possibility that neurones which innervate multiple target fields require several different neurotrophic factors for survival. Here we show that two distinct neurotrophic factors, one in the central nervous system (CNS) and the other in skeletal muscle, promote the survival of proprioceptive neurones in culture. At saturating concentrations, either factor alone supported most neurones and there was no additional survival in the presence of both factors, but at sub-saturating concentrations the combined effect was additive. The neurotrophic activity of each factor was greatest during the period of natural neuronal death. Our results demonstrate that each cultured proprioceptive neurone responds to two distinct neurotrophic factors present in its respective central and peripheral target fields, and suggest that these factors cooperate in regulating survival during development.

To investigate the specific neurotrophic requirements of neurones that innervate two distinct target fields, we studied the neurones of the embryonic chick trigeminal mesencephalic nucleus (TMN). Despite their location in the brain stem, these are unipolar, first-order, sensory neurones derived from the neural crest[7], with processes that divide into central and peripheral branches. The central branches innervate certain brainstem nuclei, including the trigeminal motor nucleus, and the peripheral branches are distributed to proprioceptors in the muscles of mastication[8]. *In vivo*, 70% of TMN neurones die during the innervation of these central and peripheral target fields[9].

We used a recently described method to establish glia-free cultures of TMN neurones[10]. The survival and growth of most of the neurones was promoted by an extract of skeletal muscle, their specific peripheral target tissue (Fig. 1). Because these neurones also project to target fields in the CNS, we sought to ascertain whether a recently purified protein[11], brain-derived neurotrophic factor (BDNF), known to act on nodose and dorsal root ganglion neurones[12], also promotes the survival of TMN neurones. As with skeletal muscle extract, we found that most TMN neurones (70-80%) survived and grew in the presence of saturating concentrations of BDNF (Fig. 1) and could be sustained in culture for more than a month with regular supplements of either factor. Virtually no neurones survived without BDNF or skeletal muscle extract. The combination of BDNF and muscle extract was additive at concentrations below saturation (Fig. 1), whereas at saturating concentrations, the combination did not promote the survival of additional neurones, indicating that all the surviving neurones responded to both factors. As the neurotrophic factor in muscle extract has not yet been purified it was necessary to show that it is functionally distinct from BDNF. This was done using explants of the ventrolateral part of the trigeminal ganglion. Although BDNF elicited profuse outgrowth from these explants, skeletal muscle extract did not (Fig. 2). In contrast, both agents were active on TMN explants (Fig. 2).

The neurite-promoting effects of BDNF and muscle extract on TMN explants showed a very similar developmental time-course (Fig. 3), which suggests that these factors are active during the same stage of neuronal development. The magnitude of neurite outgrowth in response to each factor was most marked at stages E10 and E11, which are closely related to the stage of natural neuronal death in the TMN (E9-E13)[13]. Thus, TMN neurones are most sensitive to the neurotrophic effects of BDNF and muscle extract at the same time as their survival is critically dependent on forming appropriate central and peripheral connections.

Our findings suggest that the survival of developing sensory neurones *in vivo* is normally dependent on the supply of both a neurotrophic factor from the periphery and a different

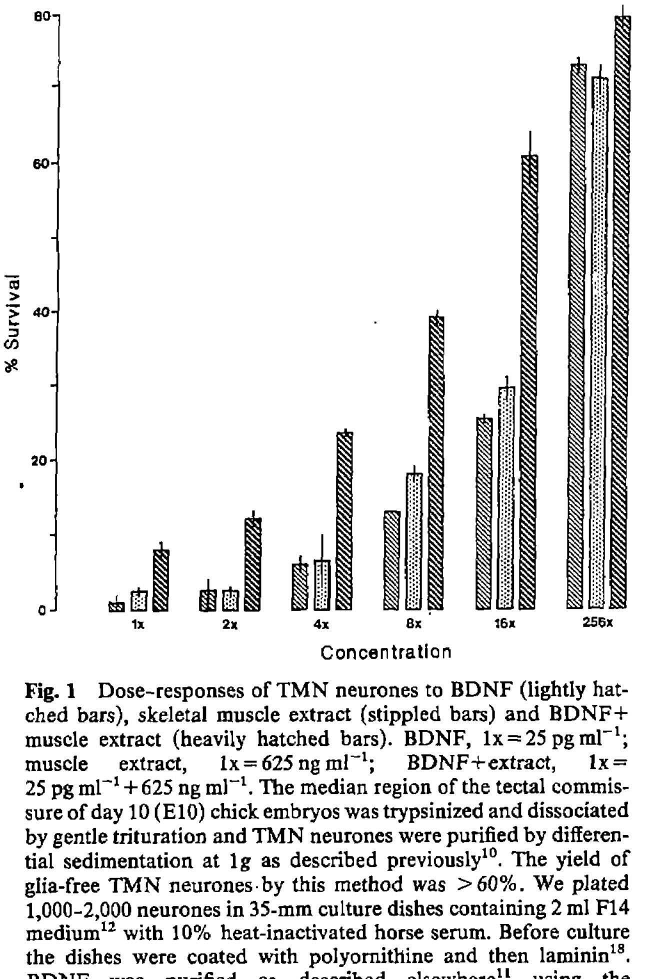

Fig. 1 Dose-responses of TMN neurones to BDNF (lightly hatched bars), skeletal muscle extract (stippled bars) and BDNF+muscle extract (heavily hatched bars). BDNF, 1x = 25 pg ml^{-1}; muscle extract, 1x = 625 ng ml^{-1}; BDNF+extract, 1x = 25 pg ml^{-1} + 625 ng ml^{-1}. The median region of the tectal commissure of day 10 (E10) chick embryos was trypsinized and dissociated by gentle trituration and TMN neurones were purified by differential sedimentation at 1g as described previously[10]. The yield of glia-free TMN neurones by this method was >60%. We plated 1,000-2,000 neurones in 35-mm culture dishes containing 2 ml F14 medium[12] with 10% heat-inactivated horse serum. Before culture the dishes were coated with polyornithine and then laminin[18]. BDNF was purified as described elsewhere[11] using the modifications described by Lindsay *et al.*[12]. Skeletal muscle extract was prepared from E18 chick pectoral muscle: 100 g muscle was homogenized in 250 ml 10 mM phosphate buffer at *p*H 7.0 containing 150 mM NaCl and 0.5 mM EDTA using a Sorvall Omnimixer. This homogenate was centrifuged at 20,000*g* for 1 h and ammonium sulphate added to the supernatant to 30% saturation. The resulting precipitate was discarded and ammonium sulphate increased to 50% saturation. This precipitate was dissolved in water and passed through a Sephadex G25 column equilibrated with F14 medium from which the void fraction containing the protein was collected. The cultures were viewed by phase-contrast microscopy after 48 h incubation and the percentage of neurones with processes >10 cell diameters was determined. The results are expressed in percentage survival, 100% being the number of cells at the time of plating. 2% of the neurones survived in the absence of BDNF and muscle extract (control cultures), and this value is subtracted from all bars. The mean and range of the percentage survival at each concentration is plotted, $n = 2$. NGF (0.2-625 ng ml^{-1}), either alone or in combination with BDNF, did not promote or influence neuronal survival (A.M.D., A. G. S. Lumsden and H. Rohrer, unpublished data).

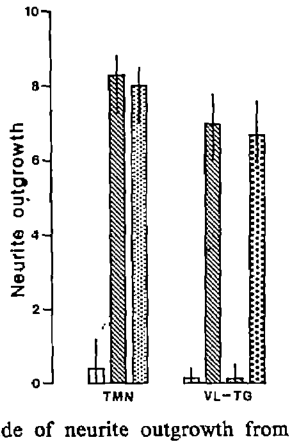

Fig. 2 Magnitude of neurite outgrowth from explants of the ventrolateral part of the trigeminal ganglion (VL-TG) and from TMN explants in control cultures (clear bars) and cultures supplemented with BDNF at 100 ng ml^{-1} (hatched bars), skeletal muscle extract at 160 μg ml^{-1} (light stippled bars) and BNDF+muscle extract (heavy stippled bars). Five explants were embedded in 250 μl collagen gel in 16-mm diameter plastic wells[19] and overlaid with 100 μl heat-inactivated horse serum and 650 μl F14 medium. The cultures were examined after 24 h incubation and the magnitude of neurite outgrowth was scored on an ordinal scale[20] from 0 to 10. The median and interquartile deviation of these scores are plotted. Although BDNF elicited marked fibre outgrowth from both VL-TG and TMN explants, skeletal muscle extract was active only on TMN explants. Note that BDNF was also active on VL-TG explants in the presence of muscle extract, showing that the lack of response of VL-TG explants to muscle extract alone is not caused by an inhibitory effect.

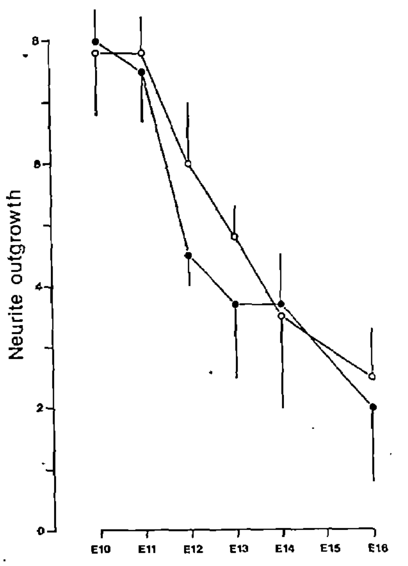

Fig. 3 Magnitude of neurite outgrowth from TMN explants of E10-E16 chick embryos after 24 h incubation with either BDNF at 100 ng ml^{-1} (solid circles) or muscle extract at 160 μg ml^{-1} (open circles). The median and an interquartile deviation are shown for each age.

neurotrophic factor from the CNS. Note that Yip and Johnson[13,14] have demonstrated that peripheral or central rhizotomy of dorsal root ganglia in neonatal rats results in the death of about half of the neurones. Furthermore, they showed that NGF administered at the time of the lesion prevented neurone death. In view of our finding that sensory neurones can be sustained by a sufficiently high concentration of either a peripheral or a central neurotrophic factor alone (Fig. 1), we suggest that NGF (found *in vivo* in the peripheral but not the central branches of dorsal root ganglia[15]) administered in high enough concentrations may rescue all NGF-responsive sensory neurones even when experimentally deprived of the supply of their CNS-derived trophic factor which we believe to be either BDNF or another, as yet uncharacterized, molecule.

Our demonstration of the response of sensory neurones to distinct central and peripheral neurotrophic factors provides the basis of a mechanism for selectively supporting the survival of only those neurones which make appropriate connections in both target fields. If the availability of each neurotrophic factor in the respective central and peripheral target fields lies below the critical threshold for maintaining survival, it would be necessary for a developing sensory neurone to make both the appropriate central and peripheral connections to procure sufficient trophic support to ensure survival. Supporting this contention is evidence from immunoassays of NGF[16] and from the purification of BDNF[11] that neurotrophic factors are normally present in only minute amounts. Furthermore, the amount of NGF present in target organs does not allow the survival of all innervating neurones because additional NGF rescues neurones that would otherwise die during development[17]. Additional NGF also increases the levels of catecholamine-synthesizing enzymes[2], indicating that the synthesis of these enzymes is not normally fully stimulated by NGF *in vivo*. Also, there is a correlation between the density of sympathetic innervation and the tissue concentration of NGF[16] and NGF messenger RNA[4,5], suggesting that the density of innervation is regulated by the availability of neurotrophic factor.

In the light of our findings it will be of interest to ascertain whether, in addition to sensory neurones, other neurones which innervate more than one target field require a different neurotrophic factor from each field for survival.

We thank the Wellcome Trust for the award of a Research Travel grant to A.M.D. and Frau Ĉáp for technical assistance.

Received 25 July; accepted 10 December 1985.

1. Levi-Montalcini, R. & Angeletti, P. U. *Physiol. Rev.* **48**, 534–569 (1968)
2. Thoenen, H. & Barde, Y.-A. *Physiol. Rev.* **60**, 1284–1335 (1980).
3. Cowan, W. M., Fawcett, J. W., O'Leary, D. D. M. & Stanfield, B B *Science* **225**, 1258 1265 (1984).
4. Heumann, R., Korsching, S., Scott, J. & Thoenen, H. *EMBO J* **3**, 3183–3189 (1984)
5. Shelton, D. L. & Reichardt, L. F. *Proc. natn. Acad. Sci. U.S.A.* **81**, 7951–7955 (1984)
6. Barde, Y.-A., Edgar, D. & Thoenen, H. *A. Rev. Physiol.* **45**, 601–612 (1983)
7. Narayanan, C. H. & Narayanan, Y. *J. embryol. exp. Morph.* **43**, 85–105 (1931)
8. Manni, E., Bortolani, R. & Azzena, G. B. *Expl Neurol.* **12**, 320–328 (1965)
9. Rogers, L. A. & Cowan, W. M. *J. comp. Neurol.* **147**, 291–320 (1973)
10. Davies, A. M. *Devl Biol.* (in the press).
11. Barde, Y.-A., Edgar, D. & Thoenen, H. *EMBO J.* **1**, 549–553 (1982)
12. Lindsay, R. M., Thoenen, H. & Barde, Y.-A. *Devl Biol.* **112**, 319–328 (1985)
13. Yip, K. H. & Johnson, E. M. *Proc. natn. Acad. Sci. U.S.A.* **81**, 6245–6249 (1984)
14. Johnson, E. M. & Yip, K. H. *Nature* **314**, 751–752 (1985)
15. Korsching, S. & Thoenen, H. *Neurosci. Lett.* **54**, 201–205 (1985).
16. Korsching, S. & Thoenen, H. *Proc. natn. Acad. Sci. U.S.A.* **80**, 3513–3516 (1983)
17. Hamburger, V., Brunso-Bechtold, J. K. & Yip, J. W. *J. Neurosci.* **1**, 60–71 (1981)
18. Edgar, D., Timpl, R. & Thoenen, H. *EMBO J.* **3**, 1463–1468 (1984)
19. Lumsden, A. G. S. & Davies, A. M. *Nature* **306**, 786–788 (1983)
20. Davies, A. M. & Lumsden, A. G. S. *J. comp. Neurol.* **223**, 124–137 (1984)

Proliferating bipotential glial progenitor cells in adult rat optic nerve

Charles ffrench-Constant & Martin C. Raff

Medical Research Council Neuroimmunology Project,
Zoology Department, University College London,
London WC1E 6BT, UK

We have shown previously that the rat optic nerve contains three types of macroglial cells—oligodendrocytes and two types of astrocytes—which develop as two distinct lineages. Type-1 astrocytes develop from one type of precursor cell beginning at embryonic day 16 (E16)[1], while oligodendrocytes and then type-2 astrocytes develop from a common, bipotential progenitor cell beginning at birth (E21) and postnatal days 7–10 (P7–10), respecively[2]. Here we report that proliferating bipotential oligodendrocyte–type-2 astrocyte (0-2A) progenitor cells are present in the adult rat optic nerve, raising the possibility that these cells are produced continually from self-renewing stem cells throughout life.

0-2A progenitor cells in cultures of perinatal optic nerve have a characteristic process-bearing morphology[3–6] and are labelled by the A2B5 monoclonal antibody, which recognizes specific angliosides[7], but not by antisera against glial fibrillary acidic protein (GFAP), which react specifically with astrocytes[8,9], or y monoclonal anti-galactocerebroside (GC) antibody[10], which eacts specifically with oligodendrocytes[10,11]. Although 0-2A progenitor cells in the perinatal optic nerve proliferate *in vivo*[12], *n vitro* they prematurely stop dividing and differentiate. In ultures containing ≥10% fetal calf serum (FCS), most acquire GFAP within 1–2 days to become A2B5$^+$, GFAP$^+$ type-2 strocytes, whereas in cultures containing ≤1% FCS most cquire GC within 2 days to become A2B5$^+$, GC$^+$ oligodenrocytes[13,14], which soon become A2B5$^-$ (ref. 5). On the other and, when cultured on a monolayer of type-1 astrocytes in .5% FCS, or in low-serum medium conditioned by type-1 astrocytes, 0-2A progenitor cells continue to proliferate and produce post-mitotic oligodendrocytes for weeks[4,5], just as they do *in vivo*[15,16]. Moreover, when E17 optic nerve cells are cultured on type-1 astrocytes in 0.5% FCS, the first oligodendrocytes appear after 4 days *in vitro*[5], equivalent to the time they first appear *in vivo*[2]. These observations led us to propose that the timing of oligodendrocyte differentiation depends on an intrinsic clock in the 0-2A progenitor cells. The clock operates by counting cell divisions, which are driven by growth factors released by type-1 astrocytes. After undergoing a certain number of divisions, the cells become unresponsive to the growth factors, stop dividing and, as a consequence, differentiate into oligodendrocytes. Type-2 astrocyte differentiation, on the other hand, we propose requires an inducing factor (which can be mimicked by 10% FCS in culture), which may not appear in the developing optic nerve until after P7[5].

The present study was undertaken to determine whether 0-2A progenitor cells are present in the adult rat optic nerve. Cells from optic nerves of adult Sprague-Dawley rats (4-6 months old, 300-350 g) were dissociated and cultured on type-1 astrocyte monolayers in low-serum conditions (<1% FCS) as described in Table 1 legend. Staining with A2B5 antibody after 2-4 days in culture revealed A2B5$^+$ cells showing a characteristic bipolar or tripolar 0-2A progenitor-cell-like morphology (Fig. 1); in double-labelling experiments these cells were GFAP$^-$ (Fig. 1) and GC$^-$ (not shown). Such cells were also seen in cultures of optic nerves from rats that were more than 1 year old. Although most GFAP$^+$ astrocytes in adult optic nerve are A2B5$^+$, very few cells with this antigenic phenotype were seen in our experiments, presumably because they were not released from the nerves by our dissociation procedure[17].

The A2B5$^+$ cells showing 0-2A progenitor-cell-like morphology usually occurred in groups of two or more (Fig. 1) and their numbers increased with time (doubling about once a day), suggesting that they were proliferating (Table 1). This was confirmed by autoradiographic studies, in which more than 60% of these cells were radiolabelled following an 18-h pulse of ^{3}H-thymidine (Table 1). Similar results were obtained when

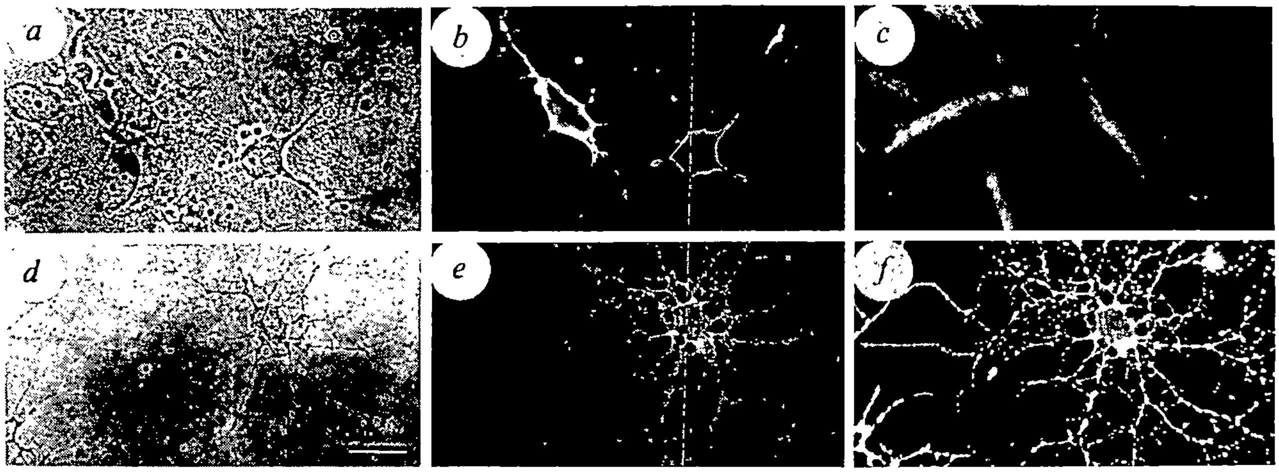

Fig. 1 *a–c*, Two A2B5$^+$, GFAP$^-$ 0-2A progenitor-like cells from adult optic nerve growing on a monolayer of type-1 astrocytes. The cells were photographed using phase contrast (*a*), rhodamine (*b*) and fluorescein (*c*) optics. Note that while the 0-2A progenitor-like cells are A2B5$^+$, GFAP$^-$, the underlying astrocytes are A2B5$^-$, GFAP$^+$. *d–f*, An A2B5$^+$, GC$^+$ oligodendrocyte in an adult optic nerve culture switched from ACM to B-S/0.5% FCS for 3 days. Note that the processes of an adjacent oligodendrocyte on the left of the photograph (whose cell body is out of the field) are GC$^+$ but A2B5$^-$. Scale bar, 20 μm.

Methods. *a–c*, The cells were prefixed in 4% paraformaldehyde in phosphate buffer and then double-labelled with A2B5 antibody[7] (culture supernatant diluted 1:2) followed by rhodamine-conjugated goat anti-mouse immunoglobulin (Cappel, diluted 1:100) and then, after fixation in acid-alcohol, with anti-GFAP serum[24] (1:1,000) followed by fluorescein-conjugated sheep anti-rabbit immunoglobulin (Wellcome, diluted 1:100). Finally the coverslips were mounted in glycerol containing 1,4-diazo-bicyclo(2,2,2)octane to inhibit fading of the fluorescence[25], examined and photographed with Tri-X film rated 400 ASA, as described previously[9]. *d–f*, Adult optic nerve cells were cultured on a PLL-coated coverslip for 3 days in astrocyte-conditioned medium and then for 3 days in B-S/0.5% FCS; the cells were labelled with monoclonal anti-GC antibody[10] (ascites fluid diluted 1:100) followed by immunoglobulin-class-specific fluorescein-conjugated goat anti-IgG3 (Nordic, diluted 1:100) and then A2B5 antibody followed by immunoglobulin-class-specific rhodamine-conjugated goat anti-IgM (Cappel, diluted 1:25), as described previously[5]. Coverslips for cell counting were prefixed with paraformaldehyde to minimize cell loss during antibody labelling. The cells were mounted and photographed as described above.

cultures were maintained in low-serum medium conditioned by type-1 astrocytes (ACM) (Table 1). On the other hand, when adult optic nerve cells were cultured directly on coverslips in low-serum medium alone, the number of A2B5$^+$ process-bearing cells did not increase with time, and less than 5% of such cells were radiolabelled by ^{3}H-thymidine (Table 1). These findings suggest that 0-2A progenitor-like cells in adult optic nerve are stimulated to proliferate by growth factors released from type-1 astrocytes, as previously shown for 0-2A progenitor cells in perinatal optic nerve[4,5].

To determine whether the A2B5$^+$, GFAP$^-$, GC$^-$ process-bearing cells in adult optic nerve cultures were 0-2A progenitor cells, adult nerve cells were cultured in ACM for 3 days followed by a further 3 days in non-conditioned medium containing either 0.5% or 10% FCS, then double-labelled with A2B5 and anti-GFAP antibodies or with A2B5 and anti-GC antibodies. After the initial period in ACM, more than 75% of the antibody-labelled cells were A2B5$^+$, GFAP$^-$, GC$^-$ (Table 2) and showed an 0-2A progenitor-cell-like morphology. (In contrast to the experiments in which cells were plated directly onto type-1 astrocytes, ~20% of the A2B5$^+$ process-bearing cells were weakly GFAP$^+$ (Table 2), suggesting that some 0-2A progenitor cells acquired GFAP in these culture conditions.) After switching into medium containing 0.5% FCS, more than 75% of the antibody-labelled cells were GC$^+$ and had a characteristic, multipolar, oligodendrocyte-like morphology. Few A2B5$^+$, GFAP$^-$, GC$^-$ cells remained, suggesting that most such cells had acquired GC to become oligodendrocytes (Table 2). This interpretation was supported by the finding that 30–40% of the GC$^+$ cells were A2B5$^+$ (Fig. 1); because oligodendrocytes rapidly become A2B5$^-$ as they mature[5,18], this finding suggests that these A2B5$^+$, GC$^+$ cells had only recently acquired GC and were newly developed oligodendrocytes. On the other hand, when cultures were placed in medium containing 10% FCS, more than 75% of the antibody-labelled cells became A2B5$^+$,GFAP$^+$ type-2 astrocytes; again few, if any, A2B5$^+$,GFAP$^-$,GC$^-$ cells remained (Table 2). Although some of the type-2 astrocytes seen in the latter cultures may have been derived from pre-existing type-2 astrocytes rather than 0-2A progenitor cells, it seems likely that most developed from 0-2A progenitor cells that acquired GFAP in the presence of 10% FCS.

The simplest interpretation of these results is that the adult rat optic nerve contains 0-2A progenitor cells that can differentiate into either oligodendrocytes or astrocytes depending on the culture conditions. Both in this respect and in their proliferative response *in vitro* to growth factors released by type-1 astrocytes, these progenitor cells resemble those in perinatal optic nerve. However, there may be important differences between these cells in adult and perinatal nerve. Wolswijk and Noble independently have found bipotential 0-2A progenitor-like cells in 1-yr-old rat optic nerve which proliferate in response to type-1-astrocyte-derived growth factors and find that only a minority of these cells are labelled by anti-vimentin antibody (G. Wolswijk and M. Noble, in preparation). This is in contrast to our earlier findings in perinatal nerve in which the majority of 0-2A progenitor cells were vimentin-positive, and appeared to lose vimentin only after they had differentiated into oligodendrocytes[14].

To determine whether 0-2A progenitor cells proliferate in adult animals, we injected ^{3}H-thymidine into adult rats 18 h and 1 h before killing them and culturing cells from their optic nerves on type-1 astrocyte monolayers for 2–3 days. Between 5 and 7% (mean 6% ± 1.2 in 3 separate animals) of the 0-2A progenitor cells were radiolabelled in such experiments (Fig. 2). Although radiolabelled 0-2A progenitor cells may have divided more often in culture than unlabelled progenitor cells, thereby increasing the labelling index, these results indicate that at least some 0-2A progenitor cells proliferate in the adult optic nerve.

What is the source of proliferating 0-2A progenitor cells in the adult rat optic nerve? It seems unlikely that the progeny of individual 0-2A progenitor cells continue to proliferate for months after developing from a pre-0-2A progenitor cell in the perinatal optic nerve, since *in vitro* experiments suggest that perinatal 0-2A progenitor cells undergo few divisions before they stop proliferating and differentiate. For example, when single 0-2A progenitor cells were cultured on type-1 astrocyte monolayers in 0.5% FCS in microwells, they divided a maximum

Table 1 Effect of type-1 astrocytes on the proliferation of, and ^{3}H-thymidine incorporation by, 0-2A progenitor-like cells in culture

Culture substrate	No. of A2B5$^+$ process-bearing cells after 2 or 4 days in culture		% Of A2B5$^+$ process-bearing cells radiolabelled by ^{3}H-thymidine
	2 days	4 days	
Poly-L-lysine	65±9	62±7	1±1
Type-1 astrocyte monolayer	79±26	336±94	62±3
Poly-L-lysine+ astrocyte conditioned medium	178±15	302±19	40±3

Cultures of adult optic nerve cells were prepared as described previously for perinatal nerves[2], with two modifications; the incubations in trypsin and collagenase were increased to 30 min and the cells were washed in Dulbecco's modified Eagle's medium (DMEM) containing 10% FCS after the dissociation. Cells from one nerve (~50,000 live cells, as assessed by counting in a haemocytomer using Trypan blue) were plated in 20 μl of the same medium. In experiments using a poly-L-lysine (PLL) substrate, the cell suspension was placed on a PLL-coated coverslip in Falcon multi-well plates, left at 37 °C for 30–60 min to allow the cells to adhere and then 500 μl of DMEM supplemented as described previously[3] (100 μg ml^{-1} bovine serum albumin, 5 μg ml^{-1} insulin, 100 μg ml^{-1} transferrin, 62 ng ml^{-1} progesterone, 16.1 μg ml^{-1} putrescine, 39.4 ng ml^{-1} selenium, 0.4 μg ml^{-1} thyroxine, 0.3 μg ml^{-1} triiodothyronine) as modified from Bottenstein and Sato[23] (B-S medium), containing 0.5% FCS (B-S/0.5% FCS), was added. In experiments using astrocyte conditioned medium, the cells were plated onto PLL-coated coverslips as described above, but after 30–60 min these coverslips were placed on glass spacers[5] in a well containing 500 μl of B-S/0.5% FCS in which a monolayer of type-1 astrocytes, prepared as described previously[5], had been growing and conditioning the medium for at least 18 h. In experiments using type-1 astrocyte monolayers as substrate, the 20-μl droplet was expelled from a pipette tip directly onto the astrocyte monolayer. All cultures were incubated for the time indicated at 37 °C in a humidified atmosphere of 5% CO_2 and 95% air. Cultures were labelled with A2B5 antibody as described in Fig. 1 legend and all antibody-labelled cells on the coverslip were counted. In autoradiography experiments, ^{3}H-thymidine (2.0 Ci mmol^{-1}) was added to the culture medium for the last 18 h, at a final concentration of 2 μCi ml^{-1}. After labelling with A2B5 antibody, cultures were dried, dipped in Ilford K5 emulsion and exposed at −70 °C for 3 days before being developed in Ilford Contrast FF. Cells with ⩾10 silver grains over the nucleus were counted as radiolabelled. These results and those in Table 2 are expressed as means±s.d. of at least three separate experiments.

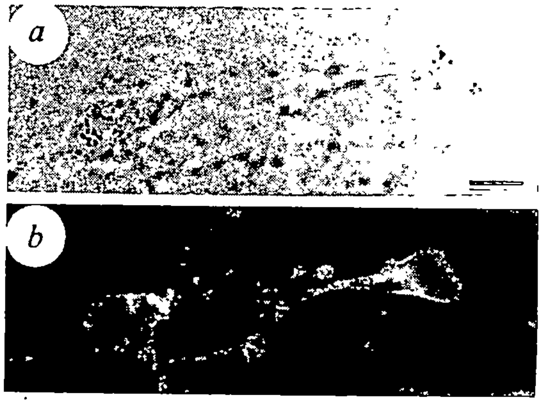

Fig. 2 Autoradiograph of a pair of ^{3}H-thymidine-labelled, A2B5$^+$ 0-2A progenitor-like cells from adult optic nerve growing on a monolayer of type-1 astrocytes. The cells were photographed using phase contrast (*a*) and rhodamine (*b*) optics. Note that both the 0-2A progenitor cells are radiolabelled; these cells were GFAP (not shown). Scale bar, 10 μm. The ^{3}H-thymidine (78 Ci mmol^{-1}, 2 μCi g^{-1}) was injected into the heart of the rat 18 h and then 1 h before death. Optic nerve cells were cultured on type-1 astrocytes, double-labelled with A2B5 and anti-GFAP antibodies, processed for autoradiography as described for Table 1 and then exposed for 6 weeks before developing.

of eight times and differentiated into oligodendrocytes within 10 days or less[6]. In these single-cell experiments the proliferative capacity of individual 0-2A progenitor cells in newborn optic nerve varied widely, although the daughter cells of a single progenitor cell tended to divide a similar number of times before differentiating, even when separated and recultured individually on type-1 astrocyte monolayers in different microwells[6]. In contrast, in bulk co-cultures of perinatal optic nerve cells on type-1 astrocytes, new oligodendrocytes continue to be produced from dividing progenitor cells for weeks[4,5]. Perhaps the simplest interpretation of these experiments is that 0-2A progenitor cells in perinatal optic nerve are produced continually from pre-0-2A progenitor cells. Taken together with the cell-division-counting model for the regulation of oligodendrocyte differentiation, this scheme would account for the heterogeneity in the proliferative capacity of 0-2A progenitor cells in nerves of a single age, as well as for the finding that oligodendrocytes are produced continually for at least several weeks after birth in the rat optic nerve[15,16]. Our present findings suggest that the putative pre-0-2A progenitor cell produces proliferating 0-2A progenitor cells throughout life and, therefore, raise the possibility that this cell is a slowly dividing, self-renewing stem cell. If this is so, then

Table 2 Differentiation of putative 02-A progenitor cells from adult optic nerve into either oligodendrocytes or type-2 astrocytes depending on the culture conditions

Culture medium	Total no. of cells per culture		
	Oligodendrocytes (GC$^+$)	Type-2 astrocytes (A2B5$^+$, GFAP$^+$)	Putative O-2A progenitor cells (A2B5$^+$, GFAP$^-$, GC$^-$)
Astrocyte conditioned medium (ACM)×3 days	6±7	44±8	161±47
ACM×3 days then B−S/0.5% FCS×3 days	150±18	20±13	19±12
ACM×3 days then B−S/10% FCS×3 days	41±30	206±95	0±12

Adult optic nerve cells were cultured in ACM for 3 days as described in Table 1 legend and then, in some cases, were switched to either B-S/0.5% FCS or to B-S/10% FCS for a further 3 days, after which they were labelled with A2B5 and anti-GFAP antibodies, or with anti-GC and A2B5 antibodies as described for Fig. 1. All antibody-labelled cells on the coverslip were counted and classified according to their antigenic phenotype. The number of putative 0-2A progenitor cells (A2B5$^+$, GFAP$^-$, GC$^-$ process-bearing cells) was calculated after counting two separate coverslips from the same experiment, one stained with A2B5 and anti-GFAP and the other with anti-GC and A2B5 antibodies. The number of A2B5$^+$, GC$^+$ cells was subtracted from the number of A2B5$^+$, GFAP$^-$ cells, and the number of A2B5$^+$, GFAP$^+$ cells was subtracted from the number of A2B5$^+$, GC$^-$ cells; the mean of these two numbers was taken as the number of putative 0-2A progenitor cells in that experiment.

in this respect at least, 0-2A progenitor cells resemble rapidly dividing haematopoietic progenitor cells, which have a limited developmental and proliferative capacity and are thought to be derived from slowly dividing, self-renewing multipotential haematopoietic stem cells[19].

The number of 0-2A progenitor cells in adult optic nerve is likely to be small. Although we do not know what proportion of these cells were liberated from the nerve by our dissociation procedures, or their plating efficiency, there were always less than 200 0-2A progenitor-like cells in cultures prepared from a single nerve and examined after 2 days. More importantly, in semi-thin frozen sections of adult rat optic nerve, less than 2% of the cells have the antigenic phenotype (A2B5$^+$, GFAP$^-$) of 0-2A progenitors[2].

The fate of the 0-2A progenitor cells in the adult optic nerve is uncertain. They may produce oligodendrocytes and/or type-2 astrocytes in association with a continuous slow turnover of these glial cells (as suggested for glial cells in other regions of the central nervous system (CNS)[20-22]), and/or in association with the continuous growth of the nerve during adult life. They may also produce new oligodendrocytes in response to demyelinating lesions. The relative inefficiency of remyelination in some demyelinating CNS diseases, such as multiple sclerosis, can have serious clinical consequences. Perhaps an understanding of the factors controlling the production, proliferation and differentiation of 0-2A progenitor cells in adult white matter will lead to the development of ways to enhance the production of new oligodendrocytes in these diseases.

We thank Dr E. Abney for performing the intracardiac injections of ^{3}H-thymidine, Dr M. Nirenburg for the A2B5 hybridoma cells, Guus Wolswijk, Mark Noble, Sally Temple, Simon Hughes and other members of the Neuroimmunology group for helpful discussion. C.ff.-C. is supported by a grant from the Multiple Sclerosis Society of Great Britain.

Received 1 October; accepted 3 December 1985.

1. Raff, M. C., Abney, E. A. & Miller, R. H. *Devl Biol.* **106**, 53-60 (1984).
2. Miller, R. H., David, S., Patel, R., Abney, E. A. & Raff, M. C. *Devl Biol.* **111**, 35-41 (1985).
3. Raff, M. C., Miller, R. H. & Noble, M. *Nature* **303**, 390-396 (1983).
4. Noble, M. & Murray, K. *EMBO J.* **3**, 2243-47 (1984).
5. Raff, M. C., Abney, E. A. & Fok-Seang, J. *Cell* **42**, 61-69 (1985).
6. Temple, S. & Raff, M. C. *Cell* (in the press).
7. Eisenbarth, G. S., Walsh, F. S. & Nirenberg, M. *Proc. natn. Acad. Sci. U.S.A.* **76**, 4913-17 (1979).
8. Bignami, A., Eng, L. F., Dahl, D. & Uyeda, C. T. *Brain Res.* **43**, 429-435 (1972).
9. Raff, M. C. *et al. Brain Res.* **174**, 283-308 (1979).
10. Ranscht, B., Clapshaw, P. A., Price, J., Noble, M. & Seifert, W. *Proc. natn. Acad. Sci. U.S.A.* **79**, 2709-2713 (1982).
11. Raff, M. C. *et al. Nature* **274**, 813-816 (1978).
12. David, S., Miller, R. H., Patel, R. & Raff, M. C. *J. Neurocytol.* **13**, 961-974 (1984).
13. Temple, S. & Raff, M. C. *Nature* **313**, 223-225 (1985).
14. Raff, M. C., Williams, B. P. & Miller, R. H. *EMBO J.* **3**, 1857-1864 (1984).
15. Skoff, R. P., Price, D. L. & Stocks, A. *J. comp. Neurol.* **169**, 291-312 (1976).
16. Skoff, R. P., Price, D. L. & Stocks, A. *J. comp. Neurol.* **169**, 313-334 (1976).
17. Miller, R. H. *et al. J. Neurosci.* (in the press).
18. Abney, E. A., Williams, B. P. & Raff, M. C. *Devl Biol.* **100**, 166-171 (1983).
19. Till, J. E. & McCulloch, E. A. *Biochim. biophys. Acta* **605**, 431-459 (1980).
20. Mares, V., Lodin, Z. & Jílek, M. *J. comp. Neurol.* **161**, 471-482 (1975).
21. Kaplan,, M. S. & Hinds, J. W. *J. comp. Neurol.* **193**, 711-727 (1980).
22. Lindsay, R. M. *Adv. Cell Neurobiol.* (in the press).
23. Bottenstein, J. & Sato, G. H. *Proc. natn. Acad. Sci. U.S.A.* **76**, 514-517 (1979).
24. Pruss, R. M. *Nature* **280**, 688-690 (1979).
25. Johnson, G. D. *et al. J. immun. Meth.* **55**, 231-242 (1982).

Restricted recognition of β_2-microglobulin by cytotoxic T lymphocytes

Hans-George Rammensee*†, Peter J. Robinson‡, Andrea Crisanti* & Michael J. Bevan†

* Basel Institute for Immunology, Grenzacherstrasse 487, Postfach, 4005 Basel, Switzerland
† Department of Immunology, Scripps Clinic & Research Foundation, La Jolla, California 92037, USA
‡ Institute for Immunology and Genetics, German Cançer Research Center, Im Neuenheimer Feld 280, D-6900, Heidelberg, FRG

Recognition of foreign antigen by cytotoxic T lymphocytes (CTL) is restricted by class I major histocompatibility complex (MHC) products. Class I heavy chains (relative molecular mass (M_r) 45,000–48,000) are reversibly and noncovalently associated with β_2-microglobulin (β_2M, $M_r = 12{,}000$) (see ref. 1). Cells expressing human or murine class I heavy chains can exchange their native β_2M for exogenously added free β_2M (refs 2–4), which is present in serum[5–7]. Two allelic forms of β_2M exist among the common laboratory mouse strains, β_2M-A and β_2M-B, which are represented in BALB and C57BL mice, respectively[8–10]. The two forms differ at a single amino acid at position 85 (ref. 11), the gene ($\beta_2 m$) is located on chromosome 2 linked to a minor histocompatibility (H) region, *H–3* (refs 12, 13). It has been proposed that one of the *H–3* loci is identical with $\beta_2 m$, and that CTL raised across certain H–3 incompatibilities are actually specific for β_2M[14,15]. Here we describe CTL raised in such a combination which recognize endogenous as well as exogenous β_2M-B in the context of $H\text{–}2K^b$. This represents a unique case of CTL recognition, as CTL usually recognize antigens inserted into the membrane, and it is the first molecular identification of the product of a minor *H* locus.

The congeneic resistant strains C57BL/10 and the partner strain B10.C-$H\text{–}3^c$ differ at the minor H region *H–3* and the $\beta_2 m$ locus on chromosome 2 (refs 12, 13, 16 and H.G.R., unpublished data). In B10.C-$H\text{–}3^c$ these genes are derived from the BALB genome. The two strains reject each other's skin grafts[16] and produce H–2K^b-restricted CTL against each other on *in vivo* immunization[15]. It has been proposed that the *H–3* region consists of several *H* loci, one of them being $\beta_2 m$[14,15,17,18]. To test the hypothesis of identity between one of the *H–3* products and β_2M, we produced a CTL line from (BALB.K × B10.C-$H\text{–}3^c$)F$_1$ ($H\text{–}2^{k\times b}$, $\beta_2 m^a$) mice immunized with (BALB.K × C57BL/10)F$_1$ ($H\text{–}2^{k\times b}$, $\beta_2 m^{a\times b}$). (We used $H\text{–}2^{k\times b}$ heterozygous animals in the hope of obtaining H–2^k-restricted β_2M-B-specific CTL, which could have been tested on L929 cells transfected with the $\beta_2 m^b$ gene[19].)

Table 1 β_2M-B-specific antibodies inhibit killing by 181B

Antibody	Dilution	Specific ^{51}Cr release of C57BL/6 blasts (%)
None	—	74.8
28-11-5S (anti-D^b) (ref. 34)	1/60	70.0
	1/300	83.0
5F1.2 (anti-K^b) (ref. 35)	1/60	40.3
	1/300	55.7
	1/1,500	67.8
S19.8 (anti-β_2M-B)	1/60	9.7
	1/300	15.2
	1/1,500	19.8

^{51}Cr-labelled C57BL/6 blasts were incubated for 4 h with the indicated antibodies[34,35] (as ascites fluid) and 181B CTL at an effector/target ratio of 38/1. Other conditions are as described in Fig. 1.

The CTL line (181B) killed stimulator-type targets and also C57BL/10 ($H\text{–}2^b$, $\beta_2 m^b$), C57BL/6 ($H\text{–}2^b$, $\beta_2 m^b$) and B10.A(5R) ($H\text{–}2K^bD^k$, $\beta_2 m^b$), but not responder-type targets nor BALB.B ($H\text{–}2^b$, $\beta_2 m^a$), B10.BR ($H\text{–}2^k$, $\beta_2 m^b$) or B10.A (2R) ($H\text{–}2K^dD^b$; $\beta_2 m^b$) (Fig. 1 and H.G.R., unpublished data), suggesting that it is specific for β_2M-B and is H–2K^b-restricted.

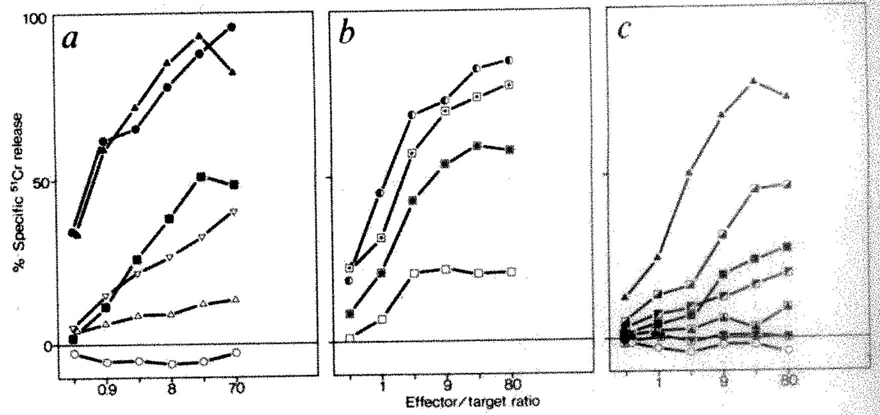

Fig. 1 Characterization of the antigen recognized by the CTL line 181B [(BALB.K × B10.C-*H-3*^{c})F$_1$ (*H-2*$^{k \times b}$, $\beta_2 m^a$) anti-(BALB.K × C57BL/10)F$_1$ (*H-2*$^{k \times b}$, $\beta_2 m^{a \times b}$)]. CTL were tested on ^{51}Cr-labelled blasts of responder (indicated as CK × H-3^c) or stimulator (CK × B10) type or of C57BL/6 (B6; $\beta_2 m^b$) or BALB.B (CB; $\beta_2 m^a$) origin. Blasts were induced for 2 days with mitogen and C57BL serum (Bl serum) or BALB serum (C serum) at 5% concentration (if not indicated otherwise) or with 10% FCS. *a*, *H-2*^{b}, $\beta_2 m^a$ cells can acquire the antigen recognized by 181B CTL from C57BL, but not BALB serum. BALB.B blasts were generated in 5% C57BL serum which had been absorbed with β_2M-B-specific monoclonal antibodies S19.8 bound to protein A-Sepharose or on protein A-Sepharose without antibody. The assay was performed in Iscove's medium containing 2% bovine serum albumin (BSA) and 1% BALB serum. Spontaneous release of targets was between 24.7 and 29.1%. ●, B6, Bl serum; ▲, B6, C serum; ■, CB, Bl serum; ▽, CB, Bl serum, protein A absorbed; △, CB, Bl serum and S198; ○, CB, C serum. *b*, Maximal killing of *H-2*^{b}, $\beta_2 m^a$ blasts with acquired serum-born antigen can be demonstrated under optimal conditions. This assay was performed in RPMI 1640 medium containing 2% bovine serum albumin (BSA) and 2.5% C57BL serum. Spontaneous release ranged between 24.2 and 37.8%. ◐, CK × B10, FCS; ⊡, CK × H-3^c, 5% Bl serum; ▣, CK × H-3^c, 1.25% Bl serum; □, CK × H-3^c, FCS. *c*, The CTL target antigen acquired by *H-2*^{b}, $\beta_2 m^a$ cells is β_2M-B. BALB.B blasts were raised in serum-free Iscove's medium containing 2% BSA and 200, 40 or 8 ng ml^{-1} purified β_2M-B or 200 ng ml^{-1} purified β_2M-A. Assay in 1% BALB serum; spontaneous release between 19.4 and 34.3%. ▲, B6, C serum; ▨, CB, 200 ng β_2M-B; ■, CB, Bl serum; ◩, CB, 40 ng β_2M-B, ◪, CB, 8 ng β_2M-B; ▩, CB, 200 ng β_2M-A; O, CB, C serum.

Methods. Production of CTL line 181B. A (BALB.K × B10.C-*H-3*^{c})F$_1$ mouse was immunized intraperitoneally 5× with 2×10^7 irradiated (3,300 rad) (BALB.K × C57BL/10)F$_1$ spleen cells suspended in 0.25 ml Hank's balanced salt solution at intervals of 3–8 weeks. Three weeks after the last injection, 2×10^7 responder splenocytes were stimulated with 2×10^7 irradiated (BALB.K × C57BL/10)F$_1$ cells for 7 days in RPMI 1640 medium containing 10% FCS, 2-mercaptoethanol, glutamine and antibiotics, and restimulated weekly in the presence of 5% interleukin-2-containing supernatant from concanavalin A (Con A)-induced rat spleen cells[33] and 50 mM α-methyl-D-mannoside to block the action of residual Con A. After several weeks, the source of stimulators was switched to a 1/1 mixture of irradiated BALB.B and C57BL/6 cells to minimize uptake of β_2M-B by responders, which would lead to self-killing. Standard ^{51}Cr-release assays were performed with 10^4 ^{51}Cr-labelled blast cells of splenic origin, which had been induced for 2 days in culture medium containing 2.5 μg ml^{-1} Con A, as described elsewhere[33]. Murine sera, bovine sera or proteins were present during these 2 days. Absorption of serum. 100 μl protein A-Sepharose slurry (Pharmacia) was incubated with 100 μl of S19.8[21] ascites fluid diluted 1/10 in phosphate-buffered saline for 3 days at 4 °C, then washed four times in phosphate-buffered saline. C57BL serum (100 μl) was mixed with protein A-Sepharose-bound antibody and incubated for 1 h at 4 °C, decanted from the centrifuged pellet and absorbed another three times on new aliquots of S19.8-Sepharose. As a control, another 100 μl of C57BL serum was absorbed four times on protein A-Sepharose without antibodies. Purification of urinary β_2M was performed as described previously[22]. An SDS-polyacrylamide gel electrophoresis analysis of the β_2M preparation used here is published elsewhere (Fig. 2, lanes 2 and 3 of ref. 22) and demonstrates the absence of detectable impurities.

The ability of anti-β_2M-B and anti-H-2K^b, but not anti-H-2D^b, antibodies to inhibit lysis by 181B is consistent with this view (Table 1).

That the line is specific for β_2M-B is shown by the following experiments. BALB.B lymphoblasts raised in medium containing 5% C57BL serum (which is known to contain free β_2M-B[20]) instead of the usual fetal calf serum (FCS) were killed by 181B, but BALB.B blasts raised in 5% BALB serum were not killed (Fig. 1*a*). C57BL/6 or B10.BR sera were both effective, sera of BALB/c, BALB.B or BALB.K were all ineffective (data not shown). The presence of β_2M-B on the surface of $\beta_2 m^a$ blasts raised with β_2M-B-containing serum was demonstrated by the binding of radiolabelled β_2M-B-specific monoclonal antibodies S19.8 (ref. 21; Table 2). Thus, sera containing β_2M-B, but not β_2M-A, can make BALB.B targets susceptible to lysis by 181B CTL, irrespective of the H-2 haplotype of the serum donor. BALB.B blasts raised in C57BL serum absorbed with β_2M-B-specific S19.8 antibodies bound to protein A-Sepharose were only weakly killed. Absorption of C57BL serum on protein A-Sepharose alone did not significantly reduce its capacity to supply the target structure to the BALB.B cells (Fig. 1*a*). Blasts raised in 1.25% C57BL serum were killed less efficiently than blasts raised in 5% serum (Fig. 1*b*). When $\beta_2 m^a$ targets raised in C57BL serum were tested in the killer assay also containing C57BL serum, the level of lysis was similar to that of $\beta_2 m^b$ targets (Fig. 1*b*). $\beta_2 m^a$ targets raised in BALB serum were also lysed at a low level if the assay was run in C57BL serum, probably through $\beta_2 m^a$ targets picking up free β_2M-B during the 4-h assay[6].

To identify unequivocally our serum-born CTL antigen, we tried to substitute the native β_2M-A on BALB.B cells with purified urinary β_2M (ref. 22). BALB.B blasts raised in serum-free medium containing 200 ng ml^{-1} purified β_2M-B were killed efficiently by 181B CTL, and lower concentrations of β_2M-B yielded lower killing (Fig. 1*c*). BALB.B blasts raised in 200 ng ml^{-1} purified β_2M-A were not lysed at all. Thus, killing comparable to that obtained by acquired serum-born antigen was demonstrated with purified β_2M-B, but not β_2M-A.

Table 2 Serum β_2M-B binds to the surface of $\beta_2 m^a$ cells

Cells	Serum source	Cell no. (×10^6)	^{3}H-labelled S19.8 antibodies bound (c.p.m.)
C57BL/6 ($\beta_2 m^b$)	FCS	1.5	16 518
		0.5	8 156
B10.C-*H-3*^{c} ($\beta_2 m^a$)	FCS	1.5	114
		0.5	93
	B10.BR	1.5	3 875
		0.5	2 512

Spleen cells of the indicated strains were cultured for 2 days in medium containing either 10% FCS or 5% B10.BR serum. The binding assay was performed as described elsewhere[36]. Briefly, cells were pelleted, incubated for 60 min with ^{3}H-labelled β_2M-B-specific S19.8 antibodies and washed twice.

In conclusion, the CTL line 181B recognizes β_2M-B in the context of K^b. This represents a unique case of CTL recognition, because 181B recognizes a soluble antigen in association with class I heavy chain. CTL usually recognize membrane-inserted antigens, that is, antigenic epitopes on class I heavy chains or class I plus virus-encoded protein; or class I plus hapten covalently coupled to cell-surface antigen; or class I plus allogeneic cell-surface antigens[23].

Of interest is the density of β_2M on the cell surface. It is well known that the reactivity of lymphocytes to a given antigen is dependent on the density of that antigen on the presenting cell[24-26]. On this basis it was proposed that the strong alloreactivity to foreign MHC products is caused by the high density of MHC on antigen-presenting cells, as opposed to the density of complexes of antigen plus MHC[27]. Because the density of β_2M on stimulator cells is at least as high as that of K and D heavy chains together, one would expect a high frequency of β_2M-reactive cells in unprimed animals, comparable to that of alloreactive cells. This is found not to be the case: no primary CTL response between MHC-identical, β_2M-incompatible strains can be demonstrated[28] and foreign β_2M does not contribute to the CTL response between class I-incompatible strains[29]. We conclude that antigen density alone cannot account for the high frequency of alloreactive T cells, and that the region of the MHC antigen affected by a change is also essential.

Our findings support the earlier hypothesis that β_2M is one of the minor H antigens encoded in the *H-3* region. Characteristics of minor H antigens are: (1) they cause slow rejection of grafts[30]; (2) they elicit CTL responses only after *in vivo* priming[28]; and (3) their recognition by CTL is class I restricted[31,32]. We have shown that the latter two points apply to β_2M; whether β_2M incompatibility can lead to graft rejection remains to be demonstrated. No other minor H antigen has so far been identified on the molecular level.

We thank U. Hämmerling, K. Fischer Lindahl and L. Sherman for antibodies, Silvie Bove for technical assistance, K. Fischer Lindahl and W. Haas for improving, and Judie Hossmann and Carolyn Harley for typing the manuscript. H.G.R. was supported by the Deutsche Forschungsgemeinschaft during part of the work. The Basel Institute for Immunology was founded and is supported by F. Hoffman-La Roche and Co., Basel, Switzerland.

Note added in proof: Since this manuscript was submitted, Kurtz *et al.*[37] have also reported that CTL raised across certain *H-3*/β_2*m* incompatibilities can be blocked by β_2M-specific antibodies.

Received 30 July; accepted 12 December 1985.

1. Klein, J. *Science* **203,** 516–521 (1979).
2. Hyafil, F. & Strominger. J. L. *Proc. natn. Acad. Sci. U.S.A.* **76,** 5834–5838 (1979).
3. Schmidt, W., Festenstein, H., Ward, P. J. & Sanderson, A. R. *Immunogenetics* **13,** 483–491 (1981).
4. Hester, R. B., Kubo, R. T. & Grey, H. M. *Scand. J. Immun.* **9,** 125–134 (1979).
5. Kefford, R. F., Calabi, F., Fearnly, I. M., Burrone, O. R. & Milstein, C. *Nature* **308,** 641–642 (1984).
6. Bernabeu, C., van de Rijn, M., Lerch, P. G. & Terhorst, C. P. *Nature* **308,** 642–645 (1984).
7. Berggard, I. & Bearn, A. G. *J. biol. Chem.* **243,** 4095–4103 (1968).
8. Goding, J. & Walker, I. *Proc. natn. Acad. Sci. U.S.A.* **77,** 7395–7399 (1980).
9. Michaelson, J., Rothenberg, E. & Boyse, E. A. *Immunogenetics* **11,** 93–95 (1980).
10. Robinson, P. J., Graf, L. & Sege, K. *Proc. natn. Acad. Sci. U.S.A.* **78,** 1167–1170 (1981).
11. Gates, F. T. III, Coligan, J. E. & Kindt, T. J. *Proc. natn. Acad. Sci. U.S.A.* **78,** 554–558 (1981).
12. Michaelson, J. *Immunogenetics* **13,** 167–171 (1981).
13. Robinson, P. J. *et al. Immunogenetics* **14,** 449–452 (1981).
14. Michaelson, J. *Immunogenetics* **17,** 219–259 (1983).
15. Rammensee, H.-G. & Klein, J. *J. Immun.* **130,** 2926–2929 (1983).
16. Graff, R. J., Brown, D. & Snell, G. D. *Transplantn Proc.* **5,** 299–302 (1973).
17. Roopenian, D. C. & Click, R. E. *Immunogenetics* **10,** 333–341 (1980).
18. Click, R. E., Schneider, D. & Roopenian, D. C. *J. Immun.* **126,** 2378–2381 (1981).
19. Margulies, D. H., Parnes, J. R., Johnson, N. A. & Seidman, J. G. *Proc. natn. Acad. Sci. U.S.A.* **80,** 2328–2331 (1983).
20. Kimura, S., Tada, N., Lin, Y. & Hämmerling, U. *Immunogenetics* **14,** 445–447 (1981).
21. Tada, N., Kimura, S., Hatzfeld, A. & Hämmerling, U. *Immunogenetics* **11,** 441–447 (1980).
22. Graf, L., Peterson, P. A., Sege, K. & Robinson, P. J. *Molec. Immun.* **19,** 877–884 (1982).
23. Zinkernagel, R. M. & Doherty, P. C. *Adv. Immun.* **27,** 51–177 (1979).
24. Pohlit, H., Haas, W. & v. Boehmer, H. *Eur. J. Immun.* **9,** 681–690 (1979).
25. Matis, L. M., Glimcher, L. H., Paul, W. E. & Schwartz, R. H. *Proc. natn. Acad. Sci. U.S.A.* **80,** 6019–6023 (1983).
26. Janeway, C. A. *et al. Nature* **306,** 80–82 (1983).
27. Bevan, M. J. *Immun. Today* **5,** 128–130 (1984).
28. Bevan, M. J. *J. exp. Med.* **143,** 1283–1288 (1979).
29. Langhorne, J. & Fischer Lindahl, K. *Eur. J. Immun.* **12,** 101–106 (1982).
30. Graff, R. J. in *Origins of Inbred Mice* (ed. Morse, H. C. III) 371–388 (Academic, New York, 1978).
31. Bevan, M. J. *J. exp. Med.* **142,** 1349–1364 (1975).
32. Gordon, R. D., Simpson,, E. & Samelson, L. E. *J. exp. Med.* **142,** 1108–1120 (1975).
33. Rammensee, H.-G., Fink, P. J. & Bevan, M. J. *J. Immun.* **133,** 2390–2396 (1984).
34. Ozato, K. & Sachs, D. H. *J. Immun.* **126,** 317–321 (1981).
35. Rüsch, E., Kuon, W. & Hämmerling, G. J. *Transplantn Proc.* **15,** 2093–2096 (1983).
36. Fischer Lindahl, K. *Immun. Meth.* **3,** 187 (1985).
37. Kurtz *et al. J. Immun.* **135,** 2847 (1985).

Two roles for guanine nucleotides in the stimulus–secretion sequence of neutrophils

M. M. Barrowman, S. Cockcroft & B. D. Gomperts

Department of Experimental Pathology, University College London, University Street, London WC1E 6JJ, UK

The term 'stimulus–secretion coupling' has, since first enunciated[1], been held to involve the mobilization of cytosol Ca^{2+}, which in turn is sufficient to trigger exocytotic secretory processes in metabolically competent cells. However, recent studies on a wide range of secretory cell types indicate that a role for Ca^{2+} can be obviated: examples are stimulation with phorbol ester (phorbol myristate acetate, PMA)[2,3] which causes the activation of protein kinase C[4] or the stimulation of platelets with collagen[5]. Ca^{2+}-independent exocytosis also occurs when analogues of GTP are injected through the lumen of patch pipettes directly into the cytosol of mast cells[6]. The results presented here suggest that GTP analogues can activate secretory processes by actions at two distinct locations: one may be at the level of the receptor[7] involving the activation of polyphosphoinositide (PPI) phosphodiesterase[8] with consequent liberation of diacylglycerol (DG)[9]; the other involves direct activation of the exocytotic mechanism. These conclusions are based on measurements of exocytotic secretion from permeabilized neutrophils into which we have been able to introduce, individually and in combination, Ca^{2+} chelators (EGTA and BAPTA), Ca^{2+} (buffered at micromolar concentrations with EGTA), analogues of GTP and GDP and the direct activator of protein kinase C, PMA.

To permeabilize rabbit neutrophils, we used 'three-day, egg-grown' Sendai virus[10]. The virus, which binds at the ubiquitous sialic acid groupings of either glycoproteins[11] or glycolipids[12] present on the surfaces of all animal cells, causes leakage of intracellular metabolites[13] and conversely it is possible to introduce normally impermeant solutes into the cytosol of such cells[14]. We have previously used Sendai virus to permeabilize rat peritoneal mast cells and introduce Ca^{2+} buffers to control cytosol Ca^{2+} at concentrations in the micromolar range: this caused the cells to undergo exocytotic secretion of histamine and *N*-acetylglucosaminidase[15].

Introduction of Ca^{2+} (buffered at concentrations in the micromolar range) into permeabilized neutrophils causes exocytotic secretion of β-glucuronidase (Fig. 1*a*, lowest curve): half-maximal secretion is achieved at *p*Ca 6.3 [0.56 ± 0.1 M ($\pm$s.d., $n = 17$ experiments)] and is independent of the concentration of EGTA (in the range 0.3–10 mM) used to buffer the Ca^{2+}. The mean extent of maximal secretion was $31 \pm 14\%$ ($\pm$s.d., $n = 57$). As with the secretion from intact cells due to receptor-directed ligands, secretion from the permeabilized neutrophils also requires brief pretreatment with cytochalasin B. There is in addition, as with other permeabilized cell systems including bovine adrenal cells[16], platelets[17] and pancreatic islet β-cells[18], a requirement for metabolic support which must be provided in the form of Mg-ATP[19]. In distinction to some of the other systems cited, we have found that the sensitivity of β-glucuronidase secretion to Ca^{2+} and other stimulatory agents (see below) declines for some 10–15 min following permeabilization with Sendai virus. This is not due to the closure of the lesions[19].

In view of the observation[20] that analogues of GTP can spare the requirement of Ca^{2+} for serotonin secretion from permeabilized platelets and so permit secretion to occur at concentrations of Ca^{2+} down to 10^{-8} M, we tested the effects of GTP-γ-S on Ca^{2+}-induced β-glucuronidase secretion from permeabilized neutrophils (Fig. 1*a*). With these cells, the effects of Ca^{2+} and the GTP analogue are additive and independent of each other. The permeabilized cells loaded with GTP-γ-S show no requirement for Ca^{2+} in the secretory process. This conclusion must of course be tempered by one's understanding of the term 'no Ca^{2+}' (ref. 21). If we accept the inescapable presence of approxi-

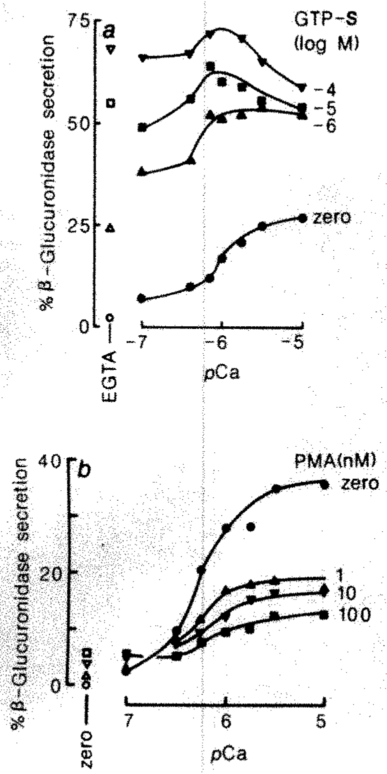

Fig. 1 Dependence on Ca^{2+} of β-glucuronidase secretion from permeabilized rabbit neutrophils in the presence of GTP-γ-S (*a*) and phorbol myristate acetate (*b*). *a*, Rabbit neutrophils were permeabilized with Sendai virus and then treated with Ca^{2+} at the concentrations indicated in the absence (●) and presence of GTP-γ-S at 10^{-6} M (▲), 10^{-5} M (■) and 10^{-4} M (▼). *b*, Rabbit neutrophils were permeabilized as in *a* and then transferred to solutions containing Ca^{2+} buffered at the concentrations indicated in the absence (●) or presence of PMA at 1 (▲), 10 (▼) and 100 (■) nM.

Methods. Rabbit peritoneal exudate neutrophils were isolated as previously described [38] and suspended at $2\text{-}5 \times 10^5\ ml^{-1}$ in a buffer (*p*H 6.8, comprising 137 mM NaCl, 2.7 mM KCl, 2 mM $MgCl_2$, 20 mM HEPES, 5.6 mM glucose, 15 µM EGTA and 1 mg ml^{-1} bovine serum albumin). After incubation for 20 min at 37 °C, cytochalasin B (5 µg ml^{-1} final concentration) was added together with Mg-ATP (final 5 mM) and EGTA 0.6 mM. After 2.5 min, Sendai virus (100 haemagglutinating units (HU) per ml final concentration) was added and after a further 2.5 min the cells were diluted twofold in tubes containing Ca^{2+} (buffered with 3 mM EGTA: final concentration) at the concentrations indicated and GTP-γ-S. *b*, The formulations for the pCa^{2+} buffers were calculated by use of the program CHELATE using appropriate dissociation constants for 37 °C derived from values of ΔH and ΔS (ref. 39). After 10 min incubation, cells were sedimented by centrifugation at 4 °C and samples of the supernatant were withdrawn for analysis of β-glucuronidase[22] and lactate dehydrogenase[15]. Leakage of lactate dehydrogenase was measured on many occasions during this work and in no instance did it exceed 5%. All data points indicate averages of duplicate determinations. Similar results were obtained on at least three occasions.

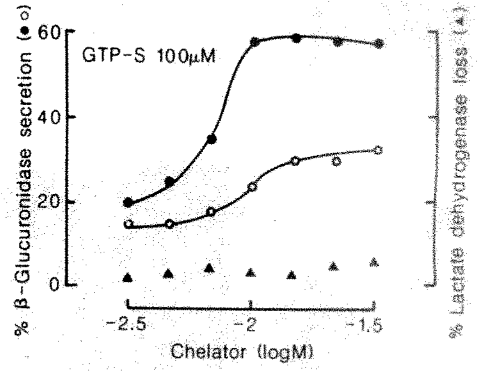

Fig. 2 Effect of extensive Ca^{2+} depletion on GTP-γ-S-induced secretion of β-glucuronidase from permeabilized neutrophils. Rabbit neutrophils (prepared as for Fig. 1) were treated with EGTA (●) or BAPTA (○) at the indicated concentrations for 2.5 min and then permeabilized by addition of Sendai virus (100 HU ml^{-1}). GTP-γ-S (100 µM) was added after a further 2.5 min and the cells were further incubated and then processed as described in Fig. 1 legend for measurement of β-glucuronidase secretion. Solid triangles indicate release of lactate dehydrogenase in the EGTA experiment. Similar results were obtained on three occasions.

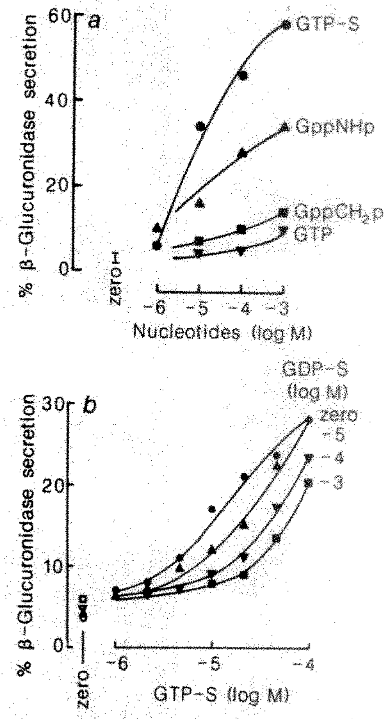

Fig. 3 Stimulation of Ca^{2+}-independent secretion by analogues of GTP and its inhibition by GDP-β-S. Rabbit neutrophils (prepared as described in Fig. 1 legend) were treated with 3 mM EGTA for 2.5 min. They were then permeabilized with Sendai virus and after a further 2.5 min, they were processed as follows: *a*, the cells were transferred to solutions containing 3 mM EGTA and GTP analogues at the concentrations indicated GTP-γ-S (●), GppNHp (▲), $GppCH_2p$ (■), GTP (▼). Similar results were obtained on three occasions. *b*, The cells were transferred to tubes containing GTP-γ-S and GDP-β-S at the concentrations indicated: zero GDP-β-S (●), 10^{-5} M (▲), 10^{-4} M (▼), 10^{-3} M (■). Similar results were obtained on four occasions. Further processing was as described in Fig. 1 legend.

nately 10 µM of contaminating Ca^{2+} (mainly present in the ovine serum albumin, a component of the buffered salt solition[22]), then under the routine conditions of our present experinents (*p*H 6.8 and 3 mM EGTA) we calculate an equilibrium oncentration of 'free' Ca^{2+} of 2×10^{-9} M. We have also carried ut similar experiments under conditions of elevated *p*H (7.4) nd EGTA (30 mM) or BAPTA (30 mM) (so reducing Ca^{2+} to $\leq 2 \times 10^{-11}$ M). In this case we find (Fig. 2) that the extent of ecretion due to GTP-γ-S is increased, not decreased, as the oncentration of either chelator is increased from 3 to 30 mM hile leakage of lactate dehydrogenase remains below 5%. We annot explain why EGTA supports a higher level of secretion than BAPTA at all concentrations. It should further be stressed that the guanine nucleotide has always been applied to the cells 2.5 min after permeabilization and introduction of the chelate ligand. We would claim that biological processes occurring under such conditions can justly be regarded as Ca^{2+}-independent.

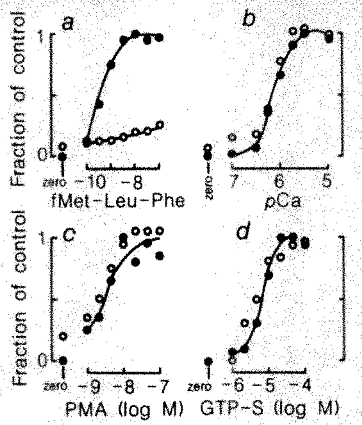

Fig. 4 Effect of pertussis toxin on secretion from intact neutrophils stimulated by fMet-Leu-Phe, and from permeabilized neutrophils stimulated by phorbol ester, Ca^{2+} or GTP-γ-S. Rabbit neutrophils were incubated in a balanced salt solution (containing 1 mM Ca^{2+}) with pertussis toxin (500 ng ml^{-1}) for 90 min. They were then processed as follows: *a*, cells were washed twice and suspended in a solution containing 1 mM Ca^{2+} and 5 μg ml^{-1} cytochalasin B and then stimulated by addition of fMet-Leu-Phe at the concentrations indicated. *b*, Cells were washed twice in a solution containing 0.6 mM EGTA and then treated with Sendai virus (100 HU ml^{-1}): after 2.5 min they were transferred to tubes containing Ca^{2+} buffered at the concentrations indicated. *c*, *d*, Cells were washed twice in a solution containing 3 mM EGTA and then further incubated for 2.5 min in 3 mM EGTA before addition of Sendai virus; they were then transferred to tubes containing phorbol ester at the indicated concentrations (*c*) or GTP-γ-S (*d*). All cells were then processed as described in Fig. 1 legend for measurement of β-glucuronidase secretion. Solid symbols (●) indicate control cells, open symbols (○) indicate pertussis-treated cells. The extent of maximal secretion due to fMet-Leu-Phe was 64±11% (±s.d., $n=14$) and 61% in the experiment illustrated (*a*); Ca^{2+}, 31±14% (±s.d., $n=57$) and 45% in the experiment illustrated (*b*); PMA (100 nM), 15±10% (±s.d., $n=18$) and 20% in the experiment illustrated (*c*); GTP-γ-S (100 μM) 35±13% (±s.d., $n=36$) and 32% in the experiment illustrated (*d*). All incubations were for 10 min. Similar results were obtained on four occasions.

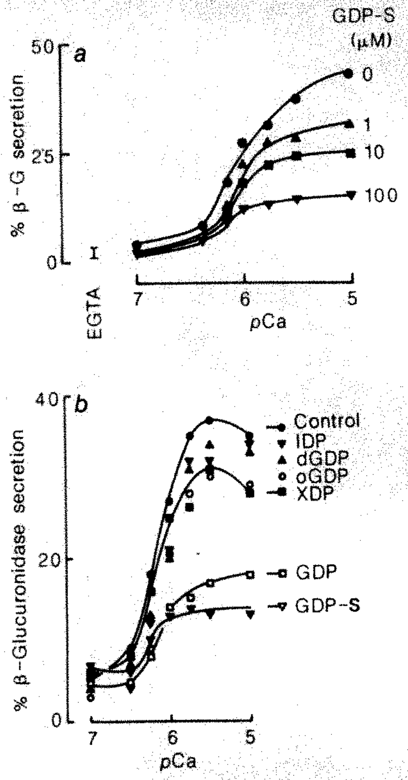

Fig. 5 Effect of GDP and GDP analogues on secretion due to Ca^{2+} from permeabilized rabbit neutrophils. Cells were prepared and permeabilized as described in Fig. 1 legend. *a*, Cells were transferred to solutions containing Ca^{2+} buffered at the concentrations indicated either in the absence (●) or in the presence of GDP-β-S at 10^{-6} M (▲), 10^{-5} M (■) and 10^{-4} M (▼). Similar results were obtained on four occasions. *b*, Cells were transferred to solutions containing Ca^{2+} buffered at the concentrations indicated in the absence (●) or in the presence of IDP (▼), dGDP (▲), oGDP (○), XDP (■), GDP (□) and GDP-β-S (▽) all at 10^{-4} M. Similar results were obtained on three occasions.

We tested other commercially available analogues of GTP for the ability to stimulate Ca^{2+}-independent secretion of β-glucuronidase (Fig. 3*a*). Of these, GppNHp induces ~60% of that achieved by GTP-γ-S at all concentrations over the range 10^{-5}–10^{-3} M. There was a small amount of secretion with $GppCH_2p$ (<25%) and GTP. Purified GTP (provided by F. Eckstein) is somewhat more active than the commercial material. GDP and GDP-β-S do not support secretion but are inhibitory of the secretion due to the GTP analogues. As the concentration of the inhibitory GDP (analogue) is increased, a higher concentration of the activator (GTP-γ-S) is needed to achieve the same amount of secretion in the manner characteristic of competitive inhibition (Fig. 3*b*).

In the knowledge[8] that GTP-γ-S can activate the PPI phosphodiesterase of isolated neutrophil membranes in the presence of normal resting levels of Ca^{2+}, we tested the ability of GTP-γ-S to cause PPI breakdown in the presence of 3 mM EGTA and no added Ca^{2+} (that is, the conditions pertaining in the permeabilized cell experiments described in this paper). In four experiments GTP-γ-S (100 μM) selectively activated the hydrolysis of 19±1% of phosphatidylinositol biphosphate and thus it is at least plausible that GTP-γ-S-induced secretion is due to its ability to activate the PPI phosphodiesterase. While it is unlikely that the water-soluble product inositol 1,4,5-trisphosphate could cause a rise of Ca^{2+} in the cytosol of the permeabilized cells to concentrations commensurate with the secretory process, the lipid-soluble product DG could be active in stimulating protein kinase C.

Protein kinase C activation can occur at concentrations of Ca^{2+} at least as low as 10^{-8} M (refs 3, 23) and we have found that secretion can occur on treating neutrophils with PMA (Fig. 4*c*) under conditions of vanishingly low concentrations of Ca^{2+}. PMA inhibited secretion due to Ca^{2+} (Fig. 1*b*): PMA (100 nM) caused 41±13% (±s.d., $n=21$) inhibition of the secretion due to 10^{-5} M Ca^{2+}. This contrasts with the combination Ca^{2+} and GTP-γ-S (Fig. 1*a*) which causes additive effects on secretion under conditions in which DG must be generated. This indicates the possibility that GTP-γ-S may act at a site insensitive to any inhibitory effect of PMA on Ca^{2+}-induced exocytosis. An alternative explanation for the difference between PMA and GTP-γ-S on Ca^{2+}-induced secretion may arise from the transient nature of the DG signal due to the guanine nucleotide compared with the persistent activation of protein kinase C due to PMA. Yet another possibility is that the inhibitory action of PMA is not expressed through activation of protein kinase C.

G-proteins can generally be modified by ADP ribosylation induced by toxins from cholera[24,25] and pertussis[26]. The neutrophil responses to fMet-Leu-Phe of Ca^{2+} mobilization, PPI hydrolysis in both intact cells[27] and plasma membranes[28], and later responses, including secretion[29,30], chemotaxis[29] and the respiratory burst[29], are all suppressed in pertussis toxin-treated cells[31]. In order to distinguish the effect of GTP-γ-S in exocytosis from its role in receptor-mediated events, we examined the effect of pertussis treatment on the secretion due to fMet-Leu-Phe from intact cells and Ca^{2+} buffers, PMA and GTP-γ-S from permeabilized cells. The results indicate that whilst secretion due to the receptor-directed ligand is prevented in toxin-treated cells, there is no effect on the secretion due to Ca^{2+}, PMA or GTP-γ-S (Fig. 4). We conclude that there are two sites of action of GTP in the stimulus-secretion sequence.

Further evidence in favour of the idea of a second site for GTP in the activation of exocytosis comes from the finding of inhibition by GDP and GDP-β-S on Ca^{2+}-induced secretion. Figure 5*a* illustrates the results of an experiment in which GDP-β-S was tested as a modulator of secretion of β-glucuronidase due to Ca^{2+}. GDP is also inhibitory to Ca^{2+}-induced secretion but higher concentrations are required (maximal inhibition at 1 mM; results not shown). Inhibition due to GDP is specific: the structurally related nucleoside diphosphates dGDP and IDP are without effect on Ca^{2+}-induced secretion (Fig. 5*b*). XDP and periodate-oxidized GDP caused inhibition to a lesser extent than GDP.

The results presented here strongly suggest that GTP and its analogues act at two sites in the control of the stimulus-secretion process. One of these has already been identified: this is the PPI phosphodiesterase[8]. The location of the second site is not known but it is concerned with the exocytotic mechanism as argued below.

GTP-γ-S can induce secretion and activate PPI phosphodiesterase in the absence of Ca^{2+}. If the sole effect of GTP-γ-S is to generate DG and so activate protein kinase C, then PMA should mimic GTP-γ-S. However, PMA only mimics GTP-γ-S in respect of inducing Ca^{2+}-independent exocytosis. The two differ in that secretion due to Ca^{2+} is inhibited by PMA whereas it is amplified by GTP-γ-S; furthermore, the extent of secretion due to PMA is always less than that due to GTP-γ-S (see Fig. 4 legend). Therefore, there is a second site of action at which GTP analogues cause secretion without intervention of the products of PPI-phosphodiesterase activation. There is the further possibility that Ca^{2+}-dependent secretion is also subject to regulation by guanine nucleotides. (Ca^{2+}-dependent secretion cannot be attributed to activation of PPI phosphodiesterase with consequent generation of DG, because the concentrations of Ca^{2+} involved are far too low to activate the enzyme[9].) The finding of inhibition of Ca^{2+}-dependent secretion by GDP and GDP-β-S further supports the idea of a GTP-regulatory system at the exocytotic site.

Although secretion from neutrophils can be activated in a variety of ways (some of which are exemplified in the present paper), the mechanism of exocytosis is likely always to be the same. Central to the mechanism of exocytosis is the fusion of the membranes of the secretory granules with the plasma membrane[32-34], the precise details of which are shrouded in obscurity. It is clear, however, that the main energy barrier to the close approach (within 2 nm) and then fusion of membranes lies in the forces which act to maintain the hydration of the membrane surfaces[35]. These are enormous and it is therefore likely that the membrane fusions which occur in the exocytotic process are catalytically regulated. While none of the molecular events are known, the second site for GTP regulation must surely be at this general level because, regardless of the mode of activation of neutrophils, GDP and GDP-β-S are inhibitory (Ca^{2+} (Fig. 5*a*), GTP analogues (Fig. 3*b*) or PMA (data not shown)). Since both membrane fusion[36] and microtubule assembly[37] are sensitive to guanine nucleotides, it is possible that one of these could be the site at which control by guanine nucleotides is exerted in the exocytotic process.

We thank Professor F. Eckstein for gifts of purified guanine nucleotides and Professor C. A. Pasternak for supplies of Sendai virus. The program CHELATE was devised by Dr Sherwin Lee. The work was supported by grants from the Vandervell Trust and the MRC.

Received 4 April; accepted 11 December 1985.

1. Douglas, W. W. *Br. J. Pharmac.* **34**, 451–474 (1968).
2. Sha'afi, R. I. *et al. Biochem. biophys. Res. Commun.* **114**, 638–645 (1983).
3. Di Virgilio, F., Lew, D. P. & Pozzan, T. *Nature* **310**, 691–693 (1984).
4. Nishizuka, Y. *Nature* **308**, 693–698 (1984).
5. Rink, T. J. & Sanchez, A. *Biochem. J.* **222**, 833–836 (1984).
6. Fernandez, J. M., Neher, E. & Gomperts, B. D. *Nature* **312**, 453–455 (1984).
7. Gomperts, B. D. *Nature* **306**, 64–66 (1983).
8. Cockcroft, S. & Gomperts, B. D. *Nature* **314**, 534–536 (1985).
9. Cockcroft, S., Baldwin, J. M. & Allan, D. *Biochem. J.* **221**, 477–482 (1984).
10. Wyke, A. M., Impraim, C. C., Knutton, S. & Pasternak, C. A. *Biochem. J.* **190**, 625–638 (1980).
11. Bachi, T., Deas, J. E. & Howe, C. *Cell Surface Rev.* **2**, 83–127 (1977).
12. Haywood, A. M. *J. molec. Biol.* **83**, 427–436 (1974).
13. Foster, K. A., Gill, K., Micklem, C. A. & Pasternak, C. A. *Biochem. J.* **190**, 639–646 (1980).
14. Impraim, C. C., Foster, K., Micklem, K. J. & Pasternak, C. A. *Biochem. J.* **186**, 847–860 (1980).
15. Gomperts, B. D., Baldwin, J. M. & Micklem, K. J. *Biochem. J.* **210**, 737–745 (1983).
16. Knight, D. E. & Baker, P. F. *J. Membrane Biol.* **68**, 107–140 (1982).
17. Knight, D. E., Niggli, V. & Scrutton, M. C. *Eur. J. Biochem.* **143**, 437–446 (1984).
18. Yaseen, M. A., Pedley, K. C. & Howell, S. L. *Biochem. J.* **206**, 81–87 (1982).
19. Barrowman, M. M., Cockcroft, S. & Gomperts, B. D. *J. Physiol., Lond.* (submitted).
20. Haslam, R. J. & Davidson, M. M. L. *FEBS. Lett.* **174**, 90–95 (1984).
21. Baker, P. F. *Nature* **310**, 629–630 (1984).
22. Cockcroft, S., Bennett, J. P. & Gomperts, B. D. *Biochem. J.* **200**, 501–508 (1981).
23. Neidel, J. E., Kuhn, L. J. & Vandenbark, G. R. *Proc. natn. Acad. Sci. U.S.A.* **80**, 263–265 (1983).
24. Cassel, D. & Pfeuffer, T. *Proc. natn. Acad. Sci. U.S.A.* **75**, 2669–2673 (1978).
25. Northup, J. K. *et al. Proc. natn. Acad. Sci. U.S.A.* **77**, 6516–6520 (1980).
26. Bokoch, G. M., Katada, T., Northup, J. K., Hewlett, E. L. & Gilman, A. G. *J. biol. Chem.* **258**, 2072–2075 (1983).
27. Verghese, M. W., Smith, C. D. & Snydermann, R. *Biochem. biophys. Res. Commun.* **127**, 450–457 (1985).
28. Smith, C. D., Lane, B. C., Kusaka, I., Verghese, M. W. & Snydermann, R. *J. biol. Chem.* **260**, 5875–5879 (1985).
29. Becker, E. L. *et al. J. Cell Biol.* **100**, 1641–1646 (1985).
30. Molski, T. F. P. *et al. Biochem. biophys. Res. Commun.* **124**, 644–650 (1984).
31. Goldman, D. W., Chang, F.-H., Gifford, L. A., Goetzl, E. J. & Bourne, H. R. *J. exp. Med.* **162**, 145–156 (1985).
32. Amsterdam, A., Ohad, I. & Schramm, M. *J. Cell Biol.* **41**, 753–773 (1969).
33. Palade, G. *Science* **189**, 347–358 (1975).
34. Chandler, D. E., Bennett, J. P. & Gomperts, B. D. *J. Ultrastruct. Res.* **83**, 221–232 (1983).
35. Parsegian, V. A., Rand, R. P. & Gingell, D. *Ciba Fdn Symp.* **103**, 9–27 (1984).
36. Paiement, J. *Biochim. biophys. Acta* **777**, 274–282; *Expl Cell Res.* **151**, 354–366 (1984).
37. Sandoval, I. V. & Weber, K. *J. biol. Chem.* **255**, 6966–6974 (1980).
38. Bennett, J. P., Cockcroft, S. & Gomperts, B. D. *Biochim. biophys. Acta* **601**, 584–591 (1980).
39. Anderegg, G. *Helv. chim. Acta* **47**, 1801–1814 (1964).

Clonal origin of haematopoietic colonies in the postnatal mouse liver

J. Rossant*‡, K. M. Vijh*‡, C. E. Grossi† & M. D. Cooper†

* Department of Biological Sciences, Brock University, St Catharines, Ontario, Canada L2S 3A1
† Cellular Immunobiology Unit of the Tumor Institute and Department of Pathology, University of Alabama, Birmingham, Alabama 35294, USA

The liver of the neonatal mouse continues to show haematopoietic activity for up to 2 weeks after birth[1,2] and morphological analysis has shown that this activity becomes focused in discrete haematopoietic colonies by the end of the first week postnatal[3]. Furthermore, each colony contains cells of one haematopoietic lineage only, that is, erythroid, myeloid or pre-B-lymphoid cells. This pattern of differentiation suggests that each colony is derived from a single committed precursor cell, which, if true, would represent the first demonstration of non-mixed haematopoietic colonies in normal development and would provide a useful system for studying the factors affecting the clonal diversity of haematopoietic stem cells and their lineage-committed progeny. Here we have analysed the haematopoietic foci in the liver of neonatal mouse chimaeras, using a newly developed ubiquitous *in situ* cell marker system which clearly demonstrates the clonal origin of these colonies.

Mouse chimaeras can be very useful for addressing problems of clonal development because they consist of a mixture of cells of two different genotypes, brought together by embryo aggregation or blastocyst injection at early stages of embryo development[4]. If a given structure in a chimaera is derived from a single progenitor cell, it will always be entirely of one genotype or the other, whereas structures with multiple progenitors will often

---

‡ Present address: Mt Sinai Hospital Research Institute, Division of Molecular and Developmental Biology, 600 University Avenue, Toronto, Ontario, Canada M5G 1X5.

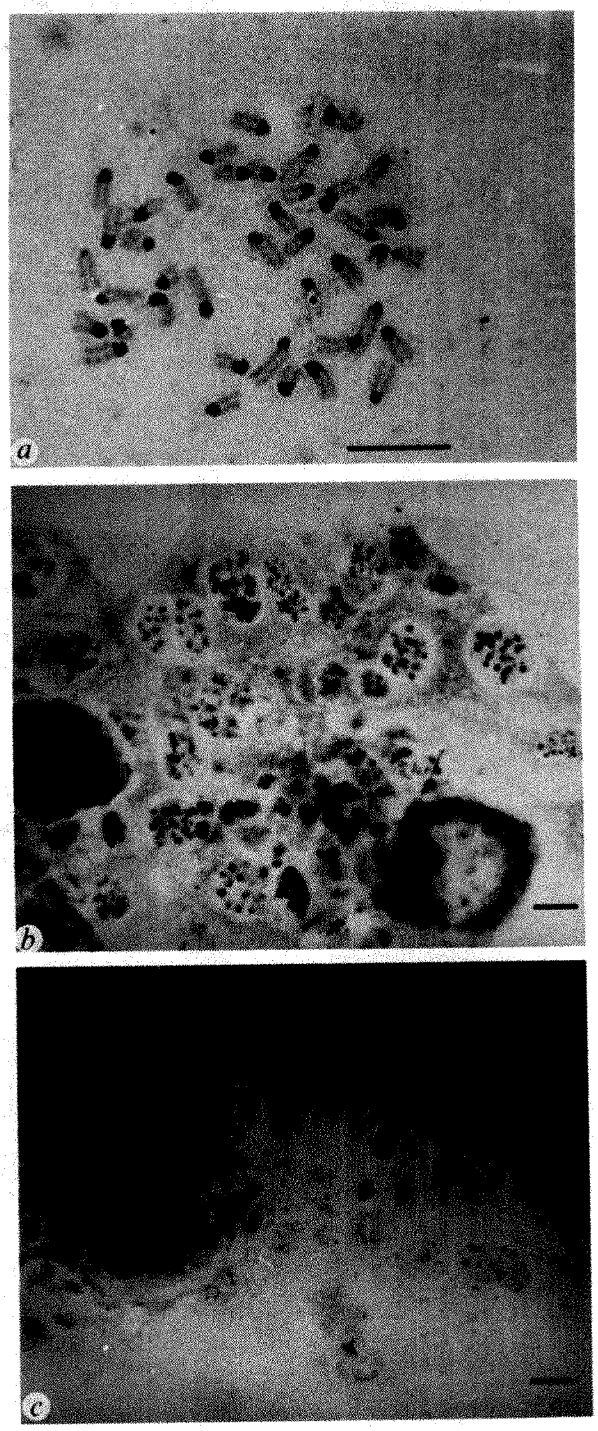

Fig. 1 Hybridization of biotinylated *M. musculus* satellite DNA to chromosomes and cell spreads. *a*, Chromosome spread from *M. musculus* showing hybridization of the probe to the centromeric regions alone. *b*, Blastocyst outgrowth from *M. musculus* showing extensive hybridization of the repetitive DNA probe as evidenced by dark clumps of staining in the nuclei. c, *M. caroli* blastocyst outgrowth showing only background staining. Scale bar, 20 μm.
Methods. The cloned probe to the *M. musculus* major satellite DNA sequence, pMR196[10], was nick-translated in the presence of Bio-16-UTP (Enzo Biochem) according to the protocol provided by the manufacturer. Unincorporated nucleotides were separated from the labelled DNA by elution through a Sephadex G-50 spun column. Incorporation of biotinylated nucleotide into DNA was assessed by spotting serial dilutions of the nick-translated probe onto nitrocellulose and heating the latter at 80 °C for 1 h under vacuum. The filter was then incubated in 4% bovine serum albumin (BSA) in phosphate-buffered saline (PBS) for 10 min at room temperature, followed by incubation with streptavidin–horseradish peroxidase (HRP) complex (Detek I HRP, Enzo Biochem) as described by the manufacturers. After washing three times in PBS, the filter was stained in the dark for 2 min with 0.5 mg ml^{-1} DAB (3,3′-diaminobenzidine tetrahydrochloride) in 0.05 M Tris-HCl *p*H 7.6, plus 0.01% hydrogen peroxide. Brown stain indicates incorporation of the biotinylated precursor and filters can be retained to allow comparison of incorporation from one batch to the next. Chromosome spreads were prepared from primary *M. musculus* embryonic fibroblast cultures in the standard manner. Blastocyst outgrowths were obtained by culturing blastocysts of the two species in chambered slides in α-modified minimal essential medium (MEM) plus 10% fetal calf serum for 4 days. Then, medium was removed and the cultures were fixed in acetic acid/ethanol (1:3) for 1 h, rinsed in ethanol and air-dried. Chromosome and cell spreads were pretreated for 1 h at 37 °C with 100 μg ml^{-1} RNase A (Boehringer Mannheim) in 2 × SSC, washed twice in 2 × SSC, dehydrated and air-dried. Slides were denatured by immersing them in 70% formamide in 2 × SSC at 70 °C for 4 min, then they were dehydrated and air-dried. Biotinylated pMR196 (final concentration 3 μg ml^{-1}) was denatured by boiling in the presence of sonicated herring sperm DNA (final concentration 250 μg ml^{-1}) for 5 min. The probe mix was quenched on ice and 50% dextran sulphate and 20× SSC were added to give a final concentration of 10% dextran sulphate and 4× SSC. Probe mix (22 μl) was placed on each spread, which was covered by an acid-cleaned coverslip. Slides were incubated overnight at 60 °C in a moist chamber. Washes were carried out at fairly high stringency to avoid cross-hybridization. Two washes in 2× SSC at room temperature were followed by two washes in 0.1× SSC, first at room temperature and then at 50 °C. The slides were then treated with the streptavidin–HRP complex and the peroxidase activity was detected with DAB as described by the manufacturer. It is very important not to let the slides dry out at any point in this procedure. Slides were lightly counterstained with Light Green.

be of mixed genotype, depending on the proportion of the two genotypes in the chimaera and the degree of cell mixing during development[4,5]. Determination of the genotype of a given structure requires sensitive genetic markers. The ideal cell marker should be ubiquitous, cell-autonomous and readily detectable in single cells in histological sections of chimaeras, so that the genotype of every cell in a structure can be determined unequivocally. There have been only a small number of *in situ* genetic marker systems described in mammals, and most have been limited to certain cell types or have not been readily detectable at the single-cell level[6].

Recently, we have described the development of an *in situ* marker system for studying clonal development in mammalian chimaeras which overcomes many of the problems of the other marker systems. Our system is based on the use of interspecific chimaeras between *Mus musculus*, the laboratory mouse, and *Mus caroli*, a wild species of mouse from South-East Asia[7]. *In situ* DNA–DNA hybridization with a cloned probe to the major satellite DNA sequence of *Mus musculus* distinguishes between the nuclei of the two species in both cell spreads and tissue sections[8,9], because *M. caroli* DNA contains very few sequences that cross-hybridize with the *M. musculus* satellite sequence[10]. This marker system has great potential for studying cell lineage in embryonic development and in the adult because it can be used in all tissues containing nucleated cells. In our original work we used a radioactively labelled probe combined with autoradiography to detect hybridization, but we have recently improved the reproducibility and resolution of the system by

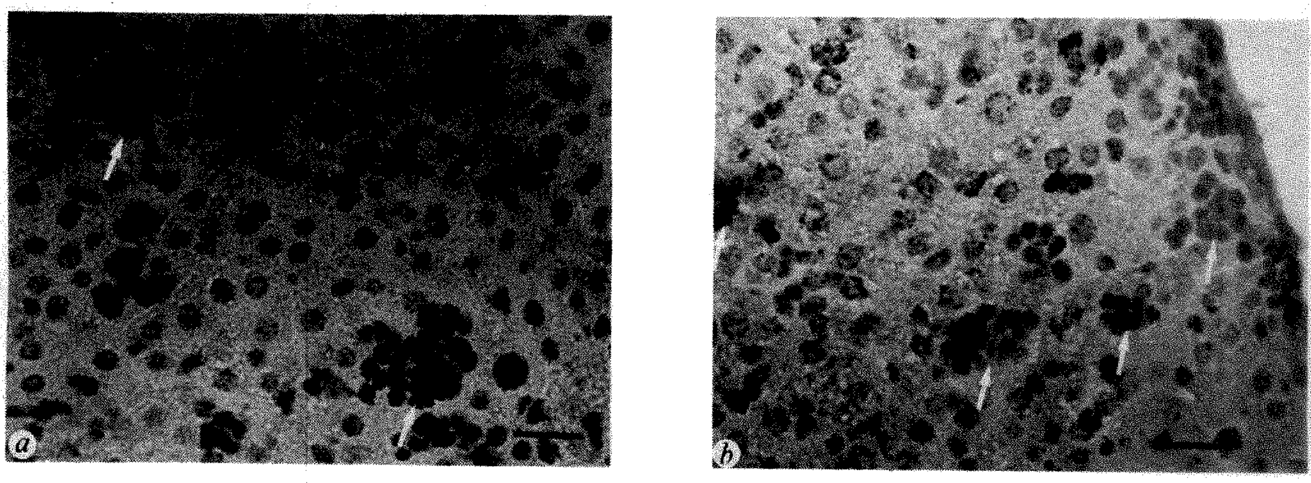

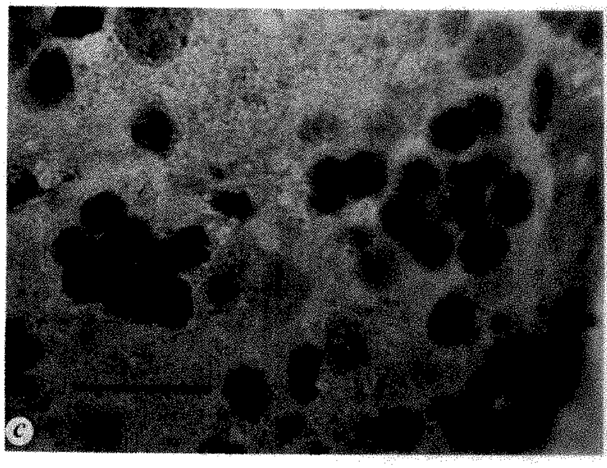

Fig. 2 Sections of liver from 6-day *M. musculus-M. caroli* chimaeras following *in situ* hybridization with *M. musculus* satellite DNA probe. *a*, Low-power photomicrograph of chimaeric liver showing two haematopoietic foci (arrows). The left-hand focus shows only purple stain and is entirely *M. caroli*, while the cells of the right-hand colony show granules of brown stain and are all *M. musculus*. *b*, Similar micrograph of a different region showing four separate foci; two *M. musculus* (extreme left and second from the right), and two *M. caroli* (second from the left and extreme right). *c*, High-power magnification of two haematopoietic colonies from *b*, showing that the left-hand colony is labelled and *M. musculus* in origin while the right-hand colony is unlabelled and *M. caroli* in origin. The granules apparent in the nuclei of the *M. caroli* colony are purple-stained heterochromatin and not brown-stained sites of hybridization. Scale bar, 20 μm.

Methods. Small pieces of liver were fixed overnight in acetic acid/ethanol (1:3) at 4 °C, washed in two changes of ethanol for 30 min each and embedded in ester wax (BDH 1960) at a temperature not exceeding 55 °C. Sections (5-μm thick) were mounted on poly-L-lysine-coated slides, then allowed to spread and dry for 1 h at 42 °C. Wax was removed using xylene and the slides were dipped in ethanol for 5 min before air-drying. Denaturation and hybridization were performed as described for the cell spreads in Fig. 1 legend. After staining for peroxidase the slides were run quickly through a haematoxylin and eosin staining series and mounted in Canada balsam. *M. musculus* nuclei show brown staining apparently associated with the heterochromatin, indicative of hybridization of the *M. musculus* satellite DNA probe. *M. caroli* nuclei stain purple with haematoxylin but show no brown staining. The difference between brown and purple stain is difficult to reproduce in a black-and-white photograph and so the distinction between labelled and unlabelled cells is not as striking in these figures as in the original slides. (Colour prints can be obtained from the authors on request.)

using biotinylated DNA[11] as the probe for hybridization (Fig. 1); this modification has transformed the marker system into one that can be used for the detailed single-cell analysis required to answer questions such as that addressed here.

Before analysing the genotype of haematopoietic foci in livers of neonatal chimaeras between *M. musculus* and *M. caroli*, we first examined the time course and nature of haematopoietic activity in *M. caroli*, to ensure that it was similar to that in *M. musculus*. Discrete haematopoietic colonies were observed slightly earlier in *M. caroli* than in *M. musculus*, but the cellular composition of the colonies in the two species was very similar (Table 1). Chimaeras between the two species were produced by injecting *M. caroli* inner cell masses into *M. musculus* blastocysts which were then transferred to *M. musculus* recipient females and allowed to proceed to term. Two chimaeras which contained approximately equal contributions from the two component species, by coat colour, were killed and their livers removed. Glucose phosphate isomerase isozyme analysis was performed on part of each liver[12] and the remainder was cut into small pieces and fixed and embedded for histological examination and *in situ* hybridization. The liver that was chosen for more extensive analysis was shown to contain ~70% *M. musculus* cells by isozyme analysis. Morphological analysis

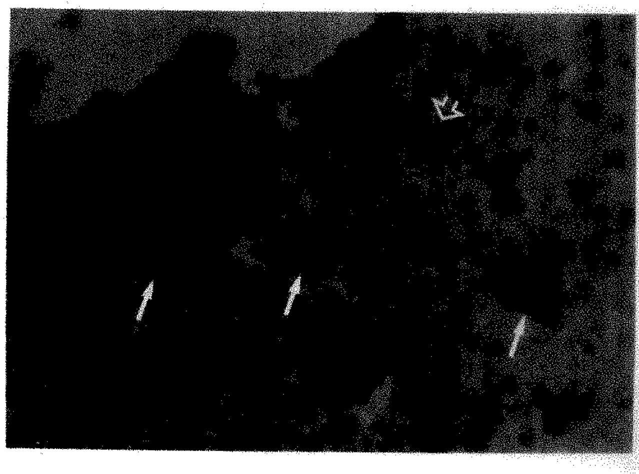

Fig. 3 Photomicrograph of chimaeric liver showing several haematopoietic foci, all of which are composed of cells of a single genotype (solid arrows). The small left-hand colony is *M. caroli* and the larger colonies are *M. musculus*. The open arrow indicates a megakaryocyte which is *M. caroli* in origin.

Table 1 Relative frequencies and cellular composition of liver haematopoietic foci as a function of day postnatal

Day postnatal	% Of colony type											
	M. musculus (BALB/c)*			Mega-kary-ocytes	*M. caroli*			Mega-karyo-ocytes	Interspecies chimaera			Mega-karyo-ocytes
	Erythroid	Myeloid	Lymphoid		Erythroid	Myeloid	Lymphoid		Erythroid	Myeloid	Lymphoid	
6	Diffuse haematopoiesis				60	22	16	2	63	20	14	3
8	44	36	16	4	55	31	10	4	ND			
10	50†	34	5	10	66	26	8	0	ND			
12	77	16	4	3	Absent				ND			
15	Absent‡				Absent				ND			

Liver samples were fixed overnight in 10% formaldehyde, dehydrated and paraffin-embedded. Sections were stained with haemotoxylin and eosin and colony types were identified on the basis of morphology. Other studies, using electron microscopy and immunofluorescence, have confirmed this morphological identification[3]. ND, not done.

* From ref. 3.

† 1% of these foci were mixed (erythroid plus myeloid).

‡ Foci no longer detectable.

Table 2 Distribution of *M. musculus* and *M. caroli* haematopoietic foci

M. musculus	71
M. caroli	19
Mixed type 1*	6
Mixed type 2†	4

Values are percentages.

* Colonies consisting of cells of the *M. caroli* type with a single cell of the *M. musculus* type.

† Colonies consisting of several cells from both species.

revealed that it contained discrete haematopoietic colonies whose cellular composition was very similar to those of non-chimaeric livers (Table 1). *In situ* hybridization with the *M. musculus* satellite DNA probe revealed roughly the expected proportion of *M. musculus* and *M. caroli* cells in the hepatocytes and also showed that there was fine intermixing of liver cells of the two genotypes, as found previously using the radioactively labelled probe on adult liver[9] and also reported from studies using enzyme activity variants as cell markers[13].

When the haematopoietic colonies in the chimaeric liver were examined for hybridization to the *M. musculus* satellite DNA probe, it was apparent that almost all colonies were entirely of one genotype or the other (Table 2, Figs 2, 3). The proportion of *M. musculus* to *M. caroli* colonies closely reflected the proportion of the two genotypes in the hepatocytes, illustrating again the high correlation coefficient between mosaic composition in different tissues of mouse chimaeras[14,15]. Of 220 colonies scored, only 10% contained cells of both genotypes. There were, on average, 8 cells per colony in a single plane of section. Thus, if the cells present in the haematopoietic foci were the result of random distribution of non-clonally related cells, approximately 6% of the colonies might appear totally *M. musculus* by chance alone and 0.0006% of the colonies would appear totally *M. caroli*. The rest of the colonies would be expected to be mixed. The results clearly differ from this prediction. A high proportion of single-genotype colonies, as observed, would result if haematopoietic progenitors of the two genotypes were non-randomly distributed in the developing liver. This seems unlikely as colonies of both genotypes were distributed widely and evenly throughout the tissue. The remaining possibility is that *M. musculus* and *M. caroli* haematopoietic cells cannot coexist in close proximity within a haematopoietic focus. However, this seems highly unlikely in view of the evidence that hepatocytes and other cell types are intermixed in chimaeras[16] and that cells of the two species interact normally even to the extent of forming chimaeric myotubes by cell fusion[16]. The most likely explanation of the large number of single-genotype foci is, therefore, that each colony contains the progeny of a single progenitor cell.

Some mixed colonies were observed; most of these consisted of a group of cells of one genotype surrounding one cell of the opposite genotype. We have shown previously that erythroid colonies in the neonatal liver often contain an accessory cell with macrophage-like features[3] and it is tempting to speculate that the mixed colonies observed represent erythroid colonies in which erythroid cells and accessory cells happen to be of different genotype. Unfortunately, the treatment of the slides for *in situ* hybridization was not compatible with the detailed morphological examination required to confirm this directly. The remaining foci were truly mixed and probably represent the result of fusion of two neighbouring colonies. Occasional colonies of mixed lineage were also observed on morphological examination[3] (Table 1).

The present study has clearly shown that the haematopoietic colonies which occur in the neonatal mouse liver are clonal in origin. As it has also been shown that each colony is derived from one haematopoietic lineage alone, it is probable that precursors committed to different lineages occur throughout the neonatal liver and give rise to discrete foci of cells. The alternative possibility that multipotential stem cells became restricted to different pathways by local environmental differences seems unlikely in the absence of any evidence for such microenvironmental variation in the liver. This represents the first demonstration of clonal development from single committed haematopoietic precursors in normal development and makes the neonatal liver system very useful for studying genetic and environmental factors that can affect the lineage preferences of haematopoietic stem cells. Our study also demonstrates the power of the *M. musculus*-*M. caroli* marker system, which provides a degree of resolution not afforded to date by any other marker system in mammals. The marker system can now be applied to many other problems of clonal analysis in mammalian chimaeras.

This work was supported by grants from the Natural Sciences and Engineering Research Council of Canada (to J.R.) and by grants CA16673 and CA13148 from the National Cancer Institute of the NIH (to M.D.C.). J.R. is an E.W.R. Steacie Memorial Fellow of NSERC.

Received 10 June; accepted 26 November 1985.

1. Kamps, W. A. & Cooper, M. D. *J. Immun.* **129**, 526-531 (1982).
2. Velardi, A. & Cooper, M. D. *J. Immun.* **133**, 672-677 (1984).
3. Grossi, C. E., Velardi, A. & Cooper, M. D. *J. Immun.* **135**, 2303-2311 (1985).
4. McLaren, A. *Mammalian Chimaeras* (Cambridge University Press, 1976).
5. West, J. D. in *Development in Mammals* Vol. 3 (ed. Johnson, M. H.) 413-460 (Elsevier/North Holland, Amsterdam, 1978).
6. West, J. D. in *Chimaeras in Developmental Biology* (eds Le Douarin, N. & McLaren, A.) 39-67 (Academic, London, 1984).
7. Rossant, J. & Frels, W. I. *Science* **208**, 419-421 (1980).
8. Siracusa, L. D. *et al. J. Embryol. exp. Morph.* **73**, 163-178 (1983).

9. Rossant, J., Vijh, K. M., Siracusa, L. D. & Chapman, V. M. *J. Embryol. exp. Morph.* **73**, 179-191 (1983).
10. Pietras, D. F. *et al. Nucleic Acids Res.* **11**, 6965-6983 (1983).
11. Langer, P. R., Waldrop, A. A. & Ward, D. C. *Proc. natn. Acad. Sci. U.S.A.* **78**, 6633-6637 (1981).
12. Peterson, A. C., Frair, P. M. & Wong, G. G. *Biochem. Genet.* **16**, 681-690 (1978).
13. West, J. D. *J. Embryol. exp. Morph.* **36**, 151-161 (1976).
14. Falconer, D. S. & Avery, P. J. *J. Embryol. exp. Morph.* **43**, 195-219 (1978).
15. West, J. D., Bucher, T., Linke, I. M. & Dunnwald, M. *J. Embryol. exp. Morph.* **84**, 309-329 (1984).
16. Rossant, J. & Chapman, V. M. *J. Embryol. exp. Morph.* **73**, 193-205 (1983).

A human osteosarcoma cell line secretes a growth factor structurally related to a homodimer of PDGF A-chains

Carl-Henrik Heldin*, Ann Johnsson*, Suzanne Wennergren*, Christer Wernstedt*, Christer Betsholtz† & Bengt Westermark†

* Department of Medical and Physiological Chemistry, Box 575, Biomedicum, S-751 23 Uppsala, Sweden
† Department of Pathology, University Hospital, S-751 85 Uppsala, Sweden

Platelet-derived growth factor (PDGF), as purified from fresh human platelets, is a protein of relative molecular mass (M_r) 30,000 composed of two disulphide-linked subunit chains of similar size, named A and B (ref. 1). The dimer structure of PDGF seems to be important for its biological effects, as reduction irreversibly inactivates the factor; it is not known, however, whether PDGF exists as a heterodimer or as a mixture of homodimers. Amino-acid sequence analysis has revealed that the A- and B-chains of human PDGF are related to each other, and that the B-chain is almost identical to part of the v-*sis* gene product of simian sarcoma virus (SSV)[2-5]. There is experimental evidence that a PDGF-like protein is indeed operational in SSV-induced transformation[6-12] and the biologically active v-*sis* product is probably structurally similar to a putative dimer of PDGF B-chains[13]. PDGF-like growth factors and/or a 4.2-kilobase (kb) c-*sis* transcript are present in several transformed mammalian cell lines[7,14-24] and in certain nontransformed cells[25-30]; cloned c-*sis* complementary DNA from human T cells transformed with human T-lymphotropic virus (HTLV)[24,31] or from human endothelial cells[32] contains the coding sequence for a putative PDGF B-chain precursor, but apparently lacks PDGF A-chain sequences. We have previously partially purified and characterized a PDGF-like growth factor from U-2 OS cells (osteosarcoma-derived growth factor, ODGF) and shown that this factor has structural, functional and immunological characteristics in common with PDGF[14]. We describe here a procedure for the preparation of homogeneous ODGF, and provide evidence that this factor, which binds to the PDGF receptor, has a structure similar to a homodimer of PDGF A-chains.

Serum-free conditioned medium was collected from U-2 OS cells[33] grown in roller bottles and used as starting material for the purification of ODGF. The growth factor activity was monitored by a ^{3}H-thymidine incorporation assay using human foreskin fibroblasts as target cells[34], and occasionally by a PDGF receptor competition assay[35]. ODGF was first concentrated and freed of glycosaminoglycans and anionic proteins by adsorption to a highly charged Sulphadex gel. The sample was then subjected to two consecutive gel chromatographies, the first at high ionic strength and neutral *p*H (Fig. 1*a*), the second at low *p*H (Fig. 1*b*). Final purification was achieved by reverse-phase chromatography on HPLC (Fig. 1*c*). This purification procedure gave a 4,000-fold purification at a yield of about 30% relative to the starting conditioned medium. Approximately 25 μg of ODGF was obtained from 8 l of conditioned medium. The purified factor had PDGF agonist activity and was recognized by antibodies against PDGF (not shown).

Purified ODGF was analysed by SDS-gel electrophoresis and silver staining, and one homogeneous component of M_r 31,000 was obtained in non-reducing conditions (Fig. 1*d*). The size of this component corresponds to the largest PDGF component, which is proteolysed in the platelets or during purification to several components of M_rs 31,000-28,000 (refs 36-40 and Fig. 1*d*). In reducing conditions ODGF appeared as a single band of M_r 17,000, whereas PDGF contained several components of M_r 17,000 and smaller (Fig. 1*d*).

The behaviour of ODGF in SDS-gel electrophoresis in the absence and presence of reducing agents indicates that, like PDGF, it has a dimer structure. Furthermore, the homogeneous appearance of ODGF after reduction suggests that it may contain only one of the two prototype chains of PDGF. To investigate this possibility, ODGF and PDGF were radioactively iodinated using two different techniques, the chloramine-T method[41] which labels tyrosine residues, and the procedure of Bolton and Hunter[42] which labels amino groups (lysine residues and the amino terminus). The structure of the labelled component was investigated by SDS-gel electrophoresis and autoradiography. Both labelling procedures led to incorporation of ^{125}I into a 31,000-M_r component of ODGF which was converted to a 17,000-M_r form after reduction (Fig. 2), that is, the same pattern as was obtained with silver staining. PDGF, however, gave different patterns by the two labelling procedures. The chloramine-T method led to the labelling of components of apparent M_r 31,000-28,000, which were converted to apparent M_rs of 17,000, 16,000 and 12,000 after reduction. The Bolton-Hunter procedure led to incorporation of radioactivity into the same components, but also into a component of apparent M_r 15,000 and into two components of M_rs <10,000 after reduction (Fig. 2). The different patterns obtained by the two labelling procedures are explained by the fact that the PDGF B-chain contains no tyrosine residues[5] and is therefore not labelled by the chloramine-T method. This conclusion was supported by experiments in which the constituent chains of ^{125}I-PDGF were separated by reverse-phase chromatography (see below); labelling of PDGF by the chloramine-T method yielded radioactivity only in the position corresponding to the PDGF A-chain (not shown). It follows from the labelling pattern of ODGF that the factor may contain the PDGF A-chain (Fig. 2).

Furthermore, reduced and alkylated ^{125}I-ODGF, labelled using the Bolton-Hunter procedure, was subjected to a reverse-phase chromatographic system capable of separating the A- and B-chains of PDGF[36]. Only one peak of radioactivity was obtained, with an elution position corresponding exactly to that of PDGF A-chains (Fig. 3*a*, *b*).

In addition to their different elution positions in reverse-phase chromatography, the A- and B-chains of PDGF differed in their susceptibilities to cleavage by formic acid and cyanogen bromide. Purified ^{125}I-labelled PDGF A-chain was cleaved by acid treatment (70% formic acid for 48 h at 37 °C) from an M_r of 17,000 to one of 15,000, while this treatment had no effect on the B-chain (Fig. 3*c*). This cleavage probably occurs at an aspartic acid-proline linkage at position 25-26 in the A-chain, since such a peptide bond is known to be susceptible to acidic conditions[43]; no such peptide bond occurs in the PDGF B-chain[5]. However, the B-chain was cleaved by CNBr in 70% formic acid, leading to the formation of two new peptides of M_rs 14,000 and 12,000 (Fig. 3*c*). The cleavages may occur at a methionine residue at position 12 and at a tryptophan residue at position 40 in the B-chain[2]. Incubation of the A-chain with CNBr in 70% formic acid produced no observable cleavage in addition to that caused by 70% formic acid only (Fig. 3*c*). This is compatible with the fact that the known sequence of the A-chain contains no methionine residues and that the only tryptophan residue is at position 36, close to the aspartic acid-proline linkage[5] at position 25-26. When reduced and alkylated

^{125}I-ODGF was subjected to acid treatment and CNBr cleavage, practically all of it was cleaved by acid to an M_r of 15,000, but CNBr had no further effect (Fig. 3*c*), that is, it behaved exactly as if it consisted entirely of PDGF A-chains.

Amino-acid sequence analysis of the N-terminus of ODGF further substantiated the presence of only A-chains in this molecule. About 200 pmol of unreduced ODGF was analysed using a solid-phase sequenator, yielding an 8-amino-acid N-terminal sequence. This contained only one major sequence, which was identical to the N-terminal sequence of the A-chain of PDGF (Fig. 4). When unreduced PDGF purified from human platelets was applied to the same analysis, sequences from both the A- and B-chains were obtained in approximately stoichiometric quantities (not shown).

We report here, for the first time, the purification to homogeneity of a PDGF-like growth factor from a human transformed cell line, the U-2 OS osteosarcoma cell line. The factor appears to be a homodimer of polypeptide chains similar to the PDGF A-chain. This is unexpected, because previous investigations have shown that the U-2 OS cells in fact express the c-*sis* gene, which encodes the B-chain precursor; a 4.2-kb messenger RNA has been identified in Northern blots using a c-*sis* probe

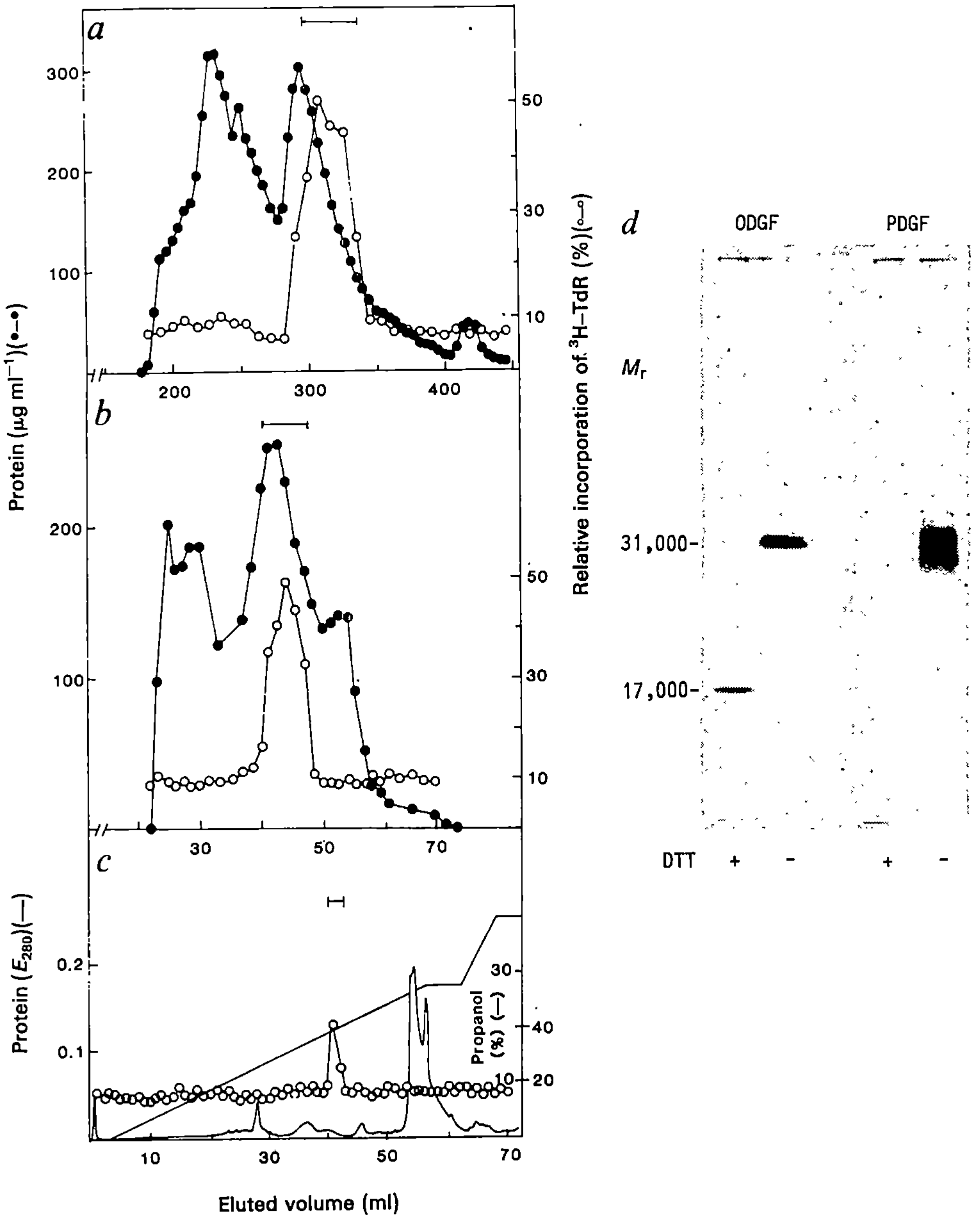

Fig. 1 Purification of ODGF. Sequential chromatography of conditioned medium from U-2 OS cells on a Sephacryl S-200 column eluted with 1 M NaCl, 0.01 M phosphate buffer *p*H 7.4 (*a*), a BioGel P-150 column eluted with 1 M acetic acid (*b*), and an HPLC RP8 column (*c*), are shown, as well as a silver-stained SDS gel of the purified ODGF (*d*). **Methods.** Conditioned medium from U-2 OS cells was collected as described previously[14]. The first step in the purification of ODGF was batch-wise adsorption to Sulphadex beads. Sulphadex gel (200 ml, synthesized as described elsewhere[48]) was added to 8 l of conditioned medium (containing ~320 mg protein) and then equilibrated overnight at 4 °C on a rocker platform. The gel was then allowed to sediment, the unadsorbed fraction discarded and the gel poured into a column (5 × 40 cm). The column was washed with 600 ml of 0.15 M NaCl, 0.01 M phosphate buffer *p*H 7.4 and then eluted with 300 ml of 1.5 M NaCl, 0.01 M phosphate buffer *p*H 7.4. The eluted fraction contained ~60 mg of protein. ODGF was then concentrated by addition of solid ammonium sulphate to 60% saturation (390 g l^{-1}). After 2 h of equilibration end over end at 4 °C, the sample was centrifuged for 20 min at 20,000 *g*. The pellet was dissolved in 5 ml of 1 M NaCl, 0.01 M phosphate buffer *p*H 7.4 and then dialysed against this buffer. After centrifugation the sample was applied to a Sephacryl S-200 column (2 × 145 cm) and eluted at 4 °C with 1 M NaCl, 0.01 M phosphate buffer *p*H 7.4 at a flow rate of 10 ml h^{-1}. Fractions (4 ml) were collected and analysed for protein and growth promoting activity (stimulation of ^{3}H-thymidine incorporation in human foreskin fibroblasts[34]). Growth promoting activity is expressed relative to that given by 10 ng ml^{-1} of PDGF (5–10 × 10^3 c.p.m., corresponding to 50–70% labelled nuclei). Active fractions were pooled as indicated in the figure (~8 mg of protein), dialysed against 1 M acetic acid and lyophilized. The sample was dissolved in 2 ml of 1 M acetic acid and applied to a BioGel P-150 column (2 × 30 cm) then eluted with 1 M acetic acid. The column was operated at room temperature, at a flow rate of 4 ml h^{-1} and 1.5-ml fractions were collected. The active fractions were pooled as indicated in the figure (~1 mg of protein) and lyophilized. The lyophilized material was then dissolved in 300 μl of 1 M acetic acid and applied to an HPLC RP8 column (Merck). The column was washed with 4 ml of 1 M acetic acid, 2 M guanidine-HCl, and then eluted with a linear gradient of propanol in 1 M acetic acid, 2 M guanidine-HCl. Fractions containing growth-promoting activity were pooled as indicated in the figure and used for further experiments. About 25 μg of ODGF was obtained from 8 l of conditioned medium. Aliquots (~0.5 μg) of ODGF, and PDGF purified from human platelets[36], were analysed on gradient gels consisting of 13–18% acrylamide, in non-reducing conditions or after reduction with dithiothreitol (DDT) and alkylation[49]. The gel was stained for protein by a silver method[50]. Note that ODGF and PDGF stain better in unreduced than reduced form. The protein concentration of purified ODGF was estimated by comparing the intensity of the ODGF band in the silver-stained SDS gel with those of known amounts of PDGF.

in stringent hybridization conditions[44,45]. If PDGF B-chains are indeed also synthesized in the U-2 OS cells, there are several possible reasons that we have not observed any such peptides in the ODGF preparation; for example, B-chains may not be properly dimerized, processed or secreted into the culture medium. Alternatively, B-chain homodimers or A- and B-chain heterodimers are formed and secreted, but are turned over rapidly, or remain associated with the cells[12,46], and are therefore not found in the conditioned medium. It is also possible that B-chain-containing molecules appear in the conditioned medium but are lost during purification.

PDGF purified from human platelets contains approximately equal quantities of A- and B-chains (ref. 5 and our data not shown). Fractionation of purified PDGF by various methods has not yielded any evidence for the presence of homodimers, and preliminary binding experiments indicate that PDGF from human platelets interacts with the PDGF receptor at higher affinity than ODGF (not shown). Taken together, these observations suggest that human PDGF may have a heterodimer structure consisting of both A- and B-chains which interacts with the PDGF receptor more avidly than the osteosarcoma-derived A-chain homodimer. However, the extensive proteolysis of

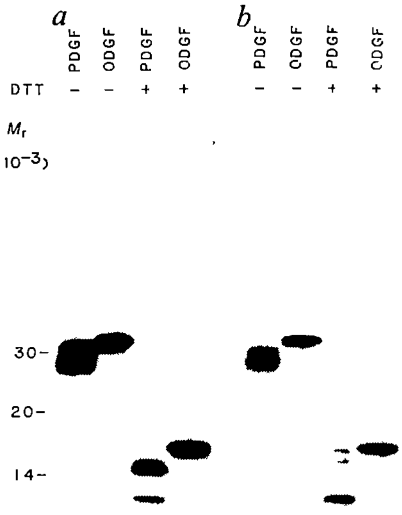

Fig. 2 Analysis by SDS-gel electrophoresis and autoradiography of ODGF and PDGF labelled with ^{125}I by two different methods: *a*, according to the method of Bolton and Hunter[42]; *b*, by the chloramine-T method[41]. Samples were analysed with or without reduction with DDT and alkylation. ODGF (1 μg) and PDGF (5 μg) were labelled by the procedure of Bolton and Hunter[42] to specific activities of 42,000 c.p.m. per ng and 32,000 c.p.m. per ng, respectively. Furthermore, 1 μg of ODGF and 5 μg of PDGF were labelled with the chloramine-T method[41], as described previously[35], to specific activities of 90,000 and 50,000 c.p.m. per ng, respectively.

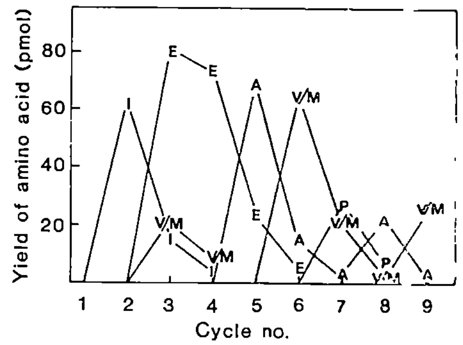

Assigned amino acid in ODGF	X	I	E	E	A	V/M	P	A	V/M
PDGF A chain	S	I	E	E	A	V	P	A	V
PDGF B chain	S	L	G	S	L	T	I	A	E

Fig. 4 Analysis of the amino-acid sequence of non-reduced ODGF. The yield of the PTH amino acids released at each step of Edman degradation is plotted against the cycle number. The solid-phase technique was used[51]. ODGF was coupled to diisothiocyanate-treated glass beads of pore size 120 Å. Data are shown from one run using ~200 pmol of ODGF. The assigned N-terminal amino-acid sequence of ODGF is compared with those of the A- and B-chains of PDGF. X denotes unidentified amino acid. V/M denotes valine or methionine (the PTH derivatives of these amino acids were not separated in the HPLC system used for identification).

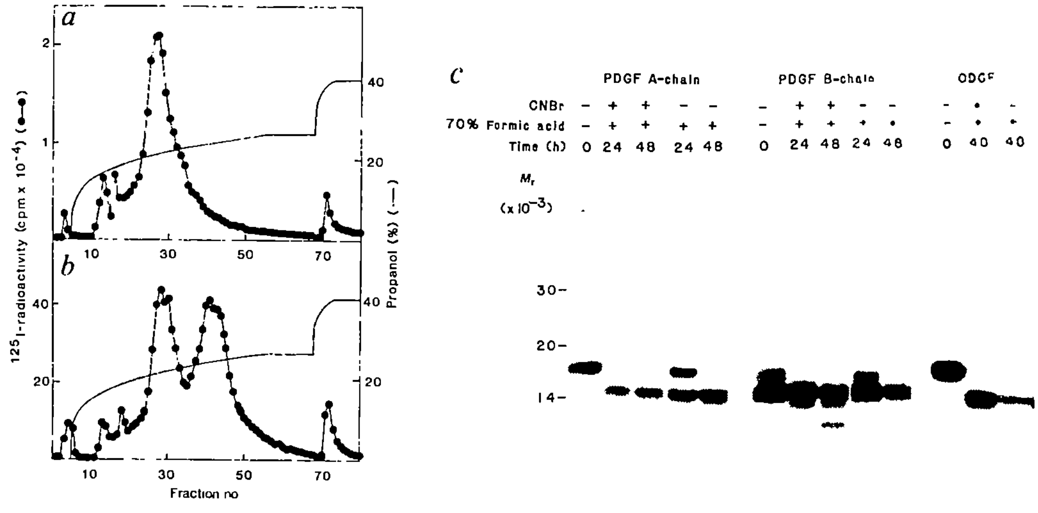

Fig. 3 Separation of the constituent polypeptide chains of ^{125}I-labelled ODGF (*a*) and ^{125}I-labelled PDGF (*b*). ^{125}I-ODGF and ^{125}I-PDGF (both labelled by the Bolton-Hunter procedure[42]) were reduced and alkylated and applied to an HPLC RP8 column (Merck). The column was eluted in 1 M acetic acid, 2 M guanidine-HCl with a nonlinear gradient of propanol, as described previously[36]. *c*, Gel showing the susceptibility of the constituent chains of PDGF and ODGF to chemical fragmentation. Separated ^{125}I-labelled A- and B-chains of PDGF, and reduced and alkylated ^{125}I-ODGF, were incubated with 70% formic acid or 30 mg ml^{-1} of CNBr in 70% formic acid for 24 or 48 h at 37 °C. Samples were then analysed by SDS-gel electrophoresis on 13-18% acrylamide gradient gels and subjected to autoradiography. The 17,000-M_r band in the B-chain preparation represents a slight contamination of A-chains.

PDGF purified from human platelets makes it difficult to form any definite conclusions about its subunit structure. Interestingly, pig PDGF seems to be a homodimer of polypeptide chains similar to the human B-chain and thus similar in structure to the PDGF-like factor from SSV-transformed cells (ref. 47 and M. Waterfield, personal communication).

The present work raises some interesting questions about the regulation of the expression of the PDGF genes. The A- and B-chains are probably encoded by different genes, and thus translated by different transcripts. Apparently, either chain can be assembled into a homodimer structure after translation, A–A in the case of ODGF and B–B in the cases of pig PDGF and the v-*sis* gene product. Activation of either PDGF gene may lead to the production of PDGF agonist activity, as both types of homodimers interact with the PDGF receptor. If this occurs in a cell that carries PDGF receptors, an autocrine loop may be formed, leading to stimulation of cell growth, as discussed for U-2 OS cells[44] and found to be the case in SSV-transformed cells[12]. It will be of particular interest to determine whether human PDGF and the PDGF-like factors produced in a regulated manner by normal cells are homodimers or heterodimers, and to compare the functional activities of the different but homologous PDGF-like growth factors from normal and malignant cells.

We thank Ulf Hellman for advice on amino-acid sequencing and Marianne Kastemar for help with cell culturing. These studies were supported by grants from the Swedish Cancer Society (689, 786 and 1794), Konung Gustaf V:s åttioårsfond and the Swedish Department of Agriculture.

Received 21 October; accepted 17 December 1985.

1. Heldin, C.-H., Wasteson, Å. & Westermark, B. *Molec. cell. Endocr.* **39**, 169–187 (1985).
2. Waterfield, M. D. *et al. Nature* **304**, 35–39 (1983).
3. Doolittle, R. F. *et al. Science* **221**, 275–277 (1983).
4. Devare, S. G., Reddy, E. P., Law, J. D., Robbins, K. C. & Aaronson, S. A. *Proc. natn. Acad. Sci. U.S.A.* **80**, 731–735 (1983).
5. Johnsson, A. *et al. EMBO J.* **3**, 921–928 (1984).
6. Deuel, T. F., Huang, J. S., Huang, S. S., Stroobant, P. & Waterfield, M. D. *Science* **221**, 1348–1350 (1983).
7. Bowen-Pope, D. F., Vogel, A. & Ross, R. *Proc. natn. Acad. Sci. U.S.A.* **81**, 2396–2400 (1984).
8. Owen, A. J., Pantazis, P. & Antoniades, H. N. *Science* **225**, 54–56 (1984).
9. Garrett, J. S. *et al. Proc. natn. Acad. Sci. U.S.A.* **81**, 7466–7470 (1984).
10. Huang, J. S., Huang, S. S. & Deuel, T. F. *Cell* **39**, 79–87 (1984).
11. Johnsson, A., Betsholtz, C., von der Helm, K., Heldin, C.-H. & Westermark, B. *Proc. natn. Acad. Sci. U.S.A.* **82**, 1721–1725 (1985).
12. Johnsson, A., Betsholtz, C., Heldin, C.-H. & Westermark, B. *Nature* **317**, 438–440 (1985).
13. Robbins, K. C., Antoniades, H. N., Devare, S. G., Hunkapiller, M. W. & Aaronson, S. A. *Nature* **305**, 605–608 (1983).
14. Heldin, C.-H., Westermark, B. & Wasteson, Å. *J. cell. Physiol.* **105**, 235–246 (1980).
15. Graves, D. T., Owen, A. J. & Antoniades, H. N. *Cancer Res.* **43**, 83–87 (1983).
16. Betsholtz, C. *et al. Biochem. biophys. Res. Commun.* **117**, 176–182 (1983).
17. Nistér, M., Heldin, C.-H., Wasteson, Å & Westermark, B. *Proc. natn. Acad. Sci. U.S.A.* **81**, 926–930 (1984).
18. Stroobant, P., Gullick, W. J., Waterfield, M. D. & Rozengurt, E. *EMBO J.* **4**, 1945–1949 (1985).
19. Betsholtz, C., Bywater, M., Westermark, B., Bürk, R. R. & Heldin, C.-H. *Biochem. biophys. Res. Commun.* **130**, 753–760 (1985).
20. Gudas, L. J., Singh, J. P. & Stiles, C. D. *Cold Spring Harb. Conf. Cell Proliferation* **10**, 229–236 (1983).
21. Van Zoelen, E. J. J. *et al. Molec. cell. Biol.* **5**, 2289–2297 (1985).
22. Eva, A. *et al. Nature* **295**, 116–119 (1982).
23. Norris, J. S. *et al. Biochem. biophys. Res. Commun.* **122**, 124–128 (1984).
24. Josephs, S. F., Guo, C., Ratner, L. & Wong-Staal, F. *Science* **223**, 487–490 (1984).
25. DiCorleto, P. E. & Bowen-Pope, D. F. *Proc. natn. Acad. Sci. U.S.A.* **80**, 1919–1923 (1983).
26. Barrett, T. B., Gajdusek, C. M., Schwartz, S. M., McDougall, J. K. & Benditt, E. P. *Proc. natn. Acad. Sci. U.S.A.* **81**, 6772–6774 (1984).
27. Jaye, M. *et al. Science* **228**, 882–885 (1985).
28. Seifert, R. A., Schwartz, S. M. & Bowen-Pope, D. F. *Nature* **34**, 669-671 (1984).
29. Nilsson, J., Sjöberg, M., Palmberg, L., Thyberg, J. & Heldin, C.-H. *Proc. natn. Acad. Sci. U.S.A.* **82**, 4418-4422 (1985).
30. Goustin, A. S. *et al. Cell* **41**, 301–312 (1985).
31. Ratner, L. *et al. Nucleic Acids Res.* **13**, 5007–5018 (1985).
32. Collins, T., Ginsburg, D., Boss, J. M., Orkin, S. H. & Pober, J. S. *Nature* **316**, 748–750 (1985).
33. Pontén, J. & Saksela, E. *Int. J. Cancer* **2**, 434–447 (1967).
34. Betsholtz, C. & Westermark, B. *J. cell. Physiol.* **118**, 203–210 (1984).
35. Heldin, C.-H., Westermark, B. & Wasteson, Å. *Proc. natn. Acad. Sci. U.S.A.* **78**, 3664–3668 (1981).
36. Johnsson, A., Heldin, C.-H., Westermark, B. & Wasteson, Å. *Biochem. biophys. Res. Commun.* **104**, 66–74 (1982).
37. Heldin, C.-H., Westermark, B. & Wasteson, Å. *Biochem. J.* **193**, 907–913 (1981).
38. Antoniades, H. N. *Proc. natn. Acad. Sci. U.S.A.* **78**, 7314–7317 (1981).
39. Deuel, T. F. *et al. J. biol. Chem.* **256**, 8896–8899 (1981).
40. Raines, E. W. & Ross, R. *J. biol. Chem.* **257**, 5154–5160 (1982).
41. Hunter, W. M. & Greenwood, F. C. *Nature* **194**, 495–496 (1962).
42. Bolton, A. E. & Hunter, W. M. *Biochem. J.* **133**, 529–539 (1973).
43. Piszkiewicz, D., Landon, M. & Smith, E. L. *Biochem. biophys. Res. Commun.* **40**, 1173–1178 (1970).
44. Betsholtz, C., Westermark, B., Ek, B. & Heldin, C.-H. *Cell* **39**, 447–457 (1984).
45. Graves, D. T. *et al. Science* **226**, 972–974 (1984).
46. Robbins, K. C., Leal, F., Pierce, J. H. & Aaronson, S. A. *EMBO J.* **4**, 1783–1792 (1985).
47. Stroobant, P. & Waterfield, M. D. *EMBO J.* **3**, 2963–2967 (1984).
48. Miletic, J. P., Broze, G. J. Jr & Majerus, P. W. *Analyt. Biochem.* **105**, 304–310 (1980).
49. Blobel, G. & Dobberstein, B. *J. Cell Biol.* **67**, 835–851 (1975).
50. Morrissey, J. H. *Analyt. Biochem.* **117**, 307–310 (1981).
51. Laurssen, R. A. & Machleidt, W. *Meth. biochem. Analysis* **26**, 201–284 (1980).

A saturable receptor for ^{32}P-inositol-1,4,5-trisphosphate in hepatocytes and neutrophils

András Spät*, Peter G. Bradford, Jerry S. McKinney, Ronald P. Rubin & James W. Putney Jr

Division of Cellular Pharmacology, Medical College of Virginia, Virginia Commonwealth University, Richmond, Virginia 23298, USA

Several receptors for neurotransmitters, hormones and growth factors cause accelerated phosphodiesteratic breakdown of polyphosphoinositides when activated[1,2]. One of the soluble products of this reaction, inositol-1,4,5-trisphosphate (Ins(1,4,5)P_3) is thought to act as a second messenger signalling the release of Ca^{2+} from intracellular stores[3]. In support of this hypothesis, several studies have shown that Ins(1,4,5)P_3 releases sequestered Ca^{2+} from permeable cells[4–6] and microsomes[7–9]. On the basis of certain structural requirements for Ca^{2+}-releasing activity by inositol phosphates, it has been postulated that Ins(1,4,5)P_3 acts by binding to a specific intracellular receptor, probably on a component of the endoplasmic reticulum[10]. Here we report that ^{32}P-Ins(1,4,5)P_3 binds to a specific saturable site in permeabilized guinea pig hepatocytes and rabbit neutrophils, and that the properties of this binding site suggest that it is the physiological receptor for Ins(1,4,5)P_3.

High-specific-activity ^{32}P-Ins(1,4,5)P_3 (~40 Ci mmol^{-1}) was prepared by phosphorylation of red cell ghosts with ^{32}P-ATP (3,000 Ci mmol^{-1}), followed by hydrolysis and purification as described in Fig. 1 legend. Binding experiments were carried out on ice and in the presence of 1 or 2 mM diphosphoglycerate to inhibit any metabolism of the ligand by, or binding of the ligand to, inositol-1,4,5-trisphosphate 5-phosphomonoesterase[11]. In a few experiments, increasing the concentration of diphosphoglycerate to 10 mM did not affect total binding, indicating that the binding site was not the 5-phosphomonoesterase. We used guinea pig hepatocytes and rabbit neutrophils whose plasma membranes were made permeable with saponin as described previously[12]. We used permeable cells rather than membranes because binding could be more readily demonstrated and correlated with Ca^{2+} release experiments performed on the same preparation. Because binding and dissociation were rapid (Fig. 1), a non-diluting technique was used to separate bound from free ligand. The technique involved centrifugation of suspensions of permeable cells through silicon oil (see Fig. 1 legend). The cells (and some trapped volume which can be corrected for with an inert marker such as ^{3}H-mannose) sediment at the bottom of the tubes, whereas the medium containing free ligand remains above the oil. No dilution of the sample is necessary, and the technique should be generally applicable to the study of binding of any ligand which dissociates rapidly.

Association of ^{32}P-Ins(1,4,5)P_3 with its specific binding site in neutrophils is rapid, even at 0–5 °C, and binding is readily reversible (Fig. 1). The binding of ^{32}P-Ins(1,4,5)P_3 to hepatocytes

---

* Present address: Department of Physiology, Semmelweis University Medical School, Budapest, Hungary.

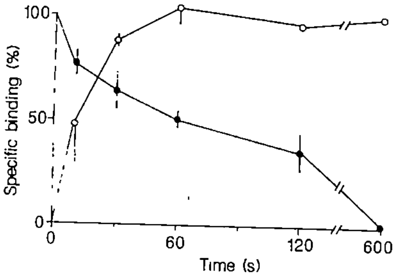

Fig. 1 Time course of: ○, binding of ^{32}P-Ins(1,4,5)P_3 to, and ●, dissociation of bound ^{32}P-Ins(1,4,5)P_3 from, saponin-permeabilized rabbit neutrophils. For the dissociation experiments 10 μM Ins(1,4,5)P_3 was added to the incubation mixtures ($t = 0$) after incubation for 10 min in the presence of ^{32}P-Ins(1,4,5)P_3 and the time course of decrease in specific binding was determined. Binding data for both curves are expressed as a percentage of specific binding at $t = 10$ min (just before the addition of non-radioactive Ins(1,4,5)P_3). Values shown are mean±s.e.m. of 3-6 separate experiments, except for the association curve at $t = 120$ s, which is the mean of two.

Methods. Rabbit neutrophils[15] and guinea pig hepatocytes[12] were prepared as described previously, permeabilized with saponin and incubated in a high-K^+ salt solution as described previously[12], with [Ca^{2+}] buffered with EGTA to 180 nM. Binding was determined by incubating permeable cells with ligand in this intracellular type medium and then at designated intervals, centrifuging the sample with a microfuge through 500 μl silicon oil (Nyosil; Nye, Inc., New Bedford, Massachusetts). Typical incubation conditions for neutrophils were 300-500 μg cellular protein and 0.02 μCi ^{32}P-Ins(1,4,5)P_3 in 500 μl, and for hepatocytes, 1-2 mg cellular protein and 0.05 μCi ^{32}P-Ins(1,4,5)P_3 in 1.0 ml. For all samples, ^{3}H-mannose was included to allow correction for trapped ^{32}P in the silicon oil pellets. Nonspecific binding was determined by including 10 μM Ins(1,4,5)P_3 in the incubation medium. Specific binding generally exceeded 100 d.p.m. All samples were counted for a sufficient interval to ensure >90% reliability in radioactivity estimates. Preparation of ^{32}P-Ins(1,4,5)P_3. Human erythrocyte ghosts were incubated for 20 min at room temperature in a solution modified from ref. 16 containing (per ml): 5 μmol $MgCl_2$, 1 μmol EGTA, 25 μmol imidazole-HCl (*p*H 7.0), 20 mCi ^{32}P-ATP (>3,000 Ci mmol^{-1}; NEN). Phosphorylation was stopped by adding 8 vol. of 1 mM EDTA in 10 mM Tris buffer (*p*H 7.5). Labelled polyphosphoinositides were hydrolysed for 10 min at room temperature in 0.18 mM $CaCl_2$ in 25 mM imidazole buffer (*p*H 7.0). The reaction was stopped with 10% perchloric acid, neutralized with KOH, and buffered to *p*H 7.5-8.5 with 50 mM Tris-phosphate buffer. ^{32}P-Ins(1,4,5)P_3 was separated from other soluble radioactivity by anion-exchange chromatography as described by Berridge *et al* [17]. Ammonium formate in the inositol trisphosphate fraction was converted to formic acid by passing over Dowex-50 (H^+). The eluate was lyophilized and stored at −76 °C. Radiochemical purity was >90% as assessed by paper chromatography[18] and HPLC[19]. Specific activity was estimated by displacement of specific binding and was 30-50 Ci mmol^{-1}.

(data not shown) was as rapid, and specific binding at 30 s was not distinguishable from that at 10 min. Nonspecific binding was taken as the residual binding in the presence of 10 μM Ins(1,4,5)P_3 (30 μM Ins(1,4,5)P_3 did not reduce binding further). After correction for free ligand in the trapped volume of the pellet, nonspecific binding was 15-20% of the total for the neutrophils and undetectable for the hepatocytes. The binding of ^{32}P-inositol-1,4-bisphosphate (^{32}P-Ins(1,4)P_2) purified from the red cell hydrolysate, was also examined; total binding to neutrophils and hepatocytes was similar to that for ^{32}P-Ins(1,4,5)P_3 but binding was not inhibited by 10 μM of either Ins(1,4)P_2 or Ins(1,4,5)P_3. Binding of ^{32}P-Ins(1,4,5)P_3 was not inhibited by 10 μM Ins(1,4)P_2, inositol 4,5-bisphosphate (Ins(4,5)P_2), inositol-1-phosphate or cyclic inositol-1,2-phosphate. In hepatocytes, omission of ATP or reduction of bovine serum albumin from 2 to 0.2% did not affect specific binding. Increasing the Ca^{2+} concentration from 180 nM to 1.0 μM slightly increased specific binding (125 ± 10% of control, $n = 4$), and reducing the Ca^{2+} concentration to 20 nM slightly reduced binding (82 ± 6% of control, $n = 6$). For hepatocytes, 100 and 300 μM Ins(4,5)P_2 inhibited binding by 45 and 85%, respectively, in two experiments.

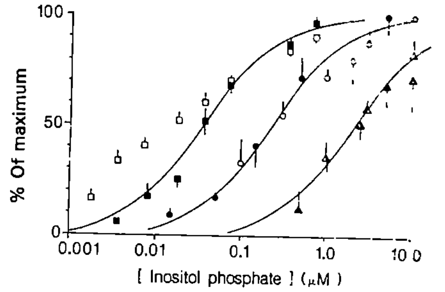

Fig. 2 Receptor occupancy (inhibition of ^{32}P-Ins(1,4,5)P_3 binding) and $^{45}Ca^{2+}$-releasing activity of Ins(1,4,5)P_3 and Ins(2,4,5)P_3 in guinea pig hepatocytes, and of Ins(1,4,5)P_3 in rabbit neutrophils. Binding to permeable cells was determined as described for Fig. 1. Occupancy was calculated as per cent inhibition of specific ^{32}P-Ins(1,4,5)P_3 binding. Release of $^{45}Ca^{2+}$ for the rabbit neutrophils was determined as described previously[10] and the data expressed as a percentage of maximal release (50 ± 5% of a total ATP-dependent $^{45}Ca^{2+}$ uptake of 1.02 ± 0.14 nmol per mg protein). The data for release of ^{45}Ca from guinea pig hepatocytes are taken from ref. 10, and are expressed as per cent maximal release with Ins(1,4,5)P_3. The curves are theoretical curves for a single-site interaction with K_D equal to the graphically estimated EC_{50} for ^{45}Ca release. △, ▲, Ins(2,4,5)P_3 in hepatocytes; ○, ●, Ins(1,4,5)P_3 in hepatocytes; □, ■, Ins(1,4,5)P_3 in neutrophils; △, ○, □, occupancy; ▲, ●, ■, ^{45}Ca release. Values shown are mean ± s.e.m. of 3-6 observations each, except for the ^{45}Ca release from the neutrophils at 3.6 nM Ins(1,4,5)P_3, which is the mean of two observations.

Figure 2 shows the concentration dependence of inhibition of binding of ^{32}P-Ins(1,4,5)P_3 (indicated as per cent occupancy) by non-radioactive Ins(1,4,5)P_3 in permeable neutrophils and hepatocytes and by inositol-2,4,5-trisphosphate (Ins(2,4,5)P_3) in hepatocytes. Also shown are the concentration dependencies of $^{45}Ca^{2+}$ release by inositol trisphosphates under similar conditions. There was a close correlation between the estimated fractional receptor occupancies of Ins(1,4,5)P_3 and Ins(2,4,5)P_3 and ^{45}Ca release in the hepatocyte. The curves in Fig. 2 were generated by taking the observed EC_{50} (50% effective concentration) for ^{45}Ca release as a dissociation constant (K_D) for binding and by assuming a single binding site with a Hill coefficient of 1. Although variability in the data may not permit detection of subtle deviations from the single-site model, the fit appears adequate for the hepatocyte.

In neutrophils, Ins(1,4,5)P_3 was more potent in releasing Ca^{2+} and in displacing bound ^{32}P-Ins(1,4,5)P_3 than in hepatocytes. However, low concentrations of Ins(1,4,5)P_3 (<30 nM) could displace proportionately greater binding than predicted either from the $^{45}Ca^{2+}$ data or from the single-site binding model. This indicates either complex binding kinetics to a single site, or binding to more than one site. Considering the latter possibility, a high-affinity site may exist which is not coupled to Ca^{2+} release; we speculate that this site indicates some other regulatory function of Ins(1,4,5)P_3 in the neutrophil not found in the hepatocyte.

The relatively low affinity of Ins(1,4,5)P_3 for its receptor when compared with more conventional ligands used in binding assays requires high-specific-activity ^{32}P-Ins(1,4,5)P_3 to detect specific binding. Because of limited quantities of the radioligand and the necessary dilution of the specific radioactivity at higher concentrations, Scatchard analysis of the data was not appropriate. Receptor density was estimated for the hepatocyte (which fits the single-site model) by extrapolating the most reliable binding data (at 100 and 300 nM) with the following relation: $B_{max} = B(K_D + [S])/[S]$ (where B_{max} is maximum binding capacity, K_D is assumed to be equal to the EC_{50} for the hepatocytes (220 nM; ref. 10) and B is the concentration of bound ligand at ligand concentration [S]). At 100 nM Ins(1,4,5)P_3, binding was 59 ± 8 ($n = 6$) fmol per mg protein, and at 300 nM, binding was 115 ± 20 ($n = 5$) fmol per mg protein. These values give receptor densities of 189 and 199 fmol per mg protein, respectively, with an average of 194 fmol per mg protein. As the guinea pig hepatocyte contains 2.18 µl intracellular water per mg protein[13], the K_D for Ins(1,4,5)P_3 (220 nM) expressed relative to cellular protein in intact cells, would be 480 fmol per mg protein. That the estimated receptor density is less than the K_D of the receptor may be significant in that the receptor would not represent a significant depot of Ins(1,4,5)P_3 binding. The intracellular concentrations of free and bound Ins(1,4,5)P_3 and resulting Ca^{2+} mobilization would thus be approximately proportional to the rate of Ins(1,4,5)P_3 production and to receptor activation, at least at submaximal concentrations of agonists.

In summary, the available data indicate that a binding site for Ins(1,4,5)P_3 can be demonstrated using high-specific-activity ^{32}P-Ins(1,4,5)P_3, and that this site is the physiological receptor for Ins(1,4,5)P_3. Binding is specific, saturable and reversible. Inositol phosphates that have Ca^{2+}-releasing activity[10] (Ins(1,4,5)P_3, Ins(2,4,5)P_3 and Ins(4,5)P_2) bind to this site, whereas those which do not release Ca^{2+} (ref. 10) do not bind. Furthermore, with the exception of some very high-affinity binding in the neutrophil, there is a close correlation between the ability of Ins(1,4,5)P_3 and Ins(2,4,5)P_3 to bind to the receptor and the abilities of these molecules to release Ca^{2+}. Receptors for ligands on the surface of cells are known to be regulated in several ways[14], and it is likely that such control mechanisms also occur at an intracellular receptor. The demonstration and quantitation of an intracellular receptor for the Ca^{2+}-mobilizing messenger, Ins(1,4,5)P_3, should open the way for future investigations into the nature and regulation of this ubiquitous site in various biological systems.

We thank R. F. Irvine for non-radioactive inositol phosphates. This research was supported by NIH grants AM-28029 and AM-32823. A.S. was supported in part by a fellowship from the Educational Commission for foreign medical graduates.

Received 16 September; accepted 3 December 1985.

1. Downes, P. & Michell, R. H. *Cell Calcium* **3**, 467-502 (1982).
2. Berridge, M. J. & Irvine, R. F. *Nature* **312**, 315-321 (1984).
3. Berridge, M. J. *Biochem. J.* **212**, 849-858 (1983).
4. Streb, H., Irvine, R. F., Berridge, M. J. & Schulz, I. *Nature* **306**, 67-68 (1983).
5. Burgess, G. M. *et al. Nature* **309**, 63-66 (1984).
6. Suematsu, E., Hirata, M., Hashimoto, T. & Kuriyama, H. *Biochem. biophys. Res. Commun.* **120**, 481-485 (1984).
7. Prentki, M. *et al. Nature* **309**, 562-564 (1984).
8. Streb, H., Bayerdorffer, E., Haase, W., Irvine, R. F. & Schulz, I. *J. Membrane Biol.* **81**, 241-253 (1984).
9. Dawson, A. P. & Irvine, R. F. *Biochem. biophys. Res. Commun.* **120**, 858-864 (1984).
10. Burgess, G. M., Irvine, R. F., Berridge, M. J., McKinney, J. S. & Putney, J. W. Jr *Biochem. J.* **224**, 741-746 (1984).
11. Downes, C. P. & Michell, R. H. *Biochem. J.* **198**, 133-140 (1981).
12. Burgess, G. M., McKinney, J. S., Fabiato, A., Leslie, B. A. & Putney, J. W. Jr *J. biol. Chem.* **258**, 15336-15345 (1983).
13. De Witt, L. M. & Putney, J. W. Jr *J. Physiol., Lond.* **346**, 395-407 (1984).
14. Czech, M. P. & Kahn, C. R. (eds) *Membrane Receptors and Cellular Regulation* (Liss, New York, 1985).
15. Bradford, P. G. & Rubin, R. P. *Molec. Pharmac.* **27**, 74-78 (1985).
16. Quist, E. *Archs Biochem. Biophys.* **236**, 140-149 (1985).
17. Berridge, M. J., Dawson, R. M. C., Downes, C. P., Heslop, J. P. & Irvine, R. F. *Biochem. J.* **212**, 473-482 (1983).
18. Desjobert, A. & Petek, F. *Bull. Soc. Chim. biol.* **38**, 871-883 (1956).
19. Irvine, R. F., Anggard, E. A., Letcher, A. J. & Downes, C. P. *Biochem. J.* **229**, 505-511 (1985).

Stimulation of bone resorption and inhibition of bone formation *in vitro* by human tumour necrosis factors

Donald R. Bertolini, Glenn E. Nedwin*†, Timothy S. Bringman*, Donna D. Smith & Gregory R. Mundy

Department of Medicine, Division of Endocrinology,
University of Texas Health Science Center, San Antonio,
Texas 78284, USA
* Genentech Inc., South San Francisco, California 94080, USA

When leukocytes are exposed to mitogens or antigens *in vitro*, they release bone-resorbing activity into the culture supernatants which can be detected by bioassay[1,2]. Like many lymphocyte–monocyte products, this activity has been difficult to purify because of its low abundance in activated leukocyte cultures and the unwieldy bioassay required to detect biological activity. Partially purified preparations of this activity inhibit bone collagen synthesis in organ cultures of fetal rat calvariae[3]. Recent data suggest that both activated lymphocytes and monocytes release factors which could contribute to this activity[2]. Recently, monocyte-derived tumour necrosis factor α (TNF-α) and lymphocyte-derived tumour necrosis factor β (TNF-β) (previously called lymphotoxin), two multifunctional cytokines which have similar cytotoxic effects on neoplastic cell lines, have been purified to homogeneity[4,5] and their complementary DNAs cloned and expressed in *Escherichia coli*[6,7]. As both of these cytokines are likely to be present in activated leukocyte supernatants, we tested purified recombinant preparations for their effects on bone resorption and bone collagen synthesis *in vitro*, and report here that both cytokines at 10^{-7} to 10^{-9} M caused osteoclastic bone resorption and inhibited bone collagen synthesis. These data suggest that at least part of the bone-resorbing activity present in activated leukocyte culture supernatants may be due to these cytokines.

Recombinant human TNF-α (rTNF-α)[7] and human TNF-β (rTNF-β)[6] used in this study were expressed in *E. coli* and the recombinant molecules purified as described previously[6,7]. The rTNF-α and rTNF-β stimulated bone-resorbing activity when incubated with fetal rat bones in which ^{45}Ca had been incorporated previously using the technique described by Raisz[8]. This bone-resorbing activity was dose-dependent from 10^{-7} to 10^{-9} M (Fig. 1). Maximal activity for both cytokines was observed at 10^{-7} M (Fig. 1). The time course of action of the cytokines was examined by incubating the bones in the presence of control medium or medium with the appropriate cytokine for 2 days and then transferring the bones to fresh control medium or medium with the cytokine for a further 3 days (data not shown). The factors released approximately equal amounts of calcium over the two time periods, similar to that shown previously for the bone-resorbing activity in non-fractionated activated leukocyte culture supernatants and parathyroid hormone (PTH)[3,9-11].

Treatment of bone cultures with rTNF-α and rTNF-β caused an increase in the number of multinucleated osteoclasts and a decrease in the amount of mineralized bone matrix (Fig. 2). In contrast, few osteoclasts were present in control bones. As further evidence that rTNF-α and rTNF-β cause resorption by osteoclast activation, their effects on bone resorption at 10^{-7} M were completely inhibited by salmon calcitonin (5 units ml^{-1}), a specific inhibitor of osteoclast activity (Table 1).

The effects of recombinant human TNF-α and TNF-β on bone collagen synthesis were determined using the method of Peterkofsky and Diegelman[12], which measures the incorporation of ^3H-proline into collagenase-digestible protein. The culture technique for studying factors which influence collagen synthesis *in vitro* has been described previously[13,14]. We used the modified procedure described by Kream *et al.*[14], which uses cultured frontal and parietal bone explants from 21-day fetal rats. Both rTNF-α and rTNF-β inhibited collagenase-digestible protein synthesis to a greater extent than they inhibited non-collagen protein synthesis (Table 1). Thus, the per cent collagen synthesis was significantly inhibited compared with corresponding bones incubated with control media.

---

† Present address: Molecular Therapeutics, Inc., 400 Morgan Lane, West Haven, Connecticut 06516, USA.

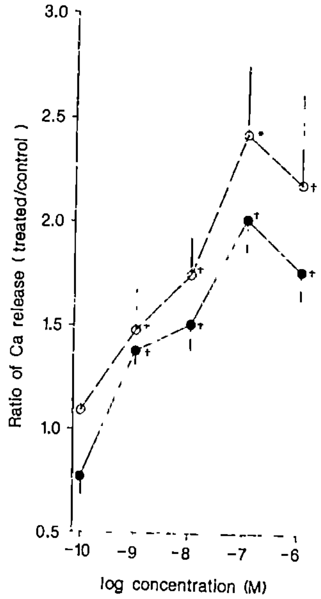

Fig. 1 Effects of recombinant TNF-α and TNF-β on bone resorption *in vitro*. rTNF-α(o) or rTNF-β(●) was diluted into fresh BGJ medium with 5% fetal bovine serum (FBS) and incubated with fetal rat long bones for 48 h. Data shown are the ratio of medium ^{45}Ca released by bones treated with test media to that released by bones treated with corresponding control media; each value represents the mean ± s.e.m. for four pairs of bone cultures. PTH (200 ng ml^{-1}) was used as a positive control in this experiment and gave a ratio of 2.33 ± 0.70. Statistical differences from 1.0 at each concentration were determined using Student's *t*-test for non-paired samples (molarity calculation based on monomer M_r). $^*P < 0.005$; $^\dagger P < 0.05$.

We also tested the effects of recombinant human cytokines on alkaline phosphatase activity in cells with the osteoblast phenotype (17/2.8 rat osteosarcoma cells) according to the method of Majeska *et al.*[15]. Alkaline phosphatase is a marker enzyme of new bone formation; agents which inhibit bone formation cause a decrease in the alkaline phosphatase content of cells of the osteoblast phenotype. The cells were incubated with the test substances for 36–72 h, and the enzyme content was assayed according to the method of Lowry *et al.*[16]. Both cytokines, in the concentration range 10^{-6}–10^{-10} M, caused a decrease in the alkaline phosphatase content of cells with the osteoblast phenotype. Enzyme content was inhibited 50% by both cytokines at 10^{-10} M, and 85% by both cytokines at 10^{-7} M. In the same experiment, PTH (50 ng ml^{-1}) also inhibited enzyme content by 85%.

The bone-resorbing activity present in activated leukocyte culture supernatants has been referred to as osteoclast activating factor (OAF), but appears to represent a family of proteins from different cellular sources. OAF was originally thought to be a lymphocyte product that required the presence of monocytes in the culture for its production[1,17] and it is possible that TNF-β is the bone-resorbing activity that was produced in these studies using separated cell populations or lymphoid cell lines. However, monocyte products such as interleukin-1 (ref. 18) and prostaglandins[19] have been shown to stimulate osteoclastic bone resorption *in vitro*[20], and these factors presumably contribute to the bone-resorbing activity present in activated leukocyte culture supernatants.

Malignant diseases of lymphoid cells such as myeloma, T-cell lymphoma and Burkitt's lymphoma are frequently associated with bone destruction and sometimes with hypercalcaemia[21]. Freshly isolated cells and cultured cell lines, such as the myeloma cell line RPMI 8226, derived from patients with these disorders, release bone-resorbing activity having similar chemical and biological characteristics to the bone-resorbing activity present in activated leukocyte culture supernatants[3,9,22]. Myeloma cell lines, including 8226, have also been shown to produce TNF-β[23]. Osteoclast activation in both organ cultures incubated with rTNF-α and rTNF-β resembles what is found in the bones of patients with myeloma. Moreover, it is characteristic of these malignancies that there is no evidence of new bone formation associated with the increased bone resorption, in contrast to what is usually seen in osteolytic bone lesions associated with solid tumours or with primary hyperparathyroidism[17]. Whether either or both of these cytokines are the only bone-resorbing factors released by malignant lymphoid cells associated with hypercalcaemia will require further study.

TNF-α and TNF-β have biochemical characteristics similar to those of the bone-resorbing activity present in activated leukocyte culture supernatants. Like TNF-α and TNF-β, OAF is produced by activated leukocytes, is heat-sensitive and is inactivated by protease[24]. OAF has a relative molecular mass (M_r) of 14,000 (14K)–25,000 (25K), estimated by gel permeation chromatography[24], but under certain conditions it can run with a M_r of between 45K and 70K[3,24]. Purified TNF-α has a M_r of 17.8K and is 157 amino acids long but elutes from gel permeation columns as a 45K protein. Purified TNF-β has a M_r of 18.7K and is 171 amino acids long but elutes from gel permeation columns as a 60K protein[5]. Natural TNF-β is a glycoprotein which is probably glycosylated at asparagine residue 62 (ref. 5). As TNF-β expressed in *E. coli* is not glycosylated, our data indicate that glycosylation is not necessary for bone-resorbing activity. It has also been demonstrated that glycosylation is not necessary for the cytotoxic effect of TNF-β on tumour cells[6].

Table 1 Effects of salmon calcitonin (CT) on bone resorption stimulated by human recombinant tumour necrosis factors

Treatment of bone cultures	Bone-resorbing activity (per cent ^{45}Ca release)
Control media	22 ± 2
Control media + CT(5 U ml^{-1})	13 ± 1*
TNF-α (10^{-7} M)	38 ± 3
TNF-α(10^{-7} M) + CT (5 U ml^{-1})	11 ± 1†
TNF-β (10^{-7} M)	33 ± 3
TNF-β (10^{-7} M) + CT(5 U ml^{-1})	12 ± 1†

The bones were cultured for 48 h. Calcitonin was added together with the cytokine at the start of the culture period. Values are means ± s.e.m for four bone cultures.

*† Significantly less ($P < 0.025$ and < 0.005, respectively) than corresponding bone cultures not incubated with CT.

Table 2 Effects of rTNF-α and rTNF-β on ^{3}H-proline incorporation into collagenase-digestible protein (CDP) and non-collagen protein (NCP) in fetal rat calvaria

Treatment		CDP (d.p.m. per µg dry wt)	NCP (d.p.m. per µg dry wt)	% Collagen synthesis*
Control		86 ± 7	171 ± 12	8.5 ± 0.3
TNF-α	10^{-7} M	19 ± 2	88 ± 7	3.9 ± 0.3†
	10^{-8} M	32 ± 6	114 ± 13	5.0 ± 0.6†
	10^{-9} M	44 ± 5	147 ± 15	5.3 ± 0.3†
TNF-β	10^{-7} M	37 ± 3	128 ± 4	5.0 ± 0.3†
	10^{-8} M	33 ± 5	116 ± 8	4.9 ± 0.6†
	10^{-9} M	51 ± 6	133 ± 8	6.6 ± 0.7‡
Insulin	10^{-6} M	180 ± 23	205 ± 17	13.9 ± 1.0†

Values are mean ± s.e.m. for six half-calvariae incubated for 48 h in the conditions indicated and pulsed with ^{3}H-proline for the final 4 h.

* Proportion of proline incorporated into collagen is corrected for the relative abundance of proline in CDP and NCP.

†‡ Significantly different from control ($P < 0.005$ and < 0.05, respectively).

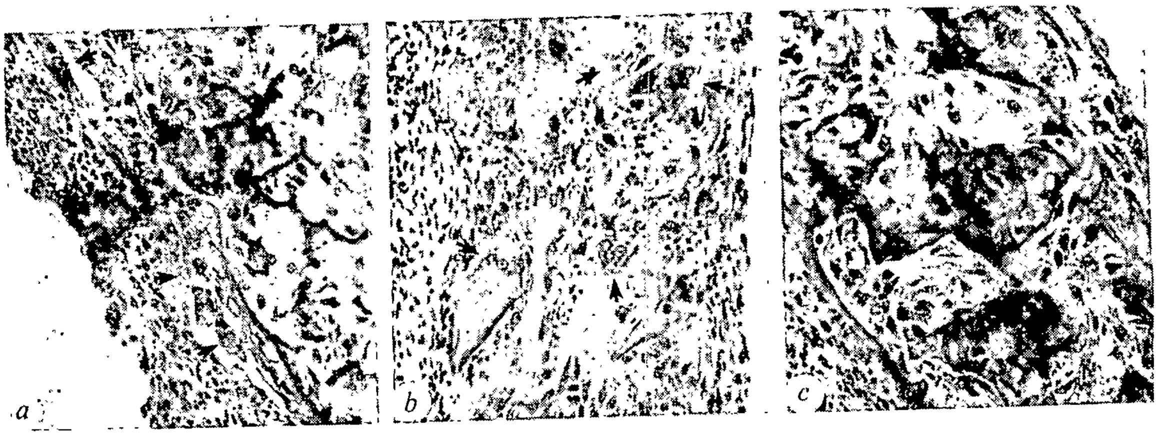

Fig. 2 Histological sections of fetal rat long bones cultured for 48 h with TNF-α (*a*), TNF-β (*b*) or control medium (*c*), showing increased osteoclast number and activity and decreased mineralized matrix in bones treated with the cytokines. Some of the obvious osteoclasts are indicated by arrows. The cytokines were incubated with the bone cultures at a concentration of 10^{-7} M.

As TNF-α and TNF-β are present in activated leukocyte cultures and both are potent bone resorbers, we suggest that they may account for a part (or all) of the bone-resorbing activity presently referred to as OAF.

Testing of rTNFs *in vitro* may reveal that they have a number of other biological activities which could be important in patients with malignant disease. Recently, it has been shown that TNF-α may be identical to cachectin[25], the macrophage product which inhibits the activity of lipoprotein lipase in adipocytes[26], and which may be responsible for the wasting that occurs in patients with malignant disease. Moreover, TNF-α may also mediate the tissue effects of the shock syndrome caused by endotoxin[27], a lipopolysaccharide component of the cell walls of some bacteria. It is imperative that any other biological activities of these molecules are identified as they are now being used in clinical trials in patients with malignant disease.

The present results may have important implications for the control of normal bone remodelling. The cellular sequence of events responsible for bone remodelling begins with a local increase in osteoclast activity. The factors responsible for this local osteoclast activation are unknown, but since activation of bone remodelling units occurs in discrete areas, it seems likely that local factors in the bone marrow microenvironment are responsible. Osteoclast activating factor has been proposed as a local mediator of osteoclast activity. The identification of specific bone-resorbing lymphokines and monokines for which cDNA probes are available may allow us to determine the role of these factors in normal bone remodelling and the increase in osteoclast activity which occurs in age-related bone loss.

We thank Genentech, Inc. for providing rTNFs, Dr Maxine Gowen for helpful criticisms and Nancy Garrett for preparing the manuscript. This work was supported by NIH grants CA29537, AM28149, AM07464 and CA40035.

Note added in proof: Since submission of this manuscript, Dewhirst *et al.*[28] have reported purification of interleukin-1 from short-term phytohaemagglutinin-activated leukocyte cultures using a bone resorption assay. However, the relative roles of interleukin-1 and the TNFs as OAFs may depend on conditions such as duration of the leukocyte culture, antigen or mitogen used as stimulant, and types of leukocytes present in the culture.

Received 30 August; accepted 2 December 1985.

1. Horton, J. E., Oppenheim, J. J., Mergenhagen, S. E. & Raisz, L. G. *J. Immun.* **113**, 1278–1287 (1974).
2. Mundy, G. R. & Bertolini, D. R. in *Endocrinology, int. Congr. Ser. 665* (eds Labrie, F. & Proulx, L.) 587–590 (Excerpta Medica, Amsterdam, 1984).
3. Raisz, L. G. *et al. J. clin. Invest.* **56**, 408–413 (1975).
4. Aggarwal, B. B., Henzel, W. J., Moffat, B., Kohr, W. J. & Harkins, R. N. *J. biol. Chem.* **260**, 2334–2344 (1985).
5. Aggarwal, B. B. *et al. J. biol. Chem.* **260**, 2345–2354 (1985).
6. Gray, P. W. *et al. Nature* **312**, 721–724 (1984).
7. Pennica, D. *et al. Nature* **312**, 724–729 (1984).
8. Raisz, L. G. *J. clin. Invest.* **44**, 103–116 (1965).
9. Mundy, G. R., Luben, R. A., Raisz, L. G., Oppenheim, J. J. & Buell, D. N. *New Engl. J. Med.* **290**, 867–871 (1974).
10. Mundy, G. R. & Raisz, L. G. *J. clin. Invest.* **60**, 122–128 (1977).
11. Horton, J. E., Raisz, L. G., Simmons, H. A., Oppenheim, J. J. & Mergenhagen, S. E. *Science* **177**, 793–795 (1972).
12. Peterkofsky, B. & Diegelmann, R. F. *Biochemistry* **10**, 988–994 (1971).
13. Dietrich, J. W., Canalis, E. M. Maina, D. M. & Raisz, L. G. *Endocrinology* **98**, 943–959 (1976).
14. Kream, B. E., Smith, M. D., Canalis, E. & Raisz, L. G. *Endocrinology* **116**, 296–302 (1985).
15. Majeska, R. J., Rodan, S. B. & Rodan, G. A. *Expl Cell Res.* **111**, 465–468 (1978).
16. Lowry, O. H. *Meth. Enzym.* **4**, 371–372 (1955).
17. Chen, P., Trummel, C., Horton, J., Baker, J. J. & Oppenheim, J. J. *Eur. J. Immun.* **6**, 732–736 (1976).
18. Gowen, M., Wood, D. D., Ihrie, E. J., McGuire, M. K. B. & Russell, R. G. G. *Nature* **306**, 378–380 (1983).
19. Dominguez, J. H. & Mundy, G. R. *Calcif. Tissue Int.* **31**, 29–34 (1980).
20. Klein, D. C. & Raisz, L. G. *Endocrinology* **86**, 1436–1440 (1970).
21. Mundy, G. R. *et al. New Engl. J. Med.* **310**, 1718–1727 (1984).
22. Mundy, G. R., Raisz, L. G., Cooper, R. A., Schechter, G. P. & Salmon, S. E. *New Engl. J. Med.* **291**, 1041–1046 (1974).
23. Nedwin, G. E., Svedersky, T. S., Bringman, T. S., Palladino, M. A. & Goeddel, D. V. *J. Immun.* **135**, 2492–2497 (1985).
24. Luben, R. A., Mundy, G. R., Trummel, C. L. & Raisz, L. G. *J. clin. Invest.* **53**, 1473–1480 (1974).
25. Beutler, B. *et al. Nature* **316**, 552–554 (1985).
26. Torti, F. M., Dieckmann, B., Beutler, B., Cerami, A. & Ringold, G. M. *Science* **229**, 867–869 (1985).
27. Beutler, B., Milsark, I. W. & Cerami, A. C. *Science* **229**, 869–871 (1985).
28. Dewhirst, F. E., Stasheuko, P. P., Mole, J. E. & Tsurumachi, T. *J. Immun.* **135**, 2562–2568 (1985).

Microanalysis gets new pulse processor

Heading this month's selection of lasers, software and new literature is an X-ray processor that can detect elements as light as boron.

KEVEX Corporation's model 4460 pulse processor (Reader Service No. 100) promises to erase the noise peaks that plagued X-ray microanalysis, giving **light element sensitivity sufficient for boron detection.** Improved signal-to-noise ratios allow all low-energy peaks, especially the carbon peak, to be more clearly resolved. Kevex improved upon conventional gaussian electronics by using triangular pulse-shaping circuitry instead. The resulting processor handles a higher X-ray throughput for better precision in less time. The Kevex model 4460, designed for the model 8000 microanalysis system, sells for $2,200 in the United States. The 4560 was developed for model 7000 analysers.

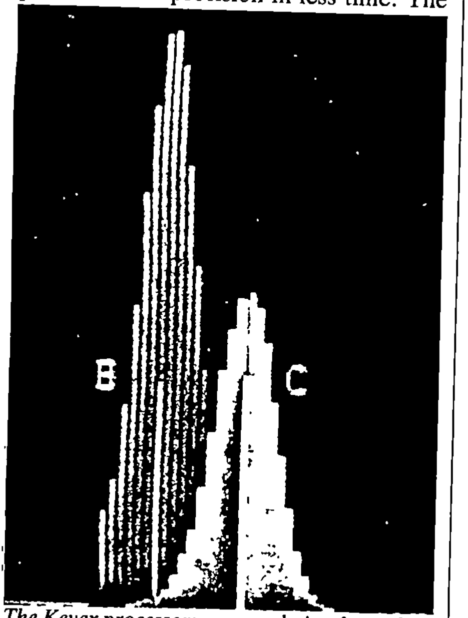

The Kevex processor: new resolution for carbon and boron

Metres and monitors

Monitoring oxygen uptake or evolution in samples with low substrate volumes is the key feature of the biological oxygen monitor from Yellow Springs Instrument Co. Inc. (Reader Service No. 101). The YSI 5300, fitted with micro or standard oxygen probes, can run 600 μl to 50 ml samples in batch or flow-through modes. The instrument can process two experiments simultaneously using two channels, displays and recorder outputs. This function allows the user to plot the differential of the two channels. YSI prices the 5300 monitor and accessory package at about $1,600.

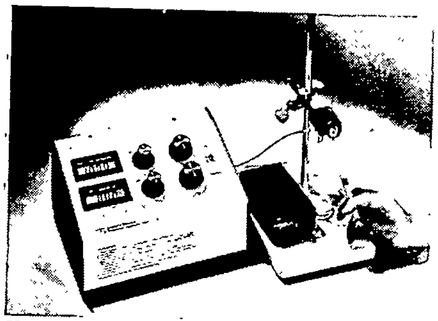
Keeping tabs on oxygen with YSI's monitor

For **relative humidity and temperature measurements** in remote and rugged environments, Hollis Geosystems Corp. has developed the durable RHT-241 (Reader Service No. 102). Originally intended for meteorological, agricultural or marine interests, the RHT-241's design incorporates low power consumption with rapid response time. A self-aspirating solar radiation shield protects the sensing elements, and the entire assembly is noncorrosive. The unit will survive dry, dusty climates or marine environments for at least one year. The RHT-241 measures 12 cm in diameter and 15 cm in height and costs about $1,200.

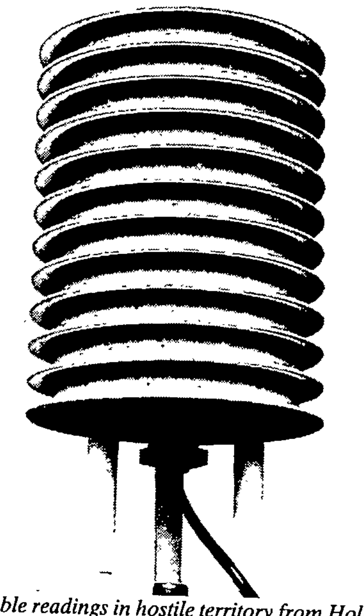
Reliable readings in hostile territory from Hollis Geosystems

A new portable concentration meter from Orion Research Inc. makes **measurement by ion-selective electrode** (ISE) as easy as *p*H determination (Reader Service No. 103). The lightweight SA 270, marketed for $650 in the United States, makes it possible to perform rapid analysis on-site. The unit prompts the user through a one- or two-point standardization, and the display reads in p.p.m., molarity, per cent and so on. Readout can be in two or three digits, depending on the speed and accuracy desired.

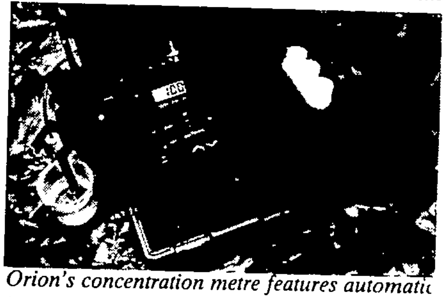
Orion's concentration metre features automatic temperature control

The light fantastic

The latest addition to Laser Science Inc.'s compact sealed nitrogen and dye lasers is the VSL-337ND **near-diffraction nitrogen laser** (Reader Service No. 104). The laser's average power (after 10 million pulses) is 3.0 mW; its peak power is 40 kW and its pulse energy greater than 150 μJ. The 4×4 mm beam is focusable to less than 5 μm, with a beam divergence of less than 0.3 mrad. The laser measures about 14×8×3 inches and operates at 337 nm. In the US, the 18-pound VSL-337ND can be had for under $5,300.

The Omnichrome 500X **air-cooled argon laser** from Lambda Photometrics Ltd. is equipped with a hard-sealed metal-ceramic plasma tube with a life expectancy of greater than 10,000 hours, and a cast resonator that can withstand three axis shock loads exceeding 30 g for 10 milliseconds with no detectable change in performance (Reader Service No. 105).

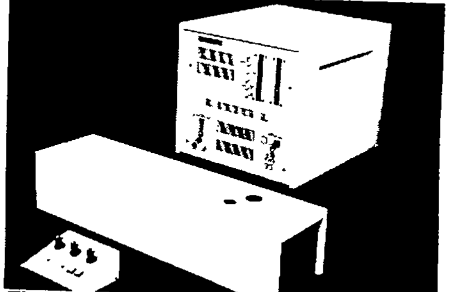
The Omnichrome laser can be refurbished for prolonged lifetime

---

These notes are based on information provided by the manufacturers. To obtain further details about these products use the reader service card bound inside the journal.

Priced at £4,911, the Omnichrome 500X is compatible with most other air-cooled argon lasers and the laser head is completely interchangeable with the Spectra-Physics 162 and ALC60X.

The Spectra-Physics DCR-11 **Nd:YAG pulsed laser** is ideal for portable applications and takes up much less space in the lab (Reader Service No. 106). The laser head is 33×9×10 inches and the power supply dimensions are 23×19×21 inches. At 1,064 nm, the DCR-11 has an output of 275 mJ and a repetition rate of 10 pulses per second. The output is nearly diffraction limited for efficient wavelength conversion: 135 mJ at 532 nm, 60 mJ at 355 nm, 30 mJ at 266 nm with the optional harmonic generator. The laser sells for $25,500 in the US.

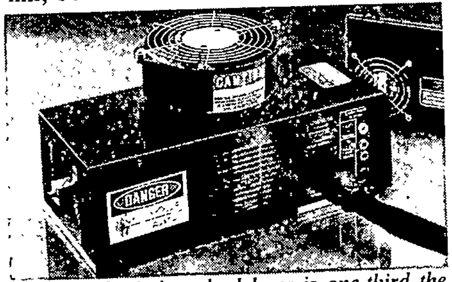
Spectra-Physics's pulsed laser is one-third the size of previous lasers

Conventional lasers must be optically straight, rigid and have accurately aligned mirrors at each end, but the Optical Fibre Research Group at Southampton University has produced **flexible lasers**, thin as human hair and carried through the core of optical fibres (Reader Service No. 107). Normally, rare earth elements in the fibre core cause large optical losses, but the group found transparent windows where the transmission is just as good as in conventional telecommunications fibres. With the particular advantages of fibre lasers, namely axial pumping, high light intensity in the core and long lengths, it is now possible to obtain laser action with new materials.

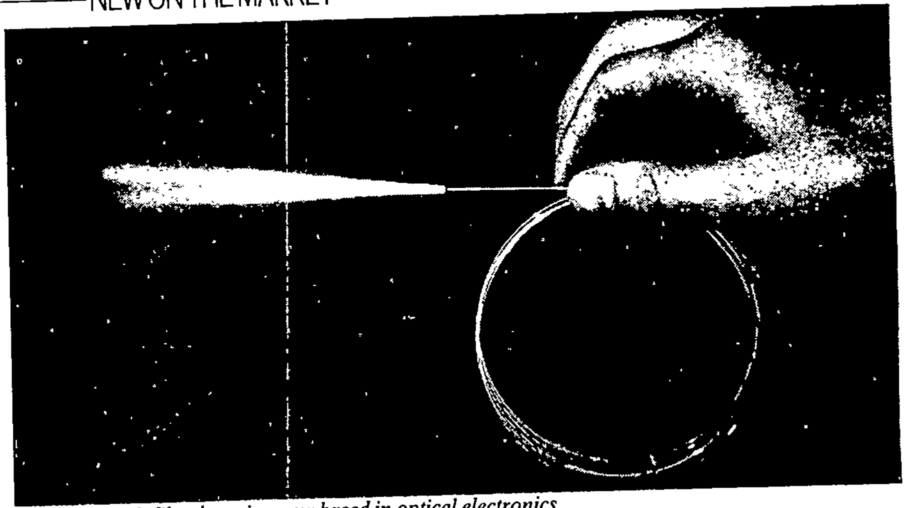
The rare-earth fibre laser is a new breed in optical electronics

The terminal enthusiast

The Continuous Flow Analyzer software from Spectra-Physics **quantitates the peaks obtained from the continuous flow analysis** of up to 120 samples at a time (Reader Service No. 108). This Autolab BASIC program requires a detector signal at regular intervals throughout a run and comes on a PROM chip for the SP4200 computing integrator. At $2,000 in the United States, the software features automatic drift correction, peak overlap correction, statistics calculations, use of both peak areas and heights and peak assignment modification.

ELISA data analysis need no longer be done by hand. Bio-Rad Laboratories's MacReader software **eliminates the manual calculations involved in ELISA screening** and quantitation, and generates printed reports such as standard curve graphics, sample extrapolations and complete statistical analyses of data (Reader Service No. 109). MacReader links the model 2550 automatic enzyme immunoassay reader with the Apple Macintosh computer and retails for $600 in the US.

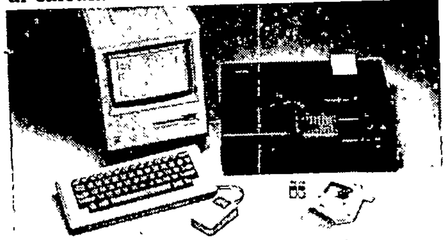
McReader software comes in several languages

Unnecessary HPLC experiments may be eliminated with Drylab I, a computer program from LC Resources Inc. that simulates chromatographic runs (Reader Service No. 110). Based on the work of Stout, Snyder *et al.* this software uses the data from an initial separation to determine the optimum parameters for further separations (column plate number, resolution, etc). DryLab I can also help troubleshoot separation problems. For $450, the software package consists of one hour of video instruction, a 100-page user's manual and the software itself.

Thermal analysis software is available from Mettler Instruments AG (Reader Service No. 111). The Mettler software combines the graphics capabilities of an IBM personal computer with the analytical precision of the TA3000 thermal analysis unit. The package costs £2,100 in the UK.

The LABS database compiles detailed **information on over 30,000 laboratories** in the United States and Canada (Reader Service No. 112). LABS records the types of research and the names of personnel at each station so that searchers can identify groups with a combination of characteristics, such as location, size and area of interest. Created by Coalesce Corp., the database encompasses scientific, engineering and medical labs. Coalesce charges $100 to $300 for initial queries.

Paperbound expertise

Kratos Analytical offers a wall chart detailing the **basic principles of mass spectrometry** and the functioning of a mass spectrometer (Reader Service No. 113).

The new **fast-affinity chromatography** (FAC) technique is the subject of a 12-page publication from Beckman Instru-

ADVERTISEMENTS

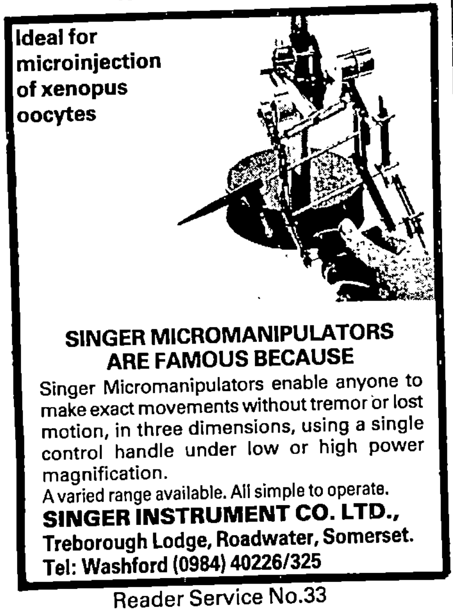
Ideal for microinjection of xenopus oocytes

SINGER MICROMANIPULATORS ARE FAMOUS BECAUSE

Singer Micromanipulators enable anyone to make exact movements without tremor or lost motion, in three dimensions, using a single control handle under low or high power magnification.
A varied range available. All simple to operate.

SINGER INSTRUMENT CO. LTD.,
Treborough Lodge, Roadwater, Somerset.
Tel: Washford (0984) 40226/325

Reader Service No.33

PHORBOL ESTERS

99 + % PURE
PMA (TPA)
PHORBOL 12-MYRISTATE
13-ACETATE
Cat. #P1680 .... 5mg/$28^00^

L C SERVICES CORPORATION
[illegible] New Boston Street
Woburn, MA 01801
[illegible]

Reader Service No.34

ments Inc. (Reader Service No. 114). Bulletin 5933 describes how to plan an FAC, with illustrations and step-by-step instructions for ligand selection, derivatization, sample loading and elution. The brochure highlights six practical examples using Beckman's Ultraffinity-EP column.

Gas, liquid or thin-layer chromatographers may want to take a look at Analytichem's **sample preparation handbook** (Reader Service No. 115). The 124-page book offers solutions to preparation problems, explains the technique of sorbent extraction, and spells out the thought processes that lead to successful development of a sample preparation method.

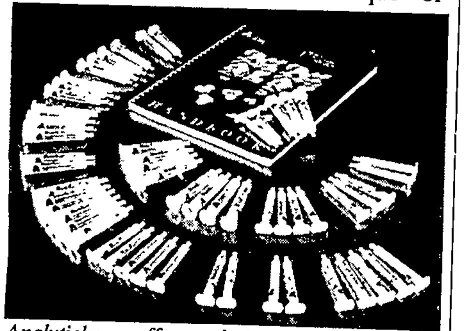
Analytichem offers solutions to preparation problems

Lecture notes on the **basic principles of recombinant DNA** technology and HPLC applications in nucleotide analysis have been introduced by Varian Associates Ltd. (Reader Service No. 116). The 42-page booklet is aimed at HPLC users and lecturers who may find the notes useful in introducing students to nucleic acid and nucleotide chromatography.

Safety firsts

For the occasional laboratory misshap, Wheaten Instruments provides a **polycarbonate safety shield** to guard against spilled chemicals and broken apparatus (Reader Service No. 117). The ¼-inch thick shield clamps to the bench top with an aluminium base. Wheaton carries two sizes, 20¼×18 inches and 26⅜×20 inches, for $92 and $144 respectively in the United States.

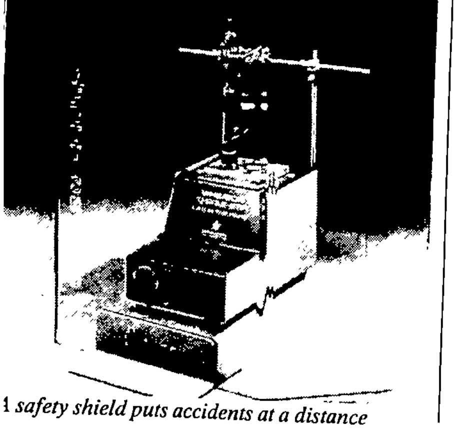
A safety shield puts accidents at a distance

The acrylic Beta Blok from Research Products International Corp. **protects fingers and hands** from overexposure to beta radiation (Reader Service No. 118). The blocks come in cases of six, each block holding four 1.5 ml or 0.25ml microcentrifuge tubes. Suitable for work with ^{32}P, the Beta Bloks sell for $57 per case in the United States.

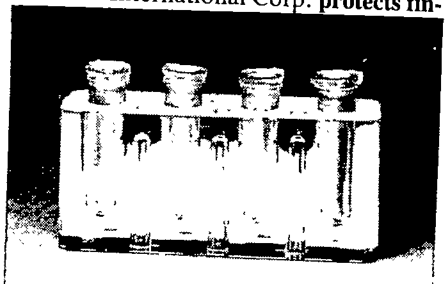
The Beta Blok makes the least of radiation

Science in motion

ExpertVision, a fully integrated computer system, **analyses and defines biochemical motion** with greater accuracy than standard film and hand digitizing methods (Reader Service No. 119). The system, designed by Motion Analysis Corp., merges computer and video technologies to enable two- or three-dimensional analysis on a high-speed graphics workstation or a personal computer. Offered at prices from $30,000 to $150,000 in the US, the system provides several advantages such as virtual elimination of marker 'drop-out', variable camera placement and programmable software.

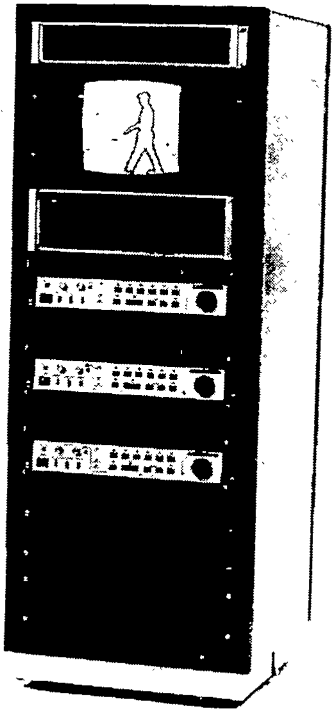
ExpertVision captures every step

Columbus Instruments markets a somewhat less complex MINI **animal activity-meter** for recording movements of creatures as small as insects or as large as rabbits (Reader Service No 120). Fifteen infrared beams span the animal cage, with adjustable receivers and emitters to accommodate a variety of cage sizes. The MINI model B separates ambulatory from stereotypic activity and uses two electronic counters to display ambulatory and total animal activity. The MINI model B sells for $1,995 in the United States and will interface with IBM-PC/XT or Apple IIe computers through software also available from Columbus Instruments.

Animal activity surveillance from Columbus

Fresh ideas, faithful methods

Separations and extractions previously performed with separatory funnels can now be carried out with a **new separation system** from Cole-Parmer Instrument Co. The Mixxor device effects separation via a mixer piston fitted into a graduated mixing reservoir and connected to a stoppered collection container (Reader Service No 121). With five strokes of the piston the sample separates, and the lower phase stays in the mixer reservoir as the upper phase goes to the stoppered collecting container. The piston becomes the divider between the upper and lower phases. Mixxor sets come in five different capacities from 2 to 50 ml, and prices range from $89 to $139 in the United States.

A novel technique for making **unilamellar liposomes** has been advanced by Xydex Technologies Inc. (Reader Service No 122). The glass Liposore cylinder creates lipid bilayers 0.1 to 1.0 μm in size in three to five minutes by forcing a phospholipid solution through capillary channels in a glass piston. The device is available in 2, 5 and 10 ml sizes, for prices ranging from $99 to $119 in the United States.

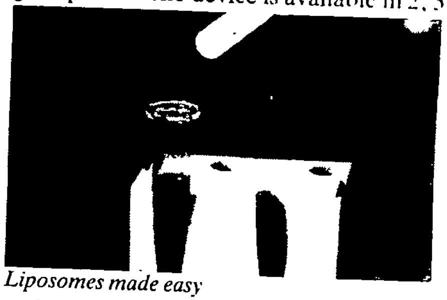
Liposomes made easy

Breaks in career — What chance for women?

from Richard Pearson

Will demographic trends and skill shortages be more effective, at least for women in professional and managerial careers, than the 1960s and 1970s legislation in support of equal opportunities?

THE proportion of women working or seeking work is now over 48%, and until the recession of the early 1980s had been steadily growing from a figure of 1 in 10 in 1921. Women now account for 43% of the labour force in the United Kingdom. While many are concentrated in part-time and low-paid jobs, they form significant and growing proportions of those in teaching, medicine, science and personnel work. They also represent 45% of those entering higher education. Technological and structural change in the economy have brought about a decline in traditionally male-dominated heavy industry and an expansion in new industrial sectors, such as electronics and services where women are more likely to be found. Likewise, the growth in managerial and highly skilled jobs, and professions such as computing is enhancing women's job prospects, particularly those qualified at graduate level. Demographic trends over the next decade are also likely to lead to an increased participation of women in professional jobs. With the number of 18-year-olds declining by one-third over the next decade, employers are likely to turn increasingly to women in their search for talent. At the same time the birth bulge of the 1950s and '60s will see increasing numbers of 30–40-year-old women returning to the labour force in the 1990s.

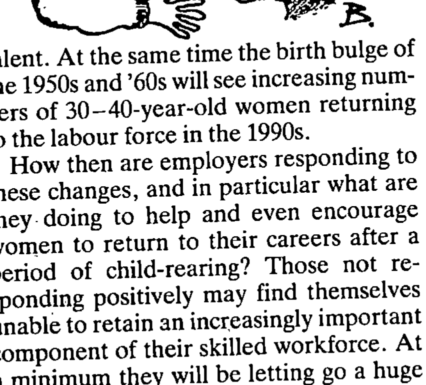
Darling—we're going to have a Maternity Leave!
DOCTOR SNODDY M.D.
B.

How then are employers responding to these changes, and in particular what are they doing to help and even encourage women to return to their careers after a period of child-rearing? Those not responding positively may find themselves unable to retain an increasingly important component of their skilled workforce. At a minimum they will be letting go a huge investment in the training and development of employees with valuable and relevant skills.

The Engineering Council are strongly promoting the need for career breaks. A report by the Institute of Manpower Studies[1] shows, however, that while employers often talk of the costs of policies to help women combine work with a family, very few have measured the costs and lost investment in letting them go.

Although many employers exceed the statutory provision in many areas of employment legislation, they do not tend to do so for maternity leave. As such, the legislative standard tends to be the norm, and most employers and employees seemed to be clear about the provisions of statutory maternity leave, which can last up to 40 weeks. However, individual companies' administrative procedures were less clear, and often poorly handled, with the presumption that the career professional or managerial women should be able to find out everything for themselves.

Data on maternity leave and women leaving from career breaks are also not easy to find, employers often recording women taking normal maternity leave as leavers when they were still technically employees. As a result, some did not know how many were on leave at any one time, which makes monitoring difficult and can inhibit the planning of the women's return to work. The available evidence about the numbers returning suggested that only a small proportion did so, one of the highest being in a computer company where 30% returned to full-time and 15% to part-time work.

One major problem in managing the career break in the uncertainty as to the intention to return. There is a legal requirement for a woman to notify her employer of her intention to return, and to reconfirm it 7 weeks after the birth. Most automatically do this to safeguard their job, yet it can inhibit an employer's planning to cover the job and the timing of the subsequent return. One enlightened company has parallel discussions about the real intentions of each individual, without affecting the legal rights, a situation that requires a high degree of trust between the parties. A defeatist attitude to the legislation is clearly avoidable. Given an uncertain duration of leave, various strategies are used to cover the vacant job, including sharing the work out, hiring temps, or in larger organizations likely to have a number of similar jobs, filling it permanently. The latter can, however, cause problems on re-entry if there is not a similar job available at the appropriate time, especially given the generally low levels of managerial turnover in most organizations. Where a woman is not returning to her original job, good practice should include early discussions and counselling as to the options; some women do not know what job they will do until they arrive, adding unnecessary anxiety to an already stressful period.

More women would return if it could be to part-time work, either as a transitional or as a more permanent arrangement. Some employers are able to accommodate this, and there are several computer software companies who operate with high percentages of part-time and often home-based, professional staff. In medicine, doctors have a national scheme which sets a quota of part-time jobs at senior registrar level, and also a retainer scheme which keeps doctors in touch with work if they wish to do very limited hours each week. In traditional organizations, attitudes of peers can be a problem. Thus, the case of a female doctor at consultant level where, in her speciality, work hours could be very flexible. It was quite acceptable for her male colleagues to organize work to allow time to play golf; it was not, however, seen as acceptable that she should organize her hours so as to collect her child from school!

To date, well-organized career breaks for women, let alone men, are still a rarity, yet they represent a missed opportunity for employers and individuals, particularly in the case of highly trained and experienced people. Barriers to change include a low realization of the costs of female wastage, and a failure to plan careers against a longer-term perspective. Resistance to women in management is still strong in many organizations, with a reluctance to accommodate flexible careers and part-time working in professional and managerial jobs. Pressure for a change from women is, however, growing, if slowly, and the more they move into such jobs and become a key source of skilled staff, the more labour market factors and economics will help reduce barriers to change. ☐

Richard Pearson is at the Institute of Manpower Studies, Mantell Building, University of Sussex, Brighton BN1 9RF, UK.

---

[1] Hirsh, W., Hutt, R. & Atkinson, J. *Women, Career Breaks and Re-entry* (Institute of Manpower Studies, Brighton 1985).

nature

NATURE VOL. 319 13 FEBRUARY 1986

Prospect of US budget chaos

The US Supreme Court is now to have a say in this year's annual budget charade in Washington. Will it be better able than the Congress to count the cost outside the United States?

THE annual tussle over the US federal budget between the US Congress and the administration will be more confused, even chaotic, this year than ever. That prospect has been on the cards for the past several months, ever since Congress passed the Gramm–Rudman Deficit Reduction Act, with the laudable objective of reducing the federal budget deficit to zero over the next five years, but by the curiously irrational process of delegating control of federal spending to a bunch of accountants at agencies such as the Office of Management and Budget if the Congress and the administration should fail to agree by deadlines specified in the act. That the Congress, which owes many of its powers over the federal budget to the eighteenth century doctrine of "no taxation without representation", should have been willing to delegate this central function as specified by the act was one of the big surprises of last year. That President Reagan should have been willing to let his hands be tied was an even greater puzzle, although the budget published last week suggests that he saw it as a chance to launch a budget free from spending of which he disapproves. The bombshell that has thrown all these calculations into disarray is the decision of a federal court last week that the Gramm–Rudman act is unconstitutional. The US Congress is to appeal to the Supreme Court, hoping that there will be some kind of decision by the early summer, in May or thereabouts. What this means is that the fierce debates about the budget that will occupy the next few months will be conducted in a vacuum. Political and economic chaos have supervened.

Last week's budget is hardly the place from which rational discussion could in any case have begun. Although the budget as a whole complies with the Gramm–Rudman act by planning to spend just less than the limit specified for the financial year beginning on 1 October, the President's package (see p.526) flies in the face of known congressional opinion. Defence spending is increased, most other forms of spending are reduced. Although basic research fares relatively well under the proposals, it is a striking measure of the skew of the package that direct support of research by civilian agencies should, under the plan, amount to only a half of what the Department of Defense would be spending on military research. In a normal year, the Congress would now embark on the familiar process of writing back into the budget items on which it considers that money should be spent; no doubt it would also repeat last year's process of cutting back the defence budget. The possibility that the Gramm–Rudman act may be unconstitutional will give heart to those who think that this year will be no different from previous years. So the result is likely to be that, by the deadline of 15 August specified under the act, Congress's version of the budget will far exceed the limit of $144,000 million. What will happen then?

Devastation

One of three things. If the Supreme Court finds the act to be constitutional, its provisions will come into effect, enforcing automatic reductions on rather less than a third of the total of planned expenditure. The effects could be devastating for some important programmes, those of agencies such as the National Science Foundation, for example. So financial chaos by the summer is one possible outcome. But the US Congress will not take well to such a prospect, and might decide that the best way of dealing with Gramm–Rudman is to get rid of it, in which case the whole episode will be seen in retrospect as having been another budgetary charade. That is the second outcome, little different from the third now in prospect that the Supreme Court will find the act unconstitutional, which will be a signal for a return to the budgetary process that has become familiar and notorious in the past decade. In theory, of course, the Congress might throw in the towel and swallow the substance of the administration's package for the sake of good government. But not in an election year.

Chaos

Where will it all end? And why, in any case, should it matter? The immediate effect of the annual confusion about the US budget is that the agencies depending on it for their spending authority do not know where they stand from one month to the next. The effects on the basic research agencies are to impede forward planning and thus the rational use of resources. That condition, now chronic, will be made worse this year. The effects of this uncertainty on the economy of the United States, and on its external monetary relations, may be even more serious. Only a few weeks ago, representatives of the five largest industrial economies meeting in London appear to have agreed that a concerted attempt to reduce money interest rates would make sense. But the capacity of the United States, which has a central influence on worldwide interest rates, to play a part in any such campaign is hamstrung by the federal deficit, which has to be financed by means of a competition for funds on the money markets of Wall Street. If it had seemed that Gramm–Rudman would have worked, it would at least have been possible to anticipate a less fierce competition. Now, with the whole issue clouded by uncertainty, the money-people will assume that the United States will remain a heavy borrower for at least the next two years. Economic growth will be held back in prosperous countries. Those, like Mexico, teetering on the edge of collapse because of a burden of foreign debt will look even more apprehensively at the future.

This is too high a price to pay for the US government's long-standing failure to agree on a mechanism for deciding how much the administration should be allowed to spend on what. The difficulty is only partly constitutional, although the convention that, in budgetary matters, the President proposes and the Congress disposes provides the opportunity for the familiar chaos. The more serious difficulties are political, stemming from the perennial conflicts between successive administrations and the Congress in questions such as the necessary cost of defence, the importance of social programmes of various kinds and the devotion of individual members of the Congress to local spending projects that may enhance their chances of re-election. What this year's budget cycle shows is that neither party to the exercise has an incentive to compromise with the other. The Gramm–Rudman shotgun will clearly not do the trick. Maybe an arrangement that no member of the Congress should be paid a salary until the budget has been agreed would be more effective. □

World Archaeological Congress

South African exclusion causes academic schism

REPORTS to the contrary notwithstanding, the World Archaeological Congress *will* take place this September in Southampton, England, without the participation of South African and Namibian scientists, but it will not enjoy the blessing of the International Union of Prehistoric and Protohistoric Sciences (IUPPS), which will instead recognize a congress at Mainz, West Germany, as its official quinquennial meeting.

At a meeting of the British executive committee for the Southampton congress at the British Museum, organizing secretary Professor Peter Ucko said plans for the congress will go ahead. But three of the five members of the executive committee, Sir David Wilson, Professor Leslie Alcock and Professor Colin Renfrew, resigned, saying they could no longer officially support the Southampton congress.

IUPPS had threatened to withdraw its support for the meeting unless the British organizers lifted their ban on South African and Namibian participation. After a meeting in Paris last month, the executive committee of IUPPS gave the British organizers until 15 February to reinvite the South Africans. The executive committee also insisted on written guarantees that groups opposing South African particiaption would not disrupt the congress.

For the past three weeks, organizers of the Southampton congress have been trying to work out a formula that would allow them to comply with the IUPPS demands. One compromise proposal would have been to seek approval of South African participation from the groups opposing it on a one-time-only basis. Once the Southampton congress received IUPPS approval, a motion would be put forward to ban South African scientists from any future meeting until South Africa's apartheid policy was lifted. But in the end, this compromise fell through, and Ucko was forced to acknowledge the he could not meet the IUPPS requirements.

According to Professor John Evans, the issue of South African participation might never have come up but for the attempts by meeting organizers to broaden the focus of the Southampton meeting. The last IUPPS international meeting was held in Mexico, the first time ever outside Europe, but hopes for a truly international meeting at that time were not realized. In trying to attract wider participation by nations outside the industrialized West, the issue of South African participation was thrown into stark relief.

Evans resigned last month as president of the executive committee of IUPPS and the British executive committee because he too did not want to be associated with a congress held without IUPPS endorsement (see *Nature* **319**, 251; 1986).

The Southampton meeting organizers now find themselves in an extremely difficult position. Encouraged initially by IUPPS to provide a broader scope to the Southampton congress by doing more to encourage participation of developing countries, they saw banning South African scientists as their only alternative. But having succeeded in attracting some formerly neglected parts of the world archaeological community, they now find they have alienated many mainstream archaeologists. Ucko estimates that the Southampton congress will attract only 1,000 of the 3,000–4,000 scientist who might otherwise have attended if IUPPS support had not been withdrawn.

Ucko maintains that the IUPPS executive committee has exacerbated the situation. At its January meeting in Paris, the committee refused to consider the positions of members from developing countries who could not be present. Ucko considers their actions "utterly scandalous", claiming the committee was only too happy to move the congress to Mainz in order to maintain the stranglehold of Western European scientists on the world archaeological community.

Opponents of the South African ban say it is an issue of academic freedom. They maintain that no *bona fide* scientist should be excluded from participating in a scientific congress for political reasons. Nobody can oppose the concept of academic freedom, says Professor Colin Renfrew, but blindly adhering to it is pointless if it causes *de facto* discrimination. In this case, including South Africans would mean not including Indians and Nigerians, among others, who have said they will not attend if the South Africans do. "I see no solution to this dilemma", says Renfrew.

There is no question that the issue of the Southampton congress has caused a split in the archaeological community. Says John Evans, "a certain amount of damage has been done, and it will take time to repair it". **Joseph Palca**

Animal welfare

Tip-off leads to NIH ban

Washington

THE National Institutes of Health (NIH) are getting tough about enforcing animal welfare rules. NIH's Office for Protection from Research Risks has started making unannounced visits to check conditions in animal laboratories using Public Health Service funds, and as a result has suspended NIH funds to the Health Sciences Division of Columbia University in New York.

The order against Columbia was made by NIH director James Wyngaarden after he received an interim report from a team that visited Columbia's Health Sciences Division on 23 and 24 January. The report identified deficiencies in four areas: veterinary care, sterility of areas where animals recuperate from surgery, housing of dogs under quarantine and methods of reducing health risks to personnel. The suspension affected only NIH funds used for research on vertebrates other than rodents, but the university has voluntarily halted all other research until the facilities are improved.

The new get-tough policy at NIH came into force formally at the end of last year, when the Public Health Service introduced new regulations that significantly tighten the requirements on grantee institutions that conduct animal research. Many of what were previously suggestions relating to animal use committees became mandatory requirements: a non-scientist must be included, and the committee must review all research proposals involving animals, to name but two. In addition, institutions were required to submit reports to NIH detailing their arrangements for meeting the new regulations. Columbia University submitted its report well before the 31 December deadline and made its failings plain, although the university had as long as a year ago been aware that "considerable improvements" were necessary and had instituted a long-range plan to achieve them. NIH were tipped off to investigate Columbia by an animal welfare group, and will be ready to listen to similar tip-offs in future.

The research that is now on hold at Columbia involves rabbits, dogs, sheep and primates. Research topics include cardiovascular disease, fertility, fetal development, immunology, birth defects (including Down's syndrome), and arthritis.

Other unannounced inspections can be expected, and NIH is not being shy about enforcing its conditions. NIH funds to the City of Hope Medical Center in Duarte, California have been suspended, and the University of Pennsylvania is barred from new NIH research funds pending agreement over requirements; head injury research at the university was suspended indefinitely last summer following discovery of serious abuses. **Tim Beardsley**

European particle physics

CERN budget scrutiny planned

An international review of the European Organisation for Nuclear Research (CERN) seems certain to go ahead this year. The result of a British initiative, the review would consider the impact on CERN of possible reductions in contributions by the 14 member states. The British have tabled a resolution to set up the review, a proposal that is likely to be adopted by CERN's council at an extraordinary session on 20 February. The British move is a first step towards implementing the recommendations of its Kendrew committee, which advocated last year that Britain should seek a cut of 25 per cent in its budget contribution or withdraw from CERN.

Short of complete withdrawal, the review is the only way that Britain may eventually reduce the cost of its membership, now six per cent of the total budget of Britain's research councils. The panel, chaired by Sir John Kendrew, concluded last year that this proportion is too high, and said that the reduction of the British contribution to CERN should be attained by 1991. The Science and Research Council (SERC) and the Advisory Board for the Research Councils subsequently endorsed this position, since when George Walden, a junior minister at the Department of Education and Science, has been trawling the capitals of Europe, testing the waters for a concerted bid to reduce the cost of CERN.

The outcome seems to have been that European ministers have agreed that it would be unobjectionable if CERN were cheaper, and that possibilities for making it so should be looked at. The council of CERN consists of ministerial representatives who are not necessarily high-energy physicists and, despite earlier misgivings, the British government is now persuaded that the council is the appropriate body to establish and monitor an independent inquiry.

The British draft resolution suggests that the review should encompass European high-energy physics and CERN, and that the effects of cuts of up to 25 per cent in CERN's budget should be assessed. While possible names for the panel — such as the director of a large German laboratory and senior industrialists — are being considered, the draft resolution leaves this aspect open. The somewhat optimistic intention is that the panel should be established within a month and should report by the end of the year. Presumably Britain would then be obliged to follow the recommendations of the panel or withdraw.

One obstacle to a reduction in CERN's funds may be the organization's success in keeping the budget as tight as it is. The construction of CERN's major new accelerator LEP (a large electron — positron collider) has been carried out within a budget that has been constant in real terms, and which will not increase at least until experiments begin in 1989. The result has been the closure of one major facility, the Intersecting Storage Rings, and the delayed refurbishment of other facilities and repayments of loans. After LEP is finished, these commitments will become due. While there may be scope for managerial change and contracting out of design or construction work, it is hard to see how a cut of 25 per cent could be achieved without devastating CERN's scientific capability.

Another obstacle to cuts is US competition. The Stanford Linear Collider (SLC) is expected to come on line in 1988 (which some CERN physicists think optimistic) and will examine, though with a lower particle production rate, some of the same phenomena as LEP. These include the production and decay of W and Z bosons. One particular goal that SLC could reach before LEP is the cataloguing of the ways in which the Z boson can decay, which should reveal, for instance, whether there are more than the three types of neutrino already known, a result that may have repercussions for cosmology as well as for particle physics. SLC may also find the "top" quark, whose possible detection at CERN last year is not yet confirmed.

A more difficult goal, which SLC almost certainly will not achieve, is the observation of the Higgs boson, a particle associated with symmetry breaking within the unified theory of electromagnetic and weak interactions and of potentially crucial importance in understanding how particles come to have mass. Higgs bosons may be produced by the decay of only one in every 100,000 Z bosons, which is why LEP's higher particle interaction rates should be crucial.

These and related phenomena would be much better investigated were LEP to achieve its full design capability by the incorporation of superconducting magnets around the 30 km circumference accelerator ring. This would permit centre-of-mass collision energies of 200 GeV to be achieved, enough to produce pairs of W bosons, for example. But it seems unlikely that the 200 million Swiss francs required could be found without an increase in the CERN budget. Perhaps this will hang on decisions about the proposed US Superconducting Supercollider, an ambitious scheme that seems unlikely to survive unscathed the current US budgetary problems.

Further ahead, there may be scope for savings at CERN in the mid-1990s, when a significant proportion of CERN staff are due to retire (at 80 per cent of their salaries). But since one of Britain's principal aims in setting up the Kendrew panel in 1984 was to find money for its hard-pressed "small science" community. that prospect may be too distant SERC has already decided to cut its domestic high-energy physics budget by 20 per cent by 1991, losing 150 of the 750-strong community. Whether there will be such economies at CERN will not be known for at least a year.

Philip Campbell

AIDS protein made

Washington

Genentech, the Californian biotechnology company, last week announced the synthesis in mammalian cells of a recombinant protein that is the favoured candidate for a vaccine against acquired immune deficiency syndrome (AIDS). Although the work marks an "unexpected modest advance" in AIDS research, it may greatly expedite the search for a safeguard against a disease that has already claimed more than 8,000 lives in the United States.

The protein, gp120, is part of the envelope of the AIDS virus, HTLV-III or LAV. Although it has been synthesized by several laboratories in bacteria and yeast cells, these systems cannot match the mammalian cell products, which Duke University's Danni Bolognesi calls "as close to the real beast as you can possibly get". Genentech's Chinese hamster ovary (CHO) cells glycosylate and secrete the protein, while microbial cultures must be engineered to do either. Despite the added expenses of maintaining mammalian cultures, Genentech's system may prove more efficient in the long run because it cuts purification costs.

Located on the viral envelope, where antibody recognition is thought to occur, gp120 has long been the focus of interest for those looking for an AIDS vaccine, but has been a devil to isolate from the virus itself. So, before Genentech's team brought its efforts to fruition, obtaining large quantities of the protein in its natural glycosylated form was both dangerous and laborious. Now senior scientist Larry Lasky and Genentech's collaborators can hasten vaccine testing, which they have just begun with rabbits, guinea pigs, rats and mice.

Genentech tried the same genetic tricks that produced its herpes vaccine last year to coax the AIDS virus protein from hamster cells; what those tricks are, the company is not saying. Although Lasky seems pleased with his latest sleight of hand, he is also cautious. As a vaccine, gp120's efficacy has yet to be proved, and it may be a year or two before monkey trials provide any data relevant to the human response. Any possible vaccine will also have to counter the many variant forms the AIDS virus is known to assume.

Karen Wright

US budget

Biosciences lose out to defence

Washington

A HUGE increase in defence spending, including defence research and development, dominates President Reagan's proposed budget for fiscal year 1987. Total federal obligations for research and development, including facilities, are estimated at $63,000 million, 16 per cent above the 1986 level of $54,000 million. Military programmes in the Departments of Defense and Energy, as in previous years, account for most of the increase. But substantial increases are also proposed for the National Science Foundation (NSF) and the National Aeronautics and Space Administration (NASA). The physical sciences in general have been relatively well treated. Biomedical research is a different story.

The budget continues all the well-known Reagan themes. Budget authority for the Strategic Defense Initiative (SDI) will increase from $2,800 million in 1986 to $4,800 million in 1987, Congress permitting. Research and development by the Department of Defense would increase to 60 per cent above its 1984 level; only $21,000 million of the $63,000 million budget for federal research and development would be non-defence, $7,600 million of that for non-military basic research. Pet Reagan hates such as the Sea Grant programme of the National Oceanic and Atmospheric Administration and the computer sciences and technology and fire and building research programmes at the National Bureau of Standards are scheduled (as they have been before) to be killed. The Environmental Protection Agency takes a 7 per cent cut.

Tension between the administration and Congress over the budget is unusually high this year, because of last year's controversial legislation setting fixed targets for reducing the federal budget deficit in each of the next five years. Under the Gramm–Rudman deficit reduction act, automatic across-the-board cuts will come into effect if Congress fails to pass budgets meeting the target.

The new 1987 budget proposal foresees total spending of $944,000 million, with a deficit of $143,600 million, just under the limit specified by Gramm–Rudman. But the administration's refusal to consider tax increases, together with a 12 per cent increase in total military spending, has meant hefty cuts to many domestic programmes, which Congress is unlikely to approve. Instead, the appropriate committees and Congress as a whole can be expected to make several changes, with the result that the actual budget for the financial year beginning on 1 October 1986 will probably look even less like the President's proposal than usual, if Gramm–Rudman stands. But further uncertainty was introduced last week when a federal judicial panel unanimously ruled the automatic cuts provision of Gramm–Rudman unconstitutional; the question will now go to the Supreme Court, which is not expected to rule before the summer.

Meanwhile, the administration's proposals are as follows.

National Science Foundation

The foundation's budget request is $1,685.7 million, an increase of 8.4 per cent. Even so, the mood at NSF is temperate. Director Erich Bloch points out that in 1983 constant dollars, the 1987 request represents a negligible increase over the 1985 amount (after a decrease in 1986). The foundation says that even if Congress should approve the full request, that would be only just good enough, in part because of the increasing complexity — and cost — of research equipment. But in the Gramm–Rudman era's scramble for funds, full approval seems unlikely.

NSF lists for "special emphases" for 1987: biotechnology, computational science and engineering, global geosciences and broadening participation in research and education. If NSF sustains budget cuts during the impending legislative fray, the foundation would probably seek to protect them.

NSF is planning to establish between two and four new multidisciplinary biotechnology research centres, as well as an undefined number of so-called mini-centres. A 50 per cent increase to $84 million is wanted for computational science and engineering; the global geosciences effort would jump from $17 million to $35 million, and would include the development of Earth-based and satellite observational instrumentation, a project for which the administration has a special enthusiasm.

NSF's plans to expand participation in science and engineering research and education include $4 million for the new Minority Research Centers of Excellence programme and a $13 million increase over the $50 million spent in 1986 to improve undergraduate research.

Two more of the agency's pet projects are seeking increased support. NSF's supercomputer centres stand to gain almost 19 per cent over their current $45.2 million, but the total, $53.6 million, will be spent on bringing on stream the five centres now being set up. NSF has chosen to push networking and software research rather than to establish new centres in 1987, even though the National Science Board's initial mandate called for 10 facilities.

The nascent engineering research centre network grabbed a $12 million increase over this year's budget of $23 million. Six centres have been established so far, and NSF hopes to have 15 by the end of 1987.

National Institutes of Health

The proposed total budget for the National Institutes of Health (NIH) is $4,936 million, a substantial drop from the $5,353 million comparable figure appropriated by Congress for 1986. This repeats a now familiar pattern: the administration proposes cuts for NIH, only to have Congress reverse them and vote huge increases a few months later. But this year, because of

US research and development budget ($ million)

	1985 actual	1986 estimated	1987 proposed
Defence-related	31,099	33,485	41,823
Health and Human Services	5,444	5,524	5,471
(NIH)	(4,824)	(4,905)	(4,672)
Energy	4,901	4,785	4,886
NASA	3,235	3,594	4,051
NSF	1,346	1,334	1,508
Agriculture	941	922	907
EPA	320	334	310
R&D facilities	1,894	1,812	1,734
All other	2,205	2,048	1,847
Total	51,385	53,836	62,537

Due process of law

IN anticipation of legal challenges to the constitutionality of Gramm-Rudman, the bill itself contains specific procedures to be followed. Rather than proceed from district court to appeals court to Supreme Court, any challenge goes first to a special panel of federal judges who issue a ruling. If there is an appeal against the panel's ruling, the case goes immediately to the Supreme Court.

In fact, challenges did arise. Several congressmen joined a suit brought by the National Treasury Employees Union. On 7 February, the panel issued its ruling declaring the automatic-cuts provision of Gramm-Rudman unconstitutional.

Now it falls to the heavily burdened Supreme Court to make a final determination. That decision is unlikely to come before July. Until then, federal agencies will have to live in fear of next fall's Gramm-Rudman axe. ☐

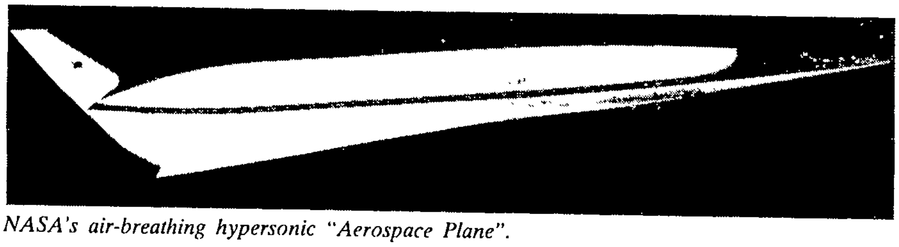

NASA's air-breathing hypersonic "Aerospace Plane".

the Gramm–Rudman Act, there is less confidence that Congress will come to the rescue, and NIH officials are acting "as if they really think it's going to happen", according to one congressional observer.

In addition to the sharply lowered budget for 1987, the administration is proposing a rescission to the NIH 1986 budget of $62 million. This is on top of $230 million that is to come out of the 1986 budget because of automatic Gramm–Rudman cuts this year. But the $62 million rescission will occur only if Congress specifically approves it within 45 days, which must be considered doubtful.

Most of the savings sought at NIH would be achieved by limiting the total number of extramural research grants to 18,000 — 776 less than Congress intended for this year. By focusing on the total number of grants, NIH hopes to shift the debate from the number of new grants awarded each year, which has been a continuing battle with Congress. But most congressional sources last week expressed incredulity that the proposed NIH budget could be taken seriously; most probably, there will at least be some restoration of the budget in the direction of last year's figure.

If not, the number of new and competing extramural grants will be 5,519 this year (6,100 had previously been agreed); this number would decrease steadily to the administration's long-sought target of 5,000 in 1989. In the short term, the rescissions may mean that NIH will have to reduce the dollar value of research grants.

A total of $213 million is proposed for research into and control of acquired immune deficiency syndrome (AIDS), to be determined as a special fund in the office of the assistant secretary for health. A sum of $46 million would go to the Centers for Disease Control, $144 million to NIH, $14 million to the Alcohol, Drug Abuse and Mental Health Administration and $10 million to the Food and Drug Administration. The total appropriated for AIDS research in the current year was $244 million, but the combined effects of Gramm–Rudman and the proposed rescission would reduce that to $193 million.

Compared with the 1986 planned allocations, relatively more AIDS funds would go to NIH (an increase of $22 million) than to the Centers for Disease Control (which would get $5 million less).

Aeronautics and Space

The budget requested for the National Aeronautics and Space Admininstration (NASA) is $7,694 million, a 5.3 per cent increase over the estimated 1986 budget after Gramm–Rudman cuts. Nevertheless, acting NASA administrator William Graham preferred to look at it another way last week: the 1987 total is still a reduction in real terms of 3.5 per cent from the level of the 1986 operating plan. In any event, NASA's budget is completely up for grabs again now with the loss of Challenger; NASA will save on shuttle operations until flights resume but will also lose part of the $704 million it had been expecting in reimbursible expenses from shuttle operations in the current year. The 1987 budget included $410 million for President Reagan's space station, the least that is plausible if the space station is to be in orbit by 1994 as the President has directed. The budget also included $29 million to "initiate" TOPEX, an oceanographic satellite being developed jointly with France. Officials declined to speculate on whether supplementary funds will be sought to build a Challenger replacement (cost estimates range up to $2,900 million), but legislation has already been introduced in the House of Representatives that would do just that. NASA already has spare parts in storage that could form the basis of new orbiter to be built quickly.

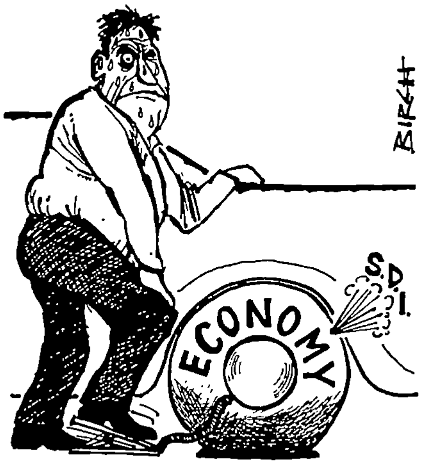

About $200 million is requested for a joint project to be carried out by NASA and the Department of Defense to develop a new class of hypersonic aerospace vehicles capable of horizontal take-off and landing on normal runways. The National Aerospace Plane, as it has been dubbed, would be mainly air-breathing and would use ramjets with hydrogen fuel, operating at speeds of between Mach 12 and Mach 25 at altitudes of up to 350,000 feet. The plan is to have a test model in the mid-1990s. The idea has been developed over the past several years by NASA and the Defense Advanced Research Projects Agency; all participants believe there is still "a high degree of technical risk". The planes would serve both civilian and military uses; ten minutes from the east coast of the United States to the west coast was one claim bandied about last week. Perhaps less frivolously, the administration may be attracted to the idea of being able to deploy US forces anywhere in the world within a few hours.

Energy

The request for the Department of Energy (DOE) in 1987 is only about 1 per cent above actual spending, a decrease in real terms. But within this total there is a 11 per cent increase for the department's nuclear weapons production and support (to $4,830 million), and a 7 per cent decrease for research and development (to $4,539 million).

As in previous years, cuts of 50 per cent and more are proposed. Magnetic fusion research is also scheduled to decrease, from $365 million to $333 million. Fossil energy research is scheduled for major cuts, but there is a new clean coal technology fund for which $150 million is requested in 1987 (1986: $100 million) and a new cooperative research and development venture pool with industry is proposed. The aim is to get industry to pay for much of the research on fossil fuels traditionally supported by DOE; if successful, conservation might be handled in the same way.

Fission research for civilian reactors (including breeder reactors) is to be phased down, while nuclear space and defence power systems (including SDI) increase from $20 million to $71 million. But high-energy physics and nuclear physics both get a boost, with first-time operating funds for the Tevatron collider at Fermilab and for the Stanford Linear Accelerator. Low level development funding continues for the Superconducting Supercollider; a decision on whether to go ahead is expected this year, and budget allocation for high-energy physics is suspended until then. Funds are requested to initiate construction of the Continuous Electron Beam Accelerator Facility at Newport News, Virginia.

Agriculture

The agricultural research service does well, with a 7 per cent increase to $497 million. The service conducts basic research in plant germplasm and biotechnology. But the cooperative state research service, which deals with more local problems, will be cut by more than 15 per cent: the administration believes local problems should be researched by state governments. The animal health and disease programme would be eliminated: in previous years Congress has reinstated it.

Tim Beardsley & Karen Wright

Japanese research

Small increase brings big gains

Tokyo

OVERALL support for academic research in Japan will not keep pace with inflation this year, according to the 1986 budget figures of the Ministry of Education, Culture and Science. The ministry is by far the largest public source of support for basic research in the universities, but it has won only a tiny overall rise (less than one per cent) in funds for the direct support of research and international exchange.

The ministry's figures compare badly with the boom in spending on research by industry, a boom that puts Japan second only to the United States in total research spending in the non-communist world. The root of the problem lies in the high priority given by the government to tackling the ever-increasing budget deficit and the austere budgets this makes necessary.

Japan's science budget (contd)

Ministry of Education, Culture and Science	Yen (thousand million)	Percentage increase or decrease
Grants in aid of research	43.5	+3.5
Maintence of scientific research system	7.8	+36.8
Research fellowships	0.8	+41.7
Energy research	20.8	−25.2
(Nuclear fusion)	(8.2)	(+9.2)
(Accelerator physics)	(5.9)	(−58.2)
Space research	12.4	+12.9
Marine science	0.5	+41.8
Earth science	2.0	+1.0
Polar research	3.1	−7.1
Cancer research	1.8	+6.0
International academic exchange	3.7	+1.9
International student exchange	11.7	+16.2

Although little has been gained overall, there are some bright spots. Direct grants-in-aid of research are up by 3.57 per cent, an annual rate of growth that has been fairly constant over the past four years, and which is ahead of the rate of inflation (about two per cent during the same period). Overall, 15,000 grants were given out, from 53,000 applicants.

Big grants tend to fall into two categories: those for "special distinguished research" likely to produce outstanding results recognized internationally, and those for "special research". The latter is an unusual category in that it is awarded to a field rather than to an individual; researchers all over Japan may apply to participate in such a project. Both types of grants go to scientists at the leading edge of research and their topics give a good idea of what are perceived as the hottest areas. As elsewhere, molecular biology and semiconductor physics are currently among the winners.

Among the 13 special research projects (total cost Y5.3 thousand million, US$26.5 million) beginning this year are those on the regulation of complex genetic systems and their responses to stresses in the intracellular and extracellular environment, the physiology of blood vessel endothelial and smooth muscle cells and changes in arteriosclerosis, biologically active substances studied through chemical synthesis and the development of biosensors in the "special distinguished" category, projects (total funding Y2.3 thousand million) have recently begun on semiconductor superlattice surface structure, the quantum Hall effect and compound semiconductor/insulator interface physics. On the biological side are those on B-lymphocyte multiplication and differentiation, the mechanism of division of animal cells, the regulation of vasoactive peptide synthesis, the regulation of enzyme synthesis in higher animals and a new protein synthesis system.

Overall, though, there has been no increase in total support for these top grants. The increase in grants-in-aid is concentrated in the smallest category of grants (up to Y3 million) available for individual projects, the small grants (up to Y1.2 million) available for researchers under 37 and the grants for cooperative research between different institutes.

Extra money has gone towards strengthening the "scientific research system" (up 36.8 per cent). Most of the increase goes towards a restructuring of the Tokyo University bibliography centre as a nationwide scientific information centre.

There is also a big increase in funds for postdoctoral fellowships, although the original amount being spent was not large.

Many of the increases are being paid for by cuts in the budget for energy research including a huge reduction in funding (−58.2 per cent) for the TRISTAN project, the construction of an electron–positron collider ring at the Institute of High-Energy Physics in Tsukuba Science City. The ring is now almost complete and will be commissioned in November, at energies around 23–25 GeV. With the addition of superconducting cavities, it should be possible to reach 36 GeV, but plans to turn the whole ring into an electron–proton collider have virtually been abandoned.

One ambitious project that does seem likely to bear fruit is the scheme developed by the Institute of Space and Astronautical Science (ISAS) designed to put a satellite into orbit around the Moon. Following the success (so far) of the first deep-space launch that sent the satellite *Suisei* towards a March encounter with Halley's comet, funds have been obtained to work on a prototype for a Moon launch (see *Nature* **315**, 173; 1985) in the early 1990s.

Another ISAS project will be supported from the funds set aside for international cooperation — several years of discussion with Chinese scientists have resulted in a high-altitude balloon launch programme which begins with a maiden flight in July.

Marine science also seems to receive a boost (+41.8 per cent). But most of this is to pay for the expensive business of full participation in the Ocean Drilling Program, even though the drill ship is not expected in Japanese waters until the 1990s.

Alun Anderson

Gorbachev's purge reaches researchers

THE Communist Party of the Soviet republic of Kirgizia has accused the Kirgiz Academy of Sciences of "serious failings". Addressing the Party Congress last month, the First Secretary of the Kirgiz Party, Absamat Masaliev, accused the academy of publicizing even routine and insignificant developments as major breakthroughs, and even reporting research work that had not been done at all. At the previous party congress, five years ago, the president of the academy, Murzabek Imanaliev, had claimed that its scientists had, "for the first time anywhere", obtained "natural iron powders, alloyed with rare earth elements", and had established with industry a semi-pilot plant for the production of such powders. This claim, Masaliev said, was simply wishful thinking.

To bolster such claims, Masaliev continued, the Kirgiz academicians have spent considerable sums on organizing symposia and conferences, and have bolstered their prestige with lavishly furnished offices. Yet the scientific standard of the Kirgiz academy is so low, he said, that not a single institute or team has been included in the new "inter-branch" scientific–technical complexes now being established union-wide, as part of the "scientific–technological revolution".

This is not the first republic academy to be attacked for slackness in the run-up to the All-Union Party Congress later this month. A few weeks ago, the Uzbek academy was accused of nepotism and general slackness, attributed to the prolonged illness of its president, who has since been replaced.

But the charge of falsifying research claims is far more serious. It is standard Soviet practice to embark on a major shake-up or purge by selecting a few smaller bodies as examples, thus giving more important institutions a chance to put their affairs in order without public censure. Indications are that the programme of reforms launched by Mr Gorbachev is taking a close look at research as well as the administrative sector.

Vera Rich

Pharmaceuticals in Britain

Drug list clouds foreign interest

Despite the recently announced decision by the Swedish pharmaceutical company Astra to develop a £2.5 million research facility in London, the climate for investment in the United Kingdom by non-British pharmaceutical companies remains poor. The chilly conditions are caused by the industry's lingering irritation over the "limited list", a scheme introduced by the British government over a year ago that determines which drugs the National Health Service (NHS) will pay for.

Pharmaceutical companies are still smarting from what they feel was an arbitrary decision to implement the limited list that effectively blacklisted certain drugs, and cut deep into profits.

Astra's plan to support the Neuroscience Research Centre at the Institute of Neurology, a part of the University of London, is a positive sign, but it is probably not the harbinger of a flood of new investments.

Before the introduction of the limited list, investment by industry in UK facilities was enjoying a fairly rosy period. The US company Merck Sharp and Dohme had established a £25 million Neuroscience Research Centre in Terling Park near Cambridge, the Swiss giant Sandoz had put up £7 million for a research unit with a staff of 50 at University College London and Parke Davis, the pharmaceutical division of US giant Warner Lambert, was building a £4 million facility on campus at the University of Cambridge.

Another US company, Wyeth, had "pens poised" to sign agreements for a £30 million research unit in Swindon, while its rival A.H. Robbins had just completed a new production facility at Langherst in West Sussex that was to be expanded to include a research facility.

But when the limited list was announced, the cries of anguish from the drug companies could be heard around the world.

Wyeth cancelled its plans for Swindon, Robbins sold off its Langherst plant, and Parke Davis made it abundantly clear that it would never have gone into the United Kingdom if it had known about the government's plans.

G.D. Searle also insisted that the closure of its High Wycombe facility was prompted by government pricing schemes, although corporate reorganization following the Monsanto takeover of Searle probably also played a major role (see *Nature* **319**, 251; 1986).

British-owned companies, by contrast, have come through the limited list ordeal nearly unscathed. On the eve of the public sale of 25 per cent of Wellcome plc, the company reported its most successful year ever, although its rate of profit on British sales was considerably less than those in other parts of the world. Glaxo, too, has done well, and was able to step in to buy Robbins' Langherst production plant. According to Glaxo research director Alan Williamson, "the climate for research and development efforts in this country is still very good".

Glaxo's impression is hardly shared by foreign pharmaceutical companies. E.J. Fullager, UK chief executive of Sandoz, says the climate is still one of "uncertainty, writ large". Unless things deteriorate substantially, Fullager says, Sandoz will continue to support its institute at University College, but he admits that Sandoz has been "disappointed" by recent government actions.

The government is aware of the disaffection it has engendered by the limited list. Health Department officials now say they are negotiating with the Association of British Pharmaceutical Industry (ABPI) on revisions to pricing schemes, "so that the industry might be offered a period of greater stability in its sales to the NHS".

But a spokesman for ABPI says "it will take a long time for the industry to forget what happened".

Joseph Palca

West German forests

Deterioration, but some recovery

Munich

The 1985 Forest Damage Inventory, the results of which were published at the end of last year, shows only a slight deterioration of West Germany's forests since the previous year. It is now estimated that 52 per cent of the total forested area is affected by the "new type forest decline", compared with 50 per cent in 1984 and 34 per cent in 1983. Damage increased at higher altitudes and notably in the Alps, but there were also the first signs of recovery in some lowland areas.

The latest inventory of forest damage is the fourth of a series of annual nationwide damage assessments initiated by the federal government but carried out by the regional governments, the *Länder*. Only the 1984 and 1985 inventories are based on a comparable assessment and classification method. Assessment areas are defined by the nodes of a 4 × 4 km plot, where a specified number of trees is classified into five damage categories ranging from category 0 (undamaged) to 4 (dead). Damage classification is based on the extent of loss of needles or leaves, with the discoloration of foliage as a second criterion.

The much disputed damage category 1 (loss of needles and leaves between 11 and 25 per cent, compared with a reference tree) is for the first time being referred to as a warning stage rather than a clear damage stage. Concentrating on the subsequent damage categories 2 to 4, the overall change between 1984 and 1985 has been a slight increase from 17 per cent to 19 per cent of the total forest area.

Broad-leaved trees such as beech and oak are now showing the same degree of damage as conifers, which were first affected by the disease. In particular oak has deteriorated markedly, with 16 per cent of oak forests being classified as medium to severely damaged.

As in previous years, there is still a distinct north–south gradient, with the southern *Länder* of Bavaria and Baden–Württemberg most severely affected. There is now also much concern for the alpine forests, where damage increased from 34 per cent in 1984 to 53 per cent in 1985 (damage categories 2–4 only). The West German concern for highland forests is shared in Switzerland. The Swiss 1985 "Sanasilva" forest damage inventory revealed marked damage at higher altitudes compared with lowland forests, for forests at an altitude of 900 m or more. 11 per cent of all trees assessed were medium to severely damaged (the Swiss damage classification is comparable to the West German). This is seen as a major threat to villages and roads, which are often protected by forests against avalanches and floods.

In contrast with the deterioration of highland forests, there is a slight recovery of some lowland forests in Germany. There is also a slight overall recovery of pine, with a decrease in the medium to severe damage from 21 per cent to 17 per cent. This local recovery, and the relatively small increase in the overall damage when comparing the 1985 results with those of the previous inventories, is largely attributed to favourable climatic conditions.

The causes of the decline are still open to debate. Regional differences in the symptomatology and the time-course of the disease have led to the suggestion that the forest decline may not be a single disease, but a series of different disease types.

These disease types may have different causes, but there is probably a common synchronizing factor triggering their onset. As regions of different pollutant levels are equally affected, it seems plausible that this synchronizing factor is an overall climatic event such as drought or frost

Lutz W. Blank

Eureka

Secretariat in search of base

PROJECT Eureka continues to make progress towards its goal of promoting European cooperation in high technolgy projects, but like most multinational cooperative ventures, some steps are disappointingly slow.

On the positive side, the Eureka High Representatives at their meeting in London late last month announced that new collaborative efforts are making "significant progress". Sixteen projects have achieved full-fledged Eureka status, with 25 more close on their heels.

But the last ministerial conference on Eureka held in Hannover set 31 January 1986 as the deadline for establishing the location and structure of the Eureka secretariat, and that deadline has passed with no decisions on location, although the group did agree on the basic structure and scope of the secretariat.

The site for the secretariat is significant for several reasons. While Brussels is favoured by a majority, some countries are concerned that Eureka should not become a satellite of the European Economic Community, especially since six of the 18 nations participating in Eureka do not belong to the Community. But a more sticky objection to Brussels has been raised by the French. France has been the moving force behind Eureka since its inception, and Strasbourg is the French choice for the headquarters.

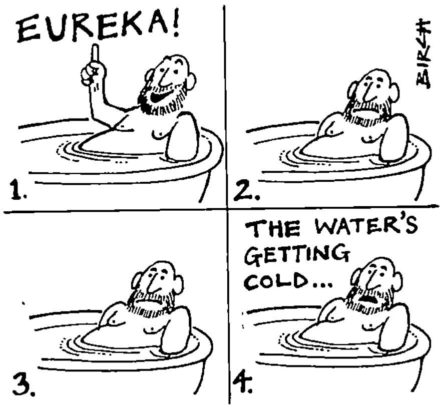

Brian Oakley, current chairman of the Eureka High Representatives, calls the delay in selecting a site "very annoying", but he believes that the situation may be resolved next March. By then the French elections will have passed, and it will politically acceptable for France to drop its insistence on Strasbourg.

The powers of the new secretariat are also important, as the smaller members are concerned to maintain some political muscle against the big four (France, Britain, West Germany and Italy). The new secretariat will consist of 12 people, half of them professional staff. Its principal function will be information dissemination and coordination of activities. One key decision of the recent meeting of Eureka High Representatives was to set approval of plans for the secretariat at the administrative level, rather than by formal treaty.

A provisional mechanism for approving projects for inclusion in the Eureka scheme is also now in place. Once two companies agree on a cooperative venture, there will be a 45-day period during which other countries may suggest their own companies as partners to the proposed project, although there is no guarantee that partnership status will in the end be granted.

Oakley sees opening up the market as a key role of Eureka. He is anxious to expand the international awareness of member companies, in part through management seminars bringing together corporate executives, financial experts and civil servants familiar with global issues.

Another important role for Eureka will be to encourage European standardization, perhaps along the lines of the British concept of "Eurotype", so as to smooth the path to market of Eureka projects.

According to Oakley, Eureka now enjoys full support from the British government. Whether it will ultimately succeed will depend not on the show of support it receives, but rather on the successful products it brings to the marketplace.

Joseph Palca

European neutrons

British aiming to share costs

THE British hope to gain substantially from attempts now being made to internationalize European neutron and synchrotron radiation sources. Hopes turn on a meeting arranged by the British Science and Engineering Research Council (SERC) for next Tuesday (18 February) at which representatives of France and Italy will discuss proposals for a substantial extension of the Spallation Neutron Source, commissioned a year ago at the Rutherford Appleton Laboratory in Oxfordshire.

The proposed extension of the Spallation Neutron Source, which goes under the new name of ISIS, would cost £60 million over ten years, of which a half would be met by SERC and the remainder by the other participants. But overseas participation in the project is a trade-off against British collaboration in the European Synchrotron Radiation Facility (ESRF) to be built at Grenoble in France, and to which the SERC contribution will be more than 15 per cent of the total construction cost of £150 million, at £24 million.

According to officials of potential partners, SERC has indicated unofficially but firmly that British participation in ESRF will be forthcoming only if the cost of the proposed ISIS project is shared with European partners. Indeed, SERC is looking not merely for a 50 per cent contribution to the cost of the extension, but for an "entry fee" of roughly a half of the cost of building the neutron source as it stands, which might amount to a total of £50 million. If these hopes materialize, SERC will be laying out £26 million less than it receives by way of contributions to ISIS.

Apart from France and Italy, other possible participants in the ISIS project include Denmark, Sweden, the Netherlands and Spain, some of whom may be represented as observers at next week's meeting. West Germany will also be in attendance, but only as an observer; the West German plan to build a superior spallation neutron source, the SNQ, was cancelled only last year.

More recently, the intriguing prospect has arisen of Australian collaboration in the British neutron projects, although the potential European partners have not yet been told of this possibility. Australia is aparently short of neutrons, and the proposed deal with SERC would give Australia free access to ISIS as a *quid pro quo* for a reduction of British spending on the Anglo-Australian Telescope, recently recommended by a SERC review committee.

Enthusiasm for an improvement of the existing spallation neutron source stems from the good performance of the machine during its first year of operation and from the circumstance that it is a rapidly pulsed machine, producing neutron beams with very high intensity. French physicists, less keen on more neutrons than the Australians, say that the existing machine offers experimentalists few advantages over the reactor-based neutron source now working at the Institut Laue–Langevin at Grenoble, but that the proposed extension could be more interesting.

The status of next week's meeting is not yet crystal clear. The goal, at that and at a nominally separate but parallel series of meetings on ESRF, is to reach intergovernmental agreements on the two projects by the middle of next year, if all goes well. But French sources say that the French interest in next week's meeting and the subsequent negotiations is to discover "what part of ISIS can be Europeanized", which would seem to offer the British less than they are looking for.

Robert Walgate

British science

Sir Keith Joseph regrets . . .

It would have been "preferable" if the great cutback of British universities since 1981 could have "gone more gently", according to Sir Keith Joseph, Secretary of State for Education and Science for the past five years. Sir Keith, just now, is in a reflective mood. Ten days ago, he announced that he would not run for re-election to the House of Commons, where he has represented a Yorkshire constituency since 1956. But in an interview last week, he denied newspaper reports that he would leave his present post before the next general election, which must be held sometime in the next 27 months, saying that that is "entirely up to her", a reference to the Prime Minister, Mrs Margaret Thatcher.

Joseph is also unrepentant. Five years ago, he said, the British academic establishment was in need of "jolts". "We inherited massive overspending on research", while the universities were "snobbishly" disdainful of "trade". The result of the 8.5 per cent reduction of university budgets, Sir Keith insisted, was that some universities are now much better than they had been. He claimed some credit for having persuaded Sir Edward Parkes, chairman of the University Grants Committee when the budget reductions were enforced, to admit as much in public.

But have not other universities been damaged? Sir Keith acknowledges that academic morale may be at a low ebb, but insists that it is not yet appreciated in Britain that there is "no god-given right" to suppose that even the present level of prosperity in Britain can be sustained. The government is, however, worried about the loss of bright young scientist from Britain, and awaits with interest and anxiety the Royal Society report on the subject due in the early summer.

Sir Keith lists the causes of the emigration now under way as the invidious comparison between Britain and other countries in respect of salaries, equipment and the chance that good research proposals will be supported by the grant-making agencies, and says he thinks the last may be the most important. He did not last week include in his list the greater intellectual stimulation now to be found at universities outside Britain.

Sir Keith is known to be the chief monetarist influence on the present British government. Indeed, he is proud of having given 150 talks at universities in the two years before the 1979 election on "the moral case for capitalism", running into rowdy trouble on only six occasions. "D'you know", he says, "I went into politics because I wanted to get rid of poverty?".

Now, with the economic "chickens coming home to roost" in Britain, "what we need are flocks and flocks of entrepreneurs". Sir Keith asks for agreement to that proposition (which is given) and to the proposition that the universities cannot produce them (which is withheld). There follows a scrappy conversation about the changing climate in British universities, and the reasons for the economic success of the United States and Japan. Sir Keith seems to be advancing two contradictory propositions, that universities cannot, because of their constitution, be a prolific source of enterprise, but that, until they are, they will not be dealt with kindly.

On one specific point, the argument of the Committee of Vice-chancellors and Principals that the demand for student places seems more buoyant than the government's demographic projections, and will be further increased if Sir Keith's own plans for improvement in the schools succeed (see *Nature* **319**, 348; 1986), the minister appears more willing to contemplate a re-expansion of British universities than previous statements would suggest. But he does not think that his plans for better schools will yield increased demand for higher education at least until the 1990s, which is probably a prudent calculation given the continuing conflict between the government and the teachers' labour unions.

On another point, Sir Keith admits failure. He points out that he has been publicly at odds with his colleagues in the government about the introduction of a scheme for suporting students at universities by means of loans. Such schemes work well elsewhere, he says; he still regrets the "honourable paternalism" and the fear that students from less prosperous backgrounds would be discouraged from seeking higher education, which appear to have been the chief reasons why the government backed away from student loans. Meanwhile, nothing seems to be happening to meet the vice-chancellors' complaint about the impoverishment of students and their families.

That complaint is one of the many critical responses to the government's discussion paper on higher education, published a year ago. Sir Keith appears to be a little chastened by the reaction to the document. "If I got the tone wrong, that's my fault." But he resents having been called a "barbarian" on account of it.

So is there any way in which the universities in Britain might work their way back into the government's good books? The minister offers three tests — the abandonment of homogeneous salary scales for academics (which he says he has already brought up with university representatives), the abolition of tenure (and "you know what we are doing about that") and the pursuit of rigour in the universities (to which end the universities' current examination of academic standards will contribute).

Much of what applies to the universities applies to Sir Keith's views of publicly supported research in Britain. Again, it would have been preferable that the "financial adjustments" required of the research councils had been spread over, say, a five-year period. Again, it would help if there were better links, both ways, with the outside world and with industry in particular. There is a case for a science minister, but not an overwhelming (or, one gathers, a persuasive) case. There is no reason to think, he says, that matters such as the British membership of the European high-energy physics community (CERN), or the question of the privatization of the Plant Breeding Institute, would have been settled any more quickly if there had been a minister responsible for getting things done.

In private, it is known that Sir Keith Joseph has in recent years been fighting hard to preserve the publicly supported research base in Britain. Aloud, he remarks on the anomaly that, when his postbag was full of letters from parents protesting at his scheme for raiding the budget for student support in the interests of research (at the end of 1984), he found only one letter of thanks from a scientist Looking back on his time in his present office, he says with pride that he is glad to have identified a number of problems of national importance (to the British); plainly, he also regrets not having done more to solve them.

So what can the research community in Britain do to win back the support of the government? No doubt a strong show of entrepreneurship would go a long way to meet Sir Kieth's demands. But he himself offers an unexptected suggestion: why not win friends in the House of Commons? Perhaps he is feeling more lonely there now than when the government to which he belongs came to office six years ago

John Maddox

Ban on South Africans

Sir—Your first leading article on the question of the South African ban (*Nature* **318**, 195; 1985) castigates the executive committee of the World Archaeological Congress for bowing precipitately to pressure from non-academic bodies. Your second (**319**, 85; 1986) fails to mention that a meeting of the full national committee, which includes most of the scholars organizing the individual academic sessions of the congress, convened on 20 November, supported the ban by a considerable majority and reiterated that this was done on grounds of principle rather than pragmatism.

It is, however, clear from the tone and content of both articles that the committee's affirmation of the ban would have had little effect on your general arguments, which could be summarized as stating that while there may be — grudgingly — a case to be made for economic or sports sanctions, there is no case for academic sanctions. The notion that "academic freedom" is an unproblematic concept, that academics have different and more elevated concerns than other people, that academic debates can be, indeed should be, divorced from historical, human and political reality requires vigorous refutation.

This archaeological congress has from the outset laid particular emphasis on being a *world* congress. Contributions from countries outside the industrialized West were particularly solicited, funds were found to make it possible for people to come to England, and themes were selected that did not simply reflect the preoccupations of "the North". The South African ban must be seen as part of this vision of what an international congress should be, and it must be recognized that failure to implement the ban would lead to the withdrawal of many participants, both from other parts of Africa and from countries expressing solidarity.

Participants at the world congress register as individuals, but their national affiliation is published. The question of admission of South Africa to an international forum cannot therefore be avoided. It might be argued that exclusion isolates and devalues the work of individual academics who have fought against apartheid from within the system. But the ban is not about individuals, it is not, indeed, about academics, it is about bringing pressure to bear on the South African government by boycotting interchanges of any sort, and this policy has the complete support of those organizations within South Africa that speak for the majority of that country's people.

It might be argued that banning South Africa is hypocritical — if South Africa, why not all the other countries that practise violent repression or genocide of "undesirable" ethnic groups? There are two reasons. First, that, unlike the other regimes, in South Africa ethnic stratification is institutionalized as the basis for formal exclusion of the majority from political rights. Second, perhaps more important, there are "historical moments" when particularly repressive action by a regime and reaction by the oppressed reach a point where positive "indignation" expressed in *every* form available to the outside world may have some effect. The state of emergency declared by the South African regime is one such moment.

One of the aims of academic research in the social sciences is to expose the realities of human social life, and to analyse the bases and causalities of what we observe, but if we restrict our discussion to academic forums, if we deem ourselves above politics, we draw the teeth of "academic freedom" and make it into something esoteric and safe. Academics cannot insulate themselves from politics. We have been asked by those within South Africa who risk their lives in opposing the regime to help them by imposing a ban. If we do so, we may also bring pressure to bear on Western governments by convincing them of the strength of their own public opinion. If, in the name of academic freedom we do nothing, we are, whether we like it or not, making a political statement — a negative one.

Your editorial called for plain speaking, and persuasion in the interests of tolerance. We all agree on the need for plain speaking. What some of us are left wondering is what it is you are asking us to tolerate.

B. Bender
J. Gledhill
M. Larsen
M. Rowlands
C. Tilley

Department of Anthropology,
University College London,
Gower Street, London WC1E 6BT, UK

Star colours

Sir—A recent paper[1] suggests that some Babylonian, Graeco-Roman and early-medieval authors considered Sirius to be red in colour. Today it shines white. I wish to argue here that, according to ancient Chinese evidence, (i) Sirius had been white all along but (ii) Betelgeuse has changed colour from yellow to red.

Volume 27, *Chronicles of Celestial Officials*, in *Historical Records* edited by Sima Qian of the Han dynasty, in the first century BC, contains the following passage: "The white is like Sirius, the red like Antares, the yellow like Betelgeuse, the blue like Bellatrix, and the dim like Mirach".

To my knowledge the above assessment was not challenged in any of the twenty-three dynastic histories compiled since, which all include chapters based on materials supplied by astronomers royal.

It is possible that the purported attribution of a red colour to Sirius in Babylonian cuneiform texts is a case of mistaken identity[2]. Assertions to the same effect in classical works may be secondary citations by non-expert authors.

In contrast to Sirius, Betelgeuse (α Orionis) does appear to have altered its colour in the light of ancient Chinese sources. It is now red, with $B-V=1.9$, comparable to the index for Antares (1.8) which the Chinese did regard as red. Being massive, however, Betelgeuse could well have cooled from yellow to red within 2,000 years, during the end of its evolution away from the main sequence into a red supergiant. For Sirius to leave the red giant and reach a white dwarf stage in a similar span of time would be an anomaly, if we accept the current models of stellar evolution[1].

Tong B. Tang

Department of Physics,
Hong Kong Baptist College,
Kowloon Tong, Hong Kong

1. Schlosser, W. & Bergmann, W. *Nature* 318, 45–46 (1985).
2. Brecher, K. & Feirtag, M. (eds.) *Astronomy of the Ancients*, 91–115 (MIT Press, Cambridge, 1979).

Radiation threshold

Sir—John Simpson's review of four books on British nuclear testing in Australia (*Nature* **318**, 319; 1985) claims that the "official view" about the relationship between radiation exposure and ill health and premature death is "that threshold values can be established to distinguish between those who are 'safe' and those 'at risk'". This is incorrect. The concept of a threshold was in common use during the 1920s and 1930s. For at least the past 35 years, however, radiological protection has been based on the assumption that there is no threshold below which it can be assumed that radiation has no harmful effects. When the International Commission on Radiological Protection was reformed after the war, it made recommendations of maximum permissible exposures at a level that involved a risk small compared with other hazards of life. Subsequent developments of radiological protection philosophy and practice have all been based on the linear no-threshold hypothesis, and it seems increasingly likely that, at least for some important types of radiation, this hypothesis results in an overestimation of the risks[1].

P. A. H. Saunders

Harwell Laboratory,
Oxfordshire OX11 0RA, UK

1. Report of the National Research Council Committee on the Biological Effects of Ionising Radiation (BEIR), National Academy Press, Washington, DC, 1980.

More tests of special relativity

Yet another experiment has provided a novel test of special relativity, one that duplicates in the laboratory phenomena for which people usually look to astrophysics.

GIVEN the zeal with which those who disbelieve the special theory of relativity go about their business, it is a comfort that experimental tests of relativity are also flourishing. One of the latest, an experiment carried out at Los Alamos by D.W. MacArthur *et al.*, has the special virtue of providing a test, successful as it happens, of the relativistic Doppler effect at velocities as great as 0.84 of that of light (see *Phys. Rev. Lett.* **56**, 282; 1986). Moreover, this laboratory experiment has all the promise of being generically novel.

The principle of the experiment is straightforward enough, as most convincing designs must be. The essential phenomenon is the excitation of quickly moving neutral hydrogen atoms by an ultraviolet laser. The atoms of the hydrogen beam have essentially a constant velocity, as does the laser. But by varying the angle at which the laser beam intercepts the moving hydrogen atoms, the interaction energy — as seen from a frame of reference in which the atoms are at rest — can be varied over a wide range.

The experiment has been made possible by the meson factory at Los Alamos, formally known as the Clinton P. Anderson Meson Physics Facility (LAMPF) and, as such, an enduring memorial of the time when members of the US Congress were among the strongest supporters of the nuclear industry in the United States. Among other things, the machine can produce a beam of negative hydrogen ions with an energy of 800 MeV, corresponding to 0.84 of the velocity of light.

Magnet

The beam is processed in three successive steps. First, a proportion of the negative hydrogen ions is converted into neutral atoms by means of an infrared laser at a frequency corresponding to that needed to shake loose one of the two electrons. The second and crucial step is the interaction with the beam of a pulsed ultraviolet laser, an yttrium aluminium garnet device doped with neodymium and yielding photons with an energy of 4.66 eV. The effect of the interaction is, naturally, to excite some of the neutral hydrogen atoms or even to ionize them completely. The final step is the separation of the three species of hydrogen atoms, the neutrals and the negatively and positively ionized atoms, by a magnet. The trick is to use a magnet whose field is strong enough to convert into protons any neutral hydrogens that have been excited above the second excited state (with principal quantum number three). Both the neutral hydrogens and the protons are counted by means of scintillators.

The cumbersome part of the equipment is the turntable that allows the laser beam to intercept the atomic beam at various angles. (There is a system of mirrors to ensure that the laser itself does not move.) The result is that the energy of the ultraviolet photons appears, from the rest-frame of the hydrogen beam, to vary by an order of magnitude between 1.4 eV and 15.8 eV. For practical purposes, the arrangement is one for allowing the measurement of the energy of the successive excitations of neutral hydrogen atoms. The authors of the experiment show convincingly that the excitation curves that they obtain (essentially the production of protons in the detection system as a function of the angle of their turntable) are indistinguishable from a gaussian curve (which is what would be expected). They have been able to record resonances corresponding to excitations from the ground state to between the fourth and the eleventh quantum level inclusive. The interpretation of the data hangs on the accuracy with which the position of the turntable can be measured, with a precision of 30 microradians, it is claimed.

Reconciling these results with what special relativity predicts requires a little subtlety. The familar Lorentz transformation between one coordinate frame and another has the time T in one frame of reference related to that, t, in the other by means of a linear relationship of the form $T = at + bx$, where x is a spatial coordinate and the factors a and b are coefficients depending on the relative velocity of the two frames, v. In practice, the prediction of special relativity is that the quantity a is the time-dilation factor given by the square root of $1/ (1 - v^2/c^2)$. MacArthur and his colleagues allow the possibility that this relationship may not be exact, that the coefficient a may be a function of velocity other than the time-dilation factor, and set out to determine from their resonance measurements just what it may be. Because of the way in which the measurements are carried out, by the interaction of atoms and photons at positions that are well-defined in both frames, the experiment cannot provide information bearing on the second coefficient, b.

Unsurprisingly, the outcome of the experiment is that the time-dilation factor is sufficient to account for the variation of the energy of the ultraviolet photons as seen from the frame in which the hydrogen atoms are at rest. That energy is the energy of the photons in the rest-frame of the laser multiplied by the time-dilation factor and by the factor that represents the influence of the strictly classical Doppler effect. This, by involving the cosine of the angle between the two beams, allows for the way in which the experiment spans a whole order of magnitude in the excitation energy of the neutral hydrogen atoms. The precision of the result is given as 27 parts in 100,000. With what would obviously be a great deal of hard work, the authors believe they could improve the precision of the experiment by a factor of as much as 1,000.

Velocity

The arresting feature of the experiment now described is not, however, its precision but the large fraction of the velocity of light at which the two frames are moving relatively to each other. It is true, of course, that most people are sufficiently persuaded of the accuracy of what has now been demonstrated about the accuracy of the time dilation factor of special relativity by the increase of the lifetime of quickly moving particles, as in cosmic rays, while the behaviour of charged particles in accelerating machines is another line of related evidence. Another novel feature of the Los Alamos experiment is that it provides a demonstration of how a laser beam, with a frequency defined in one frame of reference, can be translated into a tunable but defined frequency in another. That should be suggestive of all kinds of other measurements.

In the long run, efforts in that direction may be less rewarding than would be a successful experiment to verify that the other factors in the Lorentz transformation of coordinates behave as predicted. The obvious difficulty is that of constructing experiments in which events seen as if from two relatively moving frames are separated from each other in time and/or distance. The obvious measurements to make are those of the signals from Earth satellites and spacecraft. Much has been done already, but further efforts are needed, and not merely to keep the army of sceptics of the special theory at bay.

John Maddox

Biochemistry

Polyribonucleic acids as enzymes

from F.H. Westheimer

In the January 31 issue of *Science*, A.J. Zaug and Thomas Cech[1] published a paper entitled *The Intervening Sequence of* Tetrahymena *is an Enzyme*. This publication seems destined to take its place among the classics in biochemistry.

Sixty years ago, James Sumner crystallized urease[2] and, over the vigorous objections of Richard Willstaetter, set about proving that his crystalline protein was in fact the enzyme responsible for the hydrolysis of urea. In subsequent years, many enzymes have been purified, and the scientific community accepted — or more precisely had accepted — that all enzymes are proteins, where enzymes are defined as biological catalysts that accelerate metabolic processes by factors of 10^6–10^{12}. In keeping with the knowledge available Lubert Stryer[3], in his excellent text *Biochemistry*, states flatly that the biological catalysts "are specific proteins called enzymes". Now Cech and his co-workers at Colorado (and in complementary work, Sidney Altman and his co-workers at Yale) have established that polyribonucleotides can function as enzymes. The discovery is revolutionary in its direct impact on the theory of catalysis, in its promise for future discovery and in its implications with respect to the pathway of prebiotic chemistry. Additionally, it carries with it a series of challenges for understanding the chemistry of phosphates.

Discovery

First, a few words about the discovery itself. An RNA from the protozoon *Tetrahymena thermopila* contains, in addition to the RNA of the ribosomes, an intervening sequence (IVS) of 413 nucleotides: the mature ribosomal RNA is formed from this precursor by the precise removal of the intervening sequence at its junctions with the ribosomal sequence, and the splicing of the two ends (see Fig. 1). In 1981, Cech and his co-workers showed, astonishingly, that the excision of the intervening sequence does not require an enzyme — at least not in the conventional sense — but was initiated by the addition of micromolar quantities of GTP, or (as was later discovered) by almost any derivative of guanosine, including guanosine itself. The nucleoside initiates a series of moderately rapid reactions that lead to the excision of the intervening sequence without the need for a protein catalyst[5-7].

The guanosine (or guanosine derivative) attacks the RNA at the 5′ end of the intervening sequence of 413 nucleotides; the reaction is one of ester exchange, where the 3′ hydroxyl group of the guanosine attacks the phosphodiester bond between the 3′ end of the first exon and the first nucleotide of the intron. In the resulting product, the guanosine residue is attached to the 5′ end of the intron. Subsequently the 3′ end of the 'liberated' exon spontaneously attacks the far end of the 413-base intron to splice the two ends of the exon together (Fig. 1). Cech comments that these transesterification reactions are thermodynamically neutral, and so require no GTP or ATP to drive them forward. True, the transesterifications are essentially neutral with respect to the enthalpy of reaction, but to the extent that they go forward nearly to completion rather than coming to balanced equilibria, there must be a driving force for the overall process. In some instances, for example where a small molecule is ejected, the reactions are entropy driven; in others, the driving force must be related, at least in part, to changes in stability between reactants and products that arise from changes in the tertiary structures of the RNAs themselves.

After the intron has been extruded and the exons spliced together, the free intron undergoes a cascade of spontaneous reactions (Fig. 2). First, the 3′ end of the polyribonucleotide attacks, nearly specifically, the phosphate between the 15th and 16th nucleotides (from the 5′ end) and forms a circular polynucleotide; the process results in ejecting 15 nucleotides from the 5′ end of the intron. If the resulting circular polynucleotide is then exposed to higher *p*H (9.0 instead of 7.5), the ring is opened at precisely the same bond where it had been formed; then the active 3′ end bites again, now four nucleotides from the 5′ end, to eject a tetramer and yield a new circular polynucleotide. This ring in turn is opened by the mildly alkaline solution at precisely the bond where it closed to yield a polyribonucleotide that is 395 units long. Here the cascade of reactions stops; but it is this truncated linear intervening sequence (L-IVS-19) that has enzymic properties that are the subjects of Zaug's and Cech's paper in *Science*.

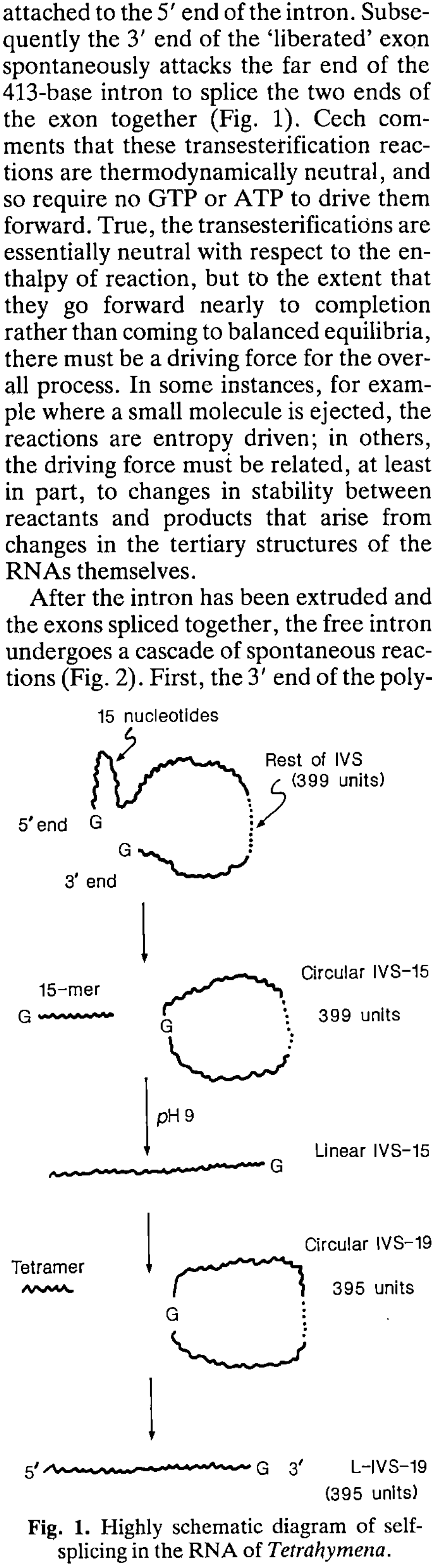

Fig. 1. Highly schematic diagram of self-splicing in the RNA of *Tetrahymena*.

Specificity

The spontaneous reactions producing the intervening sequence are remarkable enough. They are fast and quite specific, and carry strong implications of specific tertiary structures and specific binding sites in RNA. One is tempted to say that one part of the molecule is catalysing a reaction at another site within itself. But technically the reactions are not catalysis; by definition, a catalyst accelerates a reaction without undergoing change itself, or else is regenerated unchanged at the end of the process.

Many organic molecules undergo rapid internal reaction that is not catalysis. A spectacular example[8] concerns the cyclization of 2-hydroxy-phenylpropionic acids to dihydrocoumarins. A pentamethyl derivative of the acid undergoes acid-catalysed closure some 10^{10} times as fast as the unsubstituted compound does; the lactonization occurs at a rate that could be acheived by phenylpropionic acid in phenol at a hypothetical concentration of 10^{15} M. Presumably the methyl groups cause strain that is relieved on lactone formation. No one is about to call these phenolic acids enzymes, even though their rapid reactions are noteworthy. The internal reactions that Cech discovered are, of course, much more remarkable, largely because of their extraordinary specificity, and because of the distance between the reacting groups. The aromatic acids cited above have only one place to react; although the RNAs have thousands, they react at precise loci. Nevertheless a purist can maintain that, although the molecules are activated for internal reactions, they are not true catalysts. That argument — or quibble, if you prefer — does not apply to the piece of intervening sequence, L-IVS-19, that results at the end of Cech's cascade. It is a true enzyme.

In the presence of the truncated intervening sequence, various oligoribonucleo-

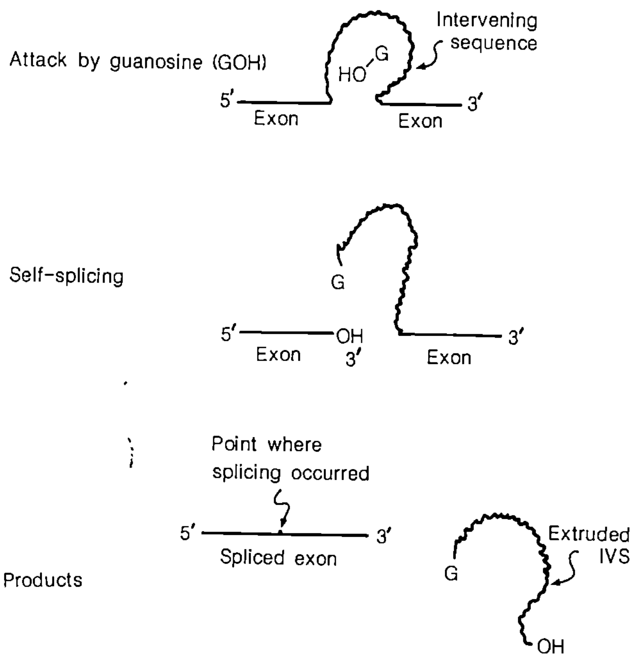

Fig. 2. The cascade of spontaneous reactions of the IVS.

tides undergo hydrolysis at rates of about 2 per minute. That is not extraordinarily rapid, but it is fast compared with the spontaneous rate of hydrolysis of RNA, and corresponds roughly to the rate of hydrolysis of DNA as catalysed by restriction enzymes, or to the rate of reaction catalysed by staphylococcal nuclease, or by a nonspecific phosphodiesterase[9–11]. Of course, RNA is generally much more liable to hydrolysis, both with alkali and with enzymes, than is DNA; pancreatic ribonuclease has a turnover number of thousands per second. But both pancreatic ribonuclease and alkali are able to use the adjacent 2′ hydroxyl group of a ribose residue to cleave the phosphate ester bond of the RNA. It is this internal attack by an adjacent residue that accounts for the rapidity of the reaction; and it is of course the absence of the 2′ hydroxyl group that makes DNA more stable to hydrolysis. The reason that Cech's IVS hydrolyses RNA relatively slowly is apparently that it fails to exploit the 2′ hydroxyl group: this is inferred from the fact that Cech's IVS yields a free 3′ hydroxyl group and leaves a phosphate at the 5′ position, whereas pancreatic ribonuclease leaves the phosphate at the 3′ position and yields a 5′ hydroxyl group as the almost inevitable consequence of the internal reaction with the 2′ hydroxyl group. This poses an interesting problem for the mechanism of catalysis.

In a series of studies with pentacytidylic acid (C_5), Zaug and Cech have now shown[1] that the truncated intervening sequence acts on this oligonucleotide to yield a mixture of polycyctidylic acids, including C_3 and C_4, together with longer molecules up to C_{30}. Here again, the transesterification reactions are probably essentially thermoneutral; here the reactions are presumably entropy driven, yielding a complex mixture from a single starting material. There can be no doubt that the IVS is acting as a true catalyst, and must be considered an enzyme.

The result is startling, but even now is not unique. First and foremost, in entirely independent but complementary research, Sidney Altman and his collaborators have also demonstrated the catalytic (the enzymic) action of particular polyribonucleic acids. They had, for many years, studied ribonuclease-P[14], an enzyme that cleaves ribonucleotides of *Escherichia coli* to create transfer RNAs, and in particular to cleave a precursor to fashion the correct 5′ terminal ends for these molecules. Ribonuclease-P, like Cech's IVS, cleaves ribonucleic acids the 'wrong' way, that is, it cleaves a 3′-5′-phosphodiester bond to leave the phosphate residue on the 5′- rather than on the 3′-position. Altman and his co-workers showed that ribonuclease-P contains ribonucleic acid as well as protein, and then discovered that the enzymic activity, although it is promoted by protein, resides in the nucleic acid component[15]. This discovery was sandwiched between Cech's finding of self-splicing in *Tetrahymena* RNA and that of the catalytic properties of the IVS.

Ribosomes

Subsequent to these two seminal discoveries — that of Cech and that of Altman — several other investigators[16,17] have found more self-splicing RNAs, following the model that Cech introduced. And other enzymes[18,19] contain both ribonucleic acid and protein, although it is not yet known whether the nucleic acid portion has catalytic properties. Furthermore, these new discoveries once again focus attention on ribosomes, where the complicated interrelationship of protein and ribonucleic acid must still be untangled[20,21]. Just when chemists were beginning to think that they could account, at least in part, for the catalytic properties of enzymes — protein enzymes, that is — in terms of structure and mechanistic principles, we are faced with new, unexpected and exciting problems. What are the tertiary structures of the active ribonucleic acids? Presumably their tertiary structures (and those of their substrates) are vitally important; without tertiary structure, the specificity of the catalytic polyribonucleotides would be hard to understand. What are the active sites of these new enzymes? What principles explain their activity? Can Cech's IVS, or Altman's catalyst, be crystallized? The IVS has about 400 residues. In a sense, this is comparable in complexity to a protein enzyme. Characteristically, proteins have 300–400 residues, and if the molecular mass of each residue is only about a third as large as that of nucleotides, the inherent diversity of the amino acids is much greater.

The new discoveries bring with them speculations about prebiotic chemistry. Bass and Cech[23] have wondered whether the ribozymes may not have preceded protein enzymes. As ribonucleotides apparently possess both the properties of self-replication and those of catalysis, could these molecules have allowed a primitive living system to function without either DNA or protein? The observation that ribonuclease-P and other enzymes contain both nucleic acids and protein suggests a pathway for prebiotic evolution. Polyribonucleic acids could have accumulated amino acids and short peptides by hydrogen-bonding them, provided that these protoproteins helped the polyribonucleic acids with respect to stability or catalysis, or both. Over time, the protein component of such mixed enzymes could have gained in complexity, and eventually the greater versatility of the amino-acid residues, compared with those of the nucleic acids, could have allowed the protein component to take over; in this scenario, in most instances the enzymes then sloughed off the nucleic acid part. Could enzymes such as ribonuclease-P be biochemical fossils, that help to illuminate for us the pathway of biochemical evolution?

But putting such speculation aside, the chemisty pioneered by Cech and Altman and their co-workers is already leading to much new biochemistry. On the one hand, several investigators are finding cascades of reactions similar to that that Cech discovered with *Tetrahymena*. On the other, the mechanistic problems in the cleavage of phosphodiester bonds and especially those problems that arise because of the cleavage of the 3′,5′-diester bond to leave the phosphate residue on the 5′ position, stand as challenges to mechanistic biochemists. □

F.H. Westheimer is in the Department of Chemistry, University of California at San Diego, La Jolla, California 92093, USA.

1. Zaug, A.J. & Cech, T.R. *Science* **231**, 470 (1986)
2. Sumner, J. *J. biol. Chem.* **69**, 435 (1926)
3. Stryer, L. *Biochemistry* (Freeman, San Francisco, 1975)
4. Cech, T.R., Zaug, A.J. & Grabowsky, P.J. *Cell* **27**, 487 (1981).
5. Kruger, K. *et al. Cell* **31**, 147 (1982)
6. Zaug, A.J., Grabowsky, P.J. & Cech, T.R. *Nature* **301** 578 (1983).
7. Zaug, A.J., Kent, J.R. & Cech, T.R. *Science* **224**, 574 (1984).
8. Milstein, S. & Cohen D. *J. biol. Chem.* **251**, 5880 (1976)
10. Kaddurah-Daouk, R., Cho, P. & Smith, H.O. *J. biol. Chem.* **260**, 15345 (1985).

11. Anfinsen, C.B. in *The Enzymes* 3rd edn (ed. Boyer, P.D.) 177 (Academic, London, 1971).
12. Gerlt, J. & Whitman, R. *J. biol. Chem.* **250**, 5053 (1973).
13. Gerlt, J. & Westheimer, F.H. *J. Am. chem. Soc.* **95**, 8166 (1973).
14. Stark, B.C., Kole, R., Bowman, E.J. & Altman, S., *Proc. natn. Acad. Sci. U.S.A.* **75**, 3719 (1977).
15. Guerrier-Takada, C., Gardiner, K., Marsh, T., Pace, N. & Altman, S. *Cell*, 849 (1983).
16. Garriga, G. & Lambowitz, A.M. *Cell* **36**, 623 (1984).
17. van der Horst, G. & Tabek, H.F. *Cell* **40**, 759 (1985).
18. Korneeva, G.A., Petrova, A.N., Venkstern, T.V. & Bayer, A.A. *Eur. J. Biochem.* **96**, 339 (1979).
19. Balasingam, K. & Ferdinand, W. *Biochem. J.* **118**, 15 (1970).
20. Moore, V.G., Atchinson. R.E., Thomas, G., Morgan, M. & Noller, H.F. *Proc. natn. Acad. Sci. U.S.A.* **72**, 844 (1975).
21. Noller, H.F. & Woese, C.R. *Science* **212**, 403 (1981).
22. Orgel, L.E. *J. molec. Biol.* **38**, 381 (1968).
23. Bass, B.L. & Cech, T.R. *Nature* **308**, 820 (1984).

---

100 years ago

Mr Johnston was early in 1884 specially commissioned by the Royal Society and the British Association to study the interesting fauna and flora of the Kilima-Njaro uplands. During the six months from May to October of that year, this experienced African traveller has succeeded under great difficulty in collecting abundant materials for illustrating the natural history and physical constitution of the "Mountain of the Snow Fiend," as its euphonious Ki-Swahili name is interpreted. These results are embodied in the work before us, which is alike admirable for its bright and graphic style, and the judicious arrangement of its varied contents. By the simple plan, consistently adhered to throughout, of treating the narrative portion separately, and confining the strictly scientific matter to the concluding chapters, all tastes are consulted, and the common mistake is avoided of sacrificing the interests of the student to those of the general reader: "The Kilima-Njaro Expedition, a Record of Scientific Exploration in Eastern Equatorial Africa." By H.H. Johnson, F.Z.S. (London: Kegan Paul, 1886).

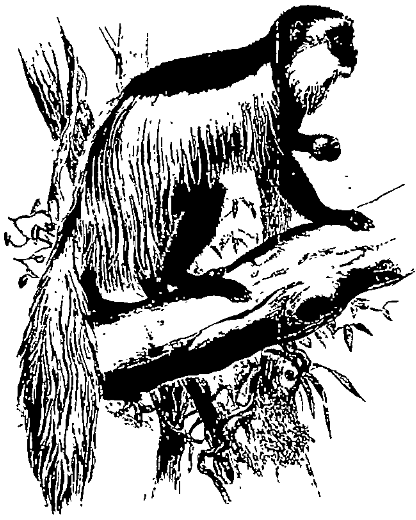

Amongst the valuable animal specimens secured was one of the new and beautiful species of Colobus (*C. guereza*, Rüpp., *var. caudatus*, var. nov.) first seen and described by Mr. Thomson, which frequents the base of Kilima-Njaro, and is apparently restricted to that region. Mr. Oldfield Thomas tells us that it is "characterised by having the white brush of the tail very much larger and finer than is the case in the true Abyssinian *C. guereza*. . . . "

From *Nature* 33 322, 4 February 1886.

Biological rhythms

Sleep researchers caught napping

from N. Mrosovsky

MINIMA in body-temperature rhythms usually occur towards the end of each night's sleep. When people live in constant conditions, without information about the time of day, sleep and temperature rhythms can become desynchronized. Initially, both rhythms free-run together with a circadian period of about 25 hours and then, in some subjects, the period of the sleep rhythm suddenly lengthens to a value near to 30 hours while the temperature rhythm retains its 25-hour period. Up until now, this has been the best example of 'internal desynchronization'; it has been used as evidence that circadian rhythmicity depends on several biological clocks, as one oscillator cannot run at two different frequencies simultaneously. The data on which the argument rests have recently been re-analysed by J. Zulley and S.S. Campbell (*Human Neurobiol.* **4**, 123; 1985 and *Sleep 84* (eds Koella, W.P., Rütter, E. & Schultz, H.) 81; Fischer, Stuttgart, 1985).

The question of whether there are one or several oscillators controlling circadian rhythms is not only of great importance to specialists on rhythms, but also has practical implications in understanding adjustment to shift work. It it also an essential ingredient of some recent theories about the role of biological rhythms in depression and cycles of mania and depression.

Both presentation and selection of data have contributed to the view that sleep and temperature can become desynchronized. Rhythm data are frequently double-plotted — a given time-segment, say 24 hours, appears twice, once below the previous segment and once beside it (on the right in Fig. 1.) This makes it easy for the viewer to see continuity in data spanning two 24-hour periods, rather than having to glance back to the start of the 24-hour segment below. The principle of double mounting is often extended to treble and multiple mounting.

Figure 2*a* shows an extended plot of data on major sleep episodes using the multiple-mounting method. In this case, however, the principle of showing continuity has been carried even further by plotting each sleep episode only once. This extended plot draws the eye across the page in a way that emphasizes differences in the periodicity of the sleep and temperature rhythms. Textbook illustrations are often in a format similar to that of Fig. 2*a*. When the sleep episodes are also plotted below each other (Fig. 2*b*), it is much less clear that the periodicity of sleep and temperature are different. But there do remain some days when sleep is apparently absent at the times of temperature minima, which is evidence for a long periodicity in the sleep rhythm.

But what is sleep? Here we come to the problem of what to include in the database. In classic diagrams showing internal desynchronization, only times that the subjects themselves considered to be major sleep episodes were included and naps were excluded. In fact, subjects were instructed not to take naps but to remain active between the times that they experienced as night. Some subjects were either unable or unwilling to follow these instructions. If they decided to sleep outside what they considered to be their major bout of night-time sleep, they pressed a button indicating they were taking a nap. But, as Zulley and Campbell point out, some of these 'naps' lasted several hours, as long as major sleep episodes. When such naps are included in the plots (see Fig. 2*c*), they cluster around the time of the temperature minima. There are also some shorter naps in the middle parts of what is perceived as day, but whatever it is called, some sleeping takes place nearly every day around the time of the temperature minima. The evidence for internal desynchronization disappears — almost.

To salvage the hypothesis, it has to be postulated that internal desynchronization occurs between what the subject per-

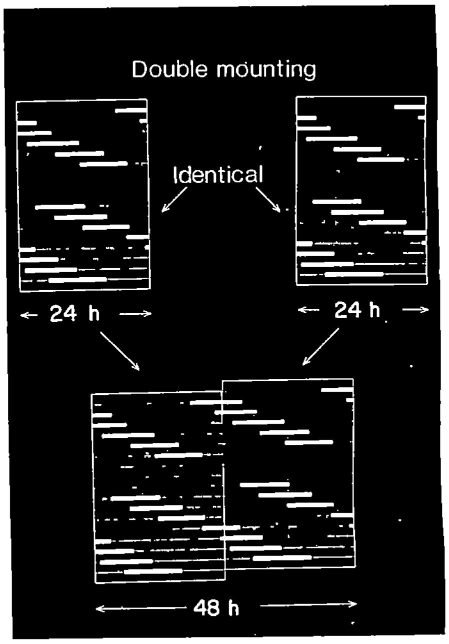

Fig. 1 Double-plotting method for showing data on biological rhythms. Two identical photographs of the same data are mounted side by side to give consecutive 24-hour spans across, as well as down, the page.

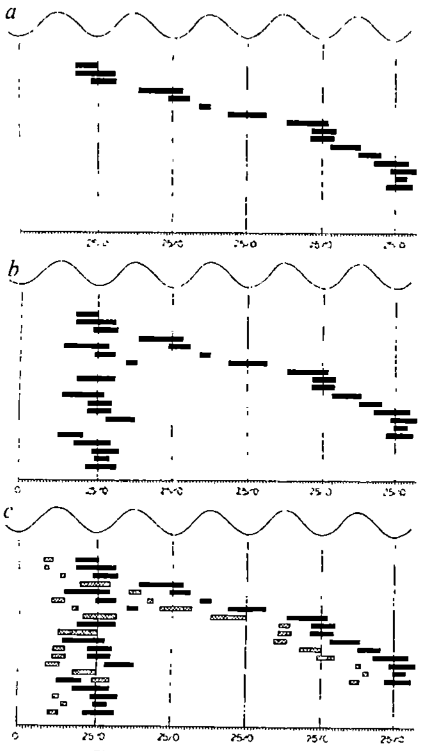

Fig. 2*a*, The body-temperature rhythm of a person in constant conditions free running at a period of 25 hours is shown schematically (line and 25-h scale on abscissa). The subjectively perceived major sleep episodes (black bars) are shown in extended plot only. *b*, The same data as *a* but with the sleep episodes plotted twice. *c*, The black bars are the same major sleep episodes as shown in *a* and *b*. The hatched bars show sleep that the subjects designated as naps. Note that some sleep occurs nearly every day around the time of temperature minima. Curved lines in *a*–*c*, body temperature (schematic). (Redrawn from Zulley and Campbell.)

ceives as the time for napping and the time for sleeping; in other words, what is perceived as day or night. Before this interpretation can be accepted, it is necessary to study the exact instructions given and the way they are interpreted. Zulley and Campbell necessarily selected subjects who napped despite instructions — perhaps internal desynchronization occurred in the other subjects, those that did not nap. To answer this it will be necessary to learn whether such subjects did not always feel sleepy when their body temperatures were low, or whether the instructions not to nap sometimes overrode sleepiness at those times.

A happy feature of Zulley and Campbell's work is that they have evidently been assisted, rather than resisted, by Jurgen Aschoff, one of the chief proponents of the phenomenon of internal desynchronization, who has made his data available and continues to exert creative leadership in the field. ☐

N. Mrosovsky is in the Departments of Zoology, Psychology and Physiology at the University of Toronto, Ontario, Canada M5S 1A1.

Neurochemistry

Peptides and Alzheimer's disease

from Alan Fine

The observation ten years ago that cholinergenic enzyme activities are reduced in the brains of patients with Alzheimer's disease[1-3] triggered a surge of interest in the biology of acetylcholine in the mammalian forebrain. Since then it has become clear that the neurochemical pathology of Alzheimer's disease, although selective, is not restricted to cholinergic pathways. New discoveries of profound decreases in cortical levels of corticotropin-releasing factor in Alzheimer's brains, reported on page 593 of this issue[4] and elsewhere[5], reinforce this conclusion. What are the implications for the pathology of Alzheimer's disease?

Corticotropin-releasing factor (CRF), a 41-amino-acid-long peptide first characterized by W.W. Vale *et al*[6], and known to be a major hypothalmic regulator of secretion of β-endorphin and adrenocorticotropic hormone from the anterior pituitary, has more recently been found in other neurones including those of the cerebral cortex. CRF-containing neurones are present in the neocortex of rodents, with cell bodies predominantly in laminae II and III and terminal fields mainly in laminae I and IV, where CRF receptors are also concentrated[7-9]. CRF is also contained in cholinergic neurones in the brainstem of rats, some of which may project to the forebrain, including the cortex.

What E.B. De Souza *et al.*[4] and G. Bissette *et al.*[5] now observe is a significant reduction in CRF (measured by radioimmunoassay) in several brain areas from Alzheimer's patients compared with matched controls. Both groups report greater than 50 per cent reductions in frontal and temporal cortex. The greatest reductions were found in occipital cortex (80 per cent) and caudate nucleus (70 per cent), at variance with the pattern of loss of cholinergic markers. Similarly surprising is that there is no significant change in CRF levels in the hippocampus, cingulate cortex, amygdala or substantia innominata, all regions where structural and cholinergic changes occur in Alzheimer's patients.

Previously, somatostatin was the only neuropeptide whose brain levels were known to be reduced in Alzheimer's disease [10,11]. Two neuropeptides other than CRF, vasoactive intestinal polypeptide and cholecystokinin, are known to have high cortical concentrations (relative to subcortical levels) in the normal brain. They are not reduced in Alzheimer's disease , which indicates a biochemical specificity in the pathology of the disease.

De Souza *et al.* have also described a proportional increase in CRF receptor levels in those areas with reduced levels of CRF. Thus, they find a twofold increase in CRF binding in the occipital cortex of Alzheimer's patients compared with controls. This up-regulation contrasts with the decreased somatostatin binding found in Alzheimer's brains[12].

It will be of interest to learn whether the distribution of CRF-containing neurones in the human brain is similar to that in rodents, and, if so, whether the observed CRF deficits reflect abnormalities of intrinsic cortical cells or of neurones that project to the brainstem. Furthermore it will be important to determine whether CRF neurones are associated with the neuritic (senile) plaques and neurofibrillary tangles that are the identifying histological abnormalities of Alzheimer's disease. Cortical somatostatin-containing neurones in Alzheimer's brains have been shown to contain tangles[13], which has led to the supposition that they are a primary focus for the disease.

There is already evidence that CRF can modulate cholinergic behavioural effects and cortical somatostatin release in rats. More extensive studies of the physiology and behavioural pharmacology of these cortical neuropeptides are now needed. Intervention in any single neurotransmitter pathway thus seems to be unlikely to provide satisfactory therapy for Alzheimer's patients. Effective therapy may need to have multiple targets, with selective M_1-agonist and M_2-antagonist cholinergic agents (the latter to maximize the efficacy of remaining cholinergic terminals) used in conjunction with appropriate peptidergic or α-adrenergic[14] agonists.

It has previously been suggested that degeneration of subcortical cholinergic (and perhaps noradrenergic and serotonergic) projection neurones of the so-called isodendritic core was the primary lesion of Alzheimer's disease[15,16]. In this hypothesis, neurofibrillary tangles, neuritic plaques and neuronal loss in target areas of hippocampus, entorhinal cortex and neocortex represent the transsynaptic consequences of this subcortical degeneration. However, as noted above, regional CRF changes are not proportional to cholinergic changes, nor does the cortical distribution of plaques accurately mirror the regional distribution of ascending cholinergic inputs (but plaques do parallel the distribution of somatostatin terminals).

Although cholinergic neurites have been identified in association with plaques in human[17] and aged monkey brains[18], so also have somatostatin-[19,20], γ-aminobutyric acid-[21] and catecholamine-containing neurites[22]. It is probable that cholinergic deafferentation of the cortex (including the hippocampus) is an important contributor to the cognitive impairments of Alzheimer's disease. However, the hypothesis that subcortical cholinergic neurones, by virtue of their particular metabolism or other molecular specialization, are the primary focus of Alzheimer's pathology seems no longer tenable. If cholinergic subcortical degeneration is not the primary focus, it may reflect a disease process acting concurrently on diverse independent structures, or it may be the result of abnormalities of the target cortical regions. The latter possibility is compatible with observations that the neuronal loss in different parts of the cholinergic basal forebrain system in Alzheimer's disease is proportional to the extent of neuritic plaque formation in their respective cortical targets[23], and with the observation of degenerative changes in cholinergic neurones of the basal forebrain following cortical lesions in rats[24,25], monkeys and humans[26]. ☐

1. Bowen, D.M. *et al. Brain* **99**, 459 (1976).
2. Davies, P. & Moloney, J.F. *Lancet* ii, 1403 (1976).
3. Perry, E.K. *et al. Lancet* i, 189 (1977).
4. De Souza, E.B. *et al. Nature* **319**, 593 (1986).
5. Bissette, G. *et al. JAMA* **254**, 3067 (1985).
6. Vale, W.W. *et al. Science* **213**, 1394 (1981).
7. Olschowka, J.A. *et al. Neuroendocrinology* **35**, 305 (1982).
8. Swanson, L.W. *et al. Neuroendocrinology* **36**, 165 (1983).
9. De Souza, E.B. *et al. Science* **224**, 1449 (1984).
10. Davies, P. *et al. Nature* **288**, 279 (1980).
11. Rossor, M. *et al. Neurosci. Lett.* **20**, 373 (1980).
12. Beal, M.F. *et al. Science* **229**, 289-291 (1985).
13. Roberts, G.W. *et al. Nature* **314**, 92 (1985).
14. Arnsten, A.F.T. & Goldman-Rakic, P.S. *Science* **230**, 1273 (1985).
15. Rossor, M. *Br. Med. J.* **283**, 1588 (1981).
16. Coyle, J.T. *et al. Science* **219**, 1184 (1983).
17. Tomlinson, B.E. *Pyschol. Med.* **12**, 449 (1982).
18. Kitt, C.A. *et al. Science* **226**, 1443 (1984).
19. Struble, R.G. *et al. Brain Res.* **324**, 394 (1984).
20. Morrison, J.H. *et al. Nature* **314**, 90 (1985).
21. Walker, L.C. *et al. Neurosci. Lett.* **59**, 165 (1985).
22. Kitt, C.A. *et al. Neuroscience* **16**, 691 (1985).
23. Arendt, T. *et al. Neuroscience* **14**, 1 (1985).
24. Sofroniew, M.V. *et al. Brain Res.* **289**, 370 (1983).
25. Stephens, P.H. *et al. J. Neurochem.* **45**, 1021 (1985).
26. Pearson, R.C.A. *et al. Brain Res.* **261**, 321 (1983).

Alan Fine is in the MRC Molecular Neurobiology Unit, University of Cambridge Medical School, Hills Road, Cambridge CB2 2QH, UK.

Atmospheric chemistry

Reservoir species discovered in the stratosphere

from Donald J. Wuebbles

It is now recognized from theoretical models that several trace constituents of the stratosphere affect the distribution of ozone. But because of difficulties in achieving enough sensitivity, the stratospheric concentrations of many of these species, particularly those termed 'reservoir' species, have remained unobserved. Now, Toon *et al.*, on page 570 of this issue[1], report the first conclusive measurement of the reservoir species N_2O_5.

Reservoir species are those trace constituents, such as HNO_3, HCl, N_2O_5 and $ClONO_2$, that are produced from the more reactive ozone-destroying species, but are longer-lived and less reactive. In a sense, these gases act as temporary reservoirs or holding tanks for the more reactive ozone-destroying forms of nitrogen-, chlorine- and hydrogen-containing species in the stratosphere. Of these reservoir species, only HNO_3 and HCl have been measured extensively. The concentration distribution observed by Toon *et al.* applies only to a particular latitude and longitude on a single day, but nonetheless represents an important step towards the validation of key aspects in the theory of ozone-controlling mechanisms.

Many recent studies have concerned the possibility that increasing concentrations of trace-gas emissions caused by human use, such as methane, nitrous oxide (N_2O) and chlorocarbons (particularly $CFCl_3$ and CF_2Cl_2) affect the distribution of stratospheric ozone. These trace gases, although emitted at the Earth's surface, are sufficiently long-lived to be transported to the upper atmosphere, where they dissociate into by-products that can react with ozone catalytically. The rate of conversion of the reactive species to the less-reactive, reservoir species largely determine the ultimate effect of these trace gases on stratospheric ozone. It has been noted that model-derived concentrations of the reservoir species are particularly sensitive to remaining uncertainties in atmospheric chemical reaction rates. For all these reasons, it was essential to measure the concentrations of reservoir species in the stratosphere.

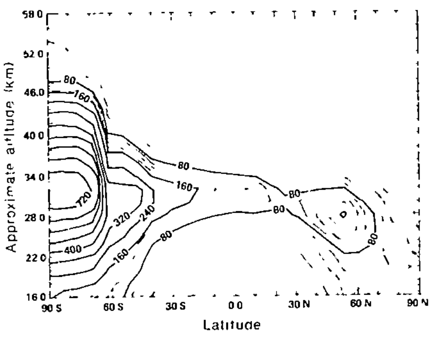

Two-dimensional model simulation of the latitudinal variation in N_2O_5 concentrations determined for May at local noon. By definition, the mixing ratio is the concentration divided by the air density. From the model of S. Solomon and R. Garcia.

N_2O_5 has long been thought to be important in the diurnal variation of NO_2, which reacts with ozone. The slow photolysis of N_2O_5 should produce NO_2 slowly during the day, while production of N_2O_5 should reduce NO_2 concentrations slowly in the night-time stratosphere. Observations of the sunrise–sunset differences in the NO_2 profile[2,3] and a recent analysis[4] of satellite-observed NO_2 at varying zenith angles have tended to verify the importance of this process. The observations by Toon *et al.*[1] are in general agreement with the expected diurnal behaviour of N_2O_5.

Model calculations suggest that N_2O_5 concentrations are particularly large in the high-latitude winter (especially in the Arctic) and that N_2O_5 is the major portion of total reactive nitrogen in the high-latitude stratosphere (see figure). Trajectory analyses[5] suggest that the conversion of NO_2 to N_2O_5 in the winter polar night explains the so-called Noxon cliff, in which sharp gradients in the total vertical column content of NO_2 are observed at high latitudes. Measurements of N_2O_5 concentrations in the polar winter stratosphere in tandem with further observations of NO_2 concentrations are needed to test this suggestion. In addition, heterogeneous mechanisms[6] have been proposed for the conversion of N_2O_5 to HNO_3 in the arctic winter. This could also be tested by observations of N_2O_5.

The observed profile of N_2O_5 in Toon *et al.*'s study is in general agreement with the expected theoretical distributions determined with models such as the Lawrence Livermore National Laboratory one-dimensional model, but a direct comparison depends on knowing the NO_2 and O_3 concentrations at the same location. As the measurements of Toon *et al.* depend on assumed profile shape, the next step is to reduce this dependence. Clearly, based on the expected diurnal behaviour and from results (see figure) that show the strong winter high-latitude gradients, observations of N_2O_5 are needed at a wide range of seasons and locations, as well as at various times throughout the day, to validate the theory. ☐

1. Toon, G.C., Farmer, C.B. & Horton, R.H. *Nature* **319**, 570 (1986).
2. Noxon, J.F., Whipple, E.C. & Hyde, R.S. *J. geophys. Res.* **84**, 5047 (1980).
3. Kerr, J.B., McElroy, C.T. & Evans, W.R.J. *Can. J. Phys.* **60**, 196 (1982).
4. Solomon, S. & Russell, J.M. *J. geophys. Res.* (in the press).
5. Solomon, S. & Garcia, R. *J. geophys. Res.* **88**, 5497 (1983).
6. Evans, W.F.J., McElroy, C.T. & Galbally, I.E. *Geophys. Res. Lett.* **12** 825 (1985).

Donald J. Wuebbles is in the Atmospheric and Geophysical Sciences Division, Lawrence Livermore National Laboratory, Livermore, California 94550, USA.

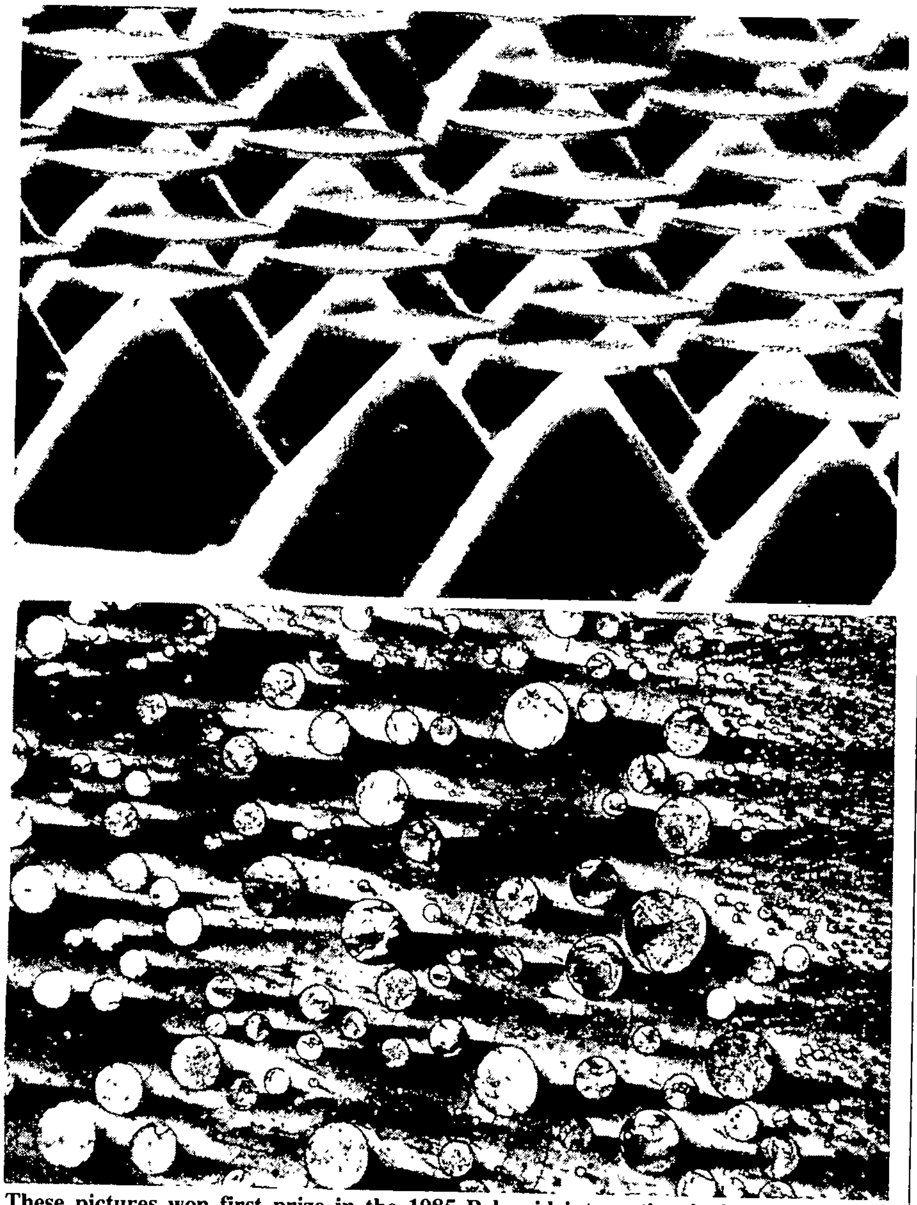

These pictures won first prize in the 1985 Polaroid international photomicrography competition. The top picture of a recrystallized mixture of sulphur and ketone was taken by William E. Schadel of Raleigh, North Carolina, using a Nikon polarizing microscope and a 35mm camera (1,680×). The bottom picture of etched silicon was taken by Anita Brandes of the Gould Research Center, with a Jeol scanning electron microscope (10×).

Distant galaxies

Pushing back the redshift limit

from C. Martin Gaskell

THE search for ever more distant galaxies has become one of the main challenges of observational cosmological research. The more distant a galaxy the greater its redshift because of the overall expansion of the Universe; astronomers generally prefer to speak of the redshift of an object rather than its distance. In this issue, J.S. Dunlop *et al.* (*Nature* **319**, 564; 1986) report the discovery of a new quasar, PKS1351−018, with a redshift (z) of 3.72. And also just recently, S. Djorgovski *et al.* (*Astrophys. J. Lett.* **299**, L1; 1985) have discovered the most distant non-quasar galaxy known. What do these discoveries mean?

Last year in these columns (*Nature* **313**, 628; 1985) I commented that the greatest known redshift for quasars had crept from 3.53 in 1974 to 3.78 in 1982, while in the same period the greatest known redshift for non-quasar galaxies shot from 0.46 to 1.82. The recent discoveries continue this trend. Djorgovski *et al.* have pushed the redshift record up to 3.218, while the quasar discovered by Dunlop *et al.* is the second most distant quasar known. There are now more than 70 quasars with redshifts greater than 3.0, but the distribution still cuts off sharply at around 3.7.

It has required much effort to measure the redshift of PKS1351−018. Dunlop *et al.* had to obtain an accurate radio position of a compact source in an apparently blank region of the sky, then deduce from infrared colours obtained with the UK infrared telescope that the object was probably a high redshift quasar, and finally obtain an optical spectrum with the Anglo–Australian telescope. It is of interest that although PKS1351−018 is considerably fainter that the previously discovered quasars with redshifts greater than 3.5, it proved to be no more distant. Does z=3.8 represent some sort of 'turn-on' epoch for quasars? The suspicion is that it does, but it will take more painstaking work to establish this.

Quasars are located in the nuclei of galaxies. Does z=3.8 represent some critical time for galaxy formation? A normal galaxy at a redshift greater than 2 is exceedingly difficult to find but the task is much easier if one knows just where to look. Extrapolating from common experience with low redshift galaxies, Djorgovski *et al.* reason that the best place to look for a galaxy is next to another galaxy. Because quasars are located in the nuclei of galaxies they decided to use quasars as signposts or beacons for their normal companion galaxies. They chose a small sample of distant quasars and used an interference filter to look for objects emitting Lyman alpha at the redshift of the quasar. In their first 20-minute exposure with the 3-metre telescope at Lick Observatory they discovered an object emitting strong Lyman alpha near a quasar. The object has the sort of spectrum expected from a mildly active galaxy at high redshift but not the sort one sees from a quasar.

The interest of this galaxy is that it is observed when the Universe was only some 14 per cent of its present age (if we assume a critical density Universe). This galaxy is probably less than 9 per cent of the present age of galaxies depending on just when galaxies formed. If galaxies formed more recently than z=4 then the Djorgovski *et al.* galaxy could be a good approximation to a 'primeval' galaxy.

The nature of this galaxy is still unknown, but perhaps the most important thing is that the method, using interference filter images of high redshift quasars to find extremely distant young galaxies, works. The technique promisies to expand studies of distant galaxies to redshifts as high as as those of the most distant known quasars and opens the door for studies of galaxies beyond z=3.

C Martin Gaskell is in the Department of Astronomy, Ohio State University, 174 West 18th Avenue, Columbus, Ohio 43210, USA

Psychophysics

Limits of visual resolution

from Graham Martin

At first sight we might expect that the limits of our ability to resolve an object in a visual scene constrains the precision with which we are able to judge the position of that object. However, psychophysical experiments suggest that this is not the case. Elsewhere in this issue, N.V. Swindale and M.S. Cynader provide an answer to this problem by measuring for the first time a physiological correlate of hyperacuity in the visual cortex (*Nature* **319**, 591; 1986). Their results suggest that the mechanism underlying hyperacuity is relatively simple, perhaps based on the well-known properties of orientation sensitivity of cortical neurones.

It is easy to demonstrate that the smallest object that we are able to resolve in a scene, determined by measuring minimum seperable visual acuity, subtends an angle at the eye of about 1 minute of arc, but we may be able to assess the position of that object in the scene (determined by measuring vernier acuity or hyperacuity) with much greater accuracy, probably about 5 seconds of arc. The reasons for this have been discussed extensively (Westheimer, G. in *Progress in Sensory Physiology* 1; Springer, Berlin, 1970) and it has been generally agreed that these two abilities and the limits on their accuracy arise from different mechanisms in the visual system.

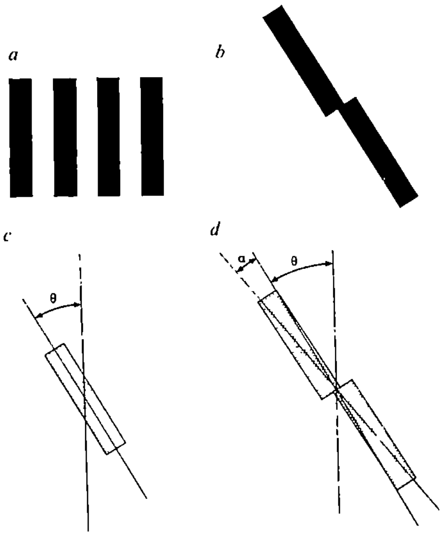

a, The type of stimulus pattern used to assess the limits of visual resolution. When using a regular grating pattern of high contrast, the smallest gap between the bars which can be detected by man subtends at the eye about 1 minute of arc. *b*, The limits of accuracy with which the position of an object in the visual scene can be assessed is measured by using a stimulus pattern consisting of two offset bars. The smallest offset in the alignment of these bars which can be discerned by man subtends only about 5 seconds of arc at the eye. Swindale and Cynader show that if such a stimulus is swept across the receptive field of a neurone in the cat's visual cortex, the response of that neurone is reduced compared with its response when a single bar of the same dimensions is used. The degree of reduction is comparable with that produced when the orientation of the single bar is changed from its optimal position, say θ (*c*) by an amount equivalent to the orientation of straight line that joins the midpoints of the two offset bars, say α (*d*).

The factors limiting visual acuity seem to lie in the eye. Here the ultimate limit on resolution is dictated by the size of the photoreceptors on which the image of the world is focused. Were photoreceptors any thinner and packed more closely together than about 2 microns, then optical cross-talk between adjacent photoreceptors would degrade the information contained in the image (Miller, W.M. in *Handbook of Sensory Physiology* VII/6A; Springer, Berlin, 1979). This sort of photoreceptor spacing, coupled with the focal length of the eye, accounts well for the measured values of maximum visual acuity in various species, including man.

The mechanisms limiting hyperacuity must, however, lie not in the eye but in the visual cortex. Theoretical explanations of hyperacuity have usually involved the idea that averaging of signals from several parts of the retina occurs within the brain, together with the notion that the visual world is represented in the cortex in a much finer grain than in the retina (Barlow, H.B. *Nature* **279**, 189; 1979). (There are several hundred times as many cells in the visual cortex as there are pathways entering from the eye.)

Swindale and Cynader show that if a vernier acuity type of stimulus is moved across the receptive field of a neurone in area 17 of the cat visual cortex, the response of that cell is significantly reduced compared with its response when a single bar is used (see figure). But the size of the offset necessary to cause this reduction is considerably smaller than the spatial resolution of the same cell. Thus, a single cortical cell can show properties that seem directly analogous to the distinction between acuity and hyperacuity.

Such an apparently straightforward correlation between the properties of single cortical cells and visual performance is in itself impressive. However, perhaps the most important aspect of the work is the similarity which Swindale and Cynader find between the vernier sensitivity of a cortical cell and its orientation selectivity. The properties of a vernier stimulus can be approximated by a single bar of the same dimensions but which has an orientation the same as that of a line joining the midpoints of the two bars that make up the vernier stimulus. Thus, hyperacuity may turn out to be subversed by the same or similar mechanisms to those which underlie our ability to detect differences in the orientation of a straight line, especially its deviation from the vertical. Mechanisms involving a hypothetical fine-grained representation of the visual world within the cortex may not be necessary to explain hyperacuity. But Swindale and Cynader's explanation does require that the nervous system has the ability to interpret fine fractional changes in the firing rates of neurones. Whether this is true will require further study, but such a property would simplify our understanding of how sensitivity thresholds measured psychophysically are related to properties of neurones in the visual cortex. ☐

Graham Martin is in the Departments of Zoology and Comparative Physiology, and of Extramural Studies at the University of Birmingham, Birmingham B15 2TT, UK.

Space science

First results from Spacelab 2

from Eugene W. Urban

The Spacelab 2 mission was launched on 29 July 1985 on the space shuttle Challenger, with a crew of seven consisting of the commander, pilot, three mission specialists who operated the spacelab systems and biological experiments, and two payload specialists, both of whom were solar scientists and operated many of the experiments. What follows is an account of the post-flight science meeting held on 14 and 15 November 1985 at the Marshall Space Flight Center at which the principal investigators of the experiments (see table) described the type, quality and status of the data and their analysis.

Spacelab 2 was originally to have been launched on 12 July 1985 for 7 days at an orbital inclination of 49·5° and a circular altitude of 385 km. This date would have given a new moon in the middle of the mission, primarily for the benefit of the infrared telescope (IRT), the plasma depletion experiment and the vehicle charging and potential (VCAP) experiment, but a technical problem caused the original lift-off to be aborted.

The launch was rescheduled for 29 July, at 1423 Eastern Daylight Time. This enabled most orbital mechanics and vehicle attitude conditions to be just as they would have been on 12 July, but coincided with a full moon rather than a new moon during the flight. However, several previously hidden active solar regions had moved around onto the solar disk, making the Sun a more interesting target for the three solar telescopes. Furthermore, the 17-day delay allowed the superfluid helium experiment (SFHE), which had suffered a component failure just before the original launch, to be repaired.

On 29 July, the launch was delayed until 1600 Eastern Daylight Time, and a technical problem left the Challenger at a lower orbital altitude (315 km) than planned, and with a significantly reduced quantity of control propellant. At first, it was necessary to cancel plans for all but two of the eight engine firings for the plasma depletion experiment and to reduce manœuvring during fly-around operations (described below) for the plasma diagnostic package (PDP). But by careful budgeting, it was possible to recover two more firings and to add an extra day to the mission.

Plasma experiments

Data analysis from all the experiments is now in progress. The three plasma physics experiments sought, by both passive and active methods, to study the properties and behaviour of the ambient ionosphere and its effects in and around the vehicle. PDP carried 14 instruments to measure electromagnetic fields and the composition and properties of the space plasma. It operated almost continuously throughout the mission, collecting data while stowed on the Spacelab pallet; while attached to the remote manipulator system (RMS) arm and being moved over the payload bay; while in an 8-hour free flight; and while being held in a parked position on the RMS outside the bay. For the free flight, the PDP was released from the RMS and spin-stabilized at 5 r.p.m. Challenger was then flown slowly around PDP in two elliptical trajectories (maximum excursion about 300 m), after which PDP was spun down and recaptured.

Several phenomena were studied during the free flight, including the undisturbed ionospheric plasma environment; wake disturbances caused by the orbiter; vehicle disturbances propagating up and down along the Earth's magnetic field lines when Challenger and PDP lay on the same flux tube; propagation along the flux tube of the electron beam ejected by the VCAP experiment beam generator (described below); and the radio frequency field profile of the orbiter's radar and communication antenna. A particularly interesting observation was made when the VCAP electron beam intercepted the PDP. The plasma wave behaviour at PDP bore a strong resemblance to earlier satellite observations of natural aurorae, indicating the value of active *in situ* plasma experiments.

Spacelab 2 experiments and their principal investigators

Ejectable plasma diagnostics package	Louis Frank, University of Iowa
Vehicle charging and potential experiment	Peter Banks, Stanford University
Plasma depletion experiments for ionospheric and radio astronomical studies	Michael Mendillo, Boston University and Paul Bernhardt, Los Alamos National Laboratory
Solar magnetic and velocity field measurement system/solar optical universal polarimeter	Alan Title, Lockheed Solar Observatory
Solar helium abundance high resolution telescope and spectograph	Guenter Brueckner, Naval Research Laboratory and Alan Gabriel, Rutherford Appleton Laboratory
Coronal helium-abundance spacelab experiment	J. Leonard Culhane, University College London
Solar ultraviolet spectral irradiance monitor	Guenter Brueckner, Naval Research Laboratory
Small helium-cooled infrared telescope	Giovanni G. Fazio, Smithsonian Astrophysical Observatory
Hard X-ray imaging of clusters of galaxies and other extended X-ray sources	A. Peter Willmore, University of Birmingham, England
Elemental composition and energy spectra of cosmic ray nuclei	Peter Meyer and Dietrich Mueller, University of Chicago
Properties of superfluid helium in zero-gravity	Peter V. Mason, Jet Propulsion Laboratory
Vitamin D metabolites and bone demineralization	Heinrich K. Schnoes, University of Wisconsin
Gravity-influenced lignification in higher plants	Joe R. Cowles, University of Houston

The VCAP experiment included passive charge, current and plasma probes and a low-energy electron-beam generator, which operated many times in both continuous and pulsed modes, emitting 50 or 100 mA beams at 1,000 V. The plasma environment and natural vehicle charging caused by the orbiter's interaction with the ambient plasma were measured frequently. Local effects of beam emission were measured by VCAP sensors; during the two PDP flux-tube connections the beam and its remote effects were detected by the free flyer. Data quality and quantity were excellent, except for low light level television and photographic images of the beam, which were overwhelmed by the bright moonlight.

The plasma depletion experiment consisted almost entirely of ground-based radio and optical observations of the large electron-depletion regions created in the ionosphere by the exhaust products from the firing of the orbiter manœuvring system engines over specified ground observatories. Although the propellant shortage and low altitude limited the number of engine burns, two were made over Millstone Hill, Massachusetts (one in daylight and one at night), and one each at night over Hobart, Tasmania and Arecibo, Puerto Rico. Significant ionospheric holes developed and were observed as they slowly recovered. Incoherent scatter radar measured the size and density of the electron-depletion regions above Millstone Hill and Arecibo, and night-time observations of the 630-nm airglow from these two burns were made despite the bright moonlight. The ionspheric radio cutoff frequency at Hobart dropped appreciably, permitting receipt on the ground of normally blocked radio astronomy signals.

Solar experiments

The three solar and one atmospheric physics experiments were mounted and co-pointed on the instrument pointing system (IPS) provided by the European Space Agency. The IPS was on its maiden flight, and could itself be considered to be an experiment. When the IPS was under pointing control of the solar instruments and later, when under control of its own optical sensor package, the required quiescent pointing stability of about 1 arc s was achieved.

The solar optical universal polarimeter (SOUP) instrument was designed to produce stable high-resolution white-light images of the Sun's surface granulation and to generate narrow-band filtergrams in polarized light to exhibit magnetic and velocity fields. Because of an unexplained hardware problem, the instrument could not be operated until the seventh day of the mission. A total of only 18 hours of solar observing by SOUP was possible, but the quality of the photographic and video data obtained is splendid.

The observing time was devoted to the diffraction-limited white-light imaging system. The video images were viewed in real time by the crew and from the ground, more than 6,000 frames of photographic film were exposed in long rapid sequences of stable high-resolution images of selected solar features. Image stability was much better than 1 arc s, thanks to an internal image motion compensation system. These filmed sequences show the evolution of extended structures and very small, previously unobservable features. Limited filtergram data were collected, but have not yet been studied.

The high-resolution telescope and spectrograph (HRTS) instrument consists of an 0.5–1.0 arc s resolution telescope, a hydrogen Lyman alpha (H_α) full disk system with both video and photographic recording, and an ultraviolet spectrograph and a full-disk ultraviolet spectroheliograph, both recording on photographic film. The H_α video image was available on board and on the ground for target selection. The objective was to study rapidly moving solar chromospheric features with high spatial and temporal resolution. Although HRTS experienced some serious thermal problems, it accomplished most of its objectives and recorded images on most of its photographic film: more than 1,300 spectroheliograph and 30,000 spectrogram images were obtained. Spectroheliograph sequences at the solar limb show details of small, rapidly evolving features which protrude into the corona. Rapid spectrograph sequences display small, short-lived, highly turbulent structures, and spectra taken in steps across the disk show larger and more stable features.

The scientific objectives of the coronal helium abundance spacelab experiment (CHASE) were to measure accurately the abundance of helium in the Sun relative to hydrogen by means of an extreme ultraviolet spectrometer looking at the intensities of several specific solar emission lines. CHASE accomplished almost all of its planned observations and produced very high quality data. By scanning both the spectrometer slit and the grazing incidence mirror, the data have generated maps at moderate resolution of much of the visible disk and the corona in several narrow spectral bands simultaneously. The maps will permit accurate determination of the helium to hydrogen abundance, and show both temperature and density in the solar atmosphere.

The solar ultraviolet spectral irradiance monitor (SUSIM), an ultraviolet spectrometer from an earlier shuttle mission and destined to fly repeatedly, is designed to measure long-term variations in the ultraviolet flux from the Sun. An internal calibration source and comparison spectrometer permit absolute flux to be measured as a function of wavelength. Despite some overheating, it accomplished more than 50 high-resolution spectral scans of the solar ultraviolet output.

High-energy experiments

The cosmic-ray nuclei experiment instrument, weighing 1,968 kg, is the heaviest scientific instrument ever carried into space. It was designed to observe and identify primary cosmic-ray particles out to energies of several TeV per nucleon, using gas Cerenkov counters and a transition radiation detector. The instrument operated smoothly throughout the mission, collecting on the order of 70 events per second for a total of 40 million cosmic-ray particles, about 0.1 per cent of which were at energies greater than 40 GeV per nucleon. Of those, only one in 50 is expected to have an energy greater than 400 GeV per nucleon. Much analysis will be necessary before the energy spectrum is known and the particles indentified atomically.

The X-ray telescope consists of two similar X-ray imaging instruments, each using a shadow mask and a multiwire proportional counter. The telescopes are carried on a two-axis pointing mount. Designed to generate images of clusters of galaxies in the 2–23 keV range, the pair of instruments, with angular resolutions of 3 and 12 arc min, observed many targets in very small increments of time. A total of at least 4 hours of data were gathered on each of six primary targets including the Perseus, Centaurus, Coma and Virgo clusters, the Milky Way galactic centre and calibration sources; several secondary targets were also observed for shorter times. Even with analysis of limited data sets, interesting maps of X-ray emitting galaxy clusters are beginning to emerge. One result is that there seems to be no X-ray source at the galactic centre in this energy range.

Infrared telescope

The scanned infrared telescope (IRT) consisted of a highly baffled herschelian telescope and 10 detectors covering wavelengths from 2 to 120 μm. The detectors and telescope were cooled to very low temperatures by helium gas delivered from a separate superfluid helium dewar so that the detector temperature was 3·1 K. When IRT observations began, a strong background saturated the intermediate wavelength bands, limiting astronomical data to the longest and shortest. Observations in these bands along the galactic plane complement earlier maps from the infrared astronomical satellite. The nature and variability of the apparent background is being studied, but may be partly explained if the water vapour density around the orbiter is higher than expected.

When the PDP was held in front and to one side of the IRT so that its base intercepted the ionospheric gases flowing past the orbiter, spacecraft glow was expected to be seen in the short wavelength channel. None was found, either because there was no glow at that wavelength or because an extended glowing volume enclosed the entire orbiter.

Performance data from the superfluid helium cooling system of IRT will be of value in the design of future cooled instruments in space. In one important test on the superfluid helium, venting from the dewar was stopped for several hours, causing the liquid to warm to the normal phase. When the venting was resumed, the liquid cooled to the superfluid phase again, confirming our ability to control a large volume of liquid helium in zero gravity, even when it is not superfluid.

Additional experiments

The SFHE was designed to study the thermal and fluid properties of bulk liquid and the fundamental interactions between the normal and superfluid constituents of very thin films of liquid. Small experiment modules within a 100-litre dewar vessel provided a stable temperature environment between 1.5 and 2.2 K. Within the bulk fluid module an array of thermometers detected the thermal response of the liquid helium to controlled heat inputs. An array of liquid/vapour sensors measured the liquid motion in response to both deliberate mechanical disturbances and periods during which equipment and crew remained silent. Flight data are being analysed. Within the quantum surface wave module, five toroidal channels, each with a different thickness of superfluid film, were excited by small heat pulses. Propagation of the pulses along the films was observed under many conditions. The results will be related to theoretical predictions.

Blood samples were taken from two payload specialists and two of the mission specialists before the flight, twice during the mission and after the flight. Analysis of the plasma, which is now in progress, will seek to add to our knowledge of spaceflight effects on vitamin D metabolism, calcium balance and bone demineralization.

Conclusions

Despite several problems, the scientific returns of the mission have clearly been very great. During the mission, the experimenters monitored and recorded portions of the data in real time. Complete data records have now been distributed for an analysis period which will take at least a year.

This summary covers only a few details of the Spacelab 2 mission but should give some idea of the quality and quantity of scientific information that was collected. The success of the experiments derives largely from the intensive efforts of the operations and science team at the Payload Operations Control Center at the NASA Johnson Space Center, Houston.

NASA is planning to fly a major portion of Spacelab 2 again in about two years time in the Sunlab/Dark Sky mission. This will allow investigators to improve their data-gathering techniques and considerably to increase the amount of astrophysical data that made Spacelab 2 such an important scientific payload. □

Eugene W. Urban was the Spacelab 2 mission scientist and is at the NASA George C. Marshall Space Flight Center, Huntsville, Alabama 35812, USA.

Accidental human vaccination with vaccinia virus expressing nucleoprotein gene

SIR—Infectious vaccinia virus recombinants that express genes of other pathogenic agents have been proposed as candidates for live vaccines[1-9]. In several cases, vaccination has been shown to effectively immunize and protect experimental or domesticated animals against a virus challenge. Here we report the physical and immunological responses in a human accidentally vaccinated while vaccinating mice with a recombinant, derived from the WR laboratory strain of vaccinia virus, which expresses the vesicular stomatitis virus serotype Indiana (VSV-IND) N protein[8]. In this incident, the vaccinated human and experimental mice had the same specific antibody response.

Vesicular stomatitis virus (VSV) is an RNA-containing, bullet-shaped, enveloped rhabdovirus that causes a highly contagious vesicular disease of cattle, horses and pigs. In humans, vesicular stomatitis (VS) causes influenza-like symptoms[10]. Epizootics of VS in US cattle occurred in 1916, 1949, 1963, 1982 and 1985. Because VS is initially indistinguishable from foot-and-mouth disease, herds with VS must be quarantined at great cost to the livestock industry.

We are investigating the immunogenicity of infectious vaccinia virus recombinants that express the G and N proteins of vesicular stomatitis virus (VSV)[8,11]. While one of us (L.J.) was injecting mice with an infectious vaccinia virus recombinant expressing the N gene of VSV (v38), a small cut on the right ring finger was inoculated with a drop of virus (3.0 × 10^6 PFU/0.05 ml). Although L.J.'s hands were washed immediately, the finger was slightly reddened and swollen 4 days later, as were similar lesions on the vaccinated mice. The swelling progressed from the base of the fingernail past the first joint of the finger, restricting movement of the joint. On day 8, the right axillary lymph node became swollen; the lymph node and finger swelling began to subside approximately 12 hours later. On day 10, the finger swelling had completely disappeared, but a single localized pock lesion appeared in the reddened area, coinciding with the appearance of similar lesions in the mice. The lymph node swelling disappeared by day 12. The lesions were completely healed by day 25 in both L.J. and the mice.

During the infection, L.J. did not experience fever or general malaise. The mildness of the infection is notable, despite the fact that a non-vaccine strain (WR) was involved in this exposure. The mildness of the infection could be related to a smallpox vaccination that L.J. had been given some 30 years before the accident, or to the attenuation of the vaccinia virus recombinant by the insertional inactivation of the thymidine kinase gene, as recently demonstrated[12].

Sera from L.J. and the mice were evaluated by immunoprecipitation of ^{35}S-methionine-labelled extracts of baby hamster kidney-21 cells infected with either VSV-IND or the VSV serotype New Jersey (VSV-NJ) and analysed on SDS-PAGE. There was only specific binding to the N protein of VSV-IND (Fig. 1). All sera were positive by ELISA against whole VSV-IND and negative against whole VSV-NJ. The absence of binding to the G protein of VSV-IND indicated that L.J. had not been infected with VSV. As expected, the sera did not have serum-neutralizing antibodies for VSV-IND or VSV-NJ since the N protein does not cause the production of serum-neutralizing antibodies. The neutralization titres to vaccinia virus of serum taken from L.J. 1 month and 4 months postinfection were 256 and 64 respectively, indicating that this was a recent infection.

These data demonstrate that the vaccinia virus recombinant can produce specific antibody to a non-vaccinia virus protein in humans as well as in mice

L. JONES*
S. RISTOW†
T. YILMA*
B. MOSS‡

*Department of Veterinary Microbiology and Pathology,
Washington State University,
Pullman, Washington 99164, USA
†USDA-ARS,
Pullman, Washington 99164, USA
‡Laboratory of Viral Diseases,
National Institutes of Allergy and Infectious Diseases,
National Institutes of Health,
Bethesda, Maryland 20205, USA

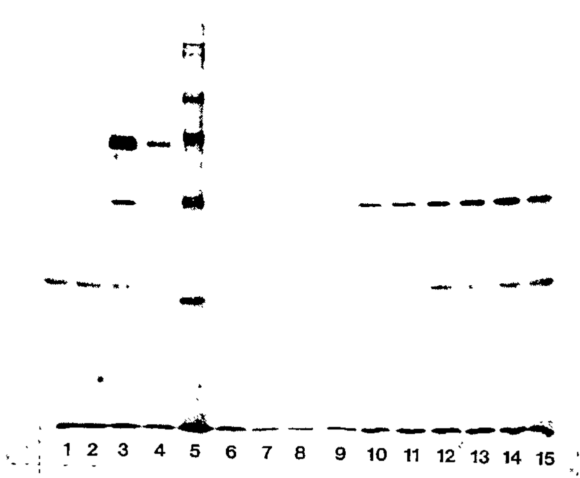

Fig. 1 An autoradiogram of SDS-PAGE analysis of sera from L.J. and vaccinated mice. The sera were immunoprecipitated as described by Kessler[13] with a lysate of ^{35}S-methionine-labelled cells infected with either VSV-IND or VSV-NJ with an MOI of 4. SDS-PAGE[14] was performed using a 10% acrylamide running gel, fixed, dried, and allowed to expose X-OMAT film for 2 days. Antigens: lanes 1–4, 6, 7, and 10–15, VSV-IND; lanes 8 and 9, VSV-NJ. Sera: lane 1, from a mouse bearing a myeloma (P3X63) for fusion; lane 2, normal BALB/c mouse; lane 3, mouse anti-VSV-IND; lane 4 is mouse anti-VSV-NJ; lane 6, mouse anti-v50 (a vaccinia recombinant bearing the gene for the VSV-NJ G protein); lanes 7 and 8, normal human; lanes 9 and 10, from L.J.; lanes 11–15, from five different BALB-c mice infected with v38. Lane 5 contains ^{14}C relative molecular mass standards (200K myosin, 100K/92.5K phosphorylase *b*, 69K bovine serum albumin, 46K ovalbumin, 30K carbonic anhydrase, 14.3K lysozyme).

1. Smith, G.L., Mackett, M. & Moss, B. *Nature* **302**, 490–493 (1983).
2. Paoletti, E., Lipinskas, B.R., Samsonoff, C., Mercer, S. & Panicali, D. *Proc. natn. Acad. Sci. U.S.A.* **81**, 193–197 (1984).
3. Panicali, D., Davis, S.W., Weinberg, R.L. & Paoletti, E. *Proc. natn. Acad. Sci. U.S.A.* **80**, 5364–5368 (1983).
4. Smith, G.L., Murphy, B.R. & Moss, B. *Proc. natn. Acad. Sci. U.S.A.* **80**, 7155–7159 (1983).
5. Kieny, M.P. *et al. Nature* **312**, 163–165 (1984).
6. Wiktor, T.F. *et al. Proc. natn. Acad. Sci. U.S.A.* **81**, 7194–7198 (1984).
7. Smith, G.L., Godson, B.N., Nussenzweig, V., Nussenzweig, R.S. & Moss, B. *Science* **224**, 397–399 (1984).
8. Mackett, M., Yilma, T., Rose, J.K. & Moss, B. *Science* **227**, 433–435 (1985).
9. Cremer, K.J., Mackett, M., Wohlenberg, C., Notkins, A.L. & Moss, B. *Science* **228**, 737–740 (1985).
10. Patterson, W.C., Mott, L.O. & Jenney, E.W. *J. Am. vet. med. Ass.* **133**, 57–62 (1958).
11. Yilma, T., Mackett, M., Rose, J.K. & Moss, B. in *Vaccinia Viruses as Vectors for Vaccine Antigens* (ed. Quinnan, G.V. Jr) 187–200 (Elsevier, New York, 1985).
12. Buller, R.M., Smith, G.L., Moss, B., Cremer, K. & Notkins, A.L. in *Vaccine 85* (eds Lerner, R.A., Chanock, R.M. & Brown, F.) 175–176 (Cold Spring Harbor, New York, 1985).
13. Kessler, S.W. *J. Immun.* **115**, 1617–1624 (1975).
14. Laemmeli, U.K. *Nature* **227**, 680–685 (1970).

Malaria — mitogens or super antigens?

SIR—The induction of a variety of immune responses by malarial infections led Greenwood[1] and Wyler[2] to propose the existence of a malaria mitogen. The activity of extracts of blood cells infected with *Plasmodium falciparum* and *Plasmodium berghei* has been studied using blast transformation of human peripheral blood lymphocytes[3,4] and rodent splenocytes . The results ranged from the demonstration of antigen-specific stimulation of previously sensitized lymphocytes[3,8] to mitogen-like stimulation of both sensitized and non-sensitized lymphocytes[4,6,7,9]. A close look at the literature and careful attention to the results obtained raises the question whether the stimulatory material in malaria parasite extracts is, in fact, a mitogen.

The points that have been put forward to support a mitogenic nature of the active factor include: (1) Ability to stimulate non-immune[4,7,10,11] and cord blood[3,7] lymphocytes; (2) the observation that a large number of immunological specificities are involved in malaria-induced autoimmunity[12–18] and (3) the belief that only a small proportion of the high serum immunoglobulins in infected individuals contains antibody activity specific for malaria parasite[4,7,19].

Results consistent with the possibility that the response to malaria extracts by normal spleen cells represents primary *in vitro* sensitization have been obtained[9]. This response exhibited delayed kinetics and reduced magnitude compared to the response by immune cells. The intense activity of the reticuloendothelial system during malarial infection[19] may result from stimulation by highly potent antigens from the parasite. This high potency of antigenic materials from plasmodia may be responsible for the response of cord blood lymphocytes. There is evidence against a functional immaturity, and for a lack of adequate triggering of surface receptors on cord B lymphocytes[20]. Also, the human fetus is able to respond immunologically to intrauterine infections[21–24].

While autoantibodies directed against a number of autoantigens have been described in malaria, an abnormal frequency of only anti-nuclear antibodies was found in a recent survey[25] carried out in a malaria endemic region in Upper Volta. Thirteen other autoantibodies studied had a normal frequency. This selective increase in the frequency of one autoantibody cannot result from a nonspecific polyclonal mitogenic activation. However, Phanuphak *et al.*[26] reported results associating acute malarial infection with high incidence of autoantibodies of both nuclear and smooth muscle antigens. Another factor that may operate in the pathogenesis of autoimmunity could be repeated stimulation of the reticuloendothelial system with parasite antigens cross-reactive with normal tissue antigens[27].

Although there is evidence to show that only a fraction (6–11%) of the high serum immunoglobulin levels in malaria is specific malaria antibody[19], there seems to be no report indicating what proportion of the total immunoglobulin produced in response to malarial infection this fraction represents.

In the light of the foregoing, is it not more appropriate to talk in terms of highly potent (or "super") antigens rather than mitogens in malarial infection?

GABRIEL O. OYEYINKA

Immunology Unit,
Department of Medicine,
Ahmadu Bello University Hospital,
Zaria, Nigeria.

1. Greenwood, B.M. *Lancet* **i**, 435–436 (1974).
2. Wyler, D.J. *Lancet* **i**, 742 (1974).
3. Wyler, D.J. & Oppenheim, J.J. *J. Immun.* **113**, 449–454 (1974).
4. Greenwood, B.M. & Vick, R.M. *Nature* **257**, 592–594 (1975).
5. Wyler, D.J. & Brown, J. *Clin. exp. Immun.* **29**, 401–407 (1977).
6. Wyler, D.J. *et al. Infect. Immun.* **24**, 106–110 (1979).
7. Greenwood, B.M. *et al. Trans. R. Soc. trop. Med. Hyg.* **73**, 178–182 (1979).
8. Troye-Blomberg, M. *et al. Clin. exp Immun.* **53**, 345–353 (1983).
9. Weinbaum, F.I. *et al. J. Immun.* **116**, 1280–1283 (1976).
10. Freeman, R.R. & Pansh, C.R. *Clin. exp. Immun.* **32**, 41–45 (1978).
11. Oyeyinka, G.O. *Immun. Lett.* **5**, 301–303 (1982).
12. Houba, V. & Allison, A.C. *Lancet* **i**, 848–852 (1966).
13. Greenwood, B.M. *et al. Clin. exp. Immun.* **7**, 75–83 (1970).
14. Greenwood, B.M. *et al. Clin. exp. Immun.* **8**, 161–173 (1971).
15. Voller, A. *et al. J. trop. Med. Hyg.* **75**, 136-139 (1972).
16. Poels, L.G. *et al. Israel J. med. Sci.* **14**, 651–654 (1978).
17. Quaki, I.A. *et al. Immun. Lett.* **1**, 153–154 (1979).
18. Poels, L.G. *et al. Expl Parasit.* **49**, 97–105 (1980).
19. Curtain, C.C. *et al. Nature* **203**, 1366–1367 (1964).
20. Unander, A.M. *et al. Clin. exp. Immun.* **53**, 703-708 (1983).
21. Van Furth, R. *et al. J. exp. Med.* **122**, 1173–1187 (1965).
22. Stiehm, E.R. *et al. N. Engl. J. Med.* **275**, 971–977 (1966).
23. Alford, C.A. *et al. N. Engl. J. Med.* **277**, 437–449 (1967).
24. Hayward, A.R. & Lydyard, P.M. *Paediatrics* **64**, 758–764 (1979).
25. Daniel-Ribeiro, C. *et al. Trans. R. Soc. trop. Med. Hyg.* **77**, 185–188 (1983).
26. Phanuphak, P. *et al. Clin. exp. Immune.* **53**, 627–633 (1983).
27. Rowley, D. & Jenkin, C.R. *Nature* **193**, 151–154 (1962).

The riddle of the magnetic doors

SIR—The Wei and Ching rivers in the northwestern part of China have their sources in Kansu province and flow into the Yellow River (Huang Ho). This river basin has been in fact the cradle of ancient Chinese civilization. It was known that the Wei is rather muddy and the water of Ching is clear; when they join together, the border line can still be seen. Sian on the south bank of the river Wei was a flourishing city during the Ch'in dynasty about 2,200 years ago.

As is generally known, the first emperor of the Ch'in dynasty (221–206 BC), Shih Huang Ti, successfully unified the country. Recently near his burial place, not far from Sian, a brigade of terracotta soldiers and horses has been found and carefully excavated. The total number of life-size figures is about 6,000. Besides many metal weapons and swords, a carriage hauled by four horses made very delicately of bronze has also been discovered. A large museum has now been built at the spot.

There has long been a tradition that the door of the tomb of Ch'in Shih Huang Ti could not be cut through by iron swords because iron was attracted to it. This may seem incredible but the records of the newly found *Yung-Lo Ta Tien* are worth mentioning. This was the world's largest known encyclopedia, and was compiled in China under the direction of the Yung-Lo emperor in 1406 (for details see *Encyclopedia Britannica* x, 847; 1980). According to Chinese literature the work contained 22,870 chapters. It was unfortunately scattered in the course of time, but a remnant of this encyclopedia, totalling 730 chapters was published in China in 1960.

Among the palaces of Ch'in Shih Huang the magnificent and splendid Ah Fang Palace was described by the famous poet Tu Mu (AD 803–853) whose rhymed description has attracted thousands of Chinese scholars. Much to our interest, another volume of the scattered *Yung-Lo Ta Tein* has been recently discovered in Yeh Hsien, a district in Shantung province. The fact that the doors of the Ah Fang Palace were built with magnetic stone is reported in this volume. We translate the description in the following passage: "There were gates of magnetic stone in Hsien-yang (a city 20 km north-west of Xian), 15 li (about 5.5 km) south-west of the city On the east and west there were bridges leading to the north gate of the Ah Fang Palace. The gate was built of magnetic stone. Warriors wearing iron armour were detained or attracted and could not pass through".

An article entitled "The Western Capital" written by Wei Su was also quoted in this volume. It states that the gates of Ah Fang Palace were made of magnetic stone so that men with swords could not enter.

Some scientific facts recently found may perhaps be connected with the above literature. A few years ago a member of the commune near Sian with modern knowledge of magnetic ferrites — which are ferrimagnetic oxides used in making devices for high frequencies in modern electronics — wrote and told me that the natural river sand from the Wei River can be sintered and used as ferrite materials with good magnetic properties. He sent me about a kilogram of the river sand from Wei. I have had the sample analysed in our laboratory. The material possesses the following chemical composition in weight percentages: Fe–69.29; Si–0.58; Mn–0.14; MgO–0.25; W– 1.0; Ti–0.55; Cr–0.20; and Al–0.30.

The oxides are black in colour. As they are highly magnetic, it may be concluded to be a mixture of magnetic Fe_3O_4, ilmenite $FeTiO_3$ and other oxides including WO_3 and $FeCr_2O_4$. The quality of the material is not inferior to the synthetic oxides used in the manufacture of ferrites in modern industry.

Unfortunately we have not yet found any direct evidence that this magnetic sand was used in ancient times.

TAI LI-CHI (L.C. TAI)

Research Institute of Iron and Steel,
Beijing, China

New Enlarged Format • Expanded Scope

CELL MOTILITY AND THE CYTOSKELETON

The success of Cell Motility during the last five years is evidenced by its growth from a quarterly to a bimonthly publication schedule. In 1986 the journal will again undergo changes: a widened scope, reflected by the new title, **Cell Motility and the Cytoskeleton**, and a new enlarged format of 8¼″ × 11″. The widening scope of the journal will provide its readers with an easily accessible source for the latest developments in the field.

The journal publishes brief communications, full-length research reports, and invited reviews. These may be accompanied by videodisc supplement contributions. Topics examined include, but are not limited to, the following areas of interest:

- molecular and supramolecular architecture
- interactions of cytoskeletal and motile proteins in normal and developmental processes
- biochemical, biophysical, and molecular aspects of cytoskeletal proteins and related control- or binding-proteins
- genetic approaches to the study of motility and/or the cytoskeleton
- the role of motility and transport in health and disease
- membrane structure and receptor transport
- prokaryotic flagellar and gliding motility
- axonal transport, microtubular gliding, and particle transport
- reticulopodial movement in foraminifera, radiolaria
- actin-based particle transport
- bulk cytoplasmic streaming (in protists, plant, animal, and fungal cells)
- amoeboid motility
- endo- and exocytosis
- cellular and molecular basis for morphogenetic movements and cell shape change
- intranuclear movements, the nuclear matrix, and nuclear cytoplasmic interchange
- mitotic movements, including karyokinesis and cytokinesis
- cytoplasmic contractility, including spasmoneme and myoneme contraction
- eukaryotic flagellar and ciliary structure and movement
- interaction of the cytoskeleton with the extracellular matrix

Please contact the publisher for further information:

ALAN R. LISS, INC.
41 East 11th Street • New York, NY 10003

EDITOR-IN-CHIEF
Robert Day Allen
Department of Biology
Dartmouth College
Hanover, NH 03755

ASSOCIATE EDITORS
B.R. Brinkley
Charles J. Brokaw
Robert D. Goldman
Yukio Hiramoto
Jeremy S. Hyams
Peter Satir
James A. Spudich

EMERITUS
Noburo Kamiya

EDITORIAL BOARD
W. Brad Amos
Howard C. Berg
Gary G. Borisy
Ian K. Buckley
Monique Cachon
Don W. Cleveland
John S. Condeelis
Benjamin Geiger
Ian R. Gibbons
Wolfgang Haupt
Elizabeth D. Hay
Peter K. Hepler
Shinya Inoué
William R. Jeffery
Raymond J. Lasek
J. Richard McIntosh
Mark S. Mooseker
N. Ronald Morris
Thomas D. Pollard
Lionel I. Rebhun
Jean-Paul Revel
Joel L. Rosenbaum
Joseph W. Sanger
Manfred Schliwa
S.J. Singer
Keiichi Takahashi
D. Lansing Taylor
Lewis Tilney
Michael Trendelenburg
Richard Vallee
J.M. Vasiliev
Dieter G. Weiss
George B. Witman

Reader Service No.7

New Books

from The Royal Society of Chemistry

Molecular Biology and Biotechnology

Edited by J. M. Walker and E. B. Gingold
The Hatfield Polytechnic

This book is aimed not at expert biotechnologists but at scientific workers with little or no previous experience in this field. The contributions in this book should thus be seen as primarily having a teaching function. The book should prove of interest both to undergraduates studying for biological or chemical qualifications and to scientific workers from other fields who need a basic introduction to this rapidly expanding area.

Contents:
Products from Micro-organisms; An Introduction to Genetic Engineering; The Expression of Foreign DNA in *Escherichia coli;* Cloning in Brewer's Yeast, *Saccharomyces cerevisiae;* Cloning in Mammalian Cells; The Genetic Manipulation of Crop Plants; The Application of Genetic Engineering to the Production of Pharmaceautical Compounds; Clinical Applications of Molecular Biology; Generation and Use of cDNA Clones for Studying Gene Expression; Enzyme Technology: Towards Usable Catalysts; Applications of Biotechnology to Chemical Production; Enzyme Recovery and Purification: Downstream Processing; Biosensors; Enzyme Engineering.

Special Publication No. 54

Softcover 348pp ISBN 0 85186 985 8 Price £25.00 ($45.00)

ORDERING:
Orders should be sent to: The Royal Society of Chemistry, Distribution Centre, Blackhorse Road, Letchworth, Herts SG6 1HN, U.K.

Pharmacokinetics of Cardiovascular, Central Nervous System, and Antimicrobial Drugs

by P. G. Welling, *Warner-Lambert Parke-Davies, USA*
and F. L. S. Tse, *Sandoz Research Institute, USA*

Three major areas of drug research and development which have undergone considerable changes in recent years include cardiovascular agents, drugs acting on the central nervous system (CNS) and antimicrobial agents.

This book reviews developments which have taken place in these subjects from 1970 to the early 1980's.

Contents:
Cardiovascular Drugs
Cardiac Glycosides and Other Cardiotonic Agents; Antiarrhythmic and Antianginal Agents; Beta-Adrenergic Receptor Antagonists; Diuretics; Other Antihypertensive Agents; Anticoagulants.

Drugs Acting on the Central Nervous System
Antidepressants; Antipsychotic Agents; Sedatives, Hypnotics, and Tranquilizers; Anticonvulsants.

Antimicrobial Agents
Penicilins; Cephalosporins and Cephamycins; Tetracyclines; Aminoglycosides; Sulfonamides; Erythromycin, Its Salts, and Ester; Other Antimicrobial Agents.

Compound Index

Hardcover 468pp ISBN 0 85186 937 8 Price £39.00 ($71.00)

Reader Service No.4

Planet Earth in Jeopardy

Environmental Consequences of Nuclear War

Lydia Dotto

A Major Contribution to the Nuclear Debate

The climatic changes which could result from a major nuclear conflict would affect combatant and non-combatant nations alike. This and other long term environmental consequences of nuclear war have been at the centre of the continuing nuclear debate in recent years, but until now there has been no comprehensive scientific basis for comment.

The recent publication of the SCOPE Report on the Environmental Consequences of Nuclear War represents the first authoritative statement on the subject. Following this study, Lydia Dotto was commissioned to write a popular account of the material which formed that particular project — "Planet Earth in Jeopardy".

Like the original project the analysis presents a rational series of scenarios without dwelling on extreme cases and likelihoods, the objective is to provide a realistic picture of the likely consequences. Moving in a logical sequence from nuclear exchange and immediate effects, the text explores the climatic and atmospheric changes induced, radiation and fallout, and then the putative biological consequences.

While readers are left to form their own opinions, the scientific case is presented in a balanced and unbiased way to give an informed and objective view.

0471 90908 4 144pp February 1986 £4.95/$8.50

John Wiley & Sons Ltd
Baffins Lane · Chichester · Sussex PO19 · England

Reader Service No.2

Yeast?
Tetrad Analysis?

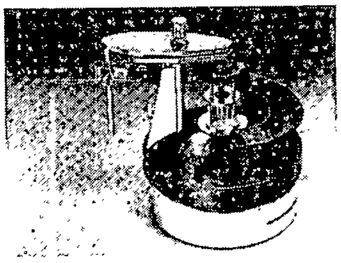

SINGER MK III Micromanipulator
With precision elevator

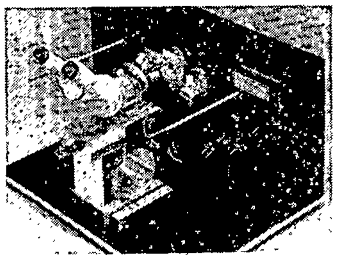

SINGER Microforge
Easy to use

Write direct to:
Singer Instrument Co. Ltd.,
Treborough Lodge, Roadwater,
Watchet, Somerset TA23 0QL
Telephone (0984) 40226

Reader Service No.9

A mind for investigation

Donald Broadbent

The Mind's New Science: A History of the Cognitive Revolution. By Howard Gardner.
Basic Books: 1985. Pp.423. $22.50.
To be published in Britain in June by Harper & Row, £15.95.

A QUIET change has come about over the past 50 years. We now have a different mode of attack on problems of "higher nervous function", or "the mind" or "behaviour". In the 1930s, the alternatives were to use concepts from the nervous system (particularly popular with physiologists, though to some extent with psychologists also); or to use refined terms from everyday language (particularly popular with philosophers); or to use direct descriptions of what people and animals were observed to do (particularly popular with psychologists, anthropologists and linguists).

Nowadays we have a fourth alternative. We can talk about operations performed on abstract symbols, where each symbol could be represented in a variety of physical ways. We can then discuss the differences between different kinds of representation and process, without for the moment knowing what neural events correspond to each symbolic description. Indeed, we can discuss kinds of intellectual operation that do not occur in human beings at all; and because it does not matter what the physical substrate of the processes may be, we can build machines to undertake them. These machines are of course computers, and therefore the five classic disciplines concerned with "the mind" have now been joined by computer science.

The change has been a quiet one, and cynics may say that this is because it is not visual. It does not make good television programmes. Another reason may be that the effects are spread over such wide fields of knowledge that it is hard to see what is happening; even people working in one of the six disciplines usually have only a slight knowledge of what is going on in the others. There has been no accessible account of the whole domain and all of its ramifications. *The Mind's New Science* is an attempt to provide such a broad view; briefly, it does so and to my knowledge has no competitor.

That alone must give the book a big claim on those wanting to find out what is meant by "cognitive science". But why should anyone do so? Well, if for no other reason, because large amounts of research funding are involved. In the past decade, the Alfred P. Sloan Foundation alone has committed twenty million dollars to the area (it was in fact the Sloan Foundation that supported the writing of this book). Other agencies, though less dedicated to the field, have added substantially to the total resources. There is a clear and visible social movement under the cognitive science banner, and scientists in general ought to make up their minds about it.

Next, the practical impact is likely to be considerable. If the field is called Information Technology, that may be more obvious. But the claims of cognitive science go further than the transformation of ways of life by the use of complicated devices. Educational methods, and social institutions, may well be deeply affected without any change in the physical technology that is employed.

Above all, the reason for finding out about these developments is because they change our view of ourselves. That may be why they sometimes arouse such strong emotions — the enthusiasm (dare one call it hype?) of some cognitive scientists on the one hand, and the counter-position exemplified by John Searle's Reith Lectures of 1984 on the other. The question is whether one is dealing with a purely temporary excitement that will expire when the fashion changes, a kind of Mesmerism or Lamarckism; or are we witnessing a lasting change such as the arrival of Darwinism? Anybody with intellectual curiosity ought to wish to find out.

Gardner has set about his task by dividing the book into three sections. In the first, the earliest roots of the movement are described in a integrated way, covering the 1950s and early 1960s. In the second, each of the six fields is discussed separately, going through from the very beginning to the present day, and outlining the main ideas of certain prominent figures. The variety is enormous, from Dennett on the legitimacy of ascribing beliefs and desires to a machine to Kandel on synaptic changes during learning in the sea-slug. On the way we pass (to take just one example from each of the other four disciplines) Sternberg on the interpretation of human reaction-times, Chomsky on transformational grammars, Newell and Simon on the role of condition-action rules in computer programs for solving problems, and Levi-Strauss on kinship-systems in a variety of societies.

In the third section, the multidisciplinary approach is illustrated by taking four specific areas of contemporary debate: visual perception, imagery, the formation of conceptual categories and classes, and reasoning. As those in the field would expect, the names to figure prominently in these areas are Marr and Gibson, Kosslyn and Pylyshyn, Rosch and Berlin, Johnson-Laird and the double act of Kahneman and Tversky. Frankly, as examples of cross-disciplinary work they reveal the nakedness of the land; no one area involves all six disciplines, and several disciplines appear in only one area each.

How well does Gardner cover this vast area? Probably better than anybody else could have done. Each field is described clearly and attractively, and, in those I know least well, I felt I had learned a lot. In the areas I know best there are errors I would describe as howlers, and I suspect that may be true in those I do not know. But that would always be true with a book of this kind. One should compare it, not with writing for specialists, but with science journalism. By that standard it rates very highly. The choice of topics and authors is good, the amount of detail about right and the writing superb.

Will it then make friends and influence people? My feeling is that the impact will be different on readers of different backgrounds. For people in the humanities, or the educated public, it should go down well. The doubt arises about the effect on scientists. The whole style of the book is to emphasize personalities, places and occasions; particular small-scale meetings, confrontations or reports. There are very few factual findings or even theories that are more than sketched in. The description is of a social movement rather than of a body of data.

Perhaps symptomatically, Gardner chides neuroscientists for their neglect of the cognitive approach. He also expresses doubt about the ultimate separate existence of psychology. These however are the disciplines with a particularly strong empirical, as opposed to theoretical, content. It is important to remember the difference between fact and theory. A computer can execute intellectual operations that human beings cannot, just as mathematicians can discuss worlds that are not physically true. We need the separate disciplines of physics and mathematics to distinguish what is, and what might be. In the same way it is no disparagement of artificial intelligence to say that it is an equal to, not a replacement for, neuroscience and psychology.

Conversely, Gardner weakens quite needlessly the case for computational models by describing the computer as a metaphor for human cognition. The whole point of the line of argument that descends from Turing is that the same abstract set of operations can be implemented in a computer or in a person, the one is no more a metaphor for the other than a falling apple is a metaphor for the Solar System. ▶

It seems, in fact, that Gardner likes best the play of ideas, discussed and adopted for their inherent appeal rather than for their truth or falsehood. This intellectualist bias may play a part in his criteria for deciding whether a particular line of work falls within the area of cognitive science. He gives a prominent place to an alleged principle that such work should not consider affect, emotion or context. There is however an enormous body of research on changes in human cognition as a function of clinical conditions, of personality, of temporary mood and of external circumstances such as the working environment. The techniques and concepts used are indistinguishable from those in the rest of cognitive psychology, but the "cognitive science" movement tends not to see them as part of the in-group. Leaving out all such work on principle has some curious side effects, however. The work of Gordon Bower of Stanford is not mentioned; it would be difficult to do so without entering Gardner's self-imposed prohibited area. Other authors such as Bartlett and Bruner (and indeed myself) are quoted prominently but without mentioning the fact that quite a lot of their work is on affect or context.

Immunologists, rheologists or acousticians, then, are likely to be worried by the minor role played by data, and will notice immediately that the six disciplines do not in fact use the *same* concepts in the way that different biological disciplines use the concept of the genetic code. Their common sense may rightly tell them that cognition without context and affect is unlikely to prove adequate; and a general distaste for bandwagons may make them resistant to the whole euphoric style. Such a backlash would be a pity. Within each of the disciplines there is a hard core of professionalism that has indeed made important advances, and will do so in the future. There is no true integrated subject of cognitive science, but there is a wide scatter of separate advances in the study of cognition which other sciences could do well to study. It is unlikely that anybody will produce a better menu than Gardner; but the menu should not be confused with the banquet. ☐

Donald Broadbent is in the Department of Experimental Psychology, University of Oxford, South Parks Road, Oxford OX1 3UD, UK.

New in paperback

- *R.A. Fisher: The Life of a Great Scientist* by Joan Fisher Box. Publisher is Wiley, price is $22.50, £23. For review see *Nature* **278**, 784 (1979).
- *The Quantum World* by J.C. Polkinghorne. Publisher is Pelican/Princeton University Press, price is £2.95, $6.95. For review see *Nature* **308**, 783 (1984).
- *Supermanifolds by Bryce De Witt. Publisher is Cambridge University Press, price is £12.95, $24.95. For review see Nature* **313**, 329 (1985).

Fictional alliance in subjugation

W.F. Bynum

The Old Brown Dog: Women, Workers, and Vivisection in Edwardian England. By Coral Lansbury. *University of Wisconsin Press:1985. Pp.212. $23.50, £23.50.*

In 1903, two Swedish medical students published a little book entitled *Shambles of Science*. It contained extracts from diaries kept of physiology classes they had attended at University College and other institutions in the University of London. Its purpose was to fan antivivisection sentiment, partly by arguing that the terms of the 1876 Act (which regulated, and still regulates, scientific research requiring vivisection) were being regularly and flagrantly contravened by physiologists. On the basis of the evidence presented by the Swedes, Stephen Coleridge, honorary secretary of the National Antivivisection Society, publicly accused Dr William Bayliss of University College of breaking the law. Bayliss sued Coleridge for libel and won substantial damages.

Three years later, Battersea Council erected a statue:

> In Memory of the Brown Terrier Dog Done to Death in the Laboratories of University College in February, 1903, after having endured Vivisection extending over more than two Months and having been handed over from one Vivisector to Another Till Death Came to his Release. Also in Memory of the 232 dogs Vivisected at the same place during the year 1902. Men and women of England, how long shall these Things be?

Deliberately provocative, the statue disturbed many at the University of London and led to a series of attempts by medical students to destroy it. Some three years later, a new Council in Battersea quietly removed it. On 12 December 1985 a new statue to the "Old Brown Dog" was unveiled in Battersea Park, complete with a repetition of the original plaque. *Plus ça change.*

The "Brown Dog Riots" are part of the lore of medical research in Britain, collectively remembered by physiologists and antivivisectionists alike. They provide the starting point for Coral Lansbury's powerful new book. She provides some additional detail about the circumstances surrounding the brown dog, particularly on the extent to which the publicity generated by the libel suit, statue and riots created a brief alliance between two traditionally disparate groups, working men and middle-class women.

In practice, however, Lansbury is less concerned with social realities than with symbolism, less preoccupied with actions than with emotions. The core of her book develops a thesis of startling bravado. It is this: that there is a symbolic identity between an experimental animal on a laboratory table, and a woman undergoing a gynaecological examination. Furthermore, both are inexorably linked to another sphere of sadistic fantasy, pornography, especially the favourite Victorian scenario in which whipping and birching are an important kind of foreplay:

> The distinction between the vivisector's experiments and the episodes of the pornographic novel is that in the latter there is never any question of failure, for the victims of the riding master always end as lascivious, demonic servants of the whip, but the animals resist to the bitter moment when they are released by death [p.127].

Times Newspapers

Emotional appeal — the new "Brown Dog" statue in Battersea Park, London, which was unveiled on 12 December last year.

We thus have a neat equation in which victim–animal–woman is subdued by pornographer–vivisector–gynaecologist. The latter three are, quite simply, dirty words.

Much of Lansbury's "evidence" is literary (she is a professor of English) and much of the volume is devoted to analysing Victorian fiction: pornography like *Birch in the Boudoir,* animal stories like *Black Beauty* (a particular favourite of hers) and novels by Wilkie Collins, George MacDonald and H.G. Wells. Her excessive reliance on literary exposition detracts from the historical persuasiveness of the exercise, as does the caricature of experimental medicine which vitiates the book.

Professor Lansbury is not required to like science, but if she wishes to write about it she does have a certain basic responsibility to her historical sources. My heart sinks when I see someone refer to *Origin of the* [sic] *Species* (p.154), as I think it is safe to assume that this person has not read, much less digested, Darwin's great work. My confidence is not strengthened when I discover Robert Koch referred to as a "physiologist", Claude Bernard (1813–1878) and Ferchault de Réaumur (1683–1757) described as "contemporaries", or Sir John Scott Burdon Sanderson rechristened "James". For Lansbury, as for nineteenth-century antivivisectionists, Claude Bernard was the chief spokesman for the new and vicious priesthood, intent on replacing the old values with the new gospel of materialism and science.

To give Professor Lansbury her due, she is aware that she has forsaken the subtle greys of historical analysis in favour of the blacks and whites of polemic: "Where emotions are the subject, quantification and statistics have proved notably deficient, and the historian is wise to defer to the poet and novelist". I doubt it. Elsewhere, she lays her cards on the table: "I know of only one law in history, and that is that people will always believe what they want to believe, despite all evidence to the contrary". This is profoundly depressing, but Lansbury's book makes me think it may be true. ☐

W.F. Bynum is at the Wellcome Institute for the History of Medicine, 183 Euston Road, London NW1 2BP, UK.

Mogi's doughnuts

Chi-Yu King

Earthquake Prediction. By Kiyoo Mogi. *Academic: 1985. Pp. 355. $64, £53.50.*

A VAST amount of information on earthquake prediction has accumulated in recent years, and has been published in several different languages in many different journals and reports. Under such circumstances, it has proved impossible for any individual to write a book on the subject that is coherent, comprehensive, up-to-date and without parochialism or personal bias. Mogi is not excepted.

The book has been translated from Japanese, with slight modification. It should, perhaps, have retained its original title, *Earthquake Prediction — A Review of the Japanese Programme*, for it mainly deals with material from Japan and Mogi's own research. Some of the older information has been covered by T. Rikitake in *Earthquake Prediction* (Elsevier, 1976), but much of the book contains newer data collected over the past decade. The translation retains a Japanese flavour, and some of the location maps are not labelled in detail so a familiarity with Japanese geography is helpful. A few technical terms (for example hypocentre, epicentre; dip, tilt) are used without discrimination. The quality of printing, however, is very good.

Mogi begins with a general discussion of the feasibility and physical basis of earthquake prediction, stressing the importance of crustal heterogeneity as a governing factor of precursor events and commenting on the success and failure of the dilatancy models and possible usefulness of the time-predictable and slip-predictable models. He then describes prediction-related studies in various disciplines, covering crustal deformation, patterns of occurrence of smaller earthquakes in space and time (including doughnut-shaped seismic gaps), seismic-wave velocity changes, electromagnetic variations, groundwater and geochemical changes, active fault movement and laboratory observation of rock fracture. The coverage is not even-handed; much space is devoted to crustal movement and seismicity, little to hydrological and geochemical studies, and none at all to observations of anomalous light, fog and animal behaviour, or to engineering and socio-economic effects.

Next comes a detailed review of interdisciplinary observations of significant earthquakes that have occurred since 1965, when the Japanese national programme on earthquake prediction began. Included here are accounts of the 1973 Nemuro-Hanto-oki earthquake (magnitude 7.4), the 1978 Miyagi-ken-oki earthquake (7.4), the 1983 Japan Sea earthquake (7.7), and the earthquakes that occurred along the Yamasaki fault and in and around the Izu region. Finally, Mogi describes the Japanese prediction efforts in the Tokai region, where a large earthquake is anticipated, and around Tokyo, and rounds things off with a discussion of strategy of long-term to short-term predictions.

The book contains no mathematics and relatively few technical details, and is thus suitable not only for experts but for nonspecialists looking for a coherent and up-to-date account of Japanese work on earthquake prediction. Those who wish to know more about research going on elsewhere (notably in the Soviet Union, China and the United States), or in disciplines not well represented, will need to consult the proceedings of international symposia such as those published by the American Geophysical Union in 1981 and by Terra Scientific Publishing for UNESCO in 1984. ☐

Chi-Yu King is at the US Geological Survey, 345 Middlefield Road, Menlo Park, California 94025, USA.

Looking for antigens

Julian Heath

An Atlas of Immunofluorescence in Cultured Cells. By Mark C. Willingham and Ira Pastan. *Academic 1985. Pp 186. $35, £31.*

IN recent years the use of fluorescently labelled antibodies to localize antigens in cells and tissues has been a prominent research tool for the cellular and molecular biologist. The compilation of an atlas of immunofluorescent images was therefore a good idea. But a truly comprehensive atlas would need to contain as many maps as there are antibodies, and would be a very large tome indeed, so Willingham and Pastan have restricted themselves to the terrain with which they are most familiar. Their small volume contains images of cultured fibroblastic and epithelioid cells stained with antibodies to 26 cytoskeletal membrane, nuclear and viral antigens many of which they have used in their own research.

Although there is a 12-page introduction discussing specimen preparation for immunofluorescence, the overall feeling is of a subjective and rather self-indulgent account of this widely used technique. Moreover, the poor reproduction of some of the plates belies the word *Atlas* in the title. Clearer images with better contrast can often be found in the original papers, and in my review copy several pages were spoilt because print was visible through the page. It is also a great pity that there are no colour plates; fluorescence microscopy is visually very appealing with the range of fluors available, an atlas of black and white plates is not.

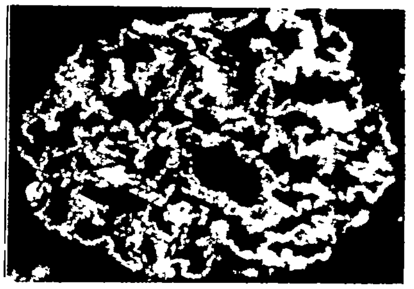

G A Andre

Immunofluorescence of the glomerular capsule showing the granular deposits of immunoglobulin characteristic of nephritis. The picture is taken from the new third edition of L. A. Sternberger's *Immunocytochemistry*, published by Wiley.

This is no hitch-hiker's guide to the galaxy of fluorescent images obtained by immunocytochemistry. But it is welcome as the first compendium of its kind and will be a useful work of reference for those new to the field and for teaching purposes.

Julian Heath is in the Department of Biology, University of Pennsylvania, Philadelphia, Pennsylvania 19104, USA.

Whitehead revealed

George Gale

Alfred North Whitehead: The Man and His Work, Vol. I 1861–1910. By Victor Lowe. *Johns Hopkins University Press: 1985. Pp.351. $27.50, £26.40.*

Science and the Modern World. By Alfred North Whitehead. Introduction by Robert M. Young. *Free Association Books, 26 Freegrove Road, London N7 9RQ, UK: 1985. Pp.265. Hbk £11.95; pbk £4.95.*

SOME works become classics of their type. Such would seem to be the destiny of the first volume of Victor Lowe's superb *Alfred North Whitehead: The Man and His Work*. Certainly, Whitehead deserves a biography. His work as a mathematician, and as partner to Bertrand Russell in creating that original of modern mathematical logic, *Principia Mathematica*, is justification enough. But when one adds to this Whitehead's later achievements following his call in 1924 to a chair in the philosophy department of Harvard University, a biography is not just warranted, it is demanded.

Unfortunately, Whitehead himself desired that no such account of his life should be given. He systematically destroyed, or had destroyed, nearly all written traces of his personal life, including letters to and from his wife and family. Moreover, he kept no journal, believing his personal life was not a fitting subject for such a record. Finally, unlike the typical scholar, he had destroyed all of his unpublished manuscripts, drafts and various manuscript editions of his published works. Thus, he reasoned, there would be no *Nachlass* for younger scholars to waste their time searching in attempts to chronicle his intellectual development. Lowe puts all of this down to Whitehead's personal reserve: "He held an almost fanatical belief in the right to privacy, and thought that the only subject of rightful public interest in him was the work he had published" (p. 7).

Given this state of affairs, it is clear that Lowe had his work cut out. Yet his 20-year-long struggle to tease out information from impoverished sources has been well worthwhile. All of the essential ingredients of successful biography are here. Whitehead's childhood, days at school, time at Cambridge as student and fellow, marriage to Evelyn Wade in 1890, and, finally, his relationship with Russell (first as teacher, then as colleague in the founding of symbolic logic and foundations of mathematics) are each carefully laid out in all the detail that could possibly be given. Even when details are missing, and Lowe must make an inference to fill in the gap, he advises us, often most diffidently, of the fact, and then goes on with no hesitation to reach a conclusion as required.

One of the more delicate of these situations concerns the beginning phases of the cooperation with Russell in 1900. Russell was apparently deeply smitten with Evelyn, and went so far as to surreptitiously support the Whitehead family to the tune of a large sum of money. Was Russell's love ever consummated? Precise details of course are lacking, yet the salient question refuses to go away. Here Lowe marshalls his evidence, warns us, and makes the inference to an answer (p.248).

One major difficulty in understanding Whitehead, especially for Americans, is lack of familiarity with the English middle-class educational culture during late Victorian times. Lowe does a fine job in laying out the entire context of public schools and Oxbridge as they existed during Whitehead's era. Indeed, whether or not interest in Whitehead alone could carry this book, Lowe's account of the educational experience would deserve our attention.

Some interesting biographical points come to light. For example, Whitehead was a supreme team player, especially at rugby. His school's journal, the *Shirburnian Magazine*, called him "the best forward the School has ever had" (p.56). Lowe finds the roots of some of Whitehead's later philosophical attitudes in these experiences on the playing field. Another rich account involves the Cambridge Conversazione Society, that select, secret discussion group more commonly known as "the Apostles". Lowe provides us with a full chapter on this subject, probably about as much as could be asked for regarding a *secret* society! Several roots of Whitehead's later philosophy are to be found in his Apostolic comradeship: years spent in intense discussion with the ebullient McTaggert certainly are sufficient to account for Whitehead's later affection for idealism of the Hegelian systematic sort.

Other Apostolic tenets perhaps account for one of the severest problems that interpreters of Whitehead must face, namely, attempting to make consistent the thinking of Whitehead the English mathematician with Whitehead the American philosopher. Lowe himself eschews the project. During his exquisitely detailed analysis of the cooperative writing of *Principia*, he cautions us so:

> But I shall not here make comparisons with the views to be found in what he published after he came to Harvard in 1924 as Professor of Philosophy, and must warn philosophers whose primary knowledge is of the later work that this is a very risky business [p.276].

Risky indeed, since in many ways the earlier Whitehead is manifestly inconsistent with the later. A possible explanation for this lies in the tradition of absolute candour imposed by the Apostles upon themselves. As Sidgewick, a fellow Apostle, has noted, "No consistency was demanded with opinions previously held — truth as we saw it then and there was what we had to embrace and maintain". This attitude went deep into Whitehead's methods. Professional philosophers, Lowe observes,

> like other scholars, show much concern about consistency with at least their own previous opinion. Whitehead did not. He wrote to formulate the truth as he saw it then and there, on the particular subject of his inquiry [p.115].

Evidence of this trait is not hard to find. Whitehead's most accessible, not to mention successful, philosophical treatise is his *Science and the Modern World* of 1926, which, after a ten-year hiatus, has just re-appeared in print, in an attractive edition from Free Association Books. From within the framework of a masterly historical account of the origin, rise and ultimate triumph of the modern scientific world-view, Whitehead deploys a contrary world-view, organic rather than material, concrete rather than abstract, dynamic rather than static, and laden with human values rather than free of them. Yet what is peculiar is that the most enduring aspect of this work, its superb and still-valuable critique of positivism, founds itself upon a philosophical view totally at odds with the position underlying *Principia*.

In *Principia*, the underlying metaphysical scheme is one of unconnected individuals, an atomistic pluralism. In harmony with this, the connecting relations between propositions in the axiomatic scheme consist of the weakest possible sort of implication, the so-called "material (or Russellian) implication", which abstracts completely from the meanings of the propositions, and attends "only to their being *either* true *or* false" (p.266).

As Lowe notes, in reference to logical atomism, "Whitehead in his mature philosophy rejected this doctrine" (p.264). Indeed, in *Science and the Modern World* Whitehead's entire critique of positivism results from his vehement attack upon Hume's philosophy, a philosophy whose notion of particular individuals and their causality are so thoroughly and well modelled by the metaphysics and logic of *Principia*.

Explanation of how this startling philosophical shift came about must await Lowe's second volume, which will begin just before Whitehead's move to America. Since this first volume will have so satisfied students of mathematics, logic, philosophy, and, indeed everyone else who has an interest in the culture of the modern world, we will all await with anticipation Lowe's account of Whitehead's transformation from English mathematician to American philosopher. □

George Gale is Professor in the Department of Philosophy, University of Missouri, Kansas City, Missouri 64110, USA.

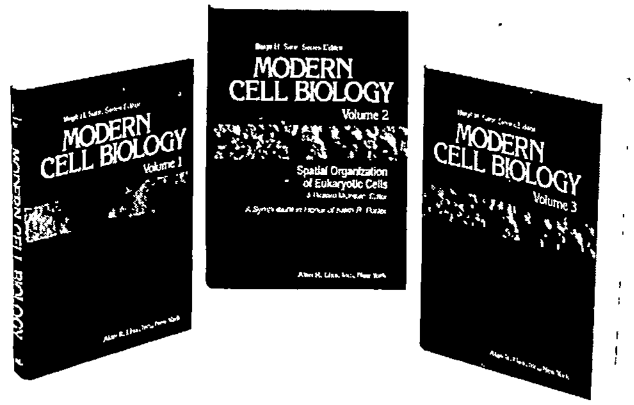

"... fulfills the need
to address the
interface between cell biology
and the recent advances
in molecular biology."

From Quarterly Review of Biology

Birgit H. Satir, Series Editor

MODERN CELL BIOLOGY

Modern Cell Biology provides researchers in cellular and molecular biology with concise articles on the biology of the cell. The series reviews the current status of research in the field and provides a base from which future investigations may develop. **Modern Cell Biology** consistently keeps its multidisciplinary audience abreast of the ongoing research in cell biology.

Contents, Volume 4: Switching Mechanisms in the Control of Ciliary Motility, **Peter Satir** • Proton-Coupled Energy Conversion: Chemiosmotic and Intramembrane Coupling, **Hagai Rottenberg** • The Role of Transferrin and Extracellular Matrix Components in Kidney Development, **Peter Ekblom and Irma Thesleff** • Mechanisms of Bacterial Taxis: Unsuspected Forms, **A.N. Glagolev and M. Yu Sherman** • The Dynamic Life Histories of Intercellular Membrane Junctions, **William James Larsen and Mary A. Risinger** • Index

ISBN 0-8451-3303-9 • ISSN 0745-3000 • Publication: December 1985 • 242 pages, $36.00

Contents, Volume 3: Export of Protein in Bacteria: Dogma and Data, **Linda L. Randall and Simon J.S. Hardy** • High Molecular Weight Microtubule Associated Proteins (MAPs), **Richard B. Vallee and George S. Bloom** • Structure and Function of the Mammalian Zona Pellucida, A Unique Extracellular Matrix, **Bonnie S. Dunbar and Debra J. Wolgemuth** • Molecular Diagnosis of Human Genetic Disease, **Vincent J. Kidd and Savio L.C. Woo** • Gap Junctions and Cell-to-Cell Coupling in Endocrine Glands, **Paolo Meda, Alain Perrelet, and Lelio Orci** • Signal Processing in Dictyostelium discoideum Slugs, **P.R. Fisher, U. Dohrmann, and K.L. Williams** • RNA Splicing and the Involvement of Small Ribonucleoproteins, **Stephen M. Mount and Joan Steitz** • Index

ISBN 0-8451-3302-0 • ISSN 0745-3000 • Publication: September 1984 • 320 pages, $49.00

Section Headings, Volume 2 • Organization of Cell Membranes and the Compartmentalization of Cytoplasm • Organization of the Fibrous Components of Cytoplasm • Cytoskeletal Action in Cytoplasmic Organization • Organization of Nuclear Structure and the Control of Gene Action • Global Organization of Cells and Extracellular Space

Volume 2: Spatial Organization of Eukaryotic Cells • J. Richard McIntosh, Editor • *Proceedings of a Symposium Held in Honor of Keith R. Porter, April 30–May 2, 1982, Boulder, Colorado* • ISBN 0-8451-3301-2 • ISSN 0745-3000 • Publication: April 1983 • LC 83-909 • 600 pages, $50.00

Contents, Volume 1 • Receptor-Mediated Endocytosis, **Richard G.W. Anderson and Jerry Kaplan** • Structure and Function of the Adhesive Glycoprotein Fibronectin, **Leo T. Furcht** • Membrane Biogenesis, Enveloped RNA Viruses and Epithelial Polarity, **Enrique Rodriguez-Boulan** • The Acetylcholine Receptor-Ion Channel Complex: Linkage Between Binding and Response, **Alfred Maelicke and Heino Prinz** • Index

ISBN 0-8451-3300-4 • ISSN 0745-3000 • Publication: March 1983 • 216 pages, $34.00

FROM THE REVIEWS

"... **[Modern Cell Biology]** *clearly fulfills Series Editor Satir's goal of containing articles 'that look to the future.'* **[Modern Cell Biology]** *should be extremely useful to students and established investigators alike.*"

Quarterly Review of Biology
Volume 59, Number 2, June 1984

ORDER FORM

☐ Send me _____ copy(ies) of **Volume 4** (Book #3303) at $36.00 U.S. per copy.
☐ Send me _____ copy(ies) of **Volume 3** (Book #3302) at $49.00 U.S. per copy.
☐ Send me _____ copy(ies) of **Volume 2**: (Book #3301) at $50.00 U.S. per copy.
☐ Send me _____ copy(ies) of **Volume 1** (Book #3300) at $34.00 U.S. per copy.
☐ Enter my standing order for the series **Modern Cell Biology.**

New York State residents please add appropriate sales tax All orders not accompanied by payment or institutional purchase order will be billed on a pro-forma basis. No postage or handling charged on prepaid orders

In Europe, the United Kingdom, and the countries of East and West Africa order from your bookseller or from *John Wiley & Sons Limited • Baffins Lane • Chichester ◦ Sussex PO19 1UD • England*

Payment must be made in U.S. dollars. Payments not drawn on a U.S. bank will be subject to bank collection charges

Return this form with payment or purchase order to **ALAN R. LISS, INC. • 41 East 11th Street ◦ New York, NY 10003**

All prices subject to change without notice.

Order NOW by Phone: We are happy to accept orders Monday–Friday, 9am–5pm at (212) 475–7700. Please have your credit card information ready.

Please charge this order to my

☐ MasterCard ☐ VISA ☐ American Express

Expiration Date ________________
Card Number ________________
Signature ________________

All orders subject to credit approval

PLEASE PRINT

Name ________________
Address ________________
____
City State Zip
Country ________________

1/86 SA-ABAA

Alan R. Liss, Inc., • 41 East 11th Street • New York, NY 10003

Reader Service No.6

WHAT IMPACT ARE NEW BIOTECHNOLOGY TECHNIQUES HAVING ON MEDICINE WORLDWIDE TODAY?

Come to Nature's 7th International Conference in London on Molecular Biology in Medicine 1986 for all the up to date facts — and a look into the near future.

NEW TECHNOLOGY
in
BIOTECHNOLOGY

MOLECULAR BIOLOGY IN MEDICINE

a survey of its achievements and its potential

JUNE 18-20 1986 – LONDON

Reader Service No.325

It is clear that the modern techniques of biotechnology are set to have a major impact on medicine. Over the next few years many new opportunities will emerge. This important conference will provide a wide-ranging survey of the most recent research in the fast changing field of molecular biology in medicine, and a look into the future. If you want an opportunity to see and hear for yourself what leading exponents have achieved in recent years — and to learn what new opportunities are on the horizon, come and join us.

JOIN US AT NATURE'S 7TH INTERNATIONAL CONFERENCE, TO BE HELD AT THE LONDON WEST HOTEL, JUNE 18-20 1986.

REGISTER NOW TO ENSURE YOUR PLACE — SPACE IS LIMITED.

The **CONFERENCE FEE** is just £189 plus VAT for the three days of the conference. This includes entrance to all sessions, mid-morning coffee, afternoon tea and reading material. Group discounts are available on application to Janine Slipman, see booking form for address and phone no.

ACCOMMODATION has been reserved in the London West Hotel for conference participants. A booking form will be sent to you as soon as we receive your registration.

TECHNICAL SEMINARS and **POSTER SESSIONS** will be held each day. Anybody wishing to present a poster should send a title and a brief synopsis.

OUR THREE DAY PROGRAMME ENABLES YOU TO ASSESS IMPORTANT NEW BIOTECHNOLOGY TECHNIQUES IN MEDICINE, MEET INTERNATIONAL RESEARCH SPECIALISTS, AND DISCUSS WHAT YOU LEARN WITH NEW CONTACTS FROM AROUND THE WORLD.

CONFERENCE PROGRAMME

Wednesday, 18 June: Immune System

9.15 **Opening**
9.20 **Vaccines – viral diseases** G. Schild, National Institute for Biological Standards & Control, London
10.15 **Vaccines – parasitic diseases** A. Capron, Institut Pasteur, Lille
11.15 **Coffee**
11.45 **Lymphokines** S. Gillis, Immunex Corporation, Washington
12.45 **Lunch**
2.00 **Engineered immunoglobulins** M. Neuberger, LMB, Cambridge
3.00 **AIDS** L. Montagnier, Institut Pasteur, Paris
4.00 **Tea**
4.30 **Technical seminar**

Thursday, 19 June: Cancer

9.15 **Oncogenes – diagnostic value** K. Sikora, Royal Postgraduate Medical School, London
10.15 **Oncogenes – therapeutic possibilities** R. Gerety, Merck Sharp & Dohme, Pennsylvania
11.15 **Coffee**
11.45 **Gene amplification and drug resistance** G. Stark, Imperial Cancer Research Fund, London
12.45 **Lunch**
2.00 **Gene probes for tumour progression** T. Waldmann, National Institutes of Health, Maryland
3.00 **Immunotoxins** R. Baldwin, University of Nottingham
4.00 **Tea**
4.30 **Technical seminar.**

Friday, 20 June: Genetic Disease

9.15 **Single gene disease** D. Weatherall, University of Oxford
10.15 **Polygenic disease** J. Scott, MRC Clinical Research Centre, Middlesex
11.15 **Coffee**
11.45 **Haemophilia** E. Tuddenham, Royal Free Hospital, London
12 45 **Lunch**
2.00 **Human gene therapy** W. F. Anderson, National Institutes of Health, Maryland
3.00 **Panel discussion: Detection and prevention of genetic diseases**
4.00 **Close**

CONFERENCE BOOKING FORM

NEW TECHNOLOGY
in
BIOTECHNOLOGY
MOLECULAR BIOLOGY
IN MEDICINE

To register for the conference, please return to Janet Mulhall
Macmillan Conferences and Exhibitions,
4 Little Essex Street, London WC2R 3LF, UK

Full name ____________________
Full job title ____________________
Address ____________________
____
____
____
____

Tel no: work __________ home __________

Please tick appropriate boxes

☐ I wish to make a firm reservation for the full duration of the conference, at £217.35 (£189 + VAT)

☐ I wish to attend the Conference Dinner on the evening of 19th June at £14.95 per person.

☐ I enclose a cheque made payable to Macmillan Journals

☐ Please charge my ☐ Visa ☐ Mastercard
account no. ____________________
expiry date ____________________
signature ____________________

☐ Please bill my organisation (please attach address and contact name if different from above)

☐ Please send me details of your group discounts.

Several social events will be organised offering a chance to chat informally with speakers and fellow delegates.

Cancellations received before May 23rd 1986 will be refunded less a processing charge. No refunds can be made after this date.

NOTES: Please complete one form per person. Extra booking forms can be obtained from the address above or by telephoning Janine Slipman on (01) 836 6633

N1

Recombinant vaccinia viruses as vaccines

from F. Brown, G. C. Schild and G. L. Ada

The prospect of live vaccines consisting of genetically modified vaccinia virus expressing foreign genes is exciting, but important issues concerning safety and efficacy need to be resolved.

THE World Health Organization (WHO) smallpox eradication programme, involving the extensive use of vaccinia virus vaccines, resulted in the late 1970s in the elimination of one of the world's most feared diseases. This achievement is a triumph for preventative medicine and for international collaboration in public health. The last reported case of smallpox was in 1977. In the early 1980s, WHO recommended that the routine use of smallpox vaccine should be stopped.

Against this background, the prospect of live vaccines consisting of genetically modified vaccinia virus expressing foreign antigens arising from the work of Moss[1] and Paoletti[2] and their colleagues has been greeted with enthusiasm. These workers have shown that genes coding for immunogenic proteins can be inserted into vaccinia virus DNA without impairing the ability of the virus to grow in tissue culture. Moreover, experimental animals infected with vaccinia virus recombinants containing genes coding for a variety of immunizing proteins have been shown to be protected against challenge infection with the corresponding infectious agent. The studies have included recombinants which express the protective antigens of hepatitis B[3], rabies[4] and malaria[5], agents causing diseases of major economic and social importance.

The observations so far involve only small numbers of laboratory animals; the development of vaccines to a stage where they can be evaluated in the field will inevitably take time and effort. But the potential attractions of such vaccines include not only their low cost and ease of production (once suitable recombinants are established), but ease of administration and a high degree of stability, which would put them within the reach of populations in developing countries. Even so, optimism that this approach will lead to inexpensive and effective vaccines against these and other major diseases must be tempered with the concern which stems from the known adverse reactions to vaccinia virus, themselves well documented[6] during the smallpox eradication programme.

Vaccinia virus

Vaccinia virus consists of a double-stranded DNA molecule of 187 kilobases complexed with structural polypeptides and transcriptional enzymes and enclosed in a lipid envelope. Transcription and replication of the genome take place untypically in the cytoplasm of infected cells, which is attributable to the possession by the virus of enzymes necessary for nucleic acid metabolism. These include DNA and RNA polymerases, enzymes to cap, methylate and polyadenylate mRNA, and a thymidine kinase (TK); however, there are no RNA-splicing enzymes.

The virus DNA is non-infectious and so large that *in vitro* manipulation is difficult, for which reasons the foreign gene must be inserted into the virus by homologous recombination (Fig. 1). A plasmid vector in which the foreign gene is placed under the control of a vaccinia promoter and flanked by non-essential vaccinia virus DNA sequences is introduced into cells infected with vaccinia virus. Recombination between the flanking vaccinia sequences of the plasmid vector and the homologous sequences in the virus genome results in the insertion of the foreign gene into a specific site of the virus genome. Since, by arrangement, the insertion occurs at a position which is not essential for virus replication, the recombinant virus genome replicates normally and is packaged into infectious progeny virus.

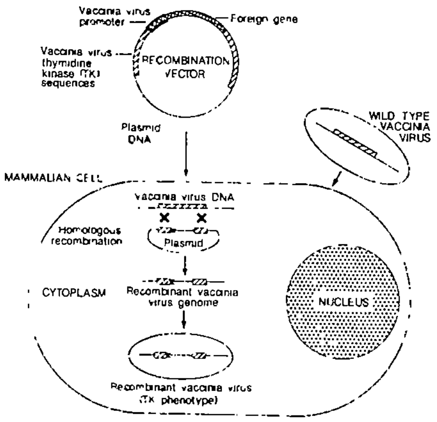

Fig. 1 Construction of vaccinia virus recombinants. The DNA sequence coding for the foreign gene is inserted into a plasmid vector downstream of a vaccinia virus promoter and flanked by vaccinia TK sequences. The resultant recombination vector is introduced into cells infected with vaccinia virus to generate a TK^- recombinant virus which expresses the foreign gene.

Recombinant viruses generated in this way are only a small proportion of the progeny, but may be distinguished from the parent virus by selective procedures: if the foreign genes are inserted within the coding sequence of the vaccinia virus TK gene this gene is inactivated and the recombinants can be selected by plaque assay on TK^- cells in the presence of 5-bromodeoxyuridine. This technique has now been used to select recombinants containing genes corresponding to antigens of medical and veterinary importance, influenza[7] and herpes simplex[8] as well as those already listed. There is little doubt that the technique is applicable to the expression of a wide range of protein or glycoprotein antigens, while several loci other than the TK gene, also inessential for virus replication, have been identified and could be valuable in constructing new recombinant viruses.

If the vaccinia virus recombinants have the same general physicochemical properties as the parent strain, they would be expected to possess the same advantages as vaccinia virus vaccines. The parent strain has a remarkable degree of stability under field conditions, a major consideration for live vaccines intended for use in tropical countries. Moreover, the vaccine can be administered easily by the dermal route, can be produced very cheaply and provides lasting immunity after a single inoculation, which is a major consideration for vaccines intended for use in developing countries. Once a suitably engineered recombinant strain of vaccinia virus has been obtained and shown to possess suitable immunogenic properties, high technology would no longer be required in vaccine production.

But before the general use of recombinant vaccinia virus vaccines is possible, several important issues concerning the safety and efficacy of vaccines of this type, will have to be resolved.

This need has been recognized by WHO, which convened two meetings, one at the US National Institutes of Health in November 1984 and a second in Geneva in September 1985. The following important conclusions were reached.

Molecular studies

Since the efficacy of the recombinants will depend on their ability to elicit a protective immunological response, further research aimed at an increased understanding of the regulation of gene expression in vaccinia virus will be required to ensure an adequate and stable level of expression of the foreign antigen. It will be necessary to define precisely the best ways of linking foreign genes to transcriptional regulatory sequences of the vaccinia virus genome and to identify the optimal sites for their insertion. The manner in which the foreign antigen is presented to the host's immune system should be investigated.

Level of attenuation

Vaccination with vaccinia virus can lead to abnormal skin eruptions, disorders affecting the central nervous system and a variety of other less severe complications. Thankfully, these severe complications are rare, so their occurrence with a genetically modified virus could be assessed only with a large-scale clinical study.

There is at present no generally accepted laboratory marker which predicts with certainty the virulence or attenuation of vaccinia virus or its recombinants for human beings. Reliable genetic markers of virulence would need to be established. Nevertheless, studies of mortality and pathogenesis in mice have been found to be of value; for example, the insertion of foreign genes in the TK gene has been found to reduce markedly the virulence of the virus[9]. Similar studies with other species would be valuable in telling whether this is a general phenomenon. It would be particularly useful to include primates and species such as cattle, which might be targets for immunization with recombinant vaccines. Moreover, it will be necessary, as with any attenuated virus vaccine, to study the virulence of the recombinant virus after several passages in the recipient species. Since successful immunization may require different routes of injection for different diseases, it will also be necessary to demonstrate that the recombinants are innocuous when administered by different routes.

Model systems

As there is no satisfactory laboratory animal model for assessing the virulence and efficacy of vaccinia virus, it is imperative to evaluate both *in vivo* and *in vitro* tests for their relevance in predicting the virulence for man of new recombinant strains. The results obtained should be compared with those obtained in the species for which the vaccine is intended. It will also be important to determine whether changes in host range or tissue tropism could occur as a result of the genetic modification of the virus and also by possible alterations in the viral envelope caused by insertion of a foreign gene product.

Assessing priorities

The use of vaccinia virus recombinants would be particularly advantageous for immunization against agents for which vaccines are not presently available, difficult to produce, ineffective and expensive. Moreover, the use of vaccinia virus offers the possibility of vaccination against several diseases by a single dose of a recombinant vaccine containing several gene inserts coding for different foreign antigens, but the extent to which the expression of one antigen may interfere with that of others encoded within the same genome will need to be evaluated. Studies of the immune responses of different hosts to each component antigen in multivalent recombinants will need to be carefully assessed.

In practice, it would be logical to use those vaccinia virus strains used extensively as vaccines in the WHO smallpox eradication programme and for which most information on satisfactory safety and efficacy is available. One or more well-characterized strains of vaccinia virus should be designated as references for use in the laboratory control and standardization of the vaccines.

Vaccine production

Vaccinia virus vaccine has been traditionally prepared in calf lymph, but this method of production is now considered by most authorities to be inappropriate. To be generally acceptable for use in man, it would be desirable to produce the vaccines in cell cultures employing the same good manufacturing practices as required for other modern live virus vaccines.

It is clear that control requirements for human vaccines using vaccinia virus as a vector for heterologous antigens would be developed progressively as more information relating to attenuation, production, safety and efficacy becomes available. Requirements applicable to live virus vaccines in general, such as the characteristics of the seed virus, use of a seed-lot system, description of the substrate and methods for production and the testing of safety, potency and stability, would be necessary. Issues peculiar to recombinant virus vaccines would thus include the description of the parent virus strain, methods for gene cloning, confirmation of the gene structure of the seed virus, the demonstration of its genetic stability and the results of clinical trials.

So that the results of research can be assessed for practical application as soon as possible, it is clear that WHO has an important role in encouraging and supporting the research work, in promoting the exchange of information and establishing technical collaboration between laboratories working on the expression of protective microbial antigens by vaccinia virus recombinants. WHO also has a role in formulating guidelines and requirements for these recombinants for the standardization, control and field use of any new vaccines developed.

While most attention has been focused on the use of vaccinia virus as the vector, similar approaches using alternative vectors, including other large DNA viruses or bacterial species, are feasible and may have advantages for some applications. For example, vectors capable of replication in the gut may be more suitable than vaccinia virus in the development of vaccines against enteric infections. Moreover, vaccinia recombinants might be used for the more efficient and safer production of antigens for the development of 'inactivated' vaccines, as exemplified by the work on rabies by a group at the Wistar Institute[4].

There is a very great potential for developing new approaches to the control of infectious disease using vaccinia virus as a vehicle, but the enthusiasm for rapid progress towards new vaccines should not be allowed to compromise the requirement for obtaining additional scientific information essential to ensure safety, efficacy and the exercise of all reasonable caution in mounting field investigations. Moreover, other approaches to vaccination are being vigorously pursued, for example controlled biosynthesis of antigens in bacterial, yeast and animal cells and site-specific mutagenesis to provide stable attenuated strains. It remains to be determined which of these approaches will provide vaccines giving optimal protection against each individual disease. ☐

Present addresses for authors: Wellcome Biotechnology Ltd, Pirbright, Surrey GU24 ONO, UK (F.B.); National Institute for Biological Standards and Controls, Holly Hill, Hampstead, London NW3 6RB, UK (G.C.S.); John Curtin School for Medical Research, Canberra, Australia (G.L.A.).

1. Mackett, M., Smith, G. L. & Moss, B. *Proc. natn. Acad. Sci. U.S.A.* **79**, 7415–7419 (1982).
2. Panicali, D. & Paoletti, E. *Proc. natn. Acad. Sci. U.S.A.* **79**, 4927–4931 (1982).
3. Smith, G. L., Mackett, M. & Moss, B. *Nature* **302**, 490–495 (1983).
4. Kieny, M. P. *et al Nature* **312**, 163–166 (1984).
5. Smith, G. L. *et al Science* **224**, 397–399 (1984).
6. Fenner, F. in *New Approaches to Vaccine Development* (eds Bell, R. & Torrigiani, G.) 187–196 (Schwake, Basel, 1984).
7. Panicali, D., Davis, S. W., Weinberg, R. L. & Paoletti, E. *Proc. natn. Acad. Sci. U.S.A.* **80**, 5364–5368 (1983).
8. Cremer, K., Mackett, M., Wohlenberg, C., Notkins, A. L. & Moss, B. *Science* **228**, 737–740 (1985).
9. Buller, R. M., Smith, G. L., Moss, B., Cremer, K. & Notkins, A. L. in *Vaccines 85* (eds Lerner, R. A., Chanook, R. M. & Brown, F.) 163–167 (Cold Spring Harbor Laboratory, New York, 1985).

Horizontal shear flow in the mantle beneath the Tonga arc

D. Giardini & J. H. Woodhouse

Harvard University, Department of Geological Sciences, Cambridge, Massachusetts 02138, USA

In the Tonga subduction zone, a systematic shear deformation, in which deep material moves relatively to the south, is superimposed on the mode of down-dip shortening which is characteristic of the region. We interpret this observation, together with a tectonic reconstruction, in terms of the interaction between the subducting lithospheric slab and a horizontal shear flow in the mantle.

THE Tonga arc forms the eastern margin of a complex 'vortex' of subduction (see Fig. 1) which has undergone major geometrical rearrangement in the past 20 Myr. The greatest changes are the rapid south-westward migration of the subduction west of Fiji from the Vityaz trench (AB; see Fig. 1), now inactive, to the current location at the New Hebrides arc[1-7]. East of Fiji the Lau Basin has opened behind the Tonga arc in the past 4-6 Myr, generating 150-250 km of new sea floor[5-6,8-12]. The northern termination of subduction (D) has migrated south-eastwards relative to the Pacific plate, its trace lying along a line (CD) joining Wallis Island to the current northern end of the Tonga Trench[1,7].

A conventional view of subduction envisages rigid slabs sinking through an essentially passive mantle. Hager and O'Connell[13,14], however, showed that the dips of Benioff zones can be approximately identified with the streamlines of an instantaneous global-flow model, indicating that, in fact, the geometry of subduction is strongly dependent on the pattern of flow in the mantle. Here we take the view that lithospheric material, subducted at the trench, becomes incorporated into the convective flow in the mantle; in a rapidly evolving region such as Tonga, therefore, we must interpret the current pattern of seismicity not as an instantaneous sample of an approximately steady state, but as the current locus of material particles injected into the flow by subduction in the past. The pattern of seismicity is thus a function of both the tectonic history of the region and the flow geometry of the mantle.

Assuming that the Pacific plate has behaved rigidly, the line BCD represents the original shape of the northern edge of the portion of the lithosphere subducted at the Tonga Trench. This portion of the lithosphere now forms the seismically active Benioff Zone dipping at ~45° from the Tonga Trench (DE) to the 'hook' shaped zone of intense deep seismicity (GH) south-east of Fiji.

The Louisville Ridge (EF) is a line of high sea-floor topography currently being subducted at the Tonga Trench[15-17]. The intersection of the ridge with the trench (E) is marked by a gap in shallow seismicity[16-18]. There is a corresponding gap in deep seismicity (H), which we identify with the intersection of the Louisville Ridge with the trench some 9 Myr ago[19]. The dipping slab DEHG represents, in this case, the current shape of the portion of the lithosphere subducted between the Louisville Ridge and the northern termination of subduction in the past 9 Myr.

The original shape of this portion of the lithosphere can be inferred by extending the line FE to intersect the Vityaz Trench at a point X between B and C. Figure 2 shows a schematic diagram of this shape, together with some approximate isochrons, indicating the time of subduction. We argue that the missing portion of the Pacific plate lying to the east of the 9 Myr isochron can be identified with the slab DEHG. The amount of distortion can be deduced by comparing the original and final shapes, yielding information on the velocity flow field in the mantle. The history of subduction in Tonga can be reconciled with the present-day distribution of seismicity if the zone has experienced a substantial horizontal shear deformation in which deep (~600 km) material has been displaced some 500 km to the south relative to surface material.

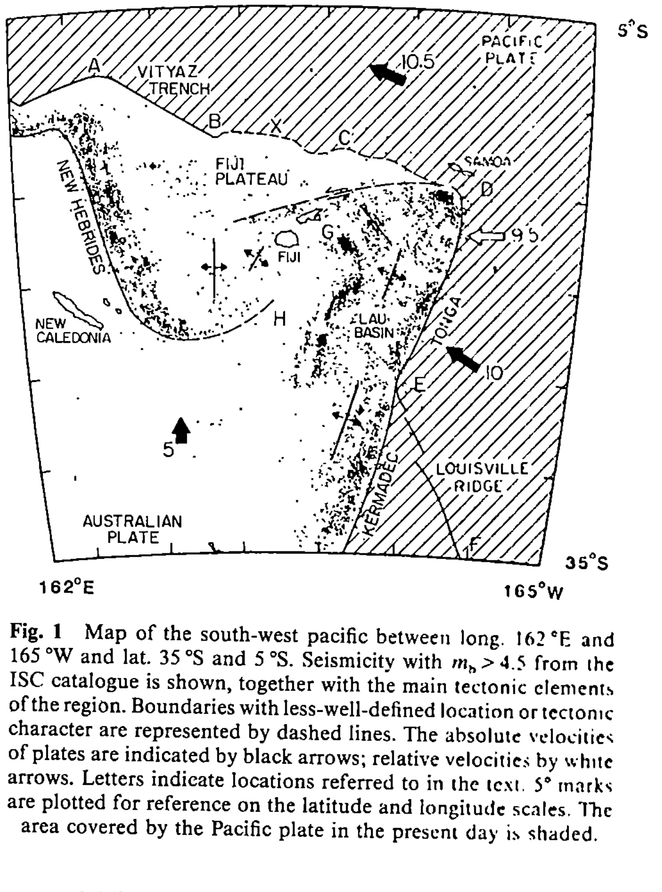

Fig. 1 Map of the south-west pacific between long. 162 °E and 165 °W and lat. 35 °S and 5 °S. Seismicity with $m_b > 4.5$ from the ISC catalogue is shown, together with the main tectonic elements of the region. Boundaries with less-well-defined location or tectonic character are represented by dashed lines. The absolute velocities of plates are indicated by black arrows; relative velocities by white arrows. Letters indicate locations referred to in the text. 5° marks are plotted for reference on the latitude and longitude scales. The area covered by the Pacific plate in the present day is shaded.

An independent observation, and, in fact, the most conclusive evidence that Tonga is undergoing such a shear deformation, is provided by the geometry of deep earthquakes in the region. Although dominated by down-dip compression[19], deep earthquakes in Tonga invariably show a component of horizontal shear in which deeper material is displaced to the south.

Seismicity of Tonga Islands region

The availability of digital data has greatly facilitated the retrieval of focal mechanisms and has improved our knowledge of active processes in subduction zones[20]. In a study focused on the deep seismicity of the Tonga Islands[19] region, it was shown how the

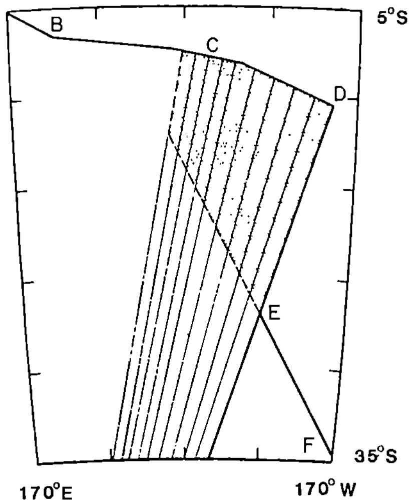

Fig. 2 Reconstruction of the Pacific lithosphere subducted at the Tonga Trench in the past 9 Myr. The tectonic elements used are depicted in Fig. 1. The geographical scale is the same as in Fig. 1. The shaded area is bounded by the Vityaz linement (BCD) and the Tonga Trench (ED), and by the extrapolation of the Louisville Ridge (FE) along its present local azimuth of 332° and the 9-Myr isochron, obtained by using a 8 cm yr^{-1} average relative velocity and a differential opening of the Lau Basin (see text for details).

combined analysis of large numbers of reliable focal mechanisms and large sets of hypocentres reveals patterns otherwise undetected. Here we make use of the same database, hypocentres from the International Seismological Centre (ISC) catalogue for the period 1964–82 and 94 moment tensor solutions for events since 1977 deeper than 400 km, obtained with the centroid moment tensor (CMT) method[21-27].

Figure 1 shows the seismicity of the south-west Pacific; the prominent tectonic features of the region are shown together with the relative and absolute velocities of the plates[7,28]. The Tonga Islands subduction zone is a region of shortening and thickening of the subducted slab, caused by the resistance encountered by the slab to penetration into the lower mantle[19,29]. Most of the deep seismicity (and all the large events) are located on parallel shear bands, which cut across the subducted slab and are inclined at ~45° to the major compression direction (which marks the direction of the slab). The orientation of the P and N axes of moment tensor solutions is strictly connected with the geometry of these shear structures[19].

In the Tonga Islands region the shear inferred from the moment tensor solutions shows a significant component in the north–south direction, perpendicular to the pattern predicted by the down-dip compression. This orientation can be seen in Fig. 3, showing a sample of typical fault plane solutions for events in the deepest part of the Tonga islands region.

The slip vectors of the solutions in Fig. 3 always have a component to the north. In the southern (events *e–j*) and northern (events *l–p*) portions of the Benioff Zone, shearing on parallel vertical bands implies motion of oceanward material relatively down, as shown by the approximately vertical fault planes (we refer to this type of focal mechanism as a type I event). It can be seen in Fig. 3, however, that the null axes of focal mechanisms on these vertical bands are systematically inclined down to the south, by an average of 18° over 36 solutions. This means that material on the oceanward side of the shear planes moves relatively down, as expected from the state of down-dip shortening, but also to the north with respect to material below (~20% of the overall shear).

In the central part, instead (events *a–d*), horizontal shear is the dominant mode of deformation, taking place on subhorizontal planes dipping to the north-west with material above moving relatively north (type II events).

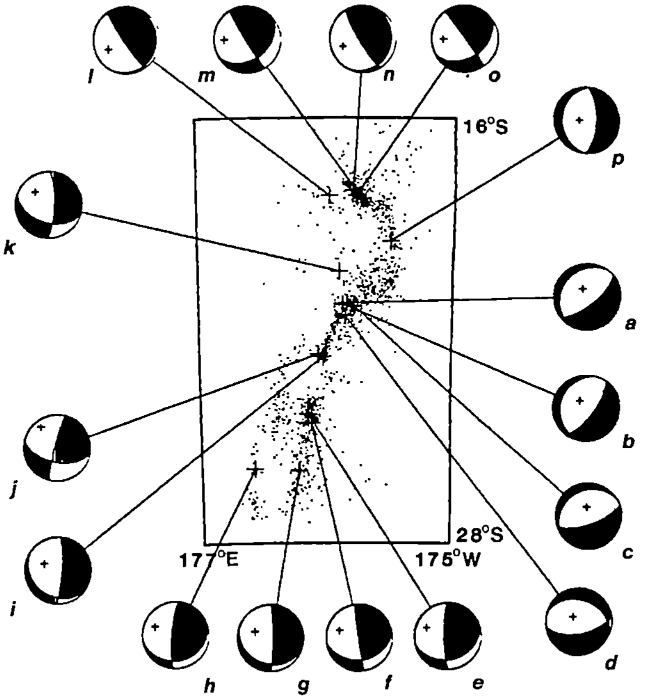

Fig. 3 Focal mechanisms for a sample of representative fault plane solutions in the Tonga Islands region. The lower hemisphere projection is shown, with the '+' indicating the direction of maximum compression. Black quadrants depict regions of extension at the source and white quadrants regions of shortening. Seismicity deeper than 400 km is shown. The events reported are: *a*, 5 July 1982; *b*, 25 November 1981; *c*, 24 April 1979; *d*, 6 February 1981; *e*, 28 April 1981; *f*, 16 September 1983; *g*, 3 November 1982; *h*, 18 April 1978; *i*, 8 July 1979; *j*, 10 April 1983; *k*, 17 June 1977; *l*, 28 January 1982; *m*, 1 January 1982; *n*, 9 November 1979; *o*, 20 July 1980; *p*, 15 May 1977.

Figure 4 shows the seismicity distribution viewed from the west, together with a representation of the moment tensors of all deep (>400 km) events in the central region. Note that the 'beachballs' of this figure do not represent the complete moment tensor solution but its projection onto the vertical meridional plane. Thus, they show only that part of the moment tensor which acts to deform vertical material planes. The boundaries between black and white quadrants are the directions of maximum shear, with the sense of motion such as would take a material particle from a white into a black quadrant. Four events show a predominance of shortening, but all others show a predominance of shear deformation. Without a single exception the direction of maximum shortening, denoted by a '+', lies to the north in the lower hemisphere, indicating a net flux of material below to the south relative to material above. For events in this region we have inferred from numerous examples[19] that the subhorizontal plane, dipping to the north, is usually the fault plane.

Figure 5*a* shows another representation of all moment tensor solutions obtained by the CMT method in the Tonga region. Each line represents the projection onto the vertical meridional plane of the axis of maximum shortening (the *P*-axis) of the complete moment tensor solution. The length of the line is governed by the degree of foreshortening. Again we note the strong tendency, for both deep and intermediate events, for maximum shortening to occur along lines dipping towards the north. Figure 5*b* shows the projections onto the vertical plane of the slip vectors of deep events, inferred by comparing moment tensor solutions with lineations in seismicity[19]. A bimodal distribution is indicated with clustering about directions dipping steeply (70°) and gently (20°) to the north, corresponding respectively to type I and II events defined above. Our previous study[19],

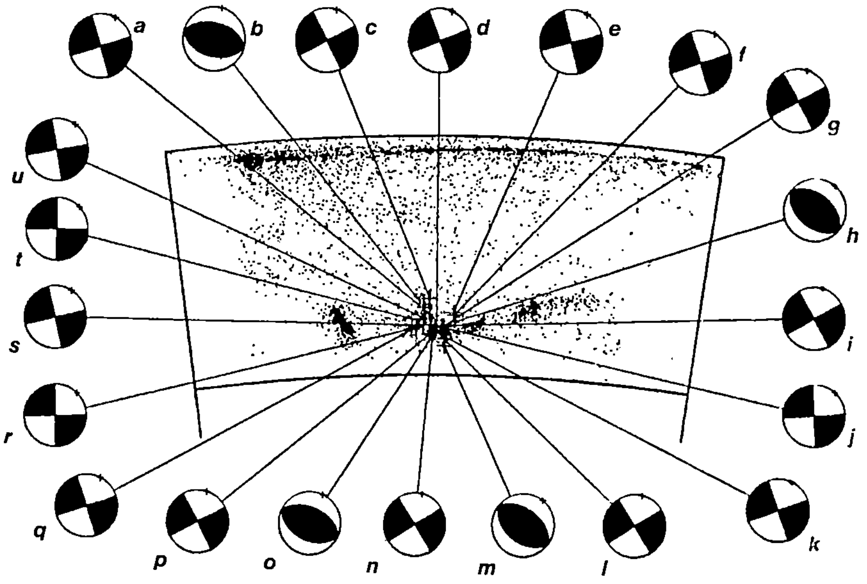

Fig. 4 Seismicity of the Tonga Islands region viewed from the west, together with a representation of the moment tensors of all the events located in the central portion of the deep Benioff Zone. The projection of the complete moment tensor onto the vertical meridional plane is shown, illustrating that part of the moment tensor which acts to deform vertical meridional planes. The events reported are: *a*, 30 November 1977; *b*, 30 November 1982; *c*, 13 November 1981; *d*, 24 April 1979; *e*, 9 November 1982; *f*, 16 July 1982; *g*, 25 March 1978; *h*, 6 July 1977; *i*, 6 November 1979; *j*, 20 October 1984; *k*, 5 July 1982; *l*, 6 February 1981; *m*, 14 December 1977; *n*, 28 May 1982; *o*, 25 November 1981; *p*, 7 October 1981; *q*, 17 June 1980; *r*, 24 December 1983; *s*, 30 October 1977; *t*, 14 March 1984; *u*, 27 November 1977.

using events occurring from 1977 to 1983, found only type I events in the northern and southern regions and type II events in the central region. If continuous over a long period of time, such a shearing pattern would induce more horizontal shear in the central region of the subducted slab. Since 1984, however, the pattern seems to be reversed; type II events have been occurring in the southern region and type I events in the central region—a startling change in the pattern of activity over such a short period. Almost invariably motion is inclined to the north in the lower hemisphere.

A second striking pattern emerges from the analysis of the hypocentre distribution. We suggest that the deep seismicity is located $\sim$500 km to the south of where it should be if the slab were subducting rigidly.

Although it is difficult to correlate a seismically-active portion of a slab with the original position on the trench at which the slab subducted, there are some cases in which this is possible; aseismic ridges, as well as corners and terminations of trenches, leave a trace in the seismicity that can be traced down the slab, sometimes to great depths[18,30]. The two tectonic features on which we focus our attention are the Louisville Ridge and the northern termination of the Tonga Trench.

The Louisville Ridge is a pronounced aseismic chain of seamounts originating at the Eltanin fracture zone on the South Pacific Ridge[15]; embedded in the Pacific plate, it has been subducting at the Tonga Trench for the past few million years[15,17]. The oblique intersection of the Louisville Ridge and the Tonga Trench marks the location of a shallow gap in seismicity[16-18]. However, attempts to locate the 'scar' left by the ridge deeper in the Benioff Zone have been unconvincing. No positive correlation with continuous gaps of seismic activity has been found on the projected location of the subducted seamount[16-18,31].

In a previous study[19], we suggested a correlation between the prominent gap in deep seismicity located at 23 °S (see Figs 1, 3) and the shallow gap located at the intersection of the Louisville Ridge with the Tonga Trench (Figs 1 and 2), on the grounds that they appear to be connected through the seismicity and because there is no known explanation for the deep gap other than its physical affinity with a similar shallow structure. The deep gap, however, is located some 500 km to the south of where the continuation of the Louisville Ridge down the slab should be[16,18].

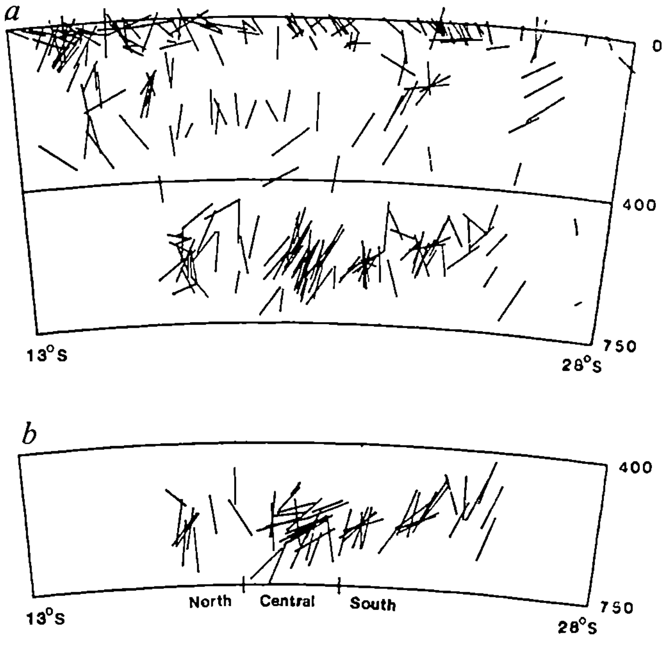

Fig. 5 *a*, All the moment tensor solutions (256) obtained with the CMT method in the Tonga Islands region are shown. Each line represents the projection onto the vertical meridional plane of the axis of maximum shortening (the P-axis) of the complete moment tensor solution. The length of each line depends on the direction of view. The 400-km depth line is shown for reference. *b*, Projection onto the vertical meridional plane of the slip vectors for all the deep events ($h > 400$ km) for which the fault plane has been identified by comparing the moment tensor solution with lineations in seismicity.

Between 10 and 20 Myr ago, the Tonga Trench (ED) and the Vityaz Trench (AB) formed a continuous arc of subduction[1-7]. Following the transfer of the subduction to the New Hebrides Arc, the Vityaz Trench, now embedded in the Pacific plate, has been translating to the west. The sequence of basins and troughs connecting the southern end of the Vityaz Trench with the northern limit of the Tonga Trench (BCD; hereafter referred to as the Vityaz linement) thus represents the track left by the northern termination of the Tonga Trench (D) in the Pacific plate since the Miocene. More recently, the Lau Basin began to open, displacing the Tonga Trench to the ESE by some 250 km in the past 4-6 Myr (refs 5, 8-12). The junction between the Vityaz and the Tonga trenches moved to the south-east, from its original position close to Wallis Island (C) to its present location (D)[1,7]. This model is also supported by seismicity trends in the Lau Basin and northern Fiji Plateau[32] and by detailed petrological,seismological and geochemical analyses of the troughs forming the Vityaz linement[7].

Based on this model, we reconstructed the shape of the lithosphere subducted at the Tonga Trench in the past 9 Myr (Fig. 2). This shape is bounded by the present location of the Tonga Trench and Vityaz linement (BCDE), the extrapolation of the Louisville Ridge (FE) along its present local azimuth of 332°, and the 9-Myr isochron based on the tectonic history of the region. The relative velocity of the Australian and Pacific plates has increased in amplitude in the past 10 Myr, from 7.1 to 9.1 cm yr^{-1} (excluding the Lau Basin spreading rate) at the northern termination of the Tonga Trench[33], because of an increase in absolute velocity by 15% for the Australian plate[34,35], and 20% for the Pacific plate[36]. The direction of the relative velocity has maintained an azimuth of 275°. To obtain the isochrons in Fig. 2 we considered an average relative velocity of 8 cm yr^{-1} over the past 9 Myr at 15° S, and 6.5 cm yr^{-1} at 28° S. Also, the opening of 250 km in the northern part of the Lau Basin, and 125 km in the South, is considered to have taken place in the past 5 Myr (ref. 6).

In Fig. 6*a* the seismicity of the Tonga Islands region is viewed from an azimuth of 266°, perpendicular to the Tonga Trench. The dashed line is the projection on a vertical plane of the shape obtained in Fig. 2. The continuous line borders the area of the Benioff zone limited to the south by a line connecting the deep seismic gap with the shallow Louisville Ridge gap.

The two shapes, observed in the seismicity and predicted from the tectonic model, should correspond if no lateral deformation was active during subduction. Instead, the difference between the two is large. The seismicity seems to be shifted to the south by an amount proportional to depth, with a maximum shift of 500 km at 650-km depth.

To test the existence and the amount of the shift, we performed a simple experiment on the seismicity (Figs 6*b*, *c*). Hypocentres are shifted to the north by an amount proportional to depth, with a maximum displacement of 300 km at 650-km depth in Fig. 6*b*, a maximum of 500 km in Fig. 6*c*. Although the shift applied in Fig. 6*b* is not quite enough to match the seismicity with the predicted profile, the agreement between the two in Fig. 6*c* is remarkable, given the shortcomings of the tectonic reconstruction and the fact that we use a planar projection for a Benioff Zone which is not truly planar.

As in the case of the earthquake moment tensors, we find in the seismicity distribution another strong indication that the slab undergoes a substantial shear deformation in the north-south direction during subduction, with the deeper part of the slab moving relatively south. We estimate that a deformation of the order of 500 km in a 9-Myr period is needed to match the observed seismicity distribution.

Plate tectonics

In the case of the Tonga Islands the existence of a north-south shear flow in the mantle, required from the seismological analysis, can be explained and predicted by looking at the absolute motion of the Australian and Pacific plates.

Absolute and relative plate velocities at trenches do not usually differ appreciably, especially at oceanic-continental boundaries and in the presence of fast subducting oceanic plates[28]. This is not always the case, however, and the Tonga Islands region provides an example of the information that can be retrieved by looking at the absolute velocities of plates.

The tectonic setting of the south-west Pacific is anomalous; the Pacific and Australian plates originate at the same ridge, and move to the north and north-west. Because the ridge is not linear and because of the large dimension of the two plates moving in a spherical geometry, the relative motion between the two plates, which move parallel south of New Zealand, becomes more and more convergent along the Melanesian border, reaching a maximum north of New Guinea, where the Pacific plate is sliding towards the west and the Australian to the north, and the relative velocity reaches 13 cm yr^{-1} (ref. 28).

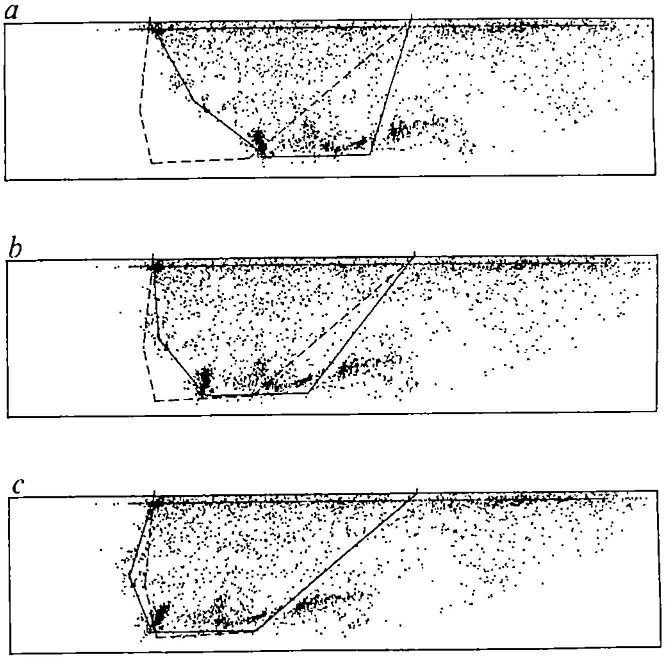

Fig. 6 *a*, Seismicity of the Tonga Islands region viewed from an azimuth of 266°, perpendicular to the Tonga Trench. The dashed line is the projection onto the vertical plane of the shape of the Pacific lithosphere subducted at the Tonga Trench in the past 9 Myr, reconstructed in Fig. 2. The solid line borders the area of the Benioff Zone limited to the south by a line connecting the deep seismic gap with the shallow Louisville Ridge gap (HE in Fig. 1). *b*, As *a*, but with the seismicity shifted to the north by an amount proportional to depth, with a 300-km maximum displacement at 600-km depth. *c*, As *b*, but with a maximum displacement of 500 km at 600-km depth.

At the Tonga Trench the Australian plate is moving to the north at ~5 cm yr^{-1} (Fig. 1), in the absolute reference velocity frame in which there is no net rotation of the lithosphere (referred to as the mean mesopheric frame)[28,33]. The Pacific plate is moving WNW[33] at 10 cm yr^{-1} (Fig. 1). This velocity can be decomposed into components of 5 cm yr^{-1} to the north and 8.5 cm yr^{-1} to the west. The westerly component is responsible for the relative velocity at the trench (a smaller contribution from the back-arc spreading in the Lau Basin accounts for the trench migration). Because the relative velocity at the trench is directed east-west and the trench itself is oriented approximately north-south, the two plates, and the trench with them, are moving in the direction perpendicular to the convergence velocity at a speed comparable with the subduction speed.

This creates a unique geometrical configuration. The Pacific lithosphere is subducting in a mantle which is likely to be moving with a different velocity. For example, in the mesopheric hypothesis[33] that the mantle is stationary at 670 km, the subducted lithosphere will undergo a shear deformation of 5 cm yr^{-1} over its entire length in the north-south direction. Assuming that the deepest part of the slab subducted ~8-10 Myr ago[17], this would produce a maximum shift of some 450 km towards the south, in agreement with the estimates derived from the seismological evidence.

We thank M. Hamburger and T. Brocher for stimulating conversations; T. Brocher for a copy of his book before publication and R. Louat for the results obtained at ORSTOM; and A. M. Dziewonski and R. J. O'Connell for discussions. This work was supported by NSF grant EAR83-07603.

15 August; accepted 11 December 1985.

se, C. G. *Bull. geol. Soc. Am.* **82,** 3087–3110 (1971).
J. B. & Gorton, M. in *The Western Pacific Islands Areas, Marginal Areas* (ed. Coleman,) 543–566 (University of Western Australia Press, Nedlands, 1973).
man, P. J. & Packham, G. H. *Earth-Sci Rev.* **12,** 197–233 (1976).
ey, D. A. *Bull. Aust. Soc. Explor. Geophys.* **9,** 117–123 (1978).
ois, J., Dupont, J. & Recy, J. *Trav. Doc. Off. Rech. Scient. Techn. Outre-Mer* **147,** 567–588 982).
J. B., Stork, A. L. & Whelan, P. M. *Tectonophysics* **102,** 207–224 (1984).
her, T. M. in *Geological Investigations of the Northern Melanesian Borderland* (ed. rocher, T. M.) (Circum-Pacific Council for Energy and Mineral Resources Earth Science eries, American Association of Petroleum Geologists, Tulsa, Oklahoma (in the press).
ig, D. E. *J. geophys. Res.* **75,** 239–254 (1970).
r, J. G., Hawkins, J. W., Mammerickx, J. & Chase, C. G. *Bull geol. Soc. Am.* **83,** 18 (1972).
A., Hawkins, J. W. & Sclater, J. G. *Earth planet. Sci. Lett.* **33,** 27–35 (1976).
K. in *Island Arcs, Deep Sea Trenches and Back-Arc Basins* (eds Talwani, M. & C., III) 429–436 (American Geophysics Union, Washington, DC, 1977).
Earth planet. Sci. Lett. **28,** 283–297 (1976).
'Connell, R. J. *Tectonophysics* **50,** 111–133 (1978).
onnell, R. J. & Raefsky, A. *Tectonophysics* **99,** 165–189 (1983).
ase, C. G. *Bull. geol. Soc. Am.* **83,** 3627–3644 (1972).
J. *Trav. Docum. Off. Rech. Scient. Techn. Outre-Mer* **147,** 299–318 (1982).
Cornell Univ. (1980).
A., Bracey, D. R. & Hey, R. N. *Geol. Soc. Am. Spec. Pap.* **172** (1976).
lhouse, J. H. *Nature* **307,** 505–509 (1984).

20. Incorporated Research Institutions for Seismology *Science Plan* (1984)
21. Dziewonski, A. M., Chou, T. A. & Woodhouse, J. H. *J. geophys. Res* **86,** 2825–2852 (1981)
22. Dziewonski, A. M. & Woodhouse, J. H. *J. geophys. Res.* **88,** 3247–3271 (1983)
23. Dziewonski, A. M., Friedman, A., Giardini, D. & Woodhouse, J. H. *Phys. Earth & planet Interiors* **33,** 76–90 (1983).
24. Dziewonski, A. M., Friedman, A. & Woodhouse, J. H. *Phys. Earth & planet Interiors* **33,** 71–75; 243–249 (1983).
25. Dziewonski, A. M., Franzen, J. E. & Woodhouse, J. H. *Phys. Earth & planet Interiors* **34,** 1–8; 129–136; 209–219 (1984).
26. Dziewonski, A. M., Franzen, J. E. & Woodhouse, J. H. *Phys. Earth & planet Interiors* **37,** 87–96; **38,** 203–213 (1985).
27. Giardini, D. *Geophys. J. R. astr. Soc.* **77,** 883–914 (1984).
28. Circum Pacific Council for Energy and Mineral Resources, *Plate Tectonic Map of the Circum-Pacific Region* (1982).
29. Isacks, B. & Molnar, P. *Rev. Geophys. Space Phys.* **9,** 103–174 (1971)
30. Kelleher, J. & McCann, W. *J. geophys. Res.* **81,** 4885–4896 (1976)
31. Isacks, B. L. & Barazangi, M., in *Island Arcs, Deep Sea Trenches and Back-Arc Basins* (eds Talwani, M. & Pitman, W. C., III) 99–114 (American Geophysics Union, Washington DC, 1977).
32. Eguchi, T., *Tectonophysics* **102,** 17–32 1984.
33. Minster, J. B. & Jordan, T. H., *J. geophys. Res.* **83,** 5331–5353 (1978)
34. Weissel, J. K. & Hayes, D. E., in *Antarctic Oceanology II: The Australian–New Zealand Sector, Antarctic Res Ser. Vol* 19 (ed. Hayes, D. E.) 165–196 (American Geophysics Union, Washington DC, 1972).
35. Weisel, J. K. & Hayes, D. E. *J. geophys. Res.* **79,** 2579–2587 (1974)
36. Molnar, P., Atwater, T., Mammerickx, J. & Smith, S. M. *Geophys. J. R. astr. Soc* **40,** 383–420 (1975).

st-transcriptional regulation accounts for the *trans*-activation of the human T-lymphotropic virus type III

Craig A. Rosen*, Joseph G. Sodroski*, Wei Chun Goh*, Andrew I. Dayton*, Judith Lippke* & William A. Haseltine*†

* Department of Pathology, Dana-Farber Cancer Institute, Harvard Medical School, 44 Binney Street, Boston, Massachusetts 01225, USA
† Department of Cancer Biology, Harvard School of Public Health, Boston, Massachusetts 02115, USA

The level of synthesis of viral proteins and heterologous proteins under the control of long terminal repeat sequences of human T-lymphotropic virus type III (HTLV-III or LAV) increases dramatically in cells that constitutively express the HTLV-III trans-*activator protein. Increased levels of protein synthesis occur without a comparable increase in the levels of corresponding messenger RNA. We propose that post-transcriptional events mediated by the HTLV-III* trans-*activator protein account for positive regulation of HTLV-III gene products in infected cells.*

A RETROVIRUS, the human T-lymphotropic virus type III (HTLV-III or LAV), is the primary aetiological agent of acquired immune deficiency syndrome[1-6] as well as other disorders, including a progressive degeneration of the central nervous system[7] and lymphadenopathy[1,2,6]. The cytopathic nature of this virus reflects the high level of virus production[8] which can be partly attributed to virus-associated *trans*-acting factors that greatly elevate the level of gene expression directed by the HTLV-III long terminal repeat (LTR)[9]. The elements of this autostimulatory pathway include an effector, the *trans*-activator protein of relative molecular mass (M_r) 14,000 (14K)[10] encoded by the bipartite *tat*-III gene[11,12] and a responder element, the *trans*-activating responsive sequence (TAR)[12,13], located within the HTLV-III LTR. Elucidation of the mechanism of this autostimulatory pathway may lead to insights important in the prevention and control of virus infection.

We have used a transient gene-expression assay to examine the mechanism of *trans*-activation. Our results demonstrate that elevation of LTR-directed gene expression in cells expressing the *tat*-III protein reflects an increase in protein synthesis without a comparable rise in the steady-state level of the respective messenger RNAs. We also find that sequences that govern the *trans*-activation response must be located at or near the 5′ terminus of the mRNA. We propose that positive regulation of HTLV-III gene expression mediated by the *trans*-activator protein occurs via post-transcriptional events.

Measurement of virus-encoded protein

Previous studies have shown that expression of the bacterial chloramphenicol acetyltransferase (*cat*) gene under control of the HTLV-III LTR is greatly elevated in cells that express the HTLV-III *tat* protein[9,11-13]. An indication that positive regulation of HTLV-III LTR-directed gene expression occurs by a post-transcriptional event was our observation that the *trans*-acting responsive sequences are mainly located immediately 3′ to the site of transcription initiation and comprise the 5′-terminal domain of the mRNA[13]. The unusually high levels of HTLV-III LTR-directed protein synthesis, an increase of expression of more than 500- to 1,000-fold relative to uninfected cells, also suggests that *trans*-activation of HTLV-III occurs by a mechanism other than an increase in transcription initiation. Specifically, we considered the possibility that increased protein expression is attributable to post-transcriptional events. A direct prediction of this hypothesis is that the ratio between the amount of protein and of corresponding mRNA will increase in the presence of the *trans*-activator protein.

To test our prediction we measured the relative levels of viral RNA and proteins in matched pairs of cell lines that differed only with respect to the expression of the HTLV-III *trans*-activator protein. The cell lines used for these experiments were the human lymphoid cell lines Raji (a B-cell line) and Jurkat (a T-cell line) that were uninfected or had been infected with

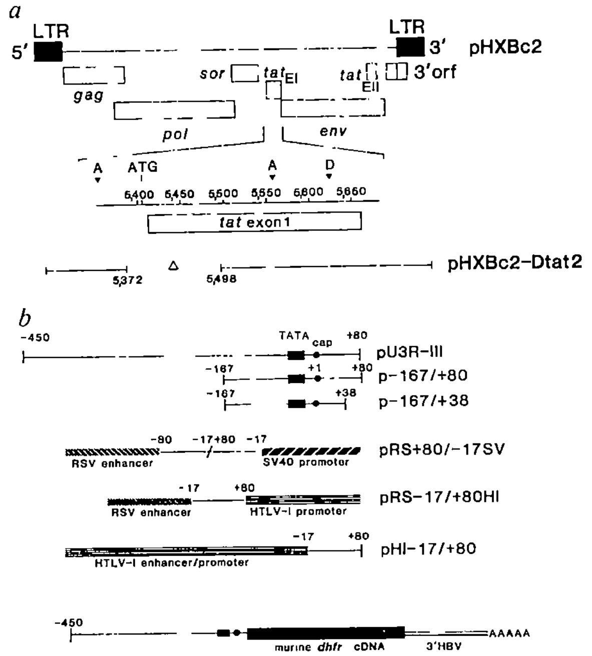

Fig. 1 Schematic diagram of plasmids used to measure *trans*-activation. *a*, Construction of plasmid pHXBc2 containing an infectious copy of HTLV-III proviral DNA has been described previously[16]. Plasmid pHXBc2-Dtat2 is identical to pHXBc2 except for deletion of nucleotides 5,372–5,498 in the first coding exon of the *tat*-III gene[40]. orf, Open reading frame. EI and EII signify exons I and II, respectively. *b*, Plasmids pU3R-III, p−167/+80, p−167/+38, pRS+80/−17SV, pRS−17/+80HI and pHI−17/+80 contain the sequences shown directing expression of the bacterial *cat* gene[23]. In each of these plasmids, polyadenylation signals obtained from the SV40 genome are present 3′ to the *cat* gene. The additional plasmid sequences are derived from plasmid pBR322 (nucleotides 2,246–4,361) and provide the origin of replication and the ampicillin resistance gene. The construction of plasmid pU3R-III and p−167/+80 has been described previously[9,13]. Plasmid p−167/+38 was constructed by deleting nucleotides +38 (*Sac* site) to +80 of the HTLV-III LTR. The RSV enhancer sequences[22] present in plasmids pRS+80/−17SV and pRS−17/+80HI encompass nucleotides −138 to −229 of the RSV LTR. Both the SV40 early promoter present in plasmid pRS+80/17SV and the HTLV-I promoter region (nucleotides −55 to +315) present in plasmid pRS−17/+80HI lack their homologous enhancer sequences. Plasmid pU3R-III-DHFR (shown at bottom) contains the cDNA[41] of the murine *dhfr* gene and HBV polyadenylation sequences 3′ to nucleotides −450 to +80 of the HTLV-III LTR. All plasmid constructions and DNA manipulations were done according to established procedures[42]. Solid lines depict HTLV-III LTR sequences.

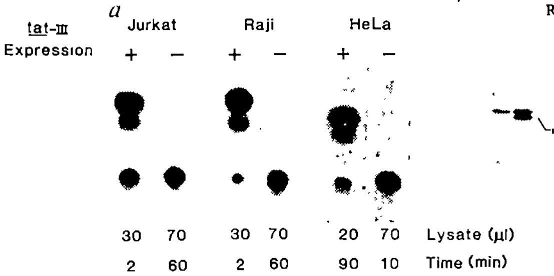

Fig. 2 Levels of HTLV-III LTR-directed CAT and DHFR synthesis in *tat*-III expressor cell lines. Cells were transfe the plasmids pU3R-III (*a*) and pU3R-III-DHFR (*b*). *a*, were prepared 48 h post-transfection and CAT assa formed as described previously[23,25]. The amount indicated was incubated with ^{14}C-chloramphenic coenzyme A for the time shown. Unreacted ^{14}C-c (bottom spot) and acetylated reaction products w ascending TLC[23]. *b*, Cells were metabolically la methionine from 48 to 58 h post-transfection. ^{35}S were immunoprecipitated[43] with anti-murine DH trophoresed on 10% polyacrylamide gels. Gels fluorography was performed using Enhance (NE endogenous human DHFR protein (upper band) DHFR protein (lower band). Cell lines that constituti the HTLV-III *tat* protein (+) were constructed as descr viously[14]. The HeLa(*tat*-III) cell line was established by co fection of plasmids p83−5365/8053–9296 (*tat*-III expressor 12) and pSV2NEO (ref. 44), followed by selection for *neo*-resista clones that expressed *tat*-III (ref. 44). The darker intensity of the background bands present in the *tat*-III lane probably reflects unequal loading.

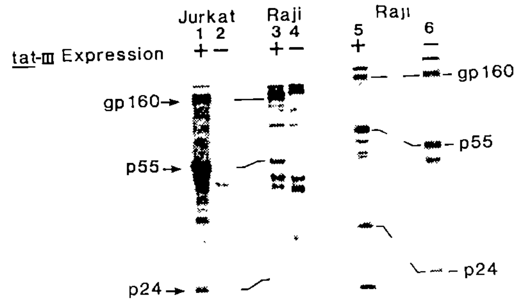

Fig. 3 Immunoprecipitation of viral proteins from transfected cells. Cell lines shown were transfected[15] with plasmids pHXBc2-Dtat2 (lanes 1–4) and pHXBc2 (lanes 5, 6). Cell lysates were prepared from cells labelled 48–58 h post-transfection with ^{35}S-methionine and ^{35}S-cysteine. The virus-specific proteins were immunoprecipitated[43] with sera from HTLV-III-infected patients and electrophoresed on 15% polyacrylamide gels.

a recombinant murine retrovirus *tat*-III expression vector[14]. These cells constitutively express a fully active HTLV-III *trans*-activator protein that stimulates HTLV-III LTR-directed gene expression. Neither the Raji (*tat*-III) nor the Jurkat (*tat*-III) cell lines express other HTLV-III-specific proteins. We have described the construction and characterization of the cell lines elsewhere[14]. Experiments were also performed in HeLa cells that constitutively express *tat*-III under control of the HTLV-III LTR (see Fig. 2 legend).

To determine the effect of the *trans*-activator protein on the level of HTLV-III viral mRNA and proteins, the cell lines were transfected[15] with HTLV-III proviral DNA. The provirus used for this study was derived from infectious proviral DNA present on plasmid pHXBc2 (ref. 16) and contained a deletion of 94 nucleotides in the first coding exon of the *tat*-III gene (pHXBc2-Dtat2; Fig. 1*a*). The deleted provirus was used to avoid the possibility that expression of the *tat*-III gene product by the transfected provirus could complicate interpretation of the experiment. The deleted provirus used for this experiment was entirely defective for expression of the *trans*-activator protein as judged by its inability to increase *cat* gene expression under the control of the HTLV-III LTR in co-transfection experiments (Table 1, expt 2).

The cells used for these experiments were simultaneously transfected with two other plasmids, pU3R-III-CAT[9], containing the *cat* gene under control of the HTLV-III LTR, and pSV2-β-globin[17], containing the rabbit β-globin gene under control of the simian virus 40 (SV40) early region promoter. The increased level of CAT enzyme activity in the *tat*-III expressor cells attests to the activity of the *trans*-activator protein (Fig. 2*a*). The level of rabbit β-globin RNA in the transfected cells serves as a control of mRNA synthesized from a promoter that is not responsive to the HTLV-III *trans*-activator[9]. The SV40 early region promoter sequences present on plasmid pSV2-β-globin are identical to those present on plasmid pSV2CAT which have previously been shown to be non-responsive to the

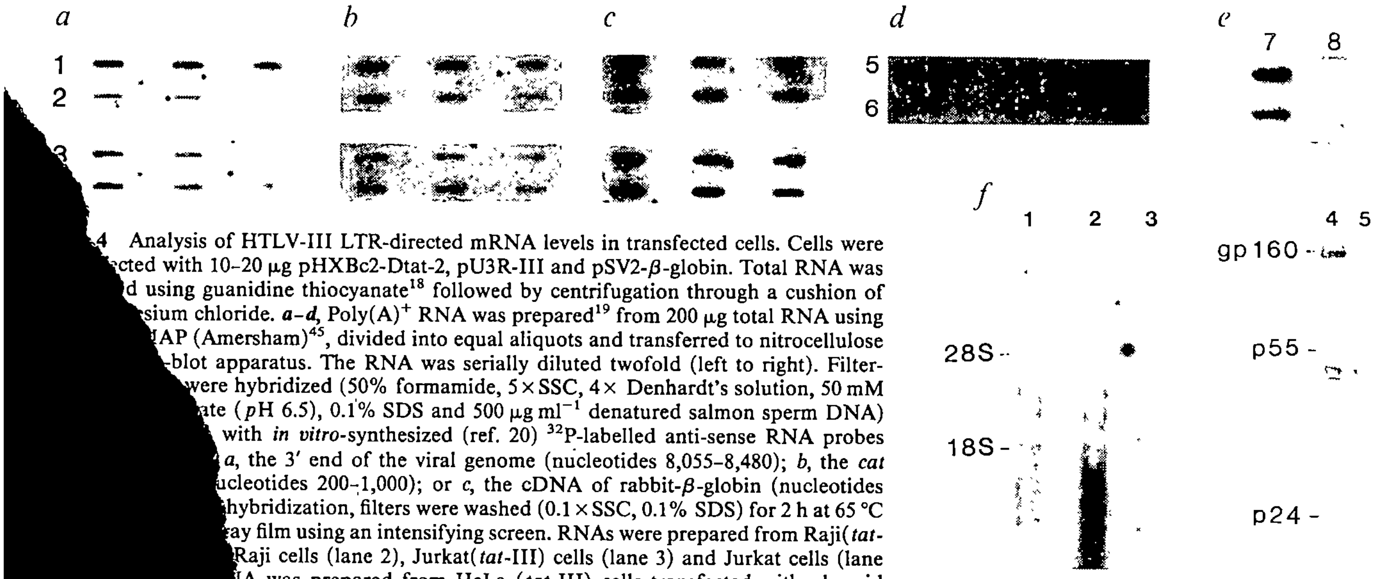

[illegible] 4 Analysis of HTLV-III LTR-directed mRNA levels in transfected cells. Cells were [illegible] cted with 10–20 μg pHXBc2-Dtat-2, pU3R-III and pSV2-β-globin. Total RNA was [illegible] d using guanidine thiocyanate[18] followed by centrifugation through a cushion of [illegible] sium chloride. ***a–d***, Poly(A)$^+$ RNA was prepared[19] from 200 μg total RNA using [illegible] AP (Amersham)[45], divided into equal aliquots and transferred to nitrocellulose [illegible] -blot apparatus. The RNA was serially diluted twofold (left to right). Filter- [illegible] were hybridized (50% formamide, 5×SSC, 4× Denhardt's solution, 50 mM [illegible] ate (*p*H 6.5), 0.1% SDS and 500 μg ml^{-1} denatured salmon sperm DNA) [illegible] with *in vitro*-synthesized (ref. 20) ^{32}P-labelled anti-sense RNA probes [illegible] *a*, the 3′ end of the viral genome (nucleotides 8,055–8,480); *b*, the *cat* [illegible] ucleotides 200–1,000); or *c*, the cDNA of rabbit-β-globin (nucleotides [illegible] hybridization, filters were washed (0.1×SSC, 0.1% SDS) for 2 h at 65 °C [illegible] ay film using an intensifying screen. RNAs were prepared from Raji(*tat*- [illegible] Raji cells (lane 2), Jurkat(*tat*-III) cells (lane 3) and Jurkat cells (lane [illegible] A was prepared from HeLa (*tat*-III) cells transfected with plasmid [illegible] ne 5) and mock-transfected HeLa *tat*-III cells (lane 6) and probed with anti-sense RNA corresponding to the *cat* coding [illegible] NA, prepared from HeLa(*tat*-III) cells transfected with plasmid pU3R-III, was treated with DNase (lanes 7, 8) and RNase [illegible] erred to nitrocellulose then hybridized with anti-sense *cat* RNA. ***f***, Northern blot analysis and protein analysis of virus-specific [illegible] protein. Total RNA was isolated from transfected cells as described above. RNA (20 μg) obtained from pHXBc2-transfected Raji [illegible] lane 1), pHXBc2-Dtat2-transfected Raji cells (lane 2) and Raji cells transfected with HTLV-I proviral DNA (plasmid pXT1env contains [illegible] TLV-I LTR directing expression of the HTLV-I *env* gene) (lane 3) was electrophoresed through 1% formaldehyde agarose gels and [illegible] nsferred to nitrocellulose filters[21]. Filter-bound RNA was hybridized for 24 h (50% formamide, 5×SSC, 4×Denhardt's solution, 50 mM sodium phosphate (*p*H 6.5), 0.1% SDS and 500 μg ml^{-1} denatured salmon sperm DNA) at 55 °C to a ^{32}P-labelled DNA probe spanning the complete genome. Filters were washed at high stringency (65 °C; 0.2×SSC, 0.1% SDS) and exposed to X-ray film and mRNA species sized using methylene blue-stained ribosomal RNA as size markers. Lanes 4 and 5 show virus-specific proteins present in the HXBc2 and HXBc2-Dtat2-transfected cells, respectively. Immunoprecipitations and protein analysis were performed as described in Fig. 3 legend.

tat-III product[9,12,13]. In a separate experiment the same cell lines were simultaneously transfected with plasmid pSV2-β-globin and plasmid pU3R-III-DHFR (Fig. 2*b*), which contains the complementary DNA of murine dihydrofolate reductase (*dhfr*) under control of the HTLV-III LTR. Figure 2*b* demonstrates that synthesis of the murine DHFR protein was greatly elevated in the *tat*-III expressor cells. The level of murine *dhfr* mRNA could not be quantitated because of co-migration on Northern gels with endogenous human *dhfr* mRNA.

The level of viral protein expression was determined by incubation of the pHXBc2-Dtat2 transfected cells with ^{35}S-methionine and ^{35}S-cysteine for 10 h, 48 h post-transfection. Virus-specific proteins were detected by immunoprecipitation with antisera from HTLV-III-infected patients followed by analysis on polyacrylamide gels. These experiments demonstrate that expression of virus-specific proteins is greatly increased in Raji(*tat*-III) compared with Raji cells (Fig. 3). Identical results were obtained on transfection of Jurkat and Jurkat(*tat*-III)-infected cells (Fig. 3). The extent of stimulation of virus-specific protein is >500-fold as determined by densitometric comparison with a host protein present in uninfected cells. No HTLV-III-specific proteins were detected upon transfection of uninfected Raji and Jurkat cells with the deleted provirus. Note that the well-characterized viral proteins gp160, p55 and p24–25 are evident in analysis of immunoprecipitates from the transfected cells. In a control experiment, pHXBc2, containing an intact infectious provirus, was transfected into uninfected Raji cells and Raji(*tat*-III) cells. Figure 3 demonstrates that the same virus-specific proteins were evident following transfection of both cell lines.

Measurement of mRNA

The level of virus-specific mRNA was determined by isolation of total cellular RNA with guanidine thiocyanate[18], centrifugation through caesium chloride and selection of poly(A)-containing RNA species[19]. The poly(A)$^+$ fraction was transferred to nitrocellulose filters and the concentration of virus-specific RNA was determined using *in vitro*-synthesized[20] ^{32}P-labelled anti-sense viral RNA corresponding to the 3′ portion of the provirus, a region of the genome not present in the retroviral vector used to introduce the HTLV-III *trans*-activator gene into the lymphoid cell lines. The steady-state level of *cat* mRNA and rabbit β-globin mRNA was also measured in these experiments using the respective ^{32}P-labelled probes. RNA and protein analysis were done using the same cell preparations at the same time.

Our results show that the level of viral mRNA relative to β-globin mRNA is similar both in uninfected cells and in cells that express the HTLV-III *trans*-activator protein (Fig. 4). The level of *cat* mRNA, also under control of the HTLV-III LTR, remains constant relative to the level of β-globin mRNA that is initiated in the SV40 promoter (Fig. 4). RNA was also prepared from untransfected cells. Figure 4*d* demonstrates that the hybridization signals are well above the background level. Digestion of the samples with RNase also eliminated the signal.

Intracellular distribution of viral mRNA

We compared the level and the length of viral mRNA species in the transfected cells by Northern blot analysis[21]. Figure 4*f* shows that similar amounts of viral mRNA species are present in Raji cells transfected with plasmid pHXBc2-Dtat2 and HXBc2. No signal was observed in control cells transfected with HTLV-I proviral DNA present on plasmid pXT1env (see Fig. 4*f* legend). Virus-specific proteins were only evident in those cells transfected with plasmid HXBc2 (Fig. 4*f*), which expresses the *tat*-III product. The proteins were extracted from ^{35}S-methionine- and ^{35}S-cysteine-labelled cells at the same time post-transfection as the RNA was extracted. The low level of viral RNA observed (Fig. 4*f*) is typical of measurements of RNA done under transient transfection conditions using cell lines that do not incorporate large amounts of DNA.

The intracellular distribution of viral RNA was determined by fractionation of the cells into nuclear and cytoplasmic components. The HeLa(*tat*-III) and Jurkat(*tat*-III) cells used for

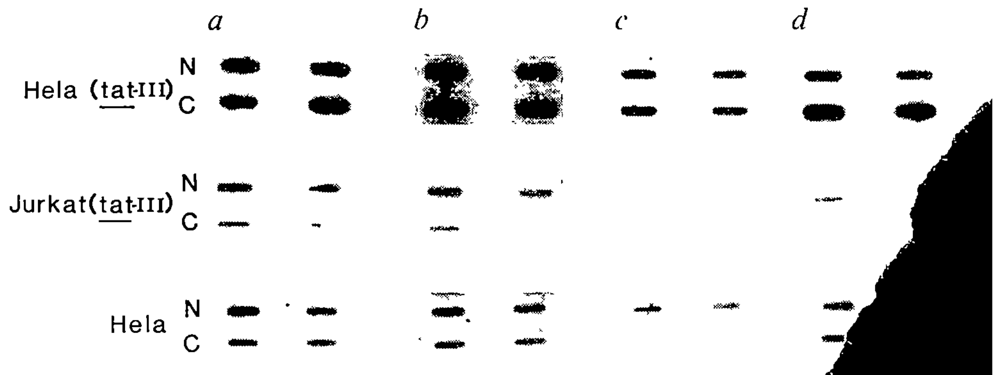

Fig. 5 Subcellular distribution of mRNA in *tat*-III expressor cells. HeLa(*tat*-III) cells, HeLa cells and Jurkat (*tat*-III) cells were transfected with pU3R-III, pSV2-β-globin and pHXBc2-Dtat2. At 48 h post-transfection, cells were lysed using the non-ionic detergent NP40 (ref. 42) and nuclear and cytoplasmic fractions were isolated, then extracted with guanidine thiocyanate. RNA was pelleted through a cushion of caesium chloride, poly(A)$^+$ RNA was prepared[19,45], diluted twofold and transferred to nitrocellulose. Hybridization and washing conditions were as described in Fig. 4 legend. *In vitro*-synthesized anti-sense RNA probes were p
DNA corresponding to:*a*, the 3′ end of the viral genome; *b*, the *cat* gene; *c*, rabbit β-globin cDNA; *d*, the murine *dhfr* cDN
1-1,115). Nuclear (N) and cytoplasmic (C) RNAs are indicated.

this study were simultaneously transfected with pHXBc2-Dtat-2, pU3R-III and pSV2-β-globin. The concentration of viral RNA, SV40-directed β-globin RNA and RNA synthesized from the cellular *dhfr* gene was measured in each fraction. Figure 5 demonstrates that the presence of the *trans*-activator protein did not affect the relative distribution of viral RNA or HTLV-III LTR-directed *cat* mRNA in the nucleus and cytoplasm in either the Jurkat(*tat*-III) or HeLa(*tat*-III) cells. The distribution of mRNAs was similar to that of the β-globin RNA synthesized from the SV40 promoter or to the endogenous *dhfr* mRNA. Similar results were obtained in parallel experiments performed with the control cells that lack *tat*-III expression (Fig. 5).

We conclude that the greatly elevated levels of virus protein and of CAT enzyme activity detected in cells that express the HTLV-III *trans*-activator protein occur without a comparable increase in the level of the corresponding mRNA and do not result from an alteration in the ratio of nuclear to cytoplasmic mRNA.

Position of TAR sequences

In a previous study, deletion analysis of the HTLV-III LTR demonstrates that the sequence necessary for *trans*-activation (the TAR sequence) is located between nucleotides −17 and +80 (initiation of viral RNA occurs at +1) (ref. 13). We next investigated the requirement for *trans*-activation of the position of the TAR sequences relative to the site of transcriptional initiation. Plasmids were constructed in which the TAR element was placed either 5′ to the site of RNA initiation, or alternatively inserted near, but not at, the 5′ end of the mRNA species (Fig. 1*b*). For these experiments the −17 to +80 HTLV-III sequences were inserted between an enhancer sequence derived from the Rous sarcoma virus (RSV)[22] and one of two promoter sequences, the SV40 promoter[23] or the HTLV-I promoter[24], each lacking the homologous enhancer. These control sequences were placed 5′ to the *cat* gene. The ability of each of these plasmids to direct *cat* gene expression in a transient expression assay was determined by transfection of either the Raji or Raji(*tat*-III) cells.

TAR sequences do not confer a responsive phenotype when placed 5′ to the heterologous promoters in these plasmids (Table 1). The lack of response of the control elements is in marked contrast to the response of heterologous promoters that contain the TAR sequences located 3′ to the site of initiation[13] (Table 1). The sequences located between +38 and +80 are required for *trans*-activation (Table 1) (compare the activity of plasmid p−167/+38 to that of p−167/+80).

The structure of the second type of plasmid (pHI−17/+80) is also shown in Fig. 1*b*. Here, the TAR sequences are located 3′ to the HTLV-I enhancer/promoter, 300 nucleotides from the natural site of initiation of the HTLV-I viral RNA. RNA transcribed from this plasmid initiates within the HTLV-I LTR sequences at a position ~300 nucleotides 5′ to the HTLV-III start site (not shown). The data in Table 1 s
of *cat* gene expression directed by plasmid p
significantly different in Raji compared wit

We conclude that *trans*-activation of HTL
the TAR sequences are located at or very nea
mRNA. The experiments also show that, consiste
results, the sequences located within the untranslate
region (+38 to +80) are required for *trans*-activat
homologous and heterologous genes.

Discussion

The strategy of replication of HTLV-III includes a positive feedback mechanism in which one product of the virus genome, the *tat*-III protein, positively regulates expression of other viral proteins. Experiments presented here suggest that positive regulation of HTLV-III genes occurs via an increased translational efficiency of virus-specific mRNA species. Our experiments also demonstrate that the increased translational efficiency requires specific sequences within the R region of the LTR, the TAR sequences, to be located at or near the 5′ terminus of the mRNA.

The simplest explanation of these data is that the *tat*-III gene product itself interacts with sequences at the 5′ terminus of mRNA species and thereby increases the translational efficiency of that mRNA. However, the experiments reported here do not exclude other mechanisms of post-transcriptional control. The

Table 1 Activity of HTLV-III LTR sequences in Raji and Raji(*tat*-III) cells and co-transfection assays

		Relative CAT activity		
Expt	Plasmid	Raji	Raji(*tat*-III)	HeLa
1	pSV2CAT	1.0	1.0	
	pU3R-III	0.3	241 (777)	1.0
	p−167/+80	0.7	1,363 (1,948)	
	p−167/+38	0.8	1.7 (2)	
	pRS+80/−17SV	0.2	0.3 (1.5)	
	pRS−17/+80HI	0.8	0.6 (0.75)	
	pHI−17/+80	1.2	1.2 (1.0)	
2	pU3R-III+HXBc2			26.0
	pU3R-III+HXBc2-Dtat2			1.2

In expt 1, cells were transfected with 2 μg of the plasmid DNA indicated and CAT assays were performed 48 h post-transfection[23,25]. The level of CAT enzyme activity was normalized to the level obtained following transfection of the same cells with pSV2CAT. The SV40 sequences directing *cat* gene expression on pSV2CAT are not responsive to the *tat*-III gene product[9]. The numbers in parentheses represent the fold stimulation in Raji (*tat*-III) compared with Raji cells. In expt 2 pU3R-III alone was transfected into HeLa cells or co-transfected with 2 μg of either pHXBc2 or pHXBc2-Dtat2. The level of CAT activity was normalized to the activity obtained following transfection with pU3R-III alone.

trans-activator protein contains a cluster of positively d amino acids, suggesting that it interacts directly with RNA[10]. Alternatively, but in our opinion less likely, a r product may be induced by the *tat*-III gene which affects slational efficiency of viral RNA.

usly reported higher levels of LTR-directed mRNA cted H9 cells compared with uninfected cells[13]. could not be determined because the rresponding mRNA in the uninfected e increased level of mRNA could rences between the cells or the HTLV-III-infected cells that the data presented here were t differ only with respect to t these results reflect more expression on virus gene in mRNA observed in some t explain the greatly elevated ed *cat* gene expression and viral essing *tat*-III.

sis n of g sion by a viral protein has been or gene directed by LTR sequences of and HTLV-I and of the bovine leukaemia virus [29,30]. The *trans*- ator protein for HTLV-I and -II is coded near the 3′ end the genomes, by the *tat*-I and *tat*-II genes, respectively[27,31]. Al ough the ultimate effect of the *trans*-activator proteins of HTLV-I, HTLV-II, BLV and HTLV-III is similar, it is likely that the mechanism of *trans*-activation differs. One indication of this difference is the disparity in sizes of the *trans*-activator proteins. The *tat*-III protein is 86 amino acids long, whereas the *tat*-I and *tat*-II proteins are >300 amino acids long. Another difference is the location of the *trans*-acting responsive sequences. The TAR-I and TAR-II sequences of HTLV-I and -II are located within the U3 regions of the respective LTRs, 5′ to the site of transcription initiation[24,32]. Finally, there is experimental evidence which demonstrates that at least part of the increase in LTR-directed gene expression in response to these *trans*-activator proteins occurs via an increased rate of transcriptional initiation and concomitant increases in the steady-state levels of mRNA species[25,27]. Evidently, different biochemical mechanisms account for *trans*-activation of gene expression mediated by the *tat*-I and *tat*-III genes of HTLV-I and HTLV-III, respectively.

Genetic regulation by alteration of the translational efficiency of mRNA has been reported for some cellular and viral genes. For example, a sequence present within the 5′-untranslated leader of the *Drosophila melanogaster* heat-shock protein (HSP70) mRNA is required for continued translation of this mRNA under conditions of stress[33,34]. Tagging of heterologous genes with the HSP70 leader sequence transfers the heat-shock translation phenotype to heterologous genes much as tagging heterologous genes with the TAR sequences of HTLV-III confers responsiveness to the type III *trans*-activator. Moreover, deletion of nucleotides within the HSP70 untranslated leader and insertion of heterologous sequences 5′ to this region abolishes selective translation[34]. Deletions within the HTLV-III leader sequence and insertions 5′ to the HTLV-III TAR sequences have a similar effect. A sequence in the untranslated leader of viral mRNAs expressed late in adenovirus infection permits continued translation of these mRNAs at times when translation of most other viral and cellular genes stops[35,36]. Translation of picornavirus mRNAs also continues at a time when translation of host genes is diminished[37,38].

Although some aspects of translational regulation are common among these disparate examples, note that high levels of protein expression mediated by the *tat*-III gene product occur in cells that retain the capacity to synthesize other proteins. Viewed from this perspective, translational control mediated by the HTLV-III *tat* gene product could serve as a prototype for a distinct category of genetic regulatory events. Perhaps similar mechanisms are involved in translational activation of mRNA in developing zygotes and the activation of specific genes in response to extracellular stimuli and to stress in situations in which large amounts of protein are made quickly[39].

We have demonstrated that the *tat*-III product is essential for virus replication in T4+ cell lines[40]. For this reason, inhibitors of HTLV-III *trans*-activation should inhibit viral replication and may moderate the effects of virus infection. The observations reported here suggest that drugs that interfere with post-transcriptional events, possibly certain antibiotics which inhibit translational processes, may specifically inhibit virus growth.

We thank Drs Robert Gallo, Flossie Wong-Staal, George Shaw and Beatrice Hahn for providing the pHXBc2 plasmid; Dr Arthur Levinson for the murine *dhfr* cDNA clone, Dr Thomas Chang for the *dhfr* antiserum; Kathryn Campbell and Renee Zaya for technical assistance; and Tanya Parks and Carol Owens for editorial assistance. This work was supported by grants to W. A. H. from the American Cancer Society and a State of Massachusetts AIDS grant. C.A.R. was supported by NIH USPHS grant CA07580; J.G.S. was supported by USPHS grant CA40658 and the Leukemia Society of America.

Received 4 November; accepted 31 December 1985.

1. Barre-Sinoussi, F. *et al. Science* **220**, 868–871 (1983).
2. Broder, S. M. & Gallo, R. C. *New Engl. J. Med.* **311**, 1292–1297 (1984).
3. Gallo, R. C. *et al. Science* **224**, 497–500 (1984).
4. Popovic, M., Sarngadharan, M. G., Read, E. & Gallo, R. C. *Science* **224**, 497–500 (1984).
5. Sarngadharan, M. G., Popovic, M., Bruch, L., Shupbach, J. & Gallo, R. C. *Science* **224**, 506–508 (1984).
6. Seligman, M. *et al. New Engl. J. Med.* **311**, 1286–1292 (1984).
7. Shaw, G. M. *et al. Science* **227**, 177–182 (1985).
8. Hahn, B. H. *et al. Nature* **312**, 166–169 (1984).
9. Sodroski, J. G., Rosen, C. A. & Haseltine, W. A. *Science* **227**, 171–173 (1985).
10. Goh, W. C., Rosen, C. A., Sodroski, J. G. & Haseltine, W. A. *J. Virol.* (submitted).
11. Arya, S., Guo, C., Josephs, S. F. & Wong-Staal, F. *Science* **229**, 69–74 (1985).
12. Sodroski, J., Patarca, R., Rosen, C., Wong-Staal, F. & Haseltine, W. A. *Science* **229**, 74–77 (1985).
13. Rosen, C. A., Sodroski, J. G. & Haseltine, W. A. *Cell* **41**, 813–823 (1985).
14. Rosen, C. A., Sodroski, J. G., Campbell, K. & Haseltine, W. A. *J. Virol.* **57**, 379–384 (1985).
15. Queen C. & Baltimore, D. *Cell* **33**, 741–748 (1983).
16. Fisher, A. C., Collati, E., Ratner, L., Gallo, R. C. & Wong-Staal, F. *Nature* **316**, 262–265 (1985).
17. Mulligan, R. C., Howard, B. H. & Berg, P. *Nature* **277**, 108–114 (1979).
18. Chirgwin, J. M., Przybyla, A. E., MacDonald, R. J. & Rutter, W. J. *Biochemistry* **18**, 5294–5299 (1979).
19. Aviv, H. & Leder, P. *Proc. natn. Acad. Sci. U.S.A.* **69**, 1408–1412 (1972).
20. Green, M. R., Maniatis, T. & Melton, D. A. *Cell* **32**, 681–694 (1983).
21. Thomas, P. *Proc. natn. Acad. Sci. U.S.A.* **77**, 5201–5202 (1980).
22. Luciw, P. A., Bishop, J. M., Varmus, H. E. & Capecchi, M. R. *Cell* **33**, 705–716 (1983).
23. Groman, C. M., Moffat, L. F. & Howard, B. H. *Molec. cell. Biol.* **2**, 1044–1051 (1982).
24. Rosen, C. A., Sodroski, J. G. & Haseltine, W. A. *Proc. natn. Acad. Sci. U.S.A.* **82**, 6502–6506 (1985).
25. Sodroski, J. G., Rosen, C. A. & Haseltine, W. A. *Science* **225**, 381–384 (1984).
26. Chen, I. S. Y. *et al. Science* **229**, 54–58 (1985).
27. Felber, B. K., Paskalis, H., Kleinman-Ewing, C., Wong-Staal, F. & Pavlakis, G. *Science* **229**, 675–679 (1985).
28. Fujiswawa, J. I., Seiki, M., Kiyokawa, T. & Yoshida, M. *Proc. natn. Acad. Sci. U.S.A.* **82**, 2277–2281 (1985).
29. Rosen, C. A., Sodroski, J. G., Kettman, R., Burny, A. & Haseltine, W. A. *Science* **227**, 320–322 (1984).
30. Derse, D., Caradonna, S. J. & Casey, J. W. *Science* **227**, 317–320 (1984).
31. Sodroski, J. G., Rosen, C. A., Goh, W. C. & Haseltine, W. A. *Science* **228**, 1430–1434 (1985).
32. Rosen, C. A., Sodroski, J. G., Kettman, R. & Haseltine, W. A. *J. Virol.* (in the press).
33. Klemenz, R., Hultmark, D. & Gehring, W. J. *EMBO J.* **4**, 2053–2060 (1985).
34. McGary, T. J. & Lindquist, S. *Cell* **42**, 903–911 (1985).
35. Thummel, C., Tijan, R., Hu, S. & Grodzicker, T. *Cell* **33**, 455–464 (1983).
36. Logan, J. & Shenk, T. *Proc. natn. Acad. Sci. U.S.A.* **81**, 3655–3659 (1984).
37. Bablanian, R. *Prog. med. Virol.* **10**, 40–83 (1975).
38. Rose, J. K., Trachsel, H., Leong, K. & Baltimore, D. *Proc. natn. Acad. Sci. U.S.A.* **75**, 2732–2736 (1978).
39. Ruderman, J. V., Rosenthal, E. T. & Tansey, T. in *Molecular Aspects of Early Development* (Malacinski, G. M. & Klein, W. H.) (Plenum, New York, 1985).
40. Dayton, A., Sodroski, J. G., Rosen, C. A., Goh, W. C. & Haseltine, W. A. *Cell* (in the press).
41. Simonsen, C. C. & Levinson, A. D. *Proc. natn. Acad. Sci. U.S.A.* **80**, 2495–2499 (1983).
42. Maniatis, T., Fritsch, W. F, & Sambrook, J. *Molecular Cloning: A Laboratory Manual* Cold Spring Harbor Laboratory, New York, 1982).
43. Lee, T. J. *et al. Proc. natn. Acad. Sci. U.S.A.* **81**, 3856–3860 (1984).
44. Southern, P. J. & Berg, P. *J. molec. appl. Genet.* **1**, 327–341 (1982).
45. Werner, D., Chemla, Y. & Herzberg, M. *Analyt. Biochem.* **141**, 329–336 (1984).

Three-dimensional structure of a specific pre-messenger RNP particle established by electron microscope tomography

U. Skoglund, K. Andersson, B. Strandberg* & B. Daneholt

Department of Medical Cell Genetics, Medical Nobel Institute, Karolinska Institutet, Box 60400, S-104 01 Stockholm, Sweden
* Department of Molecular Biology, Biomedical Center, University of Uppsala, Box 590, S-751 24 Uppsala, Sweden

Electron microscope tomography has been used to refine the structural analysis of individual RNP particles synthesized on Balbiani ring genes in Chironomus tentans. *The spherical particles have a diameter of 500 Å and are composed of a thick RNP ribbon bent into an asymmetrical, four-domain, ring-like configuration. The first domain, containing the 5′ end of the transcript, and the fourth domain, containing the 3′ end, are close to each other.*

IN eukaryotic cells messenger RNA precursors, the heterogeneous nuclear RNA (hnRNA) transcripts, are packed into ribonucleoprotein particles (hnRNP) immediately on synthesis[1,2]. The particles exhibit a monotonous polyparticle organization[3] and contain a set of 5–10 major protein components, the core proteins[2,4–7]. However, various lines of evidence suggest that each transcription product has characteristic features. For example, defined RNP particles display a specific organization of the proteins along the RNP fibre[8–10]; some of the minor protein components of hnRNP bind to specfic RNA sequences[11], whereas others are confined to certain transcription products[12–14]. At the ultrastructural level, the hnRNP particles at defined loci in polytene[15] and lampbrush[16] chromosomes show typical morphology. Because of the apparent complexity of the hnRNP population, it is important to study defined hnRNP particles and to relate their structure to the maturation processes that occur on the particles[17].

Electron microscope studies of selected chromosomal regions of insect polytene chromosomes permit analysis of specific hnRNP particles. In particular, Balbiani rings (BRs, the giant puffs in the salivary glands of *Chironomus*) have proven useful (see ref. 18 for review). The Balbiani ring (*BR*) genes encode information for the salivary polypeptides, the major protein products of the salivary gland cells. Large 75S RNA transcripts are synthesized in the BRs[19] and packed into 500 Å RNP particles[20–23]. The BR particles can be readily identified in the nuclear sap and in the nuclear pores during the translocation process[24,25]. Here we describe a general method for three-dimensional reconstruction of ultrastructural objects at the molecular level. By applying this method to the BR particles we could establish whether they attain a well-defined, higher order structure. We discuss their structure in relation to the available information on the transport, polyadenylation and splicing of the BR transcripts.

Image reconstruction

Ultrathin sections through the salivary glands of *C. tentans* were prepared according to standard procedures[21] and gold particles deposited onto the surface of the sections. A suitable nuclear area containing BR granules was identified in the electron microscope (Fig. 1), a tilt series recorded and the micrographs scanned and digitized.

Before the reconstruction was performed, the micrographs were aligned with an iterative least-squares procedure (G. Bricogne and U.S., in preparation). The gold particles on top of the section served as reference markers.

The three-dimensional reconstruction was performed according to the filtered back-projection principle where the Fourier transforms of the projections (tilts) are radially weighted[26]. The reconstruction comprised a series of two-dimensional reconstructions of circular disks perpendicular to, and repeated along, the tilt axis, forming a cylinder (Fig. 2). The completed reconstruction was presented as a series of stain density maps corresponding to the reconstructed sections through the object. The maps were subsequently used to build a balsa-wood model of the object.

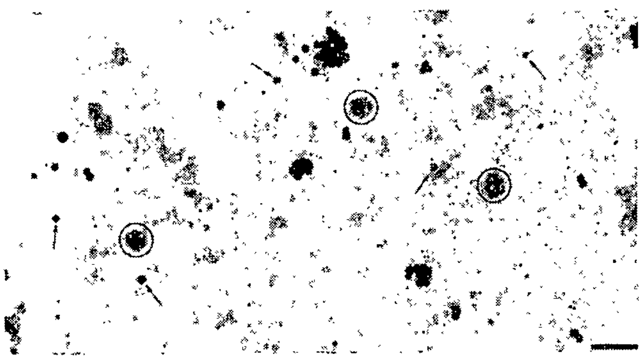

Fig. 1 Electron micrograph of a nuclear region of a salivary gland cell in *C. tentans*. Three differently orientated BR RNP particles are indicated by circles. The particles appear associated with a fibrous network. Arrows denote some of the gold particles added to the specimen. This micrograph represents 0° tilt in a ±60° series of 13 micrographs. Scale bar, 1,000 Å.

Methods. Specimen preparation, electron microscopy and image processing were performed as follows. Salivary glands from fourth instar *C. tentans* larvae were fixed in 2% glutaraldehyde and post-fixed in 1% osmium tetroxide. After embedding and sectioning, the specimens were stained with uranyl acetate and lead citrate (see ref. 21 for details). Thin sections were collected directly onto 200-mesh copper grids without a supporting plastic film. A colloidal gold suspension (Polysciences) was added to the sections, and gold particles (50–200 Å in diameter) deposited on the top. The specimens were photographed at 60 KV at a magnification of 20,000× in a JEOL TEMSCAN 100 CX electron microscope and a tilt series obtained using a standard side-entry goniometer. Micrographs were scanned and digitized in an Optronix P-1000 drum scanner. The scanning was performed with a step size of 25 μm, which corresponds to a pixel size of 12.5 Å at a magnification of ~20,000×. For each micrograph, an area ~50 mm × 50 mm was scanned, that is, 4×10^6 pixels were stored. Subsequent image processing was carried out on a VAX 11/750 minicomputer.

Evaluation of the method

Our three-dimensional reconstruction technique is based on that of Klug and coworkers, devised for symmetrical and repeating ultrastructural objects[26,27]. Here, the reconstruction is made from a series of projections that correspond to the micrographs of

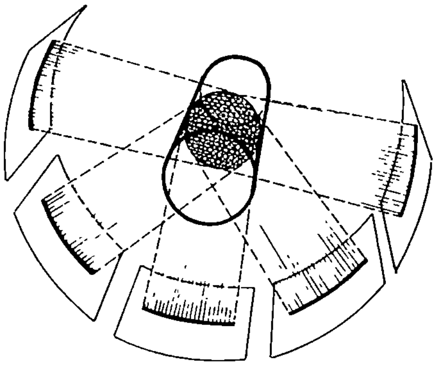

Fig. 2 The principle of three-dimensional image reconstruction from electron micrographs. Five micrographs, shown in a semicircular arrangement, represent a set of projections of a centrally placed specimen which are accurately aligned in relation to each other to allow image reconstruction. The three-dimensional reconstruction takes place as a series of two-dimensional reconstructions: in each single step, one of which is shown in the figure, a circular disk is reconstructed by back-projection (after suitable weighting) of the corresponding lines in the micrographs[47,48]. Note that the lines and the reconstructed disk are perpendicular to the tilt axis. Several consecutive disks ultimately form a cylinder in which the reconstructed object is contained.

differently tilted views of the specimen, in which any object, symmetrical or asymmetrical, can be analysed (electron microscope tomography). The feasibility of the approach has been shown previously[28,29]. The key to the success of the tomographic procedure is the proper alignment of the electron micrographs in the tilt series—the data retrieved from each micrograph must correspond to the particular object orientated in the same way (except for a modulation with the tilt angle). The use of gold markers as reference markers[30] and the development of accurate algorithms for the alignment have allowed us to restrict the average alignment errors for the gold markers between the 0° and higher tilts to ~10 Å (corresponds to <1 pixel). Care was also taken to minimize resolution loss caused by multiple resampling of the data in the computer.

The resolution of the tomographic procedure could be estimated from the reconstructed density maps computed at different resolutions. The characteristics of the maps suggested a resolution of 80–90 Å, which approaches the maximum attainable resolution calculated to be ~85 Å for a 500-Å object under optimal conditions (no background; projections available for every 10° in the range ±90°)[26]. Moreover, computation of an average structure from several reconstructions of individual but identical objects further increases the reliability of the results obtained. Preliminary results in our laboratory show that a resolution <50 Å can be reached when the number of projections are doubled. We conclude that our method is of general applicability in the analysis of objects of molecular dimensions.

Structure of individual BR particles

Three BR granules are shown in Fig. 1. The RNP particles of BR origin are of exceptional size (~500 Å) and appear roughly spherical, but their contour indicates that they are often not homogeneous. Furthermore, they frequently exhibit a bright centre, giving a ring or horseshoe appearance (see, for example, the RNP particle to the right in Fig. 1).

Information was obtained previously by direct visualization of the synthesis of the gene product[23]. It was shown that the RNP particle is formed as a thick fibre that is bent into an almost closed structure, providing a tentative explanation for the different projections observed for the completed particles. Although this study using conventional electron microscopy provided an approximate interpretation of the structure of the RNP particle, we were technically unable to describe completely the complex, spherical appearance of the particle, as neither the course of the RNP fibre nor its shape could be established. Using computer-based electron microscope tomography, we have now performed three-dimensional reconstructions of four BR particles from glands of different animals (Fig. 3*a*–*d*).

The degree of similarity between the reconstructions of the four particles was determined by a least-squares procedure that maximizes the correlation coefficients between the reconstructed densities by refining relative three-dimensional translation and rotation parameters[31,32]. When the particle in Fig. 3*a* was compared with each one of the other three particles (*b*–*d*), we obtained well-defined, maximal correlation coefficients of 0.75, 0.82 and 0.77, respectively, indicating a strong similarity between the four particles. In this type of comparison all the information in the reconstructions is considered, whereas the balsa-wood models (Fig. 3) only allow the most heavily stained features to be evaluated at the chosen contour levels (see Fig. 3 legend)

The BR particles are globular in appearance and have a diameter of ~500 Å (Fig. 3). They are asymmetrical and the contours of the particles in the various projections are similar, for example, in Fig. 3 the aligned particles exhibit a pointed bottom and a rhomboid contour. Furthermore, the particles have a central hole (with a few crossing fibres; see Fig. 3 legend) and also contain a slit at 1–2 o'clock cutting through the periphery of the particle (the position of the slit is indicated by an arrow in Fig. 3). The presence of the cleft is compatible with the horseshoe-like projections observed earlier; it is assumed that the ends of the RNP element are in proximity with each other at the cleft. Thus, we are left with a toroidal structure cut open with a narrow slit. The reconstructions indicate that the ring-shaped element is better described as a ribbon than as a fibre as it is considerably wider than it is thick.

When minor features are scrutinized, it is possible to detect differences between the particles (Fig. 3). Some of the variation can be attributed to differences in stain distribution, particularly as the balsa-wood models only represent the stain densities exceeding the selected cut-off level. Biological variation could also contribute to the differences observed; that is, the particles could be of different BR origin (BR 1 or BR 2)[18], one or more of them could be processed or partly degraded, or they could represent different dynamic states of the particle. Note, however, that at the resolution of 80–90 Å there is a striking resemblance between the four particles.

Average structure

The average structure was established by adding together the four reconstructions corrected for translation, rotation and scaling factors. *R*-values were computed as in conventional X-ray crystallography. When the individual particles (Fig. 3*a*–*d*) were related to the average, we obtained *R*-values of 0.44, 0.50, 0.41 and 0.46, respectively. These reasonably low values, as well as the high correlation numbers presented in the preceding section, provide evidence that the four BR RNP particles have the same structure at this resolution and can be represented by the computed average. The average structure is presented as a balsa-wood model in Fig. 3*e*; the toroid shape of the particle as well as the slit are clearly visible.

A more detailed description of the RNP element can be carried out with close reference to Fig. 4*a*–*f*, which displays the average particle from several views. Most conveniently, the RNP element is described by beginning at the slit, following it clockwise around the particle and finishing at the slit again. First, the RNP element, constituting the wall of the particle, has about the same thickness all around the particle (100–150 Å) and moulds itself into the general spherical shape of the particle. Second, when the particle is observed from the outside along the RNP element, it is possible to demarcate four domains, designated 1–4 (see Fig. 4*a*, *b*). Domain 1 starts as a smooth end at the slit at 1 o'clock and attains a width of ~300 Å and domain 2 begins at 3 o'clock when the RNP element rather abruptly broadens to 500–600 Å, reaches the bottom of the particle (Fig. 4*d*), makes

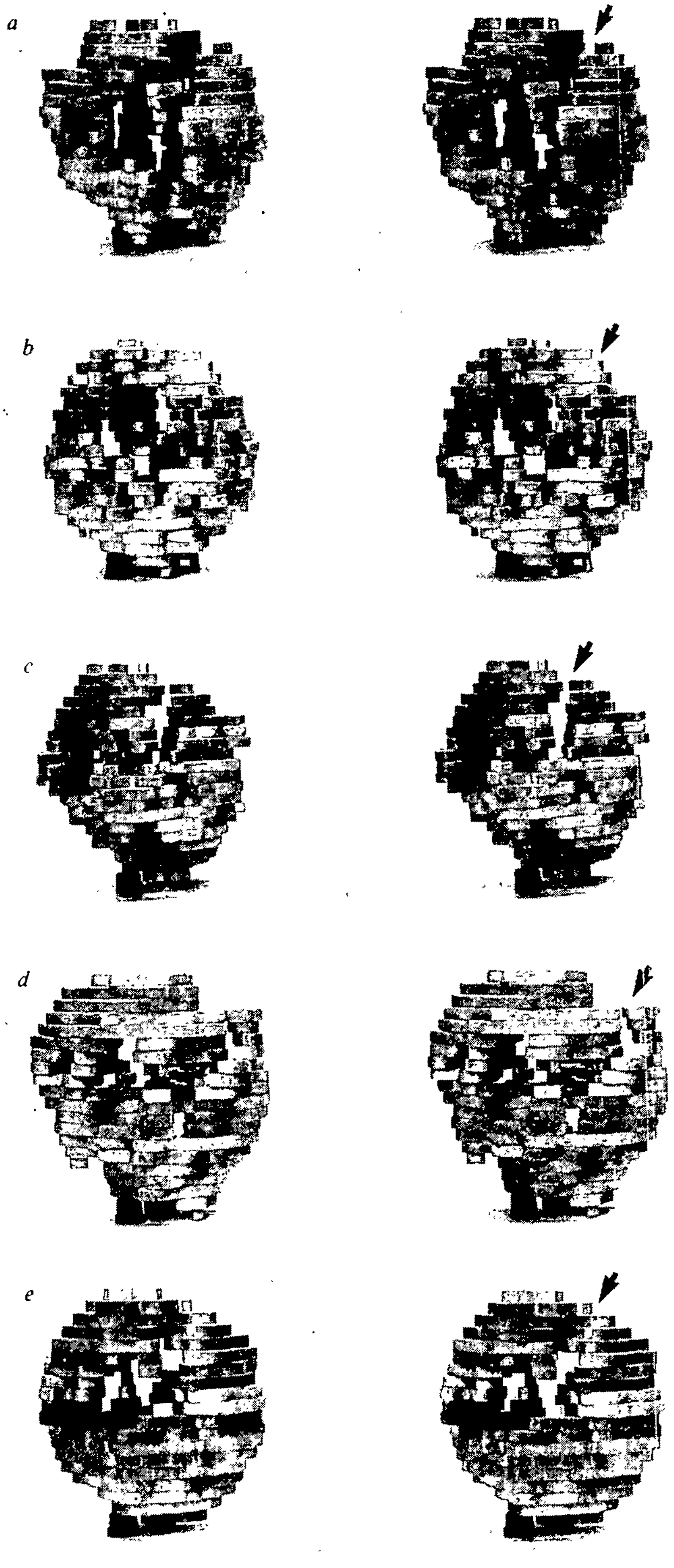

Fig. 3 Balsa-wood models of four reconstructed and aligned BR RNP particles (*a–d*) and a calculated average particle (*e*) shown as stereo pairs. The balsa-wood models of the four individual particles were built from stain density maps contoured at ~2.4 r.m.s. deviations above the mean value of the reconstructions, whereas the computed average of the four reconstructions was contoured at 1.15 r.m.s. Short arrows denote the position of the slit in the toroid-like structure. Nuclear sap fibres next to the particles have not been included in the models except for those inside the cavity of the particles. The reconstructions are compensated for a 10% reduction in thickness of the specimen during exposure.

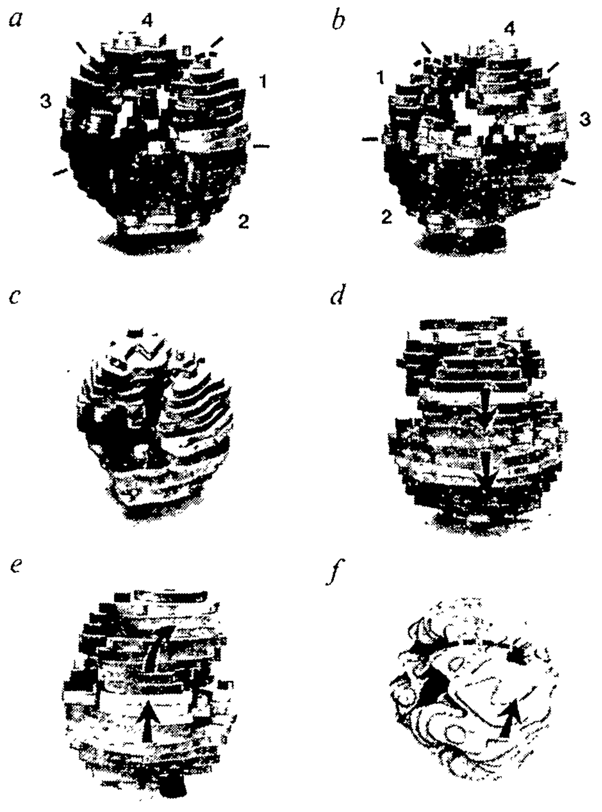

Fig. 4 Average structure of the reconstructed BR RNP particle. *a*, Front view of the particle corresponding to Fig. 4*e*. The right- and left-hand sides of the particle are defined from the view seen in *a*. In *b*, the particle is viewed on from the back, in *c* from the front and above, in *d* from the right, in *e* from the left and in *f* from the top. The slit in the ring-like structure is indicated by a broken line. In *a* and *b* the four domains have been demarcated with numbers and division lines. Arrows in *d*–*f* denote the skewed course of the ribbon-like RNP element beginning in domain 1 and ending in domain 4.

a rather sharp bend and extends almost half-way up on the other side, still keeping about the same width (Fig. 4*e*). Taken as a whole, domain 2 can be described as an asymmetrical, bowl-like structure (Fig. 4*c*). The transition to domain 3 at 8 o'clock is again distinct; the RNP element gets narrower and attains a width of 250 Å until finally, at 11 o'clock, the RNP element bends to the right (Fig. 4*e*) and passes into domain 4, which has a maximal width of 350 Å and forms a more irregular structure (Fig. 4*f*). The major part of domain 4 is dislocated to the right in Fig 4*f*, which explains the earlier notion of the particle as a short, slightly left-handed spiral[23]. Domain 4 extends towards the slit and completes the ring-like structure.

Visualization of RNP particle formation on the gene also allows us to decide the order in which the four domains are synthesized. Three consecutive growth stages of the particle, as well as a completed particle, are displayed in Fig. 5. The newly synthesized RNA fibre passes a transient thick fibre state, the stalk, before it is built into the dense portion of the RNP particle[23]. The dense RNP element on top of the stalk is gradually extended (Fig. 5*a*–*c*) and attains the structure of an open ring with the same dimensions as the completed particle (Fig. 5*d*), which suggests that the RNP element of the particle is gradually completed from one end to the other. Towards the 3′ end of the gene about three-quarters of a completed RNP particle can be seen on top of the stalk (Fig. 5*c*). Detailed comparisons with the three-dimensional reconstructed particle (Fig. 4*b*; see also Fig. 5*d*) show that the structure of the growing dense RNP particle is compatible with the assumption that the smooth end of domain 1 represents the leading edge, and that the thick domain 2 as well as the relatively thin domain 3 gradually become incorporated into the growing, dense RNP structure (Fig. 5*a*–*c*). The main alternative, that domain 4 is in the lead followed by domains 3 and 2, could not satisfy the projections of the growing particles observed. It is likely that domain 4 is formed from the stalk retracted towards the particle on release of the particle from the template. The established order of synthesis of the domains suggests that the 5′ end of the RNP transcript is located at the top of domain 1 whereas the 3′ end should reside somewhere in domain 4.

Functional implications

We have shown here that the BR RNP particle does not attain a random higher-order structure, but rather a well-defined, asymmetrical configuration comprising four major domains. This distinctive structure is probably closely related to the fate of the BR RNP particle, in particular to the transport and processing of the pre-messenger RNA molecule.

The structure of the particle could be relevant to the transport process for several reasons. The particle is remarkably compact with the dense RNP ribbon moulded into a spherical shape. Defined regions, or domains, of the particle may have specific recognition and binding functions during transport, for example, when the particle is associated with the fibrous network in the nuclear sap (see Fig. 1), or when it recognizes the nuclear pore. Finally, when the particle passes through the pore, it changes its ring-like configuration to an extended rod-like structure[24,25]. This translocation event could be dependent on the specific organization and domain structure of the particle.

One or more of the domains could be designed to participate directly in the processing of the pre-messenger molecule. A considerable portion of the *BR* RNA molecules in the nuclear sap become polyadenylated[33] and are also likely to be spliced. It is known that a *BR* 1 gene harbours a 55-base-pair (bp)-long intron ~600 bp from the poly(A) site[34]. As the members of the *BR* gene family display a strikingly similar sequence organization[35,36], it seems reasonable to assume that the other *BR* 75S RNA genes also carry an intron in the same position. In addition, U1 and U2 snRNP particles appear in all the BRs[37]. As there is good evidence that both U1 snRNP[38-40] and U2 snRNP[41] are involved in the splicing process, this observation also supports the view that the BR transcripts are spliced. The 55-bp intron is close to the 3′ end, which suggests that it resides in the particle in domain 4 (which contains about a quarter of the 37-kilobase

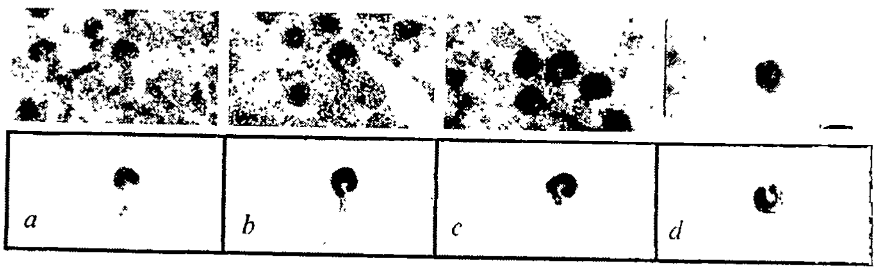

Fig. 5 Electron micrographs and schematic drawings of three growing BR particles (*a*–*c*) and of one completed and released particle (*d*). Bar, 500 Å.

(kb)-long transcript[21]). We conclude that polyadenylation and splicing occur in domain 4 of the BR particle.

Because of the ring-like configuration of the particle, domain 4 containing the 3′ poly(A) tail and the intron ends up close to domain 1 with the 5′ end of the transcript. This spatial relation could be fortuitous, but the cap structure is important for the polyadenylation and splicing processes *in vitro*[42,43]. The cap structure may exert its effect as an organizer of the RNP particle as an entity, but it could also interact more specifically with adjacent structures of the RNP particle. Further analyses of both spliceosomes in the *in vitro* systems[42,44–46] and specific pre-messenger RNP particles *in situ* are likely to shed more light on the nature and interdependence of the steps in the processing of pre-messenger RNA into mature mRNA.

We thank Dr Aaron Klug for encouragement and advice and Dr R. A. Crowther for discussions. This research was supported by Knut and Alice Wallenberg Foundation, Swedish Natural Science Research Council and National Swedish Board for Technical Development.

Received 1 October; accepted 20 December 1985.

1. Miller, O. L., Jr & Bakken, A. H. *Acta Endocr.* **168,** 155–177 (1972)
2. Economides, I. V. & Pederson, T. *Proc. natn. Acad. Sci. U.S.A.* **80,** 1599–1602 (1983).
3. Samarina, O. P., Lukanidin, E. M., Molnar, J. & Georgiev, G. P. *J. molec. Biol.* **33,** 251–263 (1968).
4. Beyer, A. L., Christensen, M. E., Walker, B. W. & Le Stourgeon, W. M. *Cell* **11,** 127–138 (1977).
5. Karn, J., Vidali, G., Boffa, L. C. & Allfrey, V. G. *J. biol. Chem.* **252,** 7307–7322 (1977).
6. Jones, R. E., Okamura, C. S. & Martin, T. E. *J. Cell Biol.* **86,** 235–243 (1980).
7. Choi, Y. D. & Dreyfuss, G. *Proc. natn. Acad. Sci. U.S.A.* **81,** 7471–7475 (1984).
8. Beyer, A. L., Miller, O. L. Jr & McKnight, S. L. *Cell* **20,** 75–84 (1980).
9. Steitz, J. A. & Kamen, R. *Molec. cell. Biol.* **1,** 21–34 (1981).
10. Ohlsson, R. I., van Eekelen, C. & Philipson, L. *Nucleic Acids Res.* **10,** 3053–3068 (1982).
11. Kish, V. M. & Pederson, T. *J. mol. Biol.* **95,** 227–238 (1975).
12. Sommerville, J. in *The Cell Nucleus* Vol. VIII (ed. Busch, H.) 1–57 (Academic, New York, 1981).
13. Dangli, A., Grond, C., Kloetzel, P. & Bautz, E. K. F. *EMBO J.* **2,** 1747–1751 (1983).
14. Risau, W., Symmons, P., Saumweber, H. & Frasch, M. *Cell* **33,** 529–541 (1983).
15. Swift, H. *In vitro* **1,** 26–49 (1965).
16. Malcolm, D. B. & Sommerville, J. *Chromosoma* **48,** 137–158 (1974).
17. Darnell, J. E., Jr *Nature* **297,** 365–371 (1982).
18. Daneholt, B. in *Insect Ultrastructure* Vol. 1 (eds King, R. & Akai, M.) 382–401 (Plenum, New York, 1982).
19. Daneholt, B. *Cell* **4,** 1–9 (1975).
20. Lamb, M. M. & Daneholt, B. *Cell* **17,** 835–848 (1979).
21. Andersson, K., Björkroth, B. & Daneholt, B. *Expl. Cell Res.* **130,** 313–327 (1980).
22. Olins, A. L., Olins, D. E. & Franke, W. W. *Eur. J. Cell Biol.* **22,** 714–723 (1980).
23. Skoglund, U., Andersson, K., Björkroth, B., Lamb, M. M. & Daneholt, B. *Cell* **34,** 847–855 (1983).
24. Beermann, W. in *Colloquium der Gesellschaft für physiologische Chemie am 3.–5. Mai 1962 in Mosbach/Baden* 64–100 (Springer, Berlin, 1962).
25. Stevens, B. J. & Swift, H. *J. Cell Biol.* **31,** 55–77 (1966).
26. Crowther, R. A., DeRosier, D. J. & Klug, A. *Proc. R. Soc.* **A317,** 319–340 (1970).
27. DeRosier, D. J. & Klug, A. *Nature* **217,** 130–134 (1968).
28. Dover, S. D., Elliot, A. & Kernaghan, A. K. J. *Microscopy* **122,** 23–33 (1981).
29. Olins, D. A. *et al. Science* **220,** 498–500 (1983).
30. Hart, R. G. *Science* **159,** 1464–1467 (1968).
31. Bricogne, G. *Acta Cryst.* **A32,** 832–847 (1976).
32. Mauguen, Y. *et al. Nature* **297,** 162–164 (1982).
33. Egyházi, E. *Eur. J. Biochem.* **107,** 315–322 (1980).
34. Höög, C., Engberg, C. & Wieslander, L. *Nucleic Acids Res.* **14,** (in the press).
35. Pustell, I., Kafatos, F. C., Wobus, U. & Bäumlein, H. *J. molec. Evol.* **20,** 281–295 (1984).
36. Wieslander, L. *et al. J. molec. Evol.* **20,** 304–312 (1984).
37. Sass, H. & Pederson, T. *J. molec. Biol.* **180,** 911–926 (1984).
38. Mount, S. M., Pettersson, I., Hinterberger, M., Karmas, A. & Steitz, J. A. *Cell* **33,** 509–518 (1983).
39. Padgett, R. A., Mount, S. M., Steitz, J. A. & Sharp, P. A. *Cell* **35,** 101–107 (1983).
40. Krämer, A., Keller, W., Appel, B. & Lührmann, R. *Cell* **38,** 299–307 (1984).
41. Black, D. L., Chabot, B. & Steitz, J. A. *Cell* **42,** 737–750 (1985).
42. Konarska, M. M., Padgett, R. A. & Sharp, P. A. *Cell* **38,** 731–736 (1984).
43. Edery, I. & Sonenberg, N. *Proc. natn. Acad. Sci. U.S.A.* **82,** 7590–7594 (1985).
44. Brody, E. & Abelson, J. *Science* **228,** 963–967 (1985).
45. Moore, C. L. & Sharp, P. A. *Cell* **41,** 845–855 (1985)
46. Grabowski, P. J., Seiler, S. R. & Sharp, P. A. *Cell* **42,** 345–353 (1985).
47. Rowland, S. W. *Topics Appl. Phys.* **32,** 9–79 (1979).
48. Robb, R. A. *A. Rev. Biophys. Bioengng.* **11,** 177–201 (1982).

LETTERS TO NATURE

A quasar with $z = 3.71$ and limits on the number of more distant objects

J. S. Dunlop*, A. J. B. Downes†, J. A. Peacock‡, A. Savage‡, S. J. Lilly§, F. G. Watson‡ & M. S. Longair*‡

* Department of Astronomy, University of Edinburgh,
Blackford Hill, Edinburgh EH9 3HJ, UK
† Mullard Radio Astronomy Observatory, Madingley Road,
Cambridge CB3 0HE, UK
‡ Royal Observatory, Blackford Hill, Edinburgh EH9 3HJ, UK
§ Princeton University Observatory, Peyton Hall, Princeton,
New Jersey 08544, USA

Spectroscopy of objects identified with radio sources from the Parkes Selected Regions has shown the compact, flat-spectrum source 1351−018 to be a quasar with redshift 3.71, the second most distant discovered to date. Compared with known quasars at such high redshifts, the object is optically very faint ($B = 20.9$), red in colour ($B - R = 1.6$) and is distinguishable photometrically from faint galaxies only by its relatively blue optical−infrared colour ($R - K = 2.1$). In common with other high-redshift, radio-loud quasars, 1351−018 has weak emission lines when compared with objects selected optically through objective-prism or grism techniques. Moreover, weak-lined objects such as this may also be missed even by surveys using broad-band optical colours, which may help to explain why such searches have failed to find faint, high-redshift quasars. Because it is a member of a complete sample, 1351−018, in fact, confirms the recent suggestion[1] that the quasar radio luminosity function declines for redshifts $z > 2$. Extrapolation of the existing data predicts that the main Parkes Survey may contain about eight 8 flat-spectrum quasars with $z > 4$.

The radio source 1351−018 lies in one of the deepest areas of the Parkes survey, the six 6.5 × 6.5° Selected Regions, which are complete to flux densities $S > 0.1$ Jy at 2.7 GHz (ref. 2). We are carrying out a detailed optical study of the 178 radio sources in the complete sample defined by these regions, with the aim of determining the high-redshift evolution of the radio source population. The 'intermediate' flux density means that powerful radio galaxies and quasars such as those found in bright, complete samples at $z \sim 1$ will be included in this sample up to $z \sim 4$, while the high selection frequency (2.7 GHz) makes possible the study of both steep- and flat-spectrum sources, the latter appearing in very small numbers in low-frequency surveys such as 3CR. We have completed the first phase of the programme—optical identifications on UK Schmidt plates, using extensive Very Large Array (VLA) observations to define accurate expected positions for optical counterparts. At this level, 56% of the sources are identified[3]. We now report the results of both deep charge-coupled device (CCD) imaging of the remaining empty fields and spectroscopic observations of sky-survey identifications. The first night of the spectroscopic programme yielded, among others, the spectrum of the quasar 1351−018, thus confirming the ability of the sample to probe high-redshift space.

PKS1351−018 is a VLA calibrator which is unresolved at 0.1 arc s resolution. The radio spectrum (Fig. 1*a*) has a broad peak over two decades in frequency, similar to that found in some other high-luminosity compact quasars[4]. Previous attempts at optical identification were initially unsuccessful[5] but later resulted in the classification of 'quasar?'[6]. We now confirm the latter identification by position coincidence: a faint red object is visible near the limits of the Palomar Sky Survey E plate and on the UK Schmidt J plate at RA 13 h 51 min 32.00 s, dec. −01°51′20.0 ± 0.3″ (1950.0), but it is too near the plate limits for its nature to be determined morphologically. The red colour, typical of faint radio galaxy identifications, was subsequently

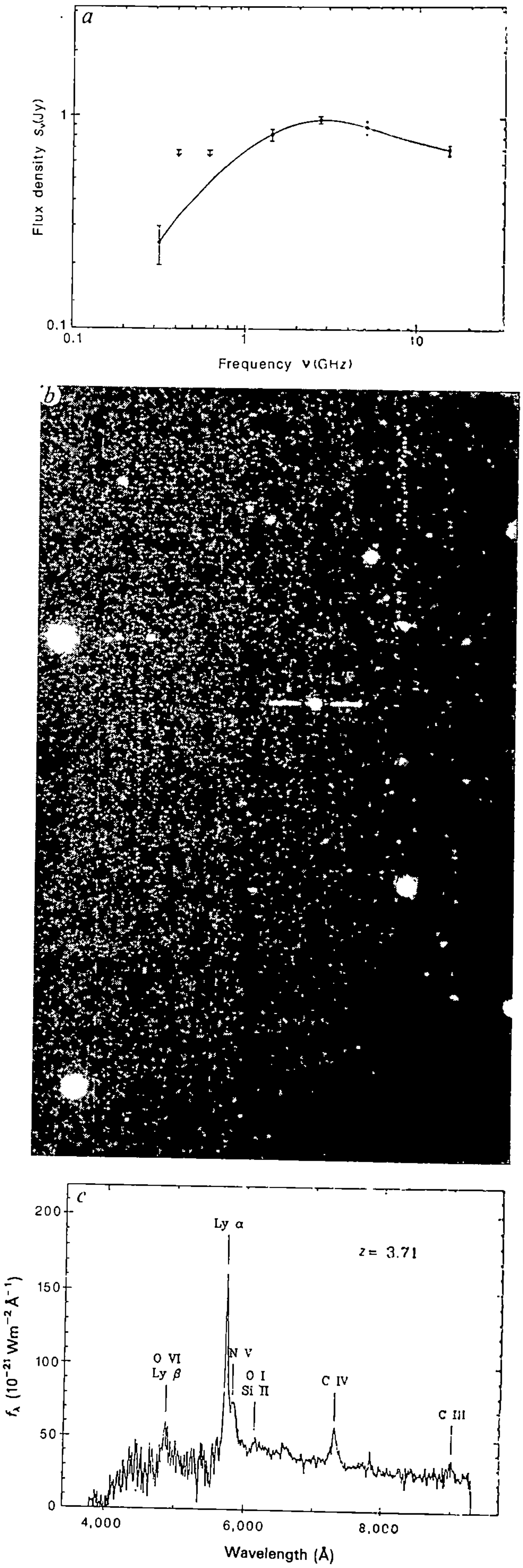

Fig. 1 *a*, The radio spectrum of PKS1351−018 (ref. 3). *b*, The optical counterpart of PKS1351−018, indicated by two bars in the centre of the field. The figure is reproduced from a *B*-band CCD image, and shows an area 2.5×4 arc min, with north to the top and east to the left. *c*, The optical spectrum of PKS1351−018 obtained on 20 April 1985 with the FORS and the RGO Spectrograph at the *f*/8 focus of the Anglo-Australian Telescope. The combined spectrum has a resolution of ~20 Å; the blue half was smoothed to a resolution similar to that of the red side, and the two spectra were joined at 5,300 Å. The absolute flux calibration was determined from the CCD *B* magnitude.

confirmed by our CCD photometry performed at the Anglo-Australian Telescope in April 1985 which gave a *B* magnitude of 20.89 (±0.03) with $B-R=1.6$ (±0.1). The Kitt Peak National Observatory (KPNO) interference filter system was used with red standards to zero-point the colours to the Cousins system. Figure 1*b* shows the *B* band CCD image taken in a 200-s exposure with the Royal Greenwich Observatory (RGO) CCD camera.

Ambiguity concerning the nature of the optical object was removed by observations with the United Kingdom Infrared Telescope (UKIRT) on 20 March 1985. An infrared study of the Parkes Selected Regions is being undertaken to enable an extension of previous work on the infrared properties of radio galaxies[7,8], both to fainter flux densities and to compact radio sources. These observations gave infrared magnitudes of $K=17.26\pm0.19$ and $J=18.32\pm0.18$ (on the Cerro Tololo Inter-American Observatory system) for 1351−018 and established it as a quasar candidate by virtue of its optical–infrared colour. This object lies among established quasars on the $(R-K)/K$ colour-magnitude diagram (Fig. 2), considerably to the blue of the well-defined radio galaxy locus. The combined properties of compact, flat-spectrum radio source, faint, red optical object, and blue optical–infrared colour thus made 1351−018 a prime candidate for a high-redshift quasar.

The optical spectrum (Fig. 1*c*) was obtained on the night of 20 April 1985 and is the result of a 1-h integration using the Faint Object Red Spectrograph (FORS) in tandem with the Image Photon Counting System (IPCS)/RGO Spectrograph at the *f*/8 Cassegrain focus of the Anglo-Australian Telescope. The observations used a 1.3-arc s slit with dichroic splitting of the beam at 5,300 Å. The grism produced a FORS spectrum with a resolution of 20 Å with the resolution in the blue camera roughly a factor of three higher. The wavelengths of the main emission features and their identifications are given in Table 1. In common with other high-redshift quasars, Lyα is the strongest line with C III, C IV, N V and O VI also clearly present. The mean redshift based on the emission lines of C III, C IV, N V, O VI, and O I/Si II is 3.709±0.003. Lyα was not used as the strong forest of absorption lines blueward of Lyα biases the centroid of the Lyα emission line to high redshifts.

The fact that 1351−018 is 2.3 mag fainter than PKS2000−330 ($z=3.78$) casts some doubt on recent suggestions that searches deeper than a magnitude of $R=18$ would be unlikely to result in the discovery of high-redshift objects[9]. With an optical absolute magnitude of $M_B=-26.8$ (assuming a Hubble constant of 50 km s^{-1} Mpc^{-1}, a density parameter $\Omega_0=1$ and flux density varying as $\nu^{-0.5}$ beyond 9,000 Å), 1351−018 is the only known quasar at $z>3.5$ to have an optical luminosity comparable with that of typical low-redshift radio-loud quasars. However, extrapolation of the radio-quasar equivalent of the Hubble diagram[10] suggests that the magnitude of 1351−018 is typical of that expected for a quasar at $z\simeq4$; high-redshift quasars in radio samples are expected to lie mainly among the fainter optical identifications.

Given the unusual nature of 1351−018, it is interesting to ask whether similar objects could be found using purely optical selection criteria. Comparison of the spectra of high-redshift quasars reveals 1351−018 (and other radio-selected quasars such as PKS2000−330)[4] to have systematically weaker emission

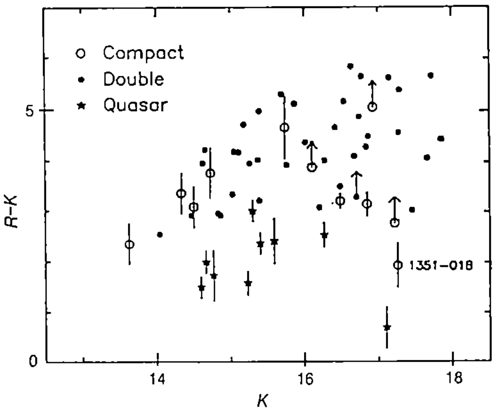

Fig. 2 The $(R-K)/K$ optical-infrared colour–magnitude diagram showing the positions of optical objects associated with different classes of radio source. Our data on Selected Region sources have been augmented by data on classical-double radio galaxies[7,8], and with additional quasar data[15,16]. The compact radio source 1351−018 lies in the region occupied by optical objects which are established quasars. Error bars are derived from the original plate photometry to indicate that such accuracy was adequate for selection of 1351−018.

Table 1 Emission lines in PKS1351−018

Observed wavelength (Å)	Identification (Å)	Redshift
4,870	[Ly β 1,025.7	3.748]
	O VI 1,033.8	3.711
5,735	Ly α 1,215.7	3.717
5,830	N V 1,240.1	3.701
6,155	[O I 1,303.5	3.722]
	Si II 1,307.6	3.707
7,295	C IV 1,549.1	3.709
9,005	C III 1,909.0	3.717

Table 2 Values of $\langle (V_e - V_0)/(V_a - V_0)\rangle$ for various values of z_0

z_0	n	$\langle (V_e - V_0)/(V_a - V_0)\rangle$ ($\Omega_0 = 1$)	$\langle (V_e - V_0)/(V_a - V_0)\rangle$ ($\Omega_0 = 0$)
1.8	30	0.375	0.424
1.9	28	0.321	0.359
2.0	22	0.304	0.345
2.1	17	0.301	0.345

lines than their optically selected counterparts[11,12]. An estimate of the rest-frame-equivalent width (W_0) of Lyα in 1351−018 yields $W_0 = 35 \pm 8$ Å, compared with $W_0 \simeq 88$ Å in 0055-2659 (the most distant optically selected quasar, $z = 3.68$)[11]. Such a bias is not unexpected in prism or grism plate surveys, but, in fact, may also affect colour-based studies such as those of Koo[13]. Using the flux-calibrated spectrum of 1351−018, we can synthesize the colours of this object for various filter systems and also work out the variation of these colours with redshift. The synthesized $B-R$ colour agrees with the photometrically measured value to within 0.1 mag, suggesting that using the spectrum in this manner is satisfactory. Using Koo's *UJF* filter system we find synthesized $U-J$ and $J-F$ colours of 2.7 ± 0.5 and 1.4 ± 0.1 respectively, the relatively large uncertainty in $U-J$ being due to the very small flux in the U band. We have also investigated the locus followed by 1351−018 on the $U-J/J-F$ colour–magnitude diagram as it varies in redshift, allowing for changes with redshift in blanketing of the Lyman continuum. The ($U-J$, $J-F$) colours are (0.4, 0.5) at $z = 3$ and (1.8, 1.2) at $z = 3.5$, which would not be classified as significantly non-stellar in Koo's faintest magnitude bin. Between $z = 3$ and $z = 3.5$, the track of 1351−018 departs from the stellar locus, but for $z > 3.5$ and $2.7 < z < 3$, faint quasars similar to 1351−018 would not have been detected. Furthermore, the spectrum of 1351−018 falls rapidly just blueward of the Lyman limit, whereas many high-redshift quasars retain significant flux at this point (for example, 0055−2659). Adding a significant fraction of ultraviolet flux to 1351−018 would make its ($U-J$, $J-F$) colours stellar at all $z > 2.5$. Conversely, by increasing the strength of the main emission lines in 1351−018, we can simulate the colours of a stronger-lined object, which we find to be clearly non-stellar at any redshift for an increase by a factor ~2 in line strength.

It therefore seems feasible that *both* prism-plate and colour selection of high-redshift quasars may be biased towards bright, strong-lined objects. If we hypothesize that most high-redshift quasars might have spectra similar to 1351−018, then the failure of faint surveys to find significant numbers of high-redshift objects could be largely a result of the selection criteria used. The conclusion that quasars were fewer but brighter in the past[11,13] may be correct but is based on searches for optically faint quasars at high redshifts which are incomplete for objects such as 1351−018. Note that all high-redshift quasars should be distinguishable on the basis of non-stellar colours, provided near-infrared (J, H, K) data are utilized in the selection procedure.

1351−018 lies in one of the two Parkes Selected Regions (centred on RA 12 h 04 min 50 s, dec. −00°31′ and RA 13 h 40 min 48 s, dec. −00°29′) on which extensive CCD imaging has been performed. This subset (55 sources) of the main sample (178 sources) is now provisionally 96% identified and can be used to draw some preliminary conclusions. Extrapolation of the observed evolution in the radio luminosity function at $z = 1$ to higher redshifts predicts that >20% of steep-spectrum sources at our flux-density level should lie at $z > 2$ (ref. 1), unless the co-moving density of objects falls at higher redshifts. With only one steep-spectrum source in the Selected Regions subsample remaining unidentified at $R \sim 24$, we now have the first indication of a redshift cutoff for these radio galaxies, since galaxies above this limiting magnitude should have redshifts $z < 2$. Extension of CCD imaging to the other regions will be needed to increase the confidence in this result.

Here we wish to concentrate on the subset of flat-spectrum sources in the Selected Regions which can be used as the faint end of a combined sample utilizing all the available complete-sample data on this class of source. Combining existing brighter datasets[1] with the 12–13 h regions discussed here, we can construct a total sample at 2.7 GHz of 151 flat-spectrum sources, of which 147 are optically identified and 119 have known redshifts. The unknown redshifts may be roughly estimated from apparent magnitude[1].

A useful way of quantifying evolution is the V_e/V_a statistic (where V_e and V_a are the cosmological volumes enclosed by, and available to, a source in the combined sample)[14], which allows analysis of such a combined sample in a generalization of the V/V_{max} test. To study evolution in specific redshift ranges, a banded version of this is required to prevent evolution at other redshifts influencing the result. We therefore evaluate $\langle (V_e - V_0)/(V_a - V_0)\rangle$ (where V_0 = cosmological volume enclosed by a redshift z_0), to study evolution beyond a redshift of z_0. The results for various values of z_0 are given in Table 2. The low values of $\langle V_e/V_a\rangle$ (that is, <0.5) reinforce the recent suggestion[1] of a deficit of high-redshift flat-spectrum objects. The basic result can be incorrect only if most objects with unknown redshift lie at $z > 3$. This seems implausible because they are generally neither very red nor faint.

To illustrate the fall in co-moving density at high redshift, we have fitted a simple parametric model of the flat-spectrum radio luminosity function to the available data. Limiting consideration to $z > 1.8$ provides a data set of 30 objects, to which we can fit a model of the form $\rho(P, z) \propto P^{-\beta}(1+z)^{-\gamma}$ (where $\rho =$

co-moving density per unit interval of P, and P = luminosity in W $\mathrm{Hz}^{-1}\,\mathrm{sr}^{-1}$); the maximum-likelihood values for the parameters are $\beta = 2.8$ and $\gamma = 3.1$ ($\Omega_0 = 1$ only was considered) corresponding to a reduction in ρ of a factor ~5 between $z = 2$ and $z = 4$. Extrapolating this model, we estimate that the main Parkes survey may contain ~8 flat-spectrum quasars with $z > 4$. To put this in context, there are ~1,200 flat-spectrum sources in the survey, of which more than half lack redshifts. If the true number were, in fact, zero, we would conclude that the luminosity function falls still more quickly at high redshifts. Nevertheless, it seems reasonable to suggest that $z > 4$ quasars might be found, and that these objects, like 1351 − 018, will lie among the faint, red optical identifications of compact radio sources.

We thank Pat Roche and the Anglo-Australian Observatory for assistance with the observations. J.S.D. is supported by a Cormack Bequest Studentship in the University of Edinburgh and S.J.L. by a SERC/NATO Fellowship.

Received 11 September; accepted 27 November 1985.

1. Peacock, J. A. *Mon. Not. R. astr. Soc.* **217**, 601-631 (1985).
2. Wall, J. V., Shimmins, A. J. & Merkelijn, K. J. *Austr. J. Phys. Astrophys. Suppl.* **19**, 1-68 (1971).
3. Downes, A. J. B., Peacock, J. A., Savage, A. & Carrie, D. R. *Mon. Not. R. astr. Soc.* **218**, 31-62 (1986).
4. Peterson, B. A., Savage, A., Jauncey, D. L. & Wright, A. E. *Astrophys. J.* **260**, L27-L29 (1982).
5. McEwan, N. J., Browne, I. W. A. & Crowther, J. H. *Mem. R. astr. Soc.* **80**, 1-59 (1975).
6. Savage, A., Bolton, J. G. & Trett, J. *Austr. J. Phys.* **35**, 207-219 (1982).
7. Lilly, S. J. & Longair, M. S. *Mon. Not. R. astr. Soc.* **211**, 833-855 (1984).
8. Lilly, S. J., Longair, M. S. & Allington-Smith, J. R. *Mon. Not. astr. Soc.* **215**, 37-57 (1985).
9. Wright, A. E. *Proc. 24th Liège Symp.* 53-58 (University of Liège, 1983).
10. Wills, D. & Lynds, R. *Astrophys. J. Suppl. Ser.* **36**, 317-358 (1978).
11. Hazard, C. & McMahon, R. *Nature* **314**, 238-240 (1985).
12. Shanks, T., Fong, R. & Boyle, B. J. *Nature* **303**, 156-158 (1983).
13. Koo, D. C., *Proc. 24th Liège Symp.*, 240-244 (University of Liège, 1983).
14. Avni, Y. & Bahcall, J. N. *Astrophys. J.* **235**, 694-716 (1980).
15. Hyland, A. R. & Allen, D. A. *Mon. Not. R. astr. Soc.* **199**, 943-952 (1982).
16. Wright, A. E., Ables, J. G. & Allen, D. A. *Mon. Not. R. astr. Soc.* **205**, 793-807 (1983).

Will cosmic strings be discovered using the Space Telescope?

Bohdan Paczyński*

Princeton University Observatory, Princeton University, Princeton, New Jersey 08544, USA

Cosmic strings are topologically stable defects in the vacuum which may be produced at a phase transition in the early Universe. Some may form closed loops, and some may be open, extending over the entire observable Universe. Although gravitational lensing of distant quasars by cosmic strings has been discussed[1–6] it is difficult to prove that a particular pair of quasar images is formed by a cosmic string. We suggest here that observations of very distant galaxies are more useful as a means for their discovery. A galaxy may appear as cut by a sharp edge if there is a cosmic string between the galaxy and the observer. We argue that if there is only one string out to a redshift $z \approx 1$, then the probability that it crosses a random image obtained with the Wide Field Camera (WFC) of the Space Telescope is $\sim 10^{-4}$. Therefore, there is a fair chance of discovering a string, after taking 10^4 images. The WFC will operate almost continuously in primary and serendipity modes, and a cosmic string, if it exists, may be discovered using the Space Telescope within the first few years of its operation.

If there is just one open cosmic string within the horizon, then the probability that the nearest part of it is at a redshift $z < 1$ is about 0.1 (ref. 6). The total length of all cosmic strings, including the loops, is logarithmically larger[4,6], so the probability of having some strings closer than at a redshift $z = 1$ is close to one. A string may lens a few quasars and separate the two images by up to a few arc minutes[4,6].

A number of known pairs or triplets of quasars have almost identical redshifts and angular separations (θ) between 1 and 4 arc min: Hazard 1146+111 B, C ($z = 1.01$, $\Delta z = 0.001$, $\Delta\theta$ = 2.6 arc min)[7], Q0952+698 A, B, C ($z = 2.05$, $\Delta z = 0.014$, $\Delta\theta$ = 3.6 arc min)[8], Q0307−195 A, B ($z = 2.13$, $\Delta z = 0.022$, $\Delta\theta$ = 1.0 arc min)[9,10], U2 and U3 near NGC2683 ($z = 1.26$, $\Delta z = 0.010$, $\Delta\theta$ = 3.6 arc min)[11], Q0107−025 A, B ($z = 0.96$, $\Delta z = 0.004$, $\Delta\theta$ = 1.3 arc min)[12]. These might be single quasars lensed by clusters or superclusters of galaxies[13,14], or in case of the pairs, these may be single quasars lensed by cosmic strings, or these may be separate quasars located in clusters or superclusters of galaxies[7,15]. How do we choose between these possibilities?

The main reason for favouring the picture with a few separate quasars located in the distant clusters or superclusters, over the gravitational imaging, is the presence of a small but significant discrepancy in redshifts between the components of all those pairs or triplets, typically ~1,000 km s^{-1}. However, if the separation between multiple images is a few arc minutes, then the time delay between various light paths is in the range of 100–1,000 yr. We have no direct observational or theoretical evidence on how stable are redshifts of quasars on such a time scale. There is some indirect observational evidence that considerable variations in the measured radial velocities might be expected. Broad emission lines in Type I Seyferts and in quasars are frequently asymmetrical, and the broad line peaks are shifted with respect to narrow lines by as much as ±2,000 km s^{-1} (refs 16–19). These shifts may vary, perhaps in 100 or 1,000 yr, and these time variations may be responsible for the redshift differences between the two images.

The following approach may resolve the present ambiguity about the nature of 'clusters of quasars'. Quasars also have forbidden emission lines which are much narrower than the broad lines[20]. They also show asymmetries[21], but systematic errors in measured redshifts may be smaller due to a smaller linewidth. Also, it is believed that forbidden lines form in regions which are a few hundred parsecs across, so their profiles should be more stable. The strongest line is [O III]5,007, a much weaker one is [O II]3,727. Both lines are redshifted into near infrared, and may be difficult to observe. However, if accurate redshifts and profiles were obtained for those lines then the present ambiguity might be resolved. If the redshifts obtained with forbidden lines are the same for both images then the case for gravitational lensing is stronger. If the redshifts are different then a cluster of quasars is more likely.

Suppose, the proposed program is carried out, and we become convinced that some widely separated pairs of quasars are, in fact, gravitationally lensed. We still would not know if the lensing were due to a cosmic string, to a cluster of faint galaxies, or to some other object. It is hard to think of a test that would demonstrate that a given pair of point-like quasars is, in fact, a single object lensed by a cosmic string, and not by something else.

The situation is entirely different for an extended object, such as a galaxy. Lensing by another galaxy, a cluster of galaxies, or a single massive object could produce multiple images and distort every image. However, some cosmic strings are expected to be straight[1,4,6], and their gravitational lensing would have a very striking signature: a background galaxy would look as though it had a sharp edge. No galaxies are known to be distorted in such a way, and the sharp edge would be a very clear indication that the galaxy is lensed by a cosmic string. By extrapolating the edge in two directions one should be able to see the same string cutting across images of other distant galaxies.

It is not clear how large the image of a galaxy should be in order to detect a sharp edge. Probably, the galaxy must be large enough to make a morphological classification possible: there should be at least 10 pixels across its image.

No cases of galaxies with sharp edges are known in the Palomar Sky Survey. As the survey covers two-thirds of the sky, this implies that no cosmic strings capable of large gravitational image splittings were discovered out to the redshift $z \approx 0.02$, or

---

[*] Permanent address: Nicholas Copernicus Astronomical Center, Polish Academy of Sciences, Poland.

so. High-resolution charge-coupled device (CCD) images obtained using the biggest telescopes cover an extremely small fraction of the sky, and do not put useful constraints on the presence of cosmic strings: even at the best CCD frames the galaxies cannot be classified by their shape beyond $z \approx 0.1$.

The Space Telescope will make a dramatic improvement. Morphological classification of galaxies will be possible out to a redshift $z \approx 1$ (ref. 22), and, therefore, sharp edges in galaxy images should be detectable out to that redshift. The ground-based observations show that there are 16,000 galaxies brighter than 24 mag in the J band per one square degree[23], and the number increases by a factor of 2.5 per magnitude. The WFC has a field-of-view 2.67×2.67 arc min (ref. 24). Therefore, there should be about 30 galaxies brighter than 24 mag, and about 200 galaxies brighter than 26 mag for each picture taken by the WFC on the Space Telescope. Any straight line which crosses the field has to cross many galaxies. It is hard to tell what fraction of those galaxies will be at a redshift > 1, but it is likely to be appreciable. I shall adopt an optimistic, but not implausible, view that if a string crosses the picture then there will be at least one very large redshift galaxy crossed by the string, and it will display a sharp edge. Thus I assume that if a string is in the field-of-view, its presence may be detected with a probability close to unity.

Let us assume that there is just one cosmic string with 100° segment close enough to have background galaxies detectable with the Space Telescope. The WFC must have the centre of its field-of-view within about 1.5 arc min of the string in order to 'see' the string. This gives the effective area for the string detection of $S \approx 100° \times 3' = 5^{\circ 2}$, roughly 10^{-4} of the whole sky. Therefore, an image taken randomly with the WFC will have a probability of 10^{-4} of falling into this strip on the sky, that is, there is a 10^{-4} probability that the string will be within the field-of-view of a random picture. About 10^4 deep images are required to have a reasonably large probability to detect the presence of the string. That many images will be obtained within the first few years of operation of the Space Telescope.

If the average image taken with the WFC shows many large redshift galaxies, then the method proposed here will be much more straightforward than the search for lines of double galaxies[4]. The angular separation between the two images of a galaxy lensed by a given cosmic string depends on the redshift of the galaxy[6]. Therefore, the emerging pattern is likely to be complicated and difficult to decipher.

I thank Roger Blandford, Richard Gott, Jim Gunn, Martin Gaskell and Edwin Turner for stimulating discussions, and the organizers of the Santa Cruz Workshop on Active Galactic Nuclei for creating a very stimulating atmosphere which helped to prepare this paper. This research was partly supported by NASA grant NAGW-765.

Received 12 September; accepted 18 November 1985.

1. Zeldovich, Ya. B. *Mon. Not. R. astr. Soc.* **192,** 663-667 (1980).
2. Vilenkin, A. *Phys. Rev.* **D23,** 852-858 (1981).
3. Vilenkin, A. *Phys. Rev. Lett.* **46,** 1169-1171 (1981).
4. Vilenkin, A. *Astrophys. J. Lett.* **282,** L51-L53 (1984).
5. Hogan, C. & Narayan, R. *Mon Not. R. astr. Soc.* **211,** 575-591 (1984).
6. Gott, J. R. *Astrophys. J.* **288,** 422-427 (1985).
7. Arp, H. & Hazard, C. *Astrophys. J.* **240,** 726-736 (1980).
8. Burbidge, E. M. *et al. Astrophys. J. Lett.* **242,** L55-L57 (1980).
9. MacAlpine, G. M. & Smith, H. E. *Astrophys. J.* **261,** 412-421 (1982).
10. Shaver, P. A. & Robertson, J. G. *Astrophys. J. Lett.* **268,** L57-L61 (1983).
11. Arp, H. *Astrophys. J.* **271,** 479-506 (1983).
12. Surdej, J., Swings, J. P., Henry, A., Arp, H., Kruszewski, A. & Pedersen, H. *Proc. 24th Liege Int. Astrophys. Colloq.* (ed. Swings, J. P.) 355-359 (1983).
13. Paczyński, B. & Górski, K. *Astrophys. J. Lett.* **248,** L101-L104 (1981).
14. Sanders, R. H., Van Albada, T. S. & Oosterloo, T. A. *Astrophys. J. Lett.* **278,** L91-L94 (1984).
15. Oort, J. H., Arp, H. & Ruiter, H. *Astr. Astrophys.* **95,** 7-13 (1981).
16. Osterbrock, D. E. & Shuder, J. M. *Astrophys. J. Suppl.* **49,** 149-174 (1982).
17. Gaskell, C. M. *Astrophys. J.* **263,** 79-86 (1982).
18. Shuder, J. M. *Astrophys. J.* **280,** 491-498 (1984).
19. Wilkes, B. J. *Mon. Not. R. astr. Soc.* **207,** 73-98 (1984).
20. Baldwin, J. A. *Astrophys. J.* **201,** 26-44 (1975).
21. Heckman, T. M., Miley, G. K. & Green, R. F. *Astrophys. J.* **281,** 525-534 (1984).
22. Gunn, J. *IAU Colloq.* No. 54, 313-319 (NASA CP-2111, 1979).
23. Tyson, J. A. & Jarvis, J. F. *Astrophys. J. Lett.* **230,** L153-L156 (1979).
24. Bahcall, J. N. & O'Dell, C. R. *IAU Colloq.* No. 54, 5-46 (NASA CP-2111, 1979).

Determination of cosmogenic ^{41}Ca in a meteorite with tandem accelerator mass spectrometry

P. W. Kubik*, D. Elmore*, N. J. Conard*, K. Nishiizumi† & J. R. Arnold†

* Nuclear Structure Research Laboratory, University of Rochester, Rochester, New York 14627, USA
† Department of Chemistry, B-017, University of California at San Diego, La Jolla, California 92093, USA

Several long-lived cosmogenic radioisotopes—^{14}C, ^{36}Cl, ^{26}Al, ^{10}Be, ^{53}Mn and ^{129}I—have been used to investigate the history of meteoric material and lunar samples. One of the most interesting results has been the determination of the residence time or 'terrestrial age' of meteorites found on ablation areas of the Antarctic ice sheets. As these ages range up to 700,000 years[1], ^{36}Cl, with a half-life of 3.01×10^5 yr has been the most useful isotope, but for reliable measurements of terrestrial ages below 300,000 yr, a radioisotope with a half-life between those of ^{36}Cl and ^{14}C ($T_{1/2} =$ 5730 yr) is needed. Calcium-41 is a suitable candidate, with $T_{1/2} = 1.03 \times 10^5$ yr, but it occurs in concentrations below the detection limit of conventional techniques. Here we report the first use of tandem accelerator mass spectrometry (TAMS) to measure ^{41}Ca in a natural sample—the Bogou iron meteorite. We find a ^{41}Ca/Ca ratio of $(3.8 \pm 0.6) \times 10^{-12}$ which corresponds to a ^{41}Ca activity of 6.9 ± 1.1 d.p.m. per kg meteorite. This implies that ^{41}Ca can be successfully used to determine the irradiation history of meteorites.

Calcium-41 has been proposed as a dating tool in palaeochronology and in dating CaCO$_3$ sediments[2]. ^{41}Ca is produced on the surface of the Earth by neutron activation of ^{40}Ca; this dominates atmospheric production rates because of the low abundance of sufficiently heavy targets in the atmosphere. The calculated saturation concentrations ^{41}Ca/Ca in the terrestrial environment are between 10^{-15} and 10^{-14} (ref. 2). Accelerator mass spectrometry is the only way to measure these low concentrations. Decay counting is not very sensitive because of the long lifetime of ^{41}Ca and because ^{41}Ca decays only by electron capture (the 3.3 keV X rays of ^{41}K are difficult to detect). The current detection sensitivity for accelerator mass spectrometry, ^{41}Ca/Ca $\approx 10^{-13}$, is still not sufficient by two orders of magnitude to measure terrestrial samples, but is high enough to measure meteorites. ^{41}Ca in meteorites is produced by cosmic ray spallation, mainly of Fe and Ni, and by the capture of thermal neutrons by ^{40}Ca.

Many of the meteorites studied with TAMS have been selected from the thousands of meteorites collected from ablation areas of the Antarctic ice sheet. Stable noble gas isotopes are used to identify meteorites with exposure times long enough to ensure saturation of the radioisotope of interest before the meteorite fell onto the earth. If the longer-lived radioisotopes ^{53}Mn ($T_{1/2} = 3.7 \times 10^6$ yr) and ^{10}Be ($T_{1/2} = 1.6 \times 10^6$ yr) are not found to be saturated, the meteorite may have originated inside a larger body that broke up following a collision in space or on entry into the earth's atmosphere[3,4]. If ^{53}Mn and ^{10}Be are saturated, a measurement of ^{14}C, ^{41}Ca and/or ^{36}Cl determines the terrestrial age of the meteorite.

The ^{41}Ca measurements were carried out with the Rochester tandem Van de Graaff accelerator. The apparatus and the general method of measuring radioisotope ratios at Rochester are described elsewhere[5] together with some initial ^{41}Ca results. Details of the method of measuring ^{41}Ca are reported here.

Negative CaO ions were produced in our scanning Hiconex (made by the General Ionex Corporation, Newburyport, Massachusetts, USA) caesium sputter ion source. Acceleration of CaO$^-$ ions was chosen over CaH$_3^-$ ions even though the latter results in a lower ^{41}K interference[6,7]. This was done because it

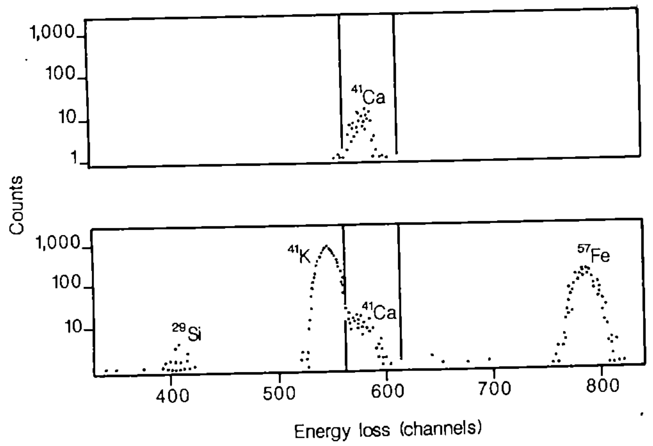

Fig. 1 ΔE spectra taken from the second plate of the ionization detector. The upper spectrum shows events that passed software gates set on four ΔE signals and the total energy signal. The lower spectrum shows the ungated events. The use of a new high-resolution injector[5] eliminated interference from ^{42}Ca^{16}O$^-$. When the injector magnet was set for mass 57, a small fraction of the high-energy tail of ^{40}Ca^{16}O$^-$, all of ^{40}Ca^{17}O$^-$ ($\approx 4\times10^{-4}$ of ^{40}CaO), and all of ^{41}K^{16}O$^-$ was transmitted into the accelerator. Except for ^{41}K, the mass resolution of the system was good enough to remove these interferences, but there was a low counting rate from two other ions having nearly the same M/q. The small ^{29}Si peak (charge state 6+) originated from ^{28}Si^{29}Si$^-$ molecules (the sample holder was made out of Si). The ^{57}Fe peak (charge state 11+) comes from stainless steel parts in the ion source. These two ions have nearly the same magnetic and electric rigidity as the ^{41}Ca in the charge states indicated but require at least one scattering or charge-changing event to be able to reach the detector, where they are well separated.

is very difficult and somewhat inefficient to prepare the small and pure metallic Ca samples necessary for producing adequate beams of CaH$_3^-$ ions. Our CaO samples had high enough radioisotope ratios and contained low enough K to allow separation of ^{41}K from ^{41}Ca in our gas ionization detector[5]. The terminal voltage was set at 10 MV. Charge state $q=8$ was chosen, since this gave the best yield from the terminal stripper foil. The ^{41}Ca/Ca ratios were determined by alternately measuring the ^{40}Ca beam current in the image Faraday cup following the accelerator and the ^{41}Ca particles in the gas counter following a 10° electrostatic analyser. Figure 1 shows a ΔE spectrum taken with the gas detector. The data analysis procedure is described in ref. 8.

The Bogou meteorite fell on 14 August 1962 in Bourkina-Fasso (Africa). The recovered mass was 8.8 kg. The following chemistry was performed to extract the calcium and to remove potassium: after adding 6.0 mg of Ca carrier, 636 mg of the Bogou meteorite was dissolved in dilute HNO$_3$. About 2% of the solution was taken as an aliquot for chemical analysis by atomic absorption spectroscopy. After separate hydroxide precipitation, 4% ammonium oxalate was added to the supernatant. The calcium oxalate was separated and dissolved in diluted HCl. The Ca was then purified through a cation exchange resin (AG 50W-X8) and precipitated as calcium oxalate. The precipitate was ignited to CaO in a quartz vial at about 1,100 °C for 10 min. The chemical procedures and analysis methods for ^{10}Be, ^{36}Cl and ^{53}Mn, which were also measured in the Bogou meteorite, were essentially the same as those reported earlier[1,3,9].

Table 1 Results of ^{41}Ca measurements

Sample	^{41}Ca counts	^{41}Ca/Ca (10^{-12})	^{41}Ca atoms per g (10^8)	^{41}Ca d.p.m. per kg
Bogou	93	3.8 ± 0.6	5.4 ± 1.0	6.9 ± 1.1
Blank	6	0.18 ± 0.08		
Standard		95.6 ± 6.1		

The ^{41}Ca standard was prepared by diluting the ^{41}Ca counting source which was used for the ^{41}Ca half-life measurement of Mabuchi *et al.*[11]. The given uncertainty is that of their ^{41}Ca half-life ($T_{1/2}=1.03\times10^5$ yr). All samples (meteorite, standard, chemistry blank) were mixed with Ag powder (CaO : Ag ≈ 1 : 4 by weight) before loading on a wheel made of ultra-pure Si. The ^{41}Ca/Ca ratio of the sample was normalized to the ^{41}Ca standard after background subtraction. The total ^{41}Ca counting times for the meteorite and the blank sample were 46 and 85 min, respectively. The quoted uncertainties are one standard deviation.

Table 2 Cosmic ray-produced radionuclides in the Bogou meteorite

Nuclide	Half-life (yr)	Activity (d.p.m. per kg sample)
^{41}Ca	1.03×10^5	6.9 ± 1.1
^{36}Cl	3.01×10^5	22.2 ± 0.7
^{10}Be	1.6×10^6	5.1 ± 0.4
^{53}Mn	3.7×10^6	471 ± 20

The results (Table 1) show that ^{41}Ca/Ca ratios in the 10^{-12} range can be measured with uncertainties of about 15%. The present background ratio for a chemistry blank is an order of magnitude lower. Improvements in the chemical removal of potassium from the samples and from the caesium should be possible. This will lower background ratios and may allow us to measure ratios in the 10^{-13} range. However, the present limitation for producing lower ratios is not the interference from ^{41}K but the difficulty of producing higher negative ion currents and the small amount of sample available. About one third of the 5.9 mg meteorite CaO sample was consumed. This gives an overall detection efficiency for ^{41}Ca of about 10^{-7}. This could be improved with the use of a high intensity and high efficiency sputter source[10]. We hope that the use of such a source with our apparatus will make measurements of terrestrial samples possible.

We normalized the ^{41}Ca/Ca ratio to a standard produced from the sample of Mabuchi *et al.*[11]. This is the sample that was used to obtain the generally accepted half-life of 1.03×10^5 years. Our earlier measurements[5] indicated that this half-life may be too low. Any error in the Mabuchi half-life would most likely arise from their estimate of the ^{40}Ca(n,γ)^{41}Ca cross section or from their activity measurement. If the uncertainty is in the cross section, this would not affect our reported value of the ^{41}Ca activity, 6.9 ± 1.1 d.p.m. per kg. However, an error in their activity measurement would affect our reported activity by a proportional amount.

For a given radioisotope, the useful range for measuring terrestrial ages of meteorites can be determined from the experimental uncertainties. The terrestrial age and its uncertainty are calculated from

$$T=-\frac{1}{\lambda}\cdot\ln(R)$$

$$\Delta T=\frac{\Delta R}{R\lambda}$$

where $\lambda=\ln 2/T_{1/2}$ and R is the ratio of measured activity to saturated activity. The uncertainty in the saturated activity is determined from the distribution in measurements for meteorites that fell recently and is usually 10–15%. At the low end of the age range, the uncertainty in R is usually dominated by the uncertainty in the saturated activity. For greater ages the activity is low and the uncertainty due to counting statistics becomes large. A young terrestrial meteorite age can be determined to ±65,000 yr using ^{36}Cl and, assuming comparable precision, we expect ±23,000 yr will be possible with ^{41}Ca. This results in approximate cross-over points of 40,000 yr for ^{14}C–^{41}Ca and about 300,000 yr for ^{41}Ca-^{36}Cl (with considerable overlap at the boundaries).

Some conclusions can be drawn from a comparison of the cosmic ray produced radionuclides ^{10}Be, ^{36}Cl, ^{41}Ca and ^{53}Mn in the Bogou meteorite (see Table 2). The recovered size of the Bogou meteorite is about 7 cm in radius. The high ^{53}Mn concentration of 471 ± 20 d.p.m. per kg suggests a pre-atmospheric radius no larger than 15 cm. The ^{36}Cl value of 22.2 ± 0.7 d.p.m. per kg, which agrees well with the average saturation value of 22.8 ± 3.1 d.p.m. per kg (ref. 9), confirms this. Not enough ^{10}Be data have been tabulated for iron meteorties to use the measured value of 5.1 ± 0.4 d.p.m. per kg for an additional constraint on the radius of this meteorite.

Both ^{36}Cl and ^{41}Ca in an iron meteorite are high-energy spallation products and therefore their production should be depth-independent for a small-sized meteorite like the Bogou iron meteorite. There is little production from neutron capture because the ^{40}Ca concentration in an iron meteorite is less than 1 p.p.m. The measured spallation cross sections for ^{41}Ca (C. Perron, personal communication which revises data from ref. 12) are lower by about a factor of 1.5 ± 0.8 as compared with those of ^{36}Cl (ref. 13). Using the average ^{36}Cl saturation value, the estimated ^{41}Ca saturation activity should be 15 ± 8 d.p.m. per kg, which is larger than, but consistent with, the measured value of 6.9 ± 1.1 d.p.m. per kg. The closest analogue to ^{41}Ca in meteorites is ^{37}Ar, whose activity averaged over an 11-yr solar cycle is about 16 d.p.m. per kg Fe (ref. 14).

Although this is the first ^{41}Ca measurement in an iron meteorite, Mabuchi *et al.*[15,16] have measured ^{41}Ca in stony meteorites using low level X-ray counting. Since ^{41}Ca in stony meteorites is produced from both Ca and Fe, these previous results can be used together with our result from an iron meteorite to obtain the production of ^{41}Ca from calcium. Using 100-200 g of meteorite Mabuchi *et al.* found 4.3 ± 1.9 d.p.m. ^{41}Ca per kg in the Granes meteorite and 48 ± 8 d.p.m. ^{41}Ca per kg in the Allende meteorite. The Granes meteorite contains 22.1% Fe, 1.35% Ca (ref. 15) and the Allende meteorite contains 23.85% Fe and 1.87% Ca (ref. 17). Using these values, we find that approximately 65% (95%) of the ^{41}Ca activity in Granes (Allende) comes from activation of ^{40}Ca. The fact that these numbers are very different in the two cases shows that ^{41}Ca is a useful nuclide for cosmic ray bombardment studies of meteorites. The ^{41}Ca activity in meteorites which are large enough to have a thermal neutron flux, such as Allende and Jilin[18], should be easily measurable by accelerator mass spectrometry.

The successful measurement of ^{41}Ca in the Bogou meteorite with tandem accelerator mass spectrometry shows that this radioisotope can now be measured in extraterrestrial samples accurately enough to help determine irradiation histories of meteorites. Calcium-41 has a half-life that falls in the gap between ^{14}C and ^{36}Cl, a range that is needed for measuring terrestrial ages of Antarctic meteorites.

We wish to thank K. Notsu *et al.*[11] for providing the ^{41}Ca standard and the US National Museum for providing the Bogou meteorite sample. We thank T. Hemmick, R. Teng and the NSRL staff for technical assistance. This work was supported by NSF grant PHY-8214295 and NASA grant NAG 9-33.

Received 16 July; accepted 20 November 1985.

1. Nishiizumi, K. *et al. Earth planet. Sci. Lett.* **52,** 31-38 (1981).
2. Raisbeck, G. M. & Yiou, F. *Nature* **277,** 42-44 (1979).
3. Nishiizumi, K. *et al. Earth planet. Sci. Lett.* **45,** 285-292 (1979).
4. Nishiizumi, K., Regnier, S. & Marti, K. *Earth planet. Sci. Lett.* **50,** 156-170 (1980).
5. Elmore, D. *et al. Nucl. Instrum. Meth.* **233** (B5 no. 2), 109-116 (1984).
6. Raisbeck, G. M., Yiou, F., Peghaire, A., Guillot, J. & Uzureau, J. *Proc. Symp. Acc. Mass Spectr. Argonne* 426-430 (1981).
7. Fink, D. *et al. Nucl. Instrum. Meth.* **233** (B5 no. 2), 123-128 (1984).
8. Elmore, D., Conard, N., Kubik, P. W. & Fabryka-Martin J. *Nucl. Instrum. Meth.* **233** (B5 no. 2), 233-237 (1984).
9. Nishiizumi, K. *et al. Earth planet. Sci. Lett.* **62,** 407-417 (1983).
10. Middleton, R. *Nucl. Instrum. Meth.* **214,** 139-150 (1983).
11. Mabuchi, H., Takahashi, H., Nakamura, Y., Notsu, K. & Hamaguchi, H. *J. inorg. nucl. Chem.* **36,** 1687-1688 (1974).
12. Perron, C. *Nature* **271,** 425-426 (1978).
13. Baros, F. & Regnier, S. *J. Physique* **45,** 855-861 (1984).
14. Begemann, F. *J. geophys. Res.* **77,** 3650-3659 (1972).
15. Mabuchi, H. Tobailem, J., Leger, C., Bibron, R. & Biettmann, D. *Geochim. cosmochim. Acta* **32,** 949-963 (1968).
16. Mabuchi, H. *et al. Meteoritics* **10,** 449 (1975).
17. Clarke, Jr. R. S. *et al. Smithson. Contr. Earth Sci.* **5,** 53 (1970).
18. Honda, M. *et al. Earth planet. Sci. Lett.* **57,** 101-109 (1978).

Detection of stratospheric N_2O_5 by infrared remote sounding

G. C. Toon, C. B. Farmer & R. H. Norton

Jet Propulsion Laboratory, California Institute of Technology,
4800 Oak Grove Drive, Pasadena, California 91109, USA

The existence of stratospheric N_2O_5, a temporary reservoir species whose photolysis products catalyse ozone destruction, has long been predicted[1] but has not previously been detected. We now report the identification of N_2O_5 absorption between 1,230 and 1,260 cm^{-1} in infrared spectra measured by the Atmospheric Trace Molecule Spectroscopy (ATMOS) experiment from orbit during the Spacelab 3 mission. Preliminary analysis of spectra recorded at sunrise on 1 May 1985 indicates a peak volume mixing ratio of 1.6×10^{-9} at 35 km altitude, or a broad concentration peak of 4×10^8 molecules cm^{-3} between 25 and 31 km. As expected, this absorption is not detectable in spectra measured at sunset because of depletion of N_2O_5 by photolysis during the daytime. This behaviour is in good agreement with predictions, and represents an important validation of current photochemical models of the stratosphere.

In the 1970s it was recognized that anthropogenic gases were the source of radicals, for example NO, Cl, OH, represented by the symbol X in the following equations, that could destroy ozone by the catalytic cycle

$$X + O_3 \rightarrow XO + O_2$$

$$XO + O \rightarrow X + O_2$$

whose net result is:

$$O + O_3 \rightarrow 2O_2$$

The catalytic cycle involving NO and NO_2 is thought to be especially efficient, with each NO radical predicted to destroy 300 ozone molecules before being trapped by one of the five following reactions:

$NO_2 + O_3 \rightarrow NO_3 + O_2$	(nitrogen trioxide)
$NO_2 + ClO \rightarrow ClONO_2$	(chlorine nitrate)
$NO_2 + OH \rightarrow HNO_3$	(nitric acid)
$NO_2 + HO_2 \rightarrow HNO_4$	(peroxynitric acid)
$NO_2 + NO_3 \rightarrow N_2O_5$	(dinitrogen pentoxide)

Like NO and NO_2, these five products are thought to be present only in parts per 10^9 and, apart from nitric acid, have not yet been detected unambiguously. Identification and measurement of these products is crucial to the confirmation of photochemical theories and hence the accurate evaluation of trends in ozone amounts.

Roscoe[2] measured the sunrise-sunset difference in the total thermal emission over the 1,230-1,250 cm^{-1} spectral region using a balloon-borne filter radiometer. However, this was not considered an unequivocal detection because Roscoe lacked the spectral resolution necessary to show that the diurnal variation was associated with the N_2O_5 absorption band.

The ATMOS instrument consisted of a suntracker and telescope which accepted a 2-mrad field-of-view from the centre of the solar disk, a double-passed Michelson interferometer, and a HgCdTe detector cooled to 77K. Measurements were made

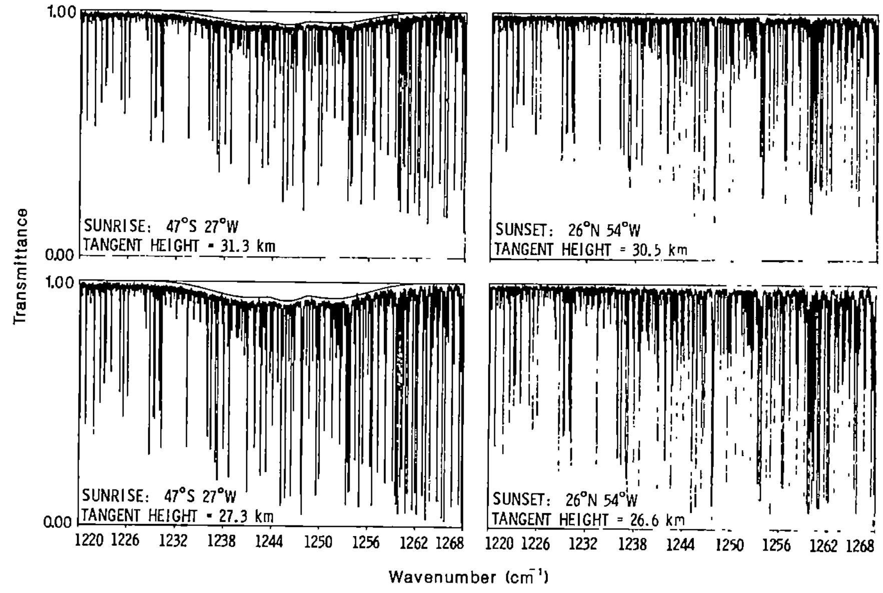

Fig. 1 Observed spectral transmittance of the atmosphere.

during the periods when the spacecraft was entering or emerging from the Earth's shadow. The solar radiation measured in successive one million point interferograms (2.2 seconds apart) had therefore passed through the Earth's atmosphere at different altitudes. After Fourier transformation, these interferograms yielded 0.015 cm^{-1} resolution spectra of the entire mid-infrared region at vertical intervals of 4 km. The high spectral resolution allowed the spectral lines of the interfering gases to be distinguished from the broad underlying absorption between 1,230 and 1,260 cm^{-1}, permitting an unambiguous identification of the ν_{12} band (symmetric NO_2 stretch[3]) of N_2O_5 to be made. The stronger, overlapping ν_1 and ν_{11} bands (antisymmetric NO_2 stretch[3]) were also evident between 1,680 and 1,760 cm^{-1}, but the heavy interference from HNO_3 spectral lines made their identification less clear-cut than that of the ν_{12} band.

In Fig. 1, spectra measured from an orbital altitude of 350 km on 1 May 1985 are presented. The sunrise was observed at 47 °S 27 °W and the sunset at 26 °N 54 °W. A broad featureless absorption band underlies the 1,230–1,260 cm^{-1} region of the sunrise spectra, but not the sunset spectra. To confirm that this absorption band corresponded to the ν_{12} band of N_2O_5, we computed the absorption of N_2O_5 alone for the same geometry as the observed spectra. Climatological temperature and pressure profiles were assumed, together with the N_2O_5 volume mixing ratio profile shown in Fig. 2. The result, the smooth curves superimposed on the sunrise spectra, completely account for the observed sunrise–sunset differences, supporting the thesis that the broad absorption band in the sunrise spectra is due to N_2O_5.

The spectral line parameters of the N_2O_5 absorption bands are not yet known. Because of the high moment of inertia of the N_2O_5 molecule, its rotational energy levels are closely spaced, giving rise to vibration–rotation bands containing large numbers of densely packed spectral lines, which are not resolved[4] even at a spectral resolution of 0.02 cm^{-1} and a pressure of 0.15 torr. It can be estimated that a full spectral characterization of the ν_{12} band and its strongest hot bands would yield over 80,000 spectral lines of significant strength, which would render line-by-line calculations of spectra tedious. We therefore sought to represent the gross features of the shape of the ν_{12} band (and its temperature dependence) with a simple empirical model. This was done by treating the molecule as linear with a vibrational constant $B = 0.1$ cm^{-1}. Each spectral line was assigned a Lorentz width of 25 cm^{-1}, and the strengths of the Q-branch lines were reduced to only 0.3 of those of the P or R branches. The spectral line positions were adjusted until the band shape at room temperature matched the laboratory measurement of Murcray *et al.*[4]. The strengths of the resulting 360 spectral lines were then scaled to give an integrated band intensity of 4.32×10^{-17} cm^{-1}/(molecules cm^{-2}). This figure was derived from absorption cross-section measurements made by Connell[5], which agree well with those of Graham and Johnston[6]. Recent measurements by Perner *et al.*[7] and Cantrell *et al.*[8] also support Connell's value. However, it should be pointed out that this value of the integrated band intensity is in disagreement with the 2.36×10^{-17} cm^{-1}/(molecules cm^{-2}) (581 cm^{-1}/(atm-cm) at 298 K) measured by Lovejoy *et al.*[9]. To resolve this discrepancy, further measurements are required, preferably at stratospheric temperatures.

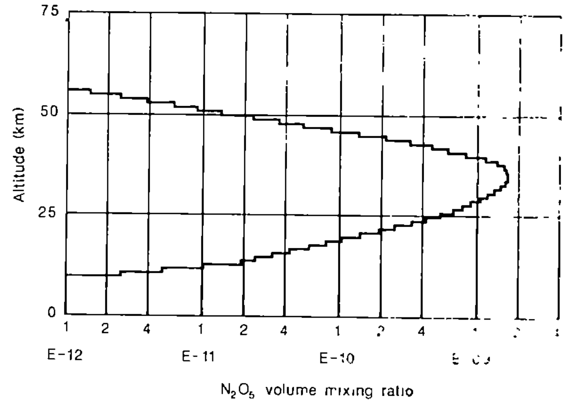

Fig. 2 Volume mixing ratio profile of N_2O_5.

This work was done while G.C.T. held a National Research Council-JPL Research Associateship. The research described here was performed by the Jet Propulsion Laboratory, California Institute of Technology, under contract with NASA.

Received 29 July; accepted 28 October 1985.

1. Johnston, H. *Science* **173**, 517–522 (1971).
2. Roscoe, H. K. *Geophys. Res. Lett.* **9**, 901–902 (1982).
3. Laane, J. & Ohlsen, J. R. *Prog. inorg. Chem.* **27**, 465–513 (1980).
4. Murcray, D. G., Goldman, A., Blatherwick, R. D., Murcray, F. J. & Bonomo, F. S. *High Resolution Infrared Laboratory Spectra* (Department of Physics, University of Denver, 1984).
5. Connell, P. S. *Lawrence Berkeley Lab. Publ.* LBL-904 (1979).
6. Graham, R. A. & Johnston, H. S., *J. phys. Chem.* **82**, 254–268 (1978).
7. Perner, D. *et al. J. geophys. Res.* **90**, 3807–3812 (1985).
8. Cantrell, C. A. *et al. J. phys. Chem.* **89**, 139–146 (1985).
9. Lovejoy, R. W., Chackerian, Jr C. & Boese, R. W. *Appl. Opt.* **19**, 744–748 (1980).

Synthetic organic chemicals in the deep Sargasso Sea

Anthony H. Knap*, Kandace S. Binkley*
& Werner G. Deuser†

* Marine and Atmospheric Programme, Bermuda Biological Station for Research, Ferry Reach, Bermuda
† Woods Hole Oceanographic Institution, Woods Hole, Massachusetts 02543, USA

The flux of chlorinated synthetic organic chemicals to the open ocean is important both to organic geochemistry and for environmental health. We have studied over a 2-yr period the deposition of polychlorinated biphenyls (PCBs), chlordanes and dieldrin by means of a sediment trap in the Sargasso Sea. We now report that the fluxes of these materials to the deep North Atlantic Ocean were 1.6 μg m^{-2} yr^{-1}, 0.02 μg m^{-2} yr^{-1} and 0.04 μg m^{-2} yr^{-1}, respectively between 1978 and 1980.

Samples were collected in a 1.5 m^2 cross-section sediment trap[1] moored 3,200 m below the surface and 1,000 m above the sea floor at 32°05′ N, 64°15′ W, ~45 km south-east of Bermuda. The amounts of material collected in the trap vary with the annual cycle of productivity in surface waters[2]. We have analysed samples collected between 1978 and 1980 over nine intervals of ~60 days for PCBs, chlordanes (the sum of *cis*- and *trans*-isomers) and dieldrin. Chlordane and dieldrin are among the most persistent chlorinated pesticides[3], while some of the PCBs are resistant to degradation and ubiquitous in the marine environment[4]. All three classes of compounds have been found in the North Atlantic atmosphere[5]; the North Atlantic Ocean may be a sink for 50–80% of PCBs in the environment[4].

The size fraction analysed (<125 μm) accounts for 75–90% of the mass collected by the deep trap[1]. The daily flux of total PCBs ranges from 1.2 to 10.8 ng m^{-2} (Table 1), corresponding to a mean yearly flux of 1.6 μg m^{-2}; the concentration on the particles ranges from 50 to 350 ng per g dry weight, or a mean of ~150 ng per g. If all PCBs are contained in the <125-μm fraction, the average concentration is 110 ng per g of total particulate matter collected.

The fluxes of chlordane and dieldrin average 58 ± 59 pg m^{-2} day^{-1} (21.4 ng m^{-2} yr^{-1}) and 114 ± 105 pg m^{-2} day^{-1} (38.4 ng m^{-2} yr^{-1}), respectively. The PCBs correlate with organic carbon ($r = 0.81$, $n = 8$) (Fig. 1), as is the case with all other constituents of this sediment-trap material[2,6,7]. Chlordane and dieldrin also correlate with organic carbon ($r = 0.72$, $r = 0.74$ respectively, $n = 7$). The concentration of chlorinated hydrocarbons in sample no. 5 was small compared with that in the other samples while the total mass and the carbon flux was the greatest[2], but we cannot tell from our limited data-set whether this total exceptionally large mass flux is the explanation. However, the relationships between the individual compounds correlate well (PCB/dieldrin, $r = 0.98$, $n = 7$; PCB/chlordane, $r = 0.90$, $n = 7$; dieldrin/chlordane, $r = 0.90$, $n = 7$). The small sample size means the analytical variability could only be tested on one sample (no. 4) by sub-sampling and independent analysis. The standard deviation of the replicate was 18%. Analytical blanks were very low as we used very small volumes of solvents. However, contamination from the sediment trap may have occurred as a satisfactory sampling blank could not be determined. We would expect to find components of the atmosphere over the Sargasso Sea[8,9] in sea water[10] and in deep-ocean sediments[11] in the trap, but not significant contamination by pesticides, chlordane and dieldrin. The presence of these organic compounds is, therefore, not caused by sampling or analytical errors.

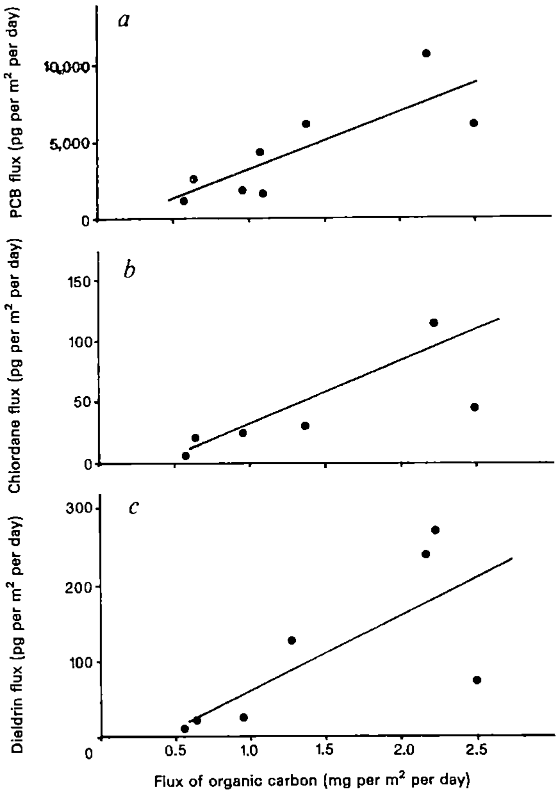

Fig. 1 *a*, Relationship of PCB flux to organic carbon flux. Regression coefficient $r = 0.83$ ($n = 8$). *b*, Chlordane to organic carbon: $r = 0.72$, $n = 7$. *c*, Dieldrin to organic carbon: $r = 0.74$, $n = 7$.

Dissolved PCB concentrations in surface waters were measured 10 km north of the trap site in January 1980 (ref. 10) at ~100 pg total PCB l^{-1}. The dissolved and particulate PCBs of an oligotrophic area of the Pacific Ocean have similar primary productivity and dissolved concentrations as in the water over our trap[12]. Tanabe and Tatsukawa[12] found that ~7–49% of the total PCB found was present on glass-fibre filters although it was not known how much was desorbed from the filter. However, PCBs have low solubility in water and high octanol/water partition coefficients, so they are readily adsorbed to suspended solids, especially those high in organic carbon[13]. In contrast, <0.5% of the α and γ isomers of hexachlorocyclohexane (HCH) were adsorbed on the filters. Lindane, the γ isomer of HCH and a widely used pesticide, is far more water-soluble (~6.1 p.p.m. 25 °C in NaCl; ref. 14) than PCBs and chlordane and is a component of North Atlantic rain water (A.H.K., in preparation) and this is presumably why we did not detect lindane in our trap, although it may have a residence time of 10 yr in the open ocean[12]. We also did not detect α-HCH on the intercepted particles.

We can compare our flux data with the more accurately known atmospheric input data[4,5,9,15]. One can predict atmospheric vapour deposition using the average concentration of the compound in the atmosphere and its deposition velocity (v_d). Although v_d is difficult to measure for the open ocean, 0.1 cm s^{-1} seems to be the best estimate[5]. We assume the atmospheric concentration of PCBs over the open North Atlantic Ocean to be 50–100 pg m^{-3} (refs 5, 9), which gives a deposition to the ocean surface of 1.6–3.1 μg m^{-2} yr^{-1}. Rainwater and dry particle deposition will remove some of this material from the atmosphere, but this process should be more effective in coastal areas than the open ocean.

Based on concentrations of PCBs in a few sediment cores taken near our trap, a similar flux of 1.6 μg m^{-2} yr^{-1} was derived[11]. A sediment trap deployment near the Tongue of the Ocean (Bahamas) yielded a flux of PCBs of 4.9 μg m^{-2} yr^{-1}; this trap was only 100 m off the bottom at 2,050 m (ref. 11).

Table 1 Flux of organochlorines at 3,200 m

Sample no.	Sampling period	Duration (days)	Flux (pg m^{-2} day^{-1}) PCB	Chlordane	Dieldrin	Flux (mg m^{-2} day^{-1}) Organic carbon
1	4 April–7 June 1978	62	6,200	31	127	1.38
2	7 June–8 August 1978	62	4,400	—	—	1.08
3	9 August–10 October 1978	62	1,600	—	—	1.10
4	12 December 1978–14 February 1979	64	10,800	165	240	2.18
5	24 March–31 May 1979	68	6,200	46	77	2.50
6	31 May–30 July 1979	60	1,900	24	25	0.96
7	10 October–3 December 1979	52	1,200	6	10	0.58
8	6 February–7 April 1980	63	—	114	274	2.22
9	15 April–17 June 1980	61	2,600	21	25	0.64
	Mean daily flux at 3,200 m	(pg m^{-2} day^{-1})	4,362 ± 3273	58 ± 59	114 ± 105	
	Mean yearly flux	(ng m^{-2} yr^{-1})	1,590	21	38	

All values are expressed on a per square metre basis. After recovery, the samples were collected from the cup of the trap and wet-sieved into five size fractions[2]. The fractions <35 μm and 35–125 μm were pooled and sub-sampled for trace organic analysis. Samples were dried at 60 °C. Sub-samples ranged from 80 to 100 mg and were extracted five times with 4-cm^3 aliquots of dichloromethane after a 15-min sonication and phase separation. These extracts were evaporated, taken up in hexane, separated into two fractions using Florisil adsorption chromatography[15] and analysed by temperature-programmed electron capture gas chromatography using splitless techniques[19]. A 25 m × 0.2 mm SE-54 column was used for separation. Confirmation of PCBs was carried out by gas chromatographic analysis before and after treatment with 7% fuming sulphuric acid[15] and identification of retention times of individual components compared with known standards[19]. Additional confirmation was carried out by selective ion monitoring gas chromatography/mass spectrometry using a Hewlett-Packard mass selective detector. Response factors were determined for these individual PCBs and quantification was carried out expressing the results as total PCB[8] rather than in terms of equivalents of commercial chemical mixtures. Dieldrin and chlordane (α and γ isomers) have been quantified using authentic standards by response factors on the ECD GC. For the present purposes both chlordane isomers have been summed.

Table 2 Individual chlorobiphenyl congener particle flux in <125 μm fraction of sediment trap material at 3,200 m

IUPAC no./name of chlorobiphenyl		PCB mix	Flux (pg m^{-2} day^{-1}) June 1978	February 1979	March 1979	July 1979	December 1979	August 1980	Flux (ng m^{-2} yr^{-1}) Mean ±s.d.	Total flux
26	2,3′,5-tri-	*a, b**	56	91	99	20	6	38	52 ± 38	19
28	2,4,4′-tri-	*a, b*	83	14	94	97	25	21	52 ± 44	19
44	2,2′,3,5′-tetra-	*a, b, c, d**	64	22	187	92	17	19	67 ± 66	24
49	2,2′,4,5′-tetra-	*a, b, c*	—	201	133	61	17	49	92 ± 74	34
52	2,2′,5,5′-tetra-	*a, b, c, d*	144	586	444	108	47	71	233 ± 225	85
101	2,2′,4,5,5′-penta-	*a, b, c, d*	111	288	181	56	55	89	130 ± 90	47
118	2,3′,4,4′,5-penta-	*a, b, c, d*	188	470	340	144	117	151	235 ± 140	85
128	2,2′,3,3′,4,4′-hexa-	*c, d*	2	24	23	7	7	0	11 ± 10	4
153	2,2′,4,4′,5,5′-hexa-	*a*, b*, c, d*	58	103	79	31	25	31	55 ± 35	8
174	2,2′,3,3′,4,5,6′-hepta-	*c*, d*	7	33	34	14	7	14	18 ± 12	6
180	2,2′,3,4,4′,5,5′-hepta-	*c, d*	25	61	56	11	21	9	31 ± 23	11
201	2,2′,3,3′,4′,5,5′,6-octa-	*d*	—	26	29	17	10	14	19 ± 11	6

These individual congeners were chosen according to their distribution in most of the samples. They are compounds that are well separated by our chromatographic techniques into single peaks and that have been identified as individual compounds by gas chromatography/mass spectrometry[15]. The only exception are peaks 28 and 153 which can sometimes co-elute with other peaks. A detailed analysis of the commercial PCB mixtures of Clophen has been carried out[18]. A series of products with different degrees of chlorination was analysed (30, 40, 50 and 60% chlorine). Compounds such as 44, 52, 101 and 118 were present in all PCB mixtures of differing chlorination. No. 49 is present in three of the four mixtures. The others are only present in two of the four products or were minor constituents in all but one mixture. *a*, Clophen A30; *b*, Clophen A40; *c*, Clophen A50; *d*, Clophen A60.

* Minor constituent in mixture.

Fluxes of PCBs measured in the Mediterranean were ~20 times greater[16] and in the Baltic Sea, in 20 m of water, 80 times greater than our Sargasso Sea values[17]. Considering the difference in magnitude of the source functions in the Mediterranean and Baltic compared with the open ocean, we consider this divergence reasonable.

Conventional analyses of PCBs are reported as the concentration in terms of commercial mixtures (Clophen or Aroclor equivalents). But this does not give information on sources, sinks and behaviour of individual PCB congeners in the environment, as each congener may behave differently[4,18]. Analysis by capillary gas chromatography is the preferred method, with calibration against accurate standards.

We have identified some individual congeners in the trap, and have quantified those for which we have standards and the correct identification. Table 2 shows that many of these individual components have different sources from various industrial mixtures and have undergone different biogeochemical modifications. The three components with the greatest flux are 52, 101 and 118 which are present in all of the most widely used commercial mixtures[18]. The other individual components have a generally lower concentration relating to the number of technical mixtures in which each compound appears.

Our data indicate that PCBs were major contaminants on particles in the open ocean up till 1980, although production in the United States ceased in 1977. The analysis of the individual components of these synthetic chemicals is important as their absence or presence in parts of the marine environment provides an insight into biogeochemical processes in the ocean.

This work was supported by a grant from British Petroleum International, and NSF grants OCE 76-21280, OCE 78-19813 and OCE 80-24130. We thank Hewlett-Packard for the donation of the mass selective detector, the Camille and Henry Dreyfus Foundation, members of the Moored Array program of the Woods Hole Oceanographic Institution, the staff of the Bermuda Biological Station and the crew of the R/V *Erline* of the US Naval Underwater Systems Center in Bermuda for help, also Professor J. Duinker for providing the individual PCB congeners, and Dr G. Harvey and Dr J. Farrington for valuable comments on the manuscript. This is contribution no. 5956 from the Woods Hole Oceanographic Institution and no. 1053 from the Bermuda Biological Station.

Received 24 May; accepted 19 November 1985.

1. Deuser, W. G., Ross, E. H. & Anderson, R. F. *Deep-Sea Res.* **28**, 495-505 (1981).
2. Deuser, W. G. & Ross, E. H. *Nature* **283**, 364-365 (1980).
3. Sanborn, J. R., Francis, B. M. & Metcalf, R. L. *U.S. NTIS PB. Rep.* PB-272353 (1977).
4. National Academy of Sciences *Polychlorinated Biphenyls* (US NAS, Washington DC, 1979).
5. Bidleman, T. F., Rice, C. P. & Olney, C. E. in *Marine Pollutant Transfer* (eds Windom, H. L. & Duce, R. A.) 323-352 (D.C. Heath, Lexington, 1976).
6. Jickells, T. D., Deuser, W. G. & Knap, A. H. *Deep-Sea Res.* **31**, 1169-1178 (1984).
7. Ittekkot, V., Deuser, W. G. & Degens, E. T. *Deep-Sea Res.* **31**, 1057-1069 (1984).
8. Knap, A. H. & Jickells, T. D. *Mar. Pollut. Bull.* **14**, 271-274 (1983).
9. Atlas, E. L. & Giam, C. S. *Science* **211**, 163-165 (1981).
10. Intergovernmental Oceanographic Commission *Tech. Ser.* No. 22, (UNESCO, 1982).
11. Harvey, G. R. & Steinhauer, W. G. in *Environmental Biochemistry* (ed. Nriagu, J. O.) 203-221 (Ann Arbor, 1976).
12. Tanabe, S. & Tatsukawa, R. *J. oceanogr. Soc. Japan* **39**, 53-62 (1983).
13. Hamelink, J. L., Waybrant, R. C. & Ball, R. C. *Trans. Am. Fish. Soc.* **100**, 207-214 (1971).
14. Masterton, W. L. & Lee, T. P. *Envir. Sci. Technol.* **6**, 919-921 (1972).
15. Bidleman, T. F., Christensen, E. J., Billings, W. N. & Leonard, R. *J. mar. Res.* **39**, 443-464 (1981).
16. Burns, K. A., Villeneuve, J. P. & Fowler, S. W. *Estuar. coast. Shelf Sci.* (in the press).
17. Osterroht, C. & Smetacek, V. *Mar. Ecol. Prog. Ser.* **2**, 27-34 (1980).
18. Duinker, J. in *Methods of Seawater Analysis* 2nd edn, Ch. 24.4 (eds Grasshoff, K., Ehrhardt, M. & Kremling, K.) 290-309 (Verlag Chemie, Wienheim, 1983).
19. Duinker, J. C. & Hillebrand, M. T. J. *Envir. Sci. Technol.* **17**, 449-456 (1983).

A lagrangian mixed layer model of Atlantic 18 °C water formation

J. D. Woods & W. Barkmann

Institut für Meereskunde an der Universität Kiel, FRG

One of the most striking features of the upper North Atlantic Ocean is an extensive layer of water with temperature close to 18 °C and salinity close to 36.5‰ (ref. 1). This 18 °C water is formed by winter convection in the Sargasso sea[2,3], but aspects of the annual rate of 18 °C water formation remain obscure[4]. We have simulated this water mass formation by integrating a one-dimensional model along a 4-yr trajectory of a water column circulating around the Sargasso Sea. Winter convection is deep (⩾200 m) in regions where the ocean suffers a net annual heat loss to the atmosphere, and shallow (⩽100 m) where the ocean gains heat each year. The origin of the thermostad (nearly isothermal layer) is a thick layer of nearly homogeneous water subducted beneath the seasonal boundary layer in the year that the water column passes through the line dividing annual cooling from annual heating. We estimate the annual production of 18 °C water to be 446,000 km^3 yr^{-1}. Downstream, more stratified central water is formed each year at a rate that depends more on Ekman pumping (wind-forced convergence) than on the decreasing depth of winter convection.

On 29 March 1873 the water temperature measurement for HMS *Challenger* station no. 28 (24°39′ N, 65°26′ W) was repeated because the water appeared to be anomalously warm at 200 fathoms. It was suspected that the thermometers were faulty, but replacements gave the same values[5,6]. That was the first encounter with 18 °C water, which has since been mapped over a large area of the North Atlantic[4]. It is now recognized to be typical of a class of water masses called mode waters, formed by deep conve
tion is sensitive to s
buoyancy flux, B (ref
winter climate in the S
production of 18 °C
estimate this variation
may be a significant
induced anomalies int
cline ventilation is an
on climate, and will h
climate prediction mo
depends on a complic
seasonal boundary lay
computed with general
results may be in error
ment of the complex p
issues that will arise in
of mode water formati

Our mixed layer mo
ment of convection[24].
integrating it with a ti
where $B=0$. Such eule
lated the observed var
such as Ocean Weathe
induced changes are s
severe problem for m
most sites. The solutio
modelling water mass
North Atlantic where
large[26]. Stommel[27] inve
ing at OWS ‘J’ usin
however, the database
sufficiently accurately
one-dimensional mode

Woods[21] proposed a
is integrated at succes
from observations or a
of climatological maps
the potential of the te
subducted in 1 yr alon
mass equation, $H=E$
placement due to Ekm
annual maximum dept
years. Central water su
to E, but according to
The theory supported t
water formation is co
now report the first test
of a mixed-layer mode

The model was integ
elevation parameteriza
pumping were taken fr
tions along a trajecto
GCM[26]. Integrations w
initial conditions[32]. Th
the mixed layer temper
(which preliminary cal
to the vertical shear o
integrated 12 times w
upstream to make the
500-km mark in Fig. 1)

Figure 1 shows the v
depth and the depths
passed through the re
maximum mixed-layer
equinox. Its value inc
$B\leqslant 0$, but then decrea
net annual buoyancy g
the integration passes t
duction of a thick laye

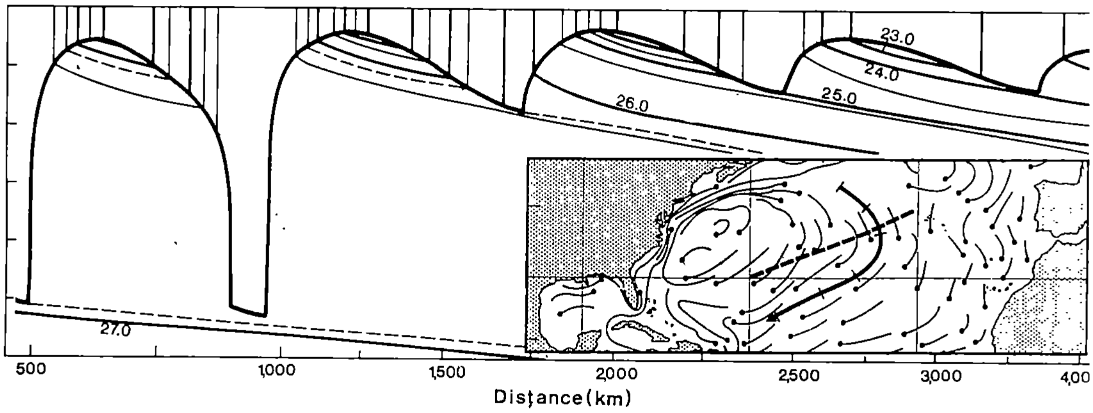

tion of mixed-layer depth and the depths of selected isopycnals (density (σ_t) values at 0.5 kg m^{-3} intervals, plus lashed) for a lagrangian integration of a mixed-layer model[24] along the trajectory shown in the inset map. The integrati the reference position 500 km from the start of the trajectory. Inset, trajectory used in the lagrangian integration wit ine); $B=0$ according to ref. 30 (dashed bold line); annual particle displacements at a depth of 159 m from ref. 26 (l

duction is effected rapidly as the mixed-layer s in the spring. The mixed-layer density decreases me, so the subducted water is statically stable. otal change in density (and temperature) is small, ed water has the characteristic pycnostad (ther- node water. In this case, the mode water has a 17.0 °C, and a salinity of 36.5‰, which lies in lass II 18 °C water[1].

de water has been formed, the model predicts s much smaller, but remains positive as long as The magnitude of D becomes smaller than E, kman pumping becomes relatively more impor- ining the annual production of central water the subduction of mode water. Figure 2 shows D and E along the trajectory, derived from the with phase lags of 1-12 months. The mode water ng a section straddling the $B=0$ line. The length uals the distance the water moves in that year. e D curve near 1,000 km arises from the differen- egrations started at 40 and 500 km. It represents of uncertainty in the method. The difference rves for integration with and without Ekman to the Ekman convergence of heat (which would, npensated by baroclinic geostrophic heat flux at were included). It does not significantly change of mode water mass production.

orth Atlantic mixed-layer depth for April, when eing formed, shows a line of maximum D close e (Fig. 3). The annual production of 18 °C water the sum of the products of the length, spacing from the 10 vectors west of the Azores in Fig. m^3 yr^{-1}; close to Worthington's[33] value of $^{-1}$ based on the surface heat flux in the Sargasso should, however, be treated with caution, given s in the vectors and the map of mixed layer depth. of 18 °C water is 1,672,000 km^3 (ref. 4), so our gives a mean renewal time of 4 yr, and Worthing- 7 yr. Independent estimates based on radioactive values <10 yr, but not precise enough to dis- en Worthington's value and ours.

he mass and temperature-salinity (T-S) proper- ter formation can also be computed by integrat- along a set of trajectories that cross the $B=0$ e, the calculation would not be more reliable uncertainties in the trajectories derived from ns[20]; (2) neglect of vertical shear in the seasonal ich may include a significant component across ectory[36]; (3) errors of up to ±50 W m^{-2} in the stimates of surface heat flux[37], making the loca- =0 line uncertain to about ±500 km; and (4) imperfections in the mixed layer model. These sour combine to give a growing deviation from the obser layer depth and temperature[32]. Furthermore, the t the mode water subducted in the year that the wate $B=0$ line depends on the assumed initial value for r depth, taken from observations[32], which depend c the method of diagnosis[21].

Despite these limitations to quantitative appli lagrangian mixed-layer model yields two conclusion is that, in common with other mode waters, 18 °C wat in a band straddling the $B=0$ line, with a downst equal to the distance water travels in that year. Th that the annual rate of water mass subduction depen D and E, with D dominating mode water, and E

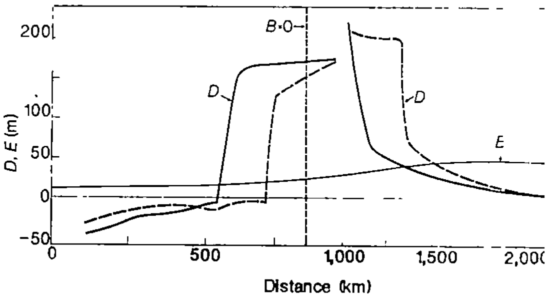

Fig. 2 Variation of D and E along the trajectory in Fig. based on a set of lagrangian integrations with monthly p The mode water is formed where D has a large value. stream extent equals the distance the integration advanc year. Solid line, with Ekman pumping; dashed line, witho pumping. The discontinuities in the two lines near 1,00 resent the different values of D computed from starting 40 and 500 km respectively. They indicate a 25% range tainty in D.

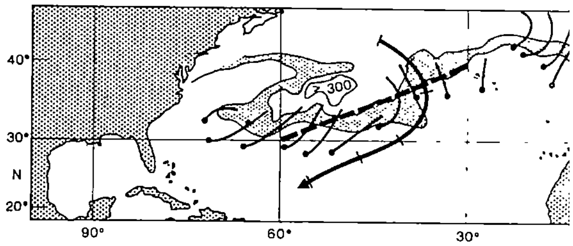

Fig. 3 The formation zone of mode water is indicated by a band between the mixed layer depths of 120 and 200 m month of April[32], when mode water is being subducted. Th line indicates $B=0$ according to ref. 30. Selected annual ment lines from Fig. 1 show where mode water is formed. the Azores it is the North Atlantic sub-polar mode wate of the Azores it is 18 °C water.

er formed downstream of the mode water. The nethod can be used generally to analyse water mass

mber; accepted 27 November 1985

L. V. in *Evolution of Physical Oceanography* (eds Warren, B. A. & Wunsch, MIT Press, Cambridge, 1981).
L. V. *Deep-Sea Res.* **5**, 297–305 (1959).
V. *Deep-Sea Res.* **7**, 384–390 (1962).
L. V. *Johns Hopkins Oceanogr. Stud.* **6**, (1976).
son, C. *The Voyage of the Challenger. The Atlantic*, (Mcmillan, London, 1877).
son, C. & Murray, J. (eds) *Challenger Report* Part 2 Vol. 1 (HMSO, London,
M. S. *Deep-Sea Res.* (Suppl.) **24**, 103–119 (1977).
M. S. *J. mar. Res.* (Suppl.) **40**, 427–464 (1982).
M. S. & Talley, L. D. *J. phys. Oceanogr.* **12**, 1169–1188 (1982).
& McCartney, M. S. *J. phys. Oceanogr.* **12**, 1189–1205 (1982).
. *Deep-Sea Res.* **16**, 463–472 (1969).
Manabe, S. in *Coupled Ocean–Atmosphere Models* (ed. Nihoul, J. C. J.) 1–6 Amsterdam, 1985).
, Barkmann, W. & Strass, V. in *The Ocean Surface: Wave Breaking, Turbulent d Radio Probing* (eds Toba, Y. & Mitsuyasu, H.) 487–507 (Reidel, Dordrecht,
M. S., Worthington, L. V. & Raymer, M. E. *J. mar. Res.* **38**, 147–172 (1980).
L. V. in *Studies in Physical Oceanography* (ed. Gordon, A. L.) 169–178 (Gordon n, New York, 1971).
., Stommel, H., Menzel, D. & Sutcliffe, W. *J. geophys. Res.* **64**, 363–366 (1959).
. *J. mar. Res.* (Suppl.) **40**, 267–290 (1982).
& Raymer, M. E. *J. mar. Res. Suppl*, **40**, 757–775 (1982).
. & Pu, S. *Prog. Oceanogr.* **14**, 443–462 (1985).
Nature **314**, 501–511 (1985).
in *Coupled Ocean–Atmosphere Models* (ed. Nihoul, J. C. J.) 543–590 (Elsevier, n, 1985).
Lewis, L. J. *J. geophys. Res.* **84**, 2503–2517 (1979).
., Han, Y.-J. & Schlesinger, M. in *Coupled Ocean–Atmosphere Models* (ed. C. J.) 131–152 (Elsevier, Amsterdam, 1985).
& Barkmann, W. *Q. J. R. met. Soc.* **112**, 1–27 (1986).
DeSzoeke, R. & Niiler, P. *Deep-Sea Res.* **28**, 1453–1476 (1981).
. *J. phys. Oceanogr.* **13**, 1924–1939 (1983).
Proc. natn. Acad. Sci. U.S.A. **76**, 2518–2521 (1979).
Proc. natn. Acad. Sci. U.S.A. **76**, 3051–3055 (1979).
. *J. phys. Oceanogr.* **13**, 1269–1274 (1983).
& Hasse, L. *The Bunker Climate Atlas of the Atlantic Ocean* (Springer, Berlin,
, A. & Reichel, E. *The World Water Balance* (Elsevier, Amsterdam, 1975).
. K., Bauer, R. A. & Schroeder, E. H. *Atlas of North Atlantic–Indian Ocean lean Temperatures and Mean Salinities of the Surface Layer* (US Naval Oceano-ffice Ref. Publ. 18, Washington DC, 1979).
, L. V. *J. phys. Oceanogr.* **2**, 205–211 (1972).
J. mar. Res. **38**, 533–569 (1980).
. L., Rooth, C. G. H. & Roether, W. *J. geophys. Res.* **87**, 8047–8056 (1982).
& Schott, F. *Deep-Sea Res.* **24**, 325–329 (1977).
. in *The Global Climate* (ed. Houghton, J. T.) 141–187 (Cambridge University 4).

---

anomalies in laboratory distillation

Esat*†, R. H. Spear* & Stuart Ross Taylor‡

t of Nuclear Physics, Research School of Physical
‡ Research School of Earth Sciences,
ational University, Canberra ACT 2601, Australia

ried out high-temperature distillation experiments at on terrestrial pyroxene crystals and measured ^{24}Mg, ^{5}Mg simultaneously using a 61-cm multi-cup mass . The raw data were corrected for isotope fractionation ower law and the Rayleigh law. Regardless of the rocedure, the sample residues are depleted in ^{26}Mg lensates are enriched in ^{26}Mg, relative to non-distilled These effects mimic the 'isotope anomalies' in Mg llende coarse- and fine-grained inclusions, previously nucleosynthetic processes involving ^{26}Al.

cted pyroxene crystals from a sample of eclogite oviet Union) to distillation. Each sample, weighing s placed in a carbon boat and heated with a radio-nduction coil in a bell-jar in a vacuum ($\sim 5 \times 10^{-5}$ torr). After melting, the samples coalesc spheres, spinning rapidly and jumping in the ca they began to vaporize at ~2,150 °C. As the vap ceeded the sample changed in colour from light pletely transparent. Chemical analysis of the resid showed that most of the iron in the sample had ized. Part of the vaporized material was collec diameter Teflon disks placed ~8 cm above the Nine samples were subjected to varying degrees for up to 30 min, and the weight of each sample before and after evaporation. Typical electron- of the pyroxenes before and after distillation Table 1.

Table 1 Electron-microprobe analyses of pyroxenes distillation

	Original (light green)	First residue (transparent)	S (
SiO_2	54.5	36.5	
TiO_2	0.2	<0.1	
Al_2O_3	2.9	10.7	
Cr_2O_3	1.0	<0.1	
FeO	1.2	<0.1	
MgO	16.5	12.5	
CaO	23.4	40.3	
Na_2O	0.5	<0.1	
Total	100.2	100.0	

Wavelength-dispersive analyses in weight per cent.

* Further vaporization of the first residue produced a white sphere. Treatment with HF and HNO_3 left a resi 2-mm diameter sphere, analysis of which showed it to $CaAl_4O_7$ with a small amount of Ti. It is interesting that calculations predict hibonite ($CaAl_{12}O_{19}$) and $CaAl_4O$ two stable calcium aluminates during condensation[14]; i be expected that they would both appear as evaporati

The evaporation residues and condensates were in a mixture of HF and HNO_3. Small aliquots of were directly loaded on V-shaped Re filaments analysis. The intermediate step of chemical separa in the direct-loading technique. There are no int species in the Mg region of the mass spectrum. other mass spectrometers[1], the ANU 61-cm multi-used does not suffer from interferences cause beams near the Mg isotopes. (The details and characteristics of this instrument in relation to the of Mg isotope abundances have been describe For each distillation sample, the raw data consis sets of simultaneous values of the intensities of ea Data collection and processing procedures have previously[2,3]. For each set a fractionation-correct ^{26}Mg-to-^{24}Mg ratio, $(^{26}\mathrm{Mg}/^{24}\mathrm{Mg})^{c}$, was obtained specific fractionation law and normalizing the (^{25}M to the National Bureau of Standards standard v (ref. 4). The fractionation-corrected value for t then compared with the fractionation-corrected using identical procedures, for a set of non-dist $((^{26}\mathrm{Mg}/^{24}\mathrm{Mg})^{c}_{s}$. The difference between these tw resented, in parts per mil (‰) by the quantity δ,

$$\delta(^{26}\mathrm{Mg}) = [(^{26}\mathrm{Mg}/^{24}\mathrm{Mg})^{c}/(^{26}\mathrm{Mg}/^{24}\mathrm{Mg})^{c}_{s} -$$

and may be regarded as a measure of the ina specific fractionation law used to account for th processes involved in the distillation. Non-z residual fractionation δ (isotope anomalies) obta for meteoritic samples have been attributed to effects[5] involving ^{26}Al, sometimes termed nonli

The Mg isotope analyses for the standards and and condensates are summarized in Table 2 and

---

Research School of Earth Sciences, Australian National University, Canberra, alia.

Table 2 Distillation-induced fractionation and residual isotope effects in Mg (±2 s.d.)

Sample and mass loss (%)	Un-normalized raw ratios* $(^{25}Mg/^{24}Mg)_{meas}$	$(^{26}Mg/^{24}Mg)_{meas}$	Fractionation† $\Delta(^{25}Mg/^{24}Mg)$‰ AMU^{-1}	δ^{26}Mg‡ (power law) ±2 s.d.	δ^{26}Mg§ (Rayleigh law) ±2 s.d.
1 Condensate	0.123684	0.134678	−1.4	+0.38±0.16	+0.36±0.16
2 Residue (23)	0.124263	0.135884	+3.3	−0.02±0.07	+0.05±0.06
Condensate	0.122352	0.132055	−12.2	+2.33±0.12	+2.09±0.12
3 Residue (42.6)	0.124930	0.137255	+8.7	−0.67±0.06	−0.50±0.07
Condensate	0.122998	0.133359	−6.9	+1.64±0.08	+1.50±0.08
4 Residue (59)	0.127204	0.142233	+27.0	−1.04±0.08	−0.51±0.07
Condensate	0.123688	0.134734	−1.4	+0.74±0.05	+0.72±0.05
5 Residue (32.7)	0.124327	0.135996	+3.8	−0.23±0.06	−0.15±0.06
Condensate	0.122176	0.131616	−13.6	+1.87±0.06	+1.60±0.07
CL condensate	0.123111	0.133525	−6.1	+1.06±0.08	+0.94±0.07
BG residue (51)	0.126094	0.139846	+18.1	−0.48±0.16	−0.12±0.16
6 First condensate	0.122136	0.131436	−13.9	+1.16±0.06	+0.88±0.05
Second condensate	0.124363	0.136154	+4.1	+0.36±0.08	+0.44±0.07
7 First condensate	0.122107	0.131327	−14.1	+0.80±0.23	+0.52±0.22
Second condensate	0.124150	0.135509	+2.4	−0.97±0.06	−0.92±0.06
Standards‖					
1	0.123858	0.134987			
2	0.123854	0.135005			
3	0.123876	0.135043			
4	0.123834	0.134953			
5	0.123863	0.135022			

Atomic masses used throughout.

* Directly measured, unnormalized raw ratios. Typical errors range from 2 to 4 in the last digit for $^{25}Mg/^{24}Mg$ and four to eight for $^{26}Mg/^{24}Mg$. Each number is the mean of ~1,200 ratios, obtained in ~1 h.

† $\Delta(^{25}Mg/^{24}Mg) = [(^{25}Mg/^{24}Mg)_{meas}/(^{25}Mg/^{24}Mg)_S - 1] \times 1,000$, where S denotes the grand mean value: $^{25}Mg/^{24}Mg = 0.123857$ for raw data determined from standards. Reproducibility for repeat runs is better than ±1.5‰.

‡ Per mil deviation of $^{26}Mg/^{24}Mg$ relative to 0.141102 (grand mean value for standards normalized using the power law) after correcting for fractionation using the power law[2,3], by normalizing $(^{25}Mg/^{24}Mg)_{meas}$ to 0.12663; errors are 2 s. d. of the mean.

§ Per mil deviation of $^{26}Mg/^{24}Mg$ relative to 0.140985 (grand mean value for standards normalized using the Rayleigh law) after correcting for fractionation using the Rayleigh law[2,3], by normalizing $(^{25}Mg/^{24}Mg)_{meas}$ to 0.12663; errors are 2 s.d. of the mean.

‖ The configuration of the mass spectrometer was altered for the present experiments by substituting three Solatron voltmeters in place of the existing Keithley voltmeters. This has reduced the dead time from 70 to <5%, but has resulted in a slight change in the mean values for our standards from those measured previously. This change does not affect our conclusions in this or any previous paper.

in Table 2 show the following: (1) Significant isotope fractionation (Δ $(^{25}Mg/^{24}Mg)$) can be induced in the laboratory by distillation; (2) the evaporation residues are enriched in the heavy Mg isotopes and the evaporation condensates in the light Mg isotopes; (3) distillation induces residual offsets (δ^{26}Mg) that are not accounted for by the simple fractionation-correction procedures used. Neither power-law nor Rayleigh-law corrections account for all of the observed effects. The application of the exponential fractionation law of Russell *et al.*[3] produces somewhat smaller values of δ^{26}Mg, but the effects remain significant; (4) the residual negative/positive effects (δ^{26}Mg) are correlated with positive/negative mass fractionation in a manner identical to that found in Allende coarse- and fine-grained inclusions[5,7]. We have plotted the variation of the residuals (δ^{26}Mg) with the degree of fractionation ($\Delta(^{25}Mg/^{24}Mg)$) obtained using the power-law correction (Fig. 1). Our corrected data are thus directly comparable with the meteoritic data for Mg isotopes[5,8], which have been almost exclusively analysed using the power law. The condensates seem to exhibit larger values of δ^{26}Mg compared with residues for a given magnitude of fractionation ($\Delta(^{25}Mg/^{24}Mg)$). Although there is an approximately linear trend for both sets, there is no precise correlation with fractionation. In a closed system, consideration of mass-balance requires that the isotope effects in the residue should complement the effects in the condensate. The significant non-complementarity in the data both for fractionation ($\Delta(^{25}Mg/^{24}Mg)$) and δ^{26}Mg between members of residue/condensate pairs is puzzling. Evidently, condensation was selective with an isotopically heterogeneous spatial distribution.

In two cases the condensing material was sampled in stages to reveal more of the isotope systematics in the distillation process (Table 2). Consideration of equipartition of energy requires that the light isotopes vaporize preferentially relative to heavy ones. The residue will gradually become enriched in the heavy isotopes and the condensate in the light. However, for a finite-sized sample, the residue will eventually be so depleted in the light isotopes that the vaporizing material will pass from being enriched in the light isotopes through normal to being enriched in the heavy isotopes. This phenomenon is observed in the differentially collected condensates; in both experiments the initial condensate is relatively enriched in the light Mg isotopes whereas the final condensate is enriched in the heavy isotopes. An identical effect was observed by Russell *et al.* using calcium[3]. Our samples show a similar but complementary effect for the residue (δ^{26}Mg) remaining after

Table 3 Complementary properties of fine- and coarse-grained Allende calcium–aluminium inclusions (CAI)

Coarse-grained CAI	Fine-grained CAI
Rim layers of fine-grained material on the outside[12]	Composed of an aggregation of small bodies (<10 µm) with similar rim layers on each one as in coarse-grained inclusions
Rare-earth element (REE) abundances mostly of Group I type. FUN inclusion[8] EK-1-4-1 is an exception with Group II-type REE	REE abundances predominantly of Group II type
Positive Mg isotope fractionation: $\Delta(^{25}Mg/^{24}Mg)$ enriched in the heavy Mg isotopes	Negative Mg isotope fractionation: $\Delta(^{25}Mg/^{24}Mg)$ enriched in the light Mg isotopes
Negative anomaly in δ^{26}Mg	Positive anomaly in δ^{26}Mg

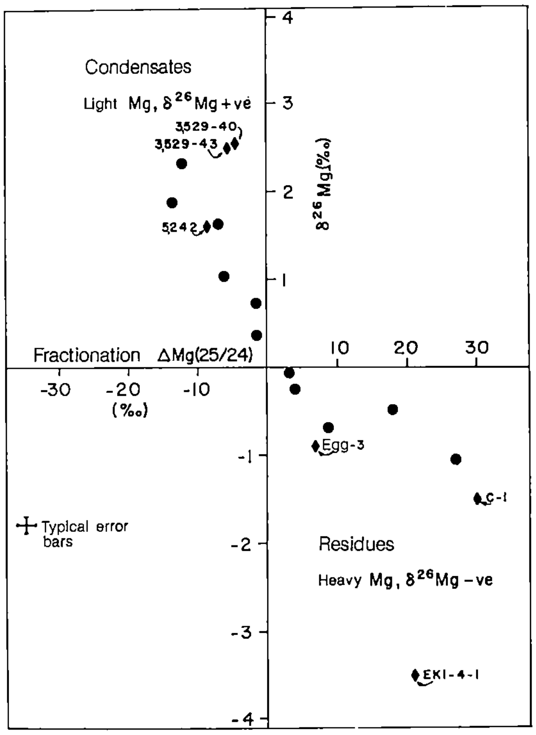

Fig. 1 Variation of δ^{26}Mg with the degree of fractionation $\Delta(^{25}Mg/^{24}Mg)$ in distillation residues and condensates. The labelled data points (diamonds) represent Allende CAI with established fractionation and residual δ^{26}Mg. Inclusions 3,529-40, 3,529-43 and 5,242 are fine-grained inclusions with Group II type REE pattern[7]. In contrast, inclusions Egg-3, C-1 and EK1-4-1 are coarse-grained[5]. With the exception of EK1-4-1, the CAI shown here lie within the field defined by the laboratory experiments. Note the correlation between coarse-grained CAI and evaporation residues, and between fine-grained CAI and evaporation condensates, with regard to both fractionation and residual δ^{26}Mg.

the fractionation correction. Isotope analyses of the residues from the differential condensation experiments were unsuccessful. The Mg signal obtained was very low ($< 10^{-14}$ A) and could not be sustained for more than 15 min, consistent with the electron-probe analyses of such samples which show no detectable amounts ($< 0.1\%$) of MgO (Table 1).

We have included some of the data from fractionated Allende inclusions in Fig. 1[5,9–12], also corrected for fractionation using the power law[2,3]. We draw attention to the complementary properties of the coarse- and fine-grained Allende inclusions (Table 3)[7]. The symmetries between the coarse- and fine-grained inclusions are replicated in the division between our distillation residues and condensates, suggesting that the coarse-grained inclusions are residues and the fine-grained inclusions are condensates. The interpretation of the excesses in the fine-grained group II aggregates could be complicated by the possible presence of ^{26}Al decay products. However, it is plausible that the observed excesses[7] in ^{26}Mg in inclusions 3,529-40, 3,529-43 and 5,242 are wholly caused by kinetic effects and not ^{26}Al, as they lie completely within the field defined by the data for condensates. Similarly, the deficits[8,13] in ^{26}Mg for the coarse-grained FUN[8] inclusions C-1, EK-1-4-1 and Egg-3 are also attributable to kinetic effects rather than to a deficient ^{26}Al component (Fig. 1). Note that EK-1-4-1 seems to be distinctly shifted from the general trend defined by the data for the residues. In summary, when we apply to distillation samples the same fractionation-correction procedures that have been applied in the past to meteoritic samples, we obtain excesses and deficits in Mg isotopes similar to those reported in the meteoritic samples. These meteoritic anomalies were previously attributed to nucleosynthetic processes. We conclude that such deductions should be made only after the effects of inadequacies in the fractionation laws used have been carefully evaluated.

Received 13 June; accepted 11 November 1985.

1. Lee, T., Papanastassiou, D. A. & Wasserburg, G. J. *Geochim. cosmochim. Acta* **41**, 1473–1485 (1977).
2. Esat, T. M. *Nucl. Instrum. Meth. Phys. Res.* **B5**, 545–553 (1984).
3. Russell, W. A., Papanastassiou, D. A. & Tombrello, T. A. *Geochim. cosmochim. Acta* **42**, 1075–1090 (1978).
4. Catanzaro, E. J., Murphy, T. J., Garner, E. L. & Shields, W. R. *J. Res. NBS* **70A**, 435–458 (1966).
5. Wasserburg, G. J. & Papanastassiou, D. A. in *Essays on Nuclear Astrophysics* (eds Barnes, C. A., Clayton, D. D. & Schramm, D. N.) 77–140 (Cambridge University Press, 1982).
6. Clayton, R. N. *et al. Geochim. cosmochim. Acta* **48**, 535–548 (1984).
7. Esat, T. M. & Taylor, S. R. *Lunar Planet. Sci.* **XV**, 252–253; 254–255 (1984).
8. Wasserburg, G. J., Lee, T. & Papanastassiou, D. A. *Geophys. res. Lett.* **4**, 299–302 (1977).
9. Lee, T. *Rev. geophys. Space phys.* **17**, 1591–1611 (1979).
10. Begemann, F. *Rep. Prog. Phys.* **43**, 1309–1356 (1980).
11. Grossman, L. *A. Rev. Earth planet. Sci.* **8**, 559–608 (1980).
12. Wark, D. A. *Astrophys. Space Sci.* **65**, 275–295 (1979).
13. Esat, T. M., Papanastassiou, D. A. & Wasserburg, G. J. *Lunar planet. Sci.* **X**, 361–363 (1979).
14. Kornacki, A. S. & Fegley, B. Jr. *J. geophys. Res.* **89**, B588–B596 (1984).

An exceptionally large late Quaternary eruption from New Zealand

P. C. Froggatt*, C. S. Nelson†, L. Carter‡, G. Griggs§ & K. P. Black†

* Centre for Continuing Education and Geology Department,
Victoria University of Wellington, Private Bag,
Wellington, New Zealand
† Department of Earth Sciences, University of Waikato, Private Bag,
Hamilton, New Zealand
‡ New Zealand Oceanographic Institute, PO Box 12346,
Wellington, New Zealand
§ Department of Earth Sciences and Centre for
Coastal Marine Studies, University of California at Santa Cruz,
California 95064, USA

A thick, widespread volcanic ash layer sampled from marine cores in the South Pacific and sub-Antarctic, has been identified using major and rare-earth element chemistry. It is the correlative of the airfall Mount Curl Tephra, the initial eruptive phase of the voluminous Whakamaru Ignimbrite from Taupo, New Zealand. Detailed oxygen-isotope analysis on the late Quaternary section of the core from Deep Sea Drilling Project Site 594, supplemented by other data, places Mount Curl Tephra within the glacial, Isotope Stage 8 and assigns an age of 254 ± 2 kyr to the tephra. The airfall tephra covers at least 10^7 km^2 with a minimum volume of 700 km^3. The Whakamaru Ignimbrite phase encompasses at least another 500–1,000 km^3. A combined volume of $>$1,200 km^3 makes this Taupo eruption the largest in the Southern Hemisphere in late Quaternary times. Mount Curl Tephra is so widespread that the eruption possibly caused disruption to the atmosphere and climate, and material from this eruption may be recognizable in sediments 10,000 km from the source.

The dispersal of volcanic ash from recent eruptions such as Tambora (1815), Krakatau (1883), Agung (1963), Mount St Helens (1982) and El Chichón (1982) has been directly observed to circle the globe[1–5]. Most of the ash from these eruptions has been dispersed through the atmosphere without leaving a distal deposit that would survive for any length of time in the geological record[1]. In contrast, studies of large prehistoric eruptions have relied on the preserved ash to demonstrate their exceptional magnitude and the global circulation patterns responsible for their dispersal (see ref. 6). To date, such studies have dealt with tephras from equatorial or Northern Hemisphere volcanoes such as Toba, Santorini and Campanian[7,8]. The extremely widespread dispersal of ash from a single Southern Hemisphere eruption has not been documented previously.

Table 1 Major element chemistry of glass shards (mean of *n* analyses with 1 s.d. in parentheses) from marine cores and land exposures, recalculated water-free

	RC9-110	RC9-113	RC12-215	DSDP 591	DSDP 594	Q203
SiO_2	78.01 (0.42)	77.73 (0.28)	77.93 (0.28)	77.14 (0.21)	77.06 (0.37)	78.22 (0.32)
Al_2O_3	12.40 (0.26)	12.59 (0.12)	12.26 (0.17)	12.42 (0.10)	12.47 (0.19)	12.30 (0.18)
TiO_2	0.14 (0.05)	0.13 (0.03)	0.12 (0.03)	0.15 (0.03)	0.15 (0.03)	0.14 (0.04)
FeO	0.94 (0.18)	1.06 (0.11)	0.87 (0.11)	1.07 (0.08)	1.03 (0.09)	1.02 (0.08)
MgO	0.12 (0.04)	0.11 (0.02)	0.12 (0.02)	0.12 (0.03)	0.11 (0.03)	0.11 (0.04)
CaO	0.79 (0.07)	0.74 (0.05)	0.78 (0.05)	0.82 (0.03)	0.81 (0.04)	0.75 (0.04)
Na_2O	3.48 (0.24)	3.49 (0.04)	3.53 (0.14)	3.60 (0.13)	3.67 (0.13)	3.24 (0.13)
K_2O	4.11 (0.32)	4.15 (0.18)	4.38 (0.18)	4.46 (0.17)	4.46 (0.12)	4.21 (1.18)
Water	4.71 (0.86)	4.64 (0.85)	4.38 (1.03)	5.21 (0.45)	6.14 (0.12)	5.42 (0.67)
n	18	11	18	14	12	13
Age	—	0.31 s[11]	0.31 s[14] 0.33 g[19]	0.24[17]	0.28 s[17]	—
CV_m	3.02	2.74	6.31	4.48	3.65	3.01
CV_t	—	—	9.41	—	—	—

	Q585	E17-10	E33-3	E33-16	038	103
SiO_2	77.74 (0.26)	75.38 (0.48)	76.14	62.93 (2.81)	77.75 (0.27)	78.09 (0.30)
Al_2O_3	12.55 (0.27)	13.14 (0.48)	12.92	14.51 (1.08)	12.59 (0.16)	12.33 (0.21)
TiO_2	0.12 (0.03)	0.21 (0.01)	ND	0.75 (0.13)	0.14 (0.03)	0.14 (0.03)
FeO	1.04 (0.07)	2.10 (0.12)	2.22	8.36 (0.48)	1.14 (0.06)	1.01 (0.08)
MgO	0.12 (0.04)	ND	ND	ND	0.11 (0.07)	0.12 (0.02)
CaO	0.74 (0.03)	0.37 (0.06)	0.36	1.39 (0.45)	0.79 (0.03)	0.79 (0.04)
Na_2O	3.42 (0.16)	4.19 (0.16)	3.87	7.22 (0.81)	3.55 (0.18)	3.30 (0.16)
K_2O	4.17 (0.20)	4.78 (0.13)	4.49	4.85 (0.23)	4.13 (0.15)	4.33 (0.15)
Water	3.61 (0.74)	11.21 (2.29)	7.53	1.57 (1.44)	4.95 (0.92)	4.55 (.125)
n	8	6	1	11	10	132
Age	—	0.37 s[13]	0.37 s[13]	—	—	0.23 g[18] 0.24 z[21] 0.25 k[18]
CV_m	4.77				4.52	1.00
CV_t	—				4.66	1.00

	122	165	166	168	207	208
SiO_2	77.82 (0.40)	78.26 (0.14)	77.65 (0.25)	78.20 (0.32)	77.91 (0.22)	78.17 (0.29)
Al_2O_3	12.58 (0.28)	12.26 (0.14)	12.41 (0.10)	12.42 (0.13)	12.31 (0.10)	12.19 (0.11)
TiO_2	0.13 (0.04)	0.16 (0.03)	0.13 (0.02)	0.13 (0.05)	0.15 (0.03)	0.14 (0.03)
FeO	1.10 (0.09)	1.11 (0.07)	1.05 (0.07)	1.02 (0.10)	1.06 (0.07)	1.05 (0.06)
MgO	0.10 (0.09)	0.14 (0.03)	0.12 (0.01)	0.12 (0.03)	0.12 (0.02)	0.12 (0.03)
CaO	0.77 (0.04)	0.75 (0.05)	0.79 (0.05)	0.77 (0.09)	0.80 (0.04)	0.75 (0.05)
Na_2O	3.50 (0.09)	2.96 (0.13)	3.73 (0.11)	3.23 (0.24)	3.35 (0.26)	3.21 (0.15)
K_2O	4.00 (0.20)	4.37 (0.13)	4.12 (0.18)	4.11 (0.18)	4.30 (0.19)	4.37 (0.21)
Water	6.06 (1.11)	2.88 (0.46)	3.13 (0.56)	5.20 (0.90)	4.71 (0.65)	3.93 (0.86)
n	10	10	12	16	20	22
Age	—	—	—	0.38 g[19] 0.37 z[43]	—	0.33 z[42]
CV_m	5.44	6.07	4.31	2.62	2.50	1.96
CV_t	—	7.44	9.26	8.71	—	9.64

Analyses were performed on a JEOL-733 microprobe using a 10-μm beam and 80-nA beam current (see ref. 16), except analyses on samples from 'E' cores, which were performed on an Etec Autoprobe fitted with an Ortec Si(Li) detector (see ref. 42 for details). Glass standards on both probes included KN-18, UA5831 and VG-99. Total Fe as FeO; water by difference; ND, not detected. Analysis on core E33-16 is representative of the phonolitic shards found in 'ash zone F' in all the 'E' cores examined. Sample numbers and identity are indicated in Fig. 1 and inset. Localities 103 and 208 are the type sections of Mount Curl Tephra[18] and Whakamaru Ignimbrite[22] respectively. Other previously named units that were sampled are 165, Rangitaiki Ignimbrite[44]; 166, Te Whaiti Ignimbrite[44]; 168, Rangitawa Pumice[19,43]; and 207, Ohinewai Ash[45]. Ages (in Myr), where determined, are (g) fission track on glass; (k) K/Ar on glass; (z) fission track on zircon; and (s) sedimentation rate based on palaeomagnetic stratigraphy, from the references cited. CV_m and CV_t are the coefficients of variation[46] for the 8 major and 12 trace elements (La, Ce, Sm Eu, Tb, Yb, Lu, Th, U, Hf, Sc, Cs) respectively, determined for each sample by comparison with Mount Curl Tephra (site 103).

We present data for the correlation, dispersal and age of a rhyolitic tephra from Taupo volcano, New Zealand. This deposit is larger than any previously reported from Taupo[9], and appears to represent the largest late Quaternary eruption in the Southern Hemisphere yet documented. As such, the results of this study are relevant to the current interest in atmospheric and climatic responses to the injection of large quantities of fine particles as discussed in recent 'nuclear winter' scenarios[10]. Detailed analysis of such responses is beyond the scope of this report.

The Plio-Pleistocene tephrostratigraphy of the south-west Pacific is broadly known[11-14], with New Zealand as the assumed source of the predominantly rhyolitic tephras[11,15]. A succession of tephra layers, originally labelled A to E, has been recorded in deep-sea cores such as RC9-113 and RC12-215, located up to 1,100 km east of New Zealand[11,14]. Suggested correlations with terrestrial deposits have been based mostly on palaeomagnetic and fission track dates[11,14,15], but glass chemistry has been used recently[16,17].

We have determined, by means of electron microprobe[16], the major elements in glass shards from tephras from seven cores taken in the New Zealand region and four cores from the sub-Antarctic (Fig. 1). Each of the seven Pacific Ocean cores has only one tephra whose chemistry matches tephra 'D' from RC9-113. Furthermore, all these 'D'-type tephras are in the same

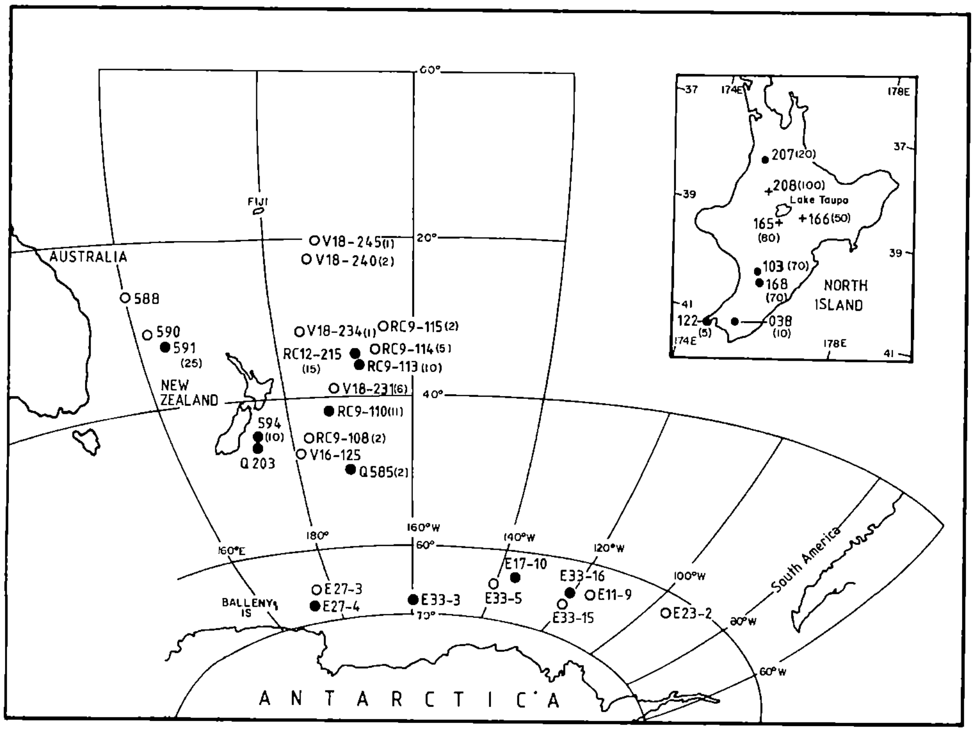
60°
20°
40°
FIJI
AUSTRALIA
NEW ZEALAND
O 588
O 590
● 591 (25)
O V18-245 (1)
O V18-240 (2)
O V18-234 (1)
O RC9-115 (2)
RC12-215 (15)
O RC9-114 (5)
● RC9-113 (10)
O V18-231 (6)
● RC9-110 (11)
594 (10)
Q 203
O RC9-108 (2)
O V16-125
● Q585 (2)
160°E
180°
160°W
140°W
120°W
100°W
80°W
60°W
60°
70°
BALLENY IS
O E27-3
● E27-4
● E33-3
E17-10
O E33-5
E33-16
O E11-9
E33-15
O E23-2
South America
ANTARCTICA
37
174E
178E
39
41
● 207 (20)
+208 (100)
Lake Taupo
165+ (80)
+166 (50)
● 103 (70)
● 168 (70)
NORTH ISLAND
122 (5)
038 (10)

palaeomagnetic age range of ~230-380 kyr (Table 1). Tephras stratigraphically above or below 'D' (rather than those with a younger or older determined age, but uncertain stratigraphy), have a different glass chemistry to the extent that 'D' is characterized uniquely (Table 1, Fig. 2). The sub-Antarctic cores also contain glass shards and part of 'ash zone F'[13] has been correlated recently with Whakamaru Ignimbrite on chronological grounds. Interestingly, most of the glass shards from 'F1', 'F2' and 'F3' in cores that we have analysed (E17-10, E27-4, E33-3 and E33-16) are phonolitic (see Table 1 for representative analyses) and did not originate in New Zealand. Less than 20% of all the shards examined are rhyolitic, but these are very fine-grained and, being hydrated, were difficult to analyse accurately. Analyses (Table 1) are similar to 'D', especially with $K_2O > Na_2O$, and are unlike any other tephras of this age[16]. We conclude that these shards are tephra 'D' but have undergone some alteration due to the high degree of hydration.

Tephra 'D' has the same major element chemistry (see Table 1; Fig. 2) as the terrestrial Mount Curl Tephra[18]—a widespread rhyolitic airfall tephra from Taupo volcano, New Zealand, and also dated at ~230-380 kyr (refs 18-21) (Table 1). As only one tephra with this chemistry and general age has been located in all the terrestrial exposures and marine cores examined, we conclude that tephra 'D' is Mount Curl Tephra, from Taupo volcano. On the basis of further chemical data, Mount Curl Tephra is here regarded as the correlative of the extensive Whakamaru Ignimbrite, a complex sheet of welded ignimbrite in central New Zealand[22]. Further evidence for this correlation is provided by the rare-earth element patterns in glass separates from samples of the tephra, ignimbrite and tephra 'D' (Fig. 3), which are distinct from those of other, similarly aged tephras.

On land, Mount Curl Tephra is an airfall ash, typified by an abundance of coarse feldspar phenocrysts that are conspicuous in the field, together with hypersthene, hornblende, Fe-Ti oxides and biotite. This same appearance and mineralogy characterizes the most basal (unwelded) portion of Whakamaru Ignimbrite, implying that the crystal-rich layer under the ignimbrite correlates with the airfall tephra. Mount Curl Tephra itself grades up to a fine vitric ash that may be the correlative of the ignimbrite (co-ignimbrite airfall ash).

Detailed carbonate and oxygen-isotope analyses are available for two adjacent tephra-bearing cores, DSDP 594 and Q203

(refs 23, 24), both taken
Based on the location of
netic boundary (730 kyr)
(ref. 25), preliminary resul
and isotope records for t
this core[26] reveal the domi
41 and 23 kyr[27-29]. Tentat
of the core, as well as ide
(Fig. 4). In particular, M
spectral age of 254 ± 2 kyr
8. This is consistent with t
in loess[18] (site 103) and in l
(site 122).

In core Q203, close to
Mount Curl Tephra is jus
the 36.5 m for DSDP 594.
ning of the sediment cov
example, Eltanin 43)[31].

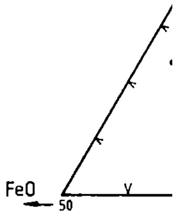

Fig. 2 Proportions of CaC
from analysed tephras. Th
Tephra and correlatives, i
tephra 'D'. The other anal
distinct from Mount Curl Te
from deep-sea cores and la
ation (CV_m and CV_t) for
with Mount Curl Tephra (
and from 17.4 to 23.8 respec

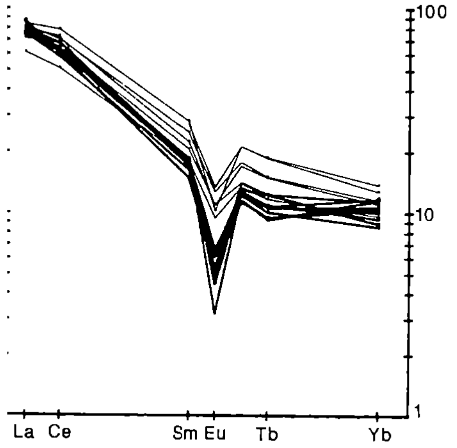

lrite-normalized rare-earth element patterns, deter-
tron-activation analysis[48], for glass separates from
ephra and correlatives (heavy lines) and for those
ly separate tephras of similar age (light lines) that
d in Fig. 2. Mount Curl Tephra is characterized by
ıtive Eu anomaly and relative depletion of mid and
th elements, probably due to feldspar and horn-
blende fractionation respectively.

; evidenced by lithological, microfaunal[33] and
analysis (Fig. 4) is complete and fully supports
of Mount Curl Tephra to Stage 8.
of cores and some terrestrial exposures of Mount
ıd Whakamaru Ignimbrite (Fig. 1) indicate an
spread distribution, presently limited by the
uitable deep-sea cores, especially west and north-
ealand. In addition to the cores that we have
cores from the Pacific contain ash layers with
phic affinity to Mount Curl Tephra. Based on
ıformation, cores V18-240 and V18-245 contain
phra[14]. From the distribution shown in Fig. 1,
at Mount Curl Tephra was deposited and pre-
least 10^7 km^2—a much greater area than that
er documented tephras, such as the 5×10^6 km^2
exceptional Toba eruption[7].
as been made to draw contours of equal tephra
ıchs), as most of the thickness data are from
ınd in these, tephra thickness is unreliable due
ional processes such as bioturbation, current
gravitational mass movement[34]. A broad esti-
yields a conservative 700 km^3. The volume of
ıimbrite is similarly difficult to estimate, but is
ı^3 (ref. 22) and probably "of the order of
e ref. 35). The minimum total volume of tephra
probably nearer 2,000 km^3, or at least 1,500 km^3
ing it, without doubt, the largest documented
ıe Southern Hemisphere and one of the largest
eruptions known. This eruption from Taupo,
lipses the extensively documented 1.8-kyr erup-
-38.

e of tephra in the deep-sea cores, both east and
aland, confirms that volcanic ash transport was
esterly winds and poleward atmospheric circula-
ful that surface sea currents, dominated by the
, could distribute such a large volume of tephra,
nse platy shards, rapidly enough to form pure,
scopic layers or concentrations of shards. Distri-
orth and west is counter to both the poleward
the prevailing westerly winds. However, direct
transport is possible by stratospheric
nds which today prevail above 20-km altitude
ıber and March (J. W. D. Hessell, personal

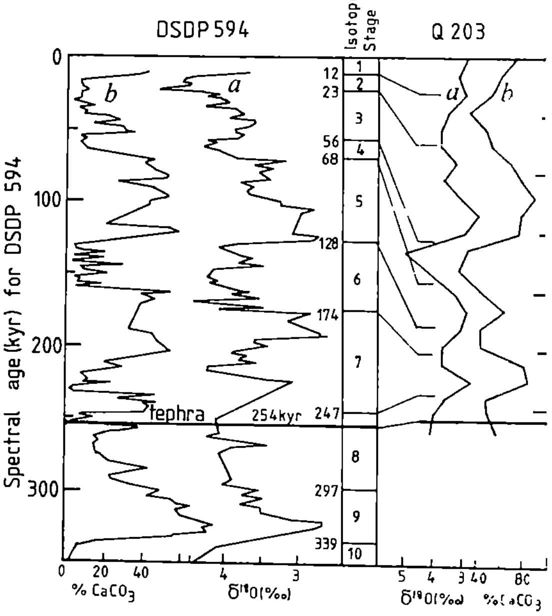

Fig. 4 A portion of the benthic foraminiferal δ^{18}O (*a*) and C
(*b*) records[24] for the late Quaternary sequence plotted as a fu
of age derived from spectral analyses for DSDP 594 anc
function of depth for core Q203. The timescale is based c
location of the Brunhes/Matuyama boundary (730 kyr) at
sub-bottom in core 594 (ref. 25) and has been tuned to the c
perturbation spectra using the forcing frequencies 100, 4
23 kyr[26]. The resulting dates of isotope stage boundaries 1
9/10 match closely those determined recently[30]. The scheme
Mount Curl Tephra at ~254 kyr.

communication), contemporaneous with lower-level
winds. The observed dispersal implies that ash reacl
stratosphere.

Injection of large quantities of material into the strato
to heights above 20 km, must have had a major impact
atmosphere and possibly the climate of the South Pa
the absence of other data, it is tempting to ascribe th
cooling event in the oxygen-isotope curve immediately
the tephra to this cause. Recent work suggests that the c
of sulphate aerosols is crucial to determining the climat
of volcanic eruptions[1,39,40], although observed temp
decreases are greatest within 1-2 months of an eruptio
the atmosphere is still laden with fine ash[41]. The quantity
ash and sulphur injected into the stratosphere by thi
eruption of Taupo is unknown, but an estimate can b
using recent analogies[40]. If as little as 0.1% formed
particles[1], 2×10^{10} tonnes would have been generated, co
with 1.6×10^8 tonnes for Krakatau and 1.2×10^9 ton
Tambora[1]. This represents more dust than is postul
nuclear scenarios[10].

Given the widespread distribution of tephra (Fig. 1)
rapidity of atmospheric transport[4], it is likely that materi
this eruption of Taupo was deposited around the gl
contention that should be tested by investigation off
America, 10,000 km from the volcano.

Analytical facilities and funding were provided by
University of Wellington (electron microprobe), and
Westgate (NSERC A3565) and the University of T
(microprobe and neutron activation). C. Hendy, A. Cuthl
and G. Jarrett (all at Waikato University) helped to es
the isotope and carbonate stratigraphy in the cores, fun
the New Zealand University Grants Committee. D. C
University of Florida provided samples from Eltanin cc
Howorth, C. G. Vucetich and J. A. Westgate reviewed d
the manuscript.

June; accepted 10 October 1985.

), M. R. & Self, S. *Quat. Res.* **18,** 127-143 (1982).
S., Sparks, R. S. J., Carey, S. N., Sigurdsson, H. & Westgate, J. A. *Nature* **301,**
19 (1983).
A. & Matson, M. *Science* **221,** 195-197 (1983).
. A., Thomas, R. J., Thomas, G. E. & Barth, C. A. *EOS* **63,** 898 (1982).
, K. E., Defoor, T. E. & Deluisi, J. *EOS* **63,** 897 (1982).
I. H. *Phil. Trans. R. Soc.* **266,** 425-533 (1970).
ch, D., Sparks, R. S. J. & Ledbetter, M. T. *Bull. volcan.* **41,** 286-298 (1978).
, N. D. *et al. Nature* **271,** 122-126 (1978).
G. P. L. *J. Volcan. geotherm. Res.* **8,** 69-94 (1980).
t. P., Toon, O. B., Ackerman, T., Pollack, J. B. & Sagan, C. *Science* **222,** 1283-1300
).
ch, D. *Earth planet. Sci. Lett.* **4,** 89-102 (1968).
T. C., Watkins, N. D., Shaw, D. M. & Kennett, J. P. *Earth planet. Sci. Lett.* **20,**
24 (1973).
T. C., Watkins, N. D. & Shaw, D. M. *Bull. geol. Soc. Am.* **86,** 1305-1315 (1975).
, N. D. & Huang, T. C. *N.Z. J. Geol. Geophys.* **20,** 179-199 (1977).
R. & Seward, D. *Geology* **12,** 487-490 (1984).
t, P. C. *Quat. Res.* **19,** 188-200 (1983).
C. S., Froggatt, P. C. & Gosson, G. J. *Init. Rep. DSDP* **90** (in the press).
I. D. G. *N.Z. J. Geol. Geophys.* **16,** 519-532 (1973).
D. *Earth planet. Sci. Lett.* **24,** 242-248 (1974).
D. *N.Z. J. Geol. Geophys.* **19,** 8-20 (1976).
D. *Geology* **7,** 479-482 (1979).
N. D. *N.Z. J. Geol. Geophys.* **19,** 463-502 (1976).
tson, A. M. thesis, Univ. Waikato (1985).
C. S., Hendy, C. H., Cuthbertson, A. M. & Jarrett, G. in *Init. Rep. DSDP* **90** (in
ress).

25. Kennett, J. P. *et al. Init. Rep. DSDP* **90** (in the press).
26. Nelson, C. S., Hendy, C. H., Jarrett, G. R. & Cuthbertson, A. M. *Natur*
27. Hays, J. D., Imbrie, J. & Shackleton, N. J. *Science* **194,** 1121-1132 (
28. Morley, J. J. & Hays, J. D. *Earth planet. Sci. Lett.* **53,** 279-295 (1981)
29. Crowley, T. J. *Rev. Geophys. Space Phys.* **21,** 828-877 (1983).
30. Imbrie, J. & Shackleton, N. J. *et al.* in *Milankovitch and Climate Cha*
    Berger, A.) (Elsevier, Amsterdam, 1985).
31. Mildenhall, D. C., Williams, D. N. & Seward, D. *N.Z. J. Geol. Geoph*
32. Hayes, D. E. & Houtz, R. *et al. Preliminary Report of Vol. 24 U.S.N.S.*
    Pt C (ed. Taiwani, M.) (Tech. Rep. CU-2-76 Columbia University,
    1976)
33. Griggs, G. B., Carter, L., Kennett, J. P. & Carter, R. M. *Bull. geol.*
    (1983).
34. Ninkovich, D. & Shackleton, N. J. *Earth planet. Sci. Lett.* **27,** 20-34
35. Wilson, C. N. J. *et al. J. geophys. Res.* **89,** 8463-8484 (1984).
36. Walker, G. P. L. *J. Volcan. geotherm. Res.* **8,** 69-94 (1980).
37. Froggatt, P. C. *N.Z. J Geol. Geophys.* **24,** 231-248 (1981).
38. Wilson, C. J. N. & Walker, G. P. L. *J. geol. Soc. Lond.* **139,** 581-592
39. Rampino, M. R. & Self, S. *Nature* **310,** 677-679 (1984).
40. Rampino, M. R. & Stothers, R. B. *Nature* **313,** 272 (1985).
41. Kelly, P. M. & Sear, C. B. *Nature* **311,** 740-742 (1984).
42. Westgate, J. A., Walter, R. C., Pearce, G. W. & Gorton, M. P. *Can. J.*
    (1985).
43. Pillans, B. J. *Geology* **11,** 292-297 (1983).
44. Grindley, G. W. *Sheet 8—Taupo. Geological Map of New Zealan*
    1960).
45. Ward, W. T. *N.Z. J. Geol. Geophys.* **10,** 1109-1135 (1967).
46. Borchardt, G. A., Aruscavage, P. J. & Millard, H. T. *J. sedim. Petr*
47. Stein, R. & Roberts, C. *Init. Rep. DSDP* **90** (in the press).
48. Barnes, S. J. & Gorton, M. P. *Geostandards Newslett.* **8,** 17-23 (198

nagnetic anomalies and tectonic s in and around enue Trough, Nigeria

jakaye*, D. H. Hall†, T. W. Millar†,
Verheijen‡, M. B. Awad* & S. B. Ojo*

nent of Physics, Ahmadu Bello University, Zaria, Nigeria
for Precambrian Studies, University of Manitoba, Winnipeg,
3T 2N2
iversity, Amsterdam, The Netherlands

jor fracture zones cutting the Atlantic sea floor off the st of Africa—St Paul's, Romanche, Chain and Charcot— n delineated offshore using bathymetric, seismic, gravity gnetic data, respectively[1]. But the extrapolation of these s onto the African Continent is uncertain. Here we analyse compiled aeromagnetic data[2] for the Benue Trough and t areas of Nigeria, and demonstrate the existence of narrow c lineaments parallel to the margins of the Benue Trough, an be matched with the oceanic fractures. Alkaline ring es which predate the opening of the Atlantic Ocean are rated along these lineaments, suggesting that they represent ting zones of weakness in the African crust which may luenced the rifting of the continental margins and the early ment of Atlantic fracture zones.

eromagnetic data extend from 7 to 12° E longitude and to 12° N latitude (Fig. 1), and were compiled from gnetic maps recently released by the Geological Survey ria[2]. A contoured map (Fig. 2) of the total magnetic field ls has magnetic values ranging from 31,995 to 33,250 nT average value of 32,860 nT. To investigate the significance data, they were filtered and continued upwards. One most striking features is a series of long sub-parallel ic anomaly belts trending ENE-WSW, designated as AA' Fig. 2). The magnetic lineaments show up as continuous belts (10-15 km in width) of negative anomalies ranging h from 10 to 650 km and in amplitude from 150 to 250 nT. re of sufficient prominence and length to suggest that probably the signatures of regional structural features nting major tectonic trends, because they cut across both nt and sedimentary rocks in the study area. MAGSAT ross West Africa also show anomaly trends over the sea verlapping the continent[3]. These aeromagnetic results therefore, be considered in the context of a continent- ctonic setting.

The Benue Trough, which lies in the centre of 1), is considered a rift valley, and is filled with >5 and Cretaceous sediments. It has very large widt when compared with widths (59±15 km) norm with rift valleys[4]. The trough is believed to hav a tensional graben system during the Cretaceou experienced a period of compressional deforma of the Cretaceous resulting in the folding of parallel to the axis of the trough[5-7]. It connects of Cretaceous troughs to the north of Niger (e to the east across Chad to Sudan[8].

The pattern of the magnetic lineaments foll margins expected for a rift. The lineaments CC' 2) mark the structural boundary of the trough. T the onshore extensions, under the Niger Delta and Charcot oceanic fractures respectively (r Charcot fracture alone as has been suggested[9,10]) supports an earlier suggestion[10] that the Benu have been initiated by the extension of the equ zones onto the continent during the early stages o of Africa and South America. Also there is a Benkhelil[10] that there exists a narrow fault z basin, which is indicated on the magnetic anom Fig. 2).

With the boundary of the trough defined by and DD' (Fig. 2), the structure of the north-ea the study area appears more complicated. Fo Tertiary Kerikeri formation lies mostly outside t (Fig. 1). The magnetic data suggest a faulted c the north-eastern Cretaceous sediments in the define it and the south-eastern boundary of th mation.

The Nigerian Basement Complex, in which th lies, consists of Precambrian rocks that were fa tured before and during the Pan-African orogen the granites yielding this latter age. The most pro direction is N-S (products of brittle deformati superposed a conjugate system of strike-slip NE SE faults believed to have resulted from tran ments[11]. The Basement Complex in the north- study area is an uplifted zone intruded by alk plexes with an age range 141-213 Myr (ref. 12)

The magmatism responsible for these ring com related to the action of mantle plumes ben sphere[13-15] or to intraplate deformation with reac fractures[9,16-18]. It has been suggested[19] that the correlation between periods of rapid plate mc

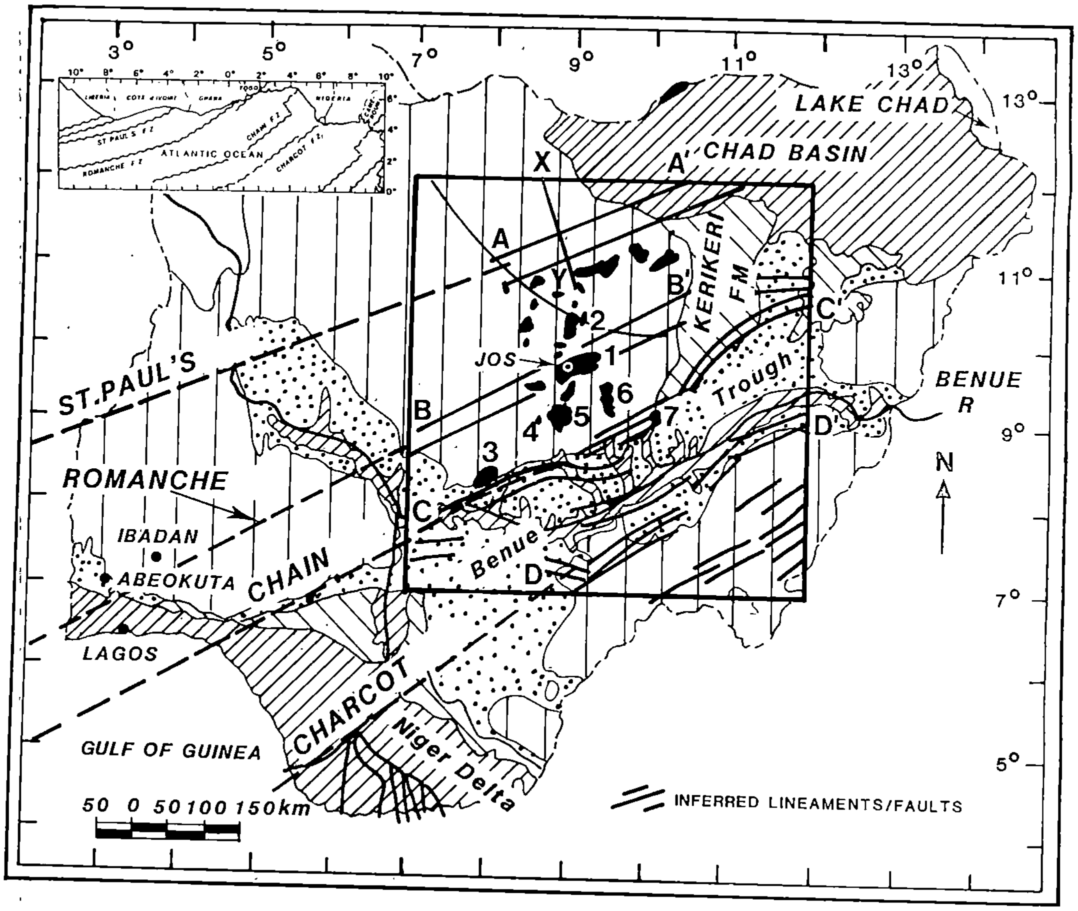

Fig. 1 Geological map of Nigeria, showing the study area, the locations of the inferred lineaments and faults, and the geological units. Younger Granite complexes: 1, Jos-Bukuru and Jarawa; 2, Amo and Buji; 3, Afu; 4, Ningishi; 5, Sha-Kaleri; 6, Pankshin; 7, Langtang. XY, Location of the profile shown in Fig. 3. ▨, Quaternary sandstone; ▧, tertiary sandstone; ▩, cretaceous sandstone; ■, younger granite series; ▥, Precambrian-Cambrian rocks; ///, inferred lineaments/faults.

plate magmatic activity which may correspond to interference and collision with the African plate[18].

Alkaline ring complexes have also been interpreted as being related to rifting[9,18,19] and to transform faulting[9,20]. Mainly because alkaline ring complexes have been found to align along transform directions[9,18], they are thought either to lie along fractures which precede and predetermine the location of oceanic transform faults, or to have occurred later during reactivation of the fractures situated at the ends of oceanic transform faults. In the case of the Nigerian ring complexes, which are a few million years older than the onset of seafloor spreading in the South Atlantic, it has been proposed[9] that the ring complexes reflect an early stage of rifting between Africa and South America that preceded the development of the first oceanic crust by a few tens of millions of years.

The magnetic data support the correlation of this intra-plate magmatism with transform faulting. In the north-eastern section of the Basement Complex of the study area (Figs 1 and 2) a major feature is depicted by a NE–SW linear zone of positive magnetic anomalies (AA', Fig. 2) flanked on either side by negative anomalies. This zone runs along the north-western boundary of the Kerikeri formation at its contact with the Chad formation and across the central crystalline shield area, where it is weakly developed. If this zone is linked to the St Paul's fracture zone, the contact must be faulted. Preliminary interpretation[21] of anomalies (Fig. 3) along this trend agrees quantitatively with this model.

The second lineament in this region (BB', Fig. 2) is aligned along a continental extension of the Romanche fracture zone in the mid-Atlantic and cuts across the Tertiary Kerikeri formation and the Cretaceous sediments. The lineament has very little surface expression. The prominent anomaly in the centre of BB' (Fig. 2) and other short-wavelength anomalies (10–30 km) over the crystalline shield and south of the line bb' have been shown to reflect surface or near-surface younger granite intrusives[2,22].

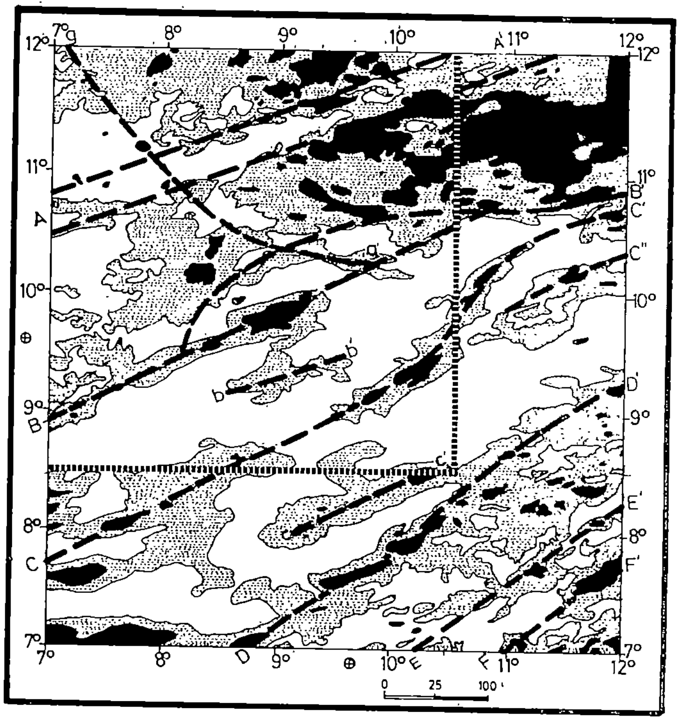

Fig. 2 Total-field aeromagnetic map of the study area, showing the lineament trends (field values are relative to a 25,000 nT base). DD', CC', BB', AA' are correlated with the Charcot, Chain, Romanche and St Paul's fracture zones in the mid-Atlantic (see also Fig. 1). All important trends are given letter designations, although not all of these are referred to in the text. The area outlined in the north-western portion of the map has been previously published[2]. The intensity ranges in nT are: □, ≥7,860; ▩, 7,780–7,860; ■, ≤7,780. ▨, Inferred lineaments/faults.

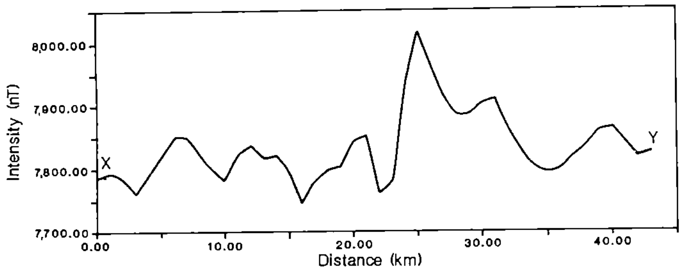

Fig. 3 Total field profile along XY (Fig. 1). A faulted contact is indicated at that location, consistent with the inferred continental lineament or fault associated with the St Paul's fracture zone.

The anorogenic alkaline ring complexes appear to be concentrated on the WSW-ENE trending magnetic lineaments. The connection between fracture zones and complexes suggests that these palaeo-megacontinental faults existed before the emplacement of the complexes and that they were reactivated in that period, either due to pressure from an underlying magma chamber or through tensional stresses in the lithosphere that allowed the release of magma to the surface. Thus, it can be inferred that the Romanche fracture zone extension along lineament BB' was reactivated on the Nigerian continental mass just before 161 Myr, which is about the age[12] of the Kagoro, Jos-Bukuru and Jarawa complexes lying along it (Fig. 1). Ages of ~151 Myr (ref. 12) for the aligned Ningishi, Sha-kaleri and Pankshin complexes may represent another such rejuvenated period (lineament bb', Fig. 2), while the period of activity around 141 Myr (ref. 12) of the Afu and Langtang complexes (lineament CC', Fig. 2) could mark a period of reactivation of the continental fracture zone associated with the Chain fracture system. This supports Sykes'[9] suggestion that various types of pre-existing zones of weakness, such as fault zones, suture zones, continental rifts, aulacogens and monoclines, have pronounced influence on the shape of subsequent continental margins and the locations of oceanic transform faults.

A further study of the magnetic anomalies centred on the complexes[2] and previous interpretations of gravity data[19] show a subsurface outline of the complexes which is commensurate with the idea that these diapirs may have risen from a common deep-seated source, possibly located in the mantle.

The existence of fracture zones extending from the continent to oceanic transform faults is also corroborated by other observations. First, the few recorded earthquakes in this area (in 1906 and 1939 in Accra, Ghana[23], and three earthquakes in 1984 near Ibadan, Nigeria) lie on faults which seem to extend from the continent to the Romanche Fault[24]. Second, this area shows up on LANDSAT imagery as a continent-wide shear system (Pelusium line) with its associated lineament system[25,26]. Third, these lineaments parallel structural trends in the oceanic crust off West Africa[2,27] and other parts of West Africa[28] and Eastern Brazil[29].

In conclusion, the Nigerian continental mass contains lineaments with definite magnetic signatures which are enhanced by the presence of anorogenic ring complexes. Further, these lineaments have a one-to-one relationship with the St Paul, Romanche, Chain and Charcot fracture zones in the continental margins of West Africa. Thus the oceanic fracture zones do not curve to the north-east on approaching the north coast of Guinea and then terminate at a relatively short distance inland as has been previously suggested[27,30]. Our evidence supports the hypothesis that major continental fracture zones tend to develop near pre-existing zones of weakness inherited from the last orogeny[9] in the continent. Thus, the magnetic lineaments could be considered to be part of the signatures of megalineament-geosutures, shear zones[20,31] or zones of weakness, that predate[32] the opening of the Atlantic Ocean. These zones were reactivated during the early stages of continental rifting, parts of which became foci of ocean spreading[32].

We thank the director of the Nigerian Geological Survey for access to some of the data; the Canadian International Development Agency, the NSERC of Canada and the Nigerian Mining Corporation for financial support.

Received 11 June; accepted 7 November 1985.

1. Sibuet, J. & Mascle, J. *J. geophys. Res.* **83,** 3401–3421 (1978).
2. Ajakaiye, D. E., Hall, D. H. & Miller, T. W. *Geophys. J.* **83,** 503–517 (1985).
3. Langel, R. A., Phillips, J. D. & Horner, R. J. *Geophys. Res. Lett.* **9,** 269–272 (1982).
4. Ajayi, C. O. & Ajakaiye, D. E. *Tectonophysics* **80,** 285–303 (1981).
5. Cratchley, C. R. & Jones, G. P. *Overseas Geological Surveys, London* (Geophysical Paper No. 1, 1965).
6. Wright, J. B. *Tectonophysics* **6,** 301–310 (1968).
7. Burke, K. & Dewey, J. F. *Nature* **249,** 313–315 (1974).
8. Burke, K. & Whiteman, A. J. in *Implications of Continental Drift to the Earth Sciences* (eds Tarling, D. A. & Runcorn, S. K.) 735–755 (Academic, London, 1973).
9. Sykes, L. R. *Rev. Geophys. Space Phys.* **16,** 621–688 (1978).
10. Benkhelil, J. *Geol. Mag.* **119,** 155–168 (1982).
11. Ball, E. *Tectonophysics* **61,** 363–379 (1980).
12. Rahaman, M. A., Van Breemen, O., Bowden, P. & Bennett, J. N. *J. Geol.* **92,** 173–184 (1984).
13. Morgan, W. J. *Nature* **230,** 42–43 (1971).
14. Briden, J. C. & Gas, I. G. *Nature* **248,** 650–653 (1974).
15. Ajakaiye, D. E. & Verheijen, P. J. T. *Geophys. Res. Lett.* **10,** 424–427 (1983).
16. Barley, P. M. *Geology* **2,** 373–376 (1974).
17. Harris, N. B. W. *Tectonophysics* **83,** 242–285 (1982).
18. Black, R., Lameyre, J. & Bonin, B. *J. Afr. Earth Sci.* **3,** 5–6 (1985).
19. Ajakaiye, D. E. *Nature* **255,** 50–52 (1970).
20. Marsh, J. S. *Earth planet. Sci. Lett.* **18,** 317–323 (1973).
21. Ajakaiye, D. E., Hall, D. H. & Millar, T. W. in *27th Int. Geological Congr.* Moscow, Abstr. Vol. (1984).
22. Ajakaiye, D. E., Hall, D. H. & Millar, T. W. *J. Afr. Earth Sci.* **1,** 355 (1983).
23. Bacon, M. & Quaah, A. O. *Bull. seism. Soc. Am.* **71,** 771–785 (1981).
24. Ajakaiye, D. E., Daniyan, M. A. & Ojo, S. B. in *2nd Symp. on Recent Crustal Movements in Africa,* Abstr. Vol. (1984).
25. Neev, D. *Tectonophysics* **38,** T1–T8 (1977).
26. Neev, D., Hall, J. K. & Saul, J. M. *J. geophys. Res.* **87,** 1015–1030 (1982).
27. Pichon, X. & Hayes, D. E. *J. geophys. Res.* **76,** 6283–6293 (1971).
28. Angoran, Y. & Kadio, E. *in Int. Symp. on Archean and Early Proterozoic Geologic Evolution and Metallogenesis,* Abstr. Vol. (1982).
29. Haralyi, N. L. E. & Hasui, Y. in *Int. Symp. on Archean and Early Proterozoic Geologic Evolution and Metallogenesis,* Abstr Vol. (1982).
30. Burke, K. G. *Nature* **222,** 655–657 (1969).
31. Moody, J. D. *Tectonophysics* **3,** 479–522 (1966).
32. McConnell, R. B. **80,** *Bull. geol. Soc. Am.* **80,** 1775–1782 (1969).

High-pressure transformation of eclogite to garnetite in subducted oceanic crust

T. Sekine*, T. Irifune, A. E. Ringwood & W. O. Hibberson

Research School of Earth Sciences, Australian National University, Canberra ACT 2601, Australia

The mineral composition of oceanic crust is a function of pressure and temperature and thus changes as a slab of crust descends a subduction zone. A knowledge of the mineralogy of subducted material would provide important constraints on its geophysical characteristics. We have sought, by means of high pressure laboratory experiments (in the pressure range 4.6–18 GPa) on a synthetic mix with the composition of mid-ocean ridge basalt (MORB), to determine the sequence of mineralogical changes. We find that at 1,200 °C, solid solution of pyroxene in garnet begins around 10 GPa, and increases substantially between 12 and 15 GPa. Complete transformation of eclogite to garnetite is achieved at 15 GPa. The garnetite has a zero-pressure density of 3.76 g cm^{-3} and accordingly would be denser than the surrounding mantle throughout its stability field, which extends to depths of ~600 km. If subducted to greater depths, garnetite may transform to perovskitite.

A model basaltic starting composition was prepared from a mixture of appropriate proportions of oxides, hydrates, carbonates and metal, and melted completely above its liquidus under an argon atmosphere before quenching in cold water to yield a glass starting material. Its composition, in weight per cent, is

---

* Present address: National Institute for Research in Inorganic Materials, Sakura-mura, Ibaraki 305, Japan.

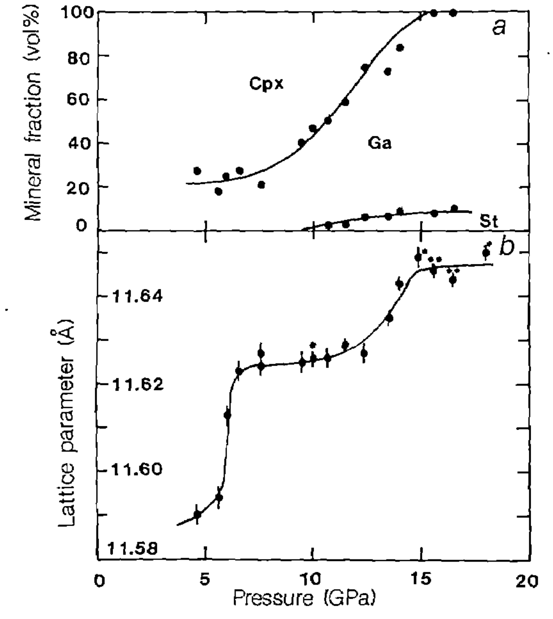

Fig. 1 *a*, Mineral proportions in a typical primitive MORB composition vary systematically with increasing pressure. *b*, Garnet lattice parameters increase non-linearly with increasing pressure. MORB composition starting materials are glass, pyroxenite (*) or amphibolite (**). Vertical bars indicate estimated uncertainties.

50.4 SiO_2, 0.6 TiO_2, 16.1 Al_2O_3, 7.7 FeO, 10.5 MgO, 13.1 CaO, 1.9 Na_2O and is equivalent to that of a typical primitive MORB[1]. The homogeneity of the glass was confirmed optically and by electron-probe microanalysis. Pyroxenite and amphibolite crystallized from the glass at 1.0-1.5 Gpa, 900 °C, were used as starting materials in some runs to minimize metastability problems (see Fig. 1).

High-pressure experiments were carried out using a pair of Bridgman anvils from 4.6 to 12 GPa and an MA-8 system at 10 GPa and above. Detailed experimental methods and procedures will be described elsewhere[2,3]. Pressure was calibrated at 1,200 °C using several well-determined phase boundaries, namely Fe_2SiO_4 olivine-spinel, coesite-stishovite, and Mg_2SiO_4 olivine-modified spinel. Uncertainty in the pressure measurement is believed to be ±0.5 GPa. Temperature was measured using Pt/Pt-10%Rh thermocouples without correcting for the effect of pressure on e.m.f. All runs were carried out at 1,200 °C except one at 6.6 GPa and 1,100 °C. Runs lasted from 30 to 90 min. Quenching was achieved by cutting off the heating power input. The products were examined optically, by X-ray diffraction and by electron microprobe. Lattice parameters of garnets were determined from the (14, 4, 0) and (14, 4, 2) reflections. The proportions of minerals in the run products were estimated from X-ray diffraction line intensities and by mass balance using electron microprobe analyses of individual phases.

Figure 1*a* summarizes how mineralogy changes as a function of pressure. Above 15 GPa the product assemblage consists of single-phase garnet, while stishovite was identified in runs between 12 and 18 GPa. Figure 1*b* illustrates how garnet lattice parameters vary with pressure. They increase sharply around 6 GPa, then pass through a plateau between about 8 and 12 GPa, followed by another increase between 12.5 and 15 Gpa, to level out between 15 and 18 GPa at ~11.65 Å.

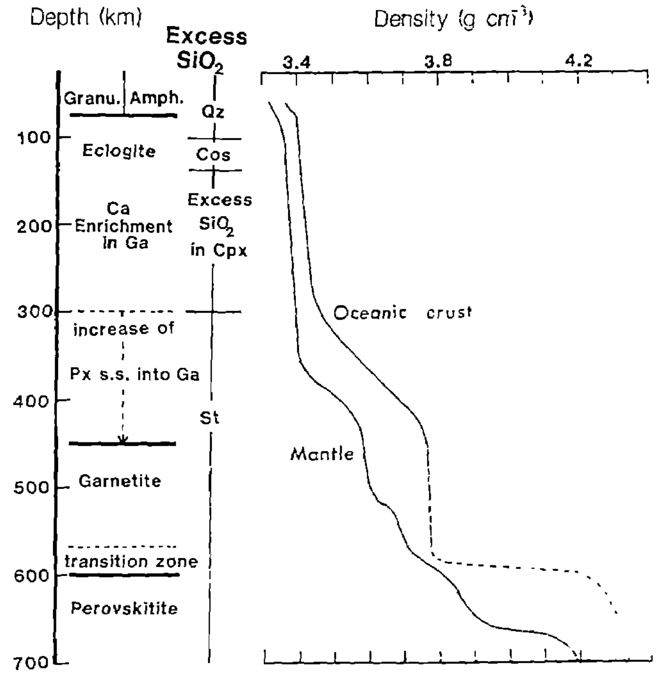

Fig. 2 Subsolidus phase changes and calculated zero-pressure densities of subducted oceanic crust are shown as a function of depth. The presence or absence of a free SiO_2 phase in the assemblage is also indicated. For comparison, the density of surrounding mantle (pyrolite composition) is shown[6]. Granu, granulite. Amph, amphibolite; Ga, garnet; Px s.s., pyroxene solid solution; Qz, quartz; Cos, coesite; Cpx, clinopyroxene; St, stishovite.

The CaO content of garnet changes in a manner analogous to the lattice parameter variations, with a rapid increase at around 6 GPa by 6 mol %, followed by a more gentle increase between 12 and 15 GPa. Solid solution of pyroxene components in garnet begins around 10 GPa and increases substantially between 12 and 15 GPa. Garnet contains <0.7 wt% Na_2O below 10 GPa, and 1.0-1.6 wt% at higher pressures. Clinopyroxenes become more jadeitic, and less aluminous with increasing pressure. The 'excess SiO_2' content of clinopyroxene, calculated as a $Ca_{0.5}AlSi_2O_6$ molecule, remains essentially constant at 16 ± 2 mol % up to 9.5 GPa, but decreases sharply thereafter. This pressure corresponds to the coesite–stishovite transition. Calculated molar volume changes (ΔVs) for the reaction.

$$0.5\ CaAl_2SiO_6\ (cpx) + 1.5\ SiO_2 = Ca_{0.5}AlSi_2O_6(cpx)$$

confirm that 'excess SiO_2' is accommodated in solid solution in clinopyroxene in the coesite stability field ($\Delta V = -2.5\ cm^3\ mol^{-1}$), but exsolves as free stishovite within the stishovite stability field ($\Delta V = +7.6\ cm^3\ mol^{-1}$).

Ringwood[4] reported lattice parameter and modal abundance variations for garnets crystallized from basaltic glasses at pressures up to 17 GPa. His data indicate a discontinuity in lattice parameter at around 5 GPa, corresponding to the sharp increase in lattice parameters and CaO content reported in this study. His experiments on an alkali-poor olivine tholeiite yielded a garnetite (>95% garnet) coexisting with a small amount of jadeitic clinopyroxene at ~13 Gpa, 900 °C, Liu[5] reported lattice parameter variations for garnets and proportions of phases crystallized from a basaltic composition very similar to that used in this study. Allowing for the large uncertainties involved in diamond-anvil pressure calibration, his data and ours are also found to be consistent. Liu reported that the ratio of garnet to clinopyroxene progressively increased with increasing pressure between 10 and 15 GPa, while X-ray diffraction studies of an 18 GPa product assemblage revealed only a weak garnet spatter, with no clinopyroxene lines. X-ray diffraction patterns of quenched 21- and 28-GPa runs contained only a few faint lines, from which he inferred that the high-pressure phase assemblage in this interval consisted of an unquenchable perovskite-type phase.

Figure 2 illustrates the subsolidus phase changes and corresponding density increases in subducted oceanic crust to a depth of 700 km, using data from this study and from Liu[5]. The MORB basaltic composition undergoes three major phase transformations: to eclogite at around 80 km, from eclogite to garnetite at around 450 km, and from garnetite to perovskitite at around 600 km. Substantial solid solution of pyroxene components in garnet begins at a depth of 300 km and is essentially completed by 450 km. The behaviour of 'excess SiO_2' is also indicated in Fig. 2. At depths shallower than 150 km, the eclogite contains free quartz or coesite. However, between 150 and 300 km, 'excess SiO_2' is accommodated in solid solution in pyroxene as a $Ca_{0.5}AlSi_2O_6$ component so that there is no free SiO_2 phase. At depths below the coesite–stishovite transition, stishovite appears in the phase assemblage.

Figure 2 also shows how the calculated density of subducted basaltic crust increases with depth. The calculations use mineral compositions as determined from electron-probe microanalysis and garnet lattice parameters (Fig. 1). The proportions of garnet and clinopyroxene were deduced from mass-balance considerations. Clinopyroxene densities were calculated using compositions determined by electron-probe microanalysis and assuming ideal solid solution between diopside, clinoenstatite, clinoferrosilite, jadeite, Ca-Tschermak and $Ca_{0.5}AlSi_2O_6$ endmembers. The individual zero-pressure densities of both garnet and clinopyroxene decrease almost linearly with increasing depth. The increase in density of the oceanic crust is caused by increasing the proportion of garnet to clinopyroxene, as shown in Fig. 1. Note that the abrupt increase in the CaO content of clinopyroxene at 6 GPa (200 km) does not result in any appreciable increase in density. Figure 2 shows that only a modest increase in density is experienced by subducted basaltic crust down to depths of ~300 km. However, between about 350 and 400 km there is a rapid increase, reaching 3.76 g cm^{-3} by 450 km where complete transformation to garnetite is attained. The density change throughout the garnetite stability field is negligible; however, the transformation of garnetite to perovskitite is probably accompanied by a substantial and rapid increase in density, as indicated by the dashed portion of the curve.

Our results demonstrate that subducted oceanic crust would remain denser than surrounding mantle (assumed to possess a pyrolite or peridotite composition) between depths of 60 and 600 km. Moreover, the results of Liu[5] imply that this situation prevails in the 600–700 km depth interval, so that gravitational body forces should cause former oceanic crust to penetrate the 670-km seismic discontinuity. According to Ringwood[6], however, harzburgite, which comprises the main part of the oceanic plate and underlies the oceanic crust, may also be denser than surrounding mantle down to around 670 km depth, but becomes less dense below this depth. Thus, the main part of a subducted lithospheric plate probably stops its further penetration at around this depth. These relationships have important geodynamic implications[6,7].

Received 14 August; accepted 20 November 1985.

1. Green, D. H., Hibberson, W. O. & Jaques, A. L. in *The Earth: Its Origin, Structure and Evolution* (ed. McElhinny, M. W.) 265–299 (Academic, London, 1979).
2. Sekine, T. & Ringwood, A. E. *Phys. Earth planet. Inter.* (in the press).
3. Irifune, T. & Hibberson, W. O. *High Temp. High Press.* (submitted).
4. Ringwood, A. E. *Earth planet. Sci. Lett.* **2**, 255–263 (1967).
5. Liu, L. *Phys. Earth planet. Inter.* **23**, 262–267 (1980).
6. Ringwood, A. E. *J. Geol.* **90**, 611–643 (1982).
7. Irifune, T., Sekine, T., Ringwood, A. E. & Hibberson, W. O. *Earth planet. Sci. Lett.* (submitted).

The pyroxene paradox in MORB glasses—a signature of picritic parental magmas?

Don Francis

Department of Geological Sciences, McGill University,
3450 University Street, Montreal, Quebec,
Canada H3A 2A7

A persistent conclusion reached in studies of glass in the chilled margins of mid-ocean ridge basalts (MORB) is that occult clinopyroxene fractionation is required in order to explain the observed variation in glass compositions[1]. Successful crystal-fractionation models commonly require crystallizing assemblages which are dominated by plagioclase and clinopyroxene rather than the plagioclase and olivine which dominate the phenocryst assemblages. The 'pyroxene paradox' arises from the observation that clinopyroxene phenocrysts are uncommon in lavas containing more than 8.5 wt% MgO (refs 2, 3) and the fact that melting experiments on liquids with such compositions indicate that clinopyroxene appears only at 20–40 °C below liquidus temperatures[4–7]. Based on a study[8] of compositional relationships between glasses and chilled margins of pillow lavas from the Baffin Bay picrite suite, I suggest here that the 'pyroxene paradox' is an illusion which arises in part because of the compositional dispersion of olivine fractionation trends from picritic parental magmas between the limiting cases of equilibrium and fractional crystallization.

The Baffin Bay volcanic province consists of a succession of Palaeocene[9] basaltic lavas that erupted during the opening of the Davis Strait separating Greenland from Baffin Island. The lavas occur as a series of outcrops between Cape Searle and Cape Dyer along the eastern coast of Baffin Island and between the Svartenhuk Peninsula and Disko Island along the western coast of Greenland. The lower part of the succession at Padloping Island[8] contains abundant pillow lavas and pillow breccias which retain fresh volcanic glass in their chilled margins. All these glasses contain millimetre-sized olivine phenocrysts, with inclusions of euhedral spinel, and plagioclase microlites but no clinopyroxene. Although there is a systematic increase in the bulk MgO content of the chilled margins with the abundance of olivine phenocrysts, there is also a general increase (Fig. 1) in the forsterite content of the olivine phenocrysts with the MgO content of both coexisting glasses and corresponding chilled margins. This correlation rules out a mechanism for formation of the more magnesian lavas involving the simple mechanical accumulation of the olivine phenocrysts observed in liquids of lowest MgO content.

I have shown[8] that despite the complications of olivine accumulation, the presence of extremely forsteritic olivine megacrysts (Fo 93+) argues for the existence of liquids whose compositions are approximated by the bulk compositions of the more magnesian lavas such as sample Pd-19 (Table 1). Fractional crystallization of olivine from a magma of the same composition as Pd-19 could produce a succession of liquid compositions which approximate the compositional spectrum of the lava chilled margins (Fig. 2, trend *a*). For example, the composition of the chilled margin of Pd-14 can be obtained by extracting 30% olivine with minor spinel from the composition of Pd-19 [Table 2, model (1)]. A strong component of equilibrium crystallization (Fig 2, trend *b*), however, is required to explain the composition of the glass actually found in the chilled margin of Pd-19. In reality, a magma of Pd-19's composition may have evolved along any path between the limiting cases of perfect fractional crystallization (trend *a*) and perfect equilibrium crystallization (trend *b*), depending on the local dynamics of the magma-chamber processes which controlled crystal/liquid separation.

The interesting question is what controls the spectrum of glass compositions. The presence of plagioclase microlites in the glasses of all the pillow lavas, regardless of bulk margin MgO content, indicates that the liquids of these lavas lay on the olivine–plagioclase cotectic at the time of their eruption. In studies of MORB, glass trends such as that from Pd-19 to Pd-14

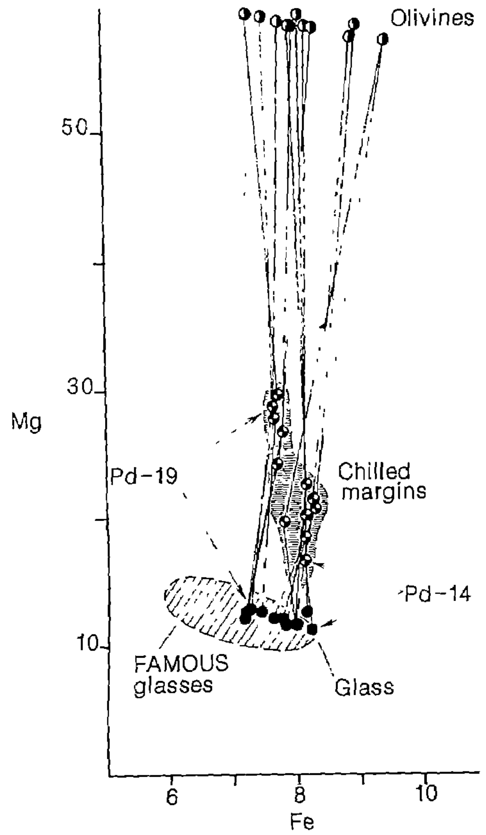

Fig. 1 Mg–Fe plot, in cation units, of the compositions of olivines (◑), glass (●) and chilled margins (⊛) of Padloping Island pillow lavas. The tie-lines join coexisting phases. The horizontally shaded field indicates the compositional range of 48 Padloping Island lava chilled margins (after Francis[8]) and the diagonally shaded field indicates the compositions of glasses from the FAMOUS project.

(Fig. 2, trend *c*) are commonly interpreted to reflect crystal fractionation trends. Model mixing calculations using only olivine and plagioclase [Table 2, model (2)] yield mineral compositions which are clearly unrealistic (that is, plagioclase is required to be pure anorthite and olivine pure forsterite) to produce the glass of Pd-14 from that of Pd-19. Finite-difference computer models[10] using instantaneous equilibrium compositions for plagioclase[11] and olivine[12] yield a rise of Ca content with fractionation, a feature which is not observed along the spectrum of glass compositions. Mixing models which include clinopyroxene are thus significantly better [Table 2, model (3)], although they involve a much larger degree of fractionation and a rather Fe-rich clinopyroxene. Such models require the extraction of significantly more pyroxene than olivine in order to prevent a build-up of Ca. Clinopyroxene is, however, absent from the Padloping glasses and we face a pyroxene paradox similar to that commonly reported in studies of MORB glasses.

The paradox arises because of the assumption that the spectrum of glass compositions represents a trend of compositional evolution. The disposition of the tie-lines in Fig. 1 suggests instead that each glass marks the arrival of an individual olivine fractionation path at the plagioclase-saturation surface. In the Padloping lavas, the length of the glass spectrum in Mg–Fe space approximates the separation, at plagioclase saturation, of the two limiting trends for olivine fractionation from an initial magma of Pd-19's composition (Fig. 2*A*). Although the presence of plagioclase microlites requires that some plagioclase crystallized from these liquids at eruption, there is no need to propose that glasses similar to Pd-14 fractionated from glasses similar to Pd-19 along the plagioclase-saturation surface. In such a model, no clinopyroxene is required to explain the lack of Ca

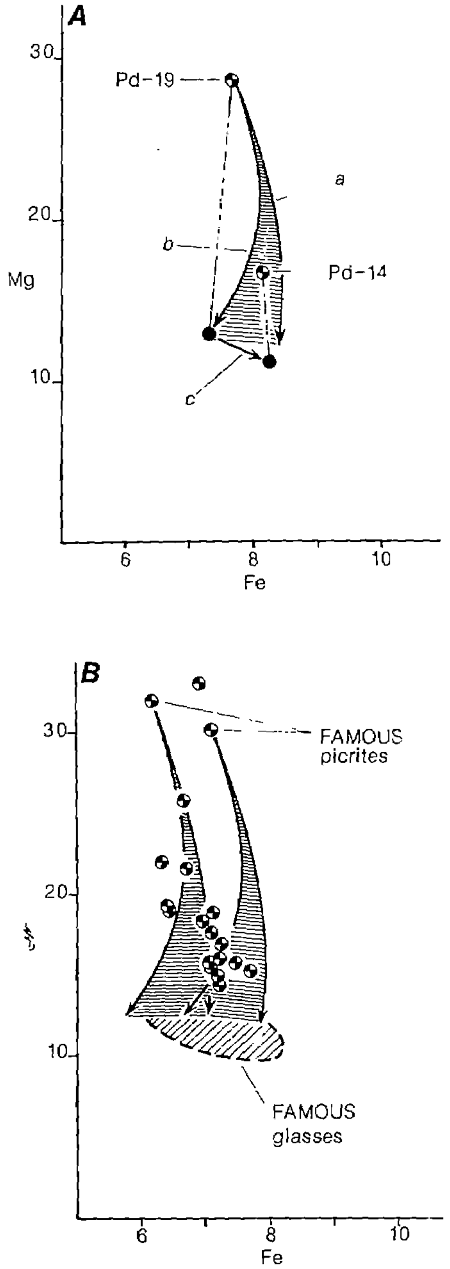

Fig. 2 *A*, Mg–Fe plot, in cation units, indicating calculated crystal fractionation paths. Trend *a* represents the path of Pd-19 undergoing perfect fractional crystallization of olivine. Trend *b* represents a perfect equilibrium olivine crystallization path for Pd-19. The low-Mg ends of paths *a* and *b* terminated at the point of plagioclase saturation, calculated using the technique of Neilson and Dungan[11] with olivine calculated after Ford *et al.*[12], and Fe^{3+}/Σ Fe fixed at 0.10. Trend *c* represents the path of crystallization of olivine, plagioclase and clinopyroxene from glass Pd-19 to glass Pd-14 as in model (3) of Table 2. *B*, Mg–Fe plot, in cation units, showing the compositions of MORB picritic lavas from FAMOUS[20,22] and DSDP[3] sites. The heavy arrows indicate the fractional and equilibrium olivine crystallization paths (calculated as in *A*) for two FAMOUS picrites to the point of plagioclase saturation. Note the correspondence between the plagioclase-saturation points at the ends of the fractionation arrows and the diagonally shaded field of FAMOUS glass compositions.

variation across the spectrum of glass compositions. Calcium essentially an incompatible element during olivine extracti and its behaviour is unaffected by the mode of fractionati Thus, with the recognition that the Padloping magmas fractic ated to the spectrum of glass compositions by the extraction olivine from picritic parents rather than along the glass spectrum via the fractionation of plagioclase, clinopyroxene and olivine, the pyroxene paradox disappears.

Accepting the above, one wonders whether a similar conceptual problem underlies the pyroxene paradox in MORB. Explanations for the pyroxene paradox have ranged from magma mixing[13,14] to clinopyroxene fractionation at depth[15]. More significantly, the work of Bryan *et al.*[16,17] indicates that the illusion of the pyroxene paradox may simply reflect the existence of multiple olivine-phyric parental magmas. The point here is that if MORB have picritic parental magmas, much of the compositional variation that is responsible for the pyroxene paradox may be attributed to the dispersion of olivine fractionation trends between the limits of equilibrium and fractional crystallization. Clarke[18] has argued that the picritic lavas of Baffin Bay could represent the parental magmas for MORB. However, as pointed out by Langmuir and Hanson[19] and indicated in Fig. 1, the Baffin picrites are too Fe-rich to be suitable parental magmas for MORB. The picritic lavas from MORB localities are, however, systematically Fe-poor compared with the Baffin picrites[8]. Figure 2*B* shows the results of assuming that two picritic lavas represent analogues of parental magmas for the glasses sampled at the FAMOUS site. In a dynamic open-system conduit system, primary magmas of compositions between these two picrite compositions could evolve to plagioclase saturation by olivine fractionation along a variety of paths between the limiting cases of equilibrium and fractional crystallization. Although a range of picritic magma compositions seems to have existed in the FAMOUS area, much of the elongation of the spectrum of FAMOUS glasses in Mg-Fe space could simply reflect this dispersion effect rather than crystal fractionation along a plagioclase-clinopyroxene-olivine cotectic. A similar observation could be made about the spectra of whole-rock compositions of aphyric lavas in other studies[22].

I propose that the very existence of the pyroxene paradox in MORB glasses and aphyric lavas is evidence of the picritic nature of parental magmas for MORB. Despite the possible complications of crystal accumulation[8], such parental magmas would have had compositions similar to those of the picritic lavas found at MORB sampling sites. Although it is difficult to specify the exact Mg content(s) of such picritic parental magmas, olivine megacrysts with forsterite contents reaching Fo 91 (ref. 3) require the existence of MORB liquids with at least 13–15 wt% MgO. A comparison of terrestrial picrite suites[8] indicates that such MORB parental magmas are rich in Al but poor in Fe with respect to the parental magmas of other tholeiitic suites.

The results of the Baffin Bay study emphasize the importance of highly porphyritic lavas to the petrogenetic interpretation of volcanic suites. A rigorous evaluation of the implications of this study for MORB would require a detailed comparison of the compositions of glass and bulk lava in picritic samples. Unfortunately, these data are scarce as such rocks have commonly been avoided because they were considered to be 'cumulates'.

Table 1 Chemical compositions of magnesian lavas

	Pd-14			Pd-19		
	Margin	Glass	Olivine	Margin	Glass	Olivine
SiO_2	46.94	50.80	39.59	44.92	49.79	40.49
TiO_2	1.17	1.46	—	0.79	0.93	—
Al_2O_3	14.22	14.22	—	10.52	15.33	—
Cr_2O_3	0.10	—	—	0.25	0.06	—
MgO	11.97	8.03	45.79	21.94	9.27	48.15
FeO	10.39	10.64	13.57	10.32	9.45	11.01
MnO	0.18	0.19	0.19	0.17	0.16	0.15
NiO	0.03	—	0.26	0.11	0.02	0.37
CaO	11.75	12.75	0.32	9.00	13.01	0.28
Na_2O	1.64	2.24	—	1.02	1.88	—
K_2O	0.05	0.21	—	0.03	0.06	—
P_2O_5	0.08	0.15	—	0.05	0.17	—
LOI	0.93	—	—	0.86	—	—
Total:	99.45	100.69	99.72	99.98	100.13	100.45
			Cation units			
Si	43.76	47.00	33.02	40.33	45.98	33.14
Ti	0.82	1.02	—	0.53	0.65	—
Al	15.62	15.51	—	11.13	16.69	—
Cr	0.07	—	—	0.18	0.04	—
Mg	16.63	11.07	56.92	29.36	12.76	58.73
Fe	8.10	8.23	9.46	7.75	7.30	7.54
Mn	0.14	0.15	0.13	0.13	0.13	0.10
Ni	0.02	—	0.17	0.08	0.01	0.24
Ca	11.74	12.64	0.29	8.66	12.87	0.25
Na	2.96	4.02	—	1.78	3.37	—
K	0.06	0.25	—	0.03	0.07	—
P	0.06	0.12	—	0.04	0.13	—
O	151.01	153.81	133.02	145.67	153.47	133.14
Oliv. Fo	87.5 (calc.)	81.3 (calc.)	85.7	93.2 (calc.)	85.1 (calc.)	88.6

Bulk pillow margin X-ray fluorescence analyses were performed by Tariq Ahmedali at McGill University with a Phillips PW 1400 instrument using fused disks and an α coefficient technique. Electron microprobe analyses of glass and olivines were performed on a Cameca CAMBAX/Micro system at McGill University using the MBXCOR/Micro software package. Total Fe was calculated as FeO and the olivine compositions were calculated according to the method of Ford *et al.*[12]. Analysis sets for 10 other Baffin pillow lavas are presented elsewhere[8]. LOI means loss on ignition.

Table 2 Fractionation models

Model (1) Bulk margin Pd-19 to bulk margin Pd-14

Pd-19 = Pd-14 + olivine (Fo 89.8) + chromite
(100) (70.0) (29.4) (0.6)
$\Sigma\ (\text{residuals})^2 = 0.23$

Model (2) Pd-19 glass to Pd-14 glass

Pd-19 = Pd-14 + olivine (Fo 100) + plagioclase (An 100)
(100) (87.9) (4.5) (7.7)
$\Sigma\ (\text{residuals})^2 = 0.23$

Model (3) Pd-19 glass to Pd-14 glass with clinopyroxene

Pd-19 = Pd-14 + olivine (Fo 81.3) + plagioclase (An 78.5)
(100) (63.5) (6.0) (19.2)
+ clinopyroxene (Wo 32.4, En 44.0, Fs 23.6)
(11.3)
$\Sigma\ (\text{residuals})^2 = 0.01$

Values in parentheses are percentages. Calculations (in cation units) were performed with the mineral distribution program of Wright and Doherty[21]. The compositions of plagioclase, olivine and clinopyroxene were calculated using the program from ideal end-members. In model (3) the olivine composition was fixed at that which would equilibrate with the glass of Pd-14.

Received 9 April; accepted 4 November 1985.

1. *Basaltic Volcanism Study Project*, 153 (Pergamon, New York, 1981).
2. Hekinian, R., Moore, J. G. & Bryan, W. B. *Contr. Miner. Petrol.* **58**, 83–110 (1976).
3. Blanchard, D. P. *et al. J. geophys. Res.* **81**, 4231–4246 (1976).
4. Bender, J. F., Hodges, F. N. & Bence, A. E. *Earth planet. Sci. Lett.* **41**, 277–302 (1978).
5. Green, D. H., Hibberson, W. O. & Jaques, A. L. in *The Earth* (ed. McElminny, M. W.) 265–299 (Academic, New York, 1979).
6. Fujii, T. & Bougault, H. *Earth planet. Sci. Lett.* **62**, 283–295 (1983).
7. Grove, T. L. & Bryan, W. B. *Contr. Miner. Petrol.* **84**, 293–309 (1983).
8. Francis, D. *Contr. Miner. Petrol.* **89**, 144–154 (1985).
9. Clarke, D. B. & Upton, B. G. J. *Can. J. Earth Sci.* **8**, 248–258 (1971).
10. Nathan, H. D. & Van Kirk, C. K. *J. Petrol.* **19**, 66–94 (1978).
11. Neilson, R. L. & Dungan, M. A. *Contr. Miner. Petrol.* **84**, 310–326 (1983).
12. Ford, C. E., Russell, D. G., Craven, J. A. & Fisk, M. R. *J. Petrol.* **24**, 256–265 (1983).
13. Rhodes, J. M., Dungan, M. A., Blanchard, D. P. & Long, P. E. *Tectonophysics* **55**, 35–61 (1979).
14. Walker, D., Shibata, T. & DeLong, S. E. *Contr. Miner. Petrol.* **70**, 111–125 (1979).
15. Bence, A. E., Bayliss, D. M., Bender, J. F. & Grove, T. L. *Deep Drilling Results in the Atlantic Ocean: Ocean Crust* (eds Talwani, M., Harrisson, C. H. & Hayes, D. E.) 331–341 (American Geophysics Union, Washington, DC, 1979).
16. Bryan, W. B., Thompson, G. & Ludden, J. G. *J. geophys. Res.* **86**, 11815–11836 (1981).

17. Bryan, W. B. *Contr. Miner. Petrol.* **83**, 62–74 (1983).
18. Clarke, D. B. *Contr. Miner. Petrol.* **25**, 203–224 (1970).
19. Langmuir, C. H. & Hanson, G. N. *Phil. Trans. R. Soc.* A**297**, 383–408 (1980).
20. Arcyana, *Deep-Sea Res.* **24**, 565–589 (1977).
21. Wright, T. L. & Doherty, P. C. *Bull. geol. Soc. Am.* **81**, 1995–2008 (1970).
22. LeRoex, A., Erlank, A. J. & Needham, H. D. *Contr. Miner. Petrol.* **77**, 24–37 (1981).

Flock-feeding on fish schools increases individual success in gulls

Frank Götmark, David W. Winkler* & Malte Andersson

Department of Zoology, University of Gothenburg, PO Box 250 59,
40031 Gothenburg, Sweden

Flock-foraging and the role of white plumage in gulls and other seabirds have been the subject of much debate[1–4]. At first sight it seems that competition within the flock would render flock formation against the interest of the bird who finds the fish school, as the fish must then be shared with birds joining the flock. However, it is also possible that flock formation is neutral or even beneficial to the individual members[5], including the bird that found the fish[4,6] (the 'first finder'). Here we show that the fishing success of individual black-headed gulls, *Larus ridibundus*, increases with flock size up to at least eight birds. Part of the reason is that the fish school is more vulnerable when attacked by several gulls. The first gull to reach a fish school therefore benefits from being joined by others, and conspicuous white upper parts in gulls may act as a means of attracting other gulls to the flock and hence improving hunting success.

Twelve black-headed gulls that had been caught in the wild (six adults and six yearlings, all in mainly white winter plumage) were monitored while hunting schooling bleak (*Alburnus alburnus*; length 6.5 ± 0.8 cm, mean ± s.d.) in a 5 × 5 m pool. The pool was situated in a 10 × 7 m room illuminated with 16 40-W fluorescent lights (at a height of 2.9 m above the pool). The pool was 14 cm deep with a light-grey bottom, and sloping at the edges over a width of 40 cm. This decrease in water depth at the periphery of the pool prevented the fish from hiding there.

Black-headed gulls are light (~275 g) and agile, hence they were able to manoeuvre easily in the room. They attacked the fish by plunging their heads under water; between attacks they flew or swam 1–3 m to locate new fish. The gulls became habituated to captivity within a few days and entered the room containing the pool to hunt when allowed to do so. For 5 days in each week, the gulls were allowed to hunt in groups of various sizes. At weekends, the birds were fed fish offal *ad libitum*. Gulls were tested singly, in flocks of three, and in flocks of six. Such triplets of tests were run 10 times for each gull; the combination of birds in each flock was chosen by drawing random numbers. Each hunting session lasted for 3 min.

On each trial day, each bird was tested in the morning and in the afternoon. After a test we re-stocked the pool with fish to maintain the number in the school at 350; this size of school covered an area of ~0.5 m^2. Handling time per fish was less than 1 s, and a gull usually caught 10–30 fish during a 3-min test. One hidden observer per gull noted each attempted and each successful attack using a tape recorder, as well as any period lasting ≥ 3 s during which the gull did not hunt (time spent searching for fish, preening or fighting). During some tests, the events in the central 6 m^2 of the pool were recorded using a video camera mounted beneath the ceiling.

During the entire 3½-week test period, the hunting success per gull was higher in triplets than in singletons, and higher in groups of six than in triplets (Fig. 1*a*; unless specified, we used two-tailed randomization tests for statistical comparisons[7]). Success increased until the sixth series of tests. After this point, success was lower after each weekend (after series 6 and 9), probably because the gulls were satiated from eating *ad libitum*; they gained weight.

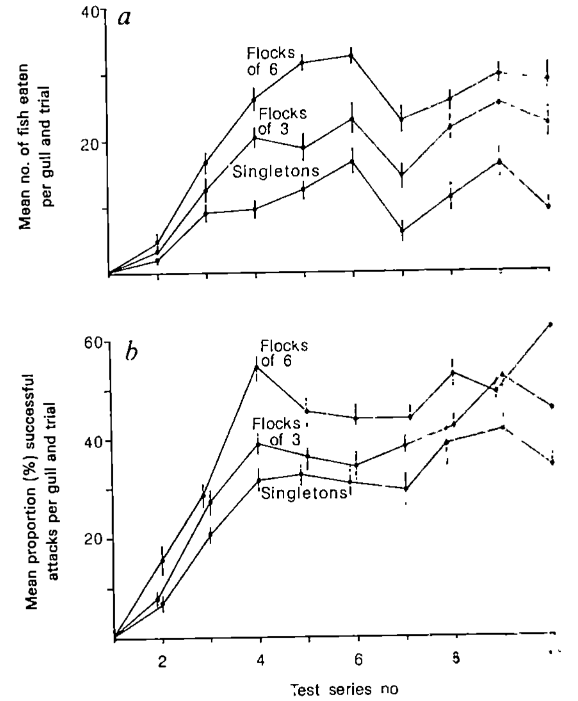

Fig. 1 *a*, The number of fish (mean ±s.e.m.) eaten per gull per 3-min trial in all test series was higher for flocks of 3 birds than for single gulls, and higher in flocks of 6 birds than in flocks of 3 birds. For test series 6–10, this trend was tested by calculating the linear regression of success in relation to flock size for every gull. The regression coefficient is positive for each of the 12 birds, with a mean of 3.18 ± 0.36 (significantly different from zero, $P = 0.0005$). The means are almost identical for adults and juveniles: 3.25 and 3.10, respectively. For each additional flock member, the hunting success per gull thus increases by an average of about three fish per 3-min hunting session. *b*, The proportions of successful attacks (mean ± s.e.m.) per gull per trial was also higher for flocks of 3 birds than for singletons, and higher in flocks of 6 birds than in flocks of 3 birds (with one exception). The trend in relation to flock size is statistically significant ($P = 0.001$; test as in *a*).

For test series 6–10, the catch per bird in flocks of six was 20–50% higher than in flocks of three birds and >100% higher than for singletons (Fig. 1*a*). The proportion of successful attacks per gull also increased with flock size (Fig. 1*b*): the averages were 34, 43 and 50% success in flocks of 1, 3 and 6 birds, respectively. Thus, on average, it was advantageous for the birds to fish in flocks.

To test directly whether the 'first finder' benefits from flock formation, we compared the success (number of fish caught) of each gull hunting as a singleton with its success as a flock member during the same test series. If every gull is better off as part of a flock than as a singleton, the first finder clearly benefits from being joined by other birds. We made this comparison for test series 6–10; the 12 gulls formed four flocks of three and two flocks of six per series. Of 20 possible comparisons for flocks of 3, each gull fared better as part of a flock than as a singleton in 14 cases; in 5 cases one gull fared worse in the flock, and in one case a gull had equal success as both a singleton and flock member. In all 10 comparisons for flocks of 6, the individual gulls fared better in the flock than as singletons. Although not amenable to statistical testing because of the dependence between the series, these results indicate that even the first finder benefits from flock formation.

During a 3-min trial, the birds hunted, on average, for 168, 172 and 175 s in flock sizes of 1, 3 and 6, respectively, which is

---

*Present address: Section of Ecology and Systematics, Cornell University, Ithaca, New York 14853-2701, USA.

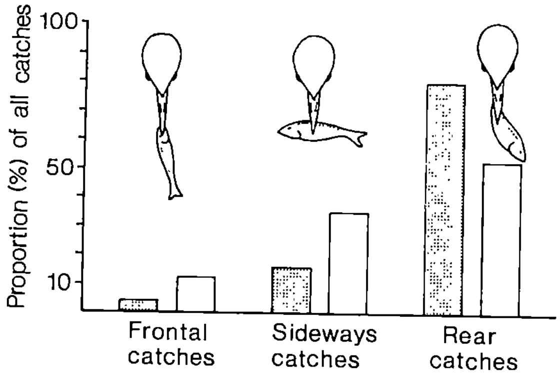

Fig. 2 Gulls in flocks (open bars) caught higher proportions of their prey from a frontal (12%) or sideways direction (35%) than did single gulls (4 and 16%; stippled bars), which captured most fish from behind ($P<0.001$, χ^2 test, d.f. = 2). For each catch visible on the video films, we measured the direction of the plunging gull in relation to the school or solitary fish just prior to the catch. Three classes of directions (each 120° wide) were scored: frontal, which means the gull met the fish within ±60° of its forward direction; sideways, within ±30° of the right angle to either side of the fish; and rear, within ±60° of the tail direction of the fish. The direction was determined for 75 catches by single gulls, and for 313 catches by members of flocks of 6.

indicative of a slightly decreased period of vigilance in the larger flocks. To allow for this possibility, we calculated hunting success per s of foraging time; again, hunting success increased with flock size ($P=0.0005$; test as in Fig. 1*a*).

Similar results were obtained in two previous test series with 6 and 8 gulls, hunting in flocks of up to 6 and 8 birds. Although these two series finally ran out of fish before hunting success reached a plateau, the success per gull increased with flock size ($P=0.06$ and 0.02, respectively). Because we monitored different individuals from those tested above, this result strengthens our conclusion and suggests that hunting success in this situation increases up to a flock size of at least eight.

The greater hunting success of gulls in flocks as determined here perhaps arose because they received more practice in flocks than alone (they were tested in flocks of two sizes, 3 and 6, for each run as a singleton). To examine this possibility, 3 weeks after the experiment we randomly split the 12 gulls into two groups of six. In 10 sessions, one group was then tested as a single flock of six; the other birds were tested individually. Again, hunting success was more than twice as high in the flock of 6 birds ($P=0.04$, one-tailed test based on the 12 individual means). The trend in success with flock size therefore is not an effect of unequal practice.

There are several possible reasons for the higher hunting success of birds in flocks[5,8]. The activity of other flock members might stimulate a bird to more intense efforts or guide it to prey sites[9]. If relevant, however, this is not the whole explanation: time spent resting, preening or searching for fish during the 3-min tests decreased ($P=0.03$) from flock size 1 to 6 by an average of only 7.5 s. This difference accounts for only a small part of the increase in the total catch.

Another, probably more important reason is altered vulnerability of the fish. The video films showed that the fish school was split into smaller and looser groups by a flock than by a single gull. We counted the number of fish in each of 30 rectangles (40×45 cm), monitored by the camera during tests with single gulls and flocks of six. Each count was done at 60 s from the start of a test, given that >75% of all fish were then visible; if not, samples were taken at 10-s intervals until this criterion was met. We then calculated the variance/mean ratio in number of fish per square. Random (Poisson) dispersion corresponds to a ratio of 1, clumping to a larger ratio. The average ratio with flocks of six was 14.1 (s.e. = 1.8; $n=9$), with single gulls 28.4 (s.e. = 2.2; $n=10$). Hence the fish became more dispersed when hunted by flocks ($P=0.0002$). This should increase the vulnerability of the fish if, as seems likely in small forms, schooling is an adaptation that reduces predation[10,11].

The gulls caught more fish from a head-on or sideways direction when hunting in flocks than when alone (Fig. 2). Some fish that were being hunted were driven from one gull towards others. It should be harder to catch a fleeing fish than one that is approaching, which must turn to escape, or one on a lateral course, which presents a larger target surface area. Consistent with this idea, a larger proportion of frontal (46%) and sideways (50%) attacks were successful compared with attacks from the rear (38%) ($n=736$, $P<0.01$, χ^2 test, d.f. = 2; data from flocks of six). No coordination was apparent among the gulls, however, nor did several together chase single fish separated from the school, as do some predatory fish[10,12].

The total catch per gull rose with flock size owing to both a higher rate and a higher success of attacks. With the rate of attacks held constant at singleton level, the increase predicted from higher success alone accounted for 30% (s.d. = 23%, range 6-76%, $n=12$) of the observed increase, while a higher attack rate (success instead held constant) accounted for 51% (s.d. = 22%, range 18-100%) of the increase.

Seabirds in the wild often encounter hunting conditions similar to those of the present experiment when schools of fish are driven to the surface by predatory fish or marine mammals[11,13,14]. As flock size becomes large, any benefits of flock fishing may be partly offset by reduced success, owing, for example, to rapid diving of the fish. However, schools can remain near the surface for several minutes, even if attacked by hundreds of birds[13]. The present trials, of 3 min duration, therefore seem realistic.

White plumage can make a bird easier to discern[15,16]. Larids are often the first to find fish schools, and conspicuous white gulls and terns attract more birds[9,11,13,17]. Our results suggest that not only the 'joiners' but also the first finder benefit from formation of a flock. Hence, conspicuous white or contrasting plumage in larids and other seabirds may provide a means, favoured by selection among individuals, of attracting other birds and hence improving hunting success. Whereas white underparts may also provide hunting camouflage[2,4,16,18], this probably is not the case for white upper parts; advantages of group foraging seem a more likely explanation.

The present results have a bearing on another aspect of foraging in seabirds. The 'information centre' hypothesis suggests that a main advantage of colony formation is that unsuccessful foragers can follow others to rich food sources[19,20]. Possible evidence in support of this hypothesis is that birds often leave colonies together, but they may do so also for other reasons[17,20-22]. If, as our results indicate, a gull that finds a fish school benefits from being joined by other birds, gulls should depart and forage together. Thus, seabirds following a 'leader' from a colony need not be heading for any particular site, but may go along simply because group foraging is beneficial. This could explain why flock leaders call more often than followers[22].

We thank many colleagues for help; Per-Åke Hägerroth and the NBL Lab, Studsvik, for catching bleak; John Krebs, Douglas Mock and Brian Partridge for valuable comments; and the Fulbright Commission, the Scandinavian-American Foundation (D.W.W.) and the Swedish Natural Sciences Research Council (M.A.) for support. On the occasion of his 60th birthday, we also thank Professor Anders Enemar for his encouragement of ornithological research.

Received 23 September; accepted 3 December 1985.

1. Darwin, C. *The Descent of Man, and Selection in Relation to Sex* (Murray, London, 1871).
2. Craik, K. J. W. *Nature* **153**, 288 (1944).
3. Tinbergen, N. *The Herring Gull's World* (Collins, London, 1953).
4. Simmons, K. E. L. *Br. Birds* **65**, 465-479, 510-521 (1972).
5. Krebs, J. R., MacRoberts, M. H. & Cullen, J. M. *Ibis* **114**, 507-530 (1972).
6. Alcock, J. *Animal Behaviour: An Evolutionary Approach* 3rd edn (Sinauer, Massachusetts, 1984).

7. Bradley, J. V. *Distribution-free Statistical Tests* (Prentice-Hall, Englewood Cliffs, 1968).
8. Scott, D. *Anim. Behav.* **32**, 1089-1100 (1984).
9. Gochfeld, M. & Burger, J. *Behavl Ecol. Sociobiol.* **10**, 15-17 (1982).
10. Partridge, B. *Scient. Am.* **246** (June), 90-99 (1982).
11. Grover, J. J. & Olla, B. L. *Auk* **100**, 979-982 (1983).
12. Major, P. F. *Anim. Behav.* **26**, 760-777 (1978).
13. Hoffman, W., Heinemann, D. & Wiens, J. A. *Auk* **98**, 437-456 (1981).
14. Evans, P. G. H. *Mammal Rev.* **12**, 187-206 (1982).
15. Kushlan, J. A. *Ibis* **119**, 361-364 (1977).
16. Mock, D. *Proc. 1st Welder Wildl. Found. Symp.*, 145-161 Welder Wildl. Found. (Sinton, Texas, 1980).
17. Andersson, M., Götmark, F. & Wiklund, C. G. *Behavl Ecol. Sociobiol.* **9**, 199-202 (1982).
18. Phillips, G. C. thesis, Univ. Oxford (1962).
19. Ward, P. & Zahavi, A. *Ibis* **115**, 517-534 (1973).
20. Krebs, J. R. *Behaviour* **51**, 99-134 (1974).
21. Bayer, R. D. *Auk* **99**, 31-40 (1982).
22. Evans, R. M. *Auk* **99**, 24-30 (1982).

Vernier acuity of neurones in cat visual cortex

N. V. Swindale & M. S. Cynader

Departments of Psychology and Physiology, Dalhousie University, Halifax, Nova Scotia, Canada B3H 4H7

The ability of human observers to detect Vernier breaks of as little as 5 s of arc has been termed hyperacuity[1] as this distance is substantially less than the angular separation of the bars of the highest spatial frequency of grating (~1 arc min) that can be detected. Although the visual cortex is a likely candidate for the location of detectors involved in this performance[2], it is not known whether there are cells sensitive enough to detect deviations from co-linearity that are small compared with their spatial resolution (defined in terms of the highest spatial frequency that the cell can detect). We report here the results of physiological experiments on single units in area 17 of the cat visual cortex in which we studied the effect of introducing a Vernier break into a bar stimulus moved across the receptive field of the cell at a constant velocity. Our results show that the responses of most simple and complex cells are significantly reduced by the introduction of a Vernier break that is substantially smaller than the spatial resolution of the cell. The most sensitive cells in our sample could discriminate Vernier offsets of 3–6 arc min with a reliability of ~70%. This was much smaller than their spatial resolution, which was in the range 25–30 arc min. We interpret these results in terms of mechanisms that could underly the orientation selectivity of cortical neurones and suggest how our results relate to human Vernier acuity.

We made recordings with extracellular platinum-iridium microelectrodes in area 17 of the cortex of 13 normal adult cats. Anaesthesia was induced with intravenous pentothal and subsequently maintained by respiration with 70% N_2O and 30% O_2. The animals were paralysed with Flaxedil, and the eyes were refracted using contact lenses with 3 mm artificial pupils onto a tangent screen 137 cm away. Two moving-bar stimuli, one from each of two computer-controlled optic benches, were projected onto the screen[3]. Each bar was typically between 1/10 and 1/4° wide and 1 and 2° long. The bars were oriented parallel with each other at the preferred orientation of the cell, and were normally placed end to end with no intervening gap. The total length of the bars was usually about the same as the length of the receptive field. In most experiments we moved the bars across the receptive field in the preferred direction of the cell and at a constant velocity close to the preferred velocity of the cell, normally between 0.5 and 3° s^{-1}. The stimuli were presented monocularly to the dominant eye. Vernier offsets of from −30 arc min to +30 arc min in 6-arc min steps were introduced, providing 11 different stimulus conditions; in a further 2 conditions each bar moved on its own through the receptive field. We normally tried to centre the stimulus in the receptive field so that each of the two bars moving on its own produced a similar response, although precise centering turned out to be unimportant. Responses were averaged over 8–16 presentations of each particular stimulus, given in random order. We often made other quantitative measurements, including a line-weighting function and orientation- and velocity-tuning curves. We measured spatial resolution either by listening to an audiomonitor or by examining computer-averaged responses from the cell as high-contrast grating stimuli of varied spatial frequency were moved across the receptive field. The bars of the gratings were the same length as that of the stimulus used to determine the Vernier acuity of the cell. All the cells in our sample had receptive fields that lay 3–15° from the area centralis. Of the 82 cells studied, 27 were classified as simple and 47 as complex; 8 could not be classified.

In most cells, the response, measured either in terms of peak firing rate or as total number of spikes per presentation, was reduced by the presence of a Vernier break (Figs 1, 2). Simple cells did not seem to differ from complex cells in this respect, and were among the most and the least sensitive cells in our sample. We found examples of cells with Vernier sensitivity in all laminae. Typically, responses were reduced by 20–50% of maximum for a Vernier offset of 30 arc min, although in the most sensitive cells the average response could be halved by a change in Vernier offset of 6 arc min.

We used an approach similar to that recently adopted by Parker and Hawken[4] to estimate the ability of a single neurone reliably to signal information about the presence of a Vernier offset. We compared the responses of a cell (measured in terms of the total number of impulses evoked) to presentations of a pair of stimuli differing in Vernier offset by a given amount. A correct response was scored if the responses of the cell differed in the expected direction, that is, if the response was greater for a smaller Vernier offset. An incorrect response was scored if the response was in the opposite direction. This comparison was carried out for all pairs of presentations in a series that took from 5 to 10 min to complete. As a means of describing the Vernier acuity of a cell this method has the advantage of taking into account the reliability of the response to a change in Vernier offset. This could be a better way to describe its performance than measuring the slope of the Vernier tuning curve averaged over many presentations.

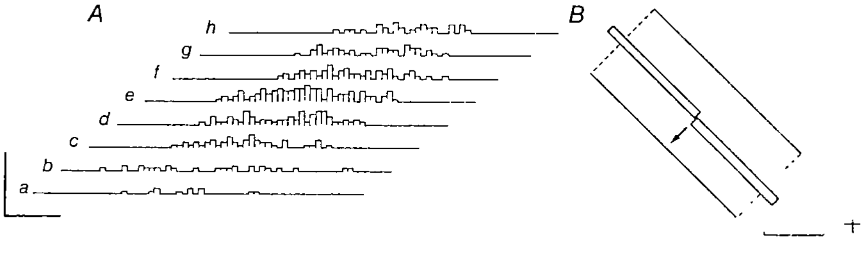

Fig. 1 *A*, *a–h*, Impulse frequency histograms from an experiment on a complex cell located in layer V of area 17; the cell had a receptive field ~3° from the area centralis. *B*, The stimulus configuration and the shape of the receptive field are drawn to scale relative to the location of the area centralis (cross). Arrow, direction of movement of the stimulus; bars are offset by ~6 arc min. Responses *a–h* are to Vernier offsets of −18, −12, −6, 0, 6, 12, 18 and 24 arc min, respectively. Each histogram shows the response to a single presentation of the stimulus. The presentations were in random order and made every 4 s. The velocity of the bars was 1° s^{-1}. Scale bars: *A*, 500 s^{-1} (vertical); 500 ms (horizontal). *B*, 1°.

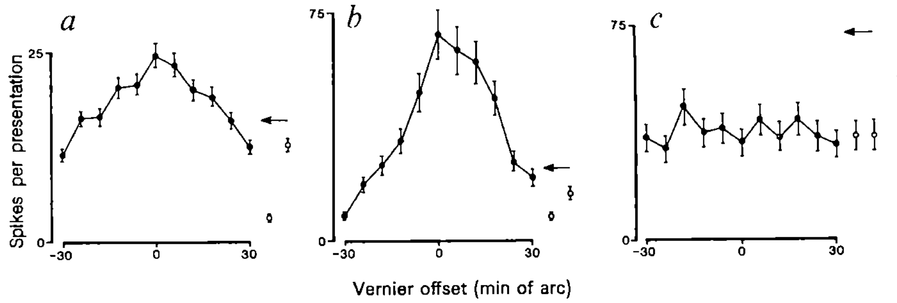

Fig. 2 Total number of impulses evoked plotted against Vernier offset for three different units. *a*, Simple; *b*, *c*, complex. The final two points in each graph (open circles) are the response to each bar presented separately. Arrow, linear sum of these responses. *a*, From a layer IV simple cell with an odd symmetrical receptive field 5° from the area centralis. The receptive field is 2° across, each bar is 0.2 × 1.1°, each response is the average of 16 presentations. *b*, From a complex cell located at the layer V/VI boundary; *c*, from a complex cell located in the upper layers of area 17 with a receptive field 10° from the area centralis. Each response is the average of eight presentations. Standard error bars are shown.

This method of analysis showed that many cells could discriminate 6–12 arc min of Vernier offset with >70% reliability. Some cells did better than this (Fig. 3); the most sensitive cell in our sample (Figs 1, 3) achieved 88% correct performance for a 6 arc min Vernier offset, implying a Vernier threshold of ~3 arc min for a 70% criterion of reliability. Figure 3 also shows one other such Vernier-discrimination curve from a cell that could detect 6 arc min of Vernier offset with 77% reliability. The spatial resolution of this cell was measured and found to be between 25 and 30 arc min. Its Vernier discrimination is thus an example of neuronal hyperacuity.

Inhibitory and, to a more variable extent, excitatory interactions between the component bars of the stimulus seem to be involved in producing these effects. In cells with good Vernier tuning, the response to the bars in the aligned condition was often greater than the sum of the responses to each bar alone (Fig. 2*a*, *b*). As Vernier offset was increased, the response decreased to a value less than this sum. The changeover from excitation to inhibition occurred typically for offsets of ~12–24 arc min. In other cells, including both simple and complex types, length summation was approximately linear, although the cells nevertheless showed good Vernier tuning. The reduction in the response caused by Vernier offset in these cells was presumably entirely caused by inhibition.

In a few cells (2 simple and 14 complex) the response was unaffected by the presence of a Vernier break. In these units, the response to the bars in the aligned condition was always similar to the response to each bar on its own (Fig. 2*c*). It was never possible to induce Vernier sensitivity in these cells by changing the stimulus properties, for example, bar length, separation, contrast or brightness of the stimulus. We recorded several cells showing some intermediate degree of Vernier sensitivity, so it could be that there are not two distinct classes of Vernier sensitivity, but rather a continuum.

We found evidence that the interaction producing the Vernier sensitivity has features in common with that responsible for the orientation selectivity of the cell. A Vernier stimulus can be approximated by a single bar of the same overall length, with an orientation the same as a line connecting the midpoints of the two component bars (Fig. 4*c*). Two observations suggest

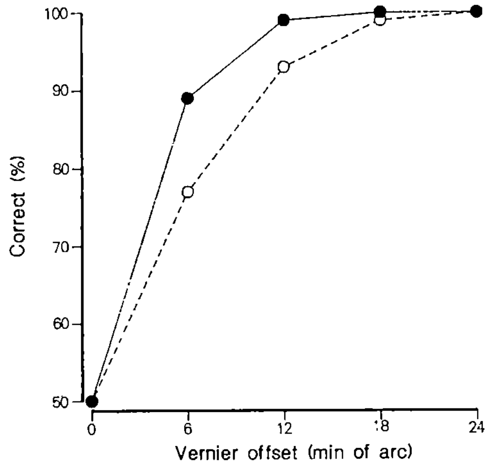

Fig. 3 Correct discriminations (%) plotted against Vernier offset for two of the most sensitive cells in our sample. A percenage discrimination of 70% for a Vernier offset of 6 arc min means that on 70% of presentations differing in Vernier offset by 6 arc min (for example, stimuli with offsets of 12 and 18 arc min), the response of the cell, measured in terms of the total number of impulses evoked, was greater for the smaller Vernier offset. Each point is based on many comparisons, for example, an experiment in which a set of nine Vernier offsets differing in 6-arc min steps were presented 16 times would yield $(9-1)\times 16^2 = 2{,}048$ comparisons for the 6 arc min point on the graph. Filled circles, results from the cell shown in Fig. 1; open circles, results from a complex cell in layer III.

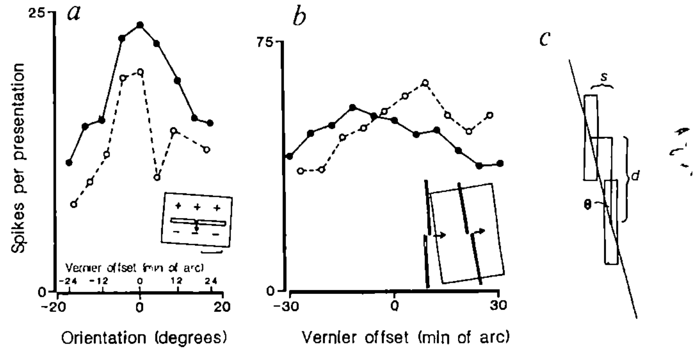

Fig. 4 *a*, Comparison between a Vernier tuning curve (filled circles) with Vernier offset re-expressed as equivalent orientation (defined in *c*), and an orientation-tuning curve (open circles) obtained for a bar of the same overall length as the Vernier stimulus. The sizes of the receptive field and the stimulus are shown. The difference in the height of the two curves is probably caused by a change in the responsiveness of the cell between experiments. Scale bar, 1°. *b*, Effect of changing the overall orientation of the Vernier stimulus on the tuning curve. Filled and open circles are for stimuli (drawn to scale relative to the receptive field size) whose overall orientation differed by 8°. The separation between the bar centres is 2.6°; the change in the orientation of the stimulus is 8° so the tuning curve should shift by 2.6° tan(8°) = 22 arc min, which is close to the shift actually observed. *c*, The definition of equivalent orientation used here; the equivalent orientation of two bars whose centres are separated by a distance *d*, and with a Vernier offset of *s*, is $\theta = \tan^{-1}(s/d)$.

that cells were treating both the Vernier stimulus and this approximation to it as equivalent. First, in several cells for which we made a quantitative measure of the orientation tuning curve (using a bar of the same overall length as the Vernier stimulus), re-expressing the Vernier tuning in terms of an equivalent orientation tuning gave a curve that was comparable in shape (Fig. 4*a*). This relationship was found to hold true for cells with both poor and good Vernier tuning. Second, changing the overall orientation of the Vernier stimulus shifted the position of the peak of the Vernier tuning curve (Fig. 4*b*). The size of this shift, re-expressed as an equivalent orientation, matched the change in the overall orientation of the stimulus.

Our results may be relevant to an understanding of Vernier acuity as measured in psychophysical experiments. Although other factors are probably involved, detection of orientation differences close to the Vernier break seems to be an important cue in Vernier tasks[5,6]. Thus, detection of Vernier offset, alignment of dots along a vertical axis, curvature or chevron distortions all have thresholds that, expressed in terms of the orientation cues available, are comparable with the ability to detect the deviation of a straight line from vertical[7,8]. This angle varies from ~1/3 to 1° (depending to some extent on the skill of the observer)[7]. Because the orientation-tuning curves of cortical cells (in monkeys) have a half-width at half-height of rather more than this (~5°), Westheimer[1] concluded that they cannot be involved in hyperacuity-type tasks. However it is arguable that the output from any kind of detector whose response is a smoothly varying function of the position or configuration of a retinal stimulus and is sufficiently noise-free, could, in principle, serve as a basis for hyperacuity-type discrimination. Thus, if two stimuli merely give rise to a statistically significant difference in the firing rate of a neurone they could, as a direct consequence, be discriminable in a behavioural task.

If this is true then a signal from a cortical cell with an orientation-tuning curve with a half-width at half-height of 5° might well subserve an orientation discrimination of $\leq 1°$. This performance could be improved on if the outputs from several cells with similar properties were averaged, although the number of cells over which an average of this sort could be taken is uncertain. Parker and Hawken[4] have recently studied the performance of neurones in monkey visual cortex and found cells with resolution and contrast sensitivity thresholds, and a predicted sensitivity to positional displacement in the hyperacuity range which is similar to that shown behaviourally by monkeys. This is evidence that the nervous system either does not average the outputs of several cortical neurones to improve its performance, or that an averaged response is degraded by noise elsewhere in the nervous system, perhaps at the level of some subsequent decision-making process. The ability of the nervous system to interpret fractional changes in the firing rates of neurones in this way, either above threshold (as we have suggested) or close to it (as Parker and Hawken[4] suggest) would eliminate the need for a fine-grain representation of positional information as hypothesized elsewhere[9,10].

Our present data show that some cells, recorded at a retinal eccentricity of 3-5°, were able to discriminate 3-6 arc min of Vernier offset with $\geq 70\%$ reliability. This was substantially less than their spatial resolution, which lay in the range 25-30 arc min. It is also less than the best resolution of retinal ganglion cells at this eccentricity, which is in the range of 15-25 arc min (ref. 11), and limits the maximum possible resolution of cortical neurones to which they provide inputs. One can extrapolate from these data to estimate the likely Vernier acuity of cells with receptive fields in the area centralis, where spatial resolution is about half that at the eccentricity from which our data came[11]. On the basis that Vernier acuity increases in proportion to resolution, some cells with receptive fields in the area centralis could be expected to have Vernier acuities as high as 1.5 arc min. This is better than the threshold of 5 arc min measured in behavioural experiments by Berkley and Sprague[2]; however, a different behavioural method shows a threshold of 1.2 arc min, which is similar to the postulated neural threshold (K. Murphy and D. E. Mitchell, personal communication). When compared with a behavioural grating resolution of ~7-8 arc min (ref. 12), the behavioural Vernier acuity of the cat is, like that of humans, well within the hyperacuity range. Berkley and Sprague's finding[2] (confirmed by Mitchell and Murphy) that lesions in area 17, but not in other visual areas, drastically reduce Vernier acuity, also supports the notion that the performance of cells with properties similar to those we have studied could be the limiting factor in the achievement of a high Vernier acuity in both cats and humans.

Received 7 October; accepted 27 November 1985.

1. Westheimer, G. *Prog. Sens. Physiol.* **1**, 1-30 (1981).
2. Berkley, M. A. & Sprague, J. M. *J. comp. Neurol.* **187**, 679-702 (1979).
3. Cynader, M. S., Mustari, M. & Gardner, J. C. *Expl Brain Res.* **53**, 384-399 (1984).
4. Parker, A. J. & Hawken, M. *J. opt. Soc. Am.* **2**, 1101-1114 (1985).
5. Watt, R. J., Morgan, M. J. & Ward, R. M. *Vision Res.* **23**, 991-995 (1983).
6. Andrews, D. P. *Vision Res.* **7**, 975-1013 (1967).
7. Sullivan, G. D., Oatley, K. & Sutherland, N. S. *Percept. Psychophys.* **12**, 433-444 (1972).
8. Andrews, D. P., Butcher, A. K. & Buckley, B. R. *Vision Res.* **13**, 599-620 (1973).
9. Barlow, H. B. *Nature* **279**, 189-190 (1979).
10. Crick, F. H. C., Marr, D. C. & Poggio, T. in *The Organisation of the Cerebral Cortex* (ed. Schmitt, F. O.) 505-533 (MIT Press, 1980).
11. Cleland, B. G., Harding, T. H. & Tulunay-Keesey, U. *Science* **205**, 1015-1017 (1979).
12. Mitchell, D. E., Murphy, K. & Kaye, M. *Invest. Opthal.* **25**, 908-917 (1984).

Reciprocal changes in corticotropin-releasing factor (CRF)-like immunoreactivity and CRF receptors in cerebral cortex of Alzheimer's disease

Errol B. De Souza*†, Peter J. Whitehouse†‡, Michael J. Kuhar*†, Donald L. Price†‡ & Wylie W. Vale§

* Neuroscience Branch, Addiction Research Center, National Institute on Drug Abuse, Baltimore, Maryland 21224, USA
† Department of Neuroscience and ‡ Neuropathology Laboratory, Department of Neurology, Johns Hopkins University School of Medicine, Baltimore, Maryland 21205, USA
§ Clayton Foundation Laboratories for Peptide Biology, Salk Institute, La Jolla, California 92037, USA

Alzheimer's disease is a progressive degenerative disease of the nervous system characterized neuropathologically by the presence of senile plaques and neurofibrillary tangles in amygdala, hippocampus and neocortex[1-4]. Dysfunction and death of basal forebrain cholinergic neurones projecting to forebrain targets[5,6] are associated with marked decreases in cholinergic markers, including the activity of choline acetyltransferase (ChAT)[2,3,7-9]. Although cortical levels of somatostatin[10-12] and somatostatin receptors[13] are reduced in Alzheimer's, no consistent changes have been reported in other neuropeptide systems[12,14-17]. We have now examined in control and Alzheimer's brain tissues pre- and postsynaptic markers of corticotropin-releasing factor (CRF), a hypothalamic peptide regulating pituitary–adrenocortical secretion[18,19] which also seems to act as a neurotransmitter in the central nervous system (CNS) (reviewed in refs 20, 21). We have found that in Alzheimer's, the concentrations of CRF-like immunoreactivity (CRF-IR) are reduced and that there are reciprocal increases in CRF receptor binding in affected cortical areas. These changes are significantly correlated with decrements in ChAT activity. Our results strongly support a neurotransmitter role for CRF in brain and demonstrate, for the first time, a modulation of CNS CRF receptors associated with altered CRF content. These observations further suggest a possible role for CRF in the pathophysiology of the dementia. Future therapies directed at increasing CRF levels in brain may prove useful for treatment.

Brains were obtained post mortem from 14 individuals with Alzheimer's disease and 11 neurologically normal controls (Table 1). One cerebral hemisphere was chosen at random for neurochemical study, the other was placed in formalin for quantitative neuropathological analysis. Standard areas of frontal pole, temporal pole, occipital pole and cingulate cortex (directly above the genu of the corpus callosum) were subdissected from the fresh brain, frozen in dry ice and stored (−70 °C) until they were processed for CRF radioimmunoassay[22], CRF receptor binding studies and ChAT assays[23]. Formalin-fixed samples of the cortex and hippocampus were embedded in paraffin, cut (10 μm) and stained with haematoxylin/eosin and silver impregnation methods. All Alzheimer's cases showed abundant neuritic plaques (>15 plaques per low-power field) and neurofibrillary tangles; the control cases showed no evidence of pathology in the brain.

Table 1 Age, sex distribution, postmortem delay and drug treatment data of controls and individuals with Alzheimer's disease

	Controls	Alzheimer's patients
Sex	7 male; 4 female	8 male; 6 female
Age (yr)	64.4±6.4 (39–96)	71.6±2.1 (57–84)
Postmortem delay (h)	10.5±2.2 (0.5–18)	8.0±1.3 (1–16)
Drug treatment		
	No. of patients	
No medication	11	6
Neuroleptics	0	3
Antidepressants	0	1
Neuroleptic/antidepressant	0	1
Anti-anxiety agents	0	1
Neuroleptic/anti-anxiety agents	0	2

Values for age and postmortem delay are mean ± s.e.m. with the range of values in parentheses. No significant differences were found between control and Alzheimer's groups.

Previous studies have defined the characteristics and distribution of CRF receptors in rat[24] and human[25] pituitary glands and in rat brain[26,27]. Here we have used a stable ^{125}I-labelled tyrosine extended analogue of rat/human CRF, ^{125}I-Tyr^0-rat/human CRF (NEN), to study the characteristics of the CRF binding site in human cerebral cortex. The binding was saturable and of high affinity, with an apparent dissociation constant (K_D) of 5.5±0.4 nM and maximum binding (B_{max}) of 170±6 fmol per mg protein (mean ±s.e.m.; $n = 3$). In competition studies, ovine CRF was equipotent with rat/human CRF in inhibiting ^{125}I-Tyr^0-rat/human CRF binding, with an inhibitor affinity constant (K_i) of 2.4±0.2 nM. The weak receptor antagonist α-helical CRF(9–41) was less potent (K_i 59.4 nM), and the rat/human CRF fragment, CRF(21–41), which is a very weak stimulator of proopiomelanocortin-derived peptide secretion, displaced only 20% of the specific binding at 1 μM concentration. At comparable 1 μM concentrations, the rat/human CRF-related fragments CRF(1–20)OH and CRF(6–33) and the unrelated peptides arginine vasopressin and angiotensin II did not inhibit ^{125}I-Tyr^0-rat/human CRF binding. The kinetics and pharmacological properties of ^{125}I-Tyr^0-rat/human CRF binding sites in human cerebral cortex are comparable to those for the biologically relevant CRF receptor in rat[24,28] and human[25] pituitary and rat brain[26,27,29].

In individuals with Alzheimer's, the concentration of CRF-IR (Fig. 1*a*) were decreased and CRF receptors (Fig. 1*b*) were reciprocally increased in the temporal, frontal and occipital cortex. The changes in CRF activity were greatest in the occipital cortex, with an 80% decrease in the content and a doubling in receptor binding; the reductions in CRF-IR and increases in
CRF receptors in the temporal and frontal cortex were all grea
than 50% of the corresponding control value. Neither CRF-
nor CRF receptors were changed significantly in the cingul
cortex. Scatchard analysis data of detailed competition cur
carried out in random samples of temporal, frontal and occipi
cortex from both control and Alzheimer's disease patients in
cate that the increase in ^{125}I-Tyr^0-rat/human CRF recep
binding reflects an up-regulation in the receptor number (B_{m}
as the affinity of the ligand for the receptor (K_D) was compara
in control and Alzheimer's groups in all the cortical ar
examined. A highly significant negative correlation ($r = -0.$
$P < 0.005$) existed between the change in CRF receptors a
CRF-IR in each cortical area.

To examine possible interactions between cholinergic defic
in Alzheimer's disease and alterations in CRF markers, Ch
activity was correlated with CRF-IR and with CRF recept
in each cortical area. Significant positive relationships exist
between ChAT activity and CRF-IR levels in the frontal (
+0.68; $P < 0.05$), temporal ($r = +0.79$; $P < 0.05$) and occipi
($r = +0.74$; $P < 0.01$) cortex, and significant negative corre
tions were detected between ChAT activity and CRF recept
in that temporal ($r = -0.61$; $P < 0.05$) and occipital ($r = -0.$
$P < 0.01$) cortex. In contrast, in both the control and AD grou
neither the age nor sex of the patient nor the postmortem inter
correlated significantly with CRF-IR, CRF receptors or Ch
activity in any of the cortical regions examined. In addition,
effect of any psychoactive drug medication was noted on C
receptors in Alzheimer's patients whereas a statistically n
significant trend towards a small increase in CRF-IR was not
in those patients treated with neuroleptics.

In rodents, CRF neurones are intrinsic to the neocortex, w
perikarya located in laminae II and III and terminal fie
concentrated in laminae I and IV (refs 30, 31), areas rich
CRF receptors[26,27]. CRF neurones probably have a similar dist
bution in the human cortex. Our finding of a decrease in CRF-
in the frontal and temporal cortex in Alzheimer's disease
similar to that observed previously[32]. The reduction in CRF-
in the cerebral cortex in Alzheimer's patients could result fr
a selective degeneration of the intrinsic cortical CRF neuron
and/or disease of CRF neurones projecting to the cortex fr
other brain areas. For example, a subpopulation of brain st
cholinergic neurones containing CRF project to various fo
brain targets including the cortex[33], and pathology of this syst
or other CRF-cholinergic neurones innervating forebrain targ
could reduce ChAT and CRF-IR. Decreased CRF content
these systems could result from cell dysfunction, that
decreased synthesis, altered processing, increased degradatio
increased release and/or cell death. Increased CRF relea
appears unlikely, as it might be expected to down-regulate t
CRF receptors rather than produce the observed up-regulatio
At present, we cannot identify the specific mechanisms leadi
to reduced CRF levels. Alterations in CRF receptors in t
cortex in Alzheimer's disease contrast with previous observ
tions of changes in the cholinergic and somatostatin systems
which reductions in presynaptic cholinergic markers[2,3,5–9] a
somatostatin content[10–12] are accompanied by inconsiste
changes in cholinergic receptors[34–36] and decreased somat
statin[13] receptors. The up-regulation of cortical CRF recepto
in Alzheimer's disease under conditions in which t
endogenous peptide is reduced is, to date, a unique finding
the study of neuropeptides in disease, and suggests that t
CRF-receptive cells may be preserved in the cortex
Alzheimer's disease. We are now investigating the immunohi
tochemical localization of CRF and the autoradiographic dist
bution of CRF receptors in normal human cortex, and t
relationship of CRF neurones to the classical features
Alzheimer's disease.

The cerebral cortical cholinergic deficiency seems to be t
most severe and consistent neurochemical deficit[3,6,7,37,38]. T
demonstration of significant correlations between changes

CRF and ChAT activity in human cortex, complemented by similar preliminary studies in rodents[33,39], suggest that the CRF and cholinergic systems interact. As mentioned above, some brain stem cholinergic neurones projecting to the frontal cortex also contain CRF[33]. In behavioural studies, CRF injected into the rat frontal cortex does not initiate, but significantly inhibits the effects of carbachol, a muscarinic cholinergic receptor agonist, on 'boxing' behaviour[39], suggesting that CRF may exert a neuromodulatory function on cholinergic systems. CRF appears to interact with somatostatin, another neuropeptide affected by Alzheimer's disease[10-12], in that it stimulates the somatostatin secretion from dispersed rat cerebral cortical cells[40]. Additional studies are necessary to define the functional importance of these cholinergic–peptidergic and peptidergic–peptidergic interactions in the pathophysiology of the disease.

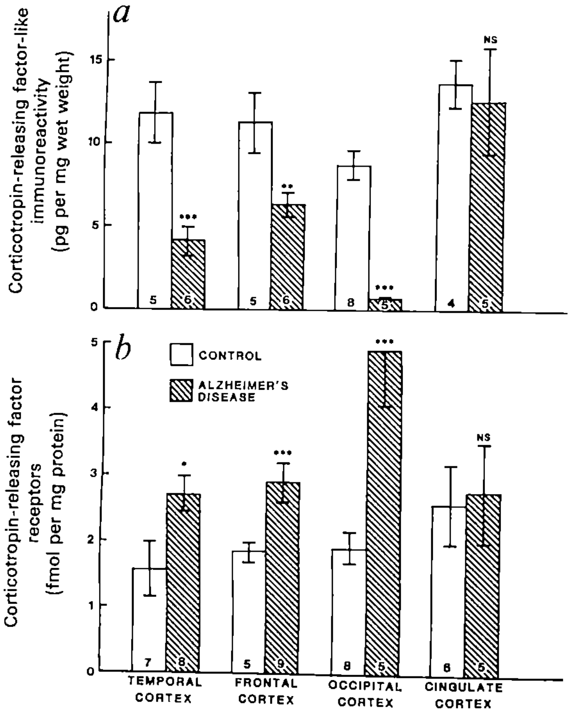

Fig. 1 CRF-like immunoreactivity (*a*) and CRF receptor binding (*b*) in discrete regions of the cerebral cortex of Alzheimer's patients and controls. All values are means ±s.e.m. The number of subjects in each group is given at the bottom of each histogram. Data were analysed for differences using a Student's *t*-test. Significant differences from control group at $P < 0.05$, $P < 0.025$ and $P < 0.005$ are denoted by *, ** and ***, respectively. NS, not significant. **Methods:** *a*, Autopsy samples were weighed, extracted in hot 1 M acetic acid/0.1 M HCl, centrifuged and then the supernatants defatted three times with 4 vols ether:petroleum ether, 1:2. The aqueous phases were applied to a BondElut C_{18} cartridge and the CRF eluted and lyophilized as described previously[22]. Reconstituted samples were assayed using HPLC-purified ^{125}I-labelled rat/human CRF analogue substituted with norleucine at amino acid residues 21 and 38, ^{125}I (Nle^{21,38})-rat/human CRF tracer, rabbit anti-rat/human CRF serum rC-68[22] and rat/human CRF as a standard. Results are expressed as pg CRF-like immunoreactivity per mg wet weight. *b*, For receptor binding studies in membrane homogenates, regions of cerebral cortex were weighed and homogenized using a Teflon pestle in 10 vol ice-cold 50 mM Tris-HCl, 10 mM $MgCl_2$, 2 mM EGTA and 0.32 M sucrose, *p*H 7.2. The homogenate was centrifuged at 4 °C for 10 min at 1,000*g*. The resulting supernatant was recentrifuged at 4 °C for 30 min at 20,000*g* and the pellet was resuspended in 50 mM Tris-HCl, 10 mM $MgCl_2$, 2 mM EGTA, 0.1% bovine serum albumin, aprotinin (100 kIU ml^{-1}) and 0.1 mM bacitracin, *p*H 7.2, at a final protein concentration of 0.3–0.6 mg ml^{-1}. The binding of ^{125}I-Tyr^0-rat/human CRF (NEN; 2,200 Ci mmol^{-1}) to CRF receptors was carried out in 1.5-ml polypropylene micro-tubes in a final volume of 300 µl with 30–60 µg protein and 40,000 c.p.m. ^{125}I-Tyr^0-rat/human CRF. Nonspecific binding was determined in the presence of 10^{-6} M rat/human CRF (Peninsula). The reaction was allowed to proceed for 2 h at room temperature. The tissue was separated from the solution by centrifugation in a Beckman Microfuge for 3 min at 12,000*g*. The resulting pellet was washed gently with 1 ml of phosphate-buffered saline, *p*H 7.4, containing 0.01% Triton-X, and the contents were recentrifuged for 3 min at 12,000*g*. The supernatant was aspirated and the radioactivity measured in a γ-counter at 80% efficiency.

Thus, CRF-IR is significantly reduced in the cortex of individuals with Alzheimer's disease and there are reciprocal increases in CRF receptor binding. The demonstration of an up-regulation of CRF receptors following a decrease in CRF-IR indicates a physiological relevance of the receptor site and is consistent with the concept that CRF acts as a neurotransmitter in normal cortical functions and that disease of this peptidergic system may be important in certain clinical manifestations of the disease.

We thank Jean Rivier (Salk Institute) for providing us with human CRF fragments, Martin Ewer and Russel Garlick (NEN) for their generous supply of ^{125}I-Tyr^0-human CRF, Shari Powell for the clinical information used in the study, Pierro Antuono and Joseph Coyle for determining the ChAT activity, Carolyn Douglas, Kendall Marcus, Theresa Kopajtic and Roberta Proctor for technical assistance and Susan Krout and Mary Flutka for preparation of the manuscript. This study was supported by PHS grants MH 25951, AG 03359, AG 05146, NS 15080 and NS 15721, grants from the McKnight, Sloan and Commonwealth Foundations and the Claster Family Fund. Research at the Clayton Foundation Laboratories for Peptide Biology was supported in part by PHS grants AM 26741 and HD 13527. Research was conducted in part by the Clayton Foundation for Research, California Division, W.W.V. is a Senior Clayton Foundation investigator.

Received 23 August; accepted 27 November 1985.

1. Terry, R. D. & Davies, P. *A. Rev. Neurosci.* **3**, 77–95 (1980).
2. Price, D. L., Whitehouse, P. J. & Struble, R. G. *A. Rev. Med.* **36**, 349–356 (1985).
3. Bowen, D. M., Smith, C. B., White, P. & Davison, A. N. *Brain* **99**, 459–496 (1976).
4. Terry, R. D. & Katzman, R. *Ann. Neurol.* **14**, 497–506 (1983).
5. Whitehouse, P. J. *et al. Science* **215**, 1237–1239 (1982).
6. Cuello, A. C. & Sofroniew, M. V. *Trends Neurosci.* **7**, 74–78 (1984).
7. Davies, P. & Maloney, A. J. R. *Lancet* **ii**, 1403 (1976).
8. Perry, E. K., Perry, R. H., Blessed, G. & Tomlinson, B. E. *Lancet* **i**, 89 (1977)
9. Rossor, M. N., Iversen, L. L., Reynolds, G. P., Mountjoy, C. Q. & Roth, M. *Br. med. J.* **288**, 961 (1984).
10. Davies, P., Katzman, R. & Terry, R. D. *Nature* **288**, 279–280 (1980)
11. Rossor, M., Emson, P. C., Mountjoy, C. G., Roth, S. M. & Iversen, L. L. *Neurosci. Le* **20**, 373–377 (1980).
12. Ferrier, I. N. *et al. J. neurol. Sci.* **62**, 159–170 (1983).
13. Beal, M. F. *et al. Science* **229**, 289–291 (1985).
14. Rossor, M. N. *et al. Life Sci.* **29**, 405–410 (1981).
15. Rossor, M. N. *et al. Brain Res.* **201**, 249–253 (1980).
16. Yates, C. M. *et al. Brain Res.* **258**, 45–52 (1983).
17. Biggins, J. A. *et al. J. neurol. Sci.* **58**, 117–122 (1983).
18. Vale, W., Spiess, J., Rivier, C. & Rivier, J. *Science* **213**, 1394–1397 (1981).
19. Rivier, C., Rivier, J. & Vale, W. W. *Science* **218**, 377–379 (1982).
20. Vale, W. *et al. Recent Prog. Horm. Res.* **39**, 245–270 (1983).
21. De Souza, E. B. *Compreh. Ther.* **11**, 3–5 (1985).
22. Vale, W. *et al. Meth. Enzym.* **103**, 565–577 (1983).
23. Bull. G. & Oderfeld-Nowak, B. *J. Neurochem.* **18**, 935–94 (1971).
24. De Souza, E. B., Perrin, M. H., Rivier, J. E., Vale, W. W. & Kuhar, M. J. *Brain Res* **296**, 202–207 (1984).
25. De Souza, E. B. *et al. Neuroendocrinology* **40**, 419–422 (1985).
26. De Souza, E. B. *et al. Science* **224**, 1449–1451 (1984).
27. De Souza, E. B. *et al. J. Neurosci.* **5**, 3189–3202 (1985).
28. Wynn, P. C., Aguilera, G., Morell, J. & Catt, K. J. *Biochem. biophys. Res. Commun* **110**, 602–608 (1983).
29. Wynn, P. C. *et al. Peptides* **5**, 1077–1084 (1984).
30. Olschowka, J. A., O'Donohue, T. L., Mueller, G. P. & Jacobowitz, D. M. *Peptides* **3**, 995–1015 (1982).
31. Swanson, L. W., Sawchenko, P. E., Rivier, J. & Vale, W. W. *Neuroendocrinology* **36**, 165–186 (1983).
32. Bissette, G., Reynolds, G. P., Kilts, C. D., Widerlov, E. & Nemeroff, C. B. *J. Am. med. Ass.* **254**, 3067–3069 (1985).
33. Jacobowitz, D. M., Skofitsch, G., Sills, M. A. & Crawley, J. N. *Neural and Endocrine Peptides and Receptors '85*, abstr., 39 (1985).
34. Whitehouse, P. J. & Au, K. S. *Prog. Neuropsychopharmacol. Biol. Psychiat.* (in the press)
35. Lang, W. & Henke, H. *Brain Res.* **267**, 271–280 (1983).
36. Mash, D. C., Flynn, D. D. & Potter, L. T. *Science* **228**, 1115–1117 (1985).
37. Bird, T. D., Stranahan, S., Sumi, S. M. & Raskind, M. *Ann. Neurol.* **14**, 284–293 (1983
38. Sims, N. R. *et al. J. Neurochem.* **40**, 503–509 (1983).
39. Crawley, J. N., Olschowska, J. A., Diz, D. & Jacobowitz, D. *Peptides* **6**, 891–901 (1985)
40. Peterfreund, R. A. & Vale, W. W. *Endocrinology* **112**, 1275–1278 (1983).

Na–Ca exchange current in mammalian heart cells

Junko Kimura, Akinori Noma & Hiroshi Irisawa

National Institute for Physiological Sciences, Myodaiji,
Okazaki 444, Japan

Electrogenic Na–Ca exchange has been known to act in the cardiac sarcolemma as a major mechanism for extruding Ca ions[1–3]. Ionic flux measurements in cardiac vesicles have recently suggested that the exchange ratio is probably 3 Na:1 Ca (refs 4, 5), although a membrane current generated by such a process has not been isolated. Using the intracellular perfusion technique[6,7] combined with the whole-cell voltage clamp[8], we were able to load Na^+ inside and Ca^{2+} outside the single ventricular cells of the guinea pig and have succeeded in recording an outward Na–Ca exchange current while blocking most other membrane currents. The current is voltage-dependent, blocked by La^{3+} and does not develop in the absence of intracellular free Ca^{2+}. This report presents the first direct measurement of the cardiac Na–Ca exchange current, and should facilitate the study of Ca^{2+} fluxes during cardiac activity, together with various electrical changes attributable to the Na–Ca exchange[9] and the testing of proposed models[10–12].

Single ventricular cells were dissociated from guinea pig hearts using collagenase. A whole-cell voltage-clamp experiment was performed using a wide-tipped (4–5 μm) glass pipette (resistance 1–2 MΩ) which facilitated the diffusion of the pipette solution into the cell. The compositions of the bath and the pipette solutions were designed to block most of the channel currents and the electrogenic Na–K pump, so that time-dependent current components largely disappeared and the current-voltage (*I–V*) relations obtained using ramp pulses became almost linear (Fig. 1*B*). The cell was initially perfused with 0 Na^+ internal solution and Ca^{2+}-free external solution, and in these conditions, superfusing Ca^{2+} (1 mM) slightly shifted the membrane current outward (Fig. 1*A*). The *I–V* curves measured before (Fig. 1*Ba*) and during (*b*) Ca^+ application illustrate that external Ca^{2+} (Ca_o^{2+}) in the absence of internal $Na^+(Na_i^+)$ did not induce a significant current change. After washing off Ca_o^{2+}, the pipette solution was changed into one containing 30 mM Na^+, which had very little effect on the membrane conductance (Fig. 1*Cc*, *d*). Subsequent superfusion of 1 mM Ca^{2+} in the presence of Na_i^+ induced a marked outward shift of the holding current. Washing off Ca_o^{2+} quickly turned off the current. The *I–V* relation taken at the peak effect (Fig. 1*Ce*) revealed a significant voltage dependence of the outward current; thus, the current was larger at more positive potentials and was almost exponential in the range between −120 and +60 mV. In the presence of 0.1 mM La_o^{3+}, which is known to block Na–Ca exchange, 1 mM Ca_o^{2+} did not activate the current (Fig. 1*A*). The magnitude of the current became larger when a higher concentration of Ca_o^{2+} was perfused and it became smaller when a lower concentration of Na^+ was in the pipette, indicating that the current depends on both Na^+ and Ca^{2+} concentrations. These results suggest that the current is generated by the exchange of internal Na^+ for external Ca^{2+}.

The Na–Ca exchange current is driven by the concentration gradients of both Na^+ and Ca^{2+} across the membrane. If the exchange ratio is 3 Na : 1 Ca, as has been suggested by others[4,5], the reversal potential of the Na–Ca exchange current (E_{NaCa}) should be given by the following thermodynamic equation[3]:

$$E_{NaCa} = 3E_{Na} - 2E_{Ca}$$

where E_{Na} and E_{Ca} are the respective reversal potentials for Na^+ and Ca^{2+}. If the ionic conditions are 140 mM Na_o^+, 30 mM Na_i^+, 1 mM Ca_o^{2+} and 73 nM Ca_i^{2+}, E_{NaCa} will be −131 mV. This value is strikingly close to the potential at which the *I–V* curves before (*d*) and in the presence of 1 mM Ca_o^{2+} (*e*) are about to meet in Fig. 1*C*. No straightforward contribution of ionic currents could give this reversal potential.

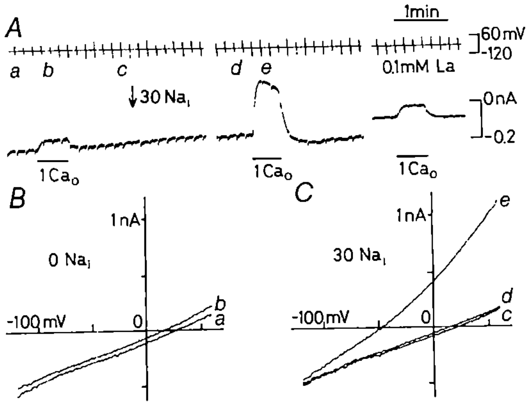

Fig. 1 *A*, Voltage-clamp records from a single myocyte showing voltage (upper trace) and current (lower trace). A ramp pulse to +60 mV and then to −120 mV was given from the holding potential of −30 mV every 10 s at a ramp speed of about 0.2 V s^{-1}. The *I–V* curves were obtained from the descending portion of this pulse from +60 mV to −120 mV. To exchange the pipette solution, a piece of tapered polyethylene tube was inserted in the pipette, through which a new solution was introduced within 1 min by applying a negative pressure inside the pipette. The arrow indicates when the solution exchange was started. The holding current shifted slightly outward on loading Na^+. The middle record shows 1 mM Ca^{2+} superfusion in the presence of Na_i^+. The Ca_o^{2+}-induced outward current appears to decay after reaching a peak. Current undershoot is seen on washing off Ca^{2+}. These phenomena may be due to Ca^{2+} accumulation immediately below the membrane or to acid induced by binding of Ca^{2+} to EGTA. The Ca^{2+}-activated current did not show a significant time dependence. The last chart record starts at 3 min after applying 0.1 mM $LaCl_3$ in the external solution. La^{3+} shifted the holding current outward and reduced the slope conductance of the background current. The *I–V* relation (not shown) taken during Ca^{2+} superfusion revealed about 90% inhibition of the Ca^{2+}-induced current by La^{3+}. The interruptions between the panels were 7 min on the left and 5 min on the right. Points *a–e* are described in parts *B* and *C*. *B*, *I–V* relations measured before (*a*) and during (*b*) 1 mM Ca^{2+} superfusion in the absence of Na_i^+. *C*, *I–V* curves before (*c*) and after (*d*) loading Na_i^+ and during subsequent 1 mM Ca_o^{2+} application (*e*). The membrane capacitance of this cell was 180 pF. A specific membrane capacitance was assumed to be 1 μF cm^{-2} to estimate the membrane area.

Methods. The external solution (34–35 °C) was Ca^{2+}-free, K^+-free Tyrode's solution containing (in mM) NaCl 140, $MgCl_2$ 2, HEPES 5 (*p*H 7.4) and the following current blockers: 1 mM $BaCl_2$ and 2 mM CsCl to block K channels, 2 μM D600 for Ca channels and 20 μM ouabain to block the Na–K pump. The control pipette solution contained 126 mM Cs^+ to replace internal K^+, 42 mM aspartic acid, 42 mM EGTA and the free Ca^{2+} was adjusted to *p*Ca 7.1 (73 nM) by adding 21 mM $CaCl_2$. The stability constant of EGTA of 1.55×10^7 (*p*H 7.4) was used[15]. The high concentration of EGTA was to prevent the cell from contracture by Ca^{2+} influx. To make a Na^+-containing pipette solution, Na^+ was replaced by equimolar Cs^+. It also contained (in mM) Mg-ATP 10, $MgCl_2$ 3, creatine phosphate 5, tetraethylammonium (TEA) 20 to block the K channel and 5 HEPES-CsOH buffer (*p*H 7.4).

Before concluding that this current is the Na–Ca exchange current, we investigated whether the current possessed a unique property found in squid axon, that is, whether the Na–Ca exchanger requires Ca_i^{2+} for its activation. This feature was described by Baker and McNaughton[13], who injected EGTA into squid axon and observed the inhibition of Ca_o^{2+}-dependent Na^+ efflux. More recently, Allen and Baker[14] confirmed this result by injecting Quin-2, another Ca chelator, into squid axon. Figure 2 illustrates that superfusion of the ventricular cell with 1 mM Ca_o^{2+} in the absence of Ca_i^{2+} (42 mM EGTA pipette solution) failed to induce an outward current even in the presence of 30 mM Na^+ in the pipette. When the internal solution

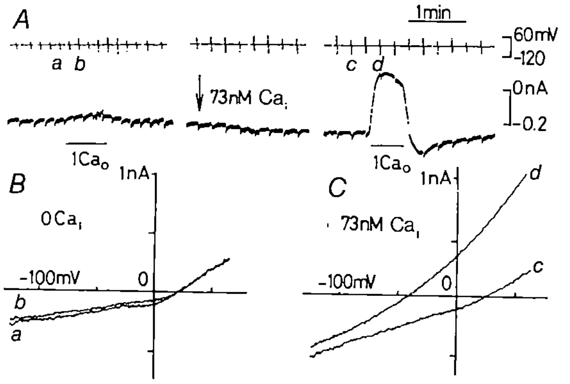

Fig. 2 *A*, Chart record of voltage (upper trace) and current (lower trace). Ramp pulses of the same shape as described in Fig. 1 were given from −30 mV every 10 or 15 s. The left panel shows the application of 1 mM Ca_o^{2+} in the absence of Ca_i^{2+}. After a 1-min interruption in the middle panel, the pipette solution was changed into one containing 73 nM Ca^{2+} (at arrow). In the right panel, after a 5-min interruption, 1 mM Ca^{2+} superfusion induced a large outward current. *B*, *I–V* curves before (*a*) and during (*b*) superfusion of 1 mM Ca^{2+} in the absence of Ca_i^{2+}. The Ca current is not completely blocked and the remaining component can be seen as a slight inward deflection at around 0 mV. *C*, *I–V* relation in the presence of 73 nM Ca^{2+} in the pipette before (*c*) and during (*d*) 1 mM Ca^{2+} superfusion. The capacitance of this cell was 246 pF.

was changed to one containing 73 nM Ca^{2+} (42 mM EGTA and 21 mM $CaCl_2$), the membrane conductance increased slightly. The subsequent superfusion of 1 mM Ca^{2+} then induced a large outward current. Reapplying Ca_o^{2+} after returning to the Ca^{2+}-free pipette solution did not induce the current. This result not only confirms that the current is generated by the Na–Ca exchange but also indicates that the requirement for Ca_i^{2+} is a general property of the Na–Ca exchanger.

The amount of Ca^{2+} influx calculated from the current at 0 mV (Figs 1*C*, 2*C*) is ~28 pM cm^{-2} s^{-1}, a larger value than that reported for squid axon[3] (0.5 pM cm^{-2} s^{-1} at 100 mV driving force) in different ionic conditions. The slope conductance of this current is ~23 μS cm^{-2} in the above ionic environment. In physiological conditions, the steady-state membrane conductance is about 1,300 μS cm^{-2} at the resting potential and about 20 μS cm^{-2} at plateau potentials[7]. The Na–Ca exchange current may therefore influence the plateau of the action potential more significantly than it does the resting potential. There is a strong possibility that the Na–Ca exchange current is involved in the arrhythmogenic potential oscillation that appears when the heart cells are overloaded with Ca^{2+}. More information about intracellular Na^+ and Ca^{2+} concentration dynamics is required to discover exactly how this current behaves during cardiac activity.

We thank Professor D. Noble for critically reading the manuscript and Dr H. Brown for correcting the English. This work was supported by grants from the Ministry of Education, Science and Culture and the Ministry of Health and Welfare of Japan. T.K. is a fellow of the Japan Society for the Promotion of Science.

Received 20 May; accepted 29 November 1985.

1. Reuter, H. & Seitz, N. *J. Physiol., Lond.* **195**, 451–470 (1968).
2. Glitsch, H. G., Reuter, H. & Scholz, H. *J. Physiol., Lond.* **209**, 25–43 (1970).
3. Mullins, L. J. *Ion Transport in Heart* (Raven, New York, 1981).
4. Pitts, B. J. *J. biol. Chem.* **254**, 6232–6235 (1979).
5. Reeves, J. P. & Hale, C. C. *J. biol. Chem.* **259**, 7733–7739 (1984).
6. Soejima, M. & Noma, A. *Pflügers Arch. ges. Physiol.* **400**, 424–431 (1984).
7. Matsuda, H. & Noma, A. *J. Physiol., Lond.* **357**, 553–573 (1984).
8. Hamill, O. P., Marty, A., Neher, E., Sakmann, B. & Sigworth, J. *Pflügers Arch. ges. Physiol.* **391**, 85–100 (1981).
9. Eisner, D. A. & Lederer, W. J. *Am. J. Physiol.* **248**, C189–C202 (1985).
0. Mullins, L. J. *J. gen. Physiol.* **70**, 681–695 (1977).
1. DiFrancesco, D. & Noble, D. *Phil. Trans. R. Soc.* **B307**, 353–398 (1985).
2. Johnson, E. A. & Kootsey, J. M. *J. Membrane Biol.* **86**, 167–187 (1985).
3. Baker, P. F. & McNaughton, P. A. *J. Physiol., Lond.* **259**, 103–144 (1976).
4. Allen, T. J. A. & Baker, P. F. *Nature* **315**, 755–756 (1985).
5. Fabiato, A. & Fabiato, F. *J. Physiol., Paris* **25**, 463–505 (1979).

Identification of Na–Ca exchange current in single cardiac myocytes

S. Mechmann & L. Pott*

Institut für Zellphysiologie, Ruhr-Universität Bochum,
Postfach 102148, D-4630 Bochum, FRG

In cardiac muscle the exchange of intracellular Ca^{2+} for extracellular Na^+ is an important transport mechanism for regulation of the intracellular free Ca^{2+} concentration ($[Ca]_i$) and hence the contractile strength of the heart (ref. 1; for reviews see refs 2–4). Due to its stoichiometry of ⩾3:1 Na^+/Ca^{2+} (refs 3, 5), Na–Ca exchange is supposed to generate a current across the cell membrane. It is thought that such a current may contribute to cardiac action potential and physiological or pathological pacemaker activity[6,7]. Although the occurrence of Na–Ca exchange is well documented, a membrane current generated by this transport has not been identified unequivocally. Previous attempts to detect such a current in multicellular preparations, for example, by measuring small current differences after varying the extracellular ionic composition[8], although providing evidence, did not rule out other possible interpretations. Here we demonstrate that a transient rise in $[Ca]_i$ caused by release of Ca from sarcoplasmic reticulum (SR) generates a membrane current in cardiac myocytes. The dependence of this current on the transmembrane gradients for Na^+ and Ca^{2+} and on membrane potential meets the criteria for a current produced by electrogenic Na–Ca exchange. Cyclic activation of this current by release of Ca from the SR can cause maintained spontaneous activity, suggesting that Na–Ca exchange contributes to certain forms of cardiac pacemaking.

Figure 1 shows inward current transients (I_{ti}) recorded from an atrial 'cardioball' at constant membrane potential (−70 mV). In the experimental conditions described in Fig. 1 legend these current transients occurred regularly for periods of up to 50 min after the start of dialysis of a cell. (If the EGTA concentration in the dialysing fluid was raised to ⩾1 mM, I_{ti} did not occur spontaneously, but could be evoked by a long-lasting or repetitive activation of voltage-dependent Ca current.) Extracellular application of caffeine (5 mM), a substance known to release Ca ions from, and to prevent their re-accumulating into, the SR of cardiac and skeletal muscle[9,10], evoked an inward current
shift of almost identical amplitude (see ref. 11). In the presen
of caffeine, I_{ti} was no longer observed (Fig. 1*a*). This re
clearly suggests that I_{ti} reflects a rise in [Ca], due to
release of Ca ions from the SR[12]. This conclusion is supp
by the observation that I_{ti} is accompanied by visible contra
of the myocytes at constant negative membrane potent
addition to the shift of the holding current, caffeine in
openings of an ionic channel with a large conductance
270 pS) which is not the elementary unit of the inward
shift[13]. Channel openings of this type can be dete
ally also during spontaneous I_{ti} (Figs 1*b*, 2*a*).

With increasing depolarization, I_{ti} was decre
and prolonged (Fig. 1*c*). After a step chan
more positive than −50 mV, only a
relaxation of which was incomplet
the current remained at a level wh
to the instantaneous current meas
ation. Relaxation of I_{ti} occurred
more negative membrane potenti
potential at which I_{ti} failed to relax
−45 mV) in 22 cells loaded with 20
the pipette contained 12 mM Na^+
(mean = −20 mV; 19 cells). This
of intracellular Na or the transm
voltage dependence of I_{ti}.

---

* To whom correspondence should be addressed.

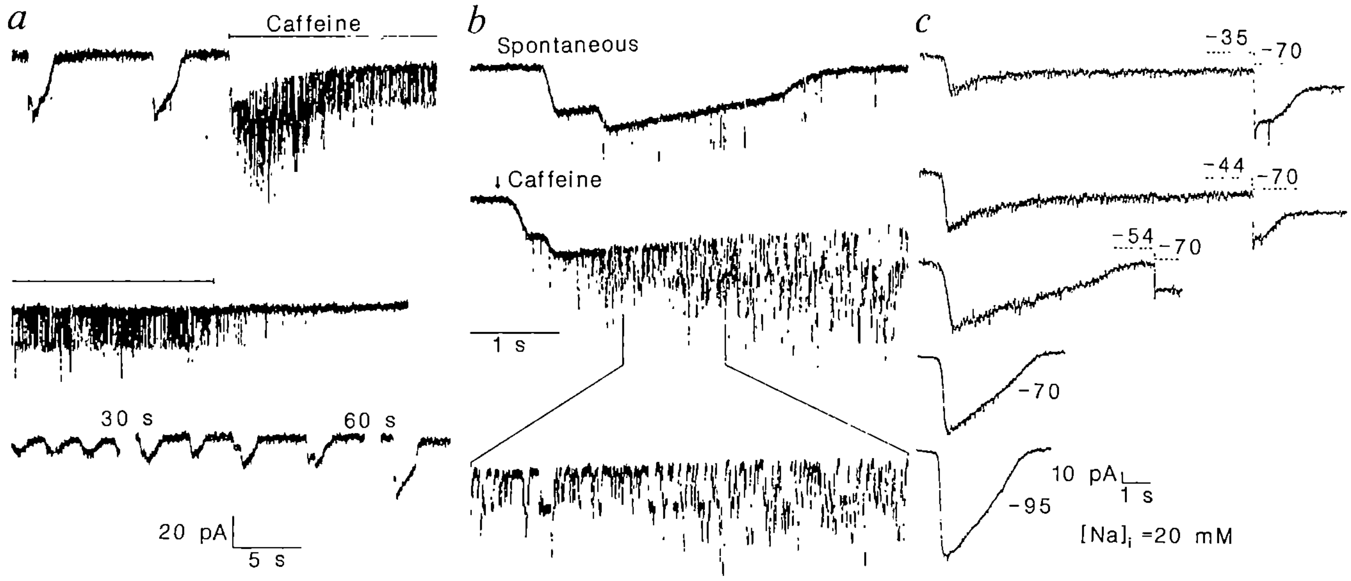

Fig. 1 *a*, Spontaneous transient inward current (I_{ti}) at constant membrane potential (−70 mV). Traces, from top to bottom, represent consecutive current recordings (interrupted at the times indicated by the gaps). The cell was dialysed with pipette-filling solution containing 12 mM Na^+ for ~10 min. That the voltage control was adequate was routinely tested by depolarizing clamp pulses into the voltage range of activation of the fast Na^+ current (I_{Na}). Voltage control was assumed to be adequate only if I_{Na} activation near threshold occurred without a distinct delay. Caffeine was applied for the time indicated, by pressure from a glass capillary (tip diameter ~5 μm) which contained the drug (5 mM) dissolved in extracellular solution. The tip of the capillary was placed ~10 μm from the surface of the cell. *b*, Spontaneous and caffeine-evoked current transient on an expanded timescale. *c*, Dependence of I_{ti} on membrane potential. From the holding potential (−70 mV), long-lasting changes of membrane potential were applied to the levels indicated. Note the transient inward current after repolarization from −35 and −44 mV but not from −54 mV.

Methods. Single cells were isolated from atria of adult guinea pig hearts by enzyme perfusion using collagenase and elastase. The cells were cultured for 3–14 days. In these conditions, spherical myocytes ('cardioballs') with a diameter of 15–25 μm are obtained[18]. Voltage-clamp experiments were performed using patch-clamp pipettes in the whole-cell recording configuration[19,20]; this allows high-resolution current recording and internal dialysis. The pipettes were filled with a solution containing (in mM): Cs-citrate 65, NaCl 20, Mg-ATP 1–2, cyclic AMP 0.1, EGTA 0.05; HEPES/CsOH 10, *p*H 7.2. In some experiments the solution also contained 12 mM NaCl and 8 mM CsCl. Pipette resistance, 2–5 MΩ. The external solution had the following composition (mM): NaCl 140, CsCl 2.0, $MgCl_2$ 1.0, $CaCl_2$ 2.0, HEPES/NaOH 10, *p*H 7.4. Experiments were performed at room temperature (21–23 °C). The current was measured by means of a patch-clamp amplifier (List LM/EPC 7), stored on analog tape and analysed later on an IBM PC at appropriate sampling rates.

Since, as demonstrated by the action of caffeine, I_{ti} is primarily
aused by a rise in $[Ca]_i$, it can be concluded from Fig. 1*c* that
decay of $[Ca]_i$ after a release is slowed by membrane
larization. $[Ca]_i$ does not decay to its resting level at mem-
potentials less negative than −45 mV (20 mM $[Na]_i$) or
V (12 mM $[Na]_i$). Thus, I_{ti} is related to a voltage-depen-
ocess of Ca extrusion from the cytoplasm. The most
andidate for such a voltage-dependent Ca extrusion is
rcolemmal Na–Ca exchange, a transport system which
inwardly directed Na gradient as an energy source for
transport of Ca^{2+} (refs 1–5). The reversal potential of
(E_{NaCa}) is given by[2,3]

$$E_{NaCa} = (nE_{Na} - 2E_{Ca})/(n-2) \quad (1)$$

the Nernst potentials for the respective
pling ratio, which is likely to b
esulting driving force is given b
a and E_m (the actual membran
relation, it follows that for a given
to activate Na–Ca exchange[14], a
f either of the ion species involved
rresponding change in membrane
ect on Na–Ca exchange: increasing
tration ($[Ca]_0$) or decreasing the
t the current in the same way as
ssuming a 3:1 stoichiometry, an
ion in the external solution from
ent to a depolarization of 23 mV.
ative experiment in which super-

fusion of the cell with a solution containing 5 mM $CaCl_2$ caused a shift of the holding current (at −70 mV) in the outward direction. The spontaneous I_{ti} was immediately reduced from 32 pA to 12 pA and was prolonged by ~3 s. A reduction of the extracellular Na concentration had a qualitatively similar effect (Fig. 2*b*): in this cell, which was loaded with 20 mM Na^+, a depolarization from −80 to −60 mV caused a slower but still complete relaxation of I_{ti}. Incomplete relaxation was observed at −40 mV. A decrease of $[Na]_0$ from 140 to 100 mM, which should be equivalent to a depolarization of 25 mV, resulted in a decreased and prolonged I_{ti} at −80 mV. Incomplete relaxation of I_{ti} was observed at −60 mV. At −100 mV, current transients with a time course similar to those observed at −80 mV at normal $[Na]_0$ were recorded. Thus, the decrease in $[Na]_0$ shifted the voltage dependence of I_{ti} by at least 20 mV.

These results show for the first time that release of calcium from SR activates a membrane current which is related to Ca removal from the cell. This current depends on membrane potential and on the transmembrane gradients for Na and Ca ions in a manner expected for electrogenic Na–Ca exchange. In the present study we have not considered the kinetic aspects of this transport. In a recent investigation, an outward current caused by Na–Ca exchange was identified in Na-loaded myocytes, and this current did not develop in the absence of intracellular Ca ions—it was not determined solely by the driving forces of the ions involved[14].

Transient inward currents due to oscillatory Ca release from SR have been described previously in Ca-overloaded multicellular preparations[15,16]. Both electrogenic Na–Ca exchange and

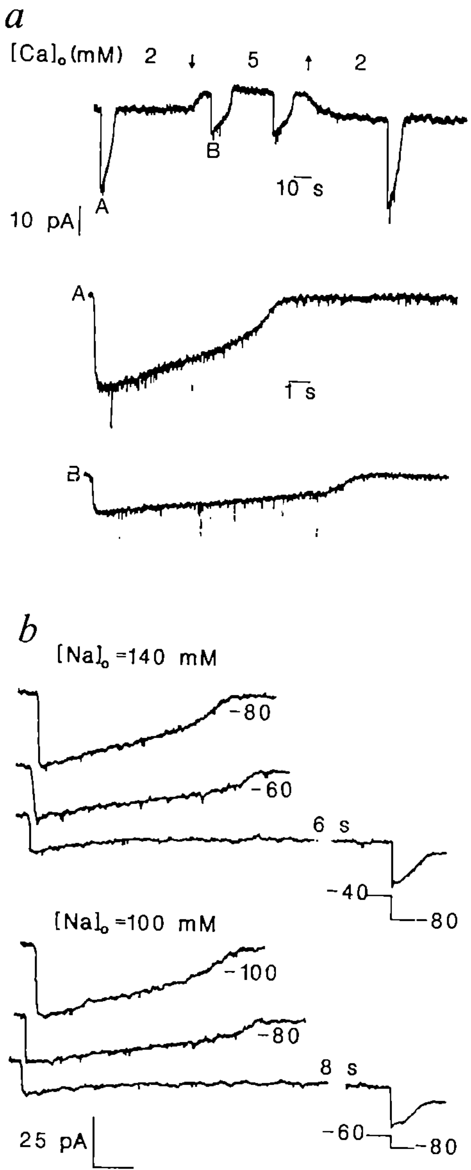

Fig. 2 Effect of changes in transmembrane Na$^+$ and Ca^{2+} gradients on spontaneous I_{ti}. *a*, Effect of increase in $[Ca]_o$ on spontaneous transient inward current. During the time indicated by the arrows the cell was superfused (see Fig. 1 legend) with a solution containing 5 mM CaCl$_2$. Note the openings (A and B) of the large-conductance channel, which are inadequately resolved at this time resolution. *b*, Effect of a reduction of $[Na]_o$ on I_{ti}. The upper three traces represent inward currents recorded in a solution containing 140 mM Na$^+$ at the membrane potentials indicated (mV). The lower traces were recorded during superfusion with a solution containing 100 mM NaCl, 40 mM being substituted by LiCl. After initiation of superfusion with the low-Na solution, the holding current was shifted in the outward direction by 16 pA.

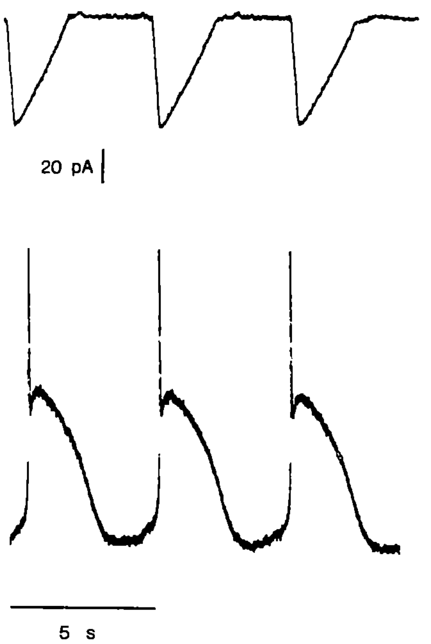

Fig. 3 Spontaneous electrical activity due to cyclic I_{ti}. The top trace shows the membrane current recorded from a cell held at a membrane potential of −70 mV (voltage clamp). The bottom trace was recorded from the same cell under current clamp conditions. To obtain a negative 'diastolic potential', a constant hyperpolarizing current of 22 pA was injected.

a Ca-activated nonspecific cation channel have been suggested as charge-carrying mechanisms. The latter interpretation was supported by the discovery of a Ca-activated nonspecific cation channel in the membrane of cultured neonatal myocytes[17]. From the results of the present study, the major mechanism behind I_{ti} is clearly a Na-Ca exchange current. Activation of a Ca-dependent ion channel could explain neither the parallel shift of the voltage dependence of I_{ti} by 20 mV on decreasing $[Na]_o$ from 140 to 100 mM, nor the effect of an increase in $[Ca]_o$ (Fig. 2). The single-channel events detected occasionally after spontaneous Ca release and which are more pronounced after release of Ca from the SR by caffeine (see Fig. 1) point to a possible contribution of gated channels to I_{ti} in multicellular preparations. Note, however, that the channel found in the present study is unlikely to be identical to the nonspecific channel described previously[17], which has a much smaller unit conductance.

A possible contribution of Na-Ca exchange to cardiac electrical activity is suggested by the result in Fig. 3. Spontaneous I_{ti} causes rhythmic action potentials consisting of a fast overshooting (Na$^+$) 'spike' and a long-lasting plateau. Although this action potential configuration is far different from any physiological one, this result indicates a role for Na-Ca exchange current in cardiac excitation.

We thank Professors H. G. Glitsch and H. Reuter for critical reading of the manuscript and Mrs U. Müller for technical assistance. This work was supported by the Deutsche Forschungsgemeinschaft (SFB 114, TPA8).

Received 11 November; accepted 30 December 1985.

1. Reuter, H. & Seitz, N. *J. Physiol., Lond.* **195**, 451-470 (1968).
2. Mullins, L. *Am. J. Physiol.* **236**, C103-110 (1979).
3. Reuter, H. in *Membranes and Transport* Vol. 1 (ed. Martonosi, A.) 623-631 (Plenum, New York, 1982).
4. Eisner, D. A. & Lederer, W. J. *Am. J. Physiol.* **248**, 189-202 (1985).
5. Reeves, J. P. & Hale, C. C. *J. biol. Chem.* **259**, 7733-7739 (1984).
6. Noble, D. *J. Physiol., Lond.* **353**, 1-50 (1984).
7. Di Francesco, D. & Noble, D. *Phil. Trans. R. Soc.* B307, 353-389 (1985).
8. Mentrard, D., Vassort, G. & Fischmeister, R. *J. gen. Physiol.* **84**, 201-220 (1984).
9. Weber, A. & Hertz, R. *J. gen. Physiol.* **52**, 750-759 (1968).
10. Jundt, H., Portzig, H., Reuter, H. & Stucki, J. W. *J. Physiol., Lond.* **246**, 229-253 (1975).
11. Clusin, T. C. *Nature* **301**, 248-250 (1983).
12. Fabiato, A. & Fabiato, F. *J. Physiol., Lond.* **249**, 469-495 (1975).
13. Mechmann, S. & Pott, L. *J. Physiol., Lond.* **366**, 80P (1985).
14. Kimura, J., Noma, A. & Irisawa, H. *Nature* (this issue).
15. Kass, R. S., Tsien, R. W. & Weingart, R. *J. Physiol., Lond.* **281**, 209-226 (1978).
16. Karagueuzian, H. S. & Katzung, B. G. *J. Physiol., Lond.* **327**, 255-271 (1982).
17. Colquhoun, D., Neher, E., Reuter, H. & Stevens, C. F. *Nature* **294**, 752-754 (1981).
18. Bechem, M., Pott, L. & Rennebaum, H. *Eur. J. Cell Biol.* **31**, 366-369 (1983).
19. Marty, A. & Neher, E. in *Single Channel Recording* (eds Sakmann, B. & Neher, E.) 107-122 (Plenum, New York, 1983).
20. Hamill, O. P., Marty, A., Neher, E., Sakmann, B. & Sigworth, F. J. *Pflügers Arch. ges. Physiol.* **391**, 85-100 (1981).

Repetitive transient rises in cytoplasmic free calcium in hormone-stimulated hepatocytes

Niall M. Woods, K. S. Roy Cuthbertson & Peter H. Cobbold

Department of Zoology, University of Liverpool, PO Box 147, Liverpool L69 3BX, UK

In the stressed animal, the vasoactive hormones vasopressin and angiotensin-II and the neurotransmitter noradrenaline induce liver cells to release glucose from glycogen. The intracellular signal that links the cell-surface receptors for noradrenaline (α_1) and vasoactive peptides to activation of glycogenolysis is known to be a rise in the cytoplasmic concentration of free calcium ions (free Ca)[1–3]. The receptors for these agonists induce the hydrolysis of phosphatidylinositol 4,5-bisphosphate, a minor plasmalemma lipid, to produce inositol trisphosphate and diacylglycerol[3–5]. Inositol trisphosphate has been shown to mobilize intracellular calcium in hepatocytes[3,6–8]. We show here, by means of aequorin measurements in single, isolated rat hepatocytes, that the free Ca response to these agonists consists of a series of transients. Each transient rose within 3 s to a peak free Ca of at least 600 nM and had a duration of approximately 7 s. The transients were repeated at intervals of 0.3–4 min, depending on agonist concentration. Between transients, free Ca returned to the resting level of ~200 nM. Clearly, the mechanisms controlling free Ca in hepatocytes are more complex than hitherto suspected.

Hepatocytes were isolated from fed, mature male rats and were kept at 37 °C in a complete culture medium for use within 10 h. Cells of about 25 μm diameter were injected with aequori (see Fig. 1 legend). Stable resting signals could be recorded fro individual hepatocytes for several hours. The mean resting signa for 55 cells was 1.2 photon counts s^{-1} above background (0. or 1.6 c.p.s.) and mean total counts per cell 2.6×10^5. Thes measurements give an upper estimate for mean resting free C of 211±9 (±s.e.m.) nM ($n = 55$), assuming 1 mM free Mg an uniform calcium distribution. Arsenazo(III) and quin2 measurements also give values of ~200 nM (refs 1, 2).

The α_1-preferring adrenergic agonist phenylephrine induce repetitive transient rises in free Ca which usually peaked above 600 nM and were blocked reversibly by phentolamin an α_1-antagonist (Fig. 1*a*). Propranolol, a β-adrenergic antagonist (2 μM), had no effect on transients induced by 2 μ phenylephrine, while yohimbine, an α_2-preferring antagoni (2 μM), reduced the frequency of transients induced by 2 μ phenylephrine (the period rose from 40 s to 60 s; data n shown). Only a proportion of the hepatocytes responded t phenylephrine (34/42 = 81%), a rather higher percentage tha respond to α_1-adrenergic stimulation by entering into DN synthesis (~30%)[9]. The frequency of the transients was depe dent on the concentration of phenylephrine (Fig. 1*b*). Low co centrations (0.6 μM), which activate phosphorylase by ~10 of maximum[1], induced transients at ~100-s intervals, whi 2 μM phenylephrine produced transients every 20–30 s (Fig. 1*b* At the higher concentrations (2–10 μM), the initial few transien were usually of higher magnitude and more frequent than tho later in the series, when the period stabilized at ~30 s. At ve high phenylephrine concentrations (100–1,000 μM), free C briefly reached 1,100 nM and fell slowly over ~2 min befo repetitive transients appeared with a period of ~20 s (Fig. 1*c* Adrenaline induced similar response patterns but was mo potent (0.3 μM adrenaline was comparable to 2 μM phenylep rine; data not shown).

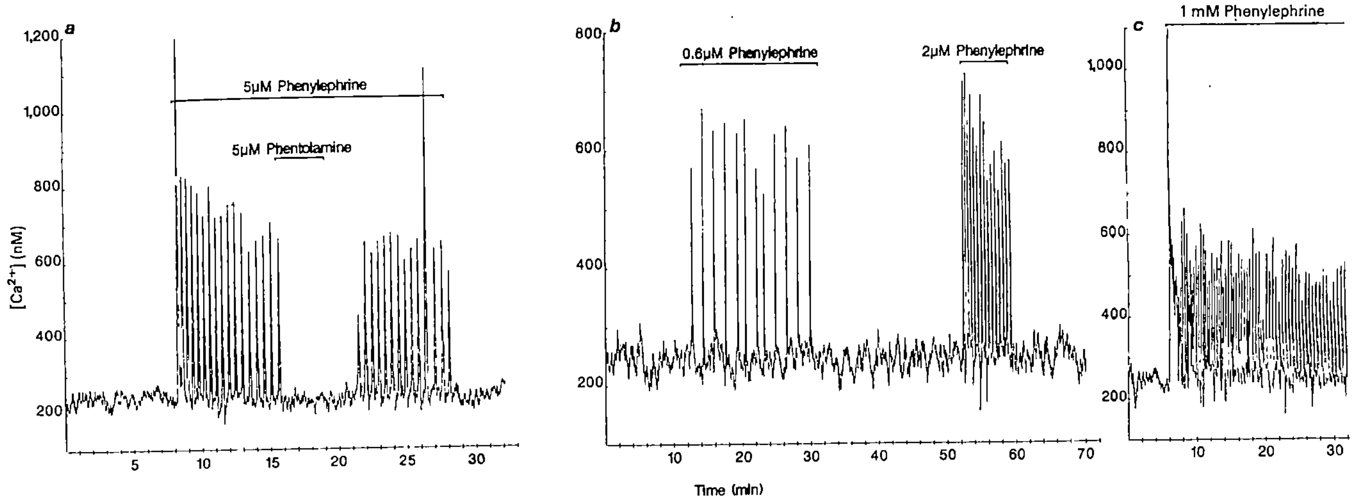

Fig. 1 Aequorin signals, transformed by microcomputer into free Ca values (nM), from individual rat hepatocytes exposed to phenylephrine. *a*, Phentolamine (5 μM) reversibly blocked free Ca transients induced by 5 μM phenylephrine. *b*, The frequency of the transients was dependent on the concentration (0.6 and 2 μM) of phenylephrine. *c*, Very high concentrations of phenylephrine (1 mM) generated a slow-falling rise, briefly reaching ~1,200 nM free Ca (peak not shown), followed by transients. (Time constants were 15 s for resting levels and 1 s for the transients.) **Methods.** Hepatocytes were prepared by perfusion of collagenase[24] (Boehringer) through livers from fed, male rats (150–250 g) and kept at 37 °C in CO_2-bicarbonate-buffered Williams' medium E (Flow Labs) containing 1.8 mM Ca, 0.05% bovine serum albumin but lacking insulin or serum. The aequorin technique was modified from refs 25 and 26 as follows. Single hepatocytes of ~25 μm diameter, selected under a ×180 stereomicroscope for their healthy appearance (no blebs, no vacuolation, distinct nuclei), were transferred to a 0.1-mm microslide (Camlab) containing a pool of 1% agarose (Sigma VII) and held at 37 °C under a layer of liquid paraffin. The cell was positioned within 100 μm of the agarose-oil interface before gelling the agarose at 4 °C for 2 min. Cells were injected on the stage of an inverted microscope (×600, Nomarski) at ~35 °C with aequorin solution from a micropipette whose tip had been filled with a 50-μm-long column of aequorin. (The tips of freshly pulled pipettes when immersed in liquid paraffin for a few seconds will subsequently allow a short column of aequorin solution to enter spontaneously.) Injected cells that had retained the distinct concave appearance of their nuclei were transferred in the microslide to a perfusable cup held at ~37 °C positioned under a low-noise photomultiplier[25]. Photon counts were sampled every 50 ms by a Sirius microcomputer. Data were plotted using exponential smoothing with time constants as indicated and calibration as before[25], except that 1 mM free Mg^{2+} was used.

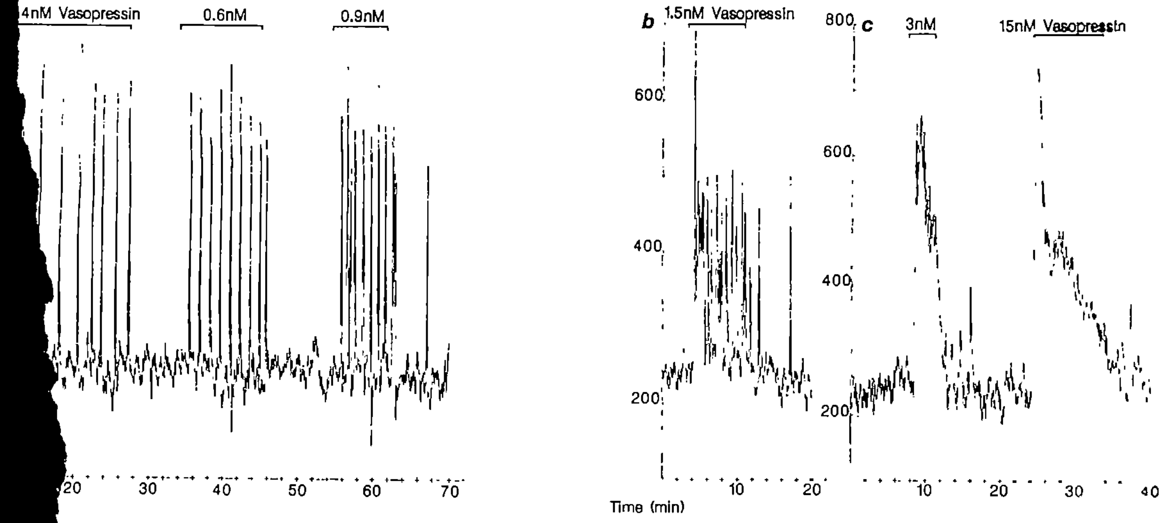

ignals plotted as free Ca (nM) from a single hepatocyte exposed to various concentrations of [Arg^8]vasopressin (time). *a*, Physiological concentrations of vasopressin (0.4, 0.6, 0.9 nM) induced free Ca transients at increasing frequencies , 80 and 60 s, respectively). Before the 0.4 nM recording, the cell had failed to generate transients when exposed to 0.2 nM .5 min. *b*, *c*, High concentrations of vasopressin (1.5, 3 and 15 nM) induced a more sustained initial free Ca rise. Repetitive urred in 1.5 nM, but not at the higher concentrations until the hormone was removed (time constants in *c* were 10 and 3 s).

and angiotensin-II at concentrations of ~1 nM, the K_m for activation of glycogen phosphory- ed a series of free Ca transients whose frequency endent on hormone concentration (Fig. 2*a*). The equency transients (period 1–4 min) was preceded parable to the period. Lags have been reported free Ca measurements on populations of [12]. Very high concentrations of peptide hormones ich would induce measurable degradation of ositol 4,5-bisphosphate and receptor occu- uced a more sustained, slowly decaying rise in peaked at 600–800 nM (Fig. 2*c*). The time course ed free Ca responses is similar to that of changes ylinositol levels and phosphorylase activation high hormone doses[13,14]. At intermediate oncentrations (1.5 nM; Fig. 2*b*), an initial sus- free Ca was followed by transients, similar to the ery high doses of phenylephrine (Fig. 1*c*). Most d to vasopressin (32/34), including 5 cells that espond to phenylephrine. Angiotensin induced a /27 cells (78%).

ws that the rate of rise of free Ca in a transient ng ~2–3 s to rise from resting levels (200 nM) to 00–1,200 nM). The peak concentration was sus- s, while the fall to resting levels took a further duration was ~7 s. No appreciable change in ers was detected at different hormone concentra- gh quin2 measurements on populations of have not revealed transient behaviour, perhaps buffering of free Ca or poor cell synchrony, have been detected in the extracellular calcium n in the perfusate from intact liver exposed to 10 μM ine (H. Sies, personal communication).

tractive possibility that the frequency of the transients the intensity of a cell's response to hormone con- within the physiological range. Calcium concentra- in the range we observe can activate phosphorylase , which contains covalently bound calmodulin. This urn activates glycogen phosphorylase, whose activity unction of the rates of phosphorylation and dephos- n. Since the frequency of the transients is the only of free Ca which varies with hormone concentration, le that frequency determines the rate of glycogenolysis vidual cell. Rasmussen and Barrett have postulated that a transient rise in free Ca to micromolar levels followed by a fall to ~500 nM would initiate and sustain calmodulin activity without promoting mitochondrial calcium overload[17]. In hepatocytes, the free Ca response is more complex than this, as free Ca falls to resting levels between transients, but our data offer a plausible explanation for the lack of mitochondrial calcium overload in chronically stimulated cells. Campbell has proposed that calcium acts as an intracellular regulator for 'threshold phenomena' that are either 'switched on' or 'switched off'[18]. Each free Ca transient conforms to this concept, while the occurrence of frequency-modulated series of transients may allow the amplitude of the glycogenolytic response in a single cell to be varied according to hormone concentration. There are indications from blowfly salivary glands[19], pancreatic islet β-cells[20] and oocytes during fertilization[21–23] that the phenomenon

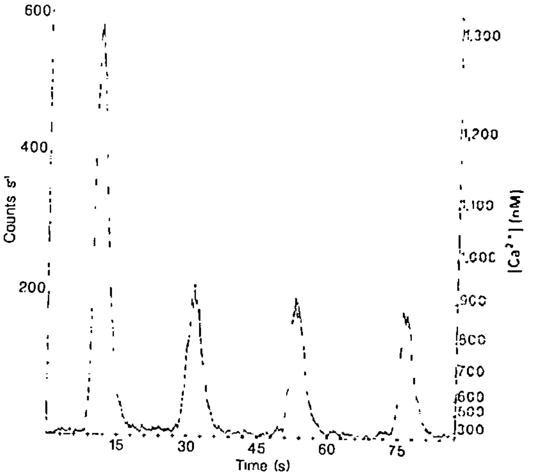

Fig. 3 The aequorin signal, expressed as photoelectron counts s^{-1} and as free Ca (nM), from a single hepatocyte responding to 5 μM phenylephrine. Time constant, 0.5 s. The signal rose from resting to peak values within 2–3 s. Owing to dead space in the perfusion chamber, the exact time of arrival of phenylephrine at the cell was unknown. The background was 1.6 counts s^{-1} and the resting level 2.4 counts s^{-1} above background, corresponding to 200 nM free Ca. The cell contained a total of 4.2×10^5 photoelectron counts

of repetitive transient rises in free Ca may be widespread in cells that use free Ca as a messenger for extracellular ligands.

We thank the Wellcome Trust for funding this work.

Received 31 October 1985; accepted 6 January 1986.

1. Murphy, E., Coll, K., Rich, T. L. & Williamson, J. R. *J. biol. Chem.* **255**, 6600–6608 (1980).
2. Charest, R., Blackmore, P. F., Berthon, B. & Exton, J. H. *J. biol. Chem.* **258**, 8769–8773 (1983).
3. Thomas, A. P., Alexander, J. & Williamson, J. R. *J. biol. Chem.* **259**, 5574–5584 (1984).
4. Creba, J. *et al. Biochem. J.* **212**, 733–747 (1983).
5. Williamson, J. R., Cooper, R. H., Joseph, S. K. & Thomas, A. P. *Am. J. Physiol.* **248**, C203–C216 (1985).
6. Berridge, M. J. & Irvine, R. F. *Nature* **312**, 315–321 (1984).
7. Burgess, G. M., Irvine, R. F., Berridge, M. J., McKinney, J. S. & Putney, J. W. *Biochem. J.* **224**, 741–746 (1984).
8. Joseph, S. K., Thomas, A. P., Williams, R. J., Irvine, R. F. & Williamson, J. R. *J. biol. Chem.* **259**, 3077–3081 (1984).
9. Cruise, J. L., Houck, K. A. & Michalopoulos, G. K. *Science* **227**, 749–751 (1985).
10. Kirk, C. J., Rodrigues, L. M. & Hems, D. A. *Biochem. J.* **178**, 493–496 (1979).
11. Campanile, C. P., Crane, J. K., Peach, M. J. & Garrison, J. C. *J. biol. Chem.* **257**, 4951–4958 (1982).
12. Cooper, R. H., Coll, K. E. & Williamson, J. R. *J. biol. Chem.* **260**, 3281–3288 (1985).
13. Kirk, C. J., Creba, J. A., Downes, C. P. & Michell, R. H. *Biochem. Soc. Trans.* **9**, 377–379 (1981).
14. Kirk, C. J. *Cell Calcium* **3**, 399–411 (1982).
15. Chrisman, T. D., Jordan, J. F. & Exton, J. H. *J. biol. Chem.* **257**, 10798–10804 (1982).
16. Erdődi, F., Gergely, P. & Bot, G. *Int. J. Biochem.* **16**, 1391–1394 (1984).
17. Rasmussen, H. & Barrett, P. Q. *Physiol. Rev.* **64**, 938–984 (1984).
18. Campbell, A. K. *Intracellular Calcium, Its Universal Role as Regulator* (Wiley, Chichester, 1983).
19. Berridge, M. J. & Prince, W. T. *J. exp. Biol.* **56**, 139–153 (1972).
20. Matthews, E. K. & O'Connor, M. D. L. *J. exp. Biol.* **81**, 75–91 (1979).
21. Cuthbertson, K. S. R., Whittingham, D. G. & Cobbold, P. H. *Nature* **294**, 754–757 (1981).
22. Poeinie, M., Alderton, J., Tsien, R. Y. & Steinhardt, R. A. *Nature* **315**, 147–149 (1985).
23. Cuthbertson, K. S. R. & Cobbold, P. H. *Nature* **316**, 541–542 (1985).
24. Burgess, G. M., Claret, M. & Jenkinson, D. H. *J. Physiol., Lond.* **317**, 67–90 (1981).
25. Cobbold, P. H., Cuthbertson, K. S. R., Goyns, M. M. & Rice, V. R. *J. Cell Sci.* **61**, 123–136 (1983).
26. Cobbold, P. H. & Bourne, P. K. *Nature* 312, 444–446 (1984).

Stable expression of two variable surface glycoproteins by cloned *Trypanosoma equiperdum*

T. Baltz*, C. Giroud*, D. Baltz*, C. Roth†,
A. Raibaud† & H. Eisen†‡

* Université de Bordeaux II, 33076 Bordeaux Cedex, France
† Institut Pasteur, 25, rue du Dr Roux, 75015 Paris, France

African trypanosomes are thought to evade the host immune system by periodically changing their variable surface glycoprotein (VSG). VSG genes are activated by a complex process involving the duplicative transposition of silent basic copy genes to one of several expression sites[1–3]. These expression-linked copies (ELCs) of the VSG genes are also subject to regulation within expression sites by as yet unknown mechanisms[4–9]. It is generally assumed that trypanosomes can express only one VSG gene at a time. Nevertheless, the finding that they contain multiple VSG gene expression sites suggests that multiple expression is possible. We show here that *Trypanosoma equiperdum* can stably express two VSG genes in a simple axenic culture system[10] and that both antigens are present on the cell surface. The two antigens do not co-cap or form heterodimers. Their corresponding genes show no cross-hybridization and are situated in different telomere-linked expression sites. Northern blot analysis reveals that both genes are active in the double expressors.

BoTat-1 (Bordeaux trypanozoon antigen type-1)[11] trypanosomes were placed in axenic tissue culture as described previously[10]. This culture system allows long-term growth of bloodstream forms with generation times comparable to those observed *in vivo*. After various intervals, the cultured trypanosomes were examined using monoclonal anti-VSG-1 antibodies.

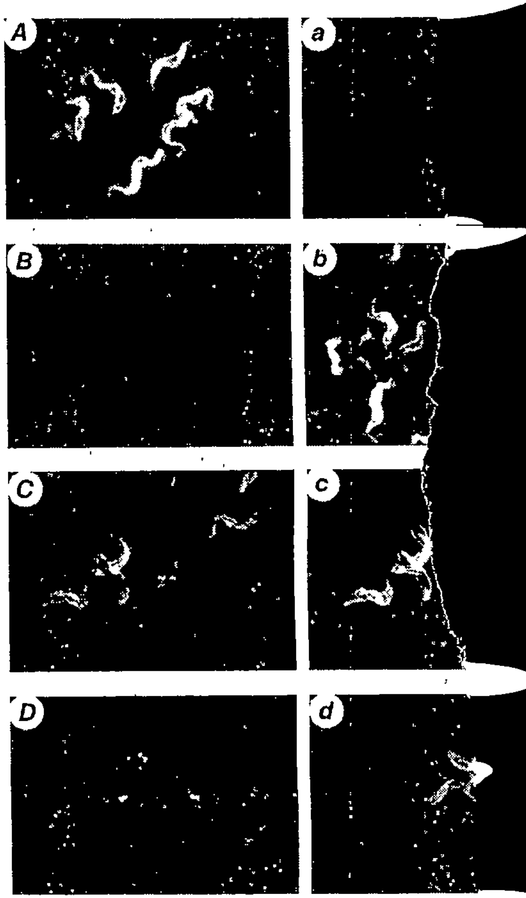

Fig. 1 Co-expression of two VSGs by cloned *T. equip* Fluorescein fluorescence (revealing VSG-1); *a–d* fluorescence (VSG-201). Trypanosomes were washed saline glucose buffer *p*H 8 (PSG)[11], deposited on micr air-dried and fixed for 1 min in 4% formaldehyde i buffered saline (PBS) and for 2 min in acetone. Afte PBS, the fixed trypanosomes were incubated for 30 temperature in a 1:1 mixture of monospecific rabbit (diluted 1:500 in PBS) and monoclonal mouse a (undiluted culture supernatant). After washing with antibodies were revealed with a 1:1 mixture of Texa gated sheep anti-mouse immunoglobulin (Amersham in PBS) and fluorescein-conjugated goat anti-rab globulin (Nordic Immunologicals, diluted 1:100 i slides were washed and examined using appropria fluorescent illumination. *A*, *a*, Pure BoTat-1; *B*, *b*, pu *C*, *c*, double expressors; *D*, *d*, live trypanosomes expr and VSG-201 were washed in PSG, resuspended in VSG-1 antiserum diluted 1:50 in PSG and incubated 20 min. They were then washed in PSG, deposited on slides, fixed and incubated with monoclonal mouse ar Bound antibodies were revealed as described a

When 5–10% of the parasites no longer expresse their surface, they were cloned in culture and non-VSG-1 trypanosomes, called BoTat-201, w Hybridomas producing anti-VSG-201 antibodies we as described elsewhere[12] and shown to react only 201. Rabbit antibodies directed against purified VS also produced. These antibodies specifically agglutin 201 parasites and in immunofluorescence te specifically with BoTat-201. Both monoclonal and antibodies were used for the analysis of variation Identical results were obtained with both. Cultures BoTat-1 were examined for the presence of VSG-1 201-bearing cells. Surprisingly, large numbers of cells both antigens were found in the cultures.

---

‡ To whom correspondence should be addressed at: Fred Hutchinson Cancer Research Center, 1124, Columbia St, Seattle, Washington 98104, USA.

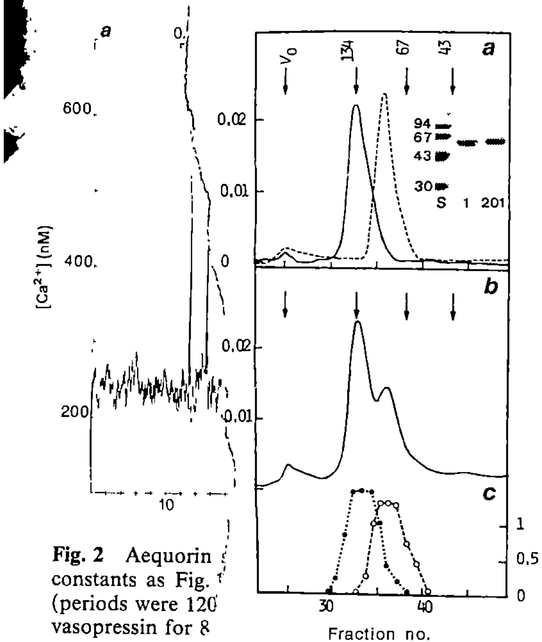

Fig. 2 Aequorin
constants as Fig.
(periods were 120
vasopressin for 8
transients occ

ltration of purified VSGs. VSGs were isolated from
populations by freezing and thawing in distilled water
Vasopressin ography of the soluble proteins on concanavalin A-
comparable to Pharmacia)[14]. The eluted VSGs were applied to a
lase[10,11], induc calibrated column of Sephacryl ACA44 and the
was again dep developed with PBS at a flow rate of 18 ml h^{-1}.
onset of low-fr arrows represent M_rs of standards (×10^{-3}). ***a***, VSG-1
by a lag com /SG-201 (- - -) isolated from mono-expressing popula-
previously in panosomes. Inset, SDS-polyacrylamide gel of purified
hepatocytes[2,3] of standards (S) are given (×10^{-3}). ***b***, VSG purified
(≥10 nM), wh expressing trypanosomes 2 days after inoculation into
phosphatidylin opulation consisted of 57% double expressors and
pancy[13,14], ind xpressors for VSG-1 (see Table 1). ***c***, Aliquots of the
free Ca which were assayed for their content of VSG-1 and VSG-201
of these sustair nked immunosorbent assay[16] using monoclonal mouse
in phosphatic ecific for each antigen. Aliquots (0.1 ml) were coated
described at s of microtitre wells (Nunc). Unbound antigen was
vasopressin c washing with 0.4% Tween 20 in PBS. Duplicate wells
tained rise in reated with 0.1 ml of either monoclonal mouse anti-
response to v or anti-VSG-201 (○). After incubation for 2 h at 37 °C
cells responde ere washed, and bound immunoglobulins revealed
had failed to r dase-conjugated sheep anti-mouse immunoglobulin
response in 21 (Pasteur) as described previously[16].

Figure 3 sho ne whether stable double expression could be
was rapid, tak he doubly expressing parasites were cloned in
peak values (hen grown either *in vitro* or in mice. The cloned
tained for ~ s were examined at various intervals with the two
3–5 s. Overall the results are presented in Fig. 1 and Table 1.
hese paramet (56 generations) in culture, more than 90% of the
tions. Altho co-expressed both antigens. By 30 days (120 gener-
hepatocytes[2,3] 16% expressed both antigens, the remainder
because of ither VSG-1 or VSG-201. Thus, *in vitro*, double VSG
oscillations is relatively stable and persists after cloning and
concentrati growth. In contrast, passage in mice resulted in the
phenyleph of parasites expressing both antigens and the appear-
It is an a opulations of pure VSG-1-expressing cells.
determin ify that the putative double VSG expression was not
centratic cross-reactivity of anti-VSG-1 and anti-VSG-201 anti-
tions w , or to the presence of a hybrid VSG, capping experiments
kinase performed. Live parasites co-expressing both antigens were
kinase ated at 25 °C for 20 min with rabbit anti-VSG-1 antibodies.
will be washing and fixation, the parasites were stained with
phoryl clonal mouse anti-VSG-201 and washed further. Bound
param odies were revealed using the appropriate fluorescent anti-
it is po (Fig. 1). Whereas the VSG-1 antigen was localized in caps
in an e poles of the cells, the VSG-201 was evenly distributed

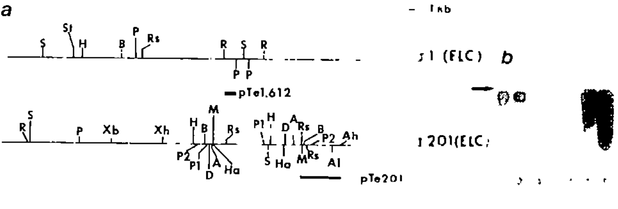

Fig. 3 *a*, Restriction maps of VSG-1 and VSG-201 gene ELCs in trypanosomes expressing both antigens and the cDNA clones used in the present study. cDNA cloning and restriction mapping were performed as described previously[2]. Symbols: S, *Sal*I, St, *Sst*I, H, *Hin*dIII; B, *Bam*HI; P, *Pst*I, Rs, *Rsa*I; R, *Eco*RI, Sa, *Sac*I, Xb, *Xba*I; Xh, *Xho*I; P1, *Pvu*I; P2, *Pvu*II; D, *Dde*I, M, *Msp*I, A, *Ava*II; Ha, *Hae*III; A1, *Ava*I; Ah, *Aha*II; T, telomere. *b*, Northern blot analysis of poly(A) RNA from BoTat-1 (lanes 1, 4), trypanosomes expressing VSG-1 and VSG-201 (lanes 2, 5) and BoTat 201 (lanes 3, 6). Lanes 1–3, probed with ^{32}P-labelled VSG-1 specific plasmid pTe1-612; lanes 4–6, probed with ^{32}P-labelled VSG 201-specific plasmid pTe201. The arrow indicates 2 kilobases. All methods were as described previously.

over the cells. This experiment definitively demonstrates that a single trypanosome can express both antigens and that each VSG behaves as an independent protein on the cell surface, thus eliminating the possibility of a hybrid protein.

Some VSGs are known to exist as dimers in solution and it has been suggested that they exist as such on the surface of the trypanosomes[13]. However, our co-capping experiments suggested that no heterodimers exist on the surface of the doubly expressing parasites. To confirm and extend this observation, variant antigen was purified from doubly expressing parasites and analysed by gel filtration chromatography[14]. Figure 2 shows that the material eluted in two peaks. The first peak, with an apparent relative molecular mass (M_r) of 134,000, corresponded to pure VSG-1 antigen, while the second peak, with an apparent M_r of 75,000, corresponds to VSG-201 antigen. While VSG-1 has a M_r of 58,000 when analysed by polyacrylamide gel electrophoresis in the presence of SDS and reducing agents, VSG 201 has an apparent M_r of 62,000. Non-denatured VSG-1 behaves like a dimer whereas VSG-201 migrates at a position closer to that expected of a monomer than of a dimer. Other methods of antigen extraction have given the same results, suggesting that VSG-1 is a dimer on the cell surface whereas VSG-201 may be a monomer. The finding that there were no heterodimers of VSG-1 and VSG-201 further confirms that the two antigens behave independently on the cell surface.

We have isolated complementary DNA clones corresponding to VSG-201. The cDNA clone pTe201 was used to determine the restriction map of the VSG-201 gene ELC, which is shown together with that of the previously characterized VSG-1 ELC from BoTat-1 (Fig. 3*a*)[2]. Note that the VSG-201 gene is in the

Table 1 Stability of double expression in tissue culture and in mice

Days of culture	Generations	% Expression of VSG 1 + 201	1	201
In vitro				
7	28	98	1	1
14	56	93	4	3
30	120	16	40	44
In mice	0	>95		
2	8	57	40	3
3	12	8	91	1

The doubly expressing trypanosomes were cloned and cultured *in vitro*, and the cultures diluted with fresh medium daily. On day 9 of culture, 10^7 parasites were inoculated into a mouse and, after 2 days, were passaged into a second mouse. At the indicated times the parasites were examined by immunofluorescence for expression of VSG-1 and VSG-201 as described in Fig. 1 legend.

previously characterized 1.78 expression site[1] and is activated without apparent duplication, as has been demonstrated for several variant antigen genes of *Trypanosoma brucei*[4,6,8,15].

RNA from pure VSG-1, pure VSG-201 and cloned doubly expressing trypanosomes was analysed with ^{32}P-labelled cDNA probes in Northern blots. Figure 3*b* shows that there is no cross-hybridization between the two RNAs and that both are present in the double expressors.

Our results demonstrate that African trypanosomes are able to express two VSGs on their surface at the same time. This double expression is relatively stable, as the parasites can be cloned and grown for over 100 generations *in vitro* presenting both antigens. It is clear that if the relatively stable expression of the two antigens reported here were to occur *in vivo*, the doubly expressing parasites would probably not be seen, as they would be killed by antibodies directed against the antigen expressed first. Also, our results (Table 1) demonstrate that trypanosomes expressing both VSG-1 and VSG-201 are rapidly lost from the population in mice, where immune selection is negligible. However, it is possible that *in vivo* double expression is a transient phase of the process of antigenic variation.

Although double antigen expression is relatively stable *in vitro*, the population slowly drifts to single expression, with no bias towards either antigen. On the other hand, when the double expressors are inoculated into mice, there is a rapid evolution towards single expression of VSG-1. Although variant antigen type (VAT)-201 grows as rapidly as VAT-1 *in vivo* when adapted to growth in the mouse, it requires a period of adaptation when transferred from culture to the mouse. This is not the case for VAT-1, which grows rapidly when transferred from culture to mouse (ref. 11 and G. Thon, unpublished). It is thus probable that, when the double expressers were injected into mice, the VAT-1s outgrew the double expressers and the VAT-201s.

The extent to which the double expression described here is specific to the two VSG genes examined is not known. We have found that another antigen, VSG-202, is co-expressed with VSG-1 in trypanosomes that have lost the VSG-201 gene (unpublished results). Double expression therefore seems to be a reasonably common phenomenon.

The two VSG genes described here and shown to be co-expressed occur in different expression sites. This demonstrates that each expression site can be regulated independently of the others and that activation of one site is not mutually exclusive of activation of others. Our results thus exclude certain models for the mechanism of variant antigen gene regulation, such as those which propose the presence of a single mobile regulatory element that moves from one expression site to another. Our findings also indicate that trypanosomes express only one antigen *in vivo* because of a selection against double antigen expression in the animal rather than because of an intrinsic genetic mechanism in the parasite.

Finally, the finding of double VSG gene expression raises questions about the functional significance of the cassette-like mechanism for VSG gene regulation. The most obvious rationale for such a mechanism is to guarantee the expression of one antigen at a time. However, this cannot be its role in *T. equiperdum*, for there are multiple expression sites and we have demonstrated here that a single trypanosome can express at least two antigen genes.

This work was supported by grants from CNRS and INSERM (France), the WHO and the European Community. C.R. was supported by fellowships from the Philipe Foundation and the Association pour la Recherche sur le Cancer.

Received 9 September; accepted 17 December 1985.

1. Longacre, S. *et al. Molec. cell. Biol.* **3,** 399–409 (1983).
2. Pays, E., Lheureux, M. & Steinert, M. *Nature* **292,** 265–267 (1981).
3. Hoeijmakers, J. H. J., Frasch, A , Bernards, A., Borst, P. & Cross, G. A. M. *Nature* **284,** 78–80 (1980).
4. Young, J. R., Miller, E., Williams, R. O. & Turner, M. J. *Nature* **306,** 196–198 (1983).
5. Buck, G. *et al. Nature* **307,** 563–566 (1984).
6. Bernards, A. *et al. Cell* **36,** 163–170 (1984).
7. Buck, G., Jacquemot, C., Baltz, T. & Eisen, H. *Gene* **32,** 329–336 (1984).
8. Laurent, M. *et al. Nucleic Acids Res.* **12,** 8319–8328 (1984).
9. Myler, P. J , Allison, J., Agabian, N. & Stewart, K. *Cell* **39,** 302–211 (1984).
10. Baltz, T., Baltz, D., Giroud, C. & Crockett, J. *EMBO J.* **4,** 1273–1277 (1985).
11. Capbern, A., Giroud, C., Baltz, T & Mattern, P. *Expl Parasit.* **42,** 6–13 (1977).
12. Esser, K. M., Schoenbechler, M. J. & Gingrich, J. B. *J. Immun.* **129,** 1715–1717 (1982).
13. Auffet, C. A. & Turner, M. G. *Biochem. J.* **193,** 647–650 (1981).
14. Baltz, I., Baltz, D. & Pautrizel, R. *Annls Immun. Inst. Pasteur, Paris* **127C,** 761–774 (1976).
15. Young, J. R., Donelson, J. E , Majiwa, P. A. O., Shapiro, S. & Williams, R. O. *Nucleic Acids Res.* **10,** 6581–6595 (1982).
16 Saunders, G. C. *Immunoassays in the Clinical Laboratory,* 99–118 (Liss, New York, 1979).

Nucleotide sequence of chicken c-*myb* complementary DNA and implications for *myb* oncogene activation

Dan Rosson & E. Premkumar Reddy

Department of Molecular Oncology, Roche Institute of Molecular Biology, Roche Research Center, Nutley, New Jersey 07110, USA

Avian myeloblastosis virus (AMV), like other acute transforming viruses, arose by recombination between its helper virus and host cellular sequences. The latter sequences, termed v-*myb*, are responsible for the oncogenic properties of the virus. AMV causes acute myeloblastic leukaemia in chickens and transforms a specific class of haematopoietic cells *in vitro*, but does not induce morphological transformation of cultured fibroblasts, suggesting that only a restricted target-cell population is responsive to its transforming gene product[1,2]. The normal cellular counterpart of v-*myb*, c-*myb*, is highly conserved and is present in all vertebrate and some invertebrate species examined[3,4]. DNA rearrangements and altered expression of the *myb* oncogene have been reported in mouse lymphoid tumours[5–7] and human myeloid[8] and colon tumours[9]. The mechanism of activation of the cellular proto-oncogenes is thought to involve the structural alteration of the coding regions that result in either the synthesis of an altered gene product or the enhanced expression of a proto-oncogene caused by alterations in its regulatory elements. To distinguish between these two mechanisms, we have cloned and sequenced the chicken c-*myb* complementary DNA and compared it with that of v-*myb* sequences. We demonstrate that during the transduction of the cellular sequences and/or viral passage a substantial portion of the coding region of the c-*myb* gene has been lost from both the 5′ and 3′ ends, resulting in the generation of a truncated gene product that mediates the transforming function of the virus.

Before cloning the normal c-*myb* cDNA sequences, we screened messenger RNA preparations from several organs of chicken and found that the proto-oncogene is expressed in substantial amounts in thymus and bursa as a 4.0-kilobase (kb)-long mRNA. Thus, for construction of a cDNA library containing the *myb* gene, thymuses from ~50 chickens were pooled and the RNA extracted as described previously[5]. After two cycles of purification on oligo(dT)-cellulose, the mRNA was used to prepare cDNA as described in Fig. 1 legend. The restriction map of the chicken c-*myb* cDNA clone that was used for sequence analysis is shown in Fig. 1. Figure 2 shows the nucleotide sequence of the coding region of this cDNA clone. The longest open reading frame extends from nucleotides 13 to 2,163 and contains an initiator codon, ATG, at position 63–65. This seems to be the true initiator codon because a terminator codon is present in-frame with this ATG at position 13–15. Furthermore, this ATG is in the sequence CCGTCCATGG which is similar to the consensus sequence CC(A/G)CCATGG for translation initiation as defined by Kozak[10]. The open reading frame shown in Fig. 2 could encode a polypeptide of 699 amino acids with an estimated relative molecular mass (M_r) of 77,000 (77K), in good agreement with the estimated size of 75K for the c-*myb*-encoded protein[11]. This open reading frame is preceded by ~500 base pairs (bp) of noncoding sequences at the 5′ end and followed by a stretch of 1,400 bp of noncoding sequences at the 3′ end.

Analysis of the predicted c-*myb* amino-acid sequence in a dot-matrix program[12] reveals a stretch of three tandem repeats in the amino-terminal end of the molecule (Fig. 3). These repeats occur in amino-acid positions 96–147, 148–199 and 200–250, the first two repeats containing more homology than the third. The role of these repeats is unknown. However, as the *myb* protein accumulates in the nucleus[13–15] and also seems to bind to DNA[15], these repeats could be involved in DNA binding or nuclear localization. A comparison of these sequences with those of mouse c-*myb*[16] shows that this region is highly conserved between the two species. Thus, it seems probable that the region encodes a critical function.

A comparison of the cDNA sequence with that of the v-*myb* sequences of AMV[17,18] reveals that the two genes are homologous from nucleotides 450 to 1,563 (Fig. 2). Sequences homologous with v-*myb*-E26 (oncogene of the E26 virus)[19] are contained in nucleotides 478–1,341. These comparisons suggest features that may be required for retroviral activation of this oncogene. In both cases similar stretches of amino- and carboxy-terminal sequences have been deleted. The AMV and E26 proteins are 142 and 150 amino acids shorter, respectively, than the normal protein at their amino-terminal ends, and 192 and 272 amino acids shorter at their carboxy-terminal ends. In AMV-transformed myeloblasts, these deletions cause the truncation of the v-*myb* gene product with a resulting M_r of 45K (refs 11, 20). The amino-terminal deletions result in the loss of the first

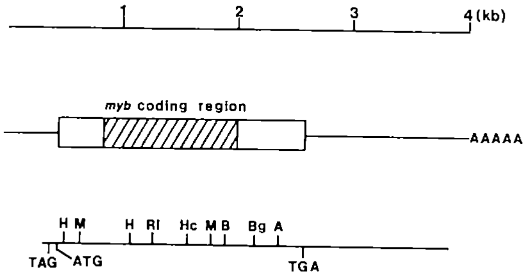

Fig. 1 Analysis of the coding region of the 4.0-kb chicken *myb* mRNA, performed on a single phage ~3.5-kb cDNA clone spanning the entire region. The cDNA library was constructed from poly(A) RNA isolated from chicken thymus. The first and second strands were synthesized by a modification of the method of Gubler and Hoffmann[22]. First-strand synthesis was accomplished using oligo(dT) primer and M-MuLV reverse transcriptase (Bethesda Research Laboratories) under conditions recommended by the manufacturer. Second-strand synthesis was performed exactly as described elsewhere[22] using RNase H and *Escherichia coli* PolI. The cDNA was then methylated with *E. coli* RI methylase and treated with T4 polymerase to blunt the ends of the cDNA before ligation to *Eco*RI linkers. After addition of linkers, the cDNA was digested with *Eco*RI and the digested linkers removed by four rounds of precipitation with 0.15 vol. of 3 M sodium acetate and 0.6 vol. of isopropanol. 200 ng of cDNA was ligated to 1 μg of λgt10 arms to obtain a library of 4 × 10⁶ recombinants. We obtained ~20 v-*myb*-hybridizing clones, one of which (clone 7) contained the entire *myb*-coding region within a 3.5-kb insert. Restriction sites shown are: H, *Hae*II; M, *Mst*II; RI, *Eco*RI; Hc, *Hinc*II; B, *Bal*I; Bg, *Bgl*II.

```
                                                   50
TTCCGGCGGC CGTAGCGGGC CATCTGCACG CGGAGCTCGC GGCCATCCAG CACGGCCCCG TCC
             ***
                                              100
ATG GCG TCC ATC GCG TCC TCG GCG TCG CGT TTG TCG TGG AAA CGG ACG AAT GCG
MET Ala Ser Ile Ala Ser Ser Ala Ser Arg Leu Ser Trp Lys Arg Thr Asn Ala
                                        150             ▼Hae II
AAC CCG CGG CTC CTC GGC ACT TCG CTG CGC GGC GGC GGA GCG CCT GGG CGC AGC
Asn Pro Arg Leu Leu Gly Thr Ser Leu Arg Gly Gly Gly Ala Pro Gly Arg Ser
                                    200
CCG GCA GCA GGG CGC GGC GGC GGG CGC GGG CTC CCC CGT CCT CTT CCC CCA GCG
Pro Ala Ala Gly Arg Gly Gly Gly Arg Gly Leu Pro Arg Pro Leu Pro Pro Ala
                               250
GCC GCC GCG AGG ATG GCC CGG AGA CCC CGG CAC AGC ATA TAC AGC AGC GAT GAC
Ala Ala Ala Arg MET Ala Arg Arg Pro Arg His Ser Ile Tyr Ser Ser Asp Asp
                          300
GAT GAA GAA GAT GTT GAG ATG TAC GAC CAC GAT TAC GAC GGC CTG CTT CCT AAG
Asp Glu Glu Asp Val Glu MET Tyr Asp His Asp Tyr Asp Gly Leu Leu Pro Lys
                     350
GCT GGG AAA CGT CAC CTA GGG AAA ACC AGG TGG ACC CGT GAA GAG GAT GAG AAA
Ala Gly Lys Arg His Leu Gly Lys Thr Arg Trp Thr Arg Glu Glu Asp Glu Lys
                400
CTG AAG AAA CTT GTG GAA CAG AAT GGC ACA GAA GAC TGG AAA GTC ATT GCC AGT
Leu Lys Lys Leu Val Glu Gln Asn Gly Thr Glu Asp Trp Lys Val Ile Ala Ser
           450▼ start AMV homology                   ▼ start E26 homology
TTC CTT CCT AAT CGG ACA GAT GTT CAG TGC CAG CAC CGG TGG CAG AAA GTA TTA
Phe Leu Pro Asn Arg Thr Asp Val Gln Cys Gln His Arg Trp Gln Lys Val Leu
   500
AAC CCA GAA CTT ATC AAA GGT CCA TGG ACT AAA GAG GAG GAT CAA AGG GTA ATA
Asn Pro Glu Leu Ile Lys Gly Pro Trp Thr Lys Glu Glu Asp Gln Arg Val Ile
                                       ▼ Hae II                 600
GAA CTC GTG CAG AAA TAC GGT CCA AAG CGC TGG TCG GTC ATT GCT AAG CAT TTG
Glu Leu Val Gln Lys Tyr Gly Pro Lys Arg Trp Ser Val Ile Ala Lys His Leu
                                                           650
AAG GGA AGG ATT GGA AAA CAG TGC AGG GAG AGG TGG CAC AAC CAT CTG AAT CCA
Lys Gly Arg Ile Gly Lys Gln Cys Arg Glu Arg Trp His Asn His Leu Asn Pro
                                                      700
GAA GTG AAG AAA ACC TCC TGG ACA GAA GAG GAA GAT AGA ATT ATT TAC CAG GCA
Glu Val Lys Lys Thr Ser Trp Thr Glu Glu Glu Asp Arg Ile Ile Tyr Gln Ala
                                                 750
CAC AAG AGA CTG GGA AAC AGA TGG GCA GAA ATT GCA AAG TTG CTG CCT GGA CGG
His Lys Arg Leu Gly Asn Arg Trp Ala Glu Ile Ala Lys Leu Leu Pro Gly Arg
                                       ▼Eco RI 800
ACT GAT AAC GCT ATC AAG AAC CAC TGG AAT TCC ACC ATG CGC CGG AAG GTC GAG
Thr Asp Asn Ala Ile Lys Asn His Trp Asn Ser Thr MET Arg Arg Lys Val Glu
                                         850
CAG GAG GGT TAC CTG CAG GAG TCC TCC AAA GCC GGC CTG CCC TCG GCA ACC ACC
Gln Glu Gly Tyr Leu Gln Glu Ser Ser Lys Ala Gly Leu Pro Ser Ala Thr Thr
                                    900
GGC TTC CAG AAG AGC AGC CAC CTG ATG GCC TTT GCC CAC AAC CCA CCT GCA GGC
Gly Phe Gln Lys Ser Ser His Leu MET Ala Phe Ala His Asn Pro Pro Ala Gly
                                950
CCG CTC CCG GGG GCC GGC CAG GCC CCG CTG GGC AGT GAC TAC CCC TAC TAC CAC
Pro Leu Pro Gly Ala Gly Gln Ala Pro Leu Gly Ser Asp Tyr Pro Tyr Tyr His
                         1000
ATT GCT GAG CCA CAA AAT GTC CCT GGT CAG ATC CCA TAT CCA GTA GCA CTG CAT
Ile Ala Glu Pro Gln Asn Val Pro Gly Gln Ile Pro Tyr Pro Val Ala Leu His
                   1050
GTA AAT ATT GTC AAT GTT CCT CAG CCA GCT GCT GCA GCT ATT CAG AGA CAC TAT
Val Asn Ile Val Asn Val Pro Gln Pro Ala Ala Ala Ala Ile Gln Arg His Tyr
              1100
AAT GAT GAA GAC CCT GAG AAA GAA AAA CGA ATA AAG GAA TTA GAG TTG CTA CTT
Asn Asp Glu Asp Pro Glu Lys Glu Lys Arg Ile Lys Glu Leu Glu Leu Leu Leu
```

```
   ▼ Sal I
 ATG TCG ACT GAG AAT GAA CTG AAA GGG CAG CAG GCA TTA CCA ACA CAG AAC CAC
 MET Ser Thr Glu Asn Glu Leu Lys Gly Gln Gln Ala Leu Pro Thr Gln Asn His
1200                                                                  1250
 ACA GCA AAC TAC CCC GGC TGG CAC AGC ACC ACG GTT GCT GAC AAT ACC AGG ACC
 Thr Ala Asn Tyr Pro Gly Trp His Ser Thr Thr Val Ala Asp Asn Thr Arg Thr
                                                               1300
 AGT GGT GAC AAT GCA CCT GTT TCC TGT TTG GGG GAA CAT CAC CAC TGT ACT CCA
 Ser Gly Asp Asn Ala Pro Val Ser Cys Leu Gly Glu His His His Cys Thr Pro
                           ▼ end E26 homology         1350
 TCT CCA CCA GTG GAT CAT GGT TGC TTA CCT GAG GAA AGT GCG TCC CCC GCA CGG
 Ser Pro Pro Val Asp His Gly Cys Leu Pro Glu Glu Ser Ala Ser Pro Ala Arg
                                                  1400
 TGC ATG ATT GTT CAC CAG AGC AAC ATC CTG GAT AAT GTT AAG AAT CTC TTA GAA
 Cys MET Ile Val His Gln Ser Asn Ile Leu Asp Asn Val Lys Asn Leu Leu Glu
                                             1450
 TTT GCA GAA ACA CTC CAG TTA ATA GAC TCC TTC TTA AAC ACA TCG TCC AAT CAC
 Phe Ala Glu Thr Leu Gln Leu Ile Asp Ser Phe Leu Asn Thr Ser Ser Asn His
                                         1500
 GAG AAT CTG AAC CTG GAC AAC CCT GCA CTA ACC TCC ACG CCA GTG TGT GGC CAC
 Glu Asn Leu Asn Leu Asp Asn Pro Ala Leu Thr Ser Thr Pro Val Cys Gly His
                                    1550           ▼end AMV homology
 AAG ATG TCT GTT ACC ACC CCA TTC CAC AGG GAC CAG ACT TTC AAA ACT CAG AAG
 Lys MET Ser Val Thr Thr Pro Phe His Arg Asp Gln Thr Phe Lys Thr Gln Lys
                               1600
 GAA AAC CAC GTT TTC AGA ACT CCT GCA ATC AAG AGG TCA ATA TTA GAG AGC TCT
 Glu Asn His Val Phe Arg Thr Pro Ala Ile Lys Arg Ser Ile Leu Glu Ser Ser
                          1650
 CCA AGA ACA CCC ACT CCA TTC AAA AAC GCA CTT GCA GCT CAG GAA ATC AAA TAT
 Pro Arg Thr Pro Thr Pro Phe Lys Asn Ala Leu Ala Ala Gln Glu Ile Lys Tyr
                     1700                                    ▼ Bgl II
 GGT CCT TTG AAG ATG CTG CCT CAA ACT CCG ACT CAT CTT GTA GAA GAT CTG CAG
 Gly Pro Leu Lys MET Leu Pro Gln Thr Pro Thr His Leu Val Glu Asp Leu Gln
                1750
 GAC GTT ATC AAG CAG GAG TCG GAG GAA TCT GCG ATA GTG GCA GGG CTA CAT GAA
 Asp Val Ile Lys Gln Glu Ser Glu Glu Ser Ala Ile Val Ala Gly Leu His Glu
           1800
 AGT GGA CCC CCT TTG CTG AAG AAA ATC AAA CAA GAG GTG GAG TCT CCT ACA GAT
 Ser Gly Pro Pro Leu Leu Lys Lys Ile Lys Gln Glu Val Glu Ser Pro Thr Asp
      1850
 AAA GCT GGA AAT TTT TTT TGC TCA AAT CAC TGG GAA GGG GAA AAC CTG AAC ACT
 Lys Ala Gly Asn Phe Phe Cys Ser Asn His Trp Glu Gly Glu Asn Leu Asn Thr
                                                                1950
 CAG CTC TTT ACA CAT GCA TCT ACC ATG GAA GAT GTG CCA AAT CTT CTT ACC AGC
 Gln Leu Phe Thr His Ala Ser Thr MET Glu Asp Val Pro Asn Leu Leu Thr Ser
                                                           2000
 TCC ATT TTA AAG ATG CCA GTG TCG GAA GAG GAG GGC AGT TTC CAC AAA GCA TTT
 Ser Ile Leu Lys MET Pro Val Ser Glu Glu Glu Gly Ser Phe His Lys Ala Phe
                                                       2050
 GCC GTA CCT AGG AAC CGG CCA CTA GCT AGC CCA CTG CAG CAT CTG AAC AAT GCT
 Ala Val Pro Arg Asn Arg Pro Leu Ala Ser Pro Leu Gln His Leu Asn Asn Ala
                                                  2100
 TGG GGG TCG GCG TCT TGC GAG AAG ACC GAG GAC CAG ATG GCC TTG ACT GAC CAG
 Trp Gly Ser Ala Ser Cys Glu Lys Thr Glu Asp Gln MET Ala Leu Thr Asp Gln
                                             2150
 GCA CGC AAG TAC ATG GCC GCG TTC CCA ACC CGG ACT CTG GTG ATG TGAAAGGGCC
 Ala Arg Lys Tyr MET Ala Ala Phe Pro Thr Arg Thr Leu Val MET ***
                               2200
 GATGGACTTC TCCGGAGAAG CATTATGGTT GGCAAACACT TCTCGTTC
```

Fig. 2 The nucleotide sequence of the coding region of the c-*myb* cDNA clone, obtained using the method of Maxam and Gilbert[23]. The amino-acid sequence predicted for the proto-oncogene product is shown below the nucleotide sequence. Pertinent restriction enzyme sites and v-*onc*-homologous regions are shown. The two terminator codons in-frame with the reading frame upstream and downstream are indicated by asterisks. Arrows indicate restriction enzyme cleavage sites or beginning and end of v-*myb*-homologous sequences.

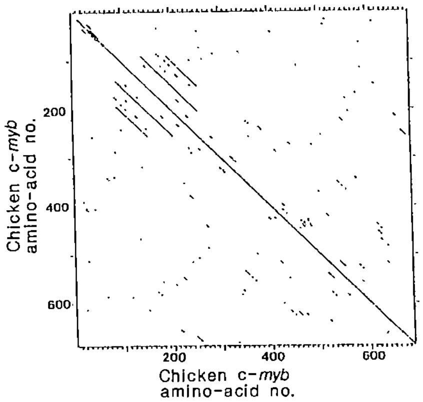

Fig. 3 Dot-matrix analysis for internal repeats within the chicken c-*myb* coding region. Segments of 25 amino acids were compared sequentially with each 25-amino-acid-long segment of the protein. A dot was placed on the matrix at the appropriate position when the total mutation data matrix score for the comparison was ≥20.

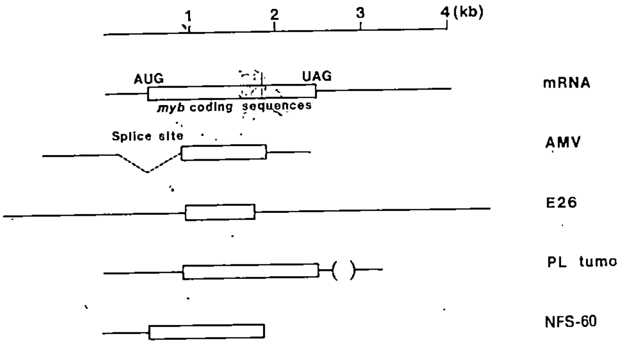

Fig. 4 Structural comparison of the *myb*-coding region of chicken c-*myb* mRNA (normal) with activated forms of *myb* mRNAs in the AMV and E26 viruses and PL and NFS-60 tumour cells. Boxes represent *myb*-coding sequences; straight lines represent flanking viral (AMV and E26) or cellular (PL tumours and NFS-60) sequences. The parentheses in PL tumour RNA indicate rearrangements at the 3′ end which have not yet been precisely defined.

of the three tandem repeats in the two v-*myb* proteins which may also be relevant for transformation.

In addition to the avian systems which suggest that deletions are important in the activation of *myb*, two other systems support this hypothesis. Analysis of the rearranged mouse c-*myb* genes in the Abelson plasmacytoid lymphosarcomas (ABPLs) induced by a mixture of Abelson murine leukaemia virus and Moloney murine leukaemia retrovirus (M-MuLV), reveals that the genomic insertion of the virus occurs in the intron immediately upstream of the sequences corresponding to nucleotide 450 in the chicken cDNA clone. This results in a deletion of the amino-terminal sequences in the aberrant c-*myb* transcripts analogous to that found in AMV (S. Lavu and E.P.R., in preparation) (Fig. 4).

A second example of activation of murine c-*myb* is seen in the NSF-60 tumour cell line induced by Cas-Br-M-MuLV[21]. In this myeloid tumour cell line the integration of the provirus has occurred at the 3′ end of the *myb* locus, which results in the synthesis of a truncated mRNA. We have recently mapped the point of integration of this virus to the point that corresponds to nucleotide 1,425 in the c-*myb* sequence presented in Fig. 2. This suggests that the *myb* protein produced in these tumour cells contains a carboxy-terminal deletion similar to that found in the AMV and E26 *myb* proteins.

Our DNA sequence comparison shows that the normal *myb* protein contains additional amino acids at the N-terminal and/or the C-terminal end when compared with any of the activated forms of this protein. The structural changes that occur as a result of these deletions probably contribute to the oncogenic potential of the proteins. The availability of chicken c-*myb* cDNA clones will allow us to make various retroviral constructs directly to test our hypothesis.

We thank Dr J. Jenson for help with computer analysis and Dr A. M. Skalka for a critical review of the manuscript.

Received 25 September; accepted 12 December 1985.

1. Baluda, M. A. & Goetz, I. E. *J. Virol.* **15,** 185–199 (1961).
2. Moscovici, C. *Curr. Topics Microbiol. Immun.* **71,** 79–96 (1975).
3. Franchini, G., Wong-Staal, F., Baluda, M. A., Lengel, C. & Tronick, S. A. *Proc. natn. Acad. Sci. U.S.A.* **80,** 7385–7389 (1983).
4. Katzen, A. L., Kornberg, T. B. & Bishop, J. M. *Cell* **41,** 449–456 (1985).
5. Mushinski, J. F., Potter, M., Bauer, S. & Reddy, E. P. *Science* **220,** 795–798 (1983).
6. Shen-Ong, G. L. C., Potter, M., Mushinski, J. F., Lavu, S. & Reddy, E. P. *Science* **226,** 1077–1080 (1984).
7. Lavu, S., Mushinski, J. F., Shen-Ong, G. L. C., Potter, M. & Reddy, E. P. *Cancer Cells* **3,** 301–306 (1985).
8. Pelicci, P.-G., Lanfrancone, L., Brathwaite, M. D., Wolman, S. R. & Dalla-Favera, R. *Science* **224,** 1117–1121 (1984).
9. Alitalo, K. *et al. Proc. natn. Acad. Sci. U.S.A.* **81,** 4534–4538 (1984).
10. Kozak, M. *Nucleic Acids Res.* **12,** 857–872 (1984).
11. Klempnauer, K. H. *et al. Cell* **33,** 345–355 (1983).
12. Maizel, J. & Leuk, R. *Proc. natn. Acad. Sci. U.S.A.* **78,** 7665–7669 (1981).
13. Klempnauer, K. H., Symonds, G., Evans, G. I. & Bishop, J. M. *Cell* **37,** 537–547 (1984).
14. Boyle, W. J., Lampert, M. A., Lipsick, J. S. & Baluda, M. A. *Proc. natn. Acad. Sci. U.S.A.* **81,** 4265–4267 (1984).
15. Moelling, K. *et al. Cell* **40,** 983–990 (1985).
16. Gonda, T. J., Gough, N. M., Dunn, A. R. & de Blaquiere, J. *EMBO J.* **4,** 2003–2008 (1985).
17. Rushlow, K. E. *et al. Science* **216,** 1421–1423 (1982).
18. Klempnauer, K. H., Gonda, T. J. & Bishop, J. M. *Cell* **31,** 453–463 (1982).
19. Nunn, M. F., Seeberg, P. H., Moscovici, C. & Duesberg, P. H. *Nature* **306,** 391–395 (1983).
20. Boyle, W. J., Lipsik, J. S., Reddy, E. P. & Baluda, M. A. *Proc. natn. Acad. Sci. U.S.A.* **80,** 2834–2839 (1983).
21. Weinstein, Y., Ihle, J. N., Lavu, S. & Reddy, E. P. *Proc. natn. Acad. Sci. U.S.A.* (submitted).
22. Gubler, U. & Hoffmann, B. J. *Gene* **5,** 263–269 (1983).
23. Maxam, A. M. & Gilbert, W. *Meth. Enzym.* **65,** 499–560 (1980).

Corrigendum

Major shear zones and autochthonous Dalradian in the north-east Scottish Caledonides

W. A. Ashcroft, B. C. Kneller, A. G. Leslie & M. Munro

Nature **310,** 760–762 (1984)

THE following reference should have appeared in support of this letter: Gallagher, J. W. thesis, Univ. Aberdeen (1983).